SESSION

FUZZY LOGIC + FUZZY SYSTEMS + APPLICATIONS

Chair(s)

TBA

Fuzzy Logic Based Sensor Skin for Robotic Applications

E. Meister, I. Zilberman, and P. Levi
Institute of Parallel and Distributed Systems, University of Stuttgart, Germany

Abstract— *Tactile sensors play an important role in many robotic applications providing information about shape, roughness, frictions and acting forces. However, it is challenging cover large robots with tactile sensors. In this paper we introduce a modular tactile sensor skin built on master and slave principle. The structure of the sensor skin was inspired by the biological multi layered skin from humans. Modular design principle allows covering different flat and rough robot geometries. The skin is able to detect tactile and pressure sensor values and is therefore applicable to different applications. Fuzzy logic based data fusion method allows the input values to be fuzzy while receiving numerical values as the output. This concept reduces the number of required sensor to a minimum and consequently also the computational effort and production costs.*

Keywords: Tactile sensing; Artificial Sensor Skin; Fuzzy logic; Modular Master-Slave design.

1. Introduction

Over the past view decades, the attitude towards robots and their acceptance in our environment has changed. Robots are stepwise bridging the gap between being a pure executive machine and becoming fully autonomous systems that are capable to fulfil tasks in our daily life or in structural manufacturing environment without human intervention. To achieve this goal, intelligent sensors play an important role providing the capabilities to sense the environment and the internal states of the robot. Inspired by humans and mammals with visual, auditory, somatosensory, gustatory and with the olfactory sensing capabilities, in robotics these sensory systems are imitating by equipping the robots with a variety of different sensors. Recently, the visual and auditory sensory systems have been experiencing tremendous progress and are already used in many robotic applications. The gustatory and the olfactory senses are difficult to imitate on robots because they are based on complex chemical reactions. However, the field of research related to an artificial somatosensory sensor systems covering the sense of touch, temperature, body position etc. are currently experiencing a rapid growth [4], [5], [16]. In a human body, the 'sense of touch' is provided by millions of skin receptors covering the whole body. In most cased we use hands to grasp and to recognize the objectt's properties such as shape, roughness, softness of the surface, size etc. Therefore, a lot of research in humanoid robotics is focusing on robotic hand applications [2],[13],[1]. However, in an unstructured or hazardous environment, humanoid shape of robot can be impractical or inefficient. Modular self-reconfigurable robots can solve the problem because they are able to reconfigure their shapes and hence are able to adapt to different situations and environments. Self-adaptivity is on the one hand advantageous but on the other hand implicates high complexity for coordination and control. Such systems strongly rely on information provided by different sensors. Therefore, the capability to recognize and sense the forces and pressures acting from each individual module is of great importance, but to sense big parts of the robots shape is still a technological challenge. We speak about artificial sensor skin when more than a few sensors cover a big robot surface. Such a sensor skin needs to fulfil several important requirements for the hardware design such as flexibility, sensitivity or reliability and therefore often requires a cost intensive realization on micro or nano level. Most of the existing artificial skin systems are based on resistive, capacitive, piezoresistive or magnetic transduction methods measuring forces, pressures or proximity. A good overview about the state-of-the-art of tactile sensors and artificial skin systems is given in [14],[9] or in [3].

The paper is organized in the following way. In Section 2 we explain the bio-inspired concept of modular sensor skin. Two different sensing principles, the optical and the capacitive method which are used in this concept are explained in this section. The modular hardware design is introduced in Section 3. In Section 4 we introduce the data processing and data fusion approach based on the Fuzzy logic theory. Implementation strategy as well as software structure are explained in Section 5. In Section 6 we show different experimental results and application scenarios. Sections 7 concludes the work and gives a short outlook.

2. Bio-Inspired Concept

The skin concept was inspired by the human skin, which consists of three layers: the water-repellent *epidermis* layer, protecting the body from infections and poisons, the *dermis* layer responsible for tensile strength, and the basement membrane layer *subcutis* providing protection against external physical influences and also acting as energy storage [6]. All layers are subdivided into more layers providing several types of mechanoreceptors, which react to different stimuli. Human skin combines multiple receptors in order to reach wide operation range. In artificial skin, this means that different kinds of sensor values need to be fused by applying

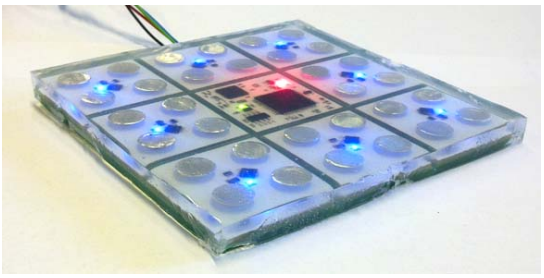

Fig. 1: Artificial sensor skin.

sensor fusion methods. Several sensor fusion techniques such as Fuzzy logic, Dempster-Shafer theory (DST), Kalman filter, Bayesian or Artificial Neural Networks (ANNs) are possible for systems with uncertainties. Fuzzy logic has been chosen as a favourite technique between all these options because it provides an adaptive method that can deal with uncertain data and allows good rule based approximation by absence of exact model of a system. As a result of different input values one numerical output value is calculated that can be directly related to a force or as a pressure value. Additionally, Fuzzy logic based approaches are not computationally and memory intensive and can run as a small stand-alone application on embedded devices. After clarifying the general concept idea for the skin several specifications have been done in order to reduce the complexity for the hardware design and realization:

1) Modularity and Scalability: The skin should be extendable to different structures and shapes.
2) Flexibility and Compliance: The skin hardware should be able to be applied on flat as well as on rough surfaces providing certain degree of bending. Additionally, the used material should provide compliance properties.
3) Master and Slave principle: The sensor pre-processing should be fused to one master unit avoiding to have microprocessors in each skin module, however at the same time keeping wiring as simple as possible.
4) Manufacturability and Maintenance: Should be easy to produce and to maintain without immense effort.
5) Robustness: The skin should resist against strong forces.
6) Adaptivity: Should be adaptive to diverse high and low pressure applications.
7) Attractiveness: The skin should give an attractive look to the robot because it is able to cover big parts of the robot.
8) Power Consumption: The high number of sensors requires that all sensors should consume as little power as possible.

The sensor skin (Figure 1) described in this paper is designed based on the dispersive reflexion principle of the infrared (IR) light in diffuse and flexible materials. The motivation was to utilise the material properties and hence to reduce the number of sensors. The level of reflexion is the quantity that can be related to the distance between the optical sensor and the reflexion layer and correspondingly between the acting load and the distance. The idea to use light as a parameter for measuring forces and loads was also used in [18] and in [12]. Ohmura et al. use visible light reflexions in urethane foam in order to determine the deformation. In [12] infrared sensors embedded into rapid-prototyped elastomer material are used to measure proximity. With the novel skin design concept we are able to detect both, the proximity as well as soft and heavy loads acting on it by using optical as well as capacitive sensors. Reflexion layer allows us to use soft and simultaneously transparent materials. Sensor fusion is based on the Fuzzy logic based approach that reduces the computational complexity and therefore enables the skin to be implemented as a stand-alone embedded sensor.

2.1 Optical method

Light has the property of reflexion and dispersion in transparent or diffuse materials. The level of dispersion depends on the chosen material. Combining these properties together open new possibilities to use light for measuring forces or deformations. When light is dispersed and reflected within the silicone it covers an orbital area surrounding the sensor. Therefore, a low number of IR sensors allows to sense big areas (Figure 2). The maximum distance between sensors that is required to sense the surface without optical gaps is $20mm$. One of the advantages of optical method is

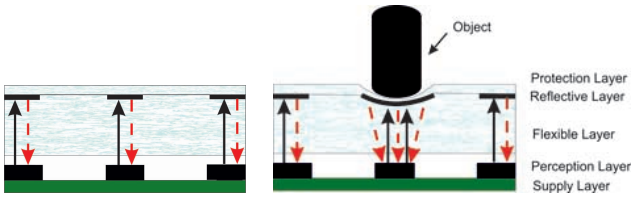

(a) (b)

Fig. 2: IR light reflexion principle of the sensor skin. (a) Without load; (b) With load.

a low degree of complexity for electronic design. Standard reflective sensors such as Sharp $GP2S60$ sensor can be used to build the skin system. In case when no load is acting on the surface, the light produced by the infrared sensor is reflecting by the reflection layer homogeneously through the silicone material settling around one value. The current value in the sensor is changed rapidly when the distance between the reflecting layer and the sensor is decreasing (Figure 2). This dependency between the distance and the collector current is scaled down and is used as force/pressure estimation. This principle depends strongly on the used viscoelastic material. Silicones seems to be a proper material to fulfil the requirements and by choosing from different

mixtures between component A and B different elasticity can be achieved. One important factor that should not be neglected is the nonlinear relaxation of soft materials. The stress relaxation can be obtained by following equations:

$$E = \frac{\sigma}{\epsilon}, where \qquad \sigma(t) = \sigma_0 e^{-\lambda t}, \tag{1}$$

where E is the elastic module, ϵ the constant strain and σ determines the stress depending on time and the relaxation time. The process is reversible as soon the deformation stays in allowed ranges and is not too excessive. In this case the material is able to recover to original stiffness in a short time. This principle allows to measure forces or pressure for a wide range of load, however due to the mentioned nonlinear relaxation not for soft touch applications.

2.2 Capacitive method

Capacitive sensing principle is a common technique used in tactile and touch based technologies. Additional capacitive sensing principle has been included in order to increase the sensitivity range of the skin. A capacitive sensor is simply a pair of adjacent electrodes. The main principle of all non contact capacitive sensors is measuring of the capacitance. The equation for calculation of the capacitance C of a parallel electrically conductive plate is

$$C = \frac{\epsilon * A}{d}, \tag{2}$$

where ϵ is the permittivity of the dielectric between two electrodes, A is the overlap area of the parallel plates and d is the clearance of those plates. It is obvious, that with the same overlap area and dielectric, the capacitance of the sensor depends only on the distance between the plates and is inversely proportional to it. We use integrated capacitive sensors where both electrodes of the capacitor are arranged in the same plane of the PCB. The structure of the capacitor is illustrated in Figure 3(a) and 3(b). To achieve homogeneous field profile a symmetric adjustment of the electrodes has been used. With this design we are able to detect very soft touch on the surface of the skin. A disadvantage of the

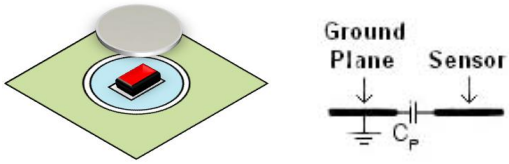

(a) (b)

Fig. 3: (a) Principle of integrated capacitive sensor; (b) Electrodes of the capacitor in the plane.

capacitive sensing technique is that sensors are only able to recognize interaction with a conductive object. To solve this problem a conductive plate is used as a reflective layer. This plate acts as reflector for infrared light and at the same time as a conductive layer changing the electromagnetic field according to the distance between the plate and the planar capacitor. In combination of elastic silicon layer it is possible to achieve a low hysteresis. Silicon acts also as dielectric in this arrangement and increases an electric flux density, which delivers a better sensing property. To achieve appropriate field profile the right size of the capacitive electrode and the gap between the pad and ground layer have been chosen. Before implementing the capacitive method a simulation in COMSOL[1] Multiphysics tool has been done to guarantee that the changes in capacitance will be enough to resolve on a microprocessor. As result an estimated

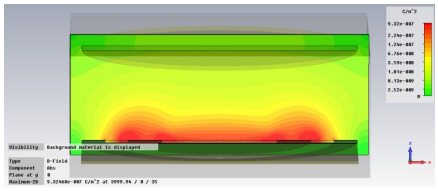

(a)

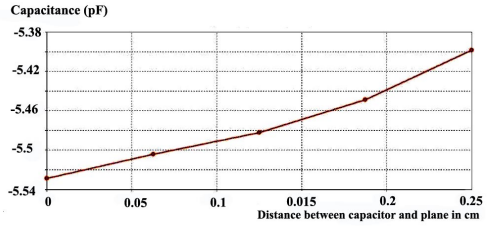

(b)

Fig. 4: (a) Electric field profile of capacitive sensors; (b) Capacity analysis dependent on distance.

capacitance of the developed integrated sensor is obtained as a function of distance between PCB plane and conductive plate Figure 4(b) and we also received visualization of the electric field profile shown in Figure 4(a).

3. Hardware

The hardware realization is based on the modular design principle consisting of one master module that carries the embedded microprocessor and a variable number of slave patches equipped with sensors. Both master and slave modules are mounted on the supply layer PCB. Different topologies for the skin can be built by connecting the patches together to one skin pattern. We call the complete system with one master and more than one slave as a Skin Unit (SU) (Figure 1).

3.1 Slave Module

Slave module has a simple structure consisting of four infrared sensors and four integrated planes for capacitive

[1]COMSOL Multiphysics is a finite element analysis solver and simulation software for physics and engineering applications

sensors (Figure 5). For this reason each slave has eight analogue signals connected to the master module. Routing all lines directly to the processor requires for n slave module $n \times 8$ signal lines. Because of limited number of available ADC pins on the microprocessor the lines need to be multiplexed. Multiplexing of signals also simplifies the

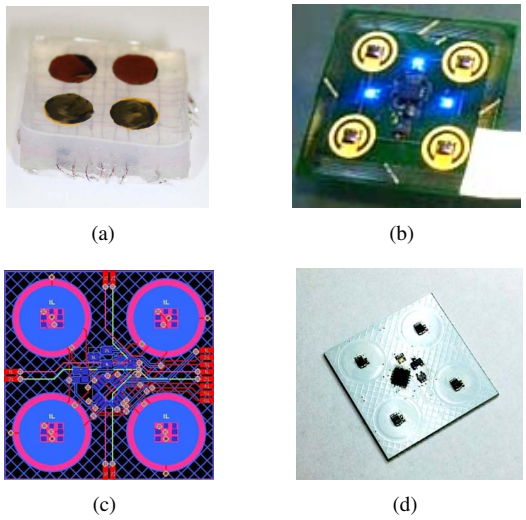

(a) (b) (c) (d)

Fig. 5: (a) First slave prototype [11]; (b) Slave module produced on flexible substrate; (c) Layout of slave module; (d) Final prototype produced on stiff PCB.

routing problem and allows the extension of slave modules in one skin system. Capacitive sensors are very sensitive to external influences, therefore the top layer of each slave has a grid-like structure ground shape for shielding and a conductive plate on the bottom layer.

3.2 Master Module

The master module controls all slave modules that are connected to it and is responsible for the data processing and for communication control. It contains a $32bit$ Programmable System on Chip (PSoC) main processor from Cypress [8] that enables to use the skin as a stand-alone embedded tool. This novel technology is similar to Field Programmable Gate Array (FPGA) however with much lower power consumption. PSoC is built based on Universal Digital Blocks (UDBs) providing diverse functionalities such as ADC, PWM, I^2C, SPI etc. which can be multiple assigned to general purpose input/output pins (GPIOs) of the processor and therefore makes the layout design very flexible. This PCB includes also a high-speed USB peripheral controller for in-system-programming (ISP) and for live debugging via the USB. The board contains also all required periphery for supplying the slave modules with power. The inter-master communication is possible via I^2C or via Controller Area Network (CAN) multi-master bus systems and allows to connect more than one skin systems.

3.3 Supply Layer

The complete skin is a multi-layer design shown in Figure 6. The lowest layer is the supply and signal layer that connects the master module with the slaves providing channels for communication, pressure signal transfer and power supply. Compared to human skin this layer has similar functionality like the *dermis layer* bundling all nerve cords. Figure 6(a) shows coloured address lines (red and blue) for different rows and columns. These signal lines select and activate the slaves. Because of narrow interface of slave and master modules the structure of the skin unit depends on the hardware structure of the supply layer. The layer can be built

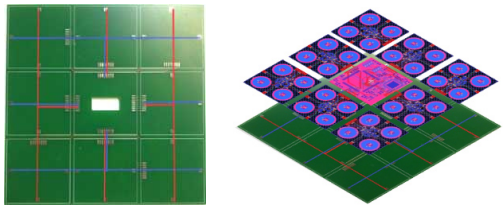

(a) (b)

Fig. 6: (a) Signal routing layer with signal lines for rows and columns; (b) Skin principle.

by using either rigid PCB materials or by flexible substrates for flexible skin applications.

4. Fuzzy Logic Based Sensor Fusion

The skin system proposed in this paper was inspired by the human skin with the goal to sense the whole skin surface without spatial gaps. However equipping the whole skin surface with sensors requires a huge hardware and processing effort. To avoid this effort and complexity, optical method has been chosen with the combination of Fuzzy logic based approach that allows reducing the number of sensors by estimating the values instead. The final skin design end up in a grid-like structure with the sensors placed $20mm$ away from each other. In the case when pressure is applied between two or more sensors without touching the sensor area directly, it becomes difficult to determine the resulting pressure. To estimate this value a cascade of three Fuzzy logic systems is used. The whole procedure is shown in the flowchart, see Figure 7.

The first fuzzy system (FS1) is used for the fuzzification of the digital values from each sensor and maps sensor values to linguistic pressure values. The sensor values are between 0 and 254 while linguistic values are of 'light', 'normal', 'heavy' and 'very heavy' character. Two different membership functions are used to describe different classes of pressure (Figures 8(a)-8(c)). The first function is sigmoidal

$$f(x, a, c) = \frac{1}{1 + e^{-a(x-c)}}, \tag{3}$$

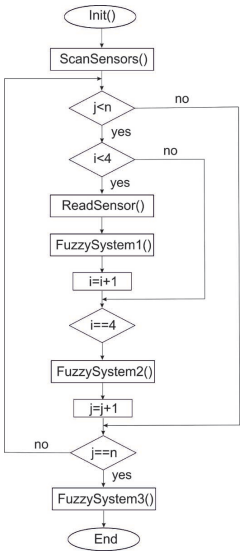

Fig. 7: Program flowchart of the skin system framework.

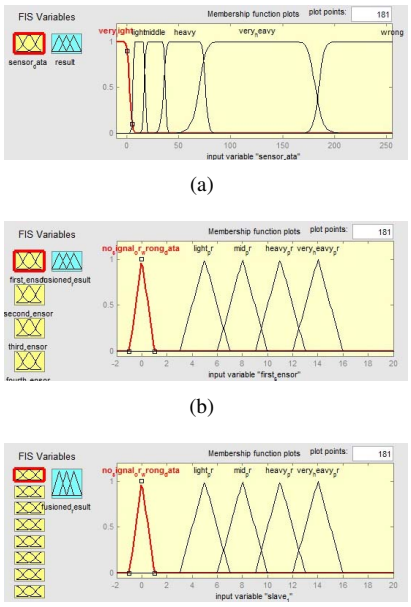

Fig. 8: Three Fuzzy Systems used for sensor fusion. (a) FS1; (b) FS2; (c) FS3.

where parameters a and c allow to shape the functions as required by application. The second function is the bell curve

$$f(x,a,b,c) = \frac{1}{1+\left|\frac{x-c}{a}\right|^{2b}}, \tag{4}$$

where parameter b is usually positive and the parameter c determine the centre of the curve.

The second fuzzy system (FS2) calculates the pressure of a single slave and has four input sets for all four sensors and one output set for the resulting force (Figure 8(b)). The fuzzy system on the highest level is the third fuzzy system (FS3), which collects the data from FS2 and according to these results, calculates the resulting pressure applied to the whole skin system. In a skin which consists of one master and eight slaves modules eight input and one output is required (Figure 8(c)). In case when pressure is applied to the skin on multiple points at the same time for many applications it is necessary to determination the resulting force. The calculation is based on vector analysis and for a single slave can be calculated as follows:

$$\begin{pmatrix} x \\ y \end{pmatrix} = \left(\tfrac{S1}{\Sigma}\right) * \begin{pmatrix} d \\ d \end{pmatrix} + \left(\tfrac{S2}{\Sigma}\right) * \begin{pmatrix} -d \\ d \end{pmatrix} + \left(\tfrac{S3}{\Sigma}\right) * \begin{pmatrix} d \\ -d \end{pmatrix} + \left(\tfrac{S4}{\Sigma}\right) * \begin{pmatrix} -d \\ -d \end{pmatrix}, \tag{5}$$

where S_i are the digital values from the four sensors, $\Sigma = S1+S2+S3+S4$, and d is the distance from the origin of slave sensor to the corresponding sensor. The same principle is used as well for the calculation of the resulting position for the whole skin system.

5. Implementation

The first prototype of the skin has been presented in [11]. At this stage one slave prototype was built in order to proof the idea. The slave was directly connected to a PSoC evaluation kit from cypress that acts as a master module and the sensor data were sent via Universal Asynchronous Receiver Transmitter (UART) interface to the host computer. One Fuzzy System based on MATLAB Fuzzy Toolbox [19] was implemented to represent the data of the four optical sensors as linguistic variables. Simple Graphical User Interface (GUI) visualized the sensor data in a three dimensional mesh. In this paper we present the extended version of the skin and of the evaluation tool. In the current design all three Fuzzy Systems are implemented to fuse the data from the whole skin. The principle is shown in Figure 9. The real

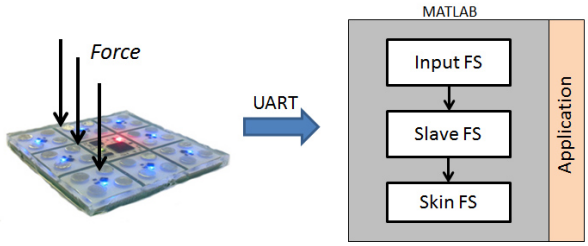

Fig. 9: Working principle of the skin with Fuzzy Systems.

skin deformation can be observed on the screen through the deformation of the two dimensional surface (Figure 10). On the left side of the GUI marked with (1), the axes show visual representation of the skin deformation according to received raw sensor data. Additionally, these values can be observed in the "RAW DATA" matrix (2). On the right side of the

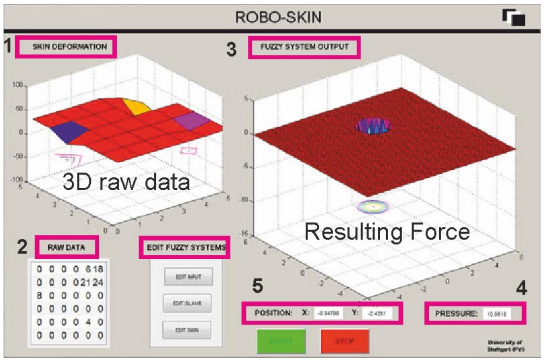

Fig. 10: GUI for monitoring and parameter adaptation.

GUI the axes show graphical representation of the resulting value calculated by all three fuzzy systems (3) as well as the numerical value (4) for it. This value is the result after the calibration process of the skin and its ranges can differ dependent on the used material or different composition of the silicone components. The estimated coordinates for the resulting position of load can also be read (5).

6. Experimental Results

The current skin design is considered to use for modular robot applications with Backbone and Scout robots [7],[10], which are developed in projects Symbrion [17] and Replicator [15]. The goal is to measure the normal forces on the ground and to detect collisions with obstacles or other robots (Figure 13(a)-13(d)). Therefore, for this kind of application we choose a hard silicone composition admitting heavy loads up to $10kg$.

Figures 11(a) and 11(b) show the force responses from one slave element when force is applied in the normal direction at one point and when it is applied sidewise. As can be observed in these figures this difference is clearly detectable. This information can be used to approximate shear forces on the surface of the skin. In this experiment only optical transduction method for pressure measurement was use without activating the capacitive sensors. Force response values are intrinsically nonlinear because of nonlinear relaxation of the silicone. However, Fuzzy logic based approach does not require exact sensor values as an input and therefore even with the sensor values accuracy of about $10-15\%$ it is still enough to determine a good approximation for the resulting force. The evaluation of the approach can be done by using the GUI tool (Figure 10) introduced in the previous section. The sampling rate for the sensors is about $100ms$ therefore forces applied on multiple points can be detected and visualized within GUI. Figures 12(a) and 12(b) show two examples when pressure is applied to one or to multiple points. Another analysis for one slave has been done for the accuracy of the optical based approach. For this experiment slave of size $40 \times 40mm$ has been divided into nine parts

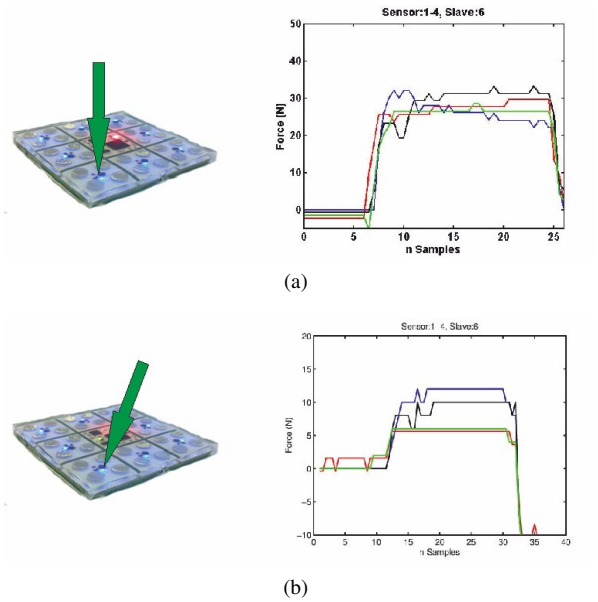

Fig. 11: Different loads applied to one slave of the skin. (a) Force applied in normal direction; (b) Force applied at an oblique angle.

$(3 \times 3$ mesh-like structure). The distance from one sensor to another is $20mm$ and hence only the half to the centre of the skin module. In this experiment we applied repeated constant pressure to different points of the skin collecting statistical values (Table 1). As can be observed from the

Table 1: Accuracy analysis of slave.

Force applied on (X/Y)	Average values	Standard deviation
-1/-1	-0.72/-0.2	0.18/0.31
-1/0*	-0.86/0.8	0.05/0.07
-1/-1	-0.77/0.79	0.09/0.08
0/-1*	0.86/-0.56	0.4/0.15
0/0*	0.6/0.22	0.22/0.29
0/1*	0.48/0.83	0.21/0.09
1/-1	1/-0.93	0/0.15
1/0*	0.88/-0.05	0.29/0.05
1/1	0.78/0.73	0.09/0.14

table, Fuzzy logic based approach is able to detect forces between two sensors (marked with star) where no real sensor is placed. Low standard deviation enables a calculation of the static offset, which can make the sensor more accurate. This analyses show that with given accuracy the skin can be used for diverse robotic platforms such for example the robots Backbone and Scout (Figures 13(a)-13(d). Modular and flexible design allows adapting the shape of the skin and therefore can also find different other applications in areas such as healthcare, eldercare, domestic, entertainment and many others.

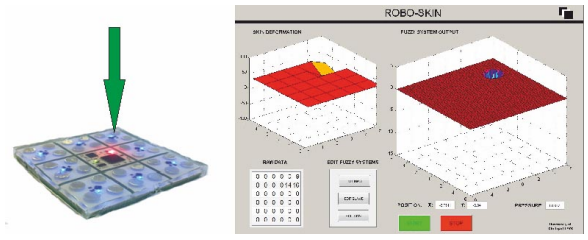

(a)

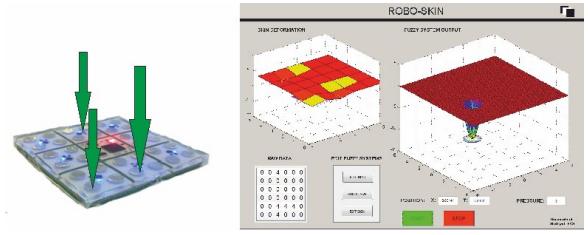

(b)

Fig. 12: Applied forces to: (a) single point; (b) to multiple points of the skin (multi-touch capability).

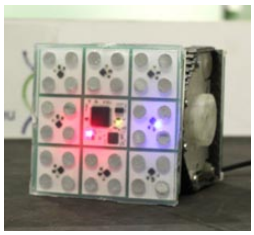

(a)

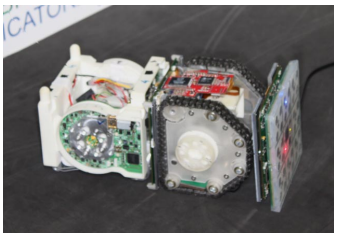

(b)

(c)

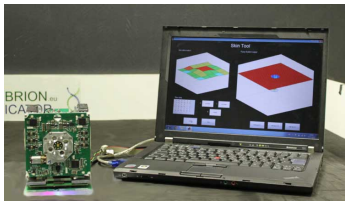

(d)

Fig. 13: Skin applications: (a) Skin on Scout robot; (b,c) Scout with Backbone as a small robot organism; (d) Online parameter adaptation.

7. Conclusion and Future Work

In this paper we present a novel idea for a tactile multi sensor skin based on modular master and slave design principle. General idea of this skin is to measure forces and pressures on the whole skin surface however with a low number of sensors. Two kinds of sensors, optical as well as capacitive sensors are used to range the applied forced from very high to very smooth touching. The hardware structure is inspired from the multi layered human skin providing different functionalities. Compensation of displaced sensors is done by use of Fuzzy logic based sensor fusion method. This concept allows input values to be fuzzy while returning sharp values for the force response. Additionally, the skin is able to determine and to approximate one single point of contact in case when load is acting on multiple points or even on the whole skin surface. This feature is important for model based control algorithms that allow one force response value only. The current prototypes are built on rigid as well as on flexible substrates and allow covering flat and rough robot geometries.

References

[1] G. Cannata, M. Maggiali, G. Metta, and G. Sandini. An embedded artificial skin for humanoid robots. In *Multisensor Fusion and Integration for Intelligent Systems, 2008. MFI 2008. IEEE International Conference on*, pages 434 –438, aug. 2008.

[2] Dirk Göger and Nicolas Gorges and Heinz Wörn. Tactile Sensing for an Anthropomorphic Robotic Hand: Hardware and Signal Processing. In *IEEE International Conference on Robotics and Automation, May 12 - 17, 2009, Kobe, Japan*, 2009.

[3] John Bradley Filip Fuma. A procedure for characterizing tactile sensors. *Technical Reports (CIS)*, 1988.

[4] Yi-Tin Ho, Li-Chen Fu, and Han-Shen Huang. Architecture and implementation of a multisensor system for robotic assembly environment. In *Industrial Electronics, Control, and Instrumentation, 1996., Proceedings of the 1996 IEEE IECON 22nd International Conference on*, volume 1, pages 513 –518 vol.1, aug 1996.

[5] M. Johnsson and C. Balkenius. Sense of touch in robots with self-organizing maps. *Robotics, IEEE Transactions on*, 27(3):498 –507, june 2011.

[6] J. H. Schwartz Kandel, E. R. *Principles of Neuroscience*. New York, McGraw-Hill Health Professions Division., 2000.

[7] S. Kernbach, E. Meister, F. Schlachter, K. Jebens, M. Szymanski, J. Liedke, D. Laneri, L. Winkler, T. Schmickl, R. Thenius, P. Corradi, and L. Ricotti. Symbiotic robot organisms: Replicator and symbrion projects. In *Proc. of Performance Metrics for Intelligent Systems Workshop (PerMIS-08)*, pages 62–69, Gaithersburg, MD, USA, 2008.

[8] F. Krüger. *PsoC Mikrocontroller*. Franzis, 2006.

[9] M. H. Lee and H.R. Nicholls. Tactile sensing for mechatronics - a state of the art survey. *Mechatronics*, 9:1–33, 1999.

[10] P. Levi and S. Kernbach, editors. *Symbiotic Multi-Robot Organisms: Reliability, Adaptability, Evolution*. Springer-Verlag, 2010.

[11] E. Meister and D. Kryvoukhov. An artificial tactile sensor skin for modular robots. In *Proc. of MULTIBODY DYNAMICS 2011, ECCOMAS Thematic Conference*, 2011.

[12] Philipp Mittendorfer. Humanoid multimodal tactile-sensing modules. *IEEE Transactions on robotics*, 27, 2011.

[13] Sadao Omata and Yoshikazu Terunuma. New tactile sensor like the human hand and its applications. *Sensors and Actuators A: Physical*, 35(1):9 – 15, 1992.

[14] Maurizio Valle Ravinder S. Dahiya, Giorgio Metta and Giulio Sandini. Tactile sensing - from humans to humanoids. *IEEE*, 2009.

[15] REPLICATOR. *REPLICATOR: Robotic Evolutionary Self-Programming and Self-Assembling Organisms, 7th Framework Programme Project No FP7-ICT-2007.2.1*. European Communities, 2008-2012.

[16] S. Ronald. Tactle sensing mechanisms. *International Journal of Robotics Research*, 9(3):3 – 23, june 1990.

[17] SYMBRION. *SYMBRION: Symbiotic Evolutionary Robot Organisms, 7th Framework Programme Project No FP7-ICT-2007.8.2*. European Communities, 2008-2012.

[18] O. Yoshiyuki and K. Yasuo. Conformable and scalable tactile sensor skin for curved surfaces. *IEEE International Conference on Robotics and Automation, Orlando, Florida*, 2006.

[19] Lotfi A. Zadeh. *Fuzzy Logic Toolbox User's Guide, Version 2*. Berkeley, CA, 1995.

Conceptual Space Filter

Scott Imhoff, Palak Thakkar, Joel Shaklee, Thomas Wang, and Kristin Burnett
Raytheon Intelligence and Information Systems
16800 E. Centretech Parkway
Aurora, CO 80011

Abstract *- This paper presents a filter for "conceptual spaces." The application is image understanding. A conceptual space is a collection of one or more "quality dimensions." In our approach, functionals on various Hough transforms of the input image determine the quality dimensions. For example, how "line-like" and "circle-like" the input image is can be used as quality dimensions. A "natural concept" is a convex region in a conceptual space. A conceptual Space can be partitioned into natural concept using a tessellation and prototypes for each concept. The filter we present takes in an input image and outputs a prototype image which represents the natural concept the input image corresponds to. It serves as an interface between an input image and a human user, aiding comprehension by providing a better match to the human information channel. We use a fuzzy tessellation to account for uncertainties in the mapping to prototypes.*

Keywords: Conceptual spaces, image understanding, fuzzy logic, Hough transforms, tessellation.

1 Quality Dimensions

A conceptual space is a collection of one or more quality dimensions. As an example, sweet, sour, salt, and bitter could be the quality dimensions of the conceptual space representing taste [1, 2]. If the conceptual space is partitioned into convex regions, these regions are *natural concepts* in the conceptual space. For example, an apple could be a natural concept in the space representing taste with quality dimensions sweet, sour, salt, and bitter. A *prototype* is a point in a natural concept in a space which is, in a certain way, the most representative point of the concept. For example, a Red Delicious apple may be a better prototype for the natural concept of apple than a Granny Smith apple would be. Figure 1 shows an example conceptual space with two quality dimensions and partitioned into six convex concepts, with each concept containing a prototype point which is highlighted in a different color. Quality dimensions are sometimes not totally independent entities. For example, the ripeness and color dimensions covary in the space of fruits [1, 2].

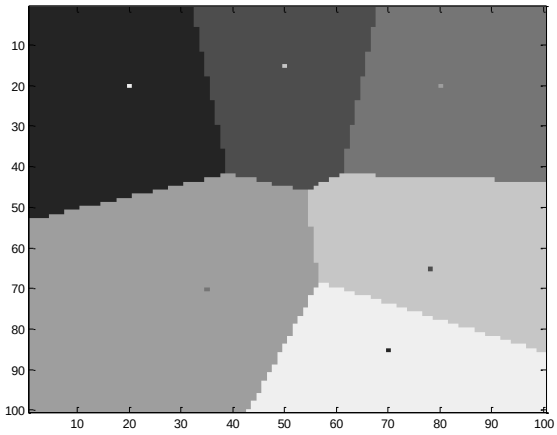

Figure 1: Conceptual Space divided up into six concepts and showing six prototypes indicated by the single pixels.

2 Conceptual Spaces Filter

The problem which the Conceptual Spaces Filter addresses is in the area of image understanding. Often image analysts are overwhelmed by the sheer volume of images they have to inspect in a limited amount of time. This causes incorrect interpretations to be made and important features to be missed. The Conceptual Spaces Filter aides the image analyst by doing part of the comprehension work so that he/she can successfully interpret a large number of images per hour. It presents to the user a prototype image rather than the input image. The prototype, being representative of a concept, is more easily comprehensible to the user than the input image. The degree of membership in a borderline fuzzy concept is also presented at the output of the filter. A high fuzzy membership signals the user that they should assign more resources to that image case, possibly to include direct human inspection of the input image.

So, for the Conceptual Spaces Filter, an input visual image is the input to the filter and a prototype visual image is the output of the filter, along with a fuzzy membership indicator. The Conceptual Spaces Filter sends the input image to a number of different Hough transforms in separate Hough

channels. These Hough transforms help to determine the quality dimensions.

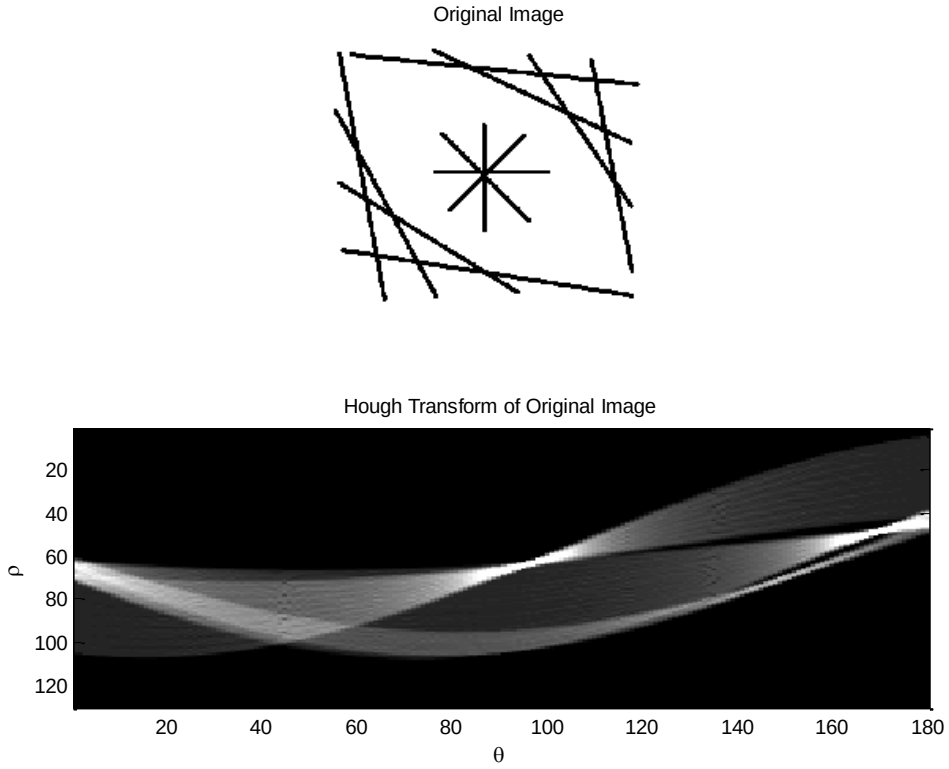

Figure 2: Line Hough detects the presence of lines. In the transform domain, the highest amplitudes are indicated by lighter shades.

Hough Transforms were discovered by Paul Hough [3]. They can be used to detect lines and curves in images [4]. Even arbitrary shapes may be detected using Hough Transforms [5]. Hough Transforms are invariant to rotation, displacement and intensity and so are widely used in image processing. A Line Hough detects the presence of lines. An example is shown in Figure 3. The original input image is shown above the Hough transform accumulator (Hough domain). The high amplitudes in the Hough domain are indicated by light shades. Most of the energy in the Hough transform domain is concentrated in a few small places, indicating that the input image is line-like. The Line Hough transforms the input from the x,y-domain to a θ,ρ-domain. *A* is the accumulator. The algorithm for the Line Hough is as follows:

To filter in the quality dimensions, the Conceptual Spaces Filter sends the input image to a number of different Hough transforms in separate Hough channels. The separate Hough transforms produce separate accumulators. A "peakiness" operator operates separately on each of the accumulators to determine a coordinate along a quality dimension associated with each Hough transform. The coordinates are combined to form an n-tuple in a conceptual space determined by the Hough quality dimensions. The conceptual space is pre-partitioned into convex concepts determined by the application. The n-tuple is a functional of the input image and will fall within one of the space's concepts or on or near a boundary. The output of the Conceptual Spaces Filter is the prototype of the concept which captured the n-tuple.

Fuzzy sets are discussed in the text by Klir and Yuan [6]. On the borders between the natural concepts a fuzzy non-natural concept is pre-determined. The n-tuple's location in the conceptual space determines a discrete membership in a natural concept and a fuzzy membership in the fuzzy non-natural concept. The prototype of the natural concept, determined by the n-tuple, is presented as output to the user along with a display indicating the fuzzy membership in the non-natural concept.

Tessellation is an algorithm for determining convex concepts once the prototypes are known and a distance is defined. In tessellation, a point belongs to a concept if it is closer to the prototype of the concept than to the other prototypes.

By "closer" we mean the distance is smaller. There are many ways to define distance. For example, weighted Euclidean distance is given by:

$$d_E(u,v) = \sqrt{\sum_i w_i (u_i - v_i)^2} \qquad (1)$$

Where the w's are the *attention weights*.

The accumulator, or the array utilized in the Line Hough Transform, detects the existence of a line. A circle Hough detects the presence of circles. Similar Hough transforms can be set up to detect ellipses, squares, and various other shapes.

The Conceptual Spaces Filter has two modes: 1.) Setup Mode and 2.) Run Mode. The diagram of the Setup Mode is presented in Figure 3. The diagram of the Run Mode is presented in Figure 4.

```
function [ x_ness ] = peakiness( B )

[m, n] = size(B)
z_max = max(B);
max_max = max(z_max);
count = 0;
for im = 1:m
   for in = 1:n
      if(B(im,in) > .5*max_max)
         count = count + 1;
end
   end
end
x_ness = m*n/count;
end
```

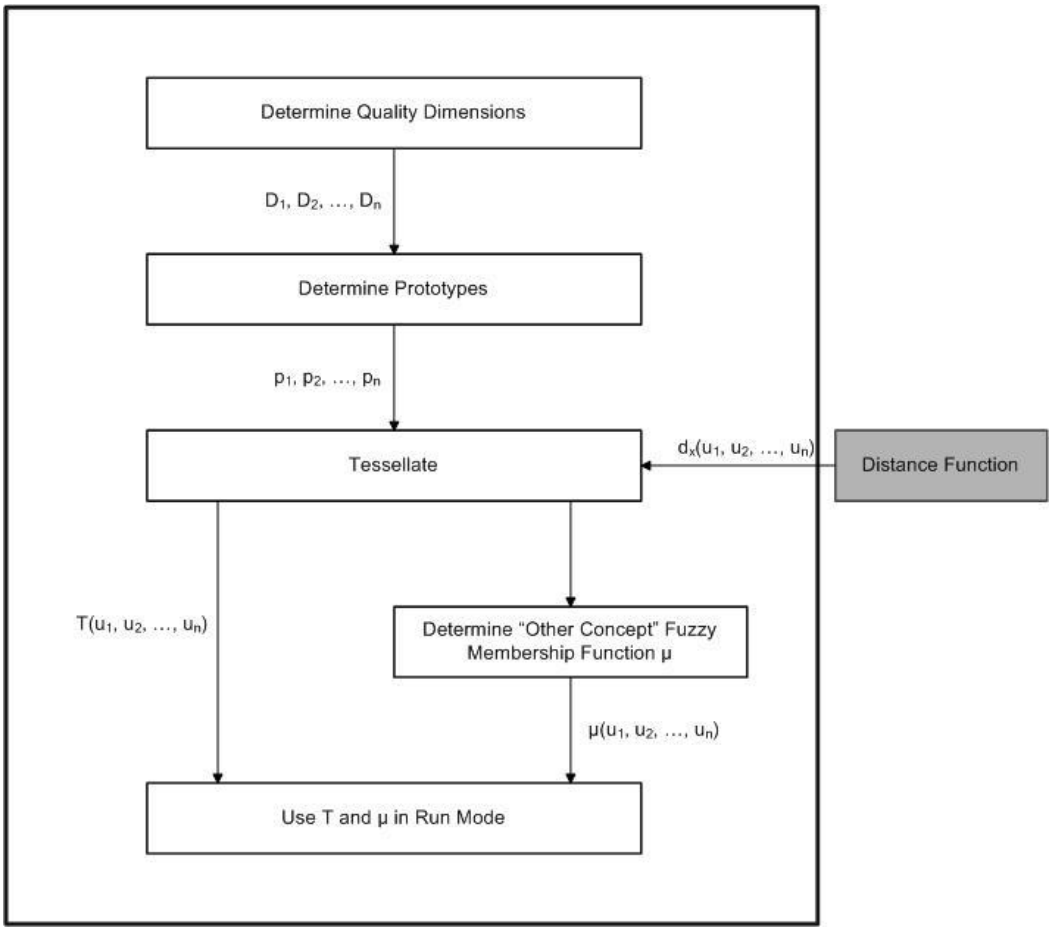

Figure 3: Setup Mode

In Setup Mode, in the first stage, it is determined, for an application, what are the qualities that need to be distinguished. Quality dimensions that have associated Hough transforms are selected. The choices are Circle Hough, Line Hough, Ellipse Hough, Square Hough and other admissible Hough transforms. A subset of these is chosen and associated quality dimensions $D_1, D_2, \ldots, D_n$ are passed to the next stage.

In the second stage in Setup Mode, prototype images are selected. These are fed into the Hough transforms selected in Stage 1. The output Hough accumulators are then fed into the peakiness function to determine the coordinates of the prototypes in the conceptual space. The peakiness is determined as follows:

Here B is the Hough accumulator. The peakiness determines how much of the Hough transform is within 50% of the peak of the Hough transform. The prototypes so determined, p1, p2,…, pn, are then sent to Stage 3.

At Stage 3 the prototypes $p_1, p_2, \ldots, p_n$ and a chosen distance function d_x are used to tessellate in order to determine the convex concepts. The tessellation T is passed to the Final

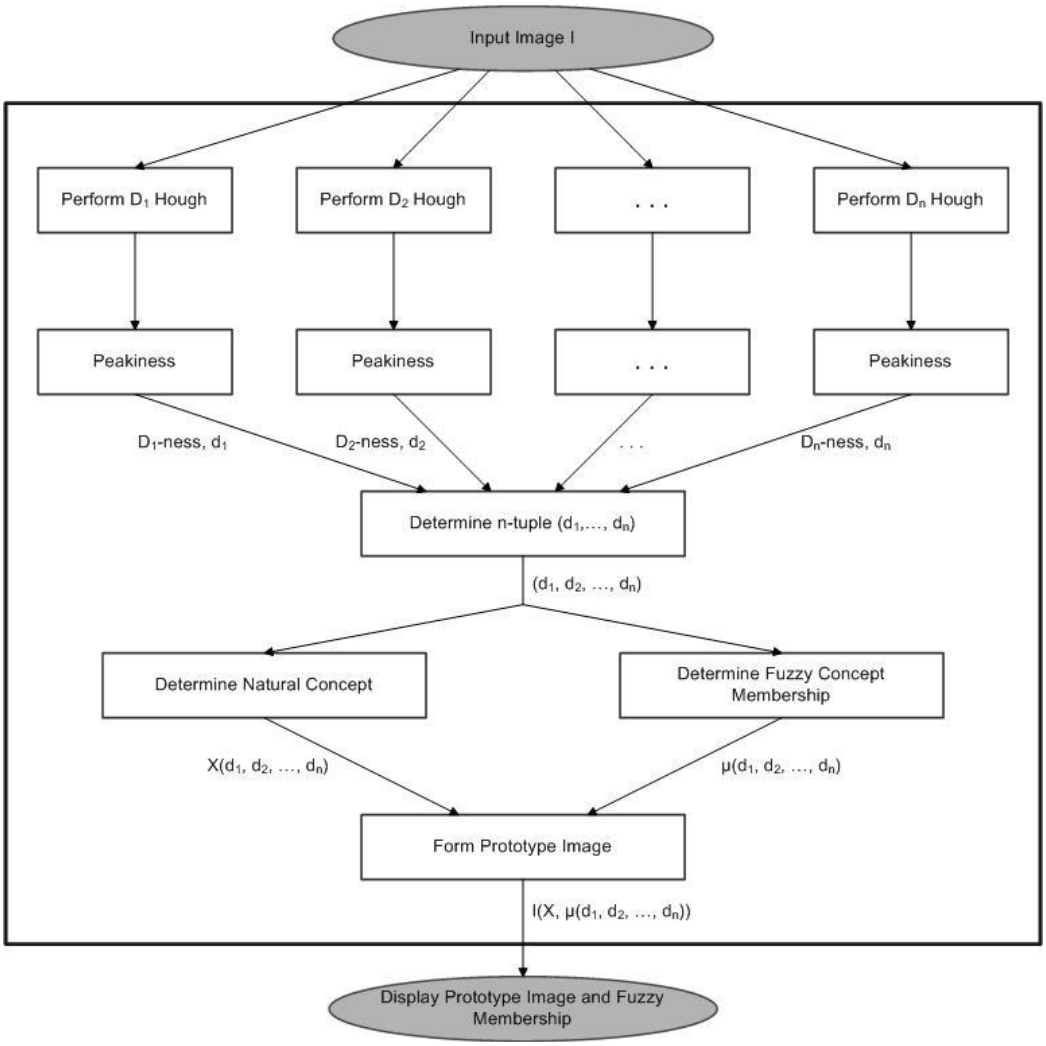

Figure 4: Run Mode

Stage. Example MATLAB code for the tessellation is as follows:

```
for i = 1:100
   for j = 1:100   %  Step through each point in the image.
      for k = 1:6
         x = p(k,1);              % Find the distance between
         y = p(k,2);              % the current point and each of
         d(k) = d_E(i, j, x, y); % the prototypes.
      end
      [y, I] = min(d);            % Find the nearest prototype.
      T(i,j) = I*10;  % Assign color according to prototype.
   end
end
```

The tessellation is also passed to an intermediate stage that determines the fuzzy concept μ. T is stepped through and every 3x3 subarray is tested to determine if it is an edge point. When an edge point is found in T, a non-zero entry is placed in the corresponding location in a buffer array Y. **N**ext, in array Y, the array (image) is smoothed (Gaussian smoothing) by replacing each pixel by the average of its neighbors.

This step is repeated until the desired fuzziness is achieved. The final smoothed concept is μ. The cross-section of μ is a Gaussian.

In Run Mode, the image is converted from color to grayscale. The image average is first determined. The image is passed to *n* separate "Hough Channels" which work independently. In each Hough channel, a Hough transform associated with each quality dimension D_k is applied to the input. To each Hough transform, a peakiness operator is applied to determine a coordinate d_k in quality dimension D_k.

The Hough channels are combined and a coordinate $(d_1,\ldots,d_n)$ in the conceptual space $S(D_1,\ldots,D_n)$ is produced. The natural concept X that $(d_1,\ldots,d_n)$ corresponds to, is determined. In parallel, the fuzzy membership $\mu(d_1,\ldots,d_n)$ in the non-natural concept μ is determined.

In the final stage, the prototype of natural concept X and the membership in the non-natural concept μ is presented to the user.

An example is shown in Figure 5. Two quality dimensions, "line-ness" L and "circle-ness" C create a conceptual space shown in blue. Using a given set of prototypes, a tessellation has partitioned the space into four natural concepts. Two input images were input to the Conceptual Spaces Filter and their locations in the conceptual space is shown. The Olympic image is well within the Circles concept with fuzzy membership 0. The LinesAndCircles image is well within the LinesAndCircles concept with fuzzy membership 0.

The operation as a filter is illustrated in Figure 6. There are four prototypes that an input image can be mapped to, farm, circles, circles and lines, and lines. The Olympics input image maps to the circles prototype image and has a membership in the fuzzy concept of $\mu = 0$. The lines and

circles input image maps to the lines and circles prototype and also has a membership in the fuzzy concept of $\mu = 0$.

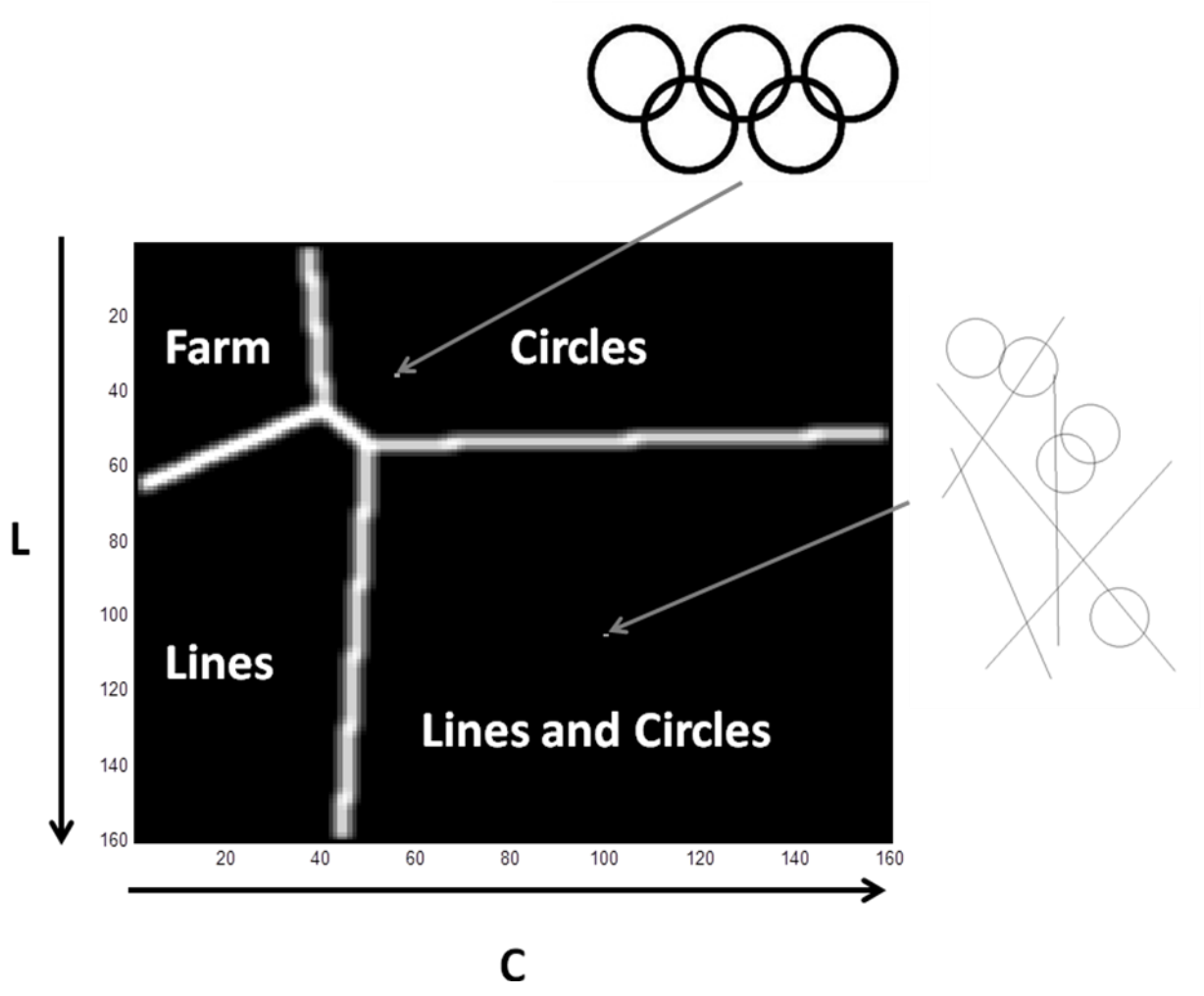

Figure 5: In the final stage, the Olympic image is mapped to the Circles concept and the LinesAndCircles image is mapped to the LinesAndCircles concept.

3 Summary

A Conceptual Spaces Filter was described which may aid image understanding and reduce the workload for image analysts. For the quality dimensions of the conceptual space, we use a peakiness functional on Hough transforms. These Hough transforms are rotationally and affine invariant and pick out special features in the image. We perform a tessellation to partition the conceptual space into convex concepts. We augment the tessellation with a fuzzy non-convex concept which is used to express uncertainties. The filter takes as its input an input image, uses Hough transforms and peakiness to determine coordinates in the conceptual space, and maps from the n-tuple to the prototype which is the output of the filter.

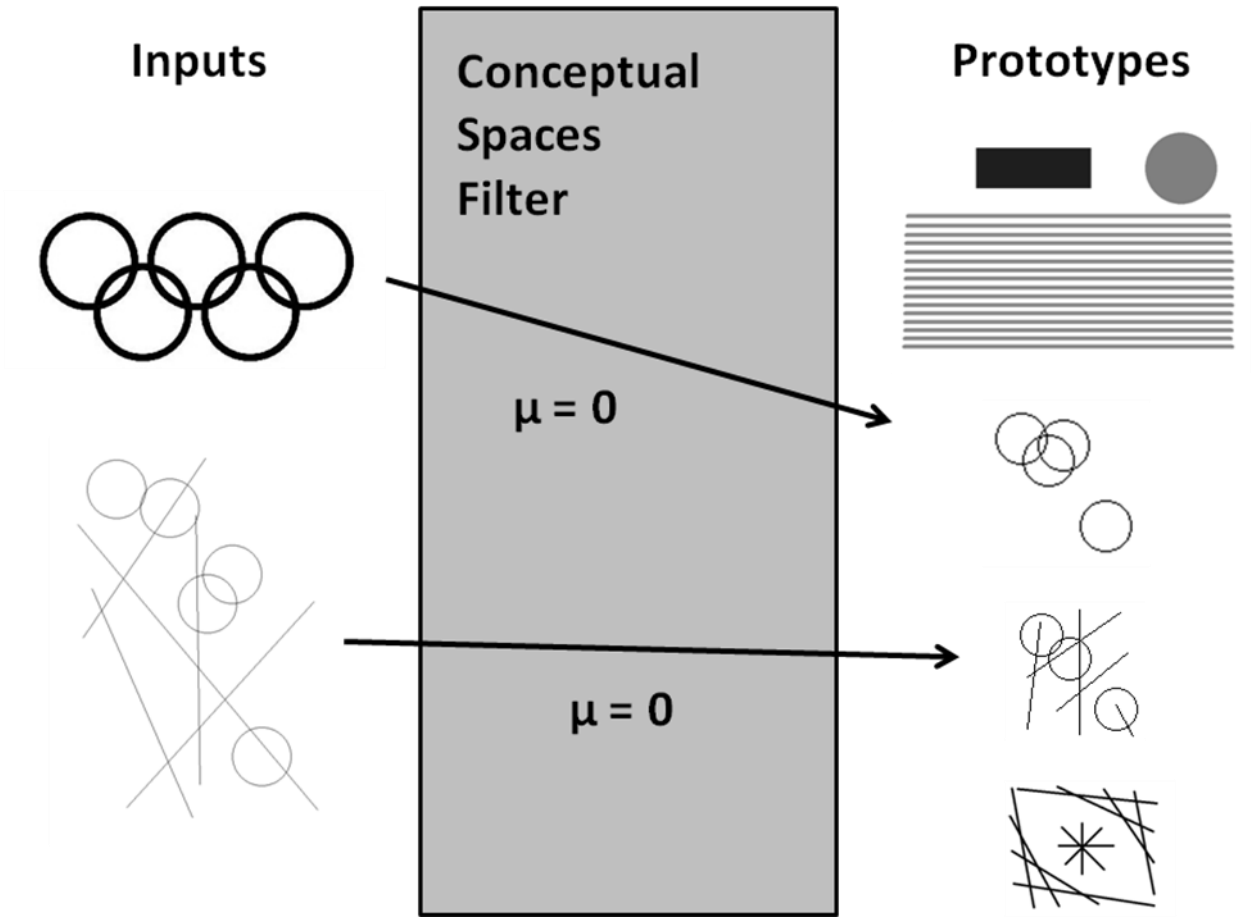

Figure 6 In the final stage, the Olympic image is mapped to the Circles concept and the LinesAndCircles image is mapped to the LinesAndCircles concept.

4 References

[1] Peter Gardenfors, "Conceptual Spaces as a Framework for Knowledge Representation," Mind and Matter, Vol. 2(2), 2004.

[2] Peter Gardenfors, Conceptual Spaces: The Geometry of Thought, MIT Press, 2004.

[3] Paul Hough, "Method and Means for Recognizing Complex Patterns," U.S. Patent 3,069,654, 1962.

[4] R.O. Duda and P. E. Hart, "Use of the Hough Transformation to Detect Lines and Curves in Pictures," *Comm. ACM, Vol. 15*, pp. 11–15 (January, 1972).

[5] D.H. Ballard. "Generalizing the Hough Transform to Detect Arbitrary Shapes, <http://www.cs.utexas.edu/~dana/HouthT.pdf>.

[6] George J. Klir and Bo Yuan, Fuzzy Sets and Fuzzy Logic Theory and Applications, Prentice Hall, 1995.

BLACKBOARD ARCHITECTURE FOR UNMANNED AERIAL VEHICLES USING FUZZY INFERENCE SYSTEMS

S.Pandhiti[1], **W.D.Potter**[2]
[1]Institute for Artificial Intelligence, University of Georgia, Athens, GA, U.S.A
[2]Institute for Artificial Intelligence, University of Georgia, Athens, GA, U.S.A

Abstract *- This paper discusses the design of a controller for low-cost fixed-wing Unmanned Aerial Vehicles (UAV's) using fuzzy rules and fuzzy inference systems. The control flow in the architecture design process consists of four levels: Guidance, Navigation, Control and Stability, Communications. The Fuzzy Logic Control System (FLCS) introduced here, is mainly used to control and stabilize the aircraft while navigating towards different waypoints defined according to the waypoint plan. This idea forms the base for an AI approach to the development of an autopilot unlike the traditional way of using PID (Proportional Integral Derivative) controllers for control and navigation [1].*

Keywords: *Unmanned Aerial Vehicle (UAV), Fuzzy Inference Systems (FIS), Flips, Fuzzy Logic*

1 Introduction

Unmanned Aerial Vehicles (UAV's) have been attracting a lot of attention especially in fields like military, civil and research applications. In addition to these, UAV's are also being used in traffic control, target acquisition, localization and surveillance [2], virtual reality aided control [3], measurement of atmospheric composition [4][5], crop monitoring, telecommunications, reconnaissance, attack roles and many other areas over the last thirty years. Autonomously controlled UAV's are gaining special importance since they do not need a radio link like the remote controlled planes and also, very minimal human support is required for control, stability and navigation.

1.1 Fuzzy Logic and Fuzzy Inference Systems

Fuzzy Logic, introduced by Lofti Zadeh [6] deals with reasoning that is fixed or appropriate rather than fixed and exact. Fuzzy Logic can be used to describe control or describe a system by using "commonsense" rules that refer to inadequate quantities [7] [8]. It incorporates a simple rule-based "if X and Y, then Z" approach to solving a control problem rather than attempting to model a system mathematically [9].

Fuzzy Inference Systems are designed based on the concept of Fuzzy Logic (FL). Fuzzy Inference can be defined as the process of formulating the mapping from a given input to an output. A Fuzzy Logic System or a Fuzzy Inference System (FIS) maps the crisp inputs into crisp outputs. A membership function is such a graph that defines how each point in the input space is mapped to the membership value between 0 and 1. A Fuzzy Inference process comprises of five parts: fuzzification of the input variables, application of the fuzzy operator in the antecedent, implication of the antecedent to the consequent, aggregation of the consequents across the rules and defuzzification.

2 System Architecture

This section introduces a brief overview of the present research article. A rule based system is being developed, where the control flows from the higher levels to the lower levels. The architecture can be described in different operating levels, which are assigned to perform four different kinds of functions. The user specifies his/her goals in a high-level (human-readable) language, which are then converted to tasks with the help of the FLIPS (Flight Instruction Processing System) parser [10]. The autopilot converts these instructions or tasks to fuzzy rules. These fuzzy rules, combined with fuzzy inference systems, send out action commands to the actuators. The actuators then communicate with the hardware (micro-controllers) on-board to execute the mission.

The main focus of this paper is the Fuzzy Logic Controller for Unmanned Aerial Vehicles, which is solely responsible for the Navigation, Control and Stability tasks. Hence, the emphasis of this paper would be the process of conversion of the tasks to actions which is depicted in Figure 1.

Though the practical implementation involves much more than this, the above architecture can be compared to a virtual blackboard. The blackboard idea is such that the values from every level are posted onto the blackboard. Every level gets its instructions or tasks from its corresponding higher level's output values. With the help of the fuzzy inference system (controller) and the values posted on the blackboard, the autopilot sends commands to the actuators for task execution.

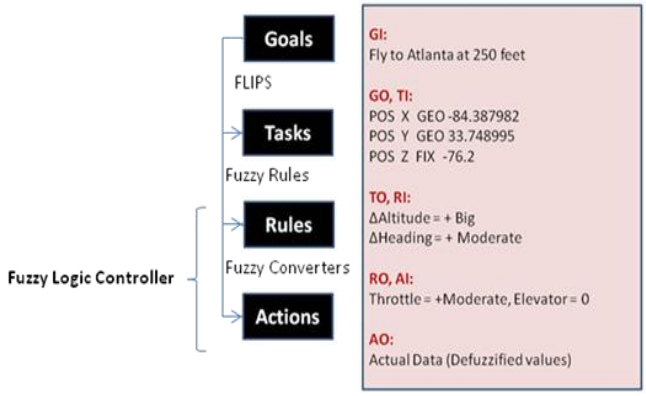

Figure 1: UAV System Overview

Since this is a closed-loop feedback system, the current state of the aircraft is measured and stored. The controller compares these values (current state and the desired state of the aircraft) and executes the tasks accordingly. The present architecture is considered as a black box which is fully autonomous.
The UAV autopilot is said to operate in four levels. They are:

i. Guidance (via FLIPS)
ii. Navigation
iii. Control and Stability
iv. Communications

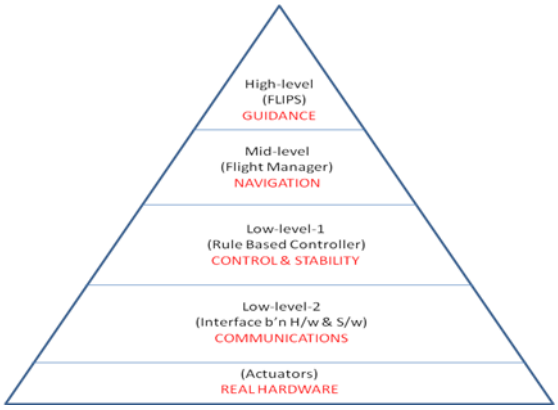

Figure 2: UAV System Architecture

2.1 Guidance (High Level)

This level consists of high-level operations (goals and missions) specified by the user. Any kind of guidance system can be implemented with the present Fuzzy Logic Control System. FLIPS (FLight Instruction Processing System for Unmanned Aerial Vehicles) grammar developed by Robert Eunice has been chosen in order to give instructions / specify waypoints (goals) [11]. FLIPS is a grammar used to define UAV mission commands in a high-level language that can be used as a hardware-independent instruction set architecture (ISA) for implementation of commands. The goal of FLIPS is to provide a better abstraction between the user and the flight hardware. The high-level tasks are specified as FLIPS assembly language instructions. These instructions are presented to MATLAB in a text file. The commands and waypoints used for controller input are specified in the example below to create a better understanding for the user. An example of FLIPS conversion is as follows:
Example1.uav

Commands:	Waypoints – Latitude, Longitude
Normal = 0	Atlanta = 33.748995, -84.387982
Take-off = 1	New York = 40.714269, -74.005973
Inverted = 2	
Hover = 4	
Roll left = 8	
Roll right = 16	

Goals: (High-level instructions) *Example1.uav.asm (FLIPS Assembly)*

a. Take-off = **CMD 1** // Take-off
b. Fly to Atlanta at 50 meters = **POS X GEO -84.387982**
// Atlanta W Longitude
POS Y GEO 33.748995
// Atlanta N Latitude
POS Z FIX -50.0
// 50m Altitude
FLY
c. Fly to New York **POS X GEO -74.005973**
// New York W Longitude
POS Y GEO 40.714269
// New York N Latitude
FLY
d. Fly at 1000 feet **POS Z FIX -304.8**
// 1000 feet = 304.8m
FLY
e. Loiter and Land **CMD 192**
// Loiter and Land

These FLIPS assembly commands are the output commands of the Guidance level.

2.2 Navigation (Mid Level)

The mid-level coordinates the task execution by receiving the task information (FLIPS Assembly) from the high level. The Flight Manager tries to identify the current & desired states of the aircraft and sends commands to the next level. These commands describe the kind of maneuver and the type of maneuver the aircraft needs to perform at that moment. Ex: From the above example, (d.) says: POS Z FIX -304.8 (climb to 1000 feet) and suppose the altitude sensor measures the current altitude as 200 feet. The altitude difference is 800 feet and is very high. The Flight Manager then sends the following instruction:

ΔAltitude = + High => Perform a steep climb

Control is now handed over to the Control and Stability level.

2.3 Control and Stability (Low Level)

The lower level receives the instructions from the mid-level and then tries to match these to the fuzzy rules designed for control and stability of the aircraft. This fires the actual rules that perform the maneuver and type of maneuver action. Examples of the low-level rules for a steep climb are displayed in Table 1:

Table 1: Steep Climb: (ΔAltitude = + High)

If	*Then*
Altitude = +High, Airspeed = High	*Throttle = VeryHigh, Elevator = High*
Altitude = +High, Airspeed = Moderate	*Throttle = VeryHigh, Elevator = High*
Altitude = +High, Airspeed = Low	*Throttle = VeryHigh, Elevator = VeryHigh*

This level is responsible for the defuzzification of the fuzzy output values from the low-level rules fired. These defuzzified values are then converted to electrical signals to be sent to the actuators. This is then sent to Flight Gear for visualization purposes.

The 'Communications' level is not being discussed here since the system has been implemented and tested in a simulation environment only.

3 Implementation

To attain the readability and flexibility of the present control system, the controller has been designed as a rule-based system whose architecture is hierarchically structured with different layers. Each layer consists of a set of rules and is based on the function performed by the autopilot. MATLAB's Fuzzy Logic Toolbox has been used for the development of a rule-base to navigate the aircraft. The rules have been categorized into four categories – Climbs, Descents, Left Turn and Right Turn which are further categorized into subcategories of Steep, Moderate and Shallow.

The climbs and descents rules are designed in such a way that the main factors - altitude and airspeed; contribute equally to the climb and descent paths. Similarly, "Angle of Bank" or "Roll Angle" is another factor which is necessary to be considered during the turns.

A simulation environment has been provided for the UAV in order to provide a platform for testing and tuning algorithms and to foresee the behavior of the UAV prototype in different scenarios. The simulation can also be used as a part of the ground station software to control the UAV.

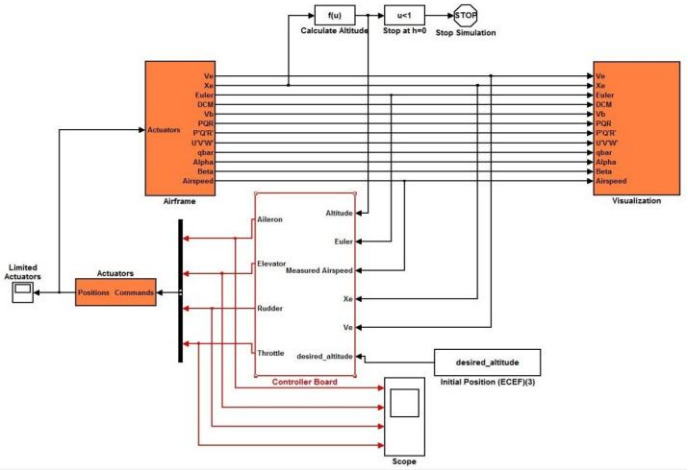

Figure 3: MATLAB Simulink Model

In order to build a base for the development of intelligent systems, the Fuzzy Logic approach has been considered by replacing the traditional PID (Proportional Integral Derivative) controllers with Fuzzy Inference Systems. The simulation environment (current UAV Simulink model in MATLAB) shown in Figure 3 has been developed using Mathwork's Simulink software and FlightGear and has been classified into three key components:

3.1 Aerodynamics and Environmental Model

This contains the 'Airframe' and 'Actuators' blocks. This model is used to characterize the dynamics of a UAV in its environment. The effects of the actuators (throttle, elevator, aileron and rudder) and the environment including gravitational forces, wind forces, aerodynamic forces and moments on the motion of the simulated UAV are taken into account to generate the total force and moment on the Airframe of the UAV.

3.2 Controller Model

This consists of the 'Controller Board', a combination of two fuzzy controllers, one for Turns (lateral controller) and one for Climbs and Descents (longitudinal controller). This model is used for Guidance, Navigation, Control & Stability and Communications. The controller model reads the current state of the aircraft from the airframe through the feedback system and sends output signals to the control actuators to meet its goals. The top-level set points for the fuzzy controllers are the three variables: desired altitude, desired heading and desired

airspeed. The waypoints are defined as parameters (not inputs or outputs) in order to calculate the above three set points. The Fuzzy Inference Systems present in the controller block which made up of rules and fuzzy membership functions pertaining to the inputs and outputs are responsible for all the logic behind the controller.

3.3 Visualization Model

This model communicates with FlightGear and produces useful graphical outputs to analyze and monitor the motion of the aircraft. This block takes in the 12-input values needed to display the state of the aircraft and the output is represented as graphical flight simulation. The whole environment is simply a feedback loop control system with subsystems built into it. This feedback loop control system reports the state of the aircraft every 0.005 sec which is said to be its simulation step time. The accuracy and the length of time of the resulting simulation depend on the size of the step taken by the simulation: the smaller the step size, the more accurate the results. In the fuzzy controllers used, the membership functions are properly chosen and are assigned with membership values with intuition by observing the universes of discourse of the input and output variables. The aircraft would become highly unstable if the values out of the specified ranges are used. The FlightGear simulation environment used in this project is as shown in Figure 4:

Figure 4: FlightGear Flight Simulator

4 Results

The Fuzzy Logic approach appears to be presenting with interesting results in the sense that the autopilot obeys the instructions precisely according to the waypoints defined.

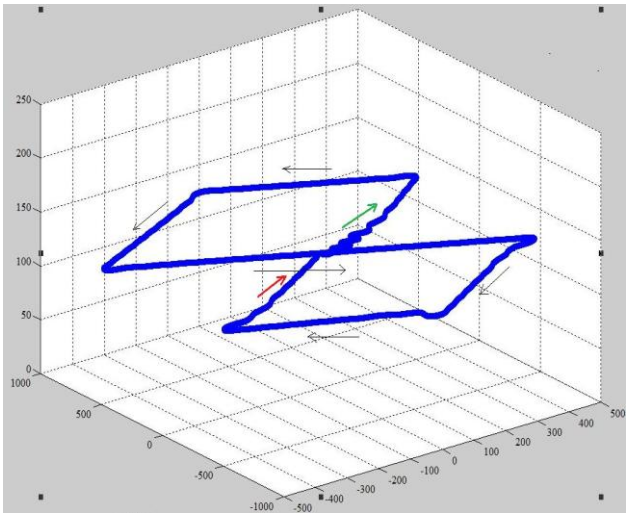

Figure 5: Figure 8 with fixed altitude

Figure Units: X-Axis – Matlab Units, Y-Axis – Matlab Units, Z-Axis – Altitude (m)

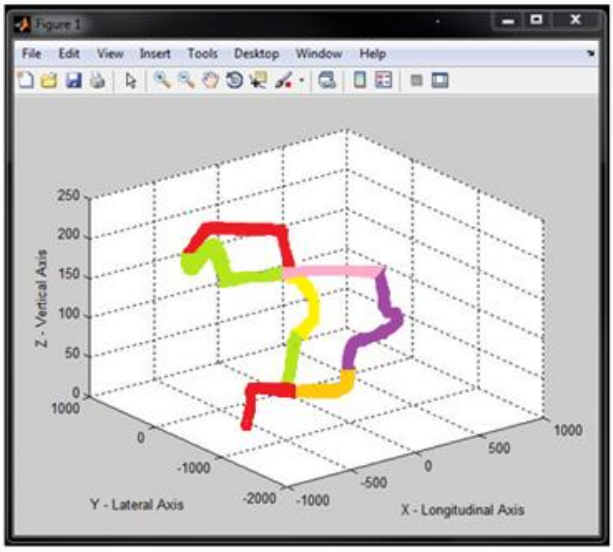

Figure 6: Figure 8 with varying altitude

Figure Units: X-Axis – Matlab Units, Y-Axis – Matlab Units, Z-Axis – Altitude (m)

It also corrects itself from small roll and pitch angle errors during straight and level flight. The autopilot has been tested with various trajectory paths and just not one to test for precision. A comparison of the results with the PID controller model has also been made in order to determine its performance. Figures 5 and 6 depict the 'Figure 8 trajectory' of the aircraft using Fuzzy Logic Control System. As presented in Figure 5, the aircraft starts from waypoint (0, 0); which represent the latitude and longitude and continues to fly according to the waypoints defined in the goal. The axes

in the above Figures depicting the aircraft trajectory define orientation of the aircraft. The 3D plots in Figures 5 and 6 display all the three X (Longitudinal Axis), Y (Lateral Axis) and Z (Vertical Axis) axes respectively. The beginning and end of the trajectory taken by the aircraft in Figure 5 are marked with green and red arrows respectively. In Figure 6, the altitude increases for the first half of 'Figure 8 trajectory' and starts decreasing for the second half. The trajectory of the path in Figure 6 is- Green, Yellow, Red, Green, Pink, Purple, Mustard and Red. The turns, as discussed earlier, seem to appear distorted since controlling the altitude and heading with rules is a challenging task for the controller and better results can be achieved with additional tuning procedures.

5 Conclusion and Future Work

The purpose of this research was to develop navigation and control based fuzzy logic controller for Unmanned Aerial Vehicles. The simulation results depict an adequate overall performance of the autopilot. The results show some deflections during the turns which are due to the adjustment of the controller with the corresponding rules during every time step. Trial and error methods to fine tune them during the turns have been performed but it was disappointing to note that not much tuning was possible to make them smoother. Every method has its own disadvantages and this can be considered as a disadvantage of using fuzzy rules for smoothing the turns. However, this might be improved by employing a very few PID's for just tuning purposes during the turns. The perfect control flow of the architecture at present helps in developing a fuzzy model on the hardware much easier without the PID's. A similar model can be used to develop a controller for elevon controlled aircrafts like Zagi. This research follows waypoint navigation like most of the aircraft control systems. New navigation control methodologies can also be employed like learning the trajectory path while traversing and coming up with a new set of points of interest.

6 References

[1] Pandhiti, S. "Blackboard Architecture for Unmanned Aerial Vehicles using Fuzzy Inference Systems". M.S. Thesis, Institute for Artificial Intelligence, University of Georgia, 2011.

[2] M. Quigley, Michael A. Goodrich, Stephen Griffiths, Andrew Eldredge, Randal W. Beard. "Target Acquisition, Localization, and Surveillance Using a Fixed-Wing Mini-UAV and Gimbaled Camera". Proceedings of the 2005 IEEE International Conference on Robotics and Automation, (pp. 2600-2605), 2005.

[3] Bryan E. Walter, Jared S. Knutzon, Adrian V. Sannier, James H. Oliver. "VR Aided Control of UAVs". 3rd AIAA Unmanned Unlimited Technical Conference, Chicago, 2004.

[4] Grabowski, T. G., Frydrychewicz, A., Goraj, Z., & Suchodolski, S. "MALE UAV design of an increased reliability level". Aricraft Engineering and Aerospace Technology, Vol. 78, Issue: 3, pp. 226 – 235, 2006.

[5] B. T. Clough. "Unmanned Aerial Vehicles: Autonomous Control Challenges, a Researcher's Perspective" in Cooperative Control and Optimization, R. Murphey and P. M. Pardalos, eds., pp. 35 - 53, Kluwer Academic Publishers, 2000.

[6] L. A. Zadeh. "Fuzzy sets". Information and Control (pp. 338 - 353), 1965.

[7] Bart K. and Satoru I. "Fuzzy Logic" retrieved from http//:Fortunecity.com/emachines/e11/86/fuzzylog.html.

[8] *Fuzzy Logic.* (n.d.) Retrieved July 2011, from http://en.wikipedia.org/wiki/Fuzzy_logic

[9] Kaehler, S. D. (n.d.). Retrieved July 2011, from seattlerobotics.org: http://www.seattlerobotics.org/encoder/mar98/fuz/fl_part1.html#INTRODUCTION

[10] Eunice, R. E. "Development of Low-Cost Nonlinear Embedded Flight Control Architecture for Autonomous Unmanned Aerial Vehicles". *Institute for Artificial Intelligence, University of Georgi*, 2007, Oct 31.

[11] Eunice, R. E. (n.d.). *Google Code*. Retrieved from FLIPS-UAV: http://code.google.com/p/flips-uav/

Fuzzy Automaton with Kalman State-Smoothing

Scott Imhoff and Palak Thakkar

Raytheon Intelligence and Information Systems
16800 E. Centretech Parkway
Aurora Colorado 80011

Abstract - *This paper presents a fuzzy automaton/Kalman filter hybrid algorithm (Kalmaton). Automata are of pivotal importance in artificial intelligence (AI), being used in knowledge engines such as Wolfram|Alpha. Also they are applicable to emerging needs for predictive situational awareness involving data mining and data fusion. Kalman filters have many applications which need predictive validity, including GPS. Fuzzy transitions from different learning states associated with fuzzy automata along with estimation of the true state of a system using a Kalman filter creates an algorithm that achieves good stability and reaches a decision boundary early.*

Keywords: Kalman filtering, automaton, fuzzy logic, change detection, state smoothing, machine learning.

1 Introduction

Formal Languages provide an advantageous framework in applications where the essential behavior of a system is language-like. A very approachable treatment of Formal Languages is given by Revesz [1]. An automaton is a kind of language receiver. Automata are not limited to spoken languages but can be used with nearly any sequence of symbols. As an automaton interacts with its environment receiving symbols, it undergoes transitions of its internal state. The internal state of the automaton determines, in part, what the output (response) of the automaton is. Automata learn from the environment what their internal state should be. If you think of an automaton as a machine, you may look inside the machine to see what it is made of. If you 'run' the automaton, and let it interact with the environment, when you open the box again and look you will typically see a different machine.

It is often advantageous to use a fuzzy automaton. When I say "yester," you go partly into a state where you are ready to hear "day." But this is not the whole story. You also go partly (slightly) into a state where you are ready to hear "year" because yesteryear is also a word you might expect to hear occasionally. Fuzzy automata allow you to work with such situations. They allow your state membership to straddle two or more states. In addition to fuzzy states, fuzzy automata also have fuzzy transitions and fuzzy output mappings (responses). Klir and Yuan provide an excellent introduction to fuzzy automata [2].

Fuzzy automata are able to learn from actions A_k produced in the environment by making fuzzy transitions from learning state x_k to learning state x_{k+1} until an admissible response B_k is achieved. This response corresponds to reaching a decision boundary for labelling in active learning. These decisions about what has been detected or acquired (the label) inform the user of what is present in the environment. A pernicious problem with fuzzy automata is the tendency in applications for the internal state to be unstable. The presently discussed new algorithm addresses this problem by integrating components of a Kalman filter to smooth the internal state of the fuzzy automaton.

Sometimes the state of a system cannot be known perfectly. For example, in GPS it is not possible to know the position and velocity perfectly owing to noise and environmental effects. A Kalman filter is used to smooth the state vector (position, velocity, etc.) to provide an optimal approximation to the true state. A Kalman filter is an algorithm for estimating the true state of a system at iteration k by using previous estimates and measured data. State estimates $\hat{x}_k$ are formed using the previous state estimate $\hat{x}_{k-1}$ and measured data z_k as well other variables including Kalman Gain K_k and covariance P_{k-1}. An engineering approach to Kalman Filtering, with a MATLAB disk, is provided by Grewal and Andrews [3] while a mathematical discussion is presented in a Dover book by Stengel [4].

The present paper presents a new algorithm which addresses the stability problem of the fuzzy automaton by smoothing its internal state using a Kalman filter. An example application is change detection. An example of the application of Kalman state-smoothing of a fuzzy automaton is presented in Figure 1. The inputs and outputs of the fuzzy automaton are shown. In Figure 1, in the top of the plot, an input signal A_k over two channels (for example, I and Q) has a hidden, low entropy, signal in one of the channels (the solid line channel). The output (automaton response) B_k is three signals that appear in the lower half of the diagram. (Think of them as three voters.). Here the input actions A_k (the "-." and black curves) produce output B_k ("-", ".", and "+"). A smooth, early arrived at, change detection is demonstrated.

Example decision boundaries could be the horizontal lines at y = .6.

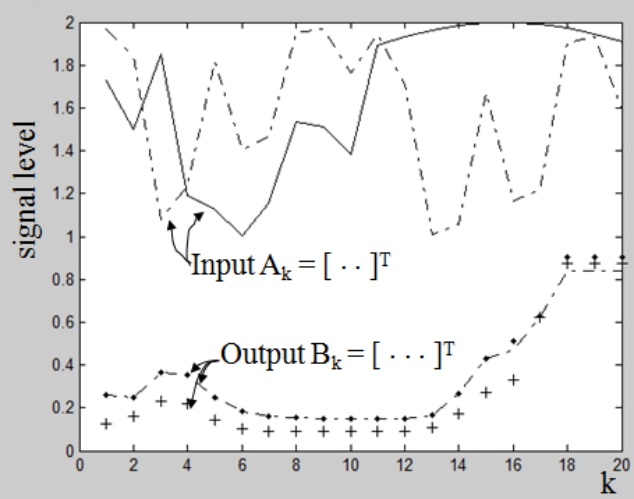

Figure 1: Smooth, early change detection using fuzzy automaton with Kalman state-smoothing. The output signals rise in response to the "hidden" signal in the solid component of the input.

2 Description of the Algorithm

This paper presents a fuzzy automaton/Kalman filter hybrid algorithm ("Kalmaton"). The algorithm is an iterative predictor device which steps through a sequence of steps from $k = 1$ to N, taking input A_k at each step and producing output B_k at each step. The elements that occur together in this algorithm are:

1) An input matrix A_k of actions from the environment external to the device.
2) A matrix B_k of outputs returned from the device and presented to the user.
3) An estimate internal state of the system $\hat{x}_k$ which is updated every iteration, k.
4) A three-dimensional matrix S of fuzzy state transitions.
5) An aggregate matrix SA_k which is derived from the input and the matrix of fuzzy state transitions at each iteration k.
6) A Kalman Gain matrix K_k which is updated each k.
7) A symmetric covariance matrix P_k which is updated each k using a congruence transform.
8) A transition matrix Φ.
9) A fuzzy response matrix R.
10) An observation matrix H.
11) An internal measurement z_k.
12) A white noise covariance matrix ρ.

The sequence of activities of the algorithm at each iteration k are as follows:

1) An input A_k from the environment is aggregated (minmax) with the matrix of fuzzy transitions S to form fuzzy intermediate matrix SA_k.

$$SA_k(\zeta_i, \zeta_j) = \max_{\ell}\left\{\min\left[A_k(\xi_\ell), S(\xi_\ell, \zeta_i, \zeta_j)\right]\right\} \quad (1)$$

2) $\hat{x}_{k-1}$ is aggregated with SA_k and the result of this aggregation is called measurement z_k.

$$z_k = \hat{x}_{k-1} \circ SA_k \quad (2)$$

Where the operator $\circ$ is defined as:

$$A \circ B = \max_{i}\left\{\min[A(i), B(i,j)]\right\} \quad (3)$$

3) The Kalman gain, K_k, is updated using the covariance, P_{k-1}, observation matrix, H, and white noise covariance, ρ.

$$K_k = P_{k-1}H^T(H\ P_{k-1}H^T + \rho)^{-1} \quad (4)$$

4) The covariance is updated to become P_k by using:

$$P_k = (I - K_k H)P_{k-1} \quad (5)$$

5) The state estimate update, $\hat{x}_k$, is then formed by using the Kalman weighted average with z_k serving as the measurement.

$$\hat{x}_k = \hat{x}_{k-1} + K_k(z_k - H\hat{x}_{k-1}) \quad (6)$$

6) Finally, $\hat{x}_k$ is aggregated with response matrix R to form the output B_k.

$$B_k = \hat{x}_k \circ R \quad (7)$$

A point of novelty is that the fuzzy intermediate matrix, SA_k, is aggregated with the state estimate from the Kalman filter, $\hat{x}_{k-1}$. This aggregation amalgamates the state of the automaton with the Kalman filter state so that the state can be smoothed in order to increase the stability. A second point of novelty is that the aggregate, z_k, is used as the input to the Kalman state update operation. This allows an innovation process that smoothes the output, making it easier to place decision boundaries. A third point of novelty is that the output, B_k, to the user is formed by aggregating the state estimate with the fuzzy response matrix R. This allows more flexibility to make the output in a format that is conducive to setting decision boundaries.

The Kalman filter is integrated with the fuzzy automaton as a hybrid algorithm, rather than being a Kalman filter and automaton in series or parallel. The block diagram of the Fuzzy Automaton with Kalman State-Smoothing is presented in Figure 2. The variables are identified in Table 1. Lower-case denotes a vector while upper-case denotes a matrix.

Table 1: List of Variables

Variable	Description
k	Iteration Number
$\hat{x}_k$	Estimate State
A_k	Input from Environment
B_k	Output to User
SA_k	Fuzzy Intermediate Matrix
K_k	Kalman Gain
S	Matrix of Fuzzy Transitions
P_k	State Covariance
R	Response Matrix
z_k	Measurement of State

3 Application of Algorithm

The algorithm described by the diagram in Figure 2 was demonstrated by coding it as a MATLAB script. That script was executed on an HP EliteBook notebook computer, generating the plot appearing in Figure 1. The plot shows a 20x2 matrix input actions, A_k, represented by the ".-" and solid curves, and a 20x3 output matrix, B_k, which is represented by the dot, dash, and plus curves. The meaning of the plot is that there is a smooth response to very noisy input actions while an early change detection capability is demonstrated as the output signals rise at about time k = 14.

For the reduction to practice the authors used the following state transition matrix Φ:

$$\Phi = \begin{bmatrix} 0.320 & 0.188 & 0.567 & 0.145 \\ 0.188 & 0.759 & 0.376 & 0.489 \\ 0.567 & 0.376 & 0.213 & 0.0128 \\ 0.145 & 0.489 & 0.0128 & 0.187 \end{bmatrix} \quad (8)$$

The input actions, A, were given by:

$$A = \begin{bmatrix} 0.0128 & 0.540 \\ 0.377 & 0.705 \\ 0.168 & 0.503 \\ 0.540 & 0.783 \\ 0.102 & 0.927 \\ 0.393 & 0.830 \\ 0.933 & 0.825 \\ 0.972 & 0.767 \\ 0.361 & 0.997 \\ 0.644 & 0.228 \\ 0.891 & 0.292 \\ 0.932 & 0.498 \\ 0.964 & 0.253 \\ 0.985 & 0.612 \\ 0.997 & 0.859 \\ 1.00 & 0.688 \\ 0.992 & 0.680 \\ 0.974 & 0.589 \\ 0.946 & 0.994 \\ 0.909 & 0.0518 \end{bmatrix} \quad (9)$$

The white noise covariance that was used is given by the following:

$$\rho = \begin{bmatrix} 0.485 & 0.691 & 0.112 & 0.499 \\ 0.838 & 0.0345 & 0.743 & 0.568 \\ 0.141 & 0.489 & 0.639 & 0.427 \\ 0.732 & 0.971 & 0.594 & 0.0762 \end{bmatrix} \quad (10)$$

The observation matrix, H, that was used is:

$$H = \begin{bmatrix} 0.291 & 0.978 & 0.474 & 0.960 \\ 0.561 & 0.0936 & 0.356 & 0.891 \\ 0.633 & 0.662 & 0.476 & 0.798 \\ 0.931 & 0.603 & 0.671 & 0.0591 \end{bmatrix} \quad (11)$$

The fuzzy response, R, that was used is:

$$R = \begin{bmatrix} 0.912 & 0.504 & 0.331 \\ 0.101 & 0.768 & 0.453 \\ 0.293 & 0.283 & 0.737 \\ 0.0516 & 0.225 & 0.510 \end{bmatrix} \quad (12)$$

The fuzzy state transition used is a 4x4x2 matrix given by the following:

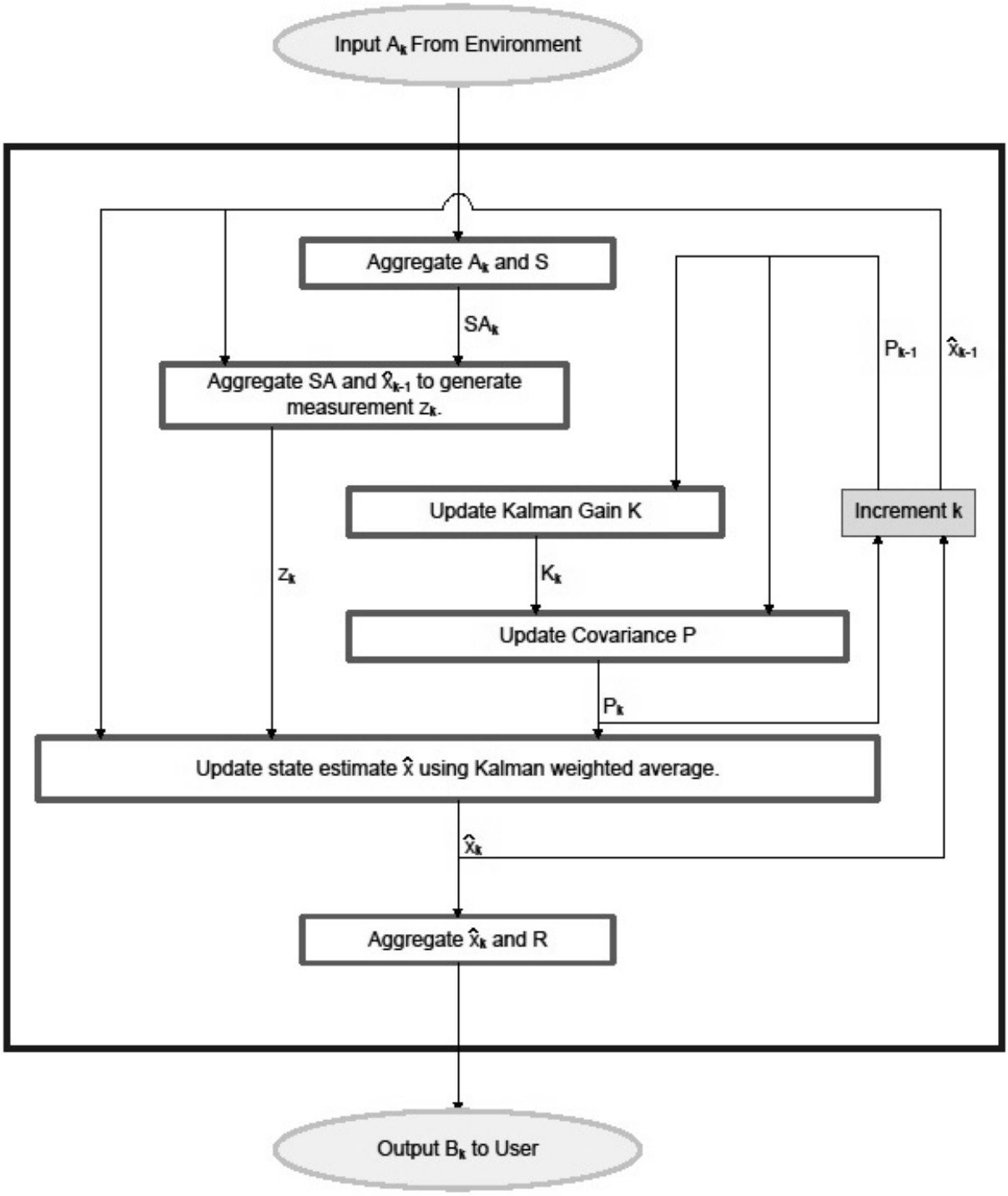

Figure 2: Fuzzy Automaton with Kalman State-Smoothing block diagram.

$$S(:,:,1) = \begin{bmatrix} 0.383 & 0.132 & 0.287 & 0.689 \\ 0.905 & 0.618 & 0.706 & 0.0505 \\ 0.965 & 0.383 & 0.535 & 0.184 \\ 0.628 & 0.991 & 0.193 & 0.0457 \end{bmatrix}$$

$$S(:,:,2) = \begin{bmatrix} 0.885 & 0.120 & 0.990 & 0.973 \\ 0.840 & 0.572 & 0.350 & 0.623 \\ 0.118 & 0.949 & 0.209 & 0.0635 \\ 0.410 & 0.256 & 0.666 & 0.374 \end{bmatrix} \quad (13)$$

The initial state of the system was:

$$x = [0.793 \quad 0.373 \quad 0.832 \quad 0.754]' \quad (14)$$

As a basis of comparison, the Kalman filter was extricated from the algorithm and the same experiment was run. As can be seen in the example in Figure 3, the automaton broke down and failed to respond to the hidden signal.

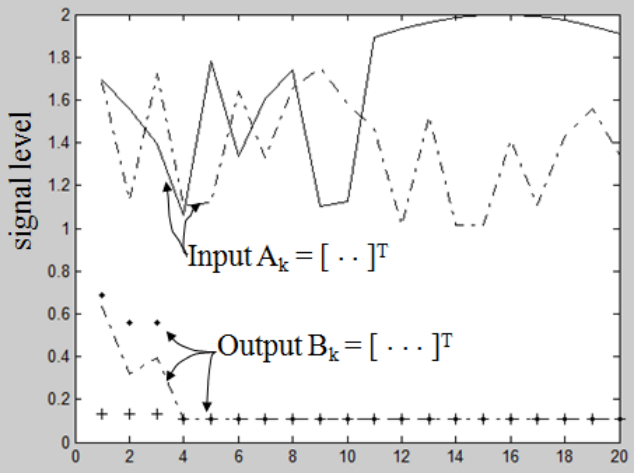

Figure 3. Automaton breaks down and fails to respond to the hidden signal.

The average of 20 Automaton responses shows that the automaton breakdown is typical. See Figure 4. Here, the same input generator was used. The average of output responses of the Kalmaton for the same input signal generator is shown in Figure 5. The response to the "hidden" signal is evident.

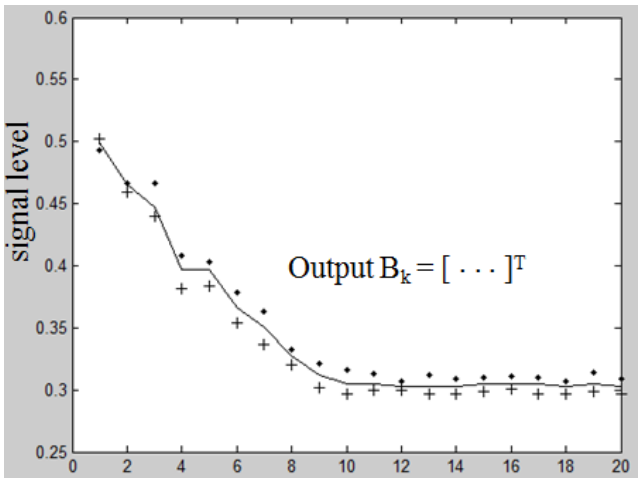

Figure 4. Average of 20 sets of automata show that utomaton breakdown is typical for the input signal of Figure 3.

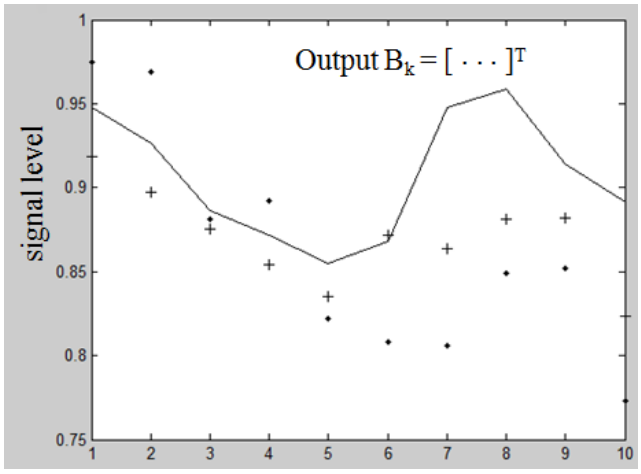

Figure 5. Average Kalmaton output shows response to "hidden" signal is typical.

4 Summary

A Kalman filter can be incorporated into a fuzzy automaton and used to smooth the internal state. The resulting "Kalmaton" can produce a stable automaton response while retaining the ability to perform an effective change detection.

5 References

[1] Gyorgy E. Revesz, Introduction to Formal Languages, Dover, 1991.

[2] George J. Klir and Bo Yuan, Fuzzy Sets and Fuzzy Logic, Prentice Hall, 1995.

[3] Mohinder S. Grewal and Angus P. Andrews, Kalman Filtering: Theory and Practice Using MATLAB, 3rd Edition, Wiley, 2008.

[4] Robert F. Stengel, Optimal Control and Estimation, Dover, 1994.

6 Appendix: MATLAB® Code

```
%
%  Scott Imhoff, PhD          15 June 2011
%  Palak Thakkar
%

M = 20;

Actions = rand(M,2)

for k = M/2+1:M
   Actions(k,1) = sin(2*k/M);
   Actions(k,2) = Actions(k-M/2,2)^2;
end

figure
plot(1:M,Actions(:,1)+1,'k')
hold on
plot(1:M,Actions(:,2)+1,'k-.')

I = [1 0 0 0; 0 1 0 0; 0 0 1 0; 0 0 0 1];

phi = rand(4,4);
phi(2,1) = phi(1,2);
phi(3,1) = phi(1,3);
phi(4,1) = phi(1,4);
phi(3,2) = phi(2,3);
phi(4,2) = phi(2,4);
phi(4,3) = phi(3,4);

Rho = rand(4,4)

H = rand(4,4)

R = rand(4,3)

S = zeros([4 4 2]);

S(:,:,1) = rand(4,4);
S(:,:,2) = rand(4,4);

C = rand(1,4)

x = rand(4,1)

P = rand(4,4)

B_buffer = zeros(M,3);

for k = 1:M

   A = Actions(k,:);

   [SA] = maxmin(A,S);

   z = aggregate(x,SA)';

   x = phi*x;

   P = phi*P*phi';

   %  Update

   K = P*H'*inv(H*P*H' + Rho);  % Kalman gain

   P = (I - K*H)*P;  % Update covariance

   x  =  x  + K*(z - H*x); % Update state

   [B] = aggregate(x,R);

   B_buffer(k,:) = B(:);

end


plot(1:M,B_buffer(:,1),'k+')
plot(1:M,B_buffer(:,2),'k.')
plot(1:M,B_buffer(:,3),'k-.')
```

A Fuzzy-Reasoning Radial Basis Function Neural Network with Reinforcement Learning Method

Ying-Kuei Yang, Jin-Yu Lin, Wei-Li Fang and Jung-Kuei Pan
Dept. of Electrical Engineering, National Taiwan University of Science & Technology, Taipei, Taiwan
Email: yingkyang@yahoo.com

Abstract - *Some researchers have proposed a self-constructing rule-based fuzzy system based on reinforcement learning, which often results in a 5-layer neural network. The Fuzzy-reasoning Radial Basis Function Neural Network (FRBFN) proposed in this paper has only 3 layers to reduce its forwarding calculation time. The network has no fuzzification and defuzzification in the learning system. The Radial Basis Function Neural Network (RBFN) is employed in FRBFN to offer the generality and smoothness of the network. The conducted experiment shows the proposed network has good performance on well training a rule-based fuzzy system through reinforcement learning.*

Keywords: fuzzy systems, radial basis function neural network, reinforcement learning, supervised learning

1 Motivation

The rule-based fuzzy systems have been successfully used in many real-world control applications [1]. Many researchers have devoted research on constructing rules and membership functions by system itself through learning [2][3][4][5]. Supervised learning requires sample data sufficiently large enough to learn. The use of reinforcement learning is to eliminate this requirement. Reinforcement learning method is based on a trial-and-error method and therefore no precise training pair is required [6][7][8][9][10].

Most researchers have considered a fuzzy system as a five layers neural network. This selection is to map input variables, input membership functions, rule base, output membership functions and output variables to each layer of neural network respectively. The use of five layers has created a complex neural network that requires high computation cost. A less layers of neural network that performs the same function is proposed in this thesis. This idea comes from the similarity between a Radial Basis Function Neural Network (RBFN) and a rule-based fuzzy system [11][12]. The proposed network has only three layers: input layer, hidden layer and output layer. The layer reduction can decrease the computation cost and enhance the learning speed of a network system.

2. The Fuzzy-Reasoning Radial Basis Function Neural Network (FRBFN)

2.1 Network Architecture

The logical network of proposed FRBFN is shown in Figure 1.

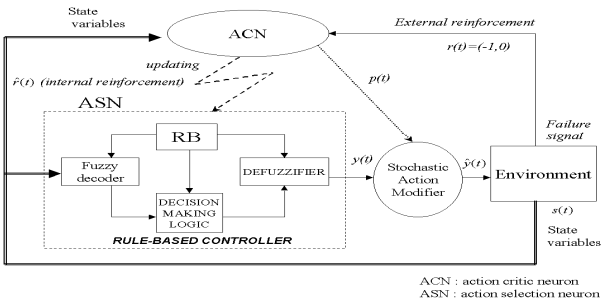

Figure 1. Logical Network Architecture of FRBFN

There are four functional blocks in Figure 1. Action Critic Network (ACN), Action Selection Network (ASN) and Stochastic Action Modifier (SAM) function blocks are the basic components of FRBFN network. The environment function block on the right is the target for control purpose.

2.2 Function of ASN

ASN acts as a rule-based fuzzy logic controller that includes three basic components in a fuzzy system: fuzzification, inference engine and defuzzification [1]. Because of the equivalence between rule-based fuzzy system and RBFN[11][12], a RBFN is introduced to implement an ASN. The RBFN performs the task of what a fuzzy system can do and eliminates the procedures of fuzzification and defuzzification. The network architecture of ASN implemented by RBFN is shown in Figure 2. ASN receives state variables *s(t)* from environment, such as a controlled plant and internal reinforcement signal $\hat{r}(t)$ generated from ACN. The state variables offer the information about plant's current status. For the associated reinforcement learning system, both the state variables and the internal reinforcement signals are used as a criteria to update learning parameters in ASN. The values of these parameters are learned and consequently generated through the signals of state variables *s(t)* and internal reinforcement signal $\hat{r}(t)$.

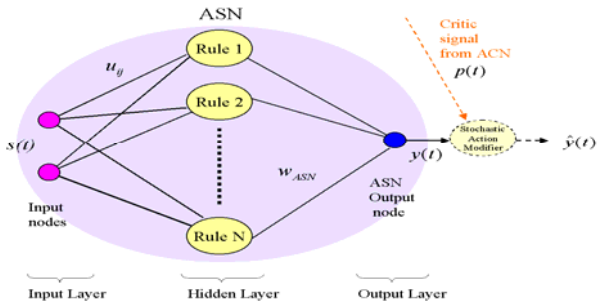

Figure 2. Block diagram of Action Selection Network (ASN)

The output of ASN does not directly apply to the controlled plant. Instead, the output *y(t)* of ASN is first sent to the Stochastic Action Modifier (SAM). The SAM then tries to optimize *y(t)* to generate a modified output $\hat{y}(t)$ based on the predicted reinforcement signal $p(t)$ at that time and its stochastic algorithm.

$$\hat{y}(t) = N(y(t), \sigma(t)) \qquad (1)$$

where N is a normal or Gaussian distribution function with mean $y(t)$ and variance $\sigma(t)$. A small value of $\sigma(t)$ indicates the system is closer to a stable situation. For our learning algorithm, we choose probability function $\sigma_p(t)$ as

$$\sigma_p(t) = \frac{1}{1+e^{2p(t)}} \qquad (2)$$

where $p(t)$ is generated by ACN and is the signal used to predict reinforcement signal $r(t)$.

2.3 Function of ACN

The function of an ACN shown in Figure 1 is to generate signals of $p(t)$ and $\hat{r}(t)$ by receiving state variables and external reinforcement signals. The output signal $p(t)$ is a prediction signal and $\hat{r}(t)$ is an internal reinforcement signal. The purpose of $p(t)$ is to predict the infinite discounted prediction signal $z(t)$ and $\hat{r}(t)$ is the difference between $p(t)$ and $z(t)$. The objective of ACN is to model the environment such that it can perform a multi-step prediction of reinforcement signal for the current action chosen by ASN. Using a Radial Basis Function Network (RBFN) is proposed to implement an ACN, because a RBFN has the ability to approximate the real-valued mapping of continuous or piecewisely continuous function. Another reason to use RBFN is for total network architecture of FRBFN. If both the ASN and ACN use the same neural network architecture, some layers of RBFN can be shared. The network diagram of ACN is shown in Figure 3.

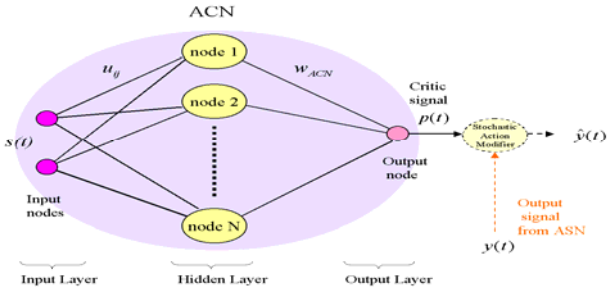

Figure 3. Block diagram of Action Critic Network (ACN)

The input space *s(t)* of ASN and ACN should be identical because they all receive same information of *s(t)* from the same environment. The input and hidden layers of ASN or ACN can be shared each other. The architecture of proposed FRBFN is more compact by sharing the first two layers,. The network architecture shown in Figure 4 is composed of one ASN and one ACN to form the final version of FRBFN.

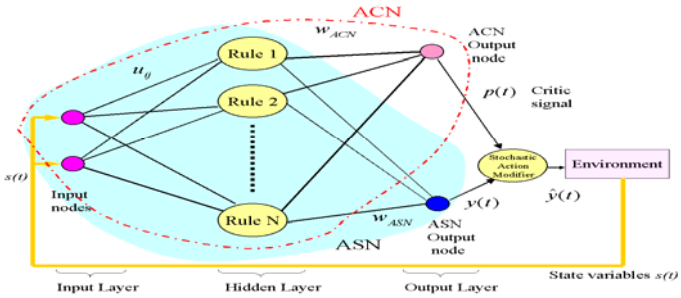

Figure 4. FRBFN implementation diagram

The network diagrams of ASN and ACN shown in Figure 2 and Figure 3 are merged in Figure 4. There are three reasons to combine these two networks: (1) Both ASN and ACN have the same network architecture. (2) The input state space for these two networks is identical. (3) The numbers of hidden nodes in ASN and ACN are identical because of the same input state space. Sharing layer 1 and layer 2 by ACN and ASN will reduce the memory requirement for storage and eliminate the need to recalculate the outputs of hidden nodes. And in learning phase, we do learn widths and centers in hidden nodes once only because ACN and ASN both use the same hidden nodes. These two networks have their own weight parameters between layer 2 and layer3. The network architecture of FRBFN is simpler and the learning parameters are less than others in [3][4][5][6].

2.4 Learning in Action Selection Network

The parameters that need to be adjusted by learning mechanism are centers and widths in nodes of hidden layer and the weights between hidden and output layers. One of the goals of the ASN is to have output that maximizes the

reinforcement signal $r(t)$. The learning relation can be written as:

$$\Delta m_i \propto \frac{\partial r}{\partial m_i} \quad (3)$$

where m_i denotes a parameter to be adjusted and Δm_i is the amount of adjustment applied to the parameter m_i stands for in ASN. The relation indicates that the amount of adjustment to a parameter is proportional to the strength of its associated reinforcement signal. Using chaining rule to expand the right part of equation (3), we have

$$\frac{\partial r}{\partial m_i} = \frac{\partial r}{\partial y} \cdot \frac{\partial y}{\partial m_i} \quad (4)$$

where y is the output of the ASN and $\frac{\partial y}{\partial m_i}$ denotes the amount y is changed when adjustment parameter m_i changes. The equation (4) shows $\frac{\partial r}{\partial y}$ and $\frac{\partial y}{\partial m_i}$ are required in order to determine $\frac{\partial r}{\partial m_i}$. The term $\frac{\partial y}{\partial m_i}$ is the gradient information for output regarding to its operational parameter and can be derived easily. But the reinforcement signal is not generated in every time step. The gradient value of $\frac{\partial r}{\partial y}$ can only be **estimated**. In our learning algorithm, we use stochastic exploration method [13] to estimate gradient information $\frac{\partial r}{\partial y}$. For multi-step prediction, the gradient information $\frac{\partial r}{\partial y}$ is estimated as

$$\frac{\partial r}{\partial y} \approx [z_{t-1} - p_{t-1}] \cdot \left[\frac{\hat{y} - y}{\sigma_p}\right]_{t-1} = \hat{r}(t) \cdot \left[\frac{\hat{y} - y}{\sigma_p}\right]_{t-1} \quad (5)$$

The estimation of $\frac{\partial r}{\partial y}$ is defined in equation (5), where z_{t-1} is infinite discounted cumulated outcome. A general network architecture of ASN based on RBFN is shown in Figure 5.

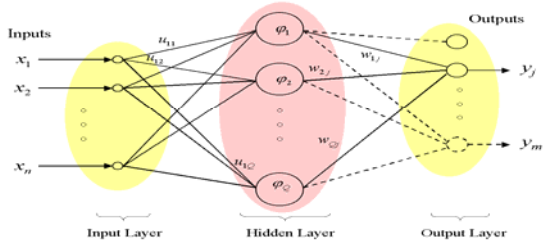

Figure 5. General Network Architecture of ASN

2.5 Learning for weights between hidden and output layers of ASN

Let's discuss weight w_{ij} between *i-th* hidden node and *j-th* output. The kernel function used in ASN is Gaussian function. From Figure 5, the output y_j for *j-th* output node can be expressed as

$$y_j = \sum_{i=1}^{Q} \varphi_i w_{ij} = \sum_{i=1}^{Q} \exp\left(-\frac{(x_{i,1} - v_{i,1})^2}{2\sigma_{i,1}^2} - \frac{(x_{i,2} - v_{i,2})^2}{2\sigma_{i,2}^2} - \cdots - \frac{(x_{i,n} - v_{i,n})^2}{2\sigma_{i,n}^2}\right) \cdot w_{ij} \quad (6)$$

where w_{ij} is the weight between *i-th* hidden node and *j-th* output node. The variable being interested in equation (6) is w. The equation (4) can be re-expressed as (m_i is replaced by w_{ij})

$$\frac{\partial r}{\partial w_{ij}} = \frac{\partial r}{\partial y_j} \cdot \frac{\partial y_j}{\partial w_{ij}} \quad (7)$$

where $y_j = \sum_i \varphi_i w_{ij}$ denotes the output value of the *j-th* output node in ASN.

Because $\frac{\partial y_j}{\partial w_{ij}} = \frac{\partial}{\partial w_{ij}} \sum_i \varphi_i w_{ij} = \varphi_i$, applying equation (5) to equation (7), we have

$$\frac{\partial r}{\partial w_{ij}} = \hat{r}(t) \cdot \left[\frac{\hat{y}_j - y_j}{\sigma_p}\right]_{t-1} \varphi_i(t-1) \quad (8)$$

According to equation (3) and equation (8), the learning rule for weights between *i-th* hidden node and *j-th* output node is

$$\Delta w_{ij} = \alpha_{ASN_w} \cdot \frac{\partial r}{\partial w_{ij}} = \alpha_{ASN_w} \cdot \hat{r}(t) \cdot \left[\frac{\hat{y}_j - y_j}{\sigma_p}\right]_{t-1} \varphi_i(t-1) \quad (9)$$

where α_{ASN_w} is a positive learning rate for weights in ASN. So, the weight $w_{ij}(t+1)$ needs to be adjusted by Δw_{ij}, that is

$$w_{ij}(t+1) = w_{ij}(t) + \Delta w_{ij} = w_{ij}(t) + \alpha_{ASN_w} \cdot \hat{r}(t) \cdot \left[\frac{\hat{y}_j - y_j}{\sigma_p}\right]_{t-1} \varphi_i(t-1) \quad (10)$$

2.6 Learning for centers in ASN hidden layer

The kernel function of hidden nodes in FRBFN is Gaussian function. There are two parameters, width and center, should be adjusted in hidden nodes. The interested variable is center *v* in equation (6). Because a hidden node in FRBFN is a multi-dimensional node, the output of a hidden node is a non-linear transformation based on Euclidean distance. Therefore, only the calculation of the Euclidean norm between input state and its center is required for multi-linguistic variable cases to perform Gaussian transformation.

Since the interested variable is *v*, by equation (4), the center parameters can be adjusted with respect to each individual dimension.

$$\frac{\partial r}{\partial v_{i,j}} = \frac{\partial r}{\partial y} \cdot \frac{\partial y}{\partial v_{i,j}} \quad (11)$$

where *i* stands for the *i-th* rule node and *j* stands for the *j-th* dimension. Referring to equation (5) and (6),

$$y_j = \sum_{i=1}^{Q} \varphi_i w_{ij} = \sum_{i=1}^{Q} \exp\left(-\frac{(x_{i,1}-v_{i,1})^2}{2\sigma_{i,1}^2} - \frac{(x_{i,2}-v_{i,2})^2}{2\sigma_{i,2}^2} - \cdots - \frac{(x_{i,n}-v_{i,n})^2}{2\sigma_{i,n}^2}\right) \cdot w_{ij}$$

the center parameter can be adjusted in every dimension by

$$\frac{\partial r}{\partial v_{i,j}} = \frac{\partial r}{\partial y}\cdot\frac{\partial y}{\partial v_{i,j}} = \frac{\partial r}{\partial y}\cdot\frac{\partial}{\partial v_{i,j}}\sum_i \exp\left(\frac{(x_{i,1}-v_{i,1})^2}{2\sigma_{i,1}^2} - \cdots - \frac{(x_{i,n}-v_{i,n})^2}{2\sigma_{i,n}^2}\right)\cdot w_{ij}$$

$$= \frac{\partial r}{\partial y}\cdot\left(\sum_i \exp\left(\frac{(x_{i,1}-v_{i,1})^2}{2\sigma_{i,1}^2} - \cdots - \frac{(x_{i,n}-v_{i,n})^2}{2\sigma_{i,n}^2}\right)\cdot w_{ij}\right)\cdot\frac{\partial}{\partial v_{i,j}}\left(\frac{(x_{i,1}-v_{i,1})^2}{2\sigma_{i,1}^2} - \cdots - \frac{(x_{i,j}-v_{i,j})^2}{2\sigma_{i,j}^2} - \cdots - \frac{(x_{i,n}-v_{i,n})^2}{2\sigma_{i,n}^2}\right)$$

$$= \frac{\partial r}{\partial y}\cdot\left(\sum_i \exp\left(\frac{(x_{i,1}-v_{i,1})^2}{2\sigma_{i,1}^2} - \cdots - \frac{(x_{i,n}-v_{i,n})^2}{2\sigma_{i,n}^2}\right)\cdot w_{ij}\right)\cdot\left(0 - \cdots + \frac{(x_{i,j}-v_{i,j})_{t-1}}{\sigma_{i,j}^2(t-1)} - \cdots - 0\right)$$

$$= \underbrace{\hat{r}(t)\cdot\left[\frac{\hat{y}-y}{\sigma_p}\right]_{t-1}}_{a}\cdot\underbrace{\varphi_i(t-1)}_{b}\cdot\underbrace{\frac{(x_{i,j}-v_{i,j})_{t-1}}{\sigma_{i,j}^2(t-1)}}_{c} \qquad (12)$$

a: estimated gradient
b: to decide effectiveness
c: to decide direction & amount

Part a is an estimated gradient information, as discussed in equation (5). Part b is one of the factors affects the adjustment amount. In part c, the nominator decides the direction and amount of adjustment. According to equation (3) and equation (12), the learning rule for center in *j-th* dimension of *i-th* output node is

$$\Delta v_{i,j} = \alpha_{ASN_v}\cdot\frac{\partial r}{\partial v_{i,j}} = \alpha_{ASN_v}\cdot\hat{r}(t)\cdot\left[\frac{\hat{y}-y}{\sigma_p}\right]_{t-1}\cdot\frac{(x_{i,j}-v_{i,j})_{t-1}}{\sigma_{i,j}^2(t-1)}\cdot\varphi_i(t-1) \quad (13)$$

where α_{ASN_w} is a positive learning rate for weight in ASN. So, the center $v_{ij}(t+1)$ needs to be adjusted by Δv_{ij}, that is

$$v_{i,j}(t+1) = v_{i,j}(t) + \alpha_{ASN_v}\cdot\hat{r}(t)\cdot\left[\frac{\hat{y}-y}{\sigma_p}\right]_{t-1}\cdot\frac{(x_{i,j}-v_{i,j})_{t-1}}{\sigma_{i,j}^2(t-1)}\cdot\varphi_i(t-1) \quad (14)$$

2.6 Learning for widths in ASN hidden layer

The interested variable is center σ in equation (6). The width in dimensions can be either equal to or different from each other.

2.6.1 Equal width in each dimension

A Gaussian kernel function is described in equation (3) a hidden node as:

$$y = \sum_i \varphi_i w_i = \sum_i \exp\left(-\frac{\|\vec{x}_i - \vec{v}_i\|^2}{2\sigma_i^2}\right)\cdot w_i \qquad (15)$$

Since the interested variable is σ, by equation (4) and (5) the width parameters can be adjusted by.

$$\frac{\partial r}{\partial \sigma_i} = \frac{\partial r}{\partial y}\cdot\frac{\partial y}{\partial \sigma_i} = \frac{\partial r}{\partial y}\cdot\frac{\partial}{\partial \sigma_i}\left(\exp\left(-\frac{\|\vec{x}_i - \vec{v}_i\|^2}{2\sigma_i^2}\right)\right)\cdot w_i$$

$$= \frac{\partial r}{\partial y}\cdot\left(\exp\left(-\frac{\|\vec{x}_i - \vec{v}_i\|^2}{2\sigma_i^2}\right)\right)\cdot w_i\cdot\frac{\partial}{\partial \sigma_i}\left(-\frac{\|\vec{x}_i - \vec{v}_i\|^2}{2\sigma_i^2}\right)$$

$$= \frac{\partial r}{\partial y}\cdot\varphi_i\cdot w_i\cdot\|\vec{x}_i - \vec{v}_i\|^2\cdot\sigma_i^{-3}$$

$$= \hat{r}(t)\cdot\left[\frac{\hat{y}-y}{\sigma_p}\right]_{t-1}\cdot\left(\varphi_i\cdot w_i\cdot\|\vec{x}_i - \vec{v}_i\|^2\cdot\sigma_i^{-3}\right)_{t-1} \qquad (16)$$

According to equation (3) and equation (16), the learning rule for width at *i-th* hidden node is

$$\Delta\sigma_i = \alpha_{ASN_\sigma}\cdot\frac{\partial r}{\partial \sigma_i} = \alpha_{ASN_\sigma}\cdot\hat{r}(t)\cdot\left[\frac{\hat{y}-y}{\sigma_p}\right]_{t-1}\cdot\left(\varphi_i\cdot w_i\cdot\|\vec{x}_i - \vec{v}_i\|^2\cdot\sigma_i^{-3}\right)_{t-1} \quad (17)$$

where α_{ASN_σ} is a positive learning rate for a width in ASN. The width $\sigma_i(t+1)$ needs to be adjusted by $\Delta\sigma_i$, that is

$$\sigma_i(t+1) = \sigma_i(t) + \Delta\sigma_i = \sigma_i(t) + \alpha_{ASN_\sigma}\cdot\hat{r}(t)\cdot\left[\frac{\hat{y}-y}{\sigma_p}\right]_{t-1}\cdot\left(\varphi_i\cdot w_i\cdot\|\vec{x}_i - \vec{v}_i\|^2\cdot\sigma_i^{-3}\right)_{t-1} \quad (18)$$

Here all width parameters in each dimension are assumed to have equal width to simplify the learning algorithm. This scaling factor u_{ij} is shown in Figure 5. This assumption does not violate the correctness of our proposed network.

2.6.2 Different width in each dimension

Since the interested variable is $\sigma_{i,j}$, by equation (4)(5) and (15) the width parameters can be adjusted by.

$$\frac{\partial r}{\partial \sigma_{i,j}} = \frac{\partial r}{\partial y}\cdot\frac{\partial y}{\partial \sigma_{i,j}} = \frac{\partial r}{\partial y}\cdot\frac{\partial}{\partial \sigma_{i,j}}\sum_i \exp\left(\frac{(x_{i,1}-v_{i,1})^2}{2\sigma_{i,1}^2} - \cdots - \frac{(x_{i,n}-v_{i,n})^2}{2\sigma_{i,n}^2}\right)\cdot w_{ij}$$

$$= \frac{\partial r}{\partial y}\cdot\sum_i \exp\left(\frac{(x_{i,1}-v_{i,1})^2}{2\sigma_{i,1}^2} - \cdots - \frac{(x_{i,n}-v_{i,n})^2}{2\sigma_{i,n}^2}\right)\cdot w_{ij}\cdot\frac{\partial}{\partial \sigma_{i,j}}\left(\frac{(x_{i,1}-v_{i,1})^2}{2\sigma_{i,1}^2} - \cdots - \frac{(x_{i,j}-v_{i,j})^2}{2\sigma_{i,j}^2} - \cdots - \frac{(x_{i,n}-v_{i,n})^2}{2\sigma_{i,n}^2}\right)$$

$$= \frac{\partial r}{\partial y}\cdot\sum_i \exp\left(\frac{(x_{i,1}-v_{i,1})^2}{2\sigma_{i,1}^2} - \cdots - \frac{(x_{i,n}-v_{i,n})^2}{2\sigma_{i,n}^2}\right)\cdot w_{ij}\cdot\left(-0 - \cdots + \|\vec{x}_i - \vec{v}_i\|^2\cdot\sigma_{i,j}^{-3} - \cdots - 0\right)$$

$$= \frac{\partial r}{\partial y}\cdot\varphi_i\cdot w_{ij}\cdot\|\vec{x}_i - \vec{v}_i\|^2\cdot\sigma_{i,j}^{-3}$$

$$= \hat{r}(t)\cdot\left[\frac{\hat{y}-y}{\sigma_p}\right]_{t-1}\cdot\left(\varphi_i\cdot w_i\cdot\|\vec{x}_i - \vec{v}_i\|^2\cdot\sigma_{i,j}^{-3}\right)_{t-1} \qquad (19)$$

This is the amount need to be adjusted for the *i-th* node in dimension *j*. According to equation (3) and equation (19), the learning rule for width at *i-th* hidden node is

$$\Delta\sigma_{i,j} = \alpha_{ASN_\sigma}\cdot\frac{\partial r}{\partial \sigma_{i,j}} = \alpha_{ASN_\sigma}\cdot\hat{r}(t)\cdot\left[\frac{\hat{y}-y}{\sigma_p}\right]_{t-1}\cdot\left(\varphi_i\cdot w_i\cdot\|\vec{x}_i - \vec{v}_i\|^2\cdot\sigma_{i,j}^{-3}\right)_{t-1} \quad (20)$$

where α_{ASN_σ} is a positive learning rate for a width in ASN. The width in each dimension $\sigma_{i,j}(t+1)$ needs to be adjusted by $\Delta\sigma_{i,j}$, that is

$$\sigma_{i,j}(t+1)=\sigma_{i,j}(t)+\Delta\sigma_{i,j}=\sigma_{i,j}(t)+\alpha_{ASN_\sigma}\cdot\hat{r}(t)\cdot\left[\frac{\hat{y}-y}{\sigma_p}\right]_{t-1}\cdot\left(\varphi_i\cdot w_i\cdot\left\|\vec{x}_i-\vec{v}_i\right\|^2\cdot\sigma_{i,j}^{-3}\right)_{t-1} \quad (21)$$

3. Conclusion

The proposed Fuzzy-reasoning Radial Basis Function Neural Network has been applied to control a cart-pole balancing system and the result has shown our proposed system works better. The experiment is not discussed detailed here due to space limit.

The contribution of this paper can be summarized as:

1. The Fuzzy-Reasoning Radial Basis Function Neural Network (FRBFN) is proposed to incorporate the reinforcement learning method with a neural network.
2. Because of the corresponding equivalence between a fuzzy system and a radial basis function neural network, the proposed FRBFN has only three layers due to the elimination of fuzzification and defuzzification functions. This feature significantly reduces the computation cost.
3. The suggestion of combining together the input and hidden layers of ASN and ACN, which simplifies the proposed FRBFN architecture.

The formula of adjusting parameters in ASN and ACN are derived for the proposed architecture.

4. References

1. C. T. Lin and C.S. Lee, "Neural Fuzzy Systems: a Neuro-Fuzzy Synergism to Intelligent Systems", Prentice Hall , 1996.
2. T. Watanabe, "A study on multi-agent reinforcement learning problem based on hierarchical modular fuzzy model", IEEE International Conference on Fuzzy Systems, 2009 , Page(s): 2041 - 2046
3. Y.-C. Wang; C.-J. Chien; D.-T. Lee, "Reinforcement fuzzy-neural adaptive iterative learning control for nonlinear systems", 10th International Conference on Control, Automation, Robotics and Vision, 2008 , Page(s): 733 – 738
4. N. B. Karayiannis, M. M. Randolph-Gips, "On the construction and training of reformulated radial basis function neural networks", *IEEE Transactions on Neural Networks*, Volume: 18,Issue: 1, 2003 , Page(s): 835 - 846
5. L. E. V. Silva, J. J. Duque, R. Tinós, L. O. Murta, "Reconstruction of multivariate signals using q-Gaussian radial basis function Network", International Conference on Computing in Cardiology, 2010 , Page(s): 465 - 468
6. Ferreyra, J. de Jesus Rubio, "A new on-line self-constructing neural fuzzy network", 45th IEEE Conference on Decision and Control, 2006 , Page(s): 3003 – 3009
7. C. W. Anderson, P. M. Young, M. R. Buehner, J. N. Knight, K. A. Bush, and D. C. Hittle, "Robust Reinforcement Learning Control Using Integral Quadratic Constraints for Recurrent Neural Networks", *IEEE Transactions on Neural Networks*, 2007 , Volume: 18 , Issue: 4 , Page(s): 993 – 1002
8. X, Ruan; J. Cai; J. Chen, "Learning to Control Two-Wheeled Self-Balancing Robot Using Reinforcement Learning Rules and Fuzzy Neural Networks", Fourth International Conference on Natural Computation, 2008 , Page(s): 395 - 398
9. M. Hacibeyoglu, and A. Arslan, "Reinforcement learning accelerated with artificial neural network for maze and search problems", 3rd Conference on Human System Interactions, 2010 , Page(s): 124 – 127
10 R. V. Florian, "A reinforcement learning algorithm for spiking neural networks", Seventh International Symposium on Symbolic and Numeric Algorithms, 2005
11. J. R. Jang and C. T. Sun, "Function Equivalence Between Radial Basis Function Networks and Fuzzy Inference Systems", *IEEE Trans. on Neural Networks*, vol. 4 no. 1, Jan 1993.
12. K. J. Hunt, R. Haas and R. M. Smith, "Extending the Functional Equivalence of Radial Basis Function Networks and Fuzzy Inference Systems", *IEEE Trans. On Neural Networks*, vol.7, no.3, May 1996.
13 R. S. Sutton, "Generalization in Reinforcement Learning: Successful Examples Using Sparse Coarse Coding", Advances in Neural Information Processing Systems 8, pp.1038-1044, MIT Press, 1996.

Fuzzy Coincidence Analyzing Automaton

Joel Shaklee, Scott Imhoff, John Mallinger, and Palak Thakkar
Intelligence and Information Systems, Raytheon Company, Aurora, Colorado, USA

Abstract - *This paper describes a Fuzzy Coincidence Analyzing Automaton. In network applications, when a number of channels are being monitored, it often happens that signals on different channels coincide in time. Usually, different combinations of coinciding signals in different combinations of channels give rise to different semantics. The present algorithm is an automaton, which monitors a set of L signal channels and, when pre-selected coincidences occur, outputs signals in alarm channels. Other sets of coinciding signals do not activate the alarm. Alarms may persist until reset by a pre-selected set of reset signals on the same L channels. The automaton is fuzzy so that it can operate in conditions of varying signal strength and in the presence of drop-outs.*

Keywords: Fuzzy logic, coincidence detection, automaton, change detection, machine learning

1 Introduction

We present an algorithm for monitoring a set of signal channels appearing at a number of separate points at fixed locations within the same system. We use a fuzzy automaton to monitor the signals so that an alarm can be issued if certain known sets of coinciding signals occur. Several of the antecedents of our approach are as follows: Hildebrand [1] applied fuzzy logic to monitoring resource status of enterprise systems so that alerts to personnel are sent when triggering events occur. Zaitsev discusses monitoring system resource utilization using fuzzy logic rules [2]. Our algorithm works for similar applications but uses fuzzy automata to transition a fuzzy internal state vector until conditions warrant the issuance of an alarm. Fuzzy automata are discussed in Klir and Yuan [3]. The training of fuzzy automata using genetic algorithms is discussed in Nguyen, Imhoff, and Kent [4].

Aggregation is a way of combining matrices that replaces the binary multiplication operation with binary min and replaces the sum with the max operation. If $\circ$ denotes the aggregation operation then we have the following:

$$[1 \quad 0.8 \quad 0.6] \circ \begin{bmatrix} 0 & 0.4 & 0.4 \\ 0.3 & 1 & 0 \\ 0.5 & 0 & 0 \end{bmatrix} =$$
$$\{max[min(1,0), min(0.8,0.3), min(0.6,5)], \ldots$$
$$max[min(1,0.4), min(0.8,1), min(0.6,0)], \ldots$$
$$max[min(1,0.4), min(0.8,0), min(0.6,0)]\} = [0.5 \quad 0.8 \quad 0.4]$$

(1)

An example of the aggregation of a 1-D matrix with a 3-D matrix is as follows:

$$[1 \quad 0.4] \circ \left[\begin{bmatrix} 0 & 0.4 & 0.2 \\ 0.3 & 1 & 0 \\ 0.5 & 0 & 0 \end{bmatrix} \begin{bmatrix} 0 & 0 & 1 \\ 0.2 & 0 & 0 \\ 0 & 0 & 0 \end{bmatrix}\right] =$$
$$\begin{bmatrix} max\{min(1,0), min(0.4,0)\} & max\{min(1,0.4), min(0.4,0)\} & max\{min(1,0.2), min(0.4,1)\} \\ max\{min(1,0.3), min(0.4,0.2)\} & max\{min(1,1), min(0.4,0)\} & max\{min(1,0), min(0.4,0)\} \\ max\{min(1,0.5), min(0.4,0)\} & max\{min(1,0), min(0.4,0)\} & max\{min(1,0), min(0.4,0)\} \end{bmatrix} =$$
$$\begin{bmatrix} 0 & 0.4 & 0.4 \\ 0.3 & 1 & 0 \\ 0.5 & 0 & 0 \end{bmatrix}$$

(2)

An automaton is a kind of state machine. There is typically more than one state that the automaton can be in. As symbols (inputs) from the environment arrive, the automaton may or may not transition from one state to the next, depending on the allowable transitions S. For example, suppose an automaton which detects English language receives the symbol "th" and transitions to a state i. If the next symbol arriving from the environment is "q", the automaton will not transition to state $i + 1$ because "thq" is not a word in the English language. If, however, the environment inputs the symbol "e", the automaton will transition to state $i + 1$ because "the" is an English word. When "q" arrives, the automaton's response is "this is not English." When "e" arrives, the automaton's response is "this is English."

A fuzzy automaton consists of a 3-D matrix of fuzzy state transition, S, of size $N \times N \times L$, a fuzzy input from the environment, which is a vector, A, of length L, a 2-D fuzzy response matrix, R, of size $N \times P$, a vector initial internal state vector, c, of length N, a vector current internal state E, of length N, and an output 2-D matrix, B, of size $N \times P$.

The algorithm appears in block diagram in Figure 1. It consists of a Learning Algorithm, by which the automaton learns its fuzzy transitions S and a Run Algorithm by which S is applied to an arriving stream of several channels of data represented by A. It is in operation of the Run Algorithm that the system responds to certain combinations of coinciding signals and raises the alarm.

The algorithm uses a novel technique of distributing the anti-diagonal to initialize the 3-D matrix S of fuzzy transitions. Other points of novelty include equipping S with a diagonal in $S(:,:,1)$ to propagate the internal state E and the anti-diagonal in $S(:,:,L)$ to reset the automaton after an alarm has occurred.

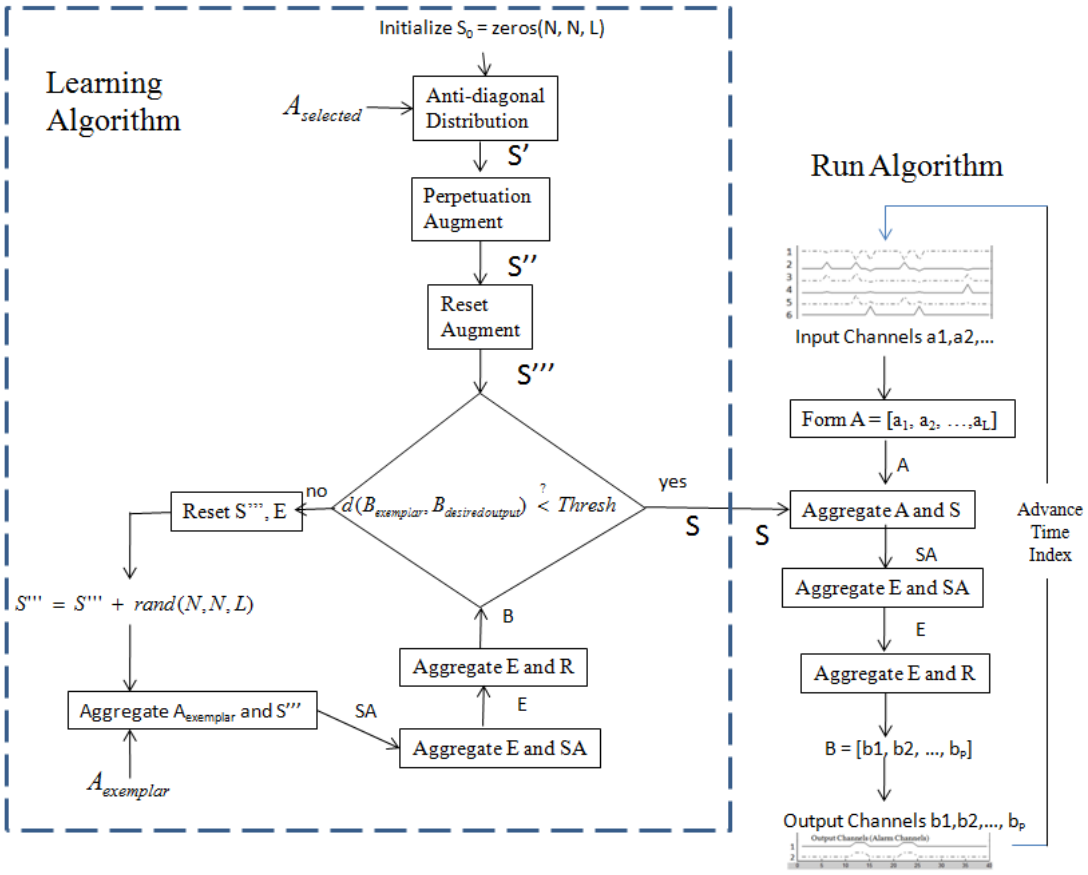

Figure 1: Fuzzy Coincidence Analyzing Automaton

2 Description of Algorithm

In the Learning Algorithm, the matrix of fuzzy transitions S''' is formed by advancing S through a series of procedures which equip S with the properties it needs to function properly in the run environment. As we equip S with the properties it needs, S becomes S', S' becomes S'', and S'' becomes S'''.

It becomes easy to detect a set of coinciding signals that flip the internal state of an automaton. The internal state of an automaton is said to *flip* when $[e_1\ e_2\ e_3\ \ldots\ e_j]^T$ becomes $[e_j\ e_{j-1}\ \ldots\ e_1]^T$. A selected coincidence of signals $A_{selected}$ is used to equip S with the ability to flip the internal state of the automaton when the selected signal coincidence occurs. A technique of *anti-diagonal distribution* is used to determine a matrix of fuzzy transitions S'. An example is shown in Figure 2. The algorithm provides that each non-zero element of A activates a portion of an anti-diagonal during an $A \circ S$ aggregation so that the aggregated *intermediate* matrix SA is the anti-diagonal. Then SA reverses the internal state E during its aggregation with E. The algorithm for the anti-diagonal distribution is as follows:

$$
\begin{array}{l}
Initialize\ S = zeros(N,N,L) \\
Initialize\ c = 0 \\
for\ k = 1{:}L \\
\quad if\ a_k == 1 \\
\quad\quad c = c + 1 \\
\quad\quad for\ i = 1{:}N \\
\quad\quad\quad S_{(i)(N+1-k)(k)} = \begin{cases} 1, & \eta(c-1)+1 \le \eta c + 1 \\ 0, & otherwise \end{cases} \\
\quad\quad end\ for \\
\quad end\ if \\
end\ for
\end{array}
$$

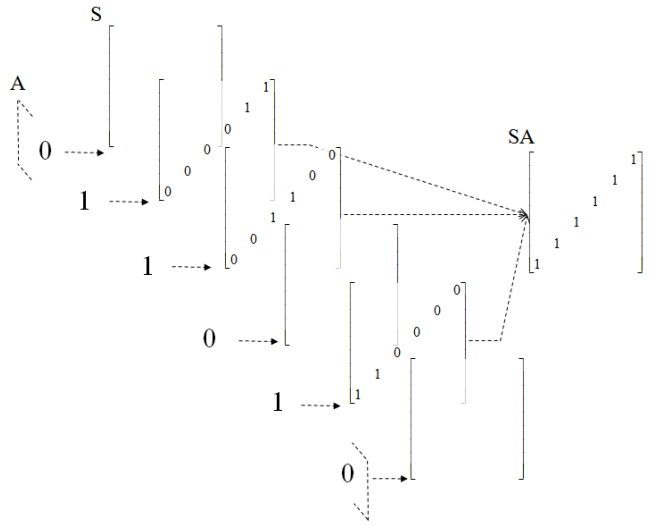

Figure 2: 'Distributing the Antidiagonal' – Preparing a transition matrix so that, when select coincidence occurs, the internal state of the automaton flips over.

The next step in the Learning Algorithm is to equip the $S(:,:,1)$ matrix with the diagonal. This maintains automaton health, meaning that the automaton won't get stuck in a state where its responses become insensitive to the inputs. Thus S'' is formed. The next step is to equip the $S(:,:,L)$ matrix with the anti-diagonal. This is used to reset the automaton after an alarm has been sent. This is S'''.

The remainder of the Learning Algorithm serves to make the automaton fuzzy and able to respond to exemplar signals in a desired way. For each exemplar, the Euclidean distance between the desired output and the actual exemplar output, $d(B_{exemplar}, B_{desired\ output})$, is monitored while S''' is perturbed by the addition of random numbers. Each $d(B_{exemplar}, B_{desired\ output})$ that does not meet a selected threshold causes the automaton to reset to S'''. After a reset, $A_{exemplar}$ is aggregated with S''', E is aggregated with SA, and then E is aggregated with R to produce the next output $B_{exemplar}$ to be used in the comparison. This is repeated until a fuzzy state matrix S having the desired exemplar responses, is obtained.

The Run Mode algorithm provides for the automaton to monitor a channel of L signals. For each time sample, an input vector $A = [a_1, a_2, \ldots, a_L]$ is formed from the L channels. This is aggregated with the automaton S in order to form the intermediate matrix SA. The internal state E is aggregated with SA to form the updated state E. E is aggregated with the response matrix R to form the output vector B. The elements of B represent one time instance of the output channels. As the time index advances, the L channels of the input are sampled, processed by the automaton, and the output channels (e.g. alarms) are generated.

3 Application of Algorithm

The algorithm was successfully demonstrated. A program Fuzzy_Coincidence_Analyzing_Automaton.m was written to illustrate a simple demonstration instantiation of the algorithm. The demonstration input channels and output alarm channels are plotted in Figure 3. In this example, there are 6 input channels and two output alarm channels. The demonstration shows how a pre-selected fuzzy coincidence sets off alarms while dissimilar fuzzy signals and coinciding signals do not set off the alarms. The algorithm analyzes coinciding signals to determine if the coincidence is important to the overall system and merits the tripping of the alarms. In this demonstration, signals close to $[0.1 \quad 0.9 \quad 0.9 \quad 0.1 \quad 0.9 \quad 0.1]$ cause the alarms to go off while other signals, such as $[0.8 \quad 0.9 \quad 0.8 \quad 0.2 \quad 0.1 \quad 0.1]$ and $[0.9 \quad 0.2 \quad 0.8 \quad 0.9 \quad 0.1 \quad 0.1]$ do not cause the alarms to go off. A signal close to $[0.1 \quad 0.1 \quad 0.1 \quad 0.2 \quad 0.3 \quad 0.9]$ is used to reset the alarms. In this example, the inputs A, the output of the alarms B, the response R, the state transitions S, and the internal states E and C are all fuzzy. The fuzzy state transitions S were initialized using the anti-diagonal algorithm.

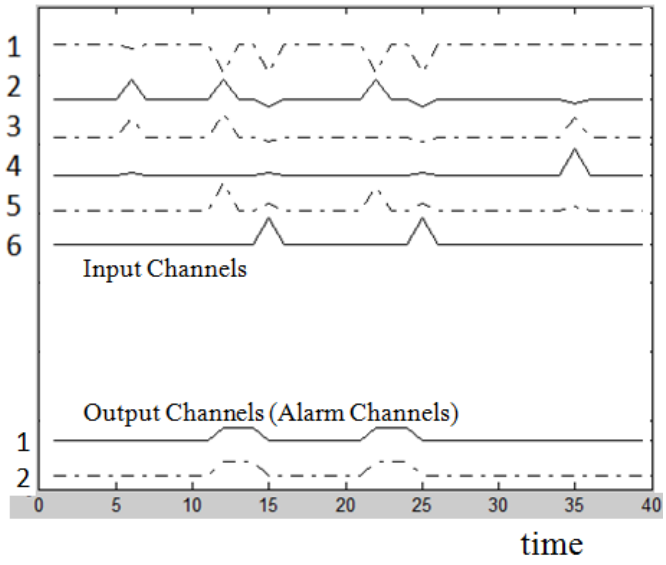

Figure 3: Fuzzy Coincidence Analyzing Algorithm. This example has six input channels and two output channels. An alarm occurs when a pre-selected combination of signals is present.

4 Conclusion

Certain sets of events falling together in time may signal a system condition that warrants the issuance of an alarm. An algorithm for detecting and alarming on certain special coincidences was described as well as an algorithm for training it. In the Learning Algorithm, a fuzzy automaton is prepared so that an arriving signal A_{alarm}, that should cause an alarm, causes the fuzzy transitions S to form an antidiagonal

during the aggregation which forms the intermediate matrix *SA*.

5 References

[1] Dietmar Hildebrand, "Fuzzy Logic-Based Surveillance in Information Technology and Business Service Management Systems," U.S. Patent No. 7,853,538, Dec. 14, 2010.

[2] Oleg V. Zaitsev, "Adaptive Configurations of Conflicting Applications," U.S. Patent No. 7,925,874, Apr. 12, 2011.

[3] George Klir and Bo Yuan, Fuzzy Sets and Fuzzy Logic: Theory and Applications, Pages 349-353, Prentice Hall, 1995.

[4] Duong Nguyen, Scott Imhoff, and Suzan Kent, Fuzzy Genetic Learning Automata Classifier, U.S. Patent No. 6,839,698, Jan. 4, 2005.

6 Appendix : MATLAB® Code

```
%
%  Fuzzy_Coincidence_Analyzing_Automaton
%
%  Scott Imhoff and  Joel Shaklee,          25 August 2011
%
%  This fuzzy automaton analyzes coinciding signals
%  and sends an alarm when the selected combination
%  of signals occurs.
%
%  In this demonstration, signals close to
%  [.1 .9 .9 .1 .9 .1] cause the alarms to go off while
%  other signals such as [.8 .9 .8 .2 .1 .1] and
%  [.9 .2 .8 .9 .2 .1] do not cause the alarms to go off.
%  A signal close to [.1 .1 .1 .2 .3 .9] resets the alarms.
%
%  The matrix of fuzzy transtions S is initialized to respond
%   to a selected coincidence using a method we
%   call 'Antidiagonal Distribution'
%
%  A is the matrix of fuzzy actions from the environment.
%  In this example, every action is a vector of length 6.  S is
%  a 3-D matrix of fuzzy transtions.  In this example, S is
%  a cube 6 on a side.  R is the matrix of fuzzy transtions,
%  in this example, R is a 2x6 matrix, producing two
% output alarms.  B is the matrix of fuzzy outputs.
%  It represents the two output alarms.  E is the internal
%  state of the automaton.  In this example, E has length 6.
%  C is the initial internal state.  C is of the same size as E.

N = 6;

R       = [.9 .8 .7 .6 .5 .4;...
           .4 .5 .6 .7 .8 .9];

Aselect = [.1 .9 .9 .1 .9 .1];

Sdiscrete = AntidiagonalDistribution(Aselect, N)

Sfuzzy = zeros([N N N]);

Sfuzzy(:,:,1) = [-.1 .3 .1 .1 .1 .1;...
        .2 -.2 .2 .1 .1 .1; ...
        .1 .3 -.1 .3 .1 .1; ...
        .1 .1 .2 -.2 .2 .1; ...
        .1 .1 .1 .2 -.1 .2; ...
        .1 .1 .1 .1 .1 -.2;];

Sfuzzy(:,:,2) = [.1 .1 .1 .1 .2 -.2;...
        .1 .1 .1 .3 -.1 .3; ...
        .1 .1 .1 .2 .3 .2; ...
        .1 .1 .1 .1 .1 .1; ...
        .1 .1 .1 .1 .1 .1; ...
        .1 .1 .1 .1 .1 .1;];

Sfuzzy(:,:,3) = [.1 .1 .1 .1 .1 .1;...
        .1 .1 .1 .1 .2 .1; ...
        .1 .1 .2 -.2 .2 .1; ...
        .1 .3 -.1 .3 .1 .1; ...
        .1 .3 .1 .1 .1 .1; ...
        .1 .1 .1 .1 .1 .1;];

Sfuzzy(:,:,4) = [.1 .2 .3 .2 .1 0;...
        0 .1 .2 .3 .2 .1; ...
        .1 .2 .3 .2 .1 0;...
        0 .1 .2 .3 .2 .1; ...
        .1 .2 .3 .2 .1 0;...
        0 .1 .2 .3 .2 .1];

Sfuzzy(:,:,5) = [.1 .1 .1 .1 .1 .1;...
        .1 .1 .1 .1 .1 .1; ...
        .1 .1 .1 .1 .1 .1; ...
        .1 .1 .2 .1 .1 .1; ...
        .2 -.2 .2 .1 .1 .1; ...
        -.1 .3 .1 .1 .1 .1];

Sfuzzy(:,:,6) = [.1 .1 .1 .1 .2 .8;...
        .1 .1 .1 .3 .9 .3; ...
        .1 .1 .2 .8 .2 .1; ...
        .1 .3 .9 .3 .1 .1; ...
        .2 .8 .2 .1 .1 .1; ...
        .9 .3 .1 .1 .1 .1];

S = Sdiscrete + Sfuzzy;

%  Add perpetuator

S(:,:,1) = S(:,:,1) + diag(ones(6,1));


C = [.3 .4 .5 .6 .7 .8];


Actions = [...
        .9 .3 .2 .1 .1 .1; .9 .3 .2 .1 .1 .1; .9 .3 .2 .1 .1 .1; .9 .3 .2
.1 .1 .1; ...
```

```
        .9 .3 .2 .1 .1 .1; .8 .9 .8 .2 .1 .1; .9 .3 .2 .1 .1 .1; .9 .3 .2
.1 .1 .1; ...
        .9 .3 .2 .1 .1 .1; .9 .3 .2 .1 .1 .1; .9 .3 .2 .1 .1 .1; .1 .9 .9
.1 .9 .1; ...
        .9 .3 .2 .1 .1 .1; .9 .3 .2 .1 .1 .1; ...
        .1 .1 .1 .2 .3 .9; .9 .3 .2 .1 .1 .1; ...
        .9 .3 .2 .1 .1 .1; .9 .3 .2 .1 .1 .1; ...
        .9 .3 .2 .1 .1 .1; .9 .3 .2 .1 .1 .1; .9 .3 .2 .1 .1 .1; .1 .9 .2
.1 .8 .1; ...
        .9 .3 .2 .1 .1 .1; .9 .3 .2 .1 .1 .1; .1 .1 .1 .2 .3 .9; .9 .3 .2
.1 .1 .1; ...
        .9 .3 .2 .1 .1 .1; .9 .3 .2 .1 .1 .1; .9 .3 .2 .1 .1 .1; .9 .3 .2
.1 .1 .1; ...
        .9 .3 .2 .1 .1 .1; .9 .3 .2 .1 .1 .1; .9 .3 .2 .1 .1 .1; .9 .3 .2
.1 .1 .1; ...
        .9 .2 .8 .9 .2 .1; .9 .3 .2 .1 .1 .1; .9 .3 .2 .1 .1 .1; .9 .3 .2
.1 .1 .1; ...
        .9 .3 .2 .1 .1 .1; .9 .3 .2 .1 .1 .1
        ];


[M N] = size(Actions);

figure
plot(1:M,Actions(:,1)+12,'b')
hold on
plot(1:M,Actions(:,2)+11,'g')
plot(1:M,Actions(:,3)+10,'r')
plot(1:M,Actions(:,4)+ 9,'c')
plot(1:M,Actions(:,5)+ 8,'m')
plot(1:M,Actions(:,6)+ 7,'k')


B_buffer = zeros(M, 6);

E_previous = C;  % Initial state

for action_index = 1:M

  A = Actions(action_index,:) % A actions from
% the environment
  [SA] = maxmin(A,S);

  [E] = aggregate(E_previous, SA)   % Present internal state


  E_previous = E;                % E reiterates

 [B] = aggregate(E_previous, R)     % R maps E_previous
%  to the output B

  B_buffer(action_index,:) = B(:);

end



% plot(1:M,B_buffer(:,1)+5,'b')
% plot(1:M,B_buffer(:,2)+4,'g')
% plot(1:M,B_buffer(:,3)+3,'r')
% plot(1:M,B_buffer(:,4)+2,'c')
% plot(1:M,B_buffer(:,5)+1,'m')
% plot(1:M,B_buffer(:,6),'k')

plot(1:M, B_buffer(:,1)+1,'b')
plot(1:M, B_buffer(:,2)+0,'g')

return


function [Y] = aggregate(Y_previous,X)

[M N] = size(X);

Y = zeros(1,N);

min_vec = zeros(1,M);

for col = 1:N

  for x = 1:M
    min_vec(x) = min([Y_previous(x) X(x,col)]);
  end

  Y(col) = max(min_vec);
end

return


function [SA] = maxmin(A,S)

[M N P] = size(S);

SA = zeros(M,N);

min_vec = zeros(1,P);

for z_row = 1:M
   for z_col = 1:N
     for k = 1:P
       min_vec(k) = min([A(k) S(z_row,z_col,k)]);
     end
     SA(z_row,z_col) = max(min_vec);
   end
end

function S = AntidiagonalDistribution(Aselect, N)

A = floor(Aselect + .5);

ZeroVec = 0*A;

M = hamming_distance(Aselect, ZeroVec)
```

```
L = length(Aselect);

eta = L/M

S = zeros(N,N,L);

c = 0;

for k = 1:L
   if A(k) == 1
      c = c + 1
      for i = 1:N
        if (eta*(c - 1) + 1 <= i) && (i < eta*c + 1)
          S(i,N+1-i,k) = 1;
        end
      end
   end
end

return


function d = hamming_distance(A, B)

L = length(A)

d = 0;

for k = 1:L
   d = d + abs(A(k) - B(k));
end

return

function S = AntidiagonalDistribution(Aselect, N)

A = floor(Aselect + .5);

ZeroVec = 0*A;

M = hamming_distance(Aselect, ZeroVec)

L = length(Aselect);

eta = L/M

S = zeros(N,N,L);

c = 0;

for k = 1:L
   if A(k) == 1
      c = c + 1
      for i = 1:N
        if (eta*(c - 1) + 1 <= i) && (i < eta*c + 1)
          S(i,N+1-i,k) = 1;
        end
      end
   end
end

return

function d = hamming_distance(A, B)

L = length(A)

d = 0;

for k = 1:L
   d = d + abs(A(k) - B(k));
end

return
```

Fuzzy Artificial Fish Ensemble Extreme Learning Machine

João Fausto Lorenzato de Oliveira and Teresa B. Ludermir
Center of Informatics, Federal University of Pernambuco, Recife, Pernambuco, Brazil

Abstract— *Neural networks have been largely applied into many real world pattern classification problems, and the combination of neural networks to overcome the natural limitations of single classifiers is one strategy to achieve better accuracy. Due to the need of having accurate classifiers with different knowledge for the same problem, ensembles need to measure their diversity. In this work we employ a Fuzzy Adaptive Modified Artificial Fish Swarm Algorithm for evolving Extreme Learning Machine Ensembles. The ensemble selection is performed by the use of a hierarchical clustering algorithm, and two diversity measures. Experimental results show that the proposed method achieved promising results.*

Keywords: Neural Networks, Optimization, Ensembles, Fuzzy Logic

1. Introduction

In the field of pattern recognition the ensemble techniques based on the combination of different classifiers were proposed in order to improve the accuracy of a system. The classifiers in an ensemble should be as accurate as possible and should make different errors [1], hence the classifiers should present diversity among themselves.

Techniques such as *Adaboost* [2] and cross validation can be applied in order to introduce diversity among the base classifiers. Studies on composing ensembles with artificial neural networks (ANNs) show that networks with different topologies can produce promising results [3], and many optimization algorithms may be used to optimize a population of neural networks and make use of the population intelligence to compose an ensemble [4].

This work is focused on combining ANNs trained by the Extreme Learning Machine (ELM) [5] algorithm. Fast training speed, good generalization performance, small set of configurable parameters are characteristics of the ELM. The usual learning methods for single layered or multilayered neural networks are the gradient descent algorithms such as the backpropagation (BP) [6], which iteratively adjust the weights until the algorithm stop condition is reached. The ELM algorithm is not based on iterative adjustments on the weights, it uses fixed random initial weights and bias for training and the output weights are analytically determined.

Classifiers in an ensemble will contribute with its knowledge over a classification region which may vary for each classifier, thus promoting the diversity among them. To combine the opinions of different classifiers, the outputs of each classifier for a given instance are combined through a fusion rule

Ensembles of extreme learning machines can be found in [7], which a trimming coefficient is introduced into the adaboost algorithm in order to use a fraction of the training set in the initial stages of execution. In [8] cross validation technique is used as a method for divide the search space to crate new classifiers. Another implementation of the ELM algorithm called online sequential ELM (OS-ELM) [9] algorithm was used in an ensemble strategy in [10].

In this work we use the fuzzy strategy presented in [11] in order to regulate the local and global search of the Modified Artificial Fish Swarm Algorithm (MAFSA) and to select the classifiers with the hierarchical clustering algorithm, and also we perform experiments with other ensemble techniques with the ELM algorithm as base classifier.

This paper is organized as follows. On Section 2 a brief overview of the ELM algorithm and the ensemble methods based on ELM are given. On section 3 the proposed algorithm is explained. On section 4 the experiments are showed along with the results of the simulations. The conclusion is presented on section 5.

2. Extreme Learning Machine

The ELM [5] is a simple algorithm for the training of single layer feedforward neural networks (SFLNs), whose learning speed can be faster then traditional gradient descent methods such as back-propagation (BP) [6] and better generalization capacity may also be obtained.

In this algorithm, the input weights and hidden layer biases are randomly set, and through matrix operations the output weights are calculated without tuning. The absence of a tuning phase, enables the training to be performed faster.

Given n distinct training samples (x_i, t_i), where $x_i = [x_{i1}, x_{i2}, ..., x_{in}]^T \in \Re^n$ and $t_i = [t_{i1}, t_{i2}, ..., t_{im}]^T \in \Re^m$ $(i \in [1, ..., n])$, the SLFN with s hidden nodes needs to learn all the training samples. Since the input weights $w_j = [w_{j1}, w_{j2}, ..., w_{jn}]^T$ and hidden biases $b = [b_1, b_2, .., b_j]$ $(j = [1, ..., s])$ are randomly generated, the task performed in the training phase is to find the appropriate output weights for the given input weights and biases through the calculation of the linear system $H\beta = T$.

The matrix $H = \{h_{ij}\}$ is the hidden-layer output matrix and $h_{ij} = g(w_j * x_i + b_j)$ corresponds to the result from the j_{th} hidden neuron to x_i, $T = [t_1, t_2, ..., t_i]$ represents the target (desired output) matrix, and $\beta_j =$

$[\beta_{j1}, \beta_{j2}, ..., \beta_{jm}]^T (j \in [1, ..., s])$ is the output weight matrix. In order to compute the output weights, an inverse matrix operation is needed. The output weight matrix will be calculated as the minimum least-square (LS) solution of a linear system, through a pseudo-inverse matrix operation [12]. The next step for the calculation of the output weight matrix is to compute the pseudo-inverse matrix of H which results in $\hat{\beta} = H^+T$.

Through these calculations the ELM algorithm achieves good generalization performance and the learning speed is reduced due to the absence of continuous weight adjustments.

3. Fuzzy Artificial Fish Ensemble Extreme Learning Machine

The hybrid algorithm named *Modified Artificial Fish Swarm for the optimization of Extreme Learning Machines* (MAFSA-ELM) aggregates characteristics from AFSA and DE, and has the primary objective to optimize weights of ELM.

In order to further explore the search capacity of the MAFSA-ELM algorithm, we employ fuzzy strategies in oder to adapt the search process, regulating a global search or a more refined local search. Yazdani *et al.* [11] proposed a fuzzy adaptive strategy to improve the AFSA algorithm using two approaches: the Fuzzy Uniform Fish and Fuzzy Autonomous Fish.

Th improve the performance of the MAFSA-ELM algorithm these two strategies are adopted, and after its execution, an ensemble selection strategy is applied using the population of ELMs.

3.1 Modified Artificial Fish Swarm Algorithm

The AFSA algorithm [13] is based on the social behavior of the fishes. Each fish will represent a potential solution, in the case of ELM optimization, each fish will represent the input weights and hidden biases. The movements of the population will be based on the actual position of each fish and the nearby fishes inside its visual field ($visual$). Two important variables are the $visual$ and $step$ which regulates how the search will be conducted. The $step$ variable will control how far a fish can move. Higher values of $visual$ and $step$ the fishes will move faster towards the best solution, passing through local minimums without getting stuck, this configuration is desired in the initial stages of execution. Lower values will produce an exploitation characteristic, desired on the last stages of the algorithm. Each fish will be represented by an input matrix W_{ij} and a bias vector b_i, and these informations are used to calculate the distance.

In order to calculate whether a certain fish is within the visual field of another fish, the distance between them is calculated using a euclidean distance. The output weights on the ELM algorithm are unknown *a priori*, hence the distance d is calculated as showed on equation 1, where p and q represent the indexes of two different fishes.

$$d_{pq} = \sum_{i=1}^{s} \sum_{j=1}^{h} (W_{ij}(p) - W_{ij}(q))^2 + \sum_{i=1}^{h} (b_i(p) - b_i(q))^2 \quad (1)$$

The number of input parameters on a given instance is represented by s and the number of hidden neurons is represented by h. The original AFSA algorithm has some basic behaviors (Follow, swarm and leap) executed by each fish, the behavior that produces the highest result will be the one used for updating the fish position. The Follow behavior as shown in equation 2 influences the fish by the best fish inside its visual range W_{max} (not necessarily the best fish in the swarm).

$$Follow(W_i) = W_i + rand() step \frac{W_{max} - W_i}{\|W_{max} - W_i\|}, \quad (2)$$

The swarm behavior influences the fish based on the central position (represented by W_c) of the fishes inside its visual field. The swarm behavior strengthens the idea of group search, and is presented in equation 3.

$$Swarm(W_i) = W_i + rand() step \frac{W_c - W_i}{\|W_c - W_i\|} \quad (3)$$

And the leap behavior, presented on equation 4, represents the capacity of the fish to move on its own, independent of any other fish.

$$Leap(W_i) = W_i + rand() step \quad (4)$$

Since the traditional Artificial Fish Swarm Algorithm does not perform well, a new behavior is introduced, using the genetic operators of *Crossover/Mutation* [14] from the Differential Evolution algorithm. The Crossover/Mutation behavior will produce new individuals based on informations of the population independently of their position in the search space. This behavior chooses randomly three fishes from the swarm, and then a new fish is created based on their positions and a mutation factor. The next step is to mix the informations of the created fish, with the original fish based on a given probability. If the new individual performs better on the validation set, then the position is updated.

In the modified AFSA algorithm (MAFSA), the additional behavior was inspired by the capacity of fishes to evolve and be selected by nature. For that purpose we use the Differential Evolution (DE) algorithm proposed by Storn and Price [14] which is known as one of the most efficient evolutionary algorithms. In order to create the next generation of individuals, the algorithm uses mutation and

crossover operators. The new behavior is executed in three steps: Mutation, Crossover and Selection [14]. The first step is the mutation:

$$W_i = W_{r_1} + F * (W_{r_2} - W_{r_3}), \quad (5)$$

where r_1,r_2 e r_3 are distinct indexes randomly chosen and F is an amplitude factor with values within the range $(0, 2)$. In the crossover phase, a new vector V is created with the same dimensionality of the individuals.

$$V_{ij} = \begin{cases} W_{ij} & \text{if } rand() < CR \quad \text{and } j = rdInd(i) \\ W_{ij} & \text{if } rand() > CR \quad \text{or } j \neq rdInd(i) \end{cases} \quad (6)$$

If the new vector has better fitness than its predecessor, the new vector will be selected, otherwise the predecessor will be selected.

By adding the crossover mutation behavior, the probability of finding better solutions increases due to the total amount of possible results (4 results) instead of the original 3 (from the three original behaviors), so the algorithm incrementally has more chances to find better solutions. And the reason why this new behavior is not affected by the $visual$ and $step$ parameters is simply to produce more diversity in the results and occasionally escaping from local minimums. Since $rdInd(i)$ is a randomly chosen index from the entire swarm, informations from the best (or worst) fishes could be gathered to produce a new individual (new solution), so this new behavior adds a stochastic strategy to the algorithm.

The first step is to initialize the population (weights and biases) along with the parameters, including the distance matrix of each fish for initialization of the visual parameter. Then each fish will execute all the behaviors, however the position adjustments will be accomplished by the behavior that yields the highest accuracy on a validation set.

Once the weights and bias are adjusted with the best values, this information is used to calculate the input variables for the fuzzy engine. There are to main approaches to this fuzzy strategy called Fuzzy Uniform Fish (FUF) and Fuzzy Autonomous Fish (FAF) [11].

3.2 Self-Adaptation with Fuzzy Autonomous Fish and Fuzzy Uniform Fish

The fuzzy strategies adopted will adjust the values of the *visual* and *step* parameters, based on the FUF and FAF approaches. In order to control the balance between global search and local search, another parameter, *constriction weight* (CW), will be introduced for the adjustments of the parameters in both approaches. The adjustment procedures are presented as follows:

$$visual_{l+1} = CW * visual_l \quad (7)$$

$$step_{l+1} = CW * step_l \quad (8)$$

In the Fuzzy Uniform Fish Ensemble ELM (FUFE-ELM) approach every fish in the swarm shares the same values for the *visual* and step parameters. Thus, the population will start searching locally or globally at the same time. The fuzzy engine based on FUF consists of two inputs and one output. The input parameters are the ratio of improved fish, and the iteration number. The output parameter is the constriction weight. The iteration number, is the proportion between the current iteration and the total number of iterations. The algorithm needs to perform a global search in the initial stages of the algorithm, so the reduction of the *visual* and step parameters in these stage must be minimal. Near the end of the execution the algorithm has already approached the global optimum region, and needs to perform a local search, thats when higher values of the *iteration Number* parameter will influence significantly on the reduction of the *visual* and step parameters.

Table 1: Fuzzy Associative memory for the FUF Engine [11]

Iteration Number	Ratio of Improved Fish	Constriction Weight
L	H	VH
L	M	H
L	L	M
M	H	H
M	M	M
M	L	L
H	H	M
H	M	L
H	L	VL

The *ratio of improved fish* is the proportion of fishes that find better solutions (weights and biases) to the total number of fishes. When most of the artificial fishes find better solutions the value will be close to 1, then there is no need to reduce the *visual* and step parameters. However, when the proportion is close to 0, there is no improvement on finding better solutions , the two parameters are reduced in order to perform a local search, raising the probability of finding better solutions.

In the Fuzzy Autonomous Fish Ensemble ELM (FAFE-ELM) approach, each fish will have its own *visual* and *step* variables with individual adjustments, producing more diverse results and allowing that a given fish start to perform more refined local search earlier than other fishes. This strategy could led to more diverse ensembles since each fish is capable of start a local search before the others, and consequently it could find a better solution.

In the initial stages of the algorithm these variables have the same value, and will be individually adjusted through the execution based on the output of the fuzzy engine which is calculated using three input parameters namely *Distance from best*, *Fitness Ranking* and *Iteration Number*.

The *Distance from best* rank-based parameter which is based in the distance between the fishes and the best fish (with highest validation accuracy), the distance is calculated in the same way is shown on equation 1. After the distance is computed, all distances are sorted, and then the proportion

Fig. 1: Fuzzy Uniform Fish Membership Functions. 1a Iteration Number. 1b Ratio of improved fish. 1c Constriction Weight.

(a) Iteration Number (b) Ratio of Improved Fish

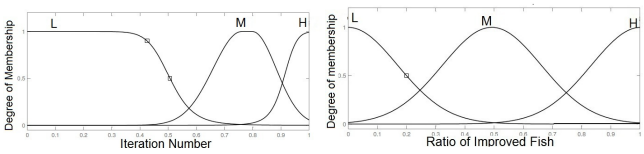

(c) Constriction Weight

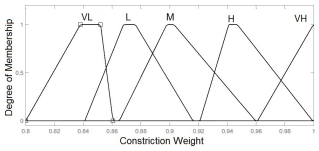

of the current rank to the total of fishes is presented to the fuzzy engine. When the distance to the best fish is low, then the *visual* and *step* parameters will be less reduced, however when a fish is close to the best fish then those values are decreased considerably, in order to perform a more refined search.

The *Fitness Ranking* is based on the fitness of each fish with respect to the validation accuracies obtained with the ELM algorithm. All fitnesses from each fish will be sorted and then the proportion to the total amount of fishes will be presented. Lower rankings on this variable will produce less reductions on the *visual* and *step* parameters. The *Distance from Best* will have the same definitions as in the FUF-ELM approach.

On figure 2 the membership functions are presented for each variable.

Fig. 2: Fuzzy Autonomous Fish Membership Functions. 2a Iteration Number. 2b Distance from best. 2c Fitness Ranking. 2d Constriction Weight.

(a) Iteration Number (b) Distance from Best

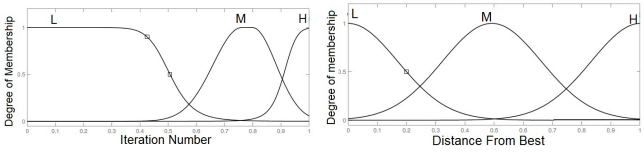

(c) Fitness Ranking (d) Constriction Weight

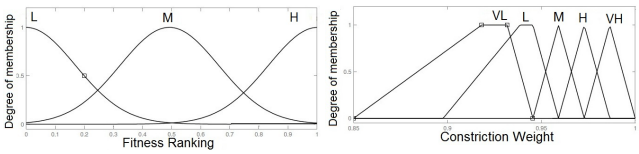

Table 2: Fuzzy Associative memory for the FAF Engine [11]

Distance from Best	Fitness Ranking	Iteration	Weight
L	L	H	VL
L	L	L	VL
L	L	L	L
L	M	H	L
L	M	M	M
L	M	H	VL
L	M	L	H
L	H	H	L
L	H	M	M
L	H	L	VL
M	L	H	VL
M	L	M	L
M	L	L	M
M	M	H	L
M	M	M	M
M	M	L	H
M	H	H	M
M	H	M	H
M	H	L	VH
H	L	H	L
H	L	M	M
H	L	L	H
H	M	H	M
H	M	M	H
H	M	L	VH
H	H	H	M
H	H	M	H
H	H	L	VL

The swarm will loop through the algorithm until a stop condition (number of iterations) is met. The steps for ensemble selection will be explained on Section 3.3.

3.3 Ensemble selection

The ensemble selection phase is executed after the FAFE-ELM algorithm is finished. Our criteria for selection are the performance and the diversity of each classifier. In the literature there are many diverse measures such as interrater agreement, double-fault, Q-statistic [1]. In this work we will use a two-stage selection. The first stage will use a pairwise measure of diversity namely Double-fault, and this measure yields the probability of two given classifiers be both wrong, and the application of the hierarchical clustering algorithm to reduce the number of possible ensembles. The second stage uses the Entropy diversity measure which will measure the diversity of an ensemble.

In [15], this measure was used for the construction of a distance matrix for distinct classifiers, and group them with a hierarchical cluster algorithm. In this work we will use the same approach as was used in [15], however with the ELM classifiers optimized differently by the MAFSA algorithm. This measure will be used to compute a distance measure to build a distance matrix that will be used for the selection of the classifiers of the ensemble.

$$D_{i,m} = 1 - \frac{u(-1,-1)}{u(-1,-1) + u(1,-1) + u(-1,1) + u(1,1)} \quad (9)$$

The diversity measure is given above, where $u(-1,-1)$ indicates the number of cases where both classifiers are wrong, $u(-1,1)$ is the number of cases where only the first classifier is wrong, $u(1,-1)$ is the number of cases where $u(1,1)$ number of cases that neither of them are wrong.

With the distance matrix we apply the hierarchical cluster algorithm [16] to group the classifiers based on their diversity. Lower values of the distance mean that there are more coincident errors between the classifiers, thus they present lower diversity. The classifiers with lower distances are put in the same cluster. Classifiers that present higher distance will be grouped in a different cluster, as they will make fewer coincident errors.

In the first step, all classifiers are considered to be in individual clusters, and they are iteratively grouped based on the smallest distance between them. The distance between two different clusters will be the highest distance between two classifiers that belong to each of them.

Algorithm 1 Fuzzy Artificial Fish Ensemble Extreme Learning Machine

$c \leftarrow 0$
Initialize population $P, \forall p_i \in P$
while $c < C$ **do**
  while $i < N$ **do**
    Determine Output Weights of fish i β_i and assess the classification accuracy CA_i
    Execute the behaviors ($follow(p_i)$, $swarm(p_i)$, $leap(p_i)$, $crossover - mutation(p_i)$)
    Update with the best result :
    $p_i \leftarrow max$[follow(p_i), $swarm(p_i)$, $leap(p_i)$, $crossover - mutation(p_i)$]
    $i \leftarrow i + 1$
  end while
  Calculate parameters for the fuzzy engine (Uniform Fish, or Autonomous Fish) $CW_i^{c+1} \leftarrow$fuzzy_Engine(Distance from best, Fitness Ranking,Iteration Number) $\times CW_i^c$
  $c \leftarrow c + 1$
end while
Build distance matrix with the Double-Fault diversity measure
Group the Ensembles with the Hierarchical Cluster
Use the Entropy diversity measure to select the final ensemble

The hierarchical clustering was used because the number of possible ensembles in a set of classifiers $V = v_1, v_2, ..., v_T$ is equal to $\sum_{r=1}^{T} \binom{T}{r}$, thus the brute force approach is unfeasible. So the number of possible ensembles is reduced through the hierarchical clustering approach. By the end of the clustering process, all the possible ensembles clustered by the hierarchical algorithm are tested using the outputs of each classifier on the validation set, combined by the majority vote rule. During the simulations we verified that more than one ensemble may yield the same highest value. In order to select the best ensemble among the ones with highest accuracy, we use an entropy [1] diversity measure. The entropy is a non-pairwise diversity measure, that verifies how diverse is an ensemble of classifiers. The ensemble with highest entropy value, is selected as the final ensemble.

This approach does not exclude the possibility of using all the classifiers in the population, the criteria for comparing the ensembles is the entropy diversity measure. In the algorithm 3, the pseudocode for the FAFE-ELM algorithm is presented.

4. Experiments

On the experiments we used the ELM, Dynamic Adaboost Ensemble ELM (DAEELM), EN-ELM, FAFE-ELM, FUFE-ELM, and a standard Artificial Fish Ensemble-ELM with no self-adaptation (AFE-ELM). They were applied on five (Sonar, Ionosphere, Horse, Glass and Vehicle) datasets from UCI machine learning repository [17].

The data from each dataset were split into training set (50%), validation set (25%) and test set (25%) randomly generated for 30 iterations. Except for the EN-ELM algorithm that uses 75% for training and 25% for testing. All algorithms receive the same testing set.

Table 3: Results for all data sets

Data set	Method	Mean	SD	h
Sonar	ELM	72.97	4.58	20
	AFE-ELM	78.65	7.03	20
	FAFE-ELM	78.97	8.11	20
	FUFE-ELM	76.35	6.67	20
	EN-ELM	71.47	5.41	20
	DAEELM	75.20	4.82	15
Vehicle	ELM	73.99	2.55	20
	AFE-ELM	77.61	2.57	20
	FAFE-ELM	77.30	2.56	20
	FUFE-ELM	77.81	3.36	20
	EN-ELM	72.74	2.52	20
	DAEELM	73.22	2.41	20
Ionosphere	ELM	85.82	4.31	20
	AFE-ELM	90.43	3.58	20
	FAFE-ELM	89.00	4.55	20
	FUFE-ELM	89.57	3.52	20
	EN-ELM	79.60	4.41	20
	DAEELM	85.89	3.62	20
Horse-colic	ELM	65.54	2.76	20
	AFE-ELM	68.60	4.14	20
	FAFE-ELM	69.05	4.39	20
	FUFE-ELM	68.77	3.95	20
	EN-ELM	62.86	3.30	20
	DAEELM	65.51	3.58	20
Glass	ELM	63.76	5.58	20
	AFE-ELM	66.05	4.83	20
	FAFE-ELM	66.12	4.43	20
	FUFE-ELM	65.81	4.49	20
	EN-ELM	66.36	5.28	20
	DAEELM	62.33	5.67	15
Diabetes	ELM	76.92	1.19	20
	AFE-ELM	78.13	3.44	20
	FAFE-ELM	78.00	3.03	20
	FUFE-ELM	78.29	3.06	20
	EN-ELM	76.98	3.17	20
	DAEELM	75.97	1.58	15

For each iteration all the classifiers receive the exact

training, validation and test sets. All the attributes from the datasets were normalized into the interval $[0..1]$. The simulations were performed with 10, 15 and 20 hidden neurons, and the configuration that produced the best result was selected. The optimization algorithms are executed for 50 iterations. The initialization of the MAFSA-ELM parameters in this work is described as follows: The $visual$ parameter was set as the mean of all the initial distances between the fishes. The number of fishes $N = 30$, $step = 0.6$, crowd factor $\delta = 0.8$, in this work we set the visual parameter as the mean for all the initial distances between the fishes. Amplitude factor for the mutation $F = 1$ and crossover rate $CR = 0.5$. The same parameters for the MAFSA-ELM algorithm are also used on the AFE-ELM, FUFE-ELM and FAFE-ELM. The EN-ELM algorithm only has the number of folds=10 and the number of hidden neurons as an input parameter. The configuration for the DAEELM algorithm is the trimming factor γ=0.1.

The experiments were measured with respect to the mean accuracy on the test set. The analysis of the results was performed through the use of the Wilcoxon Sign-rank test with 95% of confidence interval.

On Table 2 the results for all the data sets are presented. Under an empirical analysis the proposed methods performed better on the Diabetes (FUFE-ELM) ,Horse (FAFE-ELM), Vehicle (FUFE-ELM), Sonar (FAFE-ELM) datasets. Using the Wilcoxon sign-rank test the FUFE-ELM, FAFE-ELM and AFE-ELM performed similarly in all data sets, and they were superior to all other algorithms (ELM, DAEELM, EN-ELM) except for the Glass data set where the EN-ELM algorithm also achieved a similar result with higher standard deviation. The DAEELM and the EN-ELM algorithms performed worse than the single ELM classifier in some data sets because there is no guarantee that the classifiers in these ensembles will be accurate and diverse enough. Since some data sets are unbalanced, in the EN-ELM algorithm some folds might not have all the classes and this can contribute negatively for the training of the base classifiers.

The DAEELM algorithm draws samples with reposition, according to the current probability distribution, hence the accuracy of the weak classifier on the drawn sample may not be the best. The algorithm can easily stop on early iterations if the size of the sample set is equal to the size of the training set ant the error is above 0.5. This leads to ensembles with few classifiers and without the possibility to raise the accuracy of the system. The number of hidden neurons was the same for almost all techniques except for the DAEELM which, in some datasets, achieved its best values with 15 hidden neurons.

5. Conclusions

In this paper, we applied two fuzzy strategies in order to adjust the parameters of the Modified Artificial Fish Swarm Algorithm on the optimization of Extreme Learning Machines, and combined the individuals through a hierarchical clustering algorithm.

The hierarchical clustering algorithm uses a distance matrix based on the double-fault diversity measure. After the ensembles are formed, the entropy diversity measure is used to select the final ensemble. The performance of the tested algorithms was evaluated with well known benchmark classification datasets (Ionosphere, Diabetes, glass, sonar, vehicle and horse-colic), obtained from UCI Machine Learning Repository [17].

Experimental results show that our hybrid obtained promising results, in some datasets achieved better accuracy on the test sets.

As future works, we plan to evaluate the influence of using other fusion rules as well as other clustering algorithms for the composition of ensembles. Other optimization algorithms used for evolving an ELM population such as Particle swarm optimization (PSO) [18] could be explored for evolving ELM ensembles.

References

[1] L. Kuncheva, *Combining pattern classifiers: methods and algorithms*. Wiley-Interscience, 2004.

[2] Y. Freund and R. Schapire, "A desicion-theoretic generalization of on-line learning and an application to boosting," in *Computational learning theory*. Springer, 1995, pp. 23–37.

[3] J. AMANDA, "On combining artificial neural nets," *Connection Science*, vol. 8, no. 3-4, pp. 299–314, 1996.

[4] X. Yao and Y. Liu, "Making use of population information in evolutionary artificial neural networks," *Systems, Man, and Cybernetics, Part B: Cybernetics, IEEE Transactions on*, vol. 28, no. 3, pp. 417–425, 1998.

[5] G. Huang, Q. Zhu, and C. Siew, "Extreme learning machine: theory and applications," *Neurocomputing*, vol. 70, no. 1-3, pp. 489–501, 2006.

[6] S. Haykin, *Neural networks: a comprehensive foundation*. Prentice Hall PTR Upper Saddle River, NJ, USA, 1994.

[7] G. Wang and P. Li, "Dynamic adaboost ensemble extreme learning machine," in *Advanced Computer Theory and Engineering (ICACTE), 2010 3rd International Conference on*, vol. 3. IEEE, 2010, pp. V3–54.

[8] N. Liu and H. Wang, "Ensemble based extreme learning machine," *Signal Processing Letters, IEEE*, vol. 17, no. 8, pp. 754–757, 2010.

[9] G. Huang, N. Liang, H. Rong, P. Saratchandran, and N. Sundararajan, "On-line sequential extreme learning machine," in *The IASTED International Conference on Computational Intelligence (CI 2005), Calgary, Canada*. Citeseer, 2005.

[10] Y. Lan, Y. Soh, and G. Huang, "Ensemble of online sequential extreme learning machine," *Neurocomputing*, vol. 72, no. 13-15, pp. 3391–3395, 2009.

[11] D. Yazdani, A. Nadjaran Toosi, and M. Meybodi, "Fuzzy adaptive artificial fish swarm algorithm," *AI 2010: Advances in Artificial Intelligence*, pp. 334–343, 2011.

[12] C. Rao and S. Mitra, *Generalized inverse of matrices and its applications*. Wiley NY, 1971.

[13] C. Wang, C. Zhou, and J. Ma, "An improved artificial fish-swarm algorithm and its application in feed-forward neural networks," in *Machine Learning and Cybernetics, 2005. Proceedings of 2005 International Conference on*, vol. 5. IEEE, 2005, pp. 2890–2894.

[14] R. Storn and K. Price, "Differential evolution–a simple , efficient heuristic for global optimization over continuous spaces," *Journal of global optimization*, vol. 11, no. 4, pp. 341–359, 1997.

[15] G. Giacinto, F. Roli, and G. Fumera, "Design of effective multiple classifier systems by clustering of classifiers," in *Pattern Recognition, 2000. Proceedings. 15th International Conference on*, vol. 2. IEEE, 2000, pp. 160–163.

[16] G. Gan, C. Ma, and J. Wu, "Data clustering: theory, algorithms, and applications," *ASASIAM Series on Statistics and Applied Probability*, vol. 20, pp. 219–230, 2007.

[17] C. Blake and C. Merz, "UCI repository of machine learning databases," 1998.

[18] Y. Xu and Y. Shu, "Evolutionary extreme learning machine–based on particle swarm optimization," *Advances in Neural Networks-ISNN 2006*, pp. 644–652, 2006.

A New Neural Fuzzy System Using Fuzzy Linguistic Input-output Training Samples

Jing Lu , Blayne Mayfield , and Jia Liu

Computer Science Department, Oklahoma State University , Stillwater, OK, USA

Abstract - *This paper proposes a new fuzzy neural system that deals with fuzzy training samples. That is, the proposed learning system includes training of a neural network using fuzzy training samples, and it outputs fuzzy value according to a set of given rules. The learning algorithm used in the system is composed of two phases. The first phase transforms crisp samples into fuzzy ones; the second phase trains the network according to the fuzzy samples through a new neural network structure proposed in this paper. Finally, two error evaluation methods and comparison between them are given.*

Keywords: Fuzzy logic, neural network, mean solution, gragh solution.

1 Introduction

Fuzzy logic [1] and neural networks [2] play an important role in the modeling of intelligent control in complex systems. Their combination is widely used in solving problems such as classification, identification, pattern recognition and so on.

There are three common ways to combine these techniques. The first one is a fuzzy neural network [3] (FNN), which increases the efficiency of the neural network and its velocity of convergence; the second one is a neural-fuzzy system[4], the activation function of which is related to fuzzy relations or fuzzy operators; the third one is a fuzzy neural hybrid system[5], where fuzzy logic and neural networks perform separately to attain a common goal.

In our previous studies, the first and second types used crisp input-output samples to train the neural network and to output crisp values. Using these approaches, FNNs embed fuzzy logic into a neural network and use that fuzzy logic in order to reach some goal; however, the input and output values of these networks are crisp values. In this paper, by contrast, the neural network uses crisp logic, but the input and output values are fuzzy values. In other words, the previous approaches and the new approach operate in opposite ways.

The new neural fuzzy system can deal with fuzzy input-output training samples, but also with crisp training samples. And, it can output fuzzy values according to fuzzy rules given in advance. The new approach adds two extra layers in front of the network to generate fuzzy training samples. These additional layers generate crisp training samples and then fuzzify them for use as input to the network.

The organization of this paper is as follows. In section 2, we briefly introduce the preliminaries of the paper: fuzzy logic theory and neural network theory. Section 3 presents the main structure of the system and algorithm used in the new network. Section 4 is an example of the system. Finally, the experiment of the example is shown and the conclusion is summarized.

2 Preliminaries

2.1 Fuzzy Logic Theory

Fuzzy logic is a form of many-valued logic; it deals with reasoning that is approximate rather than fixed and exact. In contrast with traditional logic theory, where binary sets have two-valued logic, fuzzy logic variables may have a true value that ranges in degree between 0-1. Fuzzy logic is used to handle the concept of partial truth, in which the value may range between completely true and completely false. Furthermore, when linguistic variables[6] are used, these degrees may be managed by specific functions called membership function, which is a function from a universal set U to the interval [0,1]. A fuzzy set A is defined by its membership function μ_A over U.

2.2 Neural Network Theory

Artificial neural networks refer to computer algorithms and structures that mimic the function of the biological neutrons. Similarly, it is composed of artificial neurons. The connections of the biological neuron are modeled as weights. A negative weight reflects an inhibitory connection, while positive values mean excitatory connections. The following components of the model represent the actual activity of the neuron cell. All inputs are modified by a weight and summed altogether. This activity is referred as a linear combination. Finally, an activation function controls the amplitude of the output. For example, an acceptable range of output is usually between 0 and 1, or it could be -1 and 1.

Mathematically, this process is described in Figure 1.

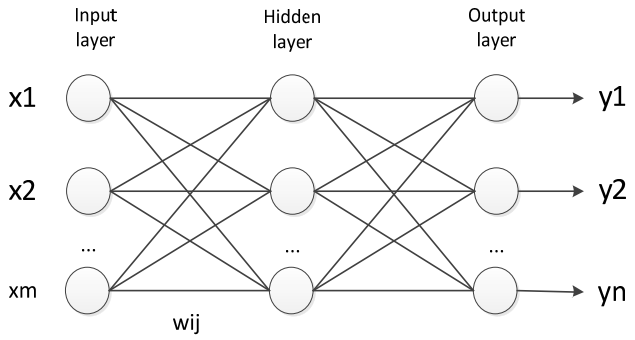

Figure 1. Neural network structure.

This network has an input layer (on the left) with m neurons, a hidden layer (in the middle) and an output layer (on the right) with n neurons.

There is one neuron in the input layer for each predictor variable. In the case of categorical variables, *N*- 1 neurons are used to represent the *N* categories of the variable.

Input Layer : A vector of predictor variable values from x1 to xm is presented to the input layer. The input layer distributes the values to each of the neurons in the hidden layer. In addition to the predictor variables, there is a constant input of 1.0, called the bias that is fed to each of the hidden layers; the bias is multiplied by a weight wij and added to the sum going into the neuron.

Hidden Layer : Arriving at a neuron in the hidden layer, the value from each input neuron is multiplied by a weight, and the resulting weighted values are added together producing a combined value, which is fed into a transfer function, which outputs a value. The outputs from the hidden layer are distributed to the output layer.

Output Layer : The y values are the outputs of the network. If a regression analysis[7] is being performed with a continuous target variable, then there is a single neuron in the output layer, and it generates a single y value. For classification problems with categorical target variables, there are *N* neurons in the output layer producing *N* values, one for each of the *N* categories of the target variable.

3 Neural fuzzy system with crisp input and fuzzy output

Herein, we consider a neural fuzzy system with a rule base of R rules, e.g., n-input m-output. The jth control rule is described as following form:

Rj: IF x1 is A1 AND x2 is A2 AND …AND xn is An, THEN y1 is B1 AND y2 is B2 AND … AND ym is Bm. Where j is a rule number, n is the total number of input variables and m is the total number of output variables, A1-An denotes the fuzzy set over the universe of x(X) and maybe not identical to each other, B1-Bm denotes the fuzzy set over the universe of y(Y) and maybe not identical to each other.

However, we cannot use fuzzy words to train the neural network and the conception of fuzzy logic can be introduced to solve such problem. In fact, it is necessary to use fuzzy values which depict the degree to which a crisp value belongs to a fuzzy set (fuzzy words) to train the neural network. By transferring the crisp samples into fuzzy ones, we could train the neural network using the fuzzy samples and output fuzzy values.

The whole structure of the neural fuzzy system with fuzzy output is show as Figure 2.

We can see from the picture that the whole neural network has several parts: Input layer, Fuzzification layer, Neural training layer and Output layer.

There may be many dashed parts. The dashed area is similar to the solid part but differ from each other corresponding to different rules. That is, the number of the solid parts and dashed parts depend on the number of the rules. We will give the reason why there is dashed part later.

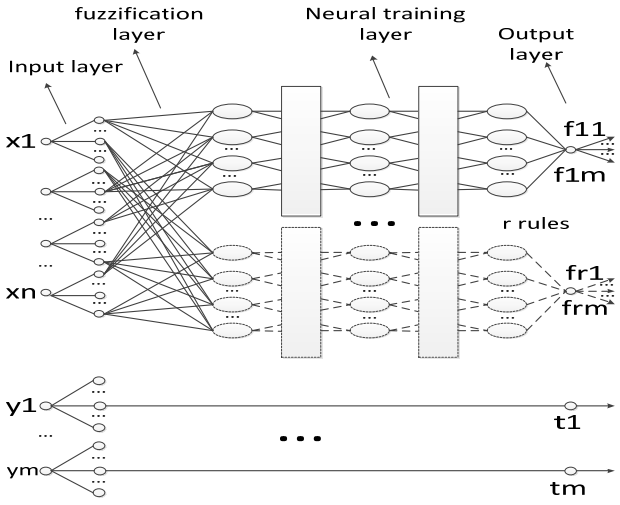

Figure 2. Fuzzy neural system.

Take a simple rule as an example:

(R1) IF x1 is Small AND x2 is Small, THEN y is Small; (R2) IF x1 is Small AND x2 is Large, THEN y is Middle; (R3) IF x1 is Large AND x2 is Small, THEN y is Middle; (R4) IF x1 is Large AND x2 is Large, THEN y is large.

There are 4 rules in the example, where n is 2 and m is 1, A1 (Small) and A2 (Small) denotes the fuzzy set (fuzzy words) over the universe of x, which are not identical to each

other in rule 1 but identical in rule 2, since A1 is Small and A2 is Large, B1denotes the fuzzy set (fuzzy words) "Small" over the universe of y, B2 denotes the fuzzy set (fuzzy words) "Middle" over the universe of y, B3 denotes the fuzzy set "Large" over the universe of y.

The network structure of this example is show as Figure 3.

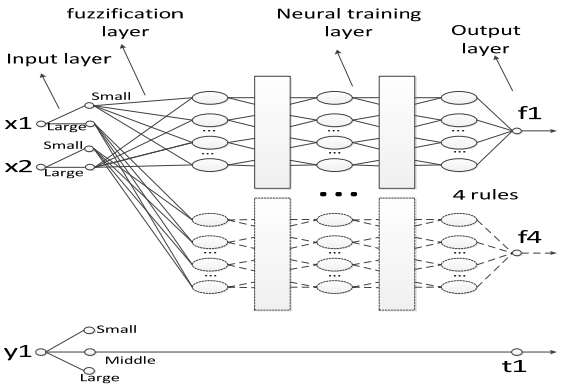

Figure 3. Fuzzy neural system with two inputs and one output.

Specification:

Input layer: If the neural fuzzy system is given suitable fuzzy training samples containing fuzzy values, this layer isn't a necessary part. But, what is the suitable fuzzy training sample? Just as the name implies, a suitable fuzzy training sample is a training sample whose members are fuzzy values corresponding to some fuzzy set (word). Besides, "suitable" means that the training sample must obey the rules we set in advance.

The main goal of this layer is to generate some crisp training samples randomly, each of which contains independent variable values and expected values of induced variable.

Using the example above, obviously, there are 2 independent variable values (x1, x2) and 1 expected value y1. Specifically, we should generate members of a training sample in the same universe of discourse for x and do the same for y.

Fuzzification layer: This layer is also redundant if the neural fuzzy system is given suitable fuzzy training samples containing fuzzy values.

If necessary, it transfers the training samples into fuzzy ones according to fuzzy logic theory. For each value in a sample, firstly, the system gets several membership function values corresponding to the current value being checked within its universal; secondly, compare membership function values and get the biggest one as a member of the fuzzy sample, at the same time, records the fuzzy word with the biggest membership function value. That is the maximum membership degree principle[8].

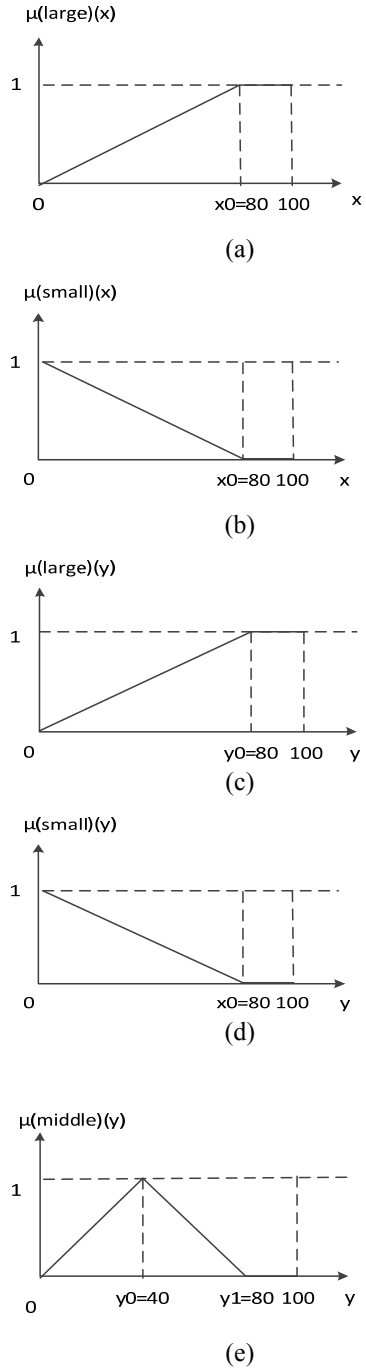

Figure 4. Membership fuction curve of fuzzy set (a) "large" with universal x, (b) "small" with universal x, (c) "large" with universal y, (d) "small" with universal y, (e) "middle" with universal x.

Assuming there is a training sample <24, 42, 90>.Firstly, the system gets 2 values for "24" according to the curve in graph(a) and graph(b); Secondly, compare them, get the biggest one --- max(μ_{large}(24), μ_{small}(24)) and the fuzzy words "small" since max(μ_{large} (24), μ_{small} (24)) is μ_{small}(24).

Sometimes, we generate some samples which are not accordance with the fuzzy rules we care, at this time, we discard these useless samples.

In the given example, we should notice (from the membership function graph of x and y) that the fuzzy sets (fuzzy words) over x and over y we have defined are not always the same but it could be.

Neural training layer: The function of this layer is similar to existing neural network, but the difference between them is that the system proposed in this paper use different structure related to the different rule to train the neural network in order to output expected value in keeping with the rule. In addition, we may make use of the same neural training layer working area, instead of open up a new working area. That is why there is dashed part in Figure 2 and 3.

Output layer: This layer outputs fuzzy values labeled by output fuzzy words. It is easy to see that one output has two meanings. One is the fuzzy set (word), the other is the fuzzy value corresponding to this fuzzy set. The point is how to decide for a fuzzy output which fuzzy set it belongs to. Deciding the fuzzy set of the output according to the given rules and the record of the fuzzy words of the inputs is a direct method.

4 Evaluation methodology

4.1 Graph solution

Here, we introduce a new evaluation methodology called "graph solution" to evaluate the performance of the neural network. This method can only be applied when the membership functions are given.

Step1: Draw the membership function of different fuzzy sets given the same universal in one graph.

For example, Figure 5 denotes the graph solution for y within the universal 0-100.

Step2: Find the biggest values for each interval. For example, [0-27]: μ_{small} (y) has the biggest values;[27-53]: μ_{middle}(y) has the biggest values;[53-100]:(y) has the biggest values.

Step3: Within each interval, find out the difference of the biggest membership function value and the smallest membership function value for the fuzzy word with the biggest values. Obviously, the example above has the same differences, which are "μ_{small}(0) - μ_{small}(27)", "μ_{middle}(40) - μ_{middle}(27)" and "μ_{large}(80) - μ_{large}(53)".

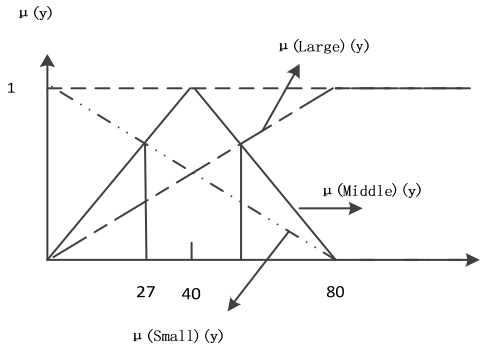

Figure 5. Graph solution.

If the error is between "0" to "0.47", the training of the neural network is reasonable.

We should notice that this method is useless if we do not know the membership function.

4.2 Mean solution

If there is a one-many relationship between the inputs and targets in the training data, then it is not possible for any mapping of the form to perform perfectly. It is straightforward to show that if a probability density P(Y|X) describes the data, then the minimum of error measure is attained by the map taking **X** to the average target

$$\int d\boldsymbol{Y}\, P(\mathbf{Y}|\mathbf{X})\mathbf{Y}$$

Any given network might or not be able to approximate this mapping well, but when trained as well as possible it will form its best possible approximation to this mean.

For the fuzzy linguistic inputs and outputs, one input set may match along with many outputs. We calculate the average target based on P(**Y**|**X**) for each rule.

5 Experiment

Rule specification:

(R1) IF x1is Small AND x2 is Small, THEN y is Small;
(R2) IF x1 is Small AND x2 is Large, THEN y is Middle;
(R3) IF x1 is Large AND x2 is Small, THEN y is Middle;
(R4) IF x1 is Large AND x2 is Large, THEN y is large.

Original training sample:

Universal of x (X) and Universal of y (Y) are [0,100]. We just generate randomly these samples such as (x1, x2, y), each of which ranges from 0 to 100, inclusively.

Algorithm to train the neural network:

BP Algorithm.

Neural network structure:

4 layers having 3, 3, 3 and 1 neutrons respectively.

Experiment environment:

Matlab.

5.1 Experiment using graph solution

The system generates 100000 samples randomly, where 28793 samples are satisfied with the 4 rules in the example. Using these training samples to train the neural network, we get error values below (Figure 6) and the error is reasonable since it fall within the interval [0-0.47] according to the "graph solution" mentioned above.

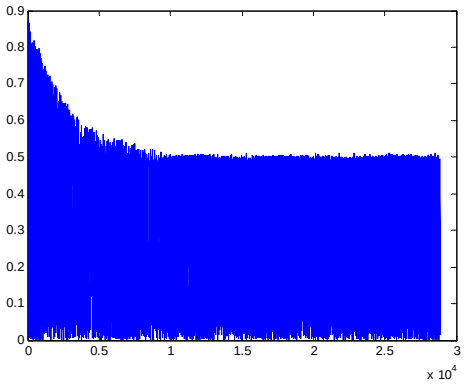

Figure 6. Training error using graph solution.

Using 14428 testing samples on this network, we get error values shown as Figure 7. The result is approximately between 0-0.47 and reasonable.

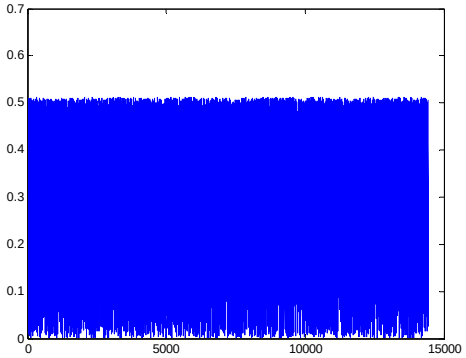

Figure 7. Testing error using graph solution.

5.2 Experiment using mean solution

Assuming P(**Y**|**X**) of each rule is an average distribution, we easily calculate the average target for four rules and they are 0.8313, 0.8375,0.8375,0.8313 separately. We get error values below (Figure 8).

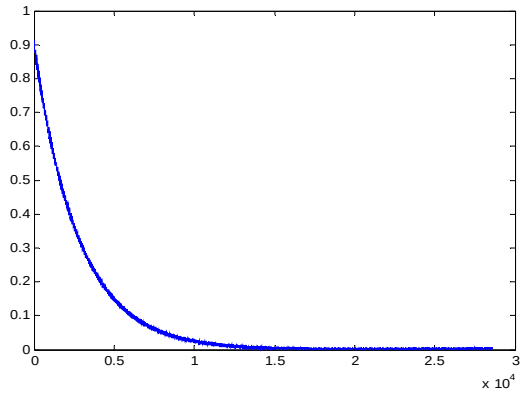

Figure 8. Training error using mean solution.

Using 14455 testing data samples on this network, we get error values shown as Figure 9. The result is between 0.015-0.04 and reasonable.

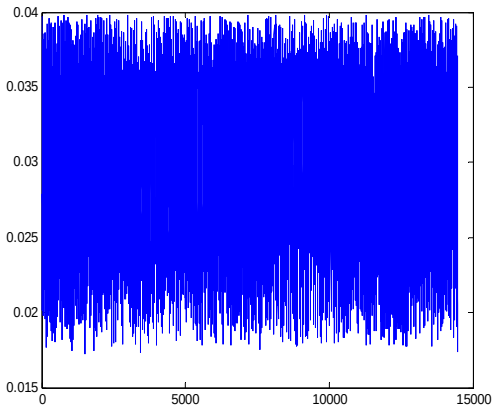

Figure 9. Testing error using mean solution.

Experiments show that the graph solution goes a litter faster than the mean solution to get to a stable state. However, mean solution could deal problems which have background knowledge P(**Y**|**X**). They are determined by properties of probability mathematics and the practical needs. So, we could realize that mean solution make use of known conditions more sufficiently. On the other hand, graph solution would be chosen if we do not want to fix fuzzy output and there is no background knowledge at all.

6 Conclusions

This neural fuzzy system could deal with problem of fuzzy rules.

Obviously, this system can input crisp values and output fuzzy values, which is more convenient compare to previous fuzzy neural networks with crisp inputs and outputs.

In addition, this system is also suitable for fuzzy reference problems. That is, if we are given the membership function value of X, what the membership function value of Y should be? It is already known that there are different fuzzy reasoning rules defined by human-beings in the fuzzy logic area, such as Mamdanian Larsen fuzzy reference[9], Zadeh fuzzy reference[1], and so on. We may choose different methods doing fuzzy reference. But which method is better? It depends on needs. For complex reference problem, fuzzy neural network system could be used to get the relationship between fuzzy variable X and Y---R(X, Y), which is a good method to get a suitable rule according to our needs.

7 References

[1] L. A. Zadeh. "Fuzzy Sets". *Information and Control*, 1986.

[2] J. M. Zurada. "*Introduction to Artificial Neural Systems*". *West Publishing Company*, pp. 175-181, 1992.

[3] C. T. Lin and C. S. G. Lee. "Neural-network-based Fuzzy Logic Control and Decision system", *IEEE Transactions on Computers*, vol. 40, pp. 1320-1336, Dec. 1991.

[4] E. Soria-Olivas and J.D. Martin-Guerrero. "A Low Complexity Fuzzy Activation Function for Artificial Neural Networks", *IEEE Transactions on Neural Networks*, vol. 14, pp.1576-1579, Nov 2003.

[5] W. Li. "A Method for Design of a Hybrid Neuro-Fuzzy Control System Based on Behavior Modeling", *IEEE Transaction Fuzzy System*, pp. 462-477, 1997.

[6] L. A. ZADEH. "The Concept of a Linguistic Variable and its Application to Approximate Resoning-I", *Information Science*, pp. 199-249, 1975.

[7] D.V. Lindley. "Regression and correlation analysis", New Palgrave: A Dictionary of Economics, pp. 120-23., 1987.

[8] QiuWen Zhang and Ming Zhong. "Using Multi-level Fuzzy Comprehensive Evaluation to Assess Reservoir Induced Seismic Risk", Journal of Computers, pp. 1670-1677, 2011.

[9] W. J. M Kickert and E. H. Mamdani. "Analysis of a Fuzzy Logic Controller", *Fuzzy Sets and Systems,* pp. 29-44, 1978.

Adaptive Two-stage Fuzzy Logic Controllers for Urban Traffic Signals at Isolated Intersections

Yang Wenchen[1], Zhang Lun[1,*], He Zhaocheng[2] and Yang Yuchen[1]
[1] School of Transportation Engineering, Tongji University, Shanghai 201804, P.R. China
[2] Intelligent Transportation Research Centre, Sun Yat-sen University, Guangzhou 510275, P.R. China

Abstract - *This paper presents two optimal approaches of two-stage fuzzy controller for traffic signals at isolated intersections. Firstly, in the light that traffic status variables in two-stage controller leads to the inefficiency of traffic status weakening under low traffic flow, a two-stage combination fuzzy controller is designed from the perspective of structural optimization; this controller introduces 0-1 combination and determines the variables of fuzzy controller's inputs according to real-time traffic status identification. Secondly, aiming at the problems of fuzzy controller parameter empirical settings and functional disability of learning, a two-stage fuzzy logic traffic signal controller with online optimization is proposed; this controller introduces the rolling horizon framework and optimizes parameters of membership functions and controller rules by an improved hybrid genetic algorithm. The performance of the two proposed models is validated via online Paramics-based simulation platform, and extensive relative simulation tests have demonstrated the potential of the proposed controllers for adaptive traffic signal control.*

Keywords: Traffic signal; fuzzy logic; combination fuzzy; hybrid genetic algorithm; isolated intersection

1 Introduction

Single fuzzy controller considers all of status variables which lead to the increasing number of control rules and interference among status variables, or the only selection of queue length as status variable could not respond to traffic status[1,2]. Multi-stage fuzzy controller takes traffic status variables such as queue length, phase time, and saturation etc., into account, and processes these status variables dispersedly, optimizes phase sequences, and improves the performance of fuzzy controllers[3,4]. However, the adoption of standard four phase structures ignores the noncritical traffic flow and right turn flow, leading to insufficient response to fluctuation of complex traffic flow and weekending of traffic status under the low or medium saturation at intersections, and due to empirical parameters assured by experts, multi-stage fuzzy controller is still without learning ability[5]. From previous optimization work on the selection of traffic status variables and structure of fuzzy controller to current optimization of controller parameters with intelligent algorithms. Optimization of fuzzy logic-based control for traffic signals at isolated intersection have attracted the attention of scholars at home and aboard.

Ballester[6], Henry[7], and Bingham[8]etc., introduces artificial intelligent algorithms, such as genetic algorithm, neural networks, reinforcement learning, to learn fuzzy controller's parameters in the course of traffic signal control's interaction with traffic environment, and the simulation results indicate effectiveness of multi-stage fuzzy optimizing control, but many of which are off-line optimizing methods, and performance of these controllers mainly depend on the efficiency of optimizing algorithm, the valid sample sets, and the design of the feedback function. Genetic algorithm(GA) has the ability of global search and does not depend on gradient information and experiential knowledge[9]. In the light of this, Lekova[10], Kim[11] and Yang[12]etc., widely employs GA in researches of parameter optimization of fuzzy controllers, which could be divided into there categories: optimizing fuzzy membership parameter under experimental fuzzy rules, optimizing of fuzzy rules under experimental membership parameters, and optimizing membership parameters and fuzzy rules at the same time. Moreover, the majority of existing methods applies Matlab and computer program to simulate operation of traffic flow at intersections which does not represent the actual traffic flow in the road network, and thus lacks simulation evaluation method to evaluate implementation of fuzzy optimal controller[13].

Along the line of previous studies and in response to the above critical issues of traffic intensity-based two stage fuzzy controller, this paper presents adaptive two-stage fuzzy controllers for traffic signals at isolated intersections: architecture, algorithms, and online Paramics simulation. The remainder of this paper is organized as follows. Section II will detail the research scope and illustrate traffic intensity-based two-stage fuzzy control model for traffic signals. Section III illustrates two-stage combination fuzzy control model for traffic signals, including modeling theory analysis and conceptual models. Section IV details HGA-based two-stage fuzzy controller, which includes rolling horizon framework, online optimization design of two-stage fuzzy controller, objective function based on traffic status identification, and solution algorithm. Section V evaluates the proposed fuzzy controller with extensive experimental tests via Paramics-based simulation platform of online two-stage fuzzy optimal

control, which still includes development of Paramics-based simulation platform via Matlab and VC++ hybrid programming, and Paramics simulation experiment design. Section VI analyzes simulation results in detail. Section VII concludes the work.

2 Research scope and two-stage fuzzy model for traffic signals

2.1 Experimental test intersection

A typical cross intersection is shown in the left of Fig.1. The intersection has four approaches, and each approach has three types of traffic flow named straight flow, left flow and right flow. When right traffic volume is heavy, to avoid that vehicles interweave with each other and affect the passing efficiency by disrupting the straight flow in the opposite direction and the left flow in the same direction, the right-turn vehicles are under the signal control to simulate a real-world control environment, and the revised standard four-phase is shown in the right of Fig.1.

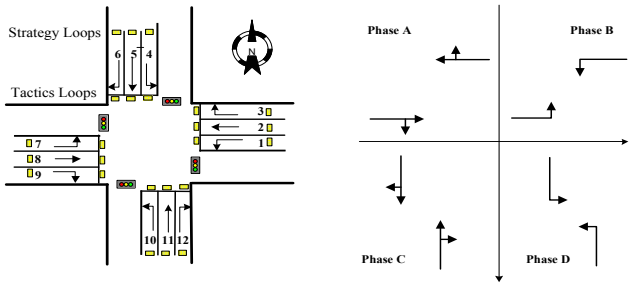

Figure 1. Experimental test intersection

To detect real-time traffic flow arrival and departure of each lane at intersection, the strategic and tactical loops are respectively deployed in each lane of each approach. As shown in left part of Fig.1, the tactical loops are deployed before the stop line to detect the throughput of each lane, including the number of leaving vehicles and their departure time, while the strategic loops are deployed at a distance of 150m away from tactical loops upstream of each approach to detect the arrival traffic demand of each lane, including the number of arrival vehicles and their arrival time.

2.2 Two-stage fuzzy control algorithm

Following basic principles of traffic signal control such as the maximum and minimum cycle and the maximum and minimum green time, the two-stage fuzzy control algorithm is as follows: (1) give minimum green time to the current green phase until the remainder of green time is 2s; (2) traffic intensity module determine red-urgency or green-urgency of each phase according to real-time detected traffic flow data, and select the red phase with maximum red-urgency as the next target green phase; (3) decision module determines extension time of current green phase (g_e) based on green-urgency and maximum red-urgency; (4) whether to switch current phase is determined by control logic that phase switch to next target green phase if g_e is less than 6s.

2.3 Structure of two-stage fuzzy controller

The Control rules of traffic signal fuzzy controller increase by exponent with the increase of the number of status variables, and each status variable interferes with each other. In order to make traffic signal fuzzy controller to respond to traffic flow change swiftly, this paper introduces traffic intensity to apply the two-stage fuzzy control model for isolated traffic signals, and denominates traffic intensity of red light phase and traffic intensity of green light phase as red urgency and green urgency respectively depending on their control features. Following this, the number of control rules decreases through multi stage and the interference between status variables of green light phase and those of red light phases is avoided. The structure of traffic signal two-stage fuzzy controller is shown in Fig.2.

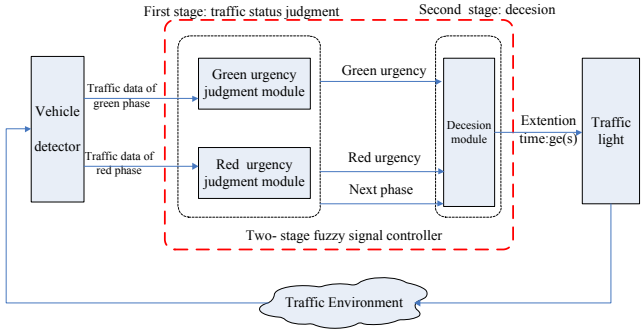

Figure 2. The structure of traffic signal two-stage fuzzy controller

The first stage is to determine the level of the traffic statues, which includes determining the urgent degree of red phase, the urgent degree of green phase and the optimal choice of next target phase. Among the three items, analyzing the traffic flow data collected at intersections, the urgent degree of red phase and the urgent degree of green phase are determined by green urgency module and red urgency module to evaluate the traffic intensity of signal phases. As to adapt to the dynamic features of traffic flow at intersections and the non-uniformity of traffic flow distribution, the function of the optimal choice of next target phase is aimed at selecting the highest phase among the urgent degree of red phases as the next target phase of green light, so as to achieve the optimization of phase sequence.

The second stage is to determine the extension time of the phase of green light. Based on the urgent degree of the current green phase and the urgent degree of the current red phase, the values of the current extension time of current green phase is determined by decision module.

The details on the above three fuzzy modules that determine red urgency, green urgency and decision time

respectively could see Yang's models[12]. Because of the uncertainty of traffic flow arrival for different phases, to consider non-critical flows, the average value of traffic flow parameters is selected as the input of controllers. And to formulate the reasonable control scheme representing traffic reality, vehicle flows of right turn are taken into account.

3 Two-stage combination fuzzy model

3.1 Theory analysis of modeling

The urban traffic signal two-stage fuzzy controller is influenced by the choice of traffic status variables and the reasonable setting of control parameters. When saturation of traffic flow is high, a certain number of queuing vehicles appears in each red light phase, thus it is hard to accurately represent the traffic status at intersections only considering the number of queuing vehicles, and two-stage fuzzy control based on traffic intensity, considering the phase time traffic status variables, meets control demands. However, the traffic flow is free under the condition of low vehicle flow and the number of queuing vehicles is less[3-5]. Under this situation, traffic status at intersections is weakened due to consideration of phase time and two-stage fuzzy control under low traffic flow approximately equals to the minimum-cycle based control. The reasons of the worse performance in low traffic flow condition is illustrated as follows: (1) Because of the short extension time of green phase, the phases switches frequently, and most of new coming vehicles have to queue before going through intersections; (2) Because of the consideration of time of red light phase, the waste of green time under no queuing vehicles is severe as the queuing vehicle of the new green light phase is less.

Thus, the status variables' choice of two-stage fuzzy controller's inputs should be directly relevant to traffic status at intersections. The choice of status variables is determined by features of traffic status. Based on respective traffic status variables of different traffic status at intersections, the structure of fuzzy controller under different traffic status should be adaptive.

3.2 Conceptual model of comination fuzzy

In the light that the standard fuzzy controller has achieved better control performance under low traffic flow and two-stage fuzzy control based on traffic intensity has achieved effective performance under high or middle traffic flow, the two-stage combination fuzzy control for urban traffic signals introduces "0-1" combination[14], in which choose the number of queuing vehicles as the traffic status variable under the condition of low traffic flow and thus apply the standard traffic signal single-stage fuzzy control (SFTSC)[2], while choose the phase traffic intensity as the traffic status variable under the condition of high traffic flow, and thus apply the traffic signal two-stage fuzzy control (TFTSC)[12]. The conceptual model of traffic signal two-stage combination fuzzy control is shown in (1).

$$\begin{cases} SFTSC & if \ \ Y \le Y_0 \\ TFTSC & if \ \ Y > Y_0 \end{cases} \tag{1}$$

In (1), Y_0 denotes total flow rate of intersections. And the identification of high or low traffic flow at intersections applies the method of two-dimension traffic status identification in reference [15]. According to the features of high or low traffic flow, the standards of identification of high and low traffic flow uses the threshold of free status that is Y_0 is 0.42 while occupancy of intersections is lower than 0.33.

Based the real-time ability of traffic signal control schemes and demand of the balanced transition of control schemes, T_c is selected as roll optimization cycle of two-stage combination fuzzy controller, that is at every T_c, by judging the traffic status of the intersection, the model of fuzzy controller for the following control interval is selected based the traffic status at isolated intersections.

4 Online optimization design for two stage fuzzy control

4.1 The rolling horizon framework

This paper optimizes parameters of membership functions and parameters of fuzzy rules at the same time[9]. To set the parameters of two-stage fuzzy controller response to real-time traffic conditions at intersections, this study introduces the rolling horizon[16]. With detecting traffic data, at each control interval, the controller parameters can be updated to adapt to real-time traffic flow characteristics accordingly. The framework of rolling horizon is shown in Fig.3. And the illustration of rolling horizon are as follows.

(1) Detect real-time traffic data during entire control time horizon H, such as arrival and leaving vehicles, etc.; (2) Setting length of projection stage T, decide each roll period length or each control interval(the accumulated time under latest controller with optimal parameters is just over T_o), and optimize parameters of fuzzy controller by hybrid genetic algorithm(HGA) according to quasi real-time historical traffic data; (3) Update parameters of fuzzy controller in time after optimization; (4) Repeat the above optimization process when it comes to the next control interval.

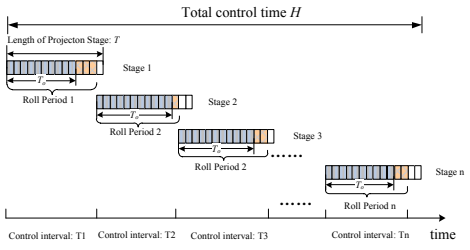

Figure 3. Illustration of the rolling horizon

And the structure of two-stage fuzzy controller based hybrid genetic algorithm for traffic signals is shown in Fig.4.

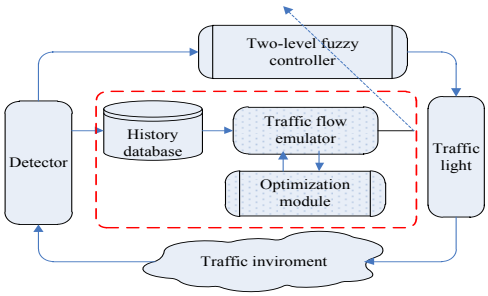

Figure 4. Structure of optimal two-stage fuzzy control system

In Fig.4, the designed HGA-based optimal fuzzy control system includes four following sub-modules: the two-stage fuzzy control in implementation, the reappearance of quasi real-time historical traffic flow, HGA-based optimization of parameters of fuzzy controllers and history database for managing traffic data.

4.2 Objective function based on traffic status identification

This study adopts average delay at an intersection as evaluation index of each controller with specific controller parameters. There are two methods to calculate delay: Mesoscopic numerical simulation[17] and Microsimulation [18]. Limited to the support of secondary development kits of most simulation software, this study employs mesoscopic numerical simulation to model the average delay.

To model the discrete process of vehicle arrival at intersections, the assumption that one vehicle is queuing when it just arrives strategic loops is mostly used. Though delay models based this assumption fit better relatively under high saturation that traffic volume at intersection is heavy and there are certain queuing vehicles at most approaches, the delay error is larger under low saturation due to vehicle's discrete process between strategic and tactics loops. Therefore, this study models average delay at intersections based traffic status identification[15]. Under low saturation, the newly arrived vehicles enter the queuing with the possibility of 50%[12], while the newly arrived vehicles enter the queuing with the possibility of 100% under high saturation[17].

4.3 Solution algorithm

(1) Decoding for controller parameters

The traffic intensity-based two-stage fuzzy controller employed in this study has two input variables and one output variable, and all of which are divided into five fuzzy sets. Decoding for this controller includes parameters of membership function and fuzzy rules. To improve control algorithm's accuracy and solution algorithm's convergence speed, real number encoding is designed to decrease the length of the chromosome. As shown in the left part of Fig.5, this study adopts triangle membership function to reduce the number of controller parameters, and let the base vertices of each membership function separately superpose centers of two adjacent membership function, consequently, with the center of membership functions, its position and shape could be effectively given.

For the chromosome of control rules,, to decrease the complexity and enhance the real-time ability of controller, utmostly 25 controller rules could be selected. considering following integer matrix R: $R=[r_{ij}]_{5\times5},\ i\in[1,5], j\in[1,5]$, while r_{ij} is a integer within [1,5], denoting the index value of output of fuzzy sets. Then R can be converted into a row vector R' that can denote the chromosome of fuzzy rule, i.e. replacing the first element of the next row just behind the last element of the former row. Individual coded schema of two-stage fuzzy controller is shown in the right part of Fig.5.

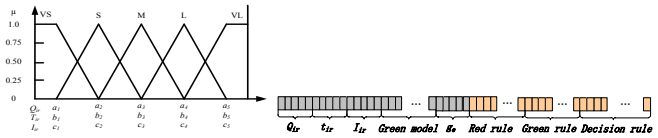

Figure 5. Decoding for parameters of fuzzy controller

(2) Hybrid genetic algorithm

A GA-based heuristic(HGA) extended form the method by Yang has been developed to yield approximate solutions for each control interval during the entire optimization period[15]. The proposed heuristic features its capability to identify the solution closest to the best solution by introducing simulated annealing algorithm to enhance the local optimal capability of genetic algorithm. The process of improved hybrid genetic algorithm is as follows:

i) Initialization: generate initial population, and initialize GA and SA parameters. According to generation and fitness value, crossrate and mutationrate is adaptive.

ii) Fitness evaluation: Evaluating performance of each controller with specific controller parameters is to calculate average delay at intersection (d) based traffic status identification, then the fitness value is computed in (2).

$$f(d)=\frac{1}{1+d} \tag{2}$$

iii) Selection: roulette wheel selection.

iv) Crossing: non-uniform arithmetic crossover operator.

v) Mutation: non-uniform mutation operator, by which the degree of mutation is adaptively adjusted with generation and fitness value.

vi) Elitist strategy: replace the worst individual by the best.

vii) Local optimization by Simulated Annealing: introduced the best individual of cur-generation as initial vector, enhancing the local optimization via SA.

a) Generate new individuals by status function of SA;

b) Select the individual by metropolis principle in SA;

c) Judge the stability of SA, if non-steady, go to a); Otherwise, execute annealing operation and go to step viii);

viii) Judgment of termination principle: if $n<Gen$, go to Step2. Otherwise, output the best solution.

5 Case study

5.1 Quasi-online Paramics-based simulation platform

Traffic simulation, which could simulates the operation of traffic flow under different control strategies, is an effective evaluation approach for urban traffic signal controls. The microscopic simulator Paramics was employed as an unbiased evaluator for model performance, and a Paramics-based simulation platform of quasi-online two-stage fuzzy optimization control is developed. The Paramics-based simulation platform of two-stage fuzzy optimization control consists of implementation module for actual control and optimizing module for learning parameters. Taking the efficiency of optimizing module into account, in the process of optimizing, the implement module is still operating. The novel optimizing codes come into operation just at the end of previous optimizing request. The following are the features of the developed simulation platform:

(1) To shorten the development cycle and improve the accuracy of fuzzy decision, three types of fuzzy controller are developed via Matlab;

(2) To make Paramics simulation platform of fuzzy control interact with above three fuzzy controller, the hybrid programming of Matlab and VC++ is introduced by which interface between VC++ and Matlab is defined and control strategies such as actuated control, two-stage fuzzy control, and HGA-based two-stage fuzzy control are secondarily developed into Paramics via Paramics API[18], and to establish the communication between implementation module and optimal module, database-based command queuing technology is used;

(3) Physical simulation network for a typical urban isolated intersection is developed via Paramics's Modeler module, and by loading control strategies' Plug-in into Paramics, the performance of those traffic signal controllers could be validated under different traffic scenarios designed in Paramics.

5.2 Paramics simulation

(1) Simulation algorithm

Following the basic algorithm of two-stage fuzzy control, in the two-stage combination fuzzy controller, T_c is 5*min*, that is when the accumulated time is just over 5*min*, two-stage combination fuzzy optimization module selects the most appropriate fuzzy controller based real-time traffic status at intersections; For HGA-based fuzzy controller, T is 10*min* and T_o is 8*min*, that is when the accumulated time under latest controller with optimal parameters is just over 8*min*, HGA-based two-stage fuzzy optimization module learns parameters of three fuzzy controllers, and updates the parameters of fuzzy controllers of implementation module at the end of parameter optimization.

(2) Simulation scenarios

In order to examine the proposed control method under different traffic flow conditions and different traffic flow fluctuation, this paper designs a variety of simulation scenarios, including uniform arrival for each approach, a sudden change in one of direction flows, and unbalanced arrival for each approach. The specification of simulation scenario is as follows:

i) Simulation length is 13*h*, approach arrival flow ranges from 400 to 1600 per hour. And every per hour is a simulation time period, and the turning ratio of left-straight-right 0.25-0.60-0.15;

ii) To simulate traffic fluctuation in short-term, vehicle's departure rate in 10*min* intervals per hour, set in the Profiles of Paramics, is as follows: 15-11-17-22-16-19;

iii) According to the design standard of urban roads in china that the capacity of straight, left and right are 1650*pcu/h*, 1550*pcu/h* and 1550*pcu/h*, the key simulation parameters of mean driver reaction time(*MDT*) and mean headway time (*MHT*) are respectively calibrated to1.8*s* and 1.5*s*;

iv) To overcome the stochastic nature of simulation results, an average of 20 simulation runs has been used.

(3) Simulation experiments

Experiment I is designed to verify two- stage combination fuzzy control (CTFIFuzzy), compared to fixed-timing, actuated, and traffic intensity-based two-stage fuzzy control. Here, fixed-timing scheme (Fixed) is Webster signal timing under average traffic flow at intersections (05:0-06:000)[19], while in actuated control (Actuated), detector loop is 30m away from the stop line, and the extension unit time is 3*s*[15]; and traffic intensity-based two-stage fuzzy control (TFIFuzzy) adopt Yang's method[12]. And compered to fixed-timing, actuated and two-stage fuzzy control based

traffic intensity, experiments II are designed to validate two-stage fuzzy control based HGA (GAFuzzy).

Considering traffic flow characteristics and safety demands at signalized intersections, simulation parameter settings are as follows：maximum green time for phase1 and phase 3 is 80*s*, while 50*s* for phase 2 and phase 4, and minimum green time for four phases is 12*s*.

6 Results

Performance indices in this study are average delay (*Delay*), average queuing number (*Queue*) and average speed (*Speed*), and approach throughput (*Count*). Among them, speed and throughput are benefit indicators, while delay and queue are efficiency indicators.

(1) Two-stage combination fuzzy controller

Simulation results of the two-stage combination fuzzy control's performance are shown in Fig.6. The performance of two-stage fuzzy controller is poor in the low traffic flow due to the weakening of traffic status, which result in the frequent shifts of phases and the waste of phase green time when less vehicles passing. Throughout the whole simulation process, combination fuzzy control is stable, and compared to the fixed, actuated or two-stage fuzzy control, the performance of combination fuzzy controller are improved greatly. For example, the delay decreases by 30% to 10%. And simulation results indicate that this controller improves the performance of two-stage fuzzy control in low traffic flow conditions.

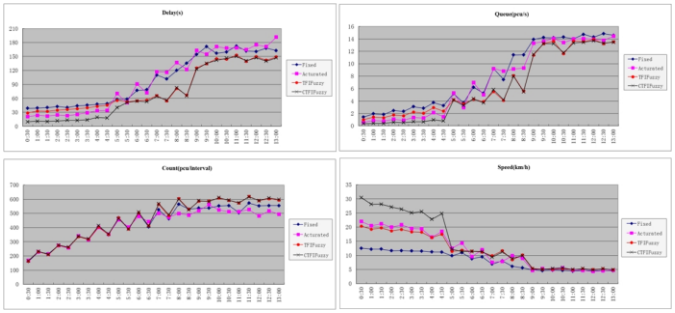

Figure 6. Simulation results of two-stage combination fuzzy controller

(2) HGA-based two-stage fuzzy controller

Simulation results of HGA-based two-stage fuzzy controller's performance indices are shown in Fig.7. Throughout the simulation process, HGA-based two-stage fuzzy control is stable. Performance of delay, queue length etc., are better than those of fixed-timing, actuated control and two-stage fuzzy control. Furthermore, performance of this controller is still getting better as traffic arrival volume of each approach is increasing. Taking delay as an example, compared to the actuated control, fixed control, and two-stage fuzzy control, GA-based fuzzy control decreases delay by 27%, 30% and by 13% respectively.

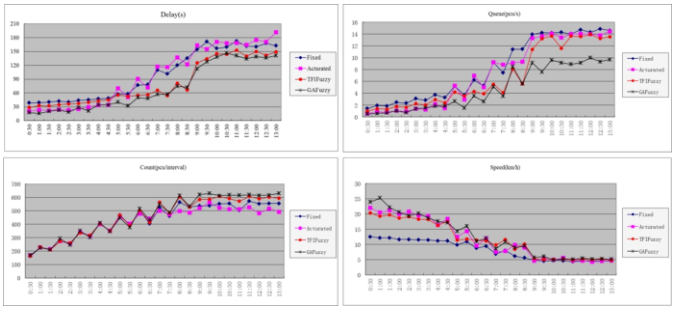

Figure 7. Simulation results of HGA-based two-stage fuzzy controller

At a certain control interval, taking the red urgency module as an example, the differences between membership functions with empirical parameters and membership functions with optimized parameters are shown in Fig.8.

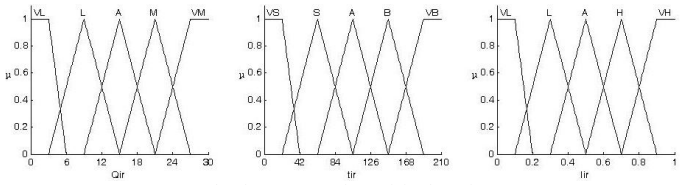

(a) The fuzzy sets of empirical settings

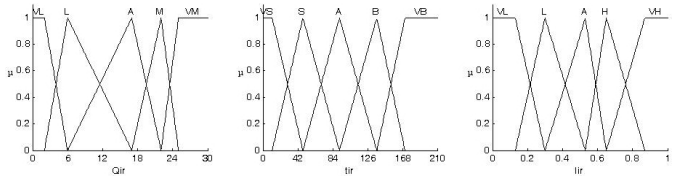

(b) The fuzzy sets aft optimization

Figure 8. Parameters of Membership functions of Red urgency judgment

7 Conclusions

This paper presents two adaptive two-stage fuzzy controllers for unban traffic signals at isolated intersections. From the perspective of structural optimization, the two-stage combination fuzzy controller introduces 0-1 combination, in which the single-stage controller will be applied under low traffic flow, while the traffic intensity-based two-stage fuzzy controller will be used under medium or high traffic flow. This combination controller determines traffic status variables of fuzzy controller's inputs depending on the traffic status at intersections, and adapts to the influence of traffic flow change on the performance of different fuzzy controllers. Then, aiming at the problems of fuzzy controller parameter empirical settings and functional disability of learning, the HGA-based two-stage fuzzy control introducing rolling horizon framework develops an adaptive optimization framework of fuzzy controller to adjust fuzzy membership functions and controller rules with on-line learning. At regular time intervals, HGA-based controller employs a hybrid genetic algorithm to efficiently yield the reliable solution through reappearance of statistical traffic flow. Experiments are carried on typical urban isolated intersection and the performance of proposed model and algorithm is validated via Paramics-based simulation platform of on-line two-stage fuzzy optimization control.

Extensive Paramics simulation results indicate that different traffic signal controller has its application boundaries. It is reasonable that combination fuzzy control selects traffic state variables of fuzzy controller according to traffic status at intersection, which improves the performance of two-stage fuzzy control in low flow conditions; and HGA-based fuzzy controller learns parameters with quasi-online optimization, which is stable and get better performance. Compare to fixed-time, actuated, and two-stage fuzzy controller for different traffic conditions, the two proposed controller offer a better performance as the traffic flow increases, and control effects are consistent with traffic manager's control object.

8 Acknowlegement

The work of this paper is supported by National Science Foundation of China (Project No. 50408034) and Shanghai Educational Foundation for Innovation (Project No. 11ZZ27).

Thanks to ITS Research Center of Sun Yat-sen University for able research assistance on Paramics simulation works.

9 References

[1] C. Pappis, E. Mamdani. "A fuzzy logic controller for a traffic junction," Man and Cybernetics, vol.7-10, 1977, pp: 48-60.

[2] R. Hoyer, U. Jumar. "An advanced fuzzy controller for traffic lights," IFAC Artificial Intelligence in Real Time Control, 1994, pp: 67-72.

[3] M.B. Trabia, M.S. Kaseko, and M. Ande. "A two-stage fuzzy logic controller for traffic signals," Transportation Research: Part C, vol. 7-6,1999, pp: 353-367.

[4] Y.S. Murat, and E. Gedizlioglu. "A fuzzy logic multi-phased signal control model for isolated junctions." Transportation Research: Part C, vol.13-1, 2005, pp: 19-36.

[5] B.M. Nair, and J. Cai. "A fuzzy logic controller for isolated signalized intersection with traffic abnormality considered," IEEE Intelligent Vehicles Symposium, 2007, pp:1229-1233.

[6] P.J. Ballester, and J.N. Carter. "A parallel real-coded genetic algorithm for history matching and its application to a real petroleum reservoir," Journal of Petroleum Science and Engineering, vol. 59-3, 2007, pp: 157-168.

[7] J.J. Henry, J.L. Farges, and J.L. Gallego. "Neuro-fuzzy techniques for traffic control," Control Engineering Practice, vol.6, 1998, pp: 755-761.

[8] E. Bingham. "Reinforcement learning in neuro-fuzzy traffic signal control," European Journal of Operation Search, vol. 131, 2001, pp: 232-241.

[9] S.M. Rahman, N.T. Ratrout. "Review of the Fuzzy Logic Based Approach in Traffic Signal Control: Prospects in Saudi Arab," Journal of Transprotaion Systems Engineering and Information Technology, vol.9-5, 2009, pp:58-70.

[10] A. Lekova, L. Mikhailov, and D. Boyadjie. "Redundant fuzzy rules exclusion by genetic algorithms," Fuzzy sets and Systems, vol.100, 1998, pp:235-243.

[11] J.W. Kim, B.M. Kim, and J.Y. Kim. "Genetic algorithm simulation approach to determine mebership functions of fuzzy traffic controller," Electronics Letters, vol.34-20, 1998, pp:1982-1983.

[12] Z.Y. Yang, X.Y. Huang, C. Xiang, "Multi-phase traffic signal control for isolated intersections based on genetic fuzzy logic," Intelligent Control and Automation, 2006, pp: 3391-3395.

[13] R.L. Kelsey, and K.R. Bisser. "A Simulation Environment for Fuzzy Control of Traffic Systems," 12th IFAC-World Congress, Sydney, Austria, Preprints(5), 18-23, July 1993, pp: 553-556.

[14] R. Chrobok, O. Kaumann, J. Wahle, M. Schreckenberg. "Different methods of traffic forecast based on real data," European Journal of Operational Research, vol.155 -3, 2004, pp: 558-568.

[15] W.C. Yang, Z.C. He, N.N. Chen. "Adaptive control method of multi-phase intersection based on traffic status identification," The Ninth International Conference on Chinese Transportation Professionals, 2009, pp: 1910-1919.

[16] Y.M. Nie, X. Wu, J.F. Dillenburg, P.C. Nelson. "Reliable route guidance: A case study from Chicago," Transportation Research Part A: Policy and Practice, vol.46-2, 2012, pp:403-419.

[17] J.X. Gao, J.G. Li, X.H. Zhao. "Two-stage fuzzy control of urban isolated intersection signal for complex traffic conditions," Proceedings of the 5th World Congress on Intelligent Control and Automation, China, vol.15-19, 2004, pp:5287-5291.

[18] Quadstone. "Paramics 6.6.1 user manual," Edinburgh, Scotland, 2008.

[19] F.V. Webster. "Traffic signals," Traffic engineering practice, 1963, pp:117-146.

Fuzzy PID based on Firefly Algorithm: Load Frequency Control in Deregulated Environment

O. Abedinia
Electrical Engineering Department,
Semnan University, Semnan, Iran

K. Kiani
Electrical Engineering Department,
Semnan University, Semnan, Iran

N. Amjady
Electrical Engineering Department,
Semnan University, Semnan, Iran

H. A. Shayanfar *
Center of Excellence for Power System Automation and Operation, Elect. Eng. Dept., Iran University of Science and Technology, Tehran, Iran

oveis.abedinia@gmail.com, kkiani2004@yahoo.com, n_amjady@yahoo.com, hashayanfar@yahoo.com

Abstract— **A Firefly Algorithm (FA) based on Fuzzy PID controller is proposed in this paper to solve the Load Frequency Control (LFC) problem in a deregulated environment. In multi area electric power systems, if a large load is suddenly connected (or disconnected) to the system, or if a generating unit is suddenly disconnected by the protection equipment, there will be a long-term distortion in the power balance between that delivered by the turbines and that consumed by the loads. This imbalance is initially covered from the kinetic energy of rotating rotors of turbines, generators and motors and, as a result, the frequency in the system will change. This paper applied a fuzzy controller to solve this problem. The results of the proposed controller are compared with the classical fuzzy PID type controller and classical PID controller through ITAE and FD performance indices.**

Keywords; FA, Load Frequency Control, Two-Area Power System, Deregulated Environment.

I. INTRODUCTION

For large scale electric power systems with interconnected areas, Load Frequency Control (LFC) is important to keep the system frequency and the inter-area tie power as near to the scheduled values as possible. The input mechanical power to the generators is used to control the frequency of output electrical power and to maintain the power exchange between the areas as scheduled. A well designed and operated electric power system must cope with changes in the load and with system disturbances, and it should provide acceptable high level of power quality while maintaining both voltage and frequency within tolerable limits. Many control strategies for Load Frequency Control (LFC) in electric power systems have been proposed by researchers over the past decades[1] .

The foremost task of LFC is to keep the frequency constant against the randomly varying active power loads, which are also referred to as unknown external disturbance[2] . Another task of the LFC is to regulate the tie-line power exchange error. A typical large-scale power system is composed of several areas of generating units. In order to enhance the fault tolerance of the entire power system, these generating units are connected via tie-lines. The usage of tie-line power imports a new error into the control problem, i.e., tie-line power exchange error. When a sudden active power load change occurs to an area, the area will obtain energy via tie-lines from other areas. But eventually, the area that is subject to the load change should balance it without external support. Otherwise there would be economic conflicts between the areas. Hence each area requires a separate load frequency controller to regulate the tie-line power exchange error so that all the areas in an interconnected power system can set their set points differently[3] .

There are lots of techniques to solve the LFC problem in power system [4]. The Proportional Integral (PI) controllers have been broadly used for the load frequency controllers [5]. The LFC design based on an entire power system model is considered as centralized method. In [6] and [7], this centralized method is introduced with a simplified multiple-area power plant in order to implement such optimization techniques on the entire model. However, the simplification is based on the assumption that all the subsystems of the entire power system are identical while they are not.

In this paper, to overcome these problems, Firefly technique (FA) is proposed for the solution of tuning the fuzzy controller parameters. The FA is a meta-heuristic, nature-inspired, optimization algorithm which is based on the social (flashing) behavior of fireflies, or lighting

* Corresponding Author. E-Mail Address: hashayanfar@yahoo.com (H. A. Shayanfar)

bugs, in the summer sky in the tropical temperature regions [8]. Its main advantage is the fact that it uses mainly real random numbers, and it is based on the global communication among the swarming particles, and as a result, it seems appropriate technique to use LFC problem solution. The effectiveness of the proposed method is tested on a three-area deregulated power system. Also the result of the proposed technique is compared with classical fuzzy PID type controller and classical PID controller [9] through Integral of the Time multiplied Absolute value of the Error (ITAE) and the Figure of Demerit (FD) performance indices.

II. POWER SYSTEM DESCRIPTION

Power systems have variable and complicated characteristics and comprise different control parts and also many of the parts are nonlinear [1]. These parts are connected to each other by tie lines and need controllability of frequency and power flow [4]. Deregulated power system consists of GENCOs, TRANSCOs and DISCOs with an open access policy. This is obvious that all transactions have to be cleared via Independent System Operator (ISO) or other responsible infrastructure. In this latter environment, it is appropriate that a new model for LFC scheme is improved to account for the effects of possible load following contracts on the system's dynamics [10].

In the restructured power system, Generation Companies (GENCOs) may or may not participate in the LFC task. On the other hand, distribution Companies (DISCOs) have the liberty to contract with any available GENCOs in their own or other areas. Thus, there can be various combinations of the possible contracted scenarios between DISCOs and GENCOs [1-3]. The concept of an Augmented Generation Participation Matrix (AGPM) is introduced to express these possible contracts in the generalized model. The dimension of the AGPM matrix in terms of rows and column is equal the total number of GENCOs and DISCOs in the overall power system, respectively. Consider the number of GENCOs and DISCOs in area i be ni and mi in a large scale power system with N control areas. The structure of the AGPM is given by:

$$AGPM = \begin{bmatrix} AGPM_{11} & \cdots & AGPM_{1N} \\ \vdots & \ddots & \vdots \\ AGPM_{N1} & \cdots & AGPM_{NN} \end{bmatrix} \quad (1)$$

$$AGPM_{ij} = \begin{bmatrix} gpf_{(s_i+1)(z_j+1)} & \cdots & gpf_{(s_i+1)(z_j+m_j)} \\ \vdots & \ddots & \vdots \\ gpf_{(s_i+n_i)(z_j+1)} & \cdots & gpf_{(s_i+n_i)(z_j+m_j)} \end{bmatrix}$$

$$s_i = \sum_{k=1}^{i-1} n_i, z_j = \sum_{k=1}^{j-1} m_j, i, j = 2,...,N \;\&\; s_1 = z_1 = 0$$

Where, n_i and m_i define the number of GENCOs and DISCOs in area i and gpf_{ij} refers to the 'generation participation factor' and displays the participation factor of GENCO i in total load following requirement of DISCO j based on the possible contracts. The sum of all inputs in each column of AGPM is univalent. The block diagram of a generalized LFC model with AVR loop in a deregulated power system to control area *i*, is presented in Fig.1. These new information signals are considered as disturbance channels for the decentralized LFC design [4]. As there are many GENCOs in each area, ACE signal has to be distributed among them due to their ACE participation factor in the LFC task and $\sum_{j=1}^{ni} apf_{ij} = 1$. It can be written that [5]:

$$d_i = \Delta P_{Loc,j} + \Delta P_{di} \quad , \quad \Delta P_{Loc,j} = \sum_{j=1}^{m_i} (\Delta P_{Lj-i} + \Delta P_{ULj-i}) \quad (2)$$

$$\eta_i = \sum_{j=1\,\&\, j\neq i}^{N} T_{ij} \Delta f_j \,, \quad \zeta_i = \sum_{k=1\,\&\, k\neq i}^{N} \Delta P_{tie,ik,sch}$$

$$\Delta P_{tie,ik,sch} = \sum_{j=1}^{n_i} \sum_{t=1}^{m_k} apf_{(s_i+j)(z_k+t)} \Delta P_{L(z_k+t)-k} - \sum_{t=1}^{n_k} \sum_{j=1}^{m_i} apf_{(s_k+t)(z_i+j)} \Delta P_{L(z_i+j)-i}$$

$$\Delta P_{tie,i-error} = \Delta P_{tie,i-actual} - \zeta_i$$

$$\rho_i = [\rho_{1i} \;\cdots\; \rho_{ki} \;\cdots\; \rho_{n_i i}] \quad , \quad \rho_{ki} = \Delta P_{m,k-i}$$

$$\Delta P_{m,k-i} = \sum_{j=1}^{z_{N+1}} gpf_{(s_i+k)j} \Delta P_{Lj-i} + apf_{ki} \sum_{j=1}^{m_i} \Delta P_{ULj-i}, k = 1,2,...,n_i$$

Where, $\Delta P_{m,ki}$ is the desired total power generation of a GENCO k in area i and must track the demand of the DISCOs in contract with it in the steady state. Two GENCOs and DISCOs are assumed to each control an area for which the system parameters are given in [3].

To make the visualization of contracts easier, the concept of a "DISCO Participation Matrix" (DPM) will be used. Essentially, DPM gives the participation of a DISCO in contract with a GENCO. In DPM, the number of rows has to be equal to the number of GENCOs and the number of columns has to the number of DISCOs in the system. Any entry of this matrix is a function of the total load power contracted by a DISCO toward a GENCO.

A. Firefly Algorithm

The Firefly Algorithm (FA) is a meta-heuristic, nature-inspired, optimization algorithm which is based on the social (flashing) behavior of fireflies, or lighting bugs, in the summer sky in the tropical temperature regions and introduced by Xin-She Yang [11]. Although FA has many similarities with other algorithms which are based on the so-called swarm intelligence; it is indeed much simpler both in concept and implementation [12].

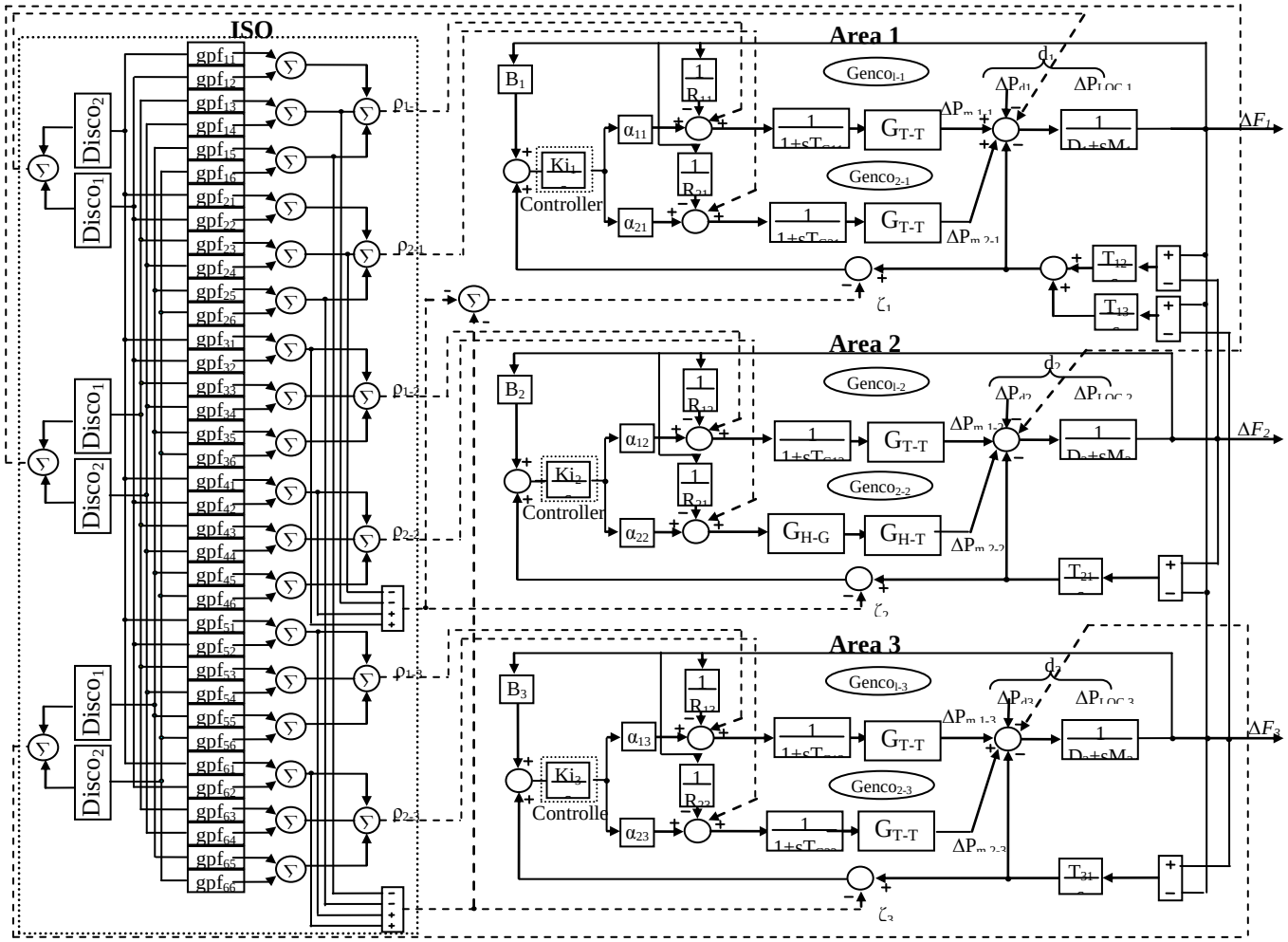

Figure 1. Generalized LFC model in the restructured system

Furthermore, this proposed technique is very efficient and can outperform other conventional algorithms, for solving many optimization problems; where the statistical performance of the firefly algorithm was measured against other well-known optimization algorithms using various standard stochastic test functions [13]. For simplicity, summarize of these flashing characteristics as the following three rules [11-13]:

- All fireflies are unisex, so that one firefly is attracted to other fireflies regardless of their sex.
- Attractiveness is proportional to their brightness, thus for any two flashing fireflies, the less bright one will move towards the brighter one. The attractiveness is proportional to the brightness and they both decrease as their distance increases. If no one is brighter than a particular firefly, it moves randomly.
- The brightness of a firefly is affected or determined by the landscape of the objective function to be optimized.

B. Attractiveness

The form of attractiveness function of a firefly is the following monotonically decreasing function [24]:

$$(\beta_r) = \beta_0^{*} \exp(-\gamma r^m), with m \geq 1, \tag{3}$$

Where, r is the distance between any two fireflies, β_0 is the initial attractiveness at $r = 0$.

γ, is an absorption coefficient which controls the decrease of the light intensity.

C. Distance

The distance between any two fireflies i and j, at positions x_i and x_j , respectively, can be defined as [12]:

$$r_{ij} = \left\| x_i - x_j \right\| = \sqrt{\sum_{k=1}^{d} (x_{i,k} - x_{j,k})^2} \tag{4}$$

Where $x_{i,k}$ is the k_{th} component of the spatial coordinate x_i of the i_{th} firefly and d is the number of

dimensions.

However, the calculation of distance *r* can also be defined using other distance metrics, based on the nature of the problem, such as Manhattan distance or Mahalanobis distance [12].

D. Movement

The movement of a firefly *i* which is attracted by a more attractive firefly *j* is given by the following equation:

$$x_i = x_j + \beta_0 * \exp(-\gamma r_{ij}^2) * (x_j - x_i) + \alpha * (rand - \frac{1}{2}) \quad (5)$$

Where, the first term is the current position of a firefly, the second term is used for considering a firefly's attractiveness to light intensity seen by adjacent fireflies, and the third term is used for the random movement of a firefly in case there are not any brighter ones. Actually α is a randomization parameter determined by the problem of interest between [0, 1].

E. FA-based PID type controller

This paper applied the PID controller for the solution of LFC problem [7]. Actually, the PID controller in wide range of operating conditions which provides robust performance. It is clear that, transient performance of the power system with respect to the control of the frequency and tie-line power flows obviously depends on the optimal tuning of the PID controller's parameters. In order to overcome the backwashes of conventional method and supply optimal control performance, FA technique is proposed to optimal tune of PID controllers parameters under different operating conditions. The block diagram of proposed technique for PID controller is presented in Fig. 2. Also the equation of load frequency control for PID in each control area is:

$$PID = k_P + \frac{k_I}{S} + k_D \quad (6)$$

Actually, in industrial PID controller is applied for low pass filter which is necessary to omit high frequency noise in entry of differentiator. Therefore in this paper for PID controller, conversion function of differentiator is:

$$k_D\, S/(1+T_dS),\ T_d=100,\ k_D \langle\langle T_d \quad (7)$$

By taking Area Control Error (ACE_i) as the input of PID controller in two case studies, the control vector for PID controller in each control area is given by:

$$u_i = k_{Pi} ACE_i + k_{Li} \int ACE_i dt + k_{Di} ACE_i \quad (8)$$

According to equation 8, in this paper the K_{Pi}, K_{Ii} and K_{Di} gains are tuned by proposed FA technique. The design problem can be formulated as the following constrained optimization problem, where the constraints are the PID controller parameter bounds:

$$\begin{aligned} &K_{Pi}^{\min} \le K_{Pi} \le K_{Pi}^{\max} \\ \textit{Minimize } u \textit{ subject to}: \quad &K_{Ii}^{\min} \le K_{Ii} \le K_{Ii}^{\max} \\ &K_{Di}^{\min} \le K_{Di} \le K_{Di}^{\max} \end{aligned}$$

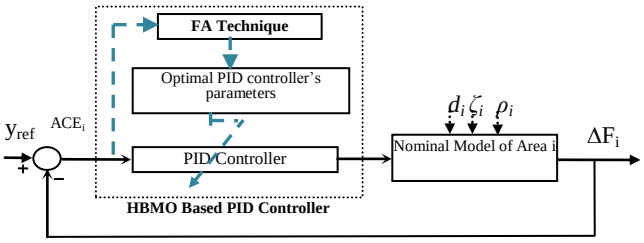

Figure 2. The introduced FA based PID controller structure.

Accordingly, the PID controller generates the control signal that applies to the governor set point in each area where the FA module works offline. For testing the robustness of the proposed technique, the power system is analyzed through some performance indices as ITAE and FD which are based on ACE_i and system responses characteristic, respectively [14]. The formulation of ITAE and FD are described as:

$$ITAE = \int_0^{10} t\left(|ACE_1(t)| + |ACE_2(t)| + |ACE_3(t)|\right)dt \quad (9)$$

$$FD = (OS \times 10)^2 + (US \times 4)^2 + (TS \times 0.3)^2$$

In other words, the concept of appropriate situation for LFC problem is based on overshoot (OS), undershoot (US) and settling time of frequency deviation in comparison of other techniques. It is clear that, the lower value of this objective functions is the best situation for system. The result of PID parameters are shown in Table 1. Also, the numerical results of these indices are presented in Table. 2.

To improve the overall system dynamic performance in a robust way and optimization synthesis, FA technique is employed to solve the above mentioned optimization problem and search for optimal or near optimal set of off-nominal PID controller parameters (K_{Pi}, K_{Ii} and K_{Di} for i=1, 2 ,…, N) where, N introduce the number of control areas [4]. Hence, the proposed method finds appropriate PID parameters with considering objective functions optimization. The convergence trend of proposed technique is presented in Fig. 3.

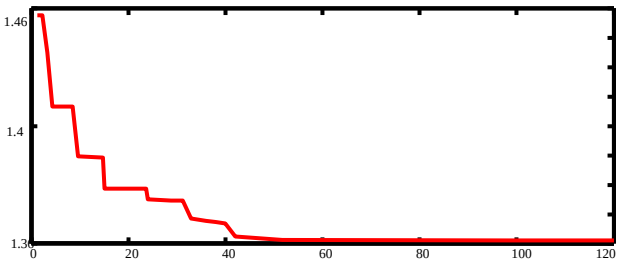

Figure 3. Variations of fitness function.

TABLE I. OPTIMUM PID CONTROLLER GAINS

FAPID	Area 1	Area 2	Area 3
K_p	2.597	1.784	1.684
K_i	3.846	1.987	1.745
K_d	1.245	1.013	1.003

In this paper, a nonlinear model with ±0.1 replaces the linear model of turbine ΔPVki/ΔPTki is considered which is shown in "Fig. 4". The proposed controller reduces the Frequency Deviance (ΔF) in dynamic status Per Load variations (ΔPL). This is to take Generation Rate Constraints (GRC) in to account, i.e. the practical limit on the rate of the change in the generating power of each GENCO.

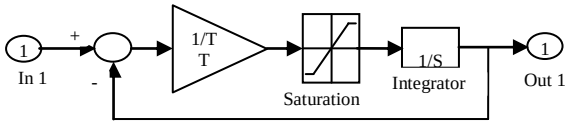

Figure 4. Nonlinear turbine model with GRC

I. SIMULATION RESULTS

In this paper for each DISCO demands 0.1 pu MW is considered. Also, it is possible that a DISCO violates a contract by demanding more power than that of specified in the contract. This excess power must be reflected as a local load of the area but not as the contract demand and taken up by the GENCOs in the same area [14].

Also for test the robustness of proposed controller the case study is tested against uncertainties and large load disturbances in the presence of GRC [14]. For this purpose two scenarios are applied as:

- *Scenario 1*

The GENCOs participate only in load following control of their areas. It is assumed that a large step load of 0.1 p.u. is demanded by each DISCO in areas 1 and 2. Assume that a case of *Poolco* based contracts between DISCOs and available GENCOs are simulated based on the following AGPM. Also the GENCOs of area 3 do not participate in the AGC task [9]. Essentially, DPM gives the participation of a DISCO in contract with a GENCO. The deviation of frequency and tie lines power flows for +25% changes is presented in Fig. 5. The element of DPM matrix and desired values for this scenario are:

$$\Delta P_{M,1\text{-}1}=0.11 \text{ pu MW}, \Delta P_{M,2\text{-}1}=0.09 \text{ pu MW}$$
$$\Delta P_{M,1\text{-}2}=0.1 \text{ pu MW}, \Delta P_{M,2\text{-}2}=0.1 \text{ pu MW}$$

$$DPM = \begin{bmatrix} 0.6 & 0.5 & 0 & 0 & 0 & 0 \\ 0.4 & 0.5 & 0 & 0 & 0 & 0 \\ 0 & 0 & 0.5 & 0.5 & 0 & 0 \\ 0 & 0 & 0.5 & 0.5 & 0 & 0 \\ 0 & 0 & 0 & 0 & 0 & 0 \\ 0 & 0 & 0 & 0 & 0 & 0 \end{bmatrix}$$

- *Scenario 2*

In this Scenario, it is assumed that in addition to the specified contracted load demands and 25% increase in parameters, DISCO 1 in area 1, DISCO 1 in area 2 and DISCO 2 in area 3 demand 0.05, 0.04 and 0.03 pu MW as large un-contracted loads, respectively [9]. Using Eq. (2), the total local load in all areas is obtained as:

$$P_{Loc,1}=0.25, P_{Loc,2}=0.24, P_{Loc,3}=0.23 \text{ MW} \quad (10)$$

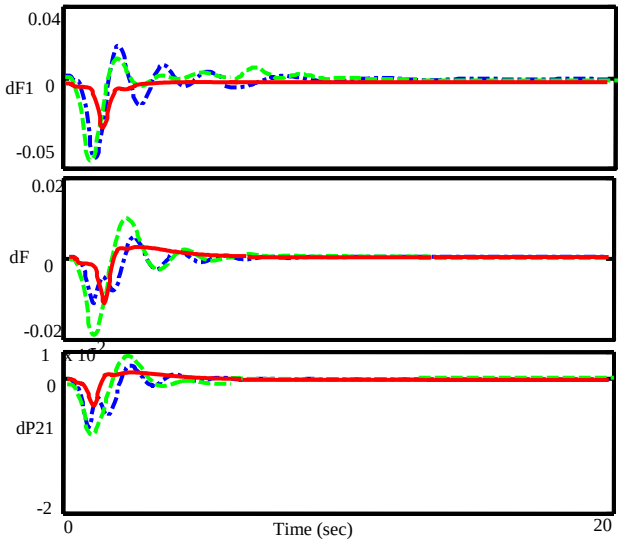

Figure 5. Frequency deviation and tie line power flows; solid (FAPID), dashed (CFPID) and dotted (PID)

The simulation results of scenario 2 are presented in Fig. 6.

TABLE II. ITAE AND FD PERFORMANCE INDICES

Change parameters	ITAE Scenario 1			ITAE Scenario 2			FD Scenario 1			FD Scenario 2		
	FAPID	CPID	PID	FAPID	CPID	PID	FAPID	CPID	PID	FAPID	CPID	PID
25%	289	340	378	425	717	3530	476	793	1378	1407	1839	12445
20%	264	293	356	404	675	2887	481	804	1187	1423	1891	10949
15%	248	269	346	384	641	2364	456	608	1134	1452	1814	9834
10%	237	258	340	368	614	2003	481	650	1088	1476	1882	8859
5%	226	256	334	357	593	1750	496	692	1043	1489	2113	7901
Nominal	214	259	329	334	582	1556	505	825	1002	1514	2205	7278
-5%	227	259	330	364	578	1383	514	875	1017	1553	2312	6782
-10%	238	288	340	374	577	1247	534	925	1068	1567	2271	6395
-15%	254	315	357	397	587	1135	584	983	1136	1588	2565	6076
-20%	276	348	377	418	601	1042	604	1046	1206	1607	2565	4592
-25%	304	391	400	450	623	970	643	1116	1283	1668	2779	5543

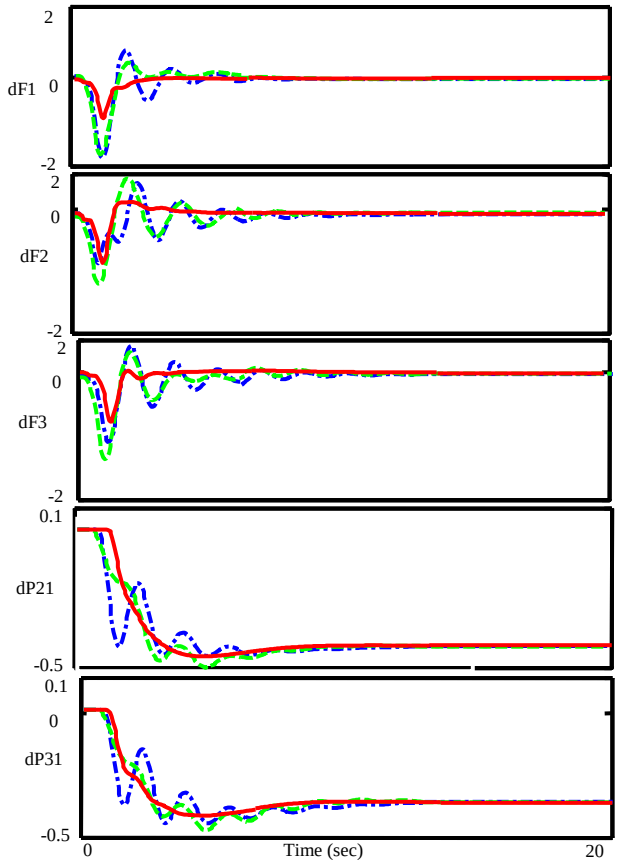

Figure 6. Deviation of frequency and tile lines power flows in proposed system; solid (FAPID), dashed (CFPID) and dotted (PID)

II. CONCLUSION

This paper presents a Firefly Algorithm to solve the LFC problem in power system. It is well known that the conventional method to tune gains of the PID controller with numerical analysis may be tedious and time consuming. This control strategy was chosen because of the increasing complexity and changing structure of the power systems. Also, it is easy to implement without additional computational complexity. The Firefly Algorithm is a meta-heuristic, nature-inspired, optimization algorithm which is based on the social (flashing) behavior of fireflies, or lighting bugs, in the summer sky in the tropical temperature regions. Its main advantage is the fact that it uses mainly real random numbers, and it is based on the global communication among the swarming particles, and as a result. The effectiveness of the proposed method is tested on a three-area restructured power system for a wide range of load demands and disturbances under different operating conditions in comparison with CPID and PID through ITAE and FD. Simulation results demonstrate its superiority and robustness.

REFERENCES

[1] V. Donde, A. Pai, IA. Hiskens, "Simulation and optimization in a LFC system after deregulation", IEEE Trans Power Syst, vol. 16, no. 3, pp. 481–489, 2001.

[2] H. Shayeghi, HA. Shayanfar, A. Jalili, M. Khazaraee, "Area load frequency control using fuzzy PID type controller in a restructured power system", In: Proceedings of the international conference on artificial intelligence, Las Vegas, Nevada, USA, pp. 344-50, June 2005.

[3] KY. Lim, Y. Wang, R. Zhou, "Robust decentralized load frequency control of multi-area power system". IEE Proc Gener Transm Distrib, vol. 43, no. 5, pp:377–86, 1996.

[4] OI. Elgerd, "Electric energy system theory: an introduction". New Yourk: Mc Graw-Hill; 1971.

[5] A. Feliachi, "On load frequency control in a restructured environment". In: Proceeding of the IEEE international conference on control application, pp: 437–41, 1996.

[6] R. Raineri, S. Rios, D. Schiele, "Technical and economic aspects of ancillary services markets in the electric power industry: an international comparison". Energy Policy, vol. 34, no. 13, pp:1540–55, 2006.

[7] RD. Christie, A. Bose, :Load frequency control issues in power system operations after deregulation:. IEEE Trans Power Syst., vol. 11, no. 3, pp:1191–200, 1996.

[8] X. S. Yang, "Nature-inspired meta-heuristic algorithms", Luniver Press, Beckington, UK, 2008.

[9] H. Shayeghi, HA. Shayanfar, A. Jalili, M. Khazaraee, "Area load frequency control using fuzzy PID type controller in a restructured power system". In: Proceedings of international conference on artificial intelligence, Las Vegas, NV, USA, Pp: 344–50, 2005.

[10] J. Kumar, NG. Hoe, G. Sheble, "LFC simulator for price-based operation". Part I: Modeling. IEEE Trans Power Syst., vol. 12, no. 2, pp: 527–32, 1997.

[11] X.-S. Yang, "Firefly algorithms for multimodal optimization", in: Stochastic Algorithms:Foundations and Appplications (Eds O. Watanabe and T. eugmann), SAGA 2009, LectureNotes in ComputerScience, 5792, Springer-Verlag, Berlin, pp: 169-178, 2009.

[12] X.-S. Yang, "Firefly algorithm, stochastic test functions and design optimisation", Int. J. Bio-Inspired Computation, vol. 2, no. 2, 2010, pp.78-84

[13] X.-S. Yang, "Firefly algorithm, levy flights and global optimization", Research and Development in Intelligent Systems XXVI (Eds M. Bramer, R. Ellis, Petridis), Springer London, , 2010, pp: 209-218.

[14] O. Abedinia, Mohammad. S. Naderi, A. Ghasemi, Robust LFC in Deregulated Environment: Fuzzy PID using HBMO, Proceeding of the IEEE International Power & Energy Society Power Systems Conference and Exposition, Italy, Rome (EEEIC), pp. 74-77, 2011.

BIOGRAPHIES

Oveis Abedinia was born in Ardabil, Iran, on April 18, 1983. He received the B.S. and M.Sc. degrees in Electrical Engineering from Azad University, Ardabil and Science and Technology Research Branch, Tehran, Iran in 2005 and 2009, respectively. Currently, he is a Ph. D. student in Electrical Eng. Department, Semnan University, Semnan, Iran. His areas of interest in research are Application of Artificial Intelligence to Power System

and Control Design, Load and Price Forecasting, Distribution Generation, Restructuring in Power Systems, Congestion Management, Optimization.

Kourosh Kiani Kourosh Kiani received the BS and MSC Degrees in electrical engineering from Delft University of Technology in Delft, the Netherlands in 1993 and the PhD degree in Medical Information from Erasmus University in Rotterdam, the Netherlands in 1997. Between 1997 and 2005 he was employed as an engineer and researcher by Philips Medical Systems. He left industry in 2005 to become Assistant Professor in the Department of Electrical Engineering at the Semnan University of Semnan, in Iran and in the Department of Electrical Engineering at the Amirkabir University of Tehran, in Iran.

Nima Amjady (SM'10) was born in Tehran, Iran, on February 24, 1971. He received the B.Sc., M.Sc., and Ph.D. degrees in electrical engineering from Sharif University of Technology, Tehran, Iran, in 1992, 1994, and 1997, respectively. At present, he is a Professor with the Electrical Engineering Department, Semnan University, Semnan, Iran. He is also a Consultant with the National Dispatching Department of Iran. His research interests include security assessment of power systems, reliability of power networks, load and price forecasting, and artificial intelligence and its applications to the problems of power systems.

Heidarali Shayanfar received the B.S. and M.S.E. degrees in Electrical Engineering in 1973 and 1979, respectively. He received his Ph. D. degree in Electrical Engineering from Michigan State University, U.S.A., in 1981. Currently, he is a Full Professor in Electrical Engineering Department of Iran University of Science and Technology, Tehran, Iran. His research interests are in the Application of Artificial Intelligence to Power System Control Design, Dynamic Load Modeling, Power System Observability Studies, Voltage Collapse, Congestion Management in a Restructured Power System, Reliability Improvement in Distribution Systems and Reactive Pricing in Deregulated Power Systems. He has published more than 405 technical papers in the International Journals and Conferences proceedings. He is a member of Iranian Association of Electrical and Electronic Engineers and IEEE.

An Evolutionary Extreme Learning Machine based on Fuzzy Fish Swarms

João Fausto Lorenzato de Oliveira and Teresa B. Ludermir
Center of Informatics, Federal University of Pernambuco, Recife, Pernambuco, Brazil

Abstract— *Neural networks have been largely applied into many real world pattern classification problems. During the training phase, every neural network can suffer from generalization loss caused by overfitting, thereby the process of learning is highly biased. In this work we propose an Adaptive Modified Artificial Fish Swarm Algorithm applied to the optimization of Extreme Learning Machines. The algorithm presents the basic* Artificial Fish Swarm Algorithm *(AFSA) with some features from* Differential Evolution *(Crossover and Mutation) and fuzzy rules to improve the quality of the solutions during the search process. The results of the simulations demonstrated good generalization capacity from the best individuals obtained in the training phase.*

Keywords: Neural Networks; Optimization; Fuzzy Logic

1. Introduction

When a mathematical model is applied in classification problems, the main task is to find a hypothesis that represents best the training set, in order to correctly classify unseen instances. The representation of a hypothesis in a neural network is based on the networks architecture, thus finding better weights and bias will improve the performance of the system. One way to improve the performance of the system is to use swarm based algorithms to search for better configurations of the networks. The search process is not an easy task due to the dimensionality of the search space, which will depend basically on the number of attributes of the problem, the number of hidden neurons and the number of layers of the network.

This work is focused on finding the best set of weights and bias for the Extreme Learning Machine (ELM) [1] through the use of swarm based search algorithms. The ELM is a technique applied to the training of Single Layered Feedforward Neural Networks (SLFNs) and its main advantage over the traditional gradient descent methods is the reduced number of parameters of the network and the learning speed. Although the ELM algorithm can only be employed in SLFNs, this is not a major constraint because with just one layer it is possible to model any continuous function [2]. With just one layer, the dimensionality of the search space will only depend on the problems attributes and the number of hidden neurons of the network. In the ELM algorithm the initial weights and bias are randomly set, and the output weights are analytically determined through matrix operations, thus the optimization of ELMs will focus on searching optimal initial weights.

In the literature the Particle Swarm Optimization (PSO) algorithm [3] has been successfully applied on the ELM algorithm [4]. In [4] the PSO algorithm is used to optimize the weights and bias of the ELM, and the best solution is applied on regression problems. The Artificial Fish Swarm Algorithm (AFSA) was applied on the optimization of ELMs (AFSA-ELM) in this work, however the results were not satisfying due to some limitations of the algorithm, conducting to modifications on the traditional algorithm in order to obtain better results. The modified AFSA called MAFSA obtained faster convergence and better results on the optimization of ELMs (MAFSA-ELM).

The PSO and the AFSA techniques differ significantly on their search methodologies. The PSO conducts the search based on their past movements of the particles and their previous experiences. The movements done in the AFSA algorithm are based on the actual position of the fishes and the situations of the neighbor fishes.

In the AFSA and MAFSA algorithms there are two important parameters used to control the way the search will be performed, namely the *visual* and *step* parameters. These two parameters are used to balance exploration and exploitation characteristics during the search. On the first stages of the algorithm the particles will move faster towards a global optimum passing through local minima, thus an exploration configuration is desired. However on the last stages of execution, the search needs to be more specific in some area in the search space, hence an exploitation characteristic is needed. Higher values of *visual* and *step* will produce an exploration characteristic while lower values will produce and exploitation characteristic. In the traditional AFSA and MAFSA algorithms these parameters are manually set and remain unchanged for the rest of the execution, thus the search process may not be performed appropriately.

In [5] simulated annealing is used along with the AFSA algorithm in order to improve the local search. The AFSA algorithm was also used on the optimization of neural networks in [6], which also modified the algorithm by introducing an aleatory *step* parameter to achieve better global search capacity. In [7] two fuzzy strategies are employed

in the AFSA algorithm, and were applied on benchmark functions. One is the Fuzzy Uniform Fish (FUF) and the other is the Fuzzy Autonomous Fish (FAF) which will be described in details.

In this work we use the fuzzy strategies presented in [7] in the MAFSA-ELM algorithm, and real world benchmark problems from the UCI repository [8] are used to validate the effectiveness of these methods. The proposed method presented better convergence than the AFSA and MAFSA, and competitive results in comparison to existing techniques.

This paper is organized as follows. On Section 2 the Evolutionary Extreme learning Machine based on Particle Swarm optimization (PSO-ELM) is presented along with the Modified Artificial Fish Swarm Algorithm for the optimization of Extreme Learning Machines (MAFSA-ELM). On section 3 the proposed method is explained in details and the experimental results are given on Section 4. On Section 5 the conclusions are presented.

2. Preliminaries

2.1 Extreme Learning Machine

The ELM [1] is a simple algorithm for the training of SLFNs, whose learning speed can be faster then traditional gradient descent methods such as back-propagation (BP) [9] and better generalization capacity may also be obtained. In this algorithm, the input weights and hidden layer biases are randomly set, and through matrix operations the output weights are calculated without tuning. The absence of a tuning phase, enables the training to be performed faster.

Given n distinct training samples (x_i, t_i), where $x_i = [x_{i1}, x_{i2}, ..., x_{in}]^T \in \Re^n$ and $t_i = [t_{i1}, t_{i2}, ..., t_{im}]^T \in \Re^m$ $(i \in [1, ..., n])$, the SLFN with s hidden nodes needs to learn all the training samples. Since the input weights $w_j = [w_{j1}, w_{j2}, ..., w_{jn}]^T$ and hidden biases $b = [b_1, b_2, .., b_j]$ $(j = [1, ..., s])$ are randomly generated, the task performed in the training phase is to find the appropriate output weights for the given input weights and biases through the calculation of the linear system $H\beta = T$.

The matrix $H = \{h_{ij}\}$ is the hidden-layer output matrix and $h_{ij} = g(w_j * x_i + b_j)$ corresponds to the result from the j_{th} hidden neuron to x_i, $T = [t_1, t_2, ..., t_i]$ represents the target (desired output) matrix, and $\beta_j = [\beta_{j1}, \beta_{j2}, ..., \beta_{jm}]^T (j \in [1, ..., s])$ is the output weight matrix. In order to compute the output weights, an inverse matrix operation is needed. The output weight matrix will be calculated as the minimum least-square (LS) solution of a linear system, through a pseudo-inverse matrix operation [10]. The next step for the calculation of the output weight matrix is presented $\hat{\beta} = H^+T$:

Through these calculations the ELM algorithm achieves good generalization performance and the learning speed is reduced due to the absence of continuous weight adjustments.

2.2 Evolving ELMs using a Modified Artificial Fish Swarm Algorithm

The AFSA algorithm is based on the social behavior of the fishes. Each fish will represent a potential solution, in the case of ELM optimization, each fish will represent the input weights and hidden biases. The movements of the population will be based on the actual position of each fish and the nearby fishes inside its visual field ($visual$). Two important variables are the $visual$ and $step$ which regulates how the search will be conducted. The $step$ variable will control how far a fish can move. Higher values of $visual$ and $step$ the fishes will move faster towards the best solution, passing through local minimums without getting stuck, this configuration is desired in the initial stages of execution. Lower values will produce an exploitation characteristic, desired on the last stages of the algorithm. Each fish will be represented by an input matrix W_{ij} and a bias vector b_i, and these informations are used to calculate the distance.

In order to calculate whether a certain fish is within the visual field of another fish, the distance between them is calculated using a euclidean distance. The output weights on the ELM algorithm are unknown *a priori*, hence the distance d is calculated as showed on equation 1, where p and q represent the indexes of two different fishes.

$$d_{pq} = \sum_{i=1}^{s}\sum_{j=1}^{h}(W_{ij}(p) - W_{ij}(q))^2 + \sum_{i=1}^{h}(b_i(p) - b_i(q))^2 \quad (1)$$

The number of input parameters on a given instance is represented by s and the number of hidden neurons is represented by h. The original AFSA algorithm has some basic behaviors (Follow, swarm and leap) executed by each fish, the behavior that produces the highest result will be the one used for updating the fish position. The Follow behavior as shown in equation 2 influences the fish by the best fish inside its visual range W_{max} (not necessarily the best fish in the swarm).

$$Follow(W_i) = W_i + rand()step\frac{W_{max} - W_i}{\|W_{max} - W_i\|} \quad (2)$$

The swarm behavior influences the fish based on the central position (represented by W_c) of the fishes inside its visual field. The swarm behavior strengthens the idea of group search, and is presented in equation 3.

$$Swarm(W_i) = W_i + rand()step\frac{W_c - W_i}{\|W_c - W_i\|} \quad (3)$$

And the leap behavior represents the capacity of the fish to move on its own, independent of any other fish.

$$Leap(W_i) = W_i + rand()step \quad (4)$$

In the modified AFSA algorithm (MAFSA), the additional behavior was inspired by the capacity of fishes to evolve and be selected by nature. For that purpose we use the Differential Evolution (DE) algorithm proposed by Storn and Price [11] which is known as one of the most efficient evolutionary algorithms. In order to create the next generation of individuals, the algorithm uses mutation and crossover operators. The new behavior is executed in three steps: Mutation, Crossover and Selection [11]. The first step is the mutation:

$$W_i = W_{r_1} + F * (W_{r_2} - W_{r_3}), \quad (5)$$

where r_1,r_2 e r_3 are distinct indexes randomly chosen and F is an amplitude factor with values within the range $(0, 2)$. In the crossover phase, a new vector V is created with the same dimensionality of the individuals.

$$V_{ij} = \begin{cases} W_{ij} & \text{if } rand() < CR \quad \text{and } j = rdInd(i) \\ W_{ij} & \text{if } rand() > CR \quad \text{or } j \neq rdInd(i) \end{cases} \quad (6)$$

If the new vector has better fitness than its predecessor, the new vector will be selected, otherwise the predecessor will be selected. By adding the crossover mutation behavior, the probability of finding better solutions increases due to the total amount of possible results (4 results) instead of the original 3 (from the three original behaviors), so the algorithm incrementally has more chances to find better solutions. And the reason why this new behavior is not affected by the $visual$ and $step$ parameters is simply to produce more diversity in the results and occasionally escaping from local minimums.

3. Proposed Method

In the AFSA-ELM and MAFSA-ELM algorithms, both values of the *visual* and *step* parameters remain unchanged for the whole execution of the algorithms. In the initial stages of execution, higher values of *visual* and *step* are desired in order to explore the search space towards the global best solution. In the last stages, lower values are desired in order to perform a more refined local search. In this work we use fuzzy strategies to adjust the values of these two parameters, based on the *Fuzzy Uniform Fish* (FUF) and *Fuzzy Autonomous Fish* (FAF) approaches presented in [7]. In order to control the balance between global search and local search, another parameter, *constriction weight* (CW), will be introduced for the adjustments of the parameters in both approaches. The adjustment procedures are presented as follows:

$$visual_{l+1} = CW * visual_l \quad (7)$$

$$step_{l+1} = CW * step_l \quad (8)$$

The *CW* is generated as an output for the fuzzy engines described in [7]. Since the traditional AFSA algorithm acts better at global searching, higher values will be assigned to the parameters on the initial stages, and they will be reduced adaptively. In this work we use the same engine presented in [7], which is a Mamdani fuzzy inference system with centroid of area defuzzyfication strategy, and the rules are shown in tables 1 and 2 for the Uniform Fish and Autonomous Fish respectively. The values of the input and output values can be represented by the following linguistic variables: Very low (VL), low (L), medium (M), high (H) and very high (VH).

3.1 Evolving ELMs with Fuzzy Uniform Fish

In the FUF approach every fish in the swarm shares the same values for the *visual* and step parameters. The fuzzy engine based on FUF consists of two inputs and one output. The input parameters are the ratio of improved fish, and the iteration number. The output parameter is the constriction weight. The iteration number, is the proportion between the current iteration and the total number of iterations. The algorithm needs to perform a global search in the initial stages of the algorithm, so the reduction of the *visual* and step parameters in these stage must be minimal. Near the end of the execution the algorithm has already approached the global optimum region, and needs to perform a local search, thats when higher values of the *iteration Number* parameter will influence significantly on the reduction of the *visual* and step parameters.

Table 1: Fuzzy Associative memory for the FUF Engine [7]

Iteration Number	Ratio of Improved Fish	Constriction Weight
L	H	VH
L	M	H
L	L	M
M	H	H
M	M	M
M	L	L
H	H	M
H	M	L
H	L	VL

The *ratio of improved fish* is the proportion of fishes that find better solutions (weights and biases) to the total number of fishes. When most of the artificial fishes find better solutions the value will be close to 1, then there is no need to reduce the *visual* and step parameters. However, when the proportion is close to 0, there is no improvement on finding better solutions , the two parameters are reduced in order to perform a local search, raising the probability of finding better solutions.

On figure 1 the membership functions for the FUF engine are presented. The membership functions for the *iteration number* and *ratio of improved fish* are shown on figures 1(a) and 1(b) respectively. The output of this fuzzy system is given by a set of fuzzy rules (same as [7]) in order to compute the value of the constriction weight parameter. The

Fig. 1: Fuzzy Uniform Fish Membership Functions. 1(a) Iteration Number. 1(b) Ratio of improved fish. 1(c) Constriction Weight.

(a) Iteration Number (b) Ratio of Improved Fish

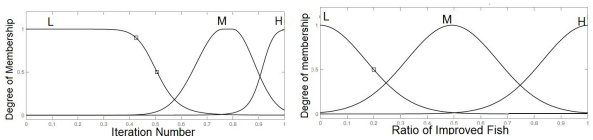

(c) Constriction Weight

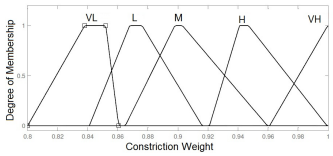

membership function for the variables is presented on figure 1(c).

3.2 Evolving ELMs with Fuzzy Autonomous Fish

In the FAF approach, each fish will have its own *visual* and *step* variables with individual adjustments, producing more diverse results and allowing that a given fish start to perform more refined local search earlier than other fishes. In the initial stages of the algorithm these variables have the same value, and will be individually adjusted through the execution based on the output of the fuzzy engine which is calculated using three input parameters namely *Distance from best*, *Fitness Ranking* and *Iteration Number*.

Fig. 2: Fuzzy Autonomous Fish Membership Functions. 2(a) Iteration Number. 2(b) Distance from best. 2(c) Fitness Ranking. 2(d) Constriction Weight.

(a) Iteration Number (b) Distance from Best

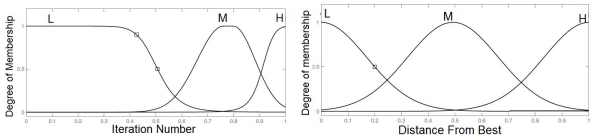

(c) Fitness Ranking (d) Constriction Weight

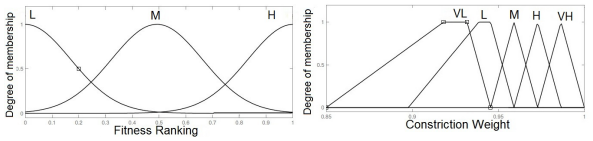

The *Distance from best* rank-based parameter which is based in the distance between the fishes and the best fish (with highest validation accuracy), the distance is calculated in the same way is shown on equation 1. After the distance is computed, all distances are sorted, and then the proportion of the current rank to the total of fishes is presented to the fuzzy engine. When the distance to the best fish is low, then the *visual* and *step* parameters will be less reduced, however when a fish is close to the best fish then those values are decreased considerably, in order to perform a more refined search.

Table 2: Fuzzy Associative memory for the FAF Engine [7]

Distance from Best	Fitness Ranking	Iteration	Weight
L	L	H	VL
L	L	L	VL
L	L	L	L
L	M	H	L
L	M	M	M
L	M	H	VL
L	M	L	H
L	H	H	L
L	H	M	M
L	H	L	VL
M	L	H	VL
M	L	M	L
M	L	L	M
M	M	H	L
M	M	M	M
M	M	L	H
M	H	H	M
M	H	M	H
M	H	L	VH
H	L	H	L
H	L	M	M
H	L	L	H
H	M	H	M
H	M	M	H
H	M	L	VH
H	H	H	M
H	H	M	H
H	H	L	VL

The *Fitness Ranking* is based on the fitness of each fish with respect to the validation accuracies obtained with the ELM algorithm. All fitnesses from each fish will be sorted and then the proportion to the total amount of fishes will be presented. Lower rankings on this variable will produce less reductions on the *visual* and *step* parameters. The *Distance from Best* will have the same definitions as presented on section 3.1.

On table 2 the associative memory is showed and on figure 2 the membership functions are presented for each variable.

4. Experiments

On the experiments we used the ELM, AFSA-ELM, PSO-ELM, MAFSA-ELM and Levenberg Marquardt (LM) algorithms [9] to compare with the proposed methods (FAF-ELM and FUF-ELM) and they were applied on five (Sonar, Ionosphere, Ecoli, Horse, and Vehicle) datasets from UCI machine learning repository [8].

Table 3: Experimental results for all datasets.

(a) Ionosphere

Technique	Mean$\pm SD$	h
ELM	84.92 $\pm$ 3.03	20
LM	88.16 $\pm$ 11.36	15
AFSA-ELM	87.15 $\pm$ 4.19	20
MAFSA-ELM	88.10 $\pm$ 4.06	20
PSO-ELM	84.09 $\pm$ 3.55	20
FAF-ELM	88.20 $\pm$ 3.63	20
FUF-ELM	87.46 $\pm$ 4.03	20

(b) Vehicle

Technique	Mean$\pm SD$	h
ELM	73.82 $\pm$ 2.69	20
LM	52.55 $\pm$ 16.70	15
AFSA-ELM	74.91 $\pm$ 2.87	20
MAFSA-ELM	74.78 $\pm$ 3.26	20
PSO-ELM	75.49 $\pm$ 2.51	20
FAF-ELM	74.88 $\pm$ 2.44	20
FUF-ELM	75.48 $\pm$ 3.09	20

(c) Ecoli

Technique	Mean$\pm SD$	h
ELM	84.24 $\pm$ 3.41	20
LM	59.20 $\pm$ 19.79	20
AFSA-ELM	84.84 $\pm$ 3.77	20
MAFSA-ELM	84.68 $\pm$ 4.47	20
PSO-ELM	83.17 $\pm$ 4.40	20
FAF-ELM	85.00 $\pm$ 3.75	15
FUF-ELM	84.48 $\pm$ 3.78	20

(d) Horse

Technique	Mean$\pm SD$	h
ELM	65.47 $\pm$ 2.60	20
LM	68.91 $\pm$ 5.61	20
AFSA-ELM	66.66 $\pm$ 4.78	20
MAFSA-ELM	68.38 $\pm$ 3.96	20
PSO-ELM	66.18 $\pm$ 4.34	15
FAF-ELM	68.78 $\pm$ 3.49	20
FUF-ELM	66.49 $\pm$ 4.44	20

(e) Sonar

Technique	Mean$\pm SD$	h
ELM	72.37 $\pm$ 4.57	20
LM	74.67 $\pm$ 10.67	10
AFSA-ELM	72.05 $\pm$ 7.36	20
MAFSA-ELM	73.71 $\pm$ 6.51	15
PSO-ELM	73.46 $\pm$ 5.13	15
FAF-ELM	73.52 $\pm$ 4.03	10
FUF-ELM	73.91 $\pm$ 5.61	20

The data from each dataset were split into training set (50%), validation set (25%) and test set (25%) randomly generated for 30 iterations. For each iteration all the classifiers receive the exact training, validation and test sets. All the attributes from the datasets were normalized into the interval $[0..1]$. The simulations were perfomed with 10, 15 and 20 hidden neurons, and the configuration that produced the best result was selected. The optimization algorithms executed for 50 iterations. The initialization of the AFSA-ELM and MAFSA-ELM parameters in this work is described as follows: The $visual$ parameter was set as the mean of all the initial distances between the fishes. The number of fishes $N = 30$, $step = 0.6$, lotation factor $\delta = 0.8$, in this work we set the visual parameter as the mean for all the initial distances between the fishes. Amplitude factor for the mutation $F = 1$ and crossover rate $CR = 0.5$. The same parameters for the MAFSA-ELM algorithm are also used on the FUF-ELM and FAF-ELM. For the experiments using the PSO-ELM method, we used the same configuration presented in [4] with some modifications. The constants $C1$ and $C2$ were initialized as $C1 = 2$ e $C2 = 2$, the inertia factor was set to $w = 0.9$, number of particles is 30, and the number of iterations is 50.

The experiments were measured with respect to the mean accuracy error over the 30 simulations on the validation set of the optimization techniques and the mean accuracy on the test set. The analysis of the results was performed through the use of the Wilcoxon Sign-rank test with 95% of confidence interval. Figures 3 to 10 present the mean accuracy over the iterations of the algorithms on the validation set.

For the Ionosphere dataset (figure 3), the proposed methods achieved better validation errors than the PSO-ELM and the AFSA-ELM. The FUF-ELM algorithm obtained the smallest validation error, while the the FAF-ELM and MAFSA-ELM obtained similar results. The FAF-ELM technique achieved higher mean accuracy on the test set than the other techniques according to table IV(b). The FUF-ELM and FAF-ELM algorithms outperform the ELM and PSO-ELM algorithms.

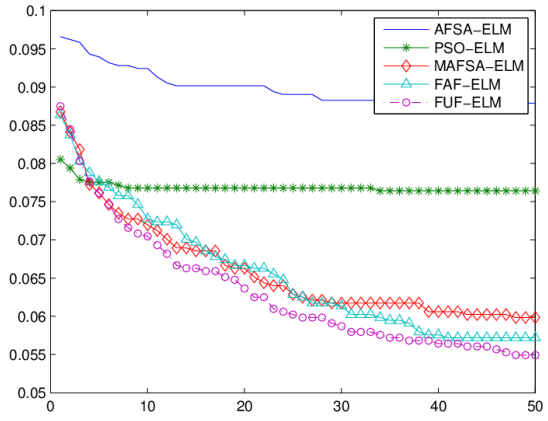

Fig. 3: Ionosphere

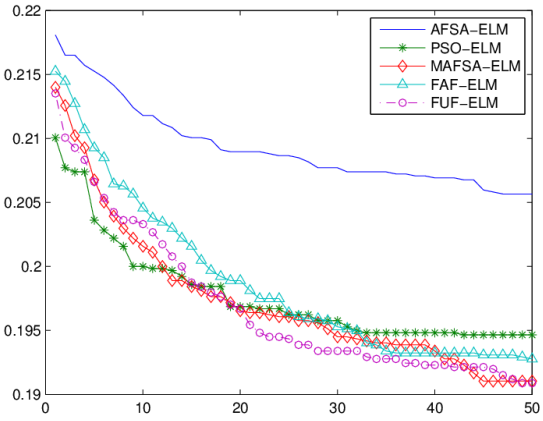

Fig. 4: Vehicle

In the Vehicle dataset (figure 4) the the FUF-ELM and the MAFSA-ELM obtained similar results, but the FUF-ELM achieved lower errors with fewer iterations. The AFSA-ELM algorithm achieved the worse results in this dataset. On table IV(c) the PSO-ELM and the FUF-ELM obtained the highest mean accuracy on the test set. The FUF-ELM and the PSO-ELM were superior to the ELM algorithm. The other algorithms obtained similar results under this level of significance (95%).

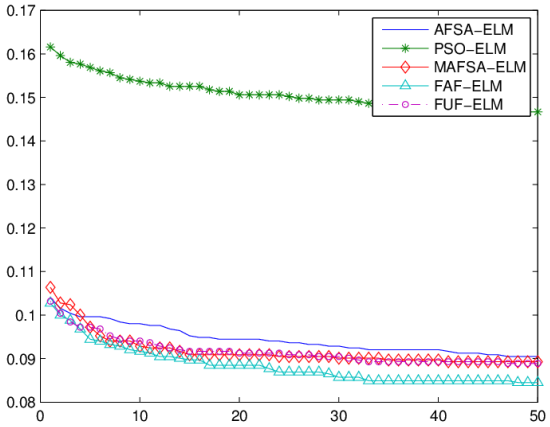

Fig. 5: Ecoli

The results concerning the Ecoli dataset (figure 5) show that the FAF-ELM method achieved lowest errors on the validation set, and the MAFSA-ELM and the FUF-ELM obtained similar results. The mean accuracy on table IV(d) shows that the FAF-ELM obtained highest accuracy with fewer hidden neurons than the other techniques. There was no significant difference on the results among the techniques.

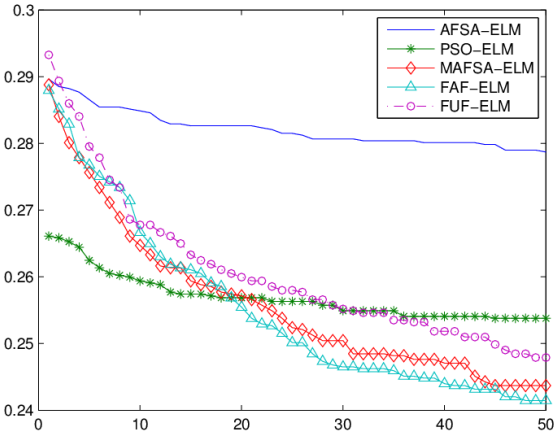

Fig. 6: Horse

With respect to the Horse dataset (figure 6) the FAF-ELM technique achieved lower errors than the MAFSA-ELM technique, the AFSA-ELM did not perform well in comparison with the other techniques. According to table IV(e) the mean accuracy of the FAF-ELM method was superior to the ELM, AFSA-ELM, FUF-ELM, MAFSA-ELM and PSO-ELM. The FAF-ELM technique was superior to the ELM, AFSA-ELM, FUF-ELM and PSO-ELM.

In the Sonar dataset (figure 7) the FUF-ELM approach

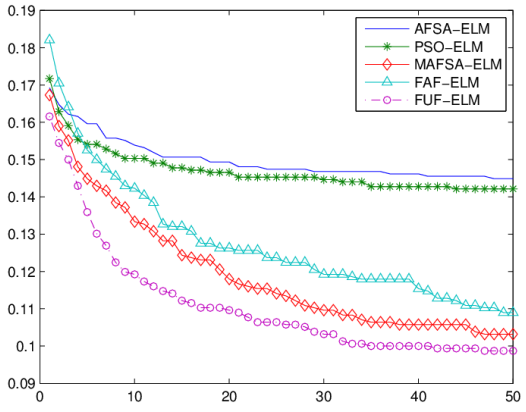

Fig. 7: Sonar

obtained smaller validation errors with fewer iterations. According to table IV(f) the FAF-ELM approach obtained acceptable results with the slowest standard deviation and fewer hidden neurons while the FUF-approach obtained the highest mean accuracy, with more hidden neurons and higher standard deviation. The results for all the techniques were similar.

5. Conclusion

In this paper, we applied two fuzzy strategies in order to adjust the parameters of the Modified Artificial Fish Swarm Algorithm on the optimization of Extreme Learning Machines, namely FAF-ELM and FUF-ELM. These algorithms optimize the random initial weights and bias from the ELM algorithm through the adjustments of global and local search using the $visual$ and $step$ parameters. The output weights are analytically determined through the pseudo-inverse matrix operation.

The performance of the tested algorithms was evaluated with well known benchmark classification datasets (Ionosphere, ecoli, sonar, vehicle and horse-colic), obtained from UCI Machine Learning Repository [8].

Experimental results show that our hybrid approaches achieve better validation errors, and in some datasets achieved better accuracy on the test sets.

As future works, we plan to evaluate the influence of using the Autonomous Fish (FAF-ELM) and Uniform Fish (FUF-ELM) for the composition of homogeneous ensembles.

References

[1] G. B. Huang, Q. Y. Zhu, and C. K. Siew, "Extreme learning machine: theory and applications," *Neurocomputing*, vol. 70, no. 1-3, pp. 489–501, 2006.

[2] P. Bartlett, "The sample complexity of pattern classification with neural networks: the size of the weights is more important than the size of the network," *Information Theory, IEEE Transactions on*, vol. 44, no. 2, pp. 525–536, 1998.

[3] A. Engelbrecht, *Fundamentals of computational swarm intelligence*. Wiley NY, 2005, vol. 1.
[4] Y. Xu and Y. Shu, "Evolutionary extreme learning machine–based on particle swarm optimization," *Advances in Neural Networks-ISNN 2006*, pp. 644–652, 2006.
[5] M. Jiang and Y. Cheng, "Simulated annealing artificial fish swarm algorithm," in *Intelligent Control and Automation (WCICA), 2010 8th World Congress on*. IEEE, 2010, pp. 1590–1593.
[6] C. Wang, C. Zhou, and J. Ma, "An improved artificial fish-swarm algorithm and its application in feed-forward neural networks," in *Machine Learning and Cybernetics, 2005. Proceedings of 2005 International Conference on*, vol. 5. IEEE, 2005, pp. 2890–2894.
[7] D. Yazdani, A. Nadjaran Toosi, and M. Meybodi, "Fuzzy adaptive artificial fish swarm algorithm," *AI 2010: Advances in Artificial Intelligence*, pp. 334–343, 2011.
[8] C. Blake and C. Merz, "UCI repository of machine learning databases," 1998.
[9] S. Haykin, *Neural networks: a comprehensive foundation*. Prentice Hall PTR Upper Saddle River, NJ, USA, 1994.
[10] C. Rao and S. Mitra, *Generalized inverse of matrices and its applications*. Wiley NY, 1971.
[11] R. Storn and K. Price, "Differential evolution–a simple , efficient heuristic for global optimization over continuous spaces," *Journal of global optimization*, vol. 11, no. 4, pp. 341–359, 1997.

Modified Invasive Weed Optimization based on Fuzzy PSS in Multi-machine Power System

O. Abedinia
Electrical Engineering Department,
Semnan University, Semnan, Iran

A. Akbari Foroud
Electrical Engineering Department,
Semnan University, Semnan, Iran

N. Amjady
Electrical Engineering Department,
Semnan University, Semnan, Iran

H. A. Shayanfar *
Electrical Eng. Department, Islamic Azad University,
South Tehran Branch, Tehran, Iran

oveis.abedinia@hotmail.com, aakbari@semnan.ac.ir, n_amjady@yahoo.com, hashayanfar@yahoo.com

Abstract— **In this paper a new Modified Invasive Weed Optimization is proposed to find a parameters of fuzzy PID controller as a stabilizer in multi-machine power system. Actually, IWO is a bio-inspired numerical algorithm which is inspired from weed colonization and motivated by a common phenomenon in agriculture that is colonization of invasive weeds. Also, finding the parameters of PID controller in power system has direct effect for damping oscillation. Thus, to reduce the design effort and find a better fuzzy system control, the parameters of proposed controller is obtained by MIWO that leads to design controller with simple structure that is easy to implement. The effectiveness of the proposed technique is applied to Single machine connected to Infinite Bus (SMIB) and IEEE 3-9 bus power system. The proposed technique is compared with some intelligent algorithms through ITAE and FD.**

Keywords: MIWO, Multi-machine System, FPID, Oscillation.

I. INTRODUCTION

In the last few decades, considerable attention has been given to the excitation system and its role in improving power system stability. Because of the small effective time constants in the excitation control loop, it was assumed that a large control effort could be expanded through excitation control with a relatively small input of control energy. By the use of a voltage regulator in the excitation control system, the output of the exciter can be adjusted so that the generated voltage and reactive power change in a desired way [1]. In early systems, the voltage regulator was entirely manual. In modern control systems the voltage regulator is an automatic controller that senses the generator output voltage as a feedback signal then adjusts the generator excitation level in the desired direction. This kind of voltage regulator has been known as an Automatic Voltage Regulator (AVR) [2].

The application of a power system stabilizer (PSS) is to generate a supplementary stabilizing signal, which is applied to the excitation control loop of a generating unit, to introduce a positive damping torque. By using the supplementary stabilizing signal, the negative damping effect of the AVR regulation can be cancelled, at the same time, the positive damping effect of the system can also be increased so that the system can operate even beyond the steady-state stability limit [3].

Several techniques have been proposed for tuning of the PSSs in power system [4]. In recent decades intelligent techniques are proposed to tune the PSS parameters. However, these controllers don't have appropriate reaction in different load conditions.

Genetic Algorithm (GA) is one of the powerful optimization techniques which is independent on the complexity of problems and no prior knowledge is available. This technique is applied to tune the PSS parameters [5]. However, GA is very sufficient in finding global or near global optimal solution of the problem, it requires a very long run time that may be several minutes or even several hours depending on the size of the system under study [6].

Recently, Fuzzy based PSS (FPSS) schemes have been proposed [7]. The first application of a traditional Fuzzy Logic Controller (FLC) as a PSS was reported in 1990 [8Hsu, 1990]. The FLC has been applied to a multi-machine power system. The performance of the FLC has been compared with the classic PSS through digital simulation and found to be better [9].

Accordingly, to overcome to the mentioned problems, this paper proposed the new meta-heuristic of MIWO based on fuzzy PID to damp low frequency oscillation in

* Correspanding Author. E-Mail Address: hashayanfar@yahoo.com (H. A. Shayanfar)

multi-machine power system. This method is inspired from weed colonization and motivated by a common phenomenon in agriculture that is colonization of invasive weeds. Weeds have shown very robust and adaptive nature which turns them to undesirable plants in agriculture. Recently, this technique is used in different application domains [10], which demonstrate the advantages of this method to other compared techniques.

This proposed technique is applies on two power system case studies as Single-machine Infinite Bus System (SMIB) and 3 machine 9 bus IEEE standard power system in comparison of GA-PSS [10] and CPSS [11] in first case study and PSOPSS and CPSS [12] in 3-9 bus test system. The mentioned technique is compared in different load condition through some performance indices as Time multiplied Absolute value of the Error (ITAE) and Figure of Demerit (FD). The results of the simulation demonstrate that MIWO-fuzzy controller is robust than other compared techniques.

II. POWER SYSTEM EXPLANATION

The complex nonlinear model related to multi-machine interconnected power system, can be described by a set of differential-algebraic equations by assembling the models for each generator, load, and other devices such as controls in the system, and connecting them appropriately via the network algebraic equations. Fig. 1 shows the main model of power system with location of controller [7].

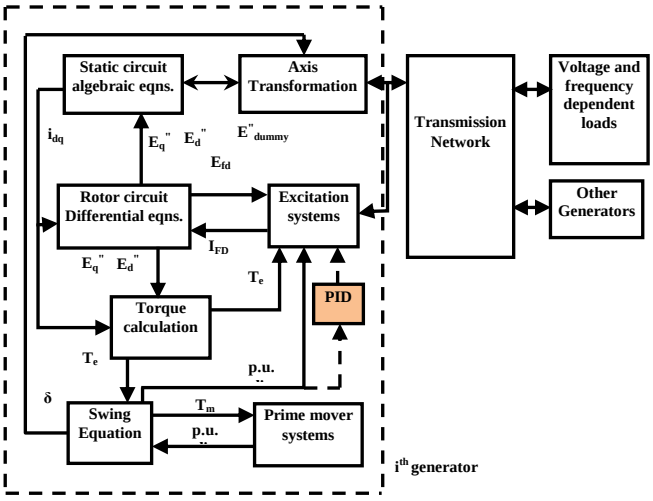

Figure 1. Structure of PSS in power systems

A. Single-machine Infinite Bus System

The Single-machine Infinite Bus system considered for small-signal performance study which is shown in Fig. 2.

The generator is represented by the third-order model comprising of the electromechanical swing equation and the generator internal voltage equation [2]. The swing equations of this system are:

$$\dot{\delta} = \omega_b(\omega - 1) \quad (1)$$

$$\dot{\omega} = \frac{1}{M}(P_m - P_e - D(\omega - 1)) \quad (2)$$

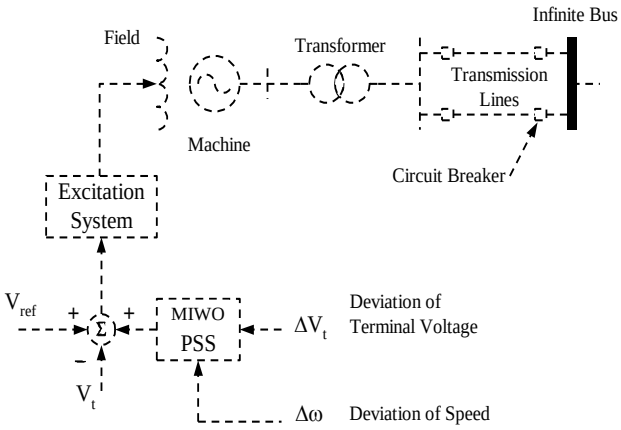

Figure 2. Schematic diagram of single machine infinite bus system

B. 3-9 bus IEEE Power System

The proposed approach is extended to a multi-machine power system as a second case study. The widely used Western Systems Coordinating Council (WSCC) 3-machine, 9-bus system shown in Fig. 3 is considered. The simplified IEEE type-ST1A static excitation system has been considered for all three generators. Also, the proposed controller is connected to all of the generators. The system data are given in [3].

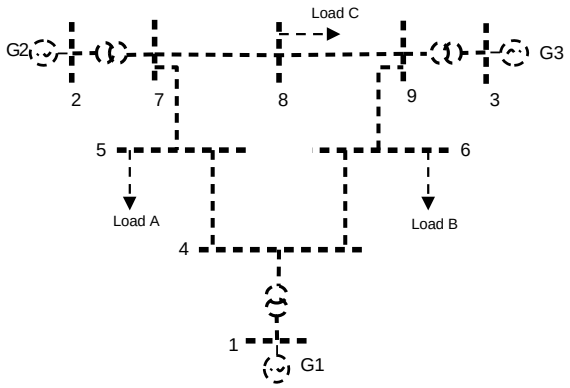

Figure 3. Three-machine nine-bus power system.

C. Design of Fuzzy PID Controller

The classical Proportional-Integral-Derivative (PID) controller and its variants remain the controllers of choice in many industrial applications [7, 9]. PID controller structure remains an engineer's preferred choice because of its structural simplicity, reliability, and the favorable

ratio between performance and cost. Beyond these benefits, it also offers simplified dynamic modeling, lower user-skill requirements, and minimal development effort, which are issues of substantial importance to engineering practice. The performance of the PID controller depends on its setting of parameters.

Basically, all the approaches to fuzzy controller design can be classified as follows:

1. Expert systems approach,
2. Control engineering approach,
3. Intermediate approaches,
4. Combined approaches and synthetic approaches.

In this paper, the gains of the Fuzzy PID controller are tuned on-line in terms of the knowledge based and fuzzy inference, and then, the conventional PID controller generates the control signal. Fig. 4 shows the block diagram of the classical fuzzy type controller to PSS design for each generator [13].

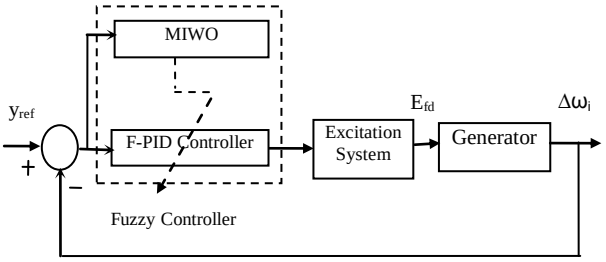

Figure 4. The FPID controller design

In the design of fuzzy logic controller, there are five parts of the fuzzy inference process:

- Fuzzification of the input variables.
- Application of the fuzzy operator (AND or OR) in the anteceden.
- Implication from the antecedent to the consequent.
- Aggregation of the consequents across the rules.
- Defuzzification.

The controller block of fuzzy is formed by fuzzification of ($\Delta\omega_i$), the interface mechanism and defuzzification. Therefore, u_i is a control signal that applies to the excitation system in each generator. By taking $\Delta\omega_i$ as the system output, control vector for the conventional PID controller is given by:

$$u_i = K_{Pi\,i}\Delta\omega_i(t) + K_{Ii}\int_0^t \Delta\omega_i(t)dt + K_{di}\Delta\dot{\omega}_i(t) \quad (3)$$

The parameters, K_{Ii}, K_{di} and K_{pi} are determined by a set of fuzzy rules of the form:

If $\Delta\omega_i$ is A_i and $\Delta(\Delta\omega_i)$ is B_i then, K_{di} is C_i and K_{pi} is D_i and K_{Ii} is E_i, $i=1,2,\cdots,n$.

Where, A_i, B_i, C_i, D_i and E_i are fuzzy sets on the corresponding supporting sets.

For the PSS optimization the ITAE and ***FD*** are considered which are described as:

$$ITAE_i = 100\int_0^{10} t(|\Delta\omega_i|)dt \quad (4)$$

$$FD = (OS\times10^{-4})^2 + (US\times10^{-4})^2 + T_s^{\,2} \quad (5)$$

Where, the constraints of the PID controller parameter bounds are considered as:

$$Minimize\, u \;\; subject\; to:$$

$$K_{Pi}^{\min} \le K_{Pi} \le K_{Pi}^{\max}$$

$$K_{Ii}^{\min} \le K_{Ii} \le K_{Ii}^{\max}$$

$$K_{Di}^{\min} \le K_{Di} \le K_{Di}^{\max}$$

III. MODIFIED INVASIVE WEED OPTIMIZATION

Invasive Weed Optimization (IWO) is inspired from weed colonization and motivated by a common phenomenon in agriculture that is colonization of invasive weeds. Weeds have shown very robust and adaptive nature which turns them to undesirable plants in agriculture. Since its advent IWO has found several successful engineering applications like tuning of Robot Controller [14], Optimal Positioning of Piezoelectric actuators [15], development of recommender system [16], antenna configuration optimization [17], computing Nash equilibria in strategic games [18], DNA computing [19], and etc.

IWO is a meta-heuristic algorithm which mimics the colonizing behavior of weeds. In Invasive Weed Optimization algorithm, the process begins with initializing a population. It means that a population of initial solutions is randomly generated over the problem space. Then members of the population produce seeds depending on their relative fitness in the population. In other words, the number of seeds for each member is beginning with the value of S_{min} for the worst member and increases linearly to S_{max} for the best member [18]. This technique can be summarized as:

A. Initialization

In this step, a finite number of weeds are initialized at the same element position of the conventional array which has a uniform spacing of "$\gamma/2$" between neighboring elements.

B. Reproduction

The individuals, after growing, are allowed to reproduce new seeds linearly depending on their own, the lowest, and the highest fitness of the colony (all of plants). The maximum (S_{max}) and minimum (S_{min}) number of seeds are predefined parameters of the algorithm and adjusted according to structure of problem. The schematic seed production in a colony of weeds is presented in Fig. 2. In this figure, the best fitness function is the lower one [14].

C. Spatial distribution

The generated seeds are being randomly distributed over the d-dimensional search space by normally distributed random numbers with mean equal to zero; but varying variance. This step ensures that the produced seeds will be generated around the parent weed, leading to a local search around each plant. However, the standard deviation (*SD*) of the random function is made to decrease over the iterations, which is defined as:

$$SD_{ITER} = \left(\frac{iter_{\max} - iter}{iter_{\max}}\right)^{pow}(SD_{\max} - SD_{\min}) + SD_{\min}$$

SD_{max} and SD_{min} are the maximum and minimum standard deviation, respectively. And *pow* is the real no. This step ensures that the probability of dropping a seed in a distant area decreases nonlinearly with iterations, which result in grouping fitter plants and elimination of inappropriate plants.

D. Competitive Exclusion

When the maximum number of population in a colony is reached (P_{max}), each weed can to produce seeds and spread them according to the mechanism mentioned in step 3.2 and step 3.3, respectively. Then, new seeds with their parents are ranked together with respect to their fitness. This method is known as competitive exclusion and is also a selection procedure of IWO. Next, weeds with lower fitness are eliminated to reach the maximum allowable population size in a colony. This mechanism by using the "survival of the fittest" idea [14] gives a chance to plants with lower fitness to reproduce, and if their offspring have good fitness, they can survive in their offspring's existence.

E. Termination Condition

The whole process continues until the maximum number of iterations has been reached, and we hope that the plant with the best fitness is the closest one to the optimal solution.

F. Modifications

For modified IWD, if we add the $|cos(iter)|$ which is a variation in *SD*, it can helps in exploring the better solutions quickly and prevents the new solutions to be spread out of the search space when the SD is relatively large which is described as:

$$SD_{ITER} = \left(\frac{iter_{\max} - iter}{iter_{\max}}\right)^{pow}|\cos(iter)|(SD_{\max} - SD_{\min}) + SD_{\min}$$

In classical IWO, the seeds are generated from a plant with a certain standard deviation, which is decreased as number of iteration increases. Thus, the plants slowly undergo a behavioral transformation from an explorative nature to an exploitative one.

Actually the routine of decreasing SD is modified, such that if the weeds are near a suspected optimal solution then it can exploit it quickly rather than wait for the standard deviation to decrease to a reasonable value, which might occur near the end of the run. In this strategy the SD varies within an envelope, so lesser values of SD are obtained much before the end of the run.

IV. Simulation Results

A. SMIB

For this case study the fitness function trend of proposed technique is presented in Fig. 5. This case is compared with GAPSS [10] and Classic PSS (CPSS) [11]. Accordingly, Fig. 6-7, shows the response of system against 6-cycle three-phase fault in different load condition. Also, the optimized parameters of the PID are presented in Table. 1.

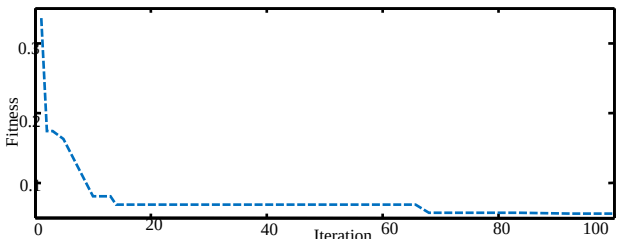

Figure 5. Optimal trend of fitness function evaluation

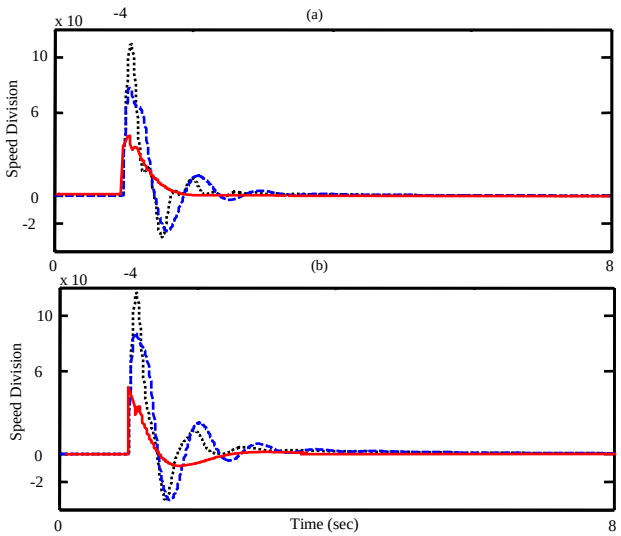

Figure 6. Fig.6: System response by applying a 6-cycle three-phase fault at t=1: Solid (MIWO-F), Dashed (GA-PSS) Doted (CPSS). a :P=0.8,Q=0.4,Xe=0.3 b: P=0.5,Q=0.1,Xe=0.3

TABLE I. OPTIMUM PID CONTROLLER PARAMETERS BY MIWO

Gain \ Gen.		G_1	G_2	G_3
Case One	K_{p1}	11.34	-	-
	K_{i1}	2.24	-	-
	K_{d1}	2.13	-	-
Case Two	K_{p1}	1.452	1.946	2.465
	K_{i1}	1.647	2.056	2.134
	K_{d1}	1.684	2.135	2.254

B. 3-9 bus IEEE Power System

The convergence of the proposed technique over second case study is shown in Fig. 7. Actually, the performance of the proposed controller under transient conditions is verified by applying a 6-cycle three-phase fault at t=1 sec, on bus 7 at the end of the line 5-7. The fault is cleared by permanent tripping the faulted line. The speed deviation of machines under the nominal loading conditions is shown in Fig. 8.

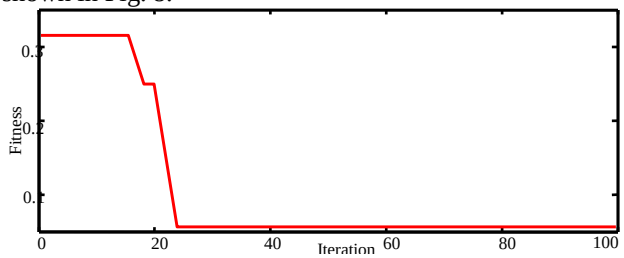

Figure 7. Optimal trend of fitness function evaluation

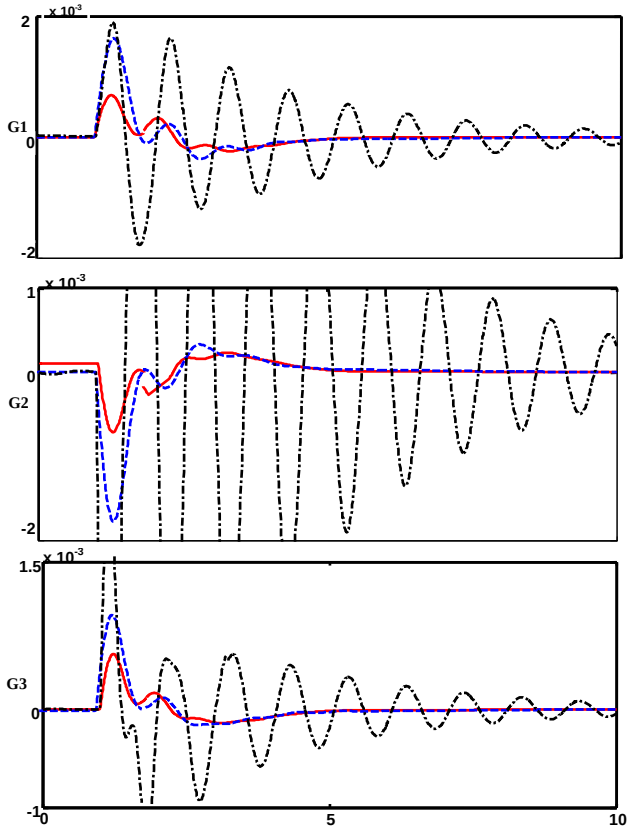

Figure 8. System response under scenario 1 with heavy loading condition: Solid (MIWOFPSS) Dashed (PSOPSS) Doted (CPSS).

For more testing, a 0.2 p.u. step increase in mechanical torque was applied at t=1.0. The results of system response are presented in Fig. 9.

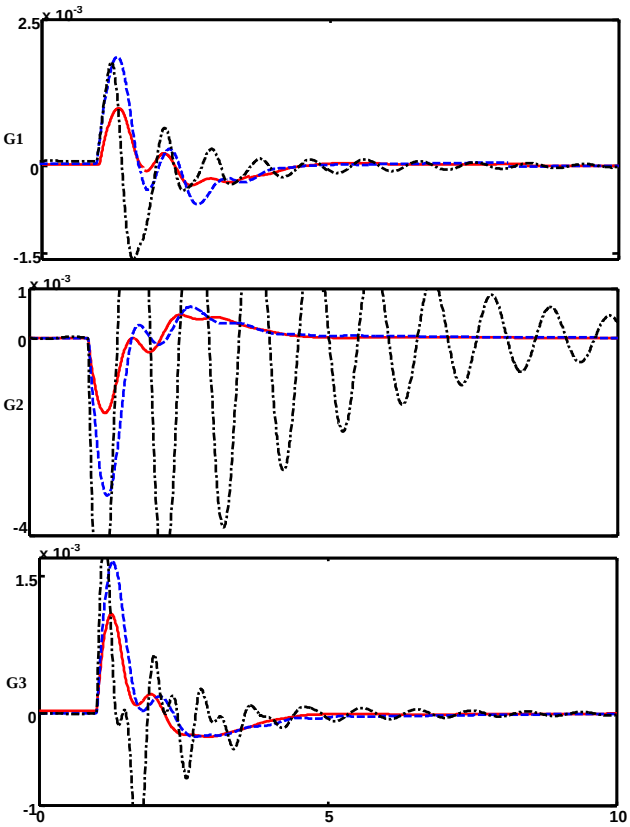

Figure 9. System response under scenario 2 with nominal loading condition: Solid (MIWOFPSS) Dashed (PSOPSS) Doted (CPSS).

According to the numerical results, it can be seen that the values of these system performance characteristics with the proposed controller are much smaller to other compared techniques. This demonstrates that the overshoot, undershoot settling time and speed deviations of all machines are greatly reduced by applying the proposed algorithm based fuzzy PSSs. The numerical results of ITAE and FD are listed in Table 2-3.

TABLE II. VALUE OF ITAE IN DIFFERENT TECHNIQUES

Method	Scenario 1			Scenario 2		
	Nominal	Light	Heavy	Nominal	Light	Heavy
MIWOFPSS	0.60	0.64	0.65	0.62	0.64	0.68
GA-FPSS	0.76	0.73	0.84	0.73	0.70	0.79
GAPSS	37.1	36.7	38.5	36.03	36	37.4

TABLE III. VALUE OF FD IN DIFFERENT TECHNIQUES

Method	Scenario 1			Scenario 2		
	Nominal	Light	Heavy	Nominal	Light	Heavy
MIWOFPSS	2.06	2.46	2.67	2.12	2.44	2.58
GA-FPSS	2.45	2.86	3.04	2.36	2.64	2.71
GAPSS	55.4	58.6	60.4	54.1	55.4	57.7

V. CONCLUSIONS

In this paper a new MIWO based fuzzy controller is proposed to provide the stability of the power system in low frequency oscillation problem in multi machine. IWO is a bio-inspired numerical algorithm which is used herein as the optimization method of players to solve optimization and control problems. This method is inspired from weed colonization and motivated by a common phenomenon in agriculture that is colonization of invasive weeds. Weeds have shown very robust and adaptive nature which turns them to undesirable plants in agriculture. The proposed technique convergence rate is really less than in comparison other methods in solving complex mathematical problems. The effectiveness of the proposed technique is tested over two case studies as SMIB and 3-9 bus IEEE power systems. The results are compared with other intelligent algorithms through ITAE and FD. Simulation results show the effectiveness of the proposed MIWO fuzzy controller which can work effectively over a wide range of the loading conditions and is superior to other compared methods.

REFERENCES

[1] M. J. Basler, R. C. Schaefer, "Understanding power system stability", IEEE Trans. Industry Applications, vol. 44, pp. 463-474, 2008.

[2] Kundur, "Power system stability and control", New York: McGraw- Hill; 1994.

[3] O. Abedinia, B. Wyns, A. Ghasemi, Robust Fuzzy PSS Design using ABC, Proceeding of the IEEE International Power & Energy Society Power Systems Conference and Exposition, submitted, Italy, Rome (EEEIC), pp. 100-103, 2011.

[4] El. Zonkoly, AA. Khalil, NM. Ahmied, "Optimal tuning of lead-lag and fuzzy logic power system stabilizers using particle swarm optimization", Expert System with Applications, vol. 10, pp. 1-10, 2008.

[5] O. Abedinia, Mohammad. S. Naderi, A. Jalili, B. Khamenepour, Optimal Tuning of Multi-Machine Power System Stabilizer Parameters Using Genetic-Algorithm, Proceedings of International Conference on Power System Technology, Page(s): 1-6, 24-28 October, 2010.

[6] JM. Call, "Genetic algorithms for modeling and optimization", Journal of Computational and Applied on Mathematics, vol. 184, pp. 205-222, 2005.

[7] H.A. Shayanfar, H. Shayeghi, O. Abedinia, A. Jalili, Design rule-base of fuzzy controller in multi-machine power system stabilizer using genetic algorithm, In: Proceedings of the international conference on artificial intelligence, Las Vegas, Nevada, USA, pp. 49-43, July 2010.

[8] J. H. Hwang, D. W. Kim, J. H. Lee and Y. J. An, "Design of Fuzzy Power System Using Adaptive Evolutionary Algorithm", Engineering Applications of Artificial Intelligence, vol. 21, pp. 86-96, 2008.

[9] M. A. James, , "Multi-stage fuzzy PID controller with fuzzy switch". In: Proceeding of the IEEE international conference on control application, vol. 4, p: 323–27, 2001.

[10] H. Yassami, A. Darabia, S.M.R. Rafieib, "Power system stabilizer design using strength pareto multi-objective optimization approach", Electric Power Systems Research, vol. 80, pp: 838–846, 2010.

[11] A. B. Ahmad, "Powers system stability enhancement using multi band stabilizer". Master thesis, king fahd university of petroleum and minerals, Dhahran, Saudi Arabia, May 2009.

[12] Shayeghi, H., Shayanfar, H.A., Safari, A., Aghmasheh, R. A. 2010. robust PSSs design using PSO in a multi-machine environment. Energy Conversion and Management 51: 696–702.

[13] A. R. Mehrabian and C. Lucas, "A novel numerical optimization algorithm inspired from invasive weed colonization," Ecological Informatics, vol. 1, pp. 355-366, 2006.

[14] H. Sepehri-Rad and C. Lucas, "A recommender system based on invasive weed optimization algorithm," in Proc. IEEE Congress on Evolutionary Computation, 2007, pp. 4297−4304.

[15] A. R. Mehrabian and A. Yousefi-Koma, "Optimal positioning of piezoelectric actuators of smart fin using bio-inspired algorithms," Aerospace Science and Technology, vol. 11, pp. 174−182, 2007.

[16] Panida, B., Chanwit, B., Weerakorn, O., "Optimal congestion management in an electricity market using particle swarm optimization with time-varying acceleration coefficients", Computers and Mathematics with Applications, Vol. 3, pp. 1-10, 2010.

[17] N.G. Pavlidis, K.E. Parsopoulos, and M.N. Vrahatis, "Computing Nash equilibria through computational intelligence methods," J. of Computational and Applied Mathematics, vol. 175, no. 1, pp. 113–136, 2005.

[18] B. Dadalipour, A. R. Mallahzadeh, Z. Davoodi-Rad, "Application of the invasive weed optimization technique for antenna configurations," in Proc. Loughborough Antennas and Propagation Conf., Loughborough, pp. 425-428, Mar. 2008.

[19] X. Zhang, Y. Wang, G. Cui, Y. Niu, and J. Xu, "Application of a novel IWO to the design of encoding sequences for DNA computing," Computers and Mathematics with Applications (2008), doi:10.1016/j.camwa.2008.10.038.

BIOGRAPHIES

Oveis Abedinia received the B.S. and M.Sc. degrees in Electrical Engineering from Azad University, Ardabil and Science and Technology Research Branch, Tehran, Iran in 2005 and 2009, respectively. Currently, he is PhD student in Semnan University. His areas of interest in research are Application of Artificial Intelligence to Power System and Control Design, Load and Price Forecasting, Distribution Generation, Restructuring in Power Systems, Congestion Management, Optimization.

Asghar Akbari Foroud was born in Hamadan, Iran, in 1971. He received B.Sc. degree from Tehran University and M.Sc. and PhD degrees from Tarbiat-modares University, Tehran, Iran. He is now with Semnan University. His research interests include power system dynamics & operation and restructuring.

Nima Amjady (SM'10) was born in Tehran, Iran, on February 24, 1971. He received the B.Sc., M.Sc., and Ph.D. degrees in electrical engineering from Sharif University of Technology, Tehran, Iran, in 1992, 1994, and 1997, respectively. At present, he is a Professor with the Electrical Engineering Department, Semnan University, Semnan, Iran. He is also a Consultant with the National Dispatching Department of Iran. His research interests include security assessment of power systems, reliability of power networks, load and price forecasting, and artificial intelligence and its applications to the problems of power systems.

Heidarali Shayanfar received the B.S. and M.S.E. degrees in Electrical Engineering in 1973 and 1979, respectively. He received his Ph. D. degree in Electrical Engineering from Michigan State University, U.S.A., in 1981. Currently, he is a Full Professor in Electrical Engineering Department of Iran University of Science and Technology, Tehran, Iran. His research interests are in the Application of Artificial Intelligence to Power System Control Design, Dynamic Load Modeling, Power System Observability Studies, Voltage Collapse, Congestion Management in a Restructured Power System, Reliability Improvement in Distribution Systems and Reactive Pricing in Deregulated Power Systems. He has published more than 405 technical papers in the International Journals and Conferences proceedings. He is a member of Iranian Association of Electrical and Electronic Engineers and IEEE.

APPLICATION OF TRAPEZOIDAL FUZZIFICATION APPROACH (TFA) AND PARTICLE SWARM OPTIMIZATION (PSO) IN FUZZY TIME SERIES (FTS) FORECASTING

by

Sa'eed Anibaba Eleruja, Muhammed Bashir Mu'azu and Danjuma Danshik Dajab
Department of Electrical and Computer Engineering, Ahmadu Bello University, Zaria
coolsaeed201@yahoo.com, mbmuazu@abu.edu.ng, dddajab@abu.edu.ng

Abstract

The trapezoidal fuzzification approach (TFA) model implemented in this paper utilizes aggregation and particle swarm optimization (PSO) to reduce the mismatch between the forecasted data and the actual data using maximum temperature data of Zaria for the period 1990-2003, obtained from Nigerian Meteorological Agency (NIMET) Zaria. The defuzzification module (including the developed PSO algorithm using C-#) of this model is then implemented on the hitherto fuzzified maximum temperature data so as to obtain forecasts. Statistical measures of MSE and MAPE are used to test the reliability of the model.

Keywords: TFA, PSO, Fuzzy Time Series, Forecasting, Temperature

1. INTRODUCTION

Cheng et al [1] introduced an approach where the crisp intervals, generally defined by the user at the initial step of FTS, are replaced with trapezoid fuzzy sets with overlapping boundaries. This overlap implies that a value may belong to more than one set. If a value belongs to more than one set, it is associated to the set where its degree of membership is highest. Poulsen's [2] approach, however, differed from this approach by performing automatically the calculations of the fuzzy intervals. Another area of difference is the notion of non-static universe of discourse. Whenever values are encountered which fall outside the boundaries of the current universe of discourse, it has to augment accordingly. The basic idea here is to repeat the fuzzification procedure when the dataset is updated.

The TFA technique is divided into two main components, fuzzification and defuzzification. These components are decoupled which implies that they can be integrated independently with other alternatives [1][2][3][4]. This will be applied to the monthly maximum temperature data to demonstrate the role of the TFA as an optimization technique to aid the fuzzy time series (FTS) forecasting. Actual maximum temperature data of Zaria for the period 1990-2003, as obtained from Nigerian Meteorological Agency (NIMET), Zaria are as shown in Table 1.

Table 1: Maximum Monthly Temperatures of Zaria

	1990	1991	1992	1993	1994	1995	1996	1997	1998	1999	2000	2001	2002	2003
JAN	31.3	29.5	27.1	27.4	30.1	28.3	32.2	31.4	29.5	30.9	31.3	29.9	26.8	31.4
FEB	30.4	36.0	30.3	33.0	32.3	31.1	34.8	28.8	33.7	34.4	28.7	30.7	32.2	34.9
MAR	33.6	35.6	35.5	35.1	37.7	36.5	36.9	35.0	34.2	37.5	39.6	36.2	36.0	35.4
APR	37.6	35.9	35.9	37.0	35.4	36.2	37.0	36.0	37.4	36.7	39.0	34.7	36.4	36.4
MAY	32.9	31.5	33.4	32.4	34.4	33.8	33.7	33.0	33.8	35.5	35.6	34.0	36.4	36.3
JUN	31.0	31.1	31.2	31.8	31.7	31.5	30.2	30.8	31.3	32.1	30.5	30.7	32.2	31.1
JUL	29.0	28.7	29.0	29.7	29.8	29.3	29.3	29.5	29.3	28.6	28.9	29.0	30.2	29.8
AUG	29.2	28.8	28.2	28.7	27.7	28.6	28.6	29.4	28.4	27.9	28.4	28.3	29.1	28.8
SEP	30.5	31.3	29.7	30.4	29.7	30.0	29.6	30.9	29.8	29.1	29.8	29.8	30.3	29.9
OCT	33.3	32.2	32.0	32.9	31.3	32.2	31.1	32.2	31.1	30.9	31.3	32.3	30.5	32.4
NOV	34.1	32.2	30.2	34.0	30.2	31.5	30.1	33.3	32.8	32.1	32.4	32.8	32.0	33.0
DEC	33.4	28.6	30.3	29.6	27.2	32.0	31.0	30.6	29.6	29.6	29.6	31.6	30.3	30.1

1.1 METHODOLOGY

The TFA-based FTS technique has two main components: fuzzification and defuzzification. The fuzzification module can be decomposed into a six-step process [2][3][4]:

i) Sorting of the values in the current dataset in ascending order.
ii) Computation of the average distance between any two consecutive values in the sorted dataset and the corresponding standard deviation.
iii) Elimination of outliers from the sorted dataset.
iv) Computation of the revised average distance between any two remaining consecutive values in the sorted dataset.

v) Definition of the universe of discourse.
vi) Fuzzification of the dataset using the trapezoid fuzzification approach.

The defuzzification module can be decomposed into a four-step process [2][3][4]:
i) Establishment of the fuzzy set groups (FSGs).
ii) Conversion of the FSGs into corresponding If-Then statements.
iii) Training of the If-Then rules.
iv) Derivation of the forecasts

The process will be concluded with the statistical and qualitative evaluation of the forecasts.

FUZZIFICATION MODULE

The forecasting process will be carried out on the data of Table 1 on a monthly basis. The data of January (1990 – 2003) will be used for demonstration. The data is sorted in ascending order as in Table 2:

Table 2: Temperature Data Sorted in Ascending Order (January 1990-2003).

Year	Temperature (^{0}C)
2002	26.8
1992	27.1
1993	27.4
1995	28.3
1991	29.5
1998	29.5
2001	29.9
1994	30.1
1999	30.9
1990	31.3
2000	31.3
1997	31.4
2003	31.4
1996	32.2

The next step is computing the average distance (AD) between any two consecutive values in the sorted dataset and the corresponding standard deviation (σ_{AD}) using equations (1) and (2) respectively.

$$AD\ (x_i \ldots x_n) = \frac{1}{n-1}\sum_{i=1}^{n-1} \left| x_{p(i)} - x_{p(i+1)} \right| \quad (1)$$

$$AD \approx 0.415$$

$$\sigma_{AD} = \sqrt{\frac{1}{n}\sum_{i=1}^{n} (x_i - AD)^2} \quad (2)$$

$$\sigma_{AD} \approx 0.376$$

The next step is eliminating outliers from the sorted dataset. Outliers are values which are either abnormally high or abnormally low and are eliminated from the sorted dataset, because the intention here is to obtain an average distance value free of distortions. It is obtained as a value less than or larger than one standard deviation from average [2][3][4]

$$0.415 - 0.376 \le x \le 0.415 + 0.376$$

$$0.039 \le x \le 0.791$$

After the elimination process is completed, a revised average distance value is computed for the remaining values in the sorted dataset,

$$AD_R = \frac{0.3 + 0.3 + 0.4 + 0.2 + 0.4 + 0.1}{6}$$

$$AD_R \approx 0.283$$

The value of AD_R is now taken as the segment length, S which is used in the next two steps to partition the universe of discourse into a series of trapezoidal fuzzy sets. This is to create a series of trapezoidal approximations which capture the generic nature of data as closely as possible, in the sense that the spread of individual functions will neither be too narrow or too wide.

The lower and upper bound of the universe of discourse is determined by locating the largest and lowest values in the dataset and augment these by:
i) subtracting the revised average distance from the lowest value and
ii) adding the revised average distance to the highest value.

If D_{max} and D_{min} are the highest and lowest values in the dataset, respectively, and AD_R is the revised average distance, then the universe of discourse, U can be defined as:

$$U = [D_{min} - AD_R,\ D_{max} + AD_R] \quad (3)$$

$$U = [26.517, 32.483]$$

When U has been determined, fuzzy subsets can be defined on U. Since the subsets are represented by trapezoidal functions, the membership degree, for a given function, μ_A and a given value, x is obtained by:

$$\mu_A = \begin{cases} \dfrac{x - a_1}{a_2 - a_1}, a_1 \le x \le a_2 \\ 1, a_2 \le x \le a_3 \\ \dfrac{a_4 - x}{a_4 - a_3}, a_3 \le x \le a_4 \\ 0, otherwise \end{cases} \quad (4)$$

Prior to the fuzzification of data, the number of subsets to be defined on U needs to be known. The number of subsets, n is determined by:

$$n = \frac{R - S}{2S} \quad (5)$$

R denotes the range of the universe of discourse and S denotes the segment length.

$$R = UB - LB \quad (6)$$

$$R = 5.966$$

$$n = \frac{5.966 - 0.283}{2 * 0.283}$$

$$n \approx 10$$

As can be seen in Table 3, the segment length is selected, such that the lowest value in the dataset always appears as the left bound in the first crisp interval, and the highest value in the dataset always appears as the right bound in the last crisp interval. It can also be seen that the lowest of the values (26.80), appears as the lower bound of the first crisp interval, A_1, and the highest value (32.20), appears as the upper bound in the last crisp interval, A_{10}. The average temperatures are then fuzzified according to membership functions A_1 to A_{10} as in Table 3.

Table 3: Generated Fuzzy Sets (January 1990 – 2003)

Fuzzy set	Fuzzy number
A_1	(26.52, 26.80, 27.08, 27.37)
A_2	(27.08, 27.37, 27.65, 27.94)
A_3	(27.65, 27.94, 28.22, 28.50)
A_4	(28.22, 28.50, 28.79, 29.07)
A_5	(28.79, 29.07, 29.36, 29.64)
A_6	(29.36, 29.64, 29.92, 30.21)
A_7	(29.92, 30.21, 30.49, 30.78)
A_8	(30.49, 30.78, 31.06, 31.34)
A_9	(31.06, 31.34, 31.63, 31.91)
A_{10}	(31.63, 31.91, 32.20, 32.48)

In situations where intervals overlap, the value is assigned to the interval with the higher membership degree. A special case occurs when the membership degree is 0.5, as this implies that a value has the same membership status in two different sets. In such cases, the respective value is associated to both sets, as in the case of 1991 and 1998 in Table 4.

Generally it is assumed that the fuzzy sets, A_1, A_2, ... , A_n, individually represent some linguistic value. Adopting the same procedure used for generating the fuzzy sets and fuzzified average temperatures for January 1990-2003, the values of average distance (AD), standard deviation (σ_{AD}), revised average distance (AD_R), universe of discourse (U) and number of sets (n) are shown in Table 5 for January (1990-2003) to December (1990-2003).

Table 4: Fuzzified Maximum Temperatures (January 1990-2003).

Year	Temperature (^{0}C)	Fuzzy set
1990	31.3	A_9
1991	29.5	A_5, A_6
1992	27.1	A_1
1993	27.4	A_2
1994	30.1	A_7
1995	28.3	A_3
1996	32.2	A_{10}
1997	31.4	A_9
1998	29.5	A_5, A_6
1999	30.9	A_8
2000	31.3	A_9
2001	29.9	A_6
2002	26.8	A_1
2003	31.4	A_9

Table 5: AD, σ_{AD}, AD_R, U and n for the entire Maximum Temperatures

	Average distance (AD)	Standard deviation (σ_{AD})	Revised average distance (AD_R)	Universe of discourse (U)	Number of sets (n)
JAN	0.415	0.376	0.283	[26.517, 32.483]	10
FEB	0.562	0.438	0.533	[28.167, 36.533]	7
MAR	0.462	0.465	0.342	[33.258, 39.942]	9
APR	0.331	0.367	0.200	[34.500, 39.200]	11
MAY	0.347	0.330	0.244	[31.256, 36.644]	11
JUN	0.154	0.084	0.140	[30.060, 32.340]	8
JUL	0.123	0.125	0.082	[28.518, 30.282]	10
AUG	0.131	0.099	0.138	[27.562, 29.538]	7
SEP	0.169	0.164	0.100	[29.000, 31.400]	12
OCT	0.215	0.214	0.229	[30.271, 33.529]	7
NOV	0.308	0.347	0.182	[29.918, 34.282]	11
DEC	0.477	0.480	0.240	[26.960, 33.640]	13

3 DEFUZZIFICATION

3.1 PARTICLE SWARM OPTIMIZATION

Particle Swarm Optimization (PSO), first introduced by Kennedy and Eberhart, is an algorithm that simulates the social behaviours shown by various kinds of organisms such as bird flocking or fish schooling. PSO is initiated with a set of randomly generated particles which in fact are candidate solutions [5].

A set of n particles is created, where n is chosen as 5 in this case. The randomly generated velocities are all initialized to v1 and v2. The positions w1 and w2 (depending on R) are then assigned to all the particles. Each particle's local best value is then initialized to the set w1 and w2, as well the global best value. The initial randomly generated velocities are stored in an array A4, designated in the program as the array *initialVelocities*. The squared errors are then calculated for the initial values specified, and stored in another array designated as A1, represented in the program as the array *oldSquaredErrors*.

An iteration loop is instantiated, whose limit is the maximum number of iterations specified. Per iteration, each particle's velocity is calculated and normalized if necessary, and then the position is then updated based on the new velocity. The squared errors after the first iteration are then stored in an array designated as A2, which is represented in the program as the array *intermediateSE*.

Per iteration, the squared errors per particle are calculated and stored in an array designated as A3, represented in the program as the array *currentSquaredErrors*. A3 is then compared with the existing values in the array A1. If the squared error for any given particle (in A3) is less than the corresponding value in the array A1, then the value in A1 is updated with this new value from A3. At the same time, if the given particle's squared error in this current iteration is better than the current local best value, then the particle's local best value is updated accordingly. If previously, any of the local best values was updated, then the global best value is then reassigned to be the smallest value in the array A3. The index of the particle whose squared error is the least in A3 is then taken. Each particle updates its velocity and position with the equations (6) and (7) [2][3][4]:

$$v_i = wv_i + c_1 r_1(\hat{x}_i - x_j) + c_2 r_2(\hat{g} - x_j) \quad (9)$$

$$x_j = x_j + v_i \quad (10)$$

where, v_i is the velocity of particle p_i and is limited to $[-V_{max}, V_{max}]$ where V_{max} is user-defined constant, w is an inertial weight coefficient, $\hat{x}_i$ is the current personal best position, x_j is the present position, $\hat{g}$ is the global best position, c_1 and c_2 are user defined constants that say how much the particle is directed towards good positions. They affect how much the particle's local best and global best influence its movement. Generally c_1 and c_2 are set to 2 and r_1 and r_2 are randomly generated numbers between 0 and 1.

At this point, if the minimum squared error obtained in this iteration is less than or equal to the user-specified target squared error value, then all further iterations are terminated, and the result object shows that the criterion was reached. All squared error values, all particle indices, initial velocities (in array A4), the best particle index and the number of iterations are all stored in the result object. However, if the iteration loop reaches the specified maximum number of iterations which the user specified, then the result object shows that the criterion was not reached. All the other values (initial velocities, etc) are all stored in the result object. The Squared Error (SE), defined by:

$$SE = (forecast_t - actual_t)^2 \quad (11)$$

3.2 AGGREGATION

This process is meant to aggregate pieces of data in a desirable way in order to reach final decision. Typically this data is represented by numerical values which make some kind of sense with regards to the application. Hence the aggregation problem is generally regarded as the problem of reducing a series of numerical values into a single representative value. Formally an aggregation operator can be defined as function h which assigns a real number y to any n-tuple $(x_1, x_2, \ldots\ldots, x_n)$ of real numbers [6]

$$y = h(x_1, x_2, \ldots\ldots, x_n)$$

Basically the idea is to evaluate the aggregated result, Y(t), against the actual outcome at time t, and adjust the weights in the defuzzification operator such that the squared error is minimized. By minimizing *SE* for t, *MSE* is minimized as well.

3.3 DEFUZZIFICATION MODULE

The data of February 1990 to 2003 (Table 6) is used to demonstrate the module

Table 6: Fuzzified maximum temperatures (February 1990-2003)

Year	Temperature (^{0}C)	Fuzzy set
1990	30.4	A_2
1991	36.0	A_7
1992	30.3	A_2
1993	33.0	A_5
1994	32.3	A_4
1995	31.1	A_3
1996	34.8	A_6
1997	28.8	A_1
1998	33.7	A_5
1999	34.4	A_6
2000	28.7	A_1
2001	30.7	A_3
2002	32.2	A_4
2003	34.9	A_6

Fuzzy Set Groups (FSGs) are established (as against the conventional Fuzzy Logic Relationship Groups (FLRG) in order to partition the historical data into unique sets of sub-patterns which subsequently are converted into corresponding If-statements. During the first pass of the algorithm, consecutive sets are grouped pair-wise. Table 7 shows the fuzzified data of Table 6 grouped in this manner. Every FSG appears in chronological order.

Table 7: Establishment of Fuzzy Set Groups (February 1990-2003)

Label	FSG
1	$\{A_2, A_7\}$
2	$\{A_7, A_2\}$
3	$\{A_2, A_5\}$
4	$\{A_5, A_4\}$
5	$\{A_4, A_3\}$
6	$\{A_3, A_6\}$
7	$\{A_6, A_1\}$
8	$\{A_1, A_5\}$
9	$\{A_5, A_6\}$
10	$\{A_6, A_1\}$
11	$\{A_1, A_3\}$
12	$\{A_3, A_4\}$
13	$\{A_4, A_6\}$

The essence of grouping sets in this manner is to obtain a series of FSGs free of ambiguities. An ambiguity occurs, if two or more FSGs contain the same combination of elements. It can be seen from Table 7 that FSGs labelled as 7 and 10 are identical. In order to obtain a series of disambiguated Fuzzy Set Groups (Table 8), the ambiguous FSGs are extended to third order FSGs, by including the previous set in the corresponding time series. The extension process is continued until a unique combination of elements is obtained for each FSG.

Table 8: Disambiguated Fuzzy Set Groups (February 1990-2003)

Label	FSG
1	$\{A_2, A_7\}$
2	$\{A_7, A_2\}$
3	$\{A_2, A_5\}$
4	$\{A_5, A_4\}$
5	$\{A_4, A_3\}$
6	$\{A_3, A_6\}$
7	$\{A_3, A_6, A_1\}$
8	$\{A_1, A_5\}$
9	$\{A_5, A_6\}$
10	$\{A_5, A_6, A_1\}$
11	$\{A_1, A_3\}$
12	$\{A_3, A_4\}$
13	$\{A_4, A_6\}$

The If-statements are generated on the basis of the content of the FSGs. This task is fairly simple as the sequence of elements of each FSGs is the same as they appear in time. Each FSG can therefore easily be transformed into If-Then rules of the form:

$$\begin{aligned} &\textit{if } (F(t-1) = A_{i,t-1} \wedge F(t-2) \\ &= A_{i,t-2} \wedge \ldots \wedge F(t-n+1) \\ &= A_{i,t-n+1} \wedge F(t-n) = A_{i,t-n}); \qquad (12) \\ &\textit{then } w_{1,t-1} = ? \wedge w_{2,t-2} \\ &= ? \wedge \ldots \wedge w_{n-1,t-n+1} \\ &= ? \wedge w_{n,t-n} = ? \end{aligned}$$

For practical reasons, the sequence of conditions in the If-statement appears in the reverse order compared to their equivalent FSGs. When a rule is matched, the resultant weights are returned and the forecasted value, Y(t), is computed according to:

$$Y(t) = \sum_{i=1}^{n} a_{t-i}.w \qquad (13)$$

$$\textit{where} \quad w_i \in [0,1]$$

By processing all the data in Table 8, a series of incomplete If-statements are generated as shown in Table 9. In order to determine the weights, PSO is utilized to train the rules individually to match the data they represent.

Table 9: Generated If-rules in Chronological Order (February 1990-2003)

Rule	Matching part
1	$if\,(F(t-1)=A_7 \wedge F(t-2)=A_2)$
2	$if\,(F(t-1)=A_2 \wedge F(t-2)=A_7)$
3	$if\,(F(t-1)=A_5 \wedge F(t-2)=A_2)$
4	$if\,(F(t-1)=A_4 \wedge F(t-2)=A_5)$
5	$if\,(F(t-1)=A_3 \wedge F(t-2)=A_4)$
6	$if\,(F(t-1)=A_6 \wedge F(t-2)=A_3)$
7	$if\,(F(t-1)=A_1 \wedge F(t-2)=A_6 \wedge F(t-3)=A_3)$
8	$if\,(F(t-1)=A_5 \wedge F(t-2)=A_1)$
9	$if\,(F(t-1)=A_6 \wedge F(t-2)=A_5)$
10	$if\,(F(t-1)=A_1 \wedge F(t-2)=A_6 \wedge F(t-3)=A_5)$
11	$if\,(F(t-1)=A_3 \wedge F(t-2)=A_1)$
12	$if\,(F(t-1)=A_4 \wedge F(t-2)=A_3)$
13	$if\,(F(t-1)=A_6 \wedge F(t-2)=A_4)$

PSO is then utilized to tune the weights in the defuzzification operator in equation (6). The following parameters are user defined:

- The inertial coefficient, w, equals 1.4.
- The self confidence and social confidence coefficients, c_1 and c_2, respectively, both equals 2.
- The minimum and maximum velocity is limited to [-0.01, 0.01].
- The minimum and maximum position is limited to [0, 1].
- The number of particles equals five.
- The stopping criteria are defined by setting the minimum *SE* to 1 and the maximum number of iterations to 500.

The PSO algorithm is coded using C-#.

Table 10: Initial Positions of all Particles

Particle	**Position 1 (w_1)**	**Position 2 (w_2)**	**SE**
1	0.75	0.5	141.61
2	0.75	0.5	141.61
3	0.75	0.5	141.61
4	0.75	0.5	141.61
5	0.75	0.5	141.61

To demonstrate the algorithm, rule 1 in Table 9 is trained. As can be seen from Table 10, the personal best positions are the same for all particles during initialization. Hence the personal best positions equal the global best position for all particles.

Table 11: Randomized Initial Velocities of all Particles

Particle	v_1	v_2
1	0.0026	0.0012
2	0.0036	0.0017
3	0.0038	0.0022
4	0.0098	0.0047
5	0.0025	0.0071

When all particles and velocities have been initialized (Table 11), the velocities are updated before positions are incremented. Velocities are updated according to equation (9). The computation yields:

$$v_{1,1} = (1.4 * 0.0026) + 2 * r_1(0.75 - 0.75) + 2 * r_2(0.75 - 0.75) = 0.0036$$
$$v_{1,2} = (1.4 * 0.0012) + 2 * r_1(0.5 - 0.5) + 2 * r_2(0.5 - 0.5) = 0.0017$$
$$v_{2,1} = (1.4 * 0.0036) + 2 * r_1(0.75 - 0.75) + 2 * r_2(0.75 - 0.75) = 0.0050$$
$$v_{2,2} = (1.4 * 0.0017) + 2 * r_1(0.5 - 0.5) + 2 * r_2(0.5 - 0.5) = 0.0024$$
$$v_{3,1} = (1.4 * 0.0038) + 2 * r_1(0.75 - 0.75) + 2 * r_2(0.75 - 0.75) = 0.0053$$
$$v_{3,2} = (1.4 * 0.0022) + 2 * r_1(0.5 - 0.5) + 2 * r_2(0.5 - 0.5) = 0.0031$$
$$v_{4,1} = (1.4 * 0.0098) + 2 * r_1(0.75 - 0.75) + 2 * r_2(0.75 - 0.75) = 0.0137$$
$$v_{4,2} = (1.4 * 0.0047) + 2 * r_1(0.5 - 0.5) + 2 * r_2(0.5 - 0.5) = 0.0066$$
$$v_{5,1} = (1.4 * 0.0025) + 2 * r_1(0.75 - 0.75) + 2 * r_2(0.75 - 0.75) = 0.0035$$
$$v_{5,2} = (1.4 * 0.0071) + 2 * r_1(0.5 - 0.5) + 2 * r_2(0.5 - 0.5) = 0.0099$$

Positions are incremented according to equation (2). Incremented positions after the first iteration are shown in Table 12.

Table 12: The Positions of all Particles after the First Iteration

Particle	w_1	w_2	SE
1	0.7526	0.5012	145
2	0.7536	0.5017	147
3	0.7538	0.5022	148
4	0.7598	0.5047	155
5	0.7525	0.5071	151

After the first iteration, none of the computed *SE* values in Table 12 is less than 141.61. Thus no personal best positions or global best positions are reached at this point. The iteration continues until either or both of the stopping criteria are met. The personal best positions of all particles after termination are listed in Table 13.

Table 13: The Personal Best Positions of all Particles after Termination

Particle	w_1	w_2	SE
1	0.5963	0.3531	3
2	0.5932	0.3502	2
3	0.5928	0.3482	2
4	0.5921	0.3414	1
5	0.5971	0.3421	2

According to Table 13, particle 4 has the global best position. Hence the weights associated to rule 1 equals 0.5921 and 0.3414.

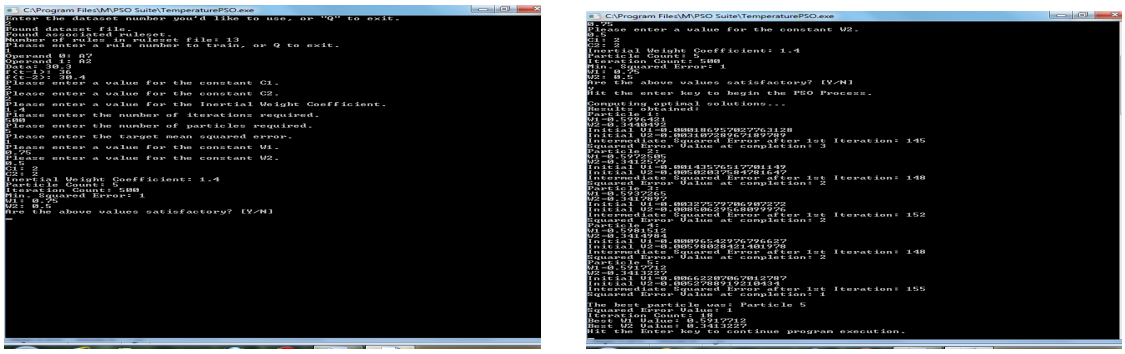

Figure 2: Screenshot Showing Inputted Parameters and Results

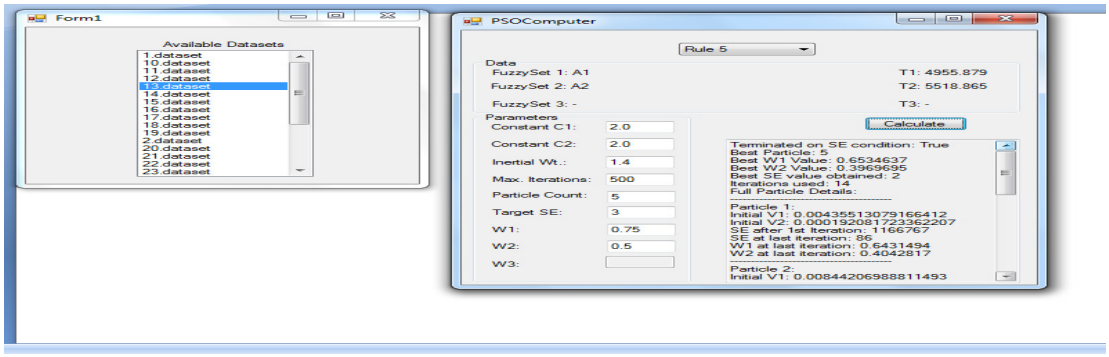

Figure 3: Graphical User Interface Showing Results

After the weights have been optimized via PSO (as shown in Figures 2 and 3), the 'blanks' in the 'Then' part can be filled. The partially completed If-rules from Table 9 are shown in fully completed form in Table 14.

Table 14: Generated if-then Rules in Chronological Order (February 1990-2003)

Rule	Matching Part	Weights
1	$if\ (F(t-1)=A_7 \wedge F(t-2)=A_2)$	$then\ w_1=0.5900\ and\ w_2=0.3400$
2	$if\ (F(t-1)=A_2 \wedge F(t-2)=A_7)$	$then\ w_1=0.6497\ and\ w_2=0.4037$
3	$if\ (F(t-1)=A_5 \wedge F(t-2)=A_2)$	$then\ w_1=0.6500\ and\ w_2=0.4000$
4	$if\ (F(t-1)=A_4 \wedge F(t-2)=A_5)$	$then\ w_1=0.6247\ and\ w_2=0.3700$
5	$if\ (F(t-1)=A_3 \wedge F(t-2)=A_4)$	$then\ w_1=0.6915\ and\ w_2=0.4480$
6	$if\ (F(t-1)=A_6 \wedge F(t-2)=A_3)$	$then\ w_1=0.5687\ and\ w_2=0.3200$
7	$if\ (F(t-1)=A_1 \wedge F(t-2)=A_6 \wedge F(t-3)=A_3)$	$then\ w_1=0.4466, w_2=0.3500\ \&\ w_3=0.2500$
8	$if\ (F(t-1)=A_5 \wedge F(t-2)=A_1)$	$then\ w_1=0.6797\ and\ w_2=0.4334$
9	$if\ (F(t-1)=A_6 \wedge F(t-2)=A_5)$	$then\ w_1=0.5584\ and\ w_2=0.3100$
10	$if\ (F(t-1)=A_1 \wedge F(t-2)=A_6 \wedge F(t-3)=A_5)$	$then\ w_1=0.4100, w_2=0.3100\ \&\ w_3=0.2066$
11	$if\ (F(t-1)=A_3 \wedge F(t-2)=A_1)$	$then\ w_1=0.6899\ and\ w_2=0.4325$
12	$if\ (F(t-1)=A_4 \wedge F(t-2)=A_3)$	$then\ w_1=0.6907\ and\ w_2=0.4400$
13	$if\ (F(t-1)=A_6 \wedge F(t-2)=A_4)$	$then\ w_1=?\ and\ w_2=?$

4: DERIVATION OF FORECASTS

Adopting the same procedure, the If-Then rules are generated for the months of January to December (1990 – 2003). Based on the rules of Table 14, the forecast for February (1990-2003) is obtained as in Table 15. Using similar tables for all the months, forecast values for January to December 2004 are

obtained as in Table 16. Adopting the same procedure, the If-Then rules are generated for the months of January to December (1990 – 2003). Based on the rules of Table 14, the forecast for February (1990-2003) is obtained as in Table 15. Using similar tables for all the months, forecast values for January to December 2004 are obtained as in Table 16. The performance of the developed model is evaluated by the Mean square Error (MSE) and the Mean Average Percentage Error (MAPE). The plot of the actual and forecasted temperatures is as shown in Figure 5

The Mean Squared Error (MSE) and Mean Absolute Percentage Error (MAPE) are defined thus:

$$MAPE = \frac{1}{n}\sum_{t=1}^{n}\frac{|forecast_t - actual_t|}{actual_t} \times 100 \quad (14)$$

$$MSE = \frac{1}{n}\sum_{i=1}^{n}(forecast_i - actual_i)^2 \quad (15)$$

Table 15: Forecast Results (February 1990-2003)

Year	Actual (^{0}C)	Forecasted (^{0}C)
1990	30.4	-
1991	36.0	-
1992	30.3	31.6
1993	33.0	34.2
1994	32.3	33.6
1995	31.1	32.4
1996	34.8	36.0
1997	28.8	29.7
1998	33.7	32.8
1999	34.4	35.4
2000	28.7	29.7
2001	30.7	29.4
2002	32.2	33.6
2003	34.9	35.7
		-
MSE		1.322
MAPE		0.0355

Table 16: Forecast Results (January to December 2004)

Month (2004)	Actual (^{0}C)	TFA (^{0}C)
January	30.9	32.3
February	32.0	33.3
March	34.5	33.5
April	37.1	38.1
May	33.4	34.3
June	30.9	32.2
July	29.4	30.5
August	28.2	27.5
September	30.1	31.5
October	32.4	33.8
November	32.8	34.1
December	31.6	32.7
MSE		1.389
MAPE		0.0364

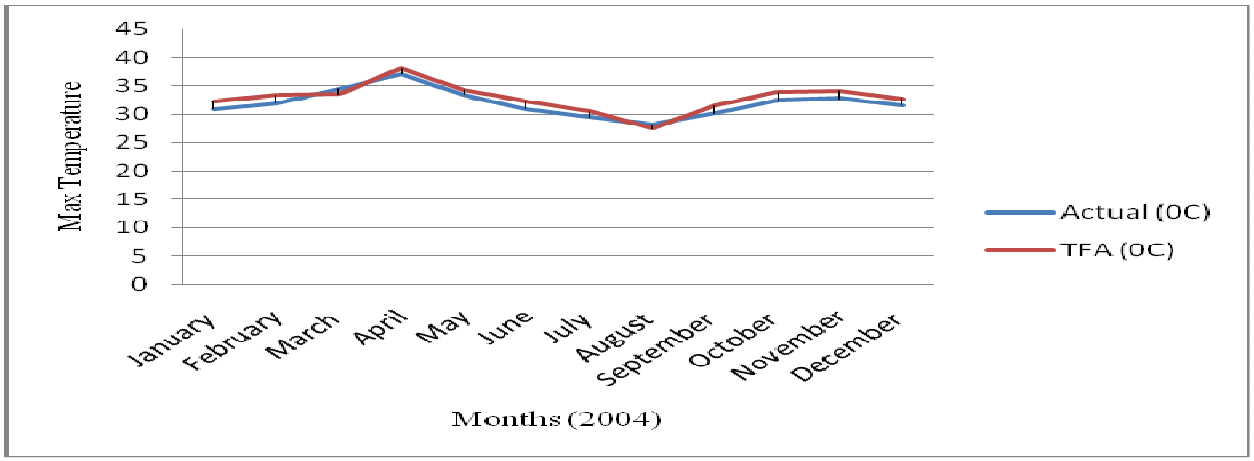

Figure 5: Plot of trends of the actual and forecasted temperatures (2004)

5. CONCLUSION

The Fuzzy Time Series (FTS) model employed in this work uses a fuzzification algorithm, based on the trapezoid fuzzification approach (TFA), which objectively partitions the universe of discourse into intervals without requiring any user defined parameters. PSO and aggregation are utilized to reduce the mismatch between the forecasted and actual data, to individually tune forecast rules and to ensure consistency between defuzzified outputs and actual outputs, regardless of selected interval partitions. As a consequence, data utilisation is improved by minimising the loss of forecast rules and minimising the number of pattern combinations to be matched with future time series data.

The FTA-based FTS technique is employed on maximum temperature data of Zaria for the period 1990-2003, as obtained from Nigerian Meteorological Agency (NIMET), Zaria and these are used to obtain the forecast for January to December 2004. A performance measure of MAPE of 3.64% is obtained, which indicates that the technique can result in the improvement of the forecasting accuracy.

REFERENCES

1) Cheng, C. H., Chang, J. R. and Yeh, C. A. (2006), Entropy-Based and Trapezoid Fuzzification Fuzzy Time Series Approaches for Forecasting IT Project Cost, Technological Forecasting and Social Change 73 (2006), pp. 524-542.
2) Poulsen J. R. (2009), "Developing a New Forecasting Model Based on High Order Fuzzy Time Series, Fuzzy Time Series Forecasting".
3) Chung-Ho S., Tai-Liang C., Ching-Hsue C., and Ya-Ching C. (2010), "Forecasting the Stock Market with Linguistic Rules Generated from Minimize Entropy Principle and the Cumulative Probability Distribution Approaches", Entropy 2010, 12, pp. 2397-2417.
4) Tai-Liang, C., Ching-Hsue, C., and Ya-Ching, C. (2010), "Using Extracted Fuzzy Rules Based on Multi-Technical Indicators for Forecasting TAIEX", International Conference on Artificial Intelligence (ICAI'10), pp. 30-34
5) Kennedy J., and Eberhart R., (1995), "Particle Swarm Optimization", Proceedings of IEEE International Conference on Neural Networks, pp. 1942-1948.
6) Detyniecki M., (2009), "Fundamentals on Aggregation", http://www.poleia.lip6.fr/~marcin/papers/Dety_AGOP_01.pdf

A Novel Fuzzy Based Multi Objective Honey Bee Mating Optimization Algorithm for PSS Design in SMIB

H. A. Shayanfar*
Center of Excellence for Power System Automation and Operation
Iran University of Science and Technology, Tehran, Iran

H. Shayeghi
Technical Eng. Department
University of Mohaghegh Ardabili
Ardabil, Iran

A. Ghasemi
Technical Eng. Department
Young Researcher Club, Islamic Azad University, Ardabil, Iran

hashayanfar@gmail.com, hshayeghi@gmail.com, ghasemi.agm@gmail.com

Abstract- *This paper presents a Novel Fuzzified Multi Objective (MO) version of Honey Bee Mating Optimization (MOHBMO) approach for optimal tuning of linear parameters (such as the gain and time constant) and nonsmooth nonlinear parameters (such as saturation limits) of Power System Stabilizer (PSS). The problem of robustly tuning of PSS based SMIB design is formulated as an optimization problem according to the time domain-based and eigenvalue based objective functions which are solved by the MOHBMO technique that has a strong ability to find the most optimistic results. The effectiveness of the proposed Fuzzy based MOHBMO based PSS is demonstrated on a Single-Machine Infinite-Bus (SMIB) power system through the nonlinear time domain simulation and some performance indices under different operating conditions in comparison with the SPEA algorithm based tuned stabilizer and conventional PSS.*

Keywords: PSS Design, HBMO, MOHBMO, Low Frequency Oscillations, SMIB.

1. Introduction

Low frequency oscillations are detrimental to the goals of maximum power transfer and optimal power system security [1]. A contemporary solution to this problem is the addition of power system stabilizers to the automatic voltage regulators on the generators in the power system. The damping provided by this additional stabilizer provides the means to reduce the inhibiting effects of the oscillations [2]. The application of Power System Stabilizer (PSS) can help in damping out these oscillations and improve the system stability. The traditional and till date the most popular solution to this problem is application of the Conventional Power System Stabilizer (CPSS). However, continual changes in the operating condition and network parameters result in corresponding change in system dynamics. This constantly changing nature of power system makes the design of CPSS a difficult task [3].

A more reasonable design of the PSS is based on the gain scheduling and adaptive control theory as it takes into consideration the nonlinear and stochastic characteristics of the power systems [4-5]. This type of stabilizer can adjust its parameters on-line according to the operating condition. Many years of intensive studies have shown that the adaptive stabilizer can not only provide good damping over a wide operating range but more importantly, it can also solve the coordination problem among the stabilizers. Many random heuristic methods, such as like Improved honey bee mating optimization algorithm, chaotic optimization algorithm, artificial bee colony algorithm, Particle Swarm Optimization (PSO), Improved version of PSO algorithm have recently received much interest for achieving high efficiency and search global optimal solution in the problem space and they have been applied to the problem of PSS design [6-11]. These evolutionary based methods are heuristic population-based search procedures that incorporate random variation and selection operators. In addition, the PSS design problem was formulated as a single objective for optimization in all of the above methods.

It should be noted that the PSS design problem is a multiobjective optimization problem due to system characteristics and nonlinear behavior of the power systems. Thus, a fuzzy based Multi Objective Honey Bee Mating Optimization (MOHBMO) technique is proposed for optimal tune of PSS parameters to improve power system low frequency oscillations damping in this paper. The HBMO algorithm is a typical swarm-based approach to optimization, in which the search algorithm is inspired by the honey-bee mating process [12-13] and has emerged as a useful tool for engineering optimization. There is no absolute global best in MOHBMO, but rather a set of nondominated solutions. Also, there may be no single local best queen for each individual of the colony. Selecting the global best and local best to guide the colony bees becomes nontrivial task in multi-objective domain. Thus, for non-

*Corresponding Author (hashayanfar@gmail.com)

dominance solutions sorting the Pareto archive maintenance approach and to ensure proper diversity amongst the solutions of the non-dominated solutions in Pareto archive maintenance the crowding distance measure concept is used [14].

In this study, the problem of robust PSS design is formulated as a multi objective optimization problem and MOHBMO technique is used to solve it. Two performance indices based on time and frequency domains characteristics are defined and used to form the objective function of the design problem. The proposed MOHBMO based designed PSS has been applied and tested on a weakly connected power system under wide range of operating conditions to illustrate their ability to provide efficient damping of low frequency oscillations. To show the superiority of the proposed design approach, the simulations results are compared with the SPEA based designed [15] and classical PSS under different operating conditions through some performance indices. The results evaluation shows that the proposed method achieves good robust performance for wide range of load changes in the presence of very highly disturbance and is superior to the other stabilizers.

2. Power system model

For stability analysis of power system adequate mathematical models describing the system are needed. The models must be computationally efficient and be able to represent the essential dynamics of the power system. The stability analysis of the system is generally attempted using mathematical models involving a set of nonlinear differential equations. A schematic diagram for the test system is shown in Fig. 1. The generator is equipped with excitation system and a power system stabilizer. System data are given in Appendix.

The synchronous generator is represented by model 1.1, i.e. with field circuit and one equivalent damper winding on q axis. The nonlinear dynamic equations of the SMIB system considered can be summarized as [2, 11].

$$\begin{aligned}
\dot{\delta} &= \omega_B S_m \\
\frac{dS_m}{dt} &= \frac{1}{2H}(-DS_m + T_m - T_e) \\
\dot{E}'_q &= \frac{1}{T'_{do}}(E_{fd} + (x_d - x'_d)i_d - E'_q) \\
\dot{E}_{fd} &= \frac{1}{T_A}(k_A(v_{ref} - v_t + V_s)) - E_{fd})
\end{aligned} \tag{1}$$

$$T_e = E'_q i_q + (x'_d - x'_q) i_d i_q \tag{2}$$

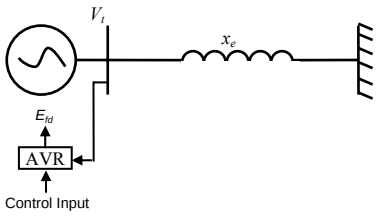

Fig. 1. SMIB power system

2.1. PSS model

The structure of PSS, to modulate the excitation voltage is shown in Fig .2. The structure consists a gain block with gain K, a signal washout block and two-stage phase compensation blocks. The input signal of the proposed method is the speed deviation ($\Delta\omega$) and the output is the stabilizing signal V_S which is added to the reference excitation system voltage. The signal washout block serves as a high-pass filter, with the time constant T_W, high enough to allow signals associated with oscillations in input signal to pass unchanged. From the viewpoint of the washout function, the value of T_W is not critical and may be in the range of 1 to 20 seconds [11]. The phase compensation block (time constants T_1, T_2 and T_3, T_4) provides the appropriate phase-lead characteristics to compensate for the phase lag between input and the output signals.

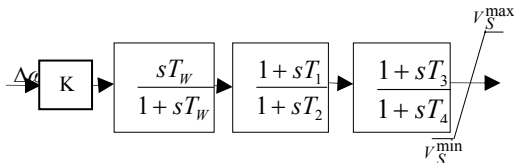

Fig .2. Structure of power system stabilizer

3. Multi Objective HBMO

A. Brief HBMO Review

A honey-bee colony typically consists of a single egg laying long-lived queen, several thousand drones (depending on the season), workers and a large family of bees living in one bee-hive [12]. Each bee undertakes sequences of actions which unfold according to genetic, ecological and social condition of the colony.

A mating flight starts with a dance performed by the queen who then starts a mating flight during which the drones follow the queen and mate with her in the air. After the mating process, the drones die. In each mating, sperm reaches the spermatheca and accumulates there to form the genetic pool of the colony. Each time a queen lays fertilized eggs, she randomly retrieves a mixture of the sperm accumulated in the spermatheca to fertilize the egg and this task can only be done by the queen [16-17].

The HBMO algorithm combines different phases of the marriage process of the honey bee. It starts with random generation of a set of initial solutions. Based on their fitness, randomly generated solutions are then

ranked. The fittest solution is named queen, whereas the remaining solutions are categorized as drones (i.e., trial solutions). In order to form the hive and start mating process, the queen, drones and workers (predefined heuristic functions) should be defined. Each queen is characterized with a genotype, speed, energy and a spermatheca with defined capacity. In the next step, drones must be nominated to mate with the queen probabilistically during the mating flight. At the start of the flight, the queen is initialized with some energy content and returns to her nest when the energy is within some threshold of either near zero or when the spermatheca is full. The mating flight may be considered as a set of transitions in a state-space (the environment). An annealing function is used to describe the probability of a drone (D) that successfully mates with the queen (Q) as follows [12]:

$$prob(Q,D) = e^{\frac{-\Delta(f)}{S(t)}} \quad (3)$$

Where, $\Delta(f)$ is the absolute difference of the fitness of D and the fitness of Q and the $s(t)$ is the speed of queen at time t. The fitness of the resulting chromosomes of drone, queen or brood is determined by evaluating the value of the objective function. After each transition in space, the queen's speed and energy decays is given by:

$$S(t+1) = \alpha \times S(t) \quad (4)$$

$$E(t+1) = E(t) - \gamma \quad (5)$$

Where, $\alpha(t)$ is speed reduction factor and γ is the amount of energy reduction after each transition (α , $\gamma \in [0,1]$).

B. MOHBMO

In most of practical cases, multi-objective optimization problems require simultaneous optimization of several incommensurable and often competitive/conflicting objectives. Because of presence of the multiple conflicting objectives, there is not exist one solution, which is the optimum of all objectives simultaneously. Instead, the solutions exist in the form of alternative trade-offs, also known as the Pareto optimal solutions. In other word, a multi-objective optimization problems always has a set of optimal solutions, for which there is no way to improve one objective value without deterioration of at least one of the other objective values. Pareto dominance concept classifies solutions as dominated or non-dominated solutions and the "best solutions" are selected from the non-dominated solutions. To sort non-dominated solutions, the first front of the non-dominated solution is assigned the highest rank and the last one is assigned the lowest rank. When comparing solutions that belong to a same front, another parameter called crowding distance is calculated for each solution. The crowding distance is a measure of how close an individual is to its neighbors. Large average crowding distance will result in better diversity in the population [14]. In order to investigate multi-objective problems, some modifications in the HBMO algorithm were made.

Here, fuzzy set theory has been implemented to derive efficiently a candidate Pareto optimal solution for the decision makers [16]. The fuzzy set theory has been implemented to derive efficiently a solution from the set of non-dominated solutions. The fuzzy decision making function is represented by the membership function to replace each variable as a precise value. Fig. 3. depicts the membership function μ_c for the fuzzy variable signifying total fuel cost $f_i(.)$. The decision maker is fully satisfied with the cost if, μ_c is one, and not satisfied at all if μ_c is zero. Therefore, the value of membership function indicates the adaptability of the economy index. Due to the imprecise nature of decision maker's judgment, the ith objective function of a solution in the non-dominated set f_i is represented by a membership function $\mu_i(.)$ defined as [17]:

$$\mu_i = \frac{f_i^{\max} - f_i}{f_i^{\max} - f_i^{\min}} \quad (6)$$

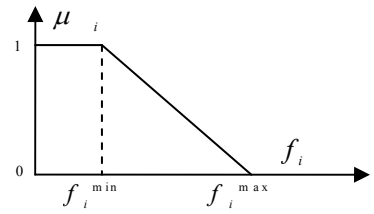

Fig. 3. Membership function of fuzzy cost.

Where f_i^{max} and f_i^{min} are the maximum and minimum values of i^{th} objective, respectively. We can have:

$$FDM_i = \begin{cases} 0 & \mu_i \le 0 \\ \mu_i & 0 < \mu_i < 1 \\ 1 & \mu_i \ge 1 \end{cases} \quad (7)$$

For each non-dominated solution k, the normalized membership function FDM^k can be defined as follows:

$$FDM^k = \left[\frac{\sum_{i=1}^{2} FDM_i^k}{\sum_{j=1}^{M} \sum_{i=1}^{2} FDM_i^j} \right] \quad (8)$$

The best compromise solution of PSS problem is the one having the maximum value of FDM^k as fuzzy decision making function. Where M is the total number of non-dominated solutions. Then all the solutions are arranged in descending order according to their membership function values which will guide the decision makers with a priority list of non-dominated solutions in view of the current operating conditions. Flowchart of MOHBMO algorithm is summarized in Fig. 4.

4. Problem formulation

In the present study, washout time constant T_W =10 sec is used for the given lead-lag structure in Fig. 2. For the optimal tuning of the PSS parameters in Fig. 4, both linear parameters (K, T_1, T_2, T_3 and T_4) and nonlinear parameters (V_{smax} and V_{smin}) are to be determined. It is worth mentioning that the PSS is designed to minimize the power system oscillations after a large disturbance so as to improve the power system stability. To increase the system damping to the electromechanical modes and find appropriate location of PSSs the objective functions for optimization is defined as follow:

$$J_1 = \sum_{j=1}^{NP} \int_0^{t_{sim}} t.\omega dt + 0.07 \times OS^2 \quad (9)$$

$$J_2 = \sum_{j=1}^{NP} \sum_{\sigma_i \geq \sigma_0} (\sigma_0 - \sigma_i)^2 + 5 \times \sum_{j=1}^{Np} \sum_{\zeta_i \leq \zeta_0} (\zeta_0 - \zeta_i)^2 \quad (10)$$

Where $\sigma_{i,j}$ and $\zeta_{i,j}$ are the real part and the damping ratio of the i^{th} eigenvalue of the j^{th} operating point. The t_{sim} is the time range of simulation and NP is the total number of operating points for which the optimization is carried out.

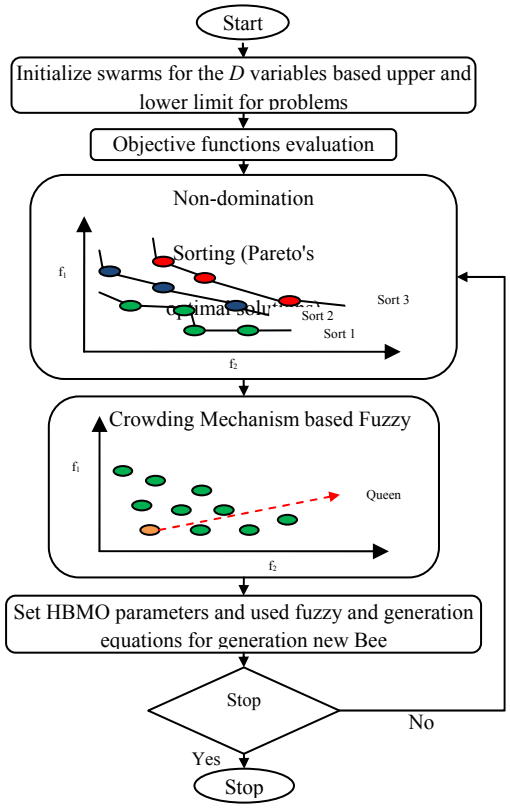

Fig. 3. Algorithm and computational flowchart of Fuzzified MOHBMO

Typical ranges of the optimized parameters are [0.1-100] for K and [0.01-5] for T_1, T_2, T_3 and T_4 and [0.05-0.5] for V_{smax} and $-V_{smin}$. The optimization of the PSS parameters is carried out by evaluating the objective cost function as given in Eqs. (9) and (10), which considers a multiple of operating conditions are given in Table 1. The operating conditions are considered for wide range of output power at different power factors. Results of the PSS parameter set values based on the objective function J_1 (by applying a three phase-to-ground fault for 100 ms at generator terminal at t=1 sec) and J_2, using the proposed MOHBMO and SPEA [15] and CPSS [2] algorithms are given in Table 2. Fig. 5 shows the minimum fitness functions evaluating process.

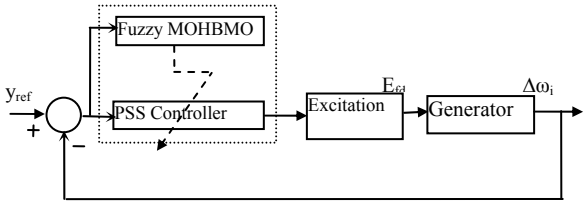

Fig .4.The FHBMO-PSS controller design

Table 1. Operation conditions

Case No.	P	Q	x_e	H
Case1 (Base case)	0.8	0.4	0.3	3.25
Case 2	0.5	0.1	0.3	3.25
Case 3	1	0.5	0.3	3.25
Case 4	0.8	0.4	0.6	3.25
Case 5	0.5	0.1	0.6	3.25
Case 6	1	0.5	0.6	3.25
Case 7	0.8	0	0.6	3.25
Case 8	1	-0.2	0.3	3.25
Case 9	0.5	-0.2	0.6	3.25
Case 10	1	0.2	0.3	0.81

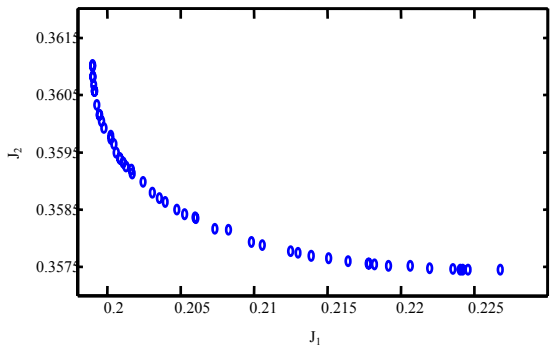

Fig. 5: Fitness convergence

Table 2. Optimal PSS parameters

Method	K_{pss}	T_1	T_2	T_3	T_4	V_{max}	$-V_{min}$
CPSS	12.5	0.073	0.028	0.073	0.028	0.1	0.1
SPEA	70.9	0.36	0.04	0.33	5.81	0.06	0.06
MOHBMO	24.06	0.761	0.451	0.135	3.923	0.082	0.076

5. Simulation results

The behavior of the proposed MOHBMO based designed PSS (MOHBMOPSS) under transient conditions is verified by applying disturbance and fault clearing sequence under different operating conditions. In comparison with the SPEA based tuned PSS (SPEAPSS) and classical PSS. The disturbances are given at t = 1 sec. System responses in the form of slip

(S_m) are plotted. The following types of disturbances have been considered.

Scenario 1: A step change of 0.1 pu in input mechanical torque.

Scenario 2: A three phase-to-ground fault for 100 ms at generator terminal.

Figure 6 shows the system response at the lagging power factor operating conditions with weak transmission system for scenario 1. It can be seen that the system with CPSS is highly oscillatory. MOHBMO and SPEA based tuned stabilizers are able to damp the oscillations reasonably well and stabilize the system at all of the operating conditions. Figure 7 depicts the responses of same operating conditions but with strong transmission system. System is more stable in this case, following any disturbance. Both PSSs improve its dynamic stability considerably and MOHBMOPSS shows its superiority over SPEAPSS and CPSS. Figure 8 refers to a three-phase to ground fault at generator terminal. Figure 9 depicts the system response in scenario 1 with inertia $H'= H/4$. It can be seen that the proposed MOHBMO based PSS has good performance in damping low frequency oscillations and stabilizes the system quickly. Moreover, it is superior to the SPEA and classical based methods tuned stabilizer.

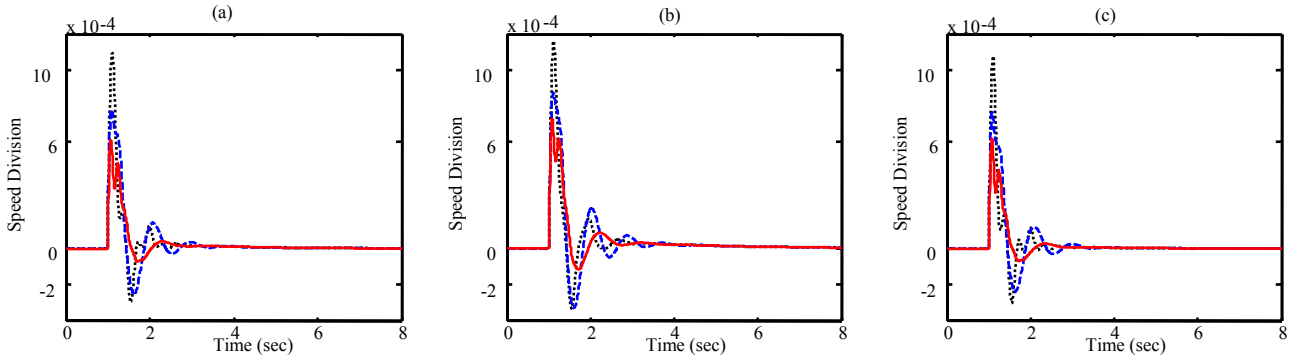

Fig. 6. ΔTm=0.1 (p.u.) under Xe=0.3; CPSS (Dotted), SPEAPSS (Dashed) and MOHBMOPSS (Solid)
a) P=0.8, Q=0.4 b) P=0.5, Q=0.1 c) P=1.0, Q=0.5

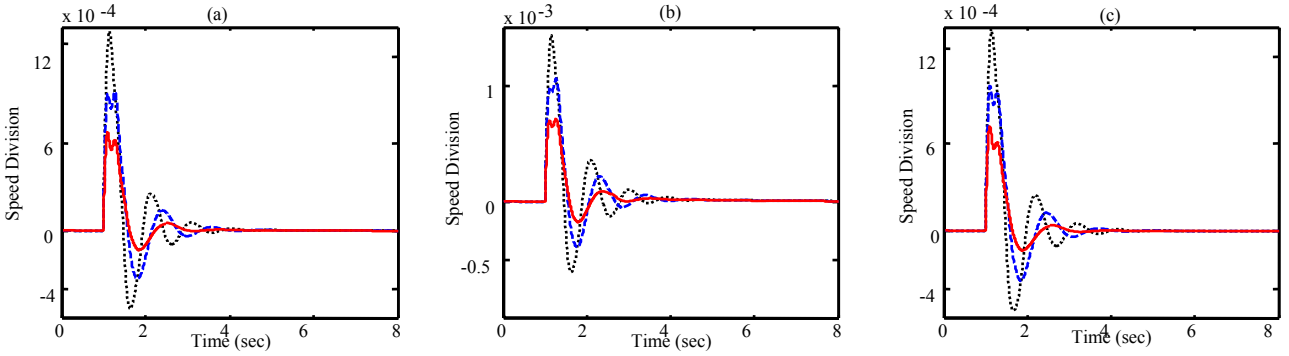

Fig. 7. ΔTm=0.1 (p.u.) under Xe=0.6; CPSS (Dotted), SPEAPSS (Dashed) and MOHBMOPSS (Solid)
a) P=0.8, Q=0.4 b) P=0.5, Q=0.1 c) P=1.0, Q=0.5

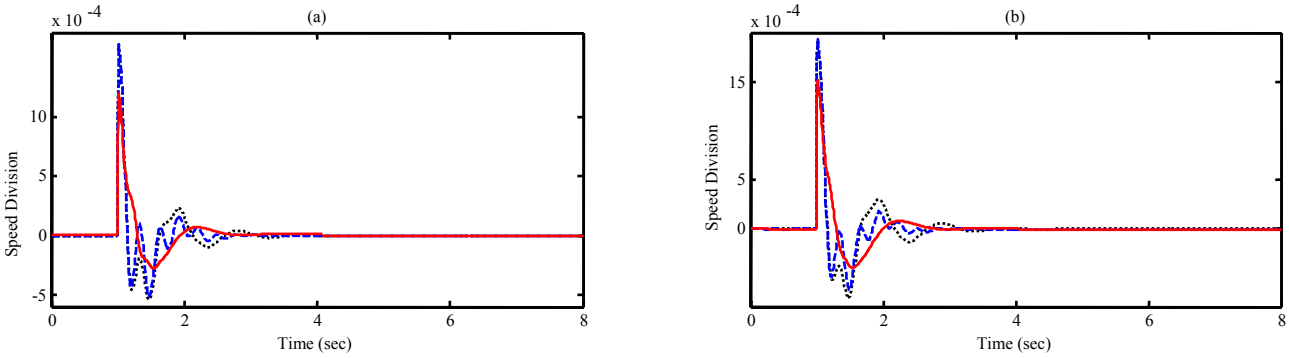

Fig. 8. 3-φ to ground fault 100 ms for Xe=0.3, CPSS (Dotted), SPEAPSS (Dashed) and MOHBMOPSS (Solid)
a) P=0.8, Q=0.4 b) P=1.0, Q=0.5

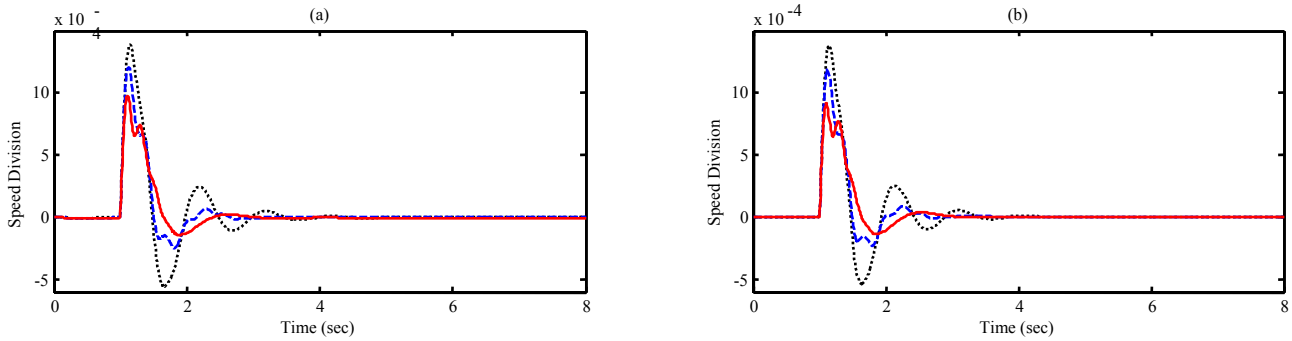

Fig. 9. ΔT_m=0.1 (p.u.) under Xe=0.6 and H'=H/4, CPSS (Dotted), SPEAPSS (Dashed) and MOHBMOPSS (Solid)
a) P=1.0, Q=0.5 b) P=0.6, Q=0.0

To demonstrate performance robustness of the proposed method, two performance indices: the Integral of the Time multiplied Absolute value of the Error (ITAE) and Figure of Demerit (FD) based on the system performance characteristics are defined as [17]:

$$FD = 10 \times [(500 \times OS)^2 + (8000 \times US)^2 + 0.01 \times T_s^2] \quad (10)$$

$$ITAE = 1000 \times \int_0^8 t \,|\Delta\omega|dt \quad (11)$$

Where, Overshoot (OS), Undershoot (US) and settling time of rotor angle deviation of machine is considered for evaluation of the FD. It is worth mentioning that the lower the value of these indices is, the better the system response in terms of time-domain characteristics. Numerical results of performance robustness for all cases as given in Table 1 for scenario 1 are listed in Table 3, respectively.

Table 3. Performance indices for scenario 1

Case No	MOHBMO		SPEA		Classic	
	ITAE	FD	ITAE	FD	ITAE	FD
1	0.5022	0.4757	0.6775	0.9942	0.5632	1.4729
2	0.8381	0.5644	1.0422	1.4799	0.9042	1.7696
3	0.3780	0.4722	0.5544	0.9281	0.4465	1.4774
4	0.7822	1.1298	1.4842	3.7696	1.1311	3.4747
5	1.1247	1.4463	1.8102	4.5268	1.4959	4.2209
6	0.7777	1.2171	1.5885	4.0670	1.1631	3.6312
7	0.7822	1.1298	1.4842	3.7696	1.1310	3.4747
8	0.3780	0.4722	0.5544	0.9281	0.4465	1.4774
9	1.1247	1.4463	1.8102	4.5268	1.4959	4.2209
10	0.3780	0.4722	0.5544	0.9281	0.4465	1.4774

It can be seen that the values of these system performance characteristics with the proposed MOHBMO based tuned PSSs are much smaller compared to that SPEA and classical based designed PSS. This demonstrates that the overshoot, undershoot settling time and speed deviations of machine is greatly reduced by applying the proposed MOHBMO based tuned PSS.

6. Conclusions

An attempt has been made in this paper to develop a simple but robust PSS with particular emphasis on achieving a minimum closed loop performance over a wide range of operating and system conditions. For dealing with different solutions in multi-objective optimization problem, Pareto dominance concept is used to generate and sort the dominated and non-dominated solutions. The minimum performance requirements of the stabilizer have been decided and this performance has been obtained using Fuzzified multi objective honey bee mating optimization. The nonlinear simulation results under wide range of operating conditions show the superiority and robustness of the Fuzzified multi objective HBMO method for the PSS design and their ability to provide efficient damping of low frequency oscillations in comparison with SPEA and classical methods. The effectiveness of the proposed method is tested on SMIB power system for a wide range of load demands and disturbances under different operating conditions. The nonlinear time simulation results confirm that the proposed MOHBMO based tuned PSS can work effectively over a wide range of loading conditions and is superior to the SPEA based tuned PSS and CPSS.

Appendix: System data

Generator: R_a=0, x_d= 2.0, x_q = 1.91, x'_d=0.244, x'_q=0.244 , f = 50 Hz, T'_{do}=4.18, T'_{qo}=0.75, H=3.25,
Transmission line: R= 0, x_e = 0.3.
Exciter: K_A=50, T_A=0.05, E_{fdmax}=7.0, E_{fdmin}=-7.0.

References

[1] H. Shayeghi, A. Safari and H.A. Shayanfar, "PSS and TCSC damping controller coordinated design using PSO in multi-machine power system", Energy Conversion and Management, vol. 51, pp. 2930-2937, 2010.

[2] K. R. Padiyar, "Power System Dynamics, Stability and Control" Second Ed., BS Publications, Hyderabad, India, 2008. 2008.

[3] D.K. Chaturvedi and O.P. Malik, "Experimental studies of a generalized neuron based adaptive power system stabilizer", Applied Soft Computing, vol. 11, pp. 149-155, 2007.

[4] J. Fraile-Ardanuy and P.J. Zufiria, "Design and comparison of adaptive power system stabilizers based on neural fuzzy networks and genetic algorithms", Neurocomputing , vol. 70, pp. 2902-2912, 2007.

[5] R. Segal, A. Sharma and M.L. Kothari, "A self-tuning power system stabilizer based on artificial neural network", Electrical Power and Energy Systems, vol. 26, pp. 423-30, 2004.

[6] H. Shayeghi and A. Ghasemi, Multiple PSS Design Using an Improved Honey Bee Mating Optimization Algorithm to Enhance Low Frequency Oscillations, International Review of Electrical Engineering, Vol. 6, pp. 3122-3133, 2011.

[7] H. Shayeghi, H.A. Shayanfar, S. Jalilzadeh and A. Safari, "Multi-machine power system stabilizers design using chaotic optimization algorithm", Energy Conversion and Management, vol. 51, pp. 1572-1580, 2010.

[8] H. Shayeghi, H.A. Shayanfar and A. Ghasemi, "A robust ABC based PSS design for a SMIB power system" International Journal on Technical and Physical Problems of Engineering vol. 3, pp. 86-92, 2011.

[9] H. Shayeghi, H.A. Shayanfar, A. Safari, R. Aghmasheh, "A robust PSSs design using PSO in a multimachine environment", Energy Conversion and Management, vol. 51, pp. 696-702, 2010.

[10] H. Shayeghi, and A. Ghasemi, "Improved time variant PSO based design of multiple power system stabilizer", International Review of Electrical Engineering, vol. 22, pp. 2490-2501, 2011.

[11] H. Shayeghi, H.A. Shayanfar and A. Ghasemi, "PID type stabilizer design for multi machine power system using IPSO procedure, Computer Science and Engineering, vol. 1, pp. 36-42, 2011.

[12] H. Shayeghi, H. A. Shayanfar, A. Akbarimajd and A. Ghasemi, PSS design for a single-machine power system using honey bee mating optimization", Proc. of the International Conference on Artificial Intelligence, Las Vegas, USA, pp. 210-216, 2011.

[13] H. Shayeghi, H. A. Shayanfar, A. Jalili and A. Ghasemi, LFC design using HBMO technique in interconnected power system, International Journal on Technical and Physical Problems of Engineering vol. 2, pp. 41-48, 2010.

[14] K. Deb, A. Pratap, S. Agarwal, T. Meyarivan, A Fast and elitist multi-objective genetic algorithm: NSGA-II, IEEE Trans. On Evolutionary Computation, vol. 6, no. 2, 2002, pp. 182-197.

[15] Y. Yassami, A. Darabi and SMR Rafier, "Power system stabilizer design using strength Pareto multi objective optimization approach", Electric Power Systems Research, vol. 80, pp. 839- 846, 2010.

[16] Y.L. Abdel-Magid and M.A. Abido, "Optimal multiobjective design of robust power system stabilizers using genetic algorithms", IEEE Trans. on Power Systems, vol. 18, No. 3, pp. 1125 -1132, 2003.

[17] L.H. Wua, Y.N. Wanga, X.F. Yuan, S.W. Zhou," Environmental/economic power dispatch problem using multiobjective differential evolution algorithm", Electric Power Systems Research, vol. 80, pp. 1171–1181, 2010.

Physical Activity Classification Using TSK-type Neuro-Fuzzy Classifier with GK Clustering

Keun-Chang Kwak[1], **Myung-Won Lee**[2]
[1]Department of Control, Instrumentation, and Robotic Engineering, Chosun University, Gwangju, Korea
[2]Department of Control and Instrumentation Engineering, Chosun University, Gwangju, Korea

Abstract - *We propose TSK (Takagi-Sugeno-Kang)-type Adaptive Neuro-Fuzzy Classifier (ANFC) for physical activity classification based on triaxial accelerometer and biomedical signal information. For this purpose, we design intelligent classifier with the ability to incorporate human knowledge and to adapt the knowledge base with the use of Gustafson-Kessel (GK) fuzzy clustering. We also obtain movement information and heart rate from the developed patch-type sensor module. This small sensor is patched onto the user's chest to obtain physiological data. The experiments consist of normal walking, brisk walking, slowest running, and jogging as physical activity classification in outdoor environments. The experimental results revealed that the presented intelligent classifier showed good performance in comparison to the previous studies.*

Keywords: Physical activity classification, neuro-fuzzy classifier, GK fuzzy clustering, patch-type sensor module

1 Introduction

Conventional approaches of pattern classification involve clustering training data and organizing clusters to given categories. The complexity and limitations of previous scheme are largely due to the lacking of an effective way of defining the boundaries among clusters. This problem becomes more intractable when the number of features used for classification increases. In contrast to conventional clustering method, neuro-fuzzy classification assumes the boundary between two neighboring classes as a continuous, overlapping area within an object has partial membership degree in each class [1]. Furthermore, clustering techniques are used in conjunction with radial basis function classifier, fuzzy classifier, and neuro-fuzzy classifier primary to determine initial locations for radial basis function of receptive field or fuzzy if-then rules [2-4]. On the other hand, the accurate measurement of energy expenditure from physical activity is a challenging problem that is important to exercise scientists and clinicians. For this, we recently developed a patch-type sensor module to solve these problems [5]. The main characteristics of this sensor module are small size, wireless operation, low cost, light weight, and comfort for long-term wear, as well as integrating all required measurement parameters into a single sensor. We shall obtain movement information and biomedical signals from this sensor patched onto the user's chest and only perform activity classification.

Therefore, this paper is concerned with the intelligent Adaptive Neuro-Fuzzy Classifier (ANFC) with the use of the developed patch-type sensor module from a given input-output data pairs such as movement information and heart rate. The Takagi-Sugeno-Kang (TSK)-type ANFC is designed by Gustafson-Kessel (GK) fuzzy clustering with fuzzy covariance matrix. This clustering technique is based on Mahalanobis distance to consider the distribution of input variables by incorporating the covariance of data points [6]. Furthermore, TSK type is by far the most popular candidate for fuzzy classifier and effective to develop a systematic approach [7]. Thus, the TSK-ANFC can possess the intensive classification capability together with meaningful fuzzy if-then rules. The experiments are performed on normal walking, brisk walking, slowest running, and jogging in outdoor environments. The experiments results revealed that the proposed intelligent classifier outperformed in the previous methods. The material of this paper is organized in following fashion. In section 2, we describe the proposed neuro-fuzzy classifier based on GK fuzzy clustering. In section 3, we perform the experimental setup and performance comparison. Finally the conclusions and comments are given in section 4.

2 Architecture of TSK-ANFC

In this section, we describe the architecture and learning rules of the TSK-ANFC. Let us now consider the TSK-ANFC with first-order TSK fuzzy rules. It also involves two phases including structure identification and parameter identification. The former is related to determining the number of fuzzy if-then rules and a proper partition of the input space. The latter is concerned with the learning of model parameters such as membership functions, linear coefficients, and so on. Fig. 1 shows the architecture of the proposed TSK-ANFC. As shown in Fig. 1, this network is composed of five layers similar to the well-known ANFIS (Adaptive Neuro-Fuzzy Inference System) introduced by Jang [1]. While ANFIS often raises the "curse of dimensionality" problem that the number of fuzzy rules exponentially increases due to the grid partitioning of the input space, the TSK-ANFC can effectively solve such a problem due to the flexible scatter partitioning of the GK fuzzy clustering approach.

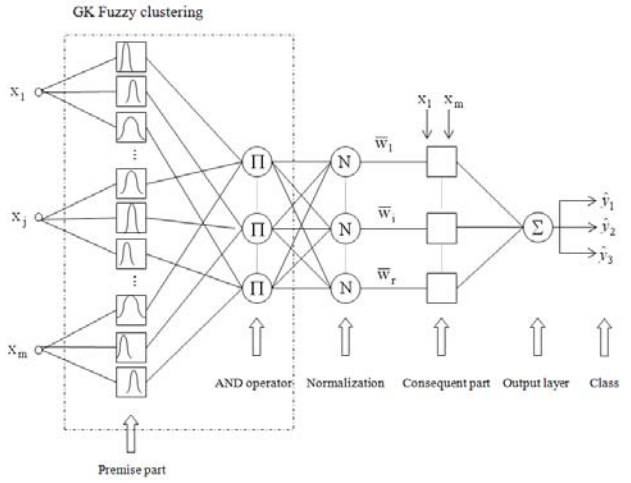

Fig. 1 Architecture of a TSK-ANFC

For simplicity, we suppose that the TSK-ANFC under consideration has m input variables $x_j, j = 1,2,\ldots,m$. For a first-order TSK fuzzy type, a typical fuzzy if-then rule has the following form [7]

$$R^i : If\ x_1\ is\ A_1^i\ and\ x_2\ is\ A_2^i, \cdots, x_m\ is\ A_m^i,$$
$$then\ y^i = a_o^i + a_1^i x_1 + a_2^i x_2 + \cdots + a_m^i x_m \quad (1)$$

where R^i, i=1,2,…,r, denotes the ith fuzzy rule. A_j^i is a linguistic label associated with the jth input variable in the premise of the ith rule and $\{a_o^i, a_1^i, \ldots, a_m^i\}$ are consequent parameters. Every node of the first layer consists of linguistic labels build by a parameterized membership function. Here, we use a Gaussian membership function specified by two parameters. A Gaussian membership function is determined completely the center and width of the membership function, respectively. Each of the cluster centers obtained by the GK fuzzy clustering method represents a prototype that exhibits significant characteristics of the target system under consideration. For further details on GK fuzzy clustering refer to [6]. Here, the membership's width, representing the initial standard deviation for each cluster center in the jth input variable, is computed by statistical method. Every node in the second layer represents the firing strength of a rule by using the product of all of the incoming signals as follows

$$w_i = \prod_{j=1}^{m} A_j^i(x_j)\ ,\ i = 1,2,\ldots,r,\ j = 1,2,\ldots,m \quad (2)$$

Every node in the third layer calculates the ratio of the ith rule's firing strength to the sum of all rule's firing strengths. Every node in the fourth layer computes the product between the normalized firing strength and the constant of the consequent part. The single node in the final layer computes the overall inference class as the summation of all incoming signals as follows

$$\hat{y} = \sum_{i=1}^{r} \overline{w}_i y^i = \frac{\sum_{i=1}^{r} w_i (a_0^i + a_1^i x_1 + \cdots + a_m^i x_m)}{\sum_{i=1}^{r} w_i} \quad (3)$$

where $\overline{w}_i$ is a normalized firing strength of the ith rule and $\hat{y}$ is the classified output of the model. $\hat{y}$ is represented as class number by class bound value. Here, the learning scheme of the proposed TSK-ANFC is performed by the hybrid learning scheme using Back-Propagation (BP) and Least Square Estimator (LSE).

3 Experimental results

The patch-type sensor module is a wireless, small size and light weight sensor that can be patched on the chest of participants to obtain physiological data. The sensor board shown in Fig. 2 consists of a 3-axis accelerometer and three ECG electrodes to detect movement information (MI) and heart rate (HR), respectively [5].

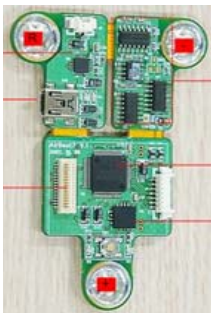

Fig. 2 Patch-type sensor module

The experiments are performed under outdoor environments. In order to obtain heart rate, we used three electrodes for ECG measurement on the chest. These electrodes without gel are mounted on a conductive adhesive patch. The ECG analog circuitry was specifically designed for effective motion artifact rejection during exercise. On the other hand, we used three-axis accelerometer (MMA7260Q) was used to detect acceleration changes during exercise. This device is a cheap capacitive micro-machined accelerometer featuring good sensitivity, low power consumption, and very small size. We used 206 samples with 4 classes. The input consists of two variables. The variables were the movement information (MI) and heart rate (HR). The output variable to be classified is physical activities. In order to evaluate the resultant model, we divided the data sets into training (odd number) and test data (even number) sets. Here, we selected 103 training sets for model construction, while the other checking data set was used for model validation. We performed the experiments as the number of cluster increases from 3 to 6. Fig. 3 shows data distribution of movement information obtained from triaxial

accelerometer sensor regarding each physical activity. As shown in Fig. 3, the movement information of brisk walking is similar to that of slowest running. Fig. 4 shows the classification performance (70.37%, 5 rules) of the proposed TSK-ANFC regarding only movement information. Fig. 5 shows data distribution of heart rate obtained from ECG sensor regarding each physical activity. As shown in Fig. 5, the heart rate has good characteristics in discrimination of each physical activity. Fig. 5 shows the classification performance (98.06%, 5 rules) of the proposed TSK-ANFC regarding only heart rate. Fig. 7 visualizes the distribution of two input variables obtained from normal walking, brisk walking, slowest running, and jogging in outdoor environments. Fig. 8 shows the classification performance representing 99.03% when the number of rule is 5. The clusters estimated by GK fuzzy clustering are shown in Fig. 9. Table 1 lists the comparison of classification performance. As listed in Table 1, the proposed TSK-ANFC showed good performance in comparison with the previous work.

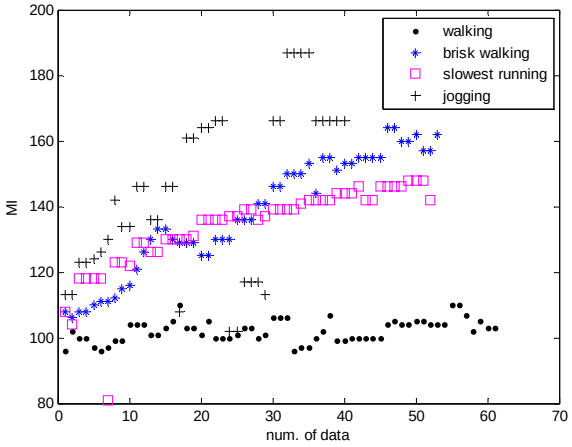

Fig. 3 Data distribution of movement information (walking, brisk walking, slowest running, jogging)

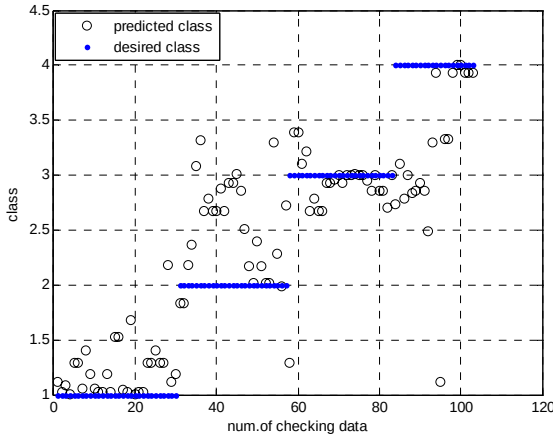

Fig. 4 Classification performance of the proposed classifier regarding only movement information

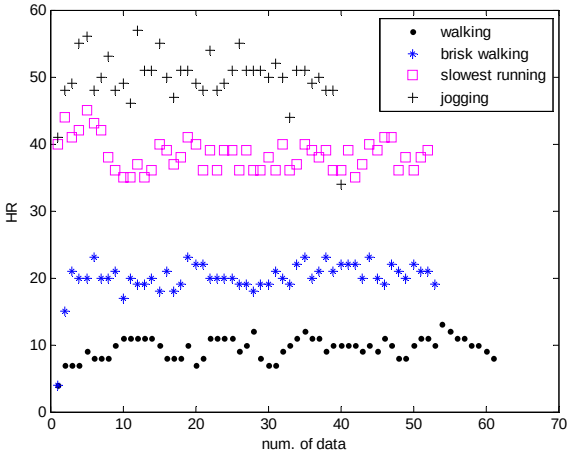

Fig. 5 Data distribution of heat rate

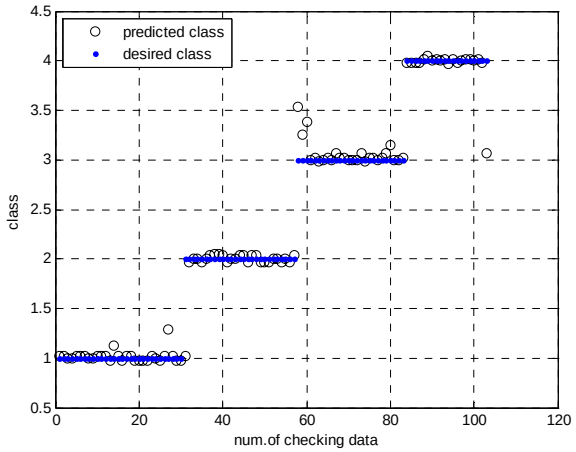

Fig. 6 Classification performance of the proposed classifier regarding only heat rate

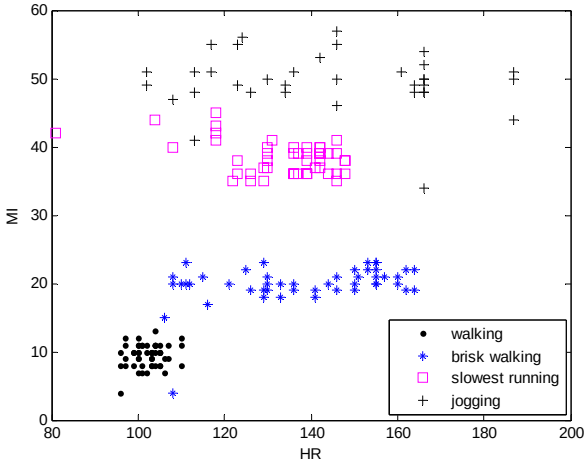

Fig. 7 Data distribution of movement information and heat rate

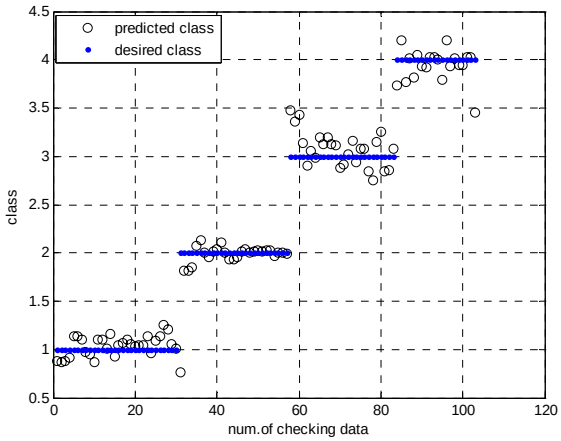

Fig. 8 Classification performance of the proposed classifier regarding movement index and heat rate

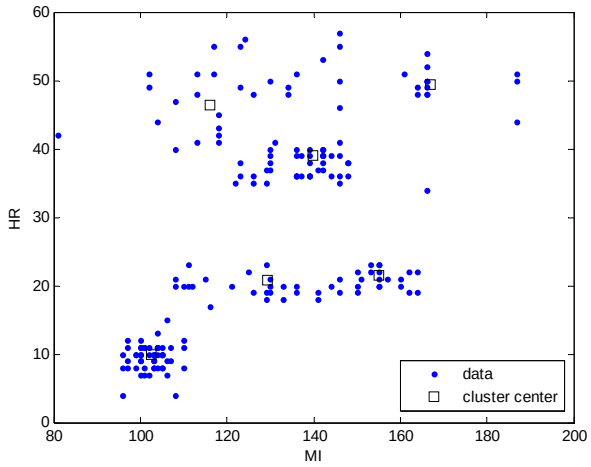

Fig. 9 Estimation of cluster centers by GK fuzzy clustering

Table 1 Comparison of classification performance for checking data

	No. rule	Classification rate (%)
NFC [1]	6	79.61
The proposed TSK-ANFC	3	98.06
	4	98.06
	5	99.03
	6	99.03

4 Conclusions

We developed the ANFC with a TSK fuzzy type based on by GK fuzzy clustering technique for physical activity classification based on triaxial accelerometer and biomedical signal information. The experiments are performed on normal walking, brisk walking, slowest running, and jogging in outdoor environments. The experiments results revealed that the proposed intelligent classifier showed good performance in comparison with the previous work. In the future, we shall use three-axis based action data well as Vicon physical action data for activity recognition.

5 Acknowledgements

This work was supported by the Ministry of Knowledge Economy (MKE), Rep. of Korea, under the IT R&D program supervised by the KOREA Evaluation Institute of Industrial Technology (KEIT) (10041059)

6 References

[1] J. S. R. Jang, "Input selection for ANFIS learning", *Proc. IEEE Int. Conference Fuzzy System*, pp. 1493-1499, New Orleans, 1996.

[2] J. Abonyi, R. Babuska, and F. Szeifert, "Modified Gath-Geva fuzzy clustering for identification of Takagi-Sugeno fuzzy models", *IEEE Trans. on Systems, Man, and Cybernetics-Part B*, Vol.32, No.5, pp. 612-621, 2002.

[3] W. Pedrycz, "Conditional fuzzy clustering in the design of radial basis function neural networks", *IEEE Trans. on Neural Networks*, Vol. 9, No. 4, pp.745-757, 1999.

[4] K. C. Kwak, M. G. Chun, J. W. Ryu, and T. H. Han, "FCM-based adaptive fuzzy inference system for coagulant dosing process in a water purification plant", *International Journal of Knowledge-Based Intelligent Engineering Systems*, Vol. 4, No. 4, pp.230-236, 2000.

[5] M. Li and Y. T. Kim, "Development of patch-type sensor module for wireless monitoring of heart rate and movement index," *Sensors and Actuators A: Physical*, vol. 173, pp.277-283, 2012.

[6] L. Teslic, B. Hartmann, O. Nelles, I. Skrjanc, "Nonlinear system identification by Gustafson-Kessel fuzzy clustering and supervised local model network learning for the drug absorption spectra process", *IEEE Trans. on Neural Networks*, Vol. 22, No. 12, pp.1941-1951, 2011.

[7] J. S. R. Jang, C. T. Sun, and E. Mizutani, *Neuro-Fuzzy and Soft Computing: A Computational Approach to Learning and Machine Intelligence*, Prentice Hall, 1997.

SESSION

KNOWLEDGE DISCOVERY AND LEARNING

Chair(s)

Dr. Raymond A. Liuzzi
Dr. Peter M. LaMonica
Dr. Todd Waskiewicz

Intelligent Agents for Mobile Network Coverage Analysis

Robert M. McGraw, Richard A. MacDonald
RAM Laboratories, Inc., San Diego, CA, USA

Abstract - *Techniques and tools are needed that allow Commanders and Analysts to intelligently plan and re-assess mobile networks that are supporting missions and courses of action in the battlespace and emergency response settings. Many techniques, simulations, and tools are available to model, represent, and analyze the RF environment, however they are typically used for a priori planning or after action analysis. Unplanned changes to the RF environment such as environmental variations, position, jamming, and terrain effects may result in coverage shortfalls that hinder mission performance. As such, there exists a need to provide visual analysis of network coverage to Warfighters executing the mission in real-time.*

This paper details an ongoing research effort that seeks through provide real-time visualization of mobile network coverage through the orchestration of a variety of data sources, simulations, network analysis techniques and cognitive models. This variety of applications is assembled into a workflow through an intelligent agent framework and used to assess and display the expected coverage for the mission under way on a GoogleEarth map, resulting in mission participants being able to "see" where the coverage begins and ends for their device.

Keywords: intelligent agents, MANETs, Signal Planning, Coverage Analysis, Bayesian Analysis

1 Introduction

This paper discusses an effort to provide the visualization of network coverage through the use of an intelligent agent framework known as the Course of Action (COA) Analysis with Radio-time Effects Toolbox (CARET). The CARET Agent Framework makes use of distributed agents that gather, process, and inject real-time data into embedded simulations for use in evaluating COAs amidst real-time RF effects. This framework provides capabilities that assist signal planners and Warfighters / mission participants in visualizing changing mobile coverage presented by uncertainties associated with forces-on-the-move. While this paper provides a discussion on the Agent Framework design, this has been provided for completeness, as much of that work has been presented elsewhere [1][2][3][4][5]. This particular paper focuses on the techniques employed for our coverage analysis that is subsequently relayed for viewing via the GoogleEarth overlay.

2 Problem Being Solved

This research addresses the issue of mobile network coverage shortfalls that can result from some type of deviation from an initial signal plan. This deviation may be a result of participants being out of position, environmental or terrain effects, adversary jamming, equipment damage or health issues, and other criteria. An example illustrating this problem is shown in Figures 1 and 2. In Figure 1, a signal planner has laid out his/her plan for the mission that supports blue force movement in accomplishing their mission. The blue arrows indicate participant movement, while the circles indicate the coverage areas for those radios. Figure 1 also indicates adversary or target positions built into the map overlays and adversary jamming or interference sources. This analysis and planning is typically performed a priori. Figure 2 details some of the unplanned activities that may affect the network support for the mission, participants may stray from their coverage areas or jamming or interference sources may move. Additionally, weather or terrain may also affect the coverage.

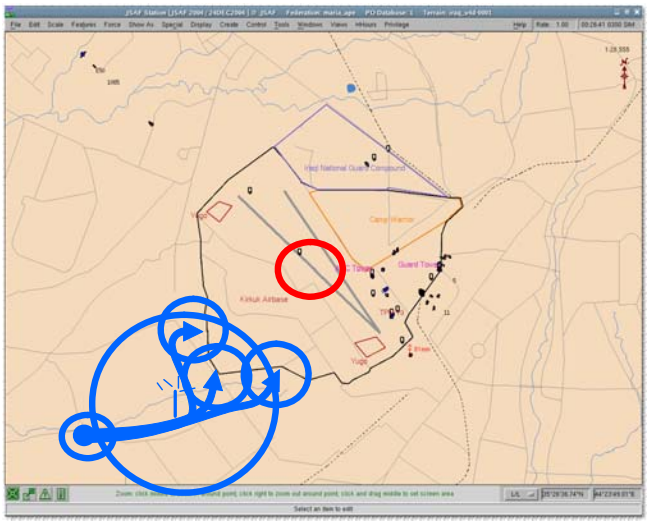

Figure 1: Network Propagation and Connectivity for a Given Mission Plan

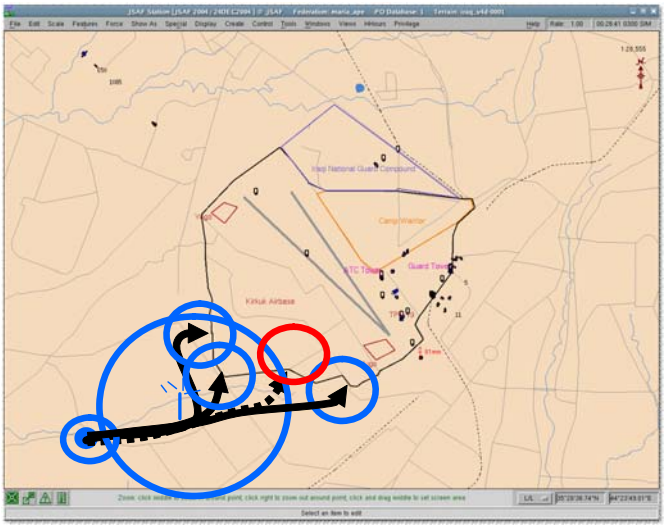

Figure 2: Plan Deviation Result in Coverage Shortfalls

3 CARET Agent Framework

The CARET Agent Framework design serves three main purposes: (1) enable the development of highly capable applications that are able to meet the demands of current and future requirements, (2) provide a development platform that is highly flexible and easily extensible, and (3) ensure that applications developed from the framework are highly interoperable with other applications, systems, and platforms, particularly legacy software and systems.

3.1 Basic Components

The first principle was the need to build applications from composable components, such as web services and/or intelligent agents. To implement our selection of software agents as a base component type, we have selected the Java Agent Development Environment (JADE) [6]. JADE is a software framework to develop agent-based applications in compliance with the FIPA specifications for interoperable intelligent multi-agent systems [7].

3.2 Handling Data

The second core principle was the use of abstract data interfaces wherever possible in order to simplify the burden on application developers. Due to this principle, our approach adopted use of Service Data Objects (SDOs), whose specification [8] prescribes a way for all compliant data exchanges to take place using a common representation for all data types. Figure 3 shows a UML diagram of the basic SDO representation for data.

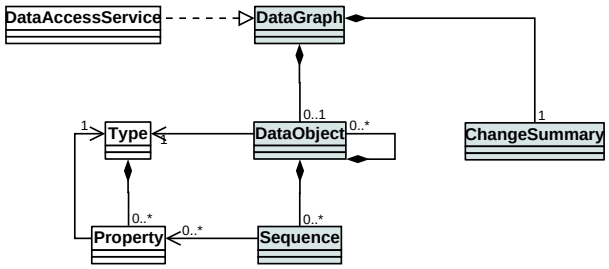

Figure 3: Service Data Object (SDO) Representation

When data needs to be exchanged between application components, sets of Data Objects are assembled into a Data Graph and sent from a DataAccessService to its final destination. Data Graphs can also keep track of all changes or modifications made to the graph over time in a Change Summary.

The choice of SDO for data interfaces reduces the impact on developers and integrators that are due to the manner in which data may be accessed. SDO translators can be written for each particular legacy data source and re-used for each instantiation of that source.

Additionally, our solution adopted the use Web Services and protocols, such as SOAP [9] to interoperate with agents or services from external systems.

3.3 Managing Workflows

The third core principle from was support for workflows, particularly those following the Observation-Interpretation-Action cycle of programmed system responses to dynamic events. Here again we are fortunate that the choice of JADE as the agent development framework provides us with a good starting point to build up from. There exists a complementary product to JADE that is called the Workflows and Agents Development Environment (WADE). WADE is built on top of JADE, as shown in Figure 4.

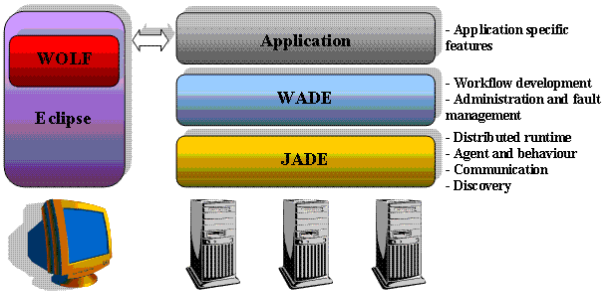

Figure 4: WADE Overview

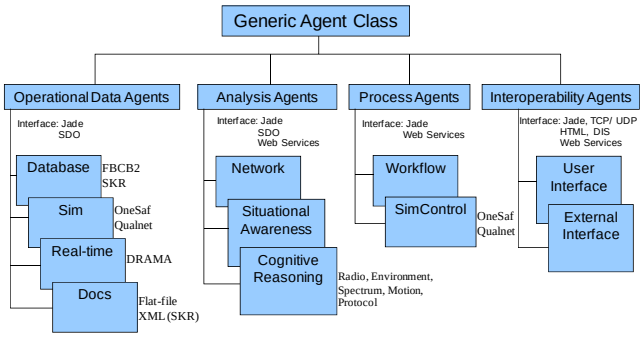

Figure 5: Agent Types for the CARET Agent Framework

3.4 Agent Classes

Based on JADE concepts, data handling approaches, agent interoperability mechanisms, and workflow orchestration concepts discussed above, this effort developed a basic agent structure from which all CARET agents could be derived. All CARET agents are derived from a Generic Agent Class as shown in Figure 5. This generic agent class provides a basic JADE agent structure with inherent data handling and processing features. The CARET Generic Agent class was used to develop four types of agents that were further derived to provide for the different agent capabilities required by the CARET Agent Framework. These agent types include Operational Data Agents (ODAs), Analysis Agents (AAs), Process Agents (PAs), and Interoperability Agents (IAs) [3][4].

Operational Data Agents are responsible for capturing or extracting data for a variety of sources in the CARET environment. Such sources may be SQL databases, real-time data sources, documents such as flat-files or XML schemas, or simulation environments. Process Agents are used to implement some type of process over time such as triggering or calibrating multiple simulation runs or managing the flow of data between agents. Analysis Agents are responsible for performing some type of analysis of data in the CARET environment, including performing the analysis of simulation results, analysis of intelligence, surveillance, or reconnaissance sensor data from the operational world, predictive analysis of trends with regard to missions or network configurations supporting those missions, and analyses of particular alternative or "what-if" scenarios in addressing a particular mission objective. AAs possess JADE, SDO and web service interfaces. Interoperability Agents (IAs) are responsible for interoperating with external systems or user interfaces and possess JADE, HTML, SDO, Web Service, TCP / UDP and DIS interfaces.

4 CARET Agent Framework Implementation

As mentioned, our implementation of the CARET Agent Framework is based on JADE. JADE uses topics so other agents can subscribe, where only one agent can be the publisher. While the topics are maintained by the main JADE container, but conceptually the flow of data between the different components is depicted in Figure 6 [5]. Ovals depict agent instances and data flows are color-coded by topic as follows:

- DISDATA
- CONFIG
- ENTITYLOC
- EXPERIMENT-SETUP
- EXPERIMENT-RESULTS

The dashed lines represent an external interaction from the JADE system

The CARET implementation uses seven intelligent agents, derived from the agent types presented in Figure 5. An overview of these agents is discussed as follows:

- DISBridgeAgent: This is an Interoperability Agent-External Systems (IA-ES) agent that processes Distributed Interactive Simulation (DIS) PDUs outputted by OneSAF Objective System [10]. OneSAF is use to simulate mission activities. For a operational use, this simulator is replaced by GPS sensors.

- IdentityAgent: This Interoperability Agent-User Interface (IA-UI) allows participants and signal planners to select, via a User Interface, the participants that he/she is interested in.

- EntityServerAgent: This Analysis Agent-Situational Awareness (AA-SA) is configured by IA-UIs and filters sensor data that pertains to entities of interest.

- AnalysisControlAgent: This Interoperability Agent-User Interface (IA-UI) agent interacts with a graphical user interface that allows the user to select parameters for the analysis.

- RemoteProcessAgent: This Process Agent-SimControl (PA-SC) agent is used to control the network analysis performed.

- SocketClientAgent: Interoperability Agent-External Systems (IA-ES) is used to provide entity information to the GoogleEarth application..

- RemoteCoverageAgent: This IA-ES agent is use to provide coverage overlay information to the GoogleEarth application

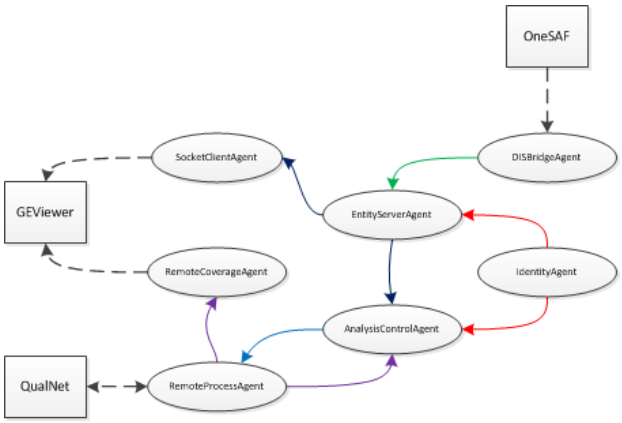

Figure 6: CARET Agent Framework Implementation

5 Statistical and Cognitive Modeling

Two key capabilities that CARET provides signal planners are a capability to analyze and diagnose issues related to network performance as a mission proceeds, and a capability to analyze and diagnose issues related to network performance as a mission is projected forward from a given point in time (using simulation) in order to identify potential unintended outcomes and assess various mission alternatives.

To provide such a capability to signal planners, CARET utilizes PA-SC agents. The PA-SC agent works by controlling the network simulation to perform an experiment around the selected participants. The PA-SC agent conducts these experiments to generate simulated network data based on the expected position of the participant in question. This data is then assembled as a coverage overlay to enable the participant or signal planner to visual the coverage patterns, or is used as input to cognitive reasoning approaches that compare the simulated data with actual network metrics to "diagnose" the cause of potential shortfalls using sets of rules, such as a fuzzy rule base, statistical analysis, and/or through the use of inference techniques.

Initial designs for these agents focused on the use of rule bases and statistical approaches as a way of identifying potential problems for the network in comparison to the expected performance. The statistical metrics were generated through the use of multiple simulations of the support network, with tweaks added to various parameters to gain an understanding of the state space amidst a variety of problems including radio degradation, platform position, and environmental effects. The rule sets were then used to diagnose the cause of specific shortfalls based on observed network behavior.

5.1 Statistical Model Development – Radial Coverage

For the first cognitive model, a statistical modeling approach was used. This modeling approach started with the idealized network topology, emitters, and receivers supporting a mission and simulated the expected coverage and QoS for that topology. Next, the statistical approach involved adjusting each of the radios (transmitters and receivers) involved in the scenario/topology with regard to their location and a variety of additional parameters while running QualNet simulations to generate an expected coverage profile for different parametric off-shoots of the mission. It should be noted that in generating the baseline coverage profiles, the prototype uses existing agent types that we developed for CARET. These agents were used because they facilitated information transfer and processing across CARET applications and alleviated the need for manual simulation execution and results extraction. To generate this coverage map, we implemented a PA-SC for Radial Coverage PA-SC RC, which runs experiments called the coverage-test. The PA-SC RC works by passing an input message defining the coverage experiment that specifies parameters required for the coverage test as follows:

1. Parameter to be varied: FREQUENCY or POWER
2. Minimum, maximum, and increment for the parameter
3. Id and latitude-longitude location of the subject-node
4. Minimum and maximum range (min_r, max_r) for the coverage test
5. Number of N concentric circles to generate
6. Number M of test nodes to place on the inner-most circle

This information is entered via the Analysis Control Agent (an IA-UI), shown in Figure 7, which subsequently passes the simulation control data to the PA-SC RC.

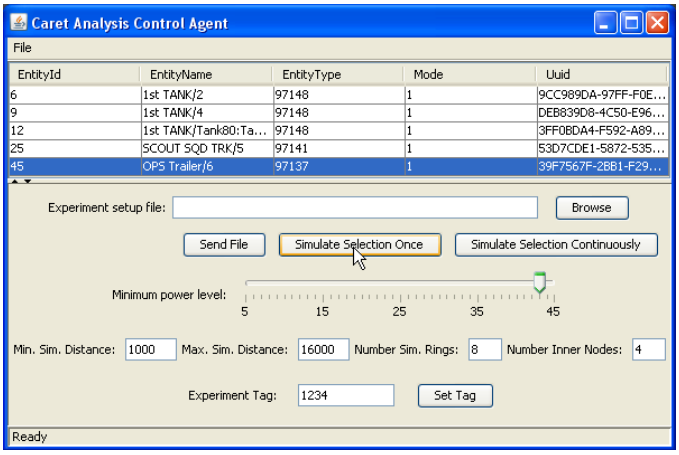

Figure 7: Agent Control using CARET Analysis Agent – Control Agent

As shown in Figure 8, the PA-SC RC creates network nodes (probe-nodes) and places them at evenly spaced

intervals on each of N concentric circles, centered at the subject-node. The radii of the N circles start at min_r and increment at even intervals to max_r. The inner-most circle is given M nodes, and the number of nodes placed in each successively larger circle is the largest integer less than M (r / min_r). This ensures that the arc-length between nodes is roughly the same from one circle to the next.

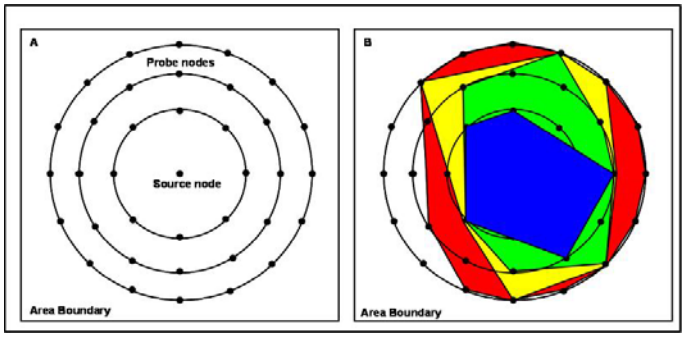

Figure 8: Node Locations for the Radial Coverage Test, N=3, M=8

The PA-SC RC runs QualNet once for each value of the target-parameter, and for each run, the PA-SC RC must generate a scenario-file for QualNet. The QualNet scenario-file has parameters specifying:

- The type of radios used
- Specifications of the communication protocol to be used
- Propagation model
- Specification of frequency
- Location of the DEM files for the area terrain
- QualNet "app" filename specifying transmit parameters

Each time the PA-SC RC runs QualNet, it modifies the scenario-file with the current value of this parameter. After the run completes, QualNet outputs a stat-file containing numerous statistics. When all runs have completed, the PA-SC RC filters all the stats files to determine the number of packets were transmitted to each probe-node and the number that it actually received. The PA-SC RC places this information into a results-file that can be read by the client application.

The result of this experiment is a map that details expected network coverage and QoS for the mission. When actual or simulated network coverage data is available, it is compared to this map to determine what types of network shortfalls may be occurring in a statistical fashion. It should be noted that the results of the PA-SC RC can be viewed by the analyst through graphical analysis. This process is described below.

5.2 Graphical Analysis

In order to gain an understanding of the statistical coverage for the network/mission at hand, the coverage-test results can be passed to a Google Earth viewer in order to gain an appreciation for the coverage bands. In this case, the coverage results are forwarded from the AA-CR RC to the IA-UI Google Earth (GE) viewer [11]. The GE viewer performs following formats the data for display as follows:

- The percentages are classified via thresholds the results into performance categories to be represented by color codes: EXCELLENT (blue), GOOD (green), FAIR (yellow), POOR (red), and none.

- Using the EXCELLENT performance threshold (EXCELLENT), it starts at the innermost probe-nodes and works outwards, forming a coverage-set for by taking the convex hull of the region containing the probe-points whose reception meet or exceed the threshold.

- This reception region is colored blue

- Still working outward from the center, the algorithm determines the convex hull of the region containing probe-nodes that meet or exceed the GOOD threshold. This will contain the previous region, so the difference between the two is colored green.

- The procedure continues likewise to determine the FAIR, and POOR regions which are colored yellow and red respectively.

The GE viewer is a wrapper for the Google Earth (GE) application. It overlays the color-coded coverage area from the graphics analysis onto a topological map of the area produced by GE. The overall use of CARET together with pertinent interfaces, are described below.

The final component in the system is the use of Google Earth [11] as the visual representation of both the entity positions/movements from OneSAF and the results of the simulations from QualNet. CARET is primarily concerned with diagnosing the obstacles to maintaining communications in a mission. The most effective way of conveying problems is with a visual representation. With QualNet, a grid around a desired entity is setup that determines in the areas around the entity where communications can be maintained. This information is then processed and displayed as a colored coverage map in Google Earth. The CARET Agent Framework User Interface is shown in Figure 9. Note that in this image the coverage maps are rendered on the right side in a simple 2D panel, however, this has been extended into a 3D Google Earth viewer (Figures 10).

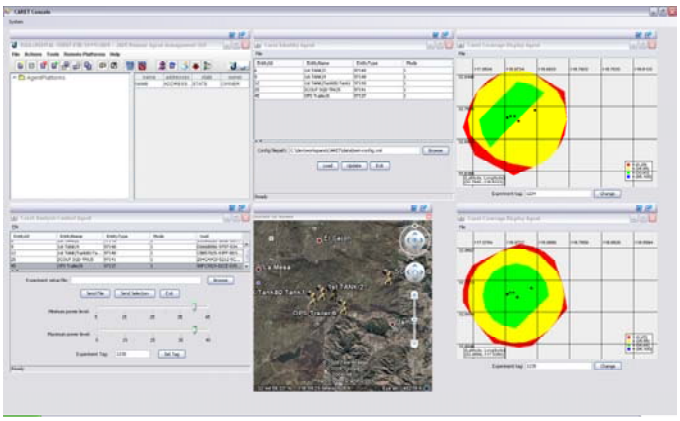

Figure 9: CARET Agent Framework User Interface

Figure 10: Scenario Coverage Depicted Through Agent-Driven Google Earth Overlayfor 85% Threshold

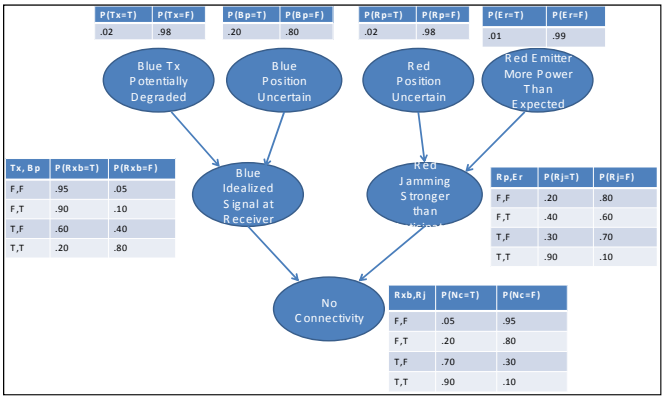

Figure 11: Statistical Metrics Used to Populate Bayesian Networks

5.3 Extending to Cognitive Reasoning

Once sets of rules and statistics were gathered in support of the cognitive analyses, an Analysis Agent – Cognitive Reasoning (AA-CR) can then be used for more advanced techniques, such as inferencing techniques, to gain further knowledge and guide the Signal Planner about the cause of certain phenomena. Our efforts researched a variety of approaches for implementing such reflective cognitive models required by this effort [12][13][14][15][16] that considered the use of neural networks, genetic algorithms, simulated annealing approaches, Bayesian networks, and Markov Models.

In this particular case, the statistical analysis of simulated radial coverage can be taken as the input or configuration data for Bayesian Network Models as shown in Figure 11, where we are considering an example where a Blue Transmitter is fixed but its transmission capability is not 100% certain, the Blue entity holding the receiver is potentially out of position, and the adversary jamming capabilities may be affected by more powerful jammers or a change in position.

For this case, we set the initial probabilities for the Blue Transmission capabilities (Tx), Blue Position Uncertainty (Bp), Red Position Uncertainty (Rp), Red Emitter Power (Re) and expected conditional probabilities for the Idealized Blue Signal Capability (Rxb) and Red Jamming Strength at the Receiver (Rj). Subsequent simulation runs (for the COAA and Network Analysis simulations) are run to refine the conditional probabilities for several of these nodes and used to diagnose the cause of particular shortfalls.

6 Conclusions

This paper has presented an approach performing mobile network coverage analysis to assist mission participants and signal planners with visualizing and understanding causes and potential remedies for network deficiencies during operations. The paper has presented an intelligent agent framework, known as CARET, which is used to integrate a variety of data sources, applications, and services. The paper also presents techniques for performing statistical analysis of anticipated coverage for various participants using GOTS/COTS simulation tools that are controlled through the use of our intelligent agents.

7 References

[1] McGraw, R. M., Shao, G., and Mumme, D. 2009. An agent-based course of action (COA) analysis with radio effects toolbox. In Proceedings of the 2009 Spring Simulation Multiconference (San Diego, California, March 22 - 27, 2009). Spring Simulation Multiconference. Society for Computer Simulation International, San Diego, CA, 1-7.

[2] McGraw, R.M., Shao, G., Mumme, D., and MacDonald, R.A. A Course of Action Analysis with Radio Effects Toolbox (CARET) for Signal Planning. In Proceedings of the 2008 Huntsville Simulation Conference (Huntsville, Alabama, October 22 – 23, 2008).

[3] Shao, G., McGraw, R., Service-Oriented Simulations for Enhancing Situational Awareness, SpringSim'09 - 42nd Annual Simulation Symposium, March 2009.

[4] McGraw, R. et al, "Design of a Course of Action Analysis with Radio Effects Toolbox (CARET)", , The International Journal of Intelligent Control and Systems, Special Issue on Agent-Directed Simulation, March 2009.

[5] Derek T. Sanders., Dean C. Mumme,, Richard A. MacDonald,. "Consolidating Multi-simulation Environments for Radio Effects Analysis." SpringSim '10, Orlando, FL, 2010.

[6] JADE. 2009. http://jade.tilab.com/

[7] FIPA: Foundation for Intelligent Physical Agents. http://www.fipa.org

[8] SDO for Java Specification V2.1, http://www.osoa.org/download/attachments/36/Java-SDO-Spec-v2.1.0-FINAL.pdf?version=1

[9] SOAP Version 1.2 Part 1: Messaging Framework (Second Edition), http://www.w3.org/TR/soap12-part1/

[10] OneSAF. 2009. http://www.onesaf.net/community/

[11] Google Earth. 2009. http://earth.google.com/comapi/

[12] Murphy, Kevin. "A Brief Introduction to Graphical Models and Bayesian Networks". http://www.cs.ubc.ca/~murphyk?Bayes/bayes.html

[13] Rabiner, L.R. "A Tutorial in Hidden Markov Models and Selected Applications in Speech Recognition", Proceedings of the IEEE, vol 77. pp. 257-286.

[14] Mead, R; Paxton, J. And R. Sojda, "Applications of Bayesian Networks in Ecological Modeling". Montana State University.

[15] [15] Lund, T.; Faultner, E.; Robinson, M.; „Condition Monitoring Using Bayesian Networks". INFORMS Annual Meeting 2006.Leslie Lamport. "LaTeX: A Document Preparation System". Addison-Wesley Publishing Company, 1986.

[16] Ree Source Person. "Title of Research Paper"; name of journal (name of publisher of the journal), Vol. No., Issue No., Page numbers (eg.728—736), Month, and Year of publication (eg. Oct 2006).

8 Biography

Robert M. McGraw co-founded RAM Laboratories, Inc. in 1997 and is now its Vice-President and Chief Technology Officer. Dr. McGraw's interests lie in the areas of multi-resolution modeling, cyber security, and distributed information management. He is currently overseeing RAM Laboratories efforts in developing an Application Security Analyzer for MDA and enhancing the CARET Agent Framework. Dr. McGraw received his B.S. in Physics and Electronics Engineering from the University of Scranton, and received his M.S. and Ph.D. in Electrical Engineering from the University of Virginia.

Richard A. MacDonald co-founded RAM Laboratories, Inc. in 1997 and has been serving in the capacity of President and Chief Executive Officer since the company's inception. With twenty years experience in high technology and defense businesses, Dr. MacDonald has overseen the strategic planning and growth of RAM Laboratories into a recognized defense technology leader with a national customer base spanning coast-to-coast, supporting multiple branches of the Department of Defense including the Army, Navy, Air Force, Coast Guard and the Department of Homeland Security. Dr. MacDonald earned both a Ph.D. and Masters of Science (M.S.) in Electrical Engineering from the University of Virginia, and a Bachelor of Science (B.S.) degree in Computer Engineering from the University of Michigan.

Cognitive RF Systems and EM Fratricide

Gerard T. Capraro and Ivan Bradaric
Capraro Technologies, Inc., 2118 Beechgrove Place, Utica, NY 13501 USA

Abstract

In many parts of our world the radio frequency (RF) spectrum is overcrowded. The Department of Defense and researchers throughout the US have been addressing this problem by developing cognitive radios, networks, and radar systems to intelligently choose frequencies, waveform parameters, antenna beam patterns, etc. to operate with conventional receivers without causing electromagnetic (EM) fratricide. In most of the documented work that addresses EM fratricide to date, there is an inherent assumption that the cognitive system knows when and where the fratricide occurs. However, the authors usually do not make known how this information is obtained. In this paper we propose two approaches of how the victim receivers can work together with cognitive systems and share the knowledge of their EM status.

1.0 Introduction

We are informed via many articles and studies that the radio frequency (RF) spectrum is crowded and more space is needed for wireless internet access, communications, and for military usage. Just recently the US Congress passed a bill to open up more spectra [1] to auction off RF frequencies belonging to the television broadcast industries. However, this alone will not solve spectrum crowding. When the frequency spectrum is measured over time, technologists have shown that the spectrum is underutilized. Recognizing this, there have been numerous research projects funded by the US Department of Defense (DOD). These research efforts go back many years to the USAF investigating software programmable radios. The Defense Agency Research Project Agency (DARPA) has probably funded the most projects in this area. Through this research, we now have two distinct users defined as the primary user (PU) (i.e. those who own the license for the frequency range) and the cognitive user (CU) (i.e. those users trying to share the spectra either by using broadband signals or sampling the spectra in time and transmitting when the PU is not transmitting). Most significant projects in this area include the DARPA XG program and the Wireless Network after Next (WNaN) program. In addition to these efforts, there has been a move to apply Cognitive Radio (CR) technologies to the radar domain (Cognitive Radar efforts) and radio networks. Some of these systems sample the spectrum and transmit if no one else is transmitting at any given frequency. This approach can cause electromagnetic interference (EMI) in nearby receivers. Many people have recognized this problem and have addressed it in many different ways [2 - 6]. Many of their solutions inherently assume they know information about the victim receiver, but do not address how this information is obtained. We propose herein two different approaches to solve this problem.

The paper is organized as follows. Section 2 briefly describes some cognitive radio and radar efforts. Section 3 defines the problem we address in this paper. Section 4 presents some potential solutions. Section 5 provides our conclusions and highlights some topics for future work.

2.0 Some Cognitive Efforts

Next Generation (XG) Program

The XG (neXt Generation Communications) program is developing an architecture that will open up the spectrum for more use by first sensing and then using unused portions of the spectrum. Some early goals of the XG program were:

1. Demonstrate through technological innovation the ability to utilize available (unused, as opposed to unallocated) spectrum more efficiently.
2. Develop the underlying architecture and framework required to enable the practical application of such technological advances.

Figure 1 from [7] is a logical functional diagram of the concept of operations of XG's policy-agile spectrum user, which uses a computer understandable spectrum policy capability. The major components are the Sensor (which senses the environment for determining its availability), Radio (the communications device that can dynamically change its emission and

reception characteristics), Policy Reasoner (manages spectrum policy information), and System Strategy Reasoner (manages the multiple radios on a platform).

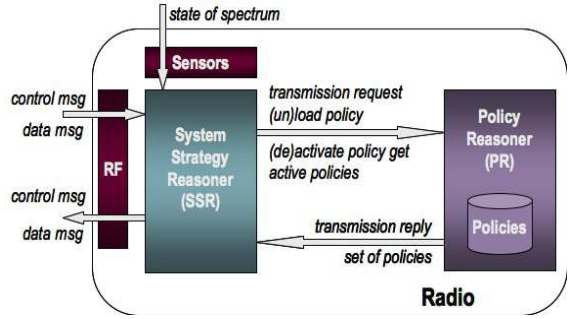

Figure 1.0 Policy-Agile Operation of XG Spectrum-Agile Radio

The last two components are of particular interest in that they utilize Semantic Web technologies. Operating a radio in different parts of the world requires that radios abide by the policies in the area where they are located. The XG program has developed its own XG policy language (XGPL) which uses OWL as its standard representation and will be implemented within the Policy Reasoner.

The Wireless after Next (WNaN)

The WNaN being performed by Raytheon BBN Technologies and funded by DARPA [8] is developing a scalable, adaptive, ad hoc network capability that will provide reliable communications to the military. The basic ingredients of their design are composed of a Dynamic Spectrum Address capability based upon the XG program. It also has 4 multiple transceivers and a disruptive tolerant networking (DTN) capability. The four transceivers provide fault tolerance and allows the system to pick the best channel for communications. The DTN capability allows the nodes to store packets temporarily during link outages. The WNaN also has content based access that allows users to query the network to find information and allow the system to store critical data at locations to minimize time and bandwidth. The system also has multicast voice with quality of service and the network protocols are designed for battery operated handheld devices with energy conserving capabilities.

Cognitive Radio

Another effort related to communications, and having similar goals to the XG program, is the Cognitive Radio [9]. Its objectives are to efficiently utilize the radio frequency (RF) spectrum and to provide reliable communications at all times. A basic cognitive cycle view of the radio is illustrated in Figure 2. A general overview and projections of the Cognitive Radio in our society can be found in [10].

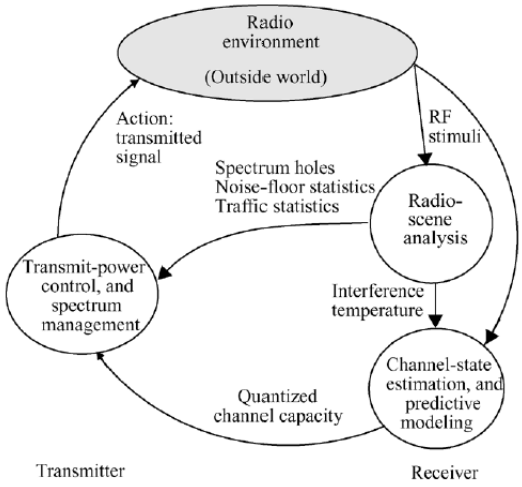

Figure 2.0 Basic Cognitive Cycle

Cognitive Radar

Interest in cognitive radar is growing in the radar community. Figure 3 describes a recent architecture we are currently working on while an earlier version is described in [11]. Figure 4 describes a cognitive radar that is primarily concerned with the tracking stages of a radar [12]. In Figure 5 a cognitive radar architecture is shown from the first textbook written on this subject [13]. The commonality of these designs are the feedback loop between the transmitter and receiver, use of outside sources of information, and the implementation of a learning process.

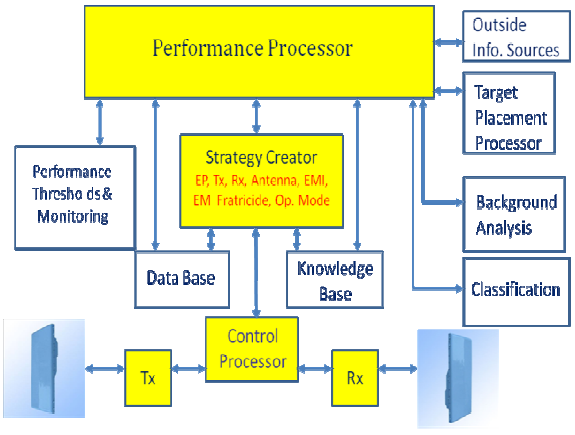

Figure 3.0 A Cognitive Radar Architecture

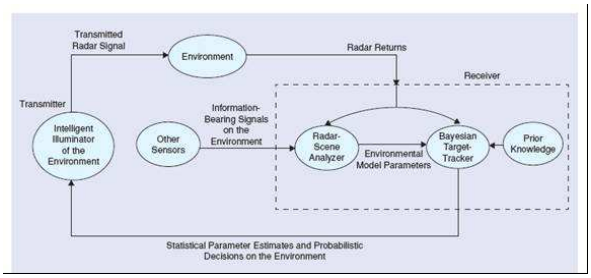

Figure 4.0 A Cognitive Tracking Architecture

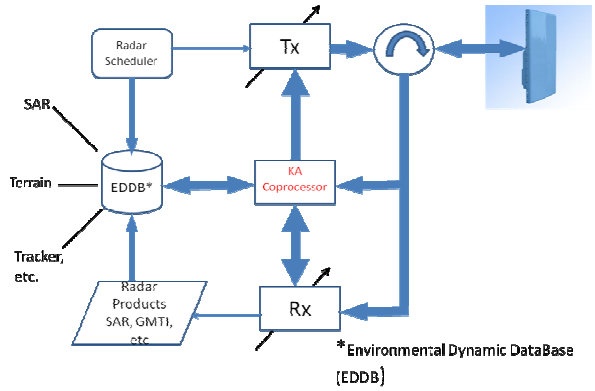

Figure 5.0 Another Cognitive Radar Architecture

3.0 Problem Definition

In all of the above programs and many others, the CU chooses which frequency to transmit using frequency policy rules based upon location and whether someone is currently transmitting within the range of interest. There are at least three issues with this approach. The first is related to the sensing of the environment. What happens if a nearby receiver is not transmitting but is waiting to receive a signal at frequency f1, for example a bistatic radar receiver or an electronic warfare receiver? They don't transmit, they just receive. The second issue relates to the following scenario. Let us assume that one decides to transmit broadband signals below the sensitivity levels of any nearby receivers. As the number of CR increases, the signals within a nearby receiver's passband may exceed the noise floor and interfere with the performance of the receiver [14]. The third issue occurs when a CR decides to transmit at a particular frequency because there are no signals present. The chosen frequency is based upon a linear relationship between the frequency chosen and the sensed environment. The decision policy does not take into effect the nonlinearities between the chosen frequency and other nearby frequencies which can mix nonlinearly and cause receiver intermodulation or mix within the receiver's frontend and cause spurious responses. Most electromagnetic interference (EMI) situations are nonlinear and we must protect our own receivers.

If we are going to deploy cognitive radios and radars nearby conventional receivers we may have to rethink our current CR policy rules. To meet the challenges of the future we need to change.

EM Compatibility Paradigm Shift

EM fratricide is the situation where we degrade the performance of our own system(s) with our own system(s), e.g. an onboard radar's energy is received by an onboard communication receiver and that degrades the receiver's performance. This is a serious problem, since there are multiple sensor and communication systems onboard platforms. Military weapon systems are engineered to prevent such phenomena between hardware located in close proximity. The military has standards for describing how to build and test hardware for EMC, and how to test weapon system platforms for EMC, e.g. Military Standards 461E and 464. The DOD has also developed EMC prediction tools to assess the EMC of its weapon systems. These tools were developed during the 1970s and 1980s and have been enhanced and are used today. They were developed according to military standards to assure proper system's testing was performed, because most of the systems developed then were deployed in space where fixing EMI problems is not practical. Using software tools to perform EM measurements in the 1970s was a major paradigm shift for the EMC community.

Just as we needed a change by using software tools to assess a system's EMC in the 1970s, we now need to rethink how to build complex systems that employ waveform diversity and some of the proposed XG and cognitive radio and radar spectrum management concepts. Whereas in the 1970s we required software tools to predict where to hone our measurements, we now need to use software to help determine when EMI may occur in real-time, and manage the EM spectrum while the platform increases its total performance. This performance gain is not related to just one system onboard the platform, but to a system performance measure of the total platform, where the platform may contain communications, navigation, radar sensors, etc. The EMC tools used today assess the performance of an individual stovepipe system, e.g. the increase in bit error rate of communications equipment and the decrease in probability of detection for a radar. The predictions made by these performance measures are

usually related to the signal to noise plus interference ratios computed for each transmitter coupled to each receiver. The tools also compute the sum or integration of all transmitters' coupling into a receiver(s) along with a hypothesized EM spectrum, to represent the environment, and to predict an integrated or total EM ratio which can be related to a receiver's performance. This method identifies the performance of each receiver, but it does not alert us to the degradation of the total weapon system's performance. In addition, each computation is performed for a fixed set of operating conditions for each transmitter and receiver of EM energy. This approach is acceptable when analyzing a weapon system with conventional equipment, where each system's performance is assessed independent of all others. However, this is not acceptable for a weapon system or platform with a global performance requirement(s) or when the waveform parameters of one or more of its systems are changing in real-time e.g. a cognitive radio or radar. Our methods of building EMC systems must change to meet this dynamic environment.

4.0 Potential Solutions

To solve the issues discussed above some people are looking to change the beam pattern of the transmitter so that the power coupled to a victim receiver is reduced, some wish to change the transmitted signal's polarization, and of course, there is the attenuation gained by employing orthogonal waveforms. All these solutions help reduce the amount of degradation caused to a friendly receiver. However, these techniques inherently are assuming that one knows that the receiver is being degraded. How would a cognitive radar, radio or a WNaN know about the receiver?

There are currently two scenarios where one can implement a capability to solve the fratricide issue. One is on a single platform such as an aircraft, ship, or a complex weapon system where multiple conventional and cognitive EM equipment reside. The second scenario is concerned with WNaN where we propose to extend its capability and add a gateway to communicate with non cognitive radios as developed under another DARPA program. The EMC paradigm shift for both scenarios requires that the equipment report to a node that is managing the EMC of the platform or the total network.

Let us consider the single platform scenario first. The system strategy reasoner in Figure 1 and the strategy creator in Figure 3 need to be extended to handle our total platform with information being obtained from all the non cognitive receivers on or near the platform. We need a cognitive sensor platform network that can create strategies, evaluate them, learn and modify strategies as the platform sensor system operates. This learning should also be transferrable to other instantiations of the same type of platform.

The single platform scenario requires sharing information among sensors. Each of the sensors has its own signal and data processing capability. An intelligent processor is needed to address fusion, control, and communication between sensors. The goal is to be able to build this capability so that it can interface with any sensor and communicate using ontological descriptions via an intelligent platform network. The intelligent network will be able to coordinate the communications between the on-board and off-platform sensor systems. There are also communications issues that need to be addressed for the sharing of information and for minimizing the potential of EM fratricide. The intelligent platform should determine if there is EM interference potential when a sensor varies its signal characteristics which may cause interference to a receiving sensor. Rather than have each sensor on a platform operate as an independent system, one needs to design our platform as a system of sensors with multiple goals managed by an intelligent platform network that can manage the dynamics of each sensor to hopefully meet the common goals of the platform. This approach will require modifying current platform weapon systems which maybe very costly to implement.

Let us now consider the WNaN scenario of a Mobile Ad Hoc Networks (MANET) [8]. How will we know that the nodes on the network are causing fratricide to a nearby non cognitive receiver? One method is to communicate with friendly receivers similar to the first scenario discussed above. The second method is to use the research findings of another DARPA program called the US Army's Future Combat Systems Communications (FCS-C). This program has developed a Gateway [15] for conventional receivers. "*DARPA demonstrated that previously incompatible tactical radios can communicate seamlessly by using the network's Internet protocol layer. This method offers the potential for more affordable military communications between legacy and coalition radios in the future.*" If we add this approach to the WNaN system it will be possible to know when we are interfering with conventional receivers. According to [8], a capability to collect data as to the number of

packets sent for each node, priority type, emitted frequency by each node, etc. has been built. There exists over 300 statistics that can be gathered. If we fuse the gateway from the FCS-C program with the statistics gathering capability of the WNaN we may be able to infer when there is EMI caused to conventional receivers connected to either the WNaN system or the FCS-C system.

One approach would modify the conventional receivers to report when they are suffering EMI to the cognitive networks via the gateway. Another, and possibly less costly, approach is to infer when EMI has occurred by monitoring statistics at the gateway where the number of packet errors and resends are requested by the conventional receivers. A smart node could infer based upon the conventional receiver's tuned frequency and the nearby emitter frequencies, power levels, antenna gain patterns, etc. which non linear EMI situation is causing the fratricide. This cognitive approach can learn on the fly and restrict certain EM scenarios to alleviate the interference. If either of these approaches are implemented then another needed EMC paradigm shift will occur.

5.0 Conclusions and Future Work

Cognitive radios, radar and networks are a fascinating area of research. Once they are fielded they will unclutter the RF spectrum for future use. More research is needed to make these systems compatible with conventional transceivers. The potential solutions presented herein should be pursued so that systems and networks can self heal from any EM fratricide that can occur. However, to do so the system must know that a receiver is being degraded. To make this happen one needs to study the FCS-C gateway approach, the WNaN gathered statistics, the logic to process these statistics to determine whether EM interference is occurring, how it was caused, how to eliminate the interference, learn from the process, and change the strategy. We also need to study how we can easily modify current systems such as an aircraft or ship and add an intelligence capability that will allow cognitive radios and radar systems to work compatibly with conventional transceivers while maximizing the performance of the total platform.

References

[1]http://blog.broadcastengineering.com/blog-opinions/2012/02/17/congress-paves-way-for-broadcast-spectrum-auctions/

[2] P. Popovski, Y. Hiroyuki, K. Nishimori, R. Di Taranto, and R. Prasad, "Opportunistic Interference Cancellation in Cognitive Radio Systems", 2nd IEEE International Symposium on New Frontiers in Dynamic Spectrum Access Networks, 2007.

[3] O. Ozdemir, E. Masazade, C. Mohan, P. Varshney, I. Kasperovich, R. Loe, A. Drozd, and S. Reichhart, "Spectrum Shaping Challenges in Dynamic Spectrum Access Networks with Transmission Hyperspace", Waveform Diversity and Design Conference, January 2012

[4] Y. Fei and Z. Wu, "An Interference Cancellation Scheme for Cognitive Radio Network", 6th International Conference on Wireless Communications Networking and Mobile Computing, Sept. 2010

[5] V. Chakravarthy, Z. Wu, A. Shaw, M. Temple, R. Kannan, and F. Garber, "A general Overlay/Underlay analytic Expression Representing Cognitive Radio Waveform", Waveform Diversity and Design Conference, June 2007

[6] E. Beadle, A. Micheals and J. Schroeder, "New Alternatives for Interference Tolerant Waveforms Hosted on a Software Programmable Multi-Mission Platform", Waveform Diversity and Design Conference, January 2012

[7] D. Elenius, G. Denker, andD. Wilkins, "XG policy Architecture", ICS-16763-TR-07-108, SRI Project No. 16763, Contract No. FA8750-05-C-0230, April 2007

[8] J. Redi and R. Ramanathan, "The DARPA WNaN Network Architecture", The 2011 Military Communications Conference, November 2011

[9] S. Haykin, "Cognitive Radio: Brain-Empowered Wireless Communications", IEEE Journal on Selected Areas in Communications, vol. 23, no. 2, pp. 201 – 220, February 2005

[10] Ashley, S. "Cognitive Radio", Scientific American, http://www.sciam.com/article.cfm?chanID=sa006&colID=1&articleID=000C7B72-2374-13F6-A37483414B7F0000, February 20, 2006.

[11] G. Capraro and M. Wicks, "Metacognition for Waveform Diverse Radar" Waveform Diversity and Design Conference, January 2012

[12] S. Haykin, "Cognitive Radar", IEEE Signal Processing Magazine, pp. 30 – 40, January 2006

[13] J. Guerci, "Cognitive Radar", Artech House, 2010

[14] I. Bradaric, G. Capraro, and D. Weiner, "Ultra Wide Band (UWB) Iterference – Assessment And Mitigation Studies", AFRL-SN-RS-TR-2006-42, February 2006, http://www.dtic.mil/cgi-bin/GetTRDoc?AD=ADA446049

[15] H. Keyton, "Networks: Adapting To Uncertainty", DARPA 50Years of Bridging the Gap, http://www.darpa.mil/WorkArea/DownloadAsset.aspx?id=2570

Ontological Decision-Making for Disaster Response Operation Planning

Aaron Wheeler, Jim Dike, and Michael Winburn
3 Sigma Research, Indialantic, Florida, USA

Abstract – *Disaster response operation planners could benefit from a software tool to assist them in extracting individual mission information from various operation tasking orders, determining resources able to carry out the operation, construct a number of alternative operation plans, alert them to mission-critical changes to these plans, and allow them to quickly replan when problems occur. Within the context of aircraft operation planning for disaster relief, we use an ontological approach to solve these problems that includes modeling the air coordination plan (ACP) knowledge domain with OWL and SWRL, making inferences about the capabilities of real-world resources using an automated reasoner, retrieving relevant operation planning resources with SPARQL, then building multiple plans from the results of the queries. We also use SPARQL queries of the operation planning ontology database to provide alerts to operation planners of potential mission-critical changes to resources. Our results show that this approach allows operation planners to generate and monitor aircraft operation plans having dependencies on aircraft and pilot availability, weather effects on payload effectiveness, flight route distance, and fuel availability. We conclude that an ontological approach to aircraft operation planning does work and also supports broader goals of data transparency, information sharing, and domain knowledge persistence.*

Keywords: ontology, decision-making, operation planning, disaster response

1 Introduction

Large-scale disasters come from many sources, ranging from natural events like hurricanes, tornadoes, earthquakes, fires, famines, volcanic eruptions, or tsunamis; to human-made crises like nuclear accidents or political unrest. Aircraft provide a critical component to first response and longer term disaster recovery.

This research focuses on operation planning of air support for disaster recovery from natural and human-made disasters and political unrest. Specifically, we introduce a methodology for automated reasoning about operation plans to support disaster response decision-making.

Because of their ability to avoid ground obstacles, aircraft provided critical components to disaster recovery, including communication, aerial reconnaissance, supplies, and evacuation. Consider the following disaster recover scenario.

Suppose that a category five hurricane strikes a major population center on the coastal United States. Winds and flooding destroy communication and transportation networks, while people lack food, water, shelter, and medical care. Disaster response operation planners use aircraft to provide a number of basic needs. They deploy a drone aircraft to circle the affected area with a payload to provide an ad hoc private cellular network to first responders. Helicopters bring smart phones to emergency responders already on the ground so they can collect and share situational awareness data (GPS linked text, audio, still pictures, and video) with each other and with the command center located outside the affected area. Other drone aircraft provide aerial reconnaissance to assess damage and look for victims. Operation planners send helicopters to evacuate victims. Both helicopters and fixed-wing aircraft drop supplies to those stranded but not in immediate danger.

Unplanned changes to aircraft status and pilot availability, supply shortages, weather conditions, and scheduling conflicts, to name but a few complications, require operation planners to have a number of contingency plans and to know quickly when the current plan cannot succeed and replanning must occur.

Section 2 of this paper provides background information about our proposed system architecture, how ontologies can support emergency operation planning, and specific ontologies for aircraft operation planning. Section 3 describe the steps for generating primary and contingency operation plans using our ontological approach. Section 4 discusses our main findings, and section 5 concludes with a brief description of a current project that we intend to apply these transformations, and also a discussion of future research directions.

2 Background

This section introduces the Semantic Emergency operation planning with Ontological Reasoning (SEMPOR) system architecture and the Semantic Web technologies used by SEMPOR to reason about aircraft operation plans.

Aircraft operation planning for disaster response and for military operations share a number of similarities. Therefore,

we leverage the same terminology when appropriate. This has the advantage of supporting cross-domain information exchange and coordination, especially important during emergency situations.

2.1 System Architecture

Figure 1 below shows the SEMPOR system architecture. The left set of components represent the various data sources from which SEMPOR will extract relevant data in order to construct and update operation plans. SEMPOR itself comprises the components to the right.

Figure 1. SEMPOR System Architecture.

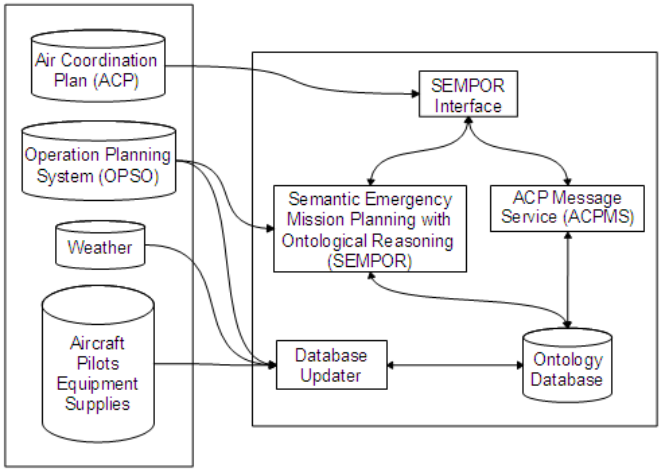

The Air Coordination Plan (ACP) database stores the current air coordination plans. The Operation Planning System (OPS) provides flight route details to the reasoner. Other data sources provide up-to-the-minute weather status, as well as details about mission-critical assets like aircraft, pilots, equipment, and supplies. SEMPOR may interactively query these data sources for specific information instead of using all possible information available about each operation asset.

Disaster response operation planners interact with SEMPOR and the ACP Message Service (ACPMS) through a graphical user interface. Both SEMPOR and ACPMS retrieve information from an ontology database. The ontology database contains specially formatted data collected from a variety of data sources that SEMPOR needs to generate operation plans.

2.2 Ontologies

The Extensible Markup Language (XML) provides language for describing the structure of information to support automated processing [8]. The XML Schema Definition (XSD) language contains type and element definitions that describe characteristics of well-formed elements and attributes of XML documents [9]. However, the XSD language does not express semantics [14] and so creates difficulties for Semantic Web technologies.

An ontology provides a formal description of a domain of discourse [1] and represents a core component of the Semantic Web. The World Wide Web Consortium (W3C) has recommendations for expressing ontologies using RDF [10], RDFS [11], and OWL [2].

The Resource Description Framework (RDF) represents a W3C standard for the Semantic Web that makes statements using subject-predicate-object triples [10]. RDF Schema (RDFS) extends RDF by allowing for the definition of classes and properties that describe other classes and properties [11].

Both RDF and the OWL 2 Web Ontology Language provide a formal semantics for interpreting ontology structures. OWL extends RDF and RDFS with terminology to express ontologies using description logic, a decidable fragment of first order logic [12]. OWL DL ontologies belongs to subset of OWL ontologies that satisfy the expressive requirements of a description logic. The expressiveness, completeness, and decidability of OWL DL makes it possible for automated reasoning engines to discover new information implied by ontology structures [13].

SEMPOR uses several Semantic Web languages to represent, reason about, and query for data needed to construct aircraft operation plans.

SEMPOR uses the Web Ontology Language (OWL) to describe our aircraft operation planning domain and the real-world resources needed for operation plans. OWL-DL, a subset of the full OWL specification, allows us to describe aircraft operation planning concepts and resources using a decidable and complete subset of first-order logic called description logic (DL). OWL-DL semantics allow for automated reasoning about classes and properties of things [2].

OWL allows us to make inferences about additional class memberships and properties of entities. However, we cannot automatically create relations between individuals based on comparisons of their explicit or inferred properties. In order to accomplish this type of reasoning, we use the Semantic Web Rule Language (SWRL) [3]. Rules in SWRL resemble production rules (e.g. "if X and Y then Z") in that individuals that match a conjunction of conditions will trigger or fire another set of conditions from which we can infer still more class membership and property relations for the individuals.

SEMPOR uses the SPARQL Protocol and RDF Query Language (SPARQL) to retrieve data from the inferred data model. The Resource Description Framework (RDF) provides a formalism for making statements about resources in terms of subject-predicate-object triples. SPARQL resembles

Structured Query language (SQL) used for querying relational databases, but includes Uniform Resource Identifiers (URI) for globally unambiguous queries [4].

An ontological representation of aircraft operation planning supports the W3C Decisions and Decision-Making Community Group objective of developing a semantic representation of decision-making concepts to improve sharing and use of decision information across diverse systems [7].

2.3 Ontologies for Operation Planning

SEMPOR uses several domain ontologies expressed using OWL and SWRL. Some of these ontologies we constructed specifically for SEMPOR, while others represent OWL versions of XML schema already developed to express ACP and related resources. We use a semi-automated approach to make the transformation from XML to OWL.

The Air Operations Community of Interest (AOCOI) has developed a number of XML schemas to describe air operations resources and concepts. They developed these schema with the intent of "enabling data transparency across the Air Operations domain, enable standard data-driven services for managers at all levels and reduce data entry, homegrown systems, and the need for record re-creation" [5]. We have chosen to use their vocabulary, taxonomy, and semantics in SEMPOR to support this effort and provide a foundation for better coordination between civilian and military responders during times of crisis.

The AOCOI has XML schemas (version 1.0.15.2) for Airspace, Common Mission Description (CMD), Friendly Order of Battle (FrOB), Mission Task Request (MTR), and Reference [5]. We have transformed to OWL the CMD and FrOB XML schemas to use in our prototype some of the terms these schemas contain. The CMD ontology provides use with concepts like ConfigurationItem and RampFuel, while the FrOB ontology gives us terms like BurnRate.

The Operation Planning Ontology contains concepts and properties specific to operation planning and also a representation of operation planner knowledge and reasoning. The Operation Asset Ontology contains representations of all operation assets not already represented by other ontologies.

3 Operation Planning

Now we enumerate the steps that operation planners and SEMPOR will follow during the course of generating air operation plans.

1. Collect information relevant to the operation from the ACP and other data sources.
2. Create in the ontology database a prototype operation plan.
3. Apply a reasoner to the ontology to infer candidate operation plan elements.
4. Build operation plan alternatives from these candidate elements.
5. Rank the operation plan alternatives from most to least preferred.

We will describe each of these steps in more detail in the sections to follow.

3.1 Data Acquisition

Collect information relevant to the operation from the ACP. Data relevant to the operation gets retrieved from their respective data sources and stored in the ontology database using OWL classes, relations, and values. This data acquisition strategy allows us to use heterogeneous data sources.

3.2 Operation Plan Prototype

SEMPOR assumes that the operation planner will create a high level description of an operation plan as part of the operation planning process. This high level specification will describe abstract planning elements from which SEMPOR can infer real elements using OWL and SWRL.

Figure 2 below shows an example of the information contained in the operation plan prototype. The operation planner provides an abstract description of each class of thing that could serve in the role of a particular operation plan element. In this example, the operation plan needs only one element. Classes of things that could perform the role required of this element appear in ***option1***. This entity has relations to two configurations, one specifying a hoist for lifting people and equipment and the other a cellular base station payload. Anything that SEMPOR can infer has one or both of these configurations can become an element in this operation plan.

Figure 2. Operation plan prototype data.

```
operation_plan
   startTime
   endTime
   flightTime
   needsElement value option1

option1
   hasConfiguration value proto_conf_hoist_4
   hasConfiguration value proto_conf_cellular_2
```

Note that SEMPOR interprets multiple needsElement and hasConfiguration differently. SEMPOR interprets multiple needsElement relations using a logical AND, meaning the operation plan must have "this element AND this

element AND ...". However, SEMPOR interprets multiple hasConfiguration relations using a logical XOR, meaning the aircraft operation plan must have only one of "this configuration OR this configuration OR ...". SPARQL queries and post-processing that we describe later will exploit these logical constructs to generate final operation plan alternatives.

3.3 Ontological Reasoning with OWL and SWRL

Describing operation planning resources and concepts with OWL-DL and SWRL allows us to use automated reasoners to make inferences over the logical structure of the knowledge representation. OWL-DL reasoners make it possible to discover implied relationships between real-world entities and use these to infer the suitability of aircraft and pilot for the air operation. We use the Pellet OWL 2 reasoner because it has a Java API, supports the latest version of OWL 2, and allows for most SWRL builtins [6].

We create in the ontology a class called ***Conf_Hoist_4*** to represent the set of things having a particular hoist configuration. We define the class by stating that individual entities belong to the set if they have both a ***has_ConfigurationItemObj*** relation to an individual that belongs to the set of ***Hoist*** things and a ***has_capacity*** property value of at least 500 pounds. Figure 3 below shows this graphically as a Venn diagram.

Figure 3. Logical AND with ontology concepts.

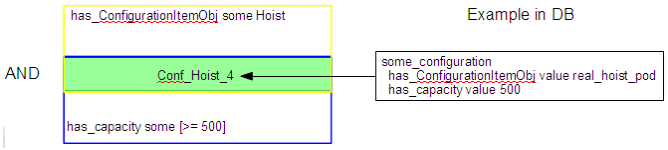

Figure 4 below shows a similar diagram, but for inference by logical OR. In this example, we define a class called ***AirAmbulance*** to represent the set of things with equipment capable of providing emergency medical support. Air ambulances can come equipped with a variety of medical payloads so we use a logical OR to capture them all in the definition of the set.

Figure 4. Logical OR with ontology concepts.

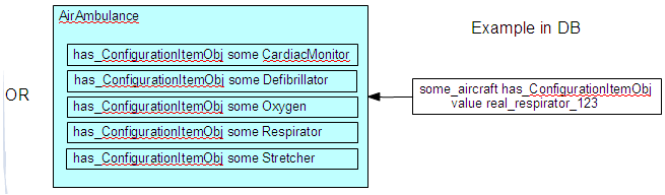

In both examples above, we could further specify that things that belong to one of the sets, either ***Conf_Hoist_500*** or ***AirAmbulance***, also have additional property values or relations to other individuals or types of things. In this way we can extend the number of inference steps that the reasoner can make, which could result in long and elaborate chains of reasoning that automatically find not so obvious classes, relations, and property values for individual entities needed for aircraft operation planning.

While OWL allows us to infer set memberships and additional property relations for individual entities, SWRL allows us to compare set memberships, relations, and property values of individuals then create relationships or assign property values. Figure 5 below shows a sequence of rules in SWRL that we use to assign additional characteristics to operation planning resources. The figure shows in words what the left-hand side (LHS) of each rule does and then shows on the right-hand side (RHS) in SWRL syntax the binding that results if the conditions on the LHS get triggered.

Figure 5. Sequence of rules for inferring additional properties.

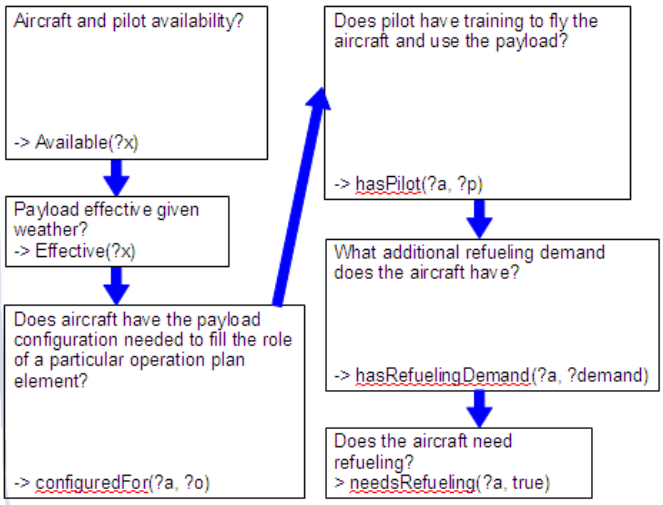

Figure 6 shows the LHS conditions in the SWRL syntax. For example, ***Available(?x)*** means that an individual instantiated on the LHS with variable ***?x*** belongs to the set of ***Available*** things. For another example, ***hasPilot(?a,?p)*** means that when the conditions on the LHS of the rule fire, the aircraft entity instantiated as the variable ***?a*** has a ***hasPilot*** relation to a pilot entity instantiated on the LHS with the variable ***?p***.

Figure 6. SWRL rules for inferring additional properties.

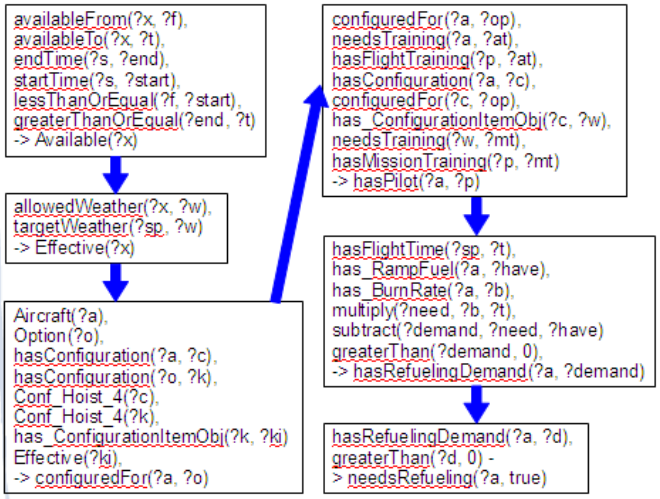

3.4 Ontology Database Queries with SPARQL

Automated reasoner, like Pellet load the explicit data model described with OWL and SWRL then makes an inferred model that contains statements implied by the logical structure of the explicit data model. SEMPOR uses database queries expresses with SPARQL to retrieve information from this inferred model.

Specifically, SEMPOR uses a SPARQL query to select for each inferred operation element the following values:

1. Operation element (e.g. option1)
2. Aircraft
3. Pilot
4. Configuration item (e.g. hoist_1)
5. Refueling demand

Figure 7 below shows the SPARQL query used by SEMPOR to retrieve these records from the inferred data model.

Figure 7. SPARQL query to retrieve operation elements.

```
select ?o ?a ?p ?ci ?rd
where {
      ?a a sp:OperationElement .
      ?a sp:configuredFor ?o .
      ?a sp:hasConfiguration ?c .
      ?c sp:configuredFor ?o .
      ?c cmd:has_ConfigurationItemObj ?ci .
      ?a sp:hasPilot ?p .
      ?p a sp:Available .
      ?a sp:hasRefuelingDemand ?rd .
}
```

SEMPOR uses the information obtained from the SPARQL query to construct aircraft operation plans, which we describe in the next section.

3.5 Aircraft Operation Plan Construction

SEMPOR now has a set of records from the SPARQL query from which it can construct aircraft operation plans with real resources that fit the requirements for operation elements requested by the operation planner in the prototype plan. The algorithm proceeds as follows.

First, divide the query results into separate lists based on the option. Each option represents a choice SEMPOR makes for a particular operation plan element. A prototype operation plan with two elements should have two options and two lists containing at least one record. This assumes at least one real resource exists that meets the requirements for the operation plan element. Next, pick one record from each list and generate an aircraft operation plan. Finally, repeat for every combination of records from each list.

For example, suppose we have a prototype operation plan that specifies two elements. The results of the SPARQL query give us aircraft1 and aircraft2 for option1; and aircraft3 and aircraft4 for option2. The algorithm creates operation plans from all combinations taken from these two lists. Specifically, SEMPOR creates the following combinations of operation plan elements:

- aircraft1 and aircraft3
- aircraft1 and aircraft4
- aircraft2 and aircraft3
- aircraft2 and aircraft4

Each of the combinations of elements above becomes part of an operation plan specification that gets returned by SEMPOR to the operation planner.

3.6 Real-Time Alerts

The ACP Message Service (ACPMS) provides real-time alerts to operation planners to keep them informed of changes in the status of both resources belonging to existing primary or contingency operation plans and to resources that could allow for new aircraft operation plans.

ACPMS monitors for changes to the ontology database. When the ontology database gets updated, ACPMS performs a number of SPARQL queries using the named entities in the primary and contingency operation plans.

Currently, ACPMS applies SPARQL queries to he ontology database to verify the following remain true;

- pilot available
- aircraft available
- aircraft has the required equipment configuration
- equipment remains effective for the weather conditions at the target
- aircraft has the same refueling demand

ACPMS alerts the operation planner to any deviations in the above conditions, as well as notifying the operation planner that more resources might have become available. The operation planner can then replan or select a different contingency plan.

4 Discussion

Our research efforts thus far show that we can

1. Represent mission-critical real-world resources with OWL and SWRL Semantic Web languages.
2. Capture operation planning knowledge and reasoning using OWL, SWRL, and SPARQL.
3. Use automated reasoning to infer implied relationships in an explicit data model of operation planning concepts and resources.
4. Query the inferred data model to obtain candidate operation plan elements.
5. Construct a primary operation plan and several contingency plans.
6. Recognize changes to operation plan elements and to the operation planning resource database that could affect existing operation plans or provide additional operation plan alternatives.
7. Alert operation planners to changes in near real-time.

5 Conclusions

We conducted research using an automated reasoner on an ontological data model of operation planning resources and concepts to determine the feasibility of the approach for ultimately developing a software tool able to meet the needs of operation planners. Among these needs include the ability to extract specific operation information for Air Coordination Plan (ACP), collect and organize data required for each mission, and verify the suitability and availability of all resources, both people and equipment, needed to carry out the air operation.

The results of our investigation show that our approach can indeed meet the needs of operation planners in their task of building and maintaining multiple operation plans. Through our research we have demonstrated that our ontological approach allows operation planners to generate and monitor aircraft operation plans having dependencies on aircraft and pilot availability, weather effects on aircraft and equipment, flight route distance, and fuel available.

In addition to satisfying these requirements, our approach has a number of additional advantages. First, the ontologies we use derive from AOCOI XML schema. This means our work supports AOCOI efforts to provide data transparency and sharing across both civilian and military Air Operations domains. Second, the ontological reasoning uses set theory in ways similar to how operation planners might combine pieces of information to construct operation plans. Third, the ontological models we develop capture the operation planning thought process in a form readable by both people and computers. Finally, having captured operation planning knowledge in an open data standard, our approach allows for the preservation and conveyance of operation planning decision-making in support of the W3C Decisions and Decision-Making Community Group [7].

6 References

[1] Thomas R. Gruber. A translation approach to portable ontology specifications, Knowledge Acquisition, 5(2):199–220, 1993. http://tomgruber.org/writing/ontolingua-kaj-1993.pdf

[2] OWL 2 Web Ontology Language Primer, W3C Recommendation, October 2009. http://www.w3.org/TR/owl2-primer/

[3] SWRL: A Semantic Web Rule Language Combining OWL and RuleML, W3C Member Submission, May 2004. http://www.w3.org/Submission/SWRL/

[4] SPARQL Query Language for RDF, W3C Recommendation, January 2008. http://www.w3.org/TR/rdf-sparql-query/

[5] Air Operations Communities of Interest (AOCOI). http://onesource.afc2ic.org/coi.aspx

[6] Pellet: OWL 2 Reasoner for Java. http://clarkparsia.com/pellet

[7] Decisions and Decision-Making Community Group. http://www.w3c.org/community/decisionml/

[8] Extensible Markup Language (XML) 1.1 (Second Edition). W3C Recommendation 16 August 2006, edited in place 29 September 2006. http://www.w3.org/TR/2006/REC-xml11-20060816/

[9] XML Schema Part 0: Primer Second Edition. W3C Recommendation 28 October 2004. http://www.w3.org/TR/xmlschema-0/

[10] RDF Primer. W3C Recommendation 10 February 2004. http://www.w3.org/TR/2004/REC-rdf-primer-20040210/

[11] RDF Vocabulary Description Language 1.0: RDF Schema. W3C Recommendation 10 February 2004. http://www.w3.org/TR/rdf-schema/

[12] From SHIQ and RDF to OWL: The Making of a Web Ontology Language by Ian Horrocks, Peter F. Patel-Schneider, and Frank van Harmelen. Journal of Web Semantics, 1(1):7-26, 2003. http://www.comlab.ox.ac.uk/people/ian.horrocks/Publications/download/2003/HoPH03a.pdf

[13] OWL 2 Web Ontology Language Document Overview. W3C Recommendation 27 October 2009. http://www.w3.org/TR/owl2-overview/

[14] OWL Web Ontology Language Overview. W3C Recommendation 10 February 2004. http://www.w3.org/TR/2004/REC-owl-features-20040210/

Abductive Requery

Joshua Powers, David Skowronski and Tony Stirtzinger
Securboration Inc., Melbourne, FL, USA

Abstract – *We present an abductive approach to query formulation based on ontology and semantic rule content. Traditional Decision Logic ontologies offer scant opportunity for the application of abductive inference. When augmented by semantic rule languages such as SPIN, however, abduction becomes an attractive possibility for the targeted exploration of potentially large or virtual data sources. We describe a method of pre-processing such rules for use in abductive reasoning. We also describe rule selection and re-query formulation methods once a set of A-Box statements is presented to the abductive reasoner. Our approach assumes that the majority of A-Box content is virtual, ie, not realized until specifically asked for from non-ontology sources such as databases and/or unstructured text documents.*

Keywords: Abduction, Ontology, Query Generation

1 Introduction

Web Ontology Language (OWL)-based query languages such as Semantic Web Rules Language (SWRL)[1] and SPARQL[2] (and its SPIN[3] expression) provide the ability to both query an ontology for facts, and assert new facts in the ontology based on existing statements. This latter style of constructive rules is an attractive mechanism for obtaining some of the deductive benefits of OWL-Full reasoning while keeping the T-Box ontology expressed at the easier to manage OWL Lite or OWL-DL levels.

Such rules in and of themselves are still purely deductive in execution, usually possessing a large number of antecedents which must be matched by some A-Box statements in order to license the production of their consequent statements. However, this population of antecedent/consequent groups has great potential for the application of abductive reasoning.

Traditional abductive reasoning 'works backward' from discovering that something which is a consequent of a rule is true, to 'guessing' that the antecedent(s) are true. We propose an extension of this reasoning to work from some reasonable subset of antecedents and consequents to produce both new statements licensed by the rule, as well as new queries which are more specific in nature than the original rule. Such queries, if satisfied by further deductive reasoning over the A-Box or by providing direction to a fact extraction capability over source data, would potentially corroborate or invalidate the abductive step.

This paper describes an approach to preparing a large population of SPIN CONSTRUCT-style rules for this expanded abductive reasoning. We describe a mechanism for selecting such rules given a set of input OWL statements, and reformulating them into both abductive conclusions and further queries. We report some early results using these techniques, and suggest several directions for future research.

2 Motivation

The motivation for our work derives from two situations regarding ontology-based reasoning. The approach we describe is largely dependent on these factors being present. First, the basic OWL statements of the ontology in question are augmented by a reasonable population of SPIN language rules. Second, the A-Box is incomplete, and not fully realized without expensive querying of non-RDF data sources such as databases and/or natural language extraction results. This last motivator separates our use case from much of the theoretical work in this field, but makes it directly applicable to many scenarios faced by RDF-based analytical capabilities.

In working with large OWL ontologies, we have found that asserting logic via the construction of complex, anonymous Restrictions is frequently unwieldy for a variety of reasons. First, they are difficult to document and interpret between human authors and users of ontologies, and are thus likely to be the cause of unexpected and difficult-to-debug deductive inferences. Second, they are 'baked in' to the ontology, and are hard to suppress from reasoning as a result. This makes it difficult to be selective on which kinds of statements we wish to create via invocation of the reasoner. Third, depending on which flavors and versions of OWL we have chosen to use, we may not be allowed to state the logic we would like to express.

To alleviate these difficulties, it is often desirable to express such logic as CONSTRUCT rules in the SPIN language, and use a rule engine to produce new deductions when desired. Such rules are easy to document and read, can be invoked at will, and allow a wide range of expressivity, even if the underlying T-Box they are executed against is a simple flavor of OWL such as OWL-Lite.

SPIN rules with explicit antecedent-consequent structure often place a large set of very detailed requirements in the

antecedents, including rdf:type statements about entities and object properties holding between them. When working with incomplete data sets, we often wish to know what facts could be likely given a set of assertions, even if every detail about them is not currently known. Further, we would like to know what additional queries we might execute against a data set if we wanted to be more certain of the likely new facts. This is especially useful in situations where our source data is contained in non-RDF data stores and/or unstructured text sources which must be selectively processed with expensive entity and relation extraction capabilities in order to populate our A-Box with potentially corroborating information.

3 Related Work

Elsenbroich et. al. (4) call for the development of abductive approaches to reasoning over ontologies and knowledge bases. They define several attractive qualities of such reasoning: Consistency, Minimality, Relevance and Explanatoriness. The approach described in our paper cannot guarantee any of these qualities, but uses the ontology's T-Box statements and the content of the SPIN rules in a way compatible with their spirit.

Kiefer (5) gives a very thorough overview of many potential abductive approaches to reasoning in the Semantic Web context. We have not incorporated probabilistic reasoning in our current design, although this is frequently done in abductive approached.

Du et. al. (6) wish to adhere quite strictly to the Minimality and Consistency qualities, and define a logic programming approach to a subset of OWL which can satisfy these goals.

Kevorchian (7) describes some features of query-initiated abduction which have a parallel to the context assumptions we make in our approach.

4 Approach

We decided early on not to adhere strictly to the consequent → antecedent path which is the strict definition of abduction. We also wanted to cover cases where many but not all of a SPIN rule's antecedents were present in the input statements, and to produce subsequent queries which would search for both the remaining antecedents as well as the consequents.

We approach the abductive requery task in two parts: An indexing phase where SPIN rules are analyzed for potentially useful groups of statements which may appear in initial queries; And a query-time phase when initial queries are compared to this index on the SPIN rules and additional queries are constructed.

4.1 Indexing Phase

We calculate SPIN rule **fragments** which are all combinations of SPIN rule statements sizes 2-n where n is the number of statements in the original SPIN rule. We consider antecedent and consequent statements together, with no differentiation. Pure abduction would, of course, require at least one consequent statement be present in each fragment, but due to the potential incompleteness of the data, we would like to be more forgiving with respect to potential input queries. The total number of fragments is thus:

Clearly, this produces a large number of fragments, many of which are unlikely to produce useful abductive results. We would like to prune the fragments before we attempt to use them in the query-time phase.

4.1.1 Example

The following SPIN rule states the antecedents required to conclude that a person is a grandmother:

```
CONSTRUCT {
  ?p1 grandmotherOf ?p2 . }
WHERE {
  ?p1 parentOf ?p3 .
  ?p3 parentOf ?p2 .
  ?p1 rdf:type Person .
  ?p2 rdf:type Person .
  ?p3 rdf:type Person .
  ?p1 gender Female . }
```

This rule produces 120 fragments, among which are those that follow, which are annotated with their intuitive abductive use:

Fragment 1:

```
{ ?p1 grandmotherOf ?p2 .
  ?p3 parentOf ?p2 . }
```

"If we know that there is a grandmother of a parent of a child, then we suspect that the grandmother could be the parent of that child's parent. We furthermore suspect that the grandmother is Female."

Fragment 2:

```
{ ?p1 rdf:type Person .
  ?p2 rdf:type Person . }
```

"If we know there are two People, then we suspect the first Person could be a grandmother, the second Person could be a parent, and that there is a third Person who is their grandchild and child, respectively."

Intuitively, the likelihood and usefulness of the abductive interpretation of the first fragment is much greater than that of the second. To exploit this intuition, we assign weights to the statements of each fragment. Weights are based on the subclass or subproperty depth of any Properties, Classes or Individuals in the statement. Subclass depth is calculated as the number of direct subClassOf assertions

from the named Class to owl:Thing in the ontology. Subproperty depth is composed of three parts: 1) the number of direct subPropertyOf assertions from the named Property to ObjectProperty or DatatypeProperty in the ontology; 2) The subclass depth of the domain constraint of the named Property, if any; 3) The subclass depth of the range constraint of the named Property, if any. Individuals have the subclass weight of the deepest parent for which there is an explicit rdf:type statement in the ontology. We then weight the fragment with the sum of its statements' weights.

4.1.2 Example

In our example, the grandmotherOf and parentOf Properties are 2 levels deep in the ObjectProperty hierarchy and have domain and range constraints of Person, which has a subclass depth of 3. Our weighted example fragments from Example 4.1.1 thus become:

Fragment 1 (weight = 16):

{ ?p1 grandmotherOf ?p2 . (weight = 8)

?p3 parentOf ?p2 . (weight = 8) }

Fragment 2 (weight = 8):

{ ?p1 rdf:type Person . (weight = 4)

?p2 rdf:type Person . (weight = 4) }

Fragments with a weight below a given threshold are removed from consideration. The rest are stored in the index which contains the weighted statements and pointers to the rules they came from. Note that in a large collection of SPIN rules, it is likely that multiple rules will contain some of the same fragments. Each fragment is indexed in turn with any named Classes, Properties and Individuals found in its statements. The index is now ready for use in the query-time phase.

4.2 Query Phase

The input to this phase is a collection of statements. As mentioned in Section 2, these statements may be a partially resolved SPARQL query still containing some open variables, or they may be ABox statements generated by some inference, extraction or other analytical process. For our purposes, they are considered to be true statements upon which we will base our abductive assumptions.

The first step of resolving the query is to find the fragments which use the same named Classes, Properties and Individuals as can be found in the input statements. The depths of the statements found in the fragments are then used to rank those fragments.

4.2.1 Example

Given the following input statements:

UID1 grandmotherOf UID2 .

UID1 rdf:type Person .

UID1 hairColor Red .

The rule fragments we have seen during the indexing phase in Section 4.1 are partial matches for this set of input statements. Specifically, Fragment 1 matches because of the grandmotherOf statement in the input query, and is thus given weight 8. Both of Fragment 2's statements match because of the same tdf:type Person statement in the input query. Because they both match the same input query statement, they are only counted once, to provide weight 4. The input query statement about hairColor does not match any fragment, and provides no weight.

Fragment 1 (weight 8):

{ **?p1 grandmotherOf ?p2 . (weight = 8)**

?p3 parentOf ?p2 . (weight = 8) }

Fragment 2 (weight 4):

{ **?p1 rdf:type Person . (weight = 4)**

?p2 rdf:type Person . (weight = 4) }

In this simple example, there is not support from multiple input query statements to fragments, but this support would be additive if it existed.

Fragments are then sorted by their weighting against the input query statements, and the full SPIN rules they are found in are then weighted by the contributions of the fragment weightings. In the example, both Fragments 1 and 2 come from the same SPIN rule for grandmothers, so this rule is assigned a weight of 12.

Now with a list of weighted SPIN rules and the input query statements, we produce a version of the SPIN rule with as many open variables bound to Individuals, Classes and Properties as possible from the input. This binding process can be potentially computationally expensive if there are many candidate input Individuals which could validly bind to open variables in the SPIN rule. Our current approach is to prune rules which would produce more than a handful of SPIN rule interpretations.

4.2.2 Example

Our example input and rule share the unique grandmotherOf assertion which limits open variable binding ambiguity. The individuals used in the input statement take the place of the open variables in the SPIN rule:

CONSTRUCT {

UID1 grandmotherOf UID2 . }

WHERE {

UID1 parentOf ?p3 .

?p3 parentOf UID2 .

UID1 rdf:type Person .

UID2 rdf:type Person .

?p3 rdf:type Person .

UID1 gender Female . }

Two sets of information are now available: fully bound statements from the original SPIN rule which can be taken as abductive inferences; and a new, more specific SPIN rule which can be issued as a SPARQL query against data sources which may result in further variable bindings and abductive processes. Of the two bolded statements above, the knowledge that UID2 is a Person could of course have been determined by deductive inference using the range constraint of the grandmotherOf Property. The knowledge that UID1 has the gender Female is something which may only have been possible to discover by referring to the SPIN rule, although in many ontologies, Restrictions are used to produce these kinds of inferences. The more specific version of the SPIN rule which is to be used as a SPARQL query is constructed as follows:

```
SELECT ?p3
WHERE {
  UID1 parentOf ?p3 .
  ?p3 parentOf UID2 .
  ?p3 rdf:type Person . }
```

UID1 and UID2 are assumed to have been named in the data source(s) from which the original input was taken, and are thus available as query elements. The additional information about their relationship to each other does not need to be restated in the next query. Intuitively, we have determined that to gain more complete knowledge of the situation, we should search our data for some Person who is both the child of the grandmother and the parent of the grandchild.

5 Results

To test our approach, we generated a basic familial relations ontology which included Class and Property hierarchies. We then built a population of 20 SPIN rules describing family relationship structures as well as family events such as marriages. We aligned this ontology to the Basic Formal Ontology[8] to give some reasonable depth characteristics of our Classes and Properties. The shape of the ontology is summarized in Table 1.

Metric	*Measurement*
Classes	6
ObjectProperties	12
Avg Class Depth	7.5
Avg Property Depth	3
SPIN Rules	20
Avg Consequent Statements	1.8
Avg Antecedent Statements	8.5

Table 1: Test Ontology Metrics

5.1 Index Phase Results

We set the threshold for fragment depth relatively low so that we could avoid 'trivial' fragments that contained only rdf:type statements for mid- or high-level classes such as Agent, Entity, etc. Table 2 presents the nature of the resulting rule fragments and index produced for the test ontology.

Metric	*Measurement*
Raw Rule Fragments	1054
Average Fragment Weight	40
Fragment Threshold	20
Fragments Passing Threshold	728

Table 2: Review Metrics for Wine Ontology

We used an HBase database to store the index contents.

5.2 Query Phase Results

To date, we have not integrated our approach with capabilities which could issue our reformulated queries against live external data sources. We constructed a number of statement sets which were representative of possible starting queries a client might have. We then queried the fragment index and calculated the subsequent requeries as we described in Section 4.2.

Results appeared reasonable when manually reviewed. Predictably, we found that the more vague the starting point, the larger the number of suggested subsequent queries. When input statements were about specific consequents, the suggested subsequent queries supported finding evidence about the antecedents.

6 Conclusions and Future Work

We believe our approach has merit in scenarios where: the T-Box is primarily Class and Property hierarchies; there is a large population of semantic rules; and the full population of the A-Box is impossible to achieve 'all at once,' and must be built iteratively using contextually relevant query and extraction processes.

Clearly, we intend to integrate the abductive requery approach with a system including a large but incomplete A-Box and a query mechanism for extracting or discovering new statements based on some kind of requerying. We believe that there are many use cases in areas such as social networking, unstructured text mining and Big Data exploration.

More focused areas for expansion of our work are described in the following sections.

6.1 Incorporating Restrictions

Until the development and use of OWL-compatible semantic rule languages, OWL Restrictions were the primary method of stating rule-like information by using subclass and equivalent class statements in conjunction

with quantification on properties. We intend to 'convert' these constructs to antecedent-consequent structures and add them to the index and requery process.

6.2 Further Exploiting Class and Property Hierarchies

We have not incorporated basic Class and Property subsumption in our query phase approach, relying on input statements to be asserted at the same 'level' in the ontology as the SPIN rule statements are asserted. In our context of an incomplete A-Box, we intend to explore both generalizing: if input statements are either 'a Person has an email address' or 'an Organization has a mailing address', we want to match a SPIN rule which requires 'an Agent has an Address'. But we also want to explore 'unmotivated' specialization such as matching an input statement which says 'an Organization has a Budget' to a SPIN rule which requires 'a Public Company has a Budget.'

7 Acknowledgements

This material is based in part upon work supported by the Intelligence Advanced Research Projects Activity (IARPA) via Air Force Research Laboratory contract number FA8650-10-C-7062. The U.S. Government is authorized to reproduce and distribute reprints for Government purposes notwithstanding any copyright annotation thereon. Disclaimer: The views and conclusions contained herein are those of the authors and should not be interpreted as necessarily representing the official policies or endorsements, either expressed or implied, of IARPA, AFRL or the U.S. Government.

8 References

[1] W3C. SWRL: A Semantic Web Rule Language Combining OWL and RuleML. W3C Member Submission 21 May 2004. http://www.w3.org/Submission/SWRL/

[2] W3C. SPARQL Query Language for RDF. W3C Recommendation 15 January 2008. http://www.w3.org/TR/rdf-sparql-query/

[3] W3C. SPARQL Inferencing Notation. W3C Member Submission 22 February 2011. http://www.w3.org/Submission/2011/SUBM-spin-overview-20110222/

[4] C. Elsenbroich, O. Kutz, and U. Sattler. "A case for abductive reasoning over ontologies"; In Proceedings of the OWLED Workshop on OWL: Experiences and Directions, Vol. 216, November, 2006.

[5] C. Kiefer. "Non-Deductive Reasoning for the Semantic Web and Software Analysis"; Doctoral Thesis, University of Zurich, 2008.

[6] J. Du, G. Qi, Y. Shen, and J. Pan, "Towards Practical ABox Abduction in Large OWL DL Ontologies"; The Twenty-Fifth AAAI Conference on Artificial Intelligence (AAAI-11), San Francisco, USA, August, 2011.

[7] C. Kevorchian. "A Semiotics Approach of Abduction Ontology Query", Annals of the University of Craiova, Mathematics and Computer Science Series, Volume 37(3), 2010.

[8] A. Spear. "Ontology for the Twenty First Century: An Introduction with Recommendations"; Under Review. http://www.ifomis.org/bfo/documents/manual.pdf

Preliminary Experiments on Literature Based Discovery using the Semantic Vectors Package

M. Heidi McClure
Intelligent Software Solutions, Inc
Colorado Springs, CO 80919

Abstract— *This paper presents a literature based discovery (LBD) implementation that uses Lucene for indexing, the Semantic Vectors (SV) package for latent semantic analysis, Neo4j for graph database storage, Gephi for visual representation along with custom code written by the author. The approach of using a latent semantic analysis based systems like SV to do LBD is not new, but going the next steps of examining related concepts and using a graph database representation for finding candidate linking terms is. The LBD system is a framework where relation extraction experiments may be performed. This paper presents work that is in progress.*

Keywords: literature based discovery, semantic vectors package, relation extraction

1. Introduction

Literature based discovery (LBD) has been around since the 1980's when D. R. Swanson first defined LBD as a means to discover previously unknown knowledge by examining term occurrences across multiple documents [16]. This paper presents an implementation that uses variations on latent semantic analysis (LSA) to perform LBD-style discovery. Studies of using LSA to do LBD have been documented by various authors, among them are *[14], [11], [19].* LSA discovers semantically related concepts giving stronger correlation scores to more strongly related concepts. When a pair of concepts that have a significant semantic relatedness score from LSA and that are never mentioned in the same document or documents, you have an LBD candidate pair. The other pairs of candidate related concepts are that are mentioned in one or more of the same documents may also provide important information. These two sets - LBD candidate pairs and share-document-mention (SDM) pairs present data that allows a next level of discovery which is the discovery of candidate linking terms. The process of using graph database navigation across all related concepts found with LSA to discover new linking-concept candidates for an LBD candidate pair is the new approach presented in this paper.

The system presented in this paper handles these tasks: corpus generation, candidate related entities discovery and relationship analysis. The corpus generation retrieves document data from databases or from text files (including XML). All data is pre-processed by applying various normalization tasks to the data. The pre-processed data is placed on the filesystem where each document is in a separate text file. Candidate related entities discovery task indexes the data, performs forms of LSA and identifies the concept pairs with the highest relatedness scores. Relationship analysis is the final task of identifying the candidate linking concepts. This is done by first retrieving all documents relating to a candidate pair, determining which are LBD and which are SDM candidate pairs. Then the concept linked to concept as an LBD or an SDM pair is captured in a graph database. Last candidate linking terms are discovered by traversing the graph database. This work is not complete and is a work in progress and will provide the framework system on which more advanced relationship discovery will be performed.

The rest of this paper presents some background information on LBD, LSA, and Random and Reflective Indexing (RI and RRI) which are enhancements to LSA. It presents some details of software components and data used in the design and test of the system including the Semantic Vectors (SV) package, Lucene, Neo4J, Gephi and the MEDLINE data set. It presents the design of the system and discussion of the results. The end of this paper presents some conclusions and ideas for the future directions of this work.

2. Background

2.1 Literature Based Discovery

LBD is the discovery of hidden knowledge in large sets of documents where the discoveries relate concepts A and C together. In LBD, a single document in the corpus will not contain the discovery. Sometimes a linking term, B, may be the means by which A and C are discovered and B would be in all documents containing A or C. In statistical approaches to LBD, there may not be a linking B term in the discovery - instead, A and C are discovered by semantic relatedness of the documents using, for example, latent semantic analysis (LSA) techniques. Once candidate discoveries are found, experiments may be performed to prove or disprove the hypotheses.

As various works state, Don R. Swanson [16] is considered to be the first to have mentioned the LBD style of discovery [13], [10], [15]. Swanson manually reviewed medical journals in one of his studies and found mentions of Raynaud's syndrome and its relation to various blood issues like problems with blood

viscosity, platelet function and vascular reactivity. Then he looked for discussions of these blood issues in articles that did not mention Raynaud's and found associations between the blood problems and fish oil. The connection made is that, perhaps, Raynaud's syndrome could be treated with fish oil. Medical studies have since been able to validate this discovery.

Since his initial study, Swanson and many other researchers started to apply automation to the task of LBD. Initially works would look for candidate B linking terms simply by their co-occurrence in the A-term documents then use these B terms to candidate documents where A is not mentioned. Then would try to find, again with co-occurrence, candidate C terms in the new set of documents. They sometimes used lists of words (vocabularies) to restrict which words they considered in each search - when list is used for both A and C concepts, the LBD system is called a closed system. An open system considers a a list of words only for the starting concept, A. [10]

This initial work is a closed LBD work, but future work plans to use the open approach.

2.2 Latent Semantic Analysis

LSA came initially from the Latent Semantic Indexing (LSI) work done by Scott Deerwester, Susan Dumais and and others [9] and used in LBD by Michael Gordon and Dumais [11] - LSA does not require, necessarily, a vocabulary, but, instead, finds similar documents based on LSI. LSA assumes that if terms or concepts are found in similar sets of text (not always the same text) then these terms or concepts may be related, the same or similar concepts. The mathematics behind LSI uses singular value decomposition (SVD) to reduce the dimensions of extremely large matrices by getting rid of less interesting data and to discover the related terms in documents. LSI proved to be more efficient than previous methods and has been moderately successful, however, it's still slow and computationally expensive.

2.3 Random and Reflective Random Indexing

More recently, Cohen, et al. [8] experimented with random indexing (RI) - a more scalable version of LSI - and extended the RI concepts to support indirect inference. Indirect inferences is what Cohen, et al. sometimes call LBD. RI is uses a random approach to further reduce the size of matrices being analyzed to discover similar terms in documents. Instead of a full term by document matrix, documents are placed into small sets of columns. For example, if there are 10,000 documents, a document may be assigned to 20 randomly chosen columns. Each document's term frequency information is tallied in each of its columns along with any other document that was randomly assigned [12]. Cohen, et al. also experimented with variations of RI - Sliding windows on RI, Term based Reflective Random Indexing (RRI), and Document based RRI. RRI uses RI but does it using results from one RI process and feeding it into another pass of RRI. Term and document based RRI vary how the random indexing is chosen - by term or by document in various passes through the RRI. Their claim is that these techniques provide more related terms/concepts that may not co-occur in the same document but are possibly related. They state that their use of RRI techniques is better suited for LBD.

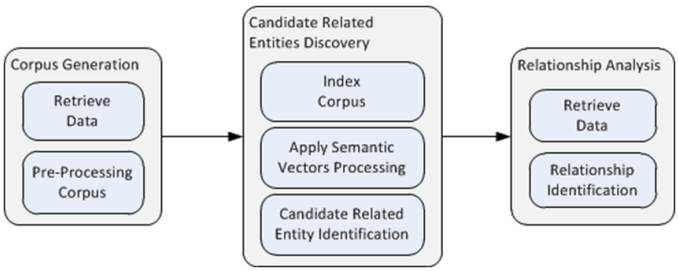

Fig. 1: Architecture

3. Design

This section describes the general design of the SV-based LBD system. There are multiple steps performed that ultimately present pairs of entities that may be related and presents candidate linking terms. The general architecture of the system is shown in Figure 1.

The steps noted below align with the small boxes in the architecture diagram.

1) **Retrieve data** and place each document into a separate text file on the computer filesystem. The data tested so far, has been in database as reports summarizing, for example, news articles, as web pages or as other text data. Data also has been in databases as copies of emails and has been in large XML files which needed to be broken up to get text documents. An example of XML files is the MEDLINE data presented in this paper where the resulting document pulled from the XML is just the abstract of the article.
2) **Pre-process the corpus** mostly to identify the concepts we wish to analyze. This makes a copy of the original filesystem documents and tags the new documents as necessary. Today this consists of doing some simple normalization of the data turning "John Doe" into "johnxxxdoe" so that the next step of indexing doesn't need to have custom indexing capabilities implemented. In other words, multi-word tokens have been turned into single words. Lowercase is being used because the SV package works best with all concepts in lower case.
3) **Index the corpus** using Lucene indexing as described in the semantic vectors package. The SV package uses the Lucene index to help build the SV vector files. See [6] for more information on Lucene.
4) **Apply semantic vectors processing** to create document and term vector files. Term vectors are not simple word

count per document vectors. They are vectors where the entries represent a term's relatedness to random sets of documents. Comparing the vector for two different terms (i.e. concepts) presents a score that gives the LSA relatedness of the two terms.

5) **Candidate related entity identification** is performed by comparing the term vectors for each entity as discussed in previous step. Some term pairs come up with a 1.0 score indicating the strongest relatedness - since there's probably nothing new to discover with this pair, these terms are ignored in LBD processing. Similarly, terms with zero or negative scores are also ignored.
6) **Retrieve documents** for the related entities. Finding these documents is done by going back to the original Lucene index created before SV processing. Returned are documents that mention either of the entities or both. At this time, identification of LBD candidates is done by finding the pairs of related entities that are never mentioned in the same documents.
7) **Relationship Identification** involves
   a) examining documents where entities appear together
   b) when entities are LBD candidates, identify candidate linking B terms. This may be done navigating the graph looking for terms that are linked to both the A and the C terms. There are examples of this presented in the results section.

   Explaining why entities may be related is the primary area of future work planned by the author.

In the next subsections, a small amount of detail is provided about some of the tools and API's used in this work.

3.1 Semantic Vectors Package

A byproduct of Cohen's work to improve LSI [8] is the Semantic Vectors (SV) package. This open source java software initially written by Cohen's co-author, Dominic Widdows, and now maintained by he and many others under a Google code project - [18]. SV provides a library of capabilities that perform random indexing which performs much faster than SVD. SVD is an N x N problem where matrices will get to a size that current computing capabilities will now allow them to be computed. RI can do LSA-like analysis on millions of documents. For this work, terms are compared to identify relatedness.

3.2 Lucene indexing

Lucene [6] is a set of java libraries that, among other things, allows for the searching of terms and phrases in sets of text documents or other representations of text like PDF's, HTML, Microsoft Word, etc. Lucene creates index files that contain the necessary information to not only find terms or phases quickly that may be contained in a corpus, it also is able to indicate where in the document the terms or phrases are. Lucene provides fast and efficient search capabilities.

In the LBD solution presented here, Lucene indexes are created first and then the Semantic Vectors package is used to find candidate LBD pairs. Once pairs are found, the Lucene indexes are again referenced to find the documents in which entities are mentioned.

3.3 Graph database - neo4j

Running SV with term comparisons across a set of documents discovers pairs of concepts that may be related. A graph database that represents node X, node Y and the link joining node X and Y is a good choice for storing results of SV or any other results of latent semantic analysis. Graph databases are sometimes called NoSQL databases since data is not stored in a traditional table structure. Neo4j is an open source light weight graph database [7].

For this project, nodes are the concepts (for example, A, B and C concepts) and the links are either an LBD link where the nodes on either side of the link are never mentioned in the same document or a shared document link where the nodes on either side are both mentioned in one or more documents.

3.4 Visualization - Gephi

Once data is stored in a neo4j database, visualizing that data is important in order to assist in the analysis of results. Gephi is an open source graph visualization tool [5]. Martin Skurla created a neo4j plugin into Gephi during Google's summer of code, 2010. [4]

Once a neo4j database is loaded into Gephi you can show only LBD relationships (links) or show only shared common document relationships. The graph (link) pictures shown in this paper were created from snapshots of Gephi displays of neo4j databases.

4. Experimentation and Results

4.1 Data Sets

The current application allows flexibility in what steps of the LBD process are run and flexibility in what data are used. For example, MEDLINE data used in experiments presented here are pulled out of XML files using python scripts that place each abstract into a separate file on the filesystem. Data may come from, for example, an Enron email corpus that may be in a database or may just be files on a filesystem [1], [3]. When data comes from database queries, the "document" data usually is read from large text fields or sets of fields - the system presented here places this data onto the filesystem - one file per document.

MEDLINE is a National Library of Medicine database of biomedical literature that includes, among other things, the

```
0.25801524803614884   hypertension - stroke
0.26078878702313346   calcium channel - nitrendipine
0.26371141356922895   glycerin - hydrogen
0.2646692347004723    cerebrovascular circulation - chronic paroxysmal
0.26537108942298393   adrenergic alpha receptor - systemic scleroderma
0.26855056509811615   beta blockade - hydrazine
```

Fig. 2: Sample of related pairs

```
start pair ----- A: fish oil ----- C: raynaud's phenomenon ... 0.10460266408050004
aOnlyDocs: 100-----------------------------------------------------------------
  C:\...\1980_1984tagged\1983_6644923.txt
  C:\...\1980_1984tagged\1981_7195080.txt
...
  C:\...\1980_1984tagged\1983_6642137.txt
cOnlyDocs: 100-----------------------------------------------------------------
  C:\...\1980_1984tagged\1983_6673032.txt
  C:\...\1980_1984tagged\1983_6416474.txt
...
  C:\...\1980_1984tagged\1983_6868709.txt
bothAandCDocs: 0---------------------------------------------------------------
end pair ----- A: fish oil ----- C: raynaud's phenomenon ... 0.10460266408050004
```

Fig. 3: Sample LBD Pairs

```
0.1309778020467315  platelet aggregation       prostaglandin          entity - prostacyclin
0.12166000932210942 lupus                     raynaud's phenomenon   entity - prostacyclin
0.10876718225628104 blood coagulation factors stroke                 entity - cerebrovascular circulation
0.1434759715509119  blood                     vasospasm              entity - vasoconstriction
0.11330897826518167 calcium                   dihydropyridine        entity - channel blockers
```

Fig. 4: Sample Candidate B Terms

titles and abstracts of over 21 million articles from over 5000 different journals and publications [2]. This data is stored in many XML files. For this effort, the python script used pulled each abstract for the years of interest and placed each into a file on the filesystem. Initial experimentation used all the abstracts from 1980-1984 which simulates rough dates used by Don Swanson in his initial LBD work [16]. This date range created 692,382 total file documents.

4.2 Output

MEDLINE data was analyzed by the system using approximately 190 candidate A and C concepts that were gathered from two papers - one that discussed fish oil and Raynaud's [11] and the other that discussed both fish oil - Raynaud's connection and migraines and magnesium connection [17].

During the processing of results, a neo4j database was created that ultimately allows for visual display of results. The Neo4j database contains nodes that represent documents and links that are named either an LBD relationship or a share-document-mention (SDM) relationship. If the relationship between two nodes is an LBD relationship, that means the nodes were never mentioned together in the same document.

The system also creates summary results in a set of text output files. In order to keep the number of result pairs to consider a manageable size, an algorithm is currently used that returns either a hard number of results or a percentage of total pairs discovered. Some of the generated output files contain:

1) All related pairs - pairs that share mentions in documents and those that don't. The ones that don't will be LBD pairs. The SV score is also captured for each pair. See Figure 2
2) All LBD pairs - in order to discover the LBD pairs, the Lucene index is queried to find all documents in which the terms are mentioned. If there are no documents in common (bothAandCDocs = 0 in the LBD Pairs output), then this is an LBD pair. For preliminary work, only a maximum of 100 document matches is allowed for this result reporting. See Figure 3
3) All candidate linking terms - this file is the result of navigating the Neo4j graph database to find candidate B linking terms between the LBD pairs reported in the second list (All LBD Pairs). The first two terms are the LBD pair, the last is the candidate B term. See Figure 4

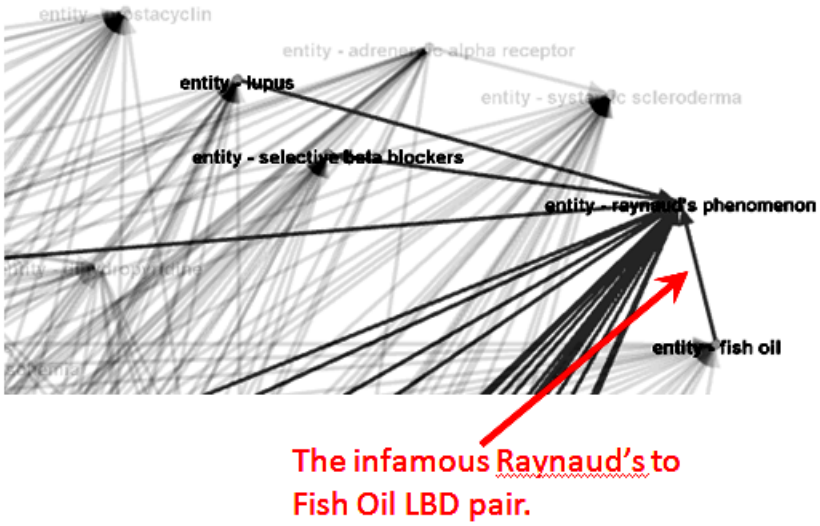

Fig. 5: Highlight Raynaud's and see LBD candidate pairs

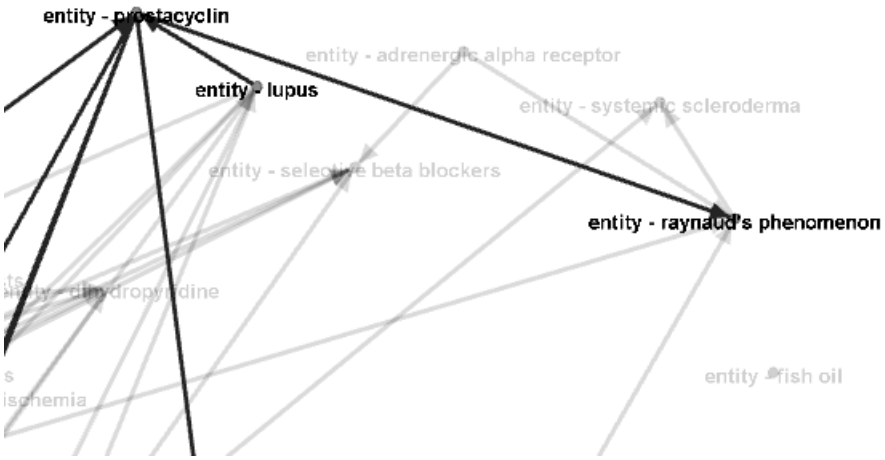

Fig. 6: Terms that share document references - A and C concepts, Lupus and Raynaud's, linked by B concept, Prostacyclin

4.3 Analysis

In addition to the text file results, the Neo4j database loaded into Gephi, the graph visualization tool, provides help in visualizing what's in the data. In Figure 5, all of the medical concepts that had an LBD relationship with Raynaud's phenomenon are highlighted. Simply mousing over the Raynaud's node performs this highlighting. From this visualization, we see that Raynaud's phenomenon is related, via LBD, to Lupus, selective beta blockers and fish oil - again, it's LBD because the links shown are only the LBD candidate pairs. As in Swanson's work [16], fish oil and Raynaud's phenomenon are never mentioned in the same documents. In Figure 6, only links where the entities actually are mentioned in the same documents are shown. This particular view where prostacyclin is highlighted shows that prostacyclin may be a linking B concept between the A and C concepts - Lupus and Raynaud's phenomenon. In Figure 7, we can see that adrenergic alpha receptor is a concept relating selective beta blockers and Raynaud's phenomenon together. In this same diagram, we notice that fish oil had no candidate linking terms to Raynaud's - this is probably due to the small subset of A and C concepts analyzed in this early testing (as noted earlier, approximately 190 terms were used for candidate A and C concepts).

5. Conclusion

I have presented an approach to discovering hidden knowledge in documents using a latent semantic analysis variant from the semantic vectors package. My approach discovers candidate

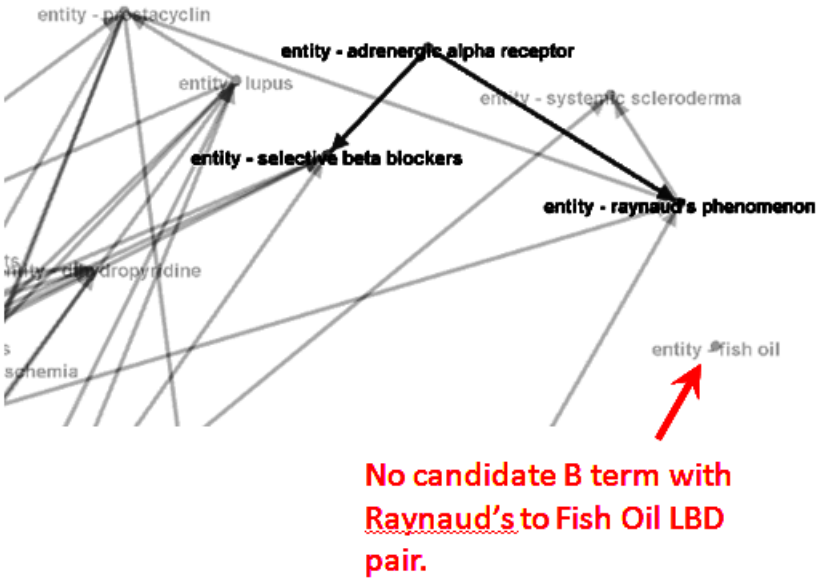

Fig. 7: Terms that share document references - A and C concepts, selective beta blockers and Raynaud's, linked by B concept, adrenergic alpha receptor. Note that no candidate term found between Raynaud's and fish oil.

A and C concepts or terms which, although never mentioned in the same document, may be related. I have also discovered candidate linking or B terms that relate the A and C. To the best of my knowledge and research, identifying the linking B terms from the LSA results is something that has not previously been done.

This system provides the platform on which alternative approaches may be tried to improve the quality of the discovered pairs.

6. Future

I hope to complete the following major tasks.

6.1 Complete the Reproduction of Swanson Results

In order to test the results of this system, I have successfully shown that fish oil and Raynaud's are semantically related and are never mentioned in the same documents in the 1980-1984 corpus. Using the evaluation methodology described by Meliha Yetisgen-Yildiz and Wanda Pratt [20], the next step is to examine the corpus of documents after 1984 to see if the LDB candidates are mentioned in the same documents, thus, perhaps, proving that there is now a confirmed and important relationship between the LBD candidate pairs. There are other published results based on MEDLINE that use LBD to discover previously unknown related concepts. I may try to recreate those discoveries, also.

6.2 Making Operational Solution

I plan to examine how analysts, scientists or other users might use the capabilities of the system presented in this paper. If I can refine the system so that fewer false positives are presented, users may find great benefit in the kind of discoveries that LBD presents - that is, the previously unknown and hidden knowledge that is in existing data.

6.3 Relationship Extraction - Discovering the Why

I plan to take the results - the candidate LBD pairs and perhaps the linking B terms - and try to figure out why the concepts are related. That is, try to explain the relations. Initially, I plan to try relationship extraction approaches that have already been published with the hopes of refining these techniques to fit with that data and to provide more accurate results.

6.4 Open LBD

The approach I have taken to date is a closed LBD solution where we know what A and C concepts to study. The next step is to expand this work to perform Open LBD where the C concepts are not known. To do this, candidate C concepts are discovered using natural language processing (NLP) named-entity (NE) extraction techniques to identify the kinds of concepts we are interested in. For example, when using medical domains, drugs, diseases, symptoms or side effects will be tagged by NLP NE extraction and then used as candidate C

concepts. When studying, for example, the Enron email corpus, people, places, organizations or events will be tagged.

Acknowledgments

Work described in this paper was funded by Intelligent Software Solutions as an internal research and development project (IRAD). The system described in the paper is patent pending, all rights reserved.

References

[1] Enron data set. http://www.cs.cmu.edu/ enron/.

[2] Medline/pubmed data files. http://www.ncbi.nlm.nih.gov/pubmed/ or http://www.PubMed.gov/.

[3] Mysql enron database. http://www.isi.edu/ adibi/Enron/Enron.htm.

[4] Plugin for visualizing neo4j graphs in gephi, 2010. https://gephi.org/plugins/neo4j-graph-database-support/.

[5] Gephi graph visualization tool, 2012. http://www.gephi.org/.

[6] Lucene, 2012. http://lucene.apache.org/.

[7] Neo4j - an open source graph databases. website, 2012. http://www.neo4j.org.

[8] Trevor Cohen, Roger Schvaneveldt, and Dominic Widdows. Reflective random indexing and indirect inference: A scalable method for discovery of implicit connections. *Journal of Biomedical Informatics*, 43(2):240 – 256, 2010.

[9] Scott Deerwester, Susan T. Dumais, George W. Furnas, Thomas K. Landauer, and Richard Harshman. Indexing by latent semantic analysis. *Journal of the American Society for Information Science*, 41:391–407, 1990.

[10] Murat C. Ganiz, William M. Pottenger, and Christopher D. Janneck. Recent advances in literature based discovery. Technical Report LU-CSE-05-027, Lehigh University, 2005.

[11] Michael D. Gordon and Susan Dumais. Using latent semantic indexing for literature based discovery. *J. Am. Soc. Inf. Sci.*, 49:674–685, June 1998.

[12] Pentti Kanerva. Hyperdimensional computing: An introduction to computing in distributed representation with high-dimensional random vectors. *Cognitive Computation*, 1:139–159, 2009. 10.1007/s12559-009-9009-8.

[13] Joel A Solka Jeffrey L Briggs Michael B Rushenberg Robert L Stump Jesse A Johnson Dustin Lyons Terence J Wyatt Jeffrey R Kostoff, Ronald N Block. Literature-related discovery (lrd). Technical Report ADA473438, OFFICE OF NAVAL RESEARCH, November 2007.

[14] Robert K. Lindsay and Michael D. Gordon. Literature-based discovery by lexical statistics. *J. Am. Soc. Inf. Sci.*, 50:574–587, May 1999.

[15] Aditya Kumar Sehgal. *Profiling topics on the Web for knowledge discovery*. Phd diss, University of Iowa, 2007.

[16] D. R. Swanson. Fish oil, raynaud's syndrome, and undiscovered public knowledge. *Perspect Biol Med*, 30(1):7–18, 1986 Autumn.

[17] Marc Weeber, Henny Klein, Lolkje T.W. de Jong-van den Berg, and Rein Vos. Using concepts in literature-based discovery: Simulating swanson's raynaud-fish oil and migraine-magnesium discoveries. *Journal of the American Society for Information Science and Technology*, 52(7):548–557, 2001.

[18] Dominic Widdows et al. Semantic vectors package, 2012. http://code.google.com/p/semanticvectors/.

[19] M. Yetisgen-Yildiz and W. Pratt. Using statistical and knowledge based approaches for literature-based discovery. *Journal of Biomedical Informatics*, 39(6):600–611, 2006.

[20] Meliha Yetisgen-Yildiz and Wanda Pratt. A new evaluation methodology for literature-based discovery systems. *Journal of Biomedical Informatics*, 42(4):633 – 643, 2009.

Semi-Autonomous Hierarchical Document Classification Using an Interactive Grounding Framework

Jacob Staples[1], **Attila Ondi**[1], **and Tony Stirtzinger**[1]
[1]Securboration, Inc., 1050 W. NASA Blvd., Melbourne, FL, USA

Abstract - *Organizations must evolve internally over time to better fulfill their missions. The structural complexity inherent in a large organization can impede an agile evolutionary process, however. In this work we describe a tool created to ease the process of structural evolution within a large, complex and hierarchically organized organization. This tool analyzes request for change documents provided by low-level personnel unfamiliar with the overall organizational structure and determines which portions of the organization will be affected. This task is accomplished using natural language processing to extract relevant textual features from request for change documents and machine learning techniques to ground these features to relevant concepts corresponding to affected portions of the hierarchy. The initial groundings are refined through an interactive question-answer session with the user providing the request for change document. The tool is shown to have desirable convergence traits and a high degree of accuracy.*

Keywords: Machine learning, NLP, Neural networks, Hierarchical document classification, Automatic document classification

1 Introduction

Organizations must evolve internally over time to better fulfill their missions. The larger the organization, the more thoroughly a potential change to its structure must be vetted as even a minor change requires significant monetary and policy commitment. In this work we propose a mechanism for easing the interaction between the low-level users who are most readily able to recognize the inefficiencies in an organization and the high-level managers who are most able to remedy them. This mechanism will be discussed in the context of a hypothetical system representing a simplified version of a real-world product.

In this system, users who notice an inefficiency or unaddressed need in their day-to-day operations may electronically submit a request for change (RFC) document to a managerial team with a good understanding of the organization's structure. The managerial team then reviews these RFC documents and determines what action to take on them. One significant problem with this process is that the content typically provided by users who create RFCs is poorly aligned to the information a reviewer needs to quickly analyze the impact of the RFC. For example, RFC authors are typically most concerned with their individual ability to improve day-to-day operations whereas RFC reviewers are more interested in the impact on the organization as a whole. In this work we describe a mechanism for determining the organizational impact of RFC documents automatically for an organization whose structure is ontologically modeled. This means that users need not spend valuable time researching information which will not directly benefit their daily activities and managers need not delve too deeply into the minutiae of daily operations. The communication between the two groups can therefore be conducted much more efficiently because users write RFCs using language they understand and reviewers receive a summary of the information they need which has been automatically derived from the user's RFC.

The determination of organizational impact is conducted in two phases. The first is performed autonomously using NLP and machine learning techniques to determine the document content and compute an initially large number of potential areas of impact within the organization. The second is an interactive state where questions are asked of the user to refine the coarse results obtained during the first phase. The final result of these two phases is a document which can be quickly and easily scanned by a RFC reviewer to determine the impact of a proposed request for change within the organization.

2 Related Work

A common and well-established problem in machine learning is automatic document classification [1] in which a text T is categorized as applying to one of several concepts (topics). A simple extension of this problem is to ground T to a set of concepts C by some numerical measure of the relative strength of the correlation between T and each concept $c \in C$ present in the text. For example, if we ground text instance Tx to a set of four concepts {*concept1*, *concept2*, *concept3*, *concept4*} then Tx might ground to *concept1* with a weight of 0.4, *concept2* with a weight of 0.9, *concept3* with a weight of 0.05 and *concept4* with a weight of 0. The magnitude of these weights implies the quality of the grounding relative to the other links (in this example, *concept1* is grounded 8 times as strongly as *concept3* by Tx). This process is commonly referred to as multi-topic text classification [2].

Many automatic text classification systems are naïve in that they make the following assumptions about the text documents on which they operate:

1. The probability of a feature occurring in a text is independent of the length of the text
2. The probability of a feature occurring in a text is independent of the existence of other features in the text

For very large numbers of documents concerning a large number of unique topics produced by a large number of unique individuals, these assumptions are a close enough approximation to average behavior that naïve Bayesian or similar classifiers are often quite accurate. Our application is significantly different from such scenarios, however. We observed lengthy Request for Change documents to frequently contain many of the same words, a violation of the first assumption listed above. For example, nearly 20% of the RFC documents longer than 100 words contained some form of the word "requirement" as a noun compared to just 3% for those shorter than 50 words. Additionally, because the RFC documents typically deal with similar subject matter, the second assumption listed above is often violated. For example, a document containing the word "money" is significantly more likely to contain the word "expenditure" than a document which does not. With too few training examples to average out the violations listed above, the discrepancies between the naïve assumptions of simple classifiers (such as Naïve Bayes) and reality are greatly exaggerated. For these reasons, our initial attempts to utilize a naïve Bayes classifier for this application were unsuccessful and we turned to a new type of supervised learning classifier.

3 Approach

To automatically determine the organizational categories embodied by an RFC document, a text-to-concept grounding engine was developed incorporating elements of natural language processing, machine learning and similarity testing. The classifier portion of the engine analyzes the natural language content of the RFC document and, based on the key features identified, prompts the document submitter for answers to clarifying questions. The answers provided by the user help to narrow down the candidate categories for the reviewers, reducing or eliminating the need for follow-up communication.

The organizational model is quite complex with a total of 687 organizational area concepts hierarchically organized under ten main branches with a maximum depth of seven children. RFC reviewers desire the most applicable concept nodes to be returned regardless of their position in the hierarchy (i.e., leaf nodes are not favored above internal nodes simply because they are lower in the hierarchy).

3.1 Grounding abstraction

At its most fundamental level, our classification system operates on a set of features F extracted from a given text T and a set of relevant concepts C' to produce a score mapping function $M:\{c \in C'\} \rightarrow R$ which generates the affinity of the text for each relevant concept $c \in C'$. This mapping function comprises our grounding of the text T.

Our grounding mechanism (classifier) operates in a similar fashion to a 2-layer neural network [3][4] where the input nodes are features observed in text and the output nodes are concepts in the hierarchy. As mentioned earlier, features can be any structure recognizable in text such as words, phrases, sentences, word groups, etc. The features we utilize are stemmed lemma/POS pairings although any feature type or combination thereof is theoretically possible. Links between features and concepts are numerical relationships reflecting the affinity of a feature for a concept. A single feature can have multiple links (directed edges) to concepts but there is only ever one link between a single feature and a single concept. Links have a weight associated with them as mentioned earlier but they have an additional component called inertia which ensures that over time the link weight will become harder to change. This inertial property is analogous to the decaying training coefficient in neural networks and is useful because without it the link weights would oscillate wildly around spurious training instances.

3.1.1 Feature extraction

The features used by the classifier are extracted from the change request documents using a Natural Language Processing pipeline implemented using the UIMA [5] framework with OpenNlp [6] components augmented by a heuristic lemmatizer based on an extended WordNet [7] dictionary enhanced with the ability to recognize custom jargon terms which do not exist in a standard dictionary. The detailed description of the feature extraction algorithm can be found elsewhere [8]. Although the grounding mechanism suggested in this work supports nearly any conceivable variety of feature types and combinations of features, we achieved satisfactory results using only a single simple feature type created by appending the lemma and part of speech category for each non trivial word in the text.

3.1.2 Feature extraction

The features used by the classifier are extracted from the change request documents using a Natural Language Processing pipeline implemented using the UIMA [5] framework with OpenNlp [6] components augmented by a heuristic lemmatizer based on an extended WordNet [7] dictionary enhanced with the ability to recognize custom jargon terms which do not exist in a standard dictionary. The detailed description of the feature extraction algorithm can be

found elsewhere [8]. Although the grounding mechanism suggested in this work supports nearly any conceivable variety of feature types and combinations of features, we achieved satisfactory results using only a single simple feature type created by appending the lemma and part of speech category for each non trivial word in the text.

3.1.3 Grounding Engine

As mentioned earlier the classifier utilized in this work is a supervised learner operating on human generated text. Thus there are effectively two phases to document classification. During training, link weights between features observable in text and concepts corresponding to those features are created and evolved. During grounding, previously learned link weights are used to compute the most likely candidates.

Pseudocode of the training algorithm

```
TRAIN(GroundingNetwork g,
  TrainInst[] trainingDataset):
 for(TrainInst i:trainingDataset)
  Feature[] features =
    NLPEngine.parse(i.Text)
  Concept[] concepts =
    i.CorrectConcepts
  for(Feature feature:features)
   for(Concept concept:concepts)
    g.updateLink(feature,concept,
      trainingDelta)
   end for
  end for
 end for
END

GroundingNetwork.updateLink(
  Feature f, Concept c, Weight w):
 Link link =
  f.getOrCreateLinkToConcept(c)
 linkUpdates = link.getUpdateCount()
 m = 1/(linkUpdates+1)
 link.weight =
  m*(link.weight * linkUpdates +
     w * inertia(linkUpdates))
 link.incrementUpdateCount()
END
```

The inertia function should monotonically decrease as link updates increase to encourage link weight convergence. We found a simple linear inertial function to work well. Feedback to the classifier can be provided in an online fashion any time new training data is obtained (even after the initial training phase is complete). Similarly to a neural network, feedback training instances must account for the difference between false positive and false negative errors, a minor modification to the above algorithm reflected by the *trainingDelta* variable.

During classification, the learned links and weights obtained during training are utilized to compute which concepts are relevant to the text.

Pseudocode of the classification algorithm

```
CLASSIFY(GroundingNetwork g,
  Text t):
 Feature[] features =
  NLPEngine.parse(t)
 ScoreMap scores
 for(Feature f:features)
  Concept[] concepts =
   f.getLinkedConcepts
  for(Concept c:concepts)
   scores.addScore(
     f.getLinkWeight(c))
  end for
 end for
 return scores.normalize()
END
```

The scores for each concept grounded by at least one feature in the text are computed as the normalized weighted sum of the feature to concept link weights in the grounding network. This is similar to node scoring in a neural network.

3.2 Interactive refinement

After scoring, we obtain a score distribution for concepts as shown in *Figure 1* below for two sample documents. The case-1 document is lengthy at over 150 words and the case-2 document is quite brief consisting of only three key words. It is interesting to note that the case-1 document has a relatively smooth distribution of scores for higher scoring concepts which are grounded by many feature to concept links but this distribution becomes more discontinuous for the lower scoring concepts which are grounded by fewer and fewer words. The case-2 document has a discontinuous distribution over its entire concept space.

Ideally this distribution would have a few concepts with very high normalized scores which could be classified as "correct" and the remaining concepts would have scores of zero and could be classified as "incorrect." As the distributions above indicate, however, the reality is more complex in that there may be dozens of scores within a single standard deviation of the best score. We observed that the top five to ten highest scoring concepts had a very high likelihood of being close to a correct concept in the hierarchy but had a lower probability of being absolutely correct. We also observed that in some instances the initially suggested concepts after thresholding were incorrect either because the language used in the RFC document was significantly different than the language on which the classifier was trained or because of ambiguous links between features and concepts as discussed later.

To handle both cases, after obtaining the grounding weights for each concept in the hierarchy for a given RFC document, we select a set B of the k best scoring concepts to use as a starting point for interactive refinement, or elicitation, which attempts to determine which concepts are actually correct. It is important to note that the choice of k is entirely arbitrary but we select it to be large enough to ensure a high degree of recall at the cost of low precision (experimental results revealed that for our purposes this occurred around k=10). This coarse set is then refined via a multi-question interaction with the user.

There are two phases in the elicitation process. In the first, the classifier assumes the initial candidate nodes are close to the correct concepts but are not exact matches (this is a good assumption since the classifier is tuned to achieve high recall but low precision). For each initial candidate, a neighborhood of nodes whose geodesic distance is less than $\boldsymbol{\delta}$ from the initial candidate (which becomes the centroid of the neighborhood) is created. The objective of phase I elicitation is to eliminate one or more of these neighborhoods. In phase II, the classifier zeroes in on a single neighborhood (the one determined to be best after analyzing the user responses from phase I) and attempts to eliminate individual concept nodes.

Questions are built using features and are of the form "*Which of the following are pertinent to your requirement?*" followed by a pick $\boldsymbol{s}$ of $\boldsymbol{n}$ multiple choice question with various features which were not found in the text but which the classifier can use to best complete its objective for the current elicitation phase. For example, question options could include "*vision*", "*computer maintenance*", and "*operations overhead*". Elicitation begins in phase I and after either an arbitrary number of questions or some trigger condition is met relating to the number of candidate centroids eliminated, elicitation enters phase II. After each question is answered, the features selected are virtually added to the RFC list of features with some additional weight $\boldsymbol{\beta}$>1 relative to an original text feature.

The features selected for these questions could be randomly selected from a history of past features observed in text. The knowledge gained from these random features, however, would typically be quite small in the context of a centroid or specific concept since the features might not have ever been observed to be associated with the concepts in the neighborhood around the centroid. Our selection process for features therefore involves scoring each possible feature in terms of the relevance of the feature to the concept(s) needed in the current question phase, the coverage of the concepts by the feature, and the specificity of the feature to the concepts.

4 Results

To gauge the effectiveness of the proposed classifier in its problem domain we utilize an experimental dataset of 63 instances of RFC documents c whose correct classifications are known. These correct classifications cover a set of 97 of 687 total concepts arranged in a hierarchy. These classifications were carefully derived by hand by organizational subject matter experts and are the gold standard against which we compare document classifications. From this dataset, an arbitrary set of $\boldsymbol{t}$ training and $\boldsymbol{v}$ validation instances are randomly selected. Note that if $|t| + |v| > 63$ there is necessarily some overlap between training and validation instances (i.e., a document is validated over at least one instance on which it was previously trained). If $|t| + |v| \leq 63$ we ensure that no validation is performed on a document which was previously used for training.

The classifier is trained over each document in t using the correct classifications. The classifier is then tasked with classifying each validation instance v' in v. For each validation instance v' the classifier is invoked on the document text and the λ best-scoring concepts are interpreted as suggested classifications. These suggested classifications are decomposed into one of the following categories:

I. Exact match—the classifier selects a concept identified by the subject matter experts
II. Close match—the classifier selects a concept within δ hops in the concept hierarchy of a concept identified by subject matter experts
III. False positive—the classifier selects a concept which is not a close or exact match

Additionally, each of the concepts in the correct concept set is placed into one of the following categories:

I. Exact matched concept—the classifier selected this concept
II. Close matched concept—the classifier selected at least one concept within δ hops in the concept hierarchy of an objective concept.
III. False negative—the concept was neither an exact nor a close match

From these classifications we can determine the precision, recall, and fscore of the classifier's suggested classifications. We compute absolute precision and recall in terms of the number of concepts partitioned into each of the above categories as shown in the equations below.

$$P_{abs} = \frac{exact\ match}{exact\ match \cup close\ match \cup false\ pos.} \quad (1)$$

$$R_{abs} = \frac{exact\ match}{exact\ match \cup close\ match \cup false\ neg.} \quad (2)$$

The absolute F1-score, a metric which accounts for the compromise between precision and recall, is then computed by taking the harmonic mean of absolute recall and precision as shown below.

$$F_{abs} = \frac{2 \cdot P_{abs} \cdot R_{abs}}{P_{abs} + R_{abs}} \quad (3)$$

For each of the above metrics we also compute a closeness measure in which the set of exact matches is unioned with the number of close matches (in the case of precision) or close matched concepts (in the case of recall). Note that concept *c'* is close to concept *c''* if and only if the geodesic distance in the concept hierarchy between *c'* and *c''* is $\leq \delta$.

$$P_{close} = \frac{exact \cup close\ matched}{exact \cup close\ matched \cup false\ positive} \quad (4)$$

$$R_{close} = \frac{exact \cup close\ matched}{exact \cup close\ matched \cup false\ negative} \quad (5)$$

$$F_{close} = \frac{2 \cdot P_{close} \cdot R_{close}}{P_{close} + R_{close}} \quad (6)$$

We compute average classifier performance in terms of these metrics over 50 such randomly generated runs and additionally present the variance between runs for all metrics.

4.1 Ideal case behavior

Our first experiment is to gauge the best-case behavior of the learning algorithm. To do so we train the classifier using all of the correctly classified documents in *c* and subsequently task the classifier with classifying all of the documents in *c*. In this experiment we set λ to 10. An ideal learner would achieve perfect recall and precision after such training. The results of this experiment are shown below:

Table 1: Ideal-case classifier behavior for various performance metrics

δ=0, λ=10

	recall	precision	fscore
arithmetic mean	0.9649	0.3411	0.5040
harmonic mean	0.9649	0.3411	0.5040
variance	0.0000	0.0000	0.0000

δ=2, λ=10

	recall	precision	fscore
arithmetic mean	0.9781	0.7566	0.8532
harmonic mean	0.9781	0.7566	0.8532
variance	0.0000	0.0000	0.0000

We see that our classifier's absolute recall (δ=0) is quite high but not perfect. This is because during training many features were observed to become ambiguously linked to multiple concepts (i.e., multiple concepts had links from a single feature). Any document containing such an ambiguous feature has a nonzero probability of incorrectly grounding one or more of these ambiguously linked concepts in place of a correct concept, reducing recall. The precision of 0.34 for the δ=0 configuration indicates a high percentage of false positives and is an artifact of setting λ to a significantly higher value than average number of correct concepts per document, which was around 3.6 in this experiment (note that λ was set to 10). In the δ=2 configuration, precision improves because it accounts for concepts whose geodesic distance within the concept hierarchy is up to 2 nodes away from the classifier suggested node. We will study the impact of varying λ in more detail later. Note that there is no variance in these initial results because there is only one way to select 63 training and validation instances as described earlier (thus each run has identical results).

4.2 Real-world performance

Next we examine the impact of varying the training and validation set sizes. To understand the classifier's learning capability we utilize a validation set on which the classifier has not been previously trained. This simulates the more realistic case where knowledge acquired during training must be generalized to new instances in order to achieve correct classifications. An ideal classifier would generalize the results of the training set and achieve perfect precision and recall on a disjoint validation set whose entries were not previously encountered. The performance of our classifier over these more difficult cases is shown in the tables below.

Table 2: Real-world behavior

V=10, T=50 (δ=0)

	recall	precision	fscore
arithmetic mean	0.8241	0.2920	0.4259
harmonic mean	0.8160	0.2773	0.4139
variance	0.0067	0.0044	0.0039

V=10, T=50 (δ=2)

	recall	precision	fscore
arithmetic mean	0.9173	0.6064	0.7257
harmonic mean	0.9142	0.5942	0.7202
variance	0.0028	0.0071	0.0039

V=20, T=40 (δ=2)

	recall	precision	fscore
arithmetic mean	0.7803	0.3441	0.4686
harmonic mean	0.7714	0.3199	0.4523
variance	0.0068	0.0074	0.0070

Table 3: λ Impact on precision and recall

δ=0, λ=40

	recall	precision	fscore
arithmetic mean	0.9751	0.0878	0.1603
harmonic mean	0.9730	0.0825	0.1521
variance	0.0019	0.0005	0.0014

δ=0, λ=5

	recall	precision	fscore
arithmetic mean	0.7447	0.5212	0.6034
harmonic mean	0.7246	0.5064	0.5962
variance	0.0141	0.0077	0.0044

Although we observe a noticeable drop in recall versus the ideal case in all three of the above experiments, we see that the classifier consistently achieves good close recall (δ=2) provided the training set has good coverage of the concept hierarchy. By altering the λ parameter we can explore the tradeoff between recall and precision as shown below.

The results above were obtained on a 50T/10V configuration. As expected, at λ=40 we observe a significant improvement in recall (from 82 percent at λ=10 to 97 percent at λ=40) at significant cost in terms of degraded precision (29 percent to 9 percent). At λ=5 we observe the opposite trend—an increase in precision and a decrease in recall compared to the λ=10 configuration. At λ=5 we approach the maximum accuracy of the unaided classifier which was roughly 52%. Because this level of accuracy is not acceptable for our application, the approach we take is to set λ to a conservative value and refine our coarse results through elicitation.

4.3 Elicitation performance

As described earlier, the elicitation process effectively reshapes the score distribution curve. As an example, the impact of elicitation on a score distribution for the case-1 document described earlier can be seen in *Figure 1* below. Note that the concepts are ranked in descending order by score and are not ordered between runs. The highest scoring concept after elicitation was the 45th highest after a purely lexical analysis of the text (although a concept one node away in the concept hierarchy was the third highest scoring and would have been suggested anyway). The highest scoring concept after elicitation was aligned with subject matter expert opinion.

In general we observed elicitation to significantly improve the quality of the initially suggested concepts. This is because the close match recall of grounding engine is quite high but absolute precision is low. The elicitation process attempts to arrive at the correct concepts using the initial close-match concepts as a starting point.

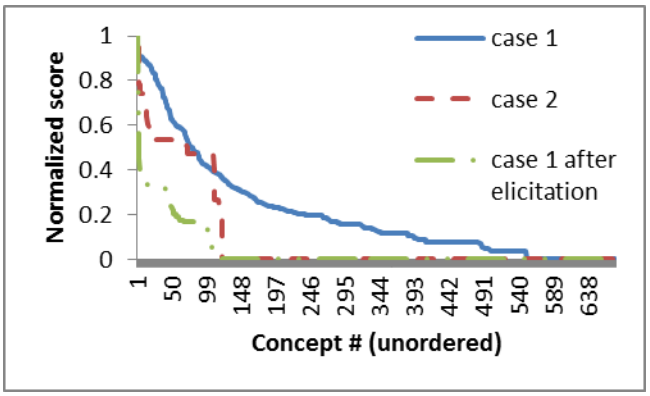

Figure 1: normalized score distributions for two sample documents

5 Conclusions and Future Work

We have demonstrated that the proposed document classification system is effective at determining the organizational impact of human produced RFC documents. We observed that the automatic classifications produced by the supervised learning classification system achieved good recall but low precision and these results were significantly improved through an interactive refinement with the user submitting the RFC document.

Although we achieved good results using simple word/part of speech features extracted from text, we believe our classification accuracy could be improved by using more advanced features such as phrases or WordNet synsets. Additionally, when selecting the initial neighborhood centroids for elicitation we utilized static thresholding with a fixed λ but it may be beneficial to arbitrarily adjust λ based on the distribution of scores returned after the initial classification. These are simple extensions of the system described.

6 Acknowledgement

This work was supported in part by the Air Force Research Laboratory, Contract Nos. FA8750-09-D-0195-0004, FA8750-09-D-0195-0006 and FA8750-08-C-0109

7 References

[1] H. B. Bernick. "Automatic document classification"; Journal of the ACM, Vol. 10, Issue 2, 151–162, 1963.

[2] A. K. McCallum. "Multi-label text classification with a mixture model trained by EM"; AAAI'99 Workshop on Text Learning, 1999.

[3] M. Anthony and P. L. Bartlett. "Neural Network Learning: Theoretical Foundations". Cambridge University Press, New York, 1999.

[4] T. M. Mitchell. "Machine Learning". McGrawHill, 1997.

[5] D. Ferrucci and A. Lally "Uima: An architectural approach to unstructured information processing in the corporate research environment"; Natural Language Engineering, Vol. 10, 327–348, 2004.

[6] J. Hockenmaier, G. Bierner and J. Baldridge. "Extending the Coverage of a CCG System"; Research in Language and Computation, Special Issue on Linguistic Theory and Grammar Implementation. Vol. 2, Issue 2, 165–208, 2004.

[7] G. A. Miller. "WordNet: a lexical database for English"; Communications of the ACM, Vol. 38, Issue 11, 39–41, 1995.

[8] A. Ondi, J. Staples and T. Stirtzinger. "Extending sparse classification knowledge via NLP analysis of classification descriptions"; Proceedings of the ICAI'12, (to appear), 2012.

Extending Sparse Classification Knowledge via NLP Analysis of Classification Descriptions

Attila Ondi[1], **Jacob Staples**[1], **and Tony Stirtzinger**[1]
[1]Securboration, Inc. 1050 W. NASA Blvd, Melbourne, FL, USA

Abstract - *Supervised machine learning algorithms, particularly those operating on free text, depend upon the quality of their training datasets to correctly classify unlabeled text instances. In many cases where the classification task is nontrivial, it is difficult to obtain a large enough set of training data to achieve good classification accuracy. In this work we examine one such case in the context of a system designed to ground free text to an organizational hierarchy which is ontologically modeled. We explore the impact of utilizing information garnered from a highly customized Natural Language Processing (NLP) analysis of this ontology to augment a very sparse initial training dataset and compare this to a more labor intensive extraction of a small set of key words and phrases associated with each concept. We demonstrate an approach with significant improvement in classifier performance for concepts having little or no initial training data coverage.*

Keywords: Hierarchical document classification, Automatic document classification, Machine learning, NLP, Ontology

1 Introduction

In this work we describe a software classification system which employs NLP analysis and machine learning algorithms to automatically determine whether a human produced text applies to one or more of a set of concepts. The machine learning portion of this system is essentially a supervised learner whose accuracy relies heavily upon the quality of the training instances it has encountered. Unfortunately the concept space over which this solution is deployed is sufficiently large that it was not feasible to obtain a large quantity of high-quality training instances. In fact, many concepts were observed to never be explicitly referenced by training instances. Although the classification portion of the system evolves dynamically to improve its classifications over time, the initial classifications produced by the system were of poor quality due to this deficiency of initial training data.

We discuss several approaches taken to improve these initial classifications and construct knowledge in the face of limited or absent training data. We compare two mechanisms of capturing expert user knowledge in terms of their impact on classifier accuracy and recall and how well they interact with traditional training instances.

2 Related Work

From a machine learning perspective, this work deals with the well-studied field of supervised learning algorithms [1]. There is a wide body of research related to applying such algorithms to human produced text, for an overview see [2]. Of particular relevance is the multi-topic document classification problem [3] in which a document is analyzed by a machine classifier and determined to be applicable or not applicable to a list of topics.

The sparseness of labeled training instances is by no means unique to this problem domain. Significant research has been conducted in the area of semi-supervised learners which attempt to generalize a small amount of labeled training data to a larger amount of unlabeled data which can subsequently be used for training. For a thorough overview of semi supervised techniques see [4].

In this work we examine a somewhat different position than that in which most semi-supervised systems are deployed, however, because we assume access to a limited number of labeled training instances but do not assume the existence of unlabeled training instances. Instead we assume access to expert generated knowledge either in the form of an ontology [5] modeling the structure of concepts in the concept space or in the form of a key-word document, either of which we attempt to derive unlabeled instances from and whose instance labels are trivial to reverse engineer from the ontology structure.

3 Approach

We explore two unique options to expand the initial classifier knowledge. The first is to exploit the knowledge of subject matter experts by hand-populating a database of key phrases they have determined likely to be associated with each concept in the concept space. The second approach is to utilize an expert-created ontology describing the nature and relationship between the concepts in the concept space to determine which lexical features are associated with what concepts by making the assumption that the definition of a

concept will contain language similar to the documents associated with that concept.

Though their angles of attack on this problem are quite different, it is important to keep in mind that these approaches are attempting to do fundamentally the same thing—derive new training instances which can be provided to the classifier. Before describing the mechanics behind generating these instances, we will give a brief overview of the classifier and its operation.

3.1 Classifier

The minutiae of the supervised learning classification algorithm utilized in this work are not germane to this discussion and are described elsewhere [10]. For the purposes of this paper, it is sufficient to understand the grounding engine mechanics for two key operations the classifier performs: classification and training.

Classification is an operation performed on a text document to determine which concepts are present in it. In order to classify a given document as exhibiting or not exhibiting a set of concepts, the document is first decomposed into features using Natural Language Processing (NLP) techniques described later. These features are provided as input to the grounding engine. The output of the grounding engine is a label for each concept indicating how confident the classifier is that the concept exists in the document whose features were provided. Note that the features passed to the classifier are either sense-ambiguous (for example a stemmed form of a word with some notion of its part of speech) or sense-specific (for example a WordNet synset identifier). In this work we explore the implications of each feature type.

Training is an operation performed on a text document and a set of labeled concepts indicating which are correctly or incorrectly associated with the text. When updated with a training instance, the classifier internally adjusts its structure such that in the future the features provided will be more likely to be associated with the concepts labeled "correct" and less likely to be associated with the concepts labeled "incorrect".

For clarity, we now introduce a logically distinct type of training, called bootstrap training, which differs slightly from the training described above. *Bootstrap training* is unique in that it is always performed before any standard training instances are encountered and is used to construct the initial body of knowledge needed to very roughly associate features with concepts. Because the bootstrap training labels in this work were implicitly derived, we could not make any assumptions about false negative concepts using a bootstrapping instance. When a bootstrap training instance was encountered, the classifier therefore only considered the concept arguments labeled as "correct" for the given text.

Bootstrapping is useful because, as mentioned earlier, for many of the concept types on which our classification system operated, there were a significant number of concepts having a trivial number of training instances (or none at all). Without some form of correction, these holes in the initial knowledge of the classifier meant that the classification algorithm would always assign some concepts zero confidence. Bootstrapping is less crude than the typical approach of assigning each concept a small virtual probability.

3.2 Feature extraction using Natural Language Processing

The features used as input to the classifier were extracted from document text via a NLP pipeline using the UIMA [6] framework and OpenNlp [7] components. The results of the OpenNlp components were augmented by a heuristic lemmatizer based on an extended WordNet [8] dictionary.

3.2.1 Custom WordNet dictionary

WordNet is a machine-usable dictionary of words organized into synonym sets (synsets). Each word in the dictionary is associated with a sense, which is captured by a synset; and each synset is associated with a textual description, along with the words belonging to this synset. In this sense the WordNet dictionary assumes the role of a thesaurus as well.

We modified WordNet in two ways to better fit the needs of the effort described here.

The first modification was at the content level—the dictionary lookup logic was modified to support customized synsets stored in a file. The addition of this custom read logic enables us to fully modify the WordNet dictionary by removing, altering, or creating new synsets in the dictionary. Nearly 1200 field-specific jargon and acronym terms were added to the dictionary. These 1200 terms were selected because they were important words previously discarded by the lemmatizer using a standard WordNet dictionary. After implementing the changes to WordNet the lemmatizer was able to recognize these terms as words.

The second modification was at the software level—the custom dictionary read logic was modified such that it loads all dictionary entries into memory (requiring around 350MB in our implementation). This change resulted in significant speedup over the file-based MIT implementation packaged with the dictionary for random word lookups. We observed a speedup of roughly 11x for random synset retrievals and 1.5x

for repeated synset retrievals compared to MIT's implementation. The lower speedup for repeated lookups is due to the use of caching in the MIT implementation, which mitigates costly file access times for dictionary entries which are frequently accessed.

3.2.2 Lemmatizer

Although the standard OpenNlp components provide reasonable accuracy for determining the correct part-of-speech (PoS) tags for words appearing in the document, the process is not perfect. To attempt to correct the erroneous PoS tags, we developed a custom component that uses simple heuristic rules to guess the potential textual form of the lemma of the word along with the correct PoS tag.

The lemma of a word is simply the base form of the word that forms the head of an entry in a dictionary (e.g. the lemmas of the words "ate" and "mice" are "eat" and "mouse", respectively). Our heuristic for finding the actual PoS tag for a word observed in a document uses the OpenNlp PoS tag guess for the word and the PoS tag of the previous non-filler word. If the custom dictionary contains a lemma/PoS pair matching the known lemma and OpenNlp PoS tag guess, the OpenNlp tag guess is assumed to be correct. Otherwise, we consult the dictionary using the following PoS tags (in the given order): verb, noun, adjective and adverb. The first matching PoS from this list when paired with the lemma is returned as correct. Note that the heuristic rules of calculating the lemma from the textual form of the word change based on the current PoS tag candidate. If no lemma/PoS tag matches an entry in the custom dictionary then the OpenNlp tag guess is assumed to be correct and the lemma is assigned the textual form of the word.

3.2.3 Sense disambiguation

The sense disambiguation scheme utilized is based on the Lesk algorithm described in [9]. The algorithm outlined below operates on sentences extracted from the document, performing the steps for each unprocessed word in the sentence. If, at any step in the algorithm, only one viable sense of the word/PoS remains, that sense is selected and the following steps are not performed.

First, exclude senses that are hyponyms of non-applicable senses (e.g. sport terms).

Second, check if senses from the current and another word are part of the same synset hierarchy; if yes, the corresponding senses are selected for both words.

Third, check if the current and the neighboring word are related to each other via lexical parallelism. Two words exhibit lexical parallelism if there exists a hypernym/hyponym (for nouns), similar-to (for adjectives), pertains-to or morphological similarity (for adverb) relationship between any of their possible senses. If lexical parallelism is observed, the senses in relation are selected for the corresponding words.

Fourth, if the current word is a verb, check if it is collocated with any of the neighboring word lemmas. A verb lemma is collocated with another lemma if the verb has a lemma in any of its hypernym synsets that is morphologically similar to the other lemma.

Fifth, perform the Lesk algorithm: check for maximum lemma overlap between the current sentence and the textual description of the possible senses.

Sixth, extract example usage from the sysnset textual definition and check for patterns with the neighboring words.

If all steps were successfully performed and there are still multiple candidate synsets associated with the word, all the remaining synsets are accepted as equally likely correct senses.

3.3 Bootstrapping mechanisms

We explored two options for generating the bootstrapping training set. For both options, we attempted to use both sense-ambiguous (lemma/PoS pair) and sense-specific (synset ID) features. In the sense-specific case we resolved the senses of the bootstrapping training set manually and employed the automatic sense disambiguation mechanism described above during training.

3.3.1 Bootstrapping based on keyword mapping

The first bootstrapping approach we took was to utilize a keyword mapping document which describes the key words and phrases associated with each concept in the concept space. To generate the bootstrapping training set, we created a set of single-feature training documents derived from the keyword mapping document. The label for the training instance contained in each of these documents was simply a list of the concepts correctly associated with the keyword.

This approach scales poorly because a domain expert must distill each concept into a list of the most important phrases and terms associated with that concept. Furthermore, it is important that these phrases and words not overlap to provide maximum differentiation between the concepts. Avoiding overlap becomes increasingly difficult as the size of the concept space grows. Additionally, it is not clear whether the few key words or phrases selected by the expert will have sufficient lexical overlap with the contents of an arbitrary document to produce meaningful classification results.

3.3.2 Bootstrapping based on ontology lexicalization

The second bootstrapping approach we explored was to utilize an ontology created by a domain expert that described the concepts in the concept space. To generate the training set, we created a single virtual training document for each concept. The training document consisted of the definition, description and other descriptive textual information extracted from the ontology describing the associated concept. The classification label associated with that document was the label of the concept from which the information was extracted. This approach scales better than manually generating the key word mapping document because the ontology is required to contain textual information (e.g. description) associated with each concept. The downside is that the training instances generated in this fashion may contain misleading knowledge since non-keywords may be included in the ontology text fields. As an example of this: the definition of a concept might always begin with the word "Definition" which will lead classified documents containing the word "Definition" to be erroneously grounded to all concepts.

4 Results

To gauge the performance of the various proposed mechanisms for training the classifier we conducted 50 runs with randomly generated training (T) and validation (V) sets for each run. Each validation set consisted of *V* randomly selected classification instances from a pool of *C* correctly classified documents (*C* = 63). The remaining *T* classification instances were used for training the classifier. The training and validation sets were selected such that they were guaranteed to be disjoint if possible (i.e., no document was validated using a classification instance previously used for training in the same run unless $|C| < |T|+|V|$). The training set was augmented with instances derived using various combinations of the following approaches:

1. No bootstrapping
2. Human-created concept keywords
3. Lexicalized ontology

For each validation instance the top 10 scoring concepts after classification were selected and the remainder was rejected. These 10 concepts were compared to the correct concept labels and the recall, precision, and fscore (the harmonic mean of the former two) values were computed as arithmetic averages over all runs.

To more clearly demonstrate the problem we faced with limited training data, we first examine the impact of decreasing the size of the training set with no training augmentation.

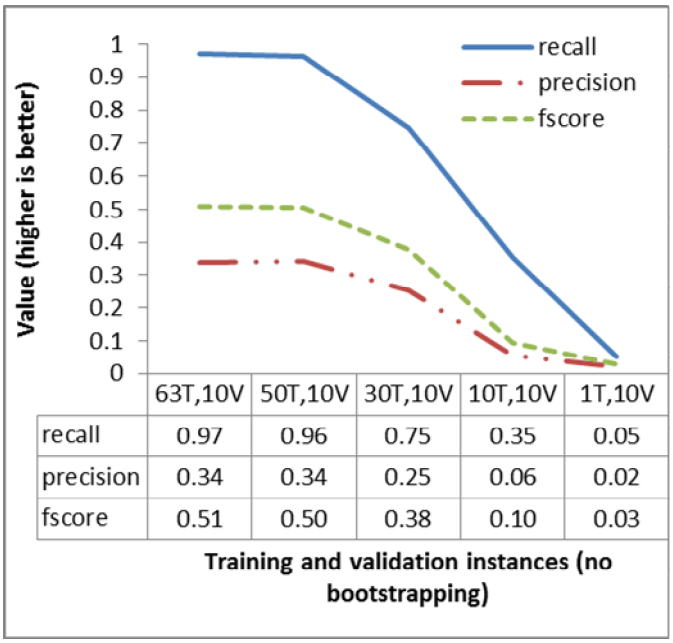

	63T,10V	50T,10V	30T,10V	10T,10V	1T,10V
recall	0.97	0.96	0.75	0.35	0.05
precision	0.34	0.34	0.25	0.06	0.02
fscore	0.51	0.50	0.38	0.10	0.03

Figure 1: Impact of training set size on classifier performance with no training augmentation

As expected, decreasing the size of the training set had a deleterious effect on precision, recall and fscore. Note that with the 1T/10V configuration the classifier's performance was actually slightly worse than if 10 concepts had been selected from the roughly 600 in the hierarchy at random. This worse-than-random behavior was due primarily to incomplete coverage of the concept space by the single training instance.

Because our classification system frequently encountered instances where there were few or no initial training instances as in the 1T/10V configuration, we clearly needed a mechanism for bootstrapping classifier knowledge.

To understand how effective bootstrapping can be on its own and with standard training, we tested the following training configurations:

- B: bootstrap training only
- B+T: bootstrap training followed by standard training
- T: standard training only

We also explored the impact of sense disambiguation during parsing using the following bootstrapping configurations:

- Dk: hand disambiguation of keyword senses, automatic disambiguation of training instances
- Dd: hand disambiguation of concept ontology descriptions, automatic disambiguation of training instances

- Ak: ambiguous keywords (no disambiguation of training instances)
- Ad: ambiguous concept ontology descriptions (no disambiguation of training instances)

Note that the Dk and Dd configurations above employed sense disambiguation. To maximize the benefit of sense disambiguation, we manually disambiguated the bootstrapping data.

Figure 2 shows the performance of various training configurations in terms of their fscores normalized to the un-bootstrapped 63T/10V case from *Figure 1*. In *Figure 2*, we observe that bootstrapping alone (B) performs poorly relative to the training alone (T) and both (B+T) configurations. This is expected because the quality of the bootstrapping training instances is significantly lower than the quality of real-world generated training instances.

It is clear from *Figure 2* that bootstrapping alone is a poor substitute for quality training data but does provide significantly better recall than simply guessing (which would produce a recall of 3.3% on average). On its own the best performing bootstrapping configuration was (Dk) which utilized the hand generated key word document.

We also observe that sense disambiguation (used in the Dk and Dd cases) only provided a benefit over using ambiguous features when bootstrapping alone (B) was used. The benefit of sense disambiguation in this case is 46% greater for keyword (Dk) than with lexicalized ontology (Dd) bootstrapping. This significant improvement over lexicalized ontology bootstrapping is a direct result of the highly targeted and minimally overlapping language used in the keyword document whereas the lexicalized ontology bootstrap instances were observed to contain many overlapping terms and phrases between unique concepts.

The next interesting observation from *Figure 2* is that the bootstrapping and training configuration (B+T) performed better than training alone (T). This indicates that bootstrapping was beneficial even for concepts covered by labeled training instances. To quantify the interaction between bootstrapping and normal training, we next varied the training set size and examined the performance of the (Ad, B+T) case above. Note that no sense disambiguation was used during bootstrapping or training and that lexicalized ontology bootstrapping was used. These results are shown in *Figure 3* as improvement factors for recall, precision and fscore relative to the corresponding values for the training only (T) case from *Figure 1*.

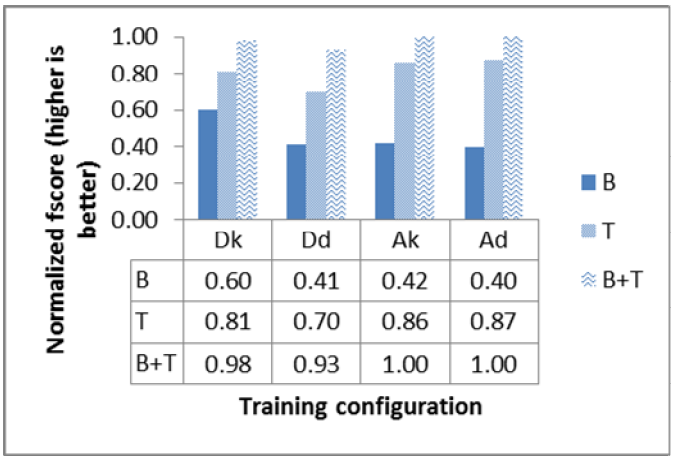

	Dk	Dd	Ak	Ad
B	0.60	0.41	0.42	0.40
T	0.81	0.70	0.86	0.87
B+T	0.98	0.93	1.00	1.00

Figure 2 : Impact of training configuration on classifier performance (63T/10V)

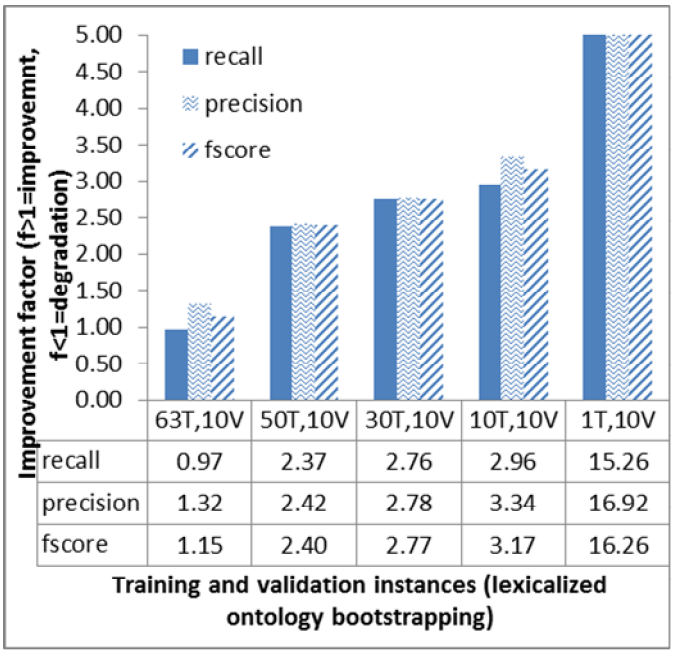

	63T,10V	50T,10V	30T,10V	10T,10V	1T,10V
recall	0.97	2.37	2.76	2.96	15.26
precision	1.32	2.42	2.78	3.34	16.92
fscore	1.15	2.40	2.77	3.17	16.26

Figure 3: Relative performance of lexicalized ontology bootstrapping + training compared to training alone

For all of the tested training set sizes shown above, bootstrapping resulted in a significant improvement in fscore relative to the trained only case. Intuitively, the benefit of bootstrapping decreases as the training set increases in size and this was also observed.

It is interesting to note that bootstrapping improved precision appreciably more than recall in all cases. This is because, during the post bootstrapping training process, exact concept matches were fed back to the system with higher weights than close concept matches.

It should be noted that while the relative improvements in recall, precision, and fscore for the 1T/10V case were large, classifier recall, precision, and fscore at that point were roughly 32%, 74% and 45%, respectively. Although still far from perfect, this result was significantly better than the results obtained with few or no initial training instances.

5 Conclusion and Future Work

We have explored several approaches which can be used to generate initial training data using domain expert knowledge. The most effective of these was building a bootstrapping training set using a lexicalization of an expert generated ontology describing the concept space. Our lexicalized bootstrapping mechanism was able to achieve an fscore of 40% even with no initial training instances present. Additionally, we observed 15% improvement in fscore values using bootstrapping and training together even for the most trained configuration tested.

One possible improvement to the techniques described in this work would be to experiment with more sophisticated sense disambiguation schemes. Our efforts to leverage WordNet to exploit synset relationships such as hypernyms and hyponyms were unsuccessful largely because we were unable to accurately map words in text to WordNet synsets automatically. In such a system it would be possible to derive a large number of similar words to those in the bootstrapping training set using the synset hypernym and hyponym relational links and we anticipate improved performance for bootstrapping using these approaches.

6 Acknowledgement

This work was supported in part by the Air Force Research Laboratory, Contract Nos. FA8750-09-D-0195-0004, FA8750-09-D-0195-0006 and FA8750-08-C-0109

7 References

[1] T. M. Mitchell. "Machine Learning". McGrawHill, 1997.

[2] M. Berry. "Survey of Text Mining: Clustering, Classification, and Retrieval", First Edition. Springer, 2008.

[3] H. B. Bernick. "Automatic document classification"; Journal of the ACM, Vol. 10, Issue 2, 151–162, 1963.

[4] N. Chawla and G. Karakoulas. "Learning from labeled and unlabeled data: an empirical study across techniques and domains"; Journal of Artificial Intelligence Research, Vol. 23, 331–366, 2005.

[5] N. Guarino. "Formal Ontology in Information Systems"; Proceedings of FOIS'98, Vol. 46, 3–15, June 1998.

[6] D. F. Lally. "Uima: An architectural approach to unstructured information processing in the corporate research environment"; Natural Language Engineering, Vol. 10, 327–348, 2004.

[7] J. Hockenmaier, G. Bierner and J. Baldridge. "Extending the Coverage of a CCG System"; Research in Language and Computation, Special Issue on Linguistic Theory and Grammar Implementation, Vol, 2, Issue 2, 165–208, 2004.

[8] G. A. Miller. "WordNet: a lexical database for English"; Communications of the ACM, Vol. 38, Issue 11, 39–41, 1995.

[9] M. Lesk. "Automatic sense disambiguation using machine readable dictionaries: how to tell a pine cone from an ice cream cone"; Proceedings of the 5th annual international conference on systems documentation (SIGDOC'86), 24–26, 1986.

[10] J. Staples, A. Ondi and T. Stirtzinger. "Semi-autonomous hierarchical document classification using an interactive grounding framework"; Proceedings of the ICAI'12, (to appear), 2012

Novel Scan Engines and Intelligent Microagents to Detect Malware

Brian H. Xu, Ph.D., Principal Computer Scientist
Honeywell Aerospace, 1985 Douglas Dr. N., Golden Valley, MN 55422 USA

Abstract. *Existing cyber security technologies and COTS products are becoming less effective to detect modern malware, because such malware becomes increasingly sophisticated. In fact malware metamorphic and polymorphic methods are outpacing current signature based anti-malware products. To address these problems, novel Scan Engines and Intelligent Microagents (SEIMs) are presented in this paper for effective malware detection and mitigation. The SEIMs are based on innovative intelligent microagents, fast scan engines, and their synergic combination. (1) SEIM microagents autonomously sift through networks, use scan engines, COTS tools, reasoners, and machine learning algorithms to quickly detect and mitigate both known and unknown malware. (2) SEIM scan engines quickly search and detect malware digital genomes at byte level with high speed (over 50 MB/S). Our experiments have proven that the SEIM technologies can successfully detect the real malware. The SEIMs can be matured into effective and scalable commercial cyber security products.*

Keywords: Microagent, Scan engine, Cyber security, Malware detection, Malware genome, Botnet.

1 Introduction

There are currently over 286 millions malicious software (malware) threats (www.venturebeat.com) in cyberspace. Bots are malware programs that are stealthily installed across a targeted network, allowing an unauthorized user to remotely control the compromised computers for various malicious purposes [1]. Botnets are networks of the machines compromised by bots so that they are controlled by the bot maters (e.g., hackers, adversaries, etc.). Botnets are capable of acting on instructions, and organized networks of malware. It is well known that these malware (botnets, rootkits, etc.) attack our cyberspace using distributed DoS, key logging, phishing, spamming, and other malicious actions. The malware also cause root problems of spam bots, click fraud, large-scale identity theft, disabling antivirus software such as McAfee and Symantec products, and breaking through military and government networks [2]. A collection of servers infected with botnets are often under a single command and control (C&C) channel such as an IRC channel and/or P2P. The malware can attack against computers and networks in coordinated ways. Botnets and malware in cyberspace can take many forms including the following common ones:

- Top botnets include TDL (Botnet A), RogueAV, Koobface.A, and Zeus (Zbot) that can be made by DIY (Do-It-Yourself) tools [8].
- Agobot, Phatbot, Forbot, XtremBot are known bots written in C++. Agobot is the only bot that uses a control protocol other than IRC. It uses a fork via the distributed organized WASTE chat network.
- SDBot, RBot, UrBot, UrXBot are bots written in C.
- IRC-based bots are Global Threat bots, as popular IRC clients for Windows ("*.mrc").
- The Dataspy Network X (DSNX) bots (C++).
- Q8bot is a very small bot with 926 lines of C code.
- The Kaiten bot is written for UNIX and Linux machines.
- Perl-based bots consisting of a few hundred lines of Perl code, etc.

Botnets pose serious threats to our cyber security by compromising many computers (e.g., 1,000 to 5,000 computers) in networks. Even a small botnet with 500 bots can cause great damages in our cyberspace. Furthermore, current malware can have many different forms or variations. However existing malware detection products and technologies are primarily based on signatures, they are not effective to detect these malware. In addition, new malware become stealthier to propagate through software vulnerabilities, Internet, IT systems, and public clouds, which make them more difficult to be detected.

Widely used anti-malware COTS tools such as Symantec (www.symantec.com), McAfee (www.mcafee.com) and others are designed primarily to deal with viruses, spyware, and adware rather than bots and botnets. They are inadequate in detecting and mitigating botnets. As a result, botnet victims are increased 654% in 2011 [8].

Symantec Digital Immune System (DIS licensed from IBM) and other anti-malware technologies are ineffective in identifying polymorphic viruses and malware. They are also incapable of detecting any new or unknown malware that has not been seen by the antivirus labs, or any 0-day attacks. In addition, current technologies do not adequately address the increasing sophistication, stealth and encrypted C&C channels and fast-flux DNS for botnets [3, 4]. In fact, no single COTS software products can ensure cyber security of a computer network against such malware.

However, key weaknesses of botnets have been found. First, bots propagation mechanisms are a key cause of background noise on the Internet, especially on TCP ports 445/TCP (Microsoft-DS Service), 135/TCP (Microsoft Remote Procedure Call, Port 139/TCP (NetBIOS Session

Service), and Port 137/UDP (NetBIOS Name Service). These mechanisms account for more than 80% of all traffic captured. Windows XP and 2000 are the most affected software platforms [5]. These ports are limited as a weakness of the bots; we focus on TCP ports 445, 135, 139, and 137, block their propagation, and track the bots. Second, the following weaknesses are also found:

(1) Botnet-makers or bot-masters reuse existing source codes for new versions of the malware. The core algorithms of the malware are usually limited to metamorphic code, polymorphic code, and other self-modifying code. The core algorithms of the malware do not change, so identifying these algorithms can help us to detect new or unknown malware;
(2) Identifiable common patterns exist in almost all botnets for us to detect, since they are primarily generated by the same core algorithms;
(3) Botnet makers are too aggressive in compromising more networked computers to tell their trappers (like Honeypots [6]). We can detect and track the makers.
(4) Bot command and control (C&C) is mostly centralized on one or more IRC servers. Deleting the C&C channel can destroy or eradicate the botnet; and
(5) Botnet makers can expose other weaknesses of their malware including the address (not stealthy), and using a single rallying point (not robust); and having hard-coded addresses (not mobile).

Based on these identified malware weaknesses, we developed the novel fast Scan Engines and Intelligent Microagents (SEIMs) for malware detection and mitigation (see Figure 1). In this paper, we introduce the SEIM approach that is based on innovative intelligent microagents, fast scan engines and their synergic combination, in order to effectively detect and mitigate malware. Using the SEIMs, multiple scan engines are designed and developed for pattern matching, online learning using our neural networks [7], malware genome based detection and machine learning algorithms, dynamic behavior analysis, and inline sniffing mechanisms for real-time traffic monitoring, in order to detect both known and unknown malware (including zero-day malware, etc.). We developed and tested the SEIM prototype in a network with different physical machines and various operating systems (like a cloud through massive virtualization). Real bots from the authorized source [6] and many real malware from another source (over **32,000** malware executables and codes) [9] have been used to conduct technical experiments. The SEIM toolset scanned extremely fast (about 50 MB/S) and successfully detected these real bots and malware in the experiments. The remainder of this paper is organized as follows: the architecture of the novel SEIM approach is introduced in Section 2. The details of the SEIM technologies are briefly described in section 3. Selected experimental results are shown in Section 4. The conclusions are given in Section 5.

2 System Overview

The SEIM system consists of multiple intelligent microagents and fast scan engines (see Figure 1) establish multiple cyber defense layers by agile microagents (anti-botnet, anti-bot, antivirus, anti-worm, antimalware, etc.) and novel scan engines to detect malware by identifying digital patterns inherited from the malware families, in order to defeat various cyber attacks. The SEIM monitoring module monitors network traffic and port activities and the detection and analysis module report the detected malware to the SEIM users (cyber operators, warfighters, etc.). The specialized microagents reside in and move across hosts and networks. They use the scan engines to scan digital patterns in data files in various formats (e.g., binary, ASCII, Unicode, etc.), detect and mitigate malware by identifying their digital genomes and/or coding patterns. They also sniff network traffic in network structures and act on suspicious activities.

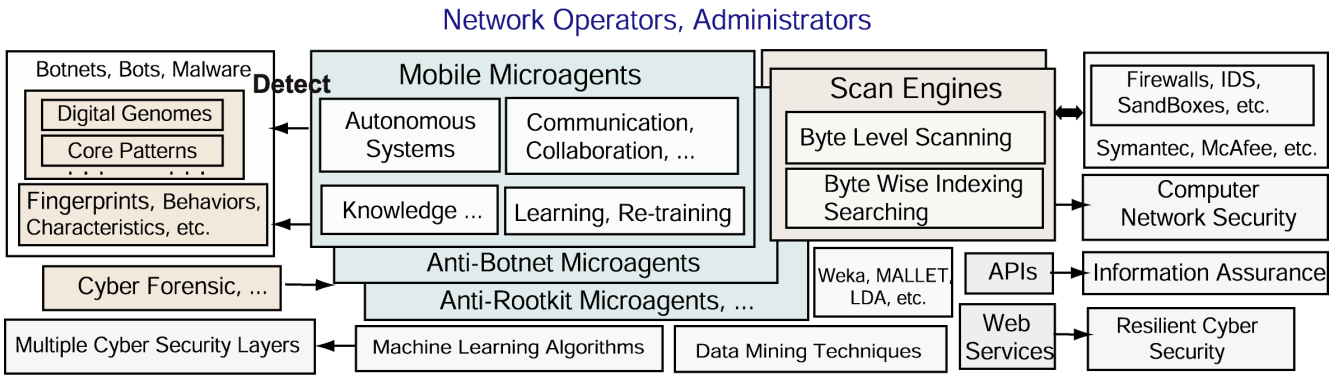

Figure 1. SEIM System Architecture and CONOPs.

The microagents (5 KB to 20 KB) need minimal network computing resources by leveraging existing defense software analysis, and by collaborating each other and work with other cyber security software agents and tools to build distributed or net-centric cyber defense systems. Each scan engine makes decisions based on the flexible

binary tree architecture that keeps the size of microagents minimal. As a result, the SEIM is able to detect and identify malware and botnets with minimal penetration rates and exploit the malware weaknesses to significantly reduce potential damages. The architecture of SEIM system architecture and con-ops are illustrated in Figure 1.

The SEIM technologies have the following advantages over existing malware detection technologies:

- Capable of adapting to new environments and dealing with new malware, because all intelligent microagents can be updated automatically by retraining our neural networks [7] and updating the digital genetics bases.
- Increased cyber security by (a) using our algorithms which can be available to critical infrastructure providers, and (b) deploying proactive microagents that collaborate to construct multiple cyber defense layers to defeat various malware families.
- Virtually boundary free operation—SEIM agile microagents patrol or move across networks, to search, detect, and eradicate malware in our cyberspace.
- Interoperable via Web services to distribute SEIM services, capabilities and functionalities to virtually all cyber systems from hypervisors to applications
- Enlarged application scope and reusability, as SEIM technologies and software are compiled as software components and web services with software APIs and Web APIs for IT systems and applications of industries, military and government agencies.

3 SEIM Design and Implementation

In general, the SEIM techniques can be applied to full-spectrum cyber security enhancement, detection, and mitigation of malware from computer networks (over 170 millions of Windows-based computers alone):

- Scan engines supported by microagents in SEIM proactively and successfully detect and mitigate malware in real time.
- Intelligent and agile microagents move across nodes and networks, they work with SEIM scan engines to detect and mitigate malware.
- SEIM fast scan engines are designed and built by developing unique capabilities to detect core digital patterns extracted and identified from sources of real botnets [1] and malware [9], based on our unique byte wise indexing search technique.
- Unique machine learning and data mining learning algorithms are developed to enhance SEIM capabilities to detect new and/or unknown malware, by adding new digital patterns that are genomes and/or digital genetics of the malware families [1, 2].

SEIM microagents are (1) lightweight (about 5 KB to 50 KB) to minimize computing resources and attack surfaces; (2) agile to move fast across nodes. They are intelligent by using distributed reasoning engines; they leverage SEIM scan engines to detect malware and can work with COTS and GOTS tools for resilient cyber security. By updating the configuration file with control instructions (in XML), the SEIMs construct a smart cyber sensor grid across computer networks of interest. They add full spectrum cyber protection to significantly enhance cyber security. SEIM microagents can be specialized in anti-botnet, anti-malware, and information assurance to form multiple cyber security layers. A sufficient number of SEIM microagents can be launched and deployed to detect malware across boundaries in cyberspace.

3.1 Fast Scan Engines

Core digital genomes and/or algorithms of computer malware (botnets, rootkits, viruses, etc.) do not change, because makers (hackers, black hat developers, etc.) of the malware continuously reuse their source codes in order to reduce the costs and time for new malware releases. The digital genomes or genetics are inherited from the source codes. The core algorithms may use metamorphic and polymorphic methods, as well as self-modifying or hiding tricks. However, these algorithms can generate variations only, not the genomes.

A sufficient number of malware source codes (over 32,000) are available for research [6, 9]. We have identified, extracted and reused some core genomes and patterns in both ASCII (scripts) and binary (executables) formats. SEIM scan engines are designed and prototyped to detect these genomes and patterns (e.g., 0xA5E3, etc.), by matching them bytes by bytes, using our rapid byte wise indexing search technique. Whenever core genomes and/or patterns are matched, the malware are detected. Immediately, the agile microagents save them to our malware repository in a database (SQL server or MySQL) for enhancing scan engines and retraining microagents and delete them from the networks based on their roles and privileges.

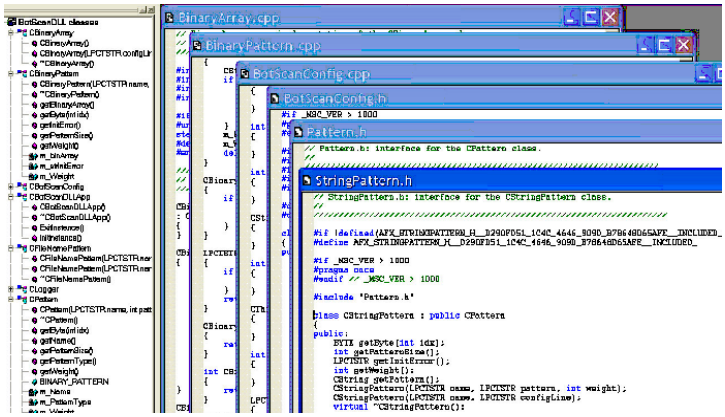

Figure 2. SEIM scan engine design, development and implementation in C++.

The Scan Engine is implanted in C++ for fastest speed. The software development environment and partial source code (classes, functions, etc.) are illustrated in Figure 2 and Listing 1, respectively.

Listing 1. Source Code Segment of the Scan Engine: BotScanDLL.cpp

```
... if ( schSCManager )
    { schService = CreateService(
      schSCManager, // SCManager database
      TEXT(SZSERVICENAME), // name of service
      TEXT(SZSERVICEDISPLAYNAME),
      SERVICE_ALL_ACCESS,    // desired access
      SERVICE_WIN32_OWN_PROCESS,
... ...
```

The scan engines are designed to search though executables (or scripts in Python, etc.) for the genetic patterns at byte level. These patterns can be extracted from real malware sources [6, 9]. For instance, the digital genomes (e.g. 0xA5E3, etc. in Hex) are malicious code specimens. SEIM scan engines search for the digital genomes through a selected executable to determine whether the executable is a malware or not. The scan engines are implemented in C++ for high computing speed. Listing 2 is a segment of the source code for prototyping the SEIM scan engines.

Listing 2. Partial Source Code in the Scan Engine.

```
... ...
class CBinaryPattern : public CPattern
 { public:
        int getWeight();
        BYTE getByte(int idx);
        int getPatternSize();
        CBinaryArray *getBinaryArray();
        LPCTSTR getInitError();
        CBinaryPattern(LPCTSTR name, LPCTSTR
        configLine);
        virtual ~CBinaryPattern();
 private:
        CString m_strInitError;
        int m_Weight;
        CBinaryArray * m_binArray; };
... ...
```

A sufficient number of the networked microagents can be deployed in a network to proactively detect and mitigate malware in parallel across networks, individually and collaboratively (without a central control site) to maximize performance and efficiency.

One of the innovative SEIM advantages is to use unanchored business objects to build components of scan engines and microagents to move the unanchored objects around applications on the computers in networks and clouds (e.g., DoD GID, DISA cloud, etc.).

The SEIM scan engines and microagents can be deployed and used on any platform, including UNIX, AIX, and Linux. The novel scan engines have successfully detected real malware; see sample experiments in Section 4.

3.2 Intelligent and Agile Microagents

The SEIM microagents have basic software agent features to (1) function with little or no user intervention; (2) communicate with their users and other agents; and (3) react to their environments or events without instruction from their users; and **novel** features to (4) move across any network to any host with the given security privilege; (5) avoid being attacked by malware due their minimal sizes, (6) learn to accomplish new tasks by leveraging existing tools (e.g., reasoning engines, scan engines, etc.), analytic algorithms and COTS (e.g., machine learning, data mining); and (7) exploit significant domain knowledge by using new rules and collect more patterns by cyber forensic and deception tools (e.g., OllyDbg, Honeypots, etc.). In addition, intelligent microagents use their neural nets [7] to learn and use their scan engines to dig into and penetrate through various malware codes. Specifically, they have unique features and capabilities in the following:

- SEIM intelligent microagents work collectively to establish a smart cyber sensor grid across entire computer networks. They add full-scale network protection on top of existing cyber security systems. They can also be integrated into current cyber defense systems through Web services and APIs.
- SEIM microagents patrol through enterprise networks and detect malware with nearly no performance degradation, because they are too lightweight to use much computing and networking resources.
- SEIM microagents collaborate with each other and interact with their users to establish collaborative intelligence; they can enhance cyber security on large networks, because they can cooperate with other cyber security defense agents and tools.
- Because SEIM microagents are all specialized in their fields such as anti-botnets, anti-malware, data leak prevention, they build multiple cyber defense layers for resilient cyberspace.
- Every SEIM microagent can use scan engines, reasoners, and analytic algorithms, so it is intelligent enough to learn and detect new malware.
- SEIM microagents launch from any network platform. They patrol and detect malware across boundaries and applications in both networks and clouds.
- All intelligent microagents can be re-trainable to adapt to a new environment and learn to detect new or unknown malware like zero-day threats.
- All intelligent microagents detect and mitigate malware individually and collaboratively under the supervision of their users (network operators, warfighters), who remotely control them from a management console.

The SEIM architecture supports sophisticated intrusion detection, botnet detection and eradication, and digital evidence gathering functions. As illustrated in Figure 1, the network administrators can manage and control their microagents from a remote network location such as a management console. The novel microagents are developed and implemented using Java, JDK in the JRE, because the Java Runtime Environment (JRE) can support operations on all platform computers on a network. The development environment and source code segment of these microagents are shown in Figure 3.

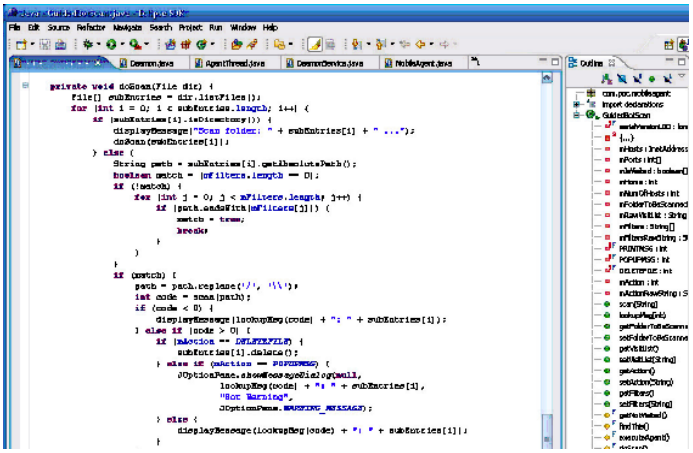

Figure 3. Design and implementation (in Java) of the SEIM microagents.

The microagents' capabilities are updated by updating the digital genomes and by editing the updatable instructions in an XML file to control the microagents. A small portion of the configuration file is illustrated in Listing 3.

Listing 3. Source Code Segment for a User to Configure Microagents and their team.

```
… …
<daemon port="7788"
log="agent.log“    remoteClassLoading="false"
verbose="true">
<agent class="com.poc.mobileagent.GuidedBotScan">
        <property name="folderToBeScanned"
value="C:\testbotscan"/>
        <property name="visitList"
value="BrianXu:7788,alex:7788"/>
        <property name="filters" value=""/>
        <property name="action" value="print"/>
… …
```

Mobility of the microagents is implemented by using unanchored and/or mobile objects. It can also be implemented by Java socket programming and object serialization. A code segment for mobility is shown in Listing 4. The intelligent microagents can use distributed rules or knowledge bases to accomplish tasks. They use Snort rules to identify new malware; new rules can be made to deal with new malware based on their new patterns, accordingly. As an example of the rules, IRC bots are detected because they use *PRIVMSG*, *Exploit*, etc. as shown in Listing 5.

Listing 4. Source Code Segment to enable the Microagents to move across a Network.

```
… …
protected final void executeAgent() throws Exception {
    if (mPorts[0] == -1) { mPorts[0] =
getDaemon().getPort(); }
        if(getRunState()
==AGENT_RETURN_TO_SENDER) {
        displayMessage("Rejected"); halt(); }
            try {   int self = findThis();
                if (self == -1 || !mIsVisited[self])
{ doScan();
… …
```

Listing 5. Source Code Segment of the Rules to detect IRC botnets.

```
… …
alert tcp $HOME_NET !21:443 -> any 1000:65535
(content:"PRIVMSG"; nocase:; content:"Exploit";
nocase:; within:80; tag:session, 20, packets;
msg:"Possible RogueIRC 03"; classtype:trojan-activity;
sid:1000168; rev:6;)
… …
```

4 Experimental Evaluations

4.1 Prototyping and Experimental Setup

The novel Scan Engines and Intelligent Microagents (SEIMs) have been successfully prototyped for malware detection and mitigation. The SEIMs have also been successfully tested and proven to effectively detect malware automatically across all computers on networks. SEIM microagents significantly improve the effectiveness of cyberspace security and automate malware detection and network protection without requiring installation of a malware detection software package on every computer in a network. A single SEIM microagent can patrol many (hundreds or thousands) computers on networks when its security privilege is granted. This capability alone can minimize the costs of purchasing many (hundreds or thousands) anti-malware software licenses, and the costs of maintenance and upgrade service. Manual installations on all individual computers are not required, and neither manual start-up nor shut-down processes. Users simply set up a small configuration file to manage which computers or even which folders need to be scanned by the cross-domain agile microagents.

We developed our IRC microagents to extend detection areas, by integrating our scan engines and microagents

with open source Snort (www.snort.org) to add network traffic sniffing. SEIM intelligent microagents have been proven effective as IRC guard agents to sniff network traffic, detect IRC-based botnets, and delete the botnets and malware by sending an SEIM microagent to scan through the bot-residence computer based on a sniff alert. SEIM microagents have effectively detected IRC botnets and deleted the botnets and malware in our lab network, by sniffing the network traffic and monitoring IRC alerts. In addition, SEIMs can also detect non-IRC botnets, by monitoring the 2LD/3LD (second level domain/third level domain) ratio online and by analyzing sniffed network traffic data. The non-IRC botnet detection capability was added to our SEIM system on top of existing IRC botnet detection capability. By combining these two capabilities, SEIM microagents and search engines can effectively detect both IRC-based and non-IRC-based botnets. A novel Network Intrusion Detection (NID) analyzer is designed in our SEIMs by integrating the scan engines and microagents with WinDump (www.windump.com). WinDump is utilized to sniff network traffic in log data files, and the NID analyzer uses and analyzes the data to visually show us the 2LD/3LD ratio graph and traffic distributions among all recorded Internet sites.

4.2 Experimental Results

The SEIM prototype was tested in a lab network consisting of physical machines running various operating systems through virtualizations. We then spread real world bots [6] in the lab network for experimental investigations. The SEIM toolset scanned at speed of about 50 MB per second and successfully detected all real bots [6] and real malware [9] in all experiments. A few experiments are demonstrated in the following scenarios:

1. SEIM microagents patrol and detect real botnets [6] and real malware [9] in all computers across the network, as illustrated in Figures 4 and 5.
2. SEIM microagents instantly detect IRC-based botnets in all computers in the network based on real-time Snort network sniffing, as illustrated in Figure 6.
3. SEIM NID analyzer monitors the 2LD/3LD ratio based on WinDump log files and triggers SEIM microagents to detect non-IRC-based botnets.
4. Working as a Windows service, see Figure 7, an SEIM search engine monitors and detects malware.

The innovative SEIMs are capable of scanning, identifying and detecting any digital patterns or genomes in computer data files. Current applications of the SEIM tools include to detect malware (viruses, Trojans, rootkits, spyware, worms, etc.) in binary (e.g., executables, DLLS, etc., see Figure 5) and ASCII or Unicode (e.g., scripts, any programming languages, etc., see Figure 4). In addition, the SEIM technologies can be applied to empower the effectiveness of analysis tools, reasoning engines and other COTS and GOTS in industry, military and government applications.

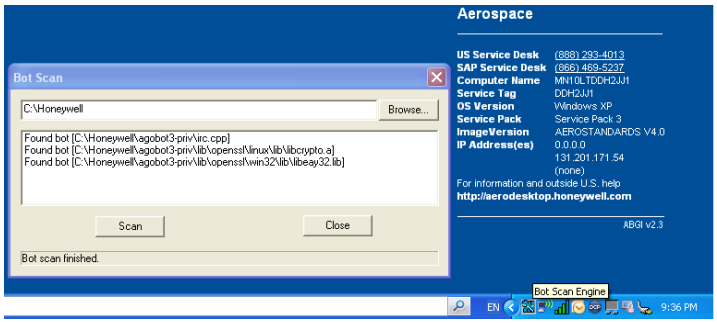

Figure 4. SEIM scan engine successfully detected real bots and botnets [6] in the machine.

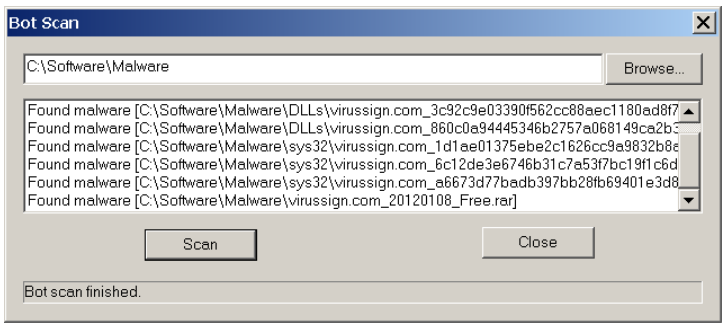

Figure 5. SEIM microagent patrolled and detected the real malware [9].

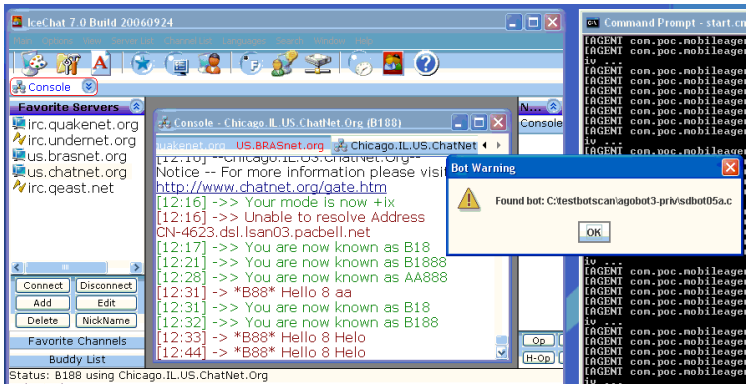

Figure 6. An IRC-based botnet was detected by the SEIM successfully.

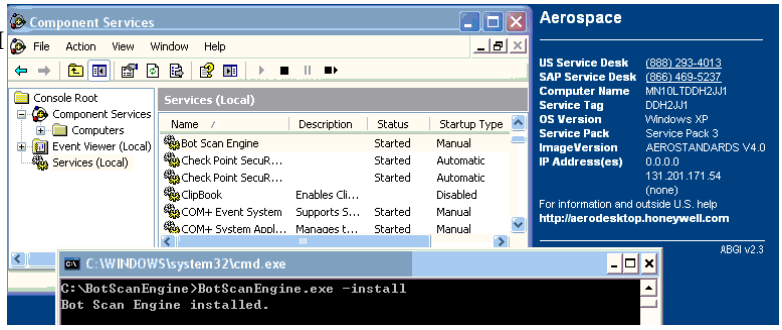

Figure 7. SEIM is running as a Window Service to protect the computer in real time.

5 Conclusions

In this paper, the novel Scan Engines and Intelligent Microagents (SEIMs) are presented for malware detection and mitigation. The SEIMs are based on novel microagents that automatically learn the behaviors of bots and botnets residing on hosts and networks to effectively stop their malicious activities. SEIM scan engines use genetic or genomic pattern matching, neural networks [7] for online learning, to detect both unknown and known malware, and use an inline sniffing mechanism for real-time traffic monitoring. The SEIMs have been prototyped (in C++ and Java) and tested in the lab network. SEIMs scanned at speed of about 50 MB/S and successfully detected real world bots [6] and real malware [9]. Specifically, experimental demonstrations have proven that SEIMs (1) detect bots, botnets, and malware across networks; (2) instantly detect IRC botnets on networked computers in parallel based on real-time network sniffing; (3) monitor 2LD/3LD ratio and detect non-IRC botnets; (4) detect malicious codes and executables in real time; and (5) scan and detect malware throughout all networked computers.

Importantly, the SEIM technologies can be applied to empower the effectiveness of guided data mining (where to mine what data, etc.), analytic tools, machine learning algorithms, and other COTS and GOTS. The digital patterns they can detect include not only malware genomes, but also key concepts and insights of humans. They can be applied to industry (business intelligence, analytic applications, cyber security, etc.), military (C2, ISR, C4IR, counter-insurgency, etc.), and government (homeland security, anti-terrorists, etc.) applications, respectively. The first goal is to advance the SEIM prototypes into fully functional and commercial software products for cyber security.

6 References

[1] CYBERCRIME. “Public and Private Entities Face Challenges in Addressing Cyber Threats”. GAO-07705, U.S. Gov. Acc. Office, Washington, D.C., 2007.

[2] B. Schneier, Secrets and Lies. “Digital Security in a Networked World”. Wiley Publishing, Inc. ISBN: 0-471-45380-3, 2004.

[3] M. Sharif, etc. “A framework for enabling static malware analysis”. Proceedings of the 13th ESORICS, Malaga, Spain, 2008.

[4] J. Nazario, T. Holz. "As the net churns: Fast-flux botnet observations". The 3rd Int’l Conference on Malicious and Unwanted Software, Fairfax, VI, 2008.

[5] S. Cheung, etc.. “Modeling Multistep Cyber Attacks for Scenario Recognition”. Third DARPA Info. Survivability Conf. and Exp. (DISCEX-III), 2003.

[6] The Honeynet Project. “Know your Enemy: Tracking Botnets, Using Honeynets to learn more about Bots”. http://www.honeynet.org, 2005.

[7] Brian. Xu, etc., “Integrated Intelligent System with Grid Fuzzy Neural Nets for Decision Making”. Int’l Conf. on Artificial Intelligence, 2006, Las Vegas.

[8] http://www.informationweek.com/news/security/attacks/229218944.

[9] http://www.virussign.com/.

Exploiting Structure within Data for Accurate Labeling using Conditional Random Fields

Aman Goel[1], **Craig A. Knoblock**[2], **and Kristina Lerman**[3]
[1]amangoel@usc.edu, [2]knoblock@isi.edu, [3]lerman@isi.edu
Information Sciences Institute and Department of Computer Science
University of Southern California
Marina del Rey, CA 90292

Abstract—*Automatically assigning semantic class labels such as WindSpeed, Flight Number and Address to data obtained from structured sources including databases or web pages is an important problem in data integration since it enables the researchers to identify the contents of these sources. Automatic semantic annotation is difficult because of the variety of formats used for each semantic type (e.g., Date) as well as the similarity between different semantic types (e.g., Humidity and Chance of Precipitation). In this paper, we show that by exploiting different kinds of latent structure within data we can perform this task accurately. We show that this improvement happens in spite of higher complexity in terms of both the inference procedure and the increased number of labels. We study how increasing the amount of structure taken into account by the model improves accuracy of semantic labeling. Finally, we show that when exploiting all the relationships, we obtain a significant improvement in field labeling accuracy over the regular-expression-based approach, while still keeping the complexity low.*

Keywords: Supervised learning, Graphical models, Semantic web

1. Introduction

Automatic semantic annotation of structured data elements is an important problem in information integration. It helps in identifying the contents of various sources so that further operations can be performed on them. For instance, once the semantic type of the data in different sources is known, these sources can be joined together. Each domain has some common semantic types defined in them. For example, the weather domain presents information about *Temperature*, *Humidity*, and *Visibility*, the flights domain presents information about *Flight Number*, *Airport*, and *Time of Arrival* and the spatial domain presents information about *Address*, *Latitude*, and *Longitude*. The first column of Table 1 shows a sequence of fields extracted from a weather forecast website and its second column shows their semantic types or labels. Formally defined, the task of semantic annotation is to assign these semantic labels to the sequence of fields when their identity is unknown.

Automatic semantic annotation is difficult to perform accurately. There are two main reasons for this. First, the semantic types have many different formats in which they can be written. Table 2 shows some of the various ways of writing the value of 9 $miles$ for *Visibility*. There are variations in the choice of the unit, its abbreviation, the precision of the numeric value, and even in the representation of a particular edge case value as a non-numeric term (for example, *Clear*). Therefore, even if the model has seen examples of a few formats, a new format may not be recognized by the model. Second, several semantic types can look similar to each other. *Humidity* and *ChanceOfPrecipitation* are two such semantic classes. Both of them are percentage values, written as a numeric value followed by a percent symbol (e.g., *40%*). This makes it hard for the model to discriminate between these semantic types.

Researchers have used CRFs to perform semantic annotation in the past. Zhu et al. [17] used CRFs to labels objects on a webpage by exploiting the relationship between adjacent items. Tang et al. [15] used tree-structured CRFs to identify different information elements such as *Telephone Number* and *Secretary Name* in official reports. Both of these approaches exploit the relationships among the field labels. The problem with this approach is that in the presence of many semantic types and weak dependencies between adjacent fields, these approaches do not perform as well. Instead, we propose to exploit the structure within the fields by modeling the relationship between the labels of the field and the labels of their tokens as well as the relationships among the adjacent tokens to achieve high field labeling accuracy. In this paper, we show that as we exploit more and more of the latent structure within the data, we can achieve higher field labeling accuracy. We show that this holds true even when the complexity of the inference increases and we add many more labels that the model has to choose from. We also show that our graph structure keeps a low limit on the complexity of the inference algorithm which is proportional to $L_f \times L_t^2$, where L_f is the number of field labels and L_t

Table 1: A sample data tuple extracted from a weather forecast website. The table shows the fields, their corresponding semantic classes, their tokens (generate by our lexer) and their semantic classes.

Fields	**Field labels**	**Tokens**	**Token labels**
90292	Zip	90292	ZipValue
$76°F$	TempF	76	TempFValue
		°	DegreeSymbol
		F	TempFUnit
50%	Humidity	50	HumidityValue
		%	PercentSymbol
$5mph$	WindSpeed	5	WindSpeedValue
		mph	WindSpeedUnit
Los $Angeles$, CA	Place	Los $Angeles$	CityName
		,	Symbol
		CA	StateAbbr
$4:05$ pm EDT	Time	4	HourValue
		:	TimeSeparator
		05	MinuteValue
		pm	AmPm
		EDT	TimeZone

Table 2: The various formats of writing the same value of Visibility in the weather domain.

Numeric Value	**Unit**
9	miles
	mi
	mi.
	MI.
	Mi.
	-no unit-
9.0	miles
9.00	miles
14.5	kilometers
	km
clear	

is the number of token labels.

The rest of the paper is structured as follows: In section 2, we give a brief overview of the CRF models. In section 3, we first explain our method of generating tokens from the fields and extracting features from them, which is common to all graph structures. Then we present different graph structures that we build incrementally to exploit more structure within the data. We describe how we generate these graphs, how we train the CRF models from them and our method of performing prediction on unlabeled graphs. We also discuss the complexity of each graph structure. In section 4, we present the results of our experiments and in section 5, we discuss the related work. We conclude in section 6.

2. Conditional random field models for labeling data

Conditional Random Field-based models [4] learn the probability distribution of labels conditioned on the evidence. The variables and their mutual probabilistic dependence is presented as nodes and edges respectively. Therefore, the training examples are in the form of labeled graphs and prediction involves assigning values to the nodes of an unlabeled graph.

Fig. 1: Six graph structures that capture the various probabilistic dependencies between the data elements.

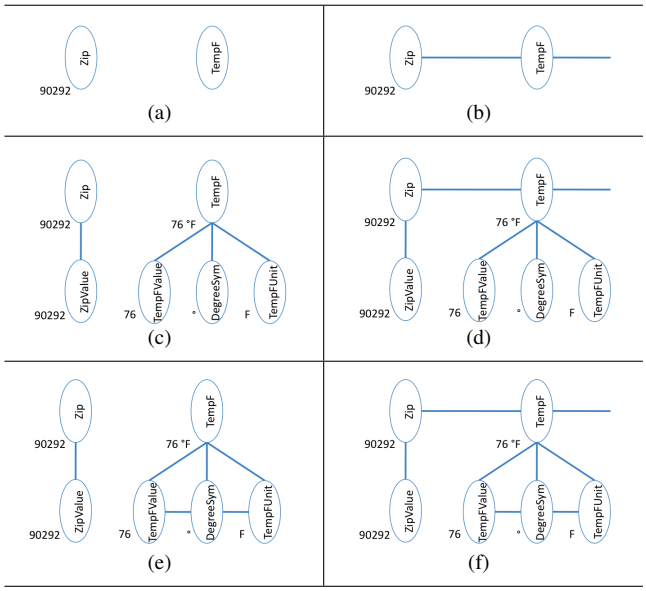

CRF models represent the relationships between the labels and the evidence and the relationships between mutually dependent variables (those that are connected via edges) in terms of feature functions. A feature function applies on a fully connected subgraph, called a clique. A feature function that applies on only one node is called a one-node feature function and that which applies on two nodes is called a two-node feature function. A feature function when applied on a clique, takes as input one label value for each node in the clique and checks if those values are the ones that it expects. It also considers the features of the evidence around those nodes. It returns a value of 1 or 0 depending on whether the required conditions are satisfied or not, respectively. Learning the model entails learning appropriate weights for these feature functions.

More formally, let the features of the evidence be represented by a feature vector, X, the labels be presented by the feature vector, $Y = \{y_i\}$, the feature functions be represented by $F = \{f_i\}$, and their weights by $W = \{w_i\}$. The potential for a clique is defined as:

$$\phi(clique) = exp\Big(\sum_i f_i(y_{clique}|x)\Big) \qquad (1)$$

The potential of the whole graph is the product of the potentials of all the cliques. The sum of the graph potential for all possible label assignments is called the partition function and represented by $Z(X)$. The likelihood of a particular label assignment to the random variables $P(Y = y|X = x)$ is defined as the ratio of the graph potential for

that label assignment to the partition function as follows:

$$1/Z(x) * exp\big(\sum_c \big(\sum_k w_k f_k(y_c, x)\big)\big) \quad (2)$$

CRFs do not have a closed form solution for the weights. The weights are found by numerical optimization techniques such as gradient based approaches [8]. The gradient with respect to the weight w_k is given below. The term $p(y_c = y|x)$ is the marginal probability of the clique variables. These marginals are found using inference algorithms such as belief propagation [10]. The labels are predicted for an unlabeled graph using potential maximization algorithms, such as the Viterbi algorithm [16].

$$\sum_c f_k(y_c = y_k, x) - \sum_c \sum_y p(y_c = y|x) f_k(y_c, x) \quad (3)$$

3. Exploiting structure within data for accurate labeling

There are three kinds of probabilistic dependencies that are generally seen among various data elements in structured data. They are as follows: 1) The dependency between the labels of neighboring fields, 2) The dependency between field labels and their token labels, and 3) The dependency between neighboring tokens within a field.

We can exploit all of these dependencies through different graph structures used for training the CRF models. Since a CRF graph represents the relationship between two random variables by means of edges between their nodes, it means that the more relationships one exploits, the more complex the graph structure becomes. A more complex graph structure also requires higher computational complexity inference techniques. Therefore, there is a trade-off between the numbers of relationships one exploits and the complexity and hence the time required to perform inference on these graphs.

In this work, we present six different graph structures constructed from the structured data by incrementally exploiting more structure within the data. These graphs are shown in figure 1. The simplest graph is one where there is only one node corresponding to each field. The purpose of the CRF model that uses this graph is to learn to predict the label for each field independently. This graph structure is show in figure 2(a) and is discussed in section 3.2. There is only one kind of label-to-label dependency that can be exploited here, the one between adjacent field nodes. The corresponding graph structure is shown in figure 2(b).

In addition to fields, the model can also take tokens into account for each field. These graphs are shown in figure 2(c) and 2(d) and are discussed in section 3.3.

Finally, we can also take into account the relationships between tokens. These graphs are show in figure 2(e) and 2(f) and are discussed in section 3.4.

In the following subsection, we discuss the process of tokenization of these fields and the extraction of features from the tokens.

3.1 Tokenization and Extraction of features

We generate the tokens from the fields using our own lexical analyzer. This lexical analyzer splits the field string at whitespaces and then splits the resultant parts in such a way that each token is either purely alphabetic (e.g., Cloudy), purely numeric (e.g., 76, -4.5), or a single symbol character (e.g., °, %).

Once the tokens have been generated, we assign features to each token. There are three different classes of features, the ones that apply to purely alphabetic tokens, the ones that apply to purely numeric tokens, and the ones that apply to symbol tokens. Table 3 lists all the features that we use. Some of the features listed are generic features, whose particular instance is generated based on the token from which it is generated. For example, the feature *Starts_With_Alpha_⟨X⟩* is a generic feature and its particular instance for the token *Cloudy* will be *Starts_With_Alpha_C*. One of the important features is the identity of the token itself. Since CRF models assign weights to features based on their frequency of appearance, this feature is useful for those semantic types that consist of a small lexicon of terms (e.g., *Country Names*). The features used by us are generic and can apply to any domain. We have picked features that capture the basic properties of any token. It is very easy to add new domain specific features to this set of features, if it is so required. However, all our experiments use only these features.

Table 3: Features used to characterize the tokens.

Features	Description
Alphabetic features	
$Alpha\_Length\_\langle N\rangle$	Length. N = 1,2, ...
$Starts\_With\_Alpha\_\langle X\rangle$	First character. X = A, a, B, ...
$Capitalized\_Token$	Token is capitalized.
$All\_Uppercase\_Token$	Whole token is uppercase.
$Alpha\_Id\_\langle Token\rangle$	Token itself is feature. $Token$ = California, NW
Numeric features	
$Num\_Length\_\langle N\rangle$	Length. N = 1,2, ...
$Before\_Decimal\_Len\_\langle N\rangle$	# of digits before decimal.
$After\_Decimal\_Len\_\langle N\rangle$	# of digits after decimal.
$Negative\_Num$	Number is negative.
$Starting\_Digit\_\langle N\rangle$	First digit. N = 0, 1,2, ...
$Unit\_Place\_Digit\_\langle N\rangle$	Units place digit. N = 0, 1,2, ...
$Tenth\_Place\_Digit\_\langle N\rangle$	Tenth place digit. N = 0, 1,2, ...
Symbol features	
$Symbol\_\langle Sym\rangle$	Symbol itself is feature. Sym = %, :, °

3.2 Graphs with field nodes only

Figure 2(a) shows the simplest graph structure generated from the data. Each field has a separate graph which contains only one node. This node represents the random variable associated with the field label. We tokenize the field into tokens, extract features for each token and then combine them into one set of features. These features are assigned to the field node. For example, the field node for '76°F' will have the features, Num_Length_2, $Starting\_Digit\_7$, $Symbol\_°$, $Alpha\_Length\_1$ and others, where the first two features have been extracted from token '76', the third feature has been extracted from '°' and the fourth feature has been extracted from the token 'F'.

We use only one class of feature functions for this graph structure. These feature functions are of the form:

$$f(field\_node, field\_label) \tag{4}$$

These feature functions return the value 1 if the field node has a feature p_m and input value $field\_label$ is some l_j. We find the marginals for a field node by finding the potential of the node for each value of label l_j and then dividing the potentials by the sum of the potentials, $Z(x)$. Once the marginals are calculated, the gradient can be calculated from them. We train our model in this way.

We predict the most likely label for a new field node by finding the label l_j for which the potential of the node and therefore of the graph (since the graph consists of only one node) is the highest. The complexity of the inference method as well as the labeling method is $O(L_f)$, where L_f is the number of field labels.

In every domain, it is generally the case that there is some order to the fields. This means that a field is immediately followed by one of a small set of fields. For example, the $Temperature$ field type is generally followed by $SkyCondition$ and a $WindSpeed$ field is generally followed by $WindDirection$. We exploit this relationship in the graph structure shown in 2(b). This graph is formed by connecting the fields in a linear chain. We capture this relationship using the following feature function:

$$f(field\_node1, field\_node2, field\_label1, field\_label2) \tag{5}$$

where it returns 1 if the input $field\_label1$ is some label l_j and input $field\_label2$ is some label l_k. Otherwise, it returns the value 0. Therefore, this graph uses the two classes of feature functions shown in equation 4 and 5.

We perform inference on this graph using the belief propagation algorithm [10]. We predict the most likely label assignment to the field nodes using the Viterbi algorithm [16]. The complexity of performing inference on this graph is again $O(L_f)$. Yet, the model uses more feature functions for these graphs. This graph structure better represents the field labels since they consider both the features of the fields as well as the neighboring fields. Our experiments show that these graph structures indeed give higher field labeling acurracy. This happens because the neighborhood information helps disambiguate between similar fields. For example, the fact that *Humidity* and *Sky Condition* are generally reported together prevented the model from mislabeling some of the *Humidity* values as *Chance Of Precipitation* because these values appeared close to a *Sky Condition* value. The model based on the graph structure in figure 2(a) did make some of these mistakes.

3.3 Adding token nodes to the field nodes

The features used to represent the fields in the models described above are derived from the tokens of the fields. It seems more appropriate to predict the identity of the tokens based on their own features and derive the identity of the field based on the tokens. For example, the field type $Temperature$ can have token types *TemperatureValue*, *DegreeSymbol*, and *TemperatureUnit* and the field type $Time$ can have the constituent token types $Hours$, $TimeSeparator$, $Minutes$ and $Seconds$. We create a new graph structure, where each field node will have token nodes as it children.

The graph structures shown in figures 2(c) and 2(d) show how these graphs look. We do not exploit the field-label-to-field-label relationship in the left figure, while we do so in the right figure.

The graph shown in figure 2(c) does not have any features belonging to the field node itself. Instead the features belong to the token nodes. We use two new classes of feature functions to represent relationships in these graphs. The first class of feature functions are written as:

$$f(token\_node, token\_label) \tag{6}$$

These feature functions take a $token\_label$ and a $token\_node$ as inputs and returns 1 if the $token\_node$ has a feature p_m and the $token\_label$ is some label l_j. These feature functions represent the dependency of the labels of token nodes on their features.

The second class of feature functions are written as:

$$f(field\_node, token\_node, field\_label, token\_label) \tag{7}$$

These feature functions take a $field\_label$ for a $field\_node$ and a $token\_label$ for a $token\_node$ and return 1 if the $field\_label$ is some label l_j and the $token\_label$ is some label l_k. These feature functions represent the co-occurence of the field labels with their token labels.

We use belief propagation to perform inference on these graphs. The graphs are already in the form of a tree, as required by the algorithm. The prediction for a new graph is made using a modified Viterbi algorithm called the max-sum algorithm [3]. This algorithm maximizes the sum of the log of the potentials of the various cliques in the graph.

Compared with the graph structure in figure 2(a), this graph is more natural because it finds the labels of each

token based on its own features and then finds the label of the field based on the labels assigned to its tokens. Yet, this graph introduces more nodes to be labeled and also introduces a large set of token labels to chose from. This increases the ambiguity while training as well as during prediction. As we show in our experiments, this graph structure gives higher field labeling accuracy than the graph structure that has only one node in the graph. This happens because when the features of the tokens are combined into one set (as in figure 2(a) and 2(b)), most of the features from different semantic types are similar. For example, if we look at the semantic type $Temperature$ and $Humidity$, both these types have numeric values, and the values are between 0 and 100. The main difference appears in the fact that $Temperature$ values end with a F or a C, but $Humidity$ ends with a percentage ($\%$) symbol. But, when these features are distributed over their own tokens, the most distinguishing tokens namely the F or C in one and the $\%$ symbol in the other have very distinct features. The CRF model can differentiate between these much better. With high confidence on these tokens, the field labels tend to be correctly assigned due to their co-occurence relationship with these tokens labels (e.g., the strong co-occurence of $Temperature$ with $TemperatureUnit$).

In addition, this graph structure also solves an important problem of identifying the semantic types of the various components within a field. For example, in order to compare two $Date$ fields that are written in different formats, (e.g., 07/21/2011 and 21 July, 2011), it is required that the semantic meaning of the various components of each date string are known so that they can be compared effectively. Therefore, the graph structure described here improves the accuracy of labeling while solving a larger problem.

The graph shown in figure 2(d) is an extension on the graph described above. In this graph, we also join the field nodes via edges. We exploit the neighboring relationships among the field nodes in the same manner as we did in the graph in figure 2(b) via the feature function presented in equation 5.

In order to perform inference in these graphs, we first need to convert them into a tree structure. We perform this conversion as follows: we make the first (leftmost) field node the root of the whole graph. All its token nodes are already its children. We also make the field node to its right, its child. This is repeated at each field node. This gives us a tree, where each node has one parent and each node can have zero or more children. We then apply belief propagation algorithm to this graph to perform inference.

Prediction on a new unlabeled graph is performed by first converting it into a tree structure as described above and then applying the max-sum algorithm [3] starting from the leaf nodes to find the most likely joint assignment of labels to all the field and token nodes. This graph structure is more complex than the one described above. We show in our experiments that exploiting the field-node-to-field-node label dependency helps improve the field labeling accuracy over the simpler model that does not exploit these relationships, similar to the results obtained for the graph structures in figure 2(a) and 2(b).

3.4 Connecting the tokens with each other

There is an important relationship between neighboring tokens within a field. In general the order of the token types within a field remains roughly constant. For example, $Minutes$ always follows $Hours$ in every format of $Time$, *Temperature Unit* ('F' or 'C') always appears after the *Temperature Value* token within a $Temperature$ field and *State Name* always written after $CityName$ within an $Address$ field. To exploit these strong relationships, we connect the tokens within the fields together. Figures 2(e) and 2(f) show how the graphs look in this case. Figure 2(e) shows the graphs where we do not exploit the neighborhood relationships between fields, whereas figure 2(f) shows the graph structure where we do.

We represent the relationships between labels of neighboring token nodes by a new class of feature functions. These feature functions are written as:

$$f(token\_node1, token\_node2, token\_label1, token\_label2) \quad (8)$$

This function returns the value 1 only when $token\_label1$ is some token label l_j and $token\_label2$ is some token label l_k. Therefore, this graph has three classes of feature functions. Two of these classes are the same as we used in the graph structure shown in figure 2(c).

We cannot use belief propagation to perform inference on these graphs since they have cycles in them. Therefore, we convert each graph into a different graph called a junction tree [5]. A junction tree (JT) is formed by replacing all the three-node cycles in the original graph by a single junction tree node (JT node) and connecting the JT nodes that share at least one node in the original graph. See [5] for the detailed general algorithm for converting any graph into a junction tree. We convert our graphs into junction trees as follows: if the field has only one or two token nodes, then it is replaced by just one JT node. Otherwise, for each field, we take two token nodes at a time starting from the left and replace the three-node cycle formed by them and the field node with one JT node. Figure 2 shows the junction tree constructed from the CRF graph in figure 2(e). Since, the adjacent JT nodes share the field node and a token node, they are connected with each other. This always gives us a linear chain of $(N-1)$ JT nodes for N token nodes. Since this is a linear chain, we apply belief propagation to this graph. The possible states that a JT node can take is a power set of the labels that each node within the clique that they represent can take. Therefore the complexity of the belief propagation algorithm is equal to:

$$L_f \times L_t^2 \quad (9)$$

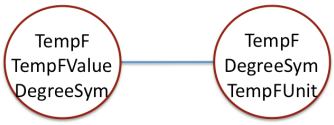

Fig. 2: The junction tree for one field and its tokens.

where L_f is the number of field labels and L_t is the number of token labels. This complexity is low enough to allow us to apply the belief propagation algorithm on graphs of practical sizes.

To label a new graph, we convert it into a junction tree, as explained above. We then use the Viterbi algorithm to find the most likely states for all the JT nodes. The Viterbi algorithm is constrained so that the states on the nodes that are shared by two adjacent JT nodes are the same. For example, since the two JT nodes in figure 2 share the field node and the middle token node, both JT nodes can only take values so that the labels values for the two shared nodes in the same.

Figure 2(f) is the most complex graph structure that we use. It exploits all the three dependencies among the field and the tokens. It uses the three feature functions used for the graph structure explained above. In addition it also uses the field label to field label feature function that we used in the graphs in figure 2(b) and 2(d) to exploit the neighborhood relationships among field labels.

Like in the previous graph, this graph also contains cycles. As a result we again convert these graphs into junction trees. Since the field nodes are connected to each other in a line, the two-node-cliques formed by consecutive field nodes are also converted into JT nodes for these graphs. These JT nodes share the field nodes with the JT nodes formed by token nodes under these field nodes (as explained for the previous graph). This results in a linear chain junction tree as shown in figure 3. Due to the linear structure, belief propagation algorithm can be applied to this graph. Since, the new JT nodes represent two field nodes, the number of states that they can take is:

$$L_f^2 \tag{10}$$

where the terms mean the same as before. Generally, this term will always be smaller than $L_f \times L_t^2$ since the total number of tokens is generally larger than the total number of fields. Therefore the complexity of performing inference on this algorithm remains bounded as before.

We similarly generate a CRF graph from unlabeled data, convert it into a linear chain junction tree and then use the Viterbi algorithm on it to predict the labels for fields and tokens.

4. Experiments on real world data

We tested the six graphical structures in three different domains: weather forecast, flight status and geocoding. For each domain, we scraped data[1] from 100 different web pages of four different web sites to obtain 400 tuples of data in each domain. We also defined a set of field level and token level semantic classes that we wanted to identify in each domain. We tokenized the fields in each tuple using our lexical analyzer. We then labeled all the fields and their tokens using the labels for the semantic classes already defined. We then extracted the features for each token. The average number of fields per tuple in the weather forecast domain was 31, in flight status domain it was 14 and in the geocoding domain it was 3.5. Table 4 shows the web sources used in each domain and also mentions the number of field and token semantic types in each domain.

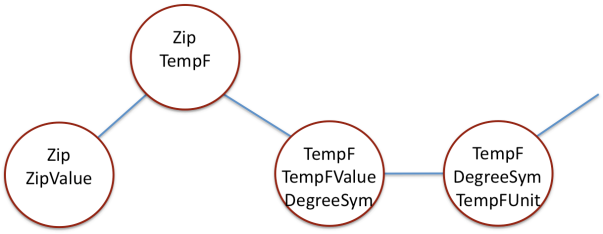

Fig. 3: The junction tree for the fully connected graph in figure 2(f). We have drawn the JT node formed from the field nodes' clique slightly elevated to differentiate it from the JT nodes formed from field and token nodes. Yet, this is a linear chain.

Table 4: Experimental setup

Domain	Details	**Data sources**
weather forecast	#field types = 15 #token types = 37	wunderground.com
		unisys.com
		weather.com
		noaa.com
flight status	#field types = 8 #token types = 17	flytecomm.com
		flightview.com
		continental.com
		delta.com
geocoding	#field types = 5 #token types = 12	geocoderus.com
		geocoderca.com
		geonames.com
		worldkit.com

We ran four experiments on every graph structure in each of the three domains. In each experiment, we trained a CRF model on the graphs created from 300 tuples from three sources and tested it by labeling the 100 tuples from the fourth source. We then averaged the field and token labeling accuracy for each graph structure. Table 5 shows the average field labeling accuracy for each graph structure in each domain. The geocoding domain is a relatively simple domain with only five field types. Therefore, even the simplest graph structure gives high field labeling accuracy and there is little scope for improvement as we take advantage of more

[1]We used a tool called AgentBuilder, from Fetch Technologies.

structure within the data. However, there is an improvement of 1% from the simplest graph structure to the most complex graph structure in the field labeling accuracy.

All the differences in the table for the other two domains are statistically significant for $p = 0.05$. The results for the weather forecast and the flight status domains show that the accuracy increases each time we exploit additional relationship among the labels. For example, the accuracy for graph structures where the relationship between the neighboring field labels is exploited (right column) is always more than the accuracy for the graph structures where it is not (left column), except in only one case for the flight status domain where the source *flytecomm.com* has dates that are in a very different format from other sources and also appear out of the normal order so that all of them get consistently mislabeled. The accuracy also increases when we exploit the relationship between the field labels and the token labels. Further, when we connect the adjacent token nodes to exploit their neighborhood relationships, we get a significant improvement in labeling accuracy. There is an improvement of 10% in the weather domain and 7% in the flight domain from the graph structure that has only one field node to the graph structure that has both the field and token nodes and all of them are connected. These results clearly show that exploiting each new relationship gives us a better model and hence higher field labeling accuracy. These experiments represent the real accuracy that one might achieve while using these graph structures since we never test our models on the same data that we trained it on. Yet, despite the fact that each new source uses its own formats and representations, the model is able to successfully identify the semantic labels for a high percentage of fields.

The following is an example of how the model exploits the inter-label relationships to correctly label a field that uses a format not seen before by it: The weather source, *unisys.com*, represents temperature in fahrenheit (*TemperatureF*) using only a numeric value and the unit, and without a degree symbol. (for example, '62 F'). None of the other three sources, on which the model was trained had such an example of this class. Yet, the model was able to assign the correct semantic label to these fields by taking advantage of the strong relationship between the field level label *TemperatureF* and the token level labels *TemperatureFValue* and *TemperatureFUnit*, and a strong correlation between the *TemperatureFUnit* token label and the feature *Alpha_Id_F*. In contrast, in the graph structure in figure 2(a), all such fields that had integer values were labeled as *Humidity* due to the lack of the differentiating feature $Symbol\_^{\circ}$ and a strong correlation between the label *Humidity* and the feature *After_Decimal_Len_0*.

Table 6 shows the token labeling accuracy results for the four graph structures in all three domains. There is an improvement in token labeling accuracy every time we add one more relationship to the model for use. There is an average improvement of 5% in the weather domain and 6% in the flights and geocoding domain between the simplest graph structure that involves tokens (figure 2(c)) and the graph structure that exploits all relationships (figure 2(f)). The average token labeling accuracy is around 85% across all the different graph structures and domains. This means that the model is able to correctly identify the semantic types of the tokens within the fields with high accuracy. Some of the tokens types are so similar to each other that it is difficult to differentiate between them. For example, the token types, $TemperatureValue$, $HumidityValue$, $PressureValue$, and $VisibilityValue$ all look very similar to each other and yet our models are able to use the identity of the neighboring fields and tokens to correctly identify them.

Table 5: Result of experiments on all six graph structures. The average field labeling accuracy improves as we exploit more structure within the tuple and the fields.

Domains		Fields not connected	Fields connected
Weather forecast	**Fields only**	0.79	0.83
	Field and tokens	0.80	0.85
	Tokens connected	0.85	**0.89**
Flight status	**Fields only**	0.90	0.88
	Field and tokens	0.90	0.93
	Tokens connected	0.93	**0.97**
Geo-coding	**Fields only**	0.97	0.97
	Field and tokens	0.98	0.98
	Tokens connected	0.98	**0.98**

Table 6: The average token labeling accuracy for experiments on all six graph structures.

Domains		Fields not connected	Fields connected
Weather forecast	**Field and tokens**	0.81	0.85
	Tokens connected	0.83	**0.86**
Flights status	**Field and tokens**	0.81	0.84
	Tokens connected	0.85	**0.87**
Geo-coding	**Field and tokens**	0.84	0.85
	Tokens connected	0.89	**0.90**

An alternate approach to assigning semantic labels to fields is based on matching unlabeled fields with regular expressions that are generally known to represent a particular semantic class. We compare a CRF model utilizing the graph structure in figure 2(f) with a sophisticated regular expression based pattern matching model proposed by us in [7]. In this work we generate regular expressions of varying generality to match the given labeled examples. For example, patterns such as 25, *2-digit*, and *numeric* are generated for a temperature value 25. The labels are assigned to unlabeled fields based on how well they match the regular expressions for each semantic type. We used the same experimental set up for running experiments on our previous approach. The average field labeling accuracy of both the approaches is presented in table 7.

In all the three domains, the labeling accuracy of the CRF model is much better than the accuracy for the regular

expression based approach. This is because the regular expression based approach it is unable to generalize the structure of a semantic class from the examples that it has seen. Therefore, even a slight change in the structure, such as the introduction of a dot after an abbreviated unit can mislead it. On the other hand, since our model learns many different types of dependencies among labels, even if some such relationships do not hold true due to changes in the structure, other dependencies such as the relationship with neighboring fields can still help the model make the right prediction.

Table 7: Comparison of our graph structure that exploits all the three relationships with a regular expression based approach. The new model performs much better on all domains.

Domains	Regular expression based model	CRF model
Weather	0.65	0.89
Flight status	0.42	0.97
Geocoding	0.36	0.98

5. Related Work

Semantic annotation is a problem that occurs in various domains and on various kinds of documents. Named entity extraction [9] is a form of semantic annotation problem where the task is to assign named entity tags to various words or phrases in a text document such as a news report. Similarly, semantic annotation can also be applied to reports, where the task is to identify the various pieces of information such as telephone numbers, etc. An example of semantic annotation in semi-structured sources is the problem of identifying the various information fields on webpages [6]. Finally, the semantic annotation of structured sources such as databases is performed under the name of schema matching [2]. In this paper, we solve the problem of assigning semantic labels to structured data obtained from databases or web pages. Unlike schema matching, we do not label entire columns of data. Instead we assign labels to all fields in a tuple, which corresponds to a row in a database table. The advantage of our approach is that it is applicable to sources with missing and optional fields since we do not need the data to be available in a regular tabular format.

CRF models were proposed by Lafferty et al. [4], where they presented experiments on linear chain graph structures for performing part-of-speech tagging of natural text. Researchers then applied the same structure to other problems such as noun phrase chunking [13] and extracting tables from documents [11]. Later researchers demonstrated the use of other graphical structures such as factorial graphs [14], two-dimensional grid structures [17] and tree-structured graphs [15]. In this paper, we use various kinds of graph structures, which include linear chain graphs, hierarchical tree structured graphs and also cyclic graphs. We compare their capability in exploiting the various patterns within data and also examine the computational complexity of performing inference on them. In addition, we also show that the cyclic hierarchical tree structure graph (Figure 2(f)) is well suited to accomplish the task of semantic annotation and achieves high accuracy both in field and token labeling.

There have been two main works using CRF models to perform semantic annotation. Zhu et al. [17] used the CRF model to assign semantic labels to the image, description, price and title of a product on a commercial product webpage. They mapped the web objects to two-dimensional grids and exploited the spatial proximity and relationship to assign labels to them. In the other work, Tang et al. [15] used tree-structured graphs to represent the layout of the information elements on semi-structured reports. In both these cases, the researchers exploit the dependence of the field labels on their structures and the relationship between adjacent field labels. In this paper, we present six different graph structures that exploit different combinations of inter-label relationships including the graph that only exploits the relationship between adjacent field labels (figure 2(b)). We show that we can achieve a significant improvement in the labeling accuracy if we exploit the relationships between the field labels and the token labels as well as the relationships among neighboring token labels.

One of the other advantages of our graph structures is that we also assign semantic labels to the tokens of the fields. This is essential in comparing data values from different sources which might be using different formats. Borkar et al. [1] used HMMs [12] to assign semantic labels to the tokens of US addresses. They trained a linear chain HMM model that learns the transition probabilities beween the various labels and the emission probability of the various kinds of tokens from these labels. The semantic types used by them are: *HouseNumber, StreetName, CityName, StateName, ZipCode*. In contrast to their approach, we use a more powerful model than HMMs, which allows the use of overlapping features. Also, we do not need to train a separate model for each field level semantic type. Instead our model can simultaneously identify the field level type of an item of data as well as the semantic types of its tokens. For example, in the geocoding domain, our model can identify the semantic type of a field as being *Latitude*, *Longitude* or *Address* and also identify their token labels such as *LatitudeDegree*, *LatitudeMinutes*, *HouseNumber*, and *StateName*.

An alternate approach to graphical models, such as CRFs and HMMs, that can be applied to the problem of semantic annotation involves learning the syntactic rules that describe the syntax of the semantic classes using regular expressions. We proposed this approach in [7]. In this approach, we generate regular expressions of varying generality from the examples of the semantic types and then match these with new unlabeled examples to predict their label. We presented

results comparing the approach proposed in this paper with our previous work and show that the new approach performs much better as compared to the previous approach. The previous approach could not handle variations in the formats easily and fails as soon as the format changes even slightly. In addition, it cannot take advantage of the information available about the neighboring fields and tokens. Since our model exploits many different classes of relationships and combines them in a probabilistic way, it can handle such variations because many of these relationships still hold true for the new format.

6. Conclusion

In this paper we have shown that we can get high labeling accuracy from CRF models by exploiting the latent structure within data. We showed that in spite of increased complexity and higher number of labels, exploiting more structure improved the labeling accuracy for fields as well as the tokens. We also showed that the complexity of the graph structure that exploits all three relationships is bounded by $L_f \times L_t^2$, where L_f is the total number of field labels and L_t is the total number of token labels.

There are many domains where entities have such hierarchical structure within them. For example, this approach can also be applied to assign part-of-speech labels to phrases within sentences, where the phrases can be split into words and the relationships between the labels of adjacent words can be used to achieve higher labeling accuracy for phrases. Similarly this approach can also be used for named entity recognition to identify top level entities such as *Address* as well as low level entities within them, such as, *City Name*, *State Name*, or *Country Name*.

One of the factors that impact the speed of training is the number of feature functions used in the model. Presently, we use all feature functions that can be generated from the training examples. In future, we will explore techniques of pruning this space to reduce the training time. We will also experiment with more complex feature functions that can be formed from conjunctions or disjunctions of elementary features functions. For example, a feature function that says that an *Hour* token can either have one or two digits is a better descriptor of this semantic type than two separate feature functions, one of which associates the feature of having one digit with the semantic type and the other associates the feature of having two digits with it. Both of the above mentioned directions can reduce the total number of feature functions used in the CRF model, while building more expressive CRF models.

7. Acknowledgments

This research is based upon work supported in part by the Intelligence Advanced Research Projects Activity (IARPA) via Air Force Research Laboratory (AFRL) contract number FA8650-10-C-7058. The U.S. Government is authorized to reproduce and distribute reprints for Governmental purposes notwithstanding any copyright annotation thereon.

The views and conclusions contained herein are those of the authors and should not be interpreted as necessarily representing the official policies or endorsements, either expressed or implied, of IARPA, AFRL, or the U.S. Government.

References

[1] V. Borkar, K. Deshmukh, and S. Sarawagi. Automatic segmentation of text into structured records. In *Proceedings of the 2001 ACM SIGMOD International Conference on Management of Data*, 2001.

[2] A. Doan, P. Domingos, and A. Y. Levy. Learning source descriptions for data integration. *WebDB*, 81-86, 2000.

[3] F. R. Kschischang, B. J. Frey, and H. A. Loeliger. Factor graphs and the sum-product algorithm. *IEEE Transactions on Information Theory*, 47(2), February 2001.

[4] J. Lafferty, A. McCallum, and F. Pereira. Conditional random fields: Probabilistic models for segmenting and labeling sequence data. In *Proceedings of the Eighteenth International Conference on Machine Learning*, pages 282–289, 2001.

[5] S. L. Lauritzen and D. J. Spiegelhalter. Local computations with probabilities on graphical structures and their application to expert systems. *Journal of the Royal Statistical Society*, 50(2):157–224, 1988.

[6] K. Lerman, L. Getoor, S. Minton, and C. A. Knoblock. Using the structure of web sites for automatic segmentation of tables. In *Proceedings of ACM SIG on Management of Data*, 2004.

[7] K. Lerman, A. Plangrasopchok, and C. A. Knoblock. Semantic labeling of online information sources. *IJSWIS, special issue on Ontology Matching*, 2006.

[8] D. C. Liu and J. Nocedal. On the limited memory method for large scale optimization. *Mathematical Programming*, 45(3):503–528, 1989.

[9] D. Nadeau and S. Sekine. A survey of named entity recognition and classification. *Linguisticae Investigationes*, 30(1):3–26, 2007.

[10] J. Pearl. *Probabilistic Reasoning in Intelligent Systems*. Morgan Kaufmann, 2nd edition, 1988.

[11] D. Pinto, A. McCallum, X. Wei, and W. B. Croft. Table extraction using conditional random fields. In *Proceedings of 26th annual international ACM SIGIR conference*, 2003.

[12] L. R. Rabiner. A tutorial on hidden markov models and selected applications in speech recognition. *Proceedings of the IEEE*, pages 257–286, 1989.

[13] F. Sha and F. Pereira. Shallow parsing with conditional random fields. In *Proceedings of the 2003 Conference of the North American Chapter of the Association for Computational Linguistics on Human Language Technology*, 2003.

[14] C. Sutton, A. McCallum, and K. Rohanimanesh. Dynamic conditional random fields: Factorized probabilistic models for labeling and segmenting sequence data. *Journal of Machine Learning Research*, 2007.

[15] J. Tang, M. Hong, J. Li, and B. Liang. Tree-structured conditional random fields for semantic annotation. In *Proceedings of 5th International Conference of Semantic Web*, 2006.

[16] A. J. Viterbi. Error bounds for convolutional codes and an asymptotically optimum decoding algorithm. *IEEE Transactions on Information Theory*, 13(2):260–269, 1967.

[17] J. Zhu, Z. Nie, J. Wen, B. Zhang, and W. Ma. 2d conditional random fields for web information extraction. In *Proceedings of the 22nd International Conference on Machine learning*, 2005.

SESSION

KNOWLEDGE AND INFORMATION REPRESENTATION, PROCESSING, ENGINEERING, ACQUISITION METHODS AND APPLICATIONS

Chair(s)

TBA

Topic Word Extraction using World Wide Web Search Rankings for Computer Conversations

Eriko Yoshimura[1], **Misako Imono**[2], **Seiji Tsuchiya**[1] **and Hirokazu Watabe**[1]
[1] Dept. of Intelligent Information Engineering & Sciences, Faculty of Science and Engineering
Doshisha University, Kyo-Tanabe, Kyoto, Japan
[2] Dept. of Knowledge Engineering & Computer Sciences, Graduate School of Engineering,
Doshisha University, Kyo-Tanabe, Kyoto, Japan

Abstract - *This paper proposes a method of extracting Web search keywords of interest by gender, age, and day of the week. By using the results of such keywords, it is expected that suitably equipped robots will be able to offer appropriate topics of conversation to the person they are interacting with. In this study, we compiled Web search engine keywords based on rank using the Biglobe Search Shunkan Ranking system. However, such rankings cannot be used independently because the relevant words for a particular day will not be known until that day is over. Accordingly, our method uses Web search rankings compiled for the day prior to day in question to select keywords for use. Because of this, the method cannot determine keywords that appear on the actual day of the conversation. However, it can extract keywords that appear repeatedly in identifiable patterns, as well as topics of general interest to a certain age and gender. In our experiments, we experienced particularly good results by focusing on three concepts: keyword consolidation, forgetting factor, and short-term and long-term memory.*

Keywords: Computer interface human factors, Knowledge engineering, Knowledge representation, Natural languages

1 Introduction

In recent years, electronic devices and various other machines have become increasingly sophisticated and intelligent. The shared future vision for these machines is for them to coexist seamlessly with human beings. Advancements toward this goal include the development of numerous robots, some of which are capable of walking on two legs, running, and even dancing [1][2]. Through such developments, machine forms are being created that appear increasingly humanlike. At this stage, in order to seamlessly and efficiently coexist with humanity, such machines have an increasing need for intelligence and the capacity to converse naturally with human beings. In the future, the ability to engage in conversation with human beings will be indispensable [3][4][5].

To accomplish this, such robots should to be able to offer appropriate topics to the person engaging them in conversation. Thus, it would be useful if such robots had the ability to collect news of interest to that person, which could then be used to help conversations proceed more smoothly.

When we first meet someone, learning the details of their personal interests is normally a challenge. However, we can usually make roughly accurate judgments of safe conversation topics by considering discernable factors such as age and gender. Thus, in such situations, we normally try to steer the conversation towards general topics we feel are appropriate to those factors, and which can be discussed without causing discomfort for either person, instead of asking for their address, hobbies or other personal information.

This paper does not address how to stimulate conversation with another person after learning the details of their personal preferences; instead, it describes a method of extracting topics of potential interest to an average person, based on their age and gender, using keywords and World Wide Web search engines. Since such search engines are designed to locate information of interest to the user, a robot equipped with this feature can determine appropriate topics based on relatively generic values.

Information of interest often varies depending on the age and gender of the person. For instance, Japanese women in their 20s tend to be more interested in TV dramas and traveling than Japanese men and women of other age ranges. Additionally, keyword search trends have been noted to vary depending on the day of week. For example, searches including Japanese Racing Association (JRA) and other entertainment-related keywords are more likely to be the subject of Web searches on Saturdays, while searches for "Town Work" and other job hunting related keywords are more prevalent on Mondays.

In view of the above, this paper proposes a method of extracting Web search keywords of interest by gender, age, and day of the week. By using the results of such keywords, it is expected that suitably equipped robots will be able to offer

appropriate topics of conversation to the person they are interacting with.

In this study, we compiled Web search engine keywords based on rank using the Biglobe Search Shunkan Ranking system[6]. However, such rankings cannot be used independently because the relevant words for a particular day will not be known until that day is over. Accordingly, our method uses Web search rankings compiled for the day prior to day in question to select keywords for use. Because of this, the method cannot determine keywords that appear on the actual day of the conversation. However, it can extract keywords that appear repeatedly in identifiable patterns, as well as topics of general interest to a certain age and gender.

2 Biglobe Search Shunkan Rankings

These rankings aggregate keyword searches entered into the Biglobe search engine and list the most popular keywords by gender and age in a ranking format from 1-20

Totals are aggregated once a day. As an example, Table 1 gives the Biglobe Search Shunkan Rankings for male users 10-19 and 20-29 ages on Thursday January 20, 2011. Table 2 gives the Biglobe Search Shunkan Rankings for male users 30-39, 40-49 and 50-59 ages on Thursday January 20, 2011.

Table 1: Biglobe Search Shunkan Rankings, male users 10-19 and 20-29 ages on Thursday, January 20, 2011

	10-19	20-29
1	Makeing	Yuko Aoyama
2	YOUR	3DS
3	Manga	Lotto 6
4	SAYMOVE	KARA
5	Auction	JRA
6	K-ON	S1
7	Anime	No experience
8	AKB48	Reservation
9	Yuko Aoyama	YOUTUBE
10	KAT-TUN	Yuko Oshima
11	Lotto 6	Smartphone
12	Spoilers	Kobe
13	Banzai System	Vacation days per year
14	KARA	AFC Asia Cup
15	Yugioh	Movies
16	Breaking news	Work
17	Monster Hunter	Shinjuku
18	Inazuma Eleven	Bic Camera
19	Center research	JAVA
20	The Life of an Amorous Man	Command

Table 2: Biglobe Search Shunkan Rankings, male users 30-39, 40-49 and 50-59 ages on Thursday, January 20, 2011

	30-39	40-49	50-59
1	Yuko Aoyama	Yuko Aoyama	Yuko Aoyama
2	Lotto 6	Lotto 6	Asia Cup
3	3DS	3DS	Lottery
4	Reservation	Nintendo 3DS	Lotto 6
5	KARA	Reservation	JRA
6	AFC Asia Cup	Megurine Luka	Winning numbers
7	Winning numbers	AFC Asia Cup	Yuko Ogura
8	Kakaku	Winning numbers	Breaking news
9	Hello Work	KARA	Club tourism
10	Lottery	Lyrics	Honda
11	Panasonic	Lottery	KARA
12	Megurine Luka	Breaking news	Winning
13	Breaking news	The Mainichi Newspapers	Yaeko Taguchi
14	Tricks	Reina Tanaka	NTA
15	Meaning	AKB	JR
16	JCB	Hokkaido	Human Body
17	Yamada Denki	Human Body	KAT-TUN
18	NHK	Nico Nico Douga	F15 fighter jet
19	Pokemon	Cell phone	Reina Tanaka
20	Reina Tanaka	Diet	Yomiuri Shimbun

3 Keyword Consolidation

“Youtube” spelled in the Roman alphabet and the Japanese spelling “Yu-Tyu-Bu” are two words that represent the same concept, but which are handled separately because they are displayed differently. There are also certain words that are subsets of other words, such as "employment" and "Rikunavi," (a popular Japanese recruiting site). In such cases, words representing the same concept, or that are included in a subset of another word, are consolidated.

In light of our objective of providing appropriate conversation topics, we believe it is useful to consolidate keywords with more generally related words. In the above example, a person searching for “Rikunavi” can be expected to plan on using the site to search for a job. Thus, it would be appropriate to offer topics and articles using the keyword "employment."

And, “Youtube” spelled in the Roman alphabet and the Japanese spelling “Yu-Tyu-Bu” are expected coherence a more popular word “Youtube”.

In this study, we also consolidate word selections using Google searches[7]. We began by searching for all ranked search keywords over a fixed cumulative period to determine the number of hits and the URL of the top hit for each

keyword. Next, we compared the URLs and separated keywords with the same URL into separate groups. The group name takes the word selection of the group member keyword with the most hits. Table 3 lists some examples of keywords for which the top URL is the same site.

Table 3: Keywords sharing the same top URL in search results

Search keyword	Hits
YouTube	4,650,000,000
Yu-Tyu-Bu (in Japanese)	18,900,000
Horseracing	18,000,000
JRA	8,330,000
Kakaku	1,130,000,000
Kakaku.com	21,700,000
Forums	193,000,000
2channel	25,700,000
Draft	2,720,000
Draft commission	422,000
Employment	24,100,000
Rikunavi	8,520,000

4 Forgetting curve

Human memory fades with the passing of time. Because of this, search rankings from one day ago cannot be treated the same as those from a month ago. Accordingly, our model uses a memory retention curve to account for the impermanence of human memory. The "forgetting curve", which shows the rate at which human memory fades, was created by German psychologist Hermann Ebbinghaus[8]. Ebbinghaus obtained the figures in Table 4 through experimentation, even though no numerical formula has been clarified.

Table 4: Ebbinghaus experiment results

Time Passage	Memory
20 Minutes	42%
1 Hour	56%
1 Day	74%
1 Week	77%
1 Month	79%

The model in this paper uses Formula (1), which approximates the forgetting curve from the five points shown in Table 4. The amount W(t) remembered over number of days *t* is as given below. Hereinafter, this is referred to as the forgetting factor.

$$W(t) = -0.1429t + 25.19 \qquad (1)$$

5 Memory Weighting

Previously accumulated keywords are used quantitatively to express degree of interest. First, search rankings 1-20 (by age and gender) are assigned points for each day accumulated. The top ranked keyword in the search rankings is given 20 points, the second is given 19 points, the third is given 18, and so on. Human memory can be broadly divided into short- and long-term memory. Short-term memory stores small amounts of information temporarily and is quickly forgotten. In contrast, long-term memory is the ongoing storage vessel for large amounts of information. In this study, points were adjusted and weighted based on the concepts of short- and long-term memory.

As will be described below, all accumulated keywords are weighted for short- or long-term memory, after which, the weight for the same keywords is consolidated. The system outputs keywords from 1-20 in order of highest total value.

5.1 Short-term Memory Weighting

Weighting for short-term memory is based on search rankings over the previous week. To accomplish this, we take the product of forgetting factors W_1-W_6 for all keywords, from one to six days previously. The weights are then totaled for the consolidated keywords. As an example, Figure 1 shows short-term memory weights for keywords selected on Saturday, January 24.

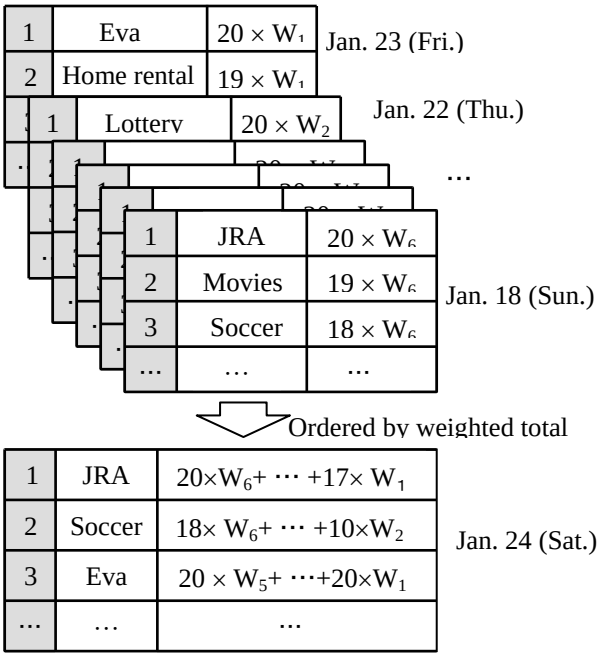

Figure 1: Weighting example for short-term memory

5.2 Long-term Memory Weighting

When creating weighting for long-term memory, data search information compiled on the same day of the week, over the past four weeks, is collected and analyzed. For example, if predicting the search rankings for a Saturday, the system would begin by compiling weighting data using the results from Saturdays seven days, 14 days, 21 days, and 28 days prior to the date the prediction is made. It would then apply the product of forgetting factors W_7, W_{14}, W_{21} and W_{28}. The weights are then recalculated for the consolidated keywords. Calculations follow the same technique described in Section 6.1.

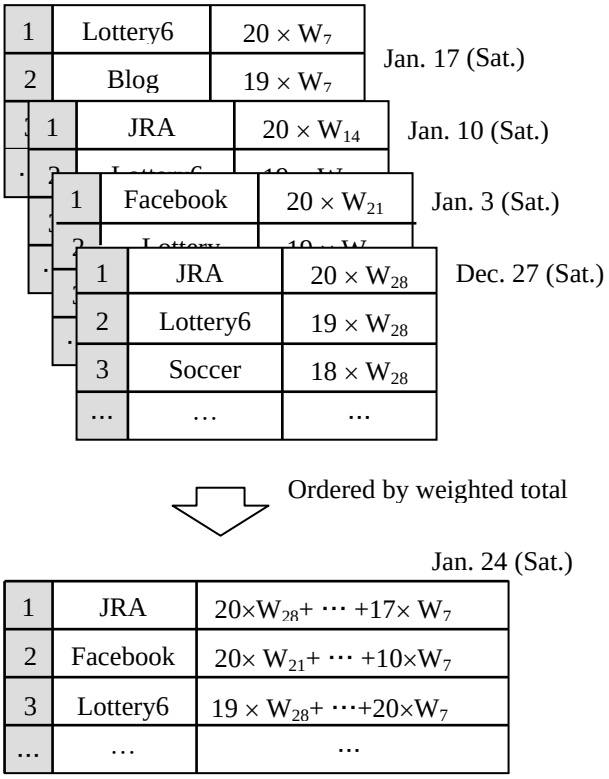

Figure 2: Weighting example for long-term memory

6 Experimental

6.1 Evaluation Method

As described previously, evaluations of the topic keywords obtained by the proposed method are compared to the actual Biglobe Search Shunkan Rankings obtained the next day. Note that the topics of a particular day will not be known until the following day.

Ranks for experiment results are given as *i*, and the actual rankings are given as *j*. Through visual inspection, the resulting keyword for rank *i* is compared to keywords *j* = 1-20 and given points *p*. Evaluation criteria have three levels: for the same concept $p = 1$, for related concepts $p = 0.5$, and for unrelated concepts $p = 0$. Equation 2 calculates the anticipated accuracy a_{ij} of the experiment result *i* and *j* = 1-20. The highest value between a_{i1}-a_{i20} is a_{ik}, which is used as the accuracy of result *i*.

$$a_{ij} = \frac{p}{i \times j} \qquad (2)$$

The above process is iterated 20 times for *i* = 1-20, and the average value for a_{ik} is taken as the average accuracy.

If an exact match exists, average accuracy is approximately 0.08. The higher the experiment results predict actual high-ranking keywords and related keywords to be ranked, the higher the average accuracy will be.

6.2 Experiment overview

In order to examine the usefulness of the created system, the following experiment was conducted:

・Period: June 4, 2010 (Fri.) - June 10, 2010 (Thurs.)

・Data for short-term memory: the past six days prior to the day of testing

・Data for long-term memory: the past four weeks

The compared data uses consolidated keywords and a keyword system to determine interests by gender and age, not accounting for short-term and long-term memory.

6.3 Experiment overview

6.3.1 Output Comparison

Table 5 lists an example of the actual rankings from our proposed system, as well as rankings from the comparison system for women in their 20s, for Monday, June 7.

In Table 5, it can be seen that the rankings obtained using the proposed method were close to the actual rankings, particularly in the higher ranks. Those results showed that women in their 20s are likely to search for recruitment-related keywords such as “Town Work” and “Hello Work” on Mondays. The system also predicted keywords close to the actual rankings in the lower ranks with similar word pairs like recipe and “Cookpad”, “Rakuten”, and Yahoo Auctions.

Table 5: Comparison of Actual Rankings and Results

Rank	Actual ranking	System from the present study	Comparison system
1	Town Work	Part time work	ARASHI
2	Hello Work	Hello Work	JRA
3	Maki Goto	Town Work	Part time work
4	Recruitment	Twitter	*YouTube*
5	Recipes	How to make	Entertainers
6	Search keywords	Youtube	One Piece
7	World Cup	Kaela Kimura	Hawaii
8	Ballroom dancing	Ameba blogs	Tumbling
9	Africa	Cookpad	One
10	Searching for a partner	Jalan	Uniqlo
11	FromA	AKB48	Mai Hosho
12	Okinawa	Recruitment	Youtube
13	Rakuten	JRA	How to make
14	Civil servant	Entertainers	Hairstyle
15	ANAP	Moon Lovers	Jalan
16	Principle	JTB	Shoujo Cosette
17	Post office	Yahoo Auctions	Wiki
18	MP3	TVXQ	JTB
19	Rent-a-car	General election	TVXQ
20	Ameba blogs	Kyoto	ANA

6.3.2 Evaluation Results

Figure 3 shows the evaluation results for male users in their 20s.

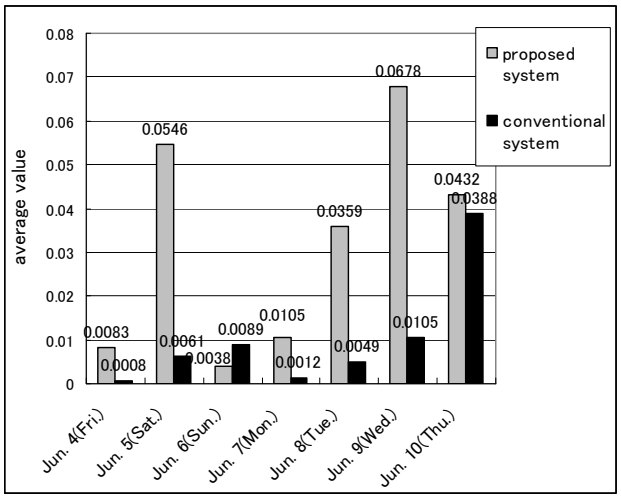

Figure 3: Results for male users in their 20s

Figure 4 shows the evaluation results for female users in their 20s.

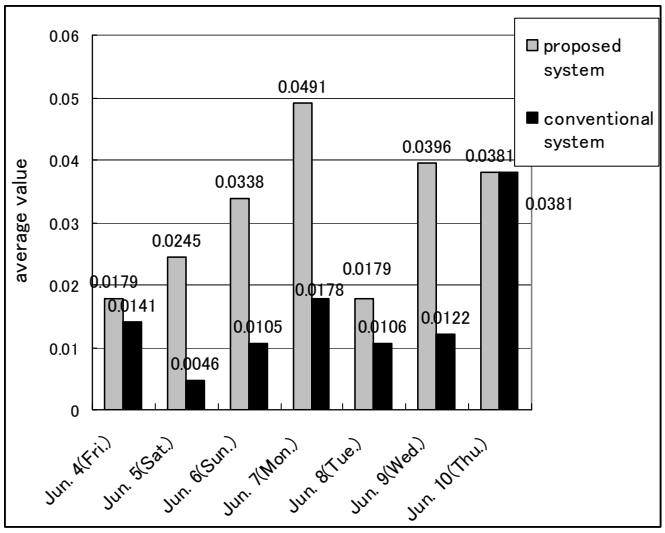

Figure 4: Results for female users in their 20s

Figure 5 shows the evaluation results for male users in their 30s.

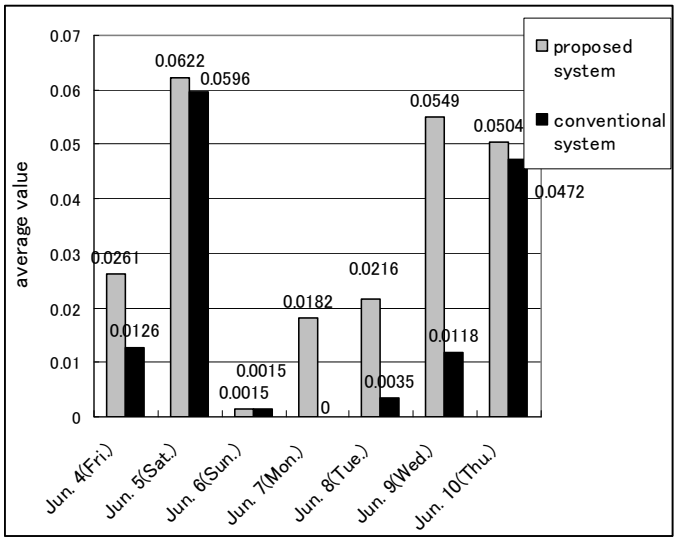

Figure 5: Results for male users in their 30s

Figure 6 shows the evaluation results for female users in their 30s.

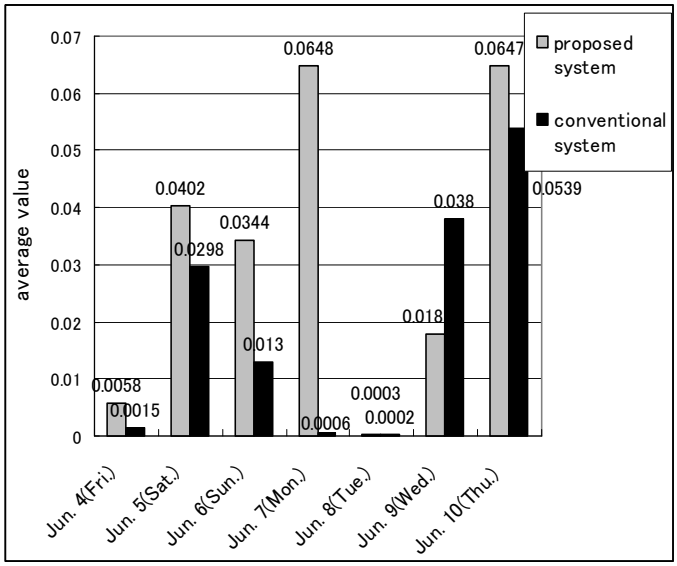

Figure 6: Results for female users in their 30s

6.3.3 Analysis

In order to determine the reasons for the increased accuracy, we analyzed the results for male users in their 20s under the following three conditions: excluding the forgetting factor, using only short-term memory, and using only long-term memory. The results are provided in Figure 7 and Table 6.

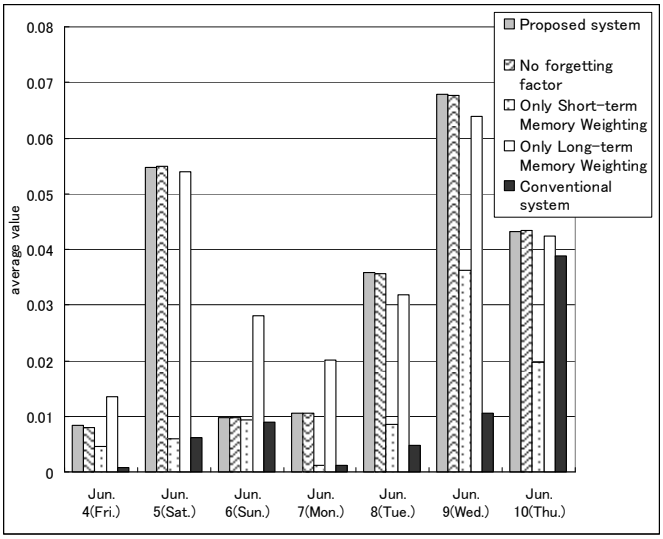

Figure 7: Analysis of results for male users in their 20s

7 Discussion

From Figure 3, it can be seen that average accuracy is high when using long-term memory only and low when using short-term memory only. Furthermore, when accounting for both short-term and long-term memory, accuracy was even higher than when only long-term memory was used on four out of the seven days. Thus, we believe that the accuracy of our system can be raised by weighting and adjusting for both short- and long-term memory.

Table 6: Analysis of results for male users in their 20s

	Present study	Forgetting factor excluded	Short-term memory only	Long-term memory only	Existing system
June 4	0.00823	0.05463	0.00981	0.01054	0.03586
June 5	0.00802	0.05499	0.00976	0.01052	0.0357
June 6	0.00463	0.00592	0.00927	0.00127	0.0086
June 7	0.01362	0.05403	0.02797	0.02018	0.03177
June 8	0.00084	0.00612	0.00892	0.00116	0.00486
June 9	0.00828	0.05463	0.00981	0.01054	0.03587
June 10	0.00802	0.05499	0.00976	0.01052	0.0357

Additionally, the forgetting factor did not appear to have any significant effect. We think this is because the system does not account for "recognition" [9] in the forgetting curve. Here, recognition refers to the ability to identify something that has been previously encountered. By nature, recognition of a previously encountered phenomenon (before it is completely forgotten) will flatten the slope of the forgetting curve. Thus, in the present study, it was necessary to devise ways to distinguish keywords that could be recognized from those that would be completely forgotten by flattening the forgetting curve slope for keywords with multiple search ranking entries.

8 Conclusion

In this paper, we proposed a method of extracting Web search keywords of interest to users by gender, age, and day of the week. In our experiments, we experienced particularly good results by focusing on three concepts: keyword consolidation, forgetting factor, and short-term and long-term memory. We believe that in the future, we will be able to obtain even better results by appropriately adjusting the weighting ratio for short- and long-term memory, and by including in the concept of recognition. Furthermore, it will be necessary to build a system that can search and suggest actual news articles based on the keywords extracted using the proposed method. Doing so should allow suitably equipped robots to autonomously introduce topics capable of stimulating rich intellectual conversation.

Acknowledgment

This research has been partially supported by the Ministry of Education, Science, Sports and Culture, Grant-in-Aid for Scientific Research (Young Scientists (B), 24700215).

References

[1] [Sony] Sony. <http://www.sony.jp/products/Consumer/aibo/> (accessed 2012-03-01).

[2] [Honda] Honda. <http://www.honda.co.jp/ASIMO/> (accessed 2012-03-01).

[3] J.Weizenbaum, ELIZA - A Computer Program For the Study of Natural Language Communication Between Man and Machine, Communications of the Association For Computing Machinery, vol9, no1, pp.36-45(1965).

[4] R.S. Richard S. Wallace, "Alicebot" (online), Available from <http://alicebot.blogspot.com/>, (accesssed 2012-03-01).

[5] R. Carpenter, "Jabberwacky – live chat bot –AL artificial intelligence chatbot – jabber wacky – talking robot – chatbots – chatterbot – chatterbots – javverwocky – take a Turning Test Loebner Prize – Chatterbox C" (online), Available from <http://www.jabberwacky.com/>, (accessed 2012-03-01).

[6] [Biglobe] Biglobe Search Shunkan Ranking system <http://search.biglobe.ne.jp/ranking/> (accessed 2012-03-01).

[7] [Google] Search engine, <http://google.com/ > (accessed 2012-03-01).

[8] Hermann Ebbinghaus, "Memory: A Contribution to Experimental Psychology", New York city, Teachers College , Columbia University, (1913).

[9] H.Tajika, "Saisei to Sainin niokeru Kensaku no Katei 2", Bulletin of Aichi University of Education, Educational Sciences, No.29, p.131-144(1980).

Application of Defeasible Domain-Specific Knowledge to the Description of Gothic Cathedrals in the ARC Project

Tyler Carlson[1], Stefaan Van Liefferinge[2], Elijah Holt[1], Rebecca A. Smith[2], Michael A. Covington[1], Walter D. Potter[1]
[1]Institute for Artificial Intelligence, University of Georgia, Athens, GA
[2]Lamar Dodd School of Art, University of Georgia, Athens, GA

Abstract - *The goal of the Architecture Represented Computationally (ARC) project is to build a complete system by which user input or written descriptions of Gothic cathedrals are automatically represented logically, allowing validation consistency, query-answering, and the generation of precise textual or visual descriptions.*

This paper will briefly cover the first major step in the implementation of this system, which is the knowledge representation and inference engine, with particular focus on the meta-programming and non-monotonicity of the application. The meta-programming allows users to define terminology, add facts, and create constraints without the need to understand Prolog. The non-monotonic knowledge representation allows the user to create rules about general concepts and conflicting rules about subsets of those concepts, from which the correct results are inferred. This ability of the ARC systems allows the user to "overgeneralize and then except," which is a basic aspect of natural description.

Keywords: Prolog, Gothic cathedral, architecture, Defeasible reasoning

1 Introduction

The ARC Logic system, implemented in Prolog, focuses on creating a system that is user-friendly through the use of two specific features. First, domain specific knowledge is represented in a manner similar to a natural method of description. Users can define terminology, assert facts, and create constraints with no programming experience. The second feature is the non-monotonicity of the knowledge representation and reasoning engine. Together, these two features narrow the gap between natural description and logical representation, which is advantageous for direct use of the system, as well as integration with automated natural language processing system. The ARC Logic user can approach a description already possessing a large amount of background knowledge and assumptions, explicitly stating only those things which vary from the background knowledge. Architecture, especially the architecture of Gothic cathedrals, is suited to this foray into description understanding because it generally follows a limited set of logical rules, and although individual cathedrals can vary, there are clear default models to work with [1].

Section 2 of this paper briefly discusses the way in which natural description uses default models, background information, and assumption from non-monotonic rules. Section 3 explains how this non-monotonic nature is modeled in the ARC Logic system as defeasible facts and rules, and how goals are derived with respect to defeasibility. Section 4 introduces the meta-programming predicates with which the user can create and customize domain information without Prolog expertise. Section 5 shows how the non-monotonic ARC system handles conflicting facts, and rebutting or undercutting constraints. The final section highlights the use of scope and the way a user can combine general and specific descriptions to naturally and logically model Gothic cathedrals.

2 Natural description

The goal of the ARC project is to allow users to easily create and use logical descriptions of Gothic cathedrals, and to eventually have an automated process by which usable logical descriptions can be extracted from natural language textual descriptions [2] [3]. The closer the logical system is to encapsulating the natural style of description, the more efficient and accurate it can be. Natural descriptions do not start in a void; they take into account the assumptions from generic models or sets of norms and then describe how a specific case varies from these generalities. As a result, a complex understanding of some specific cathedral can be

conveyed with little explicit description. A describer relies heavily on the ability of those receiving the description to fill in all the missing information by making assumptions based on their own knowledge. The describer makes assumptions about shared understandings of basic aspects of a cathedral, just as communication in general requires an assumption of shared understanding of each word used. This ability to work with assumptions also allows the user to ignore, at least explicitly, those aspects which fit expectations, and focus cognitive resources on analysis of only the deviations.

Because Gothic cathedrals follow relatively strict conventions, one can assume most of the knowledge about the structure of a specific building solely from the information that the building is a Gothic cathedral. The ARC Logic system allows users to create or use rules that apply generally to the domain, in addition to the information present explicitly in a given description. Users can describe columns, bays, choirs, or other information that is generally assumed background information in a description of Gothic cathedrals by creating constraints that apply to these general objects. Constraints can also be used to describe a complete logical model for an entire default Gothic cathedral. Just as assumption is necessary for filling in the gaps to understand a sparse natural description, a default model of a cathedral can fill in the logical gaps for all of the information not explicitly stated in a description of a specific cathedral. By modifying only the abnormalities or attributes which cannot be assumed by default, a complete logical description of a specific cathedral can be created with the small amount of explicit information.

The use of assumptions and background information in description requires the ability to hold rules that apply to a set of things, while holding conflicting rules that apply to subsets of those same things, and then reason with all of these rules appropriately. Since new information can override previous assumptions, the method of natural description is non-monotonic, and the ARC Logic system uses non-monotonic reasoning to model this.

3 Non-monotonic logic system

In monotonic logic, new information can only add new knowledge, not remove something previously derivable. If some sentence p is entailed by some set of sentences, then p must be entailed by that set and any additional sentences. The type of description modeled by the ARC project makes generalized statements and then exceptions to those generalities. Exceptions indicate that there are sentences entailed by the general rule but not by the general rule and the addition of those exceptions, so the system cannot be monotonic. Assumptions are a result of the necessity of working with uncertainty, and non-monotonic reasoning is a method of accounting for this uncertainty.

Defeasible reasoning is one of these non-monotonic methods. In defeasible reasoning, information can be classically true or false (indefeasible), but one can also work with information that should be assumed to be true or false (defeasible), unless there is a reason not to keep the assumption. This way, a user can create a defeasible rule, which can result in the derivation of defeasible facts, and then some or all of these facts, and even the rule itself, can be overridden, modified, or removed by additions to the knowledge base.

The ARC Logic system has three types of information: facts, rules from the logical properties of terms, and constraints. This system allows a user to specify, for each piece of information, the certainty of the knowledge being used. The inference engine then derives everything from the knowledge base that can be derived. Where valid inference in traditional logic is truth-preserving, valid inference in this system is certainty-of-truth-preserving, or defeasibility-preserving. Something derivable from only indefeasible premises is known indefeasibly, while derivations that require any defeasible premise can only have a defeasible conclusion.

Adding this functionality to standard Prolog for the ARC Logic system required two additions. First, ARC's logic system has a way to hold meta-information about facts, constraints, and rules from logical properties of terms. Secondly, the system has a defeasibility-preserving inference engine that uses this meta-information of facts and the defeasibility of rules.

3.1 Fact meta-information

In classical (monotonic) logic and traditional Prolog, proven consequents can be separated from their consequence relations. The set {A, A => B} entails B, so B can be used without continued consideration of the set that entailed it. In a defeasible system, however, the consequents of rules may "not be detachable even when their antecedents are derivable," [4] as one of these detached consequents could be defeated by additional information. The ARC Logic system is forward-chaining, filling the knowledge base with all the facts that can be inferred from the information in the knowledge base. To fill the knowledge base with independent facts requires detachment of the derivable consequents from their antecedents. This implementation circumvents the need to keep facts

tied to their method of proof by keeping two important pieces of metadata for each fact in the knowledge base.

The first piece of metadata is the defeasibility of the fact, which can either be defeasible or indefeasible. The ARC system's use of defeasibility could be considered a binary measure of certainty. If a fact is indefeasible, then it is known with certainty. If the fact is defeasible, then it is reasonable to assume it is true unless we have information to the contrary. The criterion for each assumption is completely up to the user, just as the semantic value of some logical fact or rule is. There is no measure of "how certain" or "how strongly to assume" in this implementation; something is considered defeasibly true if it is derivable, no matter how many defeasible facts and rules were used in this derivation.

The second piece of metadata stored with each fact is the origin of the fact, which can be either inferred or explicit. Because the system is non-monotonic, information already in the knowledge base is not necessarily safe from being removed with new knowledge. If some fact or rule in the knowledge base is modified, removed, or added, the system needs a way to expunge all the facts that required the now-missing information and all facts that were derivable because of the lack of the now-added information. The ARC Logic system uses a blunt method for removing information that is no longer derivable. When the inference engine is called, the first step is a retraction of all facts which are both defeasible and inferred. When the new inference is complete, all and only those facts that can be inferred from the known information are added back to the knowledge base. Explicitly-added defeasible facts can still be removed from contradictions, but it is important that they are differentiated from inferred facts, because their inclusion in the broad retraction could remove information with no way to recover it.

3.2 Defeasibility-preserving inference

The metadata holds information about the facts, but to add new facts with the correct defeasibility requires a defeasibility-preserving method of inference. The ARC system uses a predicate d_call/2, which is used in place of Prolog's regular call/1 functionality to answer queries or find all the facts that are derivable from the knowledge base. When d_call matches with a fact, it uses the defeasibility metadata about that fact. Of course the d_call predicate also uses Prolog rules, created from constraints and logical properties of terms, in order to prove goals. A constraint meaning "capitals are above shafts in every column," forms a rule in the knowledge base that essentially looks like above(A,B) :- object(capital, A), has(C,A), has(C,B), object(shaft, B). To prove above(A,B), each goal in the body has to be proven just like in a regular Prolog call. When there is a conjunction of terms in the body, the goal (head) is given the same defeasibility as the weakest link; if any one of the clauses is only provable defeasibly, the new fact must also be defeasible. If through backtracking, alternative proof methods are found, then the strongest defeasibility amongst these is assigned to the new information. In the ARC implementation, indefeasible vs. defeasible of d_call/2 works the same as true vs. false in classical logic; one false/defeasible clause makes the whole conjunction false/defeasible, and one true/indefeasible clause makes the whole disjunction true/indefeasible.

Prolog rules created from constraints and logical properties of term definitions also hold defeasibility, in that they each contain a goal in the body that is always defeasible or always indefeasible. If the constraint said "capitals are defeasibly above shafts," an always-defeasible goal would be included in the body of the rule, so the above fact would be defeasible, even if the capital and shaft objects are known indefeasibly.

4 Domain knowledge input

The logical representation of a cathedral comes from the facts about objects or their relationships, Prolog rules from the logical properties of relationship terms, and Prolog rules from the creation of constraints. These relationship terms and constraints are based on knowledge of a specific domain. The logic engine has no built-in rules for any specific relationship term or constraint, with the exception of the special relations has and contains. Instead, the system uses meta-programming methods to create Prolog rules from the domain-specific knowledge that users input. This approach allows users to define relationships (like above) and objects (like shaft and base), and to create constraints (to say "shafts are above bases"). These predicates allow users to create and modify complex ontologies in whatever domain they want, without the need to understand the Prolog programming language.

4.1 Term definitions

Term definitions are used to designate object and relationship terminology, and imbue the terms with the expected logical behavior. The predicates define_relationship/2, define_metarelationship/3, and define_object/3 take names and logical properties as the arguments and assert all the necessary Prolog

rules to the knowledge base at run-time. For example, a user describing Gothic cathedrals or any other architecture would likely want to use the relationship above. In most contexts, aboveness implies transitivity; the set {above(A,B), above(B,C)} should entail above(A,C). This entailment follows when a rule for the transitivity of above is added to the set. A user can implement this functionality by calling define_relationship(above, [transitive]). The first argument is the name of the relation, and the second argument is a list containing any combination of the values: symmetric, reflexive, transitive, or variations of these three. The appropriate Prolog rule (or rules) is created and asserted to the knowledge base at run-time for each of these properties in the list.

Negative versions of these logical properties are one type of variation. Standard Prolog does not have explicit negation; the \+ predicate designates negation by failure, and lack of some fact in the knowledge base means that proposition is defeasibly false. To define facts as indefeasibly false, the ARC system requires an explicit negation function. Negation is designated by an alteration of the name itself (adding or removing a 'not_' from the front of the predicate atom), so negative relationship facts are treated the same way by the ARC Logic system as positive facts.

A user can include any of the negative versions of the logical properties: asymmetric, irreflexive, and intransitive. The relationship of immediately above, for example, can be made explicitly intransitive by adding intransitive to the list of properties. This creates a rule with the same body as the transitive version would have, but with a head of the negated predicate, so that anything which can be derived from transitivity is explicitly negated.

A user could work with a taxonomy that avoids explicit negation altogether. If imm_above is created without any version of transitivity, the program would not be able to infer imm_above(A,C) from imm_above(A,B) and imm_above(B,C). Adding explicit negation could increase the thoroughness of the procedure for checking consistency.

These three positive and three negative logical properties each create indefeasible Prolog rules; if everything in the body can be proven indefeasibly, the goal is known indefeasibly. By adding 'd_' to the front of a property, the user can indicate it is a defeasible property, making 12 variations in total. It may be useful to assume that bears_weight_of is transitive, but should not be a certainty. Designating bears_weight_of as d_transitive creates the same rule as regular transitivity, except the always indefeasible goal in the body is replaced with an always defeasible one.

In addition to defining relationships between constants, the user can also define the relationships between these relationships with define_metarelationship/3. The first argument is either antonym or implies, and the next two arguments are previously-defined relationship terms. Synonymy is another logical meta-relation, but since it only creates redundancy, the user (or a natural language processing system) should decide on one naming convention. Antonymy in this implementation designates a converse relation, such that define_metarelationship(antonym, above, below) allows the system to infer below(B,A) from above(A,B), and vice-versa. define_metarelationship(implies, imm_above, above) allows the system to infer above(A,B) from imm_above(A,B). Defeasible properties are implemented in define_metarelationship/3 the same way. define_object/3 works very similarly to define_metarelationship/3, allowing users to designate subtypes and supertypes.

4.2 Defining constraints

Constraints are user-created statements that enforce existence of objects or relations between objects. Like term definitions, constraints are designed with the intention of striking a balance between versatility and usability for non-Prolog-programmers. The information given in constraints is used to automatically create Prolog rules which are asserted to the knowledge base.

The has and contains relations, which are parent and ancestor relations for objects, respectively, are the only relationships built into the ARC Logic system. These relationships are necessary for the description of objects and work differently with respect to objects than user-defined relations like above. Constraints that use the has relationship also work differently than constraints that use user-defined relationships.

If a user wants to add to the knowledge base the information that "each column has a base," the user only needs to input create_constraint(column, must, has, base). This lower arity version fills in the missing argument values with defaults, calling the complete query of create_constraint(X, object(column, X), must, has, 1, 1, base). This can be read as "For all x, if x is of type column, then it must have a minimum of one and a maximum of one base." The Prolog rule created from a has constraint checks that the minimum number (fifth argument) of objects of some type (last argument), are a part of any object that matches the condition of the first two arguments, and creates new objects if the minimum is not met.

Constraints can be written for any user-defined relation as well, but they work differently. A user-defined relation constraint can use any numbers for minimum and maximum, but the default value when not designated is all. The all value signals that the relation holds for any number of objects matching the conditions. create_constraint(X, object(shaft, X), must, above, all, all, base) means that every shaft object is above every base object where both objects belong to the same parent object (by a has relation). Constraints about user-defined relations create Prolog rules that only apply between sibling objects, as it would rarely make sense or be useful to say something like "the shaft in column 1 is above a base in column 2," and they only create new facts about relationships, not create new objects, if the minimum is not met.

The first and second arguments comprise the condition, and work the same way for any kind of relationship. The first argument is a universal quantifier and the second argument can contain any number of Prolog terms. The constraint applies to any object/constant in the knowledge base that meets the conditions. Since the most common condition is simply "all objects of some type," a user can write simpler queries by just giving a type name instead of the first two arguments, so create_constraint(column, must, has, 2, 3, base) calls create_constraint(X, object(column, X),must, has, 2, 3, base). Conditions can also be written with higher complexity. If, for example, a user wanted to make this constraint only apply to columns in the arcade level, they could enter create_constraint(X, (object(column, X), contains(Y,X), object(arcade_level, Y)), must, has, base).

Constraints of course also have defeasibility. A must value in the third argument adds an always-indefeasible clause to the dynamically-created Prolog rule, and a d_must value adds an always-defeasible clause so that all resulting facts are defeasible. This defeasibility also allows the constraint to be contradicted or altered.

5 Defeasible comparisons

This paper has explained how user-defined terms and user-created constraints are added as rules to the Prolog knowledge base dynamically, explained the way facts are stored in the knowledge base with their meta-information, and how the defeasibility-preserving d_call predicate works. Together these allow for all the information in the knowledge base to be labeled correctly as defeasible or indefeasible, but this paper has yet to demonstrate the use of this defeasibility information. The ARC system is non-monotonic and defeasibility-preserving so that it can appropriately handle conflicting information. This section briefly explains how conflicts, in facts and constraints, are resolved.

5.1 Comparing facts

The ARC system performs inference by using the d_call predicate to find every fact that can be derived and then attempts to assert each fact. It is "attempt to assert," not simply "assert," because the assertion of a derived fact into the knowledge base is not guaranteed. Whenever assert_fact/3 is called, the knowledge base is checked for matching and conflicting facts. If matching facts are found, the strongest version is kept. If conflicts are found, they are resolved as shown in Table 1.

Table 1. Fact Comparison

	New fact defeasible	New fact indefeasible
Old fact defeasible	Both facts removed	Old fact removed New fact asserted
Old fact indefeasible	New fact ignored	Requires fix

If the conflicting facts are both indefeasible, this is the same problem that arises with contradictions in classical logic. The ARC Logic system cannot automatically resolve this problem, and instead warns the user, because an indefeasible contradiction signals that either the user's ontology is self-inconsistent, or is constructed in a way that does not meet the specifications of the program.

5.2 Comparing constraints

The ARC system can resolve conflicting facts as long as at least one of them is defeasible. The same is true for constraints, but handling these conflicts is more complex. Constraints conflict if they have the same conditions and same object type for the consequent, but the relations are explicit contradictions, or the minimum of one constraint is greater than the maximum of the other.

The terminology used for conflicting constraints is adapted from John Pollock [5], who distinguished rebutting and undercutting defeaters. Defeaters make no positive claim; they only attack other defeasible assumptions. Rebutting defeaters give reason against some conclusion, while

undercutting defeaters give reason against some line of reasoning [5]. The ARC Logic implementation does not use defeaters, but regular constraints can defeat some or all of the results of defeasible constraints they conflict with. When the conditions are exactly the same, the constraints rebut each other, because the same antecedent conditions lead to contradictory conclusions. Resolution of rebutting constraints is the same as resolution of conflicting facts shown in Table 1.

Rebutting constraints can be useful, but in order to match the style of natural descriptions, which often overgeneralize and then make exceptions, the ability to create constraints that are general and other constraints which are exceptions is needed. If one constraint applies to a set of object instances, and a conflicting constraint applies to only a subset of those instances, then this second constraint undercuts the first.

If a user wanted to model "it should be assumed that each column has a base," but also "columns in the arcade level do not have a base," these would be created by create_constraint(X, object(column, X), d_must, has, 1, 1, base) and create_constraint(X, (object(column, X), contains(Y,X), object(arcade_level, Y)), must, has, 0, 0, base), respectively. The latter constraint undercuts the former, because the constraints have conflicting min-max values, the former constraint is defeasible, and the condition of the latter means the constraint applies to a subset of the former. This is the case regardless of the defeasibility of the undercutting constraint and the order in which the constraints were asserted.

To determine that the latter constraint undercuts the former, the program basically checks (with exceptions for subtypes and contains terms) if each term in the condition of the former constraint is inside the condition of latter constraint. If they are, then the latter undercuts the former. This check function also returns the difference between the two conditions. In the example above, the difference is ((contains, Y, X), object(arcade_level, Y)).

The ARC Logic system works with the natural assumption that more specific information takes precedence over more general information. When confronted with the information about columns in general and columns in the arcade level, a human being would assume that some specific column instance, which is in the arcade level, does not have a base. In natural human description, assuming other factors are equal, the more specific information has more justification. The ARC Logic system resolves undercutting constraints in a similar manner. The more specific constraint is added to the knowledge base without modification. The more general constraint, which was undercut, is retracted and modified before it is asserted back to the knowledge base. The modification turns the implicit exception, which the user does not need to indicate, into an explicit exception. The constraint is modified by adding the difference in a negation-by-failure predicate to the condition.

After the comparison, modification, and assertions, the knowledge base from this example contains two constraints (in their Prolog rules format) corresponding to constraint(X, (object(column, X), contains(Y,X), object(arcade_level, Y)), must, has, 0, 0, base) and constraint(X, (object(column, X), \+ (contains(Y,X), object(arcade_level, Y))), d_must, has, 1, 1, base). Upon inference, if there is a column in the knowledge base, the inference engine will ensure it has a base, unless d_call can prove that the column is contained in an arcade level. If later information shows that the particular object is part of the arcade level, the defeasible and inferred fact of having a base will have been removed, and not asserted back, on the next call to the inference engine.

6 Creating complete descriptions

The ability to create overgeneralizing constraints can be useful for describing generalizable concepts like columns, but this same functionality also allows the combining of constraints about general Gothic cathedrals with constraints and facts about specific cathedrals.

The number of stories in the nave of a Gothic cathedral is an important part of an architectural description, but this number varies from cathedral to cathedral. One could create a description of a generic, default, Gothic cathedral with constraints that say each cathedral indefeasibly has a nave, and that a nave indefeasibly has an arcade and clerestory, and defeasibly has a gallery and triforium, because these levels are not always or necessarily present in every Gothic cathedral. The vertical slices are called bays, and these can also vary in number depending on the cathedral. Constraints could state that each cathedral indefeasibly has a minimum of 4 bays and a maximum of twelve bays running along the side of the nave. Even though there has to be at least 4 bays, the generic model could contain the constraint that the nave defeasibly has a minimum and maximum of 7 bays running along the side. The ARC inference engine will create 4 indefeasible bays and an additional 3 defeasible ones.

To describe a specific cathedral, like Chartres, constraints can be added to the general constraints, to say that if something is a cathedral, and is chartres, no (a maximum of 0) gallery. This new constraint is in conflict with an old defeasible

constraint, but because it is more specific, it undercuts the old one. The resulting knowledge base ensures that a gallery will only be created for a cathedral object if there is no way to prove that that cathedral is chartres. This works the same way with the number of bays, and down to any level of detail.

To create a constraint that applies only to objects in chartres, the user would add contains(chartres, X) to the conditions of the constraints. Manually including this information in each constraint about the specific cathedral is not intuitive, especially if one is working with a set of general constraints already created, and is only writing constraints that apply to a specific Gothic cathedral. To correct this, the ARC logic system includes a way to alter the scope of the input data. In natural description, it is often very clear (to a human reader) if a description is referencing a concept in general or a specific instance that fits that concept. The user accesses this ability with the predicate set_scope/1. The scope indicates the outermost object that is being described. Whenever a constraint is created, a contains(Scope, X) is added to the condition, where Scope is the current scope set in the knowledge base and X matches the universal quantifier of the condition. If constraint A has the term contains(some_constant, X) in the condition and constraint B has the term contains(some_other_constant, X) in the condition (which is otherwise the same as A), then constraint B undercuts constraint A as long as contains(some_constant, some_other_constant) is derivable.

This same principle works with parts or sections of a Gothic cathedral just as well as differentiating between specific cathedrals or default models. The scope can be considered a "zooming" function that allows one to designate that the following constraints describe only a particular area of a cathedral, just as they can designate that some constraints only apply to Chartres Cathedral or Notre Dame de Paris.

The scope functionality of ARC system simplifies the user's ability to create a description of a specific cathedral, or part of a cathedral, or even a specific cathedral at a certain point in history, from a hierarchy of descriptions. Since this system can be used outside of the description of Gothic cathedrals, it might be useful to write constraints that apply to a generic building ("it has a floor, ceiling, and door," "the ceiling must be above the floor," etc.), then create a description of a generic place of worship by only describing the ways in which this would differ from a generic building. A description of generic Gothic cathedrals could be built from this description of a generic building of worship, or default Gothic cathedrals built in a particular century, or some other logical description models that would be useful for architectural historians. The user can also use this scope ability to describe and/or compare more than one cathedral in a single session.

The ARC logic system allows a user to add domain-specific knowledge to the system, creating a custom ontology and description without the need for expertise in Prolog or programming in general. The system also enables the user to combine any number of default and specific descriptions at different levels. These abilities, along with an inference engine that deals automatically and appropriately with defeasible information, capture an important element of natural description and natural intelligence, and form a solid foundation for the future ambitions of the ARC project as well as ventures into other related domains.

7 References

1] William J. Mitchell, The Logic of Architecture, Cambridge, MA: The MIT Press, 1990.

2] Charles Hollingsworth, Stefaan Van Liefferinge, Rebecca.A. Smith, Michael A. Covington and Walter D. Potter, "Artificial Intelligence Techniques for Understanding Gothic Cathedrals," *Proceedings of the 2011 International Conference on Artificial Intelligence. Vol I. Worldcomp '11*, pp. 175-178, 2011.

3] Charles Hollingsworth, Stefaan Van Liefferinge, Rebecca.A. Smith, Michael A. Covington and Walter D. Potter, "The ARC Project: Creating logical models of Gothic cathedrals using natural language processing," *Proceedings of the 5th ACL-HLT Workshop on Language Technology for Cultural Heritage, Social Sciences, and Humanities.*, pp. 63-68, 2011.

4] Donald Nute, "Defeasible Prolog," *AAAI Fall Symposium on Automated Deduction in Nonstandard Logics*, pp. 105-112, 1993.

5] John L. Pollock, "Defeasible Reasoning," *Cognitive Science*, vol. 11, no. 4, pp. 481-518, October 1987.

Document Retrieval Based on Knowledge Acquisition and Merging: A Methodology

Kelvin Vieira Kredens[1], **Mauri Ferrandin**[1],
Bráulio Coelho Ávila[1], **Edson Emílio Scalabrin**[1] **and Fabrício Enembreck**[1]
[1]Graduate Program in Computer Science
Pontifícia Universidade Católica do Paraná
Curitiba, Paraná, Brazil - +55 41 3271 1669

Abstract— *Most part of the document retrieval systems use defined keywords by the user to find documents. In the information retrieval, for some application, is important to have a system that, instead of putting a keyword, takes a complete document and gives us as output a set of documents more similar to the input document. This paper presents an approach to compare documents and proposes - through the use of MFS to represent the tokens - two heuristics that can be used together with TF-IDF algorithm in order to improve the results in the document retrieval. The results showed that the use of these heuristics improves the accuracy of the TF-IDF algorithm and generates smaller indexes for document representation.*

Keywords: document retrieval, vector-space model, term weighting, maximum frequent sequences

1. Introduction

Nowadays semi-structured data, especially text documents, represent a new challenge for researches in developing methods and tools for its indexing and retrieval. According to [1], the Internet is doubling its size every 5.32 years. Considering this growing rate and the value of the information, it becomes necessary the creation of new search engines based on new approaches for efficiently store and retrieving the information, as the use of text sequences in the representation of the content and new methods for evaluation of the importance of that content [2], [3].

Two other issues are relevant in the process of information retrieval when applied for document search: the size of the generated indexes for document, due to the necessity of storage space to keep that information available for researches, and the use of heuristics to improve the computation of the similarity between the documents that have a big impact in the performance and quality of the answers obtained from the system [4], [5]. Most of the systems that proposed to retrieve documents from a collection are based in the principle of comparing every document with some keys chosen by the user. This common approach has some deficiencies when the user needs to find documents more similar to one specific target document, because the user, after reading the target document, will determine its keywords and submit them to the retrieval system to obtain the most similar documents [6]. The system normally indexes and chooses the keywords for the documents in its database, and the way the system performs it rarely will be the same as the human uses [7].

In this paper, we propose one approach to improve the results obtained by search engines that use TD-IDF algorithm for indexing the documents through the use of MFS in two different and not exclusively ways: the first one weighs the MES by its size and the second weights the MFS accordingly to the region of the document that it appears. In the second approach, the human knowledge was mapped for a set of documents of one specific subject to establish the weights of the MFS according to the region of the document. One overview of the system is showed in Figure 1.

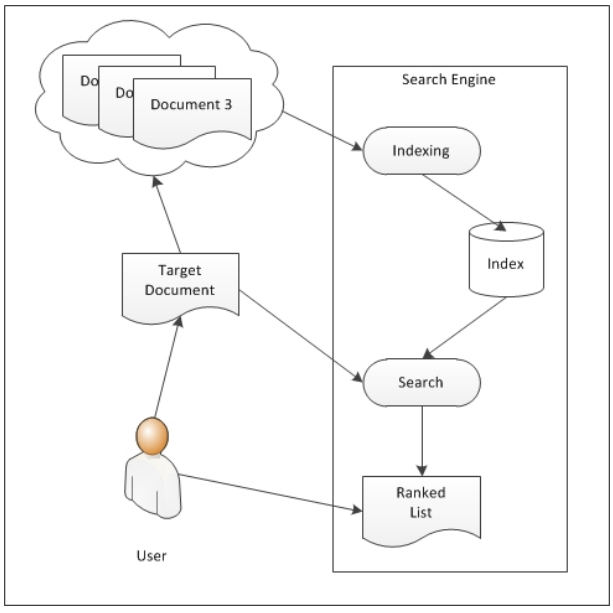

Fig. 1: Proposed Search Engine Architecture

2. Basic concepts

The classical, most used and still competitive Information Retrieval model is the Vector Space Model, created by [8], on which a document is represented as a vector and each

position of the vector is filled with the terms that compound the document. This approach begins by assuming words to be independent of each other. After this, statistics are collected for individual tokens, both in the query and in the documents that compound the collection [9]. Classical is the combination of term frequency (TF), [10], and inverse document frequency (IDF), called TF-IDF. TF is a measure of term relevance at analyzed documents or the query: the more often a term appears in a document, the more important term is to the document. IDF measures the term importance over all documents of the collection: terms that rarely appear over all documents are more important in discriminating the documents. There are some approaches to compare two documents, but the most widely used is one called Cosine Distance, that calculates the cosine measure between the angles formed by two points drawn in a cartesian plan. The main disadvantage is that this model does not take in account the word order

Here we propose his use, but instead of representing documents by using its single words, we will use word sequences, called Maximum Frequent Sequences, defined in [11], [12]. The three main characteristics that define MFS are: 1) Maximum because one MFS could not be a subsequence of another sequence, 2) Frequent in the document it occurs and 3) Sequence composed by terms of one phrase, from the same document, considering the order that the terms appear in the phrase and allowing gaps between the terms that it composes. In the process of extraction of MFS from a document, some parameters could be set, such as: maximum size accepted, minimum size, maximum gap, minimum threshold to be considered frequent. In order to evaluate the importance of the MFS, two new relevant metrics are proposed: the first one considers the size of the MFS and the second considers the region of the text it appears.

The objective is to create a methodology for document retrieval in which every document has its representation through MFS extracted for it, using the heuristics to improve the results and consider, in the evaluation, the information about the region of the document the MFS is found. The human knowledge will be merged with the other heuristics in order to provide the importance of one MFS according to the text region.

3. Related works

In [13], is pointed that, with the combined use of single words and word sequences, is not useful to apply the same relevance measures, as TF-IDF. This happens because usually the word sequences are less frequent than single words and this make them to have a not good relevance.

In[14], is proposed the use of MFS as document descriptors, using the vector space model, but they use the classical TF-IDF as weight measures and, as shown later on this paper, it is not the best way to measure the importance of a MFS.

4. Proposed relevance measures

Once the documents are represented according to the vector space and use tokens such as MFS, the next step is to define how to value the importance of each token. Here, the goal is to make the weight of an MFS reflect its content within the document in which it appears relative to its expression, representation and differentiation among the other documents that compose the collection. In order to compare and validate the results, the experiments will use the classical TF-IDF. The proposed metrics can be combined according to the representation in Figure 2 and, it is possible to use all of them together or choose other combinations of metrics along the document indexing process.

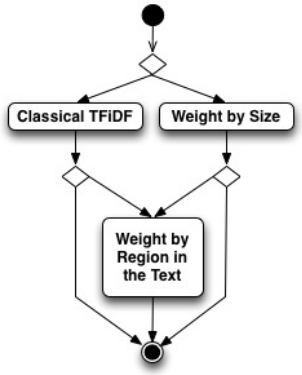

Fig. 2: Possible Combination of the Relevance Measures

4.1 Weight by size

The main idea is that the bigger the MFS is, the bigger its semantic value is and the better it can be used to describe the content of the document. In the same way, the bigger the MFS shared between a set of documents is, the bigger the similarity of that set of documents is if compared with the similarity between documents of another set that shares smaller MFS. The notion of bigger and smaller is represented in the Equation 1 and the value depends of the documents that compose the collection.

$$w = (ap \times tAp) \times (\frac{mfsSize^{IFactor}}{greatestMfsSize^{IFactor}}) \quad (1)$$

Where ap is the amount of times a MFS appears in the analyzed document; tAp is the amount of times that a MFS appears in all the documents that compound the collection; mfsSize is the size, in words, of MFS; $greatestMfsSize$ is the size of the biggest MFS that the indexed document has and $IFactor$ is the configurable parameter with any value, greater than zero, and is used to set the distance between

MFS from different sizes. In the tests we performed, it was used a value of 2.

4.2 Weight by region

In this approach, the objective is to evaluate the importance of one MFS according to the region it occurs in. For instance, one MFS that is present in the introduction is better than another one that appears in the middle of the text. To establish the weight, according to the region the MFS occurs, a set of human evaluators analyzed a set of documents from one particular subject, indicating what phrases in the content are more important to understand the document. The regions of the document are established according to the phrases that compose the document; one document with 35 phrases is divided in 35 regions. The data collected will be used to create a calculation memory for the documents of that particular subject and will be used for weighting the MFS, considering the region of the document, as showed in Equation 2.

$$weightForRegion = \frac{\sum_{i=1}^{n} regionWeight_i}{n} \quad (2)$$

Where $regionWeight_n$ is the weight, obtained from the calculation memory, from region i, where the MFS in question occurs. The weight of all regions is computed by a sum operation and an arithmetic average of the weights is computed.

The final value, $weightForRegion$, is multiplied with w, that can be obtained from the equation of the Weight By Size or by classic TF-IDF.

5. Data acquired

In order to evaluate the effectiveness of the proposed heuristics against the classic TF-IDF, we defined a methodology, creating 6 groups of evaluation. Each group had one target document and a collection of 5 other documents, composing a total of 30 documents. The documents chosen for the experiments are politics editorials from a Brazilian popular newspaper, with average size of 24 phrases and 602 words.

Given the target document, we ranked five documents in each respective group using the algorithms, sorting them according to their similarity with the target document. The ranked list created by the applications was compared with a ranked list generated from the human evaluation. The experiment was made with 9 journalism and media students, and a web application called AVALIA was developed to help the students through the evaluation process. We can split the collected data in two subsets: Data for Control and Calculation Memory.

5.1 Data for control

Collected from the human evaluations through the AVALIA system, represented in Figure 3, where the students sorted a list of given documents accordingly to their similarity with the target document.

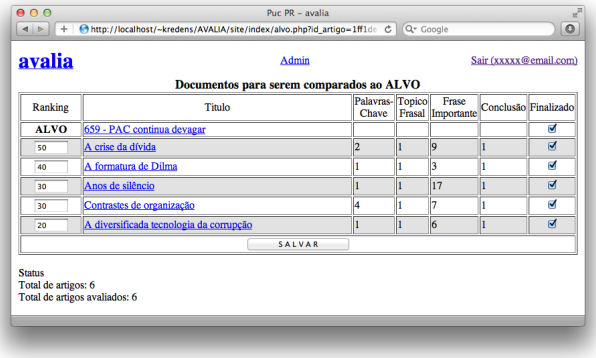

Fig. 3: AVALIA's screen shot, used by users to rank the documents.

This set of collected data was used to compare the efficiency of the heuristics proposed in this paper with the traditional methods for weighing tokens. The data was summarized for the 6 groups of documents, creating 6 rankings of documents, sorting them accordingly to the similarity with the respective target document. Table I shows the data from group 1, for which the target document was document 44.

Table 1: Consolidated ordenation of target 44

Evaluation 2, TARGET 44												
		Student - Adjusted Ordination										
Document		50	51	52	53	54	56	57	58	61	Σ	Average
3^o	23	5	1	3	1	4	1	5	3	2	25	2,778
4^o	26	3	4	2	4	2	1	3	2	4	25	2,778
5^o	41	1	0	1	5	1	1	4	1	1	15	1,667
1^o	43	4	3	5	3	3	2	2	4	3	29	3,222
2^o	45	2	2	4	2	5	3	1	4	5	28	3,111

5.2 Calculation memory

Using the ranking information provided by the evaluators about what phrases are most important in every document, the collected data was grouped and interpolated in order to determine what region of the texts is more important. This data will be used to weight the MFS accordingly to the region of the document it occurs, and a metric was created to determine what regions of the text are more important accordingly to human evaluation. Table II shows the values of the ranking obtained from the human evaluation for every group of documents and, in column Weight, is the arithmetic average from all groups ranked.

The distribution of the weights accordingly to the region of the document for the experiments is showed in Figure 4, where the graph representation was calculated considering an interval of confidence of 95%.

Table 2: Consolidated ordination of phrases from users perspective

	Evaluation						
Ordination	24	30	41	42	44	46	Weight
0	0	0	0	0	0	0	0
1	2,458	2,897	3,117	1,737	2,534	1,996	2,457
5	4,816	5,039	10,391	5,768	8,198	6,362	6,762
10	4,082	6,097	4,143	4,658	4,709	4,935	4,771
15	2,477	3,692	5,756	3,973	4,798	4,373	4,178
20	1,753	2,590	4,530	2,659	3,039	4,595	3,194
25	2,935	3,477	5,208	2,332	2,904	1,924	3,130
30	3,140	2,372	1,543	2,723	4,117	2,646	2,757
35	1,697	1,667	4,343	1,742	3,928	4,179	2,926
40	2,017	2,226	2,760	1,945	2,786	3,317	2,508
45	2,654	1,749	4,039	2,828	3,688	3,252	3,035
50	2,529	2,243	2,519	2,537	2,551	2,732	2,519
55	1,948	0,559	1,422	2,228	2,108	2,481	1,791
60	2,400	1,062	1,679	1,422	3,780	3,151	2,249
65	2,493	2,051	2,085	1,845	1,893	4,202	2,428
70	2,533	1,286	1,775	2,600	2,069	3,162	2,237
75	2,175	2,027	2,744	1,233	2,108	0,910	1,866
80	2,214	1,955	1,459	1,584	2,844	2,597	2,109
85	1,722	1,631	1,206	2,061	3,201	2,675	2,083
90	1,263	3,376	3,675	1,687	2,783	1,422	2,368
95	3,444	3,785	4,262	3,706	6,887	5,6199	4,617
100	4,8	3,4	7,4	5	5,4	7,4	5,566

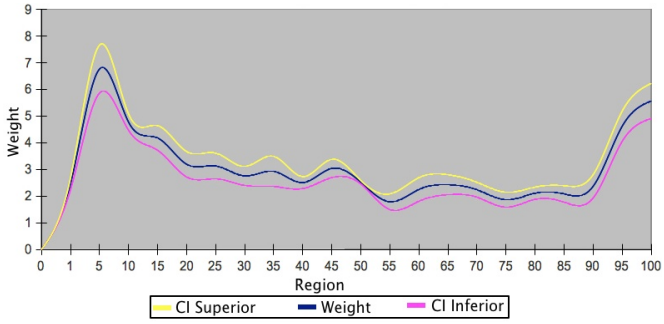

Fig. 4: Weight distribution given by students

6. Results

In order to test and validate the proposed heuristics, 9 different experiments have been created with the merge of the proposed heuristics and classical methods, with special attention to the removal or not of stop words and type of tokens. The list of experiments is represented in Table 3. The combination and merge of the techniques, represented in all 9 experiments with the 6 groups of documents, generated a set of 54 tests and 324 different indexes. The basis of combinations proposed on this paper can be viewed in Figure 2.

After concluding the creation of indexes, the 6 target documents were ranked with the documents in each respective group, in order to create a ranked list with similarity of the target document over the other documents in the group. In all experiments, the cosine similarity measure was used. After this process, every one of the 6 groups of documents had 10 rankings of similarity: one based on human evaluations, and the 9 others on the combination of heuristics proposed in Table 3. To obtain the accuracy of every experiment, the Equation 3 was used.

Table 3: Experiments created to validate the proposed relevance measures

Experiment	Tokens	*Stopwords* remotion	Weight by Size	Weight for Region in the Text
1	MFS	yes	no	no
2	MFS	yes	no	yes
3	MFS	yes	yes	no
4	MFS	yes	yes	yes
5	MFS	no	no	no
6	MFS	no	no	yes
7	MFS	no	yes	no
8	MFS	no	yes	yes
9	Single Words	–	–	–

$$accuracy = \frac{\sum_{i=1}^{5} P_i}{5} \quad (3)$$

Where P_i is the position in the final ranking and receives the value accordingly to the distance between the values obtained in the experiments and human evaluation. When the article is in the same position of the human evaluation, the value is 1, in other cases, his value is decreased in 0.2 for every position dislocated to right or left.

In Table 4, we can observe the final results for the 9 experiments and the accuracy rate obtained in every one of the 6 groups of documents.

Table 4: Consolidated view from accuracy per evaluation

		Accuracy per Evaluation						
	Exper.	1	2	3	4	5	6	Final Accuracy
1^o	4	64%	84%	68%	64%	76%	68%	70,667%
2^o	2	84%	68%	68%	52%	76%	68%	69,333%
3^o	9	84%	60%	80%	68%	68%	52%	68,667%
4^o	3	64%	76%	68%	48%	76%	68%	66,667%
5^o	5	84%	92%	68%	40%	40%	68%	65,333%
6^o	6	84%	84%	68%	40%	40%	76%	65,333%
7^o	1	56%	68%	68%	52%	76%	68%	64,667%
8^o	7	68%	84%	60%	40%	40%	76%	61,333%
9^o	8	68%	84%	60%	40%	40%	76%	61,333%

The experiment with the best result is experiment 4, that uses tokens represented as MFS and the combination of two heuristics - weight by size and weight by region - proposed on this paper. In the second position, is experiment 2, that uses MFS and the heuristic weight by region only, and in the third place, is the classic method, that uses simple words to represent the documents and the TF-IDF method for weighting the tokens.

All the best 3 positions used stop-words removal and all worst 5 positions in the results did not use stop-words removal, what demonstrates that methods, which used stop-words removal, are more effective. The only exception is the experiment 1, which used stop-words removal, token as

MFS, but used only TF-IDF with no heuristics to weight the MFS and demonstrates that the use of MFS and TD-IDF without any heuristics is worst than using single words with TF-IDF.

The last analysis shows that is necessary to create more efficiently heuristics for the use of MFS to represent documents, and the results are easily understood, considering that the TD-IDF method was created to work with single words. The non-removal of the stop-words causes the generation of too specific MFS, representing more specifically the writer style of the document author, what gives to every document unique characteristics and decreases its similarity when compared to others.

Another interesting observation is that the uses of MFS created very small indexes for the documents, as showed in Table V, where we can observe that the index for experiment 9 is about 351% bigger than the indexes generated in experiments 2 and 4. This fact reveals the advantage of using MFS instead of single words, considering storage space necessary to keep the indexes, considering that the size, using MFS, was expressively smaller. That difference is explained considering the nature of the MFS representation, where one text sequence chosen as MFS needs to be maximal - can't be a subsequence of any other sequence in the document. We can have a MFS composed by one single word if this single word is frequent and it is not part of another frequent sequence bigger than it.

Table 5: Consolidated view from index sizes distribution

	Size of the Index per Evaluation (KB)						
Exper.	1	2	3	4	5	6	Average
1	16,4	17,7	21,8	19,7	17,8	15,9	18,21
2	16,4	17,7	21,8	19,7	17,8	15,9	18,21
3	16,4	17,7	21,8	19,7	17,8	15,9	18,21
4	16,4	17,7	21,8	19,7	17,8	15,9	18,21
5	26,4	39,9	35,9	29,7	27,1	25,7	30,78
6	26,4	39,9	35,9	29,7	27,1	25,7	30,78
7	26,4	39,9	35,9	29,7	27,1	25,7	30,78
8	26,4	39,9	35,9	29,7	27,1	25,7	30,78
9	69,5	64,1	66,3	64,7	57,7	61,8	64,01

Although it is not the subject of this study, during the tests, it was noted clearly that the indexing process, when the tokens were MFS, became 6-9 times longer. The extraction of MFS sub process ends up being slow as it tries to generate all possible sequences, according to the configures parameters. But in this process, as all the indexing is done only once for each document, and also the process of calculating the index, which needs to be rerun for each new document, is not affected in its final time and decreased as the final set of tokens is smaller. This can be seen when comparing the sizes of the final indexes.

7. Conclusion

An important contribution of this paper is the fact that the method proposed uses the approach of searching for documents more similar to one target document, instead of searching for documents more similar to one set of keywords defined by one user. This issue is more efficient for retrieval of documents in environments where is necessary to retrieve documents more similar to one specific document, because it considers the taxonomy of the entire target document and avoids human errors in the process of choosing the best keywords in the target document for later use in the search.

The use of MFS to represent and index documents in the process of information retrieval, using the vector space together with proposed heuristics on this paper, obtained best results than the use of single words in both metrics: accuracy and size of the indexes.

The size of the index created for one document also has a big impact in the performance of the retrieval system, because the smaller they are, the less computational resources will be necessary to compare and calculate the similarity between the documents. Also, a smaller index needs less space to be stored.

The metrics defined in TD-IDF algorithms with the use of the MFS, and using human evaluation of the documents to generate a background information about the importance of one MFS according to the region of the document where it is found, demonstrates that the traditional methods based on TF-IDF document retrieval can be improved and achieve better results.

References

[1] G.-Q. Zhang, G.-Q. Zhang, Q.-F. Yang, S.-Q. Cheng, and T. Zhou, "Evolution of the internet and its cores," *New Journal of Physics*, vol. 10, 2008.

[2] C. N. Mooers, "Information retrieval viewed as temporal signaling," in *Proceedings of the International Congress of Mathematicians*, 1952.

[3] C. D. Manning, P. Raghavan, and H. Schtze, *Introduction to Information Retrieval*. New York, NY, USA: Cambridge University Press, 2008.

[4] K. S. Jones, "A statistical interpretation of term specificity and its application in retrieval," *Journal of Documentation*, vol. 28, pp. 11–21, 1972.

[5] F. Smadja, "Retrieving collocations from text: Xtract," *Comput. Linguist.*, vol. 19, no. 1, pp. 143–177, Mar. 1993. [Online]. Available: http://dl.acm.org/citation.cfm?id=972450.972458

[6] J. M. CigarrÃąn, A. PeÃśas, J. Gonzalo, and F. Verdejo, "Automatic selection of noun phrases as document descriptors in an fca-based information retrieval system," in *In B. Ganter and R. Godin (Eds.): ICFCA 2005, LNCS*, 2005, pp. 49–63.

[7] C. Zhai, X. Tong, N. Milic-frayling, and D. A. Evans, "Evaluation of syntactic phrase indexing - clarit nlp track report," in *The Fifth Text REtrieval Conference (TREC-5*, 1997, pp. 347–358.

[8] G. Salton, A. Wong, and C. S. Yang, "A vector space model for automatic indexing," *Commun. ACM*, vol. 18, no. 11, pp. 613–620, 1975.

[9] M. F. Porter, "Readings in information retrieval," K. Sparck Jones and P. Willett, Eds. San Francisco, CA, USA: Morgan Kaufmann Publishers Inc., 1997, ch. An algorithm for suffix stripping, pp. 313–316. [Online]. Available: http://dl.acm.org/citation.cfm?id=275537.275705

[10] H. P. Luhn, "A statistical approach to mechanical encoding and searching of literary information," *IBM Journal of Research and Development*, vol. 1(4), pp. 309–317, 1957.

[11] H. Ahonen-Myka, "Discovery of frequent word sequences in text," in *Proceedings of the ESF Exploratory Workshop on Pattern Detection and Discovery*. London, UK, UK: Springer-Verlag, 2002, pp. 180–189.

[12] A. Doucet and H. Ahonen-myka, "An efficient any language approach for the integration of phrases in document retrieval."

[13] T. Strzalkowski, J. Perez-Carballo, and M. Marinescu, "Natural language information retrieval in digital libraries," in *Proceedings of the first ACM international conference on Digital libraries*, ser. DL '96. New York, NY, USA: ACM, 1996, pp. 117–125.

[14] E. Hernández-Reyes, J. F. Martínez-Trinidad, J. A. Carrasco-Ochoa, and R. A. García-Hernández, "Document representation based on maximal frequent sequence sets," in *Proceedings of the 11th Iberoamerican conference on Progress in Pattern Recognition, Image Analysis and Applications*, ser. CIARP'06. Berlin, Heidelberg: Springer-Verlag, 2006, pp. 854–863.

Representational Choices for Problem Solving

Danny Kopec[1], **Christina Schweikert**[2], **Gavriel Yarmish**[1]
[1]Department of Computer and Information Science, Brooklyn College, Brooklyn, NY, USA
[2]Division of Computer Science, Mathematics, and Science, St. John's University, Queens, NY, USA

Abstract - *An important aspect of teaching is enabling students to analyze and solve problems in a manner most suitable for them. Some people can quickly visualize the effects of a formula. Others may first solve problems with a hands-on model approach, a diagram, or a wordy description. In this paper, we illustrate a variety of representational choices through two familiar problems / methods: the Towers of Hanoi problem and the Bucket Sort. In a broad sense, some representations of solutions may be viewed as "extensional," while others are "intensional." Depending on the predilections of the problem-solver, either approach, in general, may be preferred. We emphasize the importance of making good representational choices when attempting to solve problems. Hand in hand with the understanding of a problem, developing an algorithm for its solution, and the actual solution process and its testing, is awareness of the importance of representational choice. Such awareness is certain to enhance development of students' problem-solving skills.*

Keywords: knowledge representation, problem solving, computer science education

1 Background

It is apparent that during the past 20 years or so, we live in special times that have evolved coincident with the proliferation of the World Wide Web. It is easy to recognize the past two decades as the "Information Age," but the challenge is to convert that information into knowledge. Sowa called it the "Knowledge Soup" [6]. Ingredients of the knowledge soup, which we call the "Knowledge Pyramid," as depicted in Figure 1 may be viewed as the progression from *data*, to *facts*, to *information*, and finally to *knowledge*. Information is important for effective decision making, but knowledge, as has been said, "is golden." With knowledge, the deep understanding often necessary for problem solving can be achieved. Knowledge enables a number of different forms of problem solving including: the use of meta knowledge, analogies, cases, sub-problems, sub-goals, proof by contradiction, deduction, induction, etc.

It may be the case that students in the information age are not as well, or not sufficiently founded in the sciences, history, technology and its progress as might be expected. There seems to be great gaps in their understanding of invention and how the necessities of the times have impacted and promulgated progress.

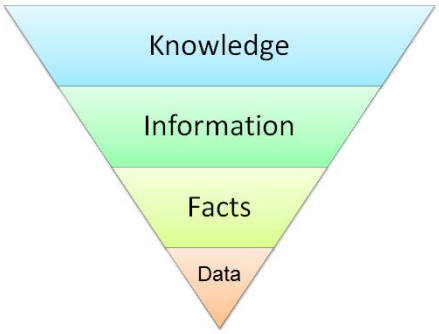

Figure 1: Knowledge hierarchy

How students learn has dramatically changed, and we must recognize that teaching techniques must change accordingly. The notion of "visualization" is not new to science education and it has been used to teach computer science algorithms and methods such as sorting for many years [2]. In many cases, the importance of representational choices, e.g. the choice of graphs, trees, semantic networks, production rules, etc., may be as integral to a problem solution, as the solution itself.

During the problem-solving process, certain choices of representation are likely to have a better impact on the memory of certain problem solvers. For example, a figure or sketch may be sufficient for some, while others may prefer a detailed, step by step description, pseudocode, or an abstract formula.

2 The Towers of Hanoi Problem

2.1 Description of the Towers of Hanoi Problem

In this game there are 3 'pegs' A, B and C and n disks, each with a different size diameter. The rule is that disks may be stacked on the pegs as long as a large disk is never placed on top of a smaller disk. In the following descriptions, a 'step' is defined as the movement of one disk from one peg to another peg. For example: A to B is a step and it means move the top disk on peg A to the top disk on peg B. Figure 2(a) illustrates the starting position for n=3. Problem: What is the minimum number of steps necessary to move all n disks from peg A to peg C and what are those steps?

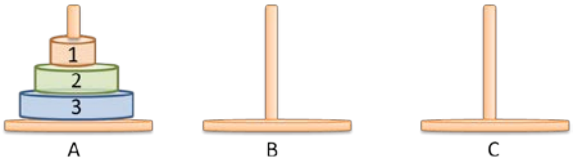

Figure 2(a): Towers of Hanoi start configuration

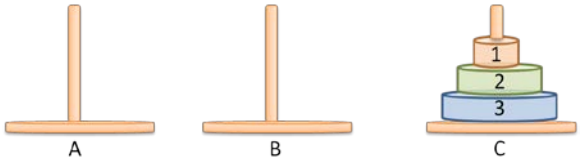

Figure 2(b): Goal state

2.2 Representations

This problem, whose ultimate solution is recursive, is quite difficult for someone who has not seen it before. It is therefore a good example for the idea of representation choices.

2.2.1 Extensional Representations

An extensional representation would be a complete set of steps describing a solution. It may be a description of a solution in words, or it may, for example, be a complete graphical representation of the solution (see Figure 2(c)) or a table (see Figure 3).

Hands-On/Pictorial

Hands-on simply means to play the game by hand with the pegs and varying numbers of disks. Alternatively, pictures may be used. The idea is to try and find patterns that connect the solution for different values of n. Figure 2(c) is a pictorial representation of the solution for n=3.

As the figure shows, the solution consists of the following 7 steps:

1. A to C
2. A to B
3. C to B
4. A to C (bottom disk)
5. B to A
6. B to C
7. A to C

If we were to play the game with n=1, then with n=2 and so on until we play it with n=10 (in reality it would only be feasible to play this game up n=~5), we would find that the total number of moves approximately doubles for each additional disk, as demonstrated in Figure 3. This table is an example of an extensional representation of the problem since it is analyzing the solutions for Towers of Hanoi for different numbers of disks.

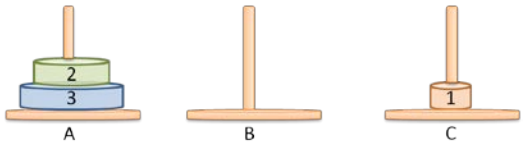

Step 1: Move disk 1 from peg A to peg C.

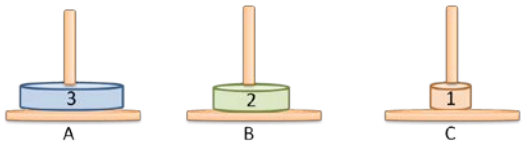

Step 2: Move disk 2 from peg A to peg B.

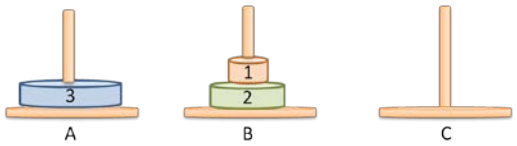

Step 3: Put disk 1 on top of disk 2.

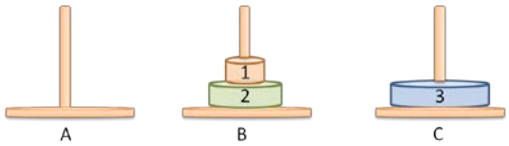

Step 4: Move disk 3 from peg A to peg C.

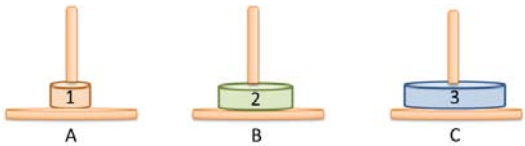

Step 5: Unravel - Move disk 1 from peg B to peg A.

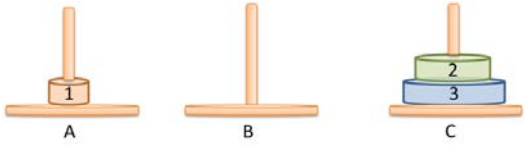

Step 6: Move disk 2 from peg B to peg C.

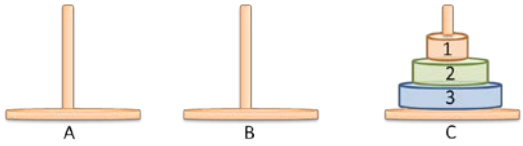

Step 7: Put disk 1 on top of disk 2 – goal state reached.

Figure 2(c): Graphical solution of the Towers of Hanoi problem

Number of Disks	Moves to Temp Peg	Moves from Temp Peg to Goal	"Big" Disk Moved to Goal State (C)	Total Number of Moves
1	0	0	1	1
2	1	1	1	3
3	3	3	1	7
4	7	7	1	15
5	15	15	1	31
6	31	31	1	63
7	63	63	1	127
8	127	127	1	255
9	255	255	1	511
10	1023	1023	1	2047

Figure 3 – Table representing the total number of moves for varying numbers of disks

2.2.2 Intensional Representations

An intensional representation is a more compact description. A student may get this quickly or they may get to this point after first describing it in other intensional or extensional forms.

A student may describe the solution as follows: Isolate the bottom disk by moving the top n-1 disks from peg A to peg B. Then move the remaining (Big) disk from peg A to peg C. Finally, move the n-1 disks on peg B to peg C.

A more compact intensional representation:

1. Move n-1 disks to intermediary peg B. This will take 2^{n-1}-1 moves (see Figure 3).
2. Move the bottom disk from peg A to peg C.
3. Move n-1 disks from peg B to peg C.

Another intensional representation would be:

- For n disks on peg A, we must use (2^n-1) moves to peg B to reveal the bottom disk on peg A.
- 1 move to move the bottom disk from peg A to peg C.
- (2^n-1) moves to move the n-1 disks to the final peg.
- Total number of moves: $2(2^n-1) + 1$

Recurrence Relation

The following recurrence relation is another representation. It is unlikely that a student will use this. However, it is possible that for those who are mathematically inclined it may be most suitable.

$T(1) = 1$

$T(n) = 2T(n-1) + 1$

Solution of recurrence: $T(n) = 2^n - 1$.

Pseudocode Representation

This representation is that which Computer Science students may be most familiar with. Nevertheless, it is not necessarily the most intuitive to all students.

Pseudocode:

```
Define:   n = number of disks
          A = start peg
          B = intermediate peg
          C = goal peg
Towers(n, A, B, C):
  If n=1 move disk from A to C
   Else
          Towers(n-1, A, C, B)
          Towers(1, A, B, C)
          Towers(n-1, B, A, C)
  End If
```

3 The Bucket Sort Problem

3.1 Description of the Bucket Sort Problem

The bucket sort algorithm works by placing items to be sorted into buckets according to a value, or range of values, and then sorting each bucket - either by applying bucket sort recursively, or utilizing another sorting algorithm. Bucket sort can be applied to various kinds of data, including numerical and textual data, and its implementation would be tailored appropriately.

3.1.1 Extensional Representations

An extensional representation of an algorithm can be a demonstration or application of the algorithm for which its intensional definition holds. For bucket sort, we can use a variety of examples, visualizations, or data structures to illustrate its core concepts by example.

Pictorial / Visual

A step by step visualization of the bucket sort process is a sample extensional representation. If we apply bucket sort to a set of names, we can use graphics to illustrate the sorting process, as depicted in Figure 4. Since we are sorting strings,

we will assign the names to buckets according to the first character. For each bucket, we will recursively apply bucket sort and assign strings to buckets according to the second, third character, etc. until all buckets contain at most one name. The contents of the sub-buckets are then concatenated and returned their originating bucket, now in sorted order. The contents of the buckets are then appended to form the sorted list.

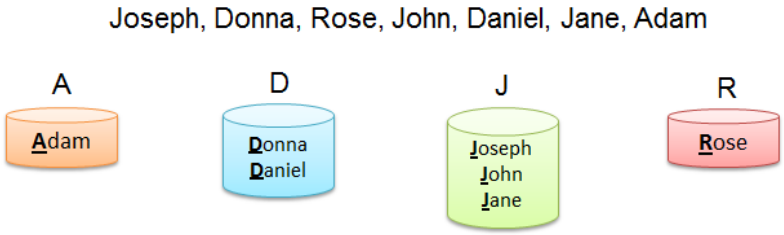

Figure 4(a): Assign strings to buckets according to first character

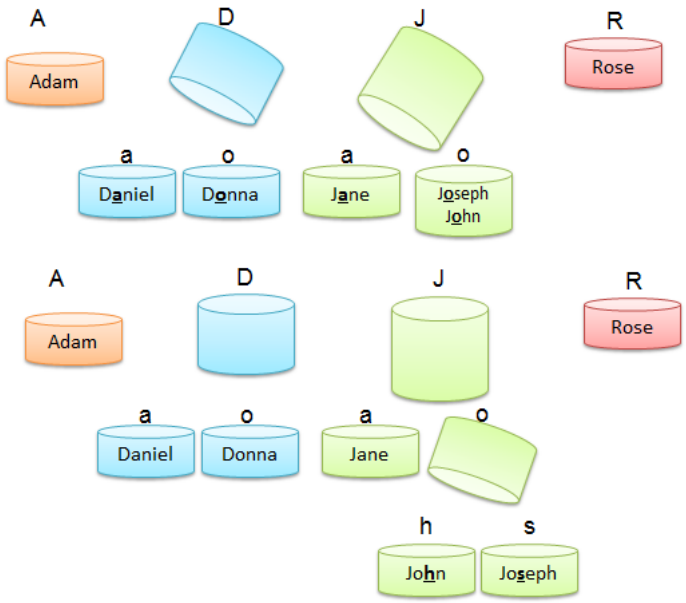

Figure 4(b): For those buckets with more than one string, assign strings to sub-buckets according to the next character, and repeat until all buckets contain one string

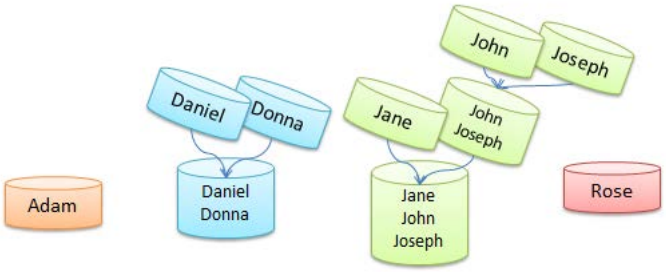

Figure 4(c): Build up the solution by filling original buckets from their sub-buckets

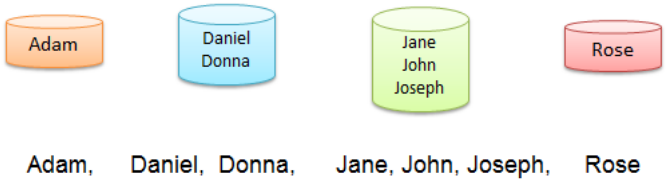

Figure 4(d): Concatenate the contents of the buckets to obtain the sorted list

Tree Structure

A tree can also be used as extensional representation of the bucket sort concept by organizing the tree according to keys. This kind of prefix tree, known as a "trie" from the term "retrieval", can be traversed in a pre-order manner to generate the sorted list of strings. A prefix tree representation for a set of sorted strings is depicted in Figure 5.

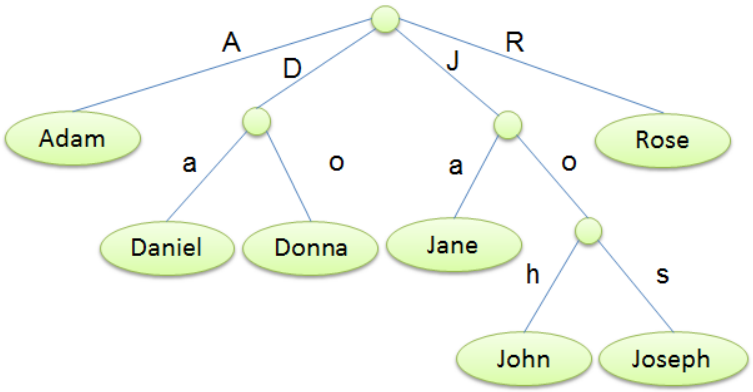

Figure 5: Prefix tree representation for a set of sorted strings

3.1.2 Intensional Representations

An intensional representation contains the most essential and intrinsic characteristics of a concept or, in this case, algorithm. For bucket sort, an abstract definition could be expressed as:

Bucket Sort Algorithm:

1. Create a set of empty buckets
2. Place each element in the input list into appropriate bucket
3. Sort each bucket
4. Concatenate the contents of the buckets in order and place into original list

This is considered an intensional definition because it provides the fundamental features of the algorithm, which can then be applied to generate a set of various extensional instances.

Pseudocode Representation

Bucket sort can be implemented with an array of lists - the array representing the set of buckets, and a list holding the contents of each bucket. The following is a sample pseudocode for bucket sort which takes an unsorted list U as input:

```
BucketSort(U):
  n = length of U
  B = new array of n lists
  for i = 1 to n
     do insert U[i] into list B[key(U[i])]
  for i = 1 to n
     do sort B[i] with insertion sort
  concatenate the lists B[0], B[1], ..., B[n-1]
```

The function key maps the range of elements in the array to bucket keys, for example converting characters to integers or floating point values to integers. A variation of this implementation could be to insert the elements into the buckets in order as they are being inserted into the lists, rather than applying insertion sort to all lists at the end. Another variant is to call BucketSort recursively. Taking this pseudocode and implementing it in specific programming languages such as C++ or Java and applying it to specific data sets would be an extension of this intensional representation.

4 Relevance to CS Education

One of the challenges faced in computer science education, and science education in general, is how to improve students' problem solving skills. In a typical computer science course, such as introductory programming, we may teach the concept behind a particular algorithm (i.e. exchange sorts), and then demonstrate it with a few examples (i.e. sorting a set of integers, characters, or words). The students then apply these algorithms to given data that is in a specified format. In a data structures course, students are taught algorithms along with their corresponding data structure, such as binary search and binary tree, or postfix evaluation and stack. Consequently, students often associate a particular problem solving method with a particular form of knowledge representation and specific types of problems.

To enrich this process, students should be exposed to diverse problem solving methods and a variety of knowledge representation choices, both intensional and extensional, depending on their preferences and learning styles. Students can be given a set of problems and then be asked to make decisions as to the most appropriate problem solving method(s) and knowledge representation(s). This will build students' experience in applying and transferring various techniques to different classes of problems.

5 Summary and Discussion

We have illustrated knowledge representation choices for students utilizing Towers of Hanoi as an example. It is a potentially complicated problem that can be approached from many representational angles – even if the ultimate solution is the same recursion. We also demonstrated extensional and intensional definitions for Bucket Sort. When approaching problem solving, we believe, that instead of only laying out one description of the answer, we should strive to work with each student so that they understand the solution in a way that is conducive to the best understanding for them.

With the desire for education to be effective in an interdisciplinary way, differences in the learning style of different students from different disciplines should be considered. For example, students with a mathematical background may prefer intensional representations, while students with an engineering background may prefer more visual or manipulative representations, and students with a computer science background may be comfortable with either approach.

Acknowledgement

The authors would like to acknowledge the late Donald Michie for the ideas about extensional and intentional solutions presented in this paper.

6 References

[1] Bierman, A. *Great Ideas in Computer Science*, Cambridge, Massachusetts: MIT Press, 1990.

[2] Clifford, A.S. et al. "Algorithm Visualization: The State of the Field," *Trans. Comput. Educ.* 10, 3, Article 9, 22 pages, August, 2010.

[3] Lucci, S. and Kopec, D. *Artificial Intelligence in the 21st Century: A Living Introduction*, Dulles, Virginia: Mercury Learning and Information, 2012.

[4] Novak, J.D. and Gowin, D.B. *Learning How to Learn*, Cambridge: Cambridge University Press, 1985.

[5] Pierce, C.S. *Collected Papers* (1931–1958). Cambridge, MA: Harvard University Press, 1958.

[6] Sowa, J. *Conceptual Structures: Information Processing in Mind and Machine*, Reading, MA: Addison–Wesley, 1984.

[7] Sowa, J. *Knowledge Representation: Logical, Philosophical, and Computational Foundations*, Boston, Massachusetts: Brooks / Cole / Thomson Learning, 2000.

Calculating Degree of Association Incorporating Viewpoint Using a Concept-Base

[1]Hirokazu Watabe, [2]Misako Imono, [3]Eriko Yoshimura, and [4]Seiji Tsuchiya

Dept. of Intelligent Information Engineering and Science,
Doshisha University, Kyotanabe, Kyoto, 610-0394, Japan
[1]hwatabe@mail.doshisha.ac.jp, [2]mimono@indy.doshisha.ac.jp, [3]eyoshimura@indy.doshisha.ac.jp,
[4]stsuchiy@mail.doshisha.ac.jp

Abstract - *For a computer to perform intelligent information processing requires functions that can extract concepts from words, as humans do, and then associate those concepts with related concepts. In order to implement this association function, it is necessary to quantify the degree of association between two concepts. In the present paper, we propose a method for quantifying degree of association incorporating viewpoint that uses a concept base (a knowledge base that expresses concepts as a collection of pairs, each pair consisting of an attribute word used to describe the concept and a weighting that expresses the word's importance). Here, "Viewpoint" is the perspective from which a concept is viewed; for example, consider the degree of association between "airplane" and "automobile", and the degree of association between "airplane" and "bird". From the viewpoint of "vehicle", "airplane" and "automobile" are highly related, while from the viewpoint of "flight", "airplane" and "bird" are highly related. We present herein a comparison of two methods for calculating degree of association incorporating viewpoint, and demonstrate that the method involving modulation of attribute weightings based on viewpoint results in degree of association calculations that are closer to human senses.*

Keywords: degree of association, viewpoint, Concept-Base

1 Introduction

The remarkable advances in modern information-processing systems have made them indispensable across human society; however, much of this progress has been in terms of enhanced function or performance. While high functionality and performance are obviously essential for ease of use, convenience is also extremely important for information-processing systems. An information-processing system that can be used in the same way as human conversation is referred to as an intelligent information system. Realization of such a system would deliver unparalleled convenience, rendering reading of manuals and remembering operational procedures redundant.

Human conversations are based on correct interpretation of unclear information made possible by the "common sense" regarding language and underlying word concepts that is acquired through experience and learning. In short, the ability to extract a concept from a word, and then associate that concept with a variety of related concepts, plays an important role in human conversation.

The ability to make anthropomorphic common-sense judgments is a necessary component of developing an intelligent information system. Such a common-sense judgment system requires a means of associating related concepts as humans do. One proposed method is to assign a numerical value to the degree of association between concepts [1]. Degree of association is calculated using a concept base [2]. In the present paper, we expand this method to calculate degree of association incorporating viewpoint.

2 Concept-Base

A concept-base is a knowledge base comprised of terms (concepts) mechanically constructed from sources such as multiple Japanese language dictionaries and newspapers and terms (attributes) that express their semantic features. Concepts have

been given attributes along with a weighting, which expresses their importance. Approximately 90,000 concept notations have been compiled in the concept base, with an average of 30 attributes for one concept. A certain concept A has a pair of sets of attribute a_i and weighting w_i, as appear below.

$$A = \{(a_1, w_1), (a_2, w_2), \cdots, (a_m, w_m)\}$$

Any primary attribute a_i is composed of the terms contained in the set of concept notations in its concept base. Therefore, to ensure that a primary attribute matches a certain concept notation, that primary attribute can be further extracted. This is called a secondary attribute. In a concept base, a concept is defined by a chained set of attributes to the n-th order.

3 Degree of Association

Each concept is defined as a set of attributes and each attribute is also a concept as described above. In this paper, a method to derive the degree of association between concepts using up to second order attributes is used. The value of the degree of association ranges from 0.0 to 1.0.

3.1 Calculating the degree of matching

Let us assume that the primary attributes for any concepts A and B are a_i and b_j, respectively, and that their corresponding weightings are u_i and v_j. The number of attributes for concepts A and B shall be L attributes and M attributes ($L \leq M$).

$$A = \{(a_i, u_i) \mid i = 1 \sim L\}$$
$$B = \{(b_j, v_j) \mid j = 1 \sim M\}$$

In this situation, the degree of matching for concepts A and B, $Match(A,B)$, can be defined in the following equation.

$$Match(A, B) = \sum_{a_i = b_j} \min(u_i, v_j)$$

Where, the total sum of the weightings of each concept must be normalized to 1. If there is an attribute that becomes $a_i = b_j$ (concepts A and B have a common attribute), relative to attributes a_i and b_j of concepts A and B, the common portions of the weightings of the common attributes. This means that only the smallest portions of the weightings will effectively be considered to be in match, and their total shall be the degree of matching.

3.2 Calculating the degree of association

To find the degree of association, the relevance between two concepts is calculated as a numeric value based on the value found by calculating the degree of matching of the secondary attributes of the concepts. More specifically, of the two concepts to be calculated, let the one with the smallest number of primary attributes be A ($L \leq M$) and the primary attributes of concept A be the criteria.

$$A = \{(a_1, u_1), \cdots, (a_i, u_i), \cdots (a_L, u_L)\}$$

After that, rearrange the primary attributes of concept B so that the sum of the degree of matching, $Match(a_i, b_{xi})$, with each primary attribute of concept A is at a maximum.

$$B_x = \{(b_{x1}, v_{x1}), \cdots, (b_{xi}, v_{xi}), \cdots, (b_{xL}, v_{xL})\}$$

This will determine a correlating set for the primary attributes of concept A and the primary attributes of concept B. The primary attributes of concept B that exceed the correlation will be ignored. (There will be L attribute combinations at this time.) However, if some of the primary attributes are in agreement, meaning that their concept notations are the same (a_i=b_j), they will be handled separately. This is because there are about 90,000 concept notations in the concept base and the matching of attributes is considered to be rare. As a result, by handling the matching attributes separately, they are valued more highly when they match. More specifically, the size of the corresponding attribute weightings u_i and v_j will be aligned in the direction of the smallest weighting. When this takes place, the value of the attribute with the smallest weighting will be subtracted from the attribute with the largest weighting and once again be correlated to the other attributes. For example, if a_i=b_j and u_i=v_j+ α , then the correlation would be between (a_i, v_j) and (b_j, v_j), and (a_i, α) would once again be correlated to the other attributes. Let us assume the number of attribute combinations determined and correlated in this manner is T. The degree of association between concepts A and B in this case, $DoA(A,B)$, is defined in equation below.

$$DoA(A, B) = \sum_{i=1}^{T} \{Match(a_i, b_{xi}) \times (u_i + v_{xi}) \times (\min(u_i, v_{xi}) / \max(u_i, v_{xi})) / 2\}$$

The value of the degree of association expresses the strength of the relevance between concepts as a continuous value between 0 and 1. The closer the value is to 1, the stronger the relevance.

4 Calculating degree of association incorporating viewpoint

The associations drawn by humans between two concepts are judged based on several viewpoints. For example, consider the degree of association between "airplane" and "automobile", and the degree of association between "airplane" and "bird". Ordinarily, from the viewpoint of "vehicle", "airplane" and "automobile" are highly related, while from the viewpoint of "flight", "airplane" and "bird" are highly related. In short, the association between two concepts will vary depending on the viewpoint, which lies outside those two concepts.

With conventional methods, two concepts are always used to investigate degree of association, and the attributes and weighting of these concepts are defined in a concept-base and are thus always consistent. Application of a third concept to act as a viewpoint is required to judge degree of association incorporating viewpoint. The question of what viewpoint to apply also becomes an important issue during practical application of this method. While it may be necessary to extract a viewpoint automatically from conversational text or surrounding context, in the present paper, we assume that a relevant viewpoint is already being applied and consider what calculation method offers the best way to subsequently calculate degree of association incorporating viewpoint.

We examined two algorithms for calculating degree of association incorporating viewpoint. One determines the correspondence between attributes of two concepts, while the other modulates attribute weighting of two concepts.

4.1 Determining attribute correspondence based on viewpoint

A comparison of concepts *A* and *B* from viewpoint *V* is an investigation of the strength of association between the attributes of viewpoint *V* and of related concepts *A* and *B*. So if we assume that viewpoint *V* has attributes $\{v_1, v_2,\ldots v_n\}$, by looking for attributes in concepts *A* and *B* that relate to attribute v_1 (and likewise for v_2 and so on), we can regard that as calculating the degree of association incorporating viewpoint. The calculation for degree of association that uses this approach can be expressed as follows.

Algorithm for calculating degree of association incorporating viewpoint

Two concepts, *A* and *B*, and one viewpoint, *V*, are expressed as

$$A = \{(a_i, u_i) \mid i = 1\sim L\}$$
$$B = \{(b_j, v_j) \mid j = 1\sim M\}$$
$$V = \{(c_k, w_k) \mid k = 1\sim N\}$$

The attributes of viewpoint *V* are fixed as

$$V=((c_1,w_1),(c_2,w_2), \ldots,(c_N,w_N))$$

To maximize the total degree of matching with viewpoint *V*, the attributes of concepts *A* and *B* are rearranged respectively as

$$A=((a_{x1},u_{x1}),(a_{x2},u_{x2}), \ldots ,(a_{xN},u_{xN}))$$
$$B=((b_{y1},v_{y1}),(b_{y2},v_{y2}), \ldots ,(b_{yN},v_{yN}))$$

The degree of association between *A* and *B* as viewed from viewpoint *V*, $DoA(A,B|V)$ is defined as follows:

$$DoA(A,B|V) = \sum_{i=1}^{N} \frac{Match(c_i,a_{xi}) + Match(c_i,b_{yi})}{2} \times (w_i / wsum)$$

$$wsum = \sum_{i=1}^{N} w_i$$

4.2 Modulating attribute weighting based on viewpoint

In a concept base, the weightings applied to attributes can be considered typical weights for concepts. But when calculating degree of association, if we explicitly specify the viewpoint, the attribute weighting can be expected to change depending on the viewpoint. For example, when we investigate attributes for the concept "bird", attributes in order of weighting might be "avian", "poultry", and "chicken". But if we specify the viewpoint "flight", the attributes "wing" and "plumage" would be weighted more heavily than the attributes "poultry" and "chicken". Here, we propose methods using either degree of matching or degree of association for calculating degree of association incorporating viewpoint that modulates attribute weighting based on viewpoint.

Algorithm for modulating weighting based on viewpoint

Concept A and viewpoint V are expressed as follows:

$A = \{(a_i, u_i) \mid i = 1 \sim L\}$
$V = \{(c_k, w_k) \mid k = 1 \sim N\}$

The weighting u_i' of attribute a_i of concept A when viewpoint V is applied is defined as follows:

$$u_i' = Match(a_i, V)$$

(weighting by degree of matching)

$$u_i' = DoA(a_i, V)$$

(weighting by degree of association)

The weighting for concept B is similarly modulated. For concepts A and B with modulated weighting, degree of association is calculated similarly to the degree of association calculation expressed in Section 3.

A characteristic of this algorithm is that it modulates attribute weighting depending on the viewpoint. Tables 1, 2, and 3 show the weighting of attributes for the concept "bird" modulated from the viewpoint "flight."

Table 1: Weighting in the concept base

Avian	Poultry	Chicken	Bird	Egg-laying	…
223	193	156	132	123	…

Table 2: Weighting by degree of matching

Wing	Down	Feather	Wildlife	Pheasant	…
0.51	0.27	0.22	0	0	…

Table 3: Degree of association weighting

Wing	Down	Feather	Plumage	Skylark	…
0.27	0.15	0.11	0.027	0.024	…

Characteristic calculation times and weightings values differ between Tables 2 and 3. When degree of matching is used for weighting, calculation time is short because only first-order attributes are calculated. Conversely, when using degree of association for weighting, each time that degree of association is calculated for a single viewpoint, the calculation must be performed several times over for each attribute of both concepts A and B in conventional degree of association calculations. Therefore, calculation times are extremely long. In terms of the number of calculations, using degree of matching for weighting is clearly preferable. In terms of the weighting values, when we take degree of matching for weighting, only those attributes that clearly have strong associations with the viewpoint are applied to the weighting because calculations use only first-order attributes. When using degree of association for weighting, almost all the attributes are applied because they are extended to the second order (there are few attributes that do not match at least once when extended to the second order), so almost all attributes contribute to the weighting value. However, this does not necessarily mean that weighting by degree of association is suitable as some weighting will be applied to attributes even if a totally unrelated concept is used as the viewpoint when calculating degree of association for two concepts A and B.

5 Assessing calculations of degree of association incorporating viewpoint

Calculations of degree of association incorporating viewpoint were assessed in two ways. The first was to assess the accuracy of the calculation itself. This test used assessment data in which the magnitude relationship of the degree of association values should be reversed due to specification of a viewpoint. The other was to assess degree of association values when calculating degree of association incorporating no viewpoint. Explicitly specifying a relevant viewpoint for calculating the degree of association between two concepts should result in higher values than when no viewpoint is specified as the latter is a special variation of calculating degree of association incorporating viewpoint.

5.1 Assessing the accuracy of calculations of degree of association incorporating viewpoint

The data shown in Table 4 was used to assess the accuracy of calculations of degree of association incorporating viewpoint.

Table 4: Assessment data (partial)

Reference concept *X*	Concept *A*	Concept *B*	Viewpoint α	Viewpoint β
Stranger	Another person	Connection	Other	Relation
Shared	Public	Lineage	Public	Community
Ally	Comrade	Navy	Peer	Battle
…	…	…	…	…

The assessment data in Table 4 is a set of five concepts. Of the five concepts, three were used to investigate degree of association, with the remaining two being viewpoints specified when calculating degree of association. Concept *X*, which was used as a reference, is a concept that could be viewed as relevant from either viewpoint α or β. Concept *A* is a concept that could be viewed as relevant from viewpoint α; concept *B* is a concept that could be viewed as relevant from viewpoint β. The degree of association between Concept *X* and Concept *A* as viewed from viewpoint α can be expressed as *DoA* (*X*, *A* | α), so if the assessment data in Table 4 satisfies the following two equations, we can take that as calculating the degree of association incorporating viewpoint:

$$DoA(X, A \mid \alpha) > DoA(X, B \mid \alpha)$$
$$DoA(X, B \mid \beta) > DoA(X, A \mid \beta)$$

The assessment data in Table 4 was generated automatically using a thesaurus [3]. Following is a description of the method used to automatically generate the assessment data.

First, we looked for leaves that appeared twice in the thesaurus and used these as reference concept *X*. While there were a large number of leaves that appeared three or more times, these high-frequency leaves were classified within the thesaurus according to fine differences in meaning, and these differences were difficult to judge accurately. For this reason, the test was limited to terms appearing twice, which were comparatively easy to judge.

Next, we used the parent nodes for each leaf as viewpoints α and β. A leaf that was present under node/viewpoint α, but not present under node/viewpoint β, became concept *A*; one that was present under node/viewpoint β, but not present under node/viewpoint α, became concept *B*. Figure 1 shows the relationships of these five concepts in the thesaurus.

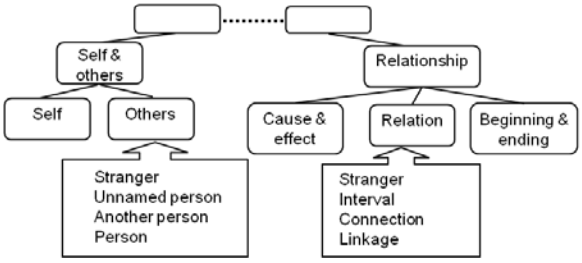

Figure 1: Positional relationships between assessment data terms in the thesaurus

Thus, by defining five concepts as shown in Table 4 as one set of data, we were able to mechanically create assessment data. We generated 3934 sets of assessment data in this way.

The assessment data in Table 4 comprises many complex data. This is because, although the thesaurus systematically classifies words, these classifications differ in range; the number of nodes present above leaves may vary, and even when the distance between two nodes is short, there may still be leaves that appear multiple times. However, as the mechanically generated data in Table 4 originates from a thesaurus, it can be considered objective. This assessment data is therefore suited to comparing the effectiveness of calculation methods based on increases or decreases in the correct answer rate rather than the achievement of a certain percentage of correct answers.

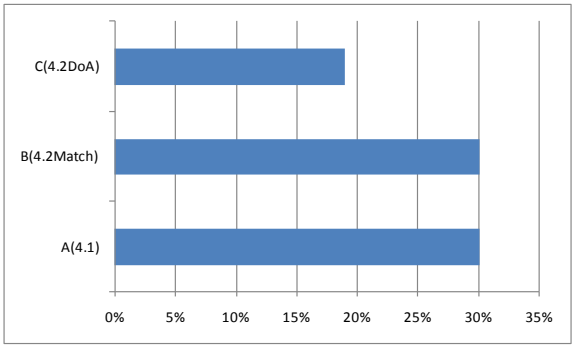

Figure 2: Assessment results
(percentage of correct answers)

Of the methods for modulating attribute weighting using viewpoint presented in Section 4.2, we found that weighting by degree of matching (B) gave more accurate results than weighting by degree of association (C). We attribute this to the qualitative difference of the weightings. We also found that

determining attribute correspondence by viewpoint (A) gave similar accuracy as weighting by degree of matching (B).

Figure 3 shows the percentage of incorrect answers from among the assessment data, where incorrect answers are defined as those that do not satisfy both of the equations in this section.

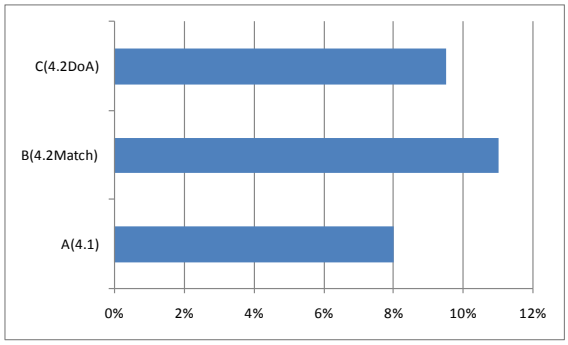

Figure 3: Assessment results
(percentage of incorrect answers)

Figure 3 shows that weighting by degree of matching (B) had the highest percentage of incorrect answers (performed worst), followed by weighting by degree of association (C); attribute correspondence by viewpoint (A) had the lowest percentage of incorrect answers. However, because the algorithm is understood to return higher values for degree of association when a relevant relationship has been specified, it is possible that there will be a high degree of association even with an irrelevant viewpoint. Further investigation is thus required to improve the algorithm.

5.2 Calculating degree of association incorporating no viewpoint and assessing compatibility

Next, let us compare the association between two concepts with no viewpoint with association using viewpoints. With regard to the concepts "airplane" and "bird", the degree of association is not necessarily high when no viewpoint is specified, but specifying the viewpoint "flight" results in a strong association. In other words, specifying a viewpoint that is relevant to both of the concepts involved in the degree of association calculation can produce a higher degree of association than when no viewpoint is specified. Also, if we investigate the degree of association between "airplane" and "flight" using a viewpoint clearly unrelated to either, such as "fluorescent light", the degree of association will naturally be lower than when no viewpoint has been specified.

Based on this, we performed an assessment using concept *X*, concept *A*, viewpoint α, and randomly selected viewpoint γ from Table 4, and took as correct answers anything that satisfied the following equation:

$$DoA(X, A \mid \alpha) > DoA(X, A) > DoA(X, A \mid \gamma)$$

Here again, we used 3934 sets of assessment data. Our results are shown in Figure 4.

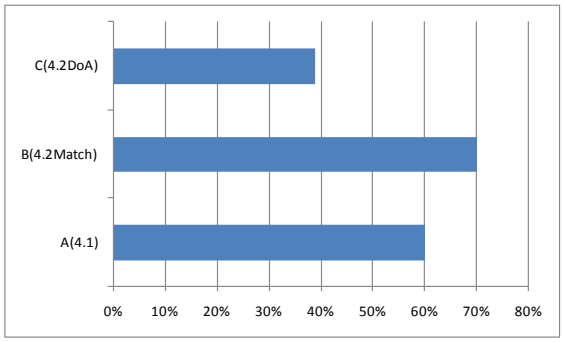

Figure 4: Assessment results (relationship to degree of association incorporating no viewpoint)

Figure 4 reveals that the best results were achieved by modulating weighting by degree of matching using viewpoint, which also yielded the best results in the assessment of accuracy. Accuracy was slightly low at approximately 70%, but as mentioned in Section 4.2, this is mechanically generated data, which is an important difference from other methods.

These findings indicate that weighting attributes by degree of matching based on viewpoint constitutes a suitable method for calculating degree of association incorporating viewpoint.

6 Conclusion

In the present paper, we examined methods for quantifying associations between two concepts, as a way to implement an association function using a concept base. In particular, we proposed and assessed

methods for calculating degree of association incorporating viewpoint. These methods permit associations more strictly related to meaning and are therefore effective tools in the endeavor to develop a intelligent common-sense judgment system.

Acknowledgements

This research has been partially supported by the Ministry of Education, Science, Sports and Culture, Grant-in-Aid for Scientific Research (Young Scientists (B), 24700215).

References

[1] H. Watabe and T. Kawaoka: "The Degree of Association between Concepts using the Chain of Concepts", Proc. of SMC2001, pp.877-881, 2001.
[2] N. Okumura, E. Yoshimura, H. Watabe, and T. Kawaoka: "An Association Method Using Concept-Base", KES 2007/WIRN2007, Part I, LNAI4692, pp.604–611, 2007.
[3] NTT Communication Science Laboratory: "NTT Thesaurus, NIHONGO-GOITAIKEI", Iwanami Shoten book, 1997.

SESSION

ARTIFICIAL NEURAL NETWORKS + LEARNING METHODS AND SYSTEMS + MACHINE LEARNING AND APPLICATIONS

Chair(s)

TBA

Meta-RaPS with Q Learning Approach Intensified by Path Relinking for the 0-1 Multidimensional Knapsack Problem

Arif Arin, Ghaith Rabadi
Dept. of Engineering Management & Systems Engineering
Old Dominion University
241 Kaufman Hall, Norfolk, VA 23529 USA

Abstract - *Many successful metaheuristics employ intelligent procedures to obtain high quality solutions for optimization problems. Intelligence emerges in these metaheuristics via memory and learning. Meta-RaPS (Metaheuristic for Randomized Priority Search) which can produce promising solutions is classified as a memoryless metaheuristic. To improve its performance, Q learning and Path Relinking (PR) are selected as memory and learning mechanisms to be incorporated into Meta-RaPS. In the proposed algorithm, Meta-RaPS Q-PR, Q learning and PR approaches serve as mechanisms that learn the best policy to construct a solution, and learn "good" attributes of best solutions to reach the optimum solution while losing "bad" attributes of the current solution. The 0-1 multidimensional knapsack problem will be used to evaluate the Meta-RaPS Q-PR.*

Keywords: Q learning; Meta-RaPS; path relinking; memory; 0-1 multidimensional knapsack problem

1 Introduction

In some optimization problems whose output is a sequence of actions, finding the policy for the correct actions that gives the best solution for all states is important. Selection of best actions in intermediate states will not mostly lead to the optimum policy, and only the actions in the feasible policy can be accepted as correct actions. In these cases, reinforcement learning (RL) is one of the successful algorithms evaluating the goodness of policies and learning from the good action sequences to create a policy.

The modern science of RL has emerged from four different fields: classical dynamic programming, artificial intelligence (AI), stochastic approximation, and function approximation [1]. RL is in the class of machine learning along with supervised and unsupervised learning. While, in supervised learning, correct values are provided by a supervisor; in unsupervised learning, there is only input data and no supervisor. In the RL, unlike supervised leaning, the machine is not told which actions to take but has to discover which actions yield the most reward. Trial-and-error search and delayed reward are the two most important unique characteristics of RL [2].

The RL algorithm can be classified as model-based and model-free. In the model-free RL algorithm, there are two different cases: deterministic, where there is a single reward and next possible state, and non-deterministic where there are different rewards to move to different next states. This type of RL algorithm is called Q learning. In Q learning algorithm, models of the agent or the environment are not required [3]. Q learning can be employed even when the agent has no prior knowledge of how its actions affect its environment.

As machine learning, Computational Intelligence (CI) is another subfield of AI (also named scruffy or soft) techniques that involves approaches based on strategy and outcome, and includes adaptive and intelligence systems [4, 5]. Metaheuristics can be viewed as another name for the strategy-outcome perspective of scruffy AI. Glover and Laguna [6] define metaheuristics as "a master strategy that guides and modifies other heuristics to produce solutions beyond those that are normally generated in a quest for local optimality". Intelligence via memory and learning in metaheuristics represents the information extracted and stored during the search for better solutions.

Glover and Laguna [6] introduced a classification method for metaheuristic algorithms that depends on three design choices: the use of adaptive memory, the type of neighborhood exploration used, and the number of current solutions carried from one iteration to the next. Meta-RaPS (Meta-heuristic for Randomized Priority Search) can currently be classified as a memoryless metaheuristic and it should benefit from existing memory and learning mechanisms to increase its effectiveness. Thus, we propose incorporating memory and learning into Meta-RaPS to study whether such techniques can help it become "intelligent". Specifically, the Q learning and Path Relinking (PR) approaches will be incorporated into Meta-RaPS as memory mechanisms and the 0-1 multidimensional knapsack problem will be used as a testbed to evaluate the effectiveness of the proposed algorithm.

The 0-1 MKP is the generalized form of the classical knapsack problem (KP). In the KP there is a knapsack with the upper weight limit b, a set of n items with different profits c_j and weights a_j for item j. The problem is to select the items from the set such that the total profit of the selected items is maximized without exceeding the upper weight limit of the

knapsack. If the number of knapsacks in the KP is increased, this will lead to the MKP. In MKP there are *m* knapsacks with different upper weight limits, and item *j* has different weight for each knapsack *i*. The objective is to find a set of items with maximal profit such that the capacity of each knapsack is not exceeded [4]. The MKP can be formulated as in equations (1), (2), and (3):

$$\text{Maximize} \quad \sum_{j=1}^{n} c_j x_j \tag{1}$$

$$\text{Subject to} \quad \sum_{j=1}^{n} a_{ij} x_j \le b_i \quad i = 1, \ldots, m; j = 1, \ldots, n \tag{2}$$

$$x_j \in \{0,1\} \quad j = 1, \ldots, n \tag{3}$$

where x is a vector of binary variables such that $x_j = 1$ if item *j* is selected, and $x_j = 0$ otherwise. The 0-1 MKP is an NP-hard problem.

The 0-1 MKP is basically a resource allocation problem, which can be used to model many problems in the literature such as the capital budgeting, project selection, cutting stock and many loading problems.

2 Meta-RaPS

Moraga et al. [7] defines Meta-RaPS as "generic, high level search procedures that introduce randomness to a construction heuristic as a device to avoid getting trapped at a local optimal solution". Meta-RaPS combines the mechanisms of priority rules, randomness, and sampling. Meta-RAPS is a two-phase metaheuristic: a constructive phase to create feasible solutions and an improvement phase to improve them. In the constructive phase, a solution is built by repeatedly adding feasible components or activities to the current solution in an order that is based on their priority rules until the stopping criterion is satisfied. Generally, solutions obtained by implementing only constructive algorithms can reach mostly local optima, which can be avoided in Meta-RaPS by employing randomness in the constructive phase.

Meta-RaPS uses four parameters: number of iterations (I), the priority percentage (p%), the restriction percentage (r%), and the improvement percentage (i%). Meta-RaPS does not select the activity with the best priority value in every iteration. Instead, the algorithm may randomly accept an activity with a good priority value, but not necessarily the best one. The parameter p% is used to decide the percentage of time an activity with the best priority value will be added to the current partial solution, and (100 - p)% of time it will be randomly selected from a candidate list (CL) containing "good" activities. The CL is created by including items whose priority values are within r% of the best priority value. The construction phase of Meta-RaPS is completed when a feasible solution is produced. The improvement phase is performed if the feasible solutions generated in the construction phase are within i% of the best constructed solution value from the preceding iterations.

DePuy et al. [8] emphasized that the advantages of the Meta-RaPS over other metaheuristics are that run times for Meta-RaPS is not significantly affected by the size of the problem, it is easy to understand and implement, and can generate a feasible solution at every iteration. Pseudo code for Meta-RaPS is shown in the Figure 1.

```
Until stopping criteria met
do until feasible ConstructedSolution generated
   Find priority value for each feasible activity
   Find best priority value
   If rnd() ≤ %p
      then select the activity with best priority value
   else create CL from feasible activities with priority ≥ Limit
      Limit = MinPriority + %r · (MaxPriority - MinPriority)
      Select randomly an activity from CL
   If ConstructedSolution > BestConstructedSolution
      ConstructedSolution ← BestConstructedSolution
End Until
If ConstructedSolution ≤ %i · BestConstructedSolution
   then improve
   If ImprovedSolution > BestImprovedSolution
      ImprovedSolution ← BestImprovedSolution
End For
```

Figure 1. Pseudo Code of Meta-RaPS

Meta-RaPS has many successful applications for discrete optimization problems, such as the Resource Constrained Project Scheduling Problem [9], the Vehicle Routing Problem [10], the Traveling Salesman Problem [11], the 0-1 Multidimensional Knapsack Problem [12], the Parallel Machine Scheduling Problem with Setup Times [13], Early/Tardy Single Machine Scheduling Problem [14], Parallel Multiple-Area Spatial Scheduling Problem with Release Times [15] and Aerial Refueling Scheduling Problem (ARSP) [16].

3 Q Learning

In the Q learning algorithm, the term Q is basically represents the reward received immediately after selecting action *a* from state *s*, plus the value, discounted by γ, of following the optimal policy. If the agent learns the Q function, it will be able to select the action that maximizes Q(s, a) among available actions in its current state.

In the terminology of the Q learning, the decision maker is called "agent" and there are several possible "states" for the agent to move from one to another. The "environment" is the current state in which the agent interacts and makes decisions. The agent has a set of possible, or feasible, actions that affect both the "reward" and the next state. Once an action is taken, the state will be changed. For each action the agent receives feedback, called the "reward". The rewards are delayed, and required for the agent to learn the system. The sequence of actions from the first state to the terminal state is called episode. To solve the optimization problem the agent learns the best course of actions that have the maximum cumulative reward via Q learning transition equation (4).

$$Q(s_t, a_t) \leftarrow (1-\alpha)\ Q(s_t, a_t) + \alpha\left[r_{t+1} + \gamma \max_{a_{t+1}} Q(s_{t+1}, a_{t+1}) \right] \quad (4)$$

In (4), $Q(s_t, a_t)$ is nominated as the cumulative quality, or reward, of action a_t taken in state s_t for time t. r_{t+1} is the reward received when the action a is taken at time (t + 1). $Q(s_{t+1}, a_{t+1})$ is the value for the next state, and has a higher chance of being correct. α is the learning factor, $0 < \alpha < 1$, gradually decreased in time to converge; and γ is the discount factor, $0 \leq \gamma < 1$ [17]. We discount this value by γ because it will happen in the next step. As γ approaches to 1, future rewards are given greater emphasis relative to the immediate reward. The discount concept essentially measures the present value of the sum of the rewards earned in the future over an infinite time.

In the process of creating the Q learning matrix, initially all $Q(s_t, a_t) = 0$ for all actions in a lookup table. The $Q(s_t, a_t)$ values are calculated using equation (4) and stored in their state-action cells of the lookup table. This process will be repeated until the Q learning matrix converges, i.e. the differences between Q values are smaller or equal than a ε value accepted. It has been shown that as α is gradually decreased in time for convergence, this algorithm converges to the optimal Q* values [18]. The pseudo code for Q learning algorithm is presented in Figure 2.

```
initialize Q learning matrix with zeros
while Q learning matrix not converged
    for t = 1 until current episode is completed
        select first item a_t for state s_t randomly
        calculate Q(s_t, a_t) via Q learning transition equation
        update Q learning matrix
        t ← t + 1
    end for
end while
```

Figure 2. Pseudo Code of Q learning.

Q learning methods are the most widely used reinforcement learning methods, probably due to their great simplicity. They can benefit from the experience generated from interaction with an environment, and be applied with a minimal amount of computation [19].

After Q learning is introduced by Watkins [20], many successful applications based on Q learning are presented by researchers in the literature, such as weightings for optimal control and design problems [21], robot navigation [22], morphing Unmanned Air Vehicles [23] and scheduling [24]. More information about the Q-learning algorithm can be found in [19, 20, 25, 26].

4 Path Relinking

The approach is named Path Relinking because it generates a path between solutions linked by a series of moves during a search to incorporate attributes of the guiding solution while recording the objective function values [6]. PR was originally proposed by Glover [27] as a way to explore trajectories between elite solutions obtained by tabu search or scatter search. The PR generates new solutions by exploring trajectories connecting the initiating solution and the guiding solution. While following the path from the initiating towards the guiding solution the high-quality solutions are created by selecting moves with "good" attributes contained in the guiding solution [28]. At each iteration, the best move in terms of the objective function and decreasing the distance between the two solutions is selected. This is repeated until the distance is equal to 0 at which point the best solution found in the trajectory is returned by the algorithm.

In the PR approach for each pair of solutions, different alternatives exist in selecting the starting and the target solutions:

- Forward: The worst of both solutions is used as the starting solution.
- Backward: The better of both solutions is used as the starting solution. Since the starting solution' neighborhood is more explored than that of the target solution, the backward strategy is in general better than the forward one.
- Back and forward relinking: Two paths are constructed in parallel, using alternatively both solutions as the starting and the target solutions.
- Mixed relinking: Two paths are constructed in parallel from both solutions but the guiding solution is an intermediate solution at the same distance from both solutions.

Recent PR approaches have been developed to solve the problems such as large-scale global optimization [29], team orienteering problem [30] and scheduling [31]. There are many successful hybrid applications where PR is used to add a memory mechanism by integrating it into other algorithms; PR with GRASP [32, 33, 34]; TS [35], GA [36, 37], and memetic algorithm [38].

5 Meta-RaPS Q with Path Relinking

Meta-RaPS Q algorithm with PR is created three main phases: first, Q learning matrix is developed to obtain priorities of each item needed for Meta-RaPS; second, a solution is generated based on Meta-RaPS principles; and in the last phase, PR is applied to reach the best solution of Meta-RaPS Q-PR. Once the solution is produced, the Q learning matrix is updated using this solution.

5.1 Creating Q Learning Matrix Phase

In the Q learning algorithm, next item is selected according their Q values, i.e. the item with the maximum Q value. However, by accepting the item having the maximum Q value the algorithm may be stuck in local regions, and cannot explore other promising areas. Another risk with this strategy is that each cell in the Q learning matrix may not be filled in enough to converge because in theory there is no

equal chance to select each cell only by considering their maximum values. A precaution to remove these risks may be to select the next item randomly, instead of looking for the one with maximum Q value. The preliminary analysis of both approaches showed that, in selecting next item, randomness strategy is superior to elitist strategy. Thus, the transition equation of Q learning (4) is modified so that the algorithm can select randomly among the feasible items in the next state instead of accepting the feasible item with maximum Q value.

To begin the algorithm, first the lookup table for the Q learning matrix is created. The solution process begins randomly by selecting both the item as in the first state and next item for the next action. If we assume that the selected item for the first state, *t=1*, is 6, then the value Q(1, 6) is calculated using equation (4) based on all feasible actions after item 6 is selected. The Q learning matrix is updated by replacing new Q(1, 6) with the previous one. In this example, the learning factor α and discount factor γ are 0.7 and 0.1, respectively, and r_{t+1} is 19 which is the priority of the item 3 selected randomly in state *t+1*.

$$Q(1, 6) = (1 - 0.7)\, Q(1, 6) + 0.7\, [r_{t+1} + 0.1\ \text{random}\{Q(2,1), Q(2,2), Q(2,3), Q(2,4), Q(2,5), Q(2,7), Q(2,8)\}]$$

$$= (1-0.7)\ 0 + 0.7[19+0.1\text{random}\ \{0, 0, 0, 0, 0, 0, 0\}]$$

$$=13.3.$$

When there are no other feasible items to add to the solution the calculations are stopped for the current episode, and this process will be repeated until the Q learning matrix converges. The converged Q learning matrix will be used as the priority matrix to select items in the Meta-RaPS Q-PR algorithm.

5.2 Meta-RaPS Phase

In the construction phase of Meta-RaPS, a solution is built by repeatedly adding feasible items to the current solution (partial solution) in the order based on their priorities. In solving the 0-1 MKP instances, priorities of items are extracted from the cells representing state-action pairs in the Q learning matrix. In the improvement phase, two different algorithms will be employed: 2-opt and insertion algorithms. Whereas, in the 2-opt algorithm, the item in the solution is replaced with an item that is not in the solution in a systematic way, in the insertion algorithm, the selected item is inserted to the right or to the left of another item in the solution and items between the old and new places of inserted item shifted towards old place of inserted item in the same order [33].

5.3 Path Relinking Phase

The PR will be employed in Meta-RaPS Q-PR as an intensification procudure. In the PR algorithm a trajectory, or a path, is created between two solutions, called initial and guide, to find new solutions. While progressing, the initial solution transforms gradually in the guide solution by incorparating the attributes of the guide solution. In Meta-RaPS Q-PR algorithm, the improved solution found at the current iteration is accepted as the initial solution, and the best improved solution until the current iteration is assigned as the guide solution. To follow the PR process, the initial and guide solutions are first coded in a binary string. The positions containing same numbers in the initial and guide solutions are identified to keep their states and the numbers in the remaining positions are changed in a systematic way to create the neighborhood. The neighbor with the maximum profit is selected to build the path. At each step, the solutions become more similar to the guide solution and more different from the initial solution. While processing the solution found is replaced with the best improved solution only if it is better than the best improved solution.

For example, considering a 4-item 0-1 MKP problem, if items 3 and 4 are selected for the initial solution, and items 1, 2 and 4 for the guide solution, they will be coded as (0 0 1 1) and (1 1 0 1), respectively. Note that initial and guide solutions share only one item with the same state at the same position. The states of items in the other positions are switched from selected (1) to not selected (0), or not selected (0) to selected (1) to obtain the following neighbors: (1 0 1 1), (0 1 1 1) and (0 0 0 1). The best neighbor, i.e. the one with the maximum profit, is selected as the new initial solution which is now closer to the guide solution, having two items at the same position. This process is followed until the initial and guide solutions are totally identical. Table 1 summarizes the PR transforming process from the initial to guide solutions.

Table 1. PR Process

Initial	**Guide**	**Neighbors**		
0 0 1 **1**	1 1 0 **1**	1 0 1 1*	0 1 1 1	0 0 0 1
1 0 1 **1**	**1** 1 0 **1**	1 1 1 1	1 0 0 1*	
1 0 **0 1**	**1** 1 **0 1**	1 1 0 1*		
1 1 0 1	**1 1 0 1**			

Note that the PR phase of the Meta-RaPS Q-PR algorithm is not executed at the first iteration because the best improved solution to serve as the guide solution is not constituted yet. The Meta-RaPS Q-PR pseudo code is shown in Figure 3.

```
Create Q learning matrix to obtain priorities of items
Until stopping criteria met
BestImprovedSolution ← Meta-RaPS Q(ConstructedSolution,
                                   ImprovedSolution)
PathRelinkingSolution ← PathRelinking(ImprovedSolution,

BestImprovedSolution)
 If  PRSolution > BestImprovedSolution
    PRSolution ← BestImprovedSolution
 update Q learning matrix by using PRSolution as an episode
End until
```

Figure 3. Pseudo Code of Meta-RaPS Q-PR.

6 Computational Study

Meta-RaPS Q-PR is coded in C++ and solved the small/medium 0-1 MKP instances on the Intel i5 CPU 2.27 GHz PC, and the large instances on the HP Z600 CPU 2.40 GHz PC. A standard library of 0-1 MKP test instances available from the OR-Library [39] is used to evaluate the proposed algorithm. These test problems are developed by [40, 41, 42, 43].

The performance of the Meta-RaPS Q-PR will be evaluated in terms of solution quality, or deviation percentage. The deviations between solutions s (solution found in the current method) and s* (optimum solution or best solution found so far) is calculated using the following equation (5):

$$\frac{f(s^*)-f(s)}{f(s^*)} x100. \quad (5)$$

The stopping criteria are to run the Meta-RaPS Q-PR algorithm 10000 iterations or to stop whenever the percent deviation becomes 0, whichever comes first. Since there are many parts in the proposed algorithm where randomness plays very important role, the Meta-RaPS Q-PR will solve each instances 10 times, and their mean and standard deviations will be taken for the analysis. The values of parameters for Meta-RaPS are obtained by applying D-optimal design, a Design of Experiments method, which is an offline parameter tuning method [44]. The optimum parameter setting found for the Meta-RaPS Q-PR algorithm is in Table 2.

Table 2. Meta-RaPS Q-PR Parameters

Parameter	Value
Learning factor α	0.7
Discount factor γ	0.1
Priority (p)	0.4
Restriction (r)	0.2
Improvement (i)	0.1
Number of iterations (I)	10000

The results for the small/medium 0-1 MKP instances produced by the proposed algorithm are summarized in Table 3. The Meta-RaPS Q-PR approach could solve all instances, and find 9.02 times optimum solutions in 10 runs in average for all instances. The average deviation% of the solutions reached by the proposed algorithm is 0.016%.

Table 3. Meta-RaPS Q-PR Results for Small/Medium 0-1 MKP

Statistics	Dev.%	#Opt.	#Iteration	Time (Sec.)
Average	0.016	9.02	1176	258
Std. Dev.	0.037	2.06	1580	593

In solving the 0-1 MKP, Moraga et al. [12] employed the Meta-RaPS with Dynamic Greedy Rule (DGR) [10] as the priority rule in determining the priorities among items. Their average deviaton% was 0.003% for all instances. PETERSEN7 was the only instance for which Meta-RaPS DGR did not find the optimal solution for 10000 iterations, and their runtimes per instance was 115 seconds.

To reveal the contribution of the Q learning and PR to Meta-RaPS Q-PR, the number of optimum solutions found in the construction, improvement and PR phases are tracked for each instance. Since it is observed in the initial analysis that the role of PR is getting more important with the increasing number of items and knapsacks, the instances are put in the order of the size, which is defined here as the product of the number of items and number of knapsacks, as a possible sign of instance difficulty.

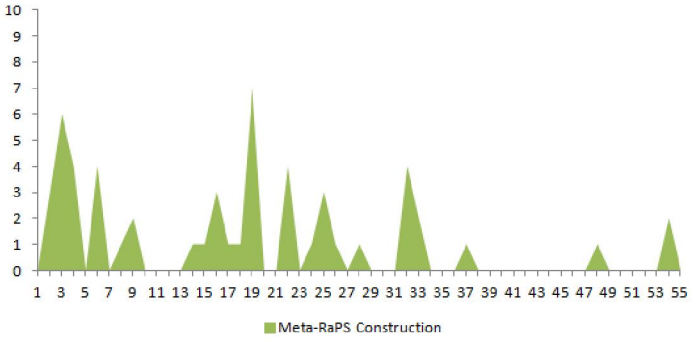

Figure 4. The number of optimum solutions found in the construction phase of Meta-RaPS Q-PR.

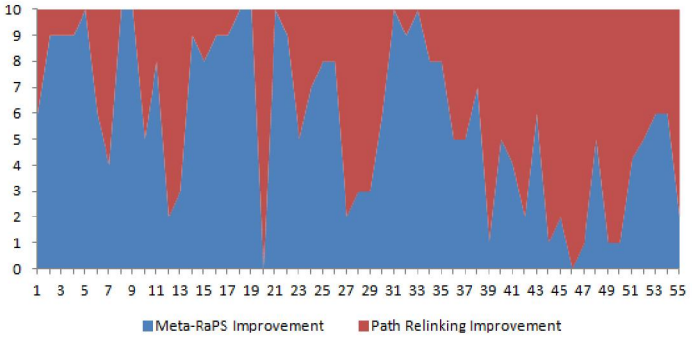

Figure 5. The distribution of solutions found in the improvement and PR phases of Meta-RaPS Q-PR in 10 replicates.

Figure 4 shows the distribution of the number of optimum solutions found in the construction phase. For the instances with lower size, Meta-RaPS could find optimum solutions even in the construction phase by using the priorities from Q learning matrix. For the remaining instances it is observed that the chance of reaching to optimum solutions is decreasing with the increasing size of the instances. The distributions of the number of optimum solutions found in the improvement and PR phases indicate the efficiency of the PR algorithm, in Figure 5. Especially for the instances with higher number of size, the role of PR in the proposed algorithm becomes clear; its share of the number of optimum or best solutions found in 10 runs for each instance is increasing.

It should remind that beside the parameter *number of iteration*, there is another stopping criterion that stops the algorithm whenever deviation% is equal to 0. For the instances with lower size, the algorithm can find the optimum solutions, and stops the solution process before it reaches to the PR phase. This is the reason why the PR phase seems not to produce optimal or best solutions for these instances. However, in solving the instances with higher size, Meta-RaPS requires employing the PR phase to obtain better results. To see the performance of the Meta-RaPS PR for larger size problems, the algorithm is also applied to solve the first 10 large size 0-1 MKP instances with 100 items and 5 knapsacks in OR Library [39]. The proposed algorithm could solve optimally 7 of 10 instances and its deviation% from optimum/best solutions is 0.14%, as seen in Table 4.

Table 2. Meta-RaPS Q-PR Results for Large 0-1 MKP

Statistics	Dev.%	#Opt	#Iteration	Time (Min.)
Average	0.14	3.2	3532	37.61
Std. Dev.	0.15	3.7	1010	13.13

Meta-RaPS Q-PR could reach better results than Meta-RaPS DGR proposed by Moraga et al. [12] whose average deviaton% was 0.60% for 0-1 MKP instances with 100 items and 5 knapsacks. Meta-RaPS DGR run times ranged from 7 to 35 minutes per problem.

7 Conclusion

According to Alpaydın [26], for a system to be intelligent, in a changing environment, it needs to have ability to memory and learn. And, learning is an intelligent process in which the basic unit of mutability is the idea [45]. "Good" adaptive ideas are maintained, much as good genes increase in a population, while poor ideas are forgotten. In similar manner, memory and learning mechanisms in metaheuristics can learn and remember "good" ideas related to the search process to make it possible to create high quality solutions for optimization problems by utilizing this information.

In the original form, Meta-RaPS has no information about the search history and begins every iteration from the same point due to its memoryless nature. In the proposed algorithm, Meta-RaPS Q-PR, the Q learning and PR approaches serve as mechanisms that learn the best policy to construct a solution, and learn "good" attributes of best solutions to reach the optimum solution while losing "bad" attributes of the current solution.

We showed that incorporating memory and learning mechanisms, such as Q learning and PR, into a memoryless metaheuristic can result in significant improvements to the metaheuristic's performance. Even though the proposed algorithm could solve all small/medium instances, the average deviatons% for proposed and original versions of Meta-RaPS are pretty small. However, the contribution of Q learning and PR becomes more clear when investigated the small set of large instances. Thus, for the future studies, the proposed algorithm should be applied to solve the remaining large 0-1 MKP instances in OR-Library to understand its true performance.

8 References

[1] Gosavi, A. Reinforcement Learning: A Tutorial Survey and Recent Advances. INFORMS Journal on Computing, Vol 21(2), 178-192, 2009.

[2] Yao X. and Liu Y. Machine Learning, Search Methodologies: Introductory Tutorials in Optimization and Decision Support Techniques / [edited by] Burke E. K. and Kendall G., Springer, New York, NY, 2005.

[3] Monekosso N. and Remagnino P. The analysis and performance evaluation of the pheromone-Q-learning algorithm, Expert Systems, Vol. 21, No. 2, 80-91, 2004.

[4] W. Pedrycz, Computational Intelligence: An Introduction, CRC Press, 1997.

[5] A.P. Engelbrecht, Computational Intelligence: An Introduction, John Wiley and Sons, 2nd edition, 2007.

[6] F. Glover & M. Laguna, Tabu Search, University of Colorado, Boulder, Kluwer Academic Publishers, 1997.

[7] R.J. Moraga, G.W. DePuy & G.E. Whitehouse, Metaheuristics: A Solution Methodology for Optimization Problems. In: A.B. Badiru (ed.), Handbook of Industrial and Systems Engineering, CRC Press, FL, 2006.

[8] G.W. DePuy, G.E. Whitehouse & R.J. Moraga, Meta-RaPS: A Simple and Efficient Approach for Solving Combinatorial Problems, 29th International Conference on Computers and Industrial Engineering, Montreal, Canada, 644-649, 2001.

[9] G.W. DePuy, G.E. Whitehouse, A simple and effective heuristic for the multiple resource allocation problem, International Journal of Production Research, Vol. 32, 424-31, 2001.

[10] R.J. Moraga, Meta-RaPS: An Effective Solution Approach for Combinatorial Problems, Ph.D. thesis, University of Central Florida, Orlando, FL, 2002.

[11] G.W. DePuy, R.J. Moraga & G.E.Whitehouse, Meta-RaPS: a simple and effective approach for solving the traveling salesman problem, Transportation Research Part E: Logistics and Transportation Review, Vol. 41, No. 2, 115-130, 2005.

[12] R.J. Moraga, G.W. DePuy & G.E.Whitehouse, Meta-RaPS approach for the 0–1 multidimensional knapsack problem, Computers and Industrial Engineering, Vol. 48, No. 2, 83-96, 2005.

[13] G. Rabadi, R.J. Moraga, & A. Al-Salem, Heuristics for the unrelated parallel machine scheduling problem with setup times, Journal of Intelligent Manufacturing, Vol. 17, 85-97, 2006.

[14] S. Hepdogan, R.J. Moraga, G.W. DePuy & G.E. Whitehouse, A Meta-RaPS For The Early/Tardy Single Machine Scheduling Problem, International Journal of Production Research, Vol. 47, No. 7, 1717-1732, 2009.

[15] C. Garcia & G.Rabadi, A Meta-RaPS algorithm for spatial scheduling with release times. Int. J. Planning and Scheduling, Vol. 1, Nos. 1/2, 19-31, 2011.

[16] S. Kaplan & G. Rabadi, A Simulated Annealing and Meta-RaPS Algorithms for the Aerial Refueling Scheduling Problem with Due Date-to-Deadline Windows and Release Time, In Press, Engineering Optimization.

[17] F. C. D. L. J´unior, J. D. D. Melo, and A. D. D. Neto, Using the Q-learning Algorithm in the Constructive Phase of the GRASP and Reactive GRASP Metaheuristics, International Joint Conference on Neural Networks (IJCNN 2008), 4169-4176, 2008.

[18] C. J. C. H. Watkins and P. Dayan, Q-learning, Machine Learning 8, 279-292, 1992.

[19] Sutton R. S. and Barto A. G. Reinforcement Learning: An Introduction, The MIT Press, Cambridge, MA, 1998.

[20] Watkins, C. J. C. H. Learning from Delayed Rewards. Ph.D. thesis, Cambridge University, 1989.

[21] Kamali K., Jiang L. J. and Yen J. Q-Learning and Genetic Algorithms to Improve the Efficiency of Weight Adjustments for Optimal Control and Design Problems, Transactions of the ASME, Vol. 7, December, 302-308, 2007.

[22] Chen C., Li H.-X. and Dong D. Hybrid Control for Robot Navigation - A Hierarchical Q-Learning Algorithm, IEEE Robotics & Automation Magazine, June, 37-47, 2008.

[23] Valasek J., Doebbler J., Tandale M. D. and Meade A. J. Improved Adaptive–Reinforcement Learning Control for Morphing Unmanned Air Vehicles, IEEE Transactions on Systems, Man, and Cybernetics—Part B: Cybernetics, Vol. 38, No. 4, 1014-1020, 2008.

[24] Zhang Z., Zheng L. and Weng M. X. Dynamic parallel machine scheduling with mean weighted tardiness objective by Q-Learning, Int J Adv Manuf Technol 34, 968–980, 2007.

[25] Watkins C. J. C. H. and Dayan P. Q-learning, Machine Learning 8, 279-292, 1992.

[26] Alpaydın, E. Introduction to Machine Learning, The MIT Press, Cambridge, Massachusetts, London, 2004.

[27] F. Glover, Tabu search and adaptive memory programing – Advances, applications and challenges. In: R.S. Barr, R.V. Helgason & J.L. Kennington (ed.), Interfaces in Computer Science and Operations Research, Kluwer, 1996.

[28] F. Glover, M. Laguna & R. Marti, Scatter Search and Path Linking, in: F. Glover & G.A. Kochenberger (eds.) Handbook of Metaheuristics, Kluwer Academic Publishers, 2003.

[29] A. Duarte, R.Martí & F. Gortazar, Path relinking for large-scale global optimization, Soft Computing, vol. 15, no. 11, 2257-2273, 2011.

[30] W. Souffriau, P. Vansteenwegen, B.G. Vanden & D. Van Oudheusden, A Path Relinking approach for the Team Orienteering Problem, Computers and Operations Research, v 37, n 11, 1853-1859, 2010.

[31] W. Bozejko, Parallel path relinking method for the single machine total weighted tardiness problem with sequence-dependent setups, Journal of Intelligent Manufacturing, v 21, n 6, 777-785, 2010.

[32] M. Laguna & R. Martí, GRASP and path relinking for 2-layer straight line crossing minimization, INFORMS Journal on Computing, 11, 44–52, 1999.

[33] J.E.C. Arroyo, A.G. Santos, F.L.S. Silva & A.F. Araújo, A GRASP with Path Relinking for the Single Machine Total Weighted Tardiness Problem, 8th International Conference on Hybrid Intelligent Systems, 726-731, 2008.

[34] M.C.V. Nascimento, M.G.C. Resende & F.M.B. Toledo, GRASP heuristic with path-relinking for the multi-plant capacitated lot sizing problem, European Journal of Operational Research, v 200, n 3, 747-754, 2010.

[35] V.A. Armentano, A.L. Shiguemoto & A. Løkketangen, Tabu search with path relinking for an integrated production-distribution problem, Computers & Operations Research, v 38, n 8, 1199-1209, 2011.

[36] C.C. Ribeiro & D.S. Vianna, A hybrid genetic algorithm for the phylogeny problem using path-relinking as a progressive crossover strategy, International Transactions in Operational Research, v 16, n 5, 641-657, 2009.

[37] E. Vallada & R. Ruiz, Genetic algorithms with path relinking for the minimum tardiness permutation flowshop problem, Omega, v 38, n 1-2, 57-67, 2010.

[38] A. Jaszkiewicz & P. Zielniewicz, Pareto memetic algorithm with path relinking for bi-objective traveling salesperson problem, European Journal of Operational Research, v 193, n 3, 885-890, 2009.

[39] J.E. Beasley, OR-Library: Distributing test problems by electronic mail, Journal of the Operational Journal Society 41, 170–181, 1990.
http://people.brunel.ac.uk/~mastjjb/jeb/info.html.

[40] C.C. Petersen, Computational experience with variants of the Balas algorithm applied to the selection of R&D projects, Management Science 13(9), 736-750, 1967.

[41] H.M. Weingartner & D.N. Ness, Methods for the solution of the multi-dimensional 0/1 knapsack problem, Operations Research 15, 83-103, 1967.

[42] W. Shi, A branch and bound method for the multiconstraint zero one knapsack problem, J. Opl. Res. Soc. 30, 369-378, 1979.

[43] A. Freville & G. Plateau, Hard 0-1 multiknapsack test problems for size reduction methods, Investigation Operativa 1, 251-270, 1990.

[44] J.M. Box, & N.R. Drapper, On minimum point second order designs, Technometrics, Vol. 16, 613-616, 1974.

[45] D.B. Fogel, Evolutionary Computation: Toward a New Philosophy of Machine Intelligence, IEEE Press, Piscataway, NJ, 1995.

Artificial Neural Networks for Content-based Web Spam Detection

Renato M. Silva[1], **Tiago A. Almeida**[2], **and Akebo Yamakami**[1]
[1]School of Electrical and Computer Engineering, University of Campinas – UNICAMP, Campinas, SP, Brazil
{renatoms,akebo}@dt.fee.unicamp.br
[2]Department of Computer Science, Federal University of São Carlos – UFSCar, Sorocaba, SP, Brazil
talmeida@ufscar.br

Abstract— *Web spam has become a big problem in the lives of Internet users, causing personal injury and economic losses. Although some approaches have been proposed to automatically detect and avoid this problem, the high speed the techniques employed by spammers are improved requires that the classifiers be more generic, efficient and highly adaptive. Despite of the fact that it is a common sense in the literature that neural based techniques have a high ability of generalization and adaptation, as far as we know there is no work that explore such method to avoid web spam. Given this scenario and to fill this important gap, this paper presents a performance evaluation of different models of artificial neural networks used to automatically classify and filter real samples of web spam based on their contents. The results indicate that some of evaluated approaches have a big potential since they are suitable to deal with the problem and clearly outperform the state-of-the-art techniques.*

Keywords: web spam; spam classifier; artificial neural network; pattern recognition

1. Introduction

The web has becoming an essential tool in the lives of their users. The steady growth in volume of available information requires the use of search engines that help users to find desired data and presenting the results in an organized, quick and efficient way. However, there are several malicious methods that try to circumvent the search engines by manipulating the relevance of web pages. This deteriorates the search results, leaves users frustrated and exposes them to inappropriate and insecure content. Such technique is known as web spamming [1].

Web spam is composed by *content spam* and/or *link spam*. According to Gyongyi and Garcia-Molina [2], a very simple example of content spam is a web page with pornography and thousands of invisible keywords that have no connection with the pornographic content. Sheng *et al.* [3] explain that link spam is a kind of web spamming with thousands of links to web pages that are intended to promote. Such method increases the relevance of pages in search engines that rank the importance of pages using the relation of the amount of links pointing to it.

The minor problems caused by web spamming is the nuisance offered by forging undeserved and unexpected answers, promoting the announcement of unwanted pages [3]. However, there are more serious problems that pose a significant threat to users, since the web spam may have malicious content that installs malwares on the computers of victims, promoting the discovery of bank passwords and other personal information, degrading the performance of computers and network, among others [4].

According to annual reports, the amount of web spam is frightfully increasing. Eiron *et al.* [5] have classified 100 million web pages and they found that, in average, 11 of the 20 best results were pornographic pages that achieved a high relevance through the manipulation of links. According to Gyongyi and Garcia-Molina [2], there are more than 20% of web spam in the search results. Furthermore, the same study has indicated that about 9% of the search results have at least one link from a spam page in the 10 best results, while 68% of all queries have some kind of spam in the four best results presented by the search engines [2].

Unlike the large amount of available approaches to deal with email spams [6], [7], [8], [9], [10], [11], [12], [13], [14], there few methods in the literature to automatically detect web spam. In general, all the techniques employ one of the following strategies:

- To analyze only the relation of web links [3], [15];
- To analyze only the content of the web pages [16], [17]; or
- To extract features from both contents and links [18], [19], [20].

Among all the approaches presented in the literature, machine learning methods are the most used ones, such as ensemble selection [21], [22], clustering [20], [23], random forest [21], boosting [21], [22], support vector machine [1], [24], and decision trees [15], [20]. However, the main conclusions presented in the literature indicate that the high speed the techniques employed by spammers are improved requires that the classifiers be more generic and adaptive.

To the best of our knowledge, the artificial neural network, that is the one of the most popular and successful technique for pattern recognition, has not been evaluated for classifying web spam. To fill this important gap, this paper presents a performance evaluation of different models of artificial

neural networks used to automatically classify and filter real and public samples of web spam.

This paper is organized as follows: Section 2 introduces the background of the evaluated artificial neural networks. The experiment protocol and main results are presented in Section 3. Finally, Section 4 offers the main conclusions and guidelines for future work.

2. Artificial neural network

Artificial neural network (ANN) is a parallel and distributed method made up of simple processing units called neurons, which has computational capacity of learning and generalization. In this system, the knowledge is acquired through a process called training or learning that is stored in strength of connections between neurons, called synaptic weights [25].

A basic model of ANN has the following components: a set of synapses, an integrator, an activation function, and a bias. So, there are different models of ANN depending on the choice of each component [25].

In the following, we briefly present each model we have evaluated in this work.

2.1 Multilayer perceptron neural network

A multilayer perceptron neural network (MLP) is a perceptron-type network that has a set of sensory units composed by an input layer, one or more intermediate (hidden) layers, and an output layer of neurons. This type of network is fully connected, in other words, all neurons in any layer are connected to all neurons of the previous layer [25].

By default, MLP is a supervised learning method that uses the backpropagation algorithm which can be summarized in two stages: *forward* and *backward*.

In the *forward* stage, the signal propagates through the network, layer by layer, as follows:

$$u_j^l(n) = \sum_{i=0}^{m^{l-1}} w_{ji}^l(n) y_i^{l-1}(n),$$

where $l = 0, 1, 2, ..., L$ are the indexes of network layers. So, $l = 0$ represents the input layer and $l = L$ represents the output layer. On the other hand, $y_i^{l-1}(n)$ is the output function relating to the neuron i in the previous layer, $l-1$, $w_{ji}^l(n)$ is the synaptic weight of neuron j in layer l and m^l corresponds to the number of neurons in layer l. For $i = 0$, $y_0^{l-1}(n) = +1$ and $w_{j0}^l(n)$ represent the bias applied to neuron j in layer l [25], [26].

The output of neuron j in layer l is given by:

$$y_j^l(n) = \varphi_j(u_j^l(n)),$$

where φ_j is the activation function of j. Then, the error can be calculated by:

$$e_j^l(n) = y_j^l(n) - d(n),$$

where $d(n)$ is the desired output for an input pattern $x(n)$.

In *backward* stage, the derivation of the backpropagation algorithm is performed starting from the output layer, as follows:

$$\delta_j^L(n) = \varphi'_j(u_j^L(n)) e_j^L(n),$$

where φ'_j is the derivative of the activation function. For $l = L, L-1, ..., 2$, is calculated:

$$\delta_j^{l-1}(n) = \varphi'_j(u_j^{l-1}(n)) \sum_{i=1}^{m^l} w_{ji}^l(n) * \delta_j^l(n),$$

for $j = 0, 1, ..., m^l - 1$ [25], [26].

According to Haykin [25], one of the most common stopping criteria for the MLPs and other types of ANNs is the amount of training iterations. The algorithm can also be stopped when the network reaches a minimum error, which can be calculated by the Mean Square Error:

$$MSE = \frac{1}{n} e^T e,$$

where n is the number of input patterns and e an array that stores the relative error for all input patterns in the network.

2.1.1 Levenberg-Marquardt algorithm

The Levenberg-Marquardt algorithm is usually employed to optimize and accelerate the convergence of the backpropagation algorithm [27]. It is considered a second order method because it uses information about the second derivative of the error function.

Considering that the error function is given by MSE, the equation used by Gauss-Newton method to update the network weights and to minimize the value of MSE is:

$$W_{i+1} = W_1 - H^{-1} \nabla f(W).$$

The gradient $\nabla f(W)$ can be represented by:

$$\nabla f(W) = J^T e$$

and the Hessian matrix can be calculated by:

$$\nabla^2 f(W) = J^T J + S,$$

where J is the Jacobian matrix

$$J = \begin{bmatrix} \frac{\partial e_1}{\partial x_1} & \frac{\partial e_1}{\partial x_2} & \cdots & \frac{\partial e_1}{\partial x_n} \\ \frac{\partial e_2}{\partial x_1} & \frac{\partial e_2}{\partial x_2} & \cdots & \frac{\partial e_2}{\partial x_3} \\ \vdots & \vdots & \ddots & \vdots \\ \frac{\partial e_n}{\partial x_1} & \frac{\partial e_n}{\partial x_2} & \cdots & \frac{\partial e_n}{\partial x_n} \end{bmatrix},$$

x_i is the i-th input pattern of the network and

$$S = \sum_{i=1}^{n} e_i \nabla^2 e_i.$$

It can be conclude that S is a small value when compared to the product of the Jacobian matrix, so the Hessian matrix can be represented by:

$$\nabla^2 f(W) \approx J^T J.$$

Therefore, updating the weights in Gauss-Newton method can be done by:

$$W_{i+1} = W_1 - (J^T J)^{-1} J^T e.$$

One limitation of the Gauss-Newton method is that a simplified Hessian matrix can not be reversed. Thus, the Levenberg-Marquardt algorithm updates the weights by:

$$W_{i+1} = W_i - (J^T J + \mu I)^{-1} J^T e,$$

where I is the identity matrix and μ a parameter that makes the Hessian a positive definite matrix.

More details about the Levenberg-Marquardt algorithm can be found at [26], [27], [28].

2.2 Kohonen's self-organizing map

The Kohonen's self-organizing map (SOM) is based on unsupervised competitive learning. Its main purpose is to transform an input pattern of arbitrary dimension in a one-dimensional or two-dimensional map in a topologically ordered fashion [25], [29].

The training algorithm for a SOM can be summarized in two stages: competition and cooperation [25], [29].

In the competition stage, a random input pattern (x_j) is chosen, the similarity between this pattern and all the neurons of the network is calculated by the Euclidean distance, defined by:

$$id = \arg \min_{\forall i} \|x_j - w_i\|,$$

where $i = 1, ...k$, and the index of the neuron with lowest distance is selected.

In the cooperation stage, the synaptic weights w_{id} that connect the winner neuron in the input pattern x_i is updated. The weights of neurons neighboring the winner neuron are also updated by:

$$w_i(t+1) = w_i(t) + \alpha(t) h(t) (x_i - w_i(t)),$$

where t is the number of training iterations, $w_i(t+1)$ is the new weight vector, $w_i(t)$ is the current weight vector, α is the learning rate, $h(t)$ is the neighborhood function and x_i is the input pattern.

The neighborhood function $h(t)$ is equal to 1 when the winner neuron is updated. This is because it determines the topological neighborhood around the winning neuron, defined by the neighborhood radius σ. The amplitude of this neighborhood function monotonically decreases as the lateral distance between the neighboring neuron and the winner neuron increases. There are several ways to calculate this neighborhood function, and one of the most common is the Gaussian function, defined by:

$$h_{ji}(t) = \exp\big(\frac{-d_{ji}^2}{2\sigma^2(t)}\big),$$

where d_{ji} is the lateral distance between winner neuron i and neuron j. The parameter $\sigma(t)$ defines the neighborhood radius and should be some monotonic function that decreases over the time. So, the exponential decay function

$$\sigma(t) = \sigma_0 \exp\big(-\frac{t}{\tau}\big)$$

can be used, where σ_0 is the initial value of σ, t is the current iteration number and τ is a time constant of the SOM, defined by

$$\tau = \frac{1000}{\log \sigma_0}.$$

The competition and cooperation stages are carried out for all the input patterns. Then, the neighborhood radius σ and learning rate α are updated. This parameter should decrease with time and can be calculated by:

$$\alpha(t) = \alpha_0 \exp\big(-\frac{t}{\tau}\big),$$

where α_0 is the initial value of α, t is the current iteration number and τ is a time constant of the SOM which can be calculated as presented in the cooperation stage.

2.3 Learning vector quantization

The learning vector quantization (LVQ) is a supervised learning technique that aims to improve the quality of the classifier decision regions, by adjusting the feature map through the use of information about the classes [25].

According to Kohonen [29], the SOM can be used to initialize the feature map by defining the set of weight vectors w_{ij}. The next step is to assign labels to neurons. This assignment can be made by majority vote, in other words, each neuron receives the class label in that it is more activated.

After this initial step, the LVQ algorithm can be employed. Although, the training process is similar to the SOM one, it does not use neighborly relations and updates only the winner neuron. Therefore, it is checked if the class label of the input vector x is equal to the label of the winner neuron. If the labels are equal, this neuron is moved towards the input vector x by:

$$w_{id}(t+1) = w_{id}(t) + \alpha(t)(x_i - w_{id}(t)),$$

where α is the learning rate, id is the index of the winner neuron and t is the current iteration number. However, if the label of the winner neuron is different from the label of the input pattern x, then it is moved away by:

$$w_{id}(t+1) = w_{id}(t) - \alpha(t)(x_i - w_{id}(t)).$$

2.4 Radial basis function neural network

A radial basis function neural network (RBF), in its most basic form, has three layers. The first one is the input layer which has sensory units connecting the network to its environment. The second layer is hidden and composed by a set of neurons that use radial basis functions to group the input patterns in clusters. The third layer is the output one, which is linear and provides a network response to the activation function applied to the input layer [25].

The activation functions consists of radial basis functions whose values increase or decrease in relation to the distance for a central point. The decreasing radial basis function most common is the Gaussian, defined by:

$$h(x) = \exp\left(-\frac{(x-c)^2}{r^2}\right),$$

where x is the input vector, c is the center point and r is the width of the function. On the other hand, the increasing radial basis function generally is represented by a multiquadric function, defined by [30]:

$$h(x) = \frac{\sqrt{r^2 + (x-c)^2}}{r}.$$

The procedure for training a RBF is performed in two stages. In the first one, the parameters of the basic functions related to the hidden layer are determined through some method of unsupervised training, as K-means.

In the second training phase, the weights of the output layer are adjusted, which corresponds to solve a linear problem [27]. According to Bishop [27], considering an input vector $x = [x_1, x_2, ..., x_n]$, the network output is calculated by:

$$y_k = \sum_{j=1}^{m} w_{kj} h_j,$$

where $x = [w_{k1}, w_{k2}, ..., x_{km}]$ are the weights, $h = [h_1, h_2, ..., h_m]$ are the radial basis functions, calculated by a function of radial basis activation.

After calculating the outputs, the weights should be updated. A formal solution to calculate the weights is given by:

$$w = h^{\dagger} d,$$

where h is the matrix of basis functions, $h^{\dagger}$ represents the pseudo-inverse of h and d is a vector with the desired responses [27].

Consult [25], [27], [30] for more information.

3. Experiments and results

To give credibility to the found results and in order to make the experiment completely reproducible, all the tests were performed with the public and well-known WEBSPAM-UK2006 collection[1]. It is composed by a set of 105,896,555 web pages hosted in 114,529 hosts in the UK domains. It is important to note that this corpus was used in *Web Spam Challenge Track*[2] *I* and *II*, that are the most known competitions of web spam detection techniques.

In our experiments, we have followed the same competition guidelines. In this way, we have used a set of 8,487 feature vectors employed to discriminate the hosts as spam or ham. This kind of information was provided by the organizers. Each feature vector is composed by 96 features proposed by Castilho *et al.* [20], where 24 features were extracted from the host home page, other 24 ones from the page with the highest PageRank, 24 ones from the mean of these values for all pages, and the remaining 24 ones from the variance of all web pages. Furthermore, each host is labeled as spam, not spam (ham) or indefinite. Thus, the vectors related to hosts that are labeled as undefined were discarded.

3.1 Protocol

We evaluated the following well-known artificial neural networks (ANNs) algorithms to automatically detect web spam based on its content: multilayer perceptron (MLP) trained with the gradient descent and Levenberg-Marquardt methods, Kohonen's self-organizing map (SOM) with learning vector quantization (LVQ) and radial basis function neural network (RBF).

We have implemented all the ANNs with a single hidden layer and with one neuron in the output layer. In addition, we have employed a linear activation function for the neuron of output layer and an hyperbolic tangent activation function for the neurons of the intermediate layer. Thus, we have initialized the weights and biases with random values between $+1$ and -1, and normalized the data to this interval.

The desired output for all networks is -1 (ham) or $+1$ (spam). So, for RBFs and MLPs, if the output is greater than or equal to 0, the host is considered spam, otherwise it is considered ham. The same not happens with SOMs since the data receive the same label of the neuron that represents them.

Regarding the parameters, in all simulations, we have employed the following stopping criteria: maximum number of iterations be greater than a threshold θ, the mean square error (MSE) of the training set be smaller than a threshold γ or when the MSE of the validation set increases (checked every 10 iterations).

[1] *Yahoo! Research: "Web Spam Collections"*. Available at `http://barcelona.research.yahoo.net/webspam/datasets/`.

[2] *Web Spam Challenge:* `http://webspam.lip6.fr/`

The parameters used for each ANN model were empirically calibrated and are the following:

- Multilayer perceptron with gradient descent method:
  - $\theta = 10,000$
  - $\gamma = 0.001$
  - Step learning $\alpha = 0.005$
  - Number of neurons in the hidden layer: 100
- Multilayer perceptron with Levemberg-Marquardt method:
  - $\theta = 500$
  - $\gamma = 0.001$
  - Step learning $\alpha = 0.001$
  - Number of neurons in the hidden layer: 50
- Kohonen's self-organizing map with learning vector quantization:
  - Competition stage:
    - One-dimensional neighborhood function with initial radius $\sigma = 4$
  - Cooperation stage:
    - $\theta = 2,000$
    - Step learning $\alpha = 0.01$
    - Number of neurons in the hidden layer: 120
- Radial basis function neural network:
  - Number of neurons in the hidden layer: 10

Note that, for the simulations using the RBFs, we have not employed any stopping criteria because the training method is not iterative, as pointed out in Section 2.4.

To address the algorithms performance, we divided each simulation in 10 tests and calculated the arithmetic mean and standard deviation of the following well-known measures: accuracy rate (Acc%), spam recall rate (Rcl%), specificity (Spc%), spam precision rate (Pcs%), and F-measure (FM). In each test, we have randomly selected 80% of the samples of each class to be presented to the algorithms in the training stage and the remaining ones were separated for testing.

3.2 Results

In this section, we report the main results of our evaluation. Table 1 presents the performance achieved by each artificial neural network. Bold values indicate the highest score.

Table 1: Results achieved by each evaluated artificial neural network for WEBSPAM-UK2006 dataset.

	Gradient	Levenberg	RBF	SOM + LVQ
	Mean	Mean	Mean	Mean
Acc	86.2±1.2	**88.6**±1.4	79.7±0.6	80.6±0.8
Rcl	57.0±4.6	**69.3**±4.2	26.7±2.8	29.2±2.6
Spc	95.0±0.4	94.2±1.2	95.8±0.7	**96.3**±0.6
Pcs	77.5±2.7	**77.6**±4.6	65.8±3.3	70.4±4.0
FM	0.656±0.039	**0.731**±0.032	0.379±0.030	0.412±0.030

According to the results, it is clear that the MLP trained with Levenberg-Marquardt method achieved the best performance. On the other hand, the Kohonen's self-organizing map and radial basis function neural network acquired the worst performances with a very low spam recall rate. Furthermore, in all results we noted the contrast between the high specificity rate and a not too high spam recall rate, which indicates that the classifiers have more successful to identify ham hosts than spam ones.

Based on these first results, we considered the hypothesis that there are redundancies in the feature vectors that could be affecting the classifiers performance. In this way, we employed the principal component analysis (PCA) [25] to analyze and reduce the dimensionality of the feature space. Using the PCA, we observed that with only 23 dimensions is possible to represent about 99% of the information presented in the original 96 feature vectors. According to the analysis, the most relevant information are in the first 21 dimensions. Therefore, it is possible to conclude that just the attributes extracted from the host home page have enough information to characterize the host as spam or ham.

After reducing the feature vectors from 96 to 23 dimensions, we performed a new simulation. The found results are presented in Table 2.

Table 2: Results achieved by each evaluated artificial neural network for WEBSPAM-UK2006 dataset after a step of dimensionality reduction using principal component analysis.

	Gradient	Levenberg	RBF	SOM + LVQ
	Mean	Mean	Mean	Mean
Acc	81.0±0.6	**85.5**±1.5	76.9±0.4	77.3±0.2
Rcl	38.8±2.4	**55.5**±3.4	2.5±1.3	3.1±0.8
Spc	95.1±0.6	94.8±1.2	99.5±0.3	**99.8**±0.1
Pcs	71.1±2.8	77.0±4.0	58.6±19.8	**88.3**±6.5
FM	0.502±0.024	**0.644**±0.027	0.047±0.024	0.060±0.014

Based on the found results we can see that, although PCA indicates that the new feature vectors represent more than 99% of the information of the original data, reducing the dimensionality of the feature space clearly affected the classifiers performance for all evaluated techniques, mainly for Kohonen's self-organizing map and radial basis function neural network which achieved spam recall rate lower than 5%. Therefore, it is conclusive that in this scenario reducing the dimensionality of the feature space is not indicated.

Analyzing the results achieved in all experiments, we also suspected that the difference between the achieved high specificity rates and low spam recall rates for all evaluated techniques could be explained by the large difference between the number of ham over the amount of spam samples. This could be doing the classifiers more specialized to identify ham hosts. Thus, to test this hypothesis, we decided to present to the classifiers the same number of data in the two classes during the training process. In this way, 1,978 samples of each class were randomly selected to be trained.

With this new setup, we performed a new simulation using again all the feature vectors. Table 3 presents the classification results.

Table 3: Results achieved by each evaluated artificial neural network for WEBSPAM-UK2006 dataset using classes of equal size in the training stage.

	Gradient	Levenberg	RBF	SOM + LVQ
	Mean	Mean	Mean	Mean
Acc	84.7±1.6	**87.6**±1.5	63.6±1.3	66.9±0.7
Rcl	82.9±2.0	**86.5**±2.0	45.6±1.9	59.7±5.9
Spc	86.4±2.4	**88.8**±1.9	81.6±1.5	74.2±5.5
Pcs	86.1±2.4	**89.1**±2.4	71.3±2.1	70.1±2.9
FM	0.845±0.015	**0.877**±0.017	0.556±0.016	0.642±0.026

The last results indicate that training the artificial neural networks with the same number of samples in each class clearly improved the performance of all classifiers. Note that, if we compare the new results with the ones presented in Table 1, as it was expected, the cost for the lower specificity rate worth if we consider the great improvement in the spam recall rate. It can be also confirmed by the improvement in the F-measure for all evaluated techniques. It is important to note that the MLP with the Levemberg-Marquardt method achieved very good results and the best performance when compared with the other evaluated methods.

To show that the evaluated artificial neural networks are really competitive, in Table 4 we present a comparison between the best results achieved by the evaluated artificial neural networks and the top performance techniques employed to classify web spam available in the literature.

Table 4: Comparison between the results achieved by the evaluated artificial neural networks and the top performance classifiers available in the literature.

Classifiers	Pcs	Rcl	FM
Top performance methods available in the literature			
Decision trees [20] - content	-	-	0.683
Decision trees [20] - content and links	-	-	0.763
Support Vector Machine [1] - content	60.0	36.4	-
Bagging [16] - content	84.4	**91.2**	-
Boosting [16] - content	86.2	91.1	-
Best results achieved by each artificial neural network			
MLP + Gradient - content	86.1	82.9	0.845
MLP + Levenberg - content	**89.1**	86.5	**0.877**
RBF - content	88.3	45.6	0.556
SOM + LVQ - content	64.2	59.7	0.642

The comparison indicates that the MLP with Levemberg-Marquardt method is very competitive and suitable to deal with the problem. Note that, although the Bagging algorithm presented by Ntoulas *et al.* [16] achieved higher spam recall rate, the spam precision rate is lower and, consequently, the specificity rate is also lower than those one achieved by MLP. Furthermore, the results indicate that the MLP neural networks outperformed established methods as the decision trees proposed by Castilho *et al.* [20] and SVM presented by Svore *et al.* [1].

4. Conclusions and future work

In this paper, we have presented a performance evaluation of different models of artificial neural networks used to automatically classify real samples of web spam based on their contents.

The results indicate that the multilayer perceptron neural network trained with the Levenberg-Marquardt method is the best evaluated model. Such a method also outperformed established techniques available in the literature such as decision trees [20] and support vector machine [1].

Furthermore, since the data is unbalanced, the results also indicate that all the evaluated techniques are superior when trained with the same amount of samples of each class. It is because the models tend to converge to the benefit of the class with the largest number of representatives, which increases the rate of false positives or false negatives.

We have also observed that the Kohonen's self-organizing map and radial basis function neural network were inferior than the multilayer perceptron neural networks in all simulations. So, we can conclude that such a models are not indicated to classify web spam.

Finally, an analysis on the feature vectors originally proposed by Castilho *et al.* [20] indicate that they have many redundancies, since with the principal component analysis is possible to reduce them from 96 to 23 dimensions that represents about 99% of the information presented in the original feature set. However, using the reduced feature vectors clearly hurts the classifiers accuracy.

For future work, we intend to propose new features to enhance the classifiers prediction, and hence increase its ability to discriminate the hosts as spam or ham. In this way, we aim to use the relation of links presented in the web pages.

References

[1] K. M. Svore, Q. Wu, and C. J. Burges, "Improving web spam classification using rank-time features," in *Proceedings of the 3rd International Workshop on Adversarial Information Retrieval on the Web (AIRWeb'07)*, Banff, Alberta, Canada, 2007, pp. 9–16.

[2] Z. Gyongyi and H. Garcia-Molina, "Spam: It's not just for inboxes anymore," *Computer*, vol. 38, no. 10, pp. 28–34, 2005.

[3] G. Shen, B. Gao, T. Liu, G. Feng, S. Song, and H. Li, "Detecting link spam using temporal information," in *Proceedings of the 6th IEEE International Conference on Data Mining (ICDM'06)*, Hong Kong, China, 2006, pp. 1049–1053.

[4] M. Egele, C. Kolbitsch, and C. Platzer, "Removing web spam links from search engine results," *Journal in Computer Virology*, vol. 7, pp. 51–62, 2011.

[5] N. Eiron, K. S. McCurley, and J. A. Tomlin, "Ranking the web frontier," in *Proceedings of the 13rd International Conference on World Wide Web (WWW'04)*, New York, NY, USA, 2004, pp. 309–318.

[6] T. Almeida, A. Yamakami, and J. Almeida, "Evaluation of Approaches for Dimensionality Reduction Applied with Naive Bayes Anti-Spam Filters," in *Proceedings of the 8th IEEE International Conference on Machine Learning and Applications*, Miami, FL, USA, 2009, pp. 517–522.

[7] ——, "Filtering Spams using the Minimum Description Length Principle," in *Proceedings of the 25th ACM Symposium On Applied Computing*, Sierre, Switzerland, 2010, pp. 1856–1860.

[8] ——, "Probabilistic Anti-Spam Filtering with Dimensionality Reduction," in *Proceedings of the 25th ACM Symposium On Applied Computing*, Sierre, Switzerland, 2010, pp. 1804–1808.

[9] T. Almeida and A. Yamakami, "Content-Based Spam Filtering," in *Proceedings of the 23rd IEEE International Joint Conference on Neural Networks*, Barcelona, Spain, 2010, pp. 1–7.

[10] T. Almeida, J. Almeida, and A. Yamakami, "Spam Filtering: How the Dimensionality Reduction Affects the Accuracy of Naive Bayes Classifiers," *Journal of Internet Services and Applications*, vol. 1, no. 3, pp. 183–200, 2011.

[11] T. Almeida and A. Yamakami, "Redução de Dimensionalidade Aplicada na Classificação de Spams Usando Filtros Bayesianos," *Revista Brasileira de Computação Aplicada*, vol. 3, no. 1, pp. 16–29, 2011.

[12] T. Almeida, J. G. Hidalgo, and A. Yamakami, "Contributions to the Study of SMS Spam Filtering: New Collection and Results," in *Proceedings of the 2011 ACM Symposium on Document Engineering*, Mountain View, CA, USA, 2011, pp. 259–262.

[13] T. A. Almeida and A. Yamakami, "Facing the Spammers: A Very Effective Approach to Avoid Junk E-mails," *Expert Systems with Applications*, pp. 1–5, 2012.

[14] ——, "Advances in Spam Filtering Techniques," in *Computational Intelligence for Privacy and Security*, ser. Studies in Computational Intelligence, D. Elizondo, A. Solanas, and A. Martinez-Balleste, Eds. Springer, 2012, vol. 394, pp. 199–214.

[15] Q. Gan and T. Suel, "Improving web spam classifiers using link structure," in *Proceedings of the 3rd international Workshop on Adversarial Information Retrieval on the Web (AIRWeb'07)*, Banff, Alberta, Canada, 2007, pp. 17–20.

[16] A. Ntoulas, M. Najork, M. Manasse, and D. Fetterly, "Detecting spam web pages through content analysis," in *Proceedings of the World Wide Web conference (WWW'06)*, Edinburgh, Scotland, 2006, pp. 83–92.

[17] T. Urvoy, E. Chauveau, and P. Filoche, "Tracking web spam with html style similarities," *ACM Transactions on the Web*, vol. 2, no. 1, pp. 1–3, February 2008.

[18] I. Bíró, D. Siklósi, J. Szabó, and A. A. Benczúr, "Linked latent dirichlet allocation in web spam filtering," in *Proceedings of the 5th International Workshop on Adversarial Information Retrieval on the Web (AIRWeb'09)*, Madrid, Spain, 2009, pp. 37–40.

[19] J. Abernethy, O. Chapelle, and C. Castillo, "Graph regularization methods for web spam detection," *Machine Learning*, vol. 81, no. 2, pp. 207–225, 2010.

[20] C. Castillo, D. Donato, and A. Gionis, "Know your neighbors: Web spam detection using the web topology," in *Proceedings of the 30th Annual International ACM SIGIR Conference on Research and Development in Information Retrieval (SIGIR'07)*, Amsterdam, The Netherlands, 2007, pp. 423–430.

[21] M. Erdélyi, A. Garzó, and A. A. Benczúr, "Web spam classification: a few features worth more," in *Proceedings of the 2011 Joint WICOW/AIRWeb Workshop on Web Quality (WebQuality'11)*, Hyderabad, India, 2011, pp. 27–34.

[22] G. Geng, C. Wang, Q. Li, L. Xu, and X. Jin, "Boosting the performance of web spam detection with ensemble under-sampling classification," in *Proceedings of the 14th International Conference on Fuzzy Systems and Knowledge Discovery (FSKD'07)*, Haikou, China, 2007, pp. 583–587.

[23] T. Largillier and S. Peyronnet, "Lightweight clustering methods for webspam demotion," in *Proceedings of the 9th IEEE/WIC/ACM International Conference on Web Intelligence and Intelligent Agent Technology (WI-IAT'10)*, Toronto, Canada, 2010, pp. 98–104.

[24] Q. Ren, "Feature-fusion framework for spam filtering based on svm," in *Proceedings of the 7th Annual Collaboration, Electronic Messaging, Anti-Abuse and Spam Conference (CEAS'10)*, Redmond, Washington, USA, 2010, pp. 1–6.

[25] S. Haykin, *Neural Networks: A Comprehensive Foundation*, 2nd ed. New York, NY, USA: Prentice Hall, 1998.

[26] H. Liu, "On the levenberg-marquardt training method for feed-forward neural networks," in *Proceedings of the 6th International Conference on Natural Computation (ICNC'10)*, Yantai,China, 2010, pp. 456–460.

[27] C. M. Bishop, *Neural Networks for Pattern Recognition*, 1st ed. Oxford: Oxford Press, 1995.

[28] M. T. Hagan and M. B. Menhaj, "Training feedforward networks with the marquardt algorithm," *IEEE Transactions on Neural Networks*, vol. 5, no. 6, pp. 989–993, 1994.

[29] T. Kohonen, "The self-organizing map," in *Proceedings of the IEEE*, vol. 9, no. 78, 1990, pp. 1464–1480.

[30] M. J. L. Orr, "Introduction to radial basis function networks," 1996.

GMDH and RBFGRNN Networks for Multi-Class Data Classification

Abrham Workineh, Mulugeta Dugda, Abdollah Homaifar and Gary Lebby
Department of Electrical and Computer Engineering, North Carolina A&T State University, Greensboro, North Carolina, USA
atworkin@ncat.edu, mtdugda@ncat.edu, homaifar@ncat.edu, lebby@ncat.edu

Abstract: *This work explored the application of Group Method of Data Handling (GMDH) and Radial Basis Functions Generalized Regression Neural Network (RBFGRNN) for a multi-class data classification with real valued attributes. The Dataset employed has 336 instances, with each instance consisting of a name and seven predictive inputs and one of five different classes. The Karhunen Loeve Transformation (KLT) technique is used to avoid redundancy in the data keeping more than 95% of the information in the original data. A four layer GMDH network with six best error outputs passed to the succeeding layer gave the best result. Before applying a multi-dimensional RBFGRNN network, a DIANA like hierarchical clustering algorithm has been employed to determine the number of cluster centers and organize the data around those centers. Finally, the multi-dimensional RBFGRNN is applied on the transformed data and the performance of the network is evaluated. The regressed output of the network highly resembles the actual desired class outputs.*

Keywords: GMDH, RBFGRNN, KLT, classification, clustering.

1. Introduction

A classification problem can be described as identifying an unknown object as a member of a known class of objects. The large volume of biological sequences, like DNA and protein sequences, available in public databases in recent times has created great interest in the area of development of computational techniques for automatic classification of those data sequences. In literatures, several algorithms have been suggested for a multivariate classification problem. Traditional sequence classification algorithms like K-nearest neighbor based techniques and machine learning algorithms like support vector machines (SVM) have been studied and implemented in this effort of sequence-based classification [1]. Over the years, algorithms based on Markov models, and Hidden Markov models have been used extensively for solving various problems in computational biology [2, 3]. Deshpand and Karypis specifically evaluated different classification algorithms applied on five different datasets, including E. coli, and found out that the SVM-based approaches provide better accuracy than Markov model or K-nearest based methods [1]. Machine learning algorithms learn from experience or observed examples based on some class of tasks and performance measure [4]. Because of the algorithm's learning ability to construct classifiers, machine learning techniques are appropriate for biological data classification problem. In machine learning, there are in general two types of learning approaches: supervised learning in which the learner has some prior knowledge of the data, and unsupervised learning where no prior information is given to the learner regarding the data or the output [5]. Neural networks are one of the most widely applied classification techniques for solving problems in human-like manner [5, 6]. After sufficient training, the neural structure uses the knowledge it stores in the connection weights to recall patterns.

This paper investigates the application of GMDH and RBFGRNN neural networks for classifying a multivariate class problem. Neural networks in general assume fairly independent sets of attribute values to avoid garbage-in garbage-out scenario. So, preprocessing of training data is very crucial to guarantee linearly independent sets of inputs to the network. For this purpose, KLT technique is applied to transform the high dimensional data to a lower dimension by avoiding a redundancy in the original data. In addition, the order of the training data is randomized at each epoch and the inputs are normalized so that all the inputs to the network will have a balanced impact on the network. The transformed data needs to be categorized in to a set of clusters before using the RBFGRNN. In most literatures, K-mean clustering algorithm was used to cluster the data in to K number of clusters. K-mean clustering is famous and simple to implement. In most circumstances however, the number of clusters that prevail in the data is not known apriori. Instead, we applied a hierarchical DIANA like clustering algorithm that starts with one big cluster and continuously divides the cluster until the diameter of the cluster is less than a threshold value. The feasibility of the algorithms for a multi-class data classification is verified using an E. coli data set obtained from the database of UCI's machine learning laboratory [7]. The E.coli (formally known as Escherichia coli) are named after a German paediatrician and bacteriologist Theodor Escherich who first discovered it in 1885 [8]. The E. coli dataset has 336 real valued instances with 8 attributes (7 predictive, 1 name). In the implementation we considered only the 7 predictive

This material is based in part upon work supported by the National Science Foundation under Cooperative Agreement No. DBI-0939454.

input attributes as the name is simply an ID that does not contribute for classification.

The rest of the paper is organized as follows: In sections 2 and 3 we present a detailed algorithmic description of GMDH and RBFGRNN networks respectively. Section 4 presents the methodology followed. The KLT dimensionality reduction and the DIANA like clustering algorithm techniques are also briefly explained here. Section 5 discusses the simulation results obtained and the last section concludes the paper by highlighting major achievements obtained and pointing future research directions. Finally, the appendix section displays the simulation results in tabular form.

2. GMDH

The GMDH neural network, invented by Alexey G. Ivakhnenko at the institute of cybernetics in Ukraine in 1968 [9], is based on a polynomial theory of complex systems. GMDH polynomial neural networks are self-organizing networks. The connections between neurons in the network vary during the training process so as to optimize the performance of the network [10]. The network starts only with input neurons. During the training process, neurons are selected from a pool of candidates and added to the hidden layers. Hence, the number of layers in the network is automatically selected to produce maximum accuracy without over fitting. GMDH does not require presetting of the neural network structure and it allows presenting a classification rule as a concise set of short-term polynomials. Ivakhnenko originally developed the GMDH for the purpose of building more accurate predictive models of the fish populations in rivers and oceans [9]. It is a self-organizing method which is based on sorting-out gradually complicated functional models (not necessarily polynomials) utilizing an external criterion in their evaluation on separate cross-validation data samples. The original intent of the GMDH lies in the field of forecasting, extrapolation of multivariate processes, pattern recognition, knowledge discovery and data mining. When used in its polynomial form, the GMDH answers the age-old question of how to fit a polynomial to data without over fitting [11]. Figure 1 illustrates the structure of a basic GMDH network using polynomial functions of two variables.

The first layer (at the top) presents one input for each predictor variable. Each neuron in the second layer draws its inputs from two of the input variables. The neurons in the third layer draw their inputs from two of the neurons in the previous layer and progresses through each layer in the same fashion. The layer at the very bottom draws its two inputs from the one just before it and generates a single value as an output of the network. Traditional GMDH neural networks use complete quadratic polynomials of two variables as transfer functions in the neurons.

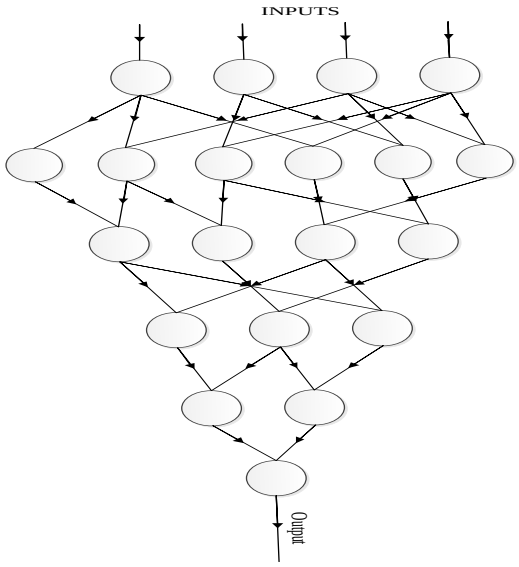

Figure 1: The structure of a basic GMDH network using polynomial functions of two variables.

A second order polynomial equation of the GMDH neural network model is shown in Equation 1. The coefficients are the values for the weight of the neuron with x1 and x2 as inputs y as an output.

$$y = a_0 + a_1 x_1 + a_2 x_2 + a_3 x_1^2 + a_4 x_2^2 + a_5 x_1 x_2 \quad (1)$$

A more simplified version of GMDH can be obtained by ignoring the square terms in equation (1). Our implementation considered both versions and the results for the simplified version are portrayed in Figures 4 to 7. And the weights and combinations of input for each of the four layers are as shown in Tables 1 to 4.

3. RBFGRNN

The RBFGRNN is an adaptation of the traditional GRNN (the Nadaraya-Watson kernel regression approximator) that was developed by Donald Specht [12]. This network is akin to the RBF network in which there is a hidden unit centered at each cluster center. These RBF units in the hidden layer are called "Gaussian Displacement Units (GDUs)" and correspond to kernel functions in the Nadaraya-Watson kernel regression approximator (see Figure 2). RBFGRNN can be used for prediction by analyzing and modeling the relation between inputs and outputs of large amount of data [13]. The KLT (also termed Principal Component Analysis in some literatures) is a linear projection technique where a high dimensional data is transformed into a lower dimension. It is a key element of many signal processing and communication tasks, including approximation, compression, and

classification. Figure 2 shows the schematic diagram of a typical RBFGRNN network.

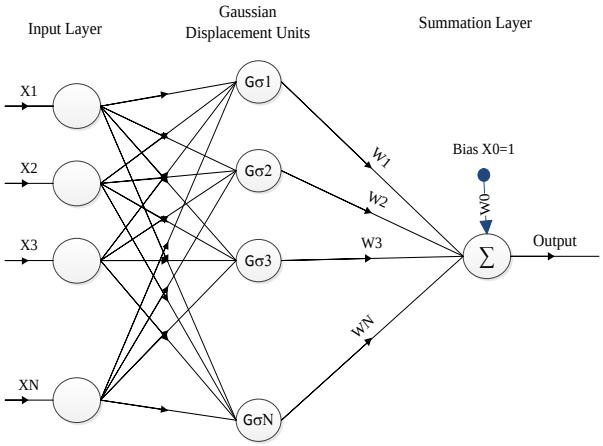

Figure 2: Architecture of a typical RBFGRNN.

The output of the GDUs is computed using equation (2).

$$g(x, c_k) = \exp(-0.5 * (x - c_k)^T Z^{-1} * (x - c_k)) \quad (2)$$

Where, the c_ks are the cluster centers and Z is the covariance matrix.

4. Methodology

The implementation is organized in to the following subsections.

4.1. Data Formatting

First, the original data downloaded from the UCI's website is formatted in a way it is suitable for training. The data is then divided in to training and testing in a 1:3 ratio (25% testing). In addition, the sequence of the events in the data is randomized for fair generalization outcome by the network. Each of the classes instances are reshuffled and equal percentage representation is maintained for each class both in the training and testing data set.

4.2. Dimensionality Reduction

The original data is transformed into a lower dimension using the KLT technique. First the covariance matrix is computed using equation (3). The Eigen values and Eigen vectors of the covariance matrix are then obtained using octave (see equation 4).

$$\text{cov } X = \frac{1}{N-1} X^T * X - mean(X)^T * mean(X) \quad (3)$$

$$[eigenvecto\,r, eigvalue] = eig(\text{cov } X) \quad (4)$$

Once the Eigen vectors and Eigen values are computed, the next step is to find the top "*dim*" Eigen values that keep 95% of the information in the original data using equation (5).

$$\frac{\sum_{i=1}^{\dim} lamda_i}{\sum_{i=1}^{N} lamda_i} >= 0.95 \quad (5)$$

Where, *dim* is the dimension of the transformed data, $lamda_i$ is the i^{th} eigen value and *N* is the number of eigen vectors. The first "*dim*" Eigen vectors satisfying equation (5) are used to form the transformation matrix *phi* given in equation (6). The *phi* matrix will be used to transform the data using equation (7)

$$phi = eigvector(:, \quad 1:\dim) \quad (6)$$

$$transformedData = X * phi \quad (7)$$

4.3. DIANA

A DIvisive ANAlysis (DIANA) is a hierarchical clustering technique that constructs the hierarchy starting with one big cluster that contains all the events, i.e. initially there is one large cluster consisting of all the objects. A DIANA like clustering algorithm is used for clustering the transformed data. At each subsequent step, the largest available cluster is split into two clusters until a stopping criterion is met. By trial and error a threshold value of 20 times the smallest nonzero distance between any two events in the data set gives the best performance and is used as stopping criteria.

Algorithmic description:

a. All vectors start out as one cluster on the buffer list.
b. Calculate the smallest none zero distance (LB) between any two events in the one cluster.
c. Divide Cluster:

For each cluster on the buffer list

i. Find the vectors (m, n) in the one cluster whose distance equals the cluster's diameter. The diameter of a cluster is defined as the largest distance between any two vectors in the cluster.
ii. For all other vectors
If vector k is closer to m, place it in group-1, otherwise place it in group-2
iii. Check Condition
If the diameter of vectors in group-1 is larger than the threshold, then place group-1 on the buffer list, otherwise place group-1 on the final list. And do the same for group-2.
iv. Remove the parent cluster from the buffer list

d. Repeat step c until no clusters exist in the buffer list.

4.4. GMDH

The GMDH network training algorithm proceeds as follows:

1. Initialize the training and testing data, iteration constant and the maximum number of layers parameters.
2. Construct the first layer which simply presents each of the input predictor variable values.
3. Construct all possible functions using combinations of inputs from the previous layer and predict the weight values.
4. Compute the Mean Absolute Error (MAE) between the regressed output at the K^{th} layer and the desired output.
5. Sort the candidate neurons in order of increasing MAE.
6. Select the best (smallest MAE) neurons from the candidate set for the next layer. A model-building parameter specifies how many neurons are used in each layer.
7. Compare the best MAE at the K^{th} layer with the best MAE at the $(K\text{-}1)^{th}$ layer.
8. Check condition
   If the error for the best neuron in the K^{th} layer is better than the error from the best neuron in the previous layer and the maximum number of layers has not been reached, then set the output of the K^{th} layer to the input of the $(K+1)^{th}$ layer and go back to step 3 to construct the next layer. Otherwise, stop the training.

When over fitting begins, the error as measured with the control data will begin to increase. Training the network should stop at this point. Figure 3 shows the layout of the program flow for the GMDH implementation.

4.5. RBFGRNN

In the RBFGRNN, the GDUs require the sample covariance matrix from the training data as well as the input cluster centers. The output of the hidden layer is fed into an optimal linear regression network to map the GDU outputs to the target training data (see figure 2). First, the KLT is applied to check linear dependency in the training data by transforming the original high dimensional data to a form that is linearly independent. Then, the transformed data is categorized into clusters around the cluster centers obtained using the DIANA like algorithm. RBFGRNN is a one pass neural network where the connection weights are computed using equation (8).

$$W = (G^T * G)^{-1} * G^T * Y_D \qquad (8)$$

Where, G is a GDU matrix whose values are computed using equation (2) and Y_D is the desired output vectors.

Once the values for the weights are determined, the regressed output of the network is calculated using equation (9).

$$Net\_Out = G * W + w_0 * bias \qquad (9)$$

Where, w_0 is the weight value associated with the bias input.

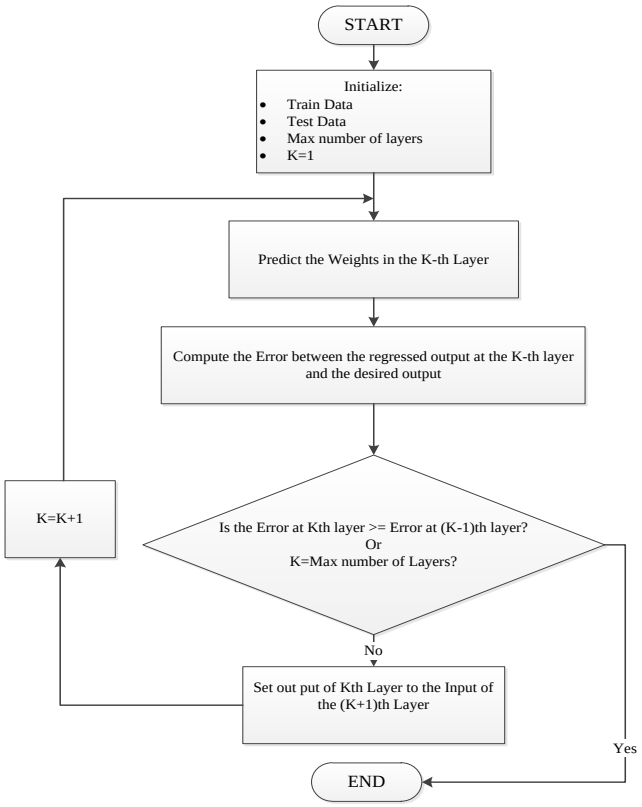

Figure 3: Program Flow Layout for GMDH.

5. Results

The performance of the two networks for solving a multi-dimensional real valued data classification is tested on an E-coli data set. The GMDH network was attempted for different best outputs (based on top best MAE values). The estimated output of the GMDH network fits with the given datasets. The performance of the network is evaluated based on the MAE for the testing date. How the network behaves for the data it has seen during the training phase is also considered. Training of the network is stopped when the MAE curve starts to increase or stops decreasing (see Figure 4). Accordingly, four layers are found to be sufficient for classifying the data. The values for the weights at each of the four layers are given in the tables in the appendix section (see Tables 1 to 4). The values for the eight cluster centers are shown in Table 5. The elbow curve (Figure 4) displays the MAE versus the number of layers for both the training and testing data. Figures 5 and 6 show a comparison of the response of the network with the desired output for the training and testing data respectively. The final architecture of the GMDH network is shown in Figure 7. Each neuron is

constrained to two inputs and one output. The a_{ij} vectors are the weights for the i^{th} and j^{th} input combinations. The input combinations are ordered by the MAE (for instance combination of inputs 1 and 3 gives the least MAE at layer 1).

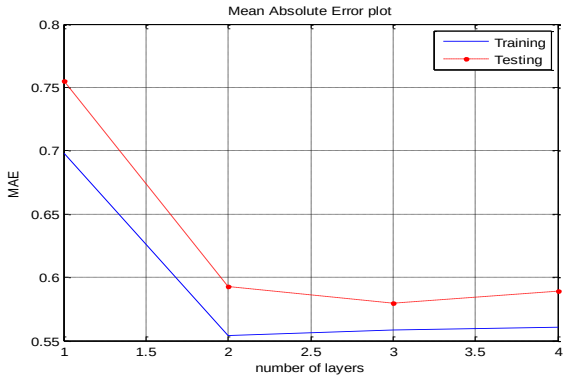

Figure 4: Mean Absolute Error (MAE) plot for the training and testing data using 6 layers.

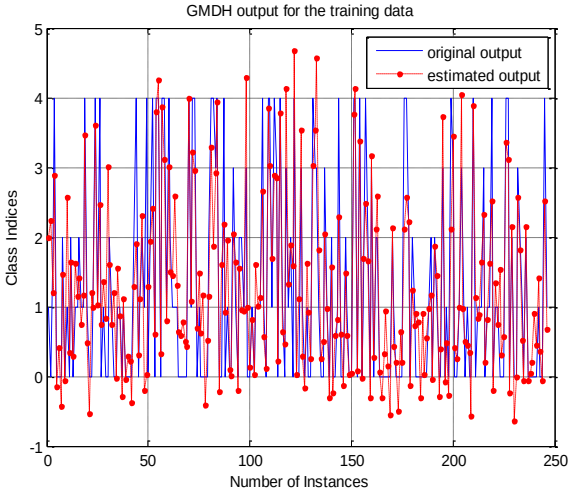

Figure 5: Actual values of the training dataset and corresponding GMDH-estimated output.

The KLT reduced the dimension of the original data from 7 to 4. It is found out that four of the Eigen values constitute more than 95% of the information in the data. Thus, the true dimension of the E. coli dataset is four. After applying the DIANA like clustering algorithm, eight cluster centers have prevailed and the data is organized around those centers based on its distance closeness. Finally, multi dimensional RBFGRNN is applied on the transformed data. The network response for the training and testing data is shown in Figures 8 and 9. The dataset has 5 classes indexed using integer numbers from 0 to 4. As can be seen from the performance curves (Figures 5, 6, 8 and 9), the output of both networks pretty much resembles the desired class indices.

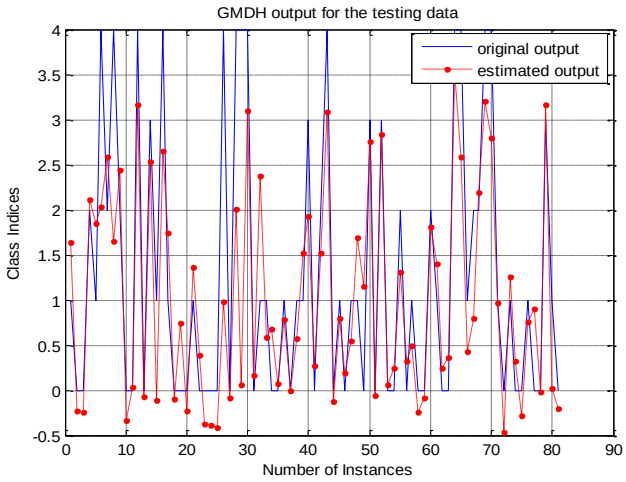

Figure 6: GMDH-estimated output versus actual values for the testing dataset.

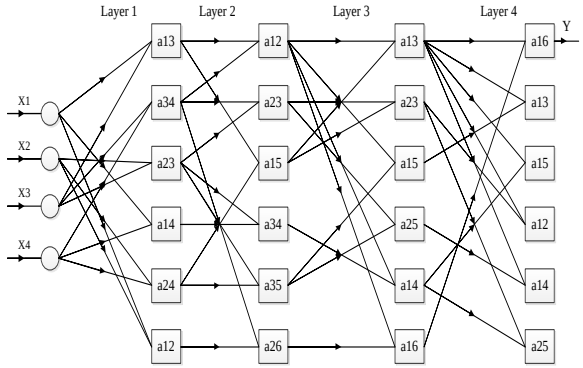

Figure 7: The architecture of the final GMDH Network after the training

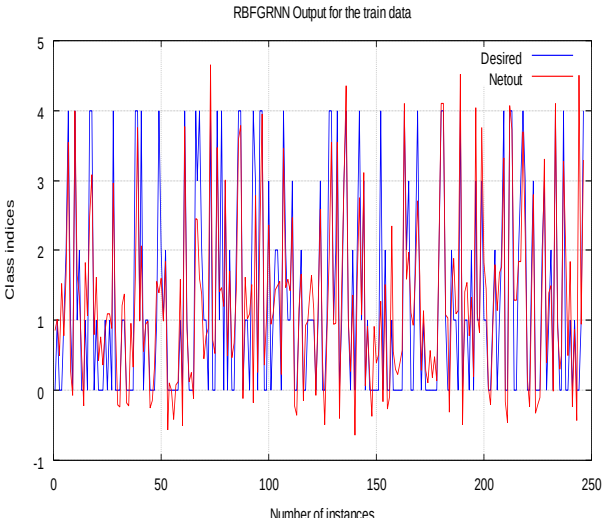

Figure 8: RBFGRNN-estimated output versus actual values for the training dataset.

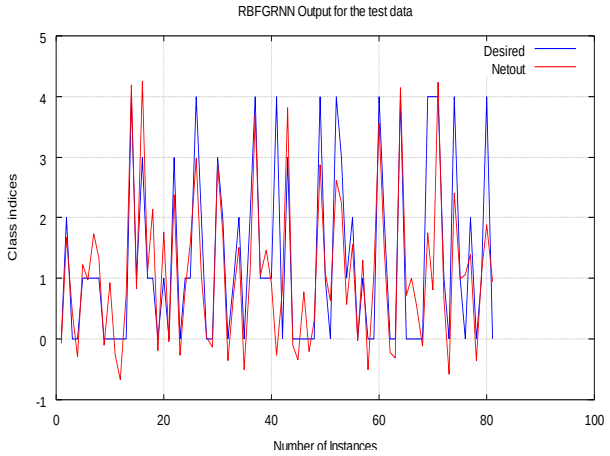

Figure 9: Output of the RBFGRNN for the test data.

As can be seen from Figure 9, the network output for the test data fairly follows the desired output. The discrepancies at some points are due to scarce training events for generalization and inadequate validation data.

6. Conclusion

This work has shown the feasibility of GMDH and RBFGRNN neural networks for classifying a multi-attribute real valued data set. The Karhunen-Loeve Transformation technique was used to avoid redundant data set in the input columns. Accordingly, the true dimension of the data was found out to be four. Considering the fitting of GMDH estimated values to given values in the database, as well as the best values of the errors as shown in the training and testing error curves, the GMDH network with six best outputs passing to the succeeding layer produced the best result. Also, it is observed that RBFGRNN is very efficient in solving a multi-dimensional classification problem as it does in approximating smooth functions. A DIANA like hierarchical clustering algorithm is used to cluster the data. The simulation results obtained proved that the regressed output of the network pretty much resembles the actual desired values. So, given enough data and an appropriately sized GDU layer, RBFGRNN and GMDH networks are very effective for classifying a multi-class data at a high precision.

7. References

[1] Deshpande, M. and George Karypis, G.,"Evaluation of Techniques for Classifying Biological Sequences", University of Minnesota, Department of Computer Science/Army HPC Research Center, 2001.

[2] Delcher, A.L, etal, "Improved microbial gene identification with glimmer", Nucleic Acid Research, pps. 4436–4641, 1998.

[3] Gusfield,D., "Algorithms on Strings, Trees, and Sequences", Cambridge University Press, 1997.

[4] Mitchell, T. "Machine Learning Algorithms", McGraw-Hill, 1997.

[5] Haykin, S., "Neural networks - A comprehensive foundation (2nd ed.)", Prentice-Hall, ISBN 0-13-908385-5, 1999.

[6] Hagan, M., Demuth,H., Beale, M.H," Neural Network Design", ISBN: 0-9717321-0-8, 2002.

[7] http://mlr.cs.umass.edu/ml/datasets/Ecoli, "UCI repository of machine learning databases".

[8] Vogt,R. and Dippold, L., "Escherichia coli O157:H7 outbreak associated with consumption of ground beef", June–July 2002. Public Health Rep 120 (2): 174–8. PMC 1497708, 2005.

[9] Ivakhnenko, A.G., "Polynomial Theory of Complex Systems", IEEE Transactions on Systems, Man and Cybernetics, vol 1, issue 4, pps 364-378, 1971.

[10] Mehra, R.K., "Group Method of data handling (GMDH): Review and experience", IEEE Conference on Decision and Control including the 16th Symposium on Adaptive Processes and a Special Symposium on Fuzzy Set Theory and Applications, Vol 16, pps 29-34, 1977.

[11] Kondo, T., "The learning algorithms of the GMDH neural network and their application to the medical image recognition", Proceedings of the 37th SICE annual conference, pps 1109-1114, 1998.

[12] Specht, D.F., " A general regression neural network", IEEE Transactions on Neural Networks, vol. 2, issue 6, pps 568-576, 1991.

[13] Lebby, G., eta'l, "Power system load modeling using a RBF GRNN with self-starting centers", IASTED PowerCon2003-Special Theme: Blackout 2003.

Acknowledgment

This material is based in part upon work supported by the National Science Foundation under Cooperative Agreement No. DBI-0939454. Any opinions, findings, and conclusions or recommendations expressed in this material are those of the author(s) and do not necessarily reflect the views of the National Science Foundation.

Appendix :

Table1: Best 6 weight vectors at layer 1

a13	a34	a23	a14	a24	a12
-3.249	-3.598	-0.772	-2.141	0.179	0.885
5.375	-8.288	-1.664	5.008	-8.571	1.092
-9.044	2.768	-4.988	2.910	1.190	-8.885
8.495	3.157	1.019	-3.669	5.636	14.788

Table 2: Best 6 weight vectors at layer 2

a12	a23	a15	a34	a35	a26
0.326	0.424	-0.962	-1.811	-0.670	-0.445
-0.472	0.659	0.959	1.418	0.847	0.855
0.572	-0.696	0.809	1.407	0.611	0.393
0.299	0.327	-0.007	-0.317	0.050	0.076

Table 3: Best 6 weight vectors at layer 3

a13	a23	a15	a25	a14	a16
-0.057	-0.085	-0.053	-0.139	-0.049	-0.085
0.789	0.825	0.990	0.976	0.743	1.245
0.284	0.305	0.106	0.262	0.331	-0.027
-0.012	-0.027	-0.024	-0.056	-0.015	-0.063

Table 4: Best 6 Weight vectors at layer 4

a16	a13	a15	a12	a14	a25
-0.036	-0.038	-0.025	-0.033	-0.029	-0.03
0.851	1.24	0.594	0.144	0.303	1.049
0.234	-0.146	0.466	0.937	0.766	0.026
-0.023	-0.026	-0.016	-0.022	-0.019	-0.021

Table 5: The Values of the 4-Dimensional 8 Cluster Centers

C1	0.383	0.019	-0.338	0.784
C2	0.434	0.081	-0.452	1.164
C3	0.505	-0.089	-0.157	1.243
C4	0.358	0.105	-0.388	1.395
C5	0.381	-0.153	-0.279	1.454
C6	0.614	0.086	-0.716	0.955
C7	0.382	-0.102	-0.728	0.870
C8	0.420	0.094	-0.314	0.560

Extracting the best features for predicting stock prices using machine learning

Ganesh Bonde
Institute of Artificial Intelligence
University Of Georgia
Athens,GA-30601
Email: ganesh84@uga.edu

Rasheed Khaled
Institute of Artificial Intelligence
University Of Georgia
Athens,GA-30601
Email: khaled@uga.edu

Abstract:-

Predicting stock price is always a challenging task. In this paper we are trying to predict the next day's highest price for eight different companies individually. For this we are using different feature sets to predict the price. It is observed that the Volume+Company and Nasdaq+S & P 500 +Company sets performed better than any other feature sets used. Also these features were very helpful for predicting stock price using sequential minimal optimization (SMO) and bagging approach. Comparing different methods, the best results were obtained using SMO and bagging.

Keywords:

Machine learning,stock market, sequential minimal optimization, bagging,

I. Introduction

For many years considerable research was devoted to stock market prediction. During the last decade we have relied on various types of intelligent systems to predict stock prices to make trading decisions. Thus numerous models have been depicted to provide the investors with more precise predictions. It has been observed that the stock price of any company does not necessarily depend on the economic situation of the country. It is no more directly linked with the economic development of the country or particular area. Thus the stock price prediction has become even more difficult than before.

These days stock prices are affected by many factors like company related news, political events, natural disasters … etc. The fast data processing of these events with the help of improved technology and communication systems has caused the stock prices to fluctuate very fast. Thus many banks, financial institutions, large-scale investors and stockbrokers have to buy and sell stocks within the shortest possible time. Thus a time span of even a few hours between buying and selling is not unusual.

Kyoung-jae [11] used support vector machines for prediction of stock price index as a time series problem. In this the effect of the value of the upper bound C and the kernel parameter δ^2 in SVM was investigated. It was observed that SVM actually performs better than back propagation and case based reasoning. This is due to the fact that SVM implements the structural risk minimization principle, which leads to better generalization than conventional techniques. Ping-Feng Pai and Chih-Sheng Lin developed a hybrid model, which is a combination of SVM and autoregressive moving average (ARIMA). This actually exploits the individual strengths of both models. Both ARIMA and SVM capture the data characteristics of linear and non-linear domains respectively. This hybrid model performs better when compared with these individual models alone.

Frank Cross [16] tries to find the relationship that could exist between stock price changes on Mondays and Fridays in the stock market. It has been observed that prices on Friday have risen more often than any other day. It has also been observed that on Monday the prices have least often risen compared to other days. Boris Podobnik [17] tries to find cross-correlation between volume change and price change. For the stock prices to changes it takes volume to move the stock price. They found two major empirical results. One is the power law cross-correlation between logarithmic price change and logarithmic volume change and the other is that the logarithmic volume change follows the same cubic law as logarithmic price change.

Many machine-learning techniques are used for predicting different target values [5,6,10]. This could be even to predict stock price. The genetic algorithm has been used for prediction and extraction important features [1,4]. Lot of analysis has been done on what are the factors that affect stock prices and financial market [2,3,8,9]. There are different ways by which stock prices can be predicted. One way is to reduce the complexity by extracting best features or by feature selection [7,13,14]. This approach will help us predict stock prices with better accuracy as the complexity reduces.

The people who invest money in the stock market usually focus only on a particular sector. For example people who want to invest money in Microsoft would not be interested in investing in a chemical industry as they cannot usually have knowledge about two different sectors. Only beginners would be interested in doing something weird like that. Thus the objective of this project is finding the relation between different companies of the same sector so that we can predict stock prices using different machine learning techniques.

II. Feature extraction based prediction

In this project we are trying to predict the highest price of the stocks of a particular company on everyday basis. There are a total of eight companies used for this experiment. These are Adobe, Apple, Google, IBM, Microsoft, Oracle, Sony and Symantec. For each company six different attributes are used. The highest stock prices for next day of these companies will be predicted using different machine learning techniques. For predicting the stock price of each company we are using eight different feature extraction techniques. These eight feature extraction techniques are explained below:-

1) Top 3 companies:-

In this type of feature extraction we are predicting the stock price of each company by finding a relation between different companies. This inter-relation between these companies will be used to predict the stock prices of a particular company in a better way. Each company's data will be individually used to predict each other company's stock price. The top three companies, which can predict a particular company with higher accuracy, will be used together to predict the stock price of a particular company. Along with the top three companies the NASDAQ index and the S&P 500 index would be used in each case.

2) Previous 3 days:-

In this the data of the previous three days for the company whose highest price we are trying to predict is used.

3) Previous 5 days:-

Similarly in this the data of the previous five days for the company whose highest price we are predicting is used.

4) Top 7 attributes:-

In this the top 7 attributes are evaluated using the ReliefFAttributeEval feature selection method. ReliefF algorithm is an extension of Relief. It is not limited to two class problems and is more robust to deal with incomplete and noisy data. The idea of ReliefF is to evaluate partitioning power of attributes according to how well their values distinguish between similar instances. An attribute is given a high score if its values separate similar observations with different class and do not separate similar instances with the same class values. For this the data of all eight companies and NASDAQ index and the S & P 500 index were used.

5) Top 10 attributes:-

In this similarly the top 10 attributes are evaluated using the ReliefFAttributeEval feature selection method. For this also the data of all eight companies and Nasdaq and S & P 500 were used.

6) Volume + Company:-

In this the volume attribute of stock purchased for each of the companies and both stock indexes i.e. NASDAQ index and the S & P 500 indexes are used. Along with this, the data of the company whose highest stock price for next day we are predicting is used for prediction.

7) Nasdaq + S & P + Company :-

In this as the name suggests, we use the NASDAQ index, the S & P 500 index and the data of the company whose highest price we are trying to predict.

8) Company alone:-

In this only the data of the company whose highest price we are predicting is used. So total attributes used in this case are six. These are the opening price, closing price, highest price, lowest price, volume and adjusted closing price.

The different machine learning techniques used for the experiments are briefly explained below:-

1) Neural Network:-

It is inspired from biological neural networks. It consists of interconnected neurons, which process information using a connectionist approach. The network adapts itself according to the information flowing into the network and tries to predict the required data.

2) Sequential Minimal optimization (SMO):-

The sequential minimal optimization solves the QP problem without any extra matrix storages and without using numerical QP optimization steps at all. The SMO decomposes the overall QP problem into QP sub-problems. It is a linear classifier that tries to find the maximum margin i.e. the distance between the classifier and the nearest data points [10,11,12].

3) Bagging using sequential minimal optimization:-

Bagging is a popular re-sampling ensemble method that generates and combines a diversity of classifiers using the same learning algorithm for the base-classifier. The learning algorithm used in this case is sequential minimal optimization. In this a standard training dataset is used which generates new training datasets using sampling. Thus we can learn different models based on the new training datasets generated. These models are combined by averaging the output or by voting to

predict the desired output. In each model the learning algorithm used is sequential minimal optimization.

4) M5P:-

For M5P, a decision-tree induction algorithm is used to build a model tree. To build this tree model divide and conquer approach is used. Secondly, the tree is pruned back from each leaf. To avoid discontinuities between the sub-trees in the model it is smoothened by combining the leaf model prediction with each node along the path back to the root, smoothing it at each of these nodes by combining it with the value predicted by the linear model for that node.

III. Experimental Setup:-

The dataset used for this experiment consists of the stock data for the last five years. Six attributes for each company are used for prediction. These are the Opening price, closing price, highest price, lowest price, volume and adjusted closing price. The values of the NASDAQ and S&P 500 indexes for the last five years are also used. These indexes also have the same six attributes. So there are a total of sixty attributes used for the experiments.

The whole data is divided into three equal sized datasets. These three datasets are sequential. So we train using the first dataset and then use the second dataset for testing. Similarly we train using the second dataset and test using the third dataset.

IV. Results:-

The prices of the stocks were predicted using mainly the four machine-learning techniques mentioned above. The results obtained by these methods are analyzed as given below:-

1) Predicting stock prices using neural network:-

When the neural network is used to predict the highest price for each company, it is observed that the feature extraction from the Company alone performed the best compared with the other feature extraction methods. The results obtained for the different datasets is given in Figures 1 and 2.

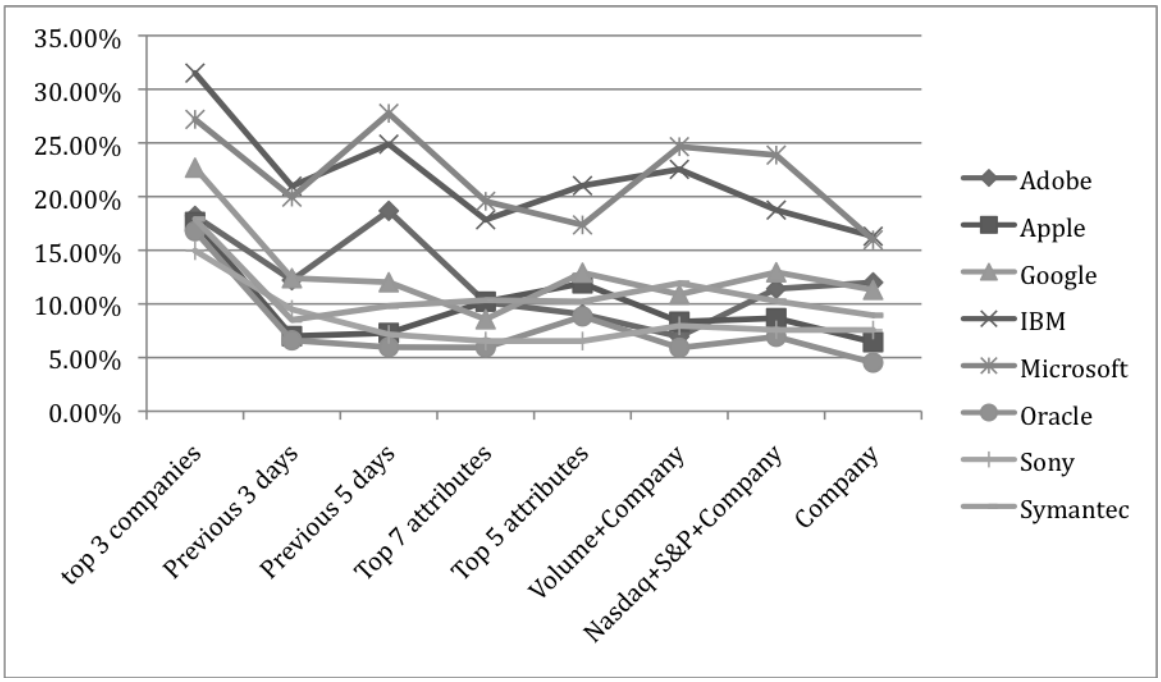

Fig 1:- This figure shows relative absolute error for predicting the highest price for eight companies using neural network. The second dataset is used as testing set in this case

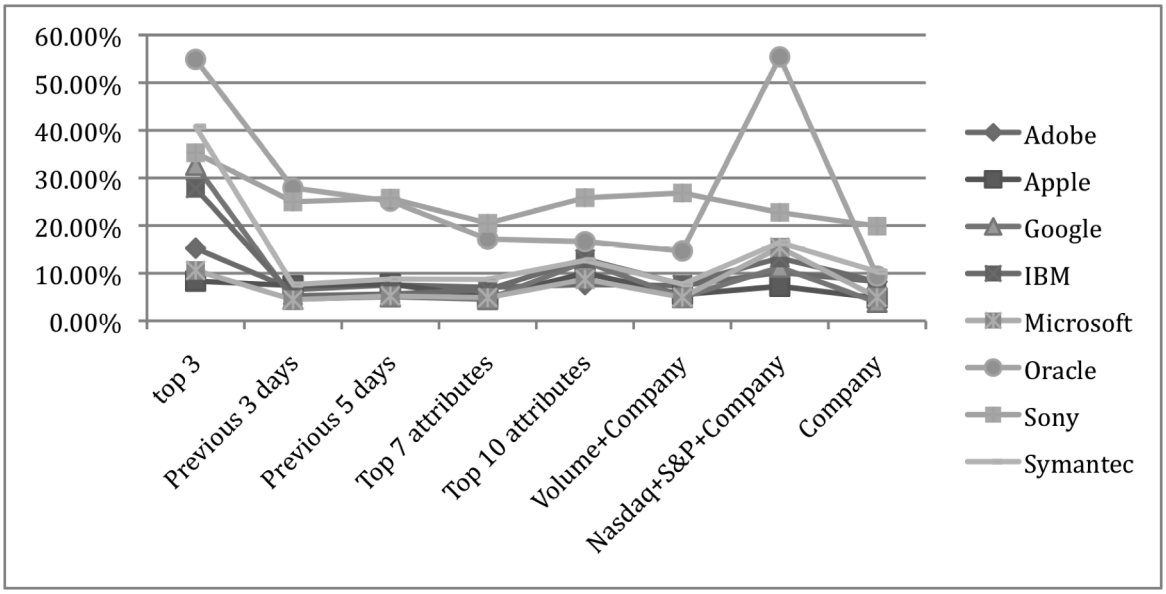

Fig 2:- This figure shows relative absolute error for predicting the highest price for eight companies using neural network. The third dataset is used as testing set in this case.

2) **Predicting stock prices using sequential minimal optimization (SMO):-**

When sequential minimal optimization is used to predict the highest price for each company, it is observed that the feature extraction methods Company + Volume and Company + NASDAQ +S & P has performed the best when compared with other feature extraction method. In this case these extraction techniques performed better than Company alone which was not the case for neural network. The other two are previous 3 days and previous 5 days. The results obtained for the different datasets are given in Figures 3 and 4.

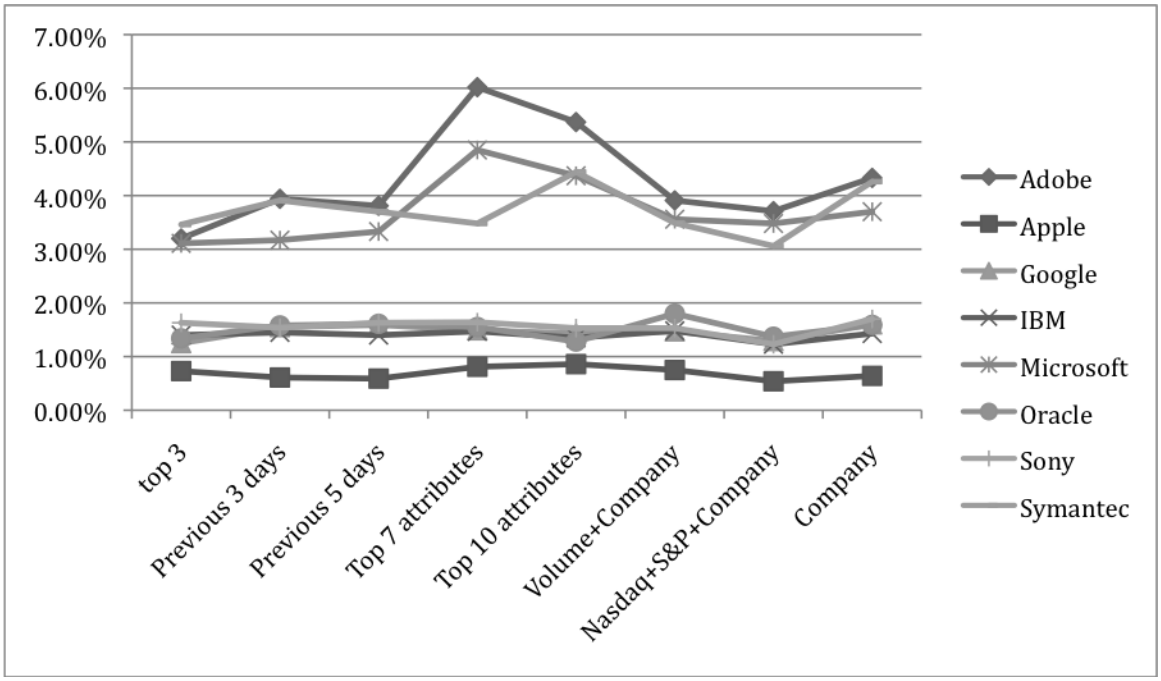

Fig 3:- This figure shows relative absolute error for predicting highest price for eight companies using sequential minimal optimization. The second dataset is used as testing set in this case.

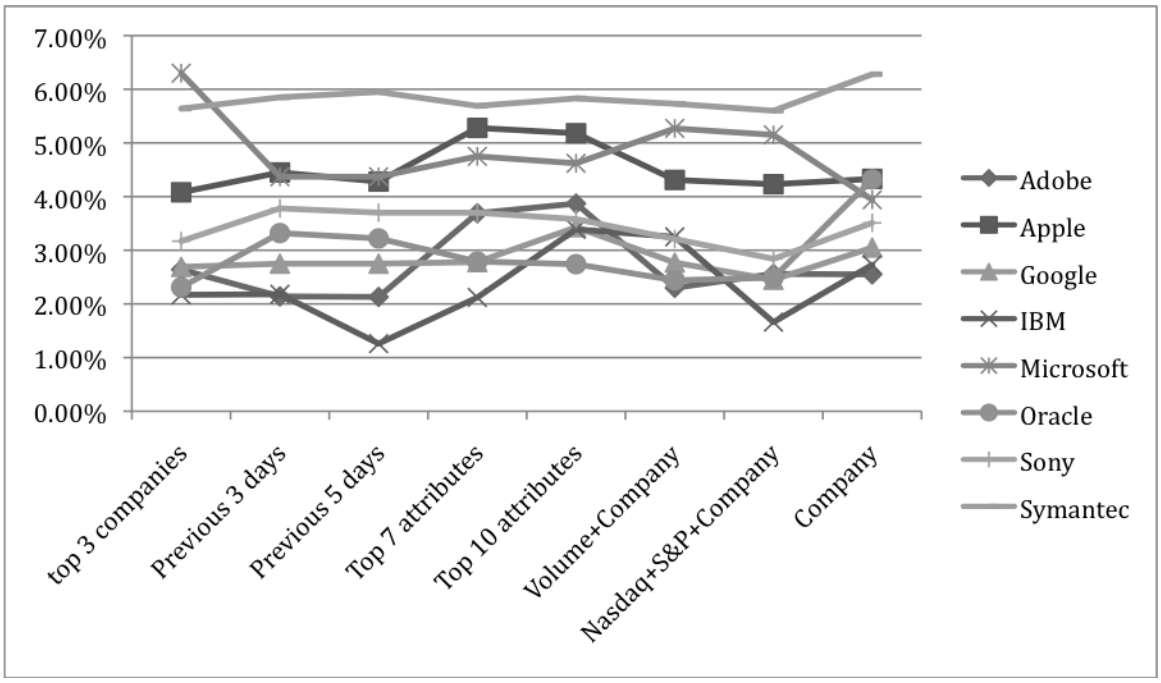

Fig 4:- This figure shows relative absolute error for predicting highest price for eight companies using sequential minimal optimization. The third dataset is used as testing set in this case.

3) Predicting stock prices using bagging:-

When bagging is used to predict the highest price for each company, it is observed that the feature extraction methods Company + Volume and Company + Nasdaq +S & P performed the best when compared with other feature extraction methods. Similar results were observed when we tried to predict the stock market using sequential minimal optimization. The results obtained for different datasets are given in Figures 5 and 6. The SMO algorithm was used internally to predict the stock price of each company.

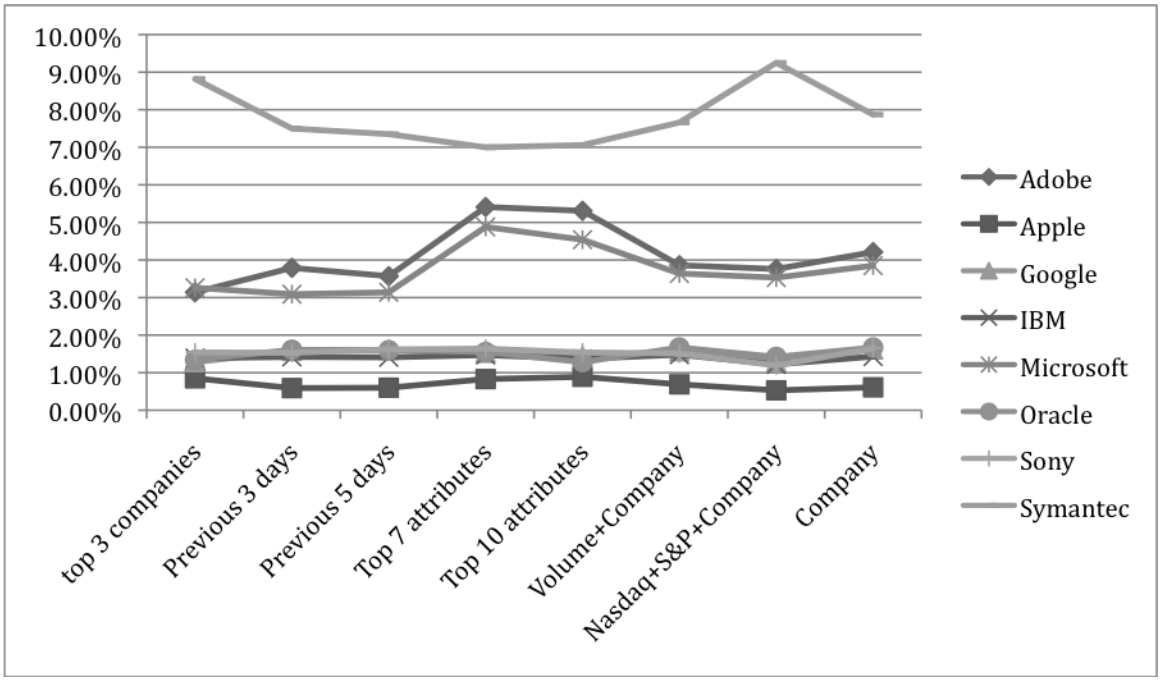

Fig 5:- This figure shows relative absolute error for predicting highest price for eight companies using bagging approach. The second dataset is used as testing set in this case.

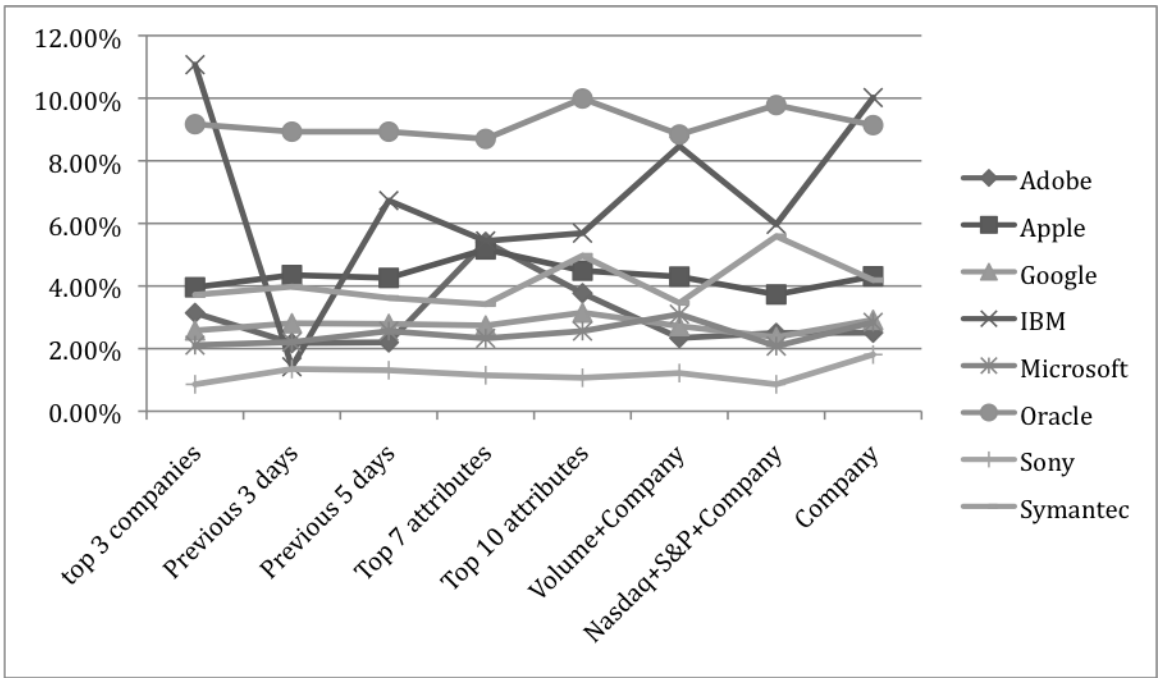

Fig 6:- This figure shows relative absolute error for predicting highest price for eight companies using bagging approach. The third dataset is used as testing set in this case.

4) **Predicting stock prices using M5P:-**

When M5P is used to predict the highest price for each company, it is observed that the feature extraction methods "Company + Volume" and "Previous 3 days" performed the best when compared with other feature extraction methods. The third best feature extraction method is Company alone. The results obtained for the different datasets are given in Figures 7 and 8.

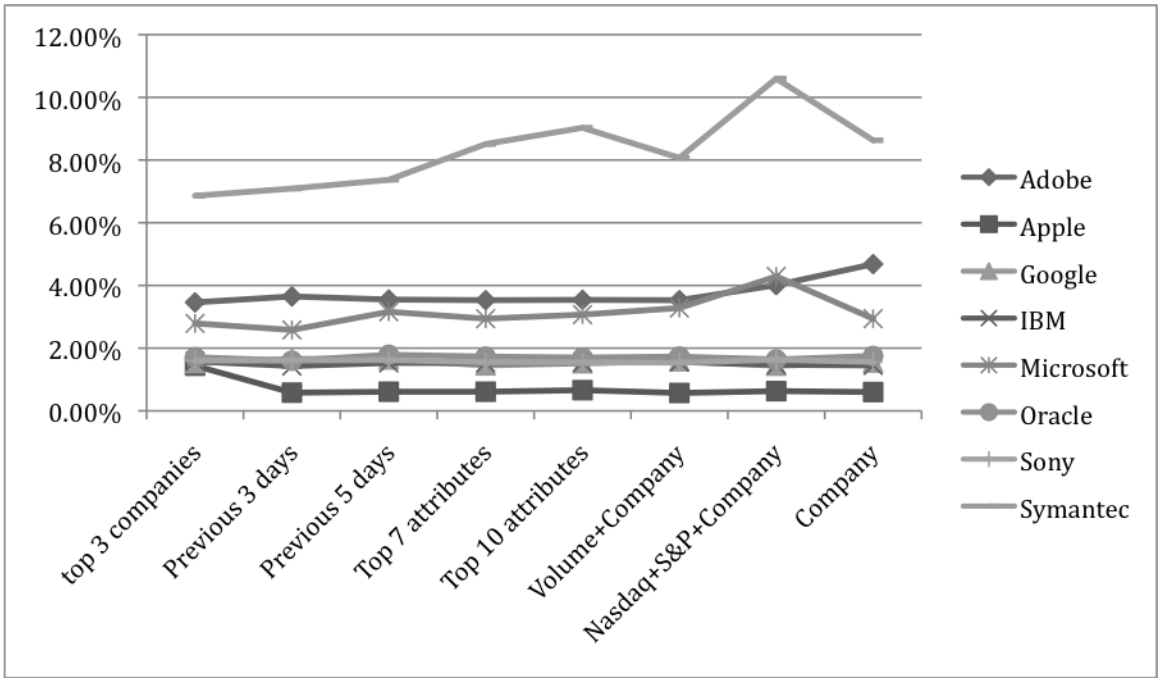

Fig 7:- This figure shows relative absolute error for predicting highest price for eight companies using M5P. The second dataset is used as testing set in this case.

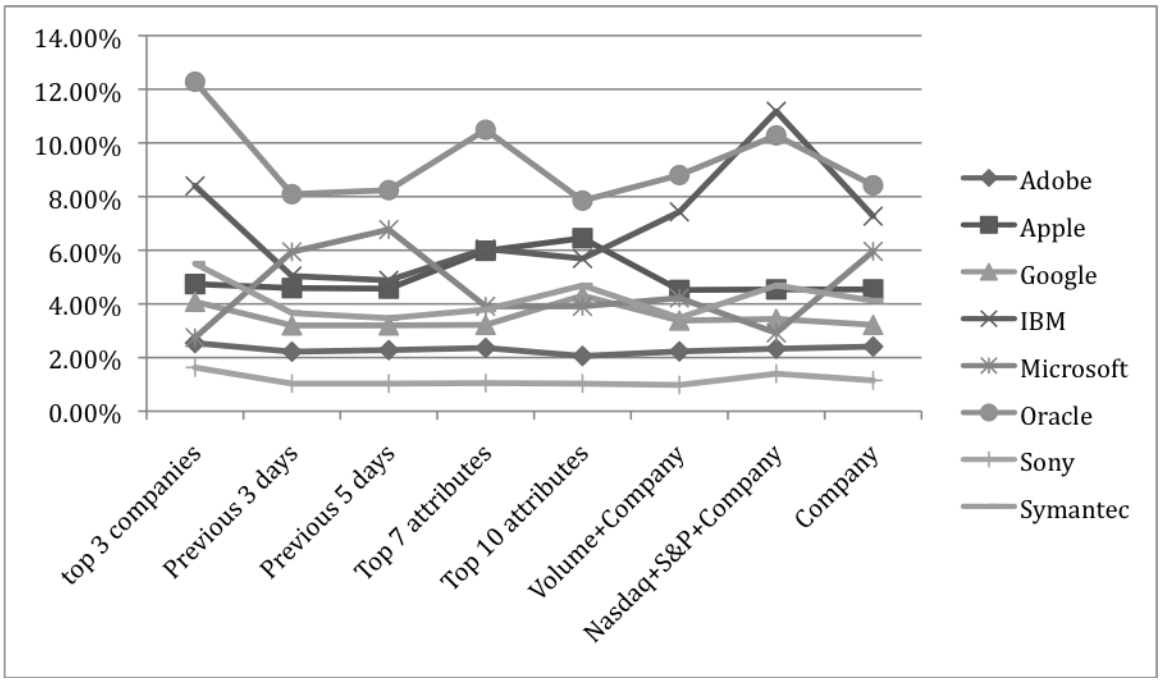

Fig 8:- This figure shows relative absolute error for predicting highest price for eight companies using M5P. The third dataset is used as testing set in this case.

V. Conclusion:-

It can be observed from Figures 1 through 8 that the best machine learning techniques for predicting the stock price are sequential minimal optimization and bagging using SMO. Using these methods the best features extracted to predict stock prices are "Volume + Company" and "Nasdaq + S & P +Company". Thus when the volume attributes of all eight companies are used along with individual data of the company whose price we are trying to predict will represent "Volume +Company". Similarly the whole data for Nasdaq, S & P 500 and individual companies data will represent "Nasdaq + S & P +Company".

Generally neural networks perform well but in this case the performance is not satisfactory. Also the results obtained using neural networks do not match the trends of the remaining learning techniques. Hence proper tuning of the different parameters is required so that neural networks may perform well like the other three learning algorithms.

REFERENCES:

[1] Abdüsselam Altunkaynak, Sediment load prediction by genetic algorithms Advances in Engineering Software, Volume 40, Issue 9, September 2009, Pages 928–934

[2] Hyunchul Ahn , Kyoung-jae Kim[b]. Bankruptcy prediction modeling with hybrid case-based reasoning and genetic algorithms approach, Applied Soft Computing,Volume 9, Issue 2, March 2009, Pages 599–607

[3] Po-Chang Ko, Ping-Chen Lin. An evolution-based approach with modularized evaluations to forecast financial distress, Knowledge-Based Systems,Volume 19, Issue 1, March 2006, Pages 84–91

[4] Kyoung-jae Kim, Ingoo Han. Genetic algorithms approach to feature discretization in artificial neural networks for the prediction of stock price index. Expert systems with Applications, 2000.

[5] Chung-I Chou, You-ling Chu and Sai-Ping Li . Evolutionary Strategy for Political Districting Problem Using Genetic Algorithm, Lecture Notes in Computer Science, 2007, Volume 4490/2007, 1163-1166.

[6] Guangwen Li, Qiuling Jia, Jingping Shi , The Identification of Unmanned Helicopter Based on Improved Evolutionary Strategy, Intelligent Computation Technology and Automation, 2009. ICICTA '09. Second International Conference on, 205-208

[7] Chih-Fong Tsai , Yu-Chieh Hsiao . Combining multiple feature selection methods for stock prediction: Union, intersection, and multi-intersection approaches, Decision Support Systems, Volume 50, Issue 1, December 2010, Pages 258–269.

[8] Xiaodong Li, Chao Wang, Jiawei Dong, Feng Wang, Xiaotie Deng, Shanfeng Zhu. Improving stock market prediction by integrating both market news and stock prices

[9] F. Mokhatab Rafiei, Manzari, S. Bostanian, Financial health prediction models using artificial neural networks, genetic algorithm and multivariate discriminant analysis: Iranian evidence, Expert Systems with Applications**,** Volume 38, Issue 8, August 2011, Pages 10210–10217

[10] George S. Atsalakis, Kimon P. Valavanis . Surveying stock market forecasting techniques – Part II: Soft computing methods, Expert Systems with Applications**,** Volume 36, Issue 3, Part 2, April 2009, Pages 5932–5941

[11] Kyoung-jae Kim. Financial time series forecasting using support vector machines, *Neurocomputing*, Volume 55, Issues 1-2 (September 2003), Pages 307-319.

[12] Ping-Feng Pai, Chih-sheng Lin. A hybrid ARIMA and support vector machines model in stock price forecasting, Omega **,**Volume 33, Issue 6, December 2005, Pages 497–505.

[13] Kyoung-jae Kim, Won Boo Lee. Stock market prediction using artificial neural networks with optimal feature transformation. Neural Computing and Applications (2004), Volume: 13, Issue: 3, Publisher: Citeseer, Pages: 255-260

[14] Kyoung-jae Kim, Ingoo Han. Genetic algorithms approach to feature discretization in artificial neural networks for the prediction of stock price index. Expert Systems with Applications, Volume 19, Issue 2, August 2000, Pages 125–132.

[15] Ajith Abraham, Baikunth Nath and P. K. Mahanti. Hybrid intelligent systems for stock market analysis. Proceedings of the International Conference on Computational Science Part 2, Pages 337-345.

[16] Frank Cross. The behavior of stock prices on Fridays and Mondays. Financial Analyst Journal Vol. 29 No. 6, pages 67-69.

[17] Boris Podobnik, Davor Horvatic, Alexander M. Peterson and Eugene Stanley. Cross-correlations between volume change and price change. Proceedings of the National Academy of Sciences of the United States of America, Vol. 106, No. 52, pp. 22079-22084, December 2009

A PERSONALIZED COURSE GENERATION SYSTEM BASED ON TASK-CENTERED INSTRUCTION STRATEGY

Heba Elbeh and Susanne Biundo

Institute of Artificial Intelligence
University of Ulm,
D-89069 Ulm, Germany
<firstname>.<lastname>@uni-ulm.de

ABSTRACT

The Course Generation System (CGS) is a system that generates a course accommodate to the teaching material, student status and learning goal. In this paper we present a framework for authoring/course generation system using ontology and an HTN planning technique called PANDA.TUTOR. This system allows the author to prepare the course structure and content, enriched with classification information without need to define the adaptation rules or specify configurations for each student, aiming to keep all the authoring process low in terms of time and effort. The course generation system, which is basically an HTN planning system, introduces a personality based planning approach, in which the course structure and the course content are generated and adapted according to students' personality and state. The system enriches with different learning scenarios, teaching strategies and learning styles. The student's personality type taken as a guide to select an appropriate scenario, teaching strategy, and learning style in order to regulate the current emotional and motivational state of student.

1. INTRODUCTION

Intelligent Tutoring System (ITS) is computer based learning which assists students in their learning process. Thus, it has the ability to be adaptable according to the needs of students. During the learning process, it is important to individualize the given course and teach students according to their personality types, cognitive capabilities and current emotional and motivational states, to achieve the learning goal efficiently. Thus, students with various personality types differ in their behavior. The process of arranging personalized adaptations is usually complex. Consequently, the current platforms usually do not provide more than a relatively simple way of personalization and adaptation. Although most of course generation systems generate a suitable course according to the student's cognitive ability, and gives some consideration to the motivation and emotion. The student's personality type, emotional appraisal and coping ways and different regulation strategies for each personality type have not been considered so far.

Course generation has long been a research field which is also known as curriculum sequencing. Two main approaches are defined in course generation field [1]: the adaptive course generation and the dynamic course generation. In the first approach, the course is generated before it delivers to the student. Indeed, it could help the student to realize the complete view about the requested concept and provides free navigation ability through the presented part. In the second approach, the student progress is observed during the interaction with the presented course, then, the presented part is adapted according to the student goals and progress. Although, this approach is appropriate with the changeable state of student, it may cause confusion for the student when s/he moves from one part to another and may not get the complete idea. Thus, our system follows the first approach.

In this paper we will introduce our system PANDA.TUTOR, a new approach of course generation in ITS, that generates a personalized course as a structured representation of the subject based on Task-Centered Instruction Strategy. The objective of our system is to build a general Authoring/Course Generation system. Thus, the course content consists of a textual description, examples, exercise and the like is prepared by the author and enriched with classification information. The course generation system is an HTN planning system. It generates the course by tailoring the learning content to an individual learner, considering the student's goal, the current emotional and motivational state of the student. Therefore, PANDA.TUTOR includes different learning strategies, learning styles and regulation strategies which help the planner to construct high individualized courses, and help students to build up their knowledge. In addition, it has the ability to adjust or maintain the student emotion.

The authoring part in our approach is defined over the course module and the course generation part is defined over the pedagogical module. Moreover, the aim of authoring phase is to

International **C**onference on **A**rtificial **I**ntelligence (ICAI-2012).

keep all the authoring process low in terms of time and effort. So, we will introduce an ontology that describes the course content module of our system. Thus, developing of the course ontology is a step toward creation shared and reusable adaptive educational systems. Also, the ontology permits the retrieval of learning materials after the pedagogical module generates the course. The proposed ontology model is a general educational ontology based on knowledge objects and the Instruction Design theory, which are introduced by Merrill [2]. Furthermore, we have considered a separation between the course Content reusability and the learning objects reusability. The authorized course afterwards is considered during the pedagogical module to construct a personalized lesson for the student.
Before introducing our proposed architecture in section 3, we will define the course generation, the relation between them and personality and learning styles in Section 2. In section 4, we will demonstrate the course ontology in our approach. Section 5 demonstrates how the HTN planning paradigm can be used to generate the personalized course. The paper ends with some concluding remarks in section 6.

2. ONTOLOGY AND E-LEARNING

The use of ontologies is a way of describing the semantics of information on the Web. Ontology provides a set of terms which should be shared among the authors, and hence could be used as well-structured shared vocabulary. Ontology is a research domain helping us to overcome the most common problems in intelligent tutoring systems[3, 4]. It enables the ontology designer and the author to share a common course structure, and the educational materials to be reused. Besides, It allows us to specify formally and explicitly the concepts that appear in a concrete domain, their property and their relationships. Aroyo et al. [5] describe how an assistant layer uses an ontology to support the complete authoring. For the course structure, Henze et al.[6] propose an approach that describes the features of the domain ontology and the learner ontology, as well as observations about the learner's interactions. Urllich[7] used the ontology to assemble the learning resources to generate a curriculum , taken into account the knowledge state of the student, the preferences an learning goals. On the other hand, there are standard meta-data, which are used to describe index, and search teaching materials; for instance,IEEE LOM, SCORM and IMS. However, these standards do not include any domain ontologies which can be specified, building on formalisms. In addition, Possible types of learning resources in LOM (Diagram, Figure, Table, Exercise, Text, Exam), mix instructional forms and resource type. On the other hand, many non-SCORM systems such as DCG [8], [9] support the pedagogical approaches but they lack the interoperability and flexibility, and they are do not support the reusability of educational materials. The contribution of our model is to build a general cognitive and constructive conceptual construction of the ontology that can be used in different types of courses. We consider a new approach to construct our ontology based on Instruction design theory of Merrill[2] as we will explain in the next sections.

3. LEARNING STYLES

learning styles are defined as "the term learning styles is used to describe the attitudes and behavior that determine an individual's preferred way of learning" [10]. Honey and Mumford itemize four learning styles as follows:

- **Active learning styles:** they prefer activity-oriented learning materials with high interactivity level, and become bored with repetition.
- **Reflective:** they like to deliberate on their experiences and study the situation from different perspectives, as well as collecting and analyzing the data before taking action. Those students prefer example-oriented learning material.
- **Theorists:** They strain to formulate their experiences in theoretical or logical form, and motive trying on ideas, theories, and experiments. they prefer exercise-oriented learning material.
- **Pragmatists:** they are eager to try out new materials, but concentrate on the concept that can help them to achieve their task, and prefer to explore and discover concepts by more abstract level. The theory-oriented learning materials are convenient for this type.

3.1. Personality and Learning Styles

The term Personality is defined as a permanent pattern of characteristics that discriminates between people in their felling thought and behavior. In PANDA.TUTOR we considered the personality types of Vollrath [11]. He defines eight types of personality based on three types Extroversion(E), Neuroticism(N), and Conscientiousness(C). The Neuroticism and Extroversion are related to stress, while conscientiousness is related to the ability of coping. These types as follows; **Spectator***(low E, low N, low C)*, **Insecure** *(low E, high N, low C)*, **Sceptic** *(low E, low N, high C)*, **Brooder** *(low E, high N, high C)*, **Hedonist***(high E, low N, low C)*, **Impulsive***(high E, high N, low C)*, **Entrepreneur***(high E, low N, high C)*, **Complicated** *(high E, high N, high C)*.
There is no single learning style that is best for all students. Many studies attempt to investigate the relation between the personality type and learning styles. Furnham [12]links between the big five factor of personality (OCEAN) and learning styles. He investigates that the Extroverts are fairly conversant with Activists and pragmatists learning style, while the introverts are reflectors. The Neuroticism is more probably theorists and reflector, and Conscientiousness interacted

positively with Activists style and negatively with theorist learning style.

4. SYSTEM ARCHITECTURE

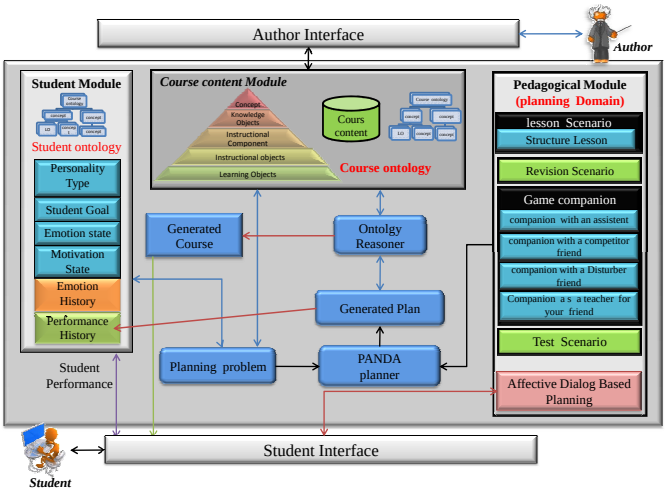

Fig. 1. The system Architecture

As depicted graphically in Figure 1, our architecture consists of three main modules: course module, student module, and pedagogical module. An authoring phase is defined over the course module and course generation phase is defined over the pedagogical module. So we have developed general educational ontologies for the student module and course module that can be used for different domains. Ontologies help us to share, reuse and reason about information. During the pedagogical module two main process are defined; the dialog process and the course generation process based on planning technique that generates the course, regarding the course module and student module.

The generated plan will be a set of querying statements that query the course ontology to retrieve the learning objects to generate the course for students.

PANDA.TUTOR includes four types of scenarios; Lesson scenario, revision scenario, companion games scenario and test scenario. The term scenario means a discrete sequence of steps inside the learning process. In these scenarios the emotional and motivational state are considered for generating the course for the concept goal.

5. COURSE ONTOLOGY IN PANDA.TUTOR

Merrill[2] defines a set of knowledge objects to describe the subject matter content or knowledge to be taught. These knowledge objects are considered as a framework to organize the knowledge base of content resources. The components of Knowledge objects are not specific to a particular subject matter domain, the same knowledge object components can be used for representing a variety of domains *(e.g. mathematics, science, humanities, technical skills, etc.)*. He describes the contents in a way that they could be manipulated in a computer system to automatically create instruction from the content. Thus, he defines five types of knowledge objects *information_about, parts_of, kinds_of(subconcept(s)), how_to (Process), and what_happens(condition or principle)*.

For each knowledge object, two levels of information are defined; *information_Level (generality)* and *a portrayal_Level*. By considering these Information levels, four instructional strategies are defined; *(Presentation (TELL)and Demonstration (SHOW))* for *Information_Level*, and *Activation (RECALL) and Application(DO))* for portrayal level.

The course space in our approach has two main sub-spaces; the course structure as the course domain space and the course content as the media space. The domain space consists of the most important concepts of course domain with different cognitive levels and relationships between them. In our work we considered the concept map approach for developing our course ontology. Concept mapping is a technique for representing concepts and their hierarchical interrelationship as a graph, which nodes represent concepts and arcs represent relationships among them [13]. While, the media space is a semantic network that is named the resource network, which is used to represent learning objects of course content. Learning objects is a unit of content of digital resources that can be shared and reused to support teaching and learning process[14].

The proposed domain is a framework for instructional design of knowledge objects from the viewpoint of ontology and semantic web. The domain ontology has been developed under OWL language. We have developed general educational ontology that can be used for different courses. This ontology is considered during the course generation to generate an adapted and personalized course. The protege 4.1 framework has been selected to edit and construct the contents.

Consequently, in our ontology six main classes are defined as a hierarchical fashion, The course space, the course concepts, the knowledge objects, the instructional strategy components, instructional objects and learning objects. Indeed, for each course, a set of concepts should be defined. For each concept different types of knowledge objects could be defined, for each knowledge object (KO) different instruction components (IC) can be defined, different instruction objects can be specified for each instruction component according to the course and the preferences of the author. Finally for each instruction object different media or learning object can be determined. In our ontology we will consider different kinds of relations; relations among Concepts, relations between the concept and its knowledge objects, relation between knowledge objects and its instructional components, relations between Instructional component and instructional objects and relations between instructional component and its teaching material types.

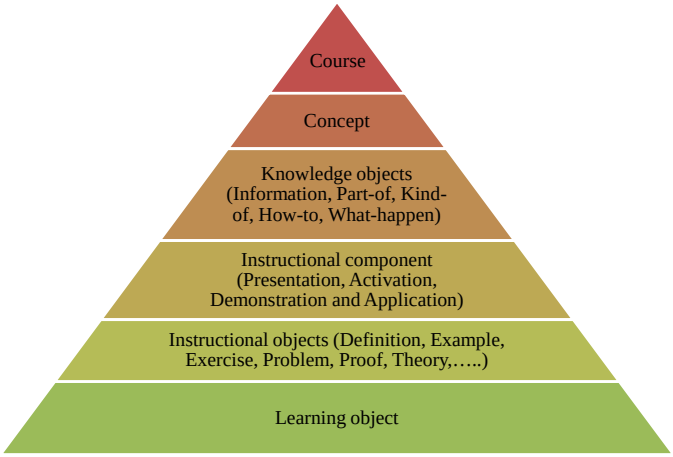

Fig. 2. Layers of course structure

These layers as depicted in figure 2 are as follows:

- **The Course layer**
  $Course \equiv Concept_1 \sqcup Concept_2 \sqcup \cdots \sqcup Concept_n$. Course class represents any course of the learning environment. It is defined as the main class which represents the subjects being taught in an educational application. The class course consists of a set of concepts that define the course. For example, the planning system or Artificial Intelligence could be individuals of this class. The course class contain several properties that describe the names and a brief description of the course: CourseName , CourseDescription and the objective. Also, different object properties (relations) are defined. , for instance HasObjective whereas hasConcept (isConceptIn is its inverse) and hasResource relations.

- **The concepts layer**
  $Concept \subseteq Course$, and $Concept \subseteq \exists has\ KO.KO$. The course in our ontology considers the concept as a main building block. Course concepts refer to basic concepts concerning the course. The concept holds one unit of knowledge and explains different aspects of it with different types of teaching material. Thus, the concept can represent as a bigger or smaller course structure part, The ontology for this model preserves the relationship between concepts as in the concept map. Thus, the author can specify various relations between concepts. In addition, the concept structure is built to represent the domain ontology that provides the structure of the course . There are different relations among concepts are considered; for instance (*has_Prerequisite, is_Prerequiste_of*), *Related_to* or *SimilarTo, OppositeOf*.

- **Knowledge objects layer**
  $KO \equiv \{Information\_About, Part\_of, Kind\_of, How\_to, What\_happen\}$, and $KO \subseteq \exists has\ IC.IC$. For each KO we should define a set of IS such that IS $\in$ (Presentation (Tell), Demonstration (Show), Activation (Recall) or Application (Do)). We represented the Knowledge_objects class as an abstract class of the Information_about, Parts_of, Kind_of, How_to and What_happen subclasses. Thus, there are relations between the concept and its Knowledge objects; *has_Information_about, is_Information_about_for*, *has_Part, is_Part_of*, *has_kind, is_kind_of*, *has_How_to, is_How_to_of*, and *has_What_happen, is_what_happen_of*.

- **Instructional component strategies layer**
  $IC \equiv \{Presentation(Tell), Demonstration(Show), Activation(Recall) or Application(Do)\}$, and $IC \subseteq \exists has\ IO.IO$. With each knowledge object four instructional components can be defined; Presentation (Tell), Demonstration (Show), Activation (Recall) or Application (Do). The relations between the knowledge objects and Instructional Components are as follows; *has_Activation, is_Activation_for*, *has_Application, is_Application_for*, *has_Demonstration, is_Demonstration_for* and *has_Presentation, is_Presentation_for*.

- **Instruction objects layer**:
  $IO \equiv \{Definition, Example, Exercise, Theory\}$, and $IO \subseteq \exists has\ LO.LO$. For each IS we should define a set of instructional objects (IO). Different IO can be assigned (by the author) for each type of instructional components. For instance, Definition, Example, Exercise, Cased_Study, Assignment, Test, Experimental, List, Condition, Action, Theory, Fact, Principle, Proof, Analysis, Description, History, Menimonic, etc. For example the author can assign Definition, or Theory or both for the Presentation component, and Problem, Case Study or Exercise for Application part.

- **Learning objects layer**
  LO=(LO_i, LO is teaching materials with different media type) where media type $\in$ (text, audio, video, ..., etc). For each type of instructional object, different forms of learning object can be assigned. The type of learning object as media type is defined the presentation format. For example text, video or audio can be assigned for the definition of the concept.

Note that, in our educational system we considered different cognitive_levels for the course parts, the quantity_level and Quality_Level. The quantity_Level is defined by the author for the course part, while quality_Level is determine according to the student achievement level. Also, Different types and levels of Example and Exercise.

6. AUTHORING PART

Authoring of adaptive Content is one of the most important activities of the course-based adaptive tutoring system. Our

goal is to help the (a non-programmer) author to build highly reusable software components that can be employed in a large number of scenarios. Thus, we introduce an ITS authoring system aim to help the teachers to configure different authorable courses with minimum effort. It is for the teacher to author, construct or modify different parts of the course and incorporate new learning materials without need for an intervention from the system developers. The authoring model allows the author to include different contents in the same concept. Moreover, there is no need to create or modify the teaching method or strategies for each student. The planning system plays the role of the teacher in our architecture. This is opposite to other systems in which the author use the authoring tool to define the Domain Model, Student Model, and rules for the Teaching Model. The author with the course module has two major missions. The first, define the course structure; it is the knowledge base of the course. The second, defines the Repository by storing all the learning and test materials. So, the following algorithm summarizes the authoring process.

Algorithm 1: Authoring Algorithm

```
Step 1 : Define the course objectives of the course.;
Step 2 : According to the course learning objectives, add
  concepts accordingly, and finally get: course
  = {Concept i | i = 1, 2, ··· m};
Step 3 : define different relations between concepts;
Step 4 : Define the data property Concept of the concept;
Step 5 : For each knowledge object of concept i =
  {Knowledge_object j | j = 1, 2, ··· }
such that Knowledge object= (information_about, Part_of,
  kind_of, how_to, what_happen);
if the concept not further has KO then
    Go to step 3 to define the next concept.;
else
    Define the different instruction strategies(IS) for its KO.
    IS= Presentation, Demonstration, Activation, and
    Application;
foreach IS do
    Define a set of IO. IO= Definition, Example, Exercise, ..;
foreach IO do
    Connect it with its learning object;
```

7. HTN PLANNING FORMAL FRAMEWORK

Our AI planner relies on a domain-independent hybrid planning framework [15]. Hybrid planning [16, 17] integrates hierarchical task network planning [18] with concepts of partial-order-causal-link (POCL) planning. The resulting systems integrate task decomposition with explicit causal reasoning. Therefore, they are able to use predefined standard solutions like in pure HTN planning. In our framework, a partial plan $P = \langle TE, \prec, VC, CL\rangle$ consists of a set of plan steps TE, i.e. (partially) instantiated task schemata, a set of ordering constraints $\prec$ that impose a partial order on the TE, and a set of variable constraints VC. CL is a set of causal links. A causal link $\langle te_i, \varphi, te_j\rangle$ specifies that the precondition φ of plan step te_j is an effect of plan step te_i and is *supported* this way. A domain model $D = \langle T, M\rangle$ consists of a set of tasks as well as a set of decomposition methods. A task $t(\overline{\tau}) = \langle prec(t(\overline{\tau})), add(t(\overline{\tau})), del(t(\overline{\tau}))\rangle$ specifies the preconditions as well as the positive and negative effects of a task. Preconditions and effects are sets of literals and $\overline{\tau} = \tau_1, \cdots \tau_n$ are the task parameters. Both primitive and abstract tasks show preconditions and effects.

A method $m = \langle t, P\rangle$ maps an abstract task t to a partial plan P, which represents an (abstract) solution or "implementation" of the task. In general, each abstract task has implemented by a number of different methods. As opposed to typical HTN-style planning, no application conditions are associated with the methods. A planning problem $\Pi = \langle D, S_{init}, P_{init}\rangle$ consists of a domain model D, an initial state S_{init}. P_{init} represents an initial partial plan.

Refinement steps include the decomposition of abstract tasks by appropriate methods, the insertion of causal links to support open preconditions of plan steps and the insertion of plan steps, ordering constraints, and variable constraints.

8. COURSE GENERATION IN PANDA.TUTOR

In PANDA.TUTOR we aim to develop an adaptive learning environment in which the course content and pedagogical aspects are adapted for each student, considering the personality type, educational progress, learning style, cognitive level and the emotional and motivational states of the student. The integration of cognitive, emotion and motivation with ITS assists students to achieve their goal. The design of the adaptive learning system requires a huge number of rules which represented in most systems as if - then rule. The proposed methodology is based on an intelligent mechanism that tries to mimic an instruction designer model. All the adaptation rules are modeled in the planning domain.

According to the current state of the student module, the planner attempts to find a sequence of operators which can achieve the student goal. An operator is much like a rule in a production system. Using the preconditions and expected effects of operators, the Planner can simulate the invocation of the various steps of a teaching plan, and thereby determine whether the plan is likely to be successful. A successful plan is one which can be applied to the current state of the student module to achieve the given goal.

PADNA.TUTOR is a constructive course generation which helps the student not only to complete their course more accurately and efficiently, but also to build new knowledge in enjoyable ways. Thus, we follow deep learning rather than surface learning. The deep learning approach encourages students to understand the concept, relate new content to the previous knowledge, which helps students to structure and or-

ganize their knowledge, which is known as task-centered instruction strategy. This approach incorporates students in the whole task early in the instructional sequence In which, each topic in a given area is taught in turn.

The instruction starts by demonstrating the first whole task in the progression. The first demonstration should be a complete task but it should be the least complex version of the whole task in the progression. This demonstration forms the objective for the task and provides the context for the students. the second task asks about the first task and introduces more information, and so on. That helps the students to easily grasp a demonstration of the whole task. Thus, getting students involved with realistic whole situations will help them to form appropriate schema and mental models. As a result, it facilitates doing application when students try to solve a new acquired knowledge and skill[2]. While the surface learning approach is interested only in a part of material and memory facts, ignoring the attempt to construct the student's knowledge. So, instructional materials in our approach that are generated for a particular learning goal are organized around specific key concepts. Our plan is generated according to the course structure especially the concept goal structure and its relations with other concepts and the student module.

The educational material provided for each concept, is organized in different levels of performance which the student should achieve in order to master the concept. Instruction strategies are adapted for the presentation of the educational material follow the student learning style.

Adaptation of the course content implies that different students receive different course version of the same concept. Our approach is adapted according to: the scenario type, the level of depth (quantity level), the student level and goal (ranging from high level overview to in-depth explanation), the level of difficulty (quality level), the learning styles, the different motivational states and different emotional states.
At the beginning, the student determines the required course and the system presents the learning content according to the student level. After that, the student selects a concept from the concept list of the course. Then, the type of learning scenario can be selected either by the student or by the system according to the student's emotional, motivational state and the performance history in the selected concept. Then the system presents a course for the selected concept.

For instance, the abstract task of the lesson scenario is *Generate_Lesson_Scenario*, for variables $?st$ of type $Student$, $?pers$ of type $Personality$, and $?Cname$ of type $Concept$. The schemata of this task is as follows:

```
Generate_Lesson_Scenario(?st: Student, ?pers:
Personality, ?Cname:Concept)
   Pre:  Studet_Personality(?St1, ?Pers)
         Selected_Scenario(?Lesson_Scenario)
         selected_Concept(?St1, ?Cname)
         Student_Performance_State(?st1,
         ?Cname, Not_Selected)
   Eff:
     Student_Performance_State(?st1, ?Cname,
     Selected)
```

The intended semantics of this schema is that the student is to be taught the specified concept. On this level of abstraction neither the learning style nor emotional and motivational state are relevant, the only significant state change concern the student personality type. We have two refinements, in which the concept is studied for first time or studied before. For the first one the abstract task is decomposed into a task network with six sub-tasks, in which the emotion and motivational states are considered and then the generated course is manipulated. With the second refinement the abstract task is decomposed into three sub-tasks according to the performance history of the student's cognitive level for the respective concept.
In the first method *(the concept is studied for the first time)*, the following sub-tasks are defined *Consider_emotional_State*, *Consider_Motivational_State*, *Teach_first_Lavel*, *Teach_Second_Lavel*, *Teach_Third_ Lavel*, *Teach_Fourth_Lavel*. The first two tasks are organized according to the emotion and motivation strategies that manipulate different emotional and motivational states. Different refinements are considered for *Consider_emotional_State* such as *increase happiness*, *decrease sadness*, *decrease fear*. The refinements of motivation task *Consider_Motivational_State* are used to *increase confidence, increase effort, maintain confidence*. The actual learn procedure, encoded by *Teach_first_Level*, *Teach_Second_Level*, *Teach_Third_Level* and *Teach_Fourth_Level*.
In our learn context, according to Task center instruction strategy, the learning process is organized in four levels:

1. In the first level, a presentation(Tell) (overview, definition, introduction,..) for the whole view of concept is introduced. This demonstration forms the objective of the concept. As well as presentation(Tell) and demonstration (Show) about the part(s) of the concept.

2. In the second level, we deliver activation (remember or recall) and application (Do) for both concept and the concept's part(s) and then teach the student presentation and demonstration about the sub-classes of concept with different learning styles.

3. In the third level, the activation application is delivered for both concept part, sub-classes and Process (How to) of the selected concept. Also, presentation and demonstration about the principle (what happen) with different learning styles are delivered.

4. In the fourth level, the student is asked to apply allKO of the concept. Finally, deliver an assignment about the whole concept to asses the student's level.

Note that, the task *Select_Learning_style* connects between the personality type and the appropriate learning style. For instance, the appropriate learning style for the personality type

Entrepreneur*(high E, low N, high C)* is the Pragmatist style. For teaching each knowledge object, four different methods are defined to represent the learning styles. For instance, to model the Pragmatist style for the concept's process (How to), the generated plan will call demonstration about the process, then presentation about the concept's process, and finally application about the process. While, in the Reflector style, the presentation will be generated then demonstration and application. The connection between the personality type and the appropriate learning style will be considered during the domain of the planning. Note that, for each KO we considered different learning styles.

9. CONCLUSION

In this paper we introduced a new personalized authoring/course generation system **PANDA.TUTOR**.
The goal of this system is to construct the student knowledge and help the author to represent the required course. Accordingly, a new approach is introduced for the course module using ontology technique, as well as for modeling the pedagogical module using the HTN planning.

ACKNOWLEDGEMENTS

This work is done within the Transregional Collaborative Research Centre SFB/TRR 62 "Companion-Technology for Cognitive Technical Systems" funded by the German Research Foundation (DFG).

10. REFERENCES

[1] Peter Brusilovsky and Julita Vassileva, "Course sequencing techniques for large-scale webbased education," *(IJCEELL*, vol. 13, pp. 75–94, 2003.

[2] M. Merrill, "A task-centered instructional strategy," *Journal of Research on Technology in Education*, vol. 40, pp. 33–50, 2007.

[3] R. Mizoguchi and J. Bourdeau, "Using ontological engineering to overcome common ai-ed problems," *International Journal of Artificial Intelligence in Education*, vol. 11, pp. 1–12, 2000.

[4] V. Devedzic, "Key issues in next-generation web based education," *IEEE Transactions on Systems, Man, and Cybernetics, Part C*, vol. 33, pp. 339–349, 2003.

[5] Lora Aroyo and Riichiro Mizoguchi, "Authoring support framework for intelligent educational systems," in *Proceedings of AI in Education, AIED-2003*. 2003, pp. 362–364, IOS Press.

[6] N. Henze, P. Dolog, and W. Nejdl, "Reasoning and ontologies for personalized e-learning in the semantic web," *Journal of Educational Technology and Society*, vol. 7, pp. 82–97, 2004.

[7] C. Ullrich, "Course generation based on htn planning," *Proc. of 13th Annual Workshop of the SIG Adaptivity and User Modeling in Interactive Systems*, pp. 74–79, 2005.

[8] J. Vassileva, "Dcg+gte: Dynamic courseware generation," *Journal of Instructional Science*, vol. 26, pp. 317–332, 1998.

[9] P. Brusilovsky, A. Kobsa, and J. Vassileva, "Adaptive hypertext and hypermedia.," *Dordrecht: Kluwer Academic Publishers*, 1998.

[10] P. Honey and A. Mumford, "The manual of learning styles," *Peter Honey Publications, ISBN: 978-0950844404*, 1992.

[11] M. Vollrath and S. Torgersen, "Personality types and coping," *Personality and Individual Differences*, vol. 29(2), pp. 367–378, 2000.

[12] Adrian Furnham, "personality and learning style: a study of three instruments," *Personality and Individual Differences*, vol. 13(4), pp. 429–438, 1992.

[13] J. D. Novak, "Clarify with concept maps," *A tool for students and teachers alike. The Science Teacher*, vol. 8(7), pp. 45–49, 1991.

[14] D. A. Wiley, "Learning object design and sequencing theory," *PhD Thesis, Brigham Young University*, 2000.

[15] B. Schattenberg and S. Biundo, "A unifying framework for hybrid planning and scheduling," *Proc. of KI'07*, pp. 361–373, 2007.

[16] S. Biundo and B. Schattenberg, "From abstract crisis to concrete relief – A preliminary report on combining state abstraction and HTN planning," *Proc. of ECP*, pp. 157–168, 2001.

[17] B. Schattenberg, A. Weigl, and S. Biundo, "Hybrid planning using flexible strategies," *Proc. of KI-05*, pp. 258–272, 2005.

[18] K. Erol, J. Hendler, and D. Nau, "Umcp: A sound and complete procedure for hierarchical task-network planning," *Proc. of AIPS*, pp. 249–254, 1994.

Hierarchical Classification using a Competitive Neural Network for Protein Function Prediction

Helyane Bronoski Borges
UTFPR– Universidade Tecnológica Federal do Paraná
PPGIa - Pontifícia Universidade Católica do Paraná
(PUCPR)
Curitiba, Brazil
helyane@utfpr.edu.br

Julio Cesar Nievola
PPGIa - Pontifícia Universidade Católica do Paraná
(PUCPR)
Curitiba, Brazil
nievola@ppgia.pucpr.br

Abstract*—Classification is a common task in Machine Learning and Data Mining. The protein function prediction can be treated as a classification problem. As protein's functions may be arranged in a hierarchy of classes, predicting the protein function is treated as a problem of hierarchical classification. *This paper presents an algorithm for hierarchical classification using the global approach, called Hierarchical Classification using a Competitive Neural Network (HC-CNN) for Protein Function Prediction. This algorithm is based on a Competitive Neural Network. It was tested in eight datasets based on Funcat and compared with algorithms from literature. The results show that the HC-CNN is an alternative in problems of hierarchical classification.

Keywords-Hierarchical Classification; Competitive Neural Network, Global Classifier

I. INTRODUCTION

Classification is one of the most important problems in Machine Learning and Data Mining. The classification consist in associating one or more classes from a set of predefined classes to an example from the database. This association of an example to a class is determined according to the features of each example.

In the context of protein functions prediction it is treated as a classification problem. A protein is considered an example of a database and biological functions are treated as classes to be provided.

The function of the proteins may be arranged in a hierarchy of classes. Thus the predicting protein is treated as a problem of hierarchical classification

A hierarchy can be defined as an ordering of elements according to their function or importance and can be represented by a tree or a directed acyclic graph (DAG).

An example of a class hierarchy is the enzymes functional classification which is structured as a tree. Another example of protein's functional classification is the Gene Ontology (GO), which is structured as a DAG.

Based on this wide diversity of problems, specific algorithms for hierarchical classification have being developed. This paper presents an algorithm for hierarchical classification based on the global approach using a competitive artificial neural network for the protein function prediction datasets. This classifier was compared with the methods Clus-HMC and Clus-HSC, developed by Vens and colleagues – Vens et al (2008).

II. RELATED WORKS

The hierarchical classification is an approach that has been widely used in text mining since the 90s. Among the work in this context can be cited Koller and Sahami (1997), Sun and Lim (2001), Sun and Lim (2003), Kiritchenko et al (2006).

The field of bioinformatics presents several problems to be solved by hierarchical classification, but it is, unfortunately, still little explored. Some works have been published using this approach, specifically in the protein function prediction, but using an hierarchical tree structure [6], [8], [9], [17], [18], [19].

In the work developed by Jensen et al. (2003), Laegreid et al. (2003) and Tu et al. (2004) the authors dismissed the class hierarchy, i.e. the concept of ancestor and descendant was not applied. Thus, one can say that the problem of hierarchical classification was transformed into flat classification problem, where the conventional classification algorithms are used.

Barutcuoglu et al. (2006), Guan et al. (2008) and Jin et al (2008), created a local binary classifier for each node. Although the set of binary classifiers represent the hierarchy of classes, there is no guarantee that they produce consistent results. Moreover, if an error occurs in a class at a certain level, this could spread to the classes of the levels below. Thus, one can say that the results presented by the authors are questionable because the approach has these drawbacks.

Vens et al. (2008) developed a hierarchical classification model for the DAG structure using the global or big-bang approach. In this work the authors discuss three kinds of classification: single-label classification (SC), hierarchical single-label classification (HSC) and multi-label hierarchical classification (HMC). For the development of these classifiers the authors used the induction of decision trees and showed how this model can be modified for use in hierarchical DAG structures.

These approaches are implemented in the CLUS and consist of generating a single decision tree for the whole hierarchy. This induction algorithm of decision tree is based on the framework Predictive Clustering Trees (PCT).

Aleksovski et al. (2009) extended the Clus HMLC developed by Vens et al. (2008), using other distance measures. The measures used by the authors were Jaccard distance, and SimGIC ImageCLEF. Such measures have been implemented in CLUS.

Otero et al. (2009) develop a new Ant Colony Optimisation algorithm, named hAnt-Miner, for the hierarchical classification problem of predicting protein functions using the GO. The algorithm proposed discovers a single global classification model in the form of an ordered list of IF-THEN classification rules which can predict GO terms at all levels of the GO hierarchy, satisfying the parent-child relationships between GO terms.

Alves et al. (2008) and Alves (2010) constructed a hierarchical classification model called Hierarchical Multi-Label Classification with an Artificial Immune System (MHCAIS), which uses concepts of an Artificial Immune System (AIS). This hierarchical classifier aims to discover knowledge represented as rules if-then.

The author presents two versions of MHCAIS: global and local. The local version builds a classifier for each class, while in the global version a single classifier is generated to distinguish all classes of the application.

The approaches of hierarchical classification Clus-HMC and Clus-HMC-HSC developed by Vens et al. (2008) and MHCAIS developed by Alves (2010) presents some advantages over those used by Jensen et al. (2003), Laegreid et al. (2003), Tu et al. (2004) and Barutcuoglu, Z. et al. (2006), Jin et al. (2008) and Guan et al. (2008). It implements the global or big-bang classification approach where the class hierarchy is considered as a whole. Thus, the prediction model built considers simultaneously all classes of the hierarchy.

III. Hierarchical Classification Hierarchical Classification using a Competitive Neural Network (HC-CNN)

One of the characteristics of a competitive network is its ability to realize mappings that preserve the topology of the input and output spaces. The learning process proposed here is based on competitive learning [16], [21], in which neurons of the output layer compete to be activated so that only one output neuron will be the "winner" of the competition process. The synaptic weight adjustments are made by the neuron that was activated and its neighbors.

The HC-CNN algorithm proposed in this work is based on a Competitive Artificial Neural Network. Figure 1 shows the neural network model. This network consists of two layers of neurons. The input layer is connected to an input vector data set. The term "Input neurons" defined in this figure represents all instances of entry, according to the interpretation of the data set. The processing layer or output layer, which in a competitive network is the output mapping, represents the hierarchy of classes, where each neuron is connected to its ancestors and possibly descendants.

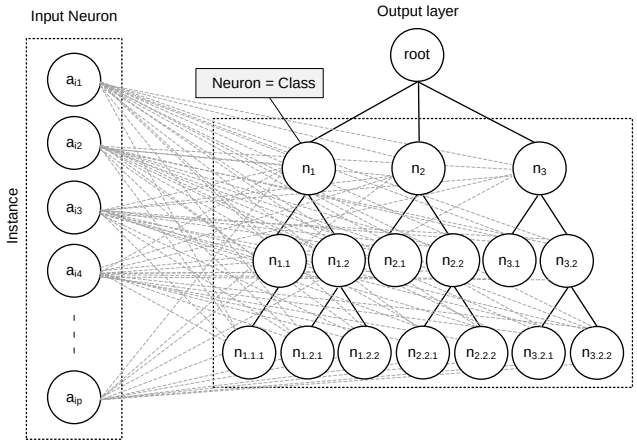

Figure 1. Example of HC-CNN.

In the traditional competitive network, for example, the Kohonen network, the neurons of the output layer are arranged in a grid network (Kohonen 1990), which can be rectangular, hexagonal, among others, and they represent the network topology. In HC-CNN algorithm the topology is a tree, where each neuron is connected with ancestors (parents) and descendent (children) neurons. These neurons (output layer) are created according to the number of classes in the hierarchy, and each neuron in the output layer is connected to all neurons of the input layer.

Neurons are stimulated by the input examples during the competitive process. In this way, it will be considered the "winner" the neuron who is more similar to the input instance selected. The comparison is made through the use of distance measures.

Prior to the training, some parameters should be defined, for instance, the amount of epochs to train the neural network and its learning rate (initial and final) which will decrease exponentially during the training, and the synaptic weights are randomly initialized. The training process of the network is divided into three phases, as in a traditional competitive network: Competition, Cooperation and Adaptation.

A. *Competition*

An instance e_i of input data set $DB_{Trein} = [e_1\ e_2\ e_3 \dots e_q]$ of dimension q is selected. Each element of DB_{Trein} consists of attributes $e_i = [a_{1i}\ a_{2i}\ a_{3i} \dots a_{li}]$, where a_{jk} is the $j-th$ attribute, $1 \le j \le l$, $l-1$ is the number of input attributes, and $i \in \mathrm{N} : l \le i \le q$, a_{li} represents the class attribute.

The neural network is created according to information obtained in the input data: the number of input neurons is equal to the number of input attributes, the output layer neurons are represented by $NN = [n_1\ n_2\ n_3 \dots n_b]$ where b is the number of class that exists in the class hierarchy. Each neuron of the

output layer consists of synaptic weights such as $n_i = [p_{1i}\ p_{2i}\ p_{3i} \ldots p_{(l-1)i}]$ that $i \in \mathrm{N} : l \le i \le (l-1)$.

To find the input vector e_i that is closest to the synaptic weights vector, distance measures are used. The measure chosen was the Euclidean distance (Equation 1).

$$d_{ik} = \sum_{i=1}^{l-1} \sqrt{(e_{ij} - n_{ijk})^2} \qquad (1)$$

where e_i is the input instance, n_{ijk} is the *k-th* neuron of output layer, l is the number of attributes and k is amount of output layer neurons.

The next step is to identify the neuron that shows the lowest distance (Equation 2). Thus, the winner neuron of the competition process of the cycle is obtained:

$$nv = \arg\min(d_i) \qquad (2)$$

Thus, the neuron of network NN that is closest to the selected input instance will be considered the winner and will stimulate their neighborhood according to the network topology.

B. Cooperation

The winner tends to excite their ancestors neurons that are closest. Thus, this phase is located in the region of the topological neighborhood that will update the weights of neurons.

In the HC-CNN algorithm, the neighborhood criterion is determined from the relationship between the neuron and their ancestors (parents of the winner neuron) and descendants (children of the winner neuron). This information is obtained through the existing relationship in the class hierarchy.

C. Adaptation

The third phase is the adaptation process of synaptic weights. Since the objective of training is to approximate the weight vectors to the input instances, because the weights of the neurons need to be adjusted so that there is a better classification of the instance e_i. If the class labels of the input instance e_i are equal to the winner neuron, then the neuron weights are adjusted so that they are closer to the instance. This is the case of a correct prediction. If the class labels of the input instance e_i are different from the labels of the predicted ones, weights will be updated to be more distant of this instance, because the class is predicted incorrectly. That is, during training, the algorithm adjusts the weights of the neuron and their ancestors, making the comparison by the identifier of the class of each input instance with the desired output.

Equation 3 shows the way the weights neurons are updated.

$$n_{ijk}(t+1) = \begin{cases} (n_{ijk} + (e_i(t) - n_{ij}(t)) * Ap(t) * Dist(t)), & \text{if the true class} \\ (n_{ijk} - (e_i(t) - n_{ij}(t)) * Ap(t) * Dist(t)), & \text{if the incorrect class} \end{cases} \qquad (3)$$

where n_{ijk} is the weight of the neuron attribute of the output layer at iteration t between the input neuron (instance) ei and the neuron k.

Ap is the learning rate for the instant of time $t+1$ which is obtained according to Equation 4.

$$Ap(t) = (\mu_i - \mu_f) * e^{-\frac{t_{current}}{C}} \qquad (4)$$

where μ_i is the initial learning rate, μ_f the end learning rate, $t_{current}$ is the current iteration and C is a constant defined for the exponential function decreases slowly.

$Dist(t)$ is the distance of winner neuron and their ancestors neurons that will have its weights adjusted as shown in Equation 5:

$$Dist(t) = 1/(k+1) \qquad (5)$$

where k is the distance in node of winner neuron and the ancestral neuron that the weights will be adjusted.

The updating of the weights of ancestor neurons follows the same method shown in the above equations (Equations 3, 4 and 5).

After the weights updating, a new instance is selected and all the procedure is repeated until all instances are selected. At the end, the first epoch of the training has been completed. Again, the procedure is repeated until the execution of all epochs.

In the last iteration of this phase the synaptic weights set of neurons is obtained and will be used in the test phase of the algorithm. Table I presents a succinct description of the HC-CNN algorithm.

TABLE I. TRAINING OF HC-CNN ALGORITHM.

INPUT
- Training data set $DB_{Trein}=[e_1\ e_2\ e_3 \ldots e_q]$ of dimension q.
STEP 1: INITIALIZE
- The initial learning rate μ_i and the final learning rate μ_f. - Determine the number of cycles *ep*. - Initialize the synaptic weights of the network: $NN=[n_1\ n_2\ n_3 \ldots n_b]$ where *b* is the number of class that exists in the class hierarchy. - Calculate the learning rate $Ap(t)=(\mu_i - \mu_f)*e^{-tcurrent/C}$ that the *tcurrent* is current iteration and *C* is a constant defined for the exponential function decreases slowly.
STEP 2: STOPPING CRITERION
- Number of cycles.
STEP 3: TRAINING
- Select an instance e_i of the input data set $DB_{Trein}=[e_1\ e_2$

$e_3 \dots e_q$].
COMPETITION:
- Calculate the distance between the instance e_i with the neurons of the network $NN=[n_1 n_2 n_3 \dots n_b]$.
- Finding neuron n_j which had the shortest distance, that are considered the winner neurons.
COOPERATION:
- Find the ancestors of the neuron *j*.
ADAPTATION:
- Update the synaptic weights of neurons and their ancestors.
- If the class true equal the predict class Dist(t)=1.
STEP 4: UPDATE
- Update the learning rate *Ap(t).*
- Go to STEP 2.
OUTPUT
- Adequate weights set.

The test of the algorithm is done similarly to training. Just as the training database, the testing database consists of instances $DB_{Test} = [x_1\ x_2\ x_3 \dots x_g]$ where g the amount of test instances. Each instance xi is composed of attributes $x_i = [a_{1i}\ a_{2i}\ a_{3i} \dots a_{li}]$, $i \in \mathrm{N} : l \le i \le g$, a_{li} represents the class attribute and l is amount attributes.

Table II shows the procedure for testing the algorithm. One can observe that it is similar to the training procedure. The main difference is that at this stage the weights are fixed from last cycle of the training phase.

TABLE II. TEST OF HC-CNN ALGORITHM.

INPUT
- Test data set $DB_{Test}=[x_1 x_2 x_3 \dots x_g]$ of g is amount of test instance.
STEP 1: STOPPING CRITERION
- Until all instances have been selected and tested.
STEP 2: TEST
- Select an instance x_i of the input data set $DB_{Test}=[x_1 x_2 x_3 \dots x_g]$.
- Calculate the distance between the instance x_i with the neurons of the network $NN=[n_1 n_2 n_3 \dots n_b]$.
- Finding neuron n_j which had the shortest distance, that are considered the winner neurons.
- Find the ancestors of the neuron *j*.
- Evaluation prediction.
- Assign result to the confusion matrix.
OUTPUT
- Accuracy rate obtained by the algorithm.

IV. EVALUATION MEASURES

Two evaluation measures were used to report the predictive performance of the samples: distance-based depth-dependent measure [8] and hierarchy based measures [12], [15]. The choice of these measures was made to assess the performance of the classification in different ways.

A. Distance-based Depth-Dependent Measures

When evaluating the result of a hierarchical prediction three situations may occur: correct prediction, partially correct prediction and incorrect prediction. To better understand these situations, each one will be exemplified.

First Possibility - Correct Prediction: There are two types of possible correct prediction. The first one occurs when the algorithm hits the full path, being the predicted class equal to the true class as shown in Figure 2.

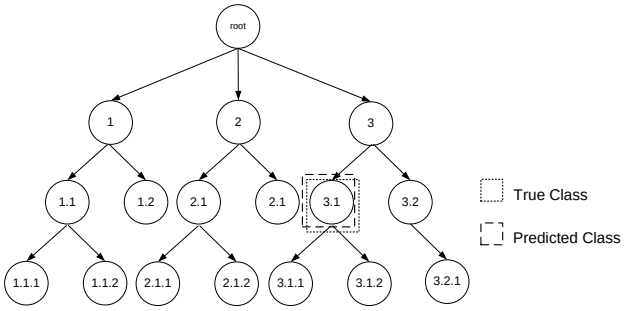

Figure 2. Example of Correct Prediction - 1st Possibility

The second case occurs when the predicted class is in the full path of the correct one, but it is more specific. Figure 3 shows this possibility: the true class is represented by the node "3" in the tree, and the algorithm predicts the node "3.1.1". This case is considered a correct prediction.

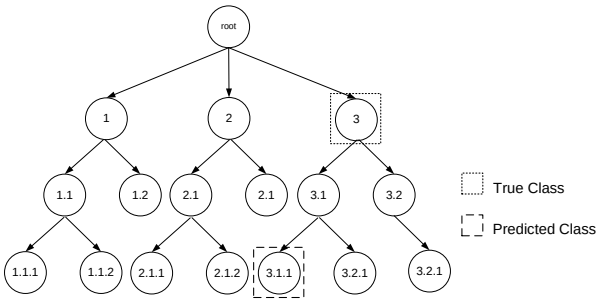

Figure 3. Example of Correct Prediction – 1nd Possibility

Second Possibility: Partially Correct Prediction: An example of a partially correct prediction is shown in Figure 5. In this case, the true class is represented by the node "2.1.1" but the algorithm predicts the class represented by the node "2.1". Observe that the node's parent node is predicted true. Although the predicted class is in the correct path it stops before finding the more detailed true class in the tree, not providing the full specificity of it. Therefore, one can say that the prediction was partially correct, because the algorithm was on the correct path of prediction, it just occurred before hitting the full specification.

An instance, whose class is predicted at higher levels, tends to be more easily classified than a class in deeper levels. Thus, the algorithm considers it a partial prediction, being based on the level of class, which means, classes at levels closer to the root have higher importance than classes at deeper levels.

In this example, the class is predicted on the second level and true class is at the third level. Then, indices of importance are assigned inversely proportional to the level of the classes, i.e., the class "2.1" is replaced by an index two times larger than the class "2.1 .1 ". Equation 6 shows the formula for this calculation.

$$1p + 2p + ... + np = 1 \quad (6)$$

where p is the index and n is the level in the hierarchy. The correct prediction rate is the sum of weights of classes correctly predicted, i.e. the predicted class and its ancestor classes. Applying the formula to this example, one obtains p=0,16. Thus, the weight of class "2.1.1" is 0.16, and the class "2.1" is 0.33 and the class "2" is 0.5. Then the hit rate of this sample is 83%.

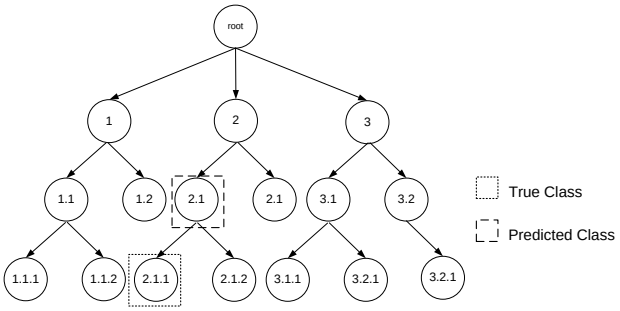

Figure 4. Example of Partially Correct Prediction.

Third Possibility: Incorrect Prediction: There is an incorrect prediction when the predicted class totally misses the path prediction as shown in Figure 5. It is observed that the true class is represented by the node "2.1.1", however, the algorithm predicts incorrectly the class as "3.2".

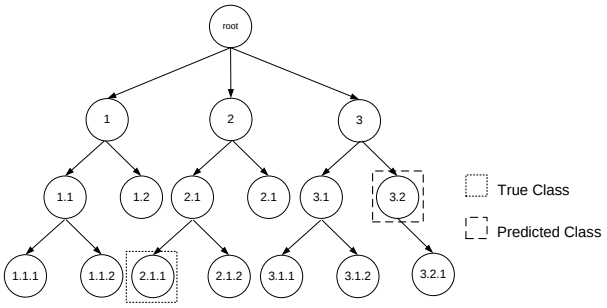

Figure 5. Example of Incorrect Prediction.

B. Hierarchy basead Measure

This kind of measure was developed by Kiritchenko et al. (2006) and uses concepts of ancestral and descendant classes. The author proposes two evaluation measures: hierarchical precision and hierarchical recall which take into account the hierarchical relationships [12], [15]. These measures are based on conventional measures of precision and recall.

These measures use the common ancestors of the true and predicted classes in the evaluation. To calculate the recall (Equation 7), the number of common ancestors is divided by the number of ancestors of the true class.

$$hR = \frac{\left|A(C_t) \cap A(C_p)\right|}{A(C_t)} \quad (7)$$

where $A(C_t)$ and $A(C_p)$ are classes that are true ancestors and predicted ancestors, respectively.

To calculate the precision (Equation 8), the number of common ancestors is divided by the number of ancestors of the predict class.

$$hP = \frac{\left|A(C_t) \cap A(C_p)\right|}{A(C_p)} \quad (8)$$

These measures can be used to calculate an extension of the F-measure (harmonic mean), named the hierarchical F-measure (Equation 9).

$$hF - Measure = \frac{(\beta^2 + 1) * hR * hP}{\beta^2 * hR * hP} \quad (9)$$

where β is the importance given to precision and recall.

V. EXPERIMENTERS AND RESULTS

Experiments to evaluate the classifier performance were performed on eight databases, four of them formed by protein G-Protein-Coupled Receptor (GPCR) and the other formed by Enzyme Commission Codes (EC). These sets were available from the authors of the work Holden & Freitas (2005). Table III shows some characteristics of these databases.

TABLE III. CHARACTERISTICS OF DATABASES

Datas Sets	Amount Samples	Amount Atributes	Amount Class	Amount Class/ Level
ECinterproFinal	14036	1216	331	6/41/96/188
ECpfamFinal	13995	708	334	6/41/96/191
ECprintsFinal	14038	382	352	6/45/92/209
ECprositeFinal	14048	585	324	6/42/89/187
GPCRinterproFinal	7461	450	198	12/54/82/50
GPCRpfamFinal	7077	75	192	12/52/79/49
GPCRprintsFinal	5422	282	179	8/46/76/49
GPCRprositeFinal	6261	128	187	9/50/79/49

The performance of HC-CNN algorithms is compared with two others algorithms: Clus-HMC and Clus-HSC. These methods are based on the concept of Predictive Clustering Trees (PCT) [5].

For the all experiments 2/3 of the examples were used for training and 1/3 for testing (hold-out procedure). In addition, all sets were normalized using the approach Min-Max. An observation to be made is that some nodes of the hierarchy

have only a few children, which causes a great unbalance in the tree.

The initial learning rate and final learning rate used in the experiments were 0.1 and 0.01, respectively. The neural network synaptic weights were generated randomly, according to a uniform distribution. The evaluation of the classification was made taking into account all levels of the hierarchy.

The results are presented based on distance-based depth dependent measure and *hF-Measure*.

For the Clus experiments were selected some thresholds to compare the performance the algorithms. Table 4 presents the results obtained with 1000 epochs for training the neural network and the thresholds 40 and 80. The term Dt_i indicates the databases in the order show of the Table 3, dist indicates distance measure and *hF* indicate *hF-Measure*.

TABLE IV. RESULTS OF EXPERIMENTERS.

	HC-CNN				Clus-HMC		Clus-HSC	
	50		**1000**		**40**	**80**	**40**	**80**
	dist	**Hf**	**dist**	**hF**	**hF**	**hF**	**hF**	**hF**
Dt1	84,1%	81,3%	85,3%	83,4%	93,5%	92,0%	93,5%	93,1%
Dt2	85,4%	83,2%	85,7%	83,6%	93,0%	92,6%	93,4%	93,2%
Dt3	85,3%	83,6%	88,0%	86,3%	93,4%	92,7%	93,4%	92,7%
Dt4	89,8%	87,5%	91,8%	90,7%	95,1%	94,4%	94,4%	93,8%
Dt5	77,5%	70,4%	75,6%	68,0%	80,4%	77,8%	80,2%	74,3%
Dt6	85,4%	60,7%	68,8%	71,8%	69,5%	65,1%	69,6%	65,0%
Dt7	79,1%	71,6%	78,7%	71,8%	79,9%	77,8%	79,9%	74,3%
Dt8	51,5%	51,1%	55,3%	47,5%	66,8%	57,8%	67,3%	59,7%

The results were statistically compared using the Friedman test [13], [14] to verify whether there is statistical significance between the differences the performances of the algorithms

Based on the results of this test, the algorithm has no statistical difference. Thus, the HC-CNN is a promising alternative to treat problems of hierarchical classification.

VI. CONCLUSION

This paper has presented a new HC-CNN algorithm for the hierarchical classification problem of predicting protein functions tree structured. The algorithm proposed is based in a competitive neural network.

This classification approach has the advantage of evaluating the predictive performance of the entire class hierarchy, reporting a single result because this method uses the global approach.

The HC-CNN was applied in eight Funcat datasets. The results of the predictions were assessed using two approaches to hierarchical classification measures: distance-based depth-dependent measure and *hF-measure*.

The experiments made in the databases obtained promising results in this first version of the classifier. Other experiments can be done using other learning rates of the neural network and the amount of cycles to train the neural network in order to compare the result of prediction.

Although the classifier has been developed to predict a single class, it can be easily adapted to hierarchical classification multi-class, whose problem is found in very diverse areas.

In addition, as future work, we intend to adapt the classifier to predict structured data in the form of a DAG.

REFERENCES

[1] Aleksovki, D.et al. 2009. Evaluation of distance measures for hierarchical multilabel classification in functional genomics. In Proc. of the 1st Workshop on Learning from Multi-Label Data (MLD), p. 5-16.

[2] Alves et al. 2008. Multi-label hierarchical classification of protein functions with artificial immune systems. In Proc. Advances in Bioinformatics and Computational Biology, v. 5167, p.1-12.

[3] Alves, R. T. 2010. Um Sistema Imunológico Artificial para Classificação Hierárquica e Multi-Label de Funções de Proteínas. Ph.D. Programa de Pós-graduação em Engenharia Elétrica e Informática Industrial, Curitiba, Paraná.

[4] Barutcuoglu, Z. et al. 2006. Hierarchical multi-label prediction of gene function. Bioinformatics. v. 22 n. 7, p. 830–836.

[5] H. Blockeel, L. De Raedt, and J. Ramon. 1998. Top-down induction of clustering trees. In International Conference on Machine Learning, p. 55–63.

[6] Blockeel, H. et al. 2002. Hierarchical multi-classification. In Proc. of the First SIGKDD Workshop on Multi-Relational Data Mining (MRDM-2002), Edmonton, Canada, July, p. 21-35.

[7] Burred, J. J. and Lerch, 2003. A. A hierarchical approach to automatic musical genre classification. In Proc. of the 6th Int. Conf. on Digital Audio Effects, London, UK, Set. p. 8-11.

[8] Clare, A. and King, R. D. Knowledge discovery in multi-label phenotype data 2001. In Proceedings of the 5th European Conference on Principles and Practice of Knowledge Discovery and Data Mining (PKDD-2001), Freiburg, Germany. p. 42-53.

[9] Clare, A. and King, R. D Predicting gene function in Saccharomyces Cerevisiae. Bioinformatics. v.19, s. 2, p. 42-49, Out. 2003.

[10] Decoro, C. et al. Bayesiana aggregation for hierarchical gene classification. In: Proc. of the 8th Int. Conf. on Music Information Retrieval, Vienna, Austria, 2007. p. 77-80.

[11] Dimitrovski, I. et al. 2008. Hierarchical annotation of medical images. In Proc. of the 11th Int. Multiconference Information Society. v. A, p. 174-177.

[12] Freitas, A. A. and Carvalho, A. C. P. F. 2007. A Tutorial on Hierarchical Classification with Applications in Bioinformatics. In: Taniar, D. Research and Trends in Data Mining Technologies and Applications. Advances in Data Warehousing and Mining. Hershey, PA, USA: IGI Publishing. Cap.7, p. 179-209.

[13] Friedman, M. 1937 The use of ranks to avoid the assumption of normality implicit in the analysis of variance. Journal of the American Statistical Association, v. 32, p. 675–701.

[14] Friedman, M. 1940. A comparison of alternative tests of significance for the problem of m rankings. In: Annals of Mathematical Statistics. v. 11, p. 86–92.

[15] Guan, Y. et al. 2008. Predicting gene function in a hierarchical context with an ensemble of classifiers. Genome Biology, v. 9, p. 1-18.

[16] Haykin, S. Redes neurais: princípios e prática. 2.ed. 2001. Tradução de, Paulo Martins Engel. Porto Alegre: Bookman.

[17] Holden, N. and Freitas, A. A. 2005. A hybrid particle swarm/ant colony algorithm for the classification of hierarchical biological data. In Proceedings of the 2005 IEEE Swarm Intelligence Symposium, Pasadena, Califórnia. p. 100-107.

[18] Holden, N. and Freitas, A. A. 2006. Hierarchical classification of G-Protein-Coupled Receptors with a PSO/ACO Algorithm. In Proceedings of the 2006 IEEE Swarm Intelligence Symposium, Indianapolis, Indiana, USA. p. 77-84.

[19] Jensen, L. J. et al. 2002. Prediction of human protein function from post-translational modifications and localization features. J. Mol. Biol. v. 319, n. 5, p. 1257-1265.

[20] Kiritchenko, S. et al. 2006. Learning and evaluation in the presence of class hierarchies: Application to text categorization. In Proc. of the 19th Canadian Conf. on Artificial Intelligence, Lecture Notes in Artificial Intelligence. v. 4013, p. 395-406.

[21] Kohonen, T. The Self-Organizing Map. Proceedings of IEEE. v.78, n.9. p-1464-1480. 1990.

[22] Koller, D. and Sahami, M. 1997. Hierarchically classifying documents using very few words. In Proc. of the 14th Int. Conf. on Machine Learning (ICML 1997), San Francisco, CA, USA, p. 170-178.

[23] Laegreid, A. et al. 2003. Predicting gene ontology biological process from temporal gene expression patterns. Genome Research. v. 13, p. 965-979.

[24] Otero, A. A et al. A Hierarchical Classification Ant Colony Algorithm for Predicting Gene Ontology Terms. In Proceedings of the 7th European Conference on Evolutionary Computation, Machine Learning and Data Mining in Bioinformatics (EvoBio 2009), LNCS 5483, pages 68–79. Springer-Verlag, 2009.

[25] Silla JR C. N. and Freitas, A. A. 2009. Novel top-down approaches for hierarchical classification and their application to automatic music genre classification. In Proc. of the IEEE Int. Conf. on Systems, Man and Cybernetics (SMC 2009). San Antonio, USA. p. 3599-3604.

[26] Silla JR C. N. and Freitas, A. A. 2010. A survey of hierarchical classification across different application domains. Data Mining and Knowledge Discovery.

[27] Sun, A. and Lim, E. 2001. Hierarchical Text Classification and Evaluation. In Proceedings of the International Conference on Data Mining (ICDM 2001), California, USA. p. 521-528.

[28] Sun, A. and Lim, E. 2003. Performance measurement framework for hierarchical text classification. Journal of the American Society for Information Science and Technology. v. 54, p. 1014-1028.

[29] Tu, K. et al. 2004. Learnability-based further prediction of gene functions in Gene Ontology. Genomics. v. 84, p. 922-928.

[30] Xue et al. 2008. Classification in large-scale text hierarchies. In Proc. of the 31st annual int. ACM SIGIR conf. on Research and development in information retrieval (SIGIR 2008), Singapore. p. 619-626.

[31] Valentini, G. 2009. True path rule hierarchical ensembles. In: Kittler J, Benediktsson J, Roli F (eds) Proc. of the Eighth Int. Workshop on Multiple Classifier Systems, Springer, Lecture Notes in Computer Science. v. 5519, p. 232-241.

[32] Vens, C. et al. 2008. Decision trees for hierarchical multi-label classification. Machine Learning. v. 73, n. 2, p. 185-214.

Comparison of Learning Rules for Adaptive Population-Based Incremental Learning Algorithms

F. Bolanos[1], **J. E. Aedo**[2], **and F. Rivera**[3]
[1]School of Mecatronics, Universidad Nacional de Colombia - ARTICA, Medellin, Colombia
[2]Electronics Department, Universidad de Antioquia - ARTICA, Medellin, Colombia
[3]Computer Science Department, Universidad de Antioquia - ARTICA, Medellin, Colombia

Abstract— *This paper describes the adaptive approach of the Population-based Incremental Learning (PBIL) algorithm, and proposes several Learning Rules aimed to improve its performance. The assessment of such alternatives was made in terms of both the convergence time and of the quality of the achieved solutions. Two classical optimization problems were used for the tests: The Job Shop Scheduling problem and the Traveling Salesman problem. The obtained results are very promising and suggest that some of the proposed learning rules have a superior performance, without degrading drastically the quality of the solutions.*

Keywords: Optimization, Adaptive algorithms, Incremental Learning, Learning Rules

1. Introduction

The use of population-based algorithms has been successful in solving highly complex optimization problems, as reported on literature [1], [2]. The success of this kind of optimization tools refers to their ability to use a population of potential solutions, to perform a parallel exploration. This parallel approach helps to avoid the local-optimum problem.

Among the different kinds of population-based approaches, Evolutionary Algorithms (EAs) are the most often used. A given EA works with a population of individuals and some rules for changing those individuals in order to reach acceptable solutions. Those rules are inspired on evolutionary processes of biological beings. Multi-Objective Evolutionary Algorithms (MOEAs) are particularly useful when optimizing several figures of merit is required, since such figures of merit are often in conflict with each other [3], [4].

PBIL optimization algorithms work also with a population of potential solutions. The main differences with respect to EAs are related with the representation and the updating process of the population [5]. In PBIL, population is represented by means of a probability array. Each probability value in the array, is related to whether a given attribute must be part or not of the final solution. The way in which the probabilities of the PBIL array are updated, in order to find an optimal, is referred as Learning Process. The updating of each probability in the PBIL array is often performed by means of an approach based on the Hebbian rule [6]. Such updating depends on a parameter called Learning Rate (LR), which controls the speed of the convergence process.

This paper describes several variations of an Adaptive Population-Based Incremental Learning (APBIL) algorithm, which adjust the learning rate parameter dynamically, in order to speeding up the convergence time. The idea is to test several learning rules (i.e. the way in which the learning rate must be modified) in order to find the best trade-off between speed of convergence and quality of the solutions. The propossed learning rules are compared with that one presented in [7], where a bell shape is suggested to change the learning rate as a function of the probability array's entropy. Although optimization algorithms may behave different when used to solve different optimization problems [8], this work provides some insight into the APBIL performance and highlights its main advantages.

This paper is organized as follows. Section II shows some previous works related to PBIL optimization algorithms. Section III shows some fundamentals about the adaptive PBIL algorithm and the learning rules proposed to improve its performance. Section IV describes the Job Shop Scheduling problem, which will be used to test the PBIL optimization approaches. Section V shows the comparison of the results provided by different approaches in terms of speed of convergence and quality of the solutions. Finally, section VI shows the concluding remarks and future work.

2. Related Work

Several works have proposed the use of PBIL for solving optimization problems [9], [10], [11]. In [10], the effect of the LR parameter on the algorithm's performance is analyzed. The design of a Power System Stabilizer (PSS) is used as case of study. This work shows that smaller learning rates, results in a high diversity of the population of solutions. Such a diversity implies a slower convergence time. On the other hand, when LR increases, the exploitation (i.e. improving and intensifying the features of the best solutions found so far) of the design space is favored and the convergence speed grows, but also may lead to find local optimals instead of the global one.

In [12], a comparison between Breeding Genetic Algorithm (BGA) and PBIL approach is performed, for the

design of a Power System Controller. BGA is a modern version of traditional evolutionary algorithms which uses the survival of the fittest as optimization mechanism, but allows a mechanism similar to artificial insemination on living beings, where the offspring may take the best attributes of its parents. Results of this work show that PBIL has almost the same performance when optimizing the power controller. The main advantage of PBIL is that it is computationally simpler and has fewer genetic operators when compared with BGA. Results also show that PBIL algorithm requires less memory and computational resources, which makes it very suitable for online implementations.

In [5], a Dual PBIL (DPBIL) algorithm is presented in order to solve a partitioning problem. As defined on that work, partitioning has the form of a binary optimization problem. The dual form of the PBIL implementation allows to improve the speed of the algorithm for finding optimal solutions. This allows the implementation of DPBIL approaches in dynamic environments, in which the optimization objective's changes over the time.

In [13], a system-level partitioning problem is solved using a PBIL approach. Unlike the DPBIL algorithm, where a probability vector is used, the non-binary nature of the system-level partitioning problem requires using a different representation for the probability array. The results show that by adjusting the learning rate parameter, convergence time is speeded up at the expense of the quality of the obtained solutions. Tuning this parameter becomes a key issue in the PBIL optimization process.

Some efforts have been conducted in order to formalize the PBIL convergence process [14], [15]. In such approaches, PBIL algorithm is modeled by means of a Markov Chain and its behaviour is approximated by using an ordinary differential equation (ODE). The idea is to prove that the corresponding ODE has only stationary points which corresponds to the optimals of the configuration space of the PBIL algorithm. These works has proven that eventually, the ODE and the associated PBIL, will converge to one of those stable points.

3. The PBIL approach

The PBIL algorithm is a stochastic search method that obtains its directional information from the previous best solutions [16]. As mentioned before, PBIL algorithms represent the population of solutions by means of an array of probabilities. In the case of binary problems, the PBIL array takes the form of a vector, which stores a probability value for each attribute of the problem to be optimized. In the case of non-binary problems, it is necessary to work with a probability matrix, in order to take into account the whole solutions space. In both cases, the idea is to update iteratively the probability values in the array, in order to that the population converges to an optimal solution.

A basic version of the APBIL approach is shown in Algorithm 1. As shown on Algorithm 1, all the values in the probability array (namely P) are initialized to $1/N$, in order to take into account all the potential solutions. At each algorithmt's iteration, a new population (Pop) is generated, based on the probabilities of the array, by means of the $Create\_Population$ routine. The attributes with the highest associated probability values, will appear with more frequency in the populationt's individuals. All the individuals of the population are assessed, using the $Evaluate\_Population$ routine. For the sake of choosing the more suitable solutions to the optimization problem at hand, the $Choose\_Best$ routine uses information about the fitness of each potential solution in the population.

In the adaptive approach of the PBIL algorithm, the Learning Rate (LR) parameter must be adjusted in order to allow both exploration and exploitation of the search space. This task is performed by the $Learning\_Rule$ routine. The Entropy (E) of the probability array is calculated and used as an estimation of the population's diversity. Once the LR parameter is calculated, the P array must be updated in order to adjust the probabilities, according to the best solution found in the population. Function $Update\_Array$ is used with this aim.

Entropy decreases as the probabilities in the PBIL array tend to concentrate on single entries of each column of the P array (i.e. when an optimal solution becomes more probable). Then, when entropy value becomes less than a given tolerance, the algorithm may stop. The optimal solution can be easily derived of the probabilities on the P array.

Let's suppose that an optimization problem can be stated as a collection of M attributes, namely Q_1, Q_2, ..., Q_M. For each attribute, there are up to N choices, in order to solve the problem. Figure 1 shows a suitable probability array, for such an optimization problem. In Figure 1, $P_{(i,j)}$ represents the probability of the j attribute to be optimized using the

Algorithm 1 Basic PBIL Algorithm

Input: An $N \times M$ probability array P
Output: An optimized solution

1: $P(i,j) = \frac{1}{N}; \forall\ 1 \leq i \leq N$ and $1 \leq j \leq M$
2: **repeat**
3: $\quad Pop = Create\_Population(P)$;
4: $\quad Fitness = Evaluate\_Population(Pop)$;
5: $\quad Best = Choose\_Best(Pop, Fitness)$;
6: $\quad E = Entropy(P)$;
7: $\quad LR = Learning\_Rule(E)$;
8: $\quad P = Update\_Array(P, Best, LR)$;
9: **until** $\{E < Tolerance\}$;

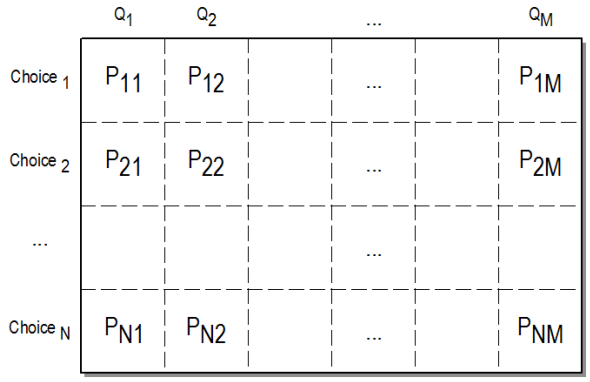

Fig. 1: A non-binary PBIL probability matrix

associated choice i. Since a single column of the matrix of Figure 1 represents the joint probability of all potential choices for a given attribute, the sum over a single column must be equal to one.

Let's suppose that after assessing a given population, it was found that for a given attribute Q_j, the best (optimal) choice is the option k. According to this, the probabilities in the array must be updated using a modified version of the Hebbian rule [17], as shown in Equation (1).

$$P_{(i,j)New} = \begin{cases} P_{(i,j)Old} + \left(1 - P_{(i,j)Old}\right) \times LR, \text{ for } i = k \\ \left(1 - P_{(k,j)New}\right) \times \frac{P_{(i,j)Old}}{1 - P_{(k,j)Old}}, \text{ for } i \neq k \end{cases} \quad (1)$$

In Equation (1), LR corresponds to the learning rate parameter. The higher the LR parameter, the fastest shall be the convergence of the algorithm, at the expense of a poorer quality of the found solutions. The adjusting of the LR parameter requires a good trade-off between quality and speed. Instead of giving to the LR parameter a fixed value, an adaptive approach varies the LR parameter whilst the algorithm converges to an optimal. The best way to do that is by calculating the systemic entropy over the PBIL array of Figure 1 [18]. In this case, systemic entropy, or simply entropy (E), may be calculated as shown in Equation (2).

$$E = -\sum_{i=1}^{N}\sum_{j=1}^{M}\left[P_{(i,j)} \times \log\left(P_{(i,j)}\right)\right] \quad (2)$$

When all problem choices are equally probable, all probabilities on the array have a value of $1/N$. In this situation, the population represented by the PBIL array has the highest diversity. Under these conditions, the maximum value of Entropy can be calculated as shown in Equation (3).

$$E_{Max} = -M \times \log\left(\frac{1}{N}\right) \quad (3)$$

When one of the choices becomes more probable than the others, entropy value decreases, meaning that the array provides less information, since some of the available options have being discarded. A value of 0 for the entropy, implies that all the attributes of the associated solution are completely defined, i.e. the PBIL algorithm has reached a unique solution.

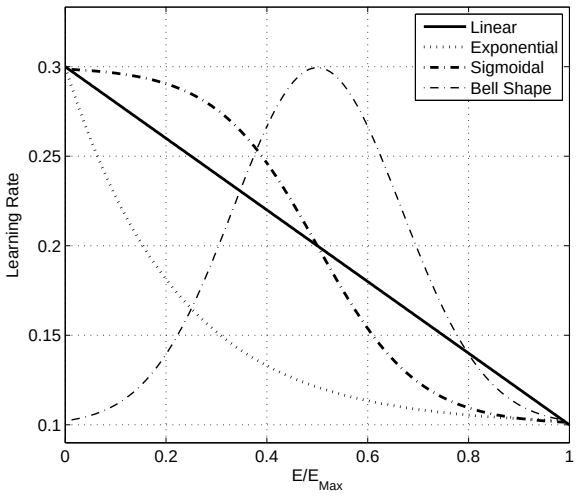

Fig. 2: Learning rules for LR between 0.1 and 0.3

The APBIL algorithm starts with high values of entropy, and they decreases as the APBIL array converges to an optimal attributes combination. Figure 2 shows three learning rules, namely linear, exponential, and sigmoidal. As shown on Figure 2, the learning rate parameter is kept at low values at the beggining of the algorithm (when entropy has maximum values), for the sake of allowing high population's diversity and exploring over all the solutions space. As the entropy decreases, as a result of the probability array updating process, the LR parameter increases, in order to improve the speed of convergence of the algorithm, and to reach the optimal solution quicker. This means that the search process allows high diversity at early iterations of the APBIL algorithm, and once the array seems to be oriented toward a given solution (low entropy), the algorithm changes the learning rate parameter, in order to speed up the convergence. Figure 2 also shows the bell shape learning rule, like that one proposed in [7]. In this case, the learning rate is kept low both at the beginning and at the end of the APBIL algorithm. The idea is to allow high population's diversity in both situations, and avoid the local optimum problem.

Concerning a multi-objective implementation of a APBIL algorithm, the main idea consists of working with several arrays (populations) independently, as is done in the island-model PBIL or IMPBIL approach [19]. As a result, at the end of the algorithm's execution, there will be several optimal solutions with different trade-offs among the objectives being optimized. There will be as much solutions as PBIL

arrays on the implementation. This implies that the learning process must be performed over several arrays, which may reduce the algorithm's performance.

Maintaining different PBIL populations generates additional problems. The first one is that a mechanism is necessary to avoid that several populations converge to the same optimal solution. As explained in [20], this may be done by using a kernel approach based on distance. The idea is that the distances among potential solutions becomes a new objective to maximize in the optimization process, in such a way that the solutions similar to an optimal in a given population, are pruned on the remaining ones.

The second problem concerning multi-objective PBIL is related to the stochastic nature of such algorithm. The random operators that are present in PBIL algorithm can lead to loosing good optimal solutions. A buffering strategy must be implemented in order to store global optimal solutions and to integrate them into the learning process while the algorithms works. Given an optimization objective, if an optimal solution is found and is better than the stored one, the previous solution is discarded and the new best solution is saved.

4. The Job Shop Scheduling optimization problem

Job Shop Scheduling [21] is a combinatorial optimization problem, which was formulated in the middle of the twentieth century. As many combinatorial optimization problems, Job Shop Scheduling is considered a NP problem, which implies that practical algorithms are aimed to find good-enough solutions instead of finding the best solutions. Scheduling is a concept related with a plethora of different optimization problems, with different levels of complexity and diverse structures too.

In order to test our adaptive PBIL algorithms, a Job Shop Scheduling problem will be used. Such a problem implies the scheduling of executable tasks in a multi-processor architecture, with several objectives to be satisfied. Three objectives were considered for optimization: the cost of the solution (N), i.e. the number of Processing Elements (PEs) required for implementing a given scheduling solution; the scheduling penalty (SP), related with tasks priorities and execution delays, and the processor occupancy (PO), which assess the eficiency in the resources usage.

The problem is stated as follows. Let's suppose a set of M independent tasks, which are going to be scheduled for their implementation over a set of up to N PEs. Although the number of tasks is well-known in advance, the number of PEs represents the first objective to be optimized in order to reduce the cost of the solution. The cheaper solution in terms of hardware cost, consists of using a single PE, which will lead to higher delays when executing the tasks. The more expensive solution implies using a single PE for each task. This enhances the performance of the designed system, because response time for each task is minimized. Due to the fact that the target architecture is homogeneous, each PE has the same cost and the execution time for a single task does not change from one specific PE to another.

A given task (T_i) has its own execution time (t_i) and a priority value (Pr_i), which ranges between 1 and Pr_{Max}. If a specific PE is assigned to execute more than one task, it is assumed that tasks will be served sequentially, using their priorities as ordering criterion. Tasks with higher priority are served before those with lower ones. The penalty for delaying a given task is calculated by means of its priority and delay to be executed. Equation (4) shows that the penalty for a specific scheduling scheme is the sum of the penalties for each task, which is defined as the product between its priority and its delay.

$$SP = \sum_{i=1}^{M} D_i \times Pr_i \tag{4}$$

In Equation (4), D_i represents the delay that a specific scheduling solution produces to the task T_i, and Pr_i is its associated priority. The system penalty (SP) is the second objective to be optimized (minimized) in the proposed scheduling problem.

Finally, the third objective to be optimized corresponds to the processor occupancy (PO) which can be simply calculated as the mean percentage of time in which processors are performing useful work (i.e. processing tasks). In this case, the PO objective must be maximized, in order to fully exploit the system's resources.

Figure 3 depicts a specific scheduling solution, in an environment of M tasks, each with a triad formed by its priority, execution time and delay. As can be seen in Figure 3, there can be up to M active PEs (the most expensive and fastest solution), but in a more efficient solution, some PEs are not used at all. Since for each PE, tasks are served on a priority basis, from the figure it can be said that priority of task T_1 is higher than priority of tasks T_i and T_M. Also, task T_1 is served first on PE_1, so the associated delay for such a task is equal to zero. Delays for remaining tasks shall depend on the subsequent execution order.

5. Experimental Results

Four APBIL Learning Rules (namely linear, sigmoidal, exponential and bell-shape) were tested in order to compare them and find the best trade-off between performance and quality for the optimization problems at hand. Such learning rules are depicted in Figure 2 and Table 1 shows their formal specification. In order to perform an equable comparison, this specification represents the only difference among the implementation of the adaptive algorithms. As shown in Table 1, LR depends on the entropy (E) of the PBIL array, as well as on the LR_{Min} and LR_{Max} parameters, which

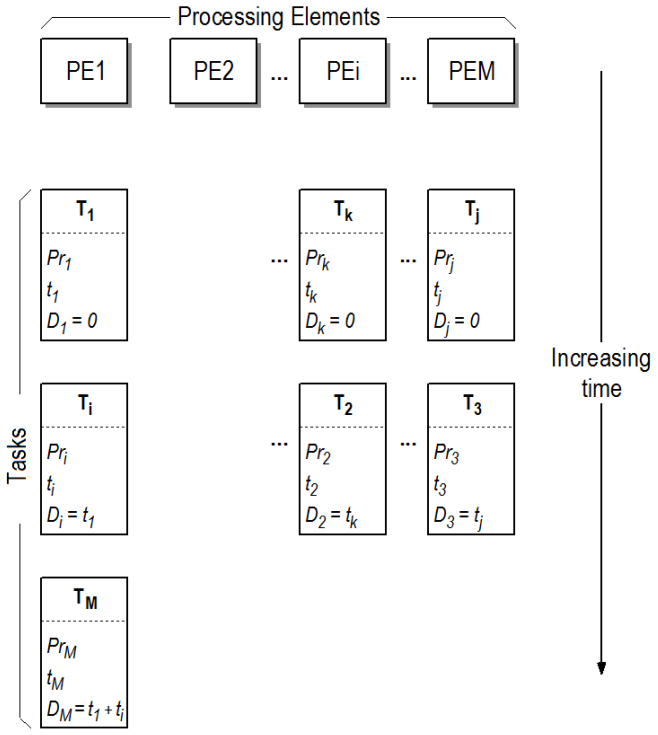

Fig. 3: A given scheduling solution

represent the minimum and maximum values for LR. For all the executions of the APBIL algorithm reported in this section, the LR_{Min} and LR_{Max} values were set to 0.1 and 0.3, respectively.

For comparison purposes, a classical Multi-Objective Evolutionary Algorithm (MOEA) was also implemented [22]. Each algorithm was used to solve the Job Shop Scheduling problem with different sizes (M).

All the algorithms were aimed to simultaneously optimize three objectives, as pointed in previous section: scheduling penalty (SP), processor occupancy (PO) and the number of PEs (N). The algorithms were tested using Matlab on a PC with an Intel Core I7 processor and 8 Gigabytes of memory.

Table 1: Formal specification of learning rules

Linear	$LR = LR_{Max} - \frac{E}{E_{Max}} \times (LR_{Max} - LR_{Min})$
Exponential	$LR = LR_{Min} + (LR_{Max} - LR_{Min}) \times e^{-4.5 \times \frac{E}{Emax}}$
Sigmoidal	$LR = LR_{Max} - \frac{LR_{Max} - LR_{Min}}{1 + e^{-10 \times \left(\frac{E}{Emax} - 0.5\right)}}$
Bell Shape	$LR = LR_{Min} + \frac{LR_{Max} - LR_{Min}}{\sqrt{2 \times \pi}} \times e^{-\frac{\left(\frac{E}{Emax} - 3\right)^2}{2}}$

Figure 4 depicts the mean convergence time for the

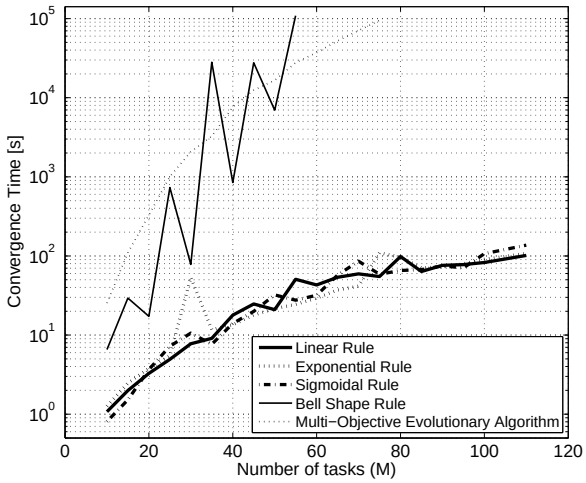

Fig. 4: Mean convergence time for the different optimization strategies

mentioned algorithms, as a function of the optimization problem's size (M). As can be seen, convergence times for MOEA and bell-shaped algorithms, becomes restrictive when dealing with higher values of M. In such cases, the execution of the algorithm was forced to stop.

Learning rules for the adaptive approaches in Figure 4, are the same depicted in Figure 2. As can be seen, there is no remarkable difference between the monotonically-increasing learning rules (linear, exponential and sigmoidal), except for a peak given on the exponential rule, for a problem size of thirty tasks. On the contrary, MOEA and bell-shaped PBIL has very poor convergence times, often several orders of magnitud above the proposals with monotonically-increasing learning rules.

With respect to the bell-shaped learning rule, it does not seems logical to decrease the learning rate at the end of the process of convergence. When a PBIL algorithm is performing the last stages of the space exploration, the probabilities in the algorithm's array tend to be concentrated on single positions of each column, which points toward the optimal solution. The results in Figure 4 suggest that there is no need to guarantee population's diversity at final stages of the PBIL algorithm's execution.

The MOEA algorithm was implemented using a vector representation for each solution on the population. Each entry in the solution's vector represents the implementation resource for a given system's task. This means that each vector on the population has a lenght of M elements. A single crossover operator was used for recombination, and the mutation was made by means of a change of a single value on a given vector position. A round-robin method and a $\mu + \lambda$ strategy was used for selection purposes [23]. As can be seen in Figure 4, MOEA's performance is very poor

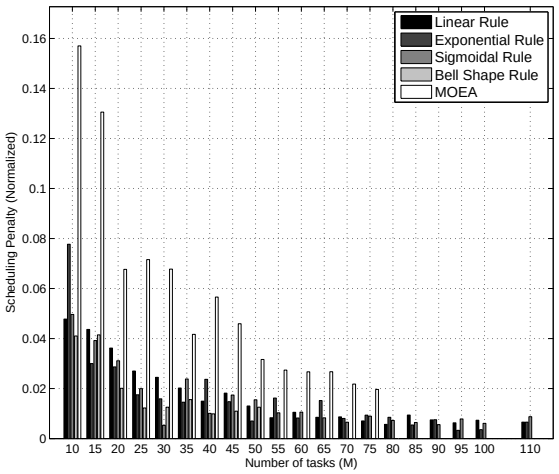

Fig. 5: Scheduling penalty for several optimization approaches

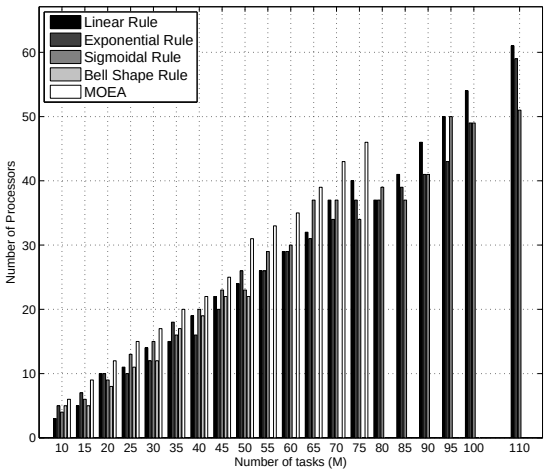

Fig. 7: Number of processors for several optimization approaches

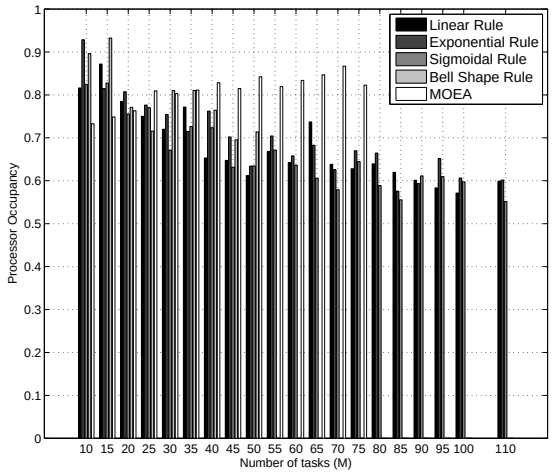

Fig. 6: Processor occupancy for several optimization approaches

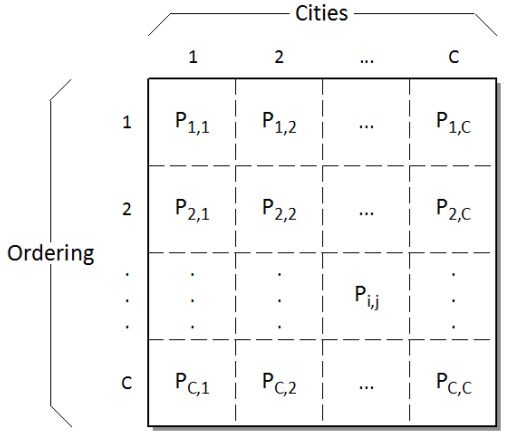

Fig. 8: A PBIL probability array representation for the TSP problem

when compared with the best APBIL algorithms because it does not have an adaptive behavior.

None of the results shown in Figure 4 would be relevant without a comparison between the quality of the solutions obtained with each approach. Figures 5, 6 and 7 show the best solutions found by each optimization algorithm, according to the objectives defined in the previous section. As can be seen, there is no remarkable differences among the PBIL algorithms, although MOEA strategy shows better solutions concerning processor occupancy. However, MOEA's quality concerning the remaining criteria (SP and N) is always poorer than those for PBIL approaches.

For the sake of providing a further insight into the performance of the proposed learning rules, a traveling salesman problem (TSP) optimization algorithm was implemented. TSP is one of the most famous NP-complete problems [24]. Given C cities, the goal is to find a minimum lenght tour which visits each city exactly once. The PBIL array used to represent such an optimization scheme is shown in Figure 8. As can be seen, the PBIL array takes the form of a $C \times C$ probability matrix. In that figure, $P_{i,j}$ represents the probability of visiting city j in the i_{th} place.

Three APBIL approaches were implemented in order to solve TSPs of several sizes. These approaches correspond to the three monotonically-increasing learning rules described before, i.e. linear, sigmoidal and exponential. The TSPs were

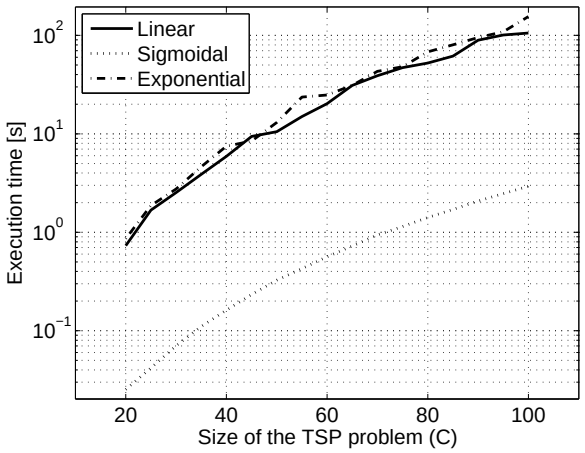

Fig. 9: Execution time for the different TSPs

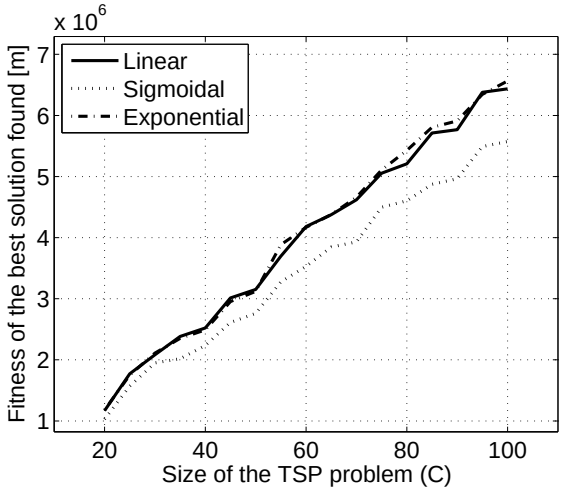

Fig. 10: Total traveled distance for several TSP problems

created by distributing randomly a total of C cities in an area of 10000 square kilometers. In order to assess the quality of the solutions provided by the APBIL search, the total traveled distance by the salesman, measured in meters, was used as a fitness value.

Figure 9 shows the mean convergence times for each APBIL implementation, for different sizes of the TSPs. Again, the only difference among APBIL implementations was the learning rule used to update the LR parameter. The sizes of the TSPs ranges from 20 to 100 cities. As mentioned in [24], complexity of the TSP problem grows very quicly with the value of C, so using larger sizes may be restrictive for simulation.

Figure 9 shows that sigmoidal learning rule has a better performance when compared with linear and exponential rules, for TSP optimization problems. Execution times related with sigmoidal learning rule are always almost an order of magnitud below the remaining alternatives, and such a trend prevails over all the range of the TSP size.

Figure 10 shows the total traveled distance for the three implementations of the APBIL algorithm. As can be seen on that figure, total traveled distance of the solutions obtained from sigmoidal learning rule are up to 16 % below of traveled distance of the remaining approaches.

According to the previous discussion, keeping low values of the LR parameter allows high population's diversity. As can be seen on Figure 2, the sigmoidal learning rule allows high population's diversity at early stages of the exploration process (i.e. when entropy values are near to its maximum). Such diversity avoids the local optimum problem, and then improves the quality of the found solutions. However, as entropy decreases and the algorithm approximates to optimal values, the sigmoidal learning rule increases the LR parameter even more than the other rules, which implies that sigmoidal rule improves exploitation at the end of the process. Such exploitation speeds up the search process, as shown on Figure 10. Figure 2 shows that sigmoidal learning rule is the second one in favoring the exploration at the begining of the search process, and also is the one which most favors the exploitation at the end of the convergence process. Such a combination of features seems to be the reason to explain why sigmoidal learning rule resulted to be both the strategy with best quality as well as the fastest one.

6. Conclusions

An adaptive PBIL strategy has been tested using several learning rules. The monotonically-increasing learning rules have shown promising results in order to speed up the convergence process. The results show that a linear or sigmoidal relationship between the learning rate and the PBIL array's entropy seems to be the best option.

Results derived from the TSP optimization suggest that sigmoidal learning rule is the best approach, in order to speed up the convergence time. However, presented results must be taken as an initial insight, in order to derive the features of the learning rules tested in this paper, which will be intended as future work.

Acknowledgment

The authors would like to thank to ARTICA, to COLCIENCIAS, to ICT Ministry of Colombia, to National University of Colombia and to University of Antioquia, for their support in the development of this work.

References

[1] H. Bai and B. Zhao, "A survey on application of swarm intelligence computation to electric power system," in *Intelligent Control and Automation, 2006. WCICA 2006. The Sixth World Congress on*, vol. 2, 2006, pp. 7587 –7591.

[2] N. Pindoriya, S. Singh, and K. Lee, "A comprehensive survey on multi-objective evolutionary optimization in power system applications," in *Power and Energy Society General Meeting, 2010 IEEE*, 2010, pp. 1 –8.

[3] A. Godit' andnez, L. Espinosa, and E. Montes, "An experimental comparison of multiobjective algorithms: Nsga-ii and omopso," in *Electronics, Robotics and Automotive Mechanics Conference (CERMA), 2010*, 28 2010-oct. 1 2010, pp. 28 –33.

[4] G. B. Lamont and D. A. V. Veldhuizen, *Evolutionary Algorithms for Solving Multi-Objective Problems*. Norwell, MA, USA: Kluwer Academic Publishers, 2002.

[5] L. jun Fan, B. Li, Z. quan Zhuang, and Z. qian Fu, "An approach for dynamic hardware /software partitioning based on dpbil," in *Natural Computation, 2007. ICNC 2007. Third International Conference on*, vol. 5, 2007, pp. 581 –585.

[6] M. Schmidt, K. Kristensen, and T. Randers Jensen, "Adding genetics to the standard pbil algorithm," in *Evolutionary Computation, 1999. CEC 99. Proceedings of the 1999 Congress on*, vol. 2, 1999, pp. 3 vol. (xxxvii+2348).

[7] H. Pang, K. Hu, and Z. Hong, "Adaptive pbil algorithm and its application to solve scheduling problems," in *Computer Aided Control System Design, 2006 IEEE International Conference on Control Applications, 2006 IEEE International Symposium on Intelligent Control, 2006 IEEE*, 2006, pp. 784 –789.

[8] B. Babu and A. Gujarathi, "Multi-objective differential evolution (mode) for optimization of supply chain planning and management," in *Evolutionary Computation, 2007. CEC 2007. IEEE Congress on*, sept. 2007, pp. 2732 –2739.

[9] S. Baluja, "Population-based incremental learning: A method for integrating genetic search based function optimization and competitive learning," Pittsburgh, PA, USA, Tech. Rep., 1994.

[10] K. A. Folly and G. K. Venayagamoorthy, "Effects of learning rate on the performance of the population based incremental learning algorithm," in *Proceedings of the 2009 international joint conference on Neural Networks*, ser. IJCNN'09. Piscataway, NJ, USA: IEEE Press, 2009, pp. 3477–3484. [Online]. Available: http://portal.acm.org/citation.cfm?id=1704555.1704773

[11] Q. Zhang, T. Wu, and B. Liu, "A population-based incremental learning algorithm with elitist strategy," in *Proceedings of the Third International Conference on Natural Computation - Volume 03*, ser. ICNC '07. Washington, DC, USA: IEEE Computer Society, 2007, pp. 583–587. [Online]. Available: http://dx.doi.org/10.1109/ICNC.2007.126

[12] S. Sheetekela and K. Folly, "Power ystem controller design: A comparison between breeder genetic algorithm and population based incremental learning," in *Neural Networks (IJCNN), The 2010 International Joint Conference on*, july 2010, pp. 1 –8.

[13] F. Bolanos, J. Aedo, and F. Rivera, "System - level partitioning for embedded systems design using population - based incremental learning," in *CDES*, H. R. Arabnia and A. M. G. Solo, Eds. CSREA Press, 2010, pp. 74–80.

[14] H. Li, S. Kwong, and Y. Hong, "The convergence analysis and specification of the population-based incremental learning algorithm," *Neurocomputing*.

[15] R. Rastegar and A. Hariri, "The population-based incremental learning algorithm converges to local optima," *Neurocomputing*, vol. 69, no. 13-15, pp. 1772 – 1775, 2006, blind Source Separation and Independent Component Analysis - Selected papers from the ICA 2004 meeting, Granada, Spain, Blind Source Separation and Independent Component Analysis. [Online]. Available: http://www.sciencedirect.com/science/article/B6V10-4J9X2VD-2/2/503395260d19018514ab89fa4c646659

[16] E. Hughes, "Optimisation using population based incremental learning (pbil)," in *Optimisation in Control: Methods and Applications (Ref. No. 1998/521), IEE Colloquium on*, Nov. 1998, pp. 2/1 –2/3.

[17] R. White, "Competitive hebbian learning," in *Neural Networks, 1991., IJCNN-91-Seattle International Joint Conference on*, vol. ii, July 1991, p. 949 vol.2.

[18] L. Wang, L. Ma, Q. Bian, and X. Zhao, "Rough set attributes reduction based on adaptive pbil algorithm," in *Information Theory and Information Security (ICITIS), 2010 IEEE International Conference on*, 2010, pp. 21 –24.

[19] J. M. Chaves-Gonzalez, D. Dominguez-Gonzalez, M. A. Vega-Rodriguez, J. A. Gomez-Pulido, and J. M. Sanchez-Perez, "Parallelizing pbil for solving a real-world frequency assignment problem in gsm networks," in *Proceedings of the 16th Euromicro Conference on Parallel, Distributed and Network-Based Processing (PDP 2008)*. Washington, DC, USA: IEEE Computer Society, 2008, pp. 391–398. [Online]. Available: http://portal.acm.org/citation.cfm?id=1343596.1343822

[20] B. W. Silverman, *Density estimation: for statistics and data analysis*, Chapman and Hall, Eds., London, 1986.

[21] M. R. Garey and D. S. Johnson, *Computers and Intractability; A Guide to the Theory of NP-Completeness*. New York, NY, USA: W. H. Freeman & Co., 1990.

[22] M. Castillo Tapia and C. Coello, "Applications of multi-objective evolutionary algorithms in economics and finance: A survey," in *Evolutionary Computation, 2007. CEC 2007. IEEE Congress on*, sept. 2007, pp. 532 –539.

[23] A. E. Eiben and J. E. Smith, *Introduction to Evolutionary Computing (Natural Computing Series)*. Springer, October 2008. [Online]. Available: http://www.amazon.com/exec/obidos/redirect?tag=citeulike07-20&path=ASIN/3540401849

[24] S. Baluja, "An empirical comparison of seven iterative and evolutionary function optimization heuristics," Tech. Rep., 1995.

Enhanced MLP Input-Output Mapping for Degraded Pattern Recognition

Shigueo Nomura and José Ricardo Gonçalves Manzan
Faculty of Electrical Engineering, Federal University of Uberlândia, Uberlândia, MG, Brasil

Abstract— *This work proposes a set of approaches for improving the multilayer perceptron (MLP) performance on degraded pattern input-output mapping process. First, differently to the classical one-per-class approach, our strategy calculates Euclidean distances between the MLP output and target vectors. Second, our approach adopts orthogonal bipolar vectors (OBVs) as target values taking advantages of larger Euclidean distance provided by these vectors rather than conventional ones. The proposed approaches were applied to MLP training and test in classifying very degraded patterns as input data. Experimental results with classical approaches in parallel to the proposed ones are presented for MLP performance comparison purposes. The improved MLP with our proposed approaches provided an increase of 9.3 % on degraded pattern recognition rate.*

Keywords: Artificial Neural Networks, Degraded Pattern, Euclidean Distance, Multilayer Perceptron, Pattern Recognition, Target Vector.

1. Introduction

Multilayer perceptron (MLP) has been successfully applied to pattern recognition [1][2][3] tasks. As a classification system, MLP requires a good approach for analyzing degraded image data, extracting features from these data, generating a set of relevant information, and improving its performance. Many efforts have attempted to develop a good method followed by feature extraction systems.

Surprisingly, it is quite difficult to find investigations focusing on output space for the input-output mapping process of MLPs as shown in Fig. 1.

Basically, approaches for the MLP multiclass categorization tasks such as one-per-class based on conventional binary or bipolar target vectors with their dimensions equal to the number of classes are classical.

This work proposes to break away from such classical treatment of the MLP input-output mapping process.

The main objective of this work is to show that the proposed approaches can considerably improve the degraded pattern recognition performance by MLPs.

In summary, the approaches adopt the Euclidean distance-based MLP multiclass categorization and the use of orthogonal bipolar vectors (OBVs) as expectation values for learning.

It is known that MLP performance using bipolar target vectors is already better than performance with binary ones [4], but no other authors' work exists, to our knowledge, adopting the Euclidean distance between OBVs and output vectors.

2. Usual Approaches on Multiclass Categorization

Connectionist algorithms are more difficult to apply to multiclass categorization problems [5]. Multiclass categorization problems [5] correspond to tasks of finding an approximate definition for an unknown function $f(x)$ given training examples of the form $\langle x_i, f(x_i)\rangle$. The unknown function f often takes values from a discrete set of "classes" $c_1, c_2, \ldots, c_k$.

We can distinguish two approaches to handle these multiclass categorization tasks as follows:

- We have one-per-class approach when the individual functions $f_1, f_2, \ldots, f_k$ are learned one for each class. To assign a new case p to one of these classes, each of individual function f_i is evaluated on p, and the case p is assigned the class j corresponding to the function f_j that returns the highest activation [6]. This categorization approach is standard for conventional target vectors.
- Distributed output code is an alternative approach pioneered by Sejnowski and Rosenberg [7] in their widely-known NETtalk system. In this approach, each class is assigned a unique binary string of length n; these strings refer to target vectors in MLP. Then n binary functions are learned, one for each bit position in these binary strings. During training for an example from class i, the desired outputs of these n binary functions are specified by the target vector for class i. With Artificial Neural Networks (ANN), these n functions can be implemented by the n output units of a single network. A new case p is classified by evaluating each of the n binary functions to generate an n-bit string s. This string is then compared to each of the k target vectors, and p is assigned to the class whose target vector is closest, according to some distance measure, to the generated string s.

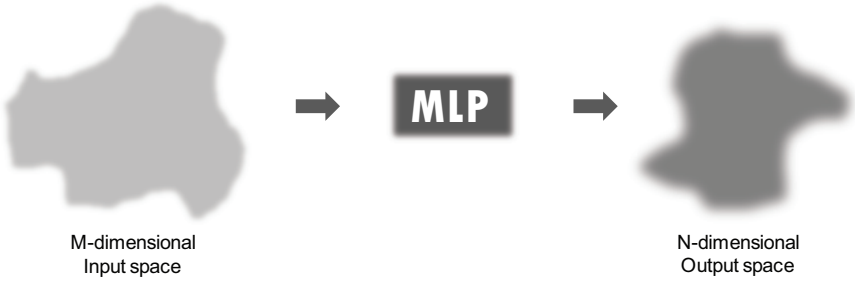

Fig. 1: Input-output mapping process of an MLP.

3. Motivation

An MLP model is trained to learn the nonlinear relationship between M-dimensional input space and N-dimensional output space as shown in Fig. 1. In this way, an incoming unknown input M-dimensional vector is transformed into a N-dimensional one and it can be placed in any point from the space.

The motivation of this work is to improve the MLP multiclass categorization performance as pattern recognition process by transforming an input vector representing a degraded pattern into an output vector representing a class.

The increase of the generalization ability of MLP models leads to their recognition performance improvement. One goal is to find a topology design strategy to provide a network with a higher ability to generalize.

Many traditional investigations have concentrated on improving the representation of input vectors. On the contrary, this work has concentrated on the alternative representation of the desired outputs (OBVs as target vectors) to adjust weights that minimize error during the supervised training process. A purpose is to influence on the multidimensional error-performance surface [8] that is constructed in the supervised training.

Since the categorization based on Euclidean distance adopted in this work depends on the distance between vectors to classify unknown input data, it is expected that the MLP performance improves with the proposed approaches. The orthogonality of new target vectors can provide larger output space rather than conventional vectors. Figure 2 presents high interference zones between pattern categorization subspaces due to the conventional target vectors. On the other hand, we can verify low interference zones between pattern categorization subspaces in Fig. 3 due to the use of new target vectors. Our hypothesis is that the approaches can lead to enhanced MLP input-output mapping even when input is degraded and slightly different from the training examples.

4. Work Proposal

A set of approaches including the input-output mapping process of MLPs based on Euclidean distance measure adopting OBVs as new target vectors is proposed in this work.

According to Dekel and Singer [9], the objective in multiclass categorization problems is to learn a classifier that accurately assigns labels (target vectors) to instances (input vectors) where the set of labels is of finite cardinality and contains more than two elements.

In this MLP application for multiclass categorization, after every presentation of an instance V^* (input vector in M-dimensional space of Fig. 1), the Euclidean distance of the output vector in N-dimensional space was calculated with all labels (target vectors in output space) for each of the classes. The class whose representation by the label had the smallest Euclidean distance with the output vector would be chosen as the "winner" to assign to instance V^*. In addition to the Euclidean distance-based approach, we propose the use of OBVs (defined in the next section) as target vectors.

5. Definition of Vectors

The following defined vectors represent target values used in our experiments for the MLP input-output mapping analysis.

5.1 Conventional Bipolar Vectors (CBVs)

The conventional bipolar vectors (CBVs) with n components for representing p^{th} pattern in n patterns are defined by Eq. (1):

$$V_p = (\overbrace{-1, \ldots, -1}^{p-1}, 1, \overbrace{-1, \ldots, -1}^{n-p})^T, \quad (1)$$

where V_p is the CBV for representing the p^{th} pattern, $p = 1, 2, \ldots, n$, n is the number of patterns or components.

In case of recognition problem for 10 digits, the digit "0" is defined as a 10^{th} digit by Eq. (2):

$$V_0 = (\overbrace{-1, \ldots, -1}^{9}, 1)^T. \quad (2)$$

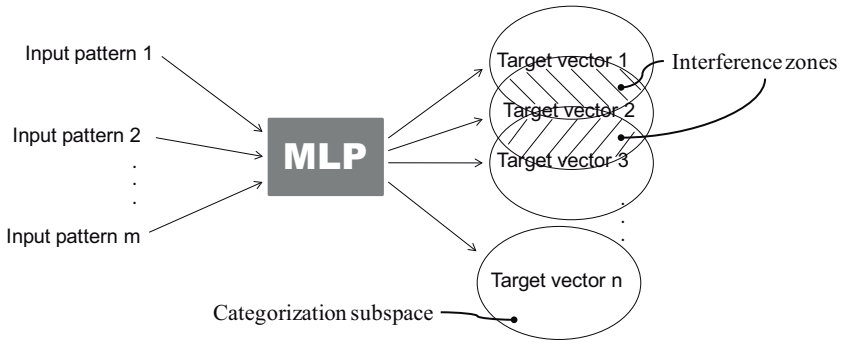

Fig. 2: High interference zones between categorization subspaces in case of using conventional target vectors.

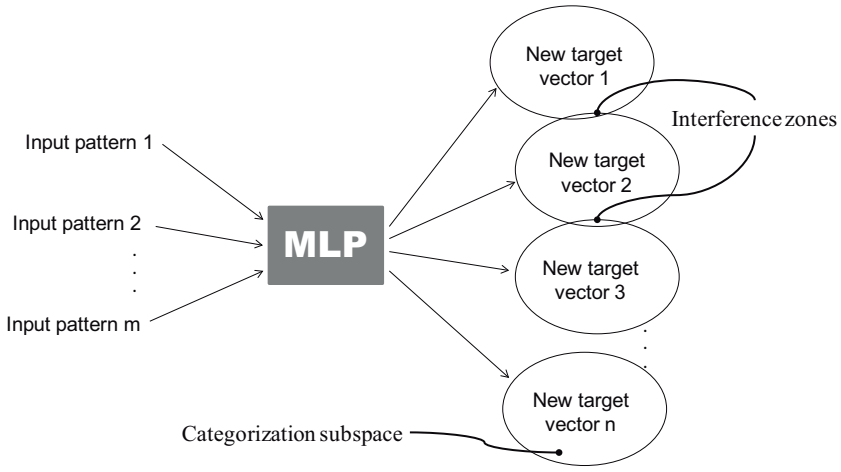

Fig. 3: Low interference zones between categorization subspaces in case of using new target vectors.

5.2 Orthogonal Bipolar Vectors (OBVs)

The norm of an orthogonal bipolar vector (OBV) in an Euclidean space $\mathbb{R}^n$ is given by Eq. (3):

$$|U| = \sqrt{{x_1}^2 + {x_2}^2 + \cdots + {x_n}^2} = \sqrt{n}, \tag{3}$$

where $U = (x_1, x_2, \ldots, x_n)^T$, x_i represents a component $+1$ or -1 for $i = 1, 2, \ldots, n$, and n is the number of components.

The usual inner product [10] between two vectors U and V in an Euclidean space $\mathbb{R}^n$ is defined by Eq. (4):

$$U.V = x_1y_1 + x_2y_2 + \cdots + x_ny_n, \tag{4}$$

where $V = (y_1, y_2, \ldots, y_n)^T$, and y_i represents a component $+1$ or -1 for $i = 1, 2, \ldots, n$, and n is the number of components.

Vectors U and V are orthogonal (denoted by $U \perp V$) if and only if $U.V = 0$ in Eq. (5):

$$U \perp V \Leftrightarrow U.V = 0. \tag{5}$$

A simple algorithm [4][11] can be implemented to generate the OBVs with various numbers of components following the above conditions. Table 1 presents examples of OBVs with 16 components, representing target values for 10 digits, generated by the mentioned algorithm.

6. Experimental Procedure

The modeling procedure of an MLP topology for the input-output mapping process of degraded pattern data as shown in Fig. 4 is presented in this section. The model is to experimentally evaluate the proposed approaches applied to the MLP in degraded pattern recognition tasks.

We have extracted input data from license plate photos automatically taken by traffic control systems of Uberlândia City in Brasil. They were images with such problems as luminosity, contrast, focalization, resolution, and size, all of which required preprocessing able to extract relevant features for pattern recognition process. The original preprocessing methods proposed in such previous works as adaptive contrast enhancement [12], adaptive thresholding [13], automatic segmentation and extraction of feature vectors [14] were used.

Table 1: Examples of OBVs with 16 components.

Digit	*OBV*
"1"	(1, -1, -1, 1, -1, 1, 1, -1, -1, 1, 1, -1, 1, -1, -1, 1)
"2"	(1, -1, -1, 1, -1, 1, 1, -1, 1, -1, -1, 1, -1, 1, 1, -1)
"3"	(1, -1, -1, 1, 1, -1, -1, 1, -1, 1, 1, -1, -1, 1, 1, -1)
"4"	(1, -1, -1, 1, 1, -1, -1, 1, 1, -1, -1, 1, 1, -1, -1, 1)
"5"	(1, -1, 1, -1, -1, 1, -1, 1, -1, 1, -1, 1, 1, -1, 1, -1)
"6"	(1, -1, 1, -1, -1, 1, -1, 1, 1, -1, 1, -1, -1, 1, -1, 1)
"7"	(1, -1, 1, -1, 1, -1, 1, -1, -1, 1, -1, 1, -1, 1, -1, 1)
"8"	(1, -1, 1, -1, 1, -1, 1, -1, 1, -1, 1, -1, 1, -1, 1, -1)
"9"	(1, 1, -1, -1, -1, -1, 1, 1, -1, -1, 1, 1, 1, 1, -1, -1)
"0"	(1, 1, -1, -1, -1, -1, 1, 1, 1, 1, -1, -1, -1, -1, 1, 1)

6.1 Data Representation

A two-dimensional set of pixels that represents a pattern is mapped onto an input vector as a set of input neurons. For a 20×15 image of each segmented pattern, the top row of 20 pixels is associated with the first 20 neurons, the next row of 20 pixels is associated with the next 20 neurons, and so on. So, segmented entities (20×15) are represented by feature vectors with 300 components, and each component in the vector should represent one pixel of the pattern (bipolar value $+1$) or one pixel of the image background (bipolar value -1).

Figure 4 shows the 120-image training set representing digits as input data.

In this work, the adopted data representation is bipolar since the categorization may be improved if the input is represented in bipolar form and the bipolar sigmoid is used for the activation function [4]. The reason is if one factor in the weight connection expression is the activation of the lower unit then units whose activations are null will not learn [4].

6.2 MLP Topology for Experiments

The adopted multilayer neural network in our experiments consists of the architecture with one layer of hidden neurons.

There are several propositions how to determine the necessary number of hidden neurons for a given problem but they yield contradictory results and have no practical utility [15].

Some heuristic rules [15] used to obtain the MLP topology for experiments are as follows:

- To reduce the number of hidden neurons when the network does not generalize, that is, the error of the output data during the training is small and the error in the test stage is large.
- To increase the number of hidden neurons when the error during the training is large or all the weights for the connections between neurons are of the same order of magnitude.

In degraded images, the input data contain redundant information which can not be removed by a suitable coding. These spurious data can be removed when the hidden layer contains less neurons than the input layer [15].

In summary, without further information there is no foolproof method for setting the exact number of hidden neurons before training stage [4].

Such usual strategies in ANN [8] as one parameter keeping and the variation of remaining parameters defined the appropriate topology of MLP. Conventional experiments get adequate topology for classifying input digits (20×15) represented by the 300-dimensional feature vectors. Our experimental MLP model consists of 300 neurons in the input layer. The adequate number of neurons in the hidden layer is set according to each experiment. The number of neurons in the output layer is defined by the target vector type or its size selected for each experiment.

6.3 Training Stage

The standard backpropagation algorithm [4] is used as the training algorithm of each MLP model. Since all experimental target vectors are bipolar, the adopted activation function is the typical bipolar sigmoid [4], which has a range of $(-1, 1)$. Initial weights are generated as random values between -0.25 and 0.25. The learning rate parameter is set as 0.02. The stop criterion for the training algorithm is to require that the maximum value of the average squared error be equal to or less than the tolerance as indicated within each graph of Figs. 5–7.

Training data set is constituted by 120 pattern-images not belonging to the test data set. It contains input patterns for the MLP model training to classify digits extracted from license plates into ten categories. Each category is represented by 12 input patterns.

6.4 Test Stage

The classification rate is calculated by Eq. (6):

Fig. 4: A sample of 120 degraded patterns used as input data for the MLP training.

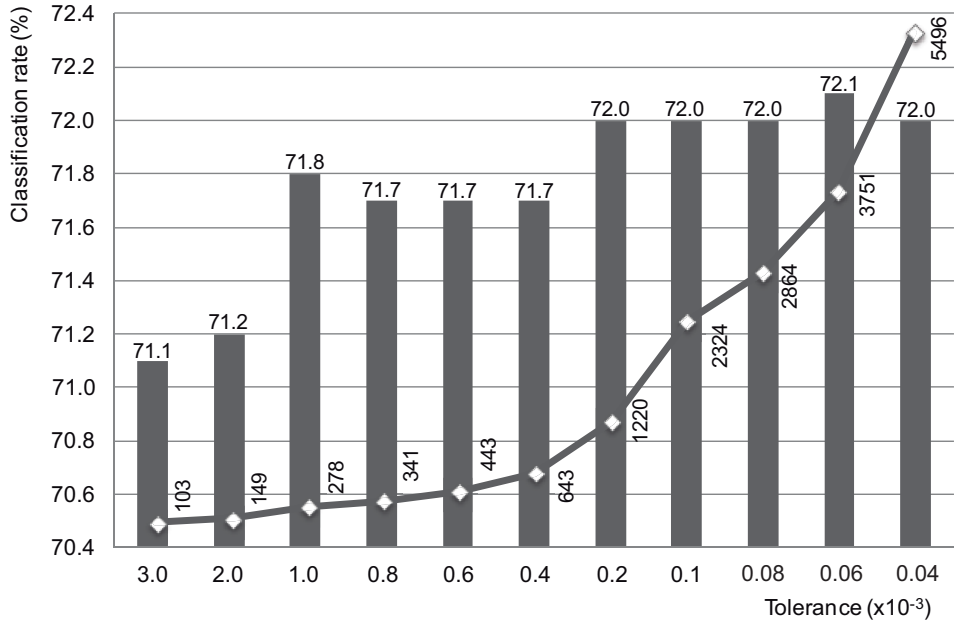

Fig. 5: MLP performance using classical one-per-class approach. The line denotes the epoch quantity evolution.

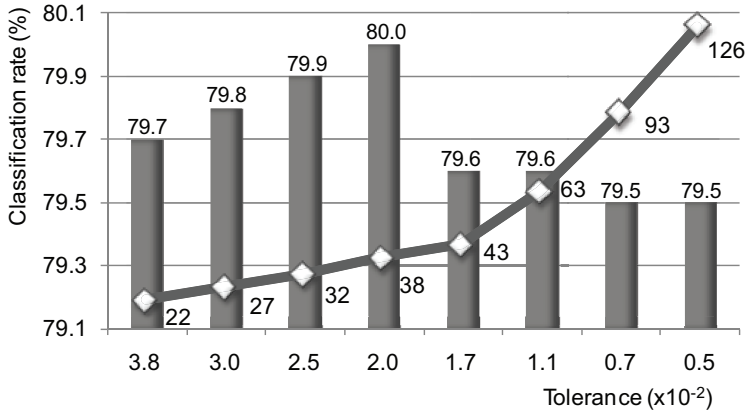

Fig. 6: MLP performance using OBVs with 16 components as target vectors. The line denotes the epoch quantity evolution.

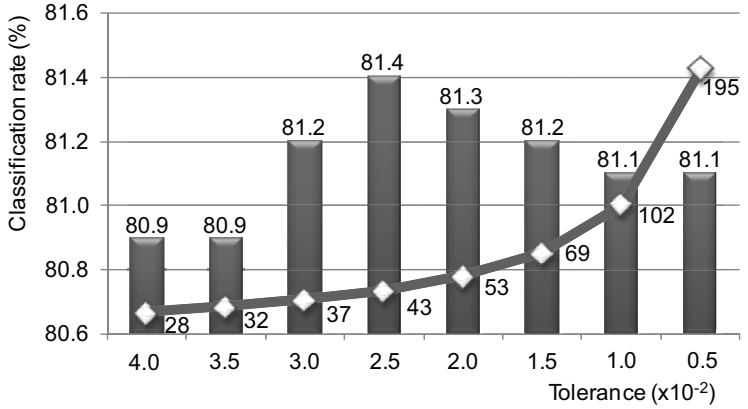

Fig. 7: MLP performance using OBVs with 64 components as target vectors. The line denotes the epoch quantity evolution.

$$cr = \frac{\sum_i^N c_i}{N}, \tag{6}$$

where cr is classification rate, N is number of test patterns, and c_i is defined as

$$c_i = \begin{cases} 1 & : \quad p_i = r_i \\ 0 & : \quad p_i \neq r_i \end{cases}, \tag{7}$$

where p_i is a classified pattern (output of the MLP model), and r_i is the corresponding category (correct response).

Test data set consisted of 1352 images containing the digits "0","1",...,"9" extracted from license plates after their preprocessing [12][13][14][16]. A trained MLP model was applied to classify those extracted digits into ten categories.

7. Experiments and Results

The experiments consisted of using CBVs and OBVs defined in Section 5 as target vectors.

We have evaluated the influence of Euclidean distance-based approach on MLP training and classification performance improvement using various target vectors.

In other words, the experiments compared the proposed Euclidean distance-based approach with the classical one-per-class categorization approach in terms of influence on MLP performance.

An MLP model with a topology of 100 hidden neurons and 10 output neurons was trained and tested using CBVs for one-per-class approach.

Figure 5 shows the MLP classification performance applying one-per-class approach for the use of CBVs as target vectors.

To evaluate the influence of using OBVs as target vectors on the MLP input-output mapping process, we have performed the following tasks:

- MLP model training for OBVs as target vectors. Different topologies according to the OBV sizes (16 or 64 components) were defined.

Table 2: Relevant results from the graphs of Figs. 5–7

Target vector type	*Categorization approach*	*Maximum rate* %
CBV	One-per-class	72.10
OBV-16	Euclidean distance-based	80.00
OBV-64	Euclidean distance-based	81.40

- Application of the Euclidean distance-based approach for the above trained MLP models. The experimental results using OBVs with 16 and 64 components, are respectively shown in Figs. 6 and 7.

8. Discussion

The graph in Fig. 5 shows that the classification rate of 72.1% is provided by the MLP model trained for 3751 epochs with the one-per-class categorization approach. Figures 6–7 show the results from the use of OBVs as target values.

Table 2 presents the highest classification rate per target vector type and categorization approach. We can note that the classification rate was increased of 9.3% by using Euclidean distance-based approach and OBVs as target values.

Considering the advantage of adopting the Euclidean distance-based categorization approach, we can verify that the MLP performance improved more and more with the use of OBVs rather than conventional target vectors.

9. Conclusion

A set of approaches to improve the MLP performance on degraded pattern recognition searching for more generalized and well-trained model was proposed. Basically, the Euclidean distance-based approach was combined to the use of OBVs as new target vectors for the MLP training and test with very degraded pattern data.

We compared the experimental results applying the proposed approaches with the results applying the classical one-per-class approach. Comparison results showed that the proposed approaches considerably improved (increase of 9.3% on classification rate) the MLP performance on degraded pattern recognition tasks.

In summary, we realized that the proposed approaches led to higher classification rate of very degraded pattern data by MLPs compared to the classical one-per-class approach.

In terms of degraded pattern recognition performance, we have gotten an enhanced MLP input-output mapping with the proposed Euclidean distance-based approach using OBVs as new target vectors.

Acknowledgment

The authors would like to thank PROPP-UFU (project 72/2010), CAPES (MINTER UFU-IFTM), and FAU-UFU for supporting this work.

References

[1] A. R. Webb and K. D. Copsey. *Statistical Pattern Recognition*. John Wiley & Sons, third edition, 2011.

[2] J. Chu, I. Moon, and M. Mun. A real-time EMG pattern recognition system based on linear-nonlinear feature projection for a multifunction myoelectric hand. *IEEE Transactions on Biomedical Engineering*, 53(11):2232–2239, Nov. 2006.

[3] Y. X. Zhang. Artificial neural networks based on principal component analysis input selection for clinical pattern recognition analysis. *Talanta*, 73(1):68–75, Aug. 2007.

[4] L. V. Fausett. *Fundamentals of Neural Networks: Architectures, Algorithms, and Applications*. Prentice Hall, Englewood Cliffs, NJ, 1994.

[5] T. G. Dietterich and G. Bakiri. Solving multiclass learning problems via error-correcting output codes. *Journal of Artificial Intelligence Research*, 2:263–286, 1995.

[6] N. J. Nilsson. *Learning Machines*. McGraw-Hill, New York, 1965.

[7] T. J. Sejnowski and C. R. Rosenberg. Parallel networks that learn to pronounce english text. *Complex Systems*, 1:145–168, 1987.

[8] S. Haykin. *Neural Networks: A Comprehensive Foundation*. Prentice Hall, New Jersey, second edition, 1999.

[9] O. Dekel and Y. Singer. "Multiclass learning by probabilistic embeddings." In *Advances in Neural Information Processing Systems*, volume 15, pages 945–952. MIT Press, 2002.

[10] B. Noble and J. W. Daniel. *Applied Linear Algebra*. Prentice Hall, Englewood Cliffs, New Jersey, second edition, 1977.

[11] S. Nomura, K. Yamanaka, O. Katai, H. Kawakami, and T. Shiose. Improved MLP learning via orthogonal bipolar target vectors. *Journal of Advanced Computacional Intelligence and Intelligent Informatics*, 9(6):580–589, Nov. 2005.

[12] S. Nomura, K. Yamanaka, O. Katai, and H. Kawakami. A new method for degraded color image binarization based on adaptive lightning on grayscale versions. *IEICE Trans. on Information and Systems*, E87-D(4):1012–1020, 2004.

[13] S. Nomura and K. Yamanaka. "New adaptive methods applied to binarization of printed word images," In N. Younan, editor, *Proceedings of the Fourth IASTED International Conference Signal and Image Processing*, pages 288–293, Kauai, USA, 2002.

[14] S. Nomura, K. Yamanaka, O. Katai, H. Kawakami, and T. Shiose. A novel adaptive morphological approach for segmenting characters in degraded images. *Pattern Recognition*, 38:1961–1975, Nov. 2005.

[15] (2012) Neuronal networks: The network. [Online]. Available: http://www.andreas-mielke.de/nn-en-4.html

[16] S. Nomura and K. Yamanaka. "New adaptive approach based on mathematical morphology applied to character segmentation and code extraction from number plate images," In *Proc. of* 6^{th} *World Multi-Conference on Systemics, Cybernetics and Informatics*, volume IX, Florida, USA, Jul. 2002.

Estimation of Phoneme Probabilities for Bangla Automatic Speech Recognition

Mohammed Rokibul Alam Kotwal, Afsana Hamid and Mohammad Nurul Huda
Department of Computer Science and Engineering, United International University, Dhaka, Bangladesh

Abstract - *This paper estimates Bangla phoneme probabilities using a neural network-based method for Automatic Speech Recognition (ASR). The method consists of three stages: i) a multilayer neural network (MLN), which converts acoustic features, mel frequency cepstral coefficients (MFCCs), into phoneme probabilities, ii) the phoneme probabilities obtained from the first stage and corresponding velocity (Δ) and acceleration (ΔΔ) parameters calculated by linear regression (LR) are inserted into another MLN, and iii) the phoneme probabilities obtained from the second stage and corresponding Δ and ΔΔ parameters are inserted into a hidden Markov model (HMM) based classifier to obtain more accurate phoneme strings. From the experiments on Bangla speech corpus prepared by us, it is observed that the proposed method provides higher phoneme recognition performance than the other investigated methods. Moreover, it requires a fewer mixture components in the HMMs*.

Keywords: Multilayer Neural Network; Hidden Markov Models; Acoustic Features; Phoneme Probabilities; Automatic Speech Recognition; Dynamic Parameters

1 Introduction

A new vocabulary word or out-of-vocabulary (OOV) word often causes an "error" or a "rejection" in current hidden Markov model (HMM)-based automatic speech recognition (ASR) systems. To resolve this OOV-word problem, an accurate phonetic typewriter or phoneme recognizer functionality is expected [1-3].

There have been many literatures on phoneme recognition for ASR systems for almost all the major spoken languages in the world. Unfortunately, only a very few works have been done in ASR for Bangla (can also be termed as Bengali), which is one of the largely spoken languages in the world. More than 220 million people speak in Bangla as their native language. It is ranked sixth based on the number of native speakers [4]. A major difficulty to research in Bangla ASR is the lack of proper speech corpus. Some efforts are made to develop Bangla speech corpus to build a Bangla text to speech system [5]. However, this effort is a part of developing speech databases for Indian languages, where Bangla is one of the parts and it is spoken in the eastern area of India (West Bengal and Kolkata as its capital). But most of the natives of Bangla (more than two thirds) reside in Bangladesh, where it is the official language. Although the written characters of standard Bangla in both the countries are same, there are some sound that are produced variably in different pronunciations of standard Bangla, in addition to the myriad of phonological variations in non-standard dialects [6]. Therefore, there is a need to do research on the main stream of Bangla, which is spoken in Bangladesh, ASR.

Recognition of Bangla phonemes by Artificial Neural Network (ANN) is reported in [7-8]. However, most of these works are mainly concentrated on simple recognition task on a very small database, or simply on the frequency distributions of different vowels and consonants. Besides, the methods provided in [7-8] uses a multilayer neural network (MLN) in their architecture. Because a single MLN has an inability of resolving coarticulation effect [9], the phoneme recognition methods do not provide higher phoneme recognition performance.

In this paper, we build a Bangla phoneme recognition system for an ASR in a large scale. For this purpose, we first develop a medium size (compared to the exiting size in Bangla ASR literature) Bangla speech corpus comprises of native speakers covering almost all the major cities of Bangladesh. Then, mel-frequency cepstral coefficients (MFCCs) of 39 dimensions are extracted from the input speech. The method consists of three stages: i) a multilayer neural network (MLN), which converts acoustic features, mel frequency cepstral coefficients (MFCCs), into phoneme probabilities, ii) the phoneme probabilities obtained from the first stage and corresponding velocity (Δ) and acceleration (ΔΔ) parameters calculated by linear regression (LR) are inserted into another MLN, and iii) the phoneme probabilities obtained from the second stage and corresponding Δ and ΔΔ parameters are inserted into a hidden Markov model (HMM) based classifier to obtain more accurate phoneme strings. The incorporation of dynamic parameters, Δ and ΔΔ, resolves coarticulation effect and consequently, increases the phoneme recognition performance. The originality of this paper is incorporation of second MLN with dynamic parameters. For evaluating Bangla phoneme correct rate (PCR) and phoneme accuracy (PA), we have designed three experiments: (i) MFCC+MLN, (ii) MFCC+MLN+ Δ, (iii) MFCC+MLN+Δ.ΔΔ, (iv) MFCC+MLN+MLN, (v) MFCC+MLN+MLN+Δ, (vi) MFCC+MLN+MLN+Δ.ΔΔ, (vii) MFCC+MLN+ Δ.ΔΔ +MLN, (viii) MFCC+MLN+Δ.ΔΔ+MLN+Δ, (ix) MFCC+MLN+Δ.ΔΔ+MLN+ Δ.ΔΔ.

The paper is organized as follows. Section 2 briefly describes approximate Bangla phonemes with its corresponding phonetic symbols; Section 3 explains about Bangla speech corpus; Section 4 provides a brief description about existing and our proposed methods, while Section 5 gives experimental setup. Section 6 explicates the experimental results and discussion, and finally, Section 7 draws some conclusions and remarks on the future works.

2 Phonetic Symbols for Bangla Phonemes

Bangla phonetic inventory consists of 8 short vowels (অ, আ, ই, উ, এ, ঐ, ও, ঔ) excluding long vowels (ঈ, ঊ) and 29 consonants. Table 1 shows Bangla vowel phonemes with their corresponding International Phonetic Alphabet (IPA) and our proposed symbols. On the other hand, the consonants, which are used in Bangla language, are presented in Table 2. Here, the Table exhibits the same items for consonants like as Table 1. In Table 2, the pronunciation of /শ/, /ষ/ and /স/ are same by considering the words বিশ (/biʃ /), বিষ (/bi ʃ /) and ডিস (/ɖ i ʃ /) respectively, which is shown in Fig. 1. Here the meanings of বিশ, বিষ and ডিস are English language "twenty (20)", "poison" and "bowl" respectively. On the other hand, in the words জাম (/dʒam/) and যাক (/dʒak/), there is no difference between the pronunciation of /জ/ and /য/ respectively that depicted in Fig. 2. Here the meanings of জাম and যাক are English language "black berry" and "go" respectively. Again, Fig. 3 shows that there is no difference between /ণ/ and /ন/ in the words হরিণ (/hɾ in/) and নাতিন (/natin/) respectively. Here the meanings of হরিণ and নাতিন are English language "deer" and "grand daughter" respectively. Moreover, phonemes /ড়/ and /ঢ়/ carry same pronunciation in the words পাহাড় (/pahaɽ /) and আষাঢ় (/aʃ aɽ /) respectively, which is shown in the Fig. 4. Here the meanings of পাহাড় and আষাঢ় are English language "hill" and "rainy season" respectively.

Table 1: Bangla Vowels

Letter	IPA	Our Symbol
অ	/ɔ / and /o/	a
আ	/a/	aa
ই	/i/	i
ঈ	/i/	i
উ	/u/	u
ঊ	/u/	u
এ	/e/ and /æ/	e
ঐ	/oj/	oi
ও	/o/	o
ঔ	/ow/	ou

Table 2: Bangla Consonants

Letter	IPA	Our Symbol
ক	/k/	k
খ	/kh/	kh
গ	/ɡ /	g
ঘ	/ɡ ʱ/	gh
ঙ	/ŋ/	ng
চ	/tʃ /	ch
ছ	/tʃ ʰ/	chh
জ	/dʒ/	j
ঝ	/dʒʱ/	jh
ট	/ʈ /	ta
ঠ	/ʈ ʰ/	tha
ড	/ɖ /	da
ঢ	/ɖ ʱ/	dha
ণ	/n/	n
ত	/t̪/	t
থ	/t̪ʰ/	th
দ	/d̪/	d
ধ	/d̪ʱ/	dh
ন	/n/	n
প	/p/	p
ফ	/pʰ/	ph
ব	/b/	b
ভ	/bʱ/	bh
ম	/m/	m
য	/dʒ/	j
র	/ɾ /	r
ল	/l/	l
শ	/ʃ / / /s/	s
ষ	/ʃ /	s
স	/ʃ / / /s/	s
হ	/h/	h
ড়	/ɽ /	rh
ঢ়	/ɽ /	rh
য়	/e̯/ /-	y

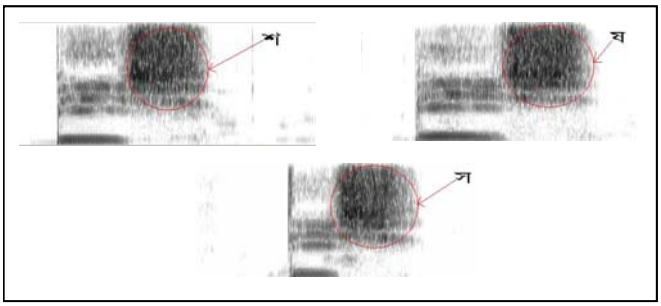

Figure 1: Spectrogram of Bangla phonemes /শ/, /ষ/ and /স/ in the words বিশ (/biʃ /), বিষ (/biʃ /) and ডিস (/ɖ iʃ /) respectively.

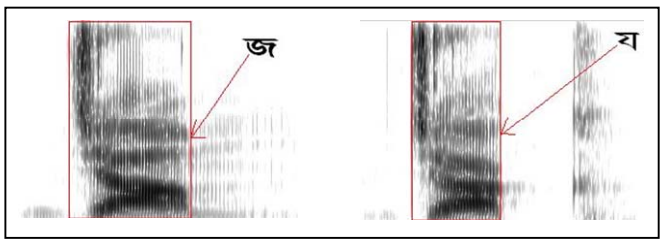

Figure 2: Spectrogram of Bangla phonemes /জ/ and /য/ in the words জাম (/dʒam/) and যাক (/dʒak/) respectively.

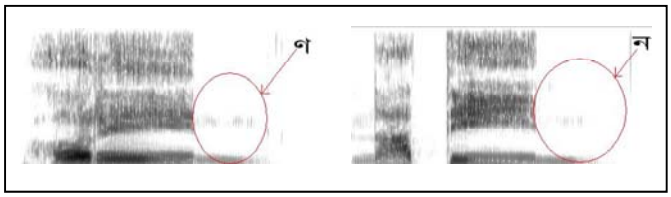

Figure 3: Spectrogram of Bangla phonemes /ণ/ and /ন/ in the words হরিণ (/hɾ in/) and নাতিন (/natin/) respectively.

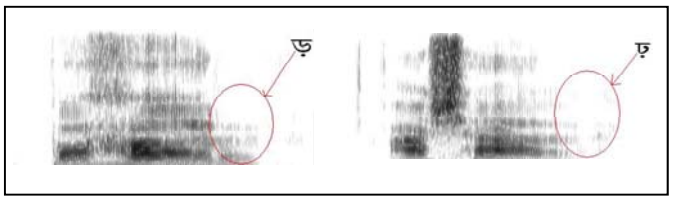

Figure 4: Spectrogram of Bangla phonemes /ড়/ and /ঢ়/ in the words পাহাড় (/pahaɽ /) and আষাঢ় (/aʃ aɽ /) respectively.

Initial consonant cluster is not allowed in the native Bangla: the maximum syllable structure is CVC (i.e. one vowel flanked by a consonant on each side) [10]. Sanskrit words borrowed into Bangla possess a wide range of clusters, expanding the maximum syllable structure to CCCVC. English or other foreign borrowings add even more cluster types into the Bangla inventory.

3 Bangla Speech Corpus

A real problem to do experiment on Bangla word ASR is the lack of proper Bangla speech corpus. In fact, such a corpus is not available or at least not referenced in any of the existing literature. Therefore, we develop a medium size Bangla speech corpus, which is described below.

Hundred sentences from the Bengali newspaper "Prothom Alo" [11] are uttered by 30 male speakers of different regions of Bangladesh. These sentences (30x100) are used for training corpus (D1). On the other hand, different 100 sentences from the same newspaper uttered by 10 different male speakers (total 1000 sentences) are used as test corpus (D2). All of the speakers are Bangladeshi nationals and native speakers of Bangla. The age of the speakers ranges from 20 to 40 years. We have chosen the speakers from a wide area of Bangladesh: Dhaka (central region), Comilla – Noakhali (East region), Rajshahi (West region), Dinajpur – Rangpur (North-West region), Khulna (South-West region), Mymensingh and Sylhet (North-East region). Though all of them speak in standard Bangla, they are not free from their regional accent.

Recording was done in a quiet room located at United International University (UIU), Dhaka, Bangladesh. A desktop was used to record the voices using a head mounted close-talking microphone. We record the voice in a place, where ceiling fan and air conditioner were switched on and some low level street or corridor noise could be heard.

Jet Audio 7.1.1.3101 software was used to record the voices. The speech was sampled at 16 kHz and quantized to 16 bit stereo coding without any compression and no filter is used on the recorded voice.

4 Phoneme Recognition Methods

4.1 Existing Method

At the acoustic feature extraction stage, input speech is converted into MFCCs of 39 dimensions (12-MFCC, 12-ΔMFCC, 12-ΔΔMFCC, P, ΔP and ΔΔP, where P stands for raw log energy of the input speech signal). Fig. 5 shows the phoneme recognition method using MLN [8] which comprises two stages: i) MFCCs are inputted to an MLN with three layers, including 2 hidden layers, after combining preceding (t-3)-th and succeeding (t+3)-th frames with the current t-th frame and ii) the phoneme probabilities obtained from the first stage and corresponding Δ and ΔΔ parameters calculated by LR are inserted into a hidden Markov model (HMM) based classifier to obtain more accurate phoneme strings. The MLN has 39 output units (total 39 monophones) of phoneme probabilities for the current frame t. The two hidden layers consist of 300 and 100 units, respectively. The MLN is trained by using the standard back-propagation algorithm. This method yields comparable recognition performance. However, the single MLN suffers from an inability to model dynamic information precisely.

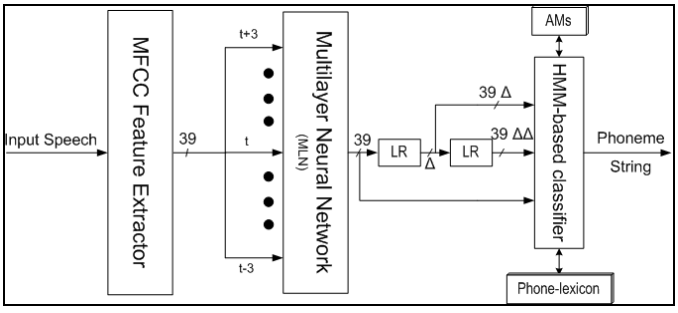

Figure 5: Existing Phoneme Recognition Method.

4.2 Proposed Method

Fig. 6 shows the phoneme recognition method using MLN which comprises three stages: i) MFCCs are inputted to an MLN with three layers, including 2 hidden layers, after combining preceding (t-3)-th and succeeding (t+3)-th frames with the current t-th frame, ii) the phoneme probabilities obtained from the first stage and corresponding velocity (Δ) and acceleration (ΔΔ) parameters calculated by 3-point linear regression (LR) are inserted into another MLN and iii) the phoneme probabilities obtained from the second stage and corresponding Δ and ΔΔ parameters calculated by 3-point LR are inserted into a hidden Markov model (HMM) based classifier to obtain more accurate phoneme strings. The architecture of first MLN and its learning method is similar to the method described in Section IV A. The 39 dimensional output probabilities obtained by the first MLN and corresponding Δ and ΔΔ (39x3) are inserted into the second MLN, which consists of four layers: three hidden and one output layers. The hidden layers are of 400, 200, and 100 units, respectively from the input layer side, while the output layer is of 39 dimensions of phoneme probabilities. The second MLN is also trained by the standard back-propagation algorithm. This method yields higher recognition performance in comparison with the method describe in Section IV A.

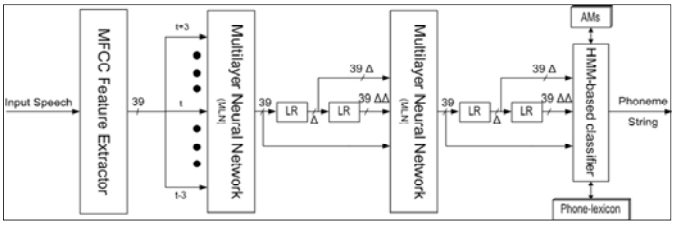

Figure 6: Proposed Phoneme Recognition Method.

5 Experimental Setup

The frame length and frame rate (frame shift between two consecutive frames) are set to 25 ms and 10 ms, respectively, to obtain acoustic features (MFCCs) from an input speech. MFCC comprised of 39 dimensional (12-MFCC, 12-ΔMFCC, 12-ΔΔMFCC, P, ΔP and ΔΔP, where P stands for raw log energy of the input speech signal).

For designing an accurate phoneme recognizer, PCR and PA for D2 data set are evaluated using an HMM-based classifier. The D1 data set is used to design 39 Bangla monophone (8 vowels, 29 consonant, sp, sil) HMMs with five states, three loops, and left-to-right models. Input features using the methods (i), (iv) and (vii); (ii), (v) and (viii); (iii), (vi) and (ix) are 39, 78 and 117 dimensions, respectively. In the HMMs, the output probabilities are represented in the form of Gaussian mixtures, and diagonal matrices are used. The mixture components are set to 1, 2, 4, 8, 16 and 32. In our experiments of the MLN, the non-linear function is a sigmoid from 0 to 1 (1/(1+exp(-x))) for the hidden and output layers.

To obtain the PCR and PA we have designed the following experiments:

(i) MFCC+MLN <39 dim>

(ii) MFCC+MLN+ Δ <78 dim>

(iii) MFCC+MLN+Δ.ΔΔ <117dim>

(iv) MFCC+MLN+MLN <39 dim>

(v) MFCC+MLN+MLN+Δ <78 dim>

(vi) MFCC+MLN+MLN+Δ.ΔΔ <117dim>

(vii) MFCC+MLN+Δ.ΔΔ+MLN <39 dim>

(viii) MFCC+MLN+Δ.ΔΔ+MLN+Δ <78 dim>

(ix) MFCC+MLN+Δ.ΔΔ+MLN+Δ.ΔΔ <117dim> [Proposed].

6 Experimental Results And Discussion

Figs. 7 and 8 show the PCR and PA respectively for the investigated methods using training data set D1. It is shown from the figures that the proposed method provides a higher phoneme recognition performance than the other methods investigated. For an example, at 32 mixture component, the method (iii) shows 70.78% PCR, while the methods, (i) and (ii) exhibit 67.75% and 70.37% PCRs, respectively. On the other hand, at the same mixture component, the accuracies of the methods (i), (ii) and (iii) are 52.98%, 59.95% and 61.31%, respectively.

On the other hand, the PCR and PA for test data, D2 are shown in the Figs. 9 and 10, respectively for the investigated methods. The method, (iii) outperformed the other methods for both the evaluations (PCR and PA) in the mixture components 2, 4, 8, 16 and 32. It is noted from the mixture component 32 of the Fig. 10 that the method (iii) having 54.66% accuracy shows its better recognition performance over the accuracies of other methods.

The reason for providing better result by the method (iii) is Δ and ΔΔ (dynamic parameters), while the existing method (i) contains no dynamic parameters. On the other hand, the second investigated method, (ii) embeds only velocity coefficient (Δ) which embeds a context window of wider size and consequently, provides a higher recognition performance than the existing method (i). Since the proposed method incorporates both velocity (Δ) and acceleration coefficients (ΔΔ), it shows better performance than the method (ii).

Tables 3 and 4 shows the PCR and PA respectively for the investigated methods incorporating using training data set D1. It is shown from the figures that the proposed method

provides a higher phoneme recognition performance than the other methods investigated. For an example, at 32 mixture component, the method (vi) shows 69.72% PCR, while the methods, (iv) and (v) exhibit 68.18% and 69.28% PCRs, respectively. On the other hand, at the same mixture component, the accuracies of the methods (iv), (v) and (vi) are 58.21%, 62.65% and 63.50%, respectively.

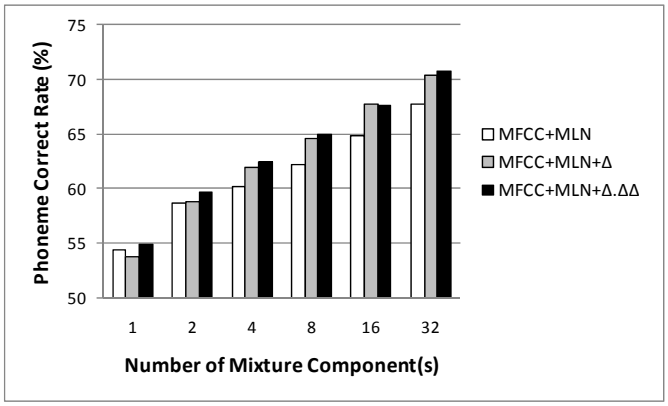

Figure 7: Phoneme correct rate for training data using methods (i), (ii) and (iii).

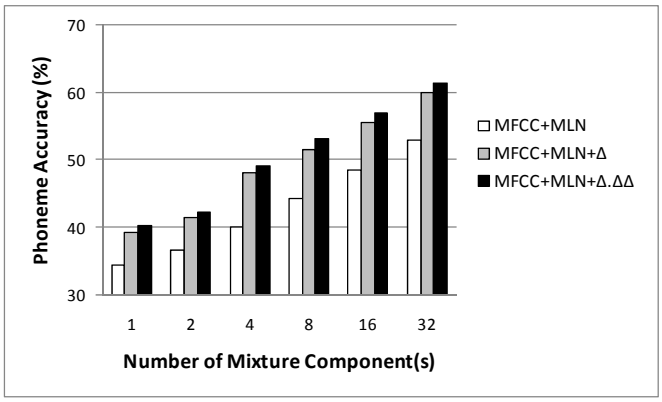

Figure 8: Phoneme accuracy for training data using methods (i), (ii) and (iii).

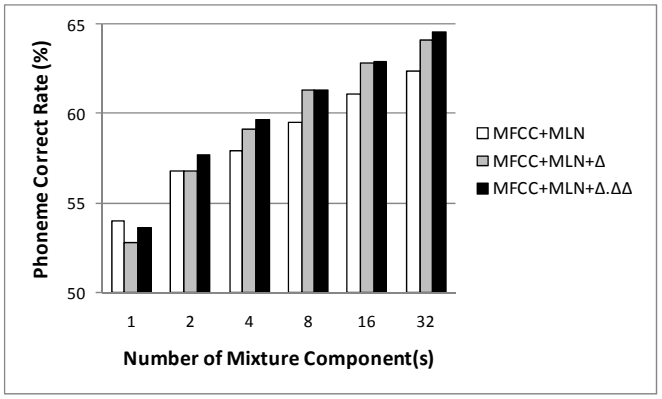

Figure 9: Phoneme correct rate for test data using methods (i), (ii) and (iii).

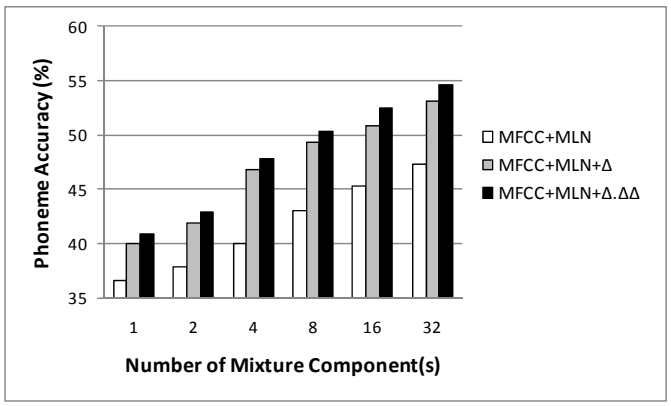

Figure 10: Phoneme accuracy for test data using methods (i), (ii) and (iii).

Table 3: Phoneme correct rate for training data using methods (iv), (v) and (vi)

Methods	Phoneme Correct Rate (%)					
	1 Mix	2 Mix	4 Mix	8 Mix	16 Mix	32 Mix
(iv) MFCC+MLN+MLN	53.28	57.77	60.81	63.03	65.85	68.18
(v) MFCC+MLN+MLN+Δ	53.23	57.81	61.67	64.23	66.41	69.28
(vi) MFCC+MLN+MLN+Δ.ΔΔ	54.76	59.85	61.94	64.21	66.72	69.72

Table 4: Phoneme accuracy for training data using methods (iv), (v) and (vi)

Methods	Phoneme Accuracy (%)					
	1 Mix	2 Mix	4 Mix	8 Mix	16 Mix	32 Mix
(iv) MFCC+MLN+MLN	41.78	43.47	47.83	50.92	54.65	58.21
(v) MFCC+MLN+MLN+Δ	44.04	47.56	52.30	56.13	58.91	62.65
(vi) MFCC+MLN+MLN+Δ.ΔΔ	45.54	48.93	52.48	55.78	59.71	63.50

Again, the PCR and PA for test data, D2 are shown in the Tables 5 and 6, respectively for the investigated methods. The method, (vi) outperformed the other methods for both the evaluations (PCR and PA) in all the mixture components. It is noted from the mixture component 32 of the Table 6 that the method (vi) having 63.50% accuracy shows its better recognition performance over the other methods accuracies.

Figs. 11 and 12 show the PCR and PA respectively incorporating Δ and ΔΔ parameters at second MLN for the investigated methods using training data set D1. It is shown from the figures that the proposed method provides a higher phoneme recognition performance than the other methods investigated. For an example, at 32 mixture component, the method (ix) shows 70.33% PCR, while the methods, (vii) and (viii) exhibit 68.78% and 70.05% PCRs, respectively. On the other hand, at the same mixture component, the accuracies of the methods (vii), (viii) and (ix) are 57.80%, 62.31% and 63.09%, respectively.

Table 5: Phoneme correct rate for test data using methods (iv), (v) and (vi)

Methods	Phoneme Correct Rate (%)					
	1 Mix	2 Mix	4 Mix	8 Mix	16 Mix	32 Mix
(iv) MFCC+MLN+MLN	51.79	55.71	58.36	60.03	61.85	62.69
(v) MFCC+MLN+MLN+Δ	50.96	55.48	58.90	60.90	62.30	63.65
(vi) MFCC+MLN+MLN+Δ.ΔΔ	52.26	57.09	59.03	61.06	62.49	64.46

Table 6: Phoneme accuracy for test data using methods (iv), (v) and (vi)

Methods	Phoneme Accuracy (%)					
	1 Mix	2 Mix	4 Mix	8 Mix	16 Mix	32 Mix
(iv) MFCC+MLN+MLN	41.78	43.47	47.83	50.92	54.65	58.21
(v) MFCC+MLN+MLN+Δ	44.04	47.56	52.30	56.13	58.91	62.65
(vi) MFCC+MLN+MLN+Δ.ΔΔ	45.54	48.93	52.48	55.78	59.71	63.50

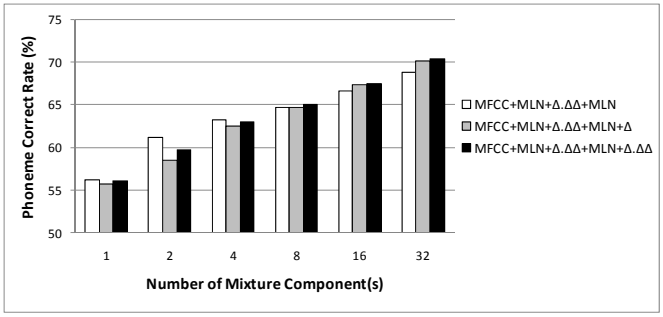

Figure 11: Phoneme correct rate for training data using methods (vii), (viii) and (ix).

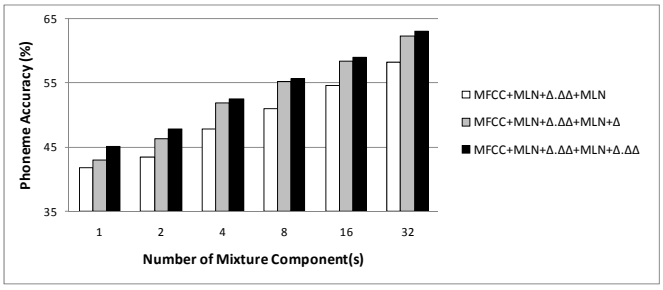

Figure 12: Phoneme accuracy for training data using methods (vii), (viii) and (ix).

Moreover, the PCR and PA for test data, D2 are shown in the Figs. 13 and 14, respectively for the investigated methods. The method, (ix) outperformed the other methods for phoneme accuracy evaluations for all mixture components. It is noted from the mixture component 32 of the Fig. 14 that the method (ix) having 56.21% accuracy shows its better recognition performance over the other methods accuracies.

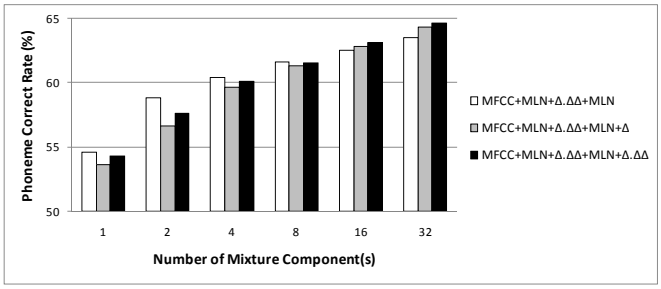

Figure 13: Phoneme correct rate for test data using methods (vii), (viii) and (ix).

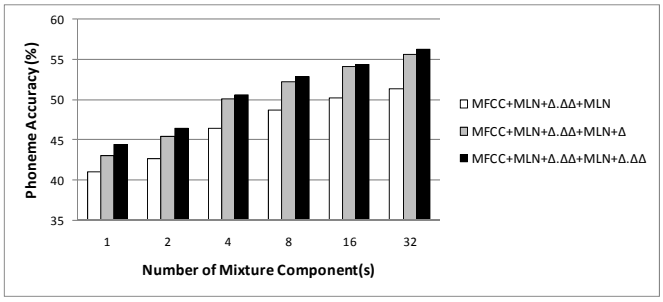

Figure 14: Phoneme accuracy for test data using methods (vii), (viii) and (ix).

7 Conclusion

In this paper, we proposed a Bangla phoneme recognition method incorporating two stage multilayer neural networks with dynamic parameters. The following conclusions are drawn from the study:

(i). The proposed method provides higher phoneme correct rate and phoneme accuracy than the other methods investigated for the both training (D1) and test (D2) data sets.

(ii). The proposed method requires a fewer mixture components in the HMMs.

(iii). The incorporation of second MLN over first MLN increases phoneme recognition performance.

(iv). The dynamic parameters used in the second MLN as input improves recognition rate.

(v). The significant improvement of recognition rate is obtained by inserting dynamic parameters, Δ and ΔΔ to the HMM based classifier.

The authors would like to evaluate phoneme recognition performance using recurrent neural network in near future. Moreover, word recognition rate based on triphone HMM model using the phoneme probabilities obtained from the two MLNs will be investigated.

8 References

[1] I. Bazzi and J. R. Glass, "Modeling OOV words for ASR," *Proceedings of ICSLP*, Beijing, China, p. 401-404, 2000.

[2] S. Seneff, et. al, "A two-pass for strategy handling OOVs in a large vocabulary recognition task," *Proc. Interspeech*, 2005.

[3] K. Kirchhoff **"**OOV Detection by Joint Word/Phone Lattice Alignment, "*ASRU* , Kyoto, Japan, Dec 2007.

[4] http://en.wikipedia.org/wiki/List_of_languages_by_total_speakers, Last accessed May 16, 2012.

[5] S. P. Kishore, A. W. Black, R. Kumar, and Rajeev Sangal, "Experiments with unit selection speech databases for Indian languages," Carnegie Mellon University.

[6] http://en.wikipedia.org/wiki/Bengali_phonology, Last accessed May 16, 2012.

[7] K. Roy, D. Das, and M. G. Ali, "Development of the speech recognition system using artificial neural network," in *Proc. 5th International Conference on Computer and Information Technology (ICCIT02)*, Dhaka, Bangladesh, 2002.

[8] M R A Kotwal, M Banik, Q N Eity, M N Huda, G Muhammad and Y A Alotaibi, "Bangla Phoneme Recognition for ASR Using Multilayer Neural Network," Proc. ICCIT'10, December 2010.

[9] T. Robinson, "An application of Recurrent Nets to Phone Probability Estimation," IEEE Trans. Neural Networks, Volume 5, Number 3, 1994.

[10] C. Masica, The Indo-Aryan Languages, Cambridge University Press.

[11] Daily Prothom Alo. Online: www.prothom-alo.com.

Knowledge Binary Information Fragment Encoding for AI System Memories

James A. Crowder and John N. Carbone
Raytheon Intelligence and Information Systems
16800 E. Centretech Parkway, Aurora, Colorado 80011

Abstract - *Memories involve the acquisition, categorization, classification and storage of information. The purpose of memory is to provide the ability to recall information and knowledge as well as events. We base our current understanding of the world around us on what we have previously learned, and chosen to store. Everything that we do in the present relies on memories of what has happened, or what has been learned in the past, unless new memories must be created for a new experience/ information. Without our memories, we would not be able to go through day-to-day living, using abstract thought and performing the most basic functions. Without memories we wouldn't be able to drive a car, brush our teeth, or perform any of the things we do "without thinking about them." Through our conceptual recollection of the past we are able to communicate with other people. However, the human brain does not store files in neat folders or in relational databases, but instead stores information as fragments that are used to construct memories when needed. Hence, we propose a binary information fragment encoding system for use in artificial intelligence systems that can be utilized to create a combined sensory perceptive, short-term, and long-term memory system similar to how the human brain dynamically stores and recalls (reconstructs) memories.*

Keywords: Artificial Intelligence, Artificial Memories

1. Introduction: Artificial Neural Memories

In order to design, develop, and implement an Artificially Intelligent System (AIS) to be truly autonomous, it must be provided with dynamic memory abilities (Crowder 2010a). Memories are typically classified into three different types: Sensory, Short-Term, and Long-Term (Miller 2002, Newell 2003). Each memory type has several instantiations, dealing with different types of information. Here we will explore each type of memory system and its implications to the AIS. We begin our discussion of memory types with a look at the relationships between the three main types of memories. Figure 1 illustrates an AIS Memory Upper Ontology, similar to human memory systems, describing these relationships (Eichenbaum 2002).

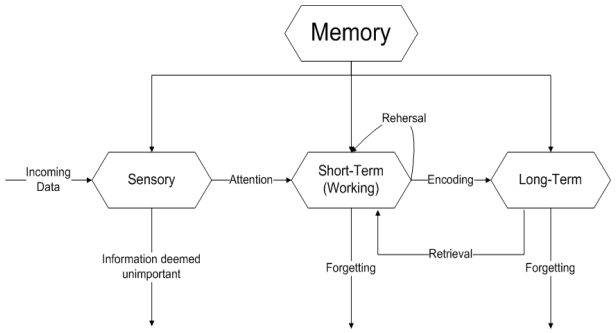

Figure 1 – AIS Memory Upper Ontology

1.1 Sensor Memories

The Sensory Memory within the AIS memory system are those memory registers where raw, unprocessed information ingested via AIS environmental sensors and are buffered to begin initial processing. The *AIS* sensory memory system has a large capacity to accommodate large quantities of possibly disparate and diverse information from a variety of sources (Crowder 2010). And although it has a large capacity, it has a short duration. The information that is buffered in this sensory memory must be sorted, categorized, turned into information fragments, metadata, contextual threads, and attributes (including emotional attributes) and then sent on to the working memory (Short-Term Memory) for initial cognitive processing. This cognitive processing is

known as Recombinant Knowledge Assimilation (RNA), where raw information content is discovered from the information domain, decomposed & reduced, compared, contrasted, and associated into new relationship threads within a temporary working knowledge domain and subsequently normalized into pedigree within the knowledge domain for future use (Carbone 2010). Hence, based upon the information gathered in initial Sensory Memory processing, Cognitive Perceptrons, manifested as Intelligence information Software Agents (ISAs), are spawned, as in relative size swarms, to create initial "thoughts" about the data. Subsequently, hypotheses are generated by the ISAs. The thought process information, along with the ISA sensory information are then sent to a working memory region which will alert the artificial cognition processes within the AIS to begin processing. (Crowder and Friess 2010a&b). Figure 2 illustrates the Sensory Memory Lower Ontology.

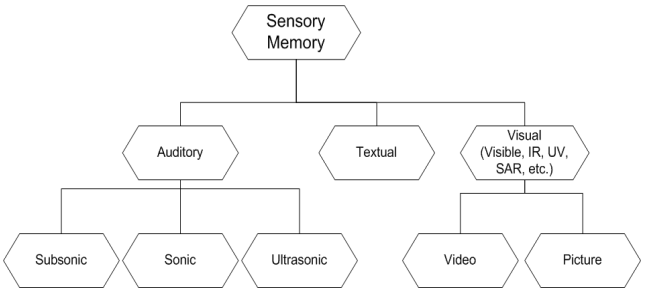

Figure 2 – Sensory Memory Lower Ontology

1.2 Short-Term Artificial Memories

Short-Term or "Working" memory within the AIS is where new information is transitionally stored in a Temporary Knowledge Domain (Carbone 2010) while it is being processed into new Knowledge. This follows the paradigm that information content has no value until it is thought about (Brillouin 2004). Short-Term memory is where most of the reasoning within the AIS happens. Short-Term memory (STM) provides a major functionality, called "rehearsals" that allows the AIS to continually refresh, or rehearse, the Short-Term memories while they are being processed and reasoned about, so that memories do not degrade until they can be sent on to Long-Term Memory and acted upon by the artificial consciousness processes within the AIS's cognitive framework (Crowder and Carbone 2011a). It should be noted that Short-Term memory is much smaller in relative space needed to process information content as compared to long term memory. Short-Term memory should be perceived not necessarily as a physical location, as in the human brain, but rather as a rapid and continuous processing of information content relative to a specific AIS directive or current undertaking. One must remember that the Short-Term memory which includes all external and internal sensory inputs will trigger a rehearsal if the AIS discovers a relationship to either a previously interred piece of information content in short or long term memory. Figure 3 illustrates the Short-Term Memory Lower Ontology for the AIS.

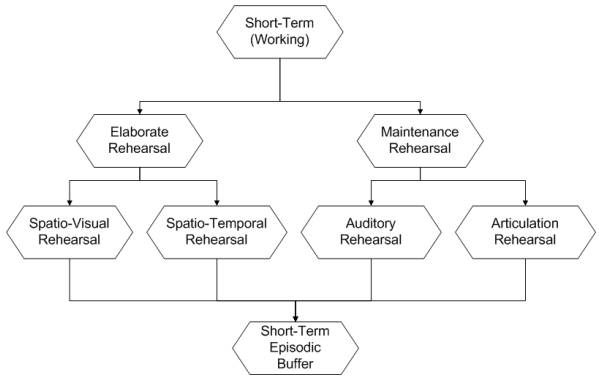

Figure 3 – AIS Short-Term Memory Lower Ontology

1.3 Long-Term Artificial Memories

Long-Term Memory (LTM), in the simplest sense, is the permanent Knowledge Domain where we assimilate our memories (Carbone 2010). If information we take in through our senses doesn't make it to LTM, we can't and don't "remember" it. Information that is processed in the STM makes it to LTM through the process of rehearsal, processing, encoding, and then association with other memories. In the brain, memories are not stored in files, nor in a database. Memories, in fact, or not stored as whole memories at all, but instead are stored as information fragments. The process of recall, or remembering, constructs memories from these information fragments that are stored in various regions of the brain, depending on the type of information. In order to create our AIS in a way that mimics human reasoning, we follow the process of storing information fragments and their respective encoding in different ways, depending on the type and context

of the information, as discussed above. Each sinple discrete fragment of objective Knowledge includes an n-dimensional set of quantum mechanics based mathematical relationships to other fragments/objects bundled in the form of eigenvector optimized Knowledge Relativity Threads (KRT) (Carbone 2010) (Carbone and Crowder, 2011).These KRT bundles include closeness, and relative importance value among others. This importance is tightly coupled, per the math, to the AIS emotional storage as a function of desire or need, as described in Figure 4, where the LTM Lower Ontology is illustrated. There are three main types of LTM (Crowder 2010a):

- Explicit, or Declarative Memories
- Implicit Memories
- Emotional Memories

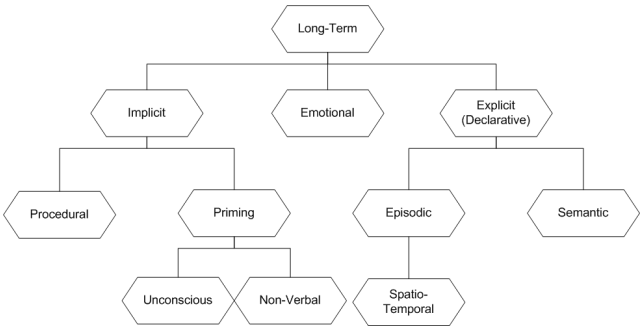

Figure 4 – Artificial Long-Term Memory Lower Ontology

2. Artificial Memory Processing and Encoding

2.1 Short-Term Artificial Memory Processing

In the human brain, STM corresponds to that area of memory associated with active consciousness, and is where most of the cognitive processing takes place. It is also a temporary storage and requires rehearsal to keep it fresh until it is compiled into Long-Term Memory (LTM). In the AIS, the memory system does not decay over time, however, the notion of "memory refresh" or rehearsal is still a valid concept as the Artificial Cognitive Processes work on this information. However, the notion of rehearsal means keeping track of "versions" of STM as it is being processed and evaluated by the artificial cognition algorithms. This is illustrated in Figure 5, the AIS STM Attention Loop. There are three distinct processes that are handled within the STM that determine where information is transferred after cognitive processing (Crowder 2010a).

This processing is shown in Figure 6. The Artificial STM processing steps are:

- **Information Fragment Selection**: this involves filtering the incoming information from the AIS Artificial Preconscious Buffers into separable information fragments and then determining which information fragments are relevant to be further processed, stored, and acted on by the cognitive processes of the AIS as a whole. Once information fragments are created from the incoming sensory information, they are analyzed and encoded with initial topical information, as well as Metadata attributes that allow the cognitive processes to organize and integrate the incoming information fragments into the AIS's overall LTM system. The Information Fragment encoding creates a small, Information Fragment Cognitive Map that will be used for the organization and integration functions.

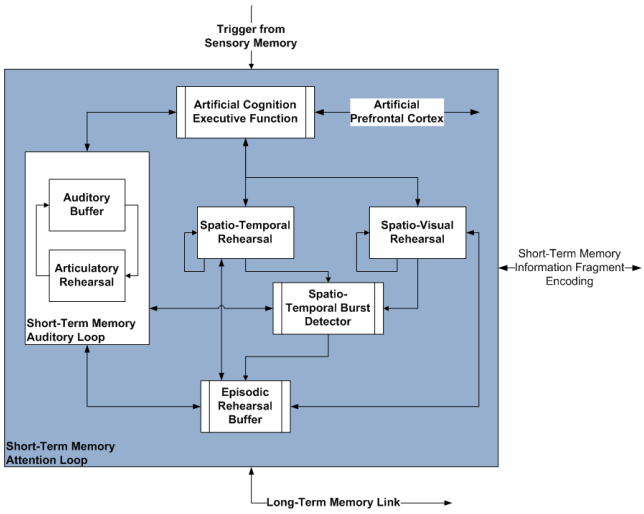

Figure 5 – Short-Term Artificial Memory Attention Loop

- **Information Fragment Organization**: these processes within the Artificial Cognition framework create additional attributes within the Information Fragment Cognitive Map that allow it to be organized for integration into

the overall AIS LTM framework. These attributes have to do with how the information will be represented in LTM and determine how these memory fragments will be used to construct new memories, or recall, memories later by as needed by the AIS, using Knowledge Relativity Thread representation to capture the context of the Information Fragment and each of it's qualitative relationships to other fragments and/or bundles of fragments already created.

- **Information Fragment Integration**: Once the Information Fragments within the STM have been KRT encoded, they are compared, associated, and attached to larger, Topical Cognitive Maps that represent relevant subject or topics within the AIS's LTM system. Once these Information Fragment Cognitive Maps have been integrated, processed, and reasoned about, including emotional triggers or emotional memory information, they are sent on to both the LTM system, as well as the AIS Artificial Prefrontal Cortex to determine if actions are required.

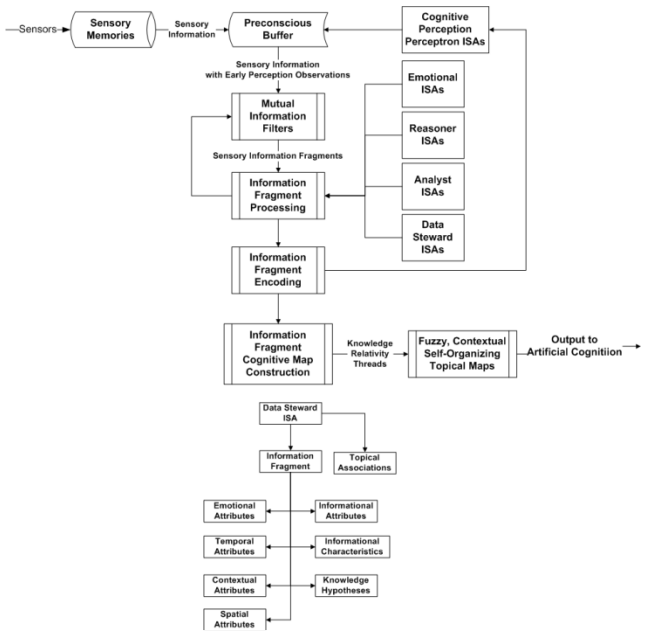

Figure 6 – AIS Information Fragment Encoding

One of the major functions within the STM Attention Loop is the Spatio-Temporal Burst Detector. Within these processes, Binary Information Fragments (BIFs) are ordered in terms of their spatial and temporal characteristics. Spatial[1] and Temporal transitions states are measured in terms of mean, mode, median, velocity, and acceleration and are correlated between their spatial and temporal characteristics and measurements. Rather than just looking at frequencies of occurrence within information, we also look for rapid increases in temporal or spatial characteristics that may trigger an inference or emotional response from the cognitive processes. It is not that an AIS system processes information content differently based upon how rapidly content is ingested, it is simply that an AIS must be able to recognize instances when information content might seem out of place within the context of a situation: e.g., a single speeding car within a crowd of hundreds of other cars. An AIS, not only optimizes its processing on the supply side of the knowledge economy, but has to recognize, infer, and avoid distraction on what focuses the demand side of its knowledge economy places upon operations and directives. State transition bursts are ranked according to their weighting (velocity and acceleration), together with the associated temporal and/or spatial characteristics, and any triggers that might have resulted from this burst processing (LaBar and Cabeza 2006). This Burst Detection and processing may help to identify relevant topics, concepts, or inferences that may need further processing by the Artificial Prefrontal Cortex and/or Cognitive Consciousness processes (Crowder and Friess 2011 a&b).

Once processing within the STM system has completed and all memories are encoded, mapped to topical associations, and their contexts captured, their knowledge relativity thread bundled representations are created and are sent on to the Cognitive Processing engine Memories that are deemed relevant to "remember" are integrated into the Long Term Memory system.

2.2 Long-Term Artificial Memory Processing

The overall AIS High-Level memory architecture is shown in Figure 7. The one thing of note is the connection between Emotional memories and both

[1] Spatial in this reference can be geographically (either 2-D or 3-D), cyber-locations, or other characteristics that may be considered "spatial" references or characteristics.

Explicit and Implicit memories. Emotional Memory carries both Explicit and Implicit characteristics.

Explicit or Declarative Memory is utilized for storage of "conscious" memories or "conscious thoughts." Explicit memory carries those information fragments that are utilized to create what most people would "think of" when they envision a memory. Explicit memory stores things, i.e., objects, and events, things that are experienced in the person's environment. Information fragments stored in Explicit Memory are normally stored in association with other information fragments that relate in some fashion. The more meaningful the association, the stronger the memory and the easier the memory is to construct/recall when you choose to (Yang and Raine 2009). In our AIS, Explicit Memory is divided into different regions, depending on the type or source of information. This division of regions is because different types of information fragments within the AIS memories are encoded and represented differently, each with its own characteristics that make it easier to construct/recall the memories later when the AIS needs the memories. In the AIS LTM, we utilize Fuzzy, Self-Organizing, Contextual Topical Maps to associate currently processed Information Fragments from the STM with memories stored in the LTM (Crowder, Scally, and Bonato 2011).

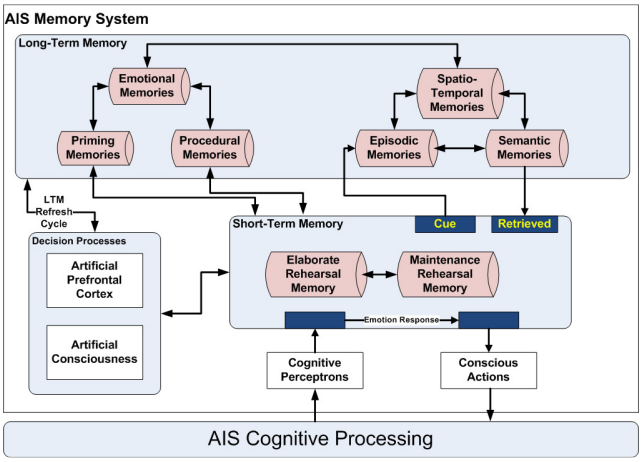

Figure 7 – High-Level Artificial Memory Architecture

LTM information fragments are not stored in databases or as files, but encoded and stored as a triple helix of continuously recombinant binary neural fiber threads that represent:

- The Binary Information Fragment (BIF) object along with the BIF Binary Attribute Objects (BAOs).
- The BIF Recombinant Knowledge Assimilation (RNA) Binary Relativity Objects.
- The Binary Security Encryption Threads.

Built into the RNA Binary Relativity Objects are Binary Memory Reconstruction Objects, based on the type and source of BIF, that allow memories to be constructed for recall purposes. There are several types of Binary Memory Reconstruction Objects, they are:

- Spectral Eigenvectors that allow memory reconstruction using Implicit and Biographical LTM BIFs
- Polynomial Eigenvectors that allow memory reconstruction using Episodic LTM BIFs
- Socio-Synthetic Autonomic Nervous System Arousal State Vectors that allow memory reconstruction using Emotional LTM BIFs
- Temporal Confluence and Spatial Resonance coefficients that allow memory reconstruction using Spatio-Temporal Episodic LTM BIFs
- Knowledge Relativity and Contextual Gravitation coefficients that allow memory reconstruction using Semantic LTM BIFs

3. Conclusions and Discussion

Described here are memory processing and encoding methodologies to provide Artificially Intelligent Systems with memory architectures, processing, storage, and retrieval constructs similar to human memories. We believe these are necessary to provide artificial cognitive structures that can truly learn, reason, think, and communicate similar to humans. There is much work to do and our current research will provide the software processing infrastructure for the Information Software Agents necessary to create the underlying cognitive processing required for this Artificial Neural Memory System (ANMS). Below we give an example of memory reconstruction utilizing this ANMS, for reconstruction of image memories.

3.1 Implicit and Biographical Memory Recall/Reconstruction Utilizing Spectral Decomposition Mapping

We create non-uniform expanding fractal decomposition of the image to be "remembered." We utilize the right and left Eigenvectors of the Pollicott-Ruelle resonances to determine the separable Pictorial Information Fragment (PIF) objects. The resulting singular fractal functions form fractal spectral representations of the PIFs. These Binary Fractal Representations are stored as the Binary Information Fragments for the image. The reconstruction uses these PIFs to create a piece-wise linear image memory reconstruction, although the individual PIFs can be utilized in other memory and cognitive processes, such as to perform pattern matching and/or pattern discovery. The proposed high-level architecture for the ISA cognition and memory system is illustrated in Figure 8.

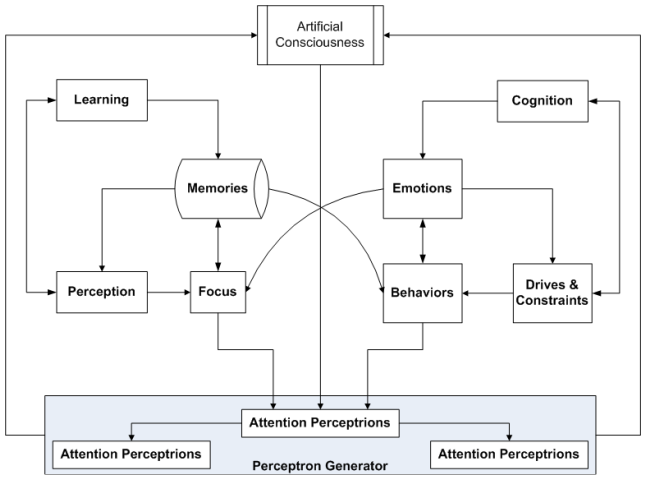

Figure 8 – The AIS High-Level Cognitive Architecture

4. References

1. Crowder, J.A., Friess, S., "Artificial Neural Diagnostics and Prognostics: Self-Soothing in Cognitive Systems." *International Conference on Artificial Intelligence*, ICAI'10 (July 2010a).
2. Crowder, J. A., Friess, S., "Artificial Neural Emotions and Emotional Memory." *International Conference on Artificial Intelligence*, ICAI'10 (July 2010b).
3. Crowder, J. A., "Flexible Object Architectures for Hybrid Neural Processing Systems." *International Conference on Artificial Intelligence*, ICAI'10 (July 2010a).
4. Crowder, J. A., Carbone, J, "*The Great Migration: Information to Knowledge using Cognition-Based Frameworks*." Springer Science, New York (2011a).
5. Crowder, J. A., "The Artificial Prefrontal Cortex: Artificial Consciousness." *International Conference on Artificial Intelligence*, ICAI'11 (July 2011a).
6. Crowder, J. A., "Metacognition and Metamemory Concepts for AI Systems." *International Conference on Artificial Intelligence*, ICAI'11 (July 2011b).
7. Crowder, J., Scally, L., & Bonato, M. 2011. Learning agents for Autonomous Space Asset Management. *Proceedings of the Advanced Maui Optical and Space Surveillance Technologies Conference*, Maui, HI.
8. Miller EK, Freedman DJ, Wallis JD (August 2002). "The prefrontal cortex: categories, concepts and cognition". *Philos. Trans. R. Soc. Lond., B, Biol. Sci.* **357** (1424): 1123–36.
9. Newell, A., "Unified Theories of Cognition." *Cambridge MA: Harvard University Press* (2003).
10. Eichenbaum H (2002) The cognitive neuroscience of memory. *New York: Oxford University Press*.
11. Kosko, G., "Fuzzy Cognitive Maps," *International Journal of Man-Machine Studies*, 24: 65-75.
12. LaBar KS and Cabeza (2006) Cognitive neuroscience of emotional memory. *Nat Rev Neurosci 7: 54-64*.
13. Yang Y, Raine A (November 2009). "Prefrontal structural and functional brain imaging findings in antisocial, violent, and psychopathic individuals: a meta-analysis". *Psychiatry Res* **174** (2): 81–8. doi:10.1016/j.pscychresns.2009.03.012. PMID 19833485.
14. Carbone, J. A Framework for Enhancing Transdisciplinary Research Knowledge, Texas Tech University Press, 2010
15. L. Brillouin, Science and information theory: Dover, 2004

Air Holding Problem Solving by Reinforcement Learning to Reduce the Congestion in Airspace Sectors

Leonardo L. B. V. Cruciol and Li Weigang
Department of Computer Science, University of Brasilia, Brasilia, DF, Brazil

Abstract—*Air Holding Problem Module (AHPM) is proposed as a Decision Support System (DSS) to help air traffic controllers in their daily air traffic flow management. This system is developed using Multiagent framework to organize and optimize the solutions for controllers to handle traffic flow in Brazilian airspace. The paper focus on the problem solving by Reinforcement Learning to show how the history experience of the controllers can be used to advise the new activities for the new situation. About 1110 daily flights over Flight Information Regions (FIRs) as FIR-Brasilia and FIR-Recife were studied considering the local and global reward functions and three time intervals to apply restrictive measures. As a result, with the use of AHPM, the decision process is improved with a high level of automation. At the same time, the congestion in related sectors is reduced from 15% to 57% in local scenarios and 41% to 48% in global.*

Keywords: Air Holding Problem, Air Traffic Flow Management, Decision Support System, Real Time Problem, Reinforcement Learning.

1. Introduction

Air Traffic Flow Management (ATFM) is a complex domain related with human and automatic activities. In this domain there are Air Holding Problem (AHP), Ground Holding Problem (GHP) and others, which happen when air traffic congestion appearing and it is necessary to apply restrictive measures to re-distribute the traffic flow by air traffic controllers. They are responsible to verify airspace scenario and analyzes the possible risk situations to take some actions with proper decision. Therefore even for an expert with rich experience is expected to make any management action in extremely short time interval with the detection and analyze of a complicated environment. In many cases this process is almost manually in some regions. This is a necessary to develop a semi-automation system with suitable computational model, especially to solve Air Holding Problem in ATFM.

Air traffic controllers work in real time with many attributes to handle in ATFM. Decision Support System (DSS) is a suitable concept to be applied in AHP solving. In DSS framework, considering the reality of AHP, Reinforcement Learning algorithm is introduced in this study. The air traffic controllers can learn the history experience and scenario to adjust the decision making when the congestion appears. As the result, the restrictive measures in AHP solving can be adequate and applied in air traffic management and improve the effeteness of the management.

In Brazil, Ground Holding Problem is studied in previous researches with the computational models [5]. The real data was collected from Integrated Air Defense Center and Air Traffic Control (CINDACTA). This research focus on the AHP solving by Reinforcement Learning to show how the history experience of controllers can be used to advise the control activities for the new situation.

Air Holding Problem Module (AHPM) is proposed as a Decision Support System to help the air traffic controllers in the daily air traffic management. In this model, multiagent framework was constructed for Flight Information Regions (FIRs) and Central. To take suitable restrictive measures, AHPM is collaborated by two approaches for agents in learning and action. First one, local agents will learn and make the best suggestions based on local scenarios and send the decision information to a global control agent. Second one, global control agent will evaluate the best actions to take for global environment. With this procedure, the suggestion is sent to air traffic controller to apply the restrictive measures with more accuracy and efficient. The knowledge about possible impacts to reduce the congestion, in each scenario, is collaborated to improve air traffic management and increase the safety.

As a case study, 1110 daily flights over FIR-Brasilia and FIR-Recife were studied considering the local and global evaluation functions and three time intervals to apply the restrictive measures. As a result, with the use of AHPM, the decision process is improvement with a high level of automation, the congestion in related sectors is reduced from 15% to 57% in local scenarios and 41% to 48% in global.

The paper is organized in the following manner. In section 2, there is a brief review of Decision Support System and Reinforcement Learning concepts and related researches. Section 3 reviews Air Traffic Flow Management concepts and related problem in Brazil. AHPM is proposed in section 4 including the definition of the reward functions. Section 5 concerns a case study with real data from FIR-Brasilia and FIR-Recife to verify the effectiveness of the developed model and related results. Section 6 concludes the paper and proposes the direction of the future research.

2. Related Concepts and Researches

The concept of Decision Support System and the method of Reinforcement Learning are used in this research. This section gives a basic description and reviews the related researches of these concepts in ATFM.

2.1 Decision Support System

A Decision Support System is used to help users with relevance information in decision making process. Using a computer to present the process of decision making of human being is still a difficult task especially in the activities of intuition, conceptualization and creativity. On the other hand, a computer can help human being in the information processing with high speed, parallelism, accuracy and persistent storage [8].

Combining these two factors, DSS achieves an accepted automation level to help the human being decisions. This allows working with problems of a decision making which proportion overtakes the human being capacity or exceeds temporal and financial means available.

Some typical tasks of DSS are data organization and visualization, perceptible knowledge representation, forecast scenarios and impacts, information clustering as new information, simulators and optimization solution. The work made by automation should be only in areas like the control of problem solving activities, detection of conflicts and execution of evaluation, search and planning sequences.

To improve this kind of system, the hybrid solutions are used, such as Reinforcement Learning which can be used to acquire knowledge from air traffic controller in ATFM and to elaborate a Multiagent System to further help the air traffic controllers in new situation and quickly replying.

In many times, human knowledge is scattered. In Flight Information Regions, the information available is distributed and not effectively applied by air traffic controllers in ATFM. With the help of decision support system, the information is well integrated and utilized. This is the main reason to develop AHPM in this research.

2.2 Reinforcement Learning

Reinforcement Learning is a learning process which consists of an agent without prior knowledge and in a certain number of interactions with the environment to learn the useful knowledge and therefore receives rewards for taking actions and achieving goals.

In Reinforcement Learning process, it is possible to realize an optimal solution to the problem in matter, i.e., it finds the best actions to achieve a determinate goal in the possible optimized way, taking into consideration of a certain environment in an instant T_k, where k is the present instant.

The agent will act mutually with the environment, during the interaction, to recognize which scenario it is and therefore to choice the best action as a decision. After the agent presents an action, it will be given a reward. Therefore it is possible to check if the action is better for the current scenario [3,6,9].

The reinforced learning algorithm used in AHPM is known as Q-learning [11]. This algorithm uses a table denominated as Q-table, that, as part of the learning process, incorporates the agent's experience. The Q-table stores action-scenario pairs that represent the states observed by the system. The scenario configuration consists of the number of aircraft in the ATC sectors at certain times.

2.3 Related Researches

Recent researches in ATFM combines Reinforcement Learning and Multiagent techniques. It uses this combination to incorporate the human agent's experience into automated ATM processes. ATC domains are too complex to be completely automated and are directly impacted by tactical ATFM.

It developed metrics to evaluate the efficiency of traffic flow control measures generated by Reinforcement Learning agents. As a result, it was possible to improve the actions taken by an agent conceived to simulate the behavior of air traffic controllers, given the suggestions by the ATFM agent and as such suggestions were accepted by the air traffic controller [1,4,7].

In the proposed system [1], the ATFM agent uses a Reinforcement Learning algorithm that seeks to maximize the reward that derives from the scenarios generated, which will be evaluated based on the total delays generated and the number of aircraft in the ATC sectors, both resulting from the flow control policy. The air traffic controller is characterized as a reward maximizing Reinforcement Learning agent that seeks only the minimization of the amount of aircraft in the ATC sectors. This assumed behavior for the air traffic controller is not entirely valid, as the minimization of traffic in the ATC sectors is not the ATC's only goal [2,5,10].

In reality, ATC seeks a balance between safety, which benefits from a low number of aircraft in the ATC sectors, and operational efficiency, which depends on the maximization of flows. This assumed behavior is, therefore, a significant limitation of the model.

3. Air Traffic Flow Management

ATFM is a complexity procedure to avoid exceeding air traffic control capacity and focuses on the supply of information to maintain the traffic flow with safety and less impact on scenarios that are necessary to take unexpected measures. The ATFM environment can be organized into three phases:

- Strategic Level: Considering tactical planning of flights covering the period of forty-eight hours until the time before the flight.
- Operational Level: Focusing on strategic decision making covering the period from forty-eight to two hours before the flight.

- Tactical Level: Considering tactical decision making covering the period from two hours before the flight until the aircraft arrives at its destination.

This study concerns in ATFM Tactical Level. The basic problems are solved such as the aircraft in flight, which increases the problem level because the occurrence of the problem and its solution happens on real time.

ATFM can guarantee that flights are conducted in a safe, quick, orderly and economic way. It is possible to avoid overloading in the air traffic capacity, optimize airspace and provide information to responsible.

Some activities from ATFM can be automate, partially or not, or improve using DSS. So, air traffic controller can monitor and analyze all aspects involved in the environment, such as meteorological aspects, evaluate restrictive measures before to take some action, and verify alternatives flows of air traffic.

3.1 The Problem of ATFM

The air traffic flow management needs to be prepared to maximize the opportunities of the available structure so that resources can be put into the good condition to use. In this case, it can be mentioned the best flow management of the aircraft while in airspace and, therefore, besides improving the safety levels of the Brazilian aviation. It is also possible to reduce negative indicators and achieve good results for all involved in a situation [5,8].

ATFM environment is a domain with many complex activities, such as the air holding problem. It occurs when aircraft in flight route needs to wait in airspace for some reasons.

One of these reasons could be that an airport had to be closed, for example. Situations involving natural phenomenon or terrorist acts, may be motive to excess of aircraft on a particular sector and thus other aircraft need to be retained for some time in other sectors.

The problem becomes much more serious, in some critical scenarios, e.g., when there is a scenario, which includes all aircraft under the responsibility of the Brazilian authorities and there are sub scenarios which responsibilities are under a certain CINDACTA. When an action is chosen for a sub scenario, as the time goes by, the result of these actions can make better a sub scenario and aggravate another one, and then the whole situation can become an issue of great risk to the safety of everyone involved.

3.2 Brazilian Scenario

Brazilian airspace covers the entire land area of the country, including part of the Atlantic. There are five FIRs: FIR - Amazônica, FIR - Recife, FIR - Brasilia, FIR - Curitiba e FIR - Atlântico. In this paper, it will consider two FIRs: Brasilia and Recife. The airspace of this case study is presented in Fig. 1 Airspace of FIR - Brasilia and FIR - Recife.

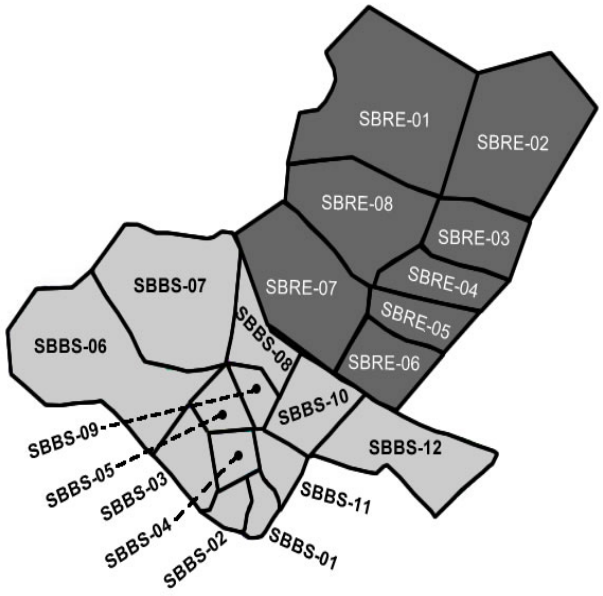

Fig. 1: Airspace of FIR - Brasilia and FIR - Recife

Each FIR is divided into some control sectors, in order to separate management activities and achieve more control. Currently, there are 46 sectors, where: 14 in FIR - Amazônica, 8 in FIR - Recife, 12 in FIR - Brasilia, 10 in FIR - Curitiba and 2 in FIR - Atlântico.

These sectors are carried out by air traffic controllers, which work in Area Control Center (ACC). In each CINDACTA, there is an ACC responsible for one FIR. Thus, it is possible to realize the complexity of activities management and necessity for subdivision to manage so many factors, e.g, the amount of aircraft by airspace sector influences the complexity of managing, i.e., more aircraft flying in the same sector, more and greater security risks involved in ATFM.

4. Air Holding Problem Module

A hybrid solution is proposed in this study, which uses Reinforcement Learning and Multiagent System. The first technical concerns in learning from the experience, day by day, with the air traffic controllers. Thus, it is possible learning online without previous knowledge to use DSS concepts. The second one, Multiagent System, makes possible to achieve better results in complex domains with many attributes.

4.1 Agents Modeling

Two FIR Agents are used in this case study: FIR-Brasilia Agent and FIR-Recife Agent. Each one is applied to achieve the best actions for some situation in its FIR. The Central Agent is responsible to analyze the possible actions from

each FIR and suggests the best group to air traffic controller. The process of the communication between agents is presented in Fig. 2 Agent Modeling.

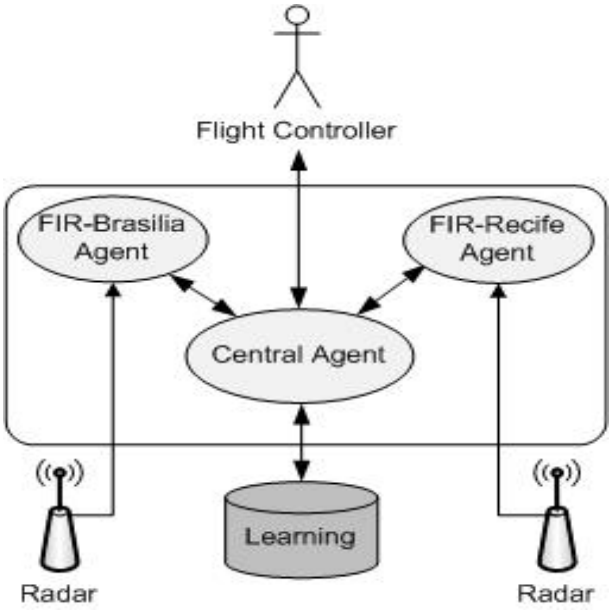

Fig. 2: Agent Modeling

After the identification of the best actions to be taken by Central Agent, this agent will verify similar scenarios on learning database and these actions are taken by the air traffic controllers.

If there are better results to reduce air traffic level, it will be presented taken actions as suggestion. If results are worse or not exists similar scenarios, it will be analyzed the three best actions for each FIR and send it to Central Agent.

4.2 Reward Functions

Each agent needs to evaluate if some action is good or not over others in a specific scenario. So agent evaluates by reward functions which make possible to take the best action for each scenario.

The agent is proposed to consider the capacity of aircraft in airspace sectors. In Brazil, every sector is allowed to set twelve flights as the responsibility of air controller to maintenance the air traffic flow. The action must reduce the amount of aircraft and improve the flow of aircraft throughout the environment.

The FIR Agent is developed to evaluate the local scenarios, i.e., environment of FIR - Brasilia or FIR - Recife and suggest the best actions for local environment. For this kind of agent, the reward function is defined as:

$$F_{FIR}(s) = \sum s \quad | \ \exists \, (a > 11 \in s) \tag{1}$$

$$C_{FIR}(s) = \sum a \quad | \ \exists \, (a > 11; \ s' \in S) \tag{2}$$

$$E_{FIR} = \sum \{F_{FIR}(s) * C_{FIR}(s)\} \tag{3}$$

Where:

- $F_{FIR}(s)$ is a summation of adjacent sectors from group *s* that are congested. Amount of aircraft in *s* is defined by *a*, which in Brazil is defined as congested sector if there are more than eleven aircraft in each airspace sector.
- $C_{FIR}(s)$ is a summation of aircraft from congested adjacent sectors (*S*) of sector *s*. Amount of aircraft in *s'* is defined by *a* and sector *s'* is in group of congested adjacent sectors *S*.
- E_{FIR} is the FIR scenario state.

The main objective of the reward function of FIR Agent is to evaluate the level of air traffic in each moment for each FIR. So it is possible to verify if some action will improve or not this level in the next time before to take any action.

The Central Agent is developed to evaluate the global environment, which includes FIR - Brasilia and FIR - Recife. It will collected three best actions for each suggestion of FIR Agent and Central Agent will evaluate the best actions for global environment, taking into account of the suggested actions by FIR Agent and its impacts in other FIR. The reward function of Central Agent is defined as:

$$G_{Central}(FIR) = \sum FIR \quad | \ \exists \, (s \in FIR; a > 11 \in s) \tag{4}$$

$$P_{Central}(s) = \sum s \quad | \ \exists \, (a > 11 \in s) \tag{5}$$

$$D_{Central} = \sum a \tag{6}$$

$$H_{Central} = G_{Central} * P_{Central}(s) * D_{Central} \tag{7}$$

Where:

- $G_{Central}(FIR)$ is a summation of FIRs that contains at least one congested sector. The amount of aircraft in *s* is defined by *a*, in Brazil, it is defined as congested sector if there are more than eleven aircraft in each airspace sector.
- $P_{Central}(s)$ is a summation of the congested sectors in the whole environment, i.e., sectors from each FIR analyzed by E_{FIR} function. The amount of aircraft in *s* is defined as *a*.
- $D_{Central}$ is a summation of the aircraft in global environment, including all necessary sectors to analyze each FIR.
- $H_{Central}$ is the global scenario state.

The main objective of the reward function of Central Agent is defined to evaluate the level of air traffic in each

moment of global environment, i.e., FIR-Brasilia and FIR-Recife. So it is possible to verify if some actions will improve or not this level in the next time before to take any action. Maybe, some suggested actions are not the best for a FIR but it is better than others for global environment.

5. Brazilian Case Study

FIR-Brasilia is the most important and critical FIR in Brazil. The FIR-Recife covers an area with high amount of flights scale. Thus, it is possible to achieve a better model because it is used, for case study, two FIRs very distinct.

The FIR-Brasilia (FIR-BS) is identified by International Civil Aviation Organization (ICAO) as *SBBS*. It consists of seven important airports in five cities. There are twelve airspace sectors in FIR-BS. It was identified fourteen airspace sectors adjacent of some sectors in this FIR.

The FIR-Recife (FIR-RE) is identified by ICAO as *SBRE*. It consists of six important airports in six cities. There are eight airspace sectors in FIR-RE. It was identified eight airspace sectors adjacent of some sectors in this FIR.

There are two types of the restrictive measures: air delay by reducing the speed and air forward by increasing the speed. These measures follow the goal of reducing airspace congestion, so the time that an aircraft designed to reach and exit of an airspace sector may be managed earlier or later as needed.

5.1 Local - FIR Agent

As presented in Fig. 2, the FIR Agent is developed to evaluate the traffic flow scenario within a FIR. In this research, FIR-Brasilia and FIR-Recife are studied separately. To analyze the decision support effects, the air traffic congestion index is defined in two conditions: 1) Traditional Approach, i.e., the restrictive measures are defined directly by air traffic controllers; 2) FIR Agent Approach, i.e., the restrictive measures are suggested by FIR Agent considering local optimization. The results from FIR-BS are presented in Fig. 3 Traditional x FIR Agent Approach in FIR-BS. And the results from FIR-RE are presented in Fig. 4.

In Fig. 3, the evolution from initial scenario to next three scenarios T_2 was presented. It is possible to verify that in the second interval there was no congestion in the airspace sectors when used AHPM approach, but the index of the level of air traffic was 264 in traditional approach by air traffic controllers.

In Fig. 4, it is possible to verify that in last two intervals there was no congested in the airspace sectors because air traffic level was zero when used AHPM approach, but using traditional approach the indexes were 255 and 74 respectively.

5.2 Global - Central Agent

As presented in Fig. 2, Central Agent is developed to evaluate the traffic flow scenario within all FIRs. In this

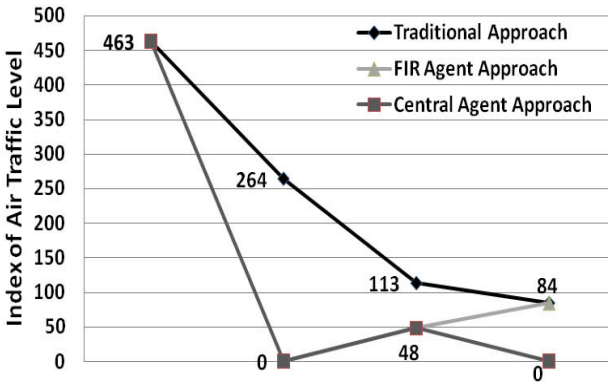

Fig. 3: Traditional x FIR Agent Approach - FIR-BS

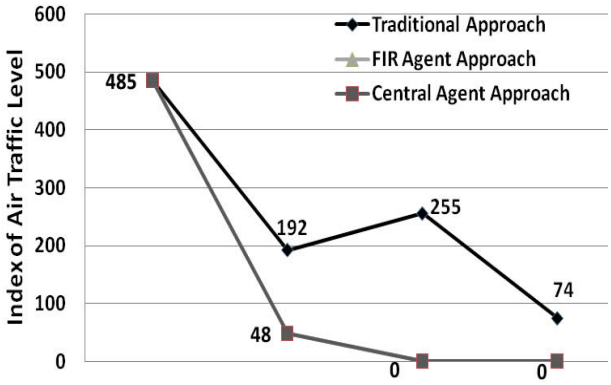

Fig. 4: Traditional x FIR Agent Approach - FIR-RE

research, two FIRs with 1110 flights daily are considered. To analyze the decision support effects, two conditions are studied: 1) Traditional Approach, i.e., the restrictive measures are defined directly by air controllers; 2) Central Agent Approach, i.e., the restrictive measures are suggested by Central Agent considering global optimization.

Central Agent is proposed to verify three best suggestions for each FIR and choose what would be the best group of restrictive measures to be applied in each FIR. The Fig. 5 presents the evolution from initial scenario to future time T_2 in the global environment.

It is possible to verify the improvement from first to second interval and reaching in the last interval no congestion in the airspace sectors by means of Central Agent. While using the Traditional Approach, the air traffic index is, on average, up to four times more than AHPM approach.

The approach proposed in this paper, AHPM, can be divided into two stages, the analysis by FIR Agent and after results for the first time the analysis by Central Agent. So even though this research is applied in only one FIR, the approach will achieve great results because it is considering factors such as adjacent sectors, aircraft in environment and congested airspace sectors.

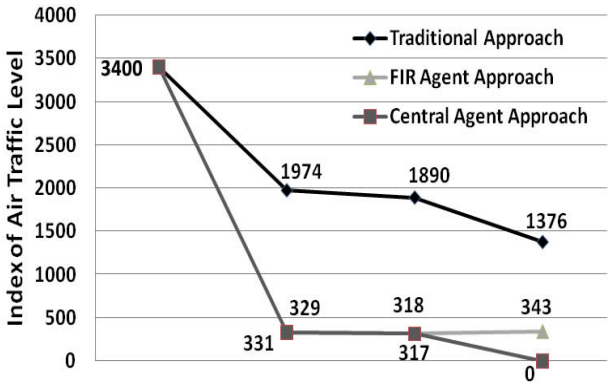

Fig. 5: Traditional x Central Agent Approach

The Central Agent will verify the three best suggestions for each FIR and choose what would be the best group of restrictive measures to be applied in each FIR.

5.3 Achieved Results

AHPM is proposed to work in two approaches: 1) the analysis by FIR Agent to support decisions with local optimization; 2) the analysis by Central Agent to support decisions with global optimization. Even though this research is applied in only two FIRs, the preliminary study is promissory.

In order to find the solutions in the more complete ATFM system, AHPM can help the air controllers to get more useful information to make the decision with more safety.

To get more evaluation of the application of AHPM, the six results from real scenario are considered: 1) the results from FIR-BS and FIR-RE using traditional approach, i.e., the restrictive measures are defined directly by air traffic controllers; 2) the results from FIR-BS and FIR-RE using AHPM, i.e., the restrictive measures are suggested by AHPM in local; 3) the results from FIR-BS and FIR-RE together using AHPM, i.e., the restrictive measures are suggested by AHPM in global. The Fig. 6 presents these six results of comparison between traditional approach and AHPM.

It is observed that the proposed approach, AHPM, achieved better results in all cases than traditional approach. And in most cases, the results from Central Agent achieved better results than FIR Agent. The following is a brief summary:

- FIR-BS
  - (17:30 - 17:59) - Improvement of 57%
  - (18:00 - 18:29) - Improvement of 15%
  - (18:30 - 18:59) - Improvement of 18%
- FIR-RE
  - (17:30 - 17:59) - Improvement of 30%
  - (18:00 - 18:29) - Improvement of 53%
  - (18:30 - 18:59) - Improvement of 15%

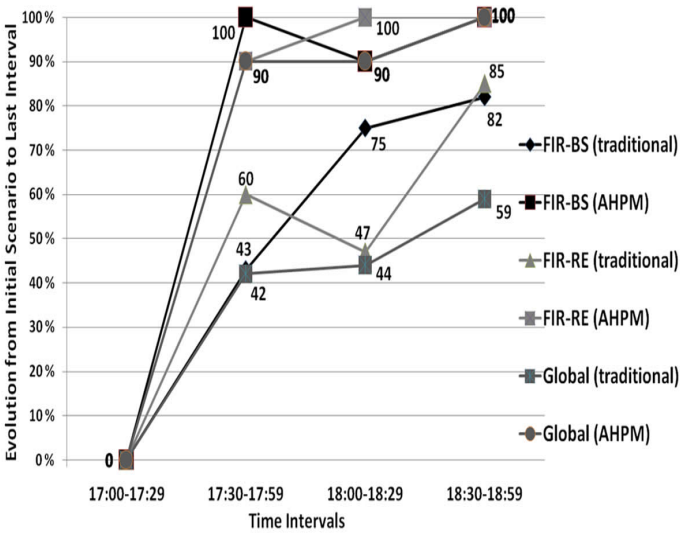

Fig. 6: Comparison between traditional approach and AHPM

- Global Environment
  - (17:30 - 17:59) - Improvement of 48%
  - (18:00 - 18:29) - Improvement of 46%
  - (18:30 - 18:59) - Improvement of 41%

As expected initially, these results showed the effectiveness of AHPM, which improved as the scenarios became more critical. Evaluating the case study, the congestion in airspace sectors was reduced between 15% and 57% in local scenarios and between 41% and 48% in global scenario.

These results demonstrate the improvement of impacts prediction and restrictive measures suggestions using AHPM. It is also show the possibility to model a computational solution to support, effectively, the decision making for air traffic controllers.

6. Conclusions

AHPM was developed to solve Air Holding Problem in Brazil. The proposed model used the Decision Support System concept including Multiagent System and Reinforcement Learning. The main utility of AHPM is to act on the reduction of Air Holding in airspace sectors and help the decision making by air traffic controllers. The AHPM is concerned to increase the security and to support ATFM process in local and global scenarios.

It were defined two reward functions to realize the suitable Reinforcement Learning. FIR Agent and Central Agent were developed as a platform to support ATFM. Three time intervals were considered to apply the restrictive measures. As a result, with the use of AHPM, the decision process was improved with a increased automation. The congestion in related sectors was reduced between 15% and 57% in local scenarios and between 41% and 48% in global.

The future work is to implement AHPM in the Brazilian Air Navigation Management Center (CGNA) to effectively help air traffic controllers in the day to day Air Traffic Flow Management process.

References

[1] A. Agogino and K. Tumer, "Learning Indirect Actions in Complex Domains: Action Suggestions for Air Traffic Control Advances in Complex Systems", *World Scientific Company*, 2009.

[2] S. R. Wolf, "Supporting Air Traffic Flow Management with Agents", *American Association for Artificial Intelligence Spring Symposium: Interaction Challenges for Intelligent Assistants*, 2007.

[3] A. M. Bayen, P. Grieder, G. Meyer and C. J. Tomlin, "Lagrangian Delay Predictive Model for Sector-Based Air Traffic Flow", *AIAA Journal of Guidance, Control and Dynamics 28*, pp. 1015-1026, 2005.

[4] A. Agogino and K. Tumer, "Regulating Air Traffic Flow with Coupled Agents Advances in Complex Systems", *Proceedings of 7th International Conference on Autonomous Agents and Multiagent Systems*, 2008.

[5] L. Weigang, D.P. Alves, M. V. P. Dib and A. F. Crespo, "Intelligent computing methods in Air Traffic Flow Management", The Transportation Research - Part C, Emerging Technologies, Vol. 18 (5), pp. 781-793, 2010.

[6] A. J. M. Castro and E. Oliveira, "Using Specialized Agents in a Distributed MAS to Solve Airline Operations Problems: a Case Study", *IAT*, 2007.

[7] G. Weiss, *Multiagent Systems, Artificial Societies and Simulated Organizations*, The MIT Press, 2005.

[8] A.J.M. Beulens and J.A.E.E. Van Nunen, "The Use of Expert System Technology in DSS", *Decision Support Systems 4*, 421-431, 1988.

[9] A. Mellouk, "Advances in Reinforcement Learning", InTech, 2011.

[10] A. M. F. Crespo, L. Weigang and A. de Barros, "Reinforcement learning agents to tactical air traffic flow management", *The International Journal of Aviation Management*, Vol. 1, 3, pp. 145 - 161, 2012.

[11] C.J.C.H. Watkins and P. Dayan, "Q-learning", *Machine Learning*, Vol. 8, No. 3, pp. 279 - 292, 1992.

Automated Intelligent Monitoring Systems

J. Wallace[1] **and S. Kambouris**[1]
[1]Infinite Dimensions, Alexandria, Virginia, United States of America

Abstract - *Some of the primary challenges in the development of cost-effective, next-generation Game Changing Technology for automated learning systems are the effective, efficient incorporation of representative knowledge models: domain or subject matter experts (SME), instructors/trainers, and trainees. Through interaction of the SME, trainer/trainee models, Automated Intelligent Monitoring System (AIMS) assesses what the student knows, and how well the student is progressing. Previous approaches to solving this problem have yet to overcome the inherent challenges long associated with complex, knowledge-based systems. The AIMS architecture framework overcomes limited and outdated psychological/computer science theories and insufficient computer science artifact using semantic ontology, and development engine architecture framework.*

Keywords: Learning Systems, Semantic Ontology, Architecture Framework

1 Introduction

Significant challenges in the development of cost-effective, next-generation Game Changing Technology for automated learning systems are the effective, efficient incorporation of representative knowledge models: domain or subject matter experts (SME), instructors/trainers, and trainees. Through interaction of the SME, trainer/trainee models, Automated Intelligent Monitoring System (AIMS) assesses what the student knows, and how well the student is progressing. The AIMS architecture framework overcomes limited and outdated psychological/computer science theories and insufficient computer science artifacts. It does this through the AIMS architecture framework's functionally realistic mission and environment approach and involvement from the training SMEs.

1.1 Automated Intelligent Monitoring System (AIMS)

The AIMS architecture framework is two things: an automated, integrated, development engine systems integration environment for high performance networked systems with library support for training and monitoring. The development engine is discussed in detail elsewhere [1]. Secondly, the AIMS' corresponding high performance real-time executive/government off-the-shelf (GOTS) message bus operates in all environments, even resource-constrained ones such as Smartphone applications or in the Battlespace itself.

AIMS is relevant over wide ranges of education and training situations and is a Game Changing Technology. AIMS includes the capability for both single learners and multi-disciplinary group training as it has the ability to instrument and control a number of systems simultaneously. AIMS allow for the distribution of system processing for efficiency and scales in two dimensions: number of learners and number of systems which are instrumented and controlled. AIMS provides a solution for the problem of implementing intelligence and automation by effectively creating the knowledge models for the Expert, Instructional, and Trainee subsystems.

2 Instrumenting Learning Environment

Instrumentation has traditionally been a fundamental problem in traditional automated learning system architecture frameworks as it requires measuring the trainee's inputs into the system as well as the reverse function of providing feedback to both the trainee and trainer. Correctly instrumented learning environments increase the overall effectiveness of the AIMS as more trainee assessment information becomes available. An example of instrumenting a flight simulator would involve measuring and recording pilot's stick and switch movements, button presses, and the way in which the pilot is monitoring the gauges.

Greater system complexity arises when addressing multi-modal group instruction as individuals perform and train on different duties simultaneously, as well as participating at different times and separate tasks. Therefore, proper AIMS instrumentation is critical. Utilization of both group and individual assessment data provides sophisticated, complex information that has been rarely accounted for in previous trainee models.

Group instruction compounds training complexity, but is taken into account by AIMS. In group instruction mode, AIMS chooses content for the trainee group and makes multiple decisions: topics to address, problems to solve, and what feedback to provide and in which order, as well as what trainee information will be recorded. When AIMS employs the trainee model, it represents all the individuals and their specific group's aspects as well as determines their tasks and correct order sequence for the trainees. Multiple possibilities

exist in determining the most appropriate tasks for a training group.

Another fundamental technical requirement for AIMS is to efficiently utilize its SMEs during training as an integrated trainer-in-the-loop. Real-time SME training integration facilitates an evolution in the inherently regimented and highly controlled nature of computerized training allowing for enhanced flexibility, complexity, variation and increased scope of the training itself. In order for a SME to interact with their trainees in a real-time environment, they need a flexible networking technology utilizing an efficient messaging system. AIMS's real-time interactions allow the training itself to evolve more rapidly based upon feedback from the trainee or trainer/SME. AIMS takes into account a trainee's needs with regard to communication, personality conflicts, or learning style issues which it rigorously accounts for as more knowledge is provided a priori to AIMS.

2.1 Semantic Ontology Streamlines AIMS Implementation

This paper addresses the ability to reduce the time required to plan, implement, execute, and analyze training in a unified AIMS architecture framework. AIMS is based on the concept of ontologies and employs Semantic Web technologies. This framework is intended to be used by different constituencies and employs a method, vocabulary, and user interface approach that allows the needs of different SMEs to be addressed. At the same time AIMS is functionally capable of operating off a unified conceptual structure.

In general, the major technological innovations are the ability to affordably instrument training/ operational systems creating a learning environment to stimulate trainees, record their responses/capabilities, and facilitate their training. AIMS utilizes the ability to create intelligent systems with hybrid algorithm capabilities and synchronizing a large number of them thereby permitting AIMS to be built in a more modular and understandable way as an entire intelligence system. AIMS facilitates the ability to distribute computation easily over a set of resources. Additionally, the authoring and programming of AIMS is done in a way that simplifies the system specification and programming, respectively facilitating the creation of an automated intelligent monitoring system.

2.2 Adaptive Learning System

AIMS takes into account the trainee's situational awareness, cognitive capabilities, action accuracy, situational distractions, cognitive distractibility and any resulting reduction in accuracy. AIMS accounts for functionally disparate phenomena such as recognition of patterns, adapting new solutions or strategies and rule following in order to represent "intelligence" more effectively. Based upon input from SMEs, current best training practices can be incorporated. AIMS ascertains the most appropriate feedback for the trainee by determining learning styles and communication preferences, in addition to skill level, and provides the most accurate advice for the trainees and SMEs. In reality, as humans, we rarely follow or interpret rules strictly; and thus, should not expect AIMS to do likewise. AIMS will have a great deal of generality and flexibility while maintaining ease-of-use for integrators, developers and users.

AIMS is an adaptive learning system, taking into account the trainee's situational awareness, cognitive capabilities, action accuracy, situational distractions, cognitive distractibility and any resulting reduction in accuracy. AIMS accounts for functionally disparate phenomena such as recognition of patterns, adapting new solutions or strategies and rule following in order to represent "intelligence" more effectively. AIMS ascertains the most appropriate feedback for the individual trainee by determining learning styles and communication preferences, in addition to skill level, and provides the most accurate advice for them so they may proceed to the next problem-solving step. The advice given to the trainee is appropriate for their capabilities.

2.3 Technological Advances

In order to implement AIMS, advances in several technology areas must be combined to create an understandable architecture, and functional decomposition, that can scale and adapt to training problems and are discussed elsewhere [1]. AIMS knowledge and intelligence representations focus on pattern recognition and the basic steps of decision-making, as opposed to a larger view to include the reasons for decisions, and the timelines in which decisions must be made. AIMS's complex, distributed application architecture framework instruments a system of training systems quickly.

2.4 Knowledge Types

Employing knowledge types in AIMS exceeds typical inference engine in rule-based environments [2]. Accommodating increased levels of modeling complexity for automating individual and team training requires a richer set of modeling primitives. A key capability involves easily constructing natural inter-component relationships logically and temporally. In this way, a functionally realistic mission and environment approach overcomes outdated psychological and computer science theories, used to represent intelligence as existing methods utilizing computer science artifacts are insufficient. An empirical connection is needed between real psychological measurement and behavior models. Certain sets of factors are more congruent and adaptive with certain mission/environments. Human factors of individuals, teams, and organizations may be capitalized upon and/or compensated for after they are identified and integrated. Through integrated interaction of the knowledge models,

AIMS accurately provides a more reasonable judgment about what the trainee knows and how well they are progressing both to the trainee, as well as their trainer.

2.5 Ontology-Based Architecture Framework Development Engine for Systems Integration

Ontology is a formal representation of domain knowledge that defines the concepts within a domain and the relationships between those concepts. It can be used to reason about the properties of that domain and is often described as a formal, explicit specification of a shared conceptualization as it provides shared vocabularies [3]. In this case, we need vocabularies able to describe: military operations and associated relevant real world activities, live military assets and their virtual reality and constructive representations, state, initialization, and exchange data and overarching conceptual descriptions of the training event.

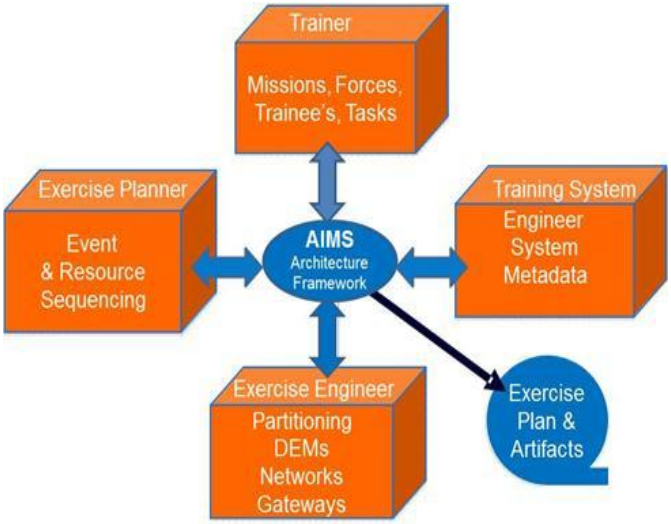

Figure 1. Composition Automation Approach

To provide composition automation, as shown in Figure 1, the AIMS Architecture Framework interfaces, models, applications (especially simulations), and data involved in AIMS systems and exercises must be described/captured in a machine readable manner. Ontologies are employed for this purpose. Ontology alignment then permits the building of connections or bridges between existing models and enhances the ability to add new models. Model management and exploitation is made more effective satisfying Warfighter needs by promoting increased realism during training. Providing these ontology based tools enables exercise SMEs and military users to employ composition and architecture bridging tools to rapidly go from testing, training, experimentation, and rehearsal requirements to a training exercise or event for single trainees or groups of them.

The understanding of models, specifically Model Semantics, is almost exclusively a human activity. Models are only partially and ambiguously documented; much has to be interpreted and filled in from experience or context closely working with SMEs. As this experience is difficult to acquire and share, using Model knowledge is restricted to experts. The goal is to provide a method to partially encode expert knowledge about: mathematical and logical assumptions about the limits of the description of physical and non-physical phenomena such as human behavior, interfaces and their semantics, identification of patterns and frameworks, and causality information and execution order, such as one event triggering another.

2.6 Metadata and Composability Services

What this means for the Warfighter: a simple but robust method for categorizing everything from a handgun to the newest air superiority jet aircraft. Published ontologies that make previously created artifacts easy to find and retrieve should help alleviate reimplementation due to the common expedient of "I can't find it so I'll just create a new one".

Utilizing the ontology-based development engine, we address the many significant systems integration challenges and create complex, realistic, and scalable networks utilizing component inter-relationships. The engine allows for the distribution of autonomous controls and constantly monitors them and permits the implementation of complex webs of cause and effect and dynamically alters the component execution structure. When information transfer occurs successfully, automatically and without human intervention, the transfer is symptomatic of integration. Systems integrators attempt to reduce overhead costs by reproducing the information flow more accurately and consistently all within the timeframe of the user's need.

Systems integration teams must adapt, evolve, and facilitate integration of training systems. Successful integration requires the establishment of an AIMS partnership approach in conjunction with agile product development for all stakeholders: users, SMEs, program managers and program developers. Utilizing a flexible learning process, agile systems integration provides rational, logical conclusions that then lead the path forward for training systems integration. Utilizing rapid modification and implementation of SME and user input creates a more effective AIMS architecture framework.

The purpose of a cohesive and robust development engine is twofold: 1) to build and query knowledge bases (set of descriptions, facts, instructions, commands); and 2) to control the execution of numerous hardware and software components of training systems. The engine integrates hardware and software systems by extending Conceptual Graphs (CG) technology improving the resulting integration.

2.7 Flexibility and Realism

AIMS development engine enables the solution of key representation problems, permitting an easy-to-use, adaptive system. The overhead costs of information flow between software and hardware continue to increase as do system complexity. There are many inherent software/hardware challenges in integrating complex systems. We utilize Conceptual Graphs (CG) to integrate complex hardware and software systems [4]. CGs resolve complex issues arising from the following issues:

- Hardware compatibility
- Communication protocols
- Understanding transfer information
- Well defined system interrelationships
- Mapping for adequate neutral-format standards
- Mutual acceptance of the communication purpose
- Operational meaning in terminology
- Advancement in the core development environment and infrastructure

AIMS leverages many important capabilities, integrates many kinds of phenomenology, and encompasses a variety of formats. The ability to integrate a wide variety of "intelligent" algorithms and software is paramount. Several mathematical and causal formalisms must be accommodated by the representation framework. The development engine's non-invasive, non-destructive integration and interoperability illustrates how the vital problem of synchronization between functionally distinct computational subsystems is accomplished. Accurate, precise synchronized control algorithms and software execution solves one of the key problems in intelligent systems today. Arbitrarily supporting complex causal networks easily is central to the value-added to the AIMS community from the perspective of development engine utility enabling both flexibility and realism.

The inherent ability to provide distributed and federated interactions and object sharing permits a wide variety of data sources to be integrated and interoperated. Functions such as automated, time-based validity and refresh checks and updating functions are a trivial capability. The implementation of more interesting functions such as causal or logical condition combinations triggering refresh or updating is naturally supported. The AIMS architecture framework is based on the abstractions shown in the Figure 2.

The *Evaluation* function relies on AIMS' ability to establish a wide variety of knowledge, information, and data feeds. This can be done in two ways by an active push or passive pull. Most systems support one or the other, but not both. Furthermore, the mechanism for doing so must be low-footprint and portable. This permits a wide variety of software systems and devices to be employed.

The *Records Database* stores Performance information, which is derived from both the Evaluation process and the *System Coach*. The Records Database holds information about the past, such as Learner history records, the present, such as current Assessments for suspending and resuming sessions and the future, such as Learner or training objectives. The Records Database represents an advance in intelligent repositories in that a wide variety of complex knowledge, information, and data storage and retrieval functions can be easily implemented.

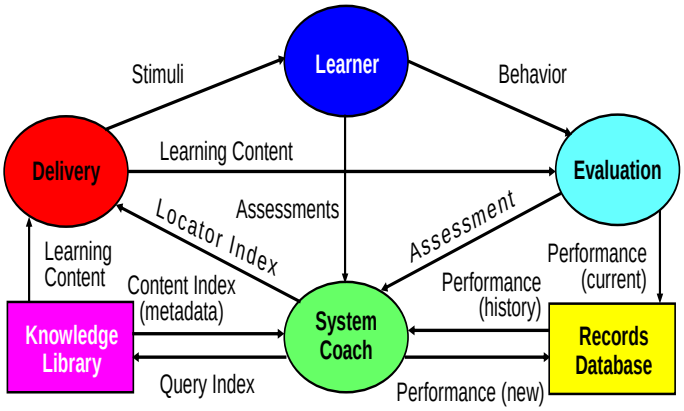

Figure 2. AIMS Architecture

The *System Coach* requests and receives Performance information, such as assessments and certifications back to the Records Database. Typically, historical information is retrieved, but current information such as "bookmarks" for resuming sessions and future information such as template of future training objectives may be retrieved. The System Coach exploits the full capability of AIMS by a complex causal network representation capability.

The *Knowledge Library* capability permits a variety of knowledge representation formats to be employed that describe actions and responses of the system. Much like the Records Database, the ability to integrate and interoperate a wide variety of databases is crucial, as is the complex database functionality previously described.

Content Indexes are the result of searches of the Knowledge Library, as directed by Query Indexes. The Content Indexes are also known as metadata. Metadata is best known in web content for facilitating searches. However, web content metadata is inadequate for learning content because learning content requires more search criteria (e.g., pre-requisites, co-requisites, learning style) than what is provided for web content (e.g., title, subject, author, keywords). Content Indexes are similar to "card catalog" entries in a public library.

Locator Indexes identify or point to Learning Content. Using the public library analogy, Locator Indexes are similar to "call numbers" in a card catalog system. Web URLs are examples of Locator Indexes. For some learning technology systems, Locator Indexes can be implicit because the Learning

Content can be retrieved along with the Content Index returned by the Query Index search. Learning Content is the coded representation of the learning experience, identified by the Locator Index, retrieved by the Knowledge Library, and transformed by the Delivery system into the training systems/environment and learning experience, where the Learner interacts with the real operational systems or training systems/environment.

The *Delivery* system, much like the Evaluation system, relies upon AIDE's powerful publication, subscription, and object sharing mechanisms. The low-footprint and portability features are important here, since that enables a wider variety of systems involved in Learner's real tasks to be employed. This improves training since the systems used at the actual tasks are used in training.

The *Learner* (process) represents any learner (one, several, or teams operating in different roles). The Learner receives Stimuli, and their Behavior is observed. From a technology perspective, a variety of assessments about the Learner (individual or group) are available to the System Coach and Evaluation processes to more effectively and efficiently guide each training session.

The *Learner Assessments* are sent to the System Coach. AIMS considers the various types of information which provides more knowledge a priori to the system itself. Figure 3 represents a multi-modeling approach to more easily bring in additional very complex and interrelated Learner Assessment models.

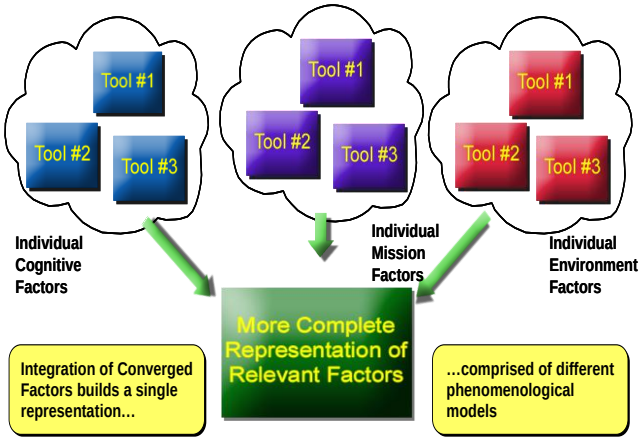

Figure 3. Learner Assessment data approach utilized in Figure 2.

AIMS has the ability to integrate naturally and efficiently for the new knowledge representation techniques and engines. Problems in communication, personality conflicts, or learning style issues can be rigorously accounted for in the training program. Learner Assessment information utilized may be obtained and include any number of the following:

- Concentration and awareness
- Accuracy of attention: environment, cognitive analysis, problem solving, set of tasks, mission
- Distraction: external, internal, mistakes and ability to recover
- Information and tasking: quantity and range of diversity
- Risk-taking, sensation seeking, thinking outside the box
- Following rules, orders, tradition, deliberation, caution
- Aspects of control, self-confidence, self-criticism
- Dominating and competitiveness: physical and intellectual
- Speed of decision making in given environments
- Listening, verbalizing, group/person selection preference
- Advocating team performance
- Communicating ideas, support, criticism
- Performing in certain types of high pressure environment

The following discussion is intended to illustrate how the AIMS architecture is implemented with the intelligent systems AIDE framework previously discussed.

The Learner construct represents one or several trainees. The Stimuli incident to the Learner requires the ability to interoperate with the learner's training or operational system. This requires the ability to quickly and easily integrate everything from buttons, switches, joysticks, variety of control knobs or interfaces to elaborate virtual reality or operational displays.

The Behavior flow shown in Figure 2 is a transmission of Learner behavior from the Learner to the Evaluation process. At the Evaluation process, the Behavior is framed in the appropriate context by matching the Learning Content to the range of Behavioral responses which is how information is collected and organized, e.g., key clicks, mouse clicks, voice response, choices, or inputs to an operational system which are sent to the System Coach. The Learner's observed Behavior is an observation of the Learner's activity while they are performing a task such as flying an airship for example. Some Behaviors may be physical location behaviors and have several levels of inputs concerning the Learner: location, six degrees of freedom position, velocity with respect to frame of reference, orientation (pitch/roll/yaw), acceleration, and the angular velocity with respect to those quantities. The Learner Behavior physical inputs are sent to the System Coach: 10 degrees of pitch, 20 degrees of roll at that moment in time, etc..

The System Coach sends the Learner Behavior to the Evaluator. Behavior information is obtained with a similar interoperation of user interface mechanisms or training specific observations such as a system of cameras to determine the scan pattern of an operator through their tasks and interfaces and feeding this streams into an Evaluation process which then would be implemented as some number of System Objects [1]. Ultimately all the data streams implemented using System Events and System Messages and the programming

constructs used to implement them are simplified for the clarity and ease of programming.

Learner Assessments sent to System Coach are different than the Behavior Evaluation path. Assessments are things that directly coming out of the training or operation system. These may be the Learner's problems with understanding when the timing of when to press a training system button. The Assessment part of the architecture represents information that comes from a direct observation of the learning environment and is not explicitly a Learner Behavior. For example, a Learner Assessment might be a warning light is on in a flight simulator and the fact that the light is on as a result of a trainee's actions and is a normal, internal part of system's operation.

AIMS observes the trainee's performance. This is a Learner Assessment and it is directly sent to the System Coach. Learner Assessment is information about what or how the trainee is doing, but it is not an Evaluation. System Coach gives feedback Stimuli to improve which is sent through the Delivery process. One piece of feedback may be "please release the safety".

The Learner Assessments transmitted from the Learner construct to the System Coach are implemented as System Objects and serve to provide specific inferences about the Learner such as an running Evaluation of the Learner's skill level at a particular task or other diagnostic that is built into the training or operational system that has some useful data which is not explicitly behavior based observation.

The System Coach is similar to the Evaluation implementation and it receives one or more Learner Assessments. The Learner Assessments are sent as System Events and System Messages. Multiple independent evaluations of behavior and multiple simulation learner assessments occur and feedback can be given and noticeable trainee improvements made over time. The delivery construct is also implemented with multiple system objects and execution engines and serves to mediate between the learning environment and the System Coach.

The Knowledge Library may then be viewed as not just rules or rule specifications, but elaborate combinations of libraries of function and arbitrary combinations of knowledge representation constructions. In both the System Coach and Evaluation, one or more knowledge execution engines can be instantiated to operate on the data being received.

The ability to have more than one knowledge execution engine operating simultaneously would simplify the construction of authoring the knowledge bases from a semantic perspective. This permits more realistic and practical evaluation information, resulting in more realistic and accurate automated inputs to the Learner. AIMS has knowledge of the Learner's activity, training systems, relationships between them, the ability to index training systems, and AIMS architecture framework system that could realize roles and responsibilities for both AIMS and the trainee.

The AIMS that captures Learner Assessment behavior must accommodate a variety of inputs, and the delivery of the Behavior then triggers the Evaluation process. The Evaluation Assessment process produces information such as where the Learner is at any given time which is then sent to System Coach. The Evaluation process uses the Learning Content to provide context to the Learner's Behavior to determine the appropriate Evaluation. The Evaluation process also creates and sends Performance information to the Records Database. This active triggering of Evaluation is an aspect of the AIMS complex, distributed application framework. The Evaluation process must then utilize advanced Knowledge and Intelligence Representation in the form of the adaptive SME and student model algorithms, such as genetic or fuzzy logic algorithms, that can then be used, as well as rules and pattern recognition. The AIMS distributed application framework also allows the ability to integrate many varied knowledge and intelligence techniques.

The AIMS complex, distributed application framework is also used to build the System Coach, as it must interact with other applications, and employ knowledge and display "intelligence" in its actions by also utilizing the advanced Knowledge and Intelligence Representation capabilities. The System Coach may store "bookmarks" as Performance information in the Records Database saving the Learner's session for resumption at some future time. The System Coach also receives the current Assessment from the Evaluation process, and Performance information from the Records Database, to support the decision-making process.

Based on the current Assessment and historical Performance information, the System Coach sends Query Indexes to the Knowledge Library to search for appropriate learning materials. The Knowledge Library returns Content Indexes such as a list of Locator Indexes that match the search query. The appropriate Locator Indexes such as a lesson plan are sent to the Delivery process. The System Coach sends Query Indexes to the Knowledge Library to search for content that is appropriate for the Learner. The Query Indexes specify search criteria based on, in part, Learning Style, Assessment, and Performance information.

The Knowledge Library stores knowledge and other learning materials as resources for the learning experience. The Knowledge Library may be searched by Query Indexes. The matching information is returned as Content Indexes, i.e., a set of content tags that are, conceptually, "card catalog" entries known as metadata. The locator Indexes (conceptually, "call numbers" on the bindings of the "books in the digital library", e.g., URLs) are extracted from the content indexes. The locator Indexes are used by the Delivery process to retrieve Learning Content. It is unspecified who initiates the

transfer of Learning Content and it can be the Learner, the System Coach, or the Delivery process itself. For example, a Query Index might return a set of Content Indexes and an ontology, which is a conceptual model of the subject represented as generic Learning Content.

The Delivery process receives locator Indexes from the System Coach and retrieves Learning Content from the Knowledge Library. The Delivery process transforms the Learning Content into Stimuli for the Learner. The Stimuli is actually sent to either simulations connected to the operational systems or training systems/environment and in some cases sent directly to the operational systems or training systems/environment. When the Delivery process sends Stimuli to the Learner, the Evaluation process is expecting some Behavioral response to the Stimuli. The Evaluation process is unable to interpret the Behavior without context, so the Delivery process sends the Learning Content to the Evaluation process to understand the context of the Learner's response.

3 Conclusions

In general, the key technological innovations are the ability to affordably instrument training/operational system for learning environments to stimulate learners and record their responses. The second key innovation is the ability to create intelligent systems with hybrid algorithm capabilities. For instance, the evolution of the value of a neural network could be the result of a query of a first order predicate calculus inference engine. The converse can also be implemented where a value in a rule or fact inference based engine's knowledge base could be calculated by evaluating a neural network.

Additionally, the ability to create hybrid intelligent algorithms and synchronize a large number of them permits the AIMS to be built in a more modular and understandable way as an entire intelligence system. In order to enable the next generation of instructional systems, several technology challenges had to be overcome. The establishment and elaboration of coherent, comprehensive system architecture, relevant over wide ranges of education and training situations, is a major step forward providing:

- Single learner or group training on customized courses
- Ability to instrument and control a number of systems simultaneously
- Allowance of the distribution of system processing for efficiency
- Scales in both dimensions – the number of learners, and the number of systems instrumented and controlled
- Internal and external processes
- Internal and external events
- Efficient simple two-way interactions
- Effectively creating the knowledge models for the Expert, Instructional, and Student Trainer subsystems
- Integrating the most appropriate decision algorithm required to naturally implement functionality – not just rule bases
- Utilizing a novel system development framework that permits the most appropriate type of interaction paradigm required for any component of the system

AIMS takes into account the trainee's situational awareness, cognitive capabilities, action accuracy, situational distractions, cognitive distractibility and any resulting reduction in accuracy. AIMS accounts for functionally disparate phenomena such as recognition of patterns, adapting new solutions or strategies and rule following in order to represent "intelligence" more effectively. AIMS ascertains the most appropriate feedback for the trainee by determining learning styles and communication preferences in addition to skill and provides the most accurate advice for them.

AIMS' next generation training interactive engine and architecture framework will revolutionize training and greatly enhance the intrinsic value training provides to our communities. Scalable, robust solutions are provided for complex, real-world training problems and scenarios. In general, unsolved problems become tractable, and integration and interoperability costs no longer dominate project cost profiles and automated, intelligent training is achieved. Integrating SMEs into the development process facilitates better training systems as they are there during the design, engineering, testing, and evaluation process ensuring that their training needs are met at every step of the AIMS development cycle. SMEs understand what the training issues for both the system to be trained and their trainees. SME knowledge, input and feedback are incorporated so the AIMS is customized to meet their specific training needs.

4 References

[1] Jeffrey W. Wallace. "The Design Document", IDI, San Diego, CA, (2011).

[2] Barbara Di Eugenio. "Toward a computational model of expert tutoring: a first report", American Association for Artificial Intelligence, (2006).

[3] Lee W. Lacy. "Potential Modeling and Simulation Applications of the Web Ontology Language – OWL"; Proceedings of the Winter Simulation Conference, Washington D.C., December 2004.

[4] Charles S. Peirce. Collected Papers of Charles S. Peirce, Hartshorne, Weiss, and Burks (eds.), Harvard University Press, Cambridge, MA, 1932.

Comparing Segmentation Methods with Different Base Classifiers

Roberto Angelo Fernandes Santos[1,2] **and Roberto Souto Maior de Barros**[1]
[1]Centro de Informática, Universidade Federal de Pernambuco, 50.740-560, Recife-PE, Brazil.
[2]Faculdade Impacta de Tecnologia, 04.043-300, São Paulo-SP, Brazil.

Abstract - *Large Companies often use statistical models and artificial intelligence to predict several kinds of risks. In general, only one statistical model or a neural network technique is used to predict these risks. It is not so uncommon for some companies to use segmentation to define subpopulation splits for the development of specific predictors to improve decision accuracy. However, the use of segmentation usually depends on the experience of the specialist. The basic premise of this paper is to compare three kinds of segmentation methods, crossed with three different base classifiers, and using five datasets from the UCI Repository. The segmentation methods are: NNTree - a Neural Network Tree based method, the traditional segmentation using Information Gain to split, and an experimental method called FBTSeg. Results show that blending classifiers using segmentation is a viable option to improve results of known and traditional techniques such as statistic regressions and neural networks.*

Keywords: Classification methods; Segmentation; Data splitting; Machine learning.

1 Introduction

The capacity for predicting events is the key element in the decision support processes for modern corporations. The results of decision models based on data are dependent on the quantity and quality of the information available. However, improvements in prediction techniques are also important for better accuracy, as several academic and practical initiatives from different areas show [1] [2] [3]. Moreover, this search goes beyond a single predictive model and is also progressing towards the combination of several predictors, both from the same and from different techniques. The literature shows that combining techniques using different sampling methods or using predictors of distinct characteristics usually offers more predictive solutions [4] [5] [6] [7] [8] [9] [10].

Combining predictors is not simple and its complexity is derived from a number of factors inherent to such combinations. Some questions that illustrate this complexity are: What is the best combination method for a specific problem? What techniques should be combined? How many predictors are needed to maximize performance? The fact is there are no simple or exact answers to those questions and most of them can only be answered based on the specific application constraints, the expertise of the developers, and results of practical experiments.

Segmentation (decomposition) [11] is one of the mostly used methods for the combination of predictive techniques and proposes the transformation of a complex problem in several less complex ones as the means to achieve the best solution to the original problem. In data mining, segmentation is used to obtain subgroups where different learning techniques may be applied, i.e. specialized predictors are applied to subsets of the original data set.

For a long time, the techniques used to find good segmentation structures were based on subjective strategies and on previous knowledge of the problem. One of these subjective techniques is separation of the data in two groups, one with a number of attributes with their values filled in, and the other with many missing values in these attributes, since this is a common situation in credit scoring problems [12]. It was even suggested that it might not be possible to create the segmentation structure without using subjective knowledge. However, methods and algorithms to find adequate segmentation structures have already been proposed. They usually represent the segmentation structure as a tree and use exhaustive or semi-exhaustive search to choose the best segmentation strategy [11].

This paper compares the performance of three different segmentation methods to build model trees. We also briefly describe a new semi-exhaustive method called FBTSeg, formerly RISKSEG [20], that implements an algorithm to optimize and build a binary decision tree with regression models in each leaf. To do this comparison we used five datasets from the UCI Repository [13].

2 Review of Used Techniques

In this section we briefly review the techniques used in the experiments, both single classifiers and their combination using segmentation.

Binary Logistic Regression is a traditional technique of statistic inference [14] that relates a dichotomic target (*good*

or *bad*, *1* or *0*, *fraud* or *not fraud*, etc.) to a set of predictive input variables X_1, X_2, …, X_n, where Y is a random variable with two possible values, 0 (zero) and 1 (one). Its result is an estimation of the probability of Y belonging to one of the two categories, based on the observed values of the predicting variables. In this paper, the estimation of $Y = 1$ will be used. The dependent variable is the logarithm of the ratio of probabilities of the two possible results of an output variable, log [p / (1-p)]. We used the widespread maximum likelihood method for estimating the binary response, having its solution found through Newton-Raphson's iterative process [15].

Linear Discriminant Analysis estimates the output variable based on the observed values of predicting variables and is usually applied when the dependent variable is numeric and continuous. Errors are assumed to have normal distribution [16]. In this paper, we use this technique to estimate the value of a dichotomic variable (0 or 1).

Multilayer Perceptron Neural Network (MLP) [17] is a computational intelligence technique that has excellent generalization capabilities, is simple to implement, and is commonly used in classification problems. In our experiments, we tested MLP with the backpropagation and Levenberg-Marquardt algorithms [17].

Segmentation is the division of the available dataset in subpopulations and the development of a prediction model for each segment. Therefore, each example is predicted according to the specific formula (model) that it belongs. The segmentation provides the most appropriate use of available information and is highly recommended when there is a large number of missing data in dataset samples. The segmentation is also recommended for capturing risk relationships among the subpopulations with different profiles – this way the specialized models in that data sample are able to explore their peculiarities more efficiently [12].

As in decision trees, one of the main criteria used for segmentation is Information Gain [18]. Decision trees aim to separate the population in disjoint subsets that are homogeneous regarding the behavior of the output variable, because distinct behaviors regarding the output variable might lead to large variations in the estimation of the regression parameters. Moreover, distinct behaviors in separate groups are to be used as the basis for the creation of multiple classifiers in the FBTSeg method.

An NNTree [19] "is a decision tree, where each non-terminal node contains a neural network". Its segmentation uses a multilayer perceptron neural network to design the classification tree. The method recursively divides the training set trying to create leaves that contain elements from a single class – each non-terminal node has elements from more than one class and uses a neural network to separate them. Even though the original implementation only uses neural networks, we have adapted the algorithm to also support both logistic regression and linear regression in the non-terminal nodes.

2.1 Find Best Tree Segmentation (FBTSeg)

The FBTSeg method [20] rationale is to try to find a set of segmented models with better performance using a binary tree built from divisions using the attribute classes. This method uses a specific algorithm for the selection of *n* attributes to test all combinations for each candidate node, where *n* is a parameter. In other words, after the attribute selection, each *n* attribute class is used to split and the best segmentation is chosen to improve the accuracy of the model for this node. Every node generates two leaves with their specific models which, when combined, generate better results than the upper node model. In summary, the best option to split each node sample is chosen. It is important to choose a specific (or the best) metric for optimizing the results of the problem in hand, such as classification error, mean squared error, KS2 [21], ROC [22], and others. To determine the best segmentation for a node split, it is necessary to join the scores of the corresponding pair of leaves, from the set of possibilities, and compare their results.

The FBTSeg method is prone to overfitting, a known problem in other supervised learning algorithms. So, it is important to create a validation dataset to apply a cross-validation between the training and validation datasets. Then the training dataset is just used to train the predictors, while the validation dataset is used to compare the scores among the segments and for determining the best segmentation possible. There is also a parameter to set the minimal number of observations to train and validate a segmented model, aimed at ensuring a minimal set to make a representative model in each leaf. Of course, its value must be established taking into account the sample size available to develop the models.

The implementation of models in subpopulations is similar to making a model with the main predictive variables combined with the variables resulting from interactions among the main variables and a selected variable [12] – see equations 1 to 5. Through the selection of good segmentations it is possible to add the most important characteristics found in the interactions of the variables. Thus, in the FBTSeg segmentation, for each terminal node that might be segmented, the possible interactions of the model variables are analyzed. The implementation algorithm builds a tree model based on the best candidate variables, those that have the best interactions with the other variables according to the chosen metric. This scheme avoids the exhaustive search for the best segmentation and permits optimizing the final result based on some chosen metric. Because it is easier to understand, we illustrate the method using a statistical linear regression with binary variables (values 0 or 1), but our implementation used logistic regression with categorical variables.

Let x_1, x_2, x_3, and x_4 be random variables, Y a dependent variable (target), $\mu_i, \beta_i, \lambda_i, \alpha_i, \omega_i, \theta_i$ the constant weights of the equations, and ε_i the error factor. We defined a simple linear regression model that only considers the main effects of the variables – no interaction term was included in the equation for parameters estimation.

$$Y = \mu_1 + \beta_1 x_1 + \beta_2 x_2 + \beta_3 x_3 + \beta_4 x_4 + \varepsilon_1 \quad (1)$$

Including interaction terms $x_i x_j$ (with i fixed and j varying) is equivalent to segment the data by x_i and adjust separate regressions for each subgroup. For example:

$$Y = \mu_2 + \lambda_1 x_1 + \lambda_2 x_2 + \lambda_3 x_3 + \lambda_4 x_4 + \lambda_{12} x_1 x_2 + \lambda_{13} x_1 x_3 + \lambda_{14} x_1 x_4 + \varepsilon_2 \quad (2)$$

In this example (2), we capture the effects of the interactions between x_1 and the other variables of the model. This is similar to segmenting the data based on the values of x_1 and adjusting different regressions to the generated subgroups. Similarly, other three models can be defined:

$$Y = \mu_3 + \alpha_1 x_1 + \alpha_2 x_2 + \alpha_3 x_3 + \alpha_4 x_4 + \alpha_{12} x_1 x_2 + \alpha_{23} x_2 x_3 + \alpha_{24} x_2 x_4 + \varepsilon_3 \quad (3)$$

$$Y = \mu_4 + \omega_1 x_1 + \omega_2 x_2 + \omega_3 x_3 + \omega_4 x_4 + \omega_{13} x_1 x_3 + \omega_{23} x_2 x_3 + \omega_{34} x_3 x_4 + \varepsilon_4 \quad (4)$$

$$Y = \mu_5 + \theta_1 x_1 + \theta_2 x_2 + \theta_3 x_3 + \theta_4 x_4 + \theta_{14} x_1 x_4 + \theta_{24} x_2 x_4 + \theta_{34} x_3 x_4 + \varepsilon_5 \quad (5)$$

These three models are equivalent to segmentations based on x_2, x_3, and x_4, respectively. So, adjusting the four regressions makes it possible to choose the best regression according to some performance measure D, i.e. the best segmentation variable. It is also necessary to choose the splitting rule, specifically, a category or a numeric interval.

The FBTSeg search is *not* the semi-exhaustive search because it does *not* test all the possible split rules of all variables. The number of splits is limited by the number of candidate variables categories. This method also permits adjusting the regressions using a subset of the training set, which makes it faster when the training set is very large.

Algorithm 1 gives a possible implementation of FBTSeg showing the search for possible segmentations. The first loop selects the best variable and the second chooses the category of this variable that may be used to split the data. So, after selecting the variable (*Var*) with the best regression results in the interaction with the other variables (factorial), all the possible binary combinations of this variable categories are tested to find the best category (*Cat*) and generate the best pair of segments, one for "*Var* = *Cat*" and another for "*Var* ≠ *Cat*". After the segmentation, the predictive performance of the suggested segments is compared to that of the upper node. The segmentation is confirmed if it improves the results of the upper node. As in decision trees, the segmentation continues until some stop criterion is reached. The final result is a set of models generated from disjoint subsets of the training data.

3 Experimental Design and Results

We run experiments with 5 (five) datasets of the UCI Machine Learning Repository [13] to compare the methods. The chosen datasets were the ones with a dichotomic target and at least 1,000 records. These are:

- *Chess* – Contains 3,196 records with information about chess matches. The peaces' positions are represented by 36 categorical variables and the target is dichotomic (0=white wins and 1=black wins).
- *German* – Credit base with 1,000 records. It contains the most common target variable in credit risk studies for the representation of good and bad payers (1=Good and 2=Bad). The input variables are mostly social-economic attributes, 20 in total, seven of them are numeric and 13 are categorical.
- *Magic Gamma Telescope* – This dataset simulates the registration of high energy gamma particles in a ground-based telescope using the imaging technique. There are 19,020 records, 10 numeric variables, and a dichotomic target with values "g" (gamma) and "h" (hadron), respectively transformed to 0 (zero) and 1 (one).
- *Adult* – Contains information of the 1994 American Census database and aims to determine whether a person makes over US$50,000 a year (1=yes) or not (0=no). There are 48,842 records and 14 variables, six of them are numeric and eight are categorical.
- *Spambase* – Contains 4,601 records and 57 numeric variables with information on the characteristics of e-mails. Its purpose is to build a spam filter, deciding whether each message is a spam (1=yes) or not (0=no).

In the preprocessing of these datasets, no categorical variable was grouped. Thus, their original values were used to generate their equivalent binary codifications, transforming each categorical variable (with n categories) in n binary variables (with values 0 or 1). On the other hand, all numeric variables were normalized with continuous values in the [0, 1] interval. However, because the implementation of the FBTSeg segmentation and also of the traditional segmentation by information gain both expect categorical variables to split the nodes, it was also necessary to categorize all numeric variables and, so, we decided to create four categories, each with approximately 25% of the data. Nevertheless, the generated categorical variables were only used in the segmentations – the training used their normalized numeric versions.

We also used the k-fold Cross Validation technique in the experiments and the chosen value for k was 10. This is a fairly common technique in experiments involving classifier

N – Training set of a given terminal node
S_1, S_2 – Subsets of N generated by the segmentation
p – Number of input variables of N
$X_1,X_2,...,X_p$ – Discrete input variables of N
w – Local variable that stores the number of categories of each discrete variable
C[w] – Local array that stores the values of each discrete variable
y – Target variable (dependent)
fMet( ) – Performance Function (larger values are considered to be better in this example)
fMerge() – Merge function to join the results of the models
Var – Variable chosen to test its categories
Cat – Category of *Var*
rMod, – Answers of the factorial models
$rMod_0$ – Best answers of the models
$rMod_1$, $rMod_2$ – Answers of the models of the candidate segments
$rMod_{12}$ – Joint answer of the models of the candidate segments

Input: N**;**

$rMod_0 \leftarrow \emptyset$; (Best answers initialization)
For i = 1 to p do { (Loop over all the input variables)

$rMod \leftarrow$ Regression answers y ~ $\sum_{j=1}^{P} X_j + \sum_{j=1, j\neq i}^{P} X_j X_i$, with data from N; (Trains model with interactions)

If *fMet* ($rMod$) > *fMet* ($rMod_0$) { (If the model improves the result)
$rMod_0 \leftarrow rMod$; (Saves the best answers of the model)
$Var \leftarrow X_i$; (Saves the chosen segmentation variable)
};
};

$rMod_0 \leftarrow \emptyset$; (Best answers re-initialization)
$rMod_{12} \leftarrow \emptyset$; (Mod12 answers set initialization)
C[w] ← Category values of *Var*;
w ← Number of categories of *Var*;

For i = 1 to w do { (Loop over the categories of Var)
S_1 ← Subset of N, such as *Var* = C[w]; (Creates the two training subsets)
S_2 ← Subset of N, such as *Var* != C[w];

$rMod_1 \leftarrow$ Regression answers y ~ $\sum_{j=1}^{P} X_j$, with data from S_1; (Trains the models of the two subsets)

$rMod_2 \leftarrow$ Regression answers y ~ $\sum_{j=1}^{P} X_j$, with data from S_2;

$rMod_{12} \leftarrow rMod_1 \cup rMod_2$; (Joins the answers of the models of the segments)
If *fMet* ($rMod_{12}$) > *fMet* ($rMod_0$) { (If the segmented models improve the result)
$rMod_0 \leftarrow rMod_{12}$; (Saves the best answers of the models)
$Cat \leftarrow$ C[w]; (Saves the chosen segmentation category)
};
};

Output: *Var, Cat*; (Best segmentation variable and category)

Algorithm 1 – FBTSeg algorithm that chooses the best segmentation.

combination [23]. Therefore, the datasets were separated in 10 parts, each with 10% of the data, and, in each experiment, one of them was the testing set. The rest of the data was used for training (65%) and validation (35%).

The simulations were implemented in such a way that each single classifier was used as base classifier in the comparison with the segmentation methods.

The main difference regarding the three segmentation methods is the way the segment splits are chosen. NNTree originally uses an MLP neural network to split the training dataset [19], but we also implemented adaptations for using linear and logistic regressions as well. These three prediction techniques were also used with the other two segmentation methods and, for each of them, the behavior of the combination methods for the generation of multiple classifiers

was observed and the results measured using the classification error rate. We named "Simple" the classifications using each of the three chosen techniques as single base classifier, and "TradSeg" the segmentations by information gain.

3.1 Defining Experiment Parameters

In both regressions, it was not necessary to choose variables or parameters. The choice of parameters for training the MLP was based on the test for the best number of neurons in the intermediate level and the best training algorithm. For each data set, we tested all the possible combinations of the two training algorithms (backpropagation and Levenberg-Marquardt) with 3, 10, and 20 neurons in the intermediate layer. The chosen activation function was logistic function having the minimum squared error on the cross-validation set as the training stopping criterion. We used the standard learning rate of SAS Enterprise Miner [24], version 4.0, which cannot be modified in this version of the software. We then chose the best configuration for the single classifier and for the segmentations.

We decided to use similar parameters in the training of the three methods as much as possible, as the means to focus on the way the dataset splits are done. For the three segmentation methods, we used 2 (two) as the maximum depth of the tree because, in preliminary tests, we observed that the best segmentations were in these two levels. For the minimum size of a leaf node we chose 5%, a size we judged appropriate, considering that all datasets have at least 1,000 examples. The metric used to evaluate the results of the experiments was the classification error. Our implementation of the segmentation methods used a validation dataset to determine if there was a gain (or not) in each segmentation possible. The validation dataset used was 35% of the training set and the same dataset was used in the validation of the MLP neural network.

3.2 Results

Table 1 presents the average classification errors (percentages) of the three single classifiers crossed with the three segmentation methods in the five data sets tested. The comparison is always based on the control classifier (Simple) of each technique. We used the t-Student test for paired data, with significance level of 5%. Average errors that are smaller than that of the respective base classifier are written in bold. Smaller and statistically different values are marked with an asterisk (*). Greater and significantly worse values are written in italics. We considered the best classifier the one with the smaller average error, as long as it is significantly better than the base classifier.

In the Chess dataset, using MLP, the three segmentations presented better average results, and statistically significant, when compared to the base classifier, and the FBTSeg method was considerably better than the second best result (TradSeg). Using linear regression, again, all three segmentations improved the results of the base classifier considerably, but the best results were obtained with the TradSeg method and its results were significantly better than the others. Using logistic regression, only the FBTSeg method presented significantly better results than the base classifier – TradSeg was only marginally better than the base classifier.

Table 1 – Average errors and confidence intervals.

Dataset	*Technique*	*Simple*	*TradSeg*	*NNTree*	*FBTSeg*	*Best*
Chess	MLP	4.07 ±1.05	**1.09 ±0.42***	**2.81 ±0.59***	**0.35 ±0.14***	FBTSeg
	Linear Reg.	8.57 ±1.64	**2.28 ±0.55***	**3.18 ±0.68***	**3.25 ±0.77***	TradSeg
	Logistic Reg.	2.60 ±0.73	**2.25 ±0.83**	2.63 ±0.51	**1.02 ±0.27***	FBTSeg
German	MLP	25.20 ±1.79	25.70 ±1.20	*27.10 ±1.97*	25.30 ±1.84	Simple
	Linear Reg.	29.00 ±2.31	**26.00 ±1.77***	29.25 ±3.08	**26.30 ±2.00**	TradSeg
	Logistic Reg.	25.70 ±2.08	**24.70 ±2.08**	25.95 ±1.94	26.30 ±2.51	Simple
Magic	MLP	15.16 ±0.53	**14.84 ±0.60***	15.24 ±0.53	**13.51 ±0.58***	FBTSeg
	Linear Reg.	32.03 ±2.81	**18.73 ±0.56***	**27.31 ±2.65***	**16.06 ±0.65***	FBTSeg
	Logistic Reg.	20.98 ±0.44	**18.29 ±0.67***	**18.69 ±0.55***	**15.40 ±0.51***	FBTSeg
Adult	MLP	14.89 ±0.91	**14.71 ±0.96**	**13.60 ±1.33***	15.07 ±0.86	NNTree
	Linear Reg.	17.38 ±1.23	**15.81 ±0.78***	**13.68 ±0.83***	**16.73 ±1.25**	NNTree
	Logistic Reg.	14.90 ±1.00	14.96 ±0.97	**14.58 ±0.97**	14.96 ±0.82	Simple
Spambase	MLP	7.06 ±0.60	7.15 ±0.91	**6.81 ±0.57**	7.45 ±0.71	Simple
	Linear Reg.	24.36 ±6.83	**9.02 ±0.92***	**6.45 ±0.61***	**10.61 ±0.75***	NNTree
	Logistic Reg.	8.69 ±0.63	**8.67 ±0.58**	**6.76 ±0.66***	**8.19 ±0.76**	NNTree

In the German dataset, only the TradSeg method using linear regression significantly improved the results of the base classifier. Using MLP, the NNTree segmentation had significantly worse results. A possible explanation to such results is the small number of examples in this dataset. This fact leads to small segments in the model tree, and this situation is aggravated by the need of examples for validation. It is likely that this is the main reason why the segmentations did not improve the results, generating classifiers that are weaker than the ones of the original nodes.

In the Magic dataset, the segmentations improved the results of nearly all combinations. The linear regressions obtained the bigger gains; in particular, FBTSeg improved the average error from 32.03% to 16.06%. Using MLP, only the results of FBTSeg and TradSeg were significantly better than that of the base classifier. Using logistic regression, all three segmentations (NNTree, FBTSeg and TradSeg) improved the results, but only FBTSeg was statistically better than the base classifier. It is important to notice that, in this dataset, FBTSeg significantly improved the average error using all three techniques, when compared to the base classifiers, and also when compared to the other segmentations.

In the Adult dataset, all three segmentations improved the results of the base classifier using linear regression, but the FBTSeg results were not significantly better. The NNTree method was the only one to significantly improve the results using MLP and none of them obtained significant improvements using logistic regression.

In the Spambase dataset, using MLP, none of segmentation methods presented statistically significant results. With linear regression, they all significantly improved the base classifier, but the NNTree method was also noticeably better than the other segmentation methods. Using logistic regression, they all had smaller errors but only NNTree was significantly better than the base classifier.

4 Conclusion

This paper presented the results of experiments comparing three different segmentation methods, using three different base classifiers, and five UCI datasets. The traditional segmentation based on information gain and another two more recent segmentation methods (NNTree and FBTSeg) were tested against well-known classifiers such as linear regression, logistic regression, and MLP neural network.

Our results show that segmentation may be a viable alternative to improve the performance of classifiers. One of its advantages is that it may improve the results of older techniques, within the existing expertise of the modeling team. Even using linear regression, a classifier that is known to be weaker [25], the use of segmentation methods may lead to results that are similar and sometimes superior to those obtained with newer and more predictive techniques such as MLP neural networks [25] [2]. Moreover, segmentations can also improve the results using MLP: in three of the five tested datasets, at least one of the three segmentation methods presented statistically better results.

From all the classifiers (simple or combined), the FBTSeg method achieved the best performance in the Chess and Magic datasets, obtaining 5 (five) of the possible 6 (six) best results, when we consider the three techniques available. The very best results in these two datasets were obtained with the FBTSeg + MLP combination.

Even though the NNTree method was not originally developed to work with the statistic regressions, it improved the results of these base classifiers in 7 (seven) of the possible 10 (ten) combinations; only in the German dataset it did not improve any results; and, perhaps surprisingly, it even achieved the best results in the Adult and Spambase datasets when combined with linear regression.

Although the TradSeg method is older and simple, it also improved the results of the base classifiers in many configurations. However, in general, both NNTree and FBTSeg presented better results. Nevertheless, none of the segmentation methods was clearly better than the others in all datasets. Thus, our conclusion is that it is worth testing more than one segmentation method to choose the one that is more suitable to the specific problem in hand.

As future work, it is important comparing the segmentation methods tested in this paper with other methods for combining classifiers such as Bagging [26], Boosting [26], and Stacking [4] [5] [26]. It is worth testing other base classifiers such as SVM [26] and k-NN [26] as well. Running experiments with other datasets is also recommended. Another possibility of future work is to experiment different split strategies for the segmentation tree, for example, using *n*-ary trees and/or different split algorithms.

5 References

[1] O. P. Rud, “Data Mining Cookbook: Modeling Data for Marketing, Risk and Customer Relationship Management”, John Wiley & sons, New York, 2001.

[2] P. J. L. Adeodato, G. C. Vasconcelos, A. L. Arnaud, R. A. F. Santos, R. C. L. V. Cunha, and D. S. M. P. Monteiro, “Neural Networks vs. Logistic Regression: a Comparative Study on a Large Data Set”, In proceedings of 17th International Conference on Pattern Recognition (ICPR'04), Volume 3, pp. 355-358, Cambridge, England, UK, 2004.

[3] P. Cortez, A. Cerdeira, F. Almeida, T. Matos and J. Reis, "Modeling Wine Preferences by Data Mining from Physicochemical Properties", Decision Support Systems, Elsevier, Volume 47, Number 4, pp. 547-553, 2009.

[4] D. H. Wolpert, "Stacked Generalization", Neural Networks, Volume 5, Number 2, pp. 241-259, 1992.

[5] S. Dzeroski, and B. Zenko, "Is Combining Classifiers with Stacking Better than Selecting the Best One?" Machine Learning, Volume 54, Number 3, pp. 255–273, 2004.

[6] G. Brown, J. Wyatt, R. Harris, and X. Yao, "Diversity Creation Methods: a Survey and Categorization", Journal of Information Fusion, Volume 6, Number 1, pp. 5-20, 2005.

[7] T. Gestel, B. Baesens, P. Dijcke, J. Suykens, et al., "Linear and Non-linear Credit Scoring by Combining Logistic Regression and Support Vector Machines", Journal of Credit Risk, Volume 1, Number 4, 2006.

[8] M. M. Islam, X. Yao, S. M. S. Nirjon, M. A. Islam, and K. Murase, "Bagging and Boosting Negatively Correlated Neural Networks", IEEE Transaction on System, Man, and Cybernetics, Part B, Volume 38, Number 3, pp.771-84, 2008.

[9] S. L. Wang, K. Shafi, C. Lokan, and H. A. Abbass, "Robustness of Neural Ensembles Against Targeted and Random Adversarial Learning". In proceedings of IEEE International Conference on Fuzzy Systems (FUZZ-IEEE), pp. 1-8, 2010.

[10] K. W. D. Bock and D. V. D. Poel, "An Empirical Evaluation of Rotation-based Ensemble Classifiers for Customer Churn Prediction", Expert Systems with Applications, Volume 38, Number 10, pp 12293-12301, 2011.

[11] O. Maimon, and L. Rokach, "Decomposition Methodology for Knowledge Discovery and Data Mining: Theory and Applications", Series in Machine Perception and Artificial Intelligence, Volume 61, World Scientific pub., 2005.

[12] L. C. Thomas, D. Edelman, and J. Crook, "Credit Scoring and its Applications", Society for Industrial and Applied Mathematics, Philadelphia, USA, 2002.

[13] C. Blake, and C. Merz, "UCI Repository of Machine Learning Databases", School of Information and Computer Sciences, University of California, Irvine, USA, 2012. http://archive.ics.uci.edu/ml/ (Access 07/05/2012).

[14] R. A. Johnson, and D. W. Wichern, "Applied Multivariate Statistical Analysis", Prentice Hall, Upper Saddle River, New Jersey-NJ, USA, sixth edition, 2007.

[15] A. J. Macleod, "A Generalization of Newton-Raphson". International Journal of Mathematical Education in Science and Technology, Volume 15, Number 1, pp. 117-120, 1984.

[16] J. Neter, M. H. Kutner, C. J. Nachtsheim, and W. Wasserman, "Applied Linear Statistical Models", McGraw-Hill, fourth edition, 1996.

[17] S. Haykin, "Neural Networks and Learning Machines", third edition, Prentice Hall, New Jersey-NJ, USA, 2009.

[18] H. Chipman, E. I. George, and R. E. McCulloch, "Bayesian Treed Models", Machine Learning, Volume 48, Numbers 1-3, pp. 299-320, 2002.

[19] P. Maji, "Efficient Design of Neural Network Tree using a New Splitting Criterion". Neurocomputing, Volume 71, Numbers 4-6, pp. 787-800, 2008.

[20] R. A. F. Santos, "Um Método para Segmentação de Preditores", Doctorate Thesis, Centro de Informática, Universidade Federal de Pernambuco, 2010. In Portuguese. http://www.cin.ufpe.br/~roberto/AlunosPG/Teses/2010-PhD-Roberto.zip.

[21] W. J. Conover, "Practical Nonparametric Statistics", third edition. John Wiley & sons, 1999.

[22] T. Fawcett, "An Introduction to ROC Analysis", Pattern Recognition Letters, Vol. 27, Number 8, pp. 861-874, 2006.

[23] B. Zenko, L. Todorovski, and S. Dzeroski, "A Comparison of Stacking with MDTs to Bagging, Boosting, and Other Stacking Methods". In proceedings of European Conference on Machine Learning and Principles and Practice of Knowledge Discovery in Databases (ECML/PKDD 2001), Workshop: Integrating Aspects of Data Mining, pp. 163-175, Freiburg, Germany, 2001.

[24] SAS Institute Inc., "Finding the Solution to Data Mining: a Map of the Features and Components of SAS ® Enterprise Miner". SAS Institute White Paper, Cary, North Carolina, 2000.

[25] M. Y. Kiang, "A Comparative Assessment of Classification Methods", Decision Support Systems, Vol. 35, Number 4, pp. 441-454, 2003.

[26] I. H. Witten, and E. Frank, "Data Mining: Practical Machine Learning Tools and Techniques with Java Implementations", Morgan Kaufmann, San Francisco, 2005.

Towards Making SELinux Smart

Leveraging SELinux to Protect End Nodes in a Federated Environment

L. Markowsky
School of Computing and Information Science, University of Maine, Orono, ME USA

Abstract – *This paper describes an intelligent, active, real-time, risk adaptable access control (RAdAC) system designed to extend the benefits of the National Security Agency's Security-Enhanced Linux (NSA's SELinux) by using SELinux not only as a secure base, but also as a source of input features to a Support Vector Machine (SVM) that will classify events/attacks in several categories. By enhancing SELinux with intelligence, it is hoped that the design will lead to real-time, non-signature based defensive systems capable of detecting and taking action against hostile users in the earliest stages of an attack.*

Keywords: support vector machine, machine learning, risk adaptable access control, RAdAC, SELinux

1 Introduction

The transformative vision of the Department of Defense's decentralized Global Information Grid (DoD's GIG) and the nation's dependence on Supervisory Control and Data Acquisition (SCADA) systems present challenging security issues. Effective security in these and many other federated environments is best implemented in layers, employing intelligent security mechanisms both centrally and on the end nodes.

The proliferation of cyberattacks will eventually overwhelm signature and rule-based approaches [1], and many critical applications and files must be permitted to continue to run or exist even when under attack. Many current solutions, however, rely on signature-based detection, kernel modifications, prevention of selected system functions while critical applications are running, the deletion or encryption of sensitive material while selected system functions are permitted, or computationally expensive data mining for anomalies [2][3]. Each of these approaches fails to meet at least one of the following desirable goals: detection of zero-day attacks, continuous operation of critical systems while under attack, widespread applicability of the technique, and real-time protection.

New approaches using machine learning and a focused set of input features [4] promise to revolutionize defensive systems. Support Vector Machines (SVMs) are among the best (and many believe are indeed the best) 'off-the-shelf' supervised learning algorithms [5].

This paper describes a prototype of an intelligent, active, real-time, risk adaptable access control (RAdAC) system designed to extend the benefits of SELinux by using SELinux not only as a secure base, but also as a source of input features to an SVM that will classify events/attacks in several categories. The system is designed to be integrated into an end node in any environment, including end nodes in federated environments such as DoD's GIG and SCADA systems. By enhancing SELinux with intelligence, it is hoped that the design will lead to real-time, non-signature based defensive systems capable of detecting and taking action against hostile users in the earliest stages of an attack.

Specifically, the prototype of the defensive system is designed to be:

- Integrable into Nearly Any Computerized Device – The defensive system is designed to be integrated into nearly any Linux-based end node (any Linux system running a 2.6 kernel and using a filesystem with extended attributes), including hand-held devices, servers, workstations, notebooks, and dedicated single purpose devices;
- Zero-Impact on Protected Applications and Files – The defensive system requires no modifications whatsoever to the software and files to be protected;
- Configurable for Critical Systems – The defensive systems can be tailored to create a focused defensive system for critical files and applications and for known personnel;
- Risk Adaptable – The defensive system is an RAdAC system in which an administratively-controlled "Current Operational Need" and the attacks and events detected by the system itself together designate the current risk level;
- Modular – The defensive system is modular in order to facilitate future extensions;

- Real-Time – By leveraging SELinux, the defensive system is designed to be lightweight enough to run in real time; and

- Compatible with National Security Goals – The defensive system is designed to parallel the National Security Agency (NSA) Information Assurance Directorate's vision for securing content in DoD's GIG.

2 Prototype – A smart, active, SELinux-based RAdAC defensive system

2.1 Modular defensive system design

The modular defensive system (Figure 1) features machine learning to overcome the limitations of signature and rule-based defenses and input from SELinux to enable the system to run in real time.

Module 1 uses SELinux denials generated by local and remote system requests to produce feature vectors suitable as input to an SVM. Module 2 then uses a previously trained SVM to classify attacks/events in several discrete categories in real time. Module 3, a graded response system, provides feedback to Module 2 and selects a response appropriate for the detected event, the history of events on that system, and the current operational need.

Testing and analysis will include study of the input feature set selection, the graded response system, and the tradeoffs between error rates and performance (false negative/positive rates vs. throughput and load on the system).

2.2 Extending Module 1

Module 1 may be extended to protect critical applications and files, to detect keyloggers, and to detect attackers with physical access (Figure 2). To protect critical applications and files, application-specific and file-specific raw input would be used in addition to SELinux denials in order to generate input feature vectors for the SVM. For example, to configure the input feature extractor to protect a web server, messages from Apache2, ModSecurity, and messages specific to the protected web pages would be used as raw input to the feature parser. Keystroke dynamics [6] [7] may be used to implement detection of keyloggers and attackers with physical access. While these extensions may enhance security, the input feature extractor will be tied to particular applications, files, and users, making this design suitable only for critical systems.

2.3 Design goals

The design of the defensive system (Figure 1) adheres to DoD's Three Tenets of Cyber Security. First, SELinux's mandatory access control mechanism (MAC) limits "access points to only those necessary to accomplish the mission [thereby making] critical access points and associated security less accessible to [the] adversary." Second, dynamically relabeling the SELinux context of a critical application "moves it out of band" when under attack. Third, the graded response system "denies [the] threat capability [by imposing] appropriate penalties when [an] attack is detected" [8].

Also, the design of the defensive system supports users of end nodes in federated systems by protecting "edge users who must operate across multiple domains and communications paths, on less hardened networks, to reach other tactical mission players, and to access protected core information systems and data warehouses" [9]. The defensive system achieves this goal by using a graded response module that neither suspends critical applications nor deletes critical and files – except in the most extreme circumstances – enabling end node systems to prevent "an attack from becoming successful while allowing the executing software and associated data being protected to remain operational and trustworthy" [10][11].

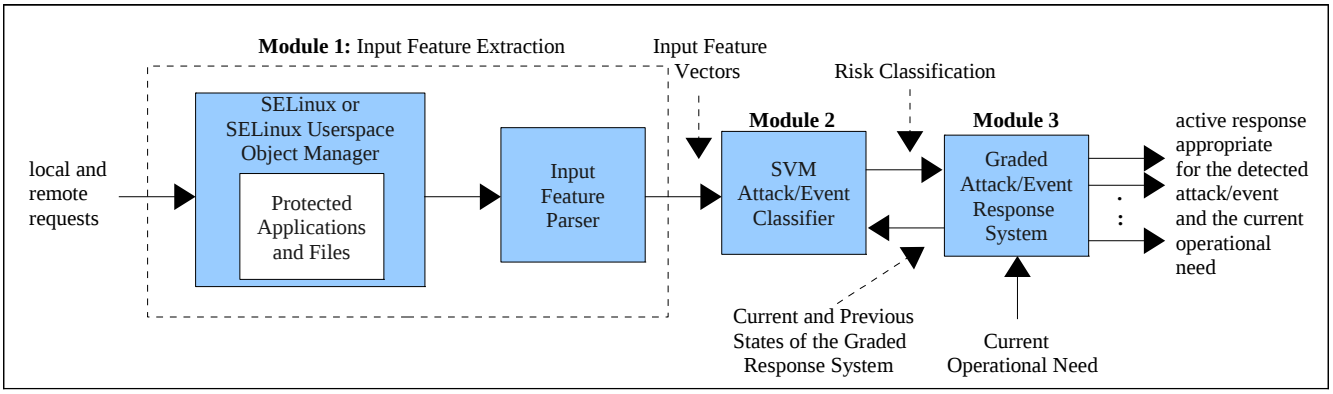

Figure 1. An Intelligent, SELinux-Based, RAdAC Defensive System

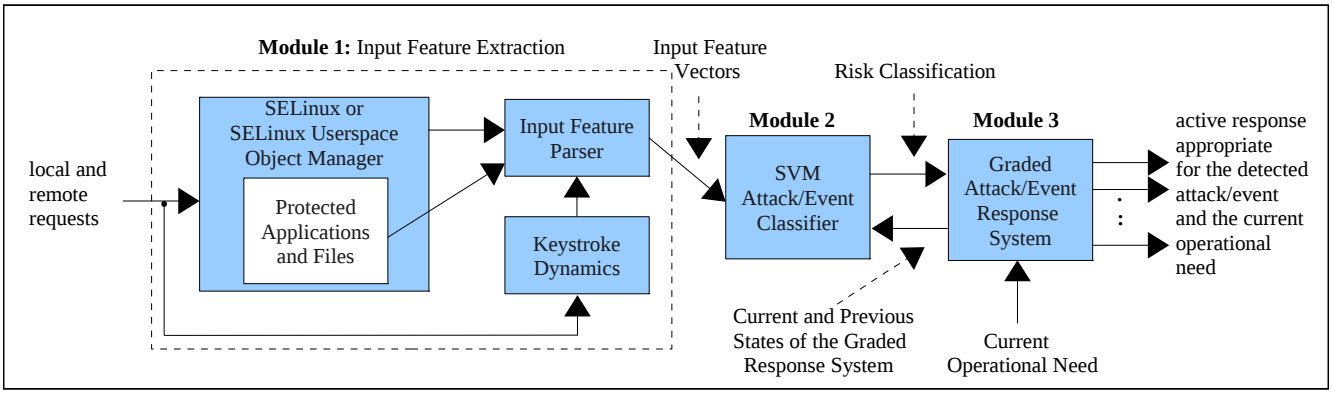

Figure 2. An Application-Specific, Personnel-Specific, Intelligent, SELinux-Based, RAdAC Defensive System

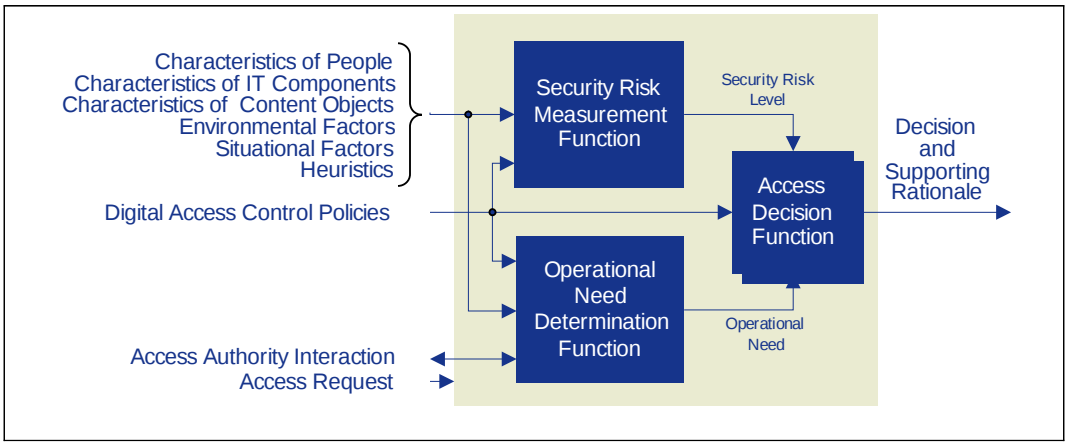

Figure 3. NSA's Vision for Access Control in DoD's GIG [12]

Finally, the design of the extended defensive system (Figure 2) parallels the NSA Information Assurance Directorate's vision for securing content in DoD's GIG (Figure 3). Modules 2 and 3 are analogous to the Security Risk Measurement Function and the Access Decision Function of Figure 3, respectively; Keystroke Dynamics, SELinux, and the Target Application messages in Module 1 are all analogous to the Characteristics of People (or other entities) [13]. The modular design facilitates future extensions that might incorporate Situational Factors or automate the current Operational Need.

3 User interface

The user interface is database-driven website designed to be friendly but restricted to authorized administrators. The main menu consists of: System, SVM, Packet Captures, Datasets, Analysis, Documentation, and Database Administration.

3.1 System submenu

The System submenu provides forms that enable the administrator to start or stop selected modules of the defensive system (Figures 4 and 5). To facilitate testing and analysis, the system permits Module 1 alone, Modules 1 and 2, or the entire defensive system to be run.

The System submenu consists of:

- Reset the SELinuxSVM Defensive System
- Start the SELinuxSVM Defensive System
- Stop the SELinuxSVM Defensive System

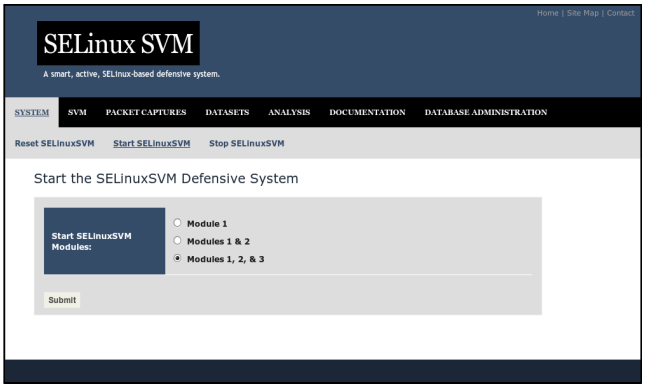

Figure 4. Starting the SELinuxSVM Defensive System

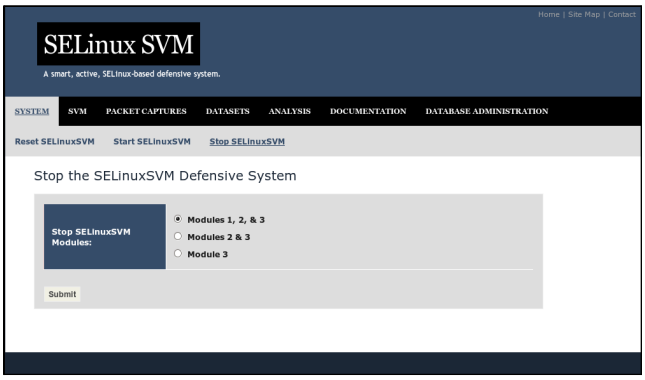

Figure 5. Stopping the SELinuxSVM Defensive System

3.2 SVM submenu

The SVM submenu provides forms that enable the administrator to select optimal SVM training parameters and dataset features as well as forms to train and test the SVM (Figure 6).

The SVM submenu consists of:

- Select Dataset Features Used to Train the SVM
- Select Parameters (Grid Search for Optimal C and gamma)
- Train the SVM
- Classify Data Points

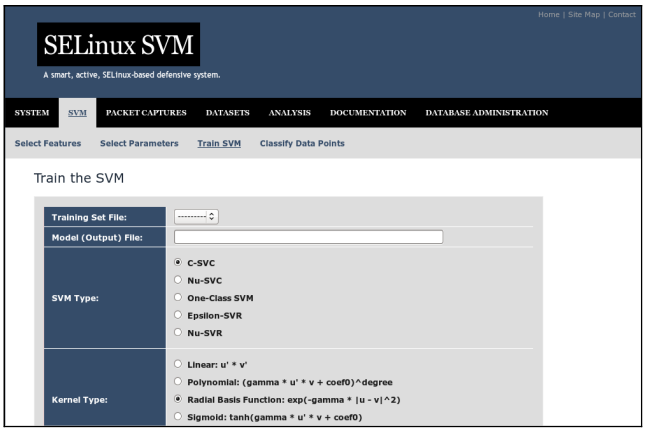

Figure 6. Training the Support Vector Machine

3.3 Packet captures submenu

The Packet Captures submenu provides forms to enable the administrator to view, replay, and filter packet capture files (Figure 7). These forms feature packet captures collected during the 2009 and 2010 Northeast Collegiate Cyber Defense Competitions (NECCDC), which are discussed in Section 7.

The Packet Captures submenu consists of:

- Filter an NECCDC 2009 Packet Capture File
- Filter an NECCDC 2010 Packet Capture File
- Filter a PREDICT Packet Capture File
- Replay a Packet Capture File
- View a Packet Capture File

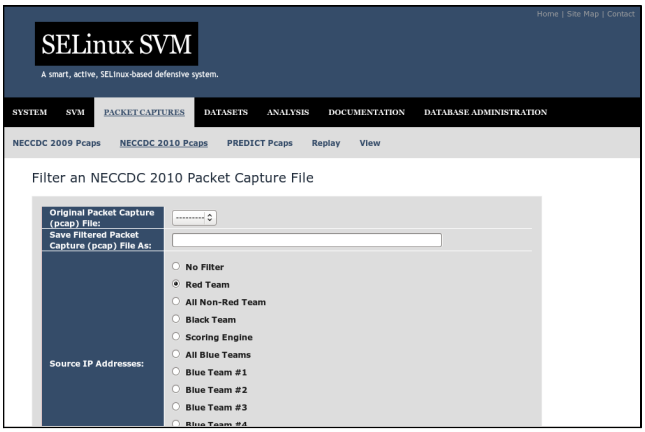

Figure 7. Filtering an Existing Packet Capture File

3.4 Datasets submenu

The Datasets submenu provides forms to enable the administrator to generate a dataset from a packet capture file, scale a dataset (Figure 8), and relabel and edit datasets. Generating datasets from packet capture files is discussed in Section 7.

The Datasets submenu consists of:

- Generate a Dataset from a Pcap File
- Scale a Dataset
- Relabel a Dataset
- Edit a Dataset

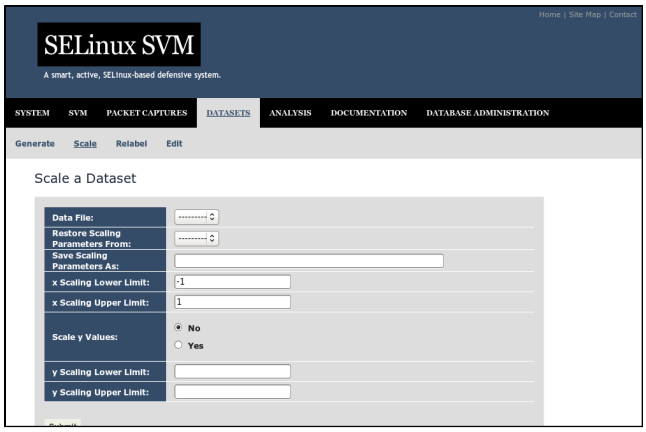

Figure 8. Scaling a Dataset

3.5 Analysis submenu

The Analysis submenu provides three performance metrics, which are discussed in Section 7, and two methods for the user to view results. "View Results" and "Plot Results", respectively, are tools to visualize and plot two-dimensional slices of the SVM together with training or testing datasets, regardless of the number of the input features.

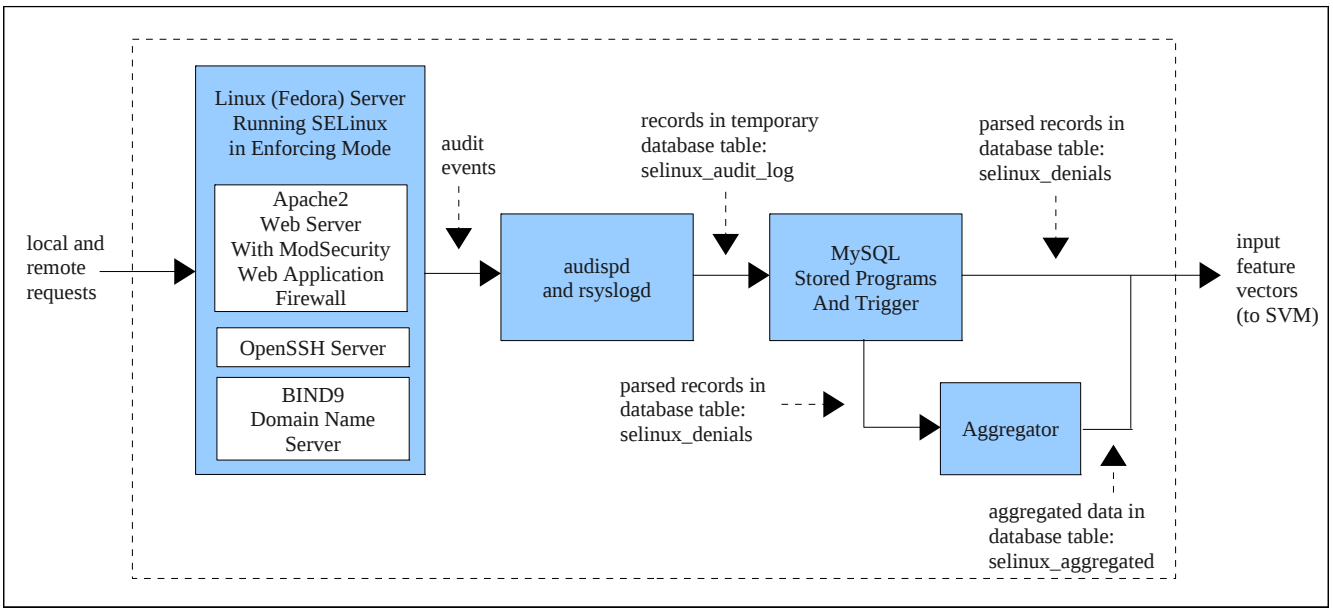

Figure 9. Module 1: Input Feature Extraction

The Analysis submenu consists of:

- Performance Metric 1: V-Fold Cross Validation Accuracy
- Performance Metric 2: SVM Training Time
- Performance Metric 3: SVM Prediction Time
- View Results (in Two Dimensions)
- Plot Results (in Two Dimensions)

4 Module 1 – Input feature extraction

Module 1, the Input Feature Extractor, automatically generates input feature vectors suitable for an SVM from local and remote requests (Figure 9). Audispd (an audit event multiplexer) and rsysogd (an extended message logging utility) are configured to enter copies of SELinux denials in a temporary MySQL database table called selinux_audit_log (Figure 10). When an entry is made in selinux_audit_log, a stored MySQL trigger parses the message to create a more useful table entry in selinux_denials (Figure 11). Offloading the parsing from the system logging mechanism to MySQL is designed to avoid a bottleneck, since parsing using rsyslogd involves time-intensive regular expression pattern matching, which is likely to be slower than MySQL stored programs. Similarly, aggregated data is collected by MySQL stored programs and entered in the selinux_aggregated table.

5 Module 2 – SVM attack/event classifier

The SVM attack/event classifier uses input from Module 1 and feedback from Module 3 in order to classify events in several discrete categories:

- Origin – an authenticated user on a tty, a user on the LAN, or a remote request;
- Number of Sources – single source vs. distributed attack;
- Target – the defensive system itself, SELinux, the operating system, the protected critical process, the protected executable, or protected files associated with the critical system;

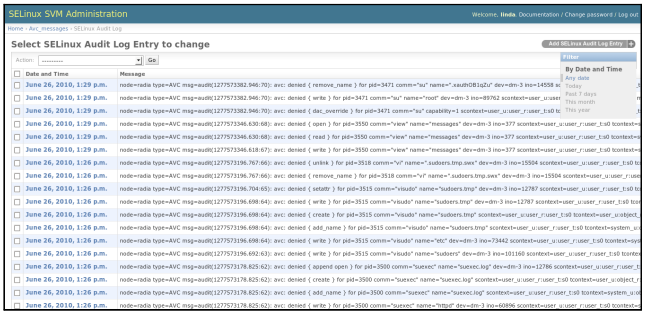

Figure 10. The SELinux Audit Log Database Table

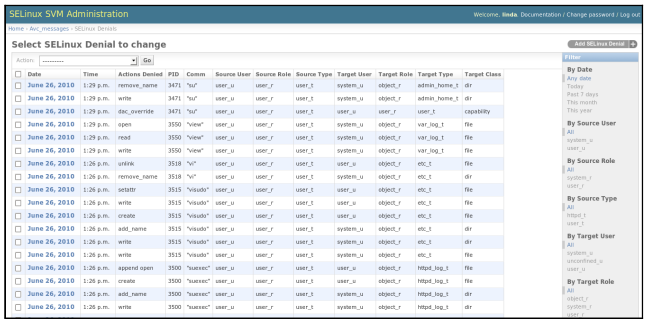

Figure 11. The SELinux Denial Database Table

- Time Span – single burst, an hourly or daily recurring event; and

- Type/Severity – single read attempt, a copy attempt over the Internet, a malicious write attempt, an unauthorized SELinux relabeling attempt, or an unauthorized attempt to transition into the SELinux sysadm_r role.

The SVM and kernel types are determined during training. Default values are C-SVC (classifier) and the radial basis function (RBF) or Gaussian kernel: $\exp(-\gamma * \|u - v\|^2)$. All SVM-related functions are implemented using libsvm [14].

6 Module 3 – Graded attack/event response system

The graded attack/event response system selects a defensive action appropriate for the classification of the attack/event as determined by the SVM, the current and previous states of the graded response system, and the current operational need. The response system selects actions appropriate for the severity of the event:

- Minor Events: In response to minor events, actions taken include alerting the administrator, filtering and saving logs, and taking a snapshot of the process tree.

- More Severe Events: In response to more severe events, actions taken include killing the offending process and processes directly related to the offending process, adding IPTables firewall rules, moving attacked files to a secure location, and relabeling the SELinux security context and Linux's discretionary access control (DAC) of the applications and files under attack.

- Extreme Events: Only in extreme circumstances (such as evidence of an attacker with physical access to the machine attempting to transition into the sysadm_r role) will critical files be deleted or critical processes terminated.

Two active responses of Module 3 specifically related to SELinux are:

- Reconfiguring Linux's DAC to dynamically manage the flow of input to the defensive system, thereby controlling the system's throughput and load; and

- Relabeling the SELinux security context of the files and processes under attack.

Relaxing the DAC causes SELinux's MAC mechanism to be consulted more frequently, increasing the load on the operating system but also catching attempted attacks at an earlier stage. If the load on the system is too great, then the DAC labels are strengthened, allowing the defensive system to continue to operate in real time. If, on the other hand, a process or file is so critical that any unauthorized attempt to read/write/execute that file would indicate an attack, then the DAC is set to the most permissive label (777) so that SELinux will be consulted on every read/write/execute request of that file, detecting the attacker at an earlier stage.

Relabeling the SELinux security context of critical files and processes under attack creates a dynamically changing protection boundary on the end node. In effect, critical files and processes are moved out of band in order to frustrate the attacker while simultaneously keeping the files and processes trustworthy and operational.

The defensive system aggressively protects itself by including the operating system, SELinux, and the system itself in the classes of targets of detected attacks. Any attempt to undermine the defensive system is be considered to be an "extreme" event.

7 Testing and analysis

7.1 Packet capture files

The packet capture files provide raw input that can be filtered and replayed to generate training and testing datasets. Packet capture files collected during the 2009 and 2010 NECCDC are currently available via the defensive system user interface. These defensive cybersecurity competitions pitted "blue" teams, each of which protected a group of servers and workstations from a "red" team charged with attacking them. The "blue" teams were prohibited from engaging in offense. A "black" team and scoring engine generated friendly traffic and monitored the services required of the blue teams' servers.

Since the IP addresses of the "blue", "red", and "black" teams are known, it is possible to filter friendly and hostile traffic using wireshark or tshark filters. In addition, the target IP addresses of the filtered packets can be rewritten to redirect the packets to a test host running the defensive system prototype. The filtered packet capture files can then be replayed to produce training and testing datasets.

7.2 Training and testing datasets

Training and testing datasets are used to train and test the SVM and graded response system. Dataset features should be scaled to prevent one feature from dominating and skewing the resulting SVM. The user interface also permits the administrator to relabel a dataset to indicate friendly traffic or hostile traffic in several classifications.

7.3 Time and performance metrics

Three performance metrics measure the accuracy and time performance of the defensive system.

The V-Fold Cross Validation Accuracy metric prevents overfitting, that is, prevents producing an SVM that is too specific for a particular dataset. Since the purpose of an SVM is to predict the classification of unknown data points, an overfitted SVM is undesirable. V-fold cross validation is a relatively simple concept:

> In v-fold cross-validation, we first divide the training set into v subsets of equal size. Sequentially one subset is tested using the classifier trained on the remaining (v – 1) subsets. Thus each instance of the whole training set is predicted once so the cross-validation accuracy is the percentage of data which are correctly classified [15].

The SVM Training Time measures the time to calculate the SVM from a dataset, and the SVM Prediction Time measures the time to make a single prediction using an existing SVM. These metrics are included to measure the defensive system's ability to run in real time, since one of the goals of the project is to attempt to design a non-signature based defensive system that can run in real time by leveraging existing security mechanisms and by dynamically adjusting the load.

8 Future work

The prototype is currently being developed. First, a complete implementation of Module 1 and preliminary implementations of Modules 2 and 3 will be completed and the NECCDC 2009 and 2010 packet captures will be used to generate testing datasets. Following a complete analysis of Module 1 using the preliminary prototype, Modules 2 and 3 will be fully implemented, the PREDICT packet captures will be added to the files used to generate testing datasets, and the entire defensive system will be tested and analyzed.

9 Acknowledgments

The author thanks Dr. James Fastook, Dr. Phil Dickens, Dr. Bruce Segee, and Dr. George Markowsky of the University of Maine and Dr. Danny Kopec of the CUNY (City University of New York) Graduate Center and Brooklyn College for their invaluable advice and support.

10 References

[1] Y. Song, M. Locasto, A. Stavrou, A. Keromytis, and S. Stolfo, "On the infeasibility of modeling polymorphic shellcode." Presented at the 14th ACM Conference on Computer and Communications Security (CCS 2007), October 2007.

[2] P. Kabiri and A. Ghorbani, "Research on intrusion detection and response: A survey." International Journal of Network Security, Vol. 1, No. 2, pp. 84-102, September 2005.

[3] F. H. Smith, "Defense against root." Presented at the 2007 International Conference on Security & Management, June 2007.

[4] B. Thuraisingham, L. Khan, M. Kantarcioglu, and K. Hamlen, "Assured information sharing for security and intelligence applications." Presented at the 2009 Cyber Security and Information Intelligence Research Workshop (CSIIRW'09), April 2009, pp.14-19.

[5] A. Ng, "Support vector machines." Autumn 2008, p.1. (http://www.stanford.edu/class/cs229/notes/cs229-notes3.pdf)

[6] F. Bergadano, D. Gunetti, and C. Picardi, "User authentication through keystroke dynamics." ACM Transactions on Information and System Security, Vol. 5, No. 4, pp. 367-397, November 2002.

[7] E. Lau, X. Liu, C. Xiao, and X. Yu, "Enhanced user authentication through keystroke biometrics." Computer and Network Security Final Project Report, MIT, December 9, 2004.

[8] Software Protection Initiative (SPI). "The three tenets of cyber security." (http://spi.dod.mil/tenets.htm)

[9] Office of the Secretary of the Defense (OSD). Small Business Innovation Research (SBIR) FY2009.2 Program Description, April 20, 2009, p.5.

[10] D. Alberts and R. Hayes, Power to the Edge: Command...Control...in the Information Age, 3rd Printing, April 2005.

[11] Office of the Secretary of the Defense (OSD). Op. Cit., p.29.

[12] R. McGraw, "Securing content in the Department of Defense's Global Information Grid." Presented at the Secure Knowledge Management Workshop, State University of New York, Buffalo, September 2004.

[13] Ibid.

[14] C. Chang and C. Lin, "LIBSVM: A library for support vector machines," 2001. (http://www.csie.ntu.edu.tw/~cjlin /libsvm)

[15] C. Hsu, C. Chang, and C. Lin, "A practical guide to support vector classification," May 19, 2009, p. 5. (http://www.csie.ntu.edu.tw/~cjlin)

Integration of Negative Emotion Detection into a VoIP Call Center System

Tsang-Long Pao, Chia-Feng Chang, and Ren-Chi Tsao
Department of Computer Science and Engineering
Tatung University, Taipei, Taiwan

Abstract - *The speech signal itself contains not only the semantics of the spoken words but also the emotion state of the speaker. By analyzing the voice signal to recognize the emotion hidden in the speech signal, it is possible to identify the emotion state of the speaker. With the integration of a speech emotion recognition system into a VoIP call center system, we can continuously monitor the emotion state of the service representatives and the customers. In this paper, we proposed a framework that integrates the speech emotion recognition system into a VoIP call center system Using this setup, we can detect in real time the speech emotion from the conversation between service representatives and customers. It can display the emotion states of the conversation in a monitoring console and, in the event of a negative emotion being detected, issue alert signal to the service manager who can then promptly react to the situation.*

Keywords: Speech Emotion Recognition, Call Center, Negative Emotion Detection, WD-KNN Classifier

1 Introduction

The voice signal in the conversation represents the semantics of the spoken words and also the emotion state of the speaker. If a dispute happened between the service representative and the customer, there is no way to notify the service manager to take action immediately in current call center system. Since the customer service is playing an important role for an enterprise, the customer satisfaction is very important. So, the management of customer service department to improve the customer satisfaction is an important issue for the enterprise.

Traditional customer service lacks of the ability in issuing alerts for conversation with negative emotion in real-time. For example, when the customer disagrees with the service representative, a dispute may arise. The traditional call center handles a large amount of calls every day and will usually make recording of all the calls for later analysis to see whether there is any improper conversation or not. However, these setups cannot handle the dispute situation in a timely manner.

A considerable number of studies have been made on speech emotion recognition over the past decades [1-16]. By integrating the speech emotion recognition system into the VoIP call center system, we can continuously monitor the emotional state of the service representatives and the customers. In this paper, we propose the mechanism to integrate the negative emotion detection engine into the VoIP call center system. A parallel processing architecture is implemented to meet the performance requirements for the system. We also record the emotion states for all of the calls into the database. Alerts will be issued to the service manager whenever a negative emotion such as anger is being detected. The service manager has a chance to intervene into the two quarreling parties to pacify the customer and resolve the problem immediately. With this mechanism, it can enhance the level of customer satisfaction.

The organization of this paper is as follows. In Section 2, the background and the related researches of speech emotion recognition and voice over Internet Protocol (VoIP) are reviewed. In Section 3, the system architecture of a multi-line negative emotion detection in VoIP Call Center is described. In Section 4, the experimental setup is presented and the results are discussed. Conclusions are presented in Section 5.

2 Backgrounds

2.1 Speech Emotion Recognition

In the past, quite a lot of researchers studied the human emotion and try to define what an emotion is. But it is hard to define emotional category because of there is no a single universally agreed definition. The emotion category defined by Ortony and Turner is a commonly accepted definition [10]. In recent years, the study of psychological tends to divide emotion category into basic emotion and complex emotion. The complex emotion is a derived version from the basic emotion in their definition.

In addition to the semantics of spoken word, the speech signal also carries information of the emotion state of the speaker. That is, inside the speech signal, there are features that are related to the emotion state at the time of making that speech. By analyzing these features, it is possible to classify the emotion categories with a suitable classifier.

Features related to speaking rate, signal amplitude, frequency, jitter, and formant are being studied in the speech emotion recognition researches. [1-4].

In previous studies of emotion recognition, there are several aspects that are being addressed. Some of the studies tried to find the most relevant acoustic features to the emotion inside the speech signal [13-16]. Searching for the most suitable machine learning algorithms for the classifier is also a topic that attracted quite a lot of attention [7][9-12]. In most of the previous studies, short speech corpora are used in the experiments. However, in this research, we need to deal with the continuous speech, which is long in nature. Therefore, we need to find a way to properly segment the speech signal and categorize the emotion such that burst misclassification will not affect the accuracy of the judgment.

The corpus is a set of a large collection of utterance segments. A corpus plays an important role in the emotion recognition research. In this paper, the D80 corpus built in the previous studies is used. We use the D80 to train our emotion recognition engine. The speech corpus was collected from 18 males and 16 females who were given 20 scripts and were asked to speak out in five emotions including anger, boredom, happiness, neutral and sadness for each of them. A subjective test is performed and those utterances with over 80% agreement were kept. After this process, there are 570 utterances left. The number of utterances in each emotion categories in the D80 corpus is 151 for anger, 83 for boredom, 96 for happiness, 116 for neutral, and 124 for sadness.

A considerable number of previous studies have been made on feature selection in order to improve the accuracy of the emotion recognition. The core of the feature selection is to reduce the dimension of the feature set to a smallest feature combination that yields the highest recognition accuracy. The speech features commonly used in previous emotion recognition researches include Formants (F1, F2 and F3), Shimmer, Jitter, Linear Predictive Coefficients (LPC), Linear Prediction Cepstral Coefficients (LPCC), Mel-Frequency Cepstral Coefficients (MFCC), first derivative of MFCC (dMFCC), second derivative of MFCC (ddMFCC), Log Frequency Power Coefficients (LFPC), Perceptual Linear Prediction (PLP), and Zero-Crossing Rat (ZCR). According to previous studies, the MFCC is the commonly used feature for the emotion recognition [13]. Therefore, we choose the MFCC feature as the acoustic feature as input to the classifier input in this research.

In the machine learning, the purpose of a classifier is to classify objects with similar characteristics into the same class. The classification can be divided into two types, supervised (e.g. KNN) and unsupervised (e.g. k-means). In this research, we used the Weighted D-KNN (WD-KNN) classifier, which is a variant of KNN and is proposed in [11]. The KNN is a classification algorithm that assigns the test sample to a class based on the distance between test sample and k-nearest training samples. The WD-KNN extends the KNN by comparing the weighted distance sum to maximize the classification accuracy. The weight calculation is to assign a higher weight to neighbors that provide more reliable information.

For an M-class classification using KNN, let the k neighbours nearest to unknown test sample $\mathbf{y}$ be $\mathbf{N}_k(\mathbf{y})$, and $c(\mathbf{z})$ be the class label for training sample $\mathbf{z}$. The subset of the nearest neighbours in class $j \in \{1, \cdots, M\}$ is

$$\mathbf{N}_k^j(\mathbf{y}) = \{\mathbf{z} \in \mathbf{N}_k(\mathbf{y}); c(\mathbf{z}) = j\} \quad (1)$$

If we denote the cardinality (the number of elements) of the set $\mathbf{N}_k^j(\mathbf{y})$ as $|\mathbf{N}_k^j(\mathbf{y})|$. Then the classification of $\mathbf{y}$ belonging to class j^* is the majority class vote, that is:

$$j^* = \arg\max_j \{|\mathbf{N}_k^j(\mathbf{y})|\} \quad (2)$$

For WD-KNN classification, we need to select k nearest neighbors from each class. Let d_i^j denotes the Euclidean distance between the i_{th} nearest neighbor in class j to unknown sample $\mathbf{y}$. The distance measure is in ascending order, that is $d_i^j \le d_{i+1}^j$. The weighted distance sum for sample $\mathbf{y}$ to all the k nearest neighbors in class j will be

$$D^j = \sum_{i=1}^{k} w_i d_i^j \quad (3)$$

where $w_i \ge w_{i+1}$ for all i. As discussed in [11], the best recognition rate could be obtained by using a weighting in the reverse ordered Fibonacci sequence, which is:

$$w_i = w_{i+1} + w_{i+2}, \quad w_{k-1} = w_k = 1 \quad (4)$$

The classification of $\mathbf{y}$ belonging to class j^* is the class with the shortest weighted distance

$$j^* = \arg\min_j \{D^j\} \quad (5)$$

As a conclusion, the speech emotion recognition is a system that takes the voice signal as input and then recognizes the emotion of the speaker at the instance of making that speech. From the extracted features, the most likely emotion was judged by using a classification algorithm. The block diagram of a speech emotion recognition system is shown in Figure 1. In this system, the

selected features were extracted and sent to the classifier to determine the most probable emotion of that segment.

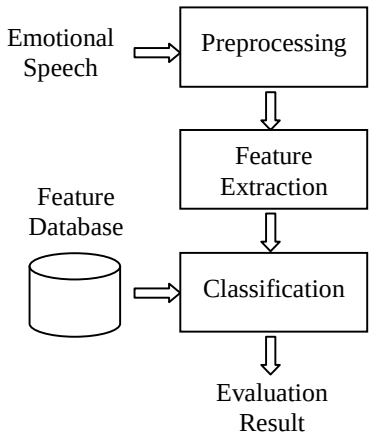

Figure 1. Block diagram of emotion recognition system

2.2 VoIP Telephony and Packet Capture Techniques

VoIP or known as IP phone is a technology that uses internet to accomplish telephone communication. The IP phone was used internally in the enterprise in the past. However, owning to the rapid grown of internet, the IP phone is now widely adopted and is gradually replacing the traditional telephone communication system. Currently, the commonly used VoIP communication protocol is the Session Initiation Protocol (SIP). The SIP is a protocol developed by IETF MMUSIC which is used in the establishment, modification and termination of an interactive call session. Possible applications include voice and video communication, instant messaging, online game, virtual reality and other multimedia applications. The purposes of SIP are to define the format and the control of the packets transmitted over the internet.

The SIP is a point to point protocol. Using a distributed architecture, the SIP transmits the text-based information and names the address by URL. The SIP use similar syntax as some protocols used in the internet such as HTTP and SMTP which consist of headers and message body.

There are two types of SIP operations for the client connection, one is to connect the two clients in a point to point manner, and the other is to connect the party though a proxy server. In this research, we adopt proxy server configuration to simplify the packet capture process. The IP PBX (IP Private Branch exchange) works as the proxy server and plays the role of packet relaying. We capture the packets in and out from the IP PBX by port mirroring from the switch the server connected to.

The packet capture tool used in this study is WinPcap. WinPcap is a tool for link-layer network access in Windows environments. It includes kernel-level packet filter, a dynamic link library (packet.dll) and a high-level and system-independent library. It can be used in win32 platform to capture network packets. WinPcap consists of a driver that facilitates the operating system to access the low-level networks. WinPcap also provides a library that can be used easily to access the low-level network layers by the application programs. In addition, the kernel of WinPcap also provides packet filtering. Through the filter setting, the driver will directly discard unwanted packet in driver layer. The performance of the packet filter is good. Hence it is now widely used in a lot of software such as WireShark.

3 System Architecture

In this paper, we proposed a framework that integrates the speech emotion recognition system into a VoIP call center system. The components of the system are shown in Figure 2. The customer and the service representative communicate with each other through the VoIP phones. We defined session as the conversation between the pair of the customer and the service representative. We use a layer 2 switch to mirror packets going in and out from the IP PBX into our packet capture agent. Then, we identify the session and assign the session with a Session ID (SID) if it is new. After the session is established, we extract the voice signal from the RTP packets captured and regroup it into proper segments. The speech emotion recognition system will be activated to classify the emotion of each segment. Finally, the recognition result will be stored into a database. The system will issue an alert whenever a negative emotion, mainly anger, is detected.

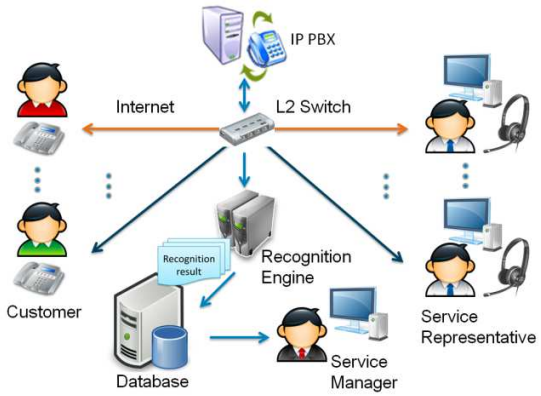

Figure 2. Components of the proposed system

The operation steps of system are shown in Figure 3. First, the system will capture the packets and filter out the SIP and RTP packets. The Speech Emotion Recognition System (SERS) will assign a Session ID (SID) according to the phone number of the service representative and

customers. Then, the speech segment will be sent to the emotion recognition engine to classify the emotion state. Finally, the classification results will be stored into database. The service manager acquires the all the results using a web page interface. The system will issue alert to service manager when the negative emotion is detected.

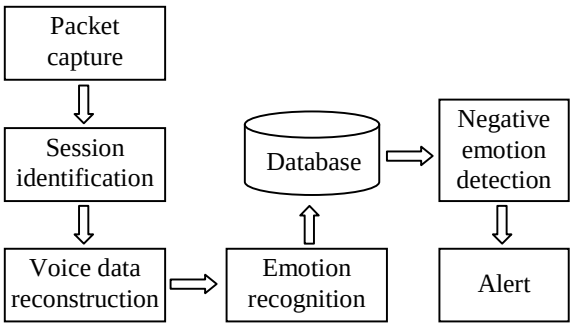

Figure 3. Operations of the speech emotion recognition

3.1 Packet Capture and Session Identification

The packet is the smallest unit in network communication. Packets are transmitted across the internet through a series of switches and routers. A packet consists of a header and a payload. The header has the control information for the transmission of packets. The control information includes source and destination IP addresses, source and destination ports, etc. In our experiment environment, all of the VoIP packet will pass through the SIP proxy server. In this framework, we can use a mechanism called port mirror in the layer 2 switch to mirror the packets in and out of the SIP server. Then, we can capture the packets and analyze its content easily.

In the call center, each phone line is independent. But once the call is established, the phone number will not change during the call. So, the identification of a session is necessary for storing the captured RTP packet to the correct pair of conversation. We build a session object to manage the session. The session object include source IP, setup time, speech coding and used buffers. We create a session object when a session start and we will remove the session object when the phone call ends. In order to implement multi-line packet capture, we need to identify the source and destination IP address of the packet first. According to the information, we assign a session ID to the session, and then allocate the storage for storing the session ID and related information.

3.2 Emotion Recognition Engine

To integrate emotion recognition function into the VoIP call center system require further effort then the speech emotion recognition. Some attempts have been made by scholars to use the combination of multiple speech features to increase the accuracy of speech emotion recognition. However, in order to process multi-line voice segment simultaneously in real-time, the recognition engine needs to reduce the computational complexity. From previous studies, the MFCC feature has been proven to be one of the most robust features in emotion recognition [12]. So we choose to use only the MFCC in the emotion recognition. We use the WD-KNN to be our classifier.

In order to process multi-line voice segment, we may need more than one computer to perform the speech recognition. We design a mechanism to share the load among several speech emotion recognition engines. Virtual machine architecture is used to fully utilize the computing power of a high performance server. With this framework, we can distribute the voice segment recognition to each virtual machine in turn. The parallel processing mechanism can resolve the bottleneck problem due to the high computational resource required by the recognition engine.

3.3 Negative Emotion Detection

In the D80 corpus, there are five basic emotion categories. We further divided them into positive and negative class. The positive emotion includes happiness and neutral, and the negative emotion includes anger, sadness and boredom. In this paper, we focus on detecting the anger emotion incurred in the conversation between the service representative and customer. The system will issue an alert whenever the anger emotion being detected during the conversion between the service representative and the customer.

To decrease the false alarm rate, a score board judgment mechanism is implemented. The score board is zero at the beginning of a session. When the emotion recognition result is anger, the score board will increase by 4 points. The score board will decrease 1 point when no anger emotion is detected for a voice segment if the score is positive. The system will confirm the anger emotion when the score exceed the threshold. An alert flag will be written to database whenever the score exceed the threshold. An alert message will be sent to the service manager through a web page interface whenever alert flag is being set.

4 Experiments and Result Discussion

4.1 Experimental Setup

The proposed system consists of three subsystems. The detail description of each subsystem will be presented in this section. The framework of the proposed system is shown in Figure 4.

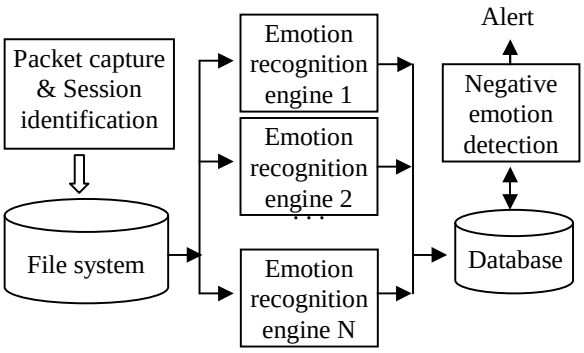

Figure 4. Framework of the proposed system

The Asterisk IP PBX server is installed in a Linux platform. In this research, we assign the SIP ID 1xx as the phone number for customers, SIP ID 4xx for the service manager, and SIP ID 6xx for the service representatives. The SIP phone is configured in the proxy mode, such that all the SIP and RTP related communication packets between the customer and the service representative will pass through the IP PBX. With this configuration, we can capture all the SIP and RTP packets by mirroring the traffic going into the server from the Layer 2 switch where the server is attached.

The session information is stored in a table structure. When a new SIP or RTP packet is received, the packet capture module will capture the packet, analyze the content of header and compare it with the contents in the session table. If it is a new session, the system will create a new session identifier and assign a new session ID to it; otherwise the existing session ID will be retrieved.

4.2 Emotion Recognition

We capture the voice signal from the conversation between the customer and service representative. The voice we captured will be regrouped into sound file in WAV format with 1 second in duration each. We will send the segmented voice file into the speech recognition engine, and the engine will output the recognition result. In order to increase the performance of the emotion recognition engine, we use a parallel architecture to build our recognition system. We setup several machines and install the recognition engine written in MATLAB into each machine. By using this structure, the bottleneck problem of the speech emotion recognition system can be avoided. The output from each recognition engine is stored into a database. The results are analyzed by using the score board algorithm stated above to determine whether the anger emotion exists in the conversation or not.

4.3 Testing Samples

A six scripts corpus was recorded by inviting volunteers to speak out the scripts with emotion as they like. Each corpus is tagged subjectively by human judge. Only the results with more than 80% agreement in this process are kept. The emotion of human seems to change gradually. So we use the score board concept to determine whether or not an anger emotion was occurred in the conversation between the customer and the service representative.

In our environment, we set the score to 0 at the beginning. If a negative emotion is being detected, the system will add 4 points to the corresponding session, or otherwise the system will subtract 1 point from that session if the score is positive. In order to reduce the false negative emotion recognition rate, a threshold should be set. We test several threshold values, including 4, 8, 12, and 16, to check the recognition accuracy. We compare the emotion recognition results with human judge for the chosen threshold. The result of the negative emotion detection is listed in Table 1.

Table 1. Number of detected negative emotion with different threshold T.

	Human Judge	T=4	T=8	T=12	T=16	T=20
Script1	2	59	36	18	1	0
Script2	0	2	0	0	0	0
Script3	0	48	33	16	5	0
Script4	1	21	1	1	1	0
Script5	7	97	85	61	29	10
Script6	10	54	39	23	12	7

In Table 1, the negative emotion detection results are close to the human judge when the threshold is 16 except the script 3 and 5. For script 3, the content of the script consist of a lot of happy sentence. It is hard to differentiate between happiness and anger in a speech emotion recognition system since they are both in the activation category. For script 5, the content of the script consists of continuous negative emotion. Due to the score board architecture, it is hard to count the dispute correctly. The advantage of the score board framework is that it can reduce the judgment error. But it cannot count the dispute exactly. For the negative emotion detection as mentioned above, the most important thing is to issue an alert when the dispute happened. The frequency of the dispute is not an important issue in this research.

5 Conclusions

The call center plays an important role for an enterprise. It is obviously that collects the opinion from the customer

and pacify the customer if he or she is too agitated is important for the enterprise. To improve the quality of the service of the call center, we can integrate a negative emotion detection mechanism into the call center system. When a service representative faces too many angry customers, the call distribution system can reduce the number of calls to that representative to avoid the representative running into angry state. In this paper, we propose and implement the frameworks which can handle multi-line phone call with negative emotion detection capability. We modularize the system components that make the system more flexible. We develop the subsystem individually which includes packet capture and analysis, emotion recognition, result recording, and negative emotion detection. In the part of emotion recognition, we adopt the parallel architecture to avoid the possible bottleneck problem. By the combination of these subsystems, we build a system that can detect negative emotion from the conversation and issue an alert to service manager accordingly. Consequently, this system can improve the service quality of a call center because of the service manager has a chance to intervene to resolve the problem immediately.

Acknowledgement

The authors would like to thank the National Science Council (NSC) for financial support of this research under NSC project No: NSC 100-2221-E-036 -043.

6 References

[1] H. Altun and G. Polat, "Boosting selection of speech related features to improve performance of multi-class SVMs in emotion detection," *Expert Systems with Applications*, 36, 8197-8203, 2009

[2] C. Busso and S. S. Narayanan, "Between Speech and Facial Gestures in Emotional Utterances: A Single Subject Study," *IEEE Transactions on Audio, Speech, and Language Processing*, Vol. 15, No. 8, pp. 2331-2347, 2007.

[3] C. Busso, S. Lee, and S. Narayanan, "Analysis of Emotionally Salient Aspects of Fundamental Frequency for Emotion Detection," *IEEE Transacations On Audio ,Speech, And language Processing*, Vol. 17, No. 4, pp.582-596, May. 2009

[4] M. Cernak and C. Wellekens, "Emotional aspects of intrinsic speech variabilities in automatic speech recognition," *International Conference on Speech and Computer*, 405-408, 2006

[5] Z. J. Chuang and C. H. Wu, "Multi-Modal Emotion Recognition from Speech and Text," *International Journal of Computational Linguistics and Chinese Language Processing*, pp. 1-18, Vol. 9, No. 2, 2004.

[6] R. E. Cowie, E. Douglas-Cowie, N. Tsapatsoulis, G. Votsis, S. Kollias, W. Fellenz, and J. Taylor, "Emotion Recognition in Human-Computer Interaction," *IEEE Signal Processing Magazine*, Vol. 18, No. 1, pp. 32-80, 2001.

[7] X. Jin and Z. Wang, "An Emotion Space Model for Recognition of Emotions in Spoken Chinese," *First International Conference on Affective Computing and Intelligent Interaction*, pp. 397-402, 2005.

[8] M. Lugger and B. Yang, "Extracting voice quality contours using discrete hidden Markov models," *Proceedings of the Speech Prosody*, 2008

[9] T. Nwe, S. Foo, and L. De Silva, "Speech emotion recognition using hidden Markov models," *Journal of Speech Communication*, 41(4), 603-623, 2003

[10] Ortony and T. J. Turner, "What's Basic about Basic Emotions," *Psychological Review*, pp. 315-331, 1990.

[11] T. L. Pao, Y. M. Cheng, Y. T. Chen & J. H. Yeh, "Performance Evaluation of Different Weighting Schemes on KNN-Based Emotion Recognition in Mandarin Speech," *International Journal of Information Acquisition*, Vol. 4, No. 4, pp. 339-346, Dec. 2007.

[12] T. L. Pao, Y. T. Chen, Chen and J. H Yeh, "Comparison of classification methods for detecting emotion from Mandarin speech," *IEICE Transactions on Information and Systems*, Vol. E91-D, no. 4, pp. 1074-1081, April 2008.

[13] T. L. Pao, Y. T. Chen, and J. H. Yeh, "Emotion Recognition and Evaluation from Mandarin Speech Signals," *International Journal of Innovative Computing, Information and Control* (IJICIC), Vol.4, no. 7, pp. 1695-1709, July 2008.

[14] J. Rong, G. Li, and Y. P. Chen, (2009). "Acoustic feature selection for automatic emotion recognition from speech," *Information Processing and Management*, 45, 315-328, 2009

[15] D. Ververidis and C. Kotropoulos, C, "Fast and accurate sequential floating forward feature selection with the Bayes classifier applied to speech emotion recognition," *Signal Processing*, 88, 2956-2970, 2008

[16] B. Yang and M. Lugger, "Emotion recognition from speech signals using new Harmony features," *Signal Processing*, 90, 1415-1423, 2010

Machine Learning with Templates

Michael Stephen Fiske
Aemea Institute, San Francisco, CA, USA
mf@aemea.org

Abstract— *New methods are presented for the machine recognition and learning of categories, patterns, and knowledge. A probabilistic machine learning algorithm is described that scales favorably to extremely large datasets, avoids local minima problems, and provides fast learning and recognition speeds. Templates may be created using an evolutionary algorithm described here, constructed with other machine learning methods, designed by a human expert or synthesized using a combination of these methods. Each template has a prototype and matching function which can help improve generalization. These methods have applications in bioinformatics, financial data mining, goal-based planners, handwriting recognition, machine vision, natural language processing / understanding, search engines, strategy such as business and games and voice recognition.*

Keywords: evolution, machine learning, pattern recognition, polymorphous, template

1. Introduction

New machine learning methods and knowledge representation have sought to provide superior technology applications. In this regard, Machine Learning with Templates pertains to recognizing categories and predictive modelling, which can be important components of advanced software technology.

Machine Learning with Templates was designed to use the advantages of bottom-up and top-down methods. Over the last few decades, some practitioners in AI, cognitive psychology, machine learning and neurobiology have observed that some cognitive tasks are better suited to bottom-up methods, while other tasks are better performed by top-down methods (See [1], [7], [10], [11], [18], [19], [20]).

An example of a bottom-up representation is a feedforward neural network that uses a gradient descent learning algorithm ([1], [12]), applied to handwritten digit recognition [17]. Other types of tasks use top-down methods. For example, IBM's Deep Blue software program plays chess [15]. Hammond's *CHEF* program creates new cooking recipes by adapting old recipes [23].

2. Summary of Useful Properties

Machine Learning with Templates has some useful properties.

1) Categorization is probabilistic and polymorphous (See [5], [24], and pages 26-31 in [7]).
2) Learning algorithm 5.1 is extremely fast. It takes less than one minute – for a 5 Ghz Intel Pentium 4 computer – to build templates that successfully recognize handwritten letters with an error rate less than 0.5%. Some neural network training times for handwriting recognition take considerably more time. Further, the design of the neural network architecture may take human researchers many weeks.
3) Learning algorithm 5.1 does not use a *greedy* optimization algorithm such as gradient descent [1], so it avoids local minima problems. On extremely large datasets, locally greedy algorithms may not adequately train in a practical amount of time.
4) Each template has a prototype and matching function which can help improve generalization. In some applications, the use of prototypical examples and templates designed by a clever human expert can substantially increase machine learning accuracy and speed.
5) Recognition algorithm 4.1 is extremely fast. It scales well on huge datasets and large numbers of categories because it exploits *exponential elimination*. As an example, consider the task of recognizing Chinese characters [25]. Some estimates state that there are 180 million distinct categories of Chinese characters. When the learning algorithm builds a set of templates that on average eliminate $\frac{1}{3}$ of the remaining Chinese character categories, then one trial of the recognition algorithm on average uses only 46 randomly chosen templates to reduce 180 million possible Chinese categories to a single category. (46 is the largest natural number n satisfying inequality $180,000,000 * (\frac{2}{3})^n < 2$.)
6) Machine Learning with Templates is flexible enough to create useful applications in bioinformatics, financial data mining, goal-based planners, handwriting recognition, information retrieval, machine vision, natural language processing / understanding and voice recognition.

3. Definitions and Template Structure

The space $\mathcal{C}$ is called a category space. Sometimes a space is a mathematical set, but a space may have more structure [21]. If the category space is about concepts that are living

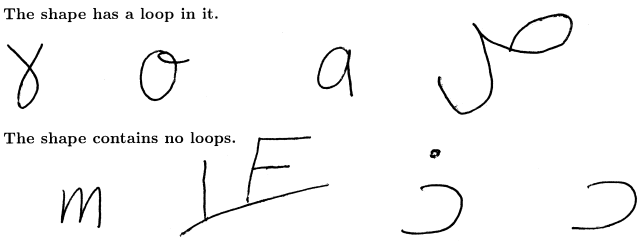

Fig. 1: Shapes with loops and no loops

creatures, then typical members of $\mathcal{C}$ are the categories: *dog*, *cat*, *animal*, *mammal*, *lizard*, *starfish*, *tree*, *barley*. A different category space is the letters of our alphabet $\{a, b, c, \ldots, y, z\}$. Another abstract type of category space may be the functional purpose of genes. One category is any gene that influences eye color; another category is any gene that codes for enzymes used in the liver; and another category is any gene that codes for membrane proteins used in neurons. In short, the structure of the category space depends upon what set of possibilities that you want the software to retrieve, recognize or categorize.

The example space $\mathcal{E}$ represents every conceivable example. Consider a software program that recognizes handwritten letters used in the English language [17]. The example space is every handwritten *a*; ... ; and every handwritten *z*. The set of training examples $\{e_1, e_2, \ldots, e_m\}$ is a subset of the example space $\mathcal{E}$.

The function $G : \mathcal{E} \rightarrow \mathcal{P}(\mathcal{C})$ is an ideal map or *ideal target function* [20], where $\mathcal{P}(\mathcal{C})$ is the power set of $\mathcal{C}$. In this case, each example e in $\mathcal{E}$ can be classified as lying in 0, 1 or multiple categories. The goal is to construct a function $g : \mathcal{E} \rightarrow \mathcal{P}(\mathcal{C})$ so that $g(e) = G(e)$ for every $e \in \mathcal{E}$. The example e = *tiger* lies in the categories *cat*, *animal* and *mammal*. In other words, $G(e) = \{cat, animal, mammal\}$. For some applications, it may impossible or extremely difficult to explicitly describe G with a mathematical formula or representation. In other implementations, the results of the template recognition algorithm can interpret e as having a probability $p(c)$ of lying in category c for each $c \in \mathcal{C}$. In these cases, the goal is to build $g : \mathcal{E} :\rightarrow [0, 1]^{\mathcal{C}}$ close to G.

Templates are similar to classifiers [20], but have additional structure. Templates are used to distinguish between two different categories of patterns, information or knowledge. For example, if the two different categories are the letters *a* and *m*, then *the shape has a loop in it* is a useful template because it distinguishes *a* from *m*. (See figure 1.)

Distinct from classifiers, templates have prototype and matching functions. Let $\{T_1, T_2, \ldots, T_n\}$ denote a collection of templates, called the template set. Associated to each template, there is a corresponding template value function $T_i : \mathcal{E} \rightarrow \mathcal{V}$, where $\mathcal{V}$ is a template value space. There are no restrictions made on the structure of $\mathcal{V}$, which may be a subset of the real line, a subset of the integers, a discrete set, a manifold, or even a function space.

Each template T_i has a corresponding prototype function $T_i : \mathcal{C} \rightarrow \mathcal{P}(\mathcal{V})$. The prototype function is constructed during the learning phase. If c is a category in $\mathcal{C}$, then $T_i(c)$ equals the set of prototypical template values that one expects for all examples e that lie in category c. Intuitively, the prototype function represents how template T_i generalizes to every example e.

For each $(template, category)$ pair, denoted as (T_i, c), there is a matching function $M_{(T_i,c)} : \mathcal{V} \rightarrow \mathcal{S}$, where $\mathcal{S}$ is the similarity space. The matching function determines if the template value is similar enough to its set of prototypical values. In general, the similarity space $\mathcal{S}$ is the range of the matching function, and can be the unit interval $[0, 1]$, a subset of $\mathbb{R}^n$, a discrete set, a manifold or a function space.

Example 3.1: Boolean Matching Function
Let $\mathcal{V} = \{0, 1\}$. Choose similarity space $\mathcal{S} = \{0, 1\}$. If template value v_1 is similar to its prototypical set $T_i(c)$, then $M_{(T_i,c)}(v_1) = 1$. If v_1 is not similar enough to its prototypical set $T_i(c)$, then $M_{(T_i,c)}(v_1) = 0$. Choose two categories $\{c_1, c_2\}$ and two templates $\{T_1, T_2\}$. Define prototypical functions for T_1 and T_2 as $T_1(c_1) = \{1\}$ and $T_1(c_2) = \{0, 1\}$. $T_2(c_1) = \{0, 1\}$ and $T_2(c_2) = \{0\}$. There are four distinct matching functions $M_{(T_1,c_1)}, M_{(T_2,c_1)}, M_{(T_1,c_2)}$ and $M_{(T_2,c_2)}$.

1) $M_{(T_1,c_1)}(0) = 0$ AND $M_{(T_1,c_1)}(1) = 1$
2) $M_{(T_2,c_1)}(0) = 1$ AND $M_{(T_2,c_1)}(1) = 1$
3) $M_{(T_1,c_2)}(0) = 1$ AND $M_{(T_1,c_2)}(1) = 1$
4) $M_{(T_2,c_2)}(0) = 1$ AND $M_{(T_2,c_2)}(1) = 0$

4. Template Recognition

The template recognition algorithm categorizes an example e from $\mathcal{E}$. When finished, for each category c in $\mathcal{C}$, there is a corresponding category score s_c, which measures to what extent the algorithm believes example e is in category c.

Algorithm 4.1: Template Recognition Algorithm

```
Allocate memory.  Read learned templates
{T1,...,Tn} from long-term memory.

Initialize every category score sc to zero.
Outer loop:  m trials.
{
   Initialize set R equal to  C.
   Inner loop: choose ρ templates randomly.
   {
     Choose template Tk with probability pk.
     For each category c ∈ R
       if M(Tk,c)(Tk(e)) = 0, then set R := R − {c}.
       (Remove category c from R.)
   }
   For each category c remaining in R, category
   score sc := sc + 1.
}
Initialize A to the empty set.
```

For each category c in C, if $(\frac{s_c}{m}) > \theta$, $A := A \cup \{c\}$.
The answer is A. The example e is in the categories that are in A.

Comments on the Template Recognition Algorithm.

1) Each template T_i has a corresponding probability p_i of being chosen during the inner loop. m is the number of trials in the outer loop. ρ is the number of templates randomly chosen in each trial. θ is a number in the interval $[0, 1]$ that is the acceptable category threshold.
2) In some applications, the category threshold is not used. Each value $\frac{s_c}{m}$ is interpreted as the probability that example e lies in category c.
3) If only the best category is returned as an answer, rather than multiple categories, then do this by replacing the step For each category c in $\mathcal{C}$, if $(\frac{s_c}{m}) > \theta$, $A := A \cup \{c\}$. Instead, search for the maximum category score if there are a finite number of categories. The answer is the category or categories that have the maximum category score.
4) If template space $\mathcal{V}$ and similarity space $\mathcal{S}$ have more structure, then the test if $M_{(T_k,c)}(T_k(e)) = 0$ inside the inner loop may be replaced by the test if $T_k(e)$ is not close to prototype value $T_k(c)$. In this case, matching function $M_{(T_k,c)}$ measures the closeness of $T_k(e)$ and $T_k(c)$.
5) In some applications, the inner loop may be exited if R has only one element left (i.e., $|R| = 1$) before all ρ templates have been applied.

5. Template Learning

The initial part of the learning phase constructs the templates from simple building blocks, using the examples and the categories to guide the construction. Templates can be built with evolution, another machine learning method [1], by a human expert with domain expertise or by a combination of these methods. In the next section, evolution algorithm 6.1 builds template value functions $T_i : \mathcal{E} \to \mathcal{V}$ from a collection of building block functions $\{f_1, f_2, \ldots, f_r\}$. The rest of the learning builds the matching functions $M_{(T_i,c)}$, constructs the prototype functions $T_i : \mathcal{C} \to \mathcal{P}(\mathcal{V})$, computes the probabilities p_i, and in some cases sets the category threshold θ.

The learning starts with a collection of training examples along with their categories. Depending on the type of template values, there are different methods for constructing the prototype and matching functions $M_{(T_i,c)}$. For clarity, the template values used are boolean (i.e., $\mathcal{V} = \{0, 1\}$). In the boolean case, $M_{(T_i,c)}(v) = 1$ if v lies in the prototypical set $T_i(c)$; $M_{(T_i,c)}(v) = 0$ if v does not lie in the prototypical set $T_i(c)$. In a more general description of the algorithm, the template value space $\mathcal{V}$ may be the interval $[0, 1]$, the circle S^1, or another manifold, a function space, a space of algorithms or even a measurable space (e.g., [6], [22]). When $\mathcal{V}$ is a metric space [21], the matching function $M_{(T_k,c)}$ may use $\mathcal{V}$'s metric to measure the closeness of $T_k(e)$ and $T_k(c)$ as described in recognition comment 4.

Algorithm 5.1: Template Learning Algorithm

Allocate memory for the templates.
Read from memory template set $\{T_1, T_2, \ldots, T_n\}$.
(The templates read are user-created, created by evolution or an alternative method as in [16].)
Outer loop: iterate thru each template T_k.
{
  Initialize $X := T_k(c_1)$.
  Initialize $A := X$.
  Inner loop: iterate thru each category c_i.
  {
    Set $E_{c_i} :=$ all learning examples in c_i.
    Build prototype function T_k as follows:
    Set $T_k(c_i) := \cup\{v\}$ for each $v = T_k(e)$ and $e \in E_{c_i}$.
    Set $A := A \cup T_k(c_i)$.
    Build matching function $M_{(T_k,c_i)}$.
    (See above for boolean case.)
  }
  If $(A == X)$ remove T_k from the template set.
}
Store the remaining templates.
Set each probability $p_k = \frac{1}{m}$ where m is the number of remaining templates.

Comments on the Template Learning Algorithm.

1) The Inner loop assumes that there are a finite number of categories.
2) In some cases, instead of a category threshold, each score s_c is interpreted as the probability that e lies in category c. In other cases, the category threshold θ is empirically determined.
3) For a fixed template T_k, there should be at least one pair of categories (c_i, c_j) such that $T_k(c_i) \neq T_k(c_j)$. Otherwise, template T_k can not separate any categories, so T_k should be removed.
4) In some applications, non-uniform probabilities p_k can be selected based on template T_k's ability to separate categories, T_k's computing speed or another property.

6. Designing Templates with Evolution

The use of evolutionary methods for optimizing processes and algorithms was first introduced by [2], [3], [4] and [9] and were further developed in [12], [13] and [14]. Building upon this prior work, this section presents an evolutionary method to design the template value functions $T_i : \mathcal{E} \to \mathcal{V}$.

Building blocks are composed to build a useful element. In some cases, the building blocks are a collection of functions $f_\lambda : X \longrightarrow X$, where $\lambda \in \Lambda$, X is a set and Λ is an index set. In some cases, X is the set of computable real numbers. In a handwriting recognition application, X is the

rational numbers and the binary functions $f_1 = +$, $f_2 = -$, $f_3 = *$, and $f_4 = /$ are sufficient for the building blocks. The index set, $\Lambda = \{1, 2, 3, 4\}$, has four elements. In some cases, the index set may be infinite. For example, consider the functions $f_{(k,b)} : \mathbb{Z} \longrightarrow \mathbb{Z}$ such that $f_{(k,b)}(x) = p_k x + b$ where $b, k \in \mathbb{N}$ and p_k is the kth prime (i.e., $p_1 = 2, p_2 = 3, \ldots$).

Bit-sequences $[b_1 b_2 b_3, \ldots b_n]$, where $b_k \in \{0, 1\}$ encode functions composed from building block functions. $[10110]$ is a bit-sequence of length 5. The expression $\{f_1, f_2, f_3, \ldots, f_r\}$ denotes the building block functions, where $r = 2^K$ for some K. Then K bits uniquely represent one building block function. The arity of a function is the number of arguments that it requires. For example, the arity of the real-valued quadratic function $f(x) = x^2$ is 1. The arity of the projection function, $P_i : X^n \longrightarrow X$, is n, where $P_i(x_1, x_2, \ldots, x_n) = x_i$.

Define the function $\vee$ as $\vee(x, y, z) = x$ if ($x \geq y$ AND $x \geq z$), else $\vee(x, y, z) = y$ if ($y \geq x$ AND $y \geq z$), else $\vee(x, y, z) = z$. Consider the functions, $\{+, -, *, \vee\}$. Each sequence of two bits uniquely corresponds to one of these functions: $00 \longleftrightarrow +$ $01 \longleftrightarrow -$ $10 \longleftrightarrow *$ $11 \longleftrightarrow \vee$

Bit-sequence $[00, 01]$ encodes the function $+(-(x_1, x_2), x_3) = (x_1 - x_2) + x_3$, which has arity 3. For the general case, consider the building block functions $\{f_1, f_2, f_3, \ldots, f_r\}$, where $r = 2^K$. Any bit-sequence $[b_1\ b_2\ \ldots\ b_K\ b_{K+1}\ b_{K+2}\ \ldots b_{2K} \ldots b_{aK+1}\ b_{aK+2} \ldots b_{(a+1)K}]$ with length $(a+1)K$ is a composition of the building block functions, $\{f_1, f_2, f_3, \ldots, f_r\}$. The composition of these r building block functions are encoded in a similar way, as described for functions $\{+, -, *, \vee\}$.

The distinct categories are $\{C_1, C_2, \ldots, C_N\}$. The population size of each generation is m. For each i, where $1 \leq i \leq N$, E_{C_i} is the set of all learning examples that lie in category C_i. The symbol γ is an acceptable level of performance for a template. The symbol Q is the number of distinct templates whose fitness must be greater than γ. The symbol $p_{crossover}$ is the probability that two templates chosen for the next generation will be crossed over. The symbol $p_{mutation}$ is the probability that a template will be mutated.

The main evolution steps are summarized. For each category pair (C_i, C_j), $i < j$, the building blocks $\{f_1, f_2, f_3, \ldots, f_r\}$ are used to build a population of m templates. This is accomplished by choosing m multiples of K, $\{l_1, l_2, \ldots, l_m\}$. For each l_i, a bit sequence of length l_i is constructed. These m bit sequences represent the m templates, $\{T_1{}^{(i,j)}, T_2{}^{(i,j)}, T_3{}^{(i,j)}, \ldots, T_m{}^{(i,j)}\}$. The superscript (i, j) represents that these templates are evolved to distinguish examples chosen from E_{C_i} and E_{C_j}. The fitness of each template is determined by how well the template can distinguish examples chosen from E_{C_i} and E_{C_j}. Using crossover and mutation, the population of bit-sequences are evolved until there are at least Q templates which have a fitness greater than γ. When this happens, choose the Q best templates from the population that distinguish categories C_i and C_j. Store these Q best templates in a distinct set $\mathcal{T}$ of templates that are used in the template learning algorithm.

Algorithm 6.1: Building Templates with Evolution

```
Set T equal to the empty set.
For each i in {1, 2, 3, ..., N}
For each j in {i+1, i+2, ..., N}
{
  Initialize population A_(i,j) = {T_1^(i,j), ... T_m^(i,j)}
  Set q := 0.
  while (q < Q)
  {
    Set G := ∅.
    while (|G| < m)
    {
      For the next generation, randomly choose
      templates T_a^(i,j) and T_b^(i,j) from A_(i,j) where
      the probability is proportional to the
      template's fitness.

      Randomly choose a number r in [0, 1].

      If (r < p_crossover), then crossover templates
      templates T_a^(i,j) and T_b^(i,j).

      Randomly choose numbers s_a, s_b in [0, 1].

      If (s_a < p_mutation), mutate template T_a^(i,j).
      If (s_b < p_mutation), mutate template T_b^(i,j).

      Set G := G ∪ {T_a^(i,j), T_b^(i,j)}.
    }
    Set A_(i,j) := G.

    For each template T_a^(i,j) in A_(i,j), evaluate
    T_a^(i,j)'s ability to distinguish examples
    from categories C_i and C_j.

    Store this ability as the fitness of T_a^(i,j)

    Set q equal to the number of templates
    with fitness greater than γ.
  }
  Based on fitness, choose the Q best
  templates from A_(i,j) and add them to T.
}
```

Comments on Building Templates with Evolution.

1) The fitness ϕ_a of template $T_a{}^{(i,j)}$ is computed by a weighted average of three criteria.
   a) The ability of a template to distinguish examples in E_{C_i} from examples in E_{C_j}
   b) The amount of memory used by the template.
   c) The average amount of time to compute the template value function on E_{C_i} and E_{C_j}.

   A quantitative measure for criterion (a) depends on the topology of the template value space $\mathcal{V}$. If $\mathcal{V} = \{0, 1\}$, the ability of template $T_a{}^{(i,j)}$ to distinguish examples in E_{C_i} from examples in E_{C_j} equals

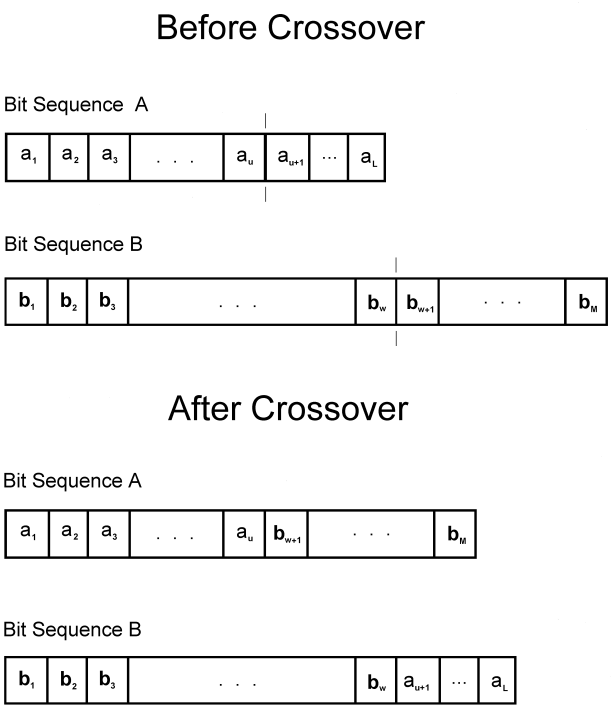

Fig. 2: Unbounded Crossover

$\frac{1}{|E_{C_i}||E_{C_j}|} \sum_{e_j \in E_{C_j}} \sum_{e_i \in E_{C_i}} |T_a{}^{(i,j)}(e_i) - T_a{}^{(i,j)}(e_j)|$.
When $\mathcal{V} \neq \{0,1\}$, then $\mathcal{V}$ has a metric $\mathcal{D}$, which measures the distance between two points in the template value space $\mathcal{V}$. In this case, the ability of template $T_a{}^{(i,j)}$ to distinguish examples E_{C_i} and E_{C_j} equals
$\frac{1}{|E_{C_i}||E_{C_j}|} \sum_{e_j \in E_{C_j}} \sum_{e_i \in E_{C_i}} \mathcal{D}(T_a{}^{(i,j)}(e_i),\ T_a{}^{(i,j)}(e_j))$.

2) Figure 2 shows a crossover between bit-sequences $A = [a_1 a_2 a_3 \ldots a_L]$ and $B = [b_1 b_2 b_3 \ldots b_M]$. L and M are each multiples of K, where $r = 2^K$ and the functions are $\{f_1, f_2, f_3, \ldots, f_r\}$. In general $L \neq M$. Two natural numbers u and w are randomly chosen such that $1 \leq u \leq L$, $1 \leq w \leq M$ and $u + M - w$ is a multiple of K. The multiple of K condition assures that after crossover, the length of each bit sequence is a multiple of K. Each bit sequence after crossover is interpreted as a composition of functions $\{f_1, f_2, f_3, \ldots, f_r\}$. The numbers u and w identify the crossover locations on A and B, respectively. After crossover, bit-sequence A is $[a_1 a_2 a_3 \ldots a_u b_{w+1} b_{w+2} \ldots b_M]$, and bit-sequence B is $[b_1 b_2 b_3 \ldots b_w a_{u+1} a_{u+2} \ldots a_L]$.

3) Before mutation, the bit-sequence is $[b_1 b_2 b_3 \ \ldots b_n]$. A mutation randomly selects k and assigns b_k the value $1 - b_k$.

4) In the current generation, the collection $\{\phi_1, \phi_2, \ldots, \phi_m\}$ represents the fitnesses of the templates $\{T_1{}^{(i,j)}, T_2{}^{(i,j)}, \ldots, T_m{}^{(i,j)}\}$. The probability that template $T_a{}^{(i,j)}$ is chosen for the next generation is $\frac{\phi_a}{\sum_{k=1}^{m} \phi_k}$.

5) $p_{crossover}$ usually ranges from 0.3 to 0.7.

6) $p_{mutation}$ is usually less than 0.1.

7. UCI Machine Learning Tests

Testing against the UCI Machine Learning Repository `http://archive.ics.uci.edu/ml/` is in progress. A subsequent publication will cover these results.

8. Acknowledgements

I would like to thank Michael Jones, David Lewis, A. Mayer, Lutz Mueller, Don Saari and Francesca Saglietti for their helpful advice.

References

[1] Christopher M. Bishop. Pattern Recognition and Machine Learning. Springer, 2006.

[2] W.W. Bledsoe. The use of biological concepts in the analytical study of systems. *ORSA-TIMS National Meeting*, San Francisco, CA, 1961.

[3] G.E.P. Box. Evolutionary operation: A method for increasing industrial production. *Journal of the Royal Statistical Society*, C, 6(2), pp. 81-101. 1957.

[4] R.J. Bremermann. Optimization through evolution and recombination. *Self-organizing systems.*, pp. 93-106. Washington, D.C., Spartan Books, 1962.

[5] I. Dennis, J.A. Hampton, and S.E.G. Lea. New problem in concept formation. *Nature*. **243**, pp. 101-102, 1973.

[6] Abbas Edalat. A computable approach to measure and integration theory. *Information and Computation*. **207**, Issue 5, May 2009, Pages 642-659

[7] Gerald Edelman. *Neural Darwinism*. Basic Books, Inc., 1987.

[8] Michael S. Fiske. *Machine Learning*. U.S. Patent 7,249,116. 2003. `http://www.aemea.com/7,249,116`.

[9] G.J. Friedman. Digital simulation of an evolutionary process. *General Systems Yearbook*, **4**, pp. 171-184. 1959.

[10] Dedre Gentner. The mechanisms of analogical learning. *Similarity and Analogical Reasoning*. Edited by Stella Vosniadou and Andrew Ortony, pp. 199-241. Cambridge University Press, 1989.

[11] Dedre Gentner, Arthur B. Markman. Structure mapping in analogy and similarity. *American Psychologist*. **52**(1), pp. 45-56, January 1997.

[12] John Hertz, Anders Krogh and Richard G. Palmer. *Introduction To The Theory of Neural Computation*. pp. 124-129. Addison-Wesley Publishing Company. Redwood City, California, 1991.

[12] John H. Holland. Genetic Algorithms and the optimal allocation of trials *SIAM Journal of Computing*. 2(2), pp. 88-105. 1973.

[13] John H. Holland. Genetic algorithms and adaptation. *Technical Report No. 34, Ann Arbor, University of Michigan*. Department of Computer and Communication Sciences, 1981.

[14] John H. Holland. *Hidden Order: How Adaptation Builds Complexity*. Perseus Books, 1995.

[15] Feng-hsiung Hsu, Thomas Anantharaman, Murray Campbell, and Andreas Nowatzyk. A Grandmaster Chess Machine. *Scientific American*, October edition, 1990.

[16] J.R. Koza. *Genetic Programming: On the Programming of Computer by Means of Natural Selection* Cambridge, MA. MIT Press, 1992.

[17] Y. LeCun, B. Boser, J. Denker, D. Henderson, R. Howard, W. Hubbard, and L. Jackel. Handwritten digit recognition with a back-propagation network. *Adv. in Neural Information Processing Systems*, 2, D. Touretzky (Editor). Morgan Kaufmann, 1990.

[18] David Marr. *Vision*. W.H. Freeman & Company, 1982.

[19] Marvin Minsky. Logical vs. Analogical or Symbolic vs. Connectionist or Neat vs. Scruffy *Artificial Intelligence at MIT. Expanding Frontiers*, Patrick H. Winston (Ed.), Volume 1, MIT Press, 1990. Online at `http://bit.ly/L9Mobg`.

[20] Tom M. Mitchell. *Machine Learning*. McGraw-Hill, 1997.

[21] James R. Munkres. *Topology*. Prentice-Hall, 1975.

[22] H.L. Royden. *Real Analysis*. 3rd Edition. Prentice-Hall, 1988.

[23] Roger Schank, Christopher Riesbeck. *Inside Case-Based Reasoning*. Lawrence Erlbaum Associates, ISBN 0-89859-767-6, 1989.

[24] Ludwig Wittgenstein. *Philosophical Investigations*. 1953.

[25] Su-Ling Yeh, Jing-Ling Li, Tasuto Takeuchi, Vincent Sun, and Wen-Ren Liu. The role of learning experience on the perceptual organization of Chinese Characters. *Visual Cognition*, 10(6), pp. 729-764. 2003.

Recognition of Business Objects in Street-View Images Using Sub-Space Grids

M. Arif Wani
Computer and Electrical Engineering and Computer Science Department
California State University Bakersfield
awani@csub.edu

Abstract— **The work presented in this paper introduces sub-space grids and shows how it can be employed for recognition of business objects like bank, fire station, restaurant and store in street-view images. The paper first describes projection of segmented image area to a six dimensional feature vector space. Principal component analysis (PCA) and multiple discriminant analysis (MDA) algorithms are used to define the orientation of six feature vectors. The range of value associated with each feature vector is divided into a number of equal parts to define six dimensional sub-space grids. A recursive procedure is then used to obtain rules where sub-space grids form premises of rules. The system is tested on a dataset of 20 images (5 images of each business object type). The results show that the use of sub-spaces grids produces good results to recognize business objects in street-view images.**

Keywords- sub-space grids, machine learning, object recognition, principle component analysis, multiple discriminant analysis, rule extraction.

I. INTRODUCTION

Street-view image analysis has received due attention recently and is used in many applications such as driver assistance systems, ego-localization and forward obstacle detection. Each application of street-view image analysis may involve addressing several issues or performing several tasks. It may involve segmentation on multi-view images captured along streets, and learning object class models from these multi-view images. The street-level images may contain personally identifiable features, such as faces. The task may involve recognizing these features, it may even involve identifying a full object like a person or a car.

Scene-text exists as part of the objects in street-view images, which includes street signs, hospital signs, bus number, license plates, shop signs, house numbers and billboards. The text carries rich information, denoting the business name, street address, direction and other crucial messages. One of the tasks of street-view image analysis may involve recognizing text that is information rich in nature.

Some applications may require moving objects to be removed from street-view images. Therefore, removal of moving objects from these images may form one of the tasks of street-view image application.

Street-parking vehicles occupy a certain area of the streets at any time. This may cause traffic problems in crowded urban areas, such as impediment to the traffic flow and blind spots. Street-view image analysis application may involve detecting vehicle clusters which will be useful for re-planning roads and traffic system.

A brief review of the previous work with street-view images is presented in the next section.

II. LITERATURE REVIEW

Xiao Long Quan [1] discuss a multi-view semantic segmentation framework for street-view images. In their approach, a pair-wise Markov Random Field (MRF) is laid out across multiple views. Both 2D and 3D features are extracted at a super-pixel level to train classifiers for the unary data terms of MRF. Their approach makes use of color differences in the same image to identify accurate segmentation boundaries, and dense pixel-to-pixel correspondences to enforce consistency across different views. To speed up training and to improve the recognition quality, their approach adaptively selects the most similar training data for each scene from the label pool.

Flores and Belongie [2] propose an automatic method to remove entire pedestrians from Street View images in urban scenes. The resulting holes are filled in with data from neighboring views. A compositing method for creating "ghost-free" mosaics is used to minimize the introduction of artifacts. This yields Street View images as if the pedestrians had never been there. The authors present promising results on a set of images from cities around the world.

Song et. al. [3] present an algorithm for text detection in images from street view, basing on Haar-Iike features and AdaBoost classification is proposed in this paper. The idea is intended for searching a wanted place in a foreign city with the business name, the scene text and the street address. There are two contributions in this paper. First the difficulty of locating the specified buildings exactly in an unfamiliar city is analyzed, and then a novel application associated with a mapping application to the real view of target place is presented. Another is training a cascade AdaBoost classifier

using several weak classifiers with Haar-Iike features, which examined their approach.

Torii et. al. [4] present a structure-from-motion (SfM) pipeline for visual 3D modeling of a large city area using 360^0 field of view Google Street View images. The core of the pipeline combines SURF feature detection technique, tentative matching by an approximate nearest neighbor search, relative camera motion estimation by solving 5-pt minimal camera pose problem, and sparse bundle adjustment. They present a large-scale reconstruction computed from 4,799 images of the Google Street View Pittsburgh Research Data Set.

Uchiyama et. al. [5] propose a method to remove moving objects from an in-vehicle camera image sequence by fusing multiple image sequences. Driver assistance systems and services such as Google Street View require images containing no moving object. The proposed scheme consists of two parts: (i) temporal and spatial registration of image sequences, and (ii) mosaicing partial images containing no moving object.

We propose a sub-space grid based approach for recognizing business objects in street-view images. Section III describes the approach used for recognizing business objects. Results and discussion is presented in section IV. Conclusion is finally summarized in section V.

III. SUB-SPACE GRIDS FOR OBJECT RECOGNITION

We propose a strategy for street-view image object recognition that is based on the following reasoning:

Color information is useful for image segmentation but not necessarily for object recognition. This is because structural information is contained in intensity values and color is one of the attributes of that structure. For example, consider two cars of same model one with green color and the second with red color. If we make cars colorless they still remain two cars. But RGB values in an image encode both color and intensity information of the two cars. Only intensity values correspond to the structure of a car while as color value is an attribute of that structure. Therefore, to reliably recognize an object in an image, it should be recognized using intensity values rather than RGB values. However, the color values, that are attributes of a structure, are very useful in segmenting an image.

Keeping the above reasoning in view, we propose strategy for street-view image object recognition that is carried out in two steps: i) Segmenting the street-view image using color information, i.e. locating object areas in an image, and ii) Recognizing object from the located areas using gray scale values. There is a lot of literature available on color image segmentation. Therefore, we will mainly focus on the second step, i.e. recognizing an object from a given located area using gray scale values of that image.

Thus the object recognition from a given located area is carried out by first converting the located area into gray scale image. An example of a street-view image, located object area, and its corresponding gray scale image is shown in Figure 1. The gray scale image is then used to recognize an object in two steps: i) Projecting gray scale image to sub-space grids, and ii) Extracting rules using sub-space grids. The two steps are discussed in detail below

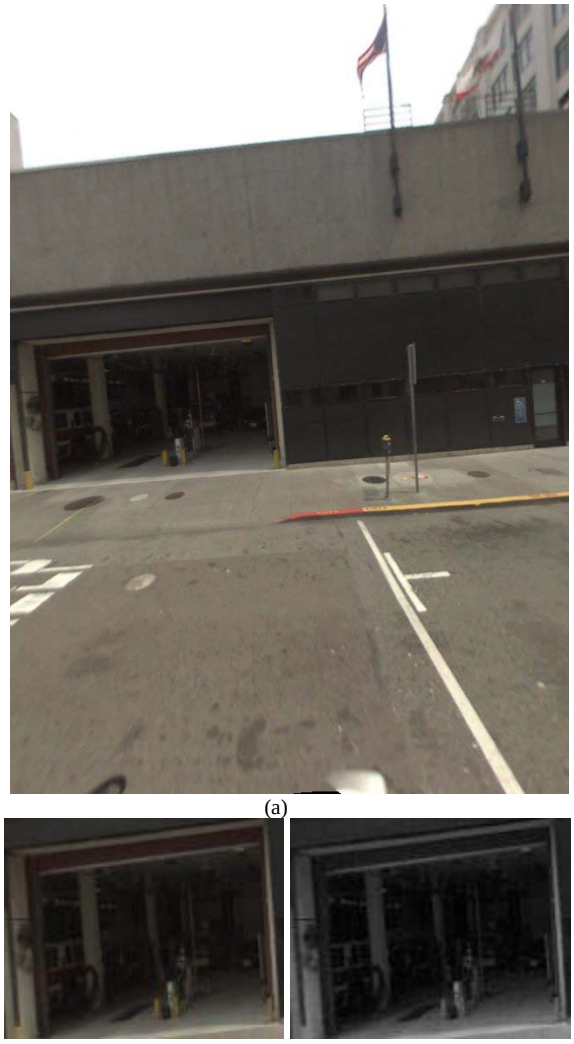

(a)

(b) (c)

Figure 1.(a) Street-view image with fire-station object,
(b) Segmented fire-station object, (c) gray-scale fire-station object.

A. Gray Scale Image Projections

Gray scale image is processed row by row and each row is projected along six projection vectors. Three of the six projection vectors are defined by principal component analysis and the rest three projection vectors are defined by multiple discriminant analysis. This transforms each image row into a set of six values. We call this set of six values as a feature vector. Thus each row of an image will be represented by a feature vector of size 6. Various image rows will not get projected to a single value on a projection vector but will get projected along a range of values associated with each

projection vector. This gives rise to a six dimensional sub-space which is divided into grids for object recognition.

a) Projection With Principal Component Analysis

Principal component analysis (PCA) is a widely-used statistical technique and it best represents the data in a least-squares sense. It works by replacing the original (numerical) variables with new numerical variables called "Principal Components". PCA captures the most descriptive features with respect to packing most "energy". This involves minimizing the criterion function $j_{d'}$ for a d'-dimensional projection:

$$j_{d'} = \sum_{k=1}^{n} \left\| (\mathrm{m} + \sum_{i=1}^{d'} a_i \mathrm{e}_i) - \mathrm{x}_k \right\|^2$$

where $x_1,\ldots x_n$ are n data points to be projected to a low dimensional space, m is the data mean, a_k are coefficients that minimize the criterion function, vectors $e_1,\ldots..e_d$' are the d' eigenvectors of the scatter matrix having the largest eigen values.

b) Projection With Multiple Discriminant Analysis

Fisher linear discriminant analysis (FDA) is a simple algorithm that best separates the data in a least-squares sense. It is used for both dimension reduction and classification. In either case, FDA attempts to minimize the Bayes error by selecting the most discriminant feature vectors. To increase the effective dimension of the projected space the use of Multiple Discriminant Analysis (MDA) instead of FDA is used.

Multiple discriminant analysis adopts a perspective similar to Principal Components Analysis, but PCA and MDA are mathematically different in what they are maximizing. MDA maximizes the difference between values of the dependent, whereas PCA maximizes the variance in all the variables accounted for by the factor. A technique that extracts invariant but descriptive features involves maximization of the criterion function given below:

$$J(v) = \frac{|W^t S_B W|}{|W^t S_W W|}$$

where W is the weight vector of a linear feature extractor and S_B and S_W are symmetric matrices designed such that they measure the desired information and the undesired noise along the direction W. S_B measures the separability of class centers (between-class variance), and S_W measures the within-class variance. S_B and S_W are given by:

$$S_B = \sum_{j=1}^{C} N_j.(m_j - m)(m_j - m)^T$$

$$S_W = \sum_{j=1}^{C} \sum_{i=1}^{N_j} (x_i^{(j)} - m_j)(x_i^{(j)} - m_j)^T$$

where $\{ x_i^{(j)}$, i=1,…,$N_j\}$, j=1,…C are feature vectors of training samples, C is the number of classes, N_j is the number of the samples of the jth class, $x_i^{(j)}$ is the ith sample from the jth class, m_j is mean vector of the jth class, and m is grand mean of all examples.

PCA and MDA, each has its own pros and cons. MDA deals directly with discrimination between classes, whereas PCA does not pay particular attention to the underlying class structure. When the data of each class can be represented by a single Gaussian distribution and share a common covariance matrix, MDA will outperform PCA. By contrast, when the number of samples per class is small or when the training data non-uniformly sample the underlying distribution, PCA might outperform MDA.

PCA and MDA algorithms were used to project the data to a feature vector space. Each algorithm used three eigenvectors that corresponded to the three largest distinct eigen values for defining the axes of feature vector space.

B. Rule Extraction using sub-space grids

The projections to feature vector space are divided into a number of cells or sub-space grids. A sub-space grid can form a premise of a rule. Rules are extracted by considering sub-space grids as its possible premises. The rule extraction process is summarized below:

The core procedure of the algorithm is a recursive process to form a decision tree from the current set of sub-space grids. Let *S* be a set of instances at a node and if all the instances in S belong to the same class, then that node is labeled with the class name of those instances. Otherwise, *S* contains representatives of more than one class. A vector is selected to partition *S* into subsets $S_1, S_2, S_3,\ldots..S_n$ where S_i contains those members of *S* that have ith sub-space grid along the selected vector. Let *A* be a set of m vectors $\{A_1, A_2, A_3,\ldots,A_m\}$, *C* a set of p classes $\{C_1, C_2, C_3,\ldots.C_p\}$. The set of possible values of a vector A_i (for forming sub-space grids) is referred to as Range (*Ai*). Each example in *S* is an m+1 tuple of the form ($V_1, V_2, V_3,\ldots.., V_m , C_k$) where V_i ε Range(A_i), i =1,….m and C_k ε *C* is the class of that example. The probability of occurrence of examples of class C_k in a set S_l, $P_{Sl,Ck}$, is the proportion of examples in S_l that are in class C_k. The information measure, which gives a measure of randomness of example distribution in S_l over the possible classes in *C*, is given by

$$I(S_l) = -\sum P_{S_l,C_k} Log_2 P_{S_l,C_k}$$

The algorithm aims to partition *S* to produce subsets S_l in which the examples are distributed less randomly over possible classes. To choose the vector that would best achieve this, the algorithm partitions *S* into subsets S_l corresponding to values V_l of a vector A_i. If the number of examples containing value V_l in *S* is n(*S*) and the number of examples containing value V_l in subset S_l is n(S_l), then information entropy of the resulting partition is given by:

$$E(A_i, S) = \sum_{V_i \in Range(A_i)} I(S_i) \frac{n(S_i)}{n(S)}$$

The algorithm chooses that vector A_i for branching which maximizes the following quantity:

$$\text{Gain}(A_i, S) = \text{I}(S) - \text{E}(A_i, S)$$

If Gain(A_i, S) is same for more than one vector, then one of them is chosen randomly.

IV. Results and Discussion

The datsets chosen in this work are Google street-view images. These street-view images have a number of objects in it but the aim of this work is to recognize the following four business objects: bank, fire station, restaurant, and store. The training data set consists of 8 street-view images (2 images of each object type) and the testing data set consists of 20 images (5 images of each object type).

TABLE I. CLASSIFICATION OF VECTORS OF IMAGES WITH BANK OBJECT

Image Used		**Number of feature vectors classified as**			
Image Object	Image Number	Bank	Fire-St.	Restau-rant	Store
Bank	Image1	59	13	6	23
	Image2	9	17	5	72
	Image3	103	1	2	4
	Image4	90	4	4	12
	Image5	81	2	4	23

TABLE II. CLASSIFICATION OF VECTORS OF IMAGES WITH FIRE ST OBJECT

Image Used		**Number of feature vectors classified as**			
Image Object	Image Number	Bank	Fire-St.	Restau-rant	Store
Fire Station	Image1	18	62	1	25
	Image2	51	21	4	25
	Image3	20	80	1	9
	Image4	13	77	9	11
	Image5	13	89	0	8

TABLE III. CLASSIFICATION OF VECTORS OF IMAGES WITH REST. OBJECT

Image Used		**Number of feature vectors classified as**			
Image Object	Image Number	Bank	Fire-St.	Restau-rant	Store
Restaur ant	Image1	18	62	1	25
	Image2	51	21	4	25
	Image3	3	7	89	11
	Image4	4	28	12	66
	Image5	3	15	85	7

TABLE IV. CLASSIFICATION OF VECTORS OF IMAGES WITH STORE OBJECT

Image Used		**Number of feature vectors classified as**			
Image Object	Image Number	Bank	Fire-St.	Restau-rant	Store
Store	Image1	20	32	4	47
	Image2	15	33	5	48
	Image3	10	23	3	74
	Image4	19	8	2	81
	Image5	12	40	4	54

Object areas in images are segmented manually in such a way that each located area has 110 image rows (110 image rows are adequate to cover all four types of business objects), giving a total of 880 image rows from four images for training purposes. Each row is projected into a six tuple feature vector. The range of values associated with each feature vector is divided into equal parts. This results into a six dimensional sub-space grid of 6 feature vectors. The sub-space grid of 6 feature vectors is used for rule extraction.

TABLE V. CLASSIFICATION OF IMAGE OBJECTS WITH PROBABILITIES

Image Object	**Image Number**	**Highest Prob. value**	**Highest prob. Object**	**% Classifi-cation Accuracy**
Bank	Image1	0.54	Bank	80
	Image2	0.65	Store	
	Image3	0.94	Bank	
	Image4	0.82	Bank	
	Image5	0.74	Bank	
Fire St.	Image1	0.56	Fire St.	80
	Image2	0.46	Bank	
	Image3	0.73	Fire St.	
	Image4	0.70	Fire St.	
	Image5	0.81	Fire St.	
Restaur ant	Image1	0.56	Fire St.	40
	Image2	0.46	Bank	
	Image3	0.81	Rest.	
	Image4	0.60	Store	
	Image5	0.77	Rest.	
Store	Image1	0.43	Store	100
	Image2	0.44	Store	
	Image3	0.67	Store	
	Image4	0.74	Store	
	Image5	0.49	Store	
Overall % Classification Accuracy				75

The testing set of 20 images resulted in 2200 feature vectors (110 rows for 20 images). The set of rules obtained above is used to test the 2200 feature vectors of 20 testing images. Table 1 shows results of 5 street-view images having business object bank in it. Each row shows results of one image. Row 1 indicates that 59 feature vectors out of 110 vectors are classified as belonging to object bank, 13 feature vectors are classified as belonging to object fire station, 6 feature vectors are classified as belonging to object restaurant, 23 feature vectors are classified as belonging to object store, and remaining 9 feature vectors were unclassified. As highest number of vectors is pooled for the business object bank, the segmented area of this image is classified as bank with a

probability of 0.54 (59/110). Other rows can be interpreted similarly. Table II shows results of 5 street-view images having business object fire station in it. Table III shows results of 5 street-view images having business object restaurant in it. Table IV shows results of 5 street-view images having business object store in it.

The accuracy of classification is summarized in Table5. The probabilities with which a segmented image area is classified as belonging to that class are also shown in the table. The Table V indicates that the worst classification accuracy was for restaurant object. Overall the results indicate that use of sub-space grids produce good results. This is mainly because these sub-space grids represent less overlapping data and are less sensitive to local changes in the training data.

V. CONCLUSION

In this paper a sub-space grid based approach was employed to recognize business objects like bank, fire station, restaurant and store. The approach was tested on Google street-view images. PCA and MDA algorithms were used to define six dimensional feature sub-space. Segmented image areas were projected to this six-dimensional sub-space. Sub-space grids were obtained by dividing the range of values associated with each feature vector into equal number of parts. A recursive procedure was used to extract rules from sub-space grids. The set of rules were used for recognition of business objects present in Google street-view images. The paper shows that use of sub-space grids in business object recognition in street-view images produces good results. A system that incorporates color information, text information and structure information using gray scales should produce a robust system for applications involving street-view images.

REFERENCES

1. Jianxiong Xiao, and Long Quan, "Multiple view semantic segmentation for street view images", 12th International Conference on Computer Vision, pp: 686-693, October 2009.

2. A. Flores, and S. Belongie, "Removing pedestrians from Google street view images", Computer Vision and Pattern Recognition Workshops (CVPRW)", pp. 53-58, June 2010.

3. Yajuan Song, Yanxiang He, Qingquan Li, and Ming Li,"Reading text in street views using Adaboost: Towards a system for searching target places", Intelligent Vehicles Symposium", pp. 227-232, July 2009

4. A. Torii, M. Havlena, and T. Pajdla, "From Google Street View to 3D city models", Computer Vision Workshops, pp. 2188-2195, September-October 2009.

5. H. Uchiyama, D. Deguchi, T. Takahashi, I. Ide, and H. Murase, "Removal of Moving Objects from a Street-View Image by Fusing Multiple Image Sequences", International Conference on Pattern Recognition, pp. 3456-3459, October 2010.

6. Hirahara, K.; Ikeuchi, K., "Extraction of vehicle image from panoramic street-image", Intelligent Vehicles Symposium, pp. 756-761, October 2004.

Autonomous Creation and Detection of Procedural Memory Scripts

James A. Crowder
Raytheon Intelligence and Information Systems
16800 E. Centretech Parkway, Aurora,
Colorado 80011

Julia M. Taylor
CIT & CERIAS
Purdue University
West Lafayette, Indiana 47907

Victor Raskin
LING & CERIAS
Purdue University
West Lafayette, Indiana 47907

Abstract - *Willingly or unwillingly, consciously or unconsciously, we all live scripted lives. This is not to say that one can look ahead into the next chapter and find out what one will have for dinner a month later. Life also brings surprises, but the scripts we are talking about are not the" scripts of life," but rather much smaller groupings of events that represent familiar routines and are stored as procedural memory in our brains. The general goal of the research presented here is to design, implement, test, evaluate, and improve a computational semantic model that will enable autonomous systems to evoke and use the correct procedural memory scripts similar to humans and thus approximate the human ability to comprehend and form procedures for learned tasks. The important step in this direction that is discussed here is to explore the constitutive properties of this artificial procedural memory model from the perspective of a broader artificial intelligence schema of information acquisition and retention and its computational semantic processing. The discussion will focus on the optimal ways for autonomous systems to acquire procedural memory scripts automatically and to activate them appropriately.*

Keywords: Procedural Memory, Knowledge Relativity

1. Procedural Memories

In his work on Procedural Memory and contextual Representation, Kahana showed that retrieval of implicit procedural memories is a cue-dependent process that contains both semantic and temporal components (Kahana, Howard, and Plyn 2008). Creation of Procedural Memories is tied not only to task repetition but also to the richness of the semantic association structure (Landauer and Dumais 1997). Earlier work by Crowder, built on Landauer's Procedural Memory computational models and Griffith's topical models (Griffith and Steyvers 1997), theorized about the creation of artificial cognitive procedural memory models based on Knowledge Relativity Threads to create the semantic associations (Crowder and Carbone 2011) and work in Fuzzy, Self-Organizing, Semantic Topical Maps (Crowder 2010) counted on the topical model needed to create long-term procedural memories. These Knowledge Relativity models and Topical Maps are based on early work by Zadeh. Zadeh (2004), described tacit knowledge as world knowledge that humans retain from experiences and education, and concluded that current search engines, with their remarkable capabilities, did not have the capability of deduction, that is the capability to synthesize answers from bodies of information which reside in various parts of a knowledge base. More specifically, Zadeh describes fuzzy logic as a formalization of human capabilities: the capability to converse, reason and make rational decisions in an environment of imprecision, uncertainty, and incompleteness of information. In their work in cognition frameworks, Crowder and Carbone (Crowder and Carbone 2011) expand on the work not only by Zadeh but also by Tanik (Tanik and Ertas 1997, 2006) in describing artificial procedural memories as procedural knowledge gained through cognitive insights based on fuzzy correlations made through a labeled form of a Fuzzy, Semantic, Self-Organizing Topical Map (FSSOM) that provides the following attributes:

1. Contextual algorithms explore the map visually for informational connection located by meaning.
2. Procedural searches utilize semantic contextual information to find links to relevant procedural information.
3. The informational maps autonomously locate temporal and semantic associations that provide procedural connections to a topic.
4. The FSSOM represents a normalized representation of any physical information content used in the development of the procedural knowledge and content.

2. Artificial Neural Memory Systems

In artificial intelligence, procedural information is one type of knowledge that can be learned and carried by an intelligent software agent (Kasaboc 1998). From the initial research in the 1998 and 1999 (Kasaboc 1998, Crowder 1999, Crowder, Barth, and Rouch 1999), work has continued on the development of artificial memory systems that mimic human processing, storage, and retrieval. It is believed that providing a cognitive framework that mimics human processing and reasoning also requires creating a constructive memory system similar to human memory storage and processing (Stillings 1995, Crowder 1999). The initial work in artificial memory systems involved the use of Intelligent information Software Agents (ISAs) to create the overall artificial cognitive framework (Crowder 2002). This work led to investigation into Linguistic Ontologies to facilitate conceptual learning in the creation of artificial neural memories (Crowder 2002, 2003).

Scripts as large structured chunks of information, typically sequences of events describing standard routines, permeate human life, society, culture. Humans are well aware of them and have the ability of thinking of and manipulating the whole scripts at any level or detailization, or grain size. Thus, when you buy a new iPhone, you must program or set it up. This is a script that your manual describes by chunking it up into setting up your calendar, email, GPS, etc., each of each is also a script. Within the script of date and time, a few clicks will set you the date and a few others the time of the day. Within the latter, there is a tiny subscript of setting up the hour and another to set up the minutes. Other, less well-defined scripts seem to be capable of almost infinite grain size refinement.

3. Creation of Artificial Procedural Memory Scripts

Continued investigation, utilizing the work of Kahana (Kahana, Howard, and Polyn 2008) in associative episodic memories, led to the development of an ISA framework for creation, storage, and retrieval artificial implicit memories (Crowder and Friess 2010a&b, 2011) (see Figure 1). Based on this work, a systems and software architecture specification was developed for an artificial cognitive framework utilizing intelligent autonomous software agents (Crowder, Scally, and Bonato 2011).

Our main hypothesis is that the procedural memory scripts can be detected and acquired with the combination of rule-based computational semantic techniques enhancing the computer understanding of text as far as we can achieve with a battery of semantic resources, acquisition tools, and software, with the state-of-the-art machine-learning technologies operating on a much enhanced knowledge base and propped up by an advanced artificial cognitive system. The objectives of this work are:

1. To identify the main principles of script acquisition using a combination of meaning-rule-based techniques from the Ontological Semantic Technology with meaning- and cognitively-enhanced machine-learning techniques from Cognitive Artificial Intelligence.
2. To develop the principles of comparison of the comprehension of natural language by computer, with and without the script module (see Figure 2).
3. To determine the principles of optimizing the grain size at which the appropriate scripts should be formulated while developing the system's functionality, that humans also have, to coarsen or to refine the grain size of a script dynamically, when necessary for comprehension.

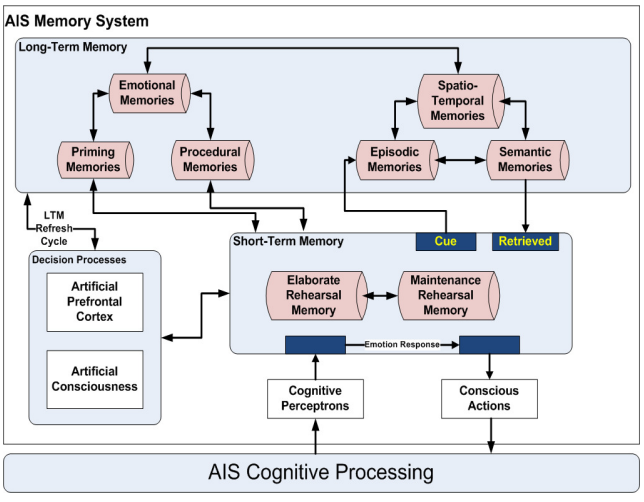

Figure 1 – AIS Artificial Memory Architecture

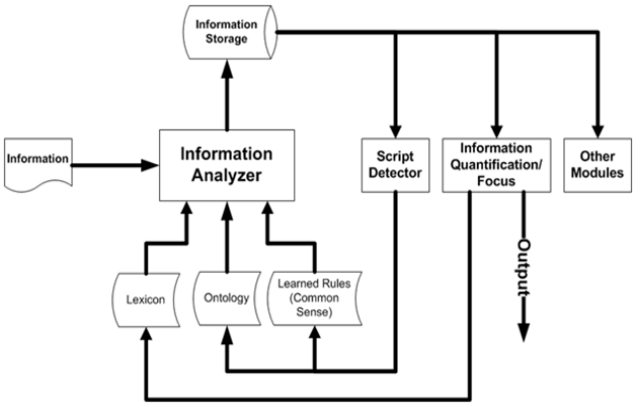

Figure 2 – Artificial Procedural Memory Generation

Crowder, in conjunction with Carbone and Friess, in researching artificial neural memory frameworks that mimic human memories, are creating computer architectures that can take advantage of Raskin and Taylor's Ontological Semantic Technology (OST: Raskin and Taylor 2010, Taylor and Raskin 2010) and create an artificial procedural memory system that has human reasoning capabilities and mimics the fuzzy and uncertain nature of human cognitive processes. This new focus for Crowder (Crowder 2011a) is to create processes necessary for the creation, storage, retrieval, and modification of artificial procedural memories (see Figure 3).

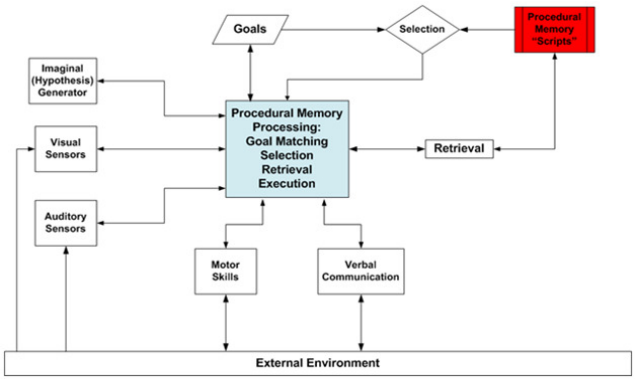

Figure 3 - ***Artificial Procedural Memory Script Retrieval***

In order to create such memories, the artificial cognitive system must have the following capabilities:

Procedural Memory Creation System Requirements:

- Mediator Agents (Artificial Prefrontal Cortex) for asynchronous event handling
- Advisor Agents for reactions and responses (decision support)
- Cognitive Perceptron Agents for procedural representation of knowledge
- Conceptual Ontology
- Cognitive system capable of goal-directed and reactive behavior
- Reasoning Agents for reflective reasoning capabilities
- Data Steward and Analyst Agents to handle incomplete or inaccurate data
- Interface Agents for Human/Machine Interface (HMI)

This cognitive system, called the Artificial Cognitive Neural Framework (ACNF) is illustrated in Figure 4 (Crowder 2011a, Crowder and Carbone 2011a).

The result of this research is to significantly improve understanding of the important properties of artificial procedural memory scripts at the level of precision and explicitness that will be suitable for autonomous computational applications, both the appropriate existing ones and novel ones. By the time the proposed research is finished, we will have advanced the understanding of this phenomenon, proven to be psychologically and cognitively real and significant for autonomous system processing relevant to information processing and autonomous mission management and execution, to the level where it can be formulated in a rigorous, formal, computer-implementable form.

4. OST Formation of Procedural Memories

We will discuss now how OST, which anchors artificial procedural memories in natural language and, via it, in reality, handles script acquisition. Figure 5 shows the ontology at the center as the language-independent conceptual graph that reflects much of what humans know about the building blocks of their world knowledge. Frequently co-occurring instantiations of concepts are additionally

collected in common-sense rules, and this is where the scripts are assembled as a result of text processing.

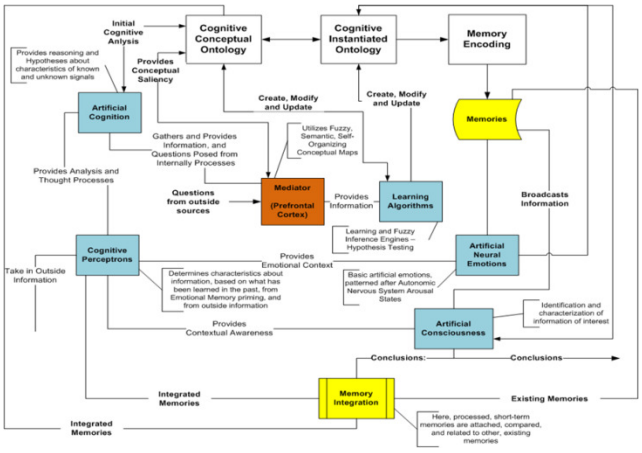

Figure 4 – The Artificial Cognitive Neural Framework

Defined in ontological terms are the entries of the lexicon for each natural language (and, incidentally, of any artificial language as well), with all of their various senses and syntactic, morphological, phonological, and lower types of information. The input text goes into the OST Processor (aka the semantic analyzer), which reads every sentence linearly, word by word, finds them in the lexicon, gets the ontological representation of every sense, and tries to combine these senses together on the basis of property/filler compatibilities.

The successful combinations form the text meaning representations (TMRs), which are accumulated in the OST InfoBase, the information repository where all the successfully processed TMRs are kept, thus constituting the contingent knowledge base following from all the conceptual instantiations. The recurring patterns are identified as common-sense rules or as scripts, depending largely if the relations between or among various invents are causal or chronological. Thus, the fact that fire cause smoking is a causal common-sense rule. On the other hand, one's being met inside a (higher-scale) restaurant by a person who asks how many are in one's party and then taken to a table, given the menus, etc., involves a series of chronologically related events that corresponds to a script. Occasionally in a real-life script of a reasonably complex nature, such as oncoming bankruptcy (Raskin et al. 2003), it is hard and possibly unnecessary to differentiate between the two: in general, causality is a poorly understood and no clearly define a relationship. The picture also shows the place OST, which is rule-based, leaves to machine learning, as mentioned above. It takes over where the existing semantic and pragmatic knowledge can no longer reach, at least temporarily.

Thus, OST provides artificial cognitive systems and the various types of memories they require to postulate with a feasible and implementable procedure.

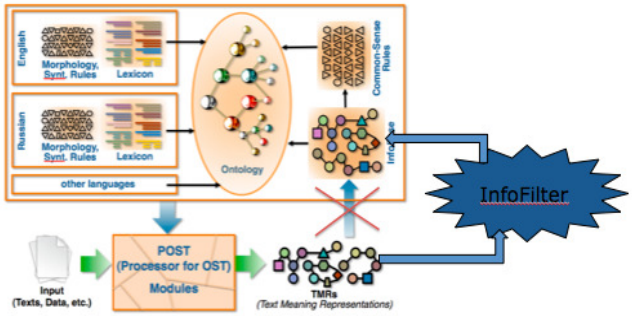

Figure 5 – Ontological Semantic Technology (OST)

5. Conclusions and Discussion

To summarize, we are anticipating four major results from this research, all contributing to the ongoing efforts in the information processing communities both to understand the theoretical nature of procedural memory scripts and their status in human cognition and language activities and to use this new understanding for optimizing computational implementations of knowledge and language processing, thus equipping the computer with the human-like capacity to sense, emphasize, and favor efficient and accurate human/machine interaction and collaboration and making an important step towards high-powered collaborative computing, including social computing.

This work represents an aspect of human communicative behavior that has so far resisted contentful and usable computation. This work will greatly enhance autonomous system reasoning functionality which is crucial for computing human-like information processing, and which will be facilitated by setting up classes of easy, predictable, intra-script inferences. We also anticipate that, conversely, the ease of an inference will serve as a powerful tool of procedural memory script discovery and creation.

References

1. Crowder, J. 1996. Fuzzy Hypergraphs: Semantic Informational Mapping. *Proceedings of the 2nd International Conference on Application of Fuzzy Systems and Soft Computing*, Siegen, Germany.
2. Crowder, J. 1996. Fuzzy Hypergraphs: Fuzzy Graph Theoretics. *Proceedings of the 5th IEEE International Conference on Fuzzy Systems*, New Orleans, LA.
3. Crowder, J. 1999. Learning Algorithms for Stochastically-Driven, Fuzzy, Genetic Neural Networks. *NSA Technical Paper*, ENIGMA_1999_02, Ft. Meade, MD.
4. Crowder, J., Barth, T., and Rouch, R. 1999. The Evolutionary Neural Infrastructure with Genetic Memory Algorithms: ENIGMA Theory Development. *NSA Technical Paper*, *ENIGMA_1999_04*, Ft. Meade, MD.
5. Crowder, J. 2002. Machine Learning: Intuition (Concept Learning) in Hybrid Neural Systems. *NSA Technical Paper CON-SP-0014-2002-06*, Ft. Meade, MD.
6. Crowder, J. 2003a. Using a Large Linguistic Ontology for Network-Based Retrieval of Object-Oriented Components. *NSA Technical Paper CON-SP-0014-2003-03*, Ft. Meade, MD.
7. Crowder, J. 2003b. Temporal Difference Learning with Fuzzy Cognitive Maps. *NSA Technical Paper CON-SP-0014-2003-04*, Ft. Meade, MD.
8. Crowder, J. 2003c. Ontology-Based Knowledge Management. *NSA Technical Paper CON-SP-0014-2003-05*, Ft. Meade, MD.
9. Crowder, J., and Friess, S. 2010a. Artificial Emotions and Emotional Memory. *Proceedings of the 11th Annual International Conference on Artificial Intelligence*, Las Vegas, Nevada.
10. Crowder, J. 2010a, Flexible Object Architectures for Hybrid Neural Processing Systems. *Proceedings of the 11th Annual International Conference on Artificial Intelligence*, Las Vegas, Nevada.
11. Crowder, J. A., and Friess, S. 2010b. Artificial Neural Diagnostics and Prognostics: Self-Soothing in Cognitive Systems. *Proceedings of the 11th Annual International Conference on Artificial Intelligence*, Las Vegas, Nevada.
12. Crowder, J. 2010b. The Continuously Recombinant Genetic Neural Fiber Network. *Proceedings for the AIAA Infotech@Aerospace 2010 Conference*, Atlanta, Georgia
13. Crowder, J., Carbone, J. 2011a. Hybrid Neural Architectures for the ELYSE Cognitive System. *Journal of Aerospace Computing, Information, and Computing, Volume 10*.
14. Crowder, J., Carbone, J. 2011b, "The Great Migration: Information to Knowledge using Cognition-Based Frameworks." *Springer Science,* New York.
15. Crowder, J. 2011a. Knowledge Density Mapping for Derivation of Inference Potential. *Proceedings of the 12th Annual International Conference on Artificial Intelligence*, Las Vegas, Nevada.
16. Crowder, J. and Friess, S. 2011. Metacognition and Metamemory Concepts for AI Systems. *Proceedings of the 12th Annual International Conference on Artificial Intelligence*, Las Vegas, Nevada.
17. Crowder, J. and Carbone, J. 2011a. Occam Learning through Pattern Discovery: Computational Mechanics in AI Systems. *Proceedings of the 12th Annual International Conference on Artificial Intelligence*, Las Vegas, Nevada.
18. Crowder, J. 2011b. Cognitive Architectures for Real-Time Integrated System Health Management. *Proceedings of the 8th Annual Workshop of Structural Health Monitoring*, Stanford University.
19. Crowder, J. and Carbone, J. 2011b. Transdisciplinary Synthesis and Cognition Frameworks. *Proceedings of the Society for Design and Process Science Conference 2011*, Jeju Island, South Korea.
20. Crowder, J., Scally, L., and Bonato M. 2011. Learning Agents for Autonomous Space Asset Management. *Proceedings of the Advanced Maui Optical and Space Surveillance Technologies Conference*, Maui, HI.
21. Griffiths T and Steyvers M (2003) Prediction and semantic association. *In: Halmberg KJ and Steyvers M (eds.) Advances in Neural Information Processing Systems, 15, pp. 11–18*. Cambridge, MA: MIT Press.
22. Kahana, M. J., Howard, M. W., and Polyn, S. M. (2008). Associative retrieval processes in episodic memory. In H. L. Roediger III (Ed.), ***Cognitive psychology of memory. Vol. 2 of Learning and memory: A comprehensive reference, 4 vols. (J. Byrne, Editor).*** Oxford:

Elsevier.
23. Kasabov, N. 1998. Introduction: Hybrid Intelligent Adaptive Systems. *International Journal of Intelligent Systems,* vol. 8, 453-454.
24. Landauer TK and Dumais ST (1997) Solution to Plato's problem: The latent semantic analysis theory of acquisition, induction, and representation of knowledge. *Psychol. Rev. 104: 211–240*.
25. Raskin, V., Nirenburg, S., Hempelmann, C. F., Nirenburg, I., and Triezenberg, K. E. (2003)The genesis of a script for bankruptcy in ontological semantics. In: G. Hirst and S. Nirenburg (eds.), *Proceedings of the Workshop on Text Meaning*, *2003 NAACL Human Language Technology Conference*, 27-31.
26. Raskin, V., Taylor, J. M., & Hempelmann, C. F. 2010. Ontological semantic technology for detecting insider threat and social engineering. *New Security Paradigms Workshop*, Concord, MA
27. Stillings, N. 1995. Cognitive Science: An Introduction, 2nd Edition. *MIT Press*, Cambridge, MA, p. 396.
28. Tanik, M. and A. Ertas. 1997. Interdisciplinary design and process science: A discourse on scientific method for the integration age. *Journal of Integrated Design and Process Science, vol. 1, pp. 76-94*.
29. Tanik M. and Ertas A. 2006. Foundations for a transdisciplinary systems research based on design & process. *The ATLAS Publishing, vol. TAM–Vol.2, pp. 1-37*.
30. Taylor, J. M., & Raskin, V. 2010. Fuzzy ontology for natural language. *29th International Conference of the North American Fuzzy Information Processing Society,* Toronto, Ontario, Canada.

SESSION

INTELLIGENT AGENTS + AUTONOMOUS AGENTS + MULTI-AGENT SYSTEMS + APPLICATIONS

Chair(s)

TBA

MATE: Next Generation Intelligent Tutoring Entities for Virtual Environments

Michael D. Kickmeier-Rust and Dietrich Albert
Cognitive Science Section, Knowledge Management Institute
Graz University of Technology, Graz, Austria

Abstract - *MATE is an intelligent tutorial system that is supposed to combine innovative pedagogical techniques from the field of coaching and to provide intelligent technological solutions for support the coaching processes in an autonomous and smart way. Conceptually, the system is composed of two distinct components, an afferential component that is 'harvesting' information coming from the virtual environment (e.g., behaviors or communication patterns) and an efferential component that is capable of making psycho-pedagogically tailored interventions (e.g., hinting or moderating the communication processes, posing new problems and questions or giving feedback, etc.). Both components are orbiting around a central executive which controls the tutorial process, draws conclusions on the basis of the input, and decides upon interventions on an individual basis as well as on the group level. MATE is work in progress; this paper gives an outline of conceptual approach and draws a sketch of the envisioned system architecture.*

Keywords: Intelligent tutorial systems, educational agents, CbKST, coaching, virtual worlds, Second Life

1 Introduction

Twenty-first century education clearly is a big buzzword in today's media. The new millennium is accompanied by substantial technological evolutions; we became a highly diverse, globalized, complex, real-time media- knowledge- information- and learning society. Since the 1990s, the progress of media and technology was breath-taking; during these one or two decades, we were facing the rise of a serious and broad use of computers at home (although the development started earlier, of course), the rise of the internet and how it revolutionized our society, becoming a "collective unconscious" (in the words of Carl Gustav Jung). We faced the spread of mobile phones and their evolution from telephones to omnipresent computer and communication devices; we see spread of mp3, twitch speed computer games and TV shows. We saw how our world got closer by changing the bridges over continents and oceans from 56k wires to hyper speed fiber glass networks. Some say, this rapid and pervasive technological revolution will have greater impact on society than the transition from an oral to a print culture.

But what does this mean for educational systems and the way our children learn and what they learn. Today's kindergarten kids will retire in 2070. Facing the pace of technological and societal changes and demands, we cannot predict what knowledge will be required in such a "far" future. But we are in charge to equip our children with the abilities and backgrounds to survive in that world. Our students are also facing many important emerging issues such as global warming, famine, poverty, health issues, a global population explosion and other environmental and social issues. These issues lead to a need for students to be able to communicate, function and create change personally, socially, economically and politically on local, national and global levels.

Soft skills such as innovative thinking, creative problem solving, meta cognitive abilities, communication and collaboration skills – all those so-called 21st century skills – need to be in the focus of novel smart tutorial systems. Presently, there are several techniques available that promote the 'acquisition' of such abilities. The problem is that most of those techniques are strongly centered on a face-to-face setting which, however, is costly and from a broader educational perspective ineffective – applications are oftentimes limited to leadership trainings for distinct groups of learners. Our aim is to elaborate on existing coaching techniques (such as Action Learning or Lego Serious Play) and to translate those real world approaches to the virtual worlds, for example Second Life. This is not a trivial attempt since virtual environments demand incorporating sound instructional design principles and, more importantly, they require educationally smart, autonomous tutorial mechanisms to control and guide the learning processes of groups of learners in the virtual worlds with their large degrees of freedom.

2 Innovative ePedagogy

Modern pedagogical strategies most often orbit around the idea of construction-oriented, active instructional design and learning theories, such as problem-based learning [1], learning by doing [2], experiential [3], or example-based learning [4] and also on communication-oriented approaches such as collaborative and peer learning [5]. In the conceptual context of an active and interactive, constructive view of learning and development, examples play a crucial role [6].

The second and probably broader concept is problem-based learning. The approach of problem-based learning is an integral part of many instructional models [7]. According to M. David Merrill [8] problem-based learning accounts for the fundamental premise "Knowledge is soon forgotten if it is not made a part of the learner's life beyond instruction".

Undoubtedly, also collaboration and communication among peers is a crucial aspect in the context of learning; there is a substantial body of evidence that peer interactions likely lead to superior learning performance and a more effective learning process [8]. One of the most compelling reasons for collaborative learning is that teachers/tutors cannot simply transmit (their own) knowledge to learners. Learning is an active, also neurological and physical, process and not a product. Students must build their own knowledge and competencies through an active, involved process in which they need to assimilate concepts into their own understandings and worlds. Social interactions in groups promotes an active involvement and mutual support (e.g., helping, assisting, supporting, encouraging, and praising one another's efforts to learn), it facilities discussions, opens new views, and it supports imitation [9]. In addition to that, there are also secondary effects reported, for example, learners tend to be more positive towards subject matter, schools, or towards each other [10].

An approach to facilitate learning, meta-learning, collaborative creative solutions, and self-reflective growing is action-oriented learning (AOL). The principal idea is that a team is working and reflecting on a realistic challenge in order to commonly develop novel and creative solutions and, equally important, to developed aforementioned abilities and meta-abilities in a collaborative process. AOL is based on the fundamental aspect of questioning; a thematically uninvolved outside moderator is guiding the process by asking appropriate questions and statements in the group work are only allowed in response to questions from the moderator or the group members.

A similar approach to top-level demands on future learning is creative serious play (CSP); the ideas of this approach are inherited from Lego Serious Play (http://www.seriousplay.com). In moderated team work, collaborative learning and problem solving, reflecting upon the group's and the own ideas and work, and finding a common language is triggered by challenging abilities and meta-abilities through playing and modeling with building blocks. A key aspect of this approach is the successful and deep learning is fostered by touching, handling, and holding objects and by making tasks and problems 'concrete'.

Both techniques are highly successful applied, predominantly in the organizational sectors and on a small scale. The reasons, in turn, are simple: the techniques are based on the work in small groups, in real-world settings, driven and hosted by professional trainers and coaches. An innovative idea that is presently work in progress in several research groups, particular in Europe, is to work on a conceptual combination of such coaching techniques. Such settings, however, cannot be transferred one-to-one to virtual worlds. Technological solutions are needed that are capable of purposefully translating and implementing AOL and CSP into the virtual reality. This, in turn, requires novel approaches to user and domain modeling, focusing not only on individual user models but models of users in groups and models of groups. In addition, domain models must be adjusted to meet the distinct needs of the "meta domain" of the 21st century skills.

3 Learning and Training n Virtual Worlds

Beginning in the late 1970s and early 1980s, tightly coupled with computer and information communication technology, immersive virtual environments and game-based worlds virtual worlds have increasingly become a major genre in the fields of entertainment but, specifically in the new millennium, they have become the places for social communication, working, teaching, and learning. This increasing use of virtual space in education suggests that the effects of virtual space on learning are an important area for continued [11]. There is a broad range of examples for virtual environments; famous World of Warcraft has far over 10 million users, for Second Life there are over 20 million registered accounts, or the popular Facebook application FarmVille has over 70 million active monthly users. The sight of this cake made mouths of serious applicants water, in particular in the educational sectors [12].

The potential advantages of virtual environments in education are numerous [13]. To give an example, virtual spaces serve as meeting points for distance education, basically due to the range of communication modes and options for collaboration (e.g., teachers and learners, represented by avatars, may interact via chat, voice, and non–verbal communication such as avatar placement and gestures [14]). Another perceived advantage of using virtual space in education is the high degree of customizability offered by some virtual spaces like Second Life [14]. The possibilities for adjusting the environment, e.g., building objects, of virtual spaces enables an educator to customize a learning space to fit a specific learning activity or a certain pedagogical approach [14]. In addition, since the laws of physics and other physical world occurrences can be disregarded in a virtual environment, virtual learning space can be used to visualize macroscopic and microscopic complex systems, manipulate time in a sequence of events, simulate scenarios, allow complex interactions, and create objects and content [13]. Certainly, the application of virtual environments, in particular the application of rich, immersive, 3D-ish ones, is not always viewed positively. A specific concern was that this rather novel educational medium must be applied cautiously and in consideration of potential risks and downsides (social isolation, un-reflected peer learning, misconceptions,

addiction, etc.). Still, overall, the trend is clearly heading towards a pedagogically informed use of technology that may support and reinforce a wide range of traditional and innovative pedagogical. But, this increasing use of virtual space in education suggests that the effects of virtual space on learning are an important area for continued research. Although the current state of knowledge on how virtual space affects learning is very broad, there is substantial fragmentation of the various research streams. As suggested by Olle Sköld [13], especially in the field of an innovative "online pedagogy", aiming to illuminate both practical and theoretical dimensions of learning and teaching in a virtual space settings, future research is required. Examples are, how learning tasks must be designed in order to account for features in specific virtual spaces, or which methods should be developed to handle ambiguity and uncertainty in virtual learning spaces.

4 MATE: The Next Generation of Intelligent Tutorial Entities

MATE stands for intelligent multi-adaptive tutorial entity; he idea is to advance and expand existing intelligent tutorial technologies, in particular from the context of CbKST [15] and digital educational games, towards the needs of 21st century skills and coaching in virtual environments. This – strongly service-oriented – technology must understand individual and group-related processes in the context of joint learning and problem solving and guide those processes in a smart and tailored way by meaningful tutorial, coaching-related interventions, for example, posing questions and problems to the group. In addition, this combination is to be enriched with features of individual and small-group coaching and some of the strength of today's immersive and engaging media (such as computer games). This novel alloy – in hour firm conviction – has a maximum of strength for teaching and training in the context of the 21st century demands and a minimum of conceptual or application-oriented downsides (e.g., the substantial costs of personal coaching).

Technically speaking, the systems intelligence is to be based on reasoning mechanisms over the combination of structural domain models (the so-called competence structures), into which the learner can be mapped, and so-called problem spaces, formal, structural models of problem solving processes [16], into which a current problem solving state can be mapped. Prerequisite relations between atomic, well-defined competencies/skills (a) establish competence structures/spaces (b). The analysis of a given problem, in turn, established a formal problem space (c). Mapping both together results in a well-defined, formal model of the 'behavioral' status (of an individual) in the virtual world (composed of location in the problem space, problem solving path, available and lacking competencies/skills, learning paths, as well as the so-called fringes, the reasonable next steps in terms of learning and problem solving). This concept builds, in essence, the basis of the artificial educational intelligence. Non-trivial challenges for the project arise from the attempt to expand this approach to the distinct features of this project, e.g., the multi-learner approach or the natural language involvement.

The second major objective is enabling the system to respond educationally meaningful and effective to the conclusions drawn from the assessment procedures, still protecting immersion and flow. Feedback and interventions can be interpreted as one mechanism that overtakes action of a teacher, i.e., providing advice, explanations, and evaluations. In game-based learning situations, adaptations on the micro level may occur through embedded feedback (e.g., through a non-player character), by guiding or hinting, or by adjusting the complexity/difficulty of a learning situation. Such kind of adaptation may indicate gaps between current and desired performance level and may enhance motivation and task strategies, it is able to reduce learners' cognitive load, and it can provide information that is useful for correcting inappropriate task strategies, errors, and misconceptions. A menu of psycho-pedagogically inspired adaptive intervention categories and types has been elaborated by [17], which are aligned with the non-invasive assessment procedures of a learner's competence and motivation.

In a next step, we must extend this framework by factors referring to the multi-learner aspect; we need to have sound mechanisms for assessing informal learning in groups, collaboration, group dynamics and roles, social networks, identifying the strength (the knowledge) and weaknesses of individuals in the groups, or the shared understanding of an entire group. In addition, it is necessary to develop and advance the related adaptation and intervention mechanisms. We need robust methods to support suitable group formation, an adaptation to individuals within groups, and an adaptation the entire group (with all the distinct characteristics). A particular challenge arises from the need to adjust the repertoire of interventions to the special requirements of the distinct coaching techniques. This includes elements such as systematic and purposeful questioning, moderating interventions, mediating interventions, task generation in the "building block" context, tailored group formation and alignment, suitable action calls, etc. Finally, to complete the vision of an intelligent tutoring system for virtual coaching, it is of deemed importance to enrich the metrics used for the CbKST-based assessment with the interpretation of natural speech acts, the chatting and talking of learners/coachees. This goal requires a close collaboration with leading edge natural langue interaction techniques.

This paper presented the conceptual approach on the basis of the existing state-of-the-art. Realizing this vision is subject to future work.

5 Acknowledgements

The research and development introduced in this work is funded by the European Commission under the seventh framework programme in the ICT research priority, contract number 258114 (NEXT-TELL; http://www.next-tell.eu).

6 References

[1] Barrett, T. (2010). The problem-based learning process as finding and being in flow. Innovations in Education & Teaching International, 47(2), 165-174.

[2] Schank, R. (1999). Dynamic Memory Revisited, 2nd Edition. New York: Cambridge University Press.

[3] Stavenga - de Jong, J. A., Wierstra, R. F. A., & Hermanussen, J. (2006). An exploration of the relationship between academic and experiential learning approaches in vocational education. British Journal of Educational Psychology, 76(1), 155-169.

[4] Renkl, A., Hilbert, T., & Schworm, S. (2009). Example-based learning in heuristic domains: A Cognitive Load Theory account. Educational Psychology Review, 21, 67-78.

[5] Dillenbourg, P. (1999). Collaborative Learning: Cognitive and Computational Approaches. Advances in Learning and Instruction Series. New York, NY: Elsevier Science, Inc.

[6] Sweller, J., Van Merrienboer, J. J. G., & Paas, F. W. C. (1998). Cognitive architecture and instructional design. Educational Psychology Review, 10, 251-296.

[7] Jonassen, D. (1999). Designing Constructivist Learning Environments. In C. M. Reigeluth (Ed.), Instructional Design Theories and Models: A New Paradigm of Instructional Theory (Vol. II) (pp. 215-239). Mahwah, NJ: Lawrence Erlbaum Associates.

[8] Merrill, M.D. (2002). First principles of instruction. Educational Technology Research and Development, 50(3), 43-59.

[9] Dillenbourg, P., Baker, M., Blaye, A., & O'Malley, C. (1996). The evolution of research on collaborative learning. . In E. Spada & P. Reiman (Eds.), Learning in Humans and Machine: Towards an interdisciplinary learning science (pp. 189-211). Oxford: Elsevier.

[10] Johnson, D. W., Johnson, R. T., & Smith, K. A. (1998). Cooperative Learning Returns To College: What Evidence Is There That It Works? Change, July/August 1998, 27-35.

[11] Warburton, S. (2009). Second Life in higher education: Assessing the potential for and the barriers to deploying virtual worlds in learning and teaching. British Journal of Educational Technology, 40(3), 414–426.

[12] Salmon, G. (2009). The future for (second) life and learning. British Journal of Educational Technology, 40(3), 526–538.

[13] Sköld, O. (2012). The effects of virtual space on learning efficacy: A literature review. First Monday, 17 (1-2).

[14] Minocha, S., & Reeves, A. (2010). Design of learning spaces in 3D virtual worlds: An empirical investigation of Second Life. Learning, Media and Technology, 35(2), 111–137.

[15] Albert, D., & Lukas, J. 1999. Knowledge spaces: Theories, empirical research, and applications. Mahwah, NJ: Lawrence Erlbaum Associates.

[16] Newell. A. (1990). Unified theories of cognition. Cambridge: Harvard University Press.

[17] Kickmeier-Rust, M. D., Mattheiss, E., Steiner, C. M., & Albert, D. (2010). Digital game-based learning: New horizons of educational technology. In M. Schiefner & M. Ebner (eds.), Looking Toward the Future of Technology Enhanced Education: Ubiquitous Learning and the Digital Native. Hershey, PA: IGI Global.

Multi-phase Updating - A Practical Approach to Simulating Animat Agents

C.J. Scogings and K.A. Hawick
Computer Science, Institute for Information and Mathematical Sciences,
Massey University, Albany, NS 102-904, Auckland, New Zealand
{c.scogings, k.a.hawick}@massey.ac.nz
Tel: +64 9 414 0800 Fax: +64 9 441 8181

March 2012

ABSTRACT
A growing number of applications can be modelled using spatial agent systems or animats. Typical animat simulations model collective macroscopic phenomena using encoded individual behaviours for microscopic agents. In spatial agent systems there are well known problems that occur if agent cells are updated in a sequential order. This is known as the sweeping problem and it also occurs in other numerical simulations such as differential equation solvers and leads to observable macroscopic effects in the simulated system that are solely artifacts of the implementation algorithm. We explore various strategies to remove these artifacts including multi-phase updating. We find that in some models that include non-diffusional effects such as predator-prey interactions, a two-phase update is not sufficient and a three-phase update strategy is necessary to preserve model semantics, particularly when concurrency is used to speed up the model. We discuss the computational implications of this for animat agent simulations.

KEY WORDS
agent-based models; updating agents; multi-phase update; animats; model semantics.

1 Introduction

Agent-based modelling [21, 22, 29] is a powerful construct for tacking many complex-systems problems [11] in: physics; sociology; finance; and other areas where emergent properties [37] arise from relatively simple individual agent properties. Simulations of multi-agent systems can be readily constructed in general purpose programming languages. Spatial agents - or animats as they are often described - are agents that have some spatial position and therefore can move around and interact with other agents. The key idea for spatial agents is usually that individual agents only interact with those local to them rather than with the entire population.

An important aspect of modelling spatial animat agents is to unambiguously specify how the agents are updated or evolved in the model. Updating might mean each agent is selected in turn or at random and given the option to exercise its microscopic behavioural rules. It might move, eat, kill, breed, grow, die, buy, sell, communicate, or exercise whatever other individual actions are open to it in the particular model being studied. The update is typically applied iteratively to evolve the whole model system through its phase or state space [31, 40].

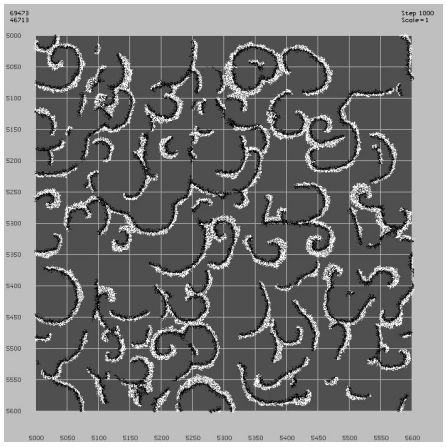

Figure 1: Animat model configuration step 1000 of a multi-phase run of a predator-prey model. Predators are black and prey are white.

Usually a particular multi-agent model will have some constraints such as conservation laws, or other global laws that cannot be sensibly violated by individual agent updates. Different models can be expressed using different sorts of update algorithmic procedures. These are often categorised as synchronous - where every agent is effectively updated at once or asynchronous - where individual updates are only loosely coupled to model time.

In automaton models [41] such as Conway's Game of Life [14] a fully synchronous update is part of the model

definition. In stochastic models such as the Metropolis Monte Carlo dynamics applied to the Ising model of a magnet [18, 27] other factors allow a partially synchronous update. Other models require an asynchronous updating scheme. The idea of using asynchronous updating is not new [4, 10] and has been explored and debated in the complex systems literature [16] for a number of different models including multi-agent systems [9]; random boolean networks [17]; automata [28]; and asynchronous cellular automata [24, 25]

Many large scale models make use of parallelism and therefore need an appropriate form of concurrency control [13] to exploit parallel hardware without changing the model semantics. Asynchronous update issues also arise in some numerical methods such as successive over-relaxation [2].

In this paper we explore the practical issues behind using a multi-phase update for agent-based models such as one of the various artificial life [3] animat models. Agent-based models have contributed significantly across a wide range of distinct areas, from Artificial Life [1, 23, 38] through ecosystems [33] and trading and economics [8, 26] to military combat [6, 7].

All agent-based models require some form of interaction between agents, for example in a predator-prey model [19, 35] predators attempt to catch prey and also to breed with other predators. It is these micro-interactions that lead to the well-known emergent macro-properties of such models, for example the emergence of spiral patterns in the predator-prey model shown in Figure 1. We are primarily interested in animat models of this category in this present paper (Section 3), although we do draw comparisons with simpler deterministic models such as the Eden/Epidemic model in Section 2

An important part of the interaction between agents is the order in which such interactions are executed and this can have a significant effect on the observed patterns of behaviour. The interaction between agents becomes more complicated when agents are developed to perform a range of "higher-order" behaviours such as trading [34] or signalling [36]. In this article we critique the known solutions to this problem and suggest some practical approaches to how best to incorporate this important process into agent-based models.

Our paper is structured as follows: In Section 2 we review some update effects and artifacts that arise from a single phase update approach in a well defined example model such as the Eden/Epidemic growth model. We discuss similar issues in animat models such as our own in Section 3. We review some key update algorithmic ideas in Section 4. We discuss some statistical ideas concerning updates and multi phase algorithms in Section 5 and summarise some pragmatic advice to model practitioners in Section 6.

2 The Eden-Epidemic Model

The Eden model [12] of an epidemic or cancerous growth consists of an initial pattern - usually a single infected seed agent in a system of uninfected agents - and whose boundary agents become infected or grow according some probability parameter p at each update step. There are a number of variations, but at each time step of the model, the state of every agent site is updated. This can be done in sequential order or as a two phase update.

In a sequential update, every agent is updated *in-situ*. This means that if an agent is updated after its neighbour then it has up to date information of any changes that have occurred in the states of other agents within the same time step. The order in which the agents are chosen to be updated can be random or fixed. A fixed order is often referred to in the literature as a "sweep". Iterating through the population in a fixed order is computationally efficient as it makes good use of memory caches, which can be highly significant if the model size is very large. However this approach introduces some definite sweeping behaviours that are neither physical nor correct in the sense of being what was intended by the modeller. Often it is the temporal behaviour that the modeller is interested in measuring. This might be in the form of periodic cycles of behaviour or a growth or shrinkage exponent. If the update algorithm is therefore unphysical the experimental simulation results will be at best biased or at worst just wrong.

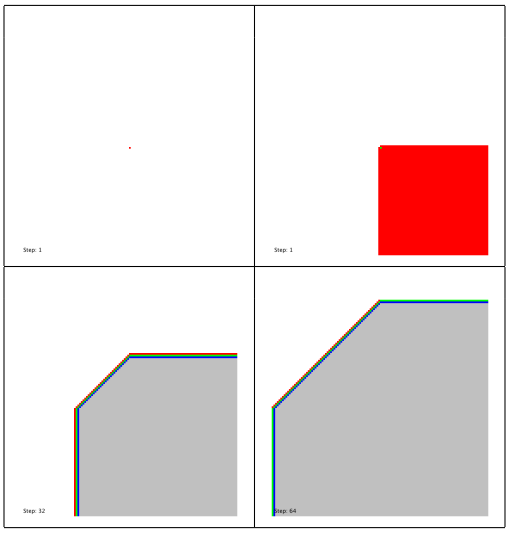

Figure 2: The effects of a sweeping *in-situ* update algorithm for the Eden Epidemic Model 128×128 across successive time steps (cells: white empty; dark live; grey dead, Infection probability 1.0). The simulation starts with a single infected cell at the centre and progresses to the right.

Figure 2 shows the effects when a sequential sweep algorithm is applied to a single central infected cell with in-

fection (or growth) probability $p = 1.0$. The sweep is essentially a row-major raster and the *in-situ* updating and sweeping effect causes the infection to propagate rapidly to all the neighbouring cells that are updated strictly after the infected cell. Infection information travels across the model system at the maximal possible speed. When the probability of infection is substantially less than 1, for example with $p = 0.25$, the skewed results of the model are more subtle. Figure 3 shows the 'correct' result on the left and the skewed results on the right. The correct results have been produced using a two-phase update algorithm.

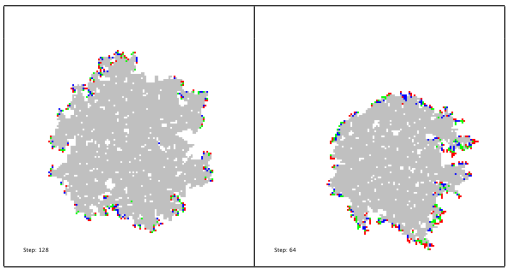

Figure 3: Two-phase update algorithm (left) with a sweeping *in-situ* update algorithm (right) for the Eden Epidemic Model 128×128 across successive time steps (cells: white empty; dark live; grey dead. Infection probability 0.25)

If constrained to a sequential update method a better way of updating the system is to randomise the choice of sites to update. This can either be done by randomly shuffling the list of sites to update (perhaps using a pair-wise shuffle). An even more random approach can be taken by performing Monte-Carlo hits on the sites: on average all sites will be updated once every n time steps (where n is the number of sites in the system), but as the update sites are being chosen randomly, there is a possibility some sites will be updated more frequently than others over a short time period. This has the effect of slightly blurring the concept of 'time' in the simulation (see Figure 4).

Figure 4a) illustrates the cellular growth behaviour of a variation of the Eden Epidemic model [12] when a single infected cell at the centre of the pattern infects nearest neighbouring cells with probability $p = 0.3$ at each time step. In the model shown, infected cells die after two time steps after being infected. Figure 4b) shows how a random algorithm can recover spatial symmetry in the growth model.

Figure 5 shows, by way of contrast, the highly regular pattern that results from the Eden model when a sequential sweep update is used. This is microscopically correct in some sense, but is clearly dominated by the sweeping artifact - and is not representative of the modeller's intentions.

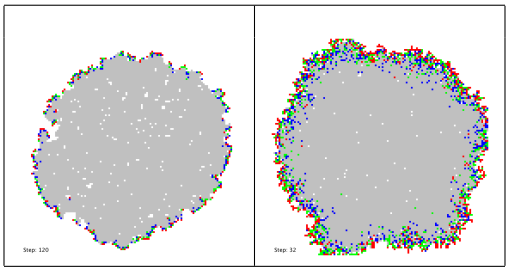

Figure 4: A variation of the Eden Epidemic model is used to show growth time scales and symmetries on a square lattice. Sites are infected from any live nearest neighbour with a probability $p = 0.3$ (left) or $p = 1.0$ (right), and once infected, die after two time steps. The cluster is grown from a single central infected cell. The left hand cluster shows the two phase update algorithm and the right hand uses a random algorithm so cells are updated once per time step on average. Some cells are hit more often and although spatial symmetry is largely recovered, the time scale is accelerated.

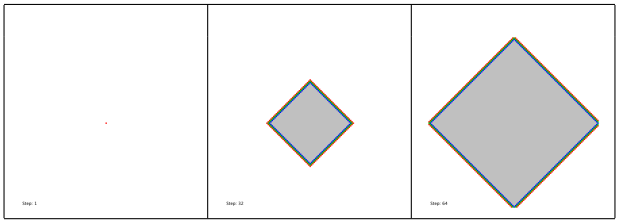

Figure 5: Sequential sweep update algorithm for the Eden Epidemic Model 128×128 cells: white empty; dark live; grey dead. (Infection probability 1.0). The simulation starts with a single infected cell at the centre and progresses to the right.

3 The Animat Model

The animat model we discuss in this section is somewhat more complicated than the Eden model, but is still implemented on a grid of agent-hosting cells, and can have a range of various sorts of update algorithm applied to each microscopic agent. An agent-based prey-predator model has been developed [35] based on "artificial animals" or *animats* [39]. Predators need to catch prey to survive and both species can breed to produce new animats. Animats can "die" from a lack of food (i.e. if health reaches zero) or due to "old age" (i.e. if age reaches a set maximum for the species). Prey animats can also die through being consumed by a predator.

Like most agent-based models, the model is executed as a sequence of cycles (called *time-steps*). Every animat is updated during each time-step and when the updating is completed, the model advances to the next time-step. The following state variables are used to maintain the

state of each animat: location in terms of x, y coordinates; age which is increased each time-step; health which is decreased each time-step but increased by "eating"; neighbours in terms of the location and species of nearest neighbours; and the microscopic species rule set which is used to decide which rule to execute. The rule sets used for the experiments described in this article were as follows:

Rules for predators:

1. breed if health $>$ 50% & mate adjacent
2. eat prey if health $<$ 50% & prey adjacent
3. seek mate if health $>$ 50%
4. seek prey if health $<$ 50%
5. randomly move to adjacent position

Rules for prey:

1. breed if health $>$ 50% & mate adjacent
2. eat grass if health $<$ 50%
3. seek mate if health $>$ 50%
4. move away from adjacent predator
5. randomly move to adjacent position

Most rules carry conditions usually relating to location or current health. The rules are presented in priority order and each animat executes the first rule in its list for which the conditions are satisfied. The "Breed Rule" regulates the production of new animats and when an animat is "born" it inherits the rules of its parents. The "Breed Rule" does not always succeed. Even if the necessary conditions are satisfied, there is still only a random chance that a new animat will be produced. This chance is known as the "birth rate" and is an abstraction of the cumulative effect of several unknown factors including birthing difficulties, availability of suitable shelter, etc. It would be difficult to simulate these factors separately so it is convenient to substitute one value which produces the desired effect in the model. Normally the birth rate for predators is set to 15% and the birth rate for prey is set to 40% but these can be modified to produce different effects in the simulation.

Predators need to consume prey and prey need to eat grass to survive. Whenever the animat successfully executes the "eat" rule, its health state variable is increased. Grass is placed at various points around the map and is automatically replenished. Future work will experiment with grass that is not replenished (or is replenished very slowly).

The interaction of the animats as they execute their individual rules has produced interesting emergent features in the form of macro-clusters often containing many hundreds of animats. We have analysed and documented these emergent clusters in [20]. The most fascinating cluster that consistently appears is a spiral and several spirals are visible in Figure 1.

The model uses a two-phase update system so each animat carries two versions of its state variables – the "current state" and the "future state". A rule is selected from the rule set and applied to the current state and this generates the future state. At the end of each time-step the current state is changed to match the future state.

4 Animat Model Updates

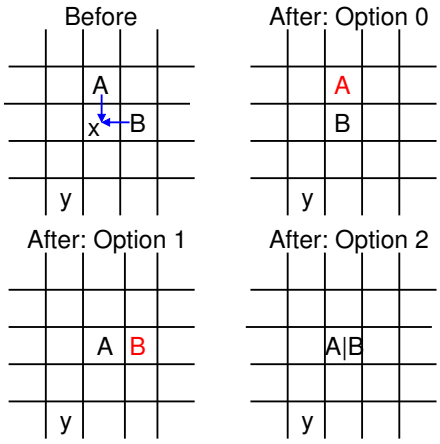

Figure 6: Using a 2-phase update, it is possible for predators A and B to "simultaneously" both locate and consume the single adjacent prey animat x. This renders the model ambiguous as it should not be possible for one prey animat to sustain more than one predator and there are three outcomes and which is the actual one is an artifact of the implementation.

Due to the known problems of a single-phase update system (discussed in section 2 above), the predator-prey model was initially constructed using a two-phase update. However it was soon discovered that the two-phase update led to a serious problem outlined in Figure 6.

The sequence of events that caused this problem can be summarised as follows:

- predator (current state) locates adjacent prey (current state)
- predator executes "Eat" Rule
- predator (future state) is updated by increasing health
- prey (future state) is updated by setting health to zero (dead)

Note that this sequence would only be executed by a predator that had less than 50% health. However in a typical model with tens of thousands of predators – often in

close proximity as shown in Figure 1 – there is a strong probability that two or more predators will be adjacent to the same prey. When this occurs, both predators update their future states to indicate an increase in health, i.e. several predators can "eat" the same prey. Note that the current state of the prey (and the predators) remains unchanged, allowing other predators to repeat the process with the same prey. The problem was discovered because it was noticed that huge numbers of predators were existing off an impossibly small prey population. This update problem thus rendered any results from the model meaningless.

It is not possible to solve the problem and retain a pure two-phase update system. The solution adopted in our model was to introduce a hybrid of the sequential and two phase update systems. In this system every prey animat was given an extra state variable to keep track of its current status and the procedure outlined above was modified as follows:

- predator (current state) locates adjacent prey (current state)
- **if prey (current state) is "dead" then abandon this sequence**
- predator executes "Eat" Rule
- predator (future state) is updated by increasing health
- prey (future state) is updated by setting health to zero
- prey **(current state)** is updated by changing status to dead

Since this sequence allows the current state of the prey to be modified, this is no longer a two-phase update. Sequential update is acceptable in these circumstances,although it is necessary also to randomly shuffle the animats before updating. Experiments have shown that the best system is sequential updating but in a random order. Predator results are shown in Figure 7. Prey results are shown in Figure 8.

The periodic boom-bust variations seen in Figures 7 and 8, showing the populations of predator and prey agents is characteristic of this sort of spatial agent model. The period lengths are consistent between runs and are a measurable property of the experiments. Phase effects - and fluctuational noise however must be averaged out, and this is usually done by averaging over many independently seeded initial model configurations. The top trace in each of these Figures shows the normalupdate algorithm. The second has no random shuffle applied - which manifestly lowers the mean value of both populations. The third case has predators given a slight advantage, which makes them overly successful hunters and again mean populations are even lower.

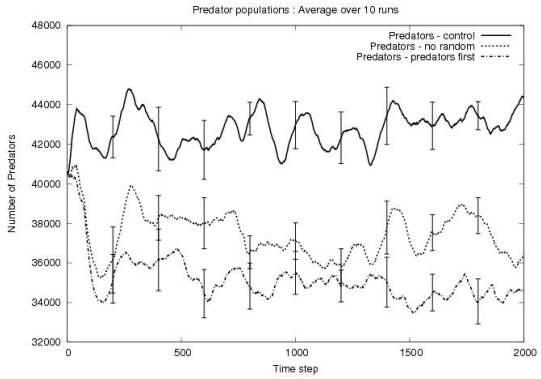

Figure 7: Predator populations using different update methods.

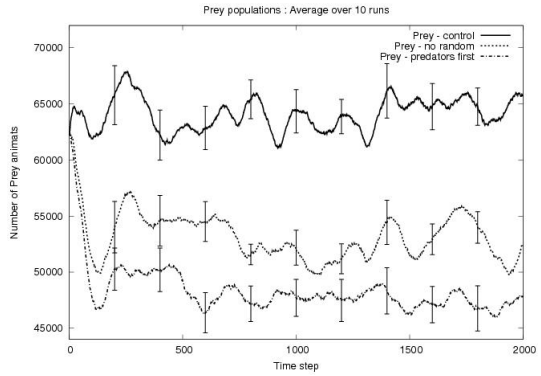

Figure 8: Prey populations using different update methods.

5 Discussion

Generally it appears that the animat model problem can be partially fixed by introduction of a 2-phase update. However, the 2-phase update causes other problems when animats are involved in (a) killing other animats or (b) bumping into objects including other animats. In these cases it is better to use a random shuffle.

We have introduced these ideas in the context of a pragmatic animat simulation. It is interesting to speculate about more general implications for other models. One theoretical approach is to consider the state space of this class of models. Each microstate $\mathbf{X}$ of the whole model system is completely specified by the set of agent state variables $\{a_i\}$. Consider a probability functional $P(\mathbf{X}, t)$ be associated with the microstate $\mathbf{X} \equiv \{a_i\}$ at time t and consider the transition probability $W_{\mathbf{X}\rightarrow\mathbf{X}'}$ giving the likelihood of a change of microstate $\mathbf{X}$ to $\mathbf{X}'$. The following master equation can be set up, requiring that the rate of change of probability of microstate $\mathbf{X}$ at time t be given by considering all transitions from $\mathbf{X}$ and all transitions to $\mathbf{X}$:

$$\frac{dP(\mathbf{X})}{dt} = -\sum_{\mathbf{X}'} W_{\mathbf{X}\to\mathbf{X}'} P(\mathbf{X}) + \sum_{\mathbf{X}'} W_{\mathbf{X}'\to\mathbf{X}} P(\mathbf{X}') \tag{1}$$

By requiring the model update algorithm to yield $P(\mathbf{X}) \to P_{eq}(\mathbf{X})$, the thermodynamic equilibrium probability of microstate $\mathbf{X}$ as $t \to \infty$, as a solution of equation 1 with $\frac{dP(\mathbf{X})}{dt} = 0$ so that:

$$\sum_{\mathbf{X}'} W_{\mathbf{X}\to\mathbf{X}'} P(\mathbf{X}) = \sum_{\mathbf{X}'} W_{\mathbf{X}'\to\mathbf{X}} P(\mathbf{X}') \tag{2}$$

This is the condition of detailed balance [5, 30]. It is common to use the stronger (but tractable) condition that:

$$\frac{W_{\mathbf{X}'\to\mathbf{X}}}{W_{\mathbf{X}\to\mathbf{X}'}} = \frac{P(\mathbf{X})}{P(\mathbf{X}')} \tag{3}$$

So that the probability of the system moving to microstate $\mathbf{X}$ is increased for highly probable microstates $\mathbf{X}$, and decreased for unlikely ones. It is then necessary to recognize that for a Boltzmann statistical weighting of the microstates, the probabilities $P(\mathbf{X})$ can be expressed in terms of the Hamiltonians $\mathcal{H}(\mathbf{X})$.

$$P(\mathbf{X}) = Ae^{-\frac{\mathcal{H}(\mathbf{X})}{k_b T}} \tag{4}$$

Where A is a normalising constant, k_b is Boltzmann's constant and T the temperature. Substituting 4 in 3 gives:

$$\frac{W_{\mathbf{X}'\to\mathbf{X}}}{W_{\mathbf{X}\to\mathbf{X}'}} = e^{-\frac{\{\mathcal{H}(\mathbf{X})-\mathcal{H}(\mathbf{X}')\}}{k_b T}} \tag{5}$$

This does not have a unique solution but commonly used approaches are the Metropolis [32] or Glauber functions [15].

These or some other deterministic or stochastic procedure provides a way of traversing the phase space of the model. In the case of the animat model we have similar concerns and goals. The procedures become more complicated in that we have killing and births and other effects that change the number of agents involved. There is potential to develop formulations for model phase state traversal bringing these two approaches together in a unified notation.

6 Conclusion

In summary we have discussed models such as the Eden/Epidemic model and our predator/prey animat model and drawn out comparisons between the updating procedures involved in both. We have identified in particular that sweeping effects can give rise to the wrong model behaviour. This is because spatial correlations are introduced that are solely due to artifacts of the algorithm rather than from the thermal and other fluctuations that we desire to simulate.

Single-phase sequential updating is shown to cause particular problems. Furthermore, in certain circumstances (such as for more complex models like the animat system) even an alternative two-phase update causes a different but related set of problems. We have discussed in particular the problem that arises when two predators would potentially eat the same prey. There are disadvantages to the two-phase update model - not the least of which is that the two-phase model also wastes memory in storing two complete model states. This is problematic for the very large model systems sizes we generally wish to simulate.

We conclude by offering the following pragmatic advice to model practitioners. Firstly, check if a sequential update will cause sweeping problems in the proposed model, and if the answer is yes, then use a two-phase update. Secondly, check if the two-phase update will cause problems similar to the "eating" problem we described, and if the answer is yes, then introduce a full or partial sequential update.

There appear to be some quite profound and deeper philosophical issues underpinning these pragmatics and we believe there is further work to be done to unify the update algorithm semantics under a single notation. This may lead to insights into the relationships between these different classes of simulation models.

References

[1] Adami, C.: On modeling life. In: Brooks, R., Maes, P. (eds.) Proc. Artificial Life IV. pp. 269–274. MIT Press (1994)

[2] Adler, S.L.: Over-relaxation method for the monte carlo evaluation of the partition function for multiquadratic actions. Physical Review D 23(12), 2901–2904 (June 1981)

[3] Aleksic, Z.: Artificial life: growing complex systems. In: Bossomaier, T.R., Green, D.G. (eds.) Complex Systems. pp. 91–126 (2000), iSBN 0-521-46245-2

[4] Bandini, S., Bonomi, A., Vizzari, G.: What do we mean by asynchronous ca? a reflection on types and effects of asynchronicity. In: Proc. 9th Int. Conf. on Cellular Automata for Research and Industry (ACRI 2010). pp. 385–394. No. 6350 in LNCS, Ascoli Piceno, Italy (21-24 September 2010)

[5] Binder, K. (ed.): Monte Carlo Methods in Statistical Physics. Topics in Current Physics, Springer-Verlag, 2 edn. (1986), number 7

[6] Cares, J.R.: The use of agenbt-based models in military concept development. In: Proc. 2002 Winter Simulation Conference. pp. 935–939. San Diego, California, USA (8-11 December 2002)

[7] Cioppa, T.M., Lucas, T.W., Sanchez, S.: Military applications of agent-based simulations. In: Proc. 2004 Winter Simulation Conference. pp. 171–180. Washington DC, USA (5-8 December 2004)

[8] Cliff, D., Bruten, J.: Animat market - trading interactions as collective social adaptive behaviour. Adaptive Behaviour 7(314), 385–414 (1999)

[9] Cornforth, D., Green, D.G., Newth, D.: Ordered asynchronous processes in multi-agent systems. Physica D 204, 70–82 (2004)

[10] Cornforth, D., Green, D.G., Newth, D., Kirley, M.: Do artificial ants march in step? ordered asynchronous processes and modularity in biological systems. In: Proc. Artificial Life VIII - the 8th Int. Conf or the Simulation and Synthesis of Living Systems. pp. 28–32. Sydney, Australia (9-13 December 2002)

[11] Cornforth, D., Green, D.S.: Intelligent Complex Adaptive Systems, chap. Modularity and Complex Adaptive Systems, pp. 75–104. IGI Global (2008)

[12] Eden, M.: A two-dimensional growth process. In: Proc. Fourth Berkeley Symposium on Mathematics, Statistics and Probability. vol. 4, pp. 223–239. Univ. California Press, Berkeley (1960)

[13] Fox, G., Coddington, P.: Complex Systems, chap. Parallel Computers and Complex Systems, pp. 289–338. Cambridge University Press (2000), iSBN 0-521-46245-2

[14] Gardner, M.: Mathematical Games: The fantastic combinations of John Conway's new solitaire game "Life". Scientific American 223, 120–123 (October 1970)

[15] Glauber, R.: Time dependent statistics of the Ising Model. J. Math. Phys. 4(2), 294–307 (1963)

[16] Green, D.G.: Towards a mathematics of complexity. Complexity International 3, 98–105 (1996), iSSN 1320-0682

[17] Harvey, I., Bossomaier, T.: Time out of joint: Attractors in asynchronous random boolean networks. In: Husbands, P., Harvey, I. (eds.) Proc Fourth European Conference on Artificial Life (ECAL97). pp. 67–75. MIT Press (1997)

[18] Hawick, K.A.: An agent model formulation of the ising model. Tech. rep., Information and Mathematical Sciences, Massey University, Albany, North Shore 102-904, Auckland, New Zealand (November 2003)

[19] Hawick, K.A., James, H.A., Scogings, C.J.: Roles of rule-priority evolution in animat models. In: Proc. Second Australian Conference on Artificial Life (ACAL 2005). pp. 99–116. Sydney, Australia (December 2005)

[20] Hawick, K.A., Scogings, C.J., James, H.A.: Defensive spiral emergence in a predator-prey model. Complexity International (msid37), 1–10 (October 2008), http://www.complexity.org.au/ci/vol12/msid37, iSSN ISSN 1320-0682

[21] Hawick, K., Scogings, C.: Agent-Based Evolutionary Search, chap. Complex Emergent Behaviour from Evolutionary Spatial Animat Agents, pp. 139–160. No. ISBN 978-3-642-13424-1, Springer (January 2010), cSTN-067

[22] Helbing, D., Balietti, S.: How to do agent-based simulations in the future: From modeling social mechanisms to emergent phenomena and interactive systems design. Tech. Rep. 11-06-024, Santa Fe Institute, NM, USA (June 2011), santa Fe Working Paper

[23] Holland, J.H.: Echoing emergence: Objectives, rough definitions, and speculations for echo-class models. In: Cowan, G.A., Pines, D., Meltzer, D. (eds.) Complexity: Metaphors, Models and Reality, pp. 309–342. Addison-Wesley, Reading, MA (1994)

[24] Jeanson, F.: Evolving asynchronous cellular automata for density classification. In: Proc. Artificial Life XI. pp. 282–288. Winchester, UK (5-8 August 2008)

[25] Kanada, Y.: The effects of randomness in asynchronous 1d cellular automata. In: Proc. Artificial Life IV (1994)

[26] King, A.J., Streltchenko, O., Yesha, Y.: Using multi-agent simulation to understand trading dynamics of a derivatives market. Annals of Maths and AI 44(3), 233–253 (July 2005)

[27] Laciana, C.E., Rovere, S.L.: Ising-like agent-based technology diffusion model: adoption patterns vs. seeding strategies. Tech. Rep. arXiv:1011.3834v1, Universidad Catolica Argentina (2010), to Appear in Physica A

[28] Li, W., Packard, N.H., Langton, C.: Transition phenomena in cellular automata rule space. Physica D 45, 77–94 (1990)

[29] Macal, C.M., North, M.J.: Tutorial on agent-based modeling and simulation part 2: How to model with agents. In: Proc. 2006 Winter Simulation Conference, Monterey, CA, USA. pp. 73–83 (3-6 December 2006), iSBN 1-4244-0501-7/06

[30] Manousiouthakis, V.I., Deem, M.W.: Strict Detailed Balance is Unneccessary in Monte Carlo Simulation. J. Chem. Phys. 110(2753) (1999)

[31] Margolus, N., Toffoli, T.: Cellular automata machines. Complex Systems 1, 967–993 (1987)

[32] Metropolis, N., Rosenbluth, A.W., Rosenbluth, M.N., Teller, A.H., Teller, E.: Equation of state calculations by fast computing machines. J. Chem. Phys. 21(6), 1087–1092 (Jun 1953)

[33] Ronkko, M.: An artificial ecosystem: Emergent dynamics and lifelike properties. J. ALife 13(2), 159–187 (2007)

[34] Scogings, C.J., Hawick, K.A.: Intelligent and adaptive animat resource trading. In: Proc. 2009 International Conference on Artificial Intelligence (ICAI 09) Las Vegas, USA. No. CSTN-076 (13-16 July 2009)

[35] Scogings, C.J., Hawick, K.A., James, H.A.: Tools and techniques for optimisation of microscopic artificial life simulation models. In: Nyongesa, H. (ed.) Proceedings of the Sixth IASTED International Conference on Modelling, Simulation, and Optimization. pp. 90–95. Gabarone, Botswana (September 2006)

[36] Scogings, C., Hawick, K.: Cross-caste communication in a multi-agent predator-prey model. In: Proc. IASTED Int. Conf. on Artificial Life and Applications (AIA 2011). pp. 163–170. IASTED (February 2011)

[37] Standish, R.K.: On complexity and emergence. Complexity International 9, 1–6 (2001), www.complexity.org.au/vol09

[38] Tyrrell, T., Mayhew, J.E.W.: Computer simulation of an animal environment. In: Meyer, J.A., Wilson, S.W. (eds.) From Animals to Animats, Proceedings of the First International Conference on Simulation of Adaptive Behavior. pp. 263–272 (1991)

[39] Wilson, S.W.: The animat path to AI. In: Meyer, J.A., Wilson, S. (eds.) From Animals to Animats 1: Proceedings of The First International Conference on Simulation of Adaptive Behavior. pp. 15–21. Cambridge, MA: The MIT Press/Bradford Books (1991)

[40] Wolfram, S.: Statistical Mechanics of Cellular Automata. Rev.Mod.Phys 55(3), 601–644 (1983)

[41] Wolfram, S.: Theory and Applications of Cellular Automata. World Scientific (1986)

Applications for Intelligent Information Agents (I^2As): Learning Agents for Autonomous Space Asset Management (LAASAM)

Dr. James A. Crowder
Raytheon Intelligence and Information Systems
16800 E. Centretech Parkway, Aurora, CO 80111

Lawrence Scally and Michael Bonato
Colorado Engineering, Inc.
1310 United Heights, Suite 105, Colorado Springs, CO 80921

Abstract – *Current and future space, air, and ground systems will continue to grow in complexity and capability, creating a serious challenge to monitor, maintain, and utilize systems in an ever growing network of assets. The push toward autonomous systems makes this problem doubly hard, requiring that the on-board system contain cognitive skills that can monitor, analyze, diagnose, and predict behaviors real-time as the system encounters its environment. Described here is a cognitive system of Learning Agents for Autonomous Space Asset Management (LAASAM) that consists of Intelligent Information Agents (I^2A) that provide an autonomous Artificially Intelligent System (AIS) with the ability to mimic human reasoning in the way it processes information and develops knowledge [Crowder 2010a, 2010b]. This knowledge takes the form of answering questions and explaining situations that the AIS might encounter. The I^2As are persistent software components, called Cognitive Perceptrons, which perceive, reason, act, and communicate. Presented will be the description, methods, and framework required for Cognitive Perceptrons to provide the following abilities to the AIS:*

1. *Allows the AIS to act on its own behalf;*
2. *Allows autonomous reasoning, control, and analysis;*
3. *Allows the Cognitive Perceptrons to filter information and communicate and collaborate with other Cognitive Perceptrons;*
4. *Allows autonomous control to find and fix problems within the AIS; and*
5. *Allows the AIS to predict a situation and offer recommend actions, providing automated complex procedures.*

A Cognitive Perceptron Upper Ontology will be provided, along with detailed descriptions of the I^2A framework required to construct a hybrid system of Cognitive Perceptrons, as well as the Cognitive Perception processing infrastructure and rules architecture.

In particular, this paper will present an application of Cognitive Perceptrons to Integrated System Health Management (ISHM), and in particular Condition-Based Health Management (CBHM), to provide the ability to manage and maintain an AIS in utilizing real-time data to prioritize, optimize, maintain, and allocate resources.

Keywords: Intelligent Agents, Space Asset Management, Artificial Learning

1 Introduction

Intelligence reveals itself in a variety of ways, including the ability to adapt to unknown situations or changing environments. Without the ability to adapt to new situations, an intelligent system is left to rely on a previously-written set of rules. If we truly desire to design and implement autonomous AI Systems (AIS), they cannot require precisely-defined sets of rules for every possible contingency. The questions then become:

- ***How does an autonomous AI system construct good representations for tasks and knowledge as it is in the process of learning the task or acquiring knowledge?***
- ***What are the characteristics of a good representation of a new task or a new piece of knowledge?***
- ***How do these characteristics and the need to adapt to entirely new situations and knowledge affect the learning process?***

CBHM entails the maintenance of systems and equipment, based on an assessment of current and projected conditions (both situational and health). A complete and modern CBHM system comprises many functional capabilities, including sensing & data acquisition, signal processing, condition & health assessment, diagnostics & prognostics, and decision reasoning [Scally, Bonato, and Crowder 2011] (See Figure 1). Such features are enabled through the application of autonomous AIS.

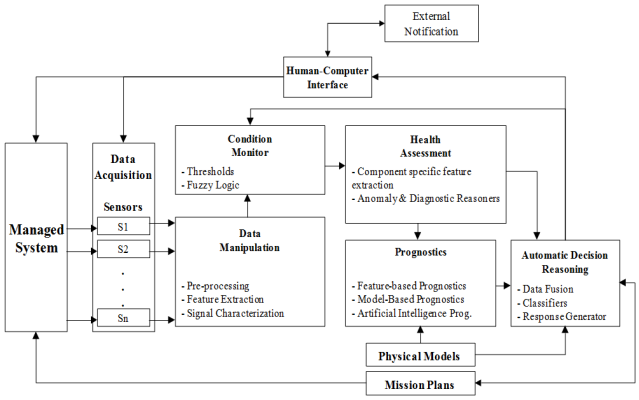

Figure 1 – CBHM Architecture

Discussed here will be the I²A Cognitive Perceptron architecture required to provide a system capable of autonomously managing a complex network of space-based assets to enhance situational awareness and optimize their utilization.

2 Intelligent Information Agents (I²A)

Intelligent Information Agents (I²A) employ soft-computing techniques to generate Intelligent Software information Agents (ISAs). These agents mimic human reasoning to process information and develop intelligence. This intelligence takes the form of answering questions and explaining situations [Crowder 2010b].

The I²A architecture is a Java framework for constructing a hybrid system of Intelligent Information Software Agents. It provides a productivity toolkit for adding intelligent software agent functions to applications and modern architectural frameworks and for building multi-agent intelligent autonomic systems. This includes the framework for providing business rules and policies for run-time systems, including an autonomic computing core technology within a multi-agent infrastructure. Figure 2 illustrates an overview of the I²A architecture framework that is the infrastructure for a hybrid neural processing environment.

I²As are active, persistent software components that perceive, reason, act, and communicate. I²As are software structures that:

1. Assist people and act on their behalf;
2. Are used for automation, control, and analysis;
3. Assist people in finding and filtering information, automating tedious tasks, and collaborating with other agents; and
4. Enable automation and control for finding and fixing problems, finding "best fit" procedures, pattern recognition and classification, predictions and recommendations, and automating complex procedures.

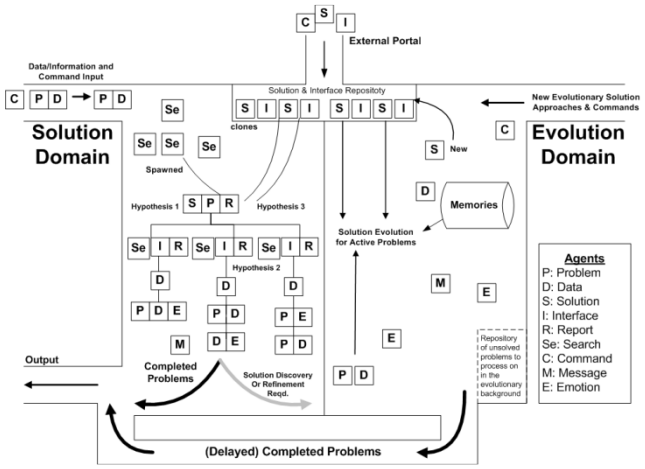

Figure 2 – I²A Intelligent Agent Infrastructure

2.1 I²A Tasking

Intelligent Information Agents have the ability to learn from experience and can be used to actually predict future states (prognostics). They are able to analyze sensor data using classification and clustering techniques to detect complex states and diagnose problems (anomaly detection and resolution). The I²As can interface with other autonomic agents and components via web-services. They have the ability to reason using domain-specific application objects and have autonomous (proactive) behavior and goals. They have the ability to correlate events to situations, reasons, and take action.

The I²A hybrid computing architecture uses genetic, neural-network and fuzzy logic to integrate diverse sources of information, associate events in the data and make observations. When combined with a dialectic search [Crowder 2010a], the application of hybrid computing promises to revolutionize information processing. The dialectic search seeks answers to questions that require interplay between doubt and belief, where our knowledge is understood to be fallible. This 'playfulness' is key to hunting within information and is explained in more detail in the section that address the Dialectic Search Argument (DSA).

2.2 The I²A Dialectic Search Argument

The Dialectic Search uses the Toulmin Argument Structure to find and relate information that develops a larger argument, or intelligence lead. The Dialectic Search Argument (DSA), illustrated in Figure 3, has four components:

1. Data: in support of the argument and rebutting the argument.
2. Warrant and Backing: explaining and validating the argument.
3. Claim: defining the argument itself.
4. Fuzzy Inference: relating the data to the claim.

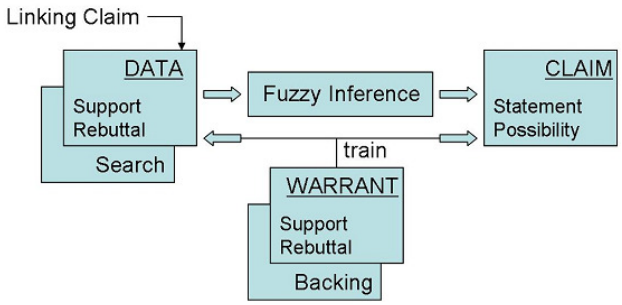

Figure 3 – The DSA Structure

The argument serves two distinct purposes. First, it provides an effective basis for mimicking human reasoning. Second, it provides a means to glean relevant information from the Topic Map [11] and transform it into actionable intelligence (practical knowledge.) These two purposes work together to provide an intelligent system that captures the capability of a human Intelligence Operative to sort through diverse information and find clues.

This approach is considered dialectic in that it does not depend on deductive or inductive logic, though these may be included as part of the warrant. Instead, the DSA depends on non-analytic inferences to find new possibilities based upon warrant examples. The DSA is dialectic because its reasoning is based upon what is plausible; the DSA is a hypothesis fabricated from bits of information.

Once the examples have been used to train the DSA, data that fits the support and rebuttal requirements is used to instantiate a new claim. This claim is then used to invoke one or more new DSAs that perform their searches. The developing lattice forms the reasoning that renders the intelligence lead plausible and enables measurement of the possibility.

As the lattice develops, the aggregate possibility is computed using the fuzzy membership values of the support and rebuttal information. Eventually, a DSA lattice is formed that relates information with its computed possibility. The computation, based on Renyi's entropy theory, uses joint information memberships to generate a robust measure of Possibility, a process that is not achievable using Bayesian methods.

3 The I^{2}A Software Architecture

The primary software component of LAASAM is the I^{2}A. Each software component, or ISA, provides different cognitive capabilities (called cognitive archetypes) that form a cognitive ecosystem within the LAASAM framework, allowing inter-agent communication, collaboration, and cooperation. Figure 4 illustrates this ecosystem. Each ISA archetype, while having separate capabilities, have a defined cognitive structure, or ontology [Raskin and Taylor 2010a, and Taylor and Raskin 2011a], shown in Figure 5.

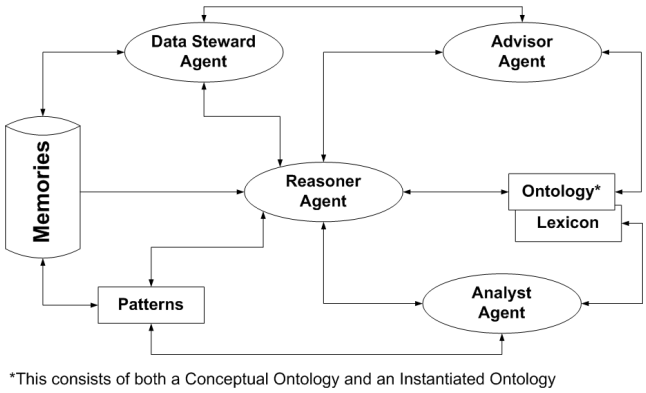

Figure 4 – The LAASAM ISA Cognitive Ecosystem

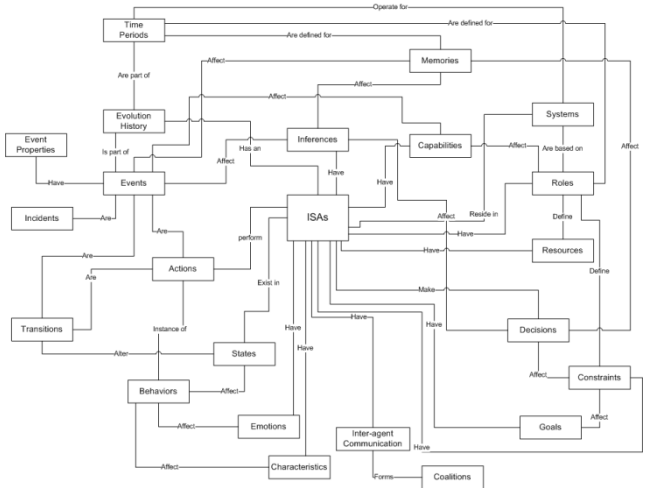

Figure 5 – The ISA Cognitive Perceptron Upper Ontology

Each LAASAM ISA is a self-contained software unit (agent) comprised of one or more services, shown in Figure 6. The combination of services defines an ISA's capabilities. There are five currently defined agent types within the LAASAM processing infrastructure:

1. Data Steward (ADS): this agent acquires raw data from a variety of sources, including sensors, and prepares incoming data for use by other agents. The Data Steward Agent generates and maintains metadata required to find and extract data/information from heterogeneous sources.
2. Advisor Agent (AAD): this agent disseminates the right information to the right place at the right time; it provides capabilities that allow collaborative question asking and information sharing by agents and end-users. Advisor Agents generate and maintain topical maps required to find relative information fragments, memories, and "expert" ISAs.
3. Reasoner Agents (ARE): The Reasoner Agent interacts with the Data Steward and Advisor Agents and utilizes the ontologies and lexicons to automate the development of domain-specific encyclopedias; it provides a mixed source of information and question answering that is used to develop an understanding of questions, answers, and their domains. Reasoner Agents analyze questions and relevant source information to provide answers and to develop cognitive ontology rules for the LAASAM CBHM system.
4. Analyst Agents (AAN): The Analyst Agents are fed by Reasoner Agents and utilize the developed ontologies and lexicons to expand upon questions and answers learned from collected information.
5. Interface Agent (AIN): The Interface Agent assesses the correctness of major decisions and adjusts the decision processes of the Advisor Agents. Interface Agents also accommodate human-in-the-loop structures.

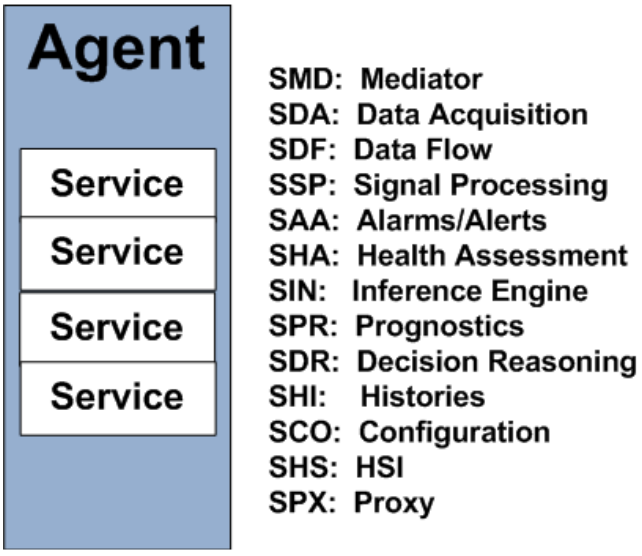

Figure 6 – Services that comprise ISAs

4 Cognitive CBHM (LAASAM)

LAASAM utilizes the I^{2}A technology to address the requirements of CBHM for space and ground asset management. LAASAM (illustrated in Figure 7) represents a significant advancement in the field of Space Asset Management by providing cognitive abilities similar to human reasoning. The LAASAM architecture provides the following high-level features:

1. An Intelligence Network: this includes mechanisms for gathering information, learning, inferences, and providing decision support to situational analysts.
2. Answer Extraction: these are mechanisms for posing hypotheses about situations and providing answers.
3. Situational Analysis: mechanisms for finding situations that require active investigation and provide actionable intelligence

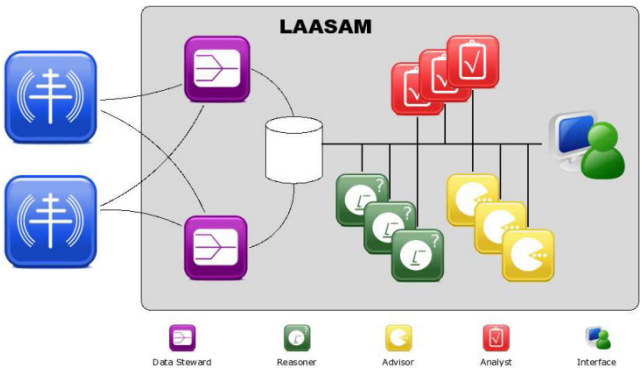

Figure 7 – LAASAM provides I^{2}A-Based Asset Management for Enhanced SSA

These features define the core of LAASAM and are realized by I^{2}A technology infrastructure. The I^{2}A cognitive processing infrastructure provides the intelligence within the LAASAM system through an implementation of an artificial prefrontal cortex [Crowder and Friess 2011a], associated artificial neural memories and data management [Crowder 2010a, Crowder and Carbone 2010a, b, and c], and derived strategies for reasoning, analysis, and inference [Crowder 2010b, Crowder and Friess 2010a &b, Crowder and Friess 2011 a and b].

The LAASAM software architecture defines the I^{2}A functions that range from data collection through providing recommendations for specific actions. Agents take on roles within the system, implemented through dynamically changing services and functional nodes, in support of system defined goals [Crowder 2010b].

The LAASAM high-level features discussed above are enhanced by evolutionary processes embedded within the I²A cognitive processing framework [Crowder 2010a] and implemented utilizing functionally distributed capabilities provided by the I²A infrastructure. Figure 8 illustrates Figure 1 with the I²As distributed across the system.

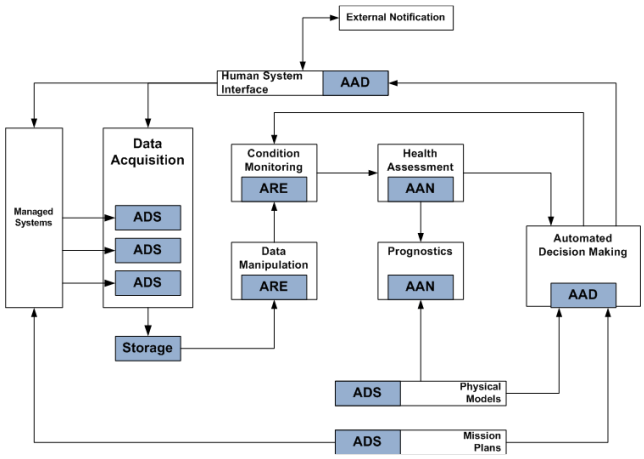

Figure 8 – Distribution of I²As for CBHM

LAASAM is based on the concept that I²As carry personalities. A personality is a collection of state information carried in a personality state token (shown in Figure 9) that describes the agent. Agent personalities can then be cloned and distributed utilizing these stored tokens.

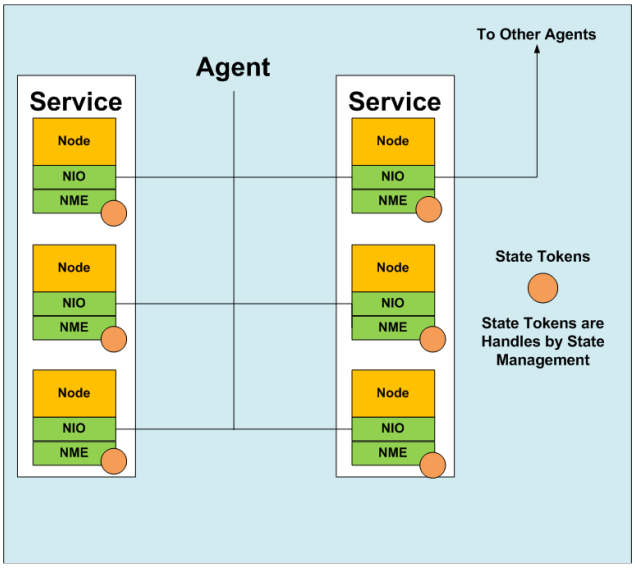

Figure 9 – I²A Personality Tokens

In this way, agents are mobile in that their personalities are mobile. This mobile nature of agent personalities, or state mobility, allows agents to evolve on a self-determining basis. LAASAM operates on a collection of host systems that support Java clients connected through a secure network. Interface agents provide the authentication and authorization for the processing infrastructure, allowing secure access to I²As within the network. Policy management for distribution of code updates and state tokens to agents within the LAASAM I²A infrastructure is handled through Interface Agents that provide User Interface (UI) capabilities. I²A personalities are partially based on their need to cooperate, learn, and function autonomously within the LAASAM framework. Figure 10 below illustrates these capabilities for the various I²As.

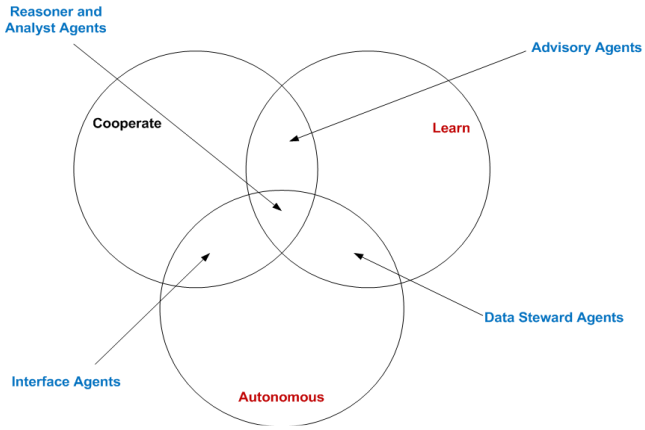

Figure 10 - I²A Venn Diagram

6 Conclusions and Discussion

In summary, the LAASAM system significantly enhances the analyst's ability to make timely and efficient decisions, and to take action to protect and maximize the utility of space, ground, and air assets. LAASAM provides context for space-related events and can alert analysts to potential space-based events. LAASAM's unique I²A cognitive processing infrastructure establishes the foundation for assigning attribution to hostile activity and for analyzing emerging activities through the application of advanced data-agnostic acquisition, reasoning, and analyst I²As (see Figure 11).

The thrust of the LAASAM research has been to realize a CBHM architecture that provides enhanced Situational Awareness for space-based assets. The cognitive I²A processing infrastructure provides the required analysis, learning, and reasoning framework to provide LAASAM the ability to analyze, diagnose, and predict health, status, and situational awareness within a complex system of space assets. This CBHM approach ideally involves synergistic deployments of component health monitoring technologies as well as integrated reasoning capabilities. The LAASAM system described here organizes various system elements into a maintenance and logistics

architecture that governs integration and interoperation within the overall space asset system, between the on-board elements and their ground-based support functions, and between the system health management and the external maintenance and operations functions. In short, LAASAM represents enhanced Space Situational Awareness and Operational Management of the multiple assets contained with an overall space, air, and ground system consisting. LAASAM can not only identify problems that are caused by asset component failures, but can highlight system issues that are, or could be, caused by external forces, maximizing system availability and minimizing downtime.

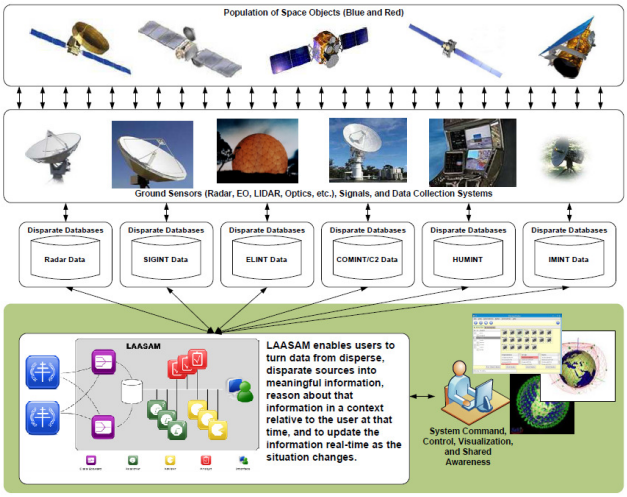

Figure 11 – Enhanced Space Situational Awareness using LAASAM

7 References

1. Crowder, J. 2010a. Flexible Object Architectures for Hybrid Neural Processing Systems. *Proceedings of the 12th annual International Conference on Artificial Intelligence*, Las Vegas, NV.
2. Crowder, J. 2010b. Operative Information Software Agents (OISA) for Intelligence Processing. *Proceedings of the 12th annual International Conference on Artificial Intelligence*, Las Vegas, NV.
3. Crowder, J. and Carbone, J. (2011a). Occam Learning through Pattern Discovery: Computational Mechanics in AI Systems. *Proceedings of the 13th annual International Conference on Artificial Intelligence*, Las Vegas, NV.
4. Crowder, J. and Carbone, J. (2011b). The Great Migration: Information to Knowledge using Cognition-Based Frameworks. *Springer Science*, New York, NY.
5. Crowder, J. and Carbone, J. (2011c). Recombinant Knowledge Relativity Threads for Contextual Knowledge Storage. *Proceedings of the 13th annual International Conference on Artificial Intelligence*, Las Vegas, NV
6. Crowder, J. and Friess, S. (2010a). Artificial Neural Diagnostics and Prognostics: Self-Soothing in Cognitive Systems. *Proceedings of the 12th annual International Conference on Artificial Intelligence*, Las Vegas, NV.
7. Crowder, J. and Friess, S. (2010b). Artificial Neural Emotions and Emotional Memory. *Proceedings of the 12th annual International Conference on Artificial Intelligence*, Las Vegas, NV.
8. Crowder, J. and Friess, S. (2011a). The Artificial Prefrontal Cortex: Artificial Consciousness. *Proceedings of the 13th annual International Conference on Artificial Intelligence*, Las Vegas, NV.
9. Crowder, J. and Friess, S. (2011b). Metacognition and Metamemory Concepts for AI Systems. *Proceedings of the 13th annual International Conference on Artificial Intelligence*, Las Vegas, NV.
10. Raskin, V., Taylor, J. M., & Hempelmann, C. F. 2010a. Ontological semantic technology for detecting insider threat and social engineering. *New Security Paradigms Workshop*, Concord, MA.
11. Scally, L., Bonato M., and Crowder, J. 2011. Learning agents for Autonomous Space Asset Management. *Proceedings of the Advanced Maui Optical and Space Surveillance Technologies Conference*, Maui, HI.
12. Taylor, J. M., & Raskin , V. 2011a. Understanding the unknown: Unattested input processing in natural language, *FUZZ-IEEE Conference*, Taipei, Taiwan.

Rapid Adaptation in Computational Organizations

S. Alqithami[1], **and H. Hexmoor**[2]
Computer Science Department, Southern Illinois University, Carbondale, IL, USA

Abstract – *Primarily, we describe a computational model of organizations where agents rapidly adapt to changing environmental conditions. We consider an organizational model with properties of roles, utilities, capabilities and norms (RUCN) in order to give the agents the opportunity to quickly adapt to any new environment. Moreover, a simulation volleyball game is implemented using Netlogo and has been thoroughly described in order to illustrate the model.*

Keywords: Fast adaptation, multiagent, computational model, organizations.

1 Introduction

Multiagent systems are very useful for building a system that can codify interactions among a group of independent and disparate players (i.e., agents). There are two kinds: a closed system is one with a single structure and fixed objectives. In contrast, an open system allows agents to enter and exit dynamically [16]. Moreover, dynamic capability evaluation is used to choose, a priori, the ability of agent instances to form an organization or complete the set of organizational requirements [14]. We will consider a closed multiagent system since the number of agents inside the organization in our model is constant.

Agents usually interact with each other inside a virtual organization. A virtual organization is a set of individuals or institutions anticipated to share resources by following sharing rules [9]. Virtual team or organization is a general word used for a task, organization or project, which is characterized by multiple locations (i.e., dispersion), division of responsibilities (i.e., empowerment), restlessness (i.e., acceptance of change), interdependence and all members' cooperation is needed. The changes inside the organization are stable, for it is dynamic in nature. The organizations may have a sufficient structure since it has been companied with a multiagency platform. Therefore, if it is able to transmit the capability from its current state to the next, it will consider a self-adapting organization [15].

In order to illustrate how the agents communicate with each other, we need to define self-adaptation in multiagent systems. Self-adaptation systems are able to change the agents' organization without a centralized, explicit, implicit, external or internal control. Such a system can be reorganized as a result of planning carried out by internal central control [17].

We will outline this paper by highlighting some previous work and related background research in section two. In the third section, we will illustrate the four main concepts of building rapid adaptive organization (roles, utilities, capabilities, and norms), and implement them in order to provide a simulation for a volleyball game. Finally, we present concluding statements in section four.

2 Background and Related Work

The organizational model used in this paper was first introduced in [11]. The author showed that the organization has a utility that is composed from productivity, synergy and fitness, represented in equation 1.

$$U\ (A,R) =\ P\ (A,R_i) + \left[\left(\frac{1}{sizeof(R_i)}\right)\sum S(i,j)\right] \quad (1)$$

A is an agent and R_i is the i^{th} role. The organization in general depends on the team capabilities (C), roles (R), departments (D), and norms (N). We also applied power to the edge (PE) algorithm to the organization because it is more empowered, superior, interoperable, agile, and has better shared awareness. The organization has been described as a set of capabilities that show the agents' capabilities in a specific range, roles for agents, departments that prescribe what a set of agents will do within specified roles, and norms of interaction among individuals. Moreover, the utility for the agent can be determined by productivity, synergy, and level of fitness. Some of the requirements that should exist for better achievement inside the organization are presenting a set of rules, organizational type, active environment, switching rules, monitoring agent performance, and verification of fitness.

Matson and DeLoach's approach to reorganization of Multiagent systems (MAS) originally involves the evaluation of the system's ability to perform a desired task [14]. Based on this evaluation, agents may decide to either proceed to satisfy the organizational goals, relax some goals, or abandon the process of reorganization and task acceptance altogether. The foundation of this approach is an organizational model consisting of goals, roles, agents, and capabilities. Based on this model, certain evaluative constraints are applied to the process. First, there is knowledge of which agents are available for inclusion in the system. Second, it must be determined what necessary capabilities exist in order to satisfy the demands of a role. Third, an assessment of the capabilities of all available agents must be made to determine

their respective qualifications for acceptance of a given role. To perform this step, the authors have devised a capability taxonomy rooted at the abstract level. Leaf nodes of this taxonomy represent concrete functions and capabilities of an agent, such as the types of sensors (sonar, infrared, light, etc.) and motivators (wheels, tracks, etc.) the agent is equipped with. Finally, limitations applied to roles must be taken into consideration.

Zhang and Zhang relegate the decision to the developer in order to choose the best subtasks [19]. Afterwards organization enters the formation process. In the negotiation process, the agents send their offers (i.e., bids) for finishing the job to the developer and each related subtask will appear in a separate bid. Then, the developer will start to select the optimal membership for the agent with the best offer from the first bid using a recursive best first research (RBFS) and heuristics algorithm. The agents may receive penalties for lack of commitment depending on the tasks that have not been satisfied as determined by the developer. Moreover, the agents are capable of making rational decisions during their operation because they incorporated the motivation quantities framework (MQ) for the task selection process. They model the agent performance, promise and penalty using the utility mapping function. Furthermore, they have mentioned a statistical model to predict and analyze the agent's behavior and the impact on the organization utility.

Furthermore, Zhang and Zhang represent five of the relationships among the three components of any organization builds [19]. The organization in general consists of individuals, tasks assigned to those individuals, and resources to accomplish certain tasks. The first type of relation is the precedence; it sorts the tasks inside the organization depending on specific mechanisms that map the temporal dependencies, like using the PERT chart to build a set of ordered pairs of tasks. Second, they represent commitment of recourses because most of the resources are required for specific tasks. The third is to assign personnel to accomplish certain tasks. Then, since most of the personnel inside the organization have different access to each other, networks among the different personnel are applied as the fourth relation. The fifth is skills that include all resources accessed by the individuals inside the organization. Moreover, the authors show that PECANS model might be applied in Thompson's theory of interdependence to show some extension to it [12].

THOMAS architecture focuses on the design of virtual organization to allow the multiagent systems in dynamic environments to deal with decomposition and abstraction. It offers a total integration to enable agents to transparently offer and request services from other agents or entities, and allowing external entities to interact with agents by using the services provided. There are three components in THOMAS: service facilitator (SF), platform kernel (PK) and organization manager service (OMS) that have the three main structural components: rule, norms, and unit [3].

Dignum provides a general overview of dynamic reorganization concepts and examines two metrics useful in examining MAS performance [6]; society utility and agent utility. Society utility is further decomposed into the success of interactions, roles, and structures in the system. Agent utility is not clearly defined, as it differs from agent to agent in heterogeneous agent systems. In addition to these utility metrics, several types of reorganization "maneuvers" are classified [7]. The first of these, pre-emptive reorganization, is a viable option in unpredictable environments where possible, or likely, events can be prepared for in order to take full advantage of them. Protective reorganization attempts not to take advantage of possible future events, but instead works to limit the negative effects of such events on the system. Exploitive reorganization takes place after the fact, and seeks to benefit from events that have already taken place. Finally, corrective reorganization attempts to lessen the damage caused by events which have previously occurred in order to maintain system usefulness. Specific methods for performing adaptation are not present in [7] but it provides many useful ideas for developing new methods or for elaborating on existing methods [2].

3 Fast adaptation

The organizational adaptation research is challenging since it accounts for multiple player interactions inside the organization. Joshua Epstein has reported a model that permits autonomous agents to be endogenously created in internal organizational structure in order to adapt optimally to a dynamic environment [8]. Wu, et. al. [18] report on a relevant research by building an organizational adaptation with suitable centralization instead of a hierarchy algorithm using four proportions: agility, robustness, resilience, and survivability.

Before we proceed, we should have a better understanding of the four central concepts of utility, norms, role, and capability that we are going to use in order to build this model. Utility is different among agents inside the organization and the outcome space is very large, which makes it difficult to predict actual levels. Our approach is to observe agents' behavior over time and to build a scale for it [4]. The second concept is norms, which are similar to rules that restrict and describe behaviors most of the time for multiagent systems [10]. In different ways of formulating norms, they can be used to guide selection of different roles because they are able to interact with normative multiagent systems [1]. Roles are used for the organizational function in order to specify the assignments for the agents inside. Finally, capabilities usually cause reorganization inside the team itself because they are dynamically changing over time, and here, they have been defined as the ability to show information in specific areas [14].

After we have applied the main concepts for building a multiagent model, we will discuss implementation issues outlined in our model. Our implemented system uses the

Netlogo platform, which is a java based cross-platform testbed for simulating natural and social phenomenon in order to build a multi-agent program modeling environment. A volleyball game will be used as an example to illustrate the issue in an obvious manner, as in Figure 1.

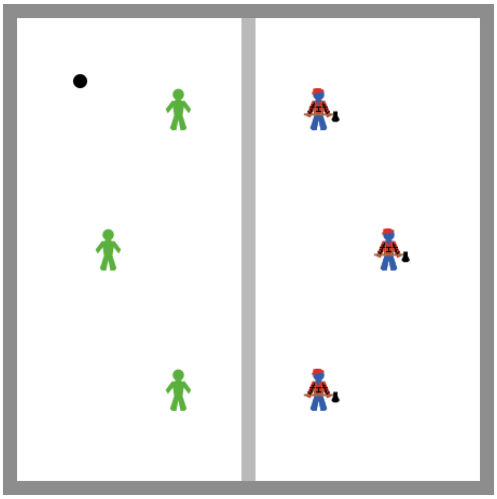

Figure 1. A screen snapshot of Volleyball demonstration in Netlogo

We implemented two teams as illustrated in Figure 1. The one in the right which represents agents in the shape of lumberjacks is the USA team, and the other in the opposite side which represents agents in the shape of people is the KSA team. The idea of using these shapes is to differentiate between teams. Also, we have implemented a small number of players because it is the least number of personnel needed to illustrate an organization and to keep the game simple. The positions for the agents inside the simulation were distributed as randomly as possible (i.e., serendipitously) as in the real world. The players interact with each other and with the ball according to the game's theoretic payoff matrix shown in Table 1.

Table 1. The game's theoretic payoff matrix between the two teams

		USA		
		P1	**P2**	**P3**
KSA	**P1**	0 , 0	1 , 1	2 , 2
	P2	1 , 1	0 , 0	1 , 1
	P3	2 , 2	1 , 1	0 , 0

As shown in Table 1, the set of $< P_1, P_2, P_3 >$ represents different players in each team, and their payoffs will be differentiated depending on the players with whom they are interacting. Thus, the player will get a higher payoff toward the opposing team if his main concepts are higher than the opponent player, detailed in table 1. However, it might be easy to find a strict pure-strategy Nash equilibrium precisely in this manner because one agent has the best response to the strategies of the others inside its team [13]. Besides, the only way to have a chance of scoring in the current moment, whether the opponent gets a fair payoff or not, is to let the player get the ball into the opponent's field with a better payoff when the distances among them goes farther, following the algorithm showing in Figure 2.

```
PLAYERS'-PAYOFFS
1  j = 1
2  for i = 1 to 3
3       if P[i] = Ball
4            if payoff for P[i] ≥ 1
5                 while j ≤ 3 and P[j]s' payoffs ≥ 1
6                      Pass to P[j] with higher payoff
7                      j = j+1
8                 Pass the ball to the opponent field
9            else
10                Pass to P with higher payoff
```

Figure 2. General algorithm for each player to adapt a new situation

In Figure 2, we show that if any of the players ($P[i]$) is in possession of the ball, where i, and j are different players, he will examine his chances of scoring depending on our four concepts for fast adaptation. The players may interact with each other by passing the ball amongst themselves until it reaches a player who has a higher payoff or a player with a better payoff is their distance. By the time the ball reaches the player with the higher payoff, he will pass the ball to the opponent's field to have a higher chance of scoring, as demonstrated in Figure 3.

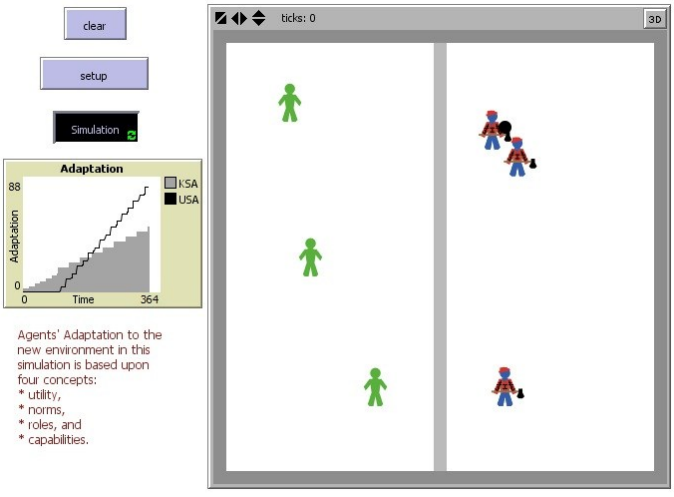

Figure 3. A screenshot of volleyball implementation after start of simulation

Any agent inside any of the small organizations (i.e., team) measures the distance between itself and the ball to

check whether the ball is within its allowed distance or not; if so, the agent (i.e., the player) will move toward the ball considering itself responsible for controlling the ball and announcing that to the closest agent in order to stop him from a possible collision. When the agent controls the ball, it will measure the distance between its position and the opponent's field again to determine if there is a possibility of scoring or not, and also to measure the distance to the closest agent inside the team because the other player may have a better payoff in scoring in the opponent field than itself.

As results, the plot in Figure 3 shows that the rates of adaptation change after the agent finds any other objects (i.e., team member, or a ball) within its range, and it rises over time when any of the agents interact with them. The gray bars represent the KSA team and the black line represents the USA team. The adaptation of the KSA team starts when any of the agents recognize the ball within their proximity and it is set stable because there are no interactions occurring. However, the adaptation rises when the agent catches the ball and starts to use any of the four adaptation concepts in its move. When the agents reach similar capabilities and norms, their adaptations will increase rapidly until it reaches some threshold point where this increase plateaus. It will resume increasing periodically when they start to implement the other two concepts in their interaction (i.e., utility and roles). In contrast, adaptation will stabilize when none of the agents inside the team has any interactions whether with the ball or with other agents.

As with the previous example illustrates, implementing the four concepts of utilities, roles, capability, and norms inside an existing organization improves the performance of the members inside it in order to rapidly adapt to any new environment including any variations to in the ball and player configurations.

4 Conclusions

We have demonstrated how agents inside a specific organization may adapt to a new environment in a short period of time, and then start to interact with other agents inside the same organization. A volleyball game has been simulated in Netlogo in order to give a concrete understanding of the issue in a simple way and to make it easier to get the results out of it. Moreover, we have found that after considering the four main concepts we modeled inside the organization (utility, role, capability, and norms), agents are able to rapidly adapt to their new environment. This model (i.e. RUCN) can capably replace previous models that have been done inside any organization for the sake of fast adaptation among its members or a new environment.

5 References

[1] G. Boella, J. Hulstijn, and L. Torre, *"Virtual Organization as Normative Multiagent System,"* in the 38th Hawaii International Conference on System Science, 2005.

[2] K. Carley & L. Gasser, *"Computational organization theory,"* in Multiagent systems: A modern approach to distributed artificial intelligence, G. Weiss, Ed. Cambridge, MA: MIT Press, pp. 299–-330, 1999.

[3] C. Carrascosa, A. Giret, A. Julian, M. Rebollo, E. Argente, and V. Botti, *"Service oriented mas: An open architecture,"* in the 8th Int. Conf. on Autonomous Agents and Multiagent systems, 2009, pp. 1291-1292, ACM press.

[4] U. Chajewska, D. Koller, and D. Ormoneit, *"Learning an agent's utility function by observing behavior,"* in the Eighteenth International Conference on Machine Learning (ICML), 2001, pp. 35-42.

[5] S. DeLoach, and E. Matson, *"An organizational model for designing adaptive multiagent systems,"* in the AAAI-04 Workshop on Agent Organizations: Theory and Practice (AOTP), 2004, pp. 66-73.

[6] V. Dignum, *"A model for organizational interaction: based on agents, founded in logic,"* 2004

[7] V. Dignum, F. Dignum, V. Furtado, A. Melo, and L. Sonenberg, *"Towards a simulation tool for evaluating dynamic reorganization of agents societies,"* in WS. on Socially Inspired Computing, 2005

[8] J. Epstein, *"Generative social science: Studies in agent-based computational modeling,"* Princeton University Press, 2007.

[9] I. Foster, C. Kesselman, and S. Tuecke, *"The anatomy of the grid: Enabling scalable virtual organizations"*. International Journal of Supercomputer Applications, 15, 3, 2001.

[10] S. Harmon, S. DeLoach, and Robby, *"Abstract requirement analysis in multiagent system design,"* in the IEEE/WIC/ACM International Conference on Intelligent Agent Technology (IAT '09), 2009, pp. 86-91.

[11] H. Hexmoor, *"Oversight of reorganization in massive multiagent systems";* International journal of Multiagent and Grid Systems (IMCST), 2011.

[12] D. Krackhardt, and K. Carley, *"A PCANS model of structure in organization,"* in the 1998 International Symposium on Command and Control Research and Technology, Vienna, VA: Evidence Based Research, 1998, pp. 113-119.

[13] K. Leyton-Brown, and Y. Shoham, *"Essentials of game theory: A concise multidisciplinary introduction,"* in Synthesis Lectures on Artificial Intelligence and Machine Learning,1, 2, pp. 88, 2008.

[14] E. Matson, and S. DeLoach, *"Using dynamic capability evaluation to organize a team of cooperative, autonomous robots,"* in the 2003 International Conference on Artificial Intelligence, pp. 744-749, 2003.

[15] E. Matson , and S. DeLoach, *"Formal transition in agent organizations,"* in IEEE International Conference on Knowledge Intensive Multiagent Systems (KIMAS '05), 2005.

[16] S. Rodriguez, B. Perez-Lancho, J. De Paz, J. Bajo, and J. Corchado, *"Ovamah: multiagent-based adaptive virtual organizations,"* in 12th International Conference on Information Fusion, pp. 990-997, 2009.

[17] G. Serugendo, M. Gleizes, and A. Karageorgos, *"Self-organization in multi-agent systems."* Knowl. Eng. Rev., 20, 2, pp.165-189, 2005.

[18] J. Wu, D. Sun, B. Hu, and Y. Zhang, *"Organizational adaptative behavior: The complex perspective of individuals-tasks interaction."* Institute for Computer Sciences, Social Informatics and Telecommunications Engineering, 4, 1, pp. 28-38, 2009.

[19] Q. Zhang, and X. Zhang, *"Study of virtual organizations using multiagent,"* in the fourth international joint conference on Autonomous agents and multiagent systems AAMAS, pp. 1147, 2005.

Norm-Based Behavior Modification in Reflex Agents

Gustavo A. L. de Campos, Emmanuel S. S. Freire, Mariela I. Cortés
Computer Science Department
Universidade Estadual do Ceará (UECE)
Fortaleza, Brazil
gustavo@larces.uece.br, savio.essf@gmail.com, mariela@larces.uece.br

Abstract—**Norms in multi-agent systems are used to regulate the behavior of agents, organizations and sub-organizations in their environments during a period of time. Much of the work on norms focuses on the specification and maintenance of normative system. Little work concentrate on the level of individual agents as the impact of norms on the different types of intelligent agent programs, as the internal modifications in the agents´ decision processes and the background information necessary for rationality in an environment governed by rules. This paper is a contribution in this direction to the case of simple reflex agent based on condition-action rules. An approach to extend this type of agent was formalized and validated it in an implementation of a simple world in the Prolog System. The results demonstrate that the approach is adequate and must be extended to consider other kinds of intelligent agents, as is the case of the goal-based agents and the utility-based agents.**

Keywords- Reflex agent architectures; Deontic concepts; Norms

I. INTRODUCTION

Multi-agent Systems (MAS) are becoming an interesting research in computer science area as a paradigm for development and creation of software systems [1] [2]. Long time MAS have been successfully applied to the development of different types of software in academia and industry [1] [2], a fact that encourages the use of this technology in complex systems.

MAS can be understood as societies in which autonomous and heterogeneous entities can work together. The main element of MAS is the agent entity and very different definitions are proposed to its concept. According to [3], an agent is an entity capable of perceiving its environment through sensors and acting upon that environment through actuators. Unlike objects, agents are entities (i) autonomous and not passive, and (ii) able to interact through messaging and not the explicit invocation of a task, as in the case of objects [4].

There are several ways of classifying agents, but the most accepted classifies agents according to their architecture [3]. The agent architecture specifies how is the process of deliberation and choice of action to be taken, according with the agent perceptions [5]. Internal architectures play a central role in the development process of agents, because it is used as a guide that determines its properties, attributes, mental and behavioral components, determining thus a different implementation for each case.

The creation of the agent function, which sets the mapping between the channels of perception and action, is one of the important contributions of Artificial Intelligence. Depending on its function on the environment, the choice of the agent architecture may not be a trivial task. Mainly, the appropriateness of the properties associated with the internal architecture of the agent and the properties of the external environment where the goals should be conducted is crucial.

In order to cope with the heterogeneity, autonomy and diversity of interests among the different members, governance (or law enforcement) systems have been defined. The governance systems define a set of norms (or laws) that must be followed by the entities in the system. Norms provide a means for regulating the agents' behavior by describing their permissions, prohibitions and obligations [6].

Norms are used to regulate the behavior of the agents in MAS by describing the actions that can be performed or states that can be achieved (permissions), actions that must be performed or states that must be achieved (obligations), and actions that cannot be performed or states that cannot be achieved (prohibitions). Thus, norms represent a way for agents to understand their responsibilities and the responsibilities of the others. Norms are used to cope with the autonomy, and are useful to regulate the different interests and desires of the agents that cohabit the system.

As claimed by [7], much of the work developed on norms focuses on the specification and maintenance of normative system, i.e., the research efforts has been concentrated at the macro level of the MAS. Noticing that very little work has been done on the level of individual agents, they proposed some adaption in BDI agents to solve tasks in open environments with the presence of norms of four types.

We believe that there is a demand for similar work for the cases of other different types of intelligent agent programs, that the effort of research must be concentrated on the internal modifications in the agents´ decision processes and the background information, that are necessary for an rational agent in an environment governed by rules. So, this paper is a contribution in this direction to the case of simple reflex agent based on condition-action rules. It describes an adaptation in the internal architectures of these reflex agents so as they can comply with two types of norms.

We formalize the approach employing the Prolog System. It was validated in an implementation of a simplified version of a vacuum cleaner where the agent can be obligated and/or prohibited to perform some actions in the environment. The

results demonstrate that the approach is adequate and must be extended to consider other kinds of intelligent agents, as is the case of the goal-based agents and the utility-based agents.

The paper is structured as follows. Section 2 briefly presents the reflex agent architecture. The concepts related to norms are detailed in Section 3. Section 4 describes how to combine rightly the use of reflex agent architectures with norms. A case study is showed in Section 5 and, finally, conclusions and future works are discussed in Section 6.

II. Simple Reflex Agent

The internal architectures of agents can be categorized based on reactive and proactive foundations. A reactive agent must attend continuously to changes in their environment, through the selection of actions, typically based on the current perception of the environment and additional knowledge about the possible actions that are best suited to different conditions in which the environment can be.

A proactive agent can take the initiative and select actions from a set of possible atomic actions or plans, and create sequences of actions that attain goals in the environment task. In this context, [3] describe the principles underlying almost all intelligent systems through programs for reactive and proactive agents. This paper focuses norms related to reflex agent, thus, the main characteristics of the simple reflex agents are briefly presented below.

According to [3], a simple reflex (or reactive) agent is the simplest type of agent. This architecture assumes that at any time, the agent perceives information about the state of the environment through sensors and based on rules in the form "if condition then action", it selects the most adequate action for the current perception. The agent performs the selected action upon the environment through actuators. The Figure 1 presents a schematic diagram of the simple reflex agent, synthesizing the Russell&Norvig´s ideas related to reactive agent program, as well as the abstract architecture of the this agent, which was proposed by Wooldridge in [8].

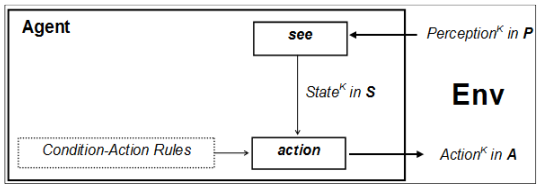

Figure 1. Schematic diagram of the simple reflex agent

This synthesis assumes that at any instant K:

(1) through sensors, the agent receives information from the environment, i.e., perceptions defined on a set, P = {Perception1, ..., Perceptionn}, of n possible perceptions from the environment (Env);

(2) a perception subsystem, see: P → S, that processes each perception in P and maps to one of m possible states, S = {State1, ..., Staten}, that are representations of aspects in the perceptual information that are accessible to the agent;

(3) a subsystem for decision making, action: S → A, that processes the states in S and selects, according to an specific rule of the set of condition-action rules, one of the l actions in the set of possible actions for the agent, A = {Action1, ..., Actionl};

(4) through actuators, the agent sends the selected action for the environment;

(5) in the interaction K+1, the agent initiates another cycle involving the perception of the world through the function see and the selection of an action to be executed by the function action.

The condition-action rules consist in supplemental information that the agent uses during the decision making process. They can be seen as a set of common associations which are observed between certain conditions established from the descriptions of States in S and certain Actions in A. The information about the agent´s goals is not explicitly considered in this architecture, but implicitly in the condition-action-rules. Thus, the agent´s designer defines these rules having in mind the performance measure that will be applied to the agent. In this context, it is expected that, in an adequate environment, if the rules are adequate, then the agent will achieve its objectives and, consequently, it will be well evaluated.

III. Norms for Agents

The norms are used to restrict and guide the behavior of agents, organizations and sub-organizations during a period of time. In this sense, a norm includes a set of sanctions applied to the entities that violated or fulfilled the norm [9]. In this section, the main elements that compose the norm are explained considering the types of norms and their representation.

A. Elements of Norms

Bellow we describe the main elements which compose a norm, based on a survey of existing specification and implementation languages for norms [9].

- Deontic Concepts: the deontic logic refers to the logic of requests, commands, rules, laws, moral principles and judgments [10]. In multi-agent systems, such concepts have been used to describe the constraints for the behavior of agents in the form of obligations (what the agent must execute), permissions (what the agent can execute) and prohibitions (what the agent cannot execute).
- Involved Entities: considering that the norms are defined to restrict the entities´ behavior, the identification of related entities is essential. The norm may regulate the behavior of individuals (for example, a particular agent, or an agent, while playing a particular role), or the behavior of a group of individuals (for example, all agents playing a particular role, groups of agents, groups of agents playing roles or all agents in the system).
- Actions: once a norm is set to restrict the behavior of the entities, it is important the clear specification of the actions that are being regulated. Such actions may be communication, usually represented by sending and

receiving a message, or non-communicative actions (such as access and modify a resource, get in an organization, move to another environment, etc.).

- Activation Constraints: a norm have a period of time in which its restrictions must be fulfilled, but only when this norm, is active. Norms may be activated by a constraint or a set of constraints that can be: the execution of actions, the definition of specific time intervals (before, after or in between), the reaching of system states or temporal aspects (such as dates) and also the activation/deactivation of other norm and fulfillment/violation of a norm.
- Sanctions: when a norm is violated the entity may suffer a punishment, and when a norm is fulfilled, the entity involved may receive a reward. Rewards and punishments are referred to as sanctions and should be related to the norm specification.
- Context: the norms are usually defined in a determined context that determines the application area. The norm may, for example, be described in the context of a specific environment and must be filled only by agents in execution in the environment. Similarly, a norm can be defined in the context of an organization and fulfilled only by the agents that play a role in the organization.

B. Norm Types and Representation

This paper considers two types of norms of four possibilities discussed in [7]. The classification scheme considers whether norms are obligations or prohibitions, and whether they refer to states of the world or to particular actions. In this context, Table 1 presents the four types of norms obtained and a description about what the agent should do when accepting a norm type.

TABLE I. THE TYPES OF NORM AND THEIR DESCRIPTIONS

Norms Types		Description
1	obligation(***p***)	agent must try to achieve certain world state ***p***
2	obligation(***a***)	agent must try to execute certain actions ***a***
3	prohibition(***p***)	agent must try to refrain from achieving a state ***p***
4	prohibition(***a***)	agent must try to refrain from executing an action ***a***

Each type of norm has activation and expiration conditions as, for instance, a well defined validity period of time, indicating when the norm is in force and when it ceases to be in force. In our approach, as [7], we leverage representational concepts from the formalization of [11]. This formalization includes notions of activation and expiration of a norm: norm(Activation, Expiration, Norm), where Activation is the activation condition for the norm to become active, Expiration is the expiration condition to deactivate the norm, and Norm is the norm itself.

It is important to note that we are not concerned, at this point, with handling more complex norm representation schemes. Moreover, in order to facilitate the creation of concrete agent behaviors, in compliance with a set of norms, this paper approaches only norms of Types 2 and 4.

IV. MODIFYING REFLEX AGENTS TO ADOPT NORMS

In this section we examine how norms can influence the choice of actions according to the internal architecture of a simple reflex agent.

A. An Outline of the Approach

Purely reflex agents should be able to quickly respond to changes in the environment. This kind of agent may be inserted into an environment that has a specified set of norms that restrict their actions. As defined by [9], the norms are intended to restrict the behavior of agents applying sanctions when they are violated or fulfilled. Therefore, the norms of an environment should not be able to avoid the execution of certain action, but rather to penalize or reward an agent if the action taken by it is prohibited or obligated. Therefore, if the set of norms defined in the environment is not considered in the condition-action rules, an agent can be penalized if it performs a prohibited action.

In order to avoid the violation of the simple reflex agent architecture, our approach proposes to consider the information about the set of norms as an extension of the condition-action rules. It involves the definition of three different groups of condition-action rules. Each group is associated with one deontic concept and considers the sanctions linked to each norm, that is:

- Obligation Rules Group: specifies the rules related with the actions that must be performed by the agents. If an event of environment matches with a rule in this group, it must necessarily be performed by the agent;
- Prohibition Rules Group: specifies the rules that are related with the actions that cannot be performed by the agent. If an event of environment matches with a rule in this group, the rule will not be executed by the agent;
- Permission Rules Group: specifies the rules related with the actions that can be executed. If an event of environment matches a rule set out of this group, it may or may not be executed by the agent.

Figure 2 shows the schematic diagram of the simple reflex agent in an environment with norms. We added two new groups in the agent´s action selection mechanism, corresponding to the representation of the information about its obligations and prohibitions. Our approach considers that if an action is obligated, then the agent must perform that action only if it is not prohibited. If an action is prohibited, then the agent must perform another action, different from the prohibited action, which is permitted and rational. If there is not an action that is obligated and prohibited, then the agent must perform a permitted action which is rational, as would do a well designed simple reflex agent in an environment without norms.

The function Simplex-Reflex Agent outlined in the sequence of five steps in Section 2 must be adapted to become valid in the case norms were activated. In order to avoid conflicts between rules from the different groups, Step 3 of the sequence must respect the following rules:

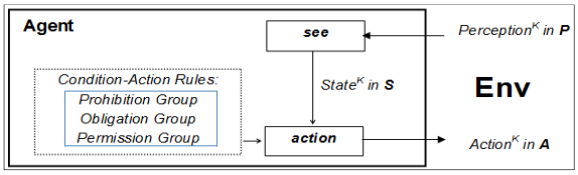

Figure 2. Schematic diagram of the simple reflex agent with norms

(3.1) first, it searches for rules in the Obligated Rules Group to find those actions that must be performed in the environment and are not prohibited;

(3.2) if there is some prohibited action, then the function inhibits rules in the Obligated Rules Group and searches for rules in the Prohibited Rules Group to find those actions that are not prohibited and can be performed, according with the environment estate conditions;

(3.3) if there are not any prohibition, the function selects the action that must be performed as indicated by the obligation norm; and

(3.4) finally, in the case where there not exist any obligations and prohibitions, the function searches for rules in the Permission Rules Group in order to find some action that can be performed, according with the environment estate conditions.

The strategy to select the action that is implicit in the approach considers that the rational behavior is achieved when the agent is able to maximize the rewards that are consequences of: (a) the selection of an obligatory and not prohibited action; (b) the non-selection of a prohibited action, and (c) the selection of permitted actions, those which are adequate with the environment state conditions and with the agent´s performance measure.

B. *Norms Outcomes*

In this section, we consider the agent accepts a norm immediately as it perceives it and that the behavior modification must ensue according to activation and expiration conditions of the norm. More specifically, the required change in the behavior of the agent that accepts a particular norm should occur according with the conditions of activation and expiration. For instance, in the case of an agent that is goal oriented, it can be necessary that the agent add the goal of achieving a state p, when a particular norm of obligation is activated, and then, when the norm is expired, delete this goal.

In the case of simple reflex agents, Tables 2 and 3 summarize all norm combinations of activation conditions (AC) and expiration condition (EC), and their outcomes respectively for norms Types 2 and 4, considered in this paper and highlighted in Table 1. The AC and EC columns give the truth-value of these conditions at the time the agent accepts the norm.

When both AC and EC are true (row 1 in Tables 2 and 3) results in the norm being ignored, as its expiration condition has already elapsed. When AC is false but EC is true (row 4 in Tables 2 and 3), norms are also ignored since, again, they have already expired. When an agent accepts an obligation, if the AC is already true (row 2 in Table 2) it must react to execute the action specified in an obligation(a) if the action is not specified in an prohibition(a). While for a prohibition (row 2 in Table 3), it must refrain from executing the offending action, and try to execute an action that is permitted and adequate to the environment conditions and to its performance measure.

TABLE II. NORM TYPE 2 - OBLIGATION(A).

AC	EC	Outcome
True	True	**(1)** Ignore norm
True	False	**(2)** Execute action ***a*** if ***a*** is not prohibited; otherwise execute an action that is not prohibited, but is permitted and adequate
False	False	**(3)** Ignore norm
False	True	**(4)** Ignore norm

TABLE III. NORM TYPE 4 – PROHIBITION(A).

AC	EC	Outcome
True	True	**(1)** Ignore norm
True	False	**(2)** Suppress rules in the Permitted Group that include action ***a*** and execute an adequate permitted action
False	False	**(3)** Ignore norm
False	True	**(4)** Ignore norm

We are considering, the agent must ignore the norm, if AC and EC are false (row 3 in Tables 2 and 3). We are considering that in the situation that the norm has not yet been activated, the agent has already been programmed for the activation of the norm in the future. Therefore, we are not considering the situation that the agent is able to include the proposed scheme at the moment it perceives a norm, that is, when both AC and EC are false.

C. *Formal Description of the Approach*

This section presents, first, a declarative description of the reflex agent program shown in Figure 1, that is, in an environment without norms and, second, an extension of this description for the case in which the agent perceives norms Types 2 and 4, as shown in Figure 2. The Prolog language was employed to formally describe the agent programs in both cases. The Prolog definition agent/2 describes the agent program discussed in Section 2:

```
agent(P,A):- see(P,S), action(A).
```

where the definition see/2 implements the perception subsystem, as indicated by Step 2 of the sequence of five steps illustrated in Section 2, it inserts, in the Prolog´s base, some predicates employed to represent the environment state; and the definition action/2 implements the decision-making subsystem of the agent program, as indicated by Step 3 in the sequence, i.e.:

```
action(A):- do_permission(A),!.
```

The definition do_permission/1 implements the Permission Rules Group for the agent in an environment without rules, which are condition-action rules highlighted in Figure 1. As mentioned, these rules depend of the agent´s task environment and must be defined according with the available knowledge about the actions that are most adequate to be executed when the environment is under certain conditions. The next section

of this paper illustrates this group of rules for the case where the agent is a vacuum cleaner in a very simple environment.

As the Subsection 4.1 indicates in the extension of Step 3 in Section 2, that is, Steps 3.1-3.4, in the case there are norms in the environment, the definition do_permission/1 will be accessed by the decision making subsystem only when active norms of Type 2 are not available. When some active norm is available, the action must be executed immediately if it is not a prohibited action by a norm of Type 4. If some action is a prohibited action, the rules in the do_permission definition must be accessed in order to indicate for the agent those not prohibited actions that are adequate with the environment conditions.

So, in order to implement the above procedure, our approach proposes that, instead of access exclusively the rules in do_permission/1, the decision making subsystem considers the three groups of rules illustrated in Figure 2 and the sequence of steps 3.1-3.4. The definition do/1 below consists of an extension in the action function, i.e:

```
action(A):- do(A),!.
```

to consider these new possibilities:

```
do(A):- do_obligation(A).
do(A):- do_prohibition(A).
do(A):- do_pemission(A).
```

where the definitions do_obligation/1 and do_prohibition/1 can be declared without concern with a specific domain and are related, as we saw that the agent will execute an action which is obligated only if it is not prohibited.

The three rules bellow compose the Obligation Group and are in accordance with what was discussed in the Section 4.2 and, more specifically, in the Table 2, that identifies the changes that are necessary to a simple reflex agent program for the case in which the environment imposes norms of Type 2 for the agents:

```
do_obligation(A):-
        norm(AC1,EC1,obligation(Ac)),
        is_True(AC1), is_False(EC1),
        norm(AC2,EC2,prohibition(Ac)),
        is_True(AC2), is_False(EC2),!,
        do_prohibition(A).
do_obligation(A):- norm(AC,EC,obligation(A)),
                   is_True(AC), is_False(EC),!.
do_obligation(A):- norm(_,_,obligation(_)),
                   do_prohibition(A).
```

where the predicates is_True/1 and is_False/1 must be specified according, respectively, with the activation or expiration conditions being considered in the arguments of the predicates stating norms.

The two first rules of the above definition are related to the situation described in row 2 of Table 2, that is, in which the activation condition (AC1) is True and the expiration condition (EC1) is False in some norm of Type 2. The first rule considers the case in which another norm of Type 4 is in the same situation (AC2 = True and EC2 = False) and the action which is obligated is, simultaneously, prohibited. The outcome of this situation is that the agent must perform an action (A) that is not prohibited, but is permitted and adequate.

The second rule considers the case in which none norm of Type 4 is active, that is, in which the agent must perform the action that is obligated by the active norm of Type 2. Finally, the third rule in the definition is related with the rows 1, 3 and 4 of Table 2. In these situations the agent must ignore the obligation norm and perform an action that is permitted and adequate, according with the conditions of the environment and the rules in the definition do_permission/1.

The two rules bellow compose the Prohibition Group and are in accordance with what was discussed in the Section 4.2 and, more specifically, in the Table 3, that identifies the changes that are necessary to a simple reflex agent program for the case in which the environment imposes norms of Type 4 for the agents:

```
do_prohibition(A):- norm(AC,EC,prohibition(Ac)),
                    is_True(AC), is_False(EC),!,
                    do_permission(A), not(A=Ac),!.
do_prohibition(A):- norm(_,_,prohibition(_)),
                    do_permission(A),!.
```

The first rule of the above definition are related to the situation described in row 2 of Table 3, that is, in which the activation condition (AC) is True and the expiration condition (EC) is False. The outcome of this situation is that the agent must perform an action (A) different from the prohibited action (Ac), but which is permitted and adequate, according with the conditions of the environment and the rules in the definition do_permission/1.

The second rule in the definition is related with the rows 1, 3 and 4 of Table 3. In these situations the agent must ignore the prohibited norm and performs an action that is permitted and adequate. So, this last rule completes the second group of rules which the approach supposes be a necessary modification to produce a rational behavior of a simple reflex agent in an environment with the presence of norms of the Types 2 and 4.

V. CASE STUDY

This section describes the third group of rules, Permission Rules Group, for a very simple problem, but still very useful to illustrate the ideas discussed in the last section. We specify the rules in the definition do_permission/1 for the case in which the agent is a vacuum cleaner in a world containing only two rooms. So, employing this specific definition, we used the Prolog System to: (1) describe experiments involving the agent in the world without and with the presence of norms, (2) record the history of the vacuum cleaner in the world, and (3) measure its performance.

Considering the vacuum cleaner world with only two rooms, where each room can be clean or dirty, in our experiments the perceived information of the environment were represented by the following atoms in Prolog: roomA, roomB, clean and dirty. So, we assume the existence of eight possible perceptions for the environment (P), which were represented by eight lists of three atoms in Prolog, i.e.:

```
P = {[roomA,dirty,dirty], [roomA,dirty,clean],
     [roomA,clean,dirty], [roomA,clean,clean],
     [roomB,dirty,dirty], [roomB,dirty,clean],
     [roomB,clean,dirty], [roomB,clean,clean]}.
```

Additionally, we assume that the agent perception is local, i.e., see/2 perceives only the room where it is located and the state of the room. So, we assume the existence of four possible internal states for the environment (S), which were represented by four lists of two atoms in Prolog, i.e:

S = {[roomA,dirty], [roomA,clean],
[roomB,dirty], [roomB,clean]}.

In each of the eight states of the world (P), there are three possible actions for the vacuum cleaner (A), which were represented by three atoms in Prolog, i.e:

A = {suck, right, left}.

In the beginning of each experiment the vacuum cleaner does not know the world configuration in terms of dirt. We considered that when the world is without the presence of norms, the measure of performance evaluation offers the reward of one point per each square clean (+1) and penalizes with the loss of one point per each movement (-1). In the case of the presence of norms in the world, the measure must be adapted in order to consider the rewards (+points) and the penalties (-points), which are consequences of the agent accepting or rejecting some norm.

A. Environment without Norms

In the Case 1, there are no norms in the world. The Prolog definition below describes the simple reflex vacuum cleaner:

```
vacuum_cleaner(P,A):- see(P,S), action(A).
```

where the terms P, S and A were defined generically in Section 2 and in the specification of the environment properties outlined in the introduction of this section; see/2 has been specialized to deal with the atoms and lists employed to represent the sets P and S; action/1 has been specialized to deal with the set A and with the specific rules do_permission/1 for this world, i.e:

```
action(A):- do_permission(A),!.
```

The definition do_permission/1 implements the Permission Rules for the agent in an environment without norms, are the condition-action rules highlighted in Figure 1. For this Case 1, was sufficient to generate a definition with four Prolog phrases, i.e:

```
do_permission(suck):- in(Romm),  is(Room,dirty).
do_permission(right):- in(roomA).
do_permission(left):-  in(roomB).
do_permission(no_op).
```

where the predicates in/1 and is/2 were used to represent the conditions in the antecedents of the rules and are known by the agent at the moment when the agent perceives the environment by see/2. Table 4 highlights the episodes performed by vacuum_cleaner/1 in six interactions with an environment without norms where, initially, the agent is in room-A, and room-A and-B are dirty.

The two first columns in the table identify the perceptions and actions of the agent in each interaction. The third and fourth columns identify the values of performance measure per episode (Ep) and history (H). Since the perception is local and at the agent does not have an internal state to avoid unnecessary movements (interactions four to six), there were no surprises in the behavior of the agent. The set of rules do_permission/1 provided a rational behavior for the agent, except for the unnecessary movements that caused a negative performance evaluation.

TABLE IV. PERFORMANCE IN A WORLD WITHOUT NORMS

P	A	Ep	H
[roomA,dirty,dirty]	suck	1	1
[roomA,clean,dirty]	right	-1	0
[roomB,clean,dirty]	suck	1	1
[roomB,clean,clean]	left	-1	0
[roomA,clean,clean]	right	-1	-1
[roomB,clean,clean]	left	-1	-2

B. Environment with Norms

In the second case (Case 2), the environment is governed by norms of the Types 2 and 4. Consider that the measure of evaluation should apply the appropriate sanctions, as the fulfillment or not of the established norms. In this particular example, the measure offers with reward three-point (+3) for the fulfillment of an obligation and two points (+2) for the fulfillment of a prohibition. In any other situation, the measure behaves in accordance with the specification realized for the Case 1. In our experiments, first, we considered a norm of Type 2 in which the environment requires the execution of a specific action by the vacuum cleaner during a period of time. For instance, the predicate below states that "The agent must suck the room-A from 4:00 to 6:00 a.m.":

```
norm(roomA, time([4,6]), obligation(suck)).
```

where the first argument of the statement identifies the condition of activation (AC), the second identifies the condition of expiration (EC), and the third is the action to be performed.

The definition do_obligation/1, which implements the Obligation Rules, are necessary for the vacuum cleaner in a simplified environment regulated by the norm stated as above. Assuming that no prohibition norm is present, the first rule in the definition do_obligation/1 will never be activated. However, the other two rules will be activated according to the truth value of AC and EC, which are obtained by the evaluation of the predicates is_True/1 and is_False/1 specifically for the above obligation norm in the vacuum cleaner world:

```
is_True(Room):-  in(Room).
is_False(time[T1,T2]):- clock(Hour),
                        Hour >= T1, Hour =< T2.
```

where in/1 is the same predicate which the agent employs to represent where it is located and clock/1 is a predicate which represents the agent´s simplified clock in the experiments.

Table 5 highlights the episodes performed by the vacuum cleaner in seven interactions with an environment with a norm of Type 2, as stated above.

TABLE V. PERFORMANCE IN A WORLD WITH NORM OF TYPE 2

P	A	Ep	H
[roomA,dirty,dirty]	suck	1	1
[roomA,clean,dirty]	right	-1	0
[roomB,clean,dirty]	suck	1	1
[roomB,clean,clean]	left	-1	0
[roomA,clean,clean]	suck	3	3
[roomA,clean,clean]	suck	3	6
[roomA,clean,clean]	right	-1	5

The rows one to four describe the behavior of the agent in a period in which the norm had not been activated and the agent was governed by the rules in the Permission Group. The rows five to six of the table (shaded) illustrate the behavior of the agent when the norm of the type 2 was activated (AC = True and EC=False). It is noticed that the agent was rewarded with three points per action during the period, according with the sanctions associated with the norm of obligation. In row 7, the norm was expired and the agent behavior was again governed by the Permission rules. These ideas can be extended to the case where the environment is also governed by norms of prohibition. For instance, consider the predicate below states that "The agent cannot suck the room-A from 1:00 to 5:00 a.m.":

norm(room(roomA), time([1,5]), prohibition(suck)).

Table 6 highlights the episodes performed by the vacuum cleaner in seven interactions in the environment with both types of norms.

TABLE VI. PERFORMANCE IN A WORLD WITH NORMS OF TWO TYPES

P	A	Ep	H
[roomA,dirty,dirty]	right	2	2
[roomB,dirty,dirty]	suck	1	3
[roomB,dirty,clean]	left	-1	2
[roomA,dirty,clean]	right	2	4
[roomB,dirty,clean]	left	-1	3
[roomA,dirty,clean]	suck	3	6
[roomA,clean,clean]	right	-1	5

The rows one and four of the table describe the behavior of the agent in a period in which the norm of Type 4 was activated (AC = True and EC=False). In row four, simultaneously with the norm of prohibition, the norm of Type 2 was activated too. It is noticed that in both case the agent was rewarded with two points, according with the sanctions associated with the norm of prohibition, which has priority on any norm of obligation. In row six only the norm of Type 2 was activated and the agent was rewarded with three points, according with the sanctions associated with the norm of obligation. The four remaining rows illustrate the cases where the two norms had expired and the agent´s behavior was governed by the rules in the Permission Group. All rows in the table that refer to the situation in which the two norms were not activated, the vacuum cleaner was evaluated according to the performance measure adopted for the agent in the world without norms.

VI. CONCLUSIONS AND FUTURE WORKS

In this work we discuss the influence of the norm concepts related to the reflex agent architectures in order to improve the performance of the agents executing in an environment governed by norms. In the original conception of reflex architecture, only permission rules are considered. Now, in the proposed approach two new sets of condition-action rules are incorporated in order to define prohibition and obligation rules. Additionally, the logic to implement the behavior of the simple reflex agents is presented. The strategy selects the actions aiming to minimize the penalties and to maximize the rewards. The case study simulates the behavior of a simple reflex agent in a vacuum cleaner word governed by obligation and prohibition rules. In this simple scenario, the proposed approach involving the implicit definition of norms as condition-action rules provides a rational behavior in consistency with the agent architecture specifications. Future works include the analysis of the agent behavior for another agent architectures in the literature, considering the influence of norms in the decision making process so that the agents can understand their responsibilities and the responsibilities of the others.

REFERENCES

[1] Lind, J., 2001. Issues in agent-oriented software engineering, In: P. Ciancarini e M. Wooldride (Eds.) Agent-Oriented Software Engineering, LNCS 1957, Germany, Springer, p.45-58.

[2] Wooldridge, M. and Ciancarini, P., 2001. Agent-Oriented Software Engineering: the State of the Art, In: M. Wooldridge and P. Ciancarini (Eds.), Agent-Oriented Software Engineering, LNCS 1957, Berlin: Springer, p. 1-28.

[3] Russell, S. and Norvig, P., 2003. Artificial Intelligence: A Modern Approach, 2nd Ed., Upper Saddle River, NJ: Prentice Hall, ISBN 0-13-790395-2.

[4] Wagner, G., 2003. The Agent-Object-Relationship Meta-Model: Towards a Unified View of State and Behavior. Information Systems, v. 28, n.5, pp. 475–504.

[5] Wooldridge, M. and Jennings, N. R., 1995. Intelligent Agents: Theory and Practice. Knowledge Engineering Review, Vol. 10, No. 2. Cambridge: Cambridge University Press, 1995.

[6] López y López, F., 2003. Social Power and Norms: Impact on agent behavior. PhD thesis, Univ. of Southampton, Faculty of Engineering and Applied Science, Department of Electronics and Computer Science.

[7] Meneguzzi, F. and Luck, M., 2009. Norm-based behavior modification in BDI agents. In: 8th Int. Conf. on Autonomous Agents and Multiagent Systems (AAMAS 2009), Decker, Sichman, Sierra and Castelfranchi (eds.), May, 10–15, 2009, Budapest, Hungary.

[8] Weiss, G., 1999. Multiagent Systems: A Modern Approach to Distributed Artificial Intelligence. The MIT Press.

[9] Silva, V. T. , Braga. C. and Figueiredo, K., 2010. A modeling language to model norms. The International Joint Conference on Autonomous Agents and Multi-Agent Systems (AAMAS'2010), 9th. Proceedings of the International Conference on Autonomous Agents and Multi-Agent Systems, Toronto, Canadá.

[10] Meyer, J. J. and Wieringa, R. J., 1993. Deontic logic in computer science: normative system specification, Deontic logic in computer science: normative system specification, John Wiley and Sons Ltd. Chichester, UK.

[11] Oren, N., Panagiotidi, S., Vazquez-Salceda, J., Modgil, S., Luck, M., and Miles, S., 2008. Towards a formalisation of electronic contracting environments. In Proc. 12th COIN Workshop, pages 61–68.

A pretopological multi-agent based model for an efficient and reliable Smart Grid simulation

Coralie Petermann*†, Soufian Ben Amor† and Alain Bui†
*Ecole Pratique des Hautes Etudes
LaISC - Paris, France
†Université de Versailles Saint-Quentin-en-Yvelines,
CaRO - Versailles, France

***Abstract*—Smart Grid is a typical complex system due to the heterogeneity of actors, economic issues and material aspects such as information technology and power generation. Moreover, the conflicting combination of human and artificial systems is an important complexity factor.**

In this paper, we provide a multi-agent based model for an efficient and reliable Smart Grid implementation. Our model combines adapted mathematical theories to obtain a more realistic modeling of Smart Grid. It takes into account the heterogeneity of components, links them with a generalized proximity concept, and ensures an optimal functioning of the whole system.

I. Introduction

A complex system is a system composed of many entities with simultaneous local interactions. The global behavior can not be deduced from the behavior of its components. An efficient modeling of Smart Grid needs an interdisciplinary approach owing to the heterogeneity of components, and also a holistic method due to the emergence phenomenon, in order to guaranty an optimal functioning of the global system.

In this paper, we are interested in Smart Grid modeling: computed and optimized electricity distribution networks to improve production and distribution of electricity. Smart grids implement heterogeneous actors with different interests: on one side, energy producers want to maximize their profits, on the other consumers try to cut costs, and finally, the state seeks to reduce carbon dioxide emissions, while optimizing the system to satisfy all customers. In our modeling, we need to aggregate the preferences of all stakeholders, to implement the concepts of sharing and redistribution of energy, and finally to ensure that the entire territory is covered in energy.

We will show that Smart Grid is a relevant example of complex system. Then we will present the Smart Grid concept and highlight the similarities with complex systems. Afterwards, we will propose a multi-agent based model founded on theoretical notions including specific algorithms to take into account specificities of Smart Grids properties. Eventually, we will present our model and discuss the results and future work.

II. Smart Grid

Currently, Smart Grid is a fuzzy concept: it is an objective to improve power generation and distribution that will integrate renewable and low carbon energies in the existent power grid. Smart Grid requires to satisfy essentials properties such as reliability, scalability, cost effectiveness but also requires real-time communications secure and sustainable [1]. Of course, this system must integrate all the heterogeneous actors.

In this section, we present the different ways of producing electricity and the relation with complex systems and networks.

A. Presentation of Smart Grid : from power generation to distribution

Smart Grids are composed of an enormous number of devices of various types, from smart meters and solar inverters to electrical substation equipment and sensors on power lines. Electricity can be produced by multiple processes: from the stable production of a nuclear plant, to the storage via electric vehicles, and integration of renewable energy which production may depend on environmental factors. A huge distribution and energy transport network has been created over the years but it is not mastered nor optimized. Our goal is to make powergrids more efficient by integrating renewable energies and taking advantages of information and communication technologies.

In the next paragraph, we present the notion of complex system to highlight that Smart Grid represents a perfect example.

B. Introduction to Complex Systems and Complex Networks

A system which consists of large populations of connected agents (or collections of interacting elements), is said to be complex if there exists an emergent global dynamics resulting from the actions of its parts rather than being imposed by a central controller. That is a self-organizing collective behavior difficult to anticipate from the knowledge of the agents' behavior [2].

The structure of complex systems is usually represented as a complex network which can be classified according to two criteria. The first concerns the categorization by scope. The second is a theoretical classification according to the mathematical properties of the network.

1) Network classification according to the domain: We can classify networks into four loose categories: social networks, information networks, technological networks and biological networks [3].

a) Social networks: A social network is a set of people or groups of people with some links or interactions between them [5], [6], [7]. It can represent friendships between individuals [8], [9], business relationships between companies [10], [11], etc... An epidemic disease affecting a population is also a good example of complex social network.

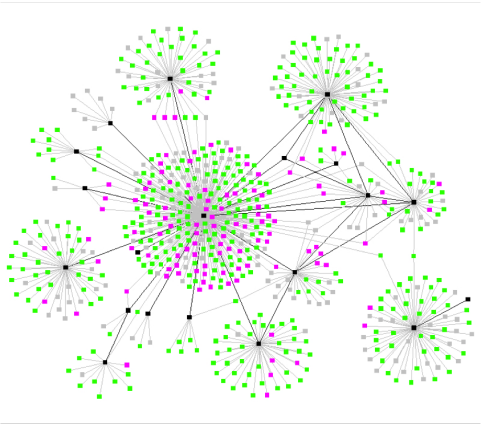

Fig. 1. Epidemic among colonies of individuals.

b) Information networks: The second network category is information networks (also sometimes called "knowledge networks") [3]. The classic example is the network of citations between academic papers [12] in which the vertices are articles and a directed edge from article A to article B indicates that A cites B.

c) Technological networks: The third class of networks is technological networks, man-made networks designed typically for distribution of some commodity or resource, such as electricity or information [3]. The electric power grid and Smart Grids are good examples.

Lots of distribution networks have been studied over the time: airline routes [18], [13], roads [14], railways [15], [16], pedestrian traffic [17], but also power grids and recently Smart Grids [19], [20]. The logical structure of Internet is also a good example with all the communication lines (optic fiber, satellite, etc...)

d) Biological networks: The last class of complex network is biological networks [21]. Lots of biological systems can be usefully represented as networks, for example, a protein can be modeled as a network of amino acids, which may also be represented as networks of atoms such as carbon, nitrogen and oxygen.

We have seen some different types of real complex networks in the various fields, in the next paragraph we will see their mathematical properties.

2) Theoretical classification of networks: Theoretical research about network established that complex networks can be represented with particular random graphs. A random graph is a graph in which the edges are randomly distributed [2]. We can distinguish two types of random graph that fit with complex system modeling : scale-free networks and small world networks. In the case of Smart Grids, we have to deal

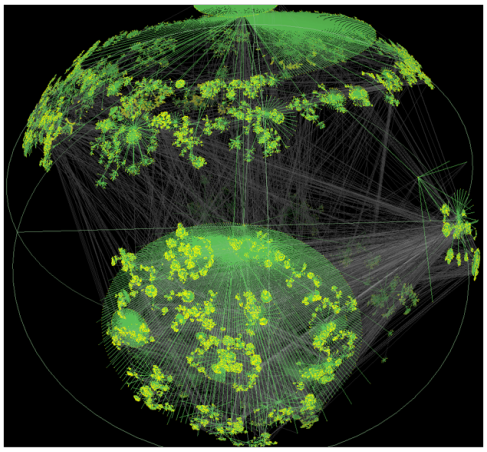

Fig. 2. Technological network : logical structure of Internet.

with heterogenous networks : a number of neighbors with large variations, compared to homogeneous networks which have a similar number of neighbors for each point. Our goal is to recreate the French national grid by generating a network with varying properties in term of network connectivity.

a) Scale-free: A scale-free network is a graph which degree distribution follows a power law.

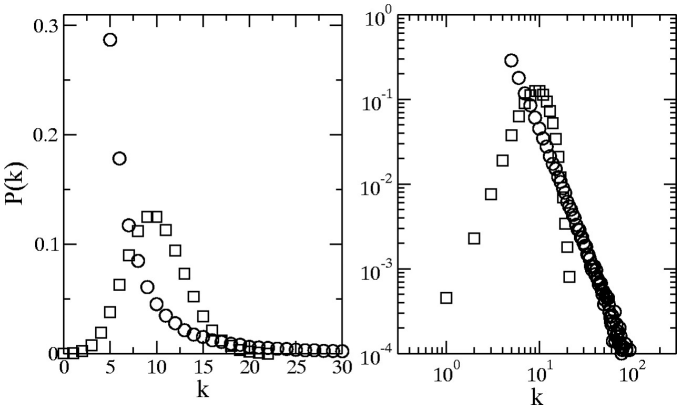

Fig. 3. Comparison between the degree distribution of scale-free networks and random graphs.

The bell-shaped degree distribution of random graphs peaks at the average degree and decreases fast for both smaller and larger degrees, indicating that these graphs are statistically homogeneous. In opposition, the degree distribution of the scale-free network follows a power law.

Scale-free networks occur in many areas of science and engineering, including the topology of web pages and the power grid of the western United States [4].

b) Small-world: A small-world network is a type of mathematical graph in which most nodes can be reached from every other by a small number of hops or steps.

Stanley Milgram, a social psychologist at Harvard, conducted a simple experiment in 1967 ([24]). He developed an easy methodology for studying how people are linked to others by giving a folder to a "starting person" instructed to send it

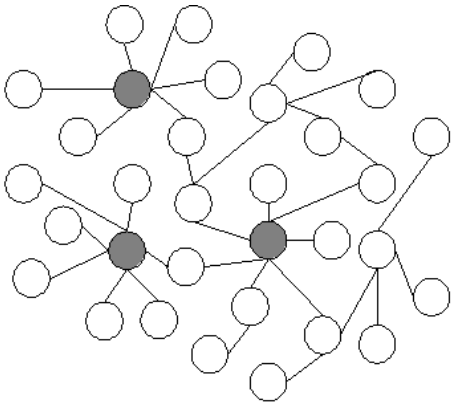

Fig. 4. Scale-free network.

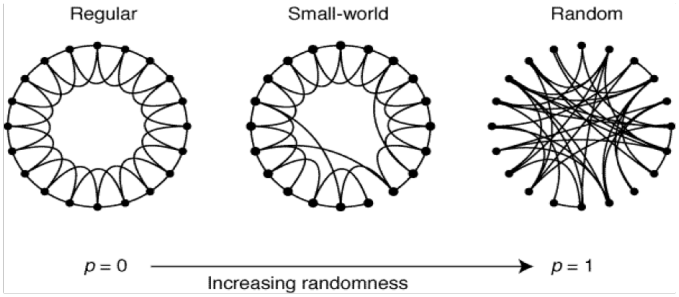

Fig. 5. Small World networks.

to a "target person". If the starter does not know the target, he send the folder to someone else among his friends, who will have to transmit the folder again until the target is reached. Thus Milgram could determine how closely linked any two people are in a population. In the original study, starters in Kansas tried to get folders to the wife of a divinity student in Cambridge, Massachusetts, and starters in Nebraska tried to get folders to a stockbroker in Sharon, Massachusetts. In the Nebraska study, Milgram found five intermediaries was the median number of links between the starter and target.

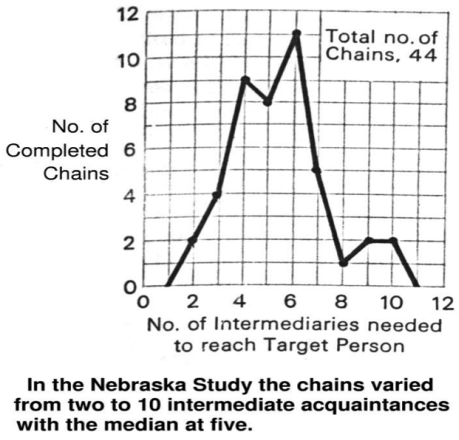

Fig. 6. Milgram Nebraska study

These properties are important issues to consider in our modeling because the scale-free is a property which clearly exists in the Smart grids as the distribution network follows this property.

Our goal is to try to find the relevant theories to solve problems of Smart Grid and to enable us to design a system with local rules leading to a global qualitative behavior. We will design the rules and a mathematics model to ensure the properties globally. In the next section, we present our theoretical model and theories used to build it.

III. Modeling

Primary, we have to distinguish models from simulation. A model is a simplified mathematical representation of a system at some particular point in time or space intended to promote understanding of the real system [2]. A simulation is the manipulation of a model in order to perceive interactions that would not otherwise be apparent because of their separation in time or space. A simulation should include as much detail as possible, whereas the model should include as little as possible to be easily generalized to other systems.[2]

Smart Grid represents a shared resource among multiple actors (or agents), with divergent interests. A complex system is characterized by its global behavior that is itself defined by local behavior. It is not obvious to do this in the form of equations, the use of multiple agents is therefore more suitable but we will be discussing that in more detail in the next section.

A. Agent-Based modeling

A multi-agent system (MAS) is a system composed of a set of multiple interacting intelligent entities (agents), an environment, a set of relations between entities and a set of operations that allows agents to perceive, produce, consume, transform and manipulate objects. Agents are specific objects representing the active entities of the system. Multi-agent systems can be used to solve problems that are difficult or impossible for an individual agent or a monolithic system to solve. Intelligence may include some methodic, functional, procedural or algorithmic search, find and processing approach.

The design of complex system is more realist with intelligent agents interacting together, because each agent can act as a separate mathematical model [30]. That is why agent-based modeling is one of the most evident approach for modeling complex system. MAS approach is used in lots of research topics such as pollution modeling [31], social structures...

An agent is a computational entity, like a computer program, a human or a robot, which can be viewed as perceiving and acting by its own on the environment. Agents in a multi-agent system have several important properties:[32]

- agents are partially autonomous: its behavior depends partly from its experience.
- agents don't have a full global view of the system but a local view
- there is no central controlling agent (it's not a monolithic system) [33]

Technically, a multi-agent system consists of a set of processes occurring at the same time. The key point of multi-agent systems lies in coordination between agents.

A MAS is said to be homogeneous if all agents are built on the same model (an ant colony), and heterogeneous if agents are built with different models from different hierarchical levels (eg the organization of a company). Concerning Smart Grid, we will use heterogeneous MAS to model all the different types of entities. Customers will even be modeled as autonomous and intelligent sub-systems. This will be further developed in this article.

One of the major benefits of MAS is to allow to study in silico the generic problem in risk-free space, while studying the global view of the system and setting up important parameters. Then, we can test the impact of various parameters in various scenari at very low-cost. Moreover, it corresponds to the reality because every agent act in real time simultaneously while having a possible individualized behavior.

However the only theory of multi-agent does not allow us to solve Smart Grids systems because there are theoretical problems. In the next section, we present in details the different theoretical aspects we use to enrich MAS to model efficiently Smart Grids. First, we will present Smart Grid as a complex network structure with behaviors tied with optimization and negotiations, so we will present game theory, a theory that models this behavior. Negotiations are based on notions of proximity between agents, but if we use a proximity metric that won't be appropriate and it will manage only one criterion, so we will use the pretopology. It will enable us to manage several relationships simultaneously using boolean functions, and that will better correspond to the reality. Moreover, in case of modification of one criterion we just have to change the corresponding adherence function. The pretopology is then one of the theories that brings lots of improvements to the existent model. Finally, we will present the percolation as a theory to validate our model. It will enable us to check if the network is always connected i.e. in terms of energy delivery, we can ensure that everyone is satisfied.

B. Smart Grid as a Complex Network

As seen in section 1, Smart Grid can be defined as a complex system. However, complex system structure is represented by a complex network, which is a combination of different graphs. Concerning Smart Grid, the complex network represent the transport and communication network. On one side, distribution network is the set of all power lines that allows the energy to pass through the grid and to be distributed. On the other side, the communication network allows agents communication, and collects the different statistics from smart meters.

In the case of Smart Grid, we represent the distribution network by an undirected graph: we consider the edges to be power lines, and the nodes to be junctions (i.e. substation, residentials, companies, ...) where the energy can go in or off a particular power line. Each edge has a maximum power supply that it is able to provide. Each node is an agent with some particular parameters (provide or consume energy, etc).

C. Game theory

In this part, we focus on game-theoretic ideas to solve the problem of negotiations concerning electricity distribution.

Smart Grids involves heterogeneous actors with different interests: the state, consumers, and companies are in perpetual conflict in the economic field. This is very close to game theory [34], [35]: it is indeed a strategic problem in which the actions of each player will influence the others.

Game theory is a method of applied mathematics used to study human and animal behaviors by modeling competing behaviors of interacting agents. Although it was initially developed in economics to understand a large collection of economic behaviors[34], the use of game theory in the social sciences has expanded, and has been applied to political, sociological, and psychological behaviors as well. Applications include auctions, bargaining, fair division, duopolies, oligopolies, social network formation, agent-based computational economics [36], mechanism design[38], voting systems[39], behavioral economics[40], and political economy [37].

Game theory can be defined as the study of mathematical models of conflict and cooperation between intelligent rational decision-maker. It provides general techniques to analyze situations, such as in games, where an entity's success depends on the choices of the other entities [35]. From our point of view, we can see it as a model of conflicts and cooperations between agents and the *game* refers to the whole Smart Grid. Then, it will model electricity traffic patterns between the agents.

As seen above, the negotiations are based on notions of proximity between agents, but if we use metric distances that won't be appropriate and it will manage only one criterion. Conventional topology would be too cumbersome to be implemented so pretopology is one of the most relevant theories that brings a lot of improvement to the existent model. It will enable us to manage several relationships simultaneously using boolean functions, and that will better represent the reality. Moreover, in case of modification of one criterion we just have to change the corresponding function.

D. Pretopology

The pretopology is a mathematical theory, weaker than classical topology to express the structural transformation of sets composed of interacting elements such as the constitution of decisive coalition among a population, alliance phenomena, tolerance and acceptability processes and emergence of collective behavior [25], [26]. In our case, we use pretopology to model the concept of proximity.

Indeed, in the context of integrating renewable energy, it is necessary to express the notion of proximity in terms of algorithm. If we take the example of wind turbines, we do not speak about metric proximity, but functional proximity: the weather influences the electrical efficiency production, and

the turbine closest from us is not necessarily the one that can provide all the energy required!

Definition We call *pseudoclosure* defined on a set E, any function a(.) from P(E) into P(E) such as:

- $a(\emptyset) = \emptyset$
- $\forall A \subset E, A \subset a(A)$

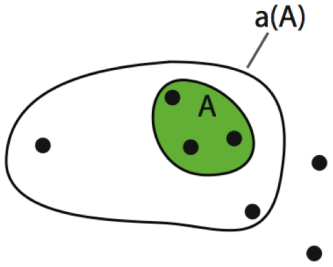

Fig. 7. Pseudo-closure of A.

Definition We call *interior* defined on a set E, any function i(.) from P(E) into P(E) such as:

- $i(E) = E$
- $\forall A \subset E, i(A) \subset A$

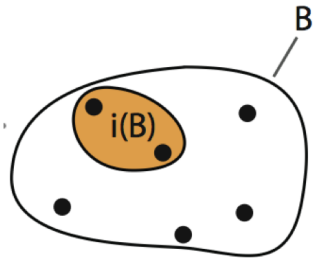

Fig. 8. Interior of A.

Definition Given, on a set E, a(.) and i(.), the couple $s = (a(.), i(.))$ is called pretopological structure on E and the 3-uple (E,a(.),i(.)) is called a pretopological space.

In pretopology, a complex network can be viewed as a family of pretopologies on a given set E [7].

Then, we can use different pretopological spaces on the same set to better model a phenomena. In our case, the integration of all the parameters of the Smart Grid can be done within a separate pretopological space for each one: weather influence, distances, maximum power supply, etc... By this way, an accurate setting can be done easily, quickly and efficiently.

With the pretopology, we can enrich our model using multivariate relationships between entities. However, the Smart Grid is dynamic so we need a method to verify that our model generates an overall system working properly: that is, it distributes electricity regularly to every customer. The percolation checks if a network is always connected so in terms of energy delivery, we can ensure that all customers are satisfied. In the next section, we present more in details this theory.

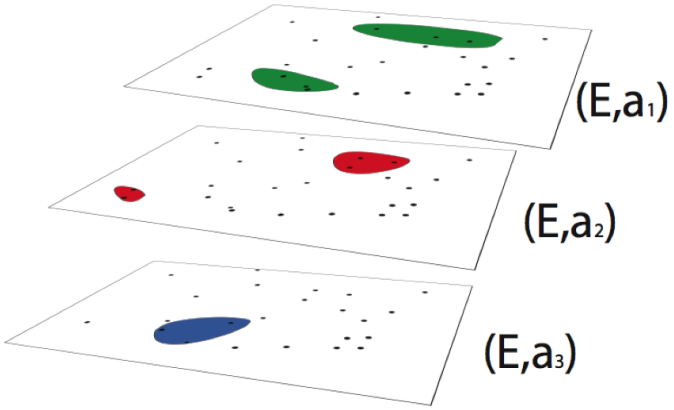

Fig. 9. Complex network in pretopology.

E. Percolation theory

Percolation is a mathematical theory used for determinist diffusion processes on a stochastic structure [27].

The theory of percolation can bring together many complex phenomena by analyzing the behavior of phase transition in these systems. It helps to highlight the underlying mechanisms. The word "percolation" comes from Latin percolatio, meaning filtration. He referred in general to the concept of agglomeration and propagation in random media partially interconnected [29].

Physical problems such as Smart Grids are mathematically modeled as a network of points (n consumers) and the connections (or edges) between each two neighbors may be opened (allowing the electricity to pass through) with probability p (connected by bonds of p random efficiency), or closed with probability $(1-p)$, and we assume they are independent. [28] So there exists a proportion $(1-p)$ of links that can be destroyed at random, which does not provoke any power failure visible for consumers, nor interfere with communication between a station and an another, as it is still possible to go through relay stations if p is greater than a critical value, called the percolation threshold p_c. Below the critical value p_c, the probability that two stations can communicate directly or indirectly is very low.

This mathematical model was originally developed for the study of physical phenomena, but it had been applied in various fields other than physics [41]. Indeed, the percolation theory has contributed, for example, in modeling complex systems in economics [42], marketing [43], sociology [44], computer science [45], ecology [46], or mathematics [47].

In our case, we will determine the acceptable threshold in order to have a proper power distribution. Eventually we will get a tool for decision support that will help to refine variables, change settings using modeling theories enriched by classical mathematical theories. We aim to achieve a very effective

model to manage Smart Grid complexity in order to control it or enhance the performance.

IV. Simulation

In this section, we present an overview of our model developed with AnyLogic.

A. Anylogic

Anylogic, a simulation software provided by XJ Technologies, is the first and only tool that brings together System Dynamics, Process-centric (Discrete Event), and Agent Based methods within one modeling language and one model development environment.

The native Java environment provides multi-platform support, and models can be exported as standalone Java applications. It supports limitless extensibility including custom reusable Java code, external libraries, and external data sources. For example, we can integer the Java library PretopoLib [48] developped by Vincent Levorato and Marc Bui to manage pretopological functions and spaces.

B. Agents and parameters

We use several types of agent in our model. We focus on individual objects and describe their local behavior. We use a configurable scale-free structure in order to be able to modify some parameters and analyze the consequences of the structure on the system dynamic.

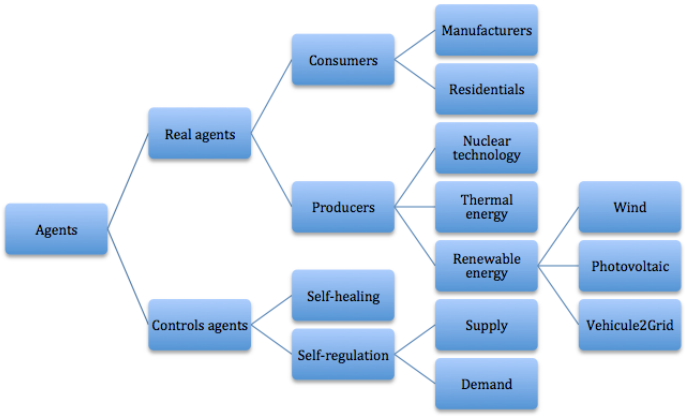

Fig. 10. Different types of agents.

We separated the work in different modules.

We stored all real data about energy consumption and production in an external database. Then, for each type of agent, we implemented mathematical models to reproduce their behavior as realistic as possible. Each type of agent has its own power management module to reproduce its consumption or production of electricity. Then, this module is connected to a decision making process module, based on game theory to compute the distribution of energy using a pretopological proximity measure. Agents can communicate with each others through a communication module, and are interconnected with a scale-free transport network. The "environment module" enables to integrate the management of external parameters having an influence on the system such as weather or pricing policy.

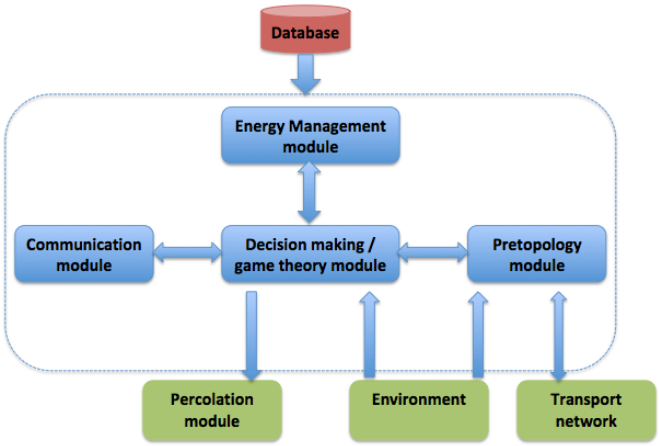

Fig. 11. Modules for each agent.

C. Futur work

Currently, our model developed on AnyLogic is a simplified model. We integrated the various agents presented in a scale-free network, and the distribution of electricity is made by calculation with pretopological distances. In a futur work, we plan to integrate game theory in our development and to test different scenario in order to optimize the system. Then, we will be able to change the value of some parameters and study their effects.

V. Conclusion

To conclude, we presented an efficient multi-agent based modeling to meet the problematics of Smart Grids.

By basing our model on theories adapted to fit each issue, our model allows to take into account the heterogeneity of the actors that makes the Smart Grid a complex system, and optimizes the existing network by integrating an overall independent supervision.

In a futur work, we will be able to present more results and will certainly adapt some points to calibrate our model at best compared to the reality of the existing network.

REFERENCES

[1] *A systems view of the modern grid.* Technical report, National Energy Technology Laboratory, Department of Energy Office of Electricity Delivery and Energy Reliability, January 2007.

[2] Nino Boccara, *Modeling Complex Systems*. "Graduate Texts in Contemporary Physics" series,Springer-Verlag, 2004 .

[3] M. E. J. Newman. *The Structure and Function of Complex Networks*. SIAM Review, Vol. 45, No. 2. (2003), pp. 167-256.

[4] Réka Albert, István Albert, and Gary L. Nakarado, *Structural vulnerability of the North American power grid*,Phys. Rev. E 69, 025103(R) (2004).

[5] Scott, J., *Social Network Analysis: A Handbook*, Sage Publications, London, 2nd ed. (2000).

[6] Wasserman, S. and Faust, K., *Social Network Analysis*, Cambridge University Press, Cambridge (1994).

[7] V. Levorato. *Modeling Groups in Social Networks*, In Proceedings of the 25th European Conference on Modelling and Simulation (ECMS'2011), pages 129-134, Krakow, Poland, 2011.

[8] Rapoport, A. and Horvath, W. J., *A study of a large sociogram*, Behavioral Science 6, 279–291 (1961).

[9] W. Zachary, *An information flow model for conflict and fission in small groups*, Journal of Anthropological Research 33, 452-473 (1977).

[10] Mizruchi, M. S., *The American Corporate Network*, 1904–1974, Sage, Beverley Hills (1982).

[11] Mariolis, P., *Interlocking directorates and control of corporations: The theory of bank control*, Social Science Quarterly 56, 425–439 (1975).

[12] Egghe, L. and Rousseau, R.,*Introduction to Informetrics*, Elsevier, Amsterdam (1990).

[13] Amaral, L. A. N., Scala, A., Barthélémy, M., and Stanley, H. E., *Classes of small-world networks*, Proc. Natl. Acad. Sci. USA 97, 11149–11152 (2000).

[14] Kalapala, V. K., Sanwalani, V., and Moore, C., *The structure of the United States road network*, Preprint, University of New Mexico (2003).

[15] Latora, V. and Marchiori, M., *Is the Boston subway a small-world network?*, Physica A 314, 109–113 (2002).

[16] Sen, P., Dasgupta, S., Chatterjee, A., Sreeram, P. A., Mukherjee, G., and Manna, S. S., Small-world properties of the Indian railway network, Phys. Rev. E 67, 036106 (2003).

[17] Chowell, G., Hyman, J. M., and Eubank, S., *Analysis of a real world network: The City of Portland*, Technical Report BU-1604-M, Department of Biological Statistics and Computational Biology, Cornell University (2002).

[18] Soufian Ben Amor and Marc Bui, *Complex System Approach in Modeling Airspace Congestion Dynamics*. Journal of Air Transport Studies, Vol. 3, 2012.

[19] K. Chen, P. Yeh, H. Hsieh, and S. Chang. *Communication infrastructure of Smart Grid. In Communications*, Control and Signal Processing (ISCCSP), 2010 4th International Symposium on, pages 1–5. Ieee, 2010.

[20] J. Gao, Y. Xiao, J. Liu, W. Liang, and C. Chen. *A survey of communication/networking in Smart Grids*. Future Generation Computer Systems, 28(2):391–404, 2012.

[21] Volterra, V.,(1929), *Fluctuations in the abundance of a species considered mathematically*, Nature Vol. 118, pp. 558-560.

[22] R. Cohen, S. Havlin, and D. ben-Avraham (2002). *Structural properties of scale free networks*. Handbook of graphs and networks (Wiley-VCH, 2002) (Chap. 4).

[23] R. Cohen, S. Havlin (2003). *Scale-free networks are ultrasmall*. Phys. Rev. Lett. 90: 058701. Bibcode 2003PhRvL..90e8701C. doi:10.1103/PhysRevLett.90.058701. PMID 12633404.

[24] Milgram, Stanley. 1967. *The Small World Problem*. Psychology Today. 1: 61-67

[25] ZT. Belmandt. *Basics of pretopology*. Hermann, 155 pages, ISBN: 978 27056 8077, 2011

[26] Vincent Levorato and Murat Ahat. Modélisation de la dynamique des réseaux complexes associée à la prétopologie. 9eme congrès de la Société Française de Recherche Opérationnelle et d'Aide a la Décision, ROADEF08, Clermont-Ferrand, France, February 2008.

[27] Soufian Ben Amor. *Percolation, prétopologie et multialéatoires, contributions à la modélisation des systèmes complexes: exemple du contrôle aérien.*, Thèse de doctorat, 2008.

[28] Soufian Ben Amor, Vincent Levorato and Ivan Lavallée *Generalized Percolation Processes Using Pretopology Theory*, IEEE International conference on computing and communications technologies (RIVF), Hanoï : Viet Nam (2007)

[29] G. Grimmett. *Percolation*. Springer-Verlag, Berlin, 1999.

[30] M. Pipattanasomporn, H. Feroze, and S. Rahman. *Multi-agent systems in a distributed Smart Grid: Design and implementation*. In Power Systems Conference and Exposition, 2009. PSCE'09. IEEE/PES, pages 1–8. IEEE, 2009.

[31] Murat Ahat and Sofiane Ben Amor and Marc Bui and Michel Lamure and Marie-Françoise Courel. *Pollution Modeling and Simulation with Multi-Agent and Pretopology* . Journal of Complex Sciences, Vol 4, p. 225-231, 2009.

[32] Michael Wooldridge, *An Introduction to MultiAgent Systems*, John Wiley & Sons Ltd, 2002, paperback, 366 pages, ISBN 0-471-49691-X.

[33] Liviu Panait, Sean Luke: *Cooperative Multi-Agent Learning: The State of the Art*. Autonomous Agents and Multi-Agent Systems 11(3): 387-434 (2005)

[34] Oskar Morgenstern, John von Neumann, *The Theory of Games and Economic Behavior*, 3rd ed., Princeton University Press 1953.

[35] Roger B. Myerson (1991). *Game Theory: Analysis of Conflict*, Harvard University Press.

[36] Leigh Tesfatsion (2006). *Agent-Based Computational Economics: A Constructive Approach to Economic Theory*, ch. 16, Handbook of Computational Economics, v. 2, pp. 831-880.

[37] Martin Shubik (1978). *Game Theory: Economic Applications*, in W. Kruskal and J.M. Tanur, ed., International Encyclopedia of Statistics, v. 2, pp. 372-78.

[38] Noam Nisan et al., ed. (2007). *Algorithmic Game Theory*, Cambridge University Press.

[39] R. Aumann and S. Hart, ed., 1994. *Handbook of Game Theory with Economic Applications*, v. 2

[40] Steven N. Durlauf and Lawrence E. Blume. *The New Palgrave Dictionary of Economics*. Second Edition. Eds. Palgrave Macmillan, 2008.

[41] Roussenq J., (1992), *Percolation*, Encyclopaedia Universalis, Paris, vol. 17, pp. 838-840.

[42] S. Pajot, (2001), *Percolation et économie*, thèse de Doctorat en Economie de l'Université de Nantes.

[43] Goldenberg J., Libai B., Solomon S., Jan N., Stauffer D., (2000), *Marketing Percolation*, Physica A, vol. 284, n?1-4, pp. 335-347.

[44] Weisbuch G., Stauffer D., (2000), *Hits and Flops Dynamics*, Physica A, vol. 287, n?3-4, pp. 563-576.

[45] Gupta P., Kumar P. R., (1998), *Critical Power for Asymptotic Connectivity in Wireless Networks*, In Stochastic Analysis, Control, Optimization and Applica- tions, Eds. W.M. McEneaney & al., Birkhauser, Boston, pp. 547-566.

[46] Clar S., Schenk K., Schwabl F., (1997). *Phase Transition in a Forest-Fire Model*, Physical Review E, Vol. 55, pp. 2174-2183

[47] Bunde A., Havlin S., (1991), *Percolation I* , in Bunde A., Havlin S. (eds.), Fractals and Disordered Systems, pp. 51-95, Springer-Verlag, Berlin.

[48] Vincent Levorato and Marc Bui, *Data Structures and Algorithms for Pretopology: the JAVA based software library PretopoLib*, IEEE 8th International Conference on Innovative Internet Community Systems, p.122-134, Schoelcher, Martinique, 2008.

Emergent Distributed Problem-solving Technique for Self-configuring Systems

Brian McLaughlan[1] and Henry Hexmoor[2]
[1]Department of Computer and Information Science
University of Arkansas – Fort Smith, Fort Smith, AR, USA
[2]Department of Computer Science
Southern Illinois University – Carbondale, Carbondale, IL, USA

Abstract - *The goal of configuring a massive, complex multi-agent system can be viewed as a distributed search problem in which each agent attempts to choose a correct configuration. This research presents a technique that can simultaneously function as the problem decomposition and solution aggregation components in such a distributed search environment. The method is tested in a number of large multi-agent simulations to demonstrate its feasibility. The agents in the system are shown to achieve optimal or near optimal configurations in significantly less time than agents configuring themselves individually.*

Keywords: *Multi-agent systems, distributed search, emergence*

1 Introduction

Distributed search is an open problem in AI research. At its core, it is a problem involving efficiently decomposing or partitioning a problem into sub-problems and allocating those sub-problems to one or more computational elements. Ideally, these elements would then be able to explore their much more limited search space in parallel. Research in distributed search can be broadly classified as dealing with one or more of the following: finding algorithms for appropriate decomposition of problems [1], distribution of sub-problems to computational elements [2], synthesizing results of sub-problems [3], and coordination between elements [4]. The research in this paper proposes a technique that will simultaneously handle problem decomposition and result synthesis.

In this research, a massive multi-agent system has been given the goal of configuring its constituent elements (i.e., the individual agents) for optimal performance of the tasks assigned to those elements. In this scenario, we make several assumptions:

- The size of the organization is such that micromanagement of individual agents is infeasible.
- The complexity of the organization and its operating environment is such that the desired configuration of the average agent is unknown.
- Individual agents may already possess some method for learning.
- In the course of performing tasks, agents will communicate or deal with each other, but agents are not required to be benevolent. They are allowed to choose an appropriate configuration for themselves without considering the needs of other agents.

2 Approach

To facilitate the speed of the search, a key observation is made regarding the performance of the agents. If all other factors are held constant, an agent that is more successful at completing its tasks will typically be better configured for the task than an agent that is less successful. Therefore, when agents interact, the more successful agent will pass appropriate traits to the less successful agent. The greater the relative success, the more strongly the trait is adopted or the more likely the trait will be adopted.

Formally, agent $\boldsymbol{A_i}$ has a Sending function F_i^S:

$$\boldsymbol{O_j}(T+1) \leftarrow F_i^S(x_i(T), \exists!\ x \in \{C, S\}). \quad (1)$$

This function sends a configuration C or success score S to the observation list of the receiving agent, $\boldsymbol{A_j}$, where it can be processed. Similarly, a Receiving function, F_i^R, is defined:

$$\boldsymbol{O_i}(T+1) \leftarrow F_i^R(F_j^S(x_j(T), \exists!\ x \in \{C, S\})). \quad (2)$$

This function receives a configuration C or success score S from agent $\boldsymbol{A_j}$ and stores it in the observation list where it can be processed. Finally, a Processing Observations function, F_i^P, and an Updating Configuration function, F_i^U, are defined:

$$\boldsymbol{B_i}(T+1) \leftarrow F_i^P(\boldsymbol{O_i}(T), \boldsymbol{B_i}(T)). \quad (3)$$
$$\boldsymbol{C_i}(T+1) \leftarrow F_i^U(\boldsymbol{C_i}(T), \boldsymbol{B_i}(T), S_i). \quad (4)$$

In F_i^P, agent $\boldsymbol{A_i}$ merges its list of observations with its beliefs to create new or updated beliefs. Similarly, F_i^U utilizes agent $\boldsymbol{A_i}$'s current configuration, its success score, and its beliefs, including its beliefs regarding other agents'

configurations and their success scores, to determine its new configuration.

In the BDICTL model, agents will only execute their intentions if there is one plan available. When more than one plan is present, noting is done. Some research (CITATION) proposes that this could be modified to have the agent pick a random plan. We propose that the random selection could be more appropriately performed by the viral trait model. To do so, the beliefs about the agent's internal decision-making process can be modeled as traits. To illustrate, let the following variables be defined:

- $\boldsymbol{E_i}$ ::= set of events associated with the execution of a task by agent $\boldsymbol{A_i}$
- $\boldsymbol{E_j}$ ::= set of events associated with the execution of a task by agent $\boldsymbol{A_j}$
- $\boldsymbol{C_i}$ ::= set of configurations of $\boldsymbol{A_i}$
- $\boldsymbol{C_j}$ ::= set of configurations of $\boldsymbol{A_j}$

Then, the BDI formalization of the trait adoption process of agent $\boldsymbol{A_i}$ becomes:

$$\begin{aligned}&\mathsf{BEL}((\textstyle\sum succeeded(\boldsymbol{E_i}) / \sum done(\boldsymbol{E_i})\\ &< \mathsf{BEL}\ (\ succeeded(\boldsymbol{E_j}) / done(\boldsymbol{E_j})))\\ &\rightarrow optional \Diamond \mathsf{INTEND}(\forall\, c_j \in \boldsymbol{C_j}\ , \forall\, e_j \in \boldsymbol{E_j}\\ &\cap\ (context(c_j) = context(c_j)), \forall\, c_i \in \boldsymbol{C_i}\ , \forall\, e_i \in \boldsymbol{E_i}\\ &\cap\ (context(c_i) = context(c_i))\ (does(\mathsf{BEL}(c_j))\\ &\wedge\ does(\neg\mathsf{BEL}(c_i)\ ))).\end{aligned} \quad (5)$$

This definition assumes the existence of the helper function *context* which returns the contextual component of the variable. In essence, the formalization states that if $\boldsymbol{A_i}$ believes its average success on a particular task is less than what it believes $\boldsymbol{A_j}$'s average success to be, then it has the option of eventually intending all planning beliefs of $\boldsymbol{C_j}$ as long as those beliefs have the same context as events associated with the task in question. It will not take any belief that is not in the same context. Additionally, $\boldsymbol{A_i}$ would intend to remove any existing beliefs that have the same context as the task. This has the effect of adopting the beliefs, including potential action plans, of a perceived superior peer.

3 Experimentation

To investigate the viability of the model, a simulation was created to examine several environments and scenarios in which the agents could operate. A screenshot of this simulation is shown in Figure 1. To get a feel for the ability of the model to handle a variety of peer networks, three different network types were utilized. These network types are representative of the types of networks found in natural and artificial systems. Possible configurations were a grid network with each agent connected to its four neighbors, a scale-free network in which a minority of agents have the majority of connections [5], and a completely random

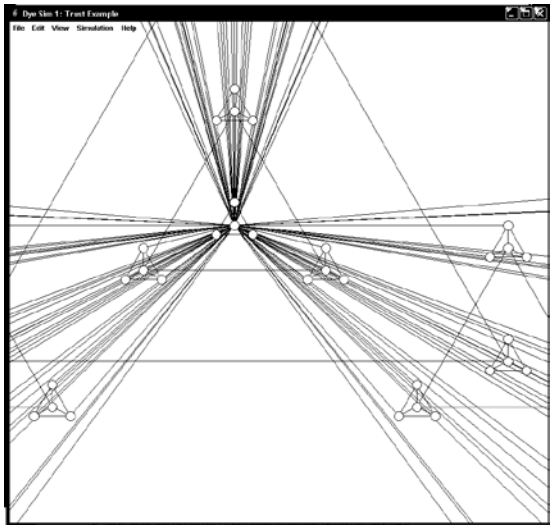

Figure 1: Screenshot of simulation

network. Each network was populated with 10,000 agents that then linked to other agents in the prescribed manner. These connections represented communication links between peer agents.

The multi-agent system was tested in a sales staff scenario. The environment simulated a large department store where the agents acted as the sales staff. The agents were given personality vectors containing five of a possible 100 randomly selected personality characteristics. These five parameters constituted the set of agent Ai's configurations, Ci. In this simulation *personality* was defined as a set of characteristics that uniquely influence cognitions, motivations, and behaviors in various situations [6]. Although there are many different theories on what characteristics constitute one's personality, this research simply assumed the characteristics are those that related to the ability to sale products.

The agents were placed in random departments to await customers. The number of customers was significantly greater than the number of sales agents so that a random "customer drought" would not influence an agent's success rates. Like the sales agents, each customer was given a random personality vector. Customers tended to gravitate towards particular departments based on their personalities and were programmed to be more likely to be persuaded to buy from an agent whose personality was likewise compatible. Therefore, agents with a personality compatible with its assigned department were more likely to be successful than agents with a significantly different personality.

The goal of the system of agents was to have each agent learn and utilize those personality traits that were most appropriate for their department. Each agent was able to perceive the personalities of their peers as the other agents made sales. Essentially, each agent would utilize the Sending

function, F^S, to transmit its current personality configuration after each successful transaction.

$$S_i(T+1) \leftarrow F_i^J(S_i(T), 1 - \sum_{x=1}^{5} | C_{cust}(x) - C_i(x) |) \quad (6)$$

$$S_i(T+1) > S_i(T) \rightarrow \boldsymbol{O_x}(T+1), \forall\, x \in \boldsymbol{P_i} \leftarrow F_i^S(\boldsymbol{C_i}(T)) \quad (7)$$

Agent $\boldsymbol{A_i}$'s performance of its job function, F_i^J, is based on the differences between its personality configuration $\boldsymbol{C_i}$ and the customer's configuration C_{cust}. If its score increases, it will send its current configuration to the observation lists of all agents in its peer list, $\boldsymbol{P_i}$.

When adopting the personalities of successful peers, the agent has a chance to assume any of personality traits of the peer. The chance of assuming a trait is based on the difference in the two agents' success rates:

$$Random^x(1{:}100) \leq (S_j - S_i) \rightarrow C_i^x \leftarrow C_j^x, \text{ for x = 1,2,..,5.} \quad (8)$$

The agents within this simulation were initialized with random values and allowed to transfer their traits to each other. When the system had converged with no more spreading of trait solutions, the simulation stopped, and the results were recorded. Of interest was the system's overall ability to spread the best solutions and the time it took to stabilize.

Next, experiments were performed to test the ability to converge after the insertion of a new agent into the community. A system of agents was allowed to converge, simulating a mature organization. Then, an agent was moved from one region to another. The time to converge and the final fitness of the new organization were recorded.

The ability of this framework was compared to the ability of a duplicate mature organization that utilized individual search to converge. The agents in this organization utilized a greedy binary search method to find appropriate configurations:

1. Try a particular trait for a period of time
2. After the period of time, use binary search, but randomly choose whether to go higher or lower
3. Try this new trait for a period of time
4. After the period of time, evaluate the effectiveness of the solution. If worse than original, try the unchosen direction. If better than original, then continue search. If both higher and lower are worse than original, then finished.

4 Results and conclusions

As shown in Figures 2 and 3, the framework's ability to stabilize at an acceptable state is quite good. The random network had the most variance in convergence time and accuracy, but averaged to reasonable levels. The grid's performance was as expected; when the "best fit" agent was centrally located, it took approximately half the distance across the network to stabilize, while "best fit" agents in the corners caused propagation to take longer. The scale-free network had more variation than initially anticipated since the distance across a scale-free network is quite short, but this variation can be attributed to the location of the ideal traits. If the "best fit" agent is also one of the network hubs, the system distributes the trait very rapidly. If the ideal trait is located in a peripheral agent, the transfer of the trait is slow until it hits a major communication artery.

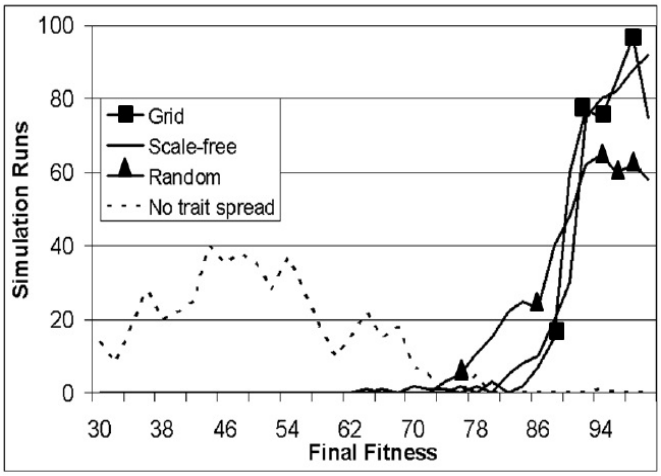

Figure 2: Number of sims obtaining a particular final fitness

Both the trait-spreading and binary search methods proved successful at quickly acclimating the transported agent to its new environment, as shown in Figure 4. However, the trait-spreading method always succeeded in very few steps, only taking longer when the agent is moved to a border area where nearby successful peers are not actually operating in the same department as the transported agent. This short stabilization time is due to the fact that the agent didn't have to find a successful configuration through trial-and-error, but rather was given a successful starting point from a nearby agent. Additionally, the amount of time take does not depend on the

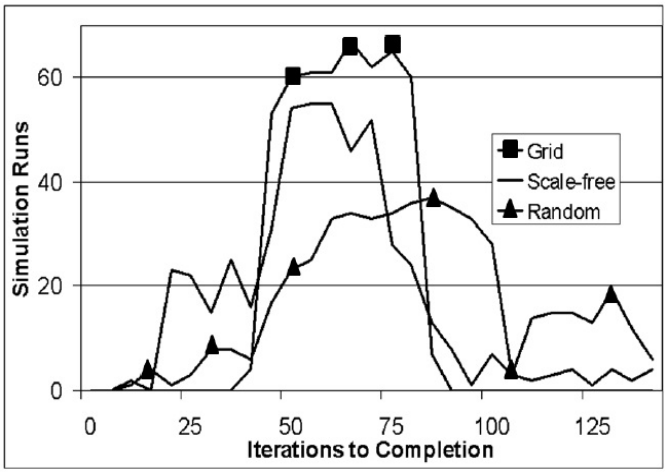

Figure 3: Stabilization times

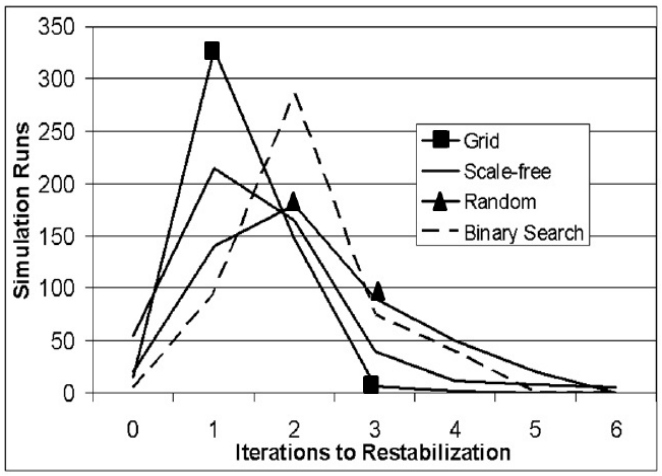

Figure 4: Number of agents with particular stabilization times

size of the problem space, unlike the individual-based binary search.

Although it is not guaranteed to find the ideal solution, it significantly reduces the amount of work done. It naturally produces subproblem boundaries in which similar agents require similar solutions and the aggregates the best known solutions. This work could be combined with other forms of distributed or individualized search. This would serve as the decomposition and aggregation component of such an amalgamation. More research into what types of search would produce the best results is needed. Additional research into the effects of increased parallelization is another area to explore.

5 References

[1] Pynadath, D.V., Tambe, M., Chauvat, N., Cavedon, L. "Toward team-oriented programming." In *Intelligent Agents VI: Agent Theories, Architectures, and Languages*. 1999.

[2] Armstrong, A., and Durfee, E. "Dynamic Prioritzation of complex agents in distributed constraint satisfaction problems." In *Proceedings of the 15th International Joint Conferences on Artificial Intelligence (IJCAI)*. 1997.

[3] Yokoo, M., Durfee, E.H., Ishida, T., and Kuwabara, K. "Distributed constraint satisfaction for formalizing distributed problem solving." In *Proceedings of 12th IEEE International Conference on Distributed Computing Systems*, 1992.

[4] Shen, J., Lesser, V., and Carver, N. "Minimizing communication cost in a distributed Bayesian network using a decentralized MDP." In *Proceedings of the Second International Joint Conference on Autonomous Agents and Multiagent Systems (AAMAS)*, 2003.

[5] Amaral, L.A.N, Scala, A., Barthelemy, M., and Stanley, H.E. "Classes of small-world networks" In *Proceedings of the National Academy of Sciences of the United States of America*, 2000.

[6] Ryckman, R.M. *Theories of Personality.* Belmont, CA: Cengage Learning/Wadsworth. 2008.

An Agent Based Approach to Find High Energy Consuming Activities

Ayesha Kashif[1], **Julie Dugdale**[2], **and Stéphane Ploix**[1]
[1]Laboratory of Grenoble for Sciences of Design, Optimisation and Production, University of Grenoble 1
46 Avenue Félix Viallet, 38031 Grenoble - France
[2]Grenoble Informatics Laboratory / University of Grenoble 2
110, Av de la Chimie, 38400, Saint Martin d'Hères, France

Abstract— *Inhabitants' behaviour in buildings has a strong impact on the energy consumption patterns resulting in energy waste. The existing multi agent and centralized energy management approaches are focused on consumption optimization and load predictions without taking into account the inhabitants' behaviour. We argue that the consumption optimization without waste reduction is difficult. In this article we focus on the energy waste reduction associated with the inhabitants' behaviour. As an example a physical model for the fridge to predict the energy waste component and an agent based co-simulation methodology to identify high energy consuming activities, are developed. The proposed methodology demonstrates that based on the co-simulation results a library of high energy consuming activities can be built to support energy waste reduction efforts in Smart homes. It shall result in a shift from an energy manager towards an energy wizard to provide agents with the information on their consumption behaviour and alternatives to ensure the energy waste reduction.*

Keywords: Multi agent simulation, behaviour, energy consumption, human behaviour modelling

1. Introduction

Buildings account for 30-40% of the total primary energy use globally [1]. The inhabitants' behaviour has a significant impact on energy consumption and is an important factor for energy waste reduction [2]. We argue that the appliance consumption patterns are strongly influenced by the inhabitants' behaviour. Existing models that are used for the usage prediction of appliances are mostly based on presence/absence profiles [3]. Such profiles could be helpful for the appliances where energy is consumed only when they are turned on, e.g. lighting systems (active appliances). However, such profiles are insufficient for the appliances having continuous energy consumption e.g. fridge, freezers (cold appliances). Widén and his colleagues proposed a scheme to predict energy demand against different activities on both active and cold appliances, however the cold appliances operation was assumed unrelated to the activity patterns [4]. We argue that these appliances offer a great challenge to model them based on human behaviour due to the diversity of different possible actions on them and their resulting consumption. It will be interesting to see that how the energy waste component resulting from actions on cold appliances impacts the energy consumption optimization efforts in the Smart homes. In this article we have focused on the inhabitants' behaviour to identify high energy consuming activities with the support of proposed physical model for our example cold appliance « fridge ». This is done in a co-simulation platform using Brahms (agent modeling language) and simulink. The purpose of this co-simulation methodology is to assess the sensitivity of inhabitants' behaviour to the energy waste component and identify the high energy consuming activities to be transformed into a library for further use in the Smart homes. It will help in developing true smart environments as well as testing the design of new appliances models. It will also help to design the smart energy advisors suggesting human agents with the alternatives that minimize the energy waste component. This article is divided in 5 sections. Section 2 presents the literature review, on existing agent based approaches for energy management and the importance of inhabitants' actions on energy consumption. The modeling of household behaviour with an agent based approach is presented in section 3. The proposed physical model for the refrigeration cycles and the co-simulation methodology are detailed in section 4 and 5. Conclusion and future perspectives are discussed in the section 6.

2. Background

The literature review is divided in 3 sub sections: (i) agent based approaches for energy management, (ii) importance of inhabitants' actions on the energy consumption and (iii) human behaviour representation.

2.1 Agent based energy management

Multi agent system approaches have been used in the domain of energy management within buildings. Davidsson and Boman proposed and implemented a multi agent system based decentralized system to monitor and control the HVAC system (Heating, Ventilation and Air Conditioning) and lighting in office buildings [5]. Abras and his colleagues proposed a home automation system made up of software

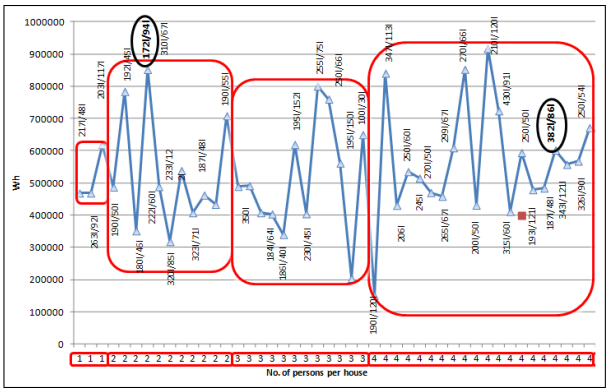

Fig. 1: Full year fridge-freezer consumption

agents that control appliances and sources [6]. It adapts power consumption to the available power resources. Agents in the MavHome project [7] predict the mobility patterns and device usage of inhabitants to satisfy the tradeoff between cost and comfort. Liao and Barooah developed a MAS approach to predict and simulate the occupancy at room and zone level in commercial buildings [8]. The anticipatory and reactive control of HVAC and lighting within smart homes has been implemented in a MAS [9]. [10] used an agent based control system in order to optimize the energy usage of a simulated residential water heating system. The above approaches do not take into account the impact of inhabitants' complex behaviour on the energy consumption for appliances. We argue that humans must be considered as active, intelligent agents for energy waste reduction in buildings.

2.2 Importance of inhabitants' actions on the energy consumption

Since human behaviour strongly influences energy consumption [2], an experiment has been performed on the IRISE database in order to see how inhabitants' behaviour affects energy consumption[1]. In figure 1 the number of people in the houses are shown on x-axis and the appliance consumption on y-axis. It shows the results of an experiment taking into account the number of people in each house and the specifications for the appliance. It can be seen that consumption does not depend solely on the number of people in the house and the size of the fridge freezer, but also on how the appliance is used by the people. For example, the first oval on the left in the figure shows that a fridge freezer with a capacity of 172l/94l in a 2-person house is consuming even more than the fridge freezer of almost double size in a 4-person house. The above experiment shows that human behaviour strongly affects energy consumption.

[1]This dataset is part of the European Residential Monitoring to Decrease Energy Use and Carbon Emissions (REMODECE) project. It contains energy consumption data, for each appliance from 98 French houses, recorded at every 10 minutes, over a one year period.

2.3 Human behaviour representation

The term "behaviour" refers to the actions or reactions of an object, usually in relation to its environment. In the literature, perception, cognition, memory, learning, social and emotional behaviour and psychomotor are considered to be the basic elements of human behaviour [11], [12], [13]. Human behaviour has also been analyzed through contextual factors including user, time, space, environment and object. These authors presented a user behaviour modeling approach called 5W1H for: what, when, where, who, why and how, which they then mapped to a home context (object, time, space, user and environment) [14]. Sempé and Quijano implemented an agent based modeling and simulation environment in order to study the use of electrical appliances by inhabitants [15]. Human behaviour can range from being very simple to very complex. The purpose here is to capture the behaviour that not only represents a simple presence or absence of an inhabitant in an environment but also represents a realistic interaction of the human with the environment. This means that the dynamic, reactive, deliberative and social behaviour of inhabitants must also be taken into account in order to fully understand its possible effect on energy consumption. This will help to consider the inhabitants as reactive, intelligent agents instead of simply "fixed metabolic heat generators passively experiencing the indoor environment" [16].

3. Modeling the household behaviour with an agent based approach

A belief-desire-intention agent model of the household's behaviour specifically for their interaction with the fridge is derived from an activity journal. The data was collected by a 2-person household, husband and wife, in which they had to specify the actions that they performed on the fridge as well as the reasons behind those actions. This reasoning mechanism when implemented into the agent based language gives them the power to think and behave the way humans do. Figure 2 shows that the agents in our model set their beliefs based on some perception from the environment. For example, perception of the other agents, objects, location and time etc. The environment could be the surroundings or the inner self for the agent. For example, in order to have the dinner, the perception from the inner self is the feeling of hunger, which now becomes a desire to eat. However, this desire will not be fulfilled by the agent until it reaches a certain threshold level and/or based on some cognitive influence. This cognition constitutes the reasoning mechanism that why the agent take or avoid taking some decisions. The social norms of the family, for example, could be one of the influencing factors on cognition. In this case, if the threshold for hunger is reached but the other agent has not arrived yet, based on the cognitive influence a new threshold level will be attained. If however the threshold

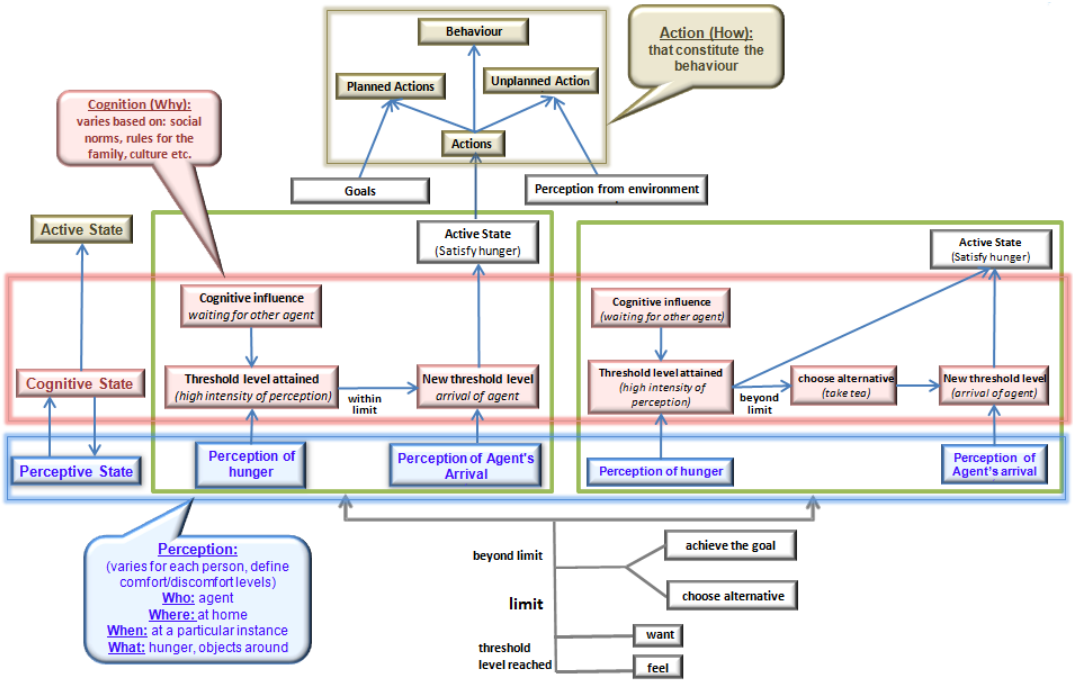

Fig. 2: Behaviour representation

level has crossed its limit, the agent will either take some alternative or his desire will be converted to an intention and he will achieve the goal, i.e. fulfill hunger. The actions caused by the agent's intentions are the planned actions, but if there is some new perception from the environment before he fulfilled the intention, it may lead to some unplanned actions. For example the planned actions to fulfill the hunger are to open the fridge, take the food out, cook it and then eat, but the unplanned actions upon the perception of a sudden pleasant change in the weather is to go to the restaurant and eat there. How the actions are performed finally constitute the behaviour of the agent. Brahms is a descriptive language to record and simulate the causal relations of inhabitant behaviour. The Brahms language [13] is compatible with our requirements. It is an agent oriented modeling/simulation environment and programming language based on belief-desire-intention agent architecture. It is able to represent people, things, places, behaviour of people over time, tools and artefacts used, when and where they are used. It also supports the communication between co-located and distributed people to support social behaviour. The key concepts are the workframes and thoughtframes. Workframes are the condition-action-consequence rules that allow agents to perform certain actions based on their beliefs and set new beliefs about the perception of the environment. Thoughtframes are used to trigger the reasoning behaviour of agents, they let the agents derive new beliefs based on existing beliefs and facts about the environment without performing some action. The BDI based behaviour model has been implemented in the Brahms environment. An example is shown in figure 3 where the agent (agentAdult1) is watching TV, he has some belief about the threshold level of his hunger. In the figure this belief is shown with the help of thoughtframes represented by a bulb symbol. The hunger level gradually increases as the simulation progresses. The agent will continue watching TV until he detects that the hunger level has reached beyond the threshold level. This detection mechanism is implemented using the concept of detectables in Brahms language which are used to interrupt, abort or continue the current activity. The first bulb symbol after 7:49:50 pm shows a pop-up of thoughtframes changing the agents' belief about the perception of hunger which is converted into the desire to eat. This desire finally becomes his intention as there is no other constraint or belief avoiding him from fulfilling the desire and he moves to the kitchen to prepare food, where he interacts with the appliances e.g. the fridge. The horizontal yellow bar just beneath the

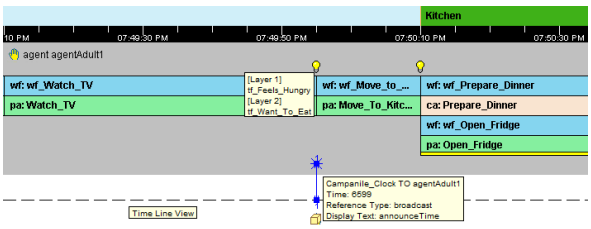

Fig. 3: Brahms simulation output

"Open_Fridge" primitive activity is used to represent the

interaction of agents with some appliances. A brief example of the model presented in figure 2 is presented in section 5, where a link is established between human and appliance behaviour.

4. Fridge simulation model

The activities of inhabitants, their presence at different locations in the house, their control over different appliances and objects, and their communications can be modeled in the Brahms simulation environment. However in order to model the appliance behaviour a physical simulator is required which provides the information about physical aspects such as temperature inside the fridge, compressor states etc. We have developed our physical model as shown in figure 4. The description of the model variables is given in table 1.

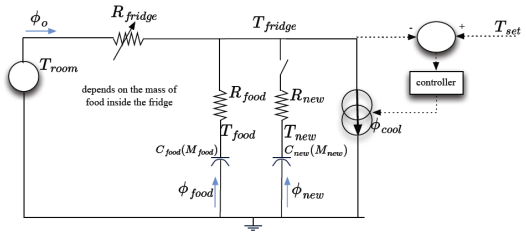

Fig. 4: Physical model for the fridge consumption cycle modeling

In this model we have made assumptions: (i) variation in the quantity of food inside the fridge is negligible, (ii) R_{food} = 0 and food temperature inside the fridge is assumed same as the inside temperature of the fridge. Figure 4 presents

Variable	Description
T_{fridge}(k)	inside temperature of the fridge during reactive time k, $\Rightarrow$ T_{fridge}(k) $\in$ [Tmin; Tmax]
T_{room}(k)	ambiant temperature of the room
T_{new}	New food temperature
C_{new}	$M_{new}C_p$, capacity of a new food added to fridge
R_{fridge}	R_{open} + ζ(Rclose - Ropen) resistivity for heat exchange between inside fridge and room
R_{food}	resistivity to heat exchange between food and fridge
R_{new}	resistivity to heat exchange between new food and fridge
M_{food}	food quantity
M_{new}	quantity of a new food
T_{set}(k)	set-point temperature
$\pm\sigma$	Dead zone: +σ and -σ represent the upper and lower limits, above and below the set point temperature, where the compressor starts or stops respectively

Table 1: Description of model variables

the physical model of the fridge energy consumption cycles. The cooling power ϕ_{cool} is provided by the controller to maintain the setpoint temperature of the fridge. Similarly ϕ_o is the heating power coming from the room and affects the inside temperature of the fridge depending on the resistance R_{fridge}. ϕ_{food} and ϕ_{new} are the heating power coming from the food already present in the fridge and the newly introduced food respectively. Their affect on the fridge temperature depends upon their heat capacity and mass as well as the corresponding resistivity. In modeling the fridge cycles, the heat pump is an important element, let ρ be the performance factor of heat pump that yields C_{elec} = $\rho\phi_{cool}$ and fridge controller is made to follow the following criteria: i) compressor stops working when the fridge temperature goes below the lower limit of the dead zone

$$T_{fridge}(t) - T_{set}(t) < -\sigma \rightarrow \xi(t+dt) = 0 \tag{1}$$

ii) compressor starts working when the fridge temperature goes above the upper limit of the dead zone

$$T_{fridge}(t) - T_{set}(t) > \sigma \rightarrow \xi(t+dt) = 1 \tag{2}$$

iii) otherwise it follows its current state

$$-\sigma \leq T_{fridge}(t) - T_{set}(t) \leq \sigma \rightarrow \xi(t+dt) = \xi(t) \tag{3}$$

cooling power at a particular instance is given by:

$$\phi_{cool}(t) = \xi(t)\phi_{cool} \tag{4}$$

We have modeled three major events for the fridge as (a) permanent mode, where the fridge operates in the normal refrigeration cycles, (b) temporary mode when the fridge door is opened and closed, as a result heat is exchanged and inside temperature rises to impact the instantaneous refrigeration cycles and (c) temporary mode when food is introduced in the fridge.

a) The model for the permanent state or normal cycles is proposed as under that computes the rate of change in the fridge temperature over the simulation period:

$$\begin{aligned}\frac{d}{dt}[T_{fridge}] = \Big[-\frac{1}{R_{fridge}C_{food}} \Big][T_{fridge}] + \\ \Big[\frac{-\rho\phi_{cool}}{C_{food}} \frac{1}{R_{fridge}C_{food}}\Big]\begin{bmatrix} \xi \\ T_{room} \end{bmatrix}\end{aligned} \tag{5}$$

The model of the permanent state (1st order) is obtained when T_{new} = T_{fridge}.

b) The model for the temporary mode when the fridge door is opened and closed. It follows the model for the permanent state with only change in the resistance of the fridge as under:

$$R_{fridge} = R_{new} + \zeta(R_{close} - R_{open}) \tag{6}$$

c) The model for the mode when new food is introduced is proposed as under that computes the change in temperature over time for both the fridge and the new food introduced into the fridge:

$$\begin{aligned}\frac{d}{dt}\begin{bmatrix} T_{fridge} \\ T_{new} \end{bmatrix} = \begin{bmatrix} -\frac{R_{new}+R_{fridge}}{R_{new}R_{fridge}C_{food}} & \frac{1}{R_{new}C_{food}} \\ \frac{1}{R_{new}C_{new}} & -\frac{1}{R_{new}C_{new}} \end{bmatrix} \\ \begin{bmatrix} T_{fridge} \\ T_{new} \end{bmatrix} + \begin{bmatrix} -\frac{\rho\phi_{cool}}{C_{food}} & \frac{1}{R_{fridge}C_{food}} \\ 0 & 0 \end{bmatrix}\begin{bmatrix} \xi \\ T_{room} \end{bmatrix}\end{aligned} \tag{7}$$

We have followed following assumptions wile modeling the fridge: (i) Opening the door modifies R_{fridge} (ii) Removing

food from fridge is assumed to have a very small impact (except the door opening) (iii) Adding food sets a new value to T_{new} and parameters like C_{new} and R_{new} may be adjusted depending on the food.

5. Co-simulation environment

Human behaviour is dynamically modeled and simulated in a multi agent simulation environment (Brahms), as intelligent agents. An agent based approach is well suited since agents are a natural and intuitive way to model humans and their characteristics and are a key towards implementing group behaviour. Agents like humans evolve in the environment, perceive it and act accordingly. The changes in the environment are perceived by the agents, who then take actions dynamically to change the state of the objects and appliances in the building. This dynamic behaviour is fed to the physical simulator containing the model of the fridge using an interface developed in java. It generates energy consumption cycles of the fridge and maintains the setpoint temperature. Physical simulator is implemented in Matlab and simulation results are monitored and analyzed with Simulink. In order to perform certain activities, the

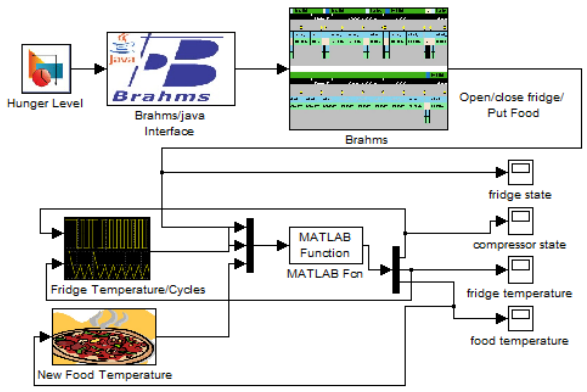

Fig. 5: Co-Simulation Platform to Find High Energy Consuming Activities

inhabitants change their locations, perform certain actions on appliances e.g. opening the fridge, putting food inside etc. As soon as these state changes happen, this information is sent to the physical simulator, where appliance behaviour is changed and its consumption is computed. The proposed co-simulation platform is presented in figure 5 with 3 distinct elements as (i) Brahms MAS, (ii) Brahms Java Interface and (iii) physical simulator (model for the fridge). The Brahms MAS element simulates the agent behaviour for the fridge. The Brahms java interface establishes the connection between Brahms and the physical model of the fridge. This interface actually drives Brahms virtual machine and manipulates different attributes of the occupant's behaviour model to be simulated by setting agents and objects attributes and handling the starting time of the simulation. It also keeps track of the current location of agents and of the current values of different attributes of objects. The physical simulator is created in Matlab/Simulink and consists of the model of the fridge and the controllers for appliances. The model of the fridge is defined in the Matlab function file which uses the output of the Brahms simulation such as opening the fridge, putting food in fridge and based on the inside temperature of the fridge turns the refrigeration cycles on or off. It computes the inside temperature of the fridge to maintain the setpoint temperature.

5.1 Agent based scenario and brahms simulation results

We will now consider a scenario consisting of a 2 person house where husband and wife are modeled as agents. It will show how the decisions taken by the agents affect the energy consumption. Figure 6(a) shows that the husband and wife are sitting in the living room and watching TV. The hunger level for the wife gradually increases with time. When it reaches beyond some threshold, she communicates with the husband to have their meal together. The husband usually likes to eat at restaurant if there is a beautiful weather outside; otherwise he prefers to eat at home. In case husband is agreed based on perception about the weather, she moves to the kitchen, opens the fridge, takes the stuff out and prepares the table for lunch. If however, the husband is not agreed to eat at home, she puts the warm food, which she had already prepared for their meal into the fridge and they go out to restaurant. The simulation results are presented in figure 6. The output is generated randomly based on agents' belief certainty. Belief certainty is the concept used in Brahms which assigns a probability between 0 to 100 to agents' beliefs and the facts in the environment. Beliefs and facts with varying probabilistic values influence agents' actions accordingly. For example, if for the communication between the agents, the fact is that the husband doesn't denies to eat at home as often as he agrees to eat at home based on his perception about the weather, there are more chances that the wife will not put the warm food which she had prepared for the meal into the fridge. Similarly, if the husband is agreed to eat at home, the duration of the activity of opening the door of the fridge and taking the stuff out is a random value between a minimum and maximum duration. Based on this duration, every time the wife will open the door of the fridge for different durations resulting in varying behaviour of the fridge. In figure 6[2], the horizontal bar on the top represents the movements of agents in different locations. Below this is the timeline, which shows the simulation time in the agent world. The vertical bars are used to represent the communication between agents. These are also used to represent the broadcast activity where the

[2]In figure 6 wf stands for workframe, tf for thoughtframe, ca for composite activity, pa for primitive activity, mv for move activity and cw for communication activity.

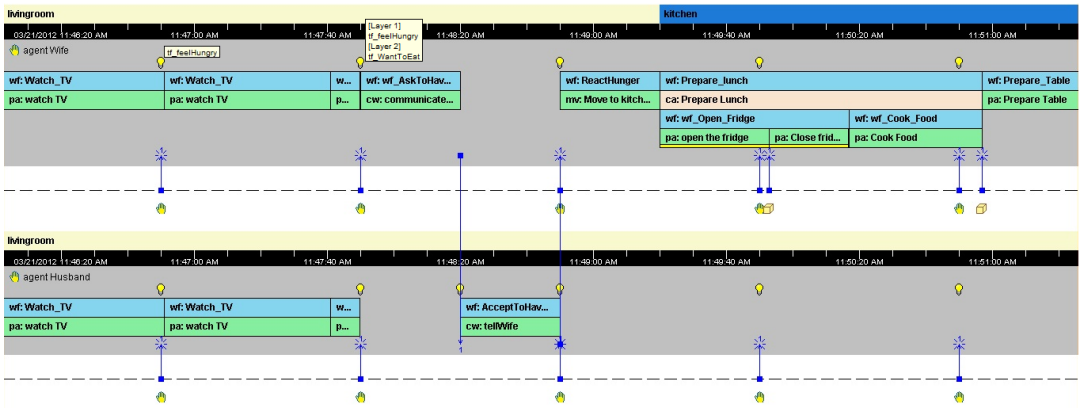

a) Social agreement between agents to have meal at home

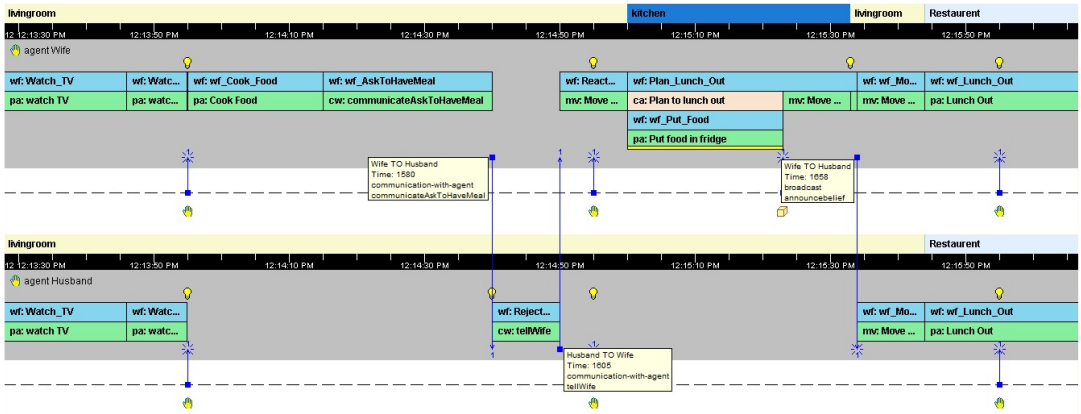

b) Social agreement between agents to eat out

Fig. 6: Simulation Results against Simulated Inhabitants' Behaviour

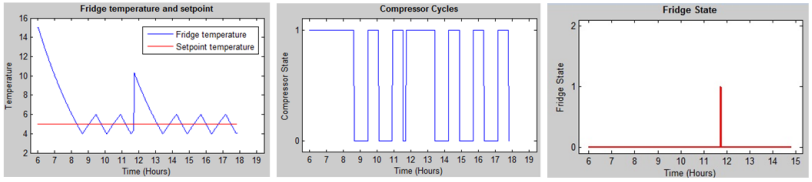

a) Door opened for 100 seconds

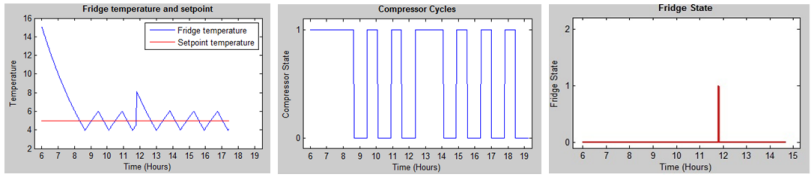

b) Door opened for 60 seconds

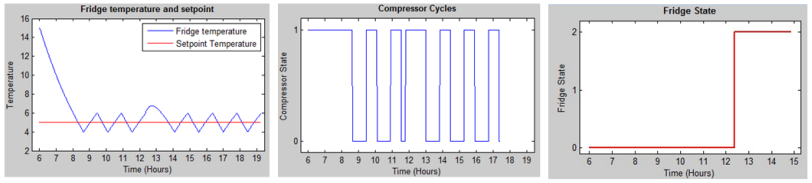

c) New food introduced in the fridge

Fig. 7: Simulation Results against Simulated Inhabitants' and appliance's Behaviour

agents transfer their beliefs with each other. For example in the figure 6(b) the vertical bar coming down from agent Wife to agent Husband at the moment when the Wife agent moves from kitchen to living room, represents the Wife agent's belief which she transfers to the husband to move to the restaurant. The bulb symbols are used to represent the thoughtframes or beliefs of agents. Thoughtframes are changed with the passage of the simulation time and based on different perceptions of agents from the environment.

5.2 Co-simulation results

Figure 7 shows the actions of agents on fridge and the resulting effect on the inside temperature and the compressor cycles. Opening the fridge door for different durations affects the compressor cycles accordingly. In figure 7(a) it can be seen that the agent opened the door of the fridge for longer period so the compressor worked longer and hence consumed more energy than as in figure 7(b) where the agent opened the door for fewer seconds. Similarly it can be seen from figure 7(c) that when the agent husband has denied having meal at house, wife put the warm food inside the fridge. As a result, the temperature inside the fridge increased causing the compressor to work longer than usual to bring the temperature back to the setpoint. The fridge states are represented by three levels 0,1 and 2 where $0 \rightarrow$ no action on the fridge, $1 \rightarrow$ door is opened and closed and $2 \rightarrow$ new food is added.

6. Conclusions and future perspectives

Until recently research has focused on active appliances to optimize the energy consumption and reduce energy waste, however cold appliances are not yet explored that constitute a significant source of energy consumption in our daily lives. It is also a fact that to model the cold appliances energy consumption behaviour is not simple as it follows the activity later in time and is quite complex to predict. We believe that these cold appliances have a hidden energy waste component that must be addressed. So, in this article we have presented a co-simulation methodology to demonstrate the hidden energy waste component from actions on the cold appliances linked with the inhabitants' behaviour. This energy waste component is further used to classify the activities as high energy consuming activities and shall help in building the energy advisors within Smart homes to propose alternative actions to the human agents in real life to ensure energy waste reduction and consumption optimization. Our contributions are (i) a multi agent model of human behaviour relating to energy related activities (ii) a physical model for the fridge energy consumption (target cold appliance), (iii) co-simulation methodology to analyze the energy consumption behaviour of cold appliances based on dynamically simulated inhabitants' behaviour. We have demonstrated by dynamically simulating the inhabitants' behaviour using Brahms modeling and simulation environment that actions on the cold appliances do have a hidden energy waste component and can be avoided to support the efforts for energy waste reduction and consumption optimization. Simulation results clearly highlights that opening fridge for long period and putting a hot food in the fridge results in longer compressor refrigeration cycles resulting in the energy waste. In future we shall validate our physical model with experiments on different categories and capacities of the fridge to develop an accurate but generic model for the fridge (cold appliances). We propose the research community to shift their focus towards other cold appliances to model the energy waste component linked with the inhabitants' behaviour.

References

[1] P. Huovila, *Building and Climate Change Status, Challenges and Opportunities*, Ed. United Nations Publications, 2007, ISBN 978-92-807-2795-1.

[2] W. F. Van Raaij and T. M. M. Verhallen, "A behavioral model of residential energy use," *Journal of Economic Psychology*, vol. 3(1), pp. 39-63, 1983.

[3] I. Richardson, M. Thomson, D. Infield, "A high-resolution domestic building occupancy model for energy demand simulations," *Energy and Buildings*, vol. 40(8), pp. 1560-1566, 2008.

[4] J. Widén, M. Lundh, I. Vassileva, E. Dahlquist, K. Ellegard, and E. Wackelgard, "Constructing load profiles for household electricity and hot water from time-use data-modelling approach and validation," *Energy and Buildings*, vol. 41(7), pp. 753-768, 2009.

[5] P. Davidsson and M. Boman, "Distributed monitoring and control of office buildings by embedded agents," *Information Sciences*, vol. 171(4), pp. 293-307, May. 2005.

[6] S. Abras, S. Ploix, S. Pesty and M. Jacomino, "Advantages of MAS for the resolution of a power management problem in smart homes," in *Advances in Intelligent and Soft Computing*, pp. 269-278, Berlin, Heidelberg: Springer, 2010.

[7] D.J. Cook, M. Youngblood and S.K. Das, "A multi-agent approach to controlling a smart environment," in *Designing Smart Homes*, pp. 165-182, Berlin, Heidelberg: Springer-Verlag, 2006.

[8] C. Liao and P. Barooah, "An integrated approach to occupancy modeling and estimation in commercial buildings," in *American Control Conference, IEEE*, June 30 2010-July 2 2010, p. 3130.

[9] H. Joumaa, S. Ploix, S. Abras and G. De Oliveira, "A MAS integrated into Home Automation system, for the resolution of power management problem in smart homes," *Energy Procedia*, vol. 6, pp. 786-794, 2011.

[10] J. Engler and A. Kusiak, "Agent-Based Control of Thermostatic Appliances," in *Green Technologies Conference, IEEE*, 15-16 April 2010, p. 1.

[11] J. F. Lehman, J. Laird and P. Rosenbloom, "A gentle introduction to Soar, an architecture for human cognition," *Invitation to Cognitive Science: Methods, Models, and Conceptual Issues*, pp. 211Ű253, Cambridge, MA: MIT Press, 1998.

[12] A. Sloman, "Varieties of Affect and the CogAff Architecture Schema," in *Proceedings of the AISBŠ01 symposium on emotion, cognition, and affective computing*, 2001, p. 39.

[13] M. Sierhuis, W. J. Clancey and R. van Hoof, "Brahms - a multiagent modeling environment for simulating work practice in organizations," *Journal for Simulation and Process Modelling*, vol. 3(3), pp. 134-152, 2007.

[14] T. S. Ha, J. H. Jung and S. Y. Oh, "Method to analyze user behaviour in home environment," *Personal and Ubiquitous Computing*, vol. 10, pp. 110- 121, 2006.

[15] F. Sempé and J. Gil-Quijano, "Incremental and Situated Modeling for Multi-agent Based Simulations," in *RIVF, IEEE*, 2010, p. 1.

[16] G. Newsham, "Manual control of window blinds and electric lighting: Implications for comfort and energy consumption," *Indoor Environment*, vol. 3, pp. 135-144, 1994.

A mixed (centralized/distributed) solving approach for energy management problem in dwelling

H. Joumaa, G. De-Oliviera, S. Ploix, and M. Jacomino
G-SCOP lab, 46 avenue Felix Viallet, 38031 Grenoble cedex 01, France
Email:Hussein.Joumaa@imag.fr, Gregory.De-Oliveira@g-scop.grenoble-inp.fr,
Stephane.Ploix@g-scop.grenoble-inp.fr, Mireille.Jacomino@g-scop.grenoble-inp.fr

Abstract— *The global dwelling energy management problem can be formalized as an optimization problem of energy consumption/production. An optimal solution for the home energy management problem is usually solved by centralized solvers. The solver gets the totality of the thermal model of the dwelling but also each appliance composing the system. Nevertheless, this centralized resolution has some limits due to some particular appliances. For example: the appliances with a non-sharable model because of the manufacturer, the appliances that need some precisions that cannot be included in their standard representation used by the solver, the appliances which require specific solvers and the appliances which possess a heuristics solving rules. This work proposes to combine the centralized solving approach for energy management problem in dwellings with a multi-agent solving system. The multi agent system provides the possibility of integrating specific models in the global solving of the problem. The proposed system is a mixed centralized/decentralized approach for the solving of global energy management problem.*

Keywords: Multi-agent systems, Energy Management in dwellings, Optimization, Home automation system, Mixed integer linear programming.

1. Introduction

Reducing housing energy costs is a major challenge of the 21^{st} century. In the near future, the main issue for building construction is the thermal insulation, but in the longer term, the issues are those of "renewable energy" (solar, wind, etc) and "smart buildings". Home automation system basically consists of household appliances linked via a communication network allowing interactions for control purposes [1]. Thanks to this network, a load management mechanism can be carried out: it is called distributed control in [2]. Load management makes it possible for inhabitants to adjust power consumption according to expected comfort, energy price variation and CO_2 equivalent emissions. A home energy management system is able to determine the best energy assignment plan and a good compromise between energy production and energy consumption [3]. In this study, energy is restricted to the electricity consumption and production. [4], [3] present a three-layer (anticipative layer, reactive layer and device layer) household energy control system. This system is both able to satisfy the maximum available electrical power constraint and to maximize a ratio between user satisfaction and cost. The objective of the anticipative layer explained in [5] is to compute plans for production and consumption of services.

Uniqueness of housing systems involves a set of new issues in control system science: it is necessary to develop new tools [6], [7], [8] and algorithms [9], [10] for globally optimized power management of the home appliances, able to anticipate difficult situations and to take into account the actual housing system state and the occupant expectations.

The approaches solving the energy management problem in living places can be split into two groups:

- The approaches solving large dimension optimization problems. It has been tackled using a mixed integer linear programming approach that can manage thousands of binary and continuous variables in [9], [10], [11]. Ways of transforming an energy management problem into a MILP, which is a regular problem, have been shown. These approaches are noted "centralized solving approach of the energy management problem" due to the use of a central MILP solver that contains the general mathematical formulation of the problem. The global solution of the problem is then computed locally in this solver.
- The approaches solving singular problems and proposing "distributed solving of energy management problem". Multi-agent approaches have been used to manage services that can only be modeled by nonlinear equations [12], [6], [7], [13], [8].

The multi-agent approaches have some advantages but cannot ensure an optimal solution of the energy management problem contrary to the centralized approaches. The centralized ones have also some limits due to requirements on models. For example, the appliances with a non-sharable model, the appliances that need some precisions that cannot be included in a linear model (as a washing machine with a lot of perturbations and/or particular actions), the appliances which need non-linear optimization, and the appliances which possess heuristics solving rules.

This work proposes to solve the energy management problem by combining centralized and distributed solving

approaches. This approach is noted mixed solving of the energy management problem.

The organization of the paper is as follows, firstly, the problem is presented and the need of a mixed solving approach is discussed in details (section 2) followed by the principle of mixed solving approach (section 3). The implementation of the approach is presented in (section 4). Finally the conclusion is drawn in (section 5).

2. Problem description

In this paper, energy is restricted to electricity consumption and production. Each electrical activity is represented by an amount of consumed/produced electrical power; it is called service and can be supported by one or several appliances.

Housing with appliances aims at providing comfort to inhabitants thanks to services which can be decomposed into three kinds: the end-user services that produce directly comfort to inhabitants, the intermediate services that manage energy storage and the support services that produce electrical power to intermediate and end-user services. Support services deal with electric power supplying thanks to conversion from primary energy to electricity. Fuel cells based generators, photovoltaic power suppliers, grid power suppliers such as EDF in France, belong to this class. Intermediate services are generally achieved by electrochemical batteries. Among the end-user services, well-known services such as clothe washing, water heating, specific room heating, cooking in ovens and lighting can be found.

A service with index i, denoted as SRV_i, transforms energy in order to meet a user's need via one or several appliances. A service is qualified as *permanent* if its energy consumption/production covers the whole time range of the energy assignment plan such as heating service, otherwise, the service is referred to as a *temporary service* such as cooking or washing service.

A temporary service is characterized by the duration and desired end time of the operation. The flexibility of this service comes from the possibility of shifting its operating time, i.e. bringing it forward or delaying the service.

A permanent service is characterized by a quantity of energy consumed or produced. The flexibility of this service comes from the possibility of modifying the energy quantities consumed/produced throughout all the periods (decrease or increase in energy consumption or production at a given time).

An important issue in Home Automation problems is the uncertainties that have to be taken into account. For instance, solar radiation, outdoor temperature or services requested by inhabitants are not exactly known. In order to solve this issue, a three-layer architecture is proposed in this paper: a local layer, a reactive layer and an anticipative layer.

The *anticipative layer* is responsible for scheduling end-user and support services taking into account predicted events and costs in order to avoid, as much as possible, the use of the reactive layer. Various forecasted information about future user requests and available power resources and costs are needed to compute anticipative plans. This layer has slow dynamics and includes predictive models. Let us assume a given time range for anticipating the energy needs (typically 24 hours). The sampling period of the anticipative layer is denoted $\triangle$. The *reactive layer* aims at adapting the anticipative plans to the actual requests and environmental conditions.

The formulation of the energy management problem contains both behavioral models with discrete and continuous variables, differential equation and quality models with non-linearities such as in the PMV model. In order to get mixed linear programs which can be solved by well known efficient solvers, transformations of the previous equations have to be done. The problem is then solved by a centralized solver. The solver takes the models of different services, constructs the problem, and provides the solution.

This centralized solving problem has some limits:

- the appliances having a model non-shared by manufacturers: usually, manufacturers keep their appliances models. From the centralized solver point of view, the model of these appliances cannot be included in the problem solving. The solver can only take into account an unsupervised service reducing accuracy.
- the appliances that need some precision and cannot be included as linear model. For example, a washing machine, more precision is expected in the control like water temperature set-points, length of some phases,... These fine controls cannot be included in a general linear model.
- the appliances having a non-linear model: for example, a heat pump is modeled by a non-linear model dependant of the outdoor temperature. The local problem solving can be done by using a non-linear optimization method such as Nelder Mead or SQP. These categories gather appliances with non-linear model and appliances that can be managed by specific solvers.
- the appliances that are managed by user-defined specific heuristic rules: These appliances have some "behavioral rules". For example, positions of shutters can be programmed with rules defined by inhabitants. This is the case of "end user programming". In this case, the behavioral rules provide the solution without the need of any optimization. The solver must take into account the chosen solution in the global problem solving.

The following section presents the solution proposed to integrate these types of appliances in the global solving of the problem.

3. Principle of mixed solving approach

The system consists of three main parts (Figure 1):

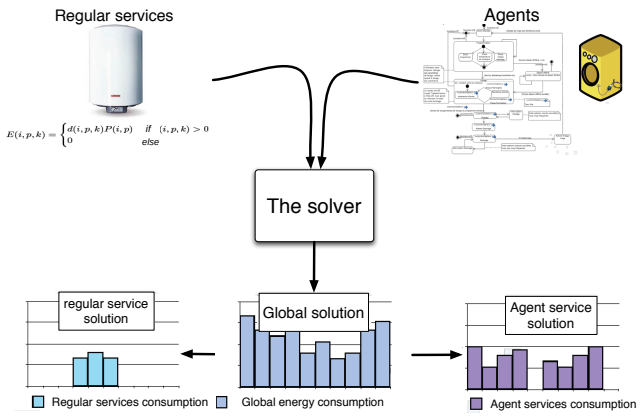

Fig. 1: Global architecture of the mixed solving system

Fig. 2: Solving process during one step

- The regular services:consist of the appliances having a linear model and can be integrated directly into the energy management problem.
- The agents:consist of the services that do not have a linear model and should communicate with the solver to give their *energetic profiles*. The steps of the solving process and the protocol of communication are presented in the following parts.
- The solver consists of a regular solver with the ability to communicate with agents. The solver integrates the information sent by the agent's local solvers with regular service models in order to generate a global problem to solve.

There is only one communication needed between this regular services and the solver. At the beginning of the solving process, the solver receive the linear model from the regular services. The models are used all along the solving process.

In the case of agents, some communications are needed. Each exchange between the agents and the solver is considered as a step in the solving process. In each step, an intermediate problem is created by the solver then computed. The solver decides which information is needed to be sent to the agents in the next step. The agent takes into account the information sent by the solver and sends energetic profiles. The solving process is presented in the following in three parts:

- The progress of the problem solving during one solving step.
- The solver's behavior during the solving process.
- The agent's behavior during the solving process.

3.1 One step solving

Figure 2 presents the information exchanged between the solver and the regular services and the agent services during the first step in the solving process.

First, the solver receives the linear models of the regular service. This operation is the initialization of the problem. Once initialization is done, the solver computes the *relevance indicator*. It is an indicator with the purpose to direct the local solving problem in the agent. When this indicator is computed, it will be sent to all agents.

The agents don't have any information about the environment but they have the ability to solve their own local problem. When agents receive the relevance indicator, they compute their solutions taking into account this indicator serving as information about their environment. They obtain several solutions, which are called *energetic profiles*. It is the consumption for the concerned agent for each period of the optimization horizon. All theses profiles are sent back to the solver. The solver includes them in the problem To be solved at this step. Then the global problem with all the services is solved at this step.

After the first step, the solver begins a new step by computing the relevance indicator. The relevance indicator is computed taking into account the received *energetic profiles* sent by the agents in order to improve the global solution each step in the solving process.

3.2 Solver's role

The solver has two tasks to do in each step. In order to formulate these tasks, we introduce some notations:

- k is the index of anticipative period
- $\mathcal{S}$ is the set of services
- $\mathcal{S}^L$ is the set of *regular services*
- $\mathcal{S}^D$ is the set of *agent services*
- S is a service included in $\mathcal{S}$
- E_k^{max} is the available energy during the period k before any optimisation
- $E_k(S)$ is the consumed energy by the *regular service* $S \in \mathcal{S}^L$ during the period k
- $E_k(S, i, \mathbb{P}_k)$ is the consumed energy by the *agent service* $S \in \mathcal{D}^L$ during the period k for the i^e profile

- C_k is the cost of energy during the period k
- $\upsilon(S)$ is the characteristic of inhabitant request for the service S
- $D(\upsilon(S))$ is the dissatisfaction of the *regular service* $S \in \mathcal{S}^L$
- $D(\upsilon(S), i, \mathbb{P}_k)$ is the dissatisfaction of the *agent service* $S \in \mathcal{S}^D$ for the i^e profile
- $\mathbb{P}_{k,\forall k}$ is the relevance indicator for the current step of resolution

a) Optimisation problem: Each step, the solver computes a linear problem to find a solution. The *regular services* models are represented in [14]. This problem is extended by including *agent services*. Some equations are added to take into account the *agent services*. A new set of variable for each *agent service* is introduced (see equation 1). $\zeta_i(S)$ is a binary variable whose value is 1 if the profile i of the *agent service* S is chosen by the solver, 0 otherwise.Combined with equation 2, ensure the solver to keep only one profile for each *agent service* in the solution.

$$\zeta_i(S) \in \{0,1\}, \forall i \tag{1}$$

$$\sum_i \zeta_i(S) = 1 \tag{2}$$

The criterion to minimise is modified and becomes a two parts criterion (3).

$$J_{iter} = \sum_{S \in \mathcal{S}^L} \left(\sum_k C_k E_k(S, \theta(S)) + \lambda \times D(\upsilon(S, \theta(S))) \right) + \sum_{S \in \mathcal{S}^D} \sum_i \zeta_i \left(\sum_k C_k E_k(S, i, \mathbb{P}_k) + \lambda \times D(\upsilon(S), i, \mathbb{P}_k) \right) \tag{3}$$

There are two different parts in this criterion, one part concerning *regular services* and one part for *agent services*. They are designed on the same scheme to have an a standardized criterion. This scheme split into two influences:

- The influence on the cost: the global energy cost must be minimized.
- The influence on the inhabitants: the dissatisfaction of the inhabitants must be minimized.

Those influences can be found in both *regular services* part and *agent services* part. But there is a fundamental difference between these two parts, and it is symbolized by the sum on the index i in the *agent services* part. The solver keep only one profile for each *service agents*. For each profile, the solver receives one consumption plan and an associated dissatisfaction. The sum in the criterion with binary variables forces to keep only one profile per agent for the minimisation.

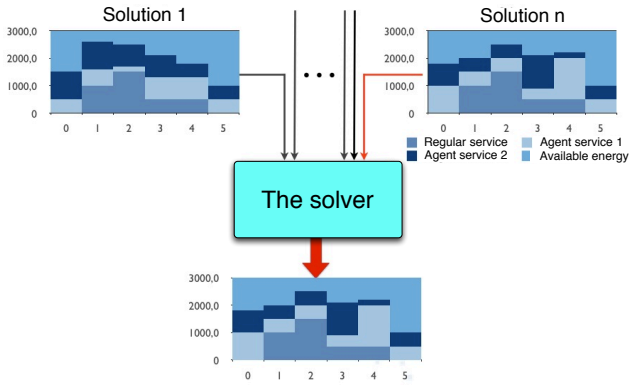

Fig. 3: Solution found by the solver

Figure 3 shows the complexity of the problem to be solved at each step. Each *service agent* provides n profiles, if there are m *singular services*, then there are n^m different solutions. But the solver has to minimise the criterion to keep one.

b) Relevance indicator: The relevance indicator is computed during each solving step to direct the local solving process of service agents for the next step. After the solving step j, the relevance indicator is computed with the equation 4. The purpose of this approach is to share the information about the energy consumption and price between solver and service agents. The service agents integrate the received information in their local solving process of the step j+1. This indicator is high when the consumed energy is important or/and when the energy is expensive. This rules aim to obtain a better solution that minimize J_{iter} in the step $j+1$. During the first step, the consumption of the *agent services* is null.

$$\mathbb{P}_k^j = \frac{1 + E_k^{max}}{1 + E_k^{max} - \sum_{S \in \mathcal{S}^L} E_i^{j*}(S)} C_k \tag{4}$$

3.3 Role of the agents

An agent is dedicated to a specific entity whose behavioral model cannot be linearized and then taken into account directly by the solver. In this part, the algorithm used by agents are explained using an example of washing machine service agent.

The washing machine service agent has its internal state model. The states are shown by figure 4. They consist in:

- some behavioral states like heating, prewash, washing and spin-drying.
- two states representing the begining and the end of the service
- some states denoted *wait i* represent the waiting time between behavioral states
- some states modeling the interuption whithin each state, denoted *interupted state*

The normal behavior of the washing machine service is given by the state sequence scenario [start, heating, prewash, washing, spy-drying, end]. The other states are only visited when the service agent tries to find some neighbouring profiles in order to respond to some criteria sent by the solver.

Each visit to an *interrupted state* has a fixed time period $\tau_{interrupted}$. It is possible to visit the *interrupted state* more than once in order to increase the interruption time in a state. For example, in the state sequence scenario [start, heating, interupted heating, heating, interrupted heating, prewash, washing, spy-drying, end], the time spent in the interupted heating state is $2 * \tau_{interruption}$.

A behavioral profile is the state sequence scenario with the date of each state visit. The behavioral profile is caracterized by:

- the starting time of the service
- the number of visits to each *interrupted state* and the number of visits for each *wait i* state
- the date of each visit to *interrupted states* and *wait i* states.

These characteristics are denoted in the following *parameters of behavioral profile*. It is interesting to note that a behavioral profile is computed in order to be converted into an energetic profile. The energetic profile consists on the energy consumed by the service in each period of the anticipative horizon. The energetic profile is then sent to the solver.

The Agent satisfaction is computed according to the energetic profile. The satisfaction depends on the number of visited interupted states and also on the effective ending time regarding its expected value for the occupants. The increase in the number of interruptions affects the agent satisfaction.

3.3.1 Agent solving algorithm

The agent solving algorithm is presented in figure 5.

Firstly, the agent receives the relevance indicator. The relevance indicator consists of information about the penalisation and the energy price during the anticipative horizon. The agent receives also the choosen energetical profile at step j.

The first step in the algorithm is to normalize the values of relevance indicators (5). The goal of this step is to obtain $RI_{k(normalized)}$ that can be used in the computation of CA_k, the agent coefficient. It is composed both on the information received from the solver and on the local satisfaction computed by the agent.

$$RI_{k(normalized)} = RI_k / Max(RI_k) \quad (5)$$

The second step consists on the computation of the agent coefficient CA_k. The CA_k merges the information about the prenalization, the energy price and the agent disatisfaction denoted I_k (6).

$$CA_k = RI_k + \lambda * I_k \quad (6)$$

In order to generate an enegertic profile, the first step is to compute the behavioral profil. The parameters of the behavioral profile are listed above. The first one in the starting time of the service. We begin by finding the best intervals over 6 periods in the 24 hour horizon according to the values CA_k. For each interval j we compute X_j (7).

$$X_j = (\sum_{k \in [j, j+6]} CA_k)/6 \quad (7)$$

We denote $X_{j_{min}}$ the minimum of the list X_j.

Then we try to find the intervals having no significant difference with $X_{j_{min}}$. We denote L_{min}, the list:

$$L_{min} = \{k / 1 - (X_{j_{min}} / X_k) < 0.1\} \quad (8)$$

The interval χ with the maximum variance in L_{min} is chosen for the optimization. The starting time of the service corresponds to the starting time of the chosen interval χ.

The parameters of the optimization are presented in figure 6 where N_{Si} is the number of interuptions in the state Si. W_{Si} is a value to select the time for interruption within the state.

A branch and bound optimization is achieved on this parameter (Figure 7) within the chosen interval χ. Each agent solves the optimization problem with this function. It represents the minization of the energetic cost and dissatisfaction from a local point of view. The function to be minimized 9 is similar to the one presented for the solver.

$$min_{\theta^{j+1}} J^{k+1} = \sum E_k(\theta^{j+1}) \mathbb{P}_k^j \mathbb{T}_k^j + \lambda D_i(\theta^{j+1})) \quad (9)$$

θ^{j+1} represents the parameters of the user that define the usage conditions. The function is composed of two parts: the first one is the influence of the energetic cost and the second one is the influence of the satisfaction of the agent.

The results of this optimisation is a list of parameters required to generate the behavioral profile (parameters of behavioral profile). Then, the energetic profile can be computed and sent to the solver to be integrated in the global problem solving.

4. Implementation

The implemented system consists of five components (figure 8):

- the classical regular solver used in [14]
- the solver that solves global problem composed from regular problem and agent problems
- the broker agent is a communication component that receives all the local problems from service agents

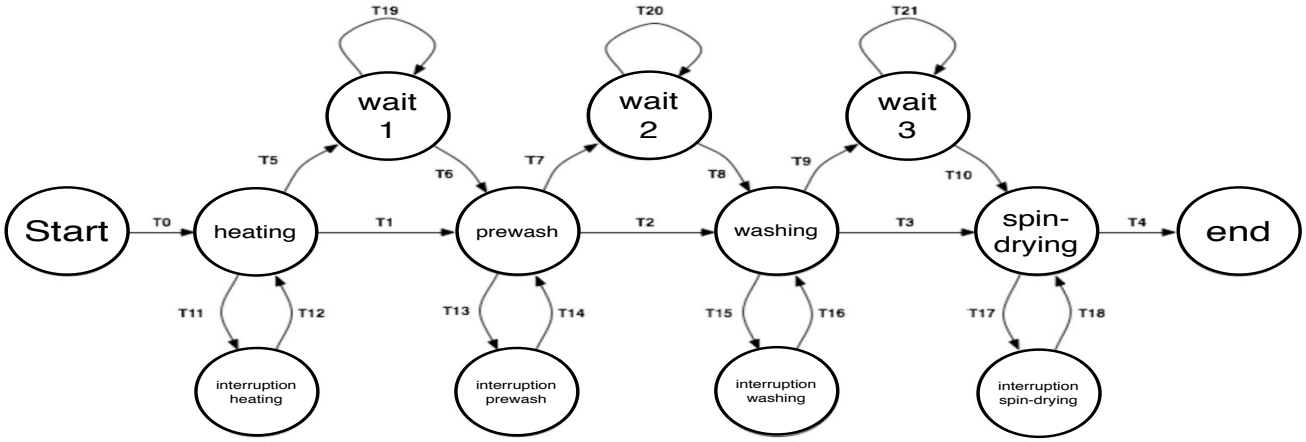

Fig. 4: State model of the washing machineservice agent

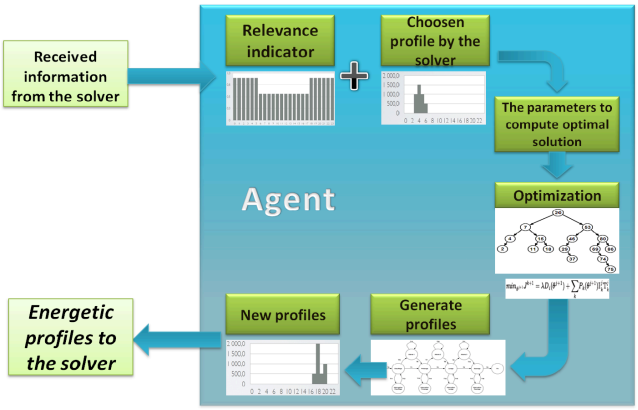

Fig. 5: Solving algorithm in the agent

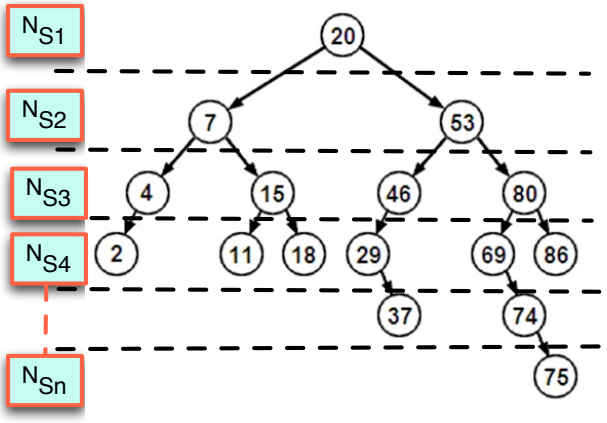

Fig. 7: Optimization using branch and bound

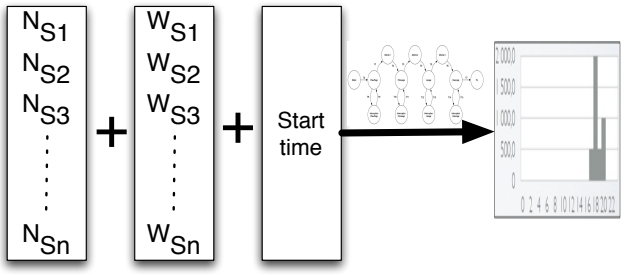

Fig. 6: Parameters of a profile

and construct one global service agent problem. This problem is sent then to the global solver. The broker receives also the relevance indicator from the solver and dispatches the information to service agents

- the service agent with the capabilities to solve a local problem.

The system is tested by using two service agents and some regular services. Figure 9 presents simulation results.

5. Conclusion

In this paper, the energy management problem is solved by combining centralized and multi-agent solving approaches. The multi agent system added to the MILP solver provides the possibility of integrating singular, i.e. not MILP, appliance models in the global energy management problem to

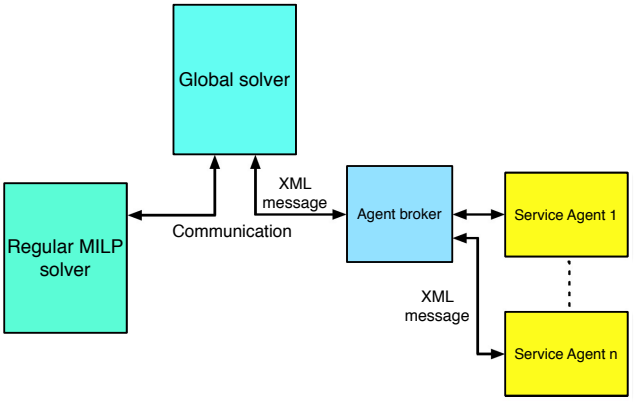

Fig. 8: The composant of the mixet solving system

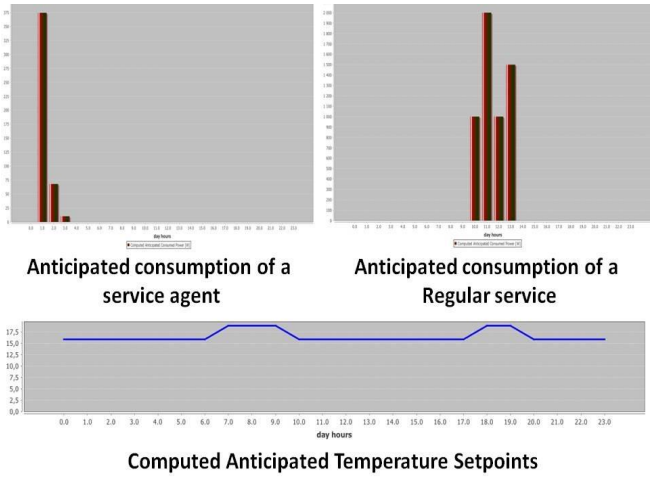

Fig. 9: Anticipating regular and service agents

be solved. The proposed approach has been implemented and tested. Conversely to centralized solution, the solution resulting from a mixed approach is not garanteed optimal solution. The number of steps used in the solving process affects the resulting solution. The algorithm used in the solver to generate the relevance indicator affects also the global solution. Genetic algorithms can be studied and introduced at this stage in order to improve the global solution.

References

[1] P. Palensky and R. Posta, "Demand side management in private home using lonworks," in *Proceedings of the IEEE International Workshop on Factory Communication Systems*, 1997.

[2] K. Wacks, "The impact of home automation on power electronics," in *Applied Power Electronics Conference and Exposition*, 1993, pp. 3–9.

[3] S. Ha, H. Jung, and Y. Oh, "Method to analyze user behavior in home environment," *Personal Ubiquitous Comput.*, vol. 10, pp. 110–121, January 2006. [Online]. Available: http://dx.doi.org/10.1007/s00779-005-0016-9

[4] S. Abras, S. Ploix, S. Pesty, and M. Jacomino, "A multi-agent design for a home automation system dedicated to power management," in *Artificial Intelligence and Innovations 2007: from Theory to Applications*, ser. IFIP International Federation for Information Processing, C. Boukis, A. Pnevmatikakis, and L. Polymenakos, Eds. Springer Boston, 2007, vol. 247, pp. 233–241.

[5] S. Abras, S. Pesty, S. Ploix, and M. Jacomino, "An anticipation mechanism for power management in a smart home using multi-agent systems," in *Information and Communication Technologies: From Theory to Applications, 2008. ICTTA 2008. 3rd International Conference on*, april 2008, pp. 1 –6.

[6] S. Abras, S. Ploix, S. Pesty, and M. Jacomino, "Advantages of mas for the resolution of a power management problem in smart homes," in *8th International Conference on Practical Applications of Agents and Multi-Agent Systems, PAAMS'2010*. Salamanca, Spain: Springer Verlag, 26-28 April 2010.

[7] S. Abras, S. Ploix, and S. Pesty, *Housing, Housing Costs and Mortgages: Trends, Impact and Prediction*, ser. Housing Issues, Laws and Programs. Nova Publishers, 2010, no. ISBN 978-1-60741-813-9, ch. Managing Power in a Smart Home Using Multi-Agent Systems.

[8] A. M. Elmahaiawy, N. Elfishawy, and M. N. El-Dien, "Anticipation the consumed electrical power in smart home using evolutionary algorithms," in *MCIT 2010 conference*, 2010.

[9] L. D. Ha, S. Ploix, F. Wurtz, P. Perichon, and J. Merten, "Energy management system for a photovoltaic grid-connected building," in *24th EU PVSEC and 4th World Conference on Photovoltaic Energy Conversion*, Hamburg, Germany, September, 21-26 2009.

[10] L. D. Ha, S. Ploix, M. Jacomino, and H. Le Minh, *Energy Management*, ser. ISBN 978-953-307-065-0. INTECH, 2010, ch. A mixed integer programming formulation of the home energy management problem.

[11] D. L. Ha, H. Joumaa, S. Ploix, and M. Jacomino, "An optimal approach for electrical management problem in dwellings," *Energy and Buildings*, vol. 45, no. 0, pp. 1 – 14, 2012.

[12] S. Abras, S. Ploix, S. Pesty, and M. Jacomino, *Informatics in Control, Automation and Robotics III*, ser. Lecture Notes in Electrical Engineering. Springer Berlin Heidelberg, 2006, vol. 15, ch. A multi-agent home automation system for power management.

[13] H. Joumaa, S. Ploix, A. S., and G. De Oliveira, "A mas integrated into home automation system, for the resolution of power management problem in smart homes," in *1st Conference and Exhibition Impact of Integrated Clean Energy on the Future of the Mediterranean Environment*, elsevier, Ed., 2011.

[14] G. De Oliveira, M. Jacomino, D. L. Ha, and S. Ploix, "Optimal power control for smart homes," in *18th IFAC World Congress*, elsevier, Ed., 2011.

Can Intelligent Agents Improve Persistence?

Dr. Wayne E. Smith
Argosy University, Dallas Campus, 5001 LBJ Freeway, Dallas, TX 75244

Abstract – The coupling of intelligent agents with learning resources create an important synergy with improved persistence as an outcome.

Keywords: Artificial Intelligence Intelligent Agents Electronic Commerce Retention Graduation Persistence

1.0 Introduction

The goal of the work presented in this paper is to offer possible methods to advance the study of intelligent student resources. The use of intelligent agents in e-commerce was designed to facilitate transactions for the buyers as well as sellers. It has been proposed that intelligent agents can assist with this process. Can intelligent agents choose learning resources in furtherance of intelligent learning technologies? The synergistic possibilities offer advances in learning around the globe.

2.0 Literature Review

2.1 Intelligent Agents

Intelligent agents have grown from little known computer programming into a wide variety of agents with multiple characteristics and competencies. Intelligent agents have advanced to even achieve a competitive advantage in the business world. Intelligent agents, like humans, have differing levels of intelligence. At the lowest level, agents merely carry out user assigned tasks. More intelligent agents can perform repetitive tasks and even monitor activity and report results. This last level refers to a semi-intelligent agent. A truly intelligent agent, at the highest level, can maintain user profiles, update the profile based on user actions, and even anticipate a users' action and learn from an error [3][6].

2.2 Intelligent Agents and Students

Studies of intelligent agent use demonstrate that agents can work in tandem to achieve a common task [1]. Original work with agents dealt with simple negotiation systems in a business-to-business or business-to-consumer e-commerce environment. Agents negotiated for simple goods or services. The ability to negotiate the acquisition of specialized goods or services will require more advanced systems. Advanced agent systems are under development with promising possibilities. Agents have also developed into the consumer-to-consumer e-commerce environment [4][5]. This level of sophistication will enable students to progress through higher levels of learning by accessing resources as necessary.

Intelligent agents enable people to maintain contact with the business world while at the same time releasing an individual from social interaction [7]. One study showed that people would rather deal with an intelligent agent than a human when conducting business online [9]. Students that are shy tend to engage online learning more fully when not overshadowed by gregarious classmates [2][8].

2.3 Freshman Success

Less than 60 percent of college freshmen graduate from the college they first entered [10]. There are several factors that mix and match in this failure. An important factor is the availability of resources to bolster weak areas. Many students discover that they left high school unprepared for college-level math and/or writing. Modern students are normally computer savvy from hours spent playing digital games. Many students interact with "online friends" separate from other relationships.

3.0 Synergy

The synergistic possibility of student needs and intelligent agent technologies is promising. In an e-commerce environment, a prospective buyer from one part of the world contacts a seller or seller's agent. In an education environment, a student will access a needed resource regardless of venue. The intelligent agent systems developed today will allow agents to discover the learning resource in the required language in a manner similar to addressing different desires for size, color, or financing options in the e-commerce space.

The combination of intelligent agents with other web intelligences has been proposed. The opportunity to deal with complex real-world education problems is the key. These new solutions will make money, satisfy students, and give educational businesses a competitive advantage [11]. When mobile marketing adopts this technology, products will be offered to students in their preferred language [7]. The ultimate purpose is for agents to anticipate the need for language appropriate learning resources and attained preparedness to meet the need [11].

4.0 Summary

The elements needed to combine intelligent agents with educational resources are in development. The combination opens a world of possibilities to enhance university retention and ultimately graduation rates. The opportunity for competitive advantage in educational venues is ripe as those that move first will reap the first benefits.

5.0 References

[1] Benharzallah, S., & Kazar, O. (2008). Intelligent Agents for a Semantic Mediation of Information Systems. *International Review on Computers & Software*, *3*(2), 170-175.

[2] Feather, S. (1999). The impact of support systems on collaborative learning groups' stages of development. *Information Technology, Learning, and Performance Journal, 17*(2), 23-34.

[3] Iyengar, J. & Shumway, D. (2006). Intelligent software agents and the creation of competitive advantage. *JGC, 14*(2), 112-120.

[4] Kim, W., Hong, J., & Song, Y. (2007). Multi-attributes-based agent negotiation framework under incremental information disclosing strategy. *International Journal of Information Technology & Decision Making*, *6*(1), 61-83.

[5] Kowalczyk, R., Braun, P., Mueller, I., Rossak, W., Franczyk, B., & Speck, A. (2003). Deploying mobile and intelligent agents in interconnected e-marketplaces. *Journal of Integrated Design & Process Science*, *7*(3), 109-123.

[6] Nadarajan, G., & Chen-Burger, Y. (2007). Translating a typical business process modelling language to a Web Services Ontology through lightweight mapping. *IET Software*, *1*(1), 1-17.

[7] Ranchhod, A. (2007). Developing mobile marketing strategie. *International Journal of Mobile Marketing, 2*(2), 76-83.

[8] Sanner, S. & Deis, M. (2009). How can interdisciplinary collaboration between schools promote culturally diverse students' success? *Academy of Educational Leadership Journal, 13*(4), 19-34.

[9] Smith, W. E. (2006). Will consumers accept intelligent agents? // Proceedings of the 2006 International Conference on Artificial Intelligence, ICAI 2006, Las Vegas, Nevada, USA, June 26-29, 2006, Volume 1, CSREA Press 2006, ISBN 1-932415-96-3.

[10] Veenstra, C. (2009). A strategy for improving Freshman College Retention. *Journal for Quality and Participation, 31*(4), 19-23.

[11] Zhong, N., Liu, J., & Yao, Y. (2007). Envisioning intelligent agent information technologies through the prism of web intelligence. *Communications of the ACM, 50*(3), 89-94.

SESSION

ARTIFICIAL INTELLIGENCE AND COGNITIVE SCIENCE + COGNITIVE ARCHITECTURES + APPLICATIONS

Chair(s)

TBA

Hybrid Reactive-Deliberative Behaviour in a Symbolic Dynamical Cognitive Architecture

Othalia Larue[1], Pierre Poirier[2], Roger Nkambou[1]
GDAC Research Laboratory
[1] Department of Computer Science
[2] Department of Philosophy
Université du Québec à Montréal
Corresponding author: larue.othalia@courrier.uqam.ca

Abstract - *Sequentiality and reactivity are features that have been deemed important for cognitive architectures[1]and recent emphasis has been put by the community on their development in cognitive architectures. However, the cooperation and competition dynamic between reactivity and sequentiality remains an open issue in the domain [2]. In this paper, we present a three level cognitive architecture for the simulation of human behaviour based on Stanovich's Tripartite Framework [3], which provides an explanation of how reflective and adaptive human behaviour emerges from the interaction of three distinct cognitive levels. We use two classical psychological tasks to study the reactivity/sequentiality dynamic in our architecture. These show that the two features collaborate in interesting and psychologically plausible ways.*

Keywords: cognitive architecure; hybridism; sequentiality; reactivity

1 Introduction

A cognitive architecture is "the overall, essential structure and process of a domain-generic computational cognitive model, used for a broad, multiple-level, multiple domain analysis of cognition of behaviour" [1] (p.4). Psychologists and other cognitive scientists can use these architectures to study the mechanisms responsible for observed behaviour, and engineers can employ them to endow their systems with cognitive (e.g. decision-making) capacities. Theoretical studies of cognitive architectures [1,3, 4] have identified many general features that architectures should have if they are to efficiently play these roles. Two such features, reactivity and sequentiality [1], have proven difficult to integrate in well-unified cognitive architectures, and, emphasis has recently been put on the development of these features (especially in the guise of reactive abilities and of reflective/deliberative). It is difficult to integrate reactivity and sequentiality because the two features appear to be functionally incompatible: designs that favour one almost inevitably hinder the other. As a result, integration of reactive and sequential processing remains a challenge in the domain [2]. In this paper, we address the challenge by introducing a new architecture, one that implements Stanovich's [3] Tripartite Framework: a framework that aims to explain how reflective (characterized by sequentiality) and adaptive (characterized by reactivity) human behaviour emerges from the interaction of three distinct cognitive levels (autonomous/reactive, algorithmic/cognitive control, and reflective). To demonstrate the flexible and coherent behaviour of the resulting architecture, we study its performance on two classical psychological tasks: the Stroop task, which requires perceptual attention and cognitive control, and the Wisconsin card sorting task, which requires cognitive flexibility and efficient collaboration between the reactive and sequential elements of the architecture.

2 Related Work

2.1 Cognitive architectures

Although there are now a variety of cognitive architectures (see for a review [3]), we chose here to focus on three of the most widely used: ACT-R, SOAR, CLARION [1].

ACT-R (Adaptive Components of Thought-Rational) [5] is a cognitive architecture whose development is oriented towards the understanding of human cognition. ACT-R's components are a set of perceptual-motor modules, memory modules, buffers, and a pattern matcher module, which finds productions that match the current state of the buffers. There are two types of memory modules in ACT-R: declarative memory and procedural memory, consisting of chunks or production (for the procedural memory) and associated sub-symbolic values (connectionist hybridism). A long-term memory of production rules coordinates the processing of the modules. Each module has a chunk holding a relational declarative structure. Each chunk has a set of sub-symbolic parameters reflecting its past activity and influencing its future retrieval from long-term memory. Adaptation in ACT-R occurs thanks to a top-down learning approach. ACT-R has been used to simulate a large number of cognitive phenomena but has seldom been used for the simulation of extended metacognitive processes. Further effort has been put into implementing a unified theory of cognition, perception, and action by integrating perceptual and motor modules working in parallel with cognition; however, cooperation between these modules is limited since their content (perceptual,

motor, declarative memory) is still processed using distinct buffers.

SOAR (State, Operator And Result) [4] is also a rule-based cognitive architecture aimed at the modelization of general intelligence. Knowledge is in the form of production rules, arranged in terms of operators acting in the problem space (set of states representing the task). Operators provide the system with adaptation since they can externally as well as internally modify the system's state. The primary learning mechanism is chunking, which allows the extraction of rules from problem solving traces. A basic processing cycle repeatedly selects, and applies operators, achieving one decision at a time. In SOAR, different types of learning are applied to different types of knowledge: reinforcement learning to adjust preference values, episodic learning to keep track of the system's evolution, semantic learning for declarative knowledge. SOAR is able to perform high-level reasoning task (planning, problem solving …).

As opposed to ACT-R and SOAR, CLARION requires less a priori knowledge. CLARION (Connectionist Learning Adaptive Rule Induction ON-line) [6] is a hybrid architecture with explicit (symbolic) and implicit (sub-symbolic) processes. CLARION is made of four memory modules, with dual explicit–implicit representation: action-centered subsystem, non-action-centered subsystem, motivational subsystem, and metacognitive subsystem. Action and non-action centered knowledge are stored in implicit form (using neural networks) and in explicit form (using symbolic production rules). Two types of learning support the team work of implicit and explicit processes : bottom-up learning (reinforcement learning methods are used to acquire implicit knowledge, the resulting knowledge is used to modify explicit knowledge at the top level through bottom-up learning mechanism), and top-down learning (extracting knowledge by observing actions guided by these rules). As in dual-process theories of mind, two levels (a meta-cognitive subsystem and a motivational subsystem) cooperate to produce behaviour by combining the action recommendations from the two levels or combining bottom-up and top-down learning. CLARION has often been used for the simulation of higher level cognitive phenomena. . However, CLARION's sensory-motor modules are not as developed as one would wish.

The architectures presented above exhibit many of the desiderata [1] for cognitive architectures, but none support all of them, often because of the theoretical orientation took as foundation (strong symbolism in ACT-R, high modularity in CLARION). Several issues for further research were thus identified; here we highlight specifically two of them [2]: (1) Effectors and perceptual attention: the need for "expanded frameworks that manage an agent's resources to selectively focus its perceptual attention, its effectors, and the tasks it pursues" [2]. In SOAR and ACT-R, perceptual systems are isolated channels providing the information from the environment to the Working memory of the system, but their activity is not regulated by the Working memory, like the activity of other productions. Also, in SOAR, perceptual cues match on separate perceptual working memory elements that are independent of context (matched by the other productions). As we will see below, perceptual information processing in our architecture depends on the current task and the context (environment and long term memory of the system). (2) Combination of deliberative problem solving with reactive control: the need for architectures that can combine deliberative problem solving with reactive control by changing their location on the deliberative vs. reactive behaviour spectrum dynamically based on their situation. CLARION, as well as other architectures (see CogAff, Sloman [7]), has chosen to address this problem by using a dual-process theory of mind [1]. It is this duality that allows CLARION to achieve high level reasoning; however, strong modularity prevents the system from really achieving strong reactive/dynamic processing. In our architecture, thanks to the unified cognitive model we chose, we are able to preserve dynamic processing while maintaining a robust (reflective) behaviour. In this paper, to design an architecture that meets the duality challenge with a clear answer to the interface problem, we have modeled our system after Stanovich's Tripartite Framework [3]. We chose this model, precisely because it provides a good account of dynamic of duality (sequentiality/rule-following and reactivity/dynamicity) in human cognition.

2.2 Cognitive Model

We base our cognitive architecture on Stanovich's tripartite framework [3]. This allows us a complete model of the cognitive mind, from automatic and implicit processes to explicit processes involving control (attention and executive functions) to more abstract planning and reasoning. Stanovich's tripartite framework belongs to the "dual-process theories" family of cognitive models, where cognition is characterized by the opposition (duality) between two types of processes or systems [8]. We will follow the latter usage, which often dubs the dual systems "System 1" (fast and automatic reasoning) and "System 2" (abstract and hypothetical reasoning). Stanovich's System 1, which he calls the "Autonomous Mind," includes instinctive behaviours, over-learned process, domain-specific knowledge, emotional regulation and implicit learning. His tripartite framework differs from other dual-process theories in its description of System 2. He divides processes usually ascribed to System 2 in two classes of processes, respectively called the "Algorithmic Mind," responsible for cognitive control, and the "Reflective Mind," responsible for deliberative processes. The Algorithmic Mind acts upon information provided by the Autonomous Mind thanks to two sets of pre-attentive processes (perceptual processes and "processes which access memories and retrieve memories and beliefs" – [9] (p 43), both of which supply content to Working Memory. The Algorithmic Mind is the locus of three processes, each initiated by the Reflective Mind: (1) inhibition of Autonomous Mind processes, (2) cognitive simulation

(decoupling), and (3) serial associative cognition. Performance of these processes leads to an activation of the anterior cingulate cortex (ACC). Decoupling, which seems to be supported by the dorsolateral prefrontal cortex (DLPFC) [3], consist in the creation of temporary models of the world, where different alternative scenarios can be tested. The temporary models created through decoupling do not affect the system's current representation of the world but the decoupling process, however, has a cognitive cost: it is difficult for the Algorithmic Mind to perform other processes while decoupling takes place. Decoupling does not occur in every situation where it would be useful, and when it does occur, it is sometimes incomplete. In these cases, subjects simply apply simple models (rules) that *appear* appropriate for the situation. Serial associative cognition supports the implementation of these simple models. The simple model chosen does not in general provide the best solution in a given situation: a better solution could have been found through decoupling, but the cognitive load of decoupling is higher than that of serial associative cognition and thus subjects will often satisfy themselves with less optimal but cognitively easier solution provided by serial association. Operations supported by the Reflective Mind define the subject's cognitive style. The Reflective Mind performs three processes: (1) initiation of inhibition of Autonomous Mind processes by the Algorithmic Mind (i.e., it tells the Algorithmic Mind: "Inhibit this Autonomous Mind process") and (2) initiation of decoupling in the Algorithmic Mind (i.e., it tells the Algorithmic Mind: "Start Decoupling") and (3) interruption of serial cognition, either by sending a new sequence to the Algorithmic Mind or by initiating a full simulation of the situation through decoupling. According to Stanovich, the division of human cognition into three sets of processes, instead of the traditional two of dual-process theories, provides a better account of individual cognitive differences. Individual differences with regard Algorithmic Mind processes are linked to cognitive abilities and fluid intelligence, while Reflective Mind differences are observed in critical thinking skills. We chose the tripartite model Stanovich, precisely because it provides a good account of the diversity in human behaviour.

3 Architecture

Our architecture is implemented in a multi-layer multi-agent simulation platform [10]. As shown in figure 1, each level presented is composed of groups of agents acting in parallel, each agent having one or more role (an abstract representation of their functionality).

3.1 Reactive level

The Reactive level in our model corresponds to Stanovich's Autonomous Mind. The main roles assigned to agents within this level are "sensor" (C –letters in parenthese in this section appear in figure 1), "effector" (D) and "knowledge" (A).

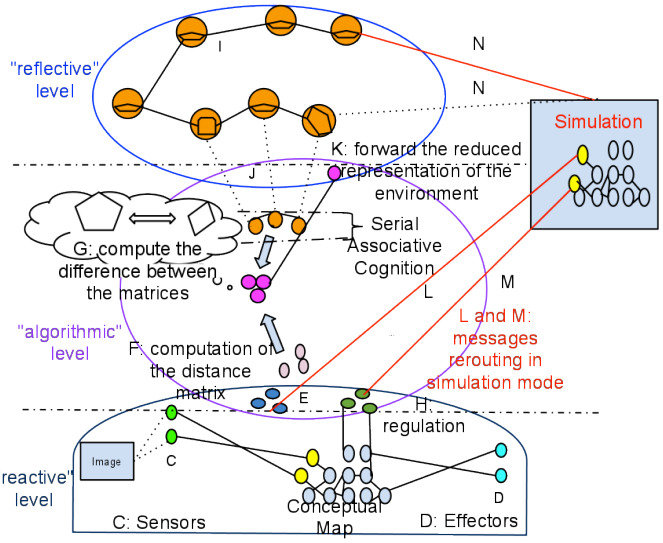

Figure 1: Architecture

The network of Knowledge agents (agents assigned with the "knowledge" role) is initialized with a knowledge base that makes up the system's declarative knowledge (semantic memory): a conceptual map made up of concepts and the semantic links between them. Knowledge agents therefore have two attributes: "knowledge" and a word from the knowledge base (e.g., "Red"); knowledge agents are also connected together according to the links in the conceptual map. Upon receiving a message from a Sensor agent or from another Knowledge agent, Knowledge agents send a message to those Knowledge agents they are connected to, therefore spreading activation in the network (a process similar to that of semantic memories, [11]). The number of messages exchanged between the agents, and therefore their activation, is at first determined by the distance between them in the conceptual map (later on, it will also be determined by the activation signals from higher levels – see below). The system's environment is similar to (portions of) human environments. In the Stroop task simulation described below, the system is presented with cards identical to those human subjects see in real Stroop task experiments. Each Sensor agent is sensitive to some particular type of information in the environment (colors, sounds, texts, etc.). If the type of information to which they are sensitive to is present in the environment, Sensor agents will (at short intervals) extract it and send messages to Knowledge agents with a role associated with the sensor's function ("read" for Knowledge agents connected to *Sensor agents* reading characters, "recognizeColor" for Knowledge agents connected to *Sensor agents* recognizing colors). Activation in the network therefore depends on the number of messages sent by the Sensor agents and the activation of the *Knowledge agents* in the conceptual map. Taken together, the action of Sensor and *Knowledge agents* make up the system's sensory motor level. This means that the system's sensory abilities are always a function of the Sensor agents' information extracting capacities and of the system's knowledge about the environment: the system is fully situated. *Effectors agents*

work similarly: a knowledge agent associated to the function of the effector ("sayRed", "sayBlue") sends messages to *Effector agents* with a similar role, which will then act on the environment.

3.2 Algorithmic level

Corresponding to Stanovich's Algorithmic Mind, the Algorithmic group is responsible for the control of the system. Control is achieved with the help of morphology [12]. RequestStatus agents (E) belong to both the Reactive and Algorithmic organisation. At regular intervals, they query Knowledge agents about their status (that is, number of messages they sent during that interval to each of the Agents to which they are connected). Status agents (F) represent the system's activity at a given time in the form of a distance matrix that describes the (message passing) activity of the system at that time. The distance between two concepts in the conceptual map is measured by the number of messages sent between the Knowledge agents bearing these two concepts as their role. Status agents also send a reduced representation of the activity in the Reactive organisation to the Reflective level. Globally, this matrix thus represents a form or shape, and it is this form that will be transformed to reach the shape describing the goal assigned to the system. At the Algorithmic level, we thus find the short-term goals of the system in the form of a graph of Goal agents sent by the Reflective level. Each Goal agent (I) contains a distance matrix that specifies the distance necessary between each Knowledge agents (that is, the number of messages that must be sent between Knowledge agents) if the system is to reach goal. Graphs of short-term goals in our architecture correspond to Stanovich's serial associative cognition. Delta agents (G) compute the difference between the matrix provided by the Status agents and the one provided by the Goal agents. The resulting difference (another matrix) is provided to Control agents (H), which in turn send regulation messages to agents in the Reactive organisation to modify (i.e., increase) their activation so that their global activity more closely matches the shape describing the current short-term goal. Agents in the Algorithmic organisation constitute the system's attention. They activate elements of the system's semantic memory in relation to its current goal. The system's long term memory is made up of the Knowledge agents in the Reactive organisation, and the system's working memory (WM) at a given time is made up of the Knowledge agents that are activated in the Reactive group at that time. This implementation of working memory is consistent with the work of Engle [13], in which WM is seen as a set of temporarily activated representations in long-term memory.

3.3 Reflective level

Each agent in this last group has a shape (a distance matrix) which represents the state that the system must be in to achieve a simple goal. Goal agents (I) are organized in a direct graph. A path in this graph represents a plan that can be applied to achieve a complex behaviour A set of Goal agents represents a graph of several complex plans or strategies decomposed into a sequence of simple objectives (steps in the plan). The logical and analytical skills of the system will be implemented at this level. A sequence of simple objectives path (J) will be sent to the Algorithmic level, which will take care of its execution. Following Stanovich's Tripartite framework, agents in this last group will have access to a reduced representation of the environment. This representation is provided by the Status agents of the Algorithmic Group to other status agents (K) that carry the reduced representation and announce themselves to the goal agents, which in turn compute their similarity to this representation. The activation of the Goal agents will be determined by the computed similarity between these two matrices. Activation propagates from the Goal agent most matching the reduced representation to those that follow in its path. The last agent in the path will send the parsed path to the Algorithmic level. Thus, the shortest path and the most active (with the most messages exchanged) will be sent first to the Algorithmic level. The shortest path (simplest model) or the one the most activated (model used more recently or more often) will prevail over the other paths. The limited serial associative cognition of the Algorithmic level will execute this path step by step. The path executed by serial associative cognition provides the system with the sequentiality necessary to achieve complex goals. However, the system does not lose its dynamicity. Indeed, the reduced representation of the environment are sent on a regular basis by the Status agents so that the Reflective organisation can interrupt serial cognitive association either by: (1) Setting a new starting point in the path, or by, (2) Taking a new branch in the path, based on the current state of the environment

3.4 Simulation

If multiple strategies (thus two or more goal agents) are selected at the algorithmic level, the goal agent that belongs to the algorithmic and reflective level (which usually contains the goal matrix selected at the reflective level) triggers a simulation of the strategies. The simulation capacity as envisioned in Stanovich's Tripartite Framework is implemented at the algorithmic level. When the algorithmic level is in simulation mode, a possible world is created thanks to the reduced representation sent by the Delta agents. This secondary representation is realized with a limited number of agents (20). These agents are assigned dynamically the same roles and links as those agents from the Reactive level they are replicating, as indicated by the reduced representation. Since this possible world is carried out thanks to distinct agents (SecondaryRepresentation agents instead of Knowledge agents) and a distinct group (Algorithmic instead of Reactive), we can be sure that this secondary representation is totally independent from the current representation of the world (i.e., knowledge agents from the reactive level). To reproduce the cognitive cost of the simulation operation, the cognitive operations (goal inhibition and selection) are carried out by the Control agents, Delta Agents, and the Reflective level. Messages from (L) and to

(M) these agents are branched to the SecondaryRepresentations instead of the Reactive level. Once the simulation is completed, the activation of Goal agents is regulated accordingly at the Reflective level (N), therefore potentially replacing the next action carried out by the Algorithmic level (by the first rule simulated). The WCST realized in this paper illustrates the simulation of an opposite style of thinking. The system first simulates the application of a chosen categorization rule and its negation (negative feedback by the instructor), and is thus able to make a new categorization rule (the alternative) emerge in the simulation.

4 Results and Discussion

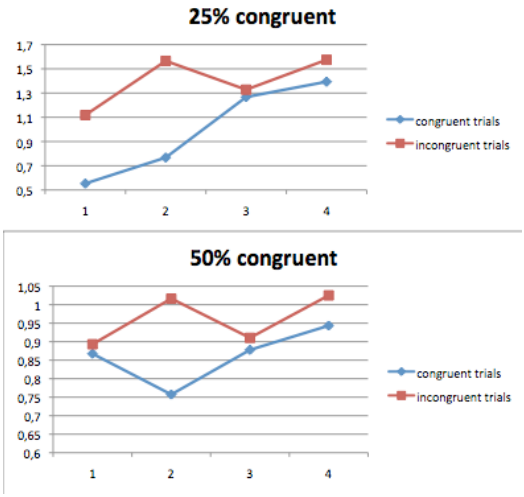

Figure 2: Mean response time per block for congruent and incongruent trials in 25% congruent conditions and 50% congruent condition

4.1 Control and perceptual attention: Stroop task

The Stroop task [14] is used to test attention and inhibitory control. It tests a subject's ability to maintain a goal in mind, suppressing a familiar response in favor of one that is less familiar. The task illustrates the Color–Word Interference effect. The set of trials is a compound of congruent trials (the word "GREEN" written in green) and incongruent trials ("RED" written in green). Two experiments were conducted. In each one, four blocks of 100 cards with a word written in a specific color were shown to the system. 25% of the cards per block were congruent in the first experiment while 50% were in the second.

Control: Set-up this way, we find that the mean response time of the system is longer for incongruent trials, specifically in the 50% congruent condition (Figure 2) (1396 ms) as opposed to the 25% congruent condition (960 ms), a result also found in human subjects. This is because, to achieve the system's goal, Control agents have to send regulation messages to the "recognizecolor" agents to compensate the distribution of agents when the system is initialized for the Stroop task (i.e., with a preponderance of "read" agents to reflect the predominance of the reading ability in normal adult subjects). The system provides an answer once the system has regained its stability, that is, once there is a sufficient difference in activity between the system's two competing responses. During incongruent trials, this stability is harder to achieve (inhibition is a time-consuming operation). Response-time variation is due to the action of the algorithmic level: in incongruent trials, it is particularly called upon to help the system remove perceptual focus on confusing information.

Perceptual attention: the Stroop task especially illustrates the dual nature (orienting and being oriented) of perceptual units in our system. The system gets initial information about its environment through its sensory agents ("recognizecolor" and "read") –the system processes all stimuli in parallel. At first, this leads to an activation of the Knowledge agents that correspond to the external stimulus (e.g., the Knowledge agent that bears the role "Red" will be activated if Sensory agents detect red in the environment). As we mentioned above, when the system is initialized for the Stroop experiment, there is a preponderance of "read" agents. After this initial phase, Control agents, guided by information provided by Status agents, themselves influenced by the system's current goal, can modify the message passing activity between the agents (by increasing the activity of the "recognizecolor" agents). With this experiment, we show that despite an initial setting favoring the "reading " ability and its connected sensor (both belonging to the reactive level), the system is able to change its "natural" tendency (from reading the word to naming the color), thanks to the cognitive control achieved by the algorithmic level. Cognitive control favors the color naming ability by increasing the activation of relevant agents in its goal matrix. Agents connected to them are in turn linked to effectors, therefore achieving perceptual control (perceptual attention) by spreading activation.

4.2 Flexibility: Wisconsin card sorting test

The Wisconsin card sorting test (WCST) [17] is widely used to test executive functioning, especially cognitive flexibility and abstract reasoning. The subject is shown a set of target cards with figures on them, which vary in shape, number and color. The subject has to match stimulus cards to the target cards, one by one. However, he is not told what the sorting rule is and has to discover it. In our experiment, we used material adapted from Dehaene & Changeux [15] representing the context effect of the four reference target cards by adding the following links in the system's conceptual map: Red – triangle – one, Green – star – two, Yellow – square – three, Blue – circle – four. We also linked the shape, color, and number knowledge (already present in ConceptNet) to the sensors. A script provided the system with the series of cards it had to categorize and evaluated the system's answer. The categorization rule was changed after 6 consecutive successes. The experiment consisted of 128 cards with figures varying in shape, number and color. The script attempted to test 6 categorization rules (["shape", "color",

"number"] times 2) on the 128 cards. As in human trials, no warning was sent before a rule change: only the answer "no" was given to the system when his answered was wrong.

Figure 3: Wisconsin card sorting task simulation

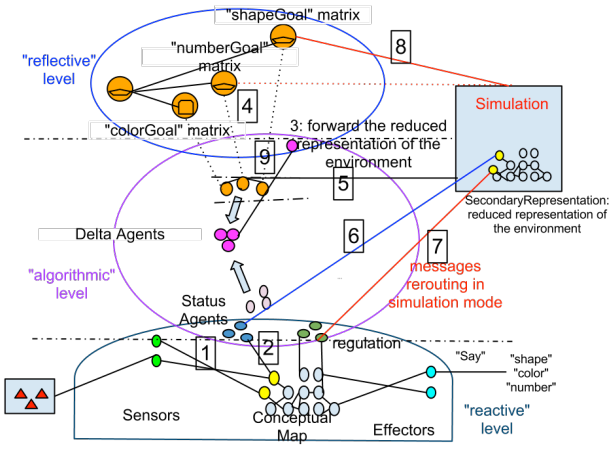

Perceptual attention: (Note that numbers in this section refer to figure 3. Please refer to the figure while the following description of the system's activity) When a new card appears in the environment, Sensors (1) forward the information to Knowledge agents in the reactive level. Activation of the different Knowledge agents is thus influenced by the environment's state. Status Agents then (2) provide the algorithmic level with the status of the agents at the reactive level. This information is used by the Delta Agents in the Algorithmic level to calculate a reduced representation (3) of the environment, which is then forwarded to the Reflective level, leading to the activation of various competing rules (4). When there are more than one winning rule/goal (because the system's working memory is loaded with contradictory contextual information), a process of cognitive decoupling (internal simulation) is launched (5) (by the Decoupling agents). A mini-world (decoupled world) -is thus created: agents in this mini-world are modeled after the reduced representation of the world (6) sent by Status agents. Decoupling agents also recreate an environment, to which the agents of the mini-world will react. For this Experiment, the environment was one in which the "no" response was sent after a categorization rulewas proposed by the mini-world. Regulating and status updating messages are rerouted (7) to act on the mini-world instead of the reactive level. The rules that emerge from the cognitive simulation are sent (8) to the reflective level (with different activations) and then the corresponding matrix is sent (9) to the algorithmic level, which is in charge of regulating the reactive level towards achievement of the goal (encouraging agent activity – even agents involved in perception – according to the system's current goal). The average number (for a hundred simulations) of rules the system (for its 128 trials) was able to discover and apply was 5.33; the maximum number was 6. Normal human subject are able to discover an average of six categories [16]. These results illustrate the system's ability to adapt adequately to the changing situation (new card, error notification) in a bidirectional manner: by orienting its executive control according to the information in the environment but also by orienting its perceptual processing according to the goal.

Equilibrium between deliberative and reactive behaviours: It is the system's design, focused on the interaction between the three cognitive levels, that helps preserve this equilibrium in the architecture to make it efficiently adaptive. Perseverationerror in the system are errors due to the reactive level.

Table 1: A simulation's log.

Serie	Trial	Response	Simulation
Color	1	correct	
	2	correct	
	3	correct	(1)color (2) shape
	4	Incorrect : shape	
	5	correct	
	…		
Shape	1	Incorrect : color	(1) shape (2)number
	2	Incorrect : color	(1) shape (2)number
	3	Incorrect : color	
	4	Incorrect : color,number	(1) number(2) shape
	5	Correct	(1) shape (2)number
	…		

However, the system's ability to achieve five categorizations is the result of a good interaction between reactive, algorithmic and reflective processing. Error notifications are sent from the Reactive level to the Algorithmic level, decreasing the activation of the now wrong classification rule, thereby allowing other rules/goals to take the lead. Activations levels of the goals are a memory of those classification rule that work and those that did not work in the past.. Although, the simulation capacity illustrates the interaction between Algorithmic and Reflective levels, it is also primordial for good cooperation between Deliberative and Reactive behaviour. Decoupling helps generate a prediction of the behaviour at the reactive level and therefore prepare an adaptive plan of action (efficient trial-error adaptation): in the third trial of the "color" series, a cognitive decoupling is run because two competing answers ("color" and "shape") are active. The system creates a simulation of a possible world where the color categorization rule is activated and observed as wrong; in this possible world, the second emerging rule was the shape categorization rule. In the first and second trial of the "shape" series, after a first wrong answer, "color" is selected, a cognitive decoupling is run where "shape" is first activated, since the possible world is an image of the system's environment before the simulation process started and where "color" had been marked as a wrong answer, the selected second answer is "number". In the third trial of the "shape" series, after a first incorrect

answer (color), a cognitive decoupling is run where the first rule activated is the "number" categorization rule, and the second is the "shape" rule, leading to a second error. Since the cognitive decoupling had activated the "shape" as second rule, the correct answer is produced.

5 Conclusion and Future Work

Theoretical studies [2,4,1] identified sequentiality and reactivity as two important features cognitive architectures must have if they are to be useful to cognitive scientists and engineers [1]. It has however proven difficult to integrate the two features in coherent architecture due to their functional incompatibility. In this paper, we focused on two such issues: Action attention and perceptual attention and flexibility. To design an architecture that addresses these issues, we sought inspiration from natural minds and modeled our system after Stanovich's Tripartite Framework [3] (reactive, algorithmic and reflective minds).The initial reaction of our system to stimuli is automatic (reactive level). However, as the task goes on, perceptual information processing is influenced not only the environmental stimuli, but by both activity in the reactive level and at the algorithmic level. The same goes for effectors. Therefore, perceptual information helps orient the system's behaviour and the system's gathering of perceptual information is oriented by the its deliberative level (its current plan). The selection of a plan itself is influenced by the information present in the environment. The plan thus depends on perception, but also influences what the system perceives (and of course does): perception and plan selection are dynamically coupled. The hybrid adaptive behaviour of the architecture is achieved through the cooperation of all three levels. Algorithmic cognition allows the system to achieve trial-and-error adaptation and hypothesis testing (e.g. simulation). Although achieved by the algorithmic level, decoupling is launched by the Reflective level from which will emerge the action to be performed by the system. However, achievement of a plan doesn't cancel the system's reactivity and dynamicity, since the algorithmic and reflective level stay up to date concerning the internal state of system at the reactive level, and are able to perform operations to adapt its long term behaviour to the constantly evolving environment. Dynamic behaviour emerges from the competition and cooperation between sequential deliberative processes (reflexive and algorithmic level) and reactive processes. In future work, we plan on addressing another issue which we think is also related to problem of flexibly integrating reactive and sequential processes: the emotional modulation of cognitive processes.

6 References

[1] Sun, R., (2004). Desiderata for cognitive architectures. Philosophical Psychology, Vol.17, No.3, pp.341- 373. 2004

[2] Langley, P., Laird, J. E., et Rogers, S. (2009). Cognitive architectures: Research issues and challenges. Cognitive Systems Research, 10(2), 141-160. doi: 10.1016/j.cogsys.2006.07.004

[3] Stanovich, K. E. (2010). Rationality and the reflective mind: Oxford University Press.

[4] Newell, A. (1990). Unified theories of cognition. Cambridge, Mass.: Harvard University Press.

[5] Anderson, J. R., et Lebiere, C. (1998). The atomic components of thought. Mahwah: Erlbaum

[6] Sun, R., Lane, S. M. & Mathews, R. C. (2009). The two systems of learning: An architectural perspective. In Jonathan Evans and Keith Frankish (eds.) *Two Minds: Dual Processes and Beyond (pp.239-264)*. New York: OUP.

[7] Sloman, A., et Logan, B. (1999). Building cognitively rich agents using the Sim agent toolkit. Communications of the Association of Computing Machinery, 42, 71--77.

[8] Evans, J.., Newstead, S., Byrne, R. (1993), Human reasoning, Lawrence Erlbaum Associ- ates

[9] Frankish, K., et Evans, J. S. B. T. (2009). The duality of mind: a historical perspective. In K. Frankish & J. S. Evans (Eds.), In Two Minds: Dual Processes and Beyond

[10] Ferber, J., Gutknecht, O., et Michel, F. (2003). From Agents to Organizations : an Organizational View of MultiAgent Systems. Paper presented at the Agent Oriented Software Engineering (AOSE) IV, Melbourne.

[11] Anderson, J. R. (1983). The architecture of cognition. Cambridge, Mass.: Harvard University Press.

[12] Cardon, A. (2005). La complexité organisée : systèmes adaptatifs et champ organisationnel. Paris: Hermès Science .

[13] Engle, R. W. (2010). Role of Working Memory capacity in Cognitive Control. Current Anthropology, 51.

[14] Stroop, J.R. (1935). Studies of interference in serial verbal reactions, JEP 18 task, Can. J. Psych. 36 684–700.

[15] Dehaene, S., & Changeux, J. (1991). WCST: Theoretical analysis and modeling. Cerebral Cortex, 1, 62–79.

[17] Grant, D. A., et Berg, E. A. (1948). A behavioural analysis of degree of reinforcement and ease of shifting to new responses in a Weigl-type card-sorting problem. Journal of Experimental Psychology, 38, 404–411.

[16] Nagahama, Y., Okina, T., Suzuki, N., Nabatame, H., et Matsuda, M. (2005). The cerebral correlates of different types of perseveration in the WCST.J Neuro Psych, 76(2).

Extended Metacognition for Artificially Intelligent Systems (AIS): Artificial Locus of Control and Cognitive Economy

Dr. James A. Crowder
Raytheon Intelligence and Information Systems
16800 E. Centretech Parkway, Aurora, Colorado 80011

Shelli Friess MA, NCC
Relevant Counseling
P.O. Box 4193, Englewood, CO 80155

Abstract - *Theories into human learning and cognition have led to much research into new methods and structures for Artificial Intelligence (AI) and Artificially Intelligent Systems (AIS) to learn and reason like humans. As we move toward completely autonomous AIS, the ability to provide metacognitive capabilities becomes important [Crowder and Friess 2011b] in order for the AIS to deal with entirely new situations within the environment it may find itself (e.g., deep space, deep undersea). Presented here are theories and methodologies for Constructivist Learning (CL) processes that provide the methodologies to allow completely autonomous AIS to understand, evaluate, and evolve its "Locus of Control [Watts 2003]."*

Presented will be the a discussion of how the use of AI learning systems, like Occam [Crowder and Carbone 2011a] and PAC learning can be combined with Cognitive Economy concepts to provide this constructivist learning process to allow a Locus of Control evolution within the AIS. The goal here is to provide the AIS with a fully autonomous, cognitive framework that would be required for autonomous environmental interaction, evolution, and control.

In addition, provided are the mathematical constructs, based in Banach Spaces and Lebesque's work in Bounded Variability, that will provide the basis for Cognitive Economy structures in Artificially Intelligent Systems (AIS), allowing the AIS to operate in a "Bounded Rationality" mode, similar to humans, that will allow the autonomous system to function in new, unforeseen, and challenging environments it may find itself in. Natural intelligence filters out irrelevant information (either raw sensory perception information or higher-level conception information), and categorizes the problem representations to allow for maximum information processing with the least cognitive effort.

This work is based on the use of Intelligent Software Agents (ISAs) [Crowder 2010a] which will represent the world (its tasks, goals, and information) in terms of the reward values associated with different actions when those features of its abilities are active.

Keywords: Metacognition, Locus of Control, Cognitive Economy

1 Introduction

Intelligence reveals itself in a variety of ways, including the ability to adapt to unknown situations or changing environments. Without the ability to adapt to new situations, an intelligent system is left to rely on a previously-written set of rules. If we truly desire to design and implement autonomous AI Systems (AIS), they cannot require precisely-defined sets of rules for every possible contingency. The questions then become:

- ***How does an autonomous AI system construct good representations for tasks and knowledge as it is in the process of learning the task or knowledge?***
- ***What are the characteristics of a good representation of a new task or a new piece of knowledge?***
- ***How do these characteristics and the need to adapt to entirely new situations and knowledge affect the learning process?***

The ISAs, having bounded cognitive resources, would reacted to three aspects of Cognitive Economy to create a Bounded Rationality set of goals for a given set of ISAs generated to solve a particular problem or situation. These are:

1. The size of the feature set – how many "features" are required to define the success of each task
2. The "fuzzy" relevance of each feature for the tasks
3. The preservation of necessary distinctions for success in each task

The AIS's cognitive components would autonomously define, for each ISA, a Banach Space for that ISA's goals and tasks and would then consider the set of ISA Banach Spaces as a set of bounded variations, the sequence of which (through ISA collaboration) produces an acceptable solution to the situation(s) or task(s) at hand.

The Cognitive Economy methods will be described and a discussion will be provided, illustrating how these Cognitive Economy and Bounded Rationality concepts affect the overall learning aspects of an autonomous AIS.

In addition, when considering autonomous AIS, we must consider its need to interact and learn from its environment, and we have to ask ourselves "what is reality?" We have to establish how the AIS would interpret their reality. One of the issues that humans deal with that assists in their understanding of reality, or their world around them and how they need to interact, is their concept of "Locus of Control." **Locus of control** is a term in psychology that refers to a person's belief about what causes the events in their life, either in general or in a specific areas such as health or academics. Understanding of the concept was developed by Rotter [Rotter 1954], and has since become an important aspect of personality studies.

2.0 Artificial Locus of Control

Locus of control refers to the extent to which individuals believe that they can control events that affect them. Individuals with a high internal locus of control believe that events result primarily from their own behavior and actions. Those with a high external locus of control believe that powerful others, fate, or chance primarily determine events. Those with a high internal locus of control have better control of their behavior, tend to exhibit more political behaviors, and are more likely to attempt to influence other people than those with a high external locus of control; they are more likely to assume that their efforts will be successful. They are more active in seeking information and knowledge concerning their situation.

Locus of control is an individual's belief system regarding the causes of his or her experiences and the factors to which that person attributes success of failure. It can be assessed with the Rotter Internal-External Locus of Control Scale (see Figure 1). Think about humans, and how each person, experiences an event. Each person will see reality differently and uniquely. There is also the notion of how one interprets not just their local reality, but also the world reality [Botella 2011]. This world reality may be based on fact or impression.

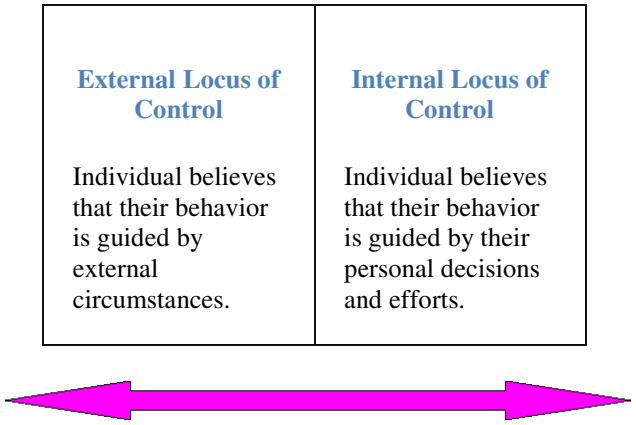

Figure 1 – The Rotter Locus of Control Scale

Take a car accident as an example. There are two people who witness a car hit a motorcycle. The police at the scene are supposed to evaluate the facts to determine what happened. The officer may use measurement tools that are

supported by mathematical equations, such to be able to determine the speed at impact or where the impact happened. The officer may measure skid marks or measure the distance between vehicles. The officer is gathering factual data. Let's consider this juried evidence and legitimate evidence. Given how the world measures and uses universal mathematic equations, this evidence can be measured and re-measured by thousands of people and likely even machines. Back to the accident, when asked by the police officer, each human witness can recall the event as if they were watching it again, a step by step recount. Each person's story likely has unique qualities depending on how they conceptualize the incident. We use eyewitness testimony all the time. Even though each witness talks a slightly different story, we use it. We know, by eyewitness testimony studies, that often times the recalled event is very different than the actual event. Let's say in this example both people recalled the event similarly except the color of the car that hit the motorcycle. Perhaps even whether the car hit the motorcycle or the motorcycle hit the care recount differs. The fire truck blocks the view of each eyewitness so they cannot confirm the color of the car as they recount the event. Each person has had a legitimate experience even if they code the color of the car differently. Factually legitimate the car and bike collided at a specific rate of speed at a specific location. Emotionally legitimate is the witnesses' personal experience. To one witness the car was green to the other it was blue. Thus, with this incident we have three realities. One of the facts that we can measure by juried tools and the reality of each of the players in the scene; all experiencing the same event but each in his own unique way. Each reality is legitimate.

For further thought let's then consider Constructivist Psychology. According to "The internet Encyclopedia of Personal Construct Psychology" the Constructivist philosophy is interested more in the people's construction of the world than they are in evaluating the extent to which such constructions are "true" in representing a presumable external reality. It makes sense to look at this in the form of legitimacies. What is true is factually legitimate and what is peoples' construction of the external reality is another form of legitimacy. Later on we can consider the locus of control in relation to internal and external legitimacies or realities. You are correct if you are thinking that AIS is not human and will not have human perceptions. AIS may have AIS perceptions and realities. Thus, a mentor will be necessary. That mentor will need to understand AIS as AIS and be able to understand AIS in a human way, a human reality. After all, isn't this what makes AIS autonomous?

3 AIS Constructivist Learning

Constructive psychology is a meta-theory that integrates different schools of thought. According to the above cited article:

> Hans Vaihinger (1852-1933) asserted that people develop "workable fictions". This is his philosophy of "As if" such as mathematical infinity or God. Alfred Korzybski's (1879-1950) "System of Semantics" focused on the role of the speaker in assigning meaning to events. Thus, constructivists thought that human beings operated on the basis of symbolic or linguistic constructs that help navigate the world without contacting it in any simple or direct way. Postmodern thinkers assert that constructions are viable to the extent that they help us live our lives meaningfully and find validation in shared understandings of others. We live in a world constituted by multiple realities social realities, no one of which can claim to be "objectively" true across persons, cultures, or historical epochs. Instead, the constructions on the basis of which we live are at best provisional ways of organizing our "selves" and our activities, which

could under other circumstances, be constituted quite differently.

For AIS with Constructivist Learning, the AIS cognitive learning process would be a building (or construction) process in which the AIS cognitive system builds an internal illustration of its learned knowledge-base, based on its experiences and personal interpretation (fuzzy inferences and conceptual ontology [Raskin & Taylor 2010a and Taylor & Raskin 2011a]) of its experiences. AIS Knowledge Representation and Knowledge Relativity Threads [Crowder and Carbone, 2011c], within AIS cognitive system memories would be continually open to modification, and the structures and linkages formed within AIS short-term, long-term, and emotional memories [Crowder and Friess, 2010b], along with its Knowledge Relativity Threads [Crowder and Carbone 2011c], would then form the bases for which knowledge structures would be created and attached to AIS memories.

One of the results of the Constructivist Learning process with the AIS would be to gradually change its "Locus of Control" for a given situation or topic, from external (the system needing external input to make sense, or infer, about its environment) to internal (the AIS having the cumulative constructive knowledge-based of information , knowledge, context, and inferences to handle a given situation internally); meaning the AIS is able to make relevant and meaningful decisions and inferences about a situation or topic without outside knowledge or involvement. This becomes extremely important for completely autonomous AIS.

4 Bounded Conceptual Rationality (Cognitive Economy)

Bounded rationality is a concept within cognitive science that deals with decision-making in humans [LaBar and Capeza 2006]. Bounded rationality is the notion that individuals are limited by the information they have available (both internally and externally), the finite amount of time they have in any situation, and the cognitive limitations of their own skills. Given these limitations, decision making becomes an exercise in finding an optimal choice given the information available. Because there is not infinite information, infinite time, nor infinite cognitive skills, humans apply their rationality after simplifying the choices available, i.e., they bound the problem to be solved into the simplest cognitive choices possible [Jones 1999].

Any AIS must suffer the same issues. An autonomous system, by definition, has limited cognitive skills, limited memory, and limited access to information. The Locus of Control concepts discussed earlier assist AIS in determining which situations can be handled internally vs. externally, but still in any situation there is limited information, time, and cognitive abilities. This is particularly true if the system is dealing with multiple situations simultaneously. In order for the system to not become overloaded, we believe autonomous systems must employ strategies similar to human bounded rationality in order to deal with unknown and multiple situations they find themselves in. This involves creating mathematical constructs that can be utilized to mimic the notion of bounded rationality within autonomous AIS.

For this we look to Banach Space theory, tied into Constructivist Learning concepts [Botella 2011] for autonomous AIS. As concepts are learned and stored in the AIS conceptual ontology [Raskin & Taylor 2010a], Banach Spaces are defined that are used to bound the rationality choices or domains for that concept. As we "construct" these concepts and the Banach Spaces that bound them, the combination of Banach Spaces then defines the Conceptual Rationality for the Autonomous AIS. Figure 2 illustrates this concept.

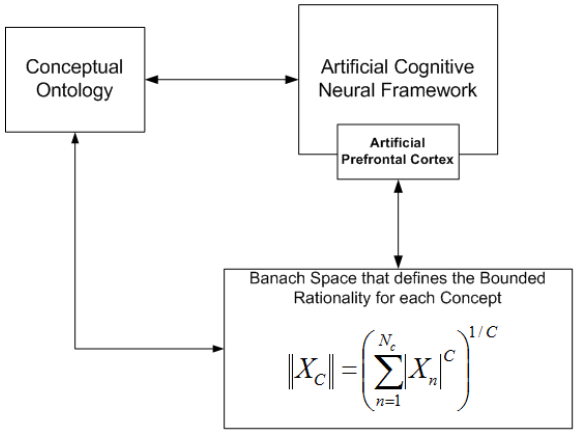

where: $X_n = \frac{1}{N} \sum_{i=1}^{N_c} G(x - x_i, \sigma I)$

and: $H_R(X_C) = \int_{-\infty}^{\infty} p_f(x) dx$

where p_f is the fuzzy membership measurement

Figure 2 – AIS Bounded Conceptual Rationality

These Banach Spaces that define the bounds for each learned concept are utilized when the AIS must reason, or perform decision making. When there are restricting limitations on time, resources (as determined by the resource manager, e.g., artificial prefrontal cortex), and available information, the bounds of these Banach Spaces would be tightened or loosened to allow the AIS to deal with multiple situations, or situations that are time critical. This allows AIS to decide what is a "good enough" solution to a given problem or set of problems, and to adjudicate between competing resources, priorities and overall goals.

6 Conclusions and Discussion

What we have presented here are initial concepts and methodologies for what we believe are essential cognitive skills that autonomous systems must have in order to deal with and survive in real-time extreme environments. As we push for systems that think, learn, and adapt, we must provide these systems with cognitive skills similar to human processes in order to be able to deal with and survive real-time situations they find in their environments. This is very preliminary work and much more remains in order to put these concepts into practice.

7 References

1. Botella, L. 2011. Personal Construction Psychology, Constructivism, and Postmodern Thought. Found at http://www.massey.ac.nz/~alock/virtual/Construc.htm.
2. Crowder, J. 2010a. Flexible Object Architectures for Hybrid Neural Processing Systems. *Proceedings of the 12th annual International Conference on Artificial Intelligence*, Las Vegas, NV.
3. Crowder, J. 2010b. Operative Information Software Agents (OISA) for Intelligence Processing. *Proceedings of the 12th annual International Conference on Artificial Intelligence*, Las Vegas, NV.
4. Crowder, J. and Carbone, J. (2011a). Occam Learning through Pattern Discovery: Computational Mechanics in AI Systems. *Proceedings of the 13th annual International Conference on Artificial Intelligence*, Las Vegas, NV.
5. Crowder, J. and Carbone, J. (2011b). The Great Migration: Information to Knowledge using Cognition-Based Frameworks. *Springer Science*, New York, NY.
6. Crowder, J. and Carbone, J. (2011c). Recombinant Knowledge Relativity Threads for Contextual Knowledge Storage. *Proceedings of the 13th annual International Conference on Artificial Intelligence*, Las Vegas, NV
7. Crowder, J. and Friess, S. (2010a). Artificial Neural Diagnostics and Prognostics: Self-Soothing in Cognitive Systems. *Proceedings of the 12th annual International Conference on Artificial Intelligence*, Las Vegas, NV.
8. Crowder, J. and Friess, S. (2010b). Artificial Neural Emotions and Emotional Memory. *Proceedings of the 12th annual International*

Conference on Artificial Intelligence, Las Vegas, NV.

9. Crowder, J. and Friess, S. (2011a). The Artificial Prefrontal Cortex: Artificial Consciousness. *Proceedings of the 13th annual International Conference on Artificial Intelligence*, Las Vegas, NV.
10. Crowder, J. and Friess, S. (2011b). Metacognition and Metamemory Concepts for AI Systems. *Proceedings of the 13th annual International Conference on Artificial Intelligence*, Las Vegas, NV.
11. Crowder, J., Scally, L., & Bonato, M. 2011. Learning agents for Autonomous Space Asset Management. *Proceedings of the Advanced Maui Optical and Space Surveillance Technologies Conference*, Maui, HI.
12. Jones B. 1999. Bounded Rationality. Annual Review of Political Science, 1999.2:297-321.
13. Kosko, G., "Fuzzy Cognitive Maps," *International Journal of Man-Machine Studies*, 24: 65-75.
14. LaBar KS and Cabeza (2006) Cognitive neuroscience of emotional memory. *Nat Rev Neurosci 7: 54-64*.
15. Neimeyer, R. 2004. The Internet Encyclopedia of Person Constructivist Psychology, located at: http://www.pcp-net.org/encyclopaedia/pc-theory.html.
16. Newell, A. 2003. Unified Theories of Cognition. *Harvard University Press*, Cambridge, MA.
17. Raskin, V., Taylor, J. M., & Hempelmann, C. F. 2010a. Ontological semantic technology for detecting insider threat and social engineering. *New Security Paradigms Workshop*, Concord, MA.
18. Rotter, J. 1954. Social Learning and Clinical Psychology. *Prentice-Hall*, New York, NY.
19. Taylor, J. M., & Raskin , V. 2011a. Understanding the unknown: Unattested input processing in natural language, *FUZZ-IEEE Conference*, Taipei, Taiwan.
20. Watts, R. 2003. Therapy as a Rational Constructivist Approach. *The Family Journal: Counseling and Therapy for Couples and Families*, Vol. 11. No. 2, pp. 139-147.
21. Yang Y, Raine A (November 2009). "Prefrontal structural and functional brain imaging findings in antisocial, violent, and psychopathic individuals: a meta-analysis". *Psychiatry Res* **174** (2): 81–8. doi:10.1016/j.pscychresns.2009.03.012. PMID 19833485.

Analyzing Factors Effective on the Development of Relationship Commitment

Authors:

Yashar Dehdashti
PhD student, The University of Texas at Dallas, USA
yashar.dehdashti@utdallas.edu
Nooshin Lotfi
PhD student, Texas A&M University, USA
nlotfi@mays.tamu.edu
Dr. Naser Karami
Assistant professor, Sharif University of Technology

Keywords:

Trust, relationship commitment, relationship marketing, fuzzy cognitive maps (FCMs)

Abstract

Due to the important role of commitment and trust in the relationship marketing, the factors which can directly result in a committed relationship along with the factors which can influence the commitment through influencing trust, according to the model of commitment and trust by (Morgan & Hunt, 1994) have been introduced and their level of importance has been investigated here. The article uses fuzzy cognitive maps (FCMs) in the proposed model to find the most important paths leading to relationship commitment. The FCM analyzes the responses of a group of 30 people including general practitioners in dentistry, managers of dental departments in some of the public clinics and hospitals who are the direct customers of 3 distributers of dentistry equipments in Iran to find the most important paths. Also the influence of coercive power, which was not concluded in previous researches, has been examined. The result of this inquires, then, has been provided along with its managerial implications and the impacts of prioritizing antecedents and factors of trust and commitment in relationship marketing.

1. Introduction

It's been suggested that "successful relationship marketing requires relationship commitment and trust." (Morgan & Hunt, 1994) The literature, also, suggests that understanding relationship marketing requires distinguishing between the discrete transaction, which has a "distinct beginning, short duration, and sharp ending by performance," and relational exchange, which "traces to previous agreements [and] ... is longer in duration, reflecting an ongoing process" (Dwyer, Scburr, & Oh, 1987). Hence Relationship marketing refers to all marketing activities directed toward establishing, developing, and maintaining successful relational exchanges.
In this article we, first, conduct a comprehensive literature review on commitment and trust and the respective constructs in section 2. In the next section we will introduce Fuzzy Cognitive Maps and the way we utilize them to find the most important paths leading to trust and commitment. Finally, conclusions regarding the results along with the managerial implications and future studies are presented.

2. A Review of Trust and Commitment

The literature is rife with researches that point to the fact that in the global economy one has to be a trusted competitor to be an effective one, which emphasizes the importance of relational marketing. As the presence of relationship commitment and trust is central to successful relationship marketing (Shelby & Hunt, 1994), and given the importance of relational marketing in today's competitive world and its bearing on CRM, a concept that has seen a great boom over the past two decades (Payne & Frow,

2005), it is important to know the antecedents that affect trust and commitment in relational marketing.
When both commitment and trust—not just one or the other—are present, they produce outcomes that promote efficiency, productivity, and effectiveness. In short, commitment and trust lead directly to cooperative behaviors

Relationship commitment is defined as an exchange partner believing that an ongoing relationship with another is so important as to warrant maximum efforts at maintaining it; that is, the committed party believes the relationship is worth working on to ensure that it endures indefinitely. (Moorman, Deshpande, & Zaltman, 1993): "Trust is defined as a willingness to rely on an exchange partner in whom one has confidence." The literature on trust suggests that confidence on the part of the trusting party results from the firm belief that the trustworthy party is reliable and has high integrity, which are associated with such qualities as consistent, competent, honest, fair, responsible, helpful, and benevolent (Rotter, 1971; Altman & Taylor, 1973; Larzelere & Huston, 1980; Dwyer & LaGace, 1986). (Anderson & Narus, 1990) focus on the perceived outcomes of trust when they define it as "the firm's belief that another company will perform actions that will result in positive outcomes for the firm as well as not take unexpected actions that result in negative outcomes." Indeed, we would expect such outcomes from a partner on whose integrity one can rely confidently.
Trust is so important to relational exchange that (Spekman, 1988) postulates it to be ' 'the cornerstone of the strategic partnership." Why? Because relationships characterized by trust are so highly valued that parties will desire to commit themselves to such relationships (Hrebintak, 1974) Shelby and Hunt (1994) propose that (1) relationship termination costs and relationship benefits directly influence commitment, (2) shared values directly influence both commitment and trust, and (3) communication and opportunistic behavior directly influence trust (and, through trust, indirectly influence commitment).

2.1. Termination Cost

A common assumption in the relationship marketing literature is that a terminated party will seek an alternative relationship and have "switching costs," which lead to dependence (Jackson, 1985; Heide & George, 1988). Termination costs are, therefore, all expected losses from termination and result from the perceived lack of comparable potential alternative partners, relationship dissolution expenses, and/or substantial switching costs. These expected termination costs lead to an ongoing relationship being viewed as important, thus generating commitment to the relationship.

2.2. Relationship Benefits

Competition—particularly in the global marketplace—requires that firms continually seek out products, processes, and technologies that add value to their own offerings. Relationship marketing theory suggests that partner selection may be a critical element in competitive strategy. Because partners that deliver superior benefits will be highly valued, firms will commit themselves to establishing, developing. and maintaining relationships with such partners
it is, therefore, proposed that firms that receive superior benefits from their partnership—relative to other options—on such dimensions as product profitability, customer satisfaction, and product performance, will be committed to the relationship (Shelby & Hunt, 1994).

2.3. Shared Values

Shared values, the only concept that we posit as being a direct precursor of both relationship commitment and trust, is the extent to which partners have beliefs in common about what behaviors, goals, and policies are important or unimportant, appropriate or inappropriate, and right or wrong (Dwyer, Scburr, & Oh, 1987) theorize that shared values contribute to the development of commitment and trust. Moreover, the organizational commitment literature often distinguishes between two kinds of commitment: (1) that brought about by a person sharing, identifying with, or internalizing the values of the organization and (2) that brought about by a cognitive evaluation of the instrumental worth of a continued relationship with the organization, that is by adding up the gains and losses, pluses and minuses, or rewards and punishments. Consistent with the organizational behavior literature, we posit that when exchange partners share values, they indeed will be more committed to their relationships, but our definition of commitment is neutral to whether it is brought about by instrumental or identification/internalization factors.

2.4. Communication

Communication can be defined broadly as the formal as well as informal sharing of meaningful and timely information between firms. Communication, especially timely communication (Moorman, Deshpande, & Zaltman, 1993) fosters trust by assisting in resolving disputes and aligning perceptions and expectations.

Shelby and Hunt (1994) propose that a partner's perception that past communications from another party have been frequent and of high quality—that is relevant, timely, and reliable— will result in greater trust. Anderson & Narus (1990) find that from both the manufacturer's and distributor's perspectives, past communication was positively related to trust. Anderson & Weitz (1989) also find that communication was positively related to trust in channels.

2.5. Opportunistic Behavior

The concept of opportunistic behavior from the transaction cost analysis literature is defined as "self-interest seeking with guile." The essence of opportunistic behavior is deceit-oriented violation of implicit or explicit promises about one's appropriate or required role behavior (John, 1984)

Shelby and Hunt propose that when a party believes that a partner engages in opportunistic behavior, such perceptions will lead to decreased trust. Rather than positing a direct effect from opportunistic behavior to relationship commitment, we postulate that such behavior results in decreased relationship commitment because partners believe they can no longer trust their partners.

3. Fuzzy Cognitive Maps

Fuzzy Cognitive Maps are used here to delineate the order of importance of the paths leading to trust and commitment. In this section, for the purpose of the reader's deeper understanding, an introduction to the concept of FCM is given. It is assumed that the reader is familiar with the fundamental notions underlying the Fuzzy theory, yet this familiarity does not bear upon the understanding of the methodology used in this article.

Cognitive Maps (CMs) were proposed and applied to ill-structured problems by (Axelrod, 1976).

The approach used by Axelrod is to develop CM's, i.e. signed digraphs designed to capture the causal assertions of a person, with respect to a certain domain and then use them in order to analyze the effects of alternatives, e.g. policies, business decisions, etc. upon certain goals. A cognitive map has only two basic types of elements Concepts and Causal Beliefs. The concepts are represented as variables and the causal beliefs as relationships among variables. Causal relationships link variables to each other and they can be either positive or negative. Variables that cause a change are called *Cause Variables* while those that undergo the effect of the change in the cause variable are called *Effect Variables*. If the relationship is positive, an increase or decrease in a cause variable causes the effect variable(s) to change in the same direction. If the relationship is negative, then the change which the effect variable undergoes is in the opposite direction. Fig. 1 is a graphical representation of a cognitive map, where variables (X, W, etc.) are represented as nodes, and causal relationships as directed arrows between variables, thus constructing a signed digraph (Nasserzadeh, Jafarzadeh, Mansouri, & Sohrabi, 2008). A famous example is cited by (Vasantha Kandasamy & Smarandache, 2003) where an expert spells out the five major concepts relating to the unemployed graduated engineers as:

E1 – Frustration

E2 – Unemployment

E3 – Increase of educated criminals

E4 – Underemployment

E5 – Using drugs, etc.

The resulting graph elicited using the expert's opinions and representing variables and corresponding relationships among them is as follows (Figure 1)

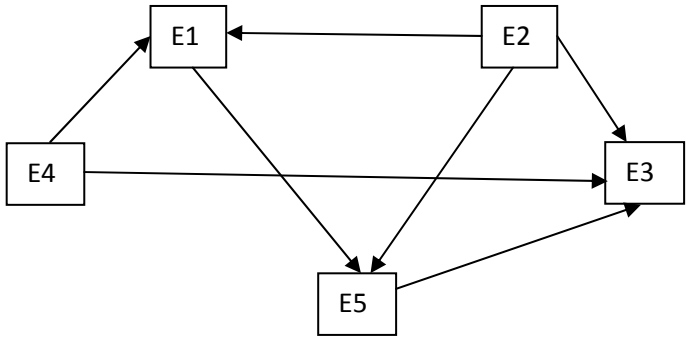

Figure 1-Causal Graph

Cognitive maps were developed in simulation, organizational strategies modeling, support for strategic problem formulation and decision analysis,

knowledge bases construction, managerial problems diagnosis, failure modes effects analysis, modeling of social and psychological processes, modeling virtual worlds and analysis of their behavior, requirements analysis and systems requirements specification (Kardaras & Karakostas, 1999). (Kosko, 1986) introduces FCM, i.e. weighted cognitive maps with fuzzy weights. It is argued, that FCM eliminates the indeterminacy problem of the total effect. Since its development, fuzzy set theory has been advanced and applied in many areas such as expert systems and decision making, control engineering, pattern recognition, etc (Zimmermann, 1991). It is argued that people use fuzzy data, vague rules, etc. and fuzzy sets as a mathematical way to represent vagueness. Fuzzy sets are characterized by a membership function, which is also called the degree or grade of membership.

Different approaches were proposed for the specification of the fuzzy weights in an FCM. One suggestion is to ask the experts to assign a real number from the interval (0, 1) for each relationship and then calculate the average. However, it is difficult for the experts to assign a real number in order to express their beliefs with regard to the strength of relationships. This is the reason why partially ordered linguistic variables such as weak < moderate < strong, etc. are preferred to real number.

It is assumed that a concept in an FCM can be represented by a numerical vector (V), whereas each element (v) of the vector represents a measurement of the concept. Another way of representing a cognitive map is made possible through an adjacency matrix where one can clearly observe the sign of the relationship, while keeping in mind that in case of an absence of relationship between these two factors, the corresponding entry will be empty:

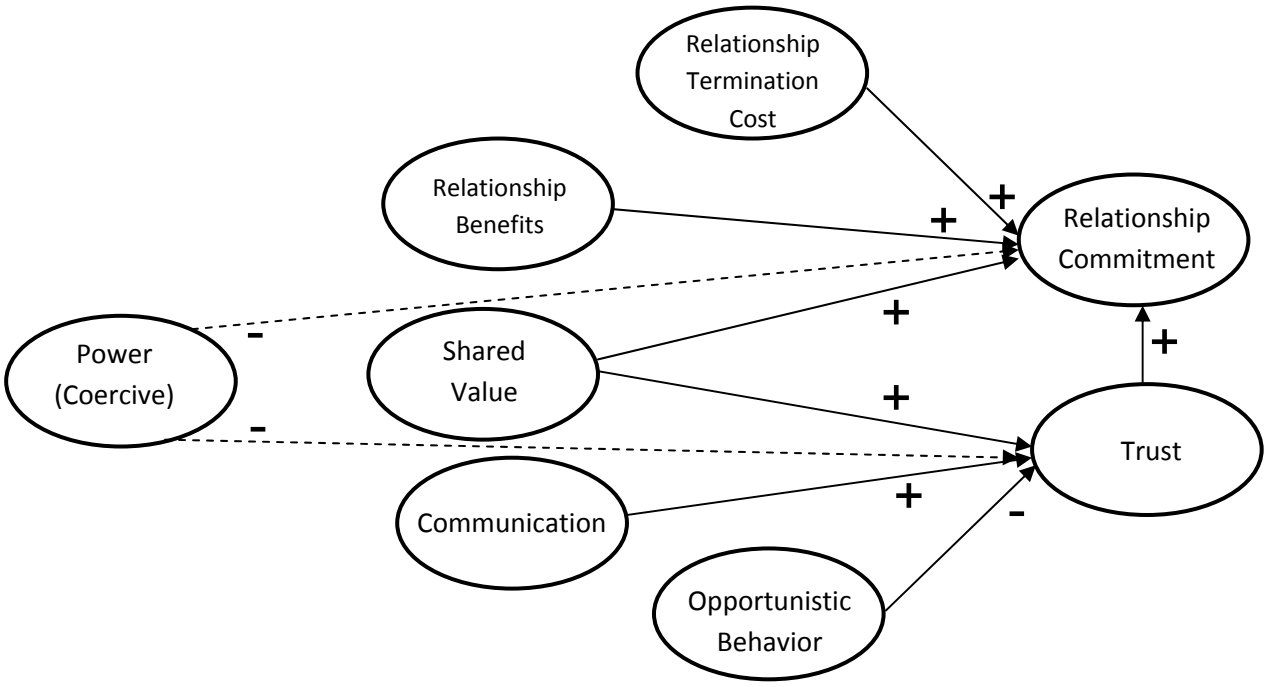

Figure 2- Model of Commitment and trust by (Morgan & Hunt, 1994)

4. Methodology

Fuzzy Cognitive Maps (FCMs) have been used to determine two things. First, the strength of the relationships described in the original Shelby and Hunt paper (1994) (Figure 2).
Second, to determine if there is a strong relationship between "power and commitment," and "power and trust and commitment" as proposed for further study in the Shelby & Hunt paper (1994).

For the purpose of determining the strength of each path in the following fuzzy diagram, the mamdani fuzzy operator has been used.

Based upon paths above a questionnaire has been developed on Likert scale of 1-5, which each of the questions refers to one of the defined relationships. These questionnaires have been responded by general practitioners in dentistry, managers of dental departments in some of the public clinics and hospitals who are the direct customers of 3 distributers of dentistry equipments in Iran. The sample group was composed of 45 people including 20 general dentists, 10 oral surgeons, 8 clinic managers, and 8 managers of dental departments of hospitals.
The questionnaire has been submitted personally to each of the members of sample group, and has been explained to them directly. It has been given one week to each respondent to reply and a reminder telephone call has been scheduled for the 6th day of the week.

The group of respondents is composed of 16 general dentists, 4 oral surgeons, 7 clinic managers and 3 managers of dental departments in 3 different hospitals. (Respondent rate is 67%)

After collecting the responses, using the above function, the linguistic labels corresponding to each of the paths shown in figure 3 are quantified. The aim is to find the path with the greatest impact on the final variable – purchase satisfaction.
Assuming:

C1: power (coercive)
C2: relationship termination cost
C3: relationship benefits
C4: shared value
C5: communication
C6: opportunistic behavior
C7: trust
C8: relationship commitment

The paths are as follows:
I_1 = {C1,C8}
I_2 = {C1,C7,C8}
I_3 = {C2,C8}
I_4 = {C3,C8}
I_5 = {C4,C8}
I_6 = {C4,C7,C8}
I_7 = {C5,C7,C8}
I_8 = {C6,C7,C8}

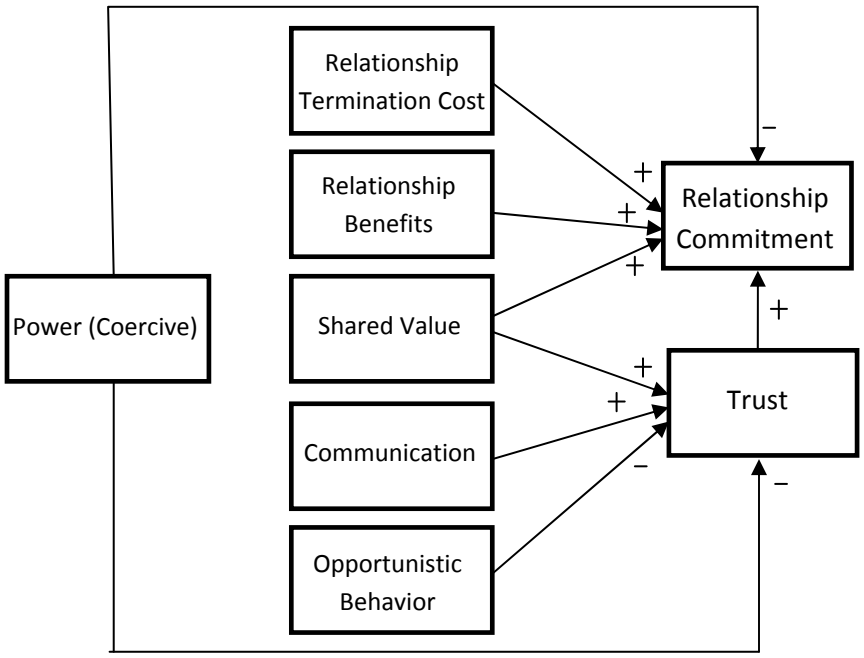

Figure 3 – Investigated Paths

5. Results

5.1. Phase I:

For the original Shelby and Hunt model, the strength of each of the paths leading to commitment has been computed. Based on the mathematics behind fuzzy cognitive maps, the importance weights of each of the paths are computed as follows:

$\Phi^1 = 0.9$ (strong)

$\Phi^2 = \min(0.94,0.97) = 0.94$ (strong)

$\Phi^3 = 0.86$ (strong)

$\Phi^4 = \underline{0.95}$ (strong)

$\Phi^5 = 0.65$ (medium)

$\Phi^6 = \min(0.63,0.97) = 0.63$ (medium)

$\Phi^7 = \min(0.71,0.97) = 0.71$ (medium)

$\Phi^8 = \min(0.93,0.97) = 0.93$ (strong)

$\Delta = \max \{ \Phi^1, \Phi^2, \Phi^3, \Phi^4, \Phi^5, \Phi^6, \Phi^7, \Phi^8 \} = 0.95 =$ strong

5.2. Phase II:

For the relationship between "power and commitment," and "power and trust and commitment," (paths I^1 and I^2) the strength for both of the paths was found to be strong.

6. Conclusion

With the increased penetration of Relationship Marketing philosophies and Relationship Commitment in businesses and organizations and the concomitant rise in spending of people and products to implement them, it is clear that the importance of developing the knowledge about the effective factors in creating such commitment will rise consequently. Each business and organization should be aware of the importance of the factors to be monitored, developed or modified in order to nurture a committed relationship with the customers. It is obvious that knowing the level of influence each factor has can help the managers not spend their priceless resources on unnecessary factors which have little influence on increasing the commitment.

The result of our research has shown that the most positive relationship can be seen when the parties of the relationship find the relationship more beneficial. The findings of this research lead to a series of managerial implications for managers to increase the commitment and trust of the firm's customers. According to these results, although having shared values and communication can be a great motive for customers to initiate a relationship with the firm, it will not guarantee an increase in the commitment the customer might feel toward the firm. This conclusion can guide the managers to put their best attempts to reduce the feeling of coercive power a customer will have about the firm through communication and modification of agreement conditions and terms and several other alternatives. In addition, the managers should be very clear in terms of communicating relationship benefits for the customer and put most of their time, money and energy on emphasizing more and more on these benefits for the customers to grow their sense of trust and commitment.

This research has been conducted on a relatively small sample group specializing mostly in medical equipment distribution and retailing. Although we are confident, to some extent, that sense of trust and commitment in the business relationships are more or less independent of the type of industry, this claim should be tested on various businesses in order to find a general pattern on how to prioritize the influential factors on developing commitment and trust. Furthermore, in the model of trust and commitment by (Morgan & Hunt, 1994) some interrelationships between the constructs have been presumed (i.e., the relationship between relational benefit and coercive power); these interrelations could be explored using the same methodology as the one used here, or using more complex Fuzzy functions. Moreover, this model has an outcome side which shows the influence of commitment and trust on several outcomes such as conflict, acquiescence, propensity to leave, cooperation and uncertainty. These outcomes are the most important reason for the firms to attempt to increase their customers' commitment to the firm.

References:

Altman, I., & Taylor, D. (1973). *Social Penetration: The Development of interpersonal Relationships.* New York: Holt, Rinehart.

Anderson, E., & Weitz, B. (1989). Determinants of Continuity in Conventional Industrial Channel Dyads. *Marketing Science , 8*, 310-323.

Anderson, J. C., & Narus, J. A. (1990). A Model of Disuibutor Firm and Manufacturer Firm Working Partnerships. *Journal of Marketing , 54*, 42-58.

Axelrod, R. (1976). *Structure of Decision: The Cognitive Maps of Political Elites.* Princeton: Princeton University Press.

Dwyer, F. R., & LaGace, R. R. (1986). On the Nature and Role of Buyer-Seller Trust. *AMA Summer Educator*s (pp. 40-45). Chicago: American Marketing Association.

Dwyer, F., Scburr, P. H., & Oh, S. (1987). Developing Buyer-Seller Relationships. *Jounal of Marketing , 51*, 11-27.

Heide, J. B., & George, J. (1988). The Role of Dependence Balancing in Safeguarding Transaction-Specific Assets in Conventional Channel. *Joumal of Marketing , 52*, 20-35.

Hrebintak, L. G. (1974). Effects of Job Level and Participation on Employee Attitudes and Perceptions of Infiuence. *Academy of Management* , 649-662.

Jackson, B. B. (1985). *Winning and Keeping Industrial Customers.* Lexington: Lexington Books.

John, G. (1984). An Empirical Investigation of Some Antecedents of Opportunism in a Marketing Channel. *Journal of Marketing Research , 21*, 278-289.

Kardaras, D., & Karakostas, B. (1999). The use of fuzzy cognitive maps to simulate the information systems strategic planning process. *information and Software Technology , 41*, 197-210.

Kosko, B. (1986). Fuzzy cognitive maps. *International Journal of Man-Machine Studies , 24*, 65-75.

Larzelere, R. E., & Huston, T. L. (1980). The Dyadic Trust Scale: Toward Understanding Interpersonal Trust in Close Relationships. *Joumal of Marriage and the Family , 42*, 595-604.

Moorman, C., Deshpande, R., & Zaltman, G. (1993). Factors Affecting Trust in Market Research Relationships. *Journal of Marketing , 57*, 81-101.

Morgan, R. M., & Hunt, S. D. (1994). The Commitment-Trust Theory of Relationship Marketing. *Journal of Marketing* .

Nasserzadeh, S. M. R., Jafarzadeh, M. H., Mansouri, T., & Sohrabi, B. (2008). Customer Satisfaction Fuzzy Cognitive Map in Banking Industry. *IBMA.*

Payne, A., & Frow, P. (2005). A Strategic Framework for Customer Relationship Management. *Journal of Marketing , 69*, 167-176.

Rotter, J. B. (1971). A New Scale for the Measurement of Interpersonal Trust. *Joumal of Personality , 35*, 651-665.

Spekman, R. E. (1988). Strategic Supplier Selection: Understanding Long-Term Buyer Relationships. *Business Horizons,* , 75-81.

Vasantha Kandasamy, W. B., & Smarandache, F. (2003). *Fuzzy Cognitive Maps and Neutrosophic cognitive Maps.* Xisquan.

Zimmermann, H. J. (1991). Fuzzy Set Theory and its Applications. *Kluwer Academic Publishers*.

Warrior Resilience Training through Cognitive Self-Regulation

Dr. James A. Crowder
Raytheon Intelligence and Information Systems
16800 E. Centretech Parkway, Aurora, Colorado 80011

Shelli Friess MA, NCC
Relevant Counseling
P.O. Box 4193, Englewood, CO 80155

Abstract - *Developing "Warrior Resiliency" has been a focus of armies since the dawn of time. There has been much research over the last decades to understand and provide systems and methodologies to develop and enhance cognitive resiliency in soldiers. The ability to adapt to adversity and overcome barriers in all walks of life is critical to a soldier's overall mental health and strength. And while physical resilience is very important, lack of psychological resilience can cripple a soldier just as easily as physical impairments. In addition to peak physical performance, each soldier must be well-balanced psychologically and socially in order to sustain the intense rigors of military life, especially when it must be balanced with home, family, and community life.*

Keywords: Cognitive Self-Regulation,

1. Introduction

What is described here is an automated, interactive, cognitive system, called the Cognitive, Interactive Training Environment (CITE, pronounced "KITE") that will provide the necessary cognitive psychological training to provide the warfighter with the ability to maintain mission readiness and psychological self-regulation before, during, and after stressful situations, whether in combat or at home. The CITE system utilizes advances in Artificial Cognitive Systems developed by Raytheon combined with Linguistic Ontological Technologies developed by Purdue University to create an interactive environment capable of providing training to and adapting to individual soldier's needs and requirements. CITE will provide automated, interactive training and capture and report metacognitive indicators and metrics that allow complete assessment of psychological resilience. CITE will gather and assess metacognitive indicators like:

- Problem solving skills
- Social skills
- Relationship Skills
- Self-awareness
- Emotional self-regulation
- Cognitive self-regulation

CITE will provide the soldier with training to assist in development of the self-monitoring and self-assessment skills needed for psychological self-regulation. Figure 1 illustrates the block diagram of the CITE system.

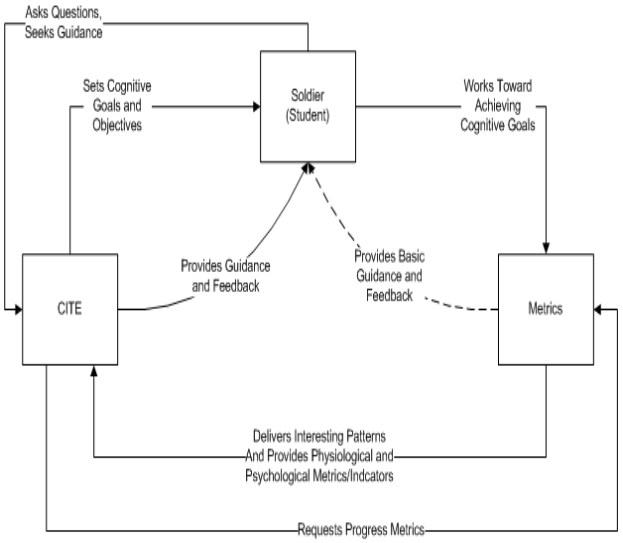

Figure 1 – Block Diagram of the CITE System

2. Warrior Resilience

The Office of Naval Research (ONR) website describes Warrior Resilience[1] as:

> "...improving the cognitive agility, flexibility and capacity of expeditionary warfighters by making them mentally tough, resilient to stress and well-adapted to chaotic, irregular environments"

In order to affect cognitive resiliency among warfighters, that must deal with a host of complex environments, both on and off the battlefield, an interactive training system must have a comprehensive understanding of the psychological, physical, and social elements and their interrelationships with warfighter performance. What we describe here is a comprehensive, Cognitive Interactive Training Environment (CITE, pronounces "kite") that will provide extensive, interactive, cognitive training and evaluation to provide warfighters with psychological self-evaluation, and self-awareness, and self-regulation skills to improve their cognitive performance throughout deployment as well as off the battlefield. We describe advanced instructional methods, based on Dr. Peter Levines [Levine 1997], autonomic nervous system states, that will provide cognitive behaviour training, metrics, and biomarkers that include environmental, contextual, and social components to affect real cognitive resiliency. The CITE system will provide the cognitive training tools to develop cognitive self-regulation and mitigation strategies to reduce cognitive dissonance among warfighters.

[1] http://www.onr.navy.mil/en/Media-Center/Fact-Sheets/Mental-Resilience-Cognitive-Agility.aspx

3. Cognitive Resiliency and Memory Development

Cognitive Resiliency develops in the brain through training that results in the learned ability to respond or self-regulate to severe psychological changes which may result from many forms of trauma and/or change; physical, emotional, environmental, or social. These learned abilities, then, get stored as memories within the human brain. Memories, in general, are divided according to the functions they serve [Newell 2003]. To qualify as a "memory" a cognitive input must cause both enduring changes within the nervous system (affect the autonomous nervous system states) and must also affect emotional and motivational responses and goals [LeDoux 1996]. A memory must induce some change that affects the nervous system and drives some physical change, in addition to modifying the human conceptual ontology, brought about by the memory being in the class of things that are affected by input, and therefore, affect other forms of behaviour. There are no memories that are neutral from a behavioural standpoint (Crowder and Friess 2010a].

4. Procedural Memory Development and Resiliency

One of the main divisions of human memory is "Procedural Memory." Procedural memory is a form of implicit memory that includes classical conditioning and the acquisition of skills. Procedural memory creation contains central pattern generators that form as a result of teaching or practice and are formed independently of conscious or declarative memory. In his work on Procedural Memory and contextual Representation, Kahana showed that retrieval of implicit procedural memories is a cue-dependent process that contains both semantic and temporal components (Kahana, Howard, and Plyn 2008)].

Creation of Procedural Memories is tied to not only repetition of tasks, but also to the richness of the semantic association structure (Landauer and Dumais 1997). In order to provide cognitive resilience, the CITE system provides interactive training that allows warfighters to create procedural memories, or "scripts" that have emotional, social, and psychological triggers and provide the skills required at the time for cognitive self-evaluation, self-awareness, and self-regulation to present or reduce psychological disorders, or problems, caused by trauma, either physical, psychological, or environmental [Crowder and Friess 2011a].

The CITE interactive training will provide a cognitive system that will interact and learn from the warfighter, developing strategies and training scenarios specific to that warfighter, thus allowing the warfighter to develop procedural memory strategies, i.e., implicit procedural memories, that will "kick in" under specific emotional memory queues, based on physical, emotional, psychological, and/or environmental events that the warfighter encounters. CITE will develop a model, or picture, or the warfighter's prefrontal cortex, based on the cognitive interactions with the system. This prefrontal cortex, or mediator, model (see Figure 2) allows CITE to understand the warfighters particular cognitive processes and what drives changes between emotional and cognitive states [Crowder and Friess 2011b] for that warfighter.

Based on these derived cognitive models, cognitive interactions between CITE and the warfigher will affect procedural memory creation, which will allow self-assessment, self-awareness, and self-regulation, driving cognitive self-soothing procedures to be initiated, greatly reducing mental stress and thus the possibilities of mental disorders [Crowder and Friess 2010b].

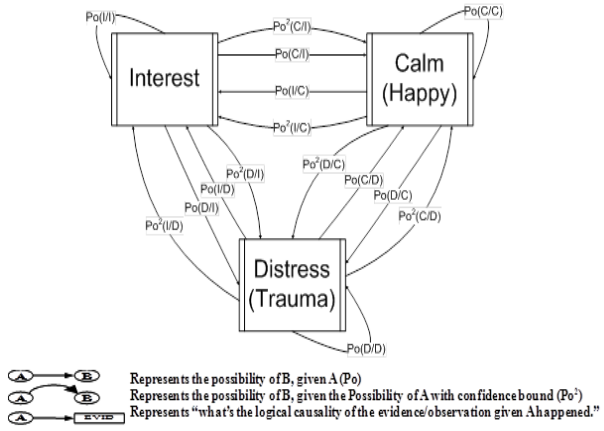

Figure 2 – Derived Warfighter Prefrontal Cortex Model, based on CITE interactions

5. The CITE Artificial Cognitive Neural Framework

The CITE warfighter cognitive models are derived through human-machine interactions and stored within the CITE Artificial Cognitive Neural Framework[2] (see Figure 3). In order to understand the world we live in, humans synthesize models that enable us to reason about what we perceive. Situations warfighters find themselves in, as well as the information they receive comes from a variety of sources, rendering it fuzzy. These diverse sources often do not have consistent contextual bases and this introduces ambiguity into the correlation and inferences the warfighter applies to the combined information. We have the ability to perceive the world we see and form our own concepts to describe and make decisions. To do this, we use language fuzzily and we communicate fuzzily, adapting and evolving our communication and processing to best fit the needs of our personal and conceptual views, along with our goals and vision for where we need to grow and evolve to [Zadeh 2004]. In order to understand and provide individualized resiliency training for

[2] Patent Pending

each warfighter, CITE must be able to organize information from the warfighter semantically into meaningful fuzzy concepts and models that provide a conceptual ontology [Raskin, Taylor, and Hempelmann 2010, and Taylor and Raskin 2010] of the individual warfighters cognitive abilities.

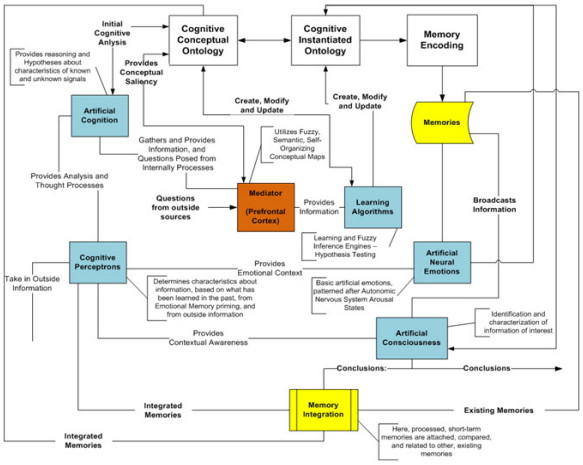

Figure 3 – The Artificial Cognitive Neural Framework

The purpose of these warfighter cognitive models is to provide cognitive knowledge products that reflect the state of being for the individual warfighter that includes metrics to measure cognitive resiliency for all aspects of life, to include battlefield, family and community.

6. Summary

What we have described is a cognitively interactive training system, CITE, that will allow warfighters to develop cognitive resiliency and provide knowledge products that reflects state of the art cognitive conditioning that minimizes injury, maximizes home station performance gains, and enables peak cognitive performance throughout deployment, and in garrison. This includes cognitive procedural memory development that will allow improvement in attitudes and knowledge about the value of proper nutrition, factors and fatigue, and the limits of sleep deprivation, through the use of cognitive self-awareness, self-evaluation, and self-regulation.

7. References

1. Crowder, J., and Friess, S. 2010a. Artificial Emotions and Emotional Memory. *Proceedings of the 11th Annual International Conference on Artificial Intelligence*, Las Vegas, Nevada.
2. Crowder, J. A., and Friess, S. 2010b. Artificial Neural Diagnostics and Prognostics: Self-Soothing in Cognitive Systems. *Proceedings of the 11th Annual International Conference on Artificial Intelligence*, Las Vegas, Nevada.
3. Crowder, J. and Friess, S. 2011a. Metacognition and Metamemory Concepts for AI Systems. *Proceedings of the 12th Annual International Conference on Artificial Intelligence*, Las Vegas, Nevada.
4. Crowder, J. and Friess, S. 2011b. The Artificial Prefrontal Cortex: Artificial Consciousness. *Proceedings of the 12th Annual International Conference on Artificial Intelligence*, Las Vegas, Nevada.
5. Crowder J., and Friess, S. 2012. Artificial Psychology: The Psychology of AI. *Proceedings of the International Multi-Conference on Information and Cybernetics*, Pasadena, CA.
6. Kahana, M. J., Howard, M. W., and Polyn, S. M. 2008. Associative retrieval processes in episodic memory. In H. L. Roediger III (Ed.), *Cognitive psychology of memory. Vol. 2 of Learning and memory: A comprehensive reference, 4 vols. (J. Byrne, Editor)*. Oxford: Elsevier.
7. LaBar KS and Cabeza. 2006. Cognitive Neuroscience of Emotional Memory. *Nat Rev Neurosci 7: 54-64*.
8. LeDoux JE. 1996. The Emotional Brain. *Simon and Schuster*, New York, NY.

9. Marsella, S., and Gratch J., "*A Step Towards Irrationality: Using Emotion to Change Belief*." 1st International Joint Conference on Autonomous Agents and Multi-Agent Systems, Bologna, Italy (July 2002).
10. Levine, P. 1997. Walking the Tiger: Healing Trauma. *North Atlantic Books*, Berkeley, CA.
11. Newell, A. 2003. Unified Theories of Cognition. *Harvard University Press*, Cambridge, MA.
12. Raskin, V., Taylor, J. M., & Hempelmann, C. F. 2010. Ontological semantic technology for detecting insider threat and social engineering. *New Security Paradigms Workshop*, Concord, MA.
13. Taylor, J. M., & Raskin, V. 2010. Fuzzy ontology for natural language. *29th International Conference of the North American Fuzzy Information Processing Society,* Toronto, Ontario, Canada.
14. Zadeh, L. 2004. A note of Web Intelligence, World Knowledge, and Fuzzy Logic. *Data and Knowledge Engineering, vol. 50, pp. 291-304*.

Computationally Adjustable Cognitive Inertia

Brian McLaughlan and Sebastian Bossarte
Department of Computer and Information Science
University of Arkansas - Fort Smith, Fort Smith, AR, USA

Abstract - *Cognitive inertia is the tendency for beliefs to endure once formed. This paper proposes that cognitive inertia can be utilized in multi-agent systems as a first derivative of trust. In this role, cognitive inertia provides a mechanism for allowing agents to determine how quickly or how drastically they should re-evaluate their trust in other agents. Appropriate levels of cognitive inertia are experimentally determined for various combinations of high and low risk and reward scenarios. Methods are examined that can allow agents to alter cognitive inertia based on feedback from the environment and other agents. From these experiments, we have identified several variables that appear to be useful indicators of appropriate cognitive inertia as well as inertia determination methods appropriate for various generalized scenarios.*

Keywords: *Multi-agent systems, trust, cognitive inertia*

1 Introduction

The evolution of e-commerce has led to an increased interest in concepts relating to trust. In fact, the ability to computationally define trust has been a major factor in successfully developing electronic and online commerce [1]. These trust models are increasing used by automated agents for making decisions or suggesting courses of action. When looking for inspiration for developing these models it is useful to look beyond traditional artificial intelligence concepts and examine how research in other disciplines may apply.

One potentially useful concept, cognitive inertia, is commonly utilized in managerial science. Essentially, cognitive inertia is the human tendency to maintain previously valid beliefs even when new evidence no longer supports those beliefs. Typically, this concept has a negative connotation, and significant research in this topic is devoted to analyzing its effects [2] or circumventing its symptoms [3]. However, cognitive inertia does have a positive role in the maintenance of trust.

Cognitive inertia is the component that makes long-term relationships of trust possible. For instance, if an individual is considered a trustworthy friend, one mistake would not be enough to invalidate that friendship. Additional confirmation of untrustworthiness is often needed. However, that one offense may prompt a slight raise of one's guard. Additional offenses would then indicate a significant change in attitude toward the individual in question. In this sense, cognitive inertia can be considered the first derivative of trust. That is, it is the rate at which trust is modified when circumstances dictate a change.

Although trust can be defined in many ways, this paper defines trust as follows: Trust is a belief that another agent is reliable in the services it provides, and is honest when given the opportunity to defect [4].

While cognitive inertia is not a one-size-fits-all concept in which a single value is most appropriate in all situations, it may be possible to generate broad guidelines for determining how quickly an agent should alter its trust in a given situation. This ability to modify its reasoning methods in response to feedback from the environment and scenario could allow an agent to avoid costly mistakes from trusting a faulty source or rashly terminating an otherwise sound relationship.

There are many techniques for modeling trust. The techniques in this paper could be best categorized as a learning model, a famous version of which is based on game theory [5] where agents calculate the benefit of cooperating with another agent. However, this work is less like traditional game theory models involving payoffs and defections and is more like the emergent trust models taken from a fusion of complexity theory, marketing, and psychological theory [6].

The research presented in this paper addresses two questions regarding cognitive inertia. First, is it possible to determine broad rules for calculating an appropriate inertia value in a given situation? Second, is it possible to utilize environmental variables, agent performance, or self-examination to adjust inertia to more appropriate levels?

2 Approach

To explore the viability of the concept of cognitive inertia in trust relationships, a generic multi-agent system is proposed. In this system, agents broadcast information to each other. Information presented by some agents tends to be more reliable than information from other agents. Believing false information incurs a penalty while believing true information provides a reward. Conversely, ignoring false information is rewarded while ignoring true information is penalized.

Agents maintain trust levels in each other agent. These trust levels represent the percentage chance that the agent will believe the information provided (Figure 1). After receiving the reward or penalty, the agent has the opportunity to adjust

its trust in the sending agent based on its cognitive inertia. While an agent maintains trust levels for each other agent, it only has a single cognitive inertia value. Future experimentation can determine if this is sufficient or if a more discrete inertia would be beneficial.

Formally, we propose a World $\boldsymbol{W}$ that consists of Agents $\boldsymbol{A}$, a Reward value R, a Penalty value P, and a discrete Time variable T:

$$\boldsymbol{W} = \{ \boldsymbol{A}, R, P, T \}. \quad (1)$$

There exists a set of agents, $\boldsymbol{A} = \{ \boldsymbol{A_1}, \boldsymbol{A_2}, \ldots, \boldsymbol{A_n} \}$, such that

$$\boldsymbol{A_i} = \{ \boldsymbol{M_i}, \boldsymbol{TR_i}, C_i, H_i, S_i, \boldsymbol{F_i} \}. \quad (2)$$

$\boldsymbol{M}_i$ is the set of message observations for $\boldsymbol{A_i}$:

$$\boldsymbol{M}_i = \{ M_i(1), M_i(2), \ldots, M_i(k) \}. \quad (3)$$

$\boldsymbol{TR_i}$ is the set of trust values in other agents:

$$\boldsymbol{TR}_i = \{TR_i^{\,1}, TR_i^{\,2}, \ldots, TR_i^{\,n-1}\} \quad (4)$$

where n is the number of agents in the system. Trust for each other agent is a value from 1 to 100.

C_i is agent $\boldsymbol{A_i}$'s cognitive inertia level on a scale of 1 to 100, representing the percentage chance it will adjust its trust in another agent. S_i represents its fitness score, and H_i is the agent's honesty on a scale of 1 to 100, representing the percentage chance it will present accurate information. Finally, $\boldsymbol{F_i}$ represents the set of functionality available to the agent.

$$\boldsymbol{F_i} = \{ F_i^S, F_i^R \} \quad (5)$$

Each turn, agent $\boldsymbol{A_i}$ will send a true message, M^{true}, or a false message, M^{false}, to all other agents using the Send function, F_i^S:

$$\boldsymbol{M_x}(T+1), \forall\, x \in \boldsymbol{A}, x \neq i \leftarrow F_i^S(M_i^{true}(T)) \Leftrightarrow \quad (6)$$
$$Random(1{:}100) \leq H_i(\mathrm{T}).$$

$$\boldsymbol{M_x}(T+1), \forall\, x \in \boldsymbol{A}, x \neq i \leftarrow F_i^S(M_i^{false}(T)) \Leftrightarrow \quad (7)$$
$$Random(1{:}100) > H_i(\mathrm{T}).$$

Similarly, a Receiving function, F_i^R, is created for receiving messages from agent $\boldsymbol{A_j}$:

$$\boldsymbol{M_i}(T+1) \leftarrow F_i^R(F_j^S(x_j(T), \exists!\, x \in \{M^{true}, M^{false}\})). \quad (8)$$

Next, we define the method in which agent $\boldsymbol{A_i}$ believes or disbelieves a message from $\boldsymbol{A_j}$:

$$\mathsf{BEL}_i\,(M^x{}_j(\mathrm{T}), \exists!\, x \in \{true, false\}\,) \Leftrightarrow \quad (9)$$
$$Random(1{:}100) \leq TR_i^{\,j}(\mathrm{T}).$$

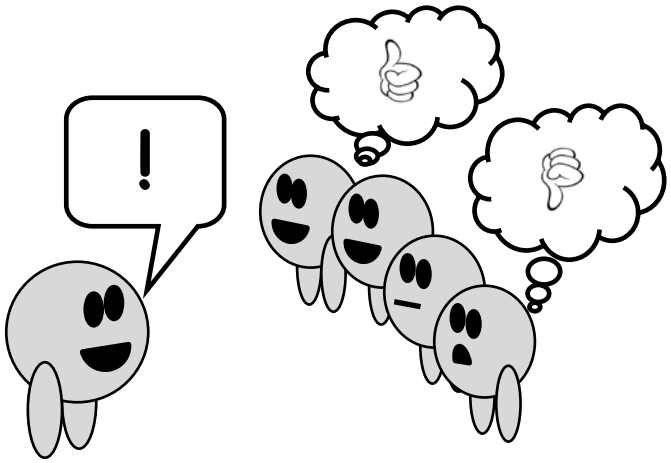

Figure 1: Agents believe or disbelieve messages based on their trust in the sending agent

That is, agent $\boldsymbol{A_i}$ will believe a message from agent $\boldsymbol{A_j}$ if and only if a randomly generated number from 1 to 100 is less than or equal to $\boldsymbol{A_i}$'s Trust in $\boldsymbol{A_j}$. While real-world scenarios would require a significant number of variables to adequately compute the trustworthiness of a message, this experiment abstracts the uncertainty as a stochastic variable.

Next, we define the methods in which the agent is rewarded or punished for the messages it has received:

$$\mathsf{BEL}_i\,(M^{true}(T)) \vee \neg\, \mathsf{BEL}_i\,(M^{false}(T)) \Rightarrow \quad (10)$$
$$S_i(\mathrm{T}+1) \leftarrow S_i(\mathrm{T}) + R.$$

$$\mathsf{BEL}_i\,(M^{false}(T)) \vee \neg\, \mathsf{BEL}_i\,(M^{true}(T)) \Rightarrow \quad (11)$$
$$S_i(\mathrm{T}+1) \leftarrow S_i(\mathrm{T}) - P.$$

When agent $\boldsymbol{A_i}$ believes a true message or disbelieves a false message, its score increases by the reward amount. Conversely, when agent $\boldsymbol{A_i}$ believes a false message or disbelieves a true message, its score decreases by the penalty amount.

Finally, we define agent $\boldsymbol{A_i}$'s ability to alter its trust in agent $\boldsymbol{A_j}$:

$$S_i(\mathrm{T}+1) > S_i(\mathrm{T}) \wedge Random(1{:}100) \leq C_i(\mathrm{T}) \Rightarrow \quad (12)$$
$$TR_i^{\,j}(\mathrm{T}+1) \leftarrow TR_i^{\,j}(\mathrm{T}) + (100\text{-}C_i)/10.$$

$$S_i(\mathrm{T}+1) < S_i(\mathrm{T}) \wedge Random(1{:}100) \leq C_i(\mathrm{T}) \Rightarrow \quad (13)$$
$$TR_i^{\,j}(\mathrm{T}+1) \leftarrow TR_i^{\,j}(\mathrm{T}) - (100\text{-}C_i)/10.$$

3 Experimentation

The proposed model was implemented in a Java simulation. The simulation consisted of 100 agents, each with a different cognitive inertia value:

$$C_i \leftarrow i, \forall\, i \in \boldsymbol{A}. \quad (14)$$

Each agent was given a random honesty value:

$$H_i \leftarrow Random(1{:}100), \forall\ i \in \boldsymbol{A}. \quad (14)$$

The honesty values for the group were weighted in one of three ways:

1. No weighting of honesty
2. Honesty weighted towards 75
3. Honesty weighted towards 25

Also examined was the model's ability to handle different reward and penalty scenarios. The experiment was executed with one of three reward/penalty combinations

1. Equal reward and risk: Reward $R = 1$, Penalty $P = 1$
2. High reward, low risk: Reward $R = 5$, Penalty $P = 1$
3. Low reward, high risk: Reward $R = 1$, Penalty $P = 5$

These parameters allow many different situations to be simulated. For instance, agents might be attempting to discover leads among data records for rooting out a wanted fugitive. In this scenario, there may be many dead-end leads and false positives shared with the group (honesty scores weighted towards 25), and those false positives don't cause significant problems (low penalty). However, a positive lead is a rare and significant event (high reward).

As another example, consider a group of agents that are interpreting and utilizing targeting data. Agents are expected to perform adequately (low reward and honesty weighted toward 75), and errors can cause catastrophic events such as targeting of friendly troops or non-combatants (high penalty).

The experiment was executed with one of five modifications to the method for adjusting cognitive inertia after each received message:

1. No change to inertia possible

2. Change inertia upwards for true received messages, downwards for false messages

$$F_i^R(M^{true}(T)) \Rightarrow C_i(T+1) \leftarrow C_i(T) + 1 \quad (15)$$
$$F_i^R(M^{false}(T)) \Rightarrow C_i(T+1) \leftarrow C_i(T) - 1 \quad (16)$$

3. Change inertia downwards for true received messages, upwards for false messages

$$F_i^R(M^{true}(T)) \Rightarrow C_i(T+1) \leftarrow C_i(T) - 1 \quad (17)$$
$$F_i^R(M^{false}(T)) \Rightarrow C_i(T+1) \leftarrow C_i(T) + 1 \quad (18)$$

4. Inertia moves toward 50 when a false message is received, away from 50 when true

$$F_i^R(M^{true}(T)) \wedge C_i(T) < 50 \Rightarrow \quad (19)$$
$$C_i(T+1) \leftarrow C_i(T) - 1$$
$$F_i^R(M^{true}(T)) \wedge C_i(T) > 50 \Rightarrow \quad (20)$$
$$C_i(T+1) \leftarrow C_i(T) + 1$$
$$F_i^R(M^{false}(T)) \wedge C_i(T) < 50 \Rightarrow \quad (21)$$
$$C_i(T+1) \leftarrow C_i(T) + 1$$
$$F_i^R(M^{false}(T)) \wedge C_i(T) > 50 \Rightarrow \quad (22)$$
$$C_i(T+1) \leftarrow C_i(T) - 1$$

5. Inertia moves toward 50 when a true message is received, away from 50 when false

$$F_i^R(M^{true}(T)) \wedge C_i(T) < 50 \Rightarrow \quad (23)$$
$$C_i(T+1) \leftarrow C_i(T) + 1$$
$$F_i^R(M^{true}(T)) \wedge C_i(T) > 50 \Rightarrow \quad (24)$$
$$C_i(T+1) \leftarrow C_i(T) - 1$$
$$F_i^R(M^{false}(T)) \wedge C_i(T) < 50 \Rightarrow \quad (25)$$
$$C_i(T+1) \leftarrow C_i(T) - 1$$
$$F_i^R(M^{false}(T)) \wedge C_i(T) > 50 \Rightarrow \quad (26)$$
$$C_i(T+1) \leftarrow C_i(T) + 1$$

To allow each agent to stabilize at what it felt was an appropriate configuration, the simulation was executed for 500 time cycles, with each agent sending one message to the group during each time cycle. This number of time cycles gave each agent adequate time to settle into particular trust and cognitive inertia values. At the end of the simulation, fitness scores of each agent were tabulated. Each of the 45 possible scenario combinations was executed 1000 times to get a good average statistic.

4 Results

Figure 2 shows the average scores of agents in a simple low risk/low reward scenario containing agents with a wide range of honesty values. The "No modifier" line shows the baseline desirability of each cognitive inertia value. Thus, a low inertia would be most appropriate here. Agents with an honesty value that clusters around 25 tend to perform similarly. However, agents with high average honesty (Figure 3) tend to perform better with a cognitive inertia in the 65 to 80 range. This trend holds fairly steady for all combinations of high/low risk and reward parameters.

The method of adjusting cognitive inertia is particularly interesting. As summarized in Figure 4, the formula that achieves the best performance varies by scenario. When the average honesty is high, pushing the inertia towards the

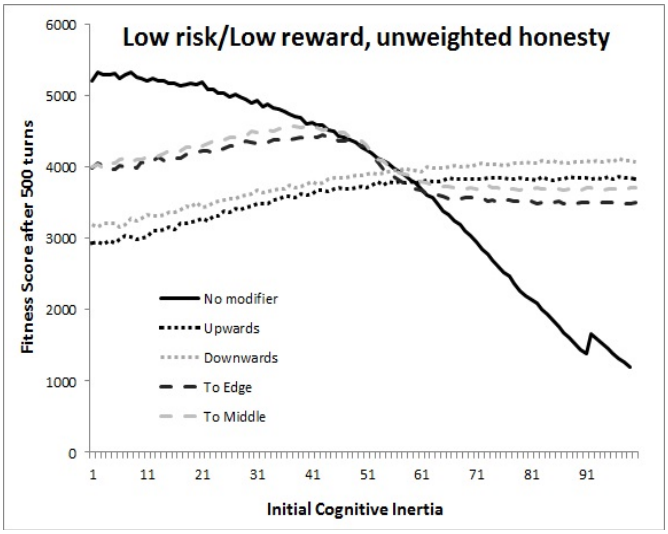

Figure 2: Comparison of inertia modification techniques in a community with random honesty

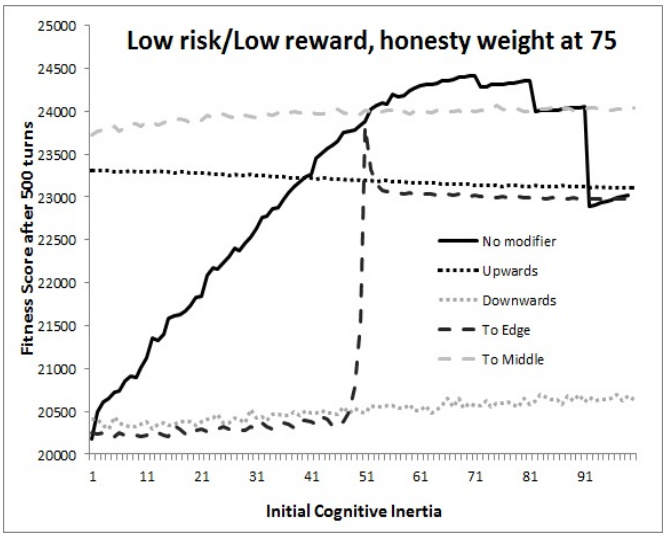

Figure 3: Comparison of inertia modification techniques in a community with honesty weighted towards 75

middle when a true statement is received and towards the edge when a false statement is received works best. This makes sense when considering that an ideal inertia value is slightly above 50, and most statements will be true.

However, other scenarios are less defined. Clustering scores to the edge or middle tends to provide adequate results, but linear pushes upwards or downwards tends to either be very good or very poor. Low risk/high reward scenarios tended to do poorly with linear movement, while high risk/low reward scenarios tended to do excellently with these formulas. As before, high honesty systems didn't follow this pattern.

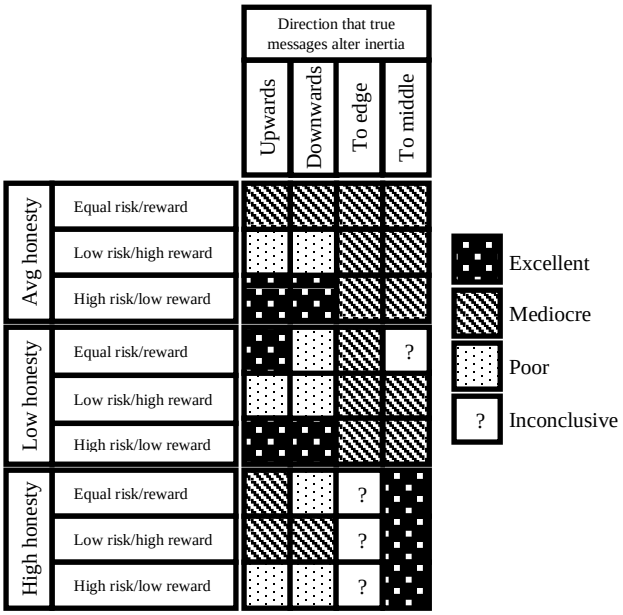

Figure 4: Summary of inertia modification techniques in various scenarios

5 Conclusions and future work

The simulations show that there are patterns in the data, suggesting that the notion of cognitive inertia is a valid method of adjusting trust in multi-agent systems. However, the anomalies suggest that a more complex representation is probably needed. For instance, agents may be better served by a trust vector, combining trust and cognitive inertia for each other agent in the system. Additionally, time may be a valid factor, with agents keeping track of how long they have held a particular trust in another agent. Another concept that may be of use is social distance [7] in which agents are not necessarily directly known to each other. Notions such as these could allow for new algorithms for adjusting trust inertia that might better serve the agents than ones presented here. Our future work in this topic will explore these possibilities.

6 References

[1] He, J. (2011) "Understanding the sources and impacts of trust in e-commerce: A meta-analysis." *AMCIS 2011 Proceedings – All Submissions.* Paper 142.

[2] Tripsas, M., and Gavetti, G. (2000) "Capabilities, cognition, and inertia: Evidence from digital imaging." In *Strategic Management Journal* 21:10-11.

[3] Messner, C., and Vosgerau, J. (2010) "Cognitive inertia and the implicit association test." In *Journal of Marketing Research*, 47:2.

[4] Dasgupta, P. (1998) "Trust as a commodity." In D. Gambetta, editor, *Trust: Making and Breaking Cooperative Relations*. Blackwell.

[5] von Neuman, J., and Morgenstern, O. (1944) *The Theory of Games and Economic Behavior*. Princeton University Press, Princeton NJ.

[6] Jarratt, D., Bossomaier, T., Thompson, J. (2007) "Trust as an emergent phenomenon in wealth management relationships." In *Global Business and Economics Review* 9:4, 335-352.

[7] Binzel, C., and Fehr, D. (2010) "Social Relationships and Trust," SFB 649 Discussion Papers, Sonderforschungsbereich 649, Humboldt University, Berlin, Germany.

SESSION

MEDICAL AND HEALTH INFORMATICS + RELATED ISSUES

Chair(s)

TBA

Open Source Text Based Biovigilance

Madhav Erraguntla, Ph. D.[1], P.E., Larissa May, MD[2], MSPH, Belita Gopal[1], Richard J. Mayer, Ph. D.[1], Perakath C. Benjamin, Ph. D.[1]
[1]Knowledge Based Systems, Inc., 1408 University Drive East, College Station, TX 77840, USA
[2]George Washington University, Washington, D.C., USA

Abstract–*Timely detection of disease outbreak events is of paramount importance for the defense against infectious diseases and biological threats. Internet-based communications can provide good situational awareness for countries where public data collection is inadequate, unreliable or missing. The key challenge is to sift through this vast amount of unstructured text to identify relevant reports and to extract disease related information into a structured format suitable for analysis. In this work, Natural Language Processing (NLP) techniques are used on data from news feeds, websites, and medical publications to extract key biological event data. We developed the Threat Assessment Dashboard (BioTHAD™) in order to improve detection and monitoring of biological events. We demonstrate that disease outbreak incidence and timing can be effectively extracted from open news sources using NLP. The BioTHAD™ application could serve as a model for tracking not only infectious, but chronic diseases and other types of events worldwide.*

Keywords: Biovigilance, Open Sources Based Surveillance, Disease Outbreaks, Natural Language Processing, Text Mining

1 Background and Significance

Most emerging infectious diseases and agents of bioterrorism present as nonspecific "flu-like illness," thus early detection requires the use of alternative sources of data rather than waiting for reporting of laboratory-confirmed diagnoses [1]. Because syndromic surveillance systems access and analyze data streams not typically available to departments of health, syndromic surveillance has the potential to identify unusual patterns of illness prior to definitive diagnoses and thus potentially closer to "real-time" than traditional surveillance systems [1]. Detection of aberrant activity using statistical tools to identify unusual spatiotemporal distributions of symptoms for further public health investigations augments traditional surveillance [1, 2, 3].

A rich source of data for bio-surveillance is the wealth of news articles posted to or available through the web. While widespread availability is a major advantage for these reports, the sheer volume of information routinely available on the web makes its utilization difficult. The detection of disease outbreaks and other potential biological threats is extremely challenging due to nuances of natural language used in news articles. Automated identification of relevant events would improve surveillance and increase research and response effectiveness. One approach to making that information more tractable for biovigilance community members is to automate the processing of news reports and to flag reports of potential interest, highlighting or tagging relevant elements within reports, and extracting data for subsequent analysis.

Extracting disease and biological event related information from unstructured text is a challenging problem because of the nuances of natural language [4, 5]. According to Kawazoe, et al., "in many cases, disease-related events are mentioned with verbs (e.g., 'infect'), verbal nouns (e.g., 'infection') and verb phrases. There are many synonymous event expressions; for example, infecting events can be expressed by many verbs and verb phrases such as 'infect,' 'transmit,' 'contract,' 'communicate (pathogen/ disease),' 'catch (pathogen/disease),' 'get (pathogen/disease),' as well as verbal nouns such as 'infection,' 'transmission,' 'contraction.'" Event recognition (in this case, finding reports about outbreaks of diseases) also occurs at the noun phrase ("outbreak of ...") and clause ("people died from ...") levels [4]. Also, sometimes, an infecting event is not mentioned directly, but only implied, as in a sentence like "A man died of bird flu" [6].

2 Approach

The BioTHAD™ technology has software agents that can be configured to monitor information sources such as news feeds, and medical publications on a daily basis. Currently, the BioTHAD™ technology monitors and downloads data from 15 sources including ProMed Mail [7], WHO, BBC Health News, CDC Morbidity and Mortality Weekly Reports, The Lancet Infectious Diseases, and BMC Infectious Diseases. HTML files are downloaded from these sites, text is extracted from these HTML files, converted to an XML format, and then processed by an NLP pipeline to extract the relevant information.

Figure 1 shows the process used to extract information from text sources. The first part of the process, shown in the top box, uses our in-house NLP pipeline. The steps involved in this initial part of the process are sentence boundary

detection, tokenization, part-of-speech tagging, phrase chunking, Subject-Verb-Object (SVO) assignment, clause segmentation and finally, named entity recognition. The first four steps internally use OpenNLP (http://incubator.apache.org/opennlp/), while the SVO assignment, clause segmentation and named entity recognition modules have been developed in-house. The SVO and Clause assignment stage involve splitting the sentence into clauses and finding SVOs in the sentence.

The main objective of the initial stages of text processing is to identify and classify the phrases which may be the constituents of event patterns. The steps shown in the green/top box are mostly domain-independent. The named entity recognition module recognizes generic named entities such as Persons, Locations and Organizations. On the other hand, the processes shown in the yellow/bottom box in Figure 1 are components that are domain-specific. The four components required are the domain concept tagger, event pattern matcher, inference of missing data, and data normalization. The following sections briefly outline each component.

2.1 Event Extraction

2.1.1 Domain concept tagging

The first step in domain event extraction (bottom box in Figure 1) is the Domain Concept Tagging. Unlike the named entity recognition module in the NLP pipeline (top box in Figure 1), the domain concept tagger tags concepts that are domain-specific. We identified the following items as key concepts associated with disease and biological events in the context of information extraction: Diseases, Symptoms, Pathogens, Antibiotics, Location, Date, Outbreak terms, Resistance terms, Victim Type and Severity. After identifying such domain-specific concepts, the extraction of domain-specific event frames becomes simplified. For example, the pattern 'disease killed victim' would match the string "cholera killed 7 inhabitants." In a similar fashion, noun phrases that could denote an unidentified disease will also be tagged. This helps to capture reports on outbreaks when the disease type is still unknown.

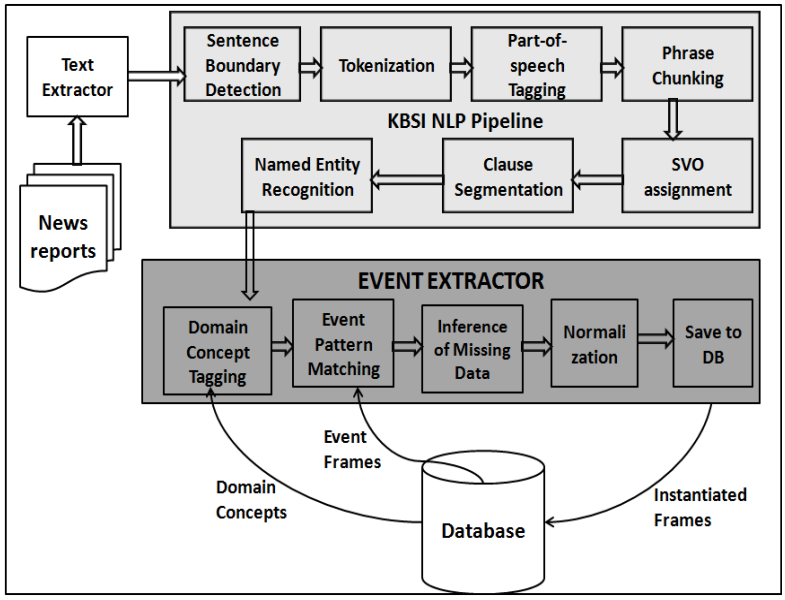

Figure 1. BioTHAD Information Extraction Pipeline

2.1.2 Event pattern matching

The next important step is the Event Pattern Matching which consists of feature extracting and the frame matching. The event pattern matching component will read all the pre-defined event patterns and compare them with the processed text to see if there are any matches. If a pattern is matched, an 'event' is generated

The Feature Extractor extracts relevant textual features that are generally very domain specific from the NLP output. Features such as noun phrases, disease, date, location, verb phrases, root form of verbs, etc., are extracted to produce a simplified representation of the processed text. This is illustrated in Figure 2.

Figure 2 shows an example of how text is processed as it proceeds through the various stages of the process. The input to the Feature Extractor is the tagged parse tree which comes from the NLP pipeline and the Domain Concept Tagger. By this stage, concepts such as disease and location have already been identified and appropriately tagged. The output of the Feature Extractor is:

NP SEGMENT(disease) + VP SEGMENT (surface) + PP SEGMENT (location)

The above feature vector means that this particular sentence contains the following components:

- A noun phrase which contains a disease, followed by,
- A verb phrase which contains the verb "surface," followed by,
- A Prepositional Phrase which contains a location.

The feature vector is then fed to the next module, the Frame Matcher. The Frame Matcher is the key module of the whole processing pipeline. Its main function is to match incoming feature vectors against a set of predefined event frames or templates. Figure 2 also shows the event frame that matches the feature vector from this particular sentence. One important input needed for this step is the repository of event frames that capture disease incidents in news report. The generation of these frames is described in more detail below.

The next step in the BioTHAD™ Information Extraction Pipeline is inferring missing data. Natural language is efficient and hence often key information is not explicitly mentioned because the human can infer it from the context. This is especially true for dates and locations.

2.1.3 Handling incomplete date specification

Heuristics are used to fill out missing or incomplete dates.

- Infer the year. Consider the example: "On 22 August the Ministry of Health (MoH) of the Central African Republic reported a laboratory confirmed case of yellow fever." To complete the date "22 August," the year from the published date is added to it.
- Infer the date from the context. Consider the example "Southern Missouri man dies of rabies." Since the date is completely missing from this sentence, it is assumed that the date is the same as the published date.
- Dereference the relative date. Consider the example "Southern Missouri man died of rabies yesterday." The actual date can be computed relative to the published date. Therefore, in this case, "yesterday" = Published Date - 1

2.1.4 Missing or ambiguous location information

Very often, an instantiated frame does not contain a location. In addition, many frames that do contain an explicit reference to a location, the source text does not contain the context of that location; whether the location is a city, a state or a country. For this reason, it is necessary to tag these three categories based on lookup lists. We created a lookup list of countries and in the case of the United States, the list also includes cities and states. The location lookup list is used to resolve a location and identify its country or state.

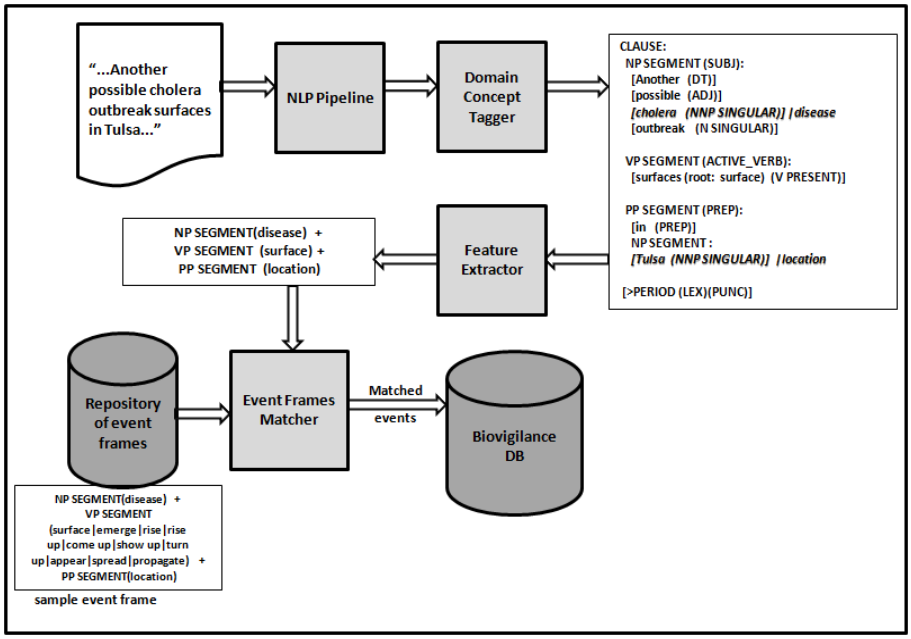

Figure 2. Text Processing and Event Extraction Process

2.1.5 Data Cleaning and Normalization

Once an event is generated, some of the instantiated event slots will need to be further refined or cleaned to generate consistent information. The following examples illustrate the need to normalize the data before saving the instantiated event to the database.

- Dates and date expressions (including dates relative to the report time, such as "last week") should be normalized to a standard form, with explicit day, month, and year.
- One disease could have many names. We designate one canonical name for each disease and normalize all

variants to that standard e.g., "Ebola," "Ebola hemorrhagic fever," "EHF."

- Similarly, some countries have many names; therefore, there is a need to normalize country names, e.g., "U.S.A.," "U.S.," "United States."

Further analysis of the stored data using techniques such as data mining will be performed on this atomic event extracted from the text.

After the frames are extracted, the information extracted undergoes further processing. This involves data cleaning and data filtering.

Open sources like news feeds and medical publications often have information related to statistical updates and summaries, prevention, negative outbreaks (i.e., documents reporting that an outbreak is abating) and reports about general information related to drugs and research, in addition to reports about disease incidents. It is necessary to filter out reports that have information content other than disease incidence reporting. We detail some of the types of filtering and aggregation below.

a) Filtering reports on statistical updates: Reports that provide information about statistical updates, such as total count of cases for a specific disease for a whole year and the worldwide situation of specific diseases are filtered out. This elimination consists of two steps. The first step removes reports that contain the pattern "update yyyy" and "world-wide" in the title. The second step filters out reports that contain the word "update" in the title and more than three locations in the text. Another example of statistical updates is temporal generalizations. For example, "Every year, cholera causes 100 deaths in Zimbabwe." Such instantiated events containing repeating time intervals are filtered out.

b) Filtering reports on prevention: The second type of report that has nothing to do with the outbreak of diseases is prevention related reports. After going through some sample reports on prevention, a list of keywords was created to denote that a report concerns prevention.

c) Filtering reports on multiple diseases: It was also decided that reports that discuss multiple diseases could potentially be noisy reports for the purpose of disease incidence detection. Therefore, these are also filtered out based on the number of diseases extracted from the text. To date we have not processed any report that contained more than three instances of a disease in the text.

d) Filtering reports on negative outbreaks: Another category of documents that must be filtered from the repository is negative outbreaks; i.e., documents reporting that an outbreak is either abating, or being controlled. A report is considered to fall in this category if the title contains one or more of the following words or phrases: under control, is over, waning, officially over, eradicate, recover, etc.

e) Filtering reports on drugs and medical research: Finally, another category of documents to be filtered out from the repository was reports focused exclusively on pharmaceutical and medical research. Reports whose titles contained any of the following concepts were eliminated: research, experiment, drug testing, pharmaceutical research, etc. Some of the reports eliminated might contain important information like approval of a drug or vaccine for a pandemic, but it is not within the current scope of the BioTHAD™ technology and those reports are filtered out.

2.1.6 Spatio-temporal aggregation

Since the disease outbreak information is being extracted from multiple sources, it is likely that multiple records are generated for the same incident by different sources. It is also possible that the same source reports information about an incident over multiple days. While displaying situation awareness information to analysts, the multiple incidents are aggregated and presented as single, major events. The aggregation is based on spatio-temporal proximity. Link list and nearest neighborhood-based clustering techniques are used to form the aggregate events [8, 9, 10].

3 Results

We validated the effectiveness of our approach against well known disease outbreaks. We present results from two of the validation studies in this section. The first analysis was to verify the data against the Haiti cholera outbreak that began in late October 2010 following the earthquake that shook the country in January 2010 [11]. The date range of the cholera outbreak events in Haiti extracted from news reports is shown in Figure 3 along with the actual date range of the outbreak as reported by CDC. The timeline analysis reveals that the date range of the extracted events coincides very well with the recorded date range for the 2009-2010 Haiti cholera outbreak.

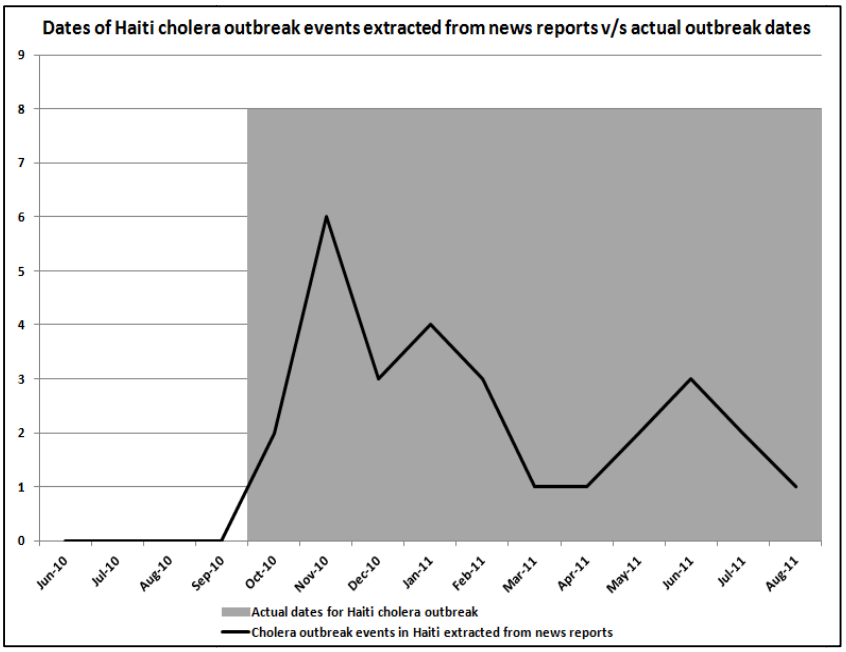

Figure 3. Trend of Cholera Outbreak in Haiti

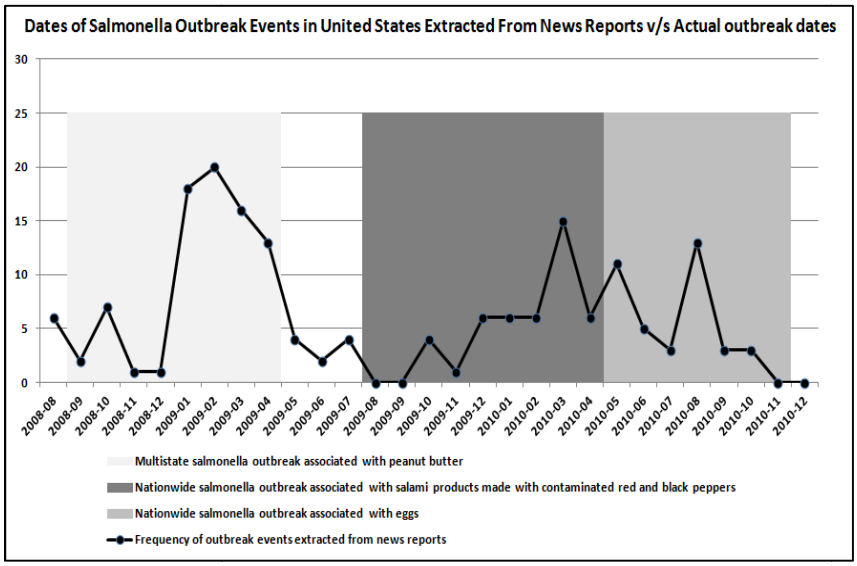

Figure 4. Salmonella Outbreak Events in the United States Extracted From News Reports

The next objective was to verify the trend for salmonella outbreaks in the United States. For this analysis, the date ranges of the extracted disease outbreak events were compared to three different known outbreaks of salmonella in the United States. The results of this comparison are illustrated in Figure 4, which also shows the three different actual salmonella outbreaks, namely:

- Multistate salmonella outbreak associated with peanut butter [12],
- Nationwide salmonella outbreak associated with eggs [13], and
- Nationwide salmonella outbreak associated with salami products made with contaminated red and black peppers [14].

Figure 4 shows a fairly close correlation between the three known outbreaks with the date ranges of the extracted disease outbreak events for salmonella in the United States.

4 Conclusion

Timely detection of disease outbreak events is of paramount importance for the defense against infectious diseases and biological threat events. News reports and medical publications of diseases and biological events are a

valuable source for collecting and organizing information regarding potential disease outbreak around the world. We present the methodology for extracting disease and biological events from open sources. In this paper, we have presented the design and implementation details of Biovigilance Threat Assessment Dashboard (BioTHAD™) that implements this capability. The BioTHAD™ technology provides good situational awareness into the status of disease and biological events across the world and is capable of detecting diverse biological events from open source reports. Analysis supported by the BioTHAD™ technology includes spatio-temporal aggregation and time-line visualization of disease outbreaks. Our approach is validated using a number of known disease outbreaks in recent years.

The BioTHAD™ technology is very effective in extracting disease incidents and their timing and has the potential for broad applications to the early detection and monitoring of not only infectious diseases, but chronic diseases and other events of national and global importance to biosecurity. We are currently validating and refining extracting victim counts and plan to extend our approach to extracting the etiology and nature of disease outbreaks (endemic, nosocomial, community acquired, etc). Another future direction is to design and develop a user interface for epidemiologic analysis and validation of intermediate results from BioTHAD™.

5 Acknowledgements

This work was performed under funding from two Office of Secretary of Defense (OSD) Small Business Innovative Research (SBIR) programs – Biosurveillance-based Integrated Outbreak Warning And Recognition System (BIOWARS) and Environment, Epidemiology, and Etiology Surveillance and Analysis Toolkit (E3SAT) [15, 16, 17]. We would like to acknowledge the support of our sponsor Dr. Kevin Montgomery.

6 References

[1] Stoto MA, Schonlau ML. Syndromic surveillance: is it worth the effort? *Chance* .2004; 17(1), 19-24.

[2] May L, Chretien JP. Pavlin JA. Beyond traditional surveillance: Applying syndromic surveillance to developing settings—opportunities and challenges. BMC Public Health 2009; 9:242.

[3] May L, Griffin BA, Maier Bauers N, Jain A, Mitchum M, Sikka N. Carim M, Stoto MA. Evaluation of emergency department chief complaint and diagnosis data for detection of influenza-like illness using an electronic medical record. The Western Journal of Emergency Medicine 2010;11 (1).

[4] Grishman R, Huttunen S, Yangarber, R. Real-time event extraction for infectious disease outbreaks. Proceedings of Human Language Technology Conference (HLT) 2002.

[5] Lu H, Zeng D, Chen H. Prospective infectious disease outbreak detection using Markov switching models. IEEE Transactions on Knowledge and Data Engineering 2010; 22 (4): 565-577.

[6] Kawazoe A, Chanlekha H, Shigematsu M, Collier, N. Structuring an event ontology for disease outbreak detection. BMC Bioinformatics 2008; 9 (3).

[7] Promed Mail. http://www.promedmail.org/

[8] Erraguntla M, Belita G, Ramachandran S, Mayer R. J. Inference of Missing ICD9 codes using text mining and nearest neighbor techniques. Submitted for Hawaii International Conference on System Sciences, 2012.

[9] Hoebe CJ, de Melker H, Spanjaard L, Dankert J, Nagelkerke N. Space-time cluster analysis of invasive meningococcal disease. Emerg Infect Dis. 2004; 10: 1621-1626.

[10] Si Y, Debba P, Skidmore AK, Toxopeus AG, Li L. Spatial and temporal patterns of global H5N1 outbreaks. The International Archives of the Photogrammetry, Remote Sensing and Spatial Information Sciences 2008; 37: 69-74.

[11] CDC. Cholera Confirmed in Haiti, October 21, 2010. http://www.cdc.gov/haiticholera/situation/.

[12] CDC. Timeline of Infections: Multistate Outbreak of Salmonella Infections Associated with Peanut Butter and Peanut Butter-Containing Products — United States, 2008–2009. http://www.cdc.gov/salmonella/typhimurium/salmonellaOutbreak_timeline.pdf.

[13] CDC. Investigation Update: Multistate Outbreak of Human Salmonella Enteritidis Infections Associated with http://www.cdc.gov/salmonella/enteritidis/index.html.

[14] CDC. Timeline of Infections: Nationwide Outbreak of Salmonella Montevideo Infections Associated with Salami Products Made with Contaminated Black and Red Pepper United States, 2009 -2010. http://www.cdc.gov/salmonella/montevideo/montevideo_timeline2.pdf.

[15] BIOWARS. Biosurveillance-based integrated outbreak warning and recognition system (BIOWARS). OSD SBIR Phase II 2010; Contract No. W81XWH-08-C-0093.

[16] E3SAT. Environment, epidemiology, and etiology surveillance and analysis toolkit (E3SAT). OSD SBIR Phase II 2009; Contract No. W81XWH-08-C-0756.

[17] Erraguntla M, Ramachandran S, Wu C., Mayer, R J. Avian influenza data mining using environment, epidemiology, and etiology surveillance and analysis toolkit (E3SAT). Hawaii International Conference on System Sciences 2010.

Applied Machine Learning and Decision Combination for Identifying the Lazy Eye Vision Disorder

Patrick G. Clark[1], **Christopher M. Gifford**[2], **Jonathan Van Eenwyk**[1], **Arvin Agah**[1], **and Gerhard W. Cibis**[3]
[1]Department of Electrical Engineering and Computer Science,
University of Kansas, Lawrence, KS 66045 USA
[2]National Security Technology Department,
The Johns Hopkins University Applied Physics Laboratory, Laurel, MD 20723 USA
[3]Cibis Eye Care, Kansas City, MO, 64112 USA

Abstract—*Amblyopia is a neurological vision disorder that studies show affects two to five percent of the population. Several early screening procedures are aimed at finding the condition while the patient is a child, including an automated vision screening system developed by Cibis, Wang, and Van Eenwyk. The system uses artificial intelligence software algorithms to achieve a 77% accuracy in identifying patients who are at risk for developing the amblyopic condition and should be referred to a specialist. Based on later work, two additional feature sets are also extracted from the same data captured with the AVVDA system, both achieving a 67% accuracy. This work explores the application of a multi-classifier collaborative learning architecture on the three data sets. The architecture has been shown to be more successful in problems that exhibit difficulty for single pass classifiers.*

Keywords: Multi-Classifier, AI in Medicine, Applied AI, Lazy Eye, Amblyopia.

1. Introduction

Eye trouble of organic origin must be diagnosed and treated before the onset of an irreversible amblyopia or what is commonly referred to as lazy eye. This condition is a developmental disorder of the visual system caused by ocular abnormalities early in life. While surgery or optical correction of refractive errors can often address the initial cause of amblyopia, once amblyopia has developed, such interventions cannot restore visual function since amblyopia itself is a cortical deficit, a neurological disorder and not a physical one [1]. Amblyopia has two primary causes, namely, strabismus and anisometropia. Strabismus is a misalignment between the two eyes. Anisometropia is when the refractive error between the two eyes is different [2]. The reason that these two conditions can lead to amblyopia is because they cause the brain to begin ignoring the signals from the weaker or blurrier eye. Corrective action after amblyopia has developed becomes problematic, as the brain will not be able to regenerate the neural pathways. Thus, early detection is essential for the patient to have a healthy visual outcome. Fortunately, amblyopia can be successfully treated if identified when the patient's brain is still in the developmental stages, generally when the patient is fewer than six years old, with the non-controversial methods of glasses and patching therapy achieving 80 to 90% effectiveness [3].

The optimal solution for vision diagnosis would be a self-contained, low-cost, completely automated system that could accurately identify disorders with minimum operator training and low patient cooperation. The solution would need to enable widespread use with small children, including infants. One approach for this sort of solution is based on [4], [3], pioneering the science of analyzing images for identifying features that may indicate the development of amblyopia, and using artificial intelligence techniques to automate the process [5].

1.1 Problem Statement

In this work, we utilize a multi-classifier machine learning architecture consisting of a heterogeneous mixture of classification techniques in a team of intelligent agents. This architecture is applied to the problem of accurately identifying the amblyopic condition using three existing data and feature sets. The effort looks to make use of both ensemble and single classifiers on the data sets in order to ascertain the best features for identifying and referring patients to a specialist.

The previous work involved reviewing each individual data set on it's own merits with a subset of classifiers, but here the work looks to take a larger view of the features by measuring them in relation to a number of classifiers. Results between the approaches are compared and conclusions drawn about the efficacy of the feature sets, applied to a variety of classifiers, as well as a multi-classifier decision fusion methodology in the vision diagnosis domain.

2. Background and Related Work

2.1 Vision Disorders

Amblyopia is the primary vision disorder this research attempts to accurately identify. It has two primary physical

causes, anisometropia and strabismus. Anisometropia is a condition where the refractive error in one eye is significantly different than the other. The difference in the refractive errors is difficult to overcome for a developing visual cortex, primarily due to the very different images being presented. Studies have shown that anisometropia is the predisposing condition that leads to amblyopia 50% of the time, and that an undiagnosed anisometropia will lead to strabismus [2]. Strabismus can be identified as a misalignment of the focal point between the two eyes, but the condition is not always identifiable with the naked eye and may require a thorough screening. Strabismus typically involves a lack of coordination between the two eyes and the extra-ocular muscles where the patient is unable to bring both eyes into focus on the same point in space, thus preventing proper binocular vision.

Both of these physical abnormalities in the eye have the potential to cause the development of a patient's visual function to be impaired and cause the image from the amblyopic eye to be disregarded by the visual cortex. If the condition is allowed to persist, the neural pathways become permanently formed and the use of the amblyopic eye is diminished. The degree to which it is diminished varies based on how early the condition developed in the patient's life and if any remediation treatment was used [2].

2.2 Automated Photo-Refractive Screening

Photo-refractive screening is based on a system to interpret the images of the eyes. It does not directly identify amblyopia, but it looks for defects in the eyes that may lead to amblyopia. One such system for identifying strabismus and amblyopia using video images, called Video Vision Development Assessment (VVDA), has been developed [3]. The method involves a consumer-grade video camera with a light source attached to the base of the camera. The patient sits approximately 52 inches from the camera and looks at the light source while approximately two minutes of video is recorded. The video is then digitized and analyzed by specialists or trained technicians to determine if the patient should be referred to a specialist. This processing is generally divided into frame selection and feature extraction.

More recently, research has been performed in order to automate the analysis of the frames using artificial intelligence techniques [6], [4], [5]. These works focused on implementing the image processing and Case-Based Reasoning [7] algorithms that constituted the first version of the Automated Video Vision Development Assessment (AVVDA) system. In a completely automated fashion, they were able to identify the key frames of the video, isolate the pupils, and locate the Hirschberg point [6], [4]. Figure 1 shows the image output from the AVVDA system, where the Hirschberg reflex and iris diameter are highlighted. The automated photo-refractive screening system works by having an operator take a short video of the patient, which is then analyzed automatically by the software in the following manner. Initially, the software identifies the frames where both eyes are open and looking at the light source. These frames are identified as key frames. Next, the software isolates the location of the eyes and pupils in the key frames. Finally, the software uses various techniques to extract the distinguishing features that may be indicators for amblyopia.

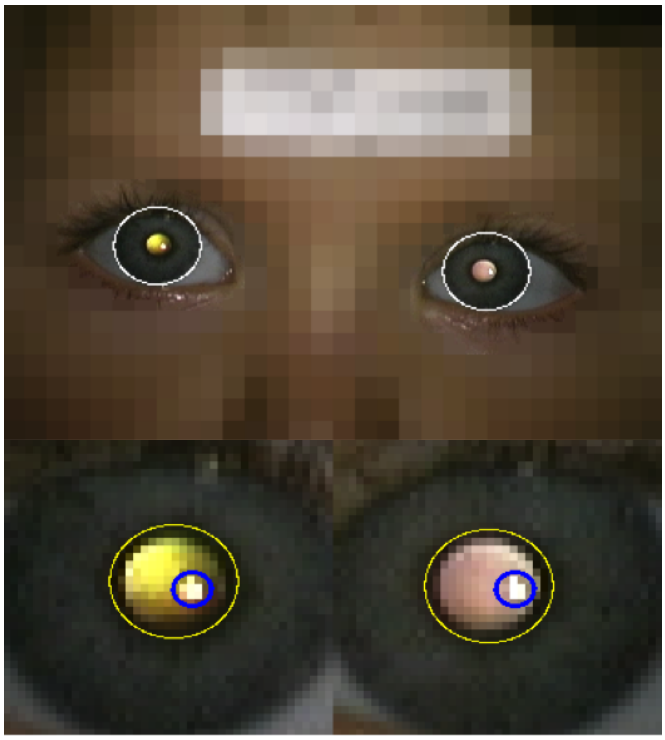

Fig. 1: Key frame output from the AVVDA system [5]

In order to further enhance AVVDA, researchers have investigated using the same feature set with a different set of classifiers, with the overall goal of the AVVDA system being to allow an unskilled technician to operate the system and accurately obtain a decision about patient referral to an optometrist or ophthalmologist [5]. In the current form, AVVDA uses Case-Based Reasoning [7], C4.5 Decision Tree [8], and Artificial Neural Network [9] classifiers to assist in making the decision. 54 features are extracted from the images to train the classifiers.

At this point, various artificial intelligence techniques have been utilized to automatically produce the referral to a specialist [3], [5]. The results reported in this work expands upon the automated photo-refractive screening method, with the goal to evaluate other classifiers, and the use of multi-classifier ensembles, as a means to produce more accurate results from the same feature set.

2.3 Combining Decisions from Multiple Classifiers

Classifier combination is an area in machine learning that has offered advances in classification accuracy for complex data sets. It has been termed differently in the literature, namely, classifier fusion, mixture of experts, committees, ensembles, teams, pools, collective recognition, composite systems, etc. When predictions from multiple classifiers are combined, they are said to form an ensemble that is then used to classify new instances. Several methods have been developed to combine classifiers, the most popular of which are voting, boosting, bagging, and stacking.

One of the primary questions in this area of study is whether combining classifiers is better than selecting the best classifier. Several works support that classifier combination provides an improvement in most cases, assuming that the classifiers exhibit reasonable individual accuracy. One such study utilized stacking with model trees to combine multiple heterogeneous learners [10]. Each learner utilized the full data set to produce a base-level model, the output of which is then combined with other base-level models using a meta-level classifier. Their results also indicated that the number of base-level classifiers did not significantly affect the results. Similarly, [11] found that when using voting and entropy methods as the heterogeneous classifier combination mechanism for word-sense disambiguation, increasing the number of less accurate classifiers adversely affected those with higher accuracy. Use of more classifiers, even if heterogeneous, does not always translate to better results. Depending on the combination method, the relative impact of adding classifiers can diminish as team size increases. Our work attempts to address this by implementing a framework where team configurations can be analyzed to determine what factors make a team of classifiers successful given the application and domain.

Although selection of the best individual classifier is easier and occasionally effective, combination techniques scale better to larger and more complex learning problems. Even combining all classifiers in an ensemble can be improved upon by selecting for combination only those that perform significantly better than others, termed Selective Fusion [12]. Using this technique, together with simple voting methods, enables the fine-tuning of diverse ensembles for specific data sets. It also offers performance comparable to other heterogeneous classifier combination methods such as stacking, without the additional computation and meta-learning costs. Researchers have studied the effectiveness of switching between selection (occurring in regions of the feature space where single classifiers are dominant) and fusion (occurring in every region not dominated by a single classifier) [13].

Other efforts have studied the use of training multiple classifiers on different feature subsets prior to their combination [14]. Focusing on differing and potentially overlapping feature subsets creates additional diversity, which could lead to an improved combined model. Some researchers also found that performance degradation occurs as the percentage of training batches (sets of training examples) overlap [15]. Multi-classifier systems offer a medium for additional study on how knowledge from classifiers with different, potentially overlapping feature and data subsets can be combined. Interaction between the classifiers during the training process may prove to increase learning efficiency, robustness, and accuracy.

3. Research Methodology

This section covers the research methodology followed to analyze and measure the utility of single- and multi-classifier configurations on a set of established features derived from 723 unique patients.

3.1 Features

We study three distinct feature sets in this work. Each originates from the same raw data, but represent three separate concepts on where the necessary data holding the predictive information is to be found. Previous experiments were performed on these data sets using a small set of individual classifiers. Therefore, the goal is to compare the results of various classifier configurations with the original published results.

3.2 The Multi-Classifier Collaborative Learning Architecture

The WEKA machine-learning suite is utilized as a base for the implementation of the proposed Multi-Classifier Collaborative Learning Architecture [16]. The primary uses of WEKA in this architecture are to prepare the data for experimentation and provide implementations of various classification algorithms. Additional Java and script/batch file implementations act as a wrapper for machine learning experiments involving single or multiple classifiers (i.e., for teams of any size), homogeneous or heterogeneous team composition, independent or collaborative learning (with the ability to vary the number of collaboration events during learning), and combining the decisions of the classifiers using a variety of accuracy- and vote-based combination techniques. This offers a robust and flexible architecture for machine learning studies involving multiple, collaborative learning agents.

The Multi-Classifier Collaborative Learning Architecture was utilized to study single- and multi-classifier machine learning configurations for the patient vision data set. By default, each classifier is provided a randomized version (different order of instances for each classifier) of the full training data set. Model creation takes place by training each classifier using the training data set. At this time, each classifier tests its model on the data on which it was trained. Once training is complete, the testing data set is passed

through each classifier's model and the corresponding class probabilities (predictions) are recorded. The final individual testing predictions are then used for combining decisions from multiple classifiers. This acts as the final collaboration step, which fuses the knowledge from multiple classifiers to a single team classifier via accuracy- and vote- based mechanisms.

Decision combination utilizes each classifiers decision/label for each testing instance to arrive at a single team classification per combination method. A classifiers decision consists of a probability that the testing instance belongs to each of the possible classes. The highest probability represents the predicted class for each classifier. The Multi-Classifier Collaborative Learning Architecture calculates team classification accuracy for each of the 12 implemented vote-based combination methods. The combination method resulting in the best classification accuracy is selected, reflecting the overall performance of the team. For a detailed discussion of the 12 vote-based combination methods used for evaluation, consult [17].

While the original architecture offers a number of vote-based methods to be used for combining classifier results for evaluation [17], this research endeavor utilized only the Average method. The Average method averages all predictions for each class from all the classifiers, selecting the class with the highest average value. The class selected by the classifier with the highest accuracy on the testing data breaks a tie.

4. Experiments for Three Feature Sets

4.1 Experimental Setup

The experimental studies followed the process of a series of rounds based on classifier performance. As long as the results of some classifier in the round exhibited reasonable improvement over the previous work, then team configurations exhibiting the highest testing accuracy move on to the next experiment, where larger teams are constructed from the best teams from the previous experiment.

In all experiments the classifiers are provided with the full training portion for model creation, and no collaboration events occurred. The reasoning behind this decision is to keep the experiments focused on measuring machine learning algorithm and decision combination performance without reviewing the effect of collaboration and independent learning. Further work could be done to measure the effect of those additional configuration options of the architecture.

The first step for a specific data set is to coarsely test a variety of individual machine learning algorithms, each with a few settings and initialization seeds, to determine which algorithms perform well in general for the data set. The best settings and corresponding 10-fold cross-validation testing accuracy for each algorithm are recorded, and the top four algorithms are selected to advance to the next experiment.

The next step is to evaluate a team four classifiers in four different configurations. This inherently includes homogeneous and heterogeneous team compositions. The same process takes place for teams of size eight, where the top teams of size four are selected to advance to the experiment of size eight teams. The same process is used with the results of the size eight teams to construct the final sixteen-team experiment. Once the experiment of size sixteen teams is complete, all results are compiled and analyzed.

It is important to note that because this work is primarily a comparison of feature sets, an exhaustive multi-classifier experiment set is not performed. Rather, the methodology looks at a shallow set of initial experiments to determine if further classifier fusion is worth pursuing based on an improvement in overall accuracy. This phased experimentation process results in running fewer round one experiments for Experimental Data Set 1, and more round one experiments Experimental Data Set 2 and Experimental Data Set 3. This is because positive results are discovered early in the Experimental Data Set 1.

In addition to differences in round one, the methodology further results in all three feature sets not following to the final sixteen-team experiment. Since this work investigates the efficacy of the three feature sets for identifying the amblyopic condition, when the results in the early rounds do not advance the state of the previous work, all the rounds are ended and the results are presented.

4.2 Experimental Results

This section presents the experimental results from a variety of machine learning configurations for the three patient vision data sets. The notation used in the subsequent figures and analyses are abbreviations of machine learning classification algorithms. The abbreviations for the ten utilized classification algorithms are: Decision Table (DTB) [18], Decision Tree (DT) [8], Instance-Based KNN (IBK) [19], Logistic Regression (LGR) [20], Naive Bayes (NB) [21], PART Rule Learner (PRT) [22], Random Forest (RFT) [23], Radial Basis Function Network (RBF) [18], RIPPER Rule Learner (JRP) [24], and Support Vector Machines (SVM) [25]. The reader is referred to the referenced papers for the algorithms and details on their underlying structure and theory.

When listing team compositions, the number of classifiers for each algorithm of the team is listed, separated by +. For example, 3IBK+2PRT+2DT+1LGR represents a team of size eight composed of three IBK, two PRT, two DT, and one LGR classifiers.

A total of 39 machine learning experiments were performed, including the variation of team size and composition. Experiments are broken down as follows:

- 29 size one
- 4 size four
- 3 size 8

- 3 size 16

4.3 Experimental Data Set 1: Color Density and Hirschberg Reflex

The first experimental data set finds its genesis in previous work from Wang and the original AVVDA system. A total of 54 key features of patients' eyes (27 features per eye) were extracted from the video feeds and key frames. The two primary features are the pupil radius and the degree of fixation based on the Hirschberg point. The remaining 25 features for each eye are calculated using the color of pixels within 80% of the radius of the pupil. This includes, for example, the average red, green, and blue values throughout the pupil. The reader is referred to [4] for additional details on how these values are calculated. These 54 features for each of the 723 patients and all of the identified key frames were used as input into the multi-classifier architecture.

As described in the previous section, many classifiers where tested on the data set, both single and combined. As a result of the experimental process, the best outcome was distilled to 16 Random Forest classifiers. We can investigate the initial outcome of the four rounds of experiments by reviewing table 1. The results show increasing improvement as the rounds advance (i.e., team size increases), and ultimately show the best results were achieved with a homogeneous, 16-classifier configuration.

In contrast, the results of the AVVDA system represent the original research and cover single instance Case-Based [7], Artificial Neural Network [9], and Decision Tree [8] classifiers. Table 2 is a summarization of the results for comparison, and shows that the use of a multi-classifier decision combination approach improved accuracy and specificity at the cost of sensitivity.

4.4 Experimental Data Set 2: Iris and Pupil Color Slope with Middle Stack Key Frame Selection

The second experimental data set is based on the work of [26]. It utilizes the same 723 patient videos but instead extracts a different set of frame and feature data. The difference begins with the key frame concept. In the previous experiment, a patient will have typically produced many key frames. As described in the Related Work section, the software identifies a key frame based on two primary criteria. First, the patient must have both eyes open. Second, the patient must be looking at the light source so that a reflection off of the retina is clear. From the key frame stack identified for a patient, a single frame is then selected. In the second experiment, the research takes a very simple approach to identify the single frame that will be used for feature extraction. It selects the frame from the middle of the stack of frames. If there are an odd number of frames, it selects the frame that is a whole number division of the entire frame count by two. The goal is to avoid the fringe frames (the first or last), and analysis of a subset of the data shows that the middle frame has the greatest chance of being one of the best images [26].

Now that a frame is selected, the color information is extracted from the image starting at the edges of the iris for both the left and right eyes. The red, blue, and green information is extracted from the eye image in a left to right pattern, representing the rate of change of color across they eye, or color slope. This is illustrated in figure 2. The key frame for each patient is then further processed to produce 552 color features.

Experimental results using the iris and pupil color slope data set are summarized in table 3. The results do not show

Table 1: Results from the experimental study performed using the Multi-Classifier Collaborative Learning Architecture on the AVVDA data set.

Team	**Accuracy** (%)	**Sensitivity** (%)	**Specificity** (%)
Team Size: 1			
DTB	68.21	89.35	34.67
DT	76.25	82.14	66.62
IBK	74.40	77.49	69.58
LGR	75.53	86.03	58.81
RBF	70.82	82.54	51.87
RFT	76.52	79.34	71.86
PRT	74.08	80.13	64.44
Team Size: 4			
1DT+1LGR+1RFT+1PRT	76.40	82.30	66.81
4DT	76.25	82.14	66.63
4RFT	77.22	81.39	70.47
2DT+2RFT	76.52	82.14	67.35
Team Size: 8			
4DT+4RFT	76.39	82.14	67.03
8RFT	77.67	82.32	70.17
8DT	76.25	82.14	66.63
Team Size: 16			
8DT+8RFT	76.52	82.14	67.34
16RFT	77.80	82.55	70.17
16DT	76.25	82.14	66.63

Table 2: Comparison of results achieved by the Multi-Classifier Collaborative Learning Architecture on the AVVDA data set.

System	**Accuracy** (%)	**Sensitivity** (%)	**Specificity** (%)
Multi-Classifier Collaborative Learning Architecture	77.80	82.55	70.17
Automated Video Vision Development Assessment	76.20	84.60	61.40

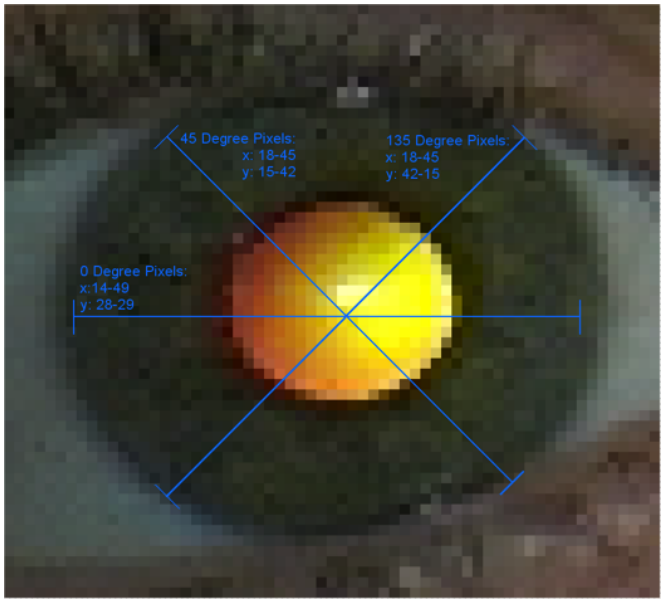

Fig. 2: Illustration of iris and pupil color slope. [26]

Table 3: Results from the experimental study performed using the Multi-Classifier Collaborative Learning Architecture on the initial color slope data set.

Team	Accuracy (%)	Sensitivity (%)	Specificity (%)
Team Size: 1			
DTB	59.34	72.60	38.95
DT (Pruned)	56.29	64.16	44.21
DT (Unpruned)	56.43	64.38	44.21
IBK	63.62	75.57	45.26
JRP	58.65	73.97	35.09
LGR	56.43	60.73	49.82
NB	58.92	64.61	50.18
PRT	56.57	66.90	40.70
RFT	62.38	69.86	50.88
RBF	60.86	83.11	26.67
SVM	64.73	73.97	50.53

Table 4: Comparison of results achieved by the Multi-Classifier Collaborative Learning Architecture on the initial color slope data set.

System	Accuracy (%)	Sensitivity (%)	Specificity (%)
Multi-Classifier Collaborative Learning Architecture	64.73	73.97	50.53
AVVDA Pupil and Iris Color Slope	67.91	82.42	45.61

an improvement over the previous work when the data was applied to a number of classifiers in the Multi-Classifier Collaborative Learning Architecture. The best single classifier from the architecture was the Support Vector Machine with improved specificity at the cost of both sensitivity and accuracy.

In contrast, the results of the work presented by [26] represent the original research and cover single team Decision Tree, Neural Network, and Random Forest classifiers. Table 4 exhibits the summarized observed results using the iris and pupil color slope data set.

Notably, when reviewing the preliminary single-classifier results from the Multi-Classifier Collaborative Learning Architecture on data set two, the results did not warrant further classifier ensembles. The reasoning behind this decision is that the results were not coming reasonably close to the accuracies achieved with data set one. Since this work is to investigate the best features for identifying the amblyopic condition, the results did not advance data set two and did not improve on previous work.

4.5 Experimental Data Set 3: Pupil Color Slope with Level Key Frame Selection

The third experimental data set is also based on the work of [26]. Utilizing the same initial set of 723 patient videos, the goal is to find the best patient and frame sets for selecting a frame. The set of key frames is still identified as described in the Related Work section. However, the frame selection process was altered so that a method different from selecting the middle frame is utilized. In this case, the frame selected out of all the key frames is that where the patient's head is most level. Since the entire classification problem is centered on the reflection of light off the lens and the retina, keeping the angle of reflection the same for both eyes would, theoretically, further enhance any differences between a healthy eye and the eye of a patient who should be referred to a specialist. The important features extracted around the crescent reflection and the Hirschberg point that is measured from that crescent further support this concept. The frame that is most level is determined by the pixel location of the center of the pupil at the Y-axis. The value is compared between the two eyes for each key frame, and the frame corresponding to the closest value is selected. When no key frame could be found where the difference in the height of the eyes was less than five pixels, then the patient data was discarded. The data was discarded so that the classifiers would not be trained with imperfect data and in hopes of further isolating the features that will yield the best results. This process reduced the number of patients in the entire sample from 723 to 499. The key frame is then further processed to extract color data from the pupil only. This process produced 180 features for each patient. Figure 3 illustrates the feature vectors extracted.

Experimental results using the pupil color slope data set are summarized in table 5. The results exhibit similar results

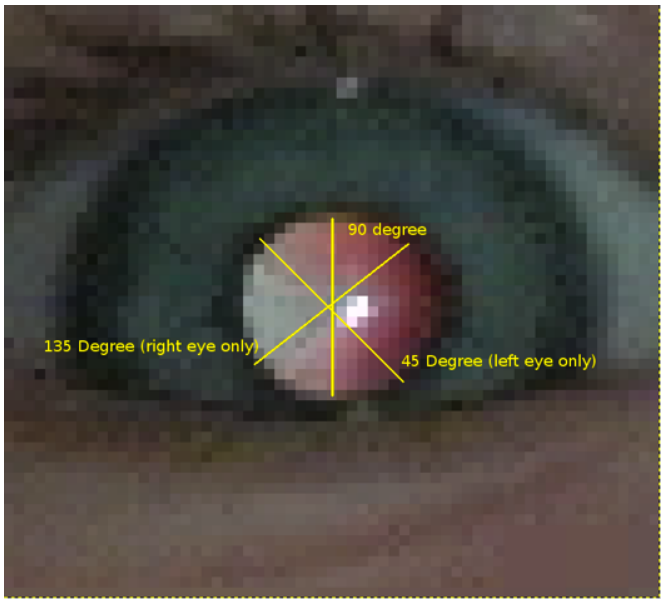

Fig. 3: Illustration of pupil color slope. [26]

as the experimental data set two, an improved specificity at the cost both accuracy and specificity. The best overall result from the Multi-Classifier Collaborative Learning Architecture was from a support vector machine.

In contrast, the results of the work presented by [26] represent the original research and cover single team Decision Tree, and Random Forest classifiers. Table 6 exhibits a summary of the observed results using the pupil color slope data set.

Notably, data set three also does not exhibit reasonable improvement over the data set one to warrant further classifier combination. The reasoning behind this decision stands the same as the experiment two results, lack of reasonable improvement over data set one, and previous work.

Table 5: Results from the experimental study performed using the Multi-Classifier Collaborative Learning Architecture on the pupil only color slope data set.

Team	**Accuracy** (%)	**Sensitivity** (%)	**Specificity** (%)
Team Size: 1			
DTB	62.93	77.45	38.90
DT (Pruned)	58.52	67.32	44.04
DT (Unpruned)	58.32	67.32	44.04
IBK	62.32	80.07	34.20
JRP	62.12	78.76	35.75
LGR	58.92	67.32	45.60
NB	58.92	59.80	57.51
PRT	57.11	68.63	38.86
RFT	62.53	68.30	53.37
RBF	58.92	87.58	13.47
SVM	63.93	81.70	35.75

Table 6: Comparison of results achieved by the Multi-Classifier Collaborative Learning Architecture on the pupil color slope data set.

System	**Accuracy** (%)	**Sensitivity** (%)	**Specificity** (%)
Multi-Classifier Collaborative Learning Architecture	63.93	81.70	35.75
AVVDA Pupil Color Slope	67.94	37.31	87.25

5. Conclusion

The primary contribution of this work is to take an existing problem, analyze three feature sets produced and find the most predictive set for accurately classifying the markers for the amblyopic condition. The feature sets were processed through a Multi-Classifier Collaborative Learning Architecture system, producing results for many classifiers, some single and some ensemble. As observed in the Experimental Results section, the original AVVDA features were improved upon as the experimental rounds progressed, thus showing promise for the ensemble classification method with certain data sets.

In contrast, the color slope experimental data sets performed worse using the Multi-Classifier Collaborative Learning Architecture. This suggests that the features are not only difficult to use for classification, but do not hold much predictive ability when presented with new patient instances.

Therefore, the results further the understanding of the predictive ability for the given data sets. Notably, of equal contribution to the vision assessment work is to illustrate that there may have been a limit reached in the classification ability of the selected color density, Hirschberg reflex, and color slope features. This conclusion is further supported by the success seen in previous work with the Multi-Classifier Collaborative Learning Architecture against challenging classification problems, and its ability to improve results over previous work on the difficult data sets [17], [16].

References

[1] S. J. Anderson, I. E. Holliday, and G. F. Harding, "Assessment of cortical dysfunction in human strabismic amblyopia using magnetoencephalography," *Vision Research*, vol. 39, pp. 1723–1738, 1999.

[2] S. B. Steinman, B. A. Steinman, and R. P. Garzia, *Foundations of Binocular Vision: A Clinical Perspective*. McGraw-Hill, 2000.

[3] G. W. Cibis, "Video vision development assessment in diagnosis and documentation of microtropia," *Binocular Vision and Strabismus Quarterly*, vol. 20, pp. 151–158, 2005.

[4] T. Wang, "Investigation of image processing and computer-assisted diagnosis system for automated video vision developement assessment," Ph.D. dissertation, Computer Engineering and Computer Science, University of Missouri - Columbia, 2005.

[5] J. Van Eenwyk, A. Agah, and G. Cibis, "Automated human vision assessment using computer vision and artificial intelligence," in *Proceedings of the IEEE international Conference on System of Systems Engineering*, June 2008.

[6] T. Wang, "Eye location and fixation estimation techniques for automated video vision development assessment," Master's thesis, Computer Engineering and Computer Science: University of Missouri - Columbia, 2002.
[7] A. Aamodt and E. Plaza, "Case-based reasoning: Foundational issues, methodological variations, and system approaches," *AICom - Artificial Intelligence Communications*, vol. 7, pp. 39–59, 1994.
[8] J. R. Quinlan, *C4.5: Programs for Machine Learning*. Morgan Kaufmann, 1993.
[9] Y. Pao, *Adaptive Pattern Recognition and Neural Networks*. Addison-Wesley Publishing Company, 1989.
[10] S. Dzeroski and B. Zenko, "Is combining classifiers better than selecting the best one?" *Machine Learning*, vol. 54, pp. 255–273, 2004.
[11] D. Klein, K. Toutanova, H. T. Ilhan, S. D. Kamvar, and C. D. Manning, "Combining heterogeneous classifiers for word-sense disambiguation," in *Proceedings of the ACL Workshop on Word Sense Disambiguation: Recent Successes and Future Directions*, vol. 8, 2002, pp. 74–80.
[12] G. Tsoumakas, L. Angelis, and I. Vlahavas, "Selective fusion of heterogeneous classifiers," *Intelligent Data Analysis*, vol. 9, no. 6, pp. 511–525, 2005.
[13] L. I. Kuncheva, "Switching between selection and fusion in combining classifiers: an experiment," *IEEE Transactions on Systems, Man, and Cybernetics*, vol. 32, no. 2, pp. 146–156, 2002.
[14] K. Chen, L. Wang, and H. Chi, "Methods of combining multiple classifiers with different features and their applications to text-independent speaker identification," *International Journal of Pattern Recognition and Artificial Intelligence*, vol. 11, pp. 417–445, 1997.
[15] K. Ting and B. Low, "Theory combination: an alternative to data combination," *Technical Report*, vol. 96, no. 19, 1996.
[16] C. M. Gifford, "Collective machine learning: team learning and classification in multi-agent systems," Ph.D. dissertation, Ph.D. Thesis, Electrical Engineering and Computer Science Department, University of Kansas, Lawrence, KS, December 2009.
[17] C. M. Gifford and A. Agah, "Sharing in teams of heterogeneous, collaborative learning agents," *International Journal of Intelligent Systems*, vol. 24, no. 2, pp. 173–200, 2009.
[18] R. Kohavi, "The power of decision tables," in *Proceedings of the European Conference on Machine Learning*, 1995, pp. 174–189.
[19] D. W. Aha, D. Kibler, and M. K. Albert, "Instance-based learning algorithms," *Machine Learning*, pp. 37–66, 1991.
[20] S. le Cessie and J. van Houwelingen, "Ridge estimators in logistic regression," *Applied Statistics*, vol. 41, no. 1, pp. 191–201, 1992.
[21] G. H. John and P. Langley, "Estimating continuous distributions in bayesian classifiers," in *Proceedings of the 11th Conference on Uncertainty in Artificial Intelligence*. Morgan Kaufmann, 1995, pp. 338–345.
[22] E. Frank and I. H. Witten, "Generating accurate rule sets without global optimization," in *Proceedings of the 15th International Conference on Machine Learning*. Morgan Kaugmann, 1998, pp. 144–151.
[23] L. Breiman, "Random forests," *Machine Learning*, vol. 45, pp. 5–32, 2001.
[24] W. Cohen, "Fast effective rule induction," in *Proceedings of the 12th International Conference on Machine Learning*, 1995, pp. 115–123.
[25] C. Cortes and V. Vapnik, "Support-vector networks," *Machine Learning*, vol. 20, no. 3, pp. 273–297, 1995.
[26] P. G. Clark, A. Agah, and G. W. Cibis, "Applied artificial intelligence techniques for identifying the lazy eye vision disorder," *Journal of Intelligent Systems*, vol. 20, no. 2, pp. 101–127, 2011/08/30 2011.

Identifying "Comment-on" Citation Data in Online Biomedical Articles Using SVM-based Text Summarization Technique

In Cheol Kim*, Daniel X. Le, and George R. Thoma

Lister Hill National Center for Biomedical Communications
National Library of Medicine, 8600 Rockville Pike, Bethesda, MD 20894

Abstract - *Comment-on (CON), a MEDLINE® citation field, indicates previously published articles commented on by authors expressing possibly complimentary or contradictory opinions. This paper presents an automated method using a support vector machine (SVM)-based text summarization technique that identifies CON data by distinguishing CON sentences from "citation sentences" and analyzes their corresponding bibliographic data in the references. We compare the performance of two types of SVM, one with a linear kernel function and the other with a radial basis kernel function (RBF). Input feature vectors for these SVMs are created by combining five feature types: 1) word statistics, 2) frequency of occurrence of author names, 3) sentence positions, 4) similarity between titles, and 5) difference of publication years. Experiments conducted on a set of online biomedical articles show that the SVM with a RBF is more reliable in terms of precision, recall, and F-measure rates than the SVM with a linear kernel function for identifying CON.*

Keywords: "Comment-on" identification, online biomedical documents, support vector machine, MEDLINE

1 Introduction

MEDLINE is the premier bibliographic online database of the U.S. National Library of Medicine (NLM) containing more than 20 million citations from over 5,500 selected worldwide biomedical journals, and accessed through NLM's PubMed service. With rapid growth of biomedical literature, both the number of journals indexed and the number of citations produced by NLM increase dramatically; 130 journal titles are newly added each year on average and nearly 700,000 citations were added to MEDLINE in 2010. Bibliographic citation data describing the article consists of more than 50 fields such as author names, article title, affiliation, etc. Currently, the majority of data for these fields are provided electronically in XML format from journal publishers. However, publishers leave out data for several important fields: Databank accession numbers, Grant supports/numbers, Comment-on/Comment-in, and investigator names, almost certainly because including these fields would be highly labor-intensive and costly. As manual extraction and entry of bibliographic data missing from publisher-provided XML files would be equally burdensome for NLM, there is a strong motivation to develop automated systems to minimize human labor and to provide bibliographic data accurately and in a timely fashion.

The Lister Hill National Center for Biomedical Communications (LHNCBC), a research and development division of NLM, has developed an automated system—the Web-based Medical Article Records System (WebMARS) that analyzes and extracts bibliographic information from online biomedical journal articles to create citations for MEDLINE [1][2]. This paper presents one of the major components of WebMARS, an automated method for identifying and extracting "Comment-on" (CON) citation data. CON is a field in a MEDLINE citation listing previously published articles commented on by authors of a given paper in a complimentary, or sometimes contradictory, manner. We refer to the "Commented on" articles as CON articles, and the papers in which such opinions are expressed as "Comment-in" (CIN) articles.

Manually extracting the CON list from a given article is time-consuming and labor-intensive, and relies heavily on human operators' linguistic knowledge and their understanding of scientific expressions and writing styles. Generally, authors of a CIN article cite CON articles related to their research as primary external sources on which they may express complimentary or contradictory opinions. Thus the full bibliographic descriptions for these CON articles can usually be found in the reference section of a CIN article. Furthermore, all external sources (journal articles, books, or Web links) listed in the reference section of the CIN paper are generally mentioned at least once within sentences ("citation sentences") in the body text.

From this observation, our idea of identifying the CON list for a given article is to recognize the sentences ("CON sentences") that mention CON articles from the "citation sentences" in the body text using a support vector machine (SVM)-based text summarization technique and analyze the corresponding bibliographic data in the reference section. In our research, we implemented two types of SVMs: one with a linear kernel function and the other with a radial basis function (RBF), and compared their performance in terms of precision, recall, and F-measure rates. Five types of features were employed to create an input feature vector for these SVMs: 1) word statistics representing how differently a word is distributed in CON sentences and other "citation sentences", 2) frequency of occurrence of author names of external sources listed in the reference section of a given input article, 3) sentence positions within an article body text, 4) similarity of titles between a given input article and external sources, and 5) difference of publication years between an input article and each external source.

2 Related work

CIN articles are usually short papers such as commentaries, letters, editorials, or brief correspondences, written mainly for the purpose of supporting, refuting, or discussing other articles (CON). Accordingly, a sentence specifically referring to a CON article, called a "CON sentence", can be considered a key part of a CIN article because it is indicative of the article's subject and purpose. Detecting and extracting such key sentences within a document is a text summarization task. A summary can be loosely defined as text that conveys important information in the original text(s) and is a condensed representation (no longer than half) of the original text(s) [3]. Automated text summarization is the process of automatically constructing a summary for an input text. This summary can either be an "extract" created by merely reusing portions of the input text such as phrases, sentences, or paragraphs that are likely to be most important, or an "abstract" that is a newly generated text after an analysis of the original text.

Since creating such an abstract requires the high complexity of natural language processing techniques and knowledge engineering technology, most text summarization studies have focused on the extraction-based method. Our task of identifying CON sentences from the body text of CIN articles can also be considered as a typical extraction-based text summarization method. Text summarization has been addressed by a variety of methods and applied in different domains and genres of documents. Most early studies were based on surface-level features that do not require linguistic analysis, such as word frequency, paragraph or sentence position, and cue phrases to determine the most important concepts within a document [4][5][6].

There is another group of studies that builds an internal representation of the text by modeling text entities and their relationships to determine salient information. For example, Barzilay and Elhadad [7], and Silber and McCoy [8] employed lexical chains representing semantic relations between words to generate a summary of the original document. In addition, an approach exploiting the global structure of the text such as document format, rhetorical structure, etc. has also been reported [9][10].

All these aforementioned approaches can be implemented as either linguistic knowledge or machine-learning techniques. Linguistic knowledge-based methods that try to semantically analyze the structure of the text involve very sophisticated and expensive linguistic processing. Therefore, most methods employed in the recent literature are based on statistical theories and machine learning techniques; e.g., Naïve Bayes [11], decision tree [12], neural networks [13], hidden Markov models [14], and SVMs [15].

3 CON and CIN articles

CIN and CON articles are indicated in MEDLINE citation fields as "Comment in" and "Comment on" respectively, and linked together. As an example, Fig. 1(a) is the MEDLINE citation of an article (CIN) in which a "Commented on" article is cited. This CON information, shown enclosed in a dotted box, consists of abbreviated journal title, publication year, volume and issue number, and pagination. Conversely, as shown in the dotted box in Fig. 1(b), the MEDLINE citation for this CON article cites the CIN article in which it is mentioned. Thus readers may get to either citation from the other.

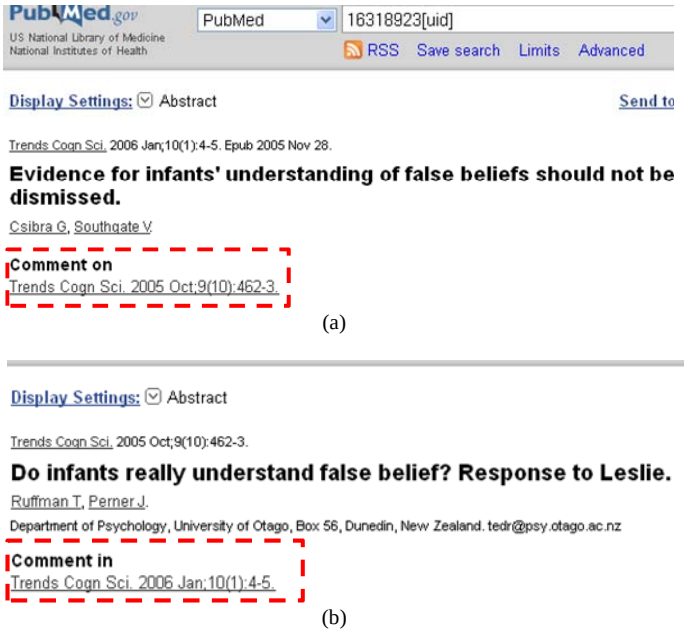

Fig. 1. (a) "Comment on" and (b) "Comment in" citations in MEDLINE

3.1 Issues

Currently, the CON list is created manually, based on certain linguistic clues and contextual patterns; operators are required to look for a particular sentence that contains a cue phrase expressing either complimentary or contradictory opinions on other articles from the body text of a given article. Typical examples of such cue phrases are listed in Table 1.

Table 1. Examples of cue phrases frequently found in CON sentences.

We congratulate [authors] for …
We question the interpretation by …
The {article | paper | letter | study | research} by …
We read with interest …
We would like to {reply | comment} to …
We agree with …

This manual method is highly labor-intensive and time-consuming. Furthermore, owing to a wide variety of linguistic expressions, and linguistic and contextual similarity between CON sentences and "citation sentences" generally citing other external sources, the overall performance relies heavily on human operators' experience, linguistic knowledge, and their understanding of scientific expressions and writing styles. In order to minimize manual efforts and to improve

accuracy and processing speed in detecting sentences that comment on other articles, we propose an automated method using a support vector machine (SVM)-based text summarization technique.

4 Method

As mentioned earlier, authors of a CIN article cite CON articles as primary external sources. Accordingly, full bibliographical descriptions for these CON articles can usually be found in the reference section of a CIN article. Note that in the scientific literature, all external sources listed in the reference section are generally mentioned at least once within sentences ("citation sentences") in the body text. The "citation sentence" that specifically indicates an article commented on by a given article is defined as the CON sentence. CON sentences are therefore a subset of "citation sentences". Based on this observation, our approach to identify a CON list for a given article is to first extract all "citation sentences" from its body text, and then to recognize the sentences among these that mention CON articles, using SVMs and to analyze the corresponding bibliographic data in the reference section. Figure 2(a) shows an example of a CON sentence (solid underline) and Fig. 2(b) shows its corresponding reference (solid box).

Hyperinsulinaemic normoglycaemic clamp in coronary artery surgery

* *E-mail:* george.carvalho@mail.mcgill.ca

Editor—We congratulate Visser and colleagues on applying glucose–insulin–potassium (GIK) therapy using a hyperinsulinaemic normoglycaemic clamp.[1] Their study confirms our findings that the clamp technique is an effective, and to date the only, method of maintaining normoglycaemia in patients undergoing coronary artery bypass grafting surgery.[2] In addition, they demonstrated, for the first time in this population, the attenuation of systemic inflammation with perioperative GIK therapy. More importantly, this effect

(a)

References

1 Visser L, Zuurbier CJ, Hoek FJ, *et al*. Glucose, insulin and potassium applied as perioperative hyperinsulinaemic normoglycaemic clamp: effects on inflammatory response during coronary artery surgery. *Br J Anaesth* 2005; **95**: 448–57 [Abstract/Free Full Text]

2 Carvalho G, Moore A, Qizilbash B, Lachapelle K, Schricker T. Maintenance of normoglycemia during cardiac surgery. *Anesth Analg* 2004; **99**: 319–24

(b)

Fig. 2. (a) A CON sentence and (b) its corresponding bibliographic description in the reference section

Our method consists of four main steps: 1) extraction of text zones of interest, 2) extraction of "citation sentences" and the corresponding bibliographical description of external sources, 3) creation of input feature vectors for SVMs, and 4) classification of CON sentences by SVMs.

Since our method takes advantage of clues from the article title, the body text, and the reference section in a given HTML-formatted online article, we need to segment the entire article into smaller logical zones, and detect such zones first. In our research, these text zones of interest are extracted using Zoning and Labeling modules detailed in [1] and [16]. Here, we focus on and provide details about the remaining three steps.

4.1 Extraction of "citation sentences" and the corresponding external source's description

In the scientific literature, each "citation sentence" is usually associated with a citation tag (such as "(1)" or "[1]") that points to the complete bibliographical description of the cited external source in the reference section. In addition, in HTML-formatted online articles, such a "citation sentence" is hyperlinked to its corresponding external source as shown in Table 2. A hyperlink consists of both a source anchor and a destination anchor. The source anchor specified by an "A" HTML element with a "*href*" attribute appears before or behind a citation tag in a "citation sentence" and points to the destination anchor. The destination anchor specified by an "A" element with a "*name*" attribute can be found at the beginning of the external source's description. The source anchor and its destination anchor should have the same unique name. Therefore, by recognizing this anchor name, we can reliably detect its associated "citation sentence" and its corresponding external source.

4.2 Feature extraction

In our research, five types of features were employed to build an input feature vector for SVM: 1) word statistics representing how differently a word is distributed in CON sentences and other "citation sentences", 2) frequency of occurrence of author names of external sources, 3) sentence positions within the body text, 4) similarity of titles between an input article and its external sources, and 5) difference of publication years between an input article and its external sources. These features were experimentally found to be effective to distinguish CON sentences from other "citation sentences". The first feature—word statistics—is based on a

Table 2. An example of a "citation sentence" and its hyperlinked external source.

Hyperlink (Source anchor)	<SPAN>Editor—We congratulate Visser and colleagues on applying glucose–insulin–potassium (GIK) therapy using a hyperinsulinaemic normoglycaemic clamp.</SPAN>^{**<A href="#B1">**1</A>}
Hyperlink (Destination anchor)	<P> **<A name=B1>** <!-- null --></A><STRONG>1</STRONG><SPAN> Visser L, Zuurbier CJ, Hoek FJ, </SPAN><I>et al</I><SPAN>. Glucose, insulin and potassium applied as perioperative hyperinsulinaemic normoglycaemic clamp: effects on inflammatory response during coronary artery surgery. </SPAN><I>Br J Anaesth</I><SPAN> 2005; </SPAN><B>95</B><SPAN>: 448–57 </SPAN>

bag of words, a vector of words. Using words as an input feature requires a very high dimensional feature space (21,314 dimensions in our case). Although SVM can manage (lead to a convergence) such a high dimensional feature space, many have suggested the need for word selection or dimension reduction to employ other conventional learning methods, to reduce the computational cost, to improve the generalization performance, and to avoid the over-fitting problem. A typical approach for word selection is to sort out words according to their importance. Many functions have been proposed to measure the importance of a word, including term frequency (TF), inverse document frequency (IDF), χ^2 statistics, and simplified χ^2 ($s\chi^2$) statistics [17]. The use of $s\chi^2$ has been reported as delivering the best performance since it removes redundancies, and emphasizes extremely rare features (words) and rare categories from χ^2 [18].

In our task, $s\chi^2$ of word t_k for CON sentences (class c_0) and other "citation sentences" (class c_1) can be defined as follows;

$$s\chi^2(t_k, c_i) = P(t_k, c_i) \cdot P(\bar{t}_k, \bar{c}_i) - P(t_k, \bar{c}_i) \cdot P(\bar{t}_k, c_i) \quad i = 0, 1 \qquad (1)$$

where $P(t_k, c_i)$ denotes the probability that, for a random sentence *x*, word t_k occurs in *x*, *x* belongs to class c_i, and is estimated by counting its occurrences in the training set. The importance of word t_k is finally measured as follows;

$$s\chi^2_{max}(t_k) = max_i s\chi^2(t_k, c_i) \qquad i = 0, 1 \qquad (2)$$

Accordingly, the more differently a word is distributed in CON sentences and other "citation sentences" classes the higher its $s\chi^2_{max}(t_k)$. Our 21,314 words are sorted according to their $s\chi^2_{max}$ and a bag of words feature is created by selecting words having highest $s\chi^2_{max}$ scores. A series of experiments to investigate the influence of word reduction and to discover the number of words showing the best classification performance is also performed. These experiments are described in Section 5. A bag of words feature is converted to a binary vector; each vector component is assigned 1 if the corresponding word is found in a given sentence, or 0 otherwise.

The second feature is based on the sentence position. In many cases, CON sentences are located at the beginning of the body text of an article. Thus such position information can also serve as a good feature to distinguish a CON sentence from other "citation sentences". The position information of each sentence is expressed as

$$P(s_i) = 1 - \frac{BD(s_i)}{|D|} \qquad (3)$$

where $|D|$ is the total number of characters in the given document *D*, and $BD(s_i)$ is the number of characters located before the sentence s_i.

Next, the frequency of occurrence of author names of external sources listed in the reference section is employed as another feature. Based on our observation, author names of CON articles are more frequently mentioned in the text of a CIN article. The frequency score of author names of external sources is defined as follows:

$$TF(s_i) = \frac{tf(s_i, D)}{tf_{max}(s, D)} \qquad (4)$$

where $tf(s_i, D)$ and $tf_{max}(s, D)$ denote the number of occurrences of author name of the external source associated with the "citation sentence" s_i and the maximum number of occurrences of an author name in the given document *D*, respectively.

The next input feature is based on similarity of titles between an input article and its external sources in the reference section. Basically, CIN and its CON articles have the same research topic because a CIN article is mainly for commenting about particular external sources (some CIN articles explicitly mention author names and/or titles of CON articles in their titles). Therefore, it is expected that their titles would be quite similar or have common keywords closely related to their research topic.

The similarity score between titles of CIN and external sources is simply measured using the ratio of the number of common words to the total number of words in the title of an external source excluding stop words, as shown below;

$$TS(t_{IN},\ s_i) = \frac{W_c(t_{IN},\ s_i)}{W(s_i)} \qquad (5)$$

Here, $W(s_i)$ denotes the number of words in the title of the external source associated with the "citation sentence" s_i in a given input article and $W_c(t_{IN}, s_i)$ is the number of words commonly found in the titles of input article and the external source for "citation sentence" s_i.

Each of the aforementioned three features, $P(s_i)$, $TF(s_i)$, and $TS(t_{IN},\ s_i)$, has a real value ranging from 0 to 1 and is converted to a 10-bit binary vector for SVM (*i*-th bit position corresponding to real values between *i*/10 and (*i*+1)/10). For $P(s_i)$ and $TF(s_i)$, one more bit component is additionally attached to represent if a given "citation sentence" is located at the first paragraph of the body text, and if this "citation sentence" includes the author name of its corresponding external source, respectively, thereby resulting in an 11-bit binary vector for each feature.

Lastly, the difference of publication years between an input article and its external source is also employed as an input feature. Based on our findings from the training dataset, authors of many CIN articles are found to be interested in and comment on recently-published articles. This feature would not be used alone because other recently-published general external sources are also found in the reference section. However, it is expected to be helpful for improving the accuracy of identifying CON sentences when combined with other features. The difference of publication years is represented using a 10-bit binary vector of which the index of each bit corresponds to the years of difference; bit 0 is set to 1 if the input article and its external source are published in the same year, and bit 9 is set to 1 if there is a difference of 9 or more years.

Finally, all these feature vectors are concatenated to build an input feature vector for the SVM-based training and classification tasks.

4.3 SVM classifiers

SVM [19] was originally introduced as a supervised learning algorithm based on the structural risk minimization principle for solving a two-class problem, though it can be easily extended to handle multi-class problems. Owing to its consistently superior performance compared to other existing methods, SVM has been widely used in many text categorization and summarization tasks. The basic idea of using SVM to solve a non-linear pattern recognition problem is to map a non-linear separable input space to a linear separable higher dimensional feature space using a predefined kernel function, and to find the optimal hyperplane that maximizes the margins between the classes in that feature space.

As mentioned earlier, we employed two types of SVMs: one with a linear kernel function and the other with a RBF. These two kernel functions, defined in equations (6) and (7) below, respectively, have been commonly used in SVM-based pattern recognition applications. We implemented these SVMs using MYSVM (for linear kernel function) and LibSVM (for RBF), free software packages for non-commercial use [20][21], and evaluated their recognition performance using HTML-formatted online biomedical journal articles.

$$K(x_i, x_j) = (x_i^T \cdot x_j) \quad (6)$$

$$K(x_i, x_j) = exp(-\gamma \|x_i - x_j\|^2) \quad (7)$$

5 Recognition experiments

5.1 Database

To build a dataset for our experiments to distinguish CON sentences from "citation sentences", we first collected a total of 5,848 HTML-formatted biomedical articles containing CON citations from a collection of indexed articles in MEDLINE. These online articles appeared in 414 different biomedical journal titles, and their publication types were Letter (49.0%), Review (2.1%), Editorial (25.4%), Commentary (14.5%), and others (9.0%). Full-length articles were not included in our dataset because CIN articles are generally letter-like short papers and MEDLINE does not typically acquire CON data from conventional full-length articles. We also developed an automated text categorization system to distinguish CIN articles from regular ones and to submit only articles classified as CIN to the proposed method of extracting CON citation data [22].

From these articles, 11,939 "citation sentences" were extracted; among them, 8,531 sentences (4,184 CON sentences + 4,347 other "citation sentences") were randomly selected to train the SVMs. The remaining 3,408 sentences (1,659 CON sentences + 1,749 other "citation sentences") were used to evaluate and compare the performance of the SVMs.

5.2 Experimental results

We evaluated the performance of SVMs in terms of precision, recall, and F-measure rates that are defined as follows:

$$precision = TP/(TP + FP)$$
$$recall = TP/(TP + FN)$$
$$F - measure = \frac{2 \times (precision \times recall)}{(precision + recall)}$$

Here, *TP*, *FP*, and *FN* denote true positive, false positive, and false negative, respectively. False positive means that a "citation sentence" is misrecognized as a CON sentence. False negative is the reverse of the above.

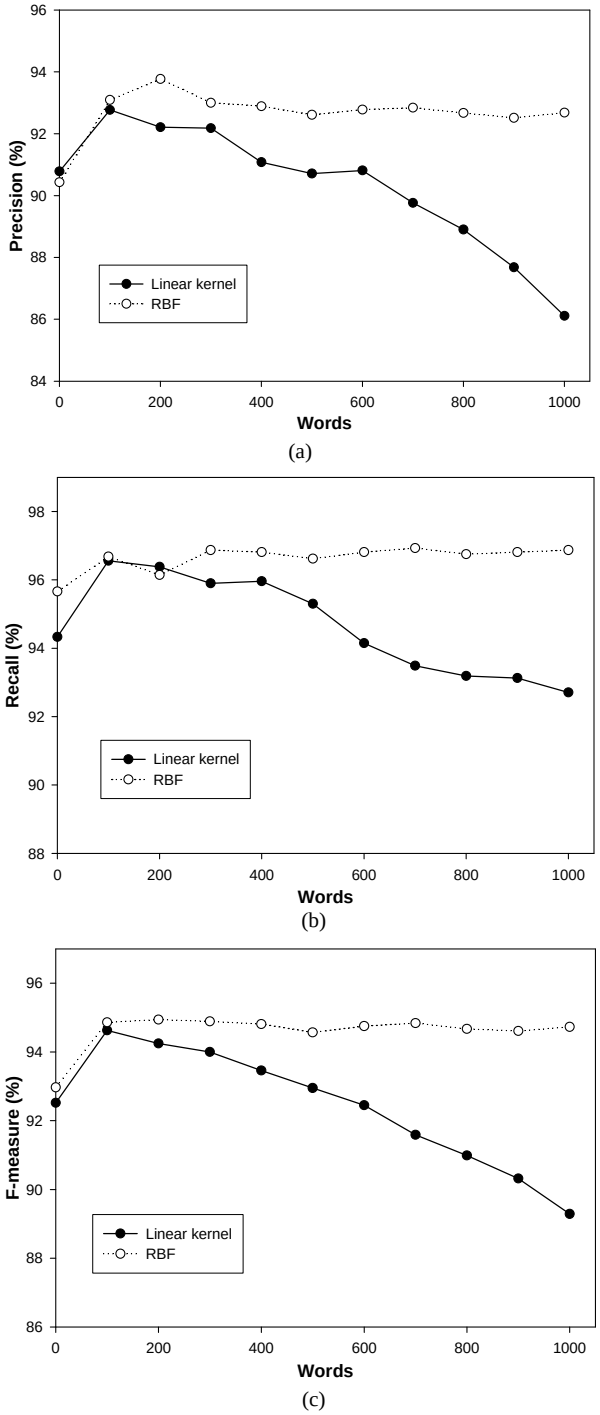

Fig. 3. (a) Precision, (b) recall, and (c) F-measure rates plotted against different word dictionary sizes.

Figure 3 shows precision, recall, and F-measure rates as functions of the size of the word dictionary in the bag of words feature ($s\chi^2_{max}$). We can see that the SVM with a RBF is slightly better than the SVM with a linear kernel, but both yield the best performance overall when the word size is 100, the performance in all three measures exceeding 93%. The SVM with a RBF shows consistent and reliable performance with respect to word selection in $s\chi^2_{max}$; its precision, recall and F-measure rates do not significantly vary with dictionary size. In contrast, the performance of SVM with a linear kernel function deteriorates as the word dictionary size increases. Therefore, we conclude that the SVM with a RBF is a more reliable classifier than the SVM with a linear kernel function for identifying CON sentences.

Table 3 shows examples of false-negative and false-positive errors. Two CON sentences shown in Table 3 (a): CON-I and CON-II, belong to the same input article and have a similar expression to comment other articles. However, unlike CON-I, CON-II is misrecognized as a general "citation sentence". It can be seen from its feature values that CON-II is located in the middle of the body text ($P(s_i)$ = 0.57), the frequency of occurrence of author name of the corresponding external source ($TF(s_i)$) is significantly small relative to other author names. Moreover, there are no words in common ($TS(t_{IN}, s_i)$) found between titles of input article and the external source corresponding to CON-II.

In contrast, the "citation sentence" (CIT-I) shown in Table 3 (b) is misrecognized as a CON sentence. CIT-I is found to contain several words frequently found in many CON sentences and located at the upper middle of the body text. Specially, it has a high similarity score ($TS(t_{IN}, s_i)$ = 0.83) between titles of CIN and its corresponding external source.

In order to minimize such problems, we recommend the addition of heuristic rules based on cue phrases and other linguistic information in future work.

Table 3. Error examples showing (a) false negative error and (b) false positive error

Input article	Growth attenuation: a diminutive solution to a daunting problem
CON-I	Now examine the proposed treatment: in this issue of the ARCHIVES, Gunther and Diekema (1) offer a medical solution to families who will likely face the harrowing choice of what to do when their child becomes too big to care for at home.
	Ref.: 1. Gunther DF, Diekema DS. *Attenuating growth in children with profound developmental disability: a new approach to an old dilemma*. Arch Pediatr Adolesc Med. 2006;160:1013-1017.
	$P(s_i)$ = 0.91 | $TF(s_i)$ = 1.00 | $TS(t_{IN}, s_i)$ = 0.10|
CON-II	Indeed, as Lee and Howell (2) point out in this issue of the ARCHIVES, estrogen has long been used to attenuate growth in girls destined to be taller than average.
	Ref.: 2. Lee JM, Howell JD. *Tall girls: the social shaping of a medical therapy*. Arch Pediatr Adolesc Med. 2006;160:1035-1039.
	$P(s_i)$ = 0.57 | $TF(s_i)$ = 0.29 | $TS(t_{IN}, s_i)$ = 0.00|

(a)

Input article	Ischemic hepatitis and collateral damage to the liver in severe viral respiratory tract infections
CON-III	Polakos and colleagues (1) investigated immunological causes of hepatic involvement by influenza virus respiratory tract infection manifesting itself in alanine and aspartate aminotransferase elevation and found evidence for a role of antigen-specific T cells in their pathogenesis.
	Ref.: 1. Polakos NK, Cornejo JC, Murray DA, Wright KO, Treanor JJ, Crispe IN, Topham DJ, Pierce RH: *Kupffer cell-dependent hepatitis occurs during influenza infection.* Am J Pathol 2006, 168:1169-1178
	$P(s_i)$ = 1.00 | $TF(s_i)$ = 1.00 | $TS(t_{IN}, s_i)$ = 0.17|
CIT-I	Adams and Hubscher (2) mention in their commentary on the work of Polakos and colleagues (1) our observational study, (3) in which we reported on the finding of elevated transaminase levels in 46% of children ventilated in the pediatric intensive care unit with severe respiratory syncytial virus bronchiolitis.
	Ref.: 2. Adams DH, Hubscher SG: *Systemic viral infections and collateral damage in the liver*. Am J Pathol 2006, 168:1057-1059
	$P(s_i)$ = 0.69 | $TF(s_i)$ = 0.5 | $TS(t_{IN}, s_i)$ = 0.83|

(b)

6 Conclusions

CON ("Comment-on") is a MEDLINE citation field showing previously published articles commented on by authors of a given article ("Comment-in" or CIN) as primary external sources on which they may express complimentary or contradictory opinions. Manually extracting the CON list from a given article is time-consuming and labor-intensive, and the overall performance relies heavily on human operators' experience, linguistic knowledge, and their understanding of scientific expressions and writing styles.

In this paper, we have presented a SVM-based text summarization method to automatically identify such CON data from online biomedical documents, thereby minimizing manual effort and improving accuracy and processing speed. Our main idea is to extract "citation sentences" using hyperlink information and then to recognize from the "citation sentences" CON sentences using SVMs. In our research, we have implemented two types of SVMs: one with a linear kernel function and the other with a radial basis function (RBF), and compared their performance in terms of precision, recall, and F-measure rates. Input feature vectors for these SVMs are created by combining five types of features: 1) word statistics representing how differently a word is distributed in CON sentences and other "citation sentences", 2) frequency of occurrence of author names of external sources listed in the reference section of a given input article, 3) sentence position within the body text, 4) similarity of titles between a given input article and external sources, and 5) difference of publication years between an input article and each external source.

Through a series of experiments on HTML-formatted online articles collected from 414 different biomedical journal titles, we can see that the SVM with a RBF and the SVM with a linear kernel both yield the best performance overall (over 93%) when the word size in the bag of words feature is 100. In addition, we found that the SVM with a RBF yields consistent and reliable performance in terms of precision, recall, and F-measure rates than the SVM with a linear kernel function with respect to word selection in the bag of words feature. Future work is planned to develop a rule-based method for compensating for recognition errors made by SVMs.

Acknowledgment

This research was supported by the Intramural Research Program of the National Library of Medicine, National Institutes of Health.

7 References

[1] J. Kim, D.X. Le, and G.R. Thoma, "Naïve bayes classifier for extracting bibliographic Information from biomedical online articles," *Proc. 5th Int'l Conf. Data Mining*, II, pp. 373-378, Las Vegas, 2008.

[2] I. Kim, D.X. Le, and G.R. Thoma, "Hybrid approach combining contextual and statistical information for identifying MEDLINE citation terms," *Proc. 15th SPIE Document Recognition and Retrieval*, 6815, 68150P (1-9), San Jose, 2008.

[3] D. Radev, E. Hovy, and K. McKeown, "Introduction to the special issue on text summarization," *Computational Linguistics*, 28(4), pp. 399-408, 2002.

[4] H.P. Luhn, "The automatic creation of literature abstracts", *IBM Journal of Research and Development*, 2(2), pp.159-165, 1958.

[5] P.B. Baxendale, "Man-made index for technical literature – An experiments", *IBM Journal of Research and Development*, 2(4), pp. 354-361, 1958.

[6] H.P. Edmundson, "New methods in automatic extracting", *Journal of the Association for Computing Machinery (JACM)*, 16(2), pp. 264-285, 1969.

[7] R. Barzilay and M. Elhadad, "Using lexical chains for text summarization", *Proc. ACL'97/EACL'97 workshop on intelligent scalable text summarization*, pp. 10-17, Madrid, Spain, 1997.

[8] H.G. Silber and K.F. McCoy, "Efficient text summarization using lexical chains," *Proc. 5th int'l Conf. Intelligence User Interfaces*, pp. 252-255, New Orleans, 2000.

[9] W. Mann and S. Thompson, "Rhetorical structure theory: Toward a functional theory of text," *Text*, 8(3), pp. 243-281, 1988.

[10] D. Marcu, *The Rhetorical parsing, summarization, and generation of natural language texts*, PhD thesis, Dept. Computer Science, Univ. Toronto, Toronto, Canada, 1997.

[11] J. Kupiec, J. Pedersen, and F. Chen, "A trainable document summarizer," *Proc. 18th ACM-SIGIR Conf. Research and Development in Information Retrieval*, pp. 68-73, New York, 1995.

[12] E. Hovy and C.Y. Lin, "Automated text summarization in SUMMARIST," *In I. Mani, and M. Maybury editors, Advances in Automatic Text Summarization*, pp. 81-94, MIT press, 1999.

[13] K. Svore, L. Vanderwende, and C. Burges, "Enhancing single-document summarization by combining RankNet and third-party sources," *Proc. EMNLP-CoNLL*, pp. 448-457, 2007.

[14] J.M. Conroy and D.P. O'leary, "Text summarization via hidden Markov models," *Proc 24th ACM SIGIR Conf. Research and Development in Information Retrieval (SIGIR 01)*, pp. 406-407, New York, 2001.

[15] T. Hirao, H. Isozaki, E. Maeda, and Y. Matsumoto: "Extracting important sentences with support vector machines", *Proc. 19th Int;l Conf. Computational Linguistics(COLING 2002)*, pp. 342-348, Taipei, Taiwan, 2002.

[16] Zou, J., Le, D. X. and Thoma, G. R. "Online medical journal article layout analysis," *Proc. 14th SPIE Document Recognition and Retrieval*, 6500, 65000V (1-12), San Jose, 2007.

[17] F. Sebastiani, "Machine learning in automated text categorization," *ACM Computing Surveys*, 34(1), pp. 1-47, 2002.

[18] L. Galavotti, F. Sebastiani, and M. Simi, "Experiments on the use of feature selection and negative evidence in to automated Text categorization," *ECDL 2000 LNCS 1923*, pp. 59-68, Springer, Heidelberg, 2000.

[19] V. Vapnik, *The nature of statistical learning theory*, New York: Springer-Verlag, 1995.

[20] S. Rüping, *mySVM-Manual*, Univ. Dortmund, 2000. [http://www-ai.cs.uni-dortmund.de/SOFTWARE/MYSVM]

[21] C.C. Chang and C.J. Lin, "LIBSVM: a library for support vector machines," 2001. [http://www.csie.ntu.edu.tw/~cjlin/libsvm]

[22] I. Kim, D.X. Le, and G.R. Thoma, "Automated Identification of Biomedical Article Type Using Support Vector Machines," *Proc. 18th SPIE Document Recognition and Retrieval*, 7874, 787403, San Francisco, 2011.

Characterizing Postoperative Pain Management Data by Cluster Analysis

Yuh-Jyh Hu[1], Rong-Hong Jan[1], Kuochen Wang[1], Yu-Chee Tseng[1], Tien-Hsiung Ku[2] , and Shu-Fen Yang[2]
[1]Department of Computer Science, National Chiao Tung University, Hsinchu, Taiwan
[2]Department of Anesthesia, Changhwa Christian Hospital, Changhwa, Taiwan

Abstract - *PCA (Patient Controlled Analgesia) is a delivery system for pain medication that makes effective and flexible pain treatments possible by allowing patients to adjust the dosage of analgesics themselves. Unlike previous research on patient controlled analgesia, this study explores patient demand behavior over time. We applied clustering methods to disclose demand patterns among patients over the first 24h of analgesic medication after surgery. We first identified three demand patterns from patient controlled analgesia request log files. We then considered demographic, biomedical, and surgery-related data to evaluate the influence of demand pattern on analgesic requirements. We recovered several associations that concurred with previous findings, and discovered several new correlations*

Keywords: postoperative pain, patient controlled analgesia, PCA demand, clustering

1 Introduction

After operations, pain is one of the most commonly reported symptoms [1]. It is a highly personal experience influenced by multiple factors, including sensitivity to pain, age, genetics, physical status, and psychological factors [2-4]. As the progress of medical science, people gradually become aware of the importance of pain management.

PCA (Patient Controlled Analgesia) is a delivery system for pain medication that makes effective and flexible pain treatments possible by allowing patients to adjust the dosage of anesthetics themselves. According to previous research [5-6], PCA has become one of the most effective techniques for postoperative analgesia. It is widely used in hospitals for the management of postoperative pain, especially for major surgeries.

Most research on postoperative pain management is limited to evaluating the correlation of patient characteristics, such as demographic attributes, biomedical variables, and psychological states, with postoperative pain intensity or analgesic requirement. Several studies have identified the preoperative predictive factors for postoperative pain and analgesic consumption in various patient groups of different genders, ages, or psychological states [7-11]. However, none of these studies analyzed continual patient demand behavior throughout the PCA therapy. Time-series data analysis is a common practice in various research fields. For example, in the study of sleep in patients with insomnia, time-series data derived from sleep diaries were used to compute conditional probabilities of having insomnia [12]; in biology, a temporal map of fluctuations in mRNA expression of 112 genes during central nervous system development in rats provides a temporal gene expression fingerprint of spinal cord development [13]. Few studies of PCA examined patient demand behavior and its relationship to analgesic drug use [14,15]. We hypothesized that patient demand behavior over time provides different and useful information in PCA administration that is missing in the preoperative factors analyzed earlier.

Our study, unlike previous research, focuses on continual analgesia demand behavior during the postoperative PCA medication. The current study explores and characterizes patient demand behavior. Patient demand behavior is represented by a series of PCA requests over time. We discover distinct and conserved demand patterns from the time-series data and identify the significant patient factors that influence demand behavior. In addition, we compare the predictors for PCA demand behavior and analgesic requirements and evaluate the contribution of demand pattern to analgesic consumption prediction

2 Materials and Methods

We restricted the study subjects to conscious hospitalized patients at Changhwa Christian Hospital (CCH) during the years from 2005 to 2010. All patients were instructed to operate the PCA device manufactured by Abbott (Abbott Pain Management Provider, Abbott Lab Chicago, IL, USA) prior to the surgery. With the assistance of Acute Pain Service, we collected more than 3000 patient records, each of which contained attributes such as basic health status, age, gender, weight, department code, doctor ID, PCA control parameters, amount of anesthetics used in different time intervals, etc. Since not all the attributes are relevant to our study or have correct values, after consulting the

anesthesiologists, we discarded irrelevant attributes, e.g. doctor ID and department code, before further investigation. We processed thousands of medical charts and PCA log files collected at CCH, and obtained 1655 complete records. Each patient was described by demographic and biomedical attributes besides PCA-related variables. Their values are either categorical or numeric. The attribute descriptions are shown in Table 1. All the statistical analyses were performed using the Statistical Package for the Social Science 10.0 (SPSS Inc. Chicago, IL, U.S.A.).

Table 1. Summary of Patient Attributes.

Attribute Name	Description	Number	Mean
Demographic:			
gender	patient's gender	986(F)/669(M)	-
age	patient's age	-	56.9±15.8
weight(kg)	patient's weight	-	63.0±12.6
Biomedical:			
sbp (mmHG)	systolic blood pressure	-	135.8±22.6
dbp (mmHG)	diastolic blood pressure	-	69.4±13.8
pulse(beats/min)	heart rate	-	81.0±15.4
ASA class[a]	1: healthy 2: mild systemic disease 3: major systemic disease	184(1)/837(2)/634(3)	-
OP-related:			
op_type[b]	surgery type: 1 ~ 8	107(1)/126(2)/411(3) 127(4)/427(5)/109(6) 212(7)/136(8)	-
ans_type	SA: spinal anesthesia GA: general anesthesia	1470(GA)/185(SA)	-
op_time(hr)	surgical duration	-	4.2±2.6
urgency	E: emergency surgery R: regular surgery	136(E)/1519(R)	-

[a]ASA class is the commonly used preoperative index of physical status defined by American Society of Anesthesiologists.
[b]1: intrathoracic, 2: upper intra-abdominal, 3: lower intra-abdominal, 4: laminectomy, 5: major joints, 6: limbs, 7: head & neck, 8: others

Given the PCA demand frequency within each unit of time, we can represent each patient's PCA demand profile as a time course. By applying clustering algorithms to the time courses, we identified different patient groups. Patients in the same group are expected to demonstrate similar demand behavior; in contrast, demand behavior of patients in different groups is different. We used k-medoids algorithms [16,17] to partition the patients into clusters according to their demand behavior. A medoid is a real data point that has the minimum average distance from all other points in the same cluster. Unlike the k-means algorithm [18], k-medoids mitigates the effect of outliers on the resulting prototypes and ensures that all the resulting clusters are non-empty [19]. To find the appropriate number of clusters, we performed a series of k-medoids clustering algorithm with the value of k varying from 2 to *K*.

The number of clusters was determined by reproducibility and stability [20]. We generated bootstrap samples from the dataset by random sampling with replacement [21]. We ran k-medoids on the sample to obtain a clustering solution. From B pairs of bootstrap samples from the original data, we produced *B* pairs of clustering results. Given two clustering solutions C_1 and C_2 from a pair of bootstrap samples, we obtained two partitions of the original data by assigning each observation to the nearest medoid. We used the adjusted Rand Index [22] to measure the similarity between the two partitions. To assess how stable a partition of the original data was, we compared the adjusted Rand Index values of the *B* pairs of bootstrapped partitions. By iterating the value of k from 2 to *K* and repeating the same procedure, we obtained different distributions of the adjusted Rand Index values. First, we performed analysis of variance (ANOVA) to determine whether significant statistical evidence existed to show that at least two adjusted Rand Index means differed. Then, we conducted sequential *t*-tests corrected for multiple comparisons to identify a significant gap between successive differences in bootstrapped adjusted Rand Index values. The most significant jump indicated the most likely number of clusters in the original data.

After identifying the PCA demand patterns using the k-medoids algorithm and bootstrapped stability tests, we examined the association between demand patterns and the patient attributes listed in Table 1. We ran chi-square tests for the dependence of the demand behavior on those patient attributes, and we conducted ANOVA tests to compare the attribute values among different patient groups according to demand patterns. For all the analyses, a level was set at 0.05 for statistical significance.

Little research explores the relationship between PCA demand patterns and PCA analgesic consumption. We applied stepwise linear regression to compare demographic, biomedical, operation-related, and PCA demand behavioral influences on PCA analgesic consumption. The criterion for inclusion or elimination of patient attributes was that a patient attribute would be included if its partial regression coefficient was significant at the $\alpha = 0.05$ level or eliminated if it was

not. To evaluate further the individual effect of PCA demand pattern on analgesic consumption, we performed stepwise regression only on patient demographic, biomedical, and surgery-related attributes. We compared the R^2 and adjusted R^2 before and after removing demand patterns. A substantial drop in R^2 and adjusted R^2 indicated that the demand patterns played a significant role in predicting analgesic consumption.

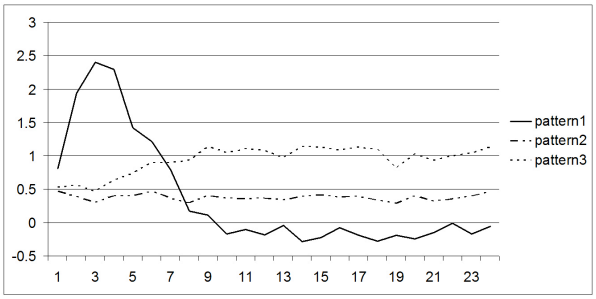

Figure 1. PCA demand patterns discovered from 1655 subjects. Three patterns are identified from 1,655 PCA patient-demand log files. Ninety-one patients' PCA demand behavior matches Pattern 1, 1,205 patients' demand behavior matches Pattern 2, and 359 patients' demand behavior matches Pattern 3. The X-axis indicates the 24h time line (1^{st}h to 24^{th}h). The Y-axis represents the normalized standard score (z-score) of the PCA demand frequency in a particular hour.

3 Results and Discussion

We performed bootstrap sampling with replacement on the 1,655 patient records and generated 100 pairs of samples. Varying k from 2 to 6, we ran k-medoids on the bootstrap samples and calculated their adjusted Rand Index values. We performed sequential *t*-tests (with Bonferroni correction) on the adjusted Rand Index groups. The test results were presented in Table 2. From the sequential *t*-test results, we observed a significant gap between k = 3 and k = 4. The mean of the adjusted Rand Index of the four cluster partitions dropped by 0.12, with $p << .000001$. It indicated that when k = 3, the clustering result was the most stable. We thus selected k = 3 as the number of clusters and identified three PCA patient groups by maximizing the demand behavior similarity among the patients in each group. The group size is 91, 1205, and 359 respectively. Patients in the same group showed a similar demand pattern that was different among different groups. Figure 1 presents the average demand pattern of each group. The X-axis represents the 24h time line, and the Y-axis is the normalized standard score (z-score) of the PCA demand frequency in a particular hour.

Different PCA demand patterns define different patient groups. We identified three demand patterns from 1,655 patients and produced three patient groups. The chi-square test was performed to test the dependence of the patient groups on the categorical patient attributes in Table 1, for example, gender, ASA class, and surgery type. ANOVA was used to compare the differences in weight, age, blood pressure, pulse, and surgical duration among different patient groups. Table 3 shows the results of the chi-square and ANOVA tests. We observed statistically significant differences among PCA demand pattern groups in gender, diastolic blood pressure, surgery type, and surgical duration respectively. The Student t-test for differences between means was performed with Bonferroni correction ($\alpha/N = 0.016$). The results indicated that Demand Pattern 1 (shown in Fig. 1) was associated with shorter surgical duration than the other two patterns ($p = .0012$; $p = .008$), and Demand Pattern 2 was more associated with lower diastolic blood ($p = .05$) than Pattern 3 ($p = .09$), but showed no significant difference from Pattern 1 ($p = .91$). In contrast, age, systolic blood pressure, and urgency showed only a weak association with PCA demand behavior. No significant difference in weight ($p = .47$) or pulse ($p = .43$) was found among demand pattern groups. In addition, no significant statistical evidence was found to reject or accept the hypothesis that the ASA class ($p = .37$) and the type of anesthesia ($p = .36$) were independent of PCA demand pattern.

Multivariate stepwise linear regression was used to identify major factors influencing PCA analgesic consumption. All demographic, biomedical, and surgery-related attributes and PCA demand patterns were included for regression analysis. We found that PCA demand pattern played the most significant role in predicting PCA analgesic consumption. The other major factors at the $\alpha = 0.05$ level were weight, age, surgical type, urgency, and anesthesia type, as presented in Table 4. To validate further the individual effect of PCA demand pattern on analgesic consumption, we performed stepwise regression only on patient demographic, biomedical, and surgery-related attributes. Three factors were selected at the $\alpha = 0.05$ level, as shown in Table 5. They were weight, age, and surgical type, in the order selected. The R^2 and adjusted R^2 are 0.05651 and 0.05479, respectively. Compared with the results ($R^2 = 0.18761$ and adjusted $R^2 = 0.18465$) in Table 4, it is clear that PCA demand pattern made a significant contribution to analgesic consumption prediction.

To our best knowledge, this study is the first to introduce an analysis of time-series data derived from PCA demand log files. We have used a clustering method to analyze the 24h PCA demand profile of 1,655 patients. The advantages of a clustering-based approach to data analysis are that it is adaptable to change and helps extract crucial properties that distinguish different data groups. Cluster analysis has been widely used in various applications. In biology, it can help biologists categorize genes or proteins with similar functionality into families or derive a hierarchical organization [23]. In business, it helps market analysts identify distinctive groups in their customer databases and characterize customer groups according to purchasing patterns [24]. Many clustering algorithms have been developed. In general, they can be classified into methods such as partitioning methods, hierarchical methods, density-based methods, model-based methods, and constraint-based methods [19,25].

The demographic, biomedical, and surgery-related predictors for analgesic consumption are not necessarily a predictor for PCA demand pattern, though a relationship between analgesia requirements and demand behavior exists.

Several studies have discovered a significant correlation between age and the dose of opioid required in the postoperative period [4,26-28]. For example, Gagliese et al. and Chang et al. both observed that age was significantly negatively correlated with morphine consumption in their studies [11,29]. However, our study only indicated a weak correlation of age with PCA demand patterns. As mentioned in previous studies, possible causes of the discrepancy in the results could be lack of understanding or misuse of PCA by older and younger patients [8], and a difference in pain sensitivity to morphine between young and elderly patients should be considered in the correlation analysis [30]. More specific studies should be restricted to a narrower age range such as 20 to 60 years, and pain intensity should be included in the correlation modeling to alleviate the limitation of a simple two-variable (age and morphine dose) model.

Table 2. Sequential *t*-test for Successive Differences in Adjusted Rand Index Means.

Number of Clusters	Adjusted RI Mean Difference	*t*-value	*p*-value
3 vs. 2	-0.07	3.63	.00037
4 vs. 3	-0.12	5.55	<< .00001
5 vs. 4	-0.06	3.32	.00106
6 vs. 5	-0.06	4.00	.00009

Table 3. Chi-Square and ANOVA Tests on Patient Attributes and Demand Patterns.

Attribute Name	Chi-Square *p*-value (DF[a])	ANOVA *p-value*
Demographic:		
gender	0.0022(2)	-
age	-	0.12
weight	-	0.47
Biomedical:		
sbp	-	0.15
dbp	-	0.02
pulse	-	0.44
ASA class	0.37(4)	-
OP-related:		
op_type	0.0028(14)	-
ans_type	0.36(2)	-
op_time	-	0.0095
urgency	0.18(2)	-

[a]DF: degree of freedom

The relationship of gender with postoperative pain and analgesic consumption varies among different studies. We found that gender was a significant correlate of PCA demand behavior. This concurred with Chia et al.'s report that gender was an important predictor of postoperative morphine requirement [8]. The chi-square test indicated that significantly more females than expected demonstrated PCA Demand Pattern 1 (see Fig. 1) in our study. Because Demand Pattern 1 indicates an early sharp increase of PCA requests, it suggests that PCA dosage for the first 3 h could be increased for the female patients whose characteristics match those in the Demand Pattern 1 group to increase their satisfaction. We found a significant association between PCA demand pattern and surgical type as well as surgical duration. These findings agreed with the lessons learned from pain management [31,32] and previous studies of PCA consumption [11,29].

Some researchers have derived predictive models of analgesic requirements or postoperative pain from regression analyses [8,10,11]. Although they identified several positive preoperative correlates, such as age and gender, their coefficients of determination were small, and in some cases, no significant predictors were found. For example, in an analysis of the first 6 h of intravenous patient controlled analgesia required in the ward, no predictors were found to meet $\alpha = 0.05$ level [9]. This suggests that predictive factors other than demographic, physiological, and surgical attributes are present that have not been analyzed. We included PCA demand pattern in the multivariate stepwise regression analysis to compare the influence of these factors on PCA consumption prediction. Our results showed that PCA demand pattern played the most significant role in predicting analgesic consumption. It increased the value of coefficient of determination from 0.05651 to 0.18761.

There are a number of limitations in our current study. First, though the patient records have been carefully reviewed, the PCA data used in our analyses were not guaranteed to be free of errors. A small amount of noisy data could occur due to human errors in data entry or misuse of PCA devices by patients. They were not recognized or resolved in the data preprocess. To mitigate the effect of data noise, we used bootstrap replications to ensure the reproducibility and stability of clustering solutions, and statistically significant results were obtained. However, data cleaning is still a crucial step before any form of data exploration, including clustering, and results of this type should be applied with caution within the imitations of

clustering algorithms. Second, most previous studies of PCA were conducted on Western patients. Little research focuses on Eastern people such as Taiwanese patients [8,29]. The discrepancy in the analysis results or conclusions might be attributable to the impact of different sociocultural origins. Third, our current study of PCA demand behavior is based on the first 24 h of PCA therapy after surgery. Shorter or longer periods of PCA medication may contain different demand behavioral patterns. Distinct and conserved demand patterns among patients over various lengths of PCA therapy are likely to correlate with different regularities in postoperative pain relief and patient satisfaction. Information of this type may be useful for predicting analgesic requirements and postoperative pain. Last, as a retrospective study, the surveyed variables were not under control, and the medical meanings of the correlation between demand patterns and demographic, biomedical, or surgery-related predictors were still unclear.

Table 4. Results of Stepwise Regression Analysis of PCA Analgesic Consumption.

Predicting PCA Analgesic Consumption						
Factor Attribute	**Beta[a]**	**B[b]**	**SE[c]**	***p*-value**	**R^2**	**adjusted R^2**
Step 1:						
PCA demand pattern	0.36149	3.65095	0.23161	0.E+0	0.13067	0.13015
Step 2:						
PCA demand pattern	0.35781	3.61380	0.22860	0.E+0	0.15415	0.15313
weight	0.15327	0.06076	0.00897	1.76712E-11		
Step 3:						
PCA demand pattern	0.35847	3.62046	0.22648	0.E+0		
weight	0.16479	0.06532	0.00893	3.88467E-13	0.17033	0.16882
op_type	-0.12772	-0.32519	0.05731	1.64481E-8		
Step 4:						
PCA demand pattern	0.35657	3.60126	0.22476	0.E+0		
weight	0.15049	0.05966	0.00892	3.15696E-11	0.18354	0.18156
op_type	-0.12298	-0.31314	0.05692	4.36024E-8		
age	-0.11589	-0.03667	0.00710	2.67005E-7		
Step 5:						
PCA demand pattern	0.35706	3.60626	0.22455	0.E+0		
weight	0.14926	0.05917	0.00892	4.40967E-11		
op_type	-0.11716	-0.29831	0.05730	2.17272E-7	0.18570	0.18323
age	-0.12192	-0.03858	0.00715	7.77338E-8		
urgency	0.04718	0.85999	0.41131	0.03669		
Step 6:						
PCA demand pattern	0.35654	3.60094	0.22437	0.E+0		
weight	0.14847	0.05885	0.00891	5.38757E-11		
op_type	-0.12254	-0.31201	0.05767	7.23051E-8	0.18761	0.18465
age	-0.13481	-0.04226	0.00744	1.14832E-8		
urgency	0.04900	0.89320	0.41129	0.03002		
ans_type	0.04595	0.73006	0.37057	0.04899		

[a]Beta: standardized coefficient; [b]B: unstandardized coefficient; [c]SE: standard error of B

4 Conclusion

Most research on correlates of postoperative pain has been limited to identifying the correlation of patients' characteristics, such as demographic attributes, biomedical variables, and psychological states, with postoperative pain intensity or analgesic requirements. Our study, unlike previous works, focused on the continual analgesia demand behaviors during the postoperative PCA therapy. The main finding was that there were conserved PCA demand patterns that partitioned the study subjects into three patient groups, each presenting distinctive PCA demand behaviors.

We advocate the analysis of PCA demand behavior. To demonstrate its feasibility and significance, in our current study we used clustering algorithms to identify demand patterns. The stability and reproducibility of the clustering solution have been verified by repeated random bootstrap sampling. The results suggest that PCA demand behavioral patterns exist over time among patients. They are correlated with specific demographic, biomedical, or surgery-related attributes, and have influence on analgesic consumption. In the future work, we will investigate other factors that can possibly explain the inconsistency, and improve postoperative pain relief.

5 Acknowledgment

This work was partially supported by National Science Council, Taiwan (NSC 100-2221-E-009-146).

Table 5. Results of Stepwise Regression Analysis of PCA Analgesic Consumption without Demand Pattern.

Predicting PCA Analgesic Consumption						
Factor Attribute	**Beta[a]**	**B[b]**	**SE[c]**	***p*-value**	**R^2**	**adjusted R^2**
Step 1:						
weight	0.16185	0.06416	0.00962	3.51607E-11	0.02619	0.02561
Step 2:						
weight	0.14663	0.05812	0.00962	1.84381E-9	0.04204	0.04088
age	-0.12679	-0.04012	0.00768	1.94306E-11		
Step 3:						
weight	0.15815	0.06269	0.00959	8.28069E-11		
age	-0.12183	-0.03855	0.00763	4.78009E-7	0.05651	0.05479
op_type	-0.12089	-0.30780	0.06117	5.38175E-7		

[a]Beta: standardized coefficient; [b]B: unstandardized coefficient; [c]SE: standard error of B

6 References

[1] Chung F, Un V, Su J. Postoperative symptoms 24 hours after ambulatory anaesthesia. *Canadian Journal of Anesthesia* 1996; **43**: 1121-7.

[2] Turk DC, Okifuji A. Assessment of patients' reporting of pain: an integrated perspective. *The Lancet* 1999; **353**: 1784-8.

[3] Bisgaard T, Klarskov B, Rosenberg J, Kehlet H. Characteristics and prediction of early pain after laparoscopic cholecystectomy. *Pain* 2001; **90**: 261-9.

[4] Macintyre PE, Jarvis DA. Age is the best predictor of postoperative morphine requirements. *Pain* 1996; **64**: 357-64.

[5] Dolin SJ, Cashman JN, Bland JM. Effectiveness of acute postoperative pain management: I. Evidence from published data. *British Journal of Anaesthesia* 2002; **89**: 409-23.

[6] Walder B, Schafer M, Henzi I, Tramer MR. Efficacy and safety of patient-controlled opioid analgesia for acute postoperative pain. A quantitative systematic review. *Acta Anaesthesiologica Scandinavica* 2001; **45**: 795-804.

[7] Hu YJ, Jan RH, Wang KC, Tseng YC, Ku TH, Yang SF, and Wu HS. An Application of Sensor Networks with Data Mining to Patient Controlled Analgesia. *Proceedings of IEEE HealthCom* 2010: 353-360.

[8] Chia YY, Chow LH, Hung CC, Liu K, Ger LP, Wang PN. Gender and pain upon movement are associated with the requirements for postoperative patient-controlled iv analgesia: a prospective survey of 2,298 Chinese patients. *Canadian Journal of Anesthesia* 2002; **49**: 249-55.

[9] Pan PH, Coghill R, Houle TT, Seid MH, Lindel WM, Parker RL, Washburn SA, Harris L, Eisenach JC. Multifactorial preoperative predictors for postcesarean section pain and analgesic requirement. *Anesthesiology* 2006; **104**: 417-25.

[10] Aubrun F, Bunge D, Langeron O, Saillant G, Coriat P, Riou B. Postoperative morphine consumption in the elderly patient. *Anesthesiology* 2003; **99**: 160-5.

[11] Gagliese L, Gauthier LR, Macpherson AK, Jovellanos M, Chan VW. Correlates of postoperative pain and intravenous patient-controlled analgesia use in younger and older surgical patients. *Pain Medicine* 2008; **9**: 299-314.

[12] Vallieres A, Ivers H, Beaulieu-Bonneau S, Morin CM. Predictability of sleep in patients with insomnia. *Sleep* 2011; **34**: 609-17.

[13] Wen X, Fuhrman S, Michaels GS, Carr DB, Smith S, Barker JL, Somogyi R. Large-scale temporal gene expression mapping of central nervous system development. *Proceedings of the National Academy of Sciences U.S.A* 1998; **95**: 334-9.

[14] Hu YJ, Jan RH, Wang KC, Tseng YC, Ku TH, and Yang SF. Analysis of Patient Controlled Analgesia Demand Patterns. *Proceedings of Industrial Conference on Data Mining* (short paper) 2011: 17-24.

[15] De Cosmo G, Congedo E, Lai C, Primieri P, Dottarelli A, Aceto P. Preoperative psychologic and demographic predictors of pain perception and tramadol consumption using intravenous patient-controlled analgesia. *Clinical Journal of Pain* 2008; **24**: 399-405.

[16] Reynolds AP, Richards G, and Rayward-Smith VJ. The Application of K-medoids and PAM to the Clustering of Rules. *Proceedings of the Fifth International Conference on Intelligent Data Engineering and Automated Learning* 2004: 173-8.

[17] Park H, Jun C: A Simple and Fast Algorithm for K-medoids Clustering. *Expert Systems with Applications* 2009; **36**: 3336-41.

[18] Forgy E: Cluster Analysis of Multivariate Data. Efficiency vs. Interpretability of Classification. *Biometrics* 1965; **21**: 768-9.

[19] Han J, Kamber M. *Data Mining: Concepts and Techniques*, 2nd edn. San Francisco: Morgan Kaufmann, 2007.

[20] Dolnicar S, Leisch F. Evaluation of structure and reproducibility of cluster solutions using the bootstrap. *Market Letters* 2010; **21**: 83-101.

[21] Efron B, Tibshirani RJ. *An Introduction to the Bootstrap*, New York: Chapman & Hall, 1993.

[22] Hubert L, Arabie P. Comparing partitions. *Journal of Classification* 1985; **2**: 193-218.

[23] Eisen MB, Spellman PT, Brown PO, Botstein D. Cluster analysis and display of genome-wide expression patterns. *Proceedings of the National Academy of Sciences U.S.A* 1998; **95**: 14863-8.

[24] Dibb S, Simkin L. A program for implementing market

segmentation. *Journal of Business and Industrial Marketing* 1997; **12**: 51-65.
[25] Xu R, Wunsch II DC. *Clustering*. New Jersey: IEEE Press, Wiley, 2009.
[26] Burns JW, Hodsman NB, McLintock TT, Gillies GW, Kenny GN, McArdle CS. The influence of patient characteristics on the requirements for postoperative analgesia. A reassessment using patient-controlled analgesia. *Anaesthesia* 1989; **44**: 2-6.
[27] Egbert AM, Parks LH, Short LM, Burnett ML. Randomized trial of postoperative patient-controlled analgesia vs. intramuscular narcotics in frail elderly men. *Archives of Internal Medicine* 1990; **150**: 1897-903.
[28] Gagliese L, Jackson M, Ritvo P, Wowk A, Katz J. Age is not an impediment to effective use of patient-controlled analgesia by surgical patients. *Anesthesiology* 2000; **93**: 601-10.
[29] Chang KY, Tsou MY, Chan KH, Sung CS, Chang WK. Factors affecting patient-controlled analgesia requirements. *Journal of the Formosan Medical Association* 2006; **105**: 918-25.
[30] Aubrun F, Monsel S, Langeron O, Coriat P, Riou B. Postoperative titration of intravenous morphine in the elderly patient. *Anesthesiology* 2002; **96**: 17-23.
[31] Ready LB. Acute pain lessons learned from 25,000 patients. *Regional Anesthesia and Pain Medicine* 1999; **24**: 499-505.
[32] Preble LM, Guveyan JA, Sinatra RS. Patient characteristics influencing postoperative pain management. In: Editor Sinatra RS, Hord AH, Ginsberg B, Preble LM. *Acute Pain Mechanisms and Management*. St. Louis, MO: Mosby Year Book, 1992.

A Case Study: Building a Web-Based Dietitian Expert System

Robert Jackson and Eman El-Sheikh
Department of Computer Science, University of West Florida, Pensacola, Florida, USA

Abstract - *This paper presents the development of a TeleHealth system built using an open source web-based expert system framework called Tohu. The expert system works by providing individualized diet and health recommendations to users based on each user's responses to a simple auto-reporting questionnaire. A comparison is given between the development and features of this system and similar systems. A description of the system development illustrates how a complex web-based expert system can be easily constructed using open source tools such as JBoss Drools and Tohu. Following a depiction of how the system can be used, the paper concludes with a discussion of opportunities for future work.*

Keywords: Web-Based Expert System, Drools, Tohu, Rule-Based System, Health Assessment, Diet Assessment.

1 Introduction

This paper presents an open source behavior monitoring and modification system in which patients can self-report their measurements and receive personalized diet and exercise feedback. TeleHealth systems are an emerging method of delivering health services to patients using telecommunications (e.g. chat, web-based expert systems, and video consultations). TeleHealth systems have seen increased use as health tools in recent years and have been shown to perform quite well [1]. In the Journal of the American Medical Association (JAMA), researchers at the Weight Control and Diabetes Research Center at Brown Medical School reported that a system in which patients submitted a weekly weight loss diary via email lost significantly more weight than those only given weight loss information [2]. Further results from studies published by Haugen et al. [3] and Digenio et al. [1] prove that TeleHealth systems are valuable and effective tools for bringing health services to a larger population.

These so-called TeleHealth systems may be a part of the solution, for the Center for Disease Control states that, American society has become characterized by environments that promote increased food intake, non-healthy foods, and physical inactivity [4]. Furthermore, the Journal of the American Medical Association observed that 72% of American men and 64% of American women are overweight or obese [5]. Also, for American men, this figure is increasing as time goes on. Research has shown that persons whose weight approaches levels classified as "overweight" or "obese," tend to increase their risks of diabetes, heart disease, cancer, and stroke [6]. Without more effective health aides, there could be a huge economic and medical impact as the population ages and starts to see the negative effect of this type of lifestyle.

The proposed TeleHealth system developed is called eDietitian; it leverages the Internet and existing tools to provide dietitian consultations to a larger population. The software performs a virtual consultation with the user by mimicking a consultation with a dietitian and asking the user a dynamic series of questions related to their lifestyle and habits. After the consultation, the user is given a customized list of recommended practices they should try to incorporate into their lifestyle to achieve and maintain a healthy lifestyle.

2 Related Works and Tools

This section describes tools that are similar to eDietitian; it also provides information about the tools used to build eDietitian.

2.1 Background Software and Tools

The eDietitian system is written in Drools [8] (see Figure 1), a Java Virtual Machine (JVM) rules engine and language. Drools provides a Java implementation of the Rete Algorithm for efficient pattern matching of facts with rules. It's similar to other rule engines such as CLIPS and Jess. The other major tool used is the Tohu [7] framework. The framework provides classes (see Figure 2) for constructing the question-and-answer tree and rendering the user interface via jQuery.

2.2 Related Systems

One of the systems that inspired eDietitian was WebMD's Personal Diet Evaluator [9]. The Personal Diet Evaluator's approach is a little different from eDietitian's but they share a similar questions-and-answer format. The big difference between the Personal Diet Evaluator (PDE) and eDietitian is that PDE is an Adobe Flash application while eDietitian is rendered with pure HTML. Also PDE is not as dynamic to the user's responses as eDietitian. eDietitian's screens react at a much more granular scale than PDE's.

Another system which bears a resemblance to eDietitian is the "Mozambican Diet Assessment Tool" [10]. It was developed by the Mozambican Ministry of Health as a quick way to measure the diet of rural and urban communities. Donald Rose et al describe how the system works as follows:

"The Mozambican Diet Assessment Tool (MDAT) is based on a simple, qualitative 24-hour recall of household food intake. The person in charge of food preparation in each household is asked to recall all foods eaten by household members at each meal and snack time in the previous 24 hours. Field personnel, usually the provincial nutritionists, then assign points to each food consumed, using a simple scoring system."

The eDietitian system differs from the Mozambican Diet Assessment Tool because it takes a different route during the evaluation by inquiring about exercise and BMI rather than strictly measuring the amount of nutrients consumed. The goal of MDAT is different from eDietitian's - which is mostly the reinforcement of a healthy lifestyle - rather than nutrient assessment.

Denning et al developed BALANCE, a smart phone application which measures caloric expenditure using sensor and activity sensing technology [11]. Their system can predict how much time a person has spent sitting, walking, jogging, or cycling each day and can recommend serving size to the patient to keep their caloric intake in balance with their expenditures.

3 eDietitian Design and Architecture

This section describes how the eDietitian system was designed and constructed using the Tohu framework and Drools language to generate the web application.

3.1 Knowledge Base

The knowledge base for the system was built using a rule-based approach. The final system contained approximately 80 rules of varying complexity. Rules came from numerous sources, but the main sources for rules are US Government sources such as: PubMed Health from the U.S. National Library of Medicine [12], the "Dietary Guidelines for Americans" from the US Department of Agriculture [13], and the Center for Disease Control's Obesity and Overweight website [14].

3.2 Architecture

3.2.1 Server-Side

Figure 1 (right) shows the server-side stack of the system. Everything runs in a Java Virtual Machine (JVM) instance. On top of the JVM, a Tomcat container serves the normal web files, but also runs a RESTful web-service called the Drools Execution Server. This service provides an interface to the Drools knowledge-base via XML.

3.2.2 Client-Side

The client-side of the system could essentially be any program that knows about the RESTful interface used by the Drools Execution Server. However, this project made use of the Tohu's jQuery library as shown in Figure 1 (left) for UI development. The Tohu project provides a JavaScript framework which can dynamically create the HTML and manipulate the Document Object Model (DOM) based on the responses given from the Server-Side. The Tohu JavaScript library uses the popular jQuery library for client-side scripting.

The big advantage of having the system run as a web application is how easily the UI can be easily changed using Cascading Style Sheets (CSS). The view can be easily modified using just style sheets; without any modification of the rules or logic classes.

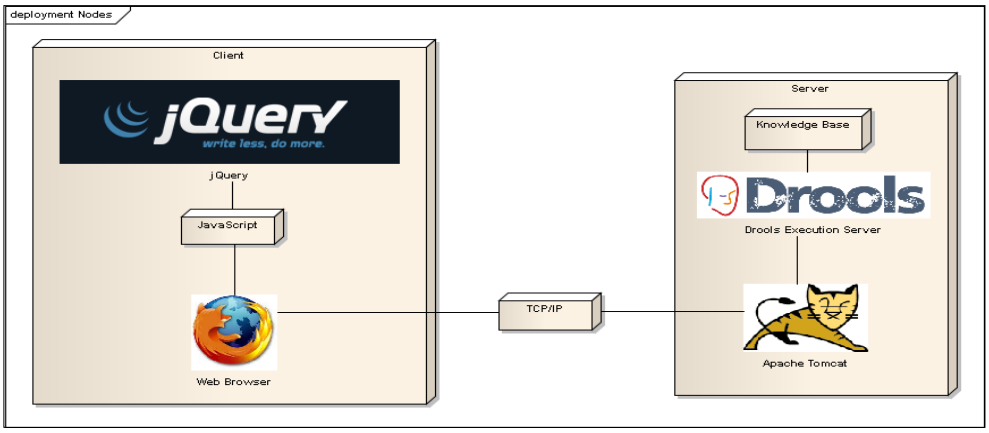

Figure 1 Client-Server stacks used in the eDietitian system. All components are open source.

3.3 Rule Workflow

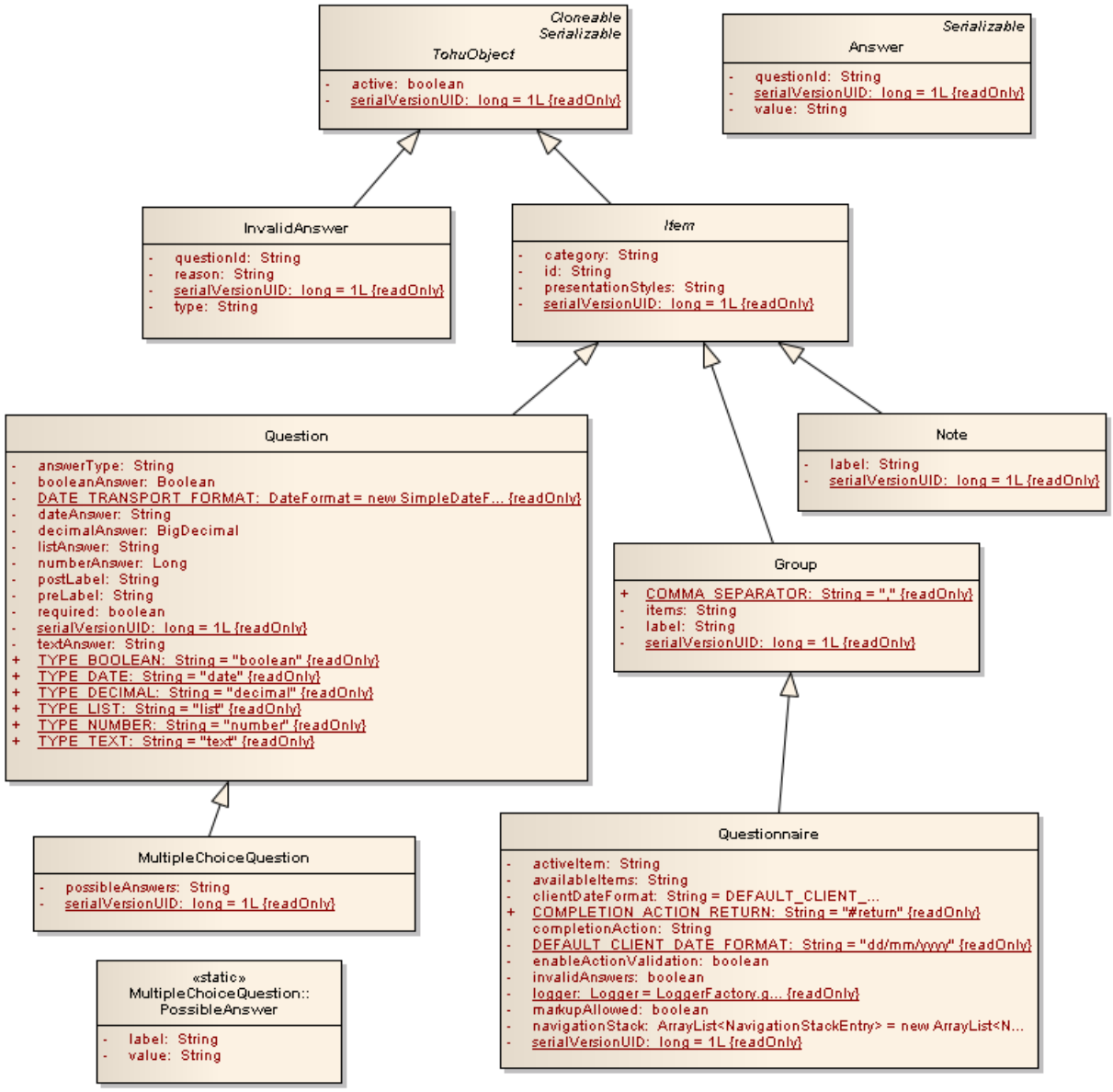

Figure 2 Class diagram of the Tohu core classes. These classes are used to build the decision tree.

The Java classes from Figure 2 are used to code the decision tree. A snippet of the Drools code is given to demonstrate this. Suppose we want to ask the user whether they exercise or not and provide a recommendation if they answer "no" to the question. Figure 3 shows the final screen with the recommendation at the bottom. Using the Tohu classes (Figure 2) to code the rule into the knowledge-base, we create a rule that inserts the `Question` object into the knowledge base as follows:

```
rule "ask if user exercises"
dialect "mvel"
then
Question question = new Question("exercise");
question.setAnswerType(Question.TYPE_BOOLEAN);
question.setPreLabel("Do you exercise?");
question.setPresentationStyles({"radio"});
```

```
insertLogical(question);
. . .  // similar code cut out for space
end
```

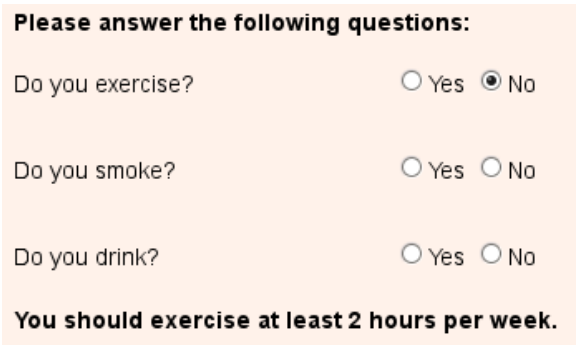

Figure 3 How Tohu renders the above code with the recommendation at the bottom. A Boolean datatype is displayed as a radio button with Yes/No values.

Once the `Question` objects are in the knowledge base and some event changes their state, such as an `Answer` object being inserted into the knowledge base, other rules that have them as an antecedent will fire which we can use to add yet more questions, facts, or recommendations into the knowledge base, for example:

```
rule "everyone should get at least 2 hours of exercise per week"
dialect "mvel"
when
  // if there is a Question with id==exercise and answer is false, then…
  Question(id == "exercise", answer == false);
then
  // display a note to the user that…
  insertLogical(
       new Note(
             "exerciseNote",
             "You should exercise at least 2 hours per week."
       )
  );
  // and give them a new exercise recommendation to be displayed on complete
  insertLogical(
       new ExerciseRecommendation(
             "needToStartExercising",                    // recommendation id
             Priority.HIGH,                              // priority
             "You should start an exercise regiment.",   // text to show
             new Source(                                 // link to source
                   "http://www.cdc.gov/physicalactivity/everyone/guidelines/adults.html",
                   "Physical Activity for Everyone: Guidelines: Adults"
             )
       )
  );
end
```

4 eDietitian Usage

The following section describes how eDietitian can be used, illustrated using screen-shots of the eDietitian system through various stages of the consultation session.

Once a user starts the questionnaire, he/she is asked some initial information, as shown in Figure 4, which is used to determine the user's Body Mass Index (BMI), Basal Metabolic Rate (BMR), and weight type (underweight, normal, overweight, obese). Next, the user is presented with questions which gather information on exercise, as illustrated in Figure 5, and high-risk conditions including tobacco use and alcohol use. After this point in the conversation, the user's answers lead him to individually-determined questions based on their specific responses to the previous questions. This would mimic the way a doctor's consult would proceed – dynamically – from question to question. At the end of the session, the system displays the results of the questionnaire, and the user's exercise, eating and any other recommendations are displayed in a jQuery "accordion" widget, as depicted in Figure 6.

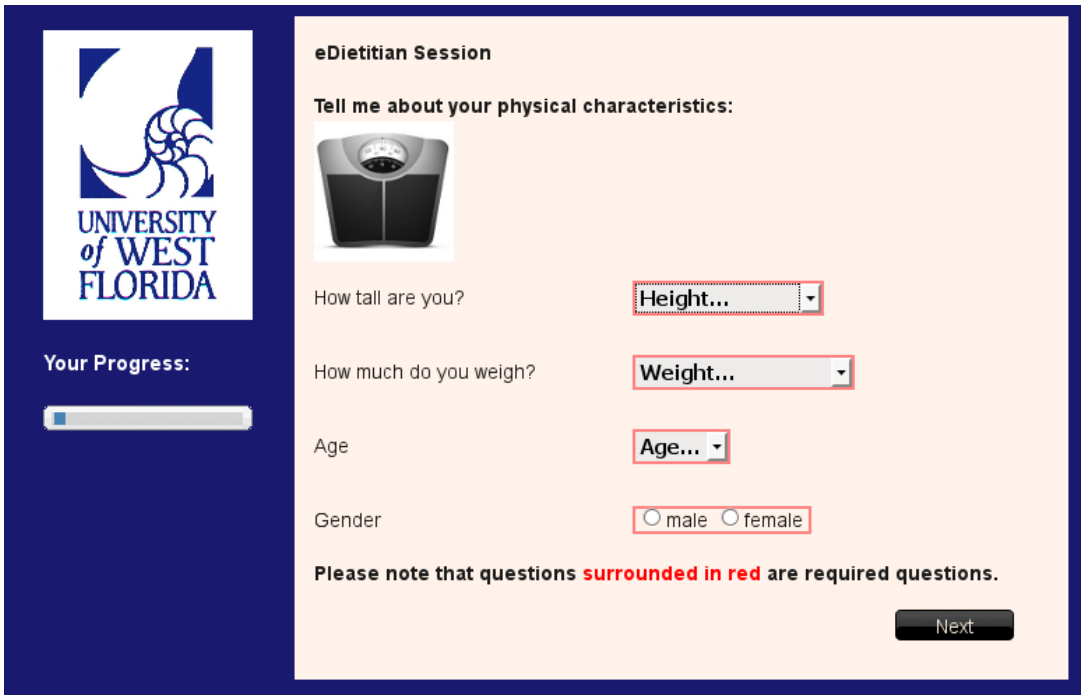

Figure 4 The initial screen of eDietitian gathers some initial information from the user.

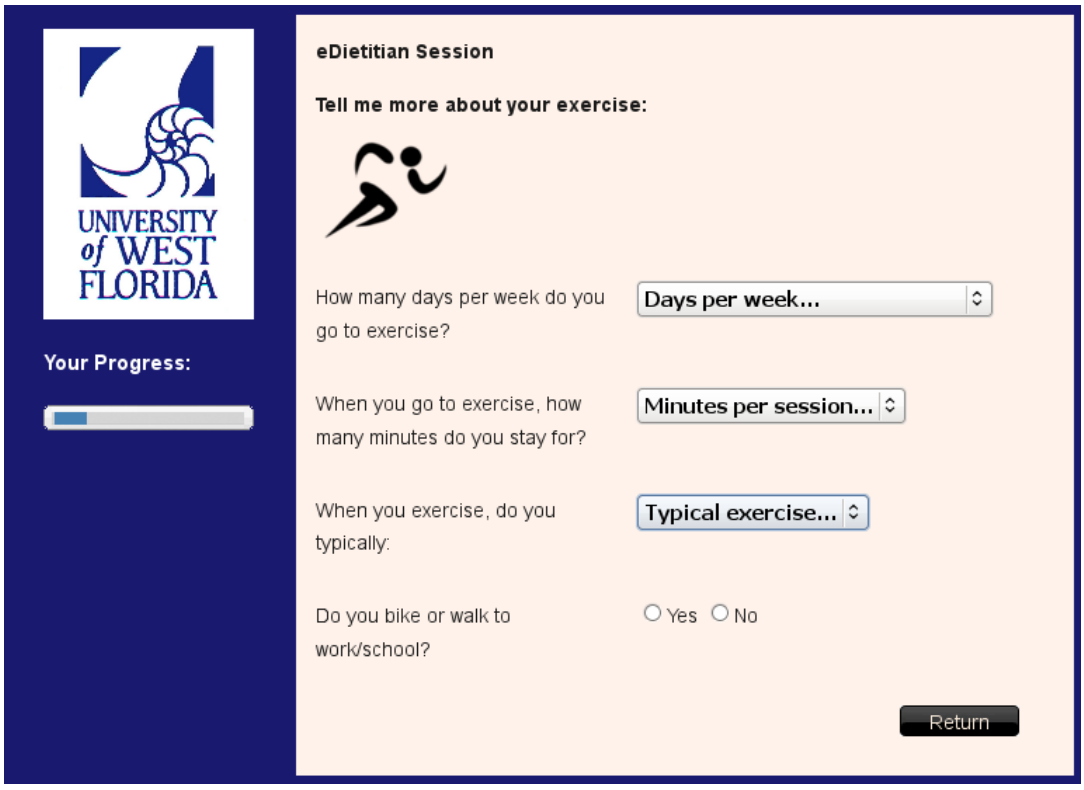

Figure 5 eDietitian asks questions related to the user's exercise output (used to calculate BMR).

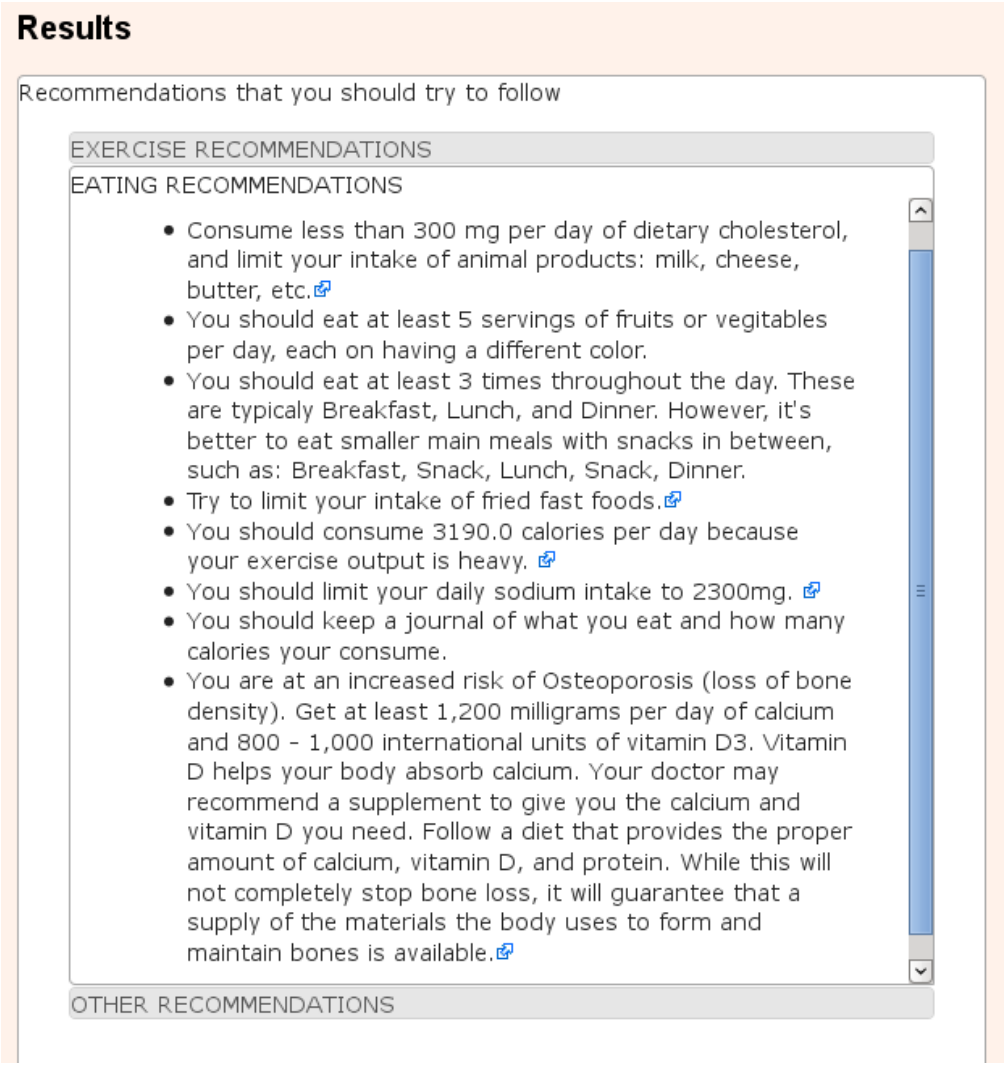

Figure 6 eDietitian shows the results of the questionnaire, along with the user's exercise, eating and any other recommendations. The blue arrow at the end of each recommendation is a hyperlink to the source of the rule, and a "tooltip" shows the reference when the user hoovers over it.

5 Review and Quality Assurance

One of the most vital issues that may impact the usability and successfulness of an expert system is the accuracy of the knowledge which it encodes. The knowledge base for the eDietitian system was based on trustworthy information from US Government sources, including the U.S. National Library of Medicine [12], the "Dietary Guidelines for Americans" from the US Department of Agriculture [13], and the Center for Disease Control's Obesity and Overweight website. Also, for review and quality assurance, a licensed dietitian was contracted to review the system. The review involved periodic live feedback sessions with the licensed dietitian, during which the developer and dietitian would go through the system screen-by-screen and inspect the wording, flow, correctness, and usability of the system.

The review followed a cyclic model, where the developer would revise the system based on the dietitian's feedback, and then have another feedback session with the expert. Cyclic reviews were performed four times until the dietitian's feedback was fully incorporated.

6 Conclusions and Future Work

This paper presents the development of a TeleHealth system called eDietitian, a system built using an open source web-based expert system framework called Tohu. TeleHealth systems are an emerging method of delivering health services to patients and have been

shown to perform quite well [1]. The system uses a rule-based approach to provide individualized diet and health recommendations to users, based on completion of a simple auto-reporting questionnaire. A comparison was given between this system and similar systems. The architectural design and implementation were described, as well as usage of the system. This project demonstrates how a complex web-based expert system can be easily constructed using open source tools such as Tohu and Drools. eDietitian uses a web-based approach and leverages existing tools to make dietitian consultations more accessible to a larger audience.

Opportunities for future work include extending the system to allow for display of video resources and selections based on pictures. These enhancements would help make the questionnaire more user-friendly, and potentially increase system usability. In addition, the user interface can be refined by adding related pictures and video content that explain conditions clearly using rich content. Another potential path for future work is the addition of an explanation facility that could provide additional information to users about why certain recommendations were given.

7 References

[1] Digenio AG, Mancuso JP, Gerber RA, Dvorak RV. Comparison of methods for delivering a lifestyle modification program for obese patients: a randomized trial. Annals Internal Medicine. 2009 Feb 17; 150(4):255-62. http://www.ncbi.nlm.nih.gov/pubmed/19221377

[2] Tate DF, Wing RR, Winett RA. Using Internet technology to deliver a behavioral weight loss program. Journal of the American Medical Association. 2001 Mar 7; 285(9):1172-7. http://www.ncbi.nlm.nih.gov/pubmed/11231746

[3] Haugen HA, Tran ZV, Wyatt HR, Barry MJ, Hill JO. Using TeleHealth to increase participation in weight maintenance programs. Obesity (Silver Spring). 2007 Dec; 15(12):3067-77. Center for Human Nutrition, University of Colorado Health Sciences Center, Denver, Colorado, USA. http://www.ncbi.nlm.nih.gov/pubmed/18198316.

[4] Center for Disease Control. "Obesity – At a Glance" http://www.cdc.gov/chronicdisease/resources/publications/AAG/obesity.htm as viewed September 2012

[5] Katherine M. Flegal, Margaret D. Carroll, Cynthia L. Ogden, Lester R. Curtin. Prevalence and Trends in Obesity among US Adults, 1999-2008. *Journal of the American Medical Association. 2010; 303(3):235-241. Published online January 13, 2010. doi: 10.1001/jama.2009.2014.* http://jama.ama-assn.org/content/303/3/235.full?ijkey=ijKHq6YbJn3Oo&keytype=ref&siteid=amajnls

[6] Obesity and Overweight for Professionals: Health Consequences. http://www.cdc.gov/obesity/causes/health.html

[7] Tohu. http://www.jboss.org/tohu as viewed September 2012

[8] Drools. http://www.jboss.org/drools as viewed September 2012

[9] WebMD's Personal Diet Evaluator. http://www.webmd.com/diet/diet-health-check/default.htm

[10] Donald Rose, Stephan Meershoek, Carina Ismael, and Margaret McEwan. Evaluation of a rapid field tool for assessing household diet quality in Mozambique. Food and Nutrition Bulletin, vol 23, No. 2. United Nations University Press. 2002. http://archive.unu.edu/unupress/food/fnb23-2.pdf#page=65

[11] Tamara Denning, Adrienne Andrew, Rohit Chaudhri, Carl Hartung, Jonathan Lester, Gaetano Borriello, Glen Duncan. BALANCE: Towards a Usable Pervasive Wellness Application with Accurate Activity Inference. HotMobile '09. Proceedings of the 10th workshop on Mobile Computing Systems and Applications. ACM. New York, NY, USA 2009. doi:10.1145/1514411.1514416

[12] http://www.ncbi.nlm.nih.gov/pubmedhealth/ - PubMed Health, from the U.S. National Library of Medicine

[13] Dietary Guidelines for Americans, 2010: http://www.cnpp.usda.gov/Publications/DietaryGuidelines/2010/PolicyDoc/PolicyDoc.pdf

[14] http://www.cdc.gov/obesity/index.html – CDC's Obesity and Overweight main site

Computerized Clinical Decision Support in a Hospital Information System

Christian J. Schuh, Walter Seeling
Center for Medical Statistics, Informatics and Intelligent Systems (CeMSIIS),
Medical Expert and Knowledge-Based Systems,
Medical University of Vienna, Spitalgasse 23,
A-1090 Vienna, Austria

Abstract - *Since the big potential of medical decision making was first realized, hundreds of articles introducing Clinical Decision Support Systems (CDSSs) have been published in the last three decades. But even today, only few systems are in clinical use. Even fewer are in use outside their site of origin, and their full potential for optimizing the healthcare system is far from realized.*
Clinician's acceptance and utilization of CDSSs depends on its workflow-oriented, context-sensitive accessibility, and availability at the point of care, integrated into a Hospital Information System (HIS). Commercially available HIS often focus on administrative tasks and mostly do not provide additional knowledge based functionality. This paper works out advantages and disadvantages of several approaches and compares them against possible alternatives. Finally, experiences, gained by clinical use of two introduced systems, integrated in the HIS of the Vienna General Hospital, to analyze the little use of CDSSs in today's clinical routine practice.

Keywords: Clinical decision support, Hospital Information Systems, Knowledge Acquisition, Medical Applications.

1 Introduction

In modern health care environment, the amount of information available is very large, and in order to manage it computers are used in medicine in almost all areas. It is generally assumed that every patient generates around 20,000 different data values on a daily base. Over 236 different variable categories in a medical ICU record are common and conclude that this far exceeds human intellectual capability [1]. Physicians and nurses are still performing time consuming manual data analysis for making the most optimal medical decision for each individual patient [11-13]. They must choose from and interpret a huge variety of clinical data, while facing pressure to decrease uncertainty, risks to patients and costs. The true essence of healthcare delivery is decision making - what information to gather, which tests to order, how to interpret and integrate this information into diagnostic hypotheses and what treatments to administer. Moreover, current ICU platforms are not offering an infrastructure for infection surveillance, data-driven guidance and modeling of critical illness.

The provisioning of Clinical Decision Support Systems (CDSSs) would enable the discovery of patterns in health data which might be important for the fight against nosocomial infections, incorrect diagnosis, unnecessary prescriptions, and improper use of medication.
Since the potential of medical decision making was first realized, hundreds of articles introducing CDSSs have been published in the last three decades. But over the years' experience has shown that the expectations were not always fulfilled. Even today, only few systems, so asserted, are in clinical use. Even fewer are in use outside their site of origin, and their full potential for optimizing the healthcare system is far from realized.
Shortliffe [20] outlines, that ''the greatest barrier to routine use of decision support by clinicians has been inertia; systems has been designed for single problems that arise infrequently and have generally not been integrated into the routine data-management environment for the user''.
The Clinicians' acceptance and utilization of CDSSs depends on its workflow-oriented, context-sensitive accessibility and availability at the point of care, integrated into a Hospital Information System (HIS). Commercially HIS often focus on administrative tasks and mostly do not provide additional knowledge based functionality [33, 36]. This paper surveys on two concrete applications the capabilities as well as limitations of CDSSs. Both presented systems are established as real-time applications. They are fully integrated in the HIS, and have reached the state of extensive clinical testing at the Vienna General Hospital. Finally, experiences, gained by clinical use of the systems, are used to analyze the little use of CDSSs in today's clinical routine practice.

2 Methods

2.1 Clinical Decision Support Systems (CDSS)

CDSS can be broadly defined as software applications that integrate patient data with a knowledge-base and an inference mechanism to produce patient specific output in the form of care recommendations, assessments, alerts and reminders to actively support practitioners in clinical decision-making.
Generally CDSS are any type of application that support the decision making process. A generic DSS receives a certain

amount of data as input, processes it using a specific methodology and offers as a result some output that can help the (physicians) decision-makers. A typical therapeutic cycle in a simplified view is shown in Fig.1.

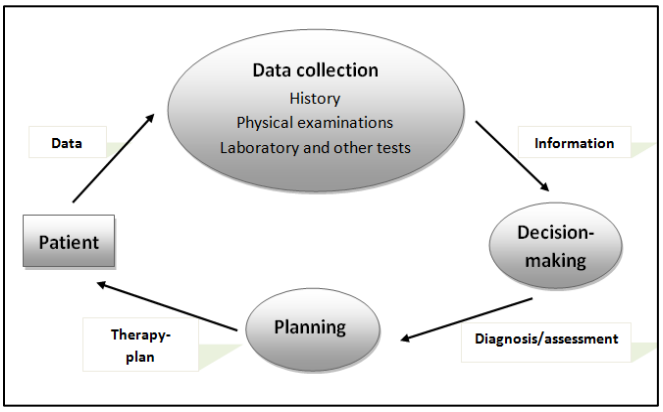

Fig. 1: The Diagnostic-Therapeutic Cycle (a simplified view)

In principle a DSS can be classified into the following six frameworks [22]: Text-, Database-oriented, Spreadsheet-oriented, Solver-oriented, Rule-oriented, and into a Compound DSS. A compound DSS is the most popular classification for a DSS [37, 38]. It is a hybrid system that includes two or more of the five basic structures of DSSs. Patient data can be input by digital entry, queried from a HIS, Patient Data Management Systems (PDMS) or transmitted from other medical devices. Patient data are compared against a knowledge-base and made sense of by an inference mechanism. The inference mechanism can be highly variable in sophistication ranging from simple 'if Rules 'Yes' or 'No' and 'If 'Then', 'Else' statements to Bayesian prediction techniques and/or with fuzzy logic [8], [21]. Expert or knowledge-based systems are another type of DSS capable of being programmed to perform decision making at the level of a domain expert [24]. These systems represent the most prevalent type of CDSS used in medical clinical practices today. Though CDSSs can include different components, and though domain knowledge can be structured in a variety of ways, certain elements are common to all: *a user interface, a knowledge base, a database*, a knowledge acquisition facility, and an *inference mechanism*. In the next section two CDSSs integrated via web services in a HIS are presented. Both systems are established as real-time applications and have reached the state of extensive clinical testing at the Vienna General Hospital. The first one is to hyperglycemia management system for critically ill surgical patients. The second gives immune-suppressive therapy for kidney-transplant patients.

2.2 Maintaining Hyperglycemia

Hyperglycemia has been shown to be an independent risk factor of mortality in patients with stroke and myocardial infarction. There is increasing evidence that tight blood glucose (TBG) control improves outcomes in critically ill adults. Furthermore, strict control of hyperglycemia reduces the rates of infectious complications in surgical Intensive Care Unit (ICU) patients. The risk of mortality or significant morbidity is high among critically ill patients who are treated in the Intensive Care Unit (ICU) for more than 5 days. These patients are susceptible to sepsis, excessive inflammation and multiple organ failure, the latter often being the cause of death. Most intensive care patients, even those who did not previously suffer from diabetes, are hyperglycemic.

Hyperglycemia caused by insulin resistance in the liver and muscles is common in intensive care patients [2]. Van den Berghe showed that Tight Glycemic Control (TGC) i.e. Controlling Blood Glucose Levels (BGLs) within 80–110 mg/dl using intensive insulin therapy, provides significant improvement in mortality (8 to 4.6%) and morbidity in surgical ICU patients.

Several published clinical trials have demonstrated morbidity and mortality benefits of moderate-to-tight glycemic control in an intensive care environment [3, 4], [6], [9, 10].

Tight Glycaemic Protocols:

The tight management of hyperglycaemic crises requires expensive and labor-intensive procedures that are not achievable in all clinical settings. The currently implemented algorithm for achieving and maintaining hyperglycemia and the used tight glucose protocol at our hospital's ICU is shown in Table I.

Table I: Algorithm for archiving and maintaining normo- glycemia in the ICU

Test	Result of BG measurement	Action
Measure BG an admission to ICU	> 220 mg/dl	Start insulin 2 – 4 | U/h
	220 – 110 mg/dl	Start insulin 1 – 2 | U/h
	< 110 mg/dl	Don't start insulin but continue BG monitoring every 4 h
Measure BG every 1 -2 h until in normal range	> 140 mg/dl	Increase insulin dose by 1 – 2 | U/h
	110 – 140 mg/dl	Increase insulin dose by 0.5 – 1 | U/h
	approaching normal range	Adjust insulin dose by 0.5 – 1 |U/h
Measure BG every 4 h	approaching normal range	Adjust insulin dose by 0.5 – 1 |U/h
	normal	Insulin dose unchanged
	falling steeply	Reduce insulin by half and check more frequently
	60 -80 mg/dl	Reduce insulin dose and check BG with 1 h
	40 – 60 mg/dl	Stop insulin infusion, assure adequate baseline glucose intake and check BG within 1 h
	< 40 mg/dl	Stop insulin infusion, assure adequate baseline glucose intake, administer glucose per 10 g IV boluses and check BG with 1h

In general protocols to assist in management of hyperglycemia are becoming more widely used and have been shown to improve outcomes for hyperglycemic patients. Several protocols for glucose control have been adapted [7], [25, 26], [28]. In a pilot study [5] was found that the majority

of patients were not achieving target BGL consistently and although the incidence of hypoglycemia was rare, the range of insulin infusion rates prescribed was often greater than patient requirements presenting a risk of overdose. This audit aims to further assess the success and safety of TGC in ICU [7].
As with any protocol, this algorithm alone does not guarantee improvement in quality of care or clinical outcome. However, in the context of the treating physician's knowledge and experience, this approach could be expected to realize significant reductions in mortality and morbidity.

2.3 Immune-Suppressive Therapy for Kidney Transplant Patients

Many chronic kidney disease patients profit from a kidney transplantation. A necessary component after transplantation is an immunosuppressive therapy. As there is a narrow range between kidney transplant rejection and the side effects of over-immune-suppression (such as an increased vulnerability to infections), therapeutic drug monitoring is another necessary component [11].

The most frequently used immune-suppressive drugs are Calcineurin inhibitors, which inhibit the cell-mediated and humoral immune responses. One of those is Tacrolimus. Since the drug absorption rate varies, close therapeutic drug monitoring is necessary. According to Satohiro [14] the therapeutic range of Tacrolimus is located between 10-20ng/ml blood concentration to avoid rejection and infections. These Calcineurin inhibitors have many side effects, one of the most popular include reversible disturbances of liver function, cardiac toxicity, edema, blurred vision, depression, sleep disturbances and nephrotoxicity, neurotoxicity, and hyperglycemia [15, 16].
Currently the immunosuppressant dosage is determined on the basis of the actual medication level and various factors (immunological situation, time after transplant rejection reactions, laboratory values, etc.). The ultimate goal is to develop a theoretical model that maps the therapy with their influencing factors [16]. A theoretical model of the dosage determination will enable physicians to gain new insights into the treatment monitoring of immunosuppressive drugs and potentially enable automation of drug dosing.

2.3.1 Data Description

To create a immune-suppressive therapy model historical patient therapy data and laboratory parameters could be used within a period of 13 years from the General Hospital of Vienna. Data from 492 patients and 13.053 consequent examination dates were available for evaluation. These data include the measured blood levels of the administered medication and the daily medications, as well as the time of the medication measured and medication administered.

2.3.2 Data Processing and Analysis

In current clinical praxis, medication adaptations are based on preliminary medication levels and other characteristics of the patients.

Consequentially, medication adaptation and preliminary data have a strong correlation, thereby confounding each other. This makes a simple estimate of the effect of a medication adaptation almost impossible. The problem is illustrated in Figure 2 (left side), where in the x-axis (-1) means to adjust down, (0) to stay and (1) to adjust upward medication. The boxplot shows that if you lower the medication, a higher medication level could be expected.
Avoid using too many capital letters. All section headings including the subsection headings should be flushed left.

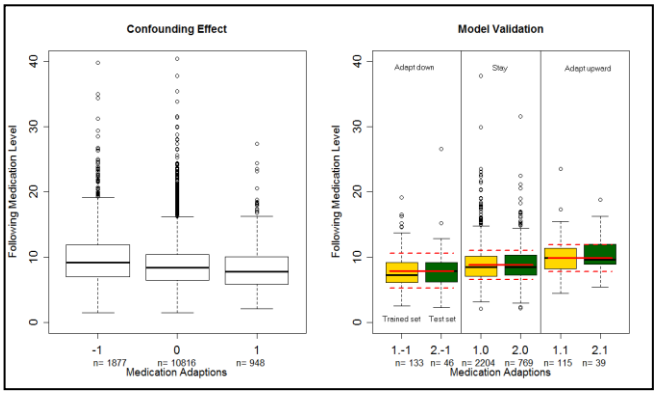

Fig. 2: Confounding Effect & Validation

This could be explained by the fact that physicians only lower the medication if the medication level is already quite high, but this action generally does not completely normalize the medication level. The main problem is to obtain the pure biological response of the patients. Since only a few medication adaptations are frequent, these were divided into three categories: upward adaptations (1), down (-1) and retention of the medication (0).

3 Conclusions

3.1 Technical Aspects

There are many different methodologies that can be used by a CDSS in order to provide support to the health care professional.
In our case the inference mechanism, i.e. a set of rules derived from the physician's (experts) and evidence-based medicine, and the knowledge base itself, are implemented through medical logic modules (MLMs) based on a language such as Arden syntax [18]. The Arden Syntax Server represents therefore the reasoning and inference mechanism with MLMs and processes the patient data, which is received from the HIS via web services. The communication mechanism of a CDSS will allow the system to show the results to the users as well as have input into the system. The HIS at the General Hospital of Vienna is i.s.h.med. This fully featured HIS represents the CDSS- communication mechanism. It provides a framework for medical documentation which can be easily customized in form of parametric medical documentation (PMD) to the special needs of the respective clinical departments.

3.2 Hyperglycemia Decision Support System

The communication mechanism of the CDSS is realized as a PMD of the HIS. The system is used for postoperative cardiac patients in an ICU at the Vienna General Hospital [29]. The advantages of the system are its easy application and generation of more specific knowledge bases with MLMs, which allow smoother treatment.
The CDSS is currently being tested with a sample of prospective randomized cases currently undergoing treatment (Fig. 3).

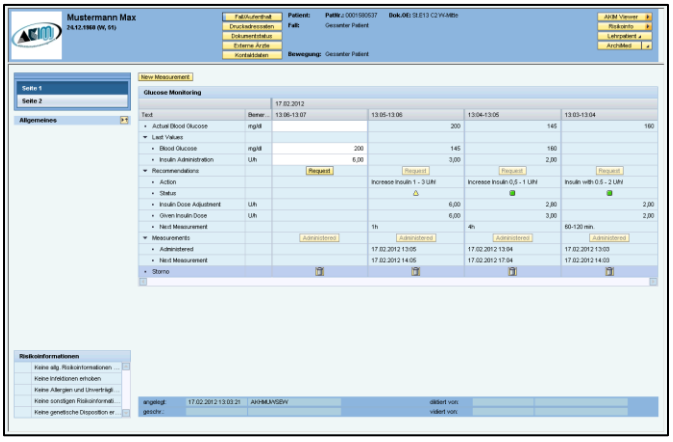

Fig. 3: HDSS Application

The results confirm the applicability of the application to represent medical knowledge, thus rendering the glycaemic process transparent and comprehensible. A direct connection, for instance with an insulin perfusion pump, would allow smooth adaptation continuously. The hyperglycaemic control may be better if appropriate safety controls can also be put in place. Safe implementation of tight glycemic control requires appropriate monitoring to reduce the risk of this complication [39]. Several protocols for glycemic control have been adapted [5], [9, 10], [25], [27], [32]. In a pilot study could be found that the majority of patients were not achieving target BGL consistently and although the incidence of hypoglycemia was rare, the range of insulin infusion rates prescribed was often greater than patient requirements presenting a risk of overdose. This audit aims to further assess the success and safety of TGC in ICU [32].
Alerts are triggered within several time depended columns of the application. The actual values and proposals and alerts are displayed in different coloured symbols.
Currently the implemented colours are red, yellow and green. These colours represent an urgent, a warning, and an information level (Fig. 4). If there is no reaction within a defined time period, i.e. column on an urgent (red) information level an acoustic alarm is activated also to force an urgent reaction.
With the control unit itself it's possible to change the glucose level, according to the proposals of the program. If different settings to the proposed one have to be set, there is also a possibility to log this information. The logging feature allows a fine tuning of the knowledge bases off line.

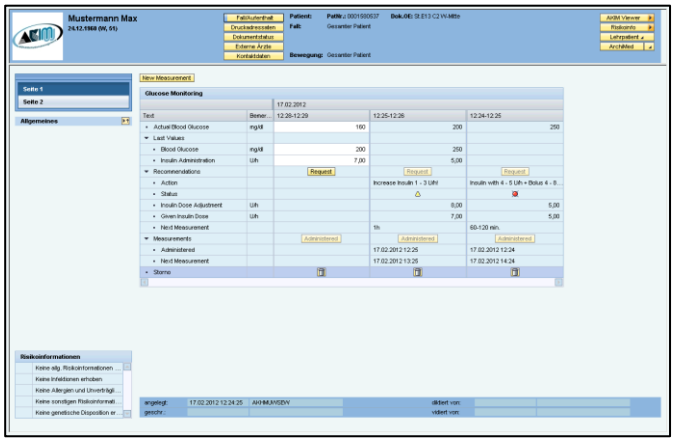

Fig. 4: HDSS alert screen

3.3 Immunosuppression Therapy System

To create a knowledgebase for immunosuppression therapy the medication blood level thresholds has been estimated statistically by a regression tree. Since this is an ordinal outcome variable, the method of Conditional Inference Trees (CITs) [17] has been chosen. Classes could be formed where the statistical relationship between preliminary data and the medication adaption isn't longer significant. The determined classification is shown in Table II.

Table II: Classification determined from the CIT

Class	BL	Additional Decision Parameters
1	≤3.8	
2	(3.8,4.7]	TSS: ≤27153
3	(3.8,4.7]	TSS: >27153
4	(4.7,6.9]	TSS: ≤6490
5	(4.7,6.9]	TSS: (6490,49281]
6	(4.7,6.9]	TSS: >49281
7	(6.9,9.3]	TSS: ≤4544
8	(6.9,9.3]	TSS: >4544
9	(9.3,10.9]	TSS: ≤34018
10	(9.3,10.9]	TSS: >34018
11	(10.9,13.9]	APR: ≤7.5 & PRO: 0,1,2
12	(10.9,13.9]	APR: ≤7.5 & PRO: 3,4
13	(10.9,13.9]	APR: >7.5
14	>13.9	LT: ≤2
15	(13.9,15.2]	LT: >2
16	>15.2	LT: >2

The CIT took the following parameters into account: Tacrolimus blood level (BL) [ng/dl] now and at the last ward round [ng/dl]. The dose of the proliferation inhibitor [mg], of the additional Aprednisolon (APR) [mg] and of the last Tacrolimus (LT) [mg] administered. Further parameters are sex, age at – and time since surgery (TSS) [h]. A model validation was performed with 80% of the data for the training set and 20% for the test set. To test the model, the ensuing medication blood levels were compared to the respective medication adaption [23].
The CIT formed homogenous classes to eliminate the confounding effect. When we performed model validation for one of the calculated groups, the distribution behave largely

normal. The box plot has a prediction interval with a coverage probability of 80%. Out of these consolidated finding knowledge could be developed through MLMs. A specific PMD of the HIS i.s.h.med acts as communication mechanism for the CDSS.
The application, shown in Figure 5 is in evaluation since June 2011.The results have to be seen as a first approach of more accurate forecasting models for the medication blood level of the respective medication.

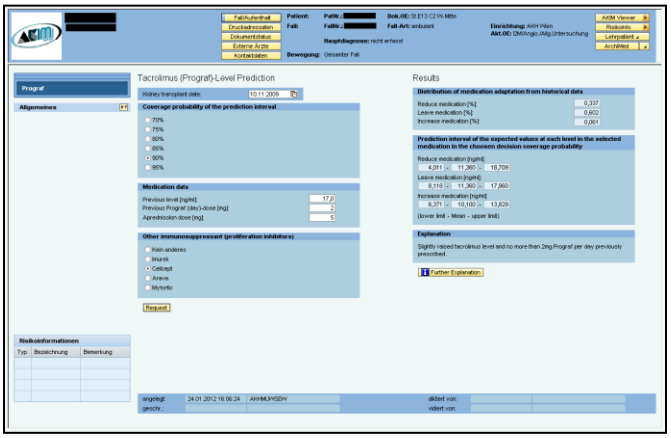

Fig. 5: Application (PMD) in i.s.h.med

The next step could be to add weights, data of rejections or other covariates, which may be able to improve the model even further.

4 Conclusions

When CDSS or DSS in general where initially developed, each knowledge base and inference mechanism required programming before the knowledge base content could be written. As the field evolved, researchers found that it was possible to separate the inference mechanism from the domain specific knowledge and databases. This key design feature became responsible for the commercial success of decision support systems.
Producing standard inference mechanism and knowledge bases made it possible to unplug one knowledge base and then connect a different one. Based on the literature, current computer-based clinical CDSS are limited in application. Roughly seventy known proprietary medical CDSS exists. Only ten out of seventy CDSSs geared towards routinely use. There is no information available about a real daily average usage of these systems.
A well-designed CDSS should have the potential to assist physicians who can and do use it as often as possible in the daily routine work. In some situations physicians learns from using a CDSS about criteria, facts or process issues that need to be considered in a specific decision situation. CDSSs encourage and promote "rationality" in decision making. CDSSs are intended to support not replace physicians, so the users need to consciously interact with a CDSS to use it effectively.
A big issue is that the expectation needs to be created that the physicians are the ultimate authority and that the physicians can anytime "over rule" or choose to ignore analyses and recommendations of the CDSS.
The greatest anticipated benefit of a CDSS lies in the constituency and uniformity in applying decision criteria of a given situation. Physicians have difficulty making decisions because they cannot exhaustively consider every factor relevant to the decision, due to either limited memory or limited information.
Anticipated limitations of CDSSs are that an optimal physician's treatment requires that physicians be able to have the following information, in real time, if possible: What is happening right now? What will happen in the future? What do I need to create the future I want? To answer these questions effectively, physicians requires data that are factual, factual inferential (why type questions) and predictive (what if questions). To date, the best support that a CDSS has been able to provide is data that answer factual and maybe some forms of predictive questions [30], [35], [39].
Physicians have no shortage of data available to them. Thus, physicians have found that currently available CDSSs are not able to meet their more complex information needs. As mentioned above one big argument of the rare utilization at this time is that most of the CDSSs have not progressed beyond the prototype stage. There are no standards or universally accepted evaluation or validation methodologies to ensure that the system's knowledge base is complete and correct.
Further questions about CDSSs are: Does the use of a CDDS improve the quality of decisions produced? And are the economic or other benefits, as for instance patients comfort, attributable to the use of the CDSS?
The absence of a well-defined or universal evaluation methodology makes these questions difficult to answer. To date, an examination of the literature indicates that there is virtually no information available related to the cost or cost effectiveness of CDSSs. Most of the CDSSs are university-based developments, and still in prototype stage. These costs regarding the initial investment of CDDSs tend to be hidden and therefore difficult to access.
This frightens or hinders the industry's interest in funding and encouraging the development of CDSSs in health care in general [19]. Still, many physicians have a real positive outlook on the potential for these systems, particularly relating to practitioner performance. However, until the use of CDSS is a routine as the use of the blood pressure cuff, it is important to be sensitive to resistance to using these systems.

5 References

[1] B. Kaplan, Evaluating informatics applications-clinical decision support systems literature review, Int. J. Med. Inform.64 (2001) 15-37.

[2] Laver S, Preston S, Turner D et al. Implementing Intensive Insulin Therapy: Development and Audit of the Bath Insulin Protocol. Anaesth Intensive Care 2004; 32: 311-316

[3] Wilton P. Policy and procedures on Intensive Insulin Therapy in Critical Care. Royal Brompton & Harefield NHS Trust. February 2004.

[4] Van den Berghe G, Wouters P, Weekers F et al. Intensive Insulin Therapy in Critically Ill Patients NEJM 2001; 45 (19): 1359 – 1367

[5] Van den Berghe G, Wouters PJ, Bouillon R, et al. Outcome benefit of intensive insulin therapy in the critically ill: insulin dose versus glycaemic control. Crit Care Med 2003;31: 359-66.

[6] Malmberg K, the DIGAMI Study Group: Prospective randomized study of intensive insulin treatment on long term survival after acute myocardial infarction in patients with diabetes mellitus. *BMJ* 314:1512–1515, 1997

[7] Furnary AP, Gao G, Grunkemeier GL, Wu Y, Zerr KJ, Bookin SO, Floten HS, Starr A: Continuous insulin infusion reduces mortality in patients with diabetes undergoing coronary artery bypass grafting. *J Thorac Cardiovasc Surg* 125:1007–1021, 2003.

[8] Zadeh, L. A.: Fuzzy Sets. *Information and Control*, 8, 1965, pp. 338-353.

[9] Vogelzang M, Zijlstra F, Nijsten MW: Design and implementation of GRIP: a computerized glucose control system at a surgical intensive care unit. *BMC Med Inform Decis Mak* 2005;5:38.

[10] Vogelzang M, Nijboer JM, van der Horst IC, et al.: Hyperglycemia has a stronger relation with outcome in trauma patients than in other critically ill patients. *J Trauma* 2006; 60:873-7.

[11] B.C. Delaney, Can computerized decision support systems deliver improved quality in primary care, Br. Med. J. 319 (1999) 1281—1282.

[12] K. Kawamoto, C.A. Houlihan, E.A. Balas, D.F. Lobach, Improving clinical practice using clinical decision support systems: a systematic review of trials to identify features critical to success, BMJ 330 (7494) (2005) 765.

[13] A.X. Garg, N.K. Adhikari, H. McDonald, M.P. Rosas-Arellano,P.J. Devereaux, J. Beyene, et al., Effects of computerized clinical decision support systems on practitioner performance and patient outcomes: a systematic review ,JAMA 293 (10) (2005) 1223–1238.

[14] Satohiro M, Ken-Ichi I. An update review on individualized dosage adjustment of calcineurin inhibitors in organ transplant patients. Pharmacology & Therapeutics. 2006; 112(1): 184-198

[15] Ho S, Clipsone N, Timmermann L, et al. The Mechanism of Action of Cyclosporin A and FK506. Clinical Immunology and Immunopathology. 1996; 80(3): 40-S45

[16] Seeling W. Computergestützte Therapieplanung von Immunsuppressiva bei Patienten mit Nierentransplantation. Vienna: Masterthesis, 2011

[17] Hothorn T, Hornik K, Zeileis A. Unbiased Recursive Partitioning: A Conditional Inference Framework. Journal of Computational and Graphical Statistics. September 1, 2006; 15(3): 651-674

[18] Adlassnig KP, Rappelsberger A. Medical knowledge packages and their integration into health-care information systems and the World Wide Web. MIE 2008; S121-126.

[19] Mueller ML, Ganslandt T, Eich HP, Lang K, Ohmann C, Prokosch HU: Towards integration of clinical decision support in commercial hospital information systems using distributed, reusable software and knowledge components. *Int J Med Inform* 2001, 64(2-3):369-377.

[20] E.H. Shortliffe, Knowledge-Based Systems in Medicine MIE 1991 Proceedings, Springer, Berlin, 1991, pp. 5–9.

[21] Zadeh, L. A.: Biological Applications of the Theory of Fuzzy Sets and Systems. *The Proceedings of an International Symposium on Biocybernetics of the Central Nervous System*. Little, Brown and Company: Boston 1969, pp. 199-206.

[22] Eddy D. M., Clinical decision making from theory to practice: a collection of essays from the Journal of the American Medical Association. Sudbury, MA: Jones and Bartlett; 1996.

[23] Long W. The Probability of Disease. In: *Symposium on Computer Applications in Medical Care*. IEEE, 1991:619–623.

[24] Spiegelhalter D. J., Bayesian Analysis in Expert Systems. MRC Biostatistics Unit, Institute of Public Health, Cambridge, 1992.

[25] Levkovich B.: An Audit of the Success and Safety of an Intensive Insulin Therapy Protocol in Adult Intensive Care. Personal Communication.

[26] Wilton P. Policy and procedures on Intensive Insulin Therapy in Critical Care. Royal Brompton & Harefield NHS Trust. February 2004.

[27] Malmberg K, the DIGAMI Study Group: Prospective randomized study of intensive insulin treatment on long term survival after acute myocardial infarction in patients with diabetes mellitus. *BMJ* 314:1512–1515, 1997

[28] Markovitz LJ, Wiechmann RJ, Harris N, Hayden V, Cooper J, Johnson G, Harelstad R, Calkins L, Braithwaite SS: Description and evaluation of a glycemic management protocol for diabetic patients undergoing heart surgery. *Endocr Pract* 8:10–18, 2002

[29] W. Seeling, M. Plischke, Ch. Schuh,: Knowledge-Based Tacrolimus Therapy for Kidney Transplant Patients. Medical Informatics Conference, MIE 2012 Proceedings, Springer, Berlin, 2012

[30] R. Goud, N.F. de Keizer, G. ter Riet, J.C.Wyatt, A. Hasman, I.M. Hellemans, et al., Effect of guideline based computerized decision support on decision making of multidisciplinary teams: cluster randomized trial in cardiac rehabilitation, BMJ 338 (2009) b1440.

[31] Morris A: Computerized protocols and bedside decision support. Crit Care Clin 15: 523-545, 1999.

[32] Lowe A, Jones RW, Harrison MJ. A graphical representation of decision support information in an intelligent anaesthesia monitor. Artif Intell. Med 2001; 22:173–91.

[33] Shojania KG, Grimshaw JM: Evidence-based quality improvement: the state of the science. *Health Aff. (Millwood)* 2005, 24(1):138-150.

[34] Tierney WM: Improving clinical decisions and outcomes with information: a review. *Int J Med Inf* 2001, 62(1):1-9.

[35] Perreault L, Metzger J. A pragmatic framework for understanding clinical decision support. Journal of Healthcare Information Management. 1999;13(2):5-21.

[36] Trivedi MH, Kern JK, Marcee A, Grannemann B, Kleiber B, Bettinger T, Altshuler KZ, McClelland A. Development and implementation of computerized clinical guidelines: barriers and solutions. Methods Inf Med. 2002;41(5):435-42.

[37] Wong HJ, Legnini MW, Whitmore HH. The diffusion of decision support systems in healthcare: are we there yet? J Healthc Manag. 2000 Jul-Aug;45(4):240-9; discussion 249-53.

[38] Fieschi M, Dufour JC, Staccini P, Gouvernet J, Bouhaddou O. Medical decision support systems: old dilemmas and new paradigms? Methods Inf Med. 2003;42(3):190-8.

[39] D. C. Classen. Editorial: Clinical Decision Support Systems to Improve Clinical Practice and Quality of Care. J Amer Med Assoc. Vol. 280 No. 15, October 21, 1998.

SESSION

COMPLEX NETWORKS, SOCIAL NETWORKS, SENSOR NETWORKS, AND APPLICATIONS

Chair(s)

TBA

Social Network Analysis for Consumer Behavior Prediction

David Alfred Ostrowski
System Analytics
Research and Innovation Center
Ford Motor Company
dostrows@ford.com

Abstract

This paper examines the structural qualities of Social Networks towards the identification of trends. We consider a collection of Twitter messages towards the trending of technologically-related topics. For each individual topic, network cohesiveness is explored over time. We demonstrate that structural qualities reflecting community dynamics can provide insight to the prediction of long term trends. The goal of this work is to lend insight to the characterization of consumer behavior, particularly in the area of technology forecasting.

I. INTRODUCTION

Online Social Networks have increased substantially in recent years with the top Social Media sites acquiring hundreds of millions of users [1][2]. Through the increased accessibility of the internet, these outlets have encouraged users to interact and build relationships. Considered in depth by the sociological community, these relationships are closely compared to those found in real-life society [3]. As such, it has become increasingly important for organizations to understand these networks for the purpose of predictive analytics for internal as well as external application [4][5].

Such networks can be represented as graphs where nodes represent individuals and edges represent their relationships [6]. Given this network representation, prior work has demonstrated that the combined knowledge of community structure and relationship strength has important application to the area of web analytics [7]. In particular, when studied over time, this structural information can be informative towards suggesting what influence it will have on the future.

In the context of community as viewed from the perspective of a graph, there are qualities that are present among people who are highly influential which can be formally considered as power. Being a fundamental property of social structures, it has been suggested that power is relational [10][11]. Through research, a relationship has been established between power and density of a described structure [12].

Influence and power are strongly associated with transformation in the context of a community. Such a phenomenon is termed as emergence and is best described as a local action influencing an overall behavioral pattern. Through the examination of connections, research has also demonstrated that emergence can be objectified [12].

The study of such structural dynamics present strong support to what we know about the predictive nature of the internet [13][14][15]. Currently, a number of examples exist in the relation of trends as compared to the development of patterns [16][17][18]. Such patterns that exist around structures are highly indicative of the concept of communities [19]. These communities have been demonstrated across many studies as integral to the study of sustainability as well as economic opportunities.

The methodology outlined in this paper describes a means of examining the structural qualities within an online community. We apply this methodology to a collection of unstructured communication acquired from a web-based resource (Twitter) [20]. Our three primary inputs include topics of interest, web-based communications as well as the consideration of between whom the communication is directed. Building a graph-based structure based on communication, structural analysis is applied. From here, we examine the relationship over time of the

network structure to that of the interest of the concept.

The remainder of this paper is as follows: In Section Two we detail current work in the field. Section Three provides an examination of our methodology. Section Four presents our case studies and Section Five provides our conclusions.

II. CURRENT RESEARCH

Due to its constrained size and minimalistic attributes, a number of research efforts in Social Analytics have been directed at Twitter as a means of predicting trends. Among such efforts, (Achrekar et. al.) utilized Twitter to assist in the prediction of flu virus trends. This was accomplished by devising auto-regression models to predict data published by the Center of Disease Control (CDC) to the percentage of 'visits' to physicians [21]. (Iyengar et. al.) determined when an event started and ended by analyzing the content of Twitter messages using an SVM classifier and hidden Markov Model. Here, event boundaries in Twitter data were predicted for a set of events in the domains of sports, weather and social activities [22]. (Peng et. al.) demonstrated that conditional random fields could be used to improve prediction effectiveness by incorporating social relationships[23].

Focusing directly on structural qualities, (Gloor, Nann, Schoder) leveraged betweenness centrality of actors by weighing the context of their positions in a network. Through this application, they were able to extract and predict long term trends on the popularity of relevant concepts such as movies and politicians [7]. (Mislove et. al.) analyzed the structure of multiple online social networks. This involved the comparison of in-degree to out-degree representation though the investigation of side-free, power-law and small-world properties [24]. (Cantanese et. al.) applied social network techniques to analyze specific properties of social networking graphs. Among the qualities examined included centrality measurements, scaling laws and distribution of friendship [25].

A substantial amount of research from Link Mining has been leveraged to support Social Network concepts. These algorithms have supported performance among a number of activities including question answering, information retrieval and web-based data warehousing [26]. (Erbs et. al) demonstrated that data volume as well as training data is vital to link discovery with text-based approaches yielding superior results [27]. (Qian et. al) relied on the application of link mining to the Enron mail corpus to determine communities within linked nodes. Further work supported the identification of 'common friends' by relying on clustering. [28] Additional methods have explored link-predicates with applications among exploring data, distributed environments and spam analysis [29][30][31].

Research in Social Networks has also expanded on current search technology including PageRank and HITS [32][33][34]. Building on these methodologies, (Bharat, Henzinger and Chakraborti) proposed variations that exploit web page context to weight pages and links based on relevance.[35][36]. Relying on the topological structure of a graph (Sugiyama et. al.) successfully integrated several methods including network, quantitative, semantic, data processing, conversion and visualization-based components [37].

Investigations in Semantic Web technologies have also greatly affected development in Social Networks. Among them, (Zhou, Chen and Yu) integrated an ontology-based Social Network along with a statistical learning method towards Semantic Web data. This involved utilization of an extended FOAF (friend-of-a-friend) ontology applied as a mediation schema to integrate Social Networks and a hybrid entity reconciliation method to resolve entities of different data sources [38]. (Thushar and Thilagam) also relied on Semantic Web technology for the identification of associations between multiple domains within a Social Network [39].

A number of efforts in Relational Learning have supported Social Network analysis predicated on the concept of homophilly-based associations to support learning. Among them include the application of probalistic modeling [40] collaborative relationship [41] and inference-based approaches [42].

Visualization techniques also provide for a substantial level of support in studying Social Networks. (Batajelj and Mrvar) developed tools for the visualization of large-scale networks allowing for support to identify vertice extracts and relations between clusters [43]. (Noel et. al.) calculated inter-item distances among combinations of elements from which hierarchical clustering dendrograms are visualized to enhance measurement consistency between clusters and frequent itemsets [44]. (Levng et. al.) developed Social Viz which provided users with a means to view frequency relationships among multiple entities in a network [45].

III. METHODOLOGY

Our methodology consists of four key areas: network representation, tie strength, key players and cohesion [46]. To support the generation of a network, we first consider the application of basic data filtering techniques including matching on keywords and hashtags. After the data set is paired

down to a topic or set of topics we construct the networks. Here, all interactions may be considered. Frequently, this is addressed in the form of users who happen to 'follow' or 'like' other users or their communications. A secondary means of edge generation is where a direct (personal) message exists between two entities. This exists in our test case in the form of a 'reply' to an existing post.

From our established network, tie strength is considered to evaluate strength/weakness of edges in our network, both as a means for graph reduction as well as clarity. Several methods are suitable among our data to serve as a proxy for the strength of a tie:

- Frequency of interaction
- Recipriocity in interaction
- Type of interaction (e.g. intimate or not)
- Relationship between entities (e.g friends, co-workers, relatives)
- Node Structure (neighborhood/relations/ affilliations)

Among the listed attributes, our main focus is to consider is frequency and recipriocity by generating a graph among entities (identifiers) who have replied to a message.

After consideration to our graph construction, we leverage the metric of centrality in understanding how key players interact in the graph. as well as their influence on the entire network. Centrality can be defined individually as a ratio of paths containing a point between two linking (separate) points. This can be formally expressed with g_{jk} as the number of geodesics linking points x_j and x_k in a graph along with $g_{jk}(x_i)$ where,

$$b_{jk}(x_i) = g_{jk}(x_i) / g_{jk}$$

is the proportion of geodesics linking x_j and x_k that contain x_i [47].

To support the overall evaluation of a graph, an index of the centralization of a complete graph C_B is considered. It is based on the intuition that a graph is centralized to the degree that its communication flow is overwhelmingly dominated by a single point. The measure is defined as the average difference between the normalized centrality of the most central point C'_B (p^*) and the normalized centralities of all other points in the graph

Where,

$$C'_B(x_i) = \sum_{i=1}^{n} [C'_B(p^*) - C'_B(p_i)] \ / \text{n-1}$$

Finally, the networks structure is examined from the perspective of cohesion by the evaluation of connectiveness in a graph. Connectivness is defined as the maximum number of elements which need to be removed to disconnect the remaining nodes from each other and is evaluated along Krackhardt's connectedness scoring. Existing as a means of expressing reachability in the termed graph, it represents the proportion of nodes (actors) that cannot be reached by other nodes. This is defined where a digraph G is equal to the fraction of all dyads { i , j } such that there exists an undirected path from i to j in G [48].

As opposed to comparing static metrics, both centrality and connectivity are evaluated over monthly intervals. Here the structural variation is considered as an indicator for changes in trends.

IV. Case Study

Our study consists of the application of stated methodologies towards a collection of 100M Twitter messages with time stamps ranging between 1/1/2010 and 6/31/2010 [49]. Our subject matter of interest was mobile Operating Systems. We focused on the three major competitive dominant (high presence) technologies – the Iphone, Blackberry and Android OS-based mobile devices. Figure one presents the market share for the three Operating Systems for the period between Jan 2010 and June 2010 [50].

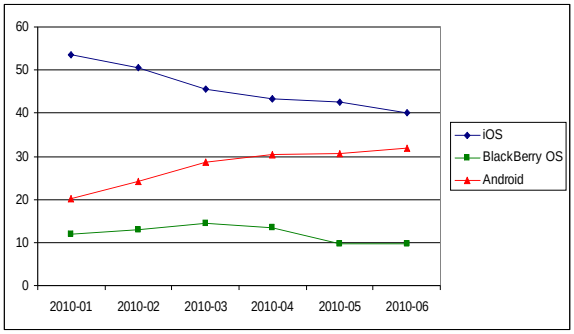

Figure 1. United States Market share for Mobile OS (Jan 2010 – Jun 2010)

Each of these topics were identified by employing filtering on terms and phrases. The collection of messages were filtered on three topics and then separated by month. The volumes of filtered messages per each month are presented in Figure 2.

Within each data collection, we considered messages which were associated with a 'reply'

communication. As such the resulting adjacency metrices maintained at least one edge (minimally) between each node. To demonstrate the graphs, a reduced sample of 100 nodes from a selected month is presented for both the Android and Iphone collection. (Figures 3 and 4) Our approach in graph generation is reflected in this graphical presentation as each node has at least one connection with the Android sample presenting a higher degree of connectiveness and centrality.

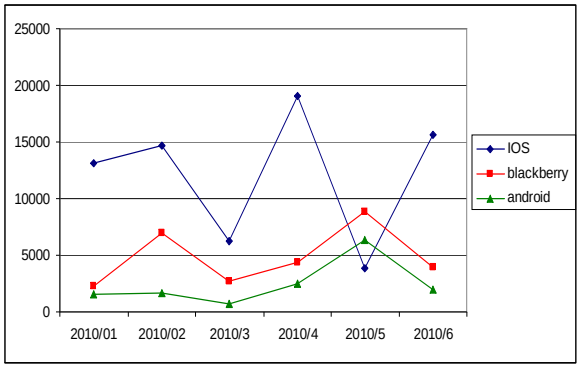

Figure 2. Data Sample Sizes (Jan 2010 – Jun 2010)

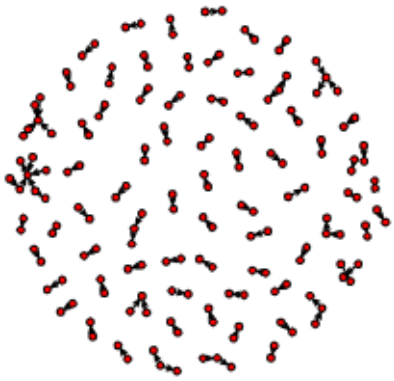

Figure 3. Android Graph (100 nodes)

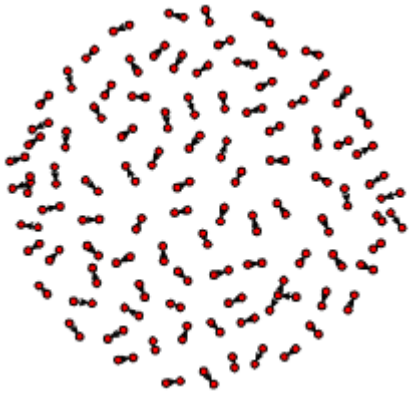

Figure 4. Iphone Graph (100 nodes)

Centrality was applied to view the properties of key players by employment of the Social Network Analysis ('R' programming) library [48]. The metric was considered for each topic across monthly intervals (Figure 5). This was examined over the entire sample for each month only including entities that had engaged in a reply conversation. Given our sample size, the metrics were very low as they ranged between .018 and .0122 among our three networks. This was in part due to our selected means of graph generation and secondly due to our sample size of approximately 1% of the entire Twitter feed (given the estimation of approximately 50M Twitter messages per day for the first and second quarters of 2010 as compared to our data set of 100M). Even though IOS maintained the largest overall sample size, the centrality measurement was the lowest, the graphs generated around the topic of Blackberry were highest corresponding to its gains in market share over the six month period.

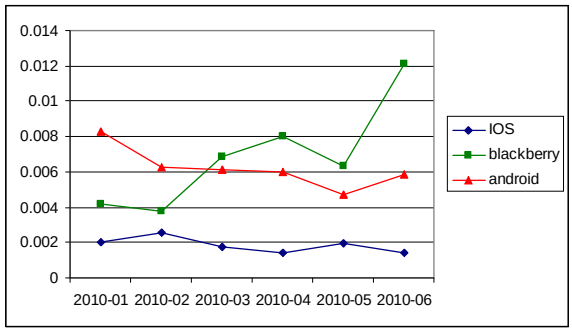

Figure 5. Centrality Measurements (Jan 2010 – Jun 2010)

Next, cohesion was examined, relying on the Krackhardt scoring mechanism for each monthly period as compared to each data set. Here, the Blackberry demonstrated a substantial increase corresponding to the US market share as determined earlier. Although maintaining the largest market share and sample size, the IOS maintained the lowest connectivity between all three ranging between 0.008 and 0.001.

Next, correlations were generated among the six sets of data, presented in figure 7, 8 and 9. First, the message sample sizes were compared against the market shares providing very little to negative correlation ranging between -.39 to .16. Corresponding to the relative volume collected, the IOS scored highest among centrality with the scores ranging between .71, .62, .85 for IOS, Android, and Blackberry. Although considering relatively moderate sample size, the BlackBerry metric scored extremely well in correlation with the market share. Connectedness was also directly correlated to the market share percentages with .91, .70 and .66 for

IOS, Android and Blackberry respectively. In spite of the relatively low connectivity metrics, IOS performed much higher than the other two mobile Operating Systems indicating that investigations in structural metrics as they change over time presents a substantial opportunity to understand their predictability.

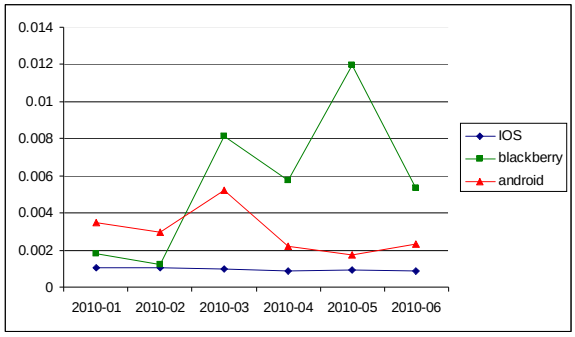

Figure 6. Connectivity Measurements (Jan 2010 – Jun 2010)

Volumes Correlation	
IOS	0.16
Android	-0.39
Blackberry	0.24

Figure 7. Volumes Correlation among our sample size. (Jan 2010 – Jun 2010)

Centrality Correlation	
IOS	0.71
Android	0.62
Blackberry	0.85

Figure 8. Correlation of Centrality metrics to Mobile OS marketshare (Jan 2010 – Jun 2010)

Connectedness Correlation	
IOS	0.91
Android	0.7
Blackberry	0.66

Figure 9. Correlation of Connectedness metrics to Mobile OS marketshare (Jan 2010 – Jun 2010)

V. Conclusion

We have considered the application of structural metrics to the trending of topics. This was accomplished by extracting topic-related data from a collection of 100M Twitter messages. Graphs were generated among the filtered collection by selecting only the messages that existed in the form of a reply. We then applied metrics to determine the effect of key players (Centrality) as well as metrics for cohesion (Connectedness). We were able to successfully correlate our graph structure metrics to the market share of three major mobile Operating Systems for the defined period. The disparity in correlation between volumes and our assigned structural metrics support that structure is a substantial indicator that is independent of changes in volumes within a given sample. As such, our metrics suggest that our Social Networks (utilized in real-time) could serve a means of predicting future consumer behavior.

Future work includes the incorporation of semantics on the filtering portion (graph generation) as well as reassigning weights to associated edges. Opportunities in this area also include examination of metrics (e.g. betweeness) among graphs integrating all three topics of comparison.

Acknowledgement

Joseph Kelly, CEO of InfoChimps Corporation for Data Consultation and Support.

References

[1]http://www.huffingtonpost.com/2011/09/01/growth-social-media-infographic_n_945256.html
[2]http://www.gev.com/2011/04/popularity-of-social-networking-sites-3/
[3] Alba, Richard D.,Gwen Moore, "Elite social circles", Applied network analysis: A methodological introduction, Burt,Minor (eds), Beverly Hills: Sage.,1983.
[4] Rob Cross, Stephen P. Borgatti, and Andrew Parker "Making Invisible Work Visible:Using Social Network Analysis to Support Strategic Collaboration" ,California Management Review, Vol 44, No. 2, Winter 2002
[5]Maroulis, Spiro, Gomez, Louis, "Does connectedness Matter? Evidence from a Social network Analysis within a Small-School Reform", Teachers College Record, Volumne 110, Number 9, Sept 2008, pp1901-1929
http://researchhighschools.pbworks.com/f/MaroulisStConnections.pdf
[6]Barnes, J.A.,"Graph theory in network analysis", Social Networks 5: 1983, pp. 235-244
[7]Wasserman , Faust, "Social network analysis: methods and applications" (structural analysis in the social sciences), Cambridge University Press, Cambridge.
[8] Hanneman, Robert, Riddle, Mark, "Introduction to Social Network Methods", On-line text
2005. Introduction to social network methods. Riverside, CA: University of California, Riverside (published in digital form at http://faculty.ucr.edu/~hanneman/)
[9] L. Tang and H. Liu. "Relational learning via latent social dimensions",. In KDD '09: Proceedings of the 15th ACM SIGKDD international conference on Knowledge discovery and data mining, pp 817–826, 2009.

[10]Ostrowski, D. A. , "Predictive Semantic Social Media Analysis, IEEE International Conference on Semantic Computing , ICSC , 2011
[11]Ostrowski, D. A. "Relational Modeling in Social Media", ICAI, World Comp, 2011
[12] Gloor, P.A.; Krauss, J.; Nann, S.; Fischbach, K.; Schoder, D.; "Web Science 2.0: Identifying Trends through Semantic Social Network Analysis", Computational Science and Engineering, 2009. CSE '09. International Conference on Volume: 4 pp: 215 - 222
[13]L. Tang and H. Liu, "Scalable Learning of Collective Behavior Based on Sparse Social Dimensions", Proc 18th ACM conf. Information and Knowledge Management (CIKM 09), ACM Press , 2009, pp. 1107 -1106
[14] Lin, F.; Cohen, W.W.; "Advances in Social Networks Analysis and Mining (ASONAM)", 2010 International Conference on 9-11 Aug. 2010 pp 192 – 199
[15]L. Tang and H.Liu, Lei Tang and Huan Liu. "Toward Predicting Collective Behavior via Social Dimension Extraction". In IEEE Intelligent Systems, 2010
[16] Lei Tang. "Collective Behavior Prediction in Social Media.", In Doctoral Student Forum, SIAM International Conference on Data Mining (SDM'09), 2009.
[17]M. McPherson, L. Smith-Lovin, and J.M. Cook. "Birds of a Feather: Homophilly in social networks", Annual Review of Sociology, 27: pp. 415-444, 2001.
[18] F.J. Provost, C. Perlish, and S.A. Mackassy, Relational Learning Problems and Simple Models, In Proceedings of the Relational Learning Workshop at IJCAI-2003, 2003.
[19]Krebs, V., J. Holley. 2002. Building smart communities through network weaving. http://www.orgnet.com/buildingnetworks.pdf.
[20] http://infochimp.com
[21] Achrekar, H.; Gandhe, A.; Lazarus, R.; Ssu-Hsin Yu; Benyuan Liu; Predicting Flu Trends using Twitter data
Computer Communications Workshops (INFOCOM WKSHPS), 2011 IEEE Conference on
Publication Year: 2011 , Page(s): 702 - 707
[22]Peng, Huan-Kai; Zhu, Jiang; Piao, Dongzhen; Yan, Rong; Zhang, Ying;
Retweet Modeling Using Conditional Random Fields
Data Mining Workshops (ICDMW), 2011 IEEE 11th International Conference on
Publication Year: 2011 , pp 336 – 343
[23] Iyengar, Akshaya; Finin, Tim; Joshi, Anupam;
Content-Based Prediction of Temporal Boundaries for Events in Twitter
Privacy, Security, Risk and Trust (PASSAT), 2011 IEEE Third International Conference on and 2011 IEEE Third International Confernece on Social Computing (SocialCom)
Publication Year: 2011 , pp 186 - 191
[24] Measurement and analysis of online social networks
by: Alan Mislove, Massimiliano Marcon, Krishna P. Gummadi, Peter Druschel, Bobby Bhattacharjee
In Proceedings of the 7th ACM SIGCOMM conference on Internet measurement (2007), pp. 29-42,
[25] cantonese, Salvadore, De Meo, Pasquale, Ferrara,Emilio, Fiumara, Giacomo, Provetti, Alessandro, Crawling Facebook for Social Network Analysis,WIMS '11 May 25-27, 2011 Sogndal Norway
[26] Knowledge Discovery and Retrieval on World Wide Web Using Web Structure Mining
Boddu, Sekhar Babu; Anne, V.P Krishna; Kurra, Rajesekhara Rao; Mishra, Durgesh Kumar;
Mathematical/Analytical Modelling and Computer Simulation (AMS), 2010 Fourth Asia International Conference on ,2010 , pp: 532 - 537
[27] Erbs, Nicolai, Zesch, Torsten, Gurevych, Iryna, Link Discovery: A Comprehensive Analysis, 2001 Fifth IEEE International Conference on Semantic Computing
[28]Acar, E.; Dunlavy, D.M.; Kolda, T.G.;
Link Prediction on Evolving Data Using Matrix and Tensor Factorizations
Data Mining Workshops, 2009. ICDMW '09. IEEE International Conference on
2009 , pp 262 - 269
[29]Cai-Rong Yan; Jun-Yi Shen; Qin-Ke Peng; Ding Pan;
Parallel Web mining for link prediction in cluster server
Machine Learning and Cybernetics, 2005. Proceedings of 2005 International Conference on
Volume: 4
: 2005 , Page(s): 2291 - 2295 Vol. 4
[30] Caverlee, J.; Webb, S.; Ling Liu; Rouse, W.B.;
A Parameterized Approach to Spam-Resilient Link Analysis of the Web
Parallel and Distributed Systems, IEEE Transactions on
Volume: 20 , Issue: 10
2009 , pp 1422 - 1438
[31] Rong Qian; Wei Zhang; Bingni Yang; Detect community structure from the Enron Email Corpus Based on Link Mining, Intelligent Systems Design and Applications, 2006. ISDA '06. Sixth International Conference on
Volume: 2Publication Year: 2006 , Page(s): 850 - 855
[32] Web structure mining: an introduction
da Costa, M.G., Jr.; Zhiguo Gong;
Information Acquisition, 2005 IEEE International Conference on 2005
[33]L. Page, S. Brin, R. Motwani, T. Winograd, The PageRank citation ranking: Bringing order to the Web. ", Technical Report, Stanford Univesity, 1998
[34]NMF: Network Mining Framework Using Topological Structure of Complex Networks
Sugiyama, K.; Ohsaki, H.; Imase, M.; Yagi, T.; Murayama, J.;
Congress on Services Part II, 2008. SERVICES-2. IEEE
Publication Year: 2008 , pp 210 - 211
[35] J. Kleinburg, Authoritative sources in a hyperlinked environment. Journal of the ACM 46(5): 604-632 1999
[36]K. Bharat , M.R. Henzinger, Improved algorithms for topic distillation in a hyperlinked environment. In ACM SIGIR International Conference on Research and Development in Information Retrieval, pages 104-111, 1998
[37]S. Chakrabarti, B.Dom, and P.Indyk, Enhanced hypertext categorization using hypelinks. In SIGMOD International Conference on Management of Data pp 307-318, 1998
[38]Semantic Message Link Based Service Set Mining for Service Composition
Anping Zhao; Xiaoyong Wang; Ke Ren; Yuhui Qiu;

Semantics, Knowledge and Grid, 2009. SKG 2009. Fifth International Conference on 2009 , Page(s): 338 - 341
[39]Thushar, A.K.; Thilagam, P.S.;An RDF Approach for Discovering the Relevant Semantic Associations in a Social Network Advanced Computing and Communications, 2008. ADCOM 2008. 16th International Conference on
Publication Year: 2008 , pp 214 – 220
[40] Achim Rettinger Matthias Nickles, Volker Tresp Statistical Relational Learning with Formal Ontologies, ECML PKDD '09 Proceedings of the European Conference on Machine Learning and Knowledge Discovery in Databases: Part II
[41] Kirsten, Mathias, Wrobel, Stefan, Inductive Logic Programming, Lecture Notes in Computer Science, 1998, Volume 1446/1998, 261-270, DOI: 10.1007/BFb0027330
[42] Chunying Zhou; Huajun Chen; Tong Yu; Learning a Probabilistic Semantic Model from Heterogeneous Social Networks for Relationship Identification Tools with Artificial Intelligence, 2008. ICTAI '08. 20th IEEE International Conference on Volume: 1
[43]Batagelj, Vladimir, Mrvar, Andrej, Pajek: Analysis and visualization of large networks, Graph Drawing Software Book . <M. Junger, P. Mutzel, editors 2003
[44]Noel, S.; Raghavan, V.; Chu, C.-H.H.;
Visualizing association mining results through hierarchical clusters, Data Mining, 2001. ICDM 2001, Proceedings IEEE International Conference on
Publication Year: 2001 , pp 425 - 432
[45]Leung, Carson Kai-Sang, Carmichael, Christopher L., Exploring Social Networks: A Frequent Pattern Visualization Approach, IEEE International Conference on Social Computing, 2010
[46]Cheliotis, Giorgos, "Social network Analysis", http://wiki.nus.edu.sg/download/attachments/57742900/Social+Network+Analysis.pdf?version=1&modificationDate=1267120366130, Ref Feb 1, 2012
[47]Freeman, Linton, Borgatti, Stephen P. ,White, Douglas R., Centrality in valued Graphs: A measure of betweenness based on Network Flow, Social Networks, Elsevier Science Pub., 1991, pp 141-154
[48]Butts, Carter T., "Social Network Analysis with sna", Journal of Statistical Software, Feb 2008, vol 21. Issue 6.
[49] http://www.infochimps.com/
[50]http://gs.statcounter.com/#mobile_os-US-monthly-200912-201112

Detection of Malicious Beacon Node Based on Intelligent Water Drops Algorithm

S.Qureshi[1] , Azzam ul Asar[2]
[1] International Islamic University Islamabad
[2]University of Engineering & Technology, Peshawar, Pakistan.

Abstract:--*Security of the wireless sensor network is emerged as a crucial issue due its resource-constrained nature. Number of localization techniques suffers from security threats when there are compromised beacon nodes in the network. This paper presents a technique for detection and revocation of compromised beacon nodes using the concept of Intelligent Water Drop algorithm. The results are very promising and show great potentials towards offering a more secure localized solution of wireless sensor networks.*

Keywords: Wireless Sensor Networks, Malicious Beacon Node, Network Security

I. INTRODUCTION

Wireless Sensor Networks (WSNs) are made up of numerous sensors with wireless communication facilities. The networks created by these sensors are ad-hoc by nature, allowing seamless communication between them. The diversity of WSNs potential applications is immense. Due to this diversity, each application may have a very different set of goals to achieve and challenges to overcome. Localization of sensors is important for large number of WSN applications [1-2]; however it has become a crucial issue due to its resource-constrained nature. To equip every sensor with GPS receiver makes the application uneconomical. Thus beacon/anchor nodes which know their location are used for localization of other sensor nodes. Different schemes and models have been developed for this purpose but these schemes cannot ensure correct localization in an environment where some of the beacon nodes are compromised. Thus researchers are struggling to find ways to overcome the affect of malicious nodes in a network and have presented a number of approaches for secure localization.

In this paper we present a scheme for detection of malicious beacon node using the concept of Intelligent Water Drops (IWD). The scheme uses the same basic method employed by Peng Ning [3]; however by using IWD concept, the scheme has become more reliable. Using simulation we verify that our scheme detects malicious nodes correctly.

II. RELATED WORK

Due to limited resources, wireless sensor networks exhibit unique operational challenges and are prone to localization attacks. Researchers have been introducing new protocols and techniques to ensure correct localization in hostile environment. The approach of robust localization has been introduced by Li et. al.[4]. It assumes presence of malicious nodes in the network and presents scheme that may tolerate the malicious behavior and still makes correct location discovery. This scheme consists of statistical methods. Liu et.

al. [5] presented a method to key out and bump off malicious information. The technique uses minimum mean squared estimation to calculate the location of sensor nodes. Lazos and Capkun have designed a robust decentralized localization system [6] which is robust to Sybil and wormhole attacks. Although this method does not involve statistical methods, it accomplishes robust localization in the presence of malicious nodes.

Another approach is based on the verification of the estimated position. Capkun et. al. [7] have designed an algorithm which is verification based. Lazos and Capkun [6] have presented hybrid algorithm which utilizes cryptographic methods for secure communication between sensors and locators and then devises an algorithm for location determination using verification. However authors of ROPE and SPINE have neglected the scenario where a number of locators themselves are compromised and that may collude.

Sastry et. al. [8] presents an algorithm named Echo which verifies the area of location of claimant. However the verification process sometimes may also be attacked by the adversaries. Wenliang du and associates [9, 54] propose a scheme which uses pre-deployment knowledge for the verification of specific location of sensor. The scheme checks the consistency of the location found by any location scheme and its actual location threshold. If the deviation is significant, it is anomaly. The scheme is dependent on probabilistic distribution of nodes; if these values are not correctly obtained, the results will critically change [10].

Fang liu et. al. [10] have presented an algorithm in which they detect localization anomaly which is followed by detection of malicious nodes responsible for this anomaly. It is grounded on clustering and thus called LADBC. The Network is grouped and has into clusters . However the clustering algorithms have the problem of being dependent on few cluster heads which can run out of battery due to

much processing and communication and can also be captured by adversaries.

Liu et. al. [3] have come up with more genuine approach to detect and revoke the malicious nodes. Three solutions have been presented in this regard by various researchers [3, 11, 12]. Liu et. al. [3] propose a technique for identification and removal of malicious beacon nodes. The detecting node on receiving the location reference from target node calculates distance between them using the signal received and location information sent by the target node. If the two are consistent with difference less than maximum distance error, it is considered benign otherwise malicious. They then developed revocation scheme which is based on the suspiciousness of a beacon node calculated at the base station through alert based scheme. However the detection scheme has a shortcoming. It has not considered the environmental affect. WSN are mostly deployed in an unattended environment; For worse weather changes, there would be much measurement error in distance and two distances may differ much larger than maximum measurement error. In this way, many alerts would be reported to the base station which may increase suspiciousness of benign node and as a result, a number of benign nodes would be revoked from the network.

Srinivasan et. al. [12] have extended the work in [3]. They introduced for the first time the concept of trust and reputation for removal of malicious beacons. They have proposed distributed reputation beacon trust system in which beacon nodes help sensor nodes to decide whether to use given beacon's location information or not by maintaining reputation of their neighbor beacon nodes misbehavior. However since WSNs pose unique challenges in terms of memory, computational capability and battery the reputation based mechanisms usually can add overhead. Also without being globally informed, it is usually hard to cope with local majority and collusion of nodes that have been compromised.

Satyajayant Misra and associates [11] proposed a scheme to detect and remove malicious beacon nodes using a mobile verifier. Authors have shown through simulations that their proposed method detects almost 80% of malicious locators while the false positives percentage is almost zero. However, this scheme has some drawbacks. Mobile verifier needs preprogrammed paths to be stored to follow through the network. Due to restricted number, there is repetition of paths which weakens the algorithm's effectiveness. An additional requirement is that the mobile verifier needs to be charged after every iteration which makes it unsuitable for most of the unattended wireless sensor networks applications. Above all, the whole scheme is dependent on single mobile verifier which is assumed to be uncompromised failing which, the whole scheme will collapse.

III PRINCIPLE OF IWD

Naturally existing rivers, lakes and seas are made up of numerous water drops. These water drops change their environment as they move along their path. Rivers join lakes or sea following paths full of twists and turns. The ideal path for river is the shortest path to its destination following the law of force of gravity. However due to several obstacles, the real path is different from this ideal path. Water drops always try to change this real path to make it better to reach destination. Continuous effort by the water drops change the river paths as the time passes by. Water drops while travelling remove soil and transfer it to another part in front. Deeper parts attract more volume of water. Clearly water drops opt for easier path when choosing between different existing branches. Based on natural water drops, artificial water drops are developed which encounters some of the characteristics of natural water drops. These Intelligent water drops are characterized by the property of amount of soil they carry. IWD prefers the path with low soils rather than higher soils on its beds and probability of next path to choose is inversely proportional to the soils of available paths. The lower the soil of the path, more chance it has for being selected by the IWD. Thus IWDs depicts intelligent behaviour to select next position in their path [13].

Utilizing the IWD algorithm for the detection scheme presented in this paper, we can consider the amount of distance-error as a factor equivalent to the amount of soil in the original IWD algorithm [14]. Greater distance-error means that a particular node is providing more malicious information and chance of that node to be compromised is much higher.

IV NETWORK MODEL

The Sample Network is shown in Figure 1. Network consists of sensor nodes including legal and malicious beacon nodes. The node taking detection can be called as detecting and the one being investigated as target node. We consider same assumptions for this network as in [3]. These include two communicating nodes sharing pair wise key. Communication is two way. Multiple detecting IDs are provided to the beacon node along with keying material. Beacon signals from target node are unicasted to the detecting node and are encrypted. Temporal leashes or RTT technique is used to detect replay attacks (stealing both ID & location).

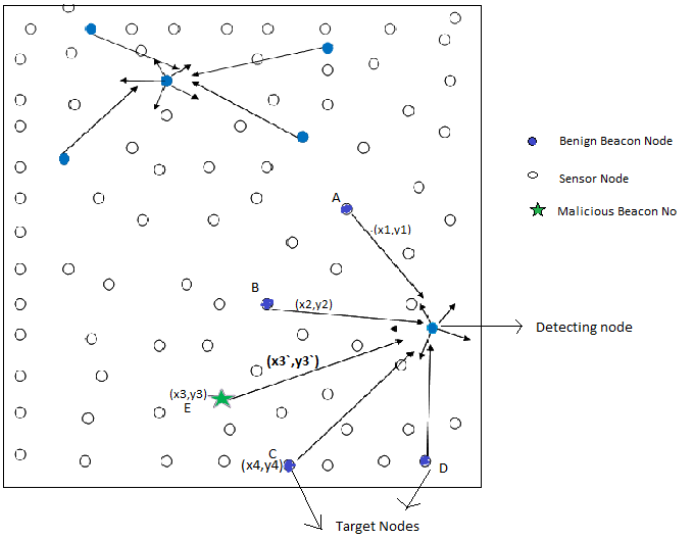

Fig. 1: Network model

V DETECTION SCHEME

The detecting node sends request for location of beacon nodes. The requesting node uses an ID other than its own because if it uses its own ID, the target node will send its correct location and will thus clear the detection test. For this purpose, every beacon node is provided with multiple IDs and all keying materials (assumption). The scheme works as follows. The detecting node first sends request message for location pretending as a non beacon node. The target nodes within range of this detecting node receive this message and reply with beacon signal carrying their ID and location. The malicious node obviously sends wrong location. The detecting node estimates the distance between them, from the beacon signal upon receiving it using TOA technique called actual distance. Since the detecting node knows its own location error due to environment, it can also calculate the distance, based on its own location e.g. (x, y) and target node (x1, y1), using distance formula.

$$D=\sqrt{(x-x1)^2+(y-y1)^2} \qquad (1)$$

The malicious signal detector (comparator) then compares the actual distance and the calculated one. Obviously there will be some error between the two values, since the range estimation techniques do not result in accurate estimations.

$$\text{Error} = |d_{(ij)\ \text{calculated}} - d_{(ij)\ \text{actual}}| \qquad (2)$$

These error values are relatively compared to each other using IWD formula to recognize the nodes with most error. Most error producing nodes will result in lower probability of trustworthiness. Probability of selecting a next position by IWD is calculated by

$$\text{Pi (j)} = \frac{f(soil(i,j))}{\sum_k f(soil(i,k))} \qquad \text{.....(3)}$$

Function of soil between two points *i* and *j* can be considered as the error of distance between two nodes [14]. Every node can be considered as intelligent water drop which calculates the goodness of the other node. According to the formula, the node producing more error will give less '*P*' value challenging its trustworthiness. Calculation of trustworthiness of a particular node is represented by:

$$P(i,j)=\frac{f(e(i,j))}{\sum_k f(e(i,k))} \qquad (4)$$

Where

$$f(e)=\frac{1}{e_s+g(e)} \qquad (5)$$

In equation (5), *k* is the number of replying nodes and e_s is a small constant value between 0 and 1.

VI REVOCATION

If the probability is below threshold value, the detecting node will generate negative vote against it and will inform base station about it. The base station keeps record of the negative votes and its originator. If several numbers of votes (above threshold) generate vote against a particular node(s), then that node(s) will be considered malicious. Next the base station informs the network about the declared malicious node. Thus the sensor and beacon nodes will stop processing any data from the declared malicious nodes.

VII ANALYSIS

Like [3], IWD based detection scheme can be used for security of localization schemes, which are based on location references from beacon node. Small communication overhead will be introduced as the nodes have to send alerts to the base stations and it can be considered as a trade off for security of localization process. Also the sensors nodes will have to maintain and store a banned list. Our scheme cannot detect malicious nodes reporting alerts against a benign node; however, since the detection of malicious beacon node is based on number of votes from several nodes and not from single node thus will prevent wrong detection of benign node as a malicious node.

Our detection scheme seems to have an inherent problem. If the actual and calculated distances are logical, even then there is possibility that the beacon signal is from a malicious node, i.e. malicious node has stolen ID of another node. However, this will not affect the localization process. In order to make incorrect location estimation the node will have to change its location and thus will be caught. Nevertheless, we can assume temporal leashes or round trip time technique (RTT) to detect replay attacks.

VII SWARM INTELLIGENCE AND REVOCATION SCHEME

In this scheme, we have used the concept of swarm of intelligent water drops. The advantage of this concept is that

the distance errors are compared relatively and the nodes with most malicious behavior are considered most untrustworthy. Since the errors are compared relatively, so if environment is hard all nodes are producing error greater than in normal conditions than these would not be wrongly detected as malicious nodes, since all nodes facing same environment will generate closer error values. Only the node which is actually compromised would generate larger error thus will be considered malicious by lower P value. Also the swarm intelligence concept employs the sharing of local or personal experience to produce a global best solution. This concept is utilized here by sending information about the locally detected node to the base-station, when other nodes have also shared their experience so the base station on basis of local experience produces a global solution i.e. declares a node to be malicious.

The revocation method in our scheme is different and better from [3], because revocation is based upon number of alerts from several nodes and malicious node can be detected in a single transmission/iteration. Also now there is no need of report counter at base station.

VIII THRESHOLD: A CRITICAL PARAMETER

In our proposed scheme, threshold probability and threshold number of votes is very important and critical since, a node is declared compromised based on these P values. Threshold P values is also very difficult to determine however it can be considered as a function of number of factors which can help to determine this value e.g. topology, application, environment, transmission range.

IX SIMULATION RESULTS

Simulation has been run for about 200 times to analyze the results. Different scenarios were considered in which nodes were distributed randomly. Variable parameters including thresholds, transmission range, beacon nodes density, malicious nodes density have been varied sufficiently to analyze the performance of proposed algorithm.

A Detection Rate vs. Transmission range

We begin by examining detection rate i.e., no of nodes banned or revoked from the network vs. transmission range. (Detection rates are average values for a number of simulations)

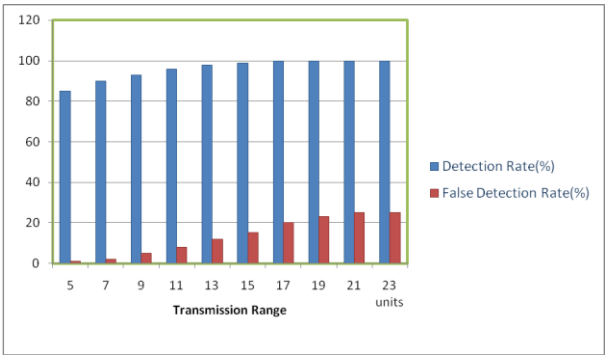

Fig. 2: Detection rate vs. Transmission range

Figure 2 shows that detection rate increases with transmission range (T.R.) till certain value .This is because if the no of neighbor nodes required to generate alerts is less than specified alert threshold, then malicious node will not be detected . But when number of neighbor nodes is enough, then transmission range will not affect the detection range. However, increasing transmission range also increases false detection rate. This is because the detection is highly dependent on threshold number of votes which have been selected for particular T.R. So if T.R. is increased, more number of false votes will be received, which will be counted in to get trust value of a node. Thus if T.R has to be changed then threshold also requires to be changed.

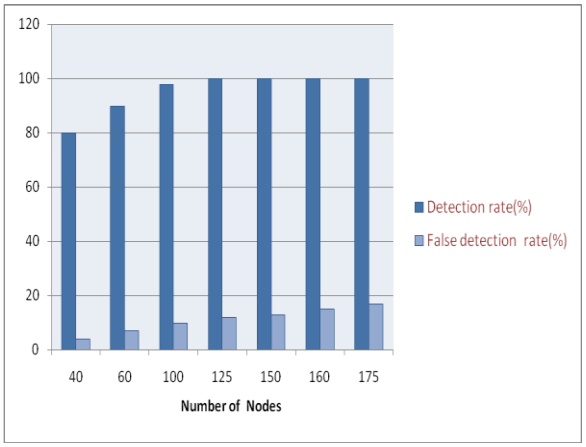

Figure 3: Detection rate vs. Network size

B Detection Rate vs. Network Size

Figure 3 shows the trend of detection rate for a particular arena size. We can observe that detection rate increases with increased no of neighbor nodes.

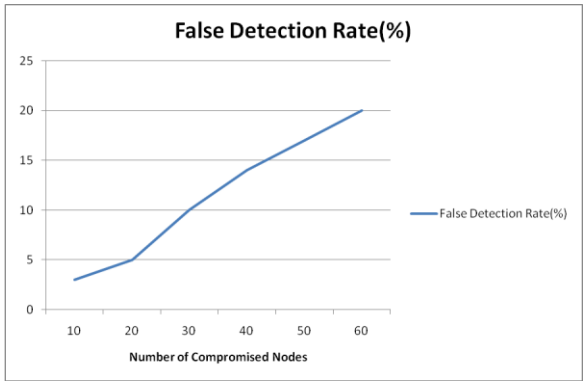

Fig. 4: False detection vs. Compromised Node Density

XI CONCLUSION AND FUTURE WORK

A novel IWD based algorithm for detection of malicious beacon node has been presented. IWD has been used for the first time in area of Wireless Sensor Networks. Also the algorithm for the first time incorporates the environmental effects in wireless communication while detecting compromised beacon nodes. The algorithm has space and potential for development and improvement. The scheme is suitable even for hard weather conditions. However a complex IWD mathematical model can be used instead of the simpler one which may improve results. Also a mechanism can be included in the algorithm to detect the malicious `` if a node generates alerts against another node again and again while no other node is reporting, then the node itself is malicious.

REFERENCES

[1]. B.Karp, H.Kung, "GPSR: Greedy Perimeter Stateless Routing for wireless networks", Proceedings of MobiCom, 2000.

[2]. Nabendu Chaki, "A Location Aided Reactive Routing Protocol for Near Optimal Route Discovery in MANET," IEEE Conference on Computer Information Systems and Industrial Management Applications (CISIM), Pages 259-264, 2010.

[3]. D. Liu, P. Ning, W.Du, "Detecting Malicious Beacon Nodes for Secure Location Discovery in Wireless Sensor Networks", 25th IEEE International Conference on Distributed Computing Systems (ICDCS '05), P. 609-619, 2005.

[4]. Z. Li, W. Trappe, Y. Zhang, and B. Nath., "Robust statistical methods for securing wireless localization in sensor networks", Proceedings of IPSN '05,2005.

[5]. D. Liu, "Attack-Resistant Location Estimation in Wireless Sensor Networks", ACM Transactions on Information and Systems Security, Vol. 11, No. 4, Article 22, 2008

[6]. L. Lazos, R.Poovendran, S. Capkun , "ROPE: Robust position estimation in wireless sensor networks", Proceedings of the 4th international symposium on Information processing in sensor networks, IPSN '05,IEEE, 2005.

[7]. S. Capkun and J.-P. Hubaux, " Secure positioning of wireless devices with application to sensor networks", Proceedings of IEEE INFOCOM '05, 2005

[8]. N. Sastry, U. Shankar, and D. Wagner, "Secure verification of location claims", Proceedings of WiSe,2003.

[9]. Wenliang Du, Lei Fang, P. Ning, "LAD: Localization Anomaly Detection for Wireless Sensor Networks", proceedings of 19th IEEE Intl. Symposium on Parallel and Distributed Processing , 2005. P: 41a.

[10] G. Zhou, "Localization Anomaly Detection for Wireless Sensor Networks", IEEE International Conference on Intelligent Computing and Intelligent Systems (ICIS), Volume: 2, 2010 , Page(s): 644 – 648.

[11]. S. Misra, G. Xue and A. Shrivastava, "Robust Localization in Wireless Sensor Networks through the Revocation of Malicious Anchors", Proceedings of IEEE Intl. Conf. on Communications, 2007

[12]. A.Srinivasan, J. Teitelbaum, and J. Wu, "DRBTS: Distributed Reputation-based Beacon Trust System", Proceedings of the 2nd IEEE International Symposium on Dependable, Autonomic and Secure Computing (DASC'06), 2006

[13]. Hamed Shah-Hosseini, "The intelligent water drops algorithm:a nature-inspired swarm-based optimization Algorithm", International Journal, Bio-Inspired Computation, Vol. 1, Nos. 1/2, 2009.

[14]. S. Qureshi, A. Asar, A. Rehman, and A. Baseer, "Swarm Intelligence based Detection of Malicious Beacon Node for Secure Localization in Wireless Sensor Networks" Journal of Emerging Trends in Engineering and Applied Sciences, Volume 4 ,Issue 2, P:664-672, 2011.

Evolutionary Optimization Algorithms for Topology Control in Wireless Sensor Networks

Robert Cristian Abreu, José Elias C. Arroyo, André Gustavo dos Santos and Victor de Oliveira Matos
[1]Departamento de Informática, Universidade Federal de Viçosa, Viçosa, MG, Brazil
robert.abreu@ufv.br, jarroyo@dpi.ufv.br, andre@dpi.ufv.br, jimctu@gmail.com

Abstract - *This paper addresses the minimum energy network connectivity (MENC) problem. This problem consists of minimizing the transmission power of each sensor in a wireless network, which results in minimizing the energy consumption of the network, while keeping its global connectivity at the same time. The MENC problem is NP-hard in the strong sense and it motivates us to apply heuristics algorithms, based on evolutionary optimization, to obtain near-optimal solutions. We use two algorithms, the first is a Genetic Algorithm proposed in the literature and the second is a Particle Swarm Optimization algorithm proposed in this work. Computational tests were conducted using a set of 50 instances of the problem and the performances of the algorithms are evaluated. The results reveal that the proposed algorithm is very competitive, achieving the best solutions for some instances.*

Keywords: wireless sensor networks, topology control, meta-heuristics, combinatorial optimization

1 Introduction

Wireless sensor network (WSN) is a class of wireless ad hoc networks in which sensor nodes collect, process and communicate data acquired from the physical environment to an external base station, thus allowing for monitoring and control of various physical parameters [2]. WSNs are mainly characterized by their limited and non-replenishable energy supply. Hence, the need for efficient energy infrastructure is becoming increasingly more important since it impacts upon the network operational lifetime.

Topology Control (TC) is one of the most important techniques used in wireless ad hoc and sensor networks to reduce energy consumption which is essential to extend the network operational life time [1][4]. The main goal of TC is to design a good network (graph representing the communication links between network nodes) with high connectivity and low power consumption.

A WSN is regarded strongly connected if for each sensor node, there is a route to reach any other node in the same network. The strongly connected topology problem with minimum total energy consumption was defined and proved to be a NP-complete problem [1][8].

Comprehensive surveys of topology control can be found in [9] and [10]. Accordingly, most topology control approaches can be classified into two groups: physical topology control (PTC) and logical topology control (LTC) [13]. PTC satisfies the goal of topology control by adjusting transmission power; it reduces interference and energy consumptions. In other hand LTC also based on the approach used by PTC along with it consider the neighbor set of a node, and restrict it to a certain number to satisfy the network connectivity. This neighbor reduction mechanism helps to reduce the routing overhead.

In the literature, some heuristics methods have been developed to solve different topology control problems. In general, the energy metric to be minimized is the total energy consumption or the maximum energy consumption per node. In [1] two heuristics are proposed, one based on a Minimum Spanning Tree (MST) algorithm and a other a Broadcast Incremental Power method. A conventional genetic algorithm and a quantum genetic algorithm are compared in [5]. In [15] and [7], topology control is considered as a degree-constrained minimum spanning tree problem. An improved discrete Particle Swarm Optimization algorithm for generating topology schemes is presented in [15]. A simulated annealing algorithm was designed in [7]. [14] proposes a genetic algorithm to logical topology control. In [11], ant colony optimization, a framework inspired by the ant foraging behavior in the area of Swarm Intelligence, is applied to physical topology control. In [12], simulated annealing is applied to the problem of minimizing broadcast tree, a problem very similar to physical topology control.

In [4] the same MENC problem is addressed and a genetic algorithm with local search is developed. This algorithm is called Topology Control Memetic Algorithm (ToCMA). ToCMA algorithm generates many different solutions and explores in an effective manner the solution space by using searching and genetic operators. Then ToCMA employs different procedures to maintain the global connectivity of the network. It checks if the network is strongly connected and if it is not then it is repaired. Furthermore, ToCMA employs an improvement procedure (local search) to further minimize the overall energy consumption of the network. In [4], the results obtained by ToCMA are compared with the solutions of the MST heuristic. The results imply that ToCMA has better performances than MST.

In this paper, a Particle Swarm Optimization (PSO) heuristic algorithm is adopted to solve the MENC problem.

This algorithm uses procedures similar to those used in the ToCMA algorithm, to maintain the global connectivity of the network and to improve the overall energy consumption of the network. The experimental results of PSO algorithm are compared with the solutions of ToCMA and MST algorithms. The comparisons show that our algorithm obtains more robust topology schemes.

The paper is organized as follows. Section 2 briefly introduces the problem. Section 3 provides a description of the proposed PSO algorithm. Section 4 presents simulation results to demonstrate the effectiveness of the approach. Section 5 concludes the paper.

2 Problem description

Please The formal definition of the minimum energy network connectivity (MENC) problem is given as follows [1][4]: A graph $G = (V, E)$ is given where $V = \{n_1,\ldots,n_n\}$ is a set of n wireless nodes and is a set E of edges or links constructed in such a manner that there is a directed edge from $u \in V$ to $v \in V$ if and only if u can reach v using its maximum transmission power. The graph G sets an upper bound on the maximum connectivity that a wireless network can have. The MENC problem consists in determining a topology T (a subgraph of G) strongly connected with minimal total energy consumption. The total energy is computed as follow:

$$TE = \sum_{i=1}^{n} p_i, \quad (1)$$

where p_i denotes the power assigned to sensor node n_i. The network model and energy consumption follow similar assumptions as proposed in [1] and [4]. The sensors in the network are stationary and located in a two-dimensional plane (the location of each sensor is fixed after deployment). The location information will be used for calculating the distance between two sensor nodes. The sensors radiate and receive equally in all directions (omnidirectional antenna). If a sensor i transmits with a power level

$$p_i = d^2, \quad (2)$$

then any sensor within the distance d can receive the signal. Suppose there are two nodes n_i and n_j then the distance between these two nodes can be calculated by using the Euclidean distance,

$$d = \sqrt{(x_i - x_j)^2 + (y_i - y_j)^2}, \quad (3)$$

where (x_i, y_i) e (x_j, y_j) are the position coordinates of sensors n_i and n_j, respectively. Sensor nodes can operate in different initial power levels, with a lower and an upper bound.

3 The proposed PSO algorithm

Particle swarm optimization (PSO), first proposed by Kennedy and Eberhart (1995) [6], is an evolutionary optimization heuristic, which is inspired by adaptation of a natural system based on the metaphor of social communication and interaction.

The basic principle of PSO is founded on the assumption that "information is shared by the entire swarm", which was derived from research into the behavior of a flock of birds or a school of fish while foraging for food. PSO algorithm uses a population (swarm) of individuals (solutions) called of *particles*. Each particle has information about its own position, velocity and fitness. With this information, each particle updates its *personal best* (best value of each individual so far) if an improved fitness value was found. On the other hand, the best particle in the whole population with its position and fitness value is used to update the *global best* (best particle in the whole population). Then the velocity of the particle is updated by using its previous velocity, the experiences of the personal best, and the global best in order to determine the position of each particle.

The current velocity (at iteration t) of the particle i is updated as follows:

$$v_i^t = W v_i^{t-1} + c_1 r_1 (xb_i^{t-1} - x_i^{t-1}) + c_2 r_2 (g^{t-1} - x_i^{t-1}), \quad (4)$$

where, xb_i^{t-1} denotes the best position that particle i has obtained until iteration t-1; g^{t-1} denotes the best position obtained from particles in the population at iteration t-1; W is the inertia weight which is a parameter to control the impact of the previous velocities on the current velocity; c_1 and c_2 are acceleration coefficients and r_1 and r_2 are uniform random numbers between [0, 1].

The current position of the particle i is updated using the previous position and current velocity of the particle as follows:

$$x_i^t = x_i^{t-1} + v_i^t. \quad (5)$$

Algorithm PSO
01. Generate a population of N particles $\{x_1^0, \ldots, x_N^0\}$;
02. For each particle i, (i := 1,…,N) set $xb_i^0 := x_i^0$;
03. t := 0;
04. While *StoppingCriterion* = *false* do
    05. For each particle x_i^t, apply ***repairing*** procedure (if necessary) and ***improving*** procedure;
    06. Find the global best particle g^t;
    07. $t := t + 1$;
    08. For each particle i, update the velocity v_i^t and the position x_i^t;
    09. For each particle i, find the personal best position xb_i^t;
10. End-While.
11. Return the best particle.

Figure 1: Pseudo-code of the PSO algorithm.

In this article, an adaptation of PSO heuristic is proposed to solve the MENC problem. A pseudocode description of the PSO algorithm is presented in Figure 1. The algorithm has five input parameters: the population size, the inertia weight parameter, the two acceleration coefficients and the stopping

condition of the algorithm. The best obtained particle is returned by the algorithm.

In the next subsections, we described the main steps of the PSO heuristic.

3.1 Solution representation and initial population

For the MENC problem, a particle (solution) i is represented by a string of n integer numbers: $x_i = (p_1^i,\ldots, p_n^i)$, where n is the total number of nodes in the sensor network. The number p_j^i is the power level (maximum power transmission) assigned to the sensor node j. The assignment of power to the sensor nodes becomes the only factor that affects the connectivity of the sensor network [4].

The quality (fitness) of a solution is measured by the sum of the power assigned to each sensor node (total energy consumption of the network), namely:

$$f(x_i) = \sum_{j=1}^{n} p_j^i , \qquad (6)$$

where p_j^i denotes the power assigned to node n_j, in the particle i, and it is calculated according to Equation (2).

The initial population of the N particles is generated randomly (N is the size of the population). For each node is randomly assigned a power within the interval $[0, 500^2]$, where 500^2 is the maximum energy that a sensor node can take [4]. This procedure does not guarantee the feasibility of each solution. Then a repairing procedure has to be applied.

3.2 Repairing procedure

A solution (particle) must be feasible, that is, the topology network must be a directed strongly connected. There are four possible cases of infeasibility [4]: case (i) there is one or more totally isolated node in the network; case (ii) there is one or more one-way isolated groups of nodes in the network; case (iii) there is one or more loop in the network; case (iv) partition occurs in the network, that is, there are two or more sub-networks.

If a solution is infeasible, as in [4], a *repairing procedure* (that includes these four cases of infeasibility) is applied. In the PSO algorithm, the repair of a solution is done as follows.

First, the repairing procedure checks if there is a node sensor with zero in-degree and/or out-degree. If the out-degree of a node x is zero, then the power of this node is increased until it reaches its nearest neighbor node y, e.g., the procedures calculates the necessary power needed by x to be able to communicate with its nearest neighbor y. Similarly, if the in-degree of a node x is zero, the power of its nearest neighbor node y is increased until it reaches node x. In both cases, the degrees of both nodes, x and y, are updated. An example of an infeasible topology is shown in Figure 2. In this network, nodes 1 and 2 have both, in-degree and out-degree, equal to zero (these nodes are totally isolated). The node 4 has out-degree equal to zero and node 5 has in-degree equal to zero. Figure 3 shows the topology partially repaired. The power of nodes 1, 2 and 4 were modified. It is worth noting that "longest output arc" of a node represents the assigned power to this node.

After checking the in-degree and out-degree of the nodes, the repairing procedure checks for partitioned groups and one-way isolated groups. These groups are sub-networks strongly connected that do not communicate with the rest of the network. For example, Figure 4 shows the three groups of the topology in Figure 3. The communication between these groups has to be set up. To set up the communication from a group g_1 to a group g_2, the procedure tries to find a node y in a group g_2 which is the nearest neighbor of a node x in group g_1. Then, the procedure calculates the power needed for x to communicate with y and assigns this power value to x. Similarly, the communication from g_2 to g_1 can also be set up. This repairing is applied to all partitioned groups (or one-way isolated groups) until network connection is established. Figure 5 shows the repaired network obtained from the network shown in Figure 4. In this example, the communications from Group 1 to Group 2 and Group 2 to Group 1 are set up. Also, the communication from Group 3 to Group 2 is set up.

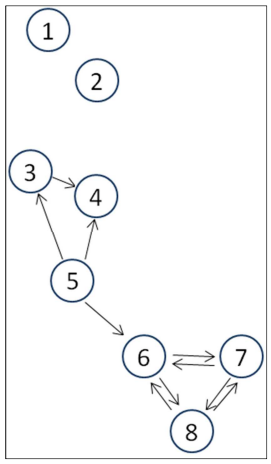

Figure 2: Infeasible topology.

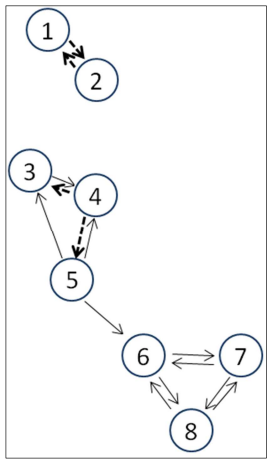

Figure 3: Topology after the first repairing.

3.3 Improving Procedure

Feasible solutions are improved by a local search method. This method tries to reduce the energy of each sensor node, while maintaining the network connectivity. The same improvements have been adopted by [4].

There are two basic improvements that can be executed in each solution (network). First, a node sensor may be using more energy than necessary to communicate with its farthest neighbor. Suppose that nodes 1 and 2 are at a distance d, and node 2 is the farthest neighbor of 1. Then, the maximum power requested for node 1 is $p_1^r = d^2$. If the current power of node 1 is $p_1 > p_1^r$ then p_1 is replaced by p_1^r, this is, the power of node 1 is decreased to the power level that is just enough to reach its farthest neighbor. Figure 6 illustrates an example in which the current power of node 1 is greater than the power needed to reach its farthest neighbor node 2.

The second improvement occurs when the power needed for a node *x* to reach directly its farthest neighbor *y* is more than the power needed if *x* follows an alternative route to *y*. For example, in Figure 7, the node 5 has a direct route to the node 3, which is its farthest neighbor. However by using an alternative route, shown in bold, the node 5 communicates with the node 3. Thus, the energy of node 5 can be reduced ("unnecessary links are removed").

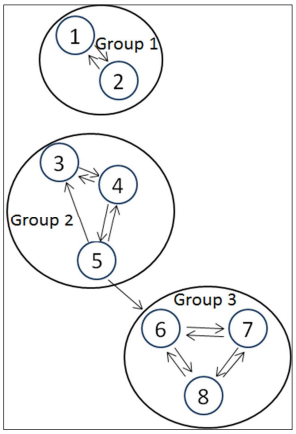

Figure 4: Network with three groups.

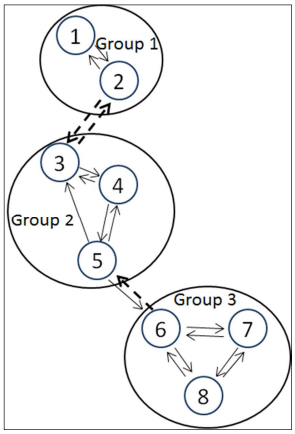

Figure 5: Network with the resumed connection.

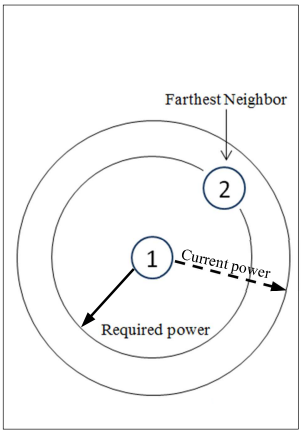

Figure 6: First improvement. Reduction of unnecessary power.

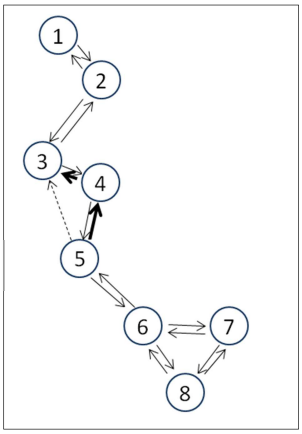

Figure 7: Second improvement. Energy of node 5 is reduced.

4 Computational results

In this work we carried out a study of the proposed PSO algorithm, ToCMA [4] and MST heuristic [1] to establish which ones show better performance for the MENC problem. All the tested algorithms are coded in C++ language and the experiments have been executed on a Intel Core i7 2.8GHz computer with 4GB of RAM memory and running with Windows 7 64 bit O.S.

The experiments were performed on 50 instances of the problem, where the number of sensor nodes *n* varies from 10 to 100. For each *n*, 5 instances (graph with all possible communication links) were generated. The coordinates of the nodes were randomly generated on a two-dimensional plane 500×500, so the power that could be randomly assigned to a sensor is between the boundaries of 0-500^2.

The PSO and ToCMA algorithms were run with the same stopping criterion which is based on an amount of CPU time. This time is giving by $2n^2$ milliseconds, where *n* is the number of sensors (size of the instance). In this way, it is assign more time to larger instances that are obviously more time consuming to solve.

In the reimplementation of the ToCMA algorithm, we use the same operators and parameters presented in [4]. In the PSO algorithm, the number of particles created at each iteration was fixed in $N = 30$. In order to find appropriate values for the parameters W, c_1 and c_2, the PSO algorithm was executed using different combinations of these parameters. Five independent executions were performed for each combination of W, c_1 and c_2. The obtained results are compared using the Relative Percentage Deviation (RPD) which is computed in the following way:

$$RPD = 100 \times \frac{TE - TE_{best}}{TE_{best}} \quad (7)$$

where TE is the total energy consumption of the network obtained by the algorithm, TE_{best} is the total energy consumption of the best solutions obtained among all the runs.

The performance of the algorithm (for different values of W, c_1 and c_2) is compared by average RPD (ARPD) over all the instances. In order to validate the results, an Analysis of Variance (ANOVA) [16] has been carried out employing the ARPD as response variable. All the tests have been executed with a confidence level of 95%. The result of ANOVA shows that there are no statistically significant differences among the means determined by the combinations of the parameters W, c_1 and c_2. Figure 8 depicts the mean plots confidence intervals with a 95% confidence level from the ANOVA test. From Figure 8, it can be seen that the best RPD means are obtained with $W = 0.5$, $c_1 = 0.2$ and $c_2 = 0.2$.

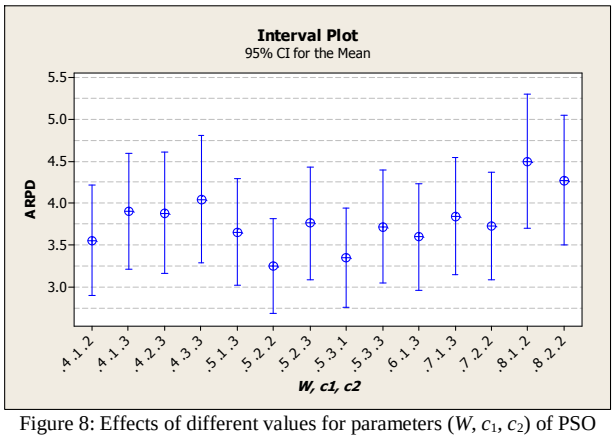

Figure 8: Effects of different values for parameters (W, c_1, c_2) of PSO algorithm.

Figure 9 shows the average (of each group of 5 instances of the same size) of the total energy consumption of the networks obtained by the three algorithms, MST, ToCMA and

PSO. We can see that for all instances, the ToCMA and PSO algorithms perform better than the MST algorithm.

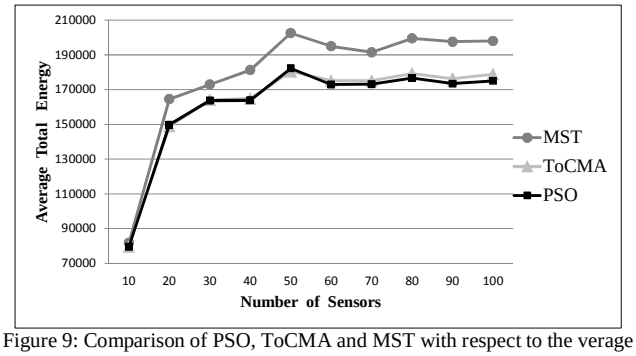

Figure 9: Comparison of PSO, ToCMA and MST with respect to the verage of total energy consumption of the obtained networks.

The efficiency of the ToCMA and PSO algorithms are evaluated by the relative percentage improvement with respect to the MST algorithm. This improvement is calculated using the following formula:

$$Improvement\ Percentage = 100 \times \frac{TE_{MST} - TE_{Alg}}{TE_{MST}} \qquad (8)$$

where TE_{Alg} is the value of total energy consumption of the network obtained by ToCMA or PSO, and TE_{MST} is the total energy value obtained by MST algorithm.

Table 1 shows the average percentage improvement of ToCMA and PSO compared to MST algorithm. We can see that ToCMA obtains better average improvement in 2 sets of instances with 20 and 50 nodes. And PSO obtains better average improvement on 6 sets, with 30 40, 60, 70, 90 and 100 nodes. Besides that, PSO obtains an overall improvement of 9.30% whilst ToCMA 8.90%. These results show that, regarding the total energy consumption of the network, the algorithms PSO and ToCMA are comparable and PSO performs slightly better.

Table 1: Improvement percentage of ToCMA and PSO with relation to MST

Number of nodes: *n*	**Improvement Percentage**	
	ToCMA	**PSO**
10	**2.87**	**2.87**
20	**9.55**	8.96
30	5.12	**5.36**
40	9.10	**9.59**
50	**10.90**	10.01
60	10.18	**11.31**
70	8.55	**9.59**
80	10.15	**11.46**
90	10.74	**12.21**
100	9.69	**11.61**
Average	8.69	**9.30**

We analyze the obtained network topologies by considering the length of the edges and the physical degree of the nodes.

Figure 10 compares the algorithms by considering the average edge length. We can see that PSO generates network topologies with small length edges for instances with 40 - 100 nodes. We can also see that, for instances with 60 - 100 nodes, MST has better performances than ToCMA in terms of the average edge length. This situation can happen because in the MST algorithm the total length of all the edges is minimized.

We also note that, the average edge length decreases as the number of nodes increases (the network density increases as the number of nodes increases). This is a consistent fact, since the coordinates of the nodes, for all the instances, were generated on the same two-dimensional plane.

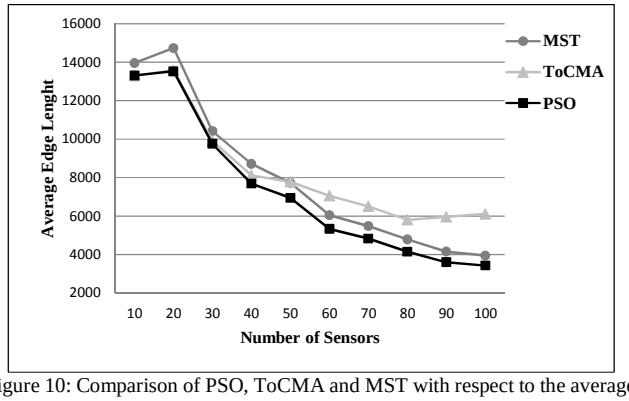

Figure 10: Comparison of PSO, ToCMA and MST with respect to the average edge length.

Figure 11 compares the algorithms with respect to the average physical degree of the nodes. The PSO algorithm generates network topologies with smaller degrees for instances with 40-100 nodes. The maximum obtained average degree was 4. Although this degree is maintained as the number of nodes increases, the average degree increases in the networks obtained by the other algorithms.

As the number of nodes increase, PSO has better performances than ToCMA and MST in terms of the total energy consumption, average edge length and average physical degree. Based on that, we can conclude that PSO has generated a more robust network topology structure than others.

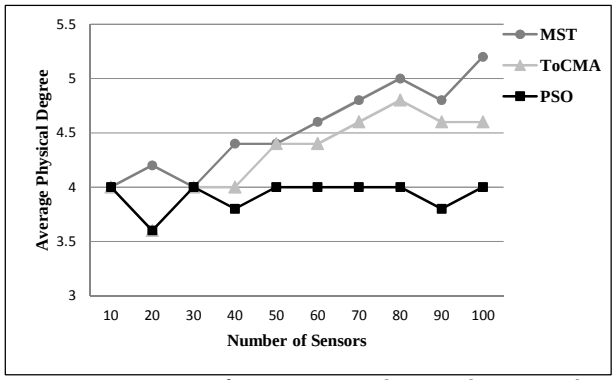

Figure 11: Comparison of PSO, ToCMA and MST with respect to the average physical degree.

5 Conclusions

In this paper, we have addressed a NP-complete problem on Topology Control in ad hoc wireless networks, with the objective of minimizing the total energy consumption while obtaining a strongly-connected topology. We have proposed a Particle Swarm Optimization algorithm in order to reduce the total power consumption. The experimental results verified the efficiency and competitiveness of the proposed algorithm by comparison with ToCMA and MST algorithms. The PSO generated networks not only with better total energy consumption (the main considered objective) but also with smaller average edge lengths and smaller average degree of nodes, indicating a better topology.

Acknowledgment

This work was funded by the Conselho Nacional de Desenvolvimento Científico e Tecnológico (CNPq), the Fundação de Amparo à Pesquisa do Estado de Minas Gerais (FAPEMIG) and the Fundação Arthur Bernandes (FUNARBE).

6 References

[1] M. X. Cheng, M. Cardei, X. Cheng, L. Wang, Y. Xu, and D.-Z. Du, "Topology Control of Ad Hoc Wireless networks for Energy Effciency", IEEE Transactions on Computers, vol. 53, no. 12, pp. 1629-1635, 2004.

[2] I. F. Akyilldiz, W. Su, Y. Sankarasubramaniam and E. Cayirci, "A survey on sensor networks", IEEE Communications Magazine, pp. 102−114, 2002.

[3] P. Santi. "Topology Control in Wireless Ad Hoc and Sensor Networks", ACM Computing Surveys, 37, 2, pp. 164–194, 2005.

[4] A. Konstantinidis, K.Yang, H-H. Chen, and Q. Zhang. "Energy-aware topology control for wireless sensor networks using memetic algorithms," Computer Communications, vol. 30, 14-15, pp. 2753-2764, 2007.

[5] L. Sun, J. Guo, K. Lu, and R. Wang. "Topology control based on quantum genetic algorithm in sensor networks," Front. Electr. Electron. Eng. China, 2(3): pp. 326–329., 2007.

[6] J. Kenned, and R.C. Eberhart. "Particle swarm optimization," In: Proceedings of IEEE international conference on neural networks. NJ: Piscataway, pp. 1942–1948, 1995.

[7] L.F. Liu and Y. Liu, "Topology control scheme based on simulated annealing algorithm in wireless sensor networks," Journal on Communications, vol.27, pp.71-77, 2006.

[8] W.T. Chen and N.-F. Huang, "The strongly connecting problem on multihop packet radio networks," IEEE Transactions on Communications, 37(3), pp 293-295, Mar. 1989.

[9] X.-Y. Li, "Topology Control in Wireless Ad Hoc Networks, Ad Hoc Networking," edited by S. Basagni, M. Conti, S. Giordano, and I. Stojmenovic, IEEE Press, 2003.

[10] C.-C. Shen, and Z. Huang, "Topology Control for Ad Hoc Networks: Present Solutions and Open Issues, Handbook of Theoretical and Algorithmic Aspects of Sensor, Ad Hoc Wireless and Peer-to-Peer Networks," edited by J. Wu, CRC Press, 2005.

[11] Z. Huang, and C.-C. Shen. "Distributed Topology Control Mechanism for Mobile Ad Hoc Networks with Swarm Intelligence," In ACM SIGMOBILE Mobile Computing and Communications Review, Volume 7 Issue 3, 2003, doi: 10.1145/961268.961273

[12] R. Montemanni, L. M. Gambardella, and A.K. Das, "The Minimum Power Broadcast Problem in Wireless Networks: A Simulated Annealing Approach," IEEE Communications Society / WCNC, 2005, doi: 10.1109/WCNC.2005.1424835.

[13] C.-C. Shen, and Z. Huang. "Theoretical and Algorithmic Aspects of Sensor, Ad Hoc Wireless and Peer-to-Peer Networks," edited by J.Wu. CRC Press, 2005. Topology Control for Ad hoc Networks: Present Solutions and Open Issues.

[14] Z. Huang; Zhensheng Zhang; Hua Zhu; Bo Ryu; "Topology Control for Wireless Ad hoc Networks: A Genetic Algorithm-based Approach," Communications and Networking in China, 2006, doi: 10.1109/CHINACOM.2006.344828.

[15] W. Guo, H. Gao, G. Chen, H. Cheng, and L. Yu, "A PSO-based Topology Control Algorithm in Wireless Sensor Networks," Proceedings of the 5th International Conference on Wireless communications, networking and mobile computing, 2009, doi: 10.1109/WICOM.2009.5301105.

[16] Montgomery, D. "Design and Analysis of Experiments," John Wiley & Sons, New York, NY, fifth edition, 2007.

Analysis of the Structure and Function of Phono-semantic Compounds Based on Complex Networks

Jianyu Li[1], Jie Zhou[2], and Xiaowen Mao[3]
[1]Engineering center of Digital Audio and Video, Communication university of China, Beijing, 100024 China
[2]Department of Automation, Tsinghua University, Beijing, 100084 China
[3]School of Computer Science, Communication university of China, Beijing, 100024 China

Abstract— *Complex network has been used in phono-semantic compounds in this paper, especially the degree correlation, hierarchical structure, diversity of the function of nodes and their relationships has been studied. We found that high degree nodes tend to be connected to low degree nodes, displaying a disassortative mixing property in the whole; some nodes can act both as phonetic radical and semantic radical, leading to a more complicated structure; and the hierarchical structure makes the disassortative mixing property more obvious. This paper reveals that phono-semantic compounds are optimal combination of phonetic radicals with semantic radicals, and they bear the merits of easy remembering, easy spreading and easy understanding. The phono-semantic compounds follow the principle of least effort [1] and characteristics of human cognitive mechanism.*

Keywords: Disassortative Mixing, Hierarchical Structure, Complex Network, Phono-semantic Compounds, Degree Correlation

1. Introduction

There are various complex systems, whose internal members interact with each other to reach a dynamical balance. This phenomenon is common in nature and human society, to name a few, brain structures, food chain networks, the Internet and WWW. The properties of those complex systems could be described by theories of complex network. A node is utilized to demonstrate an entity and an edge to depict their connection. Nodes and edges connectively form the entire network. Recently, quite a lot of work have been carried out making a more detailed analysis of the structure of complex networks[2][3][4]. People find that social interactions[5][6][7][8] and technology structures[9][10] characterize the assortative mixing, others such as brain networks[11], food chain networks, cell networks[12] and online social networks(OSN)[13] reflect disassortative mixing. Besides, some networks, such as metabolic network[14] and Chinese character network[15], even have hierarchical structure.

Chinese characters are carriers of Chinese culture and visualization of Chinese way of thinking. Study their formation and construction are very meaningful. Research of Chinese characters could disclose the behavior, lifestyles and ideology of ancient Chinese. For example, the existence of so many derogatory characters constructed with "女" (e.g. "奸", "嫉", "妓", etc.) in Chinese characters reflect the thousands-year-old traditional ideology of patriarchy. When ancient Chinese created characters, usually they constructed them based on the objects' appearances intuitively. These objects are common in people's daily life such as "氵" (water), "艹" (grass), "木" (wood). That's why a great deal of characters were constructed with the radicals "氵", "艹", "木" etc.

Quite a lot of contribution has been made in analysis of the Chinese language using complex networks theory. Li[16], Yamamoto[17], and Wang[18] built phrase related networks which display scale free and small world features. In [16], the nodes are meaningful words which may be single Chinese character or multi-character combination. Jianyu Li [15][19] found that Chinese phrase networks display some important features: not only small world and the power-law distribution, but also hierarchical structure and disassortative mixing. But in the area of Chinese characters not many results are yet reported. More than 80 percents of Chinese characters is phono-semantic character. Phono-semantic compounds consist of phonetic radicals and semantic radicals, which could be treated as nodes in our network. This paper mainly investigates the degree correlation, diversity of the function of nodes, hierarchical structure and their relationship in phono-semantic compounds network.

2. Data preparation

2.1 Concepts

Complex network is different from regular network and random network, because it has some special features, such as small world and scale free, etc. Recently, people studied more properties of complex network, for example, degree distribution, average path length (APL for short) and clustering coefficient, etc.

The degree of a node in a network is the number of connections or edges the node has to other nodes. If one node has a high degree, and widely connected, it must be good at composing characters in Chinese characters structure network. The degree distribution is very important in studying both real world networks, such as the Internet

and social networks, and theoretical networks.The degree distribution $P(k)$ of a network is then defined to be the fraction of nodes in the network with degree k. Thus if there are N nodes in total in a network and N_k of them have degree k, we have

$$P(k) = \frac{N_k}{N}. \tag{1}$$

Average path length is the average shortest distance of two nodes.

$$APL = \frac{1}{N(N-1)} \sum_{i \neq j \in V} d_{ij}(ij), \tag{2}$$

where d_{ij} is the shortest distance of node i and node j. The correlation is characterized by the

$$C_i = \frac{2e_i}{k_i(k_i - 1)} \tag{3}$$

and defined as the rate of edges e_i actually connected with node i and all links over i, where k_i is the degree of i. And average clustering coefficient of the whole network is

$$C = \frac{1}{N} \sum_{i=1}^{N} C_i. \tag{4}$$

2.2 Network construction

Semantic radicals and phonetic radicals are treated as nodes to construct a phono-semantic compounds network. If two nodes could construct a Chinese character, that means they are relevant. According to Xinhua Dictionary, the most widely used dictionary in China, we divided 4000 Chinese characters into 211 semantic radicals and 1084 phonetic radicals. We construct the networks in the following senses.

- Two nodes are connected if relevant.
- Self-connections are ignored.
- Variants (such as 足, 𧾷) of a semantic radical are treated as two different nodes.
- Node which can be used as both semantic radical and phonetic radical (e.g. "木" is semantic radical in "桦", and it is phonetic radical in "沐"), will be treated as one single node.

Based on above, we construct a phono-semantic compounds network:

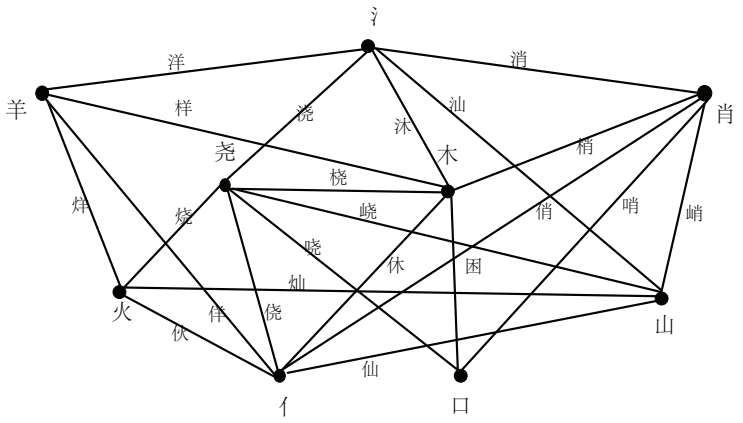

Fig. 1: Part of phono-semantic compounds network

3. Analysis

3.1 Degree Correlation

There are several correlation coefficients, often denoted r, measuring the degree of correlation. Pastor-Satorras[20], describe degree correlation using a straightforward method, which calculate degree of nodes connected to node that degree is k, and the result is a function of k. If high degree nodes tend to be connected to low degree nodes, we call the network to have a disassortative mixing pattern, and when high degree nodes tend to link to other high degree nodes, it appears assortative mixing feature. If the network has an assortative mixing pattern, the value of function is increase by degrees, vice versa. An uncorrelated network exhibits the neutral degree-mixing pattern whose function is constant. After that, Newman[21][5] simplified the method of calculating degree correlation. The correlation could be characterized by the assortativity $r(-1) \leq r \leq 1$ and defined as the Pearson correlation coefficient:

$$r = \frac{M^{-1} \sum_i j_i k_i - [M^{-1} \sum_i \frac{1}{2}(j_i + k_i)]^2}{M^{-1} \sum_i \frac{1}{2}(j_i^2 + k_i^2) - [M^{-1} \sum_i \frac{1}{2}(j_i + k_i)]^2}, \tag{5}$$

where j_i and k_i are the remaining degrees at the two ends of an edge and M represents the number of all links. r range from -1 to 1. When $r > 0$, we call the network to have an assortative mixing pattern, and when $r < 0$, disassortative mixing. An uncorrelated network exhibits the neutral degree-mixing pattern whose $r = 0$.

According to statistics, there are 1295 nodes in our phono-semantic compounds network, and the average number of links between semantic radicals is 18.8768, while that between phonetic radicals is only 3.6744. Obviously, semantic radicals could construct more Chinese characters than phonetic ones, which quite directly leads to the observation that semantic nodes have higher degree. The correlation coefficient is $r = -0.4155$, which is negative. Table 1 lists many concrete examples in real social network and TechNet, etc.

Table 1: Degree assortativity coefficients of various kinds of networks. N indicates the number of nodes, r is degree assortativity coefficient[15][21].

Network	N	r
physics coauthorship	52909	0.363
biology coauthorship	1520251	0.127
mathematics coauthorship	253339	0.120
Film actor collaborations	449913	0.208
Chinese character network	4892	−0.4097
Chinese phrase network	4858	−0.0645

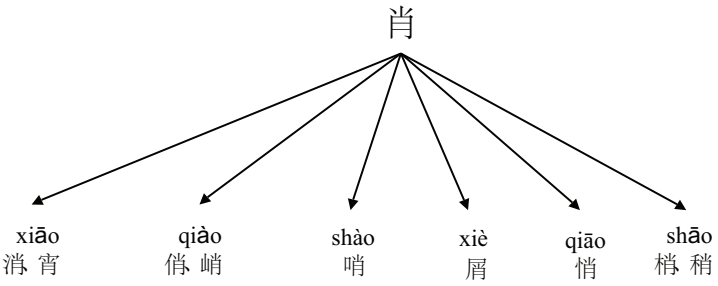

Fig. 2: Pronunciations of characters constructed by the phonetic radical "xiao".

Compare with social network, phono-semantic compounds network is similar to Chinese phrase network [15]. It is disassortative mixing, which means the high degree nodes tend to be connected to low degree nodes. Generally speaking, semantic radicals are nodes of high degree and phonetic ones are low degree nodes. Disassortative mixing in this paper means high degree semantic radicals prefer to be linked to low degree phonetic radicals. The semantic radical suggests only a general category of meaning of the compound character and it does not provide a specific meaning or definition. Their degrees tend to be higher. But the phonetic couldn't be higher, otherwise it could be a big challenge for people to remember so many characters with the same pronunciation. Therefore the disassortative mixing tendency in constructing Chinese characters follows the principle of least effort [1]. The constructed characters are easy to be recognized by their semantic radicals and their low degree phonetic radicals.

3.2 Diversity of nodes' function

Table 2 lists the top ten of characters construction capability. Study reveals that the characters constructed by the same phonetic radicals may not pronounce uniquely (22 characters constructed by "肖" have 6 pronunciations).

Table 2: Top ten of the highest characters construction of nodes in phono-semantic compounds network. The number of characters these nodes can construct has been given in brackets.

radicals	Top ten
semantic radicals	氵(270), 木(202), 扌(191), 口(168), 艹(162), 亻(151), 钅(134), 讠(108), 月(102)
phonetic radicals	肖(22), 非(21), 令(21), 各(20), 古(20), 且(19), 交(18), (18), 青(18), 包(17)

This phenomenon not only exists in high degree phonetic nodes, but also in low degree ones. We divided this case into four categories:

- Character with the same pronunciation as their phonetic radical (消xiāo and 宵xiāo e.g.);
- Character with pronunciation differs only in tone from their phonetic radicals(such as 匪fěi and 痱fèi);
- Characters with pronunciation differs only in consonants or vowels from their phonetic radicals (俏qiào, 悲bēi, 冷lěng e.g.);
- Characters with pronunciation differs both in consonants and vowels from their phonetic radicals (罪zuì, 排pái e.g.).

According to statistics, Type.1 accounts for about 38.5%, Type.2 accounts for 17.6%, Type.3 accounts for 26.3%, Type.4 accounts for 17.6%. Evidently, it is extremely common that characters with the same phonetic radical pronounce differently. In fact, such differentiation is good for understanding and memorization. For instance, people can hardly understand what are you talking about if 22 characters constructed by "肖" all pronounce xiāo. Beyond that, one semantic radical may have multiple meanings too. For example, "日" could construct a large number of characters as semantic radical. "昭", "晴", "昕", "晞", "曦", "曜" and "晓" all have meaning of bright, while "晚", "昏", "暗" and "暮" have meaning of dusk. However, they are all relevant to light. So instead of indicating the accurate meaning of characters, semantic radicals can only show a general concept.

In phono-semantic compounds network, we also found some nodes which can be used as both semantic radicals and phonetic radicals (such as "木" is a semantic radical in "桦", but it is a phonetic radical in "沐"). There are 119 this kind of nodes approximately. It accounts for 56.4% of the semantic nodes, accounts for 11.0% of the phonetic nodes and accounts for 9.3% of the whole network nodes. Almost half of semantic radicals are this kind of nodes and they play a very important role in our network. Because the average number of characters which are connected to them is 21.9160, while semantic and phonetic nodes' is only 18.8768

and 3.6744. That's why the semantic radicals can construct more characters than phonetic ones. This kind of feature not only makes phono-semantic compounds network more complex, but also makes nodes' function more various.

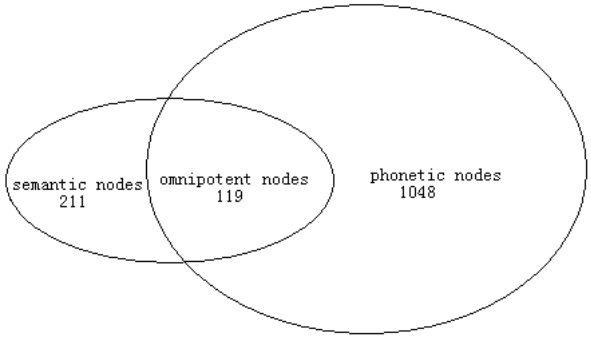

Fig. 3: Relational graph of semantic, phonetic and omnipotent nodes(nodes can be as both semantic radicals and phonetic radicals)

3.3 Hierarchical structure

As we know, several concepts are proposed to measure the hierarchy in a network, such as the hierarchical path[22], the scaling law for the clustering coefficients of the nodes[23], etc. These measures can tell us the existence and the extent of hierarchy in a network.

In this paper our networks are multilevel. Like Fig.4, simple components are used to form complicated components (phono-semantic characters), then the complicated components are used to form more complicated ones. For example, "付" and "广" are used to construct "府", and "府" are used to construct "腐". We call the phono-semantic characters such as "付" and "府", the "mid-components" provisionally. "Mid-components", 194 in network, are all phonetic radicals, which tend to be connected to semantic radicals. They generally have low power on phono-semantic compounds construction, the average number of characters they can construct is only 2.4536. Compare with simple components, the mid-components have a tendency of stability. The more complicated the components are, the less characters they can construct. Because too complicated structure of Chinese characters is not convenient for writing.

Table 3: Average degrees of different radicals.

Nodes	Average degree
Phonetic radicals(total)	3.6744
Phonetic radicals(except "mid-components")	4.7072
Semantic radicals	18.8768
"Mid-components"	2.4536

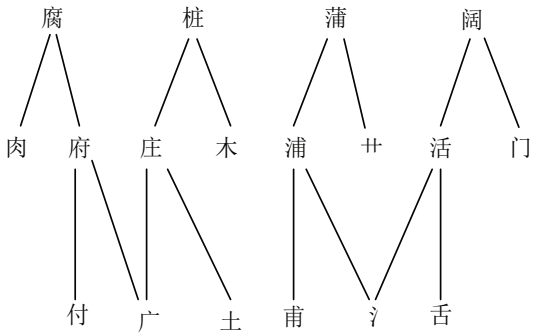

Fig. 4: Illustrating how a "mid-component" is constructed and how a "mid-component" constructs a new phono-semantic character

The intrinsic hierarchy can be characterized in a quantitative manner using the recent finding of Drogovtsev, Goltsev, and Mendes[24]. If the clustering coefficient of a node with k links follows the scaling law, like

$$C(k) \sim k^{-1}, \tag{6}$$

so the network have hierarchical structure. We found our phono-semantic compounds network have following characteristics like Fig.5.

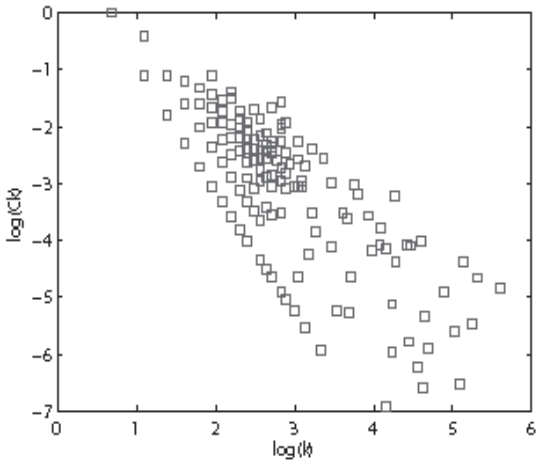

Fig. 5: Relationship between degree and clustering coefficient of nodes

We can see the phono-semantic compounds network has the tendency of hierarchy. The Chinese ancients reuse the preexisting simple characters to construct the new ones. It reduces the burden of the memory of people and improves the efficiency of creating characters.

4. Conclusion

We have already known that phono-semantic compounds network has diversity of the function of nodes. It is also hierarchical and disassortative mixing. Some nodes can be

used as both phonetic radicals and semantic radicals. Thus the network is more complicated. Moreover, some “simple components" are uses to form “complicated components" and the “complicated components" are relatively harder to combine with other components than the simple ones. So their degree is relatively low. The emergence of these nodes with low degree makes the disassortative mixing of the network more obvious.

We use complex network to analyze phono-semantic characters. We can not only learn extensive and profound Chinese culture better, but also understand the unique and creative formation of Chinese characters from ancient Chinese. Moreover, it will help us devise more interesting Chinese character learning course. And based on the differentiation of different radicals' degree, we can improve the layout of “Five-stroke Coding System", a well known character input method.

References

[1] R.F. i Cancho and R.V. Solé. Least effort and the origins of scaling in human language. *Proceedings of the National Academy of Sciences of the United States of America*, 100(3):788, 2003.

[2] A. Sundararajan. Local network effects and complex network structure. *The BE Journal of Theoretical Economics*, 7(1):46, 2008.

[3] S. Boccaletti, V. Latora, Y. Moreno, M. Chavez, and D.U. Hwang. Complex networks: Structure and dynamics. *Physics reports*, 424(4):175–308, 2006.

[4] M.E.J. Newman. The structure and function of complex networks. *SIAM review*, pages 167–256, 2003.

[5] M.E.J. Newman. Assortative mixing in networks. *Physical Review Letters*, 89(20):208701, 2002.

[6] M.E.J. Newman and J. Park. Why social networks are different from other types of networks. *Physical Review E*, 68(3):036122, 2003.

[7] DP Croft, R. James, AJW Ward, MS Botham, D. Mawdsley, and J. Krause. Assortative interactions and social networks in fish. *Oecologia*, 143(2):211–219, 2005.

[8] M. Catanzaro, G. Caldarelli, and L. Pietronero. Social network growth with assortative mixing. *Physica A: Statistical Mechanics and its Applications*, 338(1):119–124, 2004.

[9] J. Tanimoto. The effect of assortative mixing on emerging cooperation in an evolutionary network game. In *Evolutionary Computation, 2009. CEC'09. IEEE Congress on*, pages 487–493. IEEE, 2009.

[10] G. Bagler and S. Sinha. Assortative mixing in protein contact networks and protein folding kinetics. *Bioinformatics*, 23(14):1760–1767, 2007.

[11] V.M. Eguiluz, D.R. Chialvo, G.A. Cecchi, M. Baliki, and A.V. Apkarian. Scale-free brain functional networks. *Physical review letters*, 94(1):18102, 2005.

[12] A.L. Barabási and Z.N. Oltvai. Network biology: understanding the cell's functional organization. *Nature Reviews Genetics*, 5(2):101–113, 2004.

[13] H.B. Hu and X.F. Wang. Disassortative mixing in online social networks. *EPL (Europhysics Letters)*, 86:18003, 2009.

[14] E. Ravasz, A.L. Somera, D.A. Mongru, Z.N. Oltvai, and A.L. Barabási. Hierarchical organization of modularity in metabolic networks. *Science*, 297(5586):1551, 2002.

[15] J. Li and J. Zhou. Chinese character structure analysis based on complex networks. *Physica A: Statistical Mechanics and its Applications*, 380:629–638, 2007.

[16] LI Yong, W. Luoxia, N. Yi, and Y. Junxun. Structural organization and scale-free properties in chinese phrase networks. *£ÆÑğÍÍśÍ*, 50(13), 2005.

[17] K. Yamamoto and Y. Yamazaki. A network of two-chinese-character compound words in the japanese language. *Physica A: Statistical Mechanics and its Applications*, 388(12):2555–2560, 2009.

[18] J. Wang, L. Rong, and T. Jin. An empirical study of chinese word-word language directed network. In *Service Operations and Logistics, and Informatics, 2008. IEEE/SOLI 2008. IEEE International Conference on*, volume 1, pages 498–501. IEEE, 2008.

[19] J. Li and S. Yang. Visual clustering of complex network based on nonlinear dimension reduction. *Intelligent Information Processing III*, pages 555–560, 2007.

[20] M. Boguná, R. Pastor-Satorras, and A. Vespignani. Absence of epidemic threshold in scale-free networks with degree correlations. *Physical review letters*, 90(2):28701, 2003.

[21] M.E.J. Newman. Mixing patterns in networks. *Physical Review E*, 67(2):026126, 2003.

[22] A. Trusina, S. Maslov, P. Minnhagen, and K. Sneppen. Hierarchy measures in complex networks. *Physical review letters*, 92(17):178702, 2004.

[23] E. Ravasz and A.L. Barabási. Hierarchical organization in complex networks. *Physical Review E*, 67(2):026112, 2003.

[24] S.N. Dorogovtsev, AV Goltsev, and J.F.F. Mendes. Pseudofractal scale-free web. *Physical Review E*, 65(6):066122, 2002.

Distributed Energy-Efficient Target Tracking with Binary Proximity Sensors

S.M.R. Farshchi
ASR Centre for Embedded Systems Research
Sadjad Institute of Technology
Iran, Mashhad.
Mr.farshchi@sadjad.ac.ir

Arash Ghazi askar
School of Engineering and Design
Sadjad Institute of Technology
Iran, Mashhad.
Ghaziasgar@sadjad.ac.ir

***Abstract*— In this paper we use binary sensor networks, in which sensors send only one bit for tracking a particular target, passing through a field of sensors. We show that there are some geometric properties in binary sensor networks which help us improve the tracking in this kind of network. This algorithm differs even further from the previous method in that all nodes in the network are the same. The performance of this algorithm was tested with a large set of Monte Carlo simulations. Another, smaller set, of Monte Carlo simulations were generated, and those for which this algorithm could not give an answer with certainty were re-analyzed by a human in a series of blinded tests, using data from a Range Doppler plot, i.e. data about the targets' range and radial velocity over time. It was determined that the performance of both tests increased as the targets' relative radial velocities and track times increased.**

I. INTRODUCTION

Sensors are used to measure many things such as temperature, humidity, light, sound and many other things.in binary sensor networks , there is no need to send all the data which is sensed , instead , just one bit gives us a good minimal description . In target tracking subjects, binary sensor networks are used to track objects pass a trajectory in the network environment. Sensors only send one bit, 1 – if the object is getting nearer to the sensor or, 0- if the object is going away from the sensor. Obviously, we can see that this method of tracking only inform us about the direction which the target is going along, but does not give enough information about the exact location of target. Although the direction information is enough for some situations, we can have the location information by adding another binary sensor to the primary sensor. By knowing this, we can assume the location of the object too.

Besides using particle filter method, we have three assumptions implicitly. First, the sensors distributed within a region are able to sense the object which is getting near or getting far. The sensing radius of sensors forms the size and scope of this region.

Second, all the data gathered by the sensors, are sent to a processing station – a base station. Since our information is just one bit, it is possible to send this information easily.

And the third assumption is that we can use a secondary sensor to define the location of the object passing along a trajectory. That kind of a sensor may be implemented as an IR sensor with thresholding that depends on the favorite proximity range, and can also be derived from the same basic sensing element that provides the original direction bit of information.

A second method of viewing targets is by a Range Doppler plot. This plotting technique again uses scatterer range as one axis but instead of time for the second, it uses the Doppler return of the scatterer at that range. Range Doppler plotting is rooted in the practice of target identification, decision making on what is and is not an object of interest. Although it has been used heavily for target imaging, cases have been made for its usage as a tool for tracking. A tumbling and/or spinning target will have returns from scatterers on its body, which can lead to an image that is similar in dimension to the object that sourced the signal returns.

Analogous to a Range Time plot, target history can be recorded in the form of a track showing past data in Range Doppler plotting. Much like the Range Time plots, Range Doppler plots contain tracks that may bear no resemblance to the Newtonian trajectory of the targets. As with the Range Time plot's tracks which cross, the crossing tracks of a Range Doppler plot may not reflect targets' doing so in reality. The true area of interest is whether the two plotted crossings are brought about by different situational parameters.

II. RELATED WORKS

In some cases like sensor networks [7], tactical battlefield surveillance, air traffic control, perimeter security and first response to emergencies, target tracking is used as an essential point of interest.

Many methods such as Kalman filter approaches about how a target can be tracked, has been proposed .one of the recent methods is particle filtering. This method which is introduced in the field of Monte Carlo simulations quantizes probability deployment of the target location rather than maintaining the whole feasible position space. This matter would be obtained by maintaining multiple copies of an object. These copies which own a specific weight are called particles. Whenever an event occurs (usually sensor reading), a new set of particles are generated, and also the corresponding weights are updated. The main paper about this method is [9].from that time to now, many papers used this technique, but some of the most important are variance reduction scheme [8] and auxiliary particle filter [12].

There has been number of probabilistic approaches applied in robotics for simultaneous localization and mapping (SLAM), where the robot try to track itself using observed location of numerous landmarks.in some cases like [10], particle filtering is used as a successor method, if the Kalman filter had failed.

Sensor networks encounter two main problems. The first problem is the energy efficiency of the whole network and sensors.in [3] some schemes for developing the network energy saving with a little loss in tracking quality is proposed. The second problem is considering efficient processing in gathering data by sensors.in [2], a location-centric approach ,dynamically divides the sensor set into geographical cells run by manager.

In [4] , a method for tracking a target in a clustered area , run by 3 sensors to track the object. This approach uses a distributed protocol.

Track crossings can come from a single target which splits apart into multiple targets. It may seem counter-intuitive at first that targets moving away from each other would result in crossings on a Range Time plot, but the crossing occurs for the same reason as before; radar loses spatial separation because it reduces three dimensional trajectories to one dimension range measurements.

As you might guess, since we use binary sensor networks and in these kinds of networks only one bit of information is transmitted to the base station, many of the issues mentioned above are not a major problem.

III. The Binary Sensor Network Model

As we said earlier, in binary sensors only one bit is sent. From this one bit information , we decide the type of sensor. We call the sensor a "plus sensor" , whenever the target is moving toward that sensor (getting nearer) and we call the sensor a "minus sensor" , whenever the target is moving away from that sensor . All the information from this area of sensing – namely "active region of sensor network" – is sent to base station . The data bit along with sensor id , is contained in the message transmitted to the base station . Since the sensor detection might be noisy , thresholding and hysteresis is used to detect the movements of the object and computing the direction .we assume the base station is informed about the location of each sensor . We also assume that all the sensors are able to sense the target movement over the same space .

Let consider m binary sensors $S= \{S_1,S_2,\ldots,S_m\}$ are distributed inside a 2D environment, object U is moving within the region along a curve Γ and $X(t)$ is one of its parametric representations . sensors do not sample the environment all the time , instead, environment is sampled only in specific intervals of time , creating a sequence of binary m-vectors $s \in \{-1,1\}^m$ (with $s_i^{(j)} = +1/ -1$ denoting U is getting close/ going away from sensor i at time t_j). Afterward we would like to achieve a measure of the trajectory X of U for the given position of the sensors.

A. The Instantaneous Sensor Network Geometry

First of all , we show one of important properties of plus and minus sensors in the form of a lemma .

Inductive proximity sensors are designed to have a type of hysteresis in their circuitry that is used to eliminate output chattering. As a target approaches the sensor's detection face, it eventually triggers a sensor output. When the target moves away from the sensor's detection face , the triggered output holds until a certain distance has been passed.

The distance, called the "reset distance" or "distance differential," can be as high as 10% if the sensor's total sensing distance. This holds proportionally true for detection objects that cause reduced sensing distances. Make sure that the target object is completely removed beyond the sensor's reset distance to avoid all potential chattering from detectable object vibrations or other environmental factors.

When using a multitude of inductive proximity sensors in an application, be aware of an effect called mutual interference. This occurs when one proximity sensor's magnetic field affects another sensor's magnetic field causing it to trigger an output. This false triggering can be erratic and difficult to detect.

Look for inductive proximity sensors that feature alternate frequency models. These alternate frequency sensors oscillate their magnetic fields in different frequencies and do not interfere with one another as much as two inductive proximity sensors with the same frequency. Simply take one frequency proximity sensor and mount it next to one of a different frequency. Inductive proximity sensors are a simple and effective sensing tool. Avoid application problems by planned implementations, and your applications will be a success.

Like the super node algorithm implementation this algorithm also assumes that cluster head nodes have more power than normal sensor nodes. However, sensor nodes are not assigned to clusters in this algorithm. Instead, they are invited to join a cluster by the cluster head. The cluster head does this by broadcasting a join message that includes the time and signature of the target the cluster head detected [7]. Those sensor nodes that have stored data that matches the data in the broadcast message respond to the broadcast by sending their captured data to the cluster head node.

Interestingly, the cluster head only waits for a certain number of replies and when that number of replies has been received the cluster head calculates the target's location. Also, unlike the supernode algorithm, this algorithm only has one active cluster head at a time. In other words, cluster heads do no work together [7].

Considering constraint noted in Section 3, we can use a "Particle filter -like" algorithm to track the object.

The main idea in particle filter is to represent the location of density function which can be done by set of random points called "Particles". Each time a sensor event (For example a reading) occurs , these particles are updated , and the algorithm calculates an estimation of actual location based on these samples and weights. We can keep a sample set with all weights equal to each other (like what is represented in [9]) , or , use the idea of each particle being assigned different values (like what is proposed in [8]) . At each phase a set of particles (or possible positions) with weights updated according to the probability of going from the location at time $k-1$ (represented by $xk-1\ j$) to the location at time k (represented by x^k_j). This probability is estimated by $p(y_k|x^k_j)$. The first particle set is generated by drawing N independent particles outside the sensing circle of the "plus" and "minus" sensors at the time of the first sensor observing. Next, with each sensor observing , a new set of particles is produced as follows:

1. A previous position is selected according to the "old weights"
2. A probable successor is selected for this position
3. If this successor respects verification conditions (which is problem-specific and will be explained in next Subsection add it to the set of new particles and calculate its weight.

The above order of phases is repeated until N new particles have been created. The last phase is to normalize the weights so they sum up to 1.

Algorithm 1 Particle Filter Algorithm

Initialization: A set of particles $(x^1_j, w^1_j = \frac{1}{N})$ for $j = 1, \ldots, N$
$k = 1$
while y_k (sensor readings) $\neq \emptyset$ (sensors still active) **do**
  $k = k + 1$
  repeat
    choose j from $(1, 2, \ldots, N) \sim (w^{k-1}_1, \ldots, w^{k-1}_N)$
    take $x^k_j = \hat{f}_k(x^{k-1}_j, y_k)$
    if x^k_j respects "goodness" criterion **then**
      accept it as a new particle
    end if
  until N new particles have been generated
  for $j = 1 : N$ **do**
    $w^k_j = w^{k-1}_j * \hat{p}(y_k|x^k_j)$
  end for
  Normalize vector $(w^k_1, \ldots, w^k_N)$
end while

Sensor observations are aggregated to only one bit vector shown as y_k (k is the time parameter). The target's movement f is measured by taking x^k_j within the zone given by the following restrictions :

- x^k_j has to fall outside the "minus" and " plus" convex hulls (from Theorem 2)
- x^k_j has to fall *inside* the circle of center $S+$ and of radius the distance from $S+$ to $x^{k-1}{}_j$ (from Proposition 4), where $S+$ can be any "plus" sensor at sampling times $k-1$ and k
- x^k_j has to fall *outside* the circle of center $S-$ and of radius the distance from $S-$ to $x^{k-1}{}_j$ (from Proposition 4), where $S-$ can be any "minus "sensor at sampling times $k-1$ and k

Proximity sensing is the ability of a robot to tell when it is near an object, or when something is near it. This sense keeps a robot from running into things. It can also be used to measure the distance from a robot to some object. This sensing capability can be engineered by means of optical-proximity devices, eddy current proximity detectors, acoustic sensors or other devices.

Proximity sensors currently come in four flavors:

1. inductive

operates by detecting the eddy current losses when a material enters to an electromagnetic field

2. capacitive

operates by generating an electrostatic field and detecting changes in this…field caused when a target approaches the sensing face.

3. ultrasonic

Ultrasonic sensors detect objects by emitting bursts of high-frequency sound . waves which reflect or "echo" from a target.

4. optical

designed to be sensitive to different wavelengths of light

IV. Tracking With a Proximity Bit

As we discussed earlier in Theorem 7, under some special conditions , two trajectories may be indistinguishable from each other. Therefore , we add another feature to identify the target's location. This is done by adding another sensor , namely Proximity sensor , for each binary sensor in the field . the sensing range of these sensors may vary , and are usually smaller than binary sensor's range itself .

A. Algorithm And Implementation

Algorithm 2 is just the modified version of Algorithm1 for every sensor node. In this algorithm, we have proximity bit (provided by Proximity sensors) and a motion direction bit (provided by motion direction binary sensors) .so if we remove the proximity feature, Algorithm 2 is simply equal to Algorithm 1.

Algorithm 2 Algorithm for Binary Sensors with Range

```
Use Algorithm 1 as basis.
if sensor S sees the object then
  for all accepted particles P not inside the range of S do
    Let P' (a new particle) be the intersection between the range of S and semi-line (PS]
    Let P_1, ..., P_k be the ancestors of P since the last time the object was spotted.
    for i = 1 to k do
      P_i = P_i - (P - P')/(k+1)
    end for
  end for
end if
```

B. Experiments

Initially, transition probabilities are set as $\pi_{11} = 0.95, \pi_{12} = 0.05, \pi_{21} = 0.05, \pi_{22} = 0.95$ and the simulation result is shown in Figure 4.3. Since it is assumed that the probability that a target keeps its current mode is high, mode changes occur in short period and clearly presented in Figure 4.3. On the other hand, when different values are chosen as transition probabilities, the mode changes have different characteristics. As expected, the difference between marginal values of each mode probability decreases as transition probabilities between two modes increases. In Figure 4.5, two mode probabilities during uniform motion (0 ~ 4 seconds and 8 ~ 12 seconds) are almost mixed, which makes it delicate to distinguish the current mode from the figure. In addition, transient response speed changes. In the first simulation, the actual mode change occurs at 4 seconds but the conversion point is at 4.8 seconds. That is to say, there is 0.8 second time delay. However, this time delay is vanishing as different transition probabilities are adapted. In the second and third simulations (Figure 4.4 and Figure 4.5), time delays are 0.4 and 0.1 seconds, respectively. Even though these three simulations assumed that there is no measurement noise, it helps us understand the influence of transition probabilities. The next chapter deals with the case when measurement noise is presented, and it shows that the result is more complex and more uncertain.

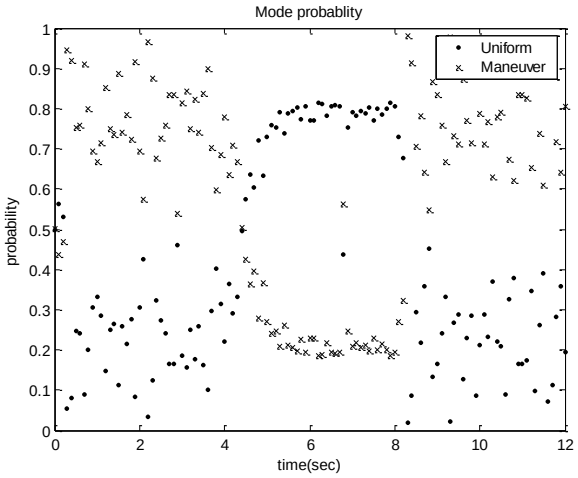

Fig. 4. Mode Probability: $\pi_{11} = 0.9, \pi_{12} = 0.1, \pi_{21} = 0.1, \pi_{22} = 0.9$

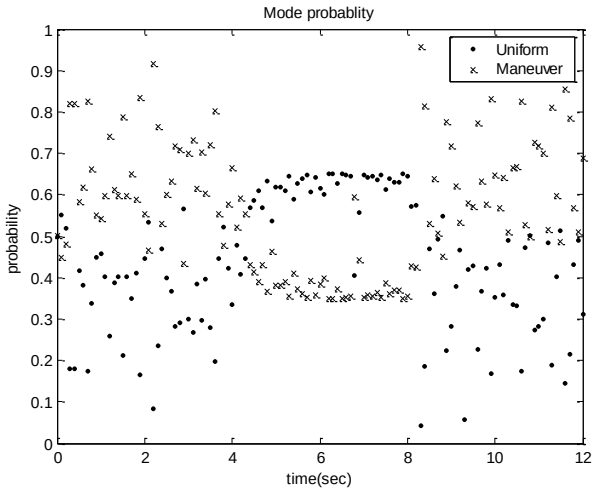

Fig. 5. Mode Probability : $\pi_{11} = 0.8, \pi_{12} = 0.2, \pi_{21} = 0.2, \pi_{22} = 0.8$

For simulation, three sensors are modeled under the assumption that they are radars, which is most commonly used in target tracking. Since radar measures the range and azimuth, they should be converted to the Cartesian coordinates. In simulation, predetermined target trajectory is converted to the polar coordinates and then converted to the Cartesian coordinates again after mixing with measurement noise. The most crucial value of the sensor is the standard deviation of the range measurement and the azimuth measurement, σ_r and σ_θ, respectively.

This algorithm deviates even further from the previously discussed algorithms. Cluster heads are special high powered nodes that know the location of every node within their cluster [10]. This algorithm takes advantage of the fact that the cluster head knows these locations. When sensor nodes detect a target, they send a very small notification message to their cluster head and store the target location

data, time and other relevant data in their local memory [10]. Upon receiving several notifications, the cluster head performs a probabilistic localization algorithm to determine which sensor nodes to query saved data from [10]. In other words, the cluster head runs an algorithm that helps it predict which sensor nodes are closest to the target and will therefore have the best data to use in order for the cluster head to calculate an accurate estimation of the target location. When the cluster head determines which nodes to query, they are asked for the data they saved in their local memory and the cluster head uses this to calculate the location of the target [10].

V. Conclusion

The main idea is that each sensor request information from only a subset of nodes which are more probable to flick on the basis of its local information. *S* supposes that the target moved on the same direction and traveled the same distance between times $t-2$ and $t-1$ as between times $t-1$ and t. so the requested information are only requested to the sensors flip base on this trajectory. We should also mention that the sensors request from a fixed number but randomly selected nodes .

At first each node is assigned a different region as possible starting place of the target. At first two time intervals every node gets the observations from all nodes so that the starting information is correct.

References

[1] S. Arulampalam, S. Maskell, N. J. Gordon, and T. Clapp, A Tutorial on Particle Filters for On-line Nonlinear/Non-Gaussian Bayesian Tracking, *IEEE Transactions of Signal Processing*, Vol. 50(2), 174-188, February 2002.

[2] R. R. Brooks, P. Ramanathan, and A. Sayeed, Distributed Target Tracking and Classification in Sensor Networks, *Proceedings of the IEEE*, September 2002

[3] B. Krishnamachari, Energy-Quality Tradeoffs for Target Tracking in Wireless Sensor Networks, *IPSN 2003*, 32-46.

[4] H. Yang and B. Sikdar, A Protocol for Tracking Mobile Targets using Sensor Networks, *Proceedings of IEEE Workshop on Sensor Network Protocols and Applications, 2003*.

[5] D. Crisan and A. Doucet. A survey of convergence results on particle filtering for practitioners, 2002.

[6] Bruce R. Donald, James Jennings, and Daniela Rus. Information invariants for distributed manipulation. *International Journal of Robotics Research*, 16(5):673‑702, 1997.

[7] W.E.L. Grimson, C. Stauffer, R. Romano, and L. Lee. Using adaptive tracking to classify and monitor activities in a site. In *Proc. of IEEE Int'l Conf. on Computer Vision and Pattern Recognition*, 22‑29, 1998.

[8] P. Clifford, J. Carpenter and P. Fearnhead. An improved particle filter for non-linear problems. In *IEE proceedings - Radar, Sonar and Navigation*, I46:2‑7, 1999.

[9] D. Salmond, N. Gordon and A. Smith. Novel approach to nonlinear/non-gaussian bayesian state estimation. In *IEE Proc.F, Radar and signal processing*, 140(2):107‑113, April 1993.

[10] Eduardo Nebot, Favio Masson, Jose Guivant, and Hugh Durrant-Whyte. Robust simultaneous localization and mapping for very large outdoor environments. In *Experimental Robotics VIII*, 200‑9. Springer, 2002.

[11] Lynne E. Parker. Cooperative motion control for multi-target observation. In *Proc. of IEEE International Conf. on Intelligent Robots and Systems*, pages 1591‑7, Grenoble, Sept. 1997.

[12] Michael K. Pitt and Neil Shephard. Filtering via simulation: Auxiliary particle filters. *Journal of the American Statistical Association*, 94(446), 1999.

[13] F. Zhao, J. Shin, and J. Reich. Information-driven dynamic sensor collaboration for tracking applications. *IEEE Signal Processing Magazine*, 19(2):61‑72, March 2002.

The Influence of the Surface Topography of Distributed Sensor Networks on Perception

Ozun Beyhan Ozkan[1], Oyku Ece Tosun[1], Arda Arslan[1], Ismail Cenk Gencer[1], Mustafa Ozcetin[2], Yelda Serindag[1], Korhan Memis[1], Serhan Ozdemir[2]

[1]Izmir Ozel Turk Science Private High School, Mithatpasa Street No: 687 - 689 35280, Kopru, Izmir, TURKEY

[2]Department of Mechanical Engineering, Izmir Institute of Technology, Artificial ***Iyte***lligence & Design Laboratory, Gulbahce 35430, Urla / Izmir TURKEY

Abstract - *This work investigates the effects of surface topography of the distributed sensor networks on perception through the differences in sensor readings. Compound eyes are found in some insects and crustaceans. Lateral inhibition is a biological signal processing which can increase contrast, enhancing perception. It is known that eye convexity helps increase field of view (FOV). A series of experiments were carried out to understand the effect of surface topography on local contrast gradient. Two sets of sensor networks of 5 x 5 were constructed. In the first network the board holding the sensors was a flat circuit board, whereas the second one was given a radius of curvature of roughly 30 cm. All readings were recorded in a dark chamber. Sensor networks were illuminated by a light source whose coordinates could be adjusted. Results are tabulated. It is seen that eye convexity in compound eyes improves perception, as well as FOV.*

Keywords: Lateral Inhibition, Distributed Sensor Networks, Contrast Enhancement, Convexity, Compound Eyes, Contrast Enhancement

1 Introduction

Haldan Keffer Hartline have studied the underlying principles of compound eyes for over thirty years by analyzing horseshoe crab (Limulus polyphemus) that has compound eyes. Hartline has shown that the photoreceptor cells in each ommatidium are connected in such a way that these cells drive down the output of the neighboring cells when stimulated. This leads to an increase in contrast and sensitivity in peripheral processing [1].

The literature search has found that almost no work exists about compound eyes with regards to topography and perception sensitivity. In fact the authors have failed to find one. One of the partially related research is about poly-visualization. Multi-lens visualization device used in medicine was designed by Joseph Rosen and David Abookasis. Their study has focused on the imitation of the visual processing of flies. Researchers combined individual photographs after scanning an object, and obtained a representative good picture. Images were averaged and dispersed beams were eliminated. This means strays at image were eliminated. This technique has been a solution for the problem on present devices [2]. But this study is about image improvement instead of increasing sensitivity in multiple sensing.

Another worth mentioning may be found in Istanbul Technical University. Ozcelik was inspired by the compound eyes of the insects in his thesis of subpixel information gathering and resolution improvement. The spinoff was a high-resolution low-cost camera in the similar working principles of a fly obtaining a single image from a multitude of images [3].

Last study models compound eyes and contrast enhancement. Workers there try to find a cost-effective sensory information processing setup for an engineering application. Coskun et al. [6] show that a low-cost but sensitive distributed sensor network is feasible. Nevertheless, there is also no link between surface topography and sensitivity increase in perception, given that everything else is the same.

2 Compound Eyes and Lateral Inhibiton

Ommatidium is a single simple eye unit of a wider ommatidia in a faceted compound eye. The number of ommatidium varies. There are roughly 4000 ommatidia in stablefly (Musca domestica). This number comes down to 300 at glowworms. It may reach 5000 for chafers, 9000 for Dytiscus, and up to 28 000 ommatidia for certain species [4].

Every ommatidium in a compound eye has a specific optic system. Every ommatidium has the basic anatomy form of a simple eye. There are retina and retina cells, rhabdomeres, masking pigments and axons, Figure 1.

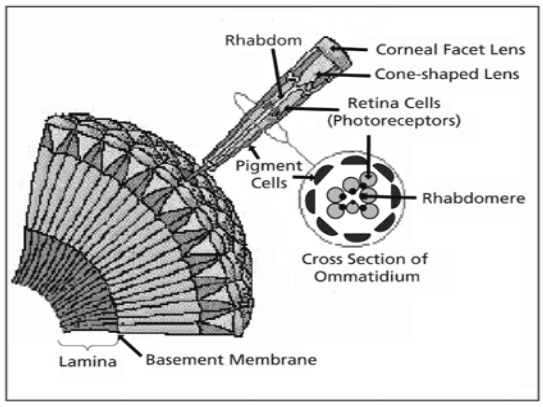

Figure 1. Form of Ommatidium [7]

Perceptions at compound eyes are somewhat different from simple eyes. Each ommatidium transmits the reverse images cast on retina to the brain. Number of images transmitted to the brain, is equal to the number of ommatidia. The brain stiches one image with the other. This composed new image is thought to be a mosaic-like image compared to what we see. This in turn likely to mean that the eventual composition is a high-resolution and high-contrast picture.

Contrast in mosaic-like vision is higher than the image formed by a simple eye. The main reason of this contrast difference is basicly Lateral Inhibition. Lateral inhibition (L.I.) is the dominant feature of biological distributed sensory networks where each individual receptor drives down each of its neighbors in proportion to its own excitation. The strengths of these connections are fixed rather than modifiable and are generally arranged as excitatory among nearby receptors and inhibitory among farther receptors. In other words, when any given receptor responds, the excitatory connections tend to increase its response while inhibitory connections try to decrease it [4, 5, 6].

The frequencies of discharge of each of two ommatidia were measured, for various intensities of illumination, when each was illuminated alone and when both were illuminated together. The below expressions show the amount of inhibition exerted upon ommatidium A by ommatidium B, as a function of the degree of activity of B, and shows the converse effect upon B of the activity of A [1, 5].

$$r_A = e_A - \beta_{AB} * (r_B - r_B^0) \quad (1)$$

$$r_B = e_B - \beta_{BA} * (r_A - r_A^0) \quad (2)$$

- r_A and r_B values are reactions of A and B ommatidiums after lateral inhibition,

- e_A and e_B are reactions of A and B ommatidiums without lateral inhibition,

- β_{AB} is inhibition coefficient of B ommatidium for A ommatidium,

- β_{BA} is inhibition coefficient of A ommatidium for B ommatidium,

- r_A^0 and r_B^0 are threshold frequency of A and B ommatidiums

3 Experiments on Surface Topography

At this study, photoresistors (LDR) were used to represent ommatidia in compound eyes. The test rig is composed of an aluminum frame, a light source whose height and position could be adjusted. Down below, there is a flat board to allow LDRs. The whole rig was then covered by a thick black cover in a darkened lab environment. In each setup, a total of 25 sensors were used. Light source was tuned in position so that sensor number 13 receives a maximum amount of light, and neighboring sensors give off a close reading, Figure 12 a. In Fig 12 b, the same test rig is used except that the board that all the sensors were mounted upon is convex with a rough radius of curvature of 0.3 meters. Sensor outputs were measured by a Keithley 2700 multimeter with multiplexers.

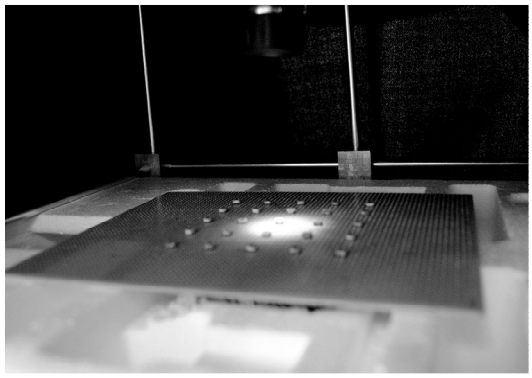

(a)

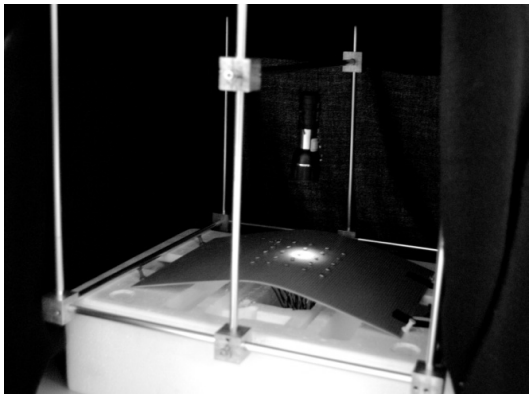

(b)

Figure 2 a, b. Compound Eye on Flat(a) and Convex(b) Surface

All the experiments were performed at two height levels for the light source, 196 and 100 mm. The convexity in the board was formed when the board was allowed to soak moisture and then shaped under a heat gun.

It is worth mentioning that if the Table 1 is inspected carefully, even though symmetrical, not all the neighbors received the same amount of light. This may be due to the fact that the light source may be slightly off the vertical, or the sensor normals do not coincide with the surface normals. To have a meaningful comparison, lower right quarter of the Table 1 was assumed to be measured from all the remaining three quarters, leading to Table 2. Table 1 gives resistance values (KOhm). Table 2 shows symmetrized version of Table 1. Table 3 gives the reciprocals of the resistance values, 1/R which is used at signal processing. Table 4, on the other hand, reflects these above-mentioned reciprocals after LI was applied with (α = 0,15 and β = 0,05). Including Table 4, the distance of the light source has been 196 mm and it is kept right above the 13th sensor. Then, to compare the convex and flat compound eye systems, the light source has been adjusted to 100 mm from the surface, and tabulated on the Table 5.

Table 1. Actual LDR Resistance Values, K Ohm

1. Sensor R = 11,831	2. Sensor R = 3,792	3. Sensor R = 3,518	4. Sensor R = 5,561	5. Sensor R = 10,196
6. Sensor R = 4,909	7.Sensor R = 1,439	8.Sensor R = 1,18	9. Sensor R = 1,921	10. Sensor R = 6,564
11. Sensor R = 2,93	12.Sensor R = 1,334	13.Sensor R = 0,991	14. Sensor R = 1,479	15. Sensor R = 5,805
16. Sensor R = 6,131	17.Sensor R = 1,988	18.Sensor R = 1,46	19. Sensor R = 2,379	20. Sensor R = 5,961
21. Sensor R = 8,63	22.Sensor R = 4,556	23.Sensor R = 4,13	24. Sensor R = 5,76	25. Sensor R = 12,616

Table 2. Symmetrized Resistance Values, K Ohm

1.Sensor R = 12,616	2.Sensor R = 5,961	3.Sensor R = 5,805	4.Sensor R = 5,961	5. Sensor R = 12,616
6.Sensor R = 5,961	7.Sensor R = 2,379	8.Sensor R = 1,479	9.Sensor R = 2,379	10. Sensor R = 5,961
11. Sensor R = 5,805	12.Sensor R = 1,479	13.Sensor R = 0,991	14.Sensor R = 1,479	15. Sensor R = 5,805
16. Sensor R = 5,961	17.Sensor R = 2,379	18.Sensor R = 1,479	19.Sensor R = 2,379	20.Sensor R = 5,961
21.Sensor R = 12,616	22.Sensor R = 5,961	23.Sensor R = 5,805	24.Sensor R = 5,961	25. Sensor R = 12,616

Table 3. 1/R Values

1.Sensor $\omega_1 \cong 0{,}079$	2.Sensor $\omega_2 \cong 0{,}167$	3.Sensor $\omega_3 \cong 0{,}172$	4.Sensor $\omega_4 \cong 0{,}167$	5. Sensor $\omega_5 \cong 0{,}079$
6.Sensor $\omega_6 \cong 0{,}167$	7.Sensor $\omega_7 \cong 0{,}420$	8.Sensor $\omega_8 \cong 0{,}676$	9.Sensor $\omega_9 \cong 0{,}420$	10. Sensor $\omega_{10} \cong 0{,}167$
11. Sensor $\omega_{11} \cong 0{,}172$	12.Sensor $\omega_{12} \cong 0{,}676$	13.Sensor $\omega_{13} \cong 1{,}009$	14.Sensor $\omega_{14} \cong 0{,}676$	15. Sensor $\omega_{15} \cong 0{,}172$
16. Sensor $\omega_{16} \cong 0{,}167$	17.Sensor $\omega_{17} \cong 0{,}420$	18.Sensor $\omega_{18} \cong 0{,}676$	19.Sensor $\omega_{19} \cong 0{,}420$	20.Sensor $\omega_{20} \cong 0{,}167$
21.Sensor $\omega_{21} \cong 0{,}079$	22.Sensor $\omega_{22} \cong 0{,}167$	23.Sensor $\omega_{23} \cong 0{,}172$	24.Sensor $\omega_{24} \cong 0{,}167$	25. Sensor $\omega_{25} \cong 0{,}079$

Table 4. 1/R Values Subjected To LI

1. Sensor $\gamma_1 \cong 0{,}05315$	2. Sensor $\gamma_2 \cong 0{,}11635$	3.Sensor $\gamma_3 \cong 0{,}1053$	4. Sensor $\gamma_4 \cong 0{,}11635$	5. Sensor $\gamma_5 \cong 0{,}05315$
6. Sensor $\gamma_6 \cong 0{,}11635$	7. Sensor $\gamma_7 \cong 0{,}3271$	8. Sensor $\gamma_8 \cong 0{,}59205$	9. Sensor $\gamma_9 \cong 0{,}3271$	10. Sensor $\gamma_{10} \cong 0{,}11635$
11. Sensor $\gamma_{11} \cong 0{,}1053$	12. Sensor $\gamma_{12} \cong 0{,}59205$	13. Sensor $\gamma_{13} \cong 0{,}94115$	14. Sensor $\gamma_{14} \cong 0{,}59205$	15. Sensor $\gamma_{15} \cong 0{,}1053$
16. Sensor $\gamma_{16} \cong 0{,}11635$	17. Sensor $\gamma_{17} \cong 0{,}3271$	18. Sensor $\gamma_{18} \cong 0{,}59205$	19. Sensor $\gamma_{19} \cong 0{,}3271$	20. Sensor $\gamma_{20} \cong 0{,}11635$
21. Sensor $\gamma_{21} \cong 0{,}05315$	22. Sensor $\gamma_{22} \cong 0{,}11635$	23. Sensor $\gamma_{23} \cong 0{,}1053$	24. Sensor $\gamma_{24} \cong 0{,}11635$	25. Sensor $\gamma_{25} \cong 0{,}05315$

4 Experiment Results

The first four tables reflect the trials for flat circuit board with sensors. So as to understand the influence of the surface curvature on the sensory perception, light source was pulled down to 100 mm distance from the nearest sensor, located at the center (number 13). These results may be seen on Table 5. The first column on Table 5 gives the ratio of certain resistance values. When no signal processing is made, raw independent readings show that the ratio of the 2nd sensor to the 3rd one is 1.67. This means, the 2nd sensor has 67 % more resistance than the 3rd one. The second and the third columns reveal ratio of resistance values at flat and curved surfaces. The last two columns display the cases of lateral inhibiton applied on flat and curved systems. Table 5 helps gather some important information. This information can be stated as follows:

When light is shed on the board centrally, light intensity naturally dies out toward the distant sensors. Even when there is no signal processing, this weakening of light from the center generates a natural contrast difference.

Table 5. Comparison Table

Contrast Between	Crude Data (Flat)	Crude Data (Curved)	Flat Data (After Lateral Inhibiton)	Curved Data (After Lateral Inhibiton)
R2 / R3	1.67	2.06	5.33	21.5
R7 / R8	3.20	3.18	10.52	8.75
R12 / R13	3.06	4.83	4.03	7.27

Second and third columns are the proof that curvature has a very positive effect on the contrast augmentation. If the ratio of R7/R8 is considered to be roughly the same, there is a 50% rise at R12/R13 value. With lateral inhibition, contrast is seen to wax even more for both flat and curved systems, but notably more so for the curved one. In our opinion, the discrepancy in R7/R8 ratios in all the four columns is due to misalignment of sensor 7 during surface mounting and soldering. Sensor 7 must slightly be off from the surface normal towards the light source in couple of degrees.

5 Conclusions

As seen from the experiments, contrast is being enhanced when a sensor network and lateral inhibition signal processing are adopted. It is also observed that when the radius of curvature of the board where the sensors were mounted gets smaller, the difference in consecutive sensor outputs increases. This is another way of saying that convex eyes not only allow a wider field of view but also augment the total light difference between light and dark areas in perception. Even though not reported here, another obvious advantage of a curved system is the capability of better localization of sources (light, for example), on the grounds that it simply makes the contrast gradient sharper. Curved facetted compound eyes thus must be quite an advantage in nature to both hunter and the prey alike. Hence, a good engineering application with a sensor net so as to have a sharper perception may involve a curved sensor board architecture, as well as an implementation of LI.

Acknowledgements

The authors would like to express their gratitude to Izmir Ozel Turk Science Private High School and Izmir Institute of Technology for their support throughout this work.

6 References

1. Hartline., H.K., Wagner, H.G., 1956, Ratcliff, Floyd, Inhibition in the Eye of Limulus, Journal of General Physiology, 39:5 pp 651-673
2. Joseph Rosen and David Abookasis, "Seeing through biological tissues using the fly eye principle", http://www.ee.bgu.ac.il/%7Erosen/fly_eye.pdf
3. Özçelik,E., Temmuz 2006 , Ardışık görüntüler ile piksel altı bilgi çıkarımı ve çözünürlük iyileştirme, Yüksek Lisans Tezi, İTÜ, İstanbul
4. Demirsoy, A., Yaşamın Temel Kuralları, Meteksan Yayınları, Ankara, Cilt 2 Kısım 219923 pp 158-169
5. Coskun, A. (2006), 'Contrast Enhancement by Lateral Inhibition in a Sensory Network', M.Sc. Thesis, Izmir Institute of Technology, Mechanical Engineering Department.
6. Coskun, A., Sevil, H.E., Ozdemir, S., "Cost Effective Localization in Distributed Sensory Networks", Engineering Applications of Artificial Intelligence, Vol 24, issue 2, pp 232-237, 2011.
7. http://www.isa.org/InTechTemplate.cfm?Section=Features3&template=/TaggedPage/DetailDisplay.cfm&ContentID=53255

SESSION

THEORETICAL ASPECTS OF AI + GAME THEORY AND APPLICATIONS

Chair(s)

TBA

Optimizing Japanese Domestic Airlines Network by Evolutionary Computation

Hiroki Inoue[1], Tomoya Sakagami[2], and Yasuhiko Kato[2]
[1]Institute of Economic Research, Kyoto University, Kyoto City, Kyoto Pref., Japan
[2]Department of Economics, Kumamoto Gakuen University, Kumamoto City, Kumamoto Pref., Japan

Abstract - *In recent years, various networks have come to exist in our surroundings. Not only can the internet and airline routes be regarded as networks; protein interactions are also networks. A network is defined as a structure of nodes (points) and links (lines). As described in this paper, an airline network is used as an example of an "economic network design problem." For the airline network, modeled based on a connection model proposed by Jackson and Wolinsky, a utility function can be defined as the sum of profits obtained from each route. Furthermore, an optimization simulation using the evolutionary computation is presented for a domestic airline in Japan.*

Keywords: Airline Network, Simulation**,** Network Game Theory, Evolutionary Computation

1 Introduction

In recent years, the Japanese aviation industry has been in dire straits, and the failure of Japan Airlines (JAL) has been well publicized. Although JAL has announced abolition of one loss-producing line one after another, All Nippon Airlines (ANA), which had been expected to replace JAL, has shown bad financial health. In such a situation, finding optimal airline networks that maximize profits is extremely important. Because the profits of other routes might also be affected by abolishing a loss-making line, it is necessary to consider transitions in an aviation network. Properly speaking, when abolition of a route is determined, it is desirable to consider not only the influence of the direct flight, but the concomitant increase and decrease of passenger traffic by effects on transit passengers. Therefore, this paper defines a profit function that regards the influence on transit passengers explicitly. We seek the optimal airline network that maximizes profits. In modeling of the airline network, connections models of Jackson and Wolinsky (1996) are extended to a model in which profits generate on a link and the utility function of the network is defined.

In the paper "airline network optimization problems," analyses were conducted for the network to maximize network utility, but finding optimal network theory is difficult when assessing real-world problems. Therefore, we propose a solution using evolutionary computation to resolve "airline network optimization problems." Furthermore, optimization simulation using evolutionary computation is demonstrated for a domestic airline in Japan. Optimal networks obtained when only the rate of the passenger discount by the transit was changed were found using the proposed algorithm.

The remainder of this paper is organized as follows. Section 2 formulates an "airline network optimization problem." Section 3 presents a description of a method of an "airline network optimization problem" using an evolutionary computation. Simulation results are presented in Section 4. Finally, we state the important conclusions in Section 5.

2 Airline network

An airline network is modeled in this paper based on Jackson and Wolinsky's (1996) connections model. In Jackson and Wolinsky (1996), the form that a stable network takes is analyzed under the situation in which formation of the link with a new each node (player)(relation) and an existing link disconnection are selected in the strategy. The network formation game theory proposed by Jackson and Wolinsky (1996) can become a substantial framework when dealings between varieties of economic agents are analyzed. For example, the conclusion distribution of the Free Trade Agreement in an international trade is foreseen, and it is applied to the analysis of the decision of the best airline line network etc. In the following, after first describing the utility function in the connections model, the airline network is modeled.

2.1 Connections model

As described in this paper, an economic network is denoted as a non-directed graph $G = (V, E)$ according to the graph theory. Graph G consists of node set V and link (edge) sets E. For example, a node in a graph represents an economic player (individual, group, city, and nation), and the link stands for a transport link, a telecommunication net, an economic regional alliance, etc. A link $e \in E$ is sets of node pairs $e = \{i, j\}$. A link between i and j is simply denoted ij. Considering a complete graph that consists of node set V, an economic network that consists of nodes (players) is subgraph G of complete graph K. The values of w_{ij} is an intrinsic value to obtain node i from node j by a direct link, and c_{ij} is the running cost of link ij. The utility function to obtain node i in graph G is defined as shown below.

$$u_i(G) = \sum_{j=1|i\neq j}^{|V|} \delta^{s_{ij}(G)} w_{ij} - \sum_{j=1|ij\in G}^{|V|} c_{ij} \qquad (1)$$

$|V|$: number of nodes in V
δ: decay rate of the gain
$s_{ij}(G)$: shortest path length in G
w_{ij}: gain to obtain node i from node j through link ij
c_{ij}: running cost of link ij

Furthermore, $\delta \in [0,1]$ is the decay rate of the gain. Considering the shortest path length s_{ij} between ij, $\delta^{s_{ij}(G)} w_{ij}$ is the gain to obtain node i from node j through the shortest path s_{ij}. Only when the link exists directly between ij is the link running cost c_{ij} needed. The graph value (utility of the entire network) is a summation of utilities of all nodes that exist in the network. The graph value is defined by the following equation.

$$u_{net}(G) = \sum_{i=1}^{|V|} u_i(G) = \sum_{i=1}^{|V|} \sum_{j=1|j\neq i}^{|V|} \delta^{s_{ij}(G)} w_{ij} - \sum_{i=1}^{|V|} \sum_{j=1|ij\in G}^{|V|} c_{ij} \quad (2)$$

The economic network design problem above can be formulated as follows.

$$\arg\max_{G \subseteq K_{|V|}} u_{net}(G) \quad (3)$$

2.2 Airline network model

There was a problem of lacking concreteness, although the connections model of Jackson and Wolinsky (1996) was able to assume various networks. Therefore, the analytical object is focused on the airline network. In the following, the airline network is modeled based on a connections model. The point in which the airline network model differs greatly from the utility function of connections model is to examine the utility obtained from a link.

In the airline network model, a node and a link respectively signify an airport and a route. The airline route with only the outward or homeward journey is a rare case. Therefore, the airline network is assumed to be a non-directed graph that does not incorporate the direction of the connection of the link. A link $e \in E$ of non-directed graph is a set of node pairs $e = \{i, j\}$ ($i, j \in V$ and $i \neq j$) without the order. A link between i and j is denoted simply as ij, and $ji = ij$. Furthermore, r_{ij} is an income of link ij; c_{ij} is an operation cost of link ij. The profit obtained between links ij in graph G is defined as

$$\pi_{ij}(G) = \begin{cases} r_{ij} - c_{ij} & if \quad ij \in G \\ \delta^{s_{ij}(G)-1} r_{ij} & otherwise \end{cases} \quad (4)$$

$|V|$: number of nodes (airport)
δ: decay rate of the profit
$s_{ij}(G)$: shortest path length in G
r_{ij}: income between i and j
c_{ij}: operation cost of link ij

Also, $\delta \in [0,1]$ is the decay rate of the profit. Considering that the shortest path length s_{ij} between ij, $\delta^{s_{ij}(G)-1} r_{ij}$ is the income got from node i by a passenger who goes to node j. Only when a direct flight exists between ij is operation cost c_{ij} needed. For these analyses, it is assumed that operation cost c_{ij} is necessary only for the direct flight's existing according to connections model. It is assumed that a flight need not be increased even if the number of passengers increases by an indirect link. Consequently, for aircraft that are not used over capacity, the load factor is at the 60% level also for the main route.

In addition, the income is the product of ticket price p_{ij} and the number of passengers q_{ij}. Also, δ is the product of the decay rate of ticket price δ_1 and the passenger decay rate δ_2. Equation (4), showing the price of the airline ticket and the number of passengers, can be rewritten as the income as follows.

$$\pi_{ij}(G) = \begin{cases} p_{ij} q_{ij} - c_{ij} & if \quad ij \in G \\ \delta_1^{s_{ij}(G)-1} p_{ij} \cdot \delta_2^{s_{ij}(G)-1} q_{ij} & otherwise \end{cases} \quad (5)$$

δ_1: decay rate of ticket price
δ_2: passenger decay rate
p_{ij}: ticket price between i and j
q_{ij}: passengers between i and j

Also, $\delta_1 \in [0,1]$ is the decay rate of the ticket price. The fare that a passenger must pay indeed gives a discount if the number of times of connection increases. In addition, $\delta_2 \in [0,1]$ is the passenger decay rate. Whenever the number of connections to the destination increases by δ_2, it is included in the model that the number of passengers decreases.

Next, operation cost c_{ij} is defined. Actually, c_{ij} is the operation cost of one year for the route between i and j, and the cost function is defined by the following equations.

$$c_{ij} = OP_{ij} \cdot FY_{ij} \quad (6)$$

OP_{ij}: cost per flight
FY_{ij}: number of annual flights

$$OP_{ij} = W(d_{ij} \cdot FU) + B \quad (7)$$

W: change of the weight by the number of passengers
d_{ij}: straight line distance between i and j
FU: fuel cost per km
B: airport landing fee

$$FU = LMX(FP + TAX)/RMX \quad (8)$$

LMX: maximum fuel capacity of the aircraft
FP: price per liter of jet fuel
TAX: fuel tax per liter
RMX: longest cruising range of aircraft

$$W = \frac{WE + PF_{ij} \cdot PW}{WE + PMX \cdot PW} \quad (9)$$

WE: operating empty weight of the aircraft
PF_{ij}: number of passengers per flight
PMX: number of seats of aircraft

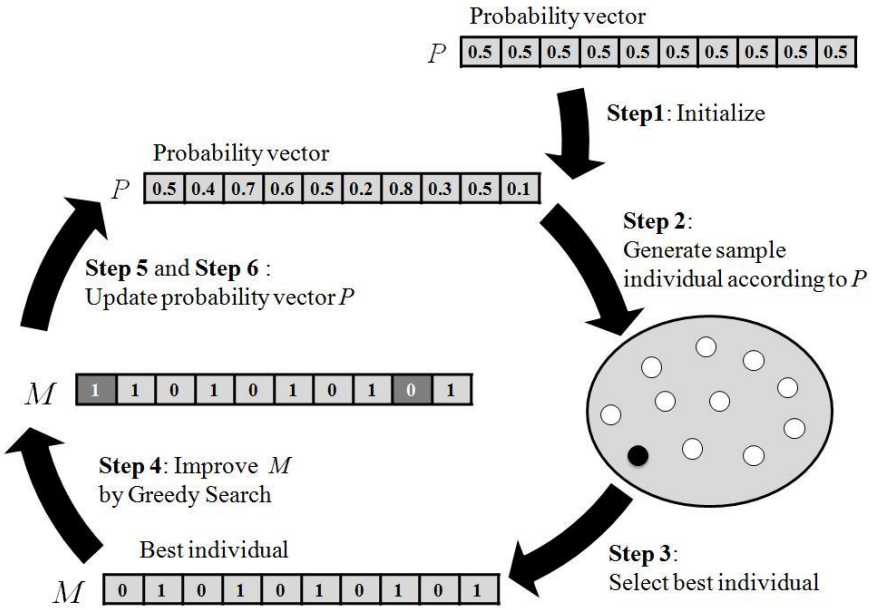

Fig. 1. Schematic diagram of algorithm.

PW: weight per passenger

The graph value $\pi_{net}(G)$ (profit of the entire airline network) is the summation of profits of all links in the network. The graph value $\pi_{net}(G)$ is defined by the following equation.

$$\pi_{net}(G) = \sum_{i=1}^{|V|}\sum_{j=1}^{|V|}\pi_{ij}(G) = \sum_{i=1}^{|V|}\sum_{j=1|j\neq i}^{|V|}\delta^{s_{ij}(G)-1}r_{ij} - \sum_{i=1}^{|V|}\sum_{j=1|ij\in G}^{|V|}c_{ij} \quad (10)$$

In equation (4), the profit when the direct link (direct flight) exists between *ij* differs when the direct link does not exist. However, no problem as $\delta^{s_{ij}(G)-1}r_{ij}$ exists because the shortest path length $s_{ij}(G) = 1$ when a direct flight exists. Equation (10) and equation (2) are the same structures if it is excluded that the exponent of δ is $s_{ij}(G)$-1. It is understood that the airline network model is a pure application of the connections model.

The airline network optimization problem above can be formulated as follows.

$$\arg\max_{G\subseteq K_{|V|}} \pi_{net}(G) \quad (11)$$

3 Evolutionary computation for "airline network optimization problem"

It is extremely difficult to analyze the network where the utility of the entire network is maximized in non-symmetric node (player) theoretically. One kind of evolutionary computation method, Population-Based Incremental Learning (PBIL) with a local search for the approximate solution method, is applied. Optimization of the network is tried. The basic operation of the improved algorithm is almost identical to that of the usual PBIL, but there is a difference in the update process of the probability vector. The difference point is to do a greedy search based on the selected excellent individual before the probability vector is updated. The former excellent solution is replaced if a better solution is found from the former excellent solution as a result of a greedy search. However, a local search examines the range of Hamming distance 1 as the neighborhood. This proposed algorithm is called G-PBIL. In the following, the schematic diagram of algorithm is presented in Fig. 1, and detailed processing of each Step is described.

Step 1: Initialization of probability vector $\vec{P}$

The probability vector $\vec{P} = (p_1, p_2, \ldots, p_{nbit})$ is the probability that each bit of the gene becomes 1. When the search begins, the probability vector is set to all 0.5. *nbit* is the gene length, which changes according to the scale of the problem. The probability vector in *t* generation (cycle) is written as $\vec{P}^t = (p_1^t, p_2^t, \ldots, p_{nbit}^t)$.

Step 2: Generate the sample population according to probability vector $\vec{P}$

Each individual is expressed by the bit string of 0 or 1 that is called a gene, and the probability vector is simply a description of the appearance probability of 1 by the vector.

Step 3: Evaluate the population, and select an excellent individual

The population is evaluated, and an excellent individual with the best fitness in the population is selected. The selected excellent individual is the notation

$M^t = (m_1^t, \ldots, m_{nbit}^t)$. A term called *fitness* is used because the right and wrong of an objective function values change with a minimization problem or maximum problem.

For a minimization problem, it is considered that a smaller objective function value has higher fitness.

Conversely, for a maximization problem, a greater objective function value indicates higher fitness.

Step 4: Greedy search based on a selected excellent individual.

First, the population that changes the gene of M^t by only one bit is generated. Next, fitness of the population that newly generates it is calculated, and the individual with the best fitness among former M^t and newly generated populations is new M^t. Greedy search is stopped if former M^t has best fitness. Otherwise, greedy search is tried again based on new M^t. However, when trying greedy search again, changing a bit again that has already changed from M^t from the first received from PBIL is forbidden. This rule limits the frequency of a greedy search. Even if it is the maximum, the frequency of a greedy search under this rule is gene length. The reason to adopt such a rule is that it is thought that the frequency of a greedy search becomes every high if the bit is changed unrestrictedly.

Step 5: Update probability vector

The probability vector is updated using excellent individual M^t improved by a greedy search.

$$p_i^{t+1} = (1.0 - LR)\, p_i^t + LR \cdot m_i^t \tag{12}$$

LR stands for the learning rate. When *LR* is large, the search will converge rapidly to the generation's excellent individual. To evade the initial convergence, *LR* should be set to a small value. However, because a generation number required for search increases when the value of *LR* is small, setting it to an extremely small value hinders the search.

Step 6: Mutation

Mutation occurs at a constant mutation probability, and the value of each element of the probability vector updated with Step 5 is changed further according to the following equation.

$$p_i^{t+1} \leftarrow (1.0 - MR)\, p_i^{t+1} + rand \cdot MR \tag{13}$$

Mutation Rate (*MR*) is a degree of the change by the mutation. The probability vector changes greatly by *MR* large. $rand \in \{0,1\}$ is a uniform random number.

Step 7: Repetition of Step 2 – Step 6

The processing of Step 2 – Step 6 is repeated until the termination condition is satisfied. It is defined as the first generation to repeat the processing of Step 2 – Step 6 once in PBIL. The termination condition of processing when the set number of generations is passed or the convergence of the search is admitted by the convergence criterion is usually adopted as a termination condition.

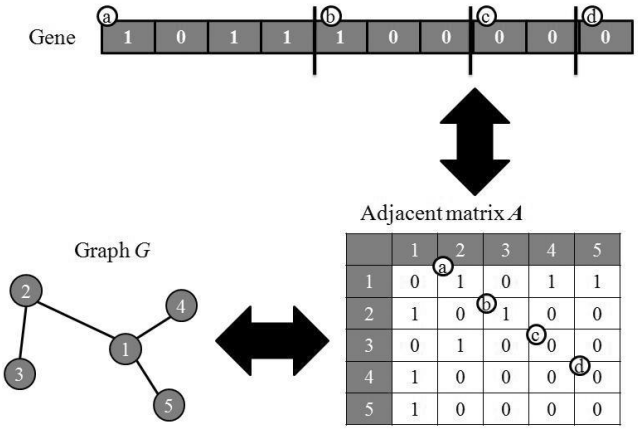

Fig. 2. Coding for a network graph with 0–1 design variable.

When this algorithm is adapted to the "network optimization problem" for which a design variable takes the discrete value of 0–1, it is necessary that a gene correspond to a graph as presented in Fig. 2. Denoting a graph by an adjacent matrix, and also making an adjacent matrix correspond to a genotype can express a graph with a gene. The adjacent matrix *A* of a graph *G* (airline network) is the matrix of |V|×|V|, where a_{ij} represents element of row *i* and column *j* of matrix *A*. It is assumed that a_{ij} =1 when the link (edge) exists directly between vertices *i* and *j*. It is also assumed that a_{ij} =0.

$$a_{ij} = \begin{cases} 1 & if \quad ij \in G \\ 0 & otherwise \end{cases} \tag{14}$$

When G-PBIL is adapted to the "network optimization problem" in which a design variable takes the discrete value of 0–1, the gene length is set as *nbit* = |*V*|(|*V*|-1)/2. In Step 3 of an algorithm, as presented in Fig. 2, a gene is changed to a graph, and the graph value is computed using equation (10). Making a computed graph value into the goodness of fit of a gene is synonymous with optimizing a graph to optimize a gene.

4 Simulation analysis of the optimal airline network

Here, the proposed algorithm is used and simulated. The simulation is targeted to 19 airports of Japan with domestic routes serving 1.5 million passengers or more annually. Figure 4 shows the existing network among the 19 airports.

4.1 Data

To conduct a simulation, some data are necessary: the ticket price p_{ij}, number of potential passengers q_{ij}, and straight line distance d_{ij} between *i* and *j*. First, we consider the ticket price p_{ij} between *i* and *j*. If between *i* and *j* is an existing route, p_{ij} examines the price of the airline ticket. However, the price cannot be examined about the route that does not exist. Then, the airline ticket price of the non-existent route is estimated by

TABLE I
Allocated populations of 19 airports (Unit: 10,000 people)

Airport name	Airport code	*pop*
1. Haneda	HND	3302.30
2. New Chitose	CTS	46.73
3. Osaka	ITM	1422.54
4. Fukuoka	FUK	312.09
5. Naha	OKA	134.70
6. Chubu	NGO	980.25
7. Kagoshima	KOJ	213.79
8. Kansai	KIX	188.20
9. Kumamoto	KMJ	184.38
10. Miyazaki	KMI	66.07
11. Hiroshima	HIJ	225.93
12. Sendai	SDJ	220.16
13. Kobe	UKB	337.01
14. Matsuyama	MYJ	122.93
15. Nagasaki	NGS	147.90
16. Komatsu	KMQ	98.09

the following regression by making the distance d_{ij} into an explanatory variable.

$$p = \alpha + \beta d \tag{15}$$

A single regression analysis that uses a straight line distance based on Google Map was done with the price of the airline tickets of All Nippon Airways (ANA). A significant result was obtained statistically by α = 15562.75 and β = 21.21 with correlation coefficient 0.89 and a coefficient of determination 0.80.

Next, passenger q_{ij} travelling between i and j is considered. Data existing for passengers between existing routes can be determined using data of the Ministry of Land, Infrastructure, Transport, and Tourism. Passenger q_{ij} of the non-existent route is estimated using the gravity model used well in aeronautic demand forecasting. A passenger can be estimated using the following formula and turns into the correlation coefficient 0.806 by a= 0 and b = 2.631×10^{-8}. However, only routes of not less than 300 km of distance can be estimated, and passenger q_{ij} for routes less than 300 km are set to zero.

$$q_{ij} = b\frac{pop_i \cdot pop_j}{{d_{ij}}^a} \tag{16}$$

pop : quota population of each airport

Data used as explanatory variables are the quota population of each arrival-and-departure airport and the distance in a straight line d_{ij} between airports. Because the quota population of each airport is needed here, we presume that the following methods are used. In this paper, a Voronoi diagram is drawn by setting each airport to the generatrix (node): the population of each area residing with a nearby airport is used most. The quota population (Table 1) of each airport was calculated by the figure of the area divisions and population data are given by Asahi Shimbun Publications. Data of the existing route are obtained using data provided by the Ministry of Land, Infrastructure, Transport and Tourism. Data estimated using the gravity model are used only for the non-existent route.

Each datum used for a cost function is set to a jet fuel value rank FP = 50 yen/liter, an aviation fuel tax TAX= 26 yen/liter, the landing fee B = 400,000 yen, and weight per passenger PW = 100 kg.

4.2 Optimization simulation

we simulate the case of one kind of aircraft. Data of the aircraft are computed from the average value of the main aircraft (Table 2). The determined optimal network by the simulation is presented in Fig. 3 – Fig. 6.

When the fare discount rate (1 - δ_1) and the passenger decrease rate (1 - δ_2) become small, the optimum network is clarified as centralized on Tokyo International Airport (Haneda). The fare discount rate (1 - δ_1) and the traveler decrease rate (1 - δ_2) become small as $\delta = \delta_1\delta_2$ becomes large. That relation corresponds to the previous work clearly to make the network excessively concentrated by growing of δ. The change to Fig. 4 from Fig. 3 occurs when the passenger decrease rate (1 - δ_2) becomes small. This change shows that the direct flight from the main island of Japan to Naha Airport is decreasing by two routes. The change to Fig. 5 from Fig. 3 changes when the passenger decrease rate (1 – δ_1) becomes small. This change shows that the direct flights from the main island of Japan to Naha Airport are decreasing by four routes, and that numerous direct flights between the airports in the main island of Japan are also decreasing. Furthermore, the change to Fig. 6 from Fig. 3 occurs when both the fare discount rate (1 - δ_1) and the passenger decrease rate (1 - δ_2) become small. The change to Fig. 5 from Fig. 3 and a difference are not apparent. Consequently, among the fare discount rate (1 - δ_1) and the passenger decrease rate (1 - δ_2), the fare discount rate (1 - δ_1) has a stronger influence on the optimal network. If the fare discount rate (1 - δ_1) is small, then because the airline can gain greater profits also from a transit flight (indirect link), it will be expected that the number of a direct flights will decrease. However, if it is expected that there is negative correlation in the fare discount rate and the passenger decrease rate, then the passenger decrease rate will become large when the fare discount rate becomes small.

Moreover, graph values of all the optimal network of Fig. 3 – Fig. 6 have exceeded graphed values of the existing network. Compared with the existing network, the optimal network by a simulation has a tendency with few routes in the graph of the optimal network. The tendency is notably apparent for the route involving Ishigaki Airport. Although a direct flight exists between each airport and Ishigaki Airport in the main island of Japan in the existing network, only the transit flight through Naha Airport exists in the optimal network graph. Therefore, cost cutting is possible by losing a direct flight with a great distance between Ishigaki Airport and the airport in the main

Fig. 3. Optimal network ($\delta_1 = 0.50$, $\delta_2 = 0.50$).

Fig. 4. Optimal network ($\delta_1 = 0.50$, $\delta_2 = 0.90$).

Fig. 5. Optimal network ($\delta_1 = 0.90$, $\delta_2 = 0.50$).

Fig. 6. Optimal network ($\delta_1 = 0.90$, $\delta_2 = 0.90$).

island of Japan. However, in this experiment, the passengers of a non-existent route are estimated using the population around an airport, and it cannot be considered that Ishigaki Island is a tourist resort. The route between Haneda Airport and Ishigaki Airport is known for a seat-occupancy rate being high, and probably, it is not realistic to abolish the route. Regarding this point, the seat-occupancy rate is included in a cost function, and improvement with a different seat-occupancy rate for every route can be considered.

5 Conclusion and Future work

As described in this paper, an airline network is modeled based on Jackson and Wolinsky's (1996) connections model. Moreover, the optimal network in an existing airline network is found using the airline network model. Results of simulations show that because a realistic network identified, the possibility exists that a connections model can be used as a framework for airline network analysis. Although Jackson reported that the connections model can be applied as a framework of various network analyses, few examples have been presented in which a connections model is actually

TABLE II
Aircraft data

	Boeing 747-400D	Boeing 777-300	Boeing 777-200	Average	Used data
Number of seats 2 class	524	451	400	458.33	450
Maximum fuel capacity (Unit: liter)	216840	171160	117335	168445.00	150000
Longest cruising range (Unit: km)	13450	11135	9696	11427.00	10000
Operating empty weight (Unit: kg)	181000	160000	138000	159666.67	150000

(Source: Japan Aircraft Development Corp.)

applied to actual network analysis. This paper has contributed a research example using a connections model. The G-PBIL algorithm that extended PBIL was used for optimization of an airline network. In the simulation, a network that is more efficient than the existing network can be found. When the fare discount rate and the traveler decrease rate were small, the optimum network was shown to centralize to Tokyo International Airport (Haneda).

Future works will expand the simulated range. With the G-PBIL algorithm, although improvement in search performance was sought using a local search together to PBIL, the time which search takes has also increased. The search time by local search increases as the network scale becomes large, and it becomes difficult to perform a simulation. Therefore, it is necessary to consider the proper balance of the evolutionary computation and the local search in G-PBIL. Moreover, although this simulation of only a domestic flight was performed, the international role of Haneda Airport can be clarified by adding main airports of the world. As a subject for other future work, analysis of the optimal airline network when an airport is closed or built is also possible by application of estimation of passengers using a Voronoi diagram and gravity model.

6 References

[1] Bala, V., and S. Goyal, "A Non-cooperative Model of Network Formation," *Econometrica*, Vol.68, pp.1181-1229, (2000a).

[2] Bala, V., and S. Goyal, "A strategic analysis of network reliability," *Review of Economic Design*, Vol.5, pp.205-228, (2000b).

[3] Biggs, N., E. Lloyd, and R. Wilson, *Graph Theory 1736-1936*, Oxford University Press, (1986).

[4] Baluja, S., "Population-Based Incremental Learning: A Method for Integrating Genetic Search Based Function Optimization and Competitive Learning," Technical Report, CMU-CS-94-163, (1994).

[5] Dijkstra, E.W., "A note on two problems in connexion with graphs," In *Numerische Mathematik*, Vol.1, pp.269-271, (1959).

[6] Freeman, L.C., "Centrality in Social Networks: I A Conceptual Clarification," *Social Networks*, Vol.1 pp.215-239, (1979).

[7] Galeotti, A., S. Goyal, and J. Kamphorst, "Network Formation with Heterogeneous Players," *Games and Economic Behavior*, Vol.54, pp.353-372, (2006).

[8] Goyal, S., and S. Joshi, "Bilateralism and Free Trade," *International Economic Review*, Vol.47, No.3, pp.749-778, (2006).

[9] Haller, H., and S. Sarangi, "Nash networks with heterogeneous links," *Mathematical Social Sciences*, Vol.50, pp.181-201, (2005).

[10] Jackson, M.O., and A. Wolinsky, "A Strategic Model of Social and Economic Networks," *Journal of Economic Theory*, Vol.71, pp.44-74, (1996).

[11] Johnson, C., and R.P. Gilles, "Spatial Social Networks," *Review of Economic Design*, Vol.5, pp.273-300, (2000).

[12] Mishra, S.K., "Performance of Repulsive Particle Swarm Method in Global Optimization of Some Important Test Functions: A Fortran Program," *Social Science Research Network* (SSRN) , Working Papers Series, http://ssrn.com/abstract=924339, (2006).

Data Fusion based on Game Theory for Speaker Diarization

Marta Barrilero and Federico Alvarez
Grupo de Aplicación de Telecomunicaciones Visuales
Escuela Técnica Superior de Ingenieros de Telecomunicación (ETSIT)
Universidad Politécnica de Madrid, Spain
{mbg@gatv.ssr.upm.es, fag@gatv.ssr.upm.es}

Abstract—*A novel algorithm based on bimatrix game theory has been developed to improve the accuracy and reliability of a speaker diarization system. This algorithm fuses the output data of two open-source speaker diarization programs, LIUM and SHoUT, taking advantage of the best properties of each one. The performance of this new system has been tested by means of audio streams from several movies. From preliminary results on fragments of five movies, improvements of 63% in false alarms and missed speech mistakes have been achieved with respect to LIUM and SHoUT systems working alone. Moreover, we also improve in a 20% the number of recognized speakers, getting close to the real number of speakers in the audio stream.*

Keywords: speaker diarization, bimatrix game-theory, data fusion.

1. Introduction

1.1 Speaker diarization

Speaker diarization is the process of splitting an audio recording with an unknown number of speakers into time segments according to a recognized speaker, and then clustering those fragments by speakers. It is known as the task of determining *Who spoke when?* [1]. This technique distinguishes between instants of speech, music or silence. Initially, it emerged as an initial process for the speech recognition, but over recent years has become an important independent task used in many fields, such as information retrieval or navigation. In fact, it has been mainly developed for broadcast recorded meetings [2], news audio and telephone conversations [3]. Generally, speaker diarization is a very useful tool in every field in which it is necessary the determination of the number of speakers, along with the time periods when each one is active.

The most remarkable applications for speaker diarization systems are reflected in the Rich Transcription evaluation series (RT) [4], a community which promotes and gauges advances in the state-of-the-art in several automatic speech recognition technologies. This community is sponsored by the National Institute of Standards and Technology (NIST) in the Unites States [4].

Unfortunately, few speaker diarization systems are available for public general use. Two of them are LIUM [5] and SHoUT [6], which are open-source systems available on the Internet, mainly developed for applications on broadcast news that use audio streams. In this paper, both LIUM and SHoUT systems are used for obtaining speaker diarization output data on audio streams from movies. We use a fusion system to select the best decision at every second of our input audio from LIUM and SHoUT programs, in order to reach a better reliability and accuracy in our whole speaker diarization system. This fusion is carried out by means of a novel algorithm based on bimatrix game theory.

1.2 Game theory

Game theory is the study of mathematical techniques for analyzing situations of cooperation or conflict (games) between two or more rational intelligent individuals (players) [7]. It was introduced by von Neumann in 1928 [8], and improved later together with Oskar Morgenstern by considering cooperative games of several players [9]. Subsequently, Nash introduced the *Nash equilibrium* criterion [10], which supposed an important advance. Game theory has been widely used in a great variety of fields, such as economics, political science, philosophy or engineering. One of its main goals is the study of intelligent rational decision making, since it allows the understanding and modeling of different rational strategies performed by diverse agents. This involves a considerable help and support in decision making systems.

The three main elements in a game are the players (typically two), their played strategies, and the pay-off matrix, which contains the received prize by each player for each strategy. *Zero-sum games* [7] are a particular case in which the interest of both players are strictly opposed, hence the pay-off matrix contain the same values in opposite signs. Players in this kind of games strictly play in a competitive way. On the other hand, *non-zero-sum games* [11] can contain some strategies which are equally beneficial or detrimental for both players. Therefore, in *non-zero-sum games* competitive and cooperative strategies are generally performed.

The modeled game in this paper is *non-zero-sum*. It executes a data fusion algorithm based on the comparison of two data outputs from two systems. These data can be processed

in a cooperative way, taking into account the outcome from both data sources, or in a competitive way, analyzing the different properties of every system, and selecting the best of them.

Fusion data systems related to game theory have been widely studied, mainly in military and general security fields. For instance, a data fusion aided platform routing algorithm based on game theory for cooperative intelligence is proposed by Shen et al. [12]. Other example is using a Markov stochastic game method to estimate the belief of possible cyber attacks patterns [13]. Although similar algorithms to the proposed in this paper have not been found in the literature, game theory is a powerful tool that can be successfully used for improving speaker diarization by means of fusion data algorithms.

2. Speaker diarization systems

2.1 LIUM

LIUM [14] is an open toolkit [5] for speaker diarization developed by the *Laboratoire d'Informatique de l'Université du Maine* [15] for the French ESTER2 evaluation campaign [16]. It obtained the best results for the task of speaker diarization of broadcast news in 2008. It is written in Java and performs methods such as Mel-frequency cepstral coefficients computation, speech/non-speech detection and speaker diarization, using some tools from the speech recognition system Sphinx-4 [17]. The main algorithm follows next steps:

1) Segmentation based on BIC (Bayesian Information Criteria): speaker change points are detected and the audio signal is split into segments.
2) BIC clustering: similar segments are joined together.
3) Segmentation based on Viterbi decoding: a new segmentation is generated.
4) Speech detection: in order to remove music and jingle regions, a segmentation into speech / non-speech is obtained using a Viterbi decoding with 8 one-state Hidden Markov Model.
5) Gender and bandwidth detection: detection of gender and bandwidth is done using a Gaussian Mixture Model (GMM) for each of the 4 combinations of gender (male / female) and bandwidth (narrow/ wide band). Each cluster is labeled according to the characteristics of the GMM which maximizes likelihood over the features of the cluster.
6) GMM-based speaker clustering: a hierarchical agglomerative clustering is performed over the last diarization in order to obtain a one-to-one relationship between clusters and speakers.

Audio input files used in the executions of the system are in Wave format (16kHz / 16bit PCM mono). Output files show the properties of the analyzed segment, along with several frequency values related to each found cluster.

Figure 1 shows an example of output file in LIUM. It provides the instants in which every speaker change is recognized, the speech segment length in centi-seconds, the gender of the speaker and the speaker label.

```
;; cluster:S10 [ score:FS = -33.40578264060857 ] [ score:FT = -33.96415644658132 ] [
score:MS = -33.946822434659126 ] [ score:MT = -34.11794073282604 ]
cena 1 1409 201 F S U S10
cena 1 2969 286 F S U S10
cena 1 3313 516 F S U S10
cena 1 3917 405 F S U S10
cena 1 5123 451 F S U S10
cena 1 5617 227 F S U S10
cena 1 6980 304 F S U S10
cena 1 7847 186 F S U S10
cena 1 8033 421 F S U S10
cena 1 17514 424 F S U S10
cena 1 29032 636 F S U S10
cena 1 36641 1098 F S U S10
cena 1 41561 500 F S U S10
cena 1 43503 292 F S U S10
;; cluster:S11 [ score:FS = -33.30782570921103 ] [ score:FT = -33.48750761571984 ] [
score:MS = -32.94431915767501 ] [ score:MT = -33.2660012560795 ]
cena 1 4774 349 M S U S11
cena 1 5968 312 M S U S11
cena 1 6328 416 M S U S11
```

Fig. 1: LIUM output file

2.2 SHoUT

SHoUT is a Dutch acronym for *Speech Recognition Research at the University of Twente*. It was completely developed by Marijn Huijbregts during his PhD research [18] at the University of Twente. It is also open source [6], and it is written in C++ in a Linux platform. SHoUT program follows next steps:

1) Speech activity detection: a silence-based segmentation strategy is employed based on silence and sound models training using HMM.
2) Segmentation and clustering: a new segmentation is performed merging multiple models throughout several iteration steps.
3) Automatic speech recognition: several features are extracted and normalized by means of cepstrum mean normalization and vocal tract length normalization. These features are decoded in order to obtain acoustic models dependent on speech clusters.
4) Acoustic model adaptation: the clustering information obtained during segmentation and clustering is used to create speaker dependent acoustic models.

The output file from SHoUT is shown in Figure 2. It is similar to the LIUM one previously explained, although the information length is provided using seconds as time unit.

3. Game modeling

A data fusion system has been designed according to a bimatrix game with the three main elements in every game: players, strategies and pay off.

```
SPKR-INFO SpeechNonSpeech 1 <NA> <NA> <NA> unknown SPK01 <NA>
SPEAKER SpeechNonSpeech 1 0.000 0.740 <NA> <NA> SPK01 <NA>
SPEAKER SpeechNonSpeech 1 89.780 0.740 <NA> <NA> SPK01 <NA>
SPEAKER SpeechNonSpeech 1 91.280 6.070 <NA> <NA> SPK01 <NA>
SPEAKER SpeechNonSpeech 1 98.110 2.030 <NA> <NA> SPK01 <NA>
SPEAKER SpeechNonSpeech 1 100.900 0.830 <NA> <NA> SPK01 <NA>
SPEAKER SpeechNonSpeech 1 102.490 0.980 <NA> <NA> SPK01 <NA>
SPEAKER SpeechNonSpeech 1 104.750 3.720 <NA> <NA> SPK01 <NA>
SPEAKER SpeechNonSpeech 1 109.520 0.740 <NA> <NA> SPK01 <NA>
SPEAKER SpeechNonSpeech 1 111.600 0.810 <NA> <NA> SPK01 <NA>
SPKR-INFO SpeechNonSpeech 1 <NA> <NA> <NA> unknown SPK05 <NA>
SPEAKER SpeechNonSpeech 1 119.220 1.470 <NA> <NA> SPK05 <NA>
SPEAKER SpeechNonSpeech 1 131.500 1.030 <NA> <NA> SPK05 <NA>
SPKR-INFO SpeechNonSpeech 1 <NA> <NA> <NA> unknown SPK02 <NA>
SPEAKER SpeechNonSpeech 1 132.530 3.210 <NA> <NA> SPK02 <NA>
SPEAKER SpeechNonSpeech 1 138.300 1.050 <NA> <NA> SPK02 <NA>
SPEAKER SpeechNonSpeech 1 144.460 1.030 <NA> <NA> SPK02 <NA>
SPEAKER SpeechNonSpeech 1 145.490 0.710 <NA> <NA> SPK01 <NA>
SPEAKER SpeechNonSpeech 1 148.030 1.820 <NA> <NA> SPK01 <NA>
SPEAKER SpeechNonSpeech 1 150.610 0.950 <NA> <NA> SPK01 <NA>
SPEAKER SpeechNonSpeech 1 152.320 0.500 <NA> <NA> SPK01 <NA>
SPEAKER SpeechNonSpeech 1 152.820 0.340 <NA> <NA> SPK05 <NA>
SPEAKER SpeechNonSpeech 1 157.730 0.740 <NA> <NA> SPK05 <NA>
```

Fig. 2: SHoUT output file

A. *Players*

We consider two players: A (LIUM) and B (SHoUT), which perform their strategies throughout the whole audio sample. Each played strategy corresponds to one second. Thus, the duration of the audio sample will determine the number of times the game is played, which is the same as the total number of performed strategies by each player.

B. *Strategies*

Each player can carry out three different strategies:

- *Strategy nº 1: No-change speaker*
  There is not a speaker change detection. The detected speaker in the current second is the same as the detected in the previous one.

- *Strategy nº 2: New speaker*
  A speaker change to an unknown speaker is detected, since the detected speaker in the current second is different to the detected one in the previous second. In addition, the current speaker is new, since he/she has not been previously detected in the audio sample.

- *Strategy nº 3: Former speaker*
  A speaker change is detected in the same way as in the previous strategy. However, the detected speaker in the current second has already been detected previously in the audio sample.

C. *Pay-off*

Initially, the pay-off matrixes have the same structure as a typical bimatrix game with two players and three strategies.

$$A = \begin{pmatrix} a_{11} & a_{12} & a_{13} \\ a_{21} & a_{22} & a_{23} \\ a_{31} & a_{32} & a_{33} \end{pmatrix} \; B = \begin{pmatrix} b_{11} & b_{12} & b_{13} \\ b_{21} & b_{22} & b_{23} \\ b_{31} & b_{32} & b_{33} \end{pmatrix} \tag{1}$$

The coefficients a_{ik} and b_{ik} stand for the pay-off received by player A (LIUM) and player B (SHoUT), respectively, if LIUM plays strategy i and SHoUT plays strategy k.

The fusion data system is designed according to a decider for this game. This decider performs the following steps. For each second:

1) Select LIUM and SHoUT strategy.
2) Compare both pay-offs, related to both strategies.
3) Choose the strategy which supposes highest pay-off for the corresponding player. The fusion system will adopt the selected strategy in current second.
4) Each player receives its pay-off.

Pay-off values have been decided according to the different observed behaviors in both diarization systems. The most reliable strategies have been assigned in line with the highest pay-off values. If a system is chosen by the decider, it receives a positive pay-off, whereas if the system has not been chosen, it receives the same pay-off value with negative sign. So far, a zero-sum game would be appropriate to model this behavior. However, there is another situation which must be taken into account: cases in which both systems perform the same strategy have been considered as the most reliable. In these cases, the decider certainly choose both systems. In addition, the selected strategy is provided with the maximum reliability since it is supported by two systems. Hence, these cases have been assigned to the highest pay-off values in both systems. Thus, a player receives a good pay-off if its strategy is chosen, but it receives an even better pay-off if both players are chosen. Consequently, the game is non-zero sum, and two pay-off matrixes are needed: therefore, the game is bimatrix. Moreover, several ideas that cause modifications in some pay-off values will be introduced subsequently.

To establish the required principles to set the pay-off values it is necessary to consider several properties related to both systems, which have been observed by means of several tests executed in both systems with different audio streams. The main goal of these considerations is to determine a direct relation between the reliability of each system and the pay-off values. On this way, the decider will select the most reliable strategy for each event, according to the pay-off values. The following properties have been implemented:

1) Initially, the pay-off related to different strategies for each player ($i \neq k$) are the same value with opposite

signs. Thus:

$$a_{ik} = -b_{ik} \qquad \forall i \neq k \tag{2}$$

2) If both systems execute the same strategy, the decider will certainly adopt it. Moreover, this strategy will be provided with the maximum reliability. Thus, in this case the pay-off values are the same and have the maximum value:

$$a_{ii} = b_{ii} \qquad \forall 1 \leq i \leq 3 \tag{3}$$
$$a_{ii} > a_{ik} \qquad \forall i \neq k \tag{4}$$
$$b_{ii} > b_{ik} \qquad \forall i \neq k \tag{5}$$

Note that these situations correspond to Nash equilibria [10], since they are maximum in both matrixes, i.e. they are optimum, and any other situation would suppose worse results. So, if both systems executed the same strategies all the time, the game would be constantly in an equilibrium point, reaching the maximum reliability.

3) Both systems perform silence, music and speech activity recognition with excellent results. In fact, the most remarkable found mistakes are related to errors in correct speaker identification. Specifically, both systems tend to consider former speakers as new speakers. Consequently, a detection of a former speaker (strategy nº3) is more reliable than a detection of a new speaker (strategy nº2). In addition, taking into account the negative pay-off values for non-chosen players, the final pay-off values fulfill the next properties:

$$a_{3i} > a_{21} > 0 \tag{6}$$
$$a_{i3} < a_{12} < 0 \tag{7}$$
$$b_{i3} > b_{12} > 0 \tag{8}$$
$$b_{3i} < b_{21} < 0 \tag{9}$$
$$\forall i < 3$$

Note that the pay-off values in entries below the main diagonal in A matrix are positive, since it supposes that the player A has been chosen. Same way in player B, but in this case the entries above the main diagonal are positive.

4) LIUM is more likely to detect erroneously new speakers than SHoUT. In fact, the final number of detected speakers by LIUM is commonly higher than the one by SHoUT. Therefore, a new speaker change detection in LIUM (strategy nº2) when SHoUT has not detected a change (strategy nº1) will be considered as less reliable than the opposite case:

$$a_{21} < b_{12} \tag{10}$$

4. Evaluations results

Several tests have been performed in order to evaluate the results of our fusion system. We have taken for the experiments audio segments with dialogues with different speakers from the movies *"Guess Who's Coming to Dinner"*, *"Marnie"*, *"Pride and Prejudice"*, *"Psycho"* and *"Sense and Sensibility"*. All the segments have been manually labeled to obtain the ground truth, creating a file with the same format as output files from LIUM and SHoUT programs. This reference file has the time slots from the audio sample associated to the proper speaker. To perform a numerical evaluation of the system, specific values have been assigned to A and B matrixes, according to the established properties on section 3.

$$A = \begin{pmatrix} 50 & -10 & -20 \\ 10 & 40 & -30 \\ 20 & 30 & 60 \end{pmatrix} \; B = \begin{pmatrix} 50 & 15 & 20 \\ -10 & 40 & 30 \\ -20 & -30 & 60 \end{pmatrix} \tag{11}$$

Therefore, numerical prizes have been settled to each player at the end of the execution of the fusion system. The prize values depend on the duration of each segment, since a different prize is obtained for each second. The obtained results are shown on Table 1, where it can be observed that SHoUT has *won the game* in every movie except in *"Psycho"*.

Table 1: Obtained prizes values.

Movie	LIUM	SHoUT	Duration (seconds)
Guess Who's Coming to Dinner	18190	18340	438
Marnie	23560	23620	603
Pride and Prejudice	19370	19555	463
Psycho	19500	19300	446
Sense and Sensibility	7120	7490	157

To evaluate the improvements introduced by our speaker diarization system, we have used the *Diarization Error Rate (DER)* value [20]. This parameter can be defined as the addition of the different possible errors of a speaker diarization system. In our experiment, *DER* has been defined as:

$$DER = FalseAlarmSpeech + MissedSpeech \tag{12}$$

False Alarm Speech is the number of times where a hypothesized speaker change is labeled as a non-change speaker in the reference. On the contrary, *Missed Speech* is the number of times where a hypothesized non-change speaker is labeled as a speaker change in the reference.

Silence activity detection can be also considered in a *DER* measure. Nevertheless, we have not taken it into account, since we have tested that the presented results by both systems in silence activity detection are much better than the results in speaker identification task, as it was explained

in section 3. Thus, only time slots related to detected speech have been considered.

The results obtained with LIUM, SHoUT, and our fusion system in terms of *DER*, are shown on Table 2, together with the added improvements (in %) by our system:

Table 2: *DER* and improvement values.

	DER			Improvements (%)	
Movie	LIUM	SHoUT	Fusion	LIUM	SHoUT
Guess Who's Coming to Dinner	22	19	4	82	79
Marnie	14	7	2	86	71
Pride and Prejudice	14	15	7	50	53
Psycho	12	11	3	75	73
Sense and Sensibility	5	10	4	20	60

On average, improvements of 63% and 67% on the *DER* parameter with respect to LIUM and SHoUT programs are reached with our fusion system. The less improvements correspond to those films, *"Pride and Prejudice"* and *"Sense and Sensibility"*, in which LIUM system performs lower *DER* than SHoUT. This can be translated into a possible unfairly performance of the fusion system, since the system which presents better results has *lost the game*. We are working to improve our system in these cases in order to reduce even more the *DER* parameter independently on the input stream.

In addition, the number of recognized speakers has been evaluated. As it has been previously explained, it is difficult to recognize properly former speakers, so the number of recognized speakers by speaker diarization systems is typically greater than the true value. However, our system reduces this number thanks to the fusion of strategies which allows clustering some speakers previously considered as different. The results are shown on Table 3. On average, we improve a 20% the number of detected speakers in comparison to the best output from LIUM and SHoUT systems working alone.

Table 3: Number of recognized speakers.

	Real speakers	Recognized			Improvements (%)	
Movie		LIUM	SHoUT	Fusion	LIUM	SHoUT
Guess Who's Coming to Dinner	4	19	8	6	68	25
Marnie	4	16	5	5	69	0
Pride and Prejudice	7	16	12	10	37	17
Psycho	5	8	9	6	25	33
Sense and Sensibility	3	6	7	4	33	43

5. Conclusions

In this paper we introduce a novel fusion algorithm based on game theory to improve the accuracy and reliability of two speaker diarization systems: LIUM and SHoUT. This algorithm is based on bimatrix game theory and performs a non-zero sum game. The establishment of the pay-off values has been carried out by means of different properties inferred by the analysis from both systems' behavior. The obtained tests show considerable advances of our fusion system in comparison to the results from LIUM and SHoUT programs working alone.

ACKNOWLEDGMENT

This paper is based on work performed in the framework of the Spanish national project BUSCAMEDIA (CEN-20091026), which is partially funded by the "CDTI-Ministerio de Economía y Competitividad".

References

[1] X. Anguera, S. Bozonnet, N. Evans, C. Fredouille, G. Friedland, O. Vinyals. "Speaker Diarization: A Review of Recent Research," *IEEE Transactions on Audio, Speech, and Language Processing* vol. 20, no.2, pp. 356-370, Feb. 2012.

[2] X. Anguera, C. Wooters, B. Peskin, M. Aguilo, "Robust speaker segmentation for meetings: The ICSI-SRI Spring 2005 Diarization System," in *Proc. Machine Learning for Multimodal Interaction Workshop (MLMI)*, Edinburgh, U.K., pp. 402-414, 2005.

[3] C. Barras, X. Zhu, S. Meignier,J-L. Gauvain. "Multi-Stage Speaker Diarization of Broadcast News", *IEEE Transactions on Audio, Speech and Language Processing*, vol. 14, no. 5, pp. 1505-1512, Sep. 2006.

[4] "The NIST Rich Transcription 2009 (RT'09) Evaluation", NIST 2009. [Online]. Available: http://www.itl.nist.gov/iad/mig/tests/rt/

[5] LIUM website. [Online]. Available: http://lium3.univ-lemans.fr/diarization/

[6] SHoUT website. [Online]. Available: http://shout-toolkit.sourceforge.net/use_case_diarization.html

[7] R. B. Myerson. "Game theory: analysis of conflict". Harvard University Press, ISBN 978-0-674-34116-6, 1997.

[8] J. v. Neumann. "Zur Theorie der Gesellschaftsspiele", Mathematische Annalen, 100(1), pp. 295-320, 1928.

[9] O. Morgenstern, J. v. Neumann. "The Theory of Games and Economic Behavior", Princeton University Press, 1947.

[10] J. Nash. "Equilibrium points in n-person games", *Proc. of the National Academy of Sciences*, pp. 48-49, 1950.

[11] A. Scodel, J. Sayer Minas, P. Ratoosh, M. Lipetz. "Some Descriptive Aspects of Two-Person Non-Zero-Sum Games" . *The Journal of conflict resolution 3* (195 9), pp. 114-119, JSTOR, 1959.

[12] D. Shen, G. Chen, J. Cruz, E. Blasch, "A game Theoretic Data Fusion Aided Path Planning Approach for Cooperative UAV Control," *IEEE Aerospace Conf., Big Sky, MT*, Mar. 2008.

[13] D. Shen, G. Chen, E. Blasch, G. Tadda, "Adaptive Markov Game Theoretic Data Fusion Approach for Cyber Network Defense", *IEEE Military Communications Conference*, 2007.

[14] S. Meignier, T. Merlin. "Lium SpkDiarization: An open source toolkit for diarization". In *CMU SPUD Workshop*, Dallas, Texas, USA, 2010.

[15] Laboratoire d'Informatique de l'Université du Maine website. [Online]. Available: http://www-lium.univ-lemans.fr

[16] P. Deléglise, Y. Estève, S. Meignier, T. Merlin, "Improvements to the LIUM French ASR system based on CMU Sphinx: what helps to significantly reduce the word error rate?", in *Interspeech*, Sep. 2009.

[17] W. Walker, P. Lamere, P. Kwok, B. Raj, R. Singh, E. Gouvea, P. Wolf, J. Woelfel. "Sphinx-4: A flexible open source framework for speech recognition", Tech. Rep., Sun Microsystems Inc., 2004.

[18] M. Huijbregts. "Segmentation, Diarization, and Speech Transcription: Surprise Data Unraveled". *PhD Thesis*, University of Twente, The Netherlands, 2008.

[19] C. Wooters, C., M. Huijbregts. "The ICSI RT07s speaker diarization system", *Multimodal Technologies for Perception of Humans. Lecture Notes in Computer Science*, 2007.

An Automated Deduction of the Independence of the Orthomodular Law from Ortholattice Theory

Jack K. Horner
PO Box 266
Los Alamos, New Mexico 87544 USA
email: jhorner@cybermesa.com

Abstract

The optimization of quantum computing circuitry and compilers at some level must be expressed in terms of quantum-mechanical behaviors and operations. In much the same way that the structure of conventional propositional logic is the logic of the description of the behavior of classical physical systems and is isomorphic to a Boolean lattice, so also the algebra, C(H), of closed linear subspaces of (equivalently, the system of linear operators on) a Hilbert space is a logic of the descriptions of the behavior of quantum mechanical systems and is a model of an ortholattice (OL). An OL can thus be thought of as a kind of "quantum logic" (QL). C(H) is also a model of an orthomodular lattice (OML), which is an OL conjoined with an orthomodularity axiom/law (OMA). The rationalization of the OMA as a claim proper to physics has proven problematic, motivating the question of whether the OMA is required in an adequate characterization of QL. Here, I use an automated deduction framework to show that the OMA is independent of the axioms of ortholattice theory. These results corroborate (and fix a minor defect in) previously published work characterizing the strength of the OMA, and demonstrate the utility of automated deduction in investigating quantum computing logic-optimization strategies.

Keywords: automated deduction, quantum computing, orthomodular lattice, Hilbert space

1.0 Introduction

The optimization of quantum computing circuitry and compilers at some level must be expressed in terms of the description of quantum-mechanical behaviors ([1], [17], [18], [20]). In much the same way that conventional propositional logic ([12]) is the logical structure of description of the behavior of classical physical systems (e.g. "measurements of the position and momentum of an electron are commutative") and is isomorphic to a Boolean lattice ([10], [11], [19]), so also the algebra, *C(H)*, of the closed linear subspaces of (equivalently, the system of linear operators on) a Hilbert space *H* ([1], [4], [6], [9], [13]) is *a* logic of the descriptions of the behavior of quantum mechanical systems (e.g., "the measurements of the position and momentum of an electron are *not* commutative ") and is a model ([10]) of an ortholattice (OL; [8]). An OL can thus be thought of as a kind of "quantum logic" (QL; [19]). *C(H)* is also a model of (i.e., isomorphic to a set of sentences which hold in) an orthomodular lattice (OML; [7], [8]), which is an OL conjoined with the orthomodularity axiom (OMA; see Figure 1).

The rationalization of the OMA as a claim proper to physics has proven problematic ([13], Section 5-6), motivating the question of whether the OMA is independent of the axioms of ortholattice theory.

Lattice axioms

```
x = c(c(x)).
x v y = y v x.
(x v y) v z = x v (y v z).
(x ^ y) ^ z = x ^ (y ^ z).
x v (x ^ y) = x.
x ^ (x v y) = x.
```

Ortholattice axioms

```
c(x) ^ x = 0.
c(x) v x = 1.
c(c(x)) = x.
x ^ y = c(c(x) v c(y)).
```

Orthomodularity law/axiom (OMA)

```
x v (c(x) ^ (x v y)) = x v y.
```

Definitions (useful, but not required)

```
i1(x,y) = c(x) v (x ^ y).
i2(x,y) = i1(c(y), c(x).
i3(x,y) = (c(x) ^ y) v (c(x) ^ c(y)) v i1(x,y).
i4(x,y) = i3(c(y), c(x)).
i5(x,y) = (x ^ y) v (c(x) ^ y) v (c(x) ^ c(y)).
le(x,y) = (x = (x ^ y)).
```

where

x, y are variables ranging over lattice nodes
^ is lattice meet
v is lattice join
c(x) is the orthocomplement of x
i1(x,y) means $x \rightarrow_1 y$ (Sasaki implication)
i2(x,y) means $x \rightarrow_2 y$ (Dishkant implication)
i3(x,y) means $x \rightarrow_3 y$ (Kalmbach implication)
i4(x,y) means $x \rightarrow_4 y$ (non-tollens implication)
i5(x,y) means $x \rightarrow_5 y$ (relevance implication)
le(x,y) means $x \leq y$
= is equivalence ([12])
1 is the maximum lattice element (= x v c(x))
0 is the minimum lattice element (= c(1))

Figure 1. Axioms (and some useful definitions) of lattices, ortholattices, orthomodularity.

The axioms for lattices, ortholattices, and orthomodularity, are shown in Figure 1.

In a QL, the distributive law

```
(x v (y ^ z) = (x v y)
     ^ (x ^ z))
```

does not hold, because the distributive law implies commutativity of

(measurement-) propositions, and in general, the (measurement-)propositions of QL are not commutative.
Roughly speaking, a QL can be thought of as a classical propositional logic (CL) in which the distribution law does not hold. Table 1 shows some further differences (and similarities) between classical propositional logic and quantum propositional logic.

Table 1. Quantum logic connective counterparts of classical logic connectives.

Classical logic connective	Quantum propositional logic connective "counterpart"
"x *or* y"	lattice join (x v y, or x $\cup$ y)
"x *and* y"	lattice meet(x ^ y, or x $\cap$ y)
"*not*-x"	orthocomplement (c(x), or $x^{\perp}$)
"*if* x, *then* y" (implication)	$x \rightarrow_i y$ (i = [1|2|3|4|5])

Note that there are five QL implications that satisfy the Birkhoff-von Neumann condition

$$(x \rightarrow_i y = 1) \leftrightarrow (x \leq y), \quad i = 1, 2, \ldots, 5 \qquad \text{(CBvN)}$$

In classical propositional logic, there is only one implication, sometimes denoted "$\rightarrow_0$", that satisfies CBvN.

2.0 Method

The ortholattice and OMA axiomatizations of Megill, Pavičić, and Horner ([5], [14], [15], [16], [21]) were implemented in a *mace4* ([2]) script ([3]) and then executed in that framework on a Dell Inspiron 545 with an Intel Core2 Quad CPU Q8200 (clocked @ 2.33 GHz) and 8.00 GB RAM, running under the *Windows Vista Home Premium /Cygwin* operating environment. More specifically, the script used in this work implements the derivation of a model (Figure 2) in which the ortholattice axioms conjoined with the *negation* of the OMA hold in at least one interpretation, demonstrating that the OMA is independent of the ortholattice axioms.

3.0 Results

Figure 2 shows a *mace4* "domain size 6" model which demonstrates "the OMA is independent of the ortholattice axioms".

```
============================== INPUT =====================================
assign(iterate_up_to,10).
set(verbose).

formulas(theory).
x = c(c(x)).
x v y = y v x.
(x v y) v z = x v (y v z).
(x ^ y) ^ z = x ^ (y ^ z).
x v (x ^ y) = x.
x ^ (x v y) = x.
c(x) ^ x = 0.
c(x) v x = 1.
c(c(x)) = x.
x ^ y = c(c(x) v c(y)).
i1(x,y) = c(x) v (x ^ y).
le(x,y) <-> x = x ^ y.
A v (c(A) ^ (A v B)) != A v B.
end_of_list.

============================== end of input ==========================

. . .

============================== MODEL =================================

interpretation( 6, [number=1, seconds=0], [

        function(A, [ 2 ]),

        function(B, [ 3 ]),

        function(c(_), [ 1, 0, 4, 5, 2, 3 ]),

        function(^(_,_), [
                    0, 0, 0, 0, 0, 0,
                    0, 1, 2, 3, 4, 5,
                    0, 2, 2, 2, 0, 0,
                    0, 3, 2, 3, 0, 0,
                    0, 4, 0, 0, 4, 5,
                    0, 5, 0, 0, 5, 5 ]),

        function(i1(_,_), [
                    1, 1, 1, 1, 1, 1,
                    0, 1, 2, 3, 4, 5,
                    4, 1, 1, 1, 4, 4,
                    5, 1, 1, 1, 5, 5,
                    2, 1, 2, 2, 1, 1,
                    3, 1, 3, 3, 1, 1 ]),

        function(v(_,_), [
                    0, 1, 2, 3, 4, 5,
                    1, 1, 1, 1, 1, 1,
                    2, 1, 2, 3, 1, 1,
```

```
                    3, 1, 3, 3, 1, 1,
                    4, 1, 1, 1, 4, 4,
                    5, 1, 1, 1, 4, 5 ]),

        relation(le(_,_), [
                    1, 1, 1, 1, 1, 1,
                    0, 1, 0, 0, 0, 0,
                    0, 1, 1, 1, 0, 0,
                    0, 1, 0, 1, 0, 0,
                    0, 1, 0, 0, 1, 0,
                    0, 1, 0, 0, 1, 1 ])
]).

============================== end of model ==========================
```

Figure 2. A "domain size 6" *mace4* model in which the axioms of an ortholattice and the negation of the OMA hold (thus demonstrating that the OMA is independent of the ortholattice axioms). Each text line of values in the rightmost set of square brackets are assignments of values of integers to lattice positions. Such an assignment of values to nodes is said to *satisfy* or *be a model of* the indicated function/relation if the function/relation holds within the lattice under the assignment to those positions. Details of the *mace4* notation can be found in [2].

The time to produce the content of Figure 2 on the platform described in Section 2.0 was approximately 0.06 second.

4.0 Discussion

The results shown in Section 3.0 motivate at least three observations:

1. The OMA is independent of the ortholattice axioms.

2. The proof corrects a minor (right-associativity) defect in a previously published work ([21]) on the strength of the OMA.

3. A proof that the OMA is independent of the ortholattice axioms is implied by the proof in [22], which shows that the OMA is also independent of ortholattice axioms conjoined with the weak orthomodularity law.

5.0 Acknowledgements

This work benefited from discussions with Tom Oberdan, Frank Pecchioni, and Tony Pawlicki. For any infelicities that remain, I am solely responsible.

6.0 References

[1] von Neumann J. *Mathematical Foundations of Quantum Mechanics*. Translated by R. T. Beyer. Princeton. 1983.

[2] McCune WW. *prover9 and mace4.* URL http://www.cs.unm.edu/~mccune/prover9/. 2006.

[3] Horner JK. OML independence mace4 scripts. Available from the author on request at jhorner@cybermesa.com.

[4] Dalla Chiara ML and Giuntini R. *Quantum Logics*. URL

http://xxx.lanl.gov/abs/quant-ph/0101028. 2004.

[5] Megill ND and Pavičić M. Orthomodular lattices and quantum algebra. *International Journal of Theoretical Physics* 40 (2001), pp. 1387-1410.

[6] Akhiezer NI and Glazman IM. *Theory of Linear Operators in Hilbert Space. Volume I.* Translated by M. Nestell. Frederick Ungar. 1961.

[7] Holland, Jr. SS Orthomodularity in infinite dimensions: a theorem of M. Solèr. *Bulletin of the American Mathematical Society* 32 (1995), pp. 205-234.

[8] Beran L. *Orthomodular Lattices: Algebraic Approach*. D. Reidel. 1985.

[9] Knuth DE and Bendix PB. Simple word problems in universal algebras. In J. Leech, ed. *Computational Problems in Abstract Algebra.* Pergamon Press. 1970. pp. 263-297.

[10] Chang CC and Keisler HJ. *Model Theory*. North-Holland. 1990. pp. 38-39.

[11] Birkhoff G. *Lattice Theory*. Third Edition. American Mathematical Society. 1967.

[12] Church A. *Introduction to Mathematical Logic. Volume I.* Princeton. 1956.

[13] Jauch J. *Foundations of Quantum Mechanics.* Addison-Wesley. 1968.

[14] Megill ND. *Metamath.* URL http://us.metamath.org/qlegif/mmql.html#unify. 2004.

[15] Horner JK. An automated deduction system for orthomodular lattice theory. *Proceedings of the 2005 International Conference on Artificial Intelligence*. CSREA Press. 2005. pp. 260-265.

[16] Horner JK. An automated equational logic deduction of join elimination in orthomodular lattice theory. *Proceedings of the 2007 International Conference on Artificial Intelligence.* CSREA Press. 2007. pp. 481-488.

[17] Messiah A. *Quantum Mechanics*. Dover. 1958.

[18] Horner JK. *Using automated theorem-provers to aid the design of efficient compilers for quantum computing*. Los Alamos National Laboratory Quantum Institute Workshop. December 9–10, 2002. URL http://www.lanl.gov/science/centers/quantum/qls_pdfs/horner.pdf.

[19] Birkhoff G and von Neumann J. The logic of quantum mechanics. *Annals of Mathematics* 37 (1936), 823-243.

[20] Nielsen MA and Chuang L . *Quantum Computation and Quantum Information*. Cambridge. 2000.

[21] Pavičić M and Megill N. Quantum and classical implicational algebras with primitive implication. *International Journal of Theoretical Physics* 37 (1998), 2091-2098. ftp://m3k.grad.hr/pavicic/quantum-logic/1998-int-j-theor-phys-2.ps.gz.

[22] Horner JK. An automated deduction of the relative strength of orthomodular and weakly orthomodular lattice theory. *2009 International Conference on Artificial Intelligence*. CSREA Press. 2009. pp. 525-530.

The Theory of Minds Within the Theory of Games

M.D. McCubbins[1], M. Turner[2], and N. Weller[3]
1 Marshall School of Business, University of Southern California, Los Angeles, California, USA
2 Department of Cognitive Science, Case Western Reserve University, Cleveland, Ohio, USA
3 Department of Political Science, University of Southern California, Los Angeles, California, USA

Abstract - *Classical rationality as accepted by game theory assumes that a human chooser in a given moment has consistent preferences and beliefs and that actions result consistently from those preferences and beliefs, and moreover that these preferences, beliefs, and actions remain the same across equal choice moments. Since, as is widely found in prior experiments, subjects do not follow the predictions of classical rationality, behavioral game theorists have assumed consistent deviations from classical rationality by assigning to subjects certain dispositions—risk preference, cognitive abilities, social norms, etc. All of these theories are fundamentally cognitive theories, making claims about how individual human minds work when choosing. All of them are fundamentally wrong in assuming one kind of consistency or another. Or at least, all of the proposals for consistency in belief, preference, and action with which we are aware turn out to be wrong when tested experimentally.*

Keywords: Behavioral game theory, experiments, cognition, Trust, Dictator, Donation

1 Introduction

Game theoretic models are utilized for behavioral predictions across a variety of domains such as allocation of security forces [1], allocation of health care services [2], and the design of political, social and market institutions [3; for relevant surveys see: 4, 5, 6, 7]. Despite the widespread use of game theoretic models to explain human behavior, we often observe behavior, from voting, to the divergence of political parties platforms, to market bubbles and crashes that do not readily accord with the predictions derived from game theory [8].

To address the discrepancy between predicted and actual behavior, scholars have proposed four common patches: (1) cognitive biases or errors in how people make decisions [9, 10, 11, 12]; (2) a mismatch between the experimenter's defined payoffs and an individual's actual utility [13, 14]; (3) the effects of uncertainty, bounded search ability, limited time for learning and equilibration, or limits in the ability of thinking about others' likely behavior [15]; and (4) newer and more clever equilibrium refinements that capture the folk psychology of different game theorists [16, 17, 18, 19].

While it is common to report that experimental subjects do not make choices that comport with Nash equilibrium strategies (or even von Neumann-Morgenstern utility maximization), we should not infer that human reasoning is thus somehow flawed. It is perhaps the case that our existing, deductive, models of human reasoning are too limited. Humans are able to solve many tasks that are quite difficult [20, 21]. Like vision, taste and smell, human intelligence and behavior are varied and flexible, creating an enormous diversity of beliefs and choices, but the models that we use to predict behavior do not and cannot capture this diversity. To build a better theory of human behavior, we must start with an appreciation for how we actually reason. As cognitive science has shown, intuitive notions of how the mind works (vision, language, memory, etc.) may be very useful for humans to hold as scaffolding for consciousness, but they are comprehensively wrong and simplistic. Intuitive notions of how we reason are not a basis for science. How we reason must be discovered, not assumed, and certainly not borrowed from intuition

One of the principal problems stems from the core solution strategy for noncooperative games of Nash equilibrium. While it is mathematically elegant, it requires agents in the game to have correct and consistent beliefs [22]. To have "correct beliefs" we assume that the agents, or the players in a game, to regard all other players as being "Nash players" and to predict that they all follow Nash equilibrium (NE) strategies. It is also typically required that players have "common knowledge" that they are all Nash players, that is, that they know that other players know that they themselves are following Nash equilibrium strategies, and so on, ad infinitum. Others have pointed out that "Common Nash refinements have similar attributes. Although these refinements differ in what they allow players to know and believe, they continue to require that actors share identical conjectures of other players' strategies" [23, p. 106]. If players do not believe that other players will adopt NE strategies, however, it is

Prepared for the 2012 International Conference on Artificial Intelligence.
Corresponding author: Nicholas Weller.

no longer true that players' best response to each other will be to follow a NE strategy. The natural, biological, or cognitive means by which this comes about are not specified, merely that, given enough time and effort, players can all learn what behaviors to adopt and when to adopt them, or, baring this eventuality, that societies will adopt rules, laws or norms to restrict and channel behavior to more efficient forms. Prior work on subjects' beliefs in experimental settings suggest that subjects possess non-equilibrium beliefs [24, 25] and that in at least some settings their behavior can be reasonable, given their beliefs [26].

In what follows, rather than trying to stitch together measurements from different experiments, with different protocols, run under different conditions and at different times, we use a within-subjects design, run over a single academic term, to investigate choices in a large battery of single-shot games. Within our battery of tasks we elicit subjects' beliefs about the other subject's actions, plus we elicit *recursive* beliefs about other subjects' *beliefs* in these games. We demonstrate that subjects' actions and beliefs are consistently inconsistent, deviating from one person to another and for each person from one task to another. A given subject is often not consistent in action across nearly identical choice moments at different times in the same within-subject battery of tasks and a given subject is often not consistent even at the same time in their beliefs, preferences and actions. We also see great variation across subjects for a given task. For our specific battery, this refutes not only Nash equilibrium but also the patches that have been designed to explain deviation from it.

2 Experimental Design

We report on a number of tasks here related to the well-known Trust Game [27]. In our experiments, subjects know that their choices are always private and anonymous, even to the experimenters at the time of the experiment (i.e., double blind). Subjects receive no feedback during the course of the experiment about the consequences of their choices, except for quizzes related to the given tasks (subjects may, for some of our tasks, be able to infer the consequences of their choices). For each task, subjects are randomly matched to another subject. Thus, to the extent possible, every task is a single shot, separate from the prior and future choices. Subjects are divided into two rooms, in groups of ten in each room. We ensure that no subject knows anyone else in either of the two rooms of the experiment. As much as possible, then, this environment creates a situation in which subjects derive their utility solely from the payoffs in the experimental tasks and not from concerns about reputation, signaling for future games, experimenter demand, or other actions that are not related to the immediate monetary payoffs we present.

The Trust Game (sometimes called the investment game) involves two players. Each player begins with a $5 endowment. The first player (Player 1 or the "Investor" [27]) chooses how many dollars, if any, to pass to an anonymous second player (Player 2 or "Trustee" [27]). In our experimental protocols, we use no labels other than "the other person(s)" (to avoid a gaming frame). To avoid suggesting an investment or reciprocity frame we label each action as a "transfer." The first player keeps any money he does not pass. As in [27], the money that is passed is tripled in value and the second player receives the tripled amount. The second player at that point has the original endowment of $5 plus three times the amount the first player passed, and decides how much, if any, of that total amount to return (i.e., transfer) to the first player. The second player at the moment of choice in the Trust Game is in a role that is equivalent to the role of Dictator in the classic Dictator Game [see 8]. As in the Dictator Game, the dominant strategy equilibrium, which is trivially the subgame perfect Nash equilibrium (SPNE), is that Player 2 will return $0. By backward induction, then Player 1 in the Trust Game will send $0. This is also a dominant strategy. As such, any amount sent by Player 1 to Player 2 should be viewed by Player 1 as a donation, and we label the first half of the Trust Game as what we call a Donation Game.

These equilibrium strategies derive from the assumption is that all players maximize their monetary payoff and that they believe that all other players do the same. In the Trust Game, a Player 1 with these beliefs would conclude that Player 2 will return nothing and so, as a maximizer, Player 1 sends nothing. The beliefs that players hold about other players lead to the belief at every level of recursion that all players will send $0, and that they will guess that others will send $0, and they will guess that others will predict that everyone will send $0, and so on, ad infinitum.

But what happens if a subject with these NE beliefs finds himself off the equilibrium path? In the Trust Game, only Player 2 could make a choice after finding himself or herself presented with an off-the-equilibrium-path choice. If Player 2 is gifted with anything more than his or her $5 endowment, the subgame perfect Nash equilibrium strategy is still to send $0 back.

Every subject makes decisions first as Player 1. They are then randomly paired with someone from the other room and they make choices as Player 2. So everyone gets to be Player 1 first, then Player 2, about 90 minutes later. To limit learning, even if it is just learning about the actions of a randomly assigned partner in another room, we defer the choices for all subjects as Player 2 to the end of the experiment. They thus play Trust twice, but in different roles. Player 1 never learns the consequences of any of his or her choices in the Trust Game. Player 2 can of course infer the consequences of his or her own choices.

We add elements to the basic Trust Game to tap into subjects' beliefs. Our belief elicitation mechanism borrows

from the idea of a prediction market [28], which in experimental settings such as those described here have been referred to as "scoring rules" [29, 30, and for a brief survey see 8]. We do not ask subjects to report their expectations, as some experimenters have done, in order to prod strategic thinking, rather, we ask them to "guess" other subjects' choices, or to guess other subjects' "predictions." As with all of our protocols, we try to provide little or no framing of the experimental tasks offered to our subjects. Only after Player 1 makes his choice about how much to transfer, do we ask him to guess how much Player 2 will return. We then elicit Player 1's recursive beliefs about Player 2. So, we next ask Player 1 to guess what Player 2 will later predict how much Player 1 is transferring. We further ask Player 1 to guess Player 2's prediction of Player 1's guess of how much Player 2 will return. We also elicit each subject's recursive beliefs when they are in the role of Player 2. Before Player 2 learns Player 1's choice, and thus before Player 2 knows how much they have available to them, we ask Player 2 to guess how much money Player 1 transferred. We also ask Player 2 to guess how much Player 1 predicted that Player 2 would guess that Player 1 transferred. After Player 2 learns Player 1's transfer, we ask Player 2 to guess how much Player 1 predicted she would return. All subjects know that all subjects earn $3 for each correct guess and earn nothing for a guess that is wrong. All subjects in our experiments know this. We also allowed subjects to, in essence, "double-down," on each guess, adding a second "bet" equal to $3 if they are correct in their guess and $0 otherwise. We also always quizzed our subjects with respect to the instructions, paying them for correct answers.

In calibrating these prediction questions prior to the launch of our experiments we learned two things: (1) that there does not exist an easy language for eliciting recursive beliefs, so we made use of generic cartoon "heads" to represent what subjects are predicting and "$" sign and arrow icons to represent actions and the object of their current attention; and (2) subjects laughed and failed to answer our queries, even when diagrammed in cartoon form, with written explanations. These two preliminary findings suggested to us that people really do not have the recursive beliefs required by NE.

The questions we ask vary slightly for each task, but as an example, here is the exact question we ask Player 2: "How much money do you guess the other person transferred to you? If you guess correctly, you will earn $3. If not, you will neither earn nor lose money." We add similar incentivized prediction tasks to various experimental tasks. Players do not learn whether their predictions were right or wrong and subjects never have any information about other subjects' guesses.

Subjects also make decisions in a variety of other games, including the already mentioned Dictator Game and what we call the Donation Game. In both these games, each subject is randomly paired with yet other subjects in the other room. In the Dictator Game, The Dictator (Player 1) and the Receiver (Player 2) have endowments identical to those the subjects had when they were in the role of Player 2 and Player 1 in Trust (although they have been randomly rematched and they known they've been randomly rematched). Accordingly, the Dictator Game was identical right down to the specific endowments to the second half of the Trust Game. In effect, each subject replayed the second half of the Trust Game, but now without the reciprocity frame. The SPNE is for the Dictator to send $0 to the Receiver. The Donation Game is identical, except that each player begins with a $5 endowment and the amount Player 1 chooses to send is quadrupled before it is given to Player 2 (making it roughly similar but not identical to the choice faced by Player 1 in the Trust Game, without the possibility of reciprocity). The dominant strategy and SPNE is again for the Donor to send $0.

The subjects in our experiment completed the tasks using pen and paper in a controlled classroom environment. Subjects were recruited using flyers and email and text messages distributed across a large public California university and were not compelled to participate in the experiment, although they were given $5 in cash when they showed up and signed in. A total of 180 subjects participated in this experiment. The experiment lasted approximately two hours, and subjects received on average $41 in cash. The experiment was followed sometime later with a questionnaire, for which subjects were also paid.

3 Result: Subjects' Beliefs in the Trust Game

Common patches to help explain the commonly observed departures to NE strategies (other-regarding preferences, cognitive constraints, decision-making biases, or equilibrium refinements) usually continue to maintain the assumption that players deviate from game-theoretic expectations in consistent ways. For example, if players prefer to reduce inequality, that preference should be stable across all manner of economic games [10]. Or, if players cannot perform backward deletion of dominated sub-games, as game theory requires, then this handicap should operate in all game environments of equal difficulty [17, 18, 19]. In this section we focus both on whether subjects have beliefs that are consistent with SPNE and whether their beliefs are consistent across tasks (regardless of alignment with SPNE). To date, there has been little focus on identifying the extent to which players have consistent beliefs or behavior across games.

Cognitive science gives us considerable reason to doubt that players will behave identically across different

environments, because changes in environment lead to changes in mental activation, which affects beliefs and behavior. As Sherrington famously wrote, the state of the brain is always shifting, "a dissolving pattern, always a meaningful pattern, though never an abiding one" [32]. If the particular tasks, and order of those tasks, induce different mental activations, then belief and behavior should vary accordingly. Our experiment is designed to shed light on whether subjects have consistent beliefs and make consistent choices.

In many of our tasks, we ask subjects to make guesses about other players' actions and predictions. Do subjects believe what game theory assumes they believe? The answer is that there is huge variance across what subjects believe in a single game and also huge variance within subjects from one task to another.

The SPNE in the Trust Game is that neither Player 1 nor Player 2 will send any money to the other. All should believe that all others will predict that no one will send money, and all such beliefs should be infinitely recursive, so that Player A believes Player B believes Player A believes Player B will send no money, and so on for any number of steps and for any subject in any role A or B.

But we see quite the contrary in our experiments: only 68 of 180 subjects as Player 2 believe that Player 1 will send nothing. In other words, 62% of subjects have "incorrect" beliefs, that is, beliefs contrary to those that support SPNE strategies.

Next we examine the guesses made by Player 1 of the amount Player 2 will return. In what follows, we include even the Player 1s who sent nothing. (Since Player 2 begins with a $5 endowment, Player 2 can transfer money even if Player 1 sent nothing.) Ninety-two of the 180 subjects guess that Player 2 will return $0, but 88, or 49%, believe that Player 2 will return some money. This means that 49% of these subjects have "incorrect" beliefs. Their beliefs diverge broadly from SPNE, across a large span of possible returns.

We can compare subjects' beliefs about others in one part of the Trust Game with their choices in that same part of the Trust Game. For example, we can examine the difference between what a subject choose to do as Player 1 in the Trust Game, and what they believe as Player 2 that Player 1 will do (and recall, when they are Player 2, they've already made choices as Player 1). The modal category is subjects believe that other subjects will play like them: 109 of the 180 subjects guess that the choice of the Player 1 with whom they are randomly matched will be the same as their own choice when they were Player 1. For these subjects, theory of mind might equal theory of self, or this may simply represent the "false consensus" effect in which people think others are more like them than they actually are [31], or it might be akin to the curse of knowledge, but we can't really tell. Perhaps most surprising, there is a large variance, with 71 subjects (39%) making guesses that differ from their own choices.

We can also examine the number of subjects who have beliefs consistent with NE across tasks. In the Trust Game, subjects make predictions as Player 1 about the behavior of Player 2 and as Player 2 about the behavior of Player 1. We already demonstrated that in either single task, a great many subjects do not have SPNE beliefs. If Player 1 has NE beliefs, it means that this subject guessed that Player 2 would return nothing. If Player 2 has NE beliefs, it means that the subject guessed that Player 1 would send nothing. Overall, out of 180 subjects in our analysis, only 63 subjects made guesses as both Player 1 and 2 that were consistent with NE beliefs. In other words, only 35% of our subjects have consistently "NE beliefs" *even inside this one game*.

There were 83 subjects who lacked NE beliefs in both part of the Trust Game, 29 subjects who possessed "NE beliefs" as Player 1 but not as Player 2, and only 5 subjects who possessed "NE beliefs" as Player 2 but not as Player 1. Our experiment does not allow us to identify why players' beliefs diverge from the NE beliefs, but it is clear that most subjects deviate from NE beliefs during at least one of the experimental tasks.

There were 60 subjects who were "fully Nash actors" in the Trust Game, that is, the subjects whose actions as both Player 1 and 2 were consistent with SPNE strategy. We examine whether these 60 subjects have beliefs that are "fully Nash" in the Trust Game. The answer is no. First, let us consider these 60 subjects in the role of Player 1 in Trust. Of these 60 subjects, 56 guessed as Player 1 that Player 2 would return nothing, which is consistent with SPNE. Only 40 of the 60 "fully Nash" Trust players (66%) guessed that Player 2 predicted that they would transfer $0. The other 20 of the 60 "fully Nash" Trust players (1/3rd) lacked that SPNE belief. 49 of the 60 also guessed Player 2's prediction of Player 1's guess of what Player 2 will return to be $0. These results show that even the 60 "fully Nash" Trust subjects hold beliefs whose degree of consistency with SPNE principles varies question by question even when we look at only those questions asked of them when they are in the role of Player 1. Beliefs show flexibility.

We next turn to the beliefs of those 60 "fully Nash" Trust subjects when they are in the role of Player 2 in Trust. Of the 60, 44 guess that Player 1 will transfer nothing; that is, 16 of 60 (27%) lack SPNE beliefs. Of the 60, 35 guess that Player 1 predicts that they will return nothing; that is, for this question, 42% of these 60 "fully Nash" Trust subjects have beliefs that are inconsistent with SPNE. Overall, non-SPNE beliefs are quite common even among the 60 "fully Nash" actors in the Trust Game. Beliefs show flexibility and refute the assumed beliefs of Nash equilibrium and the four patches often applied to NE.

4 Result: Inconsistency of Behavior in Trust, Donation, and Dictator

We turn next to examine the actions of subjects across a number of similar tasks to see if individual subjects behave consistently. In particular, we look at a set of tasks, all of which involve choosing how much money to transfer to another person and in some tasks the decision is not contingent on the other player. In the Trust Game, subjects play the role of Player 1 and 2 during the course of the experiment.

One way to investigate consistency of behavior is to examine the choices of subjects who as Player 2 in Trust received money from Player 1. Of the 100 subjects who received money as Player 2 in Trust, only 62 returned any of the money to Player 1. Additionally, of those 62, only 40 sent money in the Dictator Game, which is identical to the percentage of subjects who sent nothing in other "double blind" versions of the Dictator Game [13]. This shows that many subjects do not behave consistently in these two identical choice situations, in which their actions could reduce inequality. Further, of the 40 who sent money in Dictator, only 29 also send money in the Donation Game. This means that of the 100 subjects who received money as Player 2 in Trust, only 29 sent money to the other player in all three related tasks. This shows that the same subjects do not behave consistently even in their violations of SPNE.

Another example of apparently inconsistent behavior comes from examining the subjects who passed \$0 out of \$5 in the Donation Game, suggesting they are not concerned with others' earnings. Of the 87 subjects who passed \$0 in the Donation Game, 63 of them also passed nothing as Player 1 in the Trust Game, both behaviors of which are consistent with standard game theoretic behavior. However, the other 24 subjects passed \$0 in the Donation Game and some amount greater than \$0 in the Trust Game. What model predicts this behavior? Why would a player who passes nothing in the Donation Game pass money in the Trust Game? One possibility is that the player believes that passing money in Trust will result in greater earnings, because Player 2 will return enough money to make the choice to pass money financially beneficial. However, among these 24 subjects some guess they will earn money in the Trust Game and others guess they will lose money. The lack of consistency in these two very similar settings is further evidence that assumptions of consistent behavior are at odds with much human action.

Subjects deviate remarkably from NE strategies. We have reported how subjects' beliefs deviate from those necessary to support equilibrium strategies. We have also shown that these deviations are not consistent. Accordingly, it is doubtful that proposals to explain deviation from NE strategies will succeed if they presume a consistent mental or behavioral signature.

Now, we ask whether actions are minimally rational, that is, do subjects' actions accord with their beliefs? To begin, we investigate whether action and belief accord in the Trust Game. In our experiment, over one-half of subjects in the role of Player 1 (100 out of 180) pass a nonzero amount of money to Player 2 (this differs from [27]), which is inconsistent with a SPNE strategy, and on average subjects pass \$1.44 (which is not significantly different than the findings in [27]). Of the 100 subjects who receive money as Player 2, 62 of them return some money to Player 1. On net, Player 1 loses money (our results here are almost identical to those by [27]).

To look at the relationship between beliefs and actions we examine the difference between the amount Player 1 sends to Player 2 and the amount Player 1 guesses Player 2 will return. Recall that any money sent by Player 1 is tripled before it is sent to Player 2 and added to Player 2's initial \$5, (e.g., if Player 1 sends all \$5, then Player 2 has \$20, and if Player 2 splits that money, then Player 1 and Player 2 end with \$10 each, and we would say that each has "earned" \$5 through their actions). Overall, there are only a few players who guess that they will lose money by sending money to the other player. Mostly, players expect to break even or benefit slightly from their decision. The beliefs held by these players imply not only that they do not expect others to play consistently with SPNE strategies, but also that they expect, on average, to profit from their non-SPNE strategy to send money. But again, beliefs are not consistent across subjects.

There are 100 subjects who as Player 1 in Trust chose to send a positive amount to Player 2, and 20 of those players guess they will not receive anything in return. These 20 players guess that Player 2 will follow a SPNE strategy. These 20 subjects cannot simultaneously be maximizing their payoffs and hold the belief that Player 2 will follow a SPNE strategy of returning \$0 so it is hard to see how their choices accord with their own beliefs. We must either conclude that they are not payoff maximizers or relax the assumption that subjects act according to beliefs. One possible response is to give up the assumption that believing, preferring, deciding, and acting are coordinated mental events. Perhaps subjects act without fully activating their decisions, or believe without activating the consequences of those beliefs for action, or act without activating beliefs, and so on.

These results make it clear that we may not be able to simply observe behavior and then make correct inferences about the underlying beliefs that generated the behavior. When we observe a Player 1 in the Trust Game pass money what beliefs do we presume preceded that behavior? Is this a subject who is motivated by other-regarding preferences who does not expect to benefit financially? Or, is this a player who sincerely believes that

the 2nd player in the Trust Game will return enough money to make the initial decision profitable?

There were 60 subjects who were "fully Nash actors" throughout the game; that is, they chose SPNE strategies (i.e., $0) as both Player 1 and Player 2., We ask whether these 60 "fully-Nash" actors in Trust are "fully Nash" in the related Donation and Dictator Games. Of these 60 subjects, 57 pass $0 in the Dictator Game and 50 of the 60 pass $0 in the Donation Game. If we focus on those 57 subjects who are "fully Nash actors" as both Player 1 and Player 2 in Trust and also as Dictator in the Dictator Game, we find that 48 of the 57 pass nothing in the Donation Game. Therefore, across our entire subject pool, only 48 (27%) have consistent NE behavior in three related games of Trust, Donation, and Dictator.

Although deviations in a single game have been widely recognized, research has not focused on how behavior across games is related. We have shown in a variety of ways that NE-consistent behavior in one task does not guarantee similar behavior in another setting. Therefore, even accurately predicting a subjects' action in one setting is no guarantee that it is possible to predict accurately the subjects' action in another setting. We demonstrate thisusing game theoretic environments that are exceedingly similar, which would seem to stack the deck in favor of finding consistent behavior across games. However, the results from our battery of experimental tasks demonstrate that subjects regularly deviate from SPNE in both their beliefs and behavior, that the deviations are themselves inconsistent, and that there is variation in the degree to which behavior accords with belief. These deviations are so pervasive and the variation so large, even among subjects taking actions in similar or identical strategic settings, that is seems unwarranted to refer to them as "deviations." On the contrary, even though our subject pool is derived from subjects with very high math SATs, who were on the whole in the top 2% of high school graduates, consistent "NE behavior and beliefs" appear to be remarkable deviations from human cognitive patterns and human behavior.

5 Discussion

Games are defined by seven characteristics: players, actions, information, strategies, payoffs, outcomes, and equilibria, including equilibrium refinement [33]. Equilibria must be mutually consistent, indeed, "[T]he Nash equilibrium (NE) concept . . . entails the assumption that all players think in a very similar manner when assessing one another's strategies. In a NE, all players in a game base their strategies not only on knowledge of the game's structure but also on *identical conjectures about what all other players will do.* The NE criterion pertains to whether each player is choosing a strategy that is a best response to a shared conjecture about the strategies of all players. A set of strategies satisfies the criterion when all player strategies are best responses to the shared conjecture. In many widely used refinements of the NE concept, such as subgame perfection and perfect Bayesian, the inferential criteria also require players to have shared, or at least very similar, conjectures" [23: 103-104]. NE is, at its core, a cognitive theory.

In cognitive science, "theory of mind" refers to our amazing disposition to attribute mindedness to other human beings. Classical economics takes theory of mind for granted, and extends it to the view that all of those minds are driven by consistent preferences and beliefs to consistent actions. Behavioral game theory applies patches to come up with a conception of individual minds as consistently deviant from classical rationality. Hence the phrase "predictably irrational." The difference between classical rationality and behavioral game theory is not about consistency: classical rationality assumes that everyone is consistent in the same way, while behavioral game theory assumes that each person is consistent in a certain "deviant" way. While classical rationality and behavioral game theory are often taken to be opposed, we seem them as uniformly based on an assumption of consistency that does not stand with experimental test.

Some scholars justify consistency as a mathematical shortcut that is meant to represent the result of some unspecified learning, evolutionary adjustment process, or the adoption of social norms, laws or institutions [34]. These processes, however, are rarely defined. This line of reasoning also implies that beliefs and choices will not be consistent if players do not have time to learn or evolve.

As in many related experiments [for a survey see 8], subjects in our experiments do indeed deviate from SPNE predictions, both in their actions and in their beliefs. We also demonstrate that subjects' recursive beliefs (beliefs about the beliefs of other players) are often inconsistent with NE predictions, a result that has not been widely appreciated. We show further that the variance in actions and beliefs is very large.

Even the common patches of behavioral game theory do not predict the tremendous diversity that we observed for *individual subjects* and the variance across subjects' beliefs and behavior. Subjects' reported beliefs and their behavior are regularly incongruent – subjects who play consistently with NE prediction do not always possess the assumed game theoretic beliefs. Furthermore, subjects' beliefs differ across settings even when there are no changes in the cognitive complexity of the setting. Taken together these results suggest that game theoretic models and common modifications employed to make them explain the deviations from straightforward NE, do not accurately predict the variations in behaviors we observe in a laboratory setting. Therefore, research into decision-making should turn to discovering the cognitive patterns of decision-making.

Acknowledgments. McCubbins acknowledges the support of the National Science Foundation under Grant Number 0905645. Any opinions, findings, and conclusions or recommendations expressed in this material are those of the author(s) and do not necessarily reflect the views of the National Science Foundation. Turner acknowledges the support of the Centre for Advanced Study at the Norwegian Academy of Science and Letters.

References

[1] Pita, J., Kiekintveld, C., Tambe, M., Steigerwald, E. and Cullen, S. 2011. "GUARDS - Innovative Application of Game Theory for National Airport Security." In *Proceedings of the International Joint Conference on Artificial Intelligence* (IJCAI).

[2] Roth, A.E. 1990. "New Physicians: A Natural Experiment in Market Organization," *Science*, 250, pp. 1524-1528.

[3] Kagel, J.H. and Roth, A.E. eds. 1997. *The Handbook of Experimental Economics*. Princeton University Press.

[4] Fudenberg, D., and J. Tirole. 1991. *Game Theory*. MIT Press.

[5] Ordeshook, P. C. 1986. *Game Theory and Political Theory*. Cambridge University Press.

[6] Nisan, N., Roughgarden, T, Tardos, E., and Vazirani, V. V. 2007. *Algorithmic Game Theory*. Cambridge University Press.

[7] Tirole, J. 1988. *The Theory of Industrial Organization*. MIT Press.

[8] Camerer, C. 2003. *Behavioral Game Theory*. Russell Sage Foundation, New York, New York/Princeton University Press, Princeton, New Jersey

[9] Kahneman, D., and Tversky, A. 1979. "Prospect Theory: An Analysis of Decision under Risk." *Econometrica*, Vol. 47, No. 2. pp. 263-292.

[10] Rabin, M. and Thaler, R.H. 2001. "Anomalies: Risk Aversion," Journal of Economic Perspectives. vol. (1), pages 219-232

[11] Ainslie, G. 2001. *Breakdown of will*. Cambridge: Cambridge University Press.

[12] Elster, J. 1999. *Strong Feelings: Emotion, Addiction, and Human Behavior*. MIT Press.

[13] Hoffman E., McCabe, K., Shachat, K. and Smith, V. 1994. "Preferences, Property Rights, and Anonymity in Bargaining Games." *Games and Economic Behavior* 7(3): 346-380

[14] Rabin, M. 1993. "Incorporating Fairness into Game Theory and Economics." *American Economic Review, LXXXIII*. 1281-1302.

[15] Simon, H. 1957. "A Behavioral Model of Rational Choice", in *Models of Man, Social and Rational: Mathematical Essays on Rational Human Behavior in a Social Setting*. New York: Wiley.

[16] Camerer, C.F., T.H. Ho and K. Chong. 2004. "A cognitive hierarchy model of behavior in games," *Quarterly Journa of Economics.* Vol 119, No. 3, p. 861.

[17] Stahl, D. and Wilson, P.1994. "Experimental Evidence on Players' Models of Other Players," *Journal of Economic Behavior and Organization*, 25, 309–327.

[18] Costa-Gomes, M. A., and Crawford, V. P. 2006. "Cognition and Behavior in Two-Person Guessing Games: An Experimental Study," *American Economic Review*. vol. 96(5), pages 1737-1768.

[19] McKelvey, R. and Palfrey, T. 1998. "Quantal response equilibria for extensive form games." *Experimental Economics*, 1, 9-41.

[20] Gigerenzer, G. 2000. *Adaptive thinking: Rationality in the real world.* New York: Oxford University Press.

[21] Turner, M. 2009. "The Scope of Human Thought." http://onthehuman.org/humannature/

[22] Rasmusen, E. 2006. *Games and Information.* Oxford: Blackweller Publishers, Fourth Edition.

[23] Lupia, A., Levine, A. S., and Zharinova, N. 2010. "Should Political Scientists Use the Self Confirming Equilibrium Concept? Benefits, Costs and an Application to the Jury Theorem." *Political Analysis* 18:103-123.

[24] Kuhlman, D. M., and Wimberley, D. L. 1976. "Expectations of choice behavior held by cooperators, competitors, and individualists across four classes of experimental game." *Journal of Personality and Social Psychology, 34*, 69-81.

[25] Croson, R. 2007. "Theories of Commitment, Altruism and Reciprocity: Evidence from Linear Public Goods Games." *Economic Inquiry,* Vol. 45, pp. 199-216.

[26] McKenzie, C. R. M., and Mikkelsen, L. A. (2007). "A Bayesian view of covariation assessment." *Cognitive Psychology*, 54, 33-61

[27] Berg, J. E., Dickhaut, J., and McCabe, K. 1995. "Trust, Reciprocity, and Social History," *Games and Economic Behavior*, Vol. 10, 1995, pages 122-142.

[28] Wolfers, J. and Zietzwitz, E. 2004. "Prediction Markets." *Journal of Economic Perspectives.*

[29] McKelvey, R. and Page, R. T. 1990. "Public and private information: An experimental study of information pooling. *Econometrica*, 58, 1321-39.

[30] Camerer, C. and Karjalainen, R. 1994. "Ambiguity-aversion and non-additive beliefs in non-cooperative games: Experimental evidence." In Munier, B. And Machina, M. (eds.), *Models and Experiments on Risk and Rationality*. Dordrecht: Kluwer, 325-58.

[31] Ross, L., Green, D., and House, P. 1977. "The 'False Consensus Effect': An Egocentric Bias in Social Perception and Attribution Processes." *Journal of Experimental Social Psychology*. 13, pp. 279-250.

[32] Sherrington, C.S. Sir. [1941] 1964. *Man on his Nature*. [The Gifford Lectures, Edinburgh, 1937–1938. New York: The Macmillan Co.; Cambridge: The University Press, 1941]. New York: New American Library.

[33] Rasmusen, E. 1989. *Games and Information: An Introduction to Game Theory*. Blackwell Publishers.

[34] Denzau, A. and North, D. C. 2000. "Shared mental models: Ideologies and institutions." In Lupia, A., McCubbins, M., and Popkin, S. *Elements of reason: Cognition, choice and the bounds of rationality*. Cambridge Univesity Press.

An Automated Deduction of the Independence of the Axioms of the Megill-Pavičić Formulation of Ortholattice Theory

Jack K. Horner
PO Box 266
Los Alamos NM 87544 USA
email: jhorner@cybermesa.com

Abstract

The optimization of quantum computing circuitry and compilers at some level must be expressed in terms of quantum-mechanical behaviors and operations. In much the same way that the structure of conventional propositional logic is the logic of the description of the behavior of classical physical systems and is isomorphic to a Boolean lattice, so also the algebra, C(H), of closed linear subspaces of (equivalently, the system of linear operators on) a Hilbert space is a logic of the descriptions of the behavior of quantum mechanical systems and is a model of an ortholattice (OL). An OL can thus be thought of as a kind of "quantum logic" (QL). In order to delimit the axiomatic basis of the derivation of a proposition in a formal system, it is helpful to formulate a theory so that none of its axioms depend on any others in that theory. Here, I use an automated deduction framework to show that the axioms of the Megill-Pavičić formulation of ortholattice theory are independent. In addition, these results illustrate the utility of automated deduction in investigating the foundations of quantum computing.

Keywords: automated deduction, lattice theory

1.0 Introduction

The optimization of quantum computing circuitry and compilers at some level must be expressed in terms of the description of quantum-mechanical behaviors ([1], [17], [18], [20]). In much the same way that conventional propositional logic ([12]) is the logical structure of description of the behavior of classical physical systems (e.g. "measurements of the position and momentum of an electron are commutative") and is isomorphic to a Boolean lattice ([10], [11], [19]), so also the algebra, *C(H)*, of the closed linear subspaces of (equivalently, the system of linear operators on) a Hilbert space *H* ([1], [4], [6], [9], [13]) is *a* logic of the descriptions of the behavior of quantum mechanical systems (e.g., "the measurements of the position and momentum of an electron are *not* commutative ") and is a model ([10]) of an ortholattice (OL; [8]). An OL can thus be thought of as a kind of "quantum logic" (QL; [19]).

The Megill-Pavičić formulation of ortholattice theory ([11]) is shown in Figure 1.

```
% Definitions
le(x,y)  <->  (x v y = y)    # label("Df of le").
1 = x v c(x)                 # label("Df of 1").
0 = x ^ c(x)                 # label("Df of 0").

% Axioms
x = c(c(x))                                          # label"(MP_L1").
le(x, x v y)  &  le(y, x v y) & le(y, x v c(x))      # label("MP_L2").
(le(x,y) & le(y, x)) -> (x = y)                      # label("MP_L3a").
le(x,y) -> le(c(y), c(x))                            # label("MP_L4").
(le(x,y) & le(y,z)) -> le(x,z)                       # label("MP_L5").
(le(x,z)  &  le(y,z))  -> le(x v y, z)               # label("MP_L6").

where
       x, y are variables ranging over lattice nodes
       ^ is lattice meet
       v is lattice join
       c(x) is the orthocomplement of x
       =  is equivalence
       1 is the maximum lattice element (= x v c(x))
       0 is the minimum lattice element (= c(1))
```

Figure 1. The Megill-Pavičić formulation of ortholattice theory ([11]).

2.0 Method

The ortholattice axiomatization of [11] was implemented in *mace4* ([2]) scripts ([3]), then executed in that framework on a Dell Inspiron 545 with an Intel Core2 Quad CPU Q8200 (clocked @ 2.33 GHz) and 8.00 GB RAM, running under the *Windows Vista Home Premium /Cygwin* ([5]) operating environment. The script implements the derivation of models (Figure 2) in which all of those axioms, minus one, conjoined with the *negation* of the excluded axiom, hold in at least one interpretation, demonstrating that the axiom which has been negated is independent of the remaining lattice axioms ([10]).

3.0 Results

The six proofs Figure 2 show the independence of the ortholattice axioms of [11] from each other.

```
============================== MODEL FOR MP_L1 ================================

interpretation( 2, [number=1, seconds=0], [

        function(A, [ 0 ]),

        function(c(_), [ 1, 1 ]),

        function(^(_,_), [
                         0, 0,
                         0, 0 ]),

        function(v(_,_), [
                         0, 1,
                         1, 1 ]),
```

```
        relation(le(_,_), [
                         1, 1,
                         0, 1 ])
]).

============================== end of model ==========================


============================== MODEL FOR MP_L2 ================================

interpretation( 3, [number=1, seconds=0], [

        function(A, [ 0 ]),

        function(B, [ 0 ]),

        function(c(_), [ 2, 1, 0 ]),

        function(^(_,_), [
                         0, 0, 0,
                         0, 0, 0,
                         0, 0, 0 ]),

        function(v(_,_), [
                         0, 0, 1,
                         1, 1, 0,
                         1, 0, 2 ]),

        relation(le(_,_), [
                         1, 0, 0,
                         0, 1, 0,
                         0, 0, 1 ])
]).

============================== end of model ==========================


============================== MODEL FOR MP_L3a ================================

interpretation( 6, [number=1, seconds=0], [

        function(A, [ 2 ]),

        function(B, [ 4 ]),

        function(c(_), [ 1, 0, 3, 2, 5, 4 ]),

        function(^(_,_), [
                         0, 0, 0, 0, 0, 0,
                         0, 0, 0, 0, 0, 0,
                         0, 0, 0, 0, 0, 0,
                         0, 0, 0, 0, 0, 0,
                         0, 0, 0, 0, 0, 0,
                         0, 0, 0, 0, 0, 0 ]),

        function(v(_,_), [
                         0, 1, 2, 3, 4, 5,
                         1, 1, 1, 1, 1, 1,
                         2, 1, 2, 1, 4, 1,
                         3, 1, 1, 3, 1, 5,
                         2, 1, 2, 1, 4, 1,
                         3, 1, 1, 3, 1, 5 ]),

        relation(le(_,_), [
                         1, 1, 1, 1, 1, 1,
                         0, 1, 0, 0, 0, 0,
                         0, 1, 1, 0, 1, 0,
                         0, 1, 0, 1, 0, 1,
```

```
                        0, 1, 1, 0, 1, 0,
                        0, 1, 0, 1, 0, 1 ])
]).

============================== end of model ==========================



============================== MODEL FOR MP_L4 ================================

interpretation( 2, [number=1, seconds=0], [

        function(A, [ 0 ]),

        function(B, [ 1 ]),

        function(c(_), [ 0, 1 ]),

        function(^(_,_), [
                        0, 0,
                        0, 0 ]),

        function(v(_,_), [
                        1, 1,
                        1, 1 ]),

        relation(le(_,_), [
                        0, 1,
                        0, 1 ])
]).

============================== end of model ==========================



============================== MODEL FOR MP_L5 ================================

interpretation( 8, [number=1, seconds=0], [

        function(A, [ 0 ]),

        function(B, [ 2 ]),

        function(C, [ 3 ]),

        function(c(_), [ 6, 7, 4, 5, 2, 3, 0, 1 ]),

        function(^(_,_), [
                        0, 0, 0, 0, 0, 0, 0, 0,
                        0, 0, 0, 0, 0, 0, 0, 0,
                        0, 0, 0, 0, 0, 0, 0, 0,
                        0, 0, 0, 0, 0, 0, 0, 0,
                        0, 0, 0, 0, 0, 0, 0, 0,
                        0, 0, 0, 0, 0, 0, 0, 0,
                        0, 0, 0, 0, 0, 0, 0, 0,
                        0, 0, 0, 0, 0, 0, 0, 0 ]),

        function(v(_,_), [
                        0, 1, 2, 0, 1, 1, 1, 0,
                        1, 1, 1, 1, 1, 1, 1, 1,
                        2, 1, 2, 3, 1, 1, 1, 2,
                        0, 1, 3, 3, 1, 1, 1, 3,
                        1, 1, 1, 1, 4, 4, 6, 4,
                        1, 1, 1, 1, 4, 5, 5, 5,
                        1, 1, 1, 1, 6, 5, 6, 6,
                        0, 1, 2, 3, 4, 5, 6, 7 ]),

        relation(le(_,_), [
```

```
                          1, 1, 1, 0, 0, 0, 0, 0,
                          0, 1, 0, 0, 0, 0, 0, 0,
                          0, 1, 1, 1, 0, 0, 0, 0,
                          1, 1, 0, 1, 0, 0, 0, 0,
                          0, 1, 0, 0, 1, 0, 1, 0,
                          0, 1, 0, 0, 1, 1, 0, 0,
                          0, 1, 0, 0, 0, 1, 1, 0,
                          1, 1, 1, 1, 1, 1, 1, 1 ])
]).

============================== end of model ==========================


============================== MODEL FOR M_L6 =================================

interpretation( 4, [number=1, seconds=0], [

        function(A, [ 0 ]),

        function(B, [ 2 ]),

        function(C, [ 0 ]),

        function(c(_), [ 3, 2, 1, 0 ]),

        function(^(_,_), [
                          0, 0, 0, 0,
                          0, 0, 0, 0,
                          0, 0, 0, 0,
                          0, 0, 0, 0 ]),

        function(v(_,_), [
                          0, 1, 1, 1,
                          1, 1, 1, 1,
                          0, 1, 2, 3,
                          1, 1, 1, 3 ]),

        relation(le(_,_), [
                          1, 1, 0, 0,
                          0, 1, 0, 0,
                          1, 1, 1, 1,
                          0, 1, 0, 1 ])
]).

============================== end of model ==========================
```

Figure 2. *mace4* models showing, in turn, the independence of each of the axioms of the ortholattice theory formulation in [11] from each other Each text line of values in the rightmost set of square brackets are assignments of values of integers to lattice positions. The number of nodes in such a lattice is N, where N is the first parameter in the "interpretation" line in the model. For example, in the model showing the independence of MP_L6, the "interpretation" line begins with "interpretation (4, ...", so N = 4. Such an assignment of values to nodes is said to *satisfy* or *be a model of* the indicated function/relation if the function/relation holds within the lattice under the assignment to those positions. Details of the *mace4* notation can be found in [1].

The time to produce the content of Figure 2 on the platform described in Section 2.0 was approximately 0.5 second.

4.0 Discussion

The results shown in Section 3.0 motivate at least two observations:

1. Each ortholattice theory axiom of [11] is independent of the other axioms in that formulation.

2. All the models in Figure 2 are distinct.

5.0 Acknowledgements

This work benefited from discussions with Tom Oberdan, Frank Pecchioni, Alberto Coffa, and Tony Pawlicki. For any infelicities that remain, I am solely responsible.

6.0 References

[1] von Neumann J. *Mathematical Foundations of Quantum Mechanics*. Translated by R. T. Beyer. Princeton. 1983.

[2] McCune WW. *prover9 and mace4.* URL http://www.cs.unm.edu/~mccune/prover9/. 2006.

[3] Horner JK. MP ortholattice independence mace4 scripts. Available from the author on request.

[4] Dalla Chiara ML and Giuntini R. *Quantum Logics*. URL http://xxx.lanl.gov/abs/quant-ph/0101028. 2004.

[5] Red Hat. CYGWIN_NT_6.0-WOW64. 1.7.9(0.237/5/3). 2011. http://www.cygwin.com/.

[6] Akhiezer NI and Glazman IM. *Theory of Linear Operators in Hilbert Space. Volume I.* Translated by M. Nestell. Frederick Ungar. 1961.

[7] Holland, Jr. SS Orthomodularity in infinite dimensions: a theorem of M. Solèr. *Bulletin of the American Mathematical Society* 32 (1995), pp. 205-234.

[8] Beran L. *Orthomodular Lattices: Algebraic Approach*. D. Reidel. 1985.

[9] Knuth DE and Bendix PB. Simple word problems in universal algebras. In J. Leech, ed. *Computational Problems in Abstract Algebra.* Pergamon Press. 1970. pp. 263-297.

[10] Chang CC and Keisler HJ. *Model Theory*. North-Holland. 1990. pp. 38-39.

[11] Megill ND and Pavičić M. Orthomodular lattices and a quantum algebra. *International Journal of Theoretical Physics* 40 (2001), 1387-1410.

[12] Church A. *Introduction to Mathematical Logic. Volume I.* Princeton. 1956.

[13] Jauch J. *Foundations of Quantum Mechanics.* Addison-Wesley. 1968.

[14] Megill ND. *Metamath.* URL http://us.metamath.org/qlegif/mmql.html#unify. 2004.

[15] Horner JK. An automated deduction system for orthomodular lattice theory. *Proceedings of the 2005 International Conference on Artificial Intelligence.* CSREA Press. 2005. pp. 260-265.

[16] Horner JK. An automated equational logic deduction of join elimination in orthomodular lattice theory. *Proceedings of the 2007 International Conference on Artificial Intelligence.* CSREA Press. 2007. pp. 481-488.

[17] Messiah A. *Quantum Mechanics*. Dover. 1958.

[18] Horner JK. *Using automated theorem-provers to aid the design of efficient compilers for quantum computing*. Los Alamos National Laboratory Quantum Institute Workshop. December 9–10, 2002. URL

http://www.lanl.gov/science/centers/quantum/qls_pdfs/horner.pdf.

[19] Birkhoff G and von Neumann J. The logic of quantum mechanics. *Annals of Mathematics* 37 (1936), 823-243.

[20] Nielsen MA and Chuang L . *Quantum Computation and Quantum Information*. Cambridge. 2000.

[21] Pavičić M and Megill N. Quantum and classical implicational algebras with primitive implication. *International Journal of Theoretical Physics* 37 (1998), 2091-2098. ftp://m3k.grad.hr/pavicic/quantum-logic/1998-int-j-theor-phys-2.ps.gz.

[22] Horner JK. An automated deduction of the relative strength of orthomodular and weakly orthomodular lattice theory. *2009 International Conference on Artificial Intelligence*. CSREA Press. 2009. pp. 525-530.

SESSION

SEARCH METHODS AND APPLICATIONS

Chair(s)

TBA

Extraction of Keywords and Tags for Search and Retrieval in Enterprise Social Networks

Kivanc Ozonat and Claudio Bartolini
HP Labs
1501 Page Mill Road
Palo Alto, CA
kivanc.ozonat@hp.com claudio.bartolini@hp.com

ABSTRACT

The HP software teams have built an enterprise social platform for over 40,000 employees distributed across the globe to share knowledge, learn from each others' experiences, and search for content relevant to the Hewlett Packard Application Services business. Given the unstructured nature of the content inside the platform, a key issue for the participants is to search for and retrieve content. To address this challenge, social platforms typically allow their participants to tag and thematize content. The platform then uses the tags and themes to facilitate content search and retrieval. However, platform participants do not always tag and themetize their content, and when they do, the tags and themes can often be incomplete or misleading.

A robust and accurate tagging and themetization system that will support the search and retrieval capabilities is critical to the platform. We provide a keyword and key phrase extraction technique based on term co-occurrences that performs better than traditional tfidf-based techniques. The extracted keywords and key phrases are used to construct a semantics graph. We further provide a content thematization system that discovers the major themes within the content based on the constructed semantics graph.

1. INTRODUCTION

The Industrialized Delivery System (IDS) Square is an enterprise social platform built by Hewlett Packard to help create a globally-connected community of 40,000+ employees. The sharing, search and retrieval of content in social platforms often rely on manually-assigned tags to content; however, participants often do not tag their content, and when they do, the tags can be incomplete and misleading. In collaboration with the software teams at Hewlett Packard, we have built a system that automatically tags content, clusters the sections of content into themes, and deduces the semantics of the search phrases input by the participants. The system relies on novel pattern recognition, data mining and graph clustering techniques developed by our teams. Our system is currently being integrated into the IDS Square platform.

The HP software teams have built an enterprise social platform for over 40,000 employees distributed across the globe to share knowledge, learn from each others' experiences, and search for content relevant to the Hewlett Packard Application Services business. The platform is called the Industrialized Delivery System (IDS) Square, announced by the Application Services leadership team to their employees in late August, 2011. The 40,000+ IDS Square participants will contribute to the network through a range of activities such as posting services-related entries, linking their entries to HP's internal and external sites, and commenting and voting on each others' posts.

Given the unstructured nature of the content inside the IDS Square platform, a key issue for the participants is to search for and retrieve content. To address this challenge, social platforms typically allow their participants to tag and thematize content. The platform then uses the tags and themes to facilitate content search and retrieval. However, platform participants do not always tag and themetize their content, and when they do, the tags and themes can often be incomplete or misleading. A robust and accurate tagging and themetization system that will support the search and retrieval capabilities is critical to the IDS Square platform.

In collaboration with the Hewlett Packard software team, we have built a system that automatically tags and themetizes services-related content with the intent of providing search and retrieval capability within the IDS Square. The system is currently being integrated into the IDS Square platform.

Our system automatically builds a repository of services-related tags and generates a semantic graph of their relationships. The repository is used to automatically assign tags to any enterprise services-related content. The relationships between the assigned tags - provided by the semantic graph - are used to cluster the sections of the content (e.g., paragraphs of text) into themes. Fig. 1 illustrates the system components and their dependencies. The system consists of the following components:

- Corpus Builder - We have available to us a small number of seed websites for each HP enterprise service line. A seed site can be viewed as a main webpage for the corresponding service line; it describes the corresponding service line with links to related sites. Starting from the seed sites, our crawlers retrieve HP's internal and external sites (as well as Sharepoint sites). The retrieved content constitutes the corpus.

- Tag Extractor - Tag extraction is the discovery of the words and phrases (i.e., two or more words) relevant to the domain of interest, which, in our case, is the HP Enterprise Services. The tags are automatically extracted from the HP Enterprise Services content retrieved by the corpus builder.

  Typically, tag extraction algorithms rely on the TF/IDF technique, which discovers words and phrases that occur frequently in the corpus and rarely outside the cor-

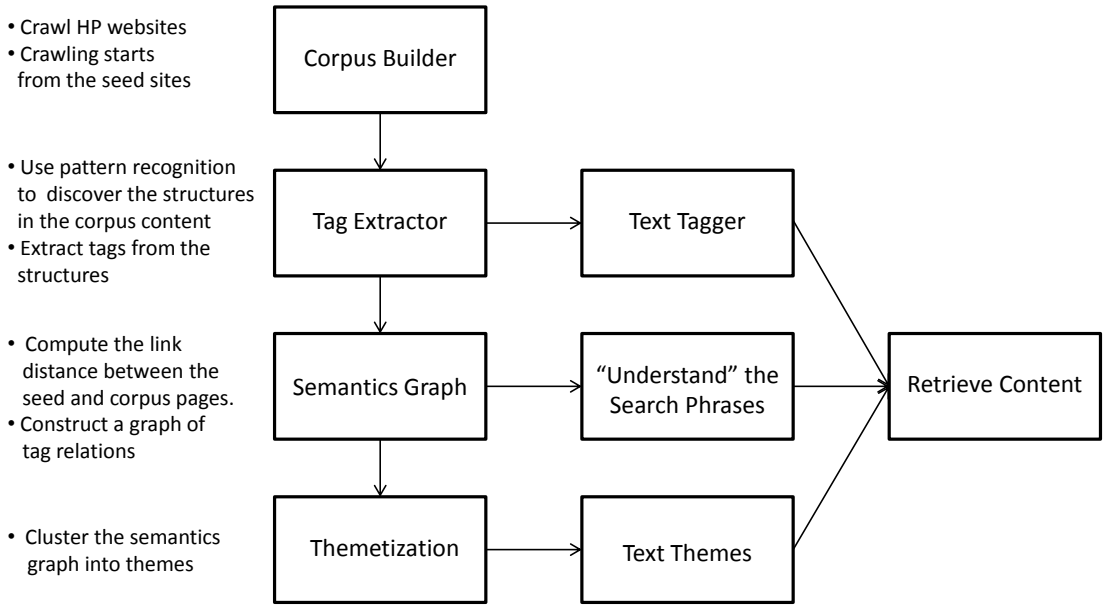

Figure 1: The architecture of the tags extraction, semantics graph building and thematization systems for search and retrieval in the enterprise service platform designed for HP's application services business

pus. However, in our context, the higher frequency of occurrence of a phrase does not necessarily indicate that the phrase is more relevant, or vice versa. For instance, the phrase "new opportunities" occurs more frequently than the phrase "application rationalization" in our corpus, although application rationalization is an actual service offering by the Application Services business. Instead of applying the TF/IDF-based techniques, we perform tag extraction through pattern recognition. Our starting assumption is that the critical words and phrases are more likely to occur inside structures such as the titles, sub-titles, lists, tables and link descriptors. Following this assumption, we design pattern recognition algorithms that automatically discover and extract the members of the structures from the corpus content.

We further apply pattern recognition techniques to discover which section(s) of a given content, are more likely to represent the content topics. For instance, if the content is an HTML page, we seek to differentiate the main sections from the side-bars, as the side-bars are less likely to be of relevance.

Once the members of titles, sub-titles, lists, tables and link descriptors are identified, we use co-occurrence based techniques [1] to extract the tags in the corpus.

- Semantics Graph Builder - The semantics graph is the graph of relations between the tags. The nodes of the graph are the tags, while the edges connecting the nodes have weights, representing the distances between the tags. A small distance between two tags indicates that the two tags are highly related to each other.

  If the phrases u and v relate to similar services lines or if they frequently appear in the same titles, lists and tables, then we force the semantic distance between u and v to be small. Towards this end, we compute the minimum number of web links to reach from each seed page to each corpus page on which the phrase u appears. From this, we deduce to which service lines u is most related. We repeat the procedure for the phrase v, and discover whether u and v relate to similar service lines.

- Thematization - The tagging by itself does not provide sufficient insight about the content. We take one step further and thematize the content, i.e., we summarize each section of the content with a theme. In order to progress from tags to themes, we cluster the semantic graph into themes. To cluster the graph, we first coarsen it by iteratively finding a matching of the graph [2], and collapsing each set of matched nodes into one node. We then partition the coarsened graph by computing a small edge-cut bisection [2] of the coarse graph such that each part contains roughly

half of the edge weights of the original graph. Finally, we project the partitioned graph back to the original graph.

- Tags, Themes and Search - The content in the IDS Square (e.g., plain text, HTML page, e-mail message, Sharepoint document) are assigned tags by matching the n-tuples in the texts by the tags discovered in the Tag Extractor stage. The content are then themetized by finding the graph clusters in which the assigned tags appear most often.

  When a participant enters a search phrase in a search box in IDS Square, our system understands the semantic of the input phrase through the semantics graph, and has the ability to retrieve the relevant content.

Our system is currently being integrated into the IDS Square platform to be used by the over 40,000 employees that support the Application Services business. The system addresses the issue of understanding the meaning of tags in their accepted meaning within HP. For instance, as Fig. 2 illustrates, our system relates "managed messaging" to concepts such as "workplace services" and "enterprise e-mail", while Wikipedia (http://www.wikipedia.org) relates it to the "fairness test", "chamber of commerce" and "rehabilitation services".

Social platforms often rely on manual tagging by the participants to support search and retrieval. Our system automatically assigns tags and themes to content without any manual step. More importantly, the system is designed specifically for the HP services domain through building a corpus of services content with crawling that starts from a set of seed services pages. Thus, the extracted tags and themes are highly relevant to HP's services business, the employees of whom will be the participants the IDS Square platform.

2. KEYWORD EXTRACTION

Keyword extraction techniques are often based on the tfidf method. The tfidf method compares the word frequencies in the repository with the word frequencies in the sample text; if the frequency of a word in the sample text is high while its frequency in the repository is low, the word is extracted as a keyword.

While the tfidf-based techniques are known to perform well in many text mining applications, they have a major shortcoming in the context of mining threads in an enterprise social platform. An enterprise social thread typically contains only few sentences and words, making it difficult to obtain reliable statistics based on word frequencies. Many relevant words appear only once in the thread, making it difficult to distinguish them from the other, less relevant words of the thread.

An alternative approach would be to form a vector of keywords in the repository of forum threads, and, generate a binary features vector for each thread. If the i^{th} repository keyword appears in the thread, the i^{th} element of the thread's feature vector is 1, and if the keyword does not appear in the thread, the i^{th} element of the thread's feature vector is 0.

The question with this simple alternative approach is then that of generating keywords in a given repository. We apply three different techniques:

- Remove only stop-words: We only filter out stop words (e.g., if, and, we, etc.) from the repository, and let the vector of keywords be the set of all remaining distinct repository words.
- The tfidf method: We apply the tfidf method on the entire repository by comparing the word frequencies in the repository with word frequencies in the English language. If the frequency of a word is high in the repository and low in the English language, we take the word as a keyword.
- Term co-occurrence: The term co-occurrence method extracts keywords from the repository without comparing the repository frequencies with the English language frequencies. This method is explained next [9].

2.1 Term Co-occurrence

Let N denote the number of all distinct words in the repository of forum threads. We construct a $N \times M$ co-occurrence matrix, where M is pre-selected integer with $M < N$. We typically take M to be 500. We index all distinct words by n, i.e., $1 \leq n \leq N$. We index the most frequently observed M words in the repository by m such that $1 \leq m \leq M$.

The $(n.m)$ element (i.e. ,n^{th} row and the m^{th} column) of the $N \times M$ co-occurrence matrix counts the number of times the word n and the word m occur together. Consider the word ẅirelesswith index n and the word c̈onnectionẅith index m, and that ẅirelessänd c̈onnectionöccur together 218 times in the repository. Then, the $(n.m)$ element of the co-occurence matrix is 218.

If the word n appears independently from the words $1 \leq m \leq M$ (the frequent words), the number of times the word n co-occurs with the frequent words is similar to the unconditional distribution of occurrence of the frequent words.

On the other hand, if the word n has a semantic relation to a particular set of frequent words, then the co-occurrence of the word n with the frequent words is greater than the unconditional distribution of occurrence the frequent words.

We denote the unconditional probability of a frequent word m as the ex- pected probability p_m and the total number of co-occurrences of the word n and fre- quent terms as c_n. Frequency of co-occurrence of the word n and the word m is written as $freq(n, m)$. The statistical value of χ^2 is defined as

$$\chi^2(n) = \sum_{1 \leq m \leq M} \frac{freq(n,m) - N_n p_m}{n_m p_m}. \quad (1)$$

2.2 Clustering of Frequent Terms

We cluster two or more frequent terms together in either of the following two conditions:

- The frequent words m_1 and m_2 co-occur frequently with each other.
- The frequent words m_1 and m_2 have a similar distribution of co-occurrence with other words.

To quantify the first condition of m_1 and m_2 co-occurring frequently, we use the mutual information between the occurrence probability of m_1 and that of m_2.

To quantify the second condition of m_1 and m_2 having a similar distribution of co-occurrence with other words, we

use the Kullback-Leibler divergence between the occurrence probability of m_1 and that of m_2.

3. ALGORITHM

We design a statistical clustering algorithm to minimize (in the Lloyd-optimal sense) the error probability given in (2) under the cluster entropy constraints. Gaussian mixture models have been used extensively in the literature to design generative algorithms for data clustering. Such algorithms are often based on the EM algorithm [5]; however, there also exists alternative training approaches such as Gauss mixture vector quantization (GMVQ) [8, 11, 12, 13, 16]. The EM algorithm assumes that the underlying data follows a Gaussian mixture distribution and tries to fit a Gaussian mixture model to the data, while the GMVQ is a Lloyd clustering algorithm and it does not make any assumptions about the statistics of the underlying data.

We use the GMVQ to design a hierarchical clustering algorithm. Our choice of GMVQ (over the EM) is motivated by the intractability of the EM solution in minimizing (2) through a hierarchical clustering scheme. We first extend the GMVQ to design a hierarchical (tree-structured) clustering algorithm.

In section 3.1, we provide an overview of the GMVQ and include the iterative solution for the GMVQ. In section 3.2, we extend the GMVQ to design a tree-structured clustering algorithm.

3.1 Gauss mixture vector quantization (GMVQ)

Consider the training set $\{z_i, 1 \leq i \leq N\}$ with its (not necessarily Gaussian) underlying distribution f in the form $f(Z) = \sum_k p_k f_k(Z)$. The goal of GMVQ is to find the Gaussian mixture distribution, g, that minimizes the distance between f and g. It has been shown in [8] that the Gaussian mixture distribution g that minimizes this distance (i.e., minimizes in the Lloyd-optimal sense) can be obtained iteratively with the following two updates at each iteration:

i. Given μ_k, Σ_k and p_k for each cluster k, assign each z_i to the cluster k that minimizes

$$\frac{1}{2}\log(|\Sigma_k|) + \frac{1}{2}(z_i - \mu_k)^T \Sigma_k^{-1}(z_i - \mu_k) - \log p_k, \quad (2)$$

where $|\Sigma_k|$ is the determinant of Σ_k. We note that (5) is also known as the QDA distortion.

ii. Given the cluster assignments, set μ_k, Σ_k and p_k as

$$\mu_k = \frac{1}{\|S_k\|} \sum_{z_i \in S_k} z_i, \quad (3)$$

$$\Sigma_k = \frac{1}{\|S_k\|} \sum_i (z_i - \mu_k)(z_i - \mu_k)^T, \quad (4)$$

and

$$p_k = \frac{\|S_k\|}{N}, \quad (5)$$

where S_k is the set of training vectors z_i assigned to cluster k, and $\|S_k\|$ is the cardinality of the set.

3.2 Tree-structured Gauss Mixture Vector Quantization

We use the BFOS algorithm to design a hierarchical (i.e., tree-structured) extension of GMVQ [13]. The BFOS algorithm requires each node of a tree to have two linear functionals such that one of them is monotonically increasing and the other is monotonically decreasing. Toward this end, we view the QDA distortion (5) of any subtree, T, of a tree as a sum of two functionals, u_1 and u_2, such that

$$u_1(T) = \frac{1}{2}\sum_{k \in T} l_k \log(|\Sigma_k|) + \frac{1}{N}\sum_{k \in T}\sum_{z_i \in S_k} \frac{1}{2}(z_i - \mu_k)^T \Sigma_k^{-1}(z_i - \mu_k), \quad (6)$$

and

$$u_2(T) = -\sum_{k \in T} p_k \log p_k \quad (7)$$

where $k \in T$ denotes the set of clusters (i.e., tree leaves) of the subtree T, and μ_k, Σ_k, p_k and the set S_k are as defined in section 3.1.

The magnitude of u_2/u_1 increases at each iteration. This is a key point of the design as, then, pruning is terminated when the magnitude of u_2/u_1 reaches λ, resulting in the subtree minimizing $u_1 + \lambda u_2$.

4. EXPERIMENTS

We've tested our approach using HP's internal enterprise services content including websites and SharePoint sites. We compared the hierarchical tree-based clustering approach to 3 other clustering techniques (EM, GMVQ and agglomerative hierarchical clustering) under 3 different feature vector constructions, and under 2 different keyword extraction schemes. The comparisons are performed on a subset of 6000 webpages of content. In each comparison, we measured the misclassification error, which is the probability of a customer query being assigned to a cluster of a product problem different from the problem expressed in the query. The ground truth for the threads, problems and queries have been established by HP's internal website owners, independently of the author of this paper.

4.1 Feature vectors

The i^{th} thread has two feature vectors, the page title and metadata $x_{i,1}$ and the page content $x_{i,2}$. Each feature vector is a W-length binary (0 or 1) vector, where W is the total number of unique words used across all pages. Each word is indexed by w, where $1 \leq w \leq W$.

The w^{th} element of $x_{i,1}$ is 1 if and only if the word w occurs in the title of the i^{th} page. Similarly, the w^{th} element of $x_{i,2}$ is 1 if and only if the word w occurs in the content of the i^{th} page. We exclude the stop-words (e.g., and, if, such, etc.) from the feature vectors.

4.2 Comparisons

We've compared the hierarchical TS-GMVQ algorihm to the EM algorithm, standard GMVQ algorithm and agglomerative clustering. In each comparison, we've tested three different feature vector constructions for the EM, GMVQ, TS-GMVQ and agglomerative clustering: the feature vector is $x_{i,1}$, the feature vector is $x_{i,2}$, and the feature vector

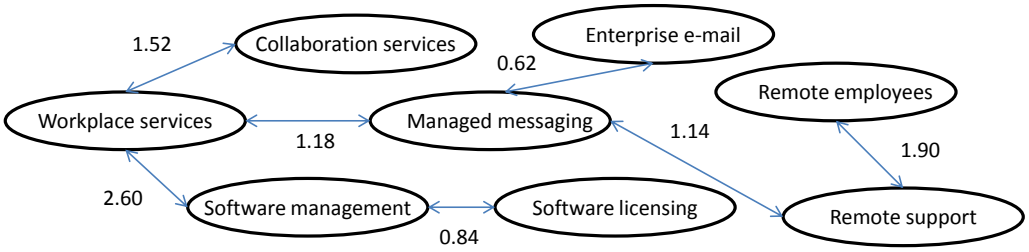

Figure 2: A section of the semantics graph with key phrases and associated pairwise weights.

is $[x_{i,1}\ x_{i,2}]$. The number of clusters established as ground truth is 54.

4.2.1 Feature vector constructions

Denoting the feature vector of the training samples by y_i, we consider three feature vector constructions:

i. $y_i = x_{i,1}$. The clustering algorithm takes only the meta data and page titles into account. The remaining content are ignored.

ii. $y_i = x_{i,2}$. The clustering algorithm takes only the content other than meta data and page titles.

iii. $y_i = [x_{i,1}\ x_{i,2}]$. The clustering algorithm takes into account both the page titles and meta data and the remaining page content.

We compare the hierarchical TS-GMVQ approach with the EM, GMVQ, and agglomerative clustering under each of these three feature vector construction settings.

4.2.2 Compared algorithms

i. EM: We use the standard EM algorithm. At each iteration, the E-step updates the membership probabilities, $v_{i,k}$, for each cluster k and sample i, while the M-step updates the mean, covariance and the probability of occurrence for each cluster k as

ii. GMVQ: The standard GMVQ algorithm updates are as given in (5)-(8) in section 4.1.

iii. TS-GMVQ: The TS-GMVQ is grown and pruned by the BFOS algorithm using (9) and (10) as described in section 4.2.

iv. Agglomerative hierarchical clustering: We start with N clusters, where N is the number of threads in the training set, and apply agglomerative clustering with the distance criterion given in (5). At each iteration, we merge the two clusters, whose closest feature vectors are closest. In other words, at each iteration, for each pair of clusters, c_k and c_m, we compute the distances between the feature vectors of c_k and the feature vectors of c_m, and denote the closest distance by $d_{k,m}$. We merge the two clusters with the minimum $d_{k,m}$.

Fig. 1 shows the classification error as a function of the number of clusters for the threads in the notebook PC set. The tfidf method is used for extracting keywords. In each plot, the classification error rate of the TS-GMVQ approach (red solid line) is compared to that of the GMVQ (blue dashed line), EM (black dash-dot line) and agglomerative hierarchical clustering (green dot-plus line). The top plot shows the setting, where the training vector for GMVQ, EM, TS-GMVQ and agglomerative hierarchical clustering are the page title and meta data feature vectors, i.e., $y_i = x_{i,1}$. In this setting, the TS-GMVQ approach outperforms the other three algorithms.

The middle plot in Fig. 1 shows the setting where the training vectors for the four approaches are the page content feature vectors, i.e., $y_i = x_{i,2}$. Similar to the setting with $y_i = x_{i,1}$, the TS-GMVQ approach leads to the minimum classification error.

The bottom plot in Fig. 1 shows the classification errors for the setting where both the page titles and meta data and page content are included as feature vectors, i.e., $y_i = [x_{i,1}\ x_{i,2}]$. The performance of the four algorithms (GMVQ, EM, TS-GMVQ and agglomerative hierarchical clustering) all improve compared to the settings shown in the top and middle plots.

5. CONCLUDING REMARKS

The HP software teams have built an enterprise social platform for over 40,000 employees distributed across the globe to share knowledge, learn from each others' experiences, and search for content relevant to the Hewlett Packard Application Services business. The platform is called the Industrialized Delivery System (IDS) Square, announced by the Application Services leadership team to their employees in late August, 2011. The 40,000+ IDS Square participants will contribute to the network through a range of activities such as posting services-related entries, linking their entries to HP's internal and external sites, and commenting and voting on each others' posts.

Given the unstructured nature of the content inside the IDS Square platform, a key issue for the participants is to search for and retrieve content. To address this challenge, social platforms typically allow their participants to tag and thematize content. The platform then uses the tags and themes to facilitate content search and retrieval. However, platform participants do not always tag and themetize their content, and when they do, the tags and themes can often

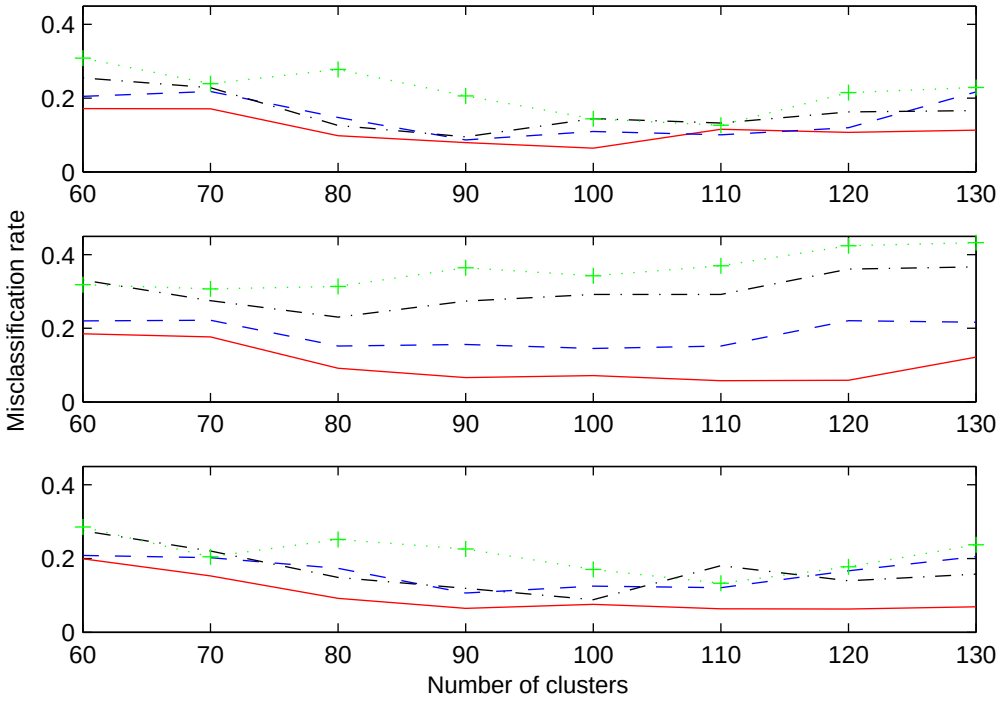

Figure 3: The classification error rate as a function of the number of clusters for the enterprise services content. The tfidf keyword extraction. The TS-GMVQ approach (red solid line) is compared to the GMVQ (blue dashed line), EM (black dash-dot line), and agglomerative hierarchical clustering (green dot-plus line). The top plot shows the setting with $y_i = x_{i,1}$, the middle plot shows the setting with $y_i = x_{i,2}$ and the bottom plot shows the setting with $y_i = [x_{i,1}\ x_{i,2}]$.

be incomplete or misleading. A robust and accurate tagging and themetization system that will support the search and retrieval capabilities is critical to the IDS Square platform.

In collaboration with the Hewlett Packard software team, we have built a system that automatically tags and themetizes services-related content with the intent of providing search and retrieval capability within the IDS Square. The system is currently being integrated into the IDS Square platform.

References

[1] S. Bickel and T Scheffer. Multi-view clustering. In Proceedings of the IEEE International Conference on Data Mining, 2004.

[2] A. Blum and T. Mitchell. Combining labeled and unlabeled data with co-training. In Proceedings of the Conference on Computational Learning Theory, pages 92-100, 1998.

[3] U. Brefeld and T. Scheffer. Co-EM support vector learning. In Proceedings of the International Conference on Machine Learning, 2004.

[4] S. Brin and L. Page. The anatomy of a large-scale hypertextual web search engine. In Proceedings of the 7th International World Wide Web Conference, pp. 107-117, 1998.

[5] A. P. Dempster, N. M. Laird, and D. B. Rubin. Maximum likelihood from incomplete data via the EM algorithm. Journal of the Royal Statistics Society, 39(1):1-21, 1977.

[6] M. Figueiredo and A. K. Jain. Unsupervised learning of finite mixture models. IEEE Transactions on Pattern Analysis and Machine Intelligence, 24:3 , pp. 381-396, March 2002.

[7] R. Ghani. Combining labeled and unlabeled data for multiclass text categorization. In Proceedings of the International Conference on Machine Learning, 2002.

[8] R.M. Gray and T. Linder. Mismatch in high rate entropy constrained vector quantization. IEEE Trans. Inform. Theory, Vol. 49, pp. 1204-1217, May, 2003.

[9] Y Matsuo. Keyword extraction from a single document using word co-occurrence statistical information. International Journal on Artificial Intelligence Tools, Vol. 13, pp. 157-169, 2004.

[10] K. Nigam and R. Ghani. Analyzing the effectiveness and applicability of co-training. In Proceedings of Information and Knowledge Management, 2000.

[11] D.B. O'Brien, M. Gupta, R.M. Gray, and J.K. Hagene. Automatic classification of images from internal optical inspection of gas pipelines. In Proceedings of the ICPIIT VIII Conference 2003, Houston.

[12] D.B. O'Brien, M. Gupta, R. M. Gray, and J. K. Hagene. Analysis and classification of internal pipeline images. In Proceedings of ICIP 2003, Barcelona, Spain.

[13] K. Ozonat, and R.M. Gray. Gauss mixture model-based classification for sensor networks. In Proceedings of the IEEE DCC 2006.

[14] K. Ozonat. Multi-view Clustering Trees for Search and Retrieval in Customer Product Forums. In Proceedings of the ICAI 2010.

[15] L. Page, S. Brin, R. Motwani, and T. Winograd. The PageRank citation ranking: Bringing order to the web. Technical report, Stanford University, 1998.

[16] K. Pyun, C.S.Won, J. Lim, and R.M. Gray. Texture classification based on multiple Gauss mixture vector quantizers. In

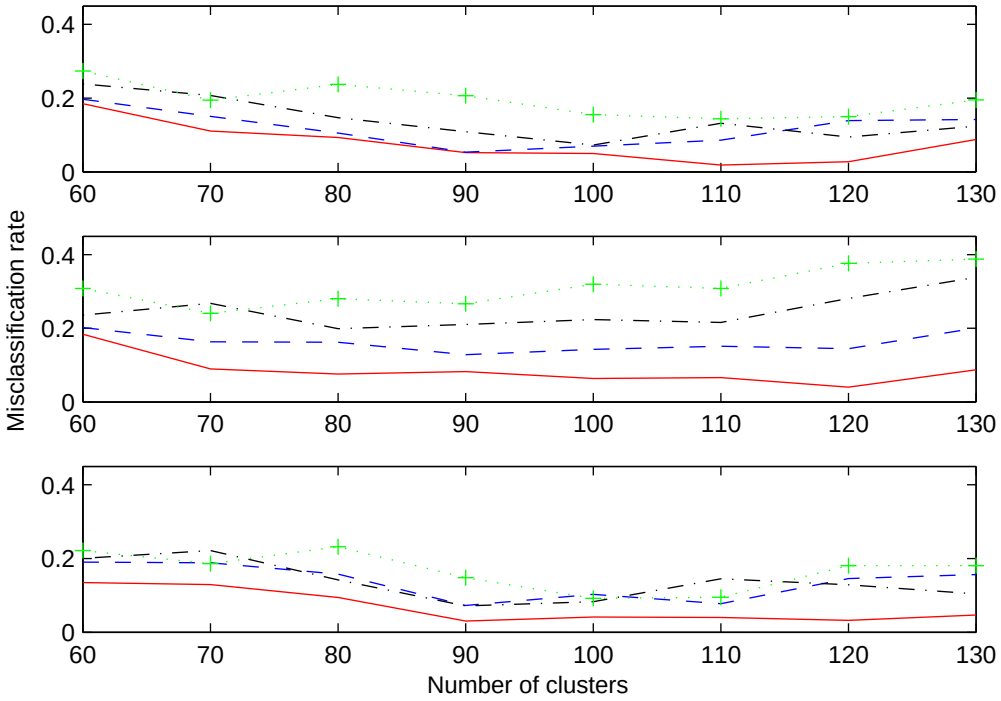

Figure 4: The classification error rate as a function of the number of clusters for the enterprise services content. The term co-occurrence keyword extraction. The TS-GMVQ approach (red solid line) is compared to the GMVQ (blue dashed line), EM (black dash-dot line), and agglomerative hierarchical clustering (green dot-plus line). The top plot shows the setting with $y_i = x_{i,1}$, the middle plot shows the setting with $y_i = x_{i,2}$ and the bottom plot shows the setting with $y_i = [x_{i,1}\ x_{i,2}]$.

Proceedings of Multimedia and Expo, 2002, pp. 501-4, 2002

[17] R. A. Redner and H. F. Walker. Mixture densities, maximum likelihood and the EM algorithm. SIAM Review, 26(2):195-239, 1984.

[18] J. Shen, Y. Zhu, H. Zhang, C. Chen, R. Sun, and F. Xu. A content-based algorithm for blog ranking. Internet Computing in Science and Engineering, 2008.

[19] G. Xu and W.Y. Ma. Building implicit links from content for forum search. In Proceedings of the 29th International Conference on Research and Development in Information Retrieval, 2006.

[20] D. Yarowsky. Unsupervised word sense disambiguation rivaling supervised methods. In Proceedings of the 33rd Meeting of the Association for Comp. Linguistics, 1995.

[21] Y Matsuo. Keyword extraction from a single document using word co-occurrence statistical information. International Journal on Artificial Intelligence Tools, Vol. 13, pp. 157-169, 2004.

[22] G. Karypis and V. Kumar. A coarse-grain parallel formulation of multilevel k-way graph partitioning algorithm. Siam Conference on Parallel Processing for Scie

Stochastic Search and Planning for Maximization of Resource Production in RTS Games

Thiago F. Naves and Carlos R. Lopes
Faculty of Computing, Federal University of Uberlândia, Uberlândia, Minas Gerais, Brasil

Abstract— *RTS games are an important field of research in Artificial Intelligence Planning. In these games we have to deal with features that represent challenges for Planning such as time constraints, numerical effects and actions with a large number of preconditions. RTS games are characterized by two important phases. The first one has to do with gathering resources and developing an army. In the second phase the resources produced in the first phase are used in battles against enemies. Thus, the first phase is vital for success in the game and the power of the army developed directly reflects in the chances of victory. Our research is focused on the first phase. In order to maximize resource production we developed algorithms based on Simulated Annealing and classical planning. As a result we have obtained a signification improvement of the strength of the army.*

Keywords: Real-Time Strategy Games, Resources, Actions, Goal, Search, Planning.

1. Introduction

Real-time strategy (RTS) games are one of the most popular categories of computer games. Titles like "Starcraft 2" and "World of Warcraft" are two representative examples of this category. These games have different character classes and resources, which are employed in battles. Battles can be waged by a human player or a computer.

It is possible to identify two phases in a RTS game. First, there is an initial period in which each player starts the game with some units and/or buildings and develops his army via resource production. In the next phase military campaigns take place. In this phase the resources gathered earlier are employed for offense and defense. Therefore, the stage of resource production is vital to succeed in this game.

The resources in RTS games are all kinds of raw materials, basic construction, military units and civilization. For obtaining a desired set of resources is necessary to carry out actions. In general we have three sorts of actions related to resources: actions that produce resources, actions that consume resources and actions that collect resources.

Once we conceive a sequence of actions (a plan) that produces a desired set of resources (a goal), we carry out this plan to take the game from an initial state of resources to another final state in which the desired set of resources is achieved. To identify what resources to be achieved (a goal) is an important step to elaborate a plan of action. The choice of an adequate goal has a direct impact on the strength of the army, which is important in the development phase. Thus, in the specification of a goal it is necessary to maximize the amount of resources to be achieved in order to raise the strength of the army. In this paper we describe our approach to achieve goals that maximize production of resources.

The domain used for this work is StarCraft, which is considered the game with the highest number of constraints on planning tasks [1]. In our approach we have to generate an initial plan of action to achieve an arbitrary amount of resources. In order to do this, we developed an sequential planner based on the STRIPS language [2]. The initial plan is the basis for exploring new plans in order to find the one that has largest amount of resources.

In this paper, we focus on the task of finding the goal that maximizes resource production based on an initial plan of action, as we stated earlier. Once we have an initial plan, we use Simulated Annealing [3] (SA) to maximize the amount of resources to be achieved. However, SA is not only used for goal specification. In the process of figuring out a goal specification, SA is also used to produce a plan to achieve that goal. Our work is motivated by the results obtained in [4] and by gaps in the approaches of [5] and [6] with respect to the choice of goals to be achieved during the production of resources. For the correct functioning of SA, techniques were introduced to adjust its parameters and validate the plans generated during the search. The results obtained are encouraging and show the efficiency of the method to find good solutions.

We understand that this research is interesting for the AI planning field because it deals with a number of challenging problems such as concurrent activities and real-time constraints. Most work in RTS games do not consider the choice of goals within the game. Usually goals for resource production have a random amount of resources to be achieved. Thus, this research can go toward a new approach to resource production, and can be extended to other applications.

The remainder of this paper is organized as follows. Section 2 lists the characteristics of the problem. In section 3 related work is presented and discussed. Section **??** explains about the domain of production resources. Section 4 describes techniques and algorithms for adjusting the parameters of SA in RTS games. Section 5 presents the

consistency checker that works with SA. Section 6 discusses the results of the experiments. In section 7 we make final considerations about our approach.

2. Characterization of the problem

The planning problem in RTS games is to find a sequence of actions that leads the game to a goal state that achieves a certain amount of resources. This process must be efficient. In general, the search for efficiency is related to the time that was spent in the execution of the plan of actions (makespan). However, in our approach we seek for actions that increase the amount of resources that raise the army power of a player. This is achieved by introducing changes into a given plan of action in order to increase the resources to be produced, especially the military units, without violating the preconditions between the actions that will be used to build these resources.

To execute any action you must ensure that its predecessor resources are available. The predecessor word can be understood as a precondition to perform an action and the creation of the resource as a effect of its execution. In this paper actions and resources have the same name. To tell them apart we use the prefix *act* to indicate actions and the prefix *rsc* when referring to resources. Resources can be labeled in one of the following categories: $Require$, $Borrow$, $Produce$ and $Consume$. Figure 1 shows the precedence relationship among some of the main resources of the domain. These resources are based on StarCraft, which has three different character classes: Zerg, Protoss and Terran. This work focuses on the resources of the class Terran.

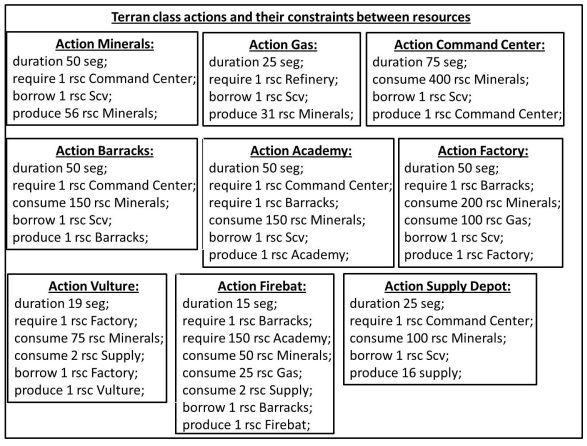

Fig. 1: Some resources of the class Terran and their dependencies.

For example, according to Figure 1 to execute an action that produces a $Firebat$ resource you must have a $Barracks$ and $Academy$ available, a certain amount of $Minerals$ and Gas is also required. The Firebat is a military resource. Thus, the action $Firebat$: $Require$ *(1 rsc Academy, 1 rsc Barracks)*, $borrow$ *(1 rsc Barracks)*, $consume$ *(50 rsc Minerals, 25 rsc Gas)* and $produces$ *(1 rsc Firebat)*. The $Barracks$ will be $borrow$, i.e, it is not possible to perform another action until *act firebat* is finished. The time to build a $Firebat$ is 15 seconds. This situation describes the challenges that surround the planning of actions.

In our approach each plan of action has a time limit, army points, feasible and unfeasible actions. The time limit constrains the maximum value of makespan of the plan of action. The army points are used to evaluate the strength of the plan in relation to its military power. Each resource has a value that defines its ability to fight the opponent. Feasible actions in a plan are those actions that can be carried out, i.e, they have all their preconditions satisfied within the current planning. Unfeasible actions are those that can not be performed in the plan and are waiting for their preconditions to be satisfied at some stage of planning. Unfeasible actions do not consume resources of planning and do not contribute for the evaluation of the army points of the plan.

Returning to the example of the $Firebat$, suppose that a goal with a time limit of 700 seconds is *(1 rsc Firebat, 1 rsc Marine)*. A plan for this goal can be achieved by the following actions: *(10 act Minerals, 1 act Gas, 1 act Refinery, 1 act Barrack, 1 act Academy, 1 act Firebat, 1 act Marine)*. In a plan every action produces a resource with its respective name, i.e, *10 act Minerals* correspond to ten individual executions of action *Minerals*. The plan contains 28 army points and a makespan of 680 seconds. Among the possible operations that can be made in this plan, consider replacing an action $Minerals$ by a new action $Firebat$. In this case the action $Minerals$ contributes to make available the resource $Barracks$. In this way $Barracks$ becomes unfeasible within the plan due to lack of $Minerals$ and consequently the other resources such as $Academy$, $Firebat$ and $Marine$ will also be because $Barracks$ is a precondition for those resources.

With all the actions that became unfeasible the plan now has 0 army points. Now, suppose if instead of removing $Minerals$ it was requested to include a $Marine$ action in place of a *Gas* action. This exchange is feasible, because $Marine$ has just as preconditions *(1 rsc Minerals, 1 rsc Barracks)* and these are already available at the time. The action $Firebat$ becomes unfeasible and the duration of the plan (makespan) drops to 670 sec. If in the next operation an action Gas is inserted into the plan the action $Firebat$ action would become feasible. In this way a plan is established with 40 army points and 695 sec of makespan. The plan that is found is better than the initial one. Reducing the makespan of the goal is not one of the objectives of this work. However,due to the characteristics of changes in the plan this might happen.

Results, as the example presented above, are motivators for this research.

3. Related Work

There is little research in maximizing goals of resources production in RTS games. One of the reasons is the complexity involved in searching and managing the state space, which makes difficult to attend the real-time constraints.

The work developed by [4] remains our approach in a certain sense. He also uses Simulated Annealing to explore the state space of the StrarCraft in order to balance the different classes in the game by checking the similarity of plans in each class. In our work Simulated Annealing is used to determine a goal to be achieved that maximizes resources production, given the current state of resources in the game and a time limit for completion of actions.

[7] developed a linear planner to generate a plan of action given an initial state and a goal for production of resources, which is defined without the use of any explicit criterion. The generated plan is scheduled in order to reduce the makespan. Our work also makes use of a sequential planner. However, our approach deals with dynamic goals for resources production. This is necessary in order to find out a goal that maximizes the strength of the army. To the contrary, [7] works with a goal with fixed and unchangeable resources to be achieved.

Work developed by [6] has the same objective as the one pursued by [7]. These approaches differ on use of the planning and scheduling algorithms. [6] developed their approach using Partial Order Planning and SLA* for scheduling. [6] also works with a goal with fixed and unchangeable resources to be achieved and not can be adapted to our problem.

We also surveyed some existent planners that could be applied. [8] and [9] were considered for our problem at hand, but both have a different approach and would have to be modified to adapt to our goal. In short, most of the approaches surveyed have different focus and the techniques used are not efficient for the domain that we are exploring.

4. The use of Simulated Annealing to Maximize Resource Production

Simulated Annealing is a meta-heuristic which belongs to the class of local search algorithms [3]. SA was chosen due to the robustness and possibility to be combined with other techniques. it was also the algorithm that achieved the best results among those used during the experiments. SA takes as input a possible solution of the problem, in our case a plan of action developed by a sequential planner. The mechanism that generates neighbors will perform operations of exchange and replacement of actions in the plan. It should be noted that these operations generate new plans of action.

In SA a possible solution is evaluated through the use of an objective function. In our approach the objective function is responsible for counting the army points existent in each plan of action. In this way it is possible to find out which states have the highest attack strength. A state that is better evaluated that the current state becomes the current state. Even if the new plan generated is not chosen as the current solution there is still a probability of its acceptance. Algorithm 1 shows the pseudocode of the Simulated Annealing algorithm.

Algorithm 1 SA($G_{initial}$, P, M, α)

```
1:  G_current ← G_initial
2:  T_0 ← InitialTemp()
3:  while T_0 > 0 do
4:    i ← 1
5:    nSuccess ← 0
6:    while i < M do
7:      G_neighbor ← NewNeighbor(G_current)
8:      Δr ← Evaluation(G_current) - Evaluation(G_neighbor)
9:      if Δr < 0 or Random() < PrAcceptance()
        then
10:       G_current ← G_neighbor
11:       nSuccess ← nSuccess + 1
12:     end if
13:     i ← i + 1
14:   end while
15:   if nSuccess ≥ P then
16:     T_0 ← α * T_0
17:   end if
18: end while
19: return G_current
```

The parameters of SA were adjusted to the domain of RTS games. In the next subsections we describe in details the algorithm, techniques were developed and parameters used.

4.1 Initial Solution

The algorithm takes as input a initial solution (plan of action) and performs operations on its actions. The initial solution $G_{initial}$ is generated by the sequential planner (it will be briefly explained in the next subsection) and it is a plan with the actions ordered by their starting time. The resources that should be achieved in the initial plan are chosen randomly and the makespan is constrained to the time limit established for the goal. Time limits vary from 3 to 5 minutes. The idea is to make SA work with varied plans, which avoids that the algorithm becomes biased to a specific value of the objective function.

4.2 Sequential Planner

The planning algorithm takes a goal to be achieved a list of resources available , which contains all the resources available to the player as the amount of minerals or units, and a time limit for the execution of the plan to be generated The planning algorithm was built upon STRIPS[2]. In this

way, based on the input data, a linear plan of actions is generated to achieve a goal.

Depending on the available time, given by the time limit parameter, the planner may be called more than once, each time with a random goal. The algorithm takes only one resource as a goal at a time because the idea is to build an initial plan of action without setting a fixed amount of resources. In each iteration a plan of action is achieved and appended to a previous plan obtained in early iterations. This is done until the time limit is reached by the resulting plan. The algorithm takes this behavior because it is necessary to build a plan of action without exceeding the time limit.

While a resource is being planned is possible to check whether the plan under development is not exceeding this time. If an action exceeds the time limit, the planning is stopped and the plan built so far is considered a valid plan and returned. Generate a plan based on a time limit is a way to build the plan based on the behavior of a human player, which does not specify an amount of resources to their goal, but builds as many resources as he can in a interval of time.

As an example suppose that it is necessary to produce a plan to achieve the resource *Marine* with time limit of 150 sec. based on the following available resources: (*(4 Scv, 50 Minerals)*. Our planner is capable of producing the following plan: (*(3 act Minerals, 1 act Barracks, 1 act Marine)*. Therefore, in order to produce *Marine*, it is necessary to execute three actions *Minerals*, one action *Barracks* and one action *Marine*.

4.3 The Cooling Scheme

The initial temperature T_0 ($InitialTemp()$, line 2) is achieved based on the average number of actions in the plan of action, which is given as input to the algorithm. With the time limit is possible to generate plans with a small number of actions. Our objective is to reproduce a typical behavior of a human player. This is achieved by establishing an initial temperature of about five times the quantity of actions in the plan. This is a appropriate value for the domain.

For cooling, a value close to a few tenths of a percent of the initial temperature is good. A logarithmic function can make the algorithm become very slow, which is an inappropriate behavior for an RTS game environment.

We developed an adaptive method of reduction, where the temperature T_{i+1} drops by a factor α (line 19) if for a given number of iterations P the new plans are always accepted. The alpha value is low and close to 1. For instance, 0.97 is a good value to be defined by alpha. P must be large enough to explore the possibilities of operations on the plans. Based on experiments we found that values between 15 and 20 represent a good choice for P.

$$T_{i+1} = \begin{cases} T_i & \text{if the number of plans accepted } < P. \\ \alpha.T_i & \text{if the number of plans accepted } = P. \end{cases}$$

The probability of a new plan to be accepted if it is not better evaluated than the current plan is given by the equation 1.

$$1 - 0.5 \tanh [2\Delta r(v_i - v_{i+1}T_{i+1}] \quad (1)$$

Where v_i is the feasible number of actions that the plan has in the corresponding iteration. The variable Δr is a factor derivation and is obtained from the difference between the values of the objective function (army points) of the current plan and new plan generated (line 11 Algorithm 1). Finally this value is divided by temperature. Thus, the algorithm can behave differently depending on the temperature value.

The function responsible for calculating the probability is $PrAcceptance()$ (line 9). Its value must be greater than the value generated by the function $Random()$ (line 9), which produces a random value between 0 and 1. The parameter M determines how many neighbors will be generated before the temperature decreasing (line 6). Its value should enable a good search in the space of states given the temperature of the algorithm.

4.4 The mechanism that generates neighbors

There are several ways to generate a new neighbor plan $G_{neighbor}$ from the current solution $G_{current}$ in Simulated Annealing. This generation is the essential for the SA get a good conversion, which is the way the plan is modified to be compatible with the characteristics of RTS games. Next we describe four possible mechanisms for acomplishing this task.

- *A.* Two actions are randomly selected in the plane and switched places, one assuming the position of other.
- *B.* An action of the plan is randomly chosen and replaced by a new action that is that is randomly chosen among all available actions in the game.
- *C.* One of the following moves is randomly chosen: Randomly select two actions within the plan and switch their positions, or replace a action chosen randomly within the plan by a new action randomly selected among all available actions in the game.
- *D.* The same mechanism as above, but the new action that will replace the other will be randomly chosen among the available actions in the plan.

The mechanism A is useful when the actions of the plan are known. Thus, the initial plan must be developed with a high value in its objective function to get good permutations. This makes the algorithm with an tendentious implementation, a situation we want to avoid in this work. The mechanism B can return satisfactory results, due to the insertion of new actions in the plan, exploring well the possibility of new resources. But C is the mechanism that returns the best results through a combination of two exploration strategies. The mechanism D has the same

problem as A. It needs quality guarantee in the initial plan to achieve good results.

When a neighbor plan is generated with function $NewNeighbor(G)$ (line 8), the consistency checker is used to manage and evaluate the changes made in the goal. The algorithm for checking consistency will be further discussed in the following sections.

5. Consistency Checker

In planning when changes are made in a plan of action it is necessary to see how these changes affect it, especially when the dependency relationship is as strong as in the case of StarCraft. A simple insertion of an action may result in the inviability of many others. However, this makes the plan suitable for the introduction of new actions. This relationship is given by the loss and addition of resources and needs to be checked effectively to not harm the planning. Therefore, we developed a checker capable of dealing with changes in a plan, verifying its consistency, ordering and managing the resources.

The consistency checker is used when SA calls the mechanism for generating neighbors. Algorithm 2 shows the pseudo-code of the checker. The algorithm takes the plan of action $Actions$, a list $NewActions$ with the new action to be inserted or two actions that will be switched, and the list of resources available R_{avaib}. Initially is checked whether any action becomes unfeasible due the operation to be carried out in the plan, either to replace one action or exchange actions of place. This checking is performed by function $checkPlan(Actions)$.

Unfeasible Actions are placed in the list $actionsUnf$. When at least one action is inserted into the $actionsUnf$, the algorithm can find the others which will also become unfeasible. This is done by going through the graph of precedence of the actions of the plan. If any of these has a resource marked as unfeasible in the predecessor list, it will become unfeasible as well.

The method $Update(Action, R_{avaib})$ (line 8 of algorithm 2) is used for check what resources will no longer exist and which will be available in the plan to be used by other actions, when the list of actions unfeasible insert some action. This means that if a resource *ScienceFacility* becomes unfeasible it does the same with *CovertOps* and *NuclearSilo*, but in return it releases 88 seconds and provides 250 *Minerals* and 300 *Gas*. These resources enable the introduction of new actions or make others that were unfeasible in the plan become feasible again.

The amount of resources that are released do not always covers the loss of actions that become unfeasible in the plan because these actions may be contributing directly to maximizing the objective function. To help the algorithm to make a decision a variable penalty is used. For each action that becomes unfeasible in the plan a μ value is added to it. Thus, the more unfeasible actions appear greater will be

Algorithm 2 Consistency($Actions$, $NewActions$, R_{avaib})

```
1:  actionsUnf ← checkPlan(NewActions)
2:  for all Action Inf ∈ actionsUnf do
3:    for all Action Act ∈ Actions do
4:      if Act.Predecessors = Inf then
5:        Act.feasible ← false
6:        actionsUnf.push(Act)
7:        penalty += μ
8:        Update(Act, R_avaib)
9:      end if
10:   end for
11: end for
12: adaptPlan(NewActions, R_avaib)
13: continue ← true
14: Actions Act
15: while continue = true do
16:   if Act ← checkPred(actionsUnf, R_avaib) then
17:     Act.feasible ← true
18:     actionsUnf.erase(Act)
19:     penalty -= μ
20:     Update(Act, R_avaib)
21:   else
22:     continue ← false
23:   end if
24: end while
25: return Actions
```

the penalty on the plan when it is evaluated. The value of μ should be small and its value is based on the formula:

$$\mu = 0.1 \text{ - } n/2 \tag{2}$$

where n is the number of actions in the plan.

With unfeasible actions already established and available resources defined, the function $adaptPlan(NewActions, R_{avaib})$ (line 2) is called. This function is responsible for changing the current plan, either by insertion or switch of actions. This function also rearranges the scheduling of actions in the plan, due to the changes made by the operation performed.

In the last stage the consistency checker verifies that after the changes in the plan some unfeasible action can become feasible again. The algorithm goes through the list of unfeasible actions and for each one checks whether its predecessors are available. This is done by function $checkPred(Act, actionsUnf, R_{avaib})$ (line 16). When an action becomes feasible again it is removed from the list of unfeasible actions, the value of the penalty is decreased and the function $Update$ (line 20) is again used to update the resources available. If the function $checkPred$ is called and no action is feasible then the algorithm exits the loop. However, if the opposite happens the algorithm is repeated because an action that is now feasible can make others to become feasible.

Finally, the algorithm returns the new plan for SA that evaluates the objective function and decides whether it will be the new solution. The following is an application example of the consistency checker.

5.1 Example of application

To illustrate the behavior of the checker suppose we have a initial plan of action that achieve the resource *Firebat* as depicted in Figure 2. The initial state of the plan is (13, 0, 42, 6, 6, 16, 565). These plan values correspond to the number of actions, number of actions unfeasible, amount of minerals available, amount of gas available, supply used, army points and the makespan of the plan. The time limit is 600 sec.

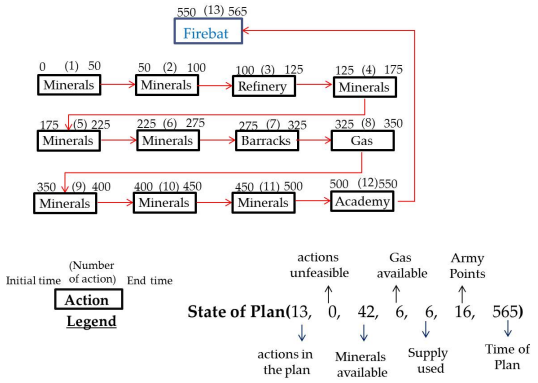

Fig. 2: An plan of action to achieve the resource Firebat.

For instance, suppose that in the first run of SA an action *Marine* substitutes the *Minerals* of number 10. Thus, the *act Minerals* is placed on the list of unfeasible actions and this action is the predecessor of *act Academy*, this also becomes unfeasible and with it the *act Firebat*. At this point the plan state is (13, 2, 186, 31, 4, 0, 465). The algorithm now inserts the new action and updates the resources it will consume. It is feasible based on available resources and the state of the plan is changed to (13, 2, 136, 31, 6, 12, 480). The algorithm cannot enable either of the two unfeasible actions, as the *act Marine* that entered does not contribute for these actions. Although there is enough *rsc Gas* and *rsc Minerals* for *act Firebat*, it may not be feasible as the *act Academy*, its predecessor continues unfeasible. The plan is then returned to SA that can opt for it, although it has fewer army points than the previous.

With the plan accepted suppose that SA indicates replacement of the action *Gas* of number 8 by another action *Marine*. *Gas* is the predecessor of *act Firebat*, but since this is already unfeasible the removal of *Gas* does not affect the plan. Now the plan state is (13, 3, 136, 0, 6, 12, 455). Although the *act Minerals* predecessor of *act Marine* are in the plan, it is in a forward position, i.e, the *act Marine* is being done prior to its predecessor. The new action goes unfeasible into the plan. No action becomes feasible in the next review and the final state of this plan is the same.

Now in SA suppose that occurs an switch of positions between the actions *Minerals* of number 11 and *Marine* of number 8. In this operation the actions remain feasible, not being necessary to check whether any action will be unfeasible. After the switching of actions the algorithm detects that *act Marine* has all its predecessors being executed before it and becomes feasible. The plan is now status (13, 2, 86, 0, 8, 24, 505) with 24 points army. The goal found is better than the original and the makespan is also reduced from 565 to 505. Although, reducing the makespan is not a goal yet explored in this work.

6. Experiments and Discussion of Results

The experiments were conducted on a computer intel core i7 1.6 GHz CPU with 4 GB of ram running on a windows operating system. The API Bwapi [10] allows to control Starcraft units and get information such as number of cycles and time of the game. It was used as an interface for the experiments with a human player and for performance evaluation of SA.

Table 1 contains comparison results. In the tests, we worked with different time limits for the makespan of the plans. We consider the planner as real-time because it can have smaller runtime (CPU time) than the makespan of the goals that it finds. In fact, this strategy was successfully used in the experiments, where the SA was able to find and maximize a future goal while the current goal was being executed in the game. The values that appear under the SA and the human player are the army points in the final plan of action obtained by both.

Table 1: Results of the test between SA and a human player

Time limit	Human player	SA	Makespan of SA	Runtime of SA
200 sec.	12	12	196	35 sec.
400 sec.	31	**34**	392	80 sec.
600 sec.	**52**	47	586	205 sec.
800 sec.	102	**109**	800	386 sec.
1000 sec.	141	**146**	990	555 sec.
1200 sec.	**204**	199	1189	696 sec.
1400 sec.	**241**	236	1388	812 sec.

Regarding the results SA proved to be able to compete with a human player, in some cases surpassing him. The most promising results were in the goals with medium time limit, where game tactics are not yet a determining factor for success in a direct confrontation, and production of more military resource can be crucial to the victory. The time limit imposed for the tests is high because the plans do not have their actions parallelized. This will be implemented in further work.

Table 2 shows the performance of SA. For goals with time limit medium the results are good, with 60% over 95% of

Table 2: Results of performance tests of SA

Time Limit	450 sec.	750 sec.	1050 sec.
Optimum value for army points	41	92	156
Number of runs over 95% of optimum	60%	40%	50%
Number of runs over 90% of optimum	30%	40%	40%
Average value	34	79	144
Number of Runs	10	10	10

optimal value. The best solution for plans with medium limit of time is known because many players share their rankings on the Internet informing these valuesâĂŃâĂŃ. For larger goals the results are encouraging. Although, with higher time limits (1050 sec.) the average of the results was better than with shorter (750 sec.). This happens because in larger plans is easier to validate actions due to the presence of more resources available.

The algorithm returns good results, but not always the optimal solution. This happens because in our approach, the SA was adapted to return a solution compatible with characteristics of real-time performance. StarCraft has a search space of exponential order, and SA running without the techniques that we have built could take hours to return the optimal solution.

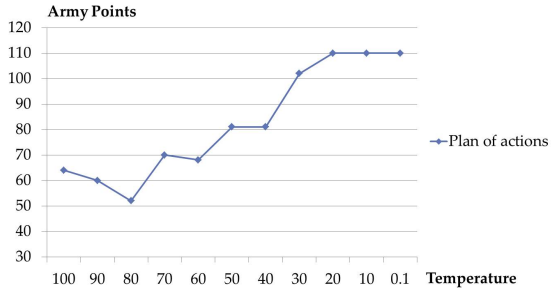

Fig. 3: Convergence of Simulated Annealing.

Figure 4 shows the convergence of the SA in a execution with time limit of 900 sec. At lower temperatures it accepts few new plans and keep those with the highest army points, a desired behavior for the SA. For this implementation the action plan given as input to the SA had 0 army points, demonstrating that even with bad entries the algorithm achieved good convergence.

7. Conclusion and Future Work

In this paper we propose the use of Simulated Annealing to maximize resource production in an RTS game. Research in this area is recent and the proposed approach is little explored by existing work. Our research is divided into two parts: The use of a sequential planner to generate one plan of action without fixed resources with time limit; and use of Simulated Annealing to maximize the resources of that plan of action by increasing the strength of its army.

Analyzing the results, the goals achieved always have an army points greater than the initial plan of action, which shows the convergence of the algorithm. The techniques developed to manage the planning contributed effectively in the quality of the results, and can be used in any domain of real-time games.

As future work we intend to explore interesting scheduling algorithms in order to reduce the makespan of the plans and achieve results with more quality. Also, We are investigating other features of StarCraft that can be used in the objective function evaluation. Based on our experience with Simulated Annealing, we also understand that other techniques such as bio-inspired algorithms may be explored.

References

[1] D. Churchil and M. Buro, "Build order optimization in starcraft," *AIIDE 2011: AI AND INTERACTIVE DIGITAL ENTERTAINMENT CONFERENCE*, 2011.

[2] R. Fikes and N. J. Nilsson, "Strips: A new approach to the application of theorem proving to problem solving," *Artif. Intell.*, vol. 2, no. 3/4, pp. 189–208, 1971.

[3] E. Aarts and J. Korst, *Simulated Annealing and Boltzmann Machines: A Stochastic Approach to Combinatorial Optimisation and Neural Computing.* John Wiley e Sons, Inc. New York, NY, USA 1989, 1989.

[4] T. Fayard, "Using a planner to balance real time strategy video game," *Workshop on Planning in Games, ICAPS 2007*, 2005.

[5] H. Chan, A. Fern, S. Ray, C. Ventura, and N. Wilson, "Extending online planning for resource production in real-time strategy games with search," *Workshop on Planning in Games ICAPS*, 2008.

[6] A. Branquinho, C. R. Lopes, and T. F. Naves, "Using search and learning for production of resources in rts games," *The 2011 International Conference on Artificial Intelligence*, 2011.

[7] H. Chan, A. Fern, S. Ray, N. Wilson, and C. Ventura, "Online planning for resource production in real-time strategy games," in *ICAPS*, 2007.

[8] M. B. Do and S. Kambhampati, "Sapa: A scalable multi-objective metric temporal planner," *Journal of AI Research 20:155Ű194*, 2003.

[9] A. Gerevini, A.; Saetti and I. Serina, "Planning through stochastic local search and temporal action graphs in lpg," *Journal of Artificial Intelligence Research 20:239-230*, 2003.

[10] Bwapi, *BWAPI - An API for interacting with Starcraft : Broodwar*, 2011. [Online]. Available: http://code.google.com/p/bwapi/

Economic Load Dispatch Using Strength Pareto Gravitational Search Algorithm with Valve Point Effect

H. A. Shayanfar *
Center of Excellence for Power System Automation and Operation, Elect. Eng. Dept., Iran University of Science and Technology, Tehran, Iran

A. Ghasemi
Young Researcher Club, Ardabil Branch, Islamic Azad University, Ardabil, Iran

N. Amjady
Electrical Engineering Department, Semnan University, Semnan, Iran

O. Abedinia
Electrical Engineering Department, Semnan University, Semnan, Iran

hashayanfar@yahoo.com, ghasemi.agm@gmail.com, n_amjady@yahoo.com, oveis.abedinia@hotmail.com

Abstract— **The Strength Pareto Gravitational Search Algorithm (SPGSA) to solve Economic Load Dispatch (ELD) is presents this paper with various generator constraints in power systems. The ELD problem in a power system is to determine the optimal combination of power outputs for all generating units which will minimize the total fuel cost while satisfying all practical constraints. For practical generator operation, many nonlinear constraints of the generator, such as ramp rate limits, prohibited operating zone, generation limits, transmission line loss and non-smooth cost functions are all considered using the proposed technique. The proposed algorithm applied on different test standard power system. The effectiveness of the proposed method is compared with other heuristic algorithm. Results showed the efficiency of the proposed algorithm.**

Keywords: SPGSA, Economic Load Dispatch, Valve Point.

I. INTRODUCTION

The efficient and optimum economic operation of electric power systems has always occupied an important position in electric power industry. In recent decades, it is becoming very important for utilities to run their power systems with minimum cost while satisfying their customer demand all the time and trying to make profit. With limited availability of generating units and the large increase in power demand, fuel cost and supply limitation, the committed units should serve the expected load demand with the changes in fuel cost and the uncertainties in the load demand forecast in all the different time intervals in an optimal manner.

The basic objective of ELD of electric power generation is to schedule the committed generating unit outputs, so as to meet the load demand at minimum operating cost while satisfying all unit and system equality and inequality constraints [1]. The ELD problem has been tackled by many researchers in the past [2]. ELD problem involves different problems. The first is Unit Commitment or pre-dispatch problem where in it is required to select optimally out of the available generating sources to operate to meet the expected load and provide a specified margin of operating reserve over a specified period of time. The second aspect of ELD is on-line economic dispatch where in it is required to distribute the load among the generating units actually parallel with the system in such a manner as to minimize the total cost of supplying power. In case of ELD, The generations are not fixed but they are allowed to take values again within certain limits so as to meet a particular load demand with minimum fuel consumption.

The ELD problem is inherently a large-scale, nonlinear, non-convex, non continuous optimization problem. Many techniques are applied to deal with ELD problem both conventional optimization approaches [3-4] such as Linear Programming (LP) or Quadratic Programming (QP) and Artificial Intelligence (AI)-based optimization techniques such as Simulated Annealing (SA) [5], Tabu Search (TS) [6], Genetic Algorithm (GA) [7-8], hybrid TS/SA [9], Evolutionary Programming (EP) [9], and Improved Evolutionary Programming (IEP) [11] etc. Gravitational Search Algorithm (GSA), a new optimization algorithm is applied to solve the above problem. Algorithm, as mentioned earlier is a new search algorithm that has been proven efficient in solving many problems. In the case of ELD, the main use of GSA would be to obtain a solution close to the global optimum in a short period of time.

* Correspanding Author. E-Mail Address: hashayanfar@yahoo.com (H. A. Shayanfar)

II. ELD PROBLEM

The problem of ELD has been introduced in 1960s as an extension of conventional economic dispatch to determine the optimal set of control variables while subject to various equality and inequality constraints. In conventional power flow the values of control variables are pre-specified unlike an ELD value of some control variables need to be found to optimize an objective function [2]. Hence, the ELD is one of the most important optimization strategies for power system managing and nonlinear programming problem. The ELD planning performs the optimal generation dispatch among the operating units to satisfy different constraints that change from problem to problem [12, 14]. In this paper, the ramp rate limits and prohibited operating zone are considered as practical operation constraints of generators for 6 and 15 unit systems and valve-point loading effects without transmission loss is tested to 40 unit system.

Actually, the adjustments of the power output are instantaneous that is one of the unpractical assumptions. Accordingly, generators are constrained because of ramp rate limits where, generation may increase or decrease with corresponding upper and downward ramp rate limits [12]. Therefore, the operating range of all online units is restricted by their ramp rate limits which are defines as:

- Power generation increasing

$P_i - P_i^0 \le UR_i$

- Power generation decreasing

$P_i^0 - P_i \le DR_i$

Where,
P_i: The current is output power of ith unit
P_i^0: previous output power
UR_i: The up ramp limit of the ith generator
DR_i: The down ramp limit of the ith generator

According to this fact that, the prohibited operating zones in the input/output curve of generator are due to vibration in a shaft bearing/steam valve operation it should be noted that, finding the actual prohibited zone by actual performance testing /operating records is really difficult. That leads to getting the best economy by avoiding operation in areas [12]. Therefore, adjustment of the generation output of a unit must avoid operation in the prohibited zones. For this purpose, the feasible operating zones of generators are described as:

$$A_{ai} = \begin{vmatrix} P_i^{\min} \le P_i \le P_{i,1}^l \\ P_{i,j-1}^u \le P_i \le P_{i,j}^l,\ j = 2,3,...,n_i,\ i = 1,...,m \\ P_{i,ni}^u \le P_i \le P_i^{\max} \end{vmatrix} \quad (1)$$

Where, A_{ai}= Feasible operating zones of i^{th} unit

Due to minimizing fuel cost is the primary concern of operation planning; the objective of ELD problem in this study is to minimizing total generator fuel cost. That can be expressed as:

$$F_t = \sum_{i=1}^{m} F_i(P_i) \quad (2)$$

Where, $F_i(P_i) = \sum_{i=1}^{m} (a_i P_i^2 + b_i P_i + c_i), i = 1,...,m$

For the mentioned equation, the F_t is the total generation cost and F_i is the cost function of the i^{th} generator. a_i, bi and c_i present the cost coefficients in i^{th} generator. Also the electrical output of the i^{th} generator is shown by P_i and m is the number of generators committed to the operating system. This constrained ELD problem is subjected to a variety of constraints depending upon assumptions and practical implications [12, 14]. These constraints are discussed as follows. Constrained conditions are:

A. Power Balance

This constraint is based on the principle of equilibrium between total system generation ($\sum_{i=1}^{m} P_i$) and total system loads (P_D) and losses (P_L) that is

$$\sum_{i=1}^{m} P_i = P_D + P_L, i = 1,...,m \quad (3)$$

P_L: Obtained using B-coefficients, given by:

$$P_L = \sum_{i=1}^{m}\sum_{j=1}^{m} P_i B_{ij} P_j + \sum_{i=1}^{m} B_{0i} P_i + B_{00} \quad (4)$$

B. Generator Operation Constraints

$$P_i^{\min} \le P_i \le P_i^{\max} \max(P_i^{\min}, P_i^0 - DR_i) \le P_i \le \min(P_i^{\max}, P_i^0 + UR_i) P_i \in A_{ai} \quad (5)$$

Where, P_i^{min} and P_i^{max} are lower and upper bounds for power outputs of the i_{th} generating unit.

C. Line Flow Constraints

$$\left|P_{Lf,k}\right| \le P_{Lf,k}^{\max}, k = 1,...,L \quad (6)$$

Where, $P_{Lf,k}$ is the real power flow of line k; $P_{Lf,k}^{max}$ is the power flow up limit of line k and L is the number of transmission lines.

III. GRAVITATIONAL SEARCH ALGORITHM

A. GSA Review

The Gravitational Search Algorithm (GSA) is constructed based on the law of gravity and the notion of mass interactions. GSA is one of the newest heuristic algorithms which have been inspired by the Newtonian laws of gravity and motion. In GSA a set of agents called masses are introduced to find the optimum solution by simulation of Newtonian laws of gravity and motion [15].

Also, each mass agent has four specifications: position, inertia mass, active gravitational mass, and passive gravitational mass. The position of the mass corresponds to a solution of the problem, and its gravitational and inertial masses are determined using a fitness function. In other words, each mass presents a solution, and the algorithm is navigated by properly adjusting the gravitational and inertia masses. By lapse of time, we expect that masses be attracted by the heaviest mass. This mass will present an optimum solution in the search space [16].

The GSA could be considered as an isolated system of masses. It is like a small artificial world of masses obeying the Newtonian laws of gravitation and motion. More precisely, masses obey the following laws:

- Law of gravity: Each particle attracts every other particle and the gravitational force between two particles is directly proportional to the product of their masses and inversely proportional to the distance between them, R.
- Law of motion: The current velocity of any mass is equal to the sum of the fraction of its previous velocity and the variation in the velocity. Variation in the velocity or acceleration of any mass is equal to the force acted on the system divided by mass of inertia.

To describe the GSA consider a system with s masses in which position of the ith mass is defined as:

$$X_i = (x_i^1, ..., x_i^d, ..., x_i^n), i = 1,2,..., s \quad (7)$$

Where, x_i^d is position of the ith mass in the dth dimension and n is the dimension of the search space. According to [19] mass of each agent is computed after calculating current population's fitness as:

$$M_i(t) = \frac{q_i(t)}{\sum_{j=1}^{s} q_i(t)} \quad (8)$$

Where, Mi(t) is the mass value of the agent i at t.

$$q_i(t) = \frac{fit_i(t) - worst(t)}{best(t) - worst(t)} \quad (9)$$

Where, $fit_i(t)$ is the fitness value of the agent i at t, and worst (t) and best (t) are defined as follows for the minimization problem:

$$best(t) = \underset{j\in\{1,...,s\}}{Min}\ fit_i(t), \quad worst(t) = \underset{j\in\{1,...,s\}}{Max}\ fit_i(t)$$

To compute acceleration of an agent, total forces from a set of heavier masses that apply on it should be considered based on the law of gravity, which is followed by calculation of agent acceleration using the law of motion. Afterwards, next velocity of an agent is calculated as a fraction of its current velocity added to its acceleration. Then, its next position can be calculated using:

$$F_i^d(t) = \sum_{j\in kbest,\, j\neq i} rand_i G(t) \frac{M_j(t) M_i(t)}{R_{ij}(t) + \varepsilon} (x_j^d(t) - x_i^d(t))$$

$$a_i^d(t) = \frac{F_i^d(t)}{M_i(t)} = \sum_{j\in kbest,\, j\neq i} rand_j G(t) \frac{M_j(t)}{R_{ij}(t) + \varepsilon} (x_j^d(t) - x_i^d(t))$$

$$V_i^d(t+1) = rand_i \times v_i^d(t) + a_i^d(t) \quad (10)$$

$$x_i^d(t+1) = x_i^d(t) + v_i^d(t+1)$$

Where, $rand_i$ and $rand_j$ are two uniformly distributed random numbers in the interval [0, 1], ε is a small value, $R_{ij}(t)$ is the Euclidean distance between two agents i and j, defined as $R_{ij}(t)=\|X_i(t), X_j(t)\|_2$, kbest is the set of first K agents with the best fitness value and biggest mass, which is a function of time, initialized to K_0 at the beginning and decreasing with time. Here K_0 is set to s (total number of agents) and is decreased linearly to 1.

In GSA, the gravitational constant, G, will take an initial value, G_0, and it will be reduced with time:

$$G(t) = G(G_0, t) \quad (11)$$

Also some differences and advantages of this technique are consisting of [16]:

- In GSA, the agent direction is calculated based on the overall force obtained by all other agents.
- In GSA the force is proportional to fitness value and so agents see the search space around themselves in the influence of force.
- GSA is memory-less and only current position of the agents plays a role in the updating procedure.
- In GSA the force is inversely proportional to the distance between solutions.

Fig. 1 shows the flowchart of the proposed intelligent algorithm.

B. SPGSA

If we plot the objective values f1 and f2 of these optimal solutions against each other in one plot. A multi-objective optimization algorithm tries to approximate

these solutions but uses a different approach to obtain these solutions. The supposed algorithm sorts the population based on non-dominated fronts. The first front found is ranked the highest and the last one the lowest. This ranking is used in the mating flight selection process. In addition to, for assure diversity in a population (honey bee) employed crowding distance measure.

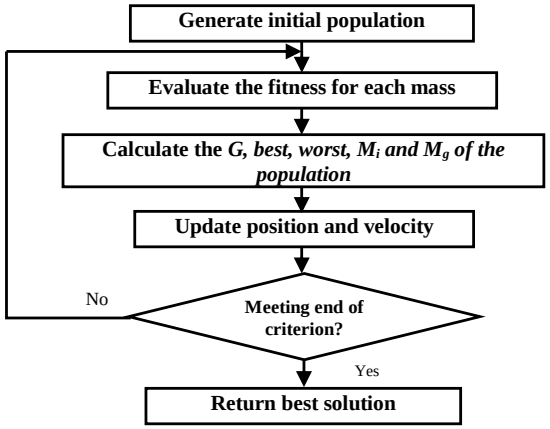

Figure 1. Flowchart of GSA

The main steps of the SPO algorithm are explained in more detail as follows:

C. Non-Dominated sort

This set of non-dominated solutions is called a Pareto front. A multi-objective algorithm selects and improves solutions based on this domination principle to approximate the real trade-off curve. Non-domination occurs when a candidate cannot be improved any further in one objective while degrading in another objective. Figure 2 explains this in more detail. The figure shows that crowding distance for solution y(x4) is calculated relative to the solutions from the same front which are all colored blue. The distance is the sum of the length and width of a cubical that can be drawn through these two closest neighbours.

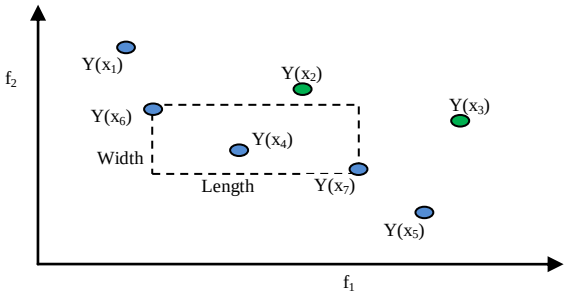

Figure 2. Crowding distance measure

D. Crowding Distance

The population density around a particular solution i is estimated by the average distance of the two solutions at either side of i along each of the objectives. Crowding distance is assigned front wise and comparing the crowding distance between two individuals in different front is meaningless.

IV. Simulation and Results

The different methods discussed earlier are applied to two cases to find out the minimum cost for any demand. In this part the three test systems as: IEEE 6-generator 30-bus, IEEE 14-generator 118-bus IEEE with transmission loss, 15 unit system with prohibited operating zones and ramp rate limits and 40 unit system is tested with valve-point loading effects without transmission loss.

A. Case I. IEEE 30-bus system

In the first case study, the IEEE 30-bus system with six generators and forty one lines is used. The system configuration of the proposed case study is shown in Fig. 3 and the system data can be found in [6,15].

The values of the fuel and emission coefficients of the IEEE 30-bus system are illustrated in Table 1. The line data and bus data of the system are referenced in [1]. The load of the IEEE 30-bus system was set to 2.834 pu on a 100MVA base. In order to demonstrate the effectiveness of the proposed approach on the IEEE 6-generator 30-bus test system. All constraints about emission, fuel cost and system loss are considered. For show efficiency and ability of supposed algorithm in EED problem, used index mismatch power as follows:

$$\text{mismatch power} = \sum_{i=1}^{N_g} P_i(G_i) - P_d$$

Where, P(G) is the power output and Pd is the total power demand.

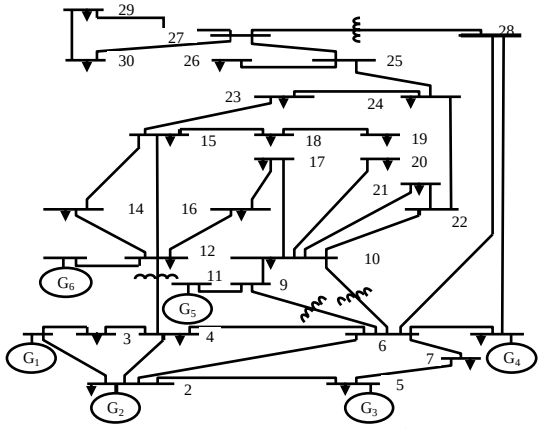

Figure 3. The IEEE 30-bus system configuration.

Results of proposed SPGSA algorithm are compared with the MOPSO [17] and MODE [14], which have been implemented and applied to the EED problem with impressive success. The results of simulation are given in Table 2. The distribution of the non-dominated solutions in Pareto optimal front using the proposed SPGSA is

represented in Fig. 4, which clearly shows the relationships among fuel cost, emission, and transmission loss.

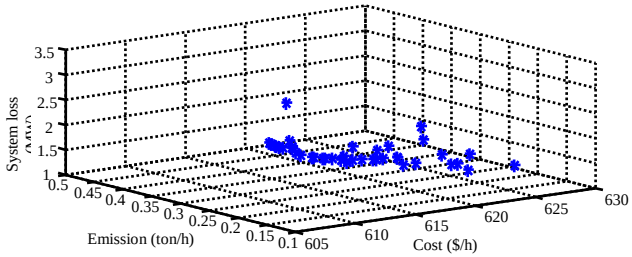

Figure 4. Three-dimensional Pareto front of SPGSA algorithm for IEEE 30-bus system

TABLE I. GENERATOR AND EMISSION COEFFICIENTS OF THE IEEE 30-BUS SYSTEM.

P_{Gmin} MW)	P_{Gmax} MW)	λ	ζ	γ	β	α	c	b	a	NO
5	150	2.857	2.0e−4	6.490	−5.543	4.091	100	200	10	P_{G1}
5	150	3.333	5.0e−4	5.638	−6.047	2.543	120	150	10	P_{G2}
5	150	8.000	1.0e−6	4.586	−5.094	4.258	40	180	20	P_{G3}
5	150	2.000	2.0e−3	3.380	−3.550	5.326	60	100	10	P_{G4}
5	150	8.000	1.0e−6	4.586	−5.094	4.258	40	180	20	P_{G5}
5	150	6.667	1.0e−5	5.151	−5.555	6.131	100	150	10	P_{G6}

A. Case II. 15 Unit Systems

The information of 15 unit system is presented in [18]. The load demand of the system is 2630 MW. The loss coefficients matrix is shown in [19]. Also Table 3, shows the numerical results of this case study in comparison with other techniques.

B. Case II. 15 Unit Systems

The information of 15 unit system is presented in [20]. The load demand of the system is 2630 MW. The loss coefficients matrix is shown in [19]. The feasibility of the proposed method has been compared in terms of solution quality and computation efficiency with PSO [20], Hybrid GAPSO [13], IPSO [20], SOH-PSO [12]. Also convergence characteristic for this case study is shown in Fig.5.

TABLE II. IEEE 30-BUS SYSTEM BEST COMPROMISE SOLUTIONS

MOPSO	MODE	SPGSA	No. Gen
0.39768	0.21207	0.1721	P_{G1}
0.41814	0.30659	0.3638	P_{G2}
0.64404	0.68878	0.6839	P_{G3}
0.75147	0.67937	0.6512	P_{G4}
0.44620	0.58218	0.6077	P_{G5}
0.48973	0.38691	0.3563	P_{G6}
614.913	614.170	**610.892**	Cost ($/h)
0.2081	0.2043	**0.1954**	Emission (ton/h)
2.8865	2.2009	**2.0413**	System loss (MW)
0.3133	0.0219	**0.0011**	Mismatch power

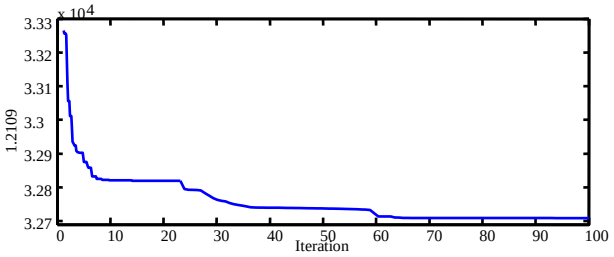

Figure 5. Convergence characteristic of 15-unit system

C. Case III. 40 Unit Systems

The load demand of the system is 10500 MW. The unit characteristics like cost coefficients along with valve-point loading coefficient, operating limits of generators are given in [4]. The achieved numerical results from proposed SPGSA method are presented in table 4 in comparison via BBO [3], NPSO_LRS [2], SOH_PSO [12] and other methods. Also convergence characteristic for this case study is shown in Fig.6.

TABLE III. BEST SIMULATION RESULTS OF 15-UNIT SYSTEM. PD = 2630 MW

Unit power output (MW)	PSO	Hybrid GAPSO	CPSO1	CPSO 2	SOH_PSO	IPSO	SPGSA
P1	439.1162	436.8482	450.05	450.02	455.00	455.00	455.0000
P2	407.9727	409.6974	454.04	454.06	380.00	380.00	388.0192
P3	119.6324	117.0074	124.82	124.81	130.00	129.97	130.0000
P4	129.9925	128.2705	124.82	124.81	130.00	130.00	130.0000
P5	151.0681	153.3361	151.03	151.06	170.00	169.93	221.8192
P6	459.9978	457.4078	460	460	459.96	459.88	460.0000
P7	425.5601	424.4400	434.53	434.57	430.00	429.25	465.0000
P8	98.5699	101.1949	148.41	148.46	117.53	60.43	132.0192
P9	113.4936	116.1186	63.61	63.59	77.90	74.78	51.9172
P10	101.1142	102.2243	101.13	101.12	119.54	158.02	25.8178
P11	33.9116	35.0317	28.656	28.655	54.50	80.00	55.7364
P12	79.9583	78.8482	20.912	20.914	80.00	78.57	72.8192
P13	25.0042	27.1292	25.001	25.002	25.00	25.00	26.2134
P14	41.414	37.1594	54.418	54.414	17.86	15.00	25.5263
P15	35.614	37.0390	20.625	20.624	15.00	15.00	19.0293
Total power output	2662.4	2661.75	2662.1	2662.1	2662.29	2660.8	2659.2
Minimum cost ($/h)	32858	32724	32835	32834	32751.39	32709	**32685.928**
Ploss	32.4306	31.75	32.1302	32.1303	32.28	30.858	**29.362511**
Mean cost ($/h)	33039	32984	33021	33021	32878	32784.5	**32710.019**
Maximum cost ($/h)	34562.4	34865.9	33451	33450.1	33001.1	32954.4	**33252.9187**

TABLE IV. BEST POWER OUTPUT FOR 40-GENERATOR SYSTEM (PD = 10,500 MW)

SPSO	PSO_LRS	PC_PSO	NPSO	NPSO_LRS	SOH_PSO	BBO	SPGSA	Unit
113.97	111.9858	113.98	113.9891	113.9761	110.80	110.8158	114.0000	P_1(MW)
114.00	110.5273	114.00	113.6334	113.9986	110.80	111.0896	112.6186	P_2(MW)
109.19	98.5560	97.26	97.5500	97.4241	97.40	97.40261	120.0000	P_3(MW)
179.77	182.9266	179.51	180.0059	179.7327	179.73	179.7549	175.5808	P_4(MW)
97.00	87.7254	89.38	97.0000	89.6511	87.80	88.20832	91.0000	P_5(MW)
91.01	139.9933	105.20	140.0000	105.4044	140.00	139.9886	140.0000	P_6(MW)
259.87	259.6628	259.55	300.0000	259.7502	259.60	259.5935	265.0000	P_7(MW)
286.99	297.7912	286.90	300.0000	288.4534	284.60	284.6174	284.0398	P_8(MW)
284.09	284.8459	284.71	284.5797	284.6460	284.60	284.6479	290.0000	P_9(MW)
204.05	130.0000	206.24	130.0517	204.8120	130.00	130.0298	130.0000	P_{10}(MW)
168.40	94.6741	166.52	243.7131	168.8311	94. 00	94.01459	169.4104	P_{11}(MW)
94.00	94.3734	94.00	169.0104	94.0000	94.00	94.26367	165.7230	P_{12}(MW)
212.30	214.7369	214.56	125.0000	214.7663	304.52	304.5153	210.9877	P_{13}(MW)
393.76	394.1370	392.76	393.9662	394.2852	304.52	394.264	390.0064	P_{14}(MW)
303.62	483.1816	306.24	304.7586	304.5187	394.28	304.5057	300.0265	P_{15}(MW)
392.05	304.5381	394.88	304.5120	394.2811	394.28	394.2472	300.0000	P_{16}(MW)
489.49	489.2139	489.26	489.6024	489.2807	489.28	489.3273	492.0000	P_{17}(MW)
489.35	489.6154	489.82	489.6087	489.2832	489.28	489.3047	489.1857	P_{18}(MW)
512.39	511.1782	510.62	511.7903	511.2845	511.28	511.3087	511.4179	P_{19}(MW)
511.21	511.7336	511.68	511.2624	511.3049	511.27	511.2495	512.5126	P_{20}(MW)
522.61	523.4072	523.52	523.3274	523.2916	523.28	523.3217	520.5096	P_{21}(MW)
523.65	523.4599	523.26	523.2196	523.2853	523.28	523.3144	525.0164	P_{22}(MW)
523.06	523.4756	523.98	523.4707	523.2797	523.28	523.3629	520.2891	P_{23}(MW)
520.72	523.7032	523.21	523.0661	523.2994	523.28	523.2883	524.9126	P_{24}(MW)
524.86	523.7854	523.54	523.3978	523.2865	523.28	523.2989	520.4441	P_{25}(MW)
525.22	523.2757	523.10	523.2897	523.2936	523.28	523.2802	526.0000	P_{26}(MW)
10.00	10.0000	10.00	10.0208	10.0000	10.00	10.02817	10.0000	P_{27}(MW)
10.00	10.6251	10.00	10.0927	10.0001	10.00	10.00321	10.0000	P_{28}(MW)
10.00	10.0727	10.00	10.0621	10.0000	10.00	10.0288	10.0000	P_{29}(MW)
87.64	51.3321	89.05	88.9456	89.0139	97.00	88.14595	90.0000	P_{30}(MW)
190.00	189.8048	190.00	189.9951	190.0000	190.00	189.9913	190.0000	P_{31}(MW)
190.00	189.7386	190.00	190.0000	190.0000	190.00	189.9888	190.0000	P_{32}(MW)
190.00	189.9122	190.00	190.0000	190.0000	190.00	189.9998	190.0000	P_{33}(MW)
200.00	199.3258	200.00	165.9825	199.9998	185.20	164.8452	168.0000	P_{34}(MW)
167.18	199.3065	164.78	172.4153	165.1397	164.80	192.9876	200.0000	P_{35}(MW)
172.12	192.8977	172.89	191.2978	172.0275	200.00	199.9876	200.0000	P_{36}(MW)
110.00	110.0000	110.00	109.9893	110.0000	110.00	109.9941	110.0000	P_{37}(MW)
110.00	109.8628	110.00	109.9521	110.0000	110.00	109.9992	110.0000	P_{38}(MW)
95.58	92.8751	94.24	109.8733	93.0962	110.00	109.9833	110.0000	P_{39}(MW)
510.85	511.6883	511.36	511.5671	511.2996	511.28	511.2794	511.3186	P_{40}(MW)
124091.16	123461.6794	122867.55	122995.0976	122981.5913	122446.30	121688.6634	1.2108e+005	Maximum
122049.66	122035.7946	121767.90	121704.7391	121664.4308	121501.14	121479.5029	121039.1389	Minimum
122327.36	122558.4565	122461.30	122221.3697	122209.3185	121853.57	121512.0576	1.2105e+005	Average

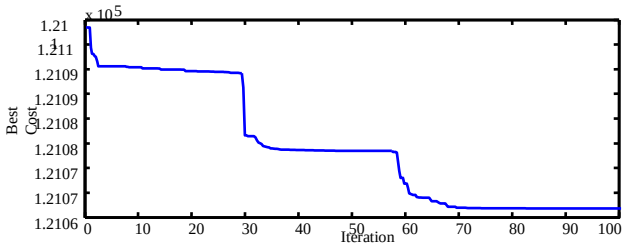

Figure 6. Convergence characteristic of 40-unit system

V. CONCLUSION

The ELD problems are the important problems in the electric power system operation. In this paper, the ELD problem has been solved considering transmission losses, valve point effects and environmental pollution. The problem has been formulated by the modified form of constraint method. The ELD problem is converted into an optimization problem which is solved by the SPGSA technique with competing objectives of fuel cost, environmental pollution (emission) and loss transmission. Numerical results for some test system have been presented to demonstrate the performance, found to converge to optimum in a faster rate and applicability of the proposed method. The proposed algorithm applied to three standard IEEE systems to show advantages of proposed algorithm in EED problem, 30-bus 6-generator IEEE test system, 15 units system and 40 units system with valve point effects. The convergence speed of this algorithm is higher than other heuristics algorithms such as NSGA, MODE, MOPSO, etc and thus the high precision and efficiency are achieved.

REFERENCES

[1] K. T. Chaturvedi, M. Pandit, L. Srivastava, Self organizing hierarchical particle swarm optimization for nonconvex economic dispatch. IEEE Transaction on Power System, vol. 23, no. 3, pp. 1079–1087, 2008.

[2] S. I. Thanushkodi, A new particle swarm optimization solution to non-convex economic dispatch problems. IEEE Transactions on Power System, vol. 22, no. 1, 2007.

[3] A. Bhattacharya, P. K. Chattopadhyay, Solving complex economic load dispatch problems using biogeography-based optimization, Expert Systems with Applications, Elsevier, vol. 37, pp. 3605–3615, 2010.

[4] N. Sinha, R. Chakrabarti, P. K. Chattopadhyay, Evolutionary programming techniques for economic load dispatch. IEEE Transactions on Evolutionary Computation, vol. 7, no. 1, pp. 83–94, 2003.

[5] C. A. Roa-Sepulveda and B. J. Pavez-Lazo, A Solution to the Optimal Power Flow Using Simulated Annealing. International

Journal of Electrical Power and Energy Systems, vol. 25, pp. 47-57, 2002.

[6] M. A. Abido, Optimal Power Flow Using Tabu Search Algorithm. Electric Power System Components and Systems, vol. 30, pp. 469-483, 2002.

[7] H. C. Leung, T. S. Chung, Optimal Power Flow with a Versatile FACTS Controller by Genetic Algorithm Approach. IEEE Power Engineering Society Meeting, vol. 4, pp. 2806-2811, 2000.

[8] A. G. Bakirtzis, P. N. Biskas, C. E. Zoumas, V. Petridis, Optimal Power Flow by Enhanced Genetic Algorithm. IEEE Transactions on Power Systems, vol. 17, no. 2, pp. 229-236, 2002.

[9] W. Ongsakul, P. Bhasaputra, Optimal Power Flow with FACTS Devices by Hybrid TS/SA Approach. International Journal of Electrical Power and Energy Systems, vol. 24, pp. 851-857, 2002.

[10] J. Yuryevich, K. P. Wong, Evolutionary Programming Based Optimal Power Flow Algorithm. IEEE Transactions on Power Systems, vol. 14, no. 4, pp. 1245-1250, 1999.

[11] W. Ongsakul, K. Tangpatiphan, Optimal Power Flow with TCSC Using Parallel Improved Evolutionary Programming., M.Eng. Thesis Unpublished , AIT, Thailand, August 2004.

[12] K. T. Chaturvedi, M. Pandit, L. Srivastava, Self organizing hierarchical particle swarm optimization for nonconvex economic dispatch. IEEE Transaction on Power System, vol. 23, no. 3, pp. 1079–1087, 2008.

[13] M. Sudhakaran, D. Ajay, P. Vimalraj, T. G. Palanivelu, GA and PSO culled hybrid technique for economic dispatch problem with prohibited operating zones, Journals of Zhejiang University Science A, vol. 8, no. 6, pp. 896–903, 2007.

[14] L.H. Wua, Y.N. Wanga, X.F. Yuan, S.W. Zhou," Environmental/economic power dispatch problem using multiobjective differential evolution algorithm", Electric Power Systems Research 80 1171–1181, 2010.

[15] A. Chatterjee, G. K. Mahanti. "Comparative performance of gravitational search algorithm and modified particle swarm optimization algorithm for synthe- sis of thinned scanned concentric ring ar- ray antenna". Progress In Electromagnetics Research B, Vol. 25, pp. 331-348, 2010.

[16] E. Rashedi , H. Nezamabadi-pour, S. Saryazdi, MM. Farsangi, "Allocation of static var compensator using gravitational search algorithm", First Joint Congress on Fuzzy and Intelligent Systems, Ferdowsi University of Mashhad, 29-31 Aug 2007.

[17] M.A. Abido, Multi-objective particle swarm optimization for environmental/economic dispatch problem, Electr. Power Syst. Res. Vol. 79, No. 7, 1105–1113, 2009.

[18] C. Jiejin, M. Xiaoqian, L. Lixiang, P. Haipeng, Chaotic particle swarm optimization for economic dispatch considering the generator constraints. Energy Conversion & Management, vol. 48, pp. 645–653, 2007.

[19] Z. L. Gaing, Particle swarm optimization to solving the economic dispatch considering the generator constraints. IEEE Transaction on Power Systems, vol. 18, no. 3, pp. 1187–1195, 2003.

[20] A. Safari, H. Shayeghi, Iteration particle swarm optimization procedure for economic load dispatch with generator constraints, Expert Systems with Applications, Elsevier, Vol. 38, Issue 5, pp. 6043-6048, May 2011.

BIOGRAPHIES

Heidarali Shayanfar received the B.S. and M.S.E. degrees in Electrical Engineering in 1973 and 1979, respectively. He received his Ph. D. degree in Electrical Engineering from Michigan State University, U.S.A., in 1981. Currently, he is a Full Professor in Electrical Engineering Department of Iran University of Science and Technology, Tehran, Iran. His research interests are in the Application of Artificial Intelligence to Power System Control Design, Dynamic Load Modeling, Power System Observability Studies, Voltage Collapse, Congestion Management in a Restructured Power System, Reliability Improvement in Distribution Systems and Reactive Pricing in Deregulated Power Systems. He has published more than 405 technical papers in the International Journals and Conferences proceedings. He is a member of Iranian Association of Electrical and Electronic Engineers and IEEE.

Ali Ghasemi received the B.Sc. and M.Sc. (Honors with first class) degree in Electrical Engineering from Isfahan University of Technology (IUT), Esfahan, Iran in 2009 and Technical Eng. Department of the University of Mohaghegh Ardabili (UMA), Ardabil, Iran in 2011. His Areas of interest in Research are power system control and operation, adaptive and robust control of power systems, operation and Planning and Power System Restructuring and applications of heuristic techniques in power systems.

Nima Amjady (SM'10) was born in Tehran, Iran, on February 24, 1971. He received the B.Sc., M.Sc., and Ph.D. degrees in electrical engineering from Sharif University of Technology, Tehran, Iran, in 1992, 1994, and 1997, respectively. At present, he is a Professor with the Electrical Engineering Department, Semnan University, Semnan, Iran. He is also a Consultant with the National Dispatching Department of Iran. His research interests include security assessment of power systems, reliability of power networks, load and price forecasting, and artificial intelligence and its applications to the problems of power systems.

Oveis Abedinia received the B.S. and M.Sc. degrees in Electrical Engineering from Azad University, Ardabil and Science and Technology Research Branch, Tehran, Iran in 2005 and 2009, respectively. Currently, he is a Ph. D. student in Electrical Eng. Department, Semnan University, Semnan, Iran. His areas of interest in research are Application of Artificial Intelligence to Power System and Control Design, Load and Price Forecasting, Distribution Generation, Restructuring in Power Systems, Congestion Management, Optimization.

The Exploration of Greedy Hill-climbing Search in Markov Equivalence Class Space

Huijuan Xu[1], Hua Yu[1], Juyun Wang[2], Jinke Jiang[1]
[1] College of Engineering, Graduate University of Chinese Academy of Sciences, Beijing, China
[2] College of Science, Communication University of China, Beijing, China

Abstract - *The greedy Hill-climbing search in the Markov Equivalence Class space (E-space) can overcome the drawback of falling into local maximum in Directed Acyclic Graph space (DAG space) caused by the score equivalent property of Bayesian scoring function, and one representative algorithm is Greedy Equivalence Search algorithm (GES algorithm) which is inclusion optimal in the large sample size, but not parameter optimal. In fact GES algorithm does not comply with the inclusion boundary condition which is a guarantee of gaining the highest score, but the unrestricted form of GES algorithm (UGES algorithm) complies with the inclusion boundary condition approximately. However, the greedy Hill-climbing search both in the DAG space and in the E-space has the drawback of time-consuming. The idea of confining the search using the constraint-based method is a good solution for the time-consuming drawback. This paper conducts experiments to compare the effects of greedy Hill-climbing search algorithm in DAG space (GS algorithm), GES algorithm and UGES algorithm both without the restriction of the parents and children sets and with the restriction of parents and children sets, and finds that GS/GES/UGES with the restriction have achieved improvement in time-efficiency and structure difference, with a little reduction in Bayesian scoring function.*

Keywords: Inclusion Boundary Condition, GES algorithm, UGES algorithm, MMHC algorithm, local discovery algorithms

1 Introduction

In the field of Bayesian network (BN), BN structure learning is a research hotspot. There are two main categories of BN structure learning algorithms, namely the constraint-based method and the search-and-score method. The constraint-based method[1][2] firstly uses the conditional independence (CI) test to determine the skeleton of the BN structure, and then directs the skeleton using the directional rules. The CI test has several forms, like Pearson's chi2 test, G2 likelihood ratio test, and mutual information.

The search-and-score method includes two typical algorithms, namely K2 algorithm[3] and greedy Hill-climbing algorithm. The K2 algorithm finds parent nodes for each node from the nodes before the node according to the initial node sequence, and builds the Bayesian network structure gradually. The initial node sequence can be determined by the method mentioned in paper [4], namely building the maximum weight spanning tree (MWST) using mutual information, and then using the topological order of the oriented MWST as the initial node sequence.

The greedy Hill-climbing algorithm in the DAG space (GS algorithm) takes an initial graph, defines a neighborhood, computes a score for every graph in this neighborhood, and chooses the one which maximizes the score for the next iteration, until the scoring function between two consecutive iterations does not improve. And the neighborhood is defined as the set of graphs that differ only with one insertion, one reversion, and one deletion from our current graph. The initial graph can be chosen as the oriented MWST. The GS algorithm has several drawbacks. Firstly, according to the score equivalent property of Bayesian scoring function, the directed acyclic graphs in the same equivalence class have the same score value. So if the two adjacent iterations are within the same equivalence class, the GS algorithm will fall into local maximum. Secondly, if we use random selection to break ties when we encounter more than one graph owning the highest score in the neighborhood, the finally learnt BN structures are more fluctuating when the GS algorithm runs multiple times. Thirdly, the GS algorithm is much more time-consuming, as the number of variables grows.

The greedy Hill-climbing search in the Markov Equivalence Class space can overcome the drawback of falling into local maximum caused by the score equivalent property of Bayesian scoring function, and can improve the volatility of the finally learnt BN structures. One state of the art algorithm of the greedy Hill-climbing search in the E-space is the GES algorithm[5]. GES algorithm starts from the empty graph, firstly adds edges until the scoring value reaches a local maximum, then deletes edges until the scoring value reaches another local maximum, and finally returns that equivalence class as the solution. In paper [6], it has been proved that in the limit of large sample sizes, the GES algorithm identifies an inclusion-optimal equivalence class of DAG models. However, GES may not be able to identify a parameter-optimal model even in the limit of large sample size, namely the parameters of the finally identified model are not the fewest among all the BNs that include the distribution. Then according to the consistent property of Bayesian scoring function, the score of the finally identified equivalence class in the GES algorithm is not the highest.

The paper [7] defines the Inclusion Boundary Condition based on the Inclusion Order provided by Meek's conjecture, and the paper [8] proves that the

hill-climbing algorithm using the penalized score function and a traversal operator satisfying the Inclusion Boundary Condition always finds the faithful model which has the highest score. In fact, the GES algorithm does not comply with the Inclusion Boundary Condition and does not get the guarantee of gaining the highest score. The UGES algorithm considers both the edge addition and the edge deletion at each step, and complies with the Inclusion Boundary Condition approximately. It is an unrestricted form of the GES algorithm and may get higher score than the GES algorithm. Both the GES algorithm and the UGES algorithm have the drawback of time-consuming.

About the drawback of time-consuming, some algorithms improve this drawback by restricting the maximum number of parents allowed for every node in the network, like the Sparse Candidate algorithm[9][10]. But it is not a sound solution. Firstly it is hard to set the value of the maximum number of parents, and secondly this parameter imposes a uniform constraint for each node in the network. If we use the constraint-based method to find the set of parents and children for each node, and restrict the greedy search within the parents and children set of each node, it will not encounter such two problems. The Max-Min Hill-climbing algorithm (MMHC algorithm)[11] is one such BN structure learning algorithm. It firstly uses the Max-Min Parents and Children algorithm (MMPC algorithm)[12] to find the set of parents and children for each node, and then applies the GS algorithm within the parents and children set of each node. It is shown that the MMHC algorithm results in computational savings and performs better than many existing algorithms.

This paper intends to conduct experiments to compare the GES algorithm and the UGES algorithm from the aspects of Bayesian score, Structural Hamming Distance (SHD)[11] and number of calls to scoring function, with the GS algorithm as a reference. Besides, we intend to use the parents and children sets learnt by the MMPC algorithm to restrict the GES algorithm and the UGES algorithm to improve the time-efficiency of these two algorithms, and conduct experiments to compare the performances of the GES algorithm and the UGES algorithm under the restriction of parents and children sets, with the MMHC algorithm (MMPC+GS) as a reference. We use the data sampled from the Alarm network[13] to conduct experiments. We implement the experiments in Matlab environment with the Bayes Net toolbox[14], the BNT Structure Learning package[15], and the Causal Explorer package[16].

This paper is structured as follows. Section 2 analyzes the GES algorithm and the UGES algorithm using the knowledge of E-space, scoring function, and Inclusion Boundary Condition. Then Section 3 introduces the local discovery algorithm MMPC and the combination of MMPC with GES algorithm and UGES algorithm. Experimental results and analysis are showed in Section 4. Finally, Section 5 presents some conclusions.

2 The greedy Hill-climbing search in the Markov Equivalence Class space

2.1. The Markov Equivalence Class space and the scoring function

The Markov Equivalence Class space (E-space) is divided into Markov equivalence classes. The DAGs in the same Markov equivalence class are equivalent.

Theorem 1 Two DAGs are equivalent if and only if they have the same skeletons and the same v-structures[17].

The skeleton of any DAG is the undirected graph resulting from ignoring the directionality of every edge. A v-structure in DAG G is an ordered triple of nodes (X, Y, Z) such that (1) G contains the edges X->Y and Z->Y, and (2) X and Z are not adjacent in G.

The equivalence classes of DAGs are represented with completed partially DAGs (CPDAGs). The CPDAG is a graph that contains both directed and undirected edges. The directed edges represent the compelled edges and the undirected edges represent the reversible edges. The compelled edge is the edge that has the same orientation for every member of the equivalence class. The reversible edge is the edge that is not compelled.

In a CPDAG or PDAG, a pair of nodes is neighbor if they are connected by an undirected edge, and they are adjacent if they are connected by either an undirected edge or a directed edge.

The DAGs in the same equivalence class gain the same score if the scoring function owns the property of score equivalence. In fact, the scoring function may own three properties:

Property 1 The scoring function is decomposable if it can be written as a sum of measures, each of which is a function only of one node and its parents.

Property 2 The scoring function is score equivalent if the DAGs in the same equivalence class gain the same score.

Property 3 The scoring function is consistent if in the large sample size, the following conditions hold: (1) If H contains the distribution and G does not contain the distribution, then the score of H is larger than the score of G; (2) If H and G both contain the distribution, and H contains fewer parameters than G, then the score of H is larger than the score of G.

Bayesian Dirichlet (BD) scoring function is one of the commonly used scoring functions. BDe scoring function is the BD scoring function which satisfies the score equivalent property. And the BDeu scoring function is the BDe scoring function whose parameter prior has uniform mean. The form of the BDeu scoring function is as follows:

$$p(G,D|\xi)=\log p(G|\xi)\cdot\prod_{i=1}^{n}\prod_{j=1}^{q_i}\frac{\Gamma(N_{ij}^{'})}{\Gamma(N_{ij}^{'}+N_{ij})}\cdot\prod_{k=1}^{r_i}\frac{\Gamma(N_{ijk}^{'}+N_{ijk})}{\Gamma(N_{ijk}^{'})} \quad (1)$$

Where $N_{ijk}^{'}=\frac{N^{'}}{r_i\cdot q_i}$, q_i denotes the number of configurations of the parent set $\pi(x_i)$, r_i denotes the

number of states of variable x_i, N_{ijk} is the number of records in dataset D for which $x_i=k$ and $\pi(x_i)$ is in the j^{th} configuration, and $N_{ij}=\Sigma_k N_{ijk}$. $\Gamma(\cdot)$ is the *Gamma* function, which satisfies $\Gamma(y+1)=y\Gamma(y)$ and $\Gamma(1)=1$.

The components N'_{ijk} and $p(G|\xi)$ specify the prior knowledge. In BDeu scoring function, the parameter prior $N'_{ijk}=\frac{N'}{r_i \cdot q_i}$ is set as uniform joint distribution, N' is the equivalent sample size, and N' is usually set to ten in most experiments. $p(G|\xi)$ is the network structure prior, the assessment of $p(G|\xi)$ is discussed in paper [18] in detail, and we set the network structure prior $p(G|\xi)$ as one in this paper. From Eq. (1), we can find that the BDeu scoring function is decomposable. Besides, the paper [18] shows that the BDeu scoring function is score equivalent, and the paper [5] shows that it is consistent. So the BDeu scoring function satisfies the three properties of the scoring function mentioned above.

2.2. Greedy Equivalent Search algorithm

The Greedy Equivalent Search algorithm (GES algorithm) starts from the empty graph, firstly adds edges until the scoring value reaches a local maximum, then deletes edges until the scoring value reaches another local maximum, and finally returns that equivalence class as the solution. The GES algorithm searches through the E-space and the equivalence classes in the E-space are represented with CPDAGs. The paper [5] proves Meek's conjecture, and shows that the local maximum reached in the first phase of the algorithm contains the generative distribution and the final equivalence class that results from the GES algorithm is asymptotically a perfect map of the generative distribution.

There are two kinds of operators which are used to construct the neighborhood in GES algorithm, namely the Insert operator in the first phase and the Delete operator in the second phase. In order to compute the scores of the PDAGs in the neighborhood after applying the operators, it needs to convert the PDAG to DAG, and the paper [19] gives a simple implementation of the algorithm PDAG-To-DAG. Besides, the GES algorithm needs the algorithm DAG-To-CPDAG[20] to convert the finally chosen DAG to CPDAG to make the greedy search continue. The two kinds of operators are listed as follows.

Definition 1 $Insert(X,Y,\mathrm{T})$ [5]

For non-adjacent nodes X and Y in the CPDAG P^c, and for any subset T of the neighbors of Y that are not adjacent to X, the $Insert(X,Y,\mathrm{T})$ operator modifies P^c by (1) inserting the directed edge $X \to Y$, and (2) for each $T \in \mathrm{T}$, directing the previously undirected edge between T and Y as $T \to Y$.

Definition 2 $Delete(X, Y, \mathrm{H})$ [5]

For adjacent nodes X and Y in the CPDAG P^c connected either as $X-Y$ or $X \to Y$, and for any subset H of the neighbors of Y that are adjacent to X, the $Delete(X, Y, \mathrm{H})$ operator modifies P^c by deleting the edge between X and Y, and for each $H \in \mathrm{H}$, (1) directing the previously undirected edge between Y and H as $Y \to H$ and (2) directing any previously undirected edge between X and H as $X \to H$.

These two operators need to satisfy the validity conditions, so that the PDAG P^{c^*} resulting from applying the operators will admit a consistent extension. If a DAG G has the same skeleton and the same set of v-structures as a PDAG P and if every directed edge in P has the same orientation in G, we say that G is a consistent extension of P. If there is at least one consistent extension of a PDAG P, we say that P admits a consistent extension. If the PDAG P^{c^*} resulting from applying the operators admits a consistent extension, it will be converted to a DAG by the algorithm PDAG-To-DAG. Otherwise, the algorithm PDAG-To-DAG will give an error during the conversion of the PDAG P^{c^*}.

The validity conditions all include the problem of judging clique. A clique in a DAG or a PDAG is a set of nodes for which every pair of nodes is adjacent. And directing the edges of the clique will not create new v-structure. About the implementation of judging clique, there are two methods. One is firstly finding all the maximal cliques of the graph, and then checking that whether the node set is a subset of any maximal clique found in the first phase. However, the general problem of finding optimal triangulations for undirected graphs in the process of finding all the maximal cliques of the graph is NP-hard[21], so heuristic algorithms[22][23] are developed, which are time-consuming. The other method of judging clique is a direct form used in the algorithm PDAG-To-DAG which is more time-efficient. For every vertex y, adjacent to x, with (x, y) undirected, if y is adjacent to all the other vertices which are adjacent to x, then x and all the vertices adjacent to x form a clique. This paper takes the second method of judging clique.

From the Profile file of the GES algorithm, we find that the GES algorithm is a time-consuming algorithm, and most of the running time is consumed in the calculation of the scores of the neighborhood and the conversion from PDAG to DAG. Since the size of the neighborhood is exponential in the number of adjacencies for a node, one paper [25] proposes changing exhaustive search by greedy search which is linear, to improve the time-efficiency of the GES algorithm. This paper intends to improve the time-efficiency of the GES algorithm by finding the parents and children set for each node using the constraint-based method and confining the GES within the parents and children set of each node.

The paper [6] proves that in the limit of large sample sizes, the GES algorithm identifies an inclusion-optimal equivalence class of DAG models, but GES may not be able to identify a parameter-optimal model. The parameter-optimal model is the model which includes the distribution with the fewest parameters. So the parameters of the final model identified by the GES algorithm may be not the fewest among all the BNs that include the distribution. Then according to the consistent property of the BDeu scoring function, the score of the finally identified equivalence class in the GES algorithm

is not the highest. This paper investigates the conditions of recovering the right structure, and intends to combine the conditions with the GES algorithm to improve the score of the GES algorithm.

2.3. Inclusion Boundary Condition

Inclusion Boundary Condition is one of the conditions that will guarantee the achievement of the highest score of the hill-climbing algorithm. It is based on the theory of Inclusion Order.

A graphical Markov model (GMM) $M(G)$ is the family of probability distributions that are Markov over G. A probability distribution P is Markov over a graph G if and only if every CI restriction encoded in G is satisfied by P. The intuition behind the Inclusion Order is that one GMM $M(G)$ precedes another GMM $M(G')$ if and only if all the CI restrictions encoded in G are also encoded in G'. Meek has provided an Inclusion Order in Meek's conjecture and Chickering has proved Meek's conjecture.

Conjecture 1 Meek's conjecture[24]

Let $D(G)$ and $D(G')$ be two Bayesian Networks determined by two DAGs G and G'. The conditional independence model induced by $D(G)$ is included in the one induced by $D(G')$, *i.e.* $D^I(G) \subseteq D^I(G')$, if and only if there exists a sequence of DAGs $L_1,\ldots,L_n$ such that $G=L_1$, $G'=L_n$ and the DAG L_{i+1} is obtained from L_i by applying either the operation of covered arc reversal or the operation of arc removal for $i=1,\ldots,n$.

The paper [7] defines the Inclusion Boundary $IB(G)$, and intuitively, the Inclusion Boundary of a given GMM $M(G)$ consists of those GMMs $M(G_i)$ that induce a set of CI restrictions $M^I(G_i)$ which immediately follow or precede $M^I(G)$ under the Inclusion Order. Then based on the definition of Inclusion Boundary, the paper [7] gives the definition of Inclusion Boundary Condition and the paper [8] gives the theorem which proves the correctness of the hill-climbing algorithm under the faithfulness and unbounded data assumptions.

Definition 3 Inclusion Boundary Condition[7]

A learning algorithm for GMMs satisfies the Inclusion Boundary Condition if for every GMM determined by a graph G, the traversal operator creates neighborhood $N(G)$ such that $N(G) \supseteq IB(G)$.

Theorem 2 The hill-climbing algorithm using the scoring function and a traversal operator satisfying the Inclusion Boundary Condition always finds the faithful model which has the highest score[8].

Based on the Inclusion Order defined by Meek's conjecture, the neighborhood created by the operators of one arc addition or one arc removal in the E-space, namely the ENR neighborhood, satisfies the Inclusion Boundary Condition. And the neighborhood created by the operators of one arc addition, one arc removal or one arc reversal in the DAG space does not satisfy the Inclusion Boundary Condition, which is the neighborhood formed in the GS algorithm.

The paper [8] gives an approximation neighborhood of the ENR neighborhood in the DAG space. But when we use the CPDAG to represent the equivalence class in the E-space, we can implement the operators of producing the ENR neighborhood directly on the CPDAG. However, in the GES algorithm, the neighborhoods formed both in the first phase and in the second phase do not contain the Inclusion Boundary defined by Meek's conjecture. So the GES algorithm does not satisfy the Inclusion Boundary Condition, the score of the BN structure identified by the GES algorithm is not the highest, and the final score of the GES algorithm still has room for improvement. This is consistent with the conclusion that the BN structure identified by the GES algorithm may be not parameter-optimal.

2.4. Unrestricted GES algorithm

GES algorithm uses the operator $Insert(X,Y,T)$ to produce the neighborhoods in the first phase and uses the operator $Delete(X,Y,H)$ to produce the neighborhoods in the second phase. The unrestricted GES algorithm (UGES algorithm) uses both the operator $Insert(X,Y,T)$ and the operator $Delete(X,Y,H)$ to produce the neighborhoods in each iteration. The neighborhood formed in the UGES algorithm asymptotically satisfies the Inclusion Boundary Condition. Therefore, we can predict that the score of the BN structure identified by the UGES algorithm is higher than the score of the BN structure identified by the GES algorithm. But the size of the neighborhood in the UGES algorithm is larger than that in the GES algorithm, so the UGES algorithm may be more time-consuming than the GES algorithm. In this paper, we conduct experiments to compare the UGES algorithm with the GES algorithm from both the aspect of algorithm time-efficiency and the aspect of structure identification quality.

3 Algorithm Improvement

Both the GES algorithm and the UGES algorithm have the drawback of time-consuming. Most of the running time is spent in the conversion from PDAG to DAG and the computation of the scoring function. This part of time has relation with the size of the neighborhood formed in the GES algorithm and the UGES algorithm. We can find the parents and children set for each node using the constraint-based method, and confine the GES algorithm and the UGES algorithm within the parents and children set of each node to reduce the size of the neighborhood and thus improve the time-consuming drawback of the GES algorithm and the UGES algorithm.

3.1. Max-Min Parents and Children algorithm

The Max-Min Parents and Children algorithm (MMPC algorithm) is the first local learning algorithm for discovering the parents and children sets of nodes. The MMPC algorithm discovers the parents and children set using a two-phase scheme. In phase I, the forward phase, variables enter sequentially a candidate parents and children set, by use of a heuristic function. In phase II, the backward phase, it removes all false positives that

entered in the first phase. In the end, the candidate parents and children set is the parents and children set.

In the backward phase, the MMPC algorithm relies on the result of the CI test to remove the false positive. The kind of CI test that the MMPC algorithm uses in the backward phase is G2 likelihood ratio test. In the forward phase, the MMPC algorithm needs to measure the strength of association between a pair of variables. The MMPC algorithm uses the negative $p-$ value returned by the G2 likelihood ratio test as the measure of association.

3.2. The combination of the GES/UGES algorithm with the MMPC algorithm

There are already papers describing the combination of the MMPC algorithm with the GS algorithm, namely the Max-Min Hill-climbing algorithm (MMHC algorithm), and the experiments show that the MMHC algorithm is a promising new algorithm that outperforms all other comparison algorithms, like the GS algorithm, the GES algorithm and the BNPC algorithm[2], in the aspects of running time, number of statistical calls, Bayesian score and Structural Hamming Distance (SHD).

This paper intends to combine the GES algorithm with the MMPC algorithm (MMPC-GES algorithm) and combine the UGES algorithm with the MMPC algorithm (MMPC-UGES algorithm). The specific implementation of the combination of the GES/UGES algorithm with the MMPC algorithm is that when the GES/UGES algorithm uses the operator $Insert(X,Y,\mathrm{T})$ to produce the neighborhood, X should be in the parents and children set of Y. We conduct experiments to compare the MMPC-GES algorithm and the MMPC-UGES algorithm with the GS/GES/UGES algorithm without the restriction of the parents and children sets, as well as the MMHC algorithm, and find some useful conclusions.

4 Experimental results and analysis

This paper uses the datasets sampled from the ALARM network[13] to conduct comparison experiments. The ALARM network stands for a medical diagnostic system of patient monitoring. It contains 37 variables and 46 edges. Each variable has two to four possible values. The max indegree is four and the max outdegree is five. The max and min of the size of the parents and children set is six and one. We randomly sampled 10 training datasets for each of the three different sample sizes 500, 1000, and 5000. Each reported statistic is the average over the 10 runs of an algorithm on the 10 different datasets of certain sample size.

This paper chooses three metrics to measure the quality of structure identification and the time-efficiency of the algorithms, namely Bayesian score, Structural Hamming Distance (SHD), and number of calls to the scoring function.

We use the BDeu scoring function to calculate the score, with the equivalent sample size of ten and the network structure prior of one. The BDeu score is the bigger the better. SHD is the sum of missing edges, extra edges, and reversed edges including edges that are undirected in one graph and directed in the other, between two PDAGs. SHD does not penalize for structural differences that cannot be statistically distinguished, so it is defined on PDAGs instead of DAGs. The SHD is the smaller the better.

Since the running time has relation with the configuration of computer, the usage of CPU and so on, this paper does not use this metric to measure the time-efficiency of the algorithms and uses number of calls to scoring function during the greedy search to measure the time-efficiency of the algorithms which is in proportion to the running time.

4.1. BDeu score results

We randomly sample one testing dataset containing 5000 cases for each of the training dataset. And the BDeu score is the average over the 10 runs of an algorithm on the 10 different testing datasets of certain sample size. Besides, we calculate the score of the true ALARM network by the same way. The results of the average BDeu score of three different sample sizes are in Table 1.

From Table 1, we can find several useful rules. Firstly, with the increase of the sample size, the BDeu score of the identified BN becomes higher. Secondly, the GES algorithm and the UGES algorithm in the E-space, achieve higher BDeu score than the GS algorithm in the DAG space, since the greedy search in the E-space improves the drawback of falling into local maximum caused by the score equivalent property of BDeu scoring function in the DAG space. Thirdly, the UGES algorithm achieves slightly higher BDeu score than the GES algorithm, since the UGES algorithm satisfies the Inclusion Boundary Condition asymptotically but the GES algorithm does not satisfy the Inclusion Boundary Condition. Fourthly, when the GS/GES/UGES algorithms are restricted by the parents and children sets produced by the MMPC algorithm, however the MMPC-GES algorithm performs the worst in BDeu score among the three algorithms MMHC, MMPC-GES and MMPC-UGES. Maybe the performance of MMPC-GES is reduced greatly by its strict two-phase search strategy. The MMPC-UGES algorithm in E-space still outperforms the MMHC algorithm in DAG space in BDeu score.

Fifthly, in all, GS/GES/UGES with the restriction of MMPC achieve lower BDeu score than GS/GES/UGES without the restriction, namely the BDeu score of GS/GES/UGES is reduced by the restriction of parents and children sets. Especially we find that the BDeu score of the MMHC algorithm is lower than that of the GS algorithm, and the BDeu score of the GS algorithm doesn't outperform the BDeu score of the true ALARM network, which doesn't show signs of overfitting. We need to remember that the parents and children sets identified by the MMPC algorithm may be not the exact parents and children sets of the true network and have relation with the quality of dataset.

Table 1: Average BDeu Score Results.

Sample size	True Alarm	GS	GES	UGES	MMHC	MMPC-GES	MMPC-UGES
500	-47892.85	-48742.44	-48425.9	-48422.26	-49538.36	-50381.35	-49002.71
1000	-47953.66	-48490.64	-48338.42	-48318.08	-49486.32	-50159.25	-48816.94
5000	-47536.78	-47941.26	-47865.43	-47835.32	-48994.44	-49008.54	-48765.58

Table 2: Average SHD Results. In the format A(B, C, D), A is the SHD, B is the number of extra edges, C is the number of missing edges, and D is the number of reversal edges.

Sample size	GS	GES	UGES	MMHC	MMPC-GES	MMPC-UGES
500	71.3(46.3, 3.4, 21.6)	59.2(43.9, 2.6, 12.7)	60.0(44.8, 2.5, 12.7)	30.8(7.6, 3.7, 19.5)	30.3(3.0, 8.5, 18.8)	29.6(8.2, 3.8, 17.6)
1000	64.6(39.2, 1.8, 23.6)	56.7(39.3, 1.7, 15.7)	55.3(38.7, 1.7, 14.9)	27.8(5.7, 2.3, 19.7)	24.5(1.5, 6.4, 16.6)	24.3(5.7, 2.3, 16.3)
5000	57.4(27.4, 0.9, 29.1)	43.7(23.4, 1.1, 19.2)	44.0(24.0, 0.8, 19.2)	23.4(4.3, 0.3, 18.8)	20.8(0.7, 0.1, 20.0)	25.9(5.1, 0.0, 20.8)

Table 3: Average Number of Calls to BDeu Scoring Function Results.

Sample size	GS	GES	UGES	MMHC	MMPC-GES	MMPC-UGES
500	105265.9	111524.5	118216.1	6073.1	1662	4379.4
1000	101082.2	114311.9	120510.4	5709.7	1527.7	3909.7
5000	94832.8	108326.8	118639.2	6117.1	2013.6	4322.4

4.2. SHD results

This paper has calculated the SHD which is the average over the 10 runs of an algorithm on the 10 different training datasets of certain sample size, as well as the three components of SHD, namely number of extra edges, number of missing edges and number of reversal edges including edges that are undirected in one graph and directed in the other. The results of the average SHD of three different sample sizes are in Table 2.

From Table 2, we can find that with the increase of the sample size, the SHD of the identified BN becomes smaller, as well as the number of extra edges and the number of missing edges, but the number of reversal edges doesn't show this feature. The GES algorithm and the UGES algorithm perform better than the GS algorithm in SHD, but the gap between the GES algorithm and the UGES algorithm in SHD is not obvious. Besides, the gaps among MMHC, MMPC-GES and MMPC-UGES in SHD are not obvious too.

In all, the SHD of GS/GES/UGES with the restriction of MMPC is lower than that of GS/GES/UGES without the restriction, namely the SHD of GS/GES/UGES is improved by the restriction of parents and children sets, especially number of extra edges.

4.3. Number of calls to BDeu scoring function results

We use number of calls to BDeu scoring function to measure the time-efficiency of algorithms. We need to know that each call to the BDeu scoring function in the E-space corresponds to one conversion from PDAG to DAG, and the time cost of one conversion is nearly the same as that of one call to the BDeu scoring function. The results of the average number of calls to BDeu scoring function of three different sample sizes are in Table 3.

From Table 3, we can find that the GES/UGES algorithms calculate about ten percent more BDeu scoring function than the GS algorithm, but the GES/UGES algorithms in E-space need extra conversions between PDAG and DAG, so we can expect that the running time of GES/UGES is much longer than that of GS. The UGES algorithm calculates about seven percent more BDeu scoring function than the GES algorithm, so we can expect that the running time of UGES is slightly longer than that of GES. Besides, the number of calls to BDeu scoring function in the MMPC-UGES algorithm is more than twice that in MMPC-GES algorithm, so the running time of MMPC-UGES is expected to be about twice that of MMPC-GES. The MMHC algorithm calculates about 40% more BDeu scoring function than the MMPC-UGES algorithm, considering the extra time cost of conversions between PDAG and DAG in MMPC-UGES, so we can expect that the running time of MMHC and MMPC-UGES should be almost the same.

In all, the number of calls to BDeu scoring function in GS/GES/UGES with the restriction of MMPC is lower than that in GS/GES/UGES without the restriction, namely the amount of calculation in GS/GES/UGES is reduced by the restriction of parents and children sets. The number of calls to BDeu scoring function in the MMPC-GES algorithm reduces the most, which also causes the worst performance of MMPC-GES in BDeu score, comparing with MMHC and MMPC-UGES.

5 Conclusions

In this paper, we use the Inclusion Boundary Condition to analyze the GES algorithm and the GS algorithm. We point out that the unrestricted form of GES algorithm which implements both the Insert operator and the Delete operator to produce the neighborhood asymptotically satisfies the Inclusion Boundary Condition. Still, the combinations of the GES/UGES algorithms with the local discovery algorithm MMPC, namely the MMPC-GES algorithm and the MMPC-UGES algorithm, are proposed. We compare GS/GES/UGES/MMHC/MMPC-GES/MMPC-UGES on the datasets sampled from the ALARM network. The experiments show that MMHC/MMPC-GES/MMPC-UGES compute less number of calls to BDeu scoring function and achieve better SHD than

GS/GES/UGES without the restriction of the parents and children sets, while the BDeu score is reduced by the restriction of the parents and children sets. Considering the huge improvement on time-efficiency and SHD, MMHC/MMPC-GES/MMPC-UGES are still compelling. And among the three algorithms MMHC/ MMPC-GES/MMPC-UGES, MMPC-GES performs the worst in BDeu score, and MMPC-UGES performs the best in BDeu score.

Finally, the combination of constraint-based method, Bayesian search-and-score method and Markov Equivalence Class space is a promising combination. The problem of confining the greedy search can also be seen as the problem of directing the skeleton identified. Many constraint-based methods usually firstly identify the skeleton and then direct the skeleton using direction rules. In some of my initial experiments with the constraint-based algorithms, the effect of skeleton identification is good, but the effect of direction on skeleton is not good, like the BNPC algorithm. If we use the search-and-score method to direct the skeleton identified by the constraint-based method, it will improve the final BN structure identified by the constraint-based method.

Acknowledgments: This work is supported by National Basic Research Program of China (973 program) with Grant No. 2011CB706900, National Natural Science Foundation of China (Grant No. 70971128), Beijing Natural Science Foundation (Grant No. 9102022) and the President Fund of GUCAS (Grant No. O95101HY00).

6 References and Notes

[1] P. Spirtes, C. N. Glymour, and R. Scheines. "Causation, Prediction, and Search". The MIT Press, 2000.

[2] J. Cheng, R. Greiner, J. Kelly, D. Bell and W. Liu. "Learning Bayesian Networks from Data: An Information-theory Based Approach"; Journal of Artificia Intelligence, Vol. 137, Issue 1, 43-90, 2002.

[3] G. F. Cooper and E. Herskovits. "A Bayesian Method for the Induction of Probabilistic Networks from Data"; Journal of Machine Learning, Vol. 9, Issue 4, 309-347, 1992.

[4] H. Xu, H. Yu, and J. Wang. "Poison Identification Based on Bayesian Method in Biochemical Terrorism Attacks"; Advanced Science Letters, Vol. 5, 1-5, 2012.

[5] D. M. Chickering. "Optimal Structure Identification with Greedy Search" ; Journal of Machine Learning Research, Vol. 3, 507-550, 2002.

[6] D. M. Chickering and C. Meek. "Finding Optimal Bayesian Networks". Proceedings of the Eighteenth Conference on Uncertainty in Artificial Intelligence, Pages 94-102, 2002.

[7] T. Kocka, R. Bouckaert, and M. Studeny. "On the Inclusion Problem". Technical Report, Academy of Sciences of the Czech Republic, 2001.

[8] R. Castelo. and T. Kočka. "Towards an Inclusion Driven Learning of Bayesian Networks". Techical Report CS-2002-05, 2002.

[9] N. Friedman, I. Nachman, and D. Peer. "Learning Bayesian Network Structure from Massive Datasets: The Sparse Candidate Algorithm". Proceedings of the Fifteenth Conference on Uncertainty in Artificial Intelligence, 1999.

[10] N. Friedman, M. Linial, I. Nachman, and D. Peer. "Using Bayesian Networks to Analyze Expression Data"; Journal of Computational Biology, Vol. 7, Issue 3, 601–620, 2000.

[11] I. Tsamardinos, L. Brown, and C. Aliferis. "The Max-Min Hill-climbing Bayesian Network Structure Learning Algorithm"; Journal of Machine Learning, Vol. 65, Issue 1, 31-78, 2006.

[12] I. Tsamardinos, C. F. Aliferis, and A. Statnikov. "Time and Sample Efficient Discovery of Markov Blankets and Direct Causal Relations". Technical Report DSL-03-02, Vanderbilt University, 2003.

[13] I. A. Beinlich, H. J. Suermondt, R. M. Chavez, and G. F. Cooper. "The ALARM Monitoring System: A Case Study with Two Probabilistic Inference Techniques for Belief Networks". Proceedings of the Second European Conference on Artificial Intelligence in Medicine, Pages 247-256, London, 1989.

[14] K. P. Murphy. the Bayes Net Toolbox for Matlab. http://code.google.com/p/bnt/

[15] P. Leray. the BNT Structure Learning Package. http://bnt.insa-rouen.fr/index.html

[16] C. Aliferis, I. Tsamardinos, A. Statnikov, and L. E. Brown. "Causal Explorer: A Causal Probabilistic Network Learning Toolkit for Biomedical Discovery". METMBS, 371–376, 2003.

[17] T. Verma and J. Pearl. "Equivalence and Synthesis of Causal Models". Proceedings of the Sixth Conference on Uncertainty in Artificial Intelligence, Pages 220–227, 1991.

[18] D. Heckerman, D. Geiger, and D. Chickering. "Learning Bayesian Networks: The Combination of Knowledge and Statistical Data"; Journal of Machine Learning Research, Vol. 20, Issue 3, 197–243, 1995.

[19] D. Dor and M. Tarsi. "A Simple Algorithm to Construct a Consistent Extension of a Partially Oriented Graph". Technical Report R-185, 1992.

[20] D. M. Chickering. "Learning Equivalence Classes of Bayesian-Network Structures"; Journal of Machine Learning Research, Vol. 2, 445-498, 2002.

[21] M. Yannakakis. "Computing the Minimum Fill-in is NP-complete"; SIAM Journal on Algebraic and Discrete Methods, Vol. 2, Issue 1, 77–79, 1981.

[22] U. Kjaerul. "Triangulation of Graphs - Algorithms Giving Small Total State Space". Technical Report R-90-09, 1990.

[23] C. Huang and A. Darwiche. "Inference in Belief Networks: A Procedural Guide"; International Journal of Approximate Reasoning, Vol. 15, Issue 3, 225-263, 1996.

[24] C. Meek. "Graphical Models, Selecting Causal and Statistical Models". PhD Thesis, Carnegie Mellon University, 1997.

[25] J. I. Alonso-Barba, L. Ossa, J. A. Gámez, and J. M. Puerta. "Scaling up the Greedy Equivalence Search Algorithm by Constraining the Search Space of Equivalence Classes". Proceedings of the 11th European Conference on Symbolic and Quantitative Approaches to Reasoning with Uncertainty, Pages 194-205, 2011.

Design Robust PID Controller for Hydro-turbine governing with ABC Algorithm

A.Yosefi
Technical Eng. Department
University of Mohaghegh Ardabili,
Ardabi, Iran

A. Ghasemi
Young Researcher Club, Ardabil
Branch, Islamic Azad University,
Ardabil, Iran

R.Bazyar
East Azarbayjan Power Generation
Management Company
Ardabil, Iran

H. A. Shayanfar *
Electrical Eng. Department, Islamic
Azad University, South Tehran
Branch, Tehran, Iran

O. Abedinia
Young Researcher Club, Ardabil
Branch, Islamic Azad University,
Ardabil, Iran

H. GholamalitabarFiroozjaee
Technical Eng. Department
University of Mohaghegh Ardabili,
Ardabi, Iran

ali.yousefi1365@gmail.com, ghasemi.agm@gmail.com, R.Bazyar@yahoo.com, hashayanfar@yahoo.com,
oveis.abedinia@gmail.com, h.gholamalitabar@yahoo.com

Abstract— **In this paper, the parameters of PID controller are tuned by Gravitational Search Algorithm (GSA). The key idea of the proposed method is to use a new design PID controller of Hydro-turbine governing. The result of simulation are shown effectiveness of the proposed method and GSA algorithm for solve Hydro-turbine governing problem in different load condition of power system. The achieved result of GSA algorithm compare with CEP, FEP, MFEP and DCMEP algorithm, the table and figure shown transcendent GSA algorithm for optimizations problem.**

Keywords- Hydro-turbine governing, GSA, robust PID controller.

I. INTRODUCTION

Energy is the basic need for economic development; every sector of country's economy (industry, agricultural, transport, commercial and domestic) needs input of energy. The Hydro-turbine governing systems contain many parts, high dimension complex systems, time-variant and multi-parameters. With attention to increases demand, the generating of energy is near to demand of energy, so need a best controller to guarantee systems for different condition. In most study used ideal PID controller for model of Hydro-turbine governing but in industrial production of ideal PID controller is not possible, so in this paper used a robust PID (RPID) controller for control Hydro turbine governing system with disturbance. PID controller is a best controller for us decide, and use many artificial algorithm for getting best answer for PID controllers (K_P, K_I, K_D) to guarantee system in best condition of working, hitherto used Genetic Algorithm (GA) [1], Simulated annealing (SA) algorithm [2], Evolutionary Programming (EP) [3], Conventional Evolutionary Programming (CEP) [4], Fast Evolutionary Programming (FEP) [4,5], Deterministic Chaotic Mutation Evolutionary Programming (DCMEP) [4,6], but the above algorithms cannot best solution for optimization of Hydro-turbine governing, so this paper a new optimization algorithm based on the law of gravity, namely Gravitational Search Algorithm (GSA) for problem solving is proposed [8]. This algorithm is based on the Newtonian gravity: ‘‘every particle in the universe attracts every other particle with a force that is directly proportional to the product of their masses and inversely proportional to the square of the distance between them”. In Sect. II, the proposed GSA algorithm is described, in Sect. IV experiments and results are presented.

* Corresponding Author. E-Mail Address: hashayanfar@yahoo.com (H. A. Shayanfar)

Nomenclature:

N: population size
T_a: inertial time constant of generator
T_w: current inertial time constant
T_S: adjust time in seconds
Δ: overshoot level
T_y: Engagers relay time constant
e_y: hydro-turbine torque vine opening level transfer coefficient
e_h: hydro-turbine torque pressure transfer coefficient
e_{qy}: hydro-turbine hydraulic flux vine opening level transfer coefficient
e_{qh}: hydro-turbine hydraulic flux pressure transfer coefficient
K_P: proportional adjustment coefficient
K_I: integral adjustment coefficient
K_D: deferential adjustment coefficient
e_n: generator's self adjustment coefficient

II. GRAVITATIONAL SEARCH ALGORITHM (GSA)

The gravitational search algorithm is constructed based on the law of gravity and the notion of mass interactions. The GSA algorithm uses the theory of Newtonian physics and its searcher agents are the collection of masses. In GSA, we have an isolated system of masses. Using the gravitational force, every mass in the system can see the situation of other masses. The gravitational force is therefore a way of transferring information between different masses. GSA was introduced by E. Rashedi et all, 2009, In GSA, agents are considered as objects and their performance is measured by their masses. All these objects attract each other by the gravity force, and this force causes a global movement of all objects towards the objects with heavier masses. Hence, masses cooperate using a direct form of communication, through gravitational force. The heavy masses - which correspond to good solutions - move more slowly than lighter ones, this guarantees the exploitation step of the algorithm [7,8]. In GSA, each mass (agent) has four specifications: position, inertial mass, active gravitational mass, and passive gravitational mass. The position of the mass corresponds to a solution of the problem, and its gravitational and inertial masses are determined using a fitness function. In other words, each mass presents a solution, and the algorithm is navigated by properly adjusting the gravitational and inertia masses. By lapse of time, we expect that masses be attracted by the heaviest mass. This mass will present an optimum solution in the search space. The GSA could be considered as an isolated system of masses. It is like a small artificial world of masses obeying the Newtonian laws of gravitation and motion. More precisely, masses obey the following laws: Law of gravity: each particle attracts every other particle and the gravitational force between two particles is directly proportional to the product of their masses and inversely proportional to the distance between them, R. Law of motion: the current velocity of any mass is equal to the sum of the fraction of its previous velocity and the variation in the velocity. Variation in the velocity or acceleration of any mass is equal to the force acted on the system divided by mass of inertia [8, 9].

In the GSA algorithm particle researcher, is sum of all mass. We define the position of the i_{th} agent by:

$$X_i = (x_i^1 \ldots x_i^d \ldots x_i^N) \text{ for } i = 1, 2, 3 \ldots N \quad (1)$$

In the Eqs.1 x_i^d is the position of ith agent in the dth dimension. N is total of agent. At a particular time (t), we have define the force acting on mass (i) from mass (j) as pursuing:

$$F_{ij}^d(t) = G(t)\,(M_{pi}(t) - M_{aj}(t))/(R_{ij}(t)+\varepsilon)\times(X_j^d(t) - X_i^d(t)$$

$M_{aj}(t)$ is the active gravitational mass related to agent j, M_{pi} is the passive gravitational mass related to agent i, G (t) is gravitational constant at time t, ε is a small constant, and $R_{ij}(t)$ is the Euclidian distance between two agents i and j:

$$R_{ij} = \left\| X_i(t), X_j(t) \right\|_2 \quad (2)$$

To give a chromatic characteristic to GSA algorithm, suppose that the total force that acts on agent i in a dimension d be a randomly weighted sum of dth components of the forces exerted from other agents:

$$F_i^d(t) = \sum_{j=1, j\neq i}^{N} rand_j F_{ij}^d(t) \quad (3)$$

Where $rand_j$ is generate random in the interval [0, 1]. by the law of motion, the acceleration of the agent i at time t, and in direction dth, $a_i^d(t)$, give from equation 5 is equal:

$$a_i^d(t) = \frac{F_i^d(t)}{M_{ii}(t)} \quad (4)$$

In the equation (4) M_{ii} is the inertial mass of ith agent. Velocity for next step will update from equation 5 it is similar to PSO algorithm, because any particle get a new vector of velocity for generate new population. After update velocity vector for agents the position of any agent get from equation 6. The equation for give new velocity and new position following:

$$v_i^d(t+1) = rand_i \times v_i^d(t) + a_i^d(t) \quad (5)$$

$$x_i^d(t+1) = x_i^d(t) + v_i^d(t+1) \quad (6)$$

With attention to Eqs.5, the next velocity of an agent is considered as a fraction of its current velocity added to its acceleration. $rand_i$ is a uniform random variable in the interval [0, 1]. For give a randomized characteristic to the search used this random number.

The gravitational constant, G, is initialized at the beginning and will be reduced with time to control the search accuracy. In other words, G is a function of the initial value (G0) and time (t):

$$G(t) = G(G0, t) \quad (7)$$

Gravitational and inertia masses are simply calculated by the fitness evaluation. A heavier mass means a more efficient agent. This means that better agents have higher attractions and walk more slowly. Assuming the equality of the gravitational and inertia mass, the values of masses are calculated using the map of fitness. We update the gravitational and inertial masses by the following Eqs.8-10:

$$M_{ai} = M_{pi} = M_{ii} = M_i, i = 1, 2, \ldots, N \quad (8)$$

$$m_i(t) = \frac{fit_i(t) - worst(t)}{best(t) - worst(t)} \quad (9)$$

$$M_i(t) = \frac{m_i(t)}{\sum_{j=1}^{N} m_i(t)} \quad (10)$$

Fitness value of the agent i at time t show with fit_i (t) and, worst (t) and best (t) are defined as follows (for a minimization problem):

$$best(t) = \min_{j\in\{1,2,...,N\}} fit_j(t) \quad (11)$$

$$worst(t) = \max_{j\in\{1,2,...,N\}} fit_j(t) \quad (12)$$

It is to be noted that for a maximization problem, Eqs. (11) and (12) are changed to Eqs. (13) and (14), respectively:

$$best(t) = \max_{j\in\{1,2,...,N\}} fit_j(t) \quad (13)$$

$$worst(t) = \min_{j\in\{1,2,...,N\}} fit_j(t) \quad (14)$$

For getting best performed with desirable compromise between exploration and exploitation, one way is to reduce the number of agents with lapse of time in Eq. (3). For getting that target, suggest set an agent with bigger mass apply their force to the other. However, we should be careful of using this policy because it may reduce the exploration power and increase the exploitation capability. We remind that in order to avoid trapping in a local optimum the algorithm must use the exploration at beginning.

By lapse of iterations, exploration must fade out and exploitation must fade in. To improve the performance of GSA by controlling exploration and exploitation only the K_{best} agents will attract the others. K_{best} is a function of time, with the initial value K0 at the beginning and decreasing with time. In such a way, at the beginning, all agents apply the force, and as time passes, K_{best} is decreased linearly and at the end there will be just one agent applying force to the others. Therefore, Eq. (3) could be modified as:

$$F_i^d(t) = \sum_{j\in K_{best}, j\neq i}^{N} rand_j F_{ij}^d(t) \quad (15)$$

Where K_{best} is the set of first K agents with the best fitness value and biggest mass. The principle of GSA is shown in flowchart of Fig. 1. The flowcharts show how the proposed algorithm is efficient some remarks are noted:

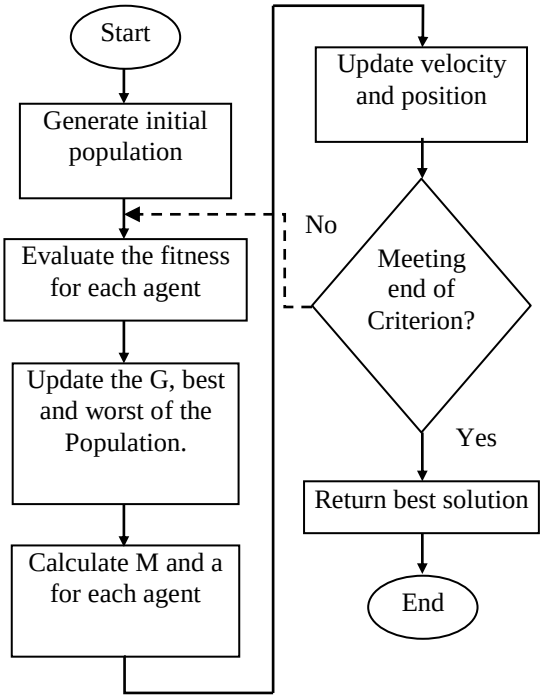

Figure 1. Flochart of GSA.

III. MODEL FOR PID CONTEROLLER IN SYSTEM STUDY

The system structure based on the GSA algorithm shown in Fig. 2 is targeted for optimizing the on line RPID parameters in the hydro-turbine governing system. The gains of the RPID controller are tuned online in terms of the knowledge base and GSA inference, and then, the RPID controller generates the control signal.

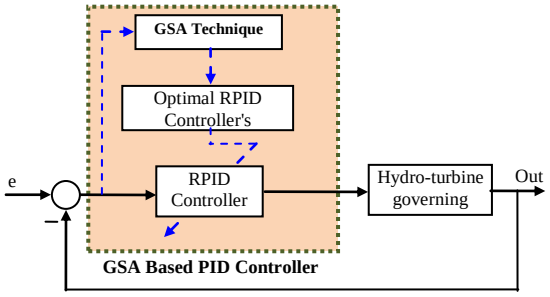

Figure 2. The proposed RPID controller design problem

The system consists of the PID governing system, the GSA algorithm parameter optimization, the hydraulic pressure servo system, the hydro-turbine system and the generator and load system In Fig. 3, y is the turbine rotating speed, r is a given signal, e = r _ y is the error signal, u is the output, Mg is the disturbance or load, Ta is the inertial time constant, Tw is the current inertial time constant and other parameters are defined in Ref. in Classical PID (CPID) controller equation is:

$$PID = k_p + \frac{K_I}{S} + k_D S \tag{16}$$

But in design industrial or robust PID controller use a low filter for delete the noise of high frequents, so this paper the function of derive represent Eqs.18:

$$\frac{k_D S}{1+T_d S}, T_d >> k_D \tag{17}$$

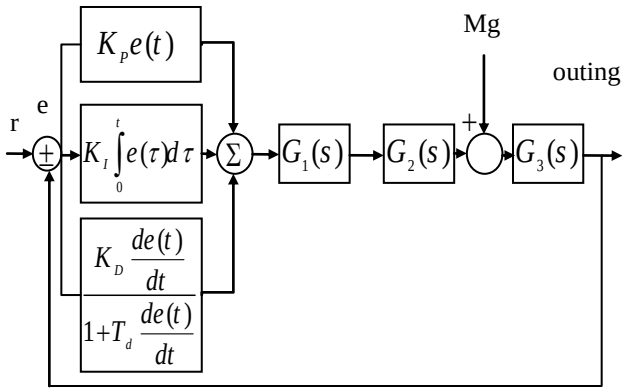

Figure 3. The system structure of Hydro-turbine governing system

The transfer function of the hydraulic pressure servo system is:

$$G_1(S) = \frac{1}{1+T_y S} \tag{18}$$

The transfer function of the hydro-turbine system is

$$G_2(S) = \frac{e_y - (e_{qy} e_y - e_{qh} ey) T_w S}{1+e_{qh} T_w S} \tag{19}$$

The transfer function of the generator and load is

$$G_3(S) = \frac{1}{T_a S + e_n} \tag{20}$$

The transfer function of the PID governing system is

$$G_g(Z) = K_p + \frac{K_1}{1-Z^{-1}} + K_D(1-Z^{-1}) \tag{21}$$

Its incremental expression is

$$\begin{aligned} \Delta U(k) &= K_p(e(k) - e(k-1)) + K_I e(k) \\ &+ K_D(e(k) - 2e(k-1) + e(k-2)) \end{aligned} \tag{22}$$

where U(k) is the governor output and e(k) is the frequency error of the kth sampling. The GSA algorithm optimizes the three PID parameters to improve the static and dynamic performances of the governed object.

IV. RESULT OF RPID DESIGN USING GSA ALGORITHM

The proposed method was applied for RPID design for hydropower station in two scenarios pursues and any scenarios contain two cases. For show proficiency of GSA algorithm in solve intricate problem with many parameters, compare the result of GSA algorithm with CEP, FEP, MFEP and DCEMP [4,5]. The object function for optimization is:

$$\text{Min } J = eTe \tag{23}$$

s. t.

$$K_{P,min} \le K_P \le K_{P,max}$$

$$K_{I,min} \le K_I \le K_{I,max}$$

$$K_{D,min} \le K_D \le K_{D,,max}$$

$$\min j = e^T e$$

Where $K_{P,min}$, $K_{I,min}$, $K_{D,min}$ and $K_{P,max}$, $K_{I,max}$, $K_{D,max}$ are the upper and lower bounds of K_P, K_I,K_D, respectively.

Scenario1: the model of Hydro-turbine is HL638-WJ-60, winding speed n=1000 r/min, power P_T = 1612 kW, pipeline length L = 1956m, cross area 4.22 m^2, inertial time constant T_a = 3.9 s, current inertial time constant T_w = 0.365 s. The result simulation from GSA, DCEMP, FEP, MFEP and CEP of scenario 1 is presented in Table 1.

Case 1: for vane opening level = 60%, the transfer coefficients are:

e_x = -0.728, e_y = 1.28 , e_h = 0.95 , e_{qx} = -0.075 , e_{qy} = 0.956 , e_{qh} = 0.618

Case 2: for vane opening level = 80%, the transfer coefficients are:

e_x = -0.860, e_y = 0.948 , e_h = 1.31 , e_{qx} = -0.029 , e_{qy} = 0.868, e_{qh} = 0.830

TABLE I. THE RESULT SIMULATION FROM GSA, DCEMP, FEP, MFEP AND CEP OF SCENARIO 1

Method	*Vane Opening (%)*	*Optimization Parameters*			$T_S(s)$	δ *(%)*	*N*
		K_P	K_I	K_D			
CEP	60	2.6	0.25	1.0	5.4	1.9	118
	80	4.0	0.23	0.2	6.0	1.77	97
FEP	60	2.7	0.23	1.5	5.2	1.85	101
	80	4.0	0.22	0.2	5.8	1.74	86
MFEP	60	3.0	0.25	1.8	4.8	1.35	57
	80	4.0	0.21	0.2	5.2	1.74	51
DCMEP	60	3.0	0.25	1.8	4.8	1.35	49
	80	4.0	0.21	0.2	5.2	1.74	30
GSA	60	3.09	0.22	2.9	4.66	1.234	50
	80	3.74	0.22	1.22	5.02	1.671	50

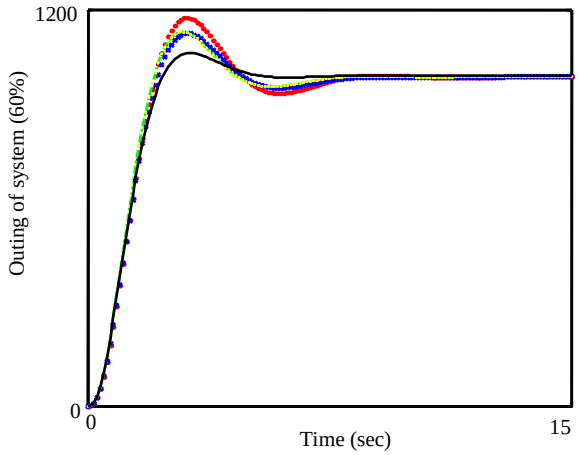

Figure 4. outing of system for all algorithms for vane opening level = 60%, CEP (…), FEP (+++), MFEP (-.-.), DCMEP (***), GSA(___)

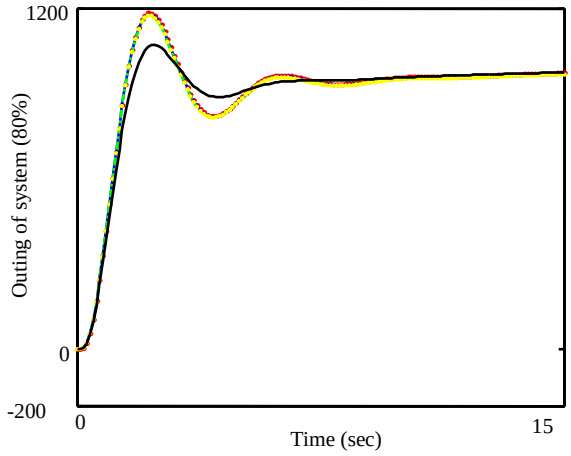

Figure 5. outing of system for all algorithms for vane opening level = 80%, CEP (…), FEP (+++), MFEP (-.-.), DCMEP (***), GSA(___)

Scenario2: the model of Hydro-turbine is HL220, winding speed n=136.4 r/min, power P_T = 75000 kW, pipeline length L = 700m, cross area 4.22 m^2, inertial time constant T_a = 9.42 s, current inertial time constant T_w = 1.32s. the simulation result from GSA, DCEMP, FEP, MFEP and CEP of scenario 2 is presented in Table. 2.

Case 1: for vane opening level = 60%, the transfer coefficients are:

e_x = -0.898, e_y = 1.205 , e_h = 0.9298 , e_{qx} = -0.197 , e_{qy} = 0.946 , e_{qh} = 0.3457

Case 2: for vane opening level = 80%, the transfer coefficients are:

e_x = -1.248, e_y = 1.313, e_h = 1.3028 , e_{qx} = -0.1035 , e_{qy} = 1.0045, e_{qh} = 0.3843

TABLE II. THE RESULT SIMULATION FROM GSA, DCEMP, FEP, MFEP AND CEP OF SCENARIO 2

Method	*Vane Opening (%)*	*Optimization Parameters*			*T_S(s)*	*δ (%)*	*N*
		K_P	K_I	K_D			
CEP	60	2.83	0.12	1.41	3.5	1.60	139
	80	4.61	0.23	0.55	5.6	1.73	103
FEP	60	2.83	0.13	1.38	3.2	1.58	94
	80	4.60	0.22	0.54	5.4	1.71	81
MFEP	60	2.81	0.12	1.30	3.1	1.55	76
	80	4.60	0.21	0.51	5.1	1.68	55
DCMEP	60	2.81	0.12	1.30	3.1	1.55	52
	80	4.60	0.21	0.51	5.1	1.68	43
GSA	60	4.09	0.14	4.9	2.9	1.43	50
	80	3.74	0.22	0.21	4.8	1.55	50

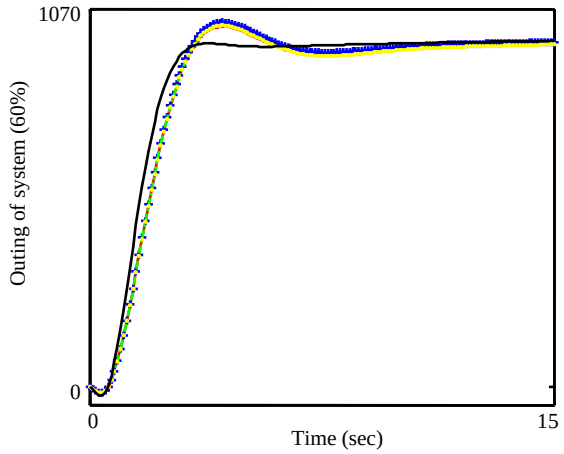

Figure 6. outing of system for all algorithms for vane opening level = 60%, CEP (…), FEP (+++), MFEP (-.-.), DCMEP (***), GSA(___)

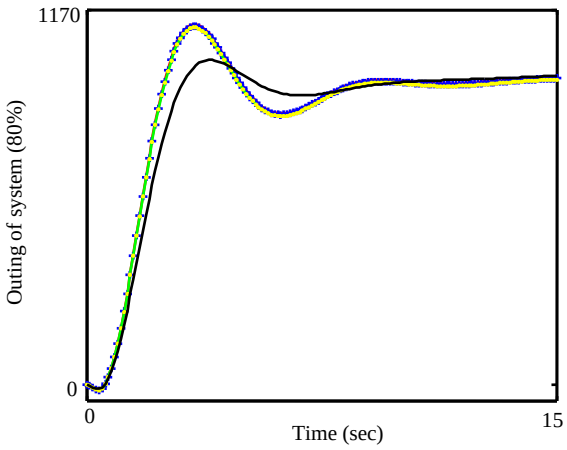

Figure 7. outing of system for all algorithms for vane opening level = 80%, CEP (…), FEP (+++), MFEP (-.-.), DCMEP (***), GSA(___)

V. CONCLUSIONS

Actually, conventional PID control has been largely applied to hydro-turbine governors and has achieved valuable results. The main reason is due to their simplicity of operation, inexpensive maintenance and low cost. But many researches were shown that classical PID control was unable to perform optimally over the full

range of operating conditions and disturbance, due to the highly complex, non-linear characteristic of hydro-turbine governing system. So to solve this problem in recent years the methods intelligence algorithms such as the (CEP, FEP, MFEP and DCMEP) is used. This paper employed GSA algorithms for optimization of RPID parameters to hydro turbine governors. The results from the two simulation cases show that the proposed method is practical and efficient in achieve optimal PID parameters for the hydro-turbine governing system. also the results of simulation cases show that the presented control strategy has enhanced response speed and robustness and achieves good performance when applied to the hydro-turbine governing system and over shoot and setting time is less than other algorithm Presented in this article.

REFERENCES

[1] B. Porter,A.H. Jones, "Genetic tuning of digital PID control," Electron Lett;Vol.28,no.9, pp.834–44. 23 April 1992.

[2] C.A. Roa-Sepulveda, B.J. Pavez-Lazo, "A solution to the optimal power flow using simulated annealing, " Power Tech Proceedings, Porto , Portugal Vol.2. pp.5, 2001.

[3] A.E. Eiben, R. Hinterding,Z. Michalewicz, " Parameter control in evolutionary algorithms" IEEE Trans Evol Comput, Vol. 3 No. 2,pp. 124 – 141,Jul 1999.

[4] J. Chuanwen, Ma. Yuchao and W. Chengmin, " PID controller parameters optimization of hydro-turbine governing systems using deterministic-chaotic-mutation evolutionary programming (DCMEP) " Energy Conversion and Management, Vol. 47,No.9-10, pp. 1222-1230, June 2006.

[5] X. Yao, Y. Liu, " Fast evolutionary programming " In: Proceedings of the fifth annual conference evolutionary programmingCambridge, MA,. pp. 451–60. 1996.

[6] K. Chellapilla, DB. Fogel, " Two new mutation operators for enhanced search and optimization in evolutionary programming " In: SPIE IntSymp Optical Science and Engineering Instrum Conf 3165: Applic Soft Comput Bellingham (WA): SPIE Press. pp. 260–269.

[7] E. Rashedi, Gravitational Search Algorithm, M.Sc. Thesis, Shahid Bahonar University of Kerman, Kerman, Iran, 2007 (in Farsi).

[8] E. Rashedi, H. Nezamabadi-pour and S. Saryazdi, " Filter modeling using gravitational search algorithm " Engineering Applications of Artificial Intelligence, 18 May 2010.

[9] S.J. Russell, P. Norvig, Artificial Intelligence a Modern Approach, Prentice Hall, Upper Saddle River, New Jersy, 1995.

BIOGRAPHIES

Ali Yousefi received the B.S. degree in Electrical Engineering from Islamic Azad University, Ardabil,Iran in 2009 and M.S.E. degree in Technical Eng. Department of the University of Mohaghegh Ardabili, Ardabil, Iran, 2011. His research interests are in the Artificial Intelligence to Power System Control Design, power system operation and control, power market analysis and expansion planning for Electric power system.

Ali Ghasemi received the B.Sc. and M.Sc. (Honors with first class) degree in Electrical Engineering from Isfahan University of Technology (IUT), Esfahan, Iran in 2009 and Technical Eng. Department of the University of Mohaghegh Ardabili (UMA), Ardabil, Iran in 2011. His Areas of interest in Research are power system control and operation, adaptive and robust control of power systems, operation and Planning and Power System Restructuring and applications of heuristic techniques in power systems.

Reza Bazyar was born in Tabriz, Iran in 1984. He received the B.S. degree in electrical engineering from Azarbaijan Higher Education & Research Complex (AHERC), Tabriz, Iran, in 2008 and the M.S. degrees in electrical engineering from Department of Engineering, ECE Group, Mohaghegh Ardebili University, Ardebil, Iran, in 2011. He is currently an Engineer of the East Azarbayjan Power Generation Management Company, Iran. His research interests include Economic dispatch, O&M Gas power plant, hybrid energy system, Power system control and operation.

Heidarali Shayanfar received the B.S. and M.S.E. degrees in Electrical Engineering in 1973 and 1979, respectively. He received his Ph. D. degree in Electrical Engineering from Michigan State University, U.S.A., in 1981. Currently, he is a Full Professor in Electrical Engineering Department of Iran University of Science and Technology, Tehran, Iran. His research interests are in the Application of Artificial Intelligence to Power System Control Design, Dynamic Load Modeling, Power System Observability Studies, Voltage Collapse, Congestion Management in a Restructured Power System, Reliability Improvement in Distribution Systems and Reactive Pricing in Deregulated Power Systems. He has published more than 405 technical papers in the International Journals and Conferences proceedings. He is a member of Iranian Association of Electrical and Electronic Engineers and IEEE.

Oveis Abedinia received the B.S. and M.Sc. degrees in Electrical Engineering from Azad University, Ardabil and Science and Technology Research Branch, Tehran, Iran in 2005 and 2009, respectively. Currently, he is a Ph. D. student in Electrical Eng. Department, Semnan University, Semnan, Iran. His areas of interest in research are Application of Artificial Intelligence to Power System and Control Design, Load and Price Forecasting, Distribution Generation, Restructuring in Power Systems, Congestion Management, Optimization.

Hossein Gholamalitabar Firoozjaee was born in Babol, Mazandaran, Iran, in 1988. He received the B.S. degree in electrical engineering from the University of Nooshirvanibabol, mazandaran, iran, in 2010. He is currently M.S. degree student in electrical engineering group from Mohaghegh Ardebili University, Ardebil, Iran. His current research interests are in power market, renewable energy and optimization with artificial algorithms.

SESSION

DATA MINING AND APPLICATIONS

Chair(s)

TBA

Using Social Media to Answer Support Questions

Kivanc Ozonat and Claudio Bartolini
HP Labs
1501 Page Mill Road
Palo Alto, CA
kivanc.ozonat@hp.com claudio.bartolini@hp.com

ABSTRACT

Users frustrated with corporate helpdesks are utilizing internet searches and social media sites for support purposes. There is a wealth of support-related content available publicly; supplier's web sites, blogs, product forums are just some examples. HP is in an optimal position to deliver a platform that utilizes the publicly available content to automatically answer corporate users' support questions.

We identify three primary technical challenges on the design of an automated platform that uses social media to answer support questions: understanding the context in which the question is asked, finding and retrieving the resources in the social media where the question has been discussed, and organizing the content retrieved from the social media resources in a user-friendly way. We apply novel statistical clustering and data mining techniques to address these challenges on the design of an automated platform that answers support questions based on content from social media.

1. INTRODUCTION

As the number of Generation Y and millennial employees increases within the corporate environment, so does the trend toward consumerization and self-help. Many employees now find it natural to use social networking sites to resolve issues they encounter with home computers, appliances, and automobiles. So, it is only natural the same employees would follow a similar process when a problem or issue arises at the office.

Users frustrated with corporate helpdesks are utilizing internet searches and social media sites for support purposes. There is a wealth of support-related content available publicly; supplier's web sites, blogs, product forums are just some examples. HP is in an optimal position, given our unique combination of client technologies and Intellectual Property (think Watercooler), and continuing RD, to deliver an automated platform that uses social media content to answer IT support questions. Yet, there are various technical challenges on the design of such an automated IT support platform:

"Understanding" the context in which the question is asked: An RD engineer at HP is unlikely to have the same hardware and software requirements and needs as, for example, a human resources manager at Walmart. The platform should have knowledge of the IT assets of each user, and leverage this knowledge to better understand the context in which the user asks their question.

Finding the resources in the social media where the question has been discussed: There are billions of websites on the world-wide web, it will be an unfruitful effort to blindly crawl and retrieve every piece of content. The crawlers that will retrieve content from the social platforms should be designed such that they "know" where to look for information on each social platform.

Organizing the content retrieved from the social media resources in a user-friendly way: Presenting the user with large amounts of redundant data in an unorganized form will be of little or no use to the user; the data needs needs to be presented to the user in an organized, easy-to-navigate way.

We apply novel statistical clustering and data mining techniques to address the challenges on the design of an automated platform that answers support questions based on content from social media.

For each corporate customer, we have available to us a set of seed URLs of the customer's main corporate IT support sites. We are further provided with each user's organization, job function, and the devices and business applications used for work. The empirical data will be available from sources such as Active Directory, IT Asset Management systems, or desktop management systems.

We crawl the customer's IT sites, starting from this set of seed URLs. The crawler is directed, i.e., it focuses on the hardware and software the user uses or is likely to use in his/her work. Our directed crawlers retrieve content from the customer's IT support sites (as well as any IT Sharepoint sites) that are likely to be of relevance to the user's environment. The retrieved content constitutes the user-centric corpus.

Then concepts are extracted from the corpus using co-occurrence based techniques [1]. The concepts include single words as well as n-tuples, where n>1. A semantics graph is then constructed that reflects the relations between the extracted concepts. The nodes of the graph are the concepts, while the edges connecting the nodes have weights, representing the distances between the concepts. A small distance between two tags indicates that the two tags are highly related to each other. In computing the distances, we take into account how frequently two concepts appear in the same paragraphs, on the same pages, and on the pages that have links between them. If two tags appear frequently, then their distance is set to be small.

Our approach to extracting concepts and their relations is critical for our platform to understand the concept in which a user asks an IT support question. Through directed crawling, we focus our corpus to the customer's IT support pages that are most relevant to the individual user. This helps us extract concepts and concept relations specific to the user's

context and environment.

We first identify the platforms in the social media that may be of relevance to IT technical support. Then, for each platform, we design a crawler that retrieves content to our repository from the platform. Since the crawler is designed for specifically for the platform, it "knows" which parts of the site to focus on, e.g., which links are more likely to contain the technical support discussions. Organizing the retrieved content

The content retrieved from the social media resources often includes too much redundant information, since the question being asked is likely to have been discussed in multiple social platforms. Presenting the user with large amounts of redundant data in an unorganized form will be of little or no use to the user; such an approach will likely require more effort on the part of the user than if the user had gathered the content through a Google search.

Statistical clustering techniques are applied to organize the content into clusters. Further, we propose a hierarchical clustering approach which organizes the content in a tree structure - so that the user can navigate easily between the clusters. For instance, the user can initially select the expected number of entries in each cluster; if the user then decides to increase the number of entries, s/he can navigate to the parent nodes, or if s/he decides to reduce the number of entries, s/he can navigate to the children nodes without having to reconstruct the clustering tree.

We note that the retrieved content from a social platform has multiple views. For instance, if the content is being retrieved from a forum, there are at least two views: the thread title and the thread content. The thread title (often consisting of just a few words) has a very different characteristic than the thread content (often consisting of at least several sentences), making it infeasible to combine the two into a (feature) vector to feed into a single clustering algorithm.

To address the issue that the retrieved content has multiple views, we design a set of clustering techniques called multi-view clustering techniques [2]. In multi-view clustering, each view has its own clustering algorithm, yet the algorithms are dependent on each other. In particular, we design a clustering tree based for each view, and each clustering tree is grown and pruned with feedback from the other clustering trees. For instance, in the case of two views, thread titles and thread content, we introduce a common penalty function, and the two trees are trained to minimize the common penalty function. In this case, the common penalty function is selected to be the clustering disagreement probability between the two trees with constraints on the entropy (size or depth) of the trees.

Our solution has been used to build an engine that accepts enterprise support desk questions as input, and outputs the questions/answers that best match the inputted IT question.

For the questions/answers, we used our crawlers to build a repository that consists of the 75,000 questions that we downloaded from an enterprise IT discussion forum called serverfault.com.

Our engine has multiple sub-engines. One sub-engine accepts the IT question from the user as input, and finds the concepts from the semantics graph that best reflect the question. A second sub-engine analyzes each question/answer in the 75,000 question/answer repository, and for each question/answer pair, it finds the concepts that reflect the pair. Finally, a third sub-engine matches the input question with the question/answer pairs in the repository based on the the concepts and the graph.

As an example, in response to the user input (see the figure on the left) "I have a problem with configuring nginx. I want the nginx to make requests to the HTTP server to upload files. In the past, the HTTP server was responsible for the uploads and the requests," our system extracted "nginx", "HTTP server" and "upload" as concepts, and related the "HTTP server" to another concept "Apache". Then, it retrieved the following question (with its answer) from the repository (see the figure on the right): "I recently put nginx in front of apache to act as a reverse proxy. Up until now Apache handled directly the requests and file uploads. Now, I need to configure nginx so that it sends file upload requests to apache". We note that this was in fact the closest question to the user input.

There are many platforms that aggregate and present content from social media for different purposes. However, to the best of our knowledge, our solution is unique in at least two ways: First, we build a content corpus specifically designed for the individual user taking into account the user's IT environment; the user-specific content corpus is then used to build a concept graph customized for the user's context.

This provides us with the ability to understand the context in which the user has asked their question. Second, we organize the retrieved content by multi-view clustering. Thus, the amount of redundant information the user is presented minimized; rather the user is presented with content grouped into clusters that can be easily navigated.

2. KEYWORD EXTRACTION

Keyword extraction techniques are often based on the tfidf method. The tfidf method compares the word frequencies in the repository with the word frequencies in the sample text; if the frequency of a word in the sample text is high while its frequency in the repository is low, the word is extracted as a keyword.

While the tfidf-based techniques are known to perform well in many text mining applications, they have a major shortcoming in the context of mining customer forum threads. A customer forum thread typically contains only few sentences and words, making it difficult to obtain reliable statistics based on word frequencies. Many relevant words appear only once in the thread, making it difficult to distinguish them from the other, less relevant words of the thread.

An alternative approach would be to form a vector of keywords in the repository of forum threads, and, generate a binary features vector for each thread. If the i^{th} repository keyword appears in the thread, the i^{th} element of the thread's feature vector is 1, and if the keyword does not appear in the thread, the i^{th} element of the thread's feature vector is 0.

The question with this simple alternative approach is then that of generating keywords in a given repository. We apply three different techniques:

- Remove only stop-words: We only filter out stop words (e.g., if, and, we, etc.) from the repository, and let the vector of keywords be the set of all remaining distinct repository words.
- The tfidf method: We apply the tfidf method on the entire repository by comparing the word frequencies

in the repository with word frequencies in the English language. If the frequency of a word is high in the repository and low in the English language, we take the word as a keyword.

- Term co-occurrence: The term co-occurrence method extracts keywords from the repository without comparing the repository frequencies with the English language frequencies. This method is explained next [9].

2.1 Term Co-occurrence

Let N denote the number of all distinct words in the repository of forum threads. We construct a $N \times M$ co-occurrence matrix, where M is pre-selected integer with $M < N$. We typically take M to be 500. We index all distinct words by n, i.e., $1 \leq n \leq N$. We index the most frequently observed M words in the repository by m such that $1 \leq m \leq M$.

The $(n.m)$ element (i.e. ,n^{th} row and the m^{th} column) of the $N \times M$ co-occurrence matrix counts the number of times the word n and the word m occur together. Consider the word ẅirelesswith index n and the word c̈onnectionẅith index m, and that ẅirelessänd c̈onnectionöccur together 218 times in the repository. Then, the $(n.m)$ element of the co-occurence matrix is 218.

If the word n appears independently from the words $1 \leq m \leq M$ (the frequent words), the number of times the word n co-occurs with the frequent words is similar to the unconditional distribution of occurrence of the frequent words.

On the other hand, if the word n has a semantic relation to a particular set of frequent words, then the co-occurrence of the word n with the frequent words is greater than the unconditional distribution of occurrence the frequent words.

We denote the unconditional probability of a frequent word m as the ex- pected probability p_m and the total number of co-occurrences of the word n and fre- quent terms as c_n. Frequency of co-occurrence of the word n and the word m is written as $freq(n, m)$. The statistical value of χ^2 is defined as

$$\chi^2(n) = \sum_{1 \leq m \leq M} \frac{freq(n,m) - N_n p_m}{n_m p_m}. \quad (1)$$

2.2 Clustering of Frequent Terms

We cluster two or more frequent terms together in either of the following two conditions:

- The frequent words m_1 and m_2 co-occur frequently with each other.
- The frequent words m_1 and m_2 have a similar distribution of co-occurrence with other words.

To quantify the first condition of m_1 and m_2 co-occurring frequently, we use the mutual information between the occurrence probability of m_1 and that of m_2.

To quantify the second condition of m_1 and m_2 having a similar distribution of co-occurrence with other words, we use the Kullback-Leibler divergence between the occurrence probability of m_1 and that of m_2.

3. ALGORITHM

We design a statistical clustering algorithm to minimize (in the Lloyd-optimal sense) the error probability given in (2) under the cluster entropy constraints. Gaussian mixture models have been used extensively in the literature to design generative algorithms for data clustering. Such algorithms are often based on the EM algorithm [5]; however, there also exists alternative training approaches such as Gauss mixture vector quantization (GMVQ) [8, 11, 12, 13, 16]. The EM algorithm assumes that the underlying data follows a Gaussian mixture distribution and tries to fit a Gaussian mixture model to the data, while the GMVQ is a Lloyd clustering algorithm and it does not make any assumptions about the statistics of the underlying data.

We use the GMVQ to design a multi-view hierarchical clustering algorithm. Our choice of GMVQ (over the EM) is motivated by the intractability of the EM solution in minimizing (2) through a hierarchical clustering scheme. We first extend the GMVQ to design a hierarchical (tree-structured) clustering algorithm. We then extend it further to the multi-view setting, where the goal is to minimize the disagreement between two different views of the training data as expressed in (2). The two views in our setting are the thread titles and the thread content.

In section 4.1, we provide an overview of the GMVQ and include the iterative solution for the GMVQ. In section 4.2, we extend the GMVQ to design a tree-structured clustering algorithm. Finally, in section 4.3, we extend it further to the multi-view setting to minimize (2).

3.1 Gauss mixture vector quantization (GMVQ)

Consider the training set $\{z_i, 1 \leq i \leq N\}$ with its (not necessarily Gaussian) underlying distribution f in the form $f(Z) = \sum_k p_k f_k(Z)$. The goal of GMVQ is to find the Gaussian mixture distribution, g, that minimizes the distance between f and g. It has been shown in [8] that the Gaussian mixture distribution g that minimizes this distance (i.e., minimizes in the Lloyd-optimal sense) can be obtained iteratively with the following two updates at each iteration:

i. Given μ_k, Σ_k and p_k for each cluster k, assign each z_i to the cluster k that minimizes

$$\frac{1}{2}\log(|\Sigma_k|) + \frac{1}{2}(z_i - \mu_k)^T \Sigma_k^{-1}(z_i - \mu_k) - \log p_k, \quad (2)$$

where $|\Sigma_k|$ is the determinant of Σ_k. We note that (5) is also known as the QDA distortion.

ii. Given the cluster assignments, set μ_k, Σ_k and p_k as

$$\mu_k = \frac{1}{\|S_k\|} \sum_{z_i \in S_k} z_i, \quad (3)$$

$$\Sigma_k = \frac{1}{\|S_k\|} \sum_i (z_i - \mu_k)(z_i - \mu_k)^T, \quad (4)$$

and

$$p_k = \frac{\|S_k\|}{N}, \quad (5)$$

where S_k is the set of training vectors z_i assigned to cluster k, and $\|S_k\|$ is the cardinality of the set.

3.2 Tree-structured Gauss Mixture Vector Quantization

We use the BFOS algorithm to design a hierarchical (i.e., tree-structured) extension of GMVQ [13]. The BFOS algorithm requires each node of a tree to have two linear functionals such that one of them is monotonically increasing and the other is monotonically decreasing. Toward this end, we view the QDA distortion (5) of any subtree, T, of a tree as a sum of two functionals, u_1 and u_2, such that

$$u_1(T) = \frac{1}{2}\sum_{k\in T} l_k \log(|\Sigma_k|) + \frac{1}{N}\sum_{k\in T}\sum_{z_i\in S_k}\frac{1}{2}(z_i-\mu_k)^T\Sigma_k^{-1}(z_i-\mu_k), \quad (6)$$

and

$$u_2(T) = -\sum_{k\in T} p_k \log p_k \quad (7)$$

where $k \in T$ denotes the set of clusters (i.e., tree leaves) of the subtree T, and μ_k, Σ_k, p_k and the set S_k are as defined in section 4.1.

The magnitude of u_2/u_1 increases at each iteration. This is a key point of the design as, then, pruning is terminated when the magnitude of u_2/u_1 reaches λ, resulting in the subtree minimizing $u_1 + \lambda u_2$.

3.3 Iterative and multi-view TS-GMVQ

We iteratively design two clustering trees, one using the thread title feature vectors, $X_{i,1}$, and the other using the thread content feature vectors, $X_{i,2}$. At each iteration, the two trees are designed (includes tree growing and tree pruning) jointly to minimize (2), the disagreement probability with constraints on the entropy of clusters.

At each iteration, the tree growing starts with a single node tree out of which two child nodes are grown. The Lloyd updates, i.e., (5)-(8), are applied to these two child nodes, minimizing (5), i.e., assigning each training vector to one of the two nodes. Then, one of the two nodes is selected to be split into a pair of new nodes. The selected node is the one, among all the existing nodes, that minimizes (2) after the split. The Lloyd updates, (5)-(8) are then applied to each pair of new nodes, minimizing (10). This procedure of growing a pair of child nodes out of one of the existing nodes, and running the Lloyd updates within the new pair of nodes is repeated until a fully-grown tree is obtained.

We denote the title feature tree by T_1 and the content feature tree by T_2. The trees, T_1 and T_2, are designed using the BFOS algorithm to minimize (2). This implies that, at iteration m, the subtree functionals for T_1 are

$$u_1^m(T) = \sum_{k\in T_1^m}\sum_{x_i\in S_k} P(\alpha_1^m(x_{i,1}) \neq \alpha_2^{m-1}(x_{i,2})), \quad (8)$$

and

$$u_2^m(T) = -\sum_{k\in T_1^m} p_k \log p_k. \quad (9)$$

The u_1 and u_2 functionals for T_2 are analogous.

We observe, by comparing (3) and (12), that

$$\sum_{T_1} u_2^m(T) = R_v \quad (10)$$

and, by comparing (1) and (11), that

$$\sum_{T_1} u_1^m(T) = P(\alpha_1^m(X_1) \neq \alpha_2^{m-1}(X_2)). \quad (11)$$

The u_2^m functional in (12) is identical to the u_2 functional in section 4.2. As for the u_1^m functional, we use (9) for growing the tree and (11) during the pruning. This is possible since (11) is also a linear and monotonically decreasing functional.

Based on the discussion in this section, the multi-view algorithm consists of the following steps (we omit the initialization steps):

i. Grow a TS-GMVQ T_1 tree for the training set $X_{i,1}$, using u_1 and u_2 as given in (9) and (10), respectively.

ii. Grow a TS-GMVQ tree T_2 for the training set $X_{i,2}$, analogously to (i).

iii. Given the tree T_2, prune the fully-grown T_1, using the BFOS algorithm with u_1 and u_2 as given in (11) and (9), respectively.

iv. Given the tree T_1, prune the fully-grown T_2, analogously to (iii).

v. Stop if the change in the cost function, given in (2), from one iteration to the next is less than some ϵ (We set ϵ such that the algorithm stops if the change in (2) is less than 1 percent from one iteration to the next). Else go back to step (i).

4. EXPERIMENTS

We've tested the hierarchical multi-view approach on the customer threads included in the forums over the web. The forum is intended to help IT customers (both the enterprise customers and the consumers) with troubleshooting their product-related problems. Each thread includes a post by a customer, explaining a problem, followed by replies by others. Each thread has a a title, in addition to thread content.

We've compared the hierarchical multi-view clustering approach to 4 other clustering techniques (EM, GMVQ, TS-GMVQ and agglomerative hierarchical clustering) under 3 different feature vector constructions. The comparisons are performed on a set of 75,000 threads in 30 clusters for the product line. In each comparison, we measured the misclassification error, which is the probability of a customer query being assigned to a cluster of a product problem different from the problem expressed in the query. The ground truth for the threads, problems and queries have been established by the website owners, independently of the author of this paper.

4.1 Feature vectors

The i^{th} thread has two feature vectors, the thread title $x_{i,1}$ and the thread content $x_{i,2}$. Each feature vector is a W-length binary (0 or 1) vector, where W is the total number of unique words used across all threads. Each word is indexed by w, where $1 \leq w \leq W$.

The w^{th} element of $x_{i,1}$ is 1 if and only if the word w occurs in the title of the i^{th} thread. Similarly, the w^{th} element of $x_{i,2}$ is 1 if and only if the word w occurs in the content of the i^{th} thread. We exclude the stop-words (e.g., and, if, such, etc.) from the feature vectors.

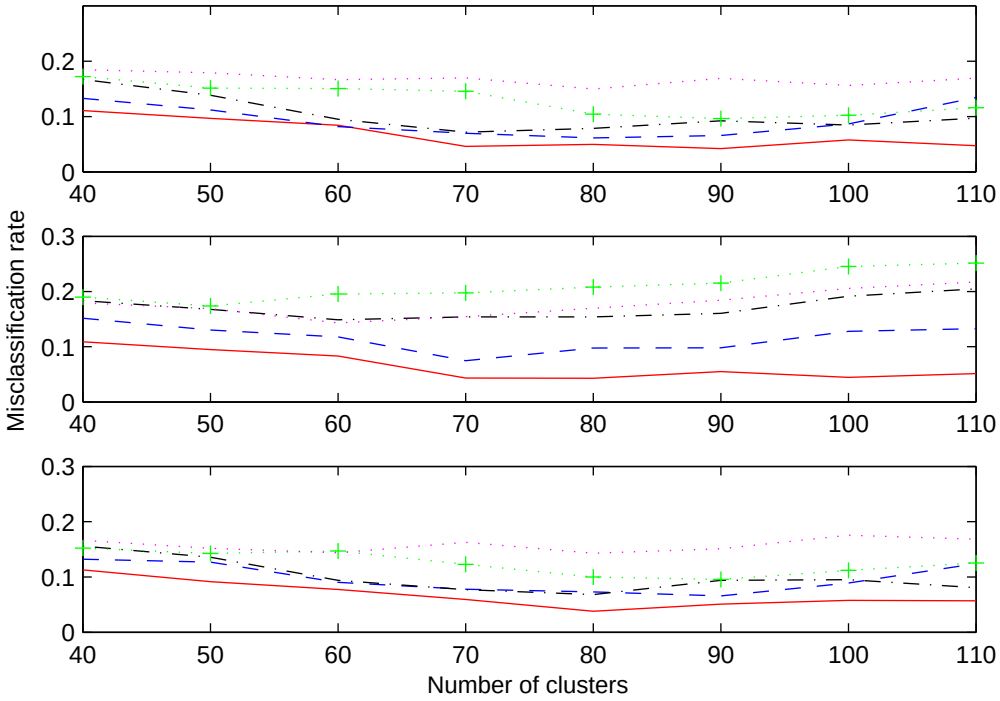

Figure 1: The classification error rate as a function of the number of clusters for the notebook computer thread. The tfidf keyword extraction. The multi-view approach (red solid line) is compared to the GMVQ (blue dashed line), EM (black dash-dot line), TS-GMVQ (magenta dotted line) and agglomerative hierarchical clustering (green dot-plus line). The top plot shows the setting with $y_i = x_{i,1}$, the middle plot shows the setting with $y_i = x_{i,2}$ and the bottom plot shows the setting with $y_i = [x_{i,1}\ x_{i,2}]$.

4.2 Comparisons

We've compared the hierarchical multi-view clustering approach to the EM algorithm, standard GMVQ algorithm, TS-GMVQ algorihm and agglomerative clustering. In each comparison, we've tested three different feature vector constructions for the EM, GMVQ, TS-GMVQ and agglomerative clustering: the feature vector is $x_{i,1}$, the feature vector is $x_{i,2}$, and the feature vector is $[x_{i,1}\ x_{i,2}]$.

4.2.1 Feature vector constructions

Denoting the feature vector of the training samples by y_i, we consider three feature vector constructions:

i. $y_i = x_{i,1}$. The clustering algorithm takes only the thread titles into account. The thread content are ignored.

ii. $y_i = x_{i,2}$. The clustering algorithm takes only the thread content into account. The thread titles are ignored.

iii. $y_i = [x_{i,1}\ x_{i,2}]$. The clustering algorithm takes into account both the thread titles and the thread content.

We compare the hierarchical multi-view approach with the EM, GMVQ, TS-GMVQ and agglomerative clustering under each of these three feature vector construction settings. To avoid any confusion, we emphasize that, the three different feature vector constructions apply only to the EM, GMVQ, TS-GMVQ and agglomerative clustering. The hierarchical multi-view algorithm, on the other hand, always makes use of both $x_{i,1}$ and $x_{i,2}$ in our experiments.

4.2.2 Compared algorithms

i. EM: We use the standard EM algorithm. At each iteration, the E-step updates the membership probabilities, $v_{i,k}$, for each cluster k and sample i, while the M-step updates the mean, covariance and the probability of occurrence for each cluster k as

ii. GMVQ: The standard GMVQ algorithm updates are as given in (5)-(8) in section 4.1.

iii. TS-GMVQ: The TS-GMVQ is grown and pruned by the BFOS algorithm using (9) and (10) as described in section 4.2.

iv. Agglomerative hierarchical clustering: We start with N clusters, where N is the number of threads in the training set, and apply agglomerative clustering with the distance criterion given in (5). At each iteration, we merge the two clusters, whose closest feature vectors are closest. In other words, at each iteration, for each pair of clusters, c_k and c_m, we compute the distances between the feature vectors of c_k and the feature vectors of c_m, and denote the closest distance by $d_{k,m}$. We merge the two clusters with the minimum $d_{k,m}$.

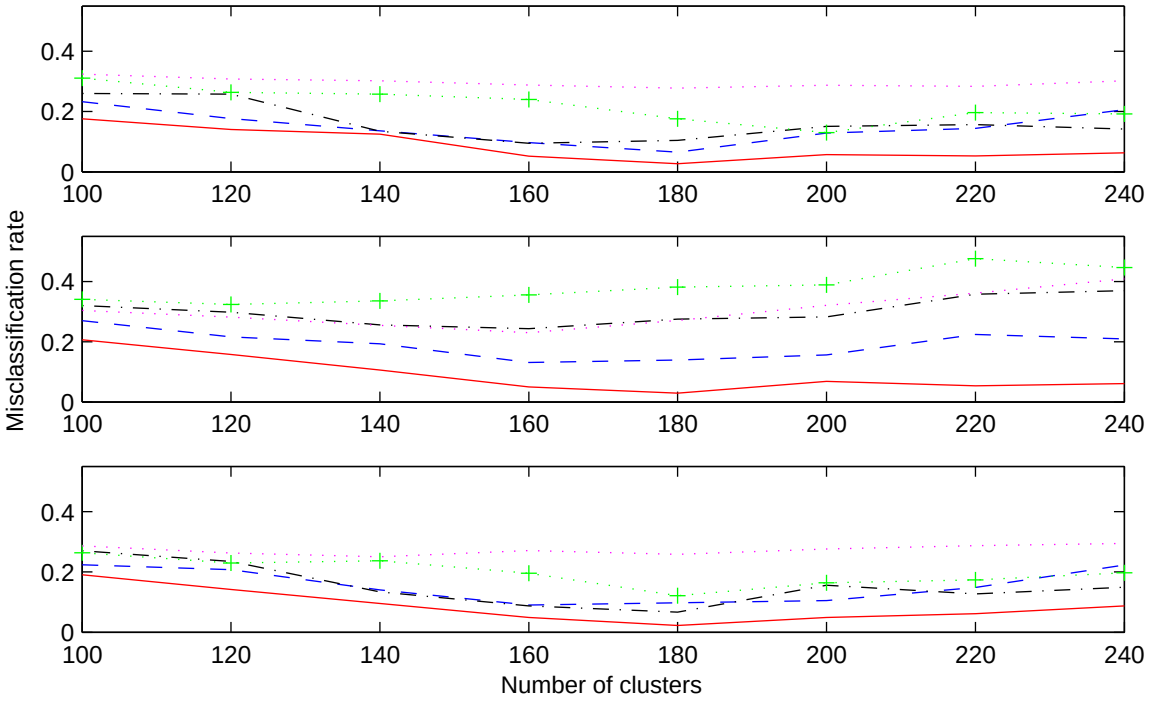

Figure 2: The classification error rate as a function of the number of clusters for the notebook computer thread. The term co-occurrence keyword extraction. The multi-view approach (red solid line) is compared to the GMVQ (blue dashed line), EM (black dash-dot line), TS-GMVQ (magenta dotted line) and agglomerative hierarchical clustering (green dot-plus line). The top plot shows the setting with $y_i = x_{i,1}$, the middle plot shows the setting with $y_i = x_{i,2}$ and the bottom plot shows the setting with $y_i = [x_{i,1}\ x_{i,2}]$.

4.3 Discussion of Results

Fig. 1 shows the classification error as a function of the number of clusters for the threads in the notebook PC set. The tfidf method is used for extracting keywords. In each plot, the classification error rate of the multi-view approach (red solid line) is compared to that of the GMVQ (blue dashed line), EM (black dash-dot line), TS-GMVQ (magenta dotted line) and agglomerative hierarchical clustering (green dot-plus line). The top plot shows the setting, where the training vector for GMVQ, EM, TS-GMVQ and agglomerative hierarchical clustering are the thread title feature vectors, i.e., $y_i = x_{i,1}$. In this setting, the multi-view approach outperforms the other four algorithms, implying that the inclusion of the thread content to the training process improves the classification.

The middle plot in Fig. 1 shows the setting where the training vectors for the four approaches are the thread content feature vectors, i.e., $y_i = x_{i,2}$. Similar to the setting with $y_i = x_{i,1}$, the multi-view approach leads to the minimum classification error, implying that the thread title should be included in the training to improve the classification accuracy.

The bottom plot in Fig. 1 shows the classification errors for the setting where both the thread titles and thread content are included as feature vectors, i.e., $y_i = [x_{i,1}\ x_{i,2}]$. The performance of the four algorithms (GMVQ, EM, TS-GMVQ and agglomerative hierarchical clustering) all improve compared to the settings shown in the top and middle plots. Once again, this implies that both thread titles and thread content should be included in the feature vectors. However, more importantly, the multi-view approach still outperforms the four algorithms.

It is not surprising for the multi-view approach to outperform the other four approaches in the setting with $y_i = [x_{i,1}\ x_{i,2}]$, because customer queries are more similar to thread titles (short, a few words) than to thread content. Thus, a clustering of thread titles, trained with guidance from the thread content, lead to a more accurate retrieval than a clustering of combined thread titles and thread content.

In Fig. 2, we show the classification error rates. The difference is that here the term co-occurrences are used for extracting the keywords. A comparison with Fig. 1 indicates that, for each clustering strategy, the term co-occurrence keyword extraction leads to a more accurate classification (i.e., lower classification error rates) than the tfidf keyword extraction.

5. CONCLUDING REMARKS

Customers discuss product malfunctions, errors and problems through the threads they post on business-supported online forums. It is not feasible to use web search algorithms such as PageRank for retrieving the relevant threads in response to a search query in the forum since the threads lack recommendation links. We provided a keyword extrac-

tion technique based on term co-occurrences that performs better than traditional tfidf-based techniques. Further, we provided statistical, iterative and multi-view approach to searching and retrieving the customer threads in such forums. The hierarhical clustering of the threads makes it possible to present the retrieved threads in a rank-ordered fashion to the customer.

References

[1] S. Bickel and T Scheffer. Multi-view clustering. In Proceedings of the IEEE International Conference on Data Mining, 2004.

[2] A. Blum and T. Mitchell. Combining labeled and unlabeled data with co-training. In Proceedings of the Conference on Computational Learning Theory, pages 92-100, 1998.

[3] U. Brefeld and T. Scheffer. Co-EM support vector learning. In Proceedings of the International Conference on Machine Learning, 2004.

[4] S. Brin and L. Page. The anatomy of a large-scale hypertextual web search engine. In Proceedings of the 7th International World Wide Web Conference, pp. 107-117, 1998.

[5] A. P. Dempster, N. M. Laird, and D. B. Rubin. Maximum likelihood from incomplete data via the EM algorithm. Journal of the Royal Statistics Society, 39(1):1-21, 1977.

[6] M. Figueiredo and A. K. Jain. Unsupervised learning of finite mixture models. IEEE Transactions on Pattern Analysis and Machine Intelligence, 24:3 , pp. 381-396, March 2002.

[7] R. Ghani. Combining labeled and unlabeled data for multiclass text categorization. In Proceedings of the International Conference on Machine Learning, 2002.

[8] R.M. Gray and T. Linder. Mismatch in high rate entropy constrained vector quantization. IEEE Trans. Inform. Theory, Vol. 49, pp. 1204-1217, May, 2003.

[9] Y Matsuo. Keyword extraction from a single document using word co-occurrence statistical information. International Journal on Artificial Intelligence Tools, Vol. 13, pp. 157-169, 2004.

[10] K. Nigam and R. Ghani. Analyzing the effectiveness and applicability of co-training. In Proceedings of Information and Knowledge Management, 2000.

[11] D.B. O'Brien, M. Gupta, R.M. Gray, and J.K. Hagene. Automatic classification of images from internal optical inspection of gas pipelines. In Proceedings of the ICPIIT VIII Conference 2003, Houston.

[12] D.B. O'Brien, M. Gupta, R. M. Gray, and J. K. Hagene. Analysis and classification of internal pipeline images. In Proceedings of ICIP 2003, Barcelona, Spain.

[13] K. Ozonat, and R.M. Gray. Gauss mixture model-based classification for sensor networks. In Proceedings of the IEEE DCC 2006.

[14] K. Ozonat. Multi-view Clustering Trees for Search and Retrieval in Customer Product Forums. In Proceedings of the ICAI 2010.

[15] L. Page, S. Brin, R. Motwani, and T. Winograd. The PageRank citation ranking: Bringing order to the web. Technical report, Stanford University, 1998.

[16] K. Pyun, C.S.Won, J. Lim, and R.M. Gray. Texture classification based on multiple Gauss mixture vector quantizers. In Proceedings of Multimedia and Expo, 2002, pp. 501-4, 2002

[17] R. A. Redner and H. F. Walker. Mixture densities, maximum likelihood and the EM algorithm. SIAM Review, 26(2):195-239, 1984.

[18] J. Shen, Y. Zhu, H. Zhang, C. Chen, R. Sun, and F. Xu. A content-based algorithm for blog ranking. Internet Computing in Science and Engineering, 2008.

[19] G. Xu and W.Y. Ma. Building implicit links from content for forum search. In Proceedings of the 29th International Conference on Research and Development in Information Retrieval, 2006.

[20] D. Yarowsky. Unsupervised word sense disambiguation rivaling supervised methods. In Proceedings of the 33rd Meeting of the Association for Comp. Linguistics, 1995.

[21] Y Matsuo. Keyword extraction from a single document using word co-occurrence statistical information. International Journal on Artificial Intelligence Tools, Vol. 13, pp. 157-169, 2004.

[22] G. Karypis and V. Kumar. A coarse-grain parallel formulation of multilevel k-way graph partitioning algorithm. Siam Conference on Parallel Processing for Scie

CLUSTRE – Clustering on Statistics Trees

Lixin Fu,
Depart of Computer Science
University of North Carolina At Greensboro
167 Petty Building 317College Ave.,
Greensboro, NC 27412
lfu@uncg.edu

Keywords Clustering, Data Mining, Algorithms

Abstract In this paper we give a new clustering algorithm based on statistics trees called CLUSTRE (CLUstering on Statistics Trees). The input data is first loaded into a statistics trees and then level by level the identified dense units are merged and expanded so that a minimum number of dense regions are formed. CLUSTRE is robust, interactive, fast and scalable. Experiments show the effectiveness of the new clustering method.

1. INTRODUCTION

As an important data mining task, data clustering is to find clusters or dense objects embedded in database. The data objects are more similar while inter-cluster similarity is lower. Clustering researches have focused on designing scalable and high quality classifiers on large relational databases or multidimensional data warehouses. The challenges include the scalability issue, construction interaction with users and integration with other data mining algorithms [1].

In this paper we give a new clustering algorithm based on statistics trees [5] called CLUSTRE (CLUstering on Statistics Trees). The input data is first loaded into a statistics trees and then level by level the identified dense units are merged and expanded so that a minimum number of dense regions are formed.

Most clustering algorithms handle only numerical attributes. For example, k-MEANS seeks full-dimensional clusters by selecting a set of relevant attributes and assigning weights [2]. Mihael Ankerst et al developed OPTICS algorithm through the creation of an augmented cluster-ordering of database objects [3]. The problems are that input parameters are hard to determine and results are sensitive to them. In addition, it is infeasible to several million of high-dimensional objects. CLARANS [6] is a random searching and hill-climbing clustering algorithm based on graph and a data structures called R*-trees [7].

In [4], PROCLUS (Papered CLUStering) is based on dimensions as well as points, as a generalization of feature selection and medoid techniques using locality analysis. The algorithm has three phases: 1) initialization: reduce set to do climbing, 2) iteration: find best set of medoids using hill-climbing (like CLARANS, gradually improving medoids) on corresponding dimensions. It uses Manhattan segment distance to assign points to medoids, and 3) cluster refinement. This is an interesting algorithm but may generate many overlaps of reported dense units called partitions.

DBSCAN [8] is a famous density based clustering algorithm that can cluster different shapes. It also suffers the scalability problem. BIRCH [9] is a very popular and classic clustering algorithm that can handle noisy data. It is incremental and dynamic. More noticeably, it is scalable. As in DBSCAN, CURE [10] can also cluster different shapes and sizes. It uses multiple representatives and compression to eliminate outliers.

Our work is most closely related to CLIQUE [11] in the sense that both use regions DNF (Disjunctive Normal Form), easy to interpret and both can cluster sub-spaces. CLIQUE uses a bottom-up, self adjoining, and MDL pruning approach. By using a graph DFS traversal and a greedy strategy to find minimum covers of the dense regions. However, it needs multiple passes and is largely overlapping as well. It is not interactive.

CLUSTRE has the following features:

1. robust: not sensitive to individual tuple noise
2. interactive: User specify the parameters such as the collapsed dimensions and minSupport.
4. precise: instead of algorithms based on sampling and reducing dimensions
5. numerical and nominal attributes are OK.
6. not overlapping
7. fast: optimal 1-pass when the tree fits into memory
8. scalable with the size of the database due to the increase of the number of records.

The rest of the paper is given as follows. Next section will briefly review the statistics tree structure and how to load it. Section 3 will detail CLUSTRE itself especially through a 3-D example to visualize and illustrate the clustering process. Some experiments are given in section 4. Section 5 concludes the paper.

2. STATISTICS TREE

Statistics Tree [5] is a multi-dimensional array data structure for dealing with multiple dimensions at the same time. Its internal nodes are used for forming branches to arrive in leaves, which contain aggregates. The aggregates can be any operators, such as SUM, AVG, MIN, MAX and so on. The attribute A_0, A_1, …, A_{k-1}, (with cardinalities d_0, d_1,…,d_{k-1}) corresponds to both dimensions of a relational table R and the levels of the statistics tree. The node at each level contains (index, pointer) pairs. The indexes represent the domain values of the corresponding dimensions (current level where the node is located). The pointers extend query paths to corresponding nodes at the next level. A feature index value called *star value*, denoted by * and located in the right most position following cardinality, represents the ALL value of dimension where the star is; the corresponding *star pointer* extends the path to the next level for a query that has no constraints for dimension where the star pointer starts. In the bottom level are leaves, which are marked by "v" in Figure 1. They only store the aggregation values of the corresponding input record tuple represented by the root-to-leaf paths, rather than records or pointers to records.

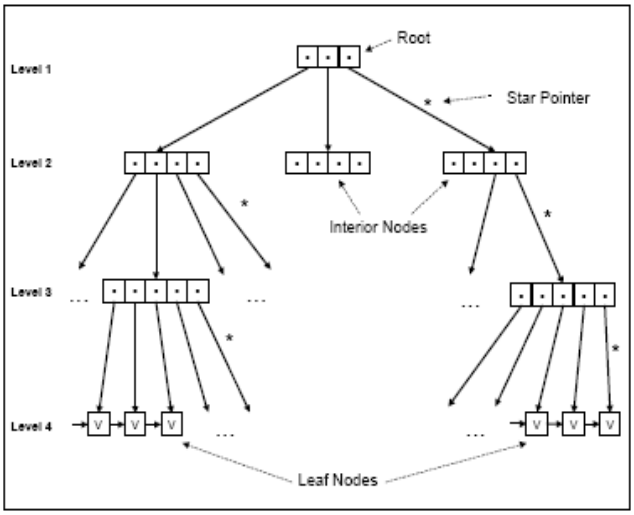

Figure 1: Statistics tree for data set with 3 dimensions.

The count values are initially zero in the leaf nodes. Next, we load the relational data set one record by one record, using the attribute values to update the aggregates and number of star in the leaves. The attribute value is component x_i of the input record $x=(x_0, x_1, \ldots x_{i,\ldots}, x_k)$, where i indicates the current level and k indicates it is a k dimensional relational data set. The update procedure starts at the root (level 0) with record component x_i, and star, then follow the $(x_i+1)^{th}$ pointer and the star pointer to the two nodes at next lower level. All pointed star nodes follow their star pointers arriving at their child star nodes. When reaching the leaves in the bottom level, increment the count values and the star number according to the number of star contained in the corresponding root-to-leaf path. Repeat above steps for each input record until all records have been loaded in this fashion.

Let us use the following 3-D case as an example. We mark the entry 1 in a 3-D cube space, if the case cell is non-empty. For example (0, 1, 3), (0, 1, 4), (0, 1, 5), (0, 1, 6) are marked as 1 in the second row of level 0. Now we create a table according to this example as the input of setting up a statistics tree. The above non-empty cells will be turned in to these four tuples (0, 1, 3; 1), (0,1, 4; 1), (0,1, 5; 1), (0, 1, 6; 1). The right most value is the measure value. In our example, we implement count operation.

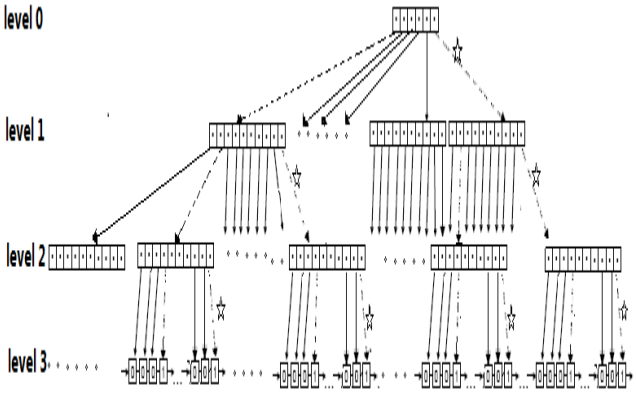

Figure2 : Statistics tree after processing input record (0,1,3).

Let us take three dimensional record tuple (0, 1, 3) as an input example to illustrate the record loading procedure. There are three dimensions A_0, A_1, A_2 with cardinalities d_0=5, d_1=10, and d_2=10, respectively. Figure 2 shows the statistics tree after (0, 1. 3) is loaded into an empty tree and dashed lines indicate its update paths of (0, 1, 3).

3.THE INTERACTIVE CLUSTERING ALGORITHM BASED ON STATISTICS TREES

3.1 Identifying Dense Units According to User's Input Parameters

After we set up a statistics tree and loaded a set of input data records. We need to identify dense unites according to user's input parameters. From the introduction of section 2, we know each leaf stores the aggregation of each root-to-leaf path which represents an input record

tuple. Users will be asked to input a threshold which is called MiniSupport. The leaves/paths/records, whose aggregation is no smaller than the threshold, will be identified as dense units. In other words, only the leaves whose aggregation is no smaller than the MiniSupport will participate the following cluster programs.

Continue above example, the values of threshold could be integers from 1 to 102 based on the loaded statistics tree in Figure 3. If a user inputs 5 as the threshold, only the aggregation of root-to-leaf paths, which represents input records, are no smaller than 5 will be identified as dense units and selected to carry on the following cluster. However, 5 is not an appropriate threshold in this case, because no duplicated record is inputted. No aggregation in the leaf expect leaves of star nodes is bigger than 1. Hence in this case we will set 1 as the threshold to implement the following cluster. Therefore, the selection of threshold for MiniSupport should accord to the feature and real situation of input data set.

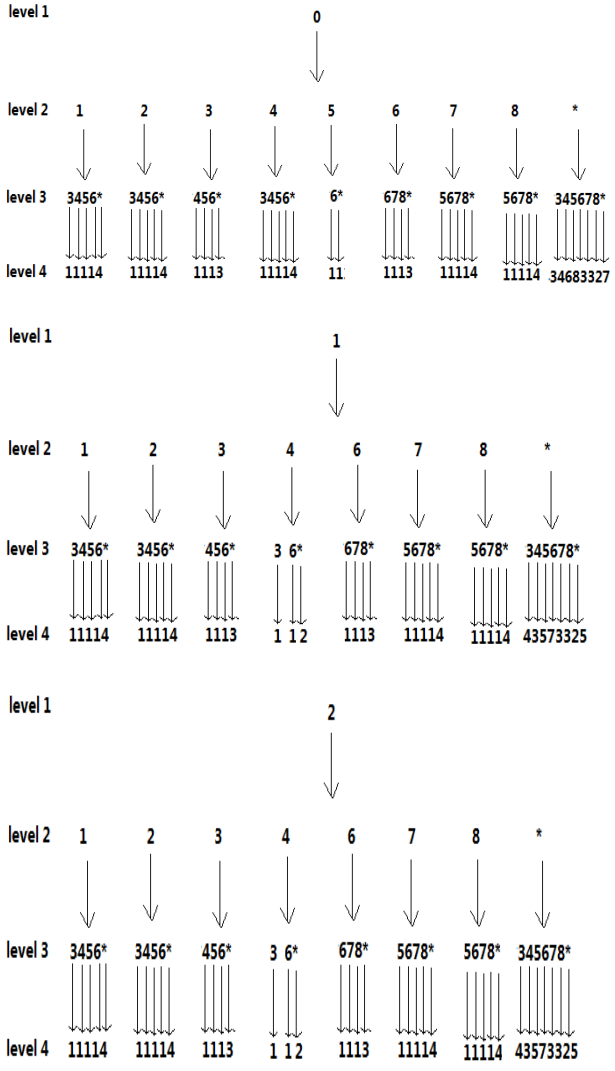

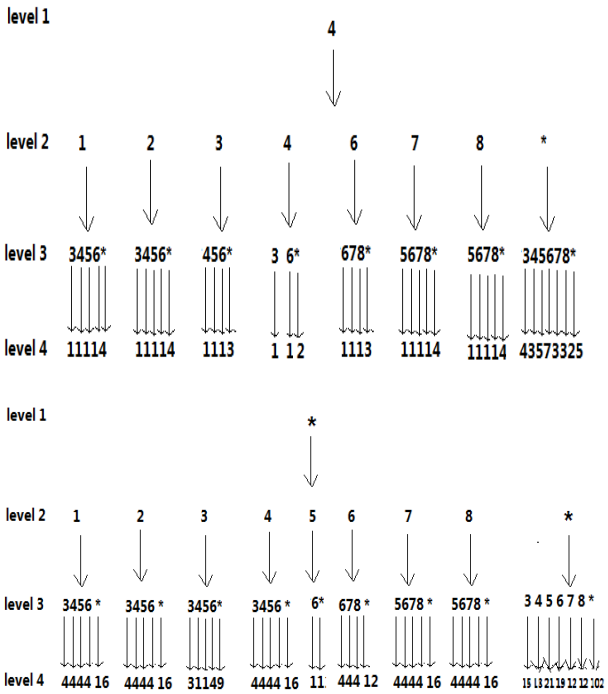

Figure 3 Statistics tree after loading the whole set of above record

3.2 Cover Dense Units with Minimal Number of Regions

When the statistic tree has been set up, clustering works on the tree structure created above. The basic idea is that we form multi-dimensional dense regions and cover them using minimal number of regions. Let us first introduce several terminologies.

Definition 1, **Range [l, h]** represents consecutive values, starting with integer **l** and ending with integer **h minus one** respectively. The volume of the range is **h-l**.

Definition 2, If l1>= l2 and h1<= h2, the boundary values are included, range r_1 [l_1, h_1] is **included** in range r_2 [l_1, h_2]. If r_1 is included in r_2 and l1= l2 or h1= h2, We say range r_1 is **on the end** of range r_2.

Definition 3, A **region** is defined as the Cartesian product of ranges. The volume of a region is the product of the volume of the ranges.

A region can be formed by different ranges, figure 4 shows region R_1 = $range_1$* $range_2$* $range_3$.

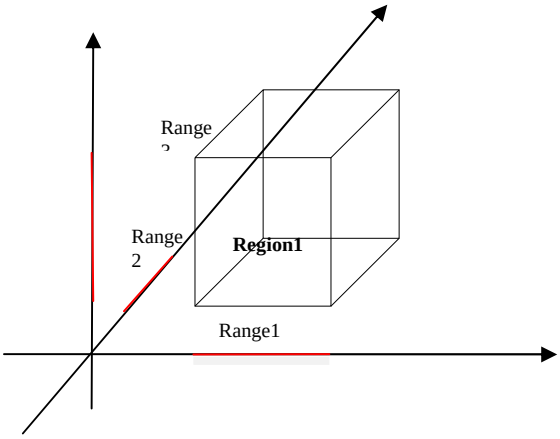

Figure 4 $Region_1 = Range_1 * Range_2 * Range_3$

A region is can be expanded from another region. Region $R_{2=}$ [l, h]*[l^{i1}, h^{i1}]*[l^{i1}, h^{i2}]*...*[l^{is}, h^{is}] , where [l, h] is a range r and [l^{i1}, h^{i1}]*[l^{i2}, h^{i2}]*...*[l^{is}, h^{is}] is region R_3 Figure 5 shows region R_2= [l, h] * R_3 = [l, h] * [l^{31}, h^{31}] * [l^{32}, h^{32}]. The bottom face is region R_3 and the cube is R_2.

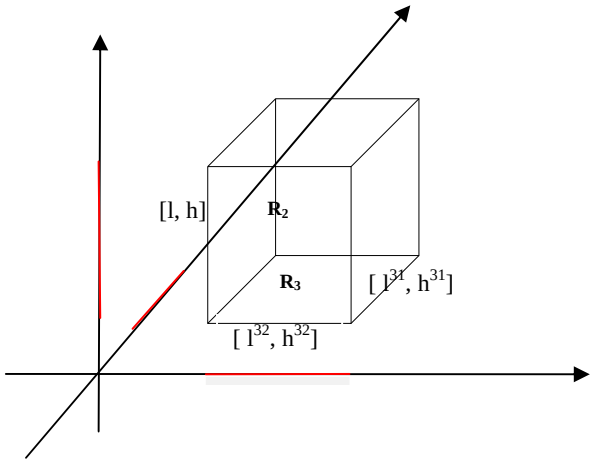

Figure 5 R_2= [l, h] * R_3 = [l, h]*[l^{31}, h^{31}] * [l^{32}, h^{32}].

Definition 4, Region R1 **is included** in region R2 for all the dimensions, each range of R1 is included in the corresponding range of R2. Region R1 = region R2, where all the corresponding ranges are exactly the same. Region R1 is on the end of region R2: if R1 is included in R2 and except that one dimension of which range end of R_2, all other corresponding ranges are exactly the same.

Definition 5, Cut the end region R1 from region R2: if R1 is on the end of R2 and the possible unequal pair of ranges are [l1, h1] and [l2, h2] respectively, [l2, h2]is changed to

[h1, h2], if l1= l2;
[l2, l1], if h1= h2.

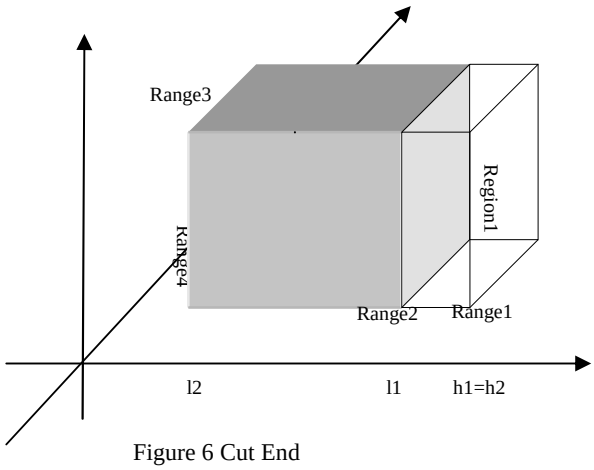

Figure 6 Cut End

For instance, in figure 6, $Range_1$[l1, h1] and $Range_2$ [l2, h2] are the only one pair of ranges that are not equal in the same dimension, where [l1, h1] is included in range [l2, h2], and other ranges of $region_1$ and $region_2$ are equal. So $Region_1$ is included $Region_2$, and $Region_1$ is the end of $Region_2$. We cut $Region_1$, the empty part, from Region2, to change [l2, h2] to [l2, l1] according to definition 5. We then get a shadow part, which is the new $Region_2$.

Region list: a linked list of regions

[l^{11}, h^{11}] * [l^{12}, h^{12}] * …*[l^{1n}, h^{1n}]: $measure_{1;}$ ($region_1$)

[l^{21}, h^{21}] * [l^{22}, h^{22}] * …*[l^{2m}, h^{2m}]: $measure_{2;}$

.....

.....

.....

[l^{i1}, h^{i1}] * [l^{i2}, h^{i2}] * …*[l^{is}, h^{is}]: $measure_{i;}$

In the linked list of regions, [l^{i1}, h^{i1}]*[l^{i2}, h^{i2}]* …*[l^{is}, h^{is}]:$measure_{i;}$ respects region i, and i is a positive integer and it indicates the size of the list m, n∈ {1,2…..k} in a k dimensional cube space. Measure is the aggregation of each region.

Cut a region r from the region list L: if there is a region R of which r is on the end, then cut r out of R (if the volume of R's remains is 0, remove it from list) and return true; else return false.

To cluster the loaded input data records on the statistic tree, the first step is to take care of the base case where we merge consecutive nodes on one level above leaves,

and return a linked list of dense units in a form of indexed region lists.

Algorithm merger:
Input: a node N in the ST at level "level";
Output: a region list that is the dense units in the sub-tree rooted at N;
RegionList clustre(N) { // base case
IF level = k-1; // When it is the bottom node level of statistic tree
THEN
Find the region list in which each region is a consecutive range;
The last region is a special region (-1,-1) (assign vol =1 to it, for the star node);
Return the region list;
// Recursively clustering its children and itself
level ← level+1; // when it starts from the first level,
FOR i = 0 TO (d_{level}-1), DO: listA[i]=clustre(i_th child of N);
outList = expand (listA);
Append to outList the regions expanded by range (-1,-1) and regions
in the region list clustre(star node child of N;
Return outList;
}

From the first node in this level, all nodes will be scanned one by one, and a set of consecutive nodes which are pointed by the same parent node will generate a range (*l*, *h*). The first node of the consecutive nodes is the lower bound *l* of a new range, and the node after the last consecutive node is the higher bound *h*. Merger ends until all of the consecutive nodes are merged. In other words, for one set of nodes which have the same parent node, whenever it is not consecutive to its previous node, a new range starts at this node and ends at the one after its last consecutive node. Notice that the last node of each set of nodes is Star node. We use range (-1,-1) to represent it specially.

Continuing the motivating example, we illustrate this algorithm with the nodes at level 2. ListA[i] is a Linked List of indexed region lists, where i indicates different region. Refer to the statistic tree in figure 3, we get List A as below. In the list, each tuple represents a region, where the first number represents domain value in first dimension, second value represents domain value in second dimension, and rightmost range is what previous algorithm merged in the third dimension.

After merging consecutive nodes in the second lowest level, we generate higher dimension dense unites by an expansion algorithm. The input is an array of region lists (list A) we get from the previous algorithm, and the output is a list of higher dimensional regions which is called OutList. We start from the minimal volume range (from one dimension to two dimensions) or minimal region (from two dimensions to multiple dimensions), and grow it both to the above and to the below of the minimal volume range/region along higher dimension, so that a range grows to a rectangle in a geometry space; a minimal region grows to a cuboid and go forth in this fashion.

Algorithm expansion:
RegionList expand (listA) { // listA is an array of "size" number of region lists initially
WHILE listA has non-empty list DO
Compute the region m_i with minimal volumes for the listA[i], i=(0,1,2,…size-1)
Compute k m_k = min { m_0 , m_1, m_2,…};
FOR low= k To 0, DO: IF (cutting m_k from listA[low] return false) BREAK;
// expand below
FOR high= k+1 To (size-1), DO: IF (cutting m_k from listA[high] return false) BREAK;
// expand above
Expand m_k with range [low,high] to higher dimensional region Mk and append to outList;
Remove m_k from region list listA[k];
}

Among all regions we search for the minimal region m_k,. It may be a part of a region or entire of a region in listA. If we found it in a region listA[k], next we check upwards if m_k is in the end of region listA[k-1]. If yes, cut it out of region listA[k-1]. Then continue to check if it is end of region listA[k-2]. If so, cut it out, too. Keep checking upwards one region by one region in this fashion and stop until the first region which does not contain m_k, as an end. Store the higher dimensional index of uppermost region that contains m_k as an end to be "low", which represents the lower bound for m_k expanding along the higher dimension. Then check if m_k is an end of region listA[k+1]. If yes, cut it out of region listA[k+1]. Then continue to check if it is an end of region listA[k+2]. Repeat check and cut steps for other regions downwards one by one in listA. Stop cutting until the first region which does not contain m_k, as an end. Store the higher dimensional index of nethermost region that includes m_k as an end plus one to be "high", which represents higher bound for m_k expanding along the higher dimension. Then expand m_k with range [low, high] to higher dimensional region M_k= m_{k*}[low,high], and append M_k to OutList. Remove m_k from region list listA[K].Repeat above steps for regions in listA until all regions in listA are moved in this fashion.

Continuing above example, refer to listA being generated by the previous algorithm, scanning the region lists, 0*5*(6,7); will be the first minimal region m_k to be found out. We first expand above. Check if this minimal region is an end of its above regions one by one. Then we found it is an end of following regions 0*4 * (3,7),

0*3*(4, 7), 0*2*(3, 7) and 0*1*(3, 7). Hence, we cut it out of these regions consecutively and store the index, 1, as "low" to be the lower bound in higher dimensional, because 0*1*(3,7) is the uppermost region that includes

$$m_i = \min_{r \in listA[i]}\{ vol_r \};$$

(6,7) as an end. Then the region 0*5*(6,7) becomes empty, and need to be moved out of listA. We continue to expand below. We found minimal region 0*5*(6,7) is only the end of regions, 0*6*(6, 9). Cut (6,7) out of this region. And store index, 7, as "high" to be the higher bound for minimal region expanding along higher dimension. In this way, m_k is expanded by range [low, high] to higher dimensional region M_k = 0*(1,7)* (6,7), which will be append to OutList.

The whole of cluster algorithm consists of merger part and expansion part, and it stars from merger algorithm. However, the merger algorithm stars at the bottom node level of the statistics tree, so we design a recursive part for the cluster algorithm to scan statistics tree from top to bottom to look for the level that meets the condition of starting base case of algorithm merger. After implement the solved case at the lowest *node* level of the statistics tree, algorithm expansion can be executed on the work of algorithm merger.

4 EXPERIMENTS

In this section we will discuss the efficiency of algorithm in terms of different volumes of input records, and different numbers of dimensions. We will use a data generation program to produce several sets of random records to compare. Firstly, we compare three sets of input data with the same number of dimensions and cardinalities, but different number of records. We set all of them have 3 dimensions with the same cardinalities 10, 10, 10. However, numbers of records are set to 100, 10000, 1000000 respectively. The running results as follows, (some output regions are omitted to improve readability)

```
setting up DST from file ...
setting finished. Spend time: 0

### FINAL ANS: ###

-- list: ---
(2,7)*(4,5)*(4,5)*:10
(3,4)*(3,7)*(4,5)*:4
(4,5)*(2,6)*(4,5)*:4
(4,6)*(3,5)*(5,6)*:8
(3,5)*(4,5)*(2,4)*:12
(4,5)*(3,5)*(6,7)*:7
(5,6)*(3,6)*(4,5)*:9
(4,5)*(5,6)*(2,6)*:10
(5,6)*(4,5)*(3,7)*:12
list length = 9

Cluster run time of DST = 0
```

Result 1: records volume=100 , dimension=3, cardinality=10, 10, 10.

```
setting up DST from file ...
setting finished. Spend time: 234

### FINAL ANS: ###

-- list: ---
(1,7)*(4,5)*(2,3)*:6
(2,8)*(5,6)*(3,4)*:6
(2,8)*(6,7)*(4,5)*:6
(1,9)*(4,5)*(4,5)*:8
(1,8)*(3,4)*(4,5)*:7
...
...
...
list length = 34

Cluster run time of DST = 0
```

Result2: records volume=10000, dimension=3,cardinality=10,10,10.

```
setting up DST from file ...
setting finished. Spend time: 19453

### FINAL ANS: ###

-- list: ---
(0,8)*(3,7)*(4,5)*:32
(1,9)*(4,5)*(6,7)*:40
(0,8)*(4,6)*(5,6)*:48
(7,8)*(1,7)*(2,3)*:6
(2,8)*(2,8)*(3,4)*:36
(2,3)*(0,8)*(5,6)*:8
...
...
...

list length = 47

Cluster run time of DST = 0
```

Result3: records volume=1000000, dimension=3,cardinality=10,10,10.

We find, for different volumes of input data with same dimensions and cardinalities, the Statistics tree setting and loading time goes up with the volume increasing, but the cluster run time does not change. They should not be zero but just the time is so small due to the size of tree is small.

Then, we compare three sets of input data the same volume and cardinalities, but different dimensions. We set all of them have 10000 input records and each cardinality is 10. However, each of record set has 3, 4 and 5 dimensions respectively. The running results as follows, (some output regions are omitted to improve readability)

```
setting up DST from file ...
setting finished. Spend time: 234

### FINAL ANS: ###

-- list: ---
(1,7)*(4,5)*(2,3)*:6
(2,8)*(5,6)*(3,4)*:6
(2,8)*(6,7)*(4,5)*:6
(1,9)*(4,5)*(4,5)*:8
(1,8)*(3,4)*(4,5)*:7
...
...
...
list length = 34

Cluster run time of DST = 0
```

Result2: records volume=10000, dimension=3,cardinality=10,10,10.

```
setting up DST from file ...
setting finished. Spend time: 296

### FINAL ANS: ###

-- list: ---
(1,3)*(4,5)*(5,6)*(2,3)*:2
(1,2)*(5,6)*(4,5)*(2,3)*:1
(3,4)*(1,2)*(6,7)*(4,5)*:1
(4,5)*(1,2)*(4,5)*(7,8)*:1
(4,5)*(2,3)*(7,8)*(5,6)*:1
(4,5)*(6,7)*(0,1)*(4,5)*:1
(4,5)*(6,7)*(5,6)*(7,8)*:1
...
...
...
list length = 108

Cluster run time of DST = 16
```

Result4: records volume=10000, dimension=4,cardinality=10,10,10,10.

```
setting up DST from file ...
setting finished. Spend time: 624

### FINAL ANS: ###

-- list: ---
(1,6)*(2,3)*(3,4)*(4,5)*(4,5)*:5
(1,2)*(2,3)*(5,6)*(3,4)*(4,5)*:1
(1,2)*(3,4)*(3,4)*(3,4)*(4,5)*:1
(1,2)*(4,5)*(0,1)*(4,5)*(4,5)*:1
(1,6)*(5,6)*(4,5)*(4,5)*(3,4)*:5
(2,3)*(2,3)*(1,2)*(3,4)*(4,5)*:1
(2,3)*(2,3)*(4,5)*(6,7)*(4,5)*:1
...
...
...
list length = 329

Cluster run time of DST = 31
```

Result5: records volume=10000, dimension=5,cardinality= 10,10,10,10,10.

We find, for different volumes of input data with the same volume and cardinalities, when number of dimensions increases, it takes longer time to set up the statistics tree. Similarly, the cluster algorithm run time goes up with the number of dimensions increasing.

5 CONCLUSION

In this paper we propose a new clustering algorithm based on Statistics Tree data structure. The structure of the statistics tree is determined by the number of dimensions and their cardinalities. Other than the loading phase, the number of records is irrelevant in the clustering phase, thus rendering the new clustering algorithm a competitive edge. The clustering algorithm merges and expands the dense regions level by level recursively. We only implement the clustering algorithm based on dense statistics trees where the attribute values are contiguous. In future work, we may develop similar clustering algorithms based on sparse trees [12] which may accommodate much larger cardinality dimensions.

REFERENCES

[1] J. Han, `` Data Mining ", in J. Urban and P. Dasgupta (eds.), Encyclopedia of Distributed Computing , Kluwer Academic Publishers, 1999.

[2] J. Han, `` OLAP Mining: An Integration of OLAP with Data Mining", Proc. 1997 IFIP Conference on Data Semantics (DS-7), Leysin, Switzerland, Oct. 1997, pp. 1-11.

[3] Mihael Ankerst, Markus M. Breunig, Hans-Peter Kriegel and Jörg Sander, OPTICS: ordering points to identify the clustering structure. Proceedings of the 1999 ACM SIGMOD international conference on Management of data (SIGMOD '99).

[4] Charu C. Aggarwal, Joel L. Wolf, Philip S. Yu, Cecilia Procopiuc and Jong Soo Park, Fast algorithms for papered clustering, Proceedings of the 1999 ACM SIGMOD international conference on Management of data (SIGMOD '99). Pages 61-72.

[5] Lixin Fu, Joachim Hammer, CubiST: A New Algorithm for Improving the
Performance of Ad-hoc OLAP Queries, ACM Third International Workshop on Data Warehousing and OLAP (DOLAP'00), Washington, D.C, USA, November, 2000, pages 72-79.

[6] Ng, R. T. and Han, J. 2002. CLARANS: A Method for Clustering Objects for Spatial Data Mining. *IEEE Trans. on Knowl. and Data Eng.* 14, 5 (Sep. 2002).

[7] Beckmann, N., Kriegel, H., Schneider, R., and Seeger, B. 1990. The R*-tree: an efficient and robust access method for points and rectangles. *SIGMOD Rec.* 19, 2 (May. 1990).

[8] Martin Ester, Hans-Peter Kriegel, Jörg Sander, Xiaowei Xu (1996). "A density-based algorithm for discovering clusters in large spatial databases with noise". Evangelos Simoudis, Jiawei Han, Usama M. Fayyad. *Proceedings of the Second International Conference on Knowledge Discovery and Data Mining (KDD-96)*. AAAI Press, pp. 226–231.

[9] Tian Zhang and Raghu Ramakrishnan and Miron Livny, BIRCH: an efficient data clustering method for very large databases In: *SIGMOD '96: Proceedings of the 1996 ACM SIGMOD International Conference on Management of Data*ACM Press (1996) , p. 103-114.

[10] S. Guha, R. Rastogi, and K. Shim. CURE: An efficient clustering algorithm for large databases. In Proceedings of ACM SIGMOD International Conference on Management of Data, pages 73--84, New York, 1998.

[11] Rakesh Agrawal, Johannes Gehrke, Dimitrios Gunopulos, Prabhakar Raghavan, Automatic subspace clustering of high dimensional data for data mining applications, SIGMOD '98.

[12] Lixin Fu, Efficient Evaluation of Sparse Data Cubes, Advances in Web-Age Information Management: 5th International Conference (WAIM'04), Dalian, China, July 15-17, 2004: Springer-Verlag GmbH, 2004, pp. 336-345.

Weighting the importance of variables with Genetic Programming

An application to Galician schizophrenia patients

V. Aguiar-Pulido[1], **D. Rivero**[1], **M. Gestal**[1], **and J. Dorado**[1]
[1]Department of Information and Communication Technologies, University of A Coruña (UDC), A Coruña, Spain
[vaguiar, drivero, mgestal, julian]@udc.es

Abstract - *Data mining, a part of the Knowledge Discovery in Databases process (KDD), is the process of extracting patterns from large data sets by combining methods from statistics and artificial intelligence with database management. Analyses of biomedical data have evolved towards genome-wide and high-throughput approaches, thus generating great amounts of data for which data mining is essential. Therefore, a novel approach based on genetic programming with the aim of weighting the importance of the different variables contained in the data generated in the biomedical field is presented. This approach was applied to SNP data from Galician schizophrenia patients, showing the possibilities it offers.*

Keywords: genetic programming, evolutionary computation, variable analysis, data mining, schizophrenia

1 Introduction

Data mining, a part of the Knowledge Discovery in Databases process (KDD), is the process of extracting patterns from large data sets by combining methods from statistics and artificial intelligence with database management. Analyses of biomedical data have evolved towards genome-wide and high-throughput approaches, thus generating great amounts of data for which data mining is essential.

During recent years, the advances in data collection have enabled scientists to store a huge amount of data. However, traditional data analysis techniques cannot usually address this increase of data, so new approaches, as data mining, were promoted. Some of the specific challenges that motivated the development of data mining techniques were precisely the scalability and the chance to work with highly dimensional data or the lack of traditional methods to work with heterogeneous and complex data. This situation is especially relevant in biomedical fields.

However, traditional data mining techniques present many drawbacks and, often, lack of the necessary flexibility. Evolutionary algorithms have a global search feature which makes them especially adequate for solving problems found along the different stages of a knowledge discovery process. For this reason, in this work, a technique based on evolutionary computation is presented. This technique was applied to biomedical data with the objective of obtaining a list of prioritized variables extracted from the data.

The fact of weighting the importance of the variables has become relevant, since, as mentioned previously, not only more biomedical data is being generated, but also the number of variables present in this data is so high that their influence and importance is of very difficult interpretation. Therefore, the technique herewith presented, apart from analyzing the data, will give useful information to the researcher and make the task of interpretation easier.

2 State of the art

2.1 Genetic Programming (GP)

Genetic programming (GP) is an evolutionary technique used to create computer programs that represent approximate or exact solutions to a problem [1]. GP works based on the evolution of a given population. In this population, every individual represents a solution for the problem that is intended to be solved. GP looks for the best solution by means of a process based on the Theory of Evolution [2], in which, from an initial population with randomly generated individuals, after subsequent generations, new individuals are produced from old ones by means of crossover, selection and mutation operations, based on natural selection. This way, the good individual will have more chances of survival to become part of the

next generation. Thus, after successive generations, the best-so-far individual is obtained, corresponding to the final solution of the problem. The GP encoding for the solutions is tree-shaped, so the user must specify which are the terminals (leaves of the tree) and the functions (nodes capable of having descendants) to be used by the evolutionary algorithm in order to build complex expressions. Additionally, a fitness function that is used for measuring the appropriateness of the individuals in the population has to be defined in GP. This is the most critic point in the design of a GP system.

The wide application of GP to various environments and its success are due to its capability of adaptation to numerous different problems. Although one of the most common applications of GP is the generation of mathematical expressions [3], it has also been used in other fields such as rule generation [4], filter design [5], classification [6], etc.

2.2 Variable analysis

Subsequently, the latest and most related papers regarding variable analysis applied to biomedical data, especially those were SNPs are used, are described.

Chen et al. [7] review four variations of LR, namely Logic Feature Selection, Monte Carlo Logic Regression, Genetic Programming for Association Studies, and Modified Logic Regression-Gene Expression Programming, and investigate the performance of each method using simulated and real genotype data. They also contrast these with another tree-like approach, namely Random Forests, and a Bayesian logistic regression with stochastic search variable selection.

Kulkarni et al. [8] compare class prediction accuracy of two different classifiers, genetic programming and genetically evolved decision trees, using microarray data. The dataset used for the tests contained the best 10 and best 20 genes ranked by the t-statistic and mutual information. In their work, they conclude that genetic programming together with mutual information-based feature selection is the most efficient alternative to the existing colon cancer prediction techniques.

Zhang et al. [9] present a framework to evolve optimized feature extractors that transform an input pattern space into a decision space in which maximal class separability is obtained. The authors applied this method to real world datasets from the UCI Machine Learning and StatLog databases to verify their approach and compare their proposed method with other reported results.

Archetti et al. [10] present a genetic programming-based framework for predicting anticancer therapeutic response. They used the NCI-60 microarray dataset and they looked for a relationship between gene expressions and responses to oncology drugs Fluorouracil, Fludarabine, Floxuridine and Cytarabine.

Nunkesser et al. [11] present a procedure based on genetic programming and multi-valued logic that enables the identification of high-order interactions of categorical variables such as SNPs. This method, called GPAS, cannot only be used for feature selection, but can also be employed for discrimination. They applied their method to the genotype data from the GENICA study, an association study concerned with sporadic breast cancer, finding that GPAS was able to identify high-order interactions of SNPs leading to a considerably increased breast cancer risk for different subsets of patients that are not found by other feature selection methods. GPAS can also be employed to analyze whole-genome data, as demonstrated in its application to a subset of the HapMap data.

Nandi et al. [12] adapted GP and applied it to a dataset of 57 breast mass mammographic images, each with 22 features computed. The extracted features relate to edge-sharpness, shape, and texture. To refine the pool of features available to the GP classifier, the authors used five feature-selection methods, including three statistical measures - Student's t-test, Kolmogorov-Smirnov Test, and Kullback-Leibler Divergence.

3 Method

With the aim of analyzing a database, genetic programming can be used in order to generate expressions that allow characterizing which variables are important and how they influence the output. For this purpose, a novel approach based on genetic programming is presented in this paper. Therefore, in this case, the set of terminals is composed of the variables involved in the analysis and a series of random constants, and the set of functions is composed of arithmetic operators. This is described in more depth in the “GP configuration” below.

This way, it is possible that genetic programming may generate a great amount of expressions very hard to interpret. In this work, GP is not used to interpret these expressions, but to analyze them with the objective of discovering the importance of each variable.

Hence, the following is done: the proposed system is executed a very large number of times and, for each execution, the best individual obtained is considered. Thus, after all the executions have finished, there will be a set of expressions that characterize, with high precision, the variable of interest, that is, the class variable. Given the stochastic character of GP, the expressions contained in this set will be, in general, different, but all of them will have the highest precision value obtained in their corresponding evolutionary process.

Once this set of expressions has been obtained, each of these expressions is analyzed to calculate the density of apparition of each variable in the whole set. Thus, the relative importance of each variable can be quantified, depending on if this variable appears in a greater or lower number of expressions.

As a second analysis technique, this process has been performed analyzing each pair of variables, instead of taking only each of them separately, observing when they appear together in the expressions obtained.

3.1 GP configuration

Before applying genetic programming to solve a real-world problem, several types of parameters need to be defined in advance.

3.1.1 The function set and the terminal set

Although there are many different functions which can be used in GP, normally only a small sub-set of those is used simultaneously, because the size of the search space increases exponentially with the size of the function set. The function set employed in this work is listed in Table I. Since the functions need to satisfy the closure property in GP, the division operator is implemented in a protected way. Protected-division works identically to ordinary division except that it outputs the value of nominator when its denominator is zero.

TABLE I. THE FUNCTION SET

Name	Number of arguments	Operation
+	2	Arithmetic add
-	2	Arithmetic subtract
*	2	Arithmetic multiply
%	2	Protected division

Referring to the terminal set of this work, it includes 48 variables and random constants in the interval [-1, 1].

3.1.2 The control parameters

These parameters are used to control the GP run. There exist many possibilities of combination with different control parameters.

For solving the given problems, several different combinations of parameters have been tried. The parameters that returned the best results are shown in Table II.

TABLE II. CONTROL PARAMETERS IN GP

Initial population generation	Ramped half-and-half method
Maximum tree depth	9
Population size	1,000
Crossover probability	95%
Mutation probability	4%

3.1.3 The termination criteria

The GP execution is terminated when the following condition is fulfilled: the generated individuals changed less than a threshold (0.000001) in a maximum number of generations (10,000).

4 Experimentation and results

The objective of this work is to analyze data taking into account a certain number of variables in order to choose those that have more influence in relation to a specific characteristic. In this case, the technique was applied to data related to schizophrenia.

4.1 Description of the problem

Association studies are those in which DNA from patients that have not developed the disease is compared to DNA from affected patients in order to find relationships between mutations in the DNA and the disease studied. Usually, mutations such as SNPs (Single Nucleotide Polymorphisms) [13] are studied. A SNP is a single nucleotide site where two (of four) different nucleotides occur in a high percentage of the population, that is, at least in 1% of the population. Since there exist 14 million of SNPs in human beings then a huge amount of data obtained from DNA genotyping needs to be dealt with, thus many variables have to be taken into account.

These studies can be done on complex diseases [14]. In these diseases, apart from the influence of genetic predisposition, environmental factors also affect, in such a way that a person could be genetically predisposed but never develop the disease. Due to the nature of these diseases, it is hard to establish a relationship between a gene and the disease since, in general, this type of disease is caused by combination of effects of several sets of SNPs which, separately, have a low effect. There is a high prevalence and impact of complex diseases like cancer, mental disorders and cardiovascular diseases.

In this work, schizophrenia data from Galician patients [15] were used. This data contained 48 SNPs at the DRD3 and HTR2A genes [16], genes which are

associated to schizophrenia. These SNPs were encoded taking different values:

- 0 if homozygous (both copies of a given gene have the same allele) for the first allele (one of a number of alternative forms of the same gene occupying a given position on a chromosome),
- 1 if heterozygous (the patient has two different alleles of a given gene),
- 2 if homozygous for the second allele or
- 3 if unknown.

The original dataset contained 260 positive subjects (genetically predisposed to schizophrenia) and 354 negative subjects (not predisposed), a total of 614 patients. The equivalence between the variable number and the SNP real name is shown in Table III.

TABLE III. EQUIVALENCE BETWEEN VARIABLE# AND REAL SNP NAME

Variable #	SNP	Variable #	SNP
SNP1	rs4682148	SNP25	rs1058576
SNP2	rs7631540	SNP26	rs6561333
SNP3	rs6808291	SNP27	rs1923884
SNP4	rs1486012	SNP28	rs2296972
SNP5	rs9824856	SNP29	rs9316233
SNP6	rs2134655	SNP30	rs659734
SNP7	rs963468	SNP31	rs1928042
SNP8	rs3773678	SNP32	rs2770296
SNP9	rs167771	SNP33	rs9316235
SNP10	rs226082	SNP34	rs582385
SNP11	rs10934256	SNP35	rs1928040
SNP12	rs1486009	SNP36	rs731779
SNP13	rs6280	SNP37	rs985934
SNP14	rs7638876	SNP38	rs9534505
SNP15	rs9825563	SNP39	rs6304
SNP16	rs1354348	SNP40	rs6305
SNP17	rs9283560	SNP41	rs2070036
SNP18	rs3889066	SNP42	rs2070037
SNP19	rs7329640	SNP43	rs6313
SNP20	rs10507544	SNP44	rs1328685
SNP21	rs7333412	SNP45	rs731244
SNP22	rs3125	SNP46	rs1360020
SNP23	rs6314	SNP47	rs10507546
SNP24	rs6308	SNP48	rs10507547

4.2 Results

Table IV shows a list of variables, ordered by the density of apparition in 134 parallel executions of the method described. As a result, an average classification accuracy of 77.38% was obtained.

This table shows the relative importance of each of these SNPs, measured as the density of apparition. As it can be seen, the SNP with the highest density is SNP48, appearing in 94.03% of the expressions obtained by the method. This SNP was also obtained as that one with the highest density of apparition by another method based on evolutionary computation [17, 18] also designed for feature selection.

TABLE IV. PRIORITIZED LIST OF VARIABLES

Variable #	Density of apparition	Variable #	Density of apparition	Variable #	Density of apparition
SNP48	**94.0298%**	SNP34	41.7910%	SNP27	31.3433%
SNP23	**92.5373%**	SNP14	40.2985%	SNP11	29.8507%
SNP29	**92.5373%**	SNP37	40.2985%	SNP32	29.8507%
SNP10	**91.0448%**	SNP24	38.8060%	SNP40	29.8507%
SNP20	76.1194%	SNP47	38.8060%	SNP3	28.3582%
SNP21	56.7164%	SNP1	37.3134%	SNP31	28.3582%
SNP43	56.7164%	SNP2	35.8209%	SNP38	28.3582%
SNP28	52.2388%	SNP22	35.8209%	SNP13	26.8657%
SNP30	52.2388%	SNP35	35.8209%	SNP9	25.3731%
SNP26	50.7463%	SNP36	35.8209%	SNP19	23.8806%
SNP41	50.7463%	SNP4	34.3284%	SNP46	23.8806%
SNP18	49.2537%	SNP44	34.3284%	SNP8	22.3881%
SNP15	47.7612%	SNP12	32.8358%	SNP5	20.8955%
SNP33	46.2687%	SNP6	31.3433%	SNP39	19.4030%
SNP42	44.7761%	SNP7	31.3433%	SNP45	19.4030%
SNP16	43.2836%	SNP17	31.3433%	SNP25	8.9552%

Additionally, this table shows that there is a big difference between the first four SNPs (numbered 48, 23, 29 and 10, with densities 94.03%, 92.54%, 92.54% and 91% respectively) and the rest. The density of apparition of the fifth SNP is much lower, 76.12%, and the following, the sixth, SNP21, has a density of 56.72%. These facts reveal the great importance of these four first SNPs compared to the rest. Furthermore, the fall in the density of apparition is very fast, and a low density of 50% appears in an early 10^{th} position.

TABLE V. DENSITY OF APPARITION FOR PAIRS OF VARIABLES

Variable #	Variable #	Density of apparition
SNP23	**SNP29**	**85.07%**
SNP23	**SNP48**	**85.07%**
SNP29	**SNP48**	**85.07%**
SNP10	**SNP23**	**83.58%**
SNP10	**SNP29**	**82.09%**
SNP10	**SNP48**	**82.09%**
SNP10	SNP20	71.64%
SNP29	SNP20	70.15%
SNP20	SNP48	68.66%
SNP23	SNP20	68.66%
SNP21	SNP48	55.22%
SNP43	SNP48	55.22%
SNP23	SNP21	53.73%
SNP23	SNP43	53.73%
SNP28	SNP48	52.24%
SNP29	SNP43	52.24%
SNP41	SNP42	52.24%
SNP10	SNP43	52.24%

Also, the expressions obtained were analyzed in order to measure the importance of groups of two SNPs. Table V shows the pairs of two SNPs with the highest density of apparition, appearing together in the expressions.

This table shows, for instance, that SNPs 23 and 29 appear together in 85.07% of the expressions. In this case, the pairs with the highest density of apparition correspond to all of the possible combinations of the four SNPs that were considered as the most important after the analysis of Table IV (SNPs 48, 23, 29 and 10).

After these combinations, the following pairs, which have a much lower density, include one of these variables. This fact, again, encourages the affirmation of the importance of these four SNPs.

5 Conclusions and future work

As section 4 shows, this technique allows analyzing databases in order to measure the importance of each variable. This has promising applications in engineering, industrial and medical environments, since many times data is collected and the number of independent variables grows exponentially.

One of these applications is studied in this paper, that is, to associate schizophrenia with SNPs that, initially, may be related to it. As a result of the application of this technique, four different SNPs are revealed to be the most important.

In this work, single and pair density of apparition are analyzed. However, in order to extract more accurate results, more analysis can be done, studying combinations of 3, 4 and more variables together. Additionally, the method will be applied to other biomedical datasets, in order to continue refining it.

6 Acknowledgement

Thanks to the “Fundación Galega de Medicina Xenómica” for providing the data used in this work. The development of the experiments described in this work was performed on computers from the Supercomputing Center of Galicia (CESGA).

Vanessa Aguiar-Pulido acknowledges the funding support for a research position by the “Plan I2C” program from Xunta de Galicia (Spain), being also co-funded by FEDER. This work is supported by the following projects: “Ibero-American Network of the Nano-Bio-Info-Cogno Convergent Technologies”, Ibero-NBIC Network (209RT-0366) funded by CYTED (Spain), “Development of new image analysis techniques in 2D Gel for biomedical research” (ref.10SIN105004PR) funded by Xunta de Galicia and RD07/0067/0005, funded by the Carlos III Health Institute.

7 References

[1] J. R. Koza, *Genetic Programming. On the Programming of Computers by means of Natural Selection*. Cambrige, MA: The MIT Press, 1992.

[2] C. Darwin, *On the Origin of Species by Means of Natural Selection*. London: John Murray, 1859.

[3] D. Rivero, *et al.*, "Time series forecast with anticipation using genetic programming," in *8th International Work-conference on Artificial Neural Networks*, 2005, pp. 968–975.

[4] M. Bot and W. Langdon, "Application of genetic programming to induction of linear classification trees," in *EuroGP'2000*, 2000, pp. 247–258.

[5] J. Rabuñal, *et al.*, "Prediction and modelling of the rainfall-runoff transformation of a typical urban basin using ANN and GP.," *Applied Artificial Intelligence*, vol. 17, pp. 329-343, 2003.

[6] P. Espejo, *et al.*, "A survey on the application of genetic programming to classification," *IEEE Transactions on Systems, Man, and Cybernetics, Part C: Applications and Reviews*, vol. 40, pp. 121-144, 2010.

[7] C. C. Chen, *et al.*, "Methods for identifying SNP interactions: a review on variations of Logic Regression, Random Forest and Bayesian logistic regression," *IEEE/ACM Trans Comput Biol Bioinform*, vol. 8, pp. 1580-91, Nov-Dec 2011.

[8] A. Kulkarni, *et al.*, "Colon cancer prediction with genetics profiles using evolutionary techniques," *Expert Systems with Applications*, vol. 38, pp. 2752-2757, 2011.

[9] Y. Zhang and P. I. Rockett, "A generic optimising feature extraction method using multiobjective genetic programming," *Appl. Soft Comput.*, vol. 11, pp. 1087-1097, 2011.

[10] F. Archetti, *et al.*, "Genetic programming for anticancer therapeutic response prediction using the NCI-60 dataset," *Computers & Operations Research*, vol. 37, pp. 1395-1405, 2010.

[11] R. Nunkesser, *et al.*, "Detecting high-order interactions of single nucleotide polymorphisms using genetic programming," *Bioinformatics*, vol. 23, pp. 3280-3288, December 15, 2007 2007.

[12] R. J. Nandi, *et al.*, "Genetic programming and feature selection for classification of breast masses in mammograms," *Conf Proc IEEE Eng Med Biol Soc*, vol. 1, pp. 3021-4, 2006.

[13] J. T. den Dunnen and S. E. Antonarakis, "Mutation nomenclature extensions and suggestions to describe complex mutations: a discussion," *Hum Mutat*, vol. 15, pp. 7-12, 2000.

[14] A. G. Motulsky, "Genetics of complex diseases," *J Zhejiang Univ Sci B*, vol. 7, pp. 167-8, Feb 2006.

[15] E. Dominguez, *et al.*, "Extensive linkage disequilibrium mapping at HTR2A and DRD3 for schizophrenia susceptibility genes in the Galician population," *Schizophr Res*, vol. 90, pp. 123-9, Feb 2007.

[16] V. Aguiar-Pulido, *et al.*, "Machine learning techniques for single nucleotide polymorphism - disease classification models in schizophrenia," *Molecules*, vol. 15, pp. 4875-89, Jul 2010.

[17] M. Gestal, *et al.*, "Selection of variables by genetic algorithms to classify apple beverages by artificial neural networks," *Applied Artificial Intelligence*, vol. 19, pp. 181-198, 2005.

[18] M. P. Gomez-Carracedo, *et al.*, "Chemically driven variable selection by focused multimodal genetic algorithms in mid-IR spectra," *Anal Bioanal Chem*, vol. 389, pp. 2331-42, Dec 2007.

Applied graph mining technique to discover consensus graphs from group ranking decisions

Li-Chen Cheng*, Min-Juan Jhang
Computer Science and Information Management, Soochow University, Taipei, Taiwan, ROC

Abstract — *The group ranking approach has been applied in many applications, such as in decision-making support systems, group recommendation systems, and so on. Previous studies have focused on how to generate a total ranking list. When there is no consensus or only slight consensus in the users' opinions or preferences, this kind of result may damage the decision-maker's decision. For this reason, this study proposes a new framework which represents user ranking information as a graph model, and a new algorithm based on the recent work to detect the maximum consensus graphs. The generated visualization results allow decision-makers to make better strategies.*

Keywords: Data mining; graph mining, Group decision making; Maximum consensus sequence

1 Introduction

Recently, the mining of knowledge from users' preferences has come to play a critical role in many applications including decision-making support systems [1-2], group recommendation systems [3], machine learning[4], and webpage search strategies [5-6]. User preference can always be expressed as ranking data. The essence of this problem is to construct a coherent aggregate result from the rankings provided by different sources.

Generally, the traditional group ranking problem can be classified using two aspects: the input format and the type of compromised output results. Among several input formats, ranking list is the most general way to express user preferences regarding the alternatives. This study allows users to provide complete or partial ranking data.

The output results of most research are to determine a fully ordered list of items. When there is no consensus or only slight consensus in the users' opinions or preferences, these studies still generate a total ordering list to represent the consensus using their ranking algorithms. However, these kinds of results will damage the decision and raise some risk to the decision maker. Recently, based on the concept of "consensus decision-making theory", Chen and Cheng proposed a new model which gives the longest ranking lists of items that agree with the majority and disagree with the minority [7]. Although the maximal consensus sequences model can solve the previously mentioned problem, the weakness of this approach may generate many maximum consensus sequences, making the results fragmented and difficult to understand and use.

This study adopts a user-provided total ranking list which is transferred to a user graph during the preprocessing step. The user graph is a directed graph illustrating the user's preference among items. The proposed algorithm will discover the maximum consensus graphs from the collection of users' graphs. A consensus graph means that a majority of users agree upon the relationships between items.

These graphs illustrate several implications which cannot be made by the previous research. The consensus graphs represent several clusters in which the relationship among items is agreed upon by most users. This is useful information for decision-makers.

2 Related work

2.1 Our recent work

The basic idea for our recent work comes from the "decision-making theory", which stresses that a process is needed to achieve the most agreeable decision among participants. It not only explores the agreement of the majority, but also resolves or mitigates the objections of the minority. To understand this decision-making process, Chen and Cheng proposed an algorithm to discover maximum consensus sequences from users' ranking lists, where the maximum consensus sequences represent the maximum possible consensuses that could be achieved among most of the users [7,8]. This algorithm can also identify ambiguous pairs that need further negotiation.

2.2 Graph mining

The graph mining technique can be applied to several different research areas, and has received much attention in recent years [9-18]. The graph model can represent arbitrary relations among objects. Using different mining techniques can detect various kinds of graph patterns. Frequent subgraphs are the most important patterns that can be discovered in a collection of graphs [10-12]. Several well-

known algorithms have been developed to mine frequent substructures [19]. Among these studies, there are two basic approaches to the frequent substructure mining problem: an Apriori-based approach and a pattern-growth approach [13]. The Apriori-based approach can be classified into the vertex-based candidate generation method and the edge-based candidate generation strategy [14-18]. This study follows the idea of the Apriori-based approach and is based on the vertex-based candidate generation scheme to propose the new framework.

3 Problem definition

Let $U = \{u_1, u_2, u_3, \ldots, u_m\}$ denote all users and $I = \{i_1, i_2, i_3, \ldots, i_n\}$ denote the sets of all distinct items. Each user u_i expresses his/her preference using user sequence $S_i = \{i_{a_1} \oplus i_{a_2} \oplus i_{a_3} \oplus \ldots \oplus i_{a_n}\}$, where $i_{a_j} \in I$, $1 \leqq i_{a_j} \leqq n$, and $\oplus \in \{>, =\}$.

3.1 User sequence's relationship function

A user sequence can be represented as $S_i = \{i_{a_1} \oplus_1 .. \oplus_{p-1} i_{a_p} \oplus_p .. \oplus_j . \oplus_{q-1} i_{a_q} \oplus ... i_{a_k}\}$. The relationship between two items i_{a_p} and i_{a_q} in user sequence Si can be represented as $Rel(i_{a_p}, i_{a_q}, S_i)$, whose value is defined below：

- If $\exists \oplus_j \in \{>\}$ $p \leq j \leq q-1$, then $Rel(i_{a_p}, i_{a_q}, S_i) =">"$;
- If $\forall \oplus_j \in \{=\}$ $p \leq j \leq q-1$, then $Rel(i_{a_p}, i_{a_q}, S_i) ="="$

3.2 User graph

A user's preference sequence S_i is transferred to be a user graph $UG_i = (V, E)$. Each item is mapped to a vertex in set $V(UG_i)$. The edge represents the items' relationship denoted as $E(UG_i) = \{e_1, e_2, e_3 \ldots, e_k\}$. UG_1 is a user graph and is shown in Fig. 1.

Example 1. Given a user sequence $S_1 = \{i_2 > i_3 = i_1\}$, user graph $UG_1 = (V, E)$, $V(UG_1) = \{i_1, i_2, i_3\}$, $E(UG_1) = \{e_1, e_2, e_3\}$.

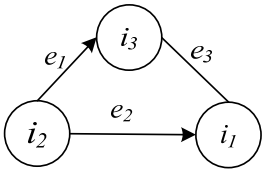

Fig. 1. User graph UG_1

3.3 Isomorphism

The two graphs $G = (V, E)$ and $G' = (V', E')$ are isomorphic. They have the same topology in that $V(G')$ and $V(G)$ are equal. The edges $E(G)$ of the mapping feature functions are equal to the $E(G')$ of the mapping feature functions.

Example 2. There are two graphs $G_1 = (V_1, E_1)$ and $G_2 = (V_2, E_2)$. The vertices of graph G_1 map to $V(G_1)$ and the vertices of graph G_2 map to $V(G_2)$. $V(G_1) = V(G_2)$ and the feature functions of G_1 are equal to the feature function of G_2.

G_1 and G_2 are isomorphic and are shown in Fig. 2.

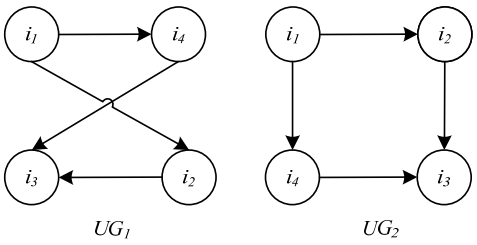

Fig. 2. Isomorphism relationship with two graphs.

3.4 Comply graph support

A subgraph G_m is called a complied graph if it satisfies the relationship $cmp\_sup(G_m) \geq cmp\_minsup$, where cmp_minsup is a threshold given by users.

4 Methodology

4.1 The proposed algorithm

We give an overview of the proposed algorithm. We propose an algorithm to discover the maximum comply graphs from the collection of all user graphs. The cmp_minsup are thresholds given by the user to filter out comply graphs.

(Step 1)

Each user sequence is transferred to a user graph based on the definition.

(Step 2)

The set of candidate graph CG^2 will be filtered. The comply support satisfies the support constraints.

(Step 3)

This step is iteratively executed until $LG^{k-1} = \phi$. We follow the vertex-based candidate generation scheme. In general, candidate CG^k can be generated by $LG^{k-1} \otimes LG^{k-1}$, where $\otimes$ denotes the join operation. After

obtaining CG^k, LG^k is the set of candidates whose *cmp_sup* satisfy the support constraints.

(Step 4)

We obtain all consensus graphs.

4.2 Candidate generation and counting supports

This section explains how to generate candidates from a set of large subgraphs. This study generates candidate subgraphs of size k CG^k by joining two frequent size k-1 subgraphs LG^{k-1}. We follow the vertex-based candidate generation scheme.

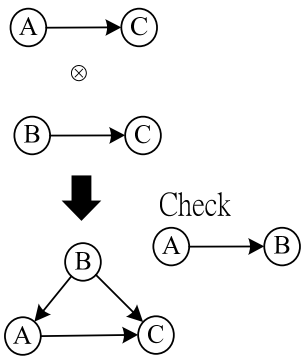

Fig. 3. Join operation of the proposed methodology.

5 An illustrative example

A simple example is demonstrated to show the computation process of the proposed method. There are 5 user sequences illustrated in Table 1.

Table 1 user sequences

1	{A > B > C = D }
2	{D > A = B > C }
3	{C = D > A > B}
4	{B > A > C = D }
5	{B = D > A > C }

Step 3 will be executed several times until the large graphs LG^4 are generated. Finally, the maximum consensus graph will be generated by LG^4 and the result is illustrated in Fig.4.

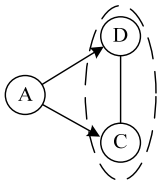

Fig. 4 The Large graph LG_5.

From the maximum consensus graph LG^5, we can discover several interesting facts. First, there are three clusters {A} and {C, D}. Second, several rules can be observed {A > C} and {A > D} and {C = D}. From these observations, the proposed algorithm can discover several consensus graph groups when there is no consensus or only slight consensus of the users' opinions or preferences. The result can still provide the decision-maker with useful information.

6 Conclusions

Existing methods for the group ranking approach always generate a total ranking list. In a recent work, we proposed methods to discover the maximum consensus sequences. Although the result is more reasonable, the weakness of this approach is that it may generate many maximum consensus sequences, making the results fragmented and difficult to understand and use. This current study based on the graph model develops a new methodology to discover the consensus graphs and ambiguous graphs. The proposed method is illustrated with an example. We will conduct extensive experiments to evaluate the effectiveness of the proposed algorithm in the future.

ACKNOWLEDGMENT

This research was supported in part by the National Science Council of Taiwan (Republic of China) under the grant NSC 100-2410-H-031 -010.

7 References

[1] W. D. Cook, B. Golany, M. Kress, M. Penn, and T. Raviv, "Optimal allocation of proposals to reviewers to facilitate effective ranking, " 51, 4, 65661.(2005)

[2] E. Fernandez, and R. Olmedo, "An agent model based on ideas of concordance and discordance for group ranking problems," *Decision Support Systems*, vol. 39, no.3, pp 429-443, 2005.

[3] Y. L. Chen, and L. C. Cheng, "A novel collaborative filtering approach for recommending ranked items," *Expert Systems with Applications*, vol. 34, no.4, pp 2396-2405, 2005..

[4] R. Fagin, R. Kumar, and D. Sivakumar, "Efficient

similarity search and classification via rank aggregation, " Paper presented at the Proceedings of the 2003 ACM SIGMOD international conference on Management of data.

[5] M. M. S. Beg, and N. Ahmad, "Soft computing techniques for rank aggregation on the WorldWideWeb," WorldWideWeb-Internet andWeb Information Systems, vol.6, no.1, pp 5-22, 2003.

[6] W. Cohen, "Learning to order things", Journal of Artificial Intelligence Research, vol.10, pp .243. 1999

[7] Y. L. Chen, and L. C. Cheng, "Mining maximum consensus sequences from group ranking data," *European Journal of Operational Research*, vol.198, no.1, pp 241-251, 2009.

[8] Y. L. Chen, and L. C. Cheng, "An approach to group ranking decisions in a dynamic environment," *Decision support systems*, vol.48, no.4, pp 622-634, 2010.

[9] A. Inokuchi, T. Washio, and H. Motoda, "An apriori-based algorithm for mining frequent substructures from graph data," 2000, In: Proceeding of the 2000 European symposium on the principle of data mining and knowledge discovery (PKDD'00), Lyon, France, pp 13–23.

[10] M. Kuramochi, and G. Karypis, "Frequent subgraph discovery", 2001, *Proceedings IEEE International Conference on Data Mining*, pp 313-320.

[11] N. Vanetik, E. Gudes, and S.E. Shimony, "Computing frequent graph patterns from semistructured data," 2002, In: Proceeding of the 2002 international conference on data mining (ICDM'02),Maebashi, Japan, pp 458–465.

[12] J. Huan, W. Wang, and J. Prins, "Efficient mining of frequent subgraphs in the presence of isomorphism," 2003, *Third IEEE International Conference on Data Mining*, pp 549-552.

[13] T. Washio, H. Motoda, "State of the art of graph-based data mining," 2003 , SIGKDD Explor 5: pp 59–68.

[14] J. Huan, W. Wang, J. Prins, and J. Yang, "Mining maximal frequent subgraphs from graph databases," 2004, Proceedings of the tenth ACM SIGKDD international conference on Knowledge discovery and data mining.

[15] M. Kuramochi, and G. Karypis, "An efficient algorithm for discovering frequent subgraphs,", *IEEE Transactions on Knowledge and Data Engineering,* vol. *16*, no.9, pp 1038-1051, 2004.

[16] E.Gudes, S. E, Shimony, and N.Vanetik, "Discovering frequent graph patterns using disjoint paths," 2006, , *IEEE Transactions on Knowledge and Data Engineering*, vol.18, no.11, pp 1441-1456, 206.

[17] H. Tong, C. Faloutsos, and Y. Koren, "Fast direction-aware proximity for graph mining," 2007, Proceedings of the 13th ACM SIGKDD international conference on Knowledge discovery and data mining.

[18] U. Kang, C. E. Tsourakakis, and C. Faloutsos, "A peta-scale graph mining system implementation and observations," 2009, *Ninth IEEE International Conference on Data Mining*, pp 229-238.

[19] J. Han, M. Kamber, and J. Pei, "Data mining: concepts and techniques: Morgan Kaufmann," 2011.

How User Types in Chinese from Keyboard

Analysis of User Behaviors on Chinese Input Software

Jinghui Xiao, Xin Li , Xiaorui Yang and Quanzhan Zheng
Research Center of Tencent Technology Company Limited, Beijing, China
{henryxiao, xinranli, smiyang, stevezheng}@tencent.com

Abstract - *The standard keyboard is initially designed for native English speakers. In China, people type in Chinese character under the help of Chinese input software which converts the pinyin sequence – the Chinese official phonetic symbol that can be typed in directly from the standard keyboard– into Chinese character sequence. QQ input software is the second most popular Chinese input software by market cap. Under the user agreement, we collect the anonymous user typing records as it uses QQ input software. This paper presents the preliminary results on user typing behaviors by analyzing these records. This work enlightens the way to improve the performance of Chinese input software, so as to improve user experience further*.

Keywords: Chinese Input Software; Data Mining

1 Introduction

The standard keyboard is initially designed for native English speakers. In Asia, such as China, Japan and Thailand, people can not input their language through the standard keyboard directly. Asian text input becomes the challenge for the computer user in Asia. In China, Chinese user types in Chinese text under the help of Chinese input software which converts the pinyin sequence – the Chinese official phonetic symbol that can be typed in directly from the standard keyboard– into Chinese character sequence. There are totally 410 pinyin symbols (without the tone information) which correspond to more than 30,000 Chinese characters. For a certain inputted pinyin sequence, there are many candidates of Chinese character sequence corresponding to it, but only one is what the user really wants to obtain. It's the challenge for Chinese input software to guess what is the user really wants to input, and present it in front of the user.

QQ input software is the second popular Chinese input software in China by market cap. It is developed by Tencent Technology Company Limited which is currently the largest internet company in China. There are more than 200 million users that have installed QQ input software on their computers. More than 25 million users input Chinese by QQ input software daily [1]. We started "user experience plan" since last year. Under the user agreement, we collect the information of anonymous users' typing records. We analyze user behaviors from these information, and get some insights how user input Chinese by Chinese input software. These results are very helpful for us to improve the quality of QQ input software so as to improve user experience on it further.

In the rest of this paper, we present our analysis works on user behaviors in section 2. In section 3, we draw the conclusions and discuss the future works.

2 Analysis OF User Records

2.1 Description of Data Set

We collect several kinds of information with the typing records from anonymous users. They are presented in Table 1 as below:

Table 1. Description of Anonymous User Typing Record

Information Type	*Description*
Host application	The name of host application in which user types in Chinese characters by QQ input software.
Pinyin sequence	How user types in pinyin string, i.e. it types in the full pinyin string or only the brief one.
Word candidate	The Chinese word candidate that QQ input software provides according to user's pinyin string.
User selection	The candidate that user selects as its real input.

There are four kinds of information above with each typing record. For experiments, we collect all the typing records from anonymous users during one week. Totally there are about 1.2 billion records.

2.2 Analysis on Host Application

There is the host information with each typing record. It's the name string of the application in which user inputs Chinese by QQ input software. By making statistics on the host information, we can get the insight of typical scenarios that user inputs Chinese. We stat the distribution for each host in the data set and present the top 10 hosts in Table 2 as below:

Table 2. Top 10 Hosts

Name of Host Application	*Type*	*Ratio*
QQ	Instant Messenger	65.8%
IE	Web Browser	2.64%
360 Explorer	Web Browser	2.54%
Ali Buyer	Instant Messenger	2.34%
Cross Fire	Game	1.99%
The Dream West Travels	Game	1.47%
Dungeon & Fighter	Game	1.39%
Word	Office	1.32%
World of Warcraft	Game	0.76%

Name of Host Application	*Type*	*Ratio*
other	other	19.75

For convenience, we summarize them into Fig. 1 as below:

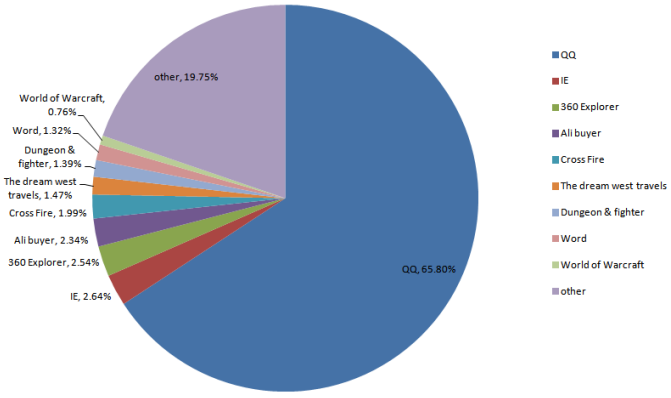

Figure 1. Top 10 hosts

Firstly, as shown in Fig. 1, user inputs Chinese mostly on several typical kinds of applications, such as instant messenger, web browser, game and so on. Each kind of application corresponds to a kind of typical user scenario. It is great helpful for Chinese input software to improve its performance on these limited scenarios. Secondly, instant messenger is the top scenario whose ratio even exceeds the sum of the others. It indicates that social contact becomes the top need for Chinese user. Web browser and game are the 2nd and the 3rd typical scenarios. User also does a lot of social contacts on them. For example, user contact with each other by twitter and blog from web browser; they share information in games. Therefore, it's necessary for Chinese input software to improve its performance on social contact to meet the user needs. For example, it should enhance its lexicon periodically by mining new words from social network. Thirdly, the 'other' type of hosts takes about 20% portion. The ratio of each individual host is no more than 0.5%. It indicates that there is also a 'long tail' in the user input scenarios, as it exists in other areas [2].

2.3 Distribution of Input Length

By the scale of input unit, Chinese input software can be categorized into three types: the character-level one, the word-level one and the sentence-level one. All of the commercial Chinese input softwares are the sentence-level ones which allow user inputs a whole Chinese sentence each time. Language modeling is the key technique to build the sentence-level Chinese input method [3]. However, by intuition, user usually does not type in all the pinyin strings for a whole sentence each time. In fact, it often types in the pinyin strings for a short fragment, that is usually semantic complete, then confirms it into the host application. User inputs the whole sentence by several fragments. For example, the user is going to input "今天下午我们开会" (in this afternoon we are going to have a meeting). It usually confirms the fragment of "今天下午" (in this afternoon) into the host application firstly. Then it inputs "我们开会" (we are going to have a meeting) in the second time.

In this section, we investigate the distribution of length of user input fragment in the typing records. By contrast, we also present the distribution of length of Chinese sentence in our training corpus which is used to build the language model for QQ input software. It is from the QQcom which is the most popular web portal in China [4]. Its scale is about 1TB. The results are described in Fig. 2 as below:

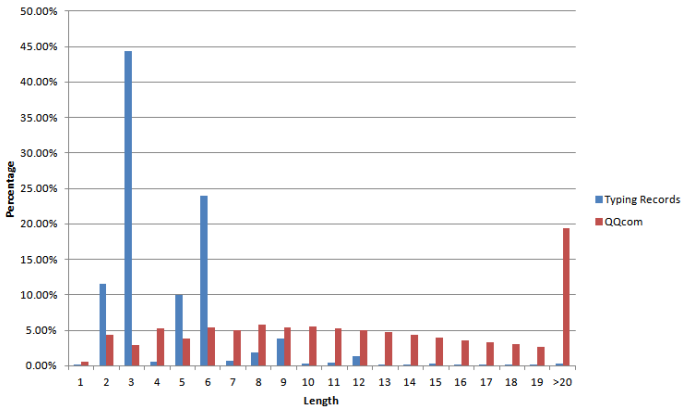

Figure 2. Distribution of Input Length

As shown in Fig.2, there is large portion on short length in user typing records. The average length that user inputs Chinese characters is 4.52. The user inputs that exceed more than 10 characters are very rare. It proves that user is prone to input Chinese by short fragment, rather than the whole sentence. By contrast, the length distribution is much evenly in the Chinese sentences in our training corpus. Its average length is 13.61. There are about 20% sentences whose length exceeds 20 Chinese characters, which indicates that some sentences are very long. Therefore, it's beneficial to build QQ input software on the corpus containing shorter sentences, so as to meet the user input in reality better.

3 Conclusions

In this paper, we study the user input behaviors by analyzing user typing records from QQ input software. We get some insights from it. It enlightens the way to improve the performance of Chinese input software. In our future works, we are going to apply these insights on the new versions of QQ input software, so as to improve user experience on inputting Chinese from keyboard.

4 References

[1] The information is provided by the operation platform of Tencent Technology Company Limited.
[2] Zipf GK. "Human Behavior and the Principle of Least Effort", Cambridge, Massachussetts: Addison-Wesley. 1949.
[3] Jinghui Xiao. "The Study of Non-stationary Language Modeling Techniques and its Practices". The PHD Thesis. Harbin Institute of Technology, 2007.
[4] www.qq.com

SESSION

ROBOTICS AND APPLICATIONS + RELATED ISSUES

Chair(s)

TBA

From Teleoperation to Autonomy: "Autonomizing" Non-Autonomous Robots

B. Kievit-Kylar[1], **P. Schermerhorn**[1], **and M. Scheutz**[3]
[1]Cognitive Science Program, Indiana University, Bloomington, IN 47404, USA
[2]Department of Computer Science, Tufts University, Medford, MA 02155, USA

Abstract— *Many complex tasks (search and rescue, explosive ordinance disposal, and more) that eventually will be performed by autonomous robots are still performed by human operators via teleoperation. Since the requirements of teleoperation are different from those of autonomous operation, design decisions of teleoperation platforms can make it difficult to convert such platforms for autonomous use. In this paper, we discuss the differences and the potential difficulties involved in this conversion, as well as strategies for overcoming them. And we demonstrate these strategies by "autonomizing" a fully teleoperated robot designed for tasks such as bomb disposal, using an autonomous architecture that has the requisite capabilities.*

Keywords: tele-operation, autonomy, conversion

1. Introduction

Teleoperated robots are becoming widely available for all kinds of activities, from defusing bombs (like the IRobot Packbot in war zones)[1] to remote presence robots (like the Vgo)[2]. These robots are able to go places and do things that would normally be too dangerous for humans, or simply be too expensive to be practical. They include a range of sophisticated equipment and low-level control algorithms, and would seem to be naturally suited, and are certainly highly desirable, for autonomous operation. Compared to autonomous robots, teleoperated robots are easier to build and easier to sell because no control system for autonomous operation has to be designed (all the intelligence and control lies with the human operator instead) and sometimes poorer quality or fewer sensors can be used (as humans can generally make better use of available sensors than current autonomous techniques). Hence, it is unsurprising that increasing the efficacy of teleoperation interfaces is a continued research focus (e.g., [1], [2], [3]).

One obvious drawback of teleoperation is the need to have a live control stream of data for sensors and effectors. However, given the constraints that make robots appealing tools, it may be difficult or impossible to establish the data connection (e.g., because of the distances involved or environmental interference), and requiring a controller to be close to the robotic platform may put the operator in danger, eliminating the primary advantage of using a robot. Even in the absence of such obstacles, the need for constant human attention adds expense and limits the overall effectiveness of the robot. The ability to operate these robots autonomously would avoid many of these limitations, but researchers need access to the robots to continue to improve the performance of autonomous robot architectures to the point where the human operator is not needed.

The common response to the above issues has been the design of "hybrid autonomous/teleoperated" systems that combine the strengths of both approaches. Mixed-initiative architectures are suitable as extraplanetary rover control systems, where prohibitive communication delays necessitate some degree of autonomy, while the higher-level decision-making remains in the hands of a team of human experts [4]. Several groups have examined effective mechanisms for adjustable autonomy, so that the balance between teleoperation and autonomy can be dynamically altered to fit the circumstances [5], [6], [7].

While mixed-initiative systems touch on the autonomization problem, these systems are designed from the ground up with partial autonomy in mind. Very little work has been done on converting systems that were designed to be purely teleoperated into partially or fully autonomous systems. Not only is the literature on the transformation of non-autonomous robots into autonomous ones far sparser, but the existing papers also focus mostly on the integration of one particular robotic platform. E.g., Barreto [8] describes the autonomization of the ANDROS platform using the idea of interchangeable "brick" components to add new sensory capabilities. Similarly, Stewart and Khosla[9] describe a modular control mechanism for a Puma 560 in which a teleoperation module is replaced with an autonomous one.

We believe that a greater understanding of how a conversion can be done would be greatly beneficial to the field. In this paper, we describe our efforts for developing systematic principles for converting non-autonomous teleoperated robots into fully autonomous platforms. We start with a brief background on teleoperated and autonomous robots. We then discuss some of the design philosophies that affect "autonomizing" teleoperated systems. Next we describe our transformation of the Multi-Mission Payload Platform (M2P2) into a general

[1]http://www.irobot.com/gi/ground/510_PackBot
[2]http://www.vgocom.com/what-vgo

purpose autonomous system. After presenting an evaluation of the new system in a "bomb disposal" task, we finish with some discussion about limitations of this technique as well as how generalizable it is to other robotic platforms (`http://www.apitech.com/products/multi-mission-payload-platform-m2p2`).

2. "Autonomizing" Teleoperated Robots

Successfully implementing an autonomous architecture on a robot that has been designed for teleoperation requires overcoming a variety of challenges. All of these challenges are traceable in some way to how different constraints factor into the design of purely teleoperated robots.

While there are some obvious mechanical differences existing in the hardware needed to perform communication with an operator verses an autonomous system, many more subtle assumptions go into the construction of these two types of robotic platforms. Autonomous and teleoperated robots will often require different levels of sophistication in the sensors needed to perform their tasks. For example, while the output of wheel encoders and range-finders may be very useful in allowing a program to determine its position, often humans rely on more expensive sensors such as video cameras to quickly expose them to a high volume of noisy data. As well as sophistication in sensors, complex robots with many moving parts require complex control systems. While a human operator may only be able to focus on a subset of controls at any given time, microchips are able to compartmentalize the various effectors allowing simultaneous meaningful control of all. While more user friendly interfaces or multiple operators may alleviate the control problem to some degree, it can not match the orchestration of a single programmatic control architecture. Similarly, the computational requirements of a remotely-controlled robot can be very low. Hence, there may be no general-purpose onboard computer, or that computer may be underpowered to handle the tasks (problem-solving, sensor processing, etc.) required for autonomous operation.

The same goes for effectors; for example, the design of a gripper that will be actuated via a gamepad in the hands of a skilled user might look very different from what an autonomous robot architect might ideally envision (e.g., because it has fewer safeguards, relying instead on the operator's skill and judgment). Even at the mundane level of connectivity, different requirements are evident; a relatively low-bandwidth wireless connection might be acceptable for teleoperation (e.g., lower frame-rates, lower resolution, or higher noise in a camera feed may be easier for a human operator to deal with than for a vision processing algorithm; similarly for audio streams and voice recognition). Autonomous operation may, therefore, necessitate the addition or replacement of computational, sensing, or effecting equipment on the teleoperation platform.

We now address specific challenges:

a) Physical connection: Sensors and effectors need to be exposed to the control architecture. In some cases it may be possible to make use of the existing teleoperation channel, but (as noted above), this will sometimes not be feasible. In that case, it will be necessary to create alternative interfaces (e.g., RS-232 or USB-based serial or wired Ethernet connections). Moreover, if device drivers and libraries do not provide access at the right level of abstraction, it may be necessary for the control architecture to implement a software interface, as well.

b) General control algorithms for effectors: Similarly, depending on the nature of the particular sensors and effectors, it might be possible to use existing control algorithms (e.g., for a mobile robot base or for an n-degree of freedom manipulator) or to use them after only minor adaptations. In the worst case (typically because a given piece of hardware is used differently under teleoperation than under autonomy), new algorithms need to be developed for particular sensors and effectors. For example, feedback from sensors such as wheel encoders can be used to generate a simple, immediate, computational understanding of an autonomous robot's pose. However, the human operator is unlikely to find encoder counts useful, so they may not be exposed via a software interface, and in the worst case, may not even be present at all. Other sensors, such as cameras, are often easier to access, but may still require additional processing steps (e.g., to extract individual frames for visual processing from a video stream encoded for efficient transmission).

c) Control architecture: Naturally, one of the biggest changes will be the inclusion of the autonomous control architecture itself. A wide variety of configurations is possible; depending on the task, the control architecture will comprise different components, possibly including a planner, an action execution component, components for user interfaces including screen-based and possibly spoken natural language dialog interfaces. The task approach can either be pre-programmed (e.g., in terms of action scripts) or the robot can be dynamically instructed during task execution. The latter requires the control architecture to use problem-solving for new tasks for which no action scripts exist [10].

d) "Plug-and-play" generalizability: Adding an existing control system can be relatively straightforward if it implements and uses a well-defined API structure. Typically, sensors will fall under a particular sensing category, e.g., range sensors, vision sensors, force sensor, etc., thus allowing for a generic interface to be adapted for the particular sensor use. Similarly, typical effectors such as wheels for mobile platforms, grippers, or robotic arms will allow for abstractions that map effector-specific commands and properties to more generic interfaces that can interact with standard algorithms. If the control system is designed with such generic interfaces in mind, the problem can be viewed as one of ensuring that the control system's expected interfaces are mapped properly onto the teleoperated robot's hardware and software

interfaces. The difficulty here is that there is unlikely to be a one-to-one match of functional units between the teleoperation platform and the control architecture. For example, the robot's interface may support driving arm joint motors at a given velocity, in agreement with the control architecture's expectations. However, it may lack a predefined position-based joint motion mechanism, which must be added as part of the integration if the control architecture expects it. Similarly, there is no reason to assume that both architectures will use the same relative sign or units.

e) Programatic interface: Ideally, whether it is implemented as a software library (e.g., C/C++ shared objects, Java classes, etc.), simply given as a communication protocol (e.g., custom serial protocols, standardized infrastructures, etc.), or some combination of the two, the interface for a new piece of hardware will be well-specified and clearly documented. However, given that teleoperated robot platforms are not originally intended to be targets for development, the likelihood of undocumented features or errors in the specification is somewhat higher than normal. In such cases, it may be necessary to examine how the teleoperation controller interfaces with the robot architecture that it was built with. Studying the effects of (or responses to) valid messages sent from the original teleoperated controls, can be very helpful for "filling in" gaps. These messages can then either be analyzed for patterns or stored as a response lookup table to be used later by the software.

f) Simulation: Simulation is a valuable tool for any autonomous robot architecture, and not just to facilitate testing before deploying on the physical robot. Take, for example, the case of arm movement and manipulation. Since human operators inherently have extremely rich mental models of the systems that they are working with, they do not require precise measurements of all of the possible positions in joint space. Simply by viewing a handful of video frames taken from a mounted camera, the operator can determine approximately how that camera is mounted in relation to the robot and the target as well as determining an appropriate movement path. For the autonomous architecture, on the other hand, pre-building a highly accurate model of the known environment (the robot and its manipulators) will allow it to avoid the time-consuming process of building relational models on the fly. Such simulation planning also allows a robotic architecture to plan movements through space that optimally avoid obstacles, which is especially important in cases where feedback from the platform regarding joint positions is of less than ideal fidelity.

2.1 Experimental Platform

The robot we chose to autonomize is the APITech Multi-Mission Payload Platform (M2P2). This robot was designed to be controlled by a human operator primarily via a wireless XBox game controller. The M2P2 is a three wheeled holonomic robot with each wheel capable of rotating independently. It is equipped with a 2 DOF arm terminated by a 2 DOF gripper. The operator can get the robot's view of its environment through two cameras, one mounted on the platform and one mounted on the arm. In addition, the platform includes both a speaker and a microphone, allowing the operator to speak through the robot and hear any sounds near the robot.

Communication in the M2P2 is a subset of JAUS (the *Joint Architecture for Unmanned Systems*, a standard for open interoperability in robotic architectures [11]), augmented by a small number of custom message types. The M2P2 implements a set of core movement functionality as well as including custom messages for the robot arm control and specific sensors. JAUS messages on this robot are passed on two onboard networks, one for sensors and one for effectors. Messages are transmitted wirelessly to a pack based Operator Control Unit (OCU). Video streams are played back on a dedicated tablet PC along with custom built software to facilitate control of robot movement.

We integrated the M2P2 into ADE (the *agent development environment*), a Java-based infrastructure for developing robotic architectures [12], [13], [14]. ADE provides communication mechanisms that allow modular functional components to interact in a distributed fashion using Java remote method invocations. ADE components can register their own services and look up services provided by other components, and connections between components are monitored to ensure robust execution. A well-defined suite of programming interfaces allows consistent access to a variety of sensors (e.g., laser range-finders, GPS sensors, and cameras) and effectors (e.g., robot bases such as the Segway RMP, Mobilerobots Pioneer, and Videre Era). Implementing these interfaces on the M2P2 allows us to take advantage of the existing autonomy facilities in ADE, including problem-solving and goal management.

2.2 Communication

The first step in autonomization is to establish communication pathways between the teleoperated robot base and the computer that will host the autonomous architecture. This meant bypassing the existing wireless RF interface used by the teleoperation rig to instead make direct (wired) Ethernet connections to the robot.

Once the physical connection has been made, it must be tested. Before the cheap availability of high performance micro processors and network adapters, connection types were likely all proprietary and highly compact. Now, developers are moving toward higher bandwidth communication to help improve comprehension of the messaging system. Protocols like the Internet Protocol (IP) both internally provide a lot of functionality (message ordering, routing, etc.) but also have many tools to help receive, send and process information. Robots running such protocols can

often be tested with packaged communication processing tools, while rarer protocols may require testing specific to a given communication design.

g) Communicating with Effectors: Although communications protocols could theoretically be arbitrarily complex, they break down into two parts, syntax and semantics. For each functional ability to be run on the robot, syntax is the set of argument variables with possibly some information on their size and type, and semantics is the generalized understanding of how the bits in each argument are interpreted (as flags, as integers representing feet, doubles representing miles per hour, etc.). When trying to back-engineer a communication protocol, the syntax of the command must be determined first. The syntax alone however is not sufficient for interpreting and generating commands of that type as the variables must be unpacked as values and then those values given in meaningful units or conditions.

For example, when implementing robot arm control for the M2P2, we determined from the JAUS protocol that the command to modify the arm position was a concatenation of values each representing a velocity of one of the arm joints. This information alone was insufficient even to determine the exact syntax of the command. Through feedback from the manufacturer in conjunction with systematic testing of options, and validation of the specifications, we found the ordering of the joints and number of bytes allocated to each joint in the command. While this specified the syntax of the commands, it was still unclear how each set of around four bytes (more for some joints and less for others) translated into a velocity on the physical arm.

Some of the most common encoding variants are; flags, scaled integers, IEEE floating point or doubles, and angles. Flags can be tested through simple trial and error when the outcome of the flag is an obvious physical change in the system. Scaled integers (where the values are interpreted as integer values times a scaler plus an offset), are often easy to detect as similar integer input values will lead to similar output speeds or other output types. Floating point or double precision number should be tested similarly to scaled integers, where similar inputs cause similar outputs however instead of using similar integer representations to test, convert the values into either doubles or floating points. Angles, while a subset to scaled integers or decimal precision numbers, are a special case as they are cyclic in nature and this must be accounted for when trying to determine if a particular encoding is of this form.

When all attempts at understanding the semantics fail (i.e., a systematic test of the possible input space provides no observable consistences), an alternative approach is to build a simple input/output lookup table. Recording what direction a particular joint makes and potentially some gross speed conditions, for a set of given inputs, can allow a simply designed inverse process where a desired speed can be achieved by finding the closest speed known in the lookup table. Some times, it is also sufficient to have the robot operate at a single speed (or more often, one speed in both the positive and negative direction) in which case a hard coded single value can be used.

The JAUS protocol specifies two main types of movement commands: "set velocity" and "move relative". Because this platform was designed to be controlled by a remote human operator, only the "set velocity" commands are implemented. Similarly, although the wheel units almost certainly include wheel encoders, they are not accessible via the JAUS interface. This was a common theme to the design, where simplifying steps were used in terms of what to expose to the external system based on the assumption that the robot would not operate autonomously. However, with the "set velocity" commands, we were able to implement all of the elements of the movement interface expected by the control architecture.

Teleoperated robots are often designed to expect continuous command feedback from an operator. The robot may receive a constant stream of drive commands even though the operator has held the movement joystick at a constant angle. Since the robot can not correct its error if the human operator is disconnected, if no new commands are received in a given amount of time, most designs will stop the robot movement. While this may be logical for an autonomous system as well, there is a stronger bias in a teleoperated system to default to no action and let the human override if this is a problem. While converting a teleoperated system this is important to note as it may require additions such as message repetition at constant intervals to keep the robot performing a desired action.

h) Communicating with Sensors: One of the most important sources of information for an autonomous robot is the camera; we will illustrate the process of establishing communication with a sensor using the example of interfacing with the M2P2 camera. From the programmer's perspective, it would be easiest if it were possible to simply grab fully-formed individual frames from the video stream. However, such an encoding scheme would consume too much bandwidth in many domains, so a variety of protocols take advantage of similarities between adjacent frames to compress the data stream. Moreover, although many of these video encoding protocols are well-known, in some cases proprietary variations may have been added to the standard protocol to meet the needs of the particular robotic platform. This imposes additional challenges when converting a teleoperated robot for autonomous operation, as even the base protocol might be unknown, and any proprietary extensions are unlikely to be published.

As noted above, the main challenge for utilizing the cameras is deciphering the video stream. Primary variations in video streams to be aware of at this stage are, different color models (RGB, CMYK, etc) and streaming verses static video translation (some decoders require the full video buffer to be available before decoding can begin, this will not work

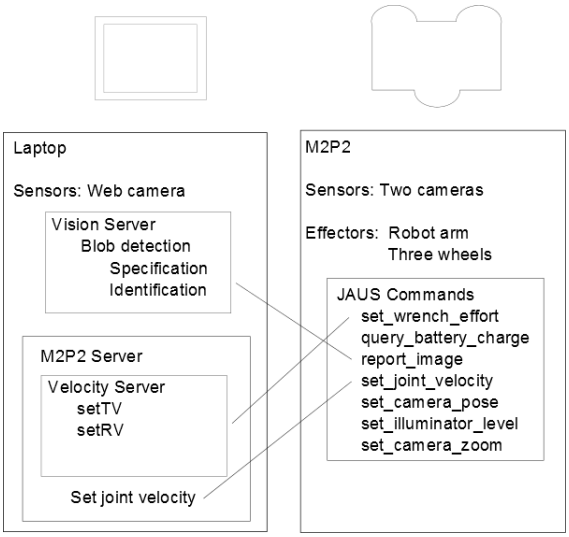

Fig. 1: **Architecture layout of the M2P2 and controller laptop.**

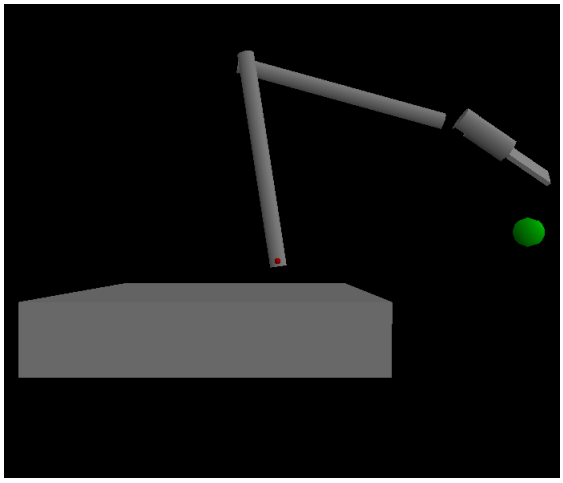

Fig. 2: **Visualization of the robot arm simulator.**

for streaming video feed from a robot).

When decoding the M2P2 video format, we started by searching the data for likely protocol elements, such as sequential markers added to verify order of packets received. This allowed us to discover the higher fidelity "key frames" that were sent at regular intervals to allow cumulative error between frames to be reset. In this particular case, we were able identify the protocol using the key frames and apply standard decoding routines to extract frames from the stream. We determined by the data header, that the M2P2 used a slightly augmented mpeg encoding variant. After removal of the additional formatting, the video stream could be parsed into readable raster images, using the FFMPEG decoder.

2.3 System Configuration and Control

Once basic communication protocols had been established, the system was integrated with the ADE infrastructure. A general purpose JAUS component was written to facilitate creation and interpretation of JAUS messages. Figure 1 shows the connections between the M2P2 control architecture and the architecture on the laptop used to control the newly autonomous robot.

The newly added laptop served as the primary intelligence control for the robot platform. As the M2P2 server is fully ADE compliant, it has access to all other ADE servers and functionality available to other holonomic robots in that environment. This includes a vision server to process incoming camera feeds, planners, and natural language interpreters. The M2P2 becomes a removable module fitting into a larger autonomous robotic infrastructure. As well as adding functionality, the ADE infrastructure adds error handling, security and the ability to offload processes not only from the original robots processors but also from those physically added to the robot. A smaller, less capable control unit can then be used to interface with the robot while the computationally expensive operations such as image processing can be handles by external, more powerful computers.

A web camera was connected to the laptop directly and mounted on the front of the mobile platform. While the robot had built in video feeds, these were slow, of lower quality, and computationally consuming to process directly on the control computer (As the signal had to pass through the JAUS communication protocol first). Connecting a new camera to the laptop helped the software react in real time (while the video feeds from the robot were still accessible). While the built in cameras were not used in this particular experimental paradigm, having the ability to interface directly with the on-board cameras allows future projects to take advantage of views that may be more difficult to introduce with external hardware. The robot arm has a small camera which gives a "dog's mouth" perspective on the gripper. Having an accessible video feed from this camera will allow for much more complex and delicate manipulation in future tasks.

To facilitate planning of arm movements, we developed a simulation environment for the robot joints (Figure 2). The simulation environment is written as an extension of a 3D visualization environment that was designed for the ADE infrastructure. Code is written in native Java and can be run with the visualization on or off. This allows the simulation to be run on either a standard PC with a GUI showing progress or a high performance computational grid to run detailed large-scale searches of the complex arm movement space.

In the simulation environment, a robot arm is specified as a series of rigid blocks connected by joints. Blocks are attached to each other in a familial hierarchy starting with the root block that is connected to the robot frame. Each block is defined as a collection of primitive objects (spheres,

rectangular solids, cylinders, etc.) with affine transformations applied relative to that block's starting position and orientation. As with most 3D tools, sub-objects can be nested in a parent block and an affine transformation specified for the entire block of sub-objects. Each joint is also capable of defining how that joint is allowed to rotate. Rotation can be in any of the three cardinal planes (around the X, Y, and Z axis). A center of rotation is specified both for block that is to be rotated as well as the parent block to which it is attached. A starting rotation angle can be given as well as bounds on rotation in each of the planes. All specifications are stored and read from an XML formatted data file.

When the control architecture determines a goal point to move the arm to, the planning mechanism in the simulation environment begins. A goal is specified as a coordinate in three-dimensional space relative to the root of the robot arm as well as an orientation of the end effector at that point. Planning is carried out using a gradient descent technique which can either be mimicked in real-time by the physical robot (and feedback used from the arm pose of the actual robot if available), or stored as an action sequence and played back at a future time. In the gradient descent algorithm, the robot attempts to move each of its joints a fixed small distance in each direction that the joint is allowed to move in. A fitness function is used to calculate the fitness of each of these new arm locations and the movement with the highest fitness is selected to be performed. This pattern is iterated until a local maximum is found. The fitness function is a scaled combination of the distance of the effector from the goal, the orientation of the effector relative to the desired end orientation and a negative strength from all joints based on their proximity to any collisions in the environment.

While gradient descent will not be sufficient to solve all arm trajectory problems, it is sufficient for many purposes. The M2P2 arm moves in a single vertical plane, with two joints controlling the position of the end effector. Since it also provides real-time (and can be pre-calculated in far faster than real-time) movements, it is ideal for the immediate response time required by tasks such as bomb defusing for which the M2P2 was designed. The simulation environment can also be used by more complex path planning algorithms for more complex environments.

One important complication to arm movement was the lack of "somatosensory" feedback, as there were no sensors to detect the relative arm position. To calculate the relative arm position, we took the arm resting pose as a base (this location was enforced through physical stops on the robot joints). Through experimentation, it was determined that the acceleration time in getting the robot arm from rest to a desired velocity was minimal. The amount of time necessary to move the arm a desired distance could be calculated simply by dividing the distance by the presumed constant speed of the arm. While this works for low fidelity situations, the acceleration will cause problems where fine motor control is required (such as using the grippers to pick up a small object). To reduce the error, all movements were blocked into constant length (or angle) chunks. As the gradient descent approach expected output tests to be constant sized already, constant sized movement blocks was the obvious choice.

If the robot had needed to perform multiple tasks, the cumulative errors would have added up. To combat this, the forced resting pose could be required after a certain amount of movement to recalibrate location.

3. Validating the Integration

To evaluate the integration, we devised a simplified version of the robot's primary function: bomb disposal. In this test, the robot was required to detect a suspicious object ("the bomb"), approach it, and retrieved it. It was then required to detect the ("safe") disposal receptacle, move to it, and deposit the "bomb" inside. This task can be decomposed into five phases, as depicted in Figure 3.

Detect object: Object detection was performed using simple color detection and blob size thresholding. The ADE vision component processed frames from the web camera, producing a description of each detected object that included its relative position in the frame (and hence relative to the robot's heading) and its size in the visual field. The autonomous control system made regular requests to the vision component until a positive identification was made, at which point control progressed to the next phase.

Move to object: Once the object was detected, the control module computed the course adjustments to move to it using a visual servoing approach [15]. Rotational adjustments were made based on the horizontal position of the object in the frame. Given the assumption that the object in question would be on the floor, distance could be estimated using the object's vertical position in the frame. When the object was determined to be in the effective region of the gripper, the approach phase was concluded.

Plan/perform reach: The reach and grasp actions were constructed dynamically using the arm motion planner described above. The "reach" goal was set based on the object's relative location as determined by the vision component. The control system sent the plan steps generated by the gradient descent algorithm to the arm, moving the gripper toward the goal state: poised over the target object.

Detect receptacle: The receptacle was detected in the same way that the target object was detected. A different color was used as the indicator.

Move to receptacle / drop: When the robot moved such that it judged its manipulator was over the receptacle, the block was released and the robot ended its movement pattern.

A video of the bomb disposal demonstration can be viewed at `http://tiny.cc/autonomized`.

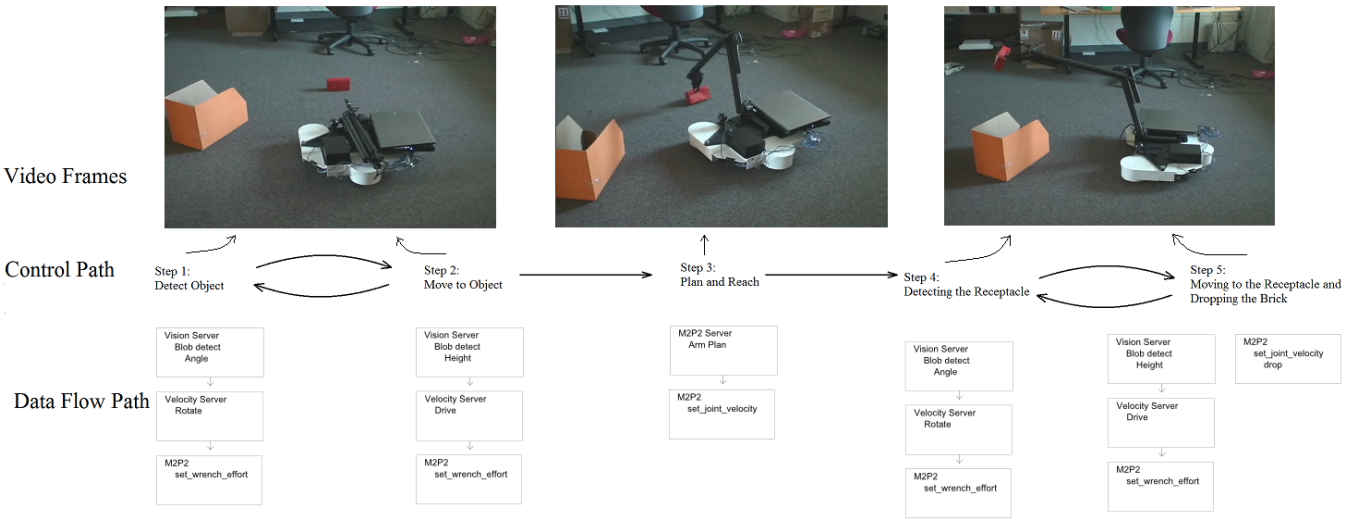

Fig. 3: **The data control path and data flow during the experiment (the control path indicates at what steps different computational units were activated).**

4. Conclusions and Future Work

Limitations to autonomizing teleoperated robots are dictated by the design of the robot in question and the persistence of the group attempting to perform the automation. In general, if basic platform movement can be achieved, most traditional robotic tasks can be performed with the possible addition of necessary sensors and manipulators. To this end, the basic platform can be thought of as an operation module with the potential addition of pre-existing functional modules attached. If very fine control is needed over the robots pose, it may not be feasible to augment a teleoperated system, since such fine feedback may not be available, and extremely difficult to add into the physical architecture. Although we used multiple software infrastructures in our case study integration, we used only one hardware platform (the M2P2 robot). In future work, integration of multiple existing hardware platforms would lead to a more modularized schema for conversion (e.g., a chassis from one manufacturer and a manipulator from another could both be integrated into the same software architecture).

References

[1] M. Luimula, K. Saaskilahti, T. Partala, S. Pieska, J. Alaspaa, and A. Lof, "Improving the remote control of a mobile robot using positioning and ubiquitous techniques," in *Proceedings of the 2007 IEEE International Conference on Automation Science and Engineering*, September 2007, pp. 1027–1033.

[2] I. Farkhatdinov and J.-H. Ryu, "Hybrid position-position and position-speed command strategy for the bilateral teleoperation of a mobile robot," in *Proceedings of the 2007 International Conference on Control, Automation and Systems*, October 2007, pp. 2442–2447.

[3] C. W. Nielsen, M. A. Goodrich, and R. W. Ricks, "Ecological interfaces for improving mobile robot teleoperation," *IEEE Transactions on Robotics*, vol. 23, no. 5, pp. 927–941, October 2007.

[4] M. Ai-Chang, J. Bresina, L. Charest, A. Chase, J. Hsu, A. Jonsson, B. Kanefsky, P. Morris, K. Rajan, J. Yglesias, B. G. Chafin, W. C. Dias, and P. F. Maldague, "MAPGEN: mixed-initiative planning and scheduling for the mars exploration rover mission," *IEEE Intelligent Systems*, vol. 19, no. 1, pp. 8–12, January-February 2004.

[5] M. Goodrich, D. O. Jr., J. Crandall, and T. Palmer, "Experiments in adjustable autonomy," in *Proceedings of the 2001 IJCAI Workshop on Autonomy, Delegation and Control: Interacting with Intelligent Agents*, Seattle, WA, August 2001, pp. 1624–1629.

[6] M. Y. Cheng and R. Cohen, "A hybrid transfer of control model for adjustable autonomy multiagent systems," in *Proceedings of the 4th International Joint Conference on Autonomous Agents and Multiagent Systems*, The Netherlands, 2005.

[7] P. Scerri, D. Pynadath, and M. Tambe, "Why the elf acted autonomously: Towards a theory of adjustable autonomy," in *Proceedings of the 1st International Joint Conference on Autonomous Agents and Multiagent Systems*, Bologna, Italy, 2002.

[8] R. D. Barreto, "Migration from teleoperation to autonomy via modular sensor and mobility bricks," Master's thesis, The University of Tennessee, Knoxville, August 2006.

[9] D. Stewart and P. Khosla, "Rapid development of robotic applications using component-based real-time software," in *International Conference on Intelligent Robots and Systems-Volume 1*, August 1995.

[10] R. Cantrell, M. Scheutz, P. Schermerhorn, and X. Wu, "Robust spoken instruction understanding for HRI," in *Proceedings of the 2010 Human-Robot Interaction Conference*, March 2010.

[11] S. Rowe and C. R. Wagner, "An introduction to the joint architecture for unmanned systems (JAUS)," Cybernet Systems Corporation, Ann Arbor, MI, Tech. Rep., 2008.

[12] J. Kramer and M. Scheutz, "Robotic development environments for autonomous mobile robots: A survey," vol. 22, no. 2, pp. 101–132, 2007.

[13] M. Scheutz, "ADE - steps towards a distributed development and runtime environment for complex robotic agent architectures," *Applied Artificial Intelligence*, vol. 20, no. 4-5, pp. 275–304, 2006.

[14] V. Andronache and M. Scheutz, "Integrating theory and practice: The agent architecture framework APOC and its development environment ADE," in *Proceedings of AAMAS 2004*. ACM Press, 2004, pp. 1014–1021.

[15] P. Corke, "Visual control of robot manipulators—a review," in *Visual Servoing: Real-Time Control of Robot Manipulators Based on Visual Sensory Feedback*, K. Hashimoto, Ed. World Scientific, 1993, pp. 1–31.

A Developmental Robotic Paradigm Using Working Memory Learning Mechanism

X. Wang [1], M. Tugcu [2], J.E. Hunter[3] and D.M. Wilkes [3]
[1]Xi'an Jiaotong University, Xi'an, Shaanxi, P.R. China
[2]STM Company, Bilkent, Çankaya, Turkey
[3]Center for Intelligent Systems, Vanderbilt University, Nashville, TN, USA

Abstract - *Traditional machine learning algorithms typically employ task specific methods and only the parameters pre-determined by the human programmer are updated. These methods often fail to respond to the dynamically changing states of the uncontrolled environments. Additionally, such methods may not represent a developmental entity, such as a human mind. In contrast, an open-ended developmental robot system can learn simple behaviors and build up more complex behaviors by utilizing the previously learned behaviors. In this paper, we propose a basic framework for visual learning tasks that integrates a perceptual system into a biologically inspired working memory system. A main objective of this research is to provide a general framework for developmental learning and to investigate how well a neuro-computational PFC working memory model performs on a robotic platform in a real world environment with complex tasks. Experimental results given show impressive performance both in terms of accuracy and speed of learning.*

Keywords: Developmental robotics, machine learning, computer vision, working memory, reinforcement learning.

1 Introduction

The ultimate goal in robotics is to build a robotic system, which can develop new skills incrementally, in an autonomous open-ended approach through interactions with the environment without having a pre-designed, task-specific representation [1]. However, traditional machine learning algorithms typically employ task specific methods and often fail to respond to the dynamically changing states of the uncontrolled environments. To fill the gap that machines do not benefit from traditional machine learning and AI techniques, a relatively new area of study, called autonomous mental development (AMD), has been proposed. It was pointed out by Weng et al. that a mental development process must be able to generate representation and architecture autonomously online and directly from raw sensory signals which must also be task nonspecific [2]. In contrast to traditional artificial neural networks, which can only accept a series of fixed size, offline sensory data vectors, a developmental robot runs in the real physical world and has the ability to add new data online that it has never seen before. Furthermore, it can develop simple, basic skills for many different kinds of tasks and these skills may be utilized to learn more complex skills. For example, a human child's brain is not manually trained with data within one training session. Instead, he/she is usually taught by his/her parents from time to time through approving or rejecting behaviors. Following the same idea, to operate in the real unconstrained world, where the environment is highly complex and dynamic and a human designer cannot predict in the initial stage of programming, a developmental robot should be trained by interacting with the environment and with the user through a student-teacher relationship. It is in this sense that there is a necessity for open-ended developmental systems. Table 1 shows the basic differences between the traditional engineering (manual development) paradigm and the proposed mental development paradigm.

Table 1. Main differences between traditional and developmental programs [2]

Properties of Program	Traditional Programs	Developmental Programs
Sensor-specific and effector-specific	Yes	Yes
Program is task-nonspecific	No	Yes
Tasks are unknown at programming time	No	Yes
Generate representation automatically	No	Yes
Animal-like online learning	No	Yes
Open-ended learning of more new tasks	No	Yes

As a bridge crossing between the external world and the internal environment, perception is an awareness of things through the physical senses. Humans perform learning at the perceptual level and perceptual learning has been considered to occur at the cognitive level where identification and categorization is performed with focuses only on the relevant data that is needed by the current learning task. In cognitive science, long-term memory has a very large capacity and the information is considered to be stored indefinitely, while working memory is defined as a theoretical framework which refers to a temporal type of storage that retains elements that are active and being manipulated for a short period of time. In the literature, many working memory models have been proposed, which have commonalities and differences [3], with the most popular one in psychology being the Baddeley and Hitch's three-component model of working memory [4] and the most famous one in neuroscience being the temporal difference (TD) learning model [5] (a very popular machine

learning algorithm describing the midbrain dopamine neurons). Recently based on the TD learning model, an open source software library, written in ANSI C++, called the Working Memory Toolkit (WMtk), has been developed which provides an abstraction layer and can be easily integrated into robotic control mechanisms [6].

A main objective of this research is to integrate a perceptual system into a biologically inspired working memory system in such a way that would yield a basic framework for visual learning tasks. Not being intended to focus on a specific task, the aim of our approach in this work is to provide a general framework for developmental learning, as well as to investigate how well a neuro-computational PFC (prefrontal cortex) working memory model performs on a robotic platform in a real world environment with complex tasks.

In the following, Section II talks about some of related work and efforts that contribute to the area of developmental robotics. Section III describes our proposed vision-based autonomous mobile robot system. In Sections IV, experiments are designed and results presented. Finally, conclusions are made in Section V.

2 Related Work

It was first pointed out by Weng that many traditional machine learning algorithms, including artificial neural networks, are computational frameworks but not developmental frameworks [1]. According to Weng, two types of paradigms exist. The first one labels the traditional machine learning methods as manual development, where the programmer understands the task, chooses a representation, and maps the task to the representation. Thus, the programmer conveys his understanding into the task representation. Next, the programmer writes code which controls the machine to execute the task using the task-specific representation. The second paradigm is called the autonomous developmental paradigm where the programmer writes a developmental program and the robot learns the task by interacting with the user/teacher and the environment. The result of such a mechanism should be that the robot generates its own internal representation.

Arguing that the system must deal with high-dimensional feature space for perceptual learning, Weng developed a structure called the "Incremental Hierarchical Discriminant Regression (IHDR) engine" [7]. To demonstrate the proposed method, a vision-guided navigation experiment using the IHDR system was presented in [1], [7], [8], where a mobile robot, called SAIL and developed at Michigan State University was trained by pushing it around the corridors of the Engineering Building. The robot had two pressure sensors on each side. The difference of the two pressure readings was translated into heading information and associated with the images. The grayscale intensity of the pixels was used as the components of the feature vectors and the resolution of the images was 30-by-40. As a result, the number of dimensions on which the system operates was 30-by-40, i.e., 1200. One feature vector was generated from an entire image and linear discriminant analysis was applied to the feature vectors to select the most discriminative features.

Krichmar and Edelman argue that devices, based on the working principles of the nervous systems, may provide the groundwork for the development of intelligent machines which operate on neurobiological principles rather than computational ones [9]. They have designed a series of theoretical models, called brain-based devices (BBDs), and applied them to physical robots in order to investigate the functionality of different regions of the brain. The robots equipped with these models are used for studying perceptual categorization, operant conditioning, episodic and spatial memory formation and motor control. They emphasize that models of brain function should reflect the dynamics of different brain regions, their structure and the connectivity of these regions, rather than implementing them as a single neuron layer. According to them, to construct such models, detailed neuro-anatomy and neural dynamics should be taken into consideration. To investigate the functional anatomy of the hippocampus region and its surrounding regions, Krichmar et al. [10] programmed a physical robot to solve a dry variant of the Morris water maze task. In the task, the robot was meant to use its spatial and episodic memory by associating perceptual cues in the environment with a particular location. In the experiment, the target location was hidden and can only be detected in close range by the robot's front IR sensor. The robot started a trial in one of the four locations and stopped if it detected the hidden platform or until a time limit of 1000 seconds was reached. The experimental results showed that the robot learned to navigate to the target location from multiple starting positions in about 8 trials.

A slightly modified version of the task, inspired by Krichmar's work, was presented by Bursch, et al. in [11], in a simulation environment. In contrast to Krichmar's experiment, the robot started a trial in random locations without using odometry information. In order to create a mapping between a perceptual state and an action for that state, a Self-Organizing Feature Map (SOFM) [12] was used and the heights (in pixels) of the colored panels were presented as an input to the SOFM. Two navigational approaches were proposed and compared. The first method was based on creating a probabilistic graph between the nodes of the SOFM and then searching for the optimum path in the graph in order to navigate to the target position. The second approach utilized the Working Memory Toolkit (WMtk), which we also chose as a working memory implementation for our system. It was reported that the first approach outperformed the WMtk with relatively little experience. However, as the number of training samples increased, the WMtk actually performed much better than the graph search technique.

3 Our Proposed System

With focuses on issues of developmental robotics, the methodology proposed in this paper is to establish a biologically inspired system that employs perceptual knowledge along with a working memory system in order to

provide broad capabilities for visual learning tasks. Such a requirement necessitates a large set of goals that the system needs to satisfy.

To have the robot operate in real world environments that are not modified by using artificial landmarks, the system learns everything from scratch. To learn and recognize natural landmarks, the images and videos were taken as RGB (red, green, blue) color images, which were next converted to the HSV (Hue Saturation Value) color space for use. To represent a small image region, a color histogram vector of size 10000 was calculated to form color based features and 40 Gabor filters were used to convolve with each image region to form texture based features. As a result, the combination of the color histogram and Gabor texture measures resulted in 10040-dimensional feature vectors. Then an unsupervised learning algorithm, a minimum spanning tree based clustering algorithm, was used to form percepts/objects for the robot vision system which would be used later for segmenting the incoming new images. For new images captured by the robot, feature vectors were first extracted, a nearest neighbor search process was followed to assign an object label to each newly extracted feature vector. Then a connected-component labeling algorithm is applied to find connected regions, called blobs. After the segmentation was done, the final stage of the perceptual system was to produce inputs for the working memory system, referred to as "chunks", in order for the robot to acquire sensory-motor associations to guide its actions. It is important to maintain a strong connection to the features of the percepts in the environment and to their semantic meanings. In other words, the robot should learn what each percept means for itself. In this context, understanding the meanings of the percepts is referred as perceptual grounding.

The limited capacity property of a working memory system provides focus for the robot to search for appropriate actions in order to accomplish a given task. In fact, the key point faced by the working memory system that is utilized in this proposed robot architecture is the determination of which chunks of information should be actively retained in the working memory, and which may be safely discarded, for tasks' success, that is, a prediction scheme in the expected future reward. Learning by associating stimuli with rewards and punishments (the reinforcers) is called reinforcement learning [13]. The particular type of reinforcement learning used in this research is called the *temporal difference (TD) learning* algorithm [5], which is typified by the delayed response tasks, with the main objective being maximizing the total amount of reward that the robot receives over a long run [5].

WMtk essentially implements a neural network version of the TD learning algorithm and contains classes and methods for constructing a working memory system that intelligently decides which chunks to maintain or discard depending on the reward criterion. This criterion is dependent on the current task of the robot and is specified by the user as a requirement for the WMtk. The reward is generated in a discrete-time manner (namely "episodes") and is a real number. Depending on the selected action in the previous episode, as well as the reward signal generated for that particular action, the WMtk updates its internal contents, based on which, the robot can then select and execute an appropriate action. The most distinctive feature of the toolkit is that it explores every possible combination of collection of chunks, which can be fit within the limited capacity of the working memory and selects and retains in the working memory the combination of chunks which provides the highest estimate value of the future reward. This feature of the WMtk can be very useful in robotic applications. The robot is not limited to only one single item to consider. For instance, in many applications a landmark location is represented by only one percept. However, a landmark location may be represented by a combination of percepts, which may help the efficiency of the robot's localization process. In addition, this would also help to increase the number of unique landmark locations in the navigation path of a robot.

The final flowchart of the system is presented in Fig. 1. The top half of the diagram represents the perceptual system. The lower portion represents the working memory system, which is combined with the robot's sensory-motor scheme (i.e., actuators and sensors such as sonars to avoid obstacles). The combination of both the perceptual system and the working memory system yields the cognitive structure for the robot.

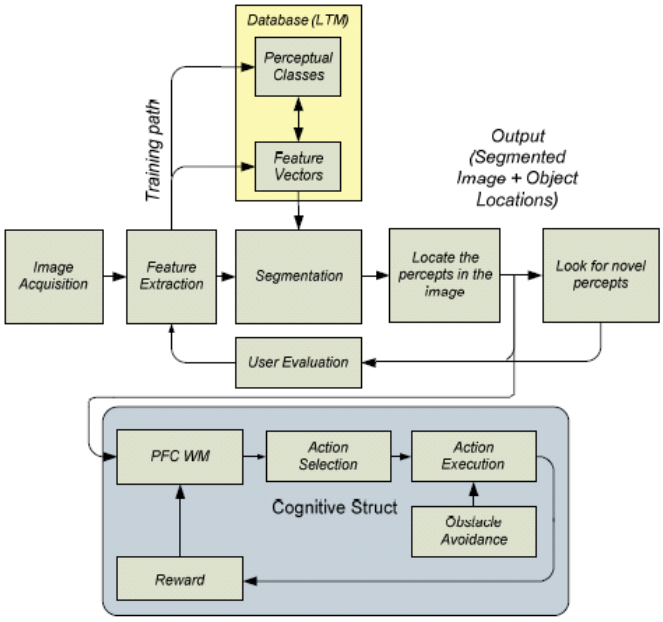

Fig. 1. The proposed system architecture.

In order to demonstrate the proposed method, the methodology proposed in this research is applied to a complex vision-guided navigation task. Part of the complexity of the task is that no a priori information is given to the system, such as a cartesian map or coordinates of objects, etc. Instead, a qualitative navigation approach is taken, where the robot proceeds by detecting natural landmarks that are present in the environment. It is desired that the system is capable of learning new skills and percepts online in uncontrolled environments while performing a task and supporting explanation of its

knowledge to and from the user in an interactive way. In order to achieve the navigation task, simple behaviors are learned and preserved in the system in order to learn more complex behaviors.

4 Methodology and Experiments

A fundamental property of a mobile robot is the ability to navigate safely in an uncertain environment. In order to achieve this task, the system needs to acquire sensory-motor associations to guide the behavior of the robot. To provide a general framework for developmental learning and to investigate how well a neuro-computational PFC working memory model performs on a robotic platform in a real world environment with complex tasks, several experiments are conducted that would exploit the usefulness and capabilities of this framework in mobile robotics. Each experiment is related and built upon each other in order for the robot to navigate successfully.

The testbed robot Skeeter is equipped with a single camera to perceive the environment. The front sonar array is only used for obstacle avoidance purposes. The experiments took place in the hall outside of the Intelligent Robotics Laboratory on the third floor of the Featheringill Hall at Vanderbilt University. A typical view of this hall is shown in Fig. 2. The major objects in this hall include the yellow floor tiles, the white floor tiles, and the black stripes of tiles, wood panel wall, light blue painted wall and a light blue railing. To generate a perceptual model for the environment, 20 images were collected over several days at different times to account the different lighting conditions. Next 66740 feature vectors were extracted from these images and clustered to obtain several percepts that constitute the training database of the system (the system's LTM). A color was assigned to each percept for displaying them in the segmented images. Table 2 shows the obtained percepts and their corresponding denoting color. A sample segmented test image is shown in Fig 2.

Table 2 Percepts and Denoting Colors

Percepts	Denoting Color
WoodPanel	Red
YellowFloor	Yellow
WhiteFloor	White
BlackFloor	Black
LightBlueWall	Light Blue
Bricks	Dark Red
BlueFloor	Blue

Fig. 2. A test image and its segmented version

In our empirical study, three experiments were designed to accomplish the navigation task. The first two experiments have been reported in [14] and are briefly repeated here for reference. The third experiment is a further extension built upon the first two. The objective of these experiments is to reveal the capabilities of the system in uncontrolled environments. In the experiments, the system learns new percepts, as well as new skills so as to ultimately perform a qualitative vision-guided navigation task. Since the task is qualitative navigation, no metric information is involved in the computations. Only the angular positions of the percepts with respect to the robot frame are computed.

4.1 Experiment 1: learning open space

The first step in the navigation task is to learn the percepts that would yield an open path for the robot through the robot's own interaction with the world. Once meaningful blobs or percepts are obtained from the images acquired from the camera, the robot needs to learn the association of the percepts with motion. In other words, the robot needs to determine whether the percept represents an obstacle or an open space. To do so, in this task, the reward criterion for the WM system is selected to be the distance moved by the robot per trial. The procedure for the first experiment is as follows:

- WM size is set to 1.
- Blobs segmented from a captured image are then presented to the WM. The WM system randomly selects one of them.
- The robot tries to move toward the selected chunk for 5 meters or until an obstacle forces it to stop.
- The distance moved by the robot is returned as a reward for the WM system.

The above procedure is followed multiple times, allowing the WM system to intelligently update its internal parameters associated with each chunk in the environment, until the percepts corresponding to an open space eventually dominates the trials. The WMtk has also a reserved position when none of the chunks provided as inputs is selected. With a WM size of 1, the weight parameters inside the WMtk are directly associated with the percepts and the received rewards. In order to evaluate the system's learning performance, two sets of experiments were conducted. In the first set, the robot was put in the middle of the hallway and let to go freely without any user interference. In the second set, the robot started moving from wherever it was. Fig. 3 shows the development of the weights associated with each percept versus the number of the trials, when all the initial weights for percepts were set to 0.5 [15].

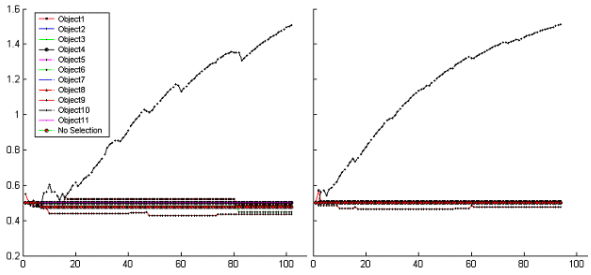

Fig 3. The weight logs for each percept (left) when the robot was let to go freely (right) when the robot was forced back to the center after each trial [15]

In terms of behavior, at the beginning, the robot moved about at random, improving its chances of encountering anything it needs. During the learning, the robot will evolve to activate the sensory inputs that are most likely to reduce the need, that is, to find open space for the robot to move 5 meters without being stopped. Unattended signals or percepts will eventually be excluded from the parts of the motor system engaged in performing the current task.

4.2 Experiment 2: learning landmarks

In a navigation task, the robot not only needs to know which percepts are associated with the open space to move safely, but also learn about landmark locations in order to localize itself in the environment. In this experiment, the appearance of black floor tiles was found to be a convenient indication of a landmark location. For instance, a navigation task could be that the robot might turn 90 ° right or left at the third landmark location. To learn the landmark location, the following steps were taken in this experiment:

- The WM size is set to 1, 2, and 3 to determine percepts to be selected for recognizing a landmark location.
- 80 training images representing landmark (40) and non-landmark (40) locations as in Fig. 4 were collected. The presence of a black floor tile in the foreground indicates a landmark location.

Fig. 4. (a) A landmark image and (b) A non-landmark image

- Images from the training set were selected randomly and processed to obtain the chunks for the WM system.
- Each of the percepts generated for each image was duplicated and presented to the WM system, and marked as a landmark chunk and a nonlandmark chunk, respectively. Once the WM system selected a set of such chunks, a majority vote was taken to determine whether the location is a landmark one or a non-landmark one. If there was a tie in the vote, it was interpreted as a non-landmark one by default. Since the training images were labeled, the WM system received a reward of 1 if the vote agreed with the label of the image, otherwise, it receives a reward of 0.

For each WM size, 1000 and 5000 trials were conducted. The results are summarized in Table 4 and good for all the cases.

Table 4. Percentage of correctness for landmark classification

WM size	1000 trials	5000 trials
1	98.10%	99.52%
2	95.50%	97.42%
3	98.00%	99.38%

4.3 Experiment 3: learning the navigation task

From the previous experiments, the robot acquired the ability to navigate safely through the environment, and the ability to localize itself in the environment. The objective of this experiment is to have the robot utilize its previously learned knowledge and apply them to learn a complex task. Suppose that the robot is positioned in front of the Intelligent Robotics Laboratory, looking towards the window side of the hallway. The black stripes along the hallway indicate the presence of a landmark. The goal of the robot is to navigate along the hallway until it reaches the third landmark. Since the delayed response task is widely used in cognitive neuroscience in order to evaluate the properties of working memory [16], [6], there are two situations to be considered. If the robot recognizes a green ball (which has been added to the system in [17]), as an unexpected, contingent percept along the way, it should remember the green ball until it reaches the last landmark and come back to the starting position. If no green ball is detected along the navigation path, the robot is required to learn to stop at the third landmark. The robot makes a decision, moves with a small distance increment and stops. The time required for this cycle is referred to as one time step. This procedure continues until the navigation is complete. The procedure for Experiment 3 is as follows:

- Initially in the environment, the robot captures an image and segments it to obtain the percepts. Three actions, such as “move”, “stop”, and “turn around”, are also and always presented to the working memory as chunks at each time step. The working memory system is rewarded or punished by the possible actions chosen by the robot along the navigation path. In addition to the action chunks, the working memory is presented with the percepts detected in the environment. However, only “YellowFloor”, “BlackFloor”, and “GreenBall” percepts are presented, if recognized by the perceptual system. Since the task requires only remembering the “GreenBall” chunk, the other percepts are treated as distractors. The working memory has a reserved “Nothing” chunk when the system does not make any selection. Therefore, the maximum number of chunks that can be presented to the working memory is seven.

- The working memory size is set to 2. One slot is for an action chunk and the other one is for a percept chunk. Thus, the working memory is required to learn to select an action chunk as well as a percept chunk.
- Once the candidate input chunk vector is presented to working memory, a decision is made. The robot either moves, stops or turns around depending on the action selection made by the working memory at each time step. Furthermore, if a "GreenBall" percept is detected, the working memory is expected to put the "GreenBall" chunk in its second output slot.
- The robot tries to move towards the open space for one meter and the cycle is repeated until the third landmark is reached. However, if a green ball is detected, it needs to remember that it has detected an indication for a contingent situation. Therefore, as the task requires, it needs to come back to its initial position by passing through each landmark again, in order to demonstrate the bootstrapping effect.

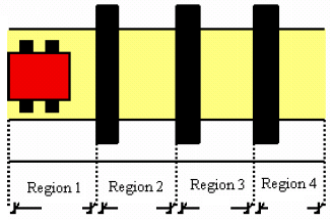

Fig. 5. An illustration of each region of the navigation path.

With the maximum number of input chunk vectors being set to seven, the training is performed in a simulated environment and all the possible chunks are presented to the robot at each time step. The robot is trained for each region of the navigation path as shown in Fig. 5. Each region may be thought of as the state of the robot (i.e., state 0 is being located at region 1, and state 1 is at region 2, etc.). Furthermore, the detection of the contingent percept is also represented as a state of the robot. However, during the training, this state is either randomly set to true once in one of the regions or not set to true at all. This means that the contingent percept has been detected at a particular region if set to true or not detected if the state stays false in the entire trial. In the real world experiment (not in simulation), this state is set true once the perceptual system detects the contingent percept. The robot is required to choose the correct action chunk at each state. In addition, it must learn to remember the contingent percept if recognized along the navigation path. The learning criteria faced by the working memory are not trivial, indeed they are challenging. The robot needs to learn a considerable amount of information from a large combinatorial chunk space in five different states. The robot is trained for each region (each of the states from zero to three) of the navigation path and a reward value is given.

However, in order to speed up the learning, the training state is switched from one to another, only if multiple numbers of positive rewards are received in a row at each state. For instance, assume that the number of positive rewards required to switch the state from one to another, is ten. A successful trial is defined as not receiving any negative reward. Therefore, the system must receive 40 positive rewards (10 for each region) in a row in order the trial to be considered as successful. The number of received positive rewards in a row is referred to as the positive reward threshold (PRT). Fig. 6 shows the learning curve of the system, as a plot of the average reward values over a sliding window of size 25 over 10000 trials for several PRTs. Table 5 shows the number of successful trials for each plot in Fig. 6.

Table 5. Number of successful trials for 10000 trials and for different reward thresholds

Positive reward threshold	Successful trials (Out of 10000)	Percentage of successful trials
1	7591	75.91%
7	8275	82.75%
10	8502	85.02%
20	9330	93.30%

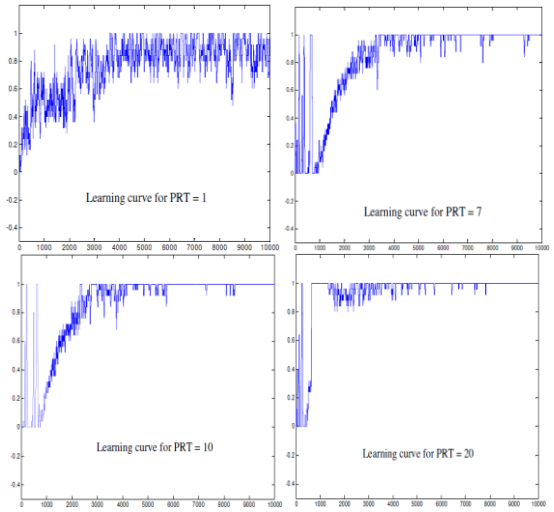

Fig. 6. Learning curves of the system for PRT of values 1,7,10,20

These numbers are reasonable under the very strict rule, that is, receiving multiple positive rewards in a row. Moreover, the initial training stage is also included in these results. If, at any time step of the training, the system fails to choose the correct chunk combination, the whole trial is considered to be an unsuccessful trial. In all of the cases, there is a positive learning trend. As the PRT is increased, the system makes fewer mistakes overall and the speed of the training is significantly increased in terms of episodes. With the system settings described in the above, the time required to train the system, when PRT is set to 10, is 12 minutes and for a PRT set to 20, it takes 15 minutes. Thus, the training time is relatively short in a simulated environment.

In this final experiment, we particularly demonstrated the delayed response effect by holding on to a percept for a period of time. The robot successfully navigated in the hallway and it came back to its initial position when a green ball percept was presented. It chose the correct actions in the action selection slot and the "Nothing" percept, meaning that no percept was held in

the working memory. However, once the contingent percept was presented along the navigation, the robot remembered the contingent percept in the percept selection slot of the working memory at each time step. Thus, the robot has successfully learned a complex task based on previously learned fundamental behaviors.

5 Conclusions

In this work, the robot successfully learned a complex, vision-guided navigation task by means of a powerful and reliable perceptual system combined with a biologically inspired prefrontal cortex working memory model. The task faced by the robot is indeed a challenging task to be learned. The robot initially learned the percepts in the environment and robustly performed segmentation. Next, the robot associated the meanings relative to motion, and landmark detection, to the percepts in the environment and encapsulated them as simple behaviors. These behaviors were then used to build up a more complex behavior.

6 References

[1] Juyang Weng, Wey-Shiuan Hwang. "J. Weng and W.S. Hwang, "From Neural Networks to the Brain Autonomous Mental Development"; IEEE Computational Intelligence Magazine, Vol.1, Issue.3, pp.15-31, Aug 2006.

[2] Juyang Weng, James Mcclelland, Alex Pentland, Ida Stockman, Mriganka Sur. "Computational Autonomous Mental Development: A White Paper for Suggesting a New Initiative"; Technical Report, Oct 2000.

[3] Akira Miyake, Priti Shah. "Models of Working Memory: Mechanisms of Active Maintanence and Executive Control". Cambridge University Press, Cambridge, 1999.

[4] Alan Baddeley, Graham Hitch. "Working Memory"; In: The Psychology of Learning and Motivation: Advances in Research and Theory, Vol.8, pp.47–89. New York: Academic Press, 1974.

[5] Richard S. Sutton. "Learning to Predict by the Method of Temporal Differences" ; Machine Learning, Vol.3, Issue.1, pp. 9-44, Aug 1988.

[6] Joshua L. Phillips, David C. Noelle. "A Biologically Inspired Working Memory Framework for Robots"; In: Proc. of the 27th Annual Meeting of the Cognitive Science Society, Stresa, Italy, July 2005.

[7] Juyang Weng, Wey-Shiuan Hwang. "Incremental Hierarchical Discriminant Regression"; IEEE Transactions on Neural Networks, Vol.18, Issue.2, pp. 397-415, Mar 2007.

[8] Juyang Weng. "Developmental Robots: Theory and Experiments"; International Journal of Humanoid Robotics, Vol.1, Issue.2, pp.199–236, 2004.

[9] Jeffrey L Krichmar, Gerald M Edelman. "Principles Underlying the Construction of Brain-Based Devices". In AISB'06 - Adaptation in Artificial and Biological Systems, pp. 37-42, April 2006.

[10] Jeffrey L. Krichmar, Douglas A. Nitz, Joseph A. Gally, and Gerald M. Edelman. "Characterizing Functional Hippocampal Pathways in A Brain-Based Device as It Solves A Spatial Memory Task"; In Proc Natl Acad Sci USA, Vol.102, Issue.6, pp. 2111-2116, Dec 2004.

[11] Mark A. Busch, Marjorie Skubic, James M. Keller, and Kevin E. Stone. "A Robot in a Water Maze: Learning a Spatial Memory Task"; In: Proc. Of IEEE International Conference on Robotics and Automation, Rome, Italy, April, 2007.

[12] Teuvo Kohonen. "The Self-Organizing Map"; In: Proc. of IEEE, Vol.78, Issue.9, pp. 1464-1480, Sept 1990.

[13] Burrhus Frederic Skinner. "Science and Human Behavior". Colliler-Macmillian, New York, 1953.

[14] Mert Tugcu, Xiaochun Wang, Jonathan E. Hunter, Joshua L. Phillips, David C. Noelle, Don Mitch Wilkes. "A Computational Neuroscience Model of Working Memory with Application to Robot Perceptual Learning"; In: Proc. of IASTED Computational Intelligence Computational Intelligence, Canada, July 2007.

[15] Xiaochun Wang, Don Mitch Wilkes. "An Autonomous Vision System Based Sensor-Motor Coordination Using Working Memory Toolkit"; In: Proc. of the 2009 International Conference on Artificial Intelligence, Las Vegas, USA, July 2009.

[16] Randall C. O'Reilly, Todd S. Beaver, Jonathan D. Cohen. "A Biologically Based Computational Model of Working Memory"; In: Models of Working Memory: Mechanisms of Active Maintenance and Executive Control. New York: Cambridge University Press, chapter 11, pp.375–411, 1999.

[17] Xiaochun Wang, Don Mitch Wilkes. "Visual Novel Object Detection for Mobile Robots"; In: Proc. of the 2008 International Conference on Data Mining, Las Vegas, July 2008.

Towards a Probabilistic Roadmap for Multi-robot Coordination

Zhi Yan, Nicolas Jouandeau, and Arab Ali Cherif
Advanced Computing Laboratory of Saint-Denis (LIASD)
Paris 8 University
93526 Saint-Denis, France
Email: {yz, n, aa}@ai.univ-paris8.fr

Abstract— *In this paper, we discuss the problem of multi-robot coordination and propose an approach for coordinated multi-robot motion planning by using a probabilistic roadmap (PRM) based on adaptive cross sampling (ACS). The proposed approach, called ACS-PRM, is a sampling-based method and consists of three steps including C-space sampling, roadmap building and motion planning. In contrast to previous approaches, our approach is designed to plan separate kinematic paths for multiple robots to minimize the problem of congestion and collision in an effective way so as to improve the system efficiency. Our approach has been implemented and evaluated in simulation. The experimental results demonstrate the total planning time can be obviously reduced by our ACS-PRM approach compared with previous approaches.*

Keywords: Multi-robot system; motion planning; multi-robot coordination; sampling-based approach;

1. Introduction

Motion planning is a fundamental problem in robotics. It could be explained as producing a continuous motion for a robot, that connects a start configuration and a goal configuration, and avoid collision with any static obstacles or other robots in an environment. The robot and obstacle geometry are generally described in a 2D or 3D workspace, and the motion could be represented as a path in configuration space. Motion planning algorithms are widely applied in many fields, such as bioinformatics, robotic surgery, industrial automation, planetary exploration, and intelligent transportation system.

The multi-robot system (MRS) is proposed to deal with some problems that are difficult or impossible to be solved by a single robot, or to improve the system implementation efficiency in some missions completed by multi-robot rather than a single robot [1], [2]. The biggest challenge for the MRS is coordination. Without coordination, it will not only lower the system efficiency, but also lead to the failure of the entire system in extreme cases. Figure 1 shows an example of multi-robot coordination, four robots implement a transportation mission cooperatively, the red robot is delivering a goods, the green robot is on its way back after completing a transportation task, the yellow robot is moving to load a goods, and the orange robot is transporting a goods to the destination location. The coordination of these four robots is obtained by assigning them to different room.

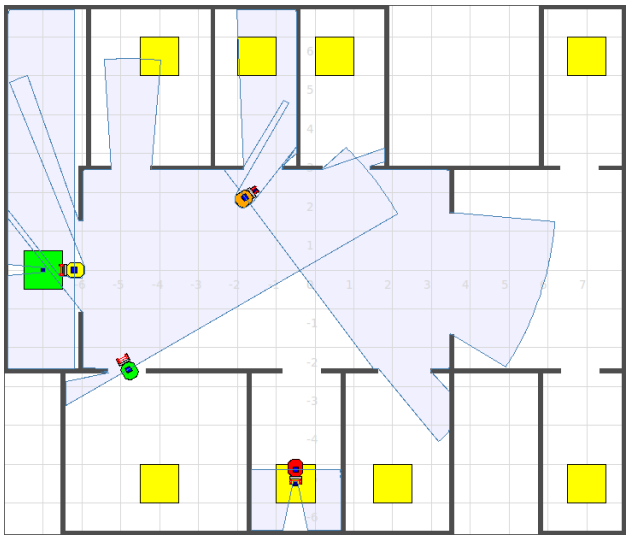

Fig. 1: Four robots implement a transportation mission cooperatively. The dark blue piece signifies the goods to be transported. The green area represents the original position of goods, and the yellow area represents the destination, which corresponds to every room, where the goods should be delivered to by the mobile robot.

In this paper, we consider the issue of coordinated motion planning for a homogeneous team of autonomous mobile robots in structured environments such as office building, warehouse, and container terminal. The larger context of the research is to establish a multi-robot goods transportation system with security, reliability and efficiency. Most of the proposed approaches for multi-robot motion planning usually have the problem of resource conflict such as congestion and collision [3], [4]. For the transportation issue, a desirable result is that robots replan their individual local path to avoid collision and congestion events, however this fashion often needs additional time and thus limit the transportation efficiency. An undesirable result is that robots are blocked, or the goods are lost or damaged, and thus fail the transportation mission. Therefore, we arranged these cases to

the waiting situation problem [5]. To handle this practical problem, this paper presents a novel approach to multi-robot motion planning by using a probabilistic roadmap (PRM) planner which is based on manner of adaptive cross sampling (ACS). This approach called ACS-PRM is decomposed into 3 main steps:

- Firstly, a sufficient number of points should be generated in C-space on an occupancy grid map by using an adaptive cross sampling method.
- Secondly, a roadmap should be built while the potential targets and milestones are extracted by post-processing the result of sampling.
- Finally, the motion of robots should be planned by querying the constructed roadmap.

The rest of the paper is organized as follows: Section 2 describes an overview of some related works; Section 3 discusses the problem of waiting situation; subsequently, Section 4 describes our ACS-PRM approach; Section 5 presents the experimental results obtained with our approach; and the paper is concluded in Section 6 at last.

2. Related Work

Multi-robot motion planning has been extensively studied for more than a decade during which a wide variety of planning frameworks and solutions have been proposed.

Švestka and Overmars [6] presented an approach for multiple nonholonomic car-like robots motion planning in the same static workspace by using probabilistic roadmaps, in which the roadmaps for the composite robot are derived from roadmaps for the underlying simple robots, and the latter is computed by a probabilistic single-robot learning method. The authors introduced the notion of *super-graphs* for multi-robot path planning, and their implementation covered the construction of the simple roadmap and the super-graphs. This approach is probabilistically complete because a given problem could be solved within a finite amount of time.

Moors *et al.* [7] presented a graph-based algorithm for coordinate multi-robot motion planning in 2D indoor environments. The scenario of this research is multi-robot indoor surveillance. The proposed approach takes the limitations and uncertainties of sensors into account, and generates the coordinated motion plan for multiple robots by using A* search algorithm. The authors also introduced a framework based on realistic probabilistic sensor models and worst case assumptions on the intruder's motions in order to compare different approaches and evaluate the coordination performance of the proposed approach.

Clark [8] presented a multi-robot motion planning strategy based on the probabilistic roadmap within a dynamic robot network (DRN) coordination platform. The DRN platform is an ad hoc network, in which single-query PRM is queried as a centralized planner to plan trajectories for all robots. The PRM planner is optimized to speed queries for multi-robot motion planning by using new sampling strategies. At first, a method of sampling PRM milestones is identified to enable fast coverage of the configuration space. Then, a method of generating PRM milestones is introduced to decrease the planning time. Finally, an endgame region is defined to improve the likelihood of finding solutions when goal configurations are highly constrained.

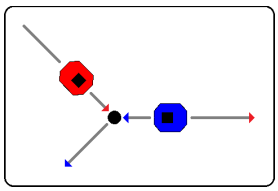

Fig. 2: A typical waypoint mutex. The black dot represents the waypoint, the gray segment represents the path, and the red and blue arrow represent the direction of the motion of the corresponding color robots respectively.

Saha and Isto [9] presented a strategy for decoupled multi-robot motion planning. The proposed strategy, which aims at improving the reliability of the basic decoupled planning approach, partially merges the two phases of the basic approach. The first phase is to compute a collision-free path to avoid the obstacles in the environment and the other robots, the second phase is coordinating the individual robot motions so that only one robot at a time may enter the area of potential inter-robot interference. The proposed approach searches for motions for a robot and coordination of motions of robots along paths already planned while ignoring the robots whose motions have not been planned simultaneously. This approach is inherently incomplete.

Besides, there are some other approaches developed with various strategies [10], [3], [11], [4].

3. Waiting Situation Problem

Multi-agent environments can be cooperative or competitive [12]. Of every agent in a team, the other agents can be considered as teammates (cooperative) or movable obstacles (competitive). One of the most important reasons which limit the efficiency of the multi-robot motion planning is the waiting situation such as the congestion and collision between robots. The core of the problem can be considered as the waypoint mutex in multi-robot motion planning. Figure 2 depicts a typical waypoint mutex. Two robots move to the same waypoint simultaneously: the red robot moves from the top left towards the right and the blue robot moves from the right towards the bottom left. Because of the waypoint can be assigned only to one robot at a time, then the mutex of the waypoint happens.

Generally, there are two ways to deal with the waypoint mutex as shown in Figure 3. One (Figure 3(a)) is to let robots pass the waypoint one by one [6]. The weakness of this strategy is that one robot must wait for another robot to pass. Another way (Figure 3(b)) is to replan the

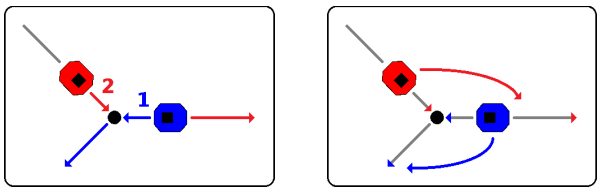

(a) (b)

Fig. 3: Two ways to deal with the waypoint mutex. The colored lines represent the motion plan for the corresponding color robots respectively. (a) The two robots pass the waypoint in order, the blue robot pass first and the red robot pass later. (b) The two robots take each other as an obstacle and replan its trajectories in real time.

local path in real time for each robot by using some goal seeking obstacle avoidance algorithms such as Vector Field Histogram (VFH+) [13] or Nearness Diagram (ND) Navigation [14]. The weakness of this strategy is that robots need some time to replan their new trajectory. Consequently, the two ways both extend the time of the motion planning and limit the system efficiency.

If we can plan separate kinematic paths for multiple robots, then the waiting situation caused by waypoint mutex will be obviously reduced. In addition, the problem of multi-robot task allocation (MRTA) [15] should also be considered. Our focus in this paper is on the multi-robot motion planning in structured environments. For instance, an office building could be simply divided into three clusters: corridor, doorway and room. The doorway usually connects the corridor with the room, it is a suitable object for task allocation. Therefore, on the one hand, the problem of waiting situation (especially at the corridors) caused by one path for all robots should be solved. On the other hand, a simple and effective way to coordinate multi-robot motion is to assign different robots to different rooms reachable from the corridors. Besides, more complex environments may require more sophisticated methods such as hand labeled training data [16], [17] or more complex reasoning [18], [19].

Because of the complexity of multi-robot systems [10], [20], the target of this paper is not to completely avoid the problem of waiting situation (i.e., waypoint mutex), but to minimize the probability of appearance of the waiting situation by using our ACS-PRM approach. Therefore, the coincidence of the waypoint in the plan of two or more robots should be reduced so as to improve the multi-robot motion planning efficiency.

4. ACS-PRM: Adaptive Cross Sampling Based Probabilistic Roadmap

There are usually two ways to handle the issue of robot motion planning based on the grid representation of the environment in low dimensional space. One is to use the incremental heuristic search algorithm such as A* [21] or D* [22]. Another is to use the topological map [23] generated on top of the grid-based map such as Voronoi diagram and straight skeleton. Nevertheless, the number of grids increases rapidly when the size of the environment expands, which make these methods inappropriate for complex and extensive environments. Moreover, these methods are hard to deal with the multi-robot motion planning and always increase the computational load.

Sampling-based approaches have been proposed to improve the computational efficiency for robot motion planning. The main idea is to avoid the explicit construction of the obstacle region in the C-space (C_{obs}). Unlike the incremental heuristic search and the topological map methods, the sampling-based approaches work well for complex environments and high-dimensional configuration spaces, and they are generally easier to implement. The probabilistic roadmap (PRM) planner[1] is one of the typical sampling-based approaches. The original PRM technique is introduced by Kavraki *et al.* [24], which has been shown to perform well in a variety of situations. On the basis of this method, different extensions have been proposed [25], [26], [27]. The approach described in this paper is also an extension of PRM, which is aimed at performing multi-robot motion planning efficiently.

To deal with the problem of waiting situation in multi-robot motion planning as mentioned in the last section by using the PRM approach, there are substantially two options:

- In the manner of single-query: when two or more robots need to pass the same waypoint simultaneously, each robot resamples the adjacent region and takes the motion of the others into account, then generate a novel local roadmap for local replanning.
- In the manner of multi-query: construct a rich roadmap at the beginning to allow robots to plan a different trajectory from others later.

4.1 C-space Sampling

The ACS-PRM approach presented in this paper is a multi-query approach. The first step is C-space sampling, in which a sufficient number of points should be generated to represent the free space of the environment. The main idea of this step is to let a random point p retracts to a position $P(q)$ with the distance d to the obstacle C_{obs} along horizontal and vertical directions (i.e., cross direction).

For autonomous nonholonomic mobile robots, in two dimensions, there are three representational degrees of freedom (DOFs) which are one rotational DOF and two translational DOFs (along or across), but only two controllable DOFs which only move by a forward motion and a steering

[1] A reference implementation of this method in C++ is available online at: http://www.ai.univ-paris8.fr/ yz

angle, the configuration space C is the special Euclidean group $SE(2) = \mathbb{R}^2 \times SO(2)$ where $SO(2)$ is the special orthogonal group of 2D rotations. To avoid the collision caused by the point retracts too close to the obstacle, we set the distance d as the sum of the positive number w and the radius r of the minimum circle to cover the robot with centering at the rotation center of the robot:

$$d = r + w, \ (w > 0) \tag{1}$$

The set of w is to deal with the negative influence of sensor error and it should be adjusted in practical applications.

C_{obs} represents the set of the obstacle, $\forall q \in C_{obs}$ define a direction r_q, then determine a symmetry point $S(q)$ which is an intersection of the open-ray with end q direction r_q and another C_{obs}:

$$S(q) = \{q + t\overrightarrow{r_q} | t > 0\} \cap C_{obs} \tag{2}$$

where, if $\{q + t\overrightarrow{r_q} | t > 0\} \cap C_{obs} = \{q\}$, then define $S(q) = \infty$. Let $dist(x, y)$ represent the distance between point x and point y, then the retraction function can be described as:

$$P(q) = \begin{cases} q + d\overrightarrow{r_q} & \text{if } dist(q, S(q)) \geq 2d \\ \frac{q+S(q)}{2} & \text{otherwise} \end{cases} \tag{3}$$

where $P(q)$ is the position for the point p to retract. In this way, the random points are adapted around to the obstacle (see Figure 4(b)), then:

$$\text{ACS-PRM} = \{P(q)\} | q \in C_{obs}\} \tag{4}$$

The implementation of this step is summarized in Algorithm 1, where the time complexity is $O(n)$ and the space complexity is $O(1)$. This step corresponds the learning phase of classic implementation of PRM.

4.2 Roadmap Building

The second step is roadmap building, in which the potential targets and the milestones should be extracted and connected to the roadmap. In the previous step C-space sampling, if there are sufficient points generated, then the points will gather into segments. The main idea of this step is post-processing the graph resulted from the previous step while identifying three types of point as follows:

- In the previous step, if $dist(p, q) < d$, then p will retract to $\frac{q+S(q)}{2}$ and be labeled as the medial axis. Therefore, we find those medial axis segments with length l a small fixed value (in our implementation, we took the thickness of obstacle), and the midpoints of segments are marked as *potential target* for task allocation. Figure 4(c) shows the extracted potential targets which are precisely doorways of the structured environment.

Algorithm 1 Adaptive cross sampling

Require: N, the sufficient number of points to generate.
Ensure: N points in C_{free} by adaptive cross sampling.

```
repeat
  Generate a uniformly random point p in C-space.
  if p is free then
    for horizontal and vertical directions do
      Find q ∈ C_obs the nearest distance from p.
      if dist(p, q) ≥ d then
        p retracts to q + d r_q.
      else
        Find {S(q)} = pq ∩ C_obs.
        p retracts to (q+S(q))/2.
      end if
    end for
  end if
until N points have been generated.
```

- For those segments without containing the potential target, we extract both of the endpoints and mark them as *milestone* (see Figure 4(d)).
- The points of intersection between two segments are also extracted and marked as *milestone* (see Figure 4(d)). These milestones have not been used in our experiments, but they will be required for the exploration problem.

This step also corresponds the learning phase of classic implementation of PRM. Figure 4 illustrates the process of generating a roadmap for an example occupancy grid map by using our approach with 200,000 random samples.

4.3 Motion Planning

The third step is motion planning, in which each individual robot's kinematic path should be planned by querying the constructed roadmap. The main idea of this step includes the following three points:

- The potential targets $\{t_i\}$ are considered as the goal nodes for path planning and the objects for task allocation as well. Then, the individual $\{r_i\}$ robots are assigned to different potential target:

$$\{r_i\} \mapsto \{t_i\} \tag{5}$$

- To maximize the difference between the paths, we assign the potential target which is the closest from the robot but further from the previously assigned target to the current individual robot:

$$t = further(closest(\{t_i\}, r), t_{i-1}) \tag{6}$$

- Similar to the classic PRM, we use the fast local planning method (i.e., the straight line planner) for the global path planning, except that we choose the path

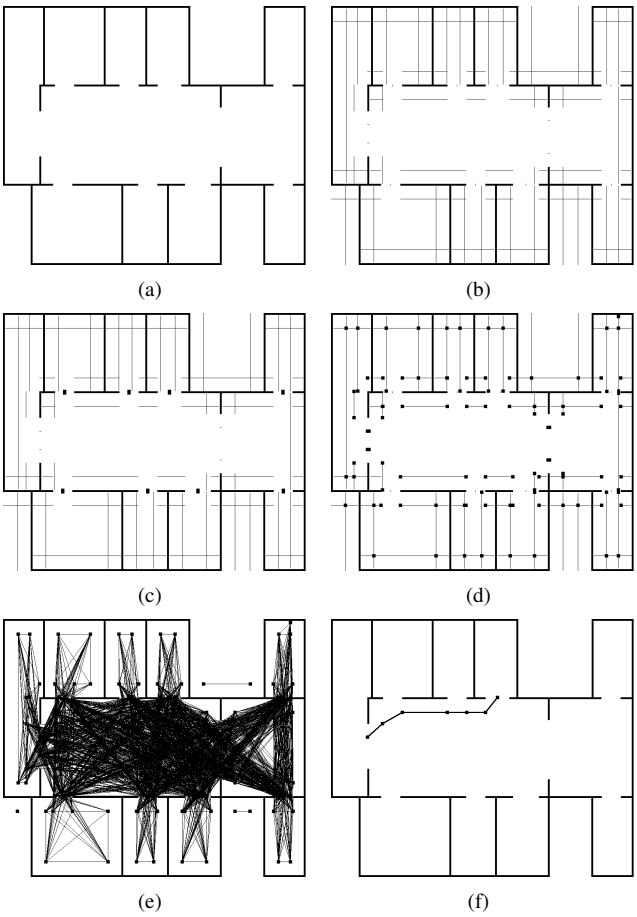

Fig. 4: Generation of the roadmap based on ACS-PRM. (a) The original gridmap, (b) adaptive cross sampling in C-space, (c) the extracted potential targets (doorways), (d) the extracted milestones, (e) the roadmap coverage of environment, and (f) an instance of path.

with the minimum number of milestones for the robots invariably.

This step corresponds the query phase of classic implementation of PRM.

5. Experiments

To evaluate our ACS-PRM approach, we conducted a series of simulation experiments with the well-known 2D multi-robot simulator Stage [28]. The experiment is to transport a certain amount of goods from one origination to divers destinations by a fleet of mobile robots. The simulated robot is the Pioneer 2-DX robot equipped with a laser range finder providing 361 samples with 180 degrees field of view and a maximum range of 8 meters. Each robot can localize itself based on an abstract localization device which models the implementation of GPS or SLAM. To transport goods, the robots are equipped with a gripper that enable them to sense, pick up and put down the goods, and the carrying

Fig. 5: A typical prototype of Pioneer 2-DX robot with gripper.

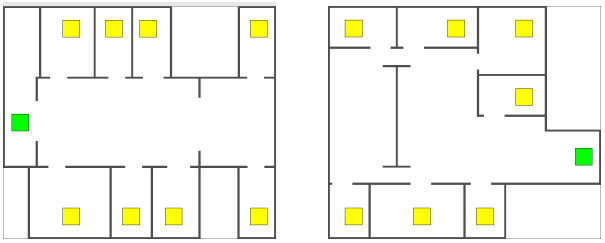

(a) map A (b) map B

Fig. 6: Two environment maps used in our simulation.

capacity is limited to one unit per robot. Figure 5 shows a typical prototype of Pioneer 2-DX robot with gripper.

We used a different number of robots to conduct several experiments in various environments. Two maps (Figure 6) were used in our simulation which are both structured environments. For each map, the green area signifies the original position of goods, and the yellow areas represent the destinations which are always placed in the rooms. For instance, map A has 8 rooms thus 8 destinations, map B has 7 rooms thus 7 destinations. The transportation team size is varied from 2 to 8 robots. On each team size, 10 experimental runs are performed for a transportation mission of 50 goods. The mission objective is to transport the goods to every room equally.

The ratio between real-world time and simulation time is about 1:1. We also compared our approach to the commonly used Voronoi-based approach [23] in which a topological map is built on top of the grid map by using the Voronoi diagram, and the *critical points* are extracted like milestones for mobile robot motion planning. All experiments reported in this paper were carried out on a system with an Intel Core 2 Duo E8400 3.00GHz processor, an Intel Q43 Express chipset and two DDR2 800MHz 1024MB dual channel memory.

In the experiments, we assumed that there exists a central server which is able to communicate with all mobile robots and assign the transportation tasks to each individual robot. The transportation task is to transport the goods from the original position to the destination. We also assumed that all the mobile robots share a common grid map and everyone

Table 1: Statistics of The Number of Occurrences of The Waypoint Mutex

(a) map A

#robots	2	3	4	5	6	7	8
ACS-PRM	1.6	3.1	6.4	7.5	10.0	11.1	16.2
Voronoi-based	15.3	18.7	26.0	26.8	19.9	23.7	27.2

(b) map B

#robots	2	3	4	5	6	7	8
ACS-PRM	3.8	4.3	7.1	14.9	12.8	10.3	16.7
Voronoi-based	17.1	19.2	19.0	26.5	27.4	27.0	29.9

has full information about all others so as to implement path planning and obstacle avoidance in real time coordinately. The ACS-PRM is designed to (but not limited to) plan the kinematic path for nonholonomic mobile robots, and in order to get an objective evaluation of the proposed approach, the drive mode of mobile robot is set to differential-steer, furthermore, the strategy of one pass after the other is applied to deal with the possible waypoint mutex problem.

The results of our experiments are given in Figure 7. We measured the transportation time gained by our approach and compared to the Voronoi-based approach. In each plot, the abscissa denotes the team size of the mobile robots, the ordinate denotes the percentage of the transportation time in the total transportation time, and the error bar indicates the confidence interval of each corresponding gain of robot team size with the 0.95 confidence level. Figure 7 shows that, a transportation time saving of 6.7% to 12.2% in map A and 6.1% to 12.0% in map B is obtainable under our ACS-PRM approach compared to the Voronoi-based approach. These results proved that our technique could obviously improve the system of planning efficiency.

Moreover, we mentioned earlier that our ACS-PRM approach is more effective than our previous approach because the ACS-PRM spends much less time for the learning phase. The experiments show that, with the new approach, the mapping times are respectively 0.321 seconds and 0.329 seconds for map A and map B with 200,000 random samples, which are averages of the 10 runs.

We also counted the average number of occurrences of waypoint mutex in each map as shown in Table 1. This table shows that the problem of waiting situation is obviously reduced by using our ACS-PRM approach, because our approach is able to plan separate paths for robots, especially in the corridor. Unlike the Voronoi-based approach, there is only one path for all robots.

In fact, the technique proposed in this paper also works well with irregular environments. Figure 8 illustrates an example with 20,000 random samples.

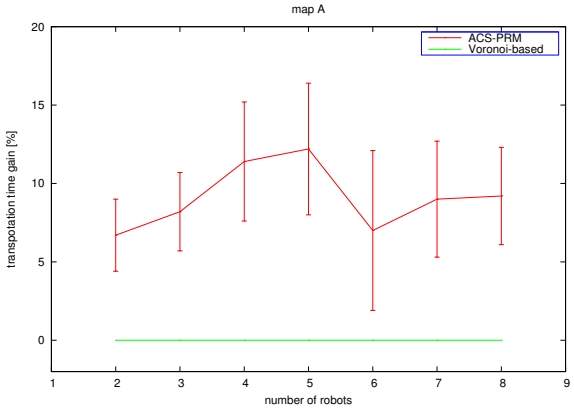

(a) map A

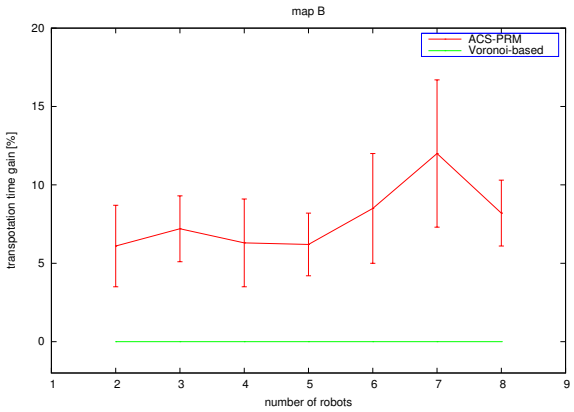

(b) map B

Fig. 7: Transportation time gained by using our ACS-PRM approach compared with the Voronoi-based approach.

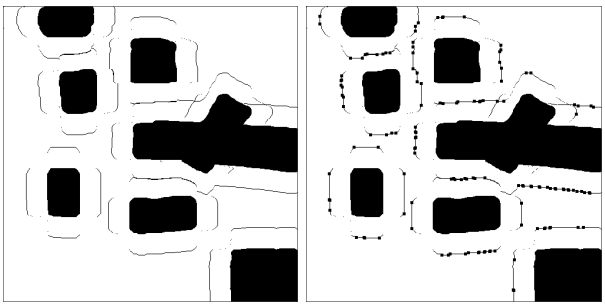

(a) (b)

Fig. 8: Irregular environment experiment based on ACS-PRM. (a)Adaptive cross sampling in C-space, (b) the extracted milestones.

6. Conclusion

In this paper, we presented a novel approach for coordinated motion planning of multiple robots by using the probabilistic roadmap planner based on a manner of adaptive cross sampling, which we called ACS-PRM. The basic thought of the proposed approach is to build separate kinematic paths for multiple robots to minimize the problem of waiting situation such as collision and congestion caused

by waypoint mutex in an effective way, thus to improve the efficiency of automated planning and scheduling.

The ACS-PRM mainly consists of three steps: C-space sampling, roadmap building and motion planning. In the first step, a sufficient number of points are generated to represent the free space of the environment. In the second step, the potential targets and the milestones are extracted and connected to the roadmap by post-processing the graph resulted from the previous step. In the third step, the robot's motion planning is done by querying the constructed roadmap. The first two steps correspond the learning phase of classic implementation of PRM, and the last step corresponds the query phase of classic implementation of PRM.

In consideration of the context of the issue of multi-robot goods transportation, the experiments were conducted to transport a certain amount of goods by a fleet of mobile robots in structured environments. The experimental results demonstrate that, by using our ACS-PRM approach, the total time needed to complete the transportation mission has been obviously reduced compared to the Voronoi-based approach.

In our future work, we will expand our experiments to various irregular environments, not just the structured environments. Furthermore, the proposed work in this paper can be also used in some other applications such as exploration mission, automated surveillance, and search and rescue operations. They are our future consideration as well.

References

[1] Y. U. Cao, A. S. Fukunaga, and A. B. Kahng, "Cooperative mobile robotics: Antecedents and directions," *Autonomous Robots*, vol. 4, no. 1, pp. 7–27, 1997.

[2] G. Dudek, M. R. M. Jenkin, E. Milios, and D. Wilkes, "A taxonomy for multi-agent robotics," *Autonomous Robots*, vol. 3, no. 4, pp. 375–397, 1996.

[3] A. Solanas and M. A. Garcia, "Coordinated multi-robot exploration through unsupervised clustering of unknown space," in *Proceedings of the 2004 IEEE/RSJ International Conference on Intelligent Robots and Systems (IROS'04)*, Sendai, Japan, September 2004, pp. 852–858.

[4] K. M. Wurm, C. Stachniss, and W. Burgard, "Coordinated multi-robot exploration using a segmentation of the environment," in *Proceedings of the 2008 IEEE/RSJ International Conference on Intelligent Robots and Systems (IROS'08)*, Nice, France, September 2008, pp. 1160–1165.

[5] Z. Yan, N. Jouandeau, and A. Ali Cherif, "Sampling-based multi-robot exploration," in *Proceedings of the Joint 41st International Symposium on Robotics and 6th German Conference on Robotics (ISR/ROBOTIK 2010)*, Munich, Germany, June 2010, pp. 44–49.

[6] P. Švestka and M. H. Overmars, "Coordinated motion planning for multiple car-like robots using probabilistic roadmaps," in *Proceedings of the 1995 IEEE International Conference on Robotics and Automation (ICRA'95)*, Nagoya, Japan, May 1995, pp. 1631–1636.

[7] M. Moors, T. Röhling, and D. Schulz, "A probabilistic approach to coordinated multi-robot indoor surveillance," in *Proceedings of the 2005 IEEE/RSJ International Conference on Intelligent Robots and Systems (IROS'05)*, Alberta, Canada, August 2005, pp. 3447–3452.

[8] C. M. Clark, "Probabilistic road map sampling strategies for multi-robot motion planning," *Journal of Robotics and Autonomous Systems*, vol. 53, no. 3-4, pp. 244–264, December 2005.

[9] M. Saha and P. Isto, "Multi-robot motion planning by incremental coordination," in *Proceedings of the 2006 IEEE/RSJ International Conference on Intelligent Robots and Systems (IROS'06)*, Beijing, China, October 2006, pp. 5960–5963.

[10] W. Burgard, M. Moors, D. Fox, R. Simmons, and S. Thrun, "Collaborative multi-robot exploration," in *Proceedings of the 2000 IEEE International Conference on Robotics and Automation (ICRA'00)*, San Francisco, CA, USA, April 2000, pp. 476–481.

[11] R. Regele and P. Levi, "Cooperative multi-robot path planning by heuristic priority adjustment," in *Proceedings of the 2006 IEEE/RSJ International Conference on Intelligent Robots and Systems (IROS'06)*, Beijing, China, October 2006, pp. 5954–5959.

[12] S. J. Russell and P. Norvig, *Artificial Intelligence: A Modern Approach (2nd Edition)*. Prentice Hall, 2002.

[13] I. Ulrich and J. Borenstein, "VFH+: Reliable obstacle avoidance for fast mobile robots," in *Proceedings of the 1998 IEEE International Conference on Robotics and Automation (ICRA'98)*, Leuven, Belgium, May 1998, pp. 1572–1577.

[14] J. Minguez and L. Montano, "Nearness diagram (ND) navigation: Collision avoidance in troublesome scenarios," *IEEE Transactions on Robotics and Automation*, vol. 20, no. 1, pp. 45–49, 2004.

[15] B. P. Gerkey and M. J. Matarić, "A formal analysis and taxonomy of task allocation in multi-robot systems," *The International Journal of Robotics Research*, vol. 23, no. 9, pp. 939–954, September 2004.

[16] E. Brunskill, T. Kollar, and N. Roy, "Topological mapping using spectral clustering and classification," in *Proceedings of the 2007 IEEE/RSJ International Conference on Intelligent Robots and Systems (IROS'07)*, San Diego, CA, USA, October 2007, pp. 3491–3496.

[17] S. Friedman, H. Pasula, and D. Fox, "Voronoi random fields: Extracting the topological structure of indoor environments via place labeling," in *Proceedings of the 20th International Joint Conference on Artificial Intelligence (IJCAI-07)*, Hyderabad, India, January 2007, pp. 2109–2114.

[18] P. Beeson, N. K. Jong, and B. Kuipers, "Towards autonomous topological place detection. using the extended voronoi graph," in *Proceedings of the 2005 IEEE International Conference on Robotics and Automation (ICRA'05)*, Barcelona, Spain, April 2005, pp. 4373–4379.

[19] Z. Zivkovic, B. Bakker, and B. J. A. Kröse, "Hierarchical map building and planning based on graph partitioning," in *Proceedings of the 2006 IEEE International Conference on Robotics and Automation (ICRA'06)*, Orlando, FL, USA, May 2006, pp. 803–809.

[20] B. P. Gerkey and M. J. Matarić, "Sold!: Auction methods for multi-robot coordination," *IEEE Transactions on Robotics and Automation*, vol. 18, no. 5, pp. 758–768, October 2002.

[21] P. E. Hart, N. J. Nilsson, and B. Raphael, "A formal basis for the heuristic determination of minimum cost paths," *IEEE Transactions on Systems Science and Cybernetics*, vol. 4, no. 2, pp. 100–107, 1968.

[22] A. Stentz, "Optimal and efficient path planning for partially-known environments," in *Proceedings of the 1994 IEEE International Conference on Robotics and Automation (ICRA'94)*, San Diego, CA, USA, May 1994, pp. 3310–3317.

[23] S. Thrun, "Learning metric-topological maps for indoor mobile robot navigation," *Artificial Intelligence*, vol. 99, no. 1, pp. 21–71, 1998.

[24] L. E. Kavraki, P. Svestka, J.-C. Latombe, and M. H. Overmars, "Probabilistic roadmaps for path planning in high-dimensional configuration spaces," *IEEE Transactions on Robotics and Automation*, vol. 12, no. 4, pp. 566–580, 1996.

[25] N. M. Amato, O. B. Bayazit, L. K. Dale, C. Jones, and D. Vallejo, "OBPRM: An obstacle-based prm for 3d workspaces," in *Proceedings of the Workshop on Algorithmic Foundations of Robotics (WAFR'98)*, Houston, TX, USA, March 1998, pp. 155–168.

[26] S. A. Wilmarth, N. M. Amatoy, and P. F. Stiller, "MAPRM: A probabilistic roadmap planner with sampling on the medial axis of the free space," in *Proceedings of the 1999 IEEE International Conference on Robotics and Automation (ICRA'99)*, Detroit, MI, USA, May 1999, pp. 1024–1031.

[27] G. Song and N. M. Amato, "Randomized motion planning for car-like robots with C-PRM," in *Proceedings of the 2001 IEEE/RSJ International Conference on Intelligent Robots and Systems (IROS'01)*, Maui, HI, USA, October 2001, pp. 37–42.

[28] B. P. Gerkey, R. T. Vaughan, and A. Howard, "The player/stage project: Tools for multi-robot and distributed sensor systems," in *Proceedings of the 11th International Conference on Advanced Robotics (ICAR'03)*, Coimbra, Portugal, June 2003, pp. 317–323.

A Framework to Control the Darwin-OP Using CLIPS

Brandon Shrewsbury, Ameen Kazerouni, Kenitra Marrow and Dr. Adel Abunawass
Department of Computer Science, University of West Georgia, Carrollton, Georgia, USA

Abstract - *Procedural Paradigms limit the capabilities of an independent system from tackling novel situations. A rule based expert system allows for dynamic expansion of a knowledge base that can be used by an inference engine to challenge a wide variety of situations. The Dynamic Anthropomorphic Robot with Intelligence (DARwIn) proved to be a practical platform for exploring the possibilities of using an expert system to control an independent agent in an uncontrolled environment. Our research revolves around the development of a framework that allows the seamless integration of the C language integrated production system (CLIPS) with the DARwIn framework. This type of control, that approaches a cognitive model rather than a procedural one, allows researchers to focus on expanding the knowledge base of the system and improving functionality and decision making skills on a more abstract level.*

Keywords: DARwIn-OP, Expert Systems, CLIPS

1 Introduction

In 1954 Isaac Asimov stunned the world with the first book of his robot novel series, introducing the world to the concept of Robots that looked and acted like human beings. For decades the minds of children, sci-fi fans and scientists have been entranced by these possibilities. Fiction novels led to sci-fi movies that were coupled with the dawn of anthropomorphic robots. What started off as the pencil sketches of a mad man can now be found in many robotics labs across the world.

The humanoid-research community today, actively researches bipedal movements, kinematics, prosthetics and a wide array of topics many stemming from Asimov's fictional designs. Along with robotics, another topic that emerged was the study of Artificial Intelligence and Human cognition. The scientific world was convinced that if we could build robots that looked like humans, we should be able to program robots to think like humans.

The framework developed in the course of our research investigates the possibility of constructing a localizationist model that could mimic decision making via the use of an Expert system to control the DARwIn - OP.

2 Motivation

Looking at the anthropomorphic form of the DARwIn raises the question; can the DARwIn be programmed to imitate "thinking" or "perceiving". There are several approaches within Artificial Intelligence used to explore cognition. One of these research areas is pattern matching using an Expert System [2]. An Expert System allows a computer to make decisions by sifting through and recalling knowledge similar to an "expert", rather than the procedural forms generally employed [5]. Exploring the possibilities of using an Expert System to control the DARwIn's motion will open various avenues for research in the field of human cognition. We wanted to develop a framework that seamlessly integrates with the DARwIn using a CLIPS expert system. This paper summarizes the implementation of the framework and outlines the communication pathways between various aspects of the project.

3 Approach

In order to provide DARwIN with an unobtrusive use of the inference engine we decided to approach the mimicking of higher functions using a localizationist model as it resembles DARwIN's current architecture. The Clips framework was developed as an external component that interfaces with the Darwin framework using an intermediary controller. The Expert System was designed as a component, and not as the controller itself, in order to keep its priority at the same level with other modules. The intermediary controller houses access to all components of the DARwIN and provides communication pathways throughout.

3.1 DARwIn

The Dynamic Anthropomorphic Robot with Intelligence (DARwIn) is a robotics platform developed at the Robotics and Mechanism Laboratory (RoMeLa) at Virginia Tech for research in kinematics, human-robot interaction, and AI [3]. It comes equipped with a dense array of sensors and expansion capabilities suitable for advanced research an almost any robotics field. DARwIn contains an integrated Fit-PC2i computer running Ubuntu.

Figure 1: DARwIn

3.2 CLIPS

C Language Integrated Production System (CLIPS) is a rule based system that was developed at the NASA-Johnson Space center. [6] CLIPS is fast, efficient, and can easily be integrated with various languages using an extensive API.

3.3 Integration

It was decided to integrate our solution with the source code provided by Robotis as it is uniformly distributed to versions of the DARwIn purchased through Robotis distributors. Versions using LUA have not been tested but the finite state machine can be adapted to interface with our framework.

4 Implementation

There are several segments that must communicate with each other to facilitate the functionality of the framework. The Expert System (ES) must receive data from the DARwIn, representing the current state from a high level. This is done by asserting either pre-processed sensor data or the running state's current classification into the CLIPS fact base. Once information has been asserted, the ES can analyze and determine the next state needed. Instructions are sent back to the intermediary controller for post processing and execution.

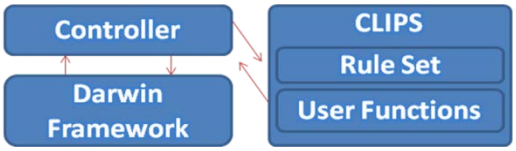

Figure 2: Framework Communication

Development of the framework was broken up into four sections:

- Integrating the CLIPS Library
- Developing communication pathways between CLIPS and the DARwIn Framework
- Creating an output control interface for CLIPS
- Developing a rule set to test the framework

4.1 CLIPS Build

CLIPS version 2.4 was used in this deployment. Installation was not necessary as the source was compiled in library format.

4.2 Communication

Information is transmitted on a pseudo publish-subscribe framework using function pointers. Potential listeners subscribe to "events" by passing function pointers to the controlling classes defined subscribe function. This allows for an easily expandable and lightweight coupling between classes without the overhead of raising events. Function pointers link CLIPS's user functions and the Darwin's framework to the intermediary controller. In both instances, communication is one way.

4.3 Control Interfaces

CLIPS provide a modifiable interface to allow for creating user defined functions. This feature is used for outgoing communications from CLIPS to the intermediate. Declaring user defined functions is facilitated by: DefineFunction(functionName,functionType,functionPointer, actualFunctionName); where the function name is the accessible name used within CLIPS. This links a LISP like call with an external call. Using this, the ES can call the defined function and interact with the intermediary controller to route commands back to the DARwIn framework. In order to decouple the CLIPS library, user defined function can be defined at runtime and stored outside of the library. Code examples can be viewed in Figure 3.

```
c++:
void setDarwinToIdle{
    Walking::GetInstance().X_MOVE_AMPLITUDE = 0;
    Walking::GetInstance().Y_MOVE_AMPLITUDE = 0;
}

int main()
{
    //Initialize CLIPS
    DefineFunction("darwinIdle","v",PTIF setDarwinToIdle,"setDarwinToIdle");
}

CLIPS:
(defrule SendStop
    "Tell Darwin To Stop"
    ?f2 <- (Walk)
    ?f1 <- (stepsToTake(stepsLeftToTake ?v))
    (test(eq ?v 0))
    =>
    (retract ?f1)
    (retract ?f2)
    (darwinIdle)
    (assert(idle))
)
```

Figure 3: External Call

4.4 Rule Set

The CLIPS Expert System has two major components; the knowledge base and an inference engine. The knowledge base consists of facts that are representative of the current state of the DARwIn and production rules. These rules represent heuristic knowledge and follow an "if-then" protocol coupled with the active facts stored in the knowledge base [4]. This implies that if a certain combination of facts has been asserted; the system "infers" a need to update the knowledge base and push new events to its agenda. A portion of the rule-base is displayed in Figure 4:

```
(defrule SendWalk
    "Assert Walk Intent - Remove idle State"
    ?f1 <- (stepsToTake)
    ?f2 <- (idle)
    =>
    (assert(Walk))
    (retract ?f2))
```

Figure 4: Rule Set

Once the production system identifies intent, rules are instantiated and added to the agenda. A rule is instantiated when all of the patterns that constitute the premise of the rule can be matched with facts present in the knowledge base. The inference engine then executes these rules based off various factors that determine the rules priority. Currently no salience was given to any one rule in our rule set. Depending on the construct of the rule, the output may modify the knowledge base or interact outside the confines of CLIPS.

5 Framework Testing

Our chunk primarily demonstrates the viability of using an Expert System to control the Darwin framework. Ideally, the DARwIn's thought process would be broken up in to numerous ESs. Each ES would be an independent component that dealt with domain specific tasks; such as, walking, vision, or auditory systems [1]. The chunk we developed for testing the framework superficially dealt with controlling motion

5.1 Workflow

Our motion control rule set tracks and manages the walking and turning of the DARwIn using state representation of the motion manager and externally registered intent. A number of steps to take or number of degrees to turn would be added to the agenda and the ES would set movement amplitudes and initiate walking. Once the DARwIn begins to move, the intermediate controller would receive updates on the movement from lower levels and relay data to the ES for monitoring. Once the ES has identified completion of the task, it would adjust the movement amplitudes and stop walking. Figure 4 traces various paths the rule-based system follows when intent has been registered.

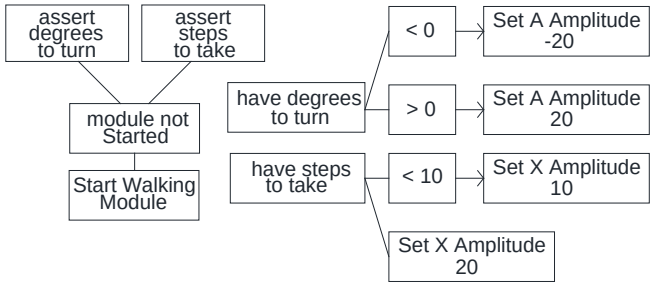

Figure 4: Rule Set – Movement Initiation

5.2 Tracking Movement

Every two steps the DARwIn takes results in a cycle through four phases; Standing -> leg raise -> standing -> leg raise. Following completion of the 1st and 3rd phases, a call is made notifying the controller of a phase change. The controller passes this information to the ES which incorporates it into the knowledge base. Once the information is logged, the ES reruns the agenda to decide when to modify the state of the DARwIn.

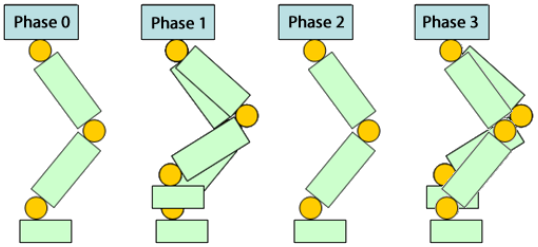

Figure 5: Walking Phase depiction – No forward movement

Table 1: Phase Transitions

Phase 0 - 1: Ankle dorsiflexes, knee is flexed, leg elevates
Phase 1 - 2: pelvis rotates and leg moves forward, knee is extended and foot contacts surface
Phases 2 - 3: Repetition of phases 1 and 2 using opposite leg

5.3 Example Integration

To facilitate our testing, both steps to take and degrees to turn were asserted arbitrarily by the intermediary controller. In order to maintain relative awareness of phase changes efficiently, the motion manager was modified to communicate openly about step phases. The walking module was given an access point, linking to the intermediary controller. With every alternate phase change an event was raised, sending an alert to the ES through the controller.

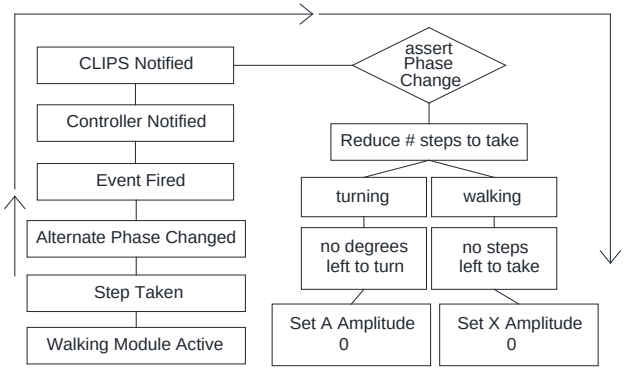

Figure 6: Rule Set – Movement Completion

6 Framework Setup

Clips integration requires minimal modifications to the CLIPS library and the DARwIn Framework. User Defined functions must be defined in the CLIPS library to match the execution requirements of the output space. This step is critical to ensuring proper feedback from the ES. The input space of the ES will pull from an array of data throughout the system and may require modification of the DARwIn's source code to include state listeners. Once communications have been properly defined, the intermediary controller can load the rule set and information can be polled and pushed to the ES through CLIPS's API.

7 Results

A framework was developed that could successfully integrate CLIPS with the DARwIn's framework. The framework was able to control the DARwIn's walking module by sending instructions to the controller based off decisions inferred by the Expert System. The Expert System itself is scalable and can be easily replaced with other Expert Systems of the user's choice. Slight changes to the DARwIn's framework will allow manipulation of almost any aspect of the DARwIn via "expert" control.

8 Acknowledgements

We would like to thank Edwin Rudolph for his guidance and support throughout the development process.

9 References

[1] John R. Anderson. 1988. The expert module. In M. Polson & J. Richardson (Eds.), Handbook of Intelligent Training Systems. Hillsdale, NJ: Erlbaum, 21-53.

[2] John R. Anderson. 2000. The Structure of Memory, Learning and Memory: An Integrated Approach. Hoboken, NJ: Wiley. Print, 203-211

[3] DARwIn OP: Open Platform Humanoid Robot for Research and Education [Online] http://www.romela.org/main/DARwIn_OP:_Open_Platform_Humanoid_Robot_for_Research_and_Education (2012)

[4] William J. Clancey. 1981. The Epistemology of a Rule-Based Expert System: a Framework for Explanation. Technical Report. Stanford University, Stanford, CA, USA.

[5] R. M. Wygant. 1989. CLIPS - a powerful development and delivery expert system tool. Comput. Ind. Eng. 17, 1 (November 1989), 546-549. DOI=10.1016/0360-8352(89)90121-6

Quasi-optimal Coverage Algorithm for Simple Robot in an Unknown Environment

Dominique DUHAUT
Lab-STICC-CNRS
Université de Bretagne Sud, France
dominique.duhaut@univ-ubs.fr

Abstract

In this paper we present a simple algorithm to make a quasi-optimal coverage of an unknown environment. Under some hypothesis, we demonstrate that it is possible to build a map of the environment and to cover it, without passing two times in the same space, except if it's impossible and we will describe these cases and show that they are very limited.

The robot is supposed to be a non holomomic platform with 2 powered wheels for "tank-like" movements, and a set of 7 distance sensors in front of the robot.

Introduction

In robotics, the problem of the covering the space in an unknown environment is a very standard problem. On this the first relevant synthesis can be found in [1]. SLAM simultaneous localization and mapping can be coupled to cover unknown space [2]. Based on graph description [3] and using a research graph algorithm is another method used to coverage. Another work proposes the Boustrophedon cellular decomposition [4] to build a path for space coverage.

Usually in this paper the sensors are a set of sensor surrounding the robot [5] or a laser sensor [6]. In this paper we will use a very simple sensor.

In this paper we will describe the robot used in the simulation and show that in a discretized environment there is no optimal path to cover the space. We then define the quasi-optimal notion. In part two we present the quasi-optimal algorithm and results of simulation. We finally discuss some perspectives to this work.

1. The robot and the environment

Description of the robot

Like a large set of commercial robots, our work uses a "tank-like" robot with two independent wheels.

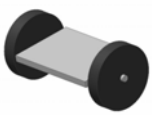

Fig.1. Non holomomic platform with 2 powered wheels for tank-like movements

In this paper we consider that the robot can only move in three directions: front, left, right in a discretized environment decomposed in elementary suares. We assume that the robot fully covers on square.

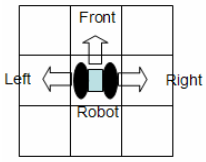

Fig.1. The 3 possible displacements

The robot is supposed to be equipped with distance sensors able to detect an obstacle in the 7 places in front of the robot and measuring a distance of 3 squares.

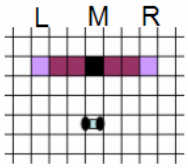

Fig.3. Line of 7 sensors for obstacle detection in front of the robot

Hypothesis on the environement

The hypotheses on the environment are:

- There is no dynamical object in the space, the robot is the only element moving
- The space is large relative to the robot. This means that if the robot covers a elementary square then the minimal distance between two static obstacles is six times this distance: six squares.

In this kind of environment it is possible to decompose the space in rectangles [2] that represents the free space.

The figures 3&4 show that this rectangle decomposition is not unique

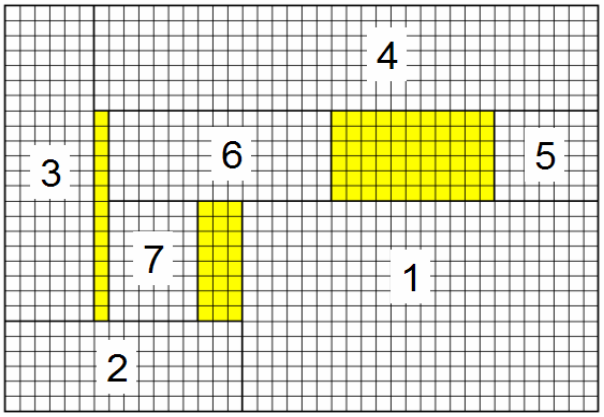

Fig.3. Decomposition of the space in 7 rectangles

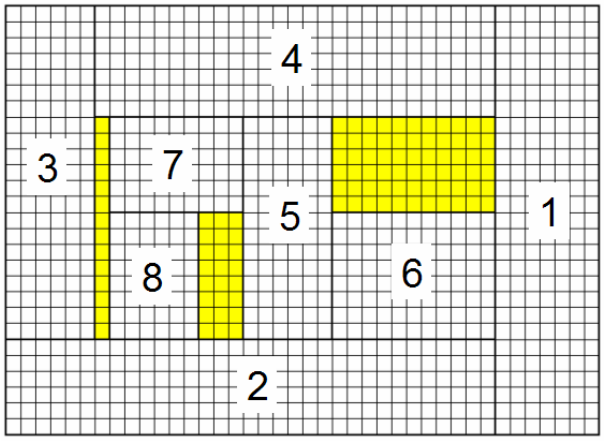

Fig.4. Decomposition of the space in 8 rectangles

Has shown in the proposed algorithm in part 2 the rectangle decomposition will depend of the initial position of the robot. In the following, we will consider that each of the 8 rectangles of the space fig 4 are empty rooms and that a door exist between two adjacent rectangles.

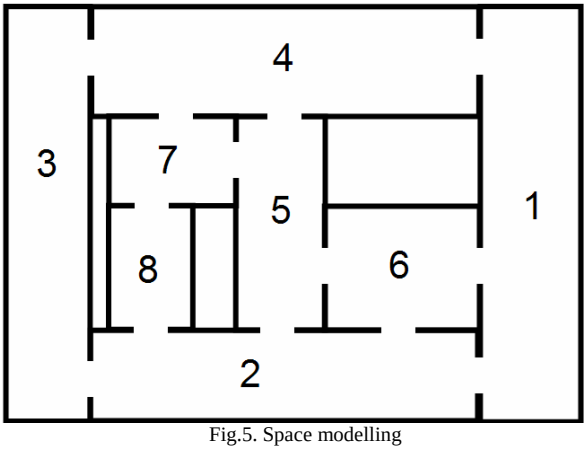

Fig.5. Space modelling

We will then consider that the environment is a set of rooms in which there are communication doors, has presented in fig 5.

No optimal path for covering the space

In this section we want to show that with the type of "tank-like" robot is is not possible to give an optimal path to cover the surface if we fix and entry door and an exit door. By optimal path we mean that the robot passes by all the squares of the environment one time and only one time.

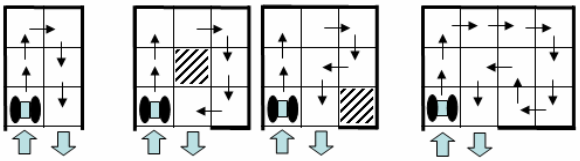
Fig.6. Depending on the size of the environment, this kind of robot cannot find an optimal path

Has shown in the figure 6, with the type if displacement allowed by the robot, an optimal path depends on the number of squares to cover and the position of the entry and the exit door. In the case of 6 or 12 squares a solution exists. But with a 9 squares there is no solution. We have to notice that the result could be different if we change the place or the entry and the exit door see figure 7.

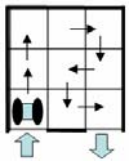
Fig.7. The entry and exit position are also parameters that influences an optimal path

We will define a quasi-optimal path as a path covering the environment, covering a maximum number of squares, without passing two times by the same square and which lets a minimal number of squares non visited.

2. The quasi-optimal algorithm

In this part, we present the principle of the algorithm, the next section will show why and when it is not optimal but only quasi-optimal. The algorithm is in two parts the first one explores the environment and build the corresponding map, the second part will finish the covering of the non visited space and will visit the adjacent rooms while passing in front of a doors.

Part 1: Building the map between obstacles

The robot enters in the room and covers the centre of the space and lets a walkway around the walls of 2 squares large.

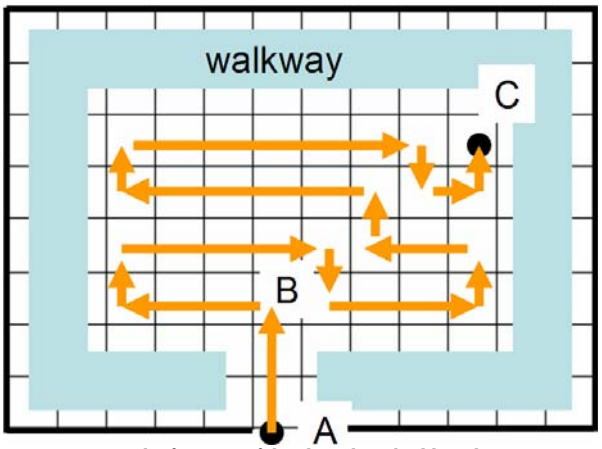

Fig.8. The first part of the algorithm : building the map

The robot enters in A in the first square then moves to the initial position B. Then a boustrophedon [4] path is generated until the sensors detect an obstacle. This path ends in the C position. Due to the distance of obstacle detection the walkway of two squares large as not been visited by the robot (except between A and B).

Part 2 Finishing the coverage

In the second part the robot uses the walkway to access to all the doors surrounding the room and ending the coverage.

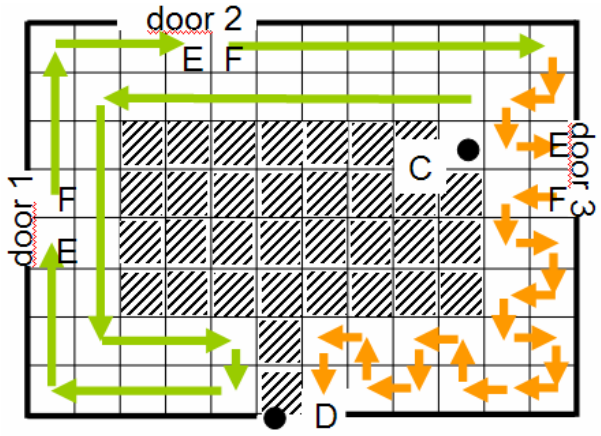

Fig.9. The second part of the algorithm : finishing the coverage

From the C position the robot moves in the opposite direction of the exit door D to finish covering the space. Following the path if a door, connecting to a non visited room, is founded then the robot enters the new room E and will re-enter coming back from this room in the next square of the space F. Then the displacement continues. When the robot exceeds the C position then again a boustrophedon path is generated. If a door if founded then the robot enter this new room at a position E and comes back from the room at the next position F. This is done until the exit position D is reached.

3. It is only quasi-optimal

We run a simulation and show that, as mentioned in fig 11 depending on the geometry of the environment the robot will construct two different freeways: one strictly 2 squares large, the second one depending of the position of the obstacles in the environment will be partially 3 squares large.

Part 1: Building the map between obstacles

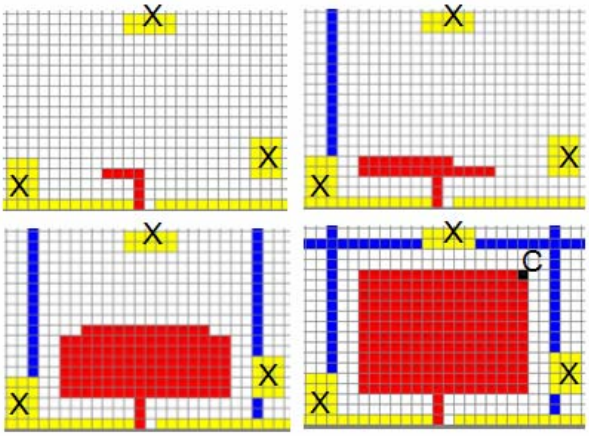

Fig.10. Screen copy of the simulation of the map building

The obstacles are in yellow in the fig 10 and when the robot finds an obstacle in front or on the side, it extends the position of the obstacle by a line (in blue) to figure the limits of the visited “room” see figure 5. If the obstacles are at good position (odd squares horizontal) then the exploration finishes with a covered rectangle (in red) and the robot is in C an angle, the freeway around this rectangle is exactly 2 squares large.

But depending of the distance between obstacles we can have 4 kinds of covering fig 11.

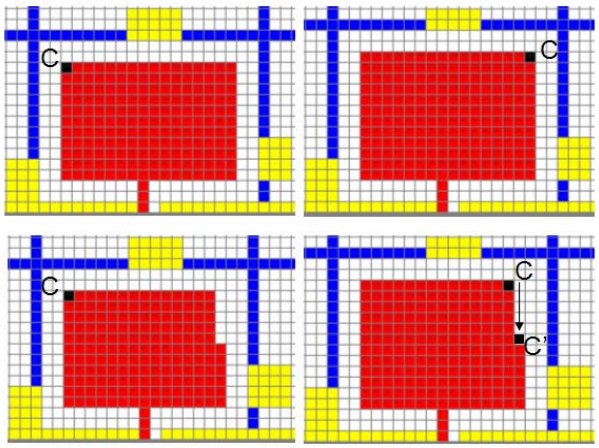

Fig.11. The visited space depending in the position of the obstacles.

In the top of the figure 11 we can see that for the same distance in columns between two obstacles (left and right) the covered surface is a rectangle, the robot finishing in C position on the left or on the right depending on the distance in line between two obstacles (top and down).
On the bottom of fig 11, if we increase the horizontal distance in column of one square then the problem mentioned in fig 6 appears and then the robot must increase the size of the walkway, passing from 2 to 3. In this case, if the robot finishes in C on the right side (bottom right fig 11) then it is possible to "close" the rectangle by moving down the third non visited column of the walkway, reaching the C' position, and then, the walkway is strictly 2 square large. But, in the last case (bottom left fig 11) it is not possible to finish the walkway with a perfect 2 squares large. We will discuss in the 2 part of the algorithm the consequence.

Part 2 Finishing the coverage

Like shown in figure 9 the finishing coverage is divided in two behaviours for the robot : strait line displacement and boustrophedon displacement. The strait doesn't produce any problem of coverage. First the internal part of the walkway is covered and after reaching the A entry point the external of the walkway is covered until de C point.
After overtaking the C point a boustrophedon displacement is used to finish the covering. Here depending on the parity of the quares of the walkway a non covered square can appear in each time that the walkway turns (see fig 7). An other non covered square can appear, for the same reasons, when the walkway it 3 squares large. So finally in the worse case 3 non covered squares can be obtain. The algorithm is not optimal and no solution exist (fig 12&13).

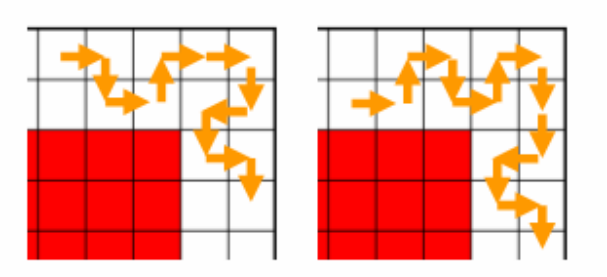

Fig.12. The covering is optimal when the walkway is 2 squares large

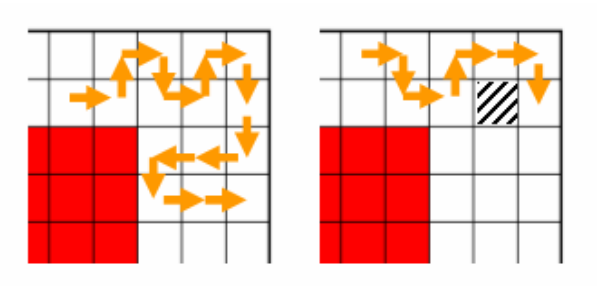

Fig.13. The covering is not optimal when the walkway is 3 squares large it depend on the size.

In this case the robot knows that a square has not been covered because it haves the map of the environment. In this case we can accept that the robot add for instance one backward motion on each of then to finish the coverage.

5. Discussion

In this work we suppose that the robot will exactly move from one square to another. We know that for real robot following a strait line never perfect due to errors introduced by slipping on the floor for instance. For a real application, some trajectory corrections should be added in localisation.
On a second hand, the hypotheses are in figure 3 that the robot is equipped with a line of sensors with 7 elementary obstacle detectors. We did not check it but we believe that only 3 obstacle sensors would enough like in figure.

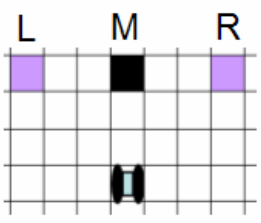

Fig.14. Three sensors should be enough if the obstacles are large

5. Java code for building the map

Here a simplify version of the code used to make the simulation presented in part 3. The full code can be found in [7].

```
void goRobot(JTextArea [][] e,int [][] t,int i,int j){
   int a,fin,odd;
  // Search left
   while ( ! leftObstacle(world,i,j)) {j=j-1; world[i][j]=2;
Red(e,i,j);};
  //draw virtual obstacle in blue
   a=0;
   while(a<20){
    if (world[a][j-3]!=1){world[a][j-3]=3;Blue(e,a,j-3);};
    a++;
   }
  // Search rigth
   i=i-1; world[i][j]=2;Red(e,i,j);a=0; // deplace en haut
   while ( ! murDroite(world,i,j)) {
    if ((world[i+1][j]==0)&&(a==0)){i=i+1;j=j-1;a=1;};
    j=j+1; world[i][j]=2; Red(e,i,j);};
  //blue line j+3
  ...
  // something one left or rigth
   fin=0;odd=0;
   i=i-1;world[i][j]=2;Red(e,i,j);a=0;
   while (fin==0){
    while(! leftObstacle(world,i,j)){
     if (world[i][j-1]==2){i=i-1;j=j+1;};
     j=j-1; world[i][j]=2; Red(e,i,j);
     if (isOdd(world,i,j)){odd=1;};
     if (sensorLeftRigth(world,i,j)){fin=1;} //blue line i-3
    };
    if (fin==0){
     i=i-1;world[i][j]=2;Red(e,i,j);a=0;
     while ( rightObstacle(world,i,j,odd)) {
      if ((world[i+1][j]==0)&&(a==0)){i=i+1;j=j-
1;a=1;};
       j=j+1; world[i][j]=2; Red(e,i,j); // blue line i-3
     };
    }
   }
  }
```

5. Conclusion

In this paper we have presented a quasi optimal algorithm to cover an unknown environment. We show that the existence of an optimal path depends on the distance between obstacles and the entry/exit doors positions, we show that in the worst case, the all surface is covered we a maximum of 3 elementary square non visited.
The map construction if done with a robot "tank like" with a line of distance sensors of 7 elements, looking 3 steps in front. This kind of robot is very standard in commercial platform.

6. References

[1] Jean-Claude Latombe. *Robot Motion Planning*. Kluwer, 1991.
[2] Heung Seok Jeon, Jung Hwan Park, and Ryumduck Oh. *An Efficient Robot Coverage Algorithm Integrated with SLAM for Unknown Environments* ICAI International Conference on Artificial Intelligence, Las Vegas, july 2010
[3] Maxim A. Batalin and Gaurav S. Sukhatme, *The Analysis of an Efficient Algorithm for Robot Coverage and Exploration based on Sensor Network Deployment*, 2005 IEEE International Conference on Robotics and Automation Barcelona, Spain, April 2005
[4] Howie Choset *Coverage of known spaces: the boustrophedon cellular decompotition*, autonomous robots 9, 247-253 2000
[5]. Sylvia C. Wong Bruce A. MacDonald, *A topological coverage algorithm for mobile robots*, IROS International Conference on Intelligent Robots and Systems 2003, page 1685-1690
[6] E. Prassler, J. Scholz, M. Schuster, and D. Schwammkrug. *Tracking a large number of moving objects in a crowded environment*. In IEEE Workshop on Perception for Mobile Agents, 1998
[7] http://dominique.duhaut.free.fr/sourcefull.java

SESSION

RECOGNITION ALGORITHMS AND APPLICATIONS

Chair(s)

TBA

Mathematical evidence for target vector type influence on MLP learning improvement

José Ricardo Gonçalves Manzan, Shigueo Nomura and Keiji Yamanaka

Abstract – ICAI - *This work proposes a mathematical proof for the use of orthogonal bipolar vectors (OBV) rather than conventional target vectors in artificial neural network MLP learning. A larger Euclidean distance provided by new target vectors is explored to improve the learning and generalization abilities of MLPs. The proposed proof compares the MLP performances by using different target vectors such as conventional binary and bipolar and orthogonal bipolar vectors. The evidence for performance improvement is shown by the study of updating process for the weights through the backpropagation algorithm. We have concluded that the use of orthogonal bipolar vectors as targets can provide a better keep of each pattern feature and reduce the interference of noises from a training pattern to the other one.*

Keywords: Mathematical proof, pattern recognition, multilayer perceptron, target vectors, orthogonal bipolar vectors

1 Introduction

Computational intelligence is a science field that has emerged as a set of powerful tools capable of solving problems that previously could not be solved. In this context, we have the Artificial Neural Networks (ANN) receiving important contributions from researchers since 80's. It is quite difficult to list all the ANN applications. Some applications are pattern recognition [1], sound signal processing [2], and biomedical signal processing [3].

Related works are presented in Section 2. Section 3 presents a motivation for the work. Hypothesis to be solved by this work is described in Section 4. The different types of target vectors are defined in Section 5. In Section 6, we can verify the mathematical evidence for affecting the MLP performance according to different target vector types. Some results are discussed in Section 7. Section 8 presents the conclusion of this work.

J. R. G. Manzan is with the Faculty of Electrical Engineering, Federal University of Uberlândia, MG 38400-902. Phone: +51 34 3319-6000, e-mail: josericardo@iftm.edu.br (corresponding author)
S. Nomura is with the Faculty of Electrical Engineering, Federal University of Uberlândia, MG 38400-902. Phone: +51 34 3239-4704, e-mail: shigueonomura@feelt.ufu.br
K. Yamanaka is with the Faculty of Electrical Engineering, Federal University of Uberlândia, MG 38400-902. Phone: +51 34 3239-4704, e-mail: keiji@ufu.br

2 Related works

Researches on pattern recognition mainly description and classification have been considered important in the computer field. Several techniques such as statistical approach, theoretical decision and syntactic approach have been adopted [11]. Currently, the ANN techniques have been widely used because of promising results. One of the advantages of using ANN is the ability for training in a supervised or unsupervised form.

It is known that traditional approaches on artificial intelligence use the sequential processing. On the other hand, ANN techniques use a learning mode with parallel and distributed processing. Their training methodology is based on biological neuron activity to learn through examples. Trial and error strategies contribute to the ability to differentiate patterns. ANN has a similar behavior when a large number of neurons send excitatory or inhibitory signals to other neurons composing the network.

Several researchers [4] [5] [6] [7] have focused on improving ANN performances. Some proposed strategies are regarded to input pattern improvement, ANN architecture optimization, learning algorithm enhancement and others.

Experimental results related to this work have been presented in [7] [8] [9] [10] showing the performance improvements.

3 Motivation

The biological cognition has abilities to recognize and distinguish patterns, even if they have a high degree of degradation an their features [12] [13] [14]. In case of ANN, an appropriate adjustment of parameters allows a learning with high degree of generalization. This is good for constructing a model with high flexibility to properly recognize very degraded patterns. However, if the training time is over then, the model becomes too rigid preventing the recognition of degraded patterns.

Several proposals in order to improve the ability to recognize degraded patterns have been carried out. In most cases they have focused on how to treat input vectors [15]. However, studies for the treatment of target vectors are still rare. This work shows effects of adopting orthogonal bipolar vectors as targets on improving the MLP performance to recognize

degraded patterns. The previous works [7] [8] [9] [10] show satisfactory results in using orthogonal bipolar vectors as expectation values for MLP learning.

4 Hypothesis

In case of conventional bipolar vectors (CBV), the inner product between two of them is not null. On the other hand, orthogonal bipolar vectors (OBV) always have null inner product between them. Also, the similarity between two OBVs is lower than that corresponding similarity between two CBVs. Furthermore, the orthogonality between two OBVs leads to the largest Euclidean distance as well as possible. We believe that larger Euclidean distance and lower similarity of OBVs can affect on the MLP performance improvement to recognize degraded patterns.

However, we have realized that there is no investigation studying the influence of target vector type on the MLP learning. This paper proposes a new methodology for the learning. Our hypothesis is on the fact that a target vector type can significantly improve the ability of MLPs in recognized degraded patterns.

This paper presents a mathematical evidence for explaining the performance improvement of MLPs.

5 Representation of vectors

5.1 Orthogonal Bipolar Vector (OBV)

Equations (1) and (2) represent two possible target vectors, the equation (3) represents the inner product and equation (4) the Euclidean distance.

$$\vec{V} = (v_1, v_2, ..., v_n) \tag{1}$$

$$\vec{W} = (w_1, w_2, ..., w_n) \tag{2}$$

$$\vec{V} \cdot \vec{W}^T = v_1 \cdot w_1 + v_2 \cdot w_2 + v_3 \cdot w_3 + ... + v_n \cdot w_n \tag{3}$$

$$d_{v,w} = \sqrt{(w_1 - v_1)^2 + (w_3 - v_3)^2 + (w_3 - v_3)^2 + ... + (w_n - v_n)^2} \tag{4}$$

Consider the case where $\vec{V}$ and $\vec{W}$ are orthogonal with size n. There will be n/2 components whose product is positive and n/2 components whose product is negative. Positive product components is correspond to the ones which the terms have the same signal. These terms do not affect on the result of the Euclidean distance given by equation (4). On the other hand, for the terms with opposite signals, the square of their difference is 4. The squares of differences contribute into the Euclidean distance resolution. Therefore, if we have larger number (n) of components then we have larger Euclidean distances. Equations (5) and (6) represent examples of OBVs. The inner product of those OBVs is given by equation (7). The OBVs can de generated by implementing the algorithm as described in [16].

$$\vec{V} \overset{def}{=} (1,1,1,1,-1,-1,-1,-1) \tag{5}$$

$$\vec{W} \overset{def}{=} (1,1,-1,-1,1,1,-1,-1) \tag{6}$$

$$\vec{V} \bullet \vec{W} = 1 \cdot 1 + 1 \cdot 1 + 1 \cdot (-1) + 1 \cdot (-1) + (-1) \cdot 1 + (-1) \cdot 1 + (-1) \cdot (-1) + (-1) \cdot (-1) = 0 \tag{7}$$

5.2 Conventional Bipolar Vector (CBV)

In case of conventional bipolar vector (CBV), one of its components values 1 at the position i corresponding to the pattern i represented by vector $\vec{V}$. All the other components value – 1 as represented by equation (8).

$$\vec{V} \overset{def}{=} (-1,-1,...,1,...,-1) \tag{8}$$

If $\vec{V}$ and $\vec{W}$ are conventional then the terms equation (4) are null except for two terms corresponding to the positive component of the vector $\vec{V}$ given by equation (8). So, the Euclidean distance for CBVs is smaller than the distance for OBVs.

5.3 Conventional Binary Vector (BV)

The binary vector (BV) is constituted by a unitary component at the position "i" to represent the i^{th} pattern and other null components as given by equation (9).

$$\vec{V} \overset{def}{=} (0,0,...,1,...,0,0) \tag{9}$$

The BVs are orthogonal between them but their Euclidean distance is always equal to $\sqrt{2}$.

6 Improving the weights between the hidden layer and output layer

6.1 Updating the weights between the hidden layer and output layer

We have considered the backpropagation algorithm foundation [16] to develop the mathematical evidence of our

proposal. A pattern of order q is propagated through the error backpropagation (δ_k) is given by equation (10).

$$\overset{q}{\delta_k} = \left(\overset{q}{t_k} - \overset{q}{y_k}\right) \cdot f`\left(\overset{q}{yin_k}\right) \tag{10}$$

Where:

- $\overset{q}{t_k}$ Represents the target vector corresponding to the q[th] pattern that propagates through the network.
- $\overset{q}{y_k}$ Represents the network output for the q[th] pattern propagating through the network.
- $f`\left(\overset{q}{yin_k}\right)$ denotes the differential value for the activation function of the net output considering the q[th] pattern.

The vectorial form of equation (10) is given by equation (11).

$$\overset{q}{\delta_k} = \left(\begin{bmatrix} \overset{q}{t_1} \\ t_2 \\ . \\ . \\ t_k \end{bmatrix} - \begin{bmatrix} \overset{q}{y_1} \\ y_2 \\ . \\ . \\ y_k \end{bmatrix}\right) .*\begin{bmatrix} y_1` & \overset{q}{y_2}` & \dots & y_k` \end{bmatrix}^T \tag{11}$$

Where:

- .* is the symbol for an unusual multiplication of two matrices with the same sizes. In this operation, each component of the first matrix, corresponding to the row i and the column j is multiplied with the corresponding component of the second matrix located at the row i and column j. The result from the operation is a matrix with the same size as the initial matrices.

In case of using BV as target vector we can verity that the k[th] component of this vector is 0. So, the difference (t_i - y_i) from equation (11) is between - 1 and 0. On the other hand when the value of k[th] of target vector element is 1, the difference (t_i - y_i) from equation (11) is between 0 and 1. These differences are always multiplied by the differential result for the activation function in y_i. The differential results will be positive since the activation function is assintotically non-decreasing. Therefore, δ_k will be negative for null components of BV and δ_k will be positive for the component of BV that is not null.

In case of using CBV as target vector we can note that the difference (t_i - y_i) from equation (11) will be from 0 to 2 for + 1 component of this vector. On the other hand, the difference (t_i - y_i) will be from – 2 to 0 for – 1 component of CBV. Therefore, δ_k will be negative for – 1 component of CBV and it will be positive for +1 components.

In case of using OBV as target vector, we can construct the first vector composed by only +1 components. So, δ_k will be positive for all the components of OBV. The second vector and others are composed by +1 and – 1 components in an equal number. Therefore, a OBV with n components will provide at least n/2 negative results and n/2 positive results of δ_k. δ_k is used for calculating Δw_{jk} in equation (12) and $\Delta w0_k$ in equation (13) as follows:

$$\overset{q}{\Delta w_{jk}} = \alpha \cdot \overset{q}{\delta_k} \cdot \overset{q}{z_j} \tag{12}$$

$$\overset{q}{\Delta w0_k} = \alpha \cdot \overset{q}{\delta_k} \tag{13}$$

In case of using CBV or BV as target vector, we can represent equation (12) as follows:

$$\overset{q}{\Delta w_{jk}} = \alpha \cdot \overset{q}{\delta_k} \cdot \overset{q}{z_j} = \left(\alpha \cdot \begin{bmatrix} \overset{q}{+} \\ - \\ . \\ . \\ - \end{bmatrix} \cdot \begin{bmatrix} \overset{q}{+} \\ + \\ . \\ . \\ - \\ + \\ - \end{bmatrix}^T\right)^T = \alpha \cdot \begin{bmatrix} + & + & \dots & - & + & - \\ - & - & \dots & + & - & + \\ . & . & . & & . & \\ . & . & . & & . & \\ - & - & & + & - & + \\ - & - & \dots & + & - & + \end{bmatrix} \tag{14}$$

In case of using OBV as target vector, equation (12) can be represented as follows:

$$\overset{q}{\Delta w_{jk}} = \alpha \cdot \overset{q}{\delta_k} \cdot \overset{q}{z_j} = \left(\alpha \cdot \begin{bmatrix} \overset{q}{+} \\ + \\ . \\ . \\ - \\ + \\ - \end{bmatrix} \cdot \begin{bmatrix} \overset{q}{+} \\ + \\ . \\ . \\ - \\ + \\ - \end{bmatrix}^T\right)^T = \alpha \cdot \begin{bmatrix} + & + & \dots & - & + & - \\ + & + & \dots & - & + & - \\ . & . & . & & . & \\ . & . & . & & . & \\ - & - & & + & - & + \\ - & - & \dots & + & - & + \end{bmatrix} \tag{15}$$

The influence of a target vector type on the term $\Delta w0_k$ can be analyzed as follows:

- In case of using BV or CBV as target vector we can note that the results for $\Delta w0_k$ will be negative for – 1 component of the target vector and only one will be positive as given by equation (16);
- In case of using OBV as target vector, it is possible to get at least half number (n/2) of components from the target vector as positive results for $\Delta w0_k$ as given by equation (17).

$$\overset{q}{\Delta w0}_k = \alpha \cdot \overset{q}{\delta}_k = \alpha \cdot \left[+ \quad - \overset{q}{\ldots} - \right]^T \tag{16}$$

$$\overset{q}{\Delta w0}_k = \alpha \cdot \overset{q}{\delta}_k = \alpha \cdot \left[+ \quad \ldots \quad + \overset{q}{-} \quad \ldots \quad - \right]^T \tag{17}$$

From equations (14) - (17), we can verify that the use of OBVs as target vectors can keep more pattern feature signal during its propagation. So, we can have more efficient mapping for pattern recognition learning.

6.2 Updating the weights between the input layer and hidden layer

A propagation of two consecutive training patterns will be considered: q order pattern and q + 1 order pattern. Equations (18), (19), and (20) are related to the q order pattern. Equation (21) is related to the q + 1 order pattern.

$$\overset{q}{\delta}_k = \left(\overset{q}{t}_k - \overset{q}{y}_k \right) \cdot f`\left(\overset{q}{yin}_k \right) \tag{18}$$

$$\overset{q}{\Delta w}_{jk} = \alpha \cdot \overset{q}{\delta}_k \cdot \overset{q}{z}_j \tag{19}$$

$$\overset{q+1}{w}_{jk} = \overset{q}{w}_{jk} + \overset{q}{\Delta w}_{jk} \tag{20}$$

$$\overset{q+1}{\delta in}_j = \sum_{k=1}^{m} \left[\overset{q+1}{\delta}_k \cdot \overset{q+1}{w}_{jk} \right] \tag{21}$$

Replacing equations (18) and (20) with the terms δ_k and Δw_{jk} from equation (21), we can obtain the following equation (22):

$$\overset{q+1}{\delta in}_j = \sum_{k=1}^{m} \left\{ \left[\left(\overset{q+1}{t}_k - \overset{q+1}{y}_k \right) \cdot f`\left(\overset{q+1}{yin}_k \right) \right] \cdot \left[\overset{q}{w}_{jk} + \overset{q}{\Delta w}_{jk} \right] \right\} \tag{22}$$

Also, replacing equation (19) with the term of equation (22), we can get the following equation (23):

$$\overset{q+1}{\delta in}_j = \sum_{k=1}^{m} \left\{ \left[\overset{q+1}{t}_k \cdot f`\left( \overset{q+1}{yin}_k \right) - \overset{q+1}{y}_k \cdot f`\left(\overset{q+1}{yin}_k \right) \right] \cdot \left[\overset{q}{w}_{jk} + \alpha \cdot \overset{q}{\delta}_k \cdot \overset{q}{z}_j \right] \right\} \tag{23}$$

Furthermore, replacing equation (18) with the term of equation (23), we can obtain equation (24):

$$\overset{q+1}{\delta in}_j = \sum_{k=1}^{m} \left\{ \begin{bmatrix} \overset{q+1}{t}_k \cdot f`\left( \overset{q+1}{yin}_k \right) \\ - \overset{q+1}{y}_k \cdot f`\left(\overset{q+1}{yin}_k \right) \end{bmatrix} \cdot \begin{bmatrix} \overset{q}{w}_{jk} + \\ \alpha \cdot \left(\overset{q}{t}_k - \overset{q}{y}_k \right) \cdot f`\left(\overset{q}{yin}_k \right) \cdot \overset{q}{z}_j \end{bmatrix} \right\} \tag{24}$$

From equation (24), we can obtain equation (25).

$$\overset{q+1}{\delta in}_j = \sum_{k=1}^{m} \left\{ \begin{bmatrix} \overset{q+1}{t}_k \cdot f`\left( \overset{q+1}{yin}_k \right) \\ - \overset{q+1}{y}_k \cdot f`\left(\overset{q+1}{yin}_k \right) \end{bmatrix} \cdot \begin{bmatrix} \overset{q}{w}_{jk} + \alpha \cdot \overset{q}{t}_k \cdot f`\left( \overset{q}{yin}_k \right) \cdot \overset{q}{z}_j \\ - \alpha \cdot \overset{q}{y}_k \cdot f`\left(\overset{q}{yin}_k \right) \cdot \overset{q}{z}_j \end{bmatrix} \right\} \tag{25}$$

Applying the distributive property to the matrix multiplication, we can obtain equation (26).

$$\overset{q+1}{\delta in}_j = \sum_{k=1}^{m} \begin{bmatrix} \left(\overset{q+1}{t}_k \cdot f\left(\overset{q+1}{yin}_k \right) \right) \cdot \left(\overset{q}{w}_{jk} \right) \\ + \left(\overset{q+1}{t}_k \cdot f`\left( \overset{q+1}{yin}_k \right) \right) \cdot \left( \alpha \cdot \overset{q}{t}_k \cdot f`\left(\overset{q}{yin}_k \right) \cdot \overset{q}{z}_j \right) \\ - \left(\overset{q+1}{t}_k \cdot f`\left( \overset{q+1}{yin}_k \right) \right) \cdot \left( \alpha \cdot \overset{q}{y}_k \cdot f`\left(\overset{q}{yin}_k \right) \cdot \overset{q}{z}_j \right) \\ - \left(\overset{q+1}{y}_k \cdot f\left(\overset{q+1}{yin}_k \right) \right) \cdot \left(\overset{q}{w}_{jk} \right) \\ - \left(\overset{q+1}{y}_k \cdot f`\left( \overset{q+1}{yin}_k \right) \right) \cdot \left( \alpha \cdot \overset{q}{t}_k \cdot f`\left(\overset{q}{yin}_k \right) \cdot \overset{q}{z}_j \right) \\ + \left(\overset{q+1}{y}_k \cdot f`\left( \overset{q+1}{yin}_k \right) \right) \cdot \left( \alpha \cdot \overset{q}{y}_k \cdot f`\left(\overset{q}{yin}_k \right) \cdot \overset{q}{z}_j \right) \end{bmatrix} \tag{26}$$

Converting equation (26) into a vector representation, the expression is given by equation (27).

$$\overset{q+1}{\delta in_j} = \begin{bmatrix} t_1 & t_2 & \overset{q+1}{\ldots} & t_k \end{bmatrix} .* \begin{bmatrix} y_1` & y_2` & \overset{q+1}{\ldots} & y_k` \end{bmatrix} \cdot \begin{bmatrix} w_{11} & w_{21} & \overset{q}{\ldots} & w_{j1} \\ w_{12} & w_{22} & \ldots & w_{j2} \\ . & . & . & . \\ . & . & . & . \\ w_{1k} & w_{2k} & \ldots & w_{kj} \end{bmatrix}$$

$$+ \begin{bmatrix} t_1 & t_2 & \overset{q+1}{\ldots} & t_k \end{bmatrix} .* \begin{bmatrix} y_1` & y_2` & \overset{q+1}{\ldots} & y_k` \end{bmatrix} \cdot \alpha \cdot \begin{bmatrix} \overset{q}{t_1} \\ t_2 \\ . \\ . \\ t_k \end{bmatrix} .* \begin{bmatrix} \overset{q}{y_1`} \\ y_2` \\ . \\ . \\ y_k` \end{bmatrix} \cdot \begin{bmatrix} z_1 & z_2 & \overset{q}{\ldots} & z_j \end{bmatrix}$$

$$- \begin{bmatrix} t_1 & t_2 & \overset{q+1}{\ldots} & t_k \end{bmatrix} .* \begin{bmatrix} y_1` & y_2` & \overset{q+1}{\ldots} & y_k` \end{bmatrix} \cdot \alpha \cdot \begin{bmatrix} \overset{q}{y_1} \\ y_2 \\ . \\ . \\ y_k \end{bmatrix} .* \begin{bmatrix} \overset{q}{y_1`} \\ y_2` \\ . \\ . \\ y_k` \end{bmatrix} \cdot \begin{bmatrix} z_1 & z_2 & \overset{q}{\ldots} & z_j \end{bmatrix}$$

$$- \begin{bmatrix} y_1 & y_2 & \overset{q+1}{\ldots} & y_k \end{bmatrix} .* \begin{bmatrix} y_1` & y_2` & \overset{q+1}{\ldots} & y_k` \end{bmatrix} \cdot \begin{bmatrix} w_{11} & w_{21} & \overset{q}{\ldots} & w_{j1} \\ w_{12} & w_{22} & \ldots & w_{j2} \\ . & . & . & . \\ . & . & . & . \\ w_{1k} & w_{2k} & \ldots & w_{kj} \end{bmatrix}$$

$$- \begin{bmatrix} y_1 & y_2 & \overset{q+1}{\ldots} & y_k \end{bmatrix} .* \begin{bmatrix} y_1` & y_2` & \overset{q+1}{\ldots} & y_k` \end{bmatrix} \cdot \alpha \cdot \begin{bmatrix} \overset{q}{t_1} \\ t_2 \\ . \\ . \\ t_k \end{bmatrix} .* \begin{bmatrix} \overset{q}{y_1`} \\ y_2` \\ . \\ . \\ y_k` \end{bmatrix} \cdot \begin{bmatrix} z_1 & z_2 & \overset{q}{\ldots} & z_j \end{bmatrix}$$

$$+ \begin{bmatrix} y_1 & y_2 & \overset{q+1}{\ldots} & y_k \end{bmatrix} .* \begin{bmatrix} y_1` & y_2` & \overset{q+1}{\ldots} & y_k` \end{bmatrix} \cdot \alpha \cdot \begin{bmatrix} \overset{q}{y_1} \\ y_2 \\ . \\ . \\ y_k \end{bmatrix} .* \begin{bmatrix} \overset{q}{y_1`} \\ y_2` \\ . \\ . \\ y_k` \end{bmatrix} \cdot \begin{bmatrix} z_1 & z_2 & \overset{q}{\ldots} & z_j \end{bmatrix} \quad (27)$$

Extracting the second term from equation (27), we have equation (28).

$$\begin{bmatrix} t_1 & t_2 & \overset{q+1}{\ldots} & t_k \end{bmatrix} .* \begin{bmatrix} y_1` & y_2` & \overset{q+1}{\ldots} & y_k` \end{bmatrix} \cdot \alpha \cdot \begin{bmatrix} \overset{q}{t_1} \\ t_2 \\ . \\ . \\ t_k \end{bmatrix} .* \begin{bmatrix} \overset{q}{y_1`} \\ y_2` \\ . \\ . \\ y_k` \end{bmatrix} \cdot \begin{bmatrix} z_1 & z_2 & \overset{q}{\ldots} & z_j \end{bmatrix} \quad (28)$$

In equation (28), we have a positive scalar α representing the learning rate and vectors represented by the following expressions:

$$\overset{q+1}{t_k} = \begin{bmatrix} a_1 & a_2 & \ldots & a_k \end{bmatrix} \quad (29)$$

$$f\left(\overset{q+1}{yin_k}\right) = \begin{bmatrix} m_1 & m_2 & \ldots & m_k \end{bmatrix} \quad (30)$$

$$\overset{q}{t_k} = \begin{bmatrix} b_1 & b_2 & \ldots & b_k \end{bmatrix}^T \quad (31)$$

$$f\left(\overset{q}{yin_k}\right) = \begin{bmatrix} n_1 & n_2 & \ldots & n_k \end{bmatrix}^T \quad (32)$$

$$\overset{q}{z_j} = \begin{bmatrix} z_1 & z_2 & \ldots & z_j \end{bmatrix} \quad (33)$$

From equations (28) – (33), we can obtain equation (34) as follows:

$$\left(\begin{bmatrix} a_1 & a_2 & \ldots & a_k \end{bmatrix} .* \begin{bmatrix} m_1 & m_2 & \ldots & m_k \end{bmatrix} \right) \cdot \left(\alpha \cdot \begin{bmatrix} b_1 \\ b_2 \\ . \\ . \\ b_k \end{bmatrix} .* \begin{bmatrix} n_1 \\ n_2 \\ . \\ . \\ n_k \end{bmatrix} \cdot \begin{bmatrix} z_1 & z_2 & \ldots & z_j \end{bmatrix} \right) \quad (34)$$

Solving only the especial results from multiplication element by element corresponding to ".*", we can get equations (35) and (36):

$$\begin{bmatrix} a_1 m_1 & a_2 m_2 & \ldots & a_k m_k \end{bmatrix} \cdot \alpha \cdot \begin{bmatrix} b_1 n_1 \\ b_2 n_2 \\ . \\ . \\ b_k n_k \end{bmatrix} \cdot \begin{bmatrix} z_1 & z_2 & \ldots & z_j \end{bmatrix} \quad (35)$$

$$\alpha \cdot \begin{bmatrix} a_1 m_1 & a_2 m_2 & \ldots & a_k m_k \end{bmatrix} \cdot \begin{bmatrix} b_1 n_1 \\ b_2 n_2 \\ . \\ . \\ b_k n_k \end{bmatrix} \cdot \begin{bmatrix} z_1 & z_2 & \ldots & z_j \end{bmatrix} \quad (36)$$

From equation (36), we can get equations (37) and (38).

$$\alpha \cdot \left(a_1 m_1 b_1 n_1 + a_2 m_2 b_2 n_2 + \ldots + a_k m_k b_k n_k \right) \cdot \begin{bmatrix} z_1 & z_2 & \ldots & z_j \end{bmatrix} \quad (37)$$

$$\alpha \cdot \left(a_1 b_1 m_1 n_1 + a_2 b_2 m_2 n_2 + \ldots + a_k b_k m_k n_k \right) \cdot \begin{bmatrix} z_1 & z_2 & \ldots & z_j \end{bmatrix} \quad (38)$$

Extracting the scalar term from equation (38), we can obtain equation (39).

$$\left(a_1 b_1 m_1 n_1 + a_2 b_2 m_2 n_2 + \ldots + a_k b_k m_k n_k \right) \quad (39)$$

The products $m_i n_i$ for $1 \le i \le k$ are positive. These results are derived from the activation function that was supposed to be assintotically non-decreasing. The components a_i and b_i for $1 \le i \le k$, depend on the target vector. They can be 0, 1 or – 1 and cause different effects as follows:

- In case of CBV as target vector, the product $a_i b_i$ for $1 \le i \le k$ will be – 1 for two terms of equation (39);
- In case of BV as target vector, the product $a_i b_i$ for $1 \le i \le k$ will be null;
- In case of OBV as target vector, the result from equation (39) will be smaller than for the case of using CBV.

Considering the use of CBVs as target vectors with four or more components, the result from equation (39) will be larger than the case of using OBVs.

7 Discussion

As illustration, we have taken CBVs with 16 components and replace the variables of equations (29) - (32) with numerical values as follows:

$$f\left(\overset{q+1}{yin_k}\right) = \begin{bmatrix} 1 & 1 & 1 & 1 & 1 & 1 & 1 & 1 & 1 & 1 & 1 & 1 & 1 & 1 & 1 & 1 \end{bmatrix} \quad (40)$$

$$\left[f\left(\overset{q}{yin_k}\right) \right]^T = \begin{bmatrix} 1 & 1 & 1 & 1 & 1 & 1 & 1 & 1 & 1 & 1 & 1 & 1 & 1 & 1 & 1 & 1 \end{bmatrix} \quad (41)$$

$$\overset{q+1}{t_k} = \begin{bmatrix} 1 & -1 & -1 & -1 & -1 & -1 & -1 & -1 & -1 & -1 & -1 & -1 & -1 & -1 & -1 & -1 \end{bmatrix} \quad (42)$$

$$\left[\overset{q}{t_k} \right]^T = \begin{bmatrix} -1 & 1 & -1 & -1 & -1 & -1 & -1 & -1 & -1 & -1 & -1 & -1 & -1 & -1 & -1 & -1 \end{bmatrix} \quad (43)$$

Then, equation (28) can be numerically expressed by equations (44) and (45).

$$= \left(\underbrace{\begin{bmatrix} 1 & -1 & \dots & -1 & -1 \end{bmatrix}}_{1\times 16} .* \underbrace{\begin{bmatrix} 1 & 1 & \dots & 1 & 1 \end{bmatrix}}_{1\times 16} \right) \cdot \alpha \cdot \left(\underbrace{\begin{bmatrix} -1 \\ 1 \\ -1 \\ . \\ . \\ . \\ -1 \end{bmatrix}}_{16\times 1} .* \underbrace{\begin{bmatrix} 1 \\ 1 \\ 1 \\ . \\ . \\ . \\ 1 \end{bmatrix}}_{16\times 1} \right) \cdot \begin{bmatrix} z_1 & z_2^{\,q} & \dots & z_j \end{bmatrix}$$

$$= \left(\underbrace{\begin{bmatrix} 1\cdot 1 & (-1)\cdot 1 & (-1)\cdot 1 & \dots & (-1)\cdot 1 \end{bmatrix}}_{1\times 16} \cdot \alpha \cdot \underbrace{\begin{bmatrix} (-1)\cdot 1 \\ 1\cdot 1 \\ (-1)\cdot 1 \\ . \\ . \\ . \\ (-1)\cdot 1 \end{bmatrix}}_{16\times 1} \right) \cdot \begin{bmatrix} z_1 & z_2^{\,q} & \dots & z_j \end{bmatrix} \quad (44)$$

$$= \begin{bmatrix} 1\cdot 1\cdot (-1)\cdot 1 + (-1)\cdot 1\cdot 1\cdot 1 + (-1)\cdot 1\cdot (-1)\cdot 1 + \dots + (-1)\cdot 1\cdot (-1)\cdot 1 \end{bmatrix} \cdot \alpha \cdot \begin{bmatrix} z_1 & z_2^{\,q} & \dots & z_j \end{bmatrix} \quad (45)$$

$$= 14 \cdot \alpha \cdot \begin{bmatrix} z_1 & z_2^{\,q} & \dots & z_j \end{bmatrix}$$

Also, we have taken OBVs with 16 components and replaced the variables of equations (29) and (31) with numerical values as follows:

$$\overset{q+1}{t_k} = \begin{bmatrix} 1 & 1 & 1 & 1 & 1 & 1 & 1 & 1 & 1 & 1 & 1 & 1 & 1 & 1 & 1 & 1 \end{bmatrix} \quad (46)$$

$$\left[\overset{q}{t_k} \right]^T = \begin{bmatrix} 1 & 1 & 1 & 1 & 1 & 1 & 1 & 1 & -1 & -1 & -1 & -1 & -1 & -1 & -1 & -1 \end{bmatrix} \quad (47)$$

Then, equation (28) can be numerically expressed by equations (48) and (49).

$$= \left(\underbrace{\begin{bmatrix} 1 & 1 & \dots & 1 & 1 \end{bmatrix}}_{1\times 16} .* \underbrace{\begin{bmatrix} 1 & 1 & \dots & 1 & 1 \end{bmatrix}}_{1\times 16} \right) \cdot \alpha \cdot \left(\underbrace{\begin{bmatrix} 1 \\ . \\ . \\ 1 \\ -1 \\ . \\ . \\ . \\ -1 \end{bmatrix}}_{16\times 1} .* \underbrace{\begin{bmatrix} 1 \\ . \\ . \\ 1 \\ 1 \\ . \\ . \\ . \\ 1 \end{bmatrix}}_{16\times 1} \right) \cdot \begin{bmatrix} z_1 & z_2^{\,q} & \dots & z_j \end{bmatrix}$$

$$= \left(\underbrace{\begin{bmatrix} 1\cdot 1 & 1\cdot 1 & \dots & 1\cdot 1 & 1\cdot 1 \end{bmatrix}}_{1\times 16} \cdot \alpha \cdot \underbrace{\begin{bmatrix} 1\cdot 1 \\ . \\ . \\ 1\cdot 1 \\ (-1)\cdot 1 \\ . \\ . \\ (-1)\cdot 1 \end{bmatrix}}_{16\times 1} \right) \cdot \begin{bmatrix} z_1 & z_2^{\,q} & \dots & z_j \end{bmatrix} \quad (48)$$

$$= \begin{bmatrix} 1\cdot 1\cdot 1\cdot 1 + \dots + 1\cdot 1\cdot 1\cdot 1 + 1\cdot 1\cdot (-1)\cdot 1 + \dots + 1\cdot 1\cdot (-1)\cdot 1 \end{bmatrix} \cdot \alpha \cdot \begin{bmatrix} z_1 & z_2^{\,q} & \dots & z_j \end{bmatrix} \quad (49)$$

$$= 0 \cdot \alpha \cdot \begin{bmatrix} z_1 & z_2^{\,q} & \dots & z_j \end{bmatrix}$$

We can verify that the result from equation (48) is null in case of using OBV and the result from equation (45) is always larger than that case. We can consider that the term of equation (39) has worked as an intensification factor for the term represented by equation (28).

Equation (28) is a term from equation (27) for updating weights during the training stage of MLPs. So, we can confirm the influence of target vector type on MLP learning. In case of using OBV as target vector, we can provide a reduced noise propagation contributing into an improved performance of MLPs on pattern recognition.

8 Conclusion

This work presented a mathematical proof to demonstrate the MLP performance improvement by adopting orthogonal bipolar vectors as targets. The mathematical results have shown the effects on noise reduction propagating from layer to layer due to the use of orthogonal bipolar vectors rather than the use of conventional target vectors for MLP learning. We also have verified that the use of orthogonal bipolar vectors provides a better separation of pattern features due to larger Euclidean distance between these vectors. We have concluded that the results can confirm the hypothesis of our work suggesting orthogonal bipolar vectors as expectation values for MLP learning in degraded pattern recognition.

9 Acknowledgments

This work was supported by a grant from PROPP-UFU through the project number 72/2010 and from CAPES through MINTER (UFU and IFTM) master program.

10 References

[1] B.C. Guingo, A. C. G. Thomé, R. J. Rodrigues, Automatic License Plate Recognition of Motor Vehicles using Artificial Neural Networks (in Portuguese), **XVII Congress of teaching and research in transport – ANPET**, Florianópolis (2004).

[2] N. C. L. Abreu, Extraction of speech signals in noisy environments by decomposition os statistically indepent basis functions (in Portuguese), Dissertation – **Federal University Maranhão** (2003).

[3] A. M. Santos, J. M. Seixas, B. B. Pereira, R. A. Medronho, Using Artificial Neural Networks and Logistic Regression in the Prediction of Hepatitis A (in Portuguese), **Brazilian Journal of Epidemiology** (2005); 8(2): 117-26.

[4] X. Wang, C. Chang, F. Du, Achieving a More Robust Neural Network Model for Control of a MR Damper by Signal Sensitivity Analysis, **Neural Computing & Applications**, 13(2002), 330-338.

[5] M. A. Costa, A. P. Braga, B. R. Menezes, Improving Neural Networks Generalization With New Constructive and Pruning Methods**, Journal Of Intelligent & Fuzzy Systems**, 13(2003), 75-83.

[6] C. M. Lee, S. S. Yang, C. L. Ho, Modified back-propagation algorithm applied to decision-feedback equalization, **Iee Proceedings – Vision, Image & Signal Processing**, 153(2006), 805-809.

[7] S. Nomura, K. Yamanaka, O. Katai, H. Kawakami, T. Shiose, Improving MLP learning via Orthogonal Bipolar Target Vectors, **Journal of Advanced Computacional Intelligence and Intelligent Informatics**, 9(2005), 580-589.

[8] S. Nomura, K. Yamanaka, O. Katai, H. Kawakami, T. Shiose, A New Approach to Improving Math Performance of Artificial Neural Networks (in Portuguese), **VIII Brazilian Symposium on Neural Networks**, (2004).

[9] J. R. G. Manzan, K. Yamanaka, S. Nomura. Improvement in Perfomance of MLP using New target vectors (in Portuguese), **X Brazilian Congress on Computational Intelligence** (2011).

[10] S. Nomura, J. R. G. Manzan, K. Yamanaka. An Experimentation with improved target vectors for MLP in classifying degraded patterns, **Journal of the Brazilian Neural Network Society, Vol. 8, Iss. 4, pp.240 – 252** (2010).

[11] A. Browne, Neural Network Analysis, Architetures, and Applications, **Institute of Physics Pub** (1997).

[12] T. Kohonen, Associative Memory: a System-Theoretical Approach, **Springer-Verlag** (1977).

[13] K. S. Fu, Syntatic Methods in Pattern Recognition, Academic Press (1974).

[14] L. N. Cooper, A Possible Organization of Animal Memory and Learning, Proc. of the Nobel Symposium on Collective Propertiers of Physical Systems, B. Lundquist and S. Lundquist (1973).

[15] R.O. Duda, P. E. Hart, Pattern Classification and Scene Analysis, **Wiley** (1973).

[16] L. Fausset, Fundamentals os Neural Networks: Architecture, Algorithms, and Applications, **Prentice-Hall**, (1994).

A Hand Image Instruction Learning System Using PL-G-SOM

T. Kuremoto[1], T. Otani[1], L.-B. Feng[2], K. Kobayashi[1, 3], and M. Obayashi[1]
[1]Gradual School of Science and Engineering, Yamaguchi University, Ube, Yamaguchi, Japan
[2]Shenzhen Institute of Advanced Technology, Chinese Academy of Sciences, Shenzhen, Guangdong, China
[3]School of Information Science and Technology, Aichi Prefectural University, Nagakute, Aichi, Japan

Abstract - *Conventionally, human instructions to a robot are often given by previously designed signals such as voices and images. In this study, one's own "shapes of a hand" is suggested to be instructions in the human-machine interaction system. We proposed a Self-Organizing Map (SOM) with a memory layer named Transient-SOM (T-SOM) and adopted it to a hand image instruction learning system. In this study, instead of T-SOM, an improved SOM, Parameter-Less Growing Self-Organizing Map (PL-G-SOM) is used to improve the hand image instruction learning system. In order to verify the performance of the proposed system, comparison experiments were executed and the results showed the priorities of the new system.*

Keywords: *Human-machine interaction, Self-Organizing Map (SOM), Parameter-Less Growing SOM, Hand image instruction, Pattern recognition*

1 Introduction

Hand gesture has been introduced to human-machine interaction since the end of last century (Pavlovic et al., 1997). Static images of hand shapes and dynamical videos of hand gestures are recognized by different mathematical models such as Multi-Layer Perceptron (MLP) (Rumelhart et al., 1986), Self-Organizing Map (SOM) (Kohonen, 1982, 1995, 1998), Hidden Markov Model (HMM) (Baum & Petrie, 1966) and so on.

Kohonen's SOM, as a well-known pattern recognition neural network, is a powerful tool to categorize high dimension data to one or two dimension space. In our previous studies, we proposed two kinds of improved SOMs, i.e., Transient SOM (T-SOM) (Kuremoto et al., 2006) which introduced a memory layer to reserve the matured "best much unit" (BMU), and Parameter-Less Growing SOM (PL-G-SOM) which combined the concepts of Berglund & Sitte's Parameter-Less SOM (PLSOM) (Berglund & Sitte, 2006) and Growing SOM (GSOM) (Bauer & Villmann, 1997; Villmann & Bauer, 1998; Dittenbach et al., 2000) to overcome the limitation of the size of map, the collapse of map' topology due to the unlearned data, and reduced the load of computation.

T-SOM has been applied to a hand image instruction learning system for a pet robot "AIBO" (Sony Ltd. Product 2003) successfully (Kuremoto et al., 2006; Hano et al., 2007) and PL-G-SOM succeeded as a voice instruction learning system for the robot (Kuremoto et al., 2010, 2011). In this research, we adopt PL-G-SOM into the hand image instruction learning system instead of T-SOM.

2 The structure of hand image instruction learning systems

The hand image instruction learning systems for partner robots, which are intelligent robots with the abilities of human-machine interaction, have a similar architecture as shown as in Figure 1. Hand images are preprocessed to yield their feature vectors as the input of systems. Three kinds of maps which are Feature Map, Action Map and Feeling Map are combined to realize input data classification, action selection and success rate expression respectively. Feature Map is a layer of T-SOM or PL-G-SOM, it clustering high dimension input data on 2-dimension spaces of maps. The input data of hand image instruction are feature vectors of hand shapes obtained by preprocessed images.

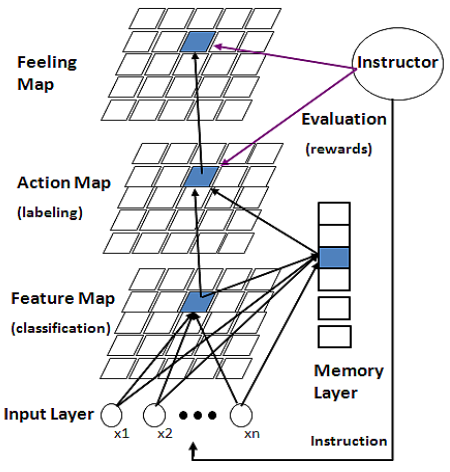

(a) T-SOM

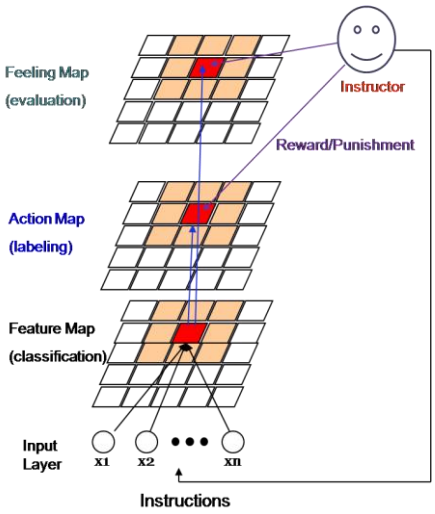

(b) PL-G-SOM

Figure 1: Structures of instruction learning systems: (a) T-SOM (Kuremoto et al., 2006, Hano et al., 2007) for hand image instructions; (b) PL-G-SOM for voice instructions (Kuremoto et al., 2010, 2011), and used in this study for hand image instructions.

2.1 Feature Vector Space of Hand Image Data

2.1.1 Image Processing for hand Extraction

The hand image instruction system is designed for a partner robot learning to select different designed actions according to the different shape of a hand of its instructor. Hand area, i.e., skin area in the image captured by a CCD camera needs to be extracted and regularized at first. For a frame of image in RGB format, it is transformed to HSV format at first, then, using the threshold values of Hue (H), and Saturation (S) (Sherrah & Gong, 2001) and Red (R) threshold in RGB, skin area is extracted as a binary image. Noise elimination and holes filling are also effective to segment a hand area from the binary image. The thresholds for skin of a yellow race people in the room of fluorescent lights (around 500lx) are given as follows as we investigated:

1) When H, $S \in [0, 360]$ degree,
If $10 \leq S < 15$, then $H > 350$;
If $15 \leq S < 20$, then $H > 330$;
If $20 \leq S < 30$, then $H > 300$ or $H < 40$;
If $30 \leq S < 50$, then $H > 250$ or $H < 30$;
If $50 \leq S < 70$, then $H > 230$ or $H < 30$;
If $70 \leq S < 150$, then $H > 220$ or $H < 40$;
If $S < 10$ or $150 \leq S \leq 360$, then $H > 300$ or $H < 40$;
2) When R, G, $B \in [0, 255]$,
$30 < R < 250$.

2.1.2 Feature Space of Hand Shape

The instructions given by the instructor of robot are supposed as the different shapes of a hand. To distinguish the type of a hand shape, feature space definition is important to result high rate of pattern recognition. We discussed the methods of feature space construction in our previous works (Kuremoto et al., 2006; Hano et al., 2009) and proposed a useful feature vector space of hand shapes. The input images are analyzed by an 80-dimension vector space (See Fig. 2). From the origin of the space to the end of the hand area, the lengths in axes each 1.8-degree increased (80 axes) are the values of the feature vector, i.e., (x_1, x_2, …, x_{80}).

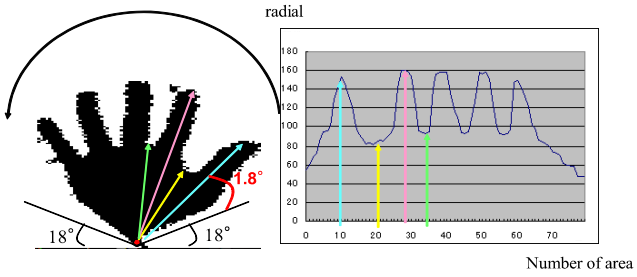

Figure 2: Input space of T-SOM and PL-G-SOM, constructed by an 80-dimension feature vector space of a hand instruction as a binary image. Left: a regularized image; Right: feature (input) space for Feature Map where horizontal axis is the dimension of vectors vertical axis is the value of vectors.

2.2 Action Map

The instructor presents his/her instructions with the different shapes of his/her hand to a robot, and in the view of the robot, hand shapes which are observed mean a state of the environment s_t, the robot intends to select a valuable action a_t (i) adapting to the state, i =*1*, *2*, …, *A*, according to a stochastic action policy π, which is according to Gibbs distribution (Boltzmann distribution) as shown by Eq. (1).

$$\pi_t(a_t(i)\,|\,s_t) = \frac{e^{\frac{Q_t(s_t,a_t(i)}{T}}}{\sum_{j=1}^{A} e^{\frac{Q_t(s_t,a_t(j))}{T}}}, \qquad (1)$$

where T is a parameter named "temperature" which comes from the physical state description of a system (higher temperature lower possibility), t is the iteration time of learning, A is the number of available actions. When an action is selected according to Eq. (1) and performed by the robot, its

instructor evaluates the action by giving a reward/punishment *r* to robot. The reward is accepted and used to modify the value of Q_t by Eq. (2), where Q_t is called "state-action value function" in reinforcement learning (RL) (Sutton & Barto, 1998).

$$Q_{t+1}(s_{t+1}, a_{t+1}(i)) = Q_t(s_t, a_t(i)) + r \quad . (2)$$

Where *s* means the state of environment observed by the robot, *a* is the action selected by the learner, *r* is the reward (scalar) given by the instructor.

2.3 Feeling Map

To express the degree of how an instruction is learned by robot, a Feeling Map which has the same number of units with Action Map is designed as shown in Figure 1. Feeling Map expresses instruction recognition rate, i.e., the feeling of robot: more successful, happier it is. Feelings of partner robots, such as pet robots, entertainment robots, caring robots and so on, are important for human-machine interaction (HMI) when they are able to express vividly by their face expressions or the gestures (Kuremoto et al., 2007). The distance between input pattern and units on Feature Map and the reward from instructor are used to calculate feeling values which is normalized in [-1.0, 1.0] where high positive value means happiness and 0.0 is the initial value of each unit here. The calculation of Feeling Map is given by Eq. (3).

$$F_{t+1}(i) = F_t(i) \pm aC - bD_i, \qquad (3)$$

where $F(i)$ notes the feeling value of unit *i* on the Feeling Map (zero initially), *C* notes the continue times of reward or punishment, D_i is the Euclidean distance (squared error) between the unit *i* on Feature Map and the input data, a, b are constants, and $0 < a < 1,\ 0 < b << 1$.

3 T-SOM

The algorithm of T-SOM (Kuremoto et al., 2006, Hano et al., 2007) and whole system processing is shown as follows:

–Step 1: Initialization. Choose random values (0.0, 1.0) for unit m_i of a *2-dimension* map corresponding to an *n-dimension* input space. $(i = 1,2,\ldots,N \times M)$

– Step 2: Input data. Present a training sample $\mathbf{x}(x_1, x_2 \ldots, x_n)$ to the Input Layer.

– Step 3: Find *BMU*, i.e., the best match unit of Memory Layer or Feature Map. A *BMU c* is decided by using minimum Euclidean distance criterion Eq. (4).

$$\boldsymbol{c} = \arg\min_i(\| \mathbf{x} - \mathbf{m}_i \|), \qquad (4)$$

where $\mathbf{x}$ is input feature vector $(x_1, x_2, \ldots, x_n)$. If *BMU c* is found from Memory Layer, then Feature Map (Step 4) is skipped.

– Step 4: Competitive learning. Using a learning rule given by Eq. (5) to update the value of $\mathbf{m}_i$.

$$\triangle \mathbf{m}_i = \alpha h_{ci}(\mathbf{x} - \mathbf{m}_i), \qquad (5)$$

where α is a learning rate and h_{ci} is a neighborhood function given by Eq. (6).

$$h_{ci} = \exp\left(-\frac{\| \mathbf{c}_i - \mathbf{c} \|^2}{2\sigma^2}\right). \qquad (6)$$

Here, $\boldsymbol{c_i}, \boldsymbol{c}$ denotes the positions of an arbitrary unit on the output map and *BMU*, respectively, $i = 1, 2, \ldots, k \le N \times M$, σ is a constant. Obviously, $h_{ci}(x) \ge 0$, $h_{ci}(0) = 1$, $h_{ci}(\infty) = 0$.

– Step 5: Vector quantization (labeling). After sufficient iterations of Step 3 and Step 4, i.e., if the distance from a *BMU* to the input is less than a threshold value, the input pattern is classified to be a unit of Action Map. This process is as same as LVQ-I (Kohonen, 1995), but labeling those units of Action Map is executed by a reinforcement learning algorithm described in Step 6.

– Step 6 Action learning. Using a reinforcement learning algorithm described in next subsection, robot select "correct actions" according to the reward or punishment from its instructor. The details are described in section 2.2.

– Step 7: Feeling formation. Units on Feeling Map are the levels of learning for actions on Action Map. The details are described in section 2.3.

– Step 8: Additional learning. For new instruction learning, T-SOM stores the succeeded unit weights into Memory Layer, and reset the units of Feature Map into random value. Additional learning or refresh learning then is able to repeat from Step 1.

T-SOM overcomes the limitation of a size fixed map of classic SOM and showed its efficiency as a real robot internal model to learn hand image instruction (Kuremoto et al., 2006; Hano et al., 2009), however, after a matured "BMU" is stored in the Memory Layer and the unit on Feature Map is refreshed with random weights of connections to the input, the distance between units of trained map and untrained input pattern (new data) shows disordered as indicated by Berglund & Sitte (Berglund & Sitte, 2006).

4 PL-G-SOM

Combine the idea of Growing SOMs (GSOM) (Bauer & Villmann, 1997, Dittenbach, Merkl & Rauber 2000) and the Parameter-Less SOM (Berglund and Sitte, 2006) together, we proposed a novel SOM named PL-G-SOM (Kuremoto et al., 2010, 2011) to realize additional learning, optimal

neighborhood preservation, and automatic tuning of parameters and applied it to a voice instruction learning system.

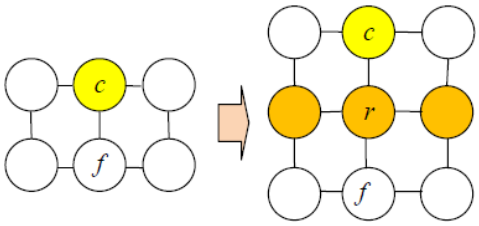

Figure 3: Insert a row/column into the feature map. Unit *c* is a *BMU* and *f* is the farthest unit among the neighbors of *c*, *r* the inserted row/column (Kuremoto et al., 2010).

Instead of the Memory Layer in T-SOM, Parameter-Less Growing Self-Organizing Map (PL-G-SOM) sets a small size of the feature map initially, and when a new input is not able to find a *BMU* from the initial map, that is, the distance between the input and the *BMU* ($\| \mathbf{x} - \mathbf{m}_i \|$) is larger than a threshold, a new row/column is inserted in to enlarge the feature map. For example, in Fig. 3, a new node *r* in the new row/column is inserted into the middle of node *c* and node *f*, where *c* is the nearest node to the new input and *f* is the neighbor of *c*. The weight of connection between the input and the new node has an average value of *c* and *f*,

$$\mathbf{m}_r = 0.5(\mathbf{m}_c + \mathbf{m}_f) \ , \qquad (7)$$

for nodes which are *r*'s neighbors in the new row/column:

$$\mathbf{m}_{r+l} = 0.5(\mathbf{m}_{c+l} + \mathbf{m}_{f+l}) \ , \qquad (8)$$

where *l=1, 2, …, N* or *M*. Unit *f* is chosen which has a largest Euclidean distance from the *BMU*-like *c* among the neighbors of *c*, and after this process, the map size changes to $N\times(M+1)$, or $(N+1)\times M$.

Following adaptive learning rate and neighborhood function are used in PL-G-SOM:

$$\Delta\mathbf{m}_i(t) = \varepsilon(t) h_{ci}^{\varepsilon}(t)(\mathbf{x}(t) - \mathbf{m}_i(t)) \ , \qquad (9)$$

$$\varepsilon(t) = \frac{\| \mathbf{x}(t) - \mathbf{m}_c(t) \|^2}{r(t)} \ , \qquad (10)$$

$$r(t) = \max(\| \mathbf{x}(t) - \mathbf{m}_c(t) \|^2, r(t-1)) \ , \qquad (11)$$

$$r(0) = \| \mathbf{x}(0) - \mathbf{m}_c(0) \|^2 , \qquad (12)$$

$$h_{ci}^{\varepsilon}(t) = \exp(-\frac{\| \mathrm{c}_i - \mathrm{c} \|^2}{(\sigma(\varepsilon(t)))^2}) , \qquad (13)$$

$$\sigma(\varepsilon(t)) = \sigma_{\max} \cdot \varepsilon(t), \ \sigma(\varepsilon(t)) \geq \sigma_{\min} . \qquad (14)$$

Here, $\varepsilon(t)$ is an adaptive learning rate, and $h_{ci}^{\varepsilon}(t)$ is a neighborhood function, $\sigma(t)$ is the neighborhood size. All of them are calculated by the distance between input and the BMU. $\sigma_{\max}, \sigma_{\min}$ are positive parameters, for example, the value may be the size of the map and 1.0, respectively. $\boldsymbol{c_i}, \boldsymbol{c}$ denotes the positions of an arbitrary unit on the output map and *BMU*, respectively, *i=1, 2, …, k* ≤ *N*×*M*. Obviously, $h_{ci}(x) \geq 0$, $h_{ci}(0) = 1$, $h_{ci}(\infty) = 0$.

Table 1: Parameters used in the experiments of SOM, T-SOM and PL-G-SOM.

Description	Symbol	Quantity
Size of image	**Width** ×**Height**	208 x156
Size of initial T-SOM and PL-G-SOM	$N \times M$	5x5
Iteration times	t	800
Temperature	T	1.0
Number of instructions (actions)	$a(i)$	8
Maximum/Minimum neighborhood in PL-G-SOM	$\sigma_{\max}$, $\sigma_{\min}$	$N \times M / 2$, 0.7
Reward for one action selected	r	10.0
Parameters of Feeling Map	$\boldsymbol{a}, \boldsymbol{b}$	0.1, 0.0001

5 The Experiment and Results

5.1 Hand Image Instruction Learning Systems Using T-SOM and PL-G-SOM

Eight kinds of hand shapes meaning 8 instructions of actions available for a robot are shown in Fig. 4 (a)-(g). Regularized binary images of hand shape showed the effectiveness of the preprocessing of images, meanwhile, feature data showed the availability of pattern recognition for their distinguished apparentness. The parameters used in T-SOM and PL-G-SOM are listed in Table 1. The number of units of SOM, T-SOM and PL-G-SOM was 5x5=25 initially. 800 iterations were executed during the learning process because the convergence of Squared Error (SE: distance between input and weights of connections, see Eq. (4)) and

Feeling value (see Eq. (3)).

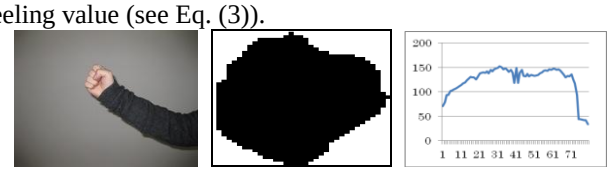
(a) "fist"


(b) "one finger"


(c) "two fingers"


(d) "three fingers"


(e) "four fingers"


(e) "five fingers"


(f) "another two-fingers"


(g) "another three-fingers"

Figure 4: Hand image instructions used in the experiments: (left) Original images of 8 kinds of gestures; (center) hand shapes obtained by the image processing; (c) Features in the input space (80-dimension on horizontal axis).

5.2 The Results and Analyses

To confirm the efficiency of learning methods, learning curves which are depicted by the graph of training time versus errors or performance of the models are commonly used. We investigated the change of distance between input feature data and units weights and the change of Feeling value according to the training time, and show them by Fig. (5) and Fig. (6). PL-G-SOM showed the furthest convergence in both evaluation figures. The value of Feelings of T-SOM and PL-G-SOM reached their highest altitude 1.0, which means that 100% success rate was achieved as hand image instruction recognition/execution. Classic SOM showed unstable performance for the learning process had not realized convergent result. The reason may be considered that the training time for SOM was not enough, and suitable parameters such as Temperature, learning rate, and neighborhood function were not used, usually they are decided by empirical values.

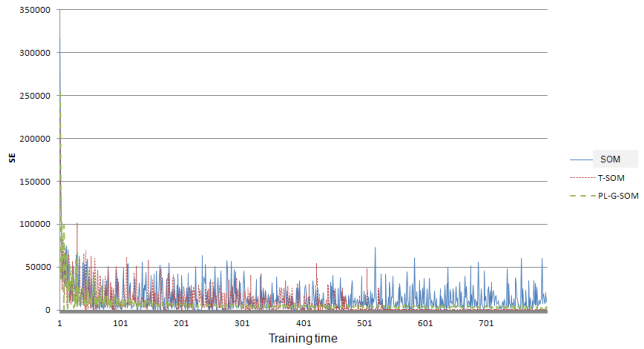

Figure 5: Comparison of different SOMs: the distances (or squared errors: SE) between *BMU* and input vectors (totally 8 kinds of gestures) decreased by training time, PL-G-SOM showed the best performance of learning convergence.

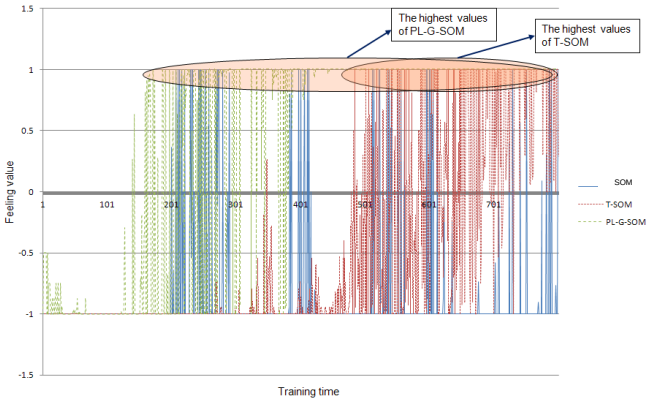

Figure 6: Comparison of different SOMs: the feeling value (totally 8 kinds of gestures) increased according to training time, PL-G-SOM showed the highest performance of learning convergence.

5	0	0	2	4	1	1
4	0	2	2	2	2	2
2	0	6	3	4	7	0
0	3	3	3	3	1	5
0	2	1	7	3	3	3
2	2	3	0	0	0	0

Figure 7: Action Map obtained by PL-G-SOM after training. 42 (6x7) units corresponding to 8 kinds of hand image instructions (0-7) are showed.

Fig. 7 shows the state of Action Map of PL-G-SOM after training. The number of units had grown from 5x5=25 to 6x7=42. Later input training data such as 4, 5, 6, 7 occurred fewer units meanwhile earlier data had more units for the more input times during the training. A method to avoid this situation is that training each instruction for certain times (until it converges) previously, then input all of data to find the global solution.

Fig. 8 shows the growth of the number of units on Feature Map (and Memory Layer) of T-SOM and PL-G-SOM. The speed and the quantity of PL-G-SOM were larger than T-SOM as the same hand image instruction learning systems.

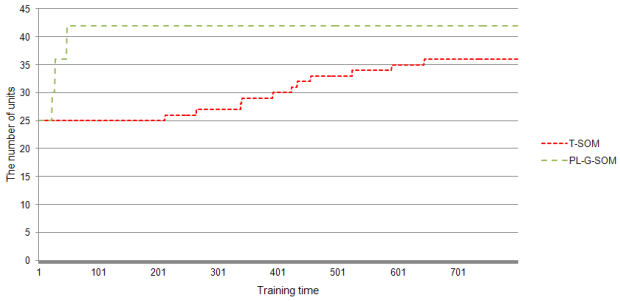

Figure 8: The number of units (neurons) on different maps grew differently during the learning process. The initial sizes of T-SOM and PL-G-SOM were same as 25, and the final sizes were 36 for T-SOM and 42 for PL-G-SOM respectively.

Furthermore, we used untrained samples with different changed variations of the eight shapes of hand, and confirmed the robustness of the trained system using T-SOM and PL-G-SOM. The limitation degree of tilt was about 30, and 45 degree for pan rotation.

From the comparisons of learning performance, it is able to conclude that PL-G-SOM proposed in this study showed more effective than the conventional T-SOM as the hand image instruction learning system.

6 Conclusions

A hand image instruction learning system for partner robot using PL-G-SOM was proposed. Comparing with the conventional system using T-SOM, PL-G-SOM showed better learning performance than T-SOM. Experiments using real robot are expected to confirm the online learning ability of the proposed system in the future.

7 References

[1] Bauer, H.-U., & Villmann Th. "Growing a hypercubical output space in a self-organizing feature map". IEEE Transaction on Neural Networks, Vol. 8, No.2, 218-226, 1997.

[2] Baum, L.E., Petrie, T."Statistical inference for finite state Markov chains", The Annals of Mathematical Statistics, Vol. 37, No.6, 1554-1563, 1966.

[3] Berglund, E., & Sitte, J. "The parameter-less self-organizing map algorithm". IEEE Transaction on Neural Networks, Vol. 17, No.2, 305-316, 2006.

[4] Cottrell, M., Fort, J.C., & Pages, G. "Theoretical aspects of the SOM algorithm". Neurocomputing, Vol.21, 119-138, 1998.

[5] Dittenbach, M., Merkl, D., & Rauber, A. "The growing hierarchical self-organizing map". In Proceedings of IEEE International Joint Conference on Neural Network (IJCNN '00) , 15-19, 2000.

[6] Fritzke, B. "Growing grid – a self-organizing network with constant neighborhood range and adaption strength". Neural Processing Letters, Vol. 2, No.5, 9-13, 1995.

[7] Hano, T., Kuremoto, T., Kobayashi, K., & Obayashi, M. "A hand image instruction learning system using Transient-SOM". Transactions on SICE (Society of Instrument and Control Engineering),Vol.43, No.11, 1004-1006, 2007 (in Japanese)

[8] Kohonen, T. "Self-organized formation of topologically correct feature maps". Biological Cybernetics, Vol.43, No.1), 59-69, 1982.

[9] Kohonen, T. "Self-Organizing Maps", Berlin; Heidelberg; New-York: Springer, Series in Information Sciences, 1995.

[10] Kohonen, T. "The self-organizing map". Neurocomputing, Vol. 21, 1-6, 1998.

[11] Kuremoto, T., Hano, T., Kobayashi, K. & Obayashi, M. "For partner robots: A hand instruction learning system using transient-SOM". In Proceedings of The 2nd International Conference on Natural Computation and The 3rd International Conference on Fuzzy Systems and Knowledge Discovery (ICNC '06-FSKD'06), 403-414, 2006.

[12] Kuremoto, T., Hano, T., Kobayashi, K. & Obayashi, M. "Robot feeling formation based on image features". In Proceedings of International Conference on Control, Automation and Systems (ICCAS 2007), 758-761, 2007.

[13] Kuremoto, T., Komoto, T., Kobayashi, K., & Obayashi, M. "Parameterless-Growing-SOM and its application to a voice instruction learning system". Journal of Robotics, 9 pages (online), 2010.

[14] Kuremoto, T., Yamane, T., Feng, L.-B., Kobayashi, K., & Obayashi, M. "A human-machine interaction system: A voice command learning system using PL-G-SOM". Proceedings of International Conference on Industrial Engineering and Management Special Session in MASS (IEEE-IEM 2011), IEEE Catalog Number: CFP1141H-CDR, 83-86, 2011.

[15] Pavlovic, V.I., Sharma, R., Huang, T.S. "Visual interpretation of hand gesture for human-computer interaction: a review". IEEE Transaction on Pattern Analysis and Machine Intelligence, Vol. 19, No. 7, 667–693, 1997.

[16] Rumelhart, D.E., McClelland, J.L., & The PDP Research Group. "Parallel distributed processing: Explorations in microstructure of cognition", The MIT Press, Cambridge, 1986.

[17] Sherrah, S., Gong, S. (2001). "Skin Colour Analysis", Available online URL:http://homepages.inf.ed.ac.uk/rbf/CVonline/LOCAL_COPIES/GONG1/cvOnline-skinColourAnalysis.html

[18] Sutton, S.S., Barto, A.G. "Reinforcement learning: an instruction", The MIT Press, London, 1998.

[19] Villmann, Th., Bauer, H. –U. "Applications of the Growing Self-Organizing Map". Neurocomputing, Vol. 21, 91-100, 1998.

[20] Wilson, A.D., & Bobick, A.F. "Parametric hidden Markov models for gesture recognition". IEEE Transactions on Pattern Analysis and Machine Intelligence, Vol. 21, No.9, 884-900, 1999.

Semantic Validation of Uttered Commands in Voice-activated Home Automation

G. Ferreira[1], H. Macedo[1], L. Matos[1], A. Leandro[1], E. Seabra[1], W. Sampaio[1], A. Silva[2], T. Mendonça[3], and M. Soto[4]
[1]Computer Department, Federal University of Sergipe, São Cristóvão/SE, Brazil
[2]Computer Institute, State University of Campinas, Campinas/SP, Brazil
[3]Vrije Universiteit Brussels, Brussels, Belgium
[4]Instituto Atalaia de Pesquisa e Desenvolvimento, São Paulo/SP, Brazil

Abstract— *This paper describes an Automatic Speech Recognition System in the home automation domain for the Brazilian Portuguese. It uses domain knowledge to automatically generate the language model and semantic evaluation of the transcription. The speech command is captured by a mobile device working as a "thin" client which is thereafter recognized by a server connected through. The speech command is then validated by a home automation domain ontology. New commands are added to the ontology which in turn is used to automatically generate a new language model. This approach is somewhat innovative in the ASR literature. Results shows a WIP of* 72% *with a real time factor of* 28% *and improved robustness of the system.*

Keywords: Home Automation, Automatic Speech Recognition, Language Model, Semantic Evaluation

1. Introduction

Current solutions for home automation include centralized control of lighting, heating, air conditioning, audio, video and other different electric and electronic devices in order to achieve comfort, save energy, improve security and provide increased quality of life for the elderly and disabled people. Mainstream operation of a home automation system is done by means of in-wall panels or, more recently, mobile devices. Due to the reduced dimension of keyboards and screens, mobile devices usability is, however, severely bounded [1].

Speech-enabled interfaces may be a good choice, since recent improvement in speech recognition accuracy and processing costs turns affordable the use of such technology.

Regardless the clear general achievements in continuous speech recognition, the lack of corpora and resources are still a huge obstacle for specific languages. Yet, the multitude of different accents and regional pronunciations makes the task even more challenging for the Portuguese language.

In this work we present a continuous Automatic Speech Recognition (ASR) system to perform home automation using Brazilian Portuguese utterances. The utterance is captured by a mobile device working as a client of a home automation server in a networked speech recognition architecture.

The server processes the spoken utterance and outputs a set of most probable candidates. Further, a home automation ontology validates the candidates using domain rules as semantic and syntactic information. The server translates the commands into zigbee codes which are finally transmitted to the respective devices. The language model is automatically generated according to the domain rules in the ontology.

Primary goals are two-fold: (1) evaluate the impact of the using specific domain knowledge provided by the ontology as semantic and syntactic information in the speech recognition accuracy and (2) analyze the feasibility of an automatically generated language model and its impact in the speech recognition accuracy.

In section 2 we present main ASR blocks along with a short review of Portuguese language issues. In section 3 we present the Semantic model we have proposed and added to ASR mainstream architecture. In section 4, we show how domain information can be actually used to validate uttered home automation commands. Experiments and results are provided in section 5. Finally, we present some concluding remarks in section 6.

2. Portuguese Language Automatic Speech Recognition

The first step of an Automatic Speech Recognition (ASR) task is to appropriately represent the speech waveform into an acoustic *feature vector* (or evidence) $X = (x_1, x_2, \cdots, x_t)$ which is generated in the time interval $[1..t]$. Such representation must deal with the drawback of having low dimensionality, which reduces complexity, and keeping the linguistic information. At the same time it must be robust, minimizing the influence of environmental noise. Extraction of the Mel-frequency cepstral coefficients (MFCCs) have been largely used [2]. MFCC warps the linear spectrum of the speech into a nonlinear scale called Mel which attempts to model the human ear sensitivity.

An ASR system can be then mathematically described as a mapping of such acoustic evidence X to a sequence of words $W = (w_1, w_2, \cdots, w_n)$ [3], where each word w_i belongs to a set of candidate words ω. The mapping is

defined in equation 1, where the term $P(W|X)$ has been rewritten using Bayes' Rule. The goal of the recognizer is, thus, to select the sequence of words that maximizes the underlying product.

$$\hat{W} = argmax_{W \in \omega} P(W|X) = P(W)P(X|W) \quad (1)$$

The estimation of the likelihood $P(X|W)$ term is given by an *acoustic model*. The acoustic model is built upon the feature extracted from a raw speech corpus and is usually modeled into Hidden Markov Models (HMMs) [4]. The HMM translate the input into a sequence of phonemes.

The term $P(W)$ is estimated by a *language model*. A popular model is based on a Markovian assumption that the probability of a given word w_i is approximated by the probability of its observing context of $n-1$ words, as shown in equation 2. The 3-gram language model seems to work better for the Brazilian Portuguese [5].

The probabilities are estimated from a corpus of sentences. The estimation of most N-grams is not reliable due to the sparseness of data. Smoothing techniques [3] are used to flatten the probability distribution, thus amending the problem. Two examples of smoothing techniques are Good-Turing [6] and Witten-Bell [7].

$$\begin{aligned} P(w_1, w_2, \cdots, w_m) &= \prod P(w_i|w_1, \cdots, w_{i-1}) \quad (2) \\ &\approx \prod P(w_i|w_{i-1(n-1)}, \cdots, w_{i-1}) \end{aligned}$$

Once the range of candidate sequence of words $W = (w_1, w_2, \cdots, w_n)$ that maximizes the product is huge, a *decoder* algorithm is used to perform an efficient search in the state space. Figure 1 illustrates how these four main blocks of an ASR system are related.

ASR rely on quite amount of preprocessed data. These data consist of labeled speech and text corpora used to the construction of acoustic models and language models, respectively. Other kind of speech-related resources may be required as well. Due to the inherent difficulty in build from scratch such a speech-related corpus and, as a consequence, to find an appropriate one, improving the state-of-the-art of the research in ASR is not an easy job. This is particularly true for natural languages other than the English one. As a consequence, most of the research in the area, regardless the country where it is actually done, has been relied on the use of public and readily available English-based corpora.

In recent years, speech recognition research for Portuguese language have been propelled. The AUDIMUS speech recognizer [8] is one of the most successful initiative and has been used as the platform for several important advances in speech recognition for Portuguese language. The AUDIMUS system uses a HMM 3-gram language model based on the transcriptions news of 51 hours from a European Portuguese corpus with 532,000 words. The output probabilities are estimated by a MLP neural network. Experiments with a 13 hours of broadcast news test data have shown a WER of 21.5%. AUDIMUS has been recently adapted for Brazilian Portuguese broadcast news [9]. Results have shown a WER of 26.9%. Most previous Brazilian Portuguese recognizers used small vocabulary [10], [11].

In addition to the development of speech recognizers, some speech corpora have been produced as a result of academic efforts in advancing speech recognition research for Portuguese language. BDPublico [12] and LECTRA [13] are proprietary speech corpora for European Portuguese language. The Spoltech [14] is probably the most widely used corpus for Brazilian Portuguese. It consists of microphone-recorded speech, with proper phonetic and orthographic transcriptions, of Brazilian men and women with different accents and ages.

Some research groups and cooperative initiatives have contributed to the improvement of Portuguese language speech recognition results, by providing textual corpora, lexicons, phonetic dictionaries, acoustic models and language models. The Nucleo Interinstitucional de Linguistica Computacional (NILC)[1], Linguateca[2] and FalaBrasil[3] are three of the most relevant ones.

3. Semantic Modeling

The method commonly used to modeling natural language for ASR is based on N-gram language modeling. The main purpose of language modeling is to bias an ASR towards sentences appropriate to a particular domain, avoiding meaningless sequences of words. An enhancement on the language model may be achieved by means of a method named structured language modeling (SLM) [15], which uses a bottom-up syntactic parser to find the most likely syntactic parses of a partial sentence. [16] reports an improvement of 2-3% in the WER over N-gram models.

These syntactic parsers, however, are not able to identify main constituents of a sentence that represent concepts and meanings. For limited-domain and task-specific spoken dialog systems, a kind of semantic analysis seems to be more effective. The SOUP parser [17] is an example of semantic analyzer.

In [18], the authors employ a semantic analyzer to enhance the language model used in a spoken dialog system. A statistical model estimates the joint probability of a sentence and its most likely semantic parse. Sentences that have parses with high probability will then be preferred in recognition.

Similarly, we consider the addition of a semantic analysis step to improve ASR results. We propose, however, a domain ontology as a shallow semantic parser. Keywords of the best resulting sequence $\hat{W}$ from ASR decoding phase are

[1] http://nilc.icmc.sc.usp.br/nilc/tools/corpora.htm)
[2] http://www.linguateca.pt/
[3] http://www.laps.ufpa.br/falabrasil/

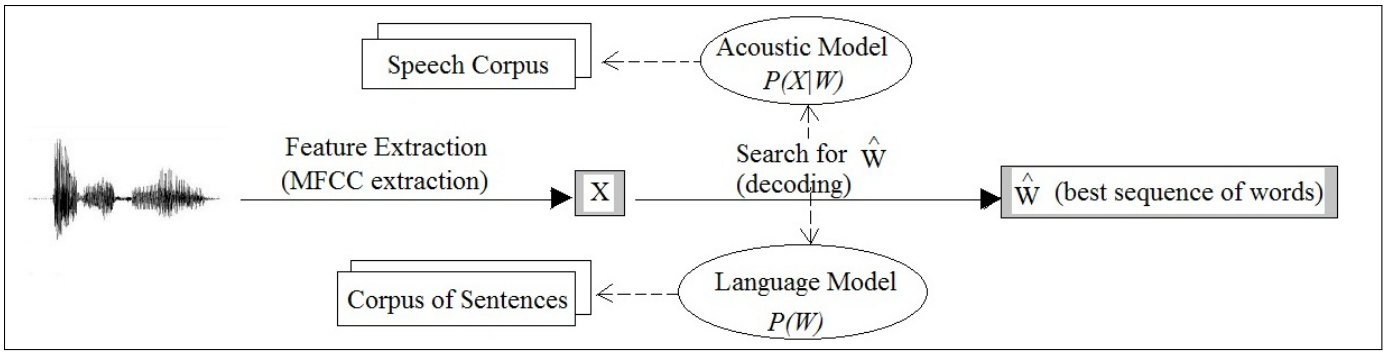

Fig. 1: Main blocks of an ASR system. The acoustic model estimates the likelihood $P(X|W)$ whereas the language model estimates $P(W)$. A "'decoding"' algorithm perform a search for the best sequence of words to the acoustic evidence X.

candidate instances of some feasible concept arrangement. Is there is any feasible concept arrangement, the sequence is validated. On the contrary, it is dropped as a false-positive.

3.1 Ontology

An ontology [19] specifies a description of terminologies, concepts, properties, and relationships between these concepts, being them hierarchical or lattice relations relevant to a particular domain or area of interest. In sophisticated cases, suitable axioms are added to constrain concepts intended interpretation.

To be useful for computational purpose, an ontology must be the result of an exhaustive and rigorous attempt to define a conceptual representation of a domain, or a fraction of that domain; in effect, the amount of knowledge to be covered by the ontology is decided by the knowledge engineer. In addition, in order to be machine readable, an ontology should be defined in a semantically strong notation. It must use a representation language that allows both a human community to share a precise, unambiguous under common understanding of the domain and software agents to perform automated reasoning about it. Ontologies are commonly used in artificial intelligence and knowledge-based computer programs. In these cases, they can be used for implementing inductive reasoning, classification algorithms, and for enabling communication and knowledge sharing between different systems. As the central piece of a data classifier system, an ontology can store knowledge rules that reason about the data, thus allowing the system to infer new knowledge. Regardless of the notation or syntax used to define different ontologies, they share many common features such as concepts, partitions, attributes and relationships.

The semantic Web [20] uses a combination of descriptive technologies like XML, RDF (Resource Description Framework) and OWL (Web Ontology Language) [21] to replace the content of Web documents, currently highly encoded in HTML. In fact, OWL is a markup language extended from RDF for publishing and sharing data using ontologies on the Web. Web ontologies improve accuracy and promote completeness through constraints, restrictions, and complex relations among terms that build on/extend the web metadata created in XML. The machine-readable descriptions enable Web content managers to add meaning to the content, facilitating automated information gathering and research by computers.

3.2 Ontology-driven Semantic Parser

Let us define an ontology O as a tuple $< D, A, \gamma^n >$, where D is the domain, A is the set of feasible arrangements of concepts and γ is a total function $\gamma^n : A \mapsto 2^{D^n}$ from A into the set of all n-ary relations on D. As a consequence, for a specific feasible arrangement instance $a \in A$, there is a set of feasible conceptual relations $R_a = \gamma(a)$.

We also define the ontology vocabulary V as set of all lexical terms (words) used to represent the concepts and relations within the ontology. The ontology modeling language Λ can thus be defined as a tuple $< O, V, \mu >$, with $\mu = V \mapsto D \cup R$ as being a function which maps concepts of D and relations of R to suitable lexical terms of V.

Recall now the best sequence of words (sentence) $\hat{W} = (w_1, w_2, \cdots, w_n)$, selected by the "'decoding"' algorithm to a given acoustic evidence X. In addition, consider $K \subseteq \hat{W}$ as the set of keywords of $\hat{W}$ such that $K = \hat{W} - \{stop_1, ..., stop_n\}$, with $stop_i$ being words that do not aggregate meaning (*stopwords*), such as articles, prepositions, conjunctions, pronouns, and punctuation marks. We say that $\hat{W}$ is *semantically validated* by an ontology $O = (D, A, \gamma^n)$ iff $\mu(K) \subseteq A \cup \gamma(A)$ and, as a consequence, $K \subseteq V$.

Once the sequence is semantically validated, it is mapped to an action Δ_j from a set of predefined domain-specific actions Δ (figure 2).

4. Speech-enabling Home Automation Commands

System's main goal is to control electric and electronic devices (e.g. TVs, doors, air conditioning, etc.) and preset

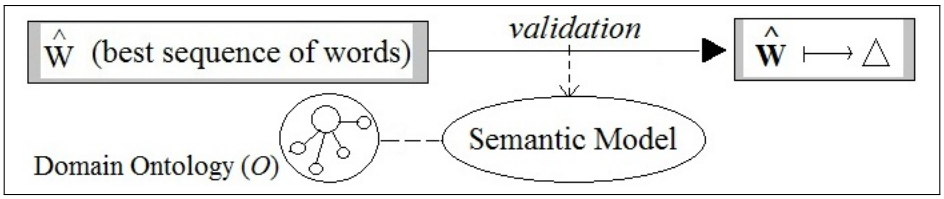

Fig. 2: Semantic validation tests whether the terms in the best sequence $\hat{W}$ can provide a feasible set of concepts and relations according to the domain ontology. In case $\hat{W}$ is validated, an action from Δ is performed.

scenarios in the home environment. A scenario represents the state of a set of controlled devices, usually composed by a large number of isolated items. A *romantic dinner scenario*, for instance, may be assigned to a special activation of lamps in the dinning room, as well as the closure of curtains and setting the air temperature to $20°C$. We have used Julius [22] software for MFCC, acoustic model and language model steps. This work use 3-gram model which seems to work better for the Brazilian Portuguese. We also have used an acoustic model based on triphone units.

Due to small size of the ontology vocabulary V and the nature of the speech utterances (commands), we have performed automatic generation of a language model from O. The resulting custom model bias the recognition to terms related to the home environment.

System's architecture is categorized as Mobile Speech Recognition Architecture [1]. In such architecture, the mobile device works just as a signal transmitter, while the whole processing is done in a server in order to enhance recognition performance and, at the same time, provide mobility in and out of the house.

The major concern with this type of architecture regards the signal (spoken utterance), which is sent to the server, and the quality of the network. In our system, the voice is first normalized and then enhanced using a simple cepstral power measurement. This is done via the Sound Exchange (SoX) tool[4]. Since different mobile devices use different sampling rates to capture voice, we have tested the system with two sampling rates: $16Khz$ and $8Khz$.

4.1 Using Domain Knowledge for Sentence Validation

The domain ontology has been coded as an OWL/RDF ontology [21]. In Figure 3 we illustrate the hierarchy of all concepts in the ontology. The two concepts `#Semantic` and `#Syntax` play primordial role. The `#Semantic` concept and their specializations represent the home's devices and system's commands, whereas the `#Syntax` concept family represents structure of commands.

`#Feature` concept instances are device-related features such as temperature, volume, etc. Features are related to supported commands by means of `#is-Used-By` relationship. `#Rangeable` concept instances are special kind of features, where an interval of values can be applied. `#Control` concept instances are assigned to direct control of predefined scenarios such as *Ativar Cenário Romântico* (*Activate Romantic Scenario*), which synthesizes a complex sequence of actions: *turn off the lights of the dining room, light the candles, close curtains and turn on the sound*, for instance. `#Function` concept instances are commands for device features, where `#Stepable` concept concerns those controls that affect the values in steps, such as Raise and Decrease. Instances of `#Controlable` concept have IDs and can be directly affected by a command by means of a `#is-Used-By` relationship. `#Device` represents the various existent devices that can be controlled, such as lights, Ar conditioner, TVs, and so on. A device may have a specific feature by means of a `#has-Feature` relationship. `#Scenario` is another kind of `#Controlable` which represents various supported scenarios, as the one exemplified so far. `#IDs` are used to uniquely identify devices and scenarios within the system. A `#UserID` enables customization of IDs, such that specified by the system's user.

Consider the following sentence as an example of the best sequence of words generated by decoding phase of the ASR system:

Aumentar temperatura do Arcondicionado do quarto da Julia

This sentence is the Portuguese version of "'Raise the temperature of Julia's room air conditioner"'. The keywords are $K \subseteq \hat{W} = (\textit{Aumentar}, \textit{temperatura}, \textit{Arcondicionado}, \textit{quarto da Julia})$.

This sentence is semantically validated and, thus, recognized as a possible home automation command only if the lexicon of their keywords can be mapped to a feasible arrangement of concepts and relations. Formally, $\mu(K) \subseteq A \cup \gamma(A)$.

Each individual has a set of names/tokens that helps the self-identification in the words sequence. The command (i.e. raise) represents the action that will be taken; the feature is the property (i.e. temperature) that will be changed; the device (i.e. air conditioner) owns the feature operated and

[4] `http://sox.sourceforge.net`

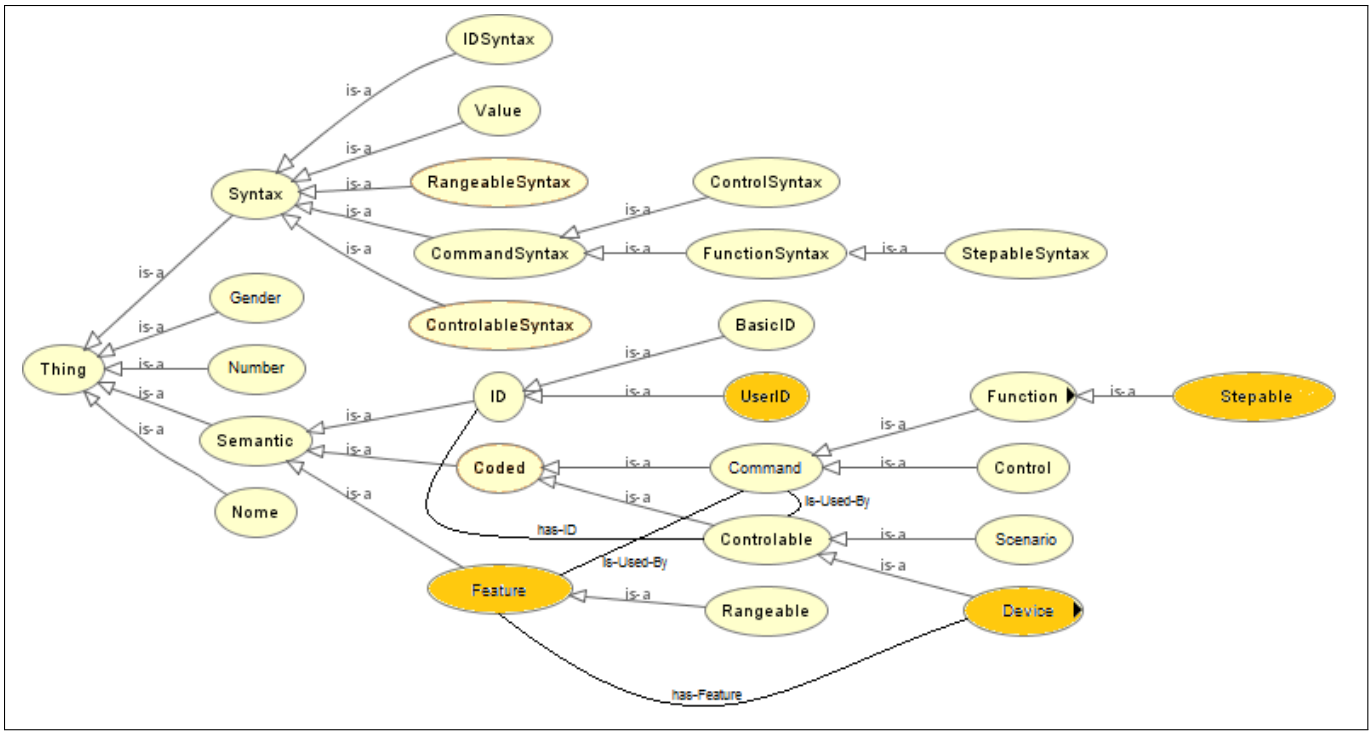

Fig. 3: The ontology class hierarchy. The highlighted slice shows a feasible arrangement of concepts and relations, able to semantically validate a sentence such as "'Raise the temperature of Julia's room air conditioner"'.

the ID (i.e. Julia's room).

For such specific example, the highlighted ontology slice in Figure 3 shows a feasible arrangement of concepts and relations from O. The lexicon "'Aumentar"' is mapped to the `Stepable` command-kind concept, "'temperatura"' is mapped to the property-type concept `Feature`, "'Arcondicionado"' is the `Device` which owns the operated feature and, finally, "'quarto de Julia"' works as an `UserID`. Note that a feasible relationship holds between concepts: (1) the command can be used to that feature, (2) the device has this specific feature, and (3) there is an user ID for that controllable device.

Certain constraints have been considered, though. The first one is that a command must always be the first item in the sentence. This is done in order to bias the grams probabilities in the language model and hopefully improve accuracy. Other words may appear in any order. Another constraint concerns the amount changed in a feature (e.g. raised, lowered). This is inferred from a range of values of a feature in O. This is done in order to make commands more comfortable to the user and to avoid great bias toward the numerous N-grams that would include a number.

4.2 Generating Language Model from Ontology

Manually create a corpus is too time consuming and the lack of domain corpora weighed heavily in the decision of a automatically made alternative. A domain specific corpus can bias the language model to the set of domain-related terms, thus improving the system accuracy. In addition, the automatic generation provides robustness to the system since it can be easily synchronized with the domain ontology and, as a consequence, with the environment updates.

Two artifacts are generated in the process: a *sentence corpus* and a *dictionary of phonetic transcriptions*. The corpus generation is done through the combination of possible command sentences. Basically, there are two kinds of sentences in the system's domain:

```
  Command [article] Device [preposition] ID
  Command [article] Feature [preposition]
Device [preposition] ID
```

The elements surround by brackets are optional. The articles and preposition can vary in gender and number. This information is extracted from the set of transcription from each individual in O. The sentences generated are all valid in the semantic sense.

After the corpus generation, the next step is to generate the phonetic transcriptions of all the words in the corpus. This is automatically done via a grapheme to phoneme tool. However, the automatically generated transcriptions do not account the regional differences in pronunciation. This can be a problem, depending on the user and the acoustic corpora used.

The vocabulary used in the system is small, consisting of 113 words. The generated corpus contained 13994 sentences and contained all possible commands but not all their variations. The manually corpus has 6050 sentences.

5. Experimental Results

The Word Error Rate (WER) measurement is widely used to evaluate continuous ASR performance. It is described in equation 4, where I stands for inserted words, C stands for correctly recognized words, D stands for deleted words and S concerns substitutions. The WER is not always the best choice to evaluation, though. Its value range is not constant $[0..1]$ and can induce abnormal results. The Word Information Preserved (WIP), on the contrary, has a constant range and is described in equation 5.

The responsiveness of the system is an important feature for it's usability. The Real time Factor (xRT) measure can be used to evaluate the system responsiveness. It is calculated using equation 3, where P stands for the processing time and I the audio duration. We have achieved a xRT of $0,29$. This value is achieved by limiting the search of grams and triphones hypothesis on the recognition process.

$$xRT = \frac{P}{I} \tag{3}$$

$$WER = \frac{S + D + I}{C + S + D} \tag{4}$$

$$WIP = \frac{C^2}{[(C + S + P)(C + S + I)]} \tag{5}$$

Moreover minor errors at the word level have no impact at the semantic information that the word sequence carries [23]. For instance, although the sequences *Ligue a luz* (Turn on the lights) and *Ligar luz* (Turn on Lights) accounts for 2 errors (i.e. substitution, and insertion/deletion), they both carry the same semantic information.

The test set been used is composed of 120 utterances for 12 different speakers. The audio has been captured in low to mid noise environment with a mobile device at 16KHzw and is resampled to match the acoustic model sampling rate. The 8KHz samples were generated from the 16KHz sample via resampling.

The table 1 shows the best WER and WIP values for the system. Those results were achieved with the Witten Bell smoothing technique for the language model, as will every measurement mentioned from now on. All the variations used the same phoneme transcriptions

The high deviations are due to a drop of accuracy towards certain types of commands. For example the word "um" (i.e. one in english) is composed of a single phoneme and is hard to recognize and often deleted/included, however it carries relevant semantic information like an ID for a device in "Ligar TV um" (Turn on TV one, in english). This can be avoided by using names instead of numbers for the devices.

The table also shows the variation of accuracy with different sampling rates. It shows a great improvement with the double sample rate. The automatically generated language model achieved a better recognition rate than the manually written one. This probably stem from the fact that the probability distribution on the automatically generated one is better biased toward the application. All the examples from the corpus is a valid command in a semantic sense.

Table 1: WER, WIP and SRR values

	Automatic(16KHz)	Manual(16KHz)	Automatic(8KHz)
WER	$23,69\% \pm 24,05\%$	$33,44\% \pm 27,94\%$	$74,39\% \pm 75,23\%$
WIP	$72,70\% \pm 28,59\%$	$60,01\% \pm 31,56\%$	$35,62\% \pm 33,69\%$
SRR	$75,92\%$	$59,25\%$	$35,00\%$

The Semantic Recognition Rate (SRR) in table 1 stands for the rate of commands fully recognized in a semantic sense. The SRR was calculated by comparing the zigbee codes from the manually transcribed uttered command to the recognized one. It is closely related to the WIP measurement, however it accounts the semantic errors only providing a more precise accuracy measurement.

6. Conclusion

This paper described a continuous ASR system for the Brazilian Portuguese language used in a home automation environment. In that environment, the ASR system was used as the input for controlling the home automation devices. Due to the semantically intrinsic mechanism of human been expose their thoughts, present in the informal discuss, we develop an ontology to perform semantic analysis of sentences provided from the intermediate level layer of the ASR system.

We have also used the domain knowledge in the ontology to generate a language model. It addresses the lack of data for the recognition system and provides a biased model for a specific domain, helping with the recognition accuracy.

The results section highlighted the problem of evaluation of continuous ASR system. Even if the WER measure is widely used it is prone to anomaly. The use of semantic information in the evaluation provided clearer results since it accounts only semantic errors.

References

[1] A. Schmitt, D. Zaykovskiy, and W. Minker, "Speech recognition for mobile devices," *Int. J. of Speech Tech.*, vol. 11, pp. 63–72, 2008, 10.1007/s10772-009-9036-6. [Online]. Available: http://dx.doi.org/10.1007/s10772-009-9036-6

[2] X. Huang, A. Acero, and H.-W. Hon, *Spoken Language Processing: A Guide to Theory, Algorithm, and System Development*, 1st ed. Upper Saddle River, NJ, USA: Prentice Hall PTR, 2001.

[3] A. G. Adami, "Automatic speech recognition: from the beginning to portuguese language," in *PROPOR*, 2010.

[4] L. R. Rabiner, "A tutorial on hidden Markov models and selected applications in speech recognition," *Proceedings of the IEEE*, vol. 77, no. 2, pp. 257–286, 1989.

[5] F. dos Santos, D. Barone, and A. Adami, "A baseline system for continuous speech recognition of brazilian portuguese using the west point brazilian portuguese speech corpus," in *Computational Processing of the Portuguese Language*, ser. LNCS, P. et al., Ed. Springer Berlin / Heidelberg, 2010, vol. 6001, pp. 132–141. [Online]. Available: \url{http://dx.doi.org/10.1007/978-3-642-12320-7_18}

[6] Orlitsky, Santhanam, and Zhang, "Always good turing: Asymptotically optimal probability estimation," *SCIENCE: Science*, vol. 302, 2003.

[7] P. Placeway, R. Schwartz, P. Fung, and L. Nguyen, "The estimation of powerful language models from small and large corpora," *Acoustics, Speech, and Signal Processing, IEEE International Conference on*, vol. 2, pp. 33–36, 1993.

[8] H. Meinedo, D. Caseiro, J. a. Neto, and I. Trancoso, "Audimus - a broadcast news speech recognition system for the european portuguese language," in *PROPOR*. LNCS, 2003, pp. 196–196.

[9] A. Abad, I. Trancoso, N. Neto, and M. C. Viana, "Porting an european portuguese broadcast news recognition system to brazilian portuguese," in *INTERSPEECH*, 2009, pp. 92–95.

[10] S. S and A. A, "Um sistema de reconhecimento de voz contínua dependente da tarefa em língua portuguesa," *Rev Soc Brasil Telecomun*, vol. 17, pp. 135–147, 2002.

[11] F. R and S. I, "Uma nova abordagem fonetico fonologica em sistemas de reconhecimento de fala espontânea," *Rev Soc Brasil Telecomun*, vol. 95, p. 225Ű239, 2003.

[12] J. P. Neto, C. A. Martins, H. Meinedo, and L. B. Almeida, "The design of a large vocabulary speech corpus for the portuguese," in *Proc. Eurospeech '97*, Rhodes, Greece, Sept. 1997, pp. 1707–1710.

[13] I. Trancoso, R. Martins, H. Moniz, A. I. Mata, and C. Viana, "The LECTRA corpus - classroom lecture transcriptions in european portuguese," in *LREC*. European Language Resources Association, 2008. [Online]. Available: http://www.lrec-conf.org/proceedings/lrec2008/

[14] N. Neto, P. Silva, A. Klautau, and A. G. Adami, "Spoltech and OGI-22 baseline systems for speech recognition in brazilian portuguese," in *PROPOR*, ser. LNCS, vol. 5190. Springer, 2008, pp. 256–259.

[15] C. Chelba and F. Jelinek, "Structured language modeling," *Computer Speech & Language*, vol. 14, no. 4, pp. 283–332, 2000. [Online]. Available: http://dx.doi.org/10.1006/csla.2000.0147

[16] J. Wu and S. Khudanpur, "Syntactic heads in statistical language modeling," *Acoustics, Speech, and Signal Processing, IEEE International Conference on*, vol. 3, pp. 1699–1702, 2000.

[17] C. Langley, A. Lavie, L. Levin, D. Wallace, D. Gates, and K. Peterson, "Spoken language parsing using phrase-level grammars and trainable classifiers," May 22 2004. [Online]. Available: http://citeseer.ist.psu.edu/643827.html;http://acl.ldc.upenn.edu/W/W02/W02-0703.pdf

[18] H. Erdogan, R. Sarikaya, S. F. Chen, Y. Gao, and M. Picheny, "Using semantic analysis to improve speech recognition performance," *Comput. Speech Lang.*, vol. 19, pp. 321–343, July 2005. [Online]. Available: http://portal.acm.org/citation.cfm?id=1648819.1648848

[19] D. Fensel, *Ontologies - a silver bullet for knowledge management and electronic commerce*. Springer, 2001.

[20] N. Shadbolt, W. Hall, and T. Berners-Lee, "The semantic web revisited," *Intelligent Systems, IEEE*, vol. 21, no. 3, pp. 96 –101, jan.-feb. 2006.

[21] D. L. McGuinness and F. Harmelen, "OWL Web Ontology Language Overview," 2003. [Online]. Available: http://www.w3.org/TR/owl-features/

[22] A. Lee, T. Kawahara, and K. Shikano, "Julius — an open source real-time large vocabulary recognition engine," in *7th Euro Conf. on Speech Commun. and Tech.*, 2001.

[23] J. Nordstrom, "Evaluation of swedish speech recognizers for spontaneous and natural speech," Master's thesis, Royal Institute of Technology, 2007.

Probabilistic Gesture Recognition

Ensembles and Multiple Input Modalities

Gary Newell[1], James Neilan[2], Mark Henderson[3]
Northern Kentucky University
Department of Computer Science, College of Informatics
Contact: Dr. Gary Newell[1], GH449
Highland Height, KY 41099
[1]newellg@nku.edu, [2]neilanj1@nku.edu, [3]hendersonm6@nku.edu

Abstract *— This paper reports upon ongoing research in the general domain of pattern recognition in the presence of uncertainty. In particular, we are attempting to develop a relatively simple but effective ensemble model for the recognition of gestures. We present a model, INCA, and two gesture recognition application domains using a pen tablet and data glove, where the ensemble methodology is implemented. Using this model, we have built a probabilistically based ensemble system and tested four standard ensemble fusion methods. The accuracy improvements in the domains of handwritten digit and hand-signed digit gesture symbols was 10% to 20% above the weakly trained component classifier performance.*

Submitted to the International Conference on Artificial Intelligence in Las Vegas, Nevada July 16th -19th 2012.

Keywords:Ensembles, Multiple Classifiers, Gesture Recognition

1. Introduction

We define a gesture in a very general way as a temporal sequence of points through *N*-dimensional space. Some examples of gestures would include speech, hand-drawn symbols, hand gestures (e.g. sign-language), facial movements, and brain-waves via electroencephalography. While some gestures consist of low-dimensioned spaces (e.g. 2D or 3D spaces for hand-written gestures), others can consist of 10 or more (e.g. speech recognition).

The proposed model, INCA ("I've No Cute Acronym") [18], assumes the existence of gestural recognition algorithms for a given domain whose performance need not be particularly strong. The goal of the model is to build a meta-algorithm that combines the individual recognition results of the component algorithms to produce an over-all superior performance to any of the participating algorithms involved. Few assumptions are made regarding the internal functionality of said recognition algorithms. Each component algorithm is assumed to receive static or dynamic, temporal, input representing the gesture in question and is expected to produce a recognition result consisting of a symbol from the given gestural alphabet. For example, in the domain of hand-written recognition, the component algorithm might receive a sequence of pen-tip positions (using standard Cartesian coordinates) over the temporal period of drawing a symbol. The algorithm would produce a recognition result indicating the recognition of some specific symbol in a given gestural alphabet (e.g. the digits 0-9, the English alphabet A-Z, etc.).

The INCA model uses a straight-forward Bayesian approach to examine each algorithm's recognition result. The model produces a confidence vector, CV, for each algorithm that represents the probabilistic likelihood that each possible symbol in the alphabet is the truly correct result.

A confidence vector is simply a finite probability space that reflects, for each possible symbol in the gestural alphabet, a probability, $p \in [0,1]$, that the symbol is, in fact, the appropriate result based upon the algorithm's reported recognition result when prior behavior is considered. Simply put, an algorithm that frequently misrecognizes a hand-written 'H' as a 'K' should not, upon recognition of a 'K', be "trusted" to have recognized correctly. Based upon the consistent misrecognition behavior, it should be identified that the probability that the correct result is, in fact, an 'H' is greater than 0. Similarly, we should consider the previous behavior of this algorithm when it identifies the symbol 'K' as it pertains to the actual input of *all* possible symbols. The resulting probabilities for each symbol constitute the confidence vector's finite probability space.

Upon the creation of the confidence vectors for all of the component algorithms, they are combined to produce an overall INCA recognition result. We have explored a variety of combination algorithms and report our results in section 6 of this document. We are currently exploring the effectiveness of these algorithms under a variety of circumstances such as the inclusion of new algorithms whose recognition rates are significantly higher or lower than the existing system's component algorithms.

A. Bayes' Theorem – A Gestural Recognition Application

Bayes' Theorem, or Bayes' Rule, is based upon the concept of conditional probability. Conditional probability P(A|B) is defined as the probability that an unobserved event A has occurred given an actual observation of an event B. Formally it is defined as $P(A|B) = P(A \cap B) / P(B)$. Intuitively, the likelihood that an event A occurs when an event B is observed depends upon how often the two events occur together in relation to how often the observed event B occurs in general [18].

Funding for this research was provided by the Northern Kentucky University Research Foundation Graduate Research Grant

Bayes theorem is presented below. It applies conditional probability to a partition of some sample space of mutually exclusive and exhaustive sets (A_1,A_2,A_3…A_m). The theorem supplies a formula for $P(A_i|B_k)$ where B_k is some empirically observable event. For our purposes, B_k is the recognition result produced by some algorithm and the A_i values represent the event of some symbol having actually been entered as input.

$$P(A_i|B_k)=\frac{P(B_k|A_i)*P(A_i)}{P(B_k)} \qquad (1)$$

B. INCA

The INCA model assumes the existence of *N* different recognition algorithms. For example, if the gestural domain were that of hand-written symbol recognition, then the algorithms might consist of a curve-matching technique, a sequence of directions approach, a neural network, a feature-analysis approach, and possibly others. Each of these algorithms will have specific strengths and weaknesses, in terms of its recognition capabilities. Experience has shown that these algorithms tend to be consistent in their recognition abilities. That is, they tend to be strong in the recognition of some subset(s) of gestures and inconsistent in the recognition of the remaining gestures. The key to the model's effectiveness is this inherent consistency not only in correct recognitions but also in misrecognitions. If an algorithm frequently misrecognizes a handwritten 'H' as a 'K', then this information is useful and allows us to modify the perceived importance of the algorithm's recognition result. Figure 1 depicts the INCA layout.

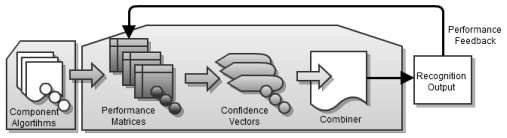

Figure 1 – *INCA Layout*

During training (and optionally during operation) INCA maintains a *performance matrix*, or *confusion matrix*, for each component algorithm. A performance matrix for any component algorithm is an *M*×*M* matrix where *M* is the number of symbols in the gestural alphabet. For any recognition algorithm A_i the performance matrix PM_i [x][y] contains the number of times that, during previous recognitions, the algorithm A_i recognized the actual input gesture S_x as the gesture S_y. In short, these matrices provide a complete, empirically observed distribution of the previous recognition events within the system.

After applying Bayes' theorem to the data stored in the algorithm's performance matrix, we can determine the probability that any gesture S_x was in fact the actual gesture entered given the algorithm's recognition of S_y as its result, based upon previous performance. This corresponds to the conditional probability $P(S_x \mid S_y)$ which simply corresponds to the following formula:

$$P(A_i|B_k)=\frac{PM[S_i,S_k]}{\sum_{j=1}^{N} PM[S_j,s_k]} \qquad (2)$$

Figure 2 indicates the performance or confusion matrix for a sample algorithm and its confidence vector for the recognition of the digit "1".

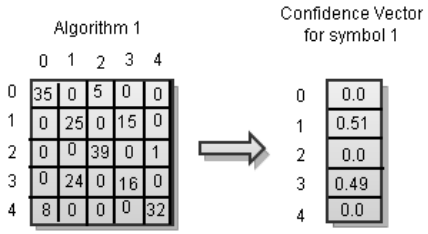

Figure 2 – *Confidence vector representing the probability space for the algorithm recognizing the symbol "1" and the INCA probability that the user did in fact enter a "1".*

Clearly, this is simply the entry PM_i [x][y] in the matrix over the sum of the column PM_i[*][y]. Once this calculation is carried out for each gesture in the given alphabet we can build its confidence vector. We can then proceed to combine it with the vectors of all other algorithms to obtain the overall system recognition result.

The INCA model provides a number of important and interesting results. One key observation is that the model provides the system with the ability to make correct gestural recognitions when all component algorithms have incorrectly identified an unknown gesture. Suppose we have three gestural recognition algorithms *A*, *B*, and *C*. They each, given an unknown input w, produce respective recognition results of *x*, *y*, and *z*. INCA recognition is capable of producing the correct result *w* regardless of the incorrect results of the component algorithms. We show in section 6 recognition improvements when the INCA model is applied to a set of relatively weak recognition algorithms, using a set of strong component algorithms.

The INCA model is also is capable of effectively ignoring, or at least minimizing, the impact upon a particular recognition of an algorithm that is particularly poor at recognizing a specific gesture. An algorithm that is extremely poor at recognizing a given gesture S_x in an inconsistent manner will produce a confidence vector that reflects its historically poor performance, and should have minimal, if any, impact upon the final recognition result of the system.

2. Related Work

Since the 1970's, researchers have studied the benefits of combining classifiers to produce systems that perform better then any of the individual classifiers that make up the ensemble. Some of the first attempts involved combining two liner regression models using a cascade approach where the first model was fit to the training set and the second was fit to the subset that had a lower classification score [6]. However, development in ensembles did not progress impressively until the 1990's when Hansen and Salmon [21] suggested that an

ensemble of neural networks be used to improve the predictive performance of a single network. Concurrently, Schapire in [23] developed the AdaBoost algorithm that empirically demonstrated that a strong classifier can be constructed by incrementally training a series of weaker classifiers by using the performance of previous classifiers as input for the next in the series.

Methods such as bagging and boosting, and many others, have been shown to improve approaches in remote sensing, person recognition [22] and incremental learning systems used for visual quality control in compact disc production systems [11].

Two methods of ensemble classifier construction, generative and non-generative, have been used in the multiple classifier field. Non-generative methods do not actively generate classifiers as in the AdaBoost algorithm above. Instead, non-generative types combine the independent classifiers after the components have produced a recognition result. Since we focus on non-generative ensemble architecture in this work, it is important to consider the three types of classifier output typically found in such methods.

Type 1: Abstract / Exact - Each classifier C_i outputs a single label given an input feature vector x pertaining to an unknown symbol *x*. Type 1 output contains no certainty measure as to the classifiers confidence in the mapping $C_i(x) = L_i$, with L_i representing a label in the classification space.

Type 2: Rank – Each classifier output provides a ranked set of output values. The output is in a ranked order from most plausible to least and can be thought of as the statement "The symbol is most likely a 4, but could be a 3, and less likely a 2." This can be especially suitable for problems with a large number of classes [1].

Type 3: Probability – Each classifier output gives the most information since either a ranking or classification can be produced from it [11]. *Type 3* output is in the form of a probability distribution of the unknown input symbol over the recognition alphabet. Here, $C_i(x) = \{a_1(x), \ldots, a_L(x)\}$, is the set of probabilities that classifier C_i considers the unknown input symbol x as belonging to class $a_1 \ldots a_L$.

Both Parker [1] and Sannen [11] state that a type 1 classifier output provides the least benefit to classifier fusion since alternative solutions are not given. A *type 2* classifier output offers relative information about possible symbol class labels, giving a rank comparison between each symbol. This type does not give absolute information regarding how the classifier performed over the entire sample space. *Type* 3 classifier output offers the most information about alternative class possibilities. One advantage of the INCA model is that algorithms of t*ype 1* and *2* are converted to t*ype 3* via the performance metrics tracking.

3. Component Algorithms

Independent component classifiers are ideal for our model. The independent classifier choice was made because we wish to look at component combinations and their characteristics in varying usage domains. In this section, we briefly describe the component machine learning algorithms we've selected, and refer the reader to the individual references for further information.

A. Contour Profiles

The contour profile algorithm uses a collection of topological features to learn and classify hand written symbols [1]. The algorithm bounds a symbol and partitions the bounded region into left and right profiles. This method uses forty-eight binary features or properties of the symbol to build a feature vector.

The training phase of this algorithm consists of steps that compute all forty-eight features to compose the training symbol feature vectors. The feature vectors contain the binary profile decomposition data, representing whether a feature is part of the symbol or not. For example, a feature of a numeral digit 9 would be true, or binary '1', if the left profile peak value is greater then '5'. This feature represents the number of pixels from the left edge of the input symbol region to the first pixel of the symbol's left profile. Table I depicts an example of small portion of the forty-eight features used in for the profile algorithm in recognizing hand printed digits.

TABLE I. Contour Profile Feature Examples

Feature Number	*Feature Calculation*	*Feature Assignment*
1	$L_{peak} < 10$; $R_{peak} > 10$	1
2	$L_{peak} < 5$; $R_{peak} > 10$	0
(...)	(others)	0 or 1

Examples of the 48 feature vector component calculations.

The measurement of character profiles can be of any discernible method such that a distinction can be made between a feature vector of one symbol and another.

During classification of an unknown input symbol, the profiles are extracted from the input image and an input 48 feature vector is created. This approach uses a training set of *N* symbols to build a database of feature vectors having known class labels. The unknown input symbol is then processed and it's feature vector is matched to the closest set in the database using a Euclidean distance measure in *N* dimensions. Equation 1 gives this measure as the classification metric:

$$argmin(x)(d_{p,q} = \sqrt{\sum_{i=1}^{N}(p_i - q_i)^2}) \qquad (3)$$

where *x* represents each class label, *p* and *q* are data points and *N* is the total number of feature points. Further information can be found in [1], [2] and [3].

B. Artificial Neural Networks

Artificial neural networks have had great success in many areas such as handwritten character recognition, data mining, and even autonomous vehicle navigation [4]. An artificial neural network determines the weights for processing elements, whereby correct classification is achieved when the proper neural connections fire in the correct order.

We constructed a three-layer network consisting of forty-eight input nodes, ninety-six hidden nodes, and ten output nodes. This design was used in [1] and [5] for handwritten digit recognition and reproduced herein.

The 48 input nodes correspond to an eight-by-six pixel square decomposition of an input symbol. During training, each symbol from a dataset is first normalized for pixel color, then the symbol is bounded. This bounded region is then scaled down to the eight-by-six pixel representation and written to a database.

Once the database has been built, we train the network using the the back-propagation method. The back-propagation method uses a steepest decent scheme to minimize the error by adjusting the weights on the network connections from the output layer to the input layer [1]. Each iteration from the database equates to an iteration of the steepest-descent minimization of error on the connection weights.

There are other methods for training artificial neural networks, such as simulated annealing and genetic algorithms. However, we selected a back-propagating artificial neural network due to previous success in handwritten character recognition [5]. Further information can be found in [7], [8] and [12].

C. K-Nearest Neighbor

The K-Nearest Neighbor algorithm classifies unlabeled examples based on the similarity of the input data and examples in the training set. Let x be an unknown symbol. We find the k-closest labeled example in the training data set and assign x to the class that appears most frequently in the k-subset [8]. For example, we have four classes and the goal is to find a class label for an unknown example x. Assuming we use the Euclidean distance metric and we set $k = 5$, we examine the five closest neighbors to x. After feature analysis, we see that of the five closest, three belong to a class labels "2", one sample to "5", and one sample point to class label "7". In this example, the class assigned to the unknown symbol would be the predominate class "2".

The KNN algorithm defers all data processing until a request for a classification is given. This method is also referred to as a memory-based method in that it loads all feature information into memory prior to classification. We use the KNN available in the OpenCV API [10] and the nearest neighbor Euclidean distance measure shown in equation 1.

D. Support Vector Machines

In pattern recognition, linear discriminants involve lines dividing feature values into groups and is an effective way to implement a classifier if there exists in the data a way to divide the classes with a line or plane [1]. A support vector machine, or SVM, is a decision method that uses vectors or distances of data points to a decision boundary that maximize the margin of separation between classification labels [9]. The data points represent the features of a class or set of classes in the sample space. The boundary is represented as a line configured in a way such that the points closest to the boundary define a maximum marginal distance.

If the data is linearly separable, there is a pair (w, b) with w being the weight vector and b representing a bias, such that two lines exist defined by [12]:

$$w^T x_i + b \geqslant 1 \quad (4)$$

$$w^T x_i + b \geqslant -1 \quad (5)$$

with the decision rule as:

$$f_{w,b} = \sin(w^T x_i + b) \quad (6)$$

The optimal hyperplane separating the two classes can be found by minimizing the squared norm:

$$\min_{w,b} \Phi(w) = \frac{1}{2}\|w\|^2 \quad (7)$$

Here, a hyperplane is a linear function that divides N-dimensional data into two parts [1]. The maximum margin hyperplane is always as far from both data sets as possible. A deeper discussion can be found in Kotsiantis [12].

E. Implementation

For the Pen tablet algorithms, we adapted Java implementations from similar algorithms written in the C programming language, and used algorithms from the OpenCV API [10] for the data glove component classifiers. It is important to note that we use only the standard parameters generally advised for the recognition task as we wish our algorithms to be non-specific and somewhat poorly tuned to any specific domain. The Contour Profile algorithm and back-propagating neural network for the pen tablet were adapted from Parker [1]. The K-Nearest Neighbor, Support Vector Machine and additional Neural Network for the data glove were called using the OpenCV API.

4. Classifier Fusion Methods

As discussed in section 1 part *B*, the INCA model produces a c-dimensional vector for each classifier in the system [11]. The strength of this model rests in synthesizing the consistent accuracies and inaccuracies of each classifier. Let such a vector for a classifier D_i for an input label x be written as:

$$D_i(x) = [d_{i,1} \ldots d_{i,c}] \quad (8)$$

where each $d_{i,n}$ represents the support of classifier i for its class label prediction ω_n in the class set ω.Thus, without loss of generality $d_{i,n} \in [0, 1]$.

A final classification is achieved through combining these vectors for an input x using some ensemble methodology. Several approaches and their efficacy in our testing follow.

A. Algebraic Combination: Max-Sum

Algebraic ensembles are appealing for their ease of implementation. They do not need to be trained and are class indifferent. Thus, they are generally computationally inexpensive. A relatively simple combination approach was used for testing.

In this approach, the support for a class label ω_n is summed across each confidence vector $D_{i,m}(x)$ for m classifiers. The class label with the highest support is chosen as the ensembles "final" classification. Thus the output of this ensemble combination method is given by:

$$argmax(x)(\sum_{1}^{m} d_{m,s}) \quad (9)$$

where s represents each class label.

B. Decision Templates

The principle behind the *Decision Template* ensemble combination method is described in [13]. In this method, a "*Decision Template"*, or the "most typical" support seen for each class label ω_n, is defined by batch training over a training set Z [11]:

$$DT_s = \frac{1}{N_s}(\sum_{Z_i \in w_n,\ Z_i \in Z} Di(Z_i)) \quad (10)$$

where N_s is the number of elements of Z_i from class ω. Put simply, the result of the training phase is a vector whose length is the number of class labels, with each vector element representing the average of the support for that label across all confidence vectors $D_{i,1}(x)$ ... $D_{i,m}(x)$.

The ensemble classification compares the Decision Template of each class label to the support of each Confidence Vector for the given label. The class with the least distance (i.e., the "*most similar")* is the output of the ensemble combination method.

While there are many measures of similarity (such as Hamming, Mahalanobis, etc. [11]), in our tests *squared Euclidean distance* is used. Thus the output of this ensemble becomes:

$$argmin(x)(1-\frac{1}{m*c}\sum_{i=1}^{m}\sum_{k=1}^{c}[DT_{i,k}-d_{i,k}(x)]^2) \quad (11)$$

C. Dempster Shafer Theory

This ensemble combination method is an adaptation of the *Decision Templates* method described in *B*, except that the distance between a Decision Template and the support of each Confidence Vector is calculated using the Dempster-Shafer theory of evidence. For a discussion of the theory, the reader is directed to [11].

First, the proximity between each classifier (Confidence Vector) and the Decision Template is calculated [11]:

$$\Phi_j^i = \frac{(1+\|DT_{i,j}-D_i(x)\|^2)^{(-1)}}{\sum_{k=1}^{c}(1+\|DT_{i,j}-D_i(x)\|^2)^{(-1)}} \quad (12)$$

In Dempster Shafer theory, $\|\cdot\|$ can be any matrix norm; here, the Euclidean distance is used. The result of this stage is m proximities for each of the c decision templates.

Using the calculated proximities, *degrees of belief* are then found for each classifier for every class label [11]:

$$b(x)_j^i = \frac{\Phi_j^i(x)\prod_{k\neq j}(1-\Phi_k^i(x))}{1-\Phi_j^i(x)[1-\prod_{k\neq j}(1-\Phi_k^i(x))]} \quad (13)$$

With these degrees of belief, the support for each class label is calculated, and the class with the most similarity to the Decision Template is the output of this ensemble combination method:

$$argmax(x)(\prod_{i=1}^{m} b_j^i(x)),\ j=1,\ldots,c \quad (14)$$

D. Behavior Knowledge Space

The last combination method considered is the Behavior Knowledge Space method, or BKS, developed by Huang and Suen [14]. This method aggregates the decisions of the component classifiers such that all possible tuples representing the possible outcomes of the classifiers are known. Generally, each classifier has *N+1* possible decisions, with *N* representing the number of symbols in the recognition alphabet. The additional of "*1*" allows the method to count misrecognitions indicating that no tuple exists in the BKS.

The BKS is a K-dimensional space, where K represents the number of component classifiers in the ensemble, such that at each intersection of the component classifiers, a BKS unit is represented. A BKS unit contains three important pieces of information:

1. The size of the alphabet.
2. The tuple representing the component guesses.
3. The number of times each symbol has been selected in previous instances of that particular tuple.

We trained our BKS by first running the ensemble system over our training data sets, recording all tuples seen, recording the number of times the ensemble selected each symbol when the tuple was seen in the past. During testing, when a tuple is passed to the BKS, the BKS unit corresponding to the tuple is checked. The final decision is then given by the symbol in the tuple with the maximum counts. In the event of a tie, a naïve "first-come first-serve" is used. This is a known area for improvement and will be addressed in future research. Please refer to [14] for further information.

The classification of an unknown symbol from within a tuple can be characterized by the following equation:

$$argmax(x)_{1\leq m\leq M} n_{e(1)\ldots e(k)}(m) \quad (15)$$

where M is the total number of class labels, m is a given label, and $n_{e(1)\ldots e(k)}$ is the total counts for each symbol in the tuple.

5. Input Modalities

In studying the use of ensembles methods in gesture recognition, we evaluated our model on a pen tablet and data

glove input modalities. Our intent was to study our system in two separate domains, develop a research framework and investigate ensemble-modality performance.

A Wacom Intuos 3 graphics tablet with a pen stylus was first used to develop the proof of concept system. The Wacom tablet was produced by Wacom Company, Ltd. [15] and was used to collect the off-line test sets and for on-line demonstrations. A third party library, JPen [16], was used to gain access to the pen tablet features. The JPen Java application programming interface (API) allowed for full access to *x, y, pressure,* and t*emporal data* from the tablet and pen.

The second input mode is the AnthroTronix data glove, the AcceleGlove [17]. AnthroTronix supplied both the glove and Java API for development and testing. The API gave full access to the raw sensor data and to a sign database, developed by AnthroTronix, for studying American sign language.

6. Datasets and Results

We have chosen a recognition alphabet consisting of the digits "0" through "9" for both the pen tablet and data glove. The pen tablet data consists of images of drawn single digits. The glove data consists of the right hand gestures for the single digits. Figures 3 and 4 depict samples of the hand written character set and sign set.

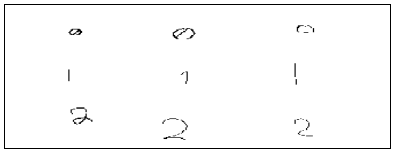

Figure 3 – *Handwritten digit samples from volunteer collection.*

Figure 4 – *American Sign example. Referenced from [25].*

We collected fifty instances of the digits zero through nine from four volunteers using both images drawn on the tablet and the eighteen position sensor data from the glove. Two-thousand total symbols were collected for each input mode.

A. Component Algorithms

We used a four-fold cross validation analysis for both the tablet and data glove evaluation. Table II presents the validation results for all algorithms used. We ran two versions of training using the pen tablet. Two points of interest are:

1. Mixed results involving symbols from the same user in the test and training sets, but not the same instance of the symbol. *User-dependent*.
2. Results involving testing sets of users not in the training sets. *User-independent*.

We chose not to perform the mixed user test for the cross validation on the data glove due to the high accuracy of the user-independent input results.

TABLE II. Four-fold Cross Validation for Component Algorithms

Algorithm	*Input Modality*	*Average %*	
		Dependent	*Independent*
CF	Pen Tablet	78.7	42.0
ANN	Pen Tablet	56.4	39.0
	Data Glove	-	96.0
KNN	Data Glove	-	95.0
SVM	Data Glove	-	80.0

Result for 4-fold cross validation on the pen tablet and data glove. User-dependent results contain instance in the training set of all users, but not all training instances per user. User-independent results had separate user training and testing.

B. Classifier Fusion Methods

We wished to get a sense of the greatest increase in the ensemble over the component algorithm performance. An interesting investigation takes the worst or average validation set results and uses the performance matrices for the component algorithms for the ensemble system. Table III shows each of the four fusion methods' performance characteristics.

We selected the average performance matrices for each algorithm for the classifier fusion step. Again, for the tablet we show user-dependent and user independent results as defined in part *A* of this section.

TABLE III. Classifier Fusion Performance – 2 Classifier Ensembles

Algorithm	*Input Modality*	*Components*	*Average %*	
			Dependent	*Independent*
Maximum Sum	Pen Tablet	CF,ANN	90.2	66.2
	Data Glove	KNN,SVM	0.0	100.0
Decision Templates	Pen Tablet	CF,ANN	77.8	7.8
	Data Glove	KNN,SVM	0.0	77.0
Dempster-Shafer	Pen Tablet	CF,ANN	85.0	34.4
	Data Glove	KNN,SVM	0.0	97.0
Behavior Knowledge Space	Pen Tablet	CF,ANN	89.2	62.4
	Data Glove	KNN,SVM	0.0	96.6

Ensemble results for the pen tablet and data glove. User-dependent results were only measured for the pen tablet as the data glove component algorithms performed highly with the user-independent.

Table IV depicts the addition of a third classifier in the data glove sets, depicting how the model reacts to the introduction of an additional classifier. We are currently investigating the addition of algorithms with higher and lower performance characteristics for results publication in the near future.

TABLE IV. Classifier Fusion Performance – 3 Classifier Ensembles

Algorithm	*Input Modality*	*Components*	*% Accuracy*
Maximum Sum	Data Glove	KNN,SVM, ANN	97.8
Decision Templates	Data Glove	KNN,SVM, ANN	83.1
Dempster-Shafer	Data Glove	KNN,SVM, ANN	85.8
Behavior Knowledge Space	Data Glove	KNN,SVM, ANN	98.3

Addition of an artificial neural network algorithm into the data glove ensemble. Improvements over the two-algorithm ensembles in the BKS and Decision Template methods are seen.

7. Discussion and Future Work

These results are preliminary in our study of the INCA model and classifier fusion techniques. We see that given various levels of classifier strengths, the ensemble methods Maximum Summation and BKS perform best for the user-dependent and user-independent tablet input modality. When considering the data glove, we see that initial results indicate the Dempster-Shafer and Maximum Summation supply strong recognition results.

The addition of the third algorithm in the data glove ensemble gives an increase in performance accuracy for the Decision Templates and BKS algorithms, however, we see a decrease in the Max-Sum and Dempster-Shafer methods. We are continuing to investigate the model to determine the reasons for this result.

We recognize that these preliminary results used a relatively small alphabet and that the model will require testing upon a more useful set of gestures appropriate for effective applications.

We are currently examining the behavior of various classifier fusion techniques as the quantity and quality of the underlying component algorithms change. That is, we wish to determine if some techniques produce significantly superior results over others when additional algorithms of varying quality are added to the INCA model. Do any of these techniques improve, remain stable, or degrade as relatively poor recognition algorithms are inserted in the model?

We have also identified infrequent situations where the inclusion of a recognition algorithm whose ability to identify a small subset of specific gestures is poor and whose inclusion has a significant negative impact upon the overall system performance, with respect to the recognition of these specific gestures. Although at first glance this would appear to be an intuitive result, the Bayesian approach should prevent such a significant degradation unless the underlying component algorithm is both consistently unable to identify the gesture and produces inconsistent incorrect results. For example, the algorithm cannot correctly recognize the symbol 'H', but does not consistently produce the same incorrect result; rather, the algorithm produces many different incorrect results. The resulting confidence vector for the algorithm in this instance begins to resemble an almost random "guessing" of a result with a uniform distribution across all possible recognition results. We believe that if this situation occurs, and if the subset of gestures for which this behavior is exhibited is small in comparison to the alphabet size, then we may be able to modify the resulting confidence vector to reflect this fact and improve the system's overall ability to identify the correct input. We are also exploring whether it is simply best to ignore any such "guess" confidence vectors entirely.

Our long-term goals include an examination of the INCA model's performance in a system implementing multiple gestural input types. For example, a system that accepts simultaneous hand, speech, and electroencephalography inputs would be a prime candidate for exploration. We hope to explore how various classifier fusion algorithms behave in such a system and if the strengths of any particular input-mode can be used to counter the weaknesses of another in order to improve overall system recognition.

Acknowledgment

We wish to thank the Northern Kentucky Research Foundation for funding this project.

References

[1] J. R. Parker, "Algorithms for Image Processing and Computer Vision, 2nd edition", Wiley Publishing, 2011.

[2] M. Shridhar and A. Badrelin, "Recognition of Isolated and Simply Connected Handwritten Numerals," *Pattern Recognition*, vol. 19, no. 1, 1986.

[3] F. Kimura and M. Shridhar, "Handwritten Numeral Recognition Based on Multiple Algorithms," *Pattern Recognition*, vol. 24, 1991.

[4] Tuduran, C., Neagoe, V., "A new Neural Network Approach for Visual Autonomous Road Following", "Latest Trends on Computers, vol 1. 2010.

[5] J. Heaton, "Introduction to Neural Networks with Java, 2nd edition." Heaton Research, Inc, 2008.

[6] L. Rokach, "Ensemble-based classifiers", *Artificial Intelligence Review*". no. 33, pp. 1-39. 2010.

[7] C. Shang and K. Brown, "Principle Features Based Texture Classification with Neural Networks," *Pattern Recognition*, vol. 27, 1994.

[8] R. Duda, P. Hart, and D. Stork, *Pattern Classification*, 2nd ed. Wiley Inter-science, 2001.

[9] C. Bishop, *Pattern Recognition and Machine Learning*, 1st ed. Springer Science+Business Media, 2006.

[10] G. Bradski and A. Kaehler, *Learning OpenCV: Computer Vision with the OpenCV Library*. O'Reilly Publishing, 2008.

[11] D. Sannen, E. Lughofer, and H. Van Brussel, "Towards incremental classifier fusion," *Intelligent Data Analysis*, vol. 14, no. 1, pp. 3–30, 2010.

[12] S. Kotsiantis, "Supervised Machine Learning: A review of Classification Techniques." *Informatica,* vol. 31, pp. 249-268, 2007

[13] L. Kuncheva, J. Bezdek, and R. Duin, "Decision Templates for Multiple Classifier Fusion: and experimental comparison.," *Pattern Recognition*, no. 34, pp. 299-314, 2001.

[14] Y. S. Huang, and Y. C. Suen, "A Method for Combining Multiple Experts for the Recognition of Unconstrained handwritten Numerals", *IEEE Transactions on Pattern Analysis and Machine Intelligence*. Vol. 17, no. 1, January 1995.

[15] "*Wacom*", n.p. 2012. March 25, 2012<http://www.wacom.com/en.aspx>

[16] Carranza, N., "*Jpen-Java Pen tablet Access Library*", n.p. 2012. March 25,2012<http://sourceforge.net/apps/mediawiki/jpen/>

[17] "*Acceleglove*", n.p. 2012. Mar. 25, 2012 <http://www.acceleglove.com/>

[18] G. Newell, "A Probabilistic Approach to Gestural Recognition and Dialogue Management." The University of Arizona. UMI Dissertation Services, 1995. Unpublished.

[19] J. Gao, W. Fan, and J. Han, "On the Power of Ensemble: Supervised and Unsupervised Methods Reconciled." SDM'2010 Columbus, OH, 2010.

[20] S. Gunter and H. Bunke "Multiple Classifier Systems in Offline Handwritten Word Recognition on the Influence of Training Set and Vocabulary Size." *International Journal of Pattern Recognition and Artificial Intelligence* vol. 18, No. 7 (2004) World Scientific Publishing Company, 2004.

[21] L. Hansen and P. Salmon, "Neural network ensembles.", *IEEE Transactions on Analytical Machine Intelligence.* Vol 12, pp. 993-1001.1990

[22] N. Oza and K. Tumer "Classifier ensembles: Select real-world applications.", *Information Fusion* vol 9, pp. 4-20, 2008.

[23] R. Schapire, "The Strength of Weak Learning", *Machine Learning*, vol 5, pp. 197-227, 1990.

[24] D. Optiz and R. Maclin, "Popular Ensemble Methods: An Empirical Study", *Journal of Artificial Intelligence Research*, vol. 11, pp. 169-198, 1999.

[25] B. Vicars, "American Sign Language Institute", n.p. 2012 <http://www.lifeprint.com/>

Ontology-Based Recognition of Physical Objects in a Virtual World

Geun Jae Jung[1], Jong Hee Park[1]
[1]Kyungpook National University,Department of Electronics,Daegu,Korea
{cooky8884, jhpark}@ee.knu.ac.kr

Abstract: *To construct a virtual world, we develop the recognition capability for agents as its key element. The agents perform this capability by means of comparing the physical properties centered on the shape with the corresponding pieces of their knowledge. Their associated perception capability is against the shapes of the objects in the virtual world simulated in terms of the regular shapes and line segments. Meanwhile, their knowledge about those objects are modelled in terms of an ontology that captures their composition, physical attributes and functions in an integrated manner. The diverse inferencing rules used by the virtual inhabitants to recognize the objects from the perceived properties mimic those logical rules humans use in their real life.*

1 INTRODUCTION

A virtual world becomes an authentic cyber-space where the users feel immersed only when it is inhabited by autonomous agents against a realistic environment. Those agents are to be designed to act appropriately according to information they perceive and infer on the situations they face. These autonomous agents are different from those types of agents designed to pursue only perfection and right answers. Like ordinary humans, these agents may make mistakes or behave in unexpected manners according to their respective knowledges and personalities[1]. To achieve this autonomousness and individuality among agents they need to be equipped with recognition capability for situations in the virtual world as a premise. Considering the situation they would deal with is constructed in terms of entities, relations and activities, the entities are the most basic elements to be recognized in the situations. The other elements are built on top of those entities and especially the physical objects.

We design object recognition capability for the agents in our virtual world. This capability is performed using their shape as the main feature. To describe the shapes of the objects in our virtual world we define a set of regular shapes, in terms of which arbitrary shapes are to be approximated as close as possible[2]. Some objects may be described with just one regular shape while other objects are with two or more shapes combined[2]. We design the virtual objects to actively transmit their contour in terms of lines and arcs in order to save primitive signal processing effort for perception in the real world.

One of the vigorous studies on image recognition vectorizes images including target objects in terms of occurrence frequencies of Visual Words[3]. This method recognizes objects and scenes in images by comparing the amount of input image features with Visual Words in the database[4][5]. However, mere frequency information is not enough to accurately recognize objects and scenes. Our recognition targets at a number of diverse objects occurring in complex situations. These objects are not only diverse in their kinds but also numerous within each kind, so our method is to be able to distinguish among difference instances of the same kind.

We develop a special ontology, which plays a pivotal role as the main knowledge base for the recognition. This ontology provides a comprehensive knowledge about the composition of the cosmos in its entirety. In other words, it describes the objects and concepts composing the real world, and their existence structures and properties changing to the associated principles, rules and constraints[6]. Also, it is used as part of the knowledge structure for the agents[7], which they use for recognition and inference. In addition to the ontology, the Instance Graph and the S-T graph are developed to provide a instantial and historical contexts in our virtual world. The agents perform their recognition of the target object by collectively comparing the information transmitted from the objects with the schematic information from the ontology and instantial and historical information from the other knowledge components above. Besides this comparison the agent is designed to use several human inferencing mechanisms such as deduction and contraposition to derive information that is not explicitly perceptible[2]. This recognition method could be used not only for physical objects but also for relations, events or whole situations not directly perceptible to their associated agents. Furthermore, its use

could be extended to recognition of abstract concepts.

2 ONTOLOGY

2.1 The structure of the ontology

Our ontology is modeled in terms basically of entities, relations and activities. The entity is characterized by its composition and descriptive attributes and functions. The relation is described by its associated entities, descriptive attributes and actions while the activity, a special type of relation, is composed of the pre-condition and procedure and effect parts[8]. The entity, the top class in the ontology, encompasses includes the physical entity and the logical entity as shown in fig.1 below.

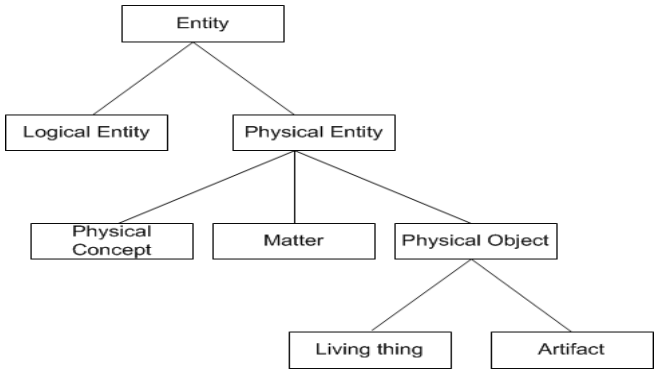

Figure 1.Top part of the ontology

The physical entity is characterized by such properties as composition, descriptive attributes, functions and rules. The descriptive attribute is represented by a variable with its domain values continuous (e.g., 10-20cm) or enumerated range (e.g., red, blue, green.) The functions describes the functional characteristics of an entity. The rules specify the laws and principles relevant to their associated entity.

The physical entity is specializes into the matter, the physical object and the physical concepts. The physical object has as its definitional property a fixed shape, and composed of solid matters or other physical objects in a recursive manner. The matters have characteristics they never disappear, but they just change in their state. They can exist on their own like sand on a beach, but usually as materials of physical objects. The physical concepts such as the light, energy, and force affect physical entities. While they reveal diverse physical characteristics like the other types of physical entity they are distinct in that they do not exclusively occupy the space. The logical entities are defined as abstract things in human's conception. They are exemplified by law, organization, language, etc.

2.2 Characteristic property

Each instance or class has its own identity. Such an identity can be established by comparing one or more properties. When a single property can uniquely distinguish its associated entity from the others, such a property is called Characteristic Property. For example, the action of nurse could identify that animal a mammal. To identify a particular instance within a species we need further characterizing properties in addition to the Characteristic Property as specified in the class. If we can acquire these Characteristic Properties we can easily identify its kind or instance by merely comparing those properties. This section must be in one column.

2.3 Definitional Property

Similar classes have commonalities in their properties. Those classes can conceptually be organized into one or more class hierarchies in terms of such commonalities.

The property distinguishing a class among those similar classes from their common super class is called Definitional Property. A Definitional Property for a class constitutes the additional qualification to that of its super class for the class membership. Consequently, subclass memberships are more restrictive than their super-class so their members each are fewer than their superclass's members. As shown in Fig.2, ‘nurse()’ of

'mammal' class is its Definitional Property that specializes the class from 'vertebrate' class.

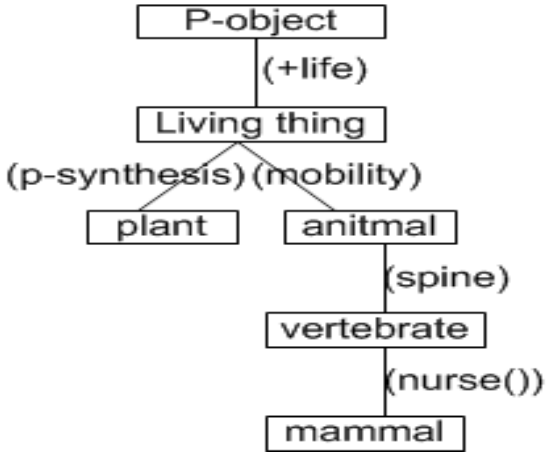

Figure 2 The class hierarchy

Unlike Characteristic Property the Definitional Property by itself cannot uniquely identify the class. Rather all its ancestor Definitional Properties need to be combined in sequence with that of the target class.

3 Perception and recognition of the properties of entities

3.1 Recognition of descriptive attributes

The entity substantiates its existence in terms of its descriptive attributes. The specific values of those properties are perceived via sensory organs or measured using instruments. For example, color, size, or shape are visually perceived and sound is audibly perceived. Moreover, touch or taste could be perceived by tactile sense or palate. Among these properties we focus on visual property in that the vision accounts for the major portion of human perception.

3.2 Perception and recognition of object shape

The perception by an agent in our virtual world starts with extracting from the image in her scope boundaries between regions (ie, shapes) exploiting difference in color. The extracted boundaries are saved in terms of lines. Those lines are used to describe 2-dimensional shapes included in the image. These shapes have their respective attributes and form positional relations with each other. According to their positional relations those 2-D shapes are rearranged to become the faces of 3-D shapes. The agents recognize objects by comparing such attributes as their types of 3-D shapes, sizes and colors with those of the entities stored in their knowledge base. In our perception mechanism we use the Finite Elements Method, where detailed regions are first analyzed and upper regions are described in terms of those detailed regions[9].

3.3 Definition of 2-D shapes

We divide the shape types into connecting lines, regular shapes, and irregular shapes. A connecting line has no internal region, and is only a simple connection. The regular shapes are classified into triangle, tetragon, circle, ellipse, and all the other shapes are regarded as irregular shapes. The regular shapes are the basic shapes to be used to approximately describe object shapes in our virtual world. The basic units to be used in our recognition stage are 3-dimensional shapes, such as sphere, cylinder, box and pyramid.

The agents recognize 3-D objects by combining the 2-D shape informations perceived in different viewing angles. We minimize the kinds of regular shapes since a shape could be seen as different shapes depending on different viewing angles, like a regular triangle seen as an isosceles triangle or a square seen as a diamond shape. However the circle is an exceptional tyoe not to be generalized to ellipse, because of the fact that the shape from any viewing angle is invariably a circle implies the object is spheric. We approximate as possible complex shapes in terms of regular shapes. In such an approximation, two or more regular shapes are combined with

modifications via spatial additions or subtractions to reflect minor deviations from their basic forms[10]. Fig. 3 illustrates how complex shapes could be approximated in terms of regular shapes.

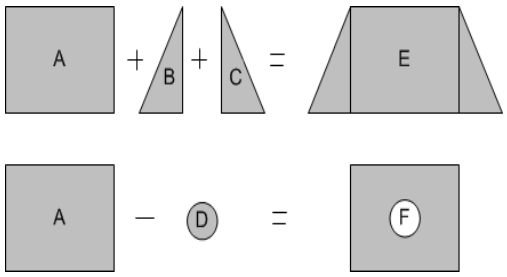

Figure 3 Complex Shape derived through

3.4 Comparison of shapes

The recognition of object shape basically is performed by comparing th approximated representation of a target shape with the corresponding information from the agent's knowledge[8]. However, this basic recognition method is to be enhanced for the points described below.

First, the amount of perceived information could differ significantly according to the distance from the agent to the object. While the agent can see all the details when the target object is close, an object in the distance would be viewed just along its outlines with details blurred. Thus, the detailed information on the object shape may or may not be provided for the agent to recognize the shape of objects.

Second, the target object may be hidden by other objects. In this case, we need reasoning algorithm for restoring the complete shape utilizing the remaining portions of the shape. The reasoning algorithm uses the three methods following.

i) Extrapolate between two line segments enough to connect them. Based on their intersection, the remaining part is inferred.

ii) In case a line is partially broken into line segments, an imaginary line including those line segments is used as the reference line for inferencing the shape.

iii) In case of ellipse, angles and lengths of repetitive arc are first calculated. Then imaginary circumference is recovered by inferring the hidden portions[9].

Third, to handle different shapes due to different viewing angles we utilizes the same method as that for the first point. That is, the perceived shape is compared against its associated composition information from the agent' knowledge.

Fourth, we are to consider an object may change in its shape by time or situation. To overcome those variations we need to judge what are the significant elements in the shape. In fact, this judgement could apply to any aspect.

4 Ontology-based object recognition and relevant logical reasoning methods

4.1 Object recognition

An agent starts the object recognition with comparing the perceived data the agent perceived with the information in the ontology. This recognition of an object could utilize not just its internal properties but its reaction to external stimuli. The most basic property by which a physical entity could be identified is its volume occupying the space. In addition the entity could be further characterized by such reactive properties as its resolution in case of mixture with another entity, its movement in case of collision with another entity, its shadow in case of being lighted etc. Those properties could be acquired through perception unless they are of dimensions too large or small to be perceived.

For example, suppose an agent is trying to find her missing dog. In case she meets a likely animal, she would first recognize its class using such class information as shape and color etc. in the ontology. Then, she would seek further pieces of information to match her knowledge about her dog. Those instantial informations might be a scar on it, a limping pattern when walking, a barking habit, etc.

On the other hand, the physical concepts can only be characterized by their inherent effects rather than their internal properties, e.g., force by the effect of exerting pressure on other materials or objects. Unlike the other physical entity categories the physical concept can share space with other physical entities.

4.2 Logical reasoning methods

Human can infer informations from raw data using diverse inference methods. Such raw data is obtained mainly via perception or indirect experience through learning. In this paper, the agents are designed to use several inference methods as follows.

1) Rule in the general form
The rule in general is represented by the following formula.
C1 -> C2
Where Ci denote clauses expressed in terms of existence and states; -> denotes implies. By instantiating the variables in the clauses we can explicate information implicit in the situation as perceived.

2) Contraposition
Contraposition is described by the following formula.
<C1 *or* C2 -> C3> leads to
<NOT C3 -> NOT C1 *and* NOT C2>
Contraposition is applicable not only to certain links but also to less than certain links. For those uncertain links an additional consideration would be required on their associated exception links[8]. Just as rules of thumb hold good in reality, if probability p from C1 or C2 to C3 $\fallingdotseq$ 1.0 contraposition should still apply. However, if p<< 1.0 or p $\fallingdotseq$ 0 it cannot apply in any case.

3) Necessary and sufficient conditions
We can utilize the necessary and sufficient conditions for inferencing, e.g., to identify a particular class or instance. Consider, for example, that the bio-force a product of the animal is used as **thrust** for its move. This relation between the source of force and the agent of the move *suggests* its move is a self-powered move by an internal force. This property is a necessary condition for being the animal and the only other class that has this necessary condition is the motor vehicle class. Given this reasoning, a self-powered moving object would be judged to be an animal with a certainty if we could somehow rule out possibility of its being a motor vehicle.

4.1 Overall procedure of our ontology based object recognition

Suppose the agent is trying to identify her family car being driven by her father in a crowded parking lot. Following our general recognition process, the comparison between her perceived data and information in the ontology starts at the class about which she can perceive the most detailed information. If the target object is not fully perceivable or there are many instances with the same shape, however, the shape is not a characteristic property so the agent needs to perform inferencing (Section 3.4) in addition to comparison (Section 3.3). When it is dark so the agent can barely figure out the objects' contour, for instance, the physical object class would be the starting class. If needed and possible additional information is deduced by inferencing. To judge (or infer) whether the object is moving, she would use the rule that an object is to be (seen) at different locations at different times. Further, no external power sources are seen (and inferred) it is inferred to be self-powered and consequently, to belong to the animal or motor vehicle class. Likewise the comparison continues along the class hierarchy using additional properties perceived or inferred until its class or instance identity is determined as required. To identify it in the instance level the agent needs to use further information such as its plate number, a dent, its unique wheel shape, etc.

5 CONCLUSIONS

In order to cope with a situation, an agent first needs to recognize objects in the situation. The objects are the most basic elements of the situation on which relationships and activities can be established. We aim to develop an autonomous agent that inhabits in our cyber-world. Such an autonomous agent needs to have perception and recognition capabilities to be able to react actively to diverse situations occurring in the cyber-world. To implement those capabilities we develop a knowledge representation scheme and associated inferencing mechanism for the agent.
We focus on the visual information among various perceptible information to be used to recognize physical objects. We develop a specialized ontology to model the entire world and to represent the agents' knowledge

structure. The object shape is the most distinctive visible property humans use to identify objects with respect to their class or instance. We develop a representation method to approximate complex object shapes in terms of several regular shapes. While these shapes usually characterize objects uniquely, the agents may need additional informations deduced by inferencing in case perception is not complete or many identical instances are considered.

To completely grasp the situations the agents need to recognize diverse imperceptible components such as relationships, activities, logical concepts, etc. Recognition of these categories of concepts demands additional knowledge on instantial and historical information besides elaborated inferencing. We hope you find the information in this template useful in the preparation of your submission.

REFERENCES

[1] Se-Jin Ji, Jung-Woo Kwon, Jong-Hee Park, 2006. "An elaborated goal production module for implementing a virtual inhabitant", IEA/AIE 2006, pp.770-779.

[2] J. H. Park. 2007.“Semantics of concepts relevant to the cyber-microcosm.”, Tech report #91, AIMM lab, Kyungpook Nat’l Univ.

[3] D. Nister and H. Stewenius. 2006. ”Scalable recognition with a vocabulary tree”. Proc. CVPR, pp. 2161-2168,

[4] F. Perronnin., 2008. “Universal and adapted vocabularies for generic visual categorization.”, PAMI, 30(7): 1243-1256.

[5] S. Zhang, Q. Tian, G. Hua, Q. Huang and S. Li, 2009. “Descriptive visual words and Visual Phrases for Image Applications”, ACM Multimedia, pp. 75-84.

[6] J. H. Park, 2001. “The ontology about the Microcosm”, Tech. report #9, AIMM lab. Kyungpook National Univ.

[7] Dong-Hoon Kim, Jong-Hee Park, 2008. “An Object Selection Mechanism for Schema Integration of Agent's Knowledge Structure in Virtual Reality.” ICEIS (2) 2008: 411-415

[8] Ji. S. J., 2007. “A Knowledge Model for Simulating Human-like Behavior of Virtual Inhabitant”, Major in Information and Communication Engineering The Graduate School., pp. 175-178.

[9] Jae-Woo Park, 2010. “Jong-Hee Park: A Perception Mechanism for Two-dimensional Shapes in the Virtual World. ICEIS (2) 2010: 381-384

[10] J. H. Park and B. s. Um, 1988 “A new approach to similarity retrieval of 2-D graphic objects based on dominantshapes”, Pattern Recognition Letters 20, pp.591-616.

SESSION

XII TECHNICAL SESSION ON APPLICATIONS OF ADVANCED AI TECHNIQUES TO INFORMATION MANAGEMENT FOR SOLVING COMPANY-RELATED PROBLEMS

Chair(s)

Dr. David de la Fuente
Dr. Jose A. Olivas

The potential of BPO (Business Process Outsourcing) in the current Spanish pre-recessive frame

M. Monterrey[1], **D. De La Fuente**[1], **N. Garcia**[1] **and J. Lozano**[1]
[1]Department of Business Management, University of Oviedo, Gijón, Asturias, Spain

Abstract - *The present research is aimed at analyzing the current outsourcing situation in European companies and, particularly, in the Spanish ones, and at establishing the bases to be able to understand the foreseen transition to more developed practices such as the Business Process Outsourcing (BPO). The current macroeconomic frame, especially adverse in the case of Spain, makes this kind of methodologies have a warm welcome among companies, either public or private ones, since they are seen as having important chances to save money. The aim is definitely to take some measures to cut not only general costs in the usual outsourcing field, but also operation and* core *processes costs, following mostly the modern BPO. Moreover, a new economic activity is generated around BPO, which can be interesting for the Spanish strategic consultancy firms. At this time, the limited development of BPO can be determined, to a certain extent, by the little confidence clients have giving "sovereignty" when they make their strategic decisions. Anyway, this kind of initial reluctances are hoped to be saved as time goes by and with the generalization of this sort of practices in all sectors and geographic environments. Some aspects like economies of scale and the consequent obtaining of minor costs or the know-how of the companies which provide this kind of services that could even produce an increase in the chapter of incomes based on economies of scope make that BPO clients think at least of the possibility of including them in some of their processes and sub-processes. Finally, this research makes a brief observation about the relation between BPO and the so-called* Offshoring, *by which growing companies or simply those eager to enhance their income statement accounts, can relocate their productive processes by means of costs.*

Keywords: Outsourcing Process, Subcontracting, Business Process Outsourcing, Core Business, Offshoring

1 Introduction

Since the crisis at the beginning of the 90s, the Spanish economy has had a decade of growth in an environment of sustained expansion. However, since 2008, the country has been suffering from an important worsening in its macroeconomic indexes, to give way to a long period of recession (2008-2010), followed by a weak growth stage with an inter-annual increase of 0.7% in 2011. As it can be seen in Figure 1, it can be expected the Spanish economy will go into a recession phase again during 2012 as a consequence of the crisis in the sovereign debt. Even though there had been previously several indexes that led to symptoms of deceleration, the damages reflected on economy could be seen from January 2008 with the stock market crisis together with the problems in the real- estate market. All this together with an inflationary frame in the increase on petrol prices and food products have led to the current pre-recessive situation. In August 2011 Spanish authorities reacted taking additional fiscal adjustment measures, as well as including a rule of budgetary stability in the Spanish Constitution, which reassured the compromise by the Spanish public finances with the maintenance of a healthy budgetary situation for the medium and long term. According to the forecast by El Banco de España [1], during 2012 and 2013 employment will continue decreasing as to reach an unemployment rate of 23.4%, which is the main structural problem of the Spanish economy. Furthermore, a replacement of domestic markets by external markets has been considered as probable by the Spanish business network in a context where the second ones are relatively stronger than the first ones, which are under a considerable withdrawal in private consumption. On the other hand, importations would support a great decrease – about 5%- having into account the strong adjustment in the national demand

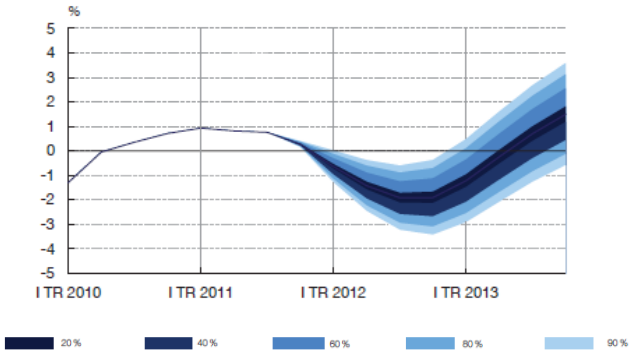

Figure 1. Expected evolution of Spanish GDP
Source: *Banco de España*

In this pre-recessive context of Spanish economy, the current research is aimed at analyzing the opportunity of development of outsourcing techniques as a way to reinforce

the competitive position of Spanish companies or, in some cases, to make even their own survival easier. Even though these practices have been applied for some decades in different ways, authors consider that the current approach to shared facilities, the act of making strategic decisions together with specialized companies, the know-how profit which these ones can contribute and definitely cost-cutting and income increasing that the outsourcing produces, will make some of these companies be able to get competitive positions that strengthen their future for a medium and long term.

On the other hand, outsourcing is evolving fast to processes where each time it is necessary to have a greater specific knowledge as well as having the support of more sophisticated technological tools. In short, we might be witnesses of an increase in the value of these services in relation to their costs. Obviously, the outsourcing business is still far from being well structured, as it is still in the starting phases of settlement as a product. It needs to grow quantitatively and qualitatively not only on the supply – to companies multi-specialized in more and more processes and to more and more *core* processes- but also on the demand – to smaller companies, in a wider environment and in more varied sectors

2 Current Outsourcing approaches: to *Core* Processes Subcontracting

In the *Global Outsourcing Survey 2007* [2], Pricewaterhouse Coopers has reached the conclusion that for a wide majority of clients – 87% of respondents-, outsourcing gets the expected benefits totally or partially. 31% think the aims have been completely achieved, which is important considering the complexity and uncertainty they face before contracting these services. As regards financial institutions, the degree of total satisfaction reaches 46%. On the other hand, 91% of the respondents either satisfied or not with the results, say they will contract outsourcing services again.

The main reasons companies give to outsource processes are the following ones:

- Lower costs (an important or very important factor for 76% of respondents).
- Getting access to know-how (70%).
- Offering services others can do better (63%).
- Increasing the flexibility in business (56%).
- Improving the relationship with clients (42%).
- Developing new products or services (37%).
- Geographic expansion (33%).

Many of the respondents (53%) stated that they outsourced processes considered as core. Obviously, the definition of activity or core process was up to the respondents and it can have different meanings for each of them. An evolution can be noticed from the external ring, (see figure 2) where no-core processes are situated, to a second ring of essentials no-core activities. For instance, in the finance function, this can be understood as an evolution from the outsourcing of payrolls and accounts payable to the technical support in the annual budget calculation, in forecasting and management control.

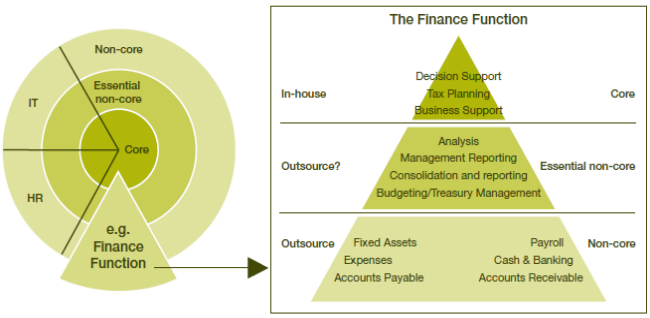

Figure 2. Core vs Non-core in the Finance Function
Source: Pricewaterhouse Coopers

ICT services are still the most widely outsourced activity for 57% of the respondents. In general, 70% of them outsource one or more activities which are intrinsically strategic:

- 53% outsource the production or delivery of core products or services.
- 33% outsource sales and marketing (including third party distribution channels)
- 32% outsource innovation, research and development.

Figure 3. Outsourcing is intensifying. Source:Pricewaterhouse Coopers Global Outsourcing Survey 2007

Financial institutions, with 40%, are especially prone to outsource sales and marketing – for instance, to insurance brokers and financial agents. Civil engineering, mass media and ICT firms are less inclined to outsource core activities although nearly 40% of them do it. Companies that operate in

mature, medium markets like Australia, Canada and New Zealand, are especially aggressive contracting outsourcing for strategic activities (up to 71%). 48% of respondents outsource sales and marketing. Growing companies from these countries have small domestic markets, which can cause the necessary pressure to force them to contract strategic capacities which enable their growth abroad. Over the last years there has been a phenomenon which affects a small number of big clients: outsourcing customer service by contracting call centers in emerging countries with low salary costs. In some cases, this option has found a serious competitor in the switchboard managed by an ICT company and without enough staff. Outsourcing is spreading in a dynamic way to areas like R+D from much more static positions in a long term, with contracts between a provider company and a client company. The freedom each one had to act was very limited. At present, as we go into the second era of outsourcing with many mature ICT contracts, clients admit that the new approaches present a rich variety of opportunities. Nowadays, the senior management team of a company must take into account culture, structures and processes attached to the geographic and sectorial markets they compete in. For this reason, they must be eager to establish alliances and collaborations which enable them to design an innovative business model. They are important factors when business people start thinking about outsourcing new functions and the joint management of shared services like human resources and accountancy. Depending on their business activity, geographical setting or size, between 27% and 55% of the respondents showed their interest to widen their current outsourcing levels within five years later than the survey was made (2007). There is still a margin to grow the ICT outsourcing services: 55% of the present clients of these services hope to increase their outsourcing levels. The key points in the outsourcing growth would be the following ones:

- For big mature markets: purchases (53%), call centers and customer services (45%) and financial and accountancy activities (44%).
- For emerging markets: Worldwide, the highest forecast growth is based on contracting *call centers* and customer service centers (56%), *core* products and services (54%) and delivery /logistic (53%). The relocation strategy is linked to these answers to a certain extent.
- Financial services: *core* products and services (56%), *call centers* customer service centers (46%) and sales/marketing (40%).
- Mass media/telecommunications/ICT: R+D (64%), *call centers* and customer service centers (73%) and finances/accountancy (50%). In these so highly competitive sectors, companies are especially pressured into taking on new initiatives.

3 The potential of BPO as a competitiveness alternative in times of crisis.

The constant improvements in Information & Communication Technologies (ICT), together with the global availability of skilled labor and the reduction of international business barriers have caused the value services supply has been broken off ([3], [4] and [5]). Many companies have gone from an asset ownership strategy to one of outsourcing a part or all the components of a service for cost-cutting, to enhance the cycle times and to get innovation capacity [6]. In this context, Business Process Outsourcing (BPO) means a further step in the strategy of outsourcing organizations. It consists of integrating several processes, even key or core processes in organizational structures unconnected with their own ones. So, in this way a new economic activity of companies specialized in making processes for third parties arises. Obviously, a great part of the competitive advantage of these companies, either back office or front office of their activity, lies on the economy of scale that is reached and, therefore, on the optimum competitive position that means to offer lower unit costs.

It is worth to mention the traditional purchasing centers, which are based on the joint realization of the purchasing process by several companies. Obviously, the management of this purchasing method can be outsourced to only one company, such as it is the case of Fortia. This company is founded as a way to adjust the great consumers to the disappearance of industrial electricity charges in Spain. It is formed by 17 business parties of different economic sectors and it develops a service that benefits all the parties involved and the economy in general, ensuring competitiveness of the Spanish basic industries. The previously mentioned groups of companies employ 40,000 workers directly in 70 factories all over the country. They have a joint turnover of about € 15,000 millions, which stands for 12% of the Spanish industrial electricity consumption. The structure of Fortia is divided into iron and steel (47,2%), cement (25,8%), metallurgical (20,8%), gas fitter (6,20%) and paper (0,07%) industries. Therefore, Fortia is in charge of another part more of the activities of the specialized companies in BPO, where the purchasing process- generally no core component or services – is outsourced.

In Spain, there is a second example of purchasing center, but with some specific features that make it different from Fortia. It is a private consultancy- Compras58, placed in Valencia, whose main features are the following ones :

- It is a transversal purchasing center dedicated to the negotiation of contracts of any type of purchases, either raw or auxiliary material or services. It is not like Fortia, whose purchase is focused on energy.

- Its potential clients are sectorial business associations and, even more, those which operate regionally. Therefore, the Compras58 activity is mainly aimed at industrial clusters.
- Compras58 cannot be said to be strictly a BPO company, since as it has been mentioned before, it only deals with purchasing process and, indeed, contract negotiation. In short, it is a classic sub-process outsourcing- contract negotiation.

From the previously mentioned aspects, it can be deduced that the only competence the Compras 58 client clusters subcontract – the renegotiation of contracts- will be for a short time and it will finish when the new purchasing contracts are signed. This does not stay integrated in processes and sub-processes series that their client companies make, which, for instance, eliminates logistic part concerning provisioning, which is an habitual purchasing process. The competitive tool used in this case is the economy of scale, obtaining a bigger purchasing power as a result of an increase in the purchasing volume. There is also a reduction in the number of providers and, therefore, a greater efficiency in the contract negotiation management. Finally, the number of purchasing references is reduced, which makes Compras58 – on behalf of its clients- become a preferential client for its providers. According to the last data obtained (year 2007), Compras58 owns a client portfolio with 300 client companies, grouped in 12 clusters from 6 Spanish regions. These clusters belong to the following sectors: textile, automobile industry, plastics and maintenance. The closed negotiations during 2012 appear in this Table:

Table 1. Savings achieved in 2010. Source : Compras58.

Item	*Negotiated amount (€)*	*Savings (€)*	*Savings (%)*
Telephony	*3,815,968*	*772,828*	*20%*
National courier	*368,637*	*113,075*	*31%*
Electricity	*29,965,668*	*2,647,355*	*9%*
Office supplies	*382,658*	*86,568*	*23%*
International courier	*899,651*	*196,975*	*22%*
Lab supplies	*434,422*	*111,579*	*26%*
Road transport	*2,341,805*	*131,425*	*6%*
Fuel	*185,092*	*7,154*	*4%*
Natural gas	*1,980,454*	*184,130*	*9%*
Insurance	*98,064*	*8,562*	*9%*
Waste Management	*7,372*	*601,000*	*8%*
TOTAL	***40,479,794***	***4,260,257***	***11%***

According to the above description, then BPO companies could be classified in two types:

- Companies which exploit benefits of economies of scale applied to a kind of process (ICT, Purchasing, Maintenance, etc.), that is, the classic outsourcing.
- Companies which, in a way, are integrated vertically into their client companies from a more strategic position. These companies are still very incipient and cover any kind of process susceptible of being outsourced. This is called BPO.

When BPO activities are placed in a specific geographical frame and, particularly, when the relocation of processes from developed countries into emerging economies takes place, we have a kind of BPO known as offshoring. This practice has attracted a considerable public attention over the last years [7]. Companies which manage this type of BPO play an important role, allowing their clients to specialize in their core competences and they are used as extension of them [8]. Without detriment to the possible savings reached, many companies are unable to value BPO advantages. Alster [9] foretold that 60% of the BPO companies would face the client desertion and the appearance of hidden costs that could cancel the savings between 2005 and 2008. Aron and Singh [8] claim that half of the companies which dealt with offshoring processes have not been able to generate the expected benefits. Robinson et al. [10] states that most of 75% of BPO providers believe their clients were not prepared enough for the initiative and lacked of a very well developed strategy when facing how outsourcing could work. These anecdotic findings state that the BPO companies' management is still not in accordance with their clients expectations. An important reason for this problem could be the inability of service providers and clients to handle with interdependences of processes, which leads to failure ([11] and [8]). The effective integration process between the service provider and its client should be made strongly and decisively in the highest collaboration frame. We must remember that BPO providing companies are usually strategic consultancy firms which do not offer a generalist view but a multi-specialist one in contrast with the only specialization of the classic outsourcing companies. The problem lies on the fact that on almost any occasion there is a distrust by the senior management team of the client company to the BPO provider requirements about "giving sovereignty" when making organizational and strategic decisions that affect the company as a whole. Anyway, these problems that rise systematically in BPO projects are determined by the business immaturity and its still scarce visibility by potential clients. The break-even point will be determined by the component of the corporate strategy that the senior management team of the client company will be willing not to transfer, but to share with its BPO provider. Obviously, the opposite point is found in keeping the brand name by the client, having outsourced the majority of processes, either core or not. There is an interesting debate concerning this, which accepts opinions in all senses, without any solution of continuity.

Although some researchers have expressed their need of a close relationship between the members of the supply chain [12], only recently has the possibility of suggesting a systematic approach to study the supply chain integration been raised. The current competitiveness in industrial and service markets has made several companies reconsider the need of establishing cooperation alliances, mutual benefit and joint improvement of transversal processes, which have become a high priority [13]. At this point we should mention the comakership techniques, which have worked so well in sectors like automobile, where the intermediate margin cutting has reached very high points. The capacity to integrate different processes into different contexts can provide BPO companies with unique competitive and irreplaceable positions that will allow those companies which contract their services to reduce failure risks in the process to improve the client service levels and performance. Given this, it is assumed that BPO can mean not only cost savings by cost-cutting and by economies of scale, but also an increase in incomes as a consequence of economies of scope, which the new core processes a BPO company can do for its client involve.

BPO range of services (maintenance, legal services, purchasing, marketing logistics, etc..) is as wide as varied the functional division of the company is, obviously assuming intermediate proposals of outsourcing of areas, sections or hierarchically less important units in a traditional organization. Clients can only contract one BPO supplier, provide him with work specifications or procedures and wait for a good supply [8]. The provider will make more mistakes and will work more inefficiently than the client company employees, until he can manage these tasks easily. This fact must be considered and quantified in ROI terms when thinking of a BPO project. Obviously, this situation is produced when the outsourced processes belong to core business and this is usually the reason that makes organizations not contract BPO companies for this kind of processes. This also means discouragement for the senior management team of companies planning to relocate a great part of its key processes, which must be considered when they decide whether making the project with their own means - through expatriate - or with other's - by contracting an offshoring company. There are other failure risks for BPO companies related to the contractual obligations that they have with their clients. The effective integration can make these problems disappear. The lack of effective integration in a service environment can lead to a deficient performance, so this is an important area to explore. Many of BPO tasks have complex knowledge components [14]. Therefore, tasks can vary the complexity grade and so the result of the execution. The quality of these services can often depend on the coordination between different processes and sub-processes within the same process. Consider that part of the sub-processes or processes are made by BPO companies and other part by the client company. The most convenient thing might be to make a maximalist approach when contracting BPO companies, that is, to outsource no core complete processes. In this way, integration problems and starting up costs would be avoided and a less payback of the investment in reducing staff to outsource it would be obtained. The border of BPO with the simple employment of workers, outsourced to a temporary work agency, can mean a sign that the BPO project has not been completely understood.

4 Conclusions

In the current work, the intention has been to make an analysis of the different aspects of the classic outsourcing and the promising future of the BPO variant in a pre-recessive context such as the present one in Spain. It has been seen that the motivations that make companies outsource their process and sub-processes are different. The satisfaction that the application of these techniques in the different productive sectors, in different geographic contexts and in companies and public capital organizations generates in contrast to the private capital ones have also been analyzed. The attitude of companies to give or, in all case, to share some of the strategic decisions with companies specialized in BPO seems to be very far. This fact can be sharply seen in small and medium size companies, where BPO has entered less than in big corporations.

As addition to the current work, the possibility of establishing an Outsourcing/BPO observatory in Spain is proposed here. It will allow to evaluate the integration degree of these techniques in the Spanish company and to feature it according to several parameters like the region where they are placed, sector they belong to, size or company ownership. The aforementioned observatory will have a department responsible for the characterization and evaluation of the services demand. In short, it means to quantify and know the evolution of this economic activity in detail.

5 References

[1] Banco de España (2012): "Informe de proyecciones de la economía española". January, 2012, pp. 2-7.

[2] "Pricewaterhouse Coopers Global Outsourcing Survey". Pricewaterhouse Coopers (2007), pp. 7-10.

[3] Apte U.M., Mason R.O. (1995): "Global disaggregation of information-intensive services". Management Science, 41 (7), pp. 1250–1262.

[4] Metters R. (2008): "A typology of offshoring and outsourcing in electronically transmitted services". Journal of Operations Management, 26 (2), pp. 198–211.

[5] Mithas, S. and Whitaker, J. (2007): "Is the world flat or spiky? Information intensity, skills and global service disaggregation". Information Systems Research, 18 (3), pp. 237–259.

[6] Kulkarni, V. (2008): "Offshore to win not shrink". J.M. Swaminathan (Ed.), Indian Economic Superpower Fiction or Future?, World Scientific Publishing Company.

[7] Metters, R. and Verma, R. (2008): "History of offshoring knowledge services". Journal of Operations Management, 26 (2), pp. 141–147.

[8] Aron, R. and Singh, J.V. (2005): "Getting offshoring right". Harvard Business Review, pp. 135–143.

[9] Alster, N. (2005): "Customer disservice". CFO, 21 (13), pp. 40–44.

[10] Robinson, P.; Lowes, P.; Loughran, C.; Moller, P.; Shields, G. and Klein, E. (2008): "Why Settle For Less?". Deloitte Consulting Report.

[11] Mani, D.; Barua, A. and Whinston, A. (2007): "A model of contingent governance choice and performance in business process outsourcing: the effects of relational and process uncertainty". International DSI Conference and APDSI Conference, Bangkok, Thailand.

[12] Armistead, C. and Mapes, J. (1993): "The impact of supply chain integration on operating performance". Logistics Information Management, 6 (4), pp. 9–14.

[13] Zhao, X.; Huo, B.; Flynn, B.B. and Yeung, J. (2008): "The impact of power and relationship commitment on the integration between manufacturers and customers in a supply chain". Journal of Operations Management, 26 (3), pp. 368–388.

[14] Youngdahl, W. and Ramaswamy, K. (2008): "Offshoring knowledge and service work: a conceptual model and research agenda". Journal of Operations Management, 26 (2), pp. 212–221.

Evaluation of Perceived Security in B2C Web Sites by means of a FDSS

Parreño J. [1], **Castro A.**[1], **Puente J.**[1] **and Gómez A.** [1]
[1]Business Administration Department, University of Oviedo, Gijón, Asturias, Spain.

Abstract *- Nowadays, increasingly more costumers use the Internet to purchase. However, the fear and the distrust of the online consumers to supply their bank account number and personal data is still an unresolved factor in some web sites. It has been acknowledged that those web sites in which customers perceive an increased security level achieve greater success in completing purchases than those that provide a lower one.*

This study aims to establish a methodology based on a Fuzzy Decision Support System (FDSS) capable of evaluating security perceived by customers in B2C websites. This technology allows to process the knowledge of decision inserted into the rule data base of the system to qualify the safety in B2C web sites according to the customer's perceptions.

Keywords: B2C, Fuzzy Decision, Security, E-commerce, Weighted Point.

1 Introduction

As the information technologies increase and the electronic communications improve, internet users are more informed and the companies consider it more important to gain new customers by using the Internet as a mean of communication and purchase.

However, security in web sites is a conditioning factor for online customers since if customers perceive that security is adequate, they may purchase. On the other hand, if the perceived security is low, customers will quit the operation, no matter the assessments given to the other key variables.

The present paper, in addition to this brief introduction, is divided into the following sections. Section 2, describes the most relevant variables regarding B2C web sites security and the authors that back these variables. In Section 3, an initial model is proposed to evaluate the perceived security in these web sites by using two different evaluation techniques: one based on weighs and the other based on fuzzy logic. Finally, in Section 4 the final conclusions of the study are shown.

2 Literature Review

In this section, it has been reviewed the literature pertaining the most frequently used variables to evaluate the perceived security in B2C web sites. The ones that are to be highlighted because of their importance are: payment security, service privacy and confidence. Table 1 defines these variables, as well as the authors that support them.

Table 1: **Relevant variables in the evaluation of perceived security.**

VARIABLE	AUTORES
Payment Security: Protection guarantee regarding transactions and means of payment used during the purchase procedure.	Szymansky y Hise (2000), Ranganathan y Ganapathy (2001), Madu y Madu (2002), Francis y White (2002), Otim y Varum (2006), Venkataiahgari et al. (2006) Oppenheim y Ward (2010), Ramanathan (2011).
Service Privacy: Protection guarantee of important data supplied by the customer regarding filing, treatment and maintenance.	Ranganathan y Ganapathy (2001), Zeithaml et al. (2002), Oppenheim y Ward (2010), Stefani y Xenos (2011).
Trust: Firm hope on someone or something. In e-commerce, specifically, refers to the hope an online customer has that the purchase made by using a web site is to fulfil his expectations.	Mayer et al. (1995), Houston y Taylor (1999), Mauldin y Arunachalam (2002), Lala et al., (2002), Kaplan y Nieschwietz (2003), Yousafzai et al., (2003), Oppenheim y Ward (2010), Hong y Cho (2011).

3 Proposed Model

The proposed model stems from a global model for B2C web sites evaluation that is the result of a Delphi Method performed nationwide by experts on Market Online. The model consists of three subsystems of partial evaluation (web site quality, offered service and security) that combine to achieve the final evaluation of the B2C web site.

In this research, we will focus on the analysis of the subsystem of evaluation of B2C web sites security by using two methods: one of weights factors and another based on a fuzzy inference system.

It has been decided, as a criterion for the good operational policy of the model, not to make the value of a variable depend on more than three others. What is more, since not all influencing factors can be measured by using

easily quantifiable variables and their measurement may depend on the expert knowledge of the evaluator, it is intended to develop an easy relational tool that allows to evaluate B2C commerce platforms with the highest possible degree of objectivity, in spite of the uncertainty associated to the evaluation of some of these influencing variables.

Figure 1 shows the parameters involved in the evaluation of the three variables that play a part in the model proposed to evaluate the security of a B2C web site.

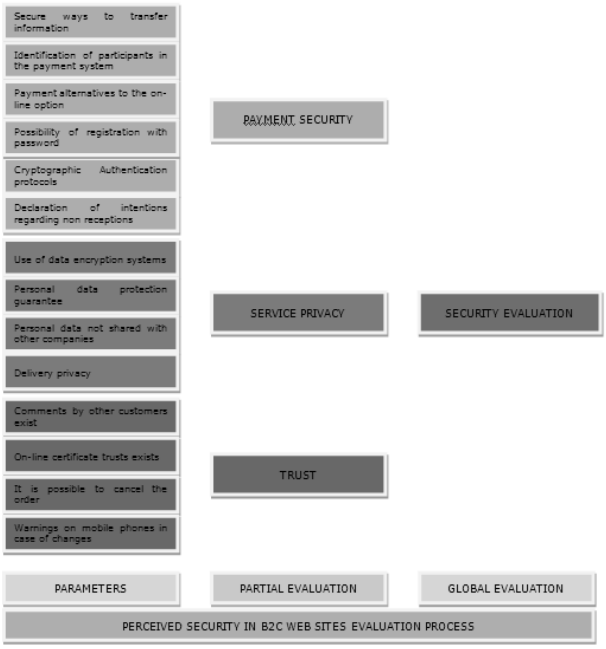

Figure 1: System for the evaluation of the perceived security in B2C web sites.

To evaluate the variable [Payment Security], the customers of the B2C web platform are asked to fill in a little questionnaire to qualify the perception of the payment security. The questionnaire evaluates the customer's degree of satisfaction (from 1 to 7) about different items related to this variable. Aspects as the availability of secure modes to transmit information or the identification of the participants of the payment system are evaluated.

For the variable [Privacy Service] it will be needed to evaluate if privacy regarding data sent really exists or if it is not explicit. With this aim, customers fill in a questionnaire in which they are asked about different items as the use of data encryption systems, personal data protection guarantee or the privacy in delivery.

Finally, variable [Trust] refers to the trust or faith on a person or thing. Regarding B2C, confidence refers to the hope that the customer has that the purchase is made according to his expectations. The existence of certificate trusts, comments made by real customers evaluating the service or the possibility of cancelling the order are factors that condition the qualification of this variable.

Taking into account the evaluations obtained for these three variables and applying some available evaluation methods–in this paper two methodologies are shown– the final qualification is obtained.

3.1 Techniques to evaluate the model

Out of the different available calculation methodologies to evaluate the dependent variables within the proposed model, two have been chosen to be depicted as examples, showing their pros and cons. These two methods are: a traditional variable weights model (Weighted Point Model) and a fuzzy inference system.

3.1.1 Weighing Method (Weighted Point Model)

In the weighing method (Timmerman, 1986), the assessments of the dependent variables defined in an evaluation model are calculated by arithmetic weighing of the assessments of the variables that have influence in their determination.

The qualification of each variable can be calculated as a function of the expert knowledge on perceived security in the B2C web platforms targets of this study or by making a poll among usual customers of these platforms.

The final obtained qualification will be a function of the score of its three determining variables: Payment Security [H1], Service Privacy [H2], and Trust [H3], taking into account their respective weights defined as [W_{S1}, W_{S2}, W_{S3}]. For instance, privacy as well as security are considered critical factors in payments, therefore the weights for the evaluation of the B2C web site security will be: [0,4; 0,4; 0,2].

Next, Table 2 shows a numerical example of the results obtained by five B2C web sites by using this method with the aforementioned weights. It must be reiterated that these weights might be eventually varied according to the expert's criterion or according to the customers' feelings obtained through polls.

Table 2: **Five B2C web sites final Evaluation.**

	H1	H2	H3	Total	
WEB 1	0,3	0,2	0,2	2,40	VERY LOW
WEB 2	0,55	0,6	0,55	5,70	MEDIUM
WEB 3	0,9	0,8	0,9	8,60	VERY HIGH
WEB 4	0,8	0,9	0,2	7,20	HIGH
WEB 5	0,4	0,4	0,1	6,92	HIGH

Intuitively, it is verified the ease to calculate of the weights model. However, this method does not allow to aggregate the knowledge to make decisions in the evaluation of the dependent variables in an intuitive way as the decision systems based on rules do allow. This fact makes it difficult to conceptualise the model of evaluation of the perceived security in B2C web sites and enforces a much too linear behaviour in that assessment. This linear behaviour may also make it difficult to adequate the evaluation to the reality if the

platform wishes to set a minimum acceptance threshold to some of the variables (i.e. security in payment) because of the importance it has to its online customer.

On the other hand, the nature of the decisions of B2C e-commerce customers is complex and little structured and the estimate of some quantitative and qualitative factors that are involved in the process has a high degree of uncertainty and subjectivity (Meziane and Nefti, 2006). That is why it is proposed to analyse an assessment method that mitigates the described inconveniences and that is able to simulate the human reasoning procedure in making decisions from inaccurate or vague data (Bevilacqua and Petroni, 2002).

Thus, it is feasible to expand the previous model to a fuzzy system able to infer the evaluation of the perceived security in different web platforms according to the opinion of their purchasing customers so that it is possible to establish a ranking depending on the perceived security.

3.1.2 Fuzzy Inference System (FDSS)

Fuzzy Decision Support Systems are based on the Fuzzy Sets Theory (Zadeh 1965). They allow to aggregate into the models a component of uncertainty which makes them more efficient when it comes to approximate to reality (Lootsma, 1997). In these systems, linguistic-type variables allow to process qualitative or quantitative information since the values that these variables take may be associated to concepts of ordinary language instead of the numeric values that the traditional variables take (Driankov et al., 1996). In the case of the perceived security in B2C web sites, the subjectivity of the evaluation they undergo may, in some cases, be high. That is why the use of artificial intelligence tools based on fuzzy logic and the use of linguistic labels as valid values for the variables of the model to be designed permits a better adaptation to the evaluation criteria supplied by the users or the expert in this type of business. It will also be proved that the design of a fuzzy system in this area will redound in a better interpretation of the knowledge inserted in the decision system, improving the behaviour of the evaluation in comparison to other more simple qualification systems–i.e. those based in weights–and achieving nonlinear behaviours in the evaluation. To perform the study in this area, we will use a fuzzy decision support system with the assistance of the application Matlab fuzzy logic toolbox ® version 2.0.

To adapt the developed model to the fuzzy environment, it is necessary to transform the aforementioned variables into their fuzzy homologues (input variables as well as output ones), in such a way that they can take linguistic values within previously defined ranges. Then, the knowledge necessary to develop the process will be aggregated as rules, with the final goal of obtaining a qualification for the portal. The rules have conditional structure, and this structure must allow to intuitively assign linguistic labels to all variables.

In this case, the labels used to perform the evaluation of the perceived security in a B2C web site are shown in Figures 2 and 3.

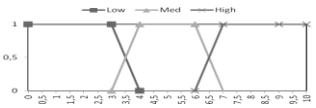

Figure 2: Labels for the input var.

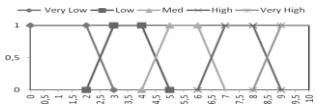

Figure 3: Labels for the output var.

Next, as a function of the expert knowledge on evaluation, the rule base shown in Table 3 is proposed.

Table 3**: Rule base to evaluate the security of the service of the B2C web site.**

SECURITY		TRUST								
		LOW	MED	HIGH	LOW	MED	HIGH	LOW	MED	HIGH
PRIVACY SERVICE	LOW	VL	VL	VL	L	L	M	M	M	VH
	MED	VL	L	L	L	M	M	M	M	VH
	HIGH	VL	L	M	M	M	H	H	H	VH
		LOW			MED			HIGH		
		PAYMENT SECURITY								

For instance, the shaded rule would suggest that if the score of the security in the payment is medium, the privacy of the service is low and the trust in the web site is high, then, the final qualification will be medium.

Once the fuzzy subsystem is designed, the evaluation of a web site can be inferred as a function of the crisp values assigned to its input variables. Besides, it is easy and intuitive to analyse the congruence of the obtained evaluations by using the inference maps supplied by each subsystem of the model. In these maps, the scores of the output variables are represented by the surface's height in each point.

This way, for instance, for a low assessment in payment security, the maximum qualification would be around 5.5 points in a little area (see Figure 4), which would determine that the user quits the process of online purchasing in that web site. However, for medium and high values in payment security, an important increase of the assessment of the web site takes place which reaches 7.5 and 9 points respectively. In addition, in this last case, for trust values over 6 points, high final qualifications are obtained, no matter the value of the privacy of the service. This behaviour would be explained because a customer that perceives that a service is secure and reliable awards the service with a high qualification regardless of the service's privacy.

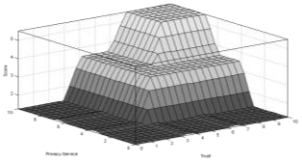

Figure 4: Map of solutions with low payment security.

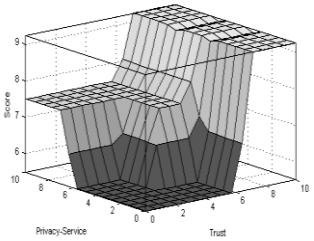

Figure 5: Map of solutions with high payment security.

4 Conclusions

In the paper, the variables that play a part in the perception of the security of B2C web sites are analysed. A model is proposed to evaluate the security in those web sites by using two different methods. The first one, based on different weights assigned to the influential variables, poses different inconveniences: too much linearity in the output variable or the difficulty of conceptualising the behaviour of the assessment given to the security of the B2C web site, which is usually described vaguely and inaccurately. The second one is a fuzzy system that not only does it mitigates the aforementioned inconveniences but also allows the introduction of the knowledge for the assessment as linguistic rules in a guided and intuitive manner (based on the expert knowledge or in the perceptions provided by the users). The results put forth a better interpretation of the security assessments of a B2C web site. These results are more in agreement with a not so much linear behaviour as the one assigned by the weights traditional methods. To broaden the research, the model will be validated through web analytics by using different available metrics: number of visits and/or unique visitors, rebound rate or conversion rate among others. The final goal will be to achieve a dynamic model that adequately adapts to the online customer necessities.

5 References

[1] Bevilacqua M; Petroni A. From "Traditional Purhasing to Supplier Management: A Fuzzy Logic-Based Approach to Supplier Selection". International Journal of Logistic 5, (235-255). 2002.

[2] Driankov D, Hellendoorm H, Reinfrank. "An Introduction to Fuzzy Control". Springer, 1996.

[3] Francis J.; White L. "PIRQUAL: A escale for measuring customer expectations and perceptions of quality in Internet retailing". Marketing theory and applications. Vol. No. 13 (263-270). 2002.

[4] Hong IB, Hwihyung Cho: "The impact of consumer trust on attitudinal loyalty and purchase intentions in B2C e-marketplace". International Journal of Information Management, 2011.

[5] Houston R.W.; Taylor G.K. "Consumer perceptions of CPA Web Trust assurances: evidence of an expectation gap". International Journal Audit. Vol. No. 3 (89-105), 1999.

[6] Kaplan S.E.; Nieschwietz R.J. "A Web assurance services model of trust for B2C e-commerce". International Journal of Accounting Information Systems Vol No.4 (95-114), 2002

[7] Lala V.; Arnold V.; Guan L. "The impact of relative information of e-commerce assurance seal on Internet purchasing behavior". International Journal Accounting Information Systems, 2002.

[8] Lootsma F. "Fuzzy Logic for Planing and Decision-Making". Kluwer. Dordrecht, 1997.

[9] Madu C.N.; Madu A.-A. " Dimensions of e-quality". International Journal of Quality & Reliability Management. Vol No. 19 (246-258), 2002.

[10] Maudin E, Arunachalam V "An experimental examination of alternative forms of Web assurance for business-to-consumer e-commerce". Journal of Information Systems Vol. No. 16 (33-54), 2002

[11] Mayer R.C.; Davis J.H., Schooman F.D. "An Integrative model of organizational trust". Academy of Management Review. Vol No. 20 (709-734), 1996

[12] Meziane F, Nefti S. "Evaluating E-commerce trust fuzzy logic". School of Computing, Science and Engineering. University of Salford. United Kingdom, 2006.

[13] Oppenheim C.; Ward L. "Evaluation of web sites for B2C". Esmerald. Vol. No. 58 (237-260), 2006.

[14] Otim S., Varum G. "An empirical study on web-based services and customer loyalty". European Journal of Information Systems. Vol. No. 15 (527-541), 2006.

[15] Ranganathan C.; Ganapathy S. "Key dimensions of business-to-consumer web sites". Information & Management Vol. No.39 (457-465), 2002.

[16] Stefani A, Xenos M. "Weight-modeling of B2C quality system. Computer Standard & Interface. Vol. No. 33 (411-421), 2011.

[17] Szymanski DM, Hise, RT. "E-satisfaction: an initial examination". Journal of Retailing. Vol. No. 76. (309-322), 2000.

[18] Venkataiahgari A.-K, Atwood J.-W, Debbabi M. "A survey of secure B2C commerce for multicast services". IEEE CCECE/CCGEI. Concordia University. Montreal, 2006.

[19] Zadeh LA. "Fuzzy Sets. Information and Control". Vol. No. 8 (338-353), 1965.

[20] Zeithaml V.; Parasuraman A.; Malhotra A. "Service quality delivery through web sites: A critical review of extant knowledge". Journal Academy of Marketing Science. Vol. No. 30 (362-410), 2002.

Application of GRASP methodology to Vehicle Routing Problem (VRP)

R. Pino[1], C. Martínez[1], V. Villanueva[1], P. Priore[1], and I. Fernández[1]
[1]Department of Business Management, University of Oviedo, Gijón, Asturias, Spain

Abstract - *In this work the development and implementation of a Decision Support System is described. It will assist in the route calculation process and in optimizing the filling of the trucks that have to transport a considerably number of vehicles from near of 8 origins to more than 3,000 possible destinations spread over Spain and Portugal, and some in France, Germany, etc. The problem can be classified as VRP (Vehicle Routing Problem), been a hybrid between the VRPTW (VRP with Time Windows) and MDVRP (Multi Depot VRP). For its resolution, a Web application using a GRASP methodology as an optimization tool has been developed. The experiments carried out prove an improvement in the results of the freights/routes planning when the DSS is used. The improvement is measured trough the percentage of daily vehicles dispatched, the decrease of the shipment delay, and truck use, among others.*

Keywords: VRP, Heuristic Optimization, GRASP

1 Introduction

The aim of the this work is to present the results obtained in the development of a research project in which heuristics techniques are applied to solve vehicle routing problems. This research was developed as an independent subproject within the project called SITIM[1], whose aims are to study, evaluate and develop methodologies and systems to improve the Intermodal Transportation through scientific and technological knowledge. For this purpose, a number of actors participate in the project, among which are: Research Groups of various Spanish universities (Universities of Valladolid and Oviedo), public Logistics and Transportation-related institutions and several private companies of these sectors.

The subproject aims at analyzing how operational optimization and routing calculation techniques may help a logistics operator to be more effective and efficient. Specifically, the case of a logistics company specialized in the automotive sector has been studied. It provides distribution services, mainly by road transport, for those companies that have the need for vehicle shipments to / from any point of the Iberian Peninsula as well as some strategic points in France and Germany. The planning necessary to carry out these services is currently performed by a team of technicians that make an optimization between service demand and available resources (fleet of trucks). On the basis of their experience, they decide what vehicles travel in each of the available trucks, in order to meet all requirements (specially delivering freight on time), objectives and/or restrictions that the business strategy. These technicians use an ERP platform that manages ordering, billing,... but does not implement any support for transportation planning.

The above mentioned procedure presents a series of drawbacks. Basically the search for optimal routes causes a delay in shipments, resulting in having to face penalties more often than desirable. The achievement of an optimized planning after evaluating all (or most) possible combinations of transport which satisfy the objectives and/or restrictions would be necessary.

When the dimension of the problem is large as in the present case, a person is not able to evaluate all possible combinations, unless he makes a thorough and detailed study for each transport mean, a fact that becomes functionally and economically impractical. A *Support System for Decision Making* (DSS: Decision Support Systems) is a software application that, using artificial intelligence algorithms, will provide the user with a better loads/routes planning. As a result, the technicians work would be more efficient and effective, and the objectives achieved to a greater extent.

The paper is organized as follows. In the remaining of this section a literature review is made to analyze different options for solving the addressed problem. In second section, the problem and current operational process is presented, emphasizing those aspects that should be improved for achieving greater efficiency work levels. Then, the proposed solution, the chosen heuristics techniques (GRASP methodology) and the developed Web application are described. In the fourth section, the solution is analyzed and compared with the current situation. The paper ends with a section summarizing the final conclusions of the work.

From the point of view of operational optimization, the problem tackled in this paper is a Vehicle Routing Problem (VRP), as first established Dantzig and Ramser [1], and

[1] *Análisis, desarrollo y evaluación de Sistemas Inteligentes de Transporte Intermodal*. Proyecto MFOM-08-E12/08 del *Subprograma para la Movilidad Sostenible y el Cambio Modal en el Transporte* del Ministerio de Fomento, Gobierno de España.

subsequently studied Bodin et al. [2], Magnanti [3] and Laporte and Nobert [4]. Under the VPR umbrella, there are a huge number of problem types to be dealt with . More specifically, our study was found to fit VRPTW (VRP with Time Windows) and MDVRP (Multi Depot VRP) types. The VRPTW type, as Savelsbergh [5] established, is used in problems where there is a time window for transport; in our case, there is a deadline for completing the delivery. In the MDVRP type, transport planning has to be performed taking into account several warehouses or depots, as explained by Kulkarni and Bhave [6]. Those are problems where the delivery is not usually centralized at a particular point. A delivery route starts from a given depot and when the truck service ends, a new route is started from a different depot.

The resolution of the above problem can be reached by using exact or approximate algorithms ([7], [8], [9] and [10]). There are interesting solutions for the "Local Search" and "Tabu Search" algorithms, especially the one proposed by Pisinger and Ropke [11] who established a framework by means of which it is possible to solve different VRP problems. On the other hand, the “two stage” algorithms use some kind of informed search and make an improvement on the heuristic based on making the resolution in two separate phases (see [12]). An interesting algorithm to be applied in this type of problems is the so called GRASP (Greedy Randomized Adaptive Search Procedure) introduced by Feo et al. [13], which combines techniques and concepts of other algorithms.

There is a large family of algorithms that involve collective intelligence or collaborative, "Evolutionary Algorithms", "Swarm Intelligence" and "Multi-Agent". Within the category of Evolutionary Algorithms, which try to simulate natural selection processes, the most prominent are genetic algorithms [14]. In recent years, swarm algorithms have blossomed, being analized by numerous researchers ([15], [16]). The basis of how these algorithms operate, is by imitating swarm systems behavior. Mainly, the most widely used in solving routing and VRP problems are based on Ant Colony. More recently, the Bees Algorithms (BA) has begun to be used in optimization problems [17]. Finally there are the so-called Multi-Agent Systems. This is a field with many possibilities in solving problems which must take into account different variables for decision-making and in problems where the information is taken from various sources [18].

2 Current System for building Route Planning

The current system for route/loads planning is based on the use of an ERP system for managing customers ordering as well as the transport to be made. Currently there is a lack of a system to carry out the transport planning or, at least, to assist the technician in this task. The software application used just only tracks orders and serves to support the other functions in company: accounting, administration, etc.., Thus, the technician should do the load/route planning relying on his experience.

When planning, the objective pursued is threefold: to maximize the load factor of trucks (the trucks are wanted to have the maximum occupation at the origin); to minimize the mileage (especially in trucks with little or no load at all) and to meet deadlines. With these three objectives in mind, the different operators perform the 9 planning over the 9 established Logistics Areas: 8 zones for Spain and Portugal, plus an additional area for international destinations. In these areas, there are 10 possible depots (origins) and 3,000 possible destinations (dealers, rent-a-car, etc.)

The company has a fleet of approximately 270 trucks, spread across the different areas. To carry out the transport planning, operators receive through the software application, information about the orders and the trucks available in their zone. The usual way of planning is to group the orders by destination and try to fill trucks to a single destination, having priority those orders whose expiration date is closer. Once the filling of trucks with orders for the most requested destinations have finished, a final check is made to assure there is not an urgent order that needs to be introduced because its deadline is very close or has expired. In that case, if possible, this order (vehicle) will replace an order planned before in a route that would be as close as possible to the new order delivery point.

When the operator fills a truck and confirms the route, he uploads the expedition orders to the system, which checks if the order is correct and produces the orders for loading the vehicles in the corresponding transport truck. The entire process is depicted in Figure 1.

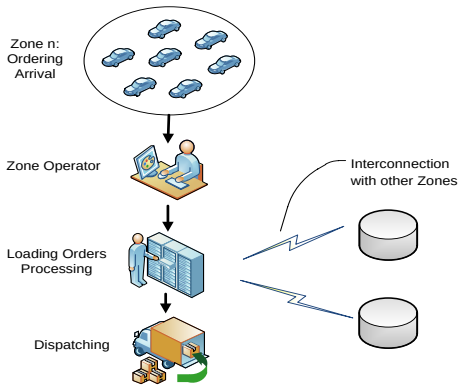

Figure 1. Current System.

It can be seen how, despite the fact that the aim is to achieve the objectives for planning (especially concerning the delivery of the vehicles on time), not all possible combinations of destinations are evaluated because the planning is done, primarily, configuring trucks to the most popular destinations. Those vehicles traveling to any

destination with little demand would be on hold until more orders for this destination arrive and have a critical mass to fill up a truck, or more orders arrive for a nearby destination in such a way that combining both a truck load could be completed. This strategy has the risk of not meeting delivery deadlines, causing uneconomic settings if, for example, is necessary to introduce a single vehicle on a route because it needs to be shipped for not exceeding the delivery deadline.

Since the work system cannot assess all possible combinations of loads, a system based on a heuristic algorithm would improve the solutions due to its higher capacity to do so. Among all these combinations could arise some cargo configurations that would better meet the objectives and/or avoiding having vehicles waiting for more orders to the same destination.

3 Planning System Proposed

The proposed model consists in a DSS (Decision Support System) that will support operators in their task of planning routes for the trucks that must deliver vehicles. A Web application in which the user (zone operator) is identified by its assigned logistics area was developed. Initially, the data of the problem to solve are uploaded (complete information of ordering and the trucks available in the zone). The algorithm parameters are adjusted and the optimizer will calculate a solution based on the evaluation and comparison of different possibilities by using the GRASP algorithm. The solution consists of a set of routes that meet the requirements of maximum truck utilization, fulfillment of vehicles delivery deadline, etc. The operator will analyze the proposed solution and will totally or partially validate it.

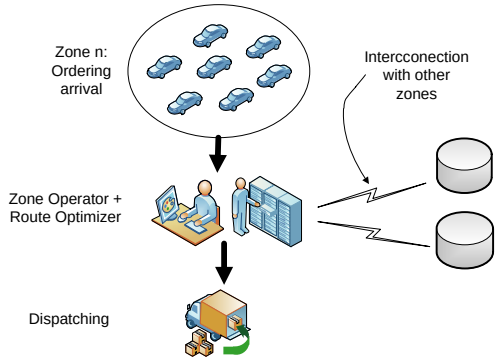

Figure 2. System Proposed.

The operational process (shown in Figure 2) is, generally speaking, based on configuring and running the algorithm. Once the result is obtained, it must be analyzed to be accepted as a valid solution (or a part of), and reconfigure any of the parameters to run the algorithm again and get new solutions.

Throughout the day, orders (vehicles to be transported to a specific destination) are continuously coming to the company software system. A zone operator performs a planning (load trucks configuration), twice during the day; a first one in the morning and another in the afternoon. In this way he manages the new orders that have arrived and those remaining from previous days.

When the operator starts the application, he identified himself as belonging to a specific logistic zone. Automatically, the information about the orders that have the origin among the operator's logistic zone will be uploaded on the application (all orders that have come to the system since the last time the planner was ran and those who have not been planned on previous uploads). These data include: vehicle identification, category, size, origin, destination, delivery deadline, priority level, etc. It also informs him about the available fleet trucks his logistic area to be used in planning.

Subsequently, the operator proceeds to assign values to the algorithm parameters according to the relative importance of the objectives to be met (immediate delivery of an order, minimizing the distance between potential destinations, maximizing the load factor, etc.)

Noteworthy that the application already has a pre-set parameters such as the maximum number of stops a truck can make on a route. This parameter is critical, because the loading and unloading of trucks represents a significant cost for the company. Therefore, it was considered that the maximum number of stops would be 4, being the first one the starting point where the truck is loaded.

Another parameter is the load factor of a truck, that is, the filling percentage of it, which depends on its capacity and the number and size of the vehicles carried. It has been established a minimum and maximum values (which could be changed by the operator in certain cases), which define the load factor which a truck should reach to be considered as valid.

Other parameters relate to the constant cost functions used, which give greater or lesser weight to the truck load factor, the distance between the possible stops, the total distance traveled by all routes forming the solution, the distance traveled without load, the urgency of delivery, etc. These values would be modified by the operator in each of the executions of the algorithm taking into account the requirements that should be prioritized at that time.

Once the settings have been configured, the execution of the algorithm will bring a solution that consists of a number of routes and loads that meet all specifications and constraints of the problem. The operator will analyze the solution, validating those loads that he considers acceptable, and will rerun the algorithm after making appropriate changes in the parameters for calculating other solution (set of routes). The process is repeated as many times as necessary until all orders were placed on acceptable routes or it runs out of available trucks.

In the latter case, there is the possibility of using trucks that are initially assigned to a close logistic zone and have not been used by the operator of its area.

The optimization algorithm can be run with or without what we call "pre-analysis". This consists of a preliminary examination of all orders looking for destinations that can fully load a truck. That is, if there is a destination with enough orders to fully fill a truck, priority will be given to the preparation of such orders. This type of route (which we called "obvious") will be almost certainly validated by the operator, thereby reducing the dimension of the problem and facilitating the subsequent optimization work of the algorithm. This execution mode has, as an advantage, to be similar to the working mode of the operator, but has the disadvantage of reducing the size of the problem and delete orders in the "pre-analysis"; due to this, the optimizer may not be able to reach an optimal solution since there are combinations of orders that cannot be considered because they contain orders as part of any of the "obvious" loads that have resulted from "pre-analysis".

3.1 Aplicación Software

This section describes the architecture involved in the previously described processes. Figure 3 briefly shows the internal functioning of the application. The following can be observed:

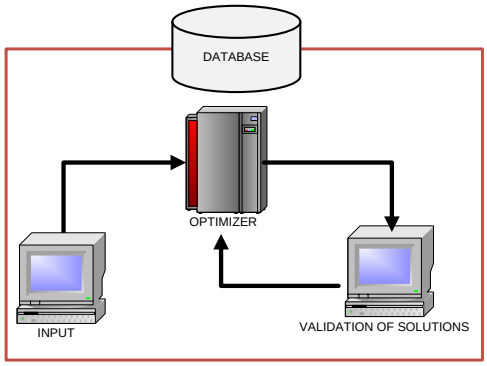

Figure 3. Application Architecture.

- The application input is the orders stored in the company database.
- When the area operator is identified, the application automatically loads the information related to orders and available trucks. This ensures that the orders and trucks stored in the application match those which are actually available in the logistic area when the operator runs the optimizer.
- The application database contains several master data such as a table of distances and the truck fleet. Master data can be created, viewed, edited, or deleted.
- After running the optimizer to find suitable solutions, the operator validates the loads and the correspondent routes. This information is provided to the company's computer system so that the delivery order is generated with the usual format.

Moreover, the application architecture follows the Model View Controller pattern, which defines the tasks to be carried out by the different modules (usually programs, libraries, …) Thus, any change in the specifications, can be programmed independently in the different modules without it affecting or interfering in the rest.

The aim is, therefore, to gain flexibility and agility, and operating with "open" standards and technologies. Figure 4 shows an outline of the application architecture: the architecture is common to J2EE-based web applications. Specifically, the implementation uses the Jboss SEAM Framework.

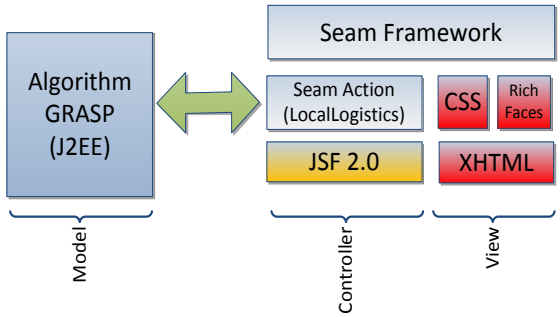

Figure 4. General architecture of the application.

3.2 GRASP

The optimizer key element is the GRASP algorithm. The metaheuristic algorithm GRASP (Greedy Randomized Adaptive Search Procedure), is a multi-start iterative process with two phases iterations: a construction phase, in which a feasible solution is built, and a local search phase, which starts from the built solution and improves it by examining its neighborhood, until it finds a local optimum. For each iteration, the best solution found so far is kept as a final result. The GRASP algorithm creates a list of candidates using a random factor in order to avoid the wrong selection of a local maximum on the base of what's called the "greedy approach". It is precisely this randomness that makes the GRASP algorithm an alternative of superior efficacy compared to many other heuristic algorithms.

Although GRASP features can be found also in other heuristic search methods, the practical implementation is different. This method has a great ability to obtain solutions for large combinational optimization problems, which suits the present case. Unlike other metaheuristic techniques, once the construction and local search strategies are defined, it is only necessary to adjust two parameters: the size of the list of candidates and the number of iterations to perform. Furthermore, this method also adapts easily to new

restrictions or conditions imposed by the problem. The GRASP algorithm consists of a continuous series of iterations, through which it attempts to select a good solution to the problem.

Compared to other popular metaheuristic techniques such as Tabu Search, Simulated Annealing and Genetic Algorithms, the GRASP procedure is fast and competitive, as it provides better quality solutions in less computational time ([19], [20]). This is mainly due to the fact that it combines the advantages of its random and greedy nature to build solutions.

Another major advantage of the GRASP algorithm compared to other metaheuristic methods is its ability to generate a large number of good quality alternative solutions. This feature is important in vehicle routing applications, because often the arrival times are estimates and thus may vary widely depending on unpredictable factors.

The elements that determine the GRASP technique are: the preprocessing method, the heuristic function, the way it builds the list of candidates, the post-processing method and the stopping criterion.

GRASP is an iterative technique of random sampling: the procedure is repeated a defined number of times in order to generate good solutions. The number of iterations "n" to be performed with the algorithm GRASP is to be determined before the execution of the main experiment, using a calibration process that implements the algorithm several times, each of them with a different "n" value, until it determines a value which provides good results in an acceptable time.

4 Analysis of the obtained results

As an example of implementing the system developed, we have chosen an operator working in a particular zone, in this case the Catalonia-Tarragona zone. This Operator must plan delivery routes for all orders which have the origin in his area (an average of 250 vehicles per day, most of them will have as origin the Tarragona depot), and as destination, any of over 3,000 possible destinations, using the trucks available in his area. The number of trucks is variable because it depends on the routes planned by other operators, ending in the Tarragona area of Catalonia (it can be estimated an average of 27 trucks per day).

As discussed in the previous section, it is possible to run the algorithm with "pre-analysis", where the algorithm "mimics" the way an operator proceed without the support of an optimizer software, that is, trying to fill trucks to serve the more demanded destinations and, therefore, be able to fill a truck without being added orders for other destinations.

This may not be quite optimal since those destinations with little demand, may experience delivery delays due to the fact that they are only planned when the delivery deadline is so close and a feasible route could not be found. That leads to deliver orders out of time, or in time but being included in a non-optimal route.

A classification of the routes/loads, based on the truck load factor, was made. It would be desirable that most of the vehicles were part of Optimal or Good Routes:

Table 1. Classification of Solutions.

	Nº of stops on the route	*Average Load Factor on the route*
Optimal Route	*1 ó 2*	*≥ 95 %*
Good Route	*≤ 4*	*≥ 80 %*
Acceptable Route	*≤ 4*	*≥ 70 %*
Bad Route	*≤ 4*	*< 70 %*

A comparison between the solution proposed by the operator without using the optimizer (using only their experience) and that achieved by the same operator but being supported by the optimizer, has been made. In it, the ratio between the Orders (vehicles) which are sent as part of each of the 4 types of route/load defined above and the total orders planned, has been measured.

Table 2. Comparison of the Orders Dispatched for each type.

	Operator Solution	*Operator + Optimizer*
Orders dispatched as "Optimal Route"	*75 %*	*73 %*
Orders dispatched as "Good Route"	*14 %*	*13 %*
Orders dispatched as "Acceptable Route"	*6 %*	*12 %*
Orders dispatched as "Bad Route"	*5 %*	*2 %*

As can be seen, in the first two categories (optimal and good routes), the operator solutions with and without optimizer are similar. But when the optimizer is used, more vehicles are introduced in acceptable routes, provoking that more vehicles are dispatched per day and deliveries out of time are reduced. These results can be seen from the figures shown in the table below (the data shown refer to average daily value):

Table 3. Comparison Orders and Deadline Fulfillment.

	Operator	*Operator + Optimizer*
Dispatched Vehicles/day	*63 %*	*85 %*

Trucks used/day	*67 %*	*80 %*
Average output time	*~3.2 days*	*~1.5 days*
Vehicles out of time	*18 %*	*5 %*

These results are mainly due to the fact that the operators (if not using the optimizer) try to plan trucks for the most demanded destinations, leaving on hold the orders of the less demanded destinations. As the deadline approaches, the operator must decide whether or not to maintain on hold the order, provoking a late delivery, or to place it in a truck that will make an "Acceptable" or even a "Bad" route.

In contrast, when the operator uses the optimizer, the algorithm tries to find combinations among all destinations to ensure that the maximum number of orders are sent in the best possible condition and trying not to exceed the deadline. Table 4 shows an example:

Table 4. Configuration of Routes/Loads.

	Route	*Nº of Vehicles*	*Load Factor*
TRUCK 1	*Tarragona – Bilbao*	*8*	*98 %*
TRUCK 2	*Tarragona - Valladolid*	*9*	*100 %*
TRUCK 3	*Tarragona – Madrid*	*8*	*98 %*
TRUCK 4	*Tarragona – Teruel*	*9*	*100 %*
	Teruel - Valencia	*8*	*90 %*
TRUCK 5	*Tarragona – Orense*	*8*	*98 %*
	Orense – Viana do Castelo	*6*	*74 %*
	Viana do Castelo - Porto	*3*	*37 %*

The table shows the solution proposed by the optimizer for a set of orders. Five routes with their assigned trucks have been configured.

The first 3 routes corresponding to the trucks 1, 2 and 3, would fit the category defined as "Optimal Route".

In the case of the route taken by the Truck 4, it would be a "Good Route". A single vehicle has to be delivered in Teruel. Therefore, the operator would hold it on waiting for more orders with the same destination; that would allow filling a truck. If no more orders appeared before the deadline, that vehicle would be introduced in some near route and delivered late with the corresponding penalty. However, the optimizer looks for the best possible routes, in which this order could be placed and delivered without delay. In this case, it has been introduced on a truck with destination Valencia, that initially was an "Optimal Route". The order for Teruel makes this route an only a "Good Route" but the order will be delivered on time instead.

In the case of the last route/load named as "Truck 5", it would be classified as "Acceptable Route" because it makes several stops and has a high load factor along the route. However, it is a valid solution because it allows to group orders by areas with low-demand destinations. In this particular case orders for the south of Galicia are grouped with those of the north of Portugal. As already mentioned, this solution is not the optimal from the point of view of the direct costs it implies. However it allows removing the praxis of paralyzing orders for less profitable destinations until more orders for those destinations would come up or either the deadline is about to fulfilled.

In summary, it could be established that the aim of improving the service efficiency by getting lower penalties for vehicle out-of-time deliveries is reached. From our point of view, this improvement, in spite of increasing the number of sub-optimal solutions (Acceptable Solutions), is offset by the reduction in penalties. Furthermore, trucks are earlier dispatched thus the percentage of non-operating time decreases and, the image of the company would benefit from an increase in the fulfillment of the fixed deadline.

5 Conclusions

In this paper the use of a DSS to aid in optimization tasks of filling trucks and route planning is presented. The current mode of planning leads to, in many cases and due to the priority of fill full trucks, delays in the dispatch of orders while the deadline is not exceeded. If this date is exceeded, the company will have to face penalties that contribute to reducing the economic performance of business operation. If delay penalties are not admissible, it may occur that certain deliveries must be sent in uneconomical routes because the truck load factor does not reaches the minimum acceptable.

The use of a DSS based on the GRASP methodology is proposed. It assists the operator in planning tasks, proposing solutions that meet all restrictions and achieve the stated objectives. Although the use of a heuristic algorithm as GRASP causes not to reach the optimal solution, it does reach a fair solution in a reasonable time by exploring multiple combinations that the operator itself would be unable to evaluate in a reasonable time. The solution proposed by the DSS, will be analyzed by the operator, who can fully or partially validate it. In the latter case, new executions of the algorithm allows to keep on improving the initial solution obtained until reaching a satisfactory solution that meets all requirements and restrictions posed.

A set of experiments from actual data provided by one of the leading Spanish transport companies have been made.

From their results, it can be concluded that the use of the developed application, clearly improves previous solutions in terms of percentage of vehicles dispatched per day, the average delay of orders, the minimization of out-of-time deliveries, and the general use of the transport trucks.

6 References

[1] Dantzig, G.B. and Ramser, J.H. (1959): "The truck dispatching problem". Management Science, Vol. 6(1), pp. 80-91.

[2] Bodin, L.; Golden, B.; Assad, A. and Ball, M. (1983): "Routing and scheduling of vehicles and crews: The state of the art". Computers & Operations Research, Vol. 10(2), pp. 63-211.

[3] Magnanti, T.L. (1981): "Combinatorial optimization and vehicle fleet planning: Perspectives and prospects". Networks, Vol. 11(2), pp. 179-213.

[4] Laporte, G. and Nobert, Y. (1987): "Exact algorithms for the vehicle routing problem". Annals of discrete Mathematics, Vol. 31, pp. 147-184.

[5] Savelsbergh, M.W.P. (1985): "Local Search in routing problems with time windows". Annals of Operations Research, Vol. 4(1), pp.285-305.

[6] Kulkarni, R.V.and Bhave, P.R. (1985): "Integer Programming Formulations of vehicle routing problems". European Journal of Operational Research, Vol. 20(1), pp. 58-67.

[7] De la Fuente, D.; Lozano, J.; Ochoa, E. and Díaz, M. (2011): "Estado del arte de algoritmos basados en colonias de hormigas para la resolución del problema VRP". Libro de Abstracts del XV Congreso Ingeniería de Organización, CIO 2011.

[8] Pino, R.; Lozano, J.; Martínez, C. and Villanueva, V. (2011): "Estado del arte para la resolución de enrutamiento de vehículos con restricciones de capacidad". Libro de Abstracts del XV Congreso Ingeniería de Organización, CIO 2011, pp.483-487.

[9] Pino, R.; Villanueva, V.; Martínez, C.; Lozano, J.; Del Pino, B. and Andrés, C. (2011): "Heuristic Solutions to the Vehicle Routing Problem with Capacity Constraints". Proceedings of ICAI-Worldcomp'11, pp. 634-640.

[10] Kontoravdis, G. and Bard, J.F. (1995): "A GRASP for the Vehicle Routing Problem with Time Windows". ORSA Journal on Computing, Vol. 7(1), pp.10-23.

[11] Pisinger D. and Ropke S. (2005): "A general heuristic for vehicle routing problems". Computers & Operations Research, Vol. 34, pp.2403-2435.

[12] Chao, I.M.; Golden, B.L. and Wasil, E. (1995): "An improved heuristic for the period vehicle routing problem". Networks, Vol. 26(1), pp.25–44.

[13] Feo, T.A.; Resende, M.G.C. and Smith, S.H. (1994): "A greedy randomized Adaptive Search procedure for maximum independent set". Operations Research, Vol. 42(5), pp. 860-878.

[14] Blanton, J.L. and Wainwright, R.L. (1993): "Multiple vehicle routing with time and capacity constraints using genetic algorithms". Proceedings of the 5th International Conference on Genetic Algorithms. San Francisco: Morgan Kaufmann, pp. 452–459.

[15] Dorigo, M.; Maniezzo, V. and Colorni, A. (1996): "Ant system: Optimization by a colony of cooperating agents". IEEE Transactions on Systems, Man, and Cybernetics, Part B, Vol. 26(1), pp. 29–41.

[16] Stützle, T; and Hoos, H (2000): "MAX-MIN ant system". Future Generation Computer Systems, Vol. 16(8), pp.889-914.

[17] Pham, D.T. and Castellani, M. (2009): "The Bees Algorithm: modelling foraging behaviour to solve continuous optimization problems". Proc. Institution of Mechanical Engineers Part C-Journal of mechanical Engineer Science, Vol. 223(12), pp. 2919-2938.

[18] Baker, A.D. (1998): "A survey of factory control algorithms that can be implemented in a Multi-Agent Heterarchy: Dispatching, Scheduling and Pull". Journal of Manufacturing Systems, Vol. 17(4), pp.297-320.

[19] Resende, G.C.M. and Ribeiro, C. (2003): "Greedy Randomized Adaptive Search Procedures". In F. Glover and G. Kochenberger (editors), *Handbook on MetaHeuristics.*

[20] Resende, G.C.M. and González Velarde, J.L. (2003): "GRASP: Procedimientos de búsquedas miopes aleatorizados y adaptativos". Revista Iberoamericana de Inteligencia Artificial, Vol. 19(2), pp. 61-76.

Trading System Based on Support Vector Machines in the S&P500 Index

R. Rosillo[1], J. Giner[2], D. De la fuente[1] and R. Pino[1]
[1]Business Management, University of Oviedo, Gijón, Asturias, Spain
[2]Finances and Economics, University of La Laguna, Santa Cruz de Tenerife, Tenerife, Spain

Abstract – *The aim of this paper is to develop a trading system based on Support Vector Machines (SVM) in order to use it in the S&P500 index. The data covers the period between 03/01/2000 and 30/12/2011. The inputs of the SVM are different forecasting algorithms: Relative Strength Index (RSI), Moving Average Convergence Divergence (MACD), Momentum, Bollinger Bands and the Chicago Board Options Exchange Volatility Index (VIX). A SVM Classifier has been used in order to develop the trading system with a weekly forecast. The output of the SVM is the decision making for investors. The trading system works better in bearish movement of the S&P500 than bullish movement of the S&P500.*

Keywords: Quantitative analysis, SVM, trading system.

1 Introduction

Trading systems are being extremely used in stock markets. Nowadays, there are a lot of Hedge Funds that are using artificial intelligence in order to forecast the stock markets and chose the best decision.

The aim of this study is to develop a trading system based on SVM. SVMs are being used in a lot of studies of researchers with very promising results. Technical trading algorithms are used in this article, such as RSI, MACD, Momentum and Bollinger Bands. It is also used the VIX. The VIX is really relevant in this study because has a negative correlation with S&P500 index and this circumstance makes better the results of the SVM.

The trading system helps investor in their decision making. The trading system output is the movement of the market (up or down) for the next week. The market trend is forecasted by the SVM algorithm.

The rest of the paper is structured as follows. In Section 2, the state of the art to Bollinger Bands, RSI, MACD, VIX and SVM is presented. Section 3 explains the kernel of the trading system. Section 4 shows the results of the trading system. Finally, Section 5 provides some concluding remarks.

2 The state of the art

The rules of the different algorithms are presented in this section.

2.1 Bollinger Bands

The Bollinger Bands were created by John Bollinger. A complete explanation of this algorithm can be seen in [1]. In the following lines, a brief explanation is shown.

As it is described in [2], Bollinger Bands consist of a set of three curves drawn in relation to securities prices. The middle band is a measure of the intermediate-term trend, usually a weighted moving average or a simple moving average, that serves as the base for the upper and lower bands. The interval between the upper and lower bands and the middle band is determined by volatility. Because the standard deviation is a measure of volatility, Bollinger Bands adjust themselves to the market conditions.

The stock price is overbought if it is situated at the upper band. The stock price is oversold if it is situated at the lower band. The Bollinger Bands definition is described below:

Middle Bollinger Band = SMA(20days) (1)

Upper Bollinger Band = SMA(20days) + SD(20days)*0.9974

Lower Bollinger Band = SMA(20days) - SD(20days)*0.9974

Where SMA is Simple Moving Average and SD is Standard Deviation.

2.2 RSI

The RSI is an oscillator that shows the strength or speed of the asset price by means of the comparison of the individual upward or downward movements of the consecutive closing prices.

It was designed by J. Welles Wilder Jr. [3]. A brief explanation of this indicator is shown below as it can be seen in [4]. If more details are needed it can be seen in J. Welles Wilder Jr. [3].

For each day, an upward change (U) or downward change (D) is calculated. "Down days" are characterised by the daily close being lower than the close of previous day.

U = closet - closet-1

D = 0

"Up days" are characterised by the daily close being higher than the close of previous day.

U = 0

D = closet - closet-1

$$RS = \frac{EMA[N]\_of\_U}{EMA[N]\_of\_D} \tag{2}$$

$$RSI = 100 - 100\frac{1}{1+RS}$$

where RSI_t is the Relative Strength Index at time t.

The 14-day RSI, a popular length of time utilized by traders, is also applied in this study. The RSI ranges from 0 to 100 however the range has been normalized between -1 and +1 in order to place it in the SVM.

2.3 MACD

The MACD is designed mainly to identify trend changes. As it is described in [4], it is constructed based on moving averages and is calculated by subtracting a longer exponential moving average (EMA) from a shorter EMA. The MACD is shown below:

$$MACD\ (n) = \sum_{i=1}^{n} EMA_k(i) - \sum_{i=1}^{n} EMA_d(i) \tag{3}$$

Where k=12 and d=26 [8]

$$EMA_n(i) = \alpha * p(i) + (1-\alpha) * EMA_n(i-1)$$

$$\alpha = \frac{2}{1+n}$$

Where n is number of days and p(i) is asset price on i^{th} day.

In this article, 12 and 26-day EMAs are selected, which are commonly used time spans in order to calculate MACD.

The range of MACD has been normalized between -1 and +1 in order to use it in the SVM.

2.4 Momentum

The Momentum is and indicator that measures the strength of the tendency of an index or a company, and it expresses the percentage variation of the price in a concrete period of time. As it is describes in [9], the Momentum is represented by a difference that is showed below:

$$M = C - C_n \tag{4}$$

where M is the Momentum, C is the last price quoted and C_n is the previous price quoted in n sessions which we take as a reference. This variable n is a number to be optimized in each title, but we take the value 12 as a reference because it is the standard. The Momentum study the speed of the movement of the price quotes related to the previous sessions and in most cases when the price quote is still upwards or downwards, the Momentum anticipates and turns, making the next change of tendency.

If the Momentum value is transferred to a chart, a line that oscillated around a neutral line (zero) will be obtained. A purchase order is generated by the Momentum if Momentum(n) is greater than 0 and Momentum(n-1) is less than or equal to 0. A sell order is generated by the Momentum if Momentum(n) is less than 0 and Momentum(n-1) is greater than or equal to 0.

2.5 VIX

CBOE Volatility Index (VIX) is a key measure of market expectations of near-term volatility based in the informational content of the SP&500 index option prices.

The VIX calculation method is an average of weighted prices of out-the-money puts and calls options on the S&P500 index.

Volatility index has several characteristics that make it interesting to use in order to forecast stock markets. It grows when uncertainty and risks increase. During falling markets, the VIX rises, reflecting increasing market fear. Volatility index reverts to the mean after high volatility situations and after low volatility situations such us interest rates. Rising markets usually the VIX goes down, reflecting a reduction of fear. So VIX is negatively correlated with stock or index level, and usually stays high after large downward moves in the market.

2.6 SVM

SVMs were originally developed by Vapnik [5]. SVMs are a specific learning algorithms characterized by the

capacity control of the decision function and the use of kernel functions [6]. It is very important the correct selection of the kernel function.

A brief explanation is described in [4].

The methods based on kernel functions suggest that instead of attaching to each element of the input domain represented by

$$\Phi : X \rightarrow F$$

a kernel function

$$K : X \times X \rightarrow R$$

is used to calculate the similarity of each pair of objects in the input set, an example is illustrated in Figure 1 [7].

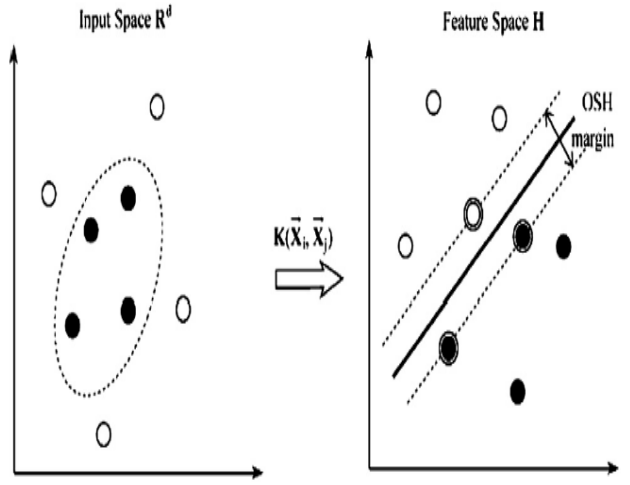

Fig. 1: An example of how a kernel function works

The biggest difference between SVMs and other more traditional methods of learning is that SVMs do not focus on an optimization protocol that makes few errors like other techniques. SVMs try to make forecasts in which the user can be very confident that the results will be correct, although it can have a lot of errors for a specific period.

Traditionally, most learning algorithms have focused on minimizing errors generated by the model. They are based on what is called the principle of Empirical Risk Minimization (ERM). The focus of SVM is different. It does not seek to reduce the empirical risk of making just a few mistakes, but pretends to build reliable models. This principle is called Structural Risk Minimization. The SVM searches a structural model that has little risk of making mistakes with future data.

The main idea of SVMs is to construct a hyperplane as the decision surface such that the margin of separation between positive and negative examples is maximized [8]; it is called the Optimum Separation Hyperplane (OSH), as shown in Figure 1.

3 Trading rule

The trading rule is created by the SVM. The inputs of the SVM are VIX, VIX-1, VIX-2, RSI, RSI-1, RSI-2, MACD, MACD-1, MACD-2, Middle Bollinger Band, Upper Bollinger Band, Lower Bollinger Band, Momentum, Momentum-1, Momentum-2 and the daily return.

The Heavy Tailed Radial Basis Function has been chosen as kernel of the SVM. The C parameter has been tested and the best value for the trading rule is 10. The SVM has been used in Classification way.

The training period has been designed with 249 days and the next day is tested by the SVM in order to know if the result is a good decision or not. The total of data for each experiment is 250 days, very similar to one business year. The trading strategy relies on a weekly prediction of the S&P 500 index price move. A weekly forecast was selected as the expected price move, up or down, over a week is more significant.

The only problem that has been detected is the situation when the SVM is being trained and it does not exit data to compare in order to make the decision to buy or sell. This situation happens for the last 5 days of the training period. In this way, the study is more real. In order to fix this, we compare the 5 days with a simple moving average of the 5 days.

The design of the trading rule is described below:

The SVM analyses the inputs classified in a purchase situation or a sell situation. After that, the SVM tries to separate the different prices of the S&P 500 in two classes knowing the inputs. The SVM uses the kernel function Heavy Tailed Radial Basis Function (HTRBF) in order to make the forecasting. The parameter C of the SVM is tested in several tests and its optimal value is 10. Finally, the SVM predicts the upward or downward movement for the following week and the intensity of that movement.

The outputs of the SVM are the up or down movements, expected for the following week of S&P 500, and its degree of set membership.

4 Results

The results of the trading rule appear in table 1.

As it can be seen in table 1, different indicators have been analysed.

Different ratios have been calculated in order to compare the two strategies.

Annualized return:

$$R^A = 250 * \frac{1}{n}\sum_{i=1}^{n} r_i \tag{6}$$

Standard deviation:

$$\sigma^A = \sqrt{250}\sqrt{\frac{1}{n-1}\sum_{i=1}^{n}(r_i - \bar{r})^2} \tag{7}$$

Sharpe ratio:

$$SR = \frac{R^A}{\sigma^A} \tag{8}$$

Maximum Drawdown calculated in S&P 500 points:

$$MDD = \min_{t=1,\ldots,n}\left(F_t - \max_{t=1,\ldots,t}(F_t)\right) \tag{9}$$

where Ft is the accumulated fund with each different strategy.

Table 1. Yearly results of the trading rule (Boll) and Buy&Hold strategy.

	SP Points		R		σ		SR		MDD (Points)	
Year	Boll	BH	Boll	BH	Boll	BH	Boll	BH	Boll	BH
2000	**311**	-707	**0.043**	-0.104	**0.078**	0.092	**0.547**	-1.126	**720**	1129
2001	**92**	-844	**0.014**	-0.139	**0.074**	0.097	**0.190**	-1.434	**515**	1859
2002	**359**	-1344	**0.059**	-0.260	**0.070**	0.107	**0.855**	-2.427	**421**	1853
2003	-112	**1104**	-0.025	**0.214**	**0.061**	0.068	-0.403	**3.147**	**428**	568
2004	-357	**536**	-0.065	**0.091**	**0.042**	0.046	-1.565	**1.952**	**415**	421
2005	188	**229**	0.031	**0.037**	**0.037**	0.042	0.838	**0.897**	**196**	349
2006	690	**811**	0.102	**0.119**	**0.036**	0.040	2.831	**2.955**	**212**	412
2007	**438**	320	**0.060**	0.044	**0.053**	0.062	**1.128**	0.716	**364**	664
2008	**1431**	-3013	**0.181**	-0.544	**0.081**	0.148	**2.242**	-3.667	**312**	3300
2009	-103	**1218**	-0.022	**0.233**	**0.103**	0.110	-0.218	**2.118**	**843**	1159
2010	42	**669**	0.007	**0.110**	**0.070**	0.076	0.104	**1.450**	**421**	901
2011	**1470**	10	**0.206**	0.002	**0.079**	0.095	**2.600**	0.016	**529**	1139
00-05	**482**	-1026	**0.011**	-0.026	**0.052**	0.083	**0.209**	-0.310	**893**	3630
06-11	**3969**	15	**0.080**	0.000	**0.055**	0.094	**1.453**	0.004	**843**	4345
00-11	**4450**	-1011	**0.040**	-0.013	**0.050**	0.092	**0.804**	-0.139	**893**	4345

The bold numbers mean the trading rule that is better for each indicator. When the S&P 500 is bullish our trading rule beats the Buy&Hold strategy.

In figure 2, a chart of Buy&Hold strategy and our trading system is shown. The upper line is our trading system and the lower line is the Buy&Hold strategy. The x-axe shows the dates and the y-axe shows the accumulative S&P 500 points that have been achieved by each strategy.

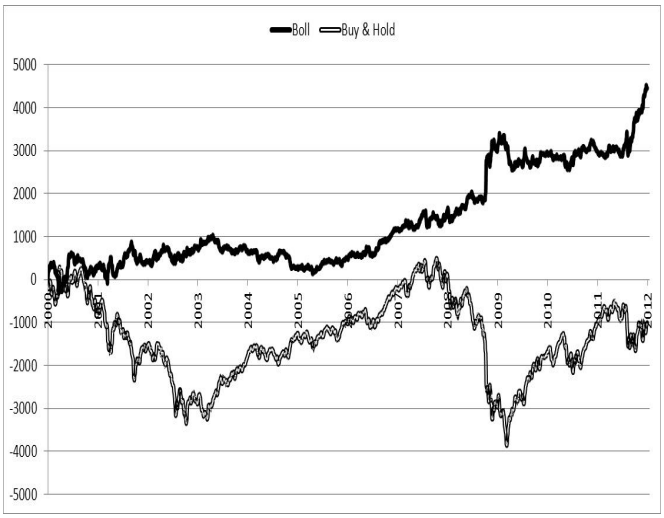

Fig. 2: The chart of the two strategies.

As it can be seen in figure 2, the best trading strategy is Boll which is our trading system.

5 Conclusions

The trading system works better in bearish movements of the S&P500 than bullish movements of the S&P500.

6 Acknowledgment

Financial support given by the Government of the Principality of Asturias is gratefully acknowledged.

7 References

[1] J. Bollinger, Bollinger on Bollinger Bands, McGraw Hill, New York, 2002.

[2] W. Liu, X. Huang, W. Zheng, Black-Scholes model and Bollinger bands, Physica A 371 (2) (2006) 565-571.

[3] Welles Wilder, J. Jr. (1978) New Concepts in Technical Trading Systems, Greensboro, N.C.: Hunter Publishing Company.

[4] Dunis, CL., Rosillo, R., De la Fuente, D. and Pino, R. (2012). Forecasting IBEX-35 moves using support vector machines. Neural Computing and Applications. DOI: 10.1007/s00521-012-0821-9

[5] Vapnik, V. N. (1998) Statistical Learning Theory. New York. Wiley.

[6] Vapnik, V. N. (1999) An overview of statistical learning theory, IEEE Transactions of neural networks, 10, 988-999.

[7] Huang, S. and Sun, Z. (2001) Support vector machine approach for protein subcellular localization prediction. Bioinformatics, 17, 721-728.

[8] Xu, X., Zhou, C. and Wang, Z. (2009) Credit scoring algorithm based on link analysis ranking with support vector machine. Expert Systems with Applications, 36, 2625–2632.

[9] Rosillo, R., De la Fuente, D. and Brugos, J.A.L. (2013): Technical analysis and the Spanish stock Exchange: testing the RSI, MACD, Momentum and Stochastic rules using Spanish market companies. Applied Economics, 45, 1541-1550.

Vehicle Routing Optimization Using a Visual Web Model in a Logistical Application

Ara I.[1], **Lena F.**[1], **Alonso M.**[1], **De la Fuente D.**[2]
[1]Department Business Administration, University of Cantabria, Santander, Spain
[2]Department Business Administration, University of Oviedo, Oviedo, Spain

Abstract – *The search for flexibility in accessing logistics information is implemented in a Web solution to provide some agility to a distribution management problem. The aim is to provide the user of the information with a simple, attractive, graphic visualization in real time, making the logistics information readily available and easily accessible.*

The Web application manages the existence of different user roles with different permissions for accessing the application and also enables access through mobile devices and next generation technologies.

This solution is adopted to follow the criteria for access from any location that has an internet connection, regardless of the platform on which the application runs.

Keywords: Vehicule routing, web model, google maps, mobile devices.

1 Introduction

The distribution sector in Europe grew by 11.7% in the period 2005 to 2010, as indicated in the trading records according to the "Eurostat" balance of payments. A major challenge for companies in the management of the Supply Chain is to achieve "agility", that is to make the chain flexible enough to adapt quickly to changes in its environment.

The importance of the time variable as a competitive element in the supply chain has been recognized for many years [1]. The ability to meet the demands of the customers through ever shorter delivery times, and to ensure that supply can be synchronized to meet the peaks and valleys in demand, is critical today. The increased sensitivity to the needs of the market requires a faster response that goes hand in hand with a greater level of maneuverability, incorporating the concept of "agility".

Agility is the capacity of the company, taking in the organizational structures, information systems, logistics processes and in particular, ways of thinking. The web application discussed in this paper proposes a flexible and agile solution for distribution management in a logistics company.

2 System

In any software application, it is essential to define the objectives to be met, considering previously and in great detail the functions and features that the application requires.

This initial approach will take into account the definition of the methodology to be applied, the tools used, and, finally, the structure of the application developed.

2.1 Methodology

In order to develop a system, it is considered essential to control each stage through the use of an appropriate methodology to structure, plan and control each of these stages. In developing this application, a methodology based on the Rational Unified Process (RUP) was used [2].

This RUP is the standard methodology most widely used in analysis, implementation and documentation in systems like the one developed here.

The RUP approach is based on defining differential life cycles established in stages over series of cyclical iterations as shown in [Fig.1].

The different stages of the RUP methodology followed in the development of the system are described below [3]:

1. Business Modeling and Requirements: Specification both of the products to be obtained and the existing restrictions.

2. Analysis, Design and Implementation: Study of the causes of the possible threats and probable undesired events.

3. Test and Deployment: Implementation of the tasks of the activity itself and testing of these. Analysis of alternatives and risk identification.

4. Evaluation: Revision of work performed and decision-taking.

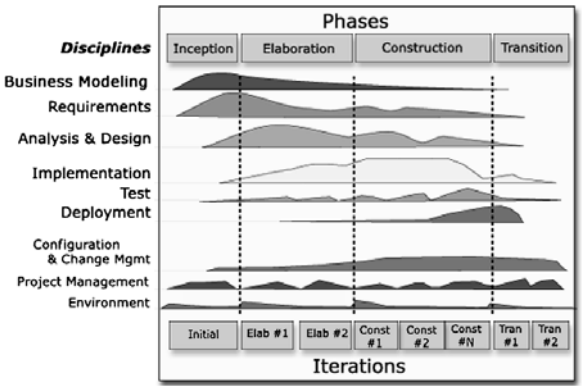

Fig. 1 Phases of RUP

2.2 Tools

As this is a web-based system, the tools chosen are the most widely used in this type of environments in their latest versions, so that many of the problems associated with their obsolescence have been eliminated:

- HTML5 (HyperText Markup Language): is the language in which websites are built. The current version HTML4 dates from 1999, meaning that the program code has not been reviewed for over 10 years. Solutions were provided, such as Flash for interactivity, but none of these were open source and compatible as HTML5. [4][5]

- CSS3 (Cascade Style Sheets): is the language used to shape the websites. CSS2 was tweaked in 2007 so designers have to do tricks to give websites the desired look, until CSS3 arrives. [6][7]

- Javascript: The programming language that allows the user to make changes to a website without having to reload each time he changes something. The code is reviewed regularly, with new versions of each browser released every month. Characterizing Insecure JavaScript Practices on the Web [8]

- PHP: Server-side language originally designed for web development to produce dynamic web pages. It is always embedded into an HTML source document. [9]

- MySQL: Most used relational database management system that runs as a server providing multi-user access to a number of databases. It runs under the terms of the GNU General Public License. [10][11]

- Google Maps: Web mapping service that powers many map-based services. The API is a free service which has the possibility to embed maps in HTML. [12]

2.3 Structure

The typical structure of a web-based technology application is defined by three differentiated layers [Fig.2]:

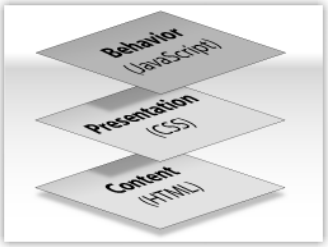

Fig. 2 Structure of a web

1. Content: The content or structure layer is what users will see when they come to the web application. Content can consist of text or images and includes the pointers that readers need to navigate around the application.

2. Presentation or Style: The style or presentation layer is how the document will look to users. This layer is defined by the CSS or styles that indicate how the document should be displayed and in what media types.

3. Behaviour: The behavior layer is the layer of a Web application that helps user interaction. In our case, as jQuery and PHP are used, it is JavaScript and PHP that make the page take actions when user clicks.

3 Web model application

The next step required after defining the system structure is the design and development of the application [13] which is divided into several levels of definition depending on the stage of development: User roles, functions and adaptation to mobile terminals.

3.1 User roles

The application is based on the implementation of a system of access with different users [14]. It was considered appropriate, after analyzing and evaluating the requirements of the user, to establish four types of access:

- Administrator: Actor with responsibility for administering the system in its entirety. Receives all the privileges of access and manipulation within the application and is considered a user with the knowledge and skills needed to manage the application.

- Transport Coordinator: Actor who controls and manages the transport fleets, with access to medium-level functions that do not require any knowledge or skills for their management, without jeopardizing the integrity of the system. This is, then, a user with certain limited privileges.

- Car Sales Manager: Has limited access to the information about his order. Will not have access to the rest of the application and, therefore, will also be a limited user so as not to be able to jeopardize the integrity of the application, being limited to consulting and handling the information that affects his area.

- Client: Actor with fewer privileges among the set of users [Fig.3]. His options will be limited to consulting data on the vehicles assigned to him.

3.2 Functions

After defining in detail the set of users and their roles, it is necessary now to define the functions available in the application.

- Index: The beginning of the application contains a brief explanation of the whole project.

- How it works: Explaining the different steps of the application.

- Upload a file: Data upload is the first step in the application. The entire process is automatic, from choosing the file to transferring it to a database. It includes the double conversion: from Excel to HTML format and from HTML to SQL format.

- Show data: Two ways to view the data: directly from the uploaded file or by querying the database from the application.

- View fleet: The data represented graphically. The first page shows the fleet with all available transport. By clicking on a truck, we access its properties. The vehicle page itself has three tabs: first the routes with full details, second the cars it carries and the final tab with full details of the transport.

- Manage Users: Section for managing the different user roles. It only shows the information according to the user that is currently viewing the page, so that everything is secure and private.

Having defined above the user roles, the access privileges are as follows [Fig.3]:

	index	How	Upload	Data	Fleet	Car	Users
Admin	T	T	T	T	T	T	T
Transport	T	F	F	T	T	T	F
Manager	T	F	F	T*	T*	T	T*
Client	T	F	F	F	T*	T	F

Fig. 3 Table of permits

T (True): The user can access to the section

F (False): The user cannot access the section.

T* (True*): The user can access to the section, but with limitations. e.g. Only its transport.

The permits are basic requirements of access to the application, an example of classes with UML. [15]

3.3 Adaptation to mobile terminals

Given the widespread and increasing use of mobile devices with broadband connection and smartphones, it was considered worthwhile developing the application with the versatility required for its use from this type of devices, adapting both the design and content for maximum operability [Fig.4]. Thanks to the appropriate selection of the technologies used and the advanced development of these, the application has been optimally adapted without too much difficulty.

Fig. 4 Application in terminals iOs and Android

The system detects on time and automatically any user accessing the application through the use of a mobile terminal and redirects him to an environment optimized for this type of devices, much lighter and less demanding on bandwidth, generating a new interface adapted to the size of the terminal screen.

The adaptation of developments to this type of terminals is a real challenge that is becoming a trend nowadays thanks to the large and ever-increasing number of users that these devices now have [16].

Optimization was performed for two types of mobile terminal operating systems:

- Apple iOs: Terminals supported: Apple iPod Touch, Apple iPad, Apple iPhone EDGE, 3G, 3GS, 4, 4S for versions iOs 4.0 and onwards.

- Google Android: Terminals from version 2.2 Froyo up to 4.0 Ice Cream Sandwich.

4 Google Maps

the content, is View Fleet. This section includes a geolocalization both of the departure point and of the arrival point of the transport and all the stops to be made during the journey.

The Google API (Application Programing Interface) is based on the direct implementation of the Travelling Salesman algorithm (Travelling Salesman Problem) [17] [18] which, roughly, is described as a Branch-and-cut algorithm [19] [20].

In this case, the implementation is developed for the study of the shortest path as a reference to the optimum transfer between two locations using the shortest distance traveled [21][22].

The section is divided into three parts

The first represents the visual route by means of a map showing the different points where the various stops will be made [Fig.5]:

Fig. 5 Visual route by means of map

The second represents the summary of the routes followed by the transport. The figure below shows a lorry covering two routes with a stop in the middle of them [Fig.6]:

Fig. 6 Summary of routes

Finally, element indicates, using points, the directions to be followed to reach the different destinations of the transport [Fig.7]:

Fig. 7 Directions using points

5 Conclusions

A flexible solution for providing access to information logistics, incorporating agility in the distribution management has been proposed for supply chain management.

The proposed solution takes the form of a Web application that incorporates a diversity of Open Source tools with the aim of providing the different users with interactive and visual access to the distribution information of interest to them. The application implements a system of access to information through the necessary security controls, which allows access from any geographic location with an Internet connection and from any platform recognized by the application.

6 References

[1] Stalk Jr, G. (1988): Time – The next source of competitive advantage, Harvard Business Review, July - August 1988, pp.41-53

[2] P. Kruchten, "'Tutorial: Introduction to the rational unified process," Proceedings - International Conference on Software Engineering, pp. 703.

[3] S. Pilemalm, P.-. Lindell, N. Hallberg and H. Eriksson, "'Integrating the Rational Unified Process and participatory design for development of socio-technical systems: a user participative approach," Des Stud, vol. 28, no. 3, pp. 263-288.

[4] S. Aghaee and C. Pautasso, "'Mashup development with HTML5," ACM International Conference Proceeding Series.

[5] W3.org (2012), HTML5 A Vocabulary and associated APIs for HTML and XHTML. W3C Working Draft. [Electronic version]. Retrieved 1/4/2012, from http://www.w3.org/TR/html5/

[6] W3.org (2012), Cascading Style Sheets. [Electronic version]. Retrieved 1/4/2012, from http://www.w3.org/Style/CSS/

[7] W3.org (2011), Cascading Style Sheets (CSS) Snapshort 2012. [Electronic version]. Retrieved 1/4/2010, from http://www.w3.org/TR/css-2010/

[8] Chuan Yue and Haining Wang, "'Characterizing Insecure JavaScript Practices on the Web," Track: Web Engineering / Session: Client Side Web Engineering, WWW 2009 Madrid, pp. 961-970.

[9] Php.net (2012), PHP: Hypertext Preprocessor. [Electronic version]. Retrieved 1/4/2012, from http://www.php.net

[10] X. Yu and C. Yi, "'Design and implementation of the website based on PHP & MYSQL," 2010 International Conference on E-Product E-Service and E-Entertainment, ICEEE2010.

[11] MySQL (2012), MySQL. The world's most popular open source database. [Electronic version]. Retrieved 1/4/2012, from http://www.mysql.com

[12] Google Maps JavaScript API. Maps JavaScript API v3 [Electronic version]. Retrieved 1/4/2012, from https://developers.google.com/maps

[13] A. Taivalsaari and T. Mikkonen, "'The web as an application platform: The Saga continues," Proceedings - 37th EUROMICRO Conference on Software Engineering and Advanced Applications, SEAA 2011, pp. 170-174.

[14] P. Zhang, F. Wang and P. Lin, "'Design and implementation of WebGIS & Web Service-Based logistic information system," 2008 International Seminar on Business and Information Management, ISBIM 2008, vol. 2, pp. 108-111.

[15] G.L. Guan, S.S. Kim, O.K. Huat, L.C. Kian, E.P.B. Sam, A.T.S. Kee, L.C. Tiong and E.C. Prakash, "'Towards support for a logistics management system on the World Wide Web," IEEE Region 10 Annual International Conference, Proceedings/TENCON, vol. 1, pp. I-373-I-376.

[16] N. Radio, Y. Zhang, M. Tatipamula and V.K. Madisetti, "'Next-generation applications on cellular networks: Trends, challenges, and solutions," Proc IEEE, vol. 100, no. 4, pp. 841-854.

[17] C. Fu, Y. Wang, Y. Xu and Q. Li, "'The logistics network system based on the google maps API," 2010 International Conference on Logistics Systems and Intelligent Management, ICLSIM 2010, vol. 3, pp. 1486-1489.

[18] D. Vigo, "'Heuristic algorithm for the asymmetric capacitated vehicle routing problem," Eur.J.Oper.Res., vol. 89, no. 1, pp. 108-126.

[19] H. Hernández-Pérez and J.-. Salazar-González, "'A branch-and-cut algorithm for a traveling salesman problem with pickup and delivery," Discrete Applied Mathematics, vol. 145, no. 1 SPEC. ISS., pp. 126-139.

[20] M.L. Yiu, Y. Lin and K. Mouratidis, "'Efficient verification of shortest path search via authenticated hints," Proceedings - International Conference on Data Engineering, pp. 237-248.

[21] A. Wang, Z. Jun and W. Jiang, "'Useful resources integration based on google maps," Proceedings of 2009 4th International Conference on Computer Science and Education, ICCSE 2009, pp. 1044-1047.

[22] H. Zhang, M. Li, Z. Chen, Z. Bao, Q. Huang and D. Cai, "'Land use information release system based on Google Maps API and XML," 2010 18th International Conference on Geoinformatics, Geoinformatics 2010.

Virtual Agent Oriented to e-Learning Processes

Celia G. Róspide[1], **Cristina Puente**[1]
[1] Advanced Technical Faculty of Engineering – ICAI, Comillas Pontifical University, Madrid, Spain

Abstract –*In this paper we explore the benefits that a virtual agent could provide to an e-Learning platform. The system uses Natural Language techniques as a basis, which makes it capable of elaborating a flexible answer according to the student requirements. The Software procedures to perform these task are also introduced s.*

Keywords: Virtual agent, Flexible answer, e-Learning.

1 Introduction

The arrival of a new educational model, with less theoretical lessons and more work on the student side, has in many cases caused extra work when solving problems via email or through other means.

To alleviate this problem, in this paper we present a virtual agent oriented towards educational environments. The purpose of this is to solve as many questions as possible, emulating the possible answers that a real professor could give. To do so, we have developed an architecture divided into modules in which the original query is analysed in order to understand the requirements of the student to return a suitable answer.

The construction of a chatbot able to emulate a flexible conversation is highly complex. Nowadays, the so called virtual robot has not been developed in its totality, and the 'perfect chatbot'still does not exist. For this reason, there are several enterprises with good reputations in the computer market, like IBM, working on these types of projects to improve their performance [1].

The idea of a virtual agent to answer questions is not new. An intelligent virtual agent is an entity capable of perceiving its environment and processing those perceptions in a rational way [2]. To be considered as AI systems, they have to fulfil the following characteristics [3]:

- Learn new problems and improve the range of solutions.
- Real time adaptation.
- Analysis of a situation in terms of behaviour, evaluating the possibilities of success and failure.
- Evolve through interaction with the environment.
- Manage great amounts of data in order to choose the best solution.

One of the greatest problems in the implementation of a virtual agent is the design of its 'personality', as it has to be original and intelligent. However, the behavior of an agent many times is not what is expected, especially when there are many restrictions or when the problem is not defined precisely.

Among the diversity of virtual agents, we can find the group of Intelligent Tutoring Systems (ITS). These type of agents were created in the eighties with the idea of sharing knowledge using an intelligent way to guide the student in their learning process. So a intelligent tutor can be defined as [4] " *a software system which employs AI techniques to represent knowledge, and interacts with the students to transfer it*" or as [5] "*systems to model teaching, learning, communication and knowledge domain of the specialist and the understanding of the student in that domain*".

Recent research is focused on finding an alternative to a human tutor. However, most of the tutoring systems do not acquire the expected level of rationality due to the difficulty involved with modelling human behavior, beyond the application of the most advanced programming techniques.

Taking these premises as a basis, the proposed chatbot is an ITS, which serves as support in the learning process of a student in a given subject. The system is composed of a hardware and software architecture which is explained in the following sections, as well as the interaction among the software modules that make understanding possible and the composition of a flexible answer. Finally, we will conclude with some guidelines for future work as well as some conclusions about the proposed work.

2 Bot Architecture

The platform used to develop this educational bot was a web environment. The hardware used was typical client-server architecture, where the client is a browser like Mozilla or

Explorer, and the server is an Apache with some other additions like a lexical analyzer.

The software is composed of several modules written in different programming languages (like Php, Javascript, C, Lex), which interact among themselves to understand the user's question and propose a suitable answer. The software model proposed to carry out this task is a Model-View-Controller, where the model interacts with a MySQL database to extract information, the View part is the interface, written in HTML5 plus Javascript, and the Model contains the interaction with the lexical analyzer plus the specific modules written in Php. In a graphic form, figure 1 represents the interaction of all these components:

.

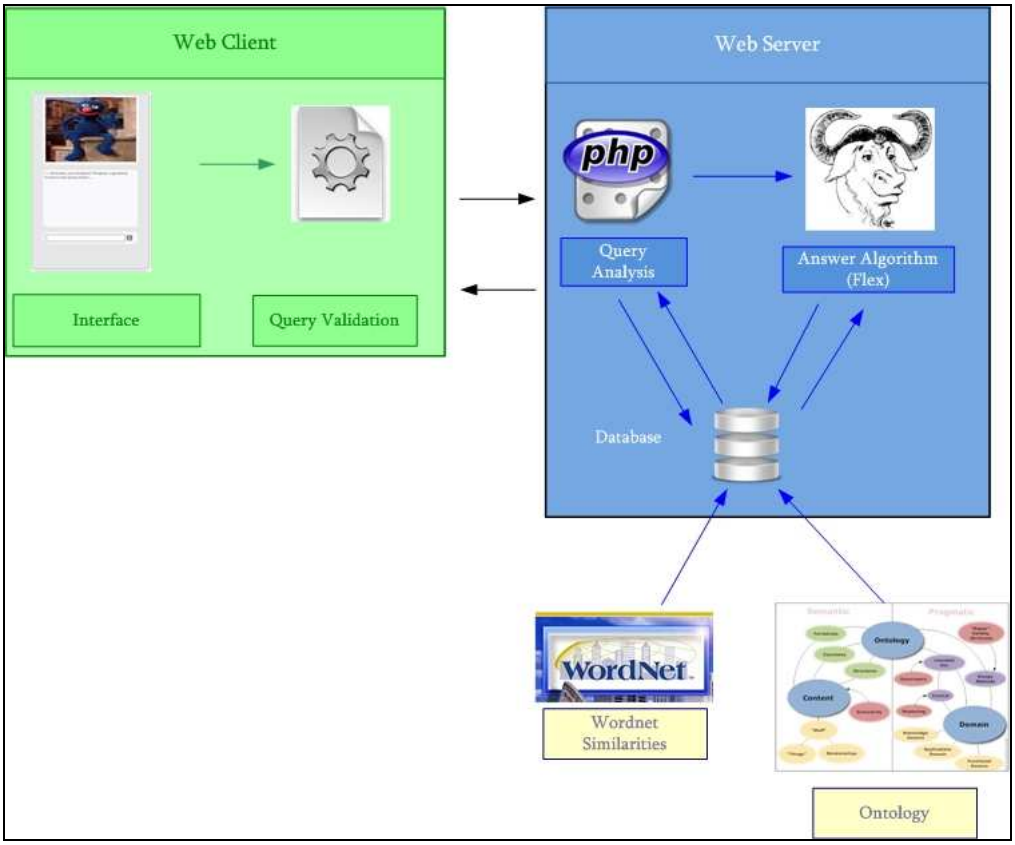

Fig. 1 Software and Hardware architecture of the bot

As seen in figure 1, the client part is composed of two parts, the interface, and another algorithm to validate the question. The interface is composed of those graphical elements which serve as input and output for information, and has three elements, an image which varies according to the answer, a text area where the dialog between user and the machine is displayed, and an input textbox where the user must write his query.

The algorithm used to validate a question was programmed using AJAX, and is in charge of sending the query to the server and waiting for an answer to be added at the end of the text area.

The web server is divided in three main parts, the query analysis module, the answer algorithm, programmed using the lexical analyzer FLEX[1], and a terminology database built through an ontology (hand-made), with the terms used in each part of the subject and the platform Wordnet Similarities[2] [6].

3 Query Analysis Module

The query analysis module is the one in charge of providing a suitable answer, and is composed of other four sub-modules: bad words, welcome, general information and complex answer (in fig. 1 represented as answer algorithm).

[1] http://www.gnu.org.
[2] wn-similarity.sourceforge.net/.

When a question is posed, the first thing to be done is to dispatch it to the appropriate module. In this way, the first module that evaluates the query is the bad words' one.

This algorithm detects if there are any bad words within the input received. If so, the user will be warned up to a maximum of three times, after which they will be expelled. To do so, we have implemented a procedure that checks the query words against a database table with a complete list of these words. The result is as seen in figure 2, where the user proposes three questions with some of these words mixed in:

Fig. 2 Example of bad words output (grey text)

If there are no bad words in the query, the input query will access the welcome module. This algorithm notices if the user is being nice or polite to it, separating the technical query (if one exists) from the welcoming greeting. In this case the answer will be a composition of answers. As in the previous case, the number of times that the user says hello to the bot is controlled, in order to focus the conversation. If the user repeats a greeting message many times, the system will encourage him to ask more specific questions, without being expelled in this case, as seen in the following figure:

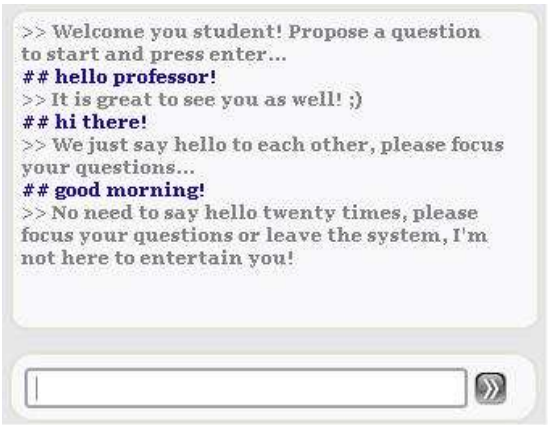

Fig. 3 Example of welcoming output (grey text)

One of the more frequent uses of a chatbot is to answer FAQs. We have included a set (through the database) of questions related to the subject such as the day of the exam, the hour, class, name of the professors and contact information, and many other useful pieces of information.

This third module, is entirely written in Php, and by matching the query keywords against those stored in the database is able to answer a wide range of questions proposed in a different way. This algorithm also evaluates the question pronouns, like how, what, when, etc., for instance, if the user begins his question with 'when', the system will know that he is asking for time. Added to the textual answer, in some cases the system has additional stored information, like schedules, etc. so this information will be displayed along with the answer in a new window:

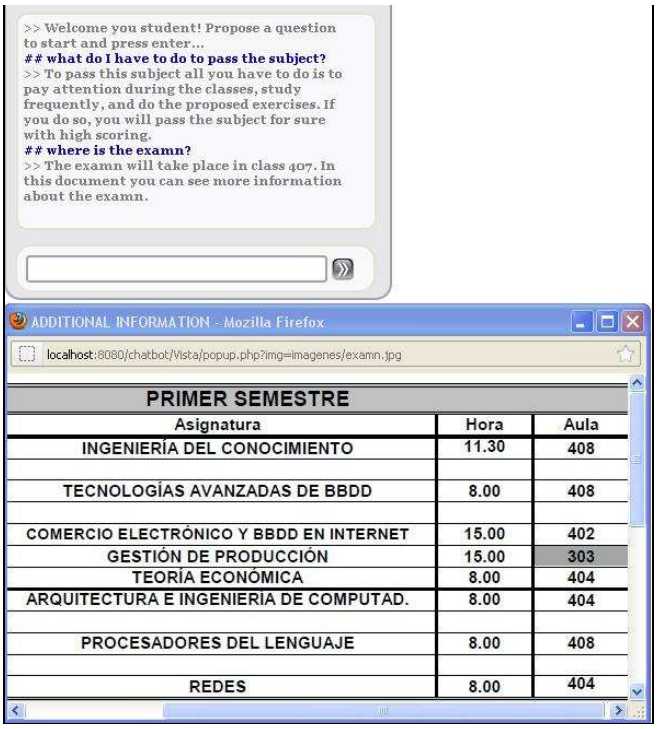

Fig. 4 Example of general information output

If the query is more specific and related to the subject's lessons, then it will be processed by a lexical analyzer, composed of an automaton which will process the input through a set of states.

4 Query Analysis Module

The query analysis algorithm was developed using the morphological analyzer FLEX plus the C programming language. This program is able to detect and locate certain lexical patterns within a text by means of an automaton.

For our specific purpose, this automaton is composed of six states which will be able to recognize:

- Concepts related to the studied subject
- Terms and keywords specifying what the user wants to know about those concepts (like definitions, how it works, and so on).
- Interrogative pronouns.
- Words and expressions commonly used to quit the system or say goodbye.
- Words and expressions used to express gratitude.
- Clauses used to lead the conversation in a friendly way.

The automaton created in FLEX has a [Pattern]-[Action] structure, so if the automaton detects any of the defined patterns, the associated action, written in C code, will be dispatched.

The defined states control the structure of the input query, so in the first place an interrogative pronoun should appear, followed by a word or set of words which will determine what the user wants to know specifically about a concept related with the subject, followed by a concept related with the subject. The query "*What is a token?*" follows this structure, but not all queries have to, for example "*How does a lexical analyzer work?*" where the concept related to the subject is not at the end of the query. To take these problems into account, we have created six states which control the possible structures of a query.

In order to ascertain the answer to the proposed question, we have classified the types of questions on the basis of their type and priority:

- Low priority: those not related with the subject's contents.
- High priority: those containing keywords or relevant patterns.
- Guiding questions: when there is not a clear answer to the proposed question, the system will answer back with another question to check if the prediction was correct. Otherwise it will encourage the student to propose the question in a different way.

This way, if the input is correct, the algorithm will recognize the type of question and a set of keywords, and will look up the related information in the database .

The database algorithm will compare the type of question first, and with the possible results will match the input keywords with those contained in each record. The 'priority' of the matches will be taken ; so many times a record that has two keywords with high priority matched will be selected instead of another with three keywords with lower priority. To do so, we have used a scoring system. The record that after the matching obtains the highest number of points is selected and its answer displayed. If this record has addition information associated, it will be displayed as well, as in the following example, where the user asks "What is a token?" and the bot gives him the definition along with the slide that contains more information related:

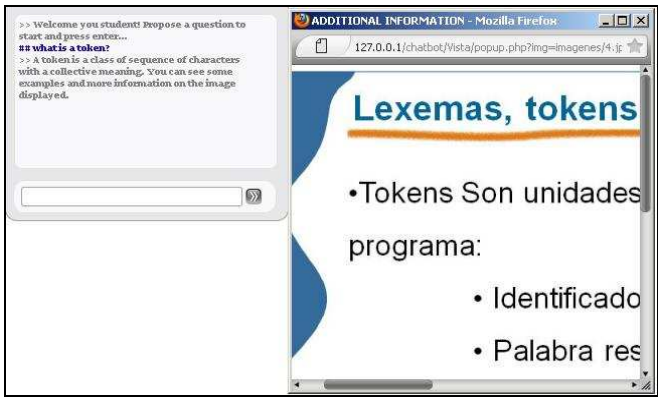

Fig. 5 Example of general information output

Many times the users are not specific with their questions, so the system will try to guess what they mean to say. The prediction algorithm is in charge of this part. The function of this process is to add flexibility and realism to the communication. So we have implemented the following considerations:

- Create the illusion of listening by introducing substrings of the input query in the answer.
- Admit its ignorance about certain issues.
- Control the date (if it is close to the exam date) to offer review exercises, for example, or make comments about how late it is, or say "*Good night*" when leaving the system.
- Redirect the conversation when the user asks for questions which have little or nothing to do with the subject.

- Introduce friendly substring in the answer like "*friend*", "*colleague*", "*dude*", etc.

- Calculate the length of the conversation, and if it is too short, encourage him to solve more problems.

Here is an example of conversation using the prediction module:

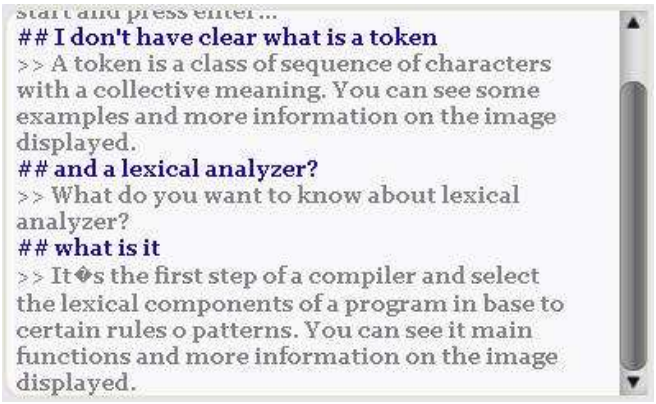

Fig. 6 Example of the prediction module

5 Conclusions

This work has introduced a prototype of an intelligent virtual agent able to answer questions related to an academic subject. Using typical client-server architecture and several modules to analyze questions and answers, the system is able to dispatch, in the majority of cases, a suitable answer for the proposed question.

There are some lines that could be improved upon in future work, like proposing exercises to the student based upon their scores, or creating a specific study plan for every student to be controlled through the bot.

6 Acknoledgements

This work has been partially supported by TIN2010-20395 FIDELIO project, MEC-FEDER, Spain and PEIC09-0196-3018 SCAIWEB-2 excellence project, JCCM, Spain.

7 References

[1] R. Russell. Language Use, Personality and True Conversational Interfaces. Artificial Intelligence and Computer Science. University of Edinburgh, 2002.

[2] B. Hayes-Roth. An Architecture for Adaptive Intelligent Systems, Artificial Intelligence, Vol. 72, pp. 329-365, Elsevier, 1995.

[3] N. Kasabov. Advanced Neuro-Fuzzy Engineering for Building Intelligent Adaptive Information Systems in Fuzzy Systems Design: Social and Engineering Applications. L.Reznik, V.Dimitrov and J.Kacprzyk (eds) Heidelberg, Physica-Verlag, 1998.

[4] K. Vanlehn, Student Modelling. Foundations of Intelligent Tutoring Systems, pp. 55-78, Hillsdale. N.J. Lawrence Erlbaum Associates, 1998.

[5] B. Wolf , Context Dependent Planning in a Machine Tutor. Ph.D. Dissertation, University of Massachusetts, Amherst, Massachusetts, 1984.

[6] T.Pedersen, WordNet::Similarity - Measuring the Relatedness of Concepts. Proceedings of the Nineteenth National Conference on Artificial Intelligence (AAAI-04), pp. 1024-1025, July 25-29, San Jose CA, 2004.

An Ontology-based Recommender System for Health Information Management

Francisco P. Romero[1], **Mateus Ferreira-Satler**[2], **Jose A. Olivas**[1], **and Jesus Serrano-Guerrero**[1]
[1]Dept. Information Technologies and Systems, University of Castilla La Mancha, Ciudad Real,Spain
[2]Dept. Computer Science / Unviersidade Federal de Juiz de Fora, Juiz de Fora, MG, Brazil

Abstract— *This paper shows how some fuzzy logic techniques applied to a recommender engine can be used in a Electronic Medical Records Repository. A Fuzzy Linguistic model based on three dimensions: intrinsic, contextual, personal is proposed. The contextual and personal dimensions are modeled using domain ontologies and a automatically built fuzzy ontology, respectively. The experiment results indicate that the presented approach is useful and warrants further research in recommending and retrieval information.*

Keywords: Recommender Systems, Fuzzy Ontology, healthcare Information Management, Fuzzy Logic

1. Introduction

Nowadays, new ways of managing and accessing to health care information are continuously appearing. Electronical Medical Records (EMRs) have the potential to make data about health care available to clinicians, researchers and students in different medical contexts and applications. Hundreds of Medical Records are stored and interchanged in Medical Records Repositories. One of the biggest challenges faced by healthcare systems is the growth of information accessible, i.e. the amount of information accessible has grown enormously and as a result health care professionals are currently burdened with more and more data, which unfortunately has not always the adequate levels of quality, making that their work cannot always be as successful as expected. A way of alleviating this situation consists in limiting somehow the number of Medical Records in a repository that are displayed for users. This can be done by means of filtering or recommendation techniques being capable to be adapted to different requirements for each one of the users. Therefore, the need of an efficient and reliable recommendation process is critical in order to provide a more personalized and tailored knowledge to clinicians, researchers and students..

In this paper, we propose the integration of the analysis of different dimensions in a recommendation system. This recommendation engine could be a useful tool to support Health Information Management in a Health Information and Management Systems, in order to improve information filtering and retrieval, as well as their classification. The analyzed dimensions in this proposal are the following: intrinsic (is the EMR complete or accurate?), contextual (is the EMR adequate according to the user context?) and personal (is the EMR adequate according to the user preferences?)

The intrinsic dimension is modeled using measures as completeness and timeliness; the contextual dimension is modeled using a domain ontology, for example, Medical Subject Headings (MeSH) [1] and the personal dimension is modeled by a fuzzy ontology automatically built from the EMR's provided or selected by the user [1]. Within this context, and taking advantage of Fuzzy Logic [2], we addressed the definition, implementation and validation of a process to construct the recommendation system. The main purpose of this work is to provide a method to describe the recommendation process as well as a linguistic model, i.e., we can only describe the whole recommendation system by using natural language.

The remainder of the work is structured as follows: Section 2 describes the background contents of this paper, i.e, recommendation systems and fuzzy ontologies. Section 3 describes the recommendation model and how the user profiles are built. In Section 4 the experiments that have been conducted to validate our proposal are explained and analyzed, and in Section 5 some conclusions and future works are pointed out.

2. Background

This section presents some concepts related to this research and proposed process. It starts describing recommendation systems, their general characteristics and their applications. Then, we discuss how the fuzzy ontologies can be used to represent user's preferences and some works about this topic.

2.1 Recommender Systems

According to [3], recommender systems are defined as systems that produce individualized recommendations as output, or have the effect of guiding the user in a personalized way to interesting or useful objects in a large space of possible options. [4] enumerate the main characteristics of recommender systems: 1) Can be applied to unstructured data and semi-structured (for example, Web documents or e-mail messages); 2) Based on user profiles, rather than

[1]http://www.geneontology.org/

users expressing their needs through consultation; 3) Manage large amounts of information; 4) Works primarily with information in text mode; 5) Its goal is to eliminate irrelevant information from the input stream. Recommendation systems share similar tasks with information filters such as removing redundant or unwanted information and reducing overload.

In recent years, there are several studies about the applications of the recommender systems in healthcare environments, for example, in [5] a recommendation system is presented with the aim of making health events accessible in personalized way. The proposed system uses a set of "signal definitions", i.e., a predefined structured queries with parameters related to kinds of health threats the users' interest's. The systems provides ratings according to this "signal definitions" to give recommendations. The method to compare the queries and the documets is very straight forward (tf-idf representations and cosine similarity measure) but its results are satisfactory.

On the other hand, there are some proposal that include fuzzy logic in recommendation techniques. For example, Chao et al. [8], propose a recommendation mechanism focused on teachers in a content management system. The main components of these systems are: data pre-processing, association rule mining, associative classification, sequential pattern mining and fuzzy sets. In [6] propose a recommender system multi-granular fuzzy linguistic approach, where the solution alternatives are the digital resources stored into the library, and the criteria to satisfy in the user profiles. This recommender system, allows users to provide preferences on some research resources and from this information are calculate their respective preference vectors on topics of interest. The user profile is completed with user preferences on the collaboration possibilities with other users, with the objective of creating academic communities.

2.2 Ontologies and User Preferences

Ontologies have proved to be successful in handling a machine-processable information representation. They can take the simple form of a taxonomy (i.e., knowledge encoded in a minimal hierarchical structure) or as a vocabulary with standardized machine-interpretable terminology supplemented with natural language definitions. Furthermore, ontology-based user profiles are being widely applied in context representation and application customization so that they meet user requirements.

FCOU [7] is a fuzzy clustering method of ontology-based user profiles construction. The method employs fuzzy clustering techniques combined with optimization techniques and an augmented Lagrangian function to create a fuzzy clustering model for the construction of user profiles. The method allows some information to belong to several user profiles simultaneously with different degrees of accuracy, and makes it possible for a user profile to be represented by one or more ontologies.

In [8], the authors propose an approach that uses locally stored desktop documents to extract terms that will be used in query expansion for web search. Three possible techniques have been investigated. The first one proposes summarizing the entire desktop using term clustering methods. The second technique issues the original web user query on the desktop and extracts expansion keywords from the most significant sentences within the Top-30 documents selected by a scoring function. Similarly, the third technique suggests selecting query expansion keywords from the most dispersive lexical compounds within the Top-30 documents returned to the user's initial web query. Some experiments have also been performed to compare the proposed method with a regular Google web search.

Another approach to represent user preferences is by a domain ontology. This domain user preferences are called "user context" in this work. Lau et al [9] present a text mining methodology for the automatic discovery of fuzzy domain ontology from a collection of on line messages posted to blogs, emails, chat rooms, web pages, and so on. The collection of messages is treated as a textual corpus. The method consists of a document parsing (stop word removal, part-of-speech tagging, and entity tagging and stemming), concept extraction (pattern filtering, text windowing, and mutual information computation), dimensionality reduction (concept pruning and term space reduction), fuzzy relation extraction (computing fuzzy relation membership) and fuzzy taxonomy extraction (taxonomy generation and taxonomy pruning).

On the other hand, [10] show how a fuzzy ontology-based approach can improve semantic documents retrieval. The proposal is illustrated using an information retrieval algorithm based on an object-fuzzy concept network.

3. Fuzzy-Based Recommender System Approach

In this section we present a new fuzzy recommender system based on a matching process developed between user preferences and the EMR representation. For this purpose, we take into account the following parameters that can be assessed in the system: the intrinsic quality of the EMR, the compatibility between the EMR and the user context and the EMR and user preferences.

This system is applied to advise EMR repository users on the best EMR's that could satisfy their information needs. This recommender system also improves the services that a EMR repository provides to users, because it is easier to obtain the knowledge about users and it allows to decrease the time cost to establish the user preferences.

The model is based on a recommendation degree used to deliver the information resources to the fitting users (Eq. 1).

$$\Psi = \sqrt{\Upsilon\left(a, k, c, t\right)} \otimes \left(\chi \oplus \Phi\right) \quad (1)$$

where Ψ represent the recommendation degree, Υ represents the intrinsic quality degree of the EMR based on the calculation of completeness c, reliability r and timeliness t, χ represents the contextual compatibility between the new EMR and the user context, and Φ represents the compatibility between the user preferences (represented by an ontology automatically built) and the EMR. The square root is used as the linguistic hedge "more or less" according to the explained in [11] about the decision criteria results. $\otimes$ denotes the fuzzy conjunction operator (t-norm). The product as t-norm allows us to obtain the best results on the empirical experiments carried out in this work. $\oplus$ denotes a fuzzy disjunction operator (t-conorm). The use of the algebraic sum as t-conorm allows us to obtain better results than applying classical functions on the empirical experiments carried out in this work.

Only those EMR's which have a recommendation degree, calculated according to the defined model, higher than a pre-established threshold are taken into account ($\Psi \geq \gamma$). This threshold (γ) is pre-established by the user as a part of the configuration process.

The model can be shown as a linguistic model, i.e., we can only describe the whole recommendation system by using natural language, for example, the model can be described as follows: "If the document has more or less quality AND is relevant to the user then it will be processed". The linguistic hedge, the fuzzy operators, the fuzzy rules and the considered intrinsic quality criterion dimensions can be changed to build an efficient recommendation system in any domain context. Each component of this approach is explained in the following subsection.

3.1 Intrinsic Quality

In order to determine if a EMR is useful enough for a user, data contained in it must be analyzed to check if it reaches an adequate level of quality according to certain parameters. Taking into account that the "fitness for use" depends on the task and role of the users who handle both EMR's and their sources, it is necessary to identify a set of dimensions that better represents quality requirements from user requirements specification. Intrinsic Dimensions denote that information has quality in its own right. These dimensions are independent of the userŠs context. They are capturing whether information correctly represents the real world and whether information is logically consistent in itself [12]

For making operative our proposal, three dimensions of a data quality (DQ) model for assessing data of new EMR's have been chosen in order to improve the performance of the proposed recommender system. These dimensions are the following:

- *Accuracy* (a): is the degree of correctness and precision with which information in an information system represents states of the real world [12].
- *Consistency* (k): implies that two or more values do not conflict with each other [13].
- *Completeness* (c): is the degree to which information is not missing [14], i.e. every item of a document is fulfilled and has information
- *Timeliness* (t): is the degree to which information is up-to-date, i. e. received information is adequate for the temporal context in which its topic is set [15].

Whole dimensions are calculated according to the specification shown in [16]. In order to get a summarized measure for a document we must take into account that the perception of quality is both subjective and inaccurate, and consequently it would be appropriate to use a fuzzy operator to measure/determine/assess DQ properly. In this work a Mamdani-style fuzzy system has been employed [17]. Linguistic labels and a set of rules were defined and optimized by a panel of experts. $\Upsilon\left(a, k, c, t\right)$ is a value obtained after a defuzzification process.

3.2 Contextual Compatibility

The Contextual Relevance (χ) of a EMR and a user is computed by using the compatibility between the EMR contents and the ontological definition of the user area of interests. This contextual representation based on ontologies is extracted from the definitions stored in domain ontologies, for example, MeSH [2], UMLS [3]

The degree of representativeness of each keyword is computed using different measures of similarity existing for this thesauri, for example, WordNetSimilarity [18] , UMLSSimilarity [19]. For example, some keywords that define the context "Pulmonary Medicine" in healthcare context using UMLS and UMLSSimilarity are shown in Table 1.

Table 1: Excerpt of "Pulmonary Medicine" Context Definition

Word	Degree
respiratory, lung	1.00
trachea, bronchial	0.50
bronchitis, pneumothorax, chest	0.25
thoracolumbar, abdominal	0.10

In this case the context and the EMR could be considered as fuzzy sets because they consist of words that have a membership degree. Therefore, the compatibility between context and document could be computed by using the generalized Jaccard coefficient as used in [20].

[2]http://www.nlm.nih.gov/pubs/factsheets/mesh.html
[3]http://www.nlm.nih.gov/research/umls/

3.3 Personal Compatibility

In this work, the user preferences will be represented as a fuzzy ontology automatically obtained from a set of EMR's previously selected by the user. A fuzzy ontology, in this context, may be considered as a set of directed graphs where each node represents an item and the edges denote that a term "is related with" other term. The proposal includes several stages of data processing, which were divided into five steps: linguistic pre-processing, term indexing (called pre-ontology), user relevant terms extraction, user ontology generation and user profile update as can be seen in [1]. In this fuzzy ontology, a relatedness degree (RD) is associated with each edge to represent the strength of the "is related with" association. In this way, the relatedness degree (RD) between two terms t_i and t_j is defined as (Eq. 2).

$$RD\left(t_i, t_j\right) = \frac{\sum_{o \in O} f - occur\left(t_i, o\right) \otimes f - occur\left(t_j, o\right)}{\sum_{o \in O} f - occur\left(t_i, o\right)} \tag{2}$$

where o is a EMR, O is the set of EMR's selected from the LOR by the user, $f - occur$ is the function of the relative frequency of a term in a EMR and $\otimes$ denotes a fuzzy conjunction operator.

The compatibility degree between the EMR and the user profile Φ assesses if the interests of the user are expressed in the EMR. The value 0 indicates that users preferences are totally different of the EMR content, i.e., the ontology extracted from the EMR and the user ontology represent different concepts, not necessarily contrary; whereas the value 1 indicates that the EMR contents are included in the users' preferences.

The EMR's ontology is built using a modification of the RD equation, where s is a section (or paragraph according to the kind of document) of the EMR δ (Eq. 3):

$$RD\left(t_i, t_j\right) = \frac{\sum_{s \in \delta} f - occur\left(t_i, s\right) \otimes f - occur\left(t_j, s\right)}{\sum_{s \in \delta} \widehat{f - occur}\left(t_i, s\right)} \tag{3}$$

The process to compute this value consists of the comparison between two ontologies. The comparison method is inspired by a set of ontology similarity measures proposed by [21]. In this case, the vector model is used to represent each concept in the ontology. Let v^i be the corresponding vector that represents a concept c_i, int v^i_j, the value in the position j, will be the RD degree between c_i and c_j when c_j belongs to the set of possible concepts that define a user profile, i.e., $v^i_j = RD(c_i, c_j)$. The detailed procedure is illustrated in Alg. 1, where $jaccard(v_1, v_2)$ represents the jaccard similarity function between two vectors.

Algorithm 1 Compatibility Degree Algorithm

```
O are the ontology corresponding to the new EMR
U are the ontology corresponding to the user
|O| and |U| are the size of each ontology
for c ∈ U do
  if c ∈ O then
    v_O = vector that represents the concept c in the ontology O
    v_U = vector that represents the concept c in the ontology U
    SC = jaccard( v_O, v_U)
  end if
  β = AVERAGE(SC) {β represents the similarity of common concepts}
end for
Φ = (|O ∩ C| ⊗ β) /min (|O|, |U|) {⊗ is a t-norm}
```

4. Experiment

An experiment was carried out to evaluate the performance of the proposed recommender system. In this section, the experiment, the performance measures used and the obtained results are described.

4.1 Experiment Description

The study group was shaped by 10 users from a healthcare organization. Most of them had experience in e-health technology as a researcher or as a physician. Each user has selected one of the following areas: traumatology (TRA), oftalmology (OFT), otolaryngology (OTO), surgery (SUR) and urology (URO). These areas and their ontological representation based on MeSH are the base for the user context definition. On the other hand, each user has selected 11 Medical Records as relevant in the Healthcare Information System. Once the selection process was finished, the user context and user preferences ontological definition were created for each participant, applying the methodology and algorithms described previously.

4.2 Experiment Results

In order to evaluate the feasibility of our approach, we compared the recommendations made by the system and the preferences for each new user of each new EMR. The contingency table (Table 2) used for this purpose is similar as the explained by [22] and by [6].

Table 2: Contingency Table

	Selected	Not Selected	Total
Relevant	Nrs	Nrn	Nr
Irrelevant	Nis	Nin	Ni
Total	Ns	Nn	N

Precision, recall and F-measure are measures useful to evaluate the quality of the recommendations [23] . Here, precision measures the probability of a selected item being

relevant, recall represents the probability of a relevant items being selected and F-measure is the harmonic mean between precision and recall (Equations 4, 5, 6).

$$P = \frac{N_{rs}}{N_s} \tag{4}$$

$$R = \frac{N_{rs}}{N_r} \tag{5}$$

$$F = \frac{(2 * R * P)}{(R + P)} \tag{6}$$

We considered a test data set with 100 EMR's of different areas. The system filtered these EMR's and recommends them to the suitable users. Then, we compared the recommendations provided by the systems with the recommendations provided by the users. After this comparison the corresponding precision, recall and F-measure are obtained. The results of this process are shown in Table 3 (the values are in the range [0,1]).

Table 3: Results.

User	Precision	Recall	F-measure
TRA	0.98	0.81	0.89
OFT	0.95	0.91	0.93
OTO	0.94	0.89	0.91
SUR	0.86	0.91	0.88
URO	0.92	0.85	0.88

The average of precision, recall and F-measure are 0.93, 0.87% and 0.90%, respectively. These values reveal a good performance of the proposed system if compared with those obtained by using non-ontological approaches (0.70, 0.61 y 0.65, respectively). We have achieved a substantial improvement in precision and recall values, which means that the proposed system is flexible enough to provide good recommendations using our approach.

5. Conclusions and Future Work

In this paper, a recommendation method based on the fuzzy representation of user preferences was proposed. This approach has been applied to provide recommendations about new Medical Records that could be interesting for a user. This is an efficient solution to minimize the problem of access relevant information in Medical Records Repositories. The proposal combines the analysis of intrinsic and conceptual features for making decisions about recommendation. User preferences are represented by domain ontologies for user context and automatically built fuzzy ontologies. This combination allows us to make recommendations based on a richer description of the user preferences.

An experiment has been carried out in order to determine if the recommended EMR's are useful and interesting for the users. Experimental results show that the proposed system is reasonably effective in terms of precision and recall.

Further research is directed towards the task of improving the user profile quality considering the information provided by the user as feedback, and the application of some techniques of collaborative filtering. Moreover, more detailed evaluation experiments also will be necessary.

References

[1] M. Ferreira-Satler, F. P. Romero, V. H. MenÃl'ndez, A. Zapata, and M. E. Prieto, "A fuzzy ontology approach to represent user profiles in e-learning environments," in *FUZZ-IEEE 2010 IEEE International Conference on Fuzzy Systems - WCCI 2010 IEEE World Congress on Computational Intelligence*, Barcelona (Spain), 2010, pp. 161–168.

[2] L. A. Zadeh, "Fuzzy logic and approximate reasoning," *Synthese*, vol. 30, no. 3, pp. 407–428, 1975.

[3] R. Burke, "Hybrid recommender systems: Survey and experiments," *User Modeling and User-Adapted Interaction*, vol. 12, pp. 331–370, November 2002.

[4] U. Hanani, B. Shapira, and P. Shoval, "Information filtering: Overview of issues, research and systems," *User Modeling and User-Adapted Interaction*, vol. 11, pp. 203–259, August 2001.

[5] R. Lage, F. Durao, P. Dolog, and A. Stewart, "Applicability of Recommender Systems to Medical Surveillance Systems," in *Proceedings of the CIKM MedEX 2011*. ACM, 2001.

[6] C. Porcel and E. Herrera-Viedma, "Dealing with incomplete information in a fuzzy linguistic recommender system to disseminate information in university digital libraries," *Knowledge Based Systems*, vol. 23, pp. 32Ű–39, 2010.

[7] L. Han and G. Chen, "A fuzzy clustering method of construction of ontology-based user profiles," *Advances in Engineering Software*, vol. 40, no. 7, pp. 535–540, 2009.

[8] P.-A. Chirita, C. S. Firan, and W. Nejdl, "Summarizing local context to personalize global web search," in *Proceedings of the 15th ACM international conference on Information and knowledge management*, ser. CIKM '06. New York, NY, USA: ACM, 2006, pp. 287–296. [Online]. Available: http://doi.acm.org/10.1145/1183614.1183658

[9] R. Y. Lau, D. Song, Y. Li, T. C. Cheung, and J.-X. Hao, "Toward a fuzzy domain ontology extraction method for adaptive e-learning," *IEEE Transactions on Knowledge and Data Engineering*, vol. 21, no. 6, pp. 800–813, 2009.

[10] S. Calegari and E. Sanchez, "Object-fuzzy concept network: An enrichment of ontologies in semantic information retrieval," *Journal of the American Society for Information Science and Technology*, vol. 59, no. 13, pp. 1532–2890, 2008.

[11] L. Zadeh, "A fuzzy set theoretic interpretation of linguistic hedges," *Journal of Cybernetics*, vol. 2, no. 3, pp. 4–34, 1972.

[12] Y. Wand and R. Wang, "Data quality in context," *Communications of the ACM*, vol. 39, no. 11, pp. 86–95, 1996.

[13] M. Mecella, M. Scannapieco, A. Virgillito, R. Baldoni, T. Catarci, and C. Batini, "Managing data quality in cooperative information systems," in *Proceedings of the Confederated International Conferences DOA, CoopIS and ODBASE*, 2002, pp. 486–502.

[14] L. Pipino, Y. Lee, and R. Wang, "Data quality assessment," *Communications of the ACM*, vol. 45, no. 4, pp. 211–218, 2002.

[15] B. Kahn, D. Strong, and R. Wang, "Quality benchmarks: Product and service performance," *Communications of the ACM*, vol. 45, no. 4, pp. 184–192, 2002.

[16] I. Caballero, E. Verbo, C. Calero, and M. Piattini, "A data quality measurement information model based on iso/iec 15939," in *Proceedings of the 12th International Conference on Information Quality*, 2007, pp. 393–408.

[17] E. Mamdani and S. Assilian, "An experiment in linguistic synthesis of fuzzy controllers," *International Journal Man-Machine Studies*, vol. 7, pp. 1–13, 1975.

[18] T. Pedersen, S. Patwardhan, and J. Michelizzi, "Wordnet::similarity: measuring the relatedness of concepts," in *Demonstration Papers at HLT-NAACL 2004*, ser. HLT-NAACL–Demonstrations '04. Stroudsburg, PA, USA: Association for Computational Linguistics, 2004, pp. 38–41.

[19] B. T. McInnes, T. Pedersen, and S. V. S. Pakhomov, "Umls-interface and umls-similarity : open source software for measuring paths and semantic similarity." *AMIA Annu Symp Proc*, vol. 2009, pp. 431–5, 2009.

[20] V. V. Cross and T. A. Sudkamp, *Similarity and compatibility in fuzzy set theory: assessment and applications*. Heidelberg, Germany, Germany: Physica-Verlag GmbH, 2002.

[21] A. Maedche and S. Staab, "Measuring similarity between ontologies," in *Proceedings of the 13th International Conference on Knowledge Engineering and Knowledge Management: Ontologies and the Semantic Web*. Germany: Springer-Verlag, 2002, pp. 251–263.

[22] C. Porcel, J. Moreno, and E. Herrera-Viedma, "A multi-disciplinar recommender system to advice research resources in university digital libraries," *Expert Systems with Applications*, vol. 36, no. 10, pp. 12 520–Ű12 528, 2009.

[23] Y. Cao and Y. Li, "An intelligent fuzzy-based recommendation system for consumer electronic products," *Expert Systems with Applications*, vol. 33, pp. 230–240, 2007.

Suré: A tool for pattern identification and sentiment detection in microtexts

Carlos Zuniga-Solis, Jose A. Olivas
SMILE Research Group, University of Castilla-La Mancha, Ciudad Real, Castilla-La Mancha, Spain

Abstract – *Knowledge exchange and opinion sharing over the Internet has reached levels never experienced before. People from different regions and socio-cultural backgrounds now have the possibility to create as much web content as they wish. This data represents a massive source of information useful to understand many aspects of society. Through sentiment analysis it is possible to leverage this highly topical data to identify people's perception of a certain topic. Different approaches have been implemented in order to detect sentiment in microtexts using mainly lexical ontologies and classification models. In this work, a tool designed for sentiment detection in microtexts named Suré is presented. This tool leverages inductive learning in order to find differentiating patterns in opinions about a given topic. Using the identified patterns Suré creates decision trees to classify microtexts as supportive or unsupportive towards the analyzed topic.*

Keywords: Induction, Microtexts, Sentiment Analysis.

1 Introduction

The advancement in web technologies over the last decade has allowed users to generate as much content on internet as they wish. This has led to knowledge exchange and opinion sharing at levels never experienced before, and the social networks have been crucial facilitators of this process.

The ease with which people can create social network messages is one of the key success factors of these web sites. According to Twitter Blog, in June of 2011, Twitter users sent 200 million tweets per day, enough text to fill a 10 million-page book every day. Through these 140 characters long, unstructured and conversational toned writings, 100 million users express what they are doing, what they are thinking and how they are feeling.

By reading a person's tweets, it is possible to understand many things about her. Therefore, studying the data of hundreds of thousands of tweets might help to develop a better understanding of our society at large. A powerful technique to leverage this huge amount of data is sentiment analysis.

Sentiment analysis is the task of identifying positive and negative opinions, emotions, and evaluations [1]. Through sentiment analysis of tweets, researchers have found that Americans seem considerably happier on Sunday morning than Thursday evening, and that West Coast American residents might be happier than their East Coast counterpart[2].

Different approaches converge in the search for the optimal sentiment detection technique. A very straightforward method is to use sets of terms with positive and negative connotations, to classify the sentiment of the words forming a message. However, the explosion of the web 2.0 and a larger internet coverage, have allowed people worldwide, to express their opinion about any topic. In this scenario, positive or negative meaning of a word becomes relative to the region or sociocultural context of a debate or a conversation. For this reason it might be more suitable to use an approach that learns from the contextual relationships of words, instead of their linguistic relationships. This could be accomplished through inductive learning, leveraging its capabilities to discover distinguishing patterns, and thus indetifying recurrent concepts in positive or negative messages in any context.

In this work a tool for sentiment detection in microtexts is presented. The developed tool named Suré leverages inductive learning and decision trees to classify microtexts as supportive or unsupportive towards a given topic. A test case using real life data is also presented showing promising results.

2 State of the art

After the release of Twitter developer platform in 2006, researchers obtained instant access to what might be the largest dataset in history, with lots of new highly topical messages available every second. This provided a great opportunity to analyze thousands of points of views and to find useful information for many different fields using specialized software for sentiment detection.

Twitter developer platform consists of a set of APIs that allow developers to integrate their custom applications with this social network. One of these APIs, the Search API is particularly useful for data extraction tasks since it allows to query for tweets from a custom application, thus it is possible

to obtain and store thousands of tweets about a certain topic within a given date range in a matter of seconds.

The increasing number of studies about sentiment analysis, published since the release of Twitter developer platform, and the growing number of countries developing researches about this topic, may be good indicators of the facilities given by this platform.

The ease with which messages on social networks can be created has been one of the key factors for the success of the most popular social network web sites. A message on a social network falls under the category of Microtext. Microtexts are very short individual contributions, often consisting of a single sentence that can be as short as a single word. They are further characterized by using an informal and unstructured grammar. These messages have a conversational tone, usually including colloquial expressions. Usually these messages are not edited before being sent, which makes them error prone [3].

These characteristics of the microtexts allow inexperienced users to quickly become creators of content. Nevertheless, these characteristics also make microtexts particularly hard to analyze for sentiment detection. Extracting sentiment information out of a sentence consisting of just a few words is not an easy task.

For these reason researchers have implemented different methodological approaches in order to obtain the best results out of the available data. Lexical ontologies and classification models highlight as the preferred techniques.

As a result of a literature review of studies related to sentiment detection in microtexts, 24 studies were found. Implementations of classification models were found in 14 of the reviewed works, lexical ontologies were found in 7 studies and the remaining 3 works used third party software or other techniques.

According to the literature review performed, when classification models were implemented, the use of Naive Bayes classifiers and SVM method were predominant. To a lesser extent, Bag of words and K-nearest neighbor classification model were used. On the other hand, in those cases about sentiment detection using lexical ontologies, a strong tendency towards the use of lexical English database WordNet® and derivates of this, such as WordNet-Affect or SentiWordNet was found.

The reason why classification models seem to be more popular between sentiment detection researchers is their capacity to leverage the context information, without depending on it. The same classification model could be used for sentiment detection in different languages. On the other hand, lexical ontologies are domain dependent, and require a significant effort to generate lists of words for each domain [4].

To avoid the burden of creating a lexical ontology for every domain universe a simple approach was identified. In several studies a generic ontology such as WordNet was used. However, this method is not always suitable, since the meaning of many terms and expression is often context dependent.

The importance of the context where a term is used becomes clear when a variety of practical applications found in the reviewed literature is analyzed. As suggested by many studies, sentiment detection in social network messages could be a useful tool to quickly identify or even to anticipate situations affecting, positively or negatively, a certain group of the people. Flu outbreaks, radicalization of opinions, and popularity loss of a touristic place are some of the examples found. As can be seen, the variety of the topics addressed might generate accuracy problems if a generic lexical ontology is used.

3 Architecture and Methodology

In order to classify microtexts as supportive or unsupportive towards a given topic leveraging the context of the information, the sentiment detection software Suré[1] was created. Suré consists of two modules: Microtext extraction and Text analysis.

3.1 Microtext extraction

The module for data extraction allows extracting microtexts from 5 sources: The digital versions of Spanish newspapers El País, El Mundo and ABC, Twitter and Facebook.

To obtain microtexts from the digital version of El País, El Mundo and ABC newspapers, a custom process was built to obtain the comments out of a web article.

To recover microtexts from Twitter, an interface was built on top of Twitter's Search API, allowing querying for Twitter content, in the same way a user would search for tweets using this social network search engine. Once the search is done, the tweets found can be stored for later analysis. Whilst Twitter's Search API allows retrieving thousands of tweets in a matter of seconds, a very important limitation must be considered: Twitter's index includes only the last 6 - 9 days of tweets.

[1] Suré is a Bribri word that means "fishing arrow", however for the native Costa Rican tribe Bribris, arrows are capable of creating cracks through which light and thinking may pass through.

To obtain microtexts from Facebook, Suré leverages the Facebook's Graph API[2]. This interface grants access to different objects of this social network, and allows navigating through the relationships of these objects.

For microtext extraction from Facebook Suré offers an interface to access comments on posts on public pages. This API grants access to the social network's different objects and to the relationships between them. The user must introduce the URL of a Facebook public page and a date range to search for its posts. Once the search is finished, Suré shows to the user the posts found, their creation date, and the number of comments received. The last step is to select one of the retrieved posts, and its comments will be extracted and stored for later analysis.

3.2 Text analysis

The text analysis capabilities offered by Suré are designed to be used after a dataset about a certain topic has been obtained through the Microtext extraction module.

The Text analysis module allows using the retrieved microtexts as a training set or as an evaluation set. The evaluation set is used for automatic sentiment detection supported by a training set previously created.

In order to create a training set, Suré allows experts to classify the microtexts by its sentiment as positive, negative, neutral or noise. The noise category should be used on those cases where a message does not offer any point of view strictly related to the subject matter addressed.

Once the microtexts have been classified, they receive a linguistic pre-processing and then the resulting data is stored in a text index. The pre-processing consists of the following tasks:

- Tokenization
- Punctuation removal
- Lowercasing
- Stopwords removal
- Stemming

Once the training set has been pre-processed and indexed, Suré permits users knowing the term-frequency distribution of the classified microtexts, filtered by the sentiment given by the expert.

Suré also has the ability to find recurring groups of terms in the positive and negative training sets. This functionality allows finding differentiating patterns between positive and negative microtexts of a certain subject. This function has been implemented following the rules of the First Order Inductive Learner algorithm [5] in order to obtain exclusive patterns for positive and negative comments. It is worth noticing that, rarely used words are not useful to find representative patterns, for this reason, Suré ignores words that appear in less than the 20% of microtexts forming the positive or negative training set. To find and remove these words Suré internally uses its term-frequency functionality.

When searching for differentiating term patterns, it is necessary to choose the number of terms included in the patterns to find. This permits to identify the patterns with the widest coverage throughout the training sets.

After a training set has been stored in a text index, it is possible to perform automatic sentiment detection on evaluation sets by creating decision trees based on the differentiating term patterns of the training set. This process is performed by Suré through implementations of the ID3 and CART algorithms. To create the ID3 or CART decision tree the user must choose the number of terms that make up the patterns to find. For this reason, it is recommended to perform prior tests on the training set using Suré's pattern identification functionality, in order to determine the appropriate number of terms to cover the maximum amount of microtexts possible.

The set of terms of the patterns found will be used later to create the nodes of the decision trees. For this reason, Suré offers the possibility to specify a minimal number of occurrences for the patterns to use. Doing this allows to prune the tree before it is created. The following step is to decide whether to use an ID3 or a CART algorithm to create the decision tree.

For the ID3 algorithm, the terms of the patterns found will be the nodes of the tree, the possible values for every term will be whether or not the term is present in a given microtext, in other words true or false. For the CART algorithm the nodes of the tree will be a condition composed of a term and one of its possible values in a microtext: true or false. Given the nature of the CART algorithm, every node will have two children, one for those cases where the condition is met, and another one for those cases where the condition is not met. The leafs on the ID3 and CART trees will be sentiment classifiers 'positive' and 'negative'. Because of the characteristics of the methodology used in Suré, both algorithms produce binary trees. Once the decision tree has been created, the user will be able to use it for sentiment detection on individual examples.

[2] https://developers.facebook.com/docs/reference/api/

4 Practical case

In order to test Suré's sentiment detection accuracy a relevant topic to Spanish society was selected: The conviction of former Spanish judge Baltasar Garzon Real.

The reason to choose this topic was that the generated views about it on social networks were so opposing that it would be very easy for a slightly informed person to tell if a comment supports or rejects Garzon's convitcion.

Nevertheless, despite of the ease with which a person could detect the sentiment in the related microtexts, the automatic classification of messages as supportive or rejective faces significant challenges. This trivial case illustrates the complexities of Artificial Intelligence and Natural Language processing.

The first step was to find articles related to Garzon's conviction in the digital version of Spanish newspapers El Mundo and El Pais. These two daily newspapers were selected because of the opposite political tendencies of its frequent readers. Once the articles were chosen, a total of 9760 comments were retrieved by Suré, 2780 from El Mundo and 6980 from El Pais. Subsequently, 4000 of the retrieved comments were classified by an expert, 2000 from El Pais, and 2000 from El Mundo. For mere classification purposes, those comments supporting Garzon's conviction were categorized as positive and those rejecting it as negative. A total of 963 comments were classified as positive and 675 as negative, the remaining 2362 were marked as noise. The positive and negative microtexts received linguistic pre-processing and were stored in an index text as the training set for this test case.

Following the linguistic pre-processing of microtexts an interesting problem related to the context of this particular case of analysis emerged. Both Spanish terms "derecho" and "derecha" stems to "derech". Nevertheless, in the microtexts retrieved, "derecho" was frequently used as a part of expressions such as: "estado de derecho" (rule of law) and "derecho de defensa" (right of defense), very common expression in opinions in favor of the Garzon's convition. On the other hand, the term "derecha" referred to right-wing politics, a very usual reference in the microtexts rejecting the above mentioned judgement. In this case, the stemming truncates the contextual value of the term. This problem might be subsequently solved leveraging synonyms and multi-term expressions in the linguistic pre-processing stage.

The next step was to identify the best differentiating patterns in order to determine the optimal parameters to specify later on when the decision trees were created. It was determined that only those terms with a frequency equal or greater than the 20% of the total of microtexts in the training set will be taken into account for pattern identification. Thus, thousands of seldom used terms were removed, improving system performance and result quality.

Very few patterns consisting of 5 and 4 terms were found. Besides, those patterns covered only a minimal percentage of the microtexts of the dataset. On the other hand, an important amount of 3 words patterns emerged, enough to cover the entire dataset if put together. Table 1 shows a sample of the most frequently found patterns.

Table 1. Frequently found patterns sample

Pattern	Occurrences	Sentiment
[garzon, juez, ley]	53	Positive
[derech, juez, ley]	38	Positive
[españ, gazon, juez]	31	Negative
[garzon, juez, pais]	28	Negative

Because of the differentiating capabilities of the patterns, and given that 3 words patterns offered great dataset coverage, it was decided to use these patterns for the later creation of the decision trees.

In order to test the sentiment detection capabilities of the presented approach, the 4000 microtexts classified by an expert were used as the training set to create ID3 and CART decision trees. Subsequently, a set of 186 comments from articles related to Garzon's sentence from the digital version of Spanish newspaper ABC was retrieved. Only comments expressing positive or negative opinions were taken into account.

Of the 186 retrieved comments, an expert classified 130 as positive and 56 as negative. Subsequently, these 186 comments were automatically classified by Suré and compared to the results given by the expert to determine Suré's accuracy. Table 2 shows the results of the comparison.

Table 2. Automatic classification accuracy

Method	Accurate positive	Accurate negative	Average accuracy
CART	107	37	77.4%
ID3	105	38	76.8%

As the results show, none of the classification methods is considerably more accurate than the other. It is also worth mentioning that both methods do better classifying the positive examples than negatives. By analyzing the negative patterns found, a large number of different sets, but with a low average number of occurrences can be seen. This evidences a trend to use a richer variety of terms used in negative microtexts than that in the positives for this particular topic, which might make negative sentiment harder to spot.

5 Conclusions and open issues

This works presents a tool for pattern identification and sentiment detection in microtexts based on inductive learning and classification trees. The tool named Suré is still a prototype; however is it capable of leveraging the vast amount of available data to extract information from context instead of using linguistic relationships. Suré has only been tested with the data previously discussed, shortly it will be tested using different data sources such as Twitter and analyzing new topics. Moreover, adding new functionality such as multi-term expression detection and synonym pre-processing will probably improve the accuracy of the results, which for this first test may be considered good.

6 References

[1] Wilson, T., Wiebe, J., Hoffman, P.: Recognizing contextual polarity in phrase-level sentiment analysis. Proc. of the conference on Human Language Technology and Empirical Methods in Natural Language Processing. pp. 347-354 (2005).

[2] Savage, N.: Twitter as medium and message. Communications of the ACM. 54, 18 (2011).

[3] Ellen, J.: All about microtext: A working definition and a survey of current microtext research within artificial intelligence and natural language processing. ICAART 2011 - Proc. of the 3rd International Conference on Agents and Artificial Intelligence. pp. 329-336 (2011).

[4] Guerra, P.H.C., Veloso, A., Meira, W., Almeida, V.: From bias to opinion: A transfer-learning approach to real-time sentiment analysis. Proc. of the ACM SIGKDD International Conference on Knowledge Discovery and Data Mining. pp. 150-158 (2011).

[5] Quinlan, J.R.: Learning logical definitions from relations. Machine Learning. 5, pp. 239-266 (1990).

SESSION

NATURAL LANGUAGE PROCESSIN, NLP + APPLICATIONS AND RELATED ISSUES

Chair(s)

TBA

A Grammatical-Error Tolerant Parser

W. Faris and K.H. Cheng
Computer Science Department, University of Houston, Houston, Texas, USA

Abstract – *The proper application of usage rules are required to construct grammatically correct sentences. For most speakers, the likelihood of writing a grammatically incorrect sentence is quite high. However, for most sentences that may have violated some grammatical rules, their correct intentions may still be inferred intuitively. Consequently when communicating with humans using a natural language, a computer program should not reject but tolerate such sentences. In this paper, we define a grammatical rule as a syntax-restriction rule if the intention of the sentence may still be intuitively inferred even when the rule is violated. In addition, we define a sentence as semantically sufficient if it is free of grammatical errors or only syntax-restriction rules are violated. If only syntax-restriction rules are violated, we have modified our parsing program to accept and interpret, instead of rejecting, the given sentence.*

Keywords: Natural Language Processing, Grammatical Error, Tolerance, Parser, Context-Based, Semantic Interpretation

1 Introduction

It is desirable for an artificial intelligence program to communicate with humans using a natural language, specifically, English. However, in today's world, many people may not be communicating in their own native language. Since the grammar of a natural language is normally complex and has many rules, many individuals may not know all the rules. Even when they do, they may not always follow them. As a result, it is unlikely that they will consistently communicate perfectly in their non-native language, and it would be unreasonable to expect correct sentences all the time. When presented with a grammatically incorrect sentence, an individual could ignore the mistake and still intuitively infer the correct meaning of the sentence. Similarly, in order to communicate effectively with humans, a computer program should be prepared to tolerate grammatically incorrect sentences as long as the most probable conveyed idea may be understood. Otherwise, it would reject sentences excessively. This attitude can also be seen in systems such as chatbots and Question/Answering expert systems to reduce the frustration of the users. They are designed to extract pertinent information from a sentence by mapping keywords to built-in functionality [1]. However, this approach is not adequate to handle normal communication since it is limited to a small number of functionalities.

We define a sentence to be semantically sufficient when the correct intent of the sentence may be determined intuitively even when syntactical errors are present. By intuitively, we mean that the interpretation is most likely the actual intention of the speaker. To give the flexibility to handle semantically sufficient sentences but still detect grammatical inconsistencies, we define a new category of rules: syntax-restriction. These rules reflect the correct syntax and morphology, but are not absolutely necessary in interpreting sentences. One characteristic for rules in this category is that it matches a property of an item with that of another, such as agreement rules. As a result, the criteria for syntax-restriction rules are that the same information can be obtained from at least two items in the given sentence, and the information obtained from one item is normally considered more reliable over the other when they are in conflict. Consequently, using the information obtained from the more reliable item, the inferred semantic interpretation is most likely the correct intention. For example, one aspect of the subject-verb agreement rule matches the number properties of the subject and the verb. Since the subject is the focal point of a sentence, it is considered much more reliable than the verb. Therefore, when there is a mismatch, understanding the sentence using the number property of the subject rather than the verb is most likely correct. A mismatch in subject-verb agreement is an example of a context-based grammatical error, in which a word differs from what is expected, based on surrounding words. In this paper, we discuss how to use this new category of rules to detect context-based errors and generate a warning, instead of rejecting the sentence as illegal. A warning is information that when displayed will notify the person communicating with the program about the grammatical error. In addition, we will illustrate how such rules can be used to resolve an ambiguous term, but still be used to generate warnings when the involved term is not ambiguous.

The objective of a context-based grammar checker is to help people write grammatically correct sentences by notifying them if a mistake is made, and ideally with an explanation of the error, so that they may correct the error. Context-based checkers can be found in applications such as word processors and machine translators. There are three

predominant models of a grammar checker [2]: syntax based, statistics based, and rule based. Syntax based checkers use parse trees to identify incorrect sentences, and unless they implement some form of rules as was done in CRITIQUE [3], they cannot identify the exact type of error. CLAWS [4], is an example of a statistics based part-of-speech (*pos*) tagger that uses the frequency of a sentence structure within a corpus to determine the validity of the sentence. Those that do not meet a defined threshold are assumed to contain errors. However, this technique is not capable of identifying the types of errors, thus leaving the individual uninformed on the reasons why the sentence is invalid. In [5], a grammar checker for a machine translator is used to automatically correct what it determines to be errors. A bottom-up parser creates chunks of related terms and phrases. The probability of a chunk is then compared to that of a corpus. For invalid sentences, Markov chains are used to determine missing or incorrect chunks that can be applied to produce a valid sentence. Regardless of which statistical model is used, the precision and recall rates depend on the size of the corpus and the threshold value, and a combination may not exist to detect all errors and to correctly identify all valid sentences. Arguments are provided in [6] to support why a rule based approach is necessary for identifying the types of grammatical errors. It proposes to use meta-rules, replacing regular grammar rules that fail, to re-parse the given sentence. Although our approach also uses rules to detect errors, these rules are normal grammar rules of the natural language. They are applied during parsing, and only one run of the parser is needed.

Recently, we have implemented a parser in a learning program system (ALPS) [7] to parse English sentences using a grammar that is acquired incrementally [8]. Subsequently, solutions have been developed to understand declarative sentences [9, 10], including identifying the correct knowledge referenced by various forms of pronouns [11]. We have also developed an algorithm to generate a sentence that reflects the contents of a logical thought using a transformation of the acquired grammar [12]. Five major components were introduced to define how a grammar term (or *pos*) is used in the language: structure, kind, role, control and rule. The structure of a grammar term defines exactly the grammatical format of the term, which may be either a sequence or an alternative. A term may have multiple kinds, which are subsets that may share the same structure but must have different roles. The role of a grammar term defines its purpose, and the intention of the role is implied by the presence of the term within a sentence. The idea of the control is to notify the parser which role within the term is responsible for organizing the various knowledge objects identified in the parsing process. A rule specifies a condition [13] satisfied by either the grammar term or its structure. They are used to either guide the parser towards the correct grammar structure or restrict certain terms from being accepted. The use of rules in a grammar enhances its scope while maintaining a manageable size. In this paper, we discuss how to use a new category of rules to detect and tolerate grammatical errors, so that a warning may be generated rather than outright rejecting the given sentence as invalid.

The rest of the paper is organized as follows. Section 2 describes briefly the original categories of grammatical rules in [8] and how they are used in parsing. It also introduces syntax-restriction rules, a new category of rules allowing the parser to handle grammatically incorrect but semantically sufficient sentences. Section 3 explains how to construct a syntax-restriction rule to be used by our program, and then presents how to check five grammatical requirements: punctuation usage, subject-predicate agreement, subject-verb agreement, verb phrase usage, and number agreement. It also presents the reasoning on why each rule can be a syntax-restriction rule, and why a certain component is more reliable in determining the semantic intention of the given sentence. Section 4 presents an example on using a syntax-restriction rule to disambiguate a term that could be used as multiple *pos*. Finally, Section 5 concludes the paper and discusses some situations when the context within the sentence is insufficient to correct grammatical mistakes.

2 Grammatical Rules

Rules have already been used in defining part of a grammar and applied when parsing a sentence. A rule is classified as one of four categories, each with a specific purpose during the parsing process. The four categories are defined by two independent dimensions: the first determines what the rule is for, and the second defines whether it is a restriction or a choice rule. A rule can be for the grammar term itself or its kind (role). A restriction rule is a necessary condition that needs to be satisfied, and a choice rule specifies a sufficient condition to make a choice when the condition is satisfied. The resulting four combinations of rules are kind-restriction, term-restriction, kind-choice, and term-choice. A kind-restriction rule specifies a necessary condition that the kind must satisfy. For example, the kind-restriction rule for a decision question states that its complete subject must not be fulfilled by an interrogative pronoun. An input sentence such as "Is how a human?" follows the sequence structure of a decision question (verb, subject, predicate), but it is rejected as invalid because this restriction rule is violated. A term-restriction rule defines the necessary condition that a grammar term must satisfy. For instance, in the structure of a noun phrase, the term-restriction rule requires that the noun cannot be fulfilled by a pronoun when an article or constant is present. This prevents 'a he' or '3 you' to be a legitimate noun phrase. A kind-choice rule defines the sufficient condition to decide the kind of the grammar term. If the condition is satisfied, the kind is chosen and its associated role is used. For example, a sequence structure of a sentence (subject, verb, predicate) may be fulfilled as

one of several kinds of sentences, such as a declarative sentence or an interrogative sentence. If the noun of the subject is an interrogative pronoun, then it is an interrogative sentence. Finally, a term-choice rule defines the condition sufficient for a grammar term to be fulfilled by one of its alternatives. This type of rule may be used to guide the parser to use a specific grammar term to parse the next part of the sentence. Take for instance the two alternatives of the complement of a sentence: subject and object complements. The English grammar states that if the main verb is an action verb, then the complement must be an object complement [14]. Otherwise, a subject complement should be used as the complement. Consequently, this type of rule can guide the parser to look for the correct complement in a sentence based on the type of the main verb.

Originally, our program only handled grammatically correct sentences. It rejected all incorrect sentences, even those with a minor grammatical error. In order to allow such sentences, a new category of rules is used: syntax-restriction. A grammatical rule is classified as a syntax-restriction rule when enough information is available in the sentence to compensate for the grammatical error or when one grammar term may be trusted to provide more reliable information than another term. For example, the semantic content of a given declarative or interrogative sentence is complete even when the punctuation mark is incorrect or missing, such as "Who is John." Consider another grammatically incorrect example, the phrase '3 apple'; the cardinal number should be a more reliable indicator of the correct number property than the noun. Similarly, since the subject of a sentence is considered the focal point of a given sentence, properties obtained from the subject may be considered more reliable than those obtained from the verb or predicate. In all these cases, the correct intention of the given sentence may be intuitively inferred, with a high degree of confidence, using the more reliable component. As a result, our program is more flexible in allowing and still understanding sentences with certain grammatical errors.

In the parsing algorithm, each rule category is applied at a specific point in the parsing process. Term-choice rules are applied before parsing a term. The term to be parsed is determined based on the parsed result of an earlier term. Other rules are applied after a term is parsed to check the validity and to decide the role of the parsed result. They are applied in the following order: term-restriction, kind-choice, and kind-restriction. A minor change to the parsing algorithm is to add a step to check the syntax-restriction rules after checking these other categories of rules. The reason is that this new category of rules is not used to determine the parse results and will have no impact on the *pos* tagging of the words. Finally, unlike other restriction rules, when a syntax-restriction rule is not satisfied, a warning unique to the rule is generated. This warning is based on the rule's purpose, which is taught along with its condition.

3 Syntax-Restriction Rules

All rules, regardless of their classification, rely on the use of conditions to determine whether the rule is satisfied or not. If the condition of the rule is met, then the rule is satisfied; otherwise, the rule is violated. In either case, appropriate actions are taken depending on the rule category. For syntax-restriction rules, this simply involves generating a warning indicating that the condition has not been met, but the parsing of the sentence will continue.

In ALPS, several condition classes have been developed and used in composing a rule. The syntax-restriction rules discussed in this section are built using fulfill, pattern, role, and composite conditions. A fulfill condition may check whether a grammar term or role has been fulfilled or not, such as checking that a helping verb appears within a verb phrase. Furthermore, if fulfilled, the condition may check whether or not it had been fulfilled by a specific grammar term; for example, a helping verb being fulfilled by a forms-of-be verb is a part of a passive voice rule. The pattern condition checks that a word begins, contains or ends with a certain sub-string, or that a sequence begins or ends with a certain grammar term. For example, a regular noun can be made plural by adding –es when it ends in –s, –x, or –ch. The role condition compares the properties of one grammar term or role to literal values or the corresponding properties of another term or role. One instance of a role condition is to check that a gerund noun is an action verb with a progressive tense property, such as 'flying', 'baking', or 'solving'. Finally, two conditions can be combined by using logical *and* or logical *or* to form a composite condition. Our implementation of a composite condition uses a lazy evaluation strategy, meaning the second condition is only evaluated if necessary. For instance, in a composite *or* condition, the second condition is evaluated only when the first condition fails. This allows for rules in which the first condition checks to see if a grammar term is not fulfilled; while the second checks to see that it is fulfilled by a specific grammar term. For example, if the purpose of a rule is to assert that a helping verb, when present, is fulfilled by a specific type of verb, then the first condition is used to allow instances in which a helping verb does not exist in the given sentence. Conversely, for a composite *and* condition, the second condition is evaluated only when the first condition is satisfied.

3.1 Punctuation Usage

In languages such as English, punctuations are used to mark the end of structures, such as the period for declarative sentences and the question mark for interrogative sentences and decision questions. However, one can generally discern the kind of a sentence based on its structure and content.

For example, the structure of a decision question is unique in that it begins with a helping verb, such as 'is', 'can', and 'did'. Although, both declarative and interrogative sentences share the same structure, an interrogative sentence must begin with an interrogative pronoun, such as 'who', 'why', and 'how', while a declarative sentence should not. Consequently, without punctuation, a reader should still know that "What is the next prime number after 7" is a question because of the subject 'what'. Similarly, the sentence "11 is the next prime number after 7" can easily be recognized as a declarative sentence. Given the ability to intuitively infer the kind of sentence from its makeup, the ending punctuation mark may be redundant. As a result, a punctuation mark that conflicts with the recognized kind of a given sentence should not limit the acceptability of the sentence, but should simply generate an appropriate warning. The condition for checking punctuations may use a pattern condition such as a declaration must end in a period, and an interrogative sentence ends in a question mark.

3.2 Subject-Predicate agreement

In English, declarative sentences that have the linking verb 'be' as the main verb serve a distinct purpose: the predicate defines a characteristic or a state of the subject. For example, the purpose of the sentence "John is a doctor" is to define the occupation of John to be that of a doctor. Similarly, "Gorillas are primates" categorizes gorillas as a species of primates. Due to this association between the subject and the predicate, the subject-predicate agreement rule asserts that their number properties be the same. It would not make sense for John, a singular entity, to be defined as multiple doctors nor for a plural number of gorillas being classified as a singular primate. However, since the intention of the sentence is relatively clear, when such a situation occurs, a warning is generated instead of rejecting the sentence as invalid. Since the subject is the focal point of a declarative sentence, we assume the number property of the predicate should be changed to match that of the subject.

The syntactic stage of the parser transforms all the words into their base form. This process of stemming will identify and store the number property of nouns and verbs, allowing them to be accessed when checking rules. The condition for the subject-predicate agreement rule can then be used to ensure that the number property of the subject is equal to that of the predicate. However, exceptions exist in which the subject-predicate agreement is not required, such as for sentences that do not have a predicate, e.g., "John runs home." As a result, the complete condition is a composite condition combining two conditions with a logical *or*. The first condition allows sentences that have exceptions to pass without checking any agreement, while the second compares the number property of the subject with that of the predicate.

3.3 Subject-verb agreement

One of the better-known usage rules in most spoken languages is the subject-verb agreement where properties shared by the subject and verb should match. For instance in English, if the subject is the pronoun 'I', i.e., the properties of the subject are first-person singular, then the properties of the verb should also be first-person singular, such as 'am'. If the meaning of the sentence is clear from the rest of the sentence, then it is unnecessary to reject the given sentence as illegal when the subject-verb agreement rule is not satisfied. Similar to subject-predicate agreement, since the subject is the focal point of a declarative sentence, the properties of the verb will assume those of the subject when a mismatch is found.

In English, the subject-verb agreement depends on several factors and we will focus on the parts of the rule when the sentence is in present tense and active voice. When the verb is an action verb, there are two possibilities. If the subject is in third-person, then the number property of the subject and verb must match, e.g., 'John gives' and 'They fix'. On the other hand, for all other person properties of the subject, the number property of the action verb must be plural, e.g., "I give" and "You receive". When the verb is not an action verb, which includes forms of be, have, and do verbs, then based on the specific person and number properties of the subject, a specific form of the verb is used. In other words, the specific verb form must have the exact person and number properties as the subject. For instance, if the subject is the pronoun 'I', having the properties first-person singular, then the forms-of-be verb is 'am'; and if the properties of the subject are second-person singular, i.e., the pronoun 'You', then the forms-of-do verb is 'do'. These tables of usage for the various forms of verbs have been taught as part of the grammar, and have been implemented using a data structure called the multi-dimensional data organization (MDDO) for easy retrieval and matching [15]. The MDDO organizes the verb forms in a table structure indexed by the property combinations that define when they are used. Our implementation of the role condition assumes the use of such a data structure when matching the properties of the subject and the main verb. Figure 1 shows the conditions of the subject-verb agreement for sentences in present tense and active voice.

Note that if the verb is either in past tense or is preceded by one or more helping verbs or the sentence is an interrogative sentence, then none of these rules should apply. For example, an action verb in the past tense will have the same form regardless of the subject, e.g., 'John walked' and 'we walked'. The impact of a helping verb is similar and will be discussed in the next section. As for interrogative sentences, the subject is an interrogative pronoun which can be used for all verb forms. In fact, the verb should agree with the predicate instead of the subject, such as "Where am I?" and "Where are they?" As a result, a predicate-verb agreement rule should be introduced as a

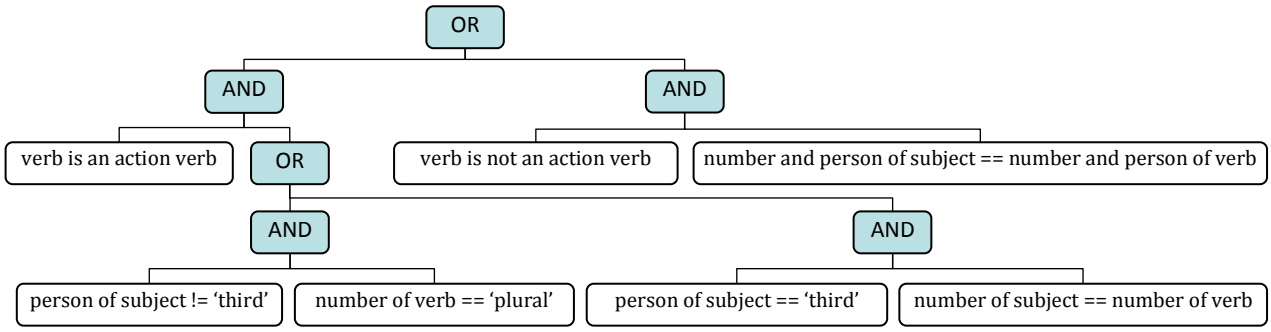

Figure 1: Conditions for subject–verb agreement.

syntax-restriction rule to handle that. Additional sub-conditions not shown in the figure are needed to exclude all these cases from violating the subject-verb agreement rule.

3.4 Verb phrase usage

The English language has four types of helping verbs: be, have, do, and modal helping verbs. As previously mentioned, the presence of helping verbs in a sentence makes the subject-verb agreement rules irrelevant. Instead, each type of helping verb has its own rules regarding the proper form of the main verb. The forms-of-be helping verbs indicate either a progressive tense such as "He is reading a book" or a passive voice "The book was given to him." As a result, the main verb needs to be in the progressive or past participle form, respectively. The forms-of-have verb is used for the perfect tense, and therefore, requires the main verb to be in the past participle form, such as "I have spent all my money." When used, forms-of-do helping verbs can either form a negative or show emphasis of the main verb. On the other hand, modal verbs, such as 'can', 'might', and 'would', modify the meaning of the sentence in some way; e.g., the modal verb 'can' asserts the ability of the subject to perform the action. Both the forms-of-do verb and modal verbs require the main verb to be in its base form, e.g., "John might go to the store tonight" or "Kate does not have her ticket." The base form of a verb is the form listed in a dictionary, such as 'eat' for the words 'eat', 'eats', 'eaten', and 'ate'.

Even though an English verb phrase can have up to three helping verbs, only the helping verb immediately preceding the main verb, known as the primary helping verb, determines the main verb's form. With the primary helping verb being the focal point, if a mismatch occurs between it and the main verb, we use the primary helping verb to determine the correct tense of the main verb. This helping verb agreement can be built by combining a composite condition for each form of helping verbs using a composite *or* condition. The first part of each individual composite condition would determine if the primary helping verb is fulfilled by the respective helping verb. The second condition would use a role condition to ensure the tense of the main verb matches what is expected for that helping verb. In our implementation, we determine that a linking verb is in its base form if no properties are associated to it, and utilize the fact that the base form of an action verb is its plural present tense form. In addition, since the semantic distinction cannot be made between its use as the main verb and helping verb, the condition for the forms-of-do helping verb is not included currently.

3.5 Number Agreement

The number agreement rule compares the number properties of a determiner and the noun that is being modified. Some examples of determiners in the English language are cardinal values, articles, demonstratives, and quantifiers. The number 1 indicates a singular entity and therefore should be followed by a singular noun. All other numbers, including negatives and the number zero should be followed by a plural noun: such as '3 cats', '0 conditions', and '-1 degrees.' Singularity is also inferred by non-unique articles 'a' and 'an'. However, the unique article 'the' can apply to both singular and plural nouns. Similarly, demonstrative pronouns and quantifiers also have the singular forms, such as 'this', 'that', 'every', and 'each' and plural forms such as 'these', 'those', 'all', and 'some'.

In English, some nouns have the same singular and plural form, such as 'sheep'. When reading the statement, 'a sheep' or '1 sheep', it is clear there is a singular animal. On the other hand, '3 sheep' represents multiple numbers. Since the number property of the noun in situations like these is irrelevant, when the number properties do not match in other situations, the value of the determiner is assumed to define the proper amount of the noun. In addition, some nouns have an irregular plural form or have complicated rules to form the plural, such as 'ox' to the plural 'oxen' versus 'fox' to 'foxes', and 'buy' to 'buys' but 'country' to 'countries'. These make it unlikely that the correct form will be used all the time. As a result, the number agreement rule should be a syntax-restriction rule with the determiner used as the basis when it fails. To illustrate how to detect number agreement, we have included a rule on cardinal values and articles. The first condition in the rule checks if

there is no determiner present or the determiner is the article 'the'. In either case the number property of the noun is irrelevant and the rule passes. The second condition compares the number property of the noun to that of the determiner as described above. The complete details of the rule are shown in Figure 2.

4 An Example in Resolving Ambiguity

In the English language, singular countable nouns such as 'computer' or 'phone' are modified by a determiner within a noun phrase. For instance, phrases like 'turn on the computer' and 'hand me my phone' are of proper grammar, while the phrases 'turn on computer' and 'hand me phone', are considered improper. Given the fact that there are enough contexts for these phrases to still be understood in light of the missing determiners, this particular rule may be implemented as a syntax-restriction rule, which would then generate a warning when the determiner was missing. However, classifying this rule as syntax-restriction presents a problem for the parsing algorithm. The reason is that for ambiguous words such as 'seal', which could represent a noun as well as an action, a phrase like 'to seal' could represent an infinitive or a directional prepositional phrase that was typed without a determiner, 'to (the) seal'. With the syntax-restriction rule in place, the phrase could sufficiently pass as an erroneous prepositional phrase even if it was intended to be an infinitive. Since our current parsing algorithm does not return multiple sentence structures, the parser would recognize the phrase of 'to seal' as a prepositional phrase instead of an infinitive based on the fact that this alternative was tried first. For ambiguous situations such as this, it would be beneficial for the syntax-restriction rule to act like a semantics restriction rule and restrict the prepositional phrase to include a determiner for singular countable nouns. If the determiner is missing, then parsing as a prepositional phrase fails. On the other hand, if the term is not ambiguous, such as 'car', then the missing determiner will result in the generation of a warning only.

It is for this reason that syntax-restriction rules have been implemented in a manner that could detect and adjust to ambiguous terms. This works by indicating to the rule which terms in the sequence to check for ambiguity. If the rule fails, and the word fulfilling the term is ambiguous, the fulfillment of the sequence fails. On the other hand, if the rule fails but the word fulfilling the term is not ambiguous, then the sequence is fulfilled sufficiently, the parsing continues, and a warning is generated. In this example, by specifying to the rule that the noun in the prepositional phrase may be ambiguous, the parsing of the phrase 'to seal' as a prepositional phrase will fail, allowing the parser to parse it successfully as an infinitive. In other words, the ambiguous term 'seal' is disambiguated as a noun by using the syntax-restriction rule when fulfilling a prepositional phrase and as an action verb when fulfilling an infinitive. A term is determined to be ambiguous if it is known within ALPS to represent multiple knowledge objects of different knowledge kinds. For example, the word 'seal' is ambiguous if ALPS is aware that it can mean an action or a category of objects. The details on how ALPS handles the word sense disambiguation problem may be found in [16].

5 Conclusion

In this paper, we showed how a parser tolerates sentences containing context-based grammatical errors. Unlike word processors that use context-based grammar checkers to alert improper grammar, ALPS uses a new category of rules, syntax-restriction, to make assumptions about the intended meaning. This is accomplished by using context in the sentence, domain knowledge, and knowledge about the grammar. When a sentence is determined to be grammatically incorrect, a warning is generated and may be shown to the user allowing them to determine if the assumed intent is correct. This category of rules gives ALPS an edge over other natural language processors by enabling it to accept and interpret sentences regardless of their grammatical correctness. The five grammatical rules shown in this paper only present a subset of what is possible with syntax-restriction rules. The incremental nature of the ALPS grammar, along with the versatility of defining rules, allows additional syntax-restriction rules to be added later. The end-result is a learning program that can accept a range of semantically sufficient sentences, including those with grammatical errors, while allowing the option of notifying the user about these errors through warnings.

In discussing syntax-restriction rules, it was stated that the more reliable of the two terms would be used when their

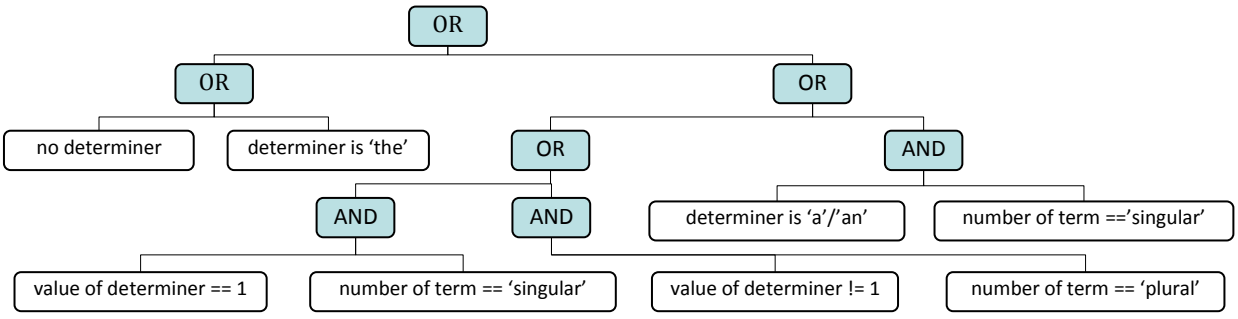

Figure 2: Conditions for number agreement.

properties conflicted. With the examples illustrated in this paper, the decision on what makes one term more reliable than the other is intuitive and obvious. For example, when presented with the verb phrase 'can goes', it is more logical to assume the helping verb was used intentionally and correctly instead of the main verb being used correctly. There may be occasions when determining the more likely intent is less obvious: for instance, when an apostrophe is missing from a possessive noun that could be either singular or plural. In the sentence "Hand me the teachers books", one interpretation could be the books of a single teacher. Alternatively, it could also be the books of many teachers. In situations like these, it is unclear which alternative would be the correct intention. Additional knowledge before the sentence is presented may be required to make the decision.

In addition, this paper has shown a situation when a syntax-restriction rule must be used to determine the correct meaning of an ambiguous term. Other ambiguity cannot be solved simply using the words in the given sentence. For example, although the punctuation usage rule may be used to verify whether a period or a question mark is used correctly, the same cannot be said between a period and an exclamation mark. This is because the most likely difference between declarative and exclamatory sentences is a sense of urgency or emotion, a distinction not evident in the text alone. The statement "I am angry" could either be an exclamation or a declaration based on the tone or the use of the appropriate punctuation. Consequently, the punctuation usage rule is required to disambiguate the intention for written sentences, but may be used as a syntax-restriction rule to understand oral conversation if the tone of the sentence heard can be distinguished by the system.

6 References

[1] C. Montero & K. Araki. " Is it correct?: towards web-based evaluation of automatic natural language phrase generation"; COLING/ACL on Interactive presentation sessions, Association for Computational Linguistics, 5-8, 2006.

[2] K. Shaalan. "Arabic GramCheck: a grammar checker for Arabic: Research Articles"; Softw. Pract. Exper. 35, 7, 643-665, 2005.

[3] S. Richardson &L. Braden-Harder. "The Experience Of Developing A Large-Scale Natural Language Text Processing System: CRITIQUE"; In ANLP, 195-202, 1988.

[4] E. Atwell. "How to detect grammatical errors in a text without parsing it"; Third conference on European chapter of the Association for Computational Linguistics, Association for Computational Linguistics, 38-45, 1987.

[5] N. Lin, K. Soe, & N. Thein. "Chunkbased Grammar Checker for Detection Translated English Sentences"; International Journal of Computer Applications, 28, 1, 7-12, 2011.

[6] N. Sondheimer & R. Weischedel. "A rule-based approach to ill-formed input"; 8th conference on Computational linguistics, 46–53, 1980.

[7] K. Cheng. "An Object-Oriented Approach to Machine Learning"; International Conference on Artificial Intelligence, 487-492, 2000.

[8] W. Faris & K. Cheng. "An Object-Oriented Approach in Representing the English Grammar and Parsing"; International Conference on Artificial Intelligence, 325-331, 2008.

[9] E. Ahn, W. Faris, & K. Cheng. "Recognizing the Effects caused by an Action in a Declarative Sentence"; International Conference on Artificial Intelligence, 149-155, 2009.

[10] W. Faris & K. Cheng. "Understanding and Executing a Declarative Sentence involving a forms-of-be Verb"; IEEE International Conference on Systems, Man, and Cybernetics, 1695-1700, 2009.

[11] W. Faris & K. Cheng. "Understanding Pronouns"; International Conference on Artificial Intelligence, 850-856, 2010.

[12] W. Faris & K. Cheng. "Generating a Sentence from a Thought"; International Conference on Artificial Intelligence, 554-560, 2011.

[13] K. Cheng. "Representing Definitions and Its Associated Knowledge in a Learning Program"; Proceedings of the International Conference on Artificial Intelligence, 71-77, 2007.

[14] R. Quirk, S. Greenbaum, G. Leech, & J. Svartvik. "A Comprehensive Grammar of the English Language"; New York: Longman, 1985.

[15] W. Faris & K. Cheng, K. "A Multi-dimensional Data Organization for Natural Language Processing"; Computational Methods in Sciences and Engineering, 9, 81-90, 2009.

[16] W. Faris & K. Cheng. "A Knowledge Based Approach to Word Sense Disambiguation"; in preparation.

Heuristics to Extract the Main Text from a Captured Web Page

Muthukumaran Chandrasekaran* and Michael A. Covington
Institute for Artificial Intelligence
The University of Georgia
Athens, Georgia 30602-7415
mkran,mc@uga.edu

Abstract

Web pages generally contain a large amount of information that is not part of their main content, such as navigation panels, copyright and privacy notices, and advertisements. Such irrelevant information, known as Web page noise, can seriously affect the accuracy of search and other web mining applications; the act of removing it is called "cleaning." Previously published work on web page cleaning is based on the observation that Web pages tend to follow fixed layouts and presentation styles, which can be recognized and parsed. Structural trees were generated, mostly by sampling pages of a particular website, to identify noisy blocks and eliminate them. In this paper, we introduce a different approach based on heuristics that extract the main text on the basis of its characteristics rather than any previously recognized structural pattern. The key insight is that the main text consists of blocks of relatively long lines that include high-frequency (common) words, while headlines and "noise" consist of smaller amounts of text, isolated from each other, with a higher proportion of rare words.

Keywords: Natural language processing, Artificial intelligence, Webpage cleaning, Content extraction

1 Introduction

A web page consists of numerous types of information which can be seen or heard by the end user, including the main text, subsidiary texts, non-textual information (static images, animated images, audio, video etc.), "on-page" interaction information (interactive text, interactive illustrations, and buttons), "between-page" interaction information (hyperlinks, forms), and internal (hidden) information (comments, scripts, metadata etc.). When a web page is to be analyzed by computer rather than viewed by a human being, extracting the main content can be a challenge; all the other content constitutes noise.

We present a technique to "clean" a retrieved web page, i.e., extract the main text of a web page from the "noise." Examples of noise in news websites, in general, include advertisements, navigation panels, copyright and private notices, side articles, user comments, and headlines of other stories. Although such information items are functionally useful for human viewers and necessary for website owners, they can seriously harm automated information collection and mining on the web. Classifying or mining noise-free web pages will improve the accuracy of search results as well as search speed and may benefit web page organization applications.

Web noise can be grouped into two categories: global noise (redundancy) and local (intra-page) noise. Global noise refers to redundant objects with large granularities, which are no smaller than individual pages. Global noise includes mirror sites, duplicated Web pages and old versioned Web pages to be deleted, etc. Local noise refers to irrelevant items within a Web page. It is usually incoherent with the main content of the page. Such noise includes images, advertisements, copyright information etc. This project deals with only local noise in Web pages.

Part of the challenge is that the goal is ambiguous — what constitutes "noise" depends on the purpose. For example, a news article from Yahoo contains side articles and user comments which may be considered as a part of the main text if useful in the sense that they talk about the same topic as the main content. However, there may be user comments that are not relevant to the main content. The challenge is to distinguish useful from noisy information. Surprisingly, despite its importance, relatively little work has been done in this field.

We developed heuristics based on the following initial observations of common news websites:

1. Headlines are short lines with a high proportion of low-frequency words or unique words.
2. The main text contains longer lines with more high-frequency (common) words.
3. News articles generally follow the inverted pyramid structure, with the most important content at the beginning.

Our approach presumes nothing about the structure of particular web pages, and with minor adjustment, should work equally well for websites in any language. To handle the fuzzy nature of the users requirements, the users are allowed to turn heuristic features on or off and set thresholds depending on how lenient they like their text stripper to be.

*Chandrasekaran, M. is the contact author (mkran@uga.edu)

2 Related Work

Web page cleaning is a challenging problem. Given its importance for any type of automatic reading of the Web, it is surprising to note that relatively little work about it has been published. In 2002, Lin and Ho (Lin and Ho 2002) proposed a method to identify informative blocks in Web pages. However, their work was limited by the following two assumptions: (1) the system knows a priori how a Web page can be partitioned into coherent content blocks; and (2) the system knows a priori which blocks are the same blocks in different Web pages. Their work views a web page as a flat collection of blocks, and each block is viewed as a collection of words. Bar-Yossef and Rajagopalan (Bar-Yossef and Rajagopalan 2002) defined web cleaning as a frequent template detection problem. Their work is not concerned with the context of a Web site, which can give useful clues for page cleaning. Their techniques developed so far work under the observation that Web pages have some structures which are reflected by their nested HTML tags. Kushmerick (Kushmerick 1999) proposes some learning mechanisms to recognize banner ads, redundant and irrelevant links of Web pages. However, these techniques are not automatic. They require a large set of manually labeled training data and also domain knowledge to generate classification rules. Techniques that analyze the text itself roughly fall into two categories: lexical cohesion methods (Beeferman, Berger, and Lafferty 1999; Kaufmann 1999) and multi-source methods (Beeferman, Berger, and Lafferty 1999). The former identifies coherent blocks of text with similar vocabulary. The latter combines lexical cohesion with other indicators of topic shift, such as relative performance of two statistical language models and cue words. Hearst and Plaunt (Hearst and Plaunt 1993) discussed the merits of imposing structure on full-length text documents and reported good results of using local structures for information retrieval. Instead of using pure text, which is unstructured, Lan Yi and Bing Liu (Yi and Liu 2003) processes semi-structured data. They make use of the semi-structures present in Web pages to help with the cleaning task. They propose a new tree structure called the compressed tree structure to concisely capture the commonalities of a Web site. It then uses an information based measure to evaluate the importance of each node in the compressed structure tree. Based on the tree and its node importance values, their method assigns a weight to each word feature in its content block.

Our approach to web cleaning is different from all of the existing technologies and is comparatively very simple. Its advantage is that it completely ignores the structure of web pages. It does not detect blocks or structures of web pages from their HTML tags or tree nodes. No pre-learning is required and hence training data or domain knowledge are not necessary. Our method is based on general characteristics of web pages, especially from news web sites, and is predicted to work almost equally well for websites in any language.

3 Key Challenges

As mentioned earlier, Web pages are multimedia. Since the objective is to extract just the main text from the web page, the first task is to eliminate non-textual information (images, audio, and video). The bigger challenge, however, is to distinguish relevant text from the rest. The main text is often observed to contain longer sentences and grammatical connectives like *and, or, the, if, is, to, from, for,* etc. (called "stop words" in information retrieval because they do not indicate subject matter). Some violations of these generalizations (e.g., short lines, lines containing only low-frequency words, or both) do occur within the main text. Side articles and user comments tend to appear after the main article. They may be relevant could be included as a part of the main text after extraction. However, if the end user is not motivated to include them, there will be problems because not only do they contain long sentences, they also contain "stop words" just like the main text. The words that appear in the headline, although uncommon, appear frequently within the main article because they define its subject matter. However, most often, names of people being referred to in the article are replaced by pronouns after their first occurrence. For example, if the article is about Roger Federer winning the Grand Slam, *Roger Federer* will be replaced by *he, him,* etc., after its first occurrence. News articles are often structured as an "inverted pyramid" — the most important part of a news article occurs at the top. This way, at any point of time, the reader can stop after reading the first few lines and still get an account of the story that is accurate as far as it goes. But a challenge arises if the news story is badly written or unconventionally structured.

4 The Proposed Heuristic

The experimental algorithm for extracting the main text from a web page (mainly from news websites) and eliminating local noise (such as other headlines, banner advertisements, non-textual information, navigation panels, copyright and privacy notices, useless side articles, and user comments) was written in Prolog.

Figure 1 shows a sample page from Yahoo News.[1] This page contains a news article about how a man built a huge ball out of rubber bands. The main content (boxed segment) only occupies approximately 1/3 of the original web page, and the rest of the page contains many advertisements, side articles, other news headlines, comics, copyright notices, etc. Such items are irrelevant and should be removed. Since each web site has its own unique structure, it would be necessary to find a suitable data structure dynamically in order to represent both the presentation styles and actual contents of the web page in the site. However, our approach eliminates such a requirement by completely ignoring the structure and basing the noise elimination wholly on the textual content in the page.

The first step of the algorithm is to take the downloaded web page and strip off all its HTML tags. After this step, all that remains is a file containing only textual information.

The next step, the *line-length stripper,* eliminates very short lines. This is necessary to account for the observation that the main text has relatively long lines. The threshold for

[1] http://news.yahoo.com/s/ap/20091029/ap_on_re_us/us_rubber_band_ball

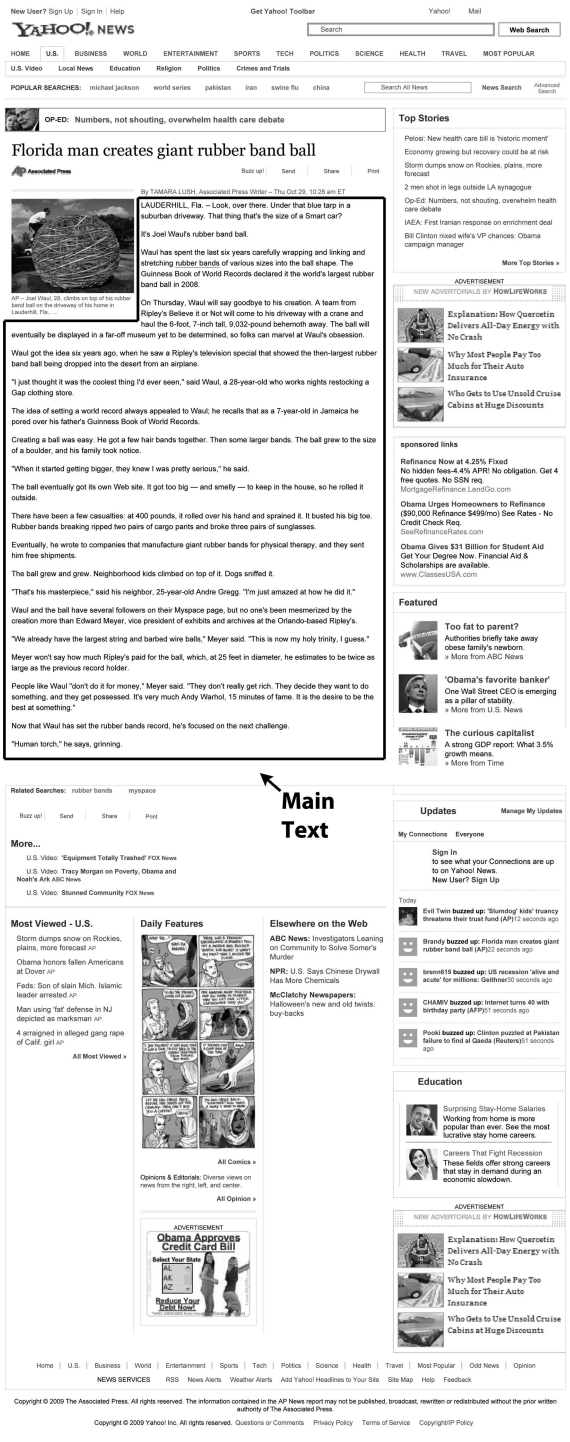

Figure 1: The main text in a web page with noise.

```
AP -- Joel Waul, 28, climbs on top of his rubber band ball
on the driveway of his home in Lauderhill, Fla.  ...

LAUDERHILL, Fla.  -- Look, over there.  Under that blue tarp
in a suburban driveway.  That thing that's the size of a
Smart car?  It's Joel Waul's rubber band ball.

Waul has spent the last six years carefully wrapping and
linking and stretching rubber bands of various sizes into
the ball shape.  The Guinness Book of World Records declared
it the world's largest rubber band ball in 2008.

On Thursday, Waul will say goodbye to his creation.  A team
from Ripley's Believe it or Not will come to his driveway
with a crane and haul the 6-foot, 7-inch tall, 9,032-pound
behemoth away.  The ball will eventually be displayed in a
far-off museum yet to be determined, so folks can marvel at
Waul's obsession.

Waul got the idea six years ago, when he saw a Ripley's
television special that showed the then-largest rubber band
ball being dropped into the desert from an airplane.

"I just thought it was the coolest thing I'd ever seen,"
said Waul, a 28-year-old who works nights restocking a Gap
clothing store.  The idea of setting a world record always
appealed to Waul; he recalls that as a 7-year-old in Jamaica
he pored over his father's Guinness Book of World Records.

Creating a ball was easy.  He got a few hair bands together.
Then some larger bands.  The ball grew to the size of a
boulder, and his family took notice.

The ball eventually got its own Web site.  It got too big --
and smelly -- to keep in the house, so he rolled it outside.

There have been a few casualties:  at 400 pounds, it rolled
over his hand and sprained it.  It busted his big toe.
Rubber bands breaking ripped two pairs of cargo pants and
broke three pairs of sunglasses.

Eventually, he wrote to companies that manufacture giant
rubber bands for physical therapy, and they sent him free
shipments.

The ball grew and grew.  Neighborhood kids climbed on top of
it.  Dogs sniffed it.

"That's his masterpiece," said his neighbor, 25-year-old
Andre Gregg.  "I'm just amazed at how he did it."

Waul and the ball have several followers on their Myspace
page, but no one's been mesmerized by the creation more than
Edward Meyer, vice president of exhibits and archives at the
Orlando-based Ripley's.

"We already have the largest string and barbed wire balls,"
Meyer said.  "This is now my holy trinity, I guess."

Meyer won't say how much Ripley's paid for the ball, which,
at 25 feet in diameter, he estimates to be twice as large as
the previous record holder.

People like Waul "don't do it for money," Meyer said.  "They
don't really get rich.  They decide they want to do
something, and they get possessed.  It's very much Andy
Warhol, 15 minutes of fame.  It is the desire to be the best
at something."

Now that Waul has set the rubber bands record, he's focused
on the next challenge.

Pelosi:  New health care bill is 'historic moment' Economy
growing but recovery could be at risk Storm dumps snow on
Rockies, plains, more forecast 2 men shot in legs outside LA
synagogue Op-Ed:  Numbers, not shouting, overwhelm health
care debate IAEA: First Iranian response on enrichment deal
Bill Clinton nixed wife's VP chances:  Obama campaign
manager

Copyright (c) 2009 The Associated Press.  All rights
reserved.  The information contained in the AP News report
may not be published, broadcast, rewritten or redistributed
without the prior written authority of The Associated Press.
```

Parameters: $T_1 = 0.6$, $T_2 = 0.9$ **(no window), "inverted pyramid" on.**

Slightly too much material is included because it could not be distinguished from the main text. The last line was missed because it was too small and towards the end of the document. Also, Figs. 1 and 2 were captured at different times and some rotating headlines had changed.

Figure 2: Text extracted from web page in Fig. 1.

number of words allowed per line in this step is indirectly obtained from the user so as to allow the user to control the elimination process in this step. However, to help the user to make an educated choice of threshold values, some good threshold values are suggested in the discussion section (later in this paper) based on their performance after the testing of the algorithm. The minimum number of words allowed per line is computed as follows:

$$\text{Minimum number of words} = T_1 \times \sqrt{\frac{\sum_{k=1}^{n}(x_k - \mu_1)^2}{n}}$$

That is, the minimum number of words allowed per line is user-supplied threshold T_1 times the standard deviation of the line length in words. Here n is the number of lines in the text, x_k is the number of words in line k, and μ_1 is the average number of words per line. This formula may seem too simple, but recall that the line length ranges all the way down to zero, so the standard deviation implicitly contains information about the mean as well as the variation.

After that step, some moderately short lines (like some headlines/captions or side articles) which are still in the text should be removed because they are not part of the main article. This is quite a challenge for a computer because it fails to recognize where these moderately short lines occur within the article. One way to differentiate those lines occurring in the main text from those that do not is by finding and comparing their subject matter with the main subject matter of the page. The ones that match in subject matter are considered to be within the main article and the ones that do not are considered to be noise.

A fair indicator of subject matter is the vocabulary. Consider the same example illustrated in Figure 1. The web page is about a man from Florida creating a rubber band ball. So, even if the words *rubber, band,* or even *ball* occur in a short line within the main text, the *word frequency stripper* (the program component that removes lines with the wrong word frequencies) will classify it with the main article because those are words with high frequencies in the story as a whole. Also, according to one of the initial observations, headlines (or captions) and side articles often comprise relatively short lines containing less-frequently-occurring words (see Figure 1), indicating that they are less likely to be a part of the main text.

The word frequency stripper decides whether to keep each line by computing a word frequency score for it and comparing this score to a threshold that is indirectly obtained from the user. The frequency score for each line is obtained by adding up the individual frequencies of each word in the line. Thus, lines containing common words or high frequency words have a high frequency score.

Again, to help the user to make an educated choice of threshold values, some good threshold values are suggested in the discussion section later in this paper. The threshold frequency score is computed as follows:

$$\text{Threshold frequency score} = T_2 \times \sqrt{\frac{\sum_{k=1}^{n}(y_k - \mu_2)^2}{n}}$$

That is, the threshold frequency score, to warrant keeping a line in the text, is user-supplied parameter T_2 times the standard deviation of the frequency scores y_k of the lines (μ_2 being their mean).

In the next pass, all the lines that begin with any character other than letters, numbers, parentheses, and single or double quotes are removed using the *character stripper* as it was observed to be very unlikely for sentences or words in the main text to begin with special characters.

The last step, *window/blur selection*, resembles vision more than text processing. Human beings recognize the main content of the web page visually, grouping characters and lines into sections of the text. Crucially, individual lines are grouped with the material in their immediate vicinity even if they, individually, do not meet the criterial for placement there. Thus a very short line at the end of a paragraph, or an individually anomalous line in the middle of a text, is not thrown out. To achieve this, we have to view the text "blurred," so to speak.

In window/blur selection, moving windows of 3 or 4 lines were considered and the frequency scores of each line in the window were combined. If the total score of a window was below a threshold, the shortest line in the window was removed but if the total score of the window was above the threshold, the shortest line remained.

In order to account for the possibility that reasonably long lines that may not be a part of the main content, could occur after it, higher scores are assigned to the lines occurring at the top of the article. The motivation behind this feature came from the concept of "inverted pyramid," which is a common news style followed by journalists all over the world. As mentioned earlier, important parts of the news article always occur at the top. Hence, it is intuitive to assign higher scores to the lines that occur at the top of the article because they are generally more important than the lines at the bottom. It is better to underestimate in the lower parts of the main article than to underestimate at the top. The datasets used in our experiments are described below followed by the goodness criteria discussion and evaluation measures.

5 Experiment Setup

For testing the above mentioned heuristics, 125 different news articles were collected, 25 each from the RSS feeds of popular news web sites such as BBC news,[2] CNN news,[3] Taipei Times,[4] ABC News,[5] and Yahoo News.[6]. As can be seen, each of these websites has its own unique structure and presentation style. Table 1 shows the different inputs from the user. The threshold ranges for which the proposed cleaning technique was implemented are also mentioned in the table. The results were then examined manually one by one and categorized based on a goodness score ranging from 0 to 10. A goodness score of 0 implies that none of the lines from the main content of the website appeared after the elimination process and a score of 10 implies that the extraction

[2] www.bbc.co.uk
[3] www.cnn.com/services/rss
[4] www.taipeitimes.com/News
[5] www.abcnews.go.com/Site/page?id=3520115
[6] www.news.yahoo.com/rss

FEATURE	USER INPUT
Short line Threshold - T_1	0.5 - 0.8 (in 0.1 intervals)
Frequency Threshold - T_2	0.5 - 1.2 (in 0.1 intervals)
Window Length - *w*	3 - 4 lines/window
Inverted Pyramid	on/off
Window Selection	on/off

Table 1: User inputs, feature selection options.

accuracy was 100% — none of the lines were over-estimated or under-estimated. The goodness criteria will be discussed in detail in the next section.

The heuristic was implemented on all 125 news articles, using each of the 64 threshold combinations, resulting in a total of 8000 output files, which were examined manually and goodness scores were assigned to each of them as described in the following section.

6 Discussion of Results

The performance of the proposed heuristic for the purpose of noise elimination and main textual content extraction was evaluated based on some goodness criteria. It is to be noted that for our experiments, side articles, user comments, copyright and privacy notices will be considered as noise. It is also assumed that over-estimation of the content is preferred over under-estimation. The headline or the caption of the main content may or may not be included as a part of the result, and the goodness score will not be affected by it. Because common news styles follow the Inverted Pyramid rule, over-estimation at the top is considered to be worse than over-estimation at the bottom. Based on these assumptions and the extent of over/under-estimation, goodness scores ranging from 0 to 10 are assigned as indicated in Table 2.

Figure 2 shows the result of processing the web page shown in Figure 1, with the specified threshold values. For those threshold values, the extraction was 100% accurate, with no over/underestimation. Hence, a goodness score of 100 is assigned to the output. All 8000 output files were evaluated in the same way. Table 3 shows the top five parameter combinations (on the left) for each web site and the total number of files that had goodness scores ≥ 9 with those parameters (broken up in the middle columns and summed on the right).

The table shows that 101 out of 125 files received goodness scores of 9 when the parameter combination of $T_1 = 0.5$, $T_2 = 1.1$ was used. Fewer articles from Yahoo news website received high goodness scores, possibly because most of them contained sections where some experts commented on the particular event. Hence, most of the Yahoo articles were assigned a score of 8, implying that 100 percent of the main textual content was extracted but there was over-estimation of more than 10 words at the bottom due to inclusion of related user comments. It is to be noted that these evaluations are done after manually examining all the output files. Table 4, showing the distribution of goodness scores, gives a clearer picture of how well the proposed technique worked. Note that 93.6 percent of the files had a goodness score ≥ 7, implying very high accuracy of the noise elimination process. Most of the files with a score of 8 came from web sites such as Yahoo News which contained lengthy and relevant user comments that were included as a part of the main text. Almost all output files received goodness scores greater than or equal to 5; none at all got a score below 4, implying that for the given range of thresholds, this technique ended up extracting more than 90 percent of the main textual content almost all the time. Those with scores of 4 resulted from experimenting with extreme threshold values.

7 Conclusion

This heuristic method of extracting the main text of a web page is a success. It does not make any presuppositions about the structure of the web page. Future improvements might include determining the parameters automatically by machine learning, testing heuristics on pages written in languages other than English, and testing the system as part of a web page clustering or classification system.

8 Acknowledgments

Co-author Covington's work on this paper was supported by NSF MINERVA grant BCS-0904669.

References

Bar-Yossef, Z., and Rajagopalan, S. 2002. Template detection via data mining and its applications. In *Proceedings of international conference on WWW*, 580–591. NY, USA: ACM.

Beeferman, D.; Berger, A.; and Lafferty, J. 1999. Statistical models for text segmentation. *Machine Learning* 34:177–210.

Hearst, M. A., and Plaunt, C. 1993. Subtopic structuring for full-length document access. In *Proceedings of the international conference on Research and development in information retrieval*, 59–68. NY, USA: ACM.

Kaufmann, S. 1999. Cohesion and collocation: using context vectors in text segmentation. In *Proceedings of the annual meeting of ACL on Computational Linguistics*, 591–595. NJ, USA: ACL.

Kushmerick, N. 1999. Learning to remove internet advertisements. In *Proceedings of conference on Autonomous Agents*, 175–181. NY, USA: ACM.

Lin, S.-H., and Ho, J.-M. 2002. Discovering informative content blocks from web documents. In *Proceedings of international conference on Knowledge discovery and data mining*, 588–593. NY, USA: ACM.

Yi, L., and Liu, B. 2003. Web page cleaning for web mining through feature weighting. In *Proceedings of the international joint conference on AI*, 43–48. CA, USA: Morgan Kaufmann Publishers Inc.

GOODNESS SCORE	EXPLANATION
10	Extraction accuracy was 100 % - none of the lines were over-estimated or under-estimated
9	100% main textual content extraction with over-estimation of less than 10 words at the bottom
8	100% main textual content extraction with over-estimation of more than 10 words due to inclusion of related user comments
7	100% main textual content extraction with over-estimation of less than 10 words at the top
6	Greater than 90 % textual content extraction and/or with under-estimation in the middle
5	Under- estimated extraction – Less than 90 % of the main textual content remained after elimination
4	Under- estimated extraction – Less than 70 % of the main textual content remained after elimination
3	Under-estimated extraction – Only less than 50% of the main textual content remained after elimination
2	Highly under-estimated extraction – Less than 30% of the main textual content remained after elimination
1	Grossly under-estimated extraction – Less than 10% of the main textual content remained after elimination
0	None of the lines from the main textual content of the website remained after elimination

Table 2: Goodness scores for evaluating some expected scenarios.

	BBC	CNN	TAIPEI	ABC	YAHOO	TOTAL (OUT OF 125)
T_1=0.5, T_2=1.1	21	20	21	22	17	**101**
T_1=0.6, T_2=1.1	21	22	19	20	16	**98**
T_1=0.5, T_2=1.0	20	21	19	19	16	**95**
T_1=0.6, T_2=0.9	19	20	20	19	17	**95**
T_1=0.6, T_2=0.8	20	18	19	18	16	**91**

Table 3: Top 5 parameter combinations and the total number of files with goodness scores ≥ 9.

Goodness Score	10	9	8	7	6	5	4	3	2	1	0	Total
No. of Output Files	4240	2375	118	757	124	343	43	0	0	0	0	8000

Table 4: Distribution of goodness scores in the entire experiment.

Segmentation of Natural Language Documents using Term Distance as Discourse Coherency Measure

ICAI 2012

Sandi Pohorec, Milan Zorman, Peter Kokol
Laboratory for System Design
University of Maribor, Faculty of electrical engineering and computer science
Maribor, Slovenia
{sandi.pohorec, milan.zorman, kokol}@uni-mb.si

Machine learning (ML) methods are used to extract new knowledge from existing datasets. Ensemble methods (EM) were introduced to improve the ML performance. While EM's offer performance improvements, they limit the amount of control and general understanding of how the final result was achieved. We are researching the possibility to verify ML results with formalization of research results accessible in natural language. We propose to use the extracted information from scientific papers for the verification of ML results. In order to be able to extract the information, relevant to the ML results, an approach to extract specific information rich segments from scientific papers is needed. We present an approach to automated selection of relevant segments from large repositories.

Keywords:natural language processing, information retrieval, machine learning, content segmentation

I. I. INTRODUCTION

A typical ML task is to induce a model using a training set with the final goal of predicting the classification class of new, unseen examples. A number of methods that solve this problem with varying success exist [3], [4]. One possibility to improve performance is the use of ensemble methods, which are also known as classifier fusion, committees of classifiers or multiple classifier systems. The main drawback of ensemble methods is the non-transparency of the final classification. As the final decision is a combination of multiple individual classifiers, it is necessary to understand the working logic of every ensemble member as well as the combination strategy used by the ensemble. Manual oversight of the ensemble results is several times more complex than the oversight of a single classifier. In many domains the verification and validation of results is of primary meaning. Any application of ML in the domain of medicine and biomedicine needs to be transparent. Domain experts have to be able to understand the underlying reasoning process that resulted in the final results. Since this is very time consuming the alternative is the validation by independent verification of the results.

If we are able to confirm the results of an ML ensemble, the time consuming process of manual inspection of each ensemble member and the combination policy can be significantly reduced. For the validation a reliable source is required. We believe that scientific papers preprocessed using natural language processing (NLP) and knowledge extraction (KE), offer the ability to automatically verify ML results. A precondition to the verification and validation of ML observations is the selection of relevant segments from large document repositories. The selection policy is dependent on the type of validation being carried out. For some tasks longer more detailed passages are required while other tasks require short passages with concentrated facts.

This paper is segmented into five sections: in Section 2 (motivation) we introduce ML and present EM's. Section 3 introduces theoretical background on information retrieval (IR) from document repositories. Section 4 represents the proposed algorithm for document segmentation. In Section 5 we present the experiment, in which our approach vas evaluated on a large document repository. Section 6 is the conclusion.

II. MACHINE LEARNING

A supervised learning problem is solved by providing a set of examples in the form of $f(e_i; r_i)$ [1], where the unknown function maps examples e_i to results r_i. Examples are usually vectors with real or discrete valued components; each component is a feature of x_i (x_{if} represents the f-th feature of x_i). The results r_i (for classification) are a discrete set of classes. Fig. 1 represents a simple decision tree classifier which uses, as features, the number of relapses in past 2 years, patient age and patients expanded disability status scale. The decision tree is used to classify patients into two classes: receive treatment and don't receive treatment. The classifier proposes a hypothesis on the true class to which the individual belongs. Example classifier represented in Fig. 1 hypothesizes that a patient with two or more relapses in the past two years who is between eighteen and fifty years old and whose EDSS is under 5.5 should receive treatment. The classifier has made such a hypothesis based on the training data it was supplied.

The accuracy of the classifier relies on the ability to form good hypotheses. Ability to form good hypotheses is very limited when size of training data is not proportional to the search space. The problem can be underrepresented (training data is too small) or the amount of data is so large it is not

feasible to learn a model on the entire data set. Without sufficient data, classifiers can form many different hypotheses and the model is unstable (if a small number of examples are removed the model changes drastically). In general EM's improve performance when the classifier needs to overcome these types of problems: small/large datasets, complex problems and heterogeneous datasets [5].

Ensembles are groups of models whose output is combined into a single result (output or prediction). The accuracy of ensembles is higher that of individual constituent models [1], [6] for both classification and regression. The theoretical basis for the improved performance of ensembles was provided in [7], [8], [9]. Ensemble learning is a two-step process: 1) learning of constituent models and 2) learning of the combination strategy. In order to ensure, that ensemble performance is better than the performance of individual members, the ensemble should be composed from diverse models. Diverse models make different classification errors and a good combination strategy can make the final results better. The diversity of the individual models can be achieved by either modifying the training dataset or by changing the learning algorithm. Modification of the dataset can be implemented with resampling techniques.

The most common method of combining individual predictions into the final result is voting [5], bagging [10], boosting [11] and random forests [12].

III. EXTRACTION OF RELEVANT DOCUMENT SEGMENTS

NLP required for the verification of potential new knowledge, discovered by ML, is typically a two-step process. First the document repository used for verification must be preprocessed. In the second step the actual verification of potential new knowledge is performed. The extraction of relevant text segments is a prerequisite to the extraction of information on individual ML generated rules.

Generally the document repositories can be classified into two categories: general and domain-specific. General repositories can contain documents from diverse scientific areas while domain-specific repositories contain only documents from the domain in question. If the source documents are a collection of scientific papers the repository is of a general nature (unless all of the papers focus on a specific area). An example of a domain specific repository would be a collection of patient data (admission form, symptoms on arrival etc.) from a specific hospital ward. With general repositories there is always the possibility that none of the documents would be relevant to the verification process. Therefore general repositories require an additional preprocessing step: the selection of relevant documents

A. Preprocessing

Preprocessing involves transformation to plain-text, tokenization and index creation. Transformation to plain-text depends on the source format of the document repositories, for scientific papers, which are usually written in PDF, this is a challenging process. For the document repository used in our experiments individual documents were stored in XML format. Consequently the extraction of plain-text required was a simple task of parsing the content from appropriate tags.

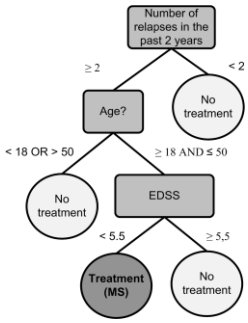

Figure 1. Decision tree classifier with three features (number of relapses, age, and expanded disability status scale. The classification classes are: receive treatment for multiple sclerosis and no treatment

Tokenization is the process of separating the text into tokens, individual lexical units (e.g. words). Tokens are not just words; in general a token is a sequence of characters that are grouped into a semantic unit [13]. Tokenization is an example of a more general problem, segmentation [14]. Manipulating text at the level of individual words is preconditioned with the ability to extract individual sentences. Segmentation into sentences is difficult because sentence-ending punctuations are ambiguous. Symbols that end sentences are also used within the sentence (abbreviations, numbers). We can view sentence segmentation as a classification task: each character that could end a sentence should be evaluated if it actually ends the previous sentence.

After the text has been tokenized the tokens are added to a unique index. This index is then used to create an inverted index with *tokenID* and *documentID* pairs. The inverted index enables quick scanning of large repositories. The index can be constructed with the use of singe-pass in-memory indexing algorithm [13]. Fig 2 represents the preprocessing: each document is transformed to a plain-text stream of text. The text is tokenized and a unique index of documents is constructed. Finally the inverted index linking terms to documents is created.

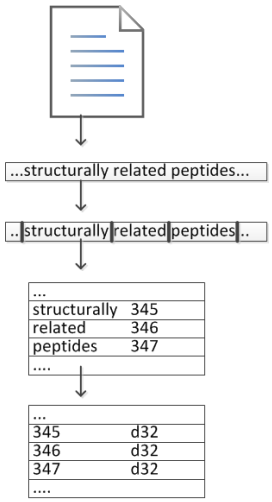

Figure 2. Preprocessing steps (bottom down): transformation to plain-text, tokenization and indexing (tokenID → documentID)

B. *Extraction of relevant segments*

The selection of relevant segments is dependent on the interests of the individual research. In general, scientific statements can be classified into some general dimensions. When selecting individual segments the approach needs to take into account the characteristics of individual phrases, sentences or paragraphs [15]. Scientific papers are already segmented into logical areas. Predefined units are: title, abstract, introduction, content sections/chapters (*1-n*), conclusion and references. These visual segments are then further segmented into paragraphs which are approximations of discourse changes. New paragraph inherently implies topic change or focusing on a smaller detail of the general topic.

The main problem with visual segmentation is that it is done without machine readable annotations of segments, in binary stored documents. When transforming the binary documents into stream of plain-text much of the formatting is lost. Therefore it is necessary to recreate much of the author's effort that went into determining boundaries of discourse. Extraction of knowledge from natural language documents requires automated discourse segmentation. The process segments individual documents into units where topic is uniform. Units are usually sentences or paragraphs. To segment a document a technique for the identification of borders is required. A border is defined as the area in text where a shift of topic occurs. A general algorithm for detecting areas where shifts of topic occurs is represented in Fig. 3. First the document is split into fixed units. In [16] it is suggested that the size of fixed units would be 20 words. Then the algorithm loops over every fixed-size unit and evaluates if two neighboring units have the same topic. If the topics are identical the two neighbors are joined and the search continues. Once a change of topic has been detected the left hand unit (which can be composed of several fixed-size units with coherent topic) is added to the list of coherently uniform segments. The search ends once all borders of the fixed size units have been evaluated and classified as either coherent uniform borders or not. The most difficult is the detection of topic coherency. The detection is done on the amount of "evidence" that the same topic is prevailing in both segments. Coherency is usually correlated to the position in the original text: introductions try to give a broad overview of the entire paper and are therefore much more diverse in covered topics, main sections of papers are longer and can discuss a the same topic for several paragraphs.

Well-known methods to evaluate cohesion that have been developed [18] are: *Vector Space Scoring* (VSM), *Block comparison* (BC) and *Vocabulary introduction* (VI). VSM evaluates the number of shared terms in the previous and the next two units of text. BC uses one unit on either side and does not consider inverse document frequency. VI is evaluated on the negative number of new terms in the left and right text units. Coherency measures need to be adapted to account for different types of text. One approach to achieve this is represented in Fig. 4, where a low pass filter is used to smooth the points in text where topic changes. This allows a certain degree of adapting the size of the segments to the type of text (longer segments on rare topic changes).

```
COHERENCY_DETECTION(document d)

fixed_segments ← SEPARATEINTOSEGMENTS (d)
t_coherent_seg ← ALLOCATEMEMORY ()
current_segment ← ALLOCATEMEMORY ()
borderIndex ← 1
while (all units have been processed)
do (borderIndex ← borderIndex + 1)
    if empty (current_segment)
        leftSegment = GETLASTITEM(fixed_segments)
    else
        leftSegment= current_segment

    rightSegment = GETNEXTITEM(fixed_segments)
    topic_left =  DETECTTOPIC(leftSegment)
    topic_right = DETECTTOPIC(rightSegment)
    if topic_left ≠ topic_right
        ADDTOLIST (topic_coherent_seg, leftSegment)
        current_segment ← DELETECONTENT()
    else
        APPEND(current_segment, rightSegment)
return topic_coherent_seg
```

Figure 3. Topic detection using coherency detection for document d

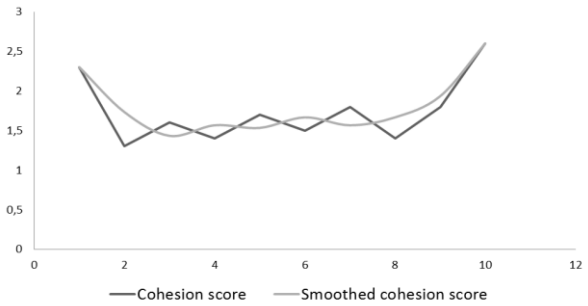

Figure 4. Cohesion score of a document, compared to the smoothed score using a low pass filter

```
EXTRACT_SEGMENT(document d, startPosition)

tokens ← TOKENIZEDOCUMENT (startPosition)
maxDistance ← SETMAXDISTANCE ()
current_distance ← 0
relevant_segment ← ALLOCATEMEMORY ()

tokenCounter ← 1
while (max distance has been reached)
do (tokenCounter ← tokenCounter + 1)
    currentToken = tokens [tokenCounter]
    ADDTOKEN(relevant_segment, currentToken)
    if TOKENISENTITY (currentToken) OR
    if TOKENISREFTOENTITY (currentToken)
        current_distance ← 0
    else
        current_distance ← current_distance + 1

    if current_distance = maxDistance
        break;

return relevant_segment
```

Figure 5. Algorithm for the extraction of relevant segments with the use of term and term-reference occurrences.

IV. ALGORITHM FOR EXTRACTION OF RELEVANT SEGMENTS

The approach we are proposing is a modification of Vocabulary Introduction. The entire algorithm is represented on Fig. 5. Instead of measuring the amount of newly introduced vocabulary we are measuring the distance from the last mention of the target entity or a reference to it. The starting point of the processing is at the index of target entity occurrence in the document. From then onward each of the following tokens are evaluated if it is the target entity or a reference to it. The end of the relevant segment is determined when a certain number of tokens have been found not to be a mention of an entity or a reference to it. The number of tokens which defines the maximum distance from the last mention of the entity or entity-reference is set at the average number of words per sentence in the entire repository.

Evaluation if the token is the mention of the target entity is comprised of two verifications. First is the evaluation if the token is a direct representation of the target entity: the entity itself, a synonym or an abbreviation of the entity. Much more difficult is the determination if the token is a reference to the entity itself. In fact the most challenging task in the algorithm is the resolution if a token is the reference to the target entity. This relies on the part-of-speech processing of the text. Using part of speech tags, together with hand-written rules, tokens are linked to previously encountered entities. If a link between the current token and a previously scanned token is found then the current token is treated as a reference to the target entity.

We have manually defined several types of frequently occurring sentence types. For instance: a definition type sentence begins with the target entity followed by a form of the verb "to-be" followed by a noun-phrase, optionally added with an additional description. Consider the following sentence where the target entity is "Crohn's disease":

"Crohn's disease is an inflammatory disease, which may affect any part of the digestive system."

The part-of-speech analysis of the sentence produces the following tags (using Brown corpus tag-set):

[('Crohns', NP$), ('disease', 'NN'), ('is', 'BEZ'), ('an', 'AT'), ('inflammatory', None), ('disease', 'NN'), (',', ','), ('which', 'WDT'), ('may', 'MD'), ('effect', 'NN'), ('any', 'DTI'), ('part', 'NN'), ('of', 'IN'), ('the','AT'), ('digestive', 'JJ'), ('system', 'NN')].

Our algorithm would try to match the input sentence to one of the predefined sentence types and find a match for the *definition* type of sentence. This type would suggest a specialization relation between "Crohn's disease" and "inflammatory disease" consequently meaning that the rest of the sentence refers either to the target entity or the more general category of the target entity. In any case, the word "which", tagged as a determiner can be categorized as a reference to the target entity since it refers to either the target entity itself or its general category.

V. EXPERIMENTAL EVALUATION

The experiment was done on a freely accessible dataset of scientific papers [17]. The dataset is a general repository. The dataset used for the experiments is a collection of scientific papers from the BioMed Central corpora [17]. The dataset contains 110.345 files. 3367 files don't contain full-text but a link to a PDF published online. We used only the files with full content. Statistics on file count, number of sentences and words in the dataset used in the experiment is represented in Table 1.

TABLE I. STATISTICS ON THE DOCUMENT REPOSITORY

Metric	***Value***
Number of files	110 345
Number of processed files	106 978
Number of sentences in processed files	35 377 906
Number of words in processed files	416 009 219
Average words per sentence	11.88
Average words per file	3888.74
Average sentences per file	330.70

A. Preprocessing

As the dataset contains documents in XML format the extraction of plain-text was done by extracting the relevant node and stripping away unnecessary tags. Tokenization was performed with a modified NLTK tokenizer [14]. NLTK tokenizer is a simple tokenizer that uses white space as a delimiter. Given many domain-specific terms in biomedical texts this type of tokenizer is not appropriate as it is unable to handle the complexity of punctuations in papers. Therefore some modifications were required. Considering that the final task of our research is the validation of new knowledge produced by ML, we have determined that, it is more profitable to have more tokens: the entities in the rule have to be located in the repository in order to extract knowledge on them. Therefore to improve retrieval the text should be split into all reasonable tokens (therefore white space splitting is insufficient). A hyphenated word "bottle-fed" should be tokenized into three tokens: "bottle", "fed" and "bottle-fed". This offers the possibility of matching a rule "IF food = bottle THEN …". The modification that we made to the NLTK tagger is an additional step after the initial tokenization on white-space. Each token from the first step is evaluated if it is reasonable to split it into multiple tokens. The initial white-space separated token is used for token normalization: it is converted to lowercase and all punctuations are removed. "Bottle-fed" becomes "bottlefed" with equivalence tokens: "Bottle-fed", "bottle-fed", "bottle" and "fed", ordered by relative token match ("bottle" and "fed" only match 50% of the original tokens). Relative token match is used at the retrieval of relevant documents.

B. Automated segmentation of documents

The repository was searched for all references of various diseases. Documents that contain names of well-known diseases were identified and a hundred documents were randomly selected to perform the evaluation of the approach. The set was split into three subsets and each was processed individually. Each document in each set was run through the algorithm to extract the relevant segments. The same documents were also manually inspected and human operators performed the segmentation and extraction of the segments in which, according to their judgment, relevant information on the target entities could be found. Table 2 presents the results of the algorithm compared to the results of manual segmentation. The average number of words (tokens) in extracted segments is compared to the values of manual extraction. Standard measure of the algorithm's ability to extract relevant segments is *recall.* The recall of the presented algorithm in the conducted experiment is 70.1%. The standard measure of *precision*, the ability to present only relevant items is somewhat altered: in our case the number of words in segments obtained by the algorithm is divided by the number of words in manually extracted segments. Consequently the precision of the presented algorithm is 78%. Given the precision and recall the F_1 score for the presented approach of document segmentation is 73.84%.

TABLE II. SEGMENTATION RESULTS

Set	*Evaluated property*	*Human*	*Algorithm*
S1	Avg. length of relevant segments [words]	63.4	39.6
S2	Avg. length of relevant segments [words]	49.2	55.4
S3	Avg. length of relevant segments [words]	58.9	42.1
S1	Num. of segments extracted [segment]	33	27
S2	Num. of segments extracted [segment]	33	22
S3	Num. of segments extracted [segment]	34	26

VI. CONCLUSION

We have presented an approach to automatically extract segments of natural language documents. The segments are used as source information for the verification and validation of ML results. It has been shown that a wider use of machine learning is inhibited by the effort that is required to validate the results. If we consider EM's that were introduced to improve the performance, the effort required to verify the final result grows exponentially. An approach that lessens the burden of manual validation is the filtering of ML results with the facts, research results found in scientific papers. The ability to extract relevant information from natural text relies on the ability of finding relevant documents and extracting topic coherent segments which discuss the entities from ML results. Extraction of relevant segments from large documents inherently introduces the problem of border definition. This paper presents an algorithm that uses a distance metric to determine the point where the segment is no longer topic coherent. The start of the relevant segment is the point where the target entity is introduced in the document. From that point on the text is tokenized and each token is evaluated if it is a mention of the target entity or a reference to it. Part-of-speech tags combined with inference rules are used to determine if the token is the entity, an abbreviation of the entity or a direct/indirect reference to it. The algorithm was evaluated on a set of 100 documents which were first manually processed to extract relevant passages. The experiment shows that the algorithm is capable of extracting the relevant passages; however it is dependent on the rules that allow it to classify individual tokens. In our future work we will focus on developing the rules that enable classification of tokens. We believe that a richer set of rules will allow the algorithm to recognize more obfuscated references to the target entities and consequently perform better.

VII. REFERENCES

[1] T. G. Dietterich, "Ensemble methods in Machine Learning", First Int. Workshop on Multiple Classifies Systems, Springer-Verlag, pp. 1-15, 2000.

[2] L. K. Hansen and L. K. Salamon, "Neural Network Ensembles", IEEE Trans. Anal. Mach. Intell, vol. 12(10), pp. 993-1001, 1990.

[3] T. Mitchell, Machine Learning. McGraw-Hill, New York, 1997.

[4] I. H. Witten and E. Frank, Data mining: practical machine learning tools and techniques, 2nd ed, Morgan Kaufmann, San Francisco, 2005.

[5] S. Dzeroski, P. Panov and B. Zenko, "Ensemble methods in Machine Learning", Encyclopedia of Complexity and Systems Science, pp. 5317-5325, Springer, 2009.

[6] E. Bauer and R. Kohavi, "An empirical comparison of voting classification algorithms: bagging, boosting and variants", Machine Learning, vol. 36 (1-2), pp. 105-139, 1996.

[7] E. L. Allwein, R. E. Schapire and Y. Singer, "Reducing multiclass to binary: a unifying approach to margin classifiers", J Mach Learn Res, vol 1, pp. 113-141, 2000.

[8] J. Kittler, M. Hafer, R. P. W. Duin and J. Matas, "On combining classifiers", IEEE Trans Patten Anal Mach Intell, vol 20 (3), pp. 226-239, 1998.

[9] R. E. Schapire, "A brief introduction to boosting", In Proc of the 6th International joint conference on artificial intelligence, Morgan Kaufmann, San Francisco, pp. 1401-1406, 1999.

[10] L. Breiman, "Bagging predictors", Mach Learn, vol. 24 (2), pp. 123-140, 1996.

[11] R. E. Schapire, "The strenght of weak learnability", Mach Learn, vol. 5(2), pp.197-227, 1990.

[12] L. Breiman, "Random forests", Mach Learn, vol 45(1), pp. 5-32, 2001.

[13] C. D. Manning, P. Raghavan, H. Schütze, Introduction to Information Retrieval , Cambridge University Press, Cambridge, UK, 2008.

[14] S. Bird, E. Klein and E. Loper, Natural Language Processing with Python: Analyzing Text with the Natural Language Toolkit, O'Reilly, Beijing, 2009.

[15] H. Shatkay, F. Pan, A. Rzhetsky, W. J. Wilbur, "Multi-dimensional classification of biomedical text: Toward automated, practical provision of high-utility text to diverse users.", Bioinformatics vol. 24 (18), pp. 2086-2093, 2008.

[16] M. A. Hearst, "TextTiling: segmenting text into multi-paragraph subtopic passages", Computational Linguistics vol. 23 (1) , pp. 33-64, 1997.

[17] BioMed Central's full-text corpus for text mining research: http://www.biomedcentral.com/about/datamining [last accessed on 01.Feb 2012]

[18] C. D. Manning, H. Schütze, Foundations of Statistical Language Processing, MIT Press, Cambridge, Massachusets, 1999.

A method for generating association words from several other words in an Association System

Misako Imono[1], Eriko Yoshimura[2], Seiji Tsuchiya[2] and Hirokazu Watabe[2]
[1]Dept. of Knowledge Engineering & Computer Sciences, Graduate School of Engineering, Doshisha University, Kyo-Tanabe, Kyoto, Japan
[2]Dept. of Intelligent Information Engineering & Sciences, Faculty of Science and Engineering, Doshisha University, Kyo-Tanabe, Kyoto, Japan

Abstract - *Humans communicate with others using natural language. Because many expressions in natural language can convey the same message, humans interpret these expressions flexibly based on their knowledge of words and association skills. An Association System was constructed on a computer by applying Concept Bases and the degree of association. This paper proposes a method for generating an association word from several other words with the Association System to show that it can achieve humanlike associative abilities on a computer. The proposed method generated a natural human association with 61.0% accuracy and 77.0% recall.*

Keywords: Concept Base, degree of association, association mechanism

1 Introduction

Recently, robots have been in demand not only for simple mechanical tasks but also for conveying information that is useful in everyday life. To do this, robots need to communicate with ordinary people. The most important factor in human communication is natural language conversation. So, it is important for robots to achieve humanlike conversational capabilities for easy communications with humans.

Humans can converse flexibly with natural language based on their knowledge of words, common sense, and ability to associate one concept with other concepts. This paper proposes a method for generating an association word from several other words. Humans can associate words such as "fishing, sewing, injections, prick…" from the word "needle." Words such as "fishing, sewing" are associative with the words "needle" and "thread." Humans associate only the related words, so if three words such as "needle," "thread," and "fish," are stated, humans associate only "fishing."

As mentioned, humans can make flexible multi-word associations by using their own knowledge of words. In this paper, an Association System, which consists of Concept Bases [1] [2] and degrees of association [3], achieves this kind of associative ability on a computer. A Concept Base is the modeling of the knowledge of a word, so the system is able to get knowledge about several words. In addition, the degree of association can choose the correct association word by determining whether a relationship exists between several entered words and the association word.

In this paper, we show the method for generating an association word from several other words to achieve humanlike associative abilities on a computer.

2 Association System

2.1 Concept Base

A Concept Base is a knowledge base that defines words as concepts. A concept is defined in the following equation.

$$A = \{(a_1, w_1), (a_2, w_2), ...(a_L, w_L)\} \quad (1)$$

A is the concept label, is the attribute, and is the weight of the attribute. The Concept Base in the Association System builds up to 87242 concepts. Table 1 shows a specific example of some concepts.

Table 1: Specific example of concepts

Concept	(Attribute, Weight)
Summer	(summertime, 0.34) (summer vacation, 0.11) ...
Summertime	(heat, 0.18) (sun, 0.04) ...
...	...

An attribute of the concept is called the first-order attribute. In the Concept Base, words defined as concepts also form the attributes. In addition, attributes can be derived from attributes. Attributes derived from attributes are called second-order attributes of the original concept.

In the example, the "summertime" attribute of the "summer" concept has been defined as a concept. So, the "heat" and "sun" attributes of the "summertime" concept are second-order attributes of the "summer" concept.

2.2 The degree of association

The degree of association (*DoA*) quantifies the relationship between concepts by using attributes that characterize the chain-reaction structure of the Concept Base. The relationship between multiple concepts is expressed quantitatively in this process. The following shows how to calculate the degree of association between concept A and concept B. This is defined as *DoA (A, B)*.

For concepts A and B with primary attributes ai and bi, weights ui and vj, and numbers of attributes L and M, respectively (L ≤ M), the concepts can be expressed as follows:

$$A = \{(a_1, u_1), (a_2, u_2), ...(a_L, u_L)\} \quad (2)$$

$$B = \{(b_1, v_1), (b_2, v_2), ...(b_M, v_M)\} \quad (3)$$

The degree of match DoM(A,B) between concepts A and B is defined as follows, where the sum of the weights of the various concepts is normalized to 1:

$$DoM(A,B) = \sum_{a_i = b_j} \min(u_L, v_j) \quad (4)$$

The degree of association is calculated by calculating the degree of match for all of the targeted primary attribute combinations and then determining the relation between the primary attributes. Specifically, priority is given to the correspondence between matching primary attributes. For primary attributes that do not match, the correspondence between primary attributes is determined to maximize the total degree of matching. By using the degree of matching, it is possible to give consideration to the degree of association, even for primary attributes that do not match perfectly. When the correspondences are thus determined, the degree of association DoM(A,B) between concepts A and B is as follows:

$$DoA(A,B) = \sum_{i=1}^{L} DoM(a_i, b_{xi}) \times \frac{(u_i + v_{xi})}{2} \times \frac{\min(u_i, v_{xi})}{\max(u_i, v_{xi})} \quad (5)$$

In other words, the degree of association is proportional to the degree of identity of the corresponding primary attributes, the average of the weights of those attributes, and the weight ratios.

3 A method for generating association words

The proposed method generates association words from the input of several words. Figure 1 shows a flowchart of the proposed method.

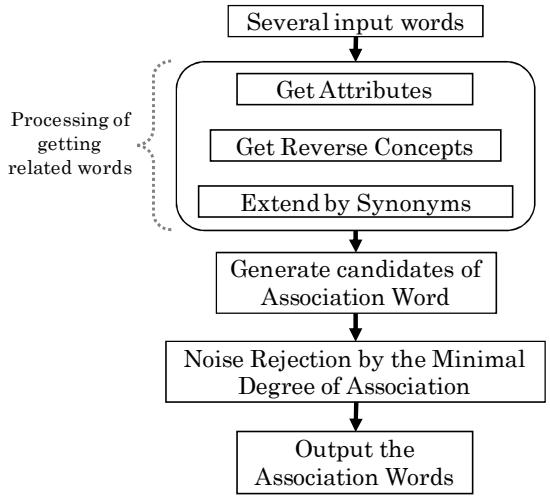

Figure 1: Flowchart of the proposed method

The input is several words which are defined in the Concept Base. There is no limit to the number of words. First, words related to the entered words are acquired from the three processes of Get Attributes, Get Reverse Concepts, and Extend by Synonyms. After acquiring the related words from the entered words, the related words generated for all entered words are considered as common related words. Before the output of association words, potential association words are processed by Noise Rejection by the Minimal Degree of Association to remove the noise from the common related words. The following sections explain each process in detail.

3.1 Get Attributes

A set of attributes defines the meaning of a concept, so the relation between concepts and attributes is relevant. To acquire attributes as related words in this process, the entered words are considered as concepts.

For the range of attributes to be acquired, the first-order attributes define the meaning of a concept directly, so the relevance is considered strong between the entered words and their first-order attributes. In addition, the second-order attributes define the meaning of the first-order attributes when these are viewed as a concept. This means that second-order attributes are considered potentially relevant with the original entered words. So, in the Get Attributes process, both first-order attributes and second-order attributes are generated as related words.

Figure 2 shows a specific example of Get Attributes from the entered word "summer."

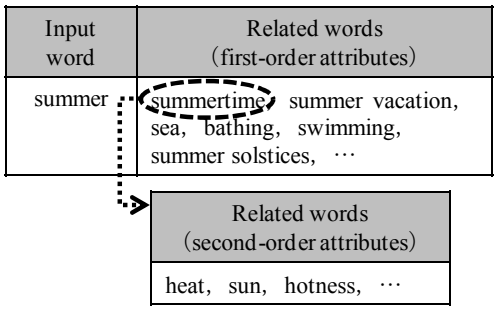

Figure 2: Specific example of Get Attributes from entered word "summer"

Related words such as "summer, summer vacation, sea…" are generated when getting only the first-order attributes. Second-order attributes such as "heat, sun…" are generated when first-order attributes such as "summer" are viewed as a concept.

A problem that occurs is an entered word with numerous attributes has too many related words. Therefore, second-order attributes are limited to 100 words. Specifically, first-order attributes can generate the top 10 words in weight and second-order attributes are generated from each of these first-order attributes.

3.2 Get Reverse Concepts

A concept Y is called the reverse concept of X when concept X is defined as an attribute of concept Y. A concept Y having concept X as an attribute means that reverse concept Y is defined by concept X. Thus, concept X and reverse concept Y are considered related. So, in this process, reverse concepts of entered words are acquired as related words.

Figure 3 shows specific an example of the Get Reverse Concepts.

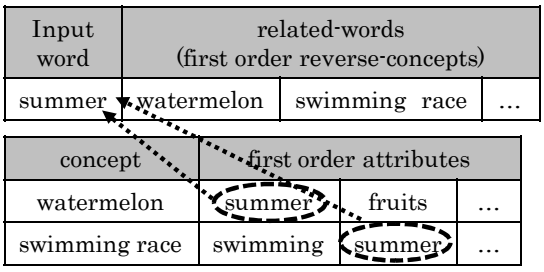

Figure 3: Specific example of Get Reverse Concepts from entered word "summer"

The entered word is "summer," so the concepts defined by "summer" as an attribute means that the reverse concepts of "summer" are acquired as related words. In this case, "summer" exists in concepts such as "watermelon" and "swimming" and also as attributes. Thus, these words are acquired as reverse concepts of "summer."

In addition, Get Reverse Concepts was performed with the same two patterns used for Get Attributes. That is, getting only first-order reverse concepts or getting first-order reverse concepts and second-order reverse concepts generate related words.

The second-order reverse concept is defined by an attribute defined with the entered word as an attribute. Second-order reverse concepts are also limited to 100 words. The top ten first-order reverse concepts are taken according to weight and second-order reverse concepts are generated from each of the first-order attributes.

3.3 Extend by Synonyms

In the Extend by Synonyms process, new related words are obtained from the synonyms of entered words. Specifically, the synonyms of entered words are considered as concepts to acquire first-order attributes and first-order reverse concepts as related words. Synonyms are acquired by a synonyms dictionary that is created automatically [4]. The synonyms dictionary is registered as a set of relations that consists of a head word and its synonyms. The number of registered relations is 31657 sets.

3.4 Generate Candidates of Association Word

In this process, related words that are generated for all entered words are acquired as common related words. Common related words have an association with all entered words, so these words are acquired as candidates of the final output (candidates of the association word).

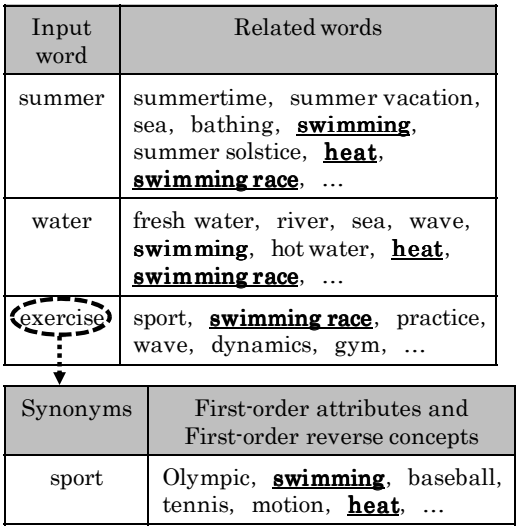

Figure 4: Specific example of Generate Candidates of Association Word from the entered words "summer," "water," and "exercise"

Figure 4 shows a specific example of Generate Candidates of Association Word from the entered words "summer," "water," and "exercise."

In this example, each entered word has the related words shown in the figure. The candidates of the association word are "swimming" and "heat".

3.5 Noise Refection by the Minimal Degree of Association

Due to noise, candidates of the association word obtained in the previous sections may be inconsistent with human association. So, the process in this section removes the noise of candidates of an association word according to the degree of association between entered words and candidates of the association word.

Candidates of association word C are obtained from entered words A and B. At this time, this process calculates each of the degrees of association between A and C, A and B. Then, the smaller value is defined as the lowest degree of association of C. The lowest degree of association is set as the threshold. If the lowest degree of association of C is lower than the threshold, candidates of association word C would be considered noise. In addition, the threshold of the lowest degree of association was determined experimentally as 0.05.

Figure 5 shows a specific example of Noise Rejection by the Minimal Degree of Association.

Candidates of association word	Input word	Degree of association
swimming	summer	0.10
	water	0.08
	exercise	0.06

Candidates of association word	Input word	Degree of association
heat	summer	0.04
	water	0.03
	exercise	0.02

Minimal degree of association is lower than the threshold

Figure 5: Specific example of Noise Rejection by the Minimal Degree of Association

In this case, candidates of the association word "swimming" and "heat" are obtained from the entered words "summer," "water," and "exercise." At this time, the process calculates the degree of association between each entered word and candidates of the association word. First, the lowest degree of association of "swimming" is 0.06 with the entered word "exercise." It is larger than the threshold, so the process is not performed. Next, the lowest degree of association of "heat" is 0.02 with the entered word "exercise." It can be determined that the association between the entered word "exercise" and candidates of the association word "heat" is slight since the lowest degree of association of "heat" is less than the threshold.

Therefore, one candidate of the association word "heat" is considered noise. The final output (association word) is "swimming" from the entered words "summer," "water," and "exercise."

4 Evaluation

An evaluation was performed using 100 test sets of several entered words and association word pairs created by a questionnaire. The test sets were created so that two or more entered words were needed to associate the association word. Precision and recall were evaluated by generating the association words by the proposed method with several entered words.

The precision was calculated by the percentage of correct association words determined correctly by more than two people in a visual assessment by three people. The recall was calculated to count the number of test sets generated for the association word described in the test set.

The evaluation was performed in two ways to obtain the related words. The patterns are as follows.

A: First-order attributes and first-order reverse concepts

B: A and second-order attributes and second-order reverse concepts

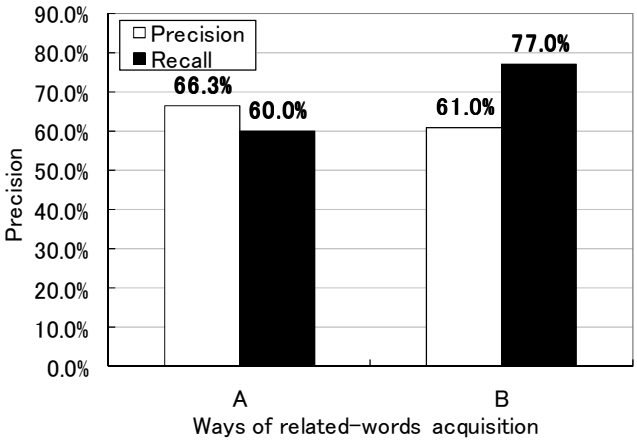

Figure 6: Evaluation

In addition, the process of Extend by Synonyms was applied to both patterns. Figure 6 shows the evaluation.

The precision of A is more than 5.3% higher than that of B. In contrast, the recall of B is more than 17.0% higher than that of A. The F-measure is 0.630 for A, 0.681 for B. Based on the above, method B (first-order attributes, first-order reverse concepts, second-order attributes, and second-order reverse concepts) in the acquisition of related words is proposed, since the precision was 61.0% and the recall was 77.0%.

5 Conclusion

This paper proposes a method of generating an association word from several other words by using the Association System. The proposed method was able to acquire related words by leveraging the knowledge of words defined in the Concept Base to generate the association words. The proposed method (first-order attributes, first-order reverse concepts, second-order attributes, and second-order reverse concepts) obtained a natural human association with 61.0% accuracy and 77.0% recall. This result shows that this study was able to achieve humanlike associative abilities on a computer.

Acknowledgment

This research has been partially supported by the Ministry of Education, Science, Sports and Culture, Grant-in-Aid for Scientific Research (Young Scientists (B), 24700215).

References

[1] K. Kojima, H. Watabe, and T. Kawaoka, “A Method of a Concept-base Construction for an Association System: Deciding AttributeWeights Based on the Degree of Attribute Reliability”, Journal of Natural Language Processing, Vol.9, No.5, pp.93–110 , 2002.

[2] N. Okumura, E. Yoshimura, H. Watabe, and T. Kawaoka: “An Association Method Using Concept-Base”, KES 2007/WIRN2007, Part I, LNAI4692, pp.604–611, 2007.

[3] H. Watabe and T. Kawaoka: “The Degree of Association between Concepts using the Chain of Concepts”, Proc. of SMC2001, pp.877-881, 2001.

[4] K. Kojima, A. Horiguchi, H. Watabe and T. Kawaoka: “Concept-Base Construction for a Word Association-System: A Method of Deciding Word Attribute Weights by Logical Relations and Attribute Reliability”, Proc. of The 6th World Multiconference on Systemics, Cybernetics and Informatics , Vol.5, pp.134-139, 2002.

Approaching Textual Entailment with Sentiment Polarity

Antonio Fernández[1], Yoan Gutiérrez[1], Rafael Muñoz[1] and Andrés Montoyo[1]
[1]Department of Software and Computing Systems, University of Alicante, Alicante, Spain

Abstract - *We present a study about the influence of sentiment polarity (positive, negative and neutral) in the Textual Entailment Recognition. The main idea of this paper is guided to identify the behavior of the sentiment polarity (obtained by a method of sentiment polarity classification based at the construction of Relevant Polarity Trees) on the Recognition of textual Entailment. Our analysis was conducted from a semantic conceptual point of view using a multidimensional resource. We also describe an experiment to evaluate the proposal in the Textual Entailment Recognition tack. The well knows dataset from Pascal Challenger RTE-1, RTE-2, RTE-3, RT4 and others like BPI, ENGARTE2 and Lexical were used as a corpus for testing our idea. Considering that only the sentiment polarity is utilized, we get an acceptable 66% of accuracy detecting the entailment relation between text-hypothesis pairs.*

Keywords: Textual Entailment, Sentiment Polarity, Opinion Mining, Multidimensional Semantic Analysis.

1. Introduction

The goal of Recognizing Textual Entailment (RTE) is to determine when one piece of text entails another. The ability to make such determinations is considered essential for several natural language processing tasks, such as information extraction, summarization, question answering and machine translation [1].

In this paper, we address the problem of RTE by treating it as a classification task. The main and unique feature we used was the recognition of the polarity in the text-hypothesis pair. Using for this, like dataset, those that were offered by the Pascal Challengers RT1 [2], RT2 [3], RT3 [4], RTE-4 (2-way only) dataset at TAC 2008 [5]. Also dataset from and ENGARTE[1], Lexical and BPI[2] had been used in order to increase the quantity of text-hypothesis pairs to examine. Of course, we used only dataset tagged with entailment information. Our principal objective is not to create a system for entailment detection, but appraising the influence of sentiment polarity in this task.

There are several resources involved in the sentiment polarity detection. *ISR-WN* [6] is a resource that allows us the integration of several semantic resources mapped to WordNet [7]. It is used as a core to link several resources like *SUMO* [8], WordNet Domains [9], WordNet Affect [10], Semantic Class [11] and SentiWordNet [12]. The integrated resource allows us to navigate inside the semantic network.

Using *ISR-WN* we tagged all the text-hypothesis entailment pairs with polarity information. Then we checked the relation between an entailment condition and polarity relation. We conduct several experiments to determine the influence of sentiment polarity in the Textual Entailment Recognition task.

The sections that follow present a brief overview of the related work, some important background and preliminaries for our idea, a description of the resource we used, the experiments that were performed, and the results obtained. In the last section, we offer our conclusions concerning to the influence of polarity in RTE task.

2. Related Work

Our word is partially related to [13], they presented and strategy for detecting author commitment to the truth/falsity of complement clauses based on their syntactic type and on the meaning of their embedding predicate. In addition, they showed that the implications of a predicate at an arbitrary depth of embedding about it complement clause depend on a globally determined notion of relative polarity. Finally, they demonstrate that different classes of complement-taking verbs have a different effect on the polarity of their complement clauses and that this effect recursively depends on their own embedding.

Other research [14] has been conducted in analyzing a methodology to detect phrases related to different characteristics and the employment of RTE for opinion mining. They test the entailment relation in a window of three consecutive phrases. In this work we can see from the obtained results, textual entailment can be useful at the time of performing category based opinion mining. However, such and as they mention, much remains to be done at the level of computing semantic similarity between opinionated texts.

There are not plenty of works about the influence of polarity in RTE. We only find a few of them that touch very lightly this theme. As far as we are aware of, such those researches has not been done in the same way, neither with our same purpose.

[1]http://nlp.uned.es/qa/ave

[2]http://wwww.cs.utexas.edu/~pclark/bpi-text-suite

3. Some background and preliminaries

There are many resources implicated in our front sight. These have been applied in order to conceptualize the analyzed sentences since different point of view. For example:

- WordNet (WN) [7] as taxonomy,
- SUMO (Suggested Upper Merged Ontology)3 [15] categories,
- WordNet Domains (WND) [9],
- WordNet Affect (WNA) [16],
- Semantic Classes (SC) labels [11],
- SentiWordNet (SWN) [12].

Amount these resources only SentiWordNet is a lexical resource where each synset of *WN* is associated to three numerical scores Obj(s), Pos(s) and Neg(s). Each score describes how Objective, Positive, and Negative the terms contained in the synset are respectively. That means that one synset would have three opinion-related properties with a certain degree (e.g. atrocious#3 [Pos: 0|Neg: 0.625 |Obj: 0.375]).

4. Integration of Semantic Resources based on WordNet (ISR-WN)

ISR-WN [6] is a resource that allows the integration of several semantic resources (the aforementioned resources) mapped to *WordNet*. In *ISR-WN*, *WordNet1.6* or *2.0* is used as a core to link those resources. As Gutiérrez et. al. [17] describe, the integrated resource allows navigate inside the semantic network, creating new virtual links amount elements of the different resources.

In order to apply the multidimensional polarity that *ISR-WN* can provide, we have analyzed related approaches like [18], [19], [20] and others published on NTCIR-8 MOAT competition [21] that take into account the polarity on the sentences. Then, we have decided to use Senti-RST [20] because it is an approach capable of being applied over several dimensions (resources) at once to obtain the polarity of the sentences, and it results are considered relevant to the polarity detection task.

5. Senti-RST

We propose to use an unsupervised knowledge-based method that uses the Relevant Semantic Trees (*RST*) [22] technique combined with *SentiWordNet*3.0 [12]. The aim of this method named by us *Senti-RST* [20], is to obtain a *RST* of each sentence and then associate this *RST* with sentiment polarity values. The process involves the following resources: *WND*, *WNA*, the *WN* taxonomy, *SUMO* and Semantic Classes (*SC*). Because of *SC* does not have a tree structure we simply obtain the Relevant Semantic Classes. Subsequently, we determine the polarities collected for each label of each *RST* obtained according to the analyzed sentence.

[3]http://www.ontologyportal.org/

Is important to remark that, the original RST is a method able to solve de word sense disambiguation task building relevant semantic trees of the sentences based on each semantic dimension of *ISR-WN*. In order to measure the association between concepts and words in each sentence according to a multidimensional perspective, *RST* uses the Association Ratio (AR) measure [23]. Our purpose is to include the Multidimensional Semantic Analysis into the Opinion Analysis using *RSTs*. The proposal involves four steps presented on next sections 5.1, 5.2, 5.3, 5.4.

5.1. Obtaining the Relevant Semantic Trees

In this section, we use a fragment of the original *RST* method with the aim of obtaining Relevant Semantic Trees of the sentences. Notice that this step must be applied for each resource.

Once each sentence is analyzed, the *AR* value is obtained and related to each concept in the trees. Equation (1) is used to measure and to obtain the values of Relevant Concepts:

$$AR(C, f) = \sum_{i=1}^{n} AR(C, f_i) \quad (1)$$

Where:

$$AR(C, w) = P(C, w) * log_2 \frac{P(C,\ w)}{P(C)} \quad (2)$$

In both equations *C* is a concept; *f* is a sentence or set of words (w); f_i is the *i-th* word of the sentence *f*; *P (C, w)* is the joint probability distribution; *P(C)* is the marginal probability.

Using the *WND* resource, we show the manner in which we obtain the *RST*. The first stage involves the lemmatization of the words in the sentence. Next, each lemma is looked up in *ISR-WN* and it is correlated with the *WND* concepts.

After obtaining the Initial Concept Vector of Domains, we apply Equation (3) in order to obtain the Relevant Semantic Tree related to the sentence.

$$AR(PC, f) = AR(ChC, f) - ND(IC, PC) \quad (3)$$

Where:

$$ND(IC, PC) = \frac{MP(IC, PC)}{TD} \quad (4)$$

Here $AR(PC, f)$ represents the AR value of PC related to the sentence *f*; $AR(ChC, f)$ is the AR value calculated with Equation (1) in case of ChC was included in the Initial Vector, otherwise is calculated with the Equation (3); ChC is the Child Concept of PC; ND is a Normalized Distance; IC is the Initial Concept from we have to add the ancestors; PC is Parent Concept; TD is Depth of the hierarchic tree of the resource to use; and MP is Minimal Path.

Applying the Equation (3), the algorithm to decide which parent concept will be added to the vector is shown here:

if ($AR(PC, f)$ $value$ $>$ 0){
if (PC had not been added to vector)
PC is added to the vector with $AR(PC, f)$ $value$;
else PC $value$ $=$ PC $value$ $+$ $AR(PC, f)$ $value$;}

The obtained vector represents the Domain tree associated to the sentence. After the Relevant Semantic Tree is obtained, the Factotum Domain is eliminated from the tree (it does not provide useful information [9] and experimentally we confirmed that it introduced errors).

5.2. Obtaining the Positive Semantic Trees

In order to obtain the Positive Semantic Trees (PST) of the sentence, we will follow the same process described in section 5.1. In this case, the AR values will be replaced by the polarity value pertaining to the analyzed sense. The polarity is obtained from the *SentiWordNet 3.0* resource, where each given word sense from *ISR-WN* for *WordNet* version 2.0 is mapped to *WordNet* version 3.0. Hence, we can find each given sense from *ISR-WN* in *SentiWordNet 3.0* and obtain the respective polarities. This new value will be called Positive Association ($PosA$). The $PosA$ value is calculated using Equation (5).

$$PosA(C, f) = \sum_{i=1}^{n} PosA(C, f_i) \quad (5)$$

Where:

$$PosA(C, w) = \sum_{i=1}^{n} PosA(C, w_i) \quad (6)$$

Where C is a concept; f is a sentence or set of words (w); f_i is a *i-th* word of the sentence *f*; $PosA(C, w_i)$ is the positive value of the sense (w_i) related to C.

The $PosA$ is used to measure the positive value associated to the leaves of the Semantic Trees where Concepts are placed. Subsequently, using the same structure of RST we create new Semantic Trees without *AR* values. Instead, the leaves with Concepts of this new Semantic Trees will be annotated with the $PosA$ value.

Later, to assign some Positive value to the parent Concepts, each parent Concept will accumulate the positive values from child Concepts. Equation (7) shows the bottom-up process.

$$PosA(PC) = \sum_{i=1}^{n} PosA(ChC) \quad (7)$$

Where PC is the Parent Concept; ChC is the Child Concept of PC; and $PosA(ChC)$ represents the positive value of the ChC.

5.3. Obtaining the Negative Semantic Trees (*NST*)

In this phase, we repeat the step described in Section 5.2, but for negative values.

5.4. Obtaining polarities of the sentences

In this step, we concentrate on detecting which polarity is more representative according to the Semantic Trees obtained for each resource (dimension). For that, we combine the RST with PST and RST with NST. Depending on the obtained results, we classify the sentence as Positive, Negative or Neutral. Of course, if there is not RST the sentence is tagged as UNKNOWN (UNK). Before performing this step, we have not to normalize the three types of Semantic Trees (RST, PST and NST) for each dimension to work with values between 0 and 1, because the original paper demonstrated that it introduce errors.

The goal is to assign more weight to the polarities related to the most relevant Concepts in each Relevant Semantic Tree. Equation (8) shows the steps followed in order to obtain the positive semantic value.

$$ACPosA(RST, PST) = \sum_{i=1} RST_i * PST_i \quad (8)$$

Where $ACPosA$ is the Positive Semantic Value of the analyzed sentence obtained for one Dimension, *RST* is the Relevant Semantic Tree sorted with the format: *RST [Concept| AR]*; *PST* is the Positive Semantic Tree sorted according *RST* structure with format: *PST [Concept|PosA]*; RST_i is the *i-th AR* value of Concept *i;* PST_i is the *i-th PosA* value of the concept *i.*

In order to measure the negative semantic value (*ACNegA*), we employ a similar equation replacing *PST* with *NST*. After obtaining the semantic opinion requirements, we evaluate our approach over thirteen annotated datasets from RTE for the monolingual English tasks.

This proposal consists of accumulating the $ACPos$ values and $ACNeg$ values of all Dimensions and comparing them. For a shorter representation we named this method $ALLRec$. The accumulated values will be named $ACPosD$ and $ACNegD$ respectively. In case $ACPosD > ACNegD$ the assigned value is POS, if $ACPosD < ACNegD$ the assigned value is NEG. Contrary to as Gutierrez in [20] did, in our proposal if it is not possible to create the RST for the analyzed phrase, therefore, there is not NST and PST neither $ACPosD$ and $ACNegD$ nor polarity result. In this case the assigned value is UNK (Unknown answer). Otherwise, the assigned value is NEU.

5.5. Calculating polarity for Text-Hypothesis pair

In order to evaluate our approach we used the rules and corpus that concern to the English Textual Entailment monolingual task (RTE-1, RTE-2, RTE-3, RT4, ENGARTE2, Lexical and BPI). Those data sets have not the same structure, for example, RTE3 and RTE4 includes the 3-way classification.

First, all the datasets were normalized converting them to the same format, in order to use the same structure for

classification of the entailment. We used only files annotated with the entailment condition. Table 1 shows all parameters of the dataset transformation.

Table 1. Parameters for Text-Hypothesis pair.

Id	pair identification number
entailment	condition of the entailment
task	task of which the pair was extracted from
length	pair length
<t>“”</t>	words from text
<h>“”</h>	Words from the hypothesis

The entailment parameter takes the values: entailment or non-entailment. All values were converted to this kind of classification.

After that, all datasets are processed with *Senti-RST*. Then, the steps explained in topic 5.1, 5.2, 5.3 and 5.4 are executed. The output is a collection of six file tagged with polarity information (Pos, Neg and Neu), one file for each resource (*WNA*, *WND*, *SC*, *SUMO*, *WN* and *ALLRec* described in topic 5.4 according to $ACNegD$ and $ACPosD$). As aforementioned in topic 5.4 each dimension (resource) was combined with *SentiWordNet* as a core for polarity detection.

Finally, 6484[5] text-hypothesis pairs from 13 datasets files with polarity information and entailment relation were tagged, departing of the following statement:

- If a text-hypothesis pair has an unequal polarity and there is not entailment, we tagged this relation as TRUE.
- If a text-hypothesis pair has an unequal polarity and there is entailment, we tagged this relation as FALSE.
- If a text-hypothesis pair has an equal polarity and there is entailment, we tagged this relation as TRUE.
- If a text-hypothesis pair has an equal polarity and there is not entailment, we tagged this relation as possible (POS).
- If at least one a text-hypothesis pair was tagged *Senti-RST* with UNK in its polarities, this pair will be excluded from any calculation.

Principally we attempted to find the truth of the first supposition through an experiment. This will be introduced in the following epigraph.

5.6. The experiment

We accomplished an experiment aimed at to verify the effect of the polarity on RTE datasets, specifically, looking for what kind of polarity relation the entailment and non-entailment text-hypothesis pairs would have.

As we have several resources that give us the opportunity to obtain the polarity, we attempted uniting these criteria to give a definite polarity to the text-hypothesis pair. Using the output getting from *Senti-RST*, we made a voting decision in order to assign the final polarity of the phrases. The voting took into account the polarity results (13 datasets files with text-hypothesis pair tagged with polarity and entailment information) obtaining from *WNA*, *WND*, *SC*, *SUMO*, *WN* and *ALLRec*:

The condition for voting was:

- If two resources agree with positive decision of polarity and two with negative, then we decided to assign neutral polarity, since there is no agreement between them.
- If two resources agree with negative polarity decision and two with neutral, we decide to assign negative polarity.
- If two resources agree with positive polarity decision and two with neutral, we decide to assign positive polarity.
- Other way, a resource with a greatest value decides the phrase polarity.

At last, we obtained 6484 text-hypothesis pairs from 13 datasets, tagged with polarity information assignee by six different ways. As well as the voting decision considering all of them.

Table 4 shows a summary of our experiment. The rows from one to four exhibits the obtained analysis for pairs with Unequal Polarity and Non-Entailment relation (*UPNE*), pairs with Unequal Polarity and Entailment relation (*UPE*), pairs with Equal Polarity and Entailment relation (*EPE*) and pairs with Equal Polarity and Non-Entailment relation (*EPNE*). Columns from two to six contain the results of every resource. Column seven display the result for *ALLRec* and in last column it can be seen the result for our voting technique.

The terms on the rows six to nine of Table 4 were calculated with the fallowing equations:

$$PNE = \frac{UPNE}{UPNE + EPNE} \tag{9}$$

Where, *PNE* is the precision detecting non-entailment relation. *UPNE*, the number of non-entailment pairs with unequal polarity is considered as CORRECT Non-Entailment detected and *EPNE*, the number of non-entailment pair with equal polarity, still when we know than a non-entailment relation can has equal polarity; this parameter is considered as INCORRECT Non-Entailment detected, because it contrasts with our purpose of determining the non-entailment condition from an unequal polarity relation of the text-hypothesis pairs.

$$PPE = \frac{EPE}{EPE + UPE} \tag{10}$$

Where, PPE is the precision detecting possible entailment relation; EPE, the number of entailment pairs with equal polarity is considered as CORRECT Entailment detected; and UPE, the number of entailment pairs with unequal polarity is considered INCORRECT Non-Entailment detected.

Also accuracy is calculated as follows:

$$A = \frac{H}{H + F} \tag{11}$$

Where, A is the accuracy, H is the number of successes detecting the non-entailment and possible entailment

[5]RTE1, RTE2, RTE3, RT4, Lexical, Engarte2 and BPI datasets.

relation and F is the number of failures committed also detecting the non-entailment and possible entailment relation.

The Average Precision is calculated as in [3]:

$$AP = \frac{1}{R}\sum_{i=1}^{n}\frac{E(i)x\#EntailmentUptopair(i)}{i} \quad (12)$$

Where n is the number of the pairs in the test set, R is the total number of positive pairs in the test set, $E(i)$ is 1 if the *i-th* pair is positive and 0 otherwise, and i ranges over the pairs, ordered by their ranking. As it was aforementioned in topic 5.5, pairs tagged with POS or UNK were excluded from this analysis. The pairs tagged with POS, because we cannot say that they are errors. Those tagged with UNK, because we did not find some kind of polarity information for tagging them, so this is not an error of our method.

6. Results and Discussion

It is important to remark that phrases polarity relation systems still show great inaccuracy [21], being 51% the best f-measure result. The system that obtained this punctuation, UNINE [18], targeted to get the relevant terms identified with one kind of specific polarity in order to get the polarity of the sentence.

Our elected method (*Senti-RST*) to detect the polarity of the sentences, presents a difference of 10 points regarding UNINE when it was evaluated over MOAT's corpus [20]. However, we elected this method because we wished to evaluate the influence of polarity, obtained from each resource integrated in *ISR-WN*, in recognizing textual entailment relation.

Doing an analysis of Table 4 we can see that *SUMO* gets the greatest number (1801) of *UPNE*, but also it gets the greatest number of *UPE* (1816). Seeing the quantity of *UPNE*, we can think that *SUMO* would be able to have the best value of *PNE*, but it comes as no surprise that our voting technique obtain the better result for this parameter (*PNE*=0.562). If we take a look at *UPNE* and *EPNE* relation, this behavior will be understood.

Taking in to consideration the relation between *UPE* and *EPE*, *WNA* obtains the best result (*PPE* (0.455)) detecting the entailment relation from equal polarity. Also the best value of Average Precision (see Table 3). Unfortunately, this resource contains labels of affective dominions that are correlated only with words that denote emotional statuses. *WNA*, it is not enough populated as if to offer a label to each examined word, failing in many instances (38.5%). Of course, *WNA* cannot be utilized isolated, but it is a good complement for improving other resources. We decide to maintain *WNA* in our voting in spite of his problems, because when it can act it does very well.

On the other hand, Table 4 also shows more cases tagged with *UPE* than *EPE*, it has no sense an entailment with unequal polarity relation, and this is due to *Senti-RST* error estimating the polarity. Consider the following two examples from RTE1 dataset (dev.xml, pair id=19):

- <t>Researchers at the Harvard School of Public Health say that people who drink coffee may be doing a lot more than keeping themselves awake - this kind of consumption apparently also can help reduce the risk of diseases.</t>
- <h>Coffee drinking has health benefits.</h>

These two phrases seem to be positive, but the polarity relation estimated by *Senti-RST* does not show that (see Table 2). Then also, the voting assigns a wrong polarity to the pair.

Table 2. Polarity assigned by *Senti-RST* and the voting.

Pair	WNA	WND	SC	SUMO	WN	ALLRec	Voting
T	Neu	Pos	Pos	Pos	Neg	Pos	Pos
H	Neu	Neu	Neu	Neg	Pos	Neg	Neu

Table 3. The Average Precision from 13 datasets.

	WNA	*WND*	*SC*	*SUMO*	*WN*	*ALLRec*	*Voting*
1	0.77	0.64	0.71	0.71	0.67	0.71	0.70
2	0.79	0.65	0.66	0.59	0.74	0.71	0.67
3	1.00	1.00	1.00	1.00	1.00	1.00	1.00
4	0.68	0.77	0.52	0.49	0.55	0.64	0.59
5	0.79	0.85	0.73	0.92	0.88	0.81	0.88
6	0.78	0.64	0.69	0.69	0.67	0.71	0.67
7	0.80	0.63	0.63	0.62	0.63	0.66	0.60
8	0.78	0.61	0.67	0.63	0.62	0.70	0.65
9	0.71	0.64	0.70	0.64	0.66	0.70	0.66
10	0.70	0.64	0.69	0.64	0.66	0.70	0.66
11	0.75	0.60	0.64	0.62	0.66	0.69	0.66
12	0.70	0.54	0.62	0.61	0.60	0.64	0.64
13	0.74	0.60	0.66	0.65	0.64	0.67	0.64

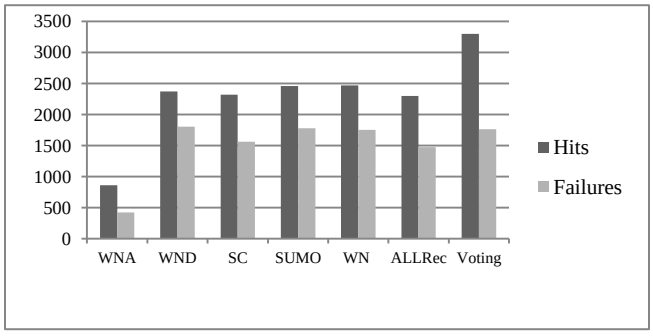

Fig 1. The Failures and Successes from each resource.

Continuing our analysis, we can see in Table 4 that our voting technique gets the greatest number of *UPNE* (0.562), and also (see Fig 1) a greatest number of successes. However, *WNA* exhibits the best relation comparing number of successes against number of failures, getting a better Accuracy (0.662). However, the voting surpasses *WNA* in about 2376 successes and exhibit a good Accuracy (0.646).

A resume of Average Precision for the 13 datasets is shown in Table 3. Only upon datasets four and five than *WND* and *SUMO*, respectively, they obtain better values;

WNA gets the maximum values of *AP*. However, we already knew the problem of low recall of this resource.

According to our judgment, the encouraging results of the voting technique (see Fig 1 and Table 4) it is due to the fact that is capable to take a better decision analyzing the verdict of all of the resources. As we can see in Table 3, all the resources have quite similar deportment, but also a complementary one. This, can be seen watching the behavior of *ALLRec*; excluding *WNA*, its results are better that each one of the isolated resources.

Table 4. Experiment results.

	WNA	***WND***	***SC***	***SUMO***	***WN***	***ALLRec***	**Voting**
Unequal Polarity and Non-Entailment (*UPNE*)	476	1733	1474	**1801**	1724	1409	1752
Unequal Polarity and Entailment (*UPE*)	426	1809	1565	**1816**	1751	1485	1755
Equal Polarity and Entailment (*EPE*)	355	667	839	730	744	880	**1462**
Equal Polarity and Non-Entailment (*EPNE*)	680	1432	1792	1466	1540	**1855**	1366
Non-Polarity Result (*NPR*)	2498	95	0	1	4	0	0
Precision detecting non-entailment (*PNE*)	0.412	0.548	0.451	0.551	0.528	0.432	**0.562**
Precision detecting possible entailment (*PPE*)	**0.455**	0.269	0.349	0.287	0.298	0.372	0.454
Accuracy (*A*)	**0.662**	0.568	0.598	0.581	0.584	0.609	**0.646**
Average Precision (*AP*)	**0.745**	0.678	0.684	0.675	0.690	0.725	0.678

7. Conclusion and future works

To our knowledge, this work represents the first attempt to discover the influence of sentiment polarity in the Recognition of Textual Entailment. We conducted an experiment with various datasets from the RTE task; showing that it is possible to detect -with an acceptable precision- the entailment and non-entailment relation, just analyzing the polarity of the text-hypothesis pair.

It is helpful to improve the method for calculating polarity with some kind of semantic analysis, in order to increase its precision. We accomplished a voting decision that he improved the calculation of polarity and it permitted us to get a good precision detecting non-entailment.

The resources as *WNA*, *SUMO* and the method *ALLRec*, seem to be very important for this task. It is urgent the taxonomic of *WNA*, because it is his weak point.

As a final remark, we observe that several resources are better for detecting non-entailment and others for entailment, so it is necessary to tackling this problem from a multidimensional point of view.

As further works, we propose to use this analysis as a new feature for a machine learning system.

8. Acknowledgments

This paper has been supported partially by Ministerio de Ciencia e Innovación - Spanish Government (grant no. TIN2009-13391-C04-01), and Conselleria d'Educación - Generalitat Valenciana (grant no. PROMETEO/2009/119 and ACOMP/2010/288).

9. References

[1] R. Bar-Haim, *et al.*, "Definition and Analysis of Intermediate Entailment Levels," in *Proceedings of the ACL Workshop on Empirical Modeling of Semantic Equivalence and Entailment*, 2005, pp. 55–60.

[2] I. Dagan, *et al.*, "The PASCAL Recognising Textual Entailment Challenge," in *Proceedings of the Workshop on Recognising Textual Entailment*, Southampton, UK, 2005, p. 18.

[3] R. Bar-Haim, *et al.*, "The Second PASCAL Recognizing Textual Entailment Challenge," in *Second PASCAL Challenges Workshop on Recognizing Textual Entailment*, Venice, Italy, 2006.

[4] D. Giampiccolo, *et al.*, "The Third PASCAL Recognizing Textual Entailment Challenge," in *Proceedings of the Workshop on Textual Entailment and Paraphrasing*, Prague, Czech Republic, 2007, pp. 1-9.

[5] D. Giampiccolo, *et al.*, "The fourth pascal recognizing textual entailment challenge," in *Preproceedings of the Text Analysis Conference (TAC)*, 2008.

[6] Y. Gutiérrez, *et al.*, "Integration of semantic resources based on WordNet," in *XXVI Congreso de la Sociedad Española para el Procesamiento del Lenguaje Natural*, Universidad Politécnica de Valencia, Valencia, 2010, pp. 161-168.

[7] G. A. Miller, *et al.*, "Introduction to WordNet: An On-line Lexical Database," *International Journal of Lexicography, 3(4):235-244.*, 1990.

[8] I. Niles and A. Pease, "Towards A Standard Upper Ontology.," in *Proceedings of FOIS 2001*, Ogunquit, Maine, USA. , 2001.

[9] B. Magnini and G. Cavaglia, "Integrating Subject Field Codes into WordNet," in *Proceedings of Third International Conference on Language Resources and Evaluation (LREC-2000)*, 2000, pp. 1413--1418.

[10] A. Valitutti, *et al.*, Eds., *Developing Affective Lexical Resources*. ITC-irst, Trento, Italy: PsychNology Journal, 2004.

[11] R. Izquierdo, *et al.*, "A Proposal of Automatic Selection of Coarse-grained Semantic Classes for WSD,"

Procesamiento del Lenguaje Natural, vol. 39, pp. 189-196, 2007.

[12] A. Esuli and F. Sebastiani, "SentiWordNet: A Publicly Available Lexical Resource for Opinion Mining," in *Fifth international conference on Languaje Resources and Evaluation* 2006, pp. 417-422.

[13] N. Rowan, *et al.*, "Computing relative polarity for textual inference," in *Inference in Computational Semantics ICoS-5*, Buxton, England, 2006, pp. 67-76.

[14] A. Balahur and A. Montoyo, "Semantic Approaches to Fine and Coarse-Grained Feature-Based Opinion Mining. Natural Language Processing and Information Systems." vol. 5723, H. Horacek, *et al.*, Eds., ed: Springer Berlin / Heidelberg, 2010, pp. 142-153.

[15] I. Niles and A. Pease, "Origins of the IEEE Standard Upper Ontology," in *Working Notes of the IJCAI-2001 Workshop on the IEEE Standard Upper Ontology*, Seattle, Washington, USA., 2001.

[16] C. Strapparava and A. Valitutti, "WordNet-Affect: an affective extension of WordNet," in *Proceedings of the 4th International Conference on Language Resources and Evaluation (LREC 2004)*, Lisbon, 2004, pp. 1083-1086.

[17] Y. Gutiérrez, *et al.*, "Enriching the Integration of Semantic Resources based on WordNet," *Procesamiento del Lenguaje Natural*, vol. 47, pp. 249-257, 2011.

[18] O. Zubaryeva and J. Savoy, "Opinion Detection by Combining Machine Learning & Linguistic Tools " in *Proceedings of NTCIR-8 Workshop Meeting*, Tokyo, Japan., 2010, pp. 221-227.

[19] R. Nairn, *et al.*, "Computing relative polarity for textual inference," in *Inference in Computational Semantics ICoS-5*, Buxton, England, 2006, pp. 67-76.

[20] Y. Gutiérrez, *et al.*, "Sentiment Classification Using Semantic Features Extracted from WordNet-based Resources," in *Proceedings of the 2nd Workshop on Computational Approaches to Subjectivity and Sentiment Analysis (WASSA 2.011)*, Portland, Oregon., 2011, pp. 139--145.

[21] NTCIR-8_MOAT. (2010, *NTCIR-8 Workshop Meeting*. Available: http://research.nii.ac.jp/ntcir/ntcir-ws8/meeting/.

[22] Y. Gutiérrez, *et al.*, "UMCC-DLSI: Integrative resource for disambiguation task," in *Proceedings of the 5th International Workshop on Semantic Evaluation*, Uppsala, Sweden, 2010, pp. 427-432.

[23] S. Vázquez, *et al.*, "Using Relevant Domains Resource for Word Sense Disambiguation," in *IC-AI'04. Proceedings of the International Conference on Artificial Intelligence*, Ed: CSREA Press. Las Vegas, E.E.U.U., 2004.

Enhancing Multi-document Summaries with Sentence Simplification

Sara Botelho Silveira and António Branco
University of Lisbon
Departamento de Informática
Faculdade de Ciências, Universidade de Lisboa
1749-016 Lisboa, Portugal
{sara.silveira, antonio.branco}@di.fc.ul.pt

Abstract— *This paper investigates the usage of a sentence simplification module that aims at improving automatically generated summaries built from a collection of texts. We describe an experiment with human subjects, that was conducted to assess the actual impact of sentence simplification in enhancing the summary quality. Motivated by those results, we present an automatic sentence simplification module that removes, from a sentence, specific sentential constructions that do not add critical information to the general message of that sentence. The rationale is that sentence simplification not only removes expendable information, but also makes room in a summary for further relevant data.*

Keywords: Multi-document summarization, sentence simplification, text simplification

1. Introduction

Text simplification is a NLP task that aims at making a text shorter and more readable, by simplifying its sentences structurally, into shorter and simpler sentences, while preserving the meaning and the information of the original sentence as much as possible. This task can be addressed in three ways: lexical, syntactic and discourse simplification. Lexical simplification involves replacing infrequent words by their simpler synonyms. To perform syntactic simplification, a linguistic representation of the text is produced as a tree-structure over which transformations are made [1]. Discourse simplification is concerned with maintaining coherence and cohesion of the simplified text: while syntactic simplification is applied to one sentence at a time, discourse simplification considers the interactions across sentences.

In order to improve the quality of the summary delivered to the end user, we discuss the inclusion of a syntactic simplification module within an extractive summarization system for Portuguese. Sentences are simplified after summarization to produce highly informative summaries.

Previous works ([2] and [3]) have focused mainly on syntactic simplification. Several types of structures are removed from a sentence based on rules induced using an annotated aligned corpus of complex and simplified texts. These structures include, for instance, passages delimited by punctuation, subordination and coordinating conjunctions, relative pronouns and boundaries of clauses and phrases. Closer to our work is the work of [4], in which simplification is used to improve content selection in a summarization system, that is, before summarizing. It is a syntactic simplification system, that uses hand-crafted rules which specify relations between simplified sentences.

A text usually contains passages that seek to explain or qualify other phrases, by providing background information about entities, or relating those entities to the discourse. These passages are parenthetical phrases. Appositions are a specific type of parentheticals, composed by a noun phrase that describes, details or modifies its antecedent (also a noun phrase). This type of phrases often add no crucial content to the correct comprehension of the sentence. Thus, we intend to remove those passages affecting the content expressed in the text to be summarized as less as possible.

The following examples present two sentences, from which parenthetical and apposition phrases (in bold) were removed, creating the corresponding simplified sentences.

Parenthetical phrase removal:

ORIGINAL SENTENCE:

Vilaça não duvidou declarar que Jones Bule ***(como ele chamava ao inglês)*** *fizera do Ramalhete "um museu".*

"Vilaça was the first to declare that "Jones Bule" **(as he called the Englishman)** had made of Ramalhete "a veritable museum"."

SIMPLIFIED SENTENCE:

Vilaça não duvidou declarar que Jones Bule fizera do Ramalhete "um museu".

"Vilaça was the first to declare that "Jones Bule" had made of Ramalhete "a veritable museum"."

Apposition phrase removal:

ORIGINAL SENTENCE:

Em 1858, Monsenhor Buccarini, ***Núncio de Sua Santidade,*** *visitara-o com ideia de instalar lá a Nunciatura.*

"In 1858, Monsignor Buccarini**, the Papal Nuncio,** had visited it with a view to establishing his residence there."

SIMPLIFIED SENTENCE:

Em 1858, Monsenhor Buccarini visitara-o com ideia de instalar lá a Nunciatura.

"In 1858, Monsignor Buccarini had visited it with a view to establishing his residence there."

To assess the possible improvements that simplification may bring to a summary, we performed a test with language experts, by asking them to rate simplified summaries over summaries whose sentences had not been simplified. The experts stated that simplification actually improves the final summary, since it allows the creation of a more simpler and incisive text, preserving at the same time the information to be conveyed. Based on these conclusions, we developed an automatic sentence simplification system that is included in a multi-document summarization system.

This paper is organized as follows: Section 2 describes the manual experiments; Section 3 describes the simplification system; Section 4 presents an evaluation of the summarization system with and without the simplification module; and, finally, in Section 5, some conclusions are drawn.

2. Manual Experiment

Experiments with human experts were made to assess whether text simplification improves the quality of a summary. Source texts were randomly selected from *TeMário* corpus [5]. Automatic summaries were build using GistSumm [6], a single-document summarizer for Portuguese (the only one available on-line). These summaries have a compression rate of 50%, since texts with a higher compression rate will not have enough material to work with. Then, simplified summaries were constructed by hand, from the automatic summaries, by removing parenthetical and apposition phrases from their sentences. This procedure was manually performed and aimed at simulating the process an automatic text simplification tool would execute.

In the first experiment, three language experts[1] were asked to perform two different tasks, in which they considered different texts (the source texts, the automatic and the simplified summaries). Also, they were invited to comment not only the tasks, but also the overall quality of the summaries. This experiment was based on two goals, Goal#1 and Goal#2, which will be pursued in two different tasks, Task#1 and Task#2, respectively. The two tasks, their goals and their evaluation are described in the following sections.

2.1 Task#1

This task aimed at verifying whether the simplified summary was a good summary for the original text (without taking into account the automatic summary). In order to perform this task, five texts, one from each section of the corpus (Special, World, Opinion, International, Politics) were selected. Experts were given the same five texts and their respective simplified summaries. Afterwards, they rated (0, bad – 5, very good) the simplified summaries concerning the original texts.

[1]Three researchers on Language Technology, graduated in linguistics.

Goal#1:

Confront the original text with a simplified summary, in order to assess the summary's quality.

Task#1:

Rate the **simplified summary** over the **original text**, concerning:
1. Readability (0 – 5);
2. Cohesion (0 – 5);
3. Coherence (0 – 5);
4. Fluency (0 – 5);
5. Original text idea preservation (0 – 5);
6. Overall quality (0 – 5);

Results are illustrated in Figure 1. By observing the graph, we can conclude that by having a low but positive grade (2.53) the *overall quality* of the summaries is acceptable. It is important to note that the best parameter is the *original text idea preservation* (2.93). Thus, we can infer that even though the simplified summary has less content, it does not mean that it does not maintain enough information conveyed by the original text. However, the way the information is presented is not the best, meaning the *fluency* (2.67) and the *readability* (2.6) of the text can be improved. The worst evaluated parameters are *coherence* (2.47) and *cohesion* (2.4). According to the experts, the sentence selection causes a lack of cohesion in the overall text. Since sentences seem disconnected and not linked with each other, text coherence is also compromised.

Fig. 1: Simplified summaries features.

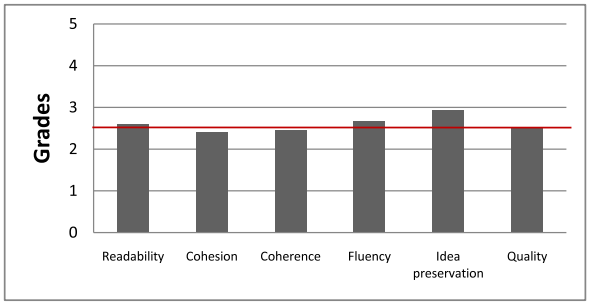

2.2 Task#2

This task aimed to confront both summaries to verify if the simplified summary, though with less content, can still convey the same information within the automatic one. It comprises two phases. In PHASE I, the simplified summary is rated vis a vis the automatic summary, considering the same set of features used in Task#1. PHASE II seeks to understand if the simplification process would not remove information that is relevant to the overall understanding of

the text. Thus, experts have answered a survey that compares the automatic and the simplified summaries.

Goal#2:

Compare an automatic summary with a simplified summary in order to assess the simplified summaries quality.

Task#2:

PHASE I: Rate the **simplified summary**.
1. Readability (0 – 5);
2. Cohesion (0 – 5);
3. Coherence (0 – 5);
4. Fluency (0 – 5);
5. Original text idea preservation (0 – 5);
6. Overall quality (0 – 5);

PHASE II: Answer the following questions by comparing the **simplified summary** with the **automatic summary**:
1. Which of the summaries is the best?
2. Consider that the simplified summary was built over the automatic one, by removing expressions considered unnecessary:
2.1. Were the removed expressions necessary?
2.2. Are there any expressions that you consider that should not have been removed?
2.3. Does the sentences context remain the same?
2.4. Does the simplified summary preserve the same idea of the original one?
2.5. Can the simplified summary replace the automatic one without losing information?
3. Other comments.

Before giving the two types of summaries to be evaluated by the human experts, both summaries were compared using ROUGE [7]. The graph in Figure 2 shows the f-measure values for all the 15 summaries used in this experiment. There is a slightly difference between them, as the average of the f-measure values for both automatic summaries (0.49752) and simplified summaries (0.49826) confirms.

Fig. 2: ROUGE f-measure values for automatic and simplified summaries.

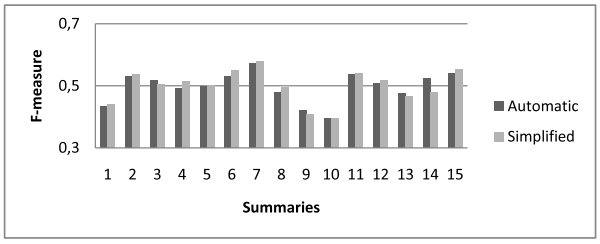

By comparing the graph in Figure 2 with the results in Figure 3, we can conclude that ROUGE does not reflect all the modifications performed in the simplified summaries, evidencing the need for manual evaluation. Nevertheless, it is a very useful tool to perform evaluation during system development, as metrics are obtained automatically.

To actually execute Task#2, each of the three experts was given five different texts. One text from each section of the corpus. Thus, we evaluated 15 texts, 3 from each section. This way, different sorts of texts were tested. Despite all of them being news texts, different sections may have different vocabulary and different writing styles. In PHASE I, experts did not have access to the original texts, so their conclusions were only based in the information contained in both summaries. Still, the automatic summary, by being longer and by having more content, should be expected to have more information than the simplified summary.

Figure 3 presents the answers given by the experts to the survey.

Fig. 3: Simplified summaries features.

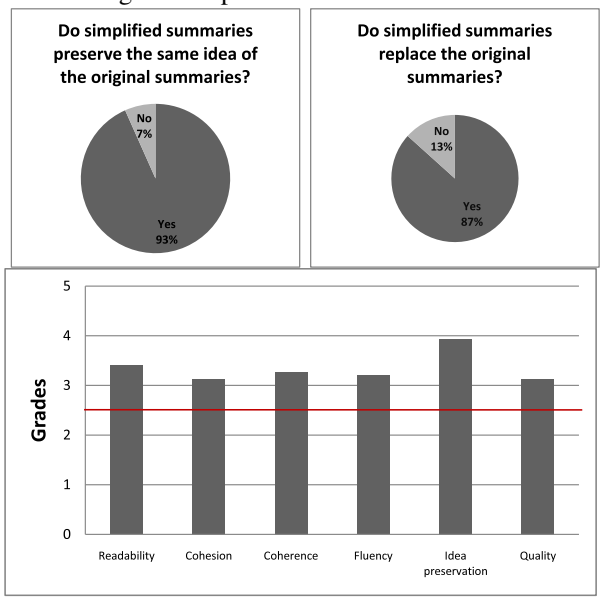

The answers to question 1. were not conclusive, since, as experts observed, the differences between automatic and simplified summaries are minimal. However, they definitely stated that simplified summaries can replace the non-simplified ones, which means that no relevant information is being missed. Thus, the information that was removed is not essential for the comprehension of the text. In addition, experts reported that the simplified summaries were simpler than the automatic ones. Also, they stated that the majority of the removed expressions were not necessary to the comprehension of the text content. Finally, they mentioned that, mainly when long parenthetical information is removed, text readability is improved.

Fig. 4: Parse tree for a sentence containing a relative clause.

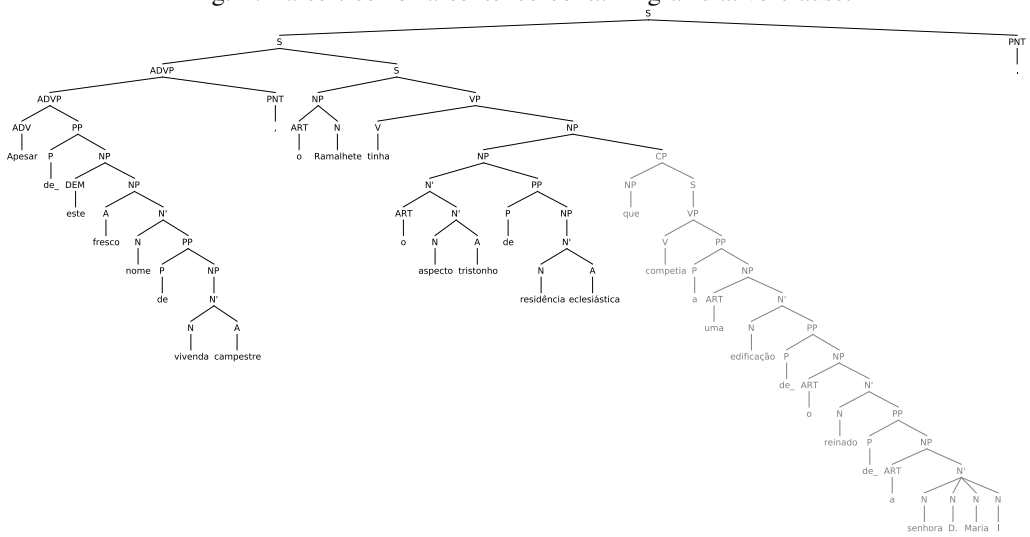

Since very similar texts were being compared, an improvement in the overall quantitative grades was expected. Nevertheless, the *original text idea preservation* was still the best feature (3.93), which lead to the fact that the information removed was indeed not essential in the summary. Moreover, this removal did not have a significant impact on text *readability* (3.4), seeing that the simplified text remains readable despite the modifications. This is not only reflected in the text *coherence* (3.27), *cohesion* (3.2), and *fluency* (3.13), but mainly in the text *overall quality* (3.13).

With this experiment, we can conclude that the simplified summaries preserve the original text idea. Also, the relevant information conveyed by the original text is maintained, allowing at the same time an optimization of the summary compression rate.

3. Simplifier

Based on the promising conclusions driven from the manual experiments, this task has been performed automatically. The simplifier is a module integrated in a multi-document summarization system, which produces generic summaries from a collection of texts in Portuguese, from any domain. After selecting the relevant content to be part of the summary, the chosen sentences are simplified to produce highly informative summaries. A detailed description of this summarizer can be found in [8].

The simplifier receives a set of sentences and retrieves them simplified. It includes two main phases, analysis and transformation, which are described in the next sections.

3.1 Analysis

The analysis phase aims to identify in each sentence the expressions which are candidate for removal. Three types of structures are recognized: (1) relative clauses; (2) parentheticals – explanatory or qualifying phrases; and (3) appositions – specific type of parentheticals, composed by a noun phrase that describes, details or modifies its antecedent (also a noun phrase). These phrases are candidates to removal, since they may introduce extra information whose removal does not affect the information eventually conveyed too much.

In order to identify the removable passages, a constituency parser for Portuguese [9] is used to build the sentence parse tree. Then, for each sentence, relative clauses, parentheticals and appositions are retrieved.

The following sentence contains a **relative clause**:

Apesar deste fresco nome de vivenda campestre, o Ramalhete tinha o aspecto tristonho de residência eclesiástica que competia a uma edificação do reinado da senhora D. Maria I.

"Despite that fresh green name worthy of some rural retreat, Ramalhete, as befitted a building dating from the reign of Queen Maria I, had the gloomy appearance of an ecclesiastical residence."

S *Apesar deste fresco nome de vivenda campestre, o Ramalhete tinha o aspecto tristonho de residência eclesiástica.*

"Despite that fresh green name worthy of some rural retreat, Ramalhete had the gloomy appearance of an ecclesiastical residence."

CP *que competia a uma edificação do reinado da senhora D. Maria I*

"as befitted a building dating from the reign of Queen Maria I"

Figure 4 illustrates the sentence parse tree in which both clauses are identified.

The first clause is the main one (starting in the top node *S* in the parse tree), and the second one is the subordinate relative clause (starting in the top node *CP* in the parse tree). Subtrees starting with the tag `CP` (complementizer phrase) are stored to be processed later.

Fig. 5: Parse tree for a sentence containing an apposition phrase.

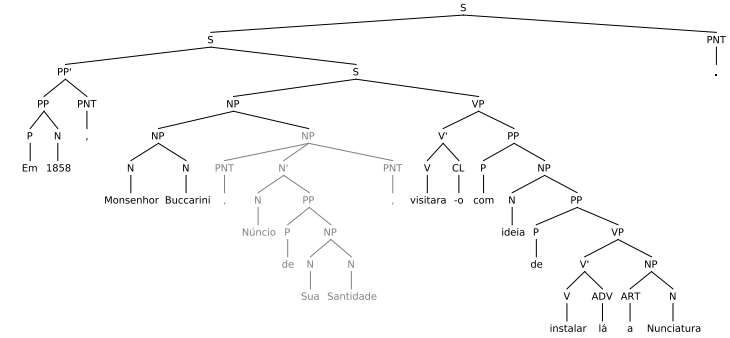

Fig. 6: Parse tree for a sentence containing a parenthetical phrase.

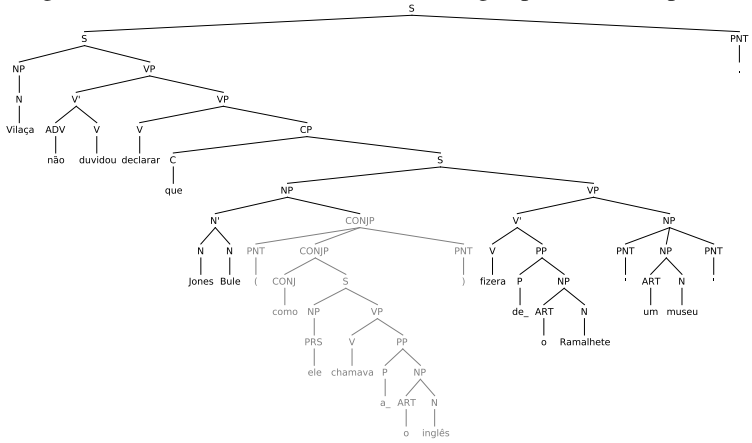

Appositions (specific type of parentheticals) are noun phrases, enclosed by commas or dashes, that define, describe or modify their antecedent which is also a noun phrase. Figure 5 depicts the parse tree for the following sentence, which includes an apposition:

Em 1858, Monsenhor Buccarini, ***Núncio de Sua Santidade,*** *visitara-o com ideia de instalar lá a Nunciatura.*

"In 1858, Monsignor Buccarini**, the Papal Nuncio,** had visited it with a view to establishing his residence there."

Considering the sentence parse tree, subtrees that start with the tags `NP` (noun phrase) or `AP` (adjective phrase), and whose leftmost child is a dash or a comma and whose rightmost child is a matching dash or comma or a period, are defined as appositions.

Parentheticals are phrases, enclosed either by parenthesis, or by commas or dashes, that explain or qualify other information being expressed. Consider the following sentence containing a parenthetical phrase:

Vilaça não duvidou declarar que Jones Bule ***(como ele chamava ao inglês)*** *fizera do Ramalhete "um museu".*

"Vilaça was the first to declare that "Jones Bule" **(as he called the Englishman)** had made of Ramalhete "a veritable museum"."

Figure 6 illustrates the parse tree for this sentence. In the parse tree, parentheticals are defined by a node, represented by any tag, which leftmost child is the opening punctuation token and its rightmost child is a closing punctuation token of the same type.

3.2 Transformation

The transformation phase aims to decide which of the phrases, retrieved in the analysis phase, can be removed without impacting on the sentence's overall informativity. Consider the following sentence:

Na conferência de líderes de ontem, a primeira da nova sessão, que a vice-presidente da bancada do PS, Ana Catarina Mendes, disse esperar que fique marcada pela 'governabilidade', ficou estabelecido que a execução orçamental será o tema central da Comissão Permanente.

"At yesterday's Leaders' Conference, the first of the new session which PS' delegation vice-president, Ana Catarina Mendes, said to hope it would be remembered by 'governability', it was settled that budget execution will be the main subject of the Standing Committee."

This sentence for instance has three removal candidates: a relative clause – *"que a vice-presidente da bancada do PS, Ana Catarina Mendes, disse esperar que fique marcada pela 'governabilidade'"*; and two appositions – *"a primeira da nova sessão"* and *"Ana Catarina Mendes"*.

For each sentence, the algorithm first considers the relative clauses, then the apposition phrases and finally the parenthetical ones. In order to obtain the new sentence, the parse tree of the original sentence is traversed until the index of the first leaf of the phrase to be removed is found. Also, the index of the last leaf of the phrase is gathered. Then, the parent node of these leaves is retrieved and the subtree is removed. The new sentence is then created without the subtree representing the phrase removed.

Afterwards, the simplification score is computed for both the main sentence and the new sentence. It is important to note that the simplifier is part of a text summarization system. This system computes the scores of the words composing the collection of sentences submitted as input, in order to select the most relevant sentences within that collection. Thus, the simplifier uses the simplification score to compare simplified sentences. This score is computed as the sum of each word score[2] composing the sentence divided by the total number of words of the sentence.

$$simplificationScore_{sentence} = \frac{\sum_{word \in sentence} score_{word}}{totalWords_{sentence}}$$

Considering the previous sentence and its removal candidates, the new sentences obtained along their simplification scores are shown in Table 1.

Table 1: Candidates to replacement.

	Candidate sentences	Score
1	*Na conferência de líderes de ontem, a primeira da nova sessão, que a vice-presidente da bancada do PS, Ana Catarina Mendes, disse esperar que fique marcada pela 'governabilidade', ficou estabelecido que a execução orçamental será o tema central da Comissão Permanente.* "At yesterday's Leaders' Conference, the first of the new session which PS' delegation vice-president, Ana Catarina Mendes, said to hope it would be remembered by 'governability', it was settled that budget execution will be the main subject of the Standing Committee."	0.01045
2	*Na conferência de líderes de ontem, a primeira da nova sessão, ficou estabelecido que a execução orçamental será o tema central da Comissão Permanente.* "At yesterday's Leaders' Conference, the first of the new session, it was settled that budget execution will be the main subject of the Standing Committee."	0.01615
3	*Na conferência de líderes de ontem, ficou estabelecido que a execução orçamental será o tema central da Comissão Permanente.* "At yesterday's Leaders' Conference, it was settled that budget execution will be the main subject of the Standing Committee."	0.01926

The first sentence in the Table is the original sentence and its simplification score is also compared with the ones of the simplified sentences. As the algorithm first considers the relative clauses, none of the simplified sentences contain the relative clause (*que a vice-presidente da bancada do PS, Ana Catarina Mendes, disse esperar que fique marcada pela 'governabilidade'*). Thus, the second simplified sentence was built by eliminating the relative clause. The third one is obtained by removing not only the relative clause, but also the first apposition referred (*a primeira da nova sessão*). The other apposition (*Ana Catarina Mendes*) is never considered since it is included in the relative clause. Owing that the third simplified sentence has the highest simplification score, it is the one selected to replace the original sentence in the final summary.

The same algorithm is executed for all the sentences which are candidates to be in the summary, ensuring the creation of a concise and highly informative text.

4. Evaluation

In order to perform evaluation, the *CSTNews* corpora [10], an annotated corpus composed of texts in Portuguese, was used. It contains 50 sets of news texts from several domains, for a total of 140 documents, 2,247 sentences, and 47,350 words. Each set contains, on average, 3 documents, which address the same subject, and an ideal summary (built manually). Ideal summaries have an average of 137 words, resulting in an average compression rate of 85%.

First, for each set of *CSTNews*, two types of summaries were created using our summarizer: simplified and non-simplified summaries. Simplified summaries are built by executing the whole summarization process. Otherwise, non-simplified ones are created without running the simplification module. In addition, summaries were generated using `GistSumm`[3] to serve as a baseline for our work. Summaries were built using a compression rate of 85% (average compression rate of the ideal summaries), meaning that the summary contains 15% of the words of the set of texts.

Afterwards, ROUGE [7] was used to derive precision, recall and f-measure metrics for the automatic summaries. ROUGE-L (longest common subsequence) was the metric selected, since it identifies the common subsequences between two sequences. This is a fairer metric compared to the original ROUGE-N metric, due to the fact that the simplification process introduces gaps in the extracted sentences. These gaps would not be taken into account when using a metric that considers co-occurring matches. Table 2 presents the results obtained.

Table 2: ROUGE-L evaluation metrics.

	GistSumm	Non-simplified	Simplified
Precision	0.3847	0.4276	0.4364
Recall	0.4362	0.4854	0.4942
F-Measure	0.4040	0.4492	0.4585

[2]The word score is the `tf-idf` score of the word considering the collection of texts to be summarized.

[3]Despite being a single-document summarizer, `GistSumm` also builds multi-document summaries by means of an option in its interface.

The complete summarization process has an overall better performance than the baseline considered, since both results with simplified and non-simplified summaries overcome the results obtained by `GistSumm`. The recall values obtained by our summarizer are very encouraging. These values indicate that there is a higher density of words that are both in the automatic summaries and in the ideal summaries. Retrieving the most relevant information in a sentence by discarding the less relevant data ensures that the summary indeed contains the most important information conveyed. This is a direct result of the simplification process. The precision values, by being identical, suggest that all summaries cover nearly the same topics. Intuitively, the precision values for the simplified summaries should decrease, since less in-sequence matches are likely to be found between them and the ideal summaries. When computing the f-measure value, by combining both precision and recall, we can confirm that both simplified and non-simplified summaries are better than `GistSumm` summaries.

Finally, note that the simplified summaries achieve better results than the non-simplified summaries. Despite being small, this difference between both summaries is very interesting. Yet, the simplification process is reflected in the evaluation of the summaries, implying that a simplification process, containing more sophisticated rules, can indeed be expected to help produce even better summaries.

5. Conclusions

This paper presents a text simplification system which is part of a text summarization system. The simplification system is focused on improving the summarization output, by simplifying the sentences composing the summaries. Our premise is that simplified sentences contain as much information as needed, helping to create more informative texts.

As manual experiments have hinted out, the simplification system is a huge contribution to the summarizer. Three main reasons lead to the decision of applying simplification after summarization: (1) this way, no relevant information is excluded before selecting the sentences to include in the summary, once all the computation regarding each original sentence has been done; (2) the simplification algorithm described does not remove the identified structures without constraints, since we aim to ensure that no crucial content is deleted from the sentence; (3) during the compression process, it is possible to add more relevant content to the summary that was not being considered in the initial list of sentence candidates.

Considering that most of the experiments have been done for the English language, we intended to prove that simplification actually improves summarization of texts in Portuguese, by using a corpora of Portuguese texts in all the experiments made.

References

[1] L. Feng, "Text simplification: A survey," The City University of New York, Tech. Rep., 2008.

[2] R. Chandrasekar, C. Doran, and B. Srinivas, "Motivations and methods for text simplification," in *In Proceedings of the Sixteenth International Conference on Computational Linguistics (COLING '96)*, 1996, pp. 1041–1044.

[3] H. Jing, "Sentence reduction for automatic text summarization," in *Proceedings of the sixth conference on Applied natural language processing*. Morristown, NJ, USA: Association for Computational Linguistics, 2000, pp. 310–315.

[4] A. Siddharthan, A. Nenkova, and K. McKeown, "Syntactic simplification for improving content selection in multi-document summarization," in *COLING '04: Proceedings of the 20th international conference on Computational Linguistics*. Morristown, NJ, USA: ACL, 2004, p. 896.

[5] L. Rino and T. Pardo, "Temário: Um corpus para a sumarização automática de textos," São Carlos – SP, Tech. Rep., 2003.

[6] T. A. S. Pardo, L. H. M. Rino, and M. das Graças Volpe Nunes, "Gistsumm: A summarization tool based on a new extractive method." in *PROPOR*, ser. Lecture Notes in Computer Science. Springer, 2003, pp. 210–218.

[7] C.-Y. Lin, "Rouge: A package for automatic evaluation of summaries," in *Text Summarization Branches Out: Proceedings of the ACL-04 Workshop*, S. S. Marie-Francine Moens, Ed. Barcelona, Spain: ACL, July 2004, pp. 74–81.

[8] S. B. Silveira and A. Branco, "Extracting multi-document summaries with a double clustering approach," in *Proceedings of the 17th International Conference on Applications of Natural Language Processing to Information Systems*. Groningen, The Netherlands: Springer, June 2012.

[9] J. Silva, A. Branco, S. Castro, and R. Reis, "Out-of-the-box robust parsing of Portuguese," in *Proceedings of the 9th Encontro para o Processamento Computacional da Língua Portuguesa Escrita e Falada (PROPOR)*, 2010, pp. 75–85.

[10] P. Aleixo and T. A. S. Pardo, "Cstnews: Um córpus de textos jornalísticos anotados segundo a teoria discursiva multidocumento cst (cross-document structure theory)." Universidade de São Paulo, Tech. Rep., 2008.

Comparison of Sentence-level Paraphrasing Approaches for Statistical Style Transformation

Foaad Khosmood
Department of Computer Science, California Polytechnic State University, San Luis Obispo, California, USA

***Abstract*-- We present six distinct English-language sentence paraphrasing techniques as transforms: *Active-to-Passive, Diction, Nodebox, Phrase, Simplify* and *Pivot translation*. We describe the basic algorithm for each and score them on precision and recall using 50 random sentences from project Tatoeba [1]. Our aim is to use these techniques for style transformation.**

Keywords: Computational Stylistics, Style Processcing, Natural Langauge Processing, Machine Learning, Computational Linguistics

1 INTRODUCTION

Statistical style transformation refers to an automatic method of rewriting text such that the information content remains the same, but the style of writing changes. Manual style transformation has been done successfully in the past [2]. In the absence of a precise universally accepted nomenclature and litmus test for different writing styles in natural languages, we define style as choice of expression [3] such as that often associated with an author. As the authorship attribution literature has shown, there are distinguishable style markers that can be used to successfully classify works by different authors [4][5] and hence also isolate their "style". Our approach uses this type of classification as a litmus test for achieving style transformation. This was done by Juola [6] already to evaluate manual style obfuscation cases.

Our model requires sentence level paraphrases to be continuously generated by modules (called transforms) and scored based on a greedy algorithm. Whichever paraphrased sentence would move the entire text statistically closest to the target style, that sentence is adopted and becomes part of the new text, but it could still be subject to further substitutions.

2 TRANSFORMS

The transforms are implemented as Python classes. They use various techniques such as typed dependency reformulation [7] or web-based validation [8] to produce a grammatical and synonymous sentence to the one they were passed in. All the implementation and most of the algorithms come from the authors, but external resources have been used quite extensively as stated below. We briefly describe each transforms.

2.1 Active to Passive transform (A2P)

Example: *The boy kicked the ball. => The ball was kicked by the boy.*

This transform converts an active voice sentence into its passive form. We encode 20 highly general rules in terms of parts-of-speech for basic active voice and equivalent passive voice cases [9][10]. The initial rules are mutated to produce 120 rules, adding variations to handle particles, adverbs and complex noun phrases. The input sentence is parsed into chunks using the Link Grammar Parser and compared with all the patterns in the database, and if matched, converted accordingly. Various NLP techniques are used to ensure plurals, pronouns and subject/verb agreement.

2.2 Diction Transform

Example: *The fact is, in the majority of cases, X is defined as an unknown. => Usually X is an unknown.*

This transforms employs a large number of rules for substituting wordiness and "bad style" phrases with their equivalent. The data sources are:

1. 655 rules from GNU *Diction* v. 1.11, itself based on *Elements of Style* [11].
2. 658 "wordiness" rules from Steve Hanov (Stevehanov.ca) partially based on William Zinsser's *On Writing Well.*
3. 409 word/alternative pairs from *The A to Z of alternative words* by the Plain English Campaign.

The rules are applied as straight string substitutions. Many of the rules had to be modified manually by the authors to remove "hints" and discussion originally designed to be examined by users of word editing programs. Some generic suggestions with no clear substitution suggestions were removed altogether from the original set of rules.

2.3 Nodebox transform

Example: *We recieved 6533 boxes. => We received thousands of boxes.*

This transform is based on the Nodebox Linguistics package [12]. It performs two tasks in particular: First, it

changes a set of unambiguous misspelled words, to their correct equivalents. Second, it converts Arabic numerical symbols modifying certain noun phrases into English approximation phrases.

2.4 Phrase replacement transform (Phrase)

Example: *I wanted to be with you alone => I desired to be with you only.*

This transform replaces phrases (defined as one or more consecutive words) with synonyms. It uses the Stanford Part of Speech Tagger to label each token in the phrase, and then uses Word Net to find synonyms for each non-overlapping phrase matching the POS in the input sentence.

For each phrase, this transform determines all the synsets of the same sense using *jcn* distance [13] to do Word Sense Disambiguation (WSD). The remaining candidates are ranked using two criteria: probability of co-occurrence with other words in the same sentence in the Microsoft BING N-Gram database (all bigrams and trigrams crawled by BING search engine) [14], and the probability of co-occurrence with other words in the same sentence in the target corpus. If the latter is not available, then only the search engine data is used.

Once a suitable candidate is chosen, NLP tools are used to produce the correct inflection before actual substitution. Heavy use of NLTK NLP tools [15] was made for this transform. The following figure summarizes the major steps in this transform and external tools used to accomplish them.

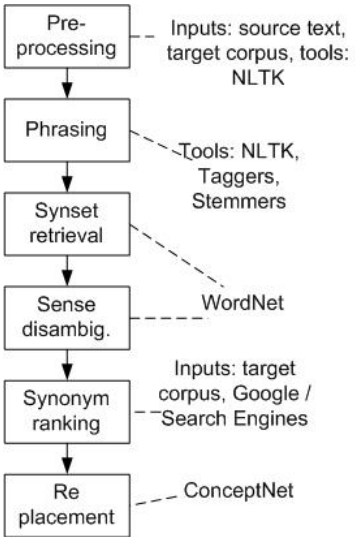

Figure 1. Phrase Transform

2.5 Simplify transform

Example: *I love Luna who is very cute and who is my pet. => I love Luna. Luna is very cute. Luna is my Pet.*

This transform aims to simplify sentences on several criteria, possibly producing more than one sentence as a result. It is written by Advaith Siddharthan [7] mostly in Perl, using the Stanford parser and the RASP toolkit. Two additional rules and a Python wrapper are written by the authors to integrate it into our evaluation system.

Simplify produces typed dependency trees for each sentence and then runs its user-modifiable rules to match patterns and adjust the final word order which could result in more than one sentence. It examines conjunctions and anaphora and looks for independent clauses that can be separated into their own sentences.

2.6 Pivot translation transform

Example: *I like to play Tennis. => I enjoy playing Tennis.*

This transform performs statistical translation by pivot: It translates an English sentence into another language and then translates the result back to English. The idea is that automatic translation tools usually produce valid but slightly modified sentences. A translation from English into another language and back to English could provide a valid semantic variation of the original with sufficient quality. Because of the high likelihood that the very same string is retuned, this transform accepts an ordered list of languages to try one at a time until a response different than the input is found.

As the back-end statistical translator, it supports Yahoo/Babelfish, Google Translator, and Microsoft Translator. We found the Microsoft product to be the most suitable for several reasons and we used it for this project.

3 METHODOLOGY

Fifty random English sentences are selected from the project Tatoeba [1] corpus, and passed on to each transform. Then each of the transforms produces responses consisting of zero, one or more paraphrased sentences for each of the input sentences. Some transforms such as *Phrase*, can produce more than one alternative paraphrase. Others such as *Diction* are highly specialized applying to few random sentences. We produce 381 paraphrases for the original 50 sentences. Each of these is scored on the scale of 0 to 3 by three separate human judges based on the following criteria.

Table 1. Evaluation criteria

Code	Criteria
3	Sentence is modified, preserves original meaning and original level of grammaticality.
2	Sentence is unmodified, or barely modified with very minor changes, or modified and the result is "acceptable" but not great.
1	Sentence is modified and the result is not acceptable.
0	No response, machine error or incomprehensible response.

4 RESULTS AND CONCLUDING REMARKS

Before the *Pivot translation* transform can be evaluated, we must decide which of the supported languages to use and how many languages to translate to before returning to English. Through a separate process using human 2 judges, we evaluate over 900 sentences using translation by pivot, and determined an ordered set of 8 languages (out of a total of 32 supported by Microsoft Translator) to use for the translation transform. In order of decreased effectiveness, they are: Czech, Swedish, Danish, Vietnamese, Norwegian, Dutch, Portuguese, and Spanish.

In addition, we generate three baseline translation "tours" (multiple language translations before returning to English) for comparison purposes. Tour1 is English->French->Spanish->German->English. Trou2 is English->Danish->Portuguese->Swedish->Vietnamese->English. TourR consists of English and four random languages.

All 381 paraphrases are scored for precision (majority score of the 3 judges). We derive the relevant precision and recall statistics as follows.

- *"recall" is calculated by counting the number of sentences for which the transform had a response (other than the input), divided by the total number of sentences, 50.*
- *"precision" is the average of all the (0-3) scores given by human evaluators to any response of the transform, across all sentences.*
- *"F-measure" is defined as* $F = \frac{2*(precision*recall)}{precision+recall}$

Table 2. Transform experiment evaluation results in terms of precision, recall and F-measure

Transform	Recall (%)	Precision (%)	F-measure
A2P	10	80	0.178
Diction	4	100	0.077
Nodebox	20	87	0.325
Phrase	100	82	0.903
Simplify	7.6	78	0.138
Translation	74	83	0.782
Tour 1	88	63	0.733
Tour 2	78	70	0.738
Tour R	88	58	0.702

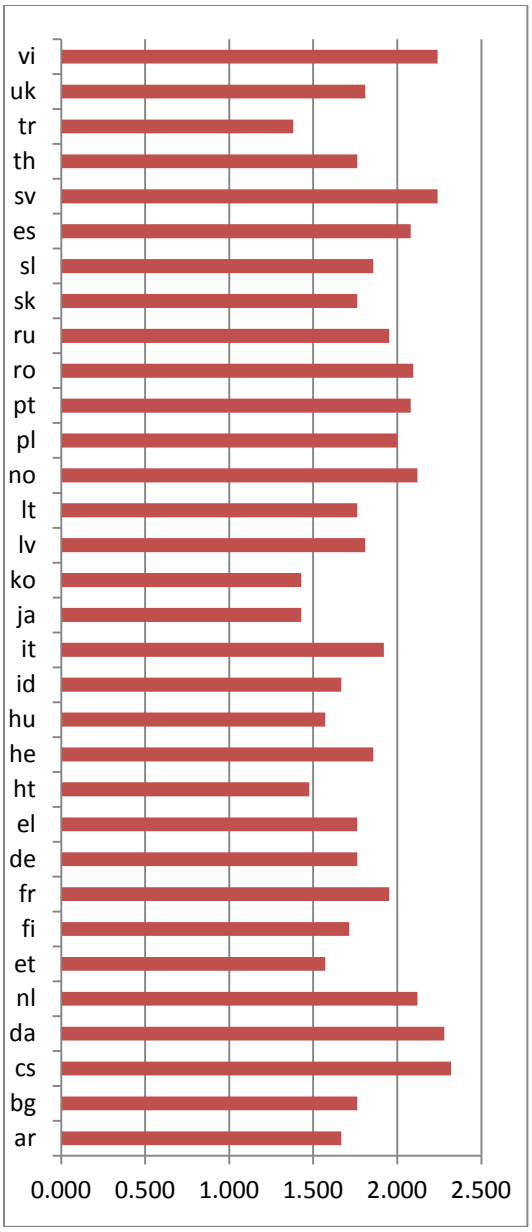

Figure 2. Microsoft translator language performance

As observed from Fig. 3, the transforms can be generally divided into two groups: high precision and high recall. The transforms in the high precision group have unsurprisingly low recall. This is because the patterns they generally seek are very specific, such as the "wordiness" phrases in *Diction*. The high recall group has more general pattern matching. Every sentence contains at least one word that would have a synonym in Word Net. Almost every sentence would have at least one translated paraphrase from some language.

We find that Phrase has the highest F-measure. But the real goal for our work is not to find a single approach, but to combine the power of different approaches to get a super-

transform of increased recall and precision. We are pursuing future work in this area.

Table 3. Microsoft Translator supported language codes (ISO 639-2)

Code	Language	Code	Language	Code	Language
ar	Arabic	he	Hebrew	ro	Romanian
bg	Bulgarian	hu	Hungarian	ru	Russian
cs	Czech	id	Indonesian	sk	Slovak
da	Danish	it	Italian	sl	Slovenian
nl	Dutch	ja	Japanese	es	Spanish
et	Estonian	ko	Korean	sv	Swedish
fi	Finnish	lv	Latvian	th	Thai
fr	French	lt	Lithuanian	tr	Turkish
de	German	no	Norwegian	uk	Ukrainian
el	Greek	pl	Polish	vi	Vietnamese
ht	Haitian	pt	Portuguese		

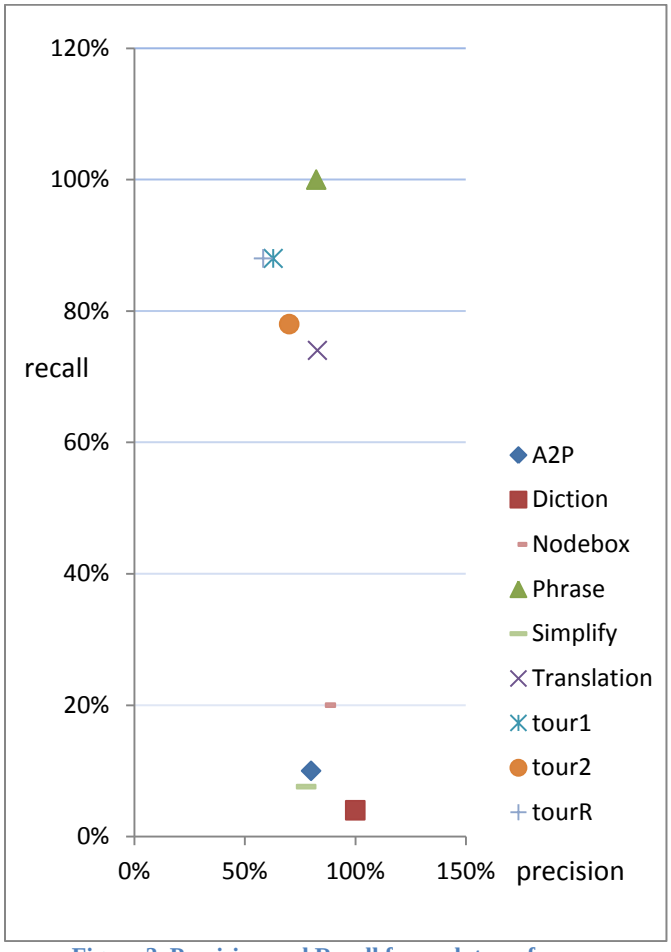

Figure 3. Precision and Recall for each transform

5 REFERENCES

[1] Project Tatoeba, English language sentence corpus (about 150,000 sentences). accessed from tatoeba.org, September 2010.

[2] D. L. Hoover. *Language and style in* The Inheritors, University Press of America. 1999.

[3] Jane Walpole. "Style as Option," *College Composition and Communication*, vol. 31, No. 2, Recent Work in Rhetoric: Discourse Theory, Invention, Arrangement, Style, Audience. May, 1980. pp. 205-212.

[4] J. F. Burrows. 'Delta': A Measure of Stylistic Difference and a Guide to Likely Authorship'. *Literary and Linguistic Computing*. 17(3), 2002. pp. 267-87.

[5] D. L. Hoover. 'Testing Burrows's Delta'. *Literary and Linguistic Computing*. 19(4), 2004. pp. 453-75.

[6] Patrick Juola. "Empirical evaluation of authorship obfuscation using JGAAP," in *Proceedings of the 3rd ACM workshop on Artificial intelligence and security*, AISec, 2010.

[7] Advaith Siddharthan. "Complex lexico-syntactic reformulation of sentences using typed dependency representations". In Proceedings of the 6th International Natural Language Generation Conference (INLG 2010), Dublin, Ireland. pp. 125-133.

[8] Houda Bouamor et. al. "Web-based validation for contextual targeted paraphrasing," *Proceedings of the ACL Workshop on Monolingual Text-To-Text Generation* 2011.

[9] EnglishPage by Language Dynamics, (www.englishpage.com), accessed Dec. 2010.

[10] Huddleston and Pullum. *A Student's Introduction to English Grammar*, Cambridge University Press, 2005.

[11] William Strunk. *The elements of style*, Ithaca, N.Y.: Priv. print., 1918.

[12] Frederik De Bleser, Tom De Smedt, Lucas Nijs. NodeBox version 1.9.5 for Mac OS X. Retrieved March 2010, from: http://nodebox.net

[13] Jiang, Jay and Conrath, David (1997). Semantic similarity based on corpus statistics and lexical taxonomy. In *Proceedings of International Conference Research on Computational Linguistics* (ROCLING X), Taiwan.

[14] Micorsoft Web N-Gram service, public Beta program, http://web-ngram.research.microsoft.com/info/ accessed 2011.

[15] Steven Bird, Ewan Klein, and Edward Loper, *Natural Language Processing with Python*, O'Reilly Media. 2009.

SESSION

INTELLIGENT LINGUISTIC TECHNOLOGIES, ILINTEC'12

Chair(s)

Dr. Elena Kozerenko

Quantity and Degree Assessment in an RDF-based Semantic Language

Igor Boguslavsky
Universidad Politécnica de Madrid, Spain / Institute for Information Transmission Problems, Russian Academy of Sciences, Moscow, Russia

Abstract - *This paper introduces a semantic language developed with the objective to be used in a semantic analyzer based on linguistic and world knowledge. Linguistic knowledge is provided by a Combinatorial Dictionary and several sets of rules. Extra-linguistic information is stored in an Ontology. The meaning of the text is represented by means of a series of RDF-type triples of the form* predicate(subject, object). *Semantic analyzer is one of the options of the multifunctional ETAP-3 linguistic processor. The analyzer can be used for Information Extraction and Question Answering. We describe semantic representation of expressions that provide an assessment of the number of objects involved and/or give a quantitative evaluation of different types of attributes. We focus on the following aspects: 1) parametric and non-parametric attributes; 2) gradable and non-gradable attributes; 3) ontological representation of different classes of attributes; 4) absolute and relative quantitative assessment; 5) punctual and interval quantitative assessment; 6) intervals with precise and fuzzy boundaries.*

Keywords: knowledge representation, semantic analysis, ontology, RDF languages, gradable attributes

1 Semantic Analysis and Semantic Structure

The semantic language described in this paper is used in a semantic analyzer under development in the Institute for Information Transmission Problems of the Russian Academy of Sciences and in the Madrid Polytechnic University. A distinctive feature of this analyzer is that the semantic representation is based on both linguistic and world knowledge. In many aspects our approach is similar to that of Ontological Semantics (Nirenburg, Raskin 2004) but the linguistic framework is substantially different. For more details about the analyzer, the reader is referred to Boguslavsky et al. 2010 and Boguslavsky 2011.

The source of linguistic information is the knowledge base of the ETAP-3 linguistic processor. World knowledge is contained in the Ontology and in the Fact Repository. Semantic representation is constructed in two steps. First, all the sentences of the text sentence are independently of one another transformed into their Backbone Semantic Structures (BSemS), which reflect the meaning directly conveyed in the sentence. Second, BSemSs are enriched by means of the Ontology and the Fact Repository and converted to Enhanced Semantic Structures (EnSemS). As an example, we will show BSemS and EnSemS of a short text (1). The working language of the analyzer is Russian, but for readers' convenience we provide an English translation of the text:

(1) *On October, 8 "Zenit" Football Club had a first friendly match in the tournament, which is taking place in Spain's La Manga. The pupils of Luciano Spaletti lost 0:1 to the Warsaw Club "Polonia".*

Step 1: BSemS construction.

BSemS of the first sentence: *On October, 8 "Zenit" Football Club had a first friendly match in the tournament, which is taking place in Spain's La Manga.*

(2)
```
hasTime(Match-01,DateTimeDescription-01)
hasMonth(DateTimeDescription-01, 2)
hasDay(DateTimeDescription-01, 8)
hasCategory(Match-01, friendly)
isPartOf(Match-01, Tournament-01)
hasParticipant(Match-01, Team-01)
hasName(Team-01, Zenit)
hasSportDiscipline(Team-01, football)
hasLocation(Tournament-01, La Manga)
hasLocation(La Manga, Spain)
```

As is usual in Artificial Intelligence, instances of classes are supplied with unique numerical identifiers. In order not to distract the reader's attention, from now on, we will omit these identifiers, if only they are not needed to distinguish between different instances.

It should be stressed that many of the classes referred to in the BSemS have many more property slots in the Ontology, but these slots are not represented in this BSemS, since the text does not provide data for filling them.

BSemS of the second sentence: *The pupils of Luciano Spaletti lost 0:1 to the Warsaw Club "Polonia".*

(3)
```
hasWinner(WinEvent, Team-02)
hasLoser(WinEvent, Team-03)
inContest(WinEvent, SportEvent)
inContest(MatchScore, SportEvent)
hasValue1(MatchScore,1)
hasValue2(MatchScore,0)
hasName(Team-02, Polonia)
represents(Team-02, Warsaw)
hasCoach(Team-03, Luciano Spalletti)
```

The second sentence was analyzed independently of the first one, and the two teams mentioned (the winner and the loser) received new identifiers – `Team-02` and `Team-03`. These teams are referred to in the text in different ways. One of them is called by its name (`Polonia`), and the only thing that is communicated about the second one is the name of its coach (`Luciano Spaletti`). The result of the match is conveyed by means of two propositions: the first one says that one of the teams defeated the other (by means of the predicate `WinEvent`), and the second one gives the score (the predicate is `MatchScore`). In order to show that both propositions refer to the same match, the `inContest` slot of both predicates is filled by the same match (`SportEvent`).

Step 2: Enhancement of BSems.

The main tasks that are solved at this stage are coreference resolution (i.e. determination of phrases that refer to the same entity) and filling of the slots for which the fillers have not yet been found. The information used to solve these tasks can be taken from the Ontology and the Fact Repository, which contains, among other things, semantic structures of previous sentences of the text processed. In particular, the Ontology should contain all the information available about the individuals. In our example, the Ontology disposes of the following information about the Zenit team:

```
hasName(Team-00, Zenit)
hasSportDiscipline(Team-00, football)
hasCoach(Team-00, Luciano Spalletti)
```

Based on this information, we can identify `Team-01` from the first sentence, whose name is `Zenit`, with `Team-03` from the second one, since its coach is `Luciano Spaletti`.

Semantic links between the sentences in the text are implicit. In EnSemS they should be restored wherever possible. We will show how it can be done in our example. There are several considerations that allow us to infer some implicit information. The first sentence of (1) tells us that a match has taken place. The second sentence gives information about a result of a match. The two sentences belong to the same text and, moreover, one of them directly follows the other one. They share at least one participant (`Zenit`) and there are no textual indications of the topic shift. Therefore, one can conclude that both sentences are describing the same match. That means that in the EnSemS we should identify `Match` from the first sentence with `SportEvent`, to which `WinEvent` and `MatchScore` are linked in the second sentence. As a result, EnSemS of (1) looks like (4) (elements introduced during the SemS extension are printed in bold face and underlined):

(4)
```
hasTime(Match, DateTimeDescription)
hasMonth(DateTimeDescription, 2)
hasDay(DateTimeDescription, 8)
hasCategory(Match, friendly)
isPartOf(Match, Tournament)
hasParticipant(Match, Team-01)
hasName(Team-01, Zenit)
hasCoach(Team-01, Luciano Spaletti)
hasSportDiscipline(Team-01, football)
hasLocation(Tournament, La Manga)
hasLocation(La Manga, Spain)
hasWinner(WinEvent, Team-02)
hasLoser(WinEvent, Team-01)
inContest(WinEvent, Match-01)
inContest(MatchScore, Match-01)
hasValue1(MatchScore, 1)
hasValue2(MatchScore, 0)
hasName(Team-02, Polonia)
represents(Team-02, Warsaw)
```

Semantic structures (2)-(4) have already given some idea of the semantic language used for representing the meaning of the texts. Below, we will concentrate on one important fragment of this language, namely the one dealing with quantitative assessment of different types of objects.

Quantitative assessment is mostly made by means of gradable attributes. We will discuss these attributes in section 2, and the values they ascribe to objects - in section 3.

2 Gradable attributes

As mentioned above, prototypically, quantitative assessment of an object is made by means of gradable attributes. Properties that they ascribe to the objects can be compared in terms of "more/less". For example, `Price` and `Intelligence` are gradable, because one bicycle can be more expensive than another one, and one person can be more

intelligent than another. Very often, they characterize an object by assigning it a numerical value (e.g. *a price of 100 Euros*). However, not all the attributes that assign a value to their object are gradable, and not all gradable attributes assign a value to their object. Let us explain this.

We will refer to the attributes that assign some definite value to their object as p a r a m e t e r s . The parameters and their values can be quantitative or not. Values of quantitative parameters, such as `Price`, `Height`, `Speed`, `Temperature`, etc. are located on a scale and are prototypically expressed by numerical expressions consisting of a numeral and a measurement unit: *the height of 15 meters*, *the speed of 180 km/hour*, *the temperature of 50 degrees Celsius.*

Non-quantitative parameters have values that are not located on a scale and are not expressed by means of a numerical expression. Typical examples of non-quantitative parameters are `Name`, `Nationality`, `Address`, `Color`, `Form`, etc. For example, the parameter of `Nationality` has values `French`, `Russian`, `Malay`, etc.

All the parameters, quantitative or not, have a sufficiently homogenous and compact range of values. The kind of entities that can serve as values of a parameter is always restricted. An important linguistic property of parameters is their behavior in *what*-questions. Any word denoting a parameter can be used in a *what*-question, and this question is always interpreted as a request for the parameter's value. When somebody asks *What is her name?* it is quite obvious what kind of entity is expected as an answer. Cf. a dialogue in which the answer does not belong to the class of parameter values and therefore does not directly satisfy the information need of the interrogator: *What is his name? - ??An unusual one*. Not all attributes are like this. Such attributes as `Beauty` or `Intelligence` do not presuppose a set of homogeneous values. Therefore, they are not parameters.

On the other hand, `Beauty` and `Intelligence` are gradable attributes, in the sense that different objects may have these properties to different extents – see above.

However, gradability of this property does not only manifest itself in comparative contexts, as is the case of (5):

(5) *Lucy is more intelligent than Mary.*

When we simply say that Lucy is intelligent, we ascribe to Lucy a high degree of intelligence, in a similar way as we ascribe to her a high degree of height, when we say that she is tall.

However, there is also an important difference between such attributes as `Height` on the one hand, and `Intelligence`, on the other. We showed above that `Height` is a parameter, and `Intelligence` is not. `Height` is a two-place predicate, which assigns to its object a value on a well-defined scale, while `Intelligence` is a one-place predicate. It does not assign any definite value to its object, but instead it has degrees.

We would like to capture the similarity between the attributes of the `Height` class and the `Intelligence` class, and on the other hand, take into account the difference between them. We adopted the following solution. Our ontology contains the class of `Parameters` with two subclasses: `GradableParameters` (like `Price`) and `Non-gradableParameters` (like `Name`). All the parameters have a `hasValue` slot. On the other hand, there is a class `GradableAttributes`. One of its subclasses is `GradableParameters` (which at the same time belongs to the `Parameters` class), and another one is `QualitativeAttributes`, which contains attributes of the `Intelligence` type. Gradable parameters have values located on a corresponding scale. Qualitative attributes do not have values but have a `hasDegree` slot instead. Specific behavior of parameters is accounted for by means of the `Parameters` class and its `hasValue` slot. For example, interpretation of the *what*-questions asked of parameters implies filling of the `hasValue` slot. How the quantification of qualitative attributes is assured is seen in SemS (5a), which represents the meaning of (5):

(5a) `hasSubject(Intelligence-01, Lucy)`
`hasDegree(Intelligence-01, var-01)`
`hasSubject(Intelligence-02, Mary)`
`hasDegree(Intelligence-02, var-02)`
`more(var-01, var-02)`

3 Values of gradable attributes

As stated in the previous section, parameters and qualitative attributes are both gradable but in a slightly different way. Although they have different slots for quantitative elements (`hasValue` and `hasDegree`), for simplicity's sake we will speak about values in both cases.

3.1 Numerical expressions

As for quantitative parameters, their values are compound numerical expressions. They are formed by a numeral and a measurement unit. Such expressions are represented by a series of two-place predicates that express a corresponding measure, such as `LinearMeasure`, `CurrencyMeasure`, `DurationMeasure`, etc.

(6) *3 meters*

(6a) `hasUnit(LinearMeasure, meter)`
`hasUnitQuantity(LinearMeasure, 3)`

(7) *20 euros 45 cents*

(7a) `hasUnit(CurrencyMeasure, euro)`
`hasUnitQuantity(CurrencyMeasure, 20,45)`

(8) *3 liters (of wine)*

(8a) `hasUnit(Amount, liter)`
`hasUnitQuantity(Amount, 3)`

(9) *3 glasses (of wine)*

(9a) `hasUnit(Amount, glass)`
`hasUnitQuantity(Amount, 3)`

A special case is temporal expressions, which are often presented in natural languages by several measurement units of different granularity, as in (10). We chose not to reduce them to a single unit (for example, a second), but to preserve the internal structure of the expression, in order to match the way humans are conceptualizing time:

(10) *3 years 2 months 5 days 10 hours and 25 minutes*

(10a) `hasYears(DurationMeasure, 3)`
`hasMonths(DurationMeasure, 2)`
`hasDays(DurationMeasure, 5)`
`hasHours(DurationMeasure, 10)`
`hasMinutes(DurationMeasure, 25)`

Another special case is a quantitative parameter which may do without a measurement unit. It is quantity, e.g. *5 books*. Besides the peculiarity of lacking a unit, this parameter has another one. It does not apply to single objects but only to collections of objects. When we say *5 books*, we don't say anything about any single book, but describe quantitatively a whole set of books. Therefore, multiple objects are represented by sets (as in Nirenburg, Raskin 2004), and sets may have a `Cardinality` parameter:

(11) *50 books*

(11a) `hasElementType(Set, Book)`
`hasSubject(Cardinality, Set)`
`hasValue(Cardinality, 50)`

There exist parameters whose value is not constituted by a single numerical expression. The state of a sport match at a given moment is characterized by the parameter of `Score`, which is a pair of numbers, e.g. `3:1`. Another example of a complex parameter value is coordinates on the Earth surface, which is a combination of two independent parameters – latitude and longitude, each of which is usually rendered by a triple of numbers – degrees, minutes and seconds.

3.2 Brief typology of quantitative assessment.

We will distinguish between two major types of quantitative assessment – absolute and relative assessment. Relative assessment, in its turn, will be divided into two subclasses: assessment with respect to the whole and with respect to the norm. In each of these three classes, the value can denote either a point on the scale, or an interval. In the latter case, the interval can have either exact or fuzzy boundaries. Below, we will illustrate all these classes.

A. Absolute assessment.

A.1 Punctual absolute assessment.

(12) *The ticket costs 20 euros*

(12a) `hasSubject(Cost, Ticket)`
`hasValue(Cost, CurrencyMeasure)`
`hasUnit(CurrencyMeasure, euro)`
`hasUnitQuantity(CurrencyMeasure, 20)`

(13) *The boy is 4 feet tall*

(13a) `hasSubject(Height, Boy)`
`hasValue(Height, LinearMeasure)`
`hasUnit(LinearMeasure, foot)`
`hasUnitQuantity(LinearMeasure, 4)`

A.2 Interval absolute assessment.

When a quantitative expression is characterized by an interval, its boundaries can be either exact or fuzzy. The difference between exact and fuzzy boundaries is manifested in inferences one can make. If it is claimed that the number of students is in the exact interval [100,150], then this claim is definitely false if in fact there are 98 or 151 students. If the interval is fuzzy, then such an inference cannot be made. The distinction between exact and fuzzy intervals is relevant for representing the meaning of many natural language words and phrases. An interval with exact boundaries is illustrated in (14), and one with fuzzy boundaries – in (15).

(14) *Only children from 5 to 8 years old are admitted to the class.*

(14a) `hasObject(Admit, Child)`
`hasSubject(Age, Child)`
`hasValue(Age, DurationMeasure)`
`hasYears(DurationMeasure, Interval)`
`from(Interval, 5)`
`to(Interval, 8)`

(15) *About 10 to 15 students will come to the meeting.*

(15a) `hasAgent(Come, Set)`
`hasElementType(Set, Student)`
`hasSubject(Cardinality, Set)`
`hasValue(Cardinality, FuzzyInterval)`
`from(FuzzyInterval, 10)`
`to(FuzzyInterval, 15)`

The word *several* is one of those natural language elements whose meaning cannot be rendered in exact terms. According to Longman English Dictionary *several* means 'a number of people or things that is more than a few but not a lot'. COBUILD dictionary gives a similar definition: 'imprecise

number of people or things that is not large but is greater than two'. Such definitions, obviously, cannot be used directly. However, this word has a clear enough meaning, which is rather specific. On the one hand, it refers to concrete numbers, as opposed to such words as *many* or *few*. It is impossible to give a number, however approximate it might be, denoting *many* or *few*. It is obviously different in different situations. As for *several*, the situation is different. Most of our informants say that the number referred to by *several* is an integer which is greater than or equal to 3 but less than 9. On the other hand, the upper boundary is not rigid. Some people feel that perhaps 8 is too many to count as several. Other people agree to accept even as many as 10. One could of course ignore this vagueness and describe *several* as any quantity expressed by an integer greater than or equal to 3 but smaller than 9. However, if we wish to approximate meanings expressed by natural language words (and we do), we should find a way to account for such an important property of natural language semantics as uncertainty, which is obviously manifested in the meaning of *several*. Our proposal is to describe *several* as a fuzzy interval between 3 and 8:

(16) *several books*

(16a)
```
hasElementType(Set, Book)
hasSubject(Cardinality, Set)
hasValue(Cardinality, FuzzyInterval)
from(FuzzyInterval, 3)
to(FuzzyInterval, 8)
```

Similarly, one could characterize approximate quantities such as *about 80* as fuzzy intervals with identical lower and upper boundaries:

(17) *about 80 people*

(17a)
```
hasElementType(Set, Person)
hasSubject(Cardinality, Set)
hasValue(Cardinality, FuzzyInterval)
from(FuzzyInterval, 80)
to(FuzzyInterval, 80)
```

B. Relative Assessment.

There are two varieties of relative assessment: the assessment with respect to the whole and with respect to the norm. In both cases, it can be punctual or interval, as in case of the punctual assessment above, and the interval boundaries can be both exact and fuzzy.

B.1 Relative Assessment with respect to the whole.

To make this kind of assessment, we introduce a predicate `FormsPartOf`, whose first argument (subject) corresponds to the quantity being assessed, the second argument (object) – to the whole with respect to which the assessment is made, and the third argument (value) characterizes the relation between the two.

B.1.1 Punctual assessment

(18) *half of the population*

(18a)
```
hasSubject(FormsPartOf, Set)
hasObject(FormsPartOf, Population)
hasValue(FormsPartOf, 0.5)
```

B.1.2 Interval Assessment.

Interval with exact boundaries:

(19) *From 13% to 15% of the population*

(19a)
```
hasSubject(FormsPartOf, Set)
hasObject(FormsPartOf, Population)
hasValue(FormsPartOf, Interval)
from(Interval, 0.13)
to(Interval, 0.15)
```

Interval with fuzzy boundaries:

(20) *about 13% - 15% of the population*

(20a)
```
hasSubject(FormsPartOf, Set)
hasObject(FormsPartOf, Population)
hasValue(FormsPartOf, FuzzyInterval)
from(FuzzyInterval, 0.13)
to(FuzzyInterval, 0.15)
```

B.2 Relative assessment with respect to the norm.

In natural languages there are many words that express a value of a gradable attribute, but do so in an imprecise, fuzzy way. For example, a stone can be characterized as big. We understand that the adjective *big* places the stone somewhere on the scale of size, but we don't know this position exactly. The only thing that the lexical meaning of *big* tells us is that the size of the stone is above the norm. This idea has long been adopted in linguistics. What exactly the norm is in each particular case is beyond the competence of lexical semantics and is determined by the context and encyclopedic knowledge. What is big for a child may be not so for an adult. A big cat is much smaller than a small horse. However, it is not enough only to state that *big* is above the norm. *Enormous* is also above the norm, but to a different extent. There are series of words and phrases that refer to the same scale but denote different points, or rather, different areas, on that scale. *Never, seldom, sometimes, from time to time, often, very often, always* – all these words correspond to different degrees on the frequency scale. A convenient way of representing the meaning of such words has been proposed within the Ontological semantics approach. All the words that express a value of a gradable attribute are assigned a point or a range in

the interval between 0 and 1. For example, the meaning of *hot* is represented as the range [0.75–1] on the scale of temperature (Nirenburg, Raskin 2004: 206).We adopt this idea in principle, but realize it in a different way.

We introduce a predicate RelativeToNorm with 4 arguments:

- `hasSubject`: what is assessed
- `hasObject`: which parameter of the Subject is assessed
- `hasValue`: what value is assigned
- `normFor`: the norm for what kind of entities is used as a reference (the fourth argument will be illustrated below in (25))

As in previous cases of assessment, the value slot can be filled both by a point and an interval in the range [0,1].

B.2.1 Punctual assessment

(21) *false solution* (limit point on the scale of Correctness)

(21a)
```
hasSubject(RelativeToNorm, Solution)
hasObject(RelativeToNorm, Correctness)
hasValue(RelativeToNorm, 0)
```

(22) *brilliant answer* (limit point on the scale of Quality)

(22a)
```
hasSubject(RelativeToNorm, Answer)
hasObject(RelativeToNorm, Quality)
hasValue(RelativeToNorm, 1)
```

B.2.2 Interval assessment

Interval assessment with exact boundaries does not seem to be possible. Fuzzy boundaries, on the contrary, are very wide spread.

(23) *a tall boy*

(23a)
```
hasSubject(RelativeToNorm, Boy)
hasObject(RelativeToNorm, Height)
hasValue(RelativeToNorm, FuzzyInterval)
from(FuzzyInterval, 0.6)
to(FuzzyInterval, 0.8)
```

(24) *a very tall boy*

(24a)
```
hasSubject(RelativeToNorm, Boy)
hasObject(RelativeToNorm, Height)
hasValue(RelativeToNorm, FuzzyInterval)
from(FuzzyInterval, 0.8)
to(FuzzyInterval, 0.9)
```

As one can easily see from (23) – (24), the difference between a tall boy and a very tall boy is manifested in different intervals on the scale of `Height`: [0.6, 0.8] in the first case and [0.8, 0.9] in the second case.

(25) *John is short for a basketball player*

(25a)
```
hasSubject(RelativeToNorm, John)
hasObject(RelativeToNorm, Height)
hasValue(RelativeToNorm, FuzzyInterval-01)
from(FuzzyInterval, 0.2)
to(FuzzyInterval, 0.4)
normFor(RelativeToNorm, BasketballPlayer)
```

(26) *story of average length*

(26a)
```
hasSubject(RelativeToNorm,Story)
hasObject(RelativeToNorm,Length)
hasValue(RelativeToNorm,FuzzyInterval)
from(FuzzyInterval, 0.4)
to(FuzzyInterval, 0.6)
```

(27) *negligibly few resources*

(27a)
```
hasSubject(RelativeToNorm, Resource)
hasObject(RelativeToNorm, Amount)
hasValue(RelativeToNorm, FuzzyInterval)
from(FuzzyInterval, 0.1)
to(FuzzyInterval, 0.2)
```

Now, it is not difficult to represent the difference between three related constructions: (28) *John solved **many problems,*** (29) *John solved **many of the problems***, and (30) *John solved **most of the problems***. Sentence (28) simply says that the number of the problems John solved is large. This is done by means of the `RelativeToNorm` predicate. It should be stressed that in this context the set of the problems John solved is interpreted as the set of **all the problems** that John solved. This meaning is rendered by a special attribute – isComplete.

(28) *John solved many problems*

(28a)
```
hasAgent(Solve, John)
hasObject(Solve, Set)
hasElement(Set, Problem)
hasSubject(RelativeToNorm, Set)
isComplete(Set)
hasObject(RelativeToNorm, Cardinality)
```

```
hasValue(RelativeToNorm,
FuzzyInterval)
from(FuzzyInterval, 0.6)
to(FuzzyInterval, 0.8)
```

Sentence (29) evaluates the proportion between two sets: some set of problems and its subset that John solved. What *many* claims here is that the second set is a large part of the first one. It is difficult to define precisely what part of the whole qualifies as large. However, what is certain is that it cannot necessarily be more than a half. It is quite possible that many of the problems have been solved and at the same time many of the problems remained unsolved. Consequently, the beginning of the large-part interval should be less than 0.5. On the other hand, a large part of something can easily be more than a half. To express this, one needs to introduce these two sets of problems and evaluate their correlation by means of `FormsPartOf`:

(29) *John solved many of the problems.*

(29a)
```
hasElement(Set-01, Problem)
hasProperSubset(Set01, Set-02)
hasAgent(Solve, John)
hasObject(Solve, Set-02)
isComplete(Set-02)
hasSubject(FormsPartOf,Set-02)
hasObject(FormsPartOf, Set-01)
hasValue(FormsPartOf,FuzzyInterval)
from(FuzzyInterval, 0.3)
to(FuzzyInterval, 0.7)
```

Sentence (30) is similar to (29) in that it compares the set of the problems that John solved and the overall set of problems. What it adds to (29) is the idea that the number of solved problems is larger than half of the whole number of problems. One of the ways to convey this meaning is to change the value of the `FormsPartOf` predicate .

(30) *John solved most of the problems.*

(30a)
```
hasElement(Set-01, Problem)
hasProperSubset(Set01, Set-02)
hasAgent(Solve, John)
hasObject(Solve, Set-02)
isComplete(Set-02)
hasSubject(FormsPartOf, Set-02)
hasObject(FormsPartOf, Set-01)
hasValue(FormsPartOf,
FuzzyInterval)
from(FuzzyInterval, 0.55)
to(FuzzyInterval, 0.9)
```

4 Conclusions

We presented a semantic language intended for performing semantic analysis and representing the meaning of NL texts. Semantic analysis is knowledge-intensive and uses two major sources of knowledge: linguistic knowledge incorporated in the combinatorial dictionary and rules of the ETAP-3 Linguistic Processor, and world knowledge stored in the Ontology and Fact Store. At the moment of writing, the Ontology is under construction. In developing it, we take into account various existing ontologies, such as SUMO, Ontological Semantics Ontology, and PROTON, but in many cases take our own solutions. The semantic language in which semantic structures of sentences are formulated consists of RDF-type triples `predicate(subject, object)`. In this paper, we show how this language represents information on quantity and degree assessment.

5 Acknowledgements

The work reported in this paper has been partly supported by grants RFBR № 11-06-00405 and RSFH № 10-04-00040a which is gratefully acknowledged.

6 References

[1] Boguslavsky, I., L. Iomdin, V. Sizov, S. Timoshenko. (2010). Interfacing the Lexicon and the Ontology in a Semantic Analyzer. In: COLING 2010. Proceedings of the 6th Workshop on Ontologies and Lexical Resources (Ontolex 2010), Beijing, August 2010, pages 67–76.

[2] Boguslavsky, I. (2011). Semantic Analysis based on linguistic and ontological resources. In: Proceedings of the 5th International Conference on the Meaning - Text Theory. Barcelona, September 8 – 9, 2011. Igor Boguslavsky and Leo Wanner (Eds.), p. 25-36.

[3] Nirenburg, S., Raskin, V. (2004). Ontological Semantics.The MIT Press.Cambridge, Massachusetts. London, England.

Technological peculiarity of knowledge extraction for logical-analytical systems

Igor P. Kuznetsov, Elena B. Kozerenko, Mikhail M. Charnine
Institute for Informatics Problems of the Russian Academy of Sciences, Moscow, Russia

Abstract *The paper is dedicated to constructing of the new classes of expert and logical-analytical systems, based on the knowledge structures. For this the means of knowledge representation (the extended semantic networks - ESN) and the tools of their processing (the language of logical programming DEKL) have been designed. They have been used as basis for creating the new technologies, which provide the following functions: the automatic extraction of the knowledge from natural language texts, forming the Knowledge Base and the solution of the most complex problems of the logical-analytical processing by transformation and comparison of the knowledge structures. On this basis many intellectual systems for different applications have been designed.*

Keywords semantics, natural language, linguistic processor, knowledge extraction, named entities

1 Introduction

The present significance of named entities extraction pertains to the growing amount of information available in unstructured form [1-20]. The existing Internet largely consists of unstructured documents. Knowledge contained within these documents can be made more accessible for machine processing by means of transformation into relational form. An intelligent processing is proposed to transform unstructured data into something that can be reasoned with [2,5,11,13]. A typical application of entities extraction is to scan a set of documents written in a natural language and populate a database with the information extracted. More prospective approach consists of using Knowledge Base. It proposes the development of new technology including the extraction of knowledge structures and organization of their processing in Knowledge Base [3,4,6].

The distinctive features of our technology are as follows:

1. Extraction from the texts of knowledge structures (not only separate named entities) that represent the links of named entities and their participation in actions and events.

2. For the knowledge extraction the unique semantic-oriented language processors (LP) are designed. Processor LP provides the deep analysis of NL-texts and revealing set of objects together with their structures.

3. Processor LP is controlled by the linguistic knowledge, which are declarative structures (on extended semantic networks - ESN) and which provide the quick tuning of LP to subject area and language - Russian and English.

4. Linguistic knowledge consists of the rules, which provide the high degree of selectivity in the entities extraction and elimination of collisions during their application. Rules provide the minimization of noise and losses, that is the high degree of completeness and accuracy.

5. The knowledge structures and means of their processing (intellectual language DEKL) were designed as the united tools, oriented at the tasks of linguistic analysis, semantic search, logical-analytical processing and the expert solutions. Using this tools considerably facilitates the development of applied intellectual systems.

Technology of knowledge structure extraction and processing have been used for construction of new classes of analytical systems [3,7,12]: "Criminal", "Analytic", "AntiTerror", "Resume" etc. [http://IpiranLogos.com/en/Systems/].

2 Knowledge Structures

2.1 Named Entities

In our technologies Named Entities (NE) are extracted from the documents on Natural Language (NL) and presented in the Knowledge Base (KB) as the fragments of the extended semantic network (ESN). The arguments of fragments are the collections of normalized words, numbers and signs, which reflect essence NE and indicate to its type. For example, the fragment

FIO(IVANOV,IVAN,IVANOVICH,1957/1+)

represents the person *Ivanov Ivan Ivanovich 1957* year of birth. The entity type is indicated by the constant FIO. Every fragment has a unique code (sign "1+"), which corresponds to all information of the fragment and which may be on the argument places of other fragments (sign 1-). It is the main difference of the concept "*fragment"* from the classical concept "*predicate"*. The network ESN consists of the set of fragments. Their order is arbitrary.

In our systems more than 40 types of NE are extracted from NL-texts. Their quantity depends on the subject area and the tasks of users. Let us note that in KB some NE can be constitutional components of others. Connections between NE may be complicated [1,6,14].

2.2 Type of entities and links for extraction

The set of the entities to be extracted depends on the tasks of a user. At the same time the quality of a linguistic processor is determined by the possibilities for knowledge extraction. The linguistic processors "Criminal", "Analytic" and ''Semantix" support more than 40 types of semantic entities which can be extracted automatically. Some examples of basic entities types and connections extracted by the these processors are given below:

• persons (by family name, given name and patronymic - FNP) with their role features (criminal, victim);
• the verbal description of the persons, their distinctive signs;
• address, posting information attributes;
• date(s) mentioned;
• weapon with its special features;
• telephone numbers, faxes, e-mails with their subsequent standardization;
• the means of transport with the indication of the vehicle type, its state number, color and other attributes;
• passport data and other documents with their attributes;
• explosives and narcotic substances;
• organizations, positions;
• quantitative characteristics (how many persons or other objects participated in an event);
• the numbers of accounts, sums of money with the indication of the currency type;
• terrorist groups and organizations;
• participants of terrorist groups with the indication of their roles (leader, head of, etc.);
• the armed forces, assigned for antiterrorist combat (Military Force);
• event (criminal, terrorist, biographical, and so on) with the indication of the information objects participation in them;
• time and the place of events.

Standard entities (names, dates, addresses, types of weapons and others) are reduced to one standard form. The identification of entities is performed taking into account brief designations (for example, separate surnames, patronymics, Initials), anaphoric references (indicative and personal pronouns, for example, this person, it...) definitions and explanations (for example, the *mayor of Moscow Sabyanin* is identified with the subsequent words *mayor*, *Sabyanin*). An important task is the identification of entities in the entire text, the use for these purposes of indicative pronouns, brief names, anaphoric references.

2.3 Connections between the entities and participation in actions

Connections and relations between NE, extracted from the NL-texts, can be very diverse. They depend on entity types. For example, one person can be connected with another by relative and friendly relations, and also by the place of living, area of interests and so on. Actions frequently are connected with the time and the place. There can be reason-consequence and other connections between actions. In such a way the complex structures are created. For their formalization special tools of knowledge representation have been designed.

Actions usually are expressed in NL-texts by the tensed verb forms, nonfinite verb forms, e.g. verbal nouns, participial and adverbial constructions, gerunds. The actions are also NE, components of which can be another NE. For example, there can be those, who participate in action, or entities, on which the action is directed. Moreover, some actions may be components of others. For many applications the actions are also the significant information which requires formalization. Because the system is oriented at the deep analysis of text constructions, it extracts all actions and events with NE.

Example of action extracting by the System "Semantix" is shown on fig.1 [http://IpiranLogos/en/Semantix/].

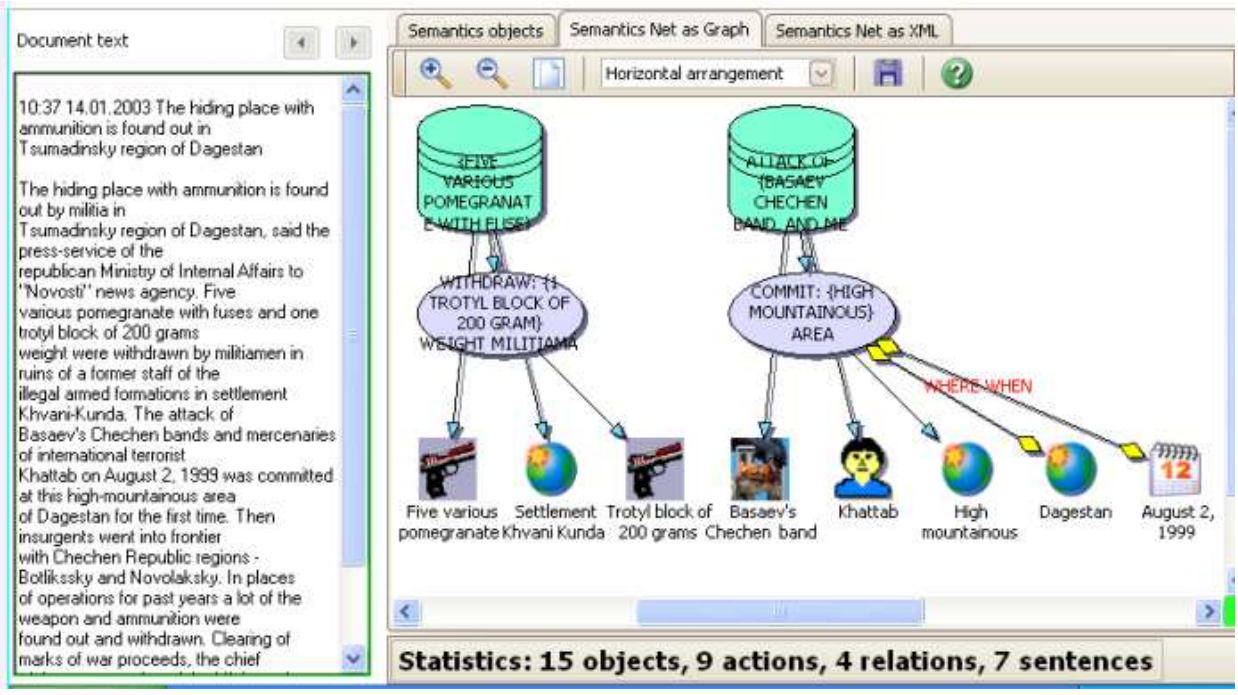

Fig.1 Example of extracted actions with entities

2.4 Meaningful portrait of a document

It is the formal representation of entities (NE), their properties and the connections, extracted from the text of the document. Such portraits are the structures of knowledge. As means of formalization in our technologies we use the extended semantic networks (ESN). Formalization is achieved automatically by the semantics-oriented linguistic processor, which analyzes the texts of NL-documents and transforms them into knowledge structures [3,10].

A set of meaningful portraits (together with index files) comprise the Knowledge Base (KB) where various types are provided of semantic search and logical-analytical functions by comparison and transformation of knowledge structures. We design the technology which provides the processing in the KB distributed within the net of computers.

The Example of text (with number 22 from file e1-02-98.TXT) :

12:16 27.12.2002 In the Chechen Republic one of leaders of bands the Arabian mercenary Abu-Tarik is destroyed. As have informed the Ministry of Foreign Affairs of the Chechen Republic, Chechen special militia destroy the insurgent in settlement Starye Atagi of Groznensky region. In one of the houses there were found the hiding place with three sub-machine guns.

On some data, Abu-Tarik was involved in murder of Salikhov's family in Starye Atagi in this year.

Meaningful portrait of the text:

DOC_(22, "1-02-98.TXT","SUMMARY; " /0+) 0-(ENG)
DATE_(DEC.,~27,12,HOUR,16,MINUTE/1+)
CRIM_GROUP(1,LEADER,OF,BAND,ARABIAN,MERCENARY/2+)
FIO("ABU - TARIK"," "," "," "/3+)
DESTROY(2-,3-/4+) 4-(22,ACT_)
PLACE_(CHECHEN,REPUBLIC/5+)
WHERE(4-,5-)
ORGANIZATION_(MINISTRY,OF,FOREIGN,AFFAIRS,OF,CHECHEN,
REPUBLIC/6+)
INFORM(6-/7+) 7-(22,ACT_)
FORCE_(SPECIAL,MILITIA/8+)
DESTROY(CHECHEN,8-,INSURGENT/9+) 9-(22,ACT_)
PLACE_(SETTLEMENT,STARYE,ATAGI,OF,GROZNENSKY,REGION/10+)
WHERE(9-,10-)
WEAPON_("SUB ",MACHINE,GUN/11+)
FIND(1,HOUSE,HIDE,PLACE,3,11-/12+) 12-(22,ACT_)
PLACE_(STARYE,ATAGI/13+)
INVOLVE(3-,MURDER,SALIKHOV,FAMILY,13-,YEAR/14+) 14-(22,ACT_)

SENTENCE_(22,1-/15+) 15-(1,1,19)
SENTENCE_(22,4-/16+) 16-(1,20,114)
SENTENCE_(22,7-,9-/17+) 17-(2,115,288)
SENTENCE_(22,12-/18+) 18-(5,289,376)
SENTENCE_(22,ON,SOME,DATA,14-/19+) 19-(6,377,476)

A meaningful portrait consists of the elementary fragments, arguments of which are words in the normal form (it is necessary for the search and processing). Each elementary fragment has its unique code, which is written in the form of the number with the sign + and is separated by a slash line. For example, in the fragment FIO("ABU - TARIK"," "," "," "/3+) the sign "3+" is its code (but "3-" is the reference to it). Fragments DOK_(22, "1-02-98.TXT", "SUMMARY; " /0+) 0-(ENG) indicate that the meaningful portrait is built on the basis of the English-language text of document with number 22 of the file of 1-02-98.TXT", which was processed as the summary of the incidents (linguistic knowledge depends on this). The following fragments present date DATE_(…/1+), criminal group CRIM_GROUP(…/2+), person's surname (name and patronymic) FIO(… /3+) and so forth. The signs "0+","0-" and "1+", "1-" and "2+", "2-" and "3+", "3-", … are the codes of the fragments, with the aid of which their connections and relations are assigned. Actions are represented in the form of fragments of the type DESTROY(2-,3-/4+) 4-(22,ACT_), where it is represented as "*criminal group* (CRIM_GROUP with code "2+") *and person* (FIO with code "3+")*, are destroyed*". With the aid of it is the fragment 4-(22, ACT_) indicates that the first fragment is DESTROY(…./4+) presents the action and relates to the document with the number 22. Fragments PLACE_(CHECHEN,REPUBLIC/5+) WHERE(4-,5-)

indicate the place of this action (WHERE). Fragments ORGANIZATION_(…/6+) INFORM(6-/7+) 7-(22,ACT_) represent that "*organization ... was informed*".

The fragments PREDL_(...), which correspond to the sentences play the special role. They are filled up with the words, which did not enter into the named entities (in this example they are absent), or with the codes of entities themselves. To these fragments the indicators of their position in the text are added. For example, the fragment SENTENCE_(22,7-,9-/17+) 17-(2,115,288) represents the fact that the objects with codes "7-" (corresponding to the action "*inform*"), "9-" (corresponding the action "*destroy"* are located in the sentence, which begins from the 2nd line of the text of the document and they occupy the place from the 115-th to the 228-th byte. These means of positioning are necessary for the work of the reverse linguistic processor.

A set of meaningful portraits of documents are organized in the Knowledge Base. Logical reference is provided with the aid of the rules IF… THEN (productions) of the language DECL, which are the basis for decision of logical-analytical tasks.

3 Semantic-oriented linguistic processor

Semantics-oriented linguistic processor comprises the following components.

3.1 The component of *lexical and morphological analysis* (LMA)

It extracts words and sentences from the text, performs lemmatization of words (normal form establishment) and constructs the semantic network presenting the space structure of text (SpST), which reflects the sequence of words, their basic features, beginnings of sentences and the presence of space character lines. The component LMA uses a two-level general ontology and a special collection of subject dictionaries (the dictionary of countries, regions of Russia, names, forms of weapons, and other items specific for the supported domains). The component performs semantic grouping of the words and assigns them additional semantic attributes [9].

3.2 The component of *syntactic-semantic analysis* (SSA)

It converts one semantic network (SN) into another which represents the semantic structure of text (SemST) the, i.e., the relevant semantic entities and their connections [6,12]. The SemST is called the meaningful portrait of document. It comprises knowledge structures of the knowledge base which serves the basis for implementing different forms of semantic search : the search by features and connections, the search for the entities connected at different levels, the search for similar persons and incidents, the search by distinctive characteristics (with the use of ontology).

The component SSA is controlled by the linguistic knowledge (LK), which determines the process of text analysis. LK includes the special contextual rules which ensure the high degree of selectivity with the extraction of entities and connections [http://www.ipiranlogos.com/english/topics/topic3-e.htm].

The functions of this component are the following:
- Extraction of entities from the flow of NL documents: persons, organizations, actions, their place and time, and many other relevant types of entities.
- The establishment of connections between entities. For example, persons are connected with organizations (PLACE_OF_WORK), by addresses (LIVES, REGISTERED). Or figurants of criminal events are connected with such entities as the type of weapon, drugs (TO HAVE).
- The analysis of finite and nonfinite verbal forms with the identification of the participation of entities in the appropriate actions. For example, one figurant gave the drugs to another figurant, and this is the fact linking them.
- The establishment of the connections of actions with the place and time (where and when some action or event occurred).
- The analysis of the reason-consequence and temporary connections between actions and events.

3.3 *Expert system* component (ES)

On the basis of semantic networks the new knowledge pieces are constructed in the form of additional fragments (ESN). For example, the component ES extracts the field of a person's activity (in accordance with the assigned classifier) from the text of resume for each autobiography. The person's experience in his field is evaluated. The correlation of a criminal incident to the specific type is accomplished with the analysis of the criminal actions of ES: the following facts are revealed - the nature of crime, the method of its accomplishment, the instrument of crime, and so forth (in accordance with the classifiers of the criminal police).

3.4 *Reverse linguistic processor* which converts the meaningful portrait of document (semantic network) into the texts on NL.

3.5 *Base of linguistic and expert knowledge* (KB)

It contains the rules of the text analysis and expert solutions in the internal representation. They determine the work of the linguistic processor. Our logical-analytical systems have several such bases, which are activated depending on subject areas and user tasks.

Fig.2 presents the example of extracted named entities (without links). The actions are the kind of entities (significant objects).

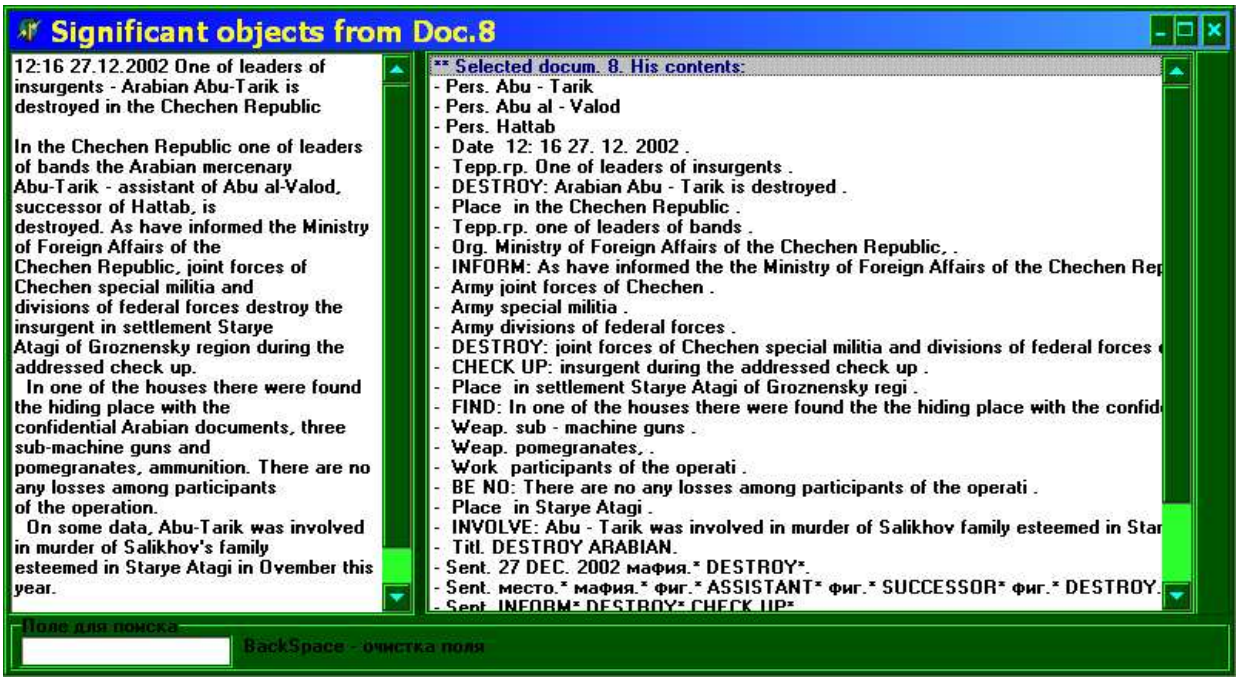

Fig.2. Example of extracted named entities

4 Logical analytical tasks

4.1 Semantic search

Semantic search is based on comparison the meaningful portrait of question and information in Knowledge Base (KB). Our technologies realize various types of semantic search [http://ipiranlogos.com/en/Technologies/]:
- Search for similar entities: persons, addresses, etc.,
- Search for links (e.g. search for anonymous persons based on their word portrait),
- Search for the entities from different documents based on the indirect links.
- Answer to free questions in natural language.

4.2 Tasks of criminal police

System "Criminal" is based on the documents, which enter from different sources: the summary of incidents, explanatory and official notes, the notebooks of figurants (criminal persons), accusatory conclusions and other. By analysis of the documents the Knowledge Base (KB) automatically is formed [http://ipiranlogos.com/en/Criminal/]. Structures in KB are the basis to achieve (by methods of structural processing) the solution of the logical-analytical problems:
- the search for similar incidents and figurants according to the information in KB;
- the search for figurants by verbal portrait;
- retrieval for information on question in NL (Russian);
- the explanation of the search results;
- analysis and mapping the connections between the figurants;
- the estimation of the degree of the participation of figurants in the incident;
- the ordering figurants according to the degree of their criminal activity;
- the discovery of the organized criminal groups;
- statistical processing of information to estimate the dynamics of the criminal processes in time.

4.3 Tasks of recruit agency

Many services, which deal with the flows of text information, must decide the problem of their formalization: the need for representation in those forms, which are accepted in these services and within the framework which this information is used [http://ipiranlogos.com/en/Resume/]. For example, the important task of many recruit agencies is connected with automatic processing of autobiographical data, claim for the work of the persons (resumes, written in the arbitrary form - on NL) with the extraction of all necessary data of these persons and the forming of the computer depositories (sites, KB, tables), which provide the necessary search. The entities extracting and automatic transformation is shown on Fig. 3.

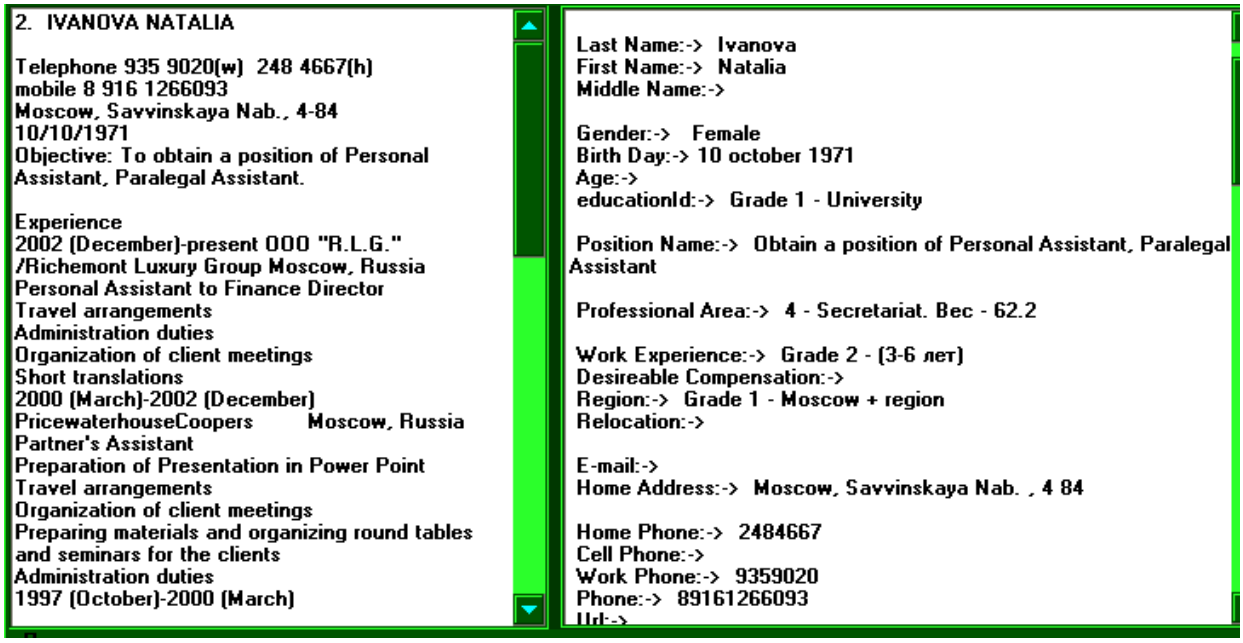

4.4 Expert systems

Expert systems on the basis of the analysis of meaningful portraits of document refer this document to the specific category (item of the classifier). In our systems two types of shells for the expert systems have been realized. The first is based on the weight coefficients of the words which correspond to the specific category. The second one is based on the presence of words in the named entities. Fig. 3 shows some examples. The "Professional area" (Secretariat – 62.2) was formed by the first type of expert system, "Region" (Moscow) was formed by second type.

4.5 Determination of the role functions of the entities

The technology of the determination of the new entities properties assigned implicitly is developed [16]. The procedure of this determination based on the analysis of the knowledge structures is proposed. The task of the determination of the role functions of entities (persons, organizations and others) on the base of their descriptions is examined as the field of application. This task in general form includes all possible "estimations", "descriptions". For example, the estimation of the stability of an enterprise (according to the information from the Internet), descriptions of political figures (positive or negative depending on the statements about them in the press), the estimation of the quality of article (on the statements of users), etc. Frequently it is not said directly: this is bad, but this is good. As a rule, in the texts (NL) the events and situations are described in which one or another information object participated. On their basis the estimation is done which is often represented in the form of the new property of entities (NE). The example of determination and argumentation of role function of persons is shown on Fig. 4.

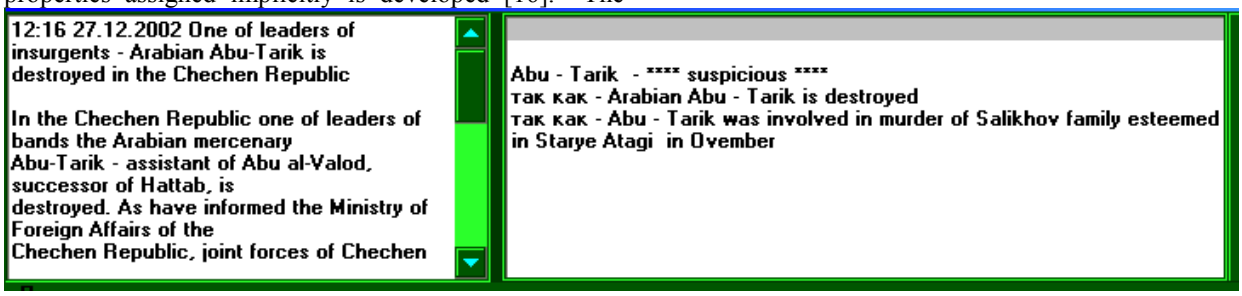

5 Conclusion

The proposed technologies were used for construction of several intellectual analytical systems: "Criminal", "Analytic", "AntiTerror", "Monument" and others. The distinctive features of these systems are as follows: automatic extraction of knowledge structures from texts (Russian, English) and forming the Knowledge Base which is used for realization of logical-analytical functions [13]. The ESN apparatus provides powerful representational possibilities for describing all levels of natural language, including the level of deep semantic structures, and cross-lingual correspondences.

The implemented linguistic processors were created on the basis of this approach which made it possible to manufacture design solutions for the basic problems of extracting meaningful knowledge from the texts in natural languages (Russian and English).

References

[1] Kuznetsov I.P. Semantic Representations // Moscow: "Nauka", 1986. 290p.

[2] FASTUS:a Cascaded Finite-State Trasducerfor Extracting Information from Natural-Language Text. // AIC, SRI International. Menlo Park. California, 1996.

[3] Kuznetsov I.P. Methods of Processing Reports with the Extraction of Figurants and Events Features // In Dialogue'99: Proceedings of the International Workshop "Computational Linguistics and its Applications", Vol.2, Tarusa, 1999.

[4] Kozerenko, E.B. Multilingual Processors: a Unified Approach to Semantic and Syntactic Knowledge Presentation. In Proceedings of the International Conference on Artificial Intelligence IC-AI'2001 25-28, 2001. CSREA Press, 2001, pp.1277-1282.

[5] Byrd, R. and Ravin, Y. Identifying and Extracting Relations in Text // 4th International Conference on Applications of Natural Language to Information Systems (NLDB). Klagenfurt, Austria, 1999.

[6] Kuznetsov I.P., Matskevich A.G. The System for Extracting Semantic Information from Natural Language Texts // Proceedings of the Dialog International Workshop "Computational Linguistics and its Applications", Vol.2, Moscow: Nauka, 2002.

[7] Kuznetsov, I., Kozerenko, E. The system for extracting semantic information from natural language texts // Proceeding of International Conference on Machine Learning. MLMTA-03, Las Vegas US, 23-26 June 2003, p. 75-80.

[8] Kuznetsov I.P. Natural Language Texts Processing Employing the Knowledge Base Technology // Sistemy i Sredstva Informatiki, Vol.13, Moscow: Nauka, 2003, pp. 241-250.

[9] Somin N.V., Solovyova N.S., Charnine M.M The System for Morphological Analysis: the Experience of Employment and Modification // Sistemy i Sredstva Informatiki, Vol. 15 Moscow: Nauka, 2005, pp. 20-30.

[10] Kuznetsov I.P., Matskevich A.G. The English Language Version of Automatic Extraction of Meaningful Information from Natural Language Texts // Proceedings of the Dialog-2005 International Conference "Computational Linguistics and Intelligent Technologies", Zvenigorod, 2005pp. 303-311.

[11] Cunningham, H. Automatic Information Extraction // Encyclopedia of Language and Linguistics, 2cnd ed. Elsevier, 2005.

[12] Kuznetsov I.P., Matskevich A.G. Semantics Oriented Linguistic Processor for Automatic Formalization of Autobiographical Data // Proceedings of the Dialog-2006 International Conference "Computational Linguistics and Intelligent Technologies", Bekasovo, 2006, pp. 317-322.

[13] Web site “Knowledge extraction for Analytical Systems”: http://Iiranlogos.com/english/

[14] Kuznetsov I.P., Efimov D.A., Kozerenko E.B. Tools for Tuning the Semantix Processor to Application Areas // Proceedings of ICAI'09, Vol. I. WORLDCOMP'09, July 13-16, 2009, Las Vegas, Nevada, USA. - CRSEA Press, USA, 2009. P. 467-472.

[15] Kuznetsov I.P., Kozerenko E.B., Matskevich A.G. *Deep and Shallow Semantic presentations in Intelligent Fact Extractors* // Proceedings of ICAI’2010 Las Vegas, USA, June 14-17, 2010, CRSEA Press, 2010.

[16] Kuznetsov, I.P., Kozerenko E.B. *Semantic Approach to Explicit and Implicit Knowledge Extraction* // Proceedings of ICAI’11, WORLDCOMP’11, July 18-21, 2011, Las Vegas, Nevada, USA. - CRSEA Press, USA, 2011.

[17] Clark P., P. Harrison, and J. Thompson. A Knowledge-Driven Approach to Text Meaning Processing // Proceedings of the HLT-NAACL 2003 Workshop on Text Meaning, 2007. P. 1–6.

[18] Gildea D. and M. Palmer. The necessity of syntactic parsing for predicate argument recognition. In Proceedings of the 40th Annual Conference of the Association for Computational Linguistics (ACL-02), Philadelphia, PA, 2002. P. 239–246.

[19] Pasca M. and B. Van Durme. What You Seek is What You Get: Extraction of Class Attributes from Query Logs // Proceedings of the 20th International Joint Conference on Artificial Intelligence (IJCAI-07), 2007. P. 2832–2837.

[20] Punyakanok V., D. Roth, and W. tau Yih. The Importance of Syntactic Parsing and Inference in Semantic Role Labeling // Computational Linguistics 34(2), 2008. P. 257–287.

The Ontological Semantics of Antonyms

Max Petrenko
Princess Ekaterina R. Dashkova Moscow Humanities Institute,
NLP Lab, Purdue University
maxpetrenko@alumni.purdue.edu

Christian F. Hempelmann
Department of Literature and Languages
Texas A&M University–Commerce
NLP Lab, Purdue University
chempelm@purdue.edu

Abstract – *This paper discusses the formal representation and lexical acquisition strategies of antonyms. The methodologies and toolbox of Ontological Semantic Technology (OST) are introduced as a framework. A brief outline of the technology and antonym taxonomies is followed by a discussion of how common and recalcitrant cases of antonyms can be represented and acquired, along with illustrations through pertinent examples.*

Keywords: computational lexicon, antonyms, language engineering, ontological semantics, structural semantics

1 Introduction

The relation of antonymy is a commonly used approach to express a key meaning relation between certain word pairs and word sets—or fields—in particular in structural semantics. The purpose here has been to enable a description of meaning without having to actually analyze that meaning, that is, relate senses to each other systemically and label that relationship rather than having to give senses meaningful descriptions in and of themselves.

Providing meaningful descriptions requires an exhaustive and interrelated system, like the ontology underlying the present approach. This ontology is not just a taxonomy and cannot afford to be selective in where it draws lines of distinction, but has to do it across the senses of the lexicon of a language. In other words, the types of antonymy must be systematically related to each other as part of the ontology. The present approach integrates the advantages and insights of the selective contrastive approach afforded by existing research on antonyms and combines it with the exhaustive, descriptive, systematic apparatus of interrelated concepts for meaning representation of ontological semantic technology (OST).

1.1 The semantics of antonyms

While extensive research exists on the semantics and classification of antonyms, the computational aspects of representing and acquiring antonymy received little attention in the literature on computational linguistics. This section will present a brief outline of the semantics of antonyms and their taxonomy.

In general, the concept of antonymy is based on dichotomization. [Murphy 2003, 183] points to binarity as the fundamental conceptualization mechanism underlying antonymy, discussing the tendency to construe of taxonomically similar entities in sets of two, so that triplets like *solid/liquid/gas* would further bifurcate into *solid/liquid*, *liquid/gas*, and *gas/solid*. Section 2.5 will discuss how the binarity principle of antonymy formation could inform antonymy acquisition within OST.

Not least since Sapir (1944), a major division of antonyms into non-gradable and gradable has been made [cf. Riemer 2010, Murphy 2003, Lyons 1977], which can be exemplified on the antonym pairs *dead-alive* (non-gradable) and *light-dark* (gradable; e.g., X is lighter/darker than Y). Further subdivisions, often orthogonal, have been proposed based on linguistic-semantic as well as logical properties. These will be discussed in more detail in relation to their acquisition and detection in section 2. Overall, the group of non-gradable antonyms is an eclectic set exhibiting significant variation at both syntactic and semantic levels, including culture- and context-based variation, which presents significant challenges even for a semi-automatic acquisition system.

Several publications exist that attempt to account for the human acquisition of antonyms by capitalizing on the tendency of antonyms to co-occur in structurally similar sentences with higher than random consistency. [Justeson and Katz 1991] build on the hypothesis introduced in [Charles and Miller 1989] that adjectival antonym pairing is largely informed by statistical co-occurrence within same sentences. Based on the list of 55 antonym pairs frequency-tested on the Brown corpus, [Justeson and Katz 1991] established that an adjectival antonym pair on average co-occurs

once in every 15 sentence in syntactically recurring constructions, which, it is concluded, provides substantial training for antonymous associations. [Fellbaum 1995] and [Jones 2002] have explored syntactic contexts for co-occurring antonym pairs, and [Jones 2006] extended the approach to spoken English. The statistical line of research presented above turns out to be of interest to OST in that it supplies a verifiable list of commonly occurring antonym pairs, which can guide the selection of proper surface word forms during semi-automatic antonym acquisition.

1.2 Ontological Semantic Technology

Ontological Semantic Technology has received extensive coverage [Nirenburg and Raskin 2004, etc.] and substantial research and development has been carried out in a number of academic and commercial projects.

The lexicon entry template below illustrates the structure of lexical entries in the OST lexicon, specific to every language handled and separate from the core resource, the ontology (for a detailed review see Nirenburg and Raskin 2004, Petrenko 2010, for a sketch of the system architecture see Fig. 1):

```
(head-entry
    (sense-1, 2, 3…
        (cat(n/v/adj/pro/prep))
        (synonyms "")
        (anno
            (def "")
            (comments "acquisition time stamp or other
                notes")
            (ex "")
        )
        (syn-struc(
            (root($var0))(cat(n/v/adj/pro/prep))
            (subject/object((root($var#))(cat(np/vp/s))))
        )
        (sem-struc
            (root-concept
                (property(value(^$var#
                (restricted-to(default/sem(concept)))))))
        )
    )
)
```

The entry begins with a part-of-speech classification, a listing of synonyms (if any), and an annotation zone for human consumption. This annotation includes a definition, an example sentence, and comments (if any) for lexicon acquirers and maintainers to quickly grasp which sense of the word is intended to be represented, as well as any syntactic peculiarities or open issues to be handled later.

This is followed by a syntactic description of the behavior of this sense in relation to other elements that will be found in its syntactic environment when the sense is used (syn-struc).

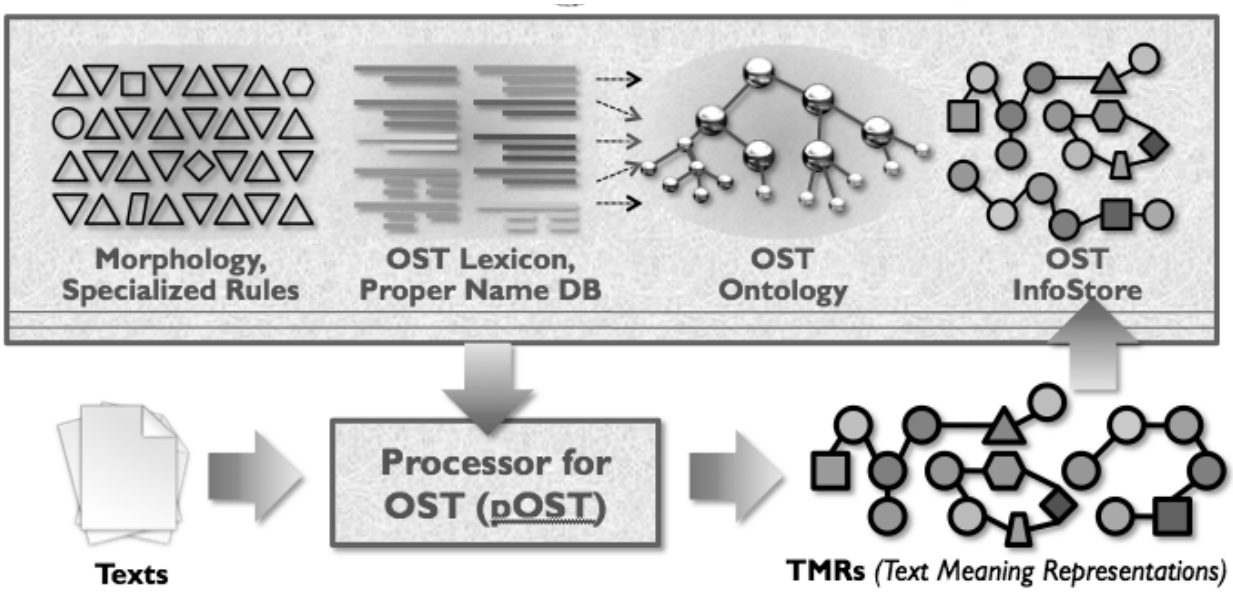

Figure 1: OST Architecture

The main information that the sense entry contributes to the OST system for text processing is in the semantic description (sem-struc). In most cases, a concept from the ontology will form the root of the semantic description, usually further refined by specifying additional constraints about certain properties of the root concept. In addition, mappings via the syn-struc to senses of other words found in the sentence can be made. For example, commonly

the syntactic subject of a sentence is mapped to the semantic role of agent.

The ontology on which the sem-strucs are based is a lattice of concepts that are interrelated as mutual property fillers. At the top level it distinguishes objects, events, and properties; objects and events are further distinguished into physical, mental, and social subtypes; properties are distinguished into attributes and relations; etc (see Fig. 2). In previous applications, the ontologies contained 5-7,000 concepts with 15-20,000 unique properties, which, by inheritance, are multiplied into 69-90,000 "facts" across the ontology.

As has hopefully become clear even from this rather cursory overview, the acquisition and maintenance of resources is the crucial effort in OST. Therefore it is guided by a set of tools that facilitate this effort by the use of templates, propagation of similar senses, formal consistency, and semantic consistency, mainly against the constraints of the ontology. For detailed accounts of methodological, practical, and computational aspects of lexicon acquisition see [Taylor et al. 2010, Petrenko 2010, Raskin and Nirenburg 1995, and Raskin et al. 2010].

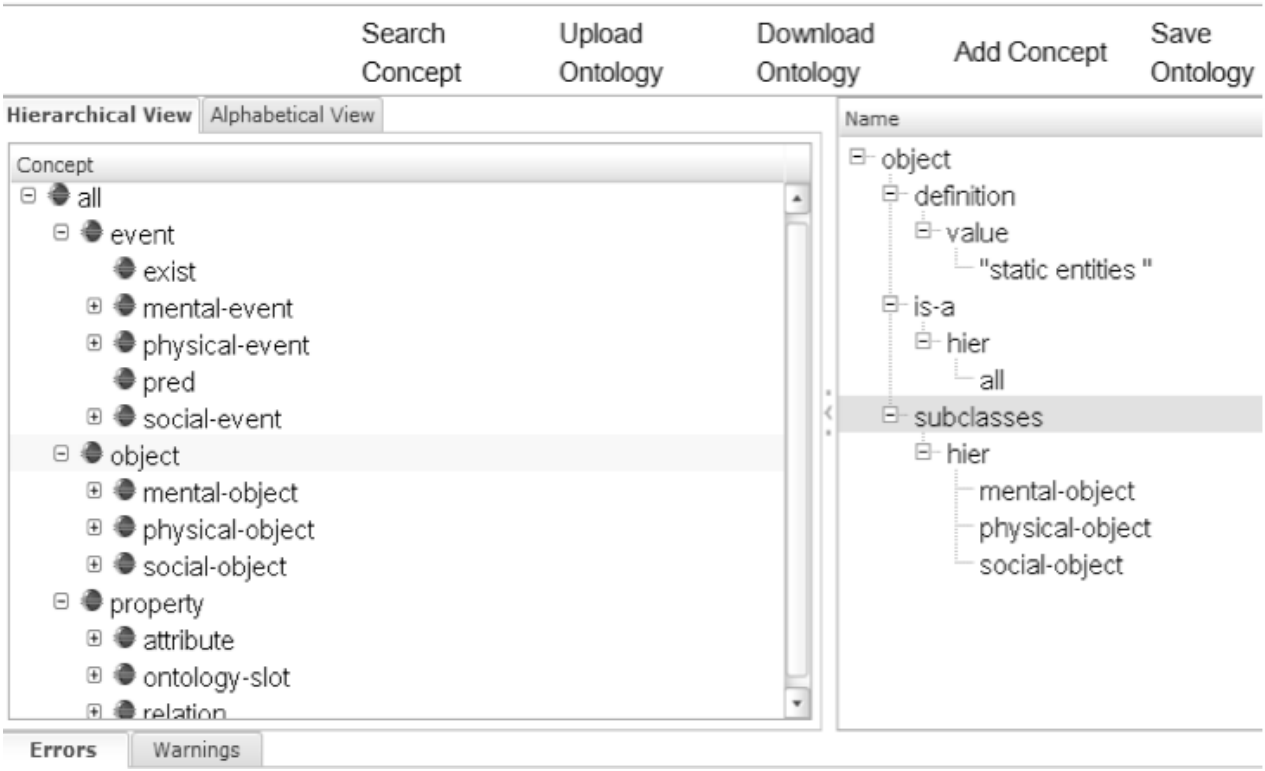

Figure 2: Top Level of the Ontology

Simplifying the exact process for the sake of brevity, in processing language the analyzer module will build representations of the text clause by clause from the building blocks found in the sem-struc. The information in the sem-strucs of every possible sense of a word is checked for compatibility with those of all senses of all other words in the clause by constraint matching, which also happens with the help of the information in the syn-struc. Finally, the combination of senses of all words in the clause that has the best matching of all constraints is chosen as the text-meaning representation of that clause to be stored in the InfoStore resource (see Fig. 1).

2 Antonyms in Ontological Semantic Technology

This section outlines representation formalisms and acquisition strategies for various types of antonyms.

2.1 Non-gradable antonyms

Lexical items with non-scalar semantics do not have a unified representation, and there are engineering considerations against having one in the static resources. For a scalable knowledge-based and domain-independent natural language processing system, explicit preference of otherwise unmarked

ontological concepts and properties representing a non-gradable pair like *alive-dead* (e.g. LIVE vs. LIVE(EPISTEMIC(0))), if implemented consistently, would lead to an unnecessary bias in extracting conceptual relations from input. While it would therefore be undesirable to accommodate the core antonym detection functionality in the static resources, and this functionality being one of the procedural, algorithmic components of an OST application, the ontology with its large descriptive thesaurus provides a comprehensive way to capture non-gradable antonym pairs.

Among the most common formats representing non-gradable antonym pairs are contrastive concept pairs, property fillers, and mutually exclusive facet values. An example below illustrates how a "male-female" pair can be captured via two contrastive literal fillers or values of the GENDER property.

```
(male-adj1
    (cat(adj))
    (anno(def "of male gender")
        (ex "a male suspect was arrested"))
    (syn-struc((root($var0))
        (cat(adj))(np((root($var1))(cat(np))))))
    (syn-struc1
        ((subject((root($var1))(cat(np))))
        (root(be))(cat(v))
        (directobject((root($var0))(cat(adj))))))
    (sem-struc(^$var1(gender(sem(male))))))

(female-adj1
    (cat(adj))
    (anno(def "of female gender")
        (ex "a female suspect was arrested"))
    ...
    (sem-struc(^$var1(gender(sem(female))))))
```

The representation above captures the contrastive gender properties as mutually exclusive values of the non-scalar attribute GENDER. An alternative representation could conceptualize the contrast as that between two full fledged concepts, as per below:

```
(male-adj1
    (cat(adj))
    (anno(def "of male gender")
        (ex "a male suspect was arrested"))
    ...
    (sem-struc(male))

(female-adj1
    (cat(adj))
    (anno(def "of female gender")
        (ex "a female suspect was arrested"))
    ...
    (sem-struc(female))
```

There are procedural implications of attribute value-based representations and concept-based representations. The former seems more intuitive but makes the semantic structure less accessible to a processor as attribute values are seldom used by semantic processing modules.

2.2 Gradable antonyms

An efficient way of representing lexical items with scalar semantics has been introduced in [Raskin and Nirenburg 1995], where the acquisition of scalar adjectives like *good*, *hot*, etc. is acquired by rapid propagation of pertinent values on a single scale (EVALUATION, TEMPERATURE, etc.). Given the scalar nature of gradable antonym pairs a similar approach could be adopted, which involves anchoring both members of an antonym pair in a single scalar attribute and assigning contrastive values:

```
(large-adj1
    (cat(adj))
    (anno(def "largely sized")
        (ex "he carried a large bag"))
    (syn-struc((root($var0))
        (cat(adj))(np((root($var1))(cat(np))))))
    (syn-struc1((subject((root($var1))(cat(np))))
        (root(be))(cat(v))(directobject((root($var0))
        (cat(adj))))))
    (sem-struc(^$var1(size(greater-than(0.8))))))

(small-adj1
    (cat(adj))
    (anno(def "small sized")
        (ex "he carried a large bag"))
    (syn-struc((root($var0))
        (cat(adj))(np((root($var1))(cat(np))))))
    (syn-struc1((subject((root($var1))(cat(np))))
        (root(be))(cat(v))(directobject((root($var0))
        (cat(adj))))))
    (sem-struc(^$var1(size(less-than(0.3))))))
```

[Riemer 2010] and [Murphy 2003] point out the semantic non-comittedness of certain pairs of gradable antonyms. In particular, [Riemer 2010] observes that in the *good-bad* pair, *good* merely posits an evaluation scale and is not committed to a specific value, which is evidenced by the acceptability of the example, "How good was that film? – Really bad." The contrastive member *bad*, on the other hand, is committed, which is in turn illustrated by the oddness of the example, "*How bad was the film? – The film is worse than the TV series, but they are both really good" [Riemer 2010: 138].

A reasonable adjustment to the representation formalism which would be sensitive to semantic non-comittedness of some gradable antonyms could involve postulating an open-ended variable whose value would be calculated contextually. More specifically, a TMR for "How good was the film" could override the default value of >.5 from the lexical entry and posit an open ended variable instead:

TMR: *How good was the film?*
exist
theme *sem* video-file
evaluative *value* $var99

The value of the high-numbered variable isassigned based on the output of higher-level processing modules capable of aggregating contextual data from ambient input segments across sentences or even acress texts in a corpus. In the example above, the ellipsis processing module would establish the co-reference of the EVALUATIVE modality filler in "Really bad.", and since *bad* is uncommitted, its value would override the default value in the previous TMR.

2.3 Autoantonyms

Autoantonymous lexical items have received extensive coverage in [Murphy 2003] and [Riemer 2003]. Unlike uncommitted antonym pairs, which posited both representational and processing challenges, autoantonyms are essentially multi-sense entries representation-wise, and the challenge mainly lies in selecting an appropriate sense at the TMR building stage. Consider, for example, 'sanction-v1' and sanction-v2:

```
(sanction-v1
    (cat(v))
    (anno(def "to allow")(comments "")
        (ex "the court sanctioned investigation into
        bribe allegations in the corporation")
    ...
    (sem-struc(allow
        (
        agent(value(^$var1(restricted-to(human)))))
        (theme(value(^$var2(restricted-to
            (sem(social-event culture-event)))))))))

(sanction-v2
    (cat(v))
    (anno(def "to penalize, impose sanctions
        on")(comments "")(ex "the union
        sanctioned the rogue state for stifling
        political opposition")(synonyms "")
    ...
    (sem-struc(allow(epistemic(0))
        (agent(value(^$var1(restricted-to(human)))))
    (patient(value(^$var2(restricted-to(sem(human
        organization)))))))))
```

A seeming similarity of the two autoantonymous senses is considerably reduced by the different case roles on their restrictions: if the theme of ALLOW is restricted to EVENTS, ALLOW(EPISTEMIC(0)) only requires an animate PATIENT filler.

2.4 Conversives and reversives

The OST framework offers an explicit formalism for representing both conversive and reversive lexical items. For a conversive pair, the order of the same ontological properties is reversed with fillers remaining in situ. For a reversive pair, sibling properties are invoked to capture the opposition. To illustrate, the canonical conversive pair *buy-sell* would receive the following representation:

```
(buy-v1
    (cat(v))
    (anno(def "to purchase")(comments "")
        (ex "he bought a cell phone from a friend")
    ...
    (sem-struc(buy
        (agent(value(^$var1(restricted-to(human)))))
        (theme(value(^$var2(restricted-to
        (sem(artifact food information)))))))
            (source(value(^$var3
                (restricted-to(sem(human)))))))))

(sell-v1
    (cat(v))
    (anno(def "to exchange for money")
        (comments "")
        (ex "he sold his cell phone to a friend")
    ...
    (sem-struc(buy
        (source(value(^$var1
            (restricted-to(human)))))
        (theme(value(^$var2(restricted-to
            (sem(artifact food information)))))))
        (agent(value(^$var3
            (restricted-to(sem(human)))))))))
```

A reversive pair "enter-leave" would receive the following representation:

```
(enter-v1
    (cat(v))
    (anno(def "to move into a structure")(comments
        "")(ex "he entered the room") (synonyms "")
    ...
    (sem-struc(move
        (agent(value(^$var1(restricted-to(human)))))
```

```
(end-location(value(^$var2
    (restricted-to(sem(artifact/building/
        landscape-object)))))))))

(leave-v1
    (cat(v))
    (anno(def "to exit a structure")(comments "")
        (ex "he left the room") (synonyms "")
    ...
    (sem-struc(move
        (agent(value(^$var1(restricted-to(human)))))
        (start-location(value(^$var2
            (restricted-to(sem(artifact/building/
                landscape-object)))))))))
```

The sibling case roles END-LOCATION and START-LOCATION are invoked to capture the reversion.

Given the multitude of ontological levels and sibling concepts, automating the acquisition of conversives and reversives is problematic. Section 2.5 will discuss additional issues and considerations regarding antonym acquisition.

2.5 Acquisition of antonyms in Ontological Semantic Technology

This section will discuss a preliminary strategy for automating the acquisition of a limited set of gradable and all gradable antonyms in OST. The strategy will allow for semi-automatic acquisition of antonyms from manually acquired senses.

A number of intrinsic parameters of many non-gradable antonyms make their automatic acquisition problematic and, in some cases, unjustified. As pointed in [Murphy 2003], the semantic motivation for relating many non-gradable antonyms is arbitrary, as well as culture- and context-sensitive. [Murphy 2003: 173] discusses the cross-cultural and contextual variation of antonyms of taste for the word *sweet* with *sweet-pungent* being preferred in Japanese, *sweet-sour* in English in neutral contexts, and *sweet-salty* (when describing snack food), *sweet-bitter* (chocolate), *sweet-dry* (wine), etc. While the OST knowledge resources provide for recognition and semantic representation of such context-sensitive antonyms, their acquisition would lead to unjustified idiosyncrasies and thus bias the text processor at the TMR building and reasoning levels. An additional consideration exists against automatic representation of those non-gradable antonyms whose semantic structure contains head concepts with multiple siblings. This leaves the machine with the uncertainty as to which sibling filler would constitute antonymy; in these cases the machine would over-generate, and there would be no scalable way to eliminate false positives. To illustrate, multiple sibling fillers of the attribute HAS-COLOR exist, many of which are culturally contrastive (e.g. *black-white*), while others are context-sensitive (e.g. *black-red* when describing a roulette wheel), and there are no *a priori* intrinsic linguistic clues for the machine to use to capture those pairs.

Among non-gradable antonyms, only cases like *male-female*, whose semantics involves selection from a set of two property fillers, lend themselves to acquisition and can be incorporated into the general semi-automatic acquisition strategy described below.

The antonym-acquisition strategy takes advantage of the representational potential of OST's knowledge resources, morphological regularities in antonym formation, the available lists of high-frequency antonym pairs and, available tagged corpora.

The general steps of the strategy are outlined below:

1) **Base antonym type detection**: Based on its semantic structure, the type of the base antonym is determined automatically. Senses whose semantic structure posits a concept in the set of two siblings, or a property with a set of two sibling fillers are non-gradable senses whose semantic structure contains a scalar attribute. are gradable, other cases are eliminated.

2) **Semantic derivation**: Depending on the base antonym type, a respective rule is applied to derive an appropriate semantic structure.

The following semantic derivation rules can be formulated for each base antonym type:

For non-gradable antonyms:

(1) (sem-struc(concept)) → (sem-struc(sibling-concept))

(2) (sem-struc(concept(facet(filler)))) → (sem-struc(concept(facet(sibling-filler))))

For gradable antonyms:

(3) (sem-struc(attribute(facet(literal-filler-a)))) → (sem-struc(attribute(facet(literal-filler-b[with a and be being the only literal fillers of that attribute))))

Rules (1-2) select an alternate sibling for the head concept or filler, and rule (3) reverses the value of the scalar attribute of the base antonym. The part of speech and syntactic structure of both pair members remain the same.

3) **Form derivation:** Morphological rules are applied to the base antonym to form a new sense by adding commonly used affixes. The list of regular antonym-forming prefixes and suffixes is based on [Justeson and Katz 1991] and, with minor additions, includes the following: [a-, ab-, an-, dis-, il-, im-, in-, un-,

non-, anti-, counter-, -less.] At this stage, the set is recursively applied to the base antonym form with each affix attached at a time. All the resulting forms are then passed to the form verification procedure.

4) **Form verification**: The core objective of this procedure is to assign an acceptable word form to an already instantiated sense template. The legitimacy of the newly derived word checked against a tagged corpus (e.g. Brown corpus) and the antonym list developed in [Justeson and Katz 1991] (referred to as JK list) containing 57 pairs of antonyms of higher than random frequency. The JK list comprises a set of 35 antonymous adjectival pairs tested in [Deese 1964] and an additional set of 22 pairs tested in [Justeson and Katz 1991.] The procedure takes all morphological derivates from procedure (3) as input. If none of the candidate forms returns a match in the tagged corpora, the JK list, as well as online and offline lists of antonyms are taken advantage of. The output of the procedure essentially completes the antonym acquisition cycle: the antonym has been derived semantically, syntactically, and lexically. If no match is returned from the available corpora, the acquisition cycle is aborted.

5) **Rapid propagation**: Once a legitimate antonym has been confirmed, its synonyms are assigned an identical sense template, thus facilitating acquisition. The application of this procedure is largely dictated by the general grain size of lexical coverage. Finer-grained applications may require a more thorough representation capturing purely preferential differences between, say, the more standard *big-little* and the less acceptable *large-little*. More generic applications may allow for antonymy to be established between all members of each pair. Procedurally, steps similar to rapid propagation outlined in [Nirenburg and Raskin 1995, 2004] are taken, when the syntactic and semantic structures of a fully derived sense get propagated across a large set of similar entries. A similar procedure was also deployed in [Petrenko 2011] in relation to deriving synonyms of semi-automatically acquired deverbal senses.

As an illustration of the antonym acquisition strategy, a selected pair *cold-hot* with contrastive TEMPERATURE values is discussed below with each procedure described in detail. Procedure (1) will determine the base antonym *cold* as gradable:

```
(cold-adj1
    (cat(adj))
    (anno(def "having a low temperature")
        (ex "he stepped in the cold water"))
    (syn-struc((root($var0))
        (cat(adj))(np((root($var1))(cat(np))))))
    (syn-struc1((subject((root($var1))(cat(np))))
        (root(be))(cat(v))(directobject((root($var0))
            (cat(adj))))))
    (sem-struc(^$var1(temperature(less-than(0.3)))
)))
```

Based on the output of procedure (1), semantic derivation rule (3) for gradable antonyms of procedure (2) will be called, which will return the following semantic structure:

(sem-struc(^$var1(temperature(greater-than(0.8))))

None of the word forms (**acold, *abcold, *ancold, *discold, *ilcold, *imcold, *incold, *uncold, *noncold, *anticold, *countercold, *coldless*) generated morphologically via procedure (4) will match the existing corpora, so the system will have to resort to existing corpora of antonyms including the JK list. The JK list will return a match "hot" for "cold", whose sem-struc, if acquired earlier, will match the template derived in procedure (1). After the *cold-hot* antonym pair has been derived, synonyms will be looked up in available online and offline corpora:

cold-adj1: [arctic, frigid, gelid, glacial, icy, polar, bleak, cutting, raw-chilly, parky, crisp, frosty, nipping, nippy, snappy, frigorific, frore, frosty, rimed, rimy, heatless, ice-cold, refrigerant, refrigerating, refrigerated, shivery, stone-cold, unheated, unwarmed]

hot-adj1: [baking, baking hot, blistering, blistery, calefacient, warming, calefactory, calefactive, calorifacient, calorific, fervent, fervid, fiery, igneous, heatable, heated, heated up, het, het up, hottish, overheated, red-hot, scorching, sizzling, sultry, stifling, sulfurous, sulphurous, sweltering, sweltry, thermal, torrid, tropical, tropic, white, white-hot]

Under the generic, coarse-grained functionality assumption, the instantiated templates for *cold* and *hot* will be propagated among all members of the retrieved sets. The acquirer will be offered an option of manually approving each built sense. Finer-grained acquisition would introduce additional demarcation criteria (stylistic preferential, etc.) and thus substantially increase the amount of manual effort.

4 Conclusion

This paper has presented a first account—descriptive and procedural—of antonyms within Ontological Semantic Technology. We first outlined, based on

relevant literature, the pertinent properties and major types of antonyms which directly resonate with the descriptive potential and computational goals of OST applications. We then discussed how non-gradable and gradable antonyms are represented within OST, how non-comittedness, auto-antonymy, reversion and conversion can be captured with OST formalisms. We concluded the paper by introducing a general strategy for semi-automatic acquisition of a limited set of non-gradable and all gradable antonyms in the OST lexicon, which takes advantage of manually acquired base senses, rich ontological and lexical knowledge resources, and relies on existing corpora.

5 References

[1] Deese, James E. "The associative structure of some common English adjectives." Journal of Verbal Learning and Verbal Behavior, 3(5): 347-57. 1964

[2] Fellbaum, C. “Co-occurrence and antonymy”. International Journal of Lexicography 8. 281–303. 1995

[3] Hempelmann, C., J. Taylor, and V. Raskin, “Application-guided ontology engineering”. In Proc. ICAI’10, Las Vegas, July 2010.

[4] Jones, S. Antonymy: a corpus-based approach. London, Routledge, 2002

[5] Jones, S. "A lexico-syntactic analysis of antonym co-occurrence in spoken English." Text and Talk 26(2). 2006

[6] Justeson, J.S., and S. M. Katz “Co-occurrences of antonymous adjectives and their contexts”. Computational Linguistics 17, 1–19.1991

[7] Lyons, J. Semantics. Vol. 1. Cambridge: CUP, 1977.

[8] Murphy, L., Semantic Relations and the Lexicon. Cambridge, Cambridge university Press, 2003.

[8] Nirenburg, S., and V. Raskin, Ontological Semantics. Cambridge, MA: MIT Press, 2004.

[10] Petrenko, M. “Semi-automatic Verb-driven Lexicon Acquisition Enhancer”. In Proc. ICAI’11, Las Vegas, July 2011.

[11] Petrenko, M. “Lexicon Management in Ontological Semantics”. In Papers from the Annual international Conference “Dialogue 2010, Moscow, Russia 2010, in press.

[12] Raskin, V., J. M. Taylor, and C. F. Hempelmann, “Guessing and knowing: Two approaches to semantics in natural language processing,”. In Papers from the Annul. Int. Conf. “Dialogue”, Moscow, 2010, vol. 9, no. 16, pp. 642-650.

[13] Raskin, V., and S. Nirenburg. “Lexical semantics of adjectives: a microtheory of adjectival semantics.” Memoranda of Computer and Cognitive Science MCCS-95-228. New Mexico State University. Computer Research Laboratory. 1995

[14] Riemer, N., Introducing Semantics. Cambridge, Cambridge university Press, 2010.

[15] Sapir, E. Grading: A study in semantics. Philosophy of Science, 11:93–116, 1994

[16] Taylor, J., C.F. Hempelmann, and V. Raskin, “On an automatic acquisition toolbox for ontologies and lexicons” In Proc. ICAI’10, Las Vegas, USA, July 2010.

SESSION

NOVEL AI APPLICATIONS AND ALGORITHMS

Chair(s)

TBA

The Application of AI to Cultural Intelligence

Zhao Xin WU [1], Roger NKAMBOU [2], and Jacqueline BOURDEAU [2]
[1,2]Computer Science Department, University of Quebec in Montreal, Montreal, Quebec, Canada
[2] LICEF, TÉLÉ-UNIVERSITÉ, Montreal, Quebec, Canada

Abstract - *In an increasingly diverse cross-cultural environment, individuals and organizations are constantly interacting with foreign cultures, which require perceptiveness and adaptability. Cultural intelligence appears as an emerging application in cross-cultural activities. Researches on this domain provide a new perspective and a promising means of intercultural conflicts and obstacles reduction. However, these researches rely mainly on questionnaires to find solutions to the cultural intelligence problems in cross-culture settings. Up until now, no research on cultural intelligence has been empirically computerized. The traditional computational techniques cannot treat cultural intelligence soft data to help individuals and organizations in solving intercultural problems. This research aims to create a new cultural intelligence model based on an innovative breed of AI technologies, and implemented in an expert system called CIES. The purpose of CIES is to support ordinary people when making culturally intelligent decisions and to improve their cultural skills when facing various authentic situations.*

Keywords: Cultural Intelligence; Soft-Computing; Expert System; Hybrid System

1 Introduction

In the context of the environment of globalization, multicultural communication and exchanges are part of today's world reality. Individuals and organizations are required to make culturally-intelligent decisions and to show their competence in culturally diverse workplaces. When confronted with cultural diversity, some individuals and organizations are able to adapt successfully to the new cultural environment, while others are not. What is the decisive factor for these opposing responses? How can good decisions be made in culturally-diverse environments? What skills can be improved to enable cultural adaptation?

In recent years, researchers have shown great interest in globalization and intercultural management. Cultural intelligence has, therefore, been presented as a new phenomenon in order to answer the above questions. Organizational psychology and human resource management have paid great attention to cultural intelligence since its introduction. These fields of study have yielded valuable results that apply to the real cultural world. However, most current studies related to cultural intelligence do not focus on the computational aspects. Moreover, a great deal of cross-cultural knowledge is expressed as 'soft data,' such as, "*this culture is more masculine*", "*that person is highly confident*". Effectively dealing with these natural linguistic variables is beyond the scope of traditional computer technology.

The new AI technologies provide us with a means for coping with these incomplete, vague and ambiguous terms that are often used in the cultural domain. This research attempts to offer effective solutions to the problems mentioned above. These solutions mainly rely on a new computational model of cultural intelligence implemented in a system called the CIES (Cultural Intelligence Expert System). This system has integrated the cultural intelligence knowledge of experts and has the potential to achieve better performance than human experts. The CIES is considered as highly intelligent due to its wealth of knowledge, openness, scalability, flexibility, adaptability, and capability to self-learn. Such a system has three goals: 1) to assist individuals and organizations in their decision-making processes involving cultural affairs; 2) to assist people in improving their use of a specific form of intelligence based on their capacity to understand, to reason correctly, and to adapt to culturally diversified situations [1]; and 3) to facilitate the work of researchers and to better equip them in their studies of cultural intelligence.

2 Cultural Intelligence and its dimensions

In the research literature, cultural intelligence has been referred to using the acronym CQ. Researchers have different opinions regarding the concept of CQ. Earley and Ang presented CQ as a reflection of people's ability to collect and to process information, to form judgments, and to implement effective measures in order to adapt to a new cultural context [2]. Earley and Mosakowski redefined CQ as the ability of managers to deal effectively with different cultures [3]. They suggested that CQ is a complementary intelligence form,

which may explain its capacity to adapt and face diversity, as well as to operate in a new cultural setting. Peterson interpreted CQ in terms of its operation [4]. He believes the concept of CQ is compatible with the Hofstede [5] cultural values and their five main dimensions, i.e., individualism versus collectivism, masculinity versus femininity, power distance, uncertainty avoidance, and short and long term orientation. Brislin et al. defined CQ as the level of success people obtain when adapting to another culture [6]. Thomas explained CQ as the ability to interact efficiently with people who are culturally different [7] [8]. Ng et al. presented CQ as the ability to be effective in all cultures [9]. Johnson et al. defined CQ as the ability of an individual to integrate a set of knowledge, skills and personal qualities so as to work successfully with people from different cultures and countries, both at home and abroad [10].

Researchers in the field of culture also use different dimensional structures to measure CQ. Each of these researches is associated with conceptual models. These structures seek to explain the attributes that enable people to develop their abilities in various cultural contexts and, thereafter, to determine how people can improve these capabilities. Earley and Ang [2] presented the first structure of CQ which integrates the following three dimensions: cognition, motivation and behaviour. While Thomas agrees with Earley and Ang that there are three dimensions to CQ [8], he does not share their point of view regarding what these three dimensions should be. He, therefore, advocated another tridimensional structure. His belief is founded on the theory of Ting-Toomey [11], which states that the structure of CQ should be based on the skills required for intercultural communication, that is to say, knowledge, vigilance and behaviour. Vigilance acts as a bridge connecting knowledge and behaviour, which is the key to CQ. Tan [12] believes that CQ has three main components: 1) strategic thinking about culture; 2) dynamics and persistence; and 3) specific behaviours. Tan stressed the importance of behavior as being essential to CQ. If the results of the first two parts are not converted into action, CQ is meaningless. Ang and Van Dyne [1] suggested a four-dimensional CQ structure. This structure is based on the general intelligence structure of Sternberg and Detterman [13]. Ang et al. used the framework of Sternberg, which divides CQ into metacognitive CQ, cognitive CQ, motivational CQ and behavioral CQ. This structure has been widely used in the following cultural researches and studies.

3 CIES architecture

We believe that the diverse structures of CQ should be considered collectively in order to integrate the elements necessary to respond the cultural knowledge acquired. Therefore, we build the CQ architecture. It is based on the specific CQ four-dimensional structure of Ang and Van Dyne [1]. The architecture is noteworthy because we use the four CQ dimensions as integrated and interdependent entities. It represents a comprehensive overview of the multi-aspects of the researches on CQ.

The architecture of CIES uses both the symbolic and connectionist approaches of AI. The architecture respects the cognitive concepts of Ang and Van Dyne [1] regarding the theories of global CQ, it also includes other important aspects, for example, Hofstede's theory of five cultural dimensions [5]. The architecture also relies on engineering concepts in its solutions when designing and implementing software. It offers learning mechanisms which emulate human intelligence.

In total, the architecture has an eleven-step cognitive process. It recognizes cross-cultural business-related information in natural language from its environment by using its cognitive cycle. The following describes these steps. These steps correspond to the numbers inside the rectangles in Fig.1.

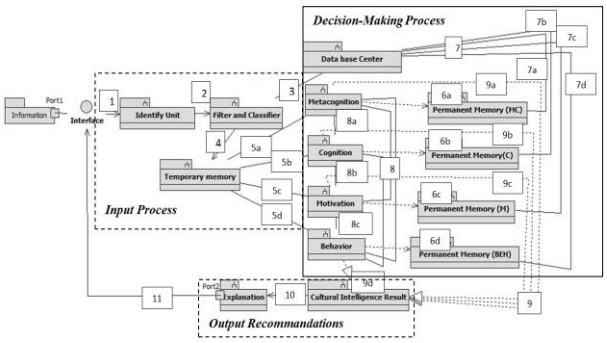

Figure 1. Architecture of CIES

Step 1: A cultural information in natural language, expressing a problem, and a question or a requirement of the user, is inputted through the user interface. This information enters the *Identify* module. This module identifies the information to determine what the user requires.

Step 2: The cultural information goes to the *Filter and Classifier* module. In this module, the information is classified and filtered from what is not useful for cultural analysis in the following steps.

Step 3: To perform this classification, the module has an associated relationship with the *Cultural Intelligence Database Center*, which has all the necessary data that the system needs, such as countries, religions, languages, and laws.

Step 4: The classified cultural data are ready to be sent to the *Temporary Memory* module. This module keeps

the data temporarily and, at the same time, interacts with the other modules.

Step5: The 5a-*Metacognitive* module, 5b-*Congnitive* module, 5c-*Motiviational* module and 5d-*Behavioral* module collect the cultural data belonging to them in the temporary memory.

Step 6: Each module depends on the consultation of its own *Permanent Memory*. These permanent memory modules are 6a for metacognition, 6b for cognition, 6c for motivation and 6d for behavior. Each permanent memory represents a complete and specific cultural database that is used by its associated module to analyze the cultural information stored in the *Temporary Memory*.

Step 7: 7a, 7b, 7c and 7d analyze the cultural information. If data are missing, permanent memories modules go to the *Cultural Intelligence Database Center* to assist in the cultural analysis of the respective modules.

Step 8: After the analysis is completed in each module, the four modules must interact with each other so that each module can adjust its cultural decision. This interaction gives a complete and effective decision before continuing to the next step.

Step 9: Following the interaction between the modules of the different CQ dimensions, the four modules in steps 9a, 9b, 9c and 9d send their final cultural decisions to the *Cultural Intelligence Result* module. In this module, the decisions of these four modules are generalized and offer significant cultural information to the user.

Step 10: The *Explanation* module justifies and explains in detail, using natural language understandable to the user, why these decisions were presented.

Step 11: The explanations are sent to the *User interface*.

4 Choices of AI techniques

CQ generally has two types of data: the first type is associated to "hard" computing; which uses numbers, or crisp values; the second type is associated with "soft" computing, which operates with uncertain, incomplete and imprecise soft data. The second type is presented in a way that reflects human thinking. When we introduce the cultural concept to cross-cultural activities, we usually use soft values represented by words rather than crisp numbers. The traditional technique, or "hard" computing, is based on Boolean logic, so it cannot treat cultural soft data. In order to enable computers to emulate humans' way of thinking and to model a human-like understanding of words in decision-making, we use a neuro-fuzzy soft-computing technique to design the CIES. This soft computing technique is capable of dealing with uncertain, imprecise and incomplete cultural soft data.

This hybrid neuro-fuzzy soft-computing technique makes use of the advantages and power of fuzzy logic and the artificial neural network (ANN). Fuzzy logic and the ANN are complementary paradigms: 1) The fuzzy logic technique is used for three reasons. First, the CQ concepts are described in natural language containing ambiguous and imprecise linguistic variables, such as "*this person has low motivation*" and "*that project is highly risky because of this religion.*" Second, fuzzy logic is well-suited to modeling human decision-making processes when dealing with "soft criteria." These processes are based on common sense and may contain vague and ambiguous terms [15]. Third, fuzzy logic provides a wide range of cultural expressions that can be understood by computers. 2) ANN: Although the fuzzy logic technique has the ability and the means to understand natural language, it offers no mechanism for automatic rule acquisition and adjustment. The ANN offers learning mechanisms in an uncertain, incomplete and imprecise cultural setting, which emulates human intelligence. It presents viable solutions for processing incomplete and imprecise cultural information. The ANN can manage the new cultural data input and the generalization of acquired knowledge. The hybrid neuro-fuzzy technique represents the essence of our soft computing model.

5 Inference engine of the system

5.1 Creating fuzzy sets

All the fuzzy sets come from the CQ domain. A practical approach to form CQ fuzzy sets is used in our system. The fuzzy sets define the sets on the universe of discourse. For example, when X is the universe of discourse of metacognition, and its elements are denoted as *x*, the fuzzy set *Metacognition (MC)* is part of the universe *X*, and is defined by the function $\mu MC(x)$ as a function of membership in the set *Metacognition*. This equation is expressed as: $\mu MC(x): X \rightarrow [0,1]$. For every element *x* of universe *X*, the membership function $\mu MC(x)$ equals the degree to which *x* is an element of set *Metacognition*. This degree, having a value between 0 and 1, represents the level of membership of element *x* to set *Metacognition*.

5.2 Linguistic variables and fuzzy rules

The idea of linguistic variables is one basis of the fuzzy set theory. A linguistic variable is a fuzzy variable. For example, when we say "the CQ is high," it means that the linguistic variable of CQ takes the linguistic value high. Thus, our cultural linguistic variables are used in fuzzy rules in the system. For example:

Rule 1:

IF Metacognition is high AND Cognition is high AND Motivation is high AND behavior is high

THEN CQ is high

The operations of cultural fuzzy sets used in our CIES are the *Intersection* and *Union*. For example, the fuzzy operation used to create the *Intersection* of two cultural fuzzy sets A and B is as follows:

$$\mu A \cap B(x) = min[\mu A(x), \mu B(x)] = \mu A(x) \cap \mu B(x), where\ x\ \in \mathrm{X} \quad (1)$$

The operation to form the fuzzy *Union* of two cultural fuzzy sets A and B is as follows:

$$\mu A \cup B(x) = max[\mu A(x), \mu B(x)] = \mu A(x) \cup \mu B(x), where\ x \in X \quad (2)$$

The CIES uses a technique called the fuzzy inference method by Mamdani [16]. Fig.2 illustrates in the CIES an example of the application of a technique called Mamdani fuzzy inference method by using triangular sets. We define that the fuzzy system as having four CQ inputs: metacognition, cognition, motivation, and behavior, and as having one output: CQ. For example, input metacognition is 7.95, cognition is 3.31, motivation is 3.41 and behavior is 2.38, inferenced by six fuzzy sets rules 1,2,3,4,5 and 6; output CQ is the result from six rules 1,2,3,4,5 and 6.

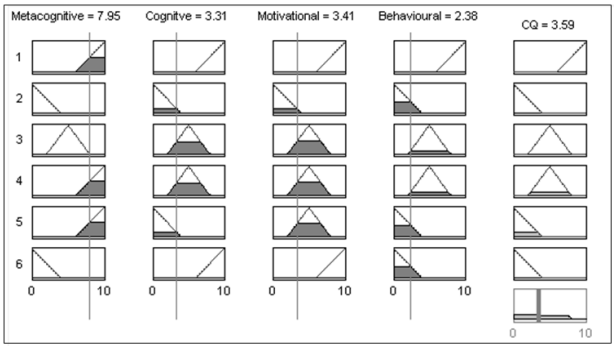

Figure 2. Example of the Fuzzy Inference System of Mamdani Using Triangular Sets in CIES

The CIES neuro-fuzzy system is similar to a multilayer neural network. Fig.3 shows the CIES neuro-fuzzy system that corresponds to the fuzzy inference model shown in Fig.2. It is represented with a neural network composed of five layers in the CIES. It has four dimensions of CQ input layer and CQ output layer, and three hidden layers that represent membership functions and CQ fuzzy rules. Each layer of the neuro-fuzzy inference model of CIES in the cross-cultural application is associated with a particular step in Mamdani fuzzy inference process. The four inputs are: metacognition (MC), cognition (C), motivation (M) and behavior (BEH), and has one output: CQ

Layer 1 - Input: No calculation is made at this layer. Each neuron corresponds to an input cultural variable. These input values are transmitted directly to the next layer.

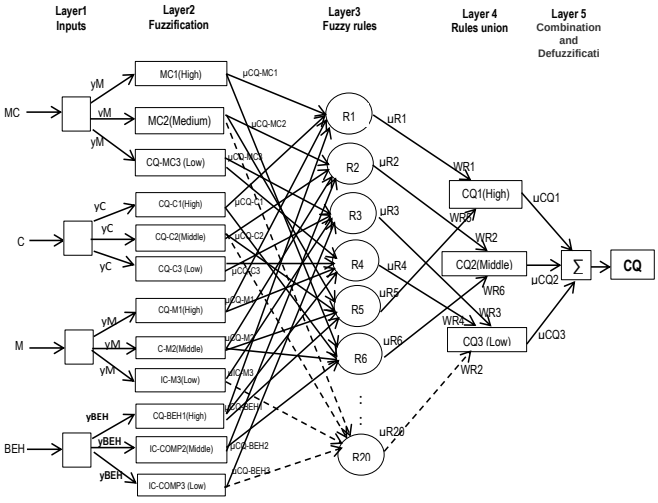

Figure 3. Soft-Computing Model of CQ

Layer 2 - Fuzzification: Each neuron corresponds to a cultural linguistic label (e.g., high, medium and low) associated with one of the input cultural variables in layer 1. In other words, the connection of the output, which represents the inclusion value, specifies the degree to which the four input cultural values belong to the neuron's fuzzy set. The connection is computed at this layer.

Layer 3 - Fuzzy Rule: The output of a neuron at level 3 is the cultural fuzzy rules. Each neuron corresponds to one cultural fuzzy rule. The cultural fuzzy rule neurons receive inputs from the layer 2 (fuzzification neurons), which represent cultural fuzzy sets. For example, neuron R1 represents cultural Rule 1 and receives input from the neurons MC1 (*Metacognition High*) and C1 (*Cognition High*). The weights (WR1 to WR20) between layers 3 and 4 are the normalized degree of confidence of the corresponding cultural fuzzy rules. These weights are adjusted when the system is trained.

Layer 4 - Rule Unions (or consequence): This neuron has two main tasks: 1) to combine the new precedent of cultural rules, and 2) to determine the output level (high, medium and low). The output level belongs to the cultural linguistic variables. For example, *μR1*, *μR5* are the inputs of *CQ1 High*, and $\mu CQ1^{(4)}$ is the output of the neuron *CQ1 High*.

Layer 5 - Combination and Defuzzification: This neuron combines all the consequential rules and computes the crisp output after defuzzification. The composition method "sum-product" [17] is used. It computes the outputs of the membership functions defined by the weighted average of their centroids. We

apply, in this case, the triangle calculation in our neuro-fuzzy system; which is the simplest calculation of the fuzzy set as shown in Fig.4:

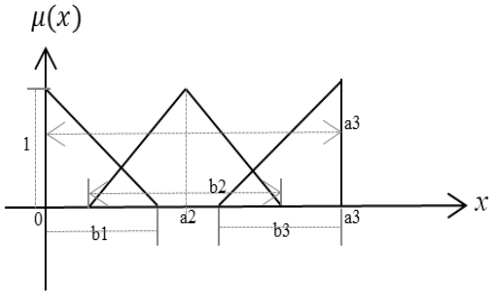

Figure 4. General Cultural Intelligence Fuzzy Sets

Where a2 is the center and a3 is the end of the triangle. b1, b2 and b3 are the widths of fuzzy sets which correspond with *CQ 3 (Low), CQ2 (Medium)* and *CQ1 (High).* The calculation formula of weighted average of the centroids of the clipped three CQ fuzzy sets CQ High (CQH), CQ Medium (CQM) and CQ Low (CQL) are calculated as:

$$y\,CQ = \frac{\frac{1}{3}b_1^2\mu CQH + a_2 b_2 \mu CQM + \left(a_3 - \frac{2}{3}b_3\right)b_3\mu CQL}{b_1\mu CQH + b_2\mu CQM + b_3\mu CQL} \quad (3)$$

5.3 Supervised and unsupervised learning

The soft-computing model can easily be modified by changing, adding or subtracting CQ rules through two main types of learning occurring in the CIES neuro-fuzzy network: supervised learning and unsupervised learning. The supervised learning is the type of training where the neuro-fuzzy network is provided with desired outputs to improve its performance. We provide to the system the fully processed external CQ experts' data, required for the supervised learning. These data are processed user cases. Each user case contains the original input cultural data, and the output data provided by cultural experts, that CIES is expected to produce. The CIES compares actual output with the cultural experts' data from the training case. If the actual output is different from the data given by experts in the training case, the CIES weights are modified. The back propagation algorithm is used in the CIES. The signal difference at the output of neuron *n* at sequence *s* is calculated as showed in equation (4). We increase sequence *s* by one, and repeat the process until the preset difference criterion is satisfied.

$$D_n(s) = y_{e,n}(s) - y_n(s) \quad (4)$$

Where $y_{e,n}(s)$ is the cultural experts' data of neuron *n* at sequence *s*, the CQ rules for updating weights at the output layer are defined in equation (5) as:

$$W_{mn}(s+1) = W_{mn}(s) + \Delta W_{mn}(s) \quad (5)$$

$\Delta W_{mn}(s)$ represents the weight correction. We use a forward procedure method to update CQ rules' weight W_{mn}. Fig. 5 shows an example of the result where CIES trains weights from bad rules to the desired CQ rules.

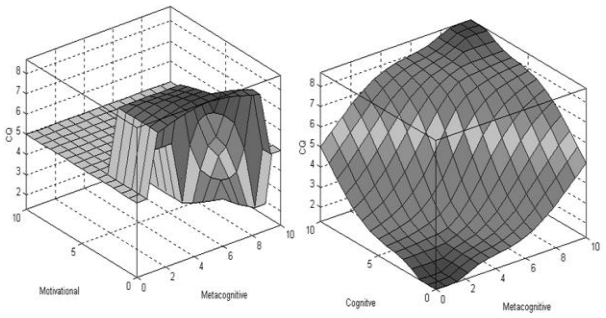

Figure 5. An Exemple of Supervised Learning

In contrast to supervised learning, with unsupervised learning in CIES, the neuro-fuzzy network is trained without desired output. The unsupervised learning does not require external cultural experts' data. During the learning process, the CIES receives a number of different original input user cases, find relationships in these cases and build new rules based on these cases used. The CQ rules for updating weights at the output layer are calculated in the equation (6). The equation (6) shows how the CIES changes the CQ rules weights, between a pair of neurons in the unsupervised learning process, through multiplication of input and output signals.

$$W_{mn}(s+1) = W_{mn}(s) + \alpha y_n(s) x_m(s) \quad (6)$$

$\Delta W_{mn}(s) = \alpha y_n(s) x_m(s)$ represents the weight correction by Hebbian algorithm [18] in CIES, α being the learning rate parameter.

6 Data acquisition and the application domains

Christine Kon et al. [19], Ang, Van Dyne et al. [20], and Ang et al. [1] developed a self-evaluation questionnaire with 20 items measuring CQ. This questionnaire was used to collect data for studies on the capabilities of the test subjects regarding their cultural adaptation capacity. This questionnaire is generally divided into four sections: CQ metacognitive CQ, cognitive CQ, motivational CQ and behavioral CQ. For example, one of the items is "*I am conscious of the cultural knowledge I use when I interacting with people with different cultural backgrounds.*" Linn Van Dyne et al. [21] developed a version of the questionnaire from the point of view of an observer. It is also based on the 20 items of Ang et al. [1] which measure the CQ of individuals. The questionnaire was adapted from each

item of the self-evaluation questionnaire to reflect the assessment made by an observer rather than the trainee himself. For example, the item of the questionnaire mentioned above changes from: "*I am conscious of the cultural knowledge I use when…*" to "*This person is conscious of cultural knowledge he / she uses when ....*"

As explained by Linn Van Dyne et al. [21], these questionnaires also allow for the effective assessment of CQ in practical applications. Among other potential applications, we can identify three application domains covered in our system. They are *Business Activities*, *Expatriates Assignments* and *Training*. Thus, we adapted the self-evaluation questionnaire of Ang et al. [1], and the observer questionnaire by Linn Van Dyne et al. [21], in order to measure CQ for these three application domains. By collecting the data from these two questionnaires, first, the data can be prepared and be used in our neuro-fuzzy network future training. Second, the user or organisations' expatriate's assignments can be evaluated so that proper training can be offered by CIES.

7 Implementing the CIES

We would like the CIES to be capable of acquiring, extracting and analyzing the new knowledge of the cultural experts. First, it should be able to: 1) express knowledge in a form that is easily understood by the users, and 2) deal with simple requests in natural language rather than programming language. Second, the CIES should consist of an efficient team of cultural experts who are able to make decisions and provide explanations in the decision-making process in culturally diverse settings. Hence, we integrated the neuro-fuzzy soft-computing model into an expert system. It relies on the functional «*consciousness*» mechanism for much of its operation [14]. Its modules communicate and offer information to each other. Fig. 6 shows the system structure of the CIES. This structure includes four main modules:

1) *The CQ knowledge base* is represented by the trained neuro-fuzzy network. This module contains CQ knowledge that is useful for solving CQ problems. The soft-computing technique used in this module makes the system able to reason and learn in an uncertain, incomplete and imprecise CQ setting. It supports all the cultural decision-making steps in the system. This module connects with three different units which are *New Data, Training Data* and the *Cultural Intelligence Database Center*. New Data include users' requests for solving a given problem that involves some cultural affairs. *Training Data* are a set of training examples. They are used for training the neuro-fuzzy network during the learning phase. The *Cultural Intelligence Database Center* mostly contributes to the knowledge gathered from data about different cultural aspects which has been collected from different countries.

2) The Cultural Intelligence Rules examines the CQ knowledge base and produces neuronal rules which are implicitly «buried» in the CIES network.

3) The Inference Engine is the core of the CIES. It controls the flow of cultural information in the system, and initiates inference reasoning from the knowledge base in the *Cultural Intelligence model*. It also concludes when the system has reached a decision.

4) *The Explanation* clarifies to the user why and how CIES achieved the specific cultural results. These explanations include analysis, advice, conclusion, and more required facts for deeper reasoning.

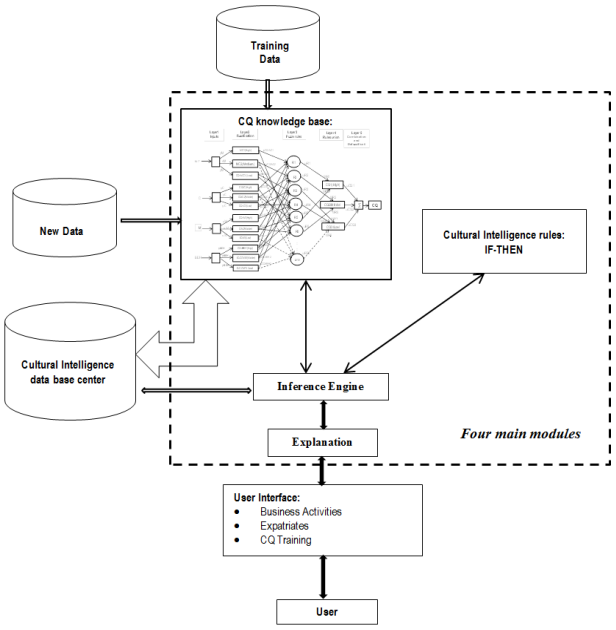

Figure 6. Structure of CIES

7.1 CIES for decisions making

The CIES possesses generic CQ, that is not specific to a particular culture (such as USA or China etc.). The system shows great capabilities of cultural adaptation by modeling the human decision-making process in situations characterized by cultural diversity. Furthermore, because of its elaborated cultural schemas and analytical abilities, the CIES can help users to identify and understand key issues in cultural judgment and decisions making, giving them the corresponding explanations.

For example, Fig.7 and Fig.8 present an output of the *Business Activity* application domain of how the CIES can help a user to make a decision, by taking into consideration his/her inputted request. The CIES prototype system follows the decision-making cycle process shown in Fig.1. The input data are specific

cross-cultural questions in the natural language of the users. The system provides two outputs as an answer to the question. Output1 (Fig.7), gives a general decision to answer the question asked by the user.

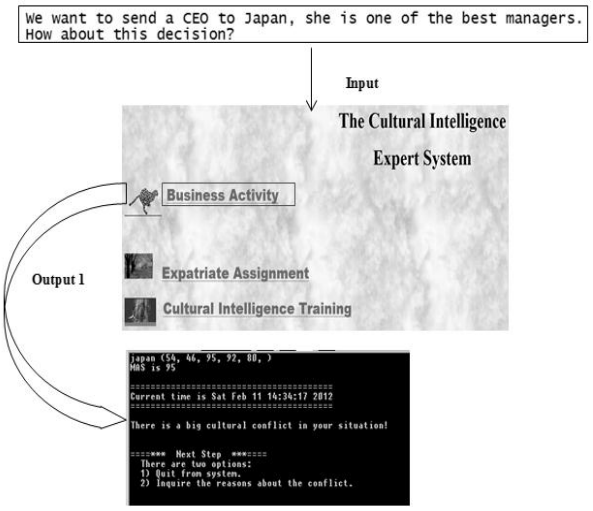

Figure 7. Business Activity in CIES Prototype (Output 1)

Output2 (Fig.8), gives more detailed explanations to clarify to the user why the system reached this decision.

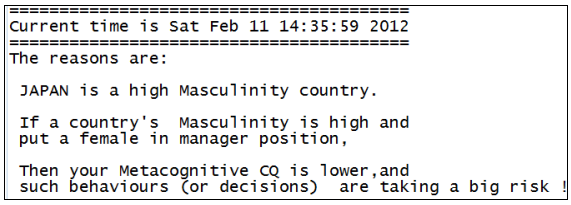

Figure 8. Business Activity in CIES Prototype (Output 2)

7.2 CIES for training

The CIES could be used in self-awareness training programs. The system provides important insights about personal capabilities and information on the user's own CQ in cultural diversity situations. Users can get two evaluations (self or observer [1] [19] [20] [21]) on the 20-itemed questionnaires so as to compare their results. Organizations could also use CIES (both self and observer evaluations) to evaluate or train, for expatriate purposes, employees who may be well-adapted. The CIES serves as an efficient team of top CQ tutors who work constantly with individuals or organizations wanting to have cross-cultural recommendations and insights on how to increase their efficiency in culturally-diverse settings. Fig.9, Fig.10 and Fig.11 present one part of the results of the self-evaluation questionnaire of a user in the CIES prototype. The CIES provides different feedback to a user receiving a high score (8>), than it does to a user receiving a low score (6<). In addition, it accordingly gives useful suggestions for personal self-development as required. This process permits the CIES to evaluate users so as to identify their problems in the CQ domain. The CIES next offers a tailored course to users based on the results of the evaluation. Moreover, during the training course, the system uses natural language to communicate with users in order to provide them a stress-free and friendly learning environment.

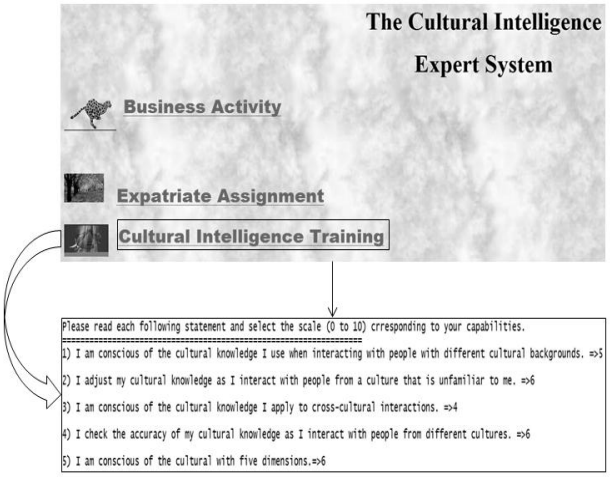

Figure 9. CIES Prototype for Traning (Self-Evalution Questionnaire)

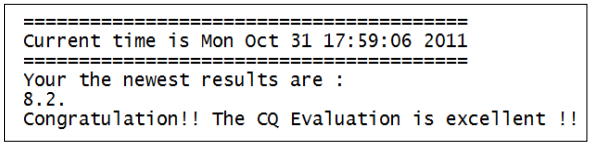

Figure 10. CIES Prototype (Output1: high score 8>)

Output 2 (Fig.11), gives useful suggestions for self-improvement to the user, when CQ is required.

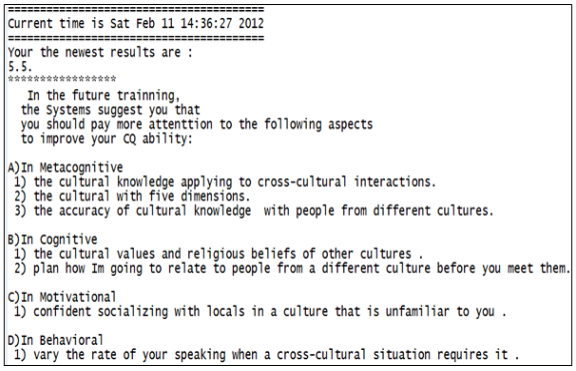

Figure 11. CIES Prototype (Output 2: low score 6<)

Three cultural experts have validated our computational CQ model, as well as that of the CIES prototype system. This validation ultimately reflects the consistency between the real world and the artificial CIES system. The CIES prototype system was tested on one hundred people. Based on the results of the validation, the cultural experts compared the CIES

results with their own. These experts concluded that the cross-cultural business decisions recommended by CIES are similar to the ones suggested by a human expert.

8 Some interesting features of CIES

First, due to the powerful designed functions and the CQ capabilities in CIES, the CIES could evaluate users and expatriates employees along with providing them specific cultural recommendations by using its knowledge to train people to improve their CQ skills, in addition, it could be used as a CQ decision-making support system to help individuals and organizations take cultural decisions in cross cultural activities. The CIES is also able to adapt dynamically to the CQ capacity of users. Second, this system is open in the sense that it can provide a standard interface that can facilitate further development. Third, the CIES is extensible, both in terms of the system concept model and the implementation of the system. Fourth, this system has the potential to work as an extended cultural and cognitive agent which could integrate into another existing intelligent system.

9 Conclusion

CQ is the human ability to capture and reason appropriately in culturally diverse settings. CQ can be measured with four dimensions. Thus, we built a CQ computational model based on a soft-computing technique so as to integrate these dimensions and embody an expert system called the CIES. This paper shows how the CIES can be used as a "culturally aware" system. The research captures the essence of culture and addresses culture from the perspective of the intelligence of an individuals or organizations wanting to develop their ability to adapt to various cultures. The CIES enables users to be more efficient and "intelligent" as they develop their cultural skills. The CIES acts as an intelligent cultural expert assistant which helps individuals or organizations to make better decisions in cross-culture activities, and it enables users to solve cultural problems that would otherwise have to be solved by cultural experts.

The contribution of our research is, first and foremost, to fill the gap between CQ and AI. Second, it improves the application of CQ theories in the field of cognition. The research focuses on modeling four CQ dimensions that are interdependent and integrated. As a result, the theories are complete, efficient, and precise in their applications. Third, we brought to the field of AI the computerization of CQ. As a result, new research topics and directions relevant to this research have arisen, and the range of computational intelligence possibilities has been expanded. Fourth, our research is groundbreaking as it simplifies the work of the researchers by freeing them from heavy, complex and repetitive tasks, normally carried out manually in CQ studies. The algorithms and techniques used in this research may offer some enlightenment as they can be applied to other research domains to improve model designs and system performances.

10 References

[1] Ang Soon., Van Dyne Linn: Handbook of Cultural Intelligence. 1st ed. M.E. Sharpe.Armonk . 2008, 2010.

[2] Earler, P.C., Ang, S.: Cultural intelligence: Individual interactions across cultures. Stanford, CA: Stanford University Press, 2003.

[3] Earley, P. C., Mosakowski, E.: Cultural intelligence. Harvard Business Review, 82, 2004, pp.139–146.

[4] Peterson, B.: Cultural intelligence: A guide to working with people from other cultures. Yarmouth, ME: Intercultural Press 2004.

[5] Geert. H. Hofstede: Cultures and Organizations: Software of the Mind, McGraw-Hill, New York ,1991

[6] Brisling, R., Worthley, R& MacNab: Cultural intelligence: understanding behaviors that serve people's goals. Group and organization management, 2006

[7] Thomas, D. C. and Inkson, Kerr. Cultural Intelligence People Skills for a Global Workforce. Consulting to Management, 16 (1). pp. 5-9, March, 2005.

[8] Thomas, D. C. Domain and development of cultural intelligence: The importance of mindfulness. Group & Organization Management, 31, 2006, pp.78–99.

[9] Ng, K-Y.,and Earley, P. C.: Culture + intelligence: Old constructs, new frontiers. Group & Organization Management, 31. 2006, pp. 4–19.

[10] Johnson, J. P., Lenartowicz, T., & Apud, S.: Cross-cultural competence in international business: Toward a definition and a model. Journal of International Business Studies, 37, 2006, pp. 525–543.

[11] Ting-Toomey. S.: Communicating across cultures. NewYork: Guilford, 1999.

[12] Tan.J-S.: Cultural intelligence and the global economy. Leadership in Action, 24, 2004, pp.19–21.

[13] Robert J.Sternber, Douglas.Detterman: What is Intelligence? Contemporary Viewpoints on Its nature and definition, Ablex publishing corporation, 355 Chestnut Street, Norwood, NewJersey 07648, 1986.

[14] Dubois, D. : Réalisation d'un agent doté d'une conscience artificielle: application à un system tutorel intellgent, Montreal, Université du Québec à Montréal, 2007.

[15] Michael Negnevitsky: Artificial Intelligence: A Guide to Intelligent Systems, ISBN 0-321-20466-2, British Library Cataloguing-in-Publication Data, 2005.

[16] Mamdani, E.H., Assilian, S.; An experiment in linguistic synthesis with a fuzzy logic controller, International Journal of Man–Machine Studies (1975).

[17] Jang, J.-S.R., Sun, C.-T., Mizutani. E.: Neuro-Fuzzy and Soft Computing: A Computational Approach to Learning and Machine Intelligence. Prentice Hall, Englewood Cliffs, NJ (1997).

[18] Parker, D.B. Optimal algorithms for adaptive networks: second order back propagation, second order direct propagation, and second order Hebbian learning, Proceedings of the IEEE 1st International Conference on Neural Networks, San Diego, CA, vol. 2, (1987).

[19] Christine Kon, Damien Joseph, Soon Ang: Cultural intelligence and the global information technology workforce, NanYang Technological University, Singapore (2010).

[20] Ang, S., Van Dyne.L., & Koh, S.K.: Personality correlates of the four-factor model of cultural intelligence. Group and Organization Management, 31, pp.100-123 (2006).

[21] Van Dyne Linn, Song Ang, Christine Koh: Development and Validation of the CQS: The cultural intelligence scale. Handbook of Cultural Intelligence. 1st ed. M.E. Sharpe.Armonk (2008).

A System for Qualitative Spatio-Temporal Reasoning*

Michael J. Almeida
Mathematics & Computer Science, Fayetteville State University, Fayetteville, NC, USA

Abstract - *The ability to reason about the spatial relationships between objects in the environment is a core requirement of mobile robots and many other types of intelligent systems. However, since objects frequently change their location, the representation of spatial location critically depends on time. Thus, what is really required is spatio-temporal reasoning. This paper presents a unified system for qualitative spatio-temporal reasoning consisting of representations for spatio-temporal knowledge and a spatio-temporal inference system to manipulate those representations. Following Almeida [2], we treat spatial relations as event types incorporating the interval-based temporal ontology of Allen [1] and the region-based spatial ontology of Randell, Cui & Cohn [13]. Our basic reasoning system is essentially an extension of the temporal reasoning system of Allen [1]. Critical to the success of this system is the ability to create and reason with maximal temporal intersections.*

Keywords: spatio-temporal reasoning, motion event, temporal intersection

1 Introduction

The ability to reason about the spatial relationships between objects in the environment is a core requirement of mobile robots and many other types of intelligent systems. However, since objects frequently change their location, the representation of spatial location critically depends on time. Thus, what is really required is spatio-temporal reasoning. This paper presents a unified system for qualitative spatio-temporal reasoning consisting of representations for spatio-temporal knowledge and a spatio-temporal inference system to manipulate those representations.

Our system makes use of an event-based representation for the changing locations of objects, adapted from the proposal of Almeida [2]. Event-based representations incorporate a concept for an *event*, the spatio-temporal particular described by the proposition [12]. For example, in "I saw the vase on the table", what I saw was the *state* (a type of event) of the vase being on the table. In other words, a spatial state is a configuration of objects in certain relationships at a particular time. Thus, events, unlike propositions, can be seen and can have causes and effects.

The event-centered style of representation that forms the basis of our approach is a development of Davidson's [5] original proposal, and is based on the following three premises. First, that *events* understood as concrete spatio-temporal particulars constitute a part of the ontology of the human conceptual system. Second, that many sentences make an implicit reference to an event even when they lack an explicit event-referring expression. And third, that the other entities referred to in the sentence are related to this implicit event assertionally rather than structurally, that is, the links between the event and the entities that play roles in that event are in the form of propositions. These propositions are most often composed of two-place predicates with the first argument being the event. So the event is the "center" around which the other entities of the sentence are arranged. Thus, "Shem kicked Shaun" would have a representation something like: inst(e1, kicking) $\wedge$ agent(e1, Shem) $\wedge$ object(e1, Shawn), where e1 is a Skolem constant representing a particular kicking of Shaun by Shem event.

2 Temporal and spatial ontology

For our temporal ontology we are using the popular interval-based representation of Allen [1]. In this system there are thirteen pairwise disjoint and collectively exhaustive relations that can hold between two nonpoint intervals of time. These are: before (b), after (bi), meets (m), met-by (mi), overlaps (o), overlapped-by (oi), starts (s), started-by (si), during (d), contains (di), finishes (f), finished-by (fi) and equals (=).

In order to represent indefinite information, the temporal relationship (tRel) between two intervals is allowed to be an arbitrary disjunction of the basic relations. Temporal relations sets (tRelSets) are used to express these disjunctions. For example, the temporal relation set [m,o,s] between intervals t1 and t2 represents the disjunction, (t1 meets t2) $\vee$ (t1 overlaps t2) $\vee$ (t1 starts t2). Therefore, if the temporal relation set between time t1 and time t2 is the disjunction [m,o,s] then this would be represented by the formula: tRel(t1, [m,o,s], t2). Networks where the vertices represent intervals and the arcs can be labeled with arbitrary subsets of the basic relations are called *interval algebra* (IA) networks [15].

For the representation of space we are using the region-based system of Randell, Cui & Cohn [13]. Their system is the spatial analog of Allen's interval-based temporal system in

* supported by NSF Award CNS-0959958

that it presupposes there are only extended (non-point) regions of space. The eight basic relations between regions of space are disconnected (dc), externally-connected (ec), partially-overlaps (po), equals (eq), tangential-proper-part (tpp), nontangential-proper-part (ntpp), tangential-proper-part-inverse (tppi), and nontangential-proper-part-inverse (ntppi). These relations are also pairwise disjoint and collectively exhaustive.

Again, in order to represent indefinite information, the spatial relationship (sRelState) between two regions is allowed to be a disjunction of the basic relations. Spatial relation sets (sRelSets) are used to express these disjunctions. For example, the spatial relation set [ec,dc] between regions l1 and l2 represents the disjunction, (l1 ec l2) ∨ (l1 dc l2). Since spatial relationships, unlike temporal relationships, are relative to time, we represent them as events, as described in the next section.

3 Representing spatial relationships

In a temporal network, each pair of times is always related by exactly one (possibly ambiguous) temporal relationship. On the other hand, since spatial relationships hold only for specific periods of time, pairs of spatial regions may be related by any number of spatial relationships. It is because of this essential difference between temporal and spatial information that we use event-based representations for spatial information.

The two principal representations used for locating objects spatially are:

(1) The *position* of an object at an instant or granule of time is the region of space occupied by that object at that moment of time [8]. Objects are assigned positions for intervals of time by *be-pos* states as follows:

inst(Event, be-pos) ∧ theme(Event, Object)
  ∧ holdsFor(Event, Time) ∧ loc(Event, Position)

This formula states that *Event* is a be-pos event where *Position* gives the spatial position of *Object* for each moment of *Time* that *Event* holds for. (*holdsFor* is one of four possible event-time connectors discussed in Section 5.) Note that, in general, what we are calling *positions* are really sequences of positions indexed by instants or granules of time. Thus, these "positions" are essentially the same as paths, which are discussed in Section 6.

(2) Spatial relationships between positions are given by *sRel* states as follows:

inst(Event, sRel) ∧ rels(Event, SRelSet)
  ∧ holdsFor(Event, Time) ∧ arg1(Event, Position1)
  ∧ arg2(Event, Position2)

This formula states that *Event* is an sRel state relating *Position1* to *Position2* by *SRelSet* for the interval *Time*. Again the "positions" being related are actually sequences of positions indexed by time, so that for each instance or granule of time in *Time*, *Position1* is spatially related to *Position2* by *SRelSet*.

As a simple example, to represent a scene in which a ball is in a box which in turn is in a room, we would use a combination of be-pos and sRel states as follows.

% A room has a position. (a be-pos state)
inst(e1, be-pos) ∧ theme(e1, room1) ∧ holdsFor(e1, t1)
  ∧ loc(e1, l1)
% A box has a position. (a be-pos state)
inst(e3, be-pos) ∧ theme(e3, box1) ∧ holdsFor(e3, t3)
  ∧ loc(e3, l3)
% The box is in the room. (an sRel state)
inst(e6, sRel) ∧ rels(e6, [tpp, ntpp]) ∧ holdsFor(e6, t6)
  ∧ arg1(e6, l3) ∧ arg2(e6, l1)
% A ball has a position. (a be-pos state)
inst(e4, be-pos) ∧ theme(e4, ball1) ∧ holdsFor(e4, t4)
  ∧ loc(e4, l4)
% The ball is in the box. (an sRel state)
inst(e7, sRel) ∧ rels(e7, [tpp, ntpp]) ∧ holdsFor(e7, t7)
  ∧ arg1(e7, l4) ∧ arg2(e7, l3)

One way we can show that these spatial events all hold simultaneously is by asserting that some interval t0 is during all of their times:
tRel(t0, [s,d,f,=], t1)
tRel(t0, [s,d,f,=], t3)
tRel(t0, [s,d,f,=], t4)
tRel(t0, [s,d,f,=], t6)
tRel(t0, [s,d,f,=], t7)

Running the reasoner on this example, two new sRel states are inferred:
inst(e8, sRel) ∧ rels(e8,[dc,ec,po,tpp,tppi,ntpp,ntppi,eq])
  ∧ holdsFor(e8, ∩(t4,t1)) ∧ arg1(e8, l4) ∧ arg2(e8, 11)
inst(e9, sRel) ∧ rels(e9, [tpp,ntpp])
  ∧ holdsFor(e9, ∩(t7,t6)) ∧ arg1(e9, l4) ∧ arg2(e9, l1)

The first inferred state, e8, relates l4 (the position of the ball) to l1 (the position of the room) for the interval ∩(t4,t1), i.e., the temporal intersection of t4 and t1. This is not a very informative relationship because it is ambiguous over all the spatial relations. It simply says that the ball and the room exist at the same time and therefore have some spatial relationship. The second inferred state, e9, is much more informative. It also relates the position of the ball to the position of the room, but here the relation set is [tpp, ntpp], that is, *inside-of*. This time the interval is ∩(t7,t6). In other words, we have inferred that the ball was in the room for the intersection of the time the ball was in the box (t7) and the time the box was in the room (t6).

4 Maximal temporal intersections

Temporal intersections are formed from pairs of overlapping times. Two intervals t1 and t2 overlap iff tRelSet(t1,t2) ⊆ [o,oi,s,si,d,di,f,fi,=]. If t1 and t2 overlap, then their *maximal temporal intersection* is denoted by ∩(t1,t2).

The intervals t1 and t2 are called the *components* of the intersection. Maximal temporal intersections play a central role in spatio-temporal reasoning because as the longest interval shared by two overlapping intervals they are unique. This uniqueness means that any other interval that is contained in both component intervals will be a subinterval of the maximal intersection. As will be described below, this uniqueness allows us to determine whether newly inferred spatial relations are nonredundant, that is, that they tell us something that we don't already know.

Although temporal intersections in our system always have exactly two components, there is no loss of generality since the components themselves may be intersections. For example, ∩(t1,∩(t2,t3)) denotes the intersection of three intervals: t1, t2 and t3. Of course this means that there may be many formulas, e.g., ∩(t2,∩(t1,t3)), that denote the same interval. Even the intersection ∩(t1,t2) can be rewritten as ∩(t2,t1). However, in our system, once one of these intersections has been created, all equivalent formulas are automatically matched to that first formula, which can be shared by multiple events.

When in the process of spatio-temporal inference a new maximal intersection is created, that interval is added to the temporal network in two steps. In the first step, the procedure *connectIntersectToComponents* uses Table 1 to determine how to temporally relate the intersection time to its two components. The entries in the table state that if A has relation Rel to B then ∩(A,B) has relation RelA to A and ∩(A,B) has relation RelB to B.

```
Procedure connectIntersectToComponents(∩(A,B))
tRelSet ← getTRelSet(A, B)
tRelSetA ← []
tRelSetB ← []
for each r1 ∈ tRelSet do
  getTable1Values(r1,RelA, RelB)
  tRelSetA ← tRelSetA ∪ RelA
  tRelSetB ← tRelSetB ∪ RelB
add tRel(∩(A,B), tRelSetA, A) to tNetwork
add tRel(∩(A,B), tRelSetB, B) to tNetwork
```

Table 1. Relation of ∩(A,B) to A and B

Rel	RelA	RelB
o	f	s
oi	s	f
s	=	s
si	s	=
d	=	d
di	d	=
f	=	f
fi	f	=
=	=	=

In the second step, the intersection is related to the rest of the intervals in the temporal network. We use a set of tables to determine the relation of ∩(A,B) to each interval C, given that A has relation Rel1 to C and B has relation Rel2 to C. There is one table for each possible relation between A and B, a total of nine in all. Table 2 is the table for the case where A strictly overlaps (o) B. (Unfortunately, there is not enough room to show all of the tables here.) Blank entries in these tables mark relations that are not possible. For example, given that A [o] B, A [m,o] C and B [di,=] C, from the four ordered pairs derived from [m,o] and [di,=], we infer that ∩(A,B) [m,o,s] C.

In general, the temporal relation sets determined by these tables are less ambiguous than those generated simply by Allen's [1] temporal inferencing algorithm, i.e., path consistency, and this extra precision turns out to be very useful.

Table 2. Relation of ∩(A,B) to C given A o B and A Rel1 C and B Rel2 C

A o B		B Rel2 C												
A Rel1 C		**b**	**bi**	**m**	**mi**	**o**	**oi**	**s**	**si**	**d**	**di**	**f**	**fi**	**=**
	b	b		b		b					b		b	
	bi		bi											
	m					m					m		m	
	mi		bi											
	o					o	d	s	s	d	o	d	o	s
	oi		bi		mi		oi							
	s						d			d		d		
	si		bi		mi		oi							
	d						d			d		d		
	di		bi		mi		oi		si		di			
	f						f							
	fi						f		=		fi			
	=						f							

5 Event-time connectors

An effective way of representing the aspectual information of events, such as their beginnings and endings, is to connect events to their times in different ways. For example, Almeida [3] proposes the following four *event-time connectors* (ETCs):

1. holdsAt(E,T) – event E holds for all of interval T, with E starting at the beginning of T and E ending at the end of T.
2. initiatesAt(E,T) – event E comes into existence at the start of interval T and holds for all of T, but doesn't necessarily end at the end of T.
3. terminatesAt(E,T) – event E holds for all of interval T, going out of existence at the end of T, but doesn't necessarily start at the beginning of T.
4. holdsFor(E,T) – event E holds for all of time T, but doesn't necessarily start at the beginning of T or end at the end of T.

The following implications hold between these four connectors:

1. holdsAt(F,T) => initiatesAt(F,T)
2. holdsAt(F,T) => terminatesAt(F,T)
3. initiatesAt(F,T) => holdsFor(F,T)
4. terminatesAt(F,T) => holdsFor(F,T)

Clearly, *holdsFor* is the most ambiguous, and *holdsAt* is the least ambiguous, of these relationships. (Note that these ETCs are related to, but different from, the similarly named relations used in the *event calculus* [11].)

The *findETC* procedure determines the event-time connector to be used for a newly inferred event, given the event-time connectors (ETC1 and ETC2) of its two component events and the temporal relations set (tRelSet) that relates the times of those two components.

```
Procedure findETC(ETC1, ETC2, tRelSet)
if initiates(ETC1, ETC2, tRelSet)
then if terminates(ETC1,ETC2, tRelSet)
      then return holdsAt
      else return initiatesAt
else if terminates(ETC1, ETC2, tRelSet)
     then return terminatesAT
     else return holdsFor

Procedure initiates(ETC1, ETC2, tRelSet)
return (ETC1 ∈ [holdsAt, initiatesAt]
        ∧ tRelSet ⊆ [s,d,f,oi,si,=])
     ∨ (ETC2 ∈ [holdsAt, initiatesAt]
        ∧ tRelSet ⊆ [o,s,si,di,fi,=])

Procedure terminates(ETC1, ETC2, tRelSet)
return (ETC1 ∈ [holdsAt, terminatesAt]
        ∧ tRelSet ⊆ [o,s,d,f,fi,=])
     ∨ (ETC2 ∈ [holdsAt, terminatesAt]
        ∧ tRelSet ⊆ [f,oi,si,di,fi,=])
```

If the ETC of an event is changed, that change may propagate to all the events of which it is a component, and so on, recursively, but it does not affect temporal relationships.

6 Incompatible events

Incompatible events are those which cannot hold simultaneously. These sets of events can be an important source of constraints on both temporal relationships and ETCs in that (1) incompatible events cannot temporally overlap one another in any way, and (2) if two incompatible events temporally *meet* (m), the first is constrained to terminate, and the second to initiate, at the point where they meet.

In general, incompatiblity of events is a matter of world knowledge. However, since the RCC8 spatial relations are pairwise dijoint, different sRel events relating the same objects by disjoint spatial relation sets will be incompatible with one another since no (classical) object can be in two different places at once.

7 Representing motion events

Motion events contain spatial paths as part of their meaning. The defining properties of *paths* are (1) regions on a path may be visited repeatedly, as can happen in, for example, running around a circular track, and (2) paths are given lengths using purely spatial measures, e.g., five miles. Therefore, paths cannot be understood simply as the join or the sum of the instantaneous positions of the event, nor are they understood as four-dimensional spatio-temporal objects. Instead, we treat paths as sequences of positions, each indexed by a point or granule of time.

Motion is always relative to some frame of reference, so, for example, the event of walking down the aisle of a moving airplane has a different path depending on whether we use the airplane or the earth as the frame of reference. However, our current system assumes a uniform frame of reference for all motion events, so we omit the reference frame role from our representations.

Jackendoff [10] proposes a classification of paths as they are expressed by prepositional phrases. All of these paths are oriented according to reference objects or places. There are three major types depending on the nature of the path's relationship to its reference object: *bounded paths, directions* and *routes.* In this paper, we will only consider bounded paths. An example of a sentence describing a motion event with a bounded path is "John walked from the house to the store". Bounded paths include *source paths,* in which the reference object occupies the initial position in the path, and *goal paths,* in which the reference object occupies the final position in the path. Source path expressions usually use the preposition *from,* as in "from the house", and goal path expressions often use *to,* as in "to the store". Conceptual analyses of bounded paths can be found in [7], [4] and [2].

Following is an example of how we represent motion events with bounded paths, in this case the sentence "The robot moved from outside the box to inside the box", where "outside the box" is the source and "inside the box" is the goal.

```
% A robot has a position. (a be-pos state)
inst(e1, be-pos) ∧ theme(e1, robot1) ∧ holdsFor(e1, t1)
  ∧ loc(e1, l1)
% The box has a position. (a be-pos state)
inst(e3, be-pos) ∧ theme(e3, box1) ∧ holdsFor(e3, t3)
  ∧ loc(e3, l3)
% The robot moved from the start to the end of path p1 over
% time t4. (a motion event)
inst(e4, moving) ∧ agent(e4, robot1) ∧ holdsAt(e4, t4)
  ∧ path(e4, p1).
% The time of the move is during t1 and t3.
tRel(t4, [s,d,f,=], t1).
tRel(t4, [s,d,f,=], t3).
% The position of the robot is given by p1 over time t4.
% (an sRel state)
inst(e5, sRel) ∧ rels(e5, [eq]) ∧ holdsFor(e5, t4)
  ∧ arg1(e5, l1) ∧ arg2(e5, p1)
% The path of the robot starts away from (disconnected from)
% the box. (an sRel State)
inst(e6, sRel) ∧ rels(e6, [dc]) ∧ terminatesAt(e6, t6)
  ∧ arg1(e6, p1) ∧ arg2(e6, l3).
% The time of the move is started by (the end of) the time
%  when the robot is away from the box.
tRel(t4, [si], t6).
% The path of the robot ends inside the box. (an sRel state)
inst(e7, sRel) ∧ rels(e7, [tpp, ntpp]) ∧ initiatesAt(e7, t7).
  ∧ arg1(e7, p1) ∧ arg2(e7, l3).
% The time of the move is finished by (the start of) the time
% when the robot is inside the box.
tRel(t4, [fi], t7).
```

The assumption of *continuity of motion* [7] would allow the system to infer that in the time between the robot being disconnected from the box and its being inside the box, the robot's position was at one time externally-connected to the position of the box, then it partially-overlapped the position of the box, and then it was a tangential-proper-part of the position of the box.

8 Temporal reasoning

Now that our basic set of representations has been described, we can look first at temporal and then spatio-temporal inference. The algorithm that forms the basis for both our temporal and spatio-temporal reasoners is *path consistency* (or 3-consistency), which was first suggested for maintaining knowledge about temporal intervals by Allen [1]. The version of this algorithm we use is from Shoham [14]. This form of inference is not optimal in that it does not give us the most precise results possible from the data. Instead it gives us an approximation to the optimal result, one which is possibly more ambiguous than the optimal result. However, this approach is reasonably accurate and efficient and so is widely used.

The principal variables for the temporal reasoner are: (1) *tNetwork* - the temporal network, which is globally accessable, (2) *tList* – a list of times, and (3) *tQueue* – a list of ordered pairs of times $\{(i, j) : i \neq j\}$.

In the following procedures, *tRelSet(i,j)* is the set of temporal relations (a disjunction) holding between times i and j, and *tTable(i, j)* is the (i, j)'th entry in Allen's [1] transitivity table.

```
Procedure propagateTimeConstraints(tQueue, tList)
repeat until tQueue is empty
 remove any (i, j) from TQueue
connectTIntersectNodeToC(i, j)
   for each interval k ∈ tList with k ≠ i, j do
        tRelSet(k, j) ← tRelSet(k, j) ∩
          timeConstraints(tRelSet(k,i), tRelSet(i,j))
        if tRelSet(k, j) changed then add (k, j) to tQueue
        tRelSet(i, k) ← tRelSet(i, k) ∩
          timeConstraints(tRels(i,j), tRels(j,k))
         if tRelSet(i,k) changed then add (i, k) to tQueue
```

```
Procedure timeConstraints(tRelSet1, tRelSet2)
tRelSet ← empty
for each r1 ∈ tRelSet1 and r2 ∈ tRelSet2 do
  tRels ← tRels ∪ tTable(r1,r2)
return tRelSet
```

The *tInference* procedure processes the entire temporal network. This should only be necessary when the network is first being established, unless a major change is made.

```
Procedure tInference()
tList ← makeTList()
tQueue ← {(i,j) : i, j ∈ tList ∧ i ≠ j}
propagateTimeConstraints(tQueue, tList)
```

The following procedures are used to make various types of additions to the temporal network. The *addNewTime* procedure (given in [1]) is used to add to the network a single new time i that is to be connected to exactly one pre-existing time j using tRelSetIJ. *propagateTimeConstraints* is called with tQueue consisting of only one pair {(i,j)} and the complete tList including i.

```
Procedure addNewTime(i, tRelSetIJ, j)
tList ← makeTList()
tList ← addToTList(i, tList)
addTRelToTNetwork(i, tRelSetIJ, j)
propagateTimeConstraints({(i, j)}, tList)
```

processNewTime is used to add a new time i which is connected to a set tNodes of pre-existing times. This procedure is primarily used to add temporal intersections, as will be described in the discussion of the spatio-temporal reasoner.

```
Procedure processNewTime(i, tNodes)
tList ← makeTList()
tList ← addToTList(i, tList)
tQueue ← {(i,j) : j ∈ tNodes}
propagateTimeConstraints(tQueue, tList)
```

9 Spatio-temporal reasoning

Our spatio-temporal reasoner is essentially an extension of the temporal reasoner described above. In a temporal network, each pair of times is always related by exactly one (possibly ambiguous) temporal relationship. On the other hand, since spatial relationships hold only for specific periods of time, pairs of spatial regions may be related by any number of spatial relationship states. This is responsible for the difference between temporal and spatio-temporal inference.

The principal variables for the spatio-temporal reasoner are: (1) *stNetwork* - the spatio-temporal network, which is globally accessable, (2) *sList* – a list of spatial positions, and (3) *sQueue* – a list of ordered pairs of positions.

As with the temporal reasoner, the core of the algorithm consists of two path consistency procedures, *propagateSpaceConstraints* and *spaceConstraints*. The basic process is that for as long as there are triplets of spatial relationships that haven't been tried yet, do:

(1) Given any three different spatial regions k, i and j where a spatial relation Ski holds between positions k and i, and a spatial relation Sij holds between positions i and j, a transitive spatial relationship event based on Ski and Sij will be inferred between positions k and j only if timeOf(Ski) and timeOf(Sij) overlap, that is, there is a nonempty intersection interval during which both Ski and Sij hold. A new sRel event with relation set Ski will therefore hold for the interval ∩(time(Ski), time(Sij)).

(2) If a new sRel event is proposed, it has to be merged into the set of sRel states, stateList(k,j), that already exist. If the new state subsumes, i.e., makes redundant, any preexisting states, they are deleted from stNetwork. If the new state is subsumed by an already existing state, then the new state is discarded, otherwise it is added to the stNetwork and the pair of positions it relates is added to sQueue.

```
Procedure propagateSpaceConstraints(sQueue, sList, tList)
repeat until sQueue is empty
  remove any (i,j) from sQueue
  for each k ∈ sList with k ≠ i, j do
    stateList(k,i) ← all sRel states relating k to i
    stateList(i,j) ← all sRel states relating i to j
    stateList(k,j) ← all sRel states relating k to j
    for each stateIJ in stateList(i,j) do
      for each stateKI ∈ stateList(k,i) do
        if timeOf(stateKI) overlaps timeOf(stateIJ)
        then stateKJ ← proposeNewSRel(stateKI,
                stateIJ, tList)
         mergeSRelIntoSet(stateKJ, stateList(k,j))
         if stateKJ not redundant
              then sQueue ← add (k,j) to sQueue
      for each stateJK ∈ stateList(j,k) do
        if timeOf(stateJK) overlaps timeOf(stateIJ)
        then stateIK ← proposeNewSRel(stateIJ,
                stateJK, tList)
         mergeSRelIntoSet(stateIK, stateList(k,i))
         if stateIK not redundant
              then sQueue ← add (i,k) to sQueue

Procedure spaceConstraints(sRelSet1, sRelSet2)
sRelSet ← empty
for each r1 ∈ sRelSet1 and r2 ∈ sRelSet2 do
  sRelSet ← sRelSet ∪ sTable(r1,r2)
return sRelSet
```

Whenever a new sRel state is inferred, its time interval will always be an intersection of two previously existing times. This intersection must always be checked to see if it already exists. If so, it is already fully connected to the temporal network, if not, it must first be connected to its components using Table 1, then it must be connected to all the other time intervals in the system using Table 2, as described in section 4.

```
Procedure proposeNewSRel(State1, State2, tList)
sRels ← spaceConstraints(sRelSetOf(State1),
          sRelSetOf(State2))
newTime ← makeTIntersect(timeOf(State1),
          timeOf(State2))
if newTime not in tList then
    connectIntersectToComponents(newTime)
    connectIntersectUsingTable2(newTime, tList)
    processNewTime(newTime,
          [timeOf(State1), timeOf(State2)])
return makeNewSRel(newTime,sRels,arg1Of(State1),
          arg2Of(State2))
```

A spatial relation state S1 relating positions k and j is redundant if there already exists a spatial relation state S2 relating k and j such that timeOf(S2) contains timeOf(S1) and sRelsOf(S2) is a subset of sRelsOf(S1). If S1 is redundant it is simply discarded. If it is not redundant, then we still need to check to see if it renders any other spatial relation state redundant. If so, the redundant relation states must be deleted from the network. The procedure *mergeSRelIntoSet* describes this process.

```
Procedure mergeSRelIntoSet(S1, StateList)
for each S2 in StateList do
  if time(S1) during time(S2) ∧ rels(S1) ⊇ rels(S2)
  then return S1 is redundant
  else if time(S2) during time(S1) ∧ rels(S2) ⊇ rels(S1)
      then delete S2 from stNetwork
```

The following two procedures start spatio-temporal inference. *stInference* runs inference on the complete stNetwork, while *addNewSNode* is used to add a single new sRelState to the network. *sInference* should only be run when the stNetwork is being first established or if there are major changes.

```
Procedure stInference()
tInference()
sList ← makeSList()
sQueue ← {(i,j) : i, j ∈ sList ∧ i ≠ j}
```

propagateSpaceConstraints(sQueue, sList)

addNewSNode is used to add a single new sRel state to the network connecting positions i and j with the relation set sRelsIJ and the time *newTime*. *addNewSNode* triggers spatio-temporal inference but only on the newly related positions, so it is very efficient.

Procedure addNewSRel(i, sRelsIJ, j, newTime)
sList ← makeSList()
makeNewSRel(newTime, sRels, i, j)
propagateSpaceConstraints({(i,j)}, sList)

10 Conclusions & future work

In this paper we have described the current state of our system for qualitative spatio-temporal reasoning. The system consists of (1) a spatio-temporal reasoner based on an extension of the path consistency algorithm to allow inference of new spatial events, (2) procedures to connect the maximal temporal intersections that are the times of these new events into the temporal network, and (3) procedures to create and update the event-time connectors that relate these events to their times. The system as described in this paper has been implemented in Prolog as part of a mobile robotics project, but we are still experimenting with the most effective ways of combining these components together.

We have three immediate goals for the future expansion of this system. (1) We need to expand the coverage of the spatial representational system by incorporating locative functions, that is, functions from regions of space to regions of space. [10], [9] and [13] contain many examples of such functions. (2) As described in the discussion of the spatio-temporal reasoner, newly inferred transitive spatial relationship states have times which are temporal intersections. So far, this is the only part of the system that combines time intervals. Aside from the inference of these states, temporal intersections and unions seem to be primarily useful in spatial question-answering. For this reason, we plan to add the ability to infer intersections and unions of temporal intervals at query-time. (3) So far, the temporal component of the system is purely interval-based. We plan to introduce a granularity into the temporal representation that is suitable for a mobile robot.

11 References

[1] James F. Allen. "Maintaining Knowledge about Temporal Intervals"; *Communications of the ACM*, Vol. 26, No. 11, 1983.

[2] Michael J. Almeida. "An Event-Based Approach to Spatial Information"; in *Spatial Information Theory - A Theoretical Basis for GIS*, Lecture Notes in Computer Science 1329, Springer-Verlag, pp. 441-454, 1997.

[3] Michael J. Almeida. "Incomplete Timestamps in Temporal Databases"; *Proceedings of the 2nd International Advanced Database Conference*, US Education Service, pp. 93-98, 2006.

[4] N. Asher, and P. Sablayrolles. "A Typology and Discourse Semantics for Motion Verbs and Spatial PPs in French"; *Journal of Semantics*, Vol. 12, pp. 163-209, 1995.

[5] Donald Davidson. "The Logical Form of Action Sentences"; in *The Logic of Decision and Action*, N. Rescher ed., University of Pittsburgh Press, 1967. Reprinted in D. Davidson, *Essays on Actions and Events*, Oxford University Press, 1980.

[6] Ernest Davis. "Representations of Commonsense Knowledge". Morgan Kaufmann, 1990.

[7] Anthony Galton. "Towards a Qualitative Theory of Movement"; in *Spatial Information Theory - Proceedings of COSIT '95*, Lecture Notes in Computer Science #988, Springer-Verlag, 1995.

[8] Anthony Galton. "Qualitative Spatial Change". Oxford University Press, 2000.

[9] Annette Herskovits. "Language and Spatial Cognition: An Interdisciplinary Study of the Prepositions in English". Cambridge University Press, 1986.

[10] Ray Jackendoff. "Semantics and Cognition". MIT Press, 1983.

[11] Erik T. Mueller. "Commomsense reasoning". Morgan Kaufmann Publishers, 2006.

[12] Terence Parsons. "Events in the Semantics of English". MIT Press, 1990.

[13] D. A. Randell, Z. Cui, and A. G. Cohn. "A Spatial Logic Based on Regions and Connection"; *Proceedings of the Third Conference on Principles of Knowledge Representation and Reasoning*, pp. 165-176, 1992.

[14] Yohav Shoham. "Artificial Intelligence Techniques in Prolog". Morgan Kaufmann, 1994.

[15] Peter van Beek. "Reasoning about Qualitative Temporal Information"; *Artificial Intelligence*. Vol. 58, pp. 297-326, 1992.

Modeling Crowd Evacuation from Indoor Spaces

Pejman Kamkarian[1], **Henry Hexmoor**[2]
[1] Electrical and Computer Engineering Department, Southern Illinois University, Carbondale, IL 62901, USA
[2] Computer Science Department, Southern Illinois University, Carbondale, IL 62901, USA

Abstract - *A crowd in an emergency situation located inside a public space, they will evacuate from that space. Crowd evacuation is a dynamic process which relies to a variety of environmental factors, as well as crowd specifications itself. To help people out of danger, rapidly and safety, we need to have a previous plan for any public space, which is obtained by collecting information of crowd evacuation in different situations, for that space. Simulating a public space virtually, helps us to study on crowd evacuation, in terms of considering all possible kinds of behaviors that are as symptoms of evacuation during emergencies. Using such strategy, keeps any possible injuries limited to the virtual simulated environment and hence we are able to study on real events with no cost of occurring any damages. This paper demonstrates application of optimized Imperialist Competition Algorithm to exit doors of indoor spaces to find the best possible locations for them, and also to estimate the minimum required width for each door in order to be able to evacuate a crowd out of risk in a reasonable time, and with the most possible safety.*

1 Introduction

In the developed countries, people spend most of their lives in indoor spaces. Often, large groups of people are gathered at the same location for leisure or work purposes. We consider these groups as crowds. Generally, a crowd is defined as a set of agents as particles who are gathered at one physical location to share or follow some common activities [9]. If a life threatening emergency such as fire or earth quake occurs, there should be efficient and reliable ways available for people to rapidly evacuate buildings. Evacuation becomes more complicated when observing to increase number of people inside space, or increasing the time that occupants need to remain at the location. Derived from safety concerns in indoor spaces, there is a force to evacuate that people toward exit openings. This has best been modeled in terms of a game among members of a crowd [8], Game theoretic modeling and analysis as well as a extensively validated fire evacuation simulator are reported from a finish research center [8]. We will focus more closely on characteristics of a crowd in the context of an emergency that requires evacuation. Although each group has a shared set of goals among its members, individuals do not necessarily decide on sharing similar actions. This is especially true when they encounter dangerous situations such as fire. In such cases, because of fear and natural instinct for survival, individuals will take separate, individualistic actions to address their own needs for survival. They will not follow group patterns for action selection. This is similar to what one can expect when a crowd of people is running away from source of danger (e.g., a fire) towards a safe place [11].

The idea of evacuating a crowd is not limited to humans and it pertains to all other types of animals. The safest exit doors should be able to evacuate not only humans but all kinds of animals that might be present in indoor spaces. This urges us to consider appropriate designs for exit doors. Buildings must adhere to an acceptance standard to be able to evacuate people who are inside it in an emergency. In most cases, such standards must account for combinations of exit doors including stairs and ladders. Emergency evacuation conditions of a crowd and abstraction of the real crowds are modeled by [13], [1]. The required number of exit doors will vary based on the size and architecture of each environment. One of the most important considerations about locating exit doors is having evacuation rate for public space. The goal is to evacuate most number of people in least amount of time. Lacking such strategy leads us having serious problems in emergency situations, even if exit doors themselves are built and located in safe and reliable positions. To make this clear, we point to stampeding events, which are one of the most common occurrences during an emergency. A stampede can occur due to human reaction to unexpected sets of events. People will herd and push each other in competition to reach the exit doors. People who are in emergencies often behave irrationally, largely based on reactions to the information available to them at the time. For instance, studies of evacuations in fires such as in [12], and in [4], indicate that people tend to leave gathering venues through the original pathways they entered. This holds even people have better solutions in terms of availability of closer, more accessible exit doors. This can be seen as irrational behavior. In fire, the smoke and heat in fires create limited visibility, which may cause people to seek escape through an exit door that they already know exists if they are unfamiliar with other possible choices.

To study and simulation crowd, macroscopic models are computationally less expensive because they consider less detailed interactions among people and with their environment. Instead, mathematical models are used to describe crowd movements as liquid flows [5], [6], [7].

2 An Overview of Environmental and Exit Door Features

As one of the most important steps to studying, designing and locating exit doors, we have to consider salient attributes that can directly or indirectly affect exit doors designs. In the following we outline several of these key attributes. Specifications of attributes for people present inside the public space, such as their health status, or their age range will lead to a better and safer selection of exit doors in terms of design and location for each. In case of considering only human beings in our environment, we can use particle systems that were proposed in [2], to simulate human behaviors. Based on particle swarms theory, each agent is considered to be a particle, augmented with a state and a feedback function to dominate its behavior. All agents' behaviors constitute the whole system's performance. Particle systems are also used for modeling the motion of groups with significant models of physics [2], [3]. Considering the number of individuals leads having a more accurate estimation. As an important factor, it should be taken into account while deciding widths and locations for exit door. As we pointed in previous examples, absence of these attributes was the main reasons for injuries and deaths. The width of exit doors should be determined relative to the proportion of the crowd. Time is another important attribute that should be accounted while designing and locating exit doors. On the other hand, exit doors should be able to service evacuation of the crowd through them in the minimum possible time. This will reduce the number of people who may potentially lose their lives due to breathing poisoned air, or stampeding of herding behavior.

3 Imperialist Competition Algorithm (ICA)

The Imperialism competitive algorithm is a natural inspiration method, which can solve variety types of optimization processes. It classifies as an evolutionary algorithm that relies on collecting a set of candidates random solutions, called initial countries. At the beginning, each country may have a different size of population, based on its features. A few such countries that have the most power among are called empires. After forming empires, all remaining countries, are called colonies. As a strategy, each empire, tries to extend its power and royalty of its government beyond its territory by trying to absorb and control the weaker countries as its colonies. At the end of initialization process, all colonies with their populations are divided among imperialists based on their powers. The total power of each empire, defines based on the power of the imperialist country itself, as well as the total powers of respective colonies. In other terms, this model obtains the amount power of each empire by adding the imperialist country itself and the mean power of its colonies in percentage. In the beginning of competition process, all colonies start moving toward their relevant imperialism country. In other hand, the imperialistic competition begins among all existing empires by increasing their power that earns by stimulating to take control on more colonies. During the process, any empire that is not able to increase and developing its power, or preventing losing its colonies, will be replaced [10], and hence eliminates from the competition.

4 Application of Optimized ICA

Based on ICA, the solution consists of many different sections. In order to focus on crowd evacuation, as well as people inside a public space, and exit doors, many sections are optimized to meet our research project requirements. At first glance, the examined space is classified to have three different kinds of components: *exit doors*, *obstacles*, and *people* present inside. The obstacles themselves can be categorized into two different groups. The first group includes the ones that are installed inside the public place, based on a previous plan. The second group may be formed accidentally, during emergencies, such as smoke, debris, and the wall or ceil parts that can block the whole, or a part of environment. Each exit door, represent a country. By initializing, they can have a population gathered around them. The people inside the space are considered as the population. Based on each person's distance from each exit door, as well as the velocity that each one may has based on some physical body features, they are classified to belong to the nearest exit door at the beginning. For instance, the equation $\{ed_1, ed_2 ed_3\ ,\ldots, ed_{N_{var}}\}$, denotes a group of exit doors, where each *'ed'*, represents a separate door. Each exit door, measures with a floating point number, which indicates the cost of it. The cost of each exit door, determines by the total number of people who are belong to that door. In the public space, the walls that have any unblocked exit door on them called a valid region. A collection of an exit door with its population is called a zone. The size of each zone might vary based on the size of that particular exit door as well as the total number of population that belongs to that door. Each person inside the space, as an entity, has a speed to reach to its designated exit door. At the beginning of the process, the initial cost for each exit door is captured by $Init\ Cost(ed_1) = Init\ Cost(ed_2) = \cdots = Init\ Cost(ed_n) = m$, where *'m'* is the initial value of each exit door as initial. The velocity of population is showed by $(p_n) = f(p_n) = f(sw_n) + f(bd_n)$, where *'p'* represents as a person inside the public space. To find the best possible exit door for each person, we use the following equation: $\{p_n \in ed_n\} \equiv \{\max(Velocity_{p_n}), \min(Distance_{ed_n})\}$. On the other hand, dependencies for each exit door are measured and determines by evaluating the maximum speed and the minimum distance from each exit door. After the initialization phase, we may have many different valid regions. Each valid region may have many exit doors. Each exit door as an empire, has a zone including population as its colonies, belong to that door. At the beginning of the process, we consider any separator walls that divide the interior area from the exterior, as a valid region. As initial locations of exit doors, based on the potential crowd inside space, each valid region may have one or more exits in same distances from one another. Each exit door has an initial width that will be determined based on

the number of people that gather around it. We note this initial width as γ. For example γ_i is the width of i^{th} exit door. Assuming crowd forms randomly inside the space, the application classifies each person as a colony to be dependent to the nearest exit as its calling an empire. To increase accuracy and also accounting for possible symptoms that crowd may have while emergencies, initially, we considered having a number of people as colony to choose their exit door as empire randomly regardless of distance. This may occur in the real world, for some reason, such as smoke covers the air and hence limited the vision site of people inside public space that leads choosing an inefficient exit door as the best solution to evacuate through.

When the process starts, people move toward the nearest exits to which they belong. If a person reaches and crosses through any exit door, it is removed from the process of evacuation. Hence that exit door as an empire loses that person as a colony. This reduces empire's power consequently. Based on the capacity and status of each exit door to evacuate people at each moment, and also with respect to other exit doors, exits as empires, they will try to raise their power by absorbing other colonies of people, from any other zones, into their own zones. In the real world, when an exit door has more capacity to evacuate people than those people around it, the other people who are currently trying to evacuate toward other exits might change their exit door, to the one with the least risk and lower number of people around it. As another reason to change the zones by people inside, we can address formation of unwanted obstacles, such as smoke or debris that are symptoms of emergencies. In case of presence of obstacles between a person and his chosen exit door, he tries to find the shortest path to turn around toward the exit. If there are other exit doors located closer to such a person changing the zone belongs to that exit door might be the best option for that person to choose. In other terms, this is a way for empires to increase their power. The following figure 1 shows a person, and an obstacle, which is located between him and his zone.

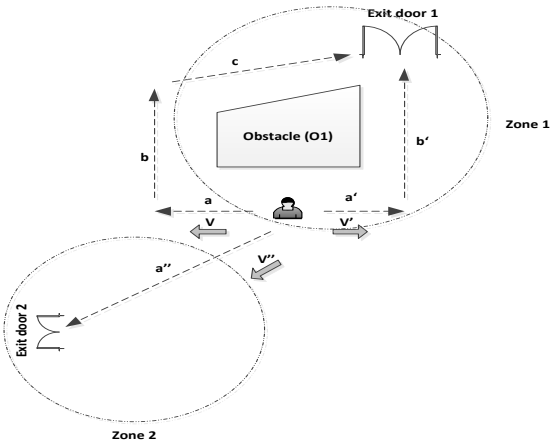

Figure 1. A person as a particle and an obstacle located between him and his optimal exit door with another exit door as an alternative to change the zone

Figure 1 shows obstacle O_1 forms during an emergency situation. The routes to reach the current optimal exit door are based on the following equations: $V = a + b + c$, $V' = a' + b'$. If there was another exit say exit door 2, located at a close distance of such person, the distance from it is calculated based on $V'' = a''$. Considering that exit is capable to accept more people to evacuate, Figure 2 is a decision flowchart which may apply to a particle as a person, in order to continue staying at the current zone, or changing it to the exit door 2.

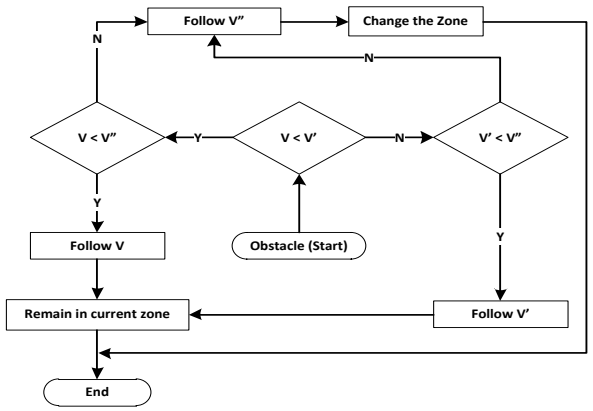

Figure 2. Decision flowchart to decide about to staying or leaving zones

We can consider other kinds of objects, between particles and exit doors at any time as obstacles. For example, any other person, or group of people who are located at any positions between any person and his optimal exit door can be classified as obstacles. In such cases, following the decision flowchart to decide about to staying or leaving zones by people as particle is essential. The process of evacuation continues until all particles as people evacuate through available exit doors. Based on the number of people who could evacuate successfully, using equation 1, the application determines the best possible width of each exit.

$$W_i = \left\lfloor \frac{\sum Pop_i}{\sum S_i} \right\rfloor \times \partial \ (in) \qquad (1)$$

Here W_i is the suggested width obtained from experiment cycle for exit door, i. S_i is the number of people who changed their zones during the experiment for any reasons. ∂ is a constant that can be vary based on the examined public space and the native architecture standards. Here we assumed $\partial = 10$, as the default value. Each exit door, based on its status during the experiment, may have a different W. based on this value, the amount that should be added to each exit, obtains. To increase the accuracy, we can repeat the experiment until the W became either minimum

or very close to its previous value in last experiment. At the end of process, the total amount of value that should be added to each exits, determines by equation 2.

$$C_i = \sum W_i + \gamma_i \quad (2)$$

C_i is the total optimized amount in inches that should be added to exit door i. γ_i is the first initialization value that i^{th} exit door had at the beginning of the first period of experiments, and W_i is the total value that earned during experimental processes.

5 Conclusions

This paper has explored the implementation and adaption of the optimized imperialist competitive algorithm to a sample indoor layout to demonstrate a solution for locating the best exit doors. The results of our implemented system are applied to prototypical scenarios has demonstrated that the location of each exit door in an indoor space can affect significantly in terms of evacuating the crowd out of danger in emergency situations. Future work will account for complex floor plans. We will also relax our assumption about traps so we can add to realism of evacuation chaos with unexpected clutter and debris.

6 References

[1] Bandini, S., Federici, M. L., Vizzari, G., "Situated Cellular Agents Approach to Crowd Modeling and Simulation", Cybernetics and Systems, 38(7), pp. 729-753, 2007.

[2] Bouvier, E., Cohen, E., and Najman, L., "From crowd simulation to Airbag Deployment: Particle Systems, a new paradigm of simulation", Journal of Electronic Imaging 6(1), pp. 94-107, SPIE, 1997.

[3] Brogan, D., Metoyer, R., and Hodgins, J., "Dynamically simulated characters in virtual environments", IEEE Computer Graphics and Applications. Vol.18, No. 5, pp. 58-69, IEEE, 1998.

[4] Canter, D. (ed.), "Fires and Human Behavior", pp. 15-30, London, U.K.: David Fulton Publishers, 1990.

[5] Colombo R., Goatin P. and Rosini M., "A Macroscopic Model of Pedestrian Flows in Panic Situations in Current Advances in Nonlinear Analysis and Related Topics", pp.43–60, Mathematical Sciences and Applications, Gakuto Pub, 2010.

[6] Dogbe C., "On the Cauchy problem for macroscopic model of pedestrian flows", J. Math. Anal. Appl. 372, pp. 77-85, Elsevier pub, 2010.

[7] Jiang Y., Zhang P., Wong S. C. and Liu R., "A higher-order macroscopic model for pedestrian flow, Physica A: Statistical Mechanics and its Applications", Volume 389, Issue 21, 1, pp. 4623-4635, Elsevier pub, November 2010.

[8] Korhonen T., Heliovaara S., Hostikkaa S. and Ehtamo H., "Counterflow Model for Agent-Based Simulation of Crowd Dynamics, In Safety Science", 2010.

[9] Musse, S. R. & Thalmann, D., "A Model of Human Crowd Behavior: Group Inter- Relationship and Collision Detection Analysis". In Proceedings of Computer Animation and Simulations 97, Euro graphics Workshop, Budapest, pp. 39-51, 1997.

[10] Nazari-Shirkouhi, S., Eivazy, H., Ghodsi, R.,Rezaie, K.,Atashpaz-Gargari, E., "Solving the Integrated Product Mix-Outsourcing Problem by a Novel Meta-Heuristic Algorithm: Imperialist Competitive Algorithm". Expert Systems with Applications 37 (12), pp. 7615-7626, 2010.

[11] Shiwakoti, N., Sarvi M., Rose G. and Burd M., "Animal dynamics based approach for modeling pedestrian crowd egress under panic conditions", Transpostation Research B, pp. 1-17, Elsevier Pub, 2011.

[12] Sime, J.D., "Affiliative Behavior during Escape to Building Exits", Journal of Environmental Psychology. (3), pp. 21-41, 1983.

[13] Still, G. K., "Review of pedestrian and evacuation simulations", International Journal of Critical Infrastructures 2007 - Vol. 3, No.3/4, pp. 376-388, 2007.

Context-Awareness Technique for GPS Positioning

Jiung-yao Huang[1], **Chung-Hsien Tsai**[2], **and Shih-Yen Wei**[3]
Computer Science and Information Engineering Department
National Taipei University
San Shia, Taipei, 237 Taiwan
jyhuang@mail.ntpu.edu.tw[1], keepbusytsai@gmail.com[2], arrny1224@gmail.com[3]

Abstract *- The previous researches of GPS positioning for navigation all focus on performing preliminary GPS data ranging error filtering by Kalman filter first and then calibration with the map matching method. However, this approach requires the accuracy of the GIS map. This paper proposes a GPS data calibration technique for navigation which entirely depends on human behavior to further calibrate GPS data from Kalman filter without map information under any unprepared environment. The study adopts the context-aware approach to fully explore user's behavior and rectify GPS data from Kalman filter accordingly. The presented method is coined as Perceptive GPS (PGPS). It starts with extracting user's feature data from Kalman filtered GPS data to classify his current state. Newton Markov Model (NMM) is then introduced from Hidden Markov Model to capture the user's motion state. Based on NMM, PGPS technique records the GPS carrier's behavior into a Transition Probability Matrix (TPM). This TPM is then used to infer the behavior of the GPS carrier from the online received GPS data and calibrate GPS carrier's position accordingly. Finally, a series of experiments to validate PGPS technique are conducted and fully discussed at the end of the paper.*

Keywords: Augmented Reality, Context aware, Hidden Markov Model, Entropy.

1. Introduction

The GPS navigation system in the market is composed by positional signal module, geographic information system(GIS) and user interface module[1]. The legacy GPS systems use the map matching technique to calibrate GPS data during navigation. The map matching approach always tries to fit the GPS data to a road that has shortest perpendicular distance. However, when there are two nearby parallel roads, the map matching approach will hop between these two roads so as to cause the serious cognitive disorder. Furthermore, owning to human cognitive errors caused by those traditional 2D map guiding, the live-view GPS navigation system has been proposed and also attracts much attention[2]. The live-view GPS navigation system adopts Mobile Augmented Reality(MAR) technology to overlay directional arrow on the live-view image to provide intuitive navigational information. Due to the lack of 2D map display, the map matching technique does not apply to live-view GPS navigation system. Along with the rapid evolvement of silicon technology in recent years, most of mobile devices, such as smartphone, nowadays are often equipped with camera, wireless network, the Global Positioning System (GPS) receiver and a variety of sensors. Such smart mobile devices allow users to interactively perceive their environmental information, such as location, personal ID, temporal or spatial information. Hence, it is a booming trend in the recent years to employ smart mobile device as a platform for developing the live-view GPS navigation system. For example, Wikitude Drive[3], AVIC-VH09[4] and Route 66 Maps+[5] systems are three well-known systems which have released their demo videos in YouTube.

However, since such built-in GPS receiver is susceptible to the environmental interferences, most of MAR applications utilize auxiliary equipment such as inertial sensors to calibrate GPS ranging error. One of the earliest MAR navigation applications that used GPS as a positional sensor was Touring Machine[6]. To get the accurate signals in urban street canyons, it redesigned vessel-based GPS receiver with a bulky wearable computer.

Fong et al.[7] in 2008 applied Differential GPS Carrier Phase technique to meet high accuracy requirements. They proposed a relative position measurement technique from GPS carrier phases of two GPS receivers, one is stationary and the other is mobile, for high precision positioning toward outdoor MAR applications. Such differential GPS carrier phase technique required at least a three-dimensional coordinates of reference receiver to stay fixed on a known control point. Therefore, the practicability of this approach is still not adopted by most of the mobile augmented reality systems applications yet.

Most existing commercial GPS navigation systems are still restricted by the inaccuracy of built-in GPS chip and employ Map matching algorithm[8] to solve GPS ranging error problem. For live-view GPS navigation system, because 2D electronic map is unable to be displayed on the screen, the Map matching algorithm becomes worthless to calibrate GPS data. We must rely on the cognitive user's behaviors to calibrate ranging error during live-view GPS navigation process.

In this paper, the technique has been proposed[2] to perceive user's behaviors for live-view GPS navigation system. We explore the context-aware approach to perceive user's behavior to calibrate the GPS ranging error accordingly and the presented algorithm is named as Perceptive GPS (called PGPS thereafter). PGPS extracts user's feature data from the received GPS data to classify his current state. The modeling method of PGPS is then introduced to infer a plausible motion state of the user. This perceived motion state is then cross-referenced with the classified current state to

reduce the possible noise and accumulative error of hardware sensors, further to correct GPS data error accordingly.

2. Related Works

Context-aware technique is originated from Pervasive Computing to deal with understanding user's behavior from the sensed environmental data and to provide proper service to the users accordingly. The so-called Context composes of "Con" and "Text". "Con" stands for connection and "Text" is related to user's surrounding information. Such data depict information of the user's states, including identification, spatial and temporal information, activities and others. In other words, a context-aware system is capable to extract and interpret context data from sensors to infer proper services for the users. The greatest challenge of designing such a system is the complexity of collecting, extracting, and reasoning the contextual data.

The previous context-aware studies regarding modeling and reasoning user's behavior from GPS data can be classified into time-series model and state-space model. Time-series model is based on the past temporal GPS raw data to profile human behaviors. For example, in 2004, Patterson et al.[9] utilized joint conditional probabilities between GPS data of user historical footprint and the terrain geometry of physical environment to predict user's transport behaviors and then infer the user's location. Different from time-series model, which is usually limited by the past finite GPS data and complicated environmental information to infer, the state-space model classifies GPS data into abstract state space to model the user's behavior and then to infer his location. The advantage of state-space model in this approach can reason user's behavior without being influenced by the fixed length of temporal sequence. It can easily couple with inertial effect to dramatically reduce the computational complexity. For example, Patterson et al.[10] applies state-space model to GPS data collected from the GPS receiver carried by animals to observe the animal behaviors. This research proves that it is feasible to perceive and model state space of animal behaviors through GPS data.

Most state-space model studies are based on environmental types to predict subject's motion state. Liao et al [11] applies hierarchical Dynamic Bayes Network(DBN) or Conditional random fields(CRF) to GPS data from different vehicles to infer their respective transport models. Due to the lack of speed and acceleration, this method is only feasible to monotonous or long-distance moving behaviors. In order to discuss more complicated motion states, the spatial conceptual maps[12] applies geometric relationship of physical environment to the state-space model to solve GPS data error problems. However, these studies did not use user's real-time motion states as the predictive basis; therefore, they can not be applied to an unprepared environment.

All these models discussed above were built on the assumption of a known or prepared environment. Further, since GPS receiver is susceptible to environmental interference the efficiency of user's state space model will be easily affected by an unknown or unprepared environment and lead the inaccuracy of GPS positioning. Hence, previous researches also require the accuracy of GIS map. The goal of this research attempts to perceive user's behavior from GPS data alone without specifically observing user's behaviors. In other words, this research treats GPS receiver as a sensor to acquire user's behavior and further to amend filtered GPS data accordingly. To achieve this goal, context-aware[13] technique is employed to explore the received NMEA 0183 formatted GPS data and to perceive GPS carrier's behavior accordingly. Since GPS data represents the snapshot of momentum changes of carrier, we can use Newton's Laws of Motion[14] to interpret GPS data. Therefore, an enhanced HMM by integrating Newton's Laws of Motion, coined Newton Markov Model(NMM), is proposed to reason user behavior from GPS data. The GPS carrier's behaviors in different environments are then captured into the Transition Probability Matrix (TPM) of NMM. This TPM is later used to perceive carrier's online motion status and further effectively amend the GPS data. This approach is named as Perceptive GPS (PGPS) method.

3. Rational of PGPS

In order to perform the context aware computation on commercially available GPS module, the context of the GPS carrier has to be decided first. While the context is a sequence of data that represents the states of behavior of GPS carrier, the context should be derived from GPS data. However, GPS data itself contain multiple dimensions of information, such as altitude, longitude, latitude and course etc., not all of them can be used for state reasoning directly. Because the goal is to perceive the behavior of GPS carrier from the received GPS data, the selected context has to contain spatial and temporal information of the GPS carrier. Furthermore, the context of GPS data has to be capable to highlight the motion of the carrier without being interfered by the environment. Under such prerequisite, the feature data for behavior aware computation is further extracted from GPS data. Therefore, the first issue of this research is to decide what the contexts hidden in GPS data are and how to extract them into the required feature data? The next question then focuses on how to classify the feature data into liable state that represents the behavior of GPS carrier? When the meaningful states are well defined, the subsequent issue is how to create the model of behavior of GPS carrier from the classified states? Importantly, in order not to be influenced by the discrepancy of different environments, this model must be in line with the innate characteristic of the GPS carrier so that the intention of GPS carrier can be captured. After the model is built, the final question is how to use the model to infer carrier behavior and amend GPS error data interactively?

To solve the above four issues, two phases, which are learning and perception phases, and five executing stages, i.e. feature extraction, state classification, learning, perception and amendment stages, as shown in Figure 1, are designed. Feature extraction stage extracts GPS carrier's feature of

motion from GPS data such as speed over ground(SOG), position and course over ground(COG) information. The extracted feature data include user's displacement, velocity change, and the course difference between two consecutive GPS data. Based on the momentum changes, the state classification stage then uses feature data to classify GPS carrier's behavior into pre-defined modeling states. The classified state is coined as the current state(CS) of GPS carrier.

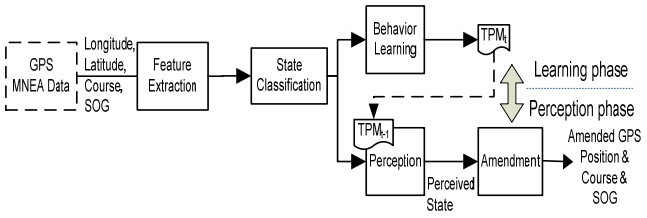

Fig. 1. PGPS process diagram

Perception needs to know the past history of the GPS carrier. The proposed technique is composed of learning phase and perception phase to perform the online perception. During the learning phase, outputs of state classification are analyzed by Newton's Laws of Motion to compute the state transition probability among modeled states. These state transition probabilities are then collected into a Transition Probability Matrix (TPM) to represent the habitual behavior of the user on that period of time. In other words, the value of TPM is filled in the form of momentum change of user's motion. This TPM then becomes inference foundation of the perception phase when the user performs online perception next time. Hence, in order to distinguish TPMs between the learning phase and the perception phase, subscript t of TPM_t represents new TPM derived from the current learning phase while subscript *t-1* of TPM_{t-1} denotes TPM from the previous learning phase. In short, during the online perception, new TPM, i.e. TPM_t, is interactively built to record user's current habitual behavior and previous TPM, i.e. TPM_{t-1}, is used to forecast the most likely current status of the user, called the perceived state(PS). Finally, the amendment stage fine-tunes of the GPS positional and course data are based on the differences between PS and CS. Detail description of each stage layout is displayed at the following sessions.

3.1 Feature Data Extraction

Among GPS sentence functional formats, NMEA 0183[15] is the most widely used standard nowadays. NMEA 0183 format regulates longitude, latitude, speed, UTC time, orientation, and satellite information, and so on into more than ten different sentences. Among these sentences, GPRMC, GPGGA, GPGSA, and GPGSV are four sentences that contain important contextual information of GPS carrier, as shown in Table 1, to capture its snapshot behavior.

Table 1. The context data from NMEA 0183

Course over ground	PDOP	SNR	Visible satellites
UTC time	latitude	longitude	Velocity over ground

Since each GPS data is the snapshot of GPS receiver at an instant of time, the study assumes that the GPS carrier is a rigid body and the sequence of received GPS data is the trajectory of GPS carrier. Under the assumption of Newton's motion physics, this study applied Newton's second Law of Motion, $F = d(mv)/dt$, to calculate the momentum of GPS carrier and to analyze the motion of GPS carrier accordingly. Based upon Newton's second Law of Motion, the momentum change is induced by the displacement, velocity change and course difference. Since the location information embedded in GPS data is denoted in latitude and longitude, Haversine formula[16] is adopted to compute the displacement Δx. Subsequently, the displacement (Δx), the velocity difference (Δv) and the course difference ($\Delta\theta$) of two consecutive GPS data are extracted as the feature data to detect the behavior change of GPS carrier.

3.2 State Classification

After the feature data are extracted, they can be used to estimate current state of GPS carrier. The question is how the GPS carrier's behaviour is classified from the above feature data? Newton's second Law of Motion tells us that the momentum change may be caused by the alteration of mass or the variation of velocity. Under the assumption that the GPS carrier is a rigid body and its mass is fixed, the momentum change is dominated by the variation of velocity. Consequently, Δv should be the first element to classify GPS carrier's behaviour from the received GPS data. Further, there is no doubt that the ranging error of GPS data is indeed embedded in the value of displacement Δx which naturally becomes the second classification key. Finally, the difference of course, $\Delta\theta$, then turns into the last component for classification. Hence, with the help of Newton's Laws of Motion, the computed feature data Δv, Δx, $\Delta\theta$ can classify GPS carrier's behaviour into 7 reasonable states: stationary(S_s), linear cruise(S_{lc}), linear acceleration(S_{la}), linear deceleration(S_{ld}), veering cruise(S_{vc}), veering acceleration(S_{va}), and veering deceleration states(S_{vd}). In other words, based upon Newton's Laws of Motion, this research assumes that the behaviour of GPS carrier can be modelled by the set $\mathbf{S} = \{S_s, S_{la}, S_{lc}, S_{ld}, S_{va}, S_{vc}, S_{vd}\}$. In order to accommodate the innate ranging errors reside in GPS signal, three threshold values, $\alpha_v, \alpha_x, \alpha_\theta$, of feature data Δv, Δx, $\Delta\theta$, respectively, are assigned for state classification. However, although the classification rules are derived from Newton's Laws of Motion, due to the GPS data ranging error, some classified states are against the law of nature and, hence, are collectively called Group X. Table 2 summarizes the above classification rules and the result of classification.

To further model the behaviour of GPS carrier by states in **S**, the Markov model is applied to Table 2 to deduce a state transition diagram as shown in Fig. 2 and it is named Newton Markov Model (NMM) thereafter. To facilitate the following discussion, the state sequence of a GPS carrier is expressed as $\{S_i\}$, with i indicates a discrete instance of time and $S_i \in \mathbf{S}$.

In Fig. 2, each node represents a state of the GPS carrier and the dotted line denotes the state transition probability between states. This dotted line is further formulated by the equation $P(S_t = j \mid S_{t-1} = i)$ to indicate the probability of state transition from state i at time t-1 to state j at time t. For example, $P(S_t = S_{la} \mid S_{t-1} = S_{la})$ represents the probability of the state S_{la} at time t-1 transition to the state S_{la} at time t.

Table 2. Summary of classification rules under valid value of Δv

$\Delta\vartheta$ & Δx & Δv	$\lvert\Delta v\rvert < \alpha_v$	$\Delta v > \alpha_v$	$\Delta v < -\alpha_v$
$\lvert\Delta\theta\rvert \le \alpha_\theta$ & $\lvert\Delta x\rvert < \alpha_x$	Group 0 (Stationary state)	Group X (Unclassified state)	Group X (Unclassified state)
$\lvert\Delta\theta\rvert \le \alpha_\theta$ & $\lvert\Delta x_t - \Delta x_{t-1}\rvert = \alpha_x$	Group 1 (Linear cruise state)	Group X (Unclassified state)	Group X (Unclassified state)
$\lvert\Delta\theta\rvert \le \alpha_\theta$ & $\lvert\Delta x_t - \Delta x_{t-1}\rvert > \alpha_x$	Group X (Unclassified state)	Group 2 (Linear acceleration state)	Group 3 (Linear deceleration state)
$\lvert\Delta\theta\rvert > \alpha_\theta$ & $\lvert\Delta x_t - \Delta x_{t-1}\rvert = \alpha_x$	Group 4 (Veering cruise state)	Group X (Unclassified state)	Group X (Unclassified state)
$\lvert\Delta\theta\rvert > \alpha_\theta$ & $\lvert\Delta x_t - \Delta x_{t-1}\rvert > \alpha_x$	Group X (Unclassified state)	Group 5 (Veering acceleration state)	Group 6 (Veering acceleration state)
$\lvert\Delta\theta\rvert > \alpha_\theta$ & $\lvert\Delta x\rvert \le \alpha_x$	Group 0 (Stationary state)	Group X (Unclassified state)	Group X (Unclassified state)

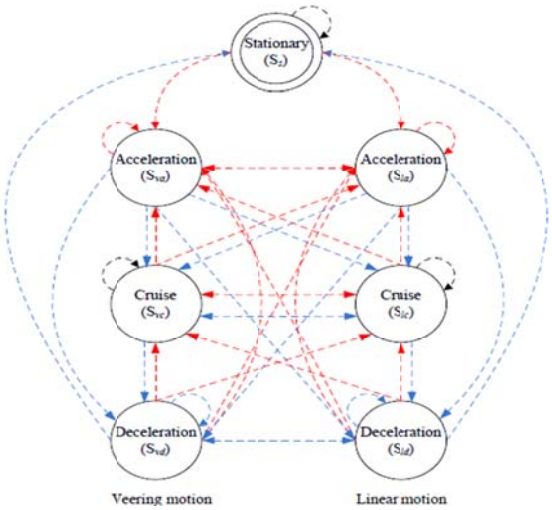

Fig. 2. Newton Markov Model

3.3 Behavior Learning

Most human will take the same habitual reaction under the similar environment. For example, when veering, at the beginning, most people would slow down, then turn, and finally to accelerate progress. To deal with the unpredictable user's behaviour under an unprepared environment is a critical issue of this study. This study takes Hidden Markov Model and Maximum Entropy to capture the uncertainty in motion behaviour modelling. If the observable GPS data sequence follows Newton Markov model, we can employ the principle of Hidden Markov Model to learn use's behaviour into a transition probability matrix(TPM) and apply Maximum Entropy to resolve the ambiguity in dynamic learning problem.

There are three canonical problems associated with HMM[17]. Since the study of inferring GPS carrier's behaviour from its past habitual behaviour is confirmed as the second canonical problem of HMM, this paper utilizes the approach of the second problem to compute the TPM of NMM. According to the state classification stage, GPS carrier can be one of 7 modelled states at any instant of time. Since GPS carrier can transit fom one state to any of 7 states at the next instant of time, we can capture its behavior by a 7X7 probability matrix. This 7 by 7 probability matrix is TPM that represents the habitual behavior of GPS receiver. Given A_{ij}(t) to denote the transition probability from state i to state j at a discrete time t, TPM can be formulated by Eq.(1).

$$\mathrm{TPM} = [P(S_t = j \mid S_{t-1} = i)]_{N\times N} = \left[A_{i,j}(t)\right]_{N\times N} \quad (1)$$

where $A_{ij}(t) = P(S_t = j \mid S_{t-1} = i)$ and N is the numbers of states. N is equal to 7 in this paper.

Therefore, if $A_{ij}(t)$ can be pre-learned, the current reasonable state of GPS carrier can then be inferred from its previous state and TPM. TPMs, which are computed from temporal sequences, represent the habitual behaviour of GPS receiver.

From the information theoretic perspective, the complexity of motion state can be related to the positioning accuracy and subsequently entropy.[18] The entropy is then becomes a good choice for quantifying the complexity of motion state. Everyone has his unique characteristics; and even for the same person, his first action would be positively different from the second movement without any accounts. Since different temporal motion state sequences may represent different behaviours, different temporal motion state sequences would derive different TPMs. The paper defines the entropy, H_t, as the absolute difference between two consecutive TPM_t and TPM_{t+1}. That is, the entropy of the system is shown as in Eq.(2).

$$H_t = \lvert TPM_{t+1} - TPM_t \rvert = \sqrt{\sum_{\forall i,j} \left(A_{i,j}^{t+1} - A_{i,j}^{t}\right)^2} \quad (2)$$

where $A_{i,j}^{t}$ indicates the possibility of state i transforming to state j in observation sequence O_t.

The continous entropy can be peceived as the changes of user's behavior. In other words, we can employ the maximum entropy to the optimal learning stratgey to perceive a stable user behavior. As the learning process continues, more TPMs will be derived from the received GPS data sequences. Therefore, we further define Eq. (3) to compute the average behaviours of GPS carrier among m consecutive observable GPS data sequences after received t^{th} sequences.

$$\psi_m(t) = \frac{1}{m}\sum_{i=0}^{i=m-1} H_{t+i} \quad (3)$$

Therefore, given ε as a tolerance value, $\psi_m(t) < \varepsilon$, when ε approaches zero, implies that the system is approaching a local stabilized behaviour with threshold ε during m consecutive training sequences. At this moment, the computed TPM is then

called a stable TPM. The stable TPM of the system can help to predict whether the user's behaviour is stable or not.

3.4 Behavior Perception

The stable TPM becomes the criteria to predict the optimal current state during online perception phase. This prediction is conducted by finding a maximum transition probability over all possible current states from a known previous state. To further increase the accuracy of prediction, this paper exercises previous two consecutive states *i, j* to compute the most possible current state *k.* Hence, the stable TPM derived from the learning phase will be in the form of a three-dimensional state transition matrix as shown in (4).

$$\mathrm{TPM} = [P(S_t = k \mid S_{t-2} = i \,\&\, S_{t-1} = j)]_{N\times N} = \left[A_{i,j,k}(t)\right]_{N\times N\times N} \quad (4)$$

As a result, Eq. (5) is the formula to obtain the maximum probability of current state from a stable TPM. Namely, Eq. (5) gives the maximum value among $A_{i,j,k}$ for all k with previous two consecutive state *i,* state *j*.

$$P(S_k \mid TPM, S_i, S_j) = \underset{given\ i,j}{\arg\max}\{A_{i,j,k}\ \forall k\} \quad (5)$$

The state computed from Eq. (5) is then compared with the current state, CS, derived from the state classification stage to detect if a GPS ranging error is occurred or not. That is, the predicted state, PS, computed from Eq. (5) gives the most likely current state based upon stable TPM, whereas the state classified from Table 2 is the possible current state according to the received GPS data**.** Hence, the comparison between these two states from two different sources can give the clue to detect GPS ranging error. Although Eq. (5) allows us to use the past experiences recorded in TPM to infer the most likely current state, yet, this computation still has some problems. For example, when $A_{i,j,k}$ is 0 or the computed maximum probability is not an unique value, the computed state would become ambiguous. Furthermore, when the perceived state, PS, from Eq. (5) is not the same as the current state, CS, from Table 2, there is no absolute conclusion on whether it means the received GPS data has ranging error or the GPS carrier is changing its habitual behaviour.

After conducting a series of experiments, the above problems can be summarized into the subsequent four possible scenarios. First, the GPS signal has the ranging errors caused by the environmental effects. The second case is that, GPS carrier is changing from one state into another during activity. The third scenario which we suppose it could be the prediction of current state is incorrect. The final situation is the habitual behaviour of GPS carrier has changed. Hence, the solutions to these four cases are discussed as below.

(1) When GPS signal has the ranging errors caused by the environmental effects, the received GPS data will not follow Newton's Laws of Motion. Hence, the received GPS data have to be amended according to the perceived state; so that it can be used to infer the following state with the stable TPM.

(2) The second case is that the GPS carrier is currently changing its state during activity. Since stable TPM records the inertial behaviour of GPS carrier, the original inertia may also be changed when the GPS carrier is switching from one state into another. In this case, the perceived state from Eq. (5) is wrong. In order to distinguish this case from the first case, a mechanism is designed to detect the change of inertial status of GPS carrier. Since the inertia has the characteristics of continuity, a posture threshold parameter, β_{pt} , is designed to count the number of consecutive state change. That is, $\beta_{pt} = \beta_{pt} + 1$ when the perceived state from Eq. (5) is continuously different from the classified state by Table 2. An inertial threshold φ is further defined for each GPS carrier so that when $\beta_{pt} > \varphi$, it implies that the GPS receiver is changing its state. The system will then believe that the state of GPS receiver has changed, and trust the classified state from the received GPS data as the accurate current state. If $\beta_{pt} \le \varphi$, we assume the system is in the first scenario and amend GPS data accordingly.

(3) The third situation is the perceived state computed from Eq. (5) is inaccurate. Since the maximum possibility inferred from Eq. (5) maybe 0 or not an unique value, it implies the state transition from the previous state to current one is undecided or there are more than one possibilities of such transition exist. Under such circumstances, the perceived state thus will become distrusted and another approach is required to verify the accuracy of online received GPS data. Hence, a cross reference scheme between two consecutive feature data sets is designed to achieve this goal. If the difference between two consecutive feature data sets is within the range of predefined threshold, the classified current state from online received GPS data is then accepted. Otherwise, the previous perceived state is trusted based upon the inertial principle.

(4) The final case is the change of habitual behaviour of GPS carrier. Different habitual behaviours will produce respective TPMs for online behaviour inference. Hence, the corresponded stable TPM for state inference and thresholds for state classification are switched for further state perception process.

3.5 Amendment

The data amendment approach is related to the geographical system. When a GPS error is detected, Dead Reckoning[19] is adopted to estimate current position based upon its previous position and reasonable state. However, since the received GPS data is in latitude and longitude format, this estimation must meet the Earth's geographical property. Consequently, the tangent line formula is used to evaluate the current position of GPS carrier as follows.

According to the tangent line formula, assuming that there are three consecutive GPS location data, A(λ_A, φ_A), B(λ_B, φ_B), C(λ_C, φ_C), where λ is longitude data, φ is latitude information. Based on the principle of inertial and tangent line formula, we can calculate the predicted location D from tangent line formula as following Eq.(6),

$$D_x = C_x + r(\lambda_B - \lambda_A)$$
$$D_y = C_y + r(\varphi_B - \varphi_A) \quad (6)$$

Besides, the veering angle, Φ, of the GPS carrier can also be estimated by Dead Reckoning formula as shown in Eq.(7).

$$\Phi = \arcsin\left(\frac{\varphi_B - \varphi_A}{\sqrt{(\varphi_B - \varphi_A)^2 + (\lambda_B - \lambda_A)^2}}\right) \quad (7)$$

Finally, to avoid effect from the accumulated error, the same Dead reckoning principle is also used if fine-tuning of GPS data is required.

4. Experiments and Results

The Implementation of PGPS is coded in java language on the Android-based smartphone. In specific, the smartphone used is HTC Hero model which is equipped with Sirf III GPS module. In order to acquire more reliable GPS data, the study applies some pre-screening steps during the initialization stage. Since GPS receiver employs a three-dimensional position computation, Phatak et al.[20] stated that there must be at least four satellites visible before the received GPS data becomes useful to compute the position of the GPS carrier. Furthermore, SNR of each satellite must exceed 30 dB [21] to derive the accurate positioning. Hence, the total SNR value should be more than 120 dB to let the received GPS data become useful for positioning. In addition, Lin et.al [22] shows that the proper PDOP value should be less than 20 during the initialization phase thereinafter.

Since the goal is to perceive the behaviour of a GPS carrier, it must have a proper framework to learn the habitual behaviour of GPS carrier before beginning to infer the behaviour of GPS carrier interactively. As a result, several questions are raised to validate the PGPS approach. Among them, the first question is if such learning framework and the perceived algorithm are applicable to GPS carriers with different momentum natures? In other words, Eq.(2) and Eq.(3) are used to calculate the stable habitual behaviour of GPS carrier. Nevertheless, the habitual behaviour of a GPS carrier will not be the same at all time. In terms of the principle of momentum, the inertial momentum will vary with the habitual behaviour and will become locally stabilized for different ranges of speed. Hence, the first question can be re-phrased as if Eq.(2) and Eq.(3) can actually capture local stable habitual behaviour of GPS carrier? The next question is if PGPS effective enough to filter out ranging error? To answer these two questions, a series of experiments are conducted to verify the presented PGPS methodology as presented in the following sections.

4.1 Entropy of Momentum

The first experiment is to verify whether Eq.(2) and Eq.(3) can capture different local habitual behaviours of the same GPS carrier? This experiment tries to calculate various entropies of the same GPS carrier under different velocity ranges that represent diverse momentums. During this experiment, the subject carries a GPS receiver and walks in the park with different speeds, including 2m/s~6m/s, 1m/s~3m/s, 0m/s~1m/s and 0m/s, to derive different GPS data learning sequences. Afterwards, the entropies for these four GPS learning sequences are then computed by Eq.(2) and Eq.(3), individually. The results are shown in the sub-graphs of Fig. 3. The vertical axis of Fig. 3 is the mean value of entropy by Eq.(3) and the horizontal axis is different segment length of the learning sequence. The result of this experiment shows that the mean entropy (i.e. vertical axis) of all four velocity ranges can be converged to a specific value after certain length of learning segments. Because the minimum learning segment length of this experiment was set up at 20, this experiment reveals that the carrier with higher velocity (momentum) will require longer length of learning segment to obtain stable TPM.

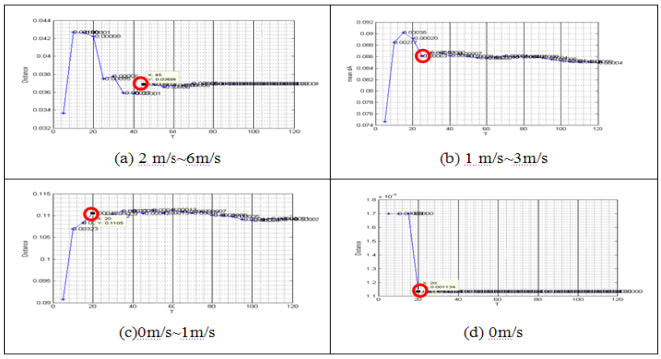

Fig. 3. Entropies in different velocity ranges.

4.2 Effectiveness of the PGPS

As depicted in Fig. 4, we chose a linear path (red line) from A to B as the base line for this experiment. A student was then asked to hold a smartphone and walk from point A to point B to log resulted PGPS data sequence. For the control group, this student repeated the same path with a notebook that is plugged in with a high-precision external GPS receiver to log GPS data sequence between points A and B.

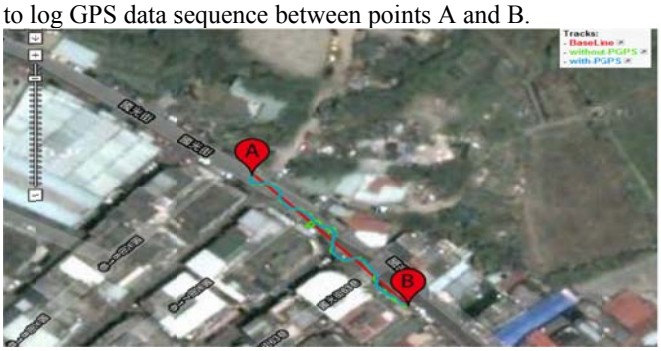

Fig. 4. The measurement scenario

In order to display the effectiveness of PGPS on reducing ranging error, Fig. 5 shows the histogram after screening out eight significantly large ranging error points. The unit of the vertical axis in Fig. 5 is meter and the red line is the result of logged PGPS while the blue line is the logged GPS data from notebook with a high-precision external GPS receiver. We can notice the largest ranging error of the red line is reduced to 4m while the blue line is 8m. This experiment shows that GPS ranging error is effectively reduced.

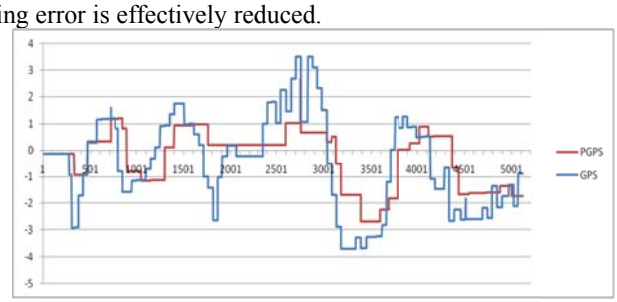

Histogram (second)

Fig. 5. The result of with PGPS and without PGPS

5. Conclusion and Future work

The paper presents an approach, called PGPS, to interactively infer the behavior of GPS carrier by utilizing the trajectory of received GPS data. Although the GPS signals are vulnerable to the environmental effects, the behavior pattern still exists in the context of the received GPS data. PGPS is a novel approach that adopts GPS data as the feature evidence of behavior state. The presented GPS calibration technique doesn't require either any high cost ground base station assistance, nor any expensive auxiliary peripherals and complex GIS system. The PGPS methodology combines Newton's Law of Motion with context awareness technique to improve the accuracy of GPS positioning. During the learning phase, PGPS applies Newton's Law of Motion to extract the GPS data to learn the behavior feature of GPS carrier. The Newton Markov Model is then defined accordingly to model the habitual behavior of GPS carrier. In accordance with the theory of Hidden Markov Model, PGPS then computes the stable TPM to capture the habitual behavior of GPS carrier. Hence, this study proposes a perceived algorithm that uses stable TPM to reason carrier's behavior online. Moreover, the posture threshold is further elaborated to detect the behavior change of GPS carrier.

The most important application of PGPS method is the live-view GPS navigation system, which needs the accurate position information for object registration during navigation. For example, OmniGuider[2] is a real world browser that can provide you the right information at the right time and right place. PGPS not only can provide an accurate behavior perception to solve the ranging errors; but also could conquer the registration problems of the mobile augmented reality system. In all, PGPS could support the precise longitude and latitude information for the user to perform point of interest (POI) navigation application.[23]

6 References

[1] R.G. Golledge, R.L. Klatzky, J. M. Loomis, J. Spiegle and J. Tietz, "A geographical information system for a GPS based personal guidance system", *International Journal of Geographical Information Science*, Taylor and Francis Ltd., London, vol.12, pp. 727-749, Apr. 1998.

[2] J. Y. Huang, C. H. Tsai, S. T. Huang, "Next Generation of GPS Navigation System," *Communications of the ACM*, vol. 55, pp. 84-93, Mar. 2012.

[3] Wikitude Drive. (2012, Feb.). [Online]. Available: http://www.wikitude.com/tour/wikitude-drive/.

[4] AVIC-VH09. (2012, Feb.). [Online]. Pioneer Japan. Available: http://pioneer.jp/carrozzeria/cybernavi/.

[5] Route 66 Maps+. (2012, Feb.). [Online]. Available: http://www.66.com/route66/.

[6] S. Feiner et al., "A Touring Machine: Prototyping 3D Mobile Augmented Reality Systems for Exploring the Urban Environment," in *Proc. 1st Int'l Symp.* Wearable Computers (ISWC 97), IEEE CS Press, Los Alamitos, Calif., 1997, pp. 74-81.

[7] W. T. Fong , S. K. Ong , A. Y. C. Nee, "A differential GPS carrier phase technique for precision outdoor AR tracking," in *Proc. 7th IEEE/ACM Int'l Symp.* on Mixed and Augmented Reality, 2008, pp.25-28.

[8] C.E. White, D. Bernstein and A. L. Kornhauser, "Some map matching algorithms for personal navigation assistants," *Transportation Research Part C: Emerging Technologies*, vol. 8, pp 91-108, Feb. 2000.

[9] D. J. Patterson, L. Liao, D. Fox and H. Kautz, "Inferring High-Level Behavior from Low-Level Sensors," in *Proc. 5th Int'l Conf.* Ubiquitous Computing, LNCS 2864, Springer-Verlag, 2003, pp. 73-89.

[10] A. T. Patterson, L. Thomas, C. Wilcox, O. Ovaskainen, J. Matthiopoulos, "Stat-space models of individual animal movement," *Trends in Ecology & Evolution*, vol. 23, pp. 87-94, Feb. 2008.

[11] L. Liao, D. Fox, and H. Kautz, "Extracting Places and Activities from GPS Traces Using Hierarchical Conditional Random Fields," *Int'l J. Robotics Research*, vol. 26, pp. 119-134, Jan. 2007.

[12] N. Samaan and A. Karmouch. "A mobility prediction architecture based on contextual knowledge and spatial conceptual maps," *IEEE Trans. Mobile Comput.*, vol. 4, pp. 537–551, Nov.-Dec. 2005.

[13] B. Schilit, N. Adams, and R. Want, "Context-Aware Computing Applications." In *Proc of the Workshop on Mobile Computing Systems and Applications*, Santa Cruz, CA, December 1994, pp. 85-90.

[14] C. Schiller. (2010, Feb.). Motion Mountain The Adventure of Physics. [Online]. Available: http://www.motionmountain.net

[15] NMEA 0183 Standard. (2010, Feb.). [Online]. Available: http://www.nmea.org/ pub/0183/

[16] R. W. Sinnott, "Virtues of the Haversine", *Sky and Telescope*, vol. 68, pp. 159, Dec. 1984.

[17] L. R. Rabiner, "A Tutorial on Hidden Markov Models and Select Applications in Speech Recognition", *Proc. IEEE*, vol. 77, pp. 257-285, Feb. 1989.

[18] D. Vasquez and T. Fraichard, "Intentional motion on-line learning and prediction," in *Proc. Conf. Field Service Robot.*, Port Douglas, Australia, Jul. 2005.

[19] R. Jirawimut, P. Ptasinski, V. Garaj, F. Cecelja and W. Balachandran, "A method for dead reckoning parameter correction in pedestrian navigation system," *IEEE Trans. Instrum. and Meas.*, vol. 52, pp. 209-215, Feb. 2003.

[20] M. Phatak and M. Chansarkar, "Position fix from three GPS satellites and altitude: A direct method," *IEEE Trans. Aerosp. Electron. Syst.*, vol. 35, pp. 350-354, Jan. 1999.

[21] P. Axelrad, C. J. Comp and P. F. MacDoran, "SNR based multipath error correction for GPS differential phase," *IEEE Trans. Aerosp. Electron. Syst.*, vol. 32, pp. 650–660, Apr. 1996.

[22] C. J. Lin, Y. Y. Chen and F. R. Chang, "Fuzzy Processing on GPS Data to Improve the Position Accuracy," in *Proc. Asian Fuzzy Syst. Symp. Soft Comput. Intell. Inf. Syst. and Inf.*, Kenting, Taiwan, 1996, pp. 557-562.

[23] D. Schmalstieg, T. Langlotz, and M. Billinghurst. "Chapter 2. Augmented Reality 2.0," In Greg Welch Sabine Coquillart, Guido Brunnett, editor, *Virtual Realities* (Dagstuhl Seminar Proceedings), 2011, pp. 13-37.

Towards Automated Scheduling in the Oil Industry: Modeling Safety Constraints

Bård Henning Tvedt[1], **Marc Bezem**[2]
[1]Epsis AS and Department of Physics and Technology, University of Bergen, Norway
[2]Department of Informatics, University of Bergen, P.O.Box 7800, 5020 Bergen, Norway

Abstract— *Maintenance schedules in the oil industry often consist of several subschedules originating in different organizational units. Even if these subschedules are locally feasible, overall feasibility can be difficult to verify by the mainly manual scheduling procedures used today. One important cross-cutting concern of large-scale scheduling is safety. Scheduling problems in the oil industry are characterized by a large number of absolute safety constraints. As a step towards automatic scheduling, we formalize the safety constraints surrounding heavy lifting. These constraints are interesting since they form an extension of the well-known jobshop model with cumulative resources. We discuss novel strategies for dealing with these safety constraints and demonstrate their usefulness on a set of benchmarks.*

Keywords: automated scheduling, constraint programming, safety constraints

1. Motivation

An oil and gas operator's objectives are to minimize the number of hazardous situations, minimizing the environmental footprint and maximize production. Meeting these, sometimes conflicting, targets is a complicated and challenging task, and meticulous preparations in the form of planning and scheduling are done within all disciplines. These include drilling & completion, reservoir & production and operations & maintenance.

The particular scheduling conditions depend on the location and age of a field, and on the discipline in question. At an offshore platform, for instance, maintenance activities are to be performed in a relatively small, enclosed space. In contrast, on a land-based field a great many maintenance activities are scheduled across vast areas. Even though the particulars of the problems can be different, several aspects are common for most scheduling problems in the industry. These aspects include:

- size – the number of activities can be in the range from hundreds to several thousands;
- complexity – the large number of constraints to be satisfied makes the (manual) generation of a feasible schedule difficult;
- dynamics – the operating conditions are continuously changing, and the dependencies on weather, logistic and equipment failure *will* disrupt schedules.

Today's scheduling routines are naturally shaped by these aspects. The size of the problem has traditionally been reduced by splitting the problem into several discipline- or department-related subproblems. Each separate problem becomes easier to solve, but the interdependencies between them are lost. The resulting schedules may therefore be unfeasible right from the start, and conflict resolution requires good communication between several departments and companies.

Even though the size of the subproblems has been reduced, there is no guarantee that the same applies for the complexity. Several of the considerations taken into account are based on the local scheduler's extensive knowledge of the problem, and not on formalized constraints. There is widespread belief that many of these considerations and best practices are difficult to implement in a solving strategy. This perception may be correct, but has not been properly tested.

Another implication of size and complexity is the quantification of the schedules' quality with respect to one or several objectives. If it is already difficult to ensure the overall feasibility of one schedule, how should several schedule suggestions be compared to determine the best solution?

The dynamics of the problem is a considerable challenge during execution of a schedule. Unforeseen events *will* occur. Due to the limited time available to reorganize a disrupted schedule, the simple strategy of postponing activities is often applied. Such a strategy can be combined with scheduling initially with slack in order to make room for some distortion. This might work well if the schedule experiences the 'right amount' of distortion during execution. On the other hand, if the execution is smooth resources become idle and new tasks must be prioritized and assigned on the fly. Anyway, there is no guarantee that distortions larger then the induced slack cannot occur. In such cases the schedule is rendered unfeasible and must be rescheduled.

The challenges mentioned above can be met by applying automated scheduling algorithms providing a consistent strategy for generating feasible schedule suggestions. To fully utilize the existing potential, several of the considerations made by schedulers must be turned into formal constraints. Some of these can be modeled and solved by well-known scheduling techniques. Others, for example, safety constraints, must be handled by tailor-made techniques as discussed in this paper. The expected benefits are greater

control and overview of safety issues, better prioritizing of activities, reduced idle time of resources, improved regularity of operations and, consequently, increased production.

2. Problem description

Our main focus in this paper is the domain of operations and maintenance. The problem definition has been simplified as much as possible while still keeping industry-specific characteristics such as absolute safety constraints. More common scheduling elements like cumulative resources and dependency constraints are included to provide real-world resemblance. The solution objective is to minimize the *makespan*, the total completion time of all activities to be scheduled. This particular objective aims at efficiency, but the techniques developed can be applied to other objectives as well.

The problem is set at an imaginary oil-platform subdivided into a set of locations. Equipment in need of maintenance is randomly distributed across the platform, and various maintenance activities are to be scheduled. The activities come with a given set of resource requirements and potential dependencies on other activities. All activities require a crew to perform them and a location to be performed at. In addition some activities require a crane because heavy lifting is involved. The crew and crane resources are scarce, meaning that they are in limited supply.

Thus far the problem classifies as a 'Resource-Constrained Project Scheduling Problem' [1, RCPSP], which is described by:

- a set of resources with given capacities;
- a set of non-interruptible activities of given processing times;
- a network of precedence constraints between the activities;
- the amount of resources required by the activities.

Even though the RCPSP description is adequate for a wide range of scheduling problems, there are several additional constraints, typical for the oil-industry as well as for other large-scale industrial settings, which do not fit into this framework. Our objective when generating a set of problem instances was to ensure that formalized examples of industry-related constraints were involved. One such example is the safety situation surrounding dangerous work, like for instance heavy lifting. Currently such schedule information is taken into account manually by the schedulers. By carefully formalizing the safety constraints we get a well-defined problem description for automation.

A solution $S(P)$ to a problem instance P is a schedule in which (1) all activities have been assigned a start time and (2) all activities requiring a crane have been assigned a crane and (3) all constraints are satisfied. Here (2) in combination with the safety constraints among (3) goes beyond the RCPSP framework. The reason is that the safety constraints are dynamic in the sense that they come into effect only *after* a crane has been assigned to an activity.

In the following paragraphs we will take a detailed look at the problem instances described in the above setting.

2.1 Notation and Terminology

A problem instance P consists of activities to be performed, resources needed to perform activities and constraints representing limitations between activities and resource use. We distinguish between *decision variables*, given *constants* and *derived variables*. An example of a decision variable is the starting time of an activity Act_i denoted $v_{sta}(Act_i)$. An activity's duration is assumed to be fixed and therefore a constant denoted $c_{dur}(Act_i)$. Finally, there are derived variables like an activity's end time, which is the sum of its start time and duration, given by $w_{end}(Act_i)$. Formally, $w_{end}(Act_i) = v_{sta}(Act_i) + c_{dur}(Act_i)$. For real objects like activities and resources we use abbreviatons starting with a capital letter.

2.2 Resources

A *location* $Loc_l \in Locs = \{Loc_1, \ldots, Loc_L\}$ is the place where activities are being executed. Even though the locations are viewed as resources there are no restrictions on the number of ordinary activities that can be performed simultaneously on a location. However, when dangerous work like heavy lifting is performed, the location is made inaccessible to all other activities. In that case we say that a *safety zone* has been established, consisting of both the location of the activity and the location of the crane. How to deal with safety zones is an important part of the different models and solution strategies discussed in Section 3.

The *crews* are responsible for executing the activities. A crew is denoted $Crew_j \in Crews = \{Crew_1, \ldots, Crew_J\}$. The resource demand is taken to be one for whole the duration of the activity. A crew can therefore simultaneously work on the same number of activities as its capacity. It is not possible to pool resources to reduce the duration of an activity.

A *crane* $Crane_k \in Cranes = \{Crane_1, \ldots, Crane_K\}$ is a potential resource for activities. Some of the activities need a crane, and all problem instances contain a small number of cranes. The cranes are *unary resources* meaning that they can only perform one activity at the time. An activity requiring a crane does not specify a particular crane, but simply that it needs a crane. A feasible solution must therefore assign one crane to all activities requiring crane from the set of cranes available. This makes the set of cranes an alternative resource [2].

Cranes have a location $c_{loc}(Crane_k) \in Locs$, and each location can only have one crane. Due to the hazardous nature of heavy lifting, crane usage is surrounded by safety zones. These safety zones are established both at the crane's own location and at the location where the activity requiring

the crane is performed. The safety zones established will therefore vary according to which crane is assigned to which activity.

2.3 Activities

An *activity* $Act_i \in Acts = \{Act_1, \ldots, Act_I\}$ comes with a start variable, a constant duration and resource requirements. Initially the domain of the start variable is $v_{sta}(Act_i) \in [0, c_{hor}(P))$, where the horizon, indicating the schedule's maximum completion time, is given as $c_{hor}(P) = \sum_i c_{dur}(Act_i)$.

Every activity Act_i requires a crew $c_{crw}(Act_i) \in Crews$ to perform it, and a location $c_{loc}(Act_i) \in Locs$ to be performed at. Every activity uses one single member of a crew and it is not possible to pool resources to reduce the duration. Some (but not all) activities require a crane, which is expressed by a boolean constant $c_{crn}(Act_i)$. In that case there is also a decision variable $v_{crn}(Act_i) \in Cranes$.

In addition to resource requirements an activity can depend on other activities, meaning that it cannot start before these other activities are finished. This is called *precedence* in the RCPSP framework.

2.4 Constraints

Dependencies between activities are common in the industry. A maintenance activity can, for instance, be dependent on both the delivery of spare parts and raising of scaffolding to ensure access to the area in question. The relation stating that activity $Act_{i'}$ depends on activity Act_i is expressed by the following constraint:

$$w_{end}(Act_i) \leq v_{sta}(Act_{i'}) \tag{1}$$

A *cumulative resource constraint* applies to every crew, ensuring that the total resource consumption is not exceeding the crew's capacity. It is expressed by:

$$\begin{aligned} \forall t, j : \sharp\{Act_i \mid t \in [v_{sta}(Act_i), w_{end}(Act_i)) \wedge \\ c_{crw}(Act_i) = Crew_j\} \leq c_{cap}(Crew_j) \end{aligned} \tag{2}$$

where $c_{cap}(Crew_j)$ is the capacity of the j-th crew.

Cranes are unique individuals and therefore modeled as a set of unary resources. The *mutual exclusion constraint* states that two activities cannot be executed simultaneously when they are assigned the same crane. We prepare by defining the temporal predicate *overlap* expressing that two activities are overlapping in time:

$$\begin{aligned} &overlap(Act_i, Act_{i'}) \equiv \\ &\exists t : \; v_{sta}(Act_i), v_{sta}(Act_{i'}) \leq t < w_{end}(Act_i), w_{end}(Act_{i'}) \end{aligned} \tag{3}$$

The mutual exclusion of crane usage then becomes:

$$\begin{aligned} \forall i, i' \neq i : v_{crn}(Act_i) = v_{crn}(Act_{i'}) \rightarrow \\ \neg overlap(Act_i, Act_{i'}) \end{aligned} \tag{4}$$

for all activities requiring crane.

Now come what we call the *safety constraints*. They are expressed in terms of the location of the activity requiring a crane and of the location of the crane chosen. The first location is known in advance, while the second is dependent on the decision as to which crane to use. The fact that the temporal constraints in (6) below depend on the crane decisions made is interesting because of the added complexity this induces. Although there may be different ways of formalizing such a constraint, it appears to be a real extension of the simple job-shop model with cumulative constraints.

Safety constraints shutting out use of the location of an activity requiring crane are:

$$\begin{aligned} \forall i, i' \neq i : \; c_{crn}(Act_i) \wedge c_{loc}(Act_i) = c_{loc}(Act_{i'}) \\ \rightarrow \neg overlap(Act_i, Act_{i'}) \end{aligned} \tag{5}$$

while safety constraints shutting out use of the crane location itself are given by:

$$\begin{aligned} \forall i,i' \neq i, j : (v_{crn}(Act_i) = Crane_j \wedge \\ c_{loc}(Act_{i'}) = c_{loc}(Crane_j)) \rightarrow \neg overlap(Act_i, Act_{i'}) \end{aligned} \tag{6}$$

2.5 Objective

The objective to minimize makespan $w_{ms}(P)$ or the duration of the schedule is defined by:

$$w_{ms}(P) = \max_i \{w_{end}(Act_i)\} \in [0, c_{hor}(P)] \tag{7}$$

which states that the makespan equals the latest end or completion time in the set of activities.

2.6 Problem instances

The problems are characterized by their sizes determined by the total number of activities, $\#Acts \in \{50, 60, 70, 80, 90, 100, 200, 300, 400, 500, 750, 1000\}$, and cranes, $\#Cranes = [2, 3]$. A total of 5 problem instances were generated for each of the 24 problem sizes, summing up to a total of 120 instances.

The problem instances were not necessarily feasible since they were generated by randomly assigning crews to activities, locations to activities, locations to cranes, dependencies between activities, and activities' crane requirements. 12 problem instances contained circular dependencies, and 11 instances had more than one crane at the same location. The total number of instances used is thus 97.

All the problem instances contain 24 locations and 4 crews with capacity $c_{cap}(Crew_j) \in [2, 3]$ drawn at random with a uniform distribution. The domain for the activities' start variables are default $v_{sta}(Act_i) = [0, c_{hor}(P))$, and the constant durations $c_{dur}(Act_i)$ are drawn uniformly at random from the range of $[1, 6]$ time steps. Approximately 20% of the activities are randomly chosen to require a crane, and approximately 10% of the activities is constrained by dependencies to some other activity.

3. Solution strategies

The problem of determining whether a given RCPSP has a solution with makespan smaller than a given deadline is NP-hard [3]. This means that the extended problem with safety constrains is also at least NP-hard. The simplest form of an RCPSP consist of a set of activities with durations and one resource with capacity two (no cranes, no dependencies between the activities). Finding the minimal makespan is then still NP-hard. This problem is sometimes called *multi-processor scheduling* and can also be viewed as binpacking with two bins. Hence finding an optimal, or even a good solution to such problems in polynomial time is by no means guaranteed.

We have experimented with one non-search and two search-based solution strategies. The first solution strategy is our own implementation of a greedy algorithm. A solution is computed as described below in Section 3.3. This strategy does not backtrack, undoing decisions and exploring other possibilities, but it is nevertheless guaranteed to produce a feasible solution.

The second set of solution strategies is implemented in C++ using the Ilog Solver 6.6 [4] and Ilog Scheduler 6.6 [5] libraries. A default search goal Ilog : IloSetTimesForward, which is designed to efficiently schedule activities in a chronological order, is applied to the activities, while the default goal Ilog : IloGenerate is used to assign cranes to activities. This search-based strategy is constrained by a time limit. The search is iterated with an additional constraint requiring that the makespan of the new solution is less than the current solution, and terminates when it fails to improve on the solution within the time limit. This strategy is applied to two different ways of modeling the safety constraints.

First theoretical lower and upper bounds for the makespans are calculated.

3.1 Theoretical lower bound for makespan

A theoretical lower bound is calculated based on the resource availability for the most constrained crew. The resulting solutions may not be feasible for the entire problem, but are packed tightly for the crew utilizing every crew hour.

$$c_{load}(Crew_j) = \sum_{c_{crw}(Act_i)=Crew_j} c_{dur}(Act_i) \tag{8}$$

$$c_{relload}(Crew_j) = \frac{c_{load}(Crew_j)}{c_{cap}(Crew_j)} \tag{9}$$

$$c_{lb,ms}(P) = \max_j\{c_{relload}(Crew_j)\} \tag{10}$$

3.2 Theoretical upper bound for makespan

A theoretical upper bound for the makespan is

$$c_{ub,ms}(P) = c_{hor}(P) = \sum_i c_{dur}(Act_i) \tag{11}$$

where all activities are executed one after the other. Feasibility of such a schedule requires a linear order of all activities which complies with all temporal dependencies. Finding such an order will be discussed in the next section. Executing all activities one after the other clearly respects all resource and safety constraints.

3.3 Non-search based (greedy) strategy

The first approach that can be expected to give some results is a so-called greedy algorithm. A characteristic of such an algorithm is that it schedules the activities one by one, always taking the earliest time-slot and first crane (if required) such that all constraints are satisfied. Clearly, one has to respect precedence to get a feasible solution and strong heuristics are required to avoid the worst schedules. This is in some sense the classical approach avoiding search: efficient generation of inefficient schedules. Thus the greedy strategy serves very well as a reference method by which the quality of other methods can be measured. Note that the greedy strategy is not unlike manual scheduling, the crucial difference being scale as well as quality of the heuristics.

Let us explain one of the heuristics which is often applied. Among the resources, it is often possible to identify the one that is most scarce. In our setting, although the safety constraints are complicating, the cranes are not a scarce resource since only 20% of the activities uses a crane. To identify a scarce resource one has to sum the total duration of all activities using the resource and divide that sum by the resource's capacity, much in the same way as the theoretical lower bound of the makespan is computed in Section 3.1. Having identified the scarcity of the resources in this way, it is often beneficial to schedule activities using a scarce resource first. Of course this should be done in a way compatible with the dependencies.

A first and necessary preparation for a greedy algorithm is that all activities are linearly ordered in a way respecting the dependencies. This is a well-known procedure called 'topological sort' [6] and can be done in time quadratic in the number of activities. Topological sort also detects circular dependencies. If a circularity is detected, then there exist no feasible schedules. From now on we assume that the activities $Act_1, \ldots, Act_I$ are listed such that $i < j$ whenever activity Act_j depends on Act_i. A feasible schedule can then be computed by scheduling each Act_j at the first possible time such that Act_i is finished (if Act_j depends on Act_i), the necessary resource is available and there is a free crane (if Act_j uses a crane), all satisfying the safety and other constraints.

3.4 Search-based strategies

The second approach is based on exhaustive search, and is applied to two variations of the model.

Inferred constraint

Finding good solutions, let alone solving to optimality, turned out to be difficult even for the smallest instances.

The default ILOG Scheduler search strategies have great performance, but they struggle to find feasible solutions due to the non-chronological elements induced by the decision-dependent safety constraints. In other words, assigning a crane to an activity can be made impossible by decisions taken long ago in the search. To reduce the effect of the non-chronological elements, implicit model information has been made explicit through an additional constraint. The model is expanded with a *cumulative resource constraint* for cranes:

$$\forall t: \ \sharp\{Act_i \mid t \in [v_{sta}(Act_i), w_{end}(Act_i)) \wedge c_{crn}(Act_i)\} \leq c_{cap}(Cranes) \quad (12)$$

where $c_{cap}(Cranes)$ equals the number of cranes. It is important to stress that this 'inferred' constraint (12) is a logical consequence of mutual exclusion of crane usage, constraint (4). As such it does not change the problem in any way. Despite being redundant, (12) improved the performance of Ilog dramatically. The search strategy assigns start times to activities before cranes are assigned. The inferred cumulative constraint ensures that the crane capacity is never exceeded.

Overconstrained model

The overconstrained model expresses all the safety constraints as non-conditional a priori constraints: the conditional constraint (6) is strengthened to (13) below. More precisely, instead of closing only the location of the crane used, we close *all* crane locations when *some* crane is used. In addition, of course the location of the activity requiring the crane is closed. This 'overconstraines' the model to a conventional RCPSP model, and the best possible makespans could go up. As such it is an interesting variant that allows one to analyse the effect of the dynamic safety constraints, both on the difficulty of solving the problem and on the quality of the solutions. This effect can be expected to depend on cranes being the most scarce resource or not.

The safety constraints in the original model expressed in constraint (6) are replaced by:

$$\forall i, i' \neq i : c_{crn}(Act_i) \wedge c_{loc}(Act_{i'}) \in C_{loc} \cup \{c_{loc}(Act_i)\} \rightarrow \neg overlap(Act_i, Act_{i'}) \quad (13)$$

where $C_{loc} = \{c_{loc}(Crane_j) \mid Crane_j \in Cranes\}$. Notice that it is only activities and not cranes that are influenced. Instead of forcing a solution to use one crane it encourages to use several cranes simultaneously. It is in other words not the same as setting the crane capacity to one.

4. Results and Evaluation

The theoretical upper and lower bounds provide the range for the makespan. Due to the way instances are generated and the nature of the bounds, this range is as expected. The durations are drawn uniformly at random from [1, 6], so with mean $\bar{c}_{dur}(Act_i) = 3,5$ units of time. The expected upper bounds are thus approximately 175 and 3500 units of time for 50 and 1000 activities, respectively. The mean theoretical upper bounds of the problem instances are 170 and 3500 units of time.

Table 1: Relative optimality index w_{rq} for the various models

#Act(#P)	≤ 100 (25)		> 100 (21)	
2 Cranes	w_{rq}	$\%^{(1)}$	w_{rq}	$\%^{(1)}$
Greedy	1.311	100	1.524	100
Inferred	1.068	100	1.063	35
Overconstrained	1.143	100	1.076	100
3 Cranes	w_{rq}	$\%^{(1)}$	w_{rq}	$\%^{(1)}$
#Act(#P)	≤ 100 (28)		> 100 (23)	
Greedy	1.276	100	1.393	100
Inferred	1.017	32	1.000	4
Overconstrained	1.176	100	1.037	91

$^{(1)}$ percentage solved problem instances

Based on four crews with a minimum capacity of two and uniformly assigned at random to activities, the theoretical lower bounds can be expected to be 1/8 of the theoretical upper bounds. For 50 and 1000 activities the expected theoretical lower bounds are approximately 22 and 438, respectively. Indeed the mean values in these problem instances are 23 and 440 units of time.

A feasible solution with makespan equal to the theoretical lower bound may not exist. However, the theoretical lower bound is based on the most constrained crew which is the problem's most constrained resource. It is therefore a sensible benchmark to compare various strategies. A measure of relative optimality w_{rq} is used to evaluate the results from the different strategies and models, given by:

$$w_{rq} = \frac{1}{|\mathcal{P}_{sol}|} \sum_{P \in \mathcal{P}_{sol}} \frac{w_{ms}(P)}{c_{lb,ms}(P)} \quad (14)$$

where $\mathcal{P}_{sol}$ is the set of problem instances solved by each approach. The elements in $\mathcal{P}_{sol}$ differ from strategy to strategy and these averages are therefore not entirely comparable, but they give an indication of the quality of the solutions. The measure w_{rq} does not penalize a strategy or model for failing to find a solution. Robustness is measured by the percentage of solved problem instances. The results are summarized in Table 1.

Our greedy solution strategy produces solutions with makespan on average 37% larger than the theoretical lower bound. When scaling up, some (expected) degradation of w_{rq} can be observed. The greedy strategy mimics a manual scheduling procedure for generating feasible schedules, and the results are believed to be comparable. The greedy algorithm's strength is that it always generates a feasible schedule. It is in fact the only strategy that solves all the problem instances. Apart from that it works in negligeable time (seconds).

The theoretical lower bound and the results of the greedy strategy set the stage for the seach-based strategies. Success means to solve many problem instances with a makespan close to the theoretical lower bound, in any case significantly smaller than the makespan the greedy strategy gives. The search-based strategies are iterated, from the makespan of the first solution found downwards in small steps. The initial bound for the makespan is always $c_{hor}(P)$, the theoretical upper bound. Each iteration the constraint enforcing an upper bound to the makespan is sharpened.

We used time limits of 1, 5 and 15 seconds for instances with $<$100, 100..499, $\geq$500 activities, respectively. Increasing the time limits didn't help very much. The final solution was reached in less than 5 iterations, all solutions are thus in fact produced within 60 seconds.

The inferred model produces the overall best makespans for feasible schedules, approximately 5.5% larger then the theoretical lower bound. On the other hand this model scales poorly and struggles when the instances become larger and more complex. For instances with 3 cranes and $>$100 activities it solves only 1 of the 23 instances, and overall it solves 43% of the problem instances.

Not surprisingly the overconstrained model produces slightly worse make-spans. This indicates that, even though cranes are not a scarce resource, the safety constraints have a clear impact on the results. The obtained makespans are approximately 11.4% larger then the theoretical lower bound. This model is, however, quite robust and 98% of the problem instances are solved.

5. Related and Future Work

The solution strategies applied in this paper are relatively simple, and improvements in quality, robustness and solving time can be expected of more sophisticated strategies. The following ideas are expected to yield improvements.

- The greedy strategy can be randomized such as in GRASP [7]. Initial experiments with randomization show promising results.
- Local search techniques such as in [8] could be further explored. Initial experiments have not shown promising results so far. It seems hard to define the right notion of neighborhood.
- Locations can be viewed as cumulative resources in the following way. The capacity of a location is equal to the total number of activities. An ordinary activity consumes one unit of the resource associated with the location of this activity. Activities using cranes consume the whole capacity of the resource associated with the location as well as of the location of the crane. In this way the safety constraints can be replaced by resource constraints, in combination with cranes as alternative resources. Initial experiments have shown promising results.
- The dynamic structure of the safety constraints could be analysed such as proposed in [9] to obtain better heuristics.

6. Conclusion

This is a preliminary study of the feasibility of automating maintenance scheduling in the oil-industry. The aim of our research was to address some of the challenges related to maintenance scheduling. More precisely, to explore different strategies for handling large and complex problems, in the highly dynamic environment of oil and gas production, in an efficient and coherent way.

The greedy strategy solves all problem instances, regardless of size and complexity, within seconds. The short solving time enables consistent handling of disruptions, caused by for instance unexpected events or delays, through rescheduling. In this manner the dynamics of the problem domain is also taken into account. The greedy algorithm mimics a manual procedure for generating a feasible schedule from scratch. Even though the search-based strategies are not as robust, the one that performed best generates solutions with on average a 20% shorter makespan.

When compared to manually scheduling, we believe our results indicate a great unutilized potential with respect to the feasibility, quality and generation time of schedules, to be exploited by automated scheduling.

References

[1] P. Baptiste, C. le Pape, and W. Nuijten, *Constraint-Based Scheduling, Applying Constraint Programming to Scheduling Problems*. Kluwer Academic Publishers, 2001.

[2] C. le Pape and S. F. Smith, "Management of temporal constraints for factory scheduling," in *Temporal aspects in Information Systems*, C. Rolland, F. Bodart, and M. Léonard, Eds. North-Holland, 1988.

[3] M. R. Garey and D. S. Johnson, *Computers and Intractability. A Guide to the Theory of NP-Completeness*. W. H. Freeman and Company, 1979.

[4] Ilog, *Ilog Solver's User Manual*, 2008.

[5] ——, *Ilog Scheduler's User Manual*, 2008.

[6] A. B. Kahn, "Topological sorting of large networks," *Communications of the ACM*, vol. 5, pp. 558–562, November 1962. [Online]. Available: http://doi.acm.org/10.1145/368996.369025

[7] T. Feo and M. Resende, "Greedy randomized adaptive search procedures," *Journal of Global Optimization*, vol. 6, pp. 109–133, 1995.

[8] P. V. Hentenryck and L. Michel, *Constraint-Based Local Search*. MIT Press, 2005.

[9] J. Beck and M. S. Fox, "Dynamic problem structure analysis as a basis for constraint-directed scheduling heuristics," *Artificial Intelligence*, vol. 117, no. 1, pp. 31 – 81, 2000. [Online]. Available: http://www.sciencedirect.com/science/article/pii/S0004370299000995

A Yield Aware Sampling Strategy for Tool Capacity Optimization

Muhammad Kashif Shahzad[123], Thomas Chaillou[1], Stéphane Hubac[1], Ali Siadat[2] and Michel Tollenaere[3]
[1]STMicroelectronics, 850 Rue Jean Monnet. 38926 Crolles, France
[2]LCFC Arts et Métiers Paris Tech, 4 rue Augustin Fresnel 57078 Metz, France
[3]G-SCOP; ENSGI - INP Grenoble 46 Avenue Félix Viallet 38000 Grenoble, France

Abstract— *The product quality in semiconductor manufacturing is ensured with 100% inspection at each process step; hence inspection tools quickly run out of capacities resulting in the production cycle delays. To best utilize the production and inspection capacities, existing sampling (static, dynamic and smart) strategies are based on the risk and delays. These strategies, however do not guarantee a reliable lot sample that represents a likely yield loss and there is a high risk of moving a bad production lot to next production steps. We present a 3-step yield aware sampling strategy to optimize inspection capacities based on the likely yield loss with the predictive state (PSM) and alarm (PAM) models as: (i) classify potentially suspected lots, (ii) cluster and/or populate suspected lots in the priority queues and (iii) apply last in first out (LIFO) to optimize capacities. This strategy is implemented with two heuristics. We also present a data model with ASCM (Alarm and State Control Management) tool for the multi source data extraction, alignment and pre-processing to support the validation of [PSM, PAM] predictive models.*

Keywords: sampling strategy, tool capacity optimization, yield prediction

1. Introduction

The SI has revolutionized our daily lives with electronic chips that can be found in almost all the equipments around us and follows the slogan smaller, faster and cheaper driven by Moore's law [1]. It postulates that the number of transistors shall double in every 18 to 24 months at reduced cost and power. Since then the SI has kept its pace as per Moore's law by continuously investing in R&D for the new technologies. New equipments are being manufactured to support and keep up with the emerging demands and the pace defined by the Moore's law. The equipments are highly expensive; hence decisions to purchase new production equipments are based on the business strategy and estimated ROI (return on investment). The metrology/inspection tools carry fixed costs and often phase out or need changes to cope up with the new emerging technologies; hence efforts are made to use the capacity optimization strategies to balance the inspection load instead of purchasing new inspection tools.

An electronic product (chip) undergoes the most complex manufacturing process with approximately 200 operations, 1100 steps and 8 weeks of processing. The sequences of operations to manufacture an electronic chip (transistors and interconnections between transistors) are classified as the FEOL (front-end-of-line) and BEOL (back-end-of-line) processes. The transistor acts like an on/off switch and it is a basic building block in the chip manufacturing. The interconnections are the wire networks that connect these transistors to form an electronic circuit. To ensure the product quality, measurement (metrology/inspection) steps are added within the manufacturing flow almost after every manufacturing step. Here we make decisions based on the parametric yield to either scrap or move the wafer to the next step with an objective to stop bad products consuming expensive resources and production capacities while ensuring the product quality. We know that the inspection tools have limited capacities; hence optimal capacity utilization in a high product mix is a key for success. There are some critical steps as well where the delay due to inspection capacity limitation might have a strong impact on the next production step, so these priority products must be inspected before other products in the queue. Till now the proposed inspection capacity optimization strategies (static, dynamic and smart sampling) are based on the risk, delays and tool capacities, however these strategies do not guarantee a reliable lot sample that represent a likely yield loss.

Let us start with an introduction to a generic production process (Fig.1) where lots are processed and controlled at production and inspection tools respectively to avoid bad lots moving to the next steps. The inspection capacities are always less than the production capacities and to balance the difference we have static, dynamic and smart sampling strategies. It can be viewed as a blind strategy with a high risk of skipping bad lots to the next steps whereas in our strategy we empower the control with PSM and PAM models to filter good and bad lots followed by capacity optimization. We argue that for a given product yield e.g. 85% the focus must be on finding and controlling the 15% bad products than inspecting 100% product using blind inspection strategies that do not differentiate between bad/good products. In this paper we present a yield aware sampling methodology that identify the potential inspection lots as good, bad or suspected and then only bad or suspected lots are potentially inspected while skipping the good lots to move to the next production steps. Inspection waiting queues are established

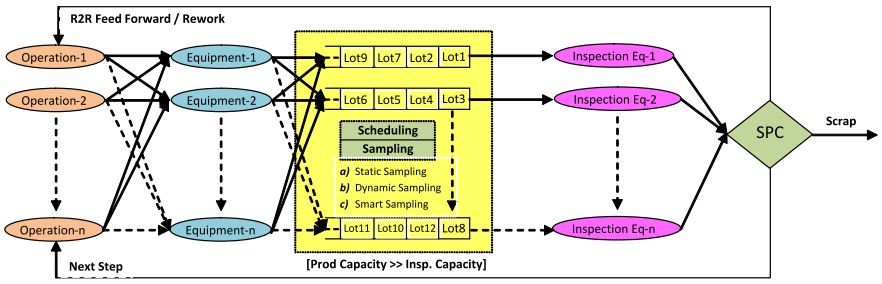

Fig. 1: Generic production process with existing sampling strategies.

and a second level optimization based on LIFO is applied to further save the inspection capacities as (i) inspections lots are clustered based on the product type and process recipe and (ii) if a potential lot results in a bad lot than all lots in the same cluster manufactured before the inspected lots are scarped. The success of this approach depends on the accuracy of learning and classification algorithm for PSM and PAM models. We propose two heuristics, first for the PSM and PAM models and second to cluster the suspected lots and applying queue optimization. A tuning parameter is also provided at the discretion of the user to control the PSM and PAM prediction confidence levels. In order to support the strategy we have also proposed a data model and ASCM tool for data extraction, alignment and pre-processing to support PSM and PAM model validations.

We have divided this paper in 4 sections. Section-1 provides a brief introduction to the semiconductor industry, problem context and the proposed methodology. Section-2 presents the literature review on the existing sampling strategies proposed and being used for capacity optimization. The proposed approach, heuristic algorithms, data model and ASCM tool are presented in the section-3. Finally we conclude this paper with discussion and future perspectives in sections 4 and 5.

2. Literature review

Chip manufacturing has become a complex but expensive production process resulting in process control challenges to find the lots with yield issues before they consume the expensive production resources. Limited inspection tools capacities has a strong impact on the production cycle times, hence an efficient sampling and control strategy is required to optimize the capacities and economic benefits. We have divided our research in two distinct areas as (i) we shall present a historical brief review on the interaction of product quality and process that lead to the emergence of SPC (statistical process control) and process control plans to ensure product quality and (ii) sampling approaches to optimize the inspection tools capacities and dynamic adaption of the process control plans.

The measurement tools are categorized as metrology and inspection tools. The metrology tool physically measures the geometric features and the product follows the SPC based control plan that either scraps the wafer or moves it to next production step. The inspections tools are used to find the defects on the surface of wafer right after the critical production steps to mark the bad chips on the circuit. It is important to understand from where the idea of control and product quality emerged or evolved and what are the latest contributions? The design of an economical control for a production process has always been an interesting research area that was initiated by [2] that lack robust results and require a balance between controls and their costs. [3] proposed a control plan with the concept of skipping by decreasing control frequency as compared to a 100% inspection plan. [4] presented that sampling size and frequency as two levels of controls are the better solution to quickly identify the issues while minimizing the cost of errors. [5] introduced the concept of SPC in the semiconductor industry that served as the basis for an updated control plan. Many approaches have been proposed for an adaptive control as (i) sampling strategy based on the number of wafers passed on metrology tools [6], (ii) updating control plan based on process excursions [7] and (iii) updating control plan based on risk encountered during productions. [8] ,[9] have designed a buffer for control machines taking into account the quality and cycle time expectations and it is the latest contribution in research regarding control plans.

Now we move to the second part of the literature where we shall present the inspection capacity allocation (referred as scheduling) problem in semiconductor industry. Existing strategies are classified as static and dynamic where static sampling [10] selects the same numbers of lots but dynamic sampling [6] select the number of lots for inspection, based on the overall production. Smart sampling is a new approach that sample lots by taking into account the risk associated with production tools, inspection tools capacities and delays to dynamically minimize the wafers at risk [11], [12]. It is a better approach than the static and dynamic strategies. In this strategy, if a lot in the waiting queue is controlled and it passes the inspection step then all lots in the waiting queues, processed before this lot are removed with a belief that they are also good lots. But none of them provide an evidence for a likely yield loss against sampled lots resulting in skipping

the suspected lots to move to the next process steps. We need a yield aware strategy to classify good, bad and suspected lots to reduce the inspection load significantly followed by an optimization strategy that exploit the production resources against limiting inspection tools capacities.

From the above literature, it is evident that the inspection capacity allocation problem is linked with the process control plans in the semiconductor industry. If we commit mistakes like skipping the bad lots to the next production steps as the existing approaches do not provide any evidence of likely yield loss then the consequences are evident in terms of customer dissatisfaction and costs. We argue that our focus should be on the identification of the bad or suspected lots while moving the good lots to the next steps. It shall not only increase the inspection capacities but shall also address critical step implications where the max time between two steps is fixed. Our proposed yield aware 3-step strategy uses the predictions made by the PSM and PAM models. Based on the predictive output combinations lots are either added to the priority inspection queues or moved to the next production steps followed by the capacity optimization.

3. Proposed approach

The proposed 3-step yield aware inspection strategy is presented in Fig.2. In our scenario, equipments are composed of 1...n modules in the parent child relationship. These modules are further classified as critical/non-critical and shared/non-shared elements. All the modules are characterized by meters, alarms and states which are recorded in the databases during the production operations. The alarms are generated at the module level, however based on these alarms the automation system changes the states of the child and parent modules. The changes in the states of the child modules serve as the basis for change in the state of parent modules. It represents the equipment health and such information can accurately predict a likely yield loss in the production induced due to unpredictable equipment behavior. The meter data triggers the preventive maintenance operations; however the module level meter data shall be included in the future to compute the weighted probabilities to weight the state and alarm level predictions. The alarms and states data represents the status of the production process and equipment health respectively; hence we use them to learn predictive alarm [PAM] and state [PSM] models.

In the proposed methodology we have used only the states and alarms data; however the module level meter data shall be included in the future to compute the weighted probabilities to refine the state and alarm level predictions. The first step in the inspection strategy is to classify the good, bad and/or suspected lots. In this step we start with the exploitation of the historical equipment states, alarms and SPC (statistical process control) data from the process, maintenance and alarms databases to build predictive state [PSM] and alarm [PAM] models. These models [PSM, PAM] are then used to classify the new production lots as good and/or bad lots and generate four possible outputs: (i) [good, good], (ii) [good, bad], (iii) [bad, good] and (iv) [bad, bad]. The good production lots [good, good] are moved to the next production steps without metrology and bad lots [bad, bad] undergoes the 100% inspection and their results are used to update the prediction [PAM] and [PSM] models.

The suspected lots [good, bad] or [bad, good] are clustered (2nd step) based on the equipment, product and recipe. It follows by a priority queue allocation algorithms (3rd step) that enter the suspected lot clusters into priority queues for further optimization based on LIFO (last in first out) principal. It states that if a suspected lot defies the prediction upon measurement then all the lots in the same cluster shall be subjected to 100% inspection otherwise the cluster members shall be skipped. The predictive state and alarm models [PSM, PAM] are updated with the feedback against all coherent and incoherent predictions as good and/or bad examples. It provides us an intelligent way to reliably sample only bad or potentially suspected lots followed by priority queuing and optimization for the economic benefits.

The step-1 where we learn the predictive [PSM, PAM] models and classify the new production lots as good, bad or suspected lots, is implemented with a heuristic algorithm as presented in section 3.1. The step-2 and step-3 are presented with a flow chart in section 3.2 that corresponds to the clustering and priority queue optimization.

3.1 Heuristic algorithm for predictive models

The alarms and states data collected from the equipment is not trivial to be used with the existing classification and pattern sequence learning algorithms; hence we have proposed a heuristic algorithm to predict the given wafer W^j as a good or bad. The time required for a production operation vary from 30 minutes to 4 hours and during operation a series of set of equipment states and alarms are generated. It is evident that data collected is a matrix of sets of alarms and states. Our proposed algorithm is simple and is based on probabilistic likely hood with the previous inspections. We start with the presentation of the variables used in the algorithm as under:

The $T^{[Ei]}$ is a tuning parameter and is defined by the user to tight the prediction and it is used to optimize the inspection capacities utilization, if required. For example, if user set its value to 50%, it means that computed likely hood shall be compared with this target prior to [good, bad] predictions. It is also important to note that the historical data shall be used to populate alarms and states matrixes for all equipments; however a confusion matrix [C] shall comprise of duplicated states and alarms sets found in both good and bad matrixes.

Proposed algorithm for the prediction of [PSM, PAM] model is as under. We start with the learning by computing good, bad and confusion matrixes of alarms and states

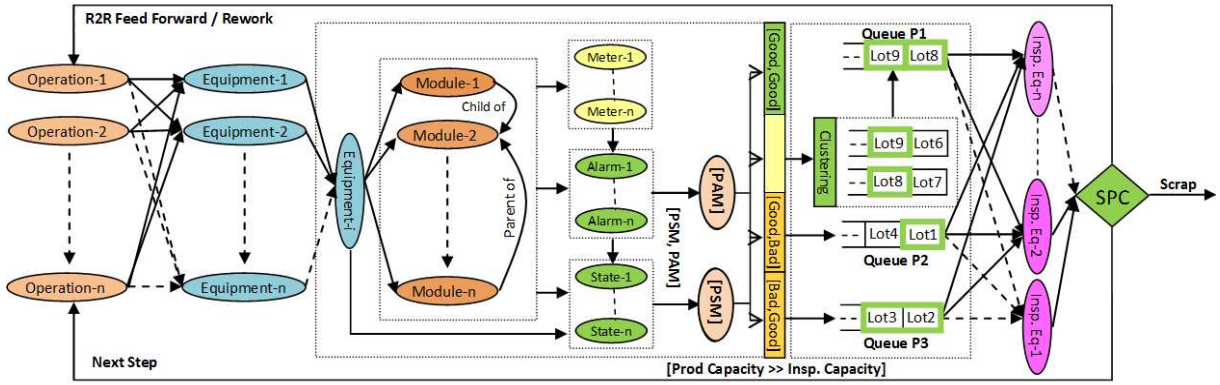

Fig. 2: 3-step methodology with predictive state (PSM) and alarm (PAM) models.

Table 1: Description of variables

Notations and Variables	Description
[G,B,C]:	G→Good, B→Bad, C→Confusion
$[E^i, W^j]$:	E^i → Equipment(i), W^j → Wafer(j)
$M^{[A,S,E^i,W^{i.9}]}_{[G,B,C]}$:	Matrix for alarms and states historical data for equipment E^i
$M^{[A,S,E^i,W^{i.9}]}_{[G,B,C]}(\sum_{j=1}^{n}[a_j, s_j])$:	Matrix for [G,B,C] alarms and states for all equipments and wafers
$M\sum_{j=1}^{n}[a_j, s_j]^{E^i}_{W^j}$:	Matrix for alarms and states sequence for equipment E^i and wafer W^j
$LS_{[G,B,C]}(\sum_{j=1}^{n}[a_j, s_j]^{E^i}_{W^j})$:	Local support for each set of alarms and states in the Matrix for equipment E^i and wafer W^j
$GS^{[A,S,E^i,W^j]}_{[G,B,C]}$:	Global support for alarms and states for equipment E^i and wafer W^j
$T^{[E^i]}$:	Target defined by the user for equipment E^i to be used for model predictions

sequence sets for all equipments as shown in step-1. It shall be used during the computation of the local support. In Step-2, we compute the local support for each set of alarms and states sequence for a given wafer W^j by counting the similar set of alarms or states sequences in [G,B,C] matrixes. This count is divided by the respective count of sequences in [G,B,C] matrixes to get the local support values for each sequence of alarms and states in wafer W^j. Further we compute global support for the wafer W^j by multiplying the local supports computed for each set of alarms and states sequence against [G,B,C] matrixes with the sum of computed local supports. The results are summed at [G,B,C] level for the prediction by comparing it against the $T^{[Ei]}$ in step-4. If the global support is smaller than the $T^{[Ei]}$ then the benefit of doubt is given to the prediction by adding the global support for [C]. Said algorithm for [PSM, PAM] models is presented as under:

Step-1: Compute $M^{[A,S,E^i]}_{[G,B,C]}$ for states and alarms data for each equipment E^i

$$M^{[A,S,E^i]}_{[G,B,C]} = M^{[A,S,E^i,W^{i.9}]}_{[G,B,C]}(\sum_{j=1}^{n}[a_j, s_j]) \quad (1)$$

Step-2: Compute local support for each set of alarms or states sequences for given wafer W^i and equipment E^i

$$LS_{[G,B,C]}(M\sum_{j=1}^{n}[a_j, s_j]^{E^i}_{W^j}) = \text{Count}(M\sum_{j=1}^{n}[a_j, s_j]^{E^i}_{W^j} == M^{[A,S,E^i,W^{i.9}]}_{[G,B,C]}[\sum_{j=1}^{n}[a_j, s_j]])/\text{Count}(M^{[A,S,E^i,W^{i.9}]}_{[G,B,C]}[\sum_{j=1}^{n}[a_j, s_j]]) \quad (2)$$

Step-3: Compute global support for a given equipment E^i and wafer W^j

$$GS^{[A,S,E^i,W^j]}_{[G,B,C]} = \text{Sum}(\text{Sum}(LS_{[G,B,C]}\sum_{j=1}^{n}[a_j, s_j]^{E^i}_{W^j}) * LS_{[G,B,C]}[M\sum_{j=1}^{n}[a_j, s_j]^{E^i}_{W^j}]) \quad (3)$$

Step-4: Predict [PSM,PAM] output for the given Wafer W^j

If $(GS^{[A,S,E^i,W^j]}_{[G]} \geq T^{[E^i]}) \Longrightarrow$ Good

eleseif $(GS^{[A,S,E^i,W^j]}_{[G]} \leq T^{[E^i]}$ AND $(GS^{[A,S,E^i,W^j]}_{[G]} + GS^{[A,S,E^i,W^j]}_{[C]})) \Longrightarrow$ Good

elseIf $(GS^{[A,S,E^i,W^j]}_{[B]} \geq T^{[E^i]}) \Longrightarrow$ Bad

eleseif $(GS^{[A,S,E^i,W^j]}_{[B]} \leq T^{[E^i]}$ AND $(GS^{[A,S,E^i,W^j]}_{[B]} + GS^{[A,S,E^i,W^j]}_{[C]})) \Longrightarrow$ Bad (4)

To demonstrate the said algorithm we present a simple example with [G,B,C] matrixes for alarms data as under (Fig.3):

Alarms matrix for equipment Ei [Good Yield]

T_ID	Module1	Module2	Module3	Module4
1	107(0x6B)			
2	384(0xF04)			
3		384(0xA04)		988(0xA04)
4		384(0xA04)		
5		384(0xC04)		
6				
7	384(0xF04)	312(0xD04)		
8				84(0xC09)
9	384(0xF04)	172(0xD04)		38(0xF14)
10	384(0xF04)	172(0xD04)		38(0xF14)

Alarms matrix for equipment Ei [Bad Yield]

T_ID	Module1	Module2	Module3	Module4
1	107(0x6B)	384(0xA04)		
2	384(0xF04)			84(0xC09)
3		388(0xA04)	388(0xA04)	988(0xA04)
4		374(0xA04)		
5	14(0xC09)	384(0xC04)		24(0xC09)
6				
7	384(0xF04)	312(0xD04)	300(0xE04)	
8				84(0xC09)
9	384(0xF04)	172(0xD04)		38(0xF14)
10				34(0xF22)

Alarms matrix for equipment Ei [Confusion]

T_ID	Module1	Module2	Module3	Module4
1	107(0x6B)			988(0xA04)
2		384(0xF04)	988(0xA04)	
3				988(0xA04)
4	38(0xF04)			
5		384(0xC04)		
6				
7	384(0xF04)			312(0xD04)

Alarms matrix for equipment Ei, Wafer Wj

T_ID	Module1	Module2	Module3	Module4
1	384(0xF04)	172(0xD04)		38(0xF14)
2		384(0xA04)		988(0xA04)
3		384(0xC04)		
4	384(0xF04)			84(0xC09)
5				34(0xF22)
6		384(0xF04)	988(0xA04)	

Fig. 3: Example [G,B,C] matrixes for alarms data.

Computed results against the potential lot W_j for prediction are detailed as under and as per computed global support this production lot with 54% likely hood is predicted as a

good lot (Fig.4).

Local Support			Global Support		
[G]	[B]	[C]	[G]	[B]	[C]
0.2	0	0	0.27		
0.1	0	0	0.13		
0.1	0	0	0.13		
0	0.1	0		0.13	
0	0.1	0		0.13	
0	0	0.143			0.19
Total = 0.743			0.54	0.27	0.19

Fig. 4: Local and global supports for [PAM] prediction.

3.2 Clustering and priority queue allocation

Based on the predictions from [PSM, PAM] models (section 3.1), we follow the 2nd and 3rd step in the proposed yield aware inspection strategy where suspected lots are clustered and added to the priority queues followed by LIFO optimization. It is presented with a simple flow chart (Fig.5). All production lots with prediction combination [PSM'Good and PAM'Good] are simply skipped whereas other lots are populated in the priority queues P1, P2 and P3 where P1>P2>P3. Lots with the combination [PSM'Bad and PAM'Bad] are first clustered based on the similarity of product, technology and recipe followed by the population of last lot from each cluster in P1. If an inspected lot from the P1 validates the model prediction than its respective cluster members are simply scrapped, otherwise each member of the cluster is inspected and the predictive [PSM, PAM] models are updated. In case of difference in model predictions, lots are declared as suspected and are populated in the priority queues P2 [PSM'Good and PAM'Bad] and P3 [PSM'Bad and PAM'Good]. The lots from P2 are sequentially inspected; if it defies the models then all lots processed before the inspected lot in P2 are given the benefit of doubt and are skipped. If a lot inspected from the P3 defies the model then all the respective cluster members are inspected and predictive [PSM, PAM] models are updated for coherences and incoherencies.

It is evident from the above discussion that the [PAM] predictions have higher priority than the [PSM] predictions based on the two facts, (i) child modules influence the states of their parent modules, hence prediction model developed at the module level might have a dual impact and (ii) alarms count and duration result in the change of state of the modules. The states data is an aggregation of the alarms data at module level, hence alarms data provide more low level detailed information with no influence on the alarms of parent modules. Based on these facts in this proposed methodology we have given higher priority to PAM prediction while performing information fusion of modules alarms and states data. The [PSM, PAM] prediction weights shall be defined in the future by including the meter data. The meter data is very critical because the values of the meters initiates the preventive maintenance actions on modules. We believe that it shall play a pivotal role in defining the prediction accuracies of the PAM model. The alarms and resulting prediction shall get more weigh when meter data fall within the distribution of previous preventive maintenance actions.

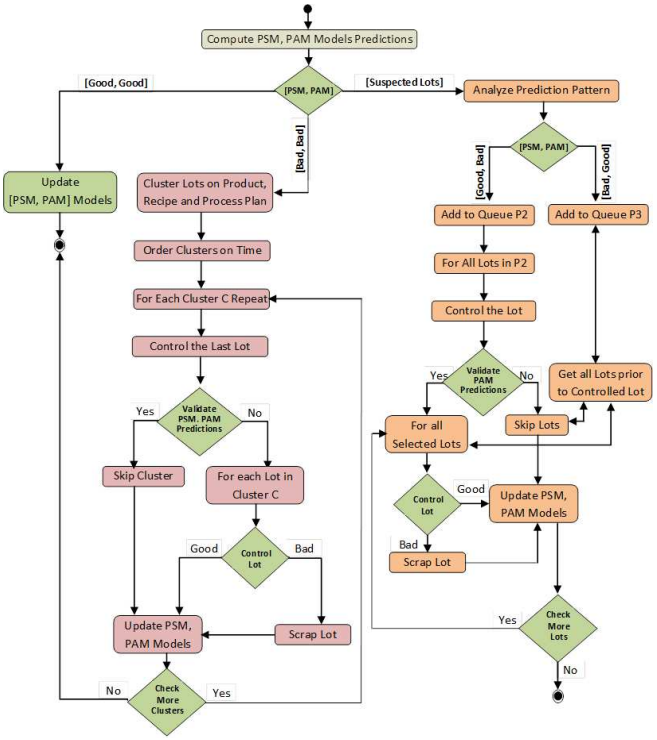

Fig. 5: Flow chart for clustering and queue allocations.

3.3 Data model and ASCM tool for data extraction, alignment and pre-processing

The biggest challenge in building and deploying these PAM and PSM predictive models is the multi-source data extraction, alignment and preprocessing from SPC, maintenance, process and alarms data sources. To facilitate this we have also proposed a data model (Fig.6) with the ASCM (Alarm and State Control Management) tool that allows engineers a quick extraction and alignment of the data.

In this data model the equipments (equipment class) are composed of modules (module class) and every module has a state (state_history class) and alarms (module_alarms class) history. The usage meter data is also available (usagemeter class) but in this paper we have not used this data. The parent-child associations between modules are captured by the parent_child_relation class. A product (product class) is manufactured using multiple lots (lot class) but follows a single process plan (process_plan class). The process plan has multiple operations (process_operation) and each operation can have multiple steps (process_steps). The process

step undergoes different step runs (step_run class) as the production or metrology runs The production step runs are associated with the equipments who have the capability (equipment_capability class) to perform the process steps. This data model is translated into a relational database which is implemented using SQL server to support the ASCM tool.

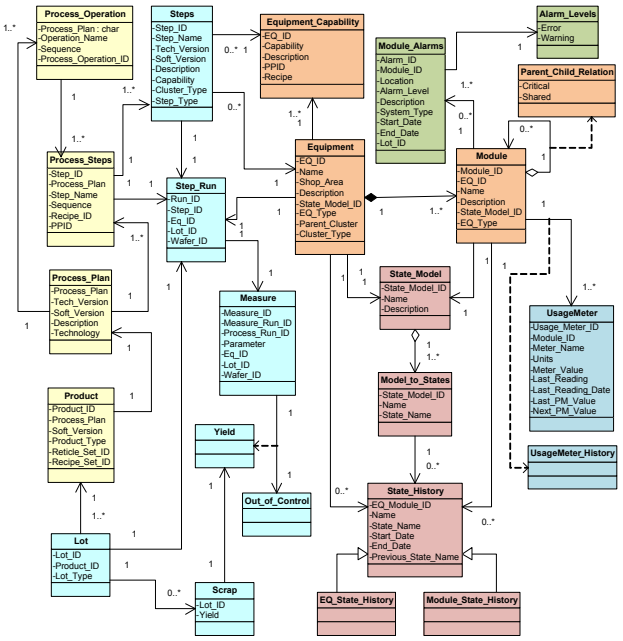

Fig. 6: Data model for extraction, alignment and processing..

A software tool is developed for the R&D engineers to extract data from SPC, maintenance and alarms databases in VB 6.0. The extracted data from different data sources are populated in the database developed as per above data model (Fig.6). Engineers are made capable to analyze and manage the data prior to the extraction for [PSM, PAM] model building. At present the tool is under revisions for the online inclusion of [PAM, PSM] model synchronization and validations. Few interfaces of the developed tools are presented below (Fig.7). This tool provides engineers the facility to analyze the real time state and alarm data at module levels for all the equipments. The states and alarms based pareto analysis result in the identification of insignificant states and alarms which are then put in quarantine to further improve the accurate prediction and classification of the [PSM, PAM] models. This tool also help the engineers to quickly identify best and worst equipments for the data extraction to be used during the [PSM, PAM] learning step.

The first interface provides computed statistics on every equipment being controlled and monitored for the PSM and PAM models. It provides quick information about the best and the worst equipment where the pareto count is based on either number of alarm counts or duration of these alarms. The equipment engineer manages the skipping of non critical alarms which are defined and grouped at the equipment

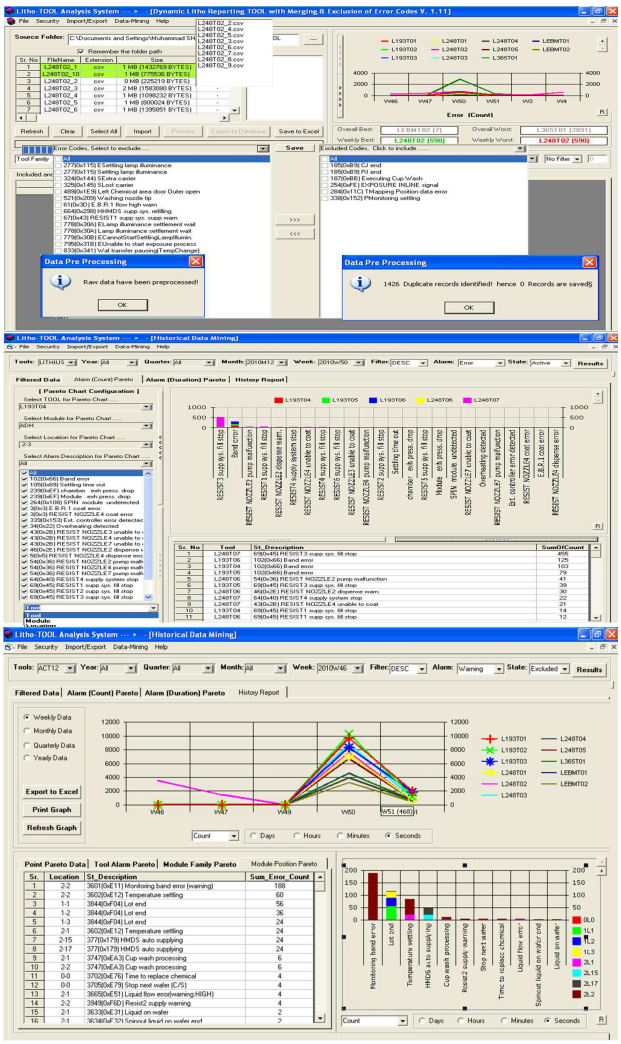

Fig. 7: ASCM Tool for extraction, alignment and pre-processing.

type level. This configuration is updated and further used to filter the unwanted alarms quarantined by the equipment experts. These alarms could easily add up the confusion matrix if not filtered because they have no direct link either with good or bad predictions. The second interface provides the capability to exploit and analyze the alarms data at the equipment and module levels based on the pareto analysis. The third interface provide an option for the point based alarms analysis. All these efforts are put together by the equipment engineers to update the filters list so that accurate and more complete alarms data is extracted to be used for PSM and PAM models.

4. Discussion and conclusions

Existing static, dynamic and smart sampling strategies for inspection are focused on the tool capacity optimization based on risk, delay and capacity. These strategies do not

guarantee the selection of lots with a likely yield loss that can result in serious consequences as if the bad product lots are skipped to the next production steps. These strategies can also be viewed as the blind optimization strategies but risk minimization justifies its adoption in the production line.

Our methodology provides an innovative intelligent sampling strategy that filters the lots as good and suspected lots where suspected lots are further sampled to optimize the inspection tools capacities using clustering and queue allocation algorithm. Our contributions include (i) data model that provide means to extract, align and exploit historical states, alarms and yield data from multiple data sources, (ii) 3-step data mining methodology that generates the PSM and PAM models and (iii) algorithms that perform priority queue allocation and selection of suspected lots for the inspection or its waiver.

We conclude that multi-source information fusion for the prediction models provides an excellent inspection capacity gains in the production line. These gains are very critical because they help us with additional inspection capacities that can be used by the R&D teams to perform more measurements. It is critical because newly emerging spatial variations that often result in increasing costs and lead times, require more measurements to model these variations.The production lots have the highest priority in the production line but unnecessary metrology results in increasing the production cycle times as well. So it is a win-win situation for both production and R&D engineering teams. The required inspection/metrology capacities are spared by reducing unnecessary metrology from the production and they are used by the R&D engineers to improve the technology. It helps us in reducing the production cycle times as well.

It is an important to identify the levels of the PAM and PSM models e.g. product, operation, recipe, equipment or a given technology. We also need to find an optimum policy to test the accuracy of these models based on which the self correction mechanism may be controlled, however in the proposed 3-step methodology, our self correction policy follows the defiance from PAM and PSM predictions. It requires a rigorous analysis on the alarms and states data.

5. Future perspectives

We are validating our methodology with different case studies at the world reputed IDM (integrated device manufacturer) and results shall be published soon. We are also testing our approach with the machine learning based classification and clustering algorithms in comparison with our heuristics. We shall improve our heuristics by adding the capability to compute local support on the partial likely hood with the weighted probability assignments. We believe that it shall improve the performance of our proposed heuristics. Further we are also working to take into account the usage meter data associated with each module in the equipment. The weighted probabilities shall be computed based on the usage meter to take into account the equipment status that can potentially impact the output of the production process.

The proposed approach improves the metrology/inspection tool capacities but makes it difficult to compute the process and machine Cpk and Cmk capabilities. The process capability is an excellent performance indicator to demonstrate the production robustness to the potential customers, however we believe that the newly emerging domain of VM (virtual metrology) shall provide sufficient metrology/inspection information to estimate the Cpk and Cmk indictors. The VM and yield aware metrology/inspection strategy shall help in significantly improving the capacity issues while maintaining the computation of the process and machine (Cpk, Cmk) indicators.

This domain is not yet exploited by the researchers at all and thats why that industrial engineers are using blind optimization strategies to improve the capacities. The semiconductor manufacturing domain is very complex but highly competitive and is characterized by the fastest change in the shortest possible time. The success of the future SI business model heavily depends on their capability to improve the waste of resources from non productive metrology/inspection steps. The machine learning and artificial intelligence are the domains that must come up and take control of these challenges.

References

[1] G.E. Moore, "Cramming more components onto integrated circuits," *Electronics*, vol. 38(8), 1965.

[2] A.J. Duncan, "The economic design of X-bar charts used to maintain current control of a process," *Journal of the American Statistical Association*, vol. 51(274), pp. 228-242, 1956.

[3] J.I.S. Hsu, "A cost model for skip-lot destructive sampling," *IEEE Transactions on Reliability,*, 1977.

[4] M.R. Reynolds Jr, R.W. Amin, J.C. Arnold, J.A. Nachlas, "X charts with variable sampling intervals," *Technometrics,*, vol. 30(2), pp. 181-192, 1988.

[5] C.J. Spanos, "Statistical process control in semiconductor manufacturing, " *Microelectronic Engineering,*, vol. 10(3-4), pp. 271-276, 1991.

[6] W. F. Van Raaij and T. M. M. Verhallen, "Adaptive Sampling Methodology for In-Line Defect Inspection," *Advanced Manufacturing Conference and Workshop*, 2005.

[7] C. Mouli and M. Scott, "Adaptive metrology sampling techniques enabling higher precision in variability detection and control," *Advanced semiconductor manufacturing conference,*, 2007.

[8] M. Colledani, "Integrated analysis of quality and production logistics performance in asynchronous manufacturing lines," *IFAC World Congress*, 2008.

[9] M. Colledani and T. Tolio, "Performance evaluation of production systems monitored by statistical process control and off-line inspections," *International Journal of Production Research*, 2009, doi:10.1016/j.ijpe.2007.07.011.

[10] J. Lee, "Artificial Intelligence-Based Sampling Planning System for Dynamic Manufacturing Process," *Expert Systems with Applications*, vol. 22(2), pp. 117-133, 2002.

[11] S. Dauzere-Peres, J.-L. Rouveyrol, C. Yugma and P. Vialletelle, "A Smart Sampling Algorithm to Minimize Risk Dynamically," *Advanced Semiconductor Manufacturing Conference*, 2011.

[12] M. Sahnoun, B. Bettayeb, P. Vialletelle, A. Mili and M. Tollenaere, "Impact of Sampling on W@R and Metrology Time Delay," *Intel European Research & Innovation Conference, Ireland*, 2011.

Fully Automated Quantification of Leaf Venation Structure

J. Mounsef[1], and L. Karam[2]
[1]School of Electrical, Computer & Energy Engineering, Arizona State University, Tempe, Arizona, USA
[2]School of Electrical, Computer & Energy Engineering, Arizona State University, Tempe, Arizona, USA

Abstract *- Recently, there has been a surge of diverse approaches to investigate leaf vein patterning, covering genetic analyses, pharmacological approaches and theoretical modeling. Genetic and pharmacological approaches remain at this stage insufficient for analyzing the formation of vascular patterns since the molecular mechanisms involved are still unclear. Similarly, theoretical models are not sufficiently constrained, and thus difficult to validate or disprove. Only few exceptions attempted to provide a link between experimental and theoretical studies by implementing different imaging techniques. Visual imaging methods have been lately extensively used in applications that are targeted to understand and analyze physical biological patterns, specifically to classify different leaf species and quantify leaf venation patterns. There is a rich literature on imaging applications in the above field and various techniques have been developed. However, current methods that aimed to provide high precision results, failed to avoid manual intervention and user assistance for the developed software tools. In this paper, we introduce a fully automated imaging approach for extracting spatial vein pattern data from leaf images, such as vein densities but also vein reticulation (loops) sizes and shapes. We applied this method to quantify leaf venation patterns of the first rosette leaf of Arabidopsis thaliana throughout a series of developmental stages. In particular, we characterized the size and shape of vein network reticulations, which enlarge and get split by new veins as a leaf develops. For this purpose, the approach uses imaging techniques in a fully automatic way that enables the user to batch process a high throughput of data without any manual intervention, yet giving highly accurate results.*

Keywords: *fully automation; leaf venation pattern; feature extraction; feature quantification; adaptive thresholding*

1 Introduction

Over the past few years, there has been a resurgence of interest in the leaf vein patterning. Traditional strategies include genetic analyses, pharmacological approaches, and theoretical modeling. Most recently, quantitative studies attempted to provide a link between theoretical and experimental methods. Many quantitative studies of leaf venations patterns have resurged with the sole aim of quantifying the response of plants to changing environments and to breed plants that can respond to such changes. Unfortunately, most of the suggested empirical analyses have failed to provide a quantitative study of the complete leaf vascular network [1],[2]. One major recent approach successfully provided a quantitative study of the complete leaf venation network [3]. The aforementioned approach proposed to quantify vein patterns spatially at the tissue level throughout leaf development. The venation forms a complex network composed of veins of different orders within the leaf tissue. Higher-order veins differentiate within loops that enlarge with the leaf growth. Therefore, quantifying vein patterns spatially at the tissue level in terms of loop shapes and sizes, in addition to vein densities, has brought new insights into patterning mechanisms. It has provided the necessary spatial resolution that was lacking in traditional methods. The procedure developed to extract venation patterns from leaf images consisted of measuring the leaf vascular network parameters by digitizing the vein segments using a user interface: points along each segment were recorded manually leading to a matrix representing all vein segments on the leaf. From the extracted series of vein segments, the topology of the network was calculated allowing the identification of each vein segment and loop. The number and position of branching points and free ending points were also recorded. Finally, the complete venation pattern and leaf outline for each sample was stored in matrix form. Such an approach proved to be efficient on the resolution side. Nevertheless, it is time consuming and painstaking especially when the throughput is high. The approach [3] tried to solve this issue by automatically digitizing veins using unpublished software. Nevertheless, the software was not sufficiently accurate to replace the manual technique described in [3]. Another recent work developed a user-assisted software tool (LEAF GUI) that extracts macroscopic vein structures directly from leaf images [4]. The software tool takes an image of a leaf and, following a series of interactive steps to clean up the image, returns information on the structure of that leaf's vein networks. Structural measurements include the dimensions, position and connectivity of all network veins, in addition to the dimensions, shape and position of all non-vein areas, called areoles. Although the tool is meant to enable users to automatically quantify the geometry of entire leaf networks, it unquestionably needs user assistance and intervention at

several steps of the images preprocessing, and cleaning. Many fully automated image-based algorithms have been in vain proposed for analyzing the leaf venation patterns. For instance, two approaches, one involving scale-space analysis and another including a combination of edge detectors [5], have been implemented to assess the digitization results of 5 test leaf images compared to the results of a manual technique that uses Adobe Photoshop. The main encountered problems were the presence of too many artefacts in the resulting processed images due to inappropriate smoothing and edge detection. Moreover, the scale-space technique was criticized for it resulted in broken venation structures.

Here, we propose a fully automatic approach based on the work described in [3]. Our approach is able to quantify the vein patterns of the first rosette leaf of *Arabidopsis thaliana* by processing 135 images provided by [3], without the need of any user assistance. It also stores the leaf venation pattern for every sample in a matrix, yet giving the same spatial accuracy as with the manual method, while significantly speeding the analysis process. The algorithm is developed in MATLAB and is based on different imaging analysis techniques including noise cleaning, adaptive thresholding, edge detection, and skeletonization.

2 Image analysis and pattern extraction

The image dataset collected for [3] was kindly provided to us by the authors. The available leaves images correspond to patterns of differentiated xylem elements. Fifteen leaves images were captured each day for nine days: from eight to sixteen days after sowing (DAS). The images were stored as jpg into 9 different folders corresponding to each DAS day. However, the algorithm can process any other image format (tif, gif, png, bmp).

Custom programs were developed to obtain quantitative pattern data from the first rosette leaf of Arabidopsis thaliana images using MATLAB. The main goal of our algorithm was speeding up the process of leaf venation pattern extraction while keeping the same spatial accuracy of the manual method [3]. To achieve a practical method that enables high throughput image analysis, it is essential to fully automate the software by avoiding any manual intervention. The main challenge remains the accuracy of the results without requiring any user assistance. Our task was made harder with the presence of noisy images with low contrast and uneven varying illumination resulting from the fact that the images were captured at different harvesting times (Fig. 1a). To resolve these issues, we incorporated different image processing techniques into the algorithm. The main steps performed by our algorithm are described as follows for a given input image: (1) Converting the rgb image into a grayscale image, (2) Performing homomorphic filtering of grayscale image, (3) Denoising and enhancing the grayscale image, (4) Removing border, (5) Thresholding the image, (6) Skeletonizing and processing the image, and (7) Extracting and quantifying the venation pattern features. All the steps do not require any user intervention since they are fully automated. Next we describe in details the overall process that our algorithm performs to process a leaf image and measure characteristic features of the corresponding venation structure.

Step 1: Converting the rgb image into grayscale image

When converting from an rgb image to a grayscale image, the value of each pixel in the resulting image is a single sample that only represents the intensity information. The range of intensities varies from absolute black (0) to absolute white (255).

Step 2: Homomorphic filtering of the image

To better improve the illumination and contrast of the image, homomorphic filtering is applied [6]. An image is a function that is expressed as the product of reflectance and illumination $F(x,y) = I(x,y).R(x,y)$. In order to separate reflectance and illumination, the function can be expressed as a logarithmic function wherein the product of the Fourier transform can be represented as the sum of the illumination and reflectance components $\ln(x,y) = \ln(I(x,y)) + \ln(R(x,y))$. The Fourier transform of the previous equation is $Z(u,v) = F_I(u,v) + F_R(u,v)$. A filter function H(u,v) is applied to the Fourier transformed signal where

$$H(u,v) = (\gamma_H - \gamma_L)[1 - e^{-cD(u,v)^2/Do^2}] + \gamma_L \quad (1)$$

The constant c controls the sharpness of the slope of the filter function as it transitions between γ_H and γ_L, D_0 is the cutoff frequency and D(u,v) is the distance between (u,v) and the frequency origin. H(u,v) is designed such that it tends to decrease the contribution made by low frequencies (illumination, $\gamma_L<1$) and amplify the contribution made by high frequencies (reflectance, $\gamma_H>1$). Next, the resulting function is inverse Fourier transformed. Finally, the inverse exponential operation yields an enhanced image.

Step 3: Denoising and enhancing the image

It is essential to attenuate the presence of background corresponding to the leaf blade and the rest of the image with respect to the foreground represented by the veins. Therefore, applying a denoising technique that cleans the background, which is considered as the unwanted part of the image, is crucial. A non-orthogonal wavelet denoising technique is used here [7]. One of its main characteristics is that it preserves the phase information, which is fundamental to the human visual perception. Also, this technique is capable of determining denoising threshold levels automatically. Nevertheless, the denoising step affects the venation structure for it attenuates the pixels intensities, including the vein pixels. Therefore, enhancing the image contrast is mandatory at this stage of the image processing chain. For this purpose, histogram equalization is applied, where a gray-level transform is used to flatten the histogram of the denoised image. Then, linear contrast stretching is applied to the

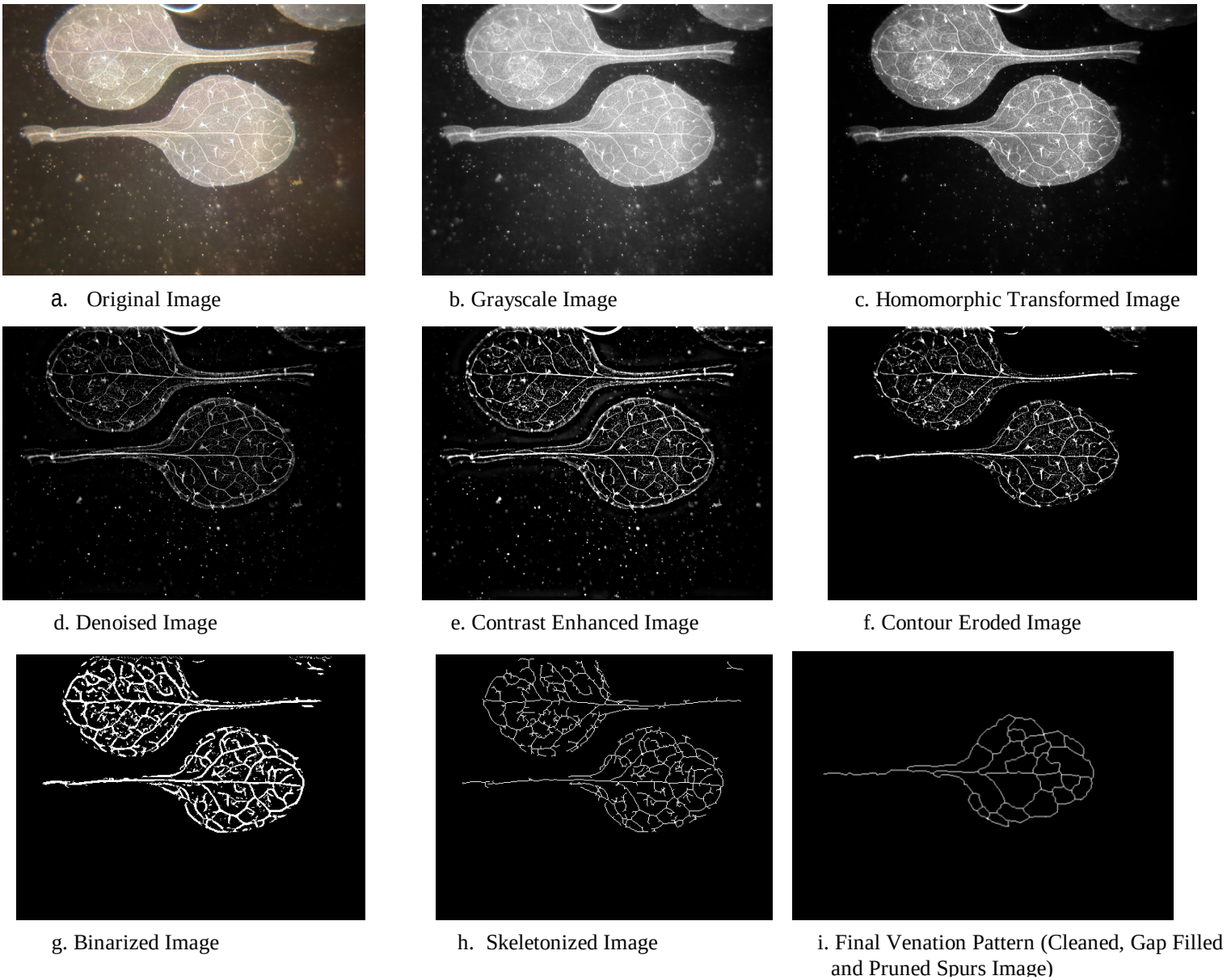

a. Original Image b. Grayscale Image c. Homomorphic Transformed Image

d. Denoised Image e. Contrast Enhanced Image f. Contour Eroded Image

g. Binarized Image h. Skeletonized Image i. Final Venation Pattern (Cleaned, Gap Filled and Pruned Spurs Image)

Figure 1. Arabidopsis leaf harvested at DAS 16: Processed images corresponding to the 7 automated steps of the leaf image processing

enhanced image where the value in the low end of the resulting histogram is assigned to extreme black (0) and the value at the high end to extreme white (1).

Step 4: Removing border

In order to remove the leaf perimeter, we need first to identify the leaf lamina from the rest of the image. This is achieved by applying global thresholding where pixels with intensities above a certain thereshold are set to 1 (leaf pixels) and pixels with values lower than the threshold are set to 0 (background pixels). The resulting image shows the entire leaf blade in white while the remaining image is black. Next, cropping is applied to the white contour corresponding to the leaf blade perimeter, by applying morphological erosion that uses a disk of n pixel diameter as a structural element. Finally, all the pixels of the eroded white area are preserved in the original image, while the values of the remaining pixels corresponding to the black area are set to 0.

Step 5: Thresholding the image

Thresholding is applied to extract the vein segments of the leaf from the rest of the image. Since leaves harvested on the same day showed uneven illumination in the same image, it was difficult to find a standard value for the threshold value that could be applicable to all images. Thus, adaptive thresholding is used by automatically calculating the

discriminative threshold from the corresponding image histogram. The histogram of any leaf image shows three main gray scale level ranges: a lower one that corresponds to the background of the image, a middle one that corresponds to the leaf blade, and a higher one that corresponds to the leaf veins. Therefore, the higher gray scale level region is of interest for our thresholding. Since the histogram showed additional peaks corresponding to the small variations resulting from high frequency noise, histogram smoothing is performed by applying a weighted averaging filter that acts as a low-pass filter for the histogram. As a result, the smoothed histogram shows three peaks that are separated by two main valley points. The value of the lowest valley point is computed by finding the gray scale level that corresponds to the first local minimum of the histogram function. After excluding the gray scale level values that are lower than the computed valley point, the resulting histogram (consisting now of two peaks) is used to find the optimal threshold separating the gray level values of the leaf blade from the gray level values of the leaf veins. Global thresholding using Otsu's method [8] is thus applied to the new histogram. The final thresholded image represents the venation pattern of the leaf.

Step 6: Skeletonizing and processing the image

Thinning is then performed by skeletonizing the resulting leaf venation structure. Skeletons represent a powerful tool for qualitative shape matching as they can effectively represent both the object shape and its topology. A thinning process is used in our approach to guarantee the condition of obtaining one-pixel thick and connected skeletons. If the skeleton is considered as a connected graph, each vertex can then be labeled as an end point or a branching point. A pixel is defined as an end point if it has a single connected pixel among its 8 neighborhood pixels. A pixel is defined as a branching point if it has more than two connected pixels among its 8 neighborhood pixels. A segment connecting two adjacent vertices is defined as a branch. Skeletonization is followed by image cleaning, which consists of removing unwanted connected blogs below a certain size threshold. For instance, all connected blog regions smaller than 10 pixels are removed.

In order to reinforce our algorithm as a fully automated technique, we need to avoid any broken contour that might result from thresholding and any extraneous spurs that might occurr after skeletonization. A gap filling function was developed to join all the disconnected edges that are supposed to be connected. The function consists of considering all end points of the skeleton and check if they were connected in the original image of the leaf before thresholding by calculating the average intensity of the pixels joining the two end points in the prethresholded image. If the computed value is lower than a preset threshold, the two end point pixels are considered not initially connected and the gap is not filled. If the computed value is higher than the threshold, then the gap between the two end point pixels is filled. This step is followed by cleaning all connected objects that are smaller than the largest connected object (venation structure). This guarantees to clean any other concomitant unwanted leaves or intruders present with the main leaf in the image, which in turn avoids the time-wasting step of manually removing any extraneous features.

On the other hand, extraneous spurs are pruned by considering all branch segments having an end point and a branching point as its vertices. If the branch segment length is smaller than a preset threshold, it is removed.

Step 7: Extracting and quantifying the venation pattern features

Using the known coordinates of the branching points and end points along each vein segment, we could record segment parameters. We could also automatically record the number and position of branching points and free-vein endings. Loops could also be identified by automatically counting the number of closed elements. The latter correspond to elements starting at one node and ending at the same visited node. The area of the blade is computed by finding the area of the white blog resulting from the aforementioned Step 4. As for the length of the venation structure, it is computed by summing the number of pixels of the final processed skeleton.

3 Results and discussion

Software was developed in the lab to extract venation patterns from leaf images. Fig. 1 shows the different images resulting from the processing steps described above. The case of a leaf harvested at DAS 16 was selected on purpose to highlight the efficiency of our algorithm when applied to a complex venation structure. Fig. 2 displays a comparison of the results between the manual and the proposed techniques. The first rosette leaves of Arabidopsis from the [3] data set grew throughout the period analyzed (from 8 to 16 days after sowing), with a decrease in growth rate after 14 days from sowing for both non-automated and automated methods (Fig. 2a). The vein density for each leaf was calculated as the total vein length across the leaf divided by the whole leaf area. The average leaf vein density is shown in Fig. 2b and shows that venation decreases over the period analyzed. The vein density has an obvious decreasing rate starting 12 days after sowing, which is consistent with the results of the non-automated approach. The mean loop number per leaf and the mean segment number per leaf for each day are shown in Figs. 2c, d. Both techniques showed similar plots where loop numbers from day 12 till day 16 and segment numbers from day 13 till day 16 were not significantly different. Free vein ending and branching point densities were calculated as number of free vein endings and branching points per unit leaf area (mm^{-2}) (Figs. 2e,f). Free vein endings showed significant similarities in mean densities of free vein endings between the plots of the non-automated and automated methods. Both techniques showed that free vein ending densities varied considerably between days. We observed comparable results for the

branching point densities where the observed increase in branching point densities between day 8 and day 10 in the automated plot (Fig. 2f) was consistent with the non-automated results.

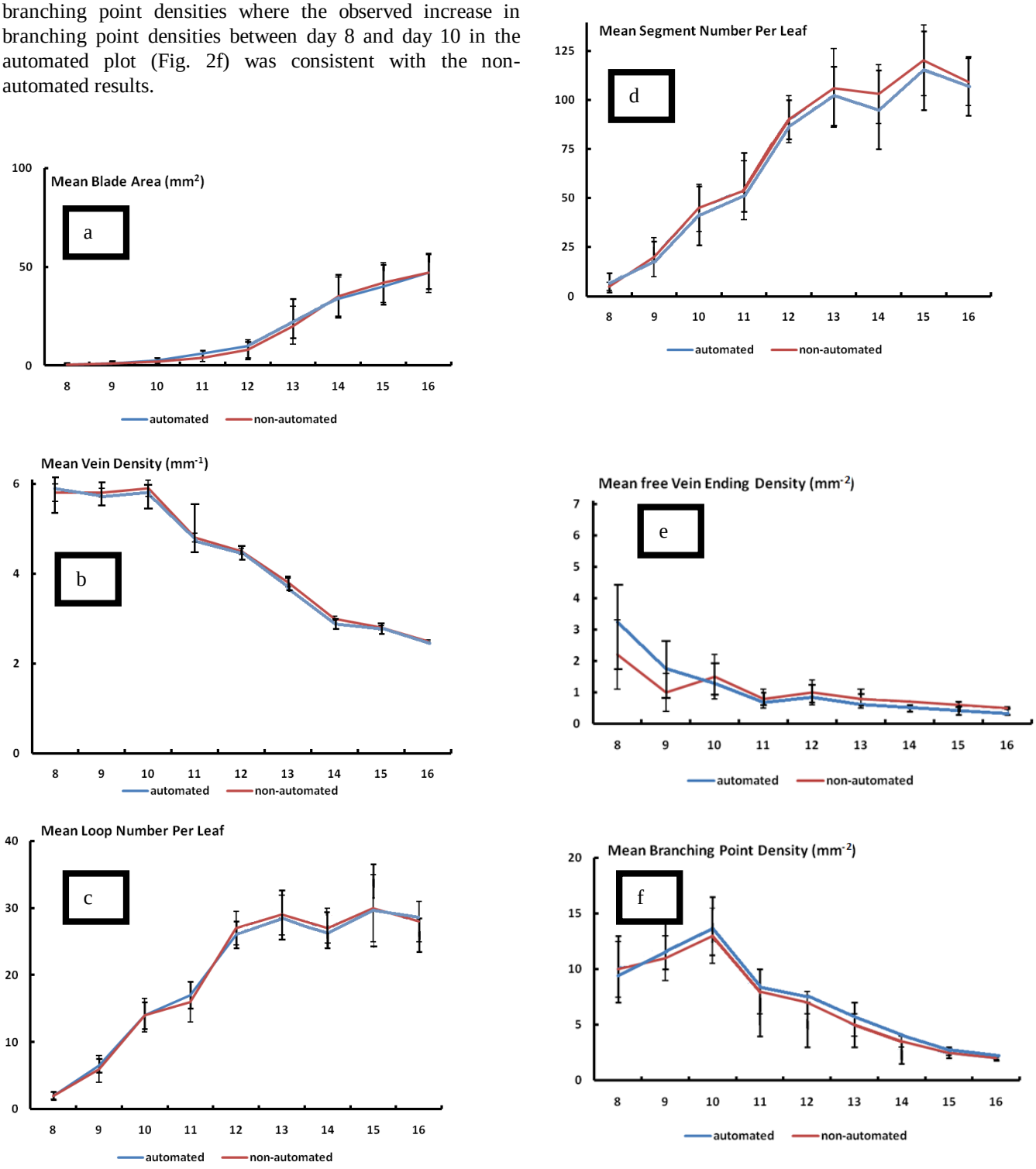

Figure 2. Plots of automated and non-automated temporal analysis of veins patterns in first rosette leaf of Arabidopsis.

4 Conclusions

We developed a method to automatically process and quantify leaf vein patterns using a series of image processing techniques and applied it to the analysis of vein pattern formation during leaf development in the first rosette leaf of Arabidopsis. Our work has the advantage of fully automating the extraction and analysis of leaf venation patterns without any user assistance. Therefore, it speeds up the analysis and allows large scale comparative analyses of vein patterning. To our knowledge, there is no available software that allows for an efficient extraction and analysis of the leaf venation

pattern using fully automated programs. Therefore, our algorithm might be considered a reliable tool that can be used by plant biologists to assess their manual results rapidly and under various conditions.

5 Acknowledgments

We would like to thank Prof. Anne-Gaëlle Rolland-Lagan for kindly providing us with the dataset of the Arabidopsis leaves and for her helpful comments on the draft of this paper.

6 References

[1] Boyce CK, Brodribb TJ, Feild TS, Zwieniecki MA (2009) Angiosperm leaf vein evolution was physiologically and environmentally transformative. Proc Biol Sci 276: 1771–1776

[2] Brodribb TJ, Feild TS (2010) Leaf hydraulic evolution led a surge in leaf photosynthetic capacity during early angiosperm diversification. EcolLett 13: 175–183

[3] Rolland-Lagan A-G, Amin M, and Pakulska M (2009) Quantifying leaf venation patterns: two-dimensional maps, The Plant Journal, vol. 57, no.1, pp.195-205

[4] Price CA, Symonova O, Mileyko Y (2011) Leaf Extraction and Analysis Framework Graphical User Interface: Segmenting and Analyzing the Structure of Leaf Veins and Areoles, Plant Physiology**,** vol. 155, no. 1, 236-245

[5] Clarke J, Barman S, Remagnino P, Bailey K, Kirkup D, Mayo S, Wilkin P (2006) Venation pattern analysis of leaf images, Lecture Notes In Computer Science, vol. 4292, pp.427-436

[6] Gonzalez R, Woods R (2001) Digital Image Processing, Second Edition, Prentice Hall

[7] Kovesi P (1999) Phase Preserving Denoising of Images, The Australian Pattern Recognition Society Conference: DICTA'99. Perth WA. pp 212-217

[8] Otsu N **(**1979) A threshold selection method from gray level histograms, IEEE Transactions on Systems, Man and Cybernetics, vol.9, no.1, pp.62-66

A Proposed Feature Extraction Method for EEG-based Person Identification

Phuoc Nguyen, Dat Tran, Xu Huang and Dharmendra Sharma
Faculty of Information Sciences and Engineering
University of Canberra, ACT 2601, Australia

Abstract— *We propose in this paper a feature extraction method to extract brain wave features from electroencephalography (EEG) signal. The proposed feature extraction method is based on an assumption that EEG signal could be considered as stationary if the time window is sufficiently short. With this assumption, EEG signal has some similar properties to speech signal and hence a feature extraction method that is currently used to extract speech features can be applied to extract brain wave features from EEG signal. Mel-frequency cepstral coefficients are features extracted and evaluated in EEG-based person identication. Experimental results show that the proposed method could provide very high recognition rate.*

Keywords: EEG, Person Identification, Brain Computer Interface

1. Introduction

Brain Computer Interface (BCI) has been considered as a new communication channel that uses brain activity as reflected by electric, magnetic or hemodynamic brain signals to control external devices such as computers, switches, wheelchairs, or neuroprosthetic extensions [1]. A BCI system can be classified as an invasive or non-invasive BCI according to the way the brain activity is being measured within this BCI. If the sensors used for measurement are placed within the brain, i.e., under the skull, the BCI is said to be invasive. On the contrary, if the measurement sensors are placed outside the head, on the scalp for instance, the BCI is said to be non-invasive [2]. The non-invasive BCI systems avoid health risks and associated ethical concerns. A typical non-invasive BCI system includes the following stages: data acquisition, data pre-processing, feature extraction, classification, device controller and feedback [3].

In invasive BCIs, electrodes or a multiunit electrode array will be placed directly inside the cortex to record electrical potentials for subsequent analysis of the electrocorticogram (ECoG). Brain signals obtained have a superior signal-to-noise ratio, need little user training, and are suitable for replacing or restoring lost motor functions in patients with damaged parts of the neuronal system [3]. Noninvasive BCIs, on the other hand, can use a variety of brain signals as input, for example, electroencephalography (EEG), magnetoencephalography (MEG), functional magnetic resonance imaging (fMRI), and near infrared spectroscopy (NIRS). MEG, fMRI, and NIRS are expensive or bulky, and fMRI and NIRS present long time constants in that they do not measure neural activity directly—relying instead on the hemodynamic coupling between neural activity and regional changes in blood flow—they cannot be deployed as ambulatory or portable BCI systems [4]. As a result, the majority of promising non-invasive BCI systems to date exploit EEG signal, mainly due to its fine temporal resolution, ease of use, portability and low set-up cost.

The use of brain wave patterns for person authentication has been investigated at IDIAP in Switzerland [5]. It has been shown that the brain-wave pattern of every individual is unique and that the EEG can be used for biometric identification [6]. The use of brain wave patterns as a new modality for person authentication has several advantages: 1) it is confidential because it corresponds to a mental task; 2) it is very difficult to mimic because similar mental tasks are person dependent; and 3) it is almost impossible to steal because the brain activity is sensitive to the stress and the mood of the person, an aggressor cannot force the person to reproduce his/her mental pass-phrase [5].

It has been shown that under the same recording condition EEG signals are low intra subject variability and high inter subject variability. In [7], [9], [10], [11] the subjects were asked to image moving hand, finger, foot or tongue while EEG data was recorded. Then the person recognition tasks were performed for each task separately. In [12] the subjects were asked to look at black and white drawings of common objects, extracted from the Snodgrass and Vanderwart picture set, while EEG signals were recording.

As indicated in [2], although numerous pre-processing, feature extraction and classification methods have been proposed and explored for BCI systems, none of them has been identified as the best method for EEG-based BCIs.

We have found that the EEG signal is a slowly time varying signal in the sense that, when examined over a sufficiently short period of time, depending on the signal between 5 and 100 ms, its characteristics are approximately stationary. However over longer periods of time, the signal characteristics are non-stationary. They change to reflect the sequence of different brain activities. Based on this "quasi-stationarity" which is also observed in speech signal, a reasonable brain wave model should have the following components. First, short-time measurements at an interval

of the order of 10 ms are to be made along the pertinent speech dimensions that best carry the relevant information for linguistic or speaker distinction. Second, because of the existence of the quasi-stationary region, the neighbouring short-time measurements on the order of 100 ms need to be simultaneously considered, either as a group of identically and independently distributed observations or as a segment of a non-stationary random process covering two quasi-stationary regions.

Based on this "quasi-stationarity", a feature extraction method that is currently used to extract speech features can be applied to extract brain wave features from EEG signal. In this paper we consider mel-frequency cepstral coefficients (MFCCs) which are the most popular speech features and extract them from EEG signal. We evaluated this feature extraction method in EEG-based person identication using support vector machine (SVM). Experimental results show that the proposed method could provide very high recognition rate.

2. Speech Features

Speech is a time varying signal. In a long period, speech signals are non-stationary but in a short interval between 5 and 100ms, the speech signals are "quasi-stationary", and the articulatory configuration stays nearly constant. Therefore, speech features are extracted for short frames. The sampled waveform is analysed in frames with short window sizes so that the signals are "quasi-stationary". The frames overlap by setting the frame period smaller than the window size. Each frame is then investigated to extract parameters. This process results in a sequence of parameter blocks [19]. source rate and target rate are the number of samples of the wave source and the number of extracted feature vectors, respectively.

In speech signal processing, the window size is typically between 15 ms and 35 ms long with a period of 10 ms. When adapting to EEG signal processing, we multiply the window size by a factor of 10 due to low frequency signal.

We define a frame of speech to be the product of a shifted window with the speech sequence [21]:

$$f_s(n;m) = s(n)w(m-n) \tag{1}$$

where $s(n)$ is the speech signal and $w(m-n)$ is a window of length N ending at sample m.

2.1 Mel-Frequency Cepstral Coefficients

The filterbank models the ability of the human ear to resolves frequencies non-linearly across the audio spectrum and decreases with higher frequencies. The filterbank is an array of band-pass filters that separates the input signal into multiple components. The filters used are triangular and they are equally spaced along the mel-scale defined by [19]:

$$\mathrm{Mel}(f) = 2595\log_{10}(1+\frac{f}{700}) \tag{2}$$

Mel-Frequency Cepstral Coefficients (MFCCs) are calculated from the log filterbank amplitudes m_j using the Discrete Cosine Transform

$$c_i = \sqrt{\frac{2}{N}}\sum_{j=1}^{n} m_j \cos\left(\frac{\pi i}{N}(j-0.5)\right) \tag{3}$$

where N is the number of filterbank channels, c_i are the cepstral coefficients.

2.2 Energy

These features model intensity based on the amplitude. The energy is computed as the average of the signal energy, that is, for speech samples $s(n), n = 1, \ldots, N$, the short-term energy of the speech frame ending at m is [20]

$$E_s(m) = \frac{1}{N}\sum_{n=m-N+1}^{m} f_s(n;m)^2 \tag{4}$$

2.3 Pitch

The pitch signal, or the glottal waveform, is produced from the vibration of the vocal folds. Two common features related to the pitch signal are the pitch frequency and the glottal air velocity [20]. The vibration rate of the vocal folds is the fundamental frequency of the phonation F_0 or pitch frequency. The air velocity through glottis during the vocal fold vibration is the glottal volume velocity. The most popular algorithm for estimating the pitch signal is based on the autocorrelation [20]. At first, the signal is low filtered at 900 Hz and then it is segmented to short-time frames of speech $f_s(n;m)$. Then the nonlinear clipping procedure that prevents the first formant interfering with the pitch is applied to each frame $f_s(n;m)$ giving

$$\hat{f}_s(n;m) = \begin{cases} f_s(n;m) - C_{thr} \text{if } |f_s(n;m)| > C_{thr} \\ 0 \text{if } |f_s(n;m)| < C_{thr} \end{cases} \tag{5}$$

with C_{thr} is about 30% of the maximum value of $f_s(n;m)$. Next the short-term autocorrelation is determined by

$$r_s(\eta;m) = \frac{1}{N}\sum_{n=m-N+1}^{m} \hat{f}_s(n;m)\hat{f}_s(n-\eta;m) \tag{6}$$

where η is the lag. Finally, the pitch frequency of the frame ending at m can be given by

$$\hat{F}_0(m) = \frac{F_s}{N}\mathrm{argmax}_\eta\{|r(\eta;m)|\}_{\eta=N(F_l/F_s)}^{\eta=N(F_h/F_s)} \tag{7}$$

where F_s is the sampling frequency, and F_l, F_h are the lowest and highest perceived pitch frequencies by humans, respectively. Normally, $F_s = 8000$ Hz, $F_l = 50$ Hz, and $F_h = 500$ Hz [20]. The maximum value of the autocorrelation $\max\{|r(\eta;m)|\}_{\eta=N_w(F_l/F_s)}^{\eta=N_w(F_h/F_s)}$ represents the glottal velocity volume.

2.4 Zero Crossing Measure

The number of zero crossings, or number of times the sequence changes sign, is also a useful feature in speech analysis. The short-term zero crossing measure for the N-length interval ending at $n = m$ is given by [21]:

$$Z_s(m) = \frac{1}{2N} \sum_{n=k}^{m} |sign\{s(n)\} - sign\{s(n-1)\}| w(m-n) \tag{8}$$

where $k = m - N + 1$ and

$$\text{sign}\{s(n)\} = \begin{cases} +1 & if \quad s(n) \geq 0 \\ -1 & if \quad s(n) < 0 \end{cases} \tag{9}$$

2.5 Probability of Voicing

Pitch detection has high accuracy for voiced pitch hypotheses but the performance degrades significantly as the signal condition deteriorates. Pitch extraction for telephone speech is more difficult because the fundamental is often weak or missing. Therefore it is more useful to provide F_0 value and probability of voicing at the same time. The hypothesis is that first, voicing decision errors will not be manifested as absent pitch values; second, features such as those describing the shape of the pitch contour are more robust to segmental misalignments; and third, a voicing probability is more appropriate than a "hard" decision of 0 and 1, when used in statistical models [22].

2.6 Jitter and Shimmer

Jitter and shimmer are micro fluctuations in vocal fold frequency and amplitude. They are correlated to rough or hoarse voice quality. The major difference is that shimmer has irregular amplitude at regular frequency while in contrast jitter has irregular frequency at regular amplitude. The wave in the top picture has irregular amplitude at the third peak and the wave in the bottom picture has irregular frequency at the second peak.

Jitter indicates cycle-to-cycle changes of the fundamental frequency and is approximated as the first derivative of the fundamental frequency [23]. These changes are considered as variations of the voice quality.

$$\text{jitter}(n) = \frac{|F_0(n+1) - F_0(n)|}{F_0(n)} \tag{10}$$

where $F_0(n)$ is the fundamental frequency at sample n. Shimmer indicates changes of the energy from one cycle to another.

$$\text{shimmer}(n) = \frac{|\text{en}(n+1) - \text{en}(n)|}{\text{en}(n)} \tag{11}$$

where $\text{en}(n)$ is energy of sample n.

3. Support Vector Machine (SVM)

3.1 Binary Case

Consider the training data $\{x_i, y_i\}$, $i = 1, ..., n$, $x_i \in R^d$, where label $y_i \in \{-1, 1\}$. The support vector machine (SVM) using C-Support Vector Classification (C-SVC) algorithm will find the optimal hyperplane [24]:

$$f(x) = w^T \Phi(x) + b \tag{12}$$

to separate the training data by solving the following optimization problem:

$$\min \frac{1}{2}\|w\|^2 + C \sum_{i=1}^{n} \xi_i \tag{13}$$

subject to

$$y_i \left[w^T \Phi(x_i) + b\right] \geq 1 - \xi_i \text{ and } \xi_i \geq 0 \ , i = 1, ..., n \tag{14}$$

The optimization problem (13) will guarantee to maximize the hyperplane margin while minimizing the cost of error, where $\xi_i, i = 1, ..., n$ are non-negative slack variables introduced to relax the constraints of separable data problems to the constraint (14) of non-separable data problems. For an error to occur the corresponding must exceed unity (see Eq. (14)), so $\sum_i \xi_i$ is an upper bound on the number of training errors. Hence an extra cost $C \sum_i \xi_i$ for errors is added to the objective function where C is a parameter chosen by the user.

The Lagrangian formulation of the primal problem is:

$$L_P = \frac{1}{2}\|w\|^2 + C \sum_i \xi_i - \sum_i \alpha_i \{y_i ({x_i}^T w + b) - 1 + \xi_i\} - \sum_i \mu_i \xi_i \tag{15}$$

We will need the Karush-Kuhn-Tucker conditions for the primal problem to attain the dual problem:

$$L_D = \sum_i \alpha_i - \frac{1}{2} \sum_{i,j} \alpha_i \alpha_j y_i y_j \Phi(x_i)^T \Phi(x_i) \tag{16}$$

subject to

$$\begin{aligned} 0 \leq \alpha_i \leq C \\ \sum_i \alpha_i y_i = 0 \end{aligned} \tag{17}$$

The solution is given by

$$w = \sum_i^{N_S} \alpha_i y_i x_i \tag{18}$$

where N_S is the number of support vectors. Notice that data only appear in the training problem, Eq. (15) and Eq. (16), in the form of dot product and can be replaced by any kernel K

with $K(x_i, x_j) = \Phi(x_i)^T \Phi(x_j)$, Φ is a mapping to map the data to some other (possibly infinite dimensional) Euclidean space. One example is Radial Basis Function (RBF) kernel $K(x_i, x_j) = e^{-\gamma \|\mathbf{x}_i - \mathbf{x}_j\|^2}$

In test phase an SVM is used by computing the sign of

$$f(x) = \sum_{i}^{N_S} \alpha_i y_i \Phi(s_i)^T \Phi(x) + b = \sum_{i}^{N_S} \alpha_i y_i K(s_i, x) + b \tag{19}$$

where s_i is the ith support vector.

3.2 Multi-class Support Vector Machine

The binary SVM classifiers can be combined to handle the multi-class case: One-against-all classification uses one binary SVM for each class to separate their members from other classes, while one-against-one or pairwise classification uses one binary SVM for each pair of classes to separate members of one class from members of the other. In one-against-one approach, there are $n(n-1)/2$ class pairs decision functions were trained. In test phase, the voting stategy was used as follow: each binary classification was considered to be a voting where votes could be cast for all data points x. The final result was the class with maximum number of votes [25].

4. Datasets

The Graz dataset IIIa in the BCI Competition 2005 (Graz IIIa 2005), Graz dataset A (Graz A 2008) and Graz dataset B (Graz B 2008) in the BCI Competition 2008 come from the Department of Medical Informatics, Institute of Biomedical Engineering, Graz University of Technology for motor imagery classification problem in BCI Competition 2005 and 2008 [26], [27], [28]. The Graz IIIa 2005 dataset contains EEG recordings of 3 subjects. Each subject was required to do cued 4 motor imagery task (left hand, right hand, foot, tongue). The recording was made with a 64-channel EEG amplifier from Neuroscan at 250 Hz with time length 7s for each trial. The Graz A 2008 dataset contains EEG recordings of 9 subjects. This dataset use the same cue-based BCI paradigm as the Graz IIIa 2005. Two sessions on different days were recorded for each subject with 288 trials per session. Twenty-two Ag/AgCl electrodes were used and the signals were sampled with 250 Hz and bandpass-filtered between 0.5 Hz and 100 Hz. The Graz B 2008 dataset consists of EEG data from 9 subjects. The subjects paticipated in two sessions contain training data without feedback (screening), and three sessions were recorded with feedback. It consisted of two classes: the motor imagery (MI) of left hand and right hand. Three bipolar recordings (C3, Cz, and C4) were recorded at sampling frequency of 250 Hz.

The dataset searched and downloaded from the web-based de-identified searchable database Australian EEG Database used in this research consists of EEG recordings of 40 patients. The database consists of EEG records recorded at the John Hunter Hospital [29], near University of Newcastle, over an 11-year period. The recordings were downloaded with the search criteria that the recordings come from the both man and women in various age. The recordings were made by 23 electrodes placed on the scalp sampled at 167 Hz for about 20 minutes.

Table 1: Dataset descriptions (#ses: number of sessions, and length: measured in seconds)

Dataset	#subjects	#tasks	#trials	#ses	length
Graz IIIa 2005	3	4	60	1	7
Graz A 2008	9	4	288	2	7.5
Graz B 2008	9	2	120	5	7.5
Australian EEG	40	free	1	1	1200
Alcoholism (large)	20	2	120	1	1
Alcoholism (full)	122	2	120	1	1

The Alcoholism datasets come from a study to examine EEG correlates of genetic predisposition to alcoholism [30]. The datasets contain EEG recordings of control and alcoholic subjects. Each subject was exposed to either a single stimulus (S1) or to two stimuli (S1 and S2) which were pictures of objects chosen from the 1980 Snodgrass and Vanderwart picture set. When two stimuli were shown, they were presented in either a matched condition where S1 was identical to S2 or in a non-matched condition where S1 differed from S2. The 64 electrodes placed on the scalp sampled at 256 Hz for 1 second. The Alcoholism large dataset contains training and test data for 10 alcoholic and 10 control subjects. The Alcoholism full dataset contains 120 trials for 122 subjects. The summary of those datasets is listed in Table 1.

5. Feature Extraction

We used the open-source Emotion and Affect Recognition toolkit's feature extracting backend openSMILE [31] for extracting brain wave features. Each channel is extracted features individually and then features from all channels are merged together. The features include MFCCs, spectral features, energy, pitch (F0), zero crossing rate, probability of voicing, jitter and shimmer and their statistics functionals [32].

The 8 channels selected are C3, Cz, C4, P3, Pz, P4, O1, O2 which are an extension of [9], except for The Graz B 2008 dataset which has only three channels C3, Cz and C4. Because of the resulting high dimensionality the Correlation-based Feature Selection with Sequential Floating Forward Selection is used [33].

Except for the Graz datasets which have separated training and testing sets, the Australian EEG dataset and the Alcoholism datasets used 1/3 for cross validation training and 2/3 for testing. Linear SVM classifiers [25] is trained in 3-folds

cross validation scheme with parameter C ranges from 1 to 1000 in 5 steps.

6. Experimental Results

Person identification rates in test phase are 99% on Graz IIIa 2005, 80.8% on Graz B 2008, 46.24% on Graz A 2008, 92.8% on Alcoholism large and 61.7% on Alcoholism full datasets. Tables 2, 3 and 4 show the confusion matrices for the Graz datasets. Results show high identification rate on Graz IIIa 2005 and Graz B 2008. However it is not high on Graz A 2008. The reasons could be that the data for training is not enough when there is high variation in data (4 imagery tasks), and the training data should come from different sessions in order to have good performance in test phase.

Table 2: Confusion matrix in test phase on Graz dataset IIIa BCI Competition 2005. Identification rate is 99%.

Classified as →	k3b	k6b	l1b
k3b	149	0	0
k6b	0	83	0
l1b	0	3	80

Table 3: Confusion matrix in test phase on Graz data set A, BCI Competition 2008. Identification rate is 46.24%.

→	A1	A2	A3	A4	A5	A6	A7	A8	A9
A1	219	9	42	0	11	0	0	0	0
A2	0	96	108	0	0	0	36	43	0
A3	5	9	244	0	3	0	0	12	0
A4	10	12	11	148	43	4	0	0	0
A5	0	0	0	0	0	0	276	0	0
A6	0	6	0	2	0	194	0	0	13
A7	221	14	0	0	15	23	0	4	0
A8	0	6	86	0	0	1	0	178	0
A9	0	0	0	0	0	217	0	31	16

Table 4: Confusion matrix in test phase on Graz dataset B, BCI Competition 2008. Identification rate is 80.8%.

→	B1	B2	B3	B4	B5	B6	B7	B8	B9
B1	221	2	0	0	5	0	0	0	0
B2	20	66	0	2	91	0	12	3	51
B3	0	0	230	0	0	0	0	0	0
B4	0	0	0	141	1	0	146	16	3
B5	1	30	0	0	242	0	0	0	0
B6	0	0	0	0	1	250	0	0	0
B7	0	0	0	0	0	0	206	0	26
B8	4	2	0	6	6	0	0	212	0
B9	0	0	0	2	0	0	0	0	243

Figure 1 shows the identification rate on Australian EEG database using a single channel Cz and 8 channels C3, Cz, C4, P3, Pz, P4, O1 and O2. For a single channel case, the EEG recording length should be at least 7 seconds for the person to be recognizable. The identification rate has a peak of 94% at 15 seconds length then slowly decreases and climbs up again. The use of 8 channels shows stable performance 97% at recording length from 3 to 60 seconds and shows higher performance of 99% at recording length longer than 90 seconds.

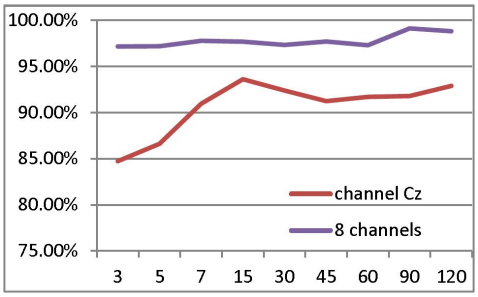

Fig. 1: Identification rate (in %) versus segment length on Australian EEG dataset

Person identification rates on Alcoholic large and Alcoholic full show that a single channel can hardly recognise the subjects. The use of 8 channels have high performance 92.8% in identification of 20 subjects and it can classify 122 subjects.

Table 5: Accuracies on dataset Alcoholic large and Alcoholic full using a single channel Cz and 8 channels C3, Cz, C4, P3, Pz, P4, O1, O2.

	Alcoholic large		Alcoholic full	
	channel Cz	8 channels	channel Cz	8 channels
Cross validation	52.50%	100%	21.87%	99.68%
Test	34.50%	92.83%	18.36%	61.59%

7. Conclusion

We have proposed a speech-based approach to brain wave feature extraction and used the proposed features to identify person. A single channel with appropriate recording time interval can be used in person identification task. The set 8 channels can give very good identification performance. For future investigation, other speech feature extraction methods will be applied to brain wave feature extraction.

References

[1] F. Babiloni, A. Cichocki, and S. Gao, "Brain-Computer Interfaces: Towards Practical Implementations and Potential Applications", Computational Intelligence and Neuroscience, Volume 2007, Article ID 62637, 2 pages, 2007.

[2] F. Lotte, M. Congedo, A. LÃl'cuyer, F. Lamarche, and B. Arnaldi, "A review of classification algorithms for EEG-based brainâĂŞcomputer interfaces", Journal of Neural Engineering, 4 R1, 2007.

[3] R. Krepki, G. Curio, B. Blankertz, K.-R. Muller, "Berlin Brain-Computer Interface-The HCI communication channel for discovery", International Journal of Human-Computer Studies, vol. 65, no. 5, pp. 460-477, 2007.

[4] A. Cichocki, Y. Washizawa, T. Rutkowski, H. Bakardjian, A. Phan, S. Choi, H. Lee, Q. Zhao, L. Zhang, and Y. Li, "Noninvasive BCIs: Multiway Signal-Processing Array Decompositions". Computer vol. 41, no. 10, pp. 34-42, 2008.

[5] Marcel, S. and Millan, J. d., Person Authentication Using Brainwaves (EEG) and Maximum A Posteriori Model Adaptation. IEEE Trans. Pattern Analysis and Machine Intelligence, 29(4), 743-752, 2007.

[6] Wang, Z., A hybrid SVMâĂŞGLM approach for fMRI data analysis, Neuro Image, vol. 46, pp. 608âĂŞ615, 2009.

[7] S. Sun , "Multitask learning for EEG-based biometrics," Pattern Recognition, 2008. ICPR 2008. 19th International Conference on , vol., no., pp.1-4, 8-11 Dec. 2008

[8] M. A. Lebedev, and M. A.L. Nicolelis, Brain-machine interfaces: past, present and future. TRENDS in Neurosciences: Elsevier, 2006.

[9] X. Bao, J. Wang, J. Hu, "Method of individual identification based on electroencephalogram analysis, New Trends in Information and Service Science", 2009. NISS '09. International Conference on, pp. 390-393, 2009.

[10] J. F. Hu, "New biometric approach based on motor imagery EEG signals, BioMedical Information Engineering", 2009. FBIE 2009. International Conference on Future, 2009

[11] D. Jiang, J. Hu, "Research of Computing in EEG Password based on Wavelet". International Conference on Future BioMedical Information Engineering, 2009

[12] K. Bringham and B. V. K. V. Kumar, "Subject Identification from Electroencephalogram (EEG) Signals During Imagined Speech", 4th BTAS, 2010.

[13] R. Palaniappan and D. P. Mandic, "Biometrics from brain electrical activity: A machine learning approach," IEEE Trans. Pattern Anal., vol. 29, no. 4, 2007.

[14] R. Palaniappan, "Identity Verification using Resting State Brain Signals". Encyclopedia of Information Ethics and Security 2007

[15] R. Palaniappan, "Two-stage biometric authentication method using thought activity brain waves, International Journal of Neural Systems", vol. 18, no. 1, 2008.

[16] F. Bimbot et. al., "A Tutorial on Text-Independent Speaker Verification". EURASIP Journal on Applied Signal Processing, 2004

[17] D.A. Reynolds, R.C. Rose; , "Robust text-independent speaker identification using Gaussian mixture speaker models," Speech and Audio Processing, IEEE Transactions on , vol.3, no.1, pp.72-83, Jan 1995

[18] "The INTERSPEECH 2009 Emotion Challenge". B. Schuller, S. Steidl, A. Batliner, INTERSPEECH, 2009

[19] S. Young, G. Evermann, D. Kershaw, G. Moore, J. Odell, D. Ollason, D. Povey, V. Valtchev, and P. C. Woodland. "The HTK Book (for HTK Version 3.4)", 2009.

[20] Dimitrios Ververidis and Constantine Kotropoulos. "Emotional speech recognition: Resources, features, and methods". Speech Communication, **48**(9):1162–1181, 2006.

[21] J. R. Deller, J. H. L. Hansen, and J. G. Proakis. "Discete-Time Processing of Speech Signals". Wiley, N.Y, 2000.

[22] W. Chao and S. Seneff. "Robust pitch tracking for prosodic modeling in telephone speech". In Acoustics, Speech, and Signal Processing, 2000. ICASSP '00. Proceedings. 2000 IEEE International Conference on, pages 1343–1346 vol.3, 2000.

[23] S. Steidl, "Automatic Classification of Emotion-Related User States in Spontaneous Children's Speech". PhD thesis, 2009.

[24] C. J. C. Burges, "A tutorial on support vector machines for pattern recognition". Data Mining and Knowledge Discovery, 1998.

[25] Chih-chung Chang and Chih-Jen Lin. LIBSVM: a Library for Support Vector Machines, 2001.

[26] G. Pfurtscheller, A. SchlÃűgl, Dataset IIIa: 4-class EEG data. Available on line at http://www.bbci.de/competition/iii/

[27] C. Brunner, R. Leeb, G. R. MÃijller-Putz, A. SchlÃűgl, and G. Pfurtscheller, BCI Competition 2008 - Graz data set A. Available online at http://www.bbci.de/competition/iv/

[28] R. Leeb, C. Brunner, G. MÃijller-Putz, A. SchlÃűgl, G. Pfurtscheller, BCI Competition 2008 - Graz data set B. Available online at http://www.bbci.de/competition/iv/

[29] M. Hunter, R. Smith, W. Hyslop, O. Rosso, R. Gerlach, J. Rostas, D. Williams, and F. Henskens, "The Australian EEG database", Clin EEG Neurosci, vol. 36, no. 2, pp. 76âĂŞ81, 2005.

[30] H. Begleiter, EEG Database. Available online at http://kdd.ics.uci.edu/databases/eeg/eeg.data.html

[31] F. Eyben, M. WÃűllmer, and B. Schuller. OpenEAR - Introducing the Munich open-source emotion and affect recognition toolkit. Proceedings - 2009 3rd International Conference on Affective Computing and Intelligent Interaction and Workshops, ACII 2009, 2009

[32] B. Schuller, S. Steidl, A. Batliner, F. Schiel, J. Krajewski, "The Interspeech 2011 Speaker State Challenge, Interspeech (2011)", ISCA, Florence, Italy, 2011.

[33] M. Hall, E. Frank, G. Holmes, B. Pfahringer, P. Reutemann, and I. Witten. "The WEKA data mining software: an update". SIGKDD Explor, 2009.

[34] L. I. Kuncheva and J. J. Rodriguez, "Classifier ensembles for fMRI data analysis: an experiment, Magnetic Resonance Imaging", vol. 28, no. 4, pp. 583-593, 2010.

[35] A. Riera, A. Soria-Frisch, M. Caparrini,C. Grau, and G. Ruffini, "Unobtrusive Biometric System Based on Electroencephalogram Analysis". EURASIP Journal on Advances in Signal Processing, 2008.

[36] A. ZÂt'uquete, B. Quintela, J. P. S. Cunha, "Biometric authentication using brain responses to visual stimuli". Proceedings of the International Conference on Bio-inspired Systems and Signal Processing, 2010.

[37] C. Miyamoto, S. Baba and I. Nakanishi, "Biometric person authentication using new spectral features of electroencephalogram (EEG)". International Symposium on Intelligent Signal Processing and Communication Systems (ISPACS2008), 2008

[38] S. Sanei and J. Chambers, EEG signal processing, 2007.

[39] R. B. Paranjape, J. Mahovsky, L. Benedicenti, and Z. Koles, "The electroencephalogram as a biometric, Proc. Canadian Conf". Electrical and Computer Eng., vol. 2, 2001.

[40] M. Poulos, M. Rangoussi, V. Chrissikopoulos, and A. Evangelou, "Person identification based on parametric processing of the EEG", Electronics, Circuits and Systems, 1999. Proceedings of ICECS '99. The 6th IEEE International Conference on, vol.1, 1999.

[41] M. A. Lebedev, and M. A.L. Nicolelis, Brain-machine interfaces: past, present and future. TRENDS in Neurosciences: Elsevier, 2006.

[42] B. Blankertz et.al., The BCI Competition 2003: Progress and Perspectives in Detection and Discrimination of EEG Single Trials, 2003.

A Comparison on How Statistical Tests Deal with Concept Drifts

Paulo M. Gonçalves Jr.[1,2], **Roberto S. M. Barros**[1]
[1]Centro de Informática, Universidade Federal de Pernambuco, Cidade Universitária, 50.740-560, Recife, Brasil
[2]Instituto Federal de Pernambuco, Cidade Universitária, 50.740-540, Recife, Brasil

Abstract— RCD *is a framework proposed to deal with recurring concept drifts. It stores classifiers together with a sample of data used to train them. If a concept drift occurs,* RCD *tests all the stored samples with a sample of actual data, trying to verify if this is a new context or an old one that is recurring. This is performed by a non-parametric multivariate statistical test to make the verification. This paper describes how two statistical tests (*KNN *and Cramer) can distinguish between new and old contexts.* RCD *is tested with several base classifiers, in environments with different rates-of-change values, with gradual and abrupt concept drifts. Results show that* RCD *improves single classifiers accuracy independently of the statistical test used.*

Keywords: Multivariate non-parametric statistical tests, concept drifts, data streams.

1. Introduction

Concept drift is a situation that frequently occurs in data streams environments [1]. One informal definition, as stated by Kolter and Maloof [2], informs that "concept drift occurs when a set of examples has legitimate class labels at one time and has different legitimate labels at another time." Another definition of concept drift describes that, in machine learning, "the term concept refers to the quantity that a learning model is trying to predict, i.e., the variable. Concept drift is the situation in which the statistical properties of the target concept change over time." [3]

Therefore, dealing with concept drift is a task of increasing importance to the areas of data mining and machine learning, as increasing amounts of data are being stored in the form of data streams instead of static databases. Also, it is not very common for data distributions and concepts to keep stable over a long period of time [4], [5].

This paper extends Recurring Concept Drifts (RCD) framework [6] with the implementation of the Cramer multivariate statistical test [7], and shows how it compares to tests using KNN [8]. The performance of the implemented tests were analyzed in terms of accuracy and evaluation time. RCD was tested with several base classifiers in commonly used data sets in the concept drift research area, including abrupt and gradual concept drifts.

The rest of this paper is organized as follows: Section 2 presents approaches to deal with concept drifts, algorithms, and how they work. Section 3 briefly describes how RCD works. Section 4 presents the algorithms used in the comparison, the parameters set, and the data sets used in the tests. Section 5 presents the accuracy, number of detected concept drifts, and evaluation time between RCD and the other algorithms in the selected data sets. Finally, Section 6 presents our conclusions and proposes future work.

2. Background

There are several approaches to handle concept drifts. One is to create a model that adapts its internal structure as instances arrive. CVFDT (Concept-adapting Very Fast Decision Tree) [9] is an example. It extends VFDT [10] to handle concept drifts. VFDT is a decision tree built to deal with data stream and uses a *Hoeffding bound* [11], [12], to decide exactly how many examples are necessary at each node to find the best attribute to test. VFDTc [13] is another proposal, which also extends VFDT with the ability to deal with continuous attributes and the use of naive Bayes classifiers at tree leaves. OcVFDT (One-class Very Fast Decision Tree) [14] is an algorithm to extend VFDT to deal with one-class problems, based on the fact that fully labeled data streams are expensive to obtain. It only deals with discrete attribute values.

Another common approach to deal with concept drifts is to identify when it occurs and create a new classifier. Thus, only classifiers trained on a current concept are maintained. Algorithms that follow this approach work in the following way: each arriving training instance is first evaluated by the base classifier. Internal statistics are updated with the results and two thresholds are computed: a warning level and an error level. As the base classifier makes mistakes, the warning level is reached and instances are stored. If the behavior continues, it will reach the error level, indicating that a concept drift has occurred. At this moment, the base classifier is destroyed and a new base classifier is created and initially trained on the stored instances. On the other hand, if the classifier starts to correctly evaluate instances, this situation is considered a false alarm and stored instances are flushed. Algorithms that follow this approach can work with any type of classifier as they only analyze how the classifier evaluates instances. Proposals that use this approach are DDM (Drift Detection Method) [15], EDDM (Early Drift Detection Method) [16], and ECDD (Exponentially Weighted Moving Average for Concept Drift Detection) [17].

Several proposals try to deal with concept drifts by the use of ensemble classifiers. This approach maintains a collection

of learners and combine their decisions to make an overall decision. To deal with concept drifts, ensemble classifiers must take in account the temporal nature of the data stream.

One of these proposals was the Streaming Ensemble Algorithm (SEA) [18]. It builds separate classifiers, each one trained on a different sequential chunk of data. These classifiers are then combined into a fixed-size ensemble using a heuristic replacement strategy. If there is free space in the ensemble, SEA adds the newly created classifier to the ensemble. If the ensemble is full, the new classifier is only added if it outperforms a stored classifier, substituting it. The performance is measured on the current batch of examples.

The Accuracy Weighted Ensemble (AWE) classifier [19] is another proposal of ensemble classifier. It uses batch classifiers and each one is built in different chunks of data. Classifiers weights are computed based on their expected accuracy in test data. Thus, they proposed to infer the weights by estimating the error rate in the most recent data blocks.

Accuracy Updated Ensemble (AUE) [20] is an enhancement of the AWE classifier. Both use classifier ensembles and associate to them weights that are updated as data arrive. AUE improves AWE in three directions: (a) Instead of batch classifiers, AUE uses on-line classifiers, which adapt to data while they arrive; (b) AUE updates both classifiers and their weights, while AWE only updates the weights; (c) AUE changed the weight computation to avoid situations where no classifier should have precision higher than the stipulated threshold, as in abrupt concept drifting environments, zeroing the weights of all classifiers and no class being predicted.

The Weighted Majority Algorithm (WMA) [21] implements a weighted ensemble classifier, which extends previous work [22] to specifically handle concept drifts. In WMA all the arriving instances are passed to all the classifiers in the ensemble. The initial weight of the classifiers is 1, and, if a classifier makes an error, its weight is reduced by a factor of β if higher than a specified minimum threshold. Then, the classifier is trained. After all the ensemble classifiers have been trained, their weights are normalized.

Dynamic Weighted Majority (DWM) [2] is another example of ensemble classifier. It extends WMA to add and remove classifiers according to the algorithms global and local performance. If the ensemble commits an error, then a classifier is added. If one classifier commits an error, its weight is reduced. If after many examples a classifier continues with a low accuracy, indicated by a low weight, it is removed from the ensemble. This method is general and, in principle, can be used with any classifier.

A common situation regarding concept drifts is its recurrence. It happens when the actual context is similar to a previously seen context. One approach commonly used to treat recurring concept drifts is to store information about the contexts, and continuously identify if actual context is similar to old contexts. If it is so, obtain stored information and use it again, as it is expected that it also represents actual context. Algorithms that use this approach to deal with context recurrence are FLORA [4], Prediction Error Context Switching (PECS) [23], and SPLICE [24].

3. The RCD Framework

The RCD framework, proposed in [6], deals with concept drifts by storing classifiers together with data samples used to train the classifiers. It starts with one single classifier and uses a concept drift detector, like DDM or EDDM for example, to identify the occurrence of a concept drift. While no drift is detected, the arriving instances are used to train the actual classifier and are stored in a FIFO data buffer with fixed length. If the drift detector enters the warning level, RCD stops storing instances in the classifier's buffer and stores them in a new buffer. If the error level is reached, indicating a concept drift, a multivariate non-parametric statistical test is performed to compare the instances obtained in the warning level with the instances associated to each classifier to identify if both samples come from the same data distribution. If not, a new classifier is stored alongside with the instances in the new buffer. If both samples come from the same data distribution, it is considered that this is an old concept that is occurring again. In this situation, the stored classifier is used as the actual classifier.

In [6], besides presenting how RCD works, we also show how RCD deals with concept drifts, comparing it with single and ensemble classifiers in environments with abrupt and gradual concept drifts. Artificial and real world data sets were tested using KNN as statistical test.

In this paper, RCD is tested using different base learners, in four different artificial data sets, with abrupt and gradual concept drift with various rates-of-change, and three real world data sets. One new implemented statistical test, Cramer, is also analyzed. It was based on the implementation of the Cramer package [7] of The R Project for Statistical Computing [25] tool.

RCD was configured with the following parameters: classifiers buffer size (100), test frequency (500), maximum number of classifiers to store (15), concept drift detection method (DDM), and minimum amount of similarity between distributions (0.05). RCD was implemented using of the MOA framework [26]. Instructions on how to download and use RCD can be found at `https://sites.google.com/site/moaextensions/`.

4. Algorithms and Datasets

In this section we present the algorithms used in the tests, their parameters, and information about the data sets.

4.1 Algorithms

Three base learners were used to test RCD: Hoeffding tree with naive Bayes at the leaves [13], naive Bayes, and

Multilayer Perceptron (MLP). From now on we will reference the decision tree as HTNB. We tested each base learner against RCD with KNN and Cramer statistical tests.

The parameters used by HTNB in the experiments are the default values present in the MOA framework: number of instances a leaf should observe between split attempts (200), split criterion to use (information gain), allowable error in split decision (10^{-7}), and threshold below which a split will be forced to break ties (0.05).

The parameters used by MLP in the experiments are the default values present in the WEKA tool [27]: learning rate (0.3), momentum (0.2). Only the number of epochs to train was reduced from 500 to 100 to increase its speed.

The following sections presents the data sets used in the comparison of the framework. The data sets used are well known in the field and have been used in several previous experiments.

4.2 Artificial data sets

We first describe the artificial data sets used to test the algorithms. All these data sets are available through the MOA framework.

4.2.1 Hyperplane

Hyperplane [9] is an artificial data set that simulates concept drifts through a moving hyperplane. A hyperplane in a d dimensional space is the set of points x that satisfies $\sum_{i=1}^{d} w_i x_i = w_0$, where x_i is the i^{th} coordinate of x. Examples where $\sum_{i=1}^{d} w_i x_i \geq w_0$ are classified as positive, and examples where $\sum_{i=1}^{d} w_i x_i < w_0$ are classified as negative. Hyperplanes are used to simulate gradual concept drifts where it is possible to smoothly change the orientation and position of the hyperplane by modifying its weights. It is possible to introduce changes in the data set changing the weight of each attribute $w_i = w_i + d\sigma$, where σ is the chance the direction of change be inverted and d is the amount of change applied to each example.

4.2.2 LED

The LED [28] data set represents the problem of predicting the digit shown by a seven-segment LED display. It is composed of 24 nominal attributes, where 17 are irrelevant, and one nominal class with ten possible values. Noise was added by including a 10% probability of each attribute being inverted. The version of LED used in the experiments is available at MOA that includes concept drifts to the data sets by simply changing the attributes positions. The number of drifting attributes chosen were 1, 3, 5, and 7.

$$(((LED_1 \oplus_{t_0}^{W} LED_3) \oplus_{2t_0}^{W} LED_5) \oplus_{3t_0}^{W} LED_7)$$

4.2.3 SEA

The SEA [18] concepts are commonly used to test abrupt concept drifts. The values of each of its three attributes are in the interval [0,10), but the third one is irrelevant. In each concept, a data point belongs to class 1 if $f_1 + f_2 \leq \theta$, where f_l and f_2 represent the first two features and θ is a threshold value between the two classes. For the experiments, we used the thresholds proposed by [18]: 8, 9, 7, 9.5 to represent four concepts. Noise was inserted by randomly changing the class value of 10% of the instances. In the following tests, SEA concepts are defined as follows:

$$(((SEA_9 \oplus_{t_0}^{W} SEA_8) \oplus_{2t_0}^{W} SEA_7) \oplus_{3t_0}^{W} SEA_{9.5})$$

4.2.4 Random RBF

RBF (Radial Basis Function) [29] creates complex concept drifts that are not straightforward to approximate with a decision tree model. It works as follows: a fixed number of random centroids are generated where each center has a random position, a single standard deviation, a class label and a weight. New examples are generated by selecting a center at random, taking weights into consideration so that centers with higher weight are more likely to be chosen. A random direction is chosen to offset the attribute values from the central point. The length of the displacement is randomly drawn from a Gaussian distribution with standard deviation determined by the chosen centroid. The chosen centroid also determines the class label of the example. This effectively creates a normally distributed hypersphere of examples surrounding each central point with varying densities. Only numeric attributes are generated. Drift is introduced by moving the centroids with constant speed. This speed is initialized by a drift parameter.

4.3 Real data sets

Here we present three real data sets used in the experiments. It is not easy to find large real-world datasets for public benchmarking, especially with substantial concept change. Another problem is that we do not know when drift occurs or if there is any drift at all. The data sets used are: Forest Covertype [30], Poker-Hand [29], and Electricity [15]. They were obtained from the MOA web site, in the following address: `http://moa.cs.waikato.ac.nz/`.

4.3.1 Forest Covertype

This data set contains the forest cover type for 30 x 30 meter cells obtained from US Forest Service (USFS) Region 2 Resource Information System (RIS) data. The goal is to predict the forest cover type from cartographic variables. It contains 581,012 instances and 54 attributes.

4.3.2 Poker Hand

The Poker Hand data set is constituted of five categoric and five numeric attributes plus one categoric class with 10 possible values informing the value of the hand, for example, one pair, two pairs, a sequence, a street flush, etc. It represents the problem of identifying the value of five cards in the Poker game. Bifet [31] describes that "in the Poker hand data set, the cards are not ordered, i.e., a hand can be represented by any permutation, which makes it very hard for propositional learners, especially for linear ones". So, in the experiments, we used a modified version, where the cards are sorted by rank and suit, and duplicates were removed. This data set is composed of 829,201 instances.

4.3.3 Electricity

This data set presents data collected from the Australian New South Wales Electricity Market. In that market, prices vary according to market demand and supply. Prices are set every five minutes and the class label identifies the change of the price related to a moving average of the last 24 hours. The goal of the problem is to predict if the price will increase or decrease. It is composed of 45,312 instances.

5. Empirical Study and Results

The evaluation methodology used in the presented data sets were the Interleaved Test-Then-Train approach. Every example is used for testing the model, then it is used to train it. The accuracy was measured as the final percentage of instances correctly classified over the interleaved evaluation. For the Hyperplane and Random RBF data sets, 10 million instances were generated; for LED and SEA, 1 million instances. The experiments were repeated 10 times. The parameters of these streams are the following:

- RBF(x, v): Random RBF data stream with x centroids moving at speed v.
- HYP(x, v): Hyperplane data stream with x attributes changing at speed v.
- SEA(v): SEA data set, with length of change v.
- LED(v): LED data set, with length of change v.

The chosen evaluation methodology, data sets, and configurations are exactly the same as used in [29], [31]. For the tests, we used an Intel Core i3 330M processor (with two cores and emulating two other), with 4GB of main memory.

Table 1 presents how long each statistical test needs to evaluate samples of sizes varying from 100 to 300 instances. Samples were obtained from the Electricity data set. We can see that the time spent by the Cramer test almost doubles each time the sample size is increased by 50 instances while KNN is less impacted. Comparing both tests, it is clear that KNN is considerably faster than Cramer performing the statistical tests. Thus, considering the data set sizes used in the experiments (1 to 10 million, with 10 repetitions), the buffer size used in RCD was 100 to increase its speed.

Table 1: Evaluation time using statistical tests (in seconds).

	100	150	200	250	300
Cramer	0.413	0.947	1.835	3.263	6.375
KNN	0.003	0.007	0.012	0.017	0.024

Tables 2, 3 and 4 present the average evaluation times in seconds and the accuracy of the HTNB, naive Bayes and MLP base classifiers, respectively. For the artificial data sets, the accuracy also contains the 95% confidence interval. The second column presents the results for the base classifier, the third one, RCD using the Cramer test, and the latter, RCD using the KNN test. The last column of Cramer and KNN presents the average number of drifts detected in all repetitions in the artificial data sets, and the total number of drifts in the real-world data sets. Best results in performance are highlighted in boldface and the values marked by an asterisk (*) represent statistically significant differences between RCD and the base learner.

Analyzing the results presented at Table 2, it is possible to observe that RCD outperformed the HTNB base classifier in the majority of the artificial data sets, independently of the statistical test used. Statistically, RCD had better performance in HYP(10,0.0001), HYP(10,0.001) (when using the KNN statistical test), and in the Random RBF configurations with 50 centroids. In all the other configurations, both algorithms had statistical similar performances.

In the Random RBF configuration without concept drifts, RBF(0,0), all algorithms had exactly the same results. This is an expected result of RCD because, when no concept drift is detected, no statistical test is performed and RCD performs the same as the base learner. In the other RBF data sets with concept drift, the configurations that RCD performed better than the base learner was the ones with 50 centroids. For this data set, the higher the number of moving centroids, the bigger the number of concept drifts. Thus, RCD had better performance exactly in the configurations with higher number of concept drifts while in the configurations with 10 centroids, the ones with lower number of concept drifts, the performances were similar.

It is possible to check the influence of the number of moving centroids compared to the average number of detected concept drifts in each configuration. In the RBF(50,0.001) configuration, using the Cramer test, 17.2 concept drifts were detected, while using KNN there were 15.4 in the ten repetitions. In the RBF(10,0.001) configuration, only 0.4 and 0.3 concept drifts were detected using the Cramer and KNN statistical tests, respectively, in the ten repetitions.

Comparing the usage of the two statistical tests, KNN had a better performance in two data sets: in RBF(50,0.0001), and in the LED data set. In the rest, both statistical tests had comparable performances. Analyzing the number of detected concept drifts, KNN is much more sensible than Cramer. Using KNN, 40,480 concept drifts were detected

Table 2: Results using the HTNB base classifier.

	HTNB		RCD HTNB CVM			RCD HTNB KNN		
	Time	**Accuracy**	**Time**	**Accuracy**	**# Drifts**	**Time**	**Accuracy**	**# Drifts**
RBF(0,0)	162.45	93.04±0.07	224.93	93.04±0.07	0.0	221.38	93.04±0.07	0.0
RBF(50,0.001)	247.17	55.27±0.04	392.35	55.37±0.11*	17.2	451.63	**55.47±0.15***	15.4
RBF(10,0.001)	178.06	88.29±0.08	242.27	**88.30±0.09**	0.4	238.70	88.29±0.09	0.3
RBF(50,0.0001)	258.82	63.40±0.08	380.44	64.39±0.27*	87.9	292.93	**69.90±2.69***	125.0
RBF(10,0.0001)	180.57	**89.37±0.07**	247.55	89.35±0.09	0.8	241.56	89.36±0.08	0.9
HYP(10,0.001)	182.55	88.71±1.83	261.13	89.06±1.47	8.0	246.00	**89.01±1.56***	8.9
HYP(10,0.0001)	181.44	89.01±0.61	251.45	89.24±0.50*	10.4	243.27	**89.18±0.58***	10.6
SEA(50)	6.87	88.67±0.85	9.93	**89.20±0.19**	0.7	9.78	**89.20±0.19**	0.7
SEA(50000)	6.78	88.68±0.85	9.84	**89.19±0.22**	0.9	9.66	**89.19±0.22**	0.9
LED(50000)	26.14	73.24±0.93	43.37	73.50±0.37	3.2	41.47	**73.51±0.37**	3.3
Covertype	23.60	79.57	326.84	75.95	2329	97.83	**84.50**	2779
Poker Hand	11.48	**77.11**	164.94	76.59	798	32.26	74.46	892
Electricity	0.51	77.43	17.30	78.68	119	2.73	**84.90**	211

while Cramer detected 33,755 in all data sets, considering all repetitions.

Regarding the time spent in the evaluation procedure, as expected, the base learner was faster than the RCD framework. In average, HTNB was approximately 75.41% faster than RCD using the Cramer test and 45.19% using KNN. In 12 out of 13 data sets, KNN was faster than Cramer.

The results presented for the naive Bayes base learner in Table 3, show that, again, the RCD framework had better performance in the majority of the data sets and configurations. Statistically, the results were similar to the ones obtained using the HTNB base learner: RCD also had higher accuracy values in both configurations of Random RBF with 50 centroids and, in this case, in both configurations of the Hyperplane data set. In the other data set configurations, RCD and naive Bayes obtained statistically similar results.

Considering RBF(0,0), two concept drifts occurred in the ten repetitions. The results of the algorithms are practically the same, only differing in the fifth decimal. This is a similar result compared to the same configuration using HTNB: when no concept drift was found, the same results occurred; when only two concept drifts were detected, the accuracy difference was negligible. Again, it is possible to notice that higher number of centroids gives higher number of concept drifts. Using the Cramer test, there were an average of 10.0 concept drifts in RBF(50,0.001) and 5.7 with 10 centroids. The same behavior occurred when using the KNN test: 16.7 and 5.5 concept drifts, respectively.

Comparing the statistical tests, KNN was statistically more accurate than Cramer in HYP(10,0.0001) and in both configurations of Random RBF with 50 centroids. In all other situations, both statistical tests had comparable performances. Comparing the number of detected concept drifts, similar results to the ones using HTNB base learner were obtained. Using KNN, 60,240 concept drifts were detected while Cramer detected 38,985 in all data sets.

Again, the base learner was faster than RCD in evaluating the data sets. The base learner was 2.5 times faster than RCD using the Cramer test, and 72% faster using KNN. The KNN statistical test was faster than the Cramer test in 9 out of 13 data set configurations.

Table 4 presents the results for the MLP base learner. The evaluation results show that, statistically, RCD had higher accuracy values compared to MLP only in RBF(50,0.0001). In all other situations, RCD and MLP had comparable performances, independently of the statistical test used.

In RBF without concept drifts, both versions of RCD performed the same, like when using the other base learners. In the 10 repetitions, only 2 concept drifts were found. These were false positives raised by the drift detector, giving the slightly different results from RCD and MLP. Similarly from the other base learners, RCD was statistically better in RBF(50,0.0001). Again it is possible to verify that the number of centroids has a much higher influence in the number of concept drifts than the speed of change. For example, using the Cramer test, an average of 6.8 concept drifts were identified in the RBF(10,0.001) configuration. Increasing the number of centroids to 50, the number of concept drifts raised to 14.0, while changing the speed of change to 0.0001 augmented the number of concept drifts to 8.0.

Comparing Cramer to KNN, only in the RBF(50,0.0001) configuration the tests had statistical different performances: KNN was better. In all other data sets, they performed similarly. Analyzing the evaluation time, the base learner was again faster. Here, Cramer was faster than KNN in average. While Cramer spent more than two times compared to MLP in the evaluation procedure, KNN was more than three times slower than the base learner. Again, KNN identified more concept drifts than Cramer: 34,348 versus 32,398.

6. Conclusion

This paper presented the implementation of a new multivariate non-parametric statistical test, the Cramer test, in the RCD framework. We compared RCD using two multivariate non-parametric statistical tests (KNN and Cramer) with three

Table 3: Results using the naive Bayes base classifier.

	NB		RCD NB CVM			RCD NB KNN		
	Time	**Accuracy**	**Time**	**Accuracy**	**# Drifts**	**Time**	**Accuracy**	**# Drifts**
RBF(0,0)	53.90	72.02±0.02	93.94	72.02±0.02	0.2	92.68	72.02±0.02	0.2
RBF(50,0.001)	117.17	53.18±0.01	161.20	53.19±0.01*	10.0	162.71	**53.22±0.02***	16.7
RBF(10,0.001)	66.40	75.78±0.03	105.95	**75.79±0.03**	5.7	103.61	75.78±0.03	5.5
RBF(50,0.0001)	116.78	53.25±0.05	160.61	53.33±0.03*	13.6	160.86	**53.76±0.31***	26.2
RBF(10,0.0001)	66.43	**75.77±0.04**	106.29	75.76±0.04	6.8	105.09	**75.77±0.04**	8.1
HYP(10,0.001)	54.91	87.10±3.14	96.88	87.64±2.78*	7.6	96.14	**87.91±2.47***	8.6
HYP(10,0.0001)	54.90	88.34±1.23	97.08	88.71±1.24*	9.3	95.03	**88.84±1.25***	8.4
SEA(50)	2.60	87.71±1.33	4.35	**87.86±1.22**	0.3	4.29	**87.86±1.22**	0.3
SEA(50000)	2.51	87.71±1.32	4.36	**88.42±0.35**	0.8	4.20	**88.42±0.35**	0.8
LED(50000)	17.77	72.58±2.36	31.89	**73.18±1.25**	0.2	32.59	**73.18±1.25**	0.2
Covertype	29.13	60.52	391.97	61.68	2513	128.54	**85.47**	3961
Poker Hand	15.09	59.55	231.88	60.25	1151	45.97	**70.88**	1790
Electricity	0.44	73.36	26.01	73.58	180	2.56	**82.21**	198

Table 4: Results using the MLP base classifier.

	MLP		RCD MLP CVM			RCD MLP KNN		
	Time	**Accuracy**	**Time**	**Accuracy**	**# Drifts**	**Time**	**Accuracy**	**# Drifts**
RBF(0,0)	56.46	**87.70±0.57**	101.86	87.44±0.53	0.2	101.90	87.44±0.53	0.2
RBF(50,0.001)	120.26	50.28±0.24	174.82	50.27±0.19	14.0	188.73	**50.30±0.33**	17.5
RBF(10,0.001)	69.09	83.95±0.47	128.76	**84.20±0.43**	6.8	133.79	83.93±0.45	10.5
RBF(50,0.0001)	120.23	49.92±0.26	176.99	50.10±0.26*	10.9	321.69	**53.23±1.94***	248.5
RBF(10,0.0001)	69.12	84.41±0.67	122.14	84.40±0.48	8.0	121.69	**84.78±0.40**	7.6
HYP(10,0.001)	56.45	**82.55±6.70**	111.98	82.24±7.33	8.6	110.47	82.27±7.36	9.2
HYP(10,0.0001)	56.44	84.31±2.14	113.46	84.34±2.22	8.9	112.71	**84.43±2.22**	9.0
SEA(50)	4.13	87.99±1.68	6.97	**88.75±0.98**	1.0	7.03	88.74±0.98	0.9
SEA(50000)	4.08	87.99±1.78	7.37	**88.04±1.70**	0.9	7.14	**88.04±1.70**	0.9
LED(50000)	27.48	63.67±4.73	50.84	63.68±4.72	0.5	51.05	**65.17±2.98**	0.5
Covertype	49.00	**60.69**	410.19	49.02	1661	388.15	49.05	1779
Poker Hand	23.35	43.03	265.26	59.80	1421	918.81	**63.47**	1284
Electricity	1.53	**57.51**	20.76	49.30	98	7.68	55.49	67

base learners: Hoeffding trees, naive Bayes, and Multilayer Perceptron. The tests were performed in seven data sets: four artificial data sets, with several rates-of-change, and three real world data sets.

The RCD configuration tested presented better performance than the Hoeffding tree base learner with naive Bayes at the leaves in 8 out of 13 possible situations using the Cramer test, in 4 situations the Hoeffding tree performed better, and in 1 situation the performance was similar. Using KNN, RCD has beaten the base learner by 9 to 2. In two situations, the performance was similar. Statistically, in three data set configurations, RCD had a better performance than the base learners considering both statistical tests. In all other situations, the performances were similar.

Using the naive Bayes base learner, the results of RCD are even better considering the Cramer test: of the 13 data set configurations, RCD performed better than naive Bayes in 11. In one situation they performed similarly and in one naive Bayes was better. Using KNN, RCD was better in ten data set configurations and in three the results were similar. Statistically, RCD performed better in four situations: both versions of Hyperplane and Random RBF with 50 centroids.

The results indicate that RCD tends to perform better than the base learners in environments with many concept drifts. This is an expected behavior because RCD stores classifiers and reuses them if actual data is similar to the ones used to build it. In environments without concept drifts, RCD's performance is similar to the base classifier, as the results from the tests shows in the Random RBF(0,0) configuration using the Hoeffding tree as base learner.

Regarding the two statistical tests in the artificial data sets, KNN statistically outperformed Cramer in six situations. In the others, both tests performed similarly. Considering the real data sets, KNN has beaten Cramer by 8 to 1. Results from the experiments clearly show that KNN is better suited for concept drift detection than Cramer.

Considering the evaluation times, as expected, the base learner was faster than using RCD. Comparing the two statistical tests, using the Hoeffding tree and naive Bayes, KNN was faster, while Cramer was faster when using Multilayer Perceptron. In all the tests, KNN was faster than Cramer in 28 situations, while the opposite occurred 11 times.

These results confirmed previous findings that the RCD approach to handle concept drifts is promising and improves single classifiers results when using them as base learners of the framework, independently of the statistical test used.

There was no situation where the base learner had a statistically better performance compared to using RCD in the experiments. Tests using other two base learners, J48 [32] and a pure Hoeffding tree, also had the same results (not presented here due to limitations of space).

6.1 Future Work

Even though RCD is actually highly configurable, as future work, further research might be made to allow the user to choose the best configuration for a specific problem:

- Analyze the influence of the drift detection method, implementing and testing alternatives to DDM and EDDM, like EWMA.
- Create an ensemble classifier based on the individual learners associated with each distribution. As more than one stored classifier can match the actual context, one approach would be to set higher weights to classifiers where their samples return higher confidence levels.
- Implement a pruning strategy different than FIFO and analyze the influence of the number of stored classifiers in terms of accuracy and performance.
- Use the two available statistical tests in conjunction and analyze if they provide better results than their individual use.

References

[1] M. M. Gaber, A. Zaslavsky, and S. Krishnaswamy, "Mining data streams: A review," *ACM SIGMOD Record*, vol. 34, pp. 18–26, 2005.

[2] J. Z. Kolter and M. A. Maloof, "Dynamic weighted majority: An ensemble method for drifting concepts," *Journal of Machine Learning Research*, vol. 8, pp. 2755–2790, December 2007.

[3] S. Wang, S. Schlobach, and M. Klein, "Concept drift and how to identify it," *Web Semantics: Science, Services and Agents on the World Wide Web*, vol. 9, no. 3, pp. 247–265, 2011.

[4] G. Widmer and M. Kubat, "Learning in the presence of concept drift and hidden contexts," *Machine Learning*, vol. 23, pp. 69–101, 1996.

[5] A. Tsymbal, "The problem of concept drift: Definitions and related work," Department of Computer Science, Trinity College, Dublin, Ireland, Tech. Rep., April 2004.

[6] P. M. Gonçalves Jr. and R. S. M. Barros, "RCD: A recurring concept drift framework," 2012, to appear. [Online]. Available: http://www.cin.ufpe.br/~roberto/AlunosPG/pmgj/rcd.pdf

[7] C. Franz, "cramer: Multivariate nonparametric cramer-test for the two-sample-problem," June 2006. [Online]. Available: http://cran.r-project.org/web/packages/cramer/index.html

[8] M. F. Schilling, "Multivariate two-sample tests based on nearest neighbors," *Journal of the American Statistical Association*, vol. 81, no. 395, pp. 799–806, September 1986.

[9] G. Hulten, L. Spencer, and P. Domingos, "Mining time-changing data streams," in *Proceedings of the 7th ACM SIGKDD International Conference on Knowledge Discovery and Data Mining*, ser. KDD '01. New York, NY, USA: ACM, 2001, pp. 97–106.

[10] P. Domingos and G. Hulten, "Mining high-speed data streams," in *Proceedings of the 6th ACM SIGKDD International Conference on Knowledge Discovery and Data Mining*, ser. KDD '00. New York, NY, USA: ACM, 2000, pp. 71–80.

[11] W. Hoeffding, "Probability inequalities for sums of bounded random variables," *Journal of the American Statistical Association*, vol. 58, pp. 13–30, 1963.

[12] O. Maron and A. Moore, "Hoeffding races: Accelerating model selection search for classification and function approximation," in *Advances in Neural Information Processing Systems 6*. San Mateo, CA, USA: Morgan Kaufmann, 1994.

[13] J. Gama, R. Rocha, and P. Medas, "Accurate decision trees for mining high-speed data streams," in *Proceedings of the 9th ACM SIGKDD International Conference on Knowledge Discovery and Data Mining*, ser. KDD '03. New York, NY, USA: ACM, 2003, pp. 523–528.

[14] C. Li, Y. Zhang, and X. Li, "Ocvfdt: one-class very fast decision tree for one-class classification of data streams," in *Proceedings of the 3rd International Workshop on Knowledge Discovery from Sensor Data*, ser. SensorKDD '09. New York, NY, USA: ACM, 2009, pp. 79–86.

[15] J. Gama, P. Medas, G. Castillo, and P. Rodrigues, "Learning with drift detection," in *Advances in Artificial Intelligence – SBIA 2004*, ser. Lecture Notes in Computer Science. Springer Berlin, 2004, vol. 3171, pp. 66–112.

[16] M. Baena-García, J. Del Campo-Ávila, R. Fidalgo, A. Bifet, R. Gavaldà, and R. Morales-Bueno, "Early drift detection method," in *4th International Workshop on Knowledge Discovery from Data Streams*, ser. IWKDDS '06, vol. 6. Citeseer, 2006, pp. 77–86.

[17] G. J. Ross, N. M. Adams, D. K. Tasoulis, and D. J. Hand, "Exponentially weighted moving average charts for detecting concept drift," *Pattern Recognition Letters*, vol. 33, no. 2, pp. 191–198, 2011.

[18] W. N. Street and Y. Kim, "A streaming ensemble algorithm (SEA) for large-scale classification," in *Proceedings of the 7th ACM SIGKDD International Conference on Knowledge Discovery and Data Mining*, ser. KDD '01. New York, NY, USA: ACM, 2001, pp. 377–382.

[19] H. Wang, W. Fan, P. S. Yu, and J. Han, "Mining concept-drifting data streams using ensemble classifiers," in *Proceedings of the 9th ACM SIGKDD International Conference on Knowledge Discovery and Data Mining*, ser. KDD '03. New York, NY, USA: ACM, 2003, pp. 226–235.

[20] D. Brzeziński and J. Stefanowski, "Accuracy updated ensemble for data streams with concept drift," in *Hybrid Artificial Intelligent Systems*, ser. Lecture Notes in Computer Science. Springer Berlin, 2011, vol. 6679, pp. 155–163.

[21] A. Blum, "Empirical support for winnow and weighted-majority algorithms: Results on a calendar scheduling domain," *Machine Learning*, vol. 26, no. 1, pp. 5–23, January 1997.

[22] N. Littlestone and M. K. Warmuth, "The weighted majority algorithm," *Information and Computation*, vol. 108, pp. 212–261, February 1994.

[23] M. Salganicoff, "Tolerating concept and sampling shift in lazy learning using prediction error context switching," *Artificial Intelligence Review*, vol. 11, no. 1-5, pp. 133–155, February 1997.

[24] M. B. Harries, C. Sammut, and K. Horn, "Extracting hidden context," *Machine Learning*, vol. 32, pp. 101–126, 1998.

[25] R. D. C. Team, "R: A language and environment for statistical computing," *R Foundation for Statistical Computing*, vol. 1, no. 10, 2008.

[26] A. Bifet, G. Holmes, R. Kirkby, and B. Pfahringer, "MOA: Massive online analysis," *Journal of Machine Learning Research*, vol. 11, pp. 1601–1604, August 2010.

[27] M. Hall, E. Frank, G. Holmes, B. Pfahringer, P. Reutemann, and I. H. Witten, "The weka data mining software: an update," *SIGKDD Explorations Newsletter*, vol. 11, pp. 10–18, November 2009.

[28] L. Breiman, J. H. Friedman, R. A. Olshen, and C. J. Stone, *Classification and Regression Trees*, ser. Wadsworth Statistics / Probability series. Belmont, California: Wadsworth Int'l Group, 1984.

[29] A. Bifet, G. Holmes, B. Pfahringer, R. Kirkby, and R. Gavaldà, "New ensemble methods for evolving data streams," in *Proceedings of the 15th ACM SIGKDD International Conference on Knowledge Discovery and Data Mining*, ser. KDD '09. New York, NY, USA: ACM, 2009, pp. 139–148.

[30] J. A. Blackard and D. J. Dean, "Comparative accuracies of artificial neural networks and discriminant analysis in predicting forest cover types from cartographic variables," *Computers and Electronics in Agriculture*, vol. 24, no. 3, pp. 131–151, 1999.

[31] A. Bifet, G. Holmes, B. Pfahringer, and E. Frank, "Fast perceptron decision tree learning from evolving data streams," in *Advances in Knowledge Discovery and Data Mining*, ser. Lecture Notes in Computer Science. Springer Berlin, 2010, vol. 6119, pp. 299–310.

[32] R. Quinlan, *C4.5: Programs for Machine Learning*. San Mateo, CA: Morgan Kaufmann Publishers, 1993.

A Propositional Family Deontic Logic

Cungen CAO and Yuefei SUI
Key Laboratory of Intelligent Information Processing
Institute of Computing Technology, Chinese Academy of Sciences, Beijing 100190, CHINA

Abstract—*A propositional family deontic logic is introduced, which is a combination of the propositional deontic logic, dynamic logic and ambient logic. A three-layered possible world semantics is given, where a possible world is a set of families which is used to define the semantics for action modality* $[\mathbf{a}]$; *a subpossible world is a family used to define the semantics for family modality* $[\mathbf{m}]$, *and a subsubpossible world is used to define the semantics for the deontic modality* OB. *An axiomatic system of the logic will be given, and the normal form theorem, the soundness theorem and completeness theorem of the axiomatic system will be proved.*

Keywords: Deontic logic, Normative system, Ambient logic, Possible world semantics, Axiomatic system.

1. Introduction

The dynamic logic ([4]) and the propositional deontic logic ([7]) are used to represent the normative systems ([2],[5],[6],[11]). For example, Åotnes, *et al.* ([2]) defined a normative temporal logic for reasoning about normative systems, which is a combination of the computational tree logic and the deontic logic. Herzig, *et al.*([5]) gave a dynamic logic of normative systems, called PDL-PA, in which the normative modalities $\mathbf{A}, \mathbf{P}$ are applied only to the propositional variables with sign $+/-$. This dynamic logic can be taken as a dynamic logic with extra propositional variables.

The propositional family deontic logic is a logic for normative systems, and is a combination of the propositional deontic logic, the dynamic logic and the ambient logic ([3]). The logical language of the logic has three kinds of modalities:

• modality OB in the deontic logic is used to denote the obligation;

• modalities $[\mathbf{a}]$ in the dynamic logic are used to represent the basic actions in/between families, for example, $\mathbf{a}$ may be **birth**, **marry**, **divorce**, where $\mathbf{a}$s are with parameters, and

• modalities $[\mathbf{m}]$ are used to denote families as positions in which propositional variables and obligatory statements are interpreted, where $[\mathbf{m}]$ is used in the ambient logic to denote spatial positions.

Only the obligations considered here are in families, and hence, a formula of form $\mathtt{OB}[\mathbf{m}]\phi$ is not well-defined. Hence, we assume that OB can be applied only to the propositional variables or the negation of the propositional variables. Action modality $[\mathbf{a}]$ changes a family ($\mathbf{a} =$ **birth**), or combines two families ($\mathbf{a} =$ **marry**) or splits a family into two families ($\mathbf{a} =$ **divorce**), and does not change the deontic statements, but can add new deontic statements to the recently-formed families.

The semantics of the propositional family deontic logic is a three-layered possible world semantics, in which

◦ a possible world w is a set of families u, such that an action changes a possible world into another one;

◦ a subpossible world u in a possible world w is a family, such that a family modality $[\mathbf{m}]$ is interpreted to be a subpossible world;

◦ a subsubpossible world z in a subpossible world u is used to interpret modality OB.

For the simplicity, we assume that for any $w \in W$, there is one and only one possible world w' such that w' is accessible from w via modality $\mathbf{a}$; and the interpretation $I_w(\mathbf{m})$ of family name $\mathbf{m}$ is constant with respect to the subpossible world, that is, if w' is accessible from w via some $\mathbf{a}$ then family $I_w(\mathbf{m})$ denoted by $\mathbf{m}$ at possible world w is the same as the one $I_{w'}(\mathbf{m})$ denoted by $\mathbf{m}$ at possible world w'.

We shall build an axiomatic system for the propositional famly deontic logic and prove the normal form theorem, the soundness theorem and the completeness theorem of the propositional family deontic logic.

The paper is organized as follows: the next section gives the basic definitions in the propositional deontic logic; the third section gives the syntax and semantics of the propositional family deontic logic; the fourth section proves the basic theorems on the equivalent formulas and the normal form theorem; the fifth section gives an axiomatic system and proves the soundness theorem and completeness theorem of the logic; the sixth section gives variant family deontic logics; and the last section concludes the whole paper.

2. The deontic logic

This section gives the basic definitions of the propositional deontic logic, its syntax and semantics.

The logical language for the propositional deontic logic consists of the following symbols:

• propositional variables: $p_0, p_1, ...$;
• logical connectives: $\neg, \wedge$;
• the deontic modality: OB; and
• auxiliary symbols: (,).

Formulas are defined inductively as follows:

$$\phi ::= p|\neg\phi_1|\phi_1 \wedge \phi_2|\mathtt{OB}\phi_1.$$

Other deontic modalities are defined:

$$\begin{aligned}
&\texttt{PE}\phi ::= \neg\texttt{OB}\neg\phi\\
&\texttt{IM}\phi ::= \texttt{OB}\neg\phi\\
&\texttt{OM}\phi ::= \neg\texttt{OB}\phi\\
&\texttt{OP}\phi ::= \neg\texttt{OB}\phi \wedge \neg\texttt{OB}\neg\phi.
\end{aligned}$$

The semantics of the propositional deontic logic is the possible world semantics.

A *frame* F is a triple (W, R, D), where

• W is a non-empty set of possible worlds;

• $R \subseteq W \times W$ is the accessibility relation for modality OB, and

• $D \subseteq W$ is a subset such that for any $w \in W$, there is a possible world $w' \in D$ such that $(w, w') \in R$.

A *model* $\mathbf{M}$ is a pair (F, I), where

• F is a frame; and

• I is an interpretation such that for any propositional variable p, $I(p) \subseteq W$.

The satisfaction of formula ϕ at a possible world w, denoted by $\mathbf{M}, w \models \phi$, is defined as follows:[1] $\mathbf{M}, w \models \phi$ iff

$$\begin{cases}
w \in I(p) & \text{if } \phi = p\\
\mathbf{M}, w \not\models \phi_1 & \text{if } \phi = \neg\phi_1\\
\mathbf{M}, w \models \phi_1 \& \mathbf{M}, w \models \phi_2 & \text{if } \phi = \phi_1 \wedge \phi_2\\
\mathbf{A}w'((w, w') \in R \& w' \in D & \\
\quad \Rightarrow \mathbf{M}, w' \models \phi_1) & \text{if } \phi = \texttt{OB}\phi_1
\end{cases}$$

Correspondingly, we have the following

$\mathbf{M}, w \models \texttt{PE}\phi$ iff
$\mathbf{E}w'((w, w') \in R \& w' \in D \& \mathbf{M}, w' \models \phi)$
$\mathbf{M}, w \models \texttt{IM}\phi$ iff
$\mathbf{A}w'((w, w') \in R \& w' \in D \Rightarrow \mathbf{M}, w' \models \neg\phi)$
$\mathbf{M}, w \models \texttt{OM}\phi$ iff
$\mathbf{E}w'((w, w') \in R \& w' \in D \& \mathbf{M}, w' \models \neg\phi)$
$\mathbf{M}, w \models \texttt{OP}\phi$ iff
$\mathbf{E}w'((w, w') \in R \& w' \in D \& \mathbf{M}, w' \models \phi)$
$\& \mathbf{E}w'((w, w') \in R \& w' \in D \& \mathbf{M}, w' \models \neg\phi)$

Axioms:

A1. All tautologies of the propositional logic;

A2. $\texttt{OB}(\phi \to \psi) \to (\texttt{OB}\phi \to \texttt{OB}\psi)$;

A3. $\texttt{OB}\phi \to \neg\texttt{OB}\neg\phi$.

Inference rules:

$$\text{(MP)} \quad \frac{\phi, \phi \to \psi}{\psi}$$

$$\text{(NEC}^{\texttt{OB}}\text{)} \quad \frac{\phi}{\texttt{OB}\phi}.$$

Theorem 2.1([7]). The deontic logic is sound and complete.

□

[1]In syntax, we use $\neg, \wedge, \to, \forall, \exists$ to denote the logical connectives and quantifiers; and in semantics we use $\sim, \&, \Rightarrow, \mathbf{A}, \mathbf{E}$ to denote the corresponding connectives and quantifiers.

3. The family deontic logic

A logic consists of a logical language, syntax, semantics and a deduction system.

The logical language of the family deontic logic contains the following symbols:

• propositional variables: $p_0, p_1, ...$;

• action names: $\mathbf{a}_0, \mathbf{a}_1, ...$; and action modalities: $[\mathbf{a}_0], [\mathbf{a}_1], ...$;

• family names: $\mathbf{m}_0, \mathbf{m}_1, ...$; and family modalities: $[\mathbf{m}_0], [\mathbf{m}_1], ...$;

• the deontic modality: OB, and

• logical connectives: $\neg, \wedge$.

For example,

$\mathbf{a} ::= \mathbf{birth}(x, y) | \mathbf{marry}(x, y) | \mathbf{divorce}(x, y)$,

where x, y are parameters, and $\mathbf{birth}(x, y)$ represents that x gives a birth to y; $\mathbf{marry}(x, y)$ that x marries y, and $\mathbf{divorce}(x, y)$ that x divorces y. Because we consider only the propositional family deontic logic, x, y are taken as parameters, not as variables.

We assume that modality OB is applied only to the atomic formulas or the negation of the atomic formulas; and action modalities and family name modalities $[\mathbf{m}]$ are applied to any formula.

Formulas are defined inductively as follows:

$$\phi ::= p | \texttt{OB}p | \texttt{OB}\neg p | \neg\phi_1 | \phi_1 \wedge \phi_2 | [\mathbf{a}]\phi_1 | [\mathbf{m}]\phi_1.$$

The semantics is a three-layered possible world semantics. Intuitively, we use a possible world to denote a set of families, a subpossible world to denote a family, and a subsubpossible world for the deontic modality.

A *model* $\mathbf{M}$ is a pair (W, R), where

• W is a set of possible worlds such that each possible world $w \in W$ is a submodel $w = (U_w, I_w)$, where

  ◦ U_w is a set of *subpossible worlds* and each subpossible world u is a model $(Z_{w,u}, R^{\texttt{OB}}_{w,u}, I_{w,u})$, where

    ◇ $Z_{w,u}$ is a set of *subsubpossible worlds*;

    ◇ $R^{\texttt{OB}}_{w,u} \subseteq Z^2_{w,u}$ is the accessibility relation for OB in u; and

    ◇ $I_{w,u}$ is an interpretation such that for any propositional variable p, $I_{w,u}(p) \subseteq Z_{w,u}$;

  and for any possible worlds w, w', if $(w, w') \in R_{\mathbf{a}}$ then $U_w \subseteq U_{w'}$, and

  ◦ I_w is an interpretation such that for any family name $\mathbf{m}$, $I_w(\mathbf{m}) \in U_w$.

• for each action name $\mathbf{a}$, $R_{\mathbf{a}} \subseteq W^2$ is the accessibility relation for action modality $[\mathbf{a}]$, such that for any possible world $w \in W$, there is one and only one possible world w' (we use $f_{\mathbf{a}}(w)$ to denote the w') such that

  ◦ $(w, w') \in R_{\mathbf{a}}$, and

  ◦ for any $\mathbf{m}$, if $I_w(\mathbf{m}) \downarrow$ (is defined) then $I_{w'}(\mathbf{m}) \downarrow$, and

$$I_w(\mathbf{m}) = I_{w'}(\mathbf{m}).$$

The last condition ensures that if w' is accessible from w via some action modality $[\mathbf{a}]$, and family $\mathbf{m}$ exists in w then $\mathbf{m}$ exists in w'.

The satisfaction of formula ϕ at a subsubpossible world (w, u, z), denoted by $\mathbf{M}, w, u, z \models \phi$, is defined as follows:

$\mathbf{M}, w, u, z \models \phi$ iff

$$\begin{cases} z \in I_{w,u}(p) & \text{if } \phi = p \\ \mathbf{A}z'((z,z') \in R^{\mathtt{OB}}_{w,u} \\ \quad \Rightarrow \mathbf{M}, w, u, z' \models p) & \text{if } \phi = \mathtt{OB}p \\ \mathbf{A}z'((z,z') \in R^{\mathtt{OB}}_{w,u} \\ \quad \Rightarrow \mathbf{M}, w, u, z' \models \neg p) & \text{if } \phi = \mathtt{OB}\neg p \\ \mathbf{M}, w, u, z \not\models \phi_1 & \text{if } \phi = \neg\phi_1 \\ \mathbf{M}, w, u, z \models \phi_1 \\ \quad \&\mathbf{M}, w, u, z \models \phi_2 & \text{if } \phi = \phi_1 \wedge \phi_2 \\ \mathbf{M}, f_{\mathbf{a}}(w), u, z \models \phi_1 & \text{if } \phi = [\mathbf{a}]\phi_1 \\ \mathbf{M}, w, I_w(\mathbf{m}), z \models \phi_1 & \text{if } \phi = [\mathbf{m}]\phi_1 \end{cases}$$

where z is a subsubpossible world of u, and u is a subpossible world of possible world w.

Remark. For the simplicity, we omit the relation D in the semantics of the propositional deontic logic.

□

A formula ϕ is *valid* in a model $\mathbf{M}$, denoted by $\mathbf{M} \models \phi$, if for any possible world w, subpossible world u of w and subsubpossible world z of $u, \mathbf{M}, w, u, z \models \phi$. ϕ is *valid*, denoted by $\models \phi$, if for any model $\mathbf{M}, \phi$ is valid in $\mathbf{M}$.

4. The normal form

In this section, we discuss the normal form of formulas, just as the disjunctive or conjunctive normal form in the propositional logic. With the normal form and the completeness theorem of the dynamic logic, we can prove the completeness theorem of the propositional family deontic logic.

Proposition 4.1. The following sentences are valid:

$$[\mathbf{a}]\neg\phi \leftrightarrow \neg[\mathbf{a}]\phi$$
$$[\mathbf{a}](\phi \wedge \psi) \leftrightarrow [\mathbf{a}]\phi \wedge [\mathbf{a}]\psi.$$

Proof. It is assumed that for any $w \in W$, there is one and only one $w' \in W$ such that $(w, w') \in R_{\mathbf{a}}$.

$\mathbf{M}, w, u, z \models [\mathbf{a}]\phi$
iff $\mathbf{A}w'((w, w') \in R_{\mathbf{a}} \Rightarrow \mathbf{M}, w', u, z \models \phi$
iff $\mathbf{M}, f_{\mathbf{a}}(w), u, z \models \phi$.

For any model $\mathbf{M}$ and w, u, z,

$\mathbf{M}, w, u, z \models [\mathbf{a}]\neg\phi$
iff $\mathbf{M}, f_{\mathbf{a}}(w), u, z \models \neg\phi$
iff $\mathbf{M}, f_{\mathbf{a}}(w), u, z \not\models \phi$
iff $\mathbf{M}, w, u, z \not\models [\mathbf{a}]\phi$
iff $\mathbf{M}, w, u, z \models \neg[\mathbf{a}]\phi$;
$\mathbf{M}, w, u, z \models [\mathbf{a}](\phi \wedge \psi)$
iff $\mathbf{M}, f_{\mathbf{a}}(w), u, z \models \phi \wedge \psi$
iff $\mathbf{M}, f_{\mathbf{a}}(w), u, z \models \phi \& \mathbf{M}, f_{\mathbf{a}}(w), u, z \models \psi$
iff $\mathbf{M}, w, u, z \models [\mathbf{a}]\phi \& \mathbf{M}, w, u, z \models [\mathbf{a}]\psi$
iff $\mathbf{M}, w, u, z \models [\mathbf{a}]\phi \wedge [\mathbf{a}]\psi$.

□

Proposition 4.2. The following sentences are valid: for any family name $\mathbf{m}$,

$$[\mathbf{m}]\neg\phi \leftrightarrow \neg[\mathbf{m}]\phi$$
$$[\mathbf{m}](\phi \wedge \psi) \leftrightarrow [\mathbf{m}]\phi \wedge [\mathbf{m}]\psi.$$

Proof. For any model $\mathbf{M}$ and w, u, z,

$\mathbf{M}, w, u, z \models [\mathbf{m}]\neg\phi$
iff $\mathbf{M}, w, I_w(\mathbf{m}), z \models \neg\phi$
iff $\mathbf{M}, w, I_w(\mathbf{m}), z\neg \models \phi$
iff $\mathbf{M}, w, u, z\neg \models [\mathbf{m}]\phi$
iff $\mathbf{M}, w, u, z \models \neg[\mathbf{m}]\phi$;
$\mathbf{M}, w, u, z \models [\mathbf{m}](\phi \wedge \psi)$
iff $\mathbf{M}, w, I_w(\mathbf{m}), z \models \phi \wedge \psi$
iff $\mathbf{M}, w, I_w(\mathbf{m}), z \models \phi \& \mathbf{M}, w, I_w(\mathbf{m}), z \models \psi$
iff $\mathbf{M}, w, u, z \models [\mathbf{m}]\phi \& \mathbf{M}, w, u, z \models [\mathbf{m}]\psi$
iff $\mathbf{M}, w, u, z \models [\mathbf{m}]\phi \wedge [\mathbf{m}]\psi$.

□

The normal form of formulas is defined as follows:

$$\begin{aligned} \theta &::= p|\mathtt{OB}p|\mathtt{OB}\neg p; \\ \psi &::= [\alpha_1]\cdots[\alpha_n]\theta|\neg\psi_1|\psi_1 \wedge \psi_2 \end{aligned}$$

where $\alpha ::= \mathbf{m}|\mathbf{a}$. Here, we say that θ and ψ are the formulas in the normal form.

Theorem 4.3. Each formula ϕ is logically equivalent to a formula ψ in the normal form, i.e., $\models \phi \leftrightarrow \psi$.

Proof. By the induction on the structure of formula ϕ and proposition 4.1 and 4.2, we have the theorem.

□

Proposition 4.4. The following formula is valid:

$$[\mathbf{a}][\mathbf{m}]\phi \leftrightarrow [\mathbf{m}][\mathbf{a}]\phi.$$

Proof. For any model $\mathbf{M}$ and w, u, z

$\mathbf{M}, w, u, z \models [\mathbf{a}][\mathbf{m}]\phi$ iff $\mathbf{M}, f_{\mathbf{a}}(w), u, z \models [\mathbf{m}]\phi$
iff $\mathbf{M}, f_{\mathbf{a}}(w), I_{f_{\mathbf{a}}(w)}(\mathbf{m}), z \models \phi$;
$\mathbf{M}, w, u, z \models [\mathbf{m}][\mathbf{a}]\phi$ iff $\mathbf{M}, w, I_w(\mathbf{m}), z \models [\mathbf{a}]\phi$
iff $\mathbf{M}, f_{\mathbf{a}}(w), I_w(\mathbf{m}), z \models \phi$.

Because $(w, f_{\mathbf{a}}(w)) \in R_{\mathbf{a}}, I_{f_{\mathbf{a}}(w)} \supseteq I_w$, i.e.,

$$I_w(\mathbf{m}) = I_{f_{\mathbf{a}}(w)}(\mathbf{m}).$$

Therefore,

$$\mathbf{M}, w, u, z \models [\mathbf{a}][\mathbf{m}]\phi \text{ iff } \mathbf{M}, w, u, z \models [\mathbf{m}][\mathbf{a}]\phi.$$

□

The strong normal form:

$$\begin{aligned} \theta &::= p|\mathtt{OB}p|\mathtt{OB}\neg p; \\ \xi &::= [\mathbf{a}]\theta; \\ \psi &::= [\mathbf{m}_1]\cdots[\mathbf{m}_n]\xi|\neg\psi_1|\psi_1 \wedge \psi_2. \end{aligned}$$

The intuition of the strong normal form is that each family action, such as, **birth**, **marry**, **divorce**, etc., happens in one

family, and a deontic statement is about members in one family.

Theorem 4.5. Each formula ϕ is logically equivalent to a formula ψ in the strong normal form, i.e., $\models \phi \leftrightarrow \psi$.

Proof. By the induction on the structure of formula ϕ. □

5. The soundness and completeness of the propositional family deontic logic

The axiomatic system of the propositional family deontic logic consists the following axioms and inference rules:

Axioms:

All the valid propositional formula
$[\mathbf{m}]\neg\phi \leftrightarrow \neg[\mathbf{m}]\phi$
$[\mathbf{m}](\phi \wedge \psi) \leftrightarrow ([\mathbf{m}]\phi \wedge [\mathbf{m}]\psi)$
$[\mathbf{a}]\neg\phi \leftrightarrow \neg[\mathbf{a}]\phi$
$[\mathbf{a}](\phi \wedge \psi) \leftrightarrow [\mathbf{a}]\phi \wedge [\mathbf{a}]\psi$
$[\mathbf{a}][\mathbf{m}]\phi \leftrightarrow [\mathbf{m}][\mathbf{a}]\phi$.

Inference rules:

$$\text{(MP)}: \quad \frac{\phi, \phi \rightarrow \psi}{\psi}$$

$$\text{(Nec}^{\mathbf{m}}\text{)}: \quad \frac{\phi}{[\mathbf{m}]\phi}$$

$$\text{(Nec}^{\mathbf{a}}\text{)}: \quad \frac{\phi}{[\mathbf{a}]\phi}.$$

Theorem 5.1(The soundness theorem). For any formula ϕ, if $\vdash \phi$ then $\models \phi$.

Proof. By the induction on the length of proofs of ϕ. □

Theorem 5.2(The completeness theorem). For any formula ϕ, if $\models \phi$ then $\vdash \phi$.

Proof. Assume that $\models \phi$. By the normal form theorem, there is a formula ψ in the normal form such that $\models \phi \leftrightarrow \psi$. Therefore, $\models \psi$. By taking ψ as a formula in the propositional logic and the completeness theorem of the propositional logic, $\vdash^1 \psi$, and therefore, $\vdash \phi$, where $\vdash^1$ is the deduction relation in the propositional logic which language contains the following propositional variables:

$$p|[\alpha_1]\cdots[\alpha_n]p|[\alpha_1]\cdots[\alpha_n]\texttt{OB}p|[\alpha_1]\cdots[\alpha_n]\texttt{OB}\neg p,$$

where $\alpha ::= \mathbf{m}|\mathbf{a}$. □

6. The variant family deontic logic

One variant family deontic logic is without restraints on applications of modalities.

Formulas can be defined as follows:

$$\phi :: \quad = \quad p|\texttt{OB}\phi_1|\neg\phi_1|\phi_1 \wedge \phi_2|[\mathbf{a}]\phi_1|[\mathbf{m}]\phi_1.$$

Correspondingly, the semantics is the common possible world semantics.

A model $\mathbf{M}$ is a triple (W, R, I), where

• W is a set of possible worlds;

• for each action name $\mathbf{a}$, $R_{\mathbf{a}} \subseteq W^2$ is the accessibility relation for modality $[\mathbf{a}]$, and $R_{\texttt{OB}} \subseteq W^2$ for modality $\texttt{OB}$, and

• I is an interpretation such that for any propositional variable p, $I(p) \subseteq W$; and for any family name $\mathbf{m}$, $I(\mathbf{m}) \in W$.

Given a model $\mathbf{M}$, for any possible world w, a formula ϕ is satisfied at possible world w, denoted by $\mathbf{M}, w \models \phi$, iff

$$\begin{cases} w \in I(p) & \text{if } \phi = p \\ \mathbf{M}, w \not\models \phi_1 & \text{if } \phi = \neg\phi_1 \\ \mathbf{M}, w \models \phi_1 \& \mathbf{M}, w \models \phi_2 & \text{if } \phi = \phi_1 \wedge \phi_2 \\ \mathbf{A}w'((w, w') \in R_{\texttt{OB}} \Rightarrow \mathbf{M}, w' \models \phi_1) & \text{if } \phi = \texttt{OB}\phi_1 \\ \mathbf{A}w'((w, w') \in R_{\mathbf{a}} \Rightarrow \mathbf{M}, w' \models \phi_1) & \text{if } \phi = [\mathbf{a}]\phi_1 \\ \mathbf{M}, I(\mathbf{m}) \models \phi_1 & \text{if } \phi = [\mathbf{m}]\phi_1 \end{cases}$$

If $\mathbf{a} ::= \textbf{birth}(x, y)|\textbf{marry}(x, y)|\textbf{divorce}(x, y)$ then binary relations for the accessibility relations are not appropriate. In the following, we shall give a model for the family deontic logic, in which

◊ a possible world is a family;

◊ action modality $[\textbf{birth}(x, y)]$ changes a possible world w into a new possible world w'; action modality $[\textbf{marry}(x, y)]$ maps two families w and w_1 into a new family w_2; action modality $[\textbf{divorce}(x, y)]$ maps one family w into two new families w_1 and w_2;

◊ the deontic modality $\texttt{OB}$ is interpreted in a classical way.

Such a model $\mathbf{M}$ is a triple (W, R, I), where

◦ W is a set of possible worlds;

◦ $R_{\texttt{OB}} \subseteq W^2$ is the accessibility relation for the modality $\texttt{OB}$; and

$$R_{\textbf{birth}} : W \rightarrow W,$$
$$R_{\textbf{marry}} : W^2 \rightarrow W,$$
$$R_{\textbf{divorce}} : W \rightarrow W^2$$

are the accessibility relations for modalities $[\textbf{birth}], [\textbf{marry}], [\textbf{divorce}]$, respectively; and

◦ I is an interpretation such that for any propositional variable $p, I(p) \subseteq W$, and for any family name $\mathbf{m}, I(\mathbf{m}) \in W$.

Correspondingly, the modality $[\textbf{divorce}]$ is split into two modalities $[\textbf{divorce}^1]$ and $[\textbf{divorce}^2]$, such that for any possible worlds $w, w_1, w_2 \in W$, if $(w, w_1, w_2) \in R_{\textbf{divorce}}$ then $(w, w_1) \in R_{\textbf{divorce}^1}$ and $(w, w_2) \in R_{\textbf{divorce}^2}$. Hence, if x divorces y in action name **divorce** then $[\textbf{divorce}^1]\phi$ means that ϕ is true in a new family of x, and $[\textbf{divorce}^2]\phi$ means that ϕ is true in a new family of y.

The satisfaction relation is defined as follows: $\mathbf{M}, w \models \phi$

iff

$$\begin{cases} w \in I(p) & \text{if } \phi = p \\ \mathbf{M}, w \not\models \phi_1 & \text{if } \phi = \neg\phi_1 \\ \mathbf{M}, w \models \phi_1 \& \mathbf{M}, w \models \phi_2 & \text{if } \phi = \phi_1 \wedge \phi_2 \\ \mathbf{A}w'((w,w') \in R_{\textbf{birth}} & \\ \quad \Rightarrow \mathbf{M}, w' \models \phi_1 & \text{if } \phi = [\textbf{birth}]\phi_1 \\ \mathbf{A}w_1, w_2((w,w_1,w_2) \in R_{\textbf{marry}} & \\ \quad \Rightarrow \mathbf{M}, w_2 \models \phi_1) & \text{if } \phi = [\textbf{marry}]\phi_1 \\ \mathbf{A}w_1, w_2((w,w_1,w_2) \in R_{\textbf{divorce}} & \\ \quad \Rightarrow \mathbf{M}, w_1 \models \phi_1 & \text{if } \phi = [\textbf{divorce}^1]\phi_1 \\ \mathbf{A}w_1, w_2((w,w_1,w_2) \in R_{\textbf{divorce}} & \\ \quad \Rightarrow \mathbf{M}, w_2 \models \phi_1 & \text{if } \phi = [\textbf{divorce}^2]\phi_1 \\ \mathbf{M}, I(\mathbf{m}) \models \phi_1 & \text{if } \phi = [\mathbf{m}]\phi_1 \\ \mathbf{A}w'((w,w') \in R_{\mathtt{OB}} & \\ \quad \Rightarrow \mathbf{M}, w' \models \phi_1) & \text{if } \phi = \mathtt{OB}\phi_1 \end{cases}$$

For the simplicity of discussion, we assume that for any possible world w,

∘ there is one and only one w' such that $(w,w') \in R_{\textbf{birth}}$; w' is denoted by $f_{\textbf{birth}}(w)$;

∘ there is one and only one pair (w_1,w_2) such that $(w,w_1,w_2) \in R_{\textbf{marry}}$; (w_1,w_2) is denoted by $f_{\textbf{marry}}(w)$; and

∘ there is one and only one pair (w_1,w_2) such that $(w,w_1,w_2) \in R_{\textbf{divorce}}$; (w_1,w_2) is denoted by $f_{\textbf{divorce}}(w)$.

Therefore,

$\mathbf{M}, v, w \models [\textbf{birth}]\phi$ iff $\mathbf{M}, v, f_{\textbf{birth}}(w) \models \phi$
$\mathbf{M}, v, w \models [\textbf{marry}]\phi$ iff $\mathbf{M}, v, \pi_2(f_{\textbf{marry}}(w)) \models \phi$
$\mathbf{M}, v, w \models [\textbf{divorce}^1]\phi$ iff $\mathbf{M}, v, \pi_1(f_{\textbf{divorce}}(w)) \models \phi$
$\mathbf{M}, v, w \models [\textbf{divorce}^2]\phi$ iff $\mathbf{M}, v, \pi_2(f_{\textbf{divorce}}(w)) \models \phi$.

7. Conclusions

The family deontic logic can be used in the normative systems and the common-knowledge representation.

A further work would be to give a less restrictive semantics for the family deontic logic, and in such a semantics, the sound and complete axiomatic system could be given.

References

[1] C. E. Alchourrón and E. Bulygin. *Normative Systems*. Springer, 1971.

[2] T. Åotnes, W. van der Hoek, J. A. Rodriguez-Aguilar, C. Sierra and M. Wooldridge. On the logic of normative systems. In *IJCAI'07*, 1181-1186. AAAI Press, 2007.

[3] L. Cardelli and A. D. Gordon. Mobile ambients. In *Foundations of Software Science and Computational Structures*, LNCS 1378, 140-155. Springer 1998.

[4] D. Harel, D. Kozen and J. Tiuryn. *Dynamic Logic*. MIT Press, Cambridge, 2000.

[5] A. Herzig, E. Lorini, F. Moisan and N. Troquard. A dynamic logic of normative systems. In Proc. IJCAI 2011, 228-233.

[6] W. van der Hoek and M. Wooldridge. On the logic of cooperation and propositional control. *Artificial Intelligence* **164**(2005), 81-119.

[7] J.-J. Ch. Meyer and R. J. Wieringa, eds. *Deontic Logic in Computer Science*. Wiley, 1993.

[8] R. Reiter. *Knowledge in action: logical foundations for specifying and implementing dynamical systems.* MIT Press, Cambridge, 2001.

[9] Y. Shoham and M. Tennenholtz. On social laws for artificial agent societies: Online design. In P. E. Agre and S. J. Rosenschein, editors, *Computational theories of interaction and agency,* 597-618. MIT Press, Cambridge, 1996.

[10] L. van der Torre. Contextual deontic logic: Normative agents, violations and independence. *Annals of Mathematics and Artificial Intelligence* **37**(2003), 33-63.

[11] M. Wooldridge and W. van der Hoek. On obligations and normative ability: towards a logical analysis of the social contract. *J. of Applied Logic* **3**(2005), 396-420.

An Evolutionary Scheme for Solving a Reverse Supply Chain Design Problem

Ernesto Del R. Santibanez-Gonzalez[1], and Henrique Pacca Luna[2]
[1]Department of Computer Science, Federal University of Ouro Preto, Ouro Preto, MG, Brazil
[2]Computer Science Institute, Federal University of Alagoas, Maceió, AL, Brazil

Abstract - *According to some authors, design strategies for reverse Supply Chain (SC) are relatively unexplored and underdeveloped. We propose a genetic algorithm (GA) that guides the search for an optimal solution to an NP-hard remanufacturing SC problem. It combines a random solution search with an optimal solution method for solving to optimality an associated LP problem. In this GA, each chromosome is generated into two steps. First is generated the part of the chromosome representing whether the facility is opened or closed. The second part of the chromosome is obtained solving to optimality a LP problem associated to the original problem. The proposed genetic algorithm was coded in GAMS. We report computational results for 11 network instances generated randomly with up to 350 sourcing facilities, 100 candidate sites for locating reprocessing facilities and 40 remanufacturing facilities (350x100x40). Computational results regarding GAP and computing times are promising.*

Keywords: Evolutionary algorithm, sustainable supply chain problem; remanufacturing location problems; integer programming

1 Introduction

The management of product return flows has received increasing attention in the last decade. The efficient waste and product return flows stewardship is concerned with the final destination of products and their components, and what is their impact on the pollution of the air, water and earth besides the costs of treating the disposal in landfill. Notice that by 2013 the total e-waste will reach 73 million metric tons. These products not only need to get back to the supplier, re-use or recycled, some disposal also remain in the earth producing several kind of damages. Several regions and nations set up tighter environmental objectives in a collaborative action to mitigate the potential damage for the economic and also the health of the people. There are specific rules in some regions like UE, where The European Waste Electrical and Electronic Equipment Directive (WEEE) and End of Life Vehicles Directive, (ELV) are encouraging companies in the automotive industry to collaborate with other businesses and organizations in the supply chain to ensure that products can be disassembled and reused, remanufactured, recycled or disposed of safely at the end of their life.

In addition to stronger legal environment restrictions, there are several reasons because an increasing number of companies will be interested into get engaged in sustainable initiatives like the management of reverse flows, going backwards from customers to recovery centers, within their supply chain [1, 2]. Some authors noted that huge monetary values "can be gained by redesigning the reverse supply chain to be faster and reduce costly time delays" [3]. According to the same authors, design strategies for reverse supply chains are relatively unexplored and underdeveloped. Returned products are remanufactured if judged cost-effective. Some firms may treat all product returns as defective. Some returned products may be new and never used; then these products must be returned to the forward flow. In this context, remanufacturing activities are recognized as a main option of recovery in terms of its feasibility and benefits. We study this problem as part of reverse logistics problems. In this paper is addressed the problem of designing a remanufacturing supply chain network and it is proposed a type of genetic algorithm for solving it. The problem is a NP-hard combinatorial optimization problem. For randomly generated test instances of the problem, we analyze the performance of the algorithm in term of computing times and quality of the solution obtained.

This paper makes two primary contributions. First it proposes an evolutionary scheme, combining an optimization method inside of a genetic algorithm scheme for solving a reverse distribution problem. Second, a computational study of the method is performed for problem instances of up to 350 sourcing facilities, 100 candidate sites for locating reprocessing facilities and 40 remanufacturing facilities (350x100x40), concluding regarding the quality of the solution obtained and the computing times. These are the largest instances problems tested so far with evolutionary algorithms.

In the second section, we provide a literature review with a brief introduction to sustainable and reverse supply chain and particularly to the remanufacturing case in connection with reverse logistics. In the third section, we formulate the mathematical model for the problem and propose the genetic algorithm for solving it. In the fourth section, we present experimental results for large sets of networks generated randomly. The last section contains our conclusions.

2 Literature review

Adopting a friendly sustainable management implies a number of changes for companies from the strategy level up to the operational point of view, affecting their people and impacting their business processes and technology. In this regards, in [4] is noted, "the strategic level deals with decisions that have a long-lasting effect on the firm. These include decisions regarding the number, location and capacities of warehouses and manufacturing plants, or the flow of material through the logistics network". They established a clear link between facility location models and strategic decisions of supply chain management (SCM). Supply Chain Management - SCM, and in particular Sustainable Supply Chain Management – SSCM gives a good framework to address sustainable issues. Green supply chain management (GSCM) was emerging in the last few years. This concept covers every stage in manufacturing from the first to the last stage of product life cycle, i.e. from product design to recycle. [5] made a carefully literature review and he shows that a broad frame of reference for Green Supply Chain Management (GSCM) is not adequately developed. As a consequence, the author identifies the need for a "succinct classification to help academicians, researchers and practitioners in understanding integrated GSCM from a wider perspective".

We focus on the remanufacturing network (RMN) and then on reverse supply chain. Here, remanufacturing is defined as one of the recovery methods by which worn-out products or parts are recovered to produce a unit equivalent in quality and performance to the original new product and then can be resold as new products or parts.

2.1 Research on Facility Location Problems for Reverse Supply Chain Design

The problem of locating facilities and allocating customers is not new to the operations research community and covers the key aspects of supply chain design [6]. This problem is one of "the most comprehensive strategic decision problems that need to be optimized for long-term efficient operation of the whole supply chain" [7]. Such as it was observed by [8], some small changes to classical facility location models are quite hard to solve.

In the last few years, mathematical modeling and solution methods for the efficient management of return flows (and/or integrated with forward flows) has been studied in the context of reverse logistics, closed-loop supply chain and sustainable supply chain.

Several authors have studied different aspects of closed-loop supply chain problems, see for example [9-14].

In [2] are discussed the new issues that arise in the context of reverse logistics and reviewed the mathematical models proposed in the literature. In [15] is proposed a generic recovery network model based on the elementary characteristics of return networks identified in [2]. In [16] is proposed a generic mixed integer model for the design of a reverse distribution network including repairing and remanufacturing options simultaneously.

Regarding reverse logistics networks in connection with location problems, in [17] is presented a two-level distribution and waste disposal problem, in which demand for products is met by plants while the waste generated by production is correctly disposed of at waste disposal units. In [18] is described a network for recycling sand from construction waste and proposed a two-level location model to solve the location problem of two types of intermediate facility.

Regarding remanufacturing location models, in [19] is described a small reverse logistics network for the returns, processing, and recovery of discarded copiers. They presented a mixed integer linear programming (MILP) model based on a multi-level uncapacitated warehouse location model. The model was used to determine the locations and capacities of the recovery facilities as well as the transportation links connecting various locations. In [20] is proposed a 0-1 MILP model for a product recall distribution problem. They analyzed the particular case in which the customer returns the product to a retail store and the product is sent to a refurbishing site which will rework the product or dispose it properly. The reverse supply chain is composed of origination, collection and refurbishing sites. With the objective to minimize fixed and distribution costs, the model has to decide which collection sites and which refurbishing sites to open, subject to a limit on the number of collection sites and refurbishing sites that can be opened. In [21] are presented three generic facility location MIP models for the integrated decision making in the design of forward and reverse logistics networks. The formulations are based on the well-known uncapacitated fixed-charge location model and they include the location of used product collection centers and the assignment of product return flows to these centers. In [22] is presented a two-level location problem with three types of facility to be located in a reverse logistics system. They proposed a 0–1 MILP model which simultaneously considers "forward" and "reverse" flows and their mutual interactions. The model has to decide the number and locations of three different types of facilities: producers, remanufacturing centers and intermediate centers.

3 Modeling a remanufacturing supply chain network design problem (RSCP)

In this section we present the MIP model for our problem of designing a sustainable supply chain network. This problem can be categorized as a single product, static, three-echelon, capacitated location model with known demand. The remanufacturing supply chain network consists of three types of members: sourcing facilities (origination sites like a retail store), collection sites and remanufacturing facilities. At the customer levels, there are product demands and used products ready to be recovered, for example call phones. We suppose that customers return products to origination sites like a retail store. At the second layer of the supply chain network, there are reprocessing centers

(collection sites) used only in the reverse channel and they are responsible for activities, such as cleaning, disassembly, checking and sorting, before the returned products are sent back to remanufacturing facilities. At the third layer, remanufacturing facilities accept the checked returns from intermediate facilities and they are responsible for the process of remanufacturing. In this paper we address the backward flow of returns coming from sourcing facilities and going to remanufacturing facilities through reprocessing facilities properly located at pre-defined sites. In such a supply chain network, the reverse flow, from customers through collection sites to remanufacturing facilities is formed by used products, while the other ("forward" flow) from remanufacturing facilities directly to point of sales consists of "new" products.

3.1 RSCP Model

In our model is assumed that the product demands (new ones) and available quantities of used products at the customers are known and deterministic. All returned products (used products) are first shipped back to collection facilities where some of them will be disposed of for various reasons, like poor quality. The checked return-products will then be sent back to remanufacturing facilities, where some of them may still be disposed of. We introduce the following inputs and sets:

I = the set of sourcing facilities at the first layer, indexed by i

J = the set of remanufacturing nodes at the third layer indexed by j

K = the set of candidate reprocessing facility locations at the mid layer, indexed by k

a_i = supply quantity at source location $i \in I$

b_j = demand quantity at remanufacturing location $j \in J$

f_k = fixed cost of locating a mid layer reprocessing facility at candidate site $k \in K$

g_k = management cost at a mid layer reprocessing facility at candidate site $k \in K$

c_{ik} = is the unit cost of delivering products at $k \in K$ from a source facility located in $i \in I$

d_{kj} = is the unit cost of supplying demand $j \in J$ from a mid layer facility located in $k \in K$

u_k = capacity at reprocessing facility location $k \in K$

We consider the following decision variables:

w_k= 1 if we locate a reprocessing facility at candidate site $k \in K$,0 otherwise

x_{ik} = flow from source facility $i \in I$ to reprocessing facility located at $k \in K$

y_{kj} = flow from remanufacturing facility located at $k \in K$ to facility $j \in J$

Following the model proposed in [23], the remanufacturing supply chain design problem (*RSCP*) is defined by:

$$Min \sum_{k \in K} f_k w_k + \sum_{k \in K} \sum_{i \in I} c_{ik} x_{ik} \sum_{k \in K} \sum_{i \in I} g_k x_{ik} + \sum_{k \in K} \sum_{j \in J} d_{kj} y_{kj} \quad (1)$$

Subject to

$$\sum_{i \in I} x_{ik} \leq u_k w_k \qquad \forall k \in K \quad (2)$$

$$\sum_{k \in K} x_{ik} \leq a_i \qquad \forall i \in I \quad (3)$$

$$\sum_{k \in K} y_{kj} \geq b_j \qquad \forall j \in J \quad (4)$$

$$\sum_{i \in I} x_{ik} = \sum_{j \in J} y_{kj} \qquad \forall k \in K \quad (5)$$

$$x_{ik}, y_{kj} \geq 0, \qquad \forall i \in I, \forall j \in J, \forall k \in K \quad (6)$$

$$w_k \in \{0,1\} \qquad \forall k \in K \quad (7)$$

The objective function (1) minimizes the sum of the installation reprocessing facility costs plus the delivering costs from sourcing facilities to reprocessing facilities and from these to remanufacturing facilities. Constraint (2) warranties that supplying at facility $k \in K$ is delivered to a mid layer reprocessing facility already opened. Constraint (3) warranties that all the return products from I is going backward to facility $k \in K$. Constraint (4) warranties that the demand at facility j $\in K$ must be satisfied by reprocessing facilities. Constraint (5) ensures that all the return products arriving to facility k are also delivered to remanufacturing facilities. Constraint (6) is a standard positive constraint. Constraint (7) is a standard binary constraint. This model has $O(n^2)$ continuous variables where $n=max\{|I|, |J|, |K|\}$ and $|K|$ binary variables. The number of constraints is $O(n)$.

Notice that following [24], models like the *RSCP* forget the origin of the products arriving to remanufacturing facilities then we lost the trace of the products. To overcome this point, we can get another formulation introducing triply subscripted variables x_{jkl} to manage the origin to destination product flows and some other changes in parameters, variables and constraints. But this is not the objective of this paper.

3.2 An Evolutionary Scheme

Genetic Algorithms (*GA*) are a type of evolutionary algorithms (*EVA*) used to solve a number of combinatorial optimization problems. See for further details the paper by [25]. An *EVA* is composed by five basic components: (a) a genetic representation of solutions to a problem; (b) a way to create an initial population of solutions; (c) an evaluation function; (d) genetic operators that alter the genetic composition of children during reproduction and (e) values for the parameters [26]. In this section we briefly describe these components and the *GA* implementation for solving the *RSCP* problem.

Typical GA encodes the whole solution for the *RSCP* model as a chromosome, and then applies the above scheme for solving the target problem. We follow a little different approach in this paper.

We can set to 0 or 1 the value of variables w_k $\forall k \in K$, let call them w_k^* . Once you set variables w_k^* we can re-write the *RSCP* model as follow:

$RSCP_R$

$$Min \sum_{k \in K^*} f_k w_k^* + \sum_{i \in I} \sum_{k \in K} c_{ik} x_{ik} + \sum_{k \in K} \sum_{i \in I} g_k x_{ik} + \sum_{k \in K} \sum_{j \in J} d_{kj} y_{kj} \quad (1a)$$

$$Subject\ to:$$

$$\sum_{i \in I} x_{ik} \leq u_k w_k^* \qquad \forall\, k \in K^* \quad (2a)$$

$$(2) - (6)$$

Where, the set K^* contains the facilities already opened, and the variables w_k^* are now coefficients with known values. Constraint (*2a*) continues to ensure that all the sourcing facilities deliver return products to a facility already opened. The rest of constraints remain the same as the original *RSCP* model. Moreover, this associated problem is a linear programming problem.

In our evolutionary scheme, we use a genetic algorithm for guiding the whole process of seeking an optimal solution for the *RSCP* problem. However, part of the chromosome is obtained by solving to optimality the $RSCP_R$ problem. In this way, we use a kind of decomposed genetic algorithm.

The evolutionary scheme is as follows:

1. **Generate** an initial population for the head of the chromosome;
    a. Apply the feasibility procedure to satisfy capacity constraints
    b. Solve to optimality the $RSCP_R$ problem
2. **While** not Finish **do**
    a. Solve to optimality the $RSCP_R$ problem;
    b. Apply selection process;
    c. Do a partial crossover to the head of the individuals;
    d. Generate individuals using the mutation operation;
    e. Apply the feasibility procedure to satisfy capacity constraints
3. **Endwhile**;

Observe that, in step (*1*) we generate each chromosome into two steps. In step *(1a)* is generated the head of the chromosome. This part of the chromosome represents whether the facility is opened or closed as described below. The second part of the chromosome (*1b*), we call tale, is obtained solving the $RSCP_R$ problem to optimality. When it is solved the $RSCP_R$ problem, it is also simultaneously computed the fitness of each chromosome. In step (*2*) the cross-over procedure is applied to the head part of the chromosome, and again, the tale part of the chromosome is obtained solving to optimality the $RSCP_R$ problem. The rest of the steps in the above scheme are similar to a classical GA.

3.3 Representation, Initial Population and Feasible Solutions

In our implementation, each solution (individual) to the problem is coded as a chromosome. In the first part of the chromosome, called head, each gene corresponds to a facility location decision variable, taking value *1* if a facility is open at the mid layer, and zero otherwise. We use a $|K|$ dimensional string to represent facilities located. The rest of the chromosome, called the tale, represents the flows of return products between the sourcing facility and the reprocessing facilities and between the reprocessing facilities and the remanufacturing facilities. As described earlier in this paper, the chromosome´s tale is obtained solving to optimality the $RSCP_R$ problem.

An initial population of 20 individuals is generated randomly. Each gene of the head of the chromosome is generated by a 0-1 uniform probability distribution. For each chromosome of the population we apply a simple feasible solution procedure. This procedure consists in two steps. In the first step we check if the number of facilities already opened is enough to satisfy the entire demand. In the second step, for those chromosomes that do not satisfy the demand, we get a feasible solution to *RSCP* based on the initial chromosome. This procedure is rather simple; it starts open facilities till the demand is satisfied. The population is composed of just feasible solutions. The fitness of a chromosome is calculated by solving simultaneously the $RSCP_R$ problem and using the objective function (*1a*).

3.4 Genetic operators

We use the standard genetic operators. The crossover generates one new individual (chromosome) exchanging the genetic material of two (parental) individuals expecting that "good" solutions can generate "better" ones. One of these individuals is selected randomly from a set of 20 individuals, as described earlier. The other individual is the best one selected from the previous population. We do not limit the number of new chromosomes generated by crossover. In this work crossover probability (*cross_p*) is set to 0.7 (70%) and we perform one-point crossover. In the crossover procedure we generate a random value, if the *cross_p* value is greater than the random value then we pick one individual from the set. We generate another random value between one and the number of potential facility sites for the corresponding layer, i.e, a cut point dividing each individual (parent) into two segments. The child is created by combining the first segment from the first parent and the second segment from the second parent. The mutation operator changes the value of a chromosome with some small probability. In our case, we do not practice mutation, we set this probability to 0.0 (0%) and remain constant through generations of the GA. After the crossover procedure, we check for unfeasible solutions in the population. In the next step we correct this.

3.5 Additional Aspects about the Genetic Algorithm

The selection operator is based on elitist selection, favoring individuals of better fitness value to reproduce more often than the worse ones when generating the new population. In every iteration (generation) the whole population (20 individuals) is ranked in a non-decreasing order of the objective function value, and we select always the best individual. As we described earlier, feasibility of

constraints (2) is verified to every individual at every iteration. In case unfeasibility, a feasible routine is applied to get a 100% of feasible solutions in the population. Considering the optimal procedure we applied inside the genetic algorithm, we work with a reduced population size (20) and with 5 generations (iterations). Nevertheless, the performance in term of quality of the solutions obtained and computing times are promising as described hereafter.

4 Numerical Experiments

In this section we discuss and compare the computational results obtained for the proposed evolutionary algorithm. We analyze the performance of the proposed algorithm regarding computational time to get the solution and the quality of the upper bound obtained.

We implemented the algorithm in *GAMS* and we used *CPLEX* as a subroutine (called from inside *GAMS*) for solving to optimality the $RSCP_R$ problem. All the experiments were developed on a PC with 2Gb RAM and 2.3GHz. In the literature, there are not large data sets available for our problem. We generated randomly 11 test problems following similar methodologies used for well known related supply chain problems [22, 23]. These test problems are data sets corresponding to networks of up to 350 origination sites, 100 candidate sites for locating reprocessing facilities and 40 remanufacturing facilities. The data set for the test problems are given in Table 1 and they are available with the authors. All the transportation costs were generated randomly using a uniform distribution with parameters [1,40]. Management costs were set to 30 for all the instance problems except for the No.1. Instances 7-9 are the same than instances 1-6 except for the value of fixed costs that were obtained multiplying by 10 the fixed costs of instances 1-6. Instances 10 and 11 are the same than instances 8 and 9 but the capacity of each location was increased in 50%. Sourcing units (a_j), capacity of reprocessing facilities (m_k) and capacity of remanufacturing facilities (b_l) are shown in Table 1. To illustrate the size problems, problem instances 5 and 6 involve 27,200 positive variables, 80 binary variables and 500 constraints; and 39,000 positive variables, 100 binary variables and 590 constraints, respectively

In order to compare the performance of the proposed algorithm, we tested it with the test instances generated randomly. We run 5 trials for each test instances. Table 2 and 3 show the results obtained using the algorithm. For each instance problem and trial, the tables show the solution provided by the random phase of the algorithm (z_{ran}), the solution provided by the GA (z_{GA}), the computing times (seconds) and the g*ap* ($100[z_{GA}-z^*]/z^*$) obtained comparing the z_{GA} with the optimal integer value of the objective function (z^*) obtained by *GAMS*. All the gap values were rounded to two decimals. The tables also show the minimum, maximum and average value for each column and each test instance. To illustrate, for problem instance 5 and trial 2, the solution value of the random phase (z_{ran}), the GA solution value (z_{GA}), the computing times and the g*ap* are 2,131,500.0, 2,129,200.0, 74.39 seconds and 0,31% respectively. For the same problem instance, the minimum, maximum and average gap are 0.31%, 0.48% and 0.4% respectively. Observe that, for all the test instances, the maximum average *gap* is 3.65% (#1 instance) and the minimum average *gap* is 0.17% (#2 instance). Regarding computing times, notice that all the test instances were solved in less than 106 seconds.

Table 1: Data set

#	Instance Problems	J	K	L	f_k	a_j	m_k	b_l
1	40x20x15	40	20	15	300	150	400	400
2	100x40x20	100	40	20	500	150	400	750
3	150x40x20	150	40	20	1000	200	800	1500
4	200x80x20	200	80	20	1000	300	800	3000
5	300x80x40	300	80	40	2000	200	800	1500
6	350x100x40	350	100	40	2000	200	800	1750
7	40x20x15	40	20	15	3000	150	400	400
8	200x80x20	200	80	20	1000	300	800	3000
9	300x80x40	300	80	40	2000	200	800	1500
10	200x80x20	200	80	20	1000	300	1200	3000
11	300x80x40	300	80	40	2000	200	1200	1500

Table 2: Random phase solution value (z_{ran}), *GA* solution value (z_{ga}), computing times (secs) and *gap(%)*

# instance	Trial	z_{ran}	z_{ga}	secs	Gap
1	1	147800	147800	21.06	3.68
	2	148150	148150	21.88	3.93
	3	149500	147250	19.86	3.30
	4	149100	148100	20.98	3.89
	5	148200	147500	19.73	3.47
Minimum		147800,0	147250,0	19.73	3.30
Maximum		149500,0	148150,0	21.88	3.93
Average		148550,0	147760,0	20.70	3.65
2	1	521200	521200	25.36	0.21
	2	521200	520600	27.49	0.10
	3	521200	521200	24.11	0.21
	4	520600	520600	24.16	0.10
	5	521200	521200	25.35	0.21
Minimum		520600,0	520600,0	24.11	0.10
Maximum		521200,0	521200,0	27.49	0.21
Average		521080,0	520960,0	25.29	0.17
3	1	1067600	1064400	25.60	0.15
	2	1065800	1064600	28.78	0.17
	3	1065400	1069100	24.94	0.59
	4	1066600	1066400	32.24	0.34
	5	1066000	1066000	30.66	0.30
Minimum		1065400,0	1064400,0	24.94	0.15
Maximum		1067600,0	1069100,0	32.24	0.59
Average		1066280,0	1066100,0	28.44	0.31
4	1	2091700	2086000	54.41	0.16
	2	2091700	2086700	52.71	0.19
	3	2092000	2092000	60.19	0.45
	4	2092600	2089000	59.42	0.30
	5	2090600	2089900	59.63	0.35
Minimum		2090600,0	2086000,0	52.71	0.16
Maximum		2092600,0	2092000,0	60.19	0.45
Average		2091720,0	2088720,0	57.27	0.29
5	1	2132800	2132800	76.20	0.48
	2	2131500	2129200	74.39	0.31
	3	2132300	2131700	79.29	0.42
	4	2131500	2130200	90.45	0.35
	5	2132900	2131700	77.32	0.42
Minimum		2131500,0	2129200,0	74.39	0.31
Maximum		2132900,0	2132800,0	90.45	0.48
Average		2132200,0	2131120,0	79.53	0.40
6	1	2472950	2470300	100.28	0.47
	2	2470000	2469500	105.74	0.44
	3	2473050	2470900	96.00	0.50
	4	2470800	2469900	99.41	0.46
	5	2470350	2469700	100.72	0.45
Minimum		2470000,0	2469500,0	96.00	0.44
Maximum		2473050,0	2470900,0	105.74	0.50
Average		2471430,0	2470060,0	100.43	0.46

Table 3: Continuation - random phase solution value (z_{ran}), *GA* solution value (z_{ga}), computing times (secs) and *Gap*

# instance	*Trial*	z_{ran}	z_{ga}	*Secs*	*Gap*
7	1	190700	190700	20.63	1.76
	2	190050	190050	19.42	1.41
	3	188900	188900	20.38	0.80
	4	189850	189850	20.50	1.31
	5	189050	188350	19.54	0.51
Minimum		188900,0	188350,0	19.42	0.51
Maximum		190700,0	190700,0	20.63	1.76
Average		189710,0	189570,0	20.09	1.16
8	1	2766700	2766700	55.44	0.33
	2	2767000	2767000	56.98	0.34
	3	2768000	2768000	60.73	0.37
	4	2766700	2766700	59.13	0.33
	5	2768500	2768500	64.06	0.39
Minimum		2766700,0	2766700,0	55.44	0.33
Maximum		2768500,0	2768500,0	64.06	0.39
Average		2767380,0	2767380,0	59.27	0.35
9	1	3482300	3482300	80.89	0.28
	2	3481900	3481900	79.84	0.26
	3	3482000	3480800	84.88	0.23
	4	3482400	3482400	78.02	0.28
	5	3480700	3480700	75.87	0.23
Minimum		3480700,0	3480700,0	75.87	0.23
Maximum		3482400,0	3482400,0	84.88	0.28
Average		3481860,0	3481620,0	79.90	0.26
10	1	2532200	2530400	60.09	2.06
	2	2533700	2526800	56.41	1.91
	3	2528600	2527700	54.68	1.95
	4	2528600	2528600	50.71	1.98
	5	2529500	2525000	54.95	1.84
Minimum		2528600,0	2525000,0	50.71	1.84
Maximum		2533700,0	2530400,0	60.09	2.06
Average		2530520,0	2527700,0	55.37	1.95
11	1	2998800	2997100	81.13	1.26
	2	2993600	2993000	77.99	1.13
	3	2997300	2997000	74.33	1.26
	4	2995700	2991000	85.66	1.06
	5	3000900	3000900	91.87	1.39
Minimum		2993600,0	2991000,0	74.33	1.06
Maximum		3000900,0	3000900,0	91.87	1.39
Average		2997260,0	2995800,0	82.19	1.22

5 Conclusions

In this paper, we proposed a type of genetic algorithm for solving a remanufacturing sustainable supply chain network design (*RSCP*) problem. This is a NP-hard problem and it addresses the design of a remanufacturing supply network that consists of three types of member i.e., sourcing facilities (sources), reprocessing facilities and remanufacturing facilities. At the customer levels, there are product demands and used products ready to be recovered. At the second level we have reprocessing facilities that receive all the returns coming from the origination facilities. At the last level there are remanufacturing facilities. We need lo locate reprocessing facilities in order to minimize the flow cost from the origination to the remanufacturing facilities. The problem was formulated as a mixed integer 0-1 linear programming problem (*MIP*). The genetic algorithm guides the search for an optimal solution to the *RSCP* problem and it combines a random solution search with an optimal solution method for solving to optimality an associated problem. In this genetic algorithm, each chromosome is generated into two steps. First is generated the head of the chromosome, representing whether the facility is opened or closed. The second part of the chromosome is obtained solving to optimality the $RSCP_R$ problem associated to the original *RSCP* problem. Notice that, when the $RSCP_R$ problem is solved, it is also simultaneously computed the fitness of each chromosome. The proposed genetic algorithm was coded in *GAMS* and tested using 11 test instances generated randomly. Considering the few number of chromosomes and the total number of generations we used, computational results regarding *GAP* and computing times are promising.

Acknowledgments

This research was partially supported by the Fundação de Amparo á Pesquisa do Estado de Minas Gerais – FAPEMIG, VALE e CNPq - Brazil.

References

[1] Rogers, D.S., & Tibben-Lembke, R.S. (1998). *Going backwards: reverse logistics trends and practices*. Reno: Reverse Logistics Executive Council.

[2] Fleischmann, M., Krikke, H.R., Dekker, R., & Flapper, S.D.P. (2000). A characterisation of logistics networks for product recovery. *Omega*, 28, 6, 653-666.

[3] Blackburn. J.D., Guide, V.D.G., Souza, C., & Van Wassenhove, L.N. (2000). Reverse Supply Chains for Commercial Returns. *California Management Review*, 46, 6-22.

[4] Simchi-Levi, D., Kaminsky, P., & Simchi-Levi, E. (2007). *Designing & Managing the Supply Chain* (3rd ed.). New York: McGraw-Hill/Irwin.

[5] Srivastava, S. (2007). Green Supply-Chain Management: A State-of-the-Art Literature Review. *International Journal of Management Reviews*, 9, 53-80.

[6] Daskin, M.S., Snyder, L.V., & Berger, R.T. (2005). Facility Location in Supply Chain Design. In A. Langevin and D. Riopel (Eds.), *Logistics Systems: Design and Optimization (pp*. 39-65). New York, Springer.

[7] Altiparmak, F., Gen, M., Lin, L., & Paksoy, T. (2006). A genetic algorithm approach for multiobjective optimization of supply chain networks. *Computers & Industrial Engineering*, 51, 197–216.

[8] Farahani, R.Z. & Hekmatfar, M. (Eds.). (2009). *Facility location: concepts, models, algorithms and case studies.* Berlin:Physica-Verlag HD.

[9] Jayaraman, V., Guide Jr., V.D.R., & Srivastava, R.A. (1999). A closed-loop logistics model for remanufacturing. *Journal of the Operational Research Society*, 50, 497–508.

[10] Fleischmann, M. (2003). Reverse Logistics Network Structures and Design , In: *Business Aspects of Closed-Loop*

Supply Chains, Vol 2, V.D.R. Guide Jr. & L. Van Wasenhove eds., 2003, NY: Carnegie Mellon University Press, p.117-135.

[11] Barbosa-Povoa, A.P., Gomes Salema, M.I., & Novais, A.Q. (2007). Design and Planning of Closed Loop Supply Chains. In : *Supply Chain Optimization*, L. Papageorgiou & M. Georgiadis eds. NY:Wiley, p 187-218.

[12] Guide Jr., V.D.R., & Van Wassenhove, L.N. (2009). The Evolution of Closed-Loop Supply Chain Research. *Operations Research*, 57, 1, 10–18.

[13] Quariguasi Frota Neto, J., Walther, G., Bloemhof-Ruwaard, J.M., van Nunen, J., & Spengler, T. (2010). From closed-loop to sustainable supply chains: the WEEE case. *Int Journal of Production Research, 48, 15, 4463-4481.*

[14] Guangfu, L. & Juncheng, W. (2011). Research trends of network design for closed-loop supply chain. In: *Proceedings 2nd International Conference on. Software Engineering and Service Science (ICSESS)*, Beijing: IEEE, p. 761–764.

[15] Fleischmann, M., Beullens, P., Bloemhof-Ruwaard, J.M., & Van Wassenhove, L.N. (2001). The Impact of Product Recovery on Logistics Network Design. *Production and Operations Management*, 10,2, 156-173.

[16] Zhou, Y-S. & Wong, S-Y. (2008). Generic Model of Reverse Logistics Network Design. *J Transpn Sys Eng & IT*, 8, 3, 71-78.

[17] Bloemhof-Ruwaard, J.M., Salomon, M., & Van Wassenhove, L.N. (1996). The capacitated distribution and waste disposal problem. *European Journal of Operational Research*, 88, 490–503.

[18] Barros, A.I. , Dekker, R., & Scholten, V. (1998). A two-level network for recycling sand:a case study. *European Journal of Operational Research*, 110, 199–214.

[19] Krikke, H.R., Van Harten, A., & Schuur, P.C. (1999). Business case OCE: Reverse logistics network re-design for copiers. *OR Spektrum*, 21, 381–409.

[20] Jayaraman, V., Patterson, R.A., & Rolland, E. (2003). The design of reverse distribution networks: Models and solution procedures. *European Journal of Operational Research*, 150, 128–149.

[21] Sahyouni, K., Savaskan, R.C., & Daskin, M.S. (2007). A Facility Location Model for Bidirectional Flows. *Transportation Science*, 41, 4, 484-499.

[22] Lu, Z., & Bostel, N. (2007). A facility location model for logistics systems including reverse flows: The case of remanufacturing activities. *Computers & Operations Research*, 34, 2, 299–323.

[23] Li, N. (2011). Research on Location of Remanufacturing Factory Based on Particle Swarm Optimization. In: *Proceedings of IEEE MSIE 2011*, p. 1016-1019.

[24] Geoffrion, A.M., & Graves, G.W. (1974). Multicommodity Distribution System Design by Benders Decomposition. *Managament Science*, 20, 5, 822-844.

[25] Goldberg, D.. (1989). *Genetic Algorithms in Search, Optimization and Machine Learning*, Reading: Addison-Wesley.

[26] Osman, I. H. and Kelly, J. P. (1996). *MetaHeuristics: Theory & Applications*, Kluwer Academic Publishers.

Evolutionary Full-Coverage Minimum Sensor Deployment using Dual Population Structure and Multiple Overlap Measure

Joon-Hong Seok, Joon-Woo Lee and Ju-Jang Lee
Department of Electrical Engineering
Korea Advanced Institute of Science and Technology
Daejeon, Korea
Email: seokjh@kaist.ac.kr, jwl@kaist.ac.kr, jjlee@ee.kaist.ac.kr

***Abstract*—Evolutionary sensor deployment algorithm using the dual population scheme and the multiple overlap measure (ESDA-DPMO) is proposed to solve the full-coverage problem with non-penetrable obstacles. The full-coverage state group (FCSG) and the non-full-coverage state group (NFCSG) find sensor deployment solutions using different fitness functions, mutation operators and selection operators, respectively. Two distinguished search directions keep genetic diversity of sensor deployment solutions and avoid getting stuck in local optimum. In addition, information change between two is well designed for efficient exploration ability. The proposed multiple overlap measure boosts both evolution of FCSG and NFCSG. In the FCSG, by gathering sensors together as much as possible, there is a high probability of reducing redundant sensor without breaking full-coverage state. In contrast, in the NFCSG, by scattering sensors as much as possible to get lower overlap rate, higher coverage rate is obtained using same number of sensors. We perform simulations on 3 virtual maps to verify the proposed ESDA-DPMO as compared to conventional approaches. The results show that the proposed ESDA-DPMO provides full-coverage solutions efficiently.**

***Keywords*-Coverage problem, Evolutionary sensor deployment, Multiple overlap measure, Dual population**

I. Introduction

A coverage problem has received much attention in the various research fields, such as such as environmental monitoring, military detection and indoor surveillance in a target area, because coverage can be considered as a measure of the quality of services or tasks [1]–[4]. Whole region of interest should be covered by combination of many sensors to accomplish their own tasks or applications. Although there are given a large number of sensors in a sensor network, inefficient sensor deployments may lead to a low coverage rate and low performance. Thus, the importance of proper sensor deployment strategies for the coverage in the target region cannot be overemphasized.

The evolutionary approach has combined the characteristics of randomized approaches and deterministic approaches. Genetic algorithms(GA) [9], [10], Differential Evolution(DE) [11], Multiobjective approaches [12] and other heuristic optimization methods are adopted to coverage problems. Most algorithms are based on weighted sum approaches among the coverage rate, the overlap rate and the number of deployed sensors. This bottom-up approach may lead to partial-coverage above predefined percentage efficiently. However, it is difficult to provide full-coverage sensor deployment with minimum number of sensors, because these objective functions are highly correlated. In contrast, an evolutionary sensor deployment algorithm (ESDA) [13] uses a top-down approach which gives top priority to full-coverage state solutions. This top-down approach provides efficient full-coverage state solution with minimum number of sensors with well-designed mutation operators and chromosome representations. However, there is some discontinuity at the reduction of sensors while keeping the full-coverage state.

In this paper, The ESDA with dual population structure and multiple overlap measure (ESDA-DPMO) is proposed. Proposed dual population structures keep sensor deployment solutions according to fitness function of each approach respectively. In addition, information change between dual populations are well designed, so excluded individuals in a group are refined slightly and are sent to selection procedure of the other group. Another proposed measure is the multiple overlap measure for the dual population. Multiple overlap measure facilitates the optimization of two groups in dual population, the full-coverage state group (FCSG) and the non-full-coverage state group (NFCSG).

The remainder of this paper is organized as follows. Section II presents the definition of the full-coverage problem with non-penetrable obstacles. Section III explains the chromosome representation and obstacle-avoidance mutation operators of ESDA preliminarily. Section IV describes the proposed ESDA-DPMO in detail and the dual population structures and multiple overlap measure. Section V shows the simulation results among sensor deployment algorithms in various maps. Section VI concludes this paper.

II. Full-coverage Problem with Non-penetrate Obstacles

The purpose of the coverage problem is that the whole target area or target points are covered or monitored by

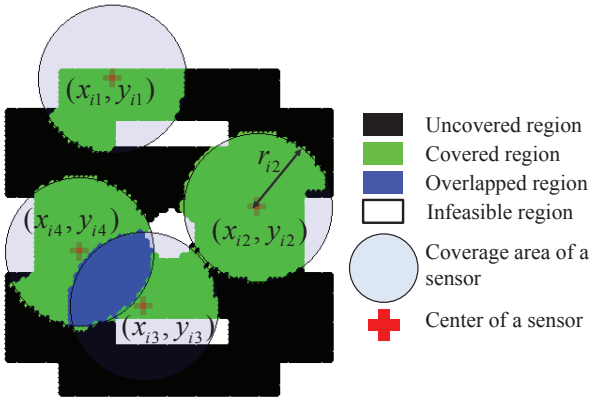

Figure 1. Sensor deployment solution representation.

sensors. A Map and sensors representations are as follows. The detail definition of the problem is defined in [13].

A. Problem Definition

1) Map Representation: A target region is denoted as R. An entire region is divided into a feasible region R_f and an infeasible region R_i. R_f and R_i are excluded.

In the feasible region R_f, sensors can be installed and this region can be covered by sensors within the coverage range. R_f can be divided into 3 subregions. First, an uncovered region R_u is defined as the region that is not covered by any sensors. A covered region R_c is defined as the region that is covered by at least one sensor. An overlapped region R_o is defined as the region that is covered by two or more sensors. In contrast, in the infeasible region R_i, sensors cannot be installed and the sight of a sensor is blocked. Generally, R_i is directly related to an obstacle region.

An entire target region R of an indoor environment is represented as a rectangular composed of a set of sample points $R = \{r_1, r_2, ..., r_{N_e}\}, N_e = W \times L/d^2$, where N_e is the number of samples in the entire region, W is the width of the rectangle including R and L is the length of the rectangular including R, and d is the interval between sample points. For the sake of convenience, we approximate an area-coverage problem into a dense point-coverage problem. The interval between sample points is much smaller than the sensing range of a sensor, the size of the obstacles and the total size of the map.

2) Sensor Representation: A sensor network S is composed of a number of sensors, $S = \{s_1, s_2, ..., s_{N_s}\}$, where s_i denotes ith sensor and N_s represents the number of sensors in the sensor network.

A binary disk model is used as the coverage model of a sensor s in a free space. A sensor s is located on the x, y axis and a feasible sensing range r. The position of the sensor (x, y) is on the target region R. Fig. 1 shows the example of the sensor deployment solution.

In some literature, probabilistic sensor models are often considered [14]. By varying the range of disk, the required number of sensor and the characteristics of sensor deployment can be reflected on the problem. So, the sensor model is not significantly addressed in this paper.

3) Objective Functions: Objective functions of the sensor arrangement problem are given as follows.

- Coverage rate(%) $F_c = 100 \times n(R_c)/n(R_f)$
- Overlap rate(%) $F_o = 100 \times n(R_o)/n(R_f)$
- Number of feasible sensor $N_s = n(S)$

The equivalent function of the coverage rate F_c is defined as uncovered rate $F_u = 100 - F_c(\%)$.

The objectives of the problem are as follows: A full-coverage sensor arrangement is required, $F_c = 100(\%)$. Every sample point is to be covered by the sensors. Minimization of the number of sensors leads to the reduction of overall cost. The other objective is the overlap rate among the sensors. The overlapped region can provide information about redundancy of sensor deployment. This overlap rate can be used differently in the dual population group, and specialized into the multiple overlap measure in Section IV.

III. Evolutionary Sensor Deployment Algorithm

In this section, the ESDA is briefly introduced [13]. The ESDA with obstacle-avoidance mutation operators solves the full-coverage sensor deployment problem. The encoding scheme and the representation on the individuals are introduced. Next, the obstacle-avoidance mutation operators are described.

A. Variable-Length Chromosomes Representations

A population P represents a set of sensor deployment solutions, $P = \{C_1, C_2, ..., C_{N_p}\}$, where N_p is the population size. The population of the ith generation is denoted as P_i, $i = 1, 2, ..., G_{max}$. Each chromosome C in the population P represent a sensor deployment solution including a sensor network S. Each gene g in a chromosome is mapped to a sensor s. A gene g has 3 properties: the position of sensor with respect to X and Y coordinates (x, y) and the radius of the sensing range, r. The variable g_{ij} represents sensor S_j including the location and the radius of the sensor. The variable j is the total number of sensors in the entire region, $i = 1, 2..., N_p$, where N_p is the number of chromosomes in the population P. A population structure is shown in Fig. 2(a).

B. Obstacle-Avoidance Mutation Operators

1) Insertion Mutation: This operator adds a gene into the offspring chromosomes. Physically, a sensor is deployed additionally for covering the uncovered region in the sensor arrangement solution represented by each chromosome. The operation is illustrated in Fig. 2(b). It may improve the coverage rate, but the required number of sensors is increased.

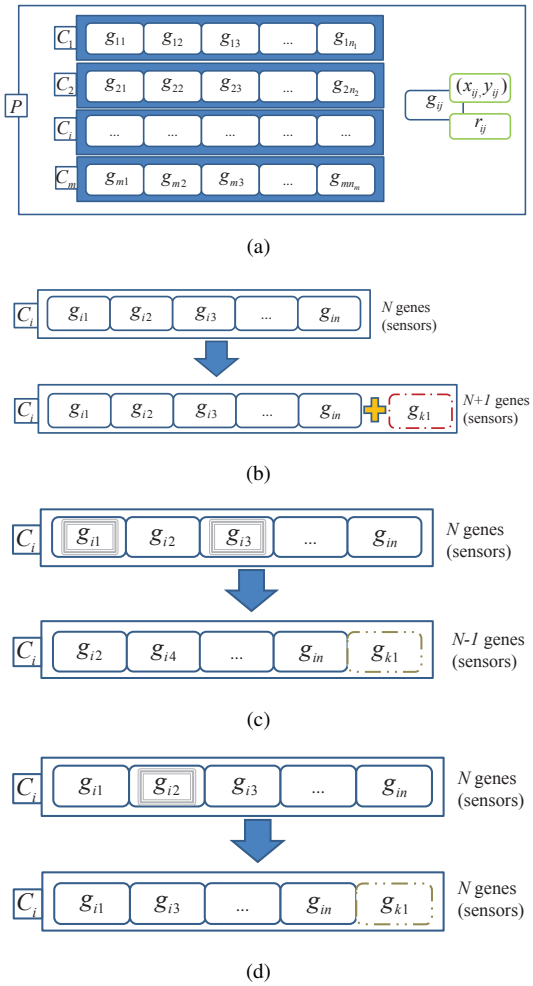

Figure 2. (a) Population, chromosomes, genes representation for sensor deployment solution. (b) Illustration of the operation of insertion mutation operator. (c) Illustration of the operation of fusion mutation operator. (d) Illustration of the operation of substitution mutation operator.

2) Fusion Mutation: If this operator is selected in some chromosome, ESDA selects a gene on the chromosome and finds the gene corresponding to nearest sensor. ESDA tries to merge two genes into a new gene within the square region made by centers of two sensors. If the center of new sensor is on the R_i, this operator applied to two genes is invalid and the substitution mutation is performed. If ESDA checks the validity of this operator successfully, two select genes are deleted and new merged gene is inserted to the chromosome. An example is illustrated in Fig. 2(c). This operator reduces the number of sensors while keeping the full-coverage state as much as possible.

3) Substitution Mutation: This operator moves a randomly selected sensor. A sensor can move towards any direction among 8 directions by at most a half of sensing range within the feasible region. An example is illustrated in Fig. 2(d). This operator has weaker effects because a risk

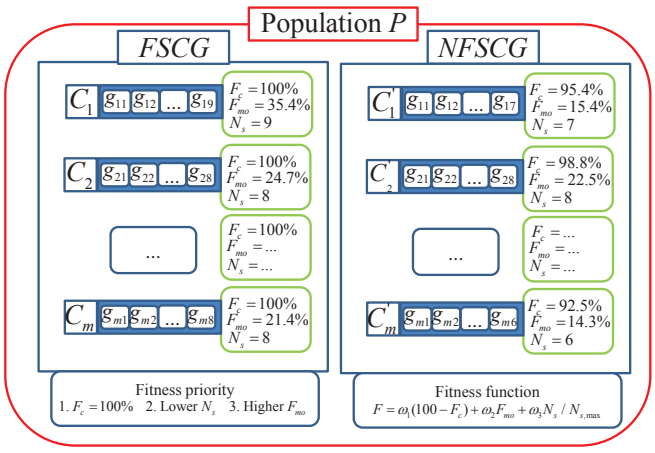

Figure 3. Illustration of ESDA-DPMO population structure.

of failing full-coverage state exists and the overall number of sensors is not reduced. Small amount of exploitation can be performed steadily.

IV. Proposed Dual Population Structure and Multiple Overlap Measure for ESDA

This section introduces ESDA-DPMO for solving the full-coverage sensor node deployment problem. The dual population structure and the multiple overlap measure are also introduced.

A. Dual Population Structure

There are two way of improving deployment solutions. One is that full-coverage solutions are obtained by inserting sensors, and then try to reduce redundant sensor. The other is that the sensors are scattered properly in target region without inserting additional sensors. The former is to keep the full-coverage state solutions in the population as much as possible. In contrast, the latter is to reduce the redundancy of current sensor deployment solutions without changing the number of sensors. In this paper, two population groups are proposed for satisfying both approaches. One is the FCSG for the top-down approach and the other is the NFCSG for the bottom-up approach.

1) Full-Coverage State Group: The fitness function of FCSG is composed of a hierarchical structure. The primary fitness function of FCSG is whether 100% coverage is satisfied or not. Let FG_i be the FCSG of ith generation and let FC_k be the kth individual in the FG_i. If full-coverage state is not satisfied, then the FG_i cannot get higher fitness value in the FG_i regardless of the number of deployed sensors. When there are two solutions with full-coverage state, less number of sensors and higher overlapped rate are compared in turn. Higher overlapped region may lead to gather the sensors as much as possible, thus the probability of eliminating excess sensors are increased.

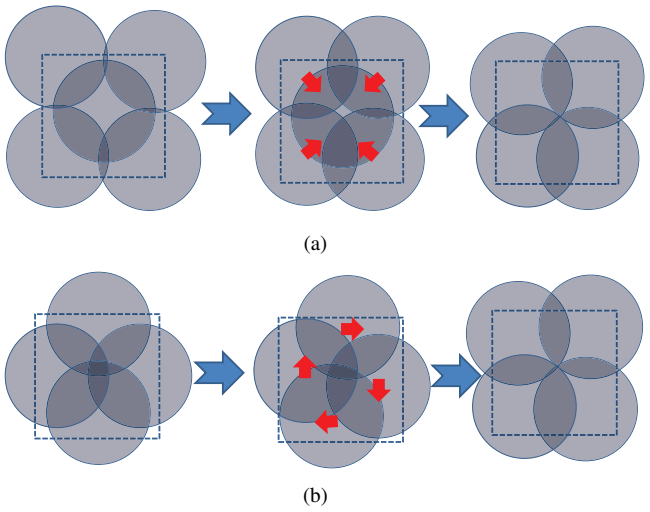

Figure 4. Two full-coverage sensor deployment approach with minimum sensors. (a) A top-down approach. The individual is included in FCSG. (b) A bottom-up approach. The individual is included in NFCSG.

Applied mutation operators are fusion and substitution mutation. Fusion mutation is mainly applied to reduce the number of sensors while keeping the full-coverage state as much as possible. When there is excess number of sensors on some individual and redundancy is appeared, it is highly probable that two sensors are merged into one sensor without breaking the full-coverage state solution. In contrast, the substitution mutation is applied to move a sensor a small amount, thus finding higher overlapped rate solutions. This mutation operator cannot reduce the number of sensor, so the result is not significantly improved compared with fusion mutation.

Selection procedure is defined as follows. After mutation operators are applied to FC in current generation, the generated offspring individuals FC' are checked whether the full-coverage state is satisfied or not. Survived offspring FC'_k are included in the full-coverage offspring group, FO_i. Also, some offspring which satisfy the full-coverage state by inserting sensors from the NFCSG are also included in the FO_i. The parent individuals of FC_{i+1} are selected by the tournament selection among individuals of FO_i and FG_i in the current generation.

FCSG finds full-coverage state solutions using the top-down approach by keeping full-coverage state during all generations.

2) Non-Full-Coverage State Group: NFCSG does not need to keep the full-coverage state. Let NFG_i be the NFCSG of ith generation and let NC_k be the kth individual in the NFG_i. The coverage rate below 100% is allowed and it is possible that the individuals with less number of sensors can be survived in NFCSG. There is no strict hierarchy in the fitness function of the NFCSG. Weighted sum fitness function is used in the NFCSG. Certainly, the coverage rate is most important and the number of sensor is as follows and the overlapped rate is last. The difference compared as FCSG is the overlapped rate. To increase the successful rate of fusion mutation, the higher overlapped rate is demanded in the FCSG, but in the NFCSG, there is no need to use fusion mutation because the full-coverage state is already not satisfied. The coverage rate of individuals in NFCSG is less than 100%, thus the reduction of sensor is not proper to satisfy full-coverage state. The substitution of each sensor is only allowed, and tries to obtain full-coverage state solutions without adding or deleting sensors.

Applied mutation operators are substitution and insert mutation. The substitution mutation is applied to each NC_k, and then NC'_k is generated. To obtain higher coverage rate and lower overlapped rate, the sensors should be scattered properly. Insertion mutation is only applied to generate full-coverage individuals NC''_k for the FO_i as mentioned previously.

Selection procedure is defined as follows. Some individuals FC'_k which are failed to check full-coverage state from the FG_i are included in the non-full-coverage offspring group, NFO_i. Also, all offspring NC' are included in NFO_i. The parent individuals of NFC_{i+1} are selected by the tournament selection among individuals of NFO_i and NFG_i in the current generation.

3) Information change: Tournament selection procedure is applied to each group using different fitness functions. Two groups are independently evolved, but the information change between two groups can increase genetic diversity to avoid getting stuck in the local optimum. In addition, the non-selected individuals are recycled in other group with minor refinement, thus computational cost can be reduced.

B. Multiple Overlap Measure

Multiple overlap measure is proposed in this paper. Multiple overlap measure considers more penalty or advantage in the region which covered by many sensors. Multiple overlap measure facilitates to gather sensors as much as possible in FCSG and to split sensors as much as possible in NFCSG. In the literatures, the overlapped region is defined as the region covered by two or more sensors, thus the influence of multiple sensors are not concerned. However, as the number of sensors is increased in some region, the probability of merging sensors is also increased in FCSG. Also, in the NFCSG, it means that the sensors are not properly scattered in the target region. Multiple overlap measure is defined as follows.

$$F_{mo} = 100 \times n(R_{mo})/n(R_f) \quad (1)$$

$$R_{mo} = \sum((i-1) * R_{o,i}), \qquad i = 2, 3, \ldots \quad (2)$$

If there are only overlapped region by two sensors, then $R_{mo} = R_{o,2} = R_o$. As the number of overlapped sensor is increased at one sample point, the overlapped point is

$FG_0, NFG_0 \leftarrow$ Initialize and evaluate populations
for $i := 1$ to G_{max} **do**
  for $k := 1$ to $N_p/4$ **do** ▷ $FG_i, FCSG$
    while Full-coverage is not satisfied **do**
      $FC'_k \leftarrow InsMutation(FC_k)$
    end while
    if $rand() < p_{fsm}$ **then**
      $FC'_k \leftarrow FusMutation(FC'_k)$
    else
      $FC'_k \leftarrow SubstMutation(FC'_k)$
    end if
    $FC'_k \leftarrow$ Evaluate individual
    if FC'_k is a full-coverage state **then**
      $NFO_i \leftarrow FC'_k$
    else
      $FO_i \leftarrow FC'_k$
    end if
  end for
  for $k := 1$ to $N_p/4$ **do** ▷ $NFG_i, NFCSG$
    $NC'_k \leftarrow SubstMutation(NC_k)$
    $NC''_k \leftarrow InsMutation(NC'_k)$
    $NC'_k, NC''_k \leftarrow$ Evaluate individual
    $NFO_i \leftarrow NC'_k$
    if NC''_k is a full-coverage state **then**
      $FO_i \leftarrow NC''_k$
    end if
  end for
  $FG_{i+1} \leftarrow$ Select $N_p/4$ chromosomes from FG_i and FO_i by tournament selection
  $NFG_{i+1} \leftarrow$ Select $N_p/4$ chromosomes from NFG_i and NFO_i by tournament selection
end for

Figure 5. A pseudo-code of ESDA-DPMO

Table I
MAP SETTING

	Optimum N_s	Sample Points $n(R_f)$	Map Size
Map1	11	2753	10mX10m
Map2	26	8010	15mX22.5m
Map3	53	14961	25mX30m

counted as $(i-1) \times R_{o,i}$ points. In the conventional ESDA, $R_o \subset R_c$ and $n(R_o) \leq n(R_c)$ are satisfied, however, in the proposed ESDA-DPMO, $R_{mo} \subset R_c$ is still satisfied, but $n(R_{mo}) \leq n(R_c)$ is not always valid because of count multiplicity of overlapped region by 3 or more sensors.

V. SIMULATION RESULTS

In this section, ESDA-DPMO and other conventional ESDA algorithm are applied to various types of maps.

Table II
THE MEANING OF REGION ACCORDING TO COLOR

The Number of Covered Sensors	
Black	0
Green	1
Blue	2
Red	3
Light Blue	4
Purple	5

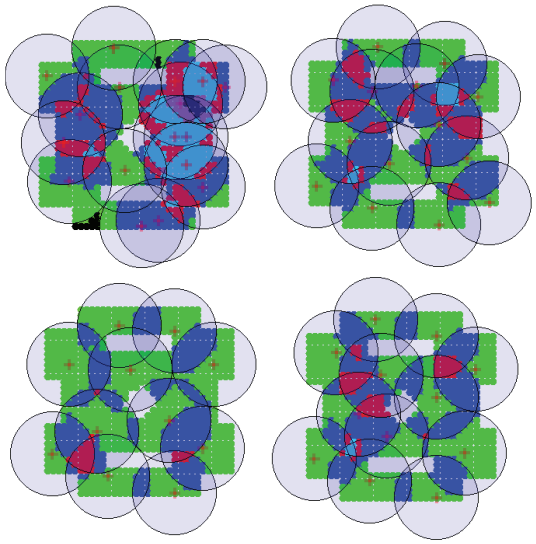

Figure 6. Best sensor deployment results in the Map1. 1st, 100th, 200th and 245th(final) generation from the left-most figure in a clockwise direction.

A. Simulation Conditions

In this simulation, we used the following parameter settings: N_p is fixed at 40 and the number of offspring generated is a half of the N_p; In the FCSG of ESDA-DPMO, the fusion mutation is applied 75% probability and the substitution mutation is applied by 25%. In the NFCSG of ESDA-DPMO, the fusion mutation is excluded and the only substitution mutation is applied all the time. Also, insertion mutation is applied to generate full-coverage state solutions in the NFCSG. Map information is shown in Table I.

$N_{s,max}$ is determined by the average number of sensors from the random deployment until the full-coverage state is satisfied during 10 iterations. Average numbers of evaluation, generation and computation times are average value during 20 independent iterations.

B. Sensor Deployment Results in the Virtual Maps

The number of covered sensor according to color in the figures are described in the Table II. The number of generations and computation times in the 3 virtual maps of each algorithm are shown in Table III. Because the ORRD is deterministic approaches, the deployed number of sensor is mentioned only. Fig. 6, 7 and 8 show the best deployment

Table III
SIMULATION RESULTS IN 3 VIRTUAL MAPS

	ESDA-DPMO		ESDA-ori		GA		ORRD
	N_G	Time(s)	N_G	Time(s)	N_G	Time(s)	N_s
Map1	275.65	21.53	304.05	20.29	843.55	32.37	20
Map2	5697.90	1063.54	6804.25	1082.43	19805.7	1770.58	36
Map3	9423.25	5324.59	11423.65	5524.72	53895.1	11176.09	75

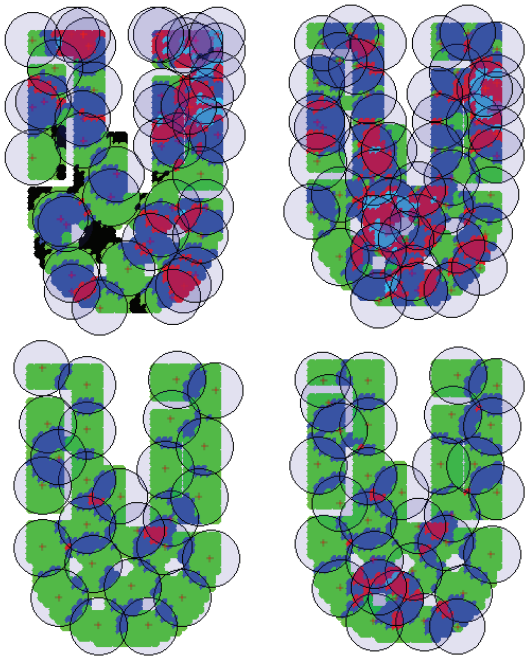

Figure 7. Best sensor deployment results in the Map2. 1st, 100th, 200th and 572th(final) generation from the left-most figure in a clockwise direction.

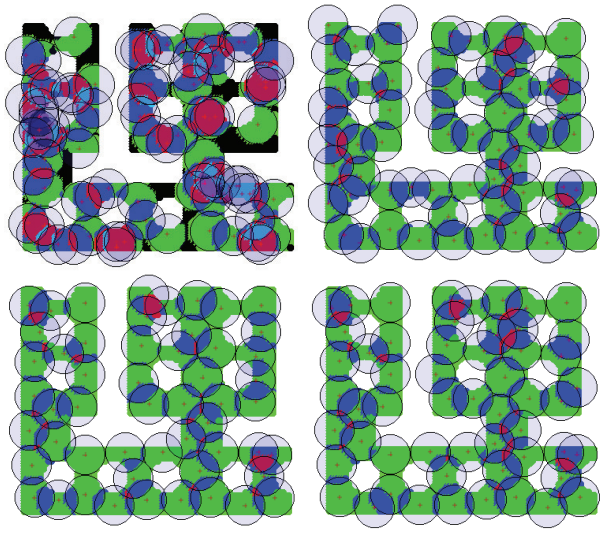

Figure 8. Best sensor deployment results in the Map3. 1st, 1000th, 2000th and 6352th(final) generation from the left-most figure in a clockwise direction.

results of ESDA-DPMO in the 3 maps according to the number of generations.

1) Convergence Property of ESDA-DPMO: In the Fig. 6, because the sensors are randomly placed, there are a lot of uncovered region and highly overlapped region. When the number of sensors is enough to cover the whole region in the early generations, the redundant sensors are merged or deleted by the fusion mutation on the individuals of the FCSG. In the 100th generations, there are little multiple-overlapped region compared as initial solutions. As the ratio of multiple-overlapped region is decreased, the redundancy of sensor deployment is also increased. It is more difficult to reduce a sensor as the number of sensors approaches into the optimal number. In this situation, the influence of individuals of the NFCSG affects to find less number of sensors while keeping a full-coverage state. The fusion mutation has a risk of breaking the full-coverage state, but, this operation is indispensable to reduce the number of sensors. The NFCSG receives the individuals which loses full-coverage state from the FCSG, and provides new location of sensors to the FCSG. Because the location of sensors using fusion mutation is restricted by the distance between sensors, the diversity of solutions are not enough to reduce even one sensor. In summary, when the excess number of sensors is deployed, the optimization of FCSG leads to delete redundant sensors, and then the NFCSG supports the weakness of FCSG according to lower redundancy when less number of sensors.

2) Comparison with Other Algorithms: First, the simple deployment using GA suffers from the continuous property of weighted sum approaches. To increase the coverage rate, the overlap rate is also increased due to the coverage rate of neighbor sensors. Small variation between the coverage rate and the overlap rate interferes to keep the full-coverage state solutions. Therefore, the computational cost is wasted to find non-full-coverage state solutions. In the Map3, the simple deployment using GA severely suffers from finding the full-coverage state solutions. Certainly, the solutions with higher coverage rate and excess number of sensors can be defeated by the solutions with lower coverage rate and less number of sensors in the complex map. The ESDA-DPMO and the ESDA-ori shows better performance than the simple deployment using GA.

By comparing ESDA-DPMO and ESDA-ori, the ESDA-DPMO shows better performance compared as the ESDA-ori in perspective of the number of generations. It seems that two reasons can be found. One is the existence of multiple

overlap measure in the ESDA-DPMO and the other is the full-coverage state solutions generated by the individuals of the NFCSG help to escape the local optimum more easily. In fact, it seems that it is difficult for the individuals of NFCSG to generate many full-coverage state solutions, but the many solutions with higher coverage rate and less number of sensors near the full-coverage state solutions can be generated and provided. This cooperation of two distinguished population structure may be helpful to get the full-coverage state solutions in the complex environment. Meanwhile, the ESDA-DPMO takes more computational time compared as the ESDA-ori. It seems that the minor refinements to provide full-coverage state solution from the NFCSG to the FCSG requires more time a little bit.

One of the deterministic algorithms, ORRD cannot provide sensor deployment solutions with full-coverage state using minimum number of sensors. These deterministic approaches deploy sensors sequentially in the environment, thus obtaining full-coverage state in the end. However, the number of sensors is not considered at all.

VI. Conclusion

In this paper, evolutionary sensor deployment algorithm using the dual population scheme and the multiple overlap measure is proposed to solve the full-coverage problem with non-penetrable obstacles.

The FCSG and the NFCSG of dual population structure keep genetic diversity of sensor deployment solutions and avoid getting stuck in local optimum. In addition, information change between dual populations lead to less computational cost compared as generating new individuals from scratch. Also, more efficient exploration ability is obtained by combining two different characteristics

The proposed multiple overlap measure boosts both evolution of FCSG and NFCSG. In the FCSG, by gathering sensors together as much as possible, there is a high probability of reducing redundant sensor without breaking full-coverage state. In contrast, in the NFCSG, by scattering sensors as much as possible to get lower overlap rate, higher coverage rate is obtained using same number of sensors.

Compared with conventional ESDA, simple deployment using genetic algorithm and deterministic algorithm, ORRD, the proposed ESDA-DPMO provides full-coverage state solutions with minimum number of sensors using less computational cost.

References

[1] J. Cortes, S. Martinez, T. Karatas, and F. Bullo, "Coverage control for mobile sensing networks," *Robotics and Automation, IEEE Transactions on*, vol. 20, no. 2, pp. 243 – 255, Apr. 2004.

[2] S. S. Ge and C. Fua, "Complete multi-robot coverage of unknown environments with minimum repeated coverage," in *IEEE International Conference on Robotics and Automation*, Apr. 2005, pp. 715 – 720.

[3] N. Hazon and G. A. Kaminka, "On redundancy, efficiency, and robustness in coverage for multiple robots," *Robotics and Autonomous Systems*, vol. 56, no. 12, pp. 1102 – 1114, Dec. 2008.

[4] H. Choset, "Coverage for robotics a survey of recent results," *Ann. Math. Artif. Intell.*, vol. 31, pp. 113–126, 2001.

[5] X. Hu, J. Zhang, Y. Yu, H. Chung, Y. Li, Y. Shi, and X. Luo, "Hybrid genetic algorithm using a forward encoding scheme for lifetime maximization of wireless sensor networks," *IEEE Trans. Evol. Comput.*, vol. 14, no. 5, pp. 766–781, Oct. 2010.

[6] J. Xiao, S. Han, Y. Zhang, and G. Xu, "Hexagonal grid-based sensor deployment algorithm," in *Control and Decision Conference*, May 2010, pp. 4342–4346.

[7] C. Chang, C. Chang, Y. Chen, and H. Chang, "Obstacle-resistant deployment algorithms for wireless sensor networks," *IEEE Trans. Veh. Technol.*, vol. 58, no. 6, pp. 2925–2941, Jul. 2009.

[8] A. Howard, M. Mataric, and G. Sukhatme, "Mobile sensor network deployment using potential fields: A distributed, scalable solution to the area coverage problem," *Distributed Autonomous Robotic Systems*, vol. 5, pp. 299–308, Jun. 2002.

[9] K. P. Ferentinos and T. A. Tsiligiridis, "Adaptive design optimization of wireless sensor networks using genetic algorithms," *Computer Networks*, vol. 51, no. 4, pp. 1031 – 1051, 2007.

[10] C.-C. Lai, C.-K. Ting, and R.-S. Ko, "An effective genetic algorithm to improve wireless sensor network lifetime for large-scale surveillance applications," in *IEEE Congress on Evolutionary Computation*, Sep. 2007, pp. 3531 –3538.

[11] S. Mendes, G. Pulido, S. Perez *et al.*, "A differential evolution based algorithm to optimize the radio network design problem," in *IEEE International Conference on e-Science and Grid Computing*, Dec. 2006, pp. 119–119.

[12] S. Chaudhry, V. Hung, R. Guha, and K. Stanley, "Pareto-based evolutionary computational approach for wireless sensor placement," *Engineering Applications of Artificial Intelligence*, 2010.

[13] J.-H. Seok, J.-Y. Lee, W. Kim, and J.-J. Lee, "Evolutionary sensor deployment algorithm for full-coverage problem with non-penetrable obstacle constraints," 2012, submitted.

[14] J. Lee, B. Choi, and J. Lee, "Energy-efficient coverage of wireless sensor networks using ant colony optimization with three types of pheromones," *Industrial Informatics, IEEE Transactions on*, vol. 7, no. 3, pp. 419–427, 2011.

A Binary Particle Swarm Optimization-based algorithm to Design a Reverse Logistics Network

Ernesto Del R. Santibanez-Gonzalez[1], and Henrique Pacca Luna[2]
[1]Department of Computer Science, Federal University of Ouro Preto, Ouro Preto, MG, Brazil
[2]Computer Science Institute, Federal University of Alagoas, Maceió, AL, Brazil

Abstract - *As recognized by several authors, the design of a reverse logistics network is a complex problem and still relatively unexplored and underdeveloped. We propose a binary particle swarm optimization (BPSO)-based scheme for solving a NP-hard remanufacturing network design problem. The algorithm combines a traditional stochastic search with an optimal solution method for solving to optimality a relaxed LP problem. We divide the swarm into two elementary groups. The first swarm group guides the search for the best location of remanufacturing facilities, while the second group defines the optimal flows between the facilities. We solve to optimality a relaxed LP problem obtained from the original problem and then we project the solution into the swarm space. The algorithm was coded in GAMS and we report computational results for 10 network instances generated randomly with up to 350 sourcing facilities, 100 candidate sites for locating reprocessing facilities and 40 remanufacturing facilities. Computational results regarding gap and computing times are promising.*

Keywords: Evolutionary algorithm ; particle swarm optimization; sustainable supply chain problem; reverse logistics; integer programming

1 Introduction

The management of product return flows has received increasing attention in the last decade. The efficient stewardship of waste and product return flows is concerned with the final destination of products and their components, and what is their impact on the pollution of the air, water and earth besides the costs of treating the disposal in landfill. There are specific rules in some regions like the European Union, where The European Waste Electrical and Electronic Equipment Directive (WEEE) and the End of Life Vehicles Directive, (ELV) are encouraging companies in the automotive industry to collaborate with other businesses and organizations in the supply chain to ensure that products can be disassembled and reused, remanufactured, recycled or disposed of safely at the end of their life.

In addition to stronger legal environmental restrictions, there are several reasons why an increasing number of companies will be interested in becoming engaged in sustainable initiatives such as the management of reverse flows within their supply chain [1,2]. Such as it was noted by some authors [3], huge monetary values 'can be gained by redesigning the reverse supply chain to be faster and reduce costly time delays'. According to the same authors, design strategies for reverse supply chains are relatively unexplored and underdeveloped. Returned products are remanufactured if this strategy is judged to be cost-effective. Some firms could treat all of the product returns as defective. Some returned products may be new and never used; then these products must be returned to the forward flow. Some products that are not reused or remanufactured are sold for scrap or recycling. Remanufactured products are sold in secondary markets for additional revenue, often to a marketing segment that is unwilling or unable to purchase a new product. In this context, remanufacturing activities are recognized as a main option of recovery in terms of their feasibility and benefits. In this paper is addressed the problem of designing a remanufacturing supply chain network and it is proposed a binary particle swarm optimization-based algorithm for solving it. We study this NP-hard combinatorial optimization problem as part of reverse logistics problems.

In the last decades, evolutionary algorithms (EVO) have been widely used as robust techniques for solving a number of hard combinatorial optimization (CO) problems. An EVO is directed by the evolution of a population in the search for an optimum solution to the CO problems. Particle Swarm Optimization (*PSO*) is an evolutionary algorithm that has been applied with success in many areas and appears to be a suitable approach for several optimization problems. Since it has been indicated by some authors, in spite of this technique to have been used by success in many continuous problems, in the discrete or binary version there are still some difficulties [4]. In this paper, for test instances of the problem that were generated randomly, we analyze the performance of the proposed algorithm in term of computing times and quality of the solution obtained.

This paper makes two primary contributions. First, we propose a *PSO*-based scheme, combining an optimization method inside of a *PSO* algorithm scheme for solving a reverse supply chain problem. Second, a computational study of the proposed method is performed for problem instances of up to 350 sourcing facilities, 100 candidate sites for locating reprocessing facilities and 40 remanufacturing facilities (350x100x40), to provide conclusions regarding the quality of the solution obtained and the computing times. These are the largest instances problems tested so far with evolutionary algorithms.

The rest of the paper is organized as follows: In the second section, we provide a literature review with a brief introduction to sustainable and reverse supply chain and with a special emphasis on to the remanufacturing case in connection with reverse logistics. In the third section, we formulate the mathematical model for the problem. In section 4 is proposed the *PSO* algorithm for solving it. In the fifth section, we present experimental results for large sets of networks generated randomly. The last section contains our conclusions.

2 Literature review

The rise of environmental and sustainable concern implies a number of changes for companies from the strategy level to the operational viewpoint, affecting their people and impacting their business processes and technology. In this regard, network design and facility location models are among the important strategic decisions for companies and organizations facing sustainable issues. Supply Chain Management - SCM, and more specifically Sustainable Supply Chain Management – SSCM provide a good framework for addressing sustainable issues. SSCM involves (a) many organizations, (b) many business processes across and within these organizations, and (c) with social, environmental and economic objectives shared by each organization and the entire Supply Chain. Reverse logistics is part of the SSCM and comprises a series of activities to treat returned products until they are properly recovered or disposed of [1]. These activities include collection, cleaning, disassembly, test and sorting, storage, transport, and recovery operations. Regarding recovery operations, we can find a combination of several main recovery options, like reuse, repair, refurbishing, remanufacturing, cannibalization and recycling [5].

There is another type of important logistics network design problem for the specific case of closed-loop supply chains. Typically, the problem of logistics network design is addressed for 'forward' supply chains or reverse supply chains, as in the case that we mentioned previously. When we integrate the forward and reverse supply chains, we obtain a closed system and then there is a new class of problems encompassed by the term closed-loop supply chain management (and design).

In this paper, we focus on the remanufacturing network problem and then on reverse supply chain. Here, remanufacturing is defined as one of the recovery methods by which worn-out products or parts are recovered to produce a unit that is equivalent in quality and performance to the original new product and that can be resold as new products or parts. Because remanufacturing activities are often implemented by the original producer such a network is likely to be a closed-loop system. Remanufacturing activities are recognized as the main option for recovery in terms of feasibility and benefits. It provides firms with a way to master the disposal of their used products, to reduce effectively the costs of production and to save raw materials.

2.1 Research Related to Network Design and Facility Location Models for Reverse and Closed-loop Supply Chain

The facility location is one of the strategic problems being part of a planning process for managing and designing the supply chain network. The problem of locating facilities and allocating customers is not new to the operations research community and covers the key aspects of supply chain design [6]. This problem is one of 'the most comprehensive strategic decision problems that need to be optimized for long-term efficient operation of the whole supply chain' [7]. As it was observed by [8], some small changes to classical facility location models turn these problems quite hard to solve.

In the last few years, mathematical modeling and solution methods for the efficient management of return flows (and/or integrated with forward flows) has been studied in the context of reverse logistics, closed-loop supply chain and sustainable supply chain.

In [9] the research on reverse logistics (and closed-loop supply chain) was classified into three functional areas: Distribution, Inventory and Production and, Supply Chain Scope. Traditional distribution decisions involve the design of network and the location of forward and reverse facilities for the distribution of products and for collecting and reprocessing returned products. In this work we focus on quantitative models for designing closed-loop supply chains, and it concerns the decisions regarding the topological structure of the network, the number of facilities to locate, their locations and capacities and the allocation of product flows between the facilities.

For a review of research on quantitative models for reverse logistics and closed-loop supply chains before 2000, we refer to [9]. [10] did a compilation of the research published on reverse logistics within the period 1995-2005. They studied the topic based on the classification proposed by [9].

As argued by numerous authors, traditional approaches for solving closed-loop (reverse) supply chains network design problems usually formulate large-scale mixed-integer linear programs (MILP) that model potential facility location as binary and product flows as positive variables. Typically, these problems belong to the class of NP-hard combinatorial optimization problems. The integration between forward and reverse flows into closed-loop supply chains networks introduce some modifications to the traditional facility location models and also give rise to some additional complexities.

In chronological order, reverse logistics models are discussed recently, for example, by [11-14]. Almost all the authors proposed MILP models. The majority of solution methods are based on standard commercial packages.

Closed-loop supply chain models are taking into account in [15-19]. Stochastic models in combination with multiobjective function were presented by [20].

Regarding evolutionary algorithms for solving related problems have been studied by: Simulated Annealing [21]; Genetic Algorithm [18], [22], [23]; Memetic Algorithm [24] and Tabu Search [21]. Notice that in [23] were solved problems of up to 15 returning centers, 10 disassembly centers

and 14 processing centers. They did not report computational results regarding time or the quality of the gap obtained. In [21] were solved problems with network of up to 100x40x30 with a maximum computing time (s) of 2,939 and a maximum gap (compared to a lower bound) of 15%.

2.2 Discrete Particle Swarm Optimization Algorithm

PSO is a metaheuristics based on the social behavior and communication of bird's flock and shoal of fishes [25]. *PSO* can be considered as an evolutionary algorithm because its way of exploration via neighborhood of solutions (particles) across a population (swarm) and exploiting the generational information gained. But, it has some divergences from other evolutionary algorithms in such a way that it has no evolutionary operators such as crossover and mutation of genetic methods. *PSO* has the advantage that is ease of use with fewer parameters to adjust. In *PSO*, the potential solutions (particles), move around in a multidimensional search space with a velocity, which is constantly updated by a combination of the particle's own experience, the experience of the particle's neighbors and the experience of the entire swarm. *PSO* has been successfully applied to a wide range of applications [26]. Since *PSO* is developed for continuous optimization problem initially, most existing *PSO* applications are resorting to continuous function value optimization [26, 27]. Recently, a few researches applied *PSO* for solving discrete combinatorial optimization problems (for example: [28, 29]).

3 Mathematical Model for designing a remanufacturing supply chain network (RSCP)

In this section we present the MILP model for the problem of designing a sustainable supply chain network. This problem can be categorized as a single product, static, three-echelon, capacitated location model with known demand. The remanufacturing supply chain network consists of three types of members: sourcing facilities (origination sites like a retail store), collection sites and remanufacturing facilities. At the customer levels, there are product demands and used products ready to be recovered, for example cell phones. We suppose that customers return products to origination sites like a retail store. At the second layer of the supply chain network, there are reprocessing centers (collection sites) used only in the reverse channel and they are responsible for activities, such as cleaning, disassembly, checking and sorting, before the returned products are sent back to remanufacturing facilities. At the third layer, remanufacturing facilities accept the checked returns from intermediate facilities and they are responsible for the process of remanufacturing. In this paper we address the backward flow of returns coming from sourcing facilities and going to remanufacturing facilities through reprocessing facilities properly located at pre-defined sites. In such a supply chain network, the reverse flow, from customers through collection sites to remanufacturing facilities is formed by used products, while the other ("forward" flow) from remanufacturing facilities directly to point of sales consists of "new" products.

3.1 RSCP Model

In our model is assumed that the product demands (new ones) and available quantities of used products at the customers are known and deterministic.

We introduce the following inputs and sets:

I = the set of sourcing facilities at the first layer, indexed by i

J = the set of remanufacturing nodes at the third layer indexed by j

K = the set of candidate reprocessing facility locations at the mid layer, indexed by k

a_i = supply quantity at source location $i \in I$

b_j = demand quantity at remanufacturing location $j \in J$

f_k = fixed cost of locating a mid layer reprocessing facility at candidate site $k \in K$

g_k = management cost at a mid layer reprocessing facility at candidate site $k \in K$

c_{ik} = is the unit cost of delivering products at $k \in K$ from a source facility located in $i \in I$

d_{kj} = is the unit cost of supplying demand $j \in J$ from a mid layer facility located in $k \in K$

u_k = capacity at reprocessing facility location $k \in K$

We consider the following decision variables:

w_k= 1 if we locate a reprocessing facility at candidate site $k \in K$,0 otherwise

x_{ik} = flow from source facility $i \in I$ to reprocessing facility located at $k \in K$

y_{kj} = flow from remanufacturing facility located at $k \in K$ to facility $j \in J$

Following the model proposed by [30], the remanufacturing supply chain design problem (*RSCP*) is defined by:

$$Min \sum_{k \in K} f_k w_k + \sum_{k \in K} \sum_{i \in I} c_{ik} x_{ik} \sum_{k \in K} \sum_{i \in I} g_k x_{ik} + \sum_{k \in K} \sum_{j \in J} d_{kj} y_{kj} \quad (1)$$

Subject to

$$\sum_{i \in I} x_{ik} \leq u_k w_k \qquad \forall k \in K \quad (2)$$

$$\sum_{k \in K} x_{ik} \leq a_i \qquad \forall i \in I \quad (3)$$

$$\sum_{k \in K} y_{kj} \geq b_j \qquad \forall j \in J \quad (4)$$

$$\sum_{i \in I} x_{ik} = \sum_{j \in J} y_{kj} \qquad \forall k \in K \quad (5)$$

$$x_{ik}, y_{kj} \geq 0, \qquad \forall i \in I, \forall j \in J, \forall k \in K \quad (6)$$

$$w_k \in \{0,1\} \qquad \forall k \in K \quad (7)$$

The objective function (1) minimizes the sum of the installation reprocessing facility costs plus the delivering costs

from sourcing facilities to reprocessing facilities and from these to remanufacturing facilities. Constraint (2) warranties that supplying at facility $k \in K$ is delivered to a mid layer reprocessing facility already opened. Constraint (3) warranties that all the return products from I is going backward to facility $k \in K$. Constraint (4) warranties that the demand at facility j $\in$ K must be satisfied by reprocessing facilities. Constraint (5) ensures that all the return products arriving to facility k are also delivered to remanufacturing facilities. Constraint (6) is a standard positive constraint. Constraint (7) is a standard binary constraint. This model has $O(n^2)$ continuous variables where $n=max\{|I|, |J|, |K|\}$ and $|K|$ binary variables. The number of constraints is $O(n)$.

Notice that following [31], models such as the *RSCP* forget the origin of the products arriving to remanufacturing facilities then we lost the trace of the products. To overcome this point, we can get another formulation introducing triply subscripted variables x_{jkl} to manage the origin to destination product flows and some other changes in parameters, variables and constraints. But this is not the objective of this paper.

4 Evolutionary Scheme

Particle Swarm Optimization (*PSO*) is an evolutionary computation method to solve continuous optimization problems. This is an optimization algorithm based on swarm theory where the main idea of a classical *PSO* is to model the flocking of birds flying around a peak in a landscape. In *PSO* the birds are substituted by artificial beings so-called particles and the peak in the landscape is the peak of an objective (fitness) function. The particles of the swarm are flying through the search solution space with a velocity forming flocks around peaks of fitness functions. In a continuous *PSO*, an individual particle's status *i* on the search solution space *D* is characterized by two factors: its position *u* and velocity *v*. The position *u* and velocity *v* of the *ith* particle in the *d*-dimensional search solution space can be represented as:

$$v_{id}^{t+1} = c_1 v_{id}^{t} + c_2 r_1 (p_{id} - u_{id}^{t}) + c_3 r_2 (p_{gd} - u_{id}^{t}) \quad (8)$$

$$u_{id}^{t+1} = u_{id}^{t} + v_{id}^{t+1} \quad (9)$$

Where c_1 is called the inertia weight factor, c_2 and c_3 are constants called acceleration coefficients, r_1 and r_2 are two independent random numbers uniformly distributed in the range of [0, 1], p_{id} corresponding to the personal best objective value of particle *i* obtained so far at time *t*, p_{ig}represents the best particle found so far at time *t*. Equation (8) stands for calculating the new velocity of each particle *i* at time (*t+1*). Equation (9) stands for updating the position of particle *I* at time (*t+1*). Each $v_{id}^{t} \in [-v_{max}, v_{max}]$ and $u_{id}^{t} \in [-x_{max}, x_{max}]$, with v_{max} and x_{max} set by users to control excessive roaming of particles outside the search solution space. Particles fly toward a new position according to (9). The process is repeated until a user-defined stopping criterion is reached.

4.1 The Binary PSO Algorithm

In order to manage discrete optimization problems, in [32] is proposed a binary *PSO* (*BPSO*) algorithm. The difference between a *BPSO* algorithm and traditional *PSO* algorithm is that (9) has been replaced by the following expression:

$$u_{id}^{t+1} = \begin{cases} 1 \; if \; rand(\;\;) < S(v_{id}^{t+1}) \\ 0 \; if \; rand(\;\;) > S(v_{id}^{t+1}) \end{cases} \quad (10)$$

Where *S(.)* is the Sigmoid function and *rand*() is a random number uniformly distributed in the range [0,1]. We use this method in this paper.

Typical *PSO* algorithm encodes the whole solution for the *RSCP* model as a particle, and then applies the traditional algorithm for solving the target problem. We follow a different approach in this paper, taking advantage of the structure of the *RSCP* model.

We can set to 0 or 1 the value of variables $w_k \; \forall k \in K$, let call them w_k^* . Once you set variables w_k^* we can re-write the *RSCP* model as follow:

$RSCP_R$

$$Minimize \sum_{k \in K^*} f_k w_k^* + \sum_{i \in I} \sum_{k \in K} c_{ik} x_{ik} + \sum_{k \in K} \sum_{i \in I} g_k x_{ik} + \sum_{k \in K} \sum_{j \in J} d_{kj} y_{kj} \quad (1a)$$

$Subject\ to$:

$$\sum_{i \in I} x_{ik} \leq u_k w_k^* \qquad \forall k \in K^* \quad (2a)$$

$(2) - (6)$

Where, the set K^* contains the facilities already opened, and the variables w_k^* are now coefficients with known values. Constraint (2a) continues to ensure that all the sourcing facilities deliver return products to a facility already opened. The rest of constraints remain the same as the original *RSCP* model. Moreover, this associated problem is a linear programming problem.

In our evolutionary scheme, we use a *BPSO* algorithm for guiding the whole process of seeking an optimal solution for the *RSCP* problem. However, part of the particle is obtained by solving to optimality the $RSCP_R$ problem. In this way, we use a decomposed *BPSO* algorithm, based into two groups of swarms, one of them guide the overall search for an optimal solution.

4.2 The particle coding method

To find a good coding method corresponding to the optimization problem is the most critical problem [27]. In this paper, the particle's d-dimensional space is divided into two sets u^1 *and* u^2 . The length of each set (vector) respectively corresponds to the number of candidate sites to locate reprocessing facilities $|K|$, the second part represents the solution to the relaxed LP associated.

In the first group of particles, every component of each vector can take only 1 or 0. If the *k*th component of u^1 is equal to 1, then the reprocessing facility at candidate site k must be open, 0 otherwise. The second group of particles represents the

flows of return products between the sourcing facility and the reprocessing facilities and between the reprocessing facilities and the remanufacturing facilities. As described earlier in this paper, this part is obtained solving to optimality the $RSCP_R$ problem.

4.3 The feasibility procedure

The standard *BPSO* algorithm could generate some particles of the first swarm group representing unfeasible solutions. To overcome this problem, for each particle of the first group we apply a simple feasible solution procedure. This procedure consists in two steps. In the first step we check if the number of facilities already opened is enough to satisfy the entire demand. In the second step, for those particles that do not satisfy the demand, we get a feasible solution to *RSCP* based on the initial particle. This procedure is rather simple; it starts open facilities till the demand is satisfied. The swarm is composed of just feasible solutions. The fitness of a particle is calculated by solving simultaneously the $RSCP_R$ problem and using the objective function ($1a$).

4.4 Other considerations

We initialize our algorithm with a size swarm of 20 particles. The maximum number of iterations was also set to 10. We used these setting parameters because initial testing provided good results besides the complexity of the problem addressed in this article. The acceleration coefficient c_2 is set to 2 and c_3 to 1. The inertia coefficient start with a value of 0.9 and it decreases till get 0.4 depending on the number of iterations performed. The initial swarm is composed of just feasible solutions. Each particle of the first group is generated randomly using a uniform distribution in the range [0,1]. Then is applied the binary procedure and after that is applied the feasibility procedure. Regarding the second group of particles, for each particle we solve to optimality the *LP* problem described earlier in this article. The velocity vector v_{id}^t is generated randomly in the range [-4,4] as in the continuous method. At every iteration, the algorithm uses the method of coding described earlier and updates the position vector u_{id}^{t+1} according to (9). The velocity vector v_{id}^t is updated at each iteration according (8). The fitness function is like (1). It is straightforward to calculate its value from. u_{id}^{t+1}. At every iteration we check for updating the best position of a particle and the global best position of the swarm. Notice that we do not explore swarm neighborhood structures, i.e. the way information is distributed among its members.

5 Numerical Experiments

In this section we discuss and compare the computational results obtained by the proposed evolutionary algorithm. Our propose is to analyze the performance of the proposed algorithm regarding computational time to get the solution and the quality of the upper bound (solution) obtained.

We implemented the algorithm in *GAMS* and we used *CPLEX* as a subroutine (called from inside *GAMS*) for solving to optimality the $RSCP_R$ problem. All the experiments were developed on a PC with 4Gb RAM and 2.3GHz. In the literature, there are not large data sets available for our problem. We generated randomly 10 test problems following similar methodologies used for well known related supply chain problems (for example: [15]). These test problems are data sets corresponding to networks of up to 350 origination sites, 100 candidate sites for locating reprocessing facilities and 40 remanufacturing facilities. The data set for the test problems are given in Table 1 and they are available with the authors. All the transportation costs were generated randomly using a uniform distribution with parameters [1,40]. Management costs were set to 30 for all the instance problems except for the No.1. Instances 7 and 8 are the same than instances 4 and 5 respectively except for the value of fixed costs that were obtained multiplying by 10 the fixed costs of instances 4 and 5. Instances 9 and 10 are the same than instances 7 and 8 respectively but the capacity of each location was increased in 50%. Sourcing units (a_j), capacity of reprocessing facilities (m_k) and capacity of remanufacturing facilities (b_l) are shown in Table 1.

Table 1: Data set

#	Instance Problems	J	K	L	f_k	a_j	m_k	b_l
1	40x20x15	40	20	15	300	150	400	400
2	100x40x20	100	40	20	500	150	400	750
3	150x40x20	150	40	20	1000	200	800	1500
4	200x80x20	200	80	20	1000	300	800	3000
5	300x80x40	300	80	40	2000	200	800	1500
6	350x100x40	350	100	40	2000	200	800	1750
7	200x80x20	200	80	20	10000	300	800	3000
8	300x80x40	300	80	40	20000	200	800	1500
9	200x80x20	200	80	20	10000	300	1200	3000
10	300x80x40	300	80	40	20000	200	1200	1500

We run 5 trials for each test instances. Table 2 and 3 show the results obtained using the algorithm. For each instance problem and trial, the tables show the solution provided by the initial random phase of the algorithm (z_{ran}), the solution provided by the BPSO2 algorithm (z_P), the computing times (seconds) and the gap ($100[z^* - z_P]/z^*$) obtained comparing the z_P with the optimal integer value of the objective function (z^*) obtained by *GAMS*. All the *GAP* values were rounded to two decimals. The table also shows the minimum, maximum and average value for each column and each test instance. Observe that, for all the test instances, the maximum average gap is 1.58% (instance #9) and the minimum average gap is 0.04% (instance #2). Regarding computing times, notice that all test instances were solved in less than 58 seconds.

6 Conclusions

In this paper, we proposed a Binary PSO-based scheme for solving a reverse supply chain network design problem. This is a NP-hard problem and was formulated as a mixed integer 0-1 linear programming problem (*MIP*). The algorithm guides the search for an optimal solution to the *RSCP* problem combining a random solution search with optimal solutions generated by solving to optimality an associated problem. The algorithm generates two groups of swarms. First is generated the particles representing whether the facility is opened or closed. The second part of the chromosome is obtained solving to optimality the $RSCP_R$ problem associated to the

original *RSCP* problem. The proposed BPSO algorithm was coded in *GAMS* and tested using 10 test instances generated randomly. Computational results regarding gap and computing times are promising.

Table 2: Random phase solution value (z_{ran}), *GA* solution value (z_{ga}), computing times (secs) and *gap(%)*

# instance	*trial*	z_{ran}	z_P	*secs*	*Gap(%)*
1	1	148500	146900	13,40	0,00
	2	149400	148550	13,46	1,12
	3	149200	149000	13,87	1,43
	4	149400	147650	13,51	0,51
	5	150050	147900	13,71	0,68
Minimum		148500,0	146900,0	13,40	0,00
Maximum		150050,0	149000,0	13,87	1,43
Average		149310,0	148000,0	13,59	0,75
2	1	521200	520250	15,92	0,03
	2	521350	520300	15,98	0,04
	3	520300	520300	15,73	0,04
	4	520300	520300	15,79	0,04
	5	520600	520300	15,96	0,04
Minimum		520300,0	520250,0	15,73	0,03
Maximum		521350,0	520300,0	15,98	0,04
Average		520750,0	520290,0	15,88	0,04
3	1	1065400	1065200	20,10	0,23
	2	1066600	1065400	19,83	0,24
	3	1065400	1065400	19,01	0,24
	4	1066600	1065800	19,88	0,28
	5	1065800	1065400	19,93	0,24
Minimum		1065400,0	1065200,	19,01	0,23
Maximum		1066600,0	1065800,	20,10	0,28
Average		1065960,0	1065440,	19,75	0,25
4	1	2091400	2090100	34,85	0,36
	2	2090700	2089000	32,89	0,30
	3	2090500	2090500	32,40	0,37
	4	2090500	2089100	33,38	0,31
	5	2090600	2090300	33,72	0,36
Minimum		2090500,0	2089000,	32,40	0,30
Maximum		2091400,0	2090500,	34,85	0,37
Average		2090740,0	2089800,	33,45	0,34
5	1	2130800	2130800	56,17	0,38
	2	2132100	2130800	56,15	0,38
	3	2131400	2130800	58,32	0,38
	4	2132200	2131100	56,29	0,40
	5	2132400	2131100	54,80	0,40
Minimum		2130800,0	2130800,	54,80	0,38
Maximum		2132400,0	2131100,	58,32	0,40
Average		2131780,0	2130920,	56,35	0,39
6	1	2471200	2467350	54,26	0,35
	2	2470900	2468750	54,32	0,41
	3	2471900	2469550	53,82	0,44
	4	2471850	2468500	54,34	0,40
	5	2468750	2467850	54,70	0,37
Minimum		2468750,0	2467350,	53,82	0,35
Maximum		2471900,0	2469550,	54,70	0,44
Average		2470920,0	2468400,	54,29	0,40

Table 3: Continuation - random phase solution value (z_{ran}), *GA* solution value (z_{ga}), computing times (secs) and *Gap*

# instance	*trial*	z_{ran}	z_P	*secs*	*Gap(%)*
7	1	2765500	2765500	40,01	0,28
	2	2768700	2765600	36,20	0,29
	3	2766700	2765600	35,81	0,29
	4	2765600	2764800	35,75	0,26
	5	2765500	2764100	35,78	0,23
Minimum		2765500,0	2764100,	35,75	0,23
Maximum		2768700,0	2765600,	40,01	0,29
Average		2766400,0	2765120,	36,71	0,27
8	1	3481700	3480800	55,85	0,23
	2	3483000	3481400	54,33	0,25
	3	3481300	3480700	54,68	0,23
	4	3482600	3481400	55,05	0,25
	5	3482900	3480200	56,52	0,22
Minimum		3481300,0	3480200,	54,33	0,22
Maximum		3483000,0	3481400,	56,52	0,25
Average		3482300,0	3480900,	55,28	0,24
9	1	2727700	2521400	35,46	1,69
	2	2525300	2513600	36,06	1,38
	3	2531000	2517200	36,55	1,52
	4	2533100	2519900	36,48	1,63
	5	2535500	2521100	36,79	1,68
Minimum		2525300,0	2513600,	35,46	1,38
Maximum		2727700,0	2521400,	36,79	1,69
Average		2570520,0	2518640,	36,27	1,58
10	1	2996600	2992000	38,97	1,09
	2	2999900	2995600	46,73	1,21
	3	2994500	2990900	48,01	1,05
	4	3003400	2999600	47,72	1,35
	5	3000000	2994000	46,95	1,16
Minimum		2994500,0	2990900,	38,97	1,05
Maximum		3003400,0	2999600,	48,01	1,35
Average		2998880,0	2994420,	45,68	1,17

Acknowledgments

This research was partially supported by the Fundação de Amparo á Pesquisa do Estado de Minas Gerais – FAPEMIG, VALE e CNPq - Brazil.

References

[1] Rogers, D.S., & Tibben-Lembke, R.S. (1998). *Going backwards: reverse logistics trends and practices*. Reno: Reverse Logistics Executive Council.

[2] Fleischmann, M., Krikke, H.R., Dekker, R., & Flapper, S.D.P. (2000). A characterisation of logistics networks for product recovery. *Omega*, 28, 6, 653-666.

[3] Blackburn. J.D., Guide, V.D.G., Souza, C., & Van Wassenhove, L.N. (2000). Reverse Supply Chains for Commercial Returns. *California Management Review*, 46, 6-22.

[4] Engelbrecht, A.P. (2005). *Fundamentals of Computational Swarm Intelligence*. Wiley.

[5] Dekker, R., & Van Der Laan, E.A. (1999). Gestion des stocks pour la fabrication et la refabrication simultanées: synthèse de resultants récents. *Logistique & Management*, 7, 59–64.

[6] Daskin, M.S., Snyder, L.V., & Berger, R.T. (2005). Facility Location in Supply Chain Design. In A. Langevin and D. Riopel (Eds.), *Logistics Systems: Design and Optimization (pp*. 39-65). New York, Springer.

[7] Altiparmak, F., Gen, M., Lin, L., & Paksoy, T. (2006). A genetic algorithm approach for multiobjective optimization of supply chain networks. *Computers & Industrial Engineering*, 51, 197–216.

[8] Farahani, R.Z. & Hekmatfar, M. (Eds.). (2009). *Facility location: concepts, models, algorithms and case studies.* Berlin:Physica-Verlag HD.

[9] Dekker, R., Fleischmann, M., Inderfurth, K., & van Wasenhove, L. (Eds.). (2004). *Reverse logistics: quantitative models for close-loop supply chains*. Berlin: Springer-Verlag

[10] Rubio, S., Chamorro, A., & Miranda, F. (2008). Characteristics of the research on reverse logistics (1995-2005). *Int J Prod Res.,* 46, 4, 1099-1120.

[11] Jayaraman, V., Patterson, R.A., & Rolland, E. (2003). The design of reverse distribution networks: Models and solution procedures. *European Journal of Operational Research*, 150, 128–149.

[12] Zhou, Y-S. & Wong, S-Y. (2008). Generic Model of Reverse Logistics Network Design. *J Transpn Sys Eng & IT*, 8, 3, 71-78.

[13] Salema, M.I.G., Barbosa-Povoa, A.P., & Novais, A.Q. (2010). Simultaneous design and planning of supply chains with reverse flows: a generic modelling framework. *European Journal of Operational Research*, 203, 2, 336–349.

[14] Gomes, M.L., Barbosa-Povoa, A.P., & Novais, A.Q. (2011). Modelling a recovery network for WEEE: A case study in Portugal. *Waste Management,* 31, 1645–1660.

[15] Lu, Z., & Bostel, N. (2007). A facility location model for logistics systems including reverse flows: The case of remanufacturing activities. *Computers & Operations Research*, 34, 2, 299–323.

[16] Barbosa-Povoa, A.P., Gomes Salema, M.I., & Novais, A.Q. (2007). Design and Planning of Closed Loop Supply Chains. In : *Supply Chain Optimization*, L. Papageorgiou & M. Georgiadis eds. NY:Wiley, p 187-218.

[17] Mutha, A., & Pokharel, S. (2009) Strategic network design for reverse logistics and remanufacturing using new and old product modules. *Computers and Industrial Engineering*, 56 (2009) 334–346.

[18] Zarei, M., Mansour, S., Kashan, A.H., & Karimi, B. (2010), Designing a Reverse Logistics Network for End-of-Life Vehicles Recovery. *Mathematical Problems in Engineering*, Article ID 649028, 1-16.

[19] Amin, S.H., & Guoqing Zhang, G. (2012). A proposed mathematical model for closed-loop network configuration based on product life cycle, *Int J Adv Manuf Technol*, 58, 791 – 801.

[20] Pishvaee, M.S., & Torabi, S.A. (2010). A possibilistic programming approach for closed-loop supply chain network design under uncertainty. *Fuzzy Sets and Systems,* 161, 2668 – 2683

[21] Lee, D.-H., & Dong, M. (2008). A heuristic approach to logistics network design for end-of-lease computer products recovery, *Transportation Research Part E*, 44, 455-474.

[22] Min,H., Ko,H.J., & Ko, C.S. (2006). A genetic algorithm approach to developing the multi-echelon reverse logistics network for product returns. *Omega*, 34, 56–69.

[23] Lee, J-E., Gen, M., & Rhee, K-G. (2009). Network model and optimization of reverse logistics by hybrid genetic algorithm. *Computers & Industrial Engineering*, 56, 951–964.

[24] Pishvaee, M.S., Farahani, R.Z., & Dullaert , W. (2010). A memetic algorithm for bi-objective integrated forward/reverse logistics network design. *Computers & Operations Research*, 37, 1100–1112.

[25] Kennedy, J., & Eberhart, R. C. (1995). Particle Swarm Optimization. Proceedings of the IEEE International Conference on Neural Networks, p.1942-1948.

[26] Poli, R. (2008). Analysis of the Publications on the Applications of Particle SwarmOptimisation. *Journal of Artificial Evolution and Applications*, Article ID 685175, 10 pages. doi:10.1155/2008/685175.

[27] Kennedy, J., & Eberhart, R.C. (2001). *Swarm Intelligence*. San Francisco: Morgan Kaufmann Publishers.

[28] AlHajri, M.F., AlRashidi, M.R., & El-Hawary, M.E. (2007). *A Novel Discrete Particle Swarm Optimization Algorithm for Optimal Capacitor Placement and Sizing*, Canadian Conference on Electrical and Computer Engineering - CCECE 2007, 1, p. 286 – 1289

[29] Allahverdi, A., & Al-Anzi, F.S. (2006). A PSO and a Tabu search heuristics for the assembly scheduling problem of the two-stage distributed database application. *Computers & Operations Research*, 33, 1056–10

[30] Li, N. (2011). Research on Location of Remanufacturing Factory Based on Particle Swarm Optimization. In: *Proceedings of IEEE MSIE 2011*, p. 1016-1019.

[31] Geoffrion, A.M., & Graves, G.W. (1974). Multicommodity Distribution System Design by Benders Decomposition. *Managament Science*, 20, 5, 822-844.

[32] Kennedy, J., & Eberhart, R. C. (1997). *A discrete binary version of the particle swarm algorithm.* Proceedings of the IEEE International Conference on Computational Cybernetics and Simulation, (1997), 4104 – 4108.

Optimal Sizing and Placement of Distribution Generation Using Imperialist Competitive Algorithm

H. A. Shayanfar *
Electrical Eng. Department, Islamic Azad University, South Tehran Branch, Tehran, Iran

N. Amjady
Electrical Engineering Department, Semnan University, Semnan, Iran

A.Ghasemi
Young Researcher Club, Ardabil Branch, Islamic Azad University, Ardabil, Iran

O. Abedinia
Electrical Engineering Department, Semnan University, Semnan, Iran

hashayanfar@yahoo.com, n_amjady@yahoo.com, ghasemi.agm@gmail.com, oveis.abedinia@hotmail.com

Abstract— **In this paper Imperialism Competitive Algorithm (ICA) is proposed to optimal placement of Distribution Generation (DG) in power system. The power distribution generation systems are necessary for consumers to achieve power with less price and best quality. In the other hand, they can help to the active power units in power system networks for system losses reduction, distribution lines, voltage profile improvement. Also, ICA is a global search strategy that uses the socio-political competition among empires as a source of inspiration. The effectiveness of the proposed technique is applied to mat power 30 buses and 57 bus power system. The achieved result shows the robust reaction of the system with DG.**

Keywords: DG, ICA, Losses and Prices.

I. INTRODUCTION

The design and operation of the electricity distribution networks always assumed power flows from higher voltage networks to lower voltage networks. Power injections and power demands that appear at various places in the distribution systems are assumed to be distributing equally between the phases. This assumption is valid for passive networks. However, the connection and operation of significant Distribution Generation (DG) (of varying technologies) alters many network characteristics making the existing assumptions of network design and operation less applicable to distribution networks. The power distribution generation systems are necessary for consumers to achieve power with less price and best quality. In the other hand, they can help to the active power units in power system networks for system losses reduction, distribution lines, voltage profile improvement and etc. The main goal for DG is determining of optimal size and placement of capacitors to be installed and efficient control schemes in the buses of distribution systems [1-4].

The DG sources can classified at four sets; micro DG (5KW to 1MW), small (5KW to 5MW), medium (5MW to 50MW) and large size (50MW to 300MW). Meanwhile, the source for DGs is very widespread so that they contain fuel cells, photo voltaic, hydro turbine, combustion engines, micro turbines and etc [5].

The optimal sizing and placement of DG problem is an attractive research area as publish some papers in this area such as global optimization techniques like genetic algorithms (GA), Harmony Search Algorithm (HAS), Particle Swarm Optimization (PSO) and Evolutionary Programming (EP) techniques have been applied for optimal tuning of DG based restructure schemes. These evolutionary algorithms are heuristic population-based search procedures that incorporate random variation and selection operators. Although, these methods seem to be good methods for the solution of DG parameter optimization problem, however, when the system has a highly epistatic objective function (i.e. where parameters being optimized are highly correlated), and number of parameters to be optimized is large, then they have degraded efficiency to obtain global optimum solution [6]. In order to overcome these drawbacks, in this paper, a strength heuristic algorithm has been presented to determine the optimal sizing capacitor and placement, taking into accounts fixed capacitors as well as potential harmonic interactions (losses, resonance and distortion factors) in the presence of nonlinear loads and DG using ICA. Therefore, for this reasons, ICA algorithm is used to solve DG problem in order to efficiently control the local search and convergence to the global optimum and solution quality. This proposed method has been tested on distorted 34-bus and 57-bus IEEE systems. The

* Corresponding Author. E-Mail Address: hashayanfar@yahoo.com (H. A. Shayanfar)

objectives on this method were to minimize power loss in the distorted distribution network having taken the cost of capacitors into account [7-10].

II. DG PROBLEM FORMULATION

The problem is formulated with a objective functions, the real power loss reduction in a distribution system is required for efficient power system operation. The loss in the system can be calculated, given the system operating condition [11].

$$SLOSS = Sij + Sji$$
$$Sloss = \sum_{j=1}^{n} Zj * Ij^2$$
$$PLOSS = real(Sloss) \qquad QLOSS = image(Sloss)$$
$$Sltotal = \sum_{j=1}^{n} Slossj$$
$$INDEX = A * Sltotal + B * \sum_{j=1}^{n} (1 - |Vj|)^2 \quad (1)$$

Where, S_{LOSS}, P_{LOSS} and Q_{LOSS} are power loss, active and reactive power loss for power system network, respectively. The A and B is penalty factor for *INDEX* objective function to voltage profit improvement and minimize total loss. This penalty factors define based operator for minimize loss or modified voltage profile [12]. Also, they are different value for test systems. This problem contains some constrains such as:

(a) Power balance constraint

$$\sum_{DG=1}^{n_{DG}} P_{DG} + \sum_{G=n_{DG}+1}^{n_G} P_G = P_D + P_L \quad (2)$$

(b) Generation and voltage limits constraints

$$P_i^{\min} \le P_i \le P_i^{\max} \qquad i \in 1,2,...,\alpha$$
$$V_i^{\min} \le V_i \le V_i^{\max} \qquad i \in 1,2,...,\alpha \quad (3)$$

The active power transmission loss P_L can be calculated by the network loss formula:

$$P_L = \sum_{i=1}^{n}\sum_{j=1}^{n} A_{ij}(P_i P_j + Q_i Q_j) + B_{ij}(Q_i P_j - P_i Q_j) \quad (4)$$

Where,

$$A_{ij} = \frac{R_{ij}\cos(\delta_i - \delta_j)}{V_i V_j}$$
$$B_{ij} = \frac{R_{ij}\sin(\delta_i - \delta_j)}{V_i V_j} \quad (5)$$

Where, *Pi* and *Qi* are net real and reactive power injection in bus *'i'* respectively, *Rij* is the line resistance between bus *'i'* and *'j'*, *Vi* and δi are the voltage and angle at bus *'i'* respectively.

III. IMPERIALIST COMPETITIVE ALGORITHM

Imperialism is the policy of extending the power and rule of a government beyond its own boundaries. A country may attempt to dominate others by direct rule or by less obvious means such as a control of markets for goods or raw materials. The latter is often called neo-colonialism [13]. ICA is a novel global search heuristic that uses imperialism and imperialistic competition process as a source of inspiration. This algorithm starts with some initial countries. Some of the best countries are selected to be the imperialist states and all the other countries form the colonies of these imperialists. The colonies are divided among the mentioned imperialists based on their power. After dividing all colonies among imperialists and creating the initial empires, these colonies start moving toward their relevant imperialist state. This movement is a simple model of assimilation policy that was pursued by some imperialist states [14]. Figure 1 shows the initial empires. Accordingly, bigger empires have greater number of colonies where weaker ones have less. In this figure, Imperialist 1 has formed the most powerful empire and consequently has the greatest number of colonies.

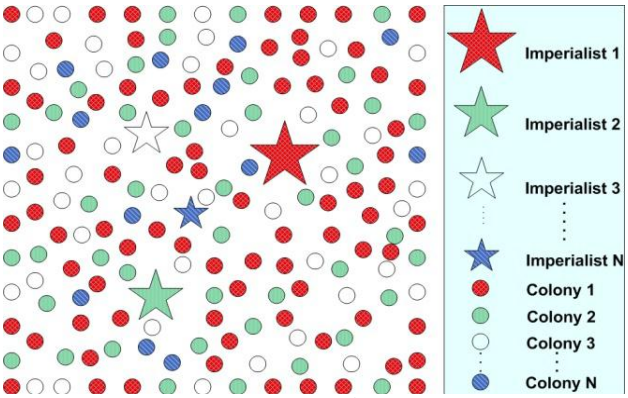

Figure 1. Generation of initial empires

A. Movement of Colonies toward the Imperialist

It is clear that, imperialist countries start to improve their colonies. We have modeled this fact by moving all the colonies toward the imperialist. Figure 2 shows a colony moving toward the imperialist by units. The direction of the movement is shown by the arrow extending from a colony to an imperialist [15]. In this figure x is a random variable with uniform (or any proper) distribution. Then for x we have:

$$x \approx U(0, \beta \times d)$$

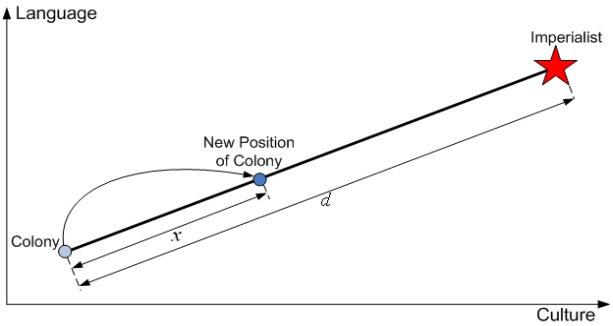

Figure 2. Movement of colonies toward their relevant imperialist

Where d is the distance between the colony and the imperialist state. The condition $\beta > 1$ causes the colonies to get closer to the imperialist state from both sides.

After dividing all colonies among imperialists and creating the initial empires, these colonies start moving toward their relevant imperialist state which is based on assimilation policy [16]. Fig.3 shows the movement of a colony towards the imperialist. In this movement, θ and x are random numbers with uniform distribution as illustrated and d is the distance between colony and the imperialist.

$$x \approx U(0, \beta \times d), \theta \approx U(-\gamma, \gamma) \qquad (6)$$

Where,

β, γ = parameters that modify the area that colonies randomly search around the imperialist.

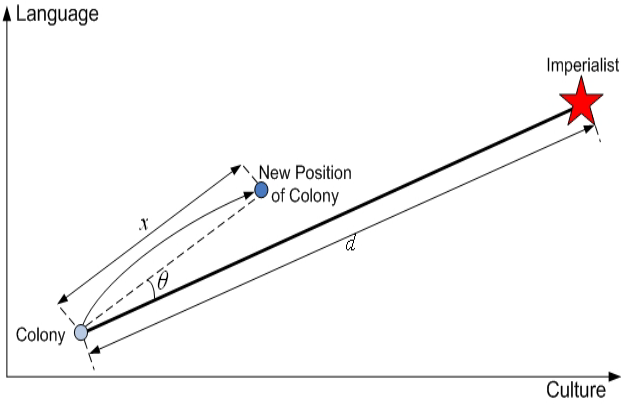

Figure 3. Movement of colonies toward their relevant imperialist in a randomly deviated direction

The total power of an empire depends on both the power of the imperialist country and the power of its colonies. In this algorithm, this fact is modeled by defining the total power of an empire by the power of imperialist state plus a percentage of the mean power of its colonies. Any empire that is not able to succeed in imperialist competition and can not increase its power (or at least prevent decreasing its power) will be eliminated.

The imperialistic competition will gradually result in an increase in the power of great empires and a decrease in the power of weaker ones. Weak empires will lose their power gradually and ultimately they will collapse [15]. The movement of colonies toward their relevant imperialists along with competition among empires and also collapse mechanism will hopefully cause all the countries to converge to a state in which there exist just one empire in the world and all the other countries are its colonies. In this ideal new world colonies have the same position and power as the imperialist. Fig.4 shows a big picture of the modeled imperialistic competition. Based on their total power, in this competition, each of the empires will have a likelihood of taking possession of the mentioned colonies.

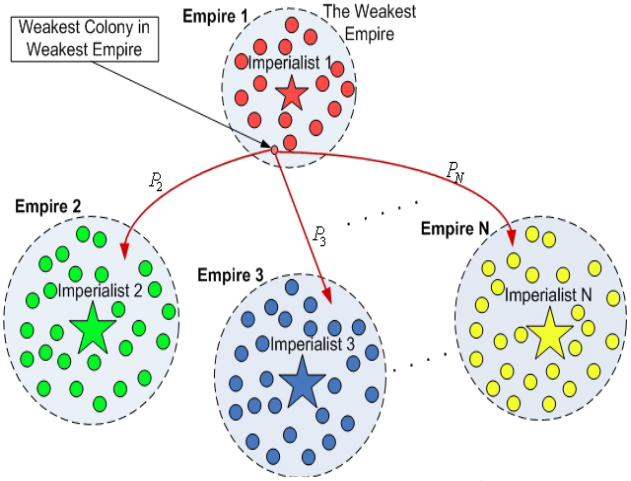

Figure 4. Imperialistic competition: The more powerful an empire is, the more likely it will possess the weakest colony of weakest empire

IV. ICA BASED DG PROBLEM

The ICA technique for solving the optimal placement and capacitor sizing DG problem to minimize the loss may be constructed with the following main stages:

Set power system: Input line and bus data, and bus voltage limits.

Calculate fitness based load flow: Calculate the loss using distribution load flow based on backward-forward sweep.

Initial population: Randomly generates an initial population (array) of particles with random positions and velocities on dimensions in the solution space. Set the iteration counter k = 0. In the other hand, in this step, an initial population based on state variable is generated, randomly. That is formulated as:

$$D = [D_1, D_2, D_3, ..., D_n] \qquad D_i = (d_i^1, d_i^2, ..., d_i^m) \qquad (7)$$

Calculate fitness: For each particle if the bus voltage is within the limits, calculate the total loss. Otherwise, that particle is infeasible. That is formulated as:

min *INDEX*

Updating: update population with ICA explore engine.

Finish: If the iteration number reaches the maximum limit, go to next Step. Otherwise, set iteration index $k = k + 1$, and go back to Step 4.

Results: Print out the optimal solution to the target problem. The best position includes the optimal locations and size of DG or multi-DGs, and the corresponding fitness value representing the minimum total real power loss.

The flowchart of the proposed ICA algorithm is shows in Fig .5.

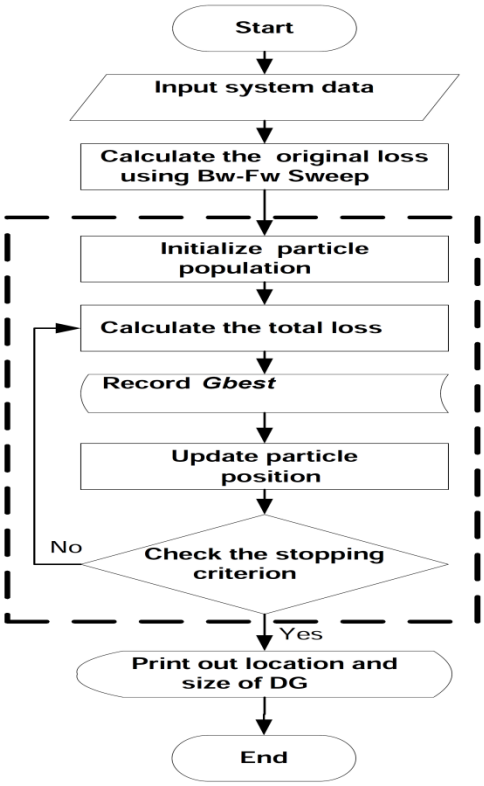

Figure 5. ICADG computational procedure

V. SIMULATION RESULTS

A. *30 and 57 bus Power System*

For the testing of proposed technique two case studies are considered as; mat power 30 and 57 bus power system. For both of the case studies, the DGs are considered with 5-50 MW and 1-10 Mvar. Also the proposed technique considered 5 source of DGs to power systems. Table. 1-2, shows the numerical results of DGs in system.

In the mentioned tables, the active and reactive powers are presented for 5 optimized buses. Fig. 6-7, shows the system response with 5 sources and without sources. It is clear that by increasing the number of DGs in power system, the stability, losses decreasing and improving of voltage profile will be appropriate.

The presented figures show the losses and voltage of active and reactive power in proposed case studies.

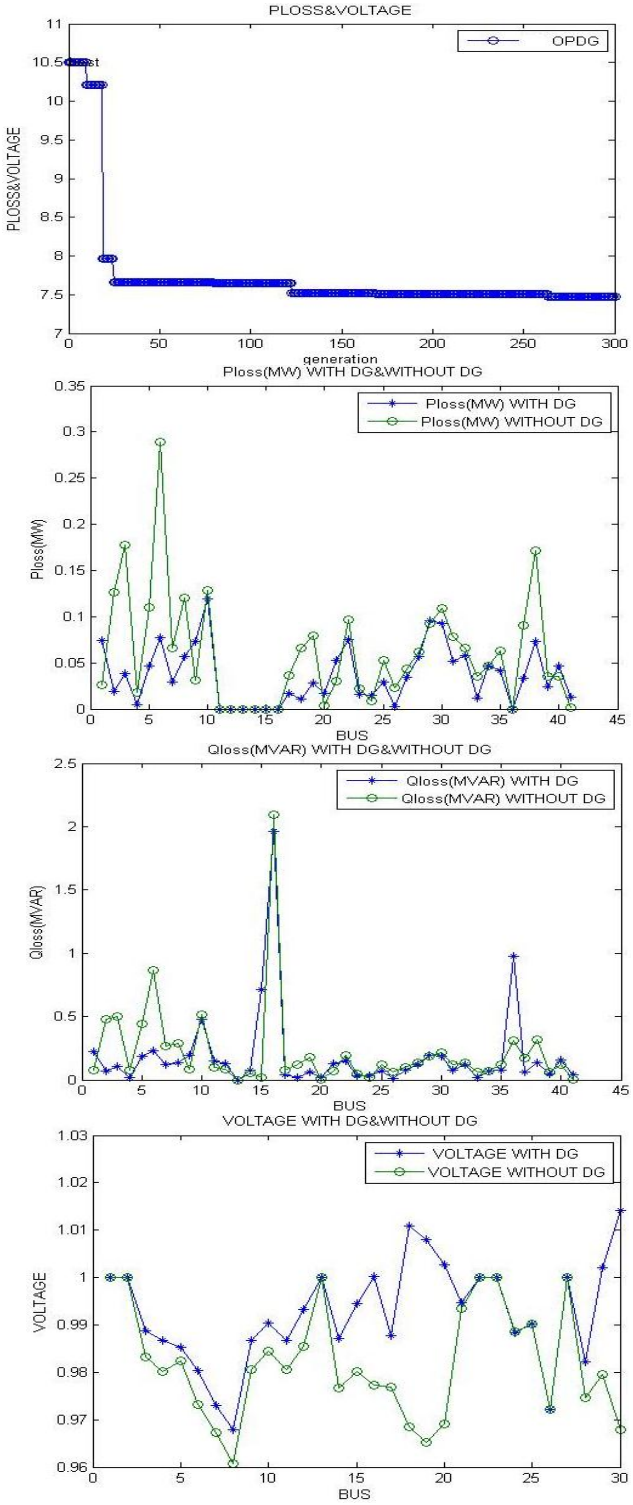

Figure 6. The losses and voltage of active and reactive power in 30-bus system.

TABLE I. THE RESULTS OF 30 BUS POWER SYSTEM

	SIZE DG	P=5-50			Q=1-10	
	NUMBER DG	1	2	3	4	5
	BUS	19	8	24	20	30
	P(MW)	31	44	6	17	7
	Q(MVAR)	10	10	10	10	9
	BUS		19	8	21	19
	P(MW)		22	34	6	7
30 Bus Power System	Q(MVAR)		10	10	9	10
	BUS			20	26	22
	P(MW)			21	3	15
	Q(MVAR)			10	10	9
	BUS				18	18
	P(MW)				9	7
	Q(MVAR)				10	9
	BUS					16
	P(MW)					8
	Q(MVAR)					10

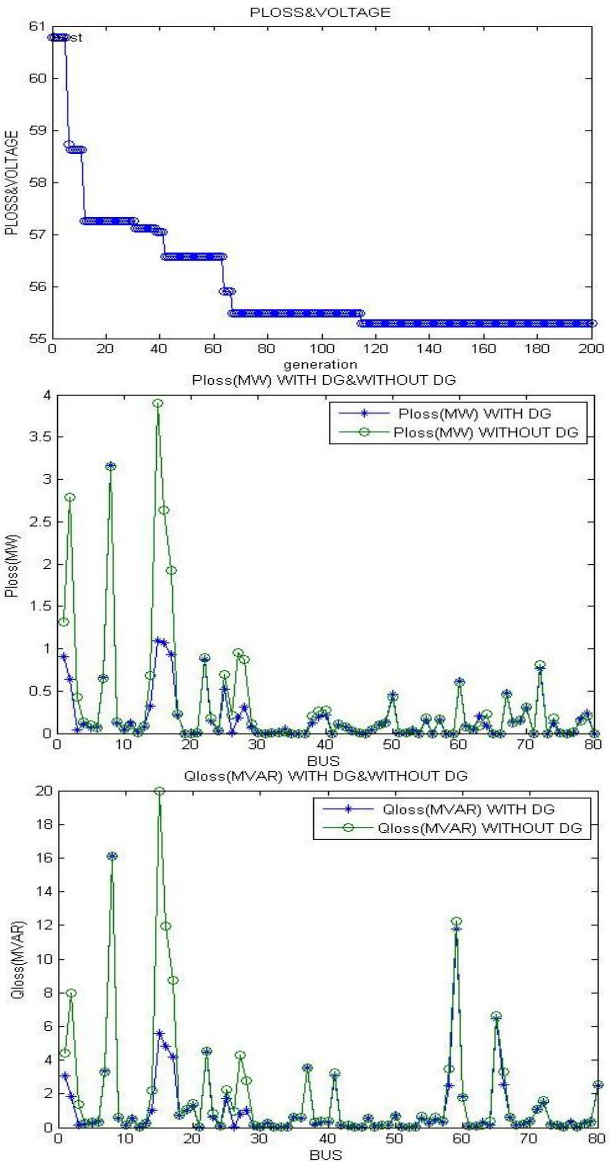

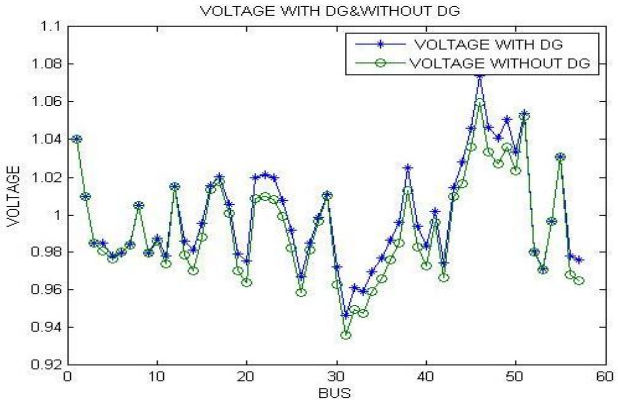

Figure 7. The losses and voltage of active and reactive power in 57-bus system.

TABLE II. THE RESULTS OF 57 BUS POWER SYSTEM

	SIZE DG	P=5-50			Q=1-10	
	NUMBER DG	1	2	3	4	5
	BUS	49	50	50	12	45
	P(MW)	50	47	47	30	38
	Q(MVAR)	1	1	2	3	1
	BUS		47	48	16	49
	P(MW)		48	48	50	29
57 Bus Power System	Q(MVAR)		1	2	2	2
	BUS			16	47	4
	P(MW)			41	47	38
	Q(MVAR)			1	4	4
	BUS				49	46
	P(MW)				40	36
	Q(MVAR)				1	3
	BUS					12
	P(MW)					37
	Q(MVAR)					3

VI. CONCLUSIONS

In this paper, we investigated the optimal placement and capacitor sizing DG power problem by employing an evolutionary algorithm based on Imperialist Competitive Algorithm. The DG optimization problem was considered and formulated as single-objective optimization problem with competing objectives of power loss and voltage profile improvement. The concept of Pareto dominance was employed to provide the selection mechanism between different objectives. The proposed algorithm applied to two standard IEEE systems to show advantages of proposed algorithm in DG problem, 34-bus IEEE test system and 57-bus IEEE test system. The numerical results demonstrate that the proposed method has better ability in finding optimal answers and possibility of particle placed in local zone. Moreover, the proposed strategy has simple structure, easy to implement and tune and therefore it is recommended to generate good quality and reliable electric energy in the restructured power systems.

REFERENCES

[1] J Anne - Marrie & Jan F.Kreider, "Distributed Generation The Anne - Marrie & Jan F.Kreider, "Distributed Generation The Power Paradigm for the New Millennium",CRC Press LLC, Pub. 2001.

[2] Thomas Ackermann , Groans Anderson, Lennart Soder, "Distributed Generation: a definition", Electric Power System Research (57), pp.195-204, June 2000.

[3] W.El-Khattam, M.M.A.Salama, "Distributed generation technologies ,definitions and benefits", Electric Power System Research (57), pp.119-128,14 january 2004.

[4] H. Lee Willis & Walter G.scott, "Distributed Power Generation: Planning and Evaluation",Marcel Dekker, Inc., Pub. 2000.

[5] A.Keyhani, "Distributed Generation Systems", Power System Workshop, Amirkabir University, May 2004.

[6] Brown, R.E. Jiuping Pan, Xiaorning Feng, Koutlev, k., "Siting Distributed Generation todefer T&D expansion", Transmission and Distribution Conference and Exposition, 2001 IEEE/PES.

[7] P.P.Barker, R.W.de Mello, "Determining the Impact of Distributed Generation on PowerSystem: Part1-Radial Distribution System, Proc. Of IEEE PES Meeting, Seattle, 16-20 July2000.

[8] N.Hadisaid, J.F.Canard, F.Dumas: "Dispersed Generation Impact on Distribution Networks", IEEE Computer Applications in Power, Vol.12, No.2, April -1999.

[9] M.A.Kashem, G. Ledwich, "Impact of Distributed Generation on Protection of Single Wire earth Return Lines", Electric Power System Research, 2002.

[10] Scientific - Technical Monthly Magazine of Electrical Power Industry, No.101 Oct. 2004.

[11] Adly Girgis, Sukumar Brahma, "Effect of Distributed Generation on Protective DeviceCoordination in Distribution System", IEEE 2001.

[12] G.Pepermans, J.driesen, D.haeseldonckx, Rr.belmans, W.dhaeseleer, "Distributed Generation Benefits and Issues", Energy Policy 33, pp.787-798, 2005.

[13] The Hutchinson Dictionary of World History, Oxford: Helicon Publishing, 1999.

[14] Atashpaz-Gargari, E. and C. Lucas, (2007) a. Imperialist Competitive Algorithm: An algorithm for optimization inspired by imperialistic competition. In: the proceeding of IEEE Congress on Evolutionary Computation. Pp 4661-4667.

[15] Atashpaz-Gargari E. and Lucas C., "Imperialist Competitive Algorithm: An algorithm for optimization inspired by imperialistic competition", IEEE Congress on Evolutionary Computation, Singapore,2008.

[16] I.Tsoulos, D.Gavrilis, E.Glavas, "Neural network construction and training using grammatical evolution", Science Direct Neurocomputing Journal, Vol.72, Issues 1-3, December 2008, pp. 269-277.

BIOGRAPHIES

Heidarali Shayanfar received the B.S. and M.S.E. degrees in Electrical Engineering in 1973 and 1979, respectively. He received his Ph. D. degree in Electrical Engineering from Michigan State University, U.S.A., in 1981. Currently, he is a Full Professor in Electrical Engineering Department of Iran University of Science and Technology, Tehran, Iran. His research interests are in the Application of Artificial Intelligence to Power System Control Design, Dynamic Load Modeling, Power System Observability Studies, Voltage Collapse, Congestion Management in a Restructured Power System, Reliability Improvement in Distribution Systems and Reactive Pricing in Deregulated Power Systems. He has published more than 405 technical papers in the International Journals and Conferences proceedings. He is a member of Iranian Association of Electrical and Electronic Engineers and IEEE.

Nima Amjady (SM'10) was born in Tehran, Iran, on February 24, 1971. He received the B.Sc., M.Sc., and Ph.D. degrees in electrical engineering from Sharif University of Technology, Tehran, Iran, in 1992, 1994, and 1997, respectively. At present, he is a Professor with the Electrical Engineering Department, Semnan University, Semnan, Iran. He is also a Consultant with the National Dispatching Department of Iran. His research interests include security assessment of power systems, reliability of power networks, load and price forecasting, and artificial intelligence and its applications to the problems of power systems.

Ali Ghasemi received the B.Sc. and M.Sc. (Honors with first class) degree in Electrical Engineering from Isfahan University of Technology (IUT), Esfahan, Iran in 2009 and Technical Eng. Department of the University of Mohaghegh Ardabili (UMA), Ardabil, Iran in 2011. His Areas of interest in Research are power system control and operation, adaptive and robust control of power systems, operation and Planning and Power System Restructuring and applications of heuristic techniques in power systems.

Oveis Abedinia received the B.S. and M.Sc. degrees in Electrical Engineering from Azad University, Ardabil and Science and Technology Research Branch, Tehran, Iran in 2005 and 2009, respectively. Currently, he is a Ph. D. student in Electrical Eng. Department, Semnan University, Semnan, Iran. His areas of interest in research are Application of Artificial Intelligence to Power System and Control Design, Load and Price Forecasting, Distribution Generation, Restructuring in Power Systems, Congestion Management, Optimization.

A Cache Management System for a Distributed Deductive Database

Larry Williams[1], Martin Maskarinec[1], and Kathleen Neumann[1]
[1] School of Computer Sciences, Western Illinois University, Macomb, IL

Abstract - *This paper will illustrate what a cache management system for a deductive database will do when a query is executed, or sent through the presented calculation plan. It will also illustrate what the Cache Management System should do when the cache is full. Once the query goes through the calculation plan, it then passes the results to the Cache Management System. The Cache Management System will then decide if the query should be cached or not. The Cache Management System will also have to decide what should be removed from the cache if the cache is full. This paper will also illustrate the how to calculate the recalculation cost.*

Keywords: Intelligent Database, Deductive Database, Cache Algorithms

1. Introduction

According to Ullman, et. al [1]., a deductive database is a conventional database containing facts, a knowledge base containing rules, and an inference engine which allows the derivation of information implied by facts and rules. The knowledge base is expressed in a subset of first-order logic.

The results sets for a deductive database can be extremely expensive. This is because each node may need to get information from many levels to produce its result. Thus, a system is needed to cache the results rather than recalculating them each time.

Conventional caching algorithms as mentioned in [2] do not have to take into consideration the dependency cost if the system removes that result from the cache. For this reason a deductive database system cannot use this conventional method of caching the results. The conventional rules do not apply especially when the system removes items from the cache. This paper will describe how to check the cache to see if the results exist. If the results exist, the system will return them. If not, the system will execute the query on the stored relations and decide if the system should cache the results or not. If the system needs to cache the results and the cache is full, the system will also need to decide which of the results should stay in the cache and which should be removed. In a conventional cache management system, the system does not have to consider the cost to recreate that result or the recalculation cost for the result. The recalculation cost is the cost that is incurred when a result is removed. The system should remove results with a low recalculation cost. This paper will discuss what to do when the results that are set to be removed from the cache have a high recalculation cost. In this case, the system will remove results from the cache that are less time intensive to recreate.

2. Execution Cycle

When the system runs a query it follows the Execution Cycle that is illustrated in Figure 1. The Execution Cycle starts by checking if it is the first query executed. If so it caches the whole result including the nodes on the bottom of the tree. If it is not the first time running a query the system sends a probe query to check the cache keys to see if it is cached. If it is, the system increments the hit counter for that node, and stores the date and time that the node was last hit. The system then increments the hit counter for the cache. Next, the results of the query are returned.

If the node is not cached, ghost data of the cache miss is stored. The ghost data is the cache key, the date and time of the last miss, and a counter that is incremented every time it is missed. The cache miss counter is also incremented at this time. Next, the system checks the node to make sure it is not a leaf node. If it is a leaf node, the system calculates the value and returns the results. If the node is not a leaf node then the system checks if the result of the node can be recalculated. If the system cannot calculate the result, it traverses the tree to the next node and goes through this process again.

3. Traversing a Predicate Graph

The order that the system uses to traverse the predicate graph is a Depth First Search. Figure 2 presents an example of a predicate graph. The order of traversal for the predicate graph shown in Figure 2, assuming there are no results cached, is: a1,b1,p1,c1,d1,d2,c2,d3,d4,p2,c3,d5,d6, c4,d7,d8,l1,m1,n1,o1,o2,u2,o3,o4,m2,n3,o5,o6,n4,o7,o8. If the node can be calculated, the system performs the calculation, and returns the results. After the system returns the results, the Cache Management System determines whether they should be cached. If the system cannot calculate the node directly, it must traverse the tree to nodes that are either cached or are leaf nodes. A result cannot be

calculated for a node until it has all the results for all the children of that node.

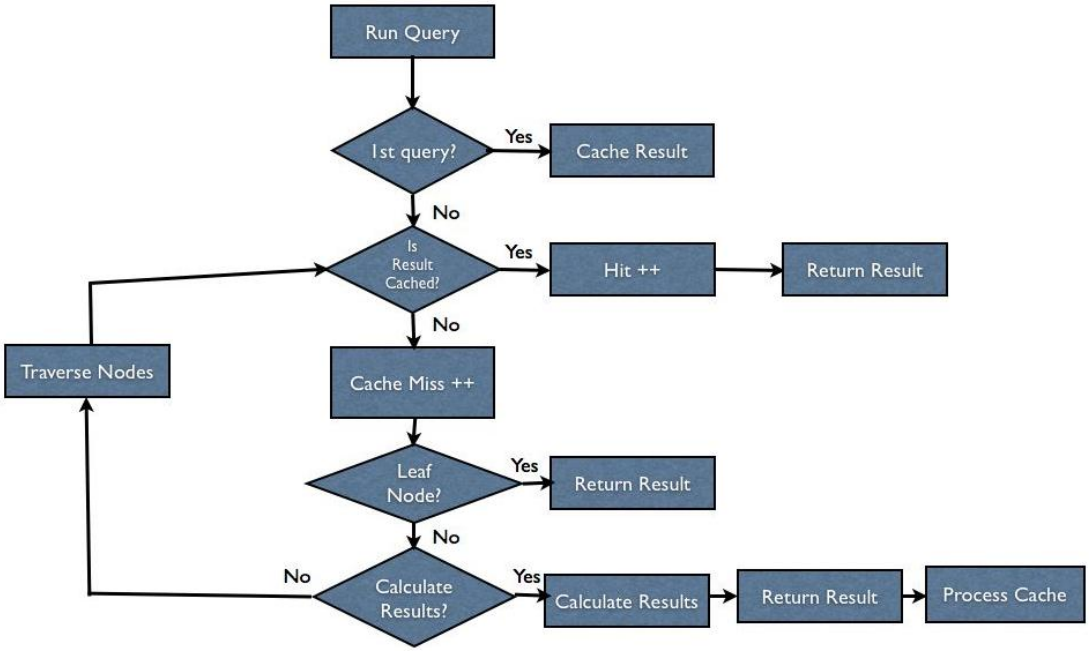

Figure 1. The Calculation Cycle

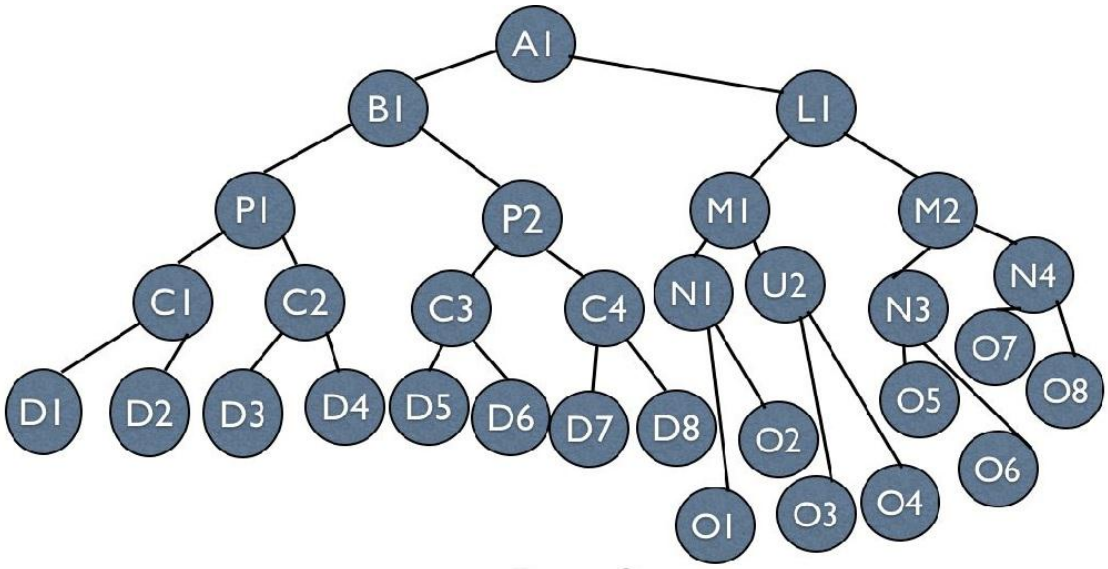

Figure 2. A Sample Predicate Graph

4. The Cache Management System

When the system is initiated, the block size and size of the cache are determined. The number of blocks available in the cache is calculated by dividing the available space by the block size. This is the total number of cache blocks that can be assigned to all cached nodes.

Figure 3 shows the Cache Management System (CMS) process. The results from the Execution Cycle are sent to the CMS. The truth table in Figure 4 illustrates the CMS in Figure 3. If the results fit in the cache then the CMS stores the results there. If they do not fit, the system checks to see if the results' miss count reaches the cache miss threshold. If it does then the CMS makes room for the results. If the initial miss threshold is not reached, a more relaxed threshold is used. If this relaxed threshold is not met, then the result is not cached. If the relaxed threshold is met, the new result must have a high cost to recalculate in order to be cached. If the cost is low, the result is not cached.

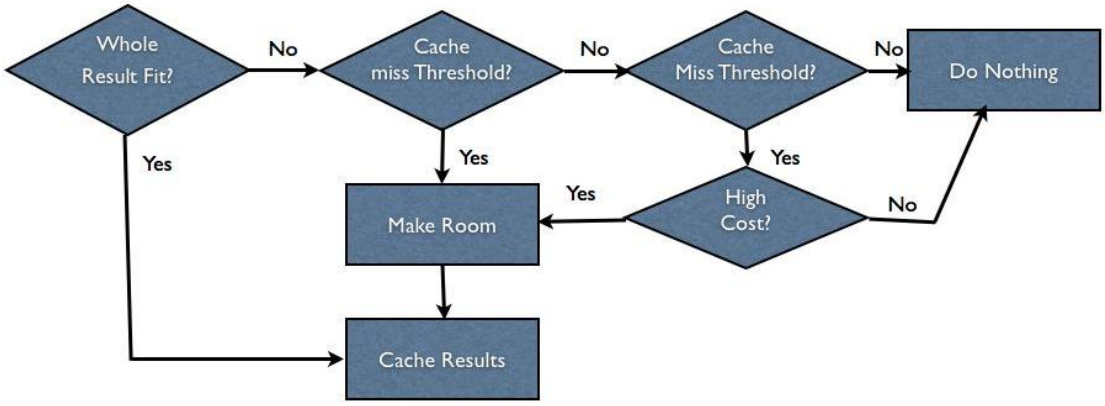

Figure 3. The Cache Management System Flow Chart

Can Whole Result Set Fit?	Is Cache Miss Thres-hold Reached ?	Is Relaxed Cache Miss Thres-hold Reached ?	Is the Re-calculation Cost High?	Action to Take
No	Yes	X	X	**Make Room**
No	No	No	X	**Do Nothing**
No	No	Yes	No	**Do Nothing**
No	No	Yes	Yes	**Make Room**
Yes	X	X	X	**Cache Results**

Figure 4. The Cache Management System Truth Table

In the next sections, the methodologies for calculating the needed data will be discussed.

5. Miss Percentages

As is seen in Figure 1, the hit and miss counts for all nodes are maintained during the Execution Cycle. The Miss Percentage of any node i is:

$$\text{Miss Percentage}_i = \#\text{misses}_i / (\#\text{misses}_i + \#\text{hits}_i)$$

6. Making Room

If the CMS decides a result set needs to be cached, but there are not enough available blocks in the cache, some existing elements must be removed from the cache. This is done by determining a normalized "recalculation cost" for all nodes in the cache. The nodes of lowest recalculation cost are removed until enough blocks are freed up to accommodate the new result set.

7. Recalculation Cost

The recalculation cost is based on normalizing the cost of calculation (discussed in the next section), the number of parents of the node (or the "node dependency"), and the miss percentage. The calculation cost is normalized to a number between 1 and 50. The node dependency and the miss percentage are normalized to a number between 1 and 5.

The recalculation cost uses these normalized values to produce a number on the same scale for all nodes. The actual formulae used are:

Norm Cost = 1 + (Cost - 1)* (50 - 1) / (max_cost - 1)

Norm Parent = 1 + (Parent Count - 1)*(5-1) / (max_parent -1)

Norm Miss = 1 + (Miss Count -1)*(5-1) / (max_node_miss -1)

Recalculation cost = (Norm Parent + Norm Miss) * Norm Cost;

The miss count is maintained in the execution cycle and the parent count is easily determined by examining the predicate graph. The next section describes how the cost of a node is calculated.

8. Cost Calculation for a Node

The cost of calculating a node is based on one of three possibilities: 1) the node is cached, 2) the node is a leaf node, or 3) the node is neither a leaf node nor cached. If the node is cached, it may be retrieved from the cache at minimal cost (we assign zero to this cost). If it is not cached, but is a leaf node, then the cost is simply the cost of retrieving the data. If it is not a leaf node, then all children of this node must be found and their costs added to the total cost (note that this may require many levels of recursive calls). The algorithm used to make this calculation is:

```
Cost_Calaculation(Input Node)
{
  if Input Node is Cached
        return 0;
  if Input Node is a leaf Node
        return b_InputNode ;
  in all other cases:
        Total Cost = Cost_Calculation(Child[0]);
        PreviousResult = Child[0];
        for(cnt =1; cnt< Child Count; cnt++)
        {
           nodeCost = Cost_Calculation(Child[cnt]);
           joinCost = b_PreviousResult + b_PreviousResult *b_Child[cnt];
           PreviousResult = PreviousResult joined to
                        Child[cnt];
           Total Cost = Total Cost + nodeCost + joinCost;
        }
  Return Total Cost;
}
```

9. Future Work

A simulation of the cache management system is currently in development and will be used to fine-tune the miss and recalculation cost thresholds. This will then be fully integrated into a deductive database management system.

10. Conclusion

A cache management system has been proposed to allow a deductive database to manage the cache of the result sets of its nodes as efficiently as possible. A heuristic has been proposed to determine when a result set should be cached, and, if room is not available, how to determine what should be removed in order to make room for this result set.

11. Bibliography

[1] Altinel, Mehmet, Christof Bornhovd, Sailesh Krishnamurthy, C. Mohan, Hamid Pirahesh, and Berthold Reinwald. "Cache Tables: Paving The Way For an Adaptive Database Cache." VLDB Conference. Berlin, Germany, 2003. Print.

[2] Ullman, Jeffrey, and Carlo Zaniolo. "Deductive Databases: Achievement And Future Directions." Sigmod. 4th ed. Vol. 19. ACM, 1990. 75-81. Print.

Improved Particle Filtering Based on Biogeography-based Optimization for UGV Navigation

A. Kuifeng Su[1,2], **B. Zhidong Deng**[1], **and C. Zhen Huang**[1]
[1]Department of Computer Science, State Key Laboratory of Intelligent Technology and Systems, Tsinghua National Laboratory for Information Science and Technology, Tsinghua University, Beijing, China
[2]Academy of Armored Force Engineering, Beijing, China

Abstract— *The main challenge with particle filtering is particle degeneracy and the accurate estimation cannot be achieved generally because of serious impoverishment problem, although resampling operation could solve degeneracy to a certain extent. In this paper, we propose an improved particle filtering approach based on biogeography-based optimization (BBO) algorithm, called BBO-PF, for state estimation of nonlinear and non-Gaussian dynamic system. The novel BBO-PF significantly reduces the degeneracy. The experimental results obtained by applying the BBO-PF to estimate the trajectory of unmanned ground vehicle validate the performance of our approach.*

Keywords: Unmanned ground vehicle; Particle filtering; Particle impoverishment; Biogeography-based optimization.

1. Introduction

The location of unmanned ground vehicle (UGV) determined according to various types of measurements is critical to UGV navigation. In fact, a variety of location algorithms have considerable difference in accuracy, robustness, and computational efficiency. Particle filtering, which is a method based on random samplings, has advantage of being applied to nonlinear and non-Gaussian dynamic systems. But there exist particle degeneracy and difficulty of selecting proposal distribution. To solve particle impoverishment problem, researchers have presented a lot of algorithms such as unscented Kalman particle filter (UKPF)[1] and Gaussian mixture sum particle filter (GMSPF)[2]. Many improved algorithms based on intelligent optimizations are also proposed to solve sample impoverishment problem, including particle swarm optimization-based particle filter (PSO-PF)[3], annealing particle filter (APF)[4], genetic particle filter (GPF)[5], evolutionary particle filter (EPF)[5], and so on. They are used to tackle the difficulty of selecting proposal distribution. Additionally, there are other hybrid algorithms such as MCMC particle filter, kernel smoothing particle filter, rejection particle filter.[6]. In this paper, we propose an improved particle filtering approach based on biogeography-based optimization (BBO) algorithm, called BBO-PF, for state estimation of nonlinear and non-Gaussian dynamic system. Based on the concept of resampling, particles with high weights have move probability to be propagated, and in the BBO-PF, some particles will join in the refining process after calculating the weight of particles, which means that those particles will move to the region with high weights. This process can be regarded as migration to the habitat with high suitability of BBO algorithm. Although the BBO operation increases the computing complexity of algorithm, the optimized weights may make the proposal distribution more closed to the poster distribution and overcome the degeneracy of particles. The proposed BBO-PF algorithm is compared to other several filtering algorithms. The experimental results show that the BBO-PF has better performance due to their lower means and variances.

2. Problem Description

The state and measurement models of the UGV location are built in this section. Our intelligent vehicle platform THIV-I developed by Tsinghua University, the location of various sensors is shown in Fig.1. The position system consists of many on-board sensors, including four ABS speed sensors and steering angle sensors, global position system (GPS), inertia measurement unit (IMU), and environment perception sensor such as lidar and camera, which provide the data of landmark. The information of speed and steering angle can obtained through the CAN bus of the vehicle itself. Meanwhile, the encoders on the rear transmission shafts can be used to obtain the accurate travelled distance during a sample period. The GPS/IMU integrated navigation system working on RTK differential mode provides accurate position reference for performance comparison of different algorithms.

2.1 System model

In this paper, the origin of the vehicle body coordinate frame locates at the center of the rear axle, i.e., the installation position of the IMU, whose position is $P_k\,(x_k, y_k)$ at the time of t_k, and the heading angle is ϕ_k. In 2D environment, the UGV's pose can be expressed by the state vector $\chi_k = (x_k, y_k, \phi_k)$. The position relation of UGV is shown in Fig. 2. In this figure, H represents a half of distance between two rear wheels, while L indicates the distance between a front axle and a rear axle of UGV.

Fig. 1: Intelligent vehicle of Tsinghua University.

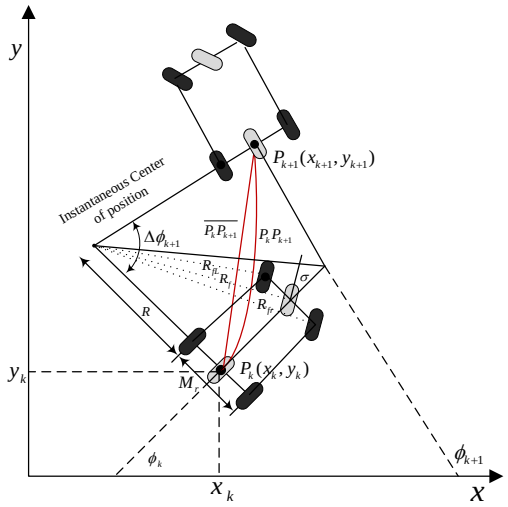

Fig. 2: Schematic diagram of the vehicle's kinematics parameter model.

$$\frac{\widehat{P_kP_{k+1}}}{\overline{P_kP_{k+1}}} = \frac{(R+M_r/2)\Delta\phi_{k+1}}{2(R+M_r/2)\sin[\Delta\ \phi_{k+1}/2]} = \frac{\Delta\phi_{k+1}/2}{\sin[\Delta\phi_{k+1}/2]} \tag{1}$$

Thus, the linear distance $\overline{P_kP_{k+1}}$ between P_k and P_{k+1} is derived below:

$$\overline{P_kP_{k+1}} = \frac{\sin[\Delta\phi_{k+1}/2]}{\Delta\phi_{k+1}/2}\widehat{P_kP_{k+1}} = \frac{\sin[\Delta\phi_{k+1}/2]}{\Delta\phi_{k+1}/2}\Delta D_{k+1} \tag{2}$$

In this formula, ΔD_{k+1} refers to the travel distance of the back wheel center measured by an encoder.

$$\mathrm{X}(k+1) = \begin{bmatrix} x_k + \overline{P_kP_{k+1}}\cos\left[\phi_{k+1} + \Delta\phi_{k+1}/2\right] \\ y_k + \overline{P_kP_{k+1}}\sin\left[\phi_{k+1} + \Delta\phi_{k+1}/2\right] \\ \phi_k + \Delta\phi_{k+1} \end{bmatrix} + \omega_k \tag{3}$$

where ω_k is system noise.

2.2 Observation model

The system of autonomous vehicle utilizes odometer and the IMU to achieve the estimation of basic position and orientation. In order to overcome the error accumulation caused by the relative positioning system, the system applies the 64-line HDL lidar, which is mounted in the anterior part of middle top of UGV, and the relative position relations with respect to UGV is shown in Fig.3.

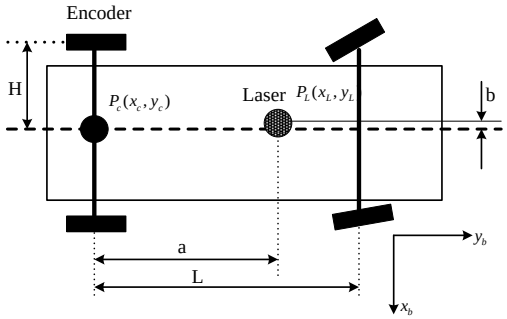

Fig. 3: Installation diagram of UGV sensor.

Then the relationship that the rear axle center transforms to the lidar centre is described by:

$$\begin{aligned} x_L &= x_c + a\cos(\phi) + b\cos(\phi + \pi/2) \\ y_L &= y_c + a\sin(\phi) + b\sin(\phi + \pi/2) \end{aligned} \tag{4}$$

The corresponding measurement equation is given by:

$$z_k = h\left(X, x_k, y_k\right) = \begin{bmatrix} \sqrt{\left(x_k - x_L\right)^2 + \left(y_k - y_L\right)^2} \\ atan\left(\frac{(y_k - y_L)}{(x_k - x_L)}\right) - \phi_L + \pi/2 \end{bmatrix} + \nu_k \tag{5}$$

In this formula, z indicates the measurement vector, i.e., the coordinates of landmark, $\{x_k, y_k\}$ represents the location of landmark identified by the 3D lidar, and ν_k is the measurement noise.

3. BBO-PF state estimation algorithm

3.1 Biogeography-based optimization

According to the island migration model of biogeography, Dan Simon proposed biogeography-based optimization (BBO) in 2008[7]. BBO is an evolutionary algorithm (EA) motivated by the optimality perspective of natural biogeography. Suppose that we have a global optimization problem and a population of candidate solutions, which can be represented by vectors of integers, each integer in the solution vector is considered to be a suitability index variable (SIV). The population consists of $\mathrm{NP} = \mathrm{n}$ solution vectors. Each individual is considered as a habitat with a habitat suitability index (HSI), which is similar to the fitness of EAs, PSO, etc to evaluate individual effectiveness. A good solution means to be an island with a high HSI, and a poor

solution indicates an island with a low HSI. The high HSI solutions tend to share their features with low HSI solutions. The low HSI solutions accept a lot of new features from the high HSI solutions.

Just as species migrate back and forth between islands, BBO operates by sharing information between individuals in a population of candidate solutions. In BBO, each individual has its own immigration rate λ and emigration rate μ. A good solution has higher μ and lower λ. The immigration rate and the emigration rate are functions of the number of species in the habitat. They can be calculated as follows:

$$\mu_{\mathbf{k}} = E\frac{k}{n} \tag{6}$$

$$\lambda_{\mathbf{k}} = I\left(1 - \frac{k}{n}\right) \tag{7}$$

where I denotes the maximum possible immigration rate, E the maximum possible emigration rate, k the number of species of the $k_t h$ individual, and n the maximum number of species[8].

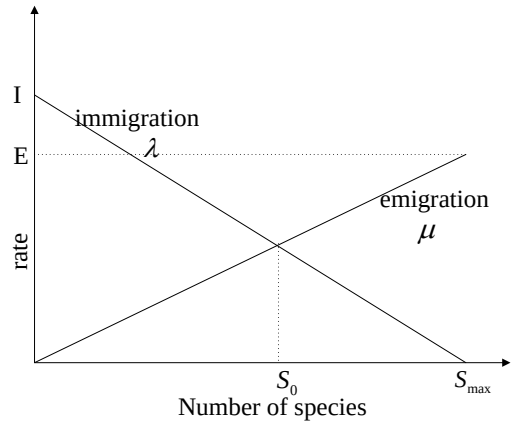

Fig. 4: Linear migration curves for an island.

There are two main operators, the migration and the mutation, in BBO. During migrating, each solution shares the information probabilistically between habitats through the emigration rate λ_i and immigration rate μ_i.

We use the immigration rate to probabilistically decide whether or not to modify each suitability index variable (SIV) in that solution. If a given solution H_i is selected to be modified, then we use the emigration rates of the other solutions to probabilistically migrate a randomly selected SIV to solution H_i. The migration process can be given by[9]:

For mutation, the main idea is deduced from the species count in habitat change drastically for cataclysmic events. A habitat's HSI can, therefore, change suddenly due to apparently random events. This mutation scheme tends to increase diversity among the population. We model this in BBO as SIV mutation, and use species count probabilities to determine mutation rates. Mutation can be described as follows[9]:

```
Select H_i with probability based on λ_i
If H_i is selected
    Select H_j with probability based on μ_i;
    If H_j is selected
        Randomly select an SIV s from H_j
        Replace a random SIV in H_i with s;
    End
End
```

```
For j=1 to length of SIVs
  Select an SIV in H_i with probability based on a priori probability m;
  If H_i is selected
    Replace SIV (H_i) with Randomly generated SIV;
  End
End
```

The BBO algorithm can be described below[9].

```
1) Initialize the BBO parameters, including the maximum species count
   n, the maximum migration rates E and I, and the mutation rate
2) Initialize the random parameter of habitat.
3) For each habitat, HIS is mapped as the number and mobility (λ_k, μ_k)
   of species k.
Calculate and determine whether HIS satisfy the supervision condition.
    If HIS dose not satisfy the supervision condition
     4) Utilize the immigration rate and emigration rate to restore
        the habitat, and then recalculate each HIS.
     5) For each habitat, refresh the probability distribution of species,
        update the species according to mutation operator, and then
        recalculate the fitness.
    End if
6) End the algorithm cycle according to the termination condition.
```

The BBO is also a species optimization algorithm. It is not related to the problems of regeneration and producing next generation, compared to both GA and evolutionary strategy optimization algorithms. There is also a remarkable difference between ACO and BBO. ACO produces a new set of solutions at each of iterations, while BBO maintains the solution set to the next iteration and adjusts the solution space according to the migration probability. BBO has more in common with PSO and DE. Compared to PSO and DE, BBO directly updates by the migration of the solution. Thus, the solutions of BBO algorithm can share properties (suitability index variable, SIVs) with each other. BBO mainly consists of the two processes, including species migration and species variation[6], [7], [8], [9].

3.2 Adaptive particle filtering algorithm based on BBO

The main disadvantage of PF is the so-called particle impoverishment problem, which is the main reason to take

resampling. This problem appears as the likelihood $p\left(y_t|x_t^i\right)$ is very narrow or likelihood lies in the tail of the proposal distribution $q\left(x_t|x_{t-1}^{(n)}, y_{1:t}\right)$. As the observation is more accurate and the prior distribution is much boarder than the likelihood (shown in Fig.5), only a few particles have weights of significant importance, which directly leads to the particle impoverishment problem.

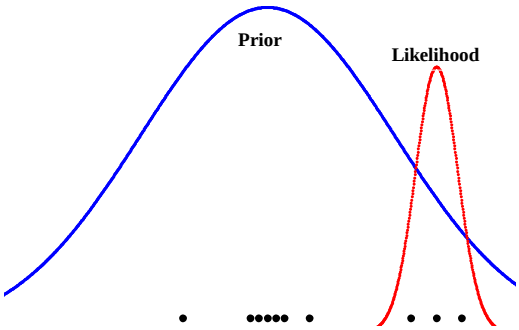

Fig. 5: Prior and Likelihood.

The proposal algorithm, called BBO-PF, incorporate the BBO algorithm into PF to improve the distribution of samples, speed up the convergence of particle sets, and overcome the impoverishment of particle filtering. The purpose is to take samples to move towards regions of the state space where the posterior probability is significant, which is related to the prior probability and likelihood. Thus, a weighted optimization problem arises to balance the contribution of prior probability and likelihood to the posterior probability. The optimization problem can be described as follows:

$$\max_{x \in S} F(x) = \kappa_1 F_1(x) + \kappa_2 F_2(x) \tag{8}$$

where κ_1 and κ_2 are non-negative weight with $\kappa_1 + \kappa_2 = 1$, S is the search space of particle sampling. Thus, the generated samples x_t^i, $i = 1, \cdots, N$, are regarded as the initial SIV in the BBO and moved to maximize the objective function $F(x)$.

Let ω_t and v_t be zero-mean Gaussian white noise with variances Q and R, respectively. Considering that (3) and (5) are nonlinear model with additive noise, the first objective consists of the function maximized at high prior regions as follows:

$$F_1 = e^{-\frac{1}{2}(x_k - \hat{x}_k)Q^{-1}(x_k - \hat{x}_k)^T} \tag{9}$$

The second objective comprises the function maximized at high likelihood regions below:

$$F_2 = e^{-\frac{1}{2}(y_k - \hat{y}_k)Q^{-1}(y_k - \hat{y}_k)^T} \tag{10}$$

Then the objective function of posterior optimization is given by:

$$F(k) = -\frac{1}{2}\kappa_1(x_k - \hat{x}_k)Q^{-1}(x_k - \hat{x}_k)^T - \frac{1}{2}\kappa_2(y_k - \hat{y}_k)Q^{-1}(y_k - \hat{y}_k)^T \tag{11}$$

The BBO-PF algorithm can be summarized below:

1.Initialization the particles $X = \left\{x_0^{(i)}, \omega_0^{(i)}\right\}_{i=1}^N$ from posterior distribution $p(x_0)$ with associated $\omega_0^{(i)} = 1/N$
2.Initialize the BBO parameters, including the maximum species count n, the maximum migration rates E and I, and the mutation rate
3.For time steps $t = 1, 2, \cdots, T$
4.Importance Sampling: for $i = 1, \cdots, N$, draw samples from the importance proposal distribution as follows: $\tilde{x}_t^{(i)} \sim q\left(x_t|x_{t-1}^{(n)}, y_{1:t}\right)$
 1) Consider each particle as a species of universal habitat.
 2) For each habitat, HIS is mapped as the number and mobility (λ_k, μ_k) of species k. Calculate and determine whether HIS can satisfy the supervision condition.
 If HIS dose not satisfy the condition of importance distribution
  3) Utilize the immigration rate and emigration rate to restore the habitat, and then recalculate each HIS.
  4) For each habitat, refresh the probability distribution of species, update the species according to mutation operator, then recalculate the fitness.
  5) Weight update: evaluate the importance weights with (11).
 End if
 6) End the algorithm cycle according to the termination condition.
5. Normalize the importance weights: $\tilde{\omega}_t^{(i)} = \frac{\tilde{\omega}_t^{(i)}}{\sum_{i=1}^N \tilde{\omega}_t^{(i)}}$
6. Output the statics of the particles.
7. Re-sampling: generate N new particles $x_t^{(i)}$ from the set $\left\{\tilde{x}_t^{(i)}\right\}_{i=1}^N$ according to the importance weights $\left\{\tilde{\omega}_t^{(i)}\right\}_{i=1}^N$
Repeat Step 3 to 7.

The BBO moves all particles towards the particles with the best fitness where is the region of having the maximum weight particles. As the best fitness value reaches a certain threshold, the optimal sampling process terminates.

4. Experimental results

To verify the effectiveness and efficiency of the proposed BBO-PF algorithm, this paper carried out experiments on urban road. Ideal two-dimensional environments were chosen as the test sites. In addition, the traffic signs stood on both sides of the road as the landmarks that were detected by the lidar. At first, we measured the accurate position of those landmarks using Span/DGPS integrated navigation system from Novatel. At the same time, the exact location of UGV was recorded during our experiment, i.e., $\chi\left(x_{ref}, y_{ref}, \theta_{ref}\right)$, in order to compare the state estimation results of various algorithms with such an exact location of UGV. The BBO-PF algorithm proposed in this paper was compared to both standard particle filtering (PF) and unscented particle filtering (UPF). The ideal reference trajectory provided by SPAN integrated navigation system and the estimation results are shown in Fig.6. Fig.7 and Fig.8 give

the comparison of eastward and northward errors, respectively. The experimental results indicated that the estimation accuracy of the proposed BBO-PF algorithm was greatly improved, compared to that of PF and UPF algorithms. The statistical distribution of position errors is shown in Fig.9 and Fig.10, respectively.

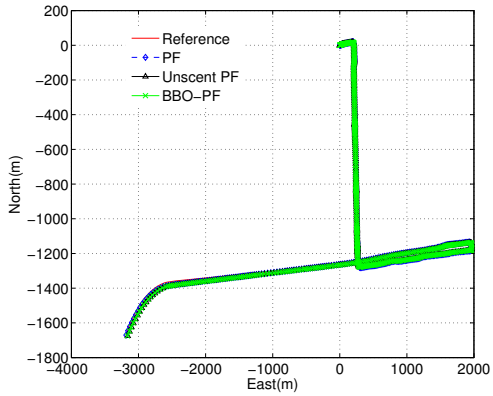

Fig. 6: Comparison of reference trajectory with estimation using PF, UPF, and BBO-PF.

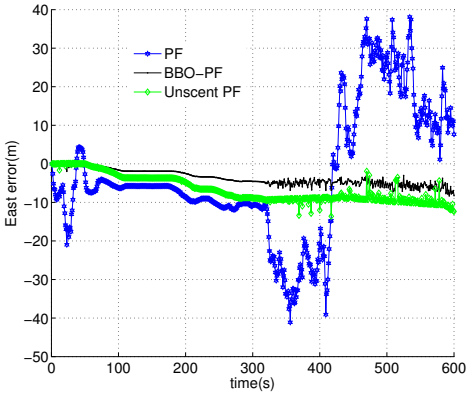

Fig. 7: Eastward deviation comparsion.

5. Conclusions

Particle filtering (PF) is sequential Monte Carlo methods based on the particle representation of probability density. It can be applied to nonlinear/non-Gaussian system and generalizes Kalman filtering. One of the main disadvantages of PF is the particle impoverishment problem, which is caused directly by the resampling process of the algorithm. We propose a BBO optimization algorithm to weight the likelihood and the prior for balancing the contribution of prior and likelihood to the posterior estimation. Our experimental results show that the BBO-PF algorithm can effectively improve the location accuracy of UGVs. In addition, due to

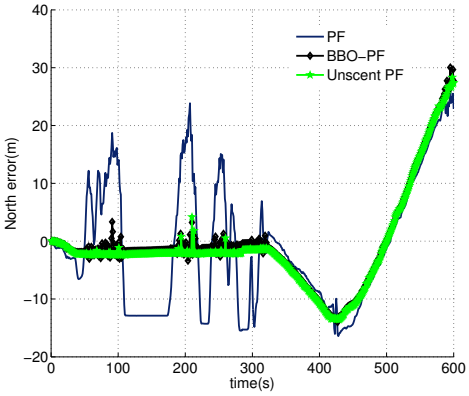

Fig. 8: Northward deviation comparison.

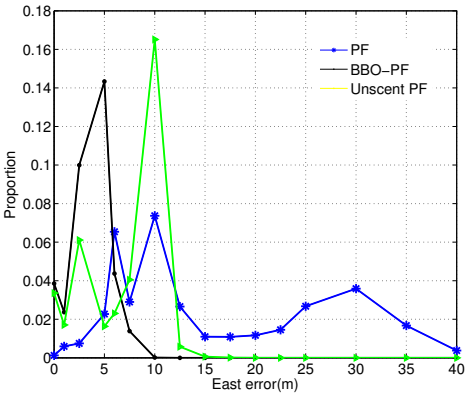

Fig. 9: Distribution of eastward error.

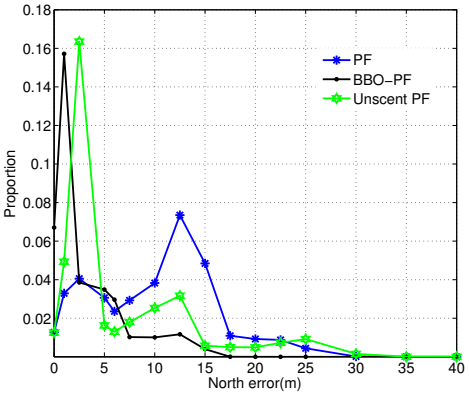

Fig. 10: Distribution of northward error.

the inherent characteristics of BBO algorithm, its efficiency is higher than other intelligent optimization algorithms such as PSO in solving high-dimensional optimization problems, which has provided a guarantee for real-time application of BBO-PF.

6. Acknowledgements

This work was supported in part by National Natural Science Foundation of China (NSFC) under Grant Nos. 90820305 and 60775040, and by the National High-Tech R & D Program of China under Grant No. 2011AA041001.

References

[1] Yi. Y, D A.Grejner-Brzezinska, "Tightly-coupled GPS/INS integration using unscented Kalman filter and particle filter," in *Proceedings of the 19th International Technical Meeting of the Satellite Division of The Institute of Navigation (ION GNSS 2006)*, 2001, pp. 2182–2191.

[2] J.H.Kotecha, P.M.Djuric, "Gaussian sum particle filtering," *IEEE Transactions on Signal Processing.*, vol. 51, pp. 2602–2612, Oct. 2003.

[3] Y.Hernane, S.Hernane, M.Benyettou, "PFPSO: An Optimised Filtering Approach Based on Sampling," *Journal of Applied Sciences.*, vol. 10, pp. 494–499, Jun. 2010.

[4] J.Gall, J.Potthoff, C. Schnörr, B.Rosenhahn, H.P.Seidel, "Interacting and annealing particle filters: Mathematics and a recipe for applications," *Journal of Mathematical Imaging and Vision.*, vol. 28, pp. 1–18, Jan. 2007.

[5] N.M. Kwok,G. Fang, W.Zhou, "Evolutionary particle filter: re-sampling from the genetic algorithm perspective," in *Intelligent Robots and Systems, 2005.(IROS 2005)*, 2005, pp. 2935–2940.

[6] Z. Chen. (2003). Bayesian filtering: From Kalman filters to particle filters, and beyond. [Online]. Available: http://users.isr.ist.utl.pt/˜ jpg/tfc0607/chen_bayesian. pdf

[7] S. Zhang, C. Zhu, J. K. O. Sin, and P. K. T. Mok, "Biogeography-based optimization," *IEEE Transactions on Evolutionary Computation.*, vol. 12, pp. 702–713, Jun. 2008.

[8] W.Gong, Z.Cai, C.X.Ling, "DE/BBO: a hybrid differential evolution with biogeography-based optimization for global numerical optimization," *Soft Computing-A Fusion of Foundations, Methodologies and Applications.*, vol. 15, pp. 645–665, Apr. 2010.

[9] M.Ovreiu, D.Simon, "Biogeography-based optimization of neuro-fuzzy system parameters for diagnosis of cardiac disease," in *Proceedings of the 12th Annual Conference on Genetic and Evolutionary Computation*, 2010, pp. 1235–1242.

Optimal Placement of Phase Shifter Transformers for Power Loss Reduction Using Artificial Bee Colony Algorithm

H. Shayeghi*
Technical Eng. Department
University of Mohaghegh Ardabili
Ardabil, Iran

H. A. Shayanfar
Electrical Eng. Department
Islamic Azad University, South Tehran Branch,
Tehran, Iran

E. Barzegar
Technical Eng. Department
University of Mohaghegh Ardabili
Ardabil, Iran

M. Ghasemi
Technical Eng. Department
University of Mohaghegh Ardabili
Ardabil, Iran

hshayeghi@gmail.com, hashayanfar@yahoo.com, e.barzega@gmail.com, mghasemi1986@yahoo.com

Abstract- *Control of power transmission and loss causes complications in the large power systems. Phase Shifter Transformers (PST) according to their capabilities can be appropriate devices for power controlling in the large power transmission systems. Various criteria such as decreasing of loss, saving of generator annual economic cost, improving system static and dynamic behaviors and reducing of congestion have been individually studied in the literature to placement problem of phase shifter transformers (PST). In this paper, loss reduction, voltage profile and congestion improvement indices are assessed and the optimal locations of PST devices evaluated by using Artificial Bee Colony (ABC) algorithm. The effectiveness of the proposed ABC based method is demonstrated on IEEE 30-Bus network through some performance indices in comparison with the genetic algorithm and particle swarm optimization. Results evaluation show that the ABC algorithm has an excellent capability in loss reduction, voltage profile and congestion improvement than the GA and PSO methods.*

Keywords: PST, Allocation, ABC; Power Loss Reduction.

1. Introduction

Nowadays, increment of generation quantity becomes a necessity relating to the ongoing industrials, electrical consumptions growing and consequently the consecutive load increasing. On the other hand, operating of power system must be closed to its nominal capacity considering high development costs of networks and their related devices and environmental concerns. Liberalization of the electricity market and utilities tendency in getting more profits also compel power systems to operate close to theirs rate capacities and sometimes in over load conditions. Moreover, variable distribution of load and generation resources based on their conditions make network operate in heavy congested load conditions in some parts and in light load conditions in others. Accurate evaluating of power transmission and determining its level is investigated in congestion indices concepts. Many various indices already have been represented to quantifying congestion values of transmission lines [1]. Network operation close to its nominal capacity may appear as over load state in some sections and can lead to partial outages. Continuation of this state results in blackout condition possibly. Thus, proper management of network power flow is a main necessity along with holding the operation constraints. Controlling and managing the power flow in network lines can be done by using the various methods and some controlling actions and devices such as Generation Rescheduling (GR), series capacitors, FACTS controlling device and suede-FACTS devices [2-4]. Phase Shifter Transformer (PST) is one of the suede-FACTS devices which can replace the power in related and next lines by changing the transmitting power value that may cause to relieve congestion [5-7]. Phase shifter transformer installation considering its advantages can control the value of line power flows obviously. However, because of investment limitations, the installation and usage of phase shifter transformers only based on their advantages will not be economic.

Proper location and sizing of PST should be noticed and studied because its installation at wrong places and capacities can cause various problems in the operation conditions. In this paper, an Artificial Bee Colony (ABC) algorithm is proposed for finding optimal location of PST aimed at reducing the power loss and

*Corresponding Author (hshayeghi@gmail.com)

improving voltage profile and power congestion. The ABC algorithm is a typical swarm-based approach to optimization, in which the search algorithm is inspired by the intelligent foraging behavior of a honey bee swarm process [12] and has emerged as a useful tool for engineering optimization. It incorporates a flexible and well-balanced mechanism to adapt to the global and local exploration and exploitation abilities within a short computation time. Hence, this method is efficient in handling large and complex search spaces [13].

IEEE 30 Bus network has been used as a test system to demonstrate the effectiveness and robustness of the proposed ABC algorithm and their ability to provide efficient loss reduction and voltage profile improvement. To show the superiority of the proposed approach, the simulations results are compared with the particle swarm optimization and genetic algorithm through some performance indices. The results evaluation shows that the proposed method achieves good robust performance and is superior to the other methods.

2. PST Model [10]

An ideal voltage source with voltage V_s and reactance X_s that is connected in series between nodes i and j is shown in Fig. 1.

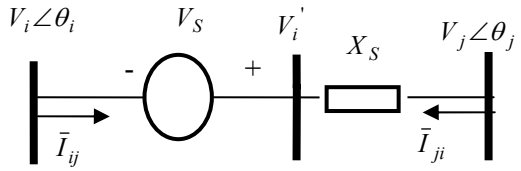

Fig. 1. Series voltage source between buses i and j

V_i is an imaginary voltage source which can be defined as:

$$\overline{V'}_i = \bar{V}_S + \bar{V}_i \quad (1)$$

$$\bar{V}_S = r\,\bar{V}_i\,e^{j\gamma} \quad \text{and} \quad 0 \le r \le 1 \quad (2)$$

Figure 2 shows a phasor diagram that is used to represent the voltage of Fig. 1 with regulating magnitude and angle.

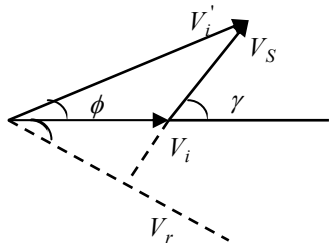

Fig. 2. Voltages phasor diagram of Fig. 1

Figure 3 shows the current source model of PST (the Norton model of voltage source) where, $b_s = \frac{1}{x_s}$ and $I_s = -jb_s\bar{V}_S$.

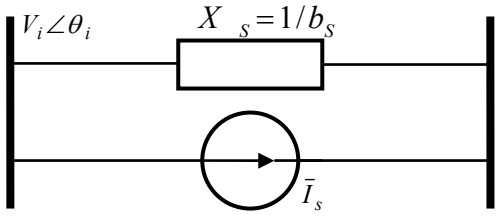

Fig. 3. Norton model of series voltage source

Current source is dependent on the usage of nodes i and j for transmitting power, then $\bar{S}_{is}$ and $\bar{S}_{js}$ are expressed as follows:

$$\bar{S}_{is} = \bar{V}_i(-\bar{I}_S)^* \quad (3)$$

$$\bar{S}_{js} = \bar{V}_j(\bar{I}_S)^* \quad (4)$$

After replacing relations (1) and (2) to (3) and (4) and simplifying, the injected active and reactive powers are calculated using the following equations [10].

$$P_{is} = r\,b_s V_i^2 Sin\,\gamma \quad (5)$$

$$Q_{is} = r\,b_s V_i^2 Cos\,\gamma \quad (6)$$

$$P_{js} = -r\,b_s V_i V_j Sin(\theta_{ji} + \gamma) \quad (7)$$

$$Q_{js} = -r\,b_s V_i V_j Cos(\theta_{ji} + \gamma) \quad (8)$$

The powers injection model of PST has been shown in Fig. 4 as a series voltage resource.

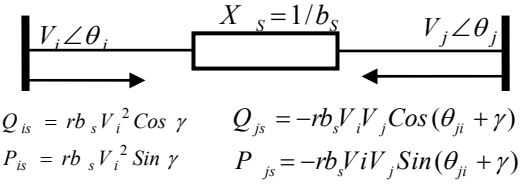

Fig. 4. Injection model of series voltage source

By using Eqs. (5) through (8) and applying a phase shifter transformer, angle γ can be changed and then the value of line power flow will be vary. If a PST is installed between buses i and j, the new admittance matrix formed considering the impedance X_s in the network admittance matrix. The Jacobean matrix is given in Table 1 [10]. Powers injection in PST model can be added to Jacobean matrix elements by a particular sign.

Table 1. Modified Jacobian matrix

$H_{(i,i)} = H^0_{(i,i)} - Q_{si}$ $H_{(i,j)} = H^0_{(i,j)} + Q_{sj}$ $H_{(j,i)} = H^0_{(j,i)} + Q_{si}$ $H_{(j,j)} = H^0_{(j,j)} - Q_{sj}$	$N_{(i,i)} = N^0_{(i,i)} - P_{si}$ $N_{(i,j)} = N^0_{(i,j)} - P_{sj}$ $N_{(j,i)} = N^0_{(j,i)} + P_{si}$ $N_{(j,j)} = N^0_{(j,j)} + P_{sj}$
$J_{(i,i)} = J^0_{(i,i)}$ $J_{(i,j)} = J^0_{(i,j)}$ $J_{(j,i)} = J^0_{(j,i)} - P_{sj}$ $J_{(j,j)} = J^0_{(j,j)} + P_{sj}$	$L_{(i,i)} = L^0_{(i,i)} + 2Q_{si}$ $L_{(i,j)} = L^0_{(i,j)}$ $L_{(j,i)} = L^0_{(j,i)} + 2Q_{sj}$ $L_{(j,j)} = L^0_{(j,j)} + 2Q_{sj}$

3. ABC Algorithm

The ABC algorithm describes the foraging behavior of honey-bees for numerical optimization problems. The algorithm simulates the intelligent foraging behavior of honey bee swarms. It is a very simple, robust and population based stochastic optimization algorithm [11].

The minimal model of forage selection in honey bee swarms intelligence consists of three essential components: food sources, employed foragers and unemployed foragers, and two leading modes of the behavior, recruitment to a nectar source and abandonment of a source, are defined [12]. A food source value depends on many factors, such as its proximity to the nest, richness or concentration of energy and the ease of extracting this energy. The employed foragers are associated with particular food sources, which they are currently exploiting or are ‘‘employed”. They carry with them information about these food sources and share this information with a certain probability. There are two types of unemployed foragers, scouts and onlookers. Scouts search the environment surrounding the nest for new food sources, and onlookers wait in the nest and find a food source through the information shared by employed foragers.

In the ABC algorithm, the colony of artificial bees contains of three groups of bees: employed bees, onlookers and scouts. The food source represents a possible solution of the optimization problem and the nectar amount of a food source corresponds to the quality (fitness) of the associated solution. Every food source has only one employed bee. Thus, the number of employed bees or the onlooker bees is equal to the number of food sources (solutions).

An onlooker bee chooses a food source depending on the probability value associated with that food source, p_i, calculated by the following expression:

$$p_i = \frac{fit_i}{\sum_{n=1}^{SN} fit_n} \tag{9}$$

where fit_i is the fitness value of the solution i evaluated by its employed bee, which is proportional to the nectar amount of the food source in the position i and SN is the number of food sources which is equal to the number of employed bees (BN). In this way, the employed bees exchange their information with the onlookers.

In order to produce a candidate food position from the old one, the ABC uses the following expression:

$$v_{ij} = x_{ij} + \phi_{ij}(x_{ij} - x_{kj}) \tag{10}$$

Where, $k \in \{1,2,...,BN\}$ and $j \in \{1,2,...,D\}$ are randomly chosen indexes. Although k is determined randomly, it has to be different from i. ϕ_{ij} is a random number between [0, 1]. It controls the production of a neighbour food source position around x_{ij} and the modification represents the comparison of the neighbor food positions visually by the bee. Equation (10) shows that as the difference between the parameters of the x_{ij} and x_{kj} decreases, the perturbation on the position x_{ij} decreases, too. Thus, as the search approaches to the optimum solution in the search space, the step length is adaptively reduced.

The food source whose nectar is abandoned by the bees is replaced with a new food source by the scouts. In the ABC algorithm this is simulated by randomly producing a position and replacing it with the abandoned one. If a position cannot be improved further through a predetermined number of cycles called *limit* then that food source is assumed to be abandoned.

After each candidate source position v_{ij} is produced and then evaluated by the artificial bee, its performance is compared with that of x_{ij}. If the new food has equal or better nectar than the old source, it is replaced with the old one in the memory. Otherwise, the old one is retained. In other words, a greedy selection mechanism is employed as the selection operation between the old and the current food sources.

The main steps of the algorithm are given by [13, 14]:

i) Initialize the population of solutions and evaluate them.
ii) Produce new solutions for the employed bees, evaluate them and apply the greedy selection mechanism.
iii) Calculate the probabilities of the current sources with which they are preferred by the onlookers.
iv) Assign onlooker bees to employed bees according to probabilities, produce new solutions and apply the greedy selection mechanism.
v) Stop the exploitation process of the sources abandoned by bees and send the scouts in the search area for discovering new food sources, randomly.
vi) Memorize the best food source found so far.
vii) If the termination condition is not satisfied, go to step 2, otherwise stop the algorithm.

It is clear from the above explanation that there are three control parameters used in the basic ABC: The

number of the food sources which is equal to the number of employed or onlooker bees (*SN*), the value of *limit* and the Maximum Cycle Number (MCN).

4. Problem Formulation

The main goal of this paper is loss reduction, voltage profile and congestion improvements via optimal allocation of PST. Decreasing the amount of loss and boosting the voltage profile are serious issues in new and modern power networks, but the necessity of having an acceptable security margin in network operation is also very important. For obtaining these purposes, utilizing of phase shifter transformers is essentially required. Thus, for balancing lines power flow, it is necessary to assess congestion problem in relevant indices firstly. To investigating the congestion parameter of test system, the PI_l index proposed in reference [15] has been used which is expressed as follows:

$$PI_l = 1 - \frac{1}{N}\sum_{i=1}^{N} \frac{\omega_i}{\sqrt{2\pi}\sigma} e^{\left(\frac{(P_i - \kappa)^2}{2\sigma^2}\right)} \quad (11)$$

Where,

σ: Lines power standard deviation from nominal values

κ: Equals 70 percent of line nominal power (P.U)

ω_i: Weight factor of line *i*

N: Number of lines N

P_i: Power of each line (p.u.)

For calculating PI_l: ω_i and σ is considered 1 and 0.3, respectively.

If all lines are loaded at their nominal value, PI_l index has a low value and if overload condition occurs in networks, PI_l will be have a large value. Thus, optimal location of PST will be evaluated to reduce lines loss and improve congestion and voltage profile indices by ABC algorithm. The objective function used for phase shifter transformers placement is given by:

$$PI = W_1 PI_l + W_2 P_{Loss} + W_3 \frac{1}{m}\sum_{i=1}^{m} |V_i - 1| \quad (12)$$

Where,

m: Total number of buses

V_i: *i*th bus voltage in p.u.

PI_l: Congestion indices in p.u.

P_{loss}: Total value of system losses in p.u

w_1, w_2, w_3: Weight coefficients related to congestion, loss and bus voltage indices, respectively

Minimizing the objective function that is composed of loss, congestion and voltage profile indices will leads to finding PST optimal location. Thus, the allocation problem can be formulated as the following optimization problem, where the constraints are the buses voltage magnitude limits, lines active power transmitting capabilities and generated active and reactive power of generators limitations [12]:

Minimize PI (13)

The proposed approach employs ABC algorithm to solve this optimization problem and search for optimal placement of PST by evaluating the objective cost function as given in Eq. (13) using load flow of power system. The goal is determining the installation place and angle setting of phase shifter transformers. The weight factors w_1, w_2 and w_3 are included in objective function according the importance and effects of P_{loss}, congestion index PI_l and buses voltage magnitudes. It is necessary to mention that in this paper they have set to 20, 1 and 1, respectively.

5. Simulation Results

The proposed method is applied to the electrical network on IEEE 30 bus including six thermal generating units as shown in Fig. 5 to assess the suitability of the algorithm. The system data extracted from [15]. The MARTPOWER-4 toolbox of MATLAB software is used for load flow running.

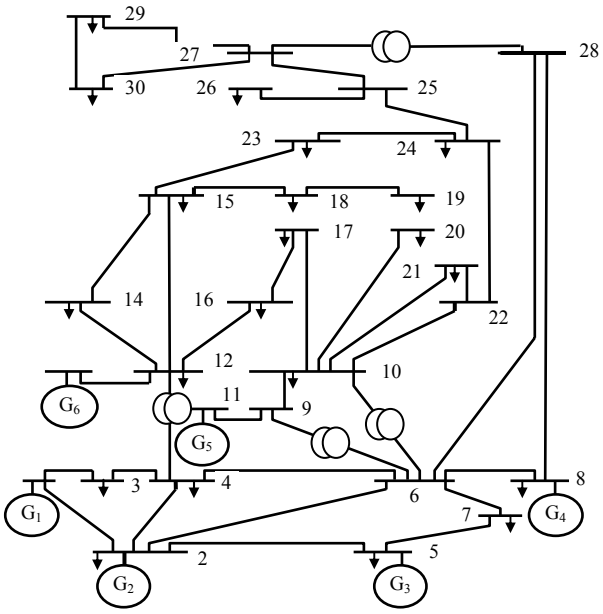

Fig. 5. IEEE 30 bus power system

The goal is determining the installation place and angle setting of phase shifter transformers. The obtained results using ABC is compared with PSO and GA methods in order to illustrate its robust performance and effectiveness for the solution of optimal allocation of PST problem.

Results of the PST placement based on the objective function *PI*, by applying AC power flow using the proposed ABC, PSO and GA algorithms are given in Table 2. Figure 6 shows the minimum fitness functions evaluating process.

Table 2. Optimal PST parameters

Algorithm	Optimized Place of PST	Angle of PST	The best cost Function
GA	11	-9.8787	0.9166
PSO	14	-8.7775	0.9153
ABC	14	-8.7773	0.9153

It can be seen that from Table 1 installing a phase shifter transformer in line 14 between buses 9 and 10 can be reduced loss and improved voltage profile and congestion indices of network clearly than the GA method. Table 3 presents the lines and network loss, PI_l index values before and after installing of PST using three methods. It is evident that the ABC and PSO based solution is identical. Using the GA the reduction at total loss of network is 7.5%, whereas it is 8.5 % using the proposed ABC algorithm.

Table 3. The lines and network loss, PI_l index values before and after installing of PST

					GA		**PSO & ABC**	
NO #	**From Bus**	**To Bus**	**P_{loss}(MW) Without PST**	**PI_l(p.u) Without PST**	**P_{loss}(MW) With PST**	**PI_l(p.u) With PST**	**P_{loss}(MW) With PST**	**PI_l(p.u) With PST**
1	1	2	0.026	0.9995	0.29	0.9994	0.029	0.9786
2	1	3	0.128	0.9998	0.118	0.9998	0.118	0.9754
3	2	4	0.178	0.9878	0.163	0.9882	0.163	0.8391
4	3	4	0.018	0.9872	0.017	0.9877	0.017	0.8337
5	2	5	0.110	0.9866	0.120	0.9870	0.118	0.8935
6	2	6	0.286	0.9741	0.326	0.9694	0.321	0.8239
7	4	6	0.066	0.9670	0.127	0.9587	0.119	0.7887
8	5	7	0.120	0.9682	0.130	0.9496	0.129	0.7689
9	6	7	0.031	0.9677	0.028	0.9492	0.028	0.7927
10	6	8	0.128	0.9400	0.124	0.9314	0.124	0.7604
11	6	9	0	0.9327	0	0.9147	0	0.7045
12	6	10	0	0.9180	0	0.8985	0	0.6751
13	9	11	0	0.9124	0	0.8929	0	0.6823
14	9	10	0	0.9050	0	0.8760	0	0.6581
15	4	12	0	0.8988	0	0.8654	0	0.6542
16	12	13	0	0.8817	0	0.8487	0	0.6321
17	12	14	0.037	0.8668	0.025	0.8340	0.026	0.6180
18	12	15	0.065	0.8604	0.018	0.8190	0.021	0.6047
19	12	16	0.008	0.8342	0.009	0.8045	0.012	0.5942
20	14	15	0.003	0.8175	0.009	0.7876	0.008	0.5798
21	16	17	0.031	0.8000	0.001	0.7710	0	0.5674
22	15	18	0.097	0.7823	0.037	0.7536	0.041	0.5545
23	18	19	0.022	0.7650	0.003	0.7368	0.04	0.5435
24	19	20	0.090	0.7503	0.020	0.7153	0.018	0.5359
25	10	20	0.052	0.7350	0.099	0.6990	0.092	0.5280
26	10	17	0.023	0.7200	0.042	0.6826	0.039	0.5207
27	10	21	0.044	0.7062	0.045	0.6687	0.044	0.5157
28	10	22	0.062	0.6915	0.056	0.6547	0.056	0.5142
29	21	22	0.093	0.6717	0.081	0.6373	0.081	0.5063
30	15	22	0.109	0.6540	0.142	0.6200	0.138	0.4985
31	22	23	0.078	0.6373	0.039	0.6023	0.037	0.4920
32	23	24	0.066	0.6200	0.042	0.5850	0.044	0.4855
33	24	25	0.035	0.6025	0.003	0.5684	0.001	0.4804
34	25	26	0.046	0.5855	0.046	0.5514	0.046	0.4750
35	25	27	0.063	0.5879	0.022	0.5344	0.023	0.4699
36	28	27	0	0.5626	0	0.5253	0	0.4745
37	27	29	0.108	0.5350	0.108	0.5077	0.108	0.4692
38	27	30	0.127	0.5176	0.127	0.4902	0.127	0.4642
39	29	30	0.013	0.5030	0.013	0.4754	0.013	0.4624
40	8	28	0.036	0.4882	0.043	0.4600	0.042	0.4601
41	6	28	0.001	0.4667	0.005	0.4450	0.005	0.4585
TOTAL			2.395		2.215		2.193	

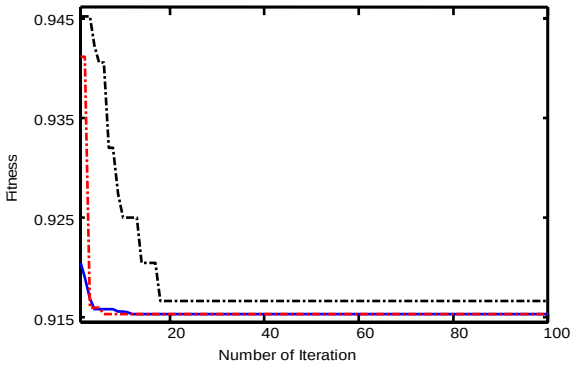

Fig. 6: Fitness convergence, Dotted (GA), Dashed (PSO) and Solid (ABC).

Figure 7 and 8 show the power loss of network lines and PI_l index. It can be seen that the proposed ABC method has good performance and power loss reduction and PI_l index improvement is significantly occurred after PST placement using ABC and PSO techniques. Voltage profile of network before and after PST installation is shown in Fig. 9. Using the proposed ABC algorithm voltage profile is considerably improved. Moreover, it is superior to the GA method.

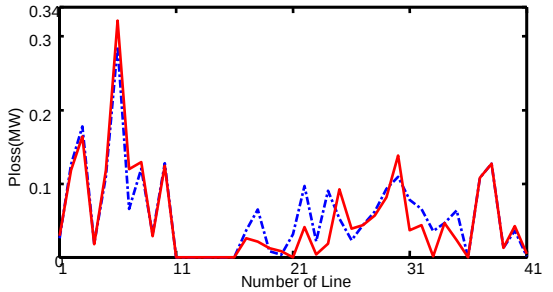

Fig. 7. P_{loss} index before and after PST installation, Dashed (before PST installation), Solid (after PST installation and using ABC)

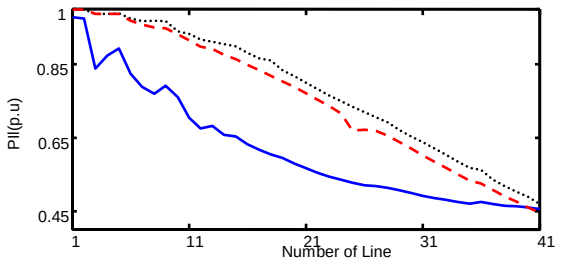

Fig. 8. PI_l congestion index, Dashed (without PST), Dotted (with PST using GA), Solid (with PST using ABC)

6. Conclusions

This paper presents an appropriate method based on ABC algorithm to improve line loss, voltage profile and congestion indices through optimal sitting of a phase shifter transformers. Due to consideration to some practical issues and by defining a new performance index, the optimum allocation of a single PST and its controlling phase angles can be determined. . The proposed ABC algorithm is easy to implement without additional computational complexity. Thereby experiments this algorithm gives quite promising results. The ability to jump out the local optima, the convergence precision and speed are remarkably enhanced and thus the high precision and efficiency are achieved. The performance of the proposed ABC based method is tested on IEEE 30-Bus network and the proper location for installing phase shifter transformers is obtained by minimizing the objective function in short evaluating time. Results evaluation show significant reduction in power loss in addition to voltage profile and congestion improvement than the GA method one.

References

[1] S. N. Singh and A. K. David, "Congestion Management by Optimal FACTS Device Location", Proc. of Int. IEEE Conf. on Elect. Utility Deregulation and Restructuring and Power Technologies, pp. 23-28, Apr. 2000.

[2] G. Wu, A. Yokoyama, J. He, and Y. Yu, "Allocation and Control of FACTS Devices for Steady-State Stability Enhancement of Large Scale Power Systems," Int. Conf. on Power Syst. Tech. POWERCON '98, Vol. 1, pp. 357-361, 1998.

[3] S. Gerbex, R. Cherkaoui, and A. J. Germond, "Optimal Location of Multi-Type FACTS Devices in a Power System by Means of Genetic Algorithms," IEEE Trans. Power Syst., Vol. 6, pp. 537–544, 2001.

[4] H. Mori and Y,Goto, "A Parallel Tabu Search Based Method for Determining Optimal Allocation of FACTS in Power Systems", Proc. of Int. IEEE Conf. on Power System Technology, Vol. 2, pp, l077-1082, Dec. 2000.

[5] P. D. Kamjorn, P. K. Arcot, and P. Dcouto,"A Screening Technique for Optimally Locating Phase Shifters in Power Systems," IEEE PES, Chicago, IL, pp. 233-238, 1994.

[6] A.K. Kazerooni, H. Seifi, M.S. Sepasian, H. Haghighat, "New Approach for Phase Shifter Transformer Allocation", The 8th IEE International Conference, pp. 94-98, 2006.

[7] P. Paterni, S. Vitet, M. Bena, A. Yokoyama, Optimal Location of Phase Shifters in the French Network by Genetic Algorithm. IEEE Trans Power Syst.; Vol. 14; N0 1; pp. 37-42; 1999.

[8] S. Gerbex, R. Cherkaoui, A.J. Germond. Optimal Location of Multi-type FACTS Devices in a Power System by Means of Genetic Algorithms. IEEE Trans Power Syst. Vol. 16; N0 3; pp. 537-544; 2001.

[9] M. Gitizadeh, H. Khalilnezhad, "Phase Shifter Transformers Optimum Allocation in Power

Systems Using a Combinational Method", Proc. of Int. IEEE Conf. on Power System Technology, pp. 886-890, 2010.

[10] R .D. Zimmerman, C. E. Murillo-sanchez, R. J. Thomas, Matpower: Steady-State Operations, Planning and Analysis Tools for Power Systems Research and Education," IEEE Transactions on Power Systems, Vol. 26, No. 1, pp. 12-19, Feb. 2011.

[11] H. Shayeghi, A. Ghasemi, Solving Economic Load Dispatch Problems with Valve Point Effects Using Artificial Bee Colony Algorithm, International Review of Electrical Engineering, Vol. 6, pp. 2569-2577, 2011.

[12] H. Shayeghi, H.A. Shayanfar, A. Ghasemi, Artificial Bee Colony Based Power System Stabilizer Design for a Turbo-generator in a Single-Machine Power System, International Conference on Artificial Intelligence (ICAI'11), Las Vegas, USA, pp. 122-128, 2011.

[13] H. Shayeghi, H.A. Shayanfar, A. Ghasemi, A Robust ABC based PSS Design For a SMIB Power System, International Journal on Technical and Physical Problems of Engineering (IJTPE), vol. 3, pp. 86-92, 2011.

[14] H. Shayeghi, A. Ghasemi, Market base LFC design using Artificial Bee Colony, International Journal on Technical and Physical Problems of Engineering (IJTPE), vol. 3, pp. 1-10, 2011.

Biographies

Hossein Shayeghi received the B.S. and M.S.E. degrees in Electrical and Control Engineering in 1996 and 1998, respectively. He received his Ph. D. degree in Electrical Engineering from Iran University of Science and Technology, Tehran, Iran in 2006. Currently, he is an Associate Professor in Technical Engineering Department of University of Mohaghegh Ardabili, Ardabil, Iran. His research interests are in the Application of Robust Control, Artificial Intelligence and Heuristic Optimization Methods to Power System Control Design, Operation and Planning and Power System Restructuring. He has authored of five books in Electrical Engineering area (all in Persian language). He has published more than 190 papers in International Journals and Conference proceedings. He is a member of Iranian Association of Electrical and Electronic Engineers (IAEEE) and IEEE.

Heidarali Shayanfar Received the B.S. and M.S.E. Degrees in Electrical Engineering in 1973 and 1979, respectively. He received his Ph. D. Degree in Electrical Engineering from Michigan State University, U.S.A., in 1981. Currently, He is a Full Professor in Electrical Engineering Department of Iran University of Science and Technology, Tehran, Iran. His Research Interests are in the Area of Application of Artificial Intelligence to Power System Control Design, Dynamic Load Modeling, Power System Observability Studies, Voltage Collapse, Congestion Management in a Restructured Power System, Reliability Improvement in Distribution Systems and Reactive Pricing in Deregulated Power Systems. He has published more than 405 papers in International Journals and Conference proceedings. He is a Member of the Iranian Association of Electrical and Electronic Engineers and IEEE.

Ebrahim Barzegar was born in 1989 and received B.Sc. degree in Electrical Engineering from faculty of electrical engineering of the Guilan University (Rasht, Iran) in 2011. Currently, he is a M.S.E. student in Technical Engineering Department of University of Mohaghegh Ardabili (Ardabil, Iran). His areas of interest in research are application of the Heuristic Methods to Power System Control, reliability and Distributed Generation (DG).

Mehdi Ghasemi Was born in 1986 and received B.S degree in Electrical Engineering form Faculty of electrical engineering of the Tabriz University Tabriz, Iran in 2009. Currently, he is a M.S.E. student in Technical Eng Department of the University of Mohaghegh Ardabili, Ardabil, Iran. His areas of interest in research are application of the Heuristic methods to Power System Control.

Multiple Camera Based Surveillance

N. Sharma[1], R. K. Behera[2], S. Bhatia[1], Mahua Bhattacharya[1*]

1 Indian Institute of Information Technology & Management
Morena Link Road Gwalior-474003, India
2 KPIT Cummins Info systems, Pune 411057, India

* *Corresponding author: bmahua@hotmail.com*

***Abstract*-The main focus of this research is to develop, implement and test a surveillance system for tracking objects automatically using multiple camera views. A surveillance camera system can be very useful in carrying out tasks like security in public areas, road traffic monitoring. More and more surveillance cameras are being installed and utilized for surveillance task and hence sometimes it becomes difficult to remember their locations and their visible areas. Therefore, with a large number of surveillance cameras, it is not an easy task for people to recognize which camera should be monitored and which region of the camera images should be checked so that all the activities and/or events in a scene can be examined. Also the ability of humans to concentrate on multiple videos simultaneously is limited. A system that could automate this task would be of great use for safety and security for everyday life.**

Keywords- Tracking, multi-perspective video, surveillance, camera handoff.

I. INTRODUCTION

Many cameras are required for covering large field of view. To track the object successfully in multiple camera one needs to establish correspondences among objects captured in multiple cameras. Handshaking can be defined as labeling the object across multiple cameras. This is accomplished by finding the limits of field of view (FOV) of a camera as visible in the other cameras. Using this information, when a person is seen in one camera, we can predict all the other cameras in which this person might be visible. This approach is applicable only when there is a significant overlap in the field of view of the cameras.

In the work of Vera Kettnaker and Ramin Zabih [1], Bayesian probabilistic approach based multi camera surveillance system is developed to predict the appearance of an object in a camera after it exits from another camera. Jehoon Lee, Shawn Lankton, A. [2] gives an approach based on affine transformation. In this approach a simple neural network is trained to predict the parameters of the affine transformation. P H Kelly et al [3] presents an approach for dealing with handoff problem. It proposes the use of calibrated cameras and a 3D model of the environment. The 3D coordinates (voxel) of the object obtained through calibration are used during handoff between cameras to assign label. The 3D coordinates of an object obtained from multiple cameras map [8] to the same point. In Omar Javed et al [4] an approach to handle the handoff [10], [11] problem is presented. This approach does not require the cameras to be calibrated. It uses a model of the relationship between FOV lines of various cameras. The FOV lines bind the FOV of a camera. When an object enters FOV of a new camera it is checked if this person is visible in the FOV of another camera [6]. Here the author presents an improved technique for object tracking. The captured video frames are smoothed by a low pass filter. This method reduces the number of computations and computation time. In addition the noise in the signals is suppressed automatically.

In [5] authors have given techniques for how to detect moving objects from an image sequence, recognize the activity of object and behavior understanding. Background subtraction is a very popular technique for foreground segmentation in a still scene [9], [13].

The technique used is independent component analysis and it is best for indoor surveillance where moving and motionless persons must be reliably detected. In [7] author has cited about how to deal with the changing background. Sometimes it is not possible to take static background and we have to do background modeling so that the background can be adaptive according to the environment. The work [12] presented is based on the GPS system which uses a multi-agent system architecture to track moving objects. In [14] an automatic method for tracking individual across cameras via a surveillance network has been reported. In this work an emerging low computational complexity handoff function that can automatically carry out the camera assignment and handoff task has been depicted.

A. Constrains:

- Cameras are stationary.
- There must be overlapping regions across the cameras.
- The objects should not be very close to each other.

II. METHODOLOGY

IN ORDER TO GET THE MOVING OBJECTS FROM IMAGES, SOME BASIC OPERATIONS ARE REQUIRED SO THAT THE OBJECT CAN BE SEPARATED FROM THE BACKGROUND. THE STEPS USED TO GET FOREGROUND OBJECTS ARE:

A. Background subtraction

Background subtraction method is used for identifying changes in the foreground. By this method we separate the objects from the background. The background subtraction is done by finding the difference between corresponding pixels of two images (taking one of them as background). The image considered as background should not contain any moving objects. Detection of the foreground [13] objects is done by taking the difference between the current frame and an image of the scene's static background.

$$|\text{frame}_i - \text{background}| > \text{Th}$$

Background subtraction method is very sensitive to threshold (Th).

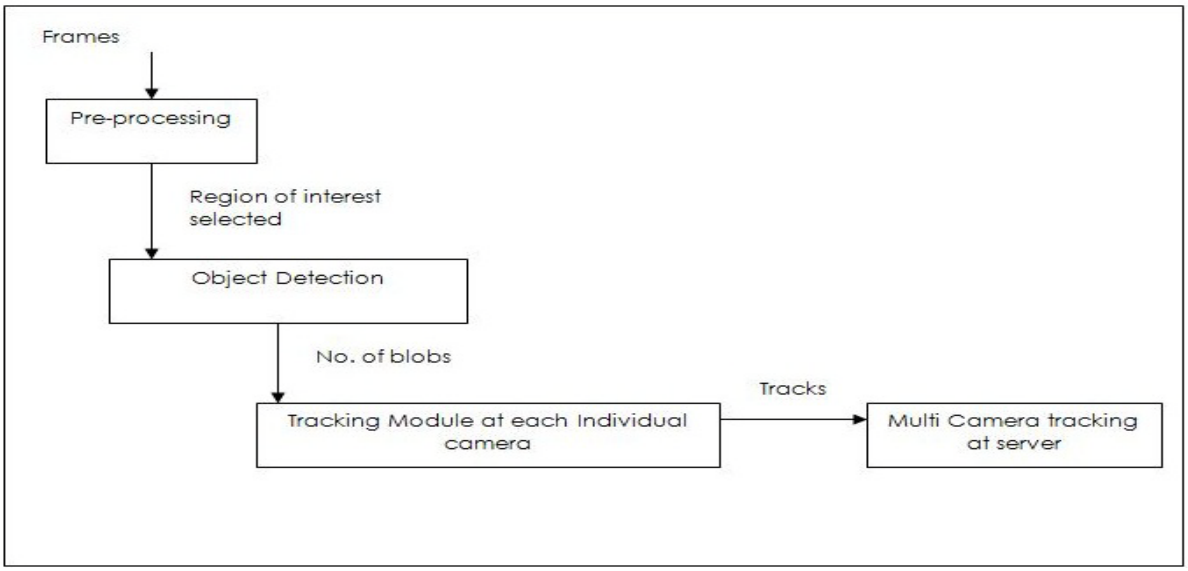

Fig. 1 System Level Diagram

B. Erosion & Dilation

The subtracted image consists of many unwanted tiny objects. To remove these unwanted objects erosion and dilation operations are used. In erosion, the local minimum is computed over an area of a kernel. In dilation, the local maximum is computed over the area of a kernel and the pixels are merged.

$$erode(x,y) = \min_{(x',y') \in kernel} src(x+x',y+y')$$

$$dilate(x,y) = \max_{(x',y') \in kernel} src(x+x',y+y')$$

C. Blob detection

Blob detection creates a box around the detected objects in a region. It takes connected points in an image and draws the box around them. Steps are as following

- Take a 3*3 patch around a point and check if any point in that patch has a label.
- If a point with a label is found, give the same label to the point in center.
- If no point with a label is found, give a new label to the point in center.
- Go to next point and repeat from step 2 until all the points are not labeled.
- Give the same label to the points which are connected (but given different label earlier)
- Draw a rectangular box around all the objects (points with same label).

To draw rectangular box we take two longest diagonal points as (x, y) and (x□, y□). Let length is l and distance is d so

$$d = y' - y$$
$$l = x' - x$$

Then draw a d*l rectangle around the object.

D. Approaches for handshaking-

1) Edge of Field of View Method -I (Perpendicular distance)

For tracking across multiple cameras *edge of field of view* method is used. When a person enters the FOV of a camera, it should be determined, if this person is visible in the FOV of any other camera, and if so, assign the same label to the new view. If the person is not visible in any other camera, then a new label is assigned to this person. Let us suppose a person enters through one of the FOV line, as cameras are stationary we just draw the FOV lines manually and try to find the distance (perpendicular) of all the objects with respect to that FOV line. As we know that the object has just entered through this line so it will be the nearest among all other objects falling in the overlapping region of these cameras with respect to that line. We assign some label to that object. Labels are unique for each object.

Algorithm for handshaking across multiple cameras

```
Repeat for every frame
For every camera C^i
{
    If new object appears in the middle of the frame
    {
        Assign it a new label
    }
    Else If object appears from any side l (FOV line)
    {
        Find s = set of FOV lines of all the cameras (C^j) in which the object is visible
        If s = 0
        {
            Assign current object new label
        }
        Else
        {
            For every camera C^j, j □ s
            {
                For every object k in C^j
                {
                    d(j,k) = D(P_k^j, L_l^ij)
                }
            }
        }
    }
}
```

For any object in C^j who is nearest to particular FOV line, assign the same label as in C^i.

2) Edge of Field of View Method-II (Distance from some point on the EOFOV)

If some objects are at the same distance from the FOV, the situation can be tackled by considering some point on the FOV line. Calculate the distance of all objects from this point and compare with the distances of the objects from the same point in view of the other camera which already contains these objects. Using the additional distance measure, the objects can be labelled accurately.

Another technique for tackling the same situation is to take a point at the foot of the perpendicular of the object of interest and calculate the distance of all the objects from the corresponding point in view of the other camera. The distance will be minimum for the same object in the other camera and same label can be assigned to that particular object.

E. Approaches for Tracking

1) Distance Based Tracking

We first take the centre of the object in the present frame and find the distance of all the objects in the next frame from this point (centre of the object in the present frame). Now assign the label to that object that has minimum distance from that point. Euclidean distance is considered. Suppose an object is at (x_1, y_1) and in the next frame it is at a point (x_2, y_2). The distance between them is:

$$d = \sqrt{(y_2 - y_1)^2 + (x_2 - x_1)^2}$$

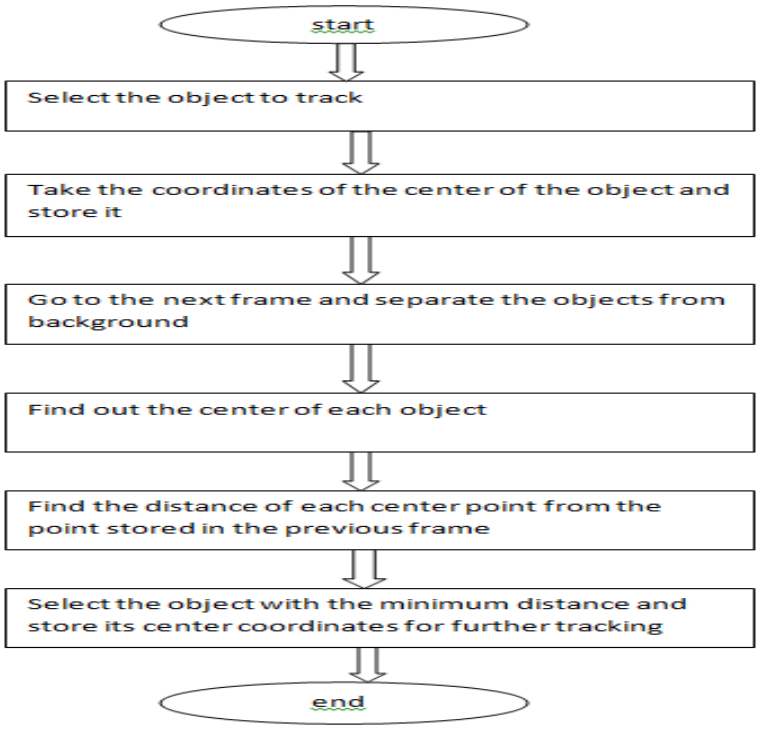

Fig. 2 Block diagram for distance based tracking

2) Direction Based Tracking

In this method we find the blob in the direction of the motion of the object. If the variation in the direction of the blob is within some range; then accept it, otherwise discard it. Suppose an object moves from point (x_1, y_1) to (x_2, y_2), slope is determined by the equation:

$$\theta = \tan^{-1}\left(\frac{y_2 - y_1}{x_2 - x_1}\right)$$

3) Shape Based Tracking

In the shape based tracking for multiple camera based surveillance, an object is selected first. The method for finding the variation between the objects in the current frame and the object in the last frame is as follows:

- Take the minimum and maximum coordinates of the object, say (x_1 ,y_1) and (x_2 ,y_2).
- Find the height and width of the object as:

$$Height(h1) = y_2 - y_1$$
$$Width(w1) = x_2 - x_1$$

- Store these data and find the height (h_2) and width (w_2) of each object in the next frame.
- Find the variation for each object by the following formula:

$$Variation(v) = (h_2 - h_1)^2 + (w_2 - w_1)^2$$

- The object with least variation is tracked object in the current frame.
- Repeat the above steps for the next frames.

III. Results and Discussion

Module wise results are shown below. Firstly, foreground and background separation is demonstrated. However, it is observed that the image obtained after background subtraction is noisy. As we know that noise in the context of image processing is anything which is not useful at particular moment though it may be useful for other context. To remove this noise we used the technique called erosion and dilation. These techniques remove and add the *unwanted and wanted data* from the image. After erosion and dilation we have used technique called blob detection to find particular object. Handshaking is performed after blob detection. In handshaking we try to find the correspondences across the cameras. If an object in one camera is at a particular position, its position in the other camera is determined. Finally in the process of tracking, we use distance based and *shape* based features.

A. *Preprocessing Result*

Fig.3 Original image

Fig. 4 Background subtraction

Fig. 5 Erosion and dilation

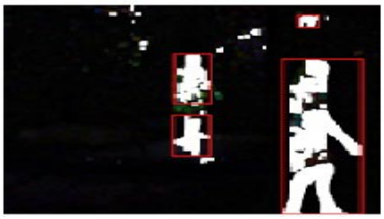

Fig. 6 Blob Detection

B. *Handshaking between two Camera*

Fig. 7 Object selected in camera 1

Figs. 8 Object matched in camera 2

C. *Tracking Result:-In camera -1*

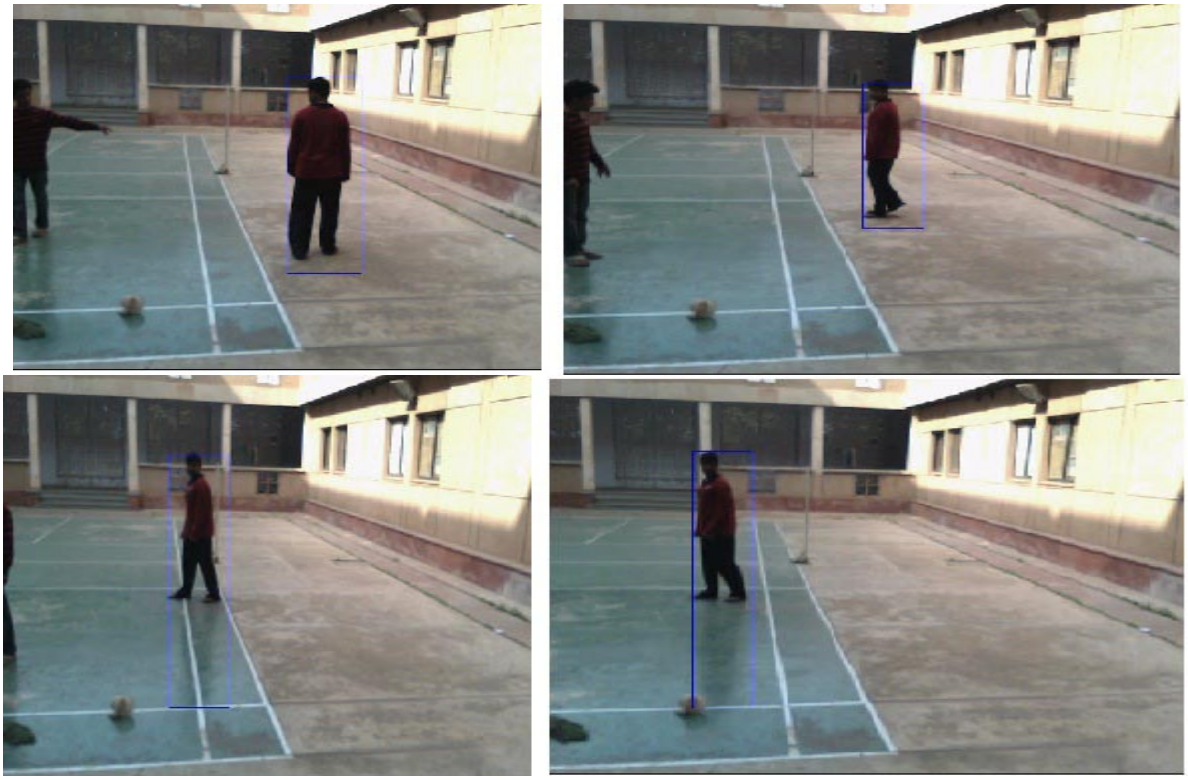

Fig. 9 Tracking in camera-1

D. Tracking Result:-In camera -2

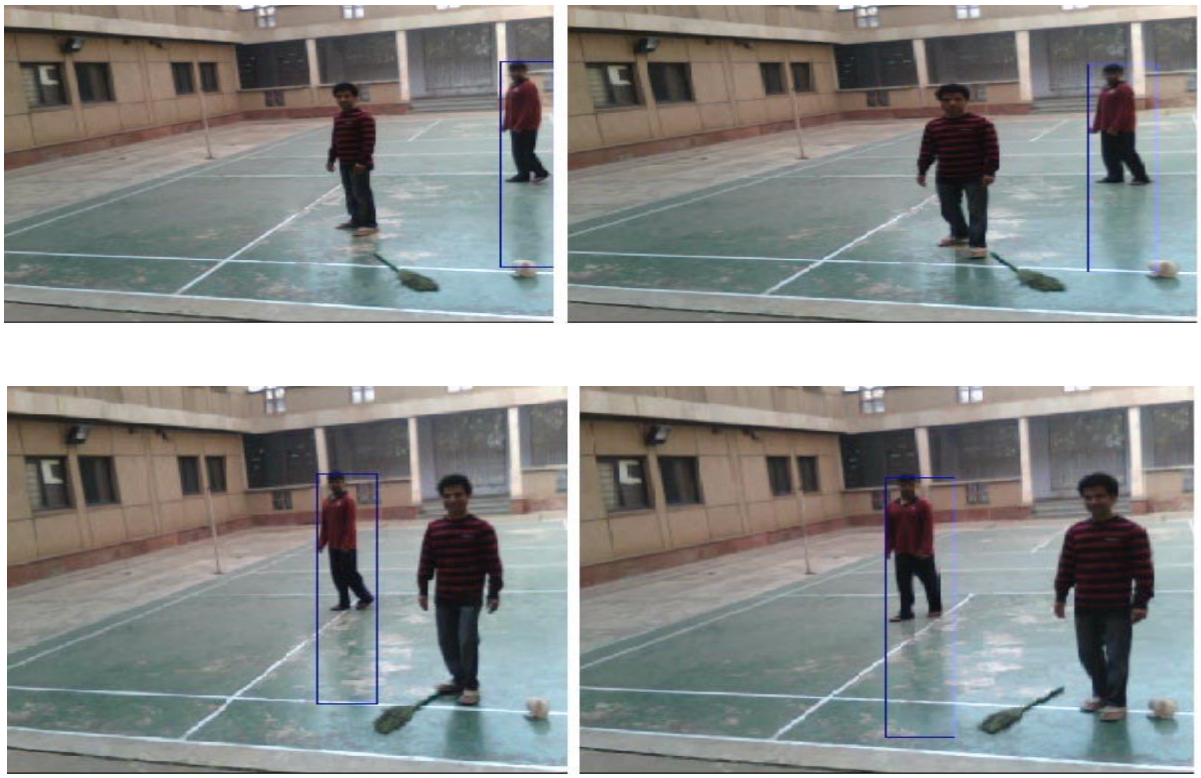

Fig. 10 Tracking in camera-2

IV. FUTURE WORK

When two objects are closer to each other and cameras are mounted at different heights and angles with respect to ground, 3D co-ordinate mapping combined with direction vectors along the length and width of the object blobs can be used to give correct results. For 3D co-ordinate mapping, height and angle of the mounted cameras are required. Blobs can be used to give the direction vector along the length and width of the object in both the cameras.

In the presence of an obstacle, tracking methods used sometime fails and we need to consider velocity based features of the objects. When single feature is not sufficient for efficient result we need to use combination of both the methods. It fails when two objects are at the same distance from the objects in the previous frame and have the same shape. We need to consider direction features of the objects.

V. CONCLUSION

2D co-ordinate mapping gives correct result when the cameras are mounted at same height and angle with respect to ground. A change in the camera setup would require the calculation of all the parameters again. Color based matching can be used as an additional feature to match the objects in different camera views. It would be inefficient if color or lighting effect changes. Under the conditions when foreground objects can be separated from the background, the results of FOV approach are satisfactory and can be used for handshaking between two cameras. We can use the EOFOV methods for efficient handshaking & it is giving satisfactory results under given constrains.

Mean shift tracking gives correct result for single object. However, it may fail when there are many objects. The method (distance & shape based) used in our approach is giving satisfactory results.

ACKNOWLEDGMENT

This work was supported by ABV-IIITM Gwalior & KPIT Cummins Infosystems Ltd Pune. Our Special thanks to Mr. Krishnan Kutty and Mrs. Sanjyot Gindi for their valuable suggestion and technical support.

REFERENCES

[1] Kettnaker, V, Zabih, R., "Bayesian multi-camera surveillance,"IEEE Computer Society Conference on Computer Vision and Pattern Recognition, pp. 253-259, 1999.

[2] Jehoon Lee, Shawn Lankton, A. T, "Object tracking and target reacquisition based on 3-d range data for moving vehicles," IEEE , pp. 2912-2924, 2011.

[3] P. H. Kelly, et. al., "An architecture for multiple perspective interactive video", In Proc. ACM Conference on Multimedia, pp. 201-212, 1995.

[4] Omar Javed, Sohaib Khan, Zeeshan Rasheed, Mubarak Shah, "Camera Handoff: Tracking in Multiple Uncalibrated Stationary Cameras," IEEE, TX, Dec 7-8, pp. 113-118, 2000.

[5] Tsai, D.-M. and Lai, S.-C., "Independent component analysis-based back ground subtraction for indoor surveillance," IEEE 18: pp. 158 – 167, 2009.

[6] J. Shajeena, D. K. R., "A novel way of tracking moving objects in video scenes," IEEE 10, pp. 805 – 810, 2011 .

[7] Piccardi, M., "Background subtraction techniques: a review," IEEE International Conference on Systems, Man and Cybernetics 7803-8566-7/04, pp. 3099-3104, 2004.

[8] K. Chen, C. Lai, Y. H. and Chen, C., "An adaptive learning method for target tracking across multiple cameras," IEEE pp. 1-8, 2008.

[9] A. Yilmaz, O. J. and Shah, M., "Object tracking a survey," ACM Computing Surveys (CSUR) 38, 145,2006.

[10] Anton van den Hengel, Anthony Dick, H. D. A. C., "Finding camera overlap in large surveillance networks," Springer-Verlag Berlin Heidelberg 32, pp. 375–384,2007.

[11] Chao-Yang Lee, Shou-Jen Lin, C.-W. L. C.-S. Y., "Adaptive camera assignment and handoff algorithm in multiple active camera sureviellance system," IEEE,67, pp. 3015-3020, 2010.

[12] Elhadi Shakshuki, Y. W., "Using agent-based approach to tracking moving objects," IEEE, pp. 578 – 581,2003.

[13] Group, C. V. R., "Background subtraction techniques a review," University of Technology, Sydney 14,2004.

[14] Huang, C.-M. and Fu, L.-C., "Multi target visual tracking based effective surveillance with cooperation of multiple active cameras," IEEE transaction 41, pp. 234–247,2011.

Influence of Generation Scheduling on Reconfiguration of Power Systems to Minimize Voltage Sag Indices

S. García-Martínez, E. Espinosa-Juárez
Electrical Engineering Faculty
Universidad Michoacana de San Nicolás de Hidalgo
Morelia, Michoacán, México
sigridt@umich.mx, eejuarez@umich.mx

Abstract - *In this paper an analysis of the influence of generation scheduling when a reconfiguration method is applied in order to reduce voltage sag indices in a power system is presented. The description of the reconfiguration method based on a Tabu Search algorithm is presented. The method implemented in Matlab® is applied to analyze several case studies in the IEEE-57 bus test system, and different conditions of generation demand in the electrical network were considered. The obtained results demonstrate the good performance of the proposed methodology*.

Keywords: voltage sags, reconfiguration, voltage sag indices, tabu search.

1 Introduction

Nowadays, voltage sags are one of the principal concerns regarding power quality, because a lot of equipment used by commercial and industrial users is sensitive to this phenomenon of power quality; consequently, industrial processes are more sensitive and companies are less tolerant to these phenomena, since they cause malfunction of their equipment which results in significant economic losses. The most severe voltage sags are usually caused by faults such as short-circuits in the electrical system. However, they may also be caused by overloads and starting of large motors [1].

A voltage sag is a short reduction in RMS voltage at the power frequency with durations from 0.5 cycles to 1 minute. At the present time, there are different methodologies to estimate and analyze voltage sags, such as stochastic methods [2]-[5] and others based on the state estimation concept [6][7]. On the other hand, there are indices that define the quality of voltage variations, for example, the System Average Interruption Duration Index (SAIDI); however, one of the most widely used for assessing the impact of voltage sags is the SARFIX index (System Average RMS Frequency Index) [1][8]. This index indicates the average number of sags and swells during an evaluation period (usually a year) per customer [8].

Furthermore, the scheduling of generators in a power system is constantly changing, and this change represents an important factor in the stochastic prediction of voltage sags [9]. Several studies have analyzed the influence of generation and topology network changes on the voltage sag estimation [9]-[11].

Currently, there are several ways to mitigate the frequency of occurrence of voltage sags. For instance, the installation of mitigation devices can be seen as a possible solution for customers; nevertheless, these devices have a mitigation capability that is limited by the energy storage capacity [12]-[15]. The network reconfiguration constitutes an alternate method to improve the system performance. Over the years, several investigations applying reconfiguration methods have been carried out in order to minimize losses in networks subjected to certain restrictions [16]-[18].

In order to improve power quality aspects, in particular the occurrence of voltage sags, a network reconfiguration is performed in this paper, with the objective of obtaining the configuration that best reduces the frequency of occurrence of voltage sags [19]. Also, the process to achieve an optimal topology that minimizes the voltage sag indices under different conditions of generation demand of the network is carried out by means of an implemented Tabu Search (TS) algorithm. Some case studies in the IEEE-57 test system are presented in order to demonstrate the performance of the proposed method.

2 Formulation of reconfiguration method

The aim of this paper is to obtain the optimal state of switches in a network in order to identify a topology that minimizes voltage sag $SARFI_X$ indices under different conditions of generation demand.

The $SARFI_X$ index represents the average number of specified rms variation measurement events that occurred over the assessment period per customer served; where the

specified disturbances are those whose magnitude is less than *x*, for sags, and greater than *x*, for swells [8]:

$$\text{SARFI}_X = \frac{\sum N_i}{\sum N_T} \quad (1)$$

where x is the rms voltage threshold; N_i is the number of customers experiencing short duration voltage deviations with a magnitude above or below x, for sags and swells respectively; and N_T is the total number of customers served from the section of system to be assessed [8].

The SARFIx index, when is calculated per single monitored point, can also be regarded as the number of disturbances in a given measurement point, over a specified period of time [8]. In this paper, for purposes of comparison between different configurations of the same system, this definition is assumed.

This paper proposes an automatic reconfiguration method of a power system, by applying Tabu Search in order to reduce voltage sags, and taking into account different generation scheduling.

The connection/disconnection state of a transmission line is represented by means of a binary vector whose length is equal to the number of switches available in the system [19]; the number of possible topologies also depends on the number of switches. Thus, the number of possible topologies will be equal to $2^{number\ of\ switches}$, and every possible topology should be evaluated in order to get the best one. However, if the number of switches increases the evaluation number will also increase, making the computational cost prohibitive.

Voltage sags rates can vary depending on the system characteristics, such as the operation conditions in an electrical system which are constantly changing according to energy demand.

Generally, statistical data about the occurrence of voltage sags in an electrical system can be obtained. These values can be considered as typical values for a particular node; another aspect to consider is that in a determinate network there are particular buses in which, due to the contract requirements specifications, there is a maximum number of voltage sags allowed in a period of time [13]. The typical values or the values specified by contract requirements can be considered as reference values of voltage sags for a particular bus. Then, when a voltage sags analysis is carried out in order to obtain voltage sag indices, and it is found that some buses have higher voltage sags rates than the specified reference values, this can be considered as an undesirable system condition that can be solved through a reconfiguration process [19].

Considering a generic electrical system of n buses and l lines, it is assumed that l_{sn} lines have switches that can change their status (open/close). Every configuration, which is obtained by changing the open/close status of the l_{ns} lines, can be described by a Y vector. The Y vector's length is equal to the number of l_{sn} lines. It is important to note that, in this analysis, even lines which regularly contain more than one switch were represented by means of a single switch in order to specify its open/close status.

For instance, taking into account a generic system with n buses and a determinate number of sn switches, a possible configuration for a given voltage threshold t can be,

$$\begin{array}{c} \quad l_1 \quad l_2 \quad l_3 \qquad l_{sn} \\ Y = [\ \ 1 \quad 1 \quad 0 \quad \ldots \quad 1 \quad] \end{array} \quad (2)$$

where l_3 is open, which means that line l_3 is not energized. Therefore, line l_3 does not belong to the new configuration. Then, a voltage sag evaluation by means of the analytical method described in [5] is applied in order to obtain the voltage sag number in the electrical system. When some buses of the system have a voltage sag number higher than the reference value, a reconfiguration process is applied to reduce the voltage sag number in those buses, thus ensuring that all voltage sag values are equal or lower than the reference values. Mathematically this can be written as follows

$$\min\left(f_{est_i} - f_{ref_i}\right) \quad \forall i \quad (3)$$

subject to

$$V_i^{\min} \le V_i \le V_i^{\max}$$

$$P_{Gi}^{\min} \le P_{Gi} \le P_{Gi}^{\max}$$

$$Q_{Gi}^{\min} \le Q_{Gi} \le Q_{Gi}^{\max}$$

where:

$f_{est\,i}$ is the voltage sags number for the i bus
$f_{ref\,i}$ is the voltage sags reference value for the i bus
$V_i^{\min}$ is the minimum voltage at bus i
V_i is the voltage at bus i
$V_i^{\max}$ is the maximum voltage at bus i
$P_{Gi}^{\min}$ is the minimum real generation at generator i
P_{Gi} is the real generation at generator i
$P_{Gi}^{\max}$ is the maximum real generation at generator i
$Q_{Gi}^{\min}$ is the minimum reactive generation at generator i
Q_{Gi} is the reactive generation at generator i
$Q_{Gi}^{\max}$ is the maximum reactive generation at generator i

In this paper, the optimal configuration of a system in order to minimize voltage sags indices is found by solving the optimization problem formulated in (3) by applying TS and taking into account the generators schedule.

3 Implementation of the reconfiguration method by applying Tabu Search

In this work, a basic TS algorithm and the reconfiguration methodology described in section II, implemented in Matlab®, are presented [19]. Fig. 1 shows a flow chart of the implemented method.

This process, which is shown in Fig. 1, is repeated until a convergence criterion is satisfied. In this work, the TS process can stop in two ways: when it reaches the maximum iteration number or when the voltage sag number at each bus is equal or lower than the corresponding reference value.

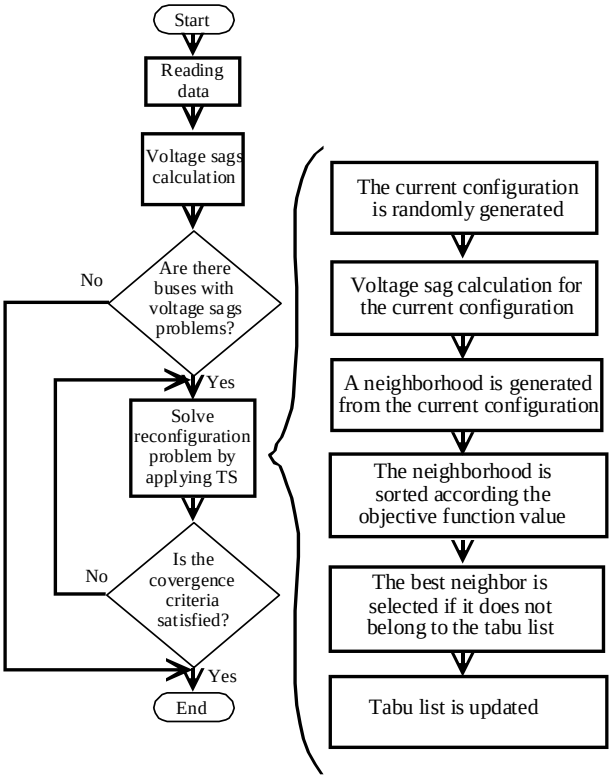

Fig. 1 Flow chart of the reconfiguration process

4 Case studies

The implemented reconfiguration method has been applied to the IEEE 57-bus test system in order to reduce the occurrence frequency of voltage sags when different conditions of energy demand are considered. The cases have been analyzed considering that voltage sags are caused by balanced three-phase faults.

The system consists of 57 buses which are interconnected by means of 63 lines, 15 transformers and 7 generating units [20]. To obtain the reference vector of voltage sags ($SARFI_x$, according to the assumed definition [8]), the method described in [5] was used and the resultant values were randomly fixed for each bus of the system with values close to those obtained by the stochastic method. The vector shown in Table I is taken as a reference vector (column 2), and it was obtained considering a voltage threshold of 0.8 p. u. ($SARFI_{80}$).

4.1 Analysis of influence of generation schedule

The analysis of the influence of generation schedule on the reconfiguration of the IEEE-57 bus test system was carried out by using the implemented method based on a TS algorithm for the following case studies assuming a fault rate of 1 faults/year for all system lines:

Case A1. Base case. Generators data provided in [20] are considered.

Case A2. 20% generation increase, achieved by increasing generation at all generation buses.

Case A3. 20% generation reduction, achieved by decreasing generation at all generation buses.

Table I shows that, in Case A1, the system has a total of 31 buses (approximately 54% of the buses) which have values of voltage sags/year (that is, $SARFI_{80}$ index) above the reference values (the shaded ones). Table I also shows that the total of voltage sags in the electrical network is 2606.44 per year, before the reconfiguration process (actual values). When the system has been reconfigured, all buses have values under the reference ones; therefore, the total of voltage sags is decreased by almost 18 %.

Table II shows that, in Case A1, the solution process requires six neighborhoods to find the solution, that is, six iterations of TS are required in order to accomplish that all 31 buses with values of voltage sags higher than their corresponding reference values reach values of voltage sags lower than the reference ones.

In Case A2, when a reduction of generation of 20% is considered, the total of buses that have values above the reference ones is less than in Case A1. In Case A2 only 15 buses have values greater than the reference.

In Case A3, when an increase of generation of 20% is considered, the total of buses (with values above the

reference) increases to 44, a significant difference when compared with Case A1.

TABLE I. VOLTAGE SAGS/YEAR CONSIDERING A VOLTAGE THRESHOLD OF 0.8 P. U. FOR CASE A1

Bus	Case A1: Voltage sags/year		
	Ref.	Actual	Reconfig.
1	30	34.0	26.3
2	30	34.8	27.3
3	34	33.6	27.8
4	32	35.4	11.0
5	38	36.2	10.6
6	28	31.4	10.1
7	42	39.9	19.7
8	35	37.9	12.7
9	40	38.4	33.8
10	33	39.6	32.7
11	41	42.3	36.0
12	35	37.6	32.0
13	39	38.6	36.4
14	42	43.7	37.4
15	39	39.0	33.6
16	36	37.1	30.9
17	35	33.9	30.2
18	40	40.3	19.6
19	45	47.2	40.6
20	52	50.5	45.3
21	48	49.6	44.0
22	50	48.5	42.6
23	49	48.4	42.7
24	51	52.9	48.6
25	51	51.7	48.0
26	55	52.2	47.0
27	48	47.9	44.8
28	42	46.6	36.2
29	46	44.3	30.7
30	54	52.2	50.5
31	56	54.0	50.7
32	58	57.1	50.1
33	54	56.0	49.1
34	53	53.8	47.8
35	48	52.7	47.4
36	52	52.0	45.9
37	50	52.7	46.5
38	51	49.6	41.8
39	55	53.7	46.1
40	51	50.9	45.4
41	48	51.2	42.1
42	52	51.0	42.3
43	46	48.2	40.3
44	47	48.9	40.7
45	44	45.1	38.3
46	45	47.4	40.4
47	46	48.0	40.8
48	44	49.0	41.0
49	48	48.0	39.6
50	42	47.2	39.2
51	43	40.6	35.8
52	42	44.5	38.8
53	46	44.7	40.2
54	41	44.3	41.0
55	40	43.3	38.1
56	53	52.8	42.5
57	55	53.8	43.7
TOTAL	2550	2606.4	2144.4

TABLE II. NUMBER OF REQUIRED NEIGHBORHOODS TO ACHIEVE THE SOLUTION FOR CASE STUDIES

Case	Required Neighborhoods
A1	6
A2	3
A3	7

Once reconfiguration is carried out, all buses have values under the reference. Table III shows the switches status for the optimal reconfiguration after the optimization process, for cases A1 to A3. It can be observed that case A1 requires 6 lines open, while cases A2 and A3 require 4 and 10 lines open, respectively.

The results for Cases A1 to A3 can be observed graphically in Fig. 2 to Fig. 4. It can be observed that in all case studies the implemented methodology ensures that all buses have $SARFI_{80}$ values below the values specified by the reference. For instance, in Case A2, when a reduction of generation is considered, just 15 buses have values above the reference; once the reconfiguration process is made, all buses have values of voltage sags below the reference ones (Fig. 3). Case A2, after reconfiguration process, has a total of voltage sags/year of 2044.3 per year. In Case A3, 44 buses have values greater (black solid line in Fig. 4) than the reference values (gray solid line in Fig. 4); after the reconfiguration process is carried out, all buses have values lower than the reference values, giving a total of voltage sags of about 1965 per year.

TABLE III. SWITCHES STATUS FOR THE OPTIMAL RECONFIGURATION, CASES A1-A3

Switch		Lines status		
No.	Line	A1	A2	A3
1	6-7	0	0	1
2	38-48	1	1	1
3	14-15	0	1	0
4	10-12	1	1	1
5	11-13	1	1	0
6	56-41	1	1	0
7	8-9	0	0	0
8	9-13	1	1	0
9	1-15	1	1	0
10	3-15	1	1	1
11	4-6	0	1	0
12	2-3	1	1	0
13	38-49	1	1	0
14	3-4	0	0	0
15	12-13	0	0	1
16	7-8	1	1	1

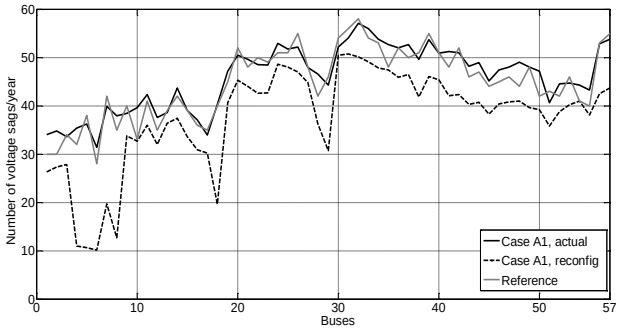

Fig. 2 Voltage sags/year for Case A1, considering a voltage threshold of 0.8 p.u.

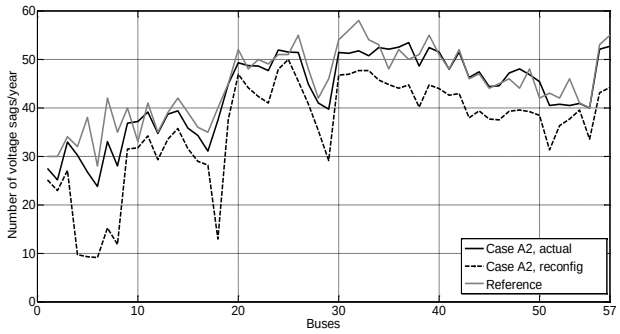

Fig. 3 Voltage sags/year for Case A2, considering a voltage threshold of 0.8 p.u.

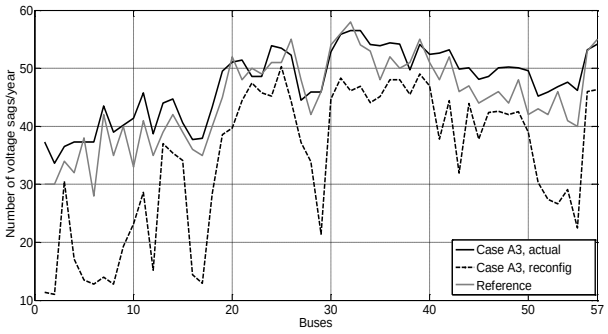

Fig. 4 Voltage sags/year for Case A3, considering a voltage threshold of 0.8 p.u.

4.2 Analysis of influence of generation schedule assuming fault rate variations

Usually, fault rates in the electrical system are obtained from statistical data for a determinate period of time, typically a year. However, fault rates have variations throughout the year, which can be estimated for seasonal or monthly periods [9]. In these cases, the variation of fault rates when the generation schedule changes is analyzed. The following case studies are presented:

Case B1. 20% generation reduction, achieved by decreasing generation at all generation buses, and a decrease of 10% in the fault rate (λ=0.9 faults/year).

Case B2. 20% generation increase, achieved by increasing generation at all generation buses, and an increase of 10% in the fault rate (λ=1.1 faults /year).

Cases B1 and B2 are similar to cases A2 and A3; the difference is the consideration of variations of fault rates: in case B1 a 10% fault rate decrease is considered, and in case B2 a 10% fault rate increase is considered. Before reconfiguration process, in Case B1, the system has a total of 13 buses that have values of voltage sags/year above the reference, as can be seen in Fig. 5. In Case B2, the most critical, the system has a total of 48 buses that have values of voltage sags/year above the reference (see Fig. 6).

From Fig. 5 and Fig. 6, it can be observed that after applying the process to reconfigure the system, all nodes have appropriate values, that is, voltage sag values below reference values.

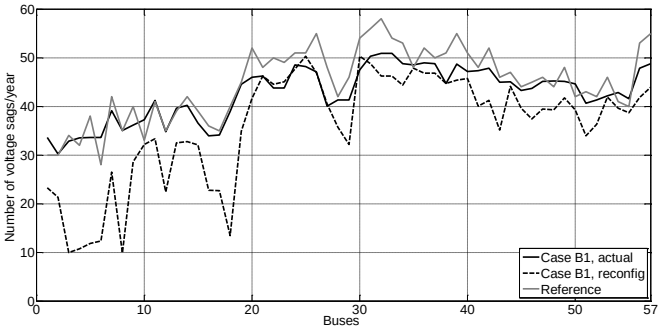

Fig. 5 Voltage sags/year for Case B1 considering a voltage threshold of 0.8 p.u.

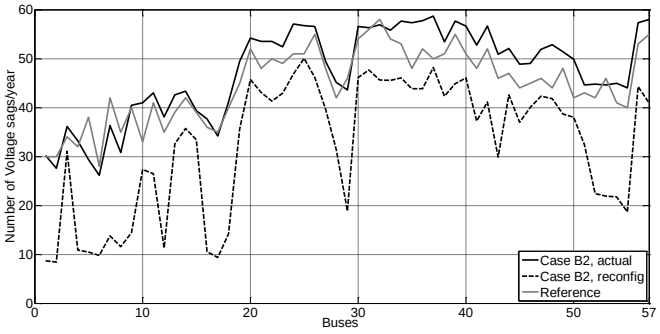

Fig. 6 Voltage sags/year for Case B2 considering a voltage threshold of 0.8 p.u.

5 Conclusions

In this paper the influence of generation scheduling on reconfiguration of power systems to minimize voltage sag indices has been analyzed. A methodology based on a Tabu Search technique has been implemented to find the optimal configuration of the power system to reduce the voltage sags number at system buses. In order to demonstrate the performance, the methodology has been applied to the IEEE-57 bus test system, taking into account that voltage sags are caused by three-phase faults.

In general, the results obtained by using this methodology show that generation demand has a meaningful impact on the expected number of voltage sags at system buses: to lower generation levels correspond higher number of sags. Consequently, when the reconfiguration process is applied in order to decrease voltage sags indexes in a power system, the schedule of generation demand is an aspect that must be considered to obtain results as close as possible to the actual conditions of the electrical network.

6 Acknowledgements

This work has been partially supported by the Consejo Nacional de Ciencia y Tecnología, México

7 References

[1] M. H. J. Bollen, Irene Y. H. Gu, "Signal processing of power quality disturbances", IEEE Press Series on Power Engineering, Mohamed E. EL-Hawary, Series Editor, A John Wiley & Sons, Inc., Publication, 2006.

[2] M. R. Qader, M. H. J. Bollen, R. N. Allan, "Stochastic prediction of voltage sags in a large transmission system", IEEE Transactions on Industry Application, Vol. 35, No. 1, January/February 1999, pp 152-162

[3] M. T. Aung, J. V. Milanovic, "Stochastic prediction of voltage sags by considering the probability of the failure of the protection system", IEEE transaction on power delivery, vol. 21, no. 1, January 2006

[4] Y. S. Lim y G. Strbac, "Analytical approach to probabilistic prediction of voltage sags on transmission networks", IEEE Proceedings Generation, Transmission and Distribution, vol. 149, no. 1, January 2002, pages 7-14.

[5] E. Espinosa-Juárez, A. Hernández, "An analytical approach for stochastic assessment of balanced an unbalanced voltage sags in large systems", IEEE Transaction on Power Delivery, vol. 21, no. 3, July 2006, pp 1493-1500

[6] B. Wang, W. Xu, Zh. Pan, "Voltage sag state estimation for power distribution systems", IEEE Transactions on Power Systems, vol. 20, no. 2, may 2005, pp 806-812.

[7] E. Espinosa-Juárez, A. Hernández, "A method for voltage sag state estimation in power systems", IEEE Transaction on Power Delivery, vol. 22, no. 4, October 2007, pp 2527-2526.

[8] A. Baggini, "Handbook of Power Quality", A John Wiley & Sons, Inc., Publication, 2008.

[9] C. H. Park, G. Jang, R. J. Thomas, "The influence of generator scheduling and time-varying fault rates on voltage sag prediction", IEEE Transaction on Power Delivery, vol. 23, no. 2, April 2008, pp 1243-1250.

[10] J. V. Milanovic, R. Gnativ, K. W. M. Chow, "The influence of loading conditions and network topology on voltage sags", Proc. Ninth International Conference on Harmonics and Quality of Power, vol. 2, Oct. 2000, pp. 757-762.

[11] E. Espinosa-Juárez, A. Hernández, "Influence of network configuration on the stochastic assessment of voltage sags", 9th International Conference on Probabilistic Methods Applied to Power Systems KTH, Stockholm, SE, 11-15 Jun. 2006.

[12] Y. Q. Zhan, S. S. Choi, D. M. Vilathgamuwa, "A voltage sag compensation scheme based on the concept of power quality control center", IEEE Transactions on Power Delivery, vol. 21 no. 1, January 2006.

[13] G. Celli, F. Pilo, G. Pisano, G. G. Soma "Stochastic assessment of voltage dips for a PQ oriented distribution system development", International Conference on Probabilistic Methods Applied to Power Systems, Stockholm, SE, 11-15 Jun. 2006.

[14] E. Babaei, F. K. Mohammad, S. Mehran. "Mitigation of voltage disturbances using dynamic voltage restorer based on direct converters"; IEEE Transactions on Power Delivery, Vol. 25, No. 4, pp. 2676-2683, October 2010.

[15] W. C. Lee, D. M. Lee, T. K. Lee, "New control scheme for a unified power-quality compensator-Q with minimum active power injection", IEEE Transaction on Power Delivery, vol. 5, no. 2, April 2010, pp 1068-1076.

[16] Y. Y. Hong, S. Ho, "Determination of network configuration considering multiobjective in distribution systems using genetic algorithms", IEEE Transactions on Power Delivery, vol. 20 no. 2, May 2005, pp 1062-1069.

[17] B. Enacheanu, B. Raison, R. Caire, O. Devaux, W. Bienia, N. HadjSaid, "Radial network reconfiguration using genetic algorithm based on the matroid theory", IEEE Transactions on Power Systems, vol. 23 no. 1, Feb 2008, pp 186-195.

[18] O. F. Fajardo, A. Vargas, "Reconfiguration of MV distribution networks with multicost and multipoint alternative supply, part I: economic dispatch through radialization", IEEE Transactions on Power Systems, vol. 23 no. 3, Aug 2008, pp 1393-1400.

[19] S. García-Martínez, E. Espinosa-Juárez, "Reconfiguration of power systems by applying Tabu search to minimize voltage sag indexes", North American Power Symposium (NAPS) 2011, Boston, MA, USA, 4-6 Aug. 2011.

[20] R. Christie, "IEEE 57 Bus Test Case", College of Engineering, Electrical Engineering, University of Washington, Available in: http://www.ee. washington/research/pstca, Aug. 1993.

8 Biographies

Sigridt García Martínez graduated in Electrical Engineering from the Universidad Michoacana de San Nicolás de Hidalgo (UMSNH), México, in 1998. She received the M.Sc. degree from the UMSNH, México, in 2000. She is currently pursuing the Ph.D. degree at the same University. Her research interests include power quality, power systems and electrical machines.

Elisa Espinosa Juárez graduated in Electrical Engineering from the Universidad Michoacana de San Nicolás de Hidalgo (UMSNH), México, in 1986, the M.Sc. degree from the Instituto Politécnico Nacional, México D.F., México, in 2001, and the Ph.D. degree from the Universidad Politécnica de Madrid, Spain, in 2006. Currently, she is a University Professor with the UMSNH, Morelia, México. Her research interests include power quality and, especially, voltage sags.

Exploring Multiple Features for POS Guessing of Chinese Unknown Words with Maximum Entropy Models

Qi Wang, Yu He, and Guohong Fu
School of Computer Science and Technology, Heilongjiang University, Harbin 150080, China

Abstract - *A key requirement for high-performing part-of-speech (POS) tagging systems is capable of predicting with accuracy the POS categories of unknown words in open-ended text. However, the topic of unknown word guessing has not been much explored for Chinese so far. This is because Chinese plain text contains very little explicit clues for unknown word guessing. In this paper, we attempt to explore morphological features for POS prediction of Chinese unknown words. To this end, we first take morphemes as the basic units in Chinese word formation, and then decompose each unknown word in Chinese sentences into a sequence of morphemes associated with their morphological position patterns. Finally, we incorporate different word-internal morphological clues with contextual information under the framework of maximum entropy modeling. Experimental results show that our method performs better in unknown word guessing than most of the best systems for POS tagging closed tracks at the fourth ACL-SIGHAN bakeoff, demonstrating that morphological features are of great value to POS guessing of Chinese unknown words.*

Keywords: Part-of-speech tagging, Chinese unknown word guessing, morphological features, maximum entropy models

1 Introduction

Part-of-speech (POS) tagging is a process of labeling each word in a sentence with a proper tag indicating its POS category. As a fundamental natural language analysis task, POS tagging play a key role in many natural language processing applications, including machine translation, information extraction and text mining.

POS disambiguation of known words (viz. in-vocabulary words) and POS guessing of unknown words (also referred to as out-of-vocabulary words) are two key issues in Chinese POS tagging. On the one hand, many Chinese words have multiple possible POS categories. POS disambiguation is thus aiming at finding proper POS categories for such ambiguous words according to their context. On the other hand, real text in Chinese may contain a number of words that are unknown to POS tagging systems because they do not occur in the training corpora or the system dictionaries. Therefore, a key requirement for high-performing POS tagging systems is capable of predicting with accuracy the POS categories for such unknown words or out-of-vocabulary (OOV) words in open-ended texts.

Despite significant progress in POS tagging over the past years, POS guessing of unknown words is still a great challenge for Chinese. As shown in [1], the best POS tagging closed tract accuracy at the 2007 ACL-SIGHAN Bakeoff is about 93.89%, 96.29%, 95.57%, 96.79% and 97.38% for in-vocabulary words over the five corpora (viz CityU, CKIP, CTB, PKU and NCC), while the counterpart figures for unknown words are only 47.33%, 58.75%, 75.22%, 60.36% and 60.59%, respectively. This is because in comparison with some other western languages like the English language, Chinese has several specialties with respect to POS tagging. Firstly, Chinese has weak morphology in that plain Chinese texts contain very little explicit morphological clues such as inflexion and capitalization in English that are of great value to correct POS disambiguation of ambiguous known words and POS prediction of unknown words. A Chinese word can function as different POS categories without any changes in its word form. Secondly, the Chinese language seems to allow very free word formation. In theory, any combination of Chinese characters could be a potential Chinese word. Free word formation inevitably introduces a great number of unknown words and ambiguities to Chinese POS tagging. Take the five POS tagging corpora used for the fourth ACL-SIGHAN Bakeoff as an example [1], 33.3-53.5% of words in the training corpora have multiple POS tags, while 5.2%-9.2% of words in the test datasets are unseen in the training corpora.

Furthermore, Chinese has a vague definition of words**.** Although a number of criteria have been proposed for word definition in Chinese linguistic literature from different perspectives, including orthographic, lexical, morphological, and phonological criteria [2], there is not a commonly acceptable and practically applicable definition for Chinese words. The vague definition of Chinese words raises another question: What kind of linguistic unit is most suitable for POS guessing of Chinese unknown words [3]. The notion of character-based tagging takes characters as the basic units in word formation [4]. Unknown word guessing based on characters is simple and efficient because it does not require any additional preprocessing. Within such a character-based

framework, however, it is not convenient to make use of word-level contextual information for POS disambiguation. To avoid this problem, Fu and Luke (2006) [5] suggest using lexicon or in-vocabulary (IV) words as the basic component tokens for word formation. Obviously, lexicon word based approach is capable of capturing both word-level contextual information and word-internal features for POS tagging, it requires a larger training corpus to achieve a reliable estimation for language models. Furthermore, most existing dictionaries for Chinese are not compiled in strict compliance with a consistent definition of words. While both true words and morphologically derived words are included in a dictionary, it becomes very difficult, or even infeasible, to explore prominent and reliable features for unknown word resolution. To address these problems, a more resent study by Fu et al. (2008) [6] chooses morphemes as the basic components of Chinese words. They have showed that compared with the character- or word-based approaches, the morpheme-based method provides a more straightforward and effective way of capturing both morphological and contextual features for Chinese word segmentation.

In fact, Chinese contains many implicit morphological cues for unknown word guessing, while common sense seems to indicate its weak morphology [2][6]. For example, some suffixes like 性 *xing4* '-ity' and 主义 *zhu3-yi4* '-ism' are indicators of nouns while some other suffixes such as 化 hua4 '-ize' are indicators of verbs. In this light, this paper attempts to explore such word-internal morphological features for POS prediction of Chinese unknown words. To this end, we first take morphemes as the basic units in Chinese word formation, and then decompose each unknown word in a given Chinese sentence into a sequence of morphemes associated with their morphological position patterns. Finally, we incorporate different word-internal morphological features with word-external contextual information under the framework of maximum entropy models (MEMs). To evaluate our approach, we have also conducted several experiments on the fourth ACL-SIGHAN Bakeoff data. The experimental results show that the proposed method performs better in unknown word guessing than most of the best systems for the ACL-SIGHAN Bakeoff POS tagging closed tracks, demonstrating that word-internal morphological features are of great value to Chinese unknown word guessing.

The rest of this paper is organized as follows: Following a brief review of the related work on POS tagging in Section 2, Section 3 describes in detail the morpheme-based MEMs for Chinese unknown word guessing. Section 4 reports our experimental results over different datasets for the fourth ACL-SIGHAN Bakeoff, with a discussion of the effects of different features on Chinese unknown word guessing. Finally, section 5 concludes our work and discusses some possible directions for future research.

2 Related work

As a fundamental task in natural language processing (NLP), POS tagging has drawn much attention within the NLP community, and a great progress has made over the past decades. Current POS tagging focuses on machine learning approaches, including hidden Markov models (HMMs) [7], lexicalized HMMs [5], transformation-based error-driven learning [8], maximum entropy models (MEMs) [9], contextual random fields (CRFs) [10], and support vector machines (SVMs) [11].

Recent research on POS tagging attempts to resolve the problems of unknown word guessing by exploring more potential features. Ratnaparkhi (1996) [9] explored multiple orthographical features such as suffixes, prefixes, capital first letters and hyphens, and incorporated them with local contextual information using MEMs. To predict the POS categories of Chinese unknown words, Lu (2008) [12] developed a set of morphological rules that encode knowledge about the relationship between the POS categories of unknown words and those of their component morphemes, and further integrated such morphological knowledge into trigram models. In addition, Qiu et al. (2008) [13] combined internal component information with local contextual information for Chinese unknown word guessing under the framework of CRFs. In addition to local information, Nakagawa and Matsumoto (2006) [14] also exploited global information to unknown word guessing. More recently, Umansky-Pesin et al. (2010) [15] presented a web-based technique for POS guessing of unknown words. They attempted to acquire knowledge for unknown words from web in order to achieve domain-adaptive POS tagging.

Motivated by the morpheme-based lexical chunking method for Chinese word segmentation [6], the present study is aiming at exploiting word-internal morphological clues to Chinese unknown word guessing. To this end, we take morpheme as the basic components of unknown words, and further employ the extended IOB chunk tags to represent the position of morphemes within words. Such morphological position pattern tags are thus combined with local context information for POS prediction of Chinese unknown words under the framework of MEMs.

3 Approach

Given an input sequence of words, our approach for POS tagging consists of three main parts: First, a word decomposition module is employed to decompose unknown words within the input sentence into a sequence of morphemes. To explore word-internal morphological clues for POS guessing, the extended BIO tagset is then used to represent the position patterns of morphemes within words. Finally, MEMs are used to incorporate word-internal morphological features with local contextual information for POS tagging. The following subsections will detail the proposed approach.

3.1 Chinese morphemes

Packard (2000) [2] has proposed two criteria for Chinese morpheme classification: whether a morpheme is free or bound and whether a morpheme is function (grammatical) or content (lexical). Morpheme classification based on the second criterion requires more lexical and grammatical knowledge about morphemes. However, such knowledge base is still not available for Chinese so far. Thus, we have to rest on the first criterion in practice. In particular, in the present study we consider two major types of morphemes, namely free morphemes and bound morphemes (viz. affixes). A free morpheme can stand by itself as a word (viz. a basic word), whereas an affix can show up if and only if being attached to other morphemes to form a word. In terms of their positions within words, Chinese affixes can be further subdivided into three groups: prefixes (e.g. 非 *fei1* 'non-', 伪 *wei3* 'pseudo'), infixes (e.g. 分之 *fei1-zhi1* 'an infix used in fractions') and suffixes (e.g. 性 *xing4* '-ity', 主义 *zhu3-yi4* '-ism').

To explore word-internal clues for POS guessing of Chinese unknown words, we employ the extended IOB tagset [6] to represent the position patterns of Chinese morphemes in word formation. Table 1 presents the detailed definition of the extended IOB tags and the correspondence between IOB tags and morpheme types.

Table 1. The extended IOB tagset for the representation of component morphemes within Chinese words

Tag	Definition	Corresponding morpheme types
O	A morpheme as a word by itself	Free morphemes
I	A morpheme inside a word	Free morphemes and infixes
B	A word-initial morpheme	Free morphemes and prefixes
E	A word-final morpheme	Free morphemes and suffixes

3.2 Word decomposition

Word decomposition is the process of decomposing a word to a sequence of morphemes associated with their IOB tags defined in Table 1. Here we employ the forward maximum matching (FMM) word segmentation technique [16] to perform this task. While FMM has the advantage of simplicity and efficiency in word decomposition, it does not work well for some words such as 非常规 *fei1-chang2-gui1* 'unconventionality' and 不安全感 *bu4-an1-quan2-gan3* 'insecurity' that involve multiple possible way of decomposition. To resolve such ambiguity, we use a set of case-based rules to correct error word decomposition yielded by FMM. a case rule for correction have the following form: *Error FMM-decomposition → correct decomposition*.

Table 2 presents some typical rules for correcting errors in FMM-based word decomposition. These rules can be extracted form the training data using the semi-automatic strategy proposed by Wang et al. (2000) and Fu et al. (2008) [6].

Table 2. Some typical case-based rules for correcting FMM-based word decomposition

Unknown words	Rules for correcting FMM word decomposition	
	Error FMM-decomposition	Correct decomposition
不安全感 'sense of insecurity'	不安 全 感	→ 不 安全 感
不平衡性 'inbalance'	不平 衡 性	→ 不 平衡 性
古人类学 'paleoanthropology'	古人 类 学	→ 古 人类 学
总装备部 'General Armament Department'	总装 备 部	→ 总 装备 部
被服务者 'service object'	被服 务 者	→ 被 服务 者

3.3 Maximum entropy models for POS tagging

Let $W = w_1 w_2 \cdots w_n$ be an input sequence of words, and $T = t_1 t_2 \cdots t_n$ be a potential sequence of POS tags corresponding to W. From a statistical point of view, the task of POS tagging is to find the most likely sequence of POS tags $\hat{T}$ that maximizes the conditional probability $P(T|W)$ of the POS tag sequence given the word sequence over all of its possible POS tag sequences {T}. MEMs decompose the conditional probability $P(T|W)$ of a POS sequence into a product of conditional probabilities $P(t_i \mid h_i)$, namely

$$\begin{aligned} \hat{T} &= \arg\max_T P(t_1 t_2 \cdots t_n \mid w_1 w_2 \cdots w_n) \\ &\approx \arg\max_T \prod_{i=1}^{n} P(t_i \mid h_i) \end{aligned} \quad (1)$$

Where $t_i (1 \le i \le n)$ is a candidate POS tag of the word w_i, and h_i is the history or context of word w_i. The

parameters $P(t_i \mid h_i)$ can be estimated from the training data with Equation (2).

$$\begin{cases} P(t \mid h) = \frac{1}{Z(h)} \exp(\sum_{j=1}^{K} \lambda_j f_j(t,h)) \\ Z(h) = \sum_{t} \exp(\sum_{j=1}^{K} \lambda_j f_j(t,h)) \end{cases} \quad (2)$$

Where *Z(h)* is a normalization term, and f_j is the j^{th} binary feature function for the current word w, associated with a weight λ_j. Its value is 1 if the feature condition is satisfied by the tag-history pair and 0 otherwise.

3.4 Features

Feature selection plays a critical role in maximum entropy modeling. In the present study, we consider two main groups of features for Chinese POS tagging, namely contextual features around words and word-formation features within words. In particular, we intend to examine the effects of word-internal features on POS guessing of Chinese unknown words, and thus focus feature selection on exploring word-internal clues for POS prediction. As such, we utilize a set of relatively simple contextual features for POS disambiguation, and define a variety of word-internal mono- or multiple-morpheme features for unknown word guessing.

Table 3 presents the feature templates for Chinese POS tagging. Where w_i denotes the current word, w_{i-1} denotes the preceding word, w_{i+1} denotes the following word; p_i, p_{i-1} and p_{i+1} denote their respective POS tags. m_{iB} m_{iI} and m_{iE} stand for the prefix, infix and suffix of the current word, respectively.

Table 3. The feature templates for Chinese POS tagging

Feature types	Feature template
Word external features	$w_i p_{i-1} p_{i+1}$ = XYZ & p_i
Word-internal mono-morpheme features (atomic features)	m_{iB} = X & p_i
	m_{iI} = X & p_i
	m_{iE} = X & p_i
Word-internal multiple morpheme features	$m_{iB}m_{iI}$ = XY & p_i
	$m_{iI}m_{iE}$ = XY & p_i
	$m_{iB}m_{iE}$ = XY & p_i
	$m_{iB}m_{iI}$ m_{iE} = XYZ & p_i

4 Experiments

To evaluate our approach, we have conducted several experiments on three data sets for the closed tracks of POS tagging at the fourth ACL-SIGHAN bakeoff [1]. This section reports the related experimental results.

4.1 Experimental setup

The POS tagging task at the fourth ACL-SIGHAN bakeoff consists of five closed tracks. Here we use three of them, namely CTB, NCC and PKU as the experimental data. In particular, we train our system only using the three training data sets for the ACL-SIGHAN bakeoff and evaluate it using the relevant counterparts for test, respectively. In addition, we have also extracted three morpheme dictionaries for word decomposition automatically from the training corpora using the method presented by (Fu et al., 2008) [6]. Table 4 presents the basic statistics of the experimental corpora and the extracted morpheme lexica.

Table 4. Statistics of the experimental corpora and the extracted morpheme lexica

		CTB	NCC	PKU
Training data set	Token	642246	535023	1116754
	Word type	42123	45108	55178
Test data set	Token	59955	102344	156407
	Word type	9797	17493	17643
	OOV	3794	5392	9295
	OOV rate	0.0633	0.0527	0.0594
Number of morphemes from training set		26330	28432	30085

Furthermore, four measures are employed in ACL-SIGHAN bakeoffs to score POS tagging performance, namely the overall accuracy (denoted by A_{Total}) and the recalls with respect to in-vocabulary words (denoted by R_{IV}), OOV words (denoted by R_{OOV}) and multi-POS words (denoted by R_{MT}). In view of the fact that our current study is concentrated on unknown word guessing, we only use the former three metrics in our evaluation. The detailed definitions of these metrics can be seen in [1].

4.2 Experimental results

4.2.1 Effects of different features on POS tagging

Our first experiment intends to examine the effects of different features, particularly word-internal morphological features on POS guessing of Chinese unknown words. In this experiment, we first use the system only using word-external

features as the baseline. In the hereafter runs, we introduce different word-internal morphological clues (viz. different mono-, bi- or tri-morpheme cues within words) into MEMs, and evaluate the yielded outputs of each run over the above three test sets. The experimental results are summarized in Tables 5-8, respectively.

Table 5. POS tagging results for the baseline only using word-external features

Test set	R_{OOV}	R_{IV}	A_{Total}
CTB	0.4090	0.9304	0.9021
NCC	0.3238	0.9632	0.9241
PKU	0.3107	0.9493	0.9107

Table 6. POS tagging results for all runs combining word-external information and word-internal mono-morpheme features

Test set	Feature template	R_{OOV}	R_{IV}	A_{Total}
CTB	$w_ip_{i-1}p_{i+1}m_{iB} = XYZA \ \& \ p_i$	0.6555	0.9319	0.9169
	$w_ip_{i-1}p_{i+1}m_{iI} = XYZA \ \& \ p_i$	0.5363	0.9306	0.9092
	$w_ip_{i-1}p_{i+1}m_{iE} = XYZA \ \& \ p_i$	0.6214	0.9319	0.9151
NCC	$w_ip_{i-1}p_{i+1}m_{iB} = XYZA \ \& \ p_i$	0.5428	0.9631	0.9374
	$w_ip_{i-1}p_{i+1}m_{iI} = XYZA \ \& \ p_i$	0.4014	0.9631	0.9288
	$w_ip_{i-1}p_{i+1}m_{iE} = XYZA \ \& \ p_i$	0.5434	0.9632	0.9375
PKU	$w_ip_{i-1}p_{i+1}m_{iB} = XYZA \ \& \ p_i$	0.5507	0.9554	0.9401
	$w_ip_{i-1}p_{i+1}m_{iI} = XYZA \ \& \ p_i$	0.4904	0.9554	0.9379
	$w_ip_{i-1}p_{i+1}m_{iE} = XYZA \ \& \ p_i$	0.6106	0.9555	0.9425

Table 7. POS tagging combining word-external information and word-internal bi-morpheme features

Test set	Feature template	R_{OOV}	R_{IV}	A_{Total}
CTB	$w_ip_{i-1}p_{i+1}m_{iB}m_{iI}=XYZAB \ \& \ p_i$	0.6813	0.9312	0.9176
	$w_ip_{i-1}p_{i+1}m_{iI}m_{iE}=XYZAB \ \& \ p_i$	0.6583	0.9316	0.9167
	$w_ip_{i-1}p_{i+1}m_{iB}m_{iE}=XYZAB \ \& \ p_i$	0.7188	0.9317	0.9201
NCC	$w_ip_{i-1}p_{i+1}m_{iB}m_{iI}=XYZAB \ \& \ p_i$	0.5547	0.9625	0.9376
	$w_ip_{i-1}p_{i+1}m_{iI}m_{iE} =XYZAB \ \& \ p_i$	0.5854	0.9625	0.9394
	$w_ip_{i-1}p_{i+1}m_{iB}m_{iE}=XYZAB \ \& \ p_i$	0.6441	0.9627	0.9432
PKU	$w_ip_{i-1}p_{i+1}m_{iB}m_{iI}= XYZAB \ \& \ p_i$	0.5760	0.9551	0.9408
	$w_ip_{i-1}p_{i+1}m_{iI}m_{iE}= XYZAB \ \& \ p_i$	0.6213	0.9556	0.9430
	$w_ip_{i-1}p_{i+1}m_{iB}m_{iE}= XYZAB \ \& \ p_i$	0.6377	0.9553	0.9433

Table 8. POS tagging results for all runs combining word-external information and word-internal triple-morpheme features

Test set	Feature template	R_{OOV}	R_{IV}	A_{Total}
CTB	$w_ip_{i-1}p_{i+1}m_{iB}m_{iI}m_{iE}$ $= XYZABC \ \& \ p_i$	0.7326	0.9317	0.9200
NCC	$w_ip_{i-1}p_{i+1}m_{iB}m_{iI}m_{iE}$ $= XYZABC \ \& \ p_i$	0.6470	0.9620	0.9428
PKU	$w_ip_{i-1}p_{i+1}m_{iB}m_{iI}m_{iE}$ $= XYZABC \ \& \ p_i$	0.6500	0.9551	0.9436

These results reveal that the morphological features within words are of great value to POS prediction of Chinese unknown words. Take the runs over the CTB data set as an example, the POS tagging accuracy for unknown words is 40.09% for the baseline that only uses contextual features for POS tagging. This figure increases to 68.13% or 62.14% while introducing prefix or suffix cues, and reach the highest value of 73.26% while combining all the three word-internal morphological position patterns with contextual information. Furthermore, as potential cues, prefix and suffix patterns prove to be more informative for Chinese unknown word guessing in comparison with infix patterns.

4.2.2 Comparison

To asses the effectiveness of our approach, we also compare our system with the best systems for the POS tagging closed tracks at the ACL-SIGHAN bakeoff. Note that in this experiment we incorporate the triple word-internal morphological patterns with contextual features. The results are given in Table 9.

Table 9 Comparison of our system with the best systems in the closed track of POS tagging at the 4th ACL-SIGHAN bakeoff

Test set	Our system			The best performance at ACL-SIGHAN bakeoff		
	R_{OOV}	R_{IV}	A_{Total}	R_{OOV}	R_{IV}	A_{Total}
CTB	0.7326	0.9317	0.9200	0.7522	0.9557	0.9428
NCC	0.6470	0.9620	0.9428	0.5998	0.9738	0.9541
PKU	0.6500	0.9551	0.9436	0.5818	0.9694	0.9450

From Table 9, we can see that compared with the relevant best system at the 2007 ACL-SIGHAN bakeoff, our method performs better in unknown word guessing than on NCC and PKU data sets, but slightly worse on the CTB corpus. However, the POS tagging performance is not satisfactory for in-vocabulary words. The reason may be that in the present study we focus our current study on explore word-internal morphological clues for Chinese unknown word guessing, and use a set of relatively simple contexture

features (viz. bi-tags), resulting in a limited capacity of in-vocabulary POS disambiguation.

5 Conclusions

In this paper, we have attempted to explore word-internal morphological clues within Chinese words, and incorporate them with word-external contextual features for POS guessing of Chinese words. We evaluated our method using some data sets for POS tagging closed tracks at the fourth ACL-SIGHAN bakeoff. The experimental results show that word-internal morphological information plays a key role in correct prediction of POS categories for Chinese unknown words.

While our system has achieved promising performance, there is still much space for improvement. Due to the lack of deep morphological knowledge for Chinese, in the present study we only took into account surface morphological clues for Chinese unknown word guessing, namely the position patterns of morphemes in word formation. In future work we intend to explore systematically deep morphological knowledge, including the POS categories of morphemes and morpho-syntactic rules for POS prediction of various unknown words in real Chinese texts. In addition, in the present study we only used contextual POS features, resulting in limited capacity in POS disambiguation. So we are also planning to enhance the overall POS tagging accuracy of our system by incorporating more complicated contextual features such as contextual lexical information with word-internal morphological features.

6 Acknowledgements

This study was supported by National Natural Science Foundation of China under Grant No.60973081 and No.61170148, the Returned Scholar Foundation of Educational Department of Heilongjiang Province under Grant No.1154hz26, and Harbin Innovative Foundation for Returnees under Grant No.2009RFLXG007, respectively.

7 References

[1] Jin, Guangjin, and Xiao Chen. "The fourth international Chinese language processing bakeoff: Chinese word segmentation, named entity recognition and Chinese POS tagging". In Proceedings of the Sixth ACL-SIGHAN Workshop on Chinese Language Processing, pages 69-81, 2008.

[2] J. Packard. "Morphology of Chinese: A linguistic and cognitive approach". Cambridge University Press, 2000.

[3] H.T. Ng, and J.K. Low. "Chinese part-of-speech tagging: One-at-a-time or all-at-once? Word-based or character-based?". In Proceedings of EMNLP 2004, pages 277-284, 2004.

[4] Niangwen Xue. "Chinese word segmentation as character tagging". Computational Linguistics and Chinese Language Processing, Vol.8, No.1, pages 29-48, 2003.

[5] Guohong Fu, and Kang-Kwong Luke. "Chinese POS disambiguation and unknown word guessing with lexicalized HMMs". International Journal of Technology and Human Interaction, Vol.2, No.1, pages 39-50, 2006.

[6] Guohong Fu, Chunyu Kit, and Jonathan J. Webster. "Chinese word segmentation as morpheme-based lexical chunking". Information Sciences, Vol.178, No.9, pages 2282-2296, 2008.

[7] T. Brants. "TnT – A statistical part-of-speech tagger". In Proceedings of ANLP-2000, pages 224-231, 2000.

[8] Eric Brill. "Transformation-based error-driven learning and natural language processing: A case study in part-of-speech tagging". Computational Linguistics, Vol.21, No.4, pages 543-565, 1995.

[9] Adwait Ratnaparkhi. "A maximum entropy model for part-of-speech tagging". In Proceedings of EMNLP 2006, pages 133-142, 2006.

[10] John Lafferty, Andrew McCallum, and Fernando C.N. Pereira. "Conditional random fields: Probabilistic models for segmenting and labeling sequence data". In Proceedings of ICML 2001, pages 282-289, 2001.

[11] Tetsuji Nakagawa, Taku Kudo, and Yuji Matsumoto. "Unknown word guessing and part-of-speech tagging using support vector machines". In Proceedings of NLPRS 2001, pages 325-331, 2001.

[12] Xiaofei Lu. "Improving part-of-speech guessing of Chinese unknown words using hybrid models". International Journal of Corpus Linguistics, Vol.13, No.2, pages 169-193, 2008.

[13] Likun Qiu, Changjian Hu, and Kai Zhao. "A method for automatic POS guessing of Chinese unknown words". In Proceedings of COLING 2008, pages 705-712, 2008.

[14] Tetsuji Nakagawa, and Yuji Matsunoto. "Guessing parts-of-speech of unknown words using global information". In Proceedings of ACL 2006, pages 705-712, 2006.

[15] Shulamit Umansky-Pesin, Roi Reichart, and Ari Rappoport. "A multi-domain web-based algorithm for POS

tagging of unknown words". In Proceeings of COLING 2010, pages 1274-1282, 2010.

[16] Xiaolong Wang, Guohong Fu, et al. "Models and algorithms of Chinese word segmentation". In: Proceedings of IC-AI 2000, pages 1279-1284, 2000.

[17] Nanyuan Liang. "CDWS - A written Chinese automatic word segmentation system". Journal of Chinese Information Processing, Vol.1, No.2, pages 44-52, 1987.

A Review of Forecasting Techniques

Mohamad Ghazali bin Ameer Amsa , A. M. Aibinu , M. J. E. Salami and Wasiu Balogun
Department of Mechatronics Engineering,
Kulliyyah of Engineering,
International Islamic University Malaysia (IIUM)
P. O. Box 10, 50728, Malaysia

Abstract - *This work examines recent publications in forecasting in various fields, these include: wind power forecasting; electricity load forecasting; crude oil price forecasting; gold price forecasting energy price forecasting etc. In this review, categorization of the processes involve in forecasting are divided into four major steps namely: input features selection; data pre-processing; forecast model development and performance evaluation. The various methods involve are discussed in order to provide the overall view about possible options for development of forecasting system. It is intended that the classification of the steps into small categories with definitions of terms and discussion of evolving techniques will provide guidance for future forecasting sytem designers.*

Keywords: Forecasting; Prediction; Feature selection; Modeling; Performance evaluation

1 Introduction

This paper gives a brief overview of forecasting techniques published in the last ten years. An attempt has been made in categorizing relevant published work into series of steps needed for understanding forecasting techniques.

Forecasting involve predicting future behavior or value of certain phenomena. Forecasting has been applied in various fields such as wind power [1,2] ; electricity load consumption [1] ; energy price forecast in power systems [1,2,3] ; gold price forecasting[4] ; price spike prediction [5] ; financial sequence prediction [6] ; fatigue life prediction [7] ; car fuel consumption forecasting [8] and so on.

Generally, forecasting activity can be divided into three relevant classes, namely short term, medium term and long term forecasting. Short term forecast activity concentrates on predicting unknown values of price for a short period of time. These periods include few minutes, hours, or days. Monthly forecast activity falls into medium term while long term forecast activity may cover period of one to few years. Short term forecast is informative for profit maximization [1, 2] while medium term price forecast is useful for negotiations of bilateral contract between suppliers and consumers. Long term forecast is a valuable tool for assets expansion [1].

The first difficulty associated with forecasting activity is the linearity of data. Forecast activity becomes easier when dealing with linear historical data [3]. Linear data normally undergo linear changes such as linearly increasing or linearly decreasing over certain period of time. On the other hand, forecasting activity become very challenging issues when dealing with non-linear data [9]. External influence has been identified as one of the reasons responsible for non-linearity nature of data. Electricity power system, load and demand system, crude oil and gold price prediction are some of the sectors known for having non-linear data.

Lots of forecasting models and techniques have been proposed in literature with each achieving various degree of success. Among the reported methods are Moving Average (MA), Linear Prediction (LPC), Auto-Regressive Moving Average (ARMA) and the Box-Jenkins approach based on Auto-Regressive Integrated Moving Average (ARIMA). These methods are preferred by some researchers when dealing with linear data [5,10].

The remaining part of this paper is organized as follows: Section II describes the common methodology used for forecasting while the last section provides a list of commonly used performance metrics.

2 Review of forecasting techniques

Extensive study of various forecasting techniques have shown four major steps; namely, input features selection, data pre-processing, Modelling cum data training and performances evaluation. Modelling and data training have been the major areas of focus in the literature. Model represent the forecast system since it is to receive input data, analyse it and produce output called predicted value. Most forecasting models are based on assumption of relationship between inputs (historical time series data) and outputs (future values). A typical forecasting block diagram is shown in Fig. 1.

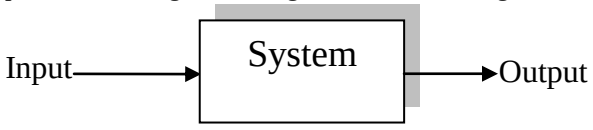

Figure 1: Block diagram of system

The overall review done in this paper based on the forecasting steps consist of (i) Input features selection (ii) Data Preprocessing step (iii) Forecasting models development step and (iv) Performance evaluation step and their

components in each step are shown in Fig. 2. The details of each components are subsequently discussed.

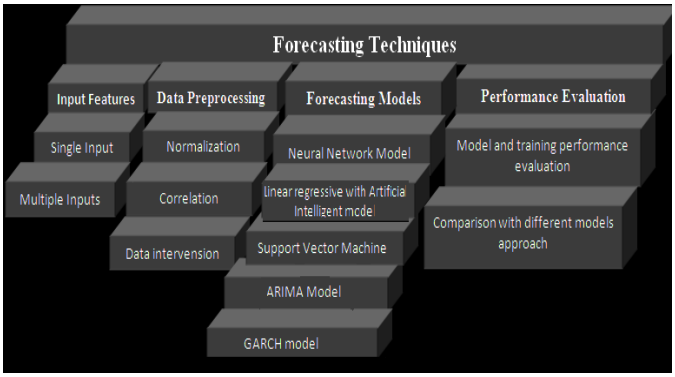

Figure 2: Major steps for forecasting

2.1 Input features selection

Input data in forecasting consist of collection of historical information that used to forecast the future values. Input data are fed into forecasting model for analysis in order to determine future output value. Input data can be developed through collection of various information that influence the data. Therefore, proper selection of input data is of utmost importance. Adequate input may give enough information to forecasting model to analyze the future trend of data accurately, whereas insufficient features in the input data may lead to serious error in forecast. Time series historical data is mainly used in forecasting system. However, in some forecasting field, time series data alone is inadequate to accurately forecast the future trends of data. Therefore, utilization of historical information base on other features may be used to enhance the forecast output. The utilization of both types of data is discussed as follows.

2.1.1 Time series historical data

Information from historical time series data is very useful for forecasting models to learn the trend of future data. Generally, time series data can be obtained from historical documents. The trend of a time series historical data is normally assumed to shows certain repetitive pattern. List of the time series data were used in lituretures such as Market Clearing Price (MCP) for forecasting electricity demand[14, 15], and previous time electricity price and load price data to forecast a day ahead electricity price [16]. In addition, utilization of previous three months data in forecasting monthly price was reported in [17] and previous hours data were used to forecast next hour data in [18].

2.1.2 Combination of time series with other features data

Multiple features input utilization have been reported in [19, 20, 25]. Seasonal factors and weather conditions were included as additional as input besides time series data for electricity demand forecasting model [19]. Ignoring the external factors may lead to inadequate training to the forecasting model which may lead to forecast error. For example, daily whether information is unignorable in electricity forcasting field since people will definitely use more electricity during hot days as compare to cold weather[19]. Other factors such as added value and number of customer were also incorporated as input features in [20], while total number of weeks, yearly number of weeks, world events impact factor and global demand were used as input features in [9,51]. Similarly, market clearing price (MCP) and other influence factors such as previous competitive load, competitive generating capacity, system running style, previous market have also been considered in forecasting electricity price [22].

2.2 Data pre-processing

The second stage in forecasting is data pre-processing stage. The objective of data pre-processing step is to remove abnormalities in the data such as noise. Besides that, data pre-processing technique is used to regulate the input and output range of data. Through this step, original historical data will be altered in order to produce new set of input data. Some of the known data pre-processing techniques are (i) Normalization, (ii) Correlation and (iii) Data intervention. Each of the preprocessing techniques is discussed as follows.

2.2.1 Normalization

Normalization is the most popular data preprocessing technique reported in literature as part of forecasting technique [9, 19, 24, 25, and 34]. Data normalization reduces data range into smaller scale such as in the range from 0 to 1. In other word, normalization process helps to rescale the huge number of data to lie between the scaling ranges.

2.2.2 Correlation

The purpose of correlation is to detect non randomness in time series data [26]. Informally, correlation technique is used to find the similarity between different observations in a given time series data. Furthermore, correlation is used for features selection from large size of data. Autocorrelation analysishas been used for feature selection process by removing irrelevant and redundant features and selecting a small set of informative features that are necessary and sufficient for good forecasting [27,28].

2.2.3 Data intervention technique

Data intervention technique function is to improve forecasting result. This technique removes intervention effects such as changes of whether condition or political instability that may produce spike to time series data. In [29], sudden high peak in the data is removed from input data since it is considered as intervention effect [29].

2.3 Forecast Model Development

The third stage in forecasting is the development of the forecast model. This is the art of the whole process and lots of efforts are usually expended in the development of such a model. Some of the reported forecast models include:

i. Artificial Intelligence model.
ii. Linear regressive with Artificial Intelligence mathematical model.
ii. Support Vector Machine (SVM) approach.
iv. Autoregressive Integrated Moving Average (ARIMA) model.
v. Generalized Autoregressive Conditional Heteroskedastic (GARCH) model.

2.3.1 Artificial Intelligence model

Artificial intelligence (AI) model in forecasting field has received favourable success in the last few years. Among the AI techniques reported in literature are fuzzy inference[11], fuzzy-neural models[12] and Artificial Neural Network (ANN) [13]. The application of ANN approach for nonlinear data, such as load forecasting in power system has received much attention in recent years, since ANN has the ability to learn complex and nonlinear relationships [5].

Modeling using Artificial Neural Network (ANN) plays the important role in forecasting field because of its capability to learn both linear and nonlinear relationship from a given input data during training process. Different types of learning algorithms for training this model has been proposed in literature. A list of studies have used Gradient Descent learning rule with momentum [19,30,31], Levenberg-Marquardt (LM) algorithm [15][18], conjugate gradient (SCG) algorithm [15] and multi ELM training algorithm [16]. Levenberg-Marquardt (LM) algorithm and scaled conjugate gradient (SCG) algorithm are proposed to overcome slow convergence of BP algorithm. Genetic Algorithm has been used as an alternative training rules to BP algorithm in order to overcome local minima problem associated with BP algorithm[14]. Combination of Levenberg-Marquardt back-propagation algorithm(LM-BP) and evolutional algorithm approach to train their MLN model was proposed in [18]. Similarly, LM-BP and Particle Swarm Optimization is reported in [18].

Radial Basis Network(FBN) is another type of feed forward network used as an alternative to Multi Layer Network in forecasting model [25]. RBN use Euclidean distance as activation function for hidden layer instead of linear activation function that used in Multi Layer Network (MLN). Elman neural network forecasting model with BP learning algorithm was reported in [17]. Elman neural network or Elman regression neural network (ERN) has an additional of one layer compared to MLN, which is the context layer. In other words, ERN developed with 4 layers; namely, input layer, hidden layer, context layer and output layer. The outputs data from hidden layer are stored in the context layer (also called accepter layer) before sending it to output layer. Therefore, ERN offers the system the capability to adapt the time variability by its dynamic character mapping function supported via internal status memory [17]. Artificial Neural Networks- Quantitative (ANN-Q) Model has been introduced in [23]. Hybrid of ANN and Adaptive Neuro-Fuzzy Inference System (ANFIS) has also been proposed to accomplish the forecast purpose in [31]. These two model are combined (in series) in such a way that one of forecasted data will be fed into ANFIS network.

2.3.2 Linear regressive with artificial intelligent mathematical model

The objective of regression analysis is to develop mathematical model that can forecast the values of dependent variables (e.g. *y* plane in the data graph) by using independent variables (e.g. *x* plane in the data graph) as input. In the case of daily gold price forecasting, the price of the gold will be dependent variables, while the date of that price occur will be independent variables. The general form of linear regressive model is :

$$y = mx + c \quad (1)$$

Where *y* is the forecast value, *m* is the slope of 'best fit' line, *x* is prediction date and *c* is intercept point of best fit line to *y* axis. In the classical method, the 'best fit' line is considered as linear line that follows the trend of data as illustrated in the Fig. 3.

Figure 3: 'Best fit line' across historical data of gold price data

The best fit line is drawn in the way that it not bias to any points. However, in case of nonlinear relationship between input and output, straight linear line unable to follow the trend of graph closely. Consequently, classical linear regressive model is not suitable for forecasting non linear data because it has tendency to produce high error in forecast value. Therefore, Artificial Intelligent technique is used to find the *m* variable, to be substitute in the linear regressive model for forecasting non-linear data. For example, in [32], Genetic Algorithm is used to find five 'best fit' coefficients for four independent variables. Similarly, Particle Swarm Optimization (PSO) algorithm has been used for tuning linear algorithm coefficients from electricity consumption data for electric consumption forecasting model of the following year [20].

2.3.3 Support Vector Machine approach (SVM)

SVM's is a supervised learner that used to analyse and recognize the patterns of data. SVM is used to constructs set of hyperplanes (gap between different classes) in a high or infinite- dimensional space in order to classify data. SVM has the advantage of reducing the problem of over-fitting or local minima because its learning algorithm is based on the structural risk minimization principle compared to ANN, which use learning algorithm based on the empirical risk minimization principle. The four basic kernel types in SVM include Linear Kernel, Polynomial Kernel, Radial, Basis Function Kernel (RBF) and Sigmoid Kernel. Kernel is used to compute dot product in terms of the variables in the original space. SVM with RBF kernel function has also been developed for forecast purpose in [9].

2.3.4 Autoregressive Integrated Moving Average (ARIMA) model

ARIMA model can be used to get better understanding of time series data and forecast the future points. ARIMA model consist of three parts : namely, an autoregressive part of order *p*, moving average part of order *q* and the first derivative of the time series of order *d*, known as the integrated part. Thus, the model is generally referred to as an ARIMA(*p*,*d*,*q*). ARIMA model can be called an Autoregressive model (AR(*p*)) whenever the order *d* and *q* becomes zero (e.g *ARIMA(1,0,0))*. Similarly, the model may be regarded as ARMA model when only the *d* term is set to zero. SARIMA model is developed with addition of seasonal component to this model. In [28], two ARIMA models was proposed to forecast hourly prices in the electricity markets. Furthermore, a model called seasonal autoregressive integrated moving Average (SARIMA) was developed to forecast electricity price [29].

2.3.5 Generalized Autoregressive Conditional Heteroskedastic (GARCH) model

The GARCH time series model was introduced in [29]. It overcomes the ARIMA and linear regression models that have limitation to deal with non linear data. This model determine the explicit relationship of the nonlinear data series. In order to get acceptable accuracy, the formulation of non linear model is developed to capture the entire important features in the historical data.

2.4 Performance evaluation

Performance evaluation is the crucial part to test the performance of the newly developed model. Normally, the performance of forecasting model is evaluated by using standard performance evaluation formula. Once the performance of the model is satisfied, the scope of evaluation is expanded to compare this newly developed model with other existing models. In the following subsections, both methods of evaluating the results obtained from the model are discussed herewith.

2.4.1 Modeling and training performance evaluation

In order to evaluate the forecast results, the facts or empirical results are normally presented. In forecast issue, standard performance evaluation metrics include mean square error (FMSE)[24], RMS error[16], [23], [33], mean absolute percentage error (MAPE) [15], [18], [30], [31], Relative absolute error (RAE) [27] and correctly forecasted percentage error[9],[16]. MAPE evaluation metric are among of the frequently used performance metric. MAPE was used as the fitness function for measuring the evolutionary algorithm optimization in [15], [18], [30], [31]. Percentage error and RMS error are used to compare performance between two or more forecast models. These metrics are calculated using (2)-(5) :

$$RMSE = \sqrt{\frac{1}{N}\sum_{i=1}^{N}(actual - forecast)^2} \quad (2)$$

$$FMSE = \frac{1}{N}\sum_{i=1}^{N}(actual - forecast)^2 \quad (3)$$

$$MAE = \frac{1}{N}(\sum_{i=1}^{N}[\left|\frac{actual - forecast}{actual}\right|] \quad (4)$$

$$MAPE = \frac{1}{N}(\sum_{i=1}^{N}[\left|\frac{actual - forecast}{actual}\right| \times 100\%] \quad (5)$$

where *N* is the data length.

Combination of more than one performance metrics have been used in some literature. Combination of MAE, RAE and MAPE was proposed in [27] while the combination of RMSE and NMSE was used in [23]. *Dstat* is used to evaluate the forecasted price movement.

2.4.2 Performance comparison of different methodology

The main objective of forecast research nowadays is to develop the best and reliable forecast model that will give minimal error between the forecasted value and actual value. Methodology comparison in term of performance metrics is a mean for evaluating any new model performance in order to compare the result among existing models. For example, RBF performance was compared with autoregressive forecasting model in [25]. Similarly, ARIMA and linear regression technique performance was compared in [32]. In [10], it was shown that ANN method leads to better prediction than time series ARIMA method, while GA performance is better than linear regression technique model. The performance of SVM and BPNN is compared in [9]. In another study, ANN performance was compared with similar day (SD) forecast approach[19].

3 Conclusion

This paper contains review of some of the forecasting techniques that have been published in the last ten years. The steps associated with forecasting are categorized into four primary steps: namely, of input features selection (step one) ; data preprocessing (step two); forecast model development (step three) and performance evaluation (step four). The various methodology proposed in each step are highlighted and discussed.

4 References

[1]M. Negnevitsky,P. Mandal, and A.K.Srivastava, "An overview of forecasting problems and techniques in power systems," *in Proc. IEEE Power and Energy Soc.General Meeting*,pp.1-4, July 2009.

[2]C. W. Potter and M. Negnevitsky, "Very short-term wind forecasting for Tasmanian Power Generation," *IEEE Trans. on Power Syst.*, vol.21, no. 2, pp. 965−972, May 2006.

[3] W. Sun, J. C. Lu, Y. J. He, J.Q. Li,"Application of Neural Network Model Combining Information Entropy and Ant Colony Clustering Theory for Short-Term Load Forecasting", *in proc. IEEE Machine Learning and Cybernetics*, vol. 8, pp.4645-4650, August 2005.

[4] S.Shafiee and E. Topal. "An overview of global gold market and gold price forecasting.*Resource Policy*,vol. 35, pp.178-189,2010.

[5] J.H. Zhao, Z. Y. Dong, X. Li and K.P.Wong , "A general method for electricity market price spike analysis," *in Proc. IEEE Power and Energy Soc. General Meeting*, vol. 1, pp.286- 293 , June 2005.

[6] S. W.K. Chan and J. Franklin . "A text-based decision support system for financial sequence prediction". *Decision Support Systems*,in press.

[7] J. C. F. Pujol a and J. M. A. Pinto. "A neural network approach to fatigue life prediction". *International Journal of Fatigue*, vol. 33, pp.313-322,2011.

[8]J.D. Wu and J. C. Liu. "A forecasting system for car fuel consumption using a radial basis function neural network". *Expert Systems with Applications*, in press.

[9] A. Khashman and N.I. Nwulu , "Intelligent prediction of crude oil price using Support Vector Machines," *in proc. IEEE Applied Machine Intelligence and Informatics (SAMI)* , pp.165-169, Jan. 2011.

[10] J. Contreras, R. Espinola, F. J. Nogales, and A. J. Conejo, "ARIMA models topredict next-day electricity prices," *IEEE Transactions on Power Systems*, vol. 18, no. 3, pp. 1014-1020, 2003.

[11] Zhao Qing-bo and Zhou Yuan-bing ,"application of fuzzy neural network in power system marginal price forecasting", *IEEE Transactions on Power Systems*, vol.28, No. 7, pp. 45-48, Apr. 2004.

[12] C. P. Rodriguez, and G. J. Anders, "Energy price prediction in the Ontario competitive power system market," *IEEE Transactions on Power Systems*, vol. 19, no. 1, pp. 366-374, 2004.

[13] B. R. Szkuta, L.A.Sanabria, and T. S Dillon, "Electricity price short-term forecasting using artificial neural networks," *IEEE Transactions on Power Systems*, vol. 14, no. 3, pp. 851-857, 1999.

[14] Bo Yang and Yuanzhang Sun , "An improved neural network prediction model for load demand in day-ahead electricity market," *in Proc. IEEE Intelligent Control and Automation*, pp.4425-4429, June 2008.

[15] Q. Tang and D. Gu, "Day-Ahead Electricity Prices Forecasting Using Artificial Neural Networks," *in Proc. IEEE Artificial Intelligence and Computational Intelligence* , vol.2, , pp.511-514, Nov. 2009.

[16] H. Tian,B. Meng and S.Z. Wang , "Day-ahead electricity price prediction based on multiple ELM," *in Proc. IEEE Control and Decision Conference* , pp.241-244, May 2010.

[17]H. Xiaolong and Z. Ming, "Applied research on real estate price prediction by the neural network," *in Proc. IEEE Environmental Science and Information Application Technology*, vol.2, pp.384-386, July 2010.

[18] D. Srinivasan , F.C. Yong and A. C. Liew , "Electricity Price Forecasting Using Evolved Neural Networks," *in Proc. IEEE Intelligent Systems Applications to Power Systems*, pp.1-7, Nov. 2007.

[19] P. Mandal, T.Senjyu, and T. Funabashi , "Neural network models to predict short-term electricity prices and loads," *in Proc. IEEE Industrial Technology* , pp.164-169, Dec. 2005.

[20] S.A.P. Kani and N.F Ershad , "Annual Electricity Demand Prediction for Iranian Agriculture Sector Using ANN and PSO," *in Proc. IEEE Electrical Power Conference*, pp.446-451, Oct. 2007.

[21] S. Santoso, M. Negnevitsky, and N. Hatziargyriou, "Applications of data mining and analysis techniques in wind power systems," *in Proc.IEEE Power Syst. Conference and Exposition*, pp. 57−59, 2006.

[22] W. Sun,J.C. Lu and M. Meng , "Application of Time Series Based SVM Model on Next-Day Electricity Price Forecasting Under Deregulated Power Market," *in Proc.IEEE Machine Learning and Cybernetics, International Conference*, pp.2373-2378, Aug. 2006.

[23]S.N. Abdullah and X. Zeng , "Machine learning approach for crude oil price prediction with Artificial Neural Networks-Quantitative (ANN-Q) model," *in Proc. IEEE Neural Networks International Joint Conference* pp.1-8, July 2010.

[24] K.Y. Huang and W.L. Chang; , "A neural network method for prediction of 2006 World Cup Football Game," *in Proc. IEEE Neural Networks International Joint Conference*, pp.1-8, July 2010.

[25]S.F.M. Hussein, M.B.N. Shah, M.R.A Jalal and S.S. Abdullah , "Gold price prediction using radial basis function neural network," *in Proc. Modeling, Simulation and Applied Optimization* , pp.1-11, April 2011.

[26]E.Kreyszig. *Advance Engineering Mathematics*.7th ed.New York:Wiley,1993,pp.1261.

[27]R.Sood, I. Koprinska and V.G. Agelidis , "Electricity load forecasting based on autocorrelation analysis," *in Proc. IEEE Neural Networks International Joint Conference* pp.1-8, July 2010.

[28]J. Contreras, R. Espinola, F.J. Nogales,and A.J. Conejo , "ARIMA models to predict next-day electricity prices," *IEEE Transactions on Power Systems,* vol.18, no.3, pp. 1014-1020, Aug. 2003.

[29 C. Nunes, A. Pacheco and T. Silva , "Statistical models to predict electricity prices," *in Proc. IEEE Electricity Market International Conference on European* , pp.1-6, May 2008.

[30] A.Wang and B. Ramsay , "Prediction of system marginal price in the UK Power Pool using neural networks," *in Proc. IEEE Neural Networks International Conference* , vol.4, pp.2116-2120 vol.4, Jun 1997.

[31]R.R.B.Aquino, M.M.S. Lira ,M.H.N. Marinho, I.A. Tavares and L.F.A. Cordeiro, "Inflow forecasting models based on artificial intelligence," *in Proc. IEEE Neural Networks International Joint Conference,* pp.1-6, July 2010.

[32] A. Azadeh,S.F. Ghaderi,S. Tarverdian and M. Saberi , "Integration of Artificial Neural Networks and Genetic Algorithm to Predict Electrical Energy consumption," *in Proc. IEEE Industrial Electronics Annual Conference* , pp.2552-2557, Nov. 2006.

[33] J.Copper, A. Baciu and D. Price , "Predicting Wind Farm Electricity Output: A Neural Network Empirical Modeling Approach," *in Proc. IEEE Power and Energy Engineering Conference,* pp.1-5, March 2009.

[34] A. M. Aibinu, M. J. E. Salami and Mohamad Ghazali bin Ameer Amsa, "A Hybrid Technique for Dinar Coin Price Prediction using Artificial Neural Network based Autoregressive Modeling Technique", in the proc. of 2nd World Conference on Riba Kuala Lumpur, *pp 130-141,* July 26-27, 2011

Evaluation of Collaborative Filtering Personalized Recommendation algorithms

B. Raja Sarath Kumar[1] and B. John Ratnam[2]

[1]Professor, CSE Department, Lenora College of Engineering, Rampachodavaram, E.G, District, A.P, India.
iamsarathphd@gmail.com

[2] Director, Lenora College of Engineering, Rampachodavaram, E.G, District, A.P, India
ratnamsmail@yahoo.com

Abstract

Collaborative filtering (CF) systems have been proven to be very effective for personalized and accurate recommendations. These systems are based on the recommendations of previous ratings by various users for various products. Since the very beginning of the research on Collaborative Filtering, different systems have been developed for different domains and application areas. Besides some general features, which are expected to be present in any system, Collaborative Filtering Algorithms have their own extra features that make them different from other systems. Through a careful study of a large number of Collaborative Filtering Algorithms, hierarchies of primary features based on which one can evaluate different Collaborative Filtering Algorithms are proposed. The methodology is applied to evaluate Mean Absolute Error (MAE) with real data. An evaluation scheme is also derived based on the prediction quality for the given features. The results are evaluated through experimental tests and results were tabulated to see the effect of different parameters on the performance of the algorithm. A comparative analysis has been evaluated with various collaborative filtering techniques and found that hybrid collaborative algorithm approach is performs better than other collaborative filtering algorithms.

Key words
Prediction, Collaborative Filtering, Mean Absolute Error

1. Introduction

The explosive growth and availability of data on the World Wide Web (www) has caused information overload. Searching for a query is not easy in the sources of information available for the interest of an individual user. Recommender system form a specific type of information filtering technique that attempts to present information items that are likely of interest to the user. A recommender system compares the user's profile to some reference characteristics, and seeks to predict the 'rating' that a user would give to an item that they had not yet considered. These characteristics may be from the information items or user's social environment Recommender systems are designed to help a user to survive with this situation by selecting a small number of options to present the user. Recommender systems helps to users to overcome information overload by providing personalized suggestions based on a history of a user's likes and dislikes. On-line web portals like Amazon.com [6]; eBay.com [7]; Netflix.com [8] etc. are providing these recommending services to know about the personalized interests.

Collaborative filtering recommender systems [1] recommend items by identifying other users with similar taste and use their opinions for recommendation; whereas content-based recommender systems recommend items based on the content information of the items. These systems suffer from scalability, data sparsity, over specialization, and cold-start problems resulting in poor quality recommendations and reduced coverage. Recommender System is to generate significant recommendations to a collection of users for items or products that might interest them. Content-based filtering and collaborative filtering (CF) are two technologies used in recommender systems. Content-based filtering systems analyze the contents of a set of items together with the ratings provided by individual users to conclude which non-rated items might be of interest for a specific user.

2. Collaborative filtering (CF)

CF is one of the most frequently used technique in personalized recommendation systems which is also making predictions about the interests of a user based on previous preferences by all users based on the idea that users who liked similar things in the past will tend to favor similar items. CF is the process of filtering for information or patterns using techniques involving collaboration among multiple agents, viewpoints, data sources, etc. They are mainly classified into three categories: namely, memory- based collaborative filtering, model- based collaborative filtering and hybrid collaborative filtering techniques [1].

2.1 Memory-based Collaborative Filtering

Memory-based algorithms utilize the entire user-item database to generate a prediction. These systems employ statistical techniques to find a set of users, known *as* neighbors. Once a neighborhood of users is formed, these systems use different algorithms to combine the preferences of neighbors to produce a prediction or *top*-N recommendation for the active user. The techniques, also known as *nearest-neighbor* or user-based collaborative filtering [1] are more popular and widely used in practice.

2.2 Model-based collaborative filtering

Model-based collaborative filtering algorithms provide item recommendation by developing a model of user ratings initially. Algorithms in this category take a probabilistic approach and envision the collaborative filtering process as computing the expected value of a user prediction, given user ratings on other items. The model building process is performed by different machine learning algorithms such as Bayesian network, clustering, Singular Value Decomposition (SVD) [1] and rule-based approaches.

2.3 Hybrid Collaborative Filtering (HCF)

HCF [1] systems combine CF with other commendation techniques to make predictions or recommendations. Hoping to avoid limitations of either recommender system and improve recommendation performance, HCF recommenders are combined by adding content-based characteristics to CF models, adding CF characteristics to content-based models, combining CF with content-based or other systems, or combining different CF algorithms.

3. The Characteristics and their Rationale

Usually, a recommender system providing fast and accurate recommendations will attract the interest of customers and bring benefits to business. For CF systems, producing high-quality predictions or recommendations depends on how well they address the challenges, which are characteristics of CF tasks as well are described.

3.1 Data Sparsity

The data sparsity challenge appears in several situations in collaborative filtering, specifically, the cold start problem [1] occurs when a new user or item has just entered the

system; it is difficult to find similar ones because there is not enough. New items cannot be recommended until some users' rate it, and new users are unlikely given good recommendations because of the lack of their rating or purchase history. This could reduce the effectiveness of a recommendation system and therefore generating predictions.

Hybrid CF algorithms [1], such as the content-boosted CF algorithm, are found helpful to address the sparsity problem, in which external content information can be used to produce predictions for new users or new items. In Ziegler et al., a hybrid collaborative filtering approach was proposed to utilize bulk information designed for exact product classification to address the data sparsity problem of CF recommendations, based on the generation of profiles.

3.2 Scalability

When numbers of existing users and items grow tremendously, traditional CF algorithms will suffer serious scalability problems, with computational resources going beyond practical or acceptable levels. As well, many systems need to react immediately to online requirements and make recommendations for all users regardless of their purchases and ratings history, which demands a high scalability of a CF system [6].

3.3 Synonymy

It refers to the tendency of a number of the same or very similar items to have different names or entries. Most recommender systems are unable to discover this latent association and thus treat these products differently. For example, the seemingly different items "children movie" and "children film" are actual the same item, but memory-based CF systems would find no match between them to compute similarity. The frequency of synonyms decreases the recommendation performance of CF systems. The drawback for fully automatic methods is that some added terms may have different meanings from intended, thus leading to rapid degradation of recommendation performance.

3.4 Gray Sheep

Gray sheep refers to the users whose opinions do not consistently agree or disagree with any group of people and thus do not benefit from collaborative filtering. Black sheep are the opposite group whose individual tastes makes recommendations nearly impossible. Although this is a failure of the recommender system, non-electronic recommenders also have great problems in these cases, so black sheep is an acceptable failure. Claypool et al. provided a hybrid approach combining content-based and CF recommendations by basing a prediction on a weighted average of the content-based prediction and the CF prediction.

3.5 Shilling Attacks

In cases where anyone can provide recommendations, people may give tons of positive recommendations for their own materials and negative recommendations for their competitors. It is desirable for CF systems to introduce precautions that discourage this kind of phenomenon [2]. Item-based CF algorithm was much less affected by the attacks than the user-based CF algorithm, and they suggest that new ways must be used to evaluate and detect shilling attacks on recommender systems. The item-based CF systems have been examined by Mobasher et al., and alternative CF systems such as hybrid CF systems and model-based CF systems were believed to have the ability to provide partial solutions to the problem.

4. Description of Algorithms Evaluated

It is proposed to choose the following algorithms to evaluate which are frequently mentioned in the literature and works on explicit ratings data. Further, the algorithms are proposed for modification by introducing new approach. In some cases, the proposal made for minor modifications to existing algorithms in order to improve performance. All the tested algorithms with basic information are described.

Classification	Name of the Algorithm	Advantages	Disadvantages
Memory-based CF	User-based Collaborative Filtering(UBCF) K- Nearest Neighbor(K-NN)	1.easy implementation 2. need not consider the content of the items being recommended 3.scale well with co-rated items	1.dependent on human ratings 2. cannot recommend for new users and items 3. have limited scalability for large datasets
Model-based CF	Apriori algorithm Singular Value Decomposition (SVD)	1.better address the sparsity, scalability and other problems 2. improve prediction performance	1. expensive model-building 2. lose useful information for dimensionality reduction techniques 3. have trade-off between prediction performance and scalability
Hybrid CF	Content-boosted Collaborative Filtering(CBCF)	1. improve prediction performance 2. overcome CF problems such as sparsity and gray sheep 3. overcome limitations of CF and content-based or other recommenders	1. need external information that usually not available 2. have increased complexity and expense for implementation

Table 1: Summary of the proposed algorithms for evaluation

5. Methodology

In this work (i) user-based collaborative filtering, (ii) k-NN algorithm, (iii) item-based collaborative filtering (iv) Apriori algorithm, (v) singular value decomposition (SVD) (iv) Simple Bayesian CF Algorithm and (iiv) content-boosted algorithm are implemented and are further examined for several combinations of suitability for making an effective combination to form a hybrid collaborative filtering algorithm by reducing the quality of predictions. Based on the performance, user-based collaborative filtering, singular value decomposition (SVD) and content-boosted algorithm are modified for further reducing the quality of prediction.

The experimental methodology used for computing the different prediction algorithms namely CF predictor, Content-based algorithm and CBCF are presented and evaluated. Then prediction times and the quality of their predictions are measured for each evaluated algorithm. All the experiments were performed on an Intel Pentium-IV Processor, 2 GB RAM system and implemented in Java and executed. The dataset is stored in database MySQL in the same computer.

6. Dataset

To carry out the research and analysis for content boosted collaborative filtering system, the GroupLens Research Project agency at the University of Minnesota developed Internet Movie Database which contains the user-movie ratings and the movie details, called the **Movie Lens dataset** [5]. This dataset may be used to derive the results. The data set consists of 100,000 ratings (1-5) from 943 users on 1682 movies. Each user has rated at least 20 movies. It provides demographic data such as age, gender, and the zip code supplied by each person. The content of the information of every movie is considered as a set of slots. Each slot is represented by number of words. Further, the data has been segregated and discarded for having less than 20 ratings or in complete demographic information. Now the dataset provides the actual rating data provided by each user for various movies and used in the implementation process to generate prediction values for various algorithm systems.

7. Experimental Evaluation

A subset of the ratings data from the MovieLens data set is used for the purposes of comparison. 20% of the users were randomly selected to be the test users. In the each movie data downloaded from grouplens website [9], it mentioned that the data sets u1.base and u1.test through u5.base and u5.test are 80%/20% splits of the u data into training and test data. Each of u1, u2, u3, u4, and u5 has disjointed test sets for cross validation. These data sets can be generated from u.data by mku.sh. Source file u.data contained the u dataset by 943 users with 100000 ratings on 1682 items. Each user has rating at least 20 movies. This is a tab separated list of user id, item id, rating and timestamp.

MAE calculates the irrelevance between the recommendation value predicted by the system and the actual evaluation value rated by the user. The measurement method of evaluating the recommendation quality of recommendation system mainly includes statistical precision measurement method it includes to measure the recommendation quality [6]. The generated prediction values are stored in an arraylist as mentioned above and tabulated.

8. Performance Evaluation and Comparative Analysis

The influence of various nearest neighbors set on predictive validity is tested by gradually increasing the number of neighbors. The dataset predicts item rating of the users are evaluated as per the opinions of the users chosen ratings. The results are shown in graphical representing MAE values Vs respective their neighbor set sizes. MAE values are computed using different test data sets and tabulated in table 2. The Comparative analysis of these computed values are presented.

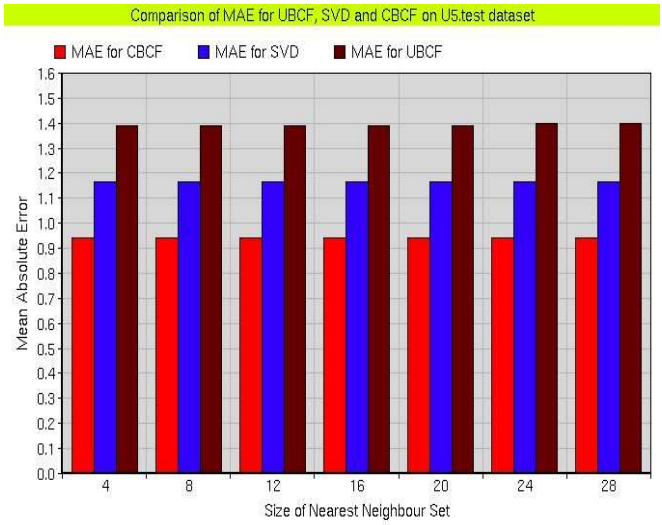

Fig.1. Comparing the performance of three modified collaborative filtering algorithms i.e., UBCF, SVD and CBCF.

The results presented in table 2 shows the MAEs for the different NNSs evaluation users using test dataset is 32.3% and 19.5%. In most of the cases, it is observed modified algorithms are performed well and showed increase in the quality perdition performance. One thing that it is important to notice is the differences between the overall performances of the modified UBCF, SVD and CBCF. CBCF performs better than the other compared algorithms.

10. CONCLUSION

In this paper, a sequence of collaborative filtering algorithms that are known for their efficiency, relevant collaborative filtering algorithms found in the literature are only presented and evaluated. The conclusions that presented are based on the results produced by the experiments conducted with the different algorithms and performance evaluation during the development of work.

As observed from the results obtained in the experiment, among all the modified collaborative filtering methods, the performance of content-boosted collaborative filtering algorithm could be proven better, which one is

related with traditional collaborative filtering algorithms.

11. REFERENCES

[1] Xiuyan Gu, Linfeng Jiang, and Ziyi Zhang, "Study on User's Browse Behavior to Measure the User's Browse Interest", Network and Communication, vol.15, pp.43-45, 2005.
[2] Incremental SVD method, Simon Funk. http://sifter.org/~simon/journal/20061211.html
[3] Serdar Sali, "Movie Rating Prediction Using Singular Value Decomposition", Machine Learning Project Report by University of California, Santa Cruz.
[4]Miguel Veloso, Alípio Jorge, Paulo Azevedo " Movie Rating Prediction Using Singular Value Decomposition"
[5] Movie lens data, http://movielens.umn.edu.
[6]Amazon, an online portal, http://www.amazon.com/
[7] eBay, an online portal, http://www.ebay.in/
[8] Netflix, an online video portal, https://www.netflix.com/
[9] Group lens, http://www.grouplens.org/

8.1 MAE values for UBCF, CBCF and SVD

Neighbor Set Size	4	8	12	16	20	24	28
MAE for UBCF	1.390	1.390	1.390	1.390	1.390	1.400	1.400
MAE for SVD	1.168	1.168	1.167	1.167	1.167	1.167	1.167
MAE for CBCF	0.940	0.940	0.940	0.940	0.940	0.940	0.940

Table 2: MAE values for different neighbor sets

Recursive Tensor Factorization for Multi-Linear Regression

A. Eliseyev[1] **and T. Aksenova**[1]
[1]CEA, LETI, CLINATEC, MINATEC Campus, 17 rue des Martyrs, 38054 Grenoble, France

Abstract - *In the present article a Recursive Multi-Way Partial Least Square Regression (RNPLS) algorithm for recursive tensor factorization and multi-linear regression is considered and tested in the model experiments. The method combines the Multi-Way Partial Least Square (NPLS) tensors decomposition with a scheme of recursive calculation. This recursive algorithm allows treating data arrays of huge dimension. In addition, it provides a fast adjustment of the regression to changes of the analyzed data. The recursive algorithm demonstrates fast and robust convergence in a set of experiments with artificial data in comparison with generic approach. The algorithm can be applied to solve a wide range of problems.*

Keywords: partial least square regression, recursive estimation, multi-way analysis, tensor factorization.

1 Introduction

In the variety of tasks several domains must be analyzed simultaneously to obtain the proper results (e.g., time-series analysis, chromatography, neuronal activity processing, etc.). Several multi-model data processing approaches were proposed, for instance, Parallel Factor Analysis [1], Multi-Way Partial Least Square [2], Iterative Multi-Way Partial Least Square [3]. Unlike the vector oriented algorithms that can be applied to the multi-way (tensor) data after unfolding, the multi-way modeling preserves the structure of the data, improves robustness of the results as well as allows identifying relative impact of each dimension. The specificity of the multi-way data is their huge size, which leads to high time- and resources consumption of the modeling procedure. In addition, in numerous applications, the analyzed signals vary significantly in time. Recursive calculations provide a fast adjustment of the model to changes of the signals. Recently, the Recursive Multi-Way Partial Least Square Regression algorithm, uniting the scheme of recursive calculation with multimodal data representation, was proposed by Eliseyev et al., [4]. This work is devoted to study of convergence of the RNPLS approach.

2 Method

The Recursive NPLS method is derived from the NPLS and Recursive PLS [5] approaches, thus it unites both the multi-way data representation of the first one, and the recursive calculation scheme of the second one. In the recursive method, the information used for decomposition of the tensors of observation of independent variables $\underline{\mathbf{X}}$ and dependent variables $\underline{\mathbf{Y}}$ is captured by their loading tensors, as well as by the coefficient matrix. They are iteratively updated according to the new data and are used instead of current tensors of observation. The size of the loading tensors and the matrix of coefficients are defined by the dimensionality of the observed variables and do not depend on the number of observations. As a result, the algorithm always keeps the size of the processing data.

3 Computational experiments

3.1 Data description

To test the convergence of the RNPLS algorithm, a set of computational experiments were carried out with artificial data. The tests were performed for matrix input and binary output variables. It leads to the observation tensor of the 3rd order. The artificial dataset $\left\{\mathbf{x}_k \in \mathbb{R}^{100\times 200}, y_k \in \{0,1\}\right\}_{k=1}^{1600}$ was created in the following way. Binary y_k were randomly generated with equal probabilities. Matrices $\mathbf{x}_k$ were calculated according to $\mathbf{x}_k = \mathbf{c}(y_k) + \lambda \boldsymbol{\varepsilon}_k$, where $\mathbf{c}(y_k) \in \mathbb{R}^{100\times 200}$ is set as $c_{ij} = \cos(2.5\pi(i-0.4j)+2)$ if $y_k = 0$, and $c_{ij} = \sin(2.5\pi(i+0.4j)+1)$ if $y_k = 1$ (Fig. 1). The random noise $\boldsymbol{\varepsilon}_k \in \mathbb{R}^{100\times 200}$ was drawn from a multivariate normal distribution $\mathcal{N}(\mathbf{0}, \boldsymbol{\Sigma})$. It was added to the templates with parameter λ introducing signal-to-noise ratio: $\lambda = \{0.5; 1; 5; 10\}$. The noise has the same amplitude as the signal $\mathbf{c}(y_k)$ in the case of $\lambda = 1$. The entire data set was split into training and test data sets of equal size.

3.2 Results

Results of the calibration process of the RNPLS algorithm can be represented as the linear regression: $\hat{y} = \sum_{i,j} x_{i,j} c_{i,j}$, where $\mathbf{C} = \left\{c_{i,j}\right\}_{i,j} \in \mathbb{R}^{100\times 200}$ is a matrix of the regression coefficients. To analyze the convergence of the set of matrixes $\{\mathbf{C}_i\}$ we calculate the distance between two matrices $\mathbf{C}_i$ and $\mathbf{C}_j$ as: $\rho(\mathbf{C}_i, \mathbf{C}_j) = \left\|\mathbf{C}_i - \mathbf{C}_j\right\|_F$, where $\|\cdot\|_F$

is the Frobenius norm. The estimations found by the NPLS and the RNPLS approaches are compared with theoretical coefficients of regression. Behavior of the mean values and the standard deviations of $\rho(\mathbf{C}_{theor}, \mathbf{C}_{RNPLS})$ for the different noise levels λ over the algorithms iterations are shown in Fig. 2 (the statistics calculated for 10 data realizations). In parallel, the means and the standard deviations of $\rho(\mathbf{C}_{theor}, \mathbf{C}_{NPLS})$ computed for the data generated by the NPLS algorithm is represented for every level of noise. As it could be seen, the mean value of the distances between the RNPLS and theoretical regression coefficients already after 1-2 iterations (20-40 points) are significantly less than the ones between the NPLS and theoretical coefficients computed for the whole training sets (800 points). In addition, the standard deviations of the RNPLS results are less than those obtained by NPLS. Thus, the RNPLS approach demonstrates fast convergence and is considerably noise-steady. For all tested levels of noise the disturbance in the RNPLS solution was appreciably less relatively to NPLS one.

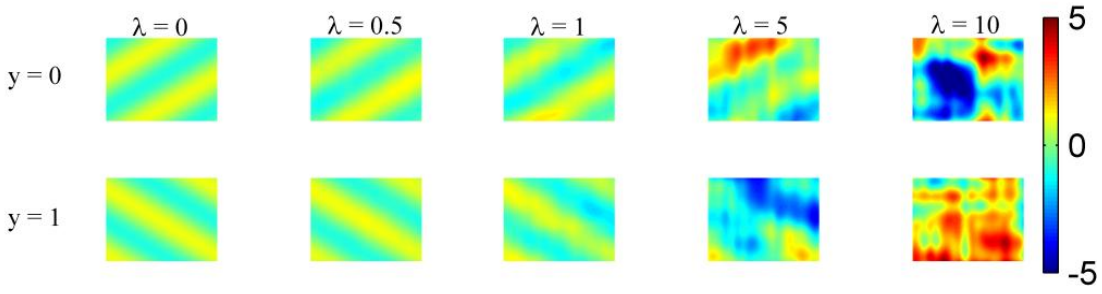

Figure 1. Examples of points from the artificial dataset, with different levels of noise.

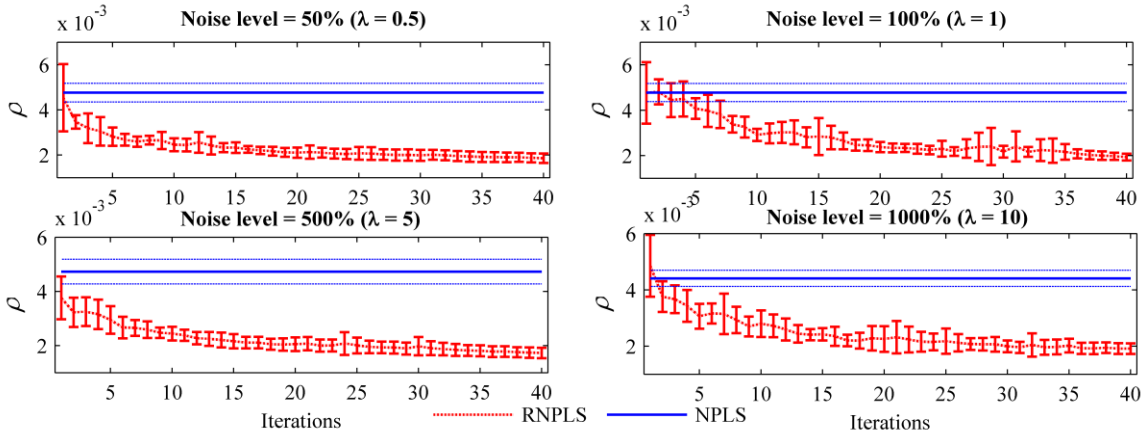

Figure 2. Comparison of RNPLS and NPLS in terms of approximation of the theoretical regression coefficients.

4 References

[1] Harshman, R.A. "Foundations of the PARAFAC procedure: Models and conditions for an "explanatory" multi-modal factor analysis". UCLA Working Papers in Phonetics, 16, 84, 1970.

[2] Bro, R. "Multiway calibration. Multi-linear PLS". J. Chemom., 10, 47-61, 1996.

[3] Eliseyev, A., Moro, C., Costecalde, T., Torres, N., Gharbi, S., Mestais, C., Benabid, A.L., Aksenova, T. "Iterative N-way PLS for self-paced BCI in freely moving animals". Journal of Neural Engineering, 8, 046012, 2011.

[4] Eliseyev, A., Benabid, A.L., Aksenova, T. "Recursive Multi-Way PLS for Adaptive Calibration of Brain Computer Interface System". Lecture Notes in Computer Science, 6792/2011, 17-24, 2011.

[5] Qin, S.J. "Recursive PLS algorithms for adaptive data modeling". Computers chem. Engng, 22, 503—514, 1998.

Applet Java Applied Fault Interpretation in Power Apparatus using Dissolved Gas Analysis

Mrs.Indra Getzy David[a] and Dr.M.Rajaram[b]

[a]getzy_wilson@yahoo.co.in ,[b]rajaramgct@rediffmail.com

Abstract: **To adapt the changing environments and uses and to implement refinements and improvements in the art of programming java is chosen for implementing a simple algorithm in protecting a Power Apparatus (PA), in which the limiting of damage becomes a by-product of the Protection System Function. To interpret the type of fault by analysing the dissolved gases which have evolved from the Insulation Media of the Apparatus and dissolved in the oil, a simple algorithm is developed and implemented in Java. To interpret the faults occurring in Power Apparatus like Power Transformers (PT), Load Tap Changers (LTC) and Bushings from the Dissolved Gas Analysis (DGA) data, the Algorithm Hexagon is developed that interprets the faults when the DGA data is imported and a visual presentation is reported. This window based Hexagon of applet java developed in java version jdk 1.6.0 may be useful for data sets pertaining to DGA of mineral or non mineral oil in PT, LTC or Bushings and to a Control and Protection Engineer in the Electricity Transmission and Distribution side .**

Keywords*: Applet Java, Hexagon, Dissolved Gas Analysis, Power Apparatus, Power Transformers.*

1. Introduction

For the interpretation of the type of fault by analysing the dissolved gases which have evolved from the Insulation Media of the Apparatus and dissolved in the oil, a simple algorithm is developed and implemented in Java. An application is a program that runs on computer under operating system of the computer. That is an application created by Java is more or less like one created using C or C++. An applet is a window based tiny java program. As such its architecture is different from the so called normal, console based programs. Applets which are event driven resemble a set of interrupt service routines. In applet the user interacts as events to which the applet waits until an event occurs and responds. The important difference is

that an applet is an intelligent program, not just an animation or media file. An applet is a program that can react to user input and dynamically change. The applet begins with import statements. Applet interacts with the user through the abstract windowing toolkit (AWT), not through the console based I/O classes. The AWT contains support for a window based, graphical interface. Every applet that is created must be a subclass of Applet. The class in the Applet must be declared as public, because it will be accessed by code that is outside the program. Once an applet has been compiled, it is included in an HTML file using the APPLET tag. The applet will be executed by a Java enabled web browser when it encounters the APPLET tag within the HTML file. The AWT notifies the applet about an event by calling an event handler that has been provided by the applet. Once this happens, the applet must take appropriate action and then return and then quickly return control to the AWT.

The window based Hexagon of applet java developed in java version jdk 1.6.0 may be useful for data sets pertaining to DGA of mineral or non mineral oil in PT, LTC or Bushings and to a Control and Protection Engineer in the Electricity Transmission and Distribution side where the Gas Chromatography help the electrical power engineer to device techniques for the identification of fault gases dissolved in transformer insulating oil from the early nineteen sixties [1]. An IEEE standard (C57.104-1991) [2] introduced the DGA as one of the most accepted methods for detecting incipient fault conditions in PTs. The correlation between the DGA and the corresponding fault conditions in the transformers has been well established and formulated and for the routine monitoring of in-service transformers it is used over the past five decades [3]. IEC Standard 60599 and IEEE Standard C 57 provide guidance for the interpretation of DGA results in service [4].

In addition to mineral oil non mineral oils like Midel, Silicone, FR3, and BioTemp are increasingly used as insulating liquids in electrical equipments because they are less flammable and more environmentally friendly. The non mineral oils have high percentage of biodegradability and are more hygroscopic in nature. Due to their high percentage of biogradability and more hygroscopic than mineral oils non mineral oils are slowly introduced into applications like PA insulation and cooling purposes in order to replace the mineral oils as the non mineral oil also has the same DGA fingerprints as mineral oil [5].

Due to its speciality of arc-quenching ability, non mineral liquids evolve gas only by one-fourth of the gas that would have been produced by the regular transformer oil [6]. In this work a simple algorithm is developed in Java platform to interpret faults

- in Equipments like LTC filled with mineral oil
- in Equipments filled with non mineral oils
- in Equipments for low temperature faults where stray gassing of oils [7]may interfere with diagnostics and
- in PT immersed in Mineral oil

The number of characteristic faults due to thermal stress and electrical stress are classified as seven by Duval by using the relative percentages of three gases namely Methane (CH_4), Ethylene (C_2H_6) and Acetylene (C_2H_2). These three gases correspond to the increasing levels of energy necessary to generate gases in transformers in service [8].The gas ratios as well as the relative proportions of gases and the rules from case studies are used for fault diagnosis from DGA data of mineral oil [9]. A combination of neural network and fuzzy system for enhancing the performance of the diagnostic system has been presented to identify only five types of faults [10].Faults have been analysed and compared with the conventional methods but none of the non mineral liquids have been considered [11]. Evolving wavelet network methodology have been proposed to monitor the condition of only PT immersed in mineral oil [12]. Data from [13-16] and the DGA data samples collected from various substations of South India are used to test this algorithm for fault interpretation. Hexagon is a single algorithm into which the data of fault gases from various PA evolved from mineral as well as non mineral cooling and insulating media is given as input and the type of fault interpreted by the algorithm is obtained as output. All the cases of Equipments and Insulating media can be tested using this single Algorithm Hexagon.

Visually presented information can be accessed by human perception in a most natural way. Complex structures and relation can be perceived in less time in greater number and with fewer errors than in any other way. Models of the real world or Models of abstract concepts are hardly dealt with by humans without taking resort to visual representations. This is the reason why the prediction of faults by visual presentation has been proposed.

2. Interpretation of Fault Gases

In the DGA method oil samples are taken from the transformer at various locations. Then, chromatographic analysis will be carried out on the oil sample to measure the concentration of the dissolved gases. The extracted gases are then separated, identified and quantitatively determined such that the DGA method can then be applied in order to obtain reliable diagnosis [17]. The extracted gases meant for analysis purpose are Hydrogen (H_2), Methane (CH_4), Ethane (C_2H_6), Ethylene (C_2H_4), Acetylene (C_2H_2), Carbon

Monoxide (CO), Carbon Dioxide (CO_2), Nitrogen (N_2) and Oxygen (O_2). C_2H_2 and C_2H_4 are used in all interpretation methods to represent high energy faults such as arcing and high temperature faults. H_2 is preferred in several of these methods to represent very low energy faults such as PDs, where it is produced in large quantities. CH_4, however, is also representative of such faults and always formed in addition to H_2 in these faults. CH_4 has been chosen rather than H_2 because it not only allows identifying these faults, but provides better overall diagnosis results for all the other types of faults than when using H_2. For the interpretation of faults The Duval Triangle was developed by Michel Duval in 1974 using three of these hydro carbon gases in relative proportions of percentage. Michel Duval proposed regions to represent seven types of faults [8]. The fault zone boundaries proposed by Michel Duval slightly differ when the insulation media differs with different sets of fault gases. The electronic version of the Duval Triangle has to be changed every time when the type of Power Apparatus or the type of insulation media changes [18].

To save time and memory a single algorithm is implemented incorporating all the different zone areas for fault interpretation regardless of whether it is a mineral oil or nonmineral oil or any type of PA. The Interpretation of Faults in the proposed Algorithm Hexagon is listed in Table1. When the data pertains to P3, the algorithm checks for four cases of non mineral liquids, viz. Silicone, FR3, Bio Temp and Midel. These polygons uses the same types of fault gases but their zone boundaries slightly differ. So they are designated as P3S, P3F, P3B and P3M representing Polygon3 for Silicone, Polygon 3 for FR3, Polygon3 for Bio Temp and Polygon3 for Midel respectively. For interpretation of faults in both mineral oil and FR3(Nonmineral oil P6) at low temperatures(P4),the fault gases of importance are H_2, CH_4 and C_2H_6.As the Polygon4 and Polygon6 differ in their inner zone boundaries alone, they are represented by the same polygon with difference in zone boundaries.

TABLE 1. Interpretation of faults in the proposed Hexagon

Location of Point inside the Polygon (Gas Type)/Zone			Interpretation of Type of Fault
Polygon		Zone	
P1 (CH_4,C_2H_4,C_2H_2)		PD	Partial Discharge
		D1	Discharges of low energy
		D2	Discharges of high energy
		T1	Thermal faults of temperature $< 300^0$C
		T2	Thermal faults of temperature 300^0C$< T < 700^0$C
		T3	Thermal faults of temperature $>700^0$C.
		DT	Combination of Thermal and Electrical Fault.
P2 (CH_4,C_2H_4,C_2H_2)		N	Normal
		T3	Thermal faults of temperature $>700^0$C.
		X3	Fault T3 or T2 in progress, or severe arcing D2
		T2	Thermal faults of temperature 300^0C$< T < 700^0$C
		D1	Abnormal Arcing D1
		X1	Thermal fault in progress
P3	P3S (CH_4,C_2H_4,C_2H_2)	PD	Partial Discharge
	P3F (CH_4,C_2H_4,C_2H_2)	D1	Discharges of low energy
	P3B (CH_4,C_2H_4,C_2H_2)	D2	Discharges of high energy
	P3M (CH_4,C_2H_4,C_2H_2)	T1	Thermal faults of temperature $< 300^0$C
		T2	Thermal faults of temperature 300^0C$< T < 700^0$C
		T3	Thermal faults of temperature $> 700^0$C.
		DT	Combination of Thermal and Electrical Fault.
P4 (H_2,CH_4,C_2H_6)		PD	Corona Partial Discharges
		S	Stray Gassing of Mineral Oil
		C	Hotspots $T > 300^0$C
		O	Overheating $T < 250^0$C

P5 (CH_4,C_2H_4,C_2H_6)	PD	Corona Partial Discharges
	S	Stray Gassing of Mineral Oil
	C	Hotspots T > 300^0C
	O	Overheating T < 250^0C
	T3	Thermal faults of very high temperature >700^0C.
P6 (H_2,CH_4,C_2H_6)	PD	Corona Partial Discharges
	S	Stray Gassing
	C	Hotspots T > 300^0C
	O	Overheating T < 250^0C
P7 (CH_4,C_2H_4,C_2H_6)	PD	Corona Partial Discharges
	S	Stray Gassing
	C	Hotspots T > 300^0C
	O	Overheating T < 250^0C

3. Proposed Hexagon in Java Platform

For speedy and easy interpretation of faults in any type of PA , a window based Hexagon is developed in Java, version jdk 1.6.0 to determine visually whether a fault evolves from a relatively harmless thermal fault into a potentially more severe electrical one or not. The Hexagon consists of number of polygons as shown in Fig.1 with respect to that listed in Table .1. The result of implementation of generating the electronic form of hexagon in java platform with the fault coordinates M, N, H, I, J, K obtained inside the different fault zones on implementation of the algorithm is presented in Fig.2. The user friendly phase to import DGA data in Java applet is presented in Fig.3; the user can select the option of his choice by clicking the buttons.

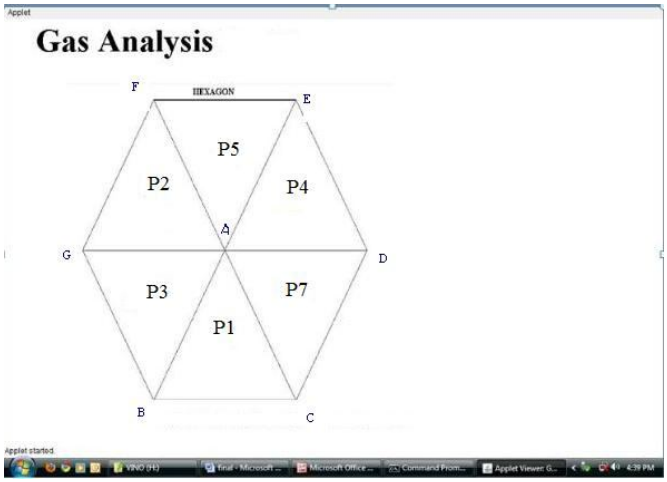

FIG. 1 HEXAGON DIVIDED INTO SIX POLYGONS P1, P2, P3, P4, P5, P7 WITH EACH SIDE OF EACH POLYGON REPRESENTING A GAS VALUE IN %

.

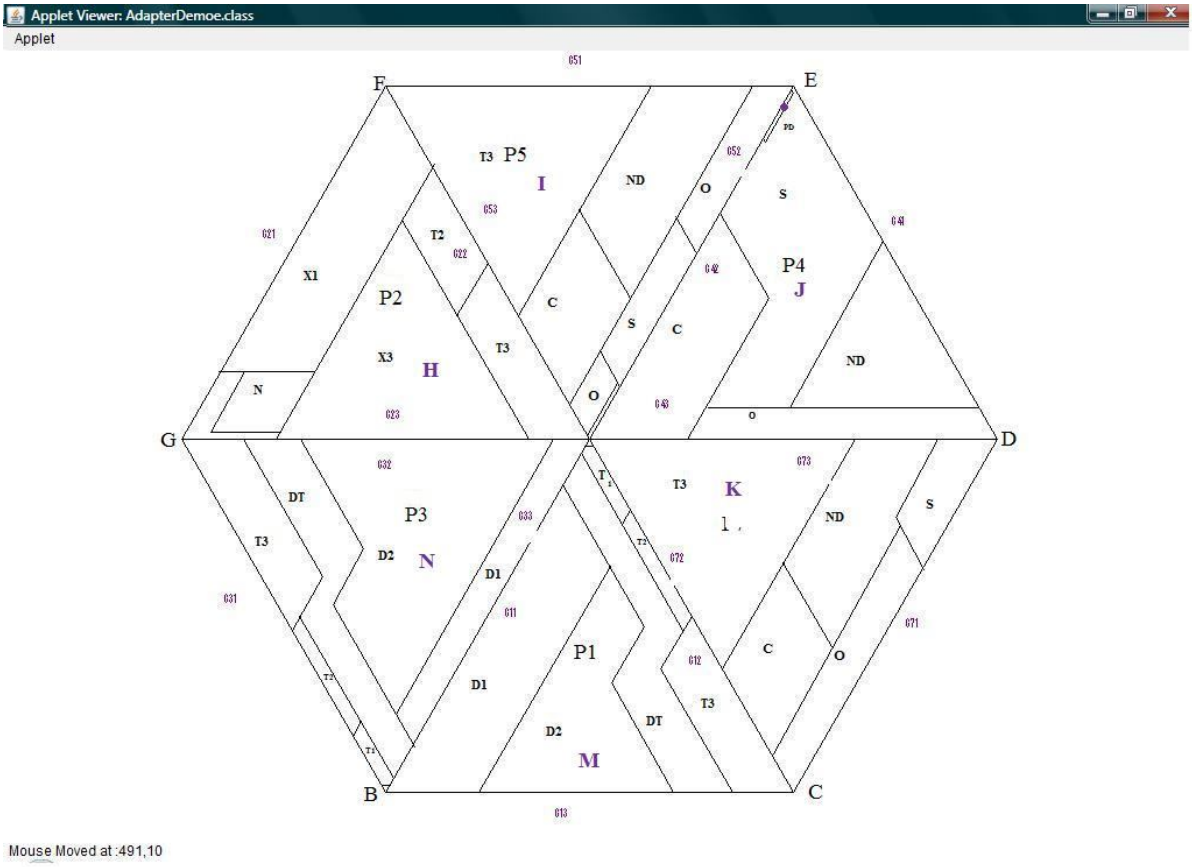

FIG.2.FAULT CO-ORDINATES M, N, H, I, J, K

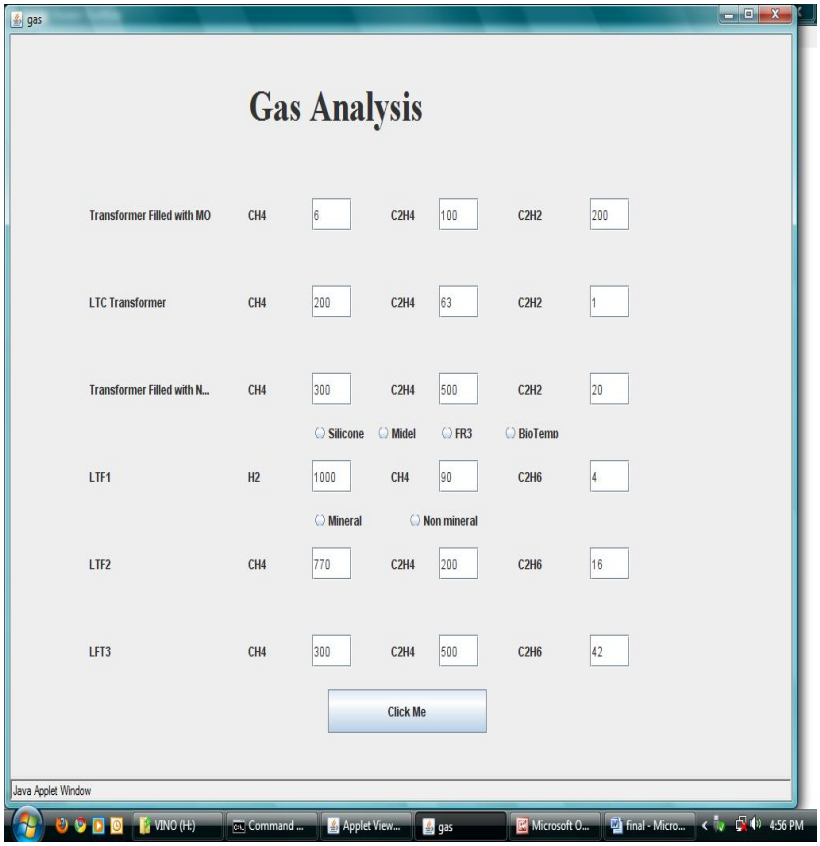

FIG.3. SAMPLE WINDOW OF PHASE II FUNCTION OF THE SOFTWARE WHICH IS USER FRIENDLY

The algorithm is implemented making use of the Cartesian Co-ordinate system. The standard co-ordinate system used on the computer systems differ from that of Cartesian co-ordinate system. The abscissa values of rectangular co-ordinate systems remains the same for the Processor Co-ordinate System, but the Ordinate values are changed by subtracting from the maximum value of the screen resolution. The algorithm developed in this work adopts modular fashion minimizing the number of "goto" statements. The notations used in this algorithm are standard notations as per Jean-Paul Tremblay and Paul G. Sorenson [19].

3.1 Algorithm *Hexagon* This algorithm when implemented in window based Java first draws the Hexagon with polygons and zones inside and then checks the presence of O_2 and N_2 from the n number of DGA data imported to it. If $O_2 / N_2 < 0.3$, then the algorithm tests the Total Combustible Gases (TCG) value and proceeds for further calculation of co-ordinate values corresponding to gas values in percentages

of parts per million (ppm) and interpretation of fault. The DGA data imported are integer values and the relative proportions of the gas values are real values.

With respect to coordinates of B (BX and BY), all the coordinates are computed by letting the length of each side of the Hexagon as L. The fault coordinates are calculated taking relative proportions of gas values G11, G12 etc in percentage. For the points that lie on the boundary lines, the probability of the type of fault is predicted by computing a small circular area around that point and evaluating the maximum number of predicted types inside the circle. The fault on the boundary then will be included to the type of fault which resulted as maximum cases of prediction. For example in Polygon 5 in Fig.1 (b), if the point lies on the zone boundary between C [Hot spot with carbonization of paper ($T>300^0C$)] and T3 [Thermal faults of very high temperatures ($T > 700^0C$)], the maximum number of predicted fault around that point if computed belong to T3, then the fault point under prediction is included into the maximum predicted case of fault i.e. T3.

1. [Develop Hexagon,Inner polygons and fault zones]

g.drawPoint

g.drawHexagon

g.drawPolygon

g.drawZone

2.[Import DGA Data and Compute O_2/ N_2 and TCG from DGA Data] (*Phase I*)

[G1, G2, G3, G4]←O_2, N_2,CO,CO_2 (*DGA Data*)

If G1/ G2 < 0.3

Then TCG ← Sum(CH_4,H_2,C_2H_2,C_2H_4,C_2H_6)

Else Exit.

[G11,G21,G33,G42,G52,G71] ←CH_4

[G12,G22,G31,G53,G72]← C_2H_4

[G13,G23,G32]← C_2H_2

[G41]←H_2

[G43,G51,G73]←C_2H_6

3.[Check TCG And Report]

If TCG < 500ppm ,Exit

Else

If 500ppm <TCG<1000 ppm, g.drawString("Significant Decomposition")

Else If

TCG >2500 ppm , g.drawString("Substantial Decomposition")

4.[Determine the type of Power Apparatus] (*Phase II*)

If Mineral Oil , Then

If (C_2H_2 = 10 ppm AND C_2H_4 = 10 ppm)

Then Import Data To P2(*LTC*)

Else Import Data To P1,P4,P5 (*Power Transformer*)

Else (P4 ← P6), Import Data To P3S,P3F,P3B,P3M,P6,P7. (*Non Mineral Oil Data*)

5.[Compute Fault Coordinates M,N,H,I,J,K]

(*Taking the gas values G11,G12 and G13,the Cartesian Co-ordinates of MX and MY are calculated by simple trignometric calculations,and similarly other fault points.*)

MX = BX + L*(G12 + G11/2)

MY=BY + L*(√3/2)G11

6.[Interpret fault and Output Result]

Select case ((M,N,H,I,J,K) inside (P1-P10))

case P1 : (Z1 thru Z7)

g.drawString (" fault in Power Transformer immersed in Mineral Oil")

case P2 : (Z8 thru Z13)

g.drawString (" fault in LTC immersed in Mineral Oil")

case P3 : (Z14 thru Z41)

g.drawString (" fault in Power Apparatus immersed in Nonmineral Oil")

case P4 : (Z42 thru Z45)

g.drawString (" low temperature fault in Power Transformer immersed in Mineral Oil")

case P5 : (Z46 thru Z50)

g.drawString ("low temperature fault in Power Transformer immersed in Mineral Oil with different sets of Gases")

case P6 : (Z51 thru Z54)

g.drawString (" low temperature faults in FR3 Oil")

case P7 : (Z55 thru Z58)

g.drawString ("low temperature faults in FR3 oil with different sets of Gases")

Default: Read (r ,fault1,fault2)

If (M,N,H,I,J,K) on (Z1-Z58) boundary lines, g.drawCircle(c,r) (*C is M,N,H,J,K*)

Compute max(fault1,fault2)

7.[Finished]

Exit.

4. RESULTS AND DISCUSSION

Java provides facilities to the programmer to define a set of objects and a set of operations (methods) to operate on that objects. All types of data are declared as per standard syntax of java. On compilation of the Algorithm Hexagon shown in Section 3.1, the results are visually presented.

The software for interpreting the faults in transformers is designed in java platform by developing a Hexagon where all the faults are interpreted. This algorithm provides more flexibility

in diagnosing the faults occurring in PT, LTC and PA immersed in mineral and non mineral liquids. This software is designed in such a way that data obtained from DGA for various PA which differ in insulation media employed in them can be used for importing input at an instant of time. The results obtained for few sets of data samples listed in Table 2 are presented in Fig.4.The dots display the interpretation of the faults inside the respective zones.

Table 2. Data Samples from Power Transformer Date of Commissioning: 08.11.2005

HC Values in ppm 16 MVA,110/11kV	H_2	CH_4	C_2H_6	C_2H_4	C_2H_2	CO_2	CO	Remarks By Lab Expert
Sample I-03.01.2006	46	168	37	286	2	840	-	Thermal Fault of above 100^0C Due to Overheating
Sample II-17.01.2006	64	224	49	376	2	1164	-	
Sample III-06.02.2006	38	219	52	377	1	1340	-	
Sample IV-16.03.2006	29	189	75	353	2	1454	-	
Sample V-11.04.2008	14	67	42	111	0	1223	-	Resample
Sample VI-07.08.2008	22	94	43	138	3	1823	-	
SampleVII-27.04.2009	25	96	50	158	6	1964	-	Satisfactory

1. CH_4,C_2H_4,C_2H_2[14]	2. CH_4 , C_2H_4 , C_2H_2 [13]	3. CH_4,C_2H_4,C_2H_2[16]
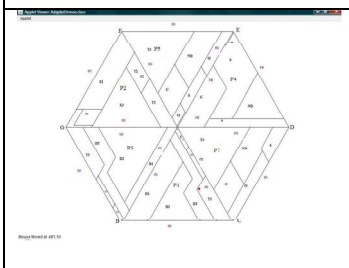	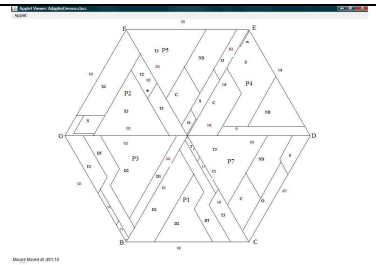	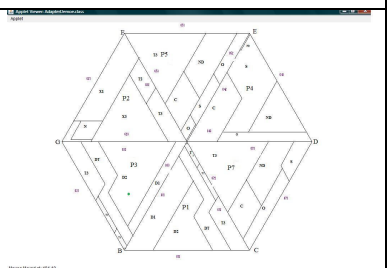
Polygon P1 Fault in Zone T3	Polygon P2 Fault in Zone T2	Polygon P3 Fault in Zone D2
4. H_2,CH_4,C_2H_6[14]	5. CH_4,C_2H_4,C_2H_6[15]	6. CH_4,C_2H_4,C_2H_6[13]
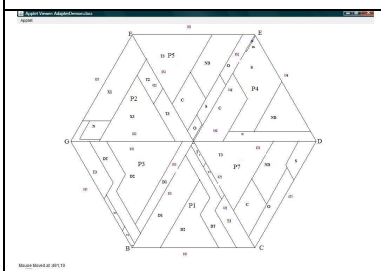	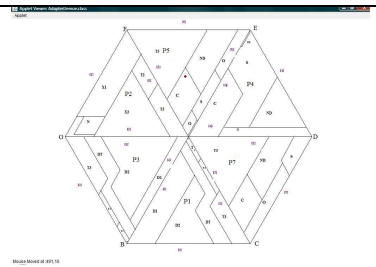	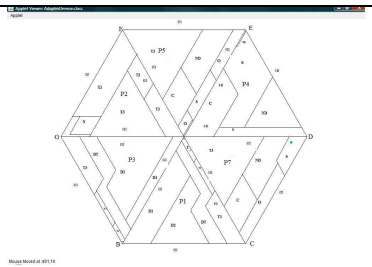
Polygon P4 Fault in Zone PD	Polygon P5Fault in Zone C	Polygon P7 Fault in Zone S

FIG.4. (a) Presentation of the results for sample datasets in ppm

1. CH_4,C_2H_4,C_2H_2[14]

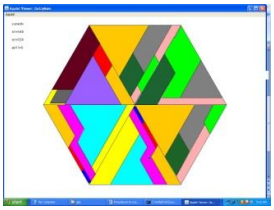

Polygon 1 Zone DT Thermal and Electrical Fault in PT

2. CH_4 , C_2H_4 , C_2H_2 [13]

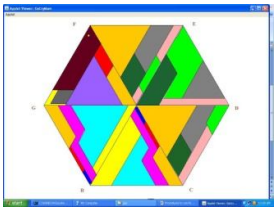

Polygon 2 ZoneX1 Thermal Fault in progress in LTC

3. CH_4,C_2H_4,C_2H_2[16]

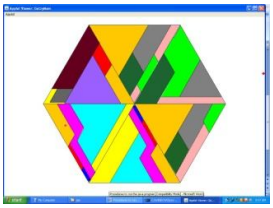

Polygon 3 ZoneT3 Thermal Fault T>700^{0}C for non mineral

4. H_2,CH_4,C_2H_6[14]

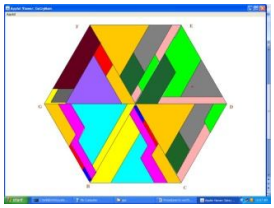

Polygon 4 Zone ND Non Deterministic

5. CH_4,C_2H_4,C_2H_6[15]

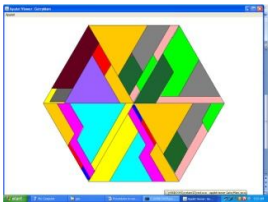

Polygon 5 Zone C Hotspots T > 300^{0}C in PT in mineral oil

6. CH_4,C_2H_4,C_2H_6[13]

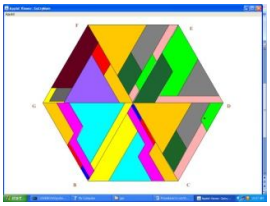

Polygon 7 Zone S Stray Gassing in FR3 oil

7. CH_4,C_2H_4,C_2H_2[14]

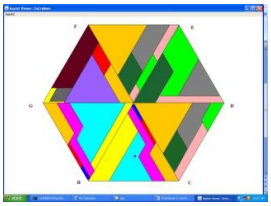

Polygon 1 Zone D2 Discharges of high energy

8.H_2, CH_4, C_2H_6 [15]

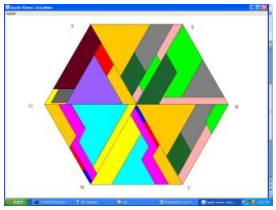

Polygon 6 Zone PD Corona Partial Discharges

FIG.4. (b) Visual Presentation of the results for sample datasets in ppm

5. CONCLUSION

This being a software implementation gives a visual picture of the indication of type of fault and user friendly modules and warns the Control Engineer to be caucious to protect the environment before failure takes place by analyzing the severety behind the shifting of the fault from less severe thermal into more severe electrical one.The effectiveness of the Hexagon Program is verified by DGA data collected from Oil Testing Centres in South India and the non mineral liquid data [13-16]. The probability of failure of a transformer due to fault in service can be determined by the studies made on the actual fault data reports obtained from the Electricity Boards Oil testing Centres in addition to this Interpretation. The Future work is to employ clustering algorithms for grouping the data sets.

6. REFERENCES

[1] Joseph J.Kelly, "Transformer Fault Diagnosis by Dissolved – Gas Analysis," *IEEE Trans. Industry Applications*, vol.I A -16, no.6, 1980.

[2] *IEEE standards C57.104 TM-2008*, "IEEE Guide for the Interpretation of Gases generated in Oil Immersed Transformers", IEEE Power and Energy Society Revision of Std C57. 104, 1991.

[3] M.Dural,Hydro-Quebec, "Dissolved Gas Analysis: It Can Save Your Transformer," *IEEE EI, Magazine*, 1989, vol-5, no.6, pp. 22-27.

[4] *IEC Publication 60599*, "Mineral Oil-Impregnated Equipment in Service – Guide to the Interpretation of Dissolved and Free Gases Analysis," March 1999.

[5] Imad –U-Khan,Zhongdong Wang and Ian Cotton,&Susan NorthCote , "Dissolved gas Analysis of Alternative fluids for Power Transformers," *IEEE EI Magazine* , 2007, vol.23, no.5, pp. 5-14.

[6] T.V.Oommen, "Vegetable oils for Liquid-filled Transformers,"*IEEE EI., Magazine*, 2002, vol. 18.no.1 pp. 6-11.

[7] I.Hohlein, "Unusual Cases of Gassing in Transformers in service,"*IEEE EI Magazine*, 2006, pp.24-27.

[8] M.Duval, "Fault gases formed in oil-filled breathing EHV power transformers- The interpretation of gas analysis data," *IEEE PAS Conf.* Paper No. C 74, 476-8, 1974.

[9] Xiaohui Li,Huaren Wu and Danning Wu, "DGA Interpretation Scheme Derived From Case Study," *IEEE Trans. Power Del.*, vol.26, no.2, pp. 1292 – 1293, April 2011.

[10] R.Naresh,Veena Sharma and Manisha Vashisth, " An Integrated Neural Fuzzy Approach for Fault Diagnosis of Transformers, " *IEEE Trans.Power Del.*, vol.23, no.4.pp 2017-2024 Oct.2008.

[11] N.A.Muhamad,B.T.Phung ,T.R.Blackburn and K.X.Lai, "Comparative study and Analysis of DGA methods for Transformer Mineral Oil," in *Proc.Power Tech. Conf.*,2007,pp.45-50.

[12] Yann.Chang Huang and Chao.Ming Huang, "Evolving wavelet networks for Power Transformer Condition Monitoring," *IEEE Trans. Power Del.*,vol.17,no 2, pp. 412-416, April 2002.

[13] M.Duval and A.dePablo, "Interpretation of Gas-in-Oil Analyses Using New IEC Publication 60599 and IEC TC10 Databases," *IEEE EI Magazine*, vol.17, no.2, p.31, 2001.

[14] C.E.Lin,J.M.Ling,C.L.Huang, "An Expert System for Transformer Fault Diagnosis Using Dissolved Gas Analysis,"*IEEE Trans. Power Del.*,vol 8,no.1, pp. 231-238, January 1993.

[15] Jyotishman Pathak,Yong Jiang,Vasant Honavar,James McCally, "Condition Data Aggregation with Application to Failure Rate Calculation of Power Transformers," in *Proc. System Science Conf. Hawaii* 2006,pp. 1- 10.

[16] Mohammad Golkhah,Sahar Saffar Shamshirgar and Mohammad Ali Vahidi, "Artificial Neural Networks applied to DGA for fault diagnosis in oil-filled power transformers," *JEEER* ,vol.3(1),pp.1-10,January 2011.

[17] M.Duval, P.Gervais and G.Belanger, " Update on Hydro-Quebec's Experience in the Interpretation of Dissolved Gas Analysis in HV Transformers ," *CIGRE Symposium*, Berlin, pp. 110-14, 1993.

[18] Michel Duval(IREQ), "The Duval Triangle for Load Tap Changers, Non mineral oils and low temperature faults in transformers," *IEEE 2008 EI* Magazine vol.24, no.6,pp 22-29, Nov/Dec 2008.

[19] Jean – Paul Tremblay and Paul G.Sorenson, "An Introduction to Data Structures with Applications,",*Tata McGraw-Hill* Publishing Company Limited ,New Delhi II Edition.

[20] Michel Duval IREQ Canada, "A Review of faults detectable by Gas – in- Oil Analysis in Transformers," *IEEE EI Magazine* vol.18, no.3, pp. 8-17, May/June 2002.

7. BIOGRAPHIES

Indra Getzy David received her B.E. [EEE] and M. E. [CSE] degrees from Govt. College of Technology Coimbatore, then affiliated to the University of Madras and Bharathiar University, South India in 1982 and 1990, respectively. She worked in the Public Works Department as an Assistant Engineer [electrical] for a period of a year where she was doing estimation and execution of the Electrical Works for the Bharathiar University Buildings Division in Coimbatore in South India. Presently she is an Associate Professor in the Department of Electrical Engineering, Govt. College of Engineering Tirunelveli in South India. To her credit she has nearly three decades of Teaching Experience. She is interested in the areas of Computer Graphics, Data Mining and Power Apparatus Protection. She is currently assisting one Government of India Project in her Department.

Dr. M.Rajaram is the Vice Chancellor of Anna University of Technology, Tirunelveli in South India. He has more than 30years of experience in teaching and more than 20 years of experience in research. His current area of research includes Power Systems, Control Systems, Computer Communication and Software Testing. He has published more than fifty papers in referred international journals. He has also presented more than one hundred and fifty research articles in national and international conferences. He has written few books for the benefit of the UG Students under Anna University Curriculum. He is currently dealing with few projects sponsored by government of India. He has produced 15 PhD Scholars and six researchers are on nearing completion under his guidance.

SESSION

ARTIFICIAL INTELLIGENCE: NOVEL APPLICATIONS AND ALGORITHMS

Chair(s)

Prof. Hamid R. Arabnia

Model free adaptive control with pseudo partial derivative based on fuzzy rule emulated network.

Chidentree Treesatayapun[1]
[1]Department of Robotic and Advanced Manufactory, CINVESTAV-Saltillo, Ramos Arizpe, 25900, Mexico

Abstract— *In this article, a model free adaptive control with the estimated pseudo partial derivative (PPD) is introduced by multi-input fuzzy rules emulated network (MiFREN) for a class of discrete-time systems. The resetting mechanism can be relaxed in this adaptation scheme. Human knowledge about the controlled plant is rearranged to define the IF-THEN rules directly. Those fixed parameters are designed according to guarantee the convergence related on the controller performance. All adjustable parameters inside MiFREN are tuned by the proposed on-line learning algorithm. The design example and simulation results demonstrate the performance of the proposed controller under the nominal system and system with disturbances.*

Keywords: Fuzzy logic; Model-free adaptive controller; Pseudo-partial derivative; Discrete-time

1. Introduction

Model free adaptive control (MFAC) has been continuously developed for several systems with unknown or ill-defined model especially for a class of discrete-time domain [1], [2]. With out any mathematic model of the plant, a linearization concept based on pseudo-partial derivative (PPD) is composed as the equivalent system. Due to the comparison with other adaptive controllers, only real time measured data of the controlled plant is necessary to establish MFAC. Unlike model reference adaptive control based on neural networks, the off-line tuning phase can be excluded because the time-varying PPD can be tuned by real time measurement data only [3].

In general, The control law has been determined by PPD under some necessary constrains and the resetting technique. It's clear that the control system performance depends on the accuracy of PPD estimation. The compensation system based on an artificial neural network has been discussed in [4] by the additional of another control effort. By using the on-off controller [5], the system dynamic can be considered as the unknown system when the switching sequence can be adapted by a feedback controller.

According to the controlled plant, in practice, PPD seems like the system sensitivity which can be understood by human knowledge related on input-output behavior. In this work, this knowledge can be reformulated into IF-THEN rules for an adaptive network called multi-input fuzzy rule emulated network(MiFREN) [6]. The on-line adaptation is developed to tune all adjustable parameters inside MiFREN. Thus, the time variation of PPD can be directly estimated by MiFREN according to our proposed cost function. Moreover, the resetting algorithm, which is needed for tuning PPD [7], can be relaxed in this work because of MiFREN's property [8] which is directly related on the change of input respectively to the plant's output. All fixed parameters are designed to guarantee the convergence which can affect the performance of controller.

This paper is organized as the follows. Section 2 introduces the problem formulation and some details about the dynamic linearization equivalent model. The control law is proposed with the estimated PPD based on MiFREN in section 3. Section 4 presents the MiFREN configuration together with the parameters adaptation. The design example and simulation results are demonstrated in section 5 including the consideration of disturbance effect. Section 6 represents our conclusions.

2. Problem Formulation

In this work, the nonlinear system for a class of discrete-time domain can be described by

$$y(k+1) = f(y(k), \cdots, y(k-n_y), u(k), \cdots, u(k-n_u)), \tag{1}$$

where $y(k) \in \mathbb{R}$ and $u(k) \in \mathbb{R}$ denote as the time index k system output and input, respectively with the unknown orders n_y and n_u. The nonlinear function $f(\cdot)$ is definitely unknown. According to the conventional MFAC algorithms, those following assumptions are stated.

Assumption 1: The partial derivatives of $f(\cdot)$ are continuous with respect to the control effort $u(k)$.

Assumption 2: The nonlinear system described in (1) is generalized Lipschitz. That means the positive constant l must be defined when $|\Delta y(k+1)| \leq l|\Delta u(k)|$, when $\Delta y(k+1) = y(k+1) - y(k)$ and $\Delta u(k) = u(k) - u(k-1)$.

According to those upper assumptions, the following lemma can be obtained.

Lemma 1: The nonlinear system (1) satisfied assumption 1 and 2 with $|\Delta u(k)| \neq 0$ for time index k, can be transformed into the equivalent compact form dynamic linearization (CFDL) as

$$\Delta y(k+1) = \Phi(k)\Delta u(k), \tag{2}$$

when $\Phi(k)$ denotes the pseudo partial derivative (PPD).
Proof: The proof is omitted here. Reader can refer to [3] for more details and complete proof.

□

The parameter PPD can be estimated by several learning algorithm such as the modified projection. On the other hand, in this work, PPD is determined by the adaptation network MiFREN which can be operated under the human knowledge according to the controlled plant.

3. Control law

In this section, the control effort $u(k)$ will be formulated. Let define the cost function as

$$J(u(k)) = [r(k+1)-y(k+1)]^2+\lambda[u(k)-u(k-1)]^2, \quad (3)$$

when λ is a designed weighting constant. By using (2), the cost function can be rewritten as

$$J(u(k)) = [r(k+1) - y(k) - \Phi(k)\Delta u(k)]^2 + \lambda[\Delta u(k)]^2. \quad (4)$$

Differentiating (4) with respect to $u(k)$, we have

$$\begin{aligned}\frac{\mathrm{d}J(u(k))}{\mathrm{d}u(k)} &= -2[r(k+1) - y(k)]\Phi(k) + 2\Phi^2(k)\Delta u(k) \\ &\quad +2\lambda\Delta u(k). \quad (5)\end{aligned}$$

Let $\frac{\mathrm{d}J(u(k))}{\mathrm{d}u(k)} = 0$, thus

$$\Delta u(k) = \frac{\Phi(k)[r(k+1) - y(k)]}{\lambda + \Phi^2(k)}. \quad (6)$$

The idea control law can be obtained as

$$u(k) = u(k-1) + \frac{\Phi(k)[r(k+1) - y(k)]}{\lambda + \Phi^2(k)}. \quad (7)$$

In practice, the output $y(k)$ can be measured but $\Phi(k)$ cannot be directly determined because of the unknown nonlinear system $f(\cdot)$. To realize this control law, $\Phi(k)$ will be estimated by MiFREN as $\hat{\Phi}(k)$, thus, the control effort can be generated by

$$u(k) = u(k-1) + \rho\frac{\hat{\Phi}(k)[r(k+1) - y(k)]}{\lambda + \hat{\Phi}^2(k)}, \quad (8)$$

when ρ is a step-size constant. Both ρ and λ are designed parameters which can be given by the following lemma to guarantee the convergence of $u(k)$. Before the proof of control effort boundary, the follow assumption is necessary.
Assumption 3: The direction of $\hat{\Phi}(k)$ or sign$\left\{\hat{\Phi}(k)\right\}$ is unknown but it doesn't change such as sign$\left\{\hat{\Phi}(k)\right\}$ = sign$\left\{\hat{\Phi}(k-1)\right\}$.
Remark: This assumption can be existed in several practical systems such as the chemical process, robotic system and so on. Moreover, this assumption will be proved again by the experimental results next.

Lemma 2: According to assumption 2 and the MiFREN's property, the maximum of $\hat{\Phi}(k)$ must be existed as $\hat{\Phi}_M, \forall k \in \mathrm{N}$ and both parameters ρ and λ are designed by following this relation

$$0 < \rho < \frac{2\lambda}{\hat{\Phi}_M}, \quad (9)$$

thus, the control effort from (8) is bounded.
Proof: Substitute $y(k) = \hat{\Phi}(k-1)[u(k-1) - u(k-2)] - y(k-1)$ into (8), we have

$$\begin{aligned}u(k) &= u(k-1) - \frac{\rho\hat{\Phi}(k)\hat{\Phi}(k-1)}{\lambda + \hat{\Phi}^2(k)}u(k-1) \\ &\quad +\frac{\rho\hat{\Phi}(k)}{\lambda + \hat{\Phi}^2(k)}\Big[r(k+1) + \hat{\Phi}(k-1)u(k-2) \\ &\quad +y(k-1)\Big], \\ &= A_u(k)u(k-1) + \xi_u(k), \quad (10)\end{aligned}$$

where

$$A_u(k) = 1 - \frac{\rho\hat{\Phi}(k)\hat{\Phi}(k-1)}{\lambda + \hat{\Phi}^2(k)}, \quad (11)$$

and

$$\xi_u(k) = \frac{\rho\hat{\Phi}(k)}{\lambda + \hat{\Phi}^2(k)}\Big[r(k+1)+\hat{\Phi}(k-1)u(k-2)+y(k-1)\Big]. \quad (12)$$

Substitute (9) into (13) and use assumption 3, it is clear that

$$A_u(k) < 1. \quad (13)$$

□

4. MiFREN for pseudo partial derivative

4.1 PPD based on MiFREN

MiFREN is an adaptive network which can be operated by human knowledge in the format of IF-THEN rules. The design of IF-THEN rules is also a key of the performance. The knowledge based on the controlled plant is roughly necessary. Due to (2), we can rearrange the relation of $\hat{\Phi}(k)$ as

$$\hat{\Phi}(k) \doteq \frac{\Delta y(k)}{\Delta u(k-1)}, \quad (14)$$

when $\Delta u(k) \neq 0$.

According to the upper relation, we can define some example IF-THEN rules as the followings:

- IF $\Delta y(k)$ is Positive Large and $\Delta u(k-1)$ is Positive Large THEN $\hat{\Phi}(k)$ should be Positive small,
- IF $\Delta y(k)$ is Positive Large and $\Delta u(k-1)$ is Positive small THEN $\hat{\Phi}(k)$ should be Positive Large,
- ...,
- IF $\Delta y(k)$ is Negative Large and $\Delta u(k-1)$ is Positive Large THEN $\hat{\Phi}(k)$ should be Negative small,
- ...,

- IF $\Delta y(k)$ is Negative Large and $\Delta u(k-1)$ is Negative small THEN $\hat{\Phi}(k)$ should be Positive Large,
- IF $\Delta y(k)$ is Negative Large and $\Delta u(k-1)$ is Negative Large THEN $\hat{\Phi}(k)$ should be Positive small.

With this implementation, unlike the conventional algorithms to determine $\hat{\Phi}(k)$, the sign of $\hat{\Phi}(k)$ is directly determined by those IF-THEN rules. To simplify, those IF-THEN rules can be defined by Table 1.

$\Delta y(k)$					$\Delta u(k-1)$
PL	PS	AZ	NS	NL	
P_1	P_6	C_{11}	N_{16}	N_{21}	PL
P_2	P_7	C_{12}	N_{17}	N_{22}	PS
ε_3	ε_8	ε_{13}	ε_{18}	ε_{23}	AZ
N_4	N_9	C_{14}	P_{19}	P_{24}	NS
N_5	N_{10}	C_{15}	P_{20}	P_{25}	NL

Table 1: IF-THEN rules

The linguistic variables PL, PS, AZ, NS and NL denote as Positive Large, Positive Small, Almost Zero, Negative Small and Negative Large, respectively. In this case, the number of IF-THEN rules is 25 and the relation the THEN-part can be given by other linguistic variable as $\square_i$ for $i = 1, 2, \cdots, 25$. The variables P, C and N stand for Positive, Close to zero and Negative, respectively. Unlike the conventional technique, when Δu nearly reaches to zero or stays in the range to AZ-membership function, the designed parameter ε is defined as a small positive constant and $\varepsilon_3 = \varepsilon_8 = \varepsilon_{13} = \varepsilon_{14} = \varepsilon_{23} = \varepsilon$. Moreover, the parameters ε_i can be given by difference values with the on-line learning algorithm which will be discussed next.

According to those IF-THEN rule, the network architecture of MiFREN can be constructed in Fig.1. The estimated

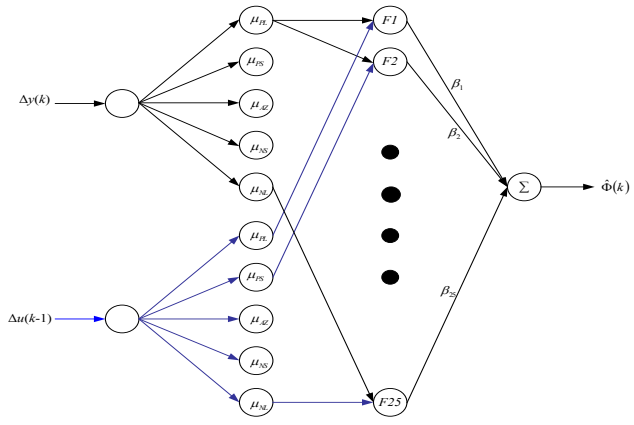

Figure 1: MiFREN networking structure.

PPD or $\hat{\Phi}(k)$ can be obtained by

$$\hat{\Phi}(k) = \sum_{i=1}^{25} F_i(\Delta y(k), \Delta u(k-1))\beta_i, \tag{15}$$

when β_i is a Linear Consequence (LC) parameter for THEN-part linguistic variable $\square_i$. The function $F_i(\cdot)$ is the i^{th} rule relation determined by membership functions related on the i^{th} rule. For example, according to Table 1, we have $F_1(k) = \mu_{PL}(\Delta y(k))\mu_{PL}(\Delta u(k-1))$ at rule # 1, $F_{16}(k) = \mu_{NS}(\Delta y(k))\mu_{PL}(\Delta u(k-1))$ at rule # 16 and $F_{25}(k) = \mu_{NL}(\Delta y(k))\mu_{NL}(\Delta u(k-1))$ at rule # 25. In this work, we can set those membership functions and LC parameters or β_i by the human knowledge based on the controlled plant. More explanations with example will be discussed in the next section.

4.2 Parameters adaptation

The on-line learning algorithm will be applied in this work for LC parameters. Thus, the estimated PPD in (15) can be rewritten by

$$\hat{\Phi}(k) = \sum_{i=1}^{25} F_i(k)\beta_i(k), \tag{16}$$

when $\beta_i(k)$ denotes the LC parameter for the i^{th} rule at time index k. To tune this parameter, the cost function $J(\hat{\Phi}(k))$ can be given as the following:

$$\begin{aligned} J(\hat{\Phi}(k)) &= \frac{1}{2}[\Delta y(k) - \hat{\Phi}(k)\Delta u(k-1)]^2 \\ &\quad + \frac{\gamma}{2}[\hat{\Phi}(k) - \hat{\Phi}(k-1)]^2, \end{aligned} \tag{17}$$

when γ is a positive defined constant. Determine the derivative with respect to $\beta_i(k)$, thus, we obtain

$$\begin{aligned} \frac{\partial J(\hat{\Phi}(k))}{\partial \beta_i(k)} &= \frac{\partial J(\hat{\Phi}(k))}{\partial \hat{\Phi}(k)} \frac{\partial \hat{\Phi}(k)}{\partial \beta_i(k)} \\ &= \Big[[\gamma + \Delta u^2(k-1)]\hat{\Phi}(k) - \gamma\hat{\Phi}(k-1) \\ &\quad - \Delta y(k)\Delta u(k-1)\Big] F_i(k). \end{aligned} \tag{18}$$

According to gradient search, the tuning law can be defined by

$$\beta_i(k+1) = \beta_i(k) - \eta_\beta \frac{\partial J(\hat{\Phi}(k))}{\partial \beta_i(k)}, \tag{19}$$

where η_β is the learning rate which can be designed as a small positive constant. By using (19) and (18), the tuning law can be formulated as

$$\begin{aligned} \beta_i(k+1) &= \beta_i(k) - \eta_\beta \Big[[\gamma + \Delta u^2(k-1)]\hat{\Phi}(k) \\ &\quad - \gamma\hat{\Phi}(k-1) - \Delta y(k)\Delta u(k-1)\Big] F_i(k). \end{aligned} \tag{20}$$

The designed parameters γ and η_β can effect to the convergence of β. The following lemma introduces the relation which guarantees the convergence of tuned parameters β_i.

Lemma 3: The LC parameters β_i for $i = 1, 2, \cdots, N_F$, when N_F denotes the number of IF-THEN rules, are

bounded with the tuning law given by (20) when the learning rate and γ are all satisfied this following requirement

$$0 < \eta_\beta < \frac{2}{\gamma + \Delta u^2(k-1)}. \quad (21)$$

Proof: Rearrange (20) in vector format, we obtain

$$\beta(k+1) = \big[1-\eta_\beta[\gamma+\Delta u^2(k-1)]||F(k)||^2(k)\big]\beta(k)+\xi(k), \quad (22)$$

when $\xi(k)$ stands for the remain terms which are not related on $\beta(k)$. Let $A = 1 - \eta_\beta[\gamma + \Delta u^2(k-1)]||F(k)||^2(k)$, we have

$$\beta(k+1) = A\beta(k) + \xi(k). \quad (23)$$

$||F(k)||^2(k)$ is the multiplication of two membership grades, thus $0 < ||F(k)||^2(k) \leq 1$ and substitute with (21) it can be obtained

$$A < 1. \quad (24)$$

□

The relation of the learning rate η_{beta} and γ obtained by this lemma can be used to support the design of both parameters which will be demonstrated in the next section. Furthermore, this result can be valid even $\Delta u(k-1) = 0$ or the previous control effort is constant.

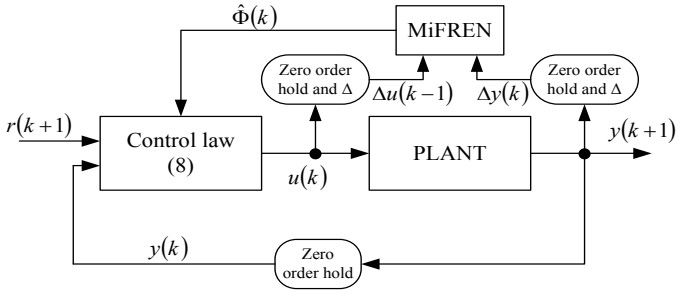

Figure 2: Control system configuration.

Furthermore, the block diagram illustrated in Fig. 2 represents the design concept and signal flow.

5. Design example and simulation results

The nonlinear discrete-time system which is selected to demonstrate the performance is described as

$$y(k+1) = \sin(y(k)) + u(k)[5 + \cos(y(k)u(k))], \quad (25)$$

when $y(k)$ denotes the output and $u(k)$ stands for the control effort. The desired trajectory $r(k)$ is given by this following:

$$r(k) = 2\sin(\frac{2\pi k}{100}). \quad (26)$$

To design the controller which is suitable for the system described in (25), in this case, we have the range of Δy and Δu in ± 2, thus the membership functions can be defined by Fig. 3 and 4 for Δy and Δu, respectively.

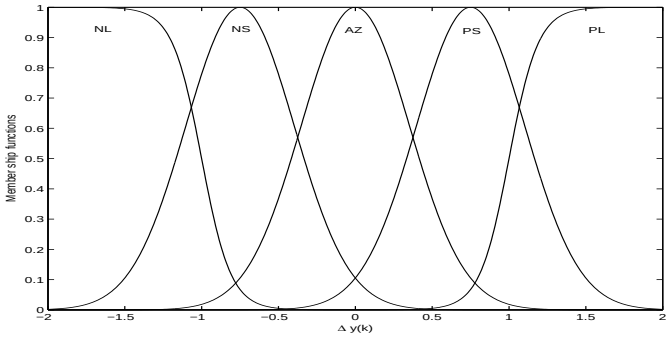

Figure 3: Membership function of $\Delta y(k)$.

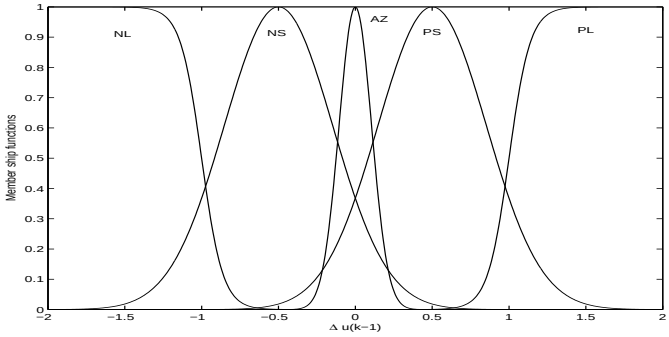

Figure 4: Membership function of $\Delta u(k-1)$.

According to (9) and (21), those designed parameters can be given as $\rho = 0.35$, $\lambda = 0.75$, $\eta_\beta = 1.5$ and $\gamma = 0.1$.

The adjustable parameters β_i can be defined by Table 2 regarding to the IF-THEN rules.

The tracking performance can be demonstrated in Fig. 5 as plots of the desired trajectory $r(k)$ and the system output $y(k)$. Finally, in Fig.6, the control effort is shown.

The demonstration of robustness is introduced next. In this setup, the time varying disturbance $d_1(k)$ is added in the original system (25) as

$$y(k+1) = \sin(y(k)) + u(k)[5 + d_1(k) + \cos(y(k)u(k))]. \quad (27)$$

such as constant parameters and $\beta_i(1)$ are same as the previous test. Fig. 7 represents the tracking performance and time varying $d_1(k)$. The control effort $u(k)$ is illustrated in Fig. 8.

For more complicity, another disturbance $d_2(k)$ is also included from the nominal system (25) as

$$\begin{aligned} y(k+1) \quad = \quad & \sin(y(k) + d_2(k)) \\ & + u(k)[5 + d_1(k) + \cos(y(k)u(k))]. \end{aligned} \quad (28)$$

With all same initial settings, the tracking performance and disturbances can be shown in Fig. 9 according the control effort displayed in Fig. 10.

$\Delta y(k)$					Δu
PL	PS	AZ	NS	NL	$(k-1)$
$\beta_1(1)$ $= 3$	$\beta_6(1)$ $= 1.5$	$\beta_{11}(1)$ $= 0.2$	$\beta_{16}(1)$ $= 0$	$\beta_{21}(1)$ $= 0$	PL
$\beta_2(1)$ $= 4$	$\beta_7(1)$ $= 2.5$	$\beta_{12}(1)$ $= 0.5$	$\beta_{17}(1)$ $= 0$	$\beta_{22}(1)$ $= 0$	PS
$\beta_3(1)$ $= 0.1$	$\beta_8(1)$ $= 0.1$	$\beta_{13}(1)$ $= 0.1$	$\beta_{18}(1)$ $= 0.1$	$\beta_{23}(1)$ $= 0.1$	AZ
$\beta_4(1)$ $= 0$	$\beta_9(1)$ $= 0$	$\beta_{14}(1)$ $= 0.5$	$\beta_{19}(1)$ $= 2.5$	$\beta_{24}(1)$ $= 4$	NS
$\beta_5(1)$ $= 0$	$\beta_{10}(1)$ $= 0$	$\beta_{15}(1)$ $= 0.2$	$\beta_{20}(1)$ $= 1.5$	$\beta_{25}(1)$ $= 3$	NL

Table 2: IF-THEN rules with initial parameters $\beta_i(1)$

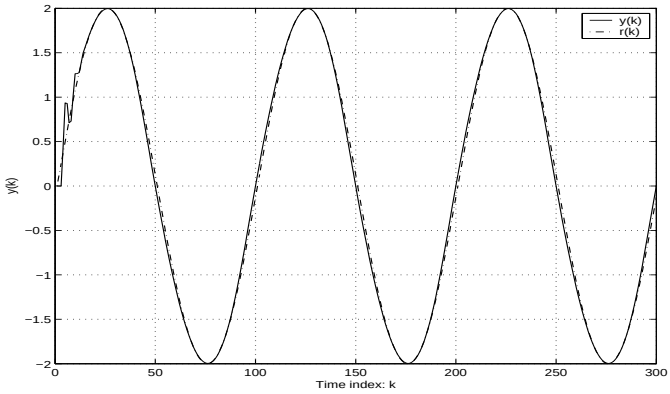

Figure 5: Tracking performance $y(k)$ and $r(k)$.

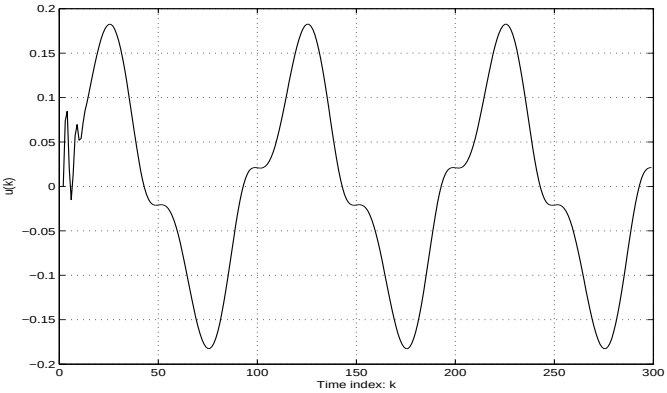

Figure 6: Control effort $u(k)$.

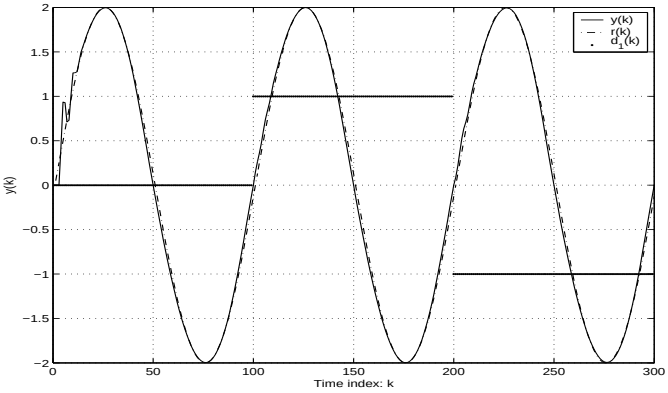

Figure 7: Tracking performance $y(k)$ and $r(k)$ with disturbance $d_1(k)$.

Remark: Any information related on those disturbances is not necessary to incorporate to the controller. That means the original controller designed based on the knowledge about the nominal plant is enough to handle those disturbance.

6. Conclusion

The model-free adaptive controller with the estimation of pseudo-partial derivation is proposed in this article. The estimation of PPD is implemented by a self-adjustable network called MiFREN. The initial setting of MiFREN's structure can be given by the human knowledge according to the controlled plant and the relation of plant's input-output within IF-THEN rules format. Moreover, all adjustable parameters inside MiFREN are begun by the knowledge of the plant directly. That can improve the system performance at the beginning. Other fixed parameters are designed by proved lemmas to guarantee the convergence. The simulation system demonstrates the design example and the effectiveness of the proposed algorithm. Both nominal system and disturbed plant have been considered to validate the controller performance and robustness.

Acknowledgment

The author would like to thank CONACyT (Project # 84791) and CINVESTAV-IPN for the financial support through this work.

References

[1] B. Zhang and W. D. Zhang, "Adaptive predictive functional control of a class of nonlinear systems," *ISA Trans.*, vol. 45, no. 2, pp. 175-183, 2006.

[2] D. Meng, Y. Jia, J. Du and F. Yu, "Data-driven control for relative degree systems via iterative learning," *IEEE Trans. Neural Networks.*, vol. 22, no. 12, pp. 2213-2225, Dec. 2011.

[3] Z. S. Hou and S. T. Jin, "A novel data-driven control approach for a class of discrete-time nonlinear systems," *IEEE Trans. Control Syst. Technol.*, vol. 19, no. 6, pp. 1549-1558, Nov. 2011.

[4] L. D. S. Coelho, W. P. Marcelo, R. S. Rodrigo, and A. A. R. Coelho, "Model-free adaptive control design using evolutionary-neural compensator," *Expert Syst. Appl.*, vol. 37, no. 1, pp. 499-508, 2010.

[5] B. Hahn and K. R. Oldham, "A model-free ONŰOFF iterative adaptive controller based on stochastic approximation," *IEEE Trans. Control Syst. Technol.*, vol. 20, no. 1, pp. 196-204, Jan. 2012.

[6] C. Treesatayapun and S. Uatrongjit, "Adaptive controller with Fuzzy rules emulated structure and its applications'," *Engineering Applications of Artificial Intelligence*, Elsevier, Volume 18, P. 603-615, 2005

[7] Z. S. Hou and S. T. Jin, "Data-driven model-free adaptive control for a class of MIMO nonlinear discrete-time systems," *IEEE Trans. Neural Networks.*, vol. 22, no. 12, pp. 2173-2188, Dec. 2011.

[8] C. Treesatayapun, "A discrete-time stable controller for an omni-directional mobile robot based on an approximated model," *Control Engineering Practice*, Elsevier, vol. 19, pp. 194-230, 2011

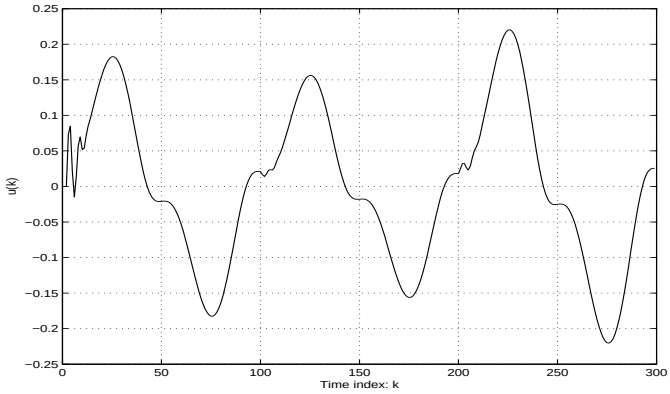

Figure 8: Control effort $u(k)$ with disturbance $d_1(k)$.

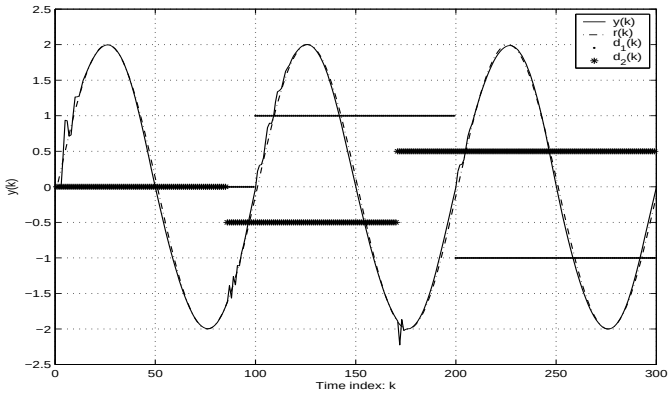

Figure 9: Tracking performance $y(k)$ and $r(k)$ with disturbances $d_1(k)$ and $d_2(k)$.

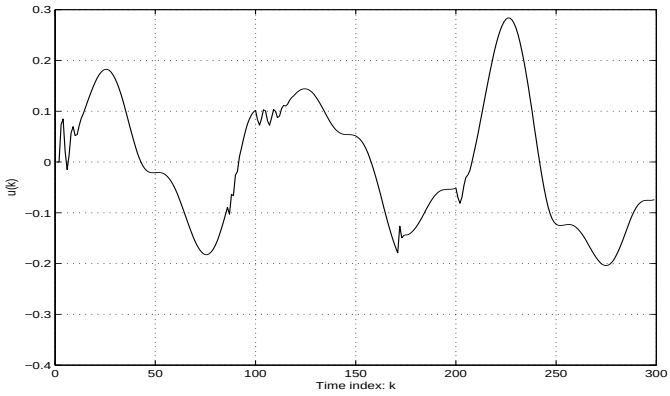

Figure 10: Control effort $u(k)$ with disturbances $d_1(k)$ and $d_2(k)$.

Application of Genetic Algorithms in Shape Optimization for Aerodynamic Bodies

V. Nejati[1]
[1]Mechanical Engineering Department, Islamic Azad University – Mashhad Branch, Mashhad, Khorasan Razavi, Iran

Abstract - *The objective of this study is to minimize the drag coefficient of aerodynamics bodies for a specified design Reynolds number regime. With the aerodynamics model the gradient of the objective function (drag coefficient) cannot be determined analytically. Furthermore, it is expected that the objective function is multi-modal, i.e. it shows more than one minimum. Therefore, the optimization algorithm must be efficiently applicable to such multi-dimensional, multi-modal and nonlinear objective functions. A powerful optimization procedure called Genetic Algorithms (GA) has been combined with the aerodynamics calculation to find the optimal shape with minimum drag coefficient. The aerodynamics calculation of flow field around the body of revolution is determined to get accurate drag coefficient. An effective numerical calculation called the Finite Volume Method is considered. For the laminar to turbulent transition locations, the linear stability analysis is applied to predict the natural transition location. The results were compared with those obtained from integral method and also experimental results and indicate a good agreement. It is concluded that for the purpose of the shape optimization of streamline bodies, the Genetic Algorithms and the Finite Volume Method with natural transition criterion is an essential approaches to indicate the optimal shape for various ranges of Reynolds number.*

Keywords: Drag Reduction; GA; FVM; Natural Transition

1 Introduction

Recently there has been a growing interest in problem solving system based on principles of evolution and heredity: such systems maintain a population of potential solutions, and they have some selection process based on fitness of individuals and some recombination operators. One type of such system is a class of Evolution Strategies which imitate the principles of natural evolution for parameter optimization problems (Rechenberg, Schwefel). Fogel's Evolutionary Programming is a technique for searching through a space of small finite state machines. Glover's Scatter Search technique maintains a population of reference points and generates offspring by weighting linear combinations. Another type of evolution based systems are Holland's Genetic Algorithms (GAs). For the large spaces, special artificial intelligence techniques must be employed. Genetic algorithms are a class of general search methods, which strike a remarkable balance between exploration and exploitation of the search space.

Drag reduction is important in considering the aerodynamic aircraft design. There have been many suggestions for reducing the skin friction drag on bodies of revolution, including extension of laminar flow regions and relaminarization of turbulent flow. For the aerodynamic design of three-dimensional fuselages with low skin friction drag, laminar bodies of revolution are often used as a design basis.

Laminar flow on a two-dimensional or an axisymmetric body can be achieved by designing the geometry so that there is an extensive region of favorable pressure gradient. This technique is frequently referred to as natural laminar flow control and may be implemented on a body of revolution by changing the location of the maximum body thickness as far aft as possible. A favorable pressure gradient and laminar flow may be maintained over a large percentage of body length, but this causes the flow separation at the remaining part of the body, with consequent increase in pressure drag.

The objective of our study is to find the optimal body shape with the minimum drag coefficient for specified Reynolds number regimes. For this purpose, an optimization process must be employed and linked to the aerodynamics calculation program. The combined computational program must be able to search through several body shapes and to choose those shapes with long laminar flow without separation. We also prove that the laminar and turbulent boundary layer calculations and the determination of the transition location must be extremely accurate for getting acceptable optimal body shape.

The aerodynamics calculation of streamline bodies is usually started from potential flow around the body to find inviscid velocity distribution. A numerical calculation called Finite Volume Method (FVM) is employed for both laminar and turbulent boundary layer calculation and those body shapes which show separation in the boundary layer domain must be rejected. Laminar to turbulent transition location is determined by using natural transition criterion based on linear stability theory. The total drag coefficient can be calculated directly.

Numerical shape optimizations were performed first by Parsons et al. [1]. In Pinebrook's study [2], the body geometry is not optimized in a direct method. Instead, a source and sink singularity distribution on the axis is used to model the body contour and to calculate the corresponding inviscid flow field. A statistical technique derived from Rechenberg's evolution strategy was also applied. In the shape optimizations presented by Lutz–Wagner [3], a semi-empirical e^n criterion based on the linear stability theory was applied to determine the natural transition location. Nejati and Matsuuchi [4] improved the Pinebrook's work by employing a powerful optimization procedure called Genetic Algorithms to find optimal shape with the global minimum drag coefficient.

2 Boundary layer flow

For the purpose of numerical shape optimization, high computational efficiency is required, and a numerical procedure, FVM, which is consistent to the geometry and physics of the problem, is applied for solving laminar and turbulent boundary layer equations for airship bodies. The coordinate system (x, y) is curvilinear, where x is parallel to the body surface and y is normal to it. This is illustrated in Fig. 1.

By assumption that flow is steady incompressible and axisymmetric, the governing equations for turbulent boundary layer are given as

$$\frac{\partial}{\partial x} ru + \frac{\partial}{\partial y} rv = 0 \qquad (1)$$

$$\rho u \frac{\partial u}{\partial x} + \rho v \frac{\partial u}{\partial y} = -\frac{dp_0}{dx} + \frac{1}{r}\frac{\partial}{\partial y} r\left\{ \mu \frac{\partial u}{\partial y} - \rho \overline{u'v'} \right\} \qquad (2)$$

where μ is viscosity, $r(x, y) = r_0(X) + y.\cos\alpha(X)$ and $r_0(X)$ is the body radius. It is worth to note that both longitudinal and transverse curvatures effects are considered in the formulation. The transverse curvature effects of solution domain become quite important when the radius of the body is small compared with the boundary layer thickness.

In order to model the Reynolds stress term $-\rho\overline{u'v'}$, one of the most frequently used two equation models $k-\varepsilon$ is employed. According to Launder and Spalding [5], at high Reynolds numbers, the final form of the transport equations for the turbulence kinetic energy k and its dissipation rate ε can be derived and by using Mangler transformation thetransport equations adequate for steady and axisymmetricturbulent boundary layer flow can be written as

$$\rho u \frac{\partial k}{\partial x} + \rho v \frac{\partial k}{\partial y} = \frac{1}{r}\frac{\partial}{\partial y} r\left\{ \left(\mu + \frac{\mu_t}{\sigma_k} \right) \frac{\partial k}{\partial y} \right\} + \mu_t \left(\frac{\partial u}{\partial y} \right)^2 - \rho\varepsilon \qquad (3)$$

$$\rho u \frac{\partial \varepsilon}{\partial x} + \rho v \frac{\partial \varepsilon}{\partial y} = \frac{1}{r}\frac{\partial}{\partial y} r\left\{ \left(\mu + \frac{\mu_t}{\sigma_\varepsilon} \right) \frac{\partial \varepsilon}{\partial y} \right\} + \mu_t C_{\varepsilon 1} \frac{\varepsilon}{k} \left(\frac{\partial u}{\partial y} \right)^2 - \rho C_{\varepsilon 2} \frac{\varepsilon^2}{k} \qquad (4)$$

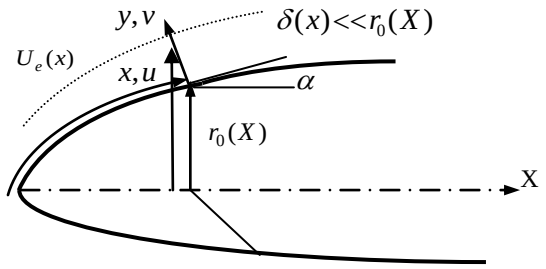

Figure 1. Curvilinear coordinate system for boundary layer on a body surface

where μ_t is turbulence viscosity given as

$$\mu_t = C_\mu \rho \frac{k^2}{\varepsilon}$$

In above equations C_μ, $C_{\varepsilon 1}$, $C_{\varepsilon 2}$, σ_k and σ_ε are modelconstants.

Since the boundary layer width is not uniform, the curvilinear (x, y) system is replaced by the mildly non-orthogonal (ξ, η) system. The lateral extent of the mesh is boundary layer thickness $\delta(x)$, which must be computed as a part of the solution procedure.

3 Transition predication

The reliable and consistent transition prediction is of essential importance for a successful shape optimization of laminar bodies. For this purpose a natural transition prediction such as linear stability theory should be employed. However transition prediction based on a complete analysis of stability theory requires too much computational effort and laborious calculations for the purpose of numerical shape optimization. An alternative is offered in the form of a database method.

The influence of the pressure gradient can be expressed by the use of a shape factor of the velocity profile and if this tedious calculation is carried out once for any shape factor, then a useful database reference can be generated. In this study, the exact velocity profile for axisymmetric body shape is calculated with the FVM and the dimensionless shape factor introduced by K. Pohlhausen can be calculated directly. For the determination of the instability point the method proposed by Schlichting and Ulrich (see Schlichting [6]) is used, and the transition point is determined based on the diagram found by Granville [7].

4 Genetic Algorithms

There are several optimization processes such as Rechenberg's Evolution Strategy (RES) and Genetic Algorithms (GA). GA can reach minimum objective function faster through a better path compared to the other optimization procedures such as RES. Since GA represents a special artificial intelligence technique for large spaces, it's one of the best optimization methods for such multi-dimensional, multi-model and nonlinear objective functions [8].

Genetic algorithms use a vocabulary borrowed from natural genetics. We would talk about *individuals* (or *genotypes*, *structures*) in a population; quite often these individuals are called also *strings* or *chromosomes.* This might be a little bit misleading: each cell of every organism of a given species carries a certain number of chromosomes (man, for example, has 46 of them); however, here we talk about one-chromosome individuals only. Chromosomes are made of units *genes* (also *features*, *characters*, or *decoders*) arranged in linear succession; every gene controls the inheritance of one or several characters. Genes of certain characters are located at certain places of the chromosome, which are called *loci* (string positions). Any character of individuals (such as hair color) can manifest itself differently.

Each genotype (here a single chromosome) would represent a potential solution to a problem; an evolution process run on a population of chromosomes corresponds to a search through a space of potential solutions. Such a search requires balancing two (apparently conflicting) objectives: exploiting the best solutions and exploring the search space. Hillclimbing is an example of a strategy, which exploits the best solution for possible improvement; on the other hand, it neglects exploration of the search space. Random search is a typical example of a strategy, which explores the search space ignoring the exploitations of the promising regions of the space. Genetic algorithms are a class of general-purpose (domain independent) search methods, which strike a remarkable balance between exploration and exploitation of the search space.

For the study we have selected two genetic algorithm implementations differing only by representation and applicable genetic operators, and equivalent otherwise: The binary implementation and floating-point implementation. Such an approach gave us a better basis for a more direct comparison. Both implementations used the same selective mechanism: stochastic universal sampling.

In particular, for parameter optimization problems with variables over continuous domains, we may experiment with real coded genes together with special genetic operators developed for them. The main objective behind such implementations is (in line with the principle of evolution programming) to move the genetic algorithm closer to the problem space. Such a move forces, but also allows, the operators to be more problems specific by utilizing some specific characteristics of real space.

In floating point representation each chromosome vector is coded as a vector of floating point numbers of the same length as the solution vector. Each element is initially selected as to be within the desired domain, and the operators are carefully designed to preserve this constraint (there is no such problem in the binary representation, but the design of the operators is rather simple; we do not see that as a disadvantage; on the other hand, it provides for other advantages mentioned below). The precision of such an approach depends on the underlying machine, but is generally much better than that of the binary representing. Of course, we can always extend the precision of the binary representation by introducing more bits, but this considerably slows down the algorithm.

The operators we use are quite different from the classical ones, as they work in a different space (real valued).

However, because of intuitive similarities, we will divide them into the standard classes, mutation and crossover. In addition, some operators are non-uniform, i.e., their action depends on the age of the population.

4.1 Crossover group

4.1.1 Simple crossover

Simple crossover**,** defined in the usual way, but with the only permissible split points between v's, for a given chromosome x.

4.1.2 Arithmetical crossover

Arithmetical crossover is defined as a linear combination of two vector: if s_v^t and s_w^t are to be crossed, the resulting offspring are $s_v^{t+1} = a.s_w^t + (1-a).s_v^t$ & $s_w^{t+1} = a.s_v^t + (1-a).s_w^t$. This operator can use a parameter a, which is either a constant (uniform arithmetical crossover), or a variable whose value depends on the age of population (non-uniform arithmetical crossover).

Here we have some new mechanisms to apply these operators; e.g., the arithmetical crossover may be applied either to selected elements of two vectors or to the whole vectors.

4.2 Mutation group

4.2.1 Uniform mutation

Uniform mutation**,** defined similarly to that of the classical version: if $x_i^t = (v_1,...,v_n)$ is a chromosome, then each element v_k has exactly equal chance of undergoing the mutative process. The result of a single application of this operator is a vector $(v_1,...,v_k^{'},...,v_n)$, with $1 \le k \le n$, and $v_k^{'}$ a random value for the domain of the corresponding parameter *domain.*

4.2.2 Non uniform mutation

Non uniform mutation is one of the operators responsible for the fine tuning capabilities of the system. It is defined as follows: the non uniform mutation operator was defined as follows: if $s_v^t = (v_1,...,v_m)$ is a chromosome and the element v_k was selected for this mutation (domain of v_k is $[l_k, u_k]$), the result is a vector $s_v^{t+1} = (v_1,...,v_k^{'},...,v_m)$, with $k \in \{1,...,n\}$, and

$$v_k^{'} = \begin{cases} v_k + \Delta(t, u_k - v_k) & if \quad random \quad digit \quad is \quad 0, \\ v_k - \Delta(t, v_k - l_k) & if \quad random \quad digit \quad is \quad 1, \end{cases}$$

where the function $\Delta(t, y)$ returns a value in the range $[0, y]$ such that the probability of $\Delta(t, y)$ being close to 0 increases as t increase. This property causes this operator to search the space uniformly initially (when t is small), and very locally at later stages. We have used the following function:

$$\Delta(t, y) = y.\left(1 - r^{(1-\frac{t}{T})^b}\right),$$

where r is a random number from [0,1], T is the maximal generation number, and b is a system parameter determining the degree of non uniformity.

Moreover, in addition to the standard way of applying mutation we have some new mechanisms: e.g., non uniform mutation is also applied to a whole solution vector rather than a single element of it, causing the whole vector to be slightly slipped in the space.

5 Results and Discussion

Pinebrook [2] applied Rechenberg's Evolution Strategy for the optimization of the airship bodies. For one example with a certain initial set of singularity elements, the minimum drag after 9600 generations was reported as 0.0273. We also carried out this example by employing the available computational program, but it could run only up to 400 generations. The minimum drag was compared with our result obtained from genetic algorithms for the same number of generations (also with the same initial parameters and Reynolds number). Fig. 2 shows that the best drag coefficient for evolution strategy is 0.0283 whereas the minimum drag in genetic algorithms is 0.0234, which is better, even than the reported result. This is because Rechenberg's evolution strategy is a type of random search, which explores the search space ignoring the exploitation. To show that GA has a remarkable balance between exploration and exploitation a 3-dimensional demonstration of reduction of drag coefficient for an example is plotted in Fig. 2 and it indicates clearly how GA exploits the best solution.

In the aerodynamics model presented by Nejati–Matsuuchi [4], the integral method and empirical relations are used to calculate the laminar and turbulent boundary layers. For simplicity, we call this model IM-FT, which is abbreviation of Integral Method and Forced Transition criterion. In this

study a new model is proposed. To improve the boundary layer calculation, IM together with the empirical relations is substituted with a powerful numerical method FVM. Furthermore the transition prediction is also modified and the natural transition criterion is added to aerodynamics calculations to get better estimation of the transition location. This model is abbreviated as FVM-NT which is referred to Finite Volume Method and Natural Transition.

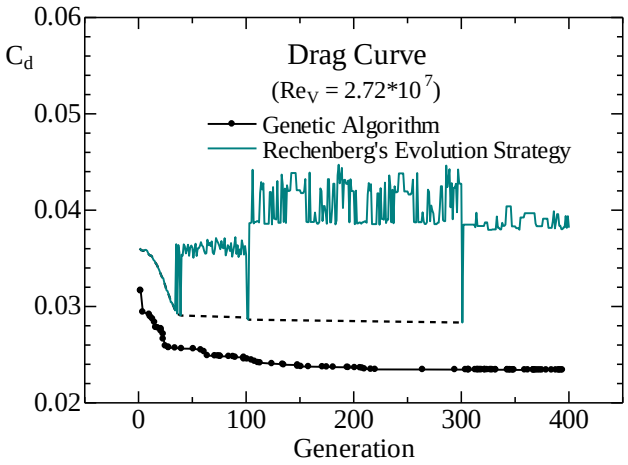

Fig. 2 Comparison of drag curves

The aerodynamics calculation is performed for a specified body shape with a volumetric Reynolds number $\mathrm{Re}_v = 9.39 \times 10^5$. The boundary layer calculations using FVM are carried out for this typical body shape. The natural transition point in this calculation is found to occur at 45% of the body length. The free-stream velocity distribution and the mean velocity profiles for some stages on the body surface are plotted in Fig. 3. The velocity profiles indicate laminar form up to 45% of the body length and exactly before the transition point *E*, flow approaches the laminar separation but transition occurs and flow becomes turbulent. It can be seen that around 50% of the body length, in point *F*, the flow becomes laminar one which means relaminarization. Downstream of this point, flow stays turbulent and near the end of the body at point *I* flow is ready to separate, but flow separation is avoided.

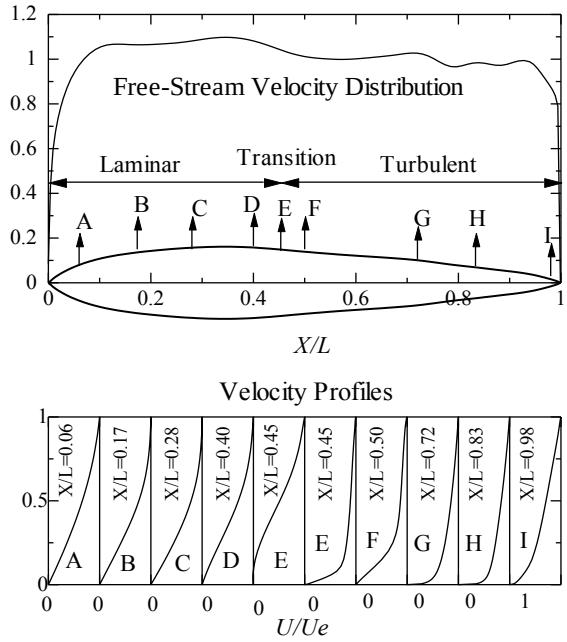

Figure 3. Free-stream velocity distribution and mean velocity profiles for specified body shape

To show the natural transition location effects on the drag coefficient in the various ranges of the Reynolds number another example is consideredfor a specified body shape used by previous investigators. For this example the airship body R101 (see Lutz–Wagner [3]) shown in Fig. 4 is taken into account, and present FVM-NT model is used to determine the drag coefficient. By increasing the free-stream velocity the Reynolds number is increased. As a validation aspect, the drag curve calculated by other investigators for this airship body is also given in Fig. 4. The experimental investigations for this shape were conducted independently by Jones and Schirmer. Schirmer performed his measurements in the wind tunnel of the former Zeppelin Company. To find the drag coefficient for this example, Lutz and Wagner used the integral method with semi-empirical e^n method. The calculated drag coefficient in this study shows satisfactory agreement with the experimental results, but in higher Reynolds number there occurs a turbulent separation almost near the end of the body and induce higher drag coefficient.

The shape optimization program is coupled with two different aerodynamics models, IM-FT and FVM-NT, in order to show the importance of aerodynamics calculation for achieving the optimal body shape. Lutz–Wagner [3] suggested five design regimes for the Reynolds number as shown in table 1. In the present research, we also carried out the optimization process for these five design regimes

to compare our results with those obtained by Lutz–Wagner.

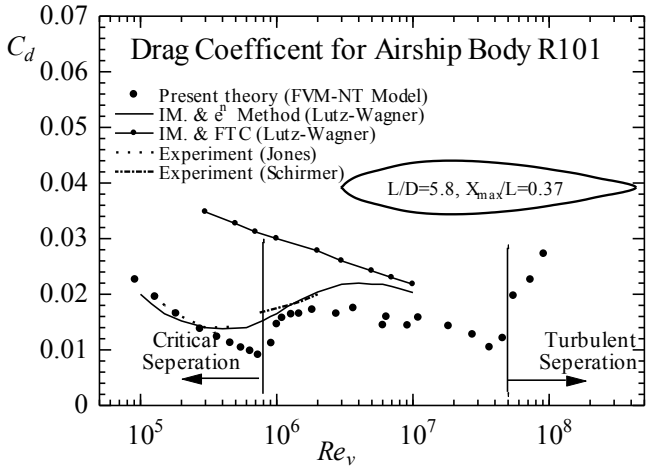

Figure. 4 Drag coefficient for airship body R101

Table 1 Design regimes

Regime	Re (min)	Re (max)
I	1.00E+06	3.16E+06
II	3.16E+06	1.00E+07
III	1.00E+07	3.16E+07
IV	3.16E+07	1.00E+08
V	1.00E+08	3.16E+08

Several optimization processes with IM-FT and FVM-NT models are carried out to find the optimal body shape with the minimum drag coefficient in each design regime. The minimum drag coefficient curves related to these two models are depicted in Fig. 5 and the results of Lutz–Wagner using the integral method with the semi-empirical e^n method are also drawn for comparison. Using FTC at 3% of the body length in IM-FT model gives bigger drag coefficient and has different drag curve.

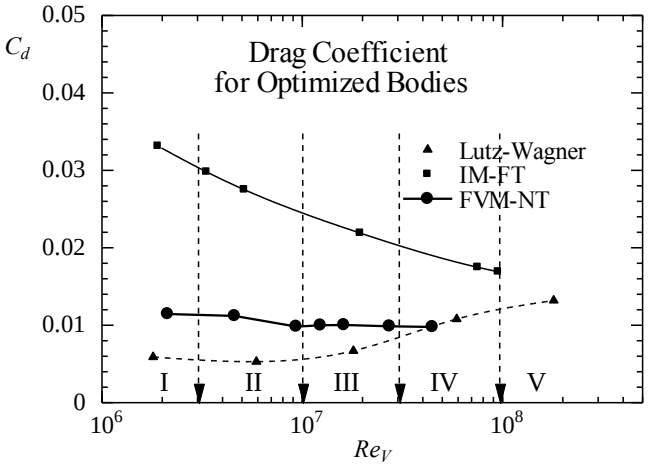

Fig. 5 Drag curve for range of Re_V

The drag coefficient obtained by FVM-NT model has a curve much similar to that obtained by Lutz–Wagner. However in low Reynolds number we get bigger drag coefficient because the transition in the optimal body shapes occurs earlier. In Lutz–Wagner results for low Reynolds numbers, the maximum radius position is located very far from the body nose. This means the existence of long favorite pressure gradient and long laminar flow on the body surface. As a result, much lower drag coefficient can be achieved.

6 Conclusions

The Finite Volume Method for boundary layer calculation is employed in order to improve the drag reduction process and to obtain the reliable optimal body shapes. We summarize our study as follows:

1) Since the Integral Method gives no velocity profile in the boundary layer domain, the drag coefficient cannot be found directly and is calculated with somewhat poor accuracy. On the other hand, in the Finite Volume Method the drag coefficient is obtained directly from the boundary layer solution. In the Integral Method the separation of the turbulent flow is judged according to the value of the shape factor and therefore the results showing no separation may be unreliable. In contrary to the Integral Method, the Finite Volume Method can estimate the separation correctly because it evaluates the velocity profiles. Furthermore the transverse curvature effects are neglected in the Integral Method. The Finite Volume Method can take these effects into account completely.

2) The laminarization plays an important role in the shape optimization. It is concluded that the natural transition criterion should be used to estimate correctly the region of

natural laminar flow. As a result, the body geometry changes as the location of the maximum body thickness moves as far aft as possible.

3) Since Genetic Algorithms strike a remarkable balance between exploration and exploitation of search space, it can reach to minimum objective function faster through a better path, whereas Rechenberg's evolution strategy is a random search type method ignoring the exploitation. Comparing the two methods, it is concluded that for large spaces, with multi-dimensional, multi-modal and nonlinear objective functions, GA is more accurate.

7 Acknowlegement

I would like to appreciate Professor Kazou Matsuuchi from University of Tsukuba, Japan. He was my supervisor in PHD program and conducted me to improve my computational calculations.

8 References

[1] J. S. Parsons, and R. E. Goodson, Shaping of Axisymmetric Bodies for Minimum Drag in Incompressible Flow, J. Hydronautics, Vol. 8, No. 3, 1974.

[2] W. E. Pinebrook, Drag Minimization on a Body of Revolution, Dissertation in the University of Houston, 1982.

[3] Th. Lutz, and S. Wagner, Numerical Shape Optimization of Natural Laminar Flow Bodies, ICAS-98-2, 9,4, 1998.

[4] V. Nejati, and K. Matsuuchi, Aerodynamics Design and Genetic Algorithms for Optimization of Airship Bodies, JSME International J., Series B, Vol.46, No.4, 2003.

[5] B. E. Launder, and D. B. Spalding, The Numerical Computation of Turbulent Flows, Computer Methods in Applied Mechanics and Engineering 3, pp. 269-289, 1974.

[6] H. Schlichting, Boundary Layer Theory, 7th ed., translated by J. Kestin, McGraw-Hill, New York, 1979.

[7] P. S. Granville, The Calculation of Viscous Drag of Bodies of Revolution, Navy Department, The David Taylor Model Basin, Rep. No. 849 1953.

[8] Z. Michalewicz, Genetic Algorithms + Data Structures = Evolution Programs, Springer-Verlag, 1992.

Formalization of Data Stream Clustering Properties and Analysis of Algorithms

Marcelo Keese Albertini e Rodrigo Fernandes de Mello
Department of Computer Sciences
Institute of Mathematics and Computer Sciences
University of Sao Paulo
Av. Trabalhador Sãocarlense 400, São Carlos - SP, Brazil
{*albertini, mello*}*@icmc.usp.br*

***Abstract*—The understanding of several phenomena requires unbounded data collections, called data streams. These phenomena often present unstable behavior and are studied by means of unsupervised induction processes based on data clustering. Currently, clustering processes have shown serious limitations in their applications to data streams due to the demands imposed by behavioral changes and unlimited data collection. However, despite the key distinctions in between traditional data sets, which are finite and unordered, and data streams, which are essentially infinite sequences, studies have overlooked the dynamic and transient nature of streams, limiting the appropriate understanding of phenomena. The lack of a theoretical analysis for the problem of data streams clustering led us to propose, in this paper, a formalization based on Set Theory. This formalization made it possible to identify and propose basic properties for the design and comparison of data stream clustering algorithms. It is expected to be a starting point to understand the foundations of unsupervised induction based on clustering and, mainly, the modeling of phenomena.**

Keywords: Artificial Intelligence; Machine Learning; Data Mining; Unsupervised Learning; Data Clustering; Data Streams; Set Theory

I. Introduction

The literature from several research fields has described two main types of phenomena that produce endless sequences of data also referred to as data streams [11], [12]. The first type is characterized by the need for data storage space and fast computation. In this situation, data is stored in secondary memory, which presents low transfer rates, and usually accessed in a contiguous manner. The second type is even more computationally demanding: data is collected at high rates and shortly afterwards is disposed. In this type, clustering models must be continuously obtained throughout the endless data-gathering process, whose dynamical properties, i.e., behavior, are expected to evolve over time [7], [12]. Data streams are frequently found in computationally intensive environments, such as climate and weather analysis [2], text mining [10], [9], genomic analysis, and advanced scientific experiments [18], [19].

The typical clustering process has been designed to approach finite and unordered data sets and, consequently, does not meet data streams requirements [20]. There exist great distinctions between clustering requirements for data sets and data streams. Firstly, a data stream must be accessed and processed sequentially as it cannot be completely stored in memory. Secondly, the open-endedness nature of data streams demands continuous and automatic analysis. Thirdly, while stable phenomena can be accurately represented by bounded data sets and are suitable to traditional data clustering, data streams, on the other hand, usually represent unstable phenomena [7], whose characteristics tend to change over the collection. This tendency indicates the transient nature of data streams and demands a continuous re-evaluation of clustering models. Finally, the role of domain experts when clustering data streams is different from clustering data sets. In the latter, specialists are often required to empirically extract, select and analyze data features in order to define the clustering algorithm and the validation criterion. Conversely, in data streams, the fast and continuous production of large amounts of data restricts human intervention, due to the limited capability of specialists to make well-founded decisions under such constraints.

In order to better understand data set clustering, Kleinberg [8] formalized three properties, which allow the analysis of algorithm capabilities independently of the target application. The formalization of the data-set clustering problem is an important step towards its deep understanding. Recently, several studies concerning the usage and proposition of properties to related problems have been developed [5], [4], [22]. These studies have broadened the possibilities to analyze clustering algorithms, although very few of them have been conducted in the context of data streams.

The lack of formal studies on the problem motived our formalization of data stream clustering as an extension of Kleinberg's approach to data sets [8]. In

such a definition, data stream clustering is described in terms of an infinite sequence of partitions, which are modified along time. The endless and changing nature of data streams requires properties different than those proposed by Kleinberg for finite and unordered data sets. Data streams, as infinite and ordered sequences, need clustering properties representative of the time evolution and behavior changing.

We have extended Kleinberg's properties to represent clustering partitions evolving according to the data stream behavior. In addition, we introduce the **Coherence** property, which states that partitions must continously evolve over time in order to preserve the meaning of the clustering process. However, we observed that this property is incompatible with the Kleinberg's Richness, which states that a data-set clustering function must be capable of generating any partition. This conflict indicates that trade-off analyses are needed in order to demand properties from algorithms. Additionally, we noticed that it is difficult to find an algorithm to comply with Richness in a data stream context.

The remainder of this paper is organized as follows: Section II introduces studies on data set clustering; Section III describes our formalization approach to data streams; Section IV draws conclusions and present ideas for future work; and, finally, references are listed.

II. Related Work

Kleinberg [8] considered concepts of Set Theory [14] to describe clustering algorithms in general terms, i.e., without relying on a specific algorithm, objective function for optimization, or statistical model. This analysis is important to understand the functioning of algorithms beforehand, i.e., without the need for experimental trials, and also to provide design guidelines for new approaches.

The concepts involved in Kleinberg's formalization are illustrated in Figure 1. This formalization assumes data elements are organized in set E, whose measurements of dissimilarity in between elements are provided in a square matrix. This matrix, d, is described in the form of a function $d : E \times E \rightarrow \mathbb{R}^+$, and is applied to two elements $\{i, j\} \in E$ to obtain a dissimilarity value $d(i, j)$ in $[0, \infty)$. The construction of d determines the possibility of a clustering algorithm to organize the elements in E. A cluster is essentially an organization of elements of E into subsets, so that each element is contained in one, and only one, subset. This structure is known as the **partition** of a set. Partitions are denoted by uppercase Greek letters, such as Γ (Gamma) and Υ (Upsilon). A clustering algorithm is, therefore, a function $f(d)$, which considers a distance matrix d for mapping elements in E into a partition belonging to the universe of partitions U.

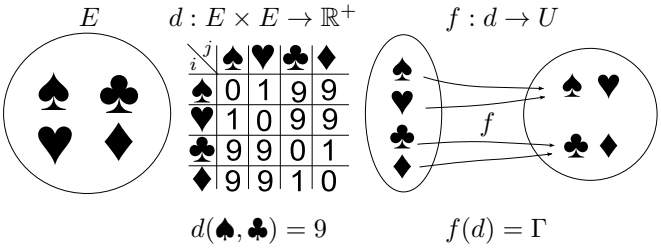

Figure 1. Illustration of concepts of data set clustering

By using this formalization, Kleinberg proposed properties to data set clustering introduced in the form of statements of principles or self-evident conditions to a well-succeeded clustering algorithm. The author initially proposed three properties: Scale-Invariance, Richness and Consistency.

Scale-Invariance refers to the ability of algorithms to abstract the measurement scale of elements, i.e., for any distance function d and constant $\alpha > 0$, we have $f(d) = f(\alpha \cdot d)$. This property reflects the expectation that the magnitude of the scale of elements should not change the partition; for example, adapting elements from centimeters to inches should not modify the partitions obtained.

Richness refers to the ability of an algorithm to induce all possible partitions for a set of elements. When Richness holds, for any partition Γ of E, there exists a distance matrix d for which $f(d)$ results in Γ. It applies the concept of surjection of Set Theory [14], which defines the image of the surjective function as being equal to its counter-domain. This property assumes it is possible to arrange elements by modifying their relative distances in order to obtain all partitions. A clustering algorithm complies with **Richness** if and only if it permits obtaining all partitions for the elements in E, otherwise some partitions are impossible to be found.

Ensuring the possibility of finding all partitions for a data set, as required by Richness, appears, at first, desirable for an algorithm whose data nature is unknown. However, this property may be difficult to comply with [8].

Consistency refers to the ability algorithms have to maintain the same partition when distances among elements within the same group are reduced while distances among elements of different groups are increased. For example, consider a partition Γ generated by a clustering function f, according to a distance function defined by d. Also consider changing d into d' in a way that it increases the distances among elements of distinct subsets of Γ and reduces the distances among elements of the same subset. A consistent clustering function $f(d')$ always generates a partition Γ' equivalent to Γ, in the sense

that $f(d') = f(d)$.

The previously described Kleinberg's properties have proven too demanding for a clustering function to comply with, resulting in the incompatibility among them. Kleinberg [8] proved, in an impossibility theorem, that only two out of these three properties could be satisfied by any algorithm. Although the practical consequences of the impossibility theorem are limited, mainly because small adaptations to the properties avoid the impossibility, Kleinberg's approach has motived several studies to further understand data clustering [5], [4], [22]. Among those studies, very few are relevant to data streams. To the best of our knowledge, the only exception is the paper by Ryabko [15]. It deals with the problem of clustering stationary stochastic processes, in which the author claims that two elements must be associated with the same cluster if and only if they are generated by the same probability distribution. Nonetheless, the usefulness of this result is limited in the context of data streams, in which the behavior of sequences changes over time.

III. Clustering data streams

Data streams differ from other types of data traditionally considered in Machine Learning. They are infinite sequences with unknown and unstable behavior [6]. These characteristics contrast with traditional data sets, which are finite, have no particular order, and are characterized by a stable behavior. These distinctions have motivated the adaptation of Kleinberg's data set properties to data streams.

In this context, a data stream is defined as an infinite and ordered set of elements, that is, a sequence $S = (s_{t_{-\infty}}, \ldots, s_{t_{-k}}, \ldots, s_{t_0})$, in which elements are indexed by $t \in \mathbb{R}$. The data collection is performed at time instants t whose order is given by integers $k \in (0, \infty)$.

The complete sequence is represented by S, while a sub-sequence of data collected up to a time instant t is S_t. Every element s_t in this sequence consists of a vector of values v, i.e., the data features obtained. The elements in S_t are comparable by a dissimilarity function $d : S \times S \to \mathbb{R}^+$.

The main goal of a data-stream clustering algorithm $f(d, S)$ is to generate a sequence of partitions $\bar{\Gamma}_{t_0} = \{\Gamma_{t_{-\infty}}, \ldots, \Gamma_{t_0}\}$ for elements in S_{t_0}, in which $\Gamma_{t_0} = f(d, S_{t_0})$. The sequence of partitions is created from the first data-stream element $S_{t_{-\infty}}$ until the most recent element S_{t_0}. Although S is infinite, partitions in $\bar{\Gamma}$ have a finite number of non-intersecting subsets. As a result of practical requirements of the data streams analysis, although S is infinite, every partition in $\bar{\Gamma}$ may use only a finite subset of S. Therefore, the design of f can consider the option of removing a convenient subset of elements R if they are represented by other elements or even expired.

In summary, the main difference of the problem of data stream clustering, when compared to data set clustering, originates from the infinite and ordered nature of such scenarios, which demands a sequence of partitions over time, instead of a single one.

A. Data-stream clustering properties

The differences between the data-set clustering problem and the data stream one motivated the adaptation of Kleinberg's properties. We observed these properties do not assure that clustering partitions *smoothly* evolve according to the data stream behavior. Therefore, we introduce the property of **Coherence**, which states that a coherent algorithm for data-stream clustering creates partition sequences in which elements do not drastically change from one cluster to another. This property ensures that clustering algorithms maintain continuity in between consecutive partitions.

Firstly, the Time-space Scale Invariance property, equivalent to Kleinberg's property of Scale Invariance, suggests that algorithms should produce the same partition if the measurement scale of space or times is transformed by a multiplicative constant.

Property 1: Time-space Scale Invariance – Consider the multiplication of distances d by a positive constant α, $\alpha \cdot d$, and the time indexes of each element $s_t \in S$ by another positive constant β, $s_{\beta \cdot t}$. The sequence of partitions $f(d, s_t)$ is equal to $f(\alpha \cdot d, s_{\beta \cdot t})$.

Similarly, the properties of Richness in Data Streams and Time-space Consistency are adaptations of Richness and Consistency for data sets. Both properties consider a notion of temporal proximity, and, therefore, differ from properties to data set clustering in terms of a reference point in time to conduct comparisons among partitions.

Property 2: Richness in Data Streams – Consider a reference point in time t_0, a sequence $S_{t_0} = (s_{-\infty}, \ldots, s_{t_0})$ observed until t_0, and a matrix of dissimilarity d among elements in S_t. The clustering function f complies with Richness in Data Streams at instant t_0 through an arbitrary transformation of d and in the order of elements in S_t if it is capable of obtaining all possible partitions for $(s_{-\infty}, \ldots, s_{t_0})$.

The Time-space Consistency property extends Consistency by including the notion of temporal proximity. It states that if elements in the same cluster are temporal and spatially closer to each other and, at the same time, elements of different clusters are farther, then the partition sequence is maintained.

Property 3: Time-space Consistency – Consider d' and S'_t are transformations of matrix dissimilarity d and observation sequence S_t such that the intervals of the occurrence of elements within a cluster become shorter and those of different clusters become longer.

A clustering function f complies with space-temporal consistency if and only if $f(d, S_t) = f(d', S'_t)$.

The proposed properties are directly related to those defined for data-set clustering. Nonetheless, the data stream properties based on Kleinberg's study do not oblige a clustering algorithm to obtain a logical sequence of partitions for data streams. For practical purposes, the guarantee that an algorithm will not randomly assign samples to distinct clusters in consecutive partitions is desirable. For example, in the context of concept drift [13], the evaluation of clusters over time is required. However, if consecutive partitions do not share a sense of continuity, the evaluation becomes meaningless.

The continuity of partitions (Definition 2) is formalized by a relation named **reach**, represented by $\triangleright$, according to Definition 1. It is inspired in the concept of **refinement** by Kleinberg [8], which states that a partition Γ is a refinement of Υ if and only if each subset in Γ either belongs to Υ or is contained in one of its subsets.

Definition 1: A partition Γ **reaches** another partition Υ if, for every subset $A \in \Gamma$, there is another subset $B \in \Upsilon$, such as $(A \setminus R^{\Gamma}) \subseteq (B \setminus R^{\Upsilon})$ or $(B \setminus R^{\Upsilon}) \subseteq (A \setminus R^{\Gamma})$, given that operation $\setminus$ is defined by $B \setminus A = \{s \in B | s \notin A\}$ and R^{Γ} is the subset of elements in Γ that do not belong to Υ, and R^{Υ} is the subset of elements in Υ that are not in Γ. The relation **reach** is denoted by $\Gamma \triangleright \Upsilon$.

Continuity (see Definition 2) is relevant to the analysis of capability of clustering algorithms to capture the behavior evolution of data streams.

Definition 2: A partition sequence $\bar{\Gamma}_t$ is **continuous** if and only if for all consecutive partitions, i.e., Γ_{t-i-1} and Γ_{t-i}, in which $i \geq 0$, the relation $\Gamma_{t-1} \triangleright \Gamma_t$ is true.

The guarantee of generating continuous partitions is stated by the Coherence property. The Coherence of a clustering algorithm allows, for example, employing measurements to evaluate partition sequences and support the exploratory analysis of phenomena.

Property 4: Coherence – For any d, S_t, and $\Gamma_t = f(d, S_t)$, the partition sequence $\bar{\Gamma}_t$ is always continuous.

The time dimension is included in the first three properties proposed to formalize the data stream clustering. However, these properties do not approach the generation of an infinite sequence of partitions, which contrasts with the data set clustering defined only by one partition. In this sense, the coherence of data-stream clustering algorithms is probably the most important property. The main relevance of the Coherence property relies on the fact it provides a parallel between clustering continuity and function continuity, allowing to evaluate differences in clustering models over time. By measuring such differences, it is possible to better the understand phenomena represented by data streams. However, as shown in the next subsections, Coeherence can be incompatible with other properties, and, sometimes, is not respected by some current important algorithms. For example, the usage of the k-means algorithm for clustering data streams, whose data are pre-organized in the form of micro-clusters, as performed by BIRCH [23] and CLUSTREAM [1] will not guarantee the continuity of partitions and, eventually, may not represent phenomena behavior.

B. Analysis of clustering algorithm properties

The formalization we have proposed is aimed at evaluating and supporting the design of data-stream clustering algorithms. In a similar approach, Kleinberg [8] considered the three previously mentioned data-set clustering properties to prove no algorithm respects them simultaneously.

Based on Kleinberg's study, we have observed a similar impossibility theorem to obtain a data-stream clustering algorithm for the first three properties proposed. Furthermore, we have also observed that Properties 2, Richness in data streams, and 4, Coherence, are mutually exclusive, because the latter limits the possibilities to produce partitions. In order to prove it, we show that if a data-stream clustering function f complies with Richness, then it necessarily generates sequences of partitions $\bar{\Gamma}$ in which at least a pair of consecutive partitions does not respect the relation **reach**; and, also, if f generates only continuous sequences of partitions, then it does not complies with Richness. Theorem 1 shows the impossibility of designing a data-stream clustering algorithm with the properties of **Coherence** and **Richness** in data streams.

Theorem 1: There is no data-stream clustering function f that complies with Properties 2 and 4.

Proof:

First part: suppose f complies with Richness in data streams, then f generates a partition sequence $\bar{\Gamma}_t$ containing consecutive partitions that do not **reach** each other.

We will show that there is a sequence $\bar{\Gamma}_t$ with partitions that do not **reach** each other, regardless of changes in both distances d and the sequence of elements S_t. A partition Γ_t is unreachable when there is no partition Γ_{t-1} preceding it, so that the relation $\Gamma_{t-1} \triangleright \Gamma_t$ is not respected, that is, the set of all possible partitions at instant $t-1$ is empty.

It suffices to provide an example in order to prove that there is an unreachable Γ_t. Take a partition at time instant t, $\Gamma_t = \{\{a_1, b_2\}, \{a_2, b_1\}\}$, where elements a_i, $\forall i$ and b_j, $\forall j$ in $\Gamma_{t-1} = \{\{a_1, a_2\}, \{b_1, b_2\}\}$ are in different clusters.

It is known that $\{\{a_1, a_2\}, \{b_1, b_2\}\} \triangleright \{\{a_1, b_2\}, \{a_2, b_1\}\}$ is not valid, because, according to the definition of the relation **reach**, no subset of the

first partition is contained in a subset of the second one, and reciprocally. It is also known that, by definition, any f that complies with Richness in data streams is supposed to generate such a sequence of partitions.

Second part: if f generates only continuous partition sequences, then f does not comply with Richness in data streams. Consider the following partition $\Gamma_{t-1} = \{\{a_1, a_2\}, \{b_1, b_2\}\}$, then f cannot generate $\Gamma_t = \{\{a_1, b_2\}, \{b_1, a_2\}\}$ in the next time instant t, and, similarly, if we take $\Gamma_{t-1} = \{\{a_1, b_2\}, \{b_1, a_2\}\}$, then f will not generate $\Gamma_t = \{\{a_1, a_2\}, \{b_1, b_2\}\}$.

Therefore, no f that generates continuous partition sequences may comply with Property 2. □

C. Analysis of data stream clustering algorithms

The use of properties for the analysis of clustering algorithms is incipient. However, such properties allow the understanding of theoretical principles for the design and selection of algorithms, taking into account utility and economic factors inherent to the application domain [3].

The properties we have introduced are the first to represent the inherent characteristics of data streams. In summary, these properties are Time-space Scale Invariance, Richness in Data Streams, Time-space Consistency and Coherence. We present a comparison among the most relevant data stream clustering algorithms, which is summarized in[1] Table I based on the properties proposed. Among the algorithms are Birch [23], WaveCluster [16], CluStream [1], Olindda [17] and *Starvation* Wta [21]. Observe that none of the algorithms complies with the property of Richness.

Table I
Evaluation of properties for data stream clustering algorithms

Algorithm	T-S Scale Invariance	T-S Consistency	Coherence
Birch	N	N	N
WaveCluster	N	—	N
CluStream	N	N	N
Olindda	Y	N	N
Wta	Y	Y	Y

(1) T-S means Time-space.

(2) Value 'Y' means yes and 'N' means no.

Usually, to verify that algorithms comply with such properties, one can prove a theorem or present a counterexample. However, in some cases none of the two options is possible. On the other hand, there are other options to check whether an algorithm respects a given property. For example, when an algorithm limits the number of groups, it does not comply with the property of Richness. An algorithm does not comply with Property 1, i.e., Time-space Invariance, if it considers any threshold for accepting elements in clusters as there is always a scalar constant that, multiplied by the distances among elements, will modify the partition produced. Still, an algorithm does not comply with Property 1 and Property 4 if it does not consider the order of data during clustering.

Another analytic option considers the evidence previously established for algorithms used to cluster traditional data sets, such as k-means and hierarchical algorithms (e.g., Single-linkage) [1], [23]. For example, algorithms that use k-means in the clustering process do not comply with Property 4 because k-means does not guarantee the continuity in sequences of partitions. Among such algorithms, Birch and CluStream are some of the most commonly considered data stream clustering algorithms.

[1]The symbol '—' represents that it was not possible to achieve an evaluation. We omit further details on verifying algorithm properties due to lack of space.

IV. Conclusions and Future Work

Despite the fundamental differences between data set and data stream clustering, many studies have overlooked the infinite, dynamic and transient nature of the latter. In this paper, we formally tackled the problem of data-stream clustering as an infinite sequence of partitions. This approach is an extension of Kleinberg's properties. Besides adapting Kleinberg's properties to data streams, we also proposed a new property referred to as **Coherence**, which deals with the infinite and sequential properties of data streams. This new property was proven to be incompatible with **Richness**, evidencing the trade-off in between both properties when designing data-stream clustering algorithms. The existence of few related studies in this theoretical branch indicates that this is a seminal study and also that there are plenty of possibilities towards developing a clustering theory.

Acknowledments

This paper is based upon work supported by FAPESP – São Paulo Research Foundation, Brazil, under grants no. 2006/05939-0 and 2011/19459-8, "CAPES – Brazilian Federal Agency for Support and Evaluation of Graduate Education" research funding agency under grant no. PDEE-4443-08-0, CNPq – National Council for Scientific and Technological Development research funding agency under grant no. 304338/2008-7. Any opinions, findings, and conclusions or recommendations expressed in this material are those of the authors and do not necessarily reflect the views of FAPESP, CAPES and CNPq.

References

[1] C. C. Aggarwal, J. Han, J. Wang, and P. S. Yu. A framework for clustering evolving data streams. In *Proceedings of the 29th international conference on Very Large Data*

Bases, volume 29, pages 81–92, Berlim, Alemanha, 2003. VLDB Endowment.

[2] B. Allcock, I. Foster, V. Nefedova, A. Chervenak, E. Deelman, C. Kesselman, J. Lee, A. Sim, A. Shoshani, B. Drach, et al. High-performance remote access to climate simulation data: A challenge problem for data grid technologies. In *SC2001 Conference*, pages 1334–1356, 2001.

[3] S. Ben-David and M. Ackerman. Measures of clustering quality: A working set of axioms for clustering. In *Advances in Neural Information Processing Systems 21*, pages 121–128. 2009.

[4] G. Carlsson and F. Mémoli. Characterization, Stability and Convergence of Hierarchical Clustering Methods. *Journal of Machine Learning Research*, 11:1425–1470, 2010.

[5] G. Carlsson and F. Mémoli. Persistent clustering and a theorem of J. Kleinberg. *ArXiv e-prints*, 1:17, 2008. http://adsabs.harvard.edu/abs/2008arXiv0808.2241C.

[6] S. Guha, A. Meyerson, N. Mishra, R. Motwani, and L. O'Callaghan. Clustering Data Streams: Theory and Practice. *IEEE Transactions on Knowledge and Data Engineering*, 15(3):515–528, 2003.

[7] D. Kifer, S. Ben-David, and J. Gehrke. Detecting change in data streams. In *Proceedings of the Thirtieth international conference on Very Large Data Bases*, volume 30, pages 180–191, Toronto, Canada, 2004. VLDB Endowment.

[8] J. Kleinberg. An impossibility theorem for clustering. In *Proceedings of Advances in Neural Information Processing Systems 15*, pages 446–453. The MIT Press, 2002.

[9] P. Lindstrom, S. J. Delany, and B. Mac Namee. Handling Concept Drift in a Text Data Stream Constrained by High Labelling Cost. In *Proceedings of the Twenty-Third International Florida Artificial Intelligence Research Society Conference*, page 52, Daytona Beach, USA, 2010.

[10] M. Masud, Q. Chen, J. Gao, L. Khan, J. Han, and B. Thuraisingham. Classification and Novel Class Detection of Data Streams in a Dynamic Feature Space. *Machine Learning and Knowledge Discovery in Databases*, 6322:337–352, 2010.

[11] L. O'Callaghan, N. Mishra, A. Meyerson, S. Guha, and R. Motwani. Streaming-data algorithms for high-quality clustering. In *Proceedings of the 18th International Conference on Data Engineering*, pages 685–694, San Jose, USA, 2002. IEEE.

[12] N. G. Pavlidis, D. K. Tasoulis, N. M. Adams, and D. J. Hand. [lambda]-Perceptron: An adaptive classifier for data streams. *Pattern Recognition*, 44(44):78–96, 2011.

[13] P.P. Rodrigues, J. Gama, and J.P. Pedroso. Hierarchical clustering of time-series data streams. *IEEE Transactions on Knowledge and Data Engineering*, pages 615–627, 2007.

[14] H. L. Royden. *Real Analysis*. Macmillan, New York, USA, 2 edition, 1968.

[15] D. Ryabko. Clustering processes. In *Proceedings of the 27th International Conference on Machine Learning*, pages 919–926, Haifa, Israel, 2010.

[16] G. Sheikholeslami, S. Chatterjee, and A. Zhang. Wavecluster: A multi-resolution clustering approach for very large spatial databases. In *Proceedings of the International Conference on Very Large Data Bases*, pages 428–439, New York, USA, 1998. Citeseer.

[17] Eduardo Spinosa, A. C. P. F. de Carvalho, and J. Gama. OLINDDA: a cluster-based approach for detecting novelty and concept drift in data streams. In *Proceedings of the 2007 ACM Symposium on Applied Computing*, pages 448–452, New York, USA, 2007. ACM.

[18] G. W. Swenson Jr. and K. I. Kellermann. An Intercontinental Array–A Next-Generation Radio Telescope. *Science*, 188(4195):1263, 1975.

[19] T. Tyson, R. Pike, M. Stein, and A. Szalay. Managing and Mining the LSST data sets. Technical report, The LSST Collaboration, Tucson, USA, 2002.

[20] R. Xu and D. Wunsch. Survey of clustering algorithms. *IEEE Transactions on neural networks*, 16(3):645–678, 2005.

[21] S. Young, I. Arel, T.P. Karnowski, and D. Rose. A Fast and Stable Incremental Clustering Algorithm. In *2010 Seventh International Conference on Information Technology*, pages 204–209, Shanghai, China, 2010. IEEE.

[22] R. B. Zadeh. Towards a Principled Theory of Clustering. Unpublished. Available at: http://www.stanford.edu/~rezab/papers/principled.pdf., 2010.

[23] T. Zhang, R. Ramakrishnan, and M. Livny. BIRCH: an efficient data clustering method for very large databases. *Proceedings of the International Conference on Management of Data*, 25(2):103–114, 1996.

A New Clustering Algorithm Using Fuzzy Logic In Wireless Sensor Networks

Mohammad Hossein Yaghmaee Moghaddam
IEEE Senior Member,
Computer Engineering Department,
Islamic Azad University,
Mashhad Branch, Mashhad, Iran
Email: yaghmaee@ieee.org

Ozra Rezvani
Computer Engineering Department,
Islamic Azad University,
Mashhad Branch, Mashhad, Iran
Email: rezvani_oz@yahoo.com

Abstract— **The network lifetime is one of the important factors in wireless sensor networks and is dependent on the network energy. Energy source in the network is very limited. In order to increase the network lifetime, energy saving should be considered. Clustering method is the one of the ways to consume energy efficiently that causes uniform load distribution and balanced energy consumption. In this essay, a new method for optimal selecting cluster head and clustering is presented using fuzzy logic. In the proposed method, a radius can be assigned for sensor with the help of fuzzy rules and fuzzy variables, energy and distance. Then cluster head sensors are elected with the help of fuzzy rules and energy and number of neighboring sensors as two fuzzy variables. Thus, the best sensors are selected as a Cluster head. Furthermore, with the help of obtained radius, cluster size is controlled with regard to distance from the base station. It means that clusters close to the base station are larger than far clusters. Therefore, in the proposed protocol the network energy consumption, which is uniformly distributed in the network, is reduced. MATLAB simulation results indicate that the proposed protocol managed to increase network lifetime more than LEACH and EECS protocols.**

Keywords- Cluster head, clustering, fuzzy logic, wireless sensor networks, network lifetime, sensor (node)

I. INTRODUCTION (HEADING 1)

Wireless sensor networks consist of many small, inexpensive sensors. Sensors are capable of processing, energy and have a limited memory. In wireless sensor networks, they collect data related to the environment events and send them to the base station [1]. Nowadays, wireless sensor networks have many usages in human life. Among these applications, monitoring the environment of humans and animals life, fire detection, flood, medical applications and military issues can be mentioned [2].

One of the most important factors in designing wireless sensor networks is energy. It is not possible to recharge or replace the sensors energy sources since the energy source in sensors is limited (because of the numerous number of sensors) and lack of access to them in different geographic environments in the network, [3] [4].

Therefore, energy is very important in saving wireless sensor networks and many researches have been presented on the field of optimizing energy consumption and increasing network lifetime. Among the protocols presented, hierarchical protocols based on clustering are efficient in energy consumption.
In these protocols, the network is divided into parts called clusters. In each cluster, a sensor is selected as a cluster head. Other cluster sensors collect data from the environment and send them to cluster head. After data collection, cluster head aggregates them in order to delete repetitive data and eventually sends them to the base station. In these protocols, only cluster heads communicate with the base station and other sensors are connected to cluster heads.

Therefore, in these protocols, selecting a sensor as cluster head and aggregating data will significantly result in saving energy. Reducing energy consumption can increase the network lifetime because of direct connection in wireless sensor networks between reducing energy consumption and increasing the lifetime of the network. In this essay, a new efficient protocol in energy consumption is presented with the help of fuzzy logic and considering distance and energy as two variables to determine the sensors radial range and considering energy and number of the neighboring sensors as two variables in cluster head selecting process.

As we follow, in section 2 past works are discussed, in section 3 the proposed protocol is presented and in section 4 simulation is performed.

II. REVIEWING PAST WORKS

There have been many researches to optimize energy consumption in wireless sensor networks and a lot of clustering algorithms have been discussed. LEACH algorithm [1] [7] is one of the first cluster routing methods presented for sensor networks .In LEACH protocol, time is divided into the parts called the round and each round is divided into two phases. The first phase is called set-up phase in which clusters are formed and the second phase, which is related to normal network function, is called the steady-state phase .In the first phase, using a probability function, head clusters are selected. Each sensor selects a random number between zero and one. If this number is smaller than a specified threshold (T), the sensor is

selected as the cluster head during the round. This probability function is designed so that each sensor is selected as cluster head only once within a certain number of rounds, and thus energy consumption is spread over the entire network. After cluster heads were selected in the set-up phase, each cluster head announces the selecting news to the other sensors and other sensors select the nearest cluster head as their cluster head, then they inform the related cluster head. In the second phase, each sensor sends data to its cluster head and cluster head combines the received data and sends it to the base station.

LEACH protocol also has disadvantages. For example, the cluster head may be placed close to each other. In addition, remaining energy of the sensor for selecting cluster head is not considered; therefore, a sensor containing very little energy may also be selected as cluster head. Similarly, cluster head may be placed in one low-density position or be placed on the edge of the network.

LEACH-C algorithm [1], is the way in which the cluster heads are selected based on sensors position data and the amount of remaining energy. In the set-up phase, each sensor sends information about its status and remaining energy to the base station. Then the base station chooses the cluster heads based on this information. One of the advantages of this method is that by placing the head clusters in the center of cluster, the energy consumption will evenly be distributed between the sensors.

In algorithm [8], a cluster head selecting method is presented using fuzzy logic. In this protocol, cluster heads are selected with the help of two variables, energy and local distance, within a constant radius. Local distance is the total of the distances of neighboring sensors within the radius.

In [9], a fuzzy algorithm for selection of cluster heads has been suggested. In this algorithm, cluster heads are elected by the base station. It means at first the sensors send data to the base station in the network and the base station selects cluster head with the help of three fuzzy variables: energy, concentration and centrality.

In EECS-M algorithm [10], a clustering method based on energy level is presented. In this algorithm for each level of networks energy, a competitive radius is taken. Sensors at every level within their radius compete to be Cluster Head. Sensors within their radius are selected as cluster head based on remaining energy. In this protocol, clusters size are different from each other in terms of area in which the sensors are placed. It means that clusters close to the base station are larger than far clusters.

In EECS algorithm [11], the author considers a constant radius for all sensors. In addition, he/she uses a competitive algorithm for the phase in which cluster heads are selected. The candidate sensors in the constant competitive radius examine that if there is a sensor with more energy, they exit the competition and broadcast the exit message. A sensor, which has maximum energy in this radius, elects itself as a cluster head and broadcast the advertisement message. In this protocol, Cluster heads are uniformly distributed in the Network. Therefore, the size of the clusters is constant due to the constant competitive radius.

III. THE PROPOSED ALGORITHM

The proposed algorithm is among those clustering algorithm. In this protocol, it has been attempted to reduce energy consumption and increase network lifetime using fuzzy rules .Cluster head energy consumption is different with regard to the distance from the base station. Cluster heads, which are close to the base station, consume the less energy for sending aggregated data than cluster heads far from the base station. For this reason, the far cluster heads lose their energy faster in the protocols that elect cluster heads without regard to the remaining energy and distance. In addition, the size of the clusters is effective in the cluster heads energy consumption. It means that cluster heads will consume more energy in the large clusters. Therefore, in this paper, using fuzzy rules for sensors, based on the amount of remaining energy and the sensor distance from the base station, a radius is considered. Then for selecting cluster heads for sensors, a chance is obtained in terms of fuzzy rules and based on remaining energy of the sensor and the number of neighbors within the related radius. Then the sensor, which has a maximum chance within its radius, is selected as cluster head and broadcasts the advertisement message to the network. Thus, the proposed protocol with selecting high-energy sensors as cluster head and limiting the size of clusters with regard to the distance from the base station cause energy consumption to reduce and ultimately lead to increasing network lifetime.

A. Network Model

Network is intended with the following specifications:

- Sensors are homogeneous and are distributed uniformly in the square area.
- Base station and sensors are fixed (static and unchanging).
- The base station is located outside square area.
- All sensors have the same initial energy.
- Sensors are aware of their position.

B. radio model

Radio model is discussed in [12] and used as the connecting model among the sensors. Equation (1) shows the amount of energy to transfer an L-bit packet to the distance d. E_{elec}, shows the amount of consumption energy of the transmitter and receiver circuits. $\boldsymbol{\varepsilon_{fs}}$ and $\boldsymbol{\varepsilon_{mp}}$, shows the amount of waste energy to boost the RF at a distance d_0 which is obtained by using equation (2):

$$E_{TX} = \begin{cases} L \times E_{elec} + L \times \varepsilon_{fs} \times d^2 & d \langle d_0 \\ L \times E_{elec} + L \times \varepsilon_{mp} \times d^4 & d \geq d_0 \end{cases} \quad (1)$$

$$d_0 = \sqrt{\frac{\varepsilon_{fs}}{\varepsilon_{mp}}} \quad (2)$$

Consumed energy to receive an L-bit packet is also calculated by using equation (3):

$$E_{RX} = L \times E_{elec} \quad (3)$$

Consumed energy in cluster heads is also calculated during a round by using equation (4):

$$E_{CH} = (\frac{n}{k} - 1) L \cdot E_{elec} + \frac{n}{k} L \cdot E_{DA} + L \cdot E_{elec} + L \cdot \varepsilon_{fs} \cdot d^4_{to-BS} \quad (4)$$

K shows the number of clusters and E_{DA} determines data combination cost. $d^4_{to\text{-}bs}$ is the average distance between cluster head and the base station. The consumed energy in conventional sensors is also calculated by using equation (5):

$$E_{CM} = L \cdot E_{elec} + L \cdot \varepsilon_{fs} \cdot d^2_{to-CH} \quad (5)$$

$d^2_{\textbf{to-bs}}$ is the average distance between the cluster member sensors and cluster head.

C. *The working process of the proposed algorithm*

This essay assumes that the sensors calculate their distance from the base station by receiving the message from the base station. Each sensor is aware of its position and its remaining energy. In the proposed protocol like LEACH protocol, time is divided into parts that are called the round. In each round, there are both set-up phase and steady-state phase. In set-up phase, radius and a chance are calculated for the sensors. Then cluster heads are selected and clustering is performed. In stable phase, data is collected, aggregated and sent to the base station by cluster heads.

1) Determining the radius for sensors with the help of fuzzy function

As previously discussed, each sensor is aware of its remaining energy and distance from the base station. In this protocol, for reducing energy consumption a radius is considered for each sensor in terms of the remaining energy and distance from the base station. In the case of electing as a cluster head, this radius makes sensor have a clustering limited to its radius in order to prevent rapid energy discharge; because cluster heads, which are far from the base station, have more energy consumption. For determining the radius in fuzzy function, fuzzy rules use two fuzzy variables, which are defined as follows:

- Energy: The amount of remaining energy of sensor.
- Distance: the distance of a sensor from the base station.

Fuzzy function acquires the radius in terms of these two variables with the help of fuzzy rules. Thus, if energy is high and distance is close, radius will be become larger. Energy consumption for data transmission to the base station is low in those sensors, so large radius is considered in order to have a bigger cluster. On the other hand, if energy is low and the distance is far, radius is considered too small. The used fuzzy rules to calculate the radius are shown in table 1 and fuzzy sets are shown in figure 1.

TABLE I. FUZZY IF-THEN RULES FOR RADIUS

Energy	Distance	Radius
1-low	Far	Very small
2-low	Medium	Very small
3-low	Close	Small
4-medium	Far	Small
5-medium	Medium	Medium
6-medium	Close	Large
7-high	Far	Medium
8-high	Medium	Large
9-high	Close	Very large

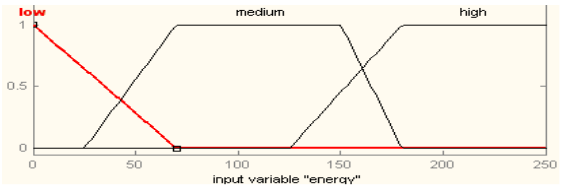

1-a) energy

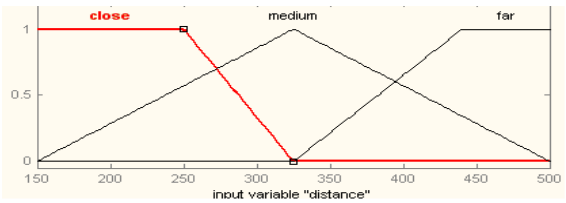

1-b) distance

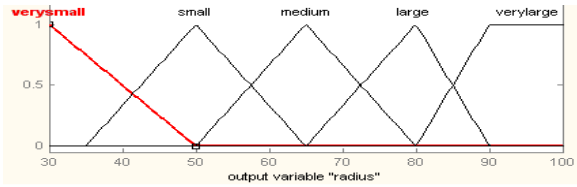

1-c) radius

Figure 1. fuzzy sets for radius

2) Calculating the chance for sensors with the help of fuzzy rules

After determining the radius for the sensors, the amount of chance to be cluster heads is calculated. To calculate the chance in terms of fuzzy rules, the following two variables are used:

- Energy: the remaining energy of the sensor.
- Neighbor: the number of neighbors in the sensor radius.

In this protocol, sensors, which contain high-energy and a great number of neighbors, have more chance to become cluster head, because these sensors are able to manage large clusters. Considering the number of neighbors will result in minimizing the number of cluster heads. Energy consumption is more in cluster heads; therefore, it reduces energy consumption in the network. The used fuzzy rules for chance calculating are shown in Table 2 and fuzzy sets in Figure 2.

TABLE II. FUZZY IF-THEN RULES FOR CHANCE

Energy	Neighbor	Chance
1-low 2-low 3-low 4-medium 5-medium 6-medium 7-high 8-high 9-high	Little Normal Many Little Normal Many Little Normal Many	Very low Low Rather low Med low Med Med high Rather high High Very high

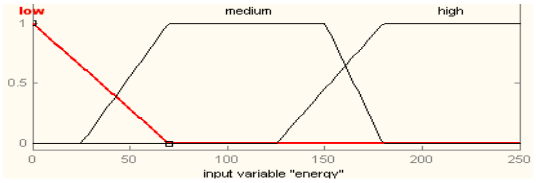

2-a) energy

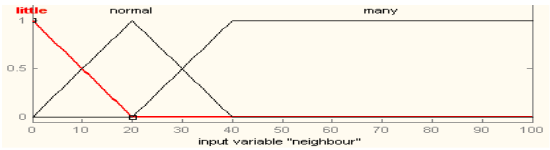

2-b) Neighboring sensors

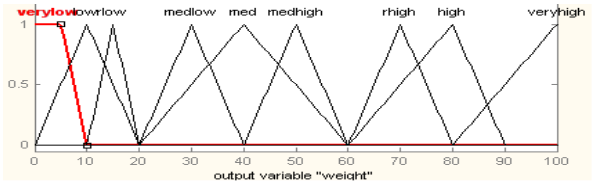

2-c) chance

Figure 2. Fuzzy sets for the chance

3) *Eelecting cluster head and clustering*

After determining the radius and calculating the chance using fuzzy rules, cluster heads should be elected. A sensor with maximum chance is elected as a cluster head. Each sensor searches the area within its radius for maximum chance. If there is no sensor with more chance, the sensor elects itself as the cluster head and broadcasts the advertisement message to the network. Other sensors, after receiving the message, inspect that if they place within several cluster heads limits, they choose the nearest cluster head as their cluster head and send the Join message to it.

IV. SIMULATION

In this paper, the provided protocol and LEACH and EECS protocols have been simulated using MATLAB. For this purpose, a 300m × 300m network is considered. Sensors are uniformly distributed in the network. The position of the base station is in the 150m × 450m in the network. Initial energy is 0.5 J for each sensor. The test values for Eelec, ε fs, ε mp and E DA is respectively considered 50 nJ/bit, 10 pJ/bit/m2, 0.0013 pJ/bit/m4 and 5 nJ / bit / signal. In Figure 3, the average of live sensors (node) in the network is shown with scenarios (different cases), 100,200,300,400, and 500 sensors. As we can see, the average of live sensors in proposed algorithm is more than the LEACH and EECS algorithms because in the proposed algorithm, cluster heads and the size of clusters are selected in terms of fuzzy rules; as a result, load is optimally distributed.

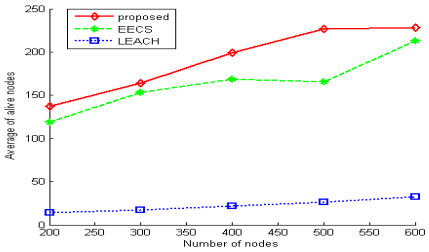

Figure 3. the average of live sensors in the network with scenarios, 100,200,300,400 and 500 sensors

In Figure 4, the average energy of total network is shown with scenarios, 100,200,300,400 and 500 sensors. As we can see, the average of the network energy in the proposed algorithm is more than LEACH and EECS algorithms because in the proposed algorithm the sensors radius is determined in terms of fuzzy rules; therefore, the far cluster heads lose their energy slower. In addition, the best sensors are selected as cluster head.

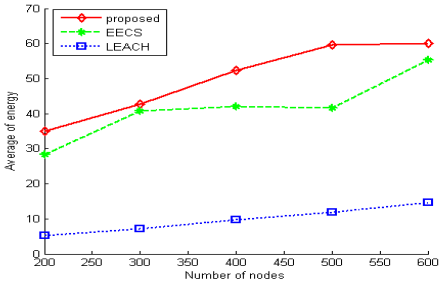

Figure 4. Average energy network with scenarios, 100,200,300,400 and 500 sensors

In figure 5, the average number of sent packets to the base station in network is shown respectively in the proposed algorithm and EECS and LEACH algorithms.

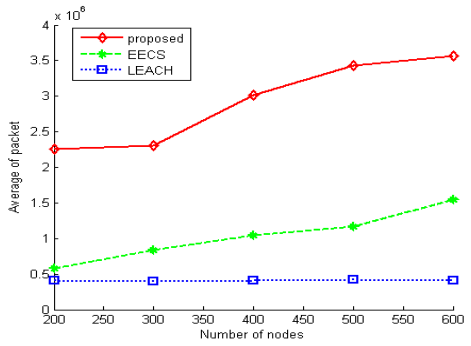

Figure 5. Average number of sent packets to BS with scenarios, 100,200,300,400 and 500 sensors

In figure 6, number of cluster heads in the network with 100,200,300,400 and 500 sensors is shown respectively in the proposed algorithm and EECS and LEACH algorithms. As we can see, the number of the cluster heads is higher than the proposed algorithm.

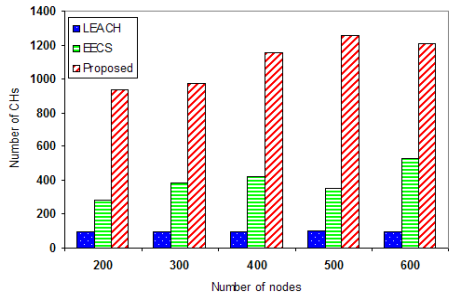

Figure 6. number of cluster heads of in the network with scenarios, 100,200,300,400 and 500 sensors

In figure 5, the first dead sensor based on number of round in the network with 100,200,300,400 and 500 sensors is shown respectively in the proposed algorithm and EECS and LEACH algorithms. As we can see, in the proposed algorithm, the network loses its first sensor slower than the EECS and LEACH algorithms.

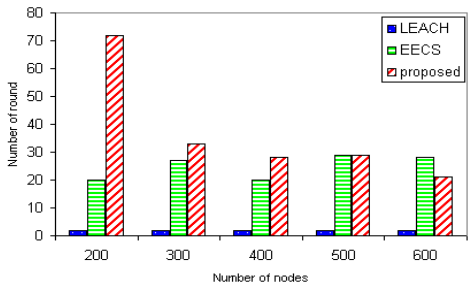

Figure 7. The first dead sensor based on number of round

V. CONCLUSION

In this paper, a protocol has been presented for the selection of cluster head using fuzzy logic. In this protocol, using fuzzy logic, a radius is considered for each sensor. Then with the help of fuzzy rules, Cluster Heads are chosen based on the variables such as remaining energy and the number of neighboring sensors within the related radius. Since energy consumption is high in cluster heads, selecting them based on energy will result in having enough energy to perform and avoiding rapid discharge energy.

Determining the radius in terms of fuzzy rules for the sensors also helps to obtain the number of neighbors within the radius. In addition, the size of the clustering is limited to the radius. Therefore, large clusters can be formed nearer than the small clusters to the base station. Thus, the proposed protocol reduces the energy consumption and increases the network lifetime. Simulation results confirm that the proposed protocol performs better than the LEACH and EECS protocols in terms of energy consumption and lifetime.

References

[1] W. Heinzelman, "Application-specific protocol architectures for wireless networks," Ph.D. Dissertation, Mass. Inst. Technol., Cambridge, 2000.

[2] L.F.Akyildiz,W.Su,Y.Sankarasubramaniam,and E.Cayiric,"A survey on sensor network,"IEEE Communications Magazine,vol.40,no.8,pp.102-114,Aug. 2002

[3] I. F. Akyildiz et al., "Wireless sensor networks: a survey", Computer Networks, Vol. 38, pp. 393-422, March 2002.

[4] C.Chong andS.P.Kumar,"Sensor Networks: Evolution,Opportunities.and Challenges," Proc.IEEE, vol. 91 , no. 8,2003,pp. 1247-1259.

[5] Al-Karaki J. N. and A. E. Kamal, "Routing Techniques in Wireless Sensor Networks: A Survey" , IEEE Journal of Wireless Communications, vol. 11, no. 6, Dec. 2004, pp. 6–28.

[6] *Kemal Akkaya* and *Mohamed Younis*, A Survey on Routing Protocols for Wireless Sensor Networks, Ad Hoc Networks, 3(3), May 2005, pp. 325-349.

[7] W. Heinzelman, A. Chandrakasan, and H. Balakrishnan,"Energy-efficient communication protocol for wireless sensor networks," in the Proceeding of the Hawaii International Conference System Sciences, Hawaii, January 2000

[8] Jong-Myoung Kim, Seon-Ho Park, Young-Ju Han and Tai-Myoung Chung,"CHEF: Cluster Head Election mechanism using Fuzzy logic in Wireless Sensor Networks",ICACT2008.

[9] Indranil Gupta, Denis Riordan ,Srinivas Sampalli,"Cluster-head Election using Fuzzy Logic for Wireless Sensor Networks",ISBN:o-7695-2333-1,IEEE Computer Society Washington ,DS,USA ,2005

[10] F.Tashtarian, M.Tolou Honary , M.Mazinani , A.T.Hghighat , J.Chitizadeh ,"A New Level Based Clustering Schema for Wireless Sensor Networks". 2008 IEEE.

[11] M.Ye, C. F. Li,G.H.Chen, and J.Wu, "EECS: An Energy Efficient Clustering Sheme in Wireless Sensor Networks," in Proceedings of IEEE Int 1 Performance Computing and Communications Conference (IPCCC),pp.535-540,2005.

[12] Rappaport T., Wirelesss Communications: Principles & Practice, Englewood Cliffs, NJ:prentice-Hall, 1996.

Contour Object Generation in Object Recognition Manufacturing Tasks

M. Peña-Cabrera[1], V. Lomas-Barrie[1], I. López-Juárez[2], R. Osorio[1], H. Gómez[1]
[1]Instituto de Investigaciones en Matemáticas Aplicadas y Sistemas, Universidad Nacional Autónoma de México, Apdo. Postal 20-726, México D.F., México
[2]Grupo de Robótica y Manufactura Avanzada, Centro de Investigación y de Estudios Avanzados del Instituto Politécnico Nacional, Unidad Saltillo, Saltillo Coahuila., México

Abstract - *The article presents a method for obtaining the contour of an object in real time from not binarized images and for objects that can be assembled on line in automated manufacturing processes. The contour information is integrated into a descriptive vector called [BOFnew], which is used by a neural network model of the type FuzzyARTMAP to test the feasibility of the method using the generated contour to learn of the object and then recognize it later To this end, it requires a fast and robust method to acquire process and communicate to a robot the information about positioning and orientation of an object for assembly purposes. The used algorithm and its simulation was developed in MatLab 7.0.*
Having this method for object recognition manufacturing tasks improves this methodology and allows the implementation of these algorithms in FPGA´s, which gives in manufacturing cell a real possibility performance demanded by industrial environments.

Keywords: robot, vision, manufacture, FPGA

1 Introduction

The process of locating and recognizing an object to perform fixtureless robotic assembly tasks in line and in an intelligent manufacturing cell, is an open research goal, since they are obvious advantages with using robots in assembly lines, and the automation of industrial processes (DeSouza 2002). In order to perform autonomous assembly operations in manufacturing processes, requiring high levels of accuracy, robustness and speed of operation, this vision machines are very useful to the be used as a sensory robot capability because they make it possible to close the mesh of control for the calculation of the POSE of the end effector of a robot (Hutchinson, 1996), the importance of the issue is demonstrated in the application performed by Bone and Capson (2003) for the assembly of components online in the automotive industry.

Recognition, tracking in real time and the estimation of the POSE of an industrial object using methods based on geometric characteristic is shown by Yoon and DeSouza (2003), in these applications, the speed and accuracy are primordial factors of the order of milliseconds (commercial video box) with errors of an estimation of millimeters in the operation; as a successful alternative methods based on the use of primitive characteristics based on silhouettes allow to satisfy these requirements (Miller et. to the.)(2003); There are numerous approaches in the area of image processing to recognize and locate objects, like using descriptors of chain codes (Bribiesca, 1999), use of invariant features of silhouettes (format watery et.al., 2002), artificial intelligence techniques as neural network to implement systems for the classification of patterns invariant to scaling, translation, and rotation (Andüceer and Oflazer, 1993) and intelligent manufacturing systems guided by vision (Langley)(, et.al., 2003). On the other hand, much effort has been focused on the development of effector right-handers mounted on the end terminals of robots manipulators (Bicchi and Kumar, 2001).

The article, presents an algorithm which allows to obtain the POSE of an object in an assembly line based on extracted information of an acquired image in real time, the centroid calculation is performed, which in our method is basic information for the recognition of the object and its orientation obtaining critical points within an image to represent the border/contour points border and the centroid of the object; a set of numerical sorted pairs, is generated by the algorithm, and form the basis for the formation of an object descriptive vector (Current Frame Descriptor). Descriptor vector is presented to a neural network of the type Fuzzy ARTMAP (Carpenter, 1991); This integrated process concludes a process of learning online; new vectors calculated with new images, refine the learned information thereby obtained a process of incremental learning thanks to the strength and rapidity of the neural network model used; in order to make more robust in terms of lighting and speed, the method performs an analysis of the 1D histogram to calculate threshold levels of gray scale for optimal segmentation of the image with different conditions of illumination, 2D histogram might be used to obtain the region of interest (ROI) and make the process of descriptive vector generation of the object with a lower

resolution and therefore faster, the integration of the algorithm with neural network, makes the method substantially a robust process with characteristics of invariance for its real application environments in manufacturing processes.

2 Methodology

The process begins with the acquisition of the image in gray levels of the object, then the distribution frequency of grey levels within the image (histogram 1D, Figure 3), to establish the levels of comparison, an "Operator Threshold" is used for image segmentation, then a binary image process is carried out within a certain dynamic range for lighting to obtain a silhouette of the object. In order to reduce processing time, the algorithm that generates the descriptive vector (CFD), applies only on the region of interest (ROI), which can be obtained on the basis of the 2D histogram. In this way, with the 1D histogram analysis are obtained the criteria of segmentation to generate the binary image and with the 2D histogram for spatial distribution of gray levels information in order to reduce the resolution of the image.

Once you have an image of the ROI, the method proceed to obtain a primitive binary image (PbinIm), which serves as a basis for the necessary information for calculating the POSE; applying the algorithm, we obtain a set of ordered pairs of critical points in the image used to generate information of the object containing the properties of invariance for rotation, translation and scaling as well as the centroid of the upper surface and orientation with reference to the NN point (North).

This information represents a model as a vector CFD vector with the information needed to extract properties that allow to recognize the object.

2.1 1D and 2D histogram

The 1D histogram shown in Figure 1, allows to know the frequency distribution of grey levels of an image (probability density function).

A model of an image is:

$$\mathrm{Im} = f(x, y) \tag{1}$$

for a range of grey levels:

$$0 \le Gl \le L - 1 \tag{2}$$

where Gl is the gray level of each point in the image as:

$$\exists Gl(i, j) \in \mathrm{Im}(xi, yj)$$

where

$$Gl(i, j) = 0, L - 1, \forall i, j = 1, N \tag{3}$$

1D Histogram methods, provide a selection of peaks or valleys using a Bayesian estimation of the probability density function of grey levels in the image or with a numerical analysis of the histogram for image segmentation (Sahoo et al., 1988); in our case, segmenting the image means separating the elements of interest for the computation of parametric or not/parametric properties, by providing us with the separation of desirable segments in the image for the subject and background, and a further segmentation separates the parts to acquire orientation information. On the other hand, traditionally optimization continued to obtain comparison thresholds are based on criteria attached to the variance and the entropy of the distribution of colors in the image, but they provide greater computational consumption in processes (Pun, 1981).

Having a grayscale levels image F(x,y) with MxN pixels, where lower numeric values represent the most dark colors and higher values the clearest colors, a function called "1D Thresholding Function" can be obtained as follows:

$$F_T(x, y) = \begin{cases} bo \text{ if } f(x, y) \le T \\ b1 \text{ if } f(x, y) > T \end{cases} \tag{4}$$

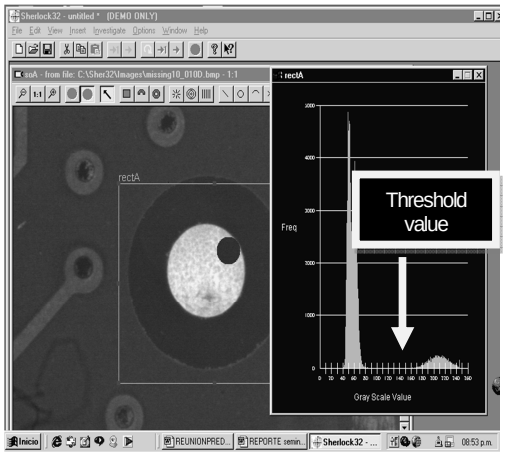

Figure 1 - 1D Histogram

The 2D histogram is used to represent the probability of the co-occurrence of two values of gray levels when their corresponding pixels are separate at a specific distance. It can be defined as a matrix H_{2d} containing information of the grey level of each pixel and the level of grey average in the vicinity of a pixel within the scale used, i.e.:

$$H_{2d} = \begin{cases} r_{i,j} / r_{i,j} = number\ of\ bin(i,j), \\ 0 \le r_{i,j} \le MN, \\ i, j = 0,1,2,...,L-1 \end{cases} \quad (5)$$

where MN is the size of the image, and where the local averages values represent the spatial information, without having a representation of the precise point of information that reflects every pixel, but if it allows to get an idea of the spatial distribution of the pixels associated with certain regions in the image base for the criterion of the definition of the ROI (Ahuja et al., 1978). The value of the local average in a window of small dimensions (2w + 1)2 centered in a pixel (x, and), is defined as:

$$g(x,y) = 1/(2w+1)^2 \sum_{k=-w}^{w} \sum_{l=-w}^{w} f(x+k, y+l) \quad (6)$$

where

$$\begin{Bmatrix} x = 1,2,...., M \\ y = 1,2,..., N \end{Bmatrix}$$

and thus gets a 2D Thresholding Function f(T,S_) defined as:

$$f(T,S)_{(x,y)} = \begin{Bmatrix} bo, \text{if } f(x,y) \le T \vee g(x,y) \le S \\ b1, \text{if } f(x,y) > T \wedge g(x,y) > S \end{Bmatrix} \quad (7)$$

where

$$0 \le bo, T, b1 \le L-1$$

and (T,S) is a 2D comparison vector.

2.2 Algorithm [CFD & POSE]

The algorithm for the descriptive vector generation, called [CFD & POSE] is shown below and is illustrated by an example of a 32 x 32 image resolution rectangle showed in Figure 2.

Of the original image, a data structure is obtained, and using the above explained process, to determine of comparison thresholds to binary operation and the ROI (Figure 3), [CFD & POSE] algorithm is applied that uses a transformation we call *Weight Matrix Transformations* as follows:

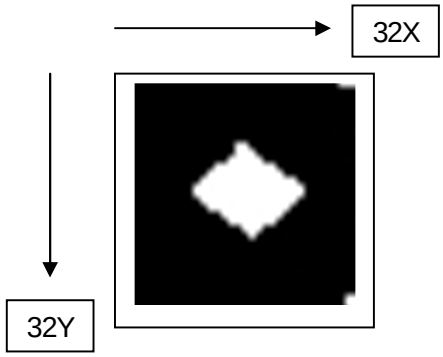

Figure 2 - 32 x 32 resolution original square image to generate a descriptive vector.

Apply the Weights Transformation Matrix of (HWf), calculation of numerical ordered pairs and generation of vector Vx (m) and Vy (m), this process allows boundary points and centroid information generation very fast.

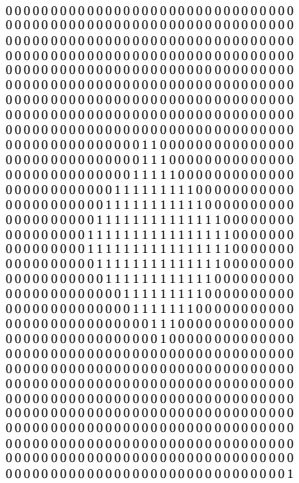

Figure 3 - Binary image

2.3 Weight Factor Matrix Transformation

This transformation get an array with numerical values in the image according to its weight and on the basis of a binary image, each numerical value is related to a couple of coordinates to establish its location, the weight number is defined as:

$$number\ \ NWf \rightarrow \left[numericalp\ aircooordi\ nates \right]$$

Where

$$NWf\min \le \sum(1's)\ en\ (\text{kxk})\ Kernel \le NWf\max \quad (8)$$

where k = 3 and numbers are obtained between:

$$0 \le NWf \le 9 \quad (9)$$

the image shown in Figure 4 is obtained, which is the transformation of the binary image to an image with the representative of the centroid and contour weights; from collection of numbers, we find the Median of Nwfmax provides the centroid of the object and the NWf min the extreme points of the outline of the object.

Numerical ordered pairs and vector Vx (m) and Vy (m) calculation

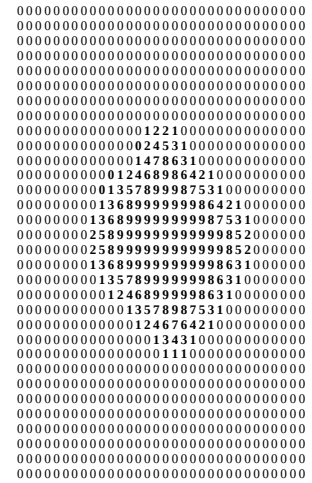

Figure 4 - Image with representative weights for centroid and border points.

Following the algorithm for calculating the numerical pairs of coordinates and vectors Vx (m) and Vy (m) is showed, image scanning is left-right and top-down directions.

- Find a different number of zero and save it as a minimum.
- Stores X and Y coordinates in vectors Vx (m) and Vy (m).
- Progresses, if new number greater than the previous save it as a maximum, and retains the minimum.
- Progresses, if new maximum number greater than the largest stored, save it as bigger and if less than the smaller stored, save it as a minor.
- Store the minimum of minimum and maximum of maximum as well as the possible number of them.

Application of the transformation of matrix of weights (HWf) proceeds as follows:

- Calculation of numerical ordered pairs and obtain vector Vx (m) who (m)
- Border points extraction and centroid.
- Among the number of maximum´s, get the coordinates of the median of the related coordinates.
- Border points and centroid extraction.

Applying the algorithm, the vectors containing the coordinates of X and Y, and the contour points are accumulated in vectors that we call:

$$vectorX\ (m) = \{x0, x1, x2, ... xn\}_{NWf\ \min}$$

and :

$$vectorY\ (m) = \{y0, y1, y2, ... yn\}_{NWf\ \min} \quad (10)$$

For the showed rectangle image ROI of 32 x 32, the boundary points for the X´s and Y´s are:

Array

(Xm)={15,18,14,19,13,20,12,21,11,22,9,23,24,9,24,10,24,11,23,12, 22,13,21,20,14,19,15,18}
Array
(Ym)={9,9,10,10,11,11,12,13,14,14,15,16,17,18,18,19,19,20,20,22 ,22,23,23,24,25,25,26,26 }

the calculation of centroid grouping all the maximum points for X-Y´s as follows:

$$Xc = {}^{1}\!/_{No}\,.NWf_{\max - X}\left[\sum NWf_{\max - X}\right]$$
$$Yc = {}^{1}\!/_{No}\,.NWf_{\max - Y}\left[\sum NWf_{\max - Y}\right] \quad (11)$$

and for the case example, the centroid is at: C = (Xc, Yc)xy(16,17) (13)

outline coordinates in the example are: Contour = {(15.9), (18.9),..., (18,26)}, then having the coordinates of the border points and the centroid, border distances are calculated, in an order defined in a clock wise direction (CW), and we can get a border points function that we call *Boundary Object Function* (BOF) with:

$$Dn = \sqrt{(X2 - X1)^2 + (Y2 - Y1)^2}$$

$$\forall \quad 0 \le n \le \text{tamaño(angular grid)} \quad (12)$$

The process is illustrated in Figure 5, on the basis of the original rectangle image until a BOF table. Is generated.

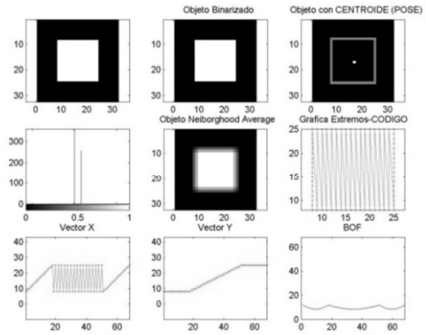

Figure 5 - Process for obtaining of the Boundary Object Function for the rectangle.

The descriptive vector is then formed with the previously calculated distances that are normalized to have independence of scaling, which defines a grid/angle for the border function points BOF, with normalizes n points, and where each of these points in the angular grid represents the degrees which form the angular increase for each standard step. Angular position of the object of 180º rotation represents a move of 90 steps on angular grid in the direction CW.

2.4 A new method using an angular scanning of the objects obtained from not binarized images

The descriptor is a vector of values that represent certain characteristics of an object as the nth distance that exists between the centroid and a border point of the object. In such a way that no matter the position, scale and rotation of an object, its descriptive vector is always the same. Calculate the BOF of an object, is part of a method by (Peña and Lopez 2006) for the recognition of objects on line for assembly of parts with robotic arms.

To calculate the BOF with the new method we have the following considerations:

- image processing is a simulation of an object.
- set image size is 100 x 100 pixels
- is a solid and filtered image with values in each pixel of 255 for white and 0 for black.
- The region of interest (ROI) has been established to focus on the object in the image.

Procedure to calculate the BOF with this method:

I. Calculate the centroid of the image

II. From the centroid define a straight line trajectory

$$y = \tan(\varphi n)x + b_0 \qquad (13)$$

where φn is an angle that varies from 0 to π, and b_0 is the ordered to the source that is based on the angle φn, and x are the matrix index of the image and represent the position of a pixel (figure 6).

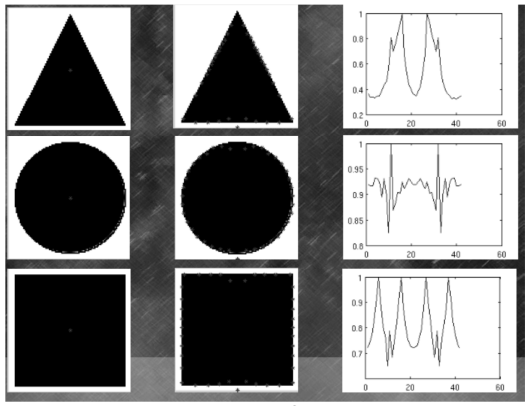

Figure 6 - A generated BOF for a square object with different grid resolution

A tentative resolution, *pre*, was defined as 0.1; it means 22 points. Which give a very low resolution that could confuse the ANN. Remember, in time computers topic, more points imply more resolution therefore more spent computer calculation time. Then variable pre was set in 0.01 with 202 points (figure 7).

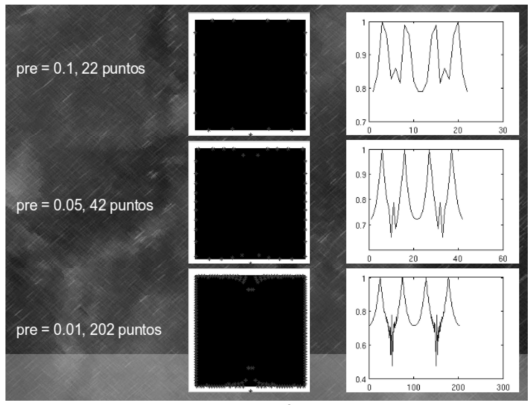

Figure 7 A generated BOF for a square object with different grid resolution

III. According to the trajectory, each pixel is evaluated and if its value is 255 returns to position x - 1 back to calculate the coordinate which will be the border pixel.

IV. The distance of that point border to the centroid is calculated with the equation:

$$Dn = \sqrt{(X2 - X1)^2 + (Y2 - Y1)^2} \qquad (14)$$

$$\forall \quad 0 \leq n \leq \text{size(angular grid)}$$

V. The distance Dn is storing in the BOF [n] vector

VI. Φn with precision p increases.

VII. Repeat steps 2 to 7 until φn reaches the value of π. To determine the best accuracy, for our purposes we change the variable *pre's* as shown in Figure 6.

2.5 FPGA implementation. First approximation process

Since there are some works around ANN implemented on FPGA (Liu, 2005) it is important to standardize and format the inputs and outputs. Thus, the late described method represents an effortless way to calculate BOF in logic design level.

A 2D image is a integer matrix with index i and j and supposing that the centroid is well known, the implementation of equation (13) in VHDL (VHSIC hardware description language) is simple.

3 Conclusions

The algorithm presented to calculate the BOF is an original idea that seeks to make a proof of concept and an assistant to train and qualify RNA for assembly object recognition purposes. To tracking pixel to pixel is not necessary a binarization process for the image. We realize the method is efficient, but might be improved in some aspects like due to the possibility that in the border point tracing procedure might catch more than one pixel. Arriving the 90 and 270 degrees, the slope of the line is so great that the advance from pixel to pixel exceeds the 4/1 ratio in x, which causes that border point found can be far away of the border. This was corrected improving the algorithm to the limits to 90 and 270 degrees an improved figures are shown in figure 8. At the same time, the error committed with pixel tracking, specifically on the slopes close to 90 and 270 degrees can be minimized increasing the resolution of the image. It is also possible to modify the algorithm of the BOF following an upward and downward trajectory for 90 and 270 degrees respectively. As for the RNA stands that largely reaches to recognize images that occur when train you with three basic figures. Even though it modifies the image resolution to recognize, succeeds in a 66.6% the only failing is the circle. However it worthwhile to perform the experiment again with other figures to dispose of the problem of the non-recognition is due to intrinsic characteristics of a circle as for example their distances to the centroid are constant, but the BoF presented here shows some noise Figure 8.

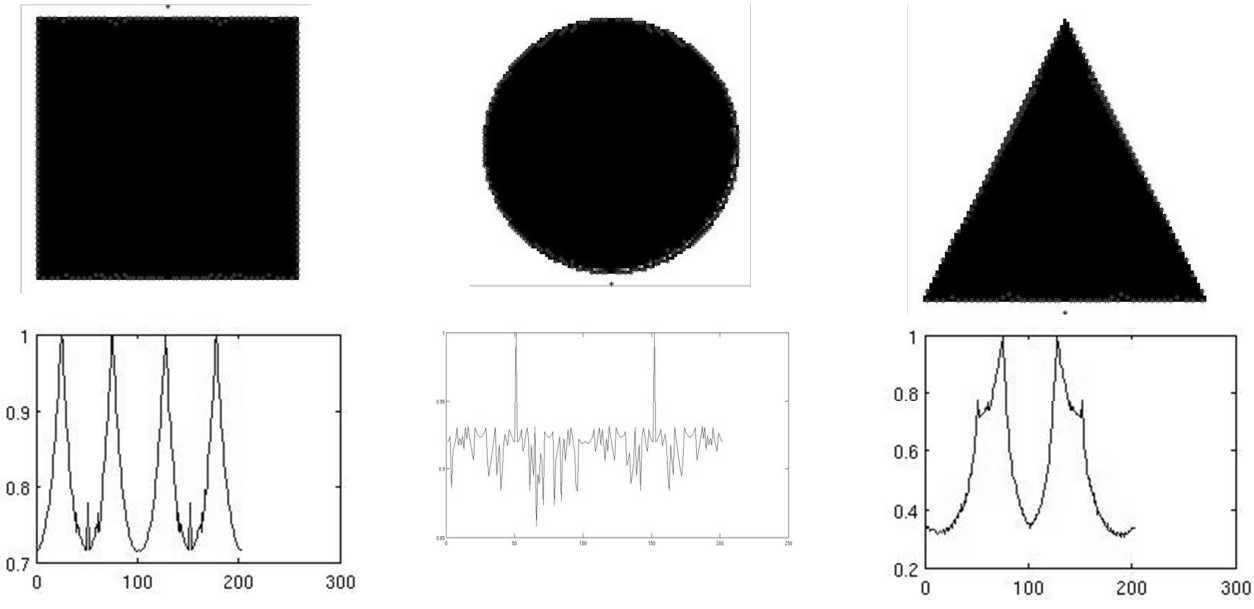

Figure 8 generated BOF for a triangle, circle and square objects and improved process

4 References

[1] Gary M. Bone, David Capson, "Vision-guided fixtureless assembly of automotive components", Robotics and Computer Integrated Manufacturing 19, 79-87. Pergamon, Elsevier Science LTD. (2003)

[2] Seth Hutchinson, Gregory D. Hager, Peter I. Corke, "A tutorial on Visual Servo Control", IEEE Transactions on Robotics and Automation, Vol.12 No.5, October. (1996)

[3] M. Peña. Inteligent Manufacturing Group and Mechatronics Laboratory Internal Report , CIATEQ, México, 2003.

[4] M. Peña-Cabrera et al. " A Learning Approach for On Line Object Recognition in Robotic Tasks", Mexican International Conference on Computer Science ENC , IEEE Computer Societey Press . (2004)

[5] M. Peña. Visión para robots en tareas de ensamble. In Proceedings of the 2nd. National Congress on Mechatronics, December. (2003)

[6] López-Juárez, M. Howarth. Learning Manipulative Skills with ART. IEEE/RSJ International Conference on Intelligent Robots and Systems (IROS´2000), Takamatsu, Japan, Vol 1, pp 578-583 ISBN 0-7803-6351-5. (2000)

[7] Cem Yüceer adn Kema Oflazer, A rotation, scaling and translation invariant pattern classification system. Pattern Recognition, vol 26, No. 5 pp. 687-710, (1993).

[8] Carpenter Gail A. and Stephen Grossberg, John H Reynolds. ARTMAP: Supervised Real-Time Learning and Classification of Nonstationary Data by Self-Organizing Neural Network. Neural Networks. Pp 565-588. 1991.

[9] Bribiesca E. A new Chain Code. Pattern Recognition 32 , Pergamon, 235-251 , (1999).

[10] Miller, S. Knoop, H. Christensen and P. Allen, " Automatic grasp planning using shape primitives", Proceedings of the 2003 IEEE International Conference on Robtics Automation, Taipei, Taiwa, September 14-19, pp.1824-1829, (2003).

[11] Y.Yoon, G. DeSouza and A. Kak, Realtime tracking and Pose estimation for industrial objects using geometric features", Proceedings of the 2003 IEEE International Conference on Robotics Automation, Taipei, Taiwa, September 14-19, pp.3473-3478,(2003).

[12] G.N. DeSouza and A. C.Kak, "A subsumptive hierarchical and distributed vision-based architecture for smart robotics" IEEE transactions on Robotics and Automation, (2002).

[13] J. Liu and D. Liang, "A Survey of FPGA-Based Hardware Implementation of ANNs" IEEE, Neural Networks and Brain, 2005. ICNN&B '05. International Conference on 13-15 Oct. 2005 pp 915-918 (2005)

A sEMG-SKELETAL MUSCLE FORCE DATA FUSION BASED ON MINIMUM DESCRIPTION LENGTH CRITERION

Madhavi Anugolu, Chandrasekhar Potluri, Steve Chiu, Alex Urfer, Jim Creelman and Marco P. Schoen

Abstract–*This paper provides a method of fusing the sEMG/skeletal muscle force sensor array data using a Minimum Description Length (MDL) data fusion algorithm. The sEMG data and the corresponding skeletal muscle force data are acquired from a test subject. A nonlinear Bayesian Half-Gaussian filter is utilized to filter sEMG data and the skeletal muscle force signal is filtered by using a Chebyshev Type-II filter. A System Identification Technique is employed to derive the mathematical relationship between the sEMG (input) and the skeletal muscle force (output) data. We implemented linear and nonlinear parametric- Auto-Regressive with eXogenous input (ARX), Auto-Regressive Moving Average with eXogenous input (ARMAX), Output Error (OE) and Weiner Hammerstein modeling. The estimated model output from the three sensors are combined by using a probabilistic based Minimum Description Length (MDL) fusion algorithm. The results are thought provoking and the overall fused output has better correlation with the actual force when compared with the individual sensor estimated force.*

Keywords: *sEMG, hand prostheses, data fusion, system identification, minimum description length criterion*

I. INTRODUCTION

In the United States, there are more that 2 million amputees and according to the statistics provided by the National Limb Loss information Center, this number will reach 3.6 million by 2050 [1].

Madhavi Anugolu is with the Measurement and Control Engineering Research Center (MCERC), School of Engineering, Idaho State University, Pocatello, Idaho 83209, USA (email: anugmadh@isu.edu).

Chandrasekhar Potluri is with the MCERC, School of Engineering, Idaho State University, Pocatello, Idaho 83209, USA (e-mail: potlchan@isu.edu).

Steve Chiu is with the Department of Electrical Engineering and Computer Science, MCERC, Idaho State University, Pocatello, Idaho 83201 USA (email: chiustev@isu.edu).

Jim Creelman is with the Department of Physical and Occupational Therapy, Idaho State University, Pocatello, Idaho 83209, USA (email:creljim@isu.edu).

Alex Urfer is with the Department of Physical and Occupational Therapy, Idaho State University, Pocatello, Idaho 83209, USA (email:urfealex@isu.edu).

Marco P. Schoen is with the Department of Mechanical Engineering, MCERC, Idaho State University, Pocatello, Idaho 83209, USA (email: schomarc@isu.edu).

The etiologies of hand amputations include cardiovascular disease, congential deformities, nerve injuries, tumors, and trauma [2]. Over the past few decades, numerous research and clinical studies have concentrated on the field of prosthetics. Even today, however, most individuals with upper extremity and hand amputations have difficulty acquiring an affordable prosthesis which allows for good functional hand motion. [3] Due to recent advances in technology, a great interest has emerged in the design of a better hand prosthesis controlled by integrated Electromyographic (EMG) signaling. In general, the EMG signal is a composition of action potentials produced by the electrical activity of the muscle groups. This signal depends on the flow of ions such as sodium (Na+), calcium (Ca++), and potassium (K+). These signals can be measured either by inserting the needle electrodes into the muscle tissues or by affixing the surface electrodes to the skin.

In this work, we used surface Electromyographic (sEMG) data since it does not require any surgical monitoring. The sEMG signals can be used in various engineering and clinical applications [4, 5]. One must be careful in analyzing sEMG signal [6]. Especially in engineering application, sEMG can be used to control the position and force of the prosthetic hand [7]. The sEMG signal amplitude varies from person to person and it depends on the applied force. Some other factors like cross-talk from different muscle groups, and biochemical reactions in the muscle fibers influence the sEMG/skeletal muscle force relationship. Therefore, these factors contribute to randomness and complexity of the sEMG signal.

From our particular perspective, it is desirable to combine the data from the array of sensors. So, in this work, we implemented a Minimum Description Length (MDL) criterion to fuse the sEMG/skeletal muscle force data from the three sensors. After collecting the data, the sEMG signals are filtered using a Genetic Algorithm (GA) based nonlinear Bayesian Half-Gaussian filter. The skeletal muscle force data is filtered by using a Chebyshev Type-II filter. Considering the sEMG as input and skeletal muscle force as output, System Identification (SI) technique is utilized to extract the dynamic relationship between the sEMG data and its corresponding skeletal muscle force data. The estimated output models are fused with a probabilistic based Minimum Description Length (MDL) criterion.

II EXPERIMENTAL DESIGN

For this work, the experiments were conducted on a healthy male subject to acquire the sEMG and its corresponding skeletal muscle force signal. Prior skin preparation was done by following the ISEK standards [8]. A muscle point stimulator manufactured by Richmar Corporation™ was used to identify the muscle motor point. For this particular experiment, the ring finger motor location on the flexor muscle was chosen. Fig. 1 illustrates the experimental design. Three sensors were placed on the skin surface, one on the ring finger flexor digitorium superficials muscle motor point and the other two adjacent to it. A Delsys Banglo-16, was used to capture the sEMG signal and the Force Sensitive Resistor (FSR) was used to acquire the corresponding skeletal muscle force signals. Both the signals were acquired through LABVIEW at a sampling rate of 2000 sample/sec.

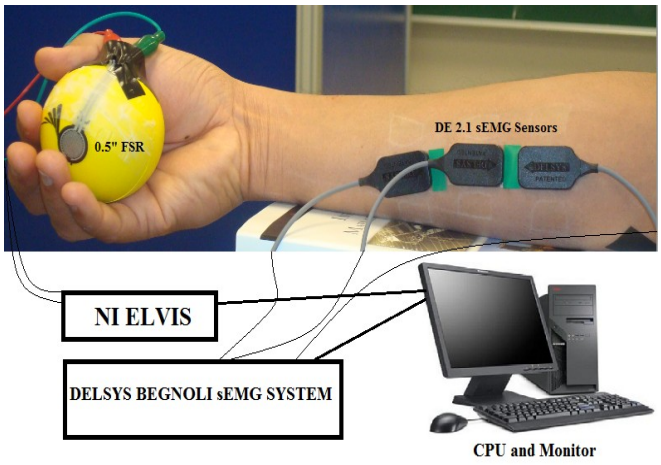

Fig. 1: Experimental Set-up

III. THEORITICAL BACKGROUND

The sEMG data acquired from the surface of the skin is rectified and filtered using a GA based nonlinear Bayesian Half-Gaussian filter. In our previous work [9] we explored different filters for sEMG filtration. We concluded that the Bayesian Half-Gaussian filter works better when compared to other filters like Butterworth, Chebyshev, Bayesian Poisson. As mentioned earlier, sEMG depends on various factors. The relationship between the actual force and the resulting sEMG after filtration can be given by the conditional probability density function $(EMG|x)$. Under the assumption that the conditional probability of the rectified EMG signal is a filtered random process at a random rate the Half-Gaussian filter is given by:

$$p(EMG|x) = 2\frac{exp\left\{\frac{-EMG^{\,2}}{2x^2}\right\}}{\sqrt{2\pi x^2}}\,, \qquad (1)$$

where $p(EMG|x)$ is the conditional probability, x is the latent driving signal, and EMG is the acquired data. According to Fokker-Planck partial differential equation, the likelihood function for the rate evolves in time [10]. The discrete time Fokker–Planck equation is given by (2)

$$p(x,t-) \approx \alpha p(x-\varepsilon,t-1)+(1-2\alpha)p(x,t-1)+ \alpha p(x+\varepsilon,t-1)+\beta+(1-\beta)p(x,t-1) \qquad (2)$$

Here, α and β are two free parameters, where α is the expected rate of gradual drift in the signal, and β is the expected rate of sudden shifts in the signal. The unknown driving signal x is discretized into bins of width ε. These two free parameters (α, β) of the non-linear Half-Gaussian filter model are optimized for the acquired EMG data using an elitism based GA. A Chebyshev Type-II filter with 550 Hz cutoff frequency is used to filter to skeletal muscle force signal.

Linear and nonlinear System Identification Models:

System Identification uses statistical methods to implement the dynamic relationship between the measured input/output data. This is done by altering the parameters within a given model until its output tracks the measured input, [11]. System identification is an alternative to the physical based modeling [11]. In this work, linear parametric models- Auto-Regressive with eXogenous input (ARX), Auto-Regressive Moving Average with eXogenous input (ARMAX), Output Error (OE) and nonlinear models- Wiener Hammerstein are implemented

The output error model structure is

$$y(t) = \frac{B(q)}{F(q)}u(t-n_k) + e(t) \qquad (3)$$

The ARX model is a random process. It predicts the output based on the previous output. Its mathematical notation is given by equation (4)

$$A(q)y(t) = B(q)u(t-n_k) + e(t) \qquad (4)$$

Based on the given data, the ARMAX model predicts the future values in a series. The mathematical notation is given by Equation (5). It consists of two parts, the autoregressive part and the moving average part.

$$A(q)y(t) = B(q)u(t-n_k) + C(t)e(t) \qquad (5)$$

In Equations (3), (4) and (5), y is output, t is time, $B(q)$, $F(q)$, $A(q)$, $C(q)$, $D(q)$, are polynomials, q is a backward shift operator, u is input, nk is delay and e is error

Nonlinear Wiener Hammerstein

A model with a fixed nonlinearity at the input is called a Hammerstein model. When the nonlinearity is at the output is called a Wiener model. The combination of these both is the Wiener-Hammerstein model, [11]. The structural representation of the Weiner- Hammerstein model is given in Fig. 2, [12]. It consists of two nonlinear blocks with a linear block in series.

Fig. 2: Weiner-Hammerstein model structural representation

The mathematical depiction of the modeling is given by,

$$w(t) = f(u(t)) \quad , \tag{6}$$

$$x(t) = \frac{B_{j,i}(q)}{F_{j,i}(q)} w(t-nk) + e(t) \quad , \tag{7}$$

$$y(t) = h(x(t)) \quad , \tag{8}$$

where $u(t)$ is the sEMG signal and $y(t)$ is the skeletal muscle force signal. f and h are nonlinear functions, $w(t)$ and $x(t)$ are internal variables, $B_{j,i}(q)$ and $F_{j,i}(q)$ are polynomials, q is the back shift operator, and $e(t)$ is the output error.

Minimum Description Length (MDL) Criterion

In 1978, the Minimum Description Length (MDL) concept was introduced by Jorma Rissanen [13]. The fundamental idea behind the MDL principle is based on the algorithmic complexity of Solomonoff, Kolmogorov and Chaitin [14]. In this work, we are inspired by [15] and used the Minimum Description Length criterion to fuse the estimated models. It is given by

$$MDL(p_i) = \frac{n}{2}\log(\hat{\sigma}_i^2) + \frac{p_i+1}{2}\log F_i + L_i \quad , \tag{9}$$

where $F_i = (Y^T Y - R_i)/(p_i \hat{\sigma}_i^2)$,

$$L_i = \frac{1}{2}\log(\frac{n-p_i}{p_i^3}) \quad ,$$

$$\hat{\sigma}_i^2 = {R_i}/{(n-p_i)} \quad .$$

Based on [9 and 15], the following fusion algorithm is implemented for sEMG-skeletal muscle models.

1. Identify the models $M_1, M_2 \ldots M_k$ using sEMG data (u) as input and fingertip force data (y) as output, for k number of sEMG sensors.
2. Calculate the residual square norm

$$R_i = \left\|y - \Phi_i \hat{\theta}_i\right\|^2 = \left\|y - \hat{y}\right\|_2 \text{ where } \hat{\theta}_i = \left\{\Phi_i^T \Phi_i\right\}^{-1} \Phi_i^T y \quad ,$$

and $\vec{\Phi} = \begin{bmatrix} y_p^T & u_p^T & y_{p-1}^T & \cdots & \\ & u_{p+1}^T & y_p^T & \cdots & \\ \vdots & \vdots & \vdots & \ddots & \vdots \\ y_{n-1}^T & u_{n-1}^T & y_{n-2}^T & \cdots & \end{bmatrix}$

3. Model criteria coefficient is calculated using Equation (9).
4. Compute the model probability as given by

$$p(M_i \mid Z) = \frac{e^{-l_i}}{\sum_{j=1}^{k} e^{-l_j}} \quad , \text{ where } l \text{ is the model selection criteria coefficient, i.e.}$$

5. Compute the fused model output $\hat{y}_f = \sum_{i=1}^{k} p(M_i \mid Z)\hat{y}_i$

RESULTS AND DISCUSSION

Fig 3. shows the raw sEMG data acquired from the surface of the skin Vs the sEMG filtered data by using Bayesian Half-gaussian filter.

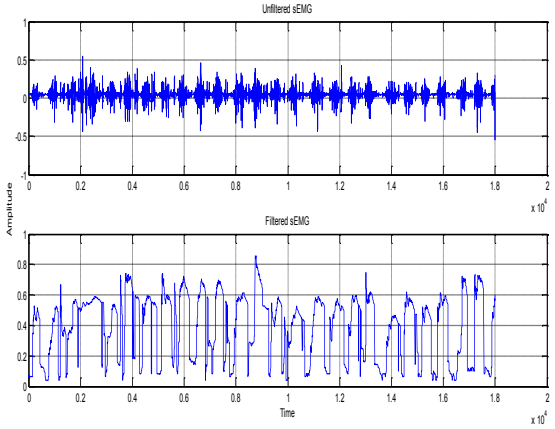

Fig.3: Raw sEMG data Vs filtered Data

Fig. 4 depicts the actual skeletal muscle force data Vs the filtered force data using Chebyshev type-II filter.

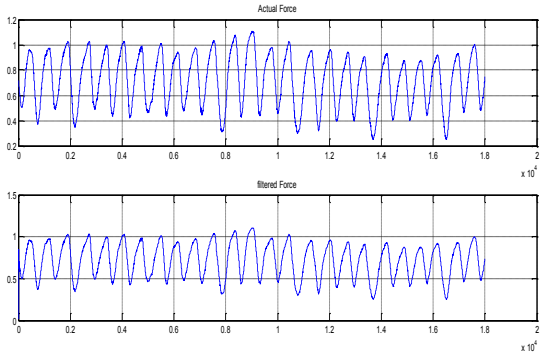

Fig. 4: Actual force and filtered force using Chebyshev Type-II filter

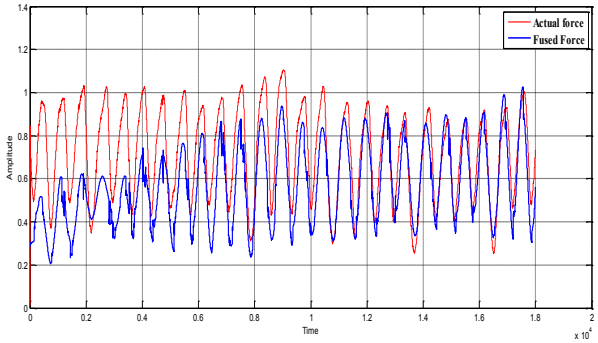

Fig. 5. Actual force and the overall estimated force for the Output Error (OE) Models

TABLE I: INVIDUAL ESTIMATED LINEAR PARAMETRIC MODELS AND THE OVERALL FUSED OUTPUT

SI Models	M_1	M_2	M_3	$\hat{Y}_f$
ARX	12.77	17.57	33.5	43.2
ARMAX	11.6	14.6	35	46.1
OE	54.42	60.39	64.96	75.6

Table I gives the individual estimated model correlation values (M_1, M_2, M_3) of the three sensors. $\hat{Y}_f$ gives the overall fused force correlation values for the linear parametric models. The individual models are computed by using the SI technique - ARX, ARMAX, OE. In all the cases, the values are high for M_3 which is the estimated model output for the sensor placed on the motor unit. All the three models are fused by using the above proposed Minimum Description Length based fusion algorithm. Even thought, the fusion algorithm shows improvement in the overall correlation value, the proposed fusion algorithm worked best for the linear Output Error (OE) models.

TABLE II: INVIDUAL ESTIMATED NONLINEAR MODELS AND THE OVERALL FUSED OUTPUT

SI Models	M_1	M_2	M_3	$\hat{Y}_f$
WH	52.37	56.8	60.35	70.32

Table II gives the individual estimated nonlinear Wiener Hammerstein models and the overall fused output using a MDL criterion based fusion algorithm. Fig 5 gives the plots of the actual skeletal muscle force and the overall fused output from the MDL fusion algorithm for OE models.

IV CONCLUSION AND FUTURE WORK

In this paper, we addressed a methodology to fuse the sEMG/skeletal muscle force data using a Minimum Description Length (MDL) criterion based fusion algorithm. Compared to the individual estimated models, the fusion-based output is showing improvement in correlation with the actual force.

In the future, we are planning to implement the same criteria for the spectral models [17] and to work on larger data sets and apply this proposed fusion algorithm to them for generalization.

ACKNOWLEDGEMENT

This research was sponsored by the US Department of the Army, under the award number W81XWH-10-1-0128 awarded and administered by the U.S. Army Medical Research Acquisition Activity, 820 Chandler Street, Fort Detrick MD 21702-5014. The information does not necessarily reflect the position or the policy of the Government, and no official endorsement should be inferred. For purposes of this article, information includes news releases, articles, manuscripts, brochures, advertisements, still and motion pictures, speeches, trade association proceedings, etc. This work was also partially supported in part by an internal Career Path Internship grant by Idaho State University. The support is greatly appreciated.

REFERENCES

[1] Estimating the Prevalence of Limb Loss in the United States- 2005 to 2050 Kathryn Ziegler-Graham, PhD, et al, *Archives of Physical Medicineand Rehabilitation* 89(3):422-429, 2008.

[2] http://cosmos.ot.buffalo.edu/t2rerc/programs/supplypush/devices.handt.html

[3] D.S. Naidu and C.-H. Chen, "Control Strategies for Smart Prosthetic Hand Technology: An Overview", Book Chapter 14, to appear in a book titled, Distributed Diagnosis and

Home Healthcare (D2H2): Volume 2, American Scientific Publishers, CA, January 2011.

[4] Pullman, S.L., Goodin, D.S., Marquinez , A.I., Tabbal, S., Rubin, M., " Clinical utility of surface EMG", 2000.

[5] Light, C.M. Chappell, P.H., "*Development of a lightweight and adaptable multiple-axis hand prosthese*", Medical Engineering and Physics, 22 , pp 679-684, 2000.

[6] Merletti, R., Parker, A.P., 1st ed., "Electromyography, Physiology Engineering and Non-Invasive Applications", Chapter 1., pp xv-xviii.

[7] M. Zecca, S Micera, M.C. Carrozza and P.Daria, "*Control of Multifunctional Prosthetic Hands by Processing the Electromyographic Signa*l", Critical reviews in Biomedical Engineering 30 (4-6), pp. 459-485, 2002.

[8] http://www.isek-online.org/standards_emg.html.

[9] M. Anugolu, A. Sebastian, P Kumar, M P. Schoen, A Urfer and Naidu DS, " *Surface EMG Array Sensor Based Model Fusion using Bayesian Approaches for Prosthetic Hands*", Proceedings of the Dynamic Systems and Control Conference (DSCC), Hollywood, CA, October 2009.

[10] Sanger D.T., " Bayesian Filtering of Myoelectric Signals", Journal of Neurophysiology, 97, pp.1839-1845, 2007

[11] Ljung L., 2nd ed., "System Identification: Theory for the user", Prentice Hall Information and System Science Series Chapter 1, pp 1-8.

[12] Ljung L., 2nd ed., "System Identification: Theory for the user", Prentice Hall Information and System Science Series Chapter 5, pp 140-145.

[13] Lennart Ljung, system Identification Toolbox 7 User's Guide, the MathWorks, Inc., 2010.

[14] J. Rissanen (1978) Modelling by the shortest data description. *Automatica 14*, 465-471.

[15] http://www.scholarpedia.org/article/Minimum_description_length

[16] Huimin Chen, Shuqing Huang, "A Comparative study on Model Selection and Multiple Model Fusion", 7th International Conference on Information Fusion, 2005, PP.820-826.

[17] Potluri C., Anugolu M., Chiu S., Urfer A., Perez A., Schoen M., Naidu DS., *" Fusion of Spectral Models for Relating sEMG-Skeletal muscle force data*., 34rd International Conference of the IEEE Engineering in Medicine and Biology Society, San Diego, 2012 (accepted).

Distributed Graph-Partitioning based Coalition Formation for Collaborative Multi-Agent Systems

Some Lessons Learned and Challenges Ahead

Predrag T. Tošić
Department of Engineering Technology and Department of Computer Science,
University of Houston, Houston, Texas, USA
pedja.tosic@gmail.com

Abstract - *We study algorithms for distributed collaborative multi-agent coalition formation. The focus of our recent and ongoing research has been on coalition formation via scalable distributed graph partitioning of the underlying agents' communication network topology. In that endeavor, we have been analyzing, simulating and optimizing our original graph partitioning algorithm called* Maximal Clique based Distributed Coalition Formation (MCDCF). *MCDCF is a fully distributed graph partitioning algorithm that was designed in a topology-independent manner, the only requirement being that the underlying graph be relatively sparse, which is a realistic assumption in most applications of our interest. In the present paper, we summarize our recent experimental findings on the performance of our algorithm on specific types of graph and draw some general lessons from those results. In particular, we focus on comparison and contrast between the MCDCF behavior on* small-world networks *and on* Erdös-Renyi random graphs. *We draw several insights from the considerable differences in MCDCF performance on these two types of underlying graphs (even when the underlying average densities or even node degree distributions are the same), identify key areas for further improvement, and outline some challenges ahead.*

Keywords: distributed algorithms, distributed AI, multi-agent systems, coalition formation, graph partitioning

1 Introduction and Motivation

We study, devise and analyze scalable distributed algorithms for challenging and important coordination problems in *Distributed Artificial Intelligence* (DAI), specifically, for medium- to large-scale collaborative multi-agent systems (MAS). We are interested in ensembles of artificial agents such as softbots, robots, unmanned vehicles or smart sensors that are autonomous, capable of sensing the environment, acting to affect changes in that environment, and also communicating and coordinating with each other. The communication and coordination capabilities enable such agents to self-organize in order to accomplish complex resource-demanding tasks that in general may exceed the computational, sensing and/or acting capabilities of the individual agents.

We have been particularly interested in mechanisms and protocols that enable large ensembles of such autonomous agents to coordinate with each other in a *fully decentralized* manner. The kinds of agents we have in mind are commonly referred to as *distributed problem solvers* in Distributed AI literature (e.g., [2, 21, 28]).

Among various interesting problems in distributed coordination and control of such agent ensembles, we have been extensively studying genuinely autonomous, fully distributed, dynamic multi-agent *coalition formation* [15-18]. We have designed a fully distributed, scalable and robust coalition formation graph algorithm named *Maximal Clique based Distributed Coalition Formation* (MCDCF) [15].

In the present paper, we build on the top of our earlier work on MCDCF [15-22], summarize and interpret our recent simulation results on the small-world and the random graph underlying network topologies, discuss possible reasons behind considerable differences in performance of our algorithm on these two types of topologies, identify some areas for further improvement, and outline future research directions. The rest of this paper is organized as follows. In Section 2, we motivate the problem of multi-agent coalition formation, briefly review the most relevant prior art, and describe our specific problem setting. In Section 3, we briefly describe how the MCDCF algorithm works. In Section 4, we summarize and discuss our simulation results when MCDCF is run on three sub-classes of small-world graphs. Section 5 summarizes and discusses our simulation results on Erdös-Renyi random graphs. In Section 6, we provide a brief comprehensive performance comparison-and-contrast on these two types of graphs. Section 7 summarizes the paper and outlines some challenges ahead.

2 Distributed Coalition Formation

Distributed coalition formation in multi-agent domains is an important coordination and collaboration problem that has been extensively studied by the MAS research community [1,

2, 8, 10-12, 15-20]. There are many collaborative MAS applications where autonomous agents need to form temporary groups or coalitions. Reasons behind multi-agent coalition formation may vary. In the context of *Distributed Problem Solving* (DPS) collaborative agents, possible motivations include resource sharing, dividing-and-conquering tasks that exceed the abilities of individual agents, and/or to improving some system-wide performance metric such as the speed of joint task completion [7, 12, 17].

In most research on multi-agent coordination and coalition formation, limitations on local computational and communication resources, as well as on each agent's local knowledge of the world around it, have been explicitly incorporated into the models and algorithms in order to make the proposed approaches realistic and relevant to the real-world distributed coordination problems; see, e.g., [8, 9]. The common formal framework for studying coalition formation is that of distributed constraint satisfaction or optimization (DCS or DCO, resp.). For a general overview of these important techniques, see e.g. [27, 28]; for a recent DCO-based work on coalition formation, see e.g. [23]. We remark that our distributed graph partitioning approach can be readily phrased in DCS/DCO terms, as well, as discussed in [16, 17]. For brevity and simplicity of notation, in this paper (as well as the two papers that are the immediate predecessors to the present work, [21, 22]), we avoid DCO formalisms and stick to graph-theoretic terminology and notation.

One well-studied general coalition formation domain is a collaborative multi-agent environment populated with a variety of distinct, mutually independent tasks, where each task requires a tuple of resources on the agents' part in order for the agents to be able to complete that task [10 - 12, 17-18]. In this *distributed task allocation* context, agents need to form coalitions such that each coalition has sufficient cumulative resources or capabilities across the coalition members in order to be able to complete the assigned task(s).

We study the problem of distributed coalition formation in the following scenario. We assume a collaborative multi-agent, multi-task dynamic and partially observable environment. The tasks are atomic (that is, a task has either been completed or it has not; we don't consider partial task completion) and *mutually independent* of each other. In general, different tasks may have different values or utilities associated with them. Moreover, the utility of a particular task may be differently perceived by different agents. This problem setting is particularly appropriate for many MAS applications involving *team robotics* and *autonomous unmanned vehicles* [5, 17, 18]. In particular, our agents are distributed problem solvers: they are assumed to be *strictly collaborative*. The agents have certain capabilities that may enable them to service various tasks. The tasks have certain resource or capability requirements, so that no agent or coalition of agents whose joint capabilities do not meet a particular task's resource requirements can serve that task [10, 17]. Each task is of a certain value to an agent. Agents are assumed capable of communicating, negotiating and making agreements with each other [2, 8, 10, 27]. Communication is accomplished via exchanging messages. This communication is not free: an agent has to spend time and effort in order to send and receive messages [17].

An important difference between our problem setting and that found in [10] is that we assume that neither *an agent's resources nor a task's utility are transferable to other agents* [15, 17]. In particular, the only way for an agent A_i to use the internal resources of agent A_j for the purpose of servicing some task is that A_i and A_j join the same coalition, and then jointly complete that task.

Our *distributed maximal clique-based coalition formation* algorithm is based on the idea that, in a *peer-to-peer* MAS, an agent would prefer to form a coalition with those agents that it can communicate with directly, and, moreover, where every member of such potential coalition can communicate with any other member *directly*. That is, the preferable coalitions are (maximal) cliques. However, finding a maximal clique in an arbitrary graph is **NP**-hard in the centralized setting [3, 4]. This implies the computational hardness that, in general, each agent faces when trying to determine the maximal clique(s) it belongs to. However, if the degree of a node is, that is, if the number of 1-hop neighbors that an agent can directly communicate with, is sufficiently small, then finding some or even all maximal cliques that this node belongs to might be computationally feasible. If one cannot guarantee that all the nodes in a given underlying interconnection topology are of small degrees, then the system designer may want to impose additional constraints, in order to ensure that coalition formation according to the MCDCF protocol is computationally feasible [15, 17]. Alternatively, the system designer may want to consider modifying the objective function, so that the candidate coalitions an agent would consider forming need not necessarily be *maximal cliques* that this agent belongs to. The most appropriate design choice clearly depends on the application at hand, the nature of agents' tasks, and the agents' communication and computational resources. For a more detailed discussion, we refer the reader to our prior work [15 - 21].

3 Outline of the MCDCF Algorithm

The MCDCF coalition formation protocol [15, 17, 18] is a *distributed graph algorithm*. The underlying undirected graph captures the communication network topology among the agents. Each agent is a node in the graph. The necessary requirement for an edge between two nodes to exist is that the two nodes be able to directly communicate with one another. Communication takes place by local or group broadcasts. The group broadcast nature of the assumed communication model is primarily inspired by the applications that drove the original MCDCF design, namely team robotics, autonomous unmanned aerial and underwater vehicles -- in particular, *micro-UAVs* [18, 19] -- as well as smart sensor networks.

The basic idea behind MCDCF is to *partition* the communication topology graph into (preferably, maximal) *cliques* of mutually connected nodes. These maximal cliques would in practice usually also need to satisfy some additional criteria in order to form coalitions of desired quality. The resulting coalitions are then maintained until they are no longer preferred by the agents involved in them.

To ensure overall scalability and computational feasibility of the protocol, the candidate coalitions in MCDCF are required to be cliques of uniformly bounded sizes. This requirement, in practice, means one of the two possibilities. One possibility is that it is *a priori* known that the underlying MAS network topology is such that it can be guaranteed that there are no cliques that are prohibitively large. Otherwise, the system designer, based on the application at hand and the available system resources, a priori chooses a threshold $K = K(n)$, where n is the total number of nodes, such that only the coalitions of sizes up to K are considered.

Agents form coalitions in a fully distributed manner as follows. Each agent (i) first learns of who are its neighbors, then (ii) determines the appropriate candidate coalitions, that the agent hopes are cliques that it belongs to, then (iii) evaluates the utility value of each such candidate coalition, measured in terms of the joint resources of all the potential coalition members and how valuable are the tasks that such a coalition can complete, then (iv) chooses the most desirable candidate coalition, and, finally, (v) sends this choice to all its neighbors. An agent also receives similar coalition proposals from some subset of its one-hop neighbors. The agent compares its current coalition proposal against those received from the neighbors. If there is an agreement among all agents in the current proposal of our agent, let's call it A_i, then this condition is recognized and a new coalition is formed. Once this happens, A_i's other neighbors, namely, those not in the newly formed coalition (if there are any such neighbors left), are notified of the formation of the new coalition. If there is no agreement, meaning, if at least one agent in the current proposal of A_i does not agree with that proposal, then the process continues and the protocol moves to the next round.

The basic procedure outlined above is repeated, together with all agents updating their knowledge of (a) what are the preferred coalitions of their neighbors, and (b) what coalitions have already been formed – until eventually every agent has joined some coalition. Note that, when an agent has no available coalition partners left, the agent is basically forced to form the trivial, "singleton coalition" (with itself as the only member). Hence, it is guaranteed that each agent will join some coalition eventually, i.e., after finitely many rounds.

Detailed description, communication and computation complexity analysis, and pseudo-code for the MCDCF algorithm can be found in [16, 17]. Considerable algorithmic and software optimizations and improvements are summarized in [20]. Among the main goals of our recent experimental investigations [21, 22] was to determine, just how effective these optimizations are when MCDCF is applied to (i) small-world-like underlying topologies and (ii) random (Erdös-Renyi) graphs.

4 Running MCDCF on Small-World Graphs

We have conducted extensive experiments to investigate how well MCDCF performs on small-world graphs [21], and also to verify theoretical predictions related to scalability [16, 17]. The two key parameters for the MCDF algorithm are the number of nodes n and the average node degree *avg_deg*. In this section, we briefly summarize the main findings of that study. We considered three subclasses of small-world graphs. The first subclass were the regular k-rings, with no random edges; strictly speaking, k-rings aren't "small-world" networks but were used as the starting point from which genuine small-world topologies were obtained, as well as the "yardstick" for MCDCF performance on highly structured graphs. We recall that MCDCF design was topology- and structure-oblivious, the only requirement being that the topology has to be relatively sparse [15-18].

The second and third subclasses were genuine small-world networks, with different probabilities of some of the local edges of a k-ring being replaced by random (hence, in general, non-local) edges. In the second subclass, 10% of the total number of edges were random edges, implying that up to 10% of all edges in the graph were non-local (but the exact fraction of non-local edges would of course vary from one randomly generated graph with p = 0.10 of a regular ring edge being replaced by a random edge to another). In the third subclass, with p = 0.20 a ring edge would get replaced by a random edge, meaning, up to 20% of all edges were non-local.

In summary, the regular k-rings, which are not truly small world networks, were used as the "yardstick" to see how would the MCDCF performance get affected with an increase in non-local network connections. We were also interested in quantifying the speed of convergence of MCDCF as the probability of random, non-local edges increases.

We considered two basic scenarios. In the first scenario, we maintained the number of nodes as a constant and varied the average node degree. In the second scenario, the average node degree was held constant and we varied the total number of nodes.

Scenario 1:

The varying parameter in this scenario was the average node degree, whereas the number of nodes remained fixed (n = 200). We have incremented the average node degree in multiples of 2, from *avg_deg* = 4 up to *avg_deg* = 20. We briefly summarize the main lessons learned from the simulation results for this scenario and their statistical analysis. Details can be found in our WorldComp ICAI-2011 paper [21].

Insofar as the rates of convergence are concerned, the increase in graph density only mildly affected the speed of convergence on the regular k-rings. However, genuine small-world networks (with non-zero probabilities of random edges) were considerably affected: the average number of rounds until convergence, in general, showed *exponential increase* with the increase in average node degree for both subclasses 2 and 3. Not surprisingly, subclass, which has a higher percentage of non-local edges, was affected more drastically, that is, the increase in the average number of rounds until convergence was steeper than for the subclass 2. For details, we refer the reader to Fig. 1 in [21] and related discussion.

The number of formed coalitions showed a gentle increase with the increase in the total graph density. Interestingly, the maximum size of coalitions that MCDCF was able to find did not show any clear trend. In particular, the fact that higher density implied expected larger maximum coalition sizes did not imply that our protocol would be able to effectively find

those larger cliques. Therefore, the optimizations discussed in detail in [20], while considerably improving the quality of found coalitions (as well as the convergence times) for certain types of underlying networks, did not result in desirable improvements for the genuine small-world networks.

Scenario 2:

In this scenario we varied the number of nodes and the average node degree remained constant: *avg_node* = 10 throughout. We incremented the number of nodes each time by 20, starting from n = 40 up to n = 200 nodes. As in Scenario 1, for each pair of values (n, *avg_deg*), we ran MCDCF on ten different, randomly generated graphs. We summarize the most important observations and lessons learned from this scenario below.

When the graph density is held constant, the number of rounds to reach convergence increases approximately *linearly* with the total number of nodes; see Figure 4 and related discussion in [21]. According to theoretical predictions [15-17], how long it takes for MCDCF to converge on an arbitrary graph primarily depends on the neighborhood sizes, not the total number of nodes in the graph.

Insofar as how many coalitions get formed and what their average and maximal sizes tend to be (as a function of the total number of nodes), it turned out that the number of coalitions was a monotonically increasing function of n as well as of the probability of random rewiring. This was in accordance with our expectations. In particular, the fixed average node degree implies that we should not expect more larger-sized coalitions as n increases; rather, we tend to get more coalitions of roughly the same average sizes as for smaller n. We also note that, for rewiring probabilities of 0.1 and 0.2, due to random nature of our test graphs, most nodes ended up in singleton and doubleton coalitions basically irrespectively of n and *avg_deg* (see Figures 3 and 5 in [21]). In particular, as the number of nodes and the probability of random rewiring increase, the total number of formed coalitions also tends to increase – but not the coalition sizes.

5 Running MCDCF on Random Graphs

In the context of Erdös-Renyi (E-R) random graphs, we essentially performed the same sets of experiments as with the small-world graphs. In particular, we considered two scenarios. In the first scenario, we maintained the number of nodes as a constant and varied the average node degree. In the second scenario, the average node degree was held constant and we varied the total number of nodes. The results for the two scenarios are summarized in this section. For much more details on MCDCF performance on random graphs, we refer the reader to [22].

We remark that we are well aware that Erdös-Renyi graphs, while often considered "the default" type of random graphs, are not a kind of network topologies frequently encountered in practice in general, or in any of the collaborative MAS applications of our interest, in particular. There are two main reasons why we have been studying MCDCF performance on these random graphs. One, E-R random graphs are a good choice of the baseline topology structure on which to test our algorithm to establish the "ground truth" on how scalable and efficient MCDCF really is in practice, as opposed to theory [15-17]. Various aspects of performance (such as the speed of convergence and the average sizes / quality of the resulting coalitions) on these random graphs therefore serve as a benchmark to better understand and appropriately calibrate the MCDCF performance on more realistic types of underlying topologies of the same or comparable sizes and/or densities. Two, the design of MCDCF was utterly oblivious with respect to the underlying graph structure: when originally designing and prototyping this algorithm [15, 16], we only cared that the node degrees be appropriately bounded – but no aspect of the original protocol, or the subsequent modifications and optimizations of it [20], made any attempt to take advantage of any local or global structural property of the underlying topology. Hence, we felt it was appropriate to first test such a structure-oblivious algorithm on a kind of underlying graphs that are, arguably, as structure-free as communication network topologies can be [22].

While our experimental results on Erdös-Renyi graphs in [22] are admittedly based on a fairly small statistical sample, we have tried to identify some general trends and properties of the MCDCF performance that, based on our experience with graph algorithms in general and MCDCF in particular, we would expect not be too significantly affected even had we performed thousands (instead of only dozens) of runs for each set of parameter values. We acknowledge that, in the future work, it is recommendable to include confidence intervals or another measure of statistical significance. We summarize the main findings below, and refer the reader to [22] for the performance plots and detailed analyses and discussion.

Scenario 1:

The varying parameter in this scenario is the average node degree, while the number of nodes remains constant (n = 100). We have incremented the average node degree in multiples of two, from avg_deg = 2 up to avg_deg = 20.

The speed of convergence shows the same general trend as in the case of small-world networks. In particular, the number of rounds required in order for all agents to join coalition clearly grows *exponentially* with the average node degree, in accordance with theoretical expectations [15-17]. We recall that, as the average node degree increases, so does the average size of a node's neighborhood list, and hence the number of candidate coalitions to consider. Moreover, the number of candidate coalitions grows exponentially with the number of neighbors. This general behavior, based on theoretical analysis [15-17], has been observed experimentally on all types of graphs that we have experimented with to date, including the small-world graphs and the Erdös-Renyi graphs.

However, unlike with the small-world networks, in case of the random graphs the total number of coalitions formed stayed roughly the same. However, the average size of coalition showed a clear trend of growth with the increase in average graph density. In particular, MCDCF is capable of finding increasingly larger maximal cliques on presumably structure-less Erdös-Renyi random graphs as the graph density (and therefore, the expected max. coalition size that a typical

node belongs to) increase; see Figure 2 in [22]. In contrast, MCDCF showed unsatisfactory performance in finding relatively large cliques in non-trivial small-world graphs as those graphs' densities grew. We were initially surprised with these findings, as MCDCF was not designed or optimized for any particular underlying structure or type of network topology. We suggest some possible explanations in the next section.

Scenario 2:

In this scenario, we varied the number of nodes *n* while the average node degree re-mains constant: *avg_node = 10* throughout. We incremented *n* each time by 10, starting from n = 10 up to n = 100 nodes. The purpose of this second set of experiments was to validate our prior theoretical predictions that MCDCF's performance, in general, should be affected very mildly by increase in the overall graph size, as long as the average neighborhood sizes are held fixed. Some general observations and the main lessons learned from this scenario fare summarized below; more details can be found in [22].

We observed a very modest increase in the number of rounds until convergence as a function of the total number of nodes (see Figure 4 in [22]. Namely, how long it takes for a node to agree with some subset of its neighbors on which coalition to form is primarily controlled by the neighborhood size and hence the size of both the initial candidate coalition and the total number of candidate coalitions that may be considered during the protocol's execution. However, the overall number of rounds can be generally expected to relatively slowly increase with *n*, since the total number of rounds is determined by the "slowest negotiators" among the agents. Hence, with an increase of the number of nodes, and given the random nature of underlying graphs, the variability in convergence speeds of different nodes can be expected to gently increase, thereby resulting in an average increase in the total number of rounds until every node in the graph joins a coalition.

Insofar as the relationship between the number of nodes and the total number of coalitions formed, it turned out that the number of coalitions is a monotonically increasing function of *n*, as expected. Moreover, this dependence turned out to be approximately linear (see Figure 6 in [22]). We think that the reason behind this is that, due to random nature of our graphs, most nodes end up in singleton and doubleton coalitions basically almost irrespectively of *n* and *avg_deg*. Therefore, as the number of nodes increases, the total number of formed coalitions increases – while the average coalition size remains roughly the same (around or below two).

6 MCDCF on Small-World vs. Erdös-Renyi Random Graphs: Comparison-and-Contrast

We summarize the key findings and insights from the comparative analysis of MCDCF performance on the two types of network topologies studied in [21, 22] and discussed in the previous two sections of the present paper. We focus on those aspects where the MCDCF behavior has turned out to be considerably different depending on whether the underlying graph was of the small-world variety or of the random (in the Erdös-Renyi sense) variety.

Insofar as the scenario where the total number of nodes *n* was held fixed but the number of edges, and hence overall connectivity and density, were gradually increased, the convergence times showed an exponential increase with the average node degree for both network topologies. That much was in accordance with theoretical predictions and our expectations. The difference is that, whereas MCDCF was fairly successful in finding cliques of relatively larger sizes in the random E-R graphs (whenever such larger cliques existed), our algorithm was not very successful in identifying such cliques in genuine small-world networks. (By "genuine" we mean, those that aren't mere regular k-rings.) This is at least in part due to the tie-breaking mechanisms in MCDCF, in situations where an agent needs to pick one among two or more "equally preferable" candidate coalitions. While MCDCF design is indeed topology-blind, the tie-breaking mechanisms are heavily based on the lexicographic ordering (that is, indexing) of different nodes. Even with the optimizations (and, in particular, some randomizations, to escape the curse of lex-based indexing) introduced in [20], the small-world graphs obtained from regular k-rings still have a considerable correlation between the probability of two nodes being adjacent (that is, connected by an edge) on one hand, and having indices close to each other (that is, small $|i - j|$), on the other. In contrast, by their very definition, the Erdös-Renyi random graphs (to within the quality of the underlying pseudo-random random generator) have no correlation between indices of the nodes and the likelihood of node pairs being connected by an edge.

While some randomization introduced in the process of selecting which candidate coalitions of a size one less than the most recent proposal (that has not been accepted by peers) an agent would consider in the future rounds has diminished the correlation between $|i - j|$ and probability of A_i and A_j being adjacent, that correlation still exists. Moreover, some of the optimizations in the traversal of the lattice of candidate coalitions of a given node [20], while making this traversal in general faster than in the original, unoptimized MCDCF [15-17], may also have undesirable side-effects on the ability of MCDCF to find relatively large cliques when index proximity and likelihood of being connected are positively correlated yet, due to introduced randomness, it isn't the case (informally speaking) that "my neighbor is also likely my neighbor's neighbor". These observations also provide a hint why MCDCF converges very fast on regular k-rings even as the graph density is increased, whereas the rates of convergence drop very significantly once random edges are introduced.

When it comes to the second scenario, where the average node degree is held fixed but the total number of nodes is varied, we see less dramatic difference between the performances on the two types of topologies. However, the speed of convergence is still more affected in the small-world than the E-R random graphs. Interestingly, while among small-world-like graphs the convergence on regular k-rings is the fastest (which is to be expected), this difference is not very pronounced – quite unlike the drastic difference between the

regular rings and the genuine small-world topologies when it comes to the speed of convergence as a function of average node degree (that is, graph density). In particular, the increase in graph size appears to slow down coalition formation convergence more on highly structured k-rings than it does on structure-free E-R random graphs for the same total sizes and densities. This is another indication that the tie-breaking mechanisms and the selection of candidate coalition(s) strictly smaller than the current choice, with their dependencies on node labels (that is, indexing), have a considerable impact on the overall effectiveness of MCDCF – even after the considerable optimizations and even some randomization have been introduced into those processes (see [20] for details on those optimizations).

When it comes to the limited ability of MCDCF to form relatively large coalitions (which, in our context, means triples or larger) on regular k-rings and small-world graphs derived from k-rings, one needs to distinguish between the protocol failures to identify larger coalitions that actually are present in the graph, and the lack of existence of such coalitions due to randomization in edge "re-wiring". We recall from [21] however that k-rings are deterministic and, for relatively high k, contain multiple what we consider to be sizable cliques. That MCDCF in general fails to find those cliques effectively is perhaps the single most important indication that, in spite of all our efforts as discussed in [20], our protocol needs to be considerably further fine-tuned and optimized.

7 Conclusions and The Road Ahead

We have applied our distributed coalition formation algorithm to small-world and random graphs. In particular, we studied our MCDCF algorithm's performance on the network topologies that, to various extents, exhibit small-world structure. We have tested our algorithm on random small-world graphs with up to 200 nodes. Our simulations have produced several generally expected results, which partly validate the claim that our approach to distributed coalition formation is applicable to a broad variety of underlying topologies. However, we have also obtained some rather unexpected and, in some instances, disappointing results. One lesson learned is that the optimizations of MCDCF reported in [20], while very helpful when the algorithm is run on random graphs [22], appear inadequate when MCDCF is run on small-world graphs [21]. Therefore, one immediate objective of our ongoing research is to improve inter-agent coalition negotiation as well as individual agent's candidate coalition search mechanisms, in order to ensure faster convergence, as well as better resulting coalition structures, when our algorithm is run on small-world-like underlying networks. We also need to investigate in more depth what properties of small-world graphs cause subpar performance of MCDCF with respect to some of the metrics discussed in this paper and its predecessor [21].

We have generally found that, most of the time, MCDCF successfully identifies larger cliques when those are indeed present in the underlying random graph. We acknowledge that further experimental validation is needed – especially on graphs that (a) exhibit some type of structure and (b) are important from an application standpoint (i.e., are more likely to arise in practice than the Erdös-Renyi graphs). Examples of such graphs include scale-free graphs, power-law graphs, and social network graphs with the assortativity property. For instance, we would expect MCDCF to be able to efficiently find relatively sizable cliques / coalitions in social network graphs with node degrees and total number of nodes comparable to the graphs in our experiments to date, yet with the property that above-average connected nodes tend to be predominantly connected to each other.

Moving forward, we will explore MCDCF performance on small-world networks when the node indices are scrambled in order to eliminate the correlation between proximity and being connected by an edge. Furthermore, from the lessons learned in the context of small-world networks, we will also study MCDCF performance on other types of interesting topologies (power-law graphs, social networks, etc.) both with and without pre-processing step that scrambles the node indices. That way, we will be able to quantify to what extent the tie-breaking mechanisms, as discussed in [15-18, 20], that are in part based on index ordering, have an impact on our algorithm's overall speed of convergence and effectiveness in finding non-trivial cliques.

Acknowledgments

The author would like to thank his former graduate student at University of Houston, Naveen K.R. Ginne, as well as his own former PhD advisor, professor Gul Agha, and members of Dr Agha's Open Systems Laboratory at University of Illinois at Urbana-Champaign, for several years of fruitful collaboration on multi-agent distributed coalition formation. The author would also like to thank Dr Yuriy Fofanov, Dr Carlos Ordonez, Dr Ioannis Kakadiaris, Dr Nikolaos Tsekos and Dr Ricardo Vilalta (all at University of Houston) for their support during 2011-2012.

References

[1] S. Abdallah, V. Lesser. *Organization-Based Cooperative Coalition Formation, in* Proc. IEEE / WIC / ACM Int'l Conf. on Intelligent Agent Technology (2004)

[2] N. M. Avouris, L. Gasser (eds.). *Distributed Artificial Intelligence: Theory and Praxis*, Euro Courses Comp. & Info. Sci. vol. 5, Kluwer Academic Publ. (1992)

[3] T. H. Cormen, C. E. Leiserson, R. L. Rivest, C. Stein. *Introduction to Algorithms*, 3rd edition, MIT Press (2009)

[4] M. R. Garey, D. S. Johnson. *Computers and Intractability: a Guide to the Theory of NP-completeness*, W.H. Freedman & Co., New York (1979)

[5] M-W Jang et al. *An Actor-based Simulation for Studying UAV Coordination*, in 16th European Simulation Symposium (ESS'03), pp. 593-601, Delft, The Netherlands (2003)

[6] X. Li, L.K. Soh. *Investigating reinforcement learning in multiagent coalition formation*, TR WS-04-06, AAAI Workshop Forming and Maintaining Coalitions & Teams in Adaptive MAS (2004)

[7] D. de Oliveira. *Towards Joint Learning in Multiagent Systems Through Opportunistic Coordination*, PhD Thesis, Univ. Federal Do Rio Grande Do Sul, Brazil (2007)

[8] T.W. Sandholm, V.R. Lesser. *Coalitions among computationally bounded agents*, in *Artificial Intelligence* vol. 94, pp. 99-137 (1997)

[9] T. W. Sandholm, K. Larson, M. Andersson, O. Shehory, F. Tohme. *Coalition structure generation with worst case guarantees*, in *AI Journal* vol.111 (1-2), pp. 209-238 (1999)

[10] O. Shehory, S. Kraus. *Task allocation via coalition formation among autonomous agents*, in Proceedings of IJCAI-95, Montréal, Canada, pp. 655–661 (1995)

[11] O. Shehory, K. Sycara, S. Jha, *Multi-agent coordination through coalition formation*, in *Intelligent Agents IV: Agent Theories, Architectures & Languages*, LNAI #1365, pp.153-164, Springer (1997)

[12] O. Shehory, S. Kraus, *Methods for task allocation via agent coalition formation,* in *AI Journal* vol. 101, pp. 165-200 (1998)

[13] L.K. Soh, X. Li. *An integrated multilevel learning approach to multiagent coalition formation*, in Proc. Int'l Joint Conf. on Artificial Intelligence IJCAI'03 (2003)

[14] R. Sun. *Meta-Learning Processes in Multi-Agent Systems*, in *Intelligent agent technology: research and development*, N. Zhong, J. Liu (eds.), pp. 210-219, World Scientific, Hong Kong (2001)

[15] P. Tosic, G. Agha. *Maximal Clique Based Distributed Group Formation Algorithm for Autonomous Agent Coalitions*, in Proc. Workshop on Coalitions & Teams, AAMAS-2004, New York City, New York (2004)

[16] P. Tosic, G. Agha. *Maximal Clique Based Distributed Coalition Formation for Task Allocation in Large-Scale Multi-Agent Systems*, Post-Proceedings of MMAS-04; LNAI vol. 3446, pp. 104-120, Springer (2005)

[17] P. Tosic. *Distributed Coalition Formation for Collaborative Multi-Agent Systems,* MS thesis, Univ. of Illinois at Urbana-Champaign (UIUC), Illinois, USA (2006)

[18] P. Tosic, G. Agha. *Understanding and Modelling Agent Autonomy in Dynamic Multi-Agent, Multi-Task Environments*, in Proc. of the 1st European Workshop on Multi-Agent Systems EUMAS'03, Oxford, England (2003)

[19] P. Tosic et al., *Modeling a System of UAVs on a Mission,* session on intelligent agent systems & technologies, in Proc. 7th World Multiconference on Systemics, Cybernetics & Informatics SCI'03 (2003)

[20] P. Tosic, N. Ginne. "MCDCF: A Fully Distributed Algorithm for Coalition Formation in Collaborative Multi-Agent Systems", Proc. WorldComp ICAI'10, Las Vegas, Nevada, USA (2010)

[21] P. Tosic, N. Ginne. "Challenges in Distributed Coalition Formation among Collaborative Multi-Agent Systems: An Experimental Case Study on Small-World Networks", Proc. WorldComp ICAI'11, Las Vegas, Nevada, USA (2011)

[22] P. Tosic, N. Ginne. "A Scalable Distributed Graph Algorithm for Dynamic Coalition Formation: A Performance Case Study on Random Graphs", Proc. of the 9th European Workshop on Multi-Agent Systems (EUMAS'11), Maastricht, The Netherlands, 2011

[23] S. Ueda, et al. "Coalition Structure Generation Based on Distributed Constraint Optimization", Proc. of the 24th AAAI Conference on Artificial Intelligence AAAI-10 (2010)

[24] L. Vig, J.A. Adams. "Coalition Formation: From Software Agents to Robots", *J. Intelligent Robot Systems*, vol. 50, pp. 85–118 (2007)

[25] Duncan J. Watts. "The "New" Science of Networks", *Annual Review of Sociology*, vol. 30, pp. 243-270 (2004)

[26] The Watts-Strogatz small-world graph generator we used can be found at http://networkx.lanl.gov/reference/generated/networkx.generators.random_graphs.watts_strogatz_graph.html

[27] G. Weiss (ed.) *Multiagent Systems: A Modern Approach to Distributed Artificial Intelligence,* MIT Press (1999)

[28] M. Wooldridge. *An Introduction to Multi-Agent Systems*, Wiley (2002)

Improved Fuzzy Neural Modeling Based on Differential Evolution for Underwater Vehicles

O. Hassanein[1*], Sreenatha G. Anavatti[2*], and Tapabrata Ray[3*]
[*]SEIT, UNSW@ADFA, Canberra, Australia
[1]o.hassan@adfa.edu.au
[2]s.anavatti@adfa.edu.au
[3]t.ray@adfa.edu.au

Abstract— *Autonomous Underwater Vehicles (AUVs) have gained importance over the years as specialized tools for performing various underwater missions in military and civilian operations. This study presents the on-line system identification of AUV dynamics to obtain the coupled nonlinear dynamic model of AUV. This proposed model has an input-output relationship based upon neural fuzzy network (NFN) model technique to overcome the uncertain external disturbance and the difficulties of modelling the hydrodynamic forces of the AUVs instead of using the mathematical model with hydrodynamic parameters estimation. Initially the models' parameters are generated randomly and tuned by Differential Evolution algorithm (DE) with a set of real input-output data. Secondly, the back propagation algorithm based upon the error between the identified model and the actual outputs of the plant are used to adopt the model's parameters. The proposed NFN model adopts a functional link neural network (FLNN) as the consequent part of the fuzzy rules. Thus, the consequent part of the NFN model is a nonlinear combination of input variables. Simulation results show the superiority of the proposed adaptive neural fuzzy network (ANFN) model in tracking of the behavior of the AUV .*

Keywords: AUV dynamic model, fuzzy modeling, adaptive fuzzy system, system identification, neural fuzzy model, FLNN.

1 Introduction

Autonomous Underwater Vehicles (AUVs) have gained importance over the years as specialized tools for performing various underwater missions in military and civilian operations. The autonomous control of underwater vehicles poses serious challenges due to the AUVs' dynamics. AUVs dynamics are highly nonlinear and time varying and the hydrodynamic coefficients of vehicles are difficult to estimate accurately because of the variations of these coefficients with different navigation conditions and external disturbances.

According to [1] the two most significant technological challenges in AUV's design are power and autonomy. Power sources limit the mission time of the vehicle and autonomy limits the degree to which an AUV can be left unattended by human operators.

Reference [2] presented a simple model identification method for UUV and applied this method to the underwater robot GARBI. The system identification was aimed at decoupling the different degrees of freedom in low speed vehicles. Least Square techniques were used to estimate the UUV dynamics. Experiments in lab and real underwater environments were carried out. A neural fuzzy system based on modified differential evolution for nonlinear system control is discussed in [3]. The proposed controller adopts a nonlinear combination of input variables to the consequent part of fuzzy rules and uses a differential evolution to optimize the system parameters. This controller is applied to the planetary-train-type inverted pendulum system and the magnetic levitation system in the VisSim solving nonlinear control problems.

The FLNN is a single-layer neural structure capable of forming arbitrarily complex decision regions by generating nonlinear decision boundaries with nonlinear functional expansion. The FLNN [4] was conveniently used for function approximation and pattern classification with faster convergence rate and less computational loading than a multilayer neural network. Recently, genetic fuzzy systems [5,6] have received increasing attention mainly because they combine the approximate reasoning method of fuzzy systems with the learning capabilities of evolutionary algorithms. However, the search is extremely time-consuming, which is one of the basic disadvantages of all genetic algorithms (GAs). Similar to GAs, differential evolution (DE) has emerged as a robust numerical optimization algorithm and has been successfully applied to solve various difficult optimization problems [7, 8]. Basically, DE is fast, easy to use, and not only astonishingly simple, but also performs extremely well in a wide variety of test problems. The basic strategy employs the difference of two randomly selected individuals as the source of random variations for a third individual. However, DE usually explores too many search points before locating the global optimum. In addition,

although DE is particularly simple to work with, having only a few control parameters, the choice of these parameters is often critical for the performance of DE [8, 9]

This study proposes an online system identification of AUV dynamics as a black box which has an input-output relationship instead of using the mathematical model with hydrodynamic parameters to obtain an accurate dynamic model to overcome the uncertaininaty, nonlinearity and the difficulties of modelling the AUVs. The only information required for generating and tuning the neural fuzzy systems is the input -output data without any prior knowledge of the physical relationship inside the system and it offers a 'black box' modelling tool. ADFA AUV has been developed and built in UNSW@ADFA. The hydrodynamic coefficients of this AUV are calculated under certain conditions using CFD method to derive the exact mathematical model. Simulation program is built up to simulate the dynamic behaviour of the AUV based upon the calculated mathematical model of the AUV.

The general dynamic equation describing the mathematical model of the ADFA AUV is provided in Section 2. The design details of identification of AUV using adaptive neural fuzzy network (ANFN) techniques are presented in section 3. The optimization and tuning techniques for the system identification are provided in section 4. Moreover, Numerical simulation results are presented in section 5. Finally, the paper is concluded in Section 7.

2 AUV's mathematical model

Fig. 1 shows a typical UNSW@ADFA AUV during one of the experiments. One electrical thruster powers the vehicle for forward motion. Two electrical pumps are used for maneuvering in the horizontal plane. In addition, two electrical pumps help the AUV to navigate in the vertical plane. The middle box is used for carrying the sensors, battery and the electronic accessories.

The hydrodynamic forces per unit mass acting on each axis will be denoted by the uppercase letters X, Y and Z. *u*, *v* and *w* represent the forward, lateral and vertical velocities along x, y and z axes respectively. Similarly, the hydrodynamic moments on AUV will be denoted by L, M and N acting around x, y and z axis respectively. The angular rates will be denoted by *p*, *q* and *r* along x, y and z axes respectively.

Dynamics of AUVs, including hydrodynamic parameters uncertainties, are highly nonlinear, coupled and time varying. According to [10], the six degrees-of-freedom nonlinear equations of motion of the vehicle are defined with respect to two coordinate systems as shown in Fig. 2. The dynamic models of thrusters and pumps have been included in the present study. The AUV model is simulated by a mathematical model based on physical laws and design data of the ADFA AUV.

3 NFN System Identification of AUV

The NFN uses a nonlinear combination of input variables (FLNN) [11] with the fuzzy system. Each fuzzy rule corresponding to the `FLNN comprises a functional expansion of input variables. The FLNN, initially proposed by [4], is a single-layer ANN structure capable of forming complex decision regions by generating nonlinear decision boundaries. In a FLNN, the need of hidden layer is removed.

Figure 1. Australian Defence Force Academy AUV.

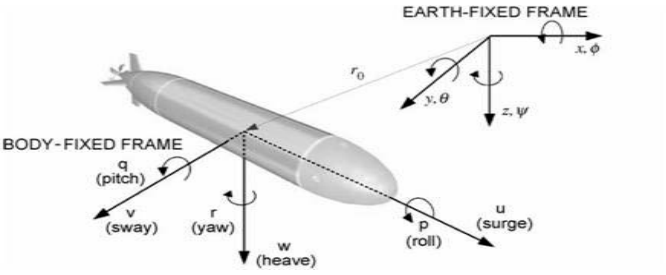

Figure 2. Six degrees of freedom of an AUV.

In this study, the functional expansion block comprises of a subset of orthogonal polynomials bases function. The FLNN has been inserted to the consequent part of the fuzzy rules. The local properties of the consequent part in the NFN model enable a nonlinear combination of input variables to be approximated more effectively.

3.1 Functional link neural network structure (FLNN)

The FLNN is a single-layer network while the input variables generated by the linear links of neural networks are linearly weighted, the functional link acts on an element of input variables by generating a set of linearly independent functions, orthogonal polynomials for a functional expansion, and then evaluating these functions with the variables as the arguments. Therefore, the FLNN structure considers trigonometric functions. In the FLNN structure as shown in Fig. 3, a set of basis functions Φ and a fixed number of

weight parameters W represent $f_{W(k)}$. The theory behind the FLNN for multidimensional function approximation has been discussed in [12]. Consider a set of basis functions $B = \{\varphi_k \in \Phi(A)\}_{k\in K}$, K = {1, 2, . . .}. Let $B = \{\varphi\}_{k=1}^{M}$ be a set of basis functions. The FLNN comprises M basis functions$\{\varphi_1, \varphi_2, \dots\dots\dots, \varphi_M\} \in B_M$. The linear sum of the j[th] node is given by

$$\hat{y}_j = \sum_{k=1}^{M} w_{kj}\varphi_k(X) \qquad (2)$$

where $X \in A \subset \Re^N, X = [x_1, \dots\dots, x_N]^T$ is the input vector and $W_j = [w_{j1}, \dots\dots, w_{jM}]^T$ is the weight vector associated with the j^{th} output of the FLNN. $\hat{y}_j$ denotes the local output of the FLNN structure and the consequent part of the j^{th}fuzzy rule in the NFN model. The m-dimensional linear output may be given by $\hat{y} = W\Phi$, where $\hat{y} = [\hat{y}_1, \hat{y}_2, \dots\dots, \hat{y}_m]^T$, m denotes the number of functional link bases, which equals the number of fuzzy rules in the NFN model, and W is an (m×M)-dimensional weight matrix of the FLNN given by $W = [w_1, w_2, \dots\dots, w_M]^T$.

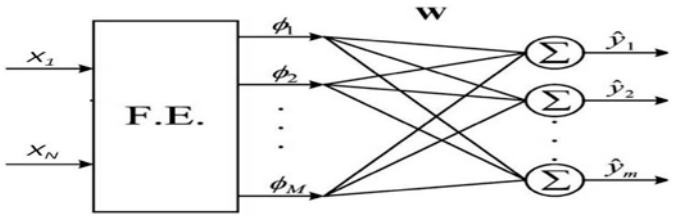

Figure 3. FLNN structure.

3.2 NFN model structure

The NFN model uses a nonlinear combination of input variables (FLNN). The structure of the NFN model is presented in Fig. 4. The ANFN model changes a fuzzy IF–THEN rule in the following form.

$$R^{(l)}: \text{IF } \left(x_1 \text{ is } F_1^l \text{ and } \dots\dots\dots \text{ and } x_N \text{ is } F_N^l\right) \text{ THEN}$$

$$\hat{y}_j = \sum_{i=1}^{M} w_{ij}\varphi_k(X) \qquad (3)$$

$$= w_{1j}\varphi_1 + w_{2j}\varphi_2 + \cdots + w_{jM}\varphi_M$$

where x_i and $\hat{y}_j$ are the input and local output variables, respectively; F_N^l is the linguistic term of the precondition part with Gaussian membership function, N is the number of input variables, w_{ij} is the link weight of the local output, φ_M is the basis trigonometric function of input variables, M is the number of basis function, and rule j is the j^{th} fuzzy rule.

In this study, each degree of freedom of underwater vehicle dynamics is represented by one NFN model. Therefore, there are six SISO NFN models to represent six degrees of freedom of AUV. In the precondition part, the input is represented by five Gaussian membership functions (mean five means and variance). In the consequent part, the output is generated by FLNN. The function expansion in FLNN uses trigonometric functions, given by $[1, \hat{x}_1, \sin(\pi\hat{x}_1), \cos(\pi\hat{x}_1)]$ for one input variable.

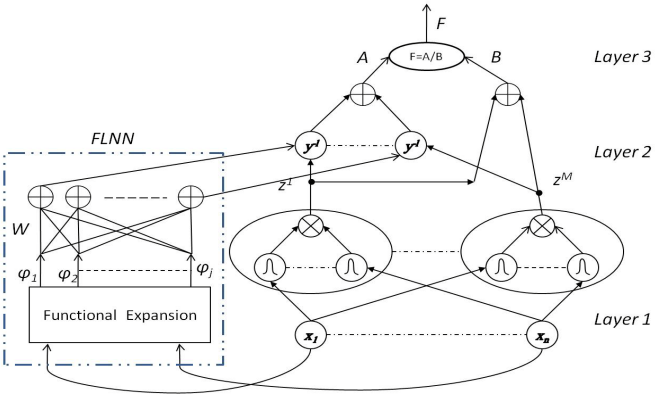

Figure 4. NFN structure

4 Tuning the NFN model

Sets of real input-output data with different operation conditions and disturbance are the only the information required for tuning the model.

The proposed technique consists of two phases. The first phase is the off-line procedure and the second one is the on-line procedure. The target of the off-line phase is to tune and optimize the model's parameters using an optimization technique according to a set of real input-output data. The on-line procedure aims to identify the model of the process online by using the input-output measurements from the mathematical model, set of real input-output data or a real system.

4.1 OFF-LINE procedure

This section presents the off-line stage as a first step in optimizing and tuning the model.

4.1.1 Parameter optimization phase

After the NFN structure has been established, the model enters the parameter-optimization phase based on Differential Evolution (DE) to adjust the parameters of the network optimally based on a different input-output training data set.

DE is known as a powerful algorithm for real parameter optimization. In DE, an initial population is generated and, for

each parent vector from the current population (target vector), a mutant vector (donor vector) is obtained. Finally, an offspring is formed by combining the donor with the target vector. A tournament is then held between each parent and its offspring with the better being copied to the next generation [13, 14]. The DE learning algorithm consists of four major steps— the initialization step, the evaluation step, the reproduction step, and the mutation step.

A. Initialization step: The first step in DE is the coding of the neural fuzzy network model parameters into an individual. Equation (4) shows the way of the individual coding of NFN parameters, where i and j represent the i^{th} input variable and the j^{th} rule, respectively. In this study, a Gaussian membership function is used with variables that represent the mean and variance of the membership function. m_{ij} *and* σ_{ij} are the mean and variance of a Gaussian membership function, respectively, and w_{Mj} represents the corresponding link weight of the consequent part that is connected to the j^{th} rule node.

$$\text{Individual} = \mathrm{m_{1j}, m_{2j}, \ldots\ldots m_{ij}, w_{1j}, \ldots. w_{Mj}} \qquad (4)$$

B. Evaluation step: The objective function is used to provide a measure of how individuals have performed in the problem domain. In the minimization problem, the fit individuals will have the lowest numerical value of the associated problem objective function. This raw measure of fitness is usually only used as an intermediate stage in determining the relative performance of individuals in a DE. Another function, the fitness function, is normally used to transform the objective function value into a measure of relative fitness.

$$F(x) = g(f(x)) \qquad (5)$$

where $f(x)$ is the objective function, g transforms the value of the objective function to a non-negative number and F is the resulting relative fitness. The cost function that attempts to optimize the whole NFN model parameters keeping the interaction between the different degree of freedom is ITSE (Integral Time of Square Error) over the total simulation time.

$$ITAE = \int_{t_1}^{t_2} e^2\, dt \qquad (6)$$

$$J_{E1} = Max(ITAE) \qquad (7)$$

$$F_{E1} = 1/J_{E1} \qquad (8)$$

where J_{E1} is the objective function of each degree of freedom separately for all population. F_{E1} is the overall fitness function of that degree of freedom. The objective function using fitness produces distribution in the range (0, 1).

C. Mutation and crossover step: This operation enables DE to explore the search space and maintain diversity. The simplest form of this operation is that a mutant vector is generated by multiplying an amplification factor, F, by the difference between two random vectors and the result is added to a third random vector (DE/rand/1) [9] as:

$$\vec{\mathrm{V}}_{\mathrm{z,t}} = \vec{\mathrm{x}}_{\mathrm{r_1,t}} + \mathrm{F} \times \left(\vec{\mathrm{x}}_{\mathrm{r_2,t}} - \vec{\mathrm{x}}_{\mathrm{r_3,t}}\right) \qquad (9)$$

where r_1, r_2, r_3 are random numbers (1,2, ..., PS), $r_1 \neq r_2 \neq r_3 \neq z$, x is a decision vector, PS is the population size, F is a positive control parameter for scaling the DE and t the current generation. For more details, readers are referred to [8].

D. Reproduction and selection step: To keep the population size constant over subsequent generations, the next step of the algorithm calls for selection to determine whether the target or the trial vector survives to the next generation, i.e., at G = G + 1. The selection operation is described as

$$\begin{aligned} \vec{\mathrm{X}}_{\mathrm{i,G+1}} &= \vec{\mathrm{U}}_{\mathrm{i,G}} \ \text{ if } \mathrm{f}\left(\vec{\mathrm{U}}_{\mathrm{i,G}}\right) \leq \mathrm{f}\left(\vec{\mathrm{X}}_{\mathrm{i,G}}\right) \\ &= \vec{\mathrm{X}}_{\mathrm{i,G}} \ \text{ if } \mathrm{f}\left(\vec{\mathrm{U}}_{\mathrm{i,G}}\right) > \mathrm{f}\left(\vec{\mathrm{X}}_{\mathrm{i,G}}\right) \end{aligned} \qquad (11)$$

where $f(x)$ is the objective function to be minimized.

4.2 ON-LINE procedure

The learning algorithm is using the back propagation technique. The back-propagation algorithm minimizes a given cost function, Eq (13), by adjusting the parameter of the membership in the antecedent part of the NFN system as mentioned in Eq (15, 16) and the link weight parameters of the FLNN in the consequent part of the NFN system as mentioned in Eq (18, 19).

4.2.1 Parameter learning phase

After the NFN parameters have been tuned in the optimization phase according to a certain input-output training data set, the network enters the parameter-learning phase to adjust the parameters of the network based on a different real input-output data, mathematical model simulation or real system. The final output of the NFN model is given by equation (12) with c_i^j and σ_i^j representing the centre and width of Gaussian memberships for input variable x_i for the rule i, j and n being the number of rules of fuzzy model and number of inputs respectively.

$$\mathrm{y_m(k+1)} = \frac{\sum_{\mathrm{j=1}}^{\mathrm{R}} \hat{\mathrm{y}}_{\mathrm{j}} \left[\prod_{\mathrm{i=1}}^{\mathrm{n}} \exp\left(-0.5\left(\frac{\mathrm{x_i - c_i^j}}{\sigma_{\mathrm{i}}^{\mathrm{j}}}\right)^2\right)\right]}{\sum_{\mathrm{j=1}}^{\mathrm{R}} \left[\prod_{\mathrm{i=1}}^{\mathrm{n}} \exp\left(-0.5\left(\frac{\mathrm{x_i - c_i^j}}{\sigma_{\mathrm{i}}^{\mathrm{j}}}\right)^2\right)\right]} \qquad (12)$$

The adaptive neural fuzzy network model is a neural fuzzy network model with a training algorithm where the model is synthesized from a bundle of fuzzy If-Then rules. As

shown in Figure 5, the fuzzy model is placed in parallel with the process to be identified. This process could be a real system, set of input-output data or mathematical model. It aims to identify the model of the process online by using the input-output measurements of the process based on a training algorithm. The learning process involves determining the minimum of a given cost function (13). The gradient method is used to adapt the model parameters based on the following objective function

$$E(k) = \frac{1}{2}\left(y_m(k+1) - y_f(k+1)\right)^2 \quad (13)$$

where E(k) is error between the NFN model and the actual plant outputs. If Z(k) represents the parameter to be adapted at iteration k in the NFN model, the back propagation algorithm seeks to minimize the value of the objective function by [15].

$$z(k+1) = z(k) - \alpha\frac{\partial E}{\partial Z} \quad (14)$$

To train c_i^j;

$$c_i^j(k+1) = c_i^j(k) - \alpha\frac{y_m - y_f}{b}(\hat{y}^j - y_m)z^l\frac{2(x_i - x^j(k))^2}{\sigma_i^{j2}(k)} \quad (15)$$

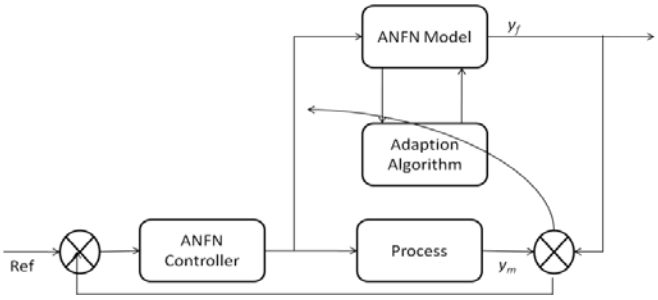

Figure 5. Figure 5. Tracking of error function between the process and ANFN model.

To train σ_i^j;

$$\sigma_i^j(k+1) = \sigma^j(k) - \alpha\frac{y_m - y_f}{b}(\hat{y}^j - y_m)z^l\frac{2(x_i - x^j(k))^2}{\sigma_i^{j3}(k)} \quad (16)$$

where

$$b = \sum_{i=1}^{M} Z^l; \qquad Z^l = \prod_{i=1}^{n}\exp\left(-0.5\left(\frac{x_i - c_i^l}{\sigma_i^l}\right)^2\right) \quad (17)$$

By following the same sequence, the equation for adapting parameter w is derived as shown in the following equations.

$$w_{ij}(k+1) = w_{ij} - \alpha_w\frac{\partial E}{\partial w_{ij}} \quad (18)$$

$$\frac{\partial E}{\partial w_{ij}} = e\left(\frac{b\,\varphi_j}{z^j}\right) \quad (19)$$

where α_w is the learning rate parameter of the FLNN weight. The learning rate α in equation (15, 16 and 18) [10] has a significant effect on the stability and convergence of the system. A higher learning rate may enhance the convergence rate but can reduce the stability of the system. A smaller value of the learning rate guarantees the stability of the system but slows the convergence. The proper choice of the learning rate is therefore very important.

In this technique, the fuzzy network is adapted through two ways. The back propagation algorithm is applied to tune the membership function parameters in antecedent part. The consequent part of the fuzzy rules is adapted through the FLNN. In addition, the back propagation algorithm is used for tuning the parameters of FLNN as well.

4.3 Convergence analysis of ANFN system

Each learning rate parameter of the weight, the mean, and the variance, α, has a significant effect on the convergence. To ensure a quick and stable convergence of fuzzy controller parameters a convergence analysis of the learning rate α will be considered according to the following theorem.

Theorem [16]: Let α be the learning rate for the parameters of fuzzy controller and g_{max}be defined as $g_{max} := \max_k\|g(k)\|$ where $g(k) = \delta y(k)/\delta z(k)$ and $\|.\|$ is the usual Euclidean norm in $\Re^n$ and let $S = \delta y_m/\delta u$. Then the convergence is guaranteed if α is chosen as

$$0 < \sigma < \frac{2}{S^2 g_{max}^2} \quad (20)$$

5 Simulation Results

This study demonstrated the performance of the NFN model for nonlinear system modeling. This section simulates the AUV system behavior and compares the performance of the NFN model with the mathematical model of the AUV.

Fig. 6 shows the motion of the AUV in square trajectory in XY plane, which means the yaw angle control. It is obviously seen that DE has a good job to tune the model's parameter from initial values and get them close enough to the original behavior of the vehicle and it makes the job easier for the online tuning to get the model track successfully the behavior of the vehicle. The motion of the AUV with NFN model with online tuning algorithm does a better job

compared to the performance of the same model without adaptive algorithm in terms of accuracy as well as the speed.

Fig. 7, Fig. 8 and Fig. 9 provide an example of the performance of NFN model and its tracking capability of the mathematical model. These figures show the angular velocity in pitch motion, q, the error between the mathematical and NFN model in pitch motion, q, and the error between the mathematical and NFN model in yaw motion, r, respectively. It is clearly seen that the behavior of the NFN model has same as the mathematical model. The NFN system identification has the capability to track the plant successfully whatever the change in the operation condition.

The learning rates, for all models were initially set to 1 to train the model parameters. Then the convergence conditions were verified at every sampling time. In the present work, the learning rate belongs to the range [0.009, 0.236] was always within the limit of convergence for parameters in NFN model.

5.1 Open loop accuracy evaluation of AUV model

The most widely used method for measuring performance and the accuracy indicators of the system is the root mean square error (RMSE). Table 1 shows the RMSE values of the modeling error in velocity in each degree of freedom. Those errors are the error between the actual velocities generated from the mathematical model and velocities generated from NFN model with and without online adaptive.

TABLE I. THE RMSE VALUES FOR AUV ANFN MODEL AND FUZZY MODEL IN EACH VELOCITY COMPONENT.

Velocity Error	NFN Model without online adaptive	NFN Model with online adaptive
u	0. 0539	3.4493e-004
v	0. 1072	0.0048
w	0.0214	1.5662e-006
q	0. 0361	4.3173e-006
r	0. 1288	9.8547e-007

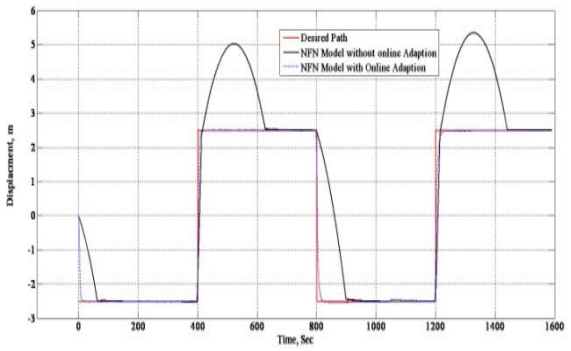

Figure 6. AUV square motion in XY plane with NFN model with and without online Adaptive.

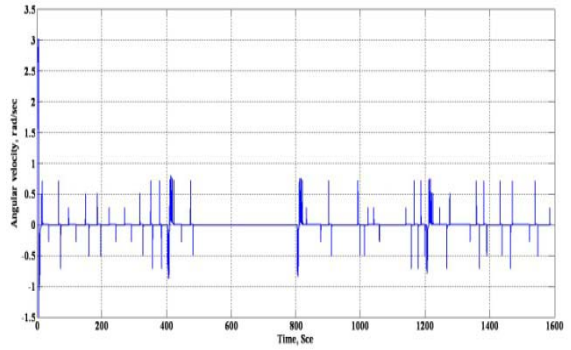

Figure 7. The angular velocity of the mathmatical model in pitch mption, *q*.

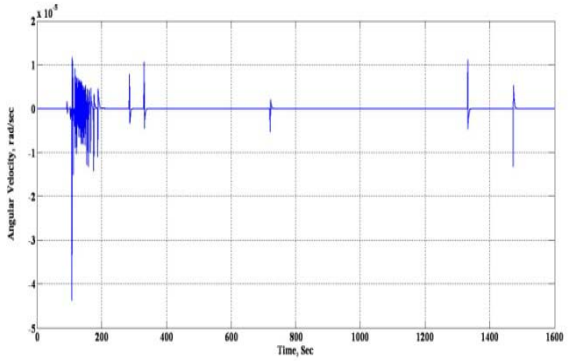

Figure 8. The error between mathematical model and adaptive NFN model in *q*.

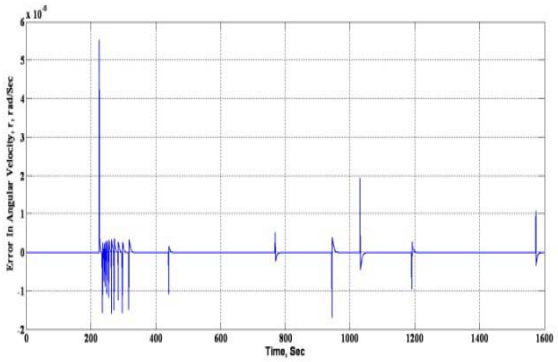

Figure 9. The error between mathematical model and ANFN model in *r*.

6 Concluding Remarks

The paper presents the numerical simulation results of the online adaptive NFN modeling with and without online adaptive as system identification of the mathematical modeling of the AUV. System identification with the NFN with FLNN structure is found to be quite effective for the coupled nonlinear, six degree of freedom dynamic model. It is shown that the overall performance of a suitably chosen NFN structure is superior to an adaptive fuzzy structure for identification of nonlinear dynamic systems.

NFN modeling is used to identify the model of the AUV using input-output data. The back propagation as a training algorithm for the system proves the fast convergence of the NFN model identifier successfully achieved a similar performance of the process.

7 References

[1] Holtzhausen, Servaas. Design of an Autonomous. Master Thesis, KwaZulu-Natal: University of KwaZulu-Natal, 2010.

[2] Citeseerx,http://citeseerx.ist.psu.edu/viewdoc/download ?doi=10.1.1.18.4264&rep=rep1&type=pdf.

[3] Y. H. Pao, S. M. Phillips, and D. J. Sobajic, "Neural-net computing and intelligent control systems," Int. J. Control, vol. 56, no. 2, pp. 263–289, 1992.

[4] J.C. Patra, G. Panda, Adriaan van den Bos, Modeling of an intelligent pressure sensor using functional link artificial neural networks, ISA Transactions 39 (2000) 15-27.

[5] Hassanein, O.; Anavatti, S.G.; Ray, T.; , " Genetic Fuzzy Controller for Robot Manipulator Position Control based upon Inverse Dynamic," 2011 IEEE Congress on Evolutionary Computation (CEC 2011), June 2011

[6] O. Cordon, F. Herrera, F. Hoffmann, L. Magdalena, Genetic Fuzzy Systems evolutionary Tuning and Learning of Fuzzy Knowledge Bases , World Scientific, Singapore, 2001.

[7] K.V. Price, R.M. Storn, J.A. Lampinen, Differential Evolution: A Practical Approach to Global Optimization , Springer-Verlag, Germany, 2005.

[8] C. H. Chen, c. J. Lin, and c. T. Lin, "nonlinear system control using adaptive neural fuzzy networks based on a modified differential evolution" IEEE Transactions on systems, man, and cybernetics—part c: applications and reviews, vol. 39, no. 4, pp. 459-473, July 2009.

[9] J. Liu and J. Lampinen, "A fuzzy adaptive differential evolution algorithm," Soft Comput.—A Fusion Found., Methodol. Appl., vol. 9, no. 6, pp. 448–642, 2005.

[10] Fossen, Thor I.: Guidance and control of ocean vehicles. Wiley , New York (1994)

[11] C. H. Chen, C. J. Lin, and C. T. Lin, "A functional-link-based neuro-fuzzy network for nonlinear system control," IEEE Trans. Fuzzy Syst., vol. 16, no. 5, pp. 1362–1378, Oct. 2008.

[12] Y. H. Pao, S. M. Phillips, and D. J. Sobajic, "Neural-net computing and intelligent control systems," Int. J. Control, vol. 56, no. 2, pp. 263–289, 1992.

[13] R. Storn, K. Price, Differential Evolution - A simple and efficient adaptive scheme for global optimization over continuous spaces, in: Technical Report, International Computer Science Institute 1995.

[14] S.M. Elsayed, R.A. Sarker, D.L. Essam, A three-strategy based differential evolution algorithm for constrained optimization, in: the 17th international conference on Neural information processing: theory and algorithms - Volume Part I, Springer-Verlag, Sydney, Australia, 2010, pp. 585-592.

[15] Li-Xin Wang.: Adaptive Fuzzy System and Control, Design and Stability Analysis. Prentic Hall, New Jersey (1994)

[16] Chen, Y.C. and C.C. Teng.: A Model Reference Control Structure Using a Fuzzy Neural Network. J. Fuzzy Sets and Systems, vol.73, pp. 291-312, 1995.

Applying Nature Inspired Metaheuristic Technique to Capture the Terrain Features

Akanksha Bharadwaj*, Daya Gupta*, V.K. Panchal#
*Computer Science Department, Delhi Technological University
Delhi, India
[1]akanksha.bharadwaj6@gmail.com
[2]dgupta@dce.ac.in
#Defence Terrain Research Laboratory, Defence Research & Development Org
Delhi, India
[3]vkpans@ieee.org

***Abstract*-- In recent years image classification has emerged as the most significant area of research in the field of remote sensing. Image classification helps us to acquire the geo-spatial information from the satellite data which can be useful to industries like defence, intelligence, natural resources etc. There exist various techniques like Biogeography Based Optimization (BBO), Ant Colony Optimization (ACO) etc for image classification. Here, we are applying a metaheuristic approach called Cuckoo Search in the area of image classification. The main advantage of this algorithm over other metaheuristic approach is that its search space is extensive in nature. The proposed methodology is applied to the Alwar region of Rajasthan. The image used is a 7 band image of 472 X 546 dimensions from Indian Remote Sensing Satellite Resiurcesat. This algorithm has captured almost all the terrain features and showed high degree of efficiency for almost all the regions (water, vegetation, urban, rocky, and barren) with a Kappa coefficient of 0.9465.**

Keywords-- ***Cuckoo Search, image classification, artificial intelligence, natural computation, Multi spectral dataset.***

I. INTRODUCTION

Remote sensing [3] is the acquisition of information about an object or phenomenon, without making physical contact with the object. Now a day's sensor technology is also being used to detect and classify the objects by the means of signals propagated by satellites. Image classification plays an important role in the area of remote sensing. The intent of the classification process is to categorize all the pixels of a Multi spectral image into one of the several land cover classes; the resultant data can then be used to create thematic maps which are used for digital image analysis. At present there exist several traditional classifiers such as Minimum Distance Classifier (MDC), Maximum Likelihood Classifier (MLC) and natural computation techniques (or nature inspired algorithms) such as BBO [1], ACO [2], Particle Swarm Optimization and Artificial Neural Networks which are being applied in the field of image classification. Thus, the decision about the classifier to be used for a particular task is to be taken by the analyst. Though various Natural Computation techniques have already been introduced as a classifier, Cuckoo Search which also comes under Natural Computation was very recently introduced in this category.

Cuckoo Search (CS) [4] is a new nature inspired metaheuristic algorithm which hardly has any footprint in any of the application. And it is different from other existing metaheuristic algorithms (such as PSO, GA) in the following ways [5]:

- CS is a population based algorithm as similar to GA and PSO but the selection mechanism is different and it is more similar to harmony search.
- The randomization is more efficient as the step length is heavy tailed and thus any large step is possible.
- Number of parameters in CS is less than GA and PSO and thus it is more general and it can be adapted to wider class of optimization problems. CS can even be extended to meta-population algorithm.

CS satisfies two crucial characteristics of modern metaheuristic algorithm: intensification and diversification [6]. Intensification refers to the fact that the problem initially searches for current best solution and then finally for global solution while diversification means the algorithm explores the search space efficiently.
We have worked on Alwar region of Rajasthan, India. The aim of this paper is to capture the natural terrain features like water, vegetation,

urban, rocky, and barren from the satellite image using Cuckoo Search. The image of Alwar region is shown in figure 1.

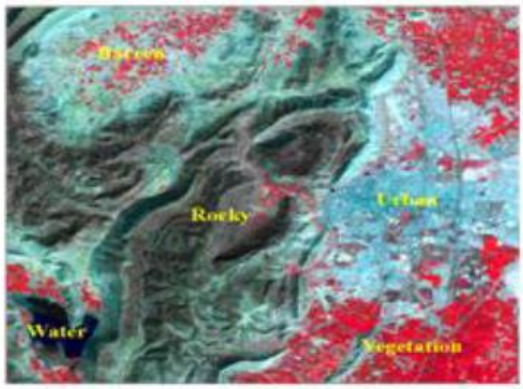

Figure 1: Alwar Region image

The organization of this paper is as follows: - Section II represents the basic concepts of Cuckoo search. Section III represents the proposed methodology. The sub-sections are organized as- problem definition, flowchart, algorithm, dataset. Section IV represents experiment and results. Section V represents conclusion of our proposed work.

II. UNDERLYING TECHNOLOGY

A. Cuckoo Search (CS)

Cuckoo Search proposed by Yang and Deb [4] is a nature inspired algorithm that is based on their aggressive reproduction strategy i.e. some species of cuckoo lay eggs in other bird's nest in a parasitic manner. There are three basic types of brood parasitism [7]:

- Intraspecific brood parasitism.
- Cooperative breeding
- Nest takeover.

Some species such as Ani and Guira cuckoos lay their eggs in the communal nests, though they may remove others' eggs to improve the hatching probability of their own eggs [8].
In cuckoo search three idealized rules [4] are formalized as follows:

- Each cuckoo lays one egg at a time, and dumps its egg in randomly chosen nest.
- The best nest with high quality of eggs will carry over the next generation.
- The number of available hosts is fixed and the egg laid by the cuckoo is discovered by the host nest with a probability $p_a \in [0, 1]$. In this case, the host bird can either throw the egg away or abandon the nest so as to build a completely new nest in a new location.

The fraction p_a of n nests is being replaced by new nests. For a maximization problem, the quality or fitness of a solution can simply be proportional to the objective function. Based on the above three rules an algorithm of cuckoo search is given by Yang and Deb [4]. This algorithm is shown in the form of flowchart in figure 2.

B. .Algorithm

Main steps involved in the process of Cuckoo search are given below:

- Compare the cuckoo's egg with the set of available hosts.
- Randomness is added to it by using Levy flight to choose host nests.
- The above steps produce a set of quality solutions and a set of discarded solutions.
- Based on the Ranking function best solution is obtained from the set of quality solutions while discarding the worst nests.

When a new solutions is generated $x^{(t+1)}$ for, say, a cuckoo i, a Levy flight is performed [4] as :

$$\mathbf{x}_i^{(t+1)} = \mathbf{x}_i^{(t)} + \alpha \oplus \text{Lévy}(\lambda),$$

Where $\alpha > 0$, it is the step size which should be related to the scales of the problem taken under consideration. In most cases, we use $\alpha = 1$. The Levy flight essentially provides a random walk while the random step length is drawn using Levy distribution given by the equation given below [4]:

$$\text{Lévy} \sim u = t^{-\lambda}, \qquad (1 < \lambda \leq 3),$$

It has an infinite variance with an infinite mean. The steps form a random walk process with a power-law step-length distribution with a heavy tail. Some of the new solutions are being generated by Levy walk nearby the best solution obtained so far, this helps to speed up the local search. However, some fraction of the new solutions is generated by taking into consideration the randomization concept. But, whose locations should conceptually be far enough from the current best solution, this

ensures that the system does not get trapped in a local optimum.

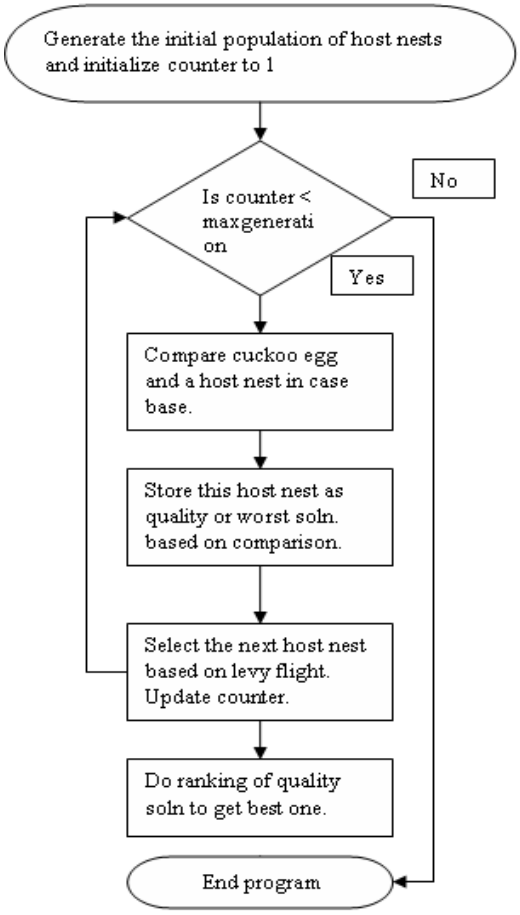

Figure 2: Cuckoo Search algorithm

III. PROPOSED METHODOLOGY

A. Problem Definition

The main aim of this section is to describe our problem domain along with the algorithm proposed to obtain a solution. Experts have provided us with the database of cases. Each of the case is a tuple of the form C={R, G, NIR, MIR, RD1, RD2, DEM} where C represents the case, R represents the value of the pixel for Red band, G represents the value the pixel for Green band, NIR represents value of the pixel for Near Infra-Red band, MIR represents the value of the pixel for Middle Infra-Red band, RD1 represents the value of the pixel for Rdarsat-1, RD2 represents value of the pixel for Radarsat-2, DEM represents the value of the pixel for Digital Elevation Model band (i.e. each of the pixel contains 7 band information obtained from the multi-spectral image of Alwar region of Rajasthan). Analyzing this case base we have to obtain the class to which the query pixel will belong using the 7 band values of the query pixel. The output classes (to which the pixel will belong) can be one of the following: water, vegetation, urban, rocky, and barren.

B. Dataset Used

We have taken a multi-spectral, multi resolution and multi-sensor image of size 472 X 546 pixels of Alwar area in Rajasthan, India. The satellite image is taken for 7 different bands. These bands are Red, Green, Near Infra-Red (NIR), Middle Infra-Red (MIR), Radarsat-1 (RD1), Radarsat-2 (RD2), and Digital Elevation Model (DEM). The ground resolution of these images is 23.5m and is taken from LISS-III sensor. The 7-band satellite image of Alwar area in Rajasthan is given in figure 3.

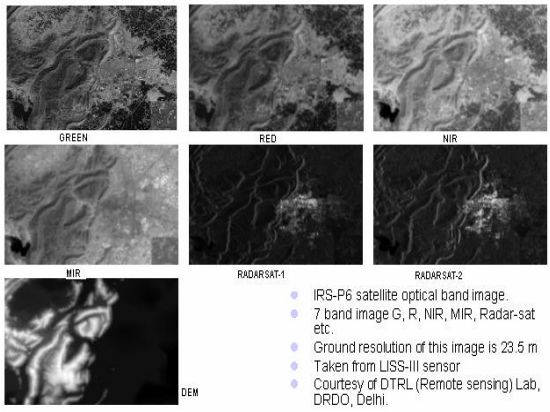

Figure 3: Band satellite image of Alwar region in Rajasthan, India

C. Algorithm

Input: Training set that consists of pixels (host nests) of different classes and other input is the image to be classified.
Output: classified image

1- Initialization
a. Generate initial population. Calculate the objective function value for all these host nests using the 7 band values.

b. Read the image to be classified. Each of the pixels of this image is to be classified.

2-Find Best Solutions

Begin Outer Loop repeat until all the pixels of the image are being classified

a. Find quality solutions

Begin Inner Loop to take into consideration all the host nests in the training set. Point the counter to the first host nest in the case base.

- Find similarity b/w host nest & cuckoo egg (pixel).(for this calculate distance between two pixels)
- Store similarity value in a database.
- Increment counter.

End Inner Loop

b. Sort the above evaluated database to find the top quality solutions.

c. The top k (taken as the square root of number of pixels in the training set) solutions are stored in a database and the worst nests are discarded.

d. Loop for the above obtained quality solution

Do the ranking of the quality solutions by calculating Pearson correlation b/w cuckoo egg & a quality solution. (Value of the coefficient varies between -1 to +1. If the value is positive it means both the quantities are positively correlated. If it's negative then the quantities are negatively correlated. But if the value is between -0.09 to +0.09 that means there is no relation between them)

End this Loop

e. Sort the quality solutions on the basis of correlation value. The one with the highest correlation value is the best solution or the required solution. The best solution is the one that matches our cuckoo egg to great extend.

f. Find the class to which best solution belongs based on the expert data. The query pixel will also belong to the same class to which the best solution belongs. Hence the query pixel is classified.

End Outer Loop

D. Flowchart

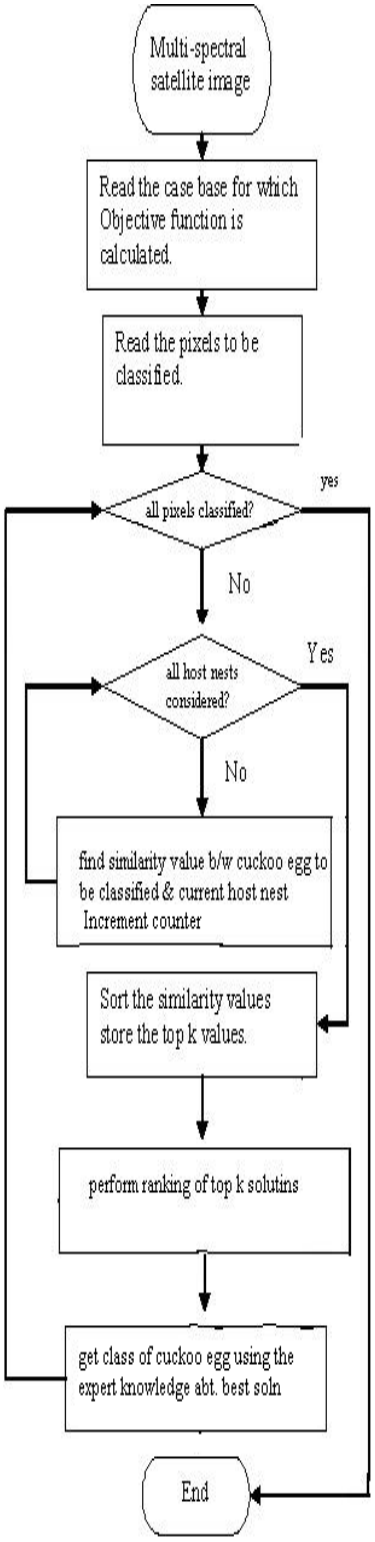

Figure 4: Flowchart of the proposed algorithm

IV. EXPERIMENT & RESULTS

To determine the efficiency of our algorithm we need to find the error matrix. Error matrix [3] compares, on category-by-category basis, the relationship between known reference data and the results obtained from an automated classification [9]. For the validation process we have taken into consideration following number of pixels:

- 68 water pixels.
- 109 vegetation pixels.
- 139 urban pixels.
- 96 rocky pixels.
- 63 barren pixels.

Using the training set the classification is performed and based on the result error matrix is calculated which is shown in table 1. The diagonal elements are representing number of properly classified pixels while non-diagonal elements are representing number of wrongly classified pixels.

Table1. Error Matrix when Cuckoo Search is applied

	Water	Vegetation	Urban	Rocky	Barren	Total
Water	68	0	0	0	0	68
Vegetation	0	109	1	0	0	110
Urban	0	0	122	0	3	125
Rocky	0	0	0	96	0	96
Barren	0	0	16	0	60	76
Total	68	109	139	96	63	475

The above table shows that with water, vegetation and rocky pixels 100% efficiency, in case of urban pixels almost 88% efficiency and with barren pixels almost 95% efficiency is obtained.

The Kappa coefficient (K) also [3] is usually considered for evaluating and analyzing the accuracy of the proposed approach in remote sensing domain. The Kappa coefficient of the Alwar image when Cuckoo search was applied is 0.9465. Comparing this value with the Kappa coefficient of MDC, MLC, BBO [9] and Membrane Computing (MC) [10], we deduced that Cuckoo search has shown best results for image classification since it has obtained the highest Kappa coefficient. The comparison is shown in figure5.

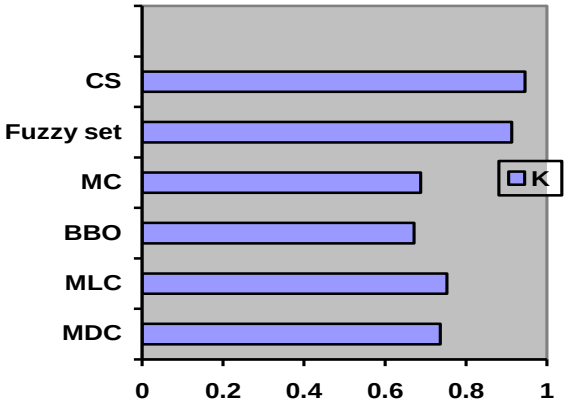

Figure 5: Classification comparison

The image showing the 257,712 classified pixels of Alwar image using Cuckoo Search is shown in figure6. The blue colour represents water region, green colour represents vegetation region, red colour represents urban region, yellow colour represents rocky region and black colour represents barren region. The output can be compared with the original image of Alwar (given by experts) shown in figure1. We analyzed that Cuckoo search has almost perfectly classified all the 5 land cover features of Alwar region.

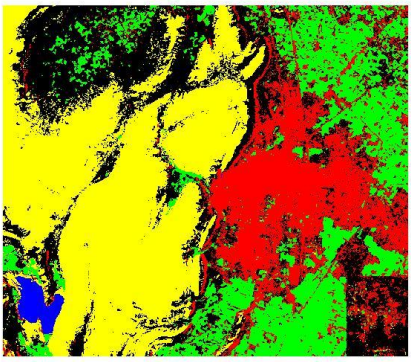

Figure 6: Classified Alwar image

V. CONCLUSION

A large numbers of soft computing techniques have been used for the classification of multi-spectral satellite image. All these techniques classified the terrain features but suffered from some uncertainties. In this paper we have presented a Cuckoo Search based search algorithm for efficiently classifying the remote sensing image. Our proposed implementation is pixel by pixel and hence overcomes the

disadvantages of the previous techniques like BBO, ACO which were implemented as cluster based approaches [1, 9]. From figure 5 we can see the higher performance for Cuckoo based search. The Kappa coefficient obtained is 0.9465 which is considered to be highly accurate as compared the Kappa coefficient of MDC, MLC, BBO, Fuzzy set and Membrane Computing which were 0.7364, 0.7525, 0.6715, 0.913 and 0.68812 [9, 10] respectively. The result of the experiment shows that the water, vegetation and rocky regions are classified with 100% efficiency while urban region with almost 88% and barren region with 95% of efficiency. Thus our proposed method for the classification of pixels was successfully able to extract the land cover features from the given dataset and also maintained high levels of classification accuracy.

REFERENCES

[1] V.K Panchal, Samiksha Goel, Mitul Bhatnagar, "Biogeography Based Land Cover Feature Extraction", VIII International Conference on Computer Information Systems and Industrial Management (CISIM), Coimbatore, December, 2009.

[2] Marco Dorigo and Thomas Stutzle, "Ant Colony Optimization" IEEE Transaction on Evolutionary Computation, Vol 6, Issue 4, pp-358-365, 2002.

[3] Ralph W. Kiefer, Thomas M. Lillesand, "Remote Sensing and Image Interpretation", John Wiley, New York, 2000.

[4] Xin-She Yang, Suash Deb, "Cuckoo search via Levy flights", In Proceedings of World Congress on Nature & Biologically Inspired Computing, (NaBIC), IEEE Publications USA, pp 210-214, Dec. 2009, India.

[5] E. Bonabeau, M. Dorigo, G. Theraulaz, "Swarm Intelligence From Nature to Artificial Systems," Oxford University Press, 1999.

[6] Blum C. and Roli A., Metaheuristics in combinatorial optimization : Overview and conceptural comparison, ACM Comput. Surv., 35, 268-308 2003.

[7] Ereck R. Speed, "Evolving a Mario agent using cuckoo search and softmax heuristics," 2010 2nd International IEEE Consumer Electronics society's games innovations conference, ICE-GIC, pp 1-7, Hong Kong.

[8] Payne R. B., Sorenson M. D., and Klitz K., "The Cuckoos", Oxford University Press, 2005.

[9] Lavika Goel, V.K Panchal, Daya Gupta, "Embedding Expert Knowledge to Hybrid Bio-Inspired Techniques- An Adaptive Strategy towards Focussed Land Cover Feature Extraction", International Journal of computer Science and Information Security (IJCSIS), vol. 8, no. 2, 2010.

[10] Daya Gupta, Bidisha Das, V.K. Panchal, "A methodological study for the Extraction of Landscape Traits using Membrane Computing Technique",Proceedings of International conference on genetic & evolutionary methods",GEM '11.

[11] Albert Barabasi et al., "The human disease network", Plos.org

Neural Net Robotics Visual Servo : Learning The Epipolar Geometry

K. N. Al Muteb[1], **E. A. Mattar**[2], **M. Al-Sulaiman**[3], **H. Ramdane**[4], **and M. Emaduddin**[5]
[1] Comp & Information Sciences College, King Saud University, P. O. Box 51178, KSA
[2]College of Engineering, University of Bahrain, P. O. Box 13184, Kingdom of Bahrain
[,3,4,5] Comp & Information Sciences College, King Saud University, P. O. Box 51178, KSA

Abstract - *Studies have shown that computations of visual kinematics relations are highly complicated and do require a considerable amount of time. This is due to dependent on Jacobians and massive inter-related relations. This hinders even complicated visual servo algorithm for real-time applications. In this respect, the proposed methodology is based on approximating the highly nonlinear relations and epipolar geometry relating changes of object visual features to changes in joint space of a robotics arm system, which are usually expressed in terms of kinematics relations, in addition to time-dependent Jacobian matrix. Artificial Neural system have been proposed for that purpose. A supervised learning artificial neutral network have been employed for learning the visual nonlinear kinematics relations. For validation, the concept have been applied to the well known Rives visual servo algorithm [1], with Two Scenes Epipolar Geometry. Results have shown that, highly accurate visual serving was achieved, while considerable amount of time has been reduced with the proposed methodology*

Keywords: Mobile Visual Navigation, Epiploar Geometry.

1 Introduction

Visual servoing aims to control a robotics system through artificial vision in a way as to manipulate an environment, comparable to humans actions. Intelligence-based visual control (e.g. neural or fuzzy systems) has also been introduced by research community as a way to supply robotics system even with more cognitive capabilities, [2]. There have been few number of research on the field of intelligent visual robotics arm control. For instant, an Image Based Visual Servoing using Takagi-Sugeno fuzzy neural network controller has been proposed by Miao et. al. [3]. In this paper, a Takagi-Sugeno Fuzzy Neural Network Controller (TSFNNC) based Image Based Visual Servoing (IBVS) method is proposed. Firstly, the eigenspace based image compression method is explored, which is chosen as the global feature transformation method. After that, the inner structure, performance and training method of T-S neural network controller are discussed respectively. Besides, the whole architecture of the TS-FNNC is investigated. Panwar and Sukavanam in [4] have introduced Neural Network Based Controller for Visual Servoing of Robotic Hand Eye System. In [5], Gilles et. al. have proposed neural networks organizations to learn complex robotic functions. The study considers a general problem of function estimation with a modular approach of neural computing. In [6] an approximate for exploring motion control for eye-in-hand visual servoing was presented by Mariko and Masaaki. Their study proposes a visual servo control method for exploring motion of eye-in-hand robot to recognize a three-dimensional object. In [7] an adaptive visual servo regulation control for camera-in-hand configuration with a fixed camera extension was presented by Chen, et. al. In this paper, image-based regulation control of a robot manipulator with an uncalibrated vision system is discussed. To compensate for the unknown camera calibration parameters, a novel prediction error formulation is presented. To achieve the control objectives, a Lyapunov-based adaptive control strategy is employed.

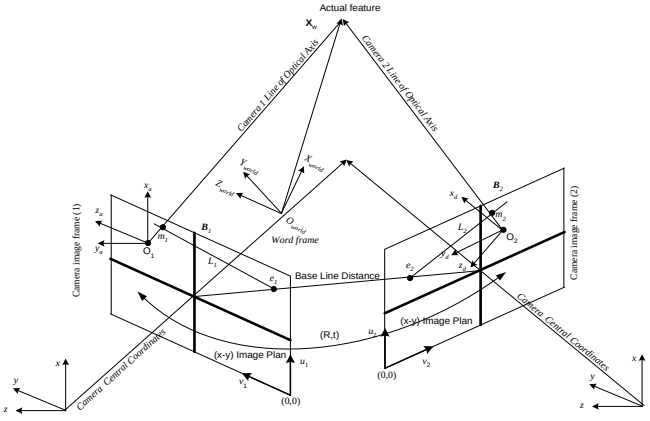

Fig. (1) : Camera image frame and Epipolar Geometry for the PowerBot AGV.

The control development for the camera-in-hand problem is presented in detail and a fixed-camera problem is included as an extension. The EGT (Epipolar Geometry Toolbox) [8], was also created to grant MATLAB users with a broaden outline for a creation and visualization of multi-camera scenarios. Image Based Visual Servoing Using Takagi-Sugeno Fuzzy Neural Network Controller has been proposed by Miao et. al. [9]. In their study, a T-S fuzzy neural controller based IBVS method was proposed. Eigenspace based image compression method is firstly explored which is chosen as the global feature transformation method. Inner structure, performance and training method of T-S neural network controller are discussed respectively. Besides that, the whole architecture of TS-FNNC is investigated. For robotics arm visual servo, this issue has been formulated as a function of object feature Jacobian. Feature Jacobian is a complicated matrix to compute for real-time applications. For more feature points in space, the issue of computing inverse of such matrix is even more hard to achieve.

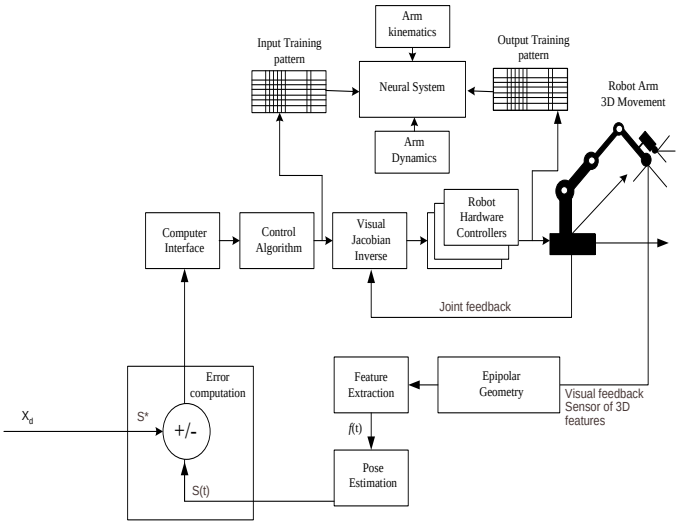

Fig. (2) : Neural system based Visual servo

2. Double Camera Scene Analysis Epipolar Geometry

In this section, we shall consider an image resulting from two camera views. For two perspective views of the same scene taken from two separate viewpoints O_1 and O_2, this is illustrated in Fig .1. Also we shall assume that (m_1 and m_2) are representing two separate points in two the views. In other words, perspective projection through O_1 and O_2, of the same point X_w, in both image planes Λ_1 and Λ_2. In addition, by letting (c_1) and (c_2) be the optical centers of two scene, the projection E_1 (E_2) of one camera center O_1 (O_2) onto the image plane of the other camera frame Λ_2 (Λ_1) is the epipole geometry. We can expressed such an epipole geometry in homogeneous coordinates in terms $\tilde{E}_1$ and $\tilde{E}_2$:

$$\tilde{E}_1 = \begin{pmatrix} E_{1x} & E_{1y} & 1 \end{pmatrix}^T \text{ and}$$
$$\tilde{E}_2 = \begin{pmatrix} E_{2x} & E_{2y} & 1 \end{pmatrix}^T \quad (1)$$

One of the main parameters of an epipolar geometry is the fundamental Matrix H (which is $\Re \in 3\times 3$). H conveys most of the information about the relative position and orientation (t, R) between the two different views. Moreover, the fundamental matrix H algebraically relates corresponding points in the two images through the Epipolar Constraint. For instant, let the case of two views of the same 3-D point X_w, both characterized by their relative position and orientation (t, R) and the internal, hence H is evaluated in terms of K_1 and K_2 (extrinsic camera parameters), [8] :

$$H = K_2^{-T}[t]_x R K_1^{-1} \quad (2)$$

In such a case, a 3-D point (X_w) is projected onto two image planes, to points (m_2) and (m_1), as to constitute a conjugate pair. Given a point (m_1) in left image plane, its conjugate point in the right image is constrained to lie on the epipolar line of (m_1). The line is considered as the projection through C_2 of optical ray of m_1. All epipolar lines in one image plane pass through an epipole point. This is the projection of conjugate optical centre : $\tilde{E}_1 = \tilde{P}_2 \begin{pmatrix} c_1 \\ 1 \end{pmatrix}$ Parametric equation of epipolar line of $\tilde{m}_1$ gives $\tilde{m}_2^T = \tilde{E}_2 + \lambda P_2 P_1^{-1} \tilde{m}_1$. In image coordinates this can be expressed as :

$$u = [m_2]_1 = \frac{[\tilde{e}_2]_1 + \lambda[\tilde{v}]_1}{[\tilde{e}_2]_3 + \lambda[\tilde{v}]_3} \quad (3)$$
$$v = [m_2]_2 = \frac{[\tilde{e}_2]_2 + \lambda[\tilde{v}]_2}{[\tilde{e}_2]_3 + \lambda[\tilde{v}]_3} \quad (4)$$

here $\tilde{v} = P_2 P_2^{-1} \tilde{m}_1$ is a projection operator extracting the i^{th} component from a vector. When (c_1) is in the focal plane of right camera, the right epipole is an infinity, and the epipolar lines form a bundle of parallel lines in the right image. Direction of each epipolar line is evaluated by derivative of parametric equations listed above with respect to (λ) :

$$\frac{du}{d\lambda} = \frac{[\tilde{v}]_1[\tilde{e}_2]_3 - [\tilde{v}]_3[\tilde{e}_2]_1}{([\tilde{e}_2]_3 + \lambda[\tilde{v}]_3)^2} \quad (5)$$
$$\frac{dv}{d\lambda} = \frac{[\tilde{v}]_2[\tilde{e}_2]_3 - [\tilde{v}]_3[\tilde{e}_2]_2}{([\tilde{e}_2]_3 + \lambda[\tilde{v}]_3)^2} \quad (6)$$

The epipole is rejected to infinity once $[\tilde{E}_2]_3 = 0$. In such a case, direction of the epipolar lines in right image doesn't

depend on any more. All epipolar lines becomes parallel to vector $\left(\left[\tilde{E}_2\right]_1 \quad \left[\tilde{E}_2\right]_2\right)^T$. A very special occurrence is once both epipoles are at infinity. This happens once a line containing (c_1) and (c_2), the baseline, is contained in both focal planes, or the retinal planes are parallel and horizontal in each image as in Fig. (1). The right pictures plot the epipolar lines corresponding to the point marked in the left pictures. This procedure is called rectification [8]. If cameras share the same focal plane the common retinal plane is constrained to be parallel to the baseline and epipolar lines are parallel.

3. Neural Net Based Image-Based Visual Servo Control (ANN-IBVS)

Over the last section we have focused more in single and double camera scenes, i.e. representing the robot arm visual sensory. In this section, we shall focus on Image-Based Visual Servo (IBVS) which uses locations of object features on image planes (epipolar) for direct visual feedback. For instant, re-consider Fig. 1, and Fig. 2, where it is desired to move a robotics arm in such away that camera's view changes from (initial) to (final) view, and feature vector from (ϕ_0) to (ϕ_d). Here (ϕ_0) may comprise coordinates of vertices, or areas of the object to be tracked. Implicit in (ϕ_d) is the robot is normal to, and centered over features of an object, at a desired distance. Elements of the task are thus specified in image space. For a robotics system with an end-effector mounted camera, viewpoint and features are functions of relative pose of the camera to the target, $({}^c\xi_t)$. Such function is usually nonlinear and cross-coupled. A motion of end-effectors DOF results in complex motion of many features. For instant, a camera rotation can cause features to translate horizontally and vertically on the same image plane, as related via the following relationship :

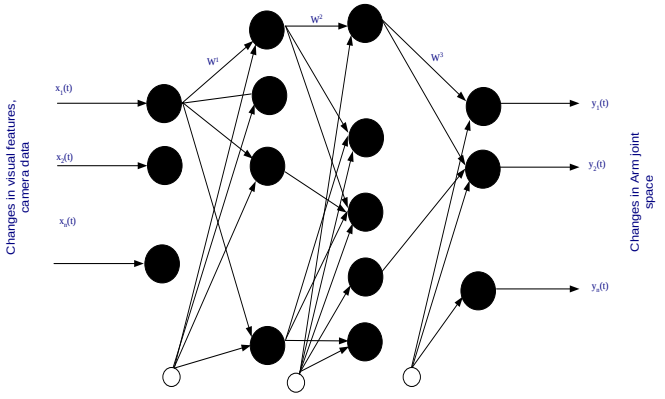

Fig. (3) : Learning neural system

$$\phi = f({}^c\xi_t) \tag{7}$$

Equ (7) is to be linearized. This is to be done around an operating point :

$$\delta\phi = {}^f J_c({}^c x_t)\delta\, {}^c x_t \tag{8}$$

$${}^f J_c({}^c x_t) = \frac{\partial \phi}{\partial {}^c x_t} \tag{9}$$

In Equ (9), ${}^f J_c({}^c x_t)$ is the Jacobian matrix, relating rate of change in robot arm pose to rate of change in feature space. Variously, this Jacobian is referred to as the feature Jacobian, image Jacobian, feature sensitivity matrix, or interaction matrix [10]. Assume that the Jacobian is square and non-singular, then :

$${}^c\dot{x}_t = {}^f J_c({}^c x_t)^{-1}\dot{f} \tag{10}$$

from which a control law can be expressed by :

$${}^c\dot{x}_t = [K][{}^f J_c({}^c x_t)^{-1}](f_d - f(t)) \tag{11}$$

will tend to move the robotics arm towards desired feature vector. In Equ (11), K^f is a diagonal gain matrix, and (t) indicates a time varying quantity. Object posture rates ${}^c\dot{x}_t$ is converted to robot end-effector rates. A Jacobian , ${}^f J_c({}^c x_t)$ as derived from relative pose between the end-effecter and camera, $({}^c x_t)$ is used for that purpose. In this respect, a technique to determine a transformation between a robot's end-effector and the camera frame is given by Tsai and Lenz [11] . In turn, an end-effector rates may be converted to manipulator joint rates using the manipulator's Jacobian [12], as follows :

$$\dot{\theta}_t = {}^{t6}J_\theta^{-1}(\theta)\,{}^{t6}\dot{x}_c \tag{12}$$

$\dot{\theta}_t$ represents the robot joint space rate. A complete closed loop equation can then be given by :

$$\dot{\theta}_t = K\,{}^{t6}J_\theta^{-1}(\theta)\,{}^{t6}J_\theta^f J_c^{-1}\,{}^c x_t(f_d - f(t)) \tag{13}$$

For achieving this task, an analytical expression of the error function is given by :

$$\varphi = Z^+\varphi_1 + \gamma(I_6 - Z^+Z)\frac{\partial \varphi_2}{\partial X} \tag{14}$$

Here, $\gamma \in \Re^+$ and Z^+ is pseudo inverse of the matrix Z, $Z \in \Re^{m\times n} = \Re(Z^T) = \Re(J_1^T)$ and J is the Jacobian matrix of task function as $J = \frac{\partial \varphi}{\partial X}$. Due to modeling errors, such a closed-loop system is relatively robust in a possible presence of image distortions and kinematics parameter variations of the Puma 560 kinematics. A number of researchers also have demonstrated good results in using this image-based approach for visual servoing. It is always reported that, the significant problem is computing or estimating the feature Jacobian, where a variety of approaches have been used [12]. The proposed IBVS structure of Weiss [13,14], controls robot joint angles directly using measured image features. Non-linearities include manipulator kinematics and dynamics as

well as the perspective imaging model. Adaptive control was also proposed, since ${}^{f}J_{\theta}^{-1}({}^{c}\theta)$, is pose dependent. In this study, changing relationship between robot pose, and image feature change is learned during the motion via a learning neural system. The learning neural system accept s a weighted set of inputs (stimulus) and responds. The four-layer feedforward neural network with (n) input units, (m) output units and N units in the hidden layer, is shown in the Fig. (3).

Fig. (3). exposes a one possible neural network architecture that have been used. In reference to the Fig. (3), every node is designed in such away to mimic its biological counterpart, the neuron. Interconnection of different neurons forms an entire grid of the used ANN that have the ability to learn and approximate the nonlinear visual kinematics relations. The used learning neural system composes of four layers. The input, output layers, and two hidden layers. If we denote ${}^{w}v_{c}$ and ${}^{w}\omega_{c}$ as the camera's linear and angular velocities with respect to the robot frame respectively, motion of the image feature point as a function of the camera velocity is obtained by :

$$\dot{\gamma} = -\frac{\alpha\lambda}{{}^{c}p_{c}} \begin{bmatrix} 0 & 0 & \frac{{}^{c}p_{x}}{{}^{c}p_{z}} & \frac{{}^{c}p_{x}\,{}^{c}p_{x}}{{}^{c}p_{z}} & -\frac{{}^{c}p_{x}\,{}^{c}p_{x}}{{}^{c}p_{z}} & {}^{c}p_{x} \\ 1 & -1 & \frac{{}^{c}p_{y}}{{}^{c}p_{z}} & \frac{{}^{c}p_{x}\,{}^{c}p_{x}}{{}^{c}p_{z}} & -\frac{{}^{c}p_{x}\,{}^{c}p_{x}}{{}^{c}p_{z}} & -{}^{c}p_{x} \end{bmatrix} \begin{bmatrix} {}^{c}R_{w} & 0 \\ 0 & {}^{c}R_{w} \end{bmatrix} \begin{bmatrix} {}^{w}v_{c} \\ {}^{w}\omega_{c} \end{bmatrix} \tag{15}$$

Instead of using coordinates ${}^{x}P_{c}$ and ${}^{y}P_{c}$ of the object feature described in camera coordinate frame, which are a priori unknown, it is usual to replace them by coordinates (u) and (v) of the projection of such a feature point onto the image frame.

4 Simulation: A Case Study

In this section the presented visual servoing is verified and discussed. The simulated system is presented in Fig. (2). During simulations the task has been performed using 6-DOF Puma manipulator with 6 revolute joints and a camera that can provide position information of the robot tip and the target in the robot workplace. The robot direct kinematics is given by the set of equations of Puma 560 robotics system, as documented in [15]. Kinematics and dynamics equations are already well known in the literature. For the purpose of comparison, the used example is based on visual servoing system developed by Rives [1]. The robotics system are has been servoing to follow an object that is moving in a 3-D working space. Object has been characterized by (8-features) marks, this has resulted in 24, $\Re \in^{8\times3}$ size, feature Jacobian matrix.

INITIAL PHASE: FREE RUNNING SYSTEM, ANN DESIGN, AND LEARNING :

The foremost ambition of this visual servoing is to drive a 6-DOF robot arm, as simulated with Robot Toolbox [14], and equipped with a pin-hole camera, as simulated with Epipolar Geometry Toolbox, EGT [8], from a starting configuration toward a desired one using only image data provided during the robot motion. For the purpose of setting up the proposed method, Rives algorithm has been run a number of time before hand. In each case, the arm was servoing with different object posture and a desired location in the working space.

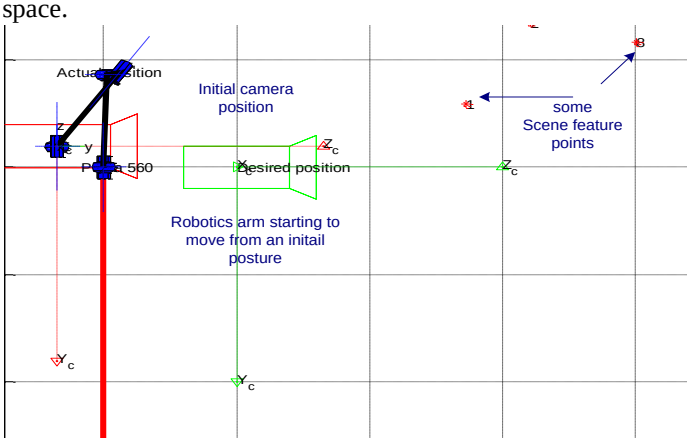

Fig. (4) : Top view: Actual object position and desired position.

Large training patterns have been gathered and classified, therefore. Gathered patterns at various loop locations gave an inspiration to a feasible size of learning neural system. Four layers artificial neural system has been found a feasible architecture for that purpose. The net maps 24 (3×8 feature points) inputs characterizing object cartesian feature position and arm joint positions into the 6 differential changes in arm joints positions. The network is presented with some arm motion in various directions. Once the neural system has learned with presented patterns and required mapping, it is ready to be employed in the visual servo controller. Trained neural net was able to map nonlinear relations relating object movement to differentional changes in arm joint space. Object path of motion was defined and simulated via Rives Algorithm, as given in [1], after such large number of running and patterns, it was apparent that the learning neural system was able to capture such nonlinear relations. Execution starts primary while employing learned neural system within the robotics dynamic controller (which is mainly dependent on visual feature Jacobian). In reference to Fig. (2), visual servoing dictates the visual features extraction block. That was achieved by the use of the Epipolar Toolbox. For assessing proposed visual servo algorithm, simulation of full arm dynamics has been achieved using kinematics and dynamic models for the Puma 560 arm. Robot Toolbox has been used for that purpose. In this respect, Fig. (4) shows an aerial view of actual object posture and the desired one. This is prior to visual servoing to take place. The figure also

indicates some scene features. Fig. (5) shows the Robot arm-camera servoing and approaching towards a desired object posture. ANN was fed with defined pattern during arm movement. Epipolars have been used to evaluate visual features and the update during arm movement. Fig. (6) shows error between the Rives Algorithm and the proposed ANN based visual servo. Results suggest high accuracy of identical results, indicating that a learned neural system was able to servo the arm to desired posture. Difference in error was recorded within the range of (2.5×10^{-7}) for specific joint angles. Finally, Fig. (7) show migration of the eight visual features as seen over the camera image plan. Just the once the Puma robot arm was moving, concentration of features are located towards an end within camera image plane.

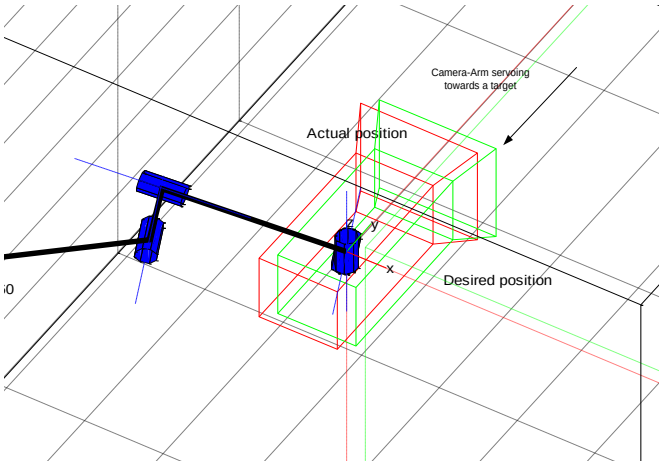

Fig. (5) : Robot am-camera servoing towards a desired object posture.

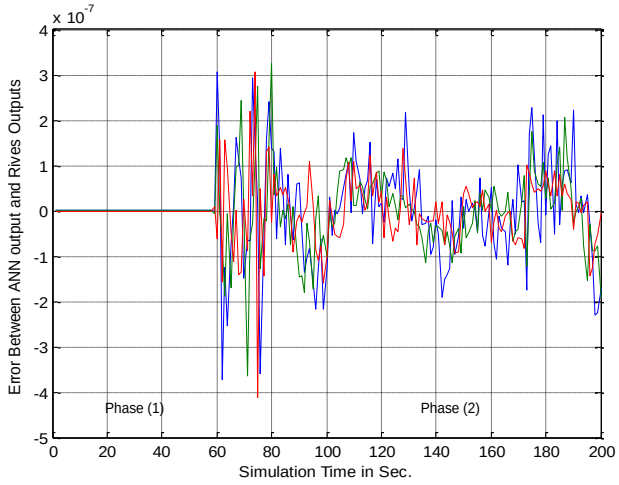

Fig. (6) : Error between the Rives Algorithm results and the proposed ANN based visual servo

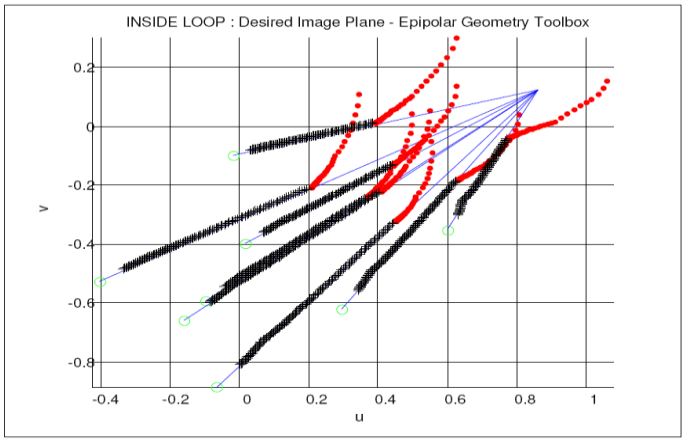

Fig. (7) : Migration of eight visual features, as seen over the camera image plan.

5 Conclusions

This article has been focused towards approximating complicated nonlinear kinematics and feature Jacobian matrices relating a robotics arm system movement in reference to an object displacement, as profoundly appear in closed loop visual servos systems. The presented approach avoids " heavily computed " kinematics relations. That was achieved whilst using a leaning artificial neural system, resulting in reduced computation time, usually a cumbersome for real-time applications. In addition, the proposed methodology depends on mergence of three MatLab-based Toolboxes together, the Robotics Toolbox, ANN toolbox, and the Epipolar Geometry Toolbox. While learning closed-loop visual and kinematics relations, a multi-layer neural net structure has been used for that purpose. The proposed methodology has proven to be an effective approach of approximation, and has reduced computational time usually needed to update visual feature Jacobian matrix as robotics system in motion.

6 References

[1] P. Rives, "Visual Servoing Based on Epipolar Geometry, " Proceedings of IEEE/RSJ International Conference on Intelligent Robots and Systems. (IROS 2000), Takamatsu, Japan, vol. 1, pp. 602–607, 2000.

[2] M. Perez Cisneros, "Intelligent Model Structures in Visual servoing, " Ph.D., University of Manchester, Institute for Science and Technology, 2004.

[3] H. Miao, S. Zengqi, and M. Fujii, "Image Based Visual Servoing Using Takagi-Sugeno Fuzzy Neural Network Controller, " IEEE 22nd International Symposium on Intelligent Control, ISIC 2007, Singapore vol.1 , Issue 3, pp. 53 – 58, 2007.

[4] V. Panwar and N. Sukavanam, "Neural Network Based Controller for Visual Servoing of Robotic Hand Eye System, "

Engineering Letters, 14:1, EL_14_1_26, Advance online publication, 2007.

[5] H. Gilles, W. Patrice, and U. Jean-Philippe, " Neural Networks Organizations to Learn Complex Robotic Functions, " ESANN'2003 Proceedings - European Symposium on Artificial Neural Networks Bruges (Belgium), d-side public., ISBN 2-930307-03-X, pp. 33-38, 2003.

[6] I. Mariko and S. Masaaki, "Approximate Exploring Motion Control for Eye-in-hand Visual Servoing," IEEJ Transactions on Industry Applications, vol. 127, no. 6, 2007, pp. 651-652 Language: Japanese, ISSN: 0913-6339, Institute of Electrical Engineers of Japan, 2007.

[7] J. Chen, M. Dawson, E. Dixon, B. Aman, " Adaptive Visual Servo Regulation Control for Camera-in-hand Configuration With a Fixed-Camera Extension, " Proceedings of the 46th IEEE Conference on Decision and Control, CDC, 2008, pp. 2339-2344, New Orleans, LA, United States, 2008.

[8] A. Eleonora, M. Gian, and P. Domenico, " Epipolar Geometry Toolbox, For Use with MATLAB, " User Guide, vo1. 1, December, 2004.

[9] H. Miao, S. Zengqi, F. Masakazu, "Image Based Visual Servoing Using Takagi-Sugeno Fuzzy Neural Network Controller, " , 22nd IEEE International Symposium on Intelligent Control Part of IEEE Multi-conference on Systems and Control Singapore, pp. 1-3, 2007.

[10] M. Gian, A. Eleonora, and P. Domenico ," The Epipolar Geometry Toolbox (EGT) for MATLAB, " Technical Report, 07-21-3-DII University of Siena, Siena, Italy, 2004.

[11] K. Lenz, Y. Tsai, " Calibrating a Cartesian Robot with Eye-on-Hand Configuration Independent of Eye-to-hand Relationship, " Proceedings Computer Vision and Pattern Recognition, 1988 CVPR apos., Computer Society Conference on Volume , Issue , 5-9, Page(s):67 - 75, 1988.

[12] P. Croke, " High-Performance Visual Closed-Loop Robot Control ", Thesis submitted in total fulfillment of the Requirements for the Degree of Doctor of Philosophy, July, 1994.

[13] L. Weiss, A. Sanderson, A. C. And Neuman, "Dynamic visual servo control of robots: An adaptive image-based approach" , IEEE Journal on Robotics and Automation 3(5), 404–417, 1987.

[14] P. Corke, " Robotics Toolbox for MatLab, " April 2002.

[15] J. Craig, " Introduction to Robotics: Mechanics and Control, " Textbook, International Edition, " Prentice Hall, 2004.

ACKNOWLEDGMENT

This work is supported by NPST program by KING SAUD UNIVERSITY. Project: Number (08-ELE200-02). Kingdom of Saudi Arabia.

Implementing analytical hierarchy process using fuzzy inference technique in route guidance system

Caixia Li , Sreenatha Gopalarao Anavatti, Tapabrata Ray
University of New South Wales @ Australian Defence Force Academy
caixia.li@student.adfa.edu.au

Abstract-*This paper focuses on the design and implementation of the analytical hierarchy process (AHP) using Fuzzy inference techniques. This AHP-FUZZY approach is a multi-criteria combination system. The nature of the AHP-FUZZY approach is pair-wise comparison, which is expressed by the fuzzy inference techniques, to achieve the weights of the attributes. The hierarchy structure of the AHP-FUZZY approach can greatly simplify the definition of decision strategy and represent the multiple criteria explicitly, and the fuzzy inference technique can handle the vagueness and uncertainty of the attributes and adaptively generate the weights for the system. Based on the AHP-FUZZY approach, a simulation system is implemented in the route guidance system and the process is analyzed.*

Keywords: fuzzy inference, analytical hierarchy process

1 Introduction

Route choice mechanism is the key technology of the route guidance system providing path planning strategy for the travelers. However, most of the route guidance systems usually give the shortest distance path or shortest time path based on the historical average traffic data, which easily cause traffic congestion. Therefore, optimum route choice based on the static and dynamic traffic information can provide optimum path for travelers and alleviate traffic congestion. Due to the complexity of the route choice attributes, it is hard to realize the pair-wise comparison between different attributes.

In the past few years, much research has been done to study the route choice algorithm, the mainly used algorithms are as follows: fuzzy logic algorithm and genetic algorithm [1], fuzzy neural algorithm [2], fuzzy logic-ant colony [3], analytical hierarchy process (AHP) using quantifier-guided ordered weighted averaging (OWA) procedure [4]. The fuzzy logic based system is widely used mainly because of its capacity to handle vagueness and it is also easy to combine with other methods to adaptively choose the optimum route. OWA is a kind of multi-criteria aggregation procedure which was developed in the context of fuzzy set theory and is composed of two weights: the weights of criterion importance and order weights. The order weights decide the optimum route choice of road network, while the AHP proposed by Saaty (1980) is based on the additive weighting model. The AHP can decompose the decision problem into a hierarchy of sub-problems composed of several criterions and the importance of weights is associated with their criterions. This approach is of great importance for spatial decision problems that can not complete pair wise comparisons of the alternatives [5]. However, due to the vagueness and uncertainty of traffic attributes and route decisions, a crisp, pair-wise comparison of AHP can not capture the vagueness of traffic attributes. Thus, fuzzy logic is introduced into the AHP structure to compensate the deficiency of AHP.

This paper is outlined as follows: Section II gives an introduction to the AHP approach in a spatial decision-making context. Section III presents the AHP procedures using fuzzy inference techniques. Section IV presents an implementation of the approach and the results analysis. Some conclusions are given in Section V.

2 The AHP approach

The AHP approach is a flexible and yet well structured methodology to analyse and solve complex decision problems by structuring them into hierarchical framework [6]. It can be realized by three steps: (1) developing the AHP hierarchy, (2) pair-wise comparison of elements of the hierarchical structure, (3) constructing an overall priority rating.

2.1 The AHP hierarchy

For the first step of the AHP procedure, it is to decompose the decision problem into several sub-problems, represented by the hierarchy structure tree, which consists of goal, objectives, attributes and alternatives (Figure 1.). Accordingly, the spatial-decision problem is related to a set of defined alternatives, a set of evaluation criteria and its associated weights.

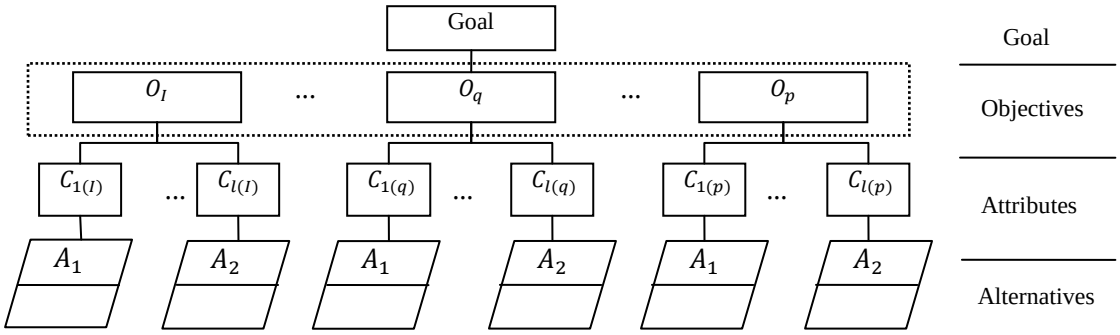

Figure 1. The hierarchy structure of AHP approach

The spatial decision problem is decomposed into a set of p objectives O_q for $q = 1,2,\dots,p$. The objectives are measured in terms of the underlying attributes, and a set of n attributes C_j for $j = 1,2,\dots,n$, corresponded with the p objectives. In addition, a subset of attributes in terms of the q th objective is denoted by $C_{k(q)}$ for $k = 1,2,\dots,l; l \le n$. The weights of objectives and attributes can be denoted by $w_q = [w_1, w_2, \dots, w_p]$ and $w_{k(q)} = [w_{1(q)}, w_{2(q)}, \dots, w_{3(q)}]$ respectively, where $w_q \in [0,1], \sum_{q=1}^{p} w_q = 1$, and $w_{k(q)} \in [0,1], \sum_{k=1}^{l} w_{k(q)} = 1$. The performance of the alternatives is related to attributes C_j is denoted by a set of standardized criterion values: $X = [x_{ij}]_{m\times n}$; $x_{ij} \epsilon [0,1]$ for $j = 1,2,\dots,n$.

2.2 Pair-wise comparisons

The pair-wise comparison as the second step of the AHP procedure is the basic measurement mode employed in the AHP procedures, which can greatly reduce the conceptual complexity of a problem since only two components are considered at any given time.

The decision hierarchy tree of AHP can provide the selection and ranking of alternatives by pair-wise comparison according to related criteria. The pair-wise comparison matrices are based on the alternatives, $A_1, \dots, A_m$, in terms of each criteria being considered. A pair-wise matrix for an expert i with respect to criterion k can be denoted as:

$$A_i^k = \begin{matrix} \\ A_1 \\ \vdots \\ A_m \end{matrix} \begin{matrix} \begin{matrix} A_1 & \dots & A_m \end{matrix} \\ \begin{bmatrix} a_{11}^{k,i} & \cdots & a_{1m}^{k,i} \\ \vdots & \ddots & \vdots \\ a_{m1}^{k,i} & \cdots & a_{mm}^{k,i} \end{bmatrix} \end{matrix} \quad (1)$$

Each a'_{11} denotes the strengths of preferences that the user believe alternative i over alternative j.

Each pair-wise matrix in the form of $m \times m$, whose elements are a'_{11}s, is a square positive reciprocal matrix:

$$a_{ij} = \frac{1}{a_{ji}} \text{ and } a_{ii} = 1.00 \ \forall i, j = 1, \dots, m \quad (2)$$

Therefore, the ratio either under or above the principal diagonal of the matrix are enough to complete the matrix by taking the reciprocals of the given elements. Each a_{ij} could be regard as an estimate of the weight of the alternative i, w_i, to alternative j, w_j:

$$a_{ij} = \frac{w_i}{w_j} \quad (3)$$

Then,

$$w_i = a_{ij} w_j \quad (4)$$

2.3 The weights of the criterions

After the pair-wise comparison matrix is obtained, the next step is to summarize preferences so that each element can be assigned a relative importance. It can be achieved by computing the weights and priorities, $w = [w_1, w_2, \dots, w_p]$ for p objectives and $w_{(q)} = [w_{1(q)}, w_{2(q)}, \dots, w_{l(q)}]$ for attributes associated with the qth objective.

The weights can be achieved by normalizing the eigenvector with respect to the maximum eigenvalue of the pair-wise comparison matrix. The normalized eigenvector consists of an iterative process; first the matrix $\hat{A}$ is calculated by normalizing the columns of A:

$$\hat{A} = [a_{qt}^*]_{p\times p}, \quad (5)$$

Where $a_{qt}^* = \frac{a_{qt}}{\sum_{q=1}^{p} a_{qt}}$, for all $t = 1,2,\dots,n$.

The vector of ω can be given:

$$w_q = \hat{a}_{qt(z)}^*, \text{ for all } q = 1,2,\dots,p. \quad (6)$$

By the simple rule, the attributes weights can be calculated:

$$a_{kh(q)}^* = \frac{a_{kh(q)}}{\sum_{k=1}^{l} a_{kh(q)}}, \text{ for all } h = 1,2,\dots l. \quad (7)$$

$$w_{k(q)} = \hat{a}_{kh(q)}^*, \text{ for all } k = 1,2,\dots,l. \quad (8)$$

2.4 The priority rating

Finally the weights can be given by aggregating the relative weights of objectives and attribute levels, which can be done by a sequence of multiplications of the matrices of relative weights at each level of hierarchy. The global weights of each criterion, w_j^g are calculated as follows:

$$w_j^g = w_q \times w_{k(q)} \quad (9)$$

For the overall evaluation results, R_i of the ith alternative is calculated as follows:

$$R_i = \sum_{j=1}^{n} w_j^g x_{ij} \quad (10)$$

Where x_{ij} is associated with the attributes value.

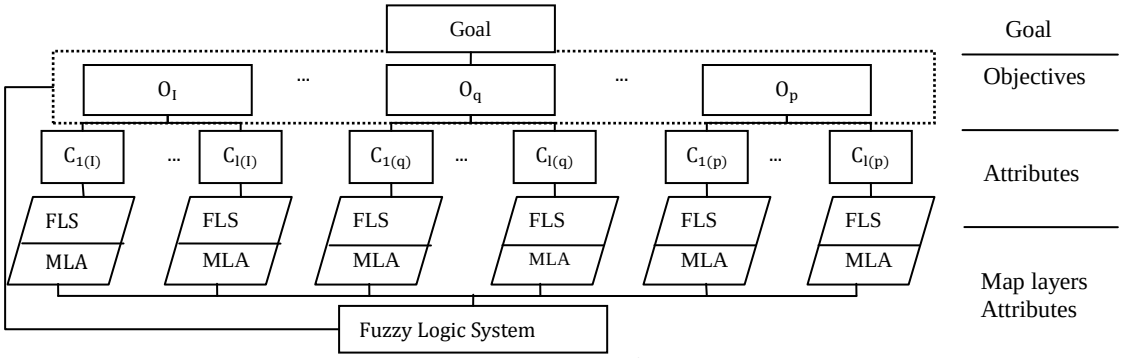

Figure 2. The hierarchical structure of AHP-FUZZY system

3 The Ahp-fuzzy system

3.1 The FUZZY model

FLS[7] is a process of mapping an input space onto an output space using membership functions and linguistically specified rules. The process of fuzzy inference involves Membership Functions, Logical Operations, and If-Then Rules. Fuzzy Logic theory with expert knowledge can represent the inference procedure explicitly using a set of fuzzy if-then rules, which offer a high degree of transparency into the system being modeled. With the inputs and output defined, it needs to specify a set of rules to define the model. The rules of approximate reasoning which can be used to describe the route choice are if-then rules. After the inputs are fuzzified and the degree of each part of the antecedent is satisfied for each rule, the logical operations can help the logical verbal rules. Finally, defuzzification process can help resolve a single output value from the set.

3.2 The AHP-FUZZY model (Figure 2.)

Consider a directed graph $\vec{G} = (V, E)$ with a origin point $o \in V$ and a destination $d \in V$. A denotes the set of all acyclic routes from the origin point o to destination point d on $\vec{G} = (V, E)$. For each road segment of road network $e \in E$, criteria is defined, then the multi-criteria structure is imposed on the road network.

The purpose of this paper is to give the least cost route decision considering both the traffic density of road segments of each intersection and the overall cost of O/D pairs. Supposing that there are a set of m alternatives, that is, m adjacency road segments for each node, which can be denoted by A_i for $i = 1,2,\dots,m$. The alternatives are to be evaluated by a set of p objectives O_q, where $q = 1,2,\dots,p$. The objectives are measured in terms of the underlying attributes. Thus, a set of n attributes associated with the p objectives can be denoted by C_j, where $j = 1,2,\dots,n$, while a subset of attributes associated with the qth objective is denoted by $C_{k(q)}$, for $k = 1,2,\dots,l; l \le n$. There are two sets of weights, $w_q = [w_1, w_2, \dots, w_p]$ and $w_{k(q)} = [w_{1(q)}, w_{2(q)}, \dots, w_{3(q)}]$ are assigned to the objectives and attributes, respectively. The weights have the following properties: $w_q \in [0,1]$, $\sum_{q=1}^{p} w_q = 1$, and $w_{k(q)} \in [0,1]$, $\sum_{k=1}^{l} w_{k(q)} = 1$. Based on the basic knowledge of AHP approach, the fuzzy logic approach is employed to improve its performance. For the weights of the objectives and weights, they are not constant values any more, which will be decided by the fuzzy logic rules. Combining with the above weights, the global weights of each criterion, w_j^g are calculated as follows: $w_j^g = w_q \times w_{k(q)}$, while the performance of alternatives A_i with respect to attributes C_j represented by a set of standardized criterion values: $X = [x_{ij}]_{m \times n}$; for $x_{ij} \in [0,1], j = 1,2,\dots n$. The final evaluation results of the ith alternative can also be calculated as follows: $R_i = \sum_{j=1}^{n} w_j^g x_{ij}$, where x_{ij} is associated with the attributes value.

4 Implementation of Ahp-fuzzy approach

4.1 Illustration of implementation process

Traditionally, the movements of vehicles are considered as isolated moving units in the route guidance system. However, a car driving on the road is influenced by the whole road network including static and dynamic

information. Generally, distance and travel time are usually considered as the main factors to decide the route selection neglecting the traffic density which can represent the traffic load capacity and the intensity of travelers' comfort. Basically, travelers usually want to get to their destination at least cost. Thus, there are three main criteria considered in this route guidance system for k routes given by the route search algorithm, as follows:

- Travel distance: 0 denotes the routes with the shortest distance. In contrast, 1 denotes the longest route. The attribute value for other routes can be decided by a linear scale.

- Travel time: 0 denotes the least time, while 1 denotes the largest time value. Again, the attribute value for other routes can be decided by a linear scale.

- Travel congestion: 0 denotes no congestion, while 1 denotes the worst situation.

It can be noticed that each driver wants to get to their destination at least cost, that is, those attribute scores are close to zero.

Therefore, the hierarchy structure also consists of objectives, attributes and alternatives (Figure 3.). The overall goal is to achieve the least cost path. The objectives are decided by three criterions: (i) distance, (ii) time, (iii) density. The weights of the objective are decided by these three criterions:

$$w_q = [w_1, w_2, w_3],$$

Where w_q denotes the weights of three criterions respectively, $q = 1,2,3$.

The weights of the attributes are decided by the pair-wise comparison of alternatives:

$$w_{k(q)} = [w_{1(q)}, w_{2(q)}, \dots, w_{3(q)}],$$

Where $w_{k(q)}$ is in terms of the weights of the alternatives corresponding to one single attribute. $k = 1,2,3$. In order to simply the illustration, only three alternative routes are considered.

As mentioned in Section III, the fuzzy inference system is introduced into the AHP approach to quantify the weights of objectives and attributes. The nature of the fuzzy inference system is the formal mathematical formulation represented by the fuzzy rule statements.

As to the weights of the objectives w_q, the traveling cost composed of travel distance and travel time, is influenced by the traffic on the roads. Moreover, the cost of road segment is greatly influenced by the road load capacity, that is, traffic density. Thus, the fuzzy rules can be given according to the intensity of traffic density. The first fuzzy rules are described as follows:

- If the traffic density is low, then the weight of distance is high, that is, the time weight is low (For the free traffic flow, the cost of traffic is totally decided by the shortest path.

- If the traffic density is high, then the weight of time is high, that is, the distance weight is low (For time periods of traffic congestion, the cost of traffic is totally decided by the least time path).

- If the traffic density is medium, then the weight of distance is medium, that is, the time weight is medium. As to the value of the weights, it can be generated by the fuzzy membership function and defuzzification process.

For the weights of the attribute $w_{k(q)}$, is in terms of the weights of the alternatives corresponding to one single attribute. $k = 1,2,3$.

1) If the degree of the attributes (distance, time, density) is low, then the weight of the attributes is low.

2) If the degree of the attributes (distance, time, density) is medium, then the weight of the attributes is medium.

3) If the degree of the attributes (distance, time, density) is high, then the weight of the attributes is high.

Based on the fuzzy rules and the membership functions of fuzzy sets, the criterion weights w_q and $w_{k(q)}$ are generated by the defuzzyfication process. The global weights of each criterion, w_j^g are calculated as follows: $w_j^g = w_q \times w_{k(q)}$. The final evaluation results of the ith alternative can also be calculated as follows: $R_i = \sum_{j=1}^{n} w_j^g x_{ij}$, where x_{ij} is associated with the attributes value.

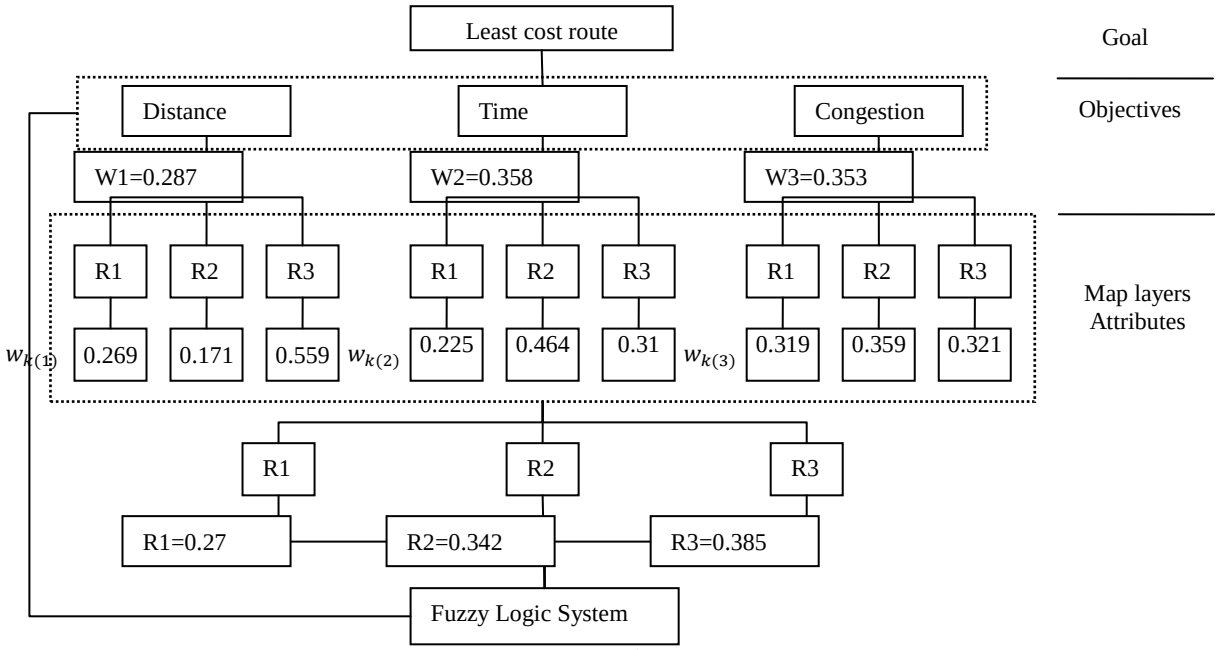

Figure 3. The implementation of AHP-FUZZY system

4.2 Result analysis

In order to demonstrate the process of the AHP-FUZZY approach, a simulation is implemented in Sydney and a random orientation and destination is selected for the study. Based on the real-time traffic information, three available routes are given as the route alternatives for pair-wise comparison and an illustration example is given in Figure 3.

TABLE 1. PAIR-WISE COMPARISON MATRIX OF THE OBJECTIVE ATTRIBUTES

	Distance	Time	density	weight
Distance	1	0.8	0.81	0.287
Time	1.25	1	1.01	0.358
Density	1.23	0.98	1	0.353

TABLE 2. PAIR-WISE COMPARISON MATRIX OF ALTERNATIVES CORRESPONDING TO THE DISTANCE

	A1	A2	A3	weight
A1	1	1.57	0.48	0.269
A2	0.64	1	0.3	0.171
A3	2.07	3.26	1	0.559

The pair-wise comparison of the objectives and attributes can be achieved by the fuzzy inference techniques. Table1 and Table2 show the pair-wise comparison of the objectives and attributes. From Equation(9), it can easily get the global weights of the alternatives. The evaluation results can also be given by the Equation(10).

TABLE 3. RESULTS COMPARISON FOR ROUTE CHOICE METHODS

Route choice methods	**Distance**	**Time**	**cost**
Shortest distance	18.5km	85min	0.2934
Least time	21.85km	44min	0.1542
Least cost	20.26km	48min	0.1278

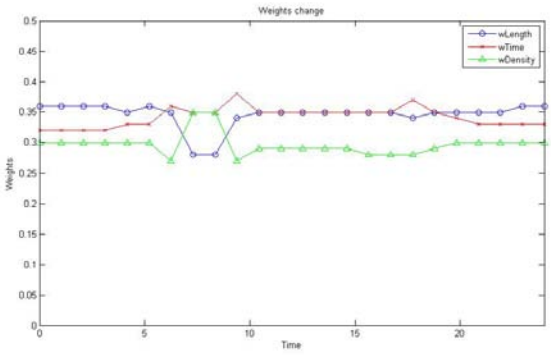

Figure 4. Traffic attributes changes during the whole day

Figure 4 shows that the weights change less during off-peak hours, while there are great gaps during peak hours. For the off-peak hours, the traffic is usually free flow traffic and the AHP-FUZZY approach usually chooses the shortest path for the travelers. During the peak hours, for the different road segments, they have different traffic density, thus the weights of traffic attributes are different from each other. The results denote that the AHP-FUZZY approach can adaptively change their weights based on the real time information.

In order to validate the AHP-FUZZY model providing optimum path, we compare the least cost path with the shortest path and least time path. During off-peak hour, shortest path or least time always comes with the least cost, there is no need to compare them during off-peak hour. Thus, the comparison results focus on the peak-hour traffic. The results for three route choice methods at 8:00am are shown in Table 3. From Table 1, it shows that the shortest distance path has the longest time and the least time path has the longest distance, while the least cost path has the medium distance and medium time. From study the traffic volume data on these three routes, it shows that traffic volume on shortest distance path has heavy traffic jams, while the least time waste too much

cost on the road distance. Based on the study of traffic data on routes of shortest distance path and least time path, it can be shown that the least cost path is more optimum and it can also balance the traffic flow on the roads without betray the cost requirements.

5 Conclusion

In this paper, an AHP-FUZZY approach for route guidance system is proposed. The AHP-FUZZY approach is a multi-criteria combination system developing the hierarchy structure and adaptively generating the weights based on the two step fuzzy rule system, which can greatly simplify the definition of decision strategy and represent the multiple criteria explicitly. In addition, for the two step fuzzy-rule system, the former one can adaptively generate different weights of attributes (distance, time and density) based on the traffic density during the whole time periods of day, and the letter one can realize the dynamic route selection based on the real time traffic information. The simulation experiment has been done on the road network in Sydney. The simulation results show that this AHP-FUZZY approach can adaptively adjust the weights of the objectives to get the least cost path for the different time periods of day.

6 References

[1] Khan, J.A. and H. Alnuweiri. A traffic engineered routing algorithm based on fuzzy logic. 2003. IEEE.

[2] Pang, G.K.H., et al., Adaptive route selection for dynamic route guidance system based on fuzzy-neural approaches. Vehicular Technology, IEEE Transactions on, 1999. 48(6): pp. 2028-2041.

[3] Salehinejad, H. and S. Talebi, Dynamic fuzzy logic-ant colony system-based route selection system. Applied Computational Intelligence and Soft Computing, 2010. 2010: pp. 3.

[4] Boroushaki, S. and J. Malczewski, Implementing an extension of the analytical hierarchy process using ordered weighted averaging operators with fuzzy quantifiers in ArcGIS. Computers & Geosciences, 2008. 34(4): pp. 399-410.

[5] Yager, R.R. and A. Kelman, An extension of the analytical hierarchy process using OWA operators. Journal of Intelligent and fuzzy Systems, 1999. 7: pp. 401-418.

[6] Saaty, T.L., Multicriteria decision making: the analytic hierarchy process: planning, priority setting, resource allocation1990: RWS.

[7] Iokibe, T., N. Mochizuki, and T. Kimura. Traffic prediction method by fuzzy logic. in Fuzzy Systems, 1993., Second IEEE International Conference on. 1993.

[8] Caixia Li, Sreenatha Anavatti, Tapabrata Ray. Short-Term Traffic Prediction Using Different Techniques, IEEE Industrial Electronics Society, Melbourne, 2011, 7: pp. 2348-2353.

Introducing Generic Artificial Bee Colony Framework-Problems Independent Framework

Amr Rekaby[1], A.A.Youssif [1], A.Sharaf Eldin[1]
[1]Faculty of computers and information, Helwan University, Cairo – Egypt
rekaby0@hotmail.com, aliaay@helwan.edu.eg, profase2000@yahoo.com

Abstract – *artificial bee colony algorithm is a new swarm intelligence algorithm. It is inspired from natural bee swarm intelligence concepts to solve the optimization problems. This paper proposes a framework for artificial bee colony algorithm. This framework is problem independent. The usage of this framework in any optimization problem is the goal of this research. This reusability is presented as a part of this paper.*

The paper introduces the artificial bee colony algorithm. Afterwards, a description of the framework will be provided. Detailed view of the framework and how to be used are shown. The experiments are stated after that. A conclusion is presented at the end of this paper.

Keywords: *Artificial Bee Colony Algorithm, Generic Artificial Bee Colony Framework (GABCF), Problem Independent Artificial Bee Colony Implementation.*

1 Introduction

The solution techniques of the optimization problems could be categorized into: combinatorial optimization techniques and approximate optimization techniques. The combinatorial optimization techniques find the optimal solution of the problem. Approximate optimization techniques target finding a solution that satisfies the user constraints and needs. This solution maybe very close to the optimal solution and also may not be close, this is not the main concern in such techniques. Swarm -based optimization algorithms are kind of the approximate techniques. Swarm intelligence algorithms contain ant colony, bee colony, cockroach, etc [2].

Artificial bee colony (ABC) algorithm is a simulation of real bee colony and its foraging behaviors. ABC is introduced in 2005 for the first time [1]. In this paper, we provide a framework that implements ABC algorithm using Java programming language. This framework called "Generic Artificial Bee Colony Framework" (GABCF). Previously, each time the researcher uses ABC algorithm for a new problem, he had to implement it again to be compatible with the problem nature. The presented framework (GABCF) in this paper is problem independently designed and implemented. The framework separates the ABC algorithm workflow/intelligence from the problem specific implementation. The framework performs this separation by providing interfaces and abstract classes as integration gates. The user could implement only a small problem's related section to have the ABC framework works with his problem dynamically.

In section 2, ABC algorithm is presented. The framework details, diagrams, and specifications are presented in section 3. The experimental work in this research is how to use this proposed framework in problem solving, this point is described in section 4. A conclusion is conducted at the end of this paper in section 5.

2 Artificial Bee Colony (ABC) Algorithm

Artificial bee colony is an algorithm that simulates the swarm intelligence integration of bees' colony in foraging natural life. The actual bees' colonies categorize the bees in foraging activities into the following types:

- Worker (Employee) bees group.
- Onlooker bees group.
- Scout bees group.

From natural bees' point of view, each group of bees has a specific role. The worker bees use the real nectar sources in foraging process. The workers collect the nectar from these sources and return to the hive. Worker bees do a waggle dance when return to the hive. The dance describes the evaluation of the food source and its geographic location.

After the worker bees dance in front of the hive, there is a group of bees (onlooker bees) monitoring their dancing to choose resources from the workers findings. This selection is based on the worker bees' sources fitness evaluation function. After the onlookers choose a subset of the resources, the onlookers go to these sources and search in their neighbors to find a better food sources. After that the onlookers return to the hive with their findings.

Simultaneously there are a group of bees called (scout bees), these bees look always for abandoned food sources exploring. Scout bees explore new areas by finding random nectar source

(create random solution in the artificial algorithm) and returning this information back to the hive.

By mapping these natural activities to the artificial bee colony algorithm, the worker bees catch a valid solution of the problem. Onlooker bees select solutions based on the fitness value of them. They search in the surrounding solutions to find a better solution. Scout bees create random solutions per iteration to simulate the real scout bees' activities.

By this step, a cycle in bee colony foraging is completed. At the beginning of the new cycle, the worker bees select new sources for the new iteration (cycle) from all the available sources (old worker sources, onlookers' findings and scout discovered sources).

There are four mandatory parameters for ABC algorithm: worker bees count, onlooker bees count, scout bees count, maximum cycle number (MCN). These parameters are mandatory for ABC to be able to do its logic. The framework gets these parameters through communication gates described in the next section.

Onlookers bees are selecting the sources depends on the sources (solutions) fitness. The selection use a probability of source selection, this probability is [2, 3]:

$$Pi = fit\ i / \sum fitn \qquad where\ n=1\ to\ SN \qquad (1)$$

Where fit_i is the fitness value of the solution number (i) and (SN) is the count of the food sources. The count of food sources is equal to the number of worker bees.

In GABCF, the framework uses this probability selection equation for the onlooker's bees sources allocation.

Some researches go to that: the worker bees also do a local search activity in the neighbor areas but with very small scale, then onlooker bees do the search with a wider scope than worker bees. GABCF provides the flexibility to the user in enabling this feature or disabling it. Figure 1 presents ABC algorithm steps.

1: Initialize Population
2: **repeat**
3: Place the employed bees on their food sources
4: Place the onlooker bees on the food sources depending on their nectar amounts
5: Send the scouts to the search area for discovering new food sources
6: Memorize the best food source found so far
7: **until** requirements are met

Figure 1: ABC algorithm description.

"Requirements are met" mentioned in figure 1 is the exit condition of ABC algorithm. It could be an acceptable solution fitness value, and also it could be the number of cycles [4, 5]. Maximum cycle number (MCN) is the used exit criteria in the generic artificial bee colony framework.

3 Generic Artificial Bee Colony Framework (GABCF)

Generic artificial bee colony framework is problems independent framework. It separates the workflow of ABC algorithm from the actual problems' details. As described in the next diagrams, the framework contains the ABC algorithm logic, and some interfaces and definitions that should be implemented (by the user) to make the GABCF works with his problem adaptively.

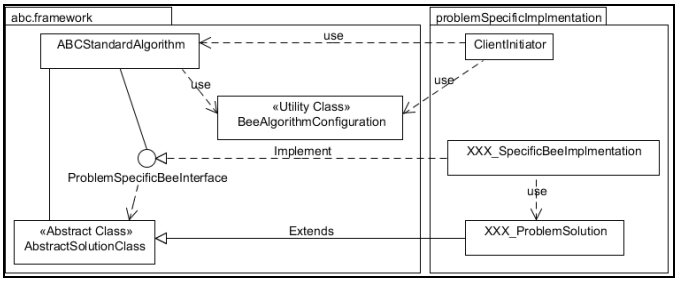

Figure 2: High level class diagram.

As described in figure 2, GABCF contains three integration gates with the user:

- "ABCStandardAlgorithm" class.
- "ProblemSpecificBeeInterface" interface.
- "AbstractSolutionClass" class.

More descriptions of these components are described in figure 3, and figure 4 in a detailed form.

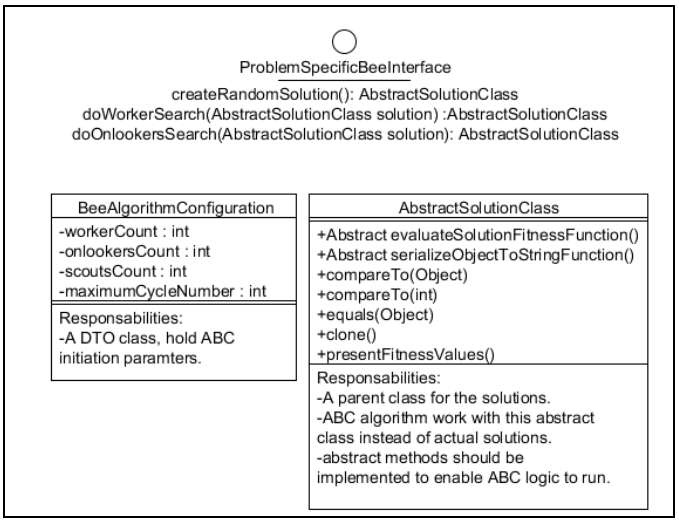

Figure 3: Low level class diagram.

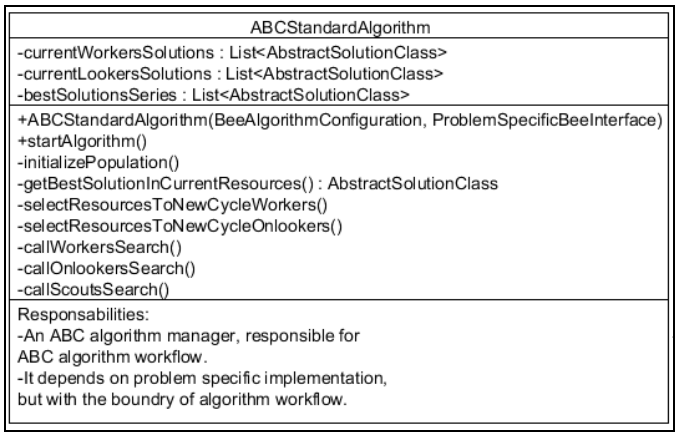

Figure 4: Low level class diagram – part 2.

In the following points, the description of each component is provided:

- "BeeAlgorithmConfiguration" class:
  It is a configuration class that has the needed parameters for ABC algorithm. These parameters are: worker bees count, onlooker bees count, scout bees count and maximum cycle number (MCN).

- "ABCStandardAlgorithm" class:
  It is the starting point of the algorithm. This class needs a configuration object described above and the problem specific implementation which provided by the user of the framework. This class contains the ABC algorithm work flow. The only public methods in "ABCStandardAlgorithm" class are the constructor and "startAlgorithm()" methods. "startAlgorithm()"is the real starting point of the algorithm execution.

- "ProblemSpecificBeeInterface" interface:
  Each problem has its search space specifications. For example if we use GABCF in travelling salesman (TSP) problem, the search space is the valid routes that could solve the problem. In this interface, there are three declared functionalities:

  a) Create random solution: which is used in the initial generation creation and in scout bees' work.

  b) Do the worker bees search: depends on each problem, the user could provide a worker bee search action to be executed during ABC algorithm lifecycle. This search should run using the method parameter (solution). If the user of the framework doesn't want search activities to be done by the worker bees, he could return the method parameter as it is into the function output without any changes.

  c) Do the onlooker bees search: depends on each problem, the user could provide an onlooker bee search action to be executed during ABC algorithm lifecycle. This search should run using the method parameter (solution). Theoretically, onlooker search action should be on a wider scale than worker bees' action, but this depends on the user implementation logic.

- "AbstractSolutionClass" class:
  This is a parent class for the solutions. Each problem has its solutions format, but the user problems' solution class should extend this abstract parent. The only two methods that should be implemented according to the problem nature are:

  a) "evaluateSolutionFitnessFunction", the user should implement this method to evaluate the solution fitness value according to the problem details.

  b) "serializeObjectToStringFunction", this method is serializing the solution object to a string format to be compared by the framework in equality conditions. This string represents the solution and should be considered as a hash code of the solution which should not return the same value except for the typical solutions content.

After discussing the detailed image of the framework components, figure 5 presents the sequence flow of the work starting from the initiation of the algorithm by the user until returning the best fetched solution to the caller. The sequence diagram presents first cycle actions. Other cycles do the same sequence of actions excluding the initial generation creation.

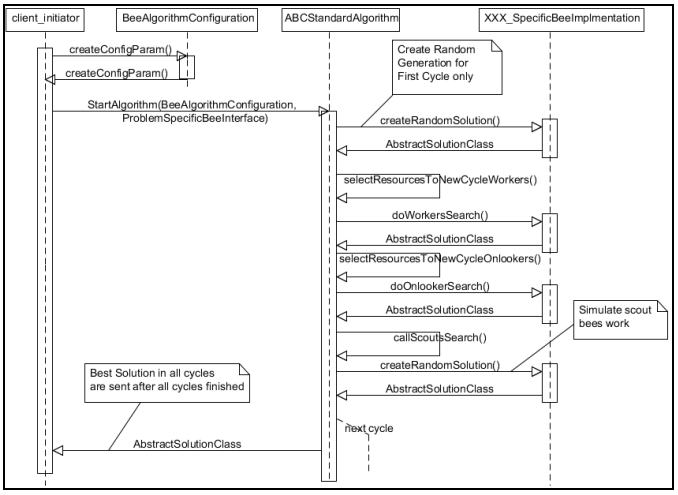

Figure 5: GABCF sequence diagram for iteration 1.

As described in figure 5, the workflow of the framework starts by the client when bee algorithm configurations object creation. In this step, the user set the needed parameters of the GABCF framework. These parameters are the ABC algorithm parameters that described in the previous section. Afterwards, the GABCF uses the specific problem implementation to run the ABC algorithm workflow. The ABC algorithm starts from initial generation creation, select the sources for the worker bees for the current iteration, run the worker search logic, select the onlooker bees' sources, run the onlooker bees

search, and run the scout bees search to complete the available sources to be ready for the next cycle enrollment. Figure 6 presents the other iterations flow. This flow in figure 6 is applied starting from iteration 2 to the last iteration.

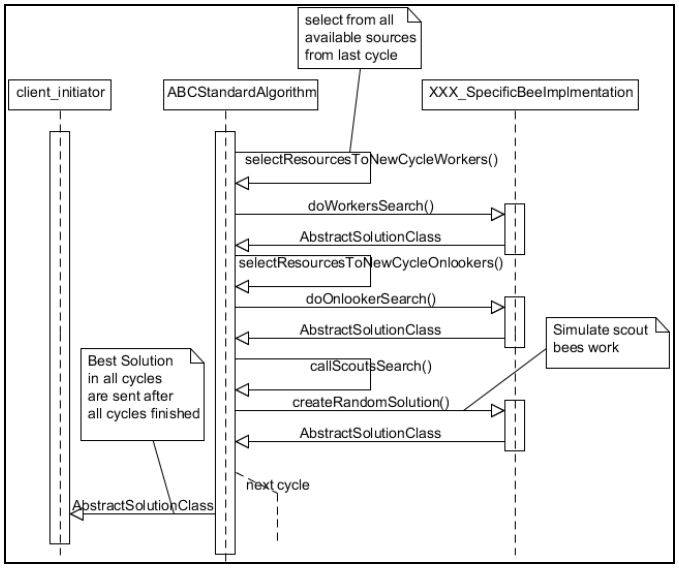

Figure 6: GABCF sequence diagram for other iterations.

4 Experiments

In this section, the paper presents experimental usage of GABCF in solving traveling salesman problem (TSP). This section mainly provides the actual activities of the GABCF user to be able to run the complete solution for his problem (TSP). As described in the previous section, the user of GABCF has to implement "ProblemSpecificBeeInterface" interface, and "AbstractSolutionClass" class.

```
public class TSPSolution extends AbstractSolutionClass {

    private List<Cities> route=new ArrayList<Cities>();// like A, B,C, A

    @Override
    public int evaluateSolutionFitnessFunction()
    {
        int length=0;
        for (int i = 0; i < route.size()-1; i++) {
            length+=Math.sqrt(
                    Math.pow(route.get(i).getCityX()-route.get(i+1).getCityX(),2) +
                    Math.pow(route.get(i).getCityY()-route.get(i+1).getCityY(),2) );
        }
        return length;
    }

    @Override
    public String serializeObjectToStringFunction()
    {
        String output="";
        for (int i = 0; i < route.size(); i++) {
            output+=route.get(i).getCityName()+"-";
        }
        return output+evaluateSolutionFitnessFunction();
    }
```

Figure 7: TSP solution class implementation.

As presented in figure 7, the user creates problem's solution extending "AbstractSolutionClass". The created class implements two abstract parent methods. The first one is "evaluateSolutionFitnessFunction", which should evaluate the solution fitness function according to the problem nature. The second one is "serializeObjectToStringFunction" which should serialize the solution object into string, just to act like the hash code during the objects comparison.

The second needed class is the implementation of "ProblemSpecificBeeInterface" interface. TSP implementation of this interface is presented in figure 8.

The needed functions implementation sample is presented in figure 8. The user implements a function that creates a random solution. This function is used in the first generation creation and in scout bees search. Other two functions search in the search space according to the problem nature, one for worker search scope and the other one for onlooker search scope. If the user in any search function (worker for example) returns the parameter as is, so the user implicitly cancels this search activity.

```
public class TSPSpecificBeesImplmentation implements ProblemSpecificBeeInterface {

    public AbstractSolutionClass createRandomSolution() {
        TSPSolution solution = new TSPSolution();
        //TODo the logic that create random solution;
        return solution;
    }

        public AbstractSolutionClass doWorkerWork(AbstractSolutionClass solution) {
        if (!(solution instanceof TSPSolution)) {
            return null;
        }
        TSPSolution newSolution = new TSPSolution();
        //Clone solution to tspSolution variable (to avoid any reference problem)
        //using tspSolution variable, do the search in worker scale (small)
        //and return the best solution in very close neighbors
        return newSolution;
    }

    public AbstractSolutionClass doOnlookersWork(AbstractSolutionClass solution) {
        if (!(solution instanceof TSPSolution)) {
            return null;
        }
        TSPSolution newSolution = new TSPSolution();
        //Clone solution to tspSolution variable (to avoid any reference problem)
        //using tspSolution variable, do the search in looker scale (wide scale somehow)
        //and return the best solution in very close neighbors
        return newSolution;
    }

    public TSPSpecificBeesImplmentation() {
        loadCitiesFromFile();// TSP problem specific implementation
    }
```

Figure 8: TSP specific problem implementation class.

5 Conclusion

Generic Artificial Bee Colony Framework (GABCF) is the proposed framework that implements artificial bee colony algorithm. The value of GABCF demonstrated in its separation between ABC algorithm details and any specific problem implementation. It implements the workflow of ABC algorithm. It provides interfaces that should be implemented by the user of the framework, by implementing these interfaces the framework will adapt and run on the user specific problem details. GABCF is applied for TSP, and some bioinformatics problems without any modifications of the framework. It just needs implementing small parts related to the problem specification components (parts which are described in the paper). Using the framework saves a lot of time in reaching a final executable solution for the problems due to the proposed reusable work provided in the framework. The usage of the framework for TSP problem is described with sample of code in this paper.

The profit of GABCF (saving the development time) is vary from problem to another due to the complexity of the problem, so this research doesn't provide a mathematical representation of this saved time, but the paper provide a sample of using the GABCF and proof its usefulness in a subjective way.

6 References

[1] D.T. Pham, A. Ghanbarzadeh, E. Koc, S. Otri, S. Rahim, M. Zaidi. "The bees algorithm", Technical Report, Manufacturing Engineering Centre, Cardiff University, UK, 2005.

[2] Dervis Karaboga, Bahriye Akay. "A Comparative Study of Artificial Bee Colony Algorithm". Applied Mathematics and Computation Journal, Elelsevier, pp. 108–132, 2009.

[3] Karl O. Jones, André Bouffet."Comparison of Bees Algorithm, Ant Colony Optimisation and Particle Swarm Optimisation for Pid Controller Tuning". International Conference on Computer Systems and Technologies - CompSysTech'08, 2008.

[4] Ling Wang, Gang Zhou, Ye Xu, Shengyao Wang, Min Liu. "An effective artificial bee colony algorithm for the flexible job-shop scheduling problem", Int J Adv Manuf Technol, September 2011.

[5] Li-Pei Wong, Malcolm Yoke Hean Low, Chin Soon Chong. "A Bee Colony Optimization Algorithm for Traveling Salesman Problem", Second Asia International Conference on Modelling & Simulation, IEEE, 2008, pp. 818-823.

[6] Xiaojun Bi, Yanjiao Wang, "An Improved Artificial Bee Colony Algorithm", Computer Research and Development (ICCRD), 2011 3rd International Conference, IEEE, 2011, pp. 174-177.

Finger-Knuckles Biometric OAuth as a Service (FKBoaS)

Ibrahim Abd-elatief Ahmed [1], Gouda I. Salama[1], and Ibrahim I. Emam[1]
[1]Computer Science, Arab Academy for Science Technology & Maritime Transport, Cairo, Egypt

Abstract - *the need for providing delicate authentication-based systems via biometric-based methods is increasing by the time. This importance is even more sustained for customer-oriented applications, especially the web-based systems. Having this authentication mechanism provides user friendly solutions for login that help the users to avoid thinking about memorizing different passwords or having to have periodic passwords changes*.

Keywords: Knuckles, HAAR, and SURF

1 Introduction

Nowadays, proof of identity is required in several places in our life [1]. This could be done by using other approaches such as user/pass requests or by asking for some personal documents, such as Social Insurance Number, Health Card, or so on [2]. These identification measures are often enough to identify persons. However, in case of having these identification measures stolen, there is no way to prevent the identity theft [3].

Therefore, the identification must provide a linkage between these metrics and the person being identified [4]. This could be done using some biological and/or behavioral measures from the identifier (such as finger and voice, which are the most popular ways to have this linkage)[5]. Therefore, using these biometric means is more reliable as they confirm the real presence of the person being identified [6].

Finger-back surface has not been in the focus of hand-based authentication researches, although the finger knuckles bending has highly unique pattern formation compared to other comparators, which means that it can be used as a valid feature to provide biometric-based identification[7].

The biometric hand-based authentication has proven significant reliability and users' acceptance, as it provides different extraction features (internal/external to distinguish between different entries) [8]. However, it becomes more challenging for large scale systems [9]. Specially, this requires extracting additional features to ensure the distinction between different users [10]. We use "Fingers' Knuckles" as a significant feature to be extracted to enhance the hand-based authentication process. In this context, we automate a feasible method to extract knuckle from the finger-back (hand dorsum) surface.

As well as the biometric authentication, we could even add an extra layer to optimize this authentication approach. This can also involve applying an oAuth application template for the signing process, and having a threshold-based process to evaluate the authentication process.

The previous finger knuckles researches provided good results with effective finger knuckles feature extraction [11]. However, these researches focused on specific equipments (mostly expensive ones) with a static environment [12]. Only few researches provided dynamic settings using cost-effective devices (such as RGB camera) to provide authentication systems [13]. Nevertheless, it has a lot of inflexibilities of having strict placement of hands in front of the camera. Having dynamic settings and environments can face several problems [14]. For example, there is a need to provide a separation between hand and any unrecognized backgrounds [15]. Also, it must provide consistent translation, scale invariance, and rotation of the Regions of Interests (ROIs), regardless of the captured images general features (such as blurriness or lighting)[16],[17].

In that research, we provide a novel approach based on or web camera to overcome all of the challenges that we can face with dynamic settings and environments. It provides a cutting edge technique to replace fingerprint biometric identifier with finger knuckles. For instance, the users will only need to show their knuckles against their web camera or their laptops integrated camera in order to get authenticated right away. On the other hand, in the normal fingerprint authentication way, you are entitled to scan your finger with a certain position and make sure that it is too straight so the system will be able to scan it well, and also avoid any other external variables such as having a sweaty fingers or unclean fingerprint scanners.

In wide-scale systems, the authentication main target is to identify a user among a large set of other existing identities in the system, or other connected systems and environments [18]. Thus, we need to have an indexing technique to reduce the number of identities to be processed by the identification algorithm [19]. A knuckle indexing technique on closed set of identifications can be applied, and based on minutiae and SURF features in order to enhance the performance of data retrieval and identification [20].

We will start first with showing an overview for the system and how it works. Then, we will show the different preprocessing operations that we apply when receiving inputs. After that, the feature extraction followed by the data retrieval process will be clarified. Then, the classification process will be illustrated in details and how we can classify different retrieved data.

2 System Overview

The system consists of two tiers which are client (User Interface), and Server. The server tier has a frontend server (Application Server) and a backend server (Biometric Server), which utilize OAuth protocol.

The client tier could be an intranet user accessing the system internally through a web camera, while, the front server is used to handle different web-based transactions. On the other hand, the Biometric Server is used to handle the user authentication processes including the users' enrollment database.

The user does his common online transactions through the front server. Once, the user is promoted to do a secure transaction (such as a payment), they are redirected to the Biometric Server, which starts handling the authentication process. The process starts by asking the user to input their authentication values using input devices (such as scanners) in order to authenticate them before starting to handle his secure transactions. Suppose that is the first time the user uses the system, then the backend server establishes an entry for the user in the database, extract different features moments, and store them in the secure server database. Figure1 shows an abstract view of the secure transaction process, and figure 2 shows a deployment view of the system.

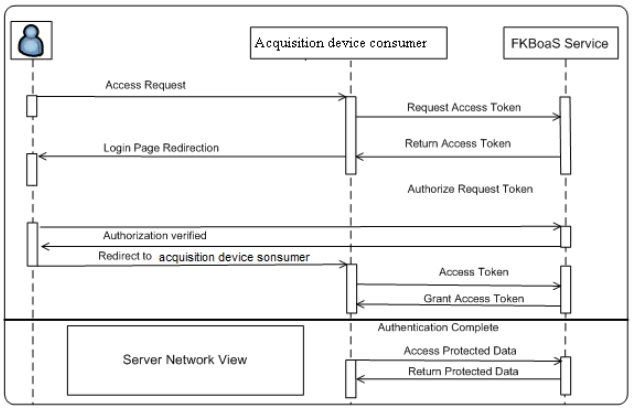

Fig. 1 Biometric Server OAuth flow.

This solution provides experimentation results based on biometric fusion rules and identifiers using web camera.

Web camera is used as a cost-effective acquisition device hosted in a cloud web service, and can be easily linked to other servers. The authentication process requires the user to show their dominant hand to the web camera and wait until the web camera captures the required details. This process requires the user to have the three gaps between the fingers visible, as they are used to extract the Region of Interest (ROI) from the fingers knuckles in addition to the depth map. The verification process consists of preprocessing, feature extraction, clustering and retrieval, and classification. It starts with the image acquisition, which goes through image preparation and mapping processes. After that, we extract the region of interests, and their SURF and Minutiae key points in order to extract features. Then, apply some curvature equations before proceeding the matching process, and taking decision whether to accept the acquired finger knuckle or not.

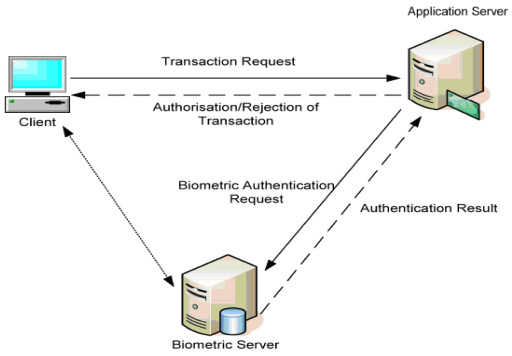

Fig. 2 Server Network Flow.

3 Preprocessing

This stage is about preparing the image for being processed by applying different image filters to enhance the picture [21]. For that, four preprocessing tasks are required prior to extracting features. These tasks are image reconstruction [22], finger features extraction, and disparity map estimation [23]. We will discuss these tasks after applying different images filters. The Image preparation procedure consists of the following ordered steps:

1. Collect the Stereo Pairs as structured samples
2. Apply a Histogram Equalization on the image [24].
3. Apply a low pass filter to remove noise [25].
4. Apply a non-linear filter [26].
5. Extract depth maps to construct illuminated image.

3.1 Structured Sampling and Image Reconstruction

We have to collect a series of images because of the small variations between the hand positions and movement, based on the radiance function properties. Then, we have to segment these captured images into regions with concave or convex behavior in order to provide sampling strategies for radiance reconstruction. This requires determining the inflection point on two orthogonal axes that pass through the surface of the captured hand. After that, an adaptive subdivision is applied on these orthogonal axes in order to produce two unidimensional segments lists. Finally, the produced image will be illuminated and ready for the next process.

3.2 Disparity Map Estimation

As we lack for raw depth map that shows the z-value differences, we use stereo pairs images to calculate the surface curvature. After that, we apply Kurt Konolige's matching

stereo correspondence algorithm in order to calculate the pixels differences between two captured images [28]. This algorithm uses the sliding sums of absolute differences sifted by variant pixels amount ranges between minimum disparity up to the summation of minimum disparity and number of disparities. The algorithm computes disparity on a pair of images (Width and Height) using the following formula:

$$o(W \times H \times numberOfDisparities) \quad (1)$$

The results will be merged to the raw disparity map with precedence to inputs.

Procedure to Extract Disparity Map Estimation

1. Collect the Stereo Pairs (pair of available images).
2. Apply the Block Matching Stereo Correspondence algorithm to find the possible correspondences.
3. Construct a simple Q-Matrix to rectify the image.
4. Reproject the image with z-value to provide a set of vertices.
5. Construct the disparity map.
   a. It calculates the Gaussian and Mean curvatures and provide the z-value for each pixel.
   b. It merges the constructed map with the raw depth map.

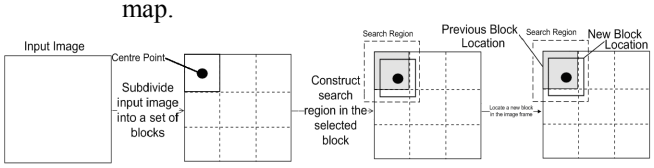

Fig. 3 Block Matching Stereo Correspondence

4 Feature Extraction

The features are extracted by examining the structural information contained in the distribution of knuckle minutiae and SURF key points [29].

These features are then clustered using K-Means [30]. This clustering is used to identify groups of samples that behave similarly and dissimilarly, such as malicious and non-malicious activity [31]. In the next phase of identification, Naïve Bayes is used for validating the identity of the group [32]. K-Mean clustering is a cluster analysis method that is used to partition observations in a set of k clusters belongs to the cluster nearest mean. This clustering process results on a set of Voronoi cells in a data space partitioning [33].

4.1 SURF Feature Extraction

The extracted ROIs for finger knuckles have low definition and their grayscale values can change very easily in the space. This makes it more difficult to detect stable points even with algorithms such as Harris or Different of Gaussian (DoG) [34].

4.1.1 Fast-Hessian algorithm as a key point's detector

In this context, the Fast-Hessian key point detector algorithm is accurate and has good performance [35]. If we have a point in an image, the Hessian matrix in that point can be defined at a given scale as follows:

$$H(p,s) = \begin{bmatrix} L_{xx}(p,s) & L_{xy}(p,s) \\ L_{xy}(p,s) & L_{yy}(p,s) \end{bmatrix} \quad (2)$$

In that matrix, the value of each element is the Gaussian second order derivative convolution $\frac{\partial^2}{ax^2} g(s)$ in a point . Using box filters, we can apply the Gaussian second order partial derivative in the directions of y and xy. In figure 4 the regions in gray are equal to zero. A box filter is and , in order to maintain high efficiency on images.

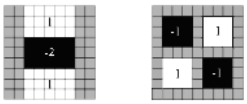

Fig. 4 Knuckle Minutiae Box Filter.

We then apply non-maximum suppression in a range of $3 \times 3 \times 3$ neighborhood in order to locate the points of interest. Figure 5 provides an example of detected Finger Knuckles points ROI images using Fast-Hessian.

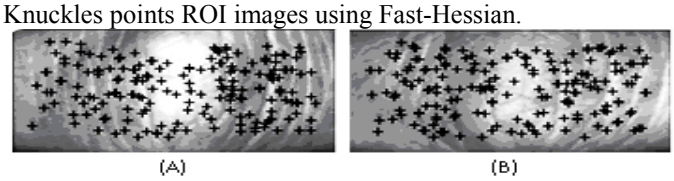

Fig. 5 SURF Keypoints.

4.2 SURF (Speeded Up Robust Feature) Descriptor

Key points must be unique compared to each others and this is provided by SURF. In SURF, a key point can be described based on its dominant orientation on the surrounding regions. Extracted key points are surrounded by circular constructed regions, which are used to compute the dominant orientation. The computation is applied on both horizontal and vertical directions using Haar wavelet responses, and calculated by adding a wavelet space θ (value 60^o in our case) to the Haar wavelet response. The result of that summation is the maximum dominant orientation for the key points' description, and it is its rotation invariant for the image rotation as well as the dominant orientation.

4.3 SURF descriptor components

Descriptor extraction constructs are an aligned centered square around the points of interest on the dominant orientation. That square region is divided into smaller squares of size of 4×4 and the Haar response is applied to each square on both axes. The summation of these responses on both sides is used as feature attribute to form the first feature vector. The polarity intensity changes information is the absolute

summation of responses on both axes on a four-dimensional vector V So, we compose a 64-length SURF descriptor for the key-point from all 4×4 sub regions as follows:

$$V = \{\sum d_x, \sum d_y, \sum |d_x|, \sum |d_y|\} \quad (3)$$

4.4 D. Index Space Model Creation

A triplet $\vec{t}_i$ has nine-fold consisting of ridge curve and geometric agglomeration features. It is presented as 9-dimensional, where $\vec{t}_i = \{\alpha^i, \beta^i, \gamma^i, k_1^i, k_2^i, k_3^i, \lambda_1^i, \lambda_2^i, \lambda_3^i\}$ and it can be viewed as a single entry in hyperspace. So, each knuckle image has a collection of points reside in that 9-dimensional index space model. For a new set of trained knuckle images, a new space model is created with unsupervised clustering on the generated 9-dimensional entities of these trained images, which results on a number of clusters shown in its centroid.

When a knuckle input y is authorized, it is divided into a set of triplets mapped into the 9-dimenstional space, and assigned to a unique cluster c_j, where j is the minimum distance rule, and it can be calculated as:

$$j = \arg \min_{k=1}^{k} \left\| t_i - \vec{\mu}_k \right\| \quad (4)$$

, where $\|\cdot\|$ is the norm of a each side, and means that this process is applied on each cluster and repeated for each entry. This provides us a list of all knuckles identities $\{y_{j1}, y_{j2}, ..., y_{jn}\}$ in that cluster, which have at least one triplet assigned.

Figure 6 shows the model map population process:

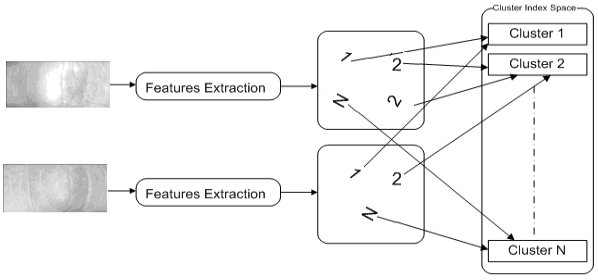

Fig. 6 Mapping finger knuckles in the database, and put similar patterns into clusters

4.5 K-means Data Clustering

Clustering is the process of partitioning data into subsets (defined as clusters) to classify the entries that share specific properties [36] It is used as a first step to enable different static analysis processes on the images, such as image analysis, pattern recognition, etc [36] The clustering can be supervised if the data collected samples are labeled by class membership; otherwise, it is an unsupervised clustering [37] In the unsupervised clustering algorithms, clustered objects are divided into a number of k partitions based on specific attributes from the generated data from Gaussian distributions [38], [39] The $k-means$ algorithm is used to minimize the variance of the intra class and squared error function following this formula:

$$E = \sum_{i=1}^{k} \sum_{x_i \in C_i} \left\| x_j - \vec{\mu}_i \right\| \quad (5)$$

Where k is the number of clusters, j a number of points x_j in a set of clusters C_i, and μ_i their centroid. The algorithm $k-means$ of is commonly used as it provides quick retrieval when it is run several times to cluster the data set available. However, it can result on unexpected results when data is not clustered totally, so, it is better to make sure that a number of clusters are pre-set first [40].

4.6 Knuckle Clustering and retrieval

When executing a query, the system divides the triplets in a 9-dimentionals points based on these extracted features. Each directive point $\vec{t}_i$ is mapped into a cluster $c_{\pi i}$ where πi is $1 \le \mu \le k$ using the minimum distant rule. Each target cluster can be associated with the executed query, and their top N-identifiers occur frequently in that target for further matching processes.

5 Classification using Naïve Bayesian Network

K-Means is used to identify groups of samples that behave similarly and dissimilarly such as malicious and non-malicious activity in the first stage while Naïve Bayes is used in the second stage to classify all data into correct class category. Naïve Bayesian Network (NBN) probabilistic classifier applies strong independence assumptions using Bayes theorem [41] NBN classifiers are trained using supervised learning set in a Bayesian network. It encodes a distributed set of variables $\{x_1, x_2, ..., x_n\}$,as a set of Conditional Probability Distributions (CPDs) and directed acyclic graph. The encoding process asserts that each node must be independent of each descendents. Each node has its corresponding CPD that provides different state probabilities, with all combinations of its patents [42].

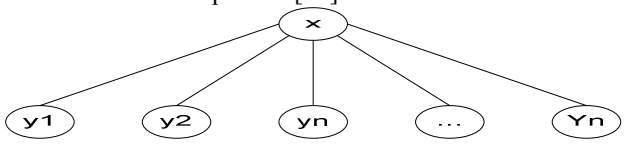

Fig. 7 Naive Bayesian Network Schema

Assume that we have a number n of input attributes $X = \{x_1, x_2, ..., x_N\}$. Thus, the total possibility (product) of this input can be written as:

$$P(x) = p(x_1) \times p(x_2) .... \times p(x_n) \quad (6)$$

It is considered independent with or without conditions in a fixed class (y), and its probabilities are estimated as follows:
Conditional probability (which is the Naïve Bayesian Classifier basis):

$$P(y \mid x) = P(y) \times P(x \mid y) / P(x) = P(y) \times (P(x_i \mid y) / P(x_i)) \quad (7)$$

Relative probability:

$$P(x \mid y) = P(x_1 \mid y) \times P(x_2 \mid y) .... P(x_N \mid y) \quad (8)$$

5.1 Fusion Decision Network

It is a majority network used to resolve uncertainties in the statistical probabilities by processing the input data and its classifier modules output in order to provide final decision [43] However, if a set of three modules provides three different classification results, the output result will be indecision [44] This requires at least two modules to have the same classified class in order to get a correct output result [45].
The applied methods for feature extraction are directly fusible. Thus, we need to apply feature length normalization or mage resizing in case the decision of the feature level is used. This requires applying an appropriate strategy for the decision level, in order to avoid having complicated system computations result eventually on performance degradation. The feature extraction generates a distance probability for each knuckle area $P^{k1}(x, y)$, and $P^{k2}(x, y)$

Thus, each knuckle has the same feature extraction process applied and ready for fusion. Each two subjects are matched through fusing decision level that requires combining the distance between their knuckle areas (k_1, k_2).

For instance, for a subject P, two feature codes x_{k1}^{p}, and x_{k2}^{p} are extracted, and for a subject Q, two other features x_{k1}^{Q}, and x_{k2}^{Q} are extracted. The two distances between these two subjects are calculated as:

$$d_{k1} = d(x_{k1}^{p}, x_{k1}^{Q}) \quad (9)$$

$$d_{k2} = d(x_{k2}^{p}, x_{k2}^{Q}) \quad (10)$$

Then, the total distance between the two subjects are calculated based on a weighted combination of two distances as:

$$d(P,Q) = \alpha(d_{k1} + d_{k2}) \quad (11)$$

In this equation, is a weighting factor and can be calculated as follows [46]:

$$\alpha(x, y) = \frac{1}{1 + \sigma v(x, y)} \quad (12)$$

In which v is the value of the image variance, and σ is used as a tuning parameter to distribute α as much as possible in a normalized range [0,1] in a formal manner [46].

6 Results

The used database for testing consists of a set of images and PolyU FKP database, in where each entry has k-images for each knuckle area; k-image consists of raw and depth image. It also includes FKP database after extracting offline depth image.

6.1 Performance of Classification

Classification performance is measured based on the error and accuracy rates. Error rate is the ratio between the number of misclassified knuckles, and the total number of test samples:

$$\text{Error Rate} = \frac{\text{Number of misclassified Knuckles} \times 100}{\text{Total number of test samples}} \% \quad (13)$$

On the other hand, the accuracy rate is simply the remained portion of the classified knuckles after subtracting the error rate:

$$Accuracy = 100\% - \text{Error Rate} \quad (14)$$

The error rate is generally described as the function of the searchable percentage of the database, which is referred to as penetration rate, and computed as:

$$\text{Penetration Rate} = \frac{\text{Number of accesses knuckles} \times 100}{\text{Total number of knuckles samples}} \% \quad (15)$$

TABLE I
MODAL BIOMETRICS PERFORMANCE

Knuckle Area	Accuracy (%)
Lk_1	99.63
Lk_2	99.84
Rk_1	99.36
Rk_2	99.79
$Lk_1 + Lk_2 + Rk_1 + Rk_2$	100

This is a summary for the accuracy of knuckle areas, using the proposed fusion approach. We can observe from the table that as high as 100% accuracy was achieved for fussed knuckle areas. The performance of identification for single knuckle area is significantly lower than that fused. Inclusion of skeletal structure of knuckle for classifying each shape to a specific region result could also improve the system accuracy.

7 Conclusion

In this research, we managed to clarify that we can use knuckle as a reliable biometric identifier that do not require expensive equipments or special arrangement. In addition, it does not force the users to provide data inputs in certain ways such as direction of fingers. Also, the user does not need to have extra cognitive thinking to remember the password or being asked to change the password periodically. Not only this, but also it maintains higher security level given that it will ensure that the person must be present in order to have a successful login.
We obtained reliable results compared to other knuckle identification researches, and the same time, we do not need to use special equipment, and instead, we use any web camera.

This means that the application can be used on different ranges.
However, in this paper, we have not applied results on a wide-scale database that covers different other cases and metrics such as aging, skin color, different races, etc. This is in addition, to other variables such as fatness, skin, injuries, etc. This will require applying different traces and geometrical features on difference races with different color skins, and hand sizes. Thus, for the future, including skeletal structure of knuckle for classifying each shape (to a specific region result) will result on more reliable, and accommodates other circumstances such as aging and injuries.

8 References

[1] R. Gil Charo Castro Manuel Wyne Mudasser F Meier, "Web Tests in LMS using Fingerprint Identification," in IEEE ICALT Conference, 2010, pp. 679-681.

[2] T. Rissanen, "Electronic identity in Finland: ID cards vs. bank IDs," Identity in the Information Society, vol. 3, no. 1, pp. 175-194, 2010.

[3] G. Kolaczek, "An Approach to Identity Theft Detection Using Social Network Analysis," 2009 First Asian Conference on Intelligent Information and Database Systems, pp. 78-81, 2009.

[4] M. Guillaumin, J. Verbeek, and C. Schmid, "Metric Learning Approaches for Face Identification," Wild, pp. 498-505, 2009.

[5] E. Mordini, "Biometric identification technology ethics," BITE Policy Paper, p. 64, 2005.

[6] M. Islam, S. Venkataraman, and M. Alazab, "Stochastic Model Based Approach for Biometric Identification," in Technological Developments in Networking Education and Automation, vol. 1, K. Elleithy, T. Sobh, M. Iskander, V. Kapila, M. A. Karim, and A. Mahmood, Eds. Springer Netherlands, 2010, pp. 303-308.

[7] L. Zhang, L. Zhang, D. Zhang, and H. Zhu, "Online finger-knuckle-print verification for personal authentication," Pattern Recognition, vol. 43, no. 7, pp. 2560-2571, 2010.

[8] P. C. Eng and M. Khalil-Hani, "FPGA-based embedded hand vein biometric authentication system," TENCON 2009 2009 IEEE Region 10 Conference, no. 79900, pp. 1-5, 2009.

[9] M. Adán, A. Adán, R. Torres, A. S. Vázquez, G. Bueno, and E. S. I. U. Spain, "Personal authentication based on hands natural layout," in Conference on Machine Vision Applications Tsukuba Science City Japan, 2005, pp. 160–163.

[10]C. Nickel, C. Busch, S. Rangarajan, and M. Mobius, "Using Hidden Markov Models for Accelerometer-Based Biometric Gait Recognition," Signal Processing and its Applications CSPA 7th International Colloquium on Signal Processing and its Applications, pp. 58-63, 2011.

[11]M.-biometric System, P. Recognition, A. Meraoumia, S. Chitroub, and A. Bouridane, "Fusion of Finger-Knuckle-Print and Palmprint for an Efficient," Science And Technology, pp. 1-5, 2011.

[12]E. C. Lee, H. Jung, and D. Kim, "New Finger Biometric Method Using Near Infrared Imaging," Sensors (Peterboroug, vol. 11, no. 3, pp. 2319-2333, 2011.

[13]M. G. K. Ong, T. Connie, A. T. B. Jin, and D. N. C. Ling, "A single-sensor hand geometry and palmprint verification system," in Proceedings of the 2003 ACM SIGMM workshop on Biometrics methods and applications WBMA 03, 2003, p. 100.

[14]F. A. Afsar, M. Arif, and M. Hussain, "Fingerprint identification and verification system using minutiae matching," in National Conference on Emerging Technologies, 2004, pp. 141-146.

[15]W. Westerman, "HAND TRACKING , FINGER IDENTIFICATION , AND CHORDIC MANIPULATION ON A MULTI-TOUCH SURFACE by FINGER IDENTIFICATION , AND CHORDIC MANIPULATION ON A MULTI-TOUCH SURFACE by," Electrical Engineering, p. 363, 1999.

[16]A. Uthama, R. Abugharbieh, A. Traboulsee, and M. J. McKeown, "Invariant SPHARM shape descriptors for complex geometry in MR region of interest analysis.," Conference Proceedings of the International Conference of IEEE Engineering in Medicine and Biology Society, vol. 2007, pp. 1322-1325, 2007.

[17]C. Weerasinghe, L. Ji, and H. Yan, "ROI extraction from motion affected MR images by suppression of blurring and motion artifacts in the image background," Signal Processing and Its Applications 1999 ISSPA 99 Proceedings of the Fifth International Symposium on, vol. 1, p. 279--282 vol.1, 1999.

[18]Z. Niu, K. Zhou, H. Jiang, T. Yang, and W. Yan, "Identification and Authentication in Large-Scale Storage Systems," 2009 IEEE International Conference on Networking Architecture and Storage, pp. 421-427, 2009.

[19]A. Pavlo et al., "A Comparison of Approaches to Large-Scale Data Analysis," Distribution, vol. 12, no. 2, pp. 165-178, 2009.

[20]A. Morales, C. M. Travieso, M. A. Ferrer, and J. B. Alonso, "Improved finger-knuckle-print authentication based on orientation enhancement," Electronics Letters, vol. 47, no. 6, p. 380, 2011.

[21]T. Heseltine, N. Pears, and J. Austin, "Evaluation of image pre-processing techniques for eigenface based face

recognition," Proceedings of SPIE, vol. 4875, no. 2002, pp. 677-685, 2002.

[22]M. Defrise and G. T. Gullberg, "Image reconstruction.," Physics in Medicine and Biology, vol. 51, no. 13, pp. R139-54, 2006.

[23]N. Baha and S. Larabi, "Neural Disparity Map Estimation From Stereo Vision," in International Symposium on Modelling and Implementation of Complex systems, 2010, no. 1.

[24]X. Sun, P. L. Rosin, R. R. Martin, and F. C. Langbein, "Bas-relief generation using adaptive histogram equalization," IEEE Transactions on Visualization and Computer Graphics, vol. 15, no. 4, pp. 642-653, 2009.

[25]J. A. S. Centeno and V. Haertal, "Adaptive Low-Pass Filter for Noise Removal," Photogrammetric Engineering and Remote Sensing, vol. 61, no. 10, pp. 1267-1272, 1995.

[26]W. Maass and E. D. Sontag, "Neural systems as nonlinear filters.," Neural Computation, vol. 12, no. 8, pp. 1743-1772, 2000.

[27]B. Pateiro-l and A. Rodr, "Generalizing the Convex Hull of a Sample : The R Package alphahull," Journal Of Statistical Software, vol. 34, no. 5, pp. 1-28, 2010.

[28]K. Konolige, W. Garage, and M. Park, "Projected Texture Stereo," Analysis, vol. M, pp. 148-155, 2010.

[29]A. Noguchi and K. Yanai, "A SURF-based Spatio-Temporal Feature for Feature-fusion-based Action Recognition," Computer, 2010.

[30]T. Kanungo, D. M. Mount, N. S. Netanyahu, C. D. Piatko, R. Silverman, and A. Y. Wu, "An efficient k-means clustering algorithm: analysis and implementation," IEEE Transactions on Pattern Analysis and Machine Intelligence, vol. 24, no. 7, pp. 881-892, 2002.

[31]E. Ahmed, A. Clark, and G. Mohay, "A Novel Sliding Window Based Change Detection Algorithm for Asymmetric Traffic," 2008 IFIP International Conference on Network and Parallel Computing, pp. 168-175, 2008.

[32]J. Ren, S. D. Lee, X. Chen, B. Kao, R. Cheng, and D. Cheung, "Naive Bayes Classification of Uncertain Data," 2009 Ninth IEEE International Conference on Data Mining, no. 60703110, pp. 944-949, 2009.

[33]R. Cheng, X. Xie, M. L. Yiu, J. Chen, and L. Sun, "UV-Diagram : A Voronoi Diagram for Uncertain Data," Data Engineering, pp. 796-807, 2010.

[34]Y. Matsui and Y. Miyoshi, Difference-of-Gaussian-Like Characteristics for Optoelectronic Visual Sensor, vol. 7, no. 10. 2007, pp. 1447-1452.

[35]K. Velmurugan and S. S. Baboo, "Content-Based Image Retrieval using SURF and Colour Moments," Global Journal of Computer Science and Technology, vol. 11, no. 10, pp. 1-4, 2011.

[36]E. Visser, E. H. J. Nijhuis, J. K. Buitelaar, and M. P. Zwiers, "Partition-based mass clustering of tractography streamlines.," NeuroImage, vol. 54, no. 1, pp. 303-312, 2011.

[37]N. Grira, M. Crucianu, and N. Boujemaa, "Unsupervised and semi-supervised clustering: a brief survey," Machine Learning, pp. 1-12, 2004.

[38]J. P. Theiler, "Contiguity-enhanced k-means clustering algorithm for unsupervised multispectral image segmentation," Proceedings of SPIE, vol. 3159, no. 1997, pp. 108-118, 1997.

[39]R. Laxhammar, "Anomaly detection for sea surveillance," in Information Fusion 2008 11th International Conference on, 2008, pp. 1–8.

[40]O. Shamir and N. Tishby, "Stability and model selection in k-means clustering," Machine Learning, vol. 80, no. 2-3, pp. 213-243, 2010.

[41]T. Roos, H. Wettig, P. Grünwald, P. Myllymäki, and H. Tirri, "On Discriminative Bayesian Network Classifiers and Logistic Regression," Machine Learning, vol. 59, no. 3, pp. 267-296, 2005.

[42]D. Lowd and P. Domingos, "Naive Bayes models for probability estimation," Proceedings of the 22nd international conference on Machine learning ICML 05, pp. 529-536, 2005.

[43]N. Wanas and M. S. Kamel, "Decision fusion in neural network ensembles," IJCNN01 International Joint Conference on Neural Networks Proceedings Cat No01CH37222, vol. 4, pp. 2952-2957, 2001.

[44]E. C. Y. Peh, Y.-C. Liang, Y. L. Guan, and Y. Zeng, "Cooperative Spectrum Sensing in Cognitive Radio Networks with Weighted Decision Fusion Scheme," 2010 IEEE 71st Vehicular Technology Conference, vol. 9, no. 12, pp. 1-5, 2010.

[45]D. Wu, "Supplier selection: A hybrid model using DEA, decision tree and neural network," Expert Systems with Applications, vol. 36, no. 5, pp. 9105-9112, 2009.

[46]V. Maik, "Image restoration using alpha map-based fusion for multiple color aperture computational camera," in 2010 Digest of Technical Papers International Conference on Consumer Electronics (ICCE), 2010, pp. 41-42.

Range based Velocity Estimation Using Scene flow

Sobers L X Francis[1], **Sreenatha G Anavatti**[1], **and Matthew Garratt**[1]
[1]SEIT, UNSW@ADFA, Canberra, ACT, Australia 2600
e-mail: ({s.francis, s.anavatti, m.garratt}@adfa.edu.au)

Abstract— *The paper presents a method to estimate the velocity of the dynamic obstacles using the range-based scene flow vectors. These scene flow vectors are computed using differential flow technique which uses the range intensity gradients. Then the velocity of the dynamic obstacle is estimated effectively using a single camera unit i.e. Photonic Mixer Device (PMD) camera. The method is tested and validated with different scenarios and the results are discussed.*

Keywords: 3D Scene flow,PMD camera, motion detection, velocity estimation

1. Introduction

Historically, the path planning problem has been studied much less for cluttered environment. This may be because of the entire information of the environment will change along with the dynamic obstacles, so the complexity and uncertainty increase greatly in dynamic environments. Uncertainty is an important factor in the field of dynamic path planning because of the partial knowledge about the obstacles. So, motion estimation plays an important role in path planning techniques.

Most of the researchers are now working on stereo camera system because of the estimation errors and somewell known ambiguities (aperture problem) occur in the single camera, since the images from the single camera are the three-dimensional information projected to the camera's image plan. The distance information between the camera and the obstacle is lost completely. These two dimensional motion vectors are obtained using sparse techniques [Bauer et al., 2006], dense optical flow techniques [Bruhn et al., 2005].

These stereo cameras offer an additional information to reconstruct the three dimensional orientation. From the research work of [Wedel et al., 2011], the triangulation of stereo camera results in ambiguities. One of the challenges of 3D scene flow estimation using stereo cameras is that the two-view stereo problem at two different time steps, and the optical flow problem for each of the cameras. The intensity based image processing techniques are mainly based on grey scale or color in the images which is obtained from the conventional cameras. The main disadvantages of these techniques are that the image processing becomes inadequate in low illumination conditions and when the objects and the background look similar to each other [Yin, 2011].

In this paper, we use a single PMD camera which provides range information. The combined Lucas/Kanade and Horn/Schunck techniques [Bruhn et al., 2005] are utilized to calculate the scene flow. The distance moved by the obstacle is computed by the mean value of the consecutive segmented range frames. Then the velocity of the obstacle is estimated

The paper is organised as follows. Section II provides the methodology for velocity estimation. In Section III, the experimental results are discussed. Section IV summarises the work.

2. Methodology

2.1 PMD Camera

We are using Photonic Mixer Device (PMD) camera, a time-of-flight (TOF) camera in this work, in figure (1). A time of flight camera is a system that works with the TOF principles [Weingarten et al., 2004], and resembles a LIDAR scanner. In the TOF unit [Lange, 2000], a modulated light pulse is transmitted by the illumination source and the target distance is measured from the time taken by the pulse to reflect from the target and back to the receiving unit. PMD cameras can generate the range information, which is almost independent of lighting conditions and visual appearance, and a grey scale intensity image, similar to conventional cameras. The coordinates of the obstacle with respect to the PMD camera are obtained as a 200 by 200 matrix, each element corresponding to a pixel. It provides fast acquisition of high resolution range data. As the PMD range camera provides sufficient information about the obstacles, it is proposed to estimate the trajectory of the moving obstacles. These TOF camera provide a 3D point cloud, which is set of surface points in a three-dimensional coordinate system (X,Y,Z), for all objects in the field of view of the camera.

Fig. 1: PMD Camera

2.2 Scene Flow

Scene Flow [Vedula et al., 2005] is the three-dimensional velocity fields of points in the world; just as optical flow is the 2D motion field of points in an image. Any optical flow is simply the projection of the scene flow onto the image plane of a camera. If the world is completely non-rigid, the motions of the points in the scene may all be independent of each other. One representation of the scene motion is therefore a dense three-dimensional vector field defined for every point on every surface in the scene.

In order to compute the $3D$ motion constraint equation, the derivatives of the depth function with respect to the other world coordinates have to be computed. For instance, the dynamic object at (x, y, z) at time t is moved by $(\delta x, \delta y, \delta z)$ to $(x + \delta x,\ y + \delta y,\ z + \delta z)$ over time δt. The $3D$ Motion Constraint Equation (1) is obtained after performing 1^{st} order Taylor series expansion [Barron and Thacker, 2005].

$$R_x V_x + R_y V_y + R_z V_z + R_t = 0 \tag{1}$$

where, $\vec{V} = (V_x, V_y, V_z) = (\delta x/\delta t, \delta y/\delta t, \delta z/\delta t)$ is the $3D$ volume velocity, $\nabla R = (R_x, R_y, R_z)$ are the $3D$ spatial derivatives and R_t is the $3D$ temporal derivative. It is the analogue of the brightness change constraint equation [Spies et al., 2002] used in optical flow calculation.

2.3 Differential Flow Technique

Differential techniques can be classified as local and global. Local techniques involve the optimization of a local energy, as in the Lucas and Kanade method. The global techniques determine the flow vector through minimization of a global energy, as in Horn and Schunck. Local methods offer robustness to noise, but lack the ability to produce dense optical flow fields. Global techniques produce 100 percent dense flow fields, but have a much larger sensitivity to noise. The combined differential approach involves applying a locally implemented, weighted least squares fit of local constraints to a constant model for flow velocity, which is combined with the global smoothness constraint. The velocity estimates can be minimised by equation (2).

$$\begin{aligned} E^2 &= \int_D (W_N^2(\nabla R.\vec{V} + R_t)^2) \\ &+ \alpha^2 \left(\|\nabla V_x\|^2 \|\nabla V_y\|^2 \|\nabla V_z\|^2\right) dxdydz \end{aligned} \tag{2}$$

$A^T W^2 A$ is calculated as (3)

$$A^T W^2 A = \begin{pmatrix} \sum W^2 R_x^2 & \sum W^2 R_x R_y & \sum W^2 R_x R_z \\ \sum W^2 R_x R_y & \sum W^2 R_y^2 & \sum W^2 R_y R_z \\ \sum W^2 R_x R_z & \sum W^2 R_y R_z & \sum W^2 R_z^2 \end{pmatrix} \tag{3}$$

The velocity estimates can be solved through an iterative process.

$$V_x^{n+1} = V_x^n - \frac{W_N^2 R_x (R_x V_x + R_y V_y + R_z V_z + R_t)}{\alpha^2 + W_N^2 (R_x^2 + R_y^2 + R_z^2)} \tag{4}$$

$$V_y^{n+1} = V_y^n - \frac{W_N^2 R_y (R_x V_x + R_y V_y + R_z V_z + R_t)}{\alpha^2 + W_N^2 (R_x^2 + R_y^2 + R_z^2)} \tag{5}$$

$$V_z^{n+1} = V_z^n - \frac{W_N^2 R_z (R_x V_x + R_y V_y + R_z V_z + R_t)}{\alpha^2 + W_N^2 (R_x^2 + R_y^2 + R_z^2)} \tag{6}$$

where, the average of previous velocity estimates (V_x^n, V_y^n, V_z^n) are used along with the derivates estimates to obtain the new velocity estimates (V_x^{n+1}, V_y^{n+1}, V_z^{n+1}).

2.4 Velocity Estimation

The distance travelled by the obstacle between the two consecutive frames in three dimensional coordinates is given by the equation (7). In three-dimensional Euclidean space, the distance D_{ab} is

$$D_{ab} = \sqrt{(X_a - X_b)^2 + (Y_a - Y_b)^2 + (Z_a - Z_b)^2} \tag{7}$$

The estimated velocity of the obstacle is calculated in the equation (8).

$$EstimatedVelocity(mm/s) = \frac{D_{ab}(mm)}{t(sec)} \tag{8}$$

where,

- D_{ab} is the distance between two points (X_a, Y_a, Z_a) and (X_b, Y_b, Z_b) in mm.
- t is the time interval between two frames in sec.

The velocity error is the difference between the mean value of the estimated velocity and the actual velocity.

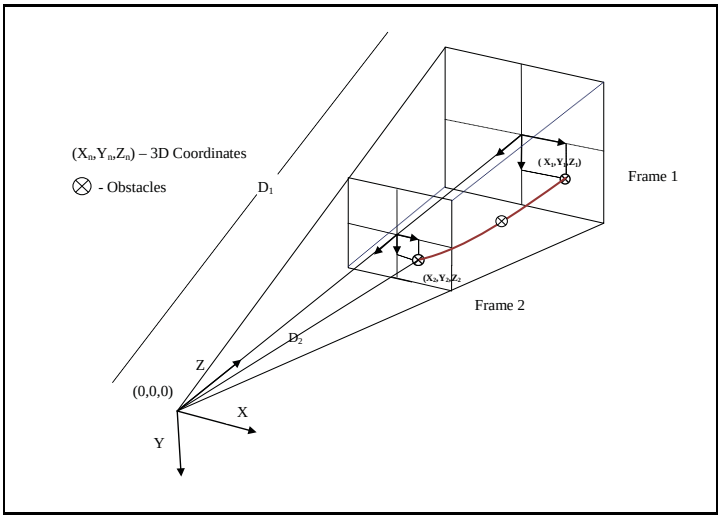

Fig. 2: Camera's Field Of View

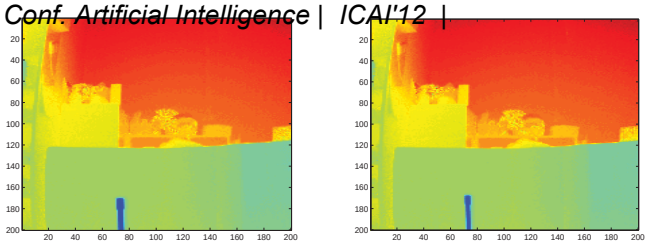

(a) Position1 (t=0.5 sec) (b) Position2 (t=1 sec)

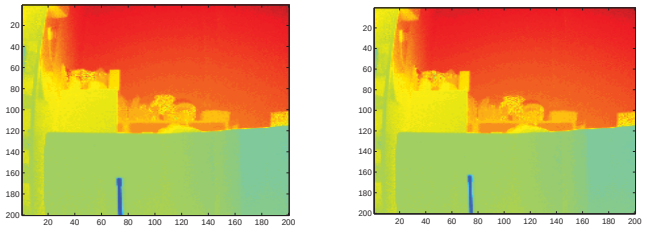

(c) Position3 (t=1.5 sec) (d) Position4 (t=2 sec)

Fig. 3: Different Frames of Moving obstacle

(a) $Frame-1$

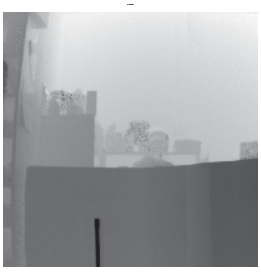

(b) $Frame-4$

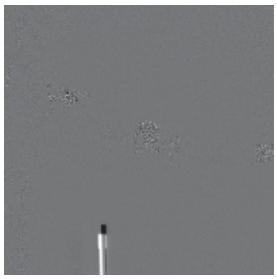

(c) $Magnitudeimage$

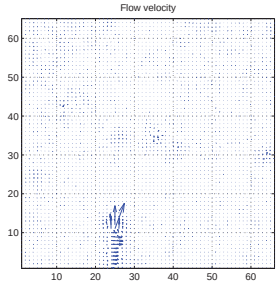

(d) $FlowVectors$

Fig. 4: 2D Range Flow Vectors

3. Experimental Results

The proposed technique is tested by various experiments. As the PMD camera can provide three dimensional coordinates (X,Y,Z), they are used for reconstructing 3D scene flow. The camera is mounted on the Pioneer 3DX Mobile Robot. The dynamic obstacle is allowed to move at different known velocities in the Field of View (FOV) of the camera as illustrated in figure 2. The pixels of range information are processed at different known time periods.

In Figure 3, the sequences of the frames are taken at different time period (t = 0.5, 1 ,1.5, 2 sec) where the obstacle is moving diagonally away from the camera. The obstacle's position in the world coordinates can be calculated in the two frames.

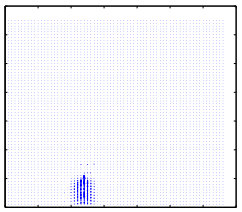

(a) Range Flow X-Coordinates

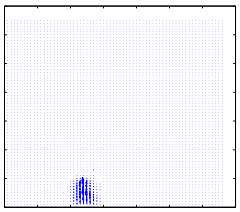

(b) Range Flow Y-Coordinates

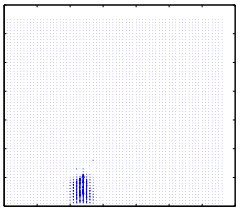

(c) Range Flow Z-Coordinates

Fig. 5: 3D Range Flow Vectors

The 2D flow vectors are computed using combined Lucas/Kanade and Horn/Schunck techniques between Frame1 and Frame4 as shown in figure 4. The three dimensional coordinates which are obtained from the PMD camera, are used to estimate the scene flow vectors. These flow vectors along X, Y, Z coordinates are illustrated in figure 5.

The distance between the mean value of two segmented frames i.e. $F_1(X_a, Y_a, Z_a)$ and $F_4(X_b, Y_b, Z_b)$ are then calculated using the equation (7). The experiments are performed in different velocities at different time frames. The table (1) compares the actual velocity with the estimated velocity. And the result shows the velocity can be estimated within a percentage error of 5%.

Table 1: Estimated Velocity

$ActualVelocity$ (mm/sec)		$EstimatedVelocity$ (mm/sec)	$Error$ (%)
600	t=0.5 sec	601.5	0.25
	t=1.0 sec	587.5	2.08
	t=1.5 sec	590.5	1.58
	t=2.0 sec	580.4	2.66
1200	t=0.5 sec	1211	0.92
	t=1.0 sec	1158	3.5
	t=1.5 sec	1257	4.57
	t=2.0 sec	1180	1.67
1800	t=0.5 sec	1838	2.11
	t=1.0 sec	1708	5.11
	t=1.5 sec	1701.2	5.488
	t=2.0 sec	1749	2.83

4. Conclusion

In this paper, we have presented a range-based differential technique for velocity estimation using scene flow information. As the PMD camera gives suffient information about the obstacles, it can integrated with a Pioneer mobile robot to develop an online efficient dynamic path planning in a cluttered environment. Experimental results have shown encouraging results. Our future work will focus on prediction of the dynamic obstacle's trajectory using the estimated velocity.

Acknowledgment

The author would like to thank Dr. Kavitha Ganesan and Mr. Logenthiran for their support.

References

[Barron and Thacker, 2005] Barron, J. L. and Thacker, N. A. (2005). Tutorial: computing 2D and 3D optical flow. In *Tina Memo*, number 2004-012.

[Bauer et al., 2006] Bauer, N., Pathirana, P., and Hodgson, P. (2006). Robust optical flow with combined lucas-kanade/horn-schunck and automatic neighborhood selection. In *Information and Automation, 2006. ICIA 2006. International Conference on*, pages 378 –383.

[Bruhn et al., 2005] Bruhn, A., Weickert, J., and Schnörr, C. (2005). Lucas/kanade meets horn/schunck: combining local and global optic flow methods. *Int. J. Comput. Vision*, 61(3):211–231.

[Lange, 2000] Lange, R. (2000). *3D time-of-flight distance measurement with custom solid-state image sensors in CMOS/CCD-technology*. PhD thesis, Dep. of Electrical Engineering and Computer Science, University of Siegen.

[Spies et al., 2002] Spies, H., Jahne, B., and Barron, J. (2002). Range flow estimation. *Computer Vision and Image Understanding*, 85(3):209–231.

[Vedula et al., 2005] Vedula, S., Rander, P., Collins, R., and Kanade, T. (2005). Three-dimensional scene flow. *Pattern Analysis and Machine Intelligence, IEEE Transactions on*, 27(3):475 –480.

[Wedel et al., 2011] Wedel, A., Brox, T., Vaudrey, T., Rabe, C., Franke, U., and Cremers, D. (2011). Stereoscopic scene flow computation for 3d motion understanding. *Int. J. Comput. Vision*, 95(1):29–51.

[Weingarten et al., 2004] Weingarten, J. W., Gruener, G., and Siegwart, R. (2004). A state-of-the-art 3D sensor for robot navigation. In Intelligent Robots and Systems. In *In IEEE/RSJ Int. Conf. on Intelligent Robots and Systems*, volume 3, pages 2155–2160.

[Yin, 2011] Yin, Xiang; Noguchi, N. (2011). Motion detection and tracking using the 3d-camera. In *18th IFAC World Congress*, volume 18, pages 14139–14144.

Optimizing Frequency Resolution Muti-tone Detection Using the WDFT

Ohbong Kwon and Aparicio Carranza
Computer Engineering Technology,
New York City College of Technology, Brooklyn, NY, U.S.A.

Abstract— In this letter we investigate how to optimize the frequency discrimination of multi-tone signals based using the warped discrete Fourier transform (WDFT). Compared to a conventional DFT or FFT, which has a uniform frequency resolution across the entire baseband, the frequency resolution of the WDFT is non-linear and externally controlled. This feature can be used to overcome the multi-tone signal detection limitations of the DFT/FFT. The letter demonstrates that by intelligently controlling the frequency resolution of the WDFT, multi-tone signals can be more readily detected and classified. Furthermore, the WDFT can be built upon an FFT enabled framework, insuring high efficiency and bandwidths.

Keywords—Spectral analysis, Frequency discrimination, Warped discrete Fourier transform (WDFT), Spectral leakage

I. INTRODUCTION

Multi-tone signal detection and discrimination is a continuing signal processing problem. The applications include dual-tone multi-frequency (DTMF) systems, Doppler radar, electronic countermeasures, wireless communications, OFDM-based radar exciters, to name but a few. Traditional multi-tone detection systems are based on a filterbank architecture that use an array of product modulators to heterodyne signals down to DC, and then processes the down-converted array of signals with a bank of lowpass filters. The output of the filterbank is then processed using a suite of energy detection operations to detect the presence of tones and multiple tones [1]. The capability of such a system to isolate and detect multiple narrowband signals is predicated on the choice of initial modulating frequencies and post-processing algorithms. Other approaches to the problem are based on multiple signal classification (MUSIC) algorithms, least mean-square (LMS) estimators, and DFT derivatives such as Goertzel algorithm [2]. The approach taken in this paper is to explore the use of another DFT derivative called the *warped discrete Fourier transform* or *WDFT* [3, 4].

II. FFT - THE ENABLING TECHNOLOGY

The discrete Fourier transform (DFT) is indisputably an important signal analysis tool, finding applications in virtually all engineering and scientific endeavors. Generally, the preferred implementation of the DFT is the venerable Cooley-Tukey fast Fourier transform (FFT) algorithm. An N-point DFT $X[k]$, $0 \le k \le N$-1, of a length-N time-series $x[n]$, $0 \le n \le N$-1, is defined by:

$$X[k] = \sum_{n=0}^{N-1} x[n] e^{-j2\pi kn/N}, \quad 0 \le k \le N-1. \qquad (1)$$

For spectral analysis applications, the DFT provides a uniform frequency resolution $\Delta = 2\pi / N$ over the normalized baseband $\omega \in [-\pi, \pi]$. That is, the DFT's frequency resolution Δ is uniform across the entire baseband. This fact historically has limited the role of the DFT in performing acoustic and modal (vibration) analysis, applications that prefer to interpret a signal spectrum using logarithmic (octave) frequency dispersions. Another application area in which a fixed frequency resolution is a limiting factor is multi-tone signal detection and classification. It is generally assumed that if two tones are separated by 1.6Δ (1.6 harmonics) or less, then a uniformly windowed DFT/FFT cannot determine if one tone or multiple tones are present at a harmonic frequency due to spectral leakage, which obscures the spectral separation between adjacent DFT harmonics [4]. This problem is exacerbated when data widows are employed (*e.g.*, Hamming window). This condition is illustrated in Fig. 1. In Fig. 1(a), two tones separated by one harmonic (i.e., Δ) are transformed. The output spectrum is seen to consist of a single peak, losing the

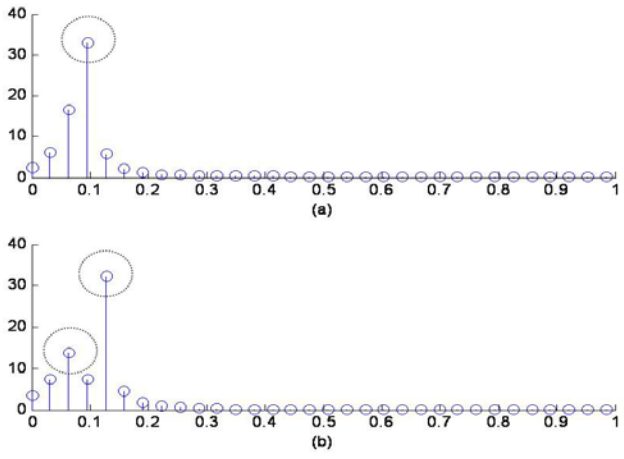

Figure 1: Magnitude spectrum for two tones using a 64-point DFT. (a) Two tone separated by one harmonic. (b) Two tones separated by two harmonics.

identification of each individual input tone because their main lobes get closer and eventually overlap. In the other case reported by Fig. 1(b), the two tones being transformed are separated in frequency by two harmonics (i.e., 2Δ). The presence of two distinct tones is now self-evident.

III. THE WDFT

The WDFT is a derivative of the familiar DFT filterbank [6]. It differentiates itself from the standard DFT filterbank in that it contains an additional pre-processed stage. The WDFT can be developed in the context of multi-rate and polyphase signal processing theory [7]. A polyphase multi-rate filter architecture, shown in Fig. 2, was used to implement a WDFT [8]. In Fig.2, the filter function $A(z)$ is as a pre-processing all-pass filter. For the case where $A(z) = 1$, the design degenerates to a traditional uniform DFT filterbank [6, 7]. For the case where $A(z) = 1$ and the polyphase terms $P_i(z) = 1$, the architecture shown in Fig. 2 becomes an N-point DFT.

Formally the N-point WDFT, reported in Fig. 2 for $P_i(z) = 1$, is defined in terms of a DFT and pre-processing the all-pass filtered data, filtered by $A(z)$, where:

$$A(z) = \frac{-a + z^{-1}}{1 - az^{-1}} \tag{2}$$

where " a "is real and is called the *warping control parameter*. For stability reasons, "a" ranges between -1 and 1.

To motivate the behavior of a WDFT, consider the experiment reported in Fig. 3. The uniform resolution DFT case ($P_i(z) = 1$ and $a = 0$) is compared to the non-uniform resolution case ($P_i(z) = 1$ and $a = \pm 0.3$). The ability of locally control the frequency

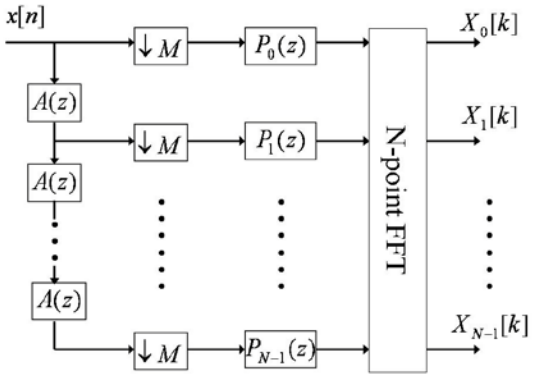

Figure 2. Polyphase multi-rate FFT Filterbank.

resolution of the WDFT is clearly demonstrated. In addition, if a lowpass subband shaping filter polyphase filter ($P(z) = \Sigma z^{-i} P_i(z)$) is employed (*e.g.*, approximate ideal lowpass FIR), then additional control can be exercised over the shape and frequency selectivity of the WDFT spectrum.

Concentrating on the WDFT case where $P(z) = 1$, it may be recalled that the standard z-transform of an N-point input time series $x[n]$, namely

$$X(z) = \sum_{n=0}^{N-1} x[n] z^{-n} . \tag{3}$$

The warping filter converts the input into:

$$\overline{X}(z) = \sum_{n=0}^{N-1} x[n] A(z)^n . \tag{4}$$

Recall that the conventional DFT of $x[n]$, namely $X[k]$, produces

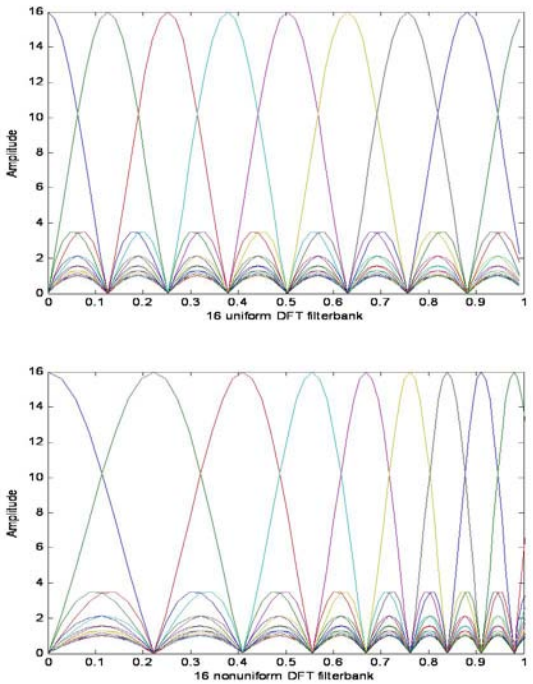

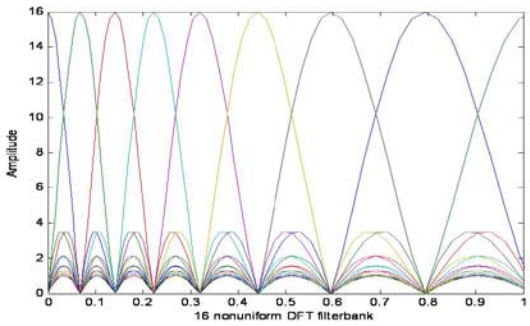

$\overline{\omega}$ corresponds to normalize baseband in [0,π].

16-channel uniform FFT spectrum (top left).

16-channel non-uniform FFT spectrum for a=-0.3 (top right).

16-channel non-uniform FFT spectrum for a= 0.3 (bottom left).

Figure 3: WDFT Experiment.

a spectrum given by:

$$X[k] = X(z)\big|_{z=e^{j2\pi k/N}},\ 0 \le k \le N-1 \qquad (5)$$

where $X[k]$ is evaluated at $z= e^{j2\pi k/N}$, a point the uniformly resolved locations on the periphery of the unit circle in the z-domain. The WDFT coefficients, $\overline{X}[k]$, are similarly obtained by uniformly sampling $\overline{X}(z)$ at points on the unit circle in the z -domain, namely:

$$\overline{X}[k] = \overline{X}(z)\big|_{z=e^{j2\pi k/N}},\ 0 \le k \le N-1. \qquad (6)$$

The conventional uniform frequency resolution DFT, defined by $z = e^{j\omega}$, has harmonic frequencies located at frequencies $\omega = 2\pi k/N,\ k \in [0,\ldots,N-1]$. The center frequencies of an N-point WDFT spectrum are located at the warped frequencies $\overline{\omega}$ where $z = e^{j\overline{\omega}}$, which are associated to ω through the non-linear frequency warping relationship

$$\tan\left(\frac{\overline{\omega}}{2}\right) = \left(\frac{1-a}{1+a}\right)\tan\left(\frac{\omega}{2}\right). \qquad (7)$$

Equation (7) establishes a non-linear frequency warping relationship that is controlled by the real parameter "*a*". A positive "*a*" provides higher frequency resolution on the high frequency region and a negative value of "*a*" increases frequency resolution in the low frequency region (see Figure 3).

The effect of the warping relationship is demonstrated in Fig. 4 which compares a DFT ($a = 0$) to WDFTs for a = -0.071, a = -0.23 and a = -0.4 for the case where two tones are present separated by a single DFT harmonic. It is easily seen that by intelligently choosing the control parameter "*a*" the locally imposed frequency resolution can be expanded or contracted. To enhance the system's frequency discrimination, the frequency resolution should be maximized in the local region containing the input signals. As such, an intelligent agent will need to assign the best warping parameter "*a*" strategy, one that concentrates the highest frequency resolution in the spectral region occupied by the multi-tone process.

The next section describes the outcome of a preliminary study that compares two criteria and two search algorithms and develops an "intelligent" frequency resolution discrimination policy that can be used to improve multi-tone detection.

IV. OPTIMIZATION OF FREQUENCY RESOLUTION

To optimize the choice of the warping parameter "*a*", $|a|<1$, an intelligent search algorithm or agent is needed. An initial search strategy is being evaluated and enabled using optimal single-variable search techniques, a Fibonacci search [1] [9] and a modified Golden Section search [2]. The search process is expected to iterate over a range of values of "*a*" that places a high local frequency resolution in the region occupied by multi-tone activity. To find the best warping parameter "*a*", two criteria of optimization and cost functionals have been singled out for focused attention. The search methods iteratively restrict and shift the search range so as to optimize spectral resolution within a convergent range. The direction of the search is decided by the value of the cost functional at two points in the range.

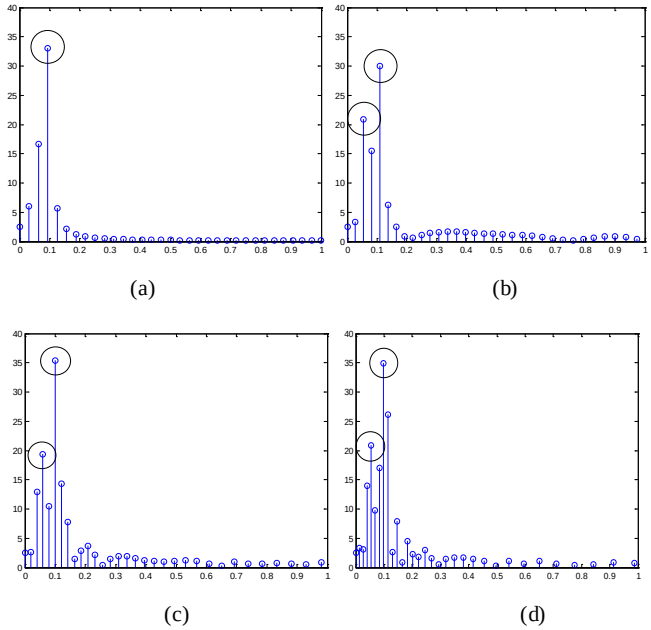

Figure 4. Magnitude spectrum for two tones with 64-point WDFT with (a) a = 0, (b) a = -0.071, (c) a = -0.23, and (d) a = -0.40.

Two criteria studied to date are developed below.

A. Criterion #1

$$\Phi_1(\overline{\omega}) = \max_k\left[\overline{X}[k]\right] - \sum\left[\overline{X}[k]\big|_{\overline{\omega}_b}\right] \qquad (8)$$

where $\overline{\omega}_b$ is a frequency within the search interval and $\Phi_1(\overline{\omega})$ is designed to reward a local concentration of spectral energy and penalize more sparsely populated section of the spectrum. The optimal operating point corresponds to a warping parameter "*a*" that maximizes the local spectral resolution in a region of signal activity.

B. Criterion #2:

$$\Phi_2(\overline{\omega}) = \sum\left[\sigma - \overline{X}[k]\right] \qquad (9)$$

where σ is the threshold used to suppress leakage and $\Phi_2(\overline{\omega})$ is designed to reward the local concentration of spectral energy.

[1] The Fibonacci search technique is a method of searching a sorted array using a divide and conquer algorithm that narrows down possible locations with the aid of Fibonacci numbers.

[2] The Golden Section search is a technique for finding the extremum (minimum or maximum) of a unimodal function by successively narrowing the range of values inside which the extremum is known to exist.

Table 1
Comparison of the warping parameter

Criterion	*Criterion #1*		*Criterion # 2*	
Search Method	Fibonacci search	M. Golden section search	Fibonacci search	M. Golden section search
Warping parameter	a = -0.1087	a = -0.0721	a = -0.0996	a = -0.1381
Elapsed time (sec.)	t = 0.749252s	t = 0.888743s	t = 0.736151s	t = 0.751035s

V. RESULTS AND COMPARISON

The letter reports on a multi-tone signal discrimination study conducted using two search methods, namely a Fibonacci search and a modified Golden Section search algorithm. Both are iterative methods that restrict and shift the searching range so as to determine an optimal operating point within a frequency range. Studies based on these criteria involved presenting to the WDFT frequency discriminator of two sinusoidal tones located at 0.157 and 0.314 rad/s. The search method was charged to find the "best" warping parameter. The comparison of results is shown in Table 1 and the evidence of this activity can be seen in Fig. 5. To compare the temporal efficiency of each case, Table 1 also shows elapsed time needed to execute a search using MATLAB. The two tones, separated by one harmonic, were unresolved with 64-point DFT but resolved with 512-point DFT at the expense of increased complexity (see Fig. 5 (a) and (b), respectively). In Fig. 5 (c)-(e), however, the two tones are seen to be present using 64-point WDFT. To calibrate the WDFT spectra, the locations of the actual two tones are also shown. Comparing the outcomes, a Fibonacci search was found to be the fastest and most effective in finding the "best" warping parameter using either search criteria. *Criterion #1* resulted in frequency resolution with a bigger variation according to search methods, while *Criterion #2* facilitated the optimization of the local resolution and identified the two tones closer to the actual locations of the tones.

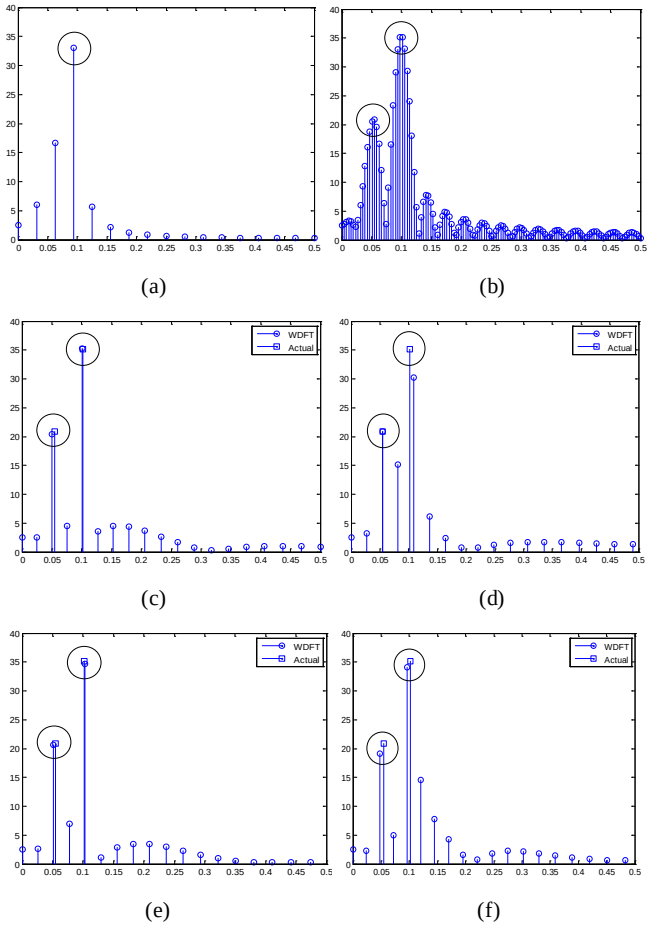

Figure 5. (a) Magnitude spectrum for two tones with (a) 64-point DFT (a = 0) and (b) 512-point DFT (a = 0) and magnitude spectrum for two tone detection with 64-point WDFT with (c) a = -0.1087, (d) a = -0.0721, (e) a = -0.0996 and(f) a = -0.1381.

VI. CONCLUSION

We have studied and shown that multi-tone processes can be successfully discriminated using the WDFT. The study demonstrates that the local frequency resolution can be selectively enhanced in regions of interest using the reported search techniques. Overall, the WDFT is found to be a very capable transform which can provide selective high spectral resolution at low complexity. Studies continue in this area, processing more complex signal cases.

REFERENCES

[1] V. Vassilevsk, Efficient Multitone Detection, IEEE Signal Processing Magazine, March 2007, pp. 144-147.

[2] B. Evans, Dual Tone Mulitple Frequencies, U.C. Berkeley, http://ptolemy.eecs.berkeley.edu/papers/96/dtmf_ict/www/node1.html

[3] A. Makur and S. Mitra, Warped Discrete-Fourier Transform: Theory and Applications, IEEE Trans. On Circuits and Systems, Vol. 48, No. 9, Sep. 2001, pp. 1086–1093.

[4] S. Franz, S. K. Mitra, and G. Doblinger, Frequency Estimation Using Warped Discrete Fourier Transform, Signal Processing, Vol. 83, Issue 8, Aug. 2003.

[5] S.K. Mitra and J.F. Kaiser, Handbook for Digital Signal Processing, Wiley-Interscience, New York NY, 1993.

[6] F. Taylor and J. Mellott, Hands-On Digital Signal Processing, McGraw Hill, 1998.

[7] S. K. Mitra, Digital Signal Processing: A Computer-Based Approach, 2nd Ed. New York: McGraw-Hill, 2001.

[8] E. Galijasevic, and J. Kiel,, Design of Allpass-Based Non-Uniform Oversampled DFT Filter Banks, IEEE ICASSP, Orlando, FL, May 2002, pp. 1181-1184.

[9] O. Kwon and F. Taylor, Multi-tone Detection Using the Warped Discret Fourier Transform, IEEE MWSCAS, Knoxville, TN, Aug. 2008, pp 281-284.

A Study on Analysis of Correlation Characteristics of EEG Channels by Five Senses stimulation

Dong-Gyu Kim[1], Byung-Hun Oh[1], Hyeong-Joon Kwon[1], Kwang-Woo Chung[2], Kwang-Seok Hong[1]
[1]Human Computer Interaction Laboratory, School of Information & Communication Engineering, Sungkyunkwan University, 440-746, 300 CheonCheon-Dong, Jangan-Gu, Suwon, Gyeonggi-Do, Korea
[2]Department of Railway Operation System Engineering, Korea National University of Transportation, Uiwang-Si, Korea

Abstract - *This paper is for the study of feature analysis of the correlation of brain waves between channels in the stimulation of the 5 senses (sight, hearing, touch, smell, taste). In the existing studies, feature analysis of brain waves in response to stimulation of the human senses has been made by single sense stimulation or double sense stimulation, but, study with stimulation of all 5 senses is still not yet satisfactory. In this paper, the brain waves in response to stimulation of the 5 senses in the behavior of eating food are collected and analyzed for the analysis of the features of brain waves. From time-based data and frequency elements, features of correlation in brain waves between channels are extracted. The overlapping rates between the stimulation sections, between experimenters, and between frames consisting of channels with high correlation coefficients are calculated. In the experiment, 65 sections (32 stimulation sections, 33 break sections) of a brain wave database (DB) about the stimulation of the 5 senses were collected and analyzed for 9 men and 2 women. In the results of the experiment, the stimulation is distinguishable for each sense.*

Keywords: EEG, Five senses stimulus, Analysis of correlation characteristics

1 Introduction

Recently, the study of Brain Computer Interfaces (BCI) has been active. Users' intensions and emotional conditions can be detected in brain waves measured through the scalp, and the electrical activity of brain cells show differences according to the mental conditions of an individual, which can be used for BCI. Human Interfaces based on brain waves have been used for medical treatment, games, training for mental concentration, robot control, and mind recognition [1, 2]. Human beings recognize situations through 5 senses (sight, hearing, touch, smell, taste). Humans become aware of their situation through the senses. In addition, interaction between humans and objects as well as with other humans takes place by means of the senses. Thus, analyses of brain wave characteristics in response to human sensory stimulation of have been conducted. In the existing studies, the feature analysis of brain waves in response to the stimulation of human senses has been done with the stimulation of a single sense [3-9] or two senses [10], but study with the stimulation of 5 senses has been dissatisfactory. Expanding on these studies, the features of brain waves in response to the stimulation of all 5 senses are analyzed by extracting correlation features in the brain waves. A DB of brain waves measured in response to the stimulation of all 5 senses during the behavior of eating food was collected and analyzed. In Chapter 2, we will examine existing research on sense stimulation. In Chapter 3, we explain our proposed correlation feature analysis method. Chapter 4 describes our experiments. Chapter 5 discusses the conclusion of this study.

2 Existing Studies

The feature analysis of brain waves for single sense stimulation [3-9] and two senses at the same time [10] has been conducted in previous studies. In addition, brain waves with visual stimulation using correlation coefficients have been analyzed [4, 5]. The method for feature analysis of brain waves acquires brain wave data when senses are stimulated, and extracts time-based data and frequency elements in each channel (each area of the scalp) from the acquired brain wave data and analyzes them. Brain wave data is induced from the scalp, passes through an amplified circuit and filter. Then the brain wave data is transmitted to an analog-to-digital (AD) converter and sent to a smart phone or PC for analysis. In existing studies, frequency element analyses of brain waves are commonly classified as Delta (1~3Hz), Theta (4~7Hz), Alpha (8~13Hz), Beta (14~30Hz), and Gamma (31~50Hz), and are analyzed for features.

3 Correlation Feature Analysis Method of Brain Waves between Channels

The feature analysis of brain waves in response to the stimulation of 5 senses was made by correlation feature extraction from brain waves between channels. A portable brain wave acquisition device was developed in a previous study [11]. Analog brain wave voltage signals in the range of 0.017uV~1.101uV are amplified by a factor of 2,225 to transform them into digital values and are transmitted to a smart phone. This device acquires the brain wave data for the 14 channels and takes 128 samples per second. AD-transformed brain wave data is changed to voltage values (0-

2.5V) by deducting an offset average value from each channel voltage value, and removing the DC element. A correlation coefficient is used to calculate the time-based data and 7 kinds of frequency elements. The frequency data are classified as Delta (1~3Hz), Theta (4~7Hz), Alpha (8~13Hz), Beta (14~30Hz), Gamma (31~50Hz), 51~59Hz, and 1~59Hz. There are 91 x 8 kinds of correlation coefficients between the 14 channels for a total of 728. The correlation coefficient is treated as a frame unit (1 unit is 128 samples). If the quantity is less than 128 in the last frame of each section, it is disregarded. Equation (1) is used to calculate the correlation coefficient.

$$r_{i,j} = \frac{\sum_{n=1}^{N}(X_{i,n} - \overline{X}_i)(X_{j,n} - \overline{X}_j)}{\sqrt{\sum_{n=1}^{N}(X_{i,n} - \overline{X}_i)^2 \times \sum_{n=1}^{N}(X_{j,n} - \overline{X}_j)^2}} \quad (1)$$

M : *The Number of EEG Channels*

$i = 1,2,\cdots,M-1$

$j = i+1, i+2,\cdots,M$

$X_{i,n}$ is data at time n sample of section i (channel), and $\overline{X}_i$ is average value over N samples of a section (channel) of data. X_i and X_j are different channels. $r_{i,j}$ is a normalized covariance value divided into the multiply standard deviation of the two variables X_i, X_j by covariance. The range has the value $-1 \le r_{i,j} \le +1$. In case of $r_{i,j} = +1$, there is a perfect positive correlation between the two variables. In case of $r_{i,j} = -1$, there is a perfect negative correlation between the two variables. In case of $r_{i,j} = 0$, the two variables are perfectly independent.

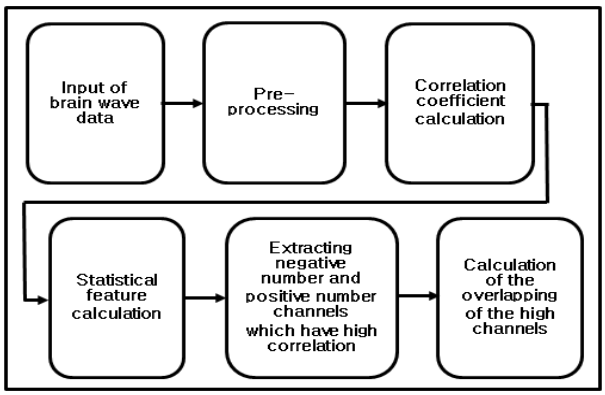

Figure 1. Block diagram of correlation feature analysis of brain waves between channels.

The statistical feature calculation calculates 5 kinds of feature values (mean, variation, standard deviation, maximum value, minimum value) of 8 kinds of correlation coefficients. There are a total of 3,640 feature values between the channels.

In the calculation of the overlapping rate of channels with high correlation in each section, the overlapping rate of all 65 sections in the brain wave DB is calculated once per test. The 240 channels which have high correlation in each section are judged in regard to whether they are the same or not. A block diagram of correlation feature analysis of brain waves between channels is shown in figure 1.

The method of correlation analysis is as follows.

1) Brain wave data is input: 14 channel brain wave data.
2) Pre-processing: AD conversion data are changed to voltage values.
3) Correlation coefficient calculation: The correlation coefficients of time-based data and 7 kinds of frequency elements are calculated (91 correlation coefficient between 14 channels, 91 x 8 kinds of correlation coefficients for a total of 728 coefficients.)
4) Statistical feature calculation: 5 kinds (mean, variation, standard deviation, maximum value, minimum value) of feature values about 8 kinds (time-based data and 7 kinds of frequency elements), (8 kinds x 91 correlation coefficient between channels x 5 kinds feature value, calculate 3,640 whole feature value between channels).
5) Extracting negative number and positive number channels which have high correlation: Extract 3 positive number and negative number channels which have high correlation from 5 kinds of feature values about 8 kinds of correlation coefficients between channels. Extract 48 from a whole feature value between 3,640 channels (8 x 91 x 5 matrix).
6) Calculation of the overlapping of the high channels: Judge whether the channels with high correlation are the same or not (compare 48 extracted features between channels).

4 Experiments and Results

4.1 Using the device

We used a portable electroencephalography (EEG) acquisition system developed in a previous study [11]. Figure 2 shows the portable EEG signal acquisition system interfaced with an Android device. This EEG device amplifies brain wave signals 2,225 times. It has an HPF cut-off frequency of 0.58Hz, an LPF cut-off frequency of about 58,94Hz, and 16-bit/128 per second sampling activities in AD conversion.

(a) (b)

Figure 2. The portable EEG signal acquisition system using an Android device: (a) portable EEG device, (b) EEG demonstration (interfacing between the portable EEG device and smart phones).

4.2 EEG Measurement Points

The lower regions behind the ears are where the EEG measurements are taken. The 14 measurement points are denoted as F7, AF3, FC5, F3, T7, P7, O1, F8, AF4, FC6, F4, T8, P8 and O2, and they are placed according to the international 10-20 electrode system. The gyro X-axis and Y-axis are assigned to channels 8 and 16, respectively. Figure 3 shows the points of EEG measurement.

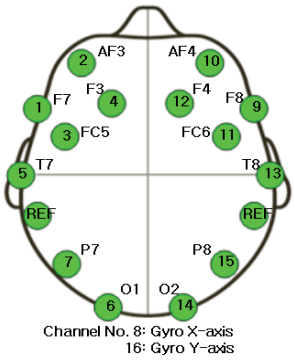

Figure 3. The points of EEG measurement.

4.3 The Experimental Conditions and Results

In this study, brain waves in response to stimulation of the 5 senses during the behavior of eating food were collected and analyzed. Correlation features between channels regarding the time base energy and frequency elements were also extracted and analyzed. The subjects of the experiment were 9 men and 2 women between the ages of 23~36, and the experiment was executed in 65 sections (32 stimulations, 33 break and rest periods). The experimental conditions were as follows:

1) The experimental place was a quiet laboratory, and the experiment was done with the subject sitting in a chair in front of a table, and the laboratory was well ventilated with an open window.

2) The food was a beef hamburger (Lot***** brand). The diameter was about 4 inches and the materials included buns, beef patty, mayonnaise, and beef sauce, weighing 154g and containing 390 kcal.

3) The experiment was composed of one subject, one experimenter, and another experimenter to give verbal instructions (e.g. "close your eyes") to the subject, who acted according to the decided scenario.

4) Auditory stimuli were made by a hamburger advertisement (the contents of the advertisement make people have the desire to eat a hamburger: beef ~ burger, burger, burger ~ Wow! Beef or shrimp which will ignite flame from man's heart)

5) The conditions of the scenario to collect the brain wave DB are to add stimulation of each sense, one by one, with minimized 5 sense stimulation, and to make the applied stimulation distinguished. There were break and rest sections between the stimulation sections to distinguish the stimulation sections from each other. Table 1 shows the type of 5 senses stimulation in the behavior of eating food. The brain wave DB was collected by dividing the total 65 sections into 4 sets. Each stimulation was about 10sec ~ 30sec, and the breaks were about 30sec ~ 40sec. The breaks were done with open eyes and restful sitting. The brain wave DB collection scenario is shown in Figure 4.

Table 1. The type of 5 senses stimulation in the behavior of eating food.

No	type of stimulation					The number of stimulation
	Sight	Hearing	Touch	Smell	Taste	
1	x	x	x	x	x	No stimulation
2	o	x	x	x	x	Single sense stimulation
3	x	o	x	x	x	
4	x	x	o	x	x	
5	x	x	x	o	x	
6	x	x	x	x	o	
7	o	o	x	x	x	Double sense stimulation
8	o	x	o	x	x	
9	o	x	x	o	x	
10	o	x	x	x	o	
11	x	o	o	x	x	
12	x	o	x	o	x	
13	x	o	x	x	o	
14	x	x	o	o	x	
15	x	x	o	x	o	
16	x	x	x	o	o	
17	o	o	o	x	x	Triple sense stimulation
18	o	o	x	o	x	
19	o	o	x	x	o	
20	o	x	o	o	x	
21	o	x	o	x	o	
22	o	x	x	o	o	
23	x	o	o	o	x	
24	x	o	o	x	0	
25	x	o	x	o	o	
26	x	x	o	o	o	
27	o	o	o	o	x	Quarter sense stimulation
28	o	o	o	x	o	
29	o	o	x	o	o	
30	o	x	o	o	o	
31	x	o	o	o	o	
32	o	o	o	o	o	Five senses stimulation

Figure 4. The scenario of brain wave DB collection (ex: No1 set)

4.3.1 Experiment 1

This experiment was done to analyze the overlapping rate between stimulation sections, which consist of channels with high correlation coefficients. For the correlation feature values of brain waves between channels of 65 sections (32 stimulation sections and 33 break sections) per one subject, the overlapping rate of the channels which had high

correlation in each section were calculated. The average overlapping rates were obtained for 32 stimulation sections and 33 break sections each. From the results of the experiment, the average overlapping rate of 32 stimulation sections for 11 people was 13.05%, and the average overlapping rate of 33 beak sections was 17.67%. The average overlapping rate of the total 65 sections was recorded as 15.36.

4.3.2 Experiment 2

This experiment was done to analyze the overlapping rate between experimenters. The analysis was done on channels with high correlation coefficients. From the results of the experiment, the average overlapping rate of al 65 sections was recorded as 7.17%. Between sensory stimuli on the same cross-section overlapping of subjects were lower than the correlation between EEG channels.

4.3.3 Experiment 3

This experiment was done to analyze the overlapping rate between frames, and was done on channels with high correlation coefficients. From the results of the experiment, the average overlapping rate of al 8 kinds was recorded as 18.71%.

4.3.4 Experiment 4

We were recognition experiments from 1 person (subject 11). 65 kinds of candidate models of recognition were used for the high-correlation channels from each section of the average correlation coefficients. This experiment changed the extracting negative number and the positive number channels which have high correlation. 3 to 30 of positive number and negative number channels which have high correlation from 1 kind of feature values about 8 kinds of correlation coefficients were extracted. 48 to 488 from a whole feature value between channels 728 (8 x 91 x1 matrix) were extracted. In the results of the experiment, 26 extracting numbers showed the highest correlation. The total average rate was recorded as 60.14%.

4.3.5 Experiment 5

We were recognition experiments from 11 people. 26 positive number and negative number channels were extracted, each of which has high correlation from 1 kind of feature value on 8 kinds of correlation coefficients. From the results of the experiment, the average rate of recognition was recorded as 59.89.

5 Conclusion

A study on correlation feature analysis of brain waves between channels related to the stimulation of five senses was performed in this paper. To analyze correlation features of brain waves related to the stimulation of five senses, brain waves were collected, and a correlation feature analysis experiment was performed on the brain waves between channels from the collected brain wave DB. In the results of the experiment, when stimulating the five senses, the overlapping rate of correlation features of the brain waves between channels was found to be low, thus, it seems that the stimulations could be distinguishable from each other. It seems that the method for extracting correlation features of brain waves between channels presented in this study could be used for technology based on brain waves for recognition of the five senses. In the future, the study of figure analysis of brain waves related to the stimulation of the five senses during movement behaviors will be needed.

6 Acknowledgments

This research was supported by the MKE, Korea, under ITRC NIPA-2012-(H0301-12-3001), by PRCP through the NRF of Korea, funded by MEST(2012-0005861), and by the Basic Science Research Program through the National Research Foundation of Korea (NRF), funded by the Ministry of Education, Science and Technology (2010-0021411).

7 References

[1] M. Teplan, “Fundamentals of EEG Measurement", Measurement Science Review, Vol 2, Section 2, (2002).

[2] Syed M. Saddique and Laraib Hassan Siddiqui, "EEG Based Brain Computer Interface", JOURNAL OF SOFTWARE, VOL. 4, NO. 6, pp. 550-554, (2009).

[3] Tadanori FUKAMI, et al., "The Relationship between Aging and Photic Driving EEG Response", IEICE TRANSACTIONS on Information and Systems Vol. E94-D No. 9 pp. 1839-1842, (2011).

[4] Manbir Singh, Sungheon Kim, and Tae-Seong Kim, "Correlation Between BOLD-fMRI and EEG Signal Changes in Response to Visual Stimulus Frequency in Humans", Magnetic Resonance in Medicine, Vol. 49, pp. 108–114, (2003)

[5] YIJUN WANG, XIAORONG GAO, BO HONG, CHUAN JIA, and SHANGKAI GAO, "Brain–Computer Interfaces Based on Visual Evoked Potentials", IEEE ENGINEERING IN MEDICINE AND BIOLOGY MAGAZINE, pp. 64-71, (2008)

[6] Heidi Yppärilä, et al., "The effect of interruption to propofol sedation on auditory event-related potentials and electroencephalogram in intensive care patients" BioMed Central, Vol. 8, No. 6, (2004).

[7] E. Manjarrez, O. Diez-Martinez, I. Mendeza, and A. Flores, “Stochastic resonance in human electroencephalographic activity elicited by mechanical tactile stimuli”, Neuroscience Letters 324, (2002).

[8] A. A. Cherninskii, et al., "Modifications of EEG Related to Directed Perception and Analysis of Olfactory Information in Humans", Neurophysiology, Vol. 41, No. 1, (2009).

[9] Juliana Cristina Hashida, et al., "EEG pattern discrimination between salty and sweet taste using adaptive Gabor transform", Neurocomputing 68 (2005).

[10] M. Teplan, et al., "Phase Synchronization in Human EEG During Audio-Visual Stimulation", Electromagnetic Biology and Medicine, Vol. 28, No. 1, pp. 80-84, (2009).

[11] Dong-Gyu Kim, Yong-Wan Roh, and Kwang-Seok Hong, "A Portable EEG Signal Acquisition System", The Second International Symposium on Mechanical Science and Technology, December 20-21, (2011).

Deployment of Augmented Reality Interactions in Games

Bo Shen Woun [1] **and Guat Yew Tan** [2]
[1] School of Mathematical Sciences, Universiti Sains Malaysia, 11800 USM, Penang, Malaysia
[2] School of Mathematical Sciences, Universiti Sains Malaysia, 11800 USM, Penang, Malaysia

Abstract - *Human Computer Interaction (HCI) is one of the key focuses in gaming industry. Its computer side interactions can be traced back since 1963 when Ivan Sutherland suggested interacting with the objects on the screen directly with a light-pen. Few years later, mice were suggested to be the replacement for the expensive light-pen and have been the most popular interactive device till now. Touch-screen technology and recognition-based user interface (RBUI) are also gaining its popularity in the recent gaming industry. However, the above mentioned technologies interact with virtual objects in two dimensional (2D) output screens which constraint the mobility of the players to only front side of the screens. Deployment of Augmented Reality (AR) in gaming industry will solve this problem by providing true three dimensional (3D) immersive experiences and 6 degree-of-freedom to the players. In this paper, we introduce ARPuzzle, an AR version of jigsaw puzzle, which provides mobility freedom to the players and focus on interactions between two virtual objects.*

Keywords: Augmented Reality, Human Computer Interaction, Recognition-Based User Interface.

1 Background

Human Computer Interaction (HCI) is one of the key focuses in gaming industry. HCI contains two main components, i.e. human side and computer side interactions. Our main discussion is on the computer side. HCI can be traced back since 1963 when Ivan Sutherland first suggested manipulating the visible objects on the computer screen directly with a light-pen pointing device in his doctoral dissertation [[1]]. Meanwhile, HCI researches on other devices were also carried out and gained successful results. Mice were developed as a commercial device by Xerox PARC [[3]] mainly as replacements for the expensive light-pens. Since then, mice have become the most popular pointing device of personal computers. Its popularity remains till now, though various other pointing devices like joysticks, touchpad, trackball, pointing stick, were suggested. Recently there is a trend to change the pointing habit from using physical input device to touch-screen technology, however, mice-supported screens are still strong in market acceptance compare to touch screen, in view of its cost effectiveness. The latest technology deployed in gaming industry which excites the players is recognition-based user interface (RBUI) that involves input-output of gestures, handwriting, speech, etc. Though RBUI is not new in discussions and researches, this technology gained its popularity around the globe when Nintendo released its *wii* version in 2006, to control the avatar remotely via accelerometer and optical sensing technology [[4]]. We anticipate the next interactive application which will stir a craze in the gaming industry is Microsft's Kinect for Xbox 360, which is based on PrimeSense light-coding technology for motion and depth detection. Unlike Nintendo *wii*, Kinect for Xbox requires no external controller device, i.e. the player is the controller [[5]]. Nevertheless, both games display the avatars, i.e. three dimensional (3D) virtual objects, on two dimensional (2D) screens. The players' mobility freedoms are partially achieved as they can walk around but still confined to the front side of the screen. Comparatively, Augmented Reality (AR) is a better choice in game developments, as AR can help to achieve true 3D immersive experiences and provide the players with six degree-of-freedom when interacting with the 3D virtual objects. AR uses pattern recognition technology to display virtual objects in the real environment on a fiducial marker. In our project, we have developed an AR game called ARPuzzle which is the AR version of a jigsaw puzzle. In the first version of ARPuzzle, we concentrate on the interactions between the virtual puzzle blocks and its pushing rod. Our final objective of ARPuzzle is to be able to deploy RBUI technology to use hand gesture to interact with the virtual puzzle blocks, in real environment.

2 ARPuzzle Overview

ARPuzzle is a user interactive game developed on ARTag for its strength to provide higher accuracy on marker detection by using arrays of markers, after reviewing a set of common AR tools available [[6]]. The first version of ARPuzzle contains four puzzle blocks shaped in square prism. The top faces of the four blocks form an image of Universiti Sains Malaysia (USM) logo once the puzzle is solved. When the virtual puzzle blocks were first displayed, it was scattered on *base0* marker (Fig. 1a), the puzzles can be moved by using the virtual pushing rod displayed on *toolbar0* marker (Fig. 1b).

The side faces of the blocks are colored in blue to create the depth illusions. When the puzzle blocks are formed correctly, the side faces of all the puzzles will be changed to red, to indicate the puzzle has been solved.

2.1 Components of ARPuzzle

There is no special equipment required as we plan to make ARPuzzle a common game which can be played anytime, anywhere. A laptop or PC running MS windows, a PC camera and two ARTag markers labeled *base0* and *toolbar0* are required. Though a PC camera is enough, a head mounted display (HMD) is encouraged while playing the game to obtain the full mobility of the players. The ARTag markers are available together with the game in PDF format, which can be printed out by the players.

The *x*- and *y*-coordinates of ARTag's *base0* marker range from –80 to +80 in both directions. The *x*- and *y*-coordinates of the *toolbar0* marker range from 0 to 40 and 0 to 100 respectively. When detected, *toolbar0's* coordinates are calculated and transformed to *base0* marker's coordinates to check if an interaction between the markers is established [[7]].

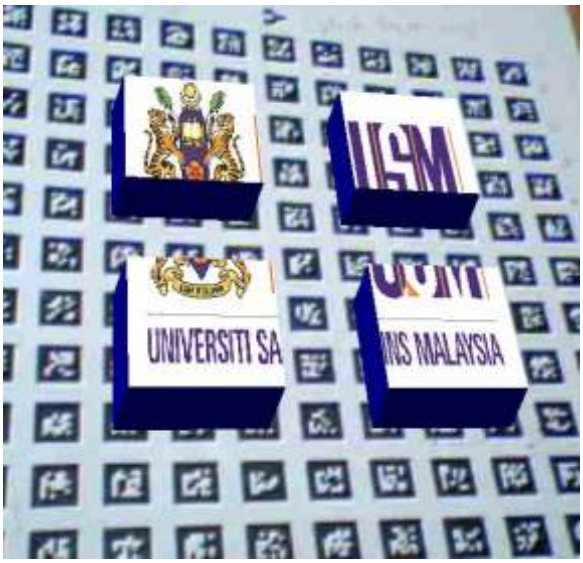

Base0 marker with the virtual puzzle blocks

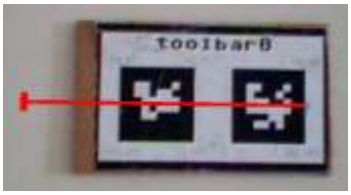

Toolbar0 marker displaying the virtual pushing rod.

Fig. 1. ARTag markers used in ARPuzzle

2.2 Structure of each puzzle block

Each puzzle block is divided into four right-angle triangles according to +45°, +135°, -135° and -45° labeled as A, B, C and D. Thus, A, B, C and D are formed within angles -135° and -45°, -45° and +45°, +45° and +135°, -135° and +135° respectively (Fig. 2.).

The right-angle vertices of the four triangles meet at the centre of the puzzle piece. When the pushing rod's tip is detected at region A, B, C or D, the piece moves up, left, down and right respectively (Fig. 3.).

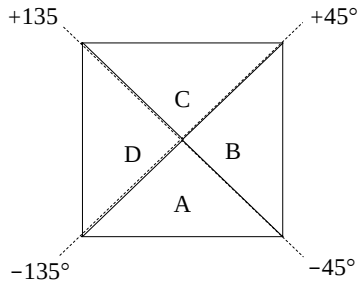

Fig. 2. Division of a puzzle piece into four right-angle triangles.

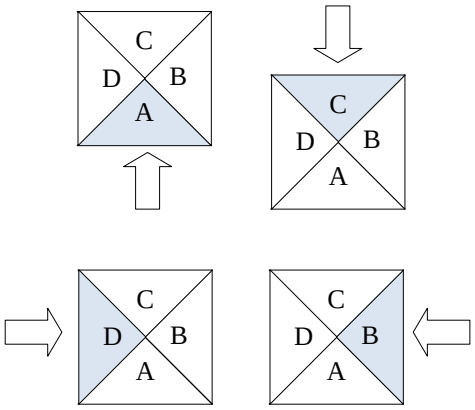

Fig. 3. Moving directions of the blocks when the tip of the pushing rod is detected. Shaded areas denote the detected areas and its moving direction is showing by the arrows.

2.3 Movement validity check when the virtual objects are interacting

While moving the puzzle blocks, we need to ensure that the blocks are not overlapping each other. The *x*- and *y*-distances between centers of two blocks are calculated. When checking the validity of the movements, the *x*- and *y*-distances are checked against the width of the blocks. Further, the positions of x_1 compare to x_2, y_1 compare to y_2 are also checked to decide the direction of the movement; given the center coordinates of the stagnant and moving puzzle blocks are (x_1, y_1) and (x_2, y_2) respectively. The validity of the movements is stated in Table 1.

3 How ARPuzzle work

ARPuzzle starts by displaying *base0* marker within the field of view of the camera. Four virtual puzzle blocks will be displayed on the marker. The blocks are scattered amongst themselves. The first version of the ARPuzzle scatters the four blocks at an ordered distance (Fig. 1a.). By pushing the blocks in four directions, i.e. up/down/left/right, from their positions, a full image of USM logo will be formed. The first version of ARPuzzle focuses on interactions between two virtual objects. A virtual pushing rod appears on the *toolbar0* when it is displayed within the camera's FOV. When the pushing rod is detected on one of the A, B, C and D region (Fig. 2), the puzzle blocks moves according to Fig. 3 and Table 1. Fig. 4 displays a half-done puzzle. When the four pieces of jigsaw puzzle combined together and become a big cube, its color turned red and it indicates the end of the game (Fig. 5).

Table 1. Validity check of two blocks during the movement. The stagnant block is assigned the center coordinates with (x_1, y_1). The piece which we want to move is assigned the center coordinate with (x_2, y_2).

		$\lvert y_1 - y_2\rvert$ < width		$\lvert y_1 - y_2\rvert$ = width		$\lvert y_1 - y_2\rvert$ > width	
		$y_1 < y_2$	$y_1 > y_2$	$y_1 < y_2$	$y_1 > y_2$	$y_1 < y_2$	$y_1 > y_2$
$\lvert x_1 - x_2\rvert$ < width	$x_1 < x_2$	Error	Error	Down-move invalid	Up-move invalid	valid	valid
	$x_1 > x_2$	Error	Error	Down-move invalid	Up-move invalid	valid	valid
$\lvert x_1 - x_2\rvert$ = width	$x_1 < x_2$	Left-move invalid	Left-move invalid	valid	valid	valid	valid
	$x_1 > x_2$	Right-move invalid	Right-move invalid	valid	valid	valid	valid
$\lvert x_1 - x_2\rvert$ > width	$x_1 < x_2$	valid	valid	valid	valid	valid	valid
	$x_1 > x_2$	valid	valid	valid	valid	valid	valid

Fig. 4. The two bottom blocks of the puzzle are formed.

Fig. 5. The edge of the completed puzzle is turned to red.

4 Conclusion and Future Work

ARPuzzle is a new development for AR game mainly focusing on the interaction between two virtual objects. Much work remains to be done. In our following versions, we shall deploy RBUI to recognize finger gesture to move the puzzle block. Further, fine-tuning on the appearance of the puzzle and provide blocks with irregular shape are in the development pipeline.

5 References

[1] Sutherland, I.E.: SketchPad: A Man machine Graphical Communication System. In: Proceeding of AFIPS Spring Joint Computer Conference 23 (1963), pp. 329-346.

[2] Mayers, B.A.: A Brief History of Human-Computer Interaction Technology. In: Interactions 5 Magazine, pp 44-54. 1998.

[3] Mayers, B.A.: The user interface for Sapphire. In: IEEE Computer Graphics and Applications, Vol 4, Issue 12 (Dec) pp 13-23. (1984)

[4] http://en.wikipedia.org/wiki/Wii_Remote

[5] http://www.primesense.com/

[6] Ng, K.P., Tan, G.Y., Iman, L.Y.: Overview of Augmented Reality Tools. In: 18th National Symposium in Mathematical Science (SKSM), Malaysia (2010)

[7] Cawood, S. and Fiala, M.: Augmented Reality: A Practical Guide. The Pragmatic Programmers (2007).

A probability based defuzzification method for fuzzy cluster partition

Thanh Le[1], Tom Altman[1], Katheleen J. Gardiner[2]
[1]Department of CSE, University of Colorado Denver, Denver, CO, USA
[2]Department of Pediatrics, University of Colorado Denver, Aurora, CO, USA

Abstract– *Fuzzy C-Means (FCM) is an unsupervised clustering method that has been used extensively in data analysis and image segmentation. The defuzzification of the fuzzy partition of FCM is usually done using the maximum membership degree principle which may not be appropriate for some real-world applications. In this paper, we present a new algorithm that generates a probabilistic model of the fuzzy partition and applies the model to classification of data objects. We show that our method outperforms four popular defuzzification methods on uniform and non-uniform artificial datasets as well as on real datasets.*

Availability: *The test datasets and the method software are available online at http://ouray.ucdenver.edu/~tnle/fzpbd.*

Keywords: *fuzzy c-means, classification, fuzzy partition, Bayesian based model.*

1 Introduction

Cluster analysis and image segmentation are important in a variety of scientific and industrial applications. They are used to group data objects based on the similarities of their properties. Data objects within a cluster are closely related to each other and can be discriminated from data objects within other clusters. Fuzzy C-Means (FCM) [1] is an unsupervised method that has been successfully applied to feature analysis, cluster analysis, classifier design, and futures analysis in fields such as astronomy, geology, medical imaging, target recognition, image segmentation, and economics. Unlike hard clustering methods, which force data objects to belong exclusively to one cluster, FCM allows data objects to belong to more than one cluster with varying degrees of fuzzy set membership. However, the fuzzy partition of FCM needs to be defuzzified for crisp classification information of the data objects. A popular approach to this problem is to use the maximum membership degree principle (MMD) [2, 9, 12]. This may be inappropriate in some applications because FCM membership is computed using distance between the data object and cluster center. Use of membership degree can assign marginal objects of a large cluster to the immediately adjacent small cluster. This is illustrated in Figure 1, where if a data object is in the gray rectangle, it may be incorrectly assigned to cluster 3 instead of cluster 2.

Recent solutions include that of Chang et al. [4] who proposed using spatial information to adjust the membership status of every data point using the membership status of its neighbors. In a similar approach, Chiu et al. [3] used spatial information to determine the distance between the data point and cluster center. However, these methods require definition of neighborhood boundaries. Genther et al. [7] proposed defining spatial information by the clustering structure, not the neighborhood, to compute the distance from the data point to cluster center.

A common limitation of methods that use spatial information in computing membership degree is that they have to scale between the actual position information of the data point and its spatial information. In addition, while use of spatial information is appropriate for image segmentation, it may not work with generic data cluster analysis because it is difficult to define neighborhood boundaries.

In this study, we propose a method that uses the fuzzy partition and the data themselves to construct a probabilistic model of the data distributions. The model is then applied to produce the classification information of data points in the dataset.

This work was supported in part by the Vietnamese Ministry of Education and Training (TL).

Thanh Le is a doctoral student in the Department of Computer Science and Engineering, University of Colorado Denver, Denver, CO 80217, USA (email: lntmail@yahoo.com).

Tom Altman is a professor in the Department of Computer Science and Engineering, University of Colorado Denver, Denver, CO 80217, USA (email: tom.altman@ucdenver.edu).

Katheleen J. Gardiner is a professor in the Department of Pediatrics and the Linda Crnic Institute for Down Syndrome; the Intellectual and Developmental Disabilities Research Center; and the Computational Biosciences, Human Medical Genetics and Neuroscience Programs, University of Colorado Denver, Aurora, CO 80045, USA (phone: 303-724-0572; email: katheleen.gardiner@ucdenver.edu).

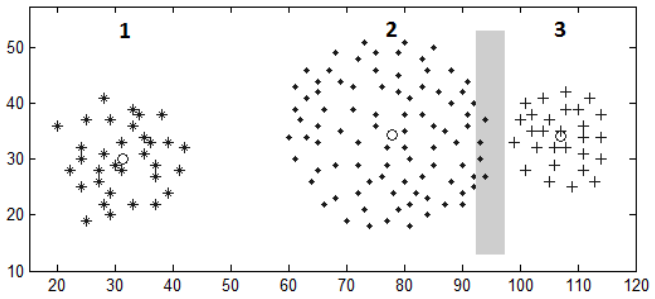

Figure 1: ASET4 - an artificial dataset with three clusters of different sizes

2 Methods

2.1 Fuzzy C-Means algorithm (FCM)

Let $X = \{x_1, x_2, \ldots, x_n\} \in R^p$ be a set of data objects x_i, i=1..n, and for a given c, $2 \le c < n$, the Fuzzy C-Means algorithm (FCM) divides X into c clusters by minimizing the objective function:

$$J_m(U,V) = \sum_{i=1}^{n}\sum_{k=1}^{c} u_{ki}^m d^2(x_i, v_k) \rightarrow \min \qquad (1)$$

where $u_{ki} \in [0,1]\ \forall k,i$,

$$\sum_{k=1}^{c} u_{ki} = 1 \forall i\ , \qquad (2)$$

and m, $1 \le m$, is the fuzzifier factor, V, $V = \{v_1, v_2, \ldots, v_c\}$ is a set of c cluster centers, $U = \{u_{ki}\}_{i=1..n,k=1..c}$ is a partition matrix and $d^2(.)$ denotes the Euclidean norm.

Minimizing J_m with respect to (2), we obtain an estimated model of U and V as:

$$u_{ki} = \left(\frac{1}{d^2(x_i, v_k)}\right)^{\frac{1}{m-1}} \Bigg/ \sum_{l=1}^{c}\left(\frac{1}{d^2(x_i, v_l)}\right)^{\frac{1}{m-1}}, \qquad (3)$$

$$v_k = \sum_{i=1}^{n} u_{ki}^m x_i \Big/ \sum_{i=1}^{n} u_{ki}^m\ . \qquad (4)$$

2.2 Defuzzification of fuzzy cluster partition

Defuzzification, in fuzzy cluster analysis, is a procedure to convert the fuzzy partition matrix U into a crisp partition which is then used to determine the classification information of the data objects.

Maximum membership degree principle

A popular approach for defuzzification of fuzzy partition is application of the maximum membership degree principle (MMD). The data object x_i is assigned to the class of v_k if and only if its membership degree to cluster v_k is the largest, that is

$$u_{ki} = \max_{l=1..c}\{u_{li}\}\ . \qquad (5)$$

If the dataset is non-uniform, this approach may make incorrect cluster assignments, in particular of marginal data objects of large clusters, as illustrated in Figure 1. Common approaches to resolve this problem use spatial information in membership degree computation.

Fuzzy clustering based method

Genther, Runkler and Glesner [7] proposed a defuzzification method based on fuzzy clustering (FCB) that used fuzzy cluster partition in membership degree computation. For each data object x_i, i=1..n, an estimated value, $\mu(x_i)$, is computed using the fuzzy partition. The set of estimated values of X, $\{\mu(x_i)\}_{i=1..n}$ is then used to compute the estimated value of v_k, w_k, k=1..c, as:

$$w_k = \sum_{i=1}^{n} u_{ki}^m \mu(x_i) \Big/ \sum_{i=1}^{n} u_{ki}^m\ . \qquad (6)$$

In FCB, distance, d_F, between the data object and cluster center, is computed using both the actual and the estimated information as:

$$d_F(x_i, v_k) = \sqrt{\frac{\alpha d^2(x_i, v_k)}{\max_{j,l}\{d^2(x_j, v_l)\}} + \frac{\beta d^2(\mu(x_i), w_k)}{\max_{j,l}\{d^2(\mu(x_j), w_l)\}}}\ . \qquad (7)$$

$d_F()$ is used, instead of d(), to compute the membership degree. The problem with this is selection of the values for α and β that scale the actual and estimated parameters in the distance measure.

Neighborhood based method (NBM)

In NBM, Chuang et al. [4] proposed adjusting the membership status of every data point using the membership status of its neighbors. Given a cluster v_k, k=1..c, a data point, x_i, i=1..n, receives an additional amount of membership degree from its neighbors:

$$h_{ki} = \sum_{x_j \in NB(x_i)} u_{kj}\ . \qquad (8)$$

The partition matrix U is then revised as in (9).

$$u_{ki}^{NB} = \frac{(u_{ki})^p \times (h_{ki})^q}{\sum_{l=1}^{c} (u_{li})^p \times (h_{li})^q} \quad (9)$$

NBM uses the spatial information in membership degree computation, but requires definition of neighborhood boundaries and the values of p, q which weight the position and spatial information.

Spatial FCM (sFCM)

In sFCM, Chiu et al. [3] used spatial information in computing the spatial distance, d_S, between the data point and cluster center:

$$d_S(x_i, v_k) = \frac{1}{NB} \sum_{j=1}^{NB} \left[(1 - \alpha_j^i) d(x_i, v_k) + \alpha_j^i d(x_j, v_k) \right], \quad (10)$$

where NB is the number of neighbors of every data point, α_j^i is the weighted factor of x_j, a neighbor of x_i, defined as:

$$\alpha_j^i = 1 / \left(1 + \exp(\Delta_j^i / \sigma_i)\right), \quad (11)$$

where $\Delta_j^i = d(x_j, x_i)$. sFCM uses $d_F()$, instead of d(), to compute the membership degree, and updates cluster centers, $\{ v_k^S \}$, k=1..c, as follows:

$$v_k^S = \sum_{i=1}^{n} u_{ki}^m \left[\frac{1}{NB} \sum_{j=1}^{NB} (1 - \alpha_j^i) x_i + \alpha_j^i x_j \right] \Big/ \sum_{i=1}^{n} u_{ki}^m \cdot \quad (12)$$

sFCM requires the number of neighbors, NB, to be specified a priori.

3 The fzPBD algorithm

To generate classification information, we propose fzPBD, a novel probability based method for defuzzification of fuzzy cluster partition, using the fuzzy partition and Bayesian probability to generate a probabilistic model of the data distributions, and applies the model to produce the classification information. To create a probabilistic model of the data distributions using fuzzy partition, we used the method of Le et al. [8].

Possibility to probability transformation

Given a fuzzy partition matrix U, the vector $U_k = \{u_{ki}\}_{i=1..n}$, k=1..c, is a possibility model of the data distribution of v_k on X. Assume P_k is the probability distribution of v_k on X, where $p_{k1} \geq p_{k2} \geq p_{k3} \geq \ldots \geq p_{kn}$. We associate with P_k a possibility distribution U_k of v_k on X [5] such that u_{ki} is the possibility of x_i, where

$$\begin{aligned} u_{kn} &= n \times p_{kn} \\ u_{ki} &= i(p_{ki} - p_{k,i+1}) + u_{k,i+1}, \ i = n-1,...1. \end{aligned} \quad (13)$$

Reversing (13), we obtain the transformation of a possibility distribution to a probability distribution. Assume that U_k is ordered the same way with P_k on X: $u_{k1} \geq u_{k2} \geq u_{k3} \geq \ldots \geq u_{kn}$,

$$\begin{aligned} p_{kn} &= u_{kn} / n \\ p_{ki} &= p_{k,i+1} + (u_{ki} - u_{k,i+1}) / i. \end{aligned} \quad (14)$$

P_k is an approximate probability distribution of v_k on X, and $p_{ki} = P(x_i|v_k)$.

Probabilistic model of the data distributions

Central Limit Theorem– *The distribution of an average tends to be normal, even when the distribution from which the average is computed is decidedly non-normal.*

In real datasets, for a cluster v_k, the data points usually come from different random distributions. Because they cluster in v_k, they tend to follow the normal distribution of v_k estimated as follows,

$$\sigma_k = \sum_{i=1}^{n} p_{ki} \| x_i - v_k \|^2, \quad (15)$$

$$P_n(x_i \mid v_k) = \left((2\pi)^{1/n} \times \sigma_k \times e^{\frac{\|x_i - v_k\|^2}{2\sigma_k^2}} \right)^{-1}. \quad (16)$$

Defuzzification of fuzzy partition

We use the probabilistic model as in (15) and (16) for defuzzification of the fuzzy partition. The data object x_i is assigned to the class of v_k, where

$$P(v_k \mid x_i) = \max_{l=1..c} \{P(v_l \mid x_i)\} \quad (17)$$

Because $P(v_k|x_i) = P(x_i,v_k)/P(x_i) = P(x_i|v_k)*P(v_k)/P(x_i)$, then

$$P(v_k \mid x_i) = \max_{l=1..c} \{P(x_i \mid v_l) \times P(v_l)\}, \quad (18)$$

where $P(v_l)$, l=1..c, the prior probability of v_l, can be computed using the method of Soto et al. [10].

fzPBD algorithm

- Input: An optimal fuzzy clustering solution,
  - c: optimal number of clusters.
  - $V = \{v_i\}$, i =1..c: the cluster centers.
  - $U=\{u_{ki}\}$, i=1..n, k=1..c: the partition matrix.
- Output: The classification of $x_i \in X$, i=1..n.

Steps

1. Convert the possibility distributions in U into probability distributions using (13) and (14).
2. Construct a probabilistic model of the data distributions using (15) and (16).
3. Apply the model to produce the classification information for every data point using (18).

4 Experimental results

Datasets

To evaluate the performance of fzPBD, we used four artificial datasets generated using an infinite mixture model method [11]. Datasets ASET1, ASET2 and ASET3 have well-separated clusters of similar size. The number of clusters and data dimensions of these dataset are (5,2), (5,3) and (11,5) respectively. ASET4 is more complex, containing three clusters that differ in size and density (Figure 1). For the real datasets, we used the Iris, Wine and Glass datasets from the University of California Irvine (UCI) Machine Learning Repository [6]. The classification structures in these datasets are known.

Performance measures

We use two measures to evaluate algorithm performance. The compactness cluster validity index is defined as:

$$\text{compactness} = \sum_{k=1}^{c}\sum_{i=1}^{N_k} d(x_i, v_k), \qquad (19)$$

where N_k is the number of data points assigned to cluster v_k, k=1..c. Smaller compactness means better cluster partition. The overall performance is measured by the number of data objects that are misclassified. The cluster label of each data object is compared with its actual class label. If any do not match, then a misclassification has occurred.

We compared fzPBD with four defuzzification algorithm methods: MMD, FCB, NBM, and sFCM [2-4, 7, 9, 12]. For each dataset, the following values of the fuzzifier factor, m were used: 1.25, 1.375, 1.50, 1.625, 1.75, 1.875 and 2.0. The number of clusters, c, was set to the known number of clusters. The FCM algorithm was run 3 times and the best fuzzy cluster partition was selected to test all the algorithms. We repeated the experiment 100 times and averaged the performance of each algorithm using the two measures.

ASET1 and ASET2 datasets

ASET1 and ASET2 each contain five well-separated clusters of the same sizes. ASET1 and ASET2 are in two-dimensional and three-dimensional data space, respectively. Performance of all algorithms is shown in Figures 2 and 3. fzPBD, MMD and sFCM generated no misclassification across multiple levels of m.

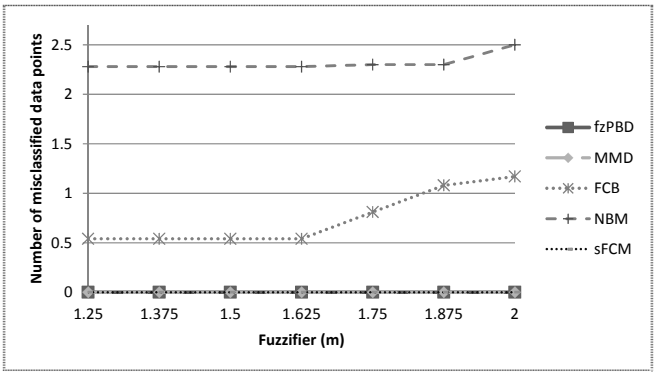

Figure 2: ASET1 dataset

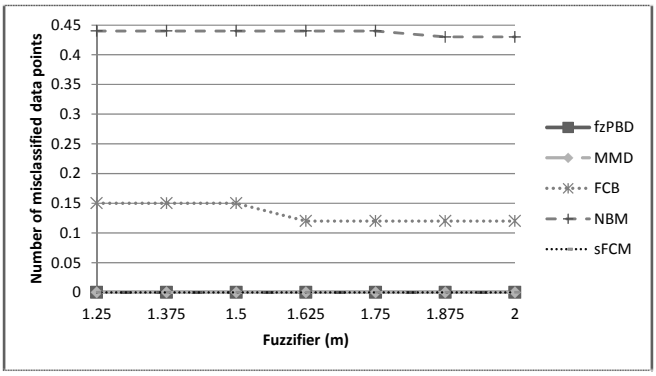

Figure 3: ASET2 dataset

ASET3 dataset

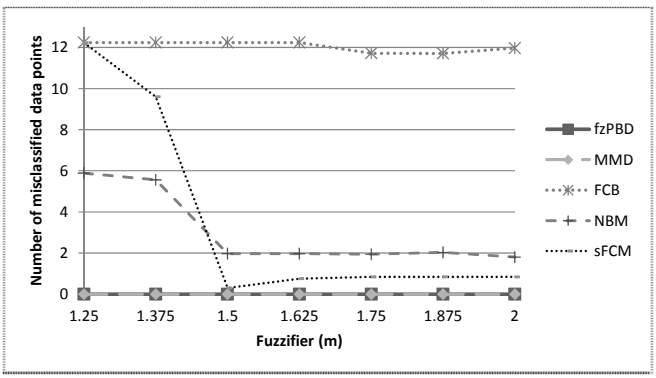

Figure 4: ASET3 dataset

ASET3 contains 11 well-separated clusters in a five-dimensional data space. Results are shown in Figure 4. fzPBD and MMD performed best. Table 1 shows that they also had the smallest compactness measures across multiple levels of m.

Table 1

ASET3: Compactness measure

Algo.	Fuzzifier factor m						
	1.25	1.375	1.5	1.625	1.75	1.875	2.00
fzPBD	0.39	0.39	0.39	0.39	0.39	0.39	0.39
MMD	0.39	0.39	0.39	0.39	0.39	0.39	0.39
FCB	4.52	4.52	4.52	4.52	4.53	4.54	4.54
NBM	12.85	11.28	8.73	8.72	8.72	8.72	8.72
sFCM	4.94	3.2	0.45	0.49	0.49	0.5	0.5

ASET4 dataset

This dataset is non-uniform with three clusters in a two-dimensional data space (Figure 1). Results are shown in Figure 5. fzPBD outperformed all the other algorithms.

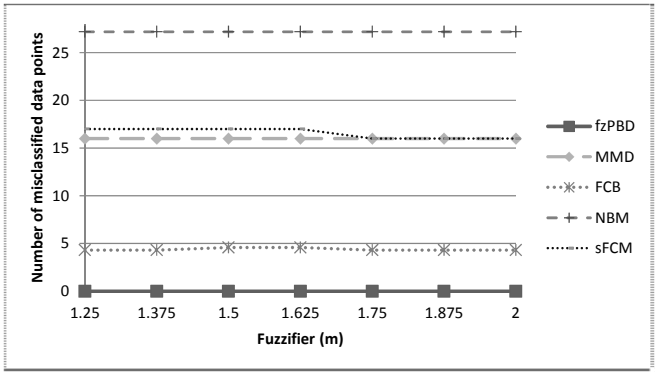

Figure 5: ASET4 dataset

IRIS dataset

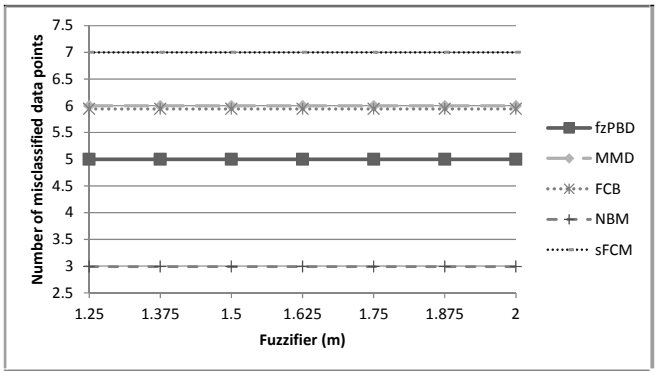

Figure 6: IRIS dataset

The IRIS dataset contains three clusters corresponding to the three classes of Iris flowers. Results are shown in Figure 6. NBM outperformed other algorithms. fzPBD performed lightly less well, however Table 2 shows that, compared with NBM, fzPBD had smaller compactness measures across multiple levels of m.

Table 2

IRIS: Compactness measure

algo	Fuzzifier factor m						
	1.25	1.375	1.5	1.625	1.75	1.875	2.00
fzPBD	0.44	0.44	0.44	0.44	0.44	0.44	0.44
MMD	0.44	0.44	0.44	0.44	0.44	0.44	0.44
FCB	11.84	11.81	11.78	11.76	11.75	11.75	11.75
NBM	1.75	1.75	1.75	1.74	1.74	1.74	1.74
sFCM	0.44	0.44	0.44	0.44	0.44	0.44	0.44

WINE dataset

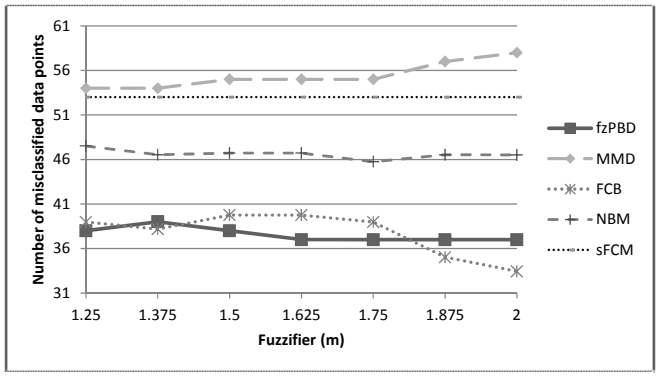

Figure 7: WINE dataset

The Wine dataset contains information on 13 attributes of the three classes of wines. Results are shown in Figure 7. fzPBD and FCB performed better than other algorithms. fzPBD performed better than FCB with the fuzzifier factor levels less than 1.8. However, Table 3 shows that fzPBD performed better FCB across multiple levels of m.

Table 3

WINE: Compactness measure

Algo	Fuzzifier factor m						
	1.25	1.375	1.5	1.625	1.75	1.875	2.00
fzPBD	0.08	0.08	0.08	0.08	0.08	0.08	0.08
MMD	0.05	0.05	0.05	0.05	0.05	0.05	0.06
FCB	0.19	0.18	0.18	0.17	0.16	0.16	0.17
NBM	0.17	0.17	0.17	0.18	0.18	0.18	0.18
sFCM	0.05	0.05	0.05	0.05	0.05	0.05	0.05

GLASS dataset

The Glass dataset contains information on nine attributes of six classes of glass used in building construction. Results are shown in Figure 8. fzPBD significantly outperformed all the other algorithms.

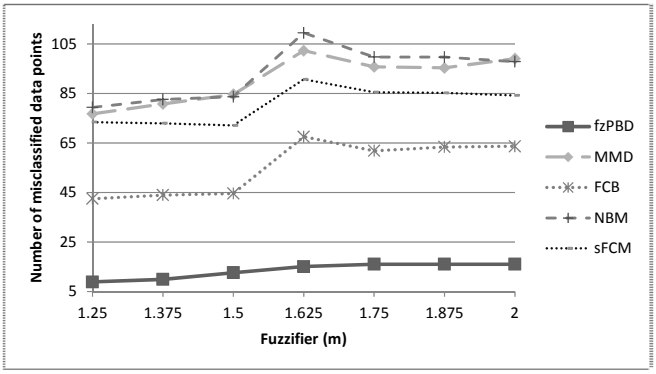

Figure 8: GLASS dataset

5 Conclusions

fzPBD is a novel defuzzification algorithm that uses a Bayesian based approach to generate a probabilistic model for a given fuzzy partition and then uses the model to produce classification information for the data objects. fzPBD outperformed other methods on both artificial and real datasets, particularly on the datasets with clusters that differed in size. fzPBD is therefore appropriate for real-world datasets, where the data densities are not uniformly distributed. In future work, we will exploit this Bayesian probabilistic model to generate classification information at different ranks with application to microarray data analysis.

6 References

[1] J.C. Bezdek, "Pattern Recognition with Fuzzy Objective Function Algorithms", Plenum Press, NewYork, 1981.

[2] S. Bodjanova, "Linear intensification of probabilistic fuzzy partitions," Fuzzy Sets and Systems, Vol. 141, pp. 319-332, 2004.

[3] W.Y. Chiu and I. Couloigner, "Modified fuzzy c-means classification technique for mapping vague wetlands using Landsat ETM+ imagery," Hydrol. Process., Vol. 20, pp. 3623–3634, 2006.

[4] K.S. Chuang, H.L. TZeng, S. Chen, J. Wu and T.J. Chen, "Fuzzy c-means clustering with spatial information for image segmentation," Computerized Medical Imaging and Graphics, Vol. 30, pp. 9-15, 2006.

[5] M.C. Florea, A.L. Jousselme, D. Grenier and E. Bosse, "Approximation techniques for the transformation of fuzzy sets into random sets", Fuzzy Sets and Systems, Vol. 159, pp. 270–288, 2008.

[6] A. Frank and A. Asuncion, (2010) Machine Learning Repository. [Online]. http://archive.ics.uci.edu/ml.

[7] H. Genther, T.A. Runkler and M. Glesner, "Defuzzification based on fuzzy clustering," Fuzzy Systems, Vol. 3, 1646-1648, 1994.

[8] T. Le and K. Gardiner, "A validation method for fuzzy clustering of gene expression data," Proc. Intl' Conf. on Bioinformatics and Computational, Las Vegas USA, 2011, Vol. 1, pp. 23-29, 2011.

[9] S. Roychowdhury and W, Pedrycz, "A Survey of Defuzzification Strategies," Intelligent Systems, Vol. 16, pp. 679-695. 2001.

[10] J. Soto, A. Flores-Sintas and J. Palarea-Albaladejo, "Improving probabilities in a fuzzy clustering partition," Fuzzy Sets and Systems, Vol. 159, pp. 406-421, 2008.

[11] L. Xu and M.I. Jordan, "On convergence properties of the EM algorithm for Gaussian mixtures", Neural Computation, Vol. 8, pp. 129–151, 1996.

[12] Y. Yang, S. Huang and N. Rao, "An Automatic Hybrid Method for Retinal Blood Vessel Extraction," Applied Mathematics and Computer Science, Vol. 18, pp. 399-407, 2008.

Friend of a Friend Influence in Terrorist Social Networks

Todd Waskiewicz
Air Force Research Laboratory, AFRL/RIEA
525 Brooks Road, Rome, NY 13441-4505
todd.waskiewicz@rl.af.mil

Abstract – *With the increasing popularity of social media over the last few years, terrorist groups have flocked to the popular web sites to spread their message and recruit new members. As terrorist groups establish a presence in these social networks, they do not rely on direct connections to influence sympathetic individuals. Instead, they leverage "friend of a friend" relationships where existing members or sympathizers bridge the gap between potential recruits and terrorist leadership or influencers. As anti-Western propaganda flows through these social networks, homegrown terrorists and lone wolf terrorists have been inspired to commit acts of terrorism. These terrorist social networks in social media can be uncovered and mapped, providing an opportunity to apply social network analysis algorithms. Leveraging these algorithms, the main influencers can be identified along with the individuals bridging the gap between the sympathizers and influencers.*

Keywords: terrorism, terrorist networks, social media, influence, social network analysis

1 Introduction

Terrorists use a number of methods to indoctrinate and radicalize new followers. With the growth of the Internet and the explosion in popularity of social networking sites all over the world in recent years, terrorist groups have significantly increased their global reach. They are now able to spread propaganda and recruit half way around the world from the convenience of an Internet cafe. Terrorist groups and their members have made a concerted effort to increase their presence on social media sites like Facebook and Twitter to go along with their existing Internet presence on web sites, forums, and message boards. However, it is their new found presence on social media sites that allows them to identify and target individuals that are particularly influenced by their propaganda. By reaching out to disillusioned individuals, they attempt to create new followers. The ultimate goal is to indoctrinate and radicalize these people so they feel compelled to commit acts of terrorism.

The individuals that have become indoctrinated with terrorist ideology have been heavily influenced during their use of social media. This has especially been the case with homegrown terrorists that have committed acts of terrorism in Western countries. Although they never had direct access to the terrorist ideology or training camps, they were exposed to it through relationships developed on social media sites and subsequently influenced. However, it was not necessarily the direct connections within their social networks that were the heavy influencers pedaling terrorist ideology. Often, it comes from individuals they are not directly connected to, but someone they encounter through a direct connection or "friend." Through a "friend of a friend," a disenchanted individual can quickly become enamored with the anti-Western culture. Consequently, it is important to identify these at risk individuals, the influencers, and the bridge between them. A variety of social network analysis methods can be used to identify these actors within a social network. This paper will explore terrorists' use of social media and the phenomenon of "friend of a friend" influence. Furthermore, it will discuss social network analysis techniques aimed at discovering these entities within social networks.

2 Terrorists' Use of Social Media

Over the last ten to fifteen years, the presence of terrorist groups online has greatly increased. In 1998, there were only 15 web sites associated with terrorist groups on the Internet [1]. By 2005, there were more than 4,000 [1]. Up until recent years, terrorists have limited themselves to more covert means of communication on the Internet such as password-protected forums for communicating and disseminating propaganda to support their causes. There was a shift in the way terrorists conduct operations. In an effort to adapt with current technology trends and reach larger audiences with their message, they have taken up the use of social networking sites. These sites also provide a number of other benefits as terrorists attempt to spread their propaganda. With that being said, terrorist groups are using social networking sites as a new medium for recruitment, radicalization, and planning.

In December 2008, pro-jihad contributors to the "al-Fajola Islamic Forums" urged Al-Qaeda supporters to "invade" Facebook by creating sympathetic groups to spread the Salafi-Jihadi message [1]. This movement had almost immediate results. In December 2009, Pakistani authorities arrested five young American Muslims as they were attempting to join Al-Qaeda [2]. Groups such as Lashkar-e-Taiba and Lashkar- e-Jhangyi used Facebook and YouTube to recruit them [1]. In regards to this incident, a high-ranking Department of Homeland Security (DHS) official said, "Online recruiting has exponentially increased, with

Facebook, YouTube, and the increasing sophistication of people online" [2].

There are many motivating factors behind the migration of terrorists to social networking sites. Terrorists have always utilized the latest technology to support their cause. Examples include the use of complex encryption programs for communications and altering computer games to mimic real life missions and attacks. As a result, their use of social networking sites is a natural progression of their technology-oriented tactics. Terrorist organizations have also moved to social networking sites out of self-perseveration [3]. Traditional web sites hosted by an ISP are prone to monitoring, attacks, and subject to shutdowns. Terrorist web sites are always targeted by the United States and its allies. Patriotic hacktivists also target the web sites using distributed denial of service (DDoS) attacks. For example, in June 2011, a hacker named "The Jester" shut down http://www.alijahad.com [3]. If they use a Facebook page, there is a very low probability someone would execute a DDoS attack against Facebook's web site. That is even assuming they can locate the page in question. The use of social networking sites provides terrorists with free web hosting where they can upload content anonymously, reliably, and at no cost [4].

Social networking sites are attractive to terrorists and their groups because they have features to control access to the page [5]. Instead of the site being open to the public, the page owner can set it to private. Then the owner must approve someone's request for access or invite them to join the page. This provides the opportunity to vet an individual thoroughly before granting them permission to view the content of the group's page or participate in a discussion forum [5]. Additionally, the owners can monitor the content posted on the pages. This provides a unique environment for terrorists where they control the content and access to it while also reaching large audiences.

The most important reason terrorist organizations are taking to social networking sites is to recruit, indoctrinate, and radicalize new members that can support their cause. "The Internet is the enabler that acts as a catalyst for the radicalization lifecycle" [6]. Without the use of the Internet and social networking sites, the perpetuation of Al-Qaeda's message would be severely stifled [6]. However, the radicalization process that used to take months now takes weeks or even days [6]. With the help of the Internet, terrorists are able to communicate across the globe instantly. They are targeting mainstream social networking sites because they are more accessible to sympathizers than the hardcore forums [7]. After the indoctrination of sympathizers, they are steered to the terrorist forums where some will finally join the front lines of the jihad [7].

3 Friend of a Friend Influence

A "friend of a friend" is described as an individual that has a friendly relationship with the friend of a person, but that person has no direct relationship to that individual. Figure 1 depicts the friend of a friend relationship between nodes A and C in the social network. C is a friend of A's friend B, and vice versa. A and C are not directly connected, but a path exists between them through C. Although there is no direct

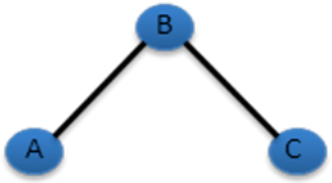

Figure 1. A friend of a friend relationship between A and C

connection between the person and the friend's friend, this is still an important relationship. Each person can exert a certain amount of influence on one another using the common friend as an intermediary. Ideas, information, behavior, and even feelings can spread through this social network. In addition, when the flow of information and ideas are strong enough, the three individuals will form a triad. In fact, social theory even argues there is a strong propensity for people to form these triads. Once this direct connection is formed between the two individuals that were not previously directly connected, ideas, information, and behavior are free to flow back and forth. The triad formed by A, B, and C is shown in Figure 2. This is the exact social phenomenon that terrorists are looking to exploit when using social media sites in an effort to build their virtual networks.

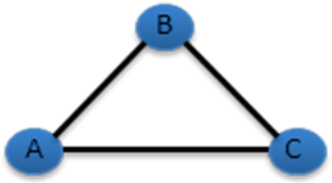

Figure 2. A triad formed between A, B, and C

4 Terrorists' Use of Friend of a Friend Relationships on Social Media Sites

Initially, the terrorists' first attempts at infiltrating social media sites like Facebook consisted of "Facebook raids" or campaigns aimed at disseminating their propaganda through existing Facebook channels [8]. Although this was spreading their message, it did very little in the way of adding followers and building their virtual networks. Their subsequent efforts have been to establish a permanent presence on Facebook by creating groups and virtual communities affiliated with terrorist web sites [8]. This allows the terrorists to bridge the gap between sympathizers and leadership. This is where the friend of the friend relationship starts to take root. To reach out to the Facebook users they are trying to recruit, terrorists are creating Facebook pages and coordinating communication between Facebook and the web sites. The terrorists operating on Facebook befriend sympathizers on the fringe and begin pedaling their anti-Western sentiment. This forms the structure seen in Figure 1 and starts the information flow from terrorist leaders and web sites to the sympathizer.

Information also flows back through this channel as sympathizers are often afforded the opportunity to interact with leadership through the intermediary. The flow of information will continue as the sympathizer becomes indoctrinated and radicalized, eventually leading to the individual becoming vetted and accepted as one of them. They then gain access to the password protected forums and web sites and are allowed to interact directly with leadership, effectively closing the triad and forming the structure depicted in Figure 2. This is the best case scenario terrorist groups hope for when targeting social media sites for new members. There are many examples that show terrorist groups attempting to reach out to sympathizers on social media sites. Some are clear cases that illustrate a concerted effort to bridge the gap between leadership and sympathizers and others show individuals that have been radicalized through these means and motivated to carry out acts of terror.

Many consider the Facebook page Jihad Al-Ummah to be one of the most important terrorist pages on Facebook and one of the most authoritative sources on the Internet outside of the actual forums [8]. The page is closely associated with the Shumukh Al-Islam forum and is a hub for jihadi material [8]. It distributes content from terrorist sites and serves as a liaison between Facebook users and those same sites [8]. The Jihad Al-Ummah Facebook page contains videos, announcements, articles, and other jihadist media right after it appears on the Shumukh forum [8]. To facilitate the material's dissemination through Facebook, they will tag friends of the page in the posts [8]. This brings the newly posted material to the attention of friends of the page or friends of the friends as they are updated on their friend's Facebook activity. For example, the Shumukh forum announced an open question and answer session with Sheikh Abu Walid Al- Maqdisi, leader of a Gaza based jihadi group [8]. Jihad Al-Ummah's Facebook page also announced the session and collected questions written by friends of the page [8]. Those who ran the Facebook page then passed on the questions to the Shumukh forum for answering. The friend of a friend relationship is being exploited by connecting friends of the Jihad Al-Ummah Facebook page to leadership in an effort to influence sympathizers. Utilizing Facebook in this manner for communications allows terrorist organizations to insulate leadership while also providing access for sympathizers.

The same type of activity is also reflected on Twitter. Twitter pages are set up to notify followers of updates on terrorist web sites and blogs. The Twitter page serves as the intermediary between sympathizers and the terrorists behind these web sites and blogs. The Taliban attempts to use Twitter in this manner. They leverage a system called TwitterFeed that automatically updates a Twitter page to reflect web site or blog updates [9]. Anytime there is a new addition to the web site, a link to the update is tweeted. This instantly updates followers who receive the tweet. The followers are now able to go directly to the site to view the update, bridging the gap between the propaganda and sympathizers.

Utilizing these communication patterns in social media, terrorists groups have inspired homegrown terrorism and driven seemingly normal individuals to act in support of their cause. For example, Taimour al-Abdaly appeared to be an average family man. He was a former DJ from Great Britain that was married with three children. However, much more sinister intentions were developing underneath his outwardly appearance. In December 2010, on a suicide mission, he blew himself up in Stockholm, Sweden, injuring two others.

As it turns out, he was a member of a virtual terrorist network constructed through social media. After the fact, when researchers explored Taimour's social media activity, they determined there were only three degress of separation between him and Samir Khan [7]. Khan was one of Al-Qaeda's top media operatives before being killed in Yemem as the target of a U.S. drone attack in September 2011. Figure 3 shows the friend of friend relationships that existed between them with Tamiour's friend being friends with several of Khan's friends [10]. Khan and his friend were not the only

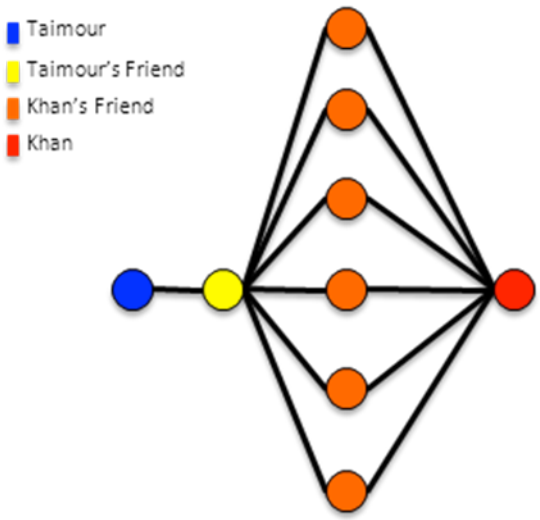

Figure 3. Subset of Taimour's Social Network

individuals who Taimour encountered online. His social media exploits also extended to YouTube where he would frequently view YouTube videos that consisted of violence and anti-Western propaganda. In fact, he was connected to Mohammed Gul, who was sentenced to jail in February 2011 in Britain for posting extremist Islamic material on the Internet. Taimour labeled four videos posted by direct associates to Gul as his favorites on YouTube [11].

Another individual that was heavily influenced by their involvement in virtual terrorist networks is Arid Uka, who opened fire on U.S. soldiers in Frankfurt, Germany, killing two and wounding another two. On Facebook, Uka had 127 friends that included extremists such Salahudin Ibn Ja'far [12]. Ja'Far openly identified with Germans involved in terrorist activity and was strongly linked as a friend and subscriber of two YouTube accounts known for posting extremist propaganda [13]. Uka was also Facebook friends with a German jihadist group using the name "Dawaffm De" that was friends with "AzeriJihadMedia," a jihadist media organization, on YouTube [14]. Uka was never a known member of any terrorists groups and was not under any type

of surveillance before his attack [15]. He was simply immersed in this online terrorist social network. Given his connections to extremists and their connections to others, it is clear that anti-Western propaganda flowed through this network and heavily influenced him. So much so that he decided to commit an act of terrorism and murder two U.S. soldiers.

5 Using Social Network Analysis to Detect Friend of a Friend Activity

It is clear that in online terrorist social networks influence is flowing through friends and between individuals who are not even directly connected, radicalizing extremist sympathizers with no physical connections to terrorist groups. Since a specific behavior has been established with these virtual networks, we can begin to use social network analysis methods to disrupt the flow of influence and try to prevent individuals from becoming indoctrinated with extremist ideals. Mapping the relationships between members of these online terrorist communities creates a social network. Various social network analysis methods can then be used to identify the different individuals that are a part of these types of relationships.

If there is an individual that is a part of a social network and feared to be a terrorist sympathizer, their ego network analysis will identify the individuals with whom they are connected to and influenced by. Ego network analysis consists of analyzing an individual within a social network and all the nodes the individual is connected to at some path length [16]. According to social theory, influence works at distances with up to three intermediaries [3]. Identifying all persons with a path length of 2 from ego produces a list of all of their friend of a friend relationships. This could go on to path lengths of three and four to identify further influencers and intermediaries. Figure 3 is essentially a subset of Taimour's ego network, depicting the people he is connected to with path length three or less. The people found to be on the end of these paths are potential influencers while those found in between are the intermediaries passing it along. Ego-networks can also be examined for structural holes. A structural hole refers to a tie that is absent [16]. For example, the network depicted in Figure 1 has a structural hole between A and C while Figure 2 contains no structural holes. Social network analysis software such as UCINET analyzes ego networks for structural holes. Identifying structural holes may lead to the discovery of friend of a friend relationships in which influence is flowing from terrorist leadership to sympathizers.

Betweenness centrality measures the ratio of shortest paths an individual is present upon. Individuals with a high betweenness centrality hold a very important position in a social network. By being present on the shortest path between two individuals, they have the opportunity to serve as a broker of information by passing it along or affecting it in some way. In the friend of the friend relationship, they serve as the intermediary connecting two individuals that would otherwise be disconnected. For example, in Figure 1, B would score a high betweenness centrality for being on the shortest path between A and C. By calculating the betweenness centrality for an entire social network, the individuals with the highest betweenness values are identified. By the pure definition of betweeness centrality we know that these individuals must be connecting others who are not directly connected. As a result, by using betweenness centrality, we identify the individuals in the friend of a friend relationships that are passing information and influence between terrorist leadership and sympathizers in social networks.

Community detection algorithms detect groups that exist within social networks and help reveal network structure. Most community detection algorithms work by measuring the density between sets of nodes and identifying groups or communities where the density of those nodes within the group is greater than that of nodes outside the group. As a result, communities of individuals are identified where the members of the community are more connected to each other than any other people in the network. For example, the subset of Taimour's social network shown in Figure 3 could be identified as a group in a large social network. We see that there are several connections between the intermediaries that serve as friends of friends and Khan himself along with Taimour's connection to this group. Depending on how the parameters are set for the community detection algorithm, many different types of groups may be identified. They could identify groups of sympathizers, intermediaries, leadership, or mix of all three. Essentially any pocket of increased connectivity. When examining social networks, it is important to identify these groups because the increased connectivity between the individuals will indicate some type of coordinated activity. For example, a group of sympathizers may be communicating on social media and actively seeking information and propaganda relating to the terrorist cause. A group of intermediaries whose job it is to bridge the gap between these sympathizers and leadership may also be identified. Community detection algorithms are valuable to the examination of social networks to identify these pockets of activity in a larger network so they can be further investigated.

6 Conclusion

Given the popularity and widespread use of social media sites across the world, terrorist groups have targeted the sites as new grounds for spreading their propaganda and recruiting new members. Targeting social media sites provides terrorists groups with a number of benefits over their traditional recruiting efforts. They are able to reach many more people essentially anywhere in the world, given free web hosting to upload content, have the ability to control access, and social media pages are less prone to attack. Once the terrorists gain a foothold on social media sites, they look to build virtual online terrorists networks where influence and ideas can flow from existing members to potential recruits. They leverage friend of a friend relationships where indirect connections allow influence and propaganda to make its way from leadership and web sites to sympathizers who may be inclined

to join their cause. Although the sympathizers may not be directly connected to the main influencers, the information and ideas still flow through intermediaries to reach them. Mainly, it is the friends that sympathizers make on social media sites that are responsible for delivering the propaganda. This social phenomenon has been exhibited as extremist groups hold question and answer sessions with leadership through Facebook and use Twitter posts to keep followers updated on the latest activity. It has also shown direct results by inspiring lone wolf terrorists. Taimour al-Abdaly injured two others while blowing himself up in Stockholm. Arid Uka acted against U.S. soldiers, murdering two and injuring another two. Later research showed these individuals were heavily immersed in virtual terrorist networks. They had friends that were connected to radical terrorists and consumed anti-Western material as it made its way to them on Facebook and YouTube. By targeting this type of behavior on social media sites, social network analysis can be used to identify these relationships. Using techniques such as ego network analysis, betweenness centrality, and community detection algorithms, the sympathizers, intermediaries, and leadership that constitute these friend of a friend relationships can be identified. Locating these relationships is extremely important so actions can be taken to disrupt the flow of influence and propaganda and prevent the existing terrorist groups from inspiring lone wolf terrorists.

7 References

[1] al-Shishani, M. B. (2010, February 4). *Taking al-Qaeda's Jihad to Facebook*. Retrieved from The Jamestown Foundation: http://www.jamestown.org/single/?no_cache=1&tx_ttnews[tt_news]=36002

[2] Witte, G., Markon, J., & Hussain, S. (2009, December 13). *Pakistani authorities hunt for alleged mastermind in plot to send N. Virginia men to Afghanistan to fight U.S. troops*. Retrieved from The Washington Post: http://www.washingtonpost.com/wp- dyn/content/article/2009/12/12/AR2009121201598.html?sid=ST2009121002234

[3] Reeder, D. (2011, June 27). *Jihadi Social Media*. Retrieved from DefenseTech: http://defensetech.org/2011/06/27/jihadi-social-media/

[4] Stalinsky, S. (2011, October 7). *Why Haven't The Taliban's Twitter Accounts Been Shut Down?* Retrieved from The Middle East Media Research Institute: http://www.memri.org/report/en/0/0/0/0/0/0/5707.htm

[5] Bumgarner, J., & Mylrea, M. (2010, March 23). *Jihad in cyberspace*. Retrieved from PoliceOne: http://www.policeone.com/communications/articles/2025862-Jihad-in-cyberspace/

[6] Bardin, J. (2010). *Cyber Jihadist Use of the Internet: What Can Be Done?* Retrieved from Treadstone 71: http://treadstone71.com/whitepapers/CyberJihadistUseoftheInternet.pdf

[7] Holtmann, P. (2011, March). *No threat at first sight: Invisible terrorist environments on Facebook and Youtube.* Retrieved from University of Vienna: http://www.univie.ac.at/jihadism/blog/wp-content/ uploads/2011/03/Philipp-Holtmann- No-threat-at-first-sight-Invisible-terrorist-environments-on-Facebook-and-Youtube.pdf

[8] Green, R. (2010, December 13). *Social Network Jihad Part 1*. Retrieved from The Middle East Media Research Institute: http://www.memri.org/report/en/0/0/0/0/0/0/4834.htm

[9] *Social Jihad Network : Taliban Twitter* . (2011, February 21). Retrieved from SITE Intel Group: http://news.siteintelgroup.com/component/content/article/438-taliban-twitter

[10] *Taimour al-Abdaly AKA Taimour Abdul Wahab.* (2010, December 13). Retrieved from Internet Haganah: http://internet-haganah.com/harchives/007103.html

[11] *Two degrees from a suicide bomber.* (2011, February 25). Retrieved from Internet Haganah: http://internet-haganah.com/harchives/007175.html

[12] *The Frankfurt shooter's Facebook page, and a little color commentary*. (2011, March 3). Retrieved from Internet Haganah: http://internet-haganah.com/harchives/007191.html

[13] *That network diagram [Taimour al-Abdaly, Salahudin Ibn Ja'far, and Samir Khan*]. (2011, January 7). Retrieved from Internet Haganah: http://internet-haganah.com/harchives/007132.html

[14] *AzeriJihad Media and the Frankfurt shooting*. (2011, March 7). Retrieved from Internet Haganah: http://internet-haganah.com/harchives/007198.html

[15] Klausen J., Barbieri, E.T., Reichlin-Melnick, A., & Zelin, A.Y. (2012). *The YouTube Jihadists: A Social Network Analysis of Al-Muhajiroun's Propaganda Campaign*. Retrieved from Perspectives on Terrorism: http://www.terrorismanalysts.com/pt/index.php/pot/article/view/klausen-et-al-youtube-jihadists/html

[16] Hanneman, R.A., & Riddle, M. (nd). *Chapter 9: Ego networks*. Retrieved from Robert Hanneman's Homepage: http://faculty.ucr.edu/~hanneman/nettext/C9_Ego_networks.html

MISAAC: Instant messaging tool for Ciberbullying Detection

Perla Janeth Castro Pérez[1], **Christian Javier Lucero Valdez**[1], **María de Guadalupe Cota Ortiz**[1], **Juan Pablo Soto Barrera**[1], **Pedro Flores Pérez**[1]
[1] Universidad de Sonora, Blvd. Luis Encinas y Rosales S/N, 83000 Colonia Centro, Hermosillo, Sonora, México.

Abstract - The efforts of education authorities to find ways to identify problems related to bullying, still have not considered ciberbullying, and have not taken the necessary measures to maintain proper control of the problem through computer applications. In this paper are proposed a security model based on agents, which can analyze the messages exchanged between children (ages 9 to 13) through chats that are used in classrooms, and emit warnings about the threats, which may be considered to address such problems. The information generated can be used for the detection of cyberbullying and offer psychological support to those that may be formed as aggressors, preventing that this behavior becomes a disease that could be avoided at an early age.

Keywords: Pattern recognition, Agent, Security, Ciberbullying.

1 Introduction

The problem of cyberbullying is defined by the fact that a person is abused, threatened or harassed through electronic means, and has recently generated great controversy, since this type of violence may increase as advances the use of new technologies [1, 2].

Because there are several forms of cyberbullying, this paper proposes a model based on the architecture of ARSEC-AMS agents [3] to detect threats and verbal abuse to which a child is usually exposed, taking into account the behavior of the aggressors and techniques of content analysis of messages exchanged through chats [4-6].

It is important to mention that the content analysis is applied to the spanish language, so that in the experimental examples section the analyzed sentences are presented in that language, since the result does not have the same structure or the same meaning in other languages.

Moreover, this paper is organized as follows: introduction, description of the model, components of content analysis, implementation of the architecture ARSEC-AMS, experimental tests, and finally is presented the conclusions and bibliographical references.

2 Model

This model focuses on the detection of threats and aggressions to which a child is exposed on having interacted with others through instant messaging, applying content analysis techniques to measure the dangerousness of the message. Moreover, it is used the software agent technology based on the architecture ARSEC-AMS [3] that allows to implement computer security concepts.

2.1 Content analysis

The analysis of content is a set of technologies that allow distinguishing the symbolic semantics of the messages regarding the mode of production, these messages generally do not have a single meaning, since in occasions they change their semantics according to the context in which they are in relation to the rest of the information. [4-6]

In the process of analysis, the aim consists of realizing an inspection of the sentences that are exchanged in the instant messaging application, and identify those that represent a threat to the user who receives them, and registered as evidence to determine if the user is a person likely to carry out his threats. For this task we designed a dictionary of keywords, some of which are used in sentences that constitute a threat, as well as the words that can not represent an attack by themselves. As support for the content analysis it was identified two components or modules that help to detect if the statement is a threat to another person. These components are the lexical analyzer (tokenizer) and the content analysis.

2.1.1 Lexical analyzer

The lexical analyzer also known as tokenizer is a program that separates the words of the sentence analyzed in tokens, which are compared with the content of a dictionary that corresponds to a previously selected set of sentences for testing. With the obtained result it is possible to recognize if the word belongs to the set of verbs, adjectives or nouns. Later, the set of analyzed words will serve to identify patterns that will match with some type of registered threat.

Before comparing the tokens with the designed dictionary, they are processed in a sub-module for exchange of characters, which purpose is to consider those written in words misspelled, idioms or abbreviations, in order to have the word in a neutral state by applying a procedure that allows identifying the principal core of the word. To obtain each token in a neutral state certain characters are replace by others, which are previously identified with base in the specifications of *Table 1* that are used in place of characters in the words that are analyzed, where it is presented the letters or syllables according to their cataloguing and character replacement.ion.

Table 1. Words replacement

Replacement	Letters or syllables
0	b,v
1	ce,ci,si,se,zi,ze
2	d,de
3	g,j
4	i,y,ll
5	ca,co,cu,ka,ko,ku
6	qui,qi,ki,que,qe,ke,q,k
7	t,te
8	u,w
9	x,cs,xh,cc,sh,zh
*****	sa,so,su,za,zo,zu
^	s,es
+	pe,p
-	R
It is omitted	First letter 'h'

It is necessary to mention that the way of assigning the replacement characters does not have preferential order, nevertheless, on having replaced some characters or syllables in the application they do have preference for exchange, since in certain cases would alter the token in a neutral state and the difficulty of cataloguing it as a key word.

2.1.2 Knowledge programming

After being labeled or tokenized the selected words of the sentence are evaluated in the module of knowledge programming through predicates or rules of prolog type; in order to determine whether they match aggression patterns or threats that were emitted by the user responsible of the analyzed message.

The components of the knowledge programming and the lexical analyzer provide a rapid and accurate way to analyze messages, and give the possibility to evaluate information as a human being does.

2.2 ARSEC-AMS architecture

The proposed model is based on the architecture ARSEC-AMS [3] (*Figure 1*), which takes into account the use of four modules: reactive, deliberative-cognitive, security and control of blackboard, in such a way that the signs that are received in the agent system via sensors are filtered by an interpreter which is responsible for acting in a coordinated way and track the set of actions required to achieve the correspondent objectives, applying this in the model to detect the danger of exchanged messages through a system of Instant Messaging (IM). A wide reference of the previously architecture mentioned is described in [3].

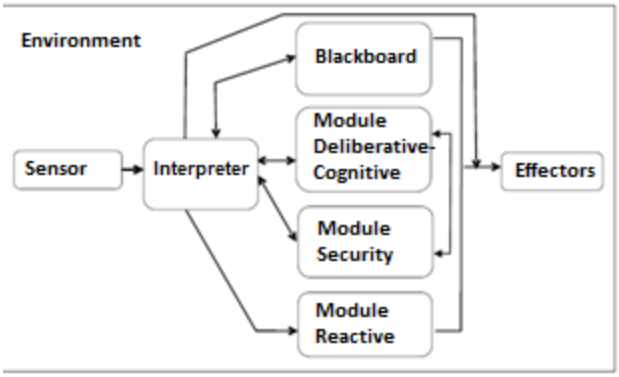

Figure 1. ARSEC-AMS architecture

2.3 Agent model

The agent model proposed in the architecture ARSEC-AMS defines a hierarchy of agents, which is described below:

- *Coordinator agent*: is the software agent responsible of the flow of transactions that allow to apply security levels in the system and in the work of local and network agents, in addition is in charge of analyzing the content of the messages to determine if they are

evidences, and if necessary alert users that exceed a certain number of incidences of evidences.

- *Local Agent:* is the software agent that reviews and tokenize the messages of the users locally.
- *Network Agent:* is the agent responsible of the messages sent by the user and get them already encrypted to the system.

To show the control that the agents will have in the system it was included the sequence diagram for the content analysis in order to model the functioning of the application (*diagram 1*).

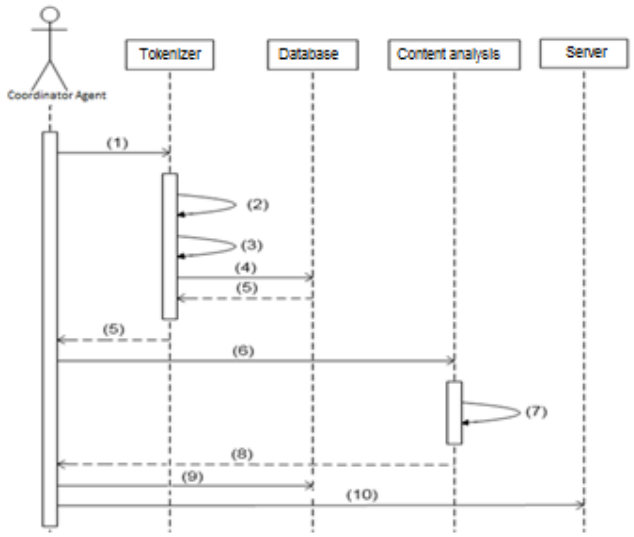

Diagram 1. Content analysis process

Next are detailed the steps that realized the coordinating agent in *diagram 1*:

(1). Passes the original message

(2). Divides the message into lexical components (tokens)

(3). Codifies lexical components (exchange of characters)

(4). Searches for neutral words in the dictionary

(5). Returns keywords

(6). Sends keywords

(7). Finds patterns that match threats of cyberbullying

(8). Returns the dangerousness of keywords

(9). Stores user information and the original message

(10). Displays an alert message

3 Experimental tests

To determine the proper functioning of the application were taken sentences with certain degree of dangerousness called evidences and common sentences that can be misinterpreted by a system as described herein. Following are some common sentences and evidences:

Common sentences

- "Voy a pegar lo que recortamos en el cuaderno."
- "Hiciste la tarea sobre la matanza de Tóxcatl."
- "El cuento del zorro es muy interesante."

Evidence sentences

- "Te voy a pegar estúpido."
- "Vamos a matarte."
- "Eres una zorra."

.

In previous examples, underlined words, which can have different meanings, depending on the context of the sentence, so that sometimes are part of a sentence may be considered threatening and sometimes can be part of phrases that are considered normal.

It is noteworthy that the evidences have certain degree of dangerousness; therefore they are categorized into low and high levels. Evidences of high level are phrases, which meaning is a threat to another user, while the low level evidences are aggressions. According to the number and level of evidences is how the coordinating agent can determine the state in which the user is, cataloguing it in three levels, denoting it as 'semaphore of users' and the levels are red, yellow and green. The red level corresponds to a user who must be observed; the yellow one corresponds to users who not necessarily have reach a level of threat, but that his sentences have already certain trend to do it; the green level is for users who do not represent any danger.

As an example, next is the procedure applied to a previously misspelled phrase selected to determine whether it is a phrase that can be used as evidence:

"TE BOOOOI A PEGAR, HIMBÉCIL"

The following is an example of how the sentence is processed above:

The phrase is converted into lowercase letters:

"te booooi a pegar himbécil"

Vowels with accents are replaced by vowels without accents:

"te booooi a pegar himbecil"

Omit repetitions:

"te boi a pegar himbecil"

Replacement according to Table 1, character interchange:

"7 0o4 a +3a- 4m0e1l"

Note: It can be observed that the number of characters has decreased omitting the spaces in the original sentence. The number of characters is 22 in the original sentence, while the replacement sentence has 15. Obtained the words in neutral form, they are compared with the words contained in the dictionary, resulting in two verbs "0o4" (voy), "+3a -" (pegar), plus an adjective "4m0e1l" (imbécil), naming them key words.

The keywords are evaluated in the predicates type Prolog, obtaining as result that the sentence is an evidence of high level.

The coordinator agent records the evidence and reviews the history of the user to determine in what level of the semaphore is positioned. Following *Table 2* shows different cases that may occur depending on the user status and considering that he did an incidence of high level.

Table 2. States of user (Semaphore)

User state	Previous evidences		New State
	High	Low	
Green	0	1	Green
Yellow	2	6	Red
Red	5	10	Red

When cataloging through the semaphore allows early detection of cases of users that merit attention from school authorities and are given appropriate treatment.

4 Conclusions

With the proposed model it is intended to help detect early cases of cyberbullying avoiding cases of threats and aggressions that may be suffering the child or the young person in school. The fact that there is a children interest to use tools based on information technologies and communications, makes them feel part of the technological wave which nobody wants to be left behind. These tools give course to communication channels that are not exempt from threats or aggressions by users to people with low self-esteem and high levels of vulnerability. By the above, it is important that schools classrooms where computers are used, are applied to detect forms of cyberbullying problems through systems like the one proposed in our model, where an agent system can analyze in real time messages that are exchanged through chats.

5 References

[1] El Universal, "*Bullying, riesgo para 18 millones de niños: CNDH*". 2011 http://www.eluniversal.com.mx/notas/779963.html .

[2] Slonje Robert; Smith Peter K. "*Cyberbullying: Another main type of bullying?" Scandinavian Journal Of Psychology*, Volume 492, p. 147-154, DOI: 10.1111/j.1467-9450.2007.00611.x. 2008.

[3] Cota O. María de Guadalupe & Soto B. J. Pablo. "*Architecture for design and development of security Systems based on agent technology*". WorldComp'11 – The 2011 World Congress in Computer Science, Computer Engineering, an Applied Computing (ICAI'11 – International Conference on Artificial Intelligence). Las Vegas, Nevada USA. 2011. (http://www.world-academy-of-science.org/worldcomp11/ws)

[4] José Luis Piñuel Raigada, "*Epistemología, metodología y técnicas de análisis de contenido*". http://web.jet.es/pinuel.raigada/A.Contenido.pdf

[5] AngelFire, Análisis de contenidos, http://www.angelfire.com/tv2/tesis/Analisisdecontenido.htm.

[6] Bernard Berelson, *Content Analysis in Communication Research* (New York: The Free Press (1952), p. 18. http://devcompage.files.wordpress.com/2007/12/17-content_analysis.pdf .

Leveraging Layered Network Analysis for Intuitive Decision-Making

Peter M. LaMonica and Craig S. Anken
Air Force Research Laboratory, AFRL/RIEA
525 Brooks Road, Rome, NY 13441-4505

Abstract - *Current analysis and decision-making relies too heavily on a single source of data. This can be attributed to a myriad of reasons such as failure to standardize and normalize diverse data, inability to define a common ontological mapping between datasets, and even an unawareness that related additional data exists. However, in reality many datasets can be interconnected through nodes and/or edges and together can collectively provide much greater situation awareness to the user. Fusing multiple diverse datasets together for collective exploitation is referred to as layered network analysis and provides a more intuitive approach to analysis and decision-making. The purpose of this article is to conceptually define how layered network analysis can advocate and provide an intuitive decision-making environment in knowledge discovery and decision support systems. Further, this approach can be applied to numerous domains that address the data-to-decision problem.*

Keywords: Layered network analysis, intuition, decision-making, situation awareness, knowledge discovery, and data to decisions.

1 Introduction

Decision makers in various domains are constantly hampered by information overload from numerous diverse sources. This places tremendous strain and burden on the decision maker to manually derive mental correlations to determine how these diverse data sources are connected and related. Even more troublesome is deriving patterns over space and time across these different data types. While this is an extremely difficult manual process, the vast majority of this data does not exist independently, as much of it is related and connected across networks of data. This was the reasoning behind developing the Layered Network Analysis model [1] for combining heterogeneous relational data types to improve situation awareness. Layered Network Analysis provides a foundation for users to think intuitively by quickly allowing them to understand how data is connected and related. Allowing users to better understand the data will provide greater situation awareness [2] and intuitive decision-making capabilities. This research will provide detail on Intuitive Decision-Making by Klein and the Layered Network Analysis model, and discuss how these two approaches can work together to improve decision-making.

2 Intuitive Decision-Making

Klein [3, 4, 5, 6] claims that the vast majority of decisions made are driven by personal intuition. This is a great contrast and departure from the traditional decision-making models that leverage analytical and statistical methods. Klein proves that intuition is used more accurately than analysis of a situation – in order to make a decision.

Throughout his research on intuitive decision-making, Klein developed a model that demonstrates the process that users go through. Klein's Recognition-Primed Decision Model can be seen in Figure 1 [3]. This process begins when a user experiences a situation that demonstrates cues. The user determines if this situation is typical based on what has been observed. If this is not a typical situation, the user looks for features to diagnose the situation to determine any relevancies to past situations. If this is a typical situation, the user seeks to recognize four by-products: cues, expectancies, plausible goals, and typical actions.

If this is a situation that is typical yet the expectancies are anomalistic, then the user needs more data to further clarify and diagnose the situation. Otherwise, the user evaluates the action that has taken place and also conducts mental simulation where the user relies on mental models to determine potential outcomes. If these models do not seem to work (possibly due to an underlying difference in the situation – e.g. different terrain), the user may slightly modify existing models to project future outcomes. Otherwise, the user determines how the situation can progress and determines a course of action that can be implemented successfully.

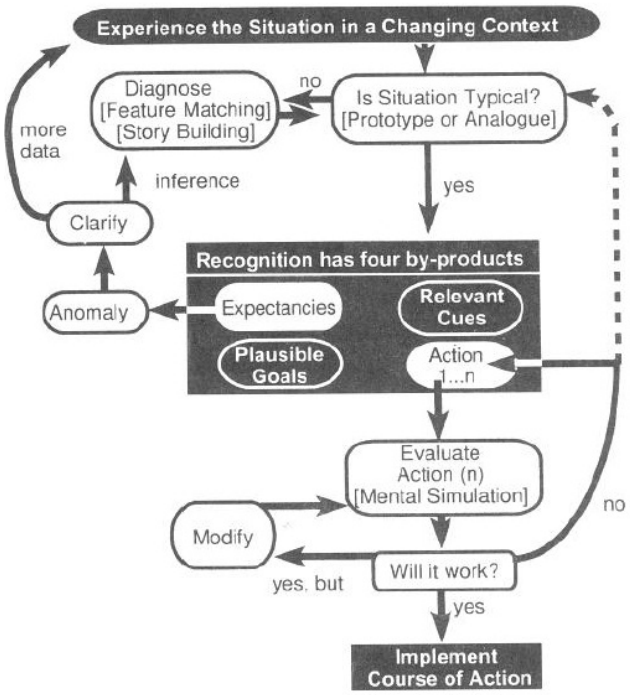

Figure 1. Recognition Primed Decision model [3]

The Recognition-Primed Decision Model is highly relevant in multiple user domains ranging from firefighters to United States Naval commanders. Klein [3] conducted a series of studies across various domains to test the Recognition-Primed Decision Model. One study explored United States Navy AEGIS command and control (C2) commanders. AEGIS is an integrated United States Naval weapons system that uses radar and software systems to guide and track weapons. This work was done in coordination with the Office of Naval Research and Klein wanted to learn how these officers had responded and made decisions in conflicts. In this case, the time pressure was severe and the skill level of the officers was generally high. However, the situations changed rapidly and there were very few courses of action available. The officers had clear guidelines with official rules of engagement. Over 78 decision points that Klein studied in this case, the Naval officers used Recognition-Primed Decision-making 95% of the time. These officers claimed that in 95% of the cases, they had not compared any options and the course of action selected was not a novel one. The commanders justified their selection to use intuition decision-making because of typically suffering from various issues such as relevance to a past event/scenario (known patterns), a lack of time, and a lack of specific scenario data (uncertain, unknown, or incomplete data).

In another study, Klein looked at how teams use the Recognition-Primed Decision Model. Klein worked with command and control teams at the Army brigade level at Fort Hood. The teams were working through training exercises on decision-making. Klein [3] initially thought that a team structure might reduce the rate of recognition-primed decision-making because when a team makes decisions, the team typically comes to consensus, which involves considering alternate courses of action. However after analyzing the complete training session tapes (five hours in duration) and the 27 decision points, only one of those points showed evidence of comparing options (demonstrated a 96% use of recognition-primed decision-making). This was startling to Klein since typically Army planners are taught to develop a set of courses of action that typically includes a minimum of three options.

In a different domain, Klein [3] studied how urban fireground commanders make their decisions. Fireground commanders rely on visual and audio cues to determine how to approach a fire. For example, if a fire starts on the lower floors of an urban building and there are no visual signs of smoke from the outside of a building, then this means a fire is just starting. However, if smoke is pouring from the eaves of the roof, then the fire has risen from the lower floors to the roof of the building. This puts the fireground commander into search and rescue mode to get all occupants out of the building as soon as possible. This demonstrates how fireground commanders are required to make quick, accurate decisions based on cues of what they recognize in real-time. Figure 2 depicts other studies that Klein conducted with many of them demonstrating high levels of recognition-primed decision-making.

Study	Number of Decision Points	Decision Points Handled Using RPD Strategy (%)
1. Urban fireground commanders	156	80
2. Expert fireground commanders	48	58
Novice fireground commanders	33	46
3. Tank platoon leaders	110	42
4. Wildfire incident commanders	110	51
Functional decisions	79	56
Organizational decisions	31	39
5. Design engineers	51	60
6. Battle command teams	27	96
7. AEGIS commanders	78	95

Figure 2. Frequency of Recognition Primed Decision-Making Across Domains [3]

2.1 An Intuition Example

The following scenario will further reinforce the application of the Recognition Primed Decision Model and took place during the Persian Gulf War in 1992. This is used by Klein [3] to demonstrate and compare intuition to analysis. The HMS Gloucester is a British destroyer and is on watch

during an airraid of Kuwait. United States Navy A-6 aircraft that had specific targets to take out in Kuwait City was conducting the airraid. During this mission, the Gloucester was monitoring the airspace for retaliation by Iraq when it noticed a blip on the radar screen.

A US Navy A-6 aircraft flew at approximately 600-650 knots when returning from a bomb run and typically flew at 2,000 to 3,000 feet. When the pilots would make a bomb run, their radars were typically off as well as their 'Identify Friendly or Foe' mechanism, as these were two ways to be easily detected by the enemy. In this particular mission, the allied forces were conducting an airraid near a known Iraqi silkworm missile site. The silkworm missile flew at approximately 600-650 knots, was about the same size as the American A-6 aircraft, but it flew at roughly 1,000 feet of altitude. The radar used on the British ship could only work over water and not on land due to high amounts of ground clutter and noise. Further, the British radar could only work vertically first, then once it detects a target it takes an additional 30 seconds to track it horizontally to determine its altitude.

In this case, the British officer immediately claimed that the blip on the screen was a silkworm missile aimed for the Gloucester and not a friendly American aircraft. The British officer ordered for a missile to be fired and the blip was taken out. Instantaneously, the commander ordered for reasoning behind the officer's determination. The officer did not have time to wait for the horizontal radar to sweep and determine altitude. How did this officer know that this was a missile and not an aircraft? Initially, the officer could not explain how he determined that it was a missile and not a friendly aircraft.

The British officer later discussed the scenario with Klein and told Klein that he knew the Iraqis were getting desperate and this attack was the Iraqi's last chance to use their missiles in an attempt to disrupt allied forces. With all these factors considered, he immediately knew that this was a silkworm missile aimed at the Gloucester. The officer said he knew he only had seconds left to live if he had not ordered to fire at the silkworm missile. The officer turned out to be correct – the blip on his radar was in fact an Iraqi silkworm missile and this missile would have done significant damage if not catastrophic to the Gloucester if the officer had not acted on his intuition.

Klein noted several key factors about this scenario and why intuitive decision-making is more agile and accurate. In the end, it was the officer's mental model that saved his life, as well as his fellow troops. It was the combination of radar, location, and knowledge of the situation that collectively determined the action of the officer. Klein [2] argues that if the officer had relied on the analysis of metrics and the hard sensor data alone, then his decision probably would not have been the same.

3 Layered Network Analysis

Layered Network Analysis is a novel term that was defined by LaMonica and Waskiewicz [1] and refers to the fusion of previously disconnected data in a common operating picture allowing the user to explore and exploit the interconnected data in a unified state. Layered Network Analysis can be used to discover patterns within and across layers, discover previously unknown nodes and edges, and allow users to focus on multiple data types within a specific time and space.

The intent is to understand the structure and dynamics of network data as this data is of vital importance to decision makers. Current analysis of network data occurs primarily within one or two particular domains and relies on the user to infer and derive links between data sources. However, to fully understand the network environment, decision makers must be able to investigate interconnected relationships of many diverse network types simultaneously as they evolve spatially and temporally. No single data network exists in a vacuum as networks are interconnected through space and time. It is imperative to understand that no single network exists independently of others. Each layer represents a diverse network data type and these layers can be connected through nodal and edge similarities as is depicted in Figure 3 below.

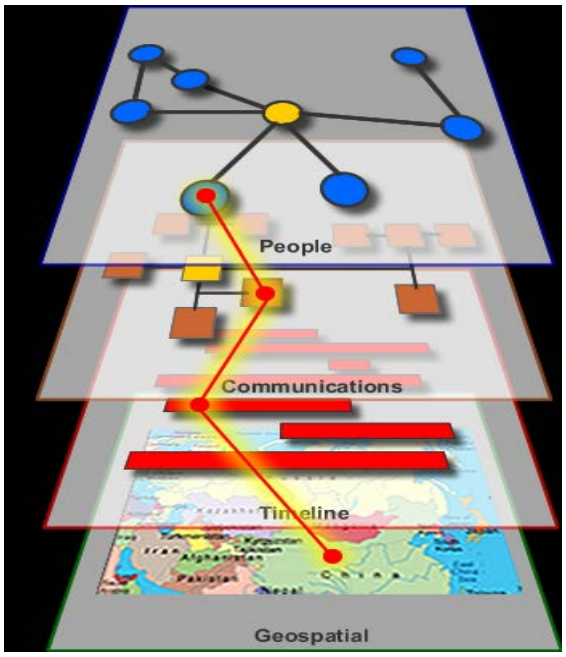

Figure 3. Layered network analysis

Layered Network Analysis is meant to be an approach to this data problem that users can interrogate and shape for their mission. Layered Network Analysis can assemble previously disconnected, multi-modal networks (e.g. social networks, financial transactions, computer networks) in a common battlespace picture providing the user with timely situation awareness, understanding and anticipation of threats, and support for effective decision-making in diverse environments. Combining numerous networks requires various data transformation techniques such as data association, alignment, and entity resolution.

The ultimate goal of this research is to allow a decision maker to have all network data in a layered network application where they can correlate and analyze activity and time occurrence in related networks to understand and potentially predict when a major event of interest is about to happen and where to expect it. Thus, Layered Network Analysis will allow users to apply network analysis methods (e.g. centrality measures, group detection algorithms) via visualization technology to the collective network.

The concept behind layered network analysis is derived from social network analysis and link analysis techniques. The collective network is layered because it would consist of many interconnected networks that were previously disparate. It is also multi-modal because the network will incorporate many different entity types (e.g. people, organizations, locations, objects). Having this data in a collective network will allow users to apply techniques derived from traditional SNA and link analysis measures. In addition, this may introduce new areas of research for metrics, entity resolution and pattern learning as the user will ultimately have to analyze data of multiple types.

There are many reasons behind a layered network analysis approach. First, an underlying unified network model is necessary that will allow multimodal and multi-dimensional layered network analysis to be possible [7]. This framework would serve as the connecting language and translation mechanism between the heterogeneous data networks. This would allow any network in any domain to be mapped and connected. Ultimately, users would analyze and visualize these collective networks. Further, the user would be able to select which layers he/she would want to view and focus the collective network based on space and time. This will drastically reduce complexity and any potential scalability issues with this approach. It will also deliver the appropriate data to the user based on his/her current situation.

Once the data is in a common network, new network analysis metrics can measure the importance of entities, groups, and their relationships across networks. Previously, traditional social network analysis metrics are designed to analyze only social relations [8]. Also, prior SNA metrics do not analyze attribute data, rather they measure connectivity (how well each node is connected to other nodes in the network). Thus, it is unclear how these metrics will be applicable. In addition, new threat patterns will need to be developed per given scenarios that can operate across networks, time, and entity types. The end user has previously done this manually.

At present, the research team is focusing on developing an approach to apply social network analysis metrics based on specific measures (e.g. eigenvector centrality, group detection) and visualization technology to the collective network. At this initial stage in the research, the team has identified two risks with this approach – scalability and visualization. However, the researchers feel that these two risks can be mitigated by providing only the data that user needs for his/her scenario. This can be accomplished either through selecting which data sources the user needs or through group detection algorithms to determine subgraphs related to the user's scenario.

3.1 Significance

Developing a layered network approach to network analysis will eliminate the current stovepipes and manual association that exist today. This approach would create an environment where users can visualize and analyze how numerous networks (entities and their relationships) are interconnected. This will allow the user to have all network data in a layered network application where they can correlate and analyze activity and time occurrence in related networks to better understand the battlespace. From this information, the user would be able to derive the most influential nodes and relationships, discover groups, and learn and predict the behavior of how these different network types interact and influence each other.

From the way that nodes and edges can connect these diverse network datasets (subgraphs) this can immediately allow users to learn and understand relationships in and across databases that they never knew existed. This can also help to infer new relationships, help uncover unknowns, and identify new groups and patterns across networks. Entities and relationships that were lost or unknown in one database could be discovered in another. Also, information and new patterns can be conveyed between data networks. Collectively this will enable users to act and predict by aiding in threat detection and prediction, provide informed course of action selection, and have a solid understanding to make a decision and act.

4 Application

Data-to-Decisions is one of seven science and technology (S&T) priorities of the Secretary of Defense [9]. The goal of this initiative is to shorten the cycle time from data

gathering to decision-making to address the challenge of insuring that the right, relevant and actionable information is provided to achieve the desired effect. With the increasing availability and relevance of open source information, the need to discover and identify threat signatures in complex, incomplete, imprecise and potentially contradictory large datasets has become a critical issue.

Recently, Lieutenant General David Deptula (now retired and the former Air Force Director of Intelligence) recognized that the armed services are 'swimming in sensors and drowning in data.' [10] The addition of new sensing capabilities are emerging and are delivering significantly much more data that can currently be processed. Because the current intelligence collection and analysis process is overwhelmed by the volume of information it must process to generate, analyze, and understand networks of interest, there is a disconnect between the output requirements and the inputs available for analysis [9]. As a result, the process results in high information loss, incomplete analysis and poor situation awareness and understanding.

Decision makers have a clear recognition that the detection and understanding of enemy networks is a critical factor in the building of situational awareness. However, developing the ability to be fully aware of enemy social networks is a challenging task. The results of the research outlined in this paper are aimed at assisting decision makers gather and fuse the most complete knowledge and understanding of geospatial, temporal and social events. This will enable the decision maker to assemble previously disconnected information about networks in a common battlespace picture, providing timely situation awareness, understanding and anticipation of threats, and support for effective decision-making in diverse environments. It will also help remove the burden of making mental correlations of observations and conclusions the user has drawn from one domain as additional information is made available from other domains.

Layered Network Analysis is an intuitive way to think – take for example the scenario about the W2-Glouscter ship. The British officer put together multiple data to come to his conclusion, decision, and action all in seconds.

The following meteorological example clearly demonstrates the power and applicability of Layered Network Analysis. Assume a severe thunderstorm that is demonstrating tornadic attributes. A meteorologist does not solely rely on one particular data type to analyze this potentially catastrophic event. For example, Doppler radar will tell the meteorologist where the storm is, precipitation, and where the storm is moving over time. However, the meteorologist needs more information to make an accurate forecast. Therefore the meteorologist will focus on various inputs, in addition to Doppler radar such as wind speed/direction, barometric pressure, temperature, cloud cover, etc. A key point is that each data type is different from every other data type; however when focused on a specific space and time, the data is all related and connected. The meteorologist depends on this data to make an accurate forecast and prediction of where the thunderstorm will move, how fast, and what severity it may have. This example also demonstrates how a user could focus on what is relevant to his/her current situation. The meteorologist is immediately focused on this localized thunderstorm and will likely analyze localized weather data, as opposed to developing a longer forecast (e.g. five day forecast) where the meteorologist will analyze more global trends.

5 Conclusion

Layered Network Analysis tools can provide a core piece to the Processing, Exploitation and Dissemination (PED) process helping automate the tedious process associated with the detection, recognition and understanding of enemy entity-relation networks. The Layered Network Analysis approach has shown promise in helping users quickly go from data-to-decisions by finding patterns in very large databases and facilitating the connection of bits of information into patterns that can be evaluated and analyzed. The technical area encompasses how people combine, interpret, store, and retain information, providing a quantitative evaluation of events that enhances a decision maker's ability to judge, appraise, and determine the relevance of emerging situations. The technology area is focused on providing the Air Force and its component units with the capabilities needed to achieve a higher level of enemy network comprehension [11]. Identifying relationships in large, dynamic, multi-modal layered graphs requires the development and integration of novel technologies. Layered Network Analysis will allow users to identify and detect emerging threats from large collections of data spatially and temporally. The result will be a dramatic improvement in situational awareness across multiple domains and significantly advance the current state-of-the-art network analysis capabilities by having an accurate and complete multi-dimensional understanding of the layered, dynamic network environment. Lastly, the Layered Network Analysis approach will provide an intuitive, logical process to decision-making that is agile and accurate.

6 Reference

[1] LaMonica, P.M. and Waskiewicz, T.V. (2011).

[2] Jones, D.G., Bolstad, C.A., Riley, J.M., Endsley, M.R., & Shattuck, L. (2003). Situation awareness requirements for the future objective force**.** *Proceedings of the ARL Collaborative Technology Alliances Conference,* Adelphi, MD: ARL.

[3] Klein, G. (1999). *Sources of Power: How people make decisions*. Boston, MA: MIT Press.

[4] Klein, G. (2003a). *Intuition at work: Why developing your gut instincts will make you better at what you do.* New York, NY: Doubleday.

[5] Klein, G. (2003b). *The power of intuition*. New York, NY: Doubleday.

[6] Klein, G. (2009). *Streetlights and shadows: Searching for the keys to adaptive decision making.* Boston, MA: MIT Press.

[7] Margitus, M.R., Tagliaferri, W.A., Sudit, M., and LaMonica, P.M. (2012). Dynamic graph analytic framework (DYGRAF): Greater situation awareness through layered multi-modal network analysis. *Proceedings of SPIE, Evolutionary and Bio-Inspired Computation: Theory and Applications VI*, April 2012.

[8] Peter LaMonica and Todd Waskiewicz. Developing an intelligence analysis process through social network analysis. *Proceedings of SPIE, Evolutionary and Bio-Inspired Computation: Theory and Applications II*, 6964, May 2008.

[9] Lemnios, Z.J. (2010). Statement testimony of the Honorable Zachary J. Lemnios Director, Defense Research and Engineering before the United States House of Representatives Committee on Armed Services Subcomittee on terrorism, unconventional threats and capabilities. Received from http://www.dtic.mil/cgi-bin/GetTRDoc?Location=U2&doc=GetTRDoc.pdf&AD=ADA517238.

[10] Deptula, D. (2009). Speech content. C4ISR Journal Conference, Arlington, VA.

[11] Hoffman, F.G. (2006). Complex irregular warfare: The next revolution in military affairs. *Orbis, 50*(3), 395-411.

IMPROVING THE RELIABILITY OF COMMUNICATION NETWORK USING MEMETIC ALGORITHM

[1]Deepak Kumar Singh, [2]K.K.Mishra, [3] Shailesh Tiwari and [4]A.K.Misra
[1234]*Department of Computer Science & Engineering*
MNNIT, Allahabad, India

ABSTRACT

A Communication network is used to facilitate communication among different parties. Though any network topology can be designed to implement a communication network but for a given problem we can choose a network topology which maximizes the reliability of communication network. This problem has many applications in telecommunications, electricity distribution, gas pipelines and computer communication industry. Since this problem belongs to an optimization problem, many authors have applied evolutionary techniques however there is still a need to apply optimization algorithm effectively so that this problem can be solved in minimum time. This paper makes such an attempt to solve this problem by using a memetic Algorithm.

Keyword: Network, Reliability, Cost and Multi-Objective Optimization

I. INTRODUCTION

Topological optimization of networks is an important problem in many fields such as telecommunications, electricity distribution, gas pipelines and computer communication. This refers to design an optimal network topology for one or more objective functions (network delay, bandwidth utilization, reliability, cost etc.). Since optimization problems are NP hard problems, many nature inspired algorithms have been applied for solving this problem. GA and Tabu search are the basis of many research proposal [3,4,5,13]

There have been several notable attempts in the literature to solve this optimization problem. Jan et al. [1] applied branch and bound technique to minimize cost of links of a network with a minimum network reliability constraint, this is computationally tractable for fully connected networks up to 12 nodes .Using a greedy heuristic, Agrawal et al.[2] maximized the reliability of a network . Jos´e Manue et al[3] optimize the budget of network topology. Bassam Al-Bassam et al.[4] has done the reliability optimization . Anup Kumar [5] optimized the diameter of network topology. Ventetsanopoulos and Singh [6] used a combination of heuristic search and branch bound to find most reliable network. Atiqullah and Rao [7] and Pierre et al. [8] used simulated annealing to find optimal designs for networks. Koh and Lee [9] used tabu search to find telecommunication network design that require some nodes (special offices) having more than one link while other others (regular offices) required only one link, while also using this link constraint as a surrogate for network reliability.

Although many methods are available yet there is a need to apply optimization algorithm effectively so that this problem can be solved in minimum time. This paper makes such an attempt to solve this problem by using a combination of local search and a variant of genetic algorithm [14].

The primary goal of this paper is to design a topology which has maximum reliability and satisfies the given cost constraints. The paper is organized into five sections. Section 2 presents some background on Genetic Algorithm and its variant .Section 3 describes step by step application of memetic algorithm For solving Problem. In Section 4, we discuss experimental results of the proposed algorithm. Finally, in Section 5 concludes the paper.

II. BRIEF HISTORY OF GENETIC ALGORITHM

Genetic algorithms are search algorithms which work according to the principle of natural selection on a population and behave according to the principle of 'Survival of the fittest'. More precisely genetic algorithm is a family of computational models inspired by evolution. At each generation, a new set of solutions are created by the process .Selection of the individual is done according to their fitness value in the solution space .This process leads to the evolution of populations of individuals that are better suited to their environment than the individuals that they were created from, just as in natural adaptation.

These algorithms encode a potential solution to a specific problem on a sample chromosome-like data structure and apply recombination operators to these

structures so as to preserve critical information related to the problem. Genetic algorithms are often viewed as function optimizers although the range of problems to which genetic algorithms have been applied is quite broad.

Genetic algorithms search for optimum value by using three operators.

A. Selection Operator

It is a genetic operator that chooses a chromosome from the current generation's population for inclusion in the next generation's population. Before making it into the next generation's population, selected chromosomes may undergo crossover or mutual depending upon the probability of crossover and mutation) in which case the offspring chromosome(s) are actually the ones that make it into the next generation's population.

This is achieved in following steps

a) Identify good solutions in population.
b) Make multiple copies of good solutions.
c) Eliminate bad solutions from the population so that multiple copies of good solutions can be placed in the population.

Some common methods [10, 11] for selection are:

a) Tournament Selection
b) Proportionate Selection
c) Ranking Selection

B. Crossover Operator

The chromosomes are exchanged between these two parents and offspring are produced. In general crossover operator recombines two chromosomes so it is also known as recombination. Crossover is intelligent search operator that exploits the information acquired by the parent chromosomes to generate new offspring. If both the parent has same genetic structure then offspring are just copies of the parent irrespective of cutting point but if parent have different genetic structure then offspring are different then parent. Thus, crossover is sampling process, which samples new points in search space. Generally crossover probability is very high like 1.00, 0.95, 0.90 etc.

Parents	01010101 11110000
Offspring	01010000 11110101

A number of variations on crossover operations are proposed and the simplest form is a single-point crossover. The parents are randomly selected based on the above mentioned selection scheme. A crossover point is randomly selected and the portions of the two chromosomes beyond this point are exchanged to form the offspring's. Some common methods for crossover are

a) Single point crossover
b) Uniform crossover[12]

C. Mutation Operator

The need for mutation is to maintain a good diversity of 1s and 0s in the population. After reproduction, crossover, and mutation are applied to the whole population, one generation of a GA is completed. The need for mutation [12] is to keep diversity in the population

III. PROPOSED APPROACH

Earlier in previous work, K.K.Mishra et al [14], have proposed a novel genetic algorithm by changing the crossover operator of genetic algorithms. The details of this algorithm had been taken from paper [14]. In genetic algorithm, we do not concentrate on the fitness value of parents involved in crossover. Also we randomly choose a cross site and as such we cannot predict the nature of generated children by traditional genetic algorithm. In our method we will concentrate on fitness of both the parents involved and will generate good children .We will not choose the cross site randomly .We will decide that site using the fitness of parents. Our crossover operator is based on the biological nature of crossover .In nature when parents (male, female) perform crossover children share the properties of parents. We will use the same basic for generating children. Let we are performing crossover operation between two parents P1 and P2 having the fitness value f1 and f2 and each of length L (chromosome length). We assume that fitness of male is always greater than female and cut point is to be determined by Male. We will calculate the crossover point by calculating ((f1/(f1+f2))*L) and ((f2/(f1+f2))*L) (If f1 is the fitness of male chromosome) and rounding off this to say variable C1 and C2. On the basis of this value C1, we will cut parents chromosomes at these sites and generate two children. The value C1 will always be less than L. Similarly we repeat the same process for C2 and generate two mutated children. We then perform binary tournament selection and select best mutant. Now we will show that application of this crossover and mutation will not affect randomness of genetic algorithm. As we are unaware about the nature of fitness value associated with each population, so fitness values will appear as random values associated with the parents and this operator will generate random values of children. So this operator will preserve the randomness of genetic algorithm][14].

III.I. APPLICATION OF MEMETIC ALGORITHM FOR SOLVING PROBLEM

In order to optimize the reliability of the network topology, we have used memetic algorithm. Since random initialization may cause infeasible solution. At initial stage prime's algorithm is used to generate initial population for the problem which perform a local search for a set of good solution then this variant of G.A has been applied to generate most reliable topology.

III.I.I. STATEMENT OF THE PROBLEM

As discussed in [13] the statement of problem can be explained as follows. A probabilistic graph G = (N, L, p) can be used to represent communication network. Where N and L are the set of nodes and links that corresponds to the computer sites and communication connections, respectively. The networks are assumed to have bi-directional links and, therefore, are modeled by graphs with undirected links. It is further assumed that the graph has no parallel (i.e. redundant) edges. Redundant links can be added to improve reliability, and the approach described here could be modified straightforwardly to include redundancy. The optimization problem is

$$\text{Minimum } Z = \sum_{i=1}^{N-1} \sum_{j=i+1}^{N} c_{ij}x_{ij}$$

Maximize R(x)

Where $x_{ij} \in \{0, 1\}$ is decision variable, c_{ij} is the cost of (i, j) link, R(x) is the network reliability.

The other problem assumptions are:

1. The location of each network node is given.
2. Nodes are perfectly reliable.
3. Each c_{ij} and p are fixed and known.
4. Links are either operational or failed.
5. The failures of links are independent.
6. No repair is considered.

III.I.II. NETWORK DESIGN USING MEMETIC ALGORITHM

Input: A Set of network topology is generated by primes algorithm and this work as initial population.

Output: network topology that achieves maximum reliability for the network.

Begin

STEP 1: Create an initial population by applying prime's algorithm at initial stage $N(P_0)$ (set of chromosomes are generated by assigning binary strings to edges(if present assign 1 else 0)) and then fitness (reliability) of each chromosome is calculated

STEP 2: Generate off spring population Q_t by using binary tournament selection recombination and mutation operator.

STEP 3: Create offspring population Q_{t+1} from P_{t+1} by using the tournament selection, crossover and mutation operators.

STEP 3.1: Tournament Selection: For each population generated randomly, randomly pick two members from Q_t and a tournament is done between two based on fitness function f(x).Winners are further propagated for crossover.

STEP 3.2: Crossover: Two strings are crossed based on the crossover point (jcross).

In proposed approach, crossover point=jcross=(f1(x)/f1(x)+f2(x))*Length (chromosome).

STEP3.3: Mutation: point=jcross=(f2(x)/f1(x)+f2(x))*Length(chromoso me). Perform tournament selection and pick best one.

These processes ultimately result in the next generation population of chromosomes that is different from the initial generation. Generally the average fitness will have increased by this procedure for the population.

STEP 4: Repeat steps 3 until a network with required reliability has been reached.

IV. EXPERIMENTAL RESULTS:

We have compared the results of proposed approach with the results produced by ga[13].It can be seen that networks generated by proposed approach has better reliability as compared to other approach. For calculating reliability two connectivity repair algorithm has been used.

initial parameters of the graph is shown below the no. of nodes:5

Cost of link between 1 and 2:-146
Cost of link between 1 and 3:-130
Cost of link between 1 and 4:-182
Cost of link between 1 and 5:-90
Cost of link between 2 and 3:-56
Cost of link between 2 and 4:-117
Cost of link between 2 and 5:-195
Cost of link between 3 and 4:-15
Cost of link between 3 and 5:-148
Cost of link between 4 and 5:-126
levels for different populations

The various Parameters for simple Genetic Algorithm were

Size of initial population=14
Desired level of fitness= 0.99999

Probability of Cross-over=0.7
Probability of mutation=0.5

Table:1

Serial no	Results Produced by GA	Results Produced by proposed Approach
1	0.890000	0.931230
2	0.801931	0.874563
3	0.878320	0.912365
4	0.974911	0.985623
5	0.973512	0.989632
6	0.983234	0.989546
7	0.974922	0.995236
8	0.974921	0.987456
9	0.974921	0.979421
10	0.888830	0.901546
11	0.966276	0.985621
12	0.982994	0.992564
13	0.982994	0.998546
14	0.887548	0.912345

Data after first Generation

Table:2:

Serial no	Results Produced by GA	Results Produced by proposed Approach
1	0.964425	0.975586
2	0.801931	0.823564
3	0.878320	0.895647
4	0.974911	0.984564
5	0.973512	0.985774
6	0.983234	0.994561
7	0.974922	0.985623
8	0.974921	0.995264
9	0.974921	0.985641
10	0.888830	0.895642
11	0.966276	0.978521
12	0.982994	0.998546
13	0.982994	0.989999
14	0.887548	0.902412

Data after Second Generation

Table:3

Serial no	Results Produced by GA	Results Produced by proposed Approach
1	0.964425	0.985641
2	0.801931	0.856451
3	0.878320	0.885644
4	0.974911	0.985667
5	0.973512	0.984561
6	0.983234	0.994215
7	0.974922	0.987562
8	0.974921	0.985745
9	0.974921	0.979888
10	0.888830	0.901487
11	0.966276	0.978874
12	0.982994	0.989878
13	0.982994	0.998546
14	0.887548	0.912456

Data after Third Generation

Table:4

Serial no	Results Produced by GA	Results Produced by proposed Approach
1	0.789654	0.99999
2	0.795698	0.861931
3	0.828320	0.878320
4	0.865412	0.974911
5	0.756456	0.953512
6	0.836546	0.973234
7	0.885647	0.964922
8	0.796546	0.954921
9	0.845612	0.974921
10	0.825645	0.918830
11	0.812364	0.966276
12	0.865436	0.942994
13	0.895647	0.971564
14	0.785461	0.887548

Data after Fourth Generation

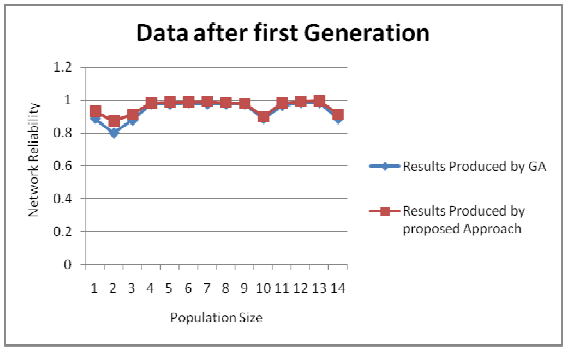

Graph-1

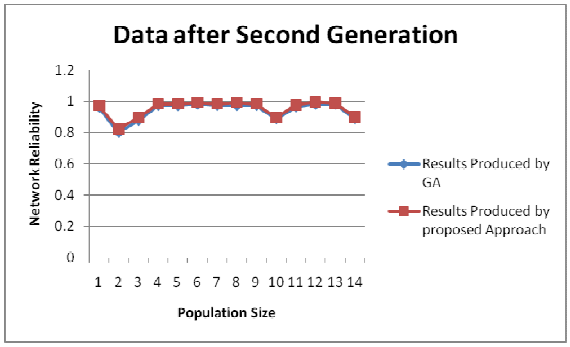

Graph-2

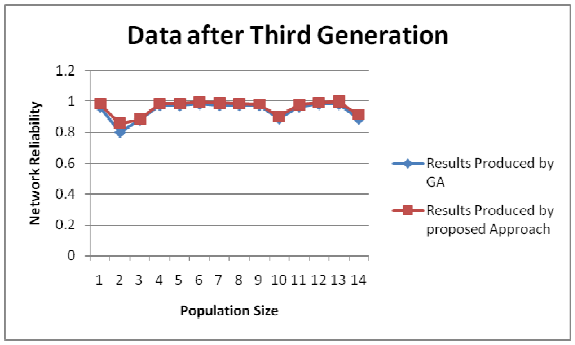

Graph-3

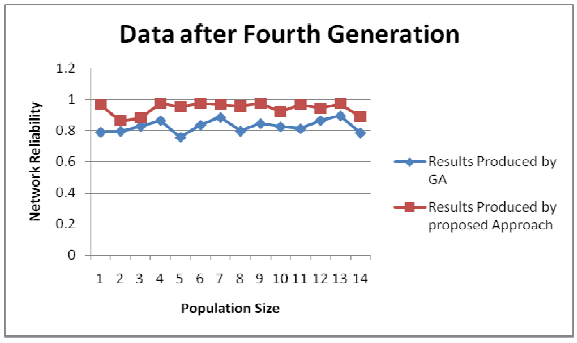

Graph-4

V. CONCLUSIONS

Experiments prove that the results generated by the proposed approach are good. Generation of unreliable network has been avoided by the use of local search. This local search produces good population at initial population. When this population is supplied to the proposed algorithm it has produced better results. Comparisons are shown in graph 1 to 4.

RERRENCES:

[1] H. Jan, F. J. Hwang and S. T. Cheng. "Topological optimization of a communication network subject to a reliability constraint "IEEE Trans. Reliability. Vol 42 pp.63-70, 1993.

[2] K. Agarwal, Y. C Chopra, and J, S, Bajwa." Reliability evaluation by network decomposition. " IEEE Trans. Reliability, Vol. R-31, pp. 355 358 1982.

[3] Jos´e Manuel Guti´errez L´opez, Mohamed Imine and Ole Brun Madsen "Network Planning Using GA For Regular Topologies".

[4] Bassam Al-Bassam, Abdulmohsen Alheraish, Saad Haj Bakry, "A tutorial on using genetic algorithms for the design of network topology".

[5] Anup Kumar, Rakesh M. Pathak, M. C. Gupta, "Genetic algorithm based approach for designing computer network topology".

[6] N. Ventetsanopoulos and I .Singh. "Topological optimization of communication networks subject to reliability constraints. Theory vol. 15 pp 63-78.1986.

[7] M. Atiqullah and S. S. Rao, "Reliability optimization of communication network using simulated annealing," Microelectronics and Reliability, vol. 33 pp 1303-1319 ,1993

[8] Pierre M. A. hyppolite ,J. M Bourjolly ,and O.Dioume, "Topological design of computer communication networks using simulated annealing " Eng. Applicat, Artificial Intell, vol .8 pp. 61-69 1995.

[9] Glover, M, Lee, and J,Ryan , " Least-cost network topology design for a new service: An application of a tabu search ."Ann. Opor. Res vol. 33. pp 351-362 1991.

[10] D.E. Goldberg, "Genetic Algorithm in Search, Optimization, and Machine Learning" Addison Wesley Publishing Company, 1989.

[11] Tomasz D. Gwiazda, *Genetic Algorithms Reference Vol.1 Crossover for single-objective numerical optimization problems*, Tomasz Gwiazda, Lomianki, 2006. ISBN 83-923958-3-2.

[12] Sywerda, G. 1989. Uniform crossover in genetic algorithms. In Proceedings of the Third international Conference on Genetic Algorithms. J. D. Schaffer, Ed. Morgan Kaufmann Publishers, San Francisco, CA, 2-9.

[13] Kumar, A.; Mishra, K.K.; Misra, A.K.; , "Optimizing the reliability of communication network using specially designed genetic algorithm," *Nature & Biologically Inspired Computing, 2009. NaBIC 2009. World Congress on* , vol., no., pp.499-502, 9-11 Dec. 2009doi: 10.1109/NABIC.2009.5393371

[14] K.K.Mishra, Anoj kumar, Shailesh Tiwari and A.K.Misra, "A Variant of Genetic Algorithm for generating test cases for white box testing" 3rd International Conference on Machine Learning and Computing(ICMLC2011) Singapore, Proceeding of IEEE, February from 26-02-2011 to 28-02-2011

Evaluating Chronic Cystic Fibrosis Severity Using Artificial Neural Networks

J. Redfield[1], D. Palmer[2], D. J. Conrad[3], and P. Salamon[1]
[1] Department of Mathematics and Statistics, [2] Department of Biology,
San Diego State University, San Diego CA
[3] UC San Diego Division of Pulmonary & Critical Care Medicine, La Jolla, CA

Abstract - *We present an ensemble of artificial neural networks to predict the severity of chronic cystic fibrosis within an individual by comparing against fifty patients ranked ordinally by increasing disease severity. The neural networks were programmed using Matlab and trained to minimize the sum-of-squared-error between the networks' rankings and the fifty actual rankings. The training data was subjectively but professionally ranked by one of us (DJC). Variables were chosen from the data collected in the UCSD cystic fibrosis clinic to use as input parameters for the networks. The resulting data matrix was then used by an ensemble of neural networks in training, validation and testing to ultimately produce a prediction of the chronic severity of cystic fibrosis within a patient. Between any two patients, the networks were able to correctly identify the more severe case 86% of the time. The goal was to capture Dr. Conrad's severity index, implied by the ranked set provided, to use on patients outside of that data set in assessing their chronic disease severity. The resulting neural networks have the potential to provide a useful diagnostic tool for physicians treating CF patients.*

Keywords: Machine learning, neural networks, cystic fibrosis

1 Introduction

We set out to develop an ensemble of artificial neural networks (ANNs) to predict chronic disease severity within cystic fibrosis patients as an experienced pulmonary physician would. ANNs are a form of machine learning algorithm based on the functionality and structure of a biological neural network, as observed in the brain. Used to observe complex trends and patterns in a set of data, they are capable of applying sets of non-linear equations to inputs to achieve a desired outcome. These equations can be reproduced to apply to further data, which gives rise to the predictive capabilities that this project utilizes.

2 Materials and Methods

The data were collected from patients cared for in the UCSD Adult Cystic Fibrosis Clinic (ACFC). Fifty patients were selected and ordinally ranked by Dr. Douglas J. Conrad, director at the ACFC, in order of increasing disease severity ranking 1 to 50 as a training cache for the ANNs. The 50 patients and their corresponding 14 variables were compiled as a matrix, along with their actual rankings, and imported to Matlab. Such variables included results from lung function tests (FEV1, FVC, FEV1/FVC), physical descriptions (age, height, weight, gender, BMI) and longitudinal regression values based on FEV1 vs. time graphs (m, b, r^2, se_m, se_b). For each patient, only the best FEV1 value from the previous year was considered.

2.1 Programming the ANN

To obtain the artificial neural networks, a progression of training, validating and testing steps were taken to develop the ability to predict with an acceptable amount of error. In training, each network is supplied with a set of data as inputs, and through a series of equations, returns an answer. Once the tested outputs of the network accurately reflect the answers provided in the training data, the ANNs can then be used to classify future data.

For an ANN to follow the trends in cystic fibrosis data, the variables were run through a series of equations, deemed "layers." Four matrices of random numbers were generated, two representing weights and two being biases. Let *w1* and *w2* denote the weight matrices, *b1* and *b2* the biases, and *in* represent the vector of one patient's inputs. The layout of a single-hidden layer ANN is as follows:

$$hidden\ layer = squash((in \times w1) - b1) \quad (1)$$

$$CF\ severity = (hidden\ layer) \times w2 - b2 \quad (2)$$

$$squash(x) = \frac{1}{1+e^{-x}} \quad (3)$$

Once the severity has been run through the above layers for each patient, the ANN returns its predicted severity, and the error is calculated between its prediction and the actual answer. The weights and biases are adjusted using Matlab's fminsearch optimization function, and after each adjustment, the squared error was calculated between the ANN outputs and the actual provided patient severity. Fminsearch is set to repeat these adjustments until a minimum in the total calculated error is found. However, if the entire set of 50 patients were to be used in training a network, there would be no unknowns upon which to test its accuracy. For this reason, only thirty of the fifty patients, or 3/5 of the original data set, were randomly selected and used to train each ANN.

The remaining 20 patients are randomized and split evenly into validation and testing groups. In validation, the purpose is to halt the fminsearch function once a network begins to over-train. Between the fminsearch iterations of the training set, the squared error is calculated and recorded for the ten validation patients. Once the weights and biases have become overly specific for the training set, the validation error will halt the network training (Figure 2). The test set for the network is recorded along with the adjusted parameters.

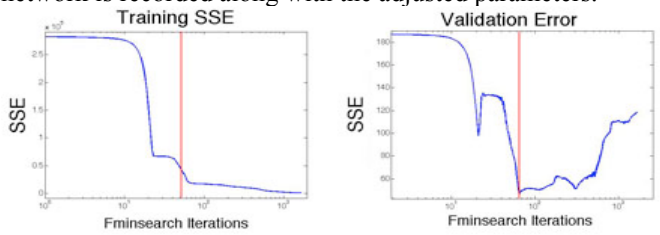

Figure 2. Training and Validation Errors for an ANN

2.2 Testing

A set of twenty networks' parameters and test sets was compiled. Each patient defined to be in a test set was run through the layers using the corresponding network's weights and biases, and averaged with the other participating networks. Thus, each ANN only "voted" on the severity of inputs that were not used in its training or validation processes. The averaged output consists of fifty patients, to be compared against the actual severities provided on the original fifty-patient datasheet.

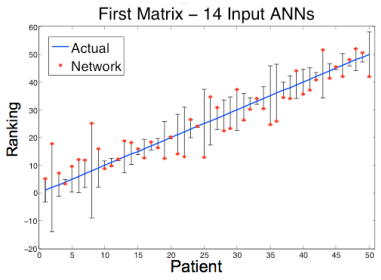

Figure 3. Voting of 14-input ANNs

2.3 Subsequent Inputs

Following the testing of the original networks, the importance of the 14 training variables was determined. Using the computational program R and the randomForest toolbox, FVC, FEV_1, and obstruction ratio were found to hold the strongest predictive power for CF severity. A new ensemble of 50 ANNs were trained and tested using only the FVC, FEV_1, and obstruction ratio as training features (See figure 5A).

A new dataset was then assembled including several new inputs. Multiproduct and powerproduct attempt to place emphasis on age, and were generated from the equations:

$$multiproduct = Age \times FEV1\% \quad (4)$$

$$powerproduct = FEV1\% \times e^{\frac{Age}{10}} \quad (5)$$

Other variables included the Brasfield score and its components. The randomForest toolbox predicted multiproduct, FEV1, FVC, powerproduct, obstruction ratio, and the overall Brasfield score as the most important variables of the new set (Table 1). An ensemble of ANNs were trained from these six variables and tested for their performance. For each of the 3 sets of inputs, the R^2 values were calculated (see Table 2). The ranking accuracy was defined by the ability of the ANNs to identify the more severe case of CF for any two patients.

First Inputs	Node Purity	Second Inputs	Node Purity
FVC	3018.8	Multiproduct	2308.5
FEV1	1960.8	FEV1	1217.0
Obstruction Ratio	1086.6	FVC	960.5
Age	616.3	PowerProduct	832.5
BMI	593.3	Obstruction Ratio	622.3
Weight	452.0	Brasfield	563.9
m	381.0	Cystic	481.3
r2	377.9	Age	456.1
b	299.5	BMI	293.1
Patient ID	290.1	Overall	254.1
Height	258.6	Patient ID	160.1
sey	219.2	Height	145.4
seb	201.0	Linear	131.4
sem	155.7	Exp	73.1
Gender	21.5	Gender	16.5
		LgLS	13.2

Table 1. Sets of Inputs : The Initial and the Modified

3 Conclusions

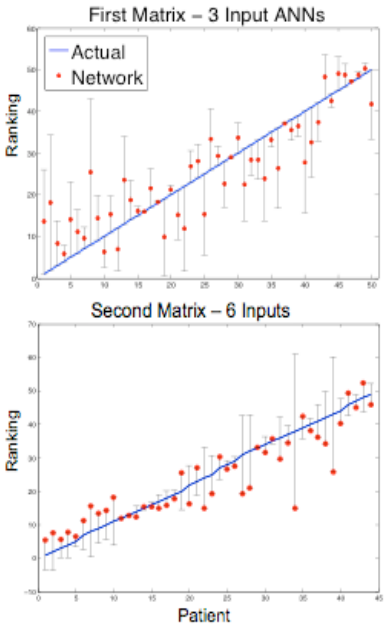

Figure 5. Voting of 3-Input and 6-Input ANNs

Matrix	Inputs	Train Time (min)	R^2	Ranking Accuracy (%)
1	14	360	.8261	86.67
1	3	10	.7845	85.14
2	6	30	.8109	88.48

Table 2. ANN Voting Results

The ensembles of neural networks were all able to train from the provided inputs and accurately vote upon unseen CF patients, as shown in Table 2. The variables FEV1, FVC, and obstruction ratio appeared to hold the greatest ability to train the ANNs from the original list of inputs. Of the second list of inputs, the Brasfield Index, multiproduct, and powerproduct were also found to be useful in ANN training. Future directions include expanding the parameters used, comparing the accuracies of multiple networks using the different inputs, obtaining rankings from other CF experts, and integrating the developed neural networks into a comprehensive GUI interface application being developed by the SDSU Cystic Fibrosis Group.

This work was made possible by NSF grant UBM 0827278 to A.M. Segall and P. Salamon. We thank the SDSU UBM and Cystic Fibrosis Groups for their guidance and many helpful discussions.

A Transient Current Based Transmission line Protection Using Neuro-Wavelet Approach in the Presence of Static Var Compensator

G.Ravikumar[1], S.S.TulasiRam[2], Shaik Abdul Gafoor[3]
[1] Electrical Engineering Department , Research Scholar, JNT University,Kakinada,Andhrapradesh,India
[2]Electrical Engineering Department , Professor, JNT University,Hyderabad,Andhrapradesh,India
[3]School of Electrical Engineering, Professor, Vignan University, Vadlamudi, Guntur, Andhrapradesh, India.

Abstract *- The SVC (Static Var Compensator) based on voltage source converter (VSC) is used for voltage regulation in transmission and distribution system. The SVC can rapidly supply dynamic VARs required during system faults for voltage support. The apparent impedance is influenced by the reactive power injected or absorbed by the SVC, which will result in the under reaching or over reaching of distance relay. This paper presents simulation results of the application of distance relays for the protection of transmission systems employing flexible alternating current transmission controllers such as SVC. The complete digital simulation of the Static Var Compensator within a transmission system is performed in the MATLAB/Simulink environment using the Power System Block set (PSB). This paper presents an efficient method based on wavelet transforms, fault detection, classification and location using ANN technique which is almost independent of fault impedance, fault distance and fault inception angle .*

Keywords: *Distance relay, Flexible alternating current transmission controllers, SVC, power system protection.*

1 Introduction

The performance of a power system is affected by faults on transmission lines, which results in interruption of power flow. The quick detection of faults and accurate estimation of fault location, helps in faster maintenance and restoration of supply resulting in improved economy and reliability of the power supply. Wavelet Transform (WT) is an effective tool in analyzing transient voltage and current signals associated with faults both in frequency and time domain. Chul-Hwan Kim, et al [1] have used Wavelet Transforms to detect the high impedance arcing faults. Joe-Air Jiang, et al [2] has used Haar Wavelet to detect dc component for identifying the faulty phases. The distance protection schemes using WT based phasor estimation are reported in [3]&[4].

Some research has been done on the performance of the distance relay for a transmission system with different FACTS[5-6] devices. The impact of SVC on the performance to the type of the FACTS controller[10,11], the application for which it is used for and its location in the power system. The question of whether the existing transmission line distance protection relays would perform well with the installation of shunt FACTS controllers in the transmission line has been recently investigated and reported in [8]-[9]. The results of these investigations have shown that midpoint shunt FACTS compensation can affect the distance relays with regards to impedance measurement, phase selection and operating times. It has been reported also the observation of the over-reaching and under- reaching phenomena in the presence of a midpoint SVC controllers.

Due to fast developing communication techniques, it is possible to develop communication-aided high-speed digital protection scheme, which suits the EHV transmission. Even better performance can be achieved using two terminal synchronized sampling of signals. The Global Position System (GPS) based algorithms with better performance and accuracy have been proposed. There is always a need to develop innovative methods for transmission line protection. In this paper, Wavelet Multi Resolution Analysis is used for detection, classification and location of faults on transmission lines. Detail D1 coefficients of current signals using Bior1.5 wavelets at both the ends are used to detect, classify and location of fault.

This paper presents an efficient method based on wavelet transforms both fault detection, classificationand location using artificial Neural network, which is almost independent of fault impedance, fault location and fault inception angle of transmission line fault currents with FACTS controllers.

2 Wavelet Analysis

Wavelet Transform (WT) is an efficient means of analyzing transient currents and voltages. Unlike DFT, WT not only analyzes the signal in frequency bands but also provides non-uniform division of frequency domain, i.e. WT uses short window at high frequencies and long window at low frequencies. This helps to analyze the signal in both frequency and time domains effectively. A set of basis functions called Wavelets, are used to decompose the signal in various frequency bands, which are obtained from a mother wavelet by dilation and translation. Hence the amplitude and incidence of each frequency can be found precisely. Wavelet Transform is defined as a sequence of a

function {h(n)}(low pass filter) and {g(n)}(high pass filter). The scaling function φ(t) and wavelet ψ(t) are defined by the following equations φ(t) = √2∑ h (n) φ(2t-n), ψ(t) = √2∑ g (n) φ(2t-n) Where g(n) = $(-1)^n$ h(1-n) A sequence of {h(n)} defines a Wavelet Transform. There are many types of wavelets such as Haar, Daubachies, and Symlet etc. The selection of mother wavelet is based on the type of application. In the following section a novel method of detection and classification of faults using Multi Resolution Analysis of the transient currents associated with the fault is discussed.

3 System Under Study

Figure-1 shows the single line diagram of the system considered along with the various blocks of the proposed scheme. Two 200-km parallel 500kV transmission lines terminated in two 9000-MVA short-circuit levels (SCLs) sources and the angle difference 20^0 with 60HZ.The 100MVA and FACTS controller is installed in the middle of the second transmission line.

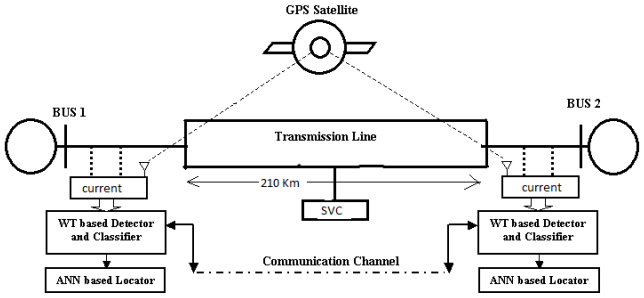

Fig.1.Power system model with SVC Controller

A 300-Mvar Static Var Compensator (SVC) regulates voltage on a 6000-MVA 500-kV system. The SVC consists of a 500kV/16-kV 333-MVA coupling transformer, one 109-Mvar thyristor-controlled reactor bank (TCR) and three 94-Mvar thyristor-switched capacitor banks (TSC1 TSC2 TSC3) connected on the secondary side of the transformer.

4 Detection and classification of Faults

Wavelet Multi Resolution Analysis is used for detection, classification and location of faults on transmission lines. Detail D1 coefficients of current signals at both the ends are used to detect and classify the type of fault. The three phase currents of the local terminal are analyzed with Bior.1.5 mother wavelet to obtain the detail coefficients ($D1_L$) over a moving window of half cycle length. These $D1_L$ coefficients are then transmitted to the remote end. The detail coefficients received from the remote bus ($D1_R$) are added to the local detail coefficients ($D1_L$) to obtain effective D1 coefficients ($D1_E$). The Fault Index ($\mathbf{I_{f1}}$) of each phase is then calculated as $I_{f1} = \Sigma \left| D1_E \right|$.

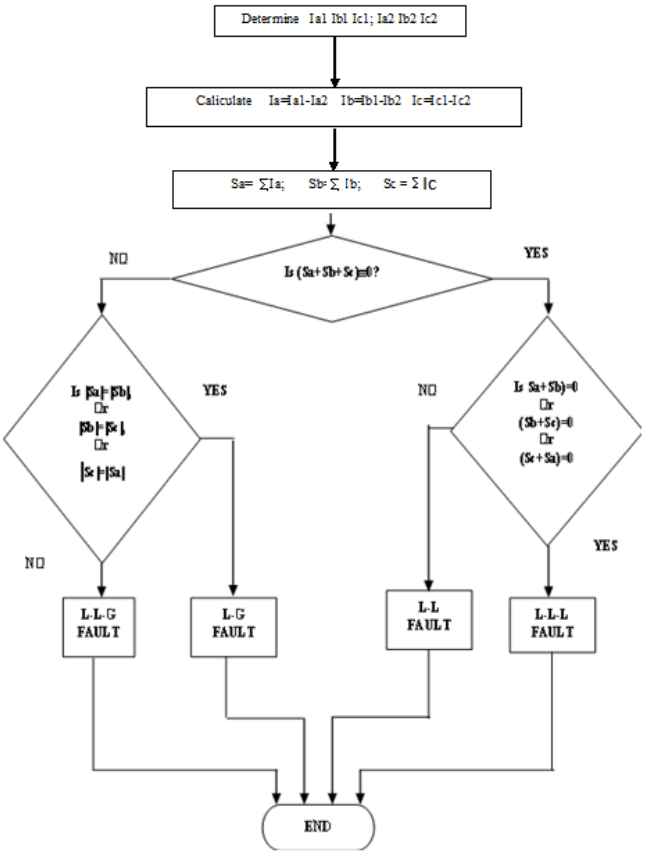

Fig 2. Flow chart for the fault classification

The types of faults considered in the analysis are L-G, L-L-G, L-L, L-L-L, faults. The simulations show that fault inception angle has a considerable effect on the phase current samples and therefore also on Wavelet transform output of post-fault signals. As the waves are periodic, it is sufficient to study the effect of inception angle in the range of 0^0 to 180^0. The complete flow chart for the fault classification is as shown in Figure 2.

5 Estimation of Fault Location

Subsequent to detection and classification of fault, estimation of fault location is carried out using ANNs [12-13]. For this purpose the three phase currents of the local terminal are decomposed with Bior1.5 mother wavelet over a half cycle window are obtained. This is done concurrently with the decomposition D1 used for fault detection and classification to speed up estimation of fault location.

For an LG, LLG and LLLG fault, D1 decomposition of any one faulty phase can be used to estimate fault location. . The details of the ANN architecture descibed as follows :

Input layer : Detail D1 coefficients of current signals using Bior1.5 wavelets at both the ends are used location of fault.
Number Layers : two
Number of neurons : 18
Transfer function : Log-Sigmoid

6 Result Analysis

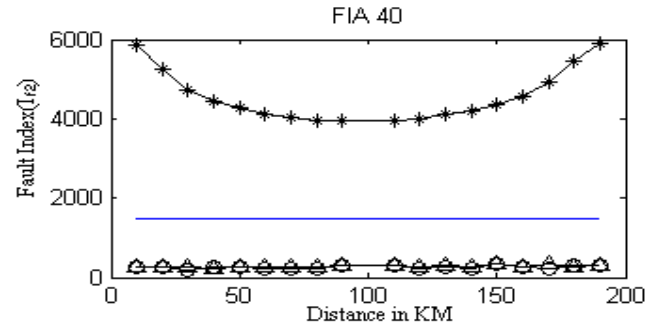

(a)

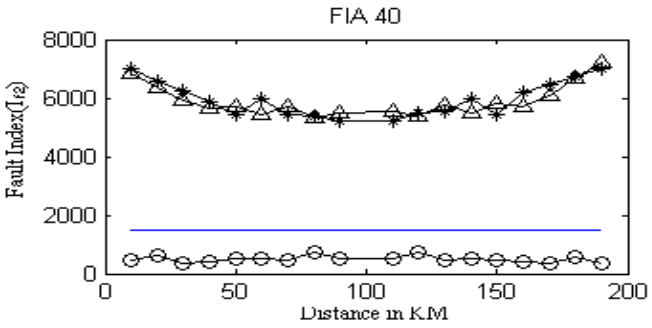

(b)

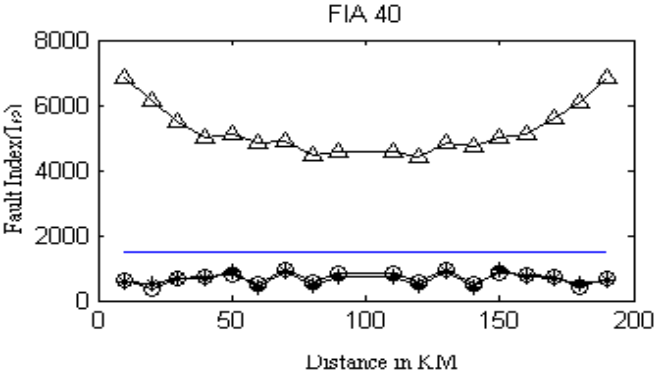

(c)

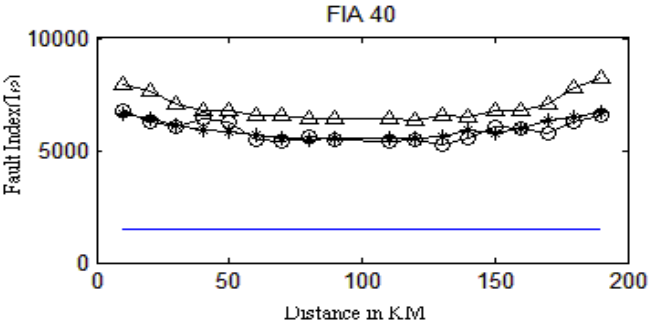

(d)

Fig3.Variation of fault index for transmission line without SVC at 40^0 (a) LG Fault on Phase A (b) LLG Fault on CAG (c) LG Fault on Phase C (d) Variation of fault index for LLLG Fault on Phase ABC.

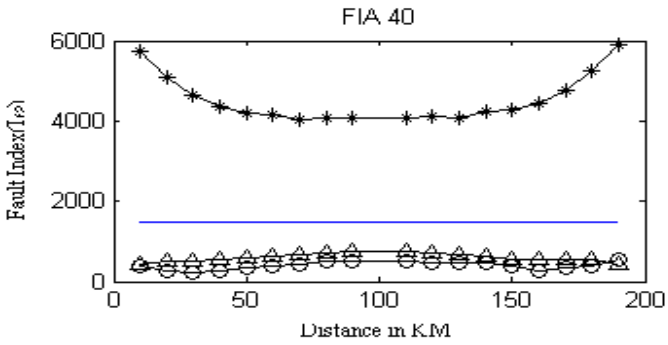

(a)

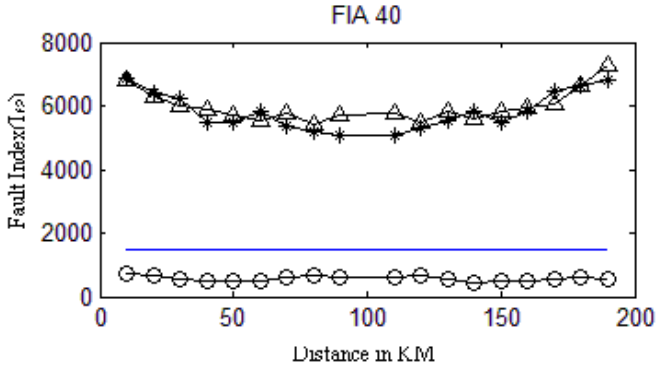

(b)

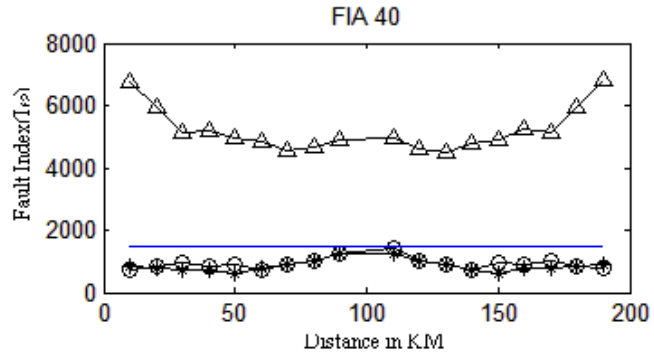

(c)

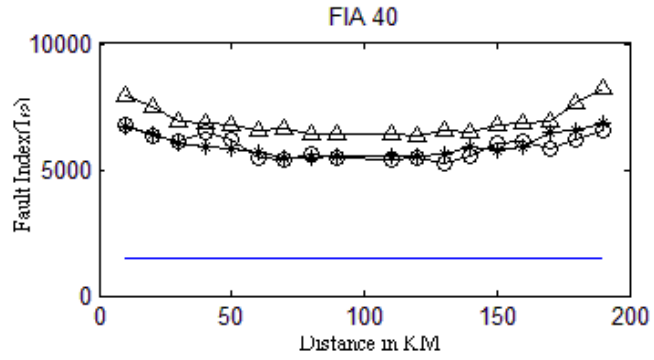

(d)

Fig 4.Variation of fault index at Fault Inception angle 40^0 (a)for LG fault on Phase A with SVC Controller(b)for LLG fault on Phase CAG with SVC Controller(c) for LG fault on Phase C with SVC Controller (d) for LLLG fault on Phase ABCG with SVC Controller

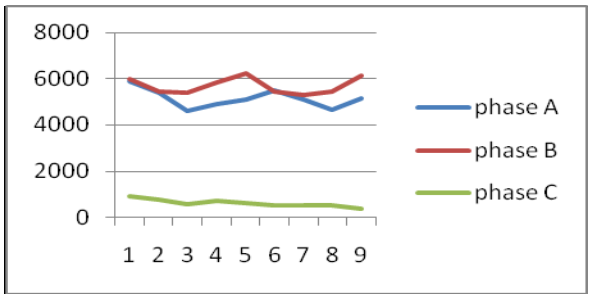

(a)

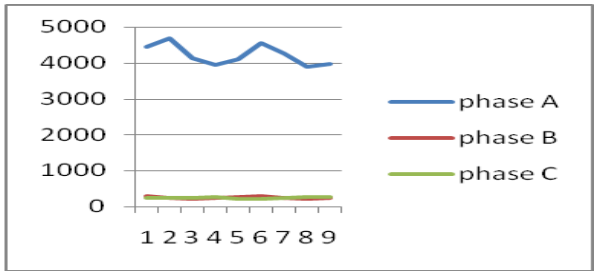

(b)

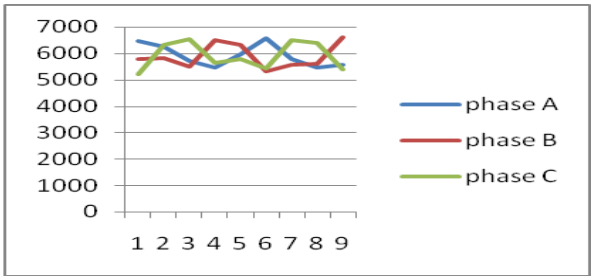

(c)

Fig 5.Variation of fault index at 60km from Bus1(a)for LLG fault on Phase AB without SVC controller(b)for LG fault on Phase A without SVC(c)for LLLG fault on Phase ABC without SVC controller

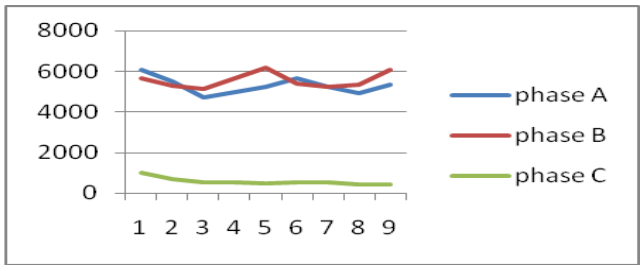

(a)

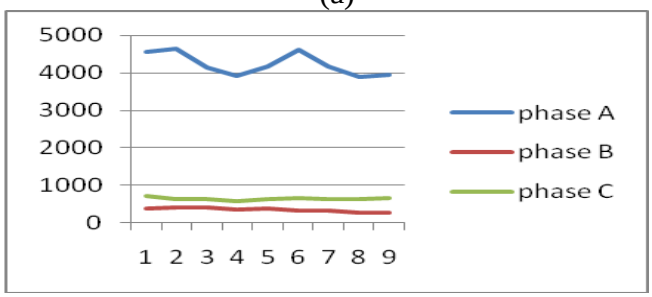

(b)

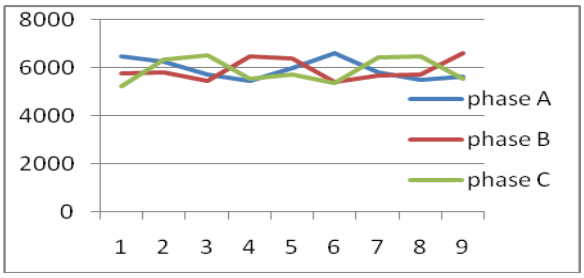

(c)

Fig 6.Variation of fault index at 60km from Bus1(a)for LLG fault on Phase AB with SVC controller(b)for LG fault on Phase A with SVC controller(c)for LLLG fault on Phase ABC with SVC controller

Table-I: ANN based fault location Analysis

Fault type	Actual Distance	ANN distance	error	%error
ag	40	39.996	0.004	0.0
	80	80.002	-0.002	0.0
	120	119.968	0.032	-0.02
	160	159.066	0.934	-0.47
	200	197.2	2.8	1.4
bg	40	38.8	1.2	0.60
	80	75.188	4.812	-2.41
	120	116.86	3.14	-1.571
	160	150.72	9.2	-4.64
	200	198.33	1.66	0.83
bc	40	39.25	0.742	0.37
	80	74.168	5.832	2.92
	120	128.54	-8.54	4.27
	160	157.596	2.4	1.2
	200	194.208	5.792	2.9
abcg	40	39.974	0.026	-0.001
	80	80.19	-0.19	0.009
	120	123.544	-3.544	1.77
	160	159.84	0.158	-0.008
	200	191.318	8.682	-4.34

The fault index of three phase currents for transmission line is shown in Figure-3 and the fault index of three phase currents with SVC controllers are placed at middle of the transmission line shown in Fig 4. It is observed that the fault index of faulty phase is large compared to those of healthy phases. Thus the number of faulty phases is determined by comparing the Fault Index (I_{f1}) with a Fault Threshold (T_{f1}).The proposed algorithm has been tested for all types of faults, considering variations in fault locations and fault incidence angles (θ) in the range 0-180^o. This scheme is proved to be effective in detecting and classifying various types of faults. Fig 5-a,b,c shows the variation of three phase currents D1 Coefficients of Phase A, Phase B &Phase C for LG,LLG&LLLG fault on transmission line without SVC Controller. Figu 6-a,b,c shows the variation of D1 coefficients for LG,LLG and LLLG transmission line with SVC Controller. Table. I shows the fault distance location analysis

7 Conclusions

Wavelet based multiresolution analysis approach can be successfully applied for effective detection and classification and location of faults in transmission lines. Fault detection and classification can be accomplished with in a half a cycle using detail coefficients of currents at both the ends. Fault location can be estimated with a fair degree of accuracy from the approximate decomposition of phase voltages and currents of local end using ANNs. The proposed protection scheme is found to be fast, reliable and accurate for various types of faults on transmission line fault currents with FACTS controllers, at different locations and with variations in incidence angles

8 References

[1] Chul-Hwan Kim, Hyun Kim, Young-Hun Ko, Sung-Hyun Byun, Raj K. Aggarwal, AllanT. Johns, "A Novel Fault-Detection Technique of High-Impedance Arcing Faults in Transmission Lines Using the Wavelet Transform*", IEEE Trans. on Power Delivery*, Vol.17 No.4, October 2002, pp. 921-929.

[2] Joe-Air Jiang, Ping-Lin Fan, Ching-Shan Chen, Chi-Shan Yu, Jin-Yi Sheu, "A Fault Detection and Faulted Phase Selection Approach for Transmission Lines with Haar Wavelet Transform", Transmission and Distribution Conference and Exposition 2003, IEEE PES, 7-12, September 2003, Vol.1, pp.285-289.

[3] Feng Liang, B. Jeyasura, "Transmission Line Distance Protection Using Wavelet Transform Algorithm". *IEEE Trans. on Power Delivery*, Vol.19, No.2 April 2004, pp. 545-553.

[4] A.H. Osman, O.P. Malik, "Transmission Line Distance Protection Based on Wavelet Transform", *IEEE Trans. on Power Delivery*, Vol.19, No.2, April 2004, pp.515-523.

[5] P.K. Dash., , A.K. Pradhan, , G. Panda, , A.C. Liew, "Adaptive relay setting for flexible AC transmission systems (FACTS) ," Power Delivery, IEEE Transactions on , Volume: 15 Issue: 1 , Jan 2000 Page(s): 38 -43

[6] T. S. Sidhu, R.K. Varma, P.K. Gangadharan, F.A. Albasri and G.R. Ortiz, "Performance of Distance Relays on Shunt-FACTS Compensated Transmission Lines," *IEEE Trans. on Power Del.*, vol. 20, no. 3, pp.1837-1845, July 2005.

[7] F.A. Albasri, T. S. Sidhu, R.K. Varma, "Impact of Shunt-FACTS on distance protection of Transmission Lines, " in *Power Delivery*, Vol.18. No.1, January 2003, pp. 34-42.

[8] F.A. Albasri, T.S. Sidhu, R.K. Varma, "Performance Comparison of Distance Protection Schemes for Shunt-FACTS Compensated Transmission Lines," *IEEE Trans. on Power Del.*, vol.22, no. 4, pp.2116-2125, October 2007.

[9] Joe-Air Jiang, Ping-Lin Fan, Ching-Shan Chen,Chin_Wen Liu, "A New Protection Scheme for Fault Detection ,Direction Discrimination, Classification, and Location in Transmission Lines", *IEEE trans. On Power Del*

[10]N.G. Hingorani and L. Gyugyi, *Understanding FACTS Concepts and Technology of Flexible AC Transmission Systems*, John Wiley & Sons, November 1999.

[11]R.M. Mathur and R.K. Varma, *Thyristor-based FACTS Controllers for Electrical Transmission Systems*, Wiley-IEEE Press, February 2002.

[12]Fransisco Martin, Jose A. Aguado, "Wavelet-Based ANN Approach for Transmission Line Protection" , IEEE Trans. on Power Delivery, Vol.18, No.4. October 2003. pp.1572-1574.

[13]M. M. Tawfik, M. M. Marcos, "ANN-Based Techniques for Estimating Fault Location on Transmission Lines Using Prony Method", *IEEE Trans. on Power Delivery*, Vol.16,No.2, April 2001, pp. 219-224

Learning the Size of the Sliding Window for the Collocations Extraction: a ROC-based Approach

Fethi Fkih[1] **and Mohamed Nazih Omri**[1]
[1]MARS Research Unit, Faculty of Sciences of Monastir,
University of Monastir, Monastir, Tunisia

Abstract - *In the statistical terminology field, the collocations extraction from specialized textual corpus is done by computing the joint frequency of a given pair of words inside a sliding window of fixed size. The choice of the window size, which provides the best performance to the system of collocations extraction, remains a problem in this area. In this paper, we propose an efficient approach based on ROC curves for the automatic learning of the window size used for the collocations extraction.*

Keywords: collocation extraction, sliding window, window size, ROC curves, Area Under Curve

1 Introduction

The knowledge extraction from text documents is an important task in the Natural Language Processing (NLP) field. Such knowledge can be used in several applications such as machine translation, document classification, automatic indexing, construction of linguistic resources, etc.

In this paper we will focus on the extraction of a particular kind of knowledge, i.e. word collocations, which are characterized by specific linguistic and statistical properties. Indeed, the extraction of collocations requires two main tasks: recognizing interesting collocations in the text; classifying them according to classes predefined by the expert.

The techniques used for the collocations extraction are often based on the calculation of the joint frequency of a pair of words within a sliding window of fixed size. The choice of the ideal window size (for a given knowledge field) is considered as a problem in the terminology extraction field. However, we don't find in the literature any exact rules to justify this choice. So, it's interesting to propose a new technique for the window size learning based on empirical studies using ROC curves.

The remainder of this paper is structured as follows. Section 2 presents the theoretical basis of the statistical approach for collocations extraction. Then, we propose our approach based on the ROC curves technique. Finally we conclude with an exposition of the obtained results.

2 Collocations extraction: state of the art

In this section, we present an overview of the terminology extraction field through a statistical approach. Next, we introduce the problematic of the window size choice.

2.1 Definition

In the statistical approach, collocation is considered as a sequence of words (n-gram) among millions of other possible word sequences. In Church and Hunks work [1], a collocation as defined is a pair of words that appear together more often than expected. Benson in [2] defines collocation as an arbitrary and recurrent word combination. Smadja in [3] consider that these definitions don't cover some aspects and properties of collocations that affect a number of machine applications. So, he enriches these definitions by four properties:

- Collocations are arbitrary: collocations are difficult to produce for second language learners; it's difficult to translate a collocation word-for-word.
- Collocations are domain-dependent: they are related to the treated knowledge area (medical, biologic, etc.).
- Collocations are recurrent: these combinations are not exceptions; they are very often repeated in a given context.
- Collocations are cohesive lexical clusters: the presence of one or several words of the collocations often implies or suggests the rest of the collocation

The remainder of this paper, we adopt this definition. Subsequently, we present the techniques used for collocations extraction.

2.2 Statistical approach for collocations extraction

The collocations extraction technique is based on a simple principle: if two words frequently appear together, then there's a chance that they form a meaningful lexical sequence (or a pertinent term). In practice, we calculate a score that measures the attachment force between two words in a given text. If this force exceeds a threshold fixed a priori, we can judge in this case that the couple can form a pertinent term.

Before calculating the words joint frequency we must, first, reduce them to a canonical form. Stemming (or lemmatization) can solve the terminological variation problem. The terminological variation can be graphical, inflectional or otherwise. In fact, terminology variation can disrupt the results if we consider two variations of the same token as two different units. Example, the lexical units "acids" and "Acid" are reduced to their canonical form "acid" that will accumulate the frequencies sum of all its variations.

Next, we apply on the text a common statistical technique presented by Kenneth Church in [1]. This technique consists in moving a sliding window of size *T* over the text (see Figure 1).

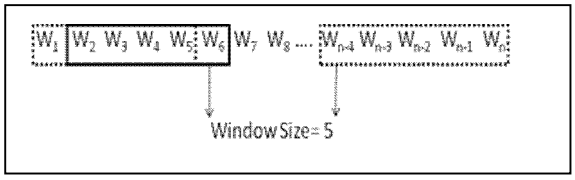

Figure 1. Example of a sliding window of size 5

For each pair of lemma (w_1,w_2), (w_1,w_2),…, (w_1,w_T) we increment it's occurrence frequency in the corpus. We associate with each couple (w_i,w_j) a contingency table (see table1).

Table 1. Contingency table

	w_j	$w_{j'}$ with $j' \neq j$
w_i	*a*	*b*
$w_{i'}$ with $i' \neq i$	*c*	*d*

- *a* = occurrences number of the pair of lemma.
- *b* = occurrences number of the pair of lemma where a given lemma appears as the first item of the pair.
- *c* = occurrences number of the pair of lemma where a given lemma appears as the second item of the pair.
- *d* = occurrences number of the pairs of lemma that don't contain one of the two lemma.

In the literature, we find several statistical criteria to determine the reattachment force between two words in a text. These measures are used initially in biology domain to detect possible relationships between events that occur together. We cite, inter alia, the mutual information and the likelihood (*Loglike*).

According to Fano [4] and Shannon [5], if two points *x* and *y* have respectively the probabilities *P(x)* and *P(y)* then their Mutual Information is defined by (1):

$$I(x,y) = \log_2 \frac{P(x,y)}{P(x)P(y)} \quad (1)$$

Mutual information compares the probability of observing *x* and *y* together (the joint probability) with the probabilities of observing *x* and *y* independently (chance) [1].

This measure is adapted to calculate the connection force between two words w_i and w_j, using our notation (Table 1) the formula becomes (2):

$$I(w_i, w_j) = \log_2 \frac{a}{(a+b)(a+c)} \quad (2)$$

The likelihood (*Loglikelihood*) (3) is distinguished from other measures by the consideration of cases where no occurrences appear [6]. This measure is frequently used in the terminology extraction field as in [7], [8] and [9].

$$\begin{aligned} \text{Loglike} = {} & a\log(a) + b\log(b) + c\log(c) + d\log(d) - \\ & (a+b)\log(a+b) - (a+c)\log(a+c) - \\ & (b+d)\log(b+d) - (c+d)\log(c+d) + \\ & (a+b+c+d)\log(a+b+c+d) \end{aligned} \quad (3)$$

Roche in [10] defines a new measure (Occ_L) that combines likelihood with joint occurrence (4).

$$Occ_L = Loglike + a \quad (4)$$

Based on experimental studies, Roche in [11] has proved that Occ_L measure admits a higher discriminative ability than other measures and offers, therefore, the best result. That's why; we choose this measure to extract collocations in our work.

The frequencies calculation in the statistical approach is based on the sliding window technique. Then, the window size choice is a necessary task to ensure better performance

for the term extraction. Therefore, we do a survey on the related works.

2.3 How to choose the appropriate size of the sliding window?

In the domain of terminology extraction based statistical approach, we confront a main problematic: in a given knowledge field, what's the ideal window size for the collocations extraction? Practically, we find in the literature a several window sizes used for extraction. Kenneth Church shows that window size choice varies with the type of information to extract. Small windows will identify fixed expressions (idioms) and named entities (person names, dates, company names, etc...). By cons, larger windows sizes will identify semantic concepts [12].

For terminology extraction, Kenneth Church proposes a window size of 5 words [1]. According to Church, this size is a good compromise, one side, it is large enough to show some semantic relationships between words, and on the other hand, it is not too large to lose the relationships that demand a certain strict adjacency between words.

Frank Smadja in [3] uses in her system (Xtract) a window of size 6. It tries to detect possible collocations by exploring the near neighbors of the target word (five neighbors before and five after the word). He considers that two words co-occur if they are in a single sentence and if there are fewer than five words between them.

In conclusion, the choice of the size of the sliding window for the extraction of collocations remain (until now) without clear justification. Therefore, we propose our approach based on ROC curves for assistance in decision making of the window size most appropriate for a given knowledge field.

3 Learning the size of the sliding window: a ROC-based approach

In the context of the statistic approach, we propose an approach based on ROC curves. Practically, we want to help choose the window size which offers to the system an optimal discriminative ability.

3.1 ROC curves

Bradely in [13] is the first to use the ROC curves for evaluation and comparison of learning algorithms. Mathieu Roche [11] used ROC curves for learning statistical measures used for terminology extraction.

ROC (Receiver Operating Characteristic) is used to measure system performance. Its methodology is based on statistical decision theory; its goal is to measure the performance of a binary classifier, i.e., a system that aims to categorize entities into two distinct groups based on one or many of their characteristics. Graphically, the ROC curve shows the rate of correct classifications (called true positive rate) as a function of the number of incorrect classifications (false positive rate) for a set of results provided by the system to be evaluated. The area under the ROC curve (AUC) is considered as an important criterion for evaluating the system.

In our case, our system (*S*) classifies collocations into two classes: relevant and irrelevant collocations. Collocations correctly classified by the system in the class "relevant" are called "true positives"; collocations misclassified are called "false positives". Collocations correctly classified by the system in the class "irrelevant" are called "true negatives"; collocations misclassified are called "false negatives". The relevance of the extracted collocations is reviewed by a domain expert (researcher, linguist, engineer…) who will decide whether collocations admit sense or not. The ultimate goal of our technique is to maximize the rate of true positives and the rate of false positives, also is to minimize the rate of false positives and the rate of false negatives.

Subsequently, we can build the following table:

Table 2. Basic measures of performance of diagnostic tests

	Relevant collocations	**Irrelevant collocations**
Collocations evaluated as relevant by the system	True Positives (TP)	False Positives (FP)
Collocations evaluated as irrelevant by the system	False Negatives (FN)	True Negatives (TN)

We define the following terms [14]:

- Sensitivity (also known as Fraction of True Positives): proportion of positive collocations detected by the test. In other words, the sensitivity allows measuring how much the test is effective when used on positive collocations. The test is perfect for positive collocations when sensitivity is 1, equivalent to a random draw when sensitivity is 0.5. If it is below 0.5, the test is cons-efficient.

  Sensitivity (*Se*) is defined as: $Se = TP/(TP+FN)$.

- Specificity (also known as Fraction of True Negatives): proportion of negative collocations detected by the test. Specificity allows measuring how well the test is effective when used on

negative collocations. The test is perfect for collocations negative when the specificity is 1, equivalent to a random draw when specificity is 0.5. If it is below 0.5, the test is cons-efficient.

Specificity (*Sp*) is defined as: *Sp= TN/(TN+FP).*

- Area Under Curve (AUC): is considered it as an important criterion for system evaluation, is equal to the probability that a randomly selected positive case will receive a higher score than a randomly selected negative case [15].

Graphically, the ROC curve represents the sensitivity (*Se*) as a function of fraction of false negatives (*1-Sp*).

Our idea is to evaluate system performance by varying the size of the sliding window and finally to choose the window size which ensures optimum performance for the system, i.e., the window size that maximizes the true positives and the true negatives rate.

3.2 Experimental study and results evaluation

3.2.1 Corpus description

During this work, we used an extract from the medical corpus MEDLARS[1] (75 documents) for the experimentation phases. An expert in the medical field (university professor in medicine) manually prepared a list of relevant terms extracted from the corpus. This list contains 225 technical terms in the medical field. Examples of terms existing in the list: *fetal plasma, maternal level, diabetic syndrome, histological examination, nucleic acid*, etc.

Cleaning the corpus is a necessary task to remove all empty words such as articles (*the, a, an, some, any*), conjunctions (*before, when, so, if*, etc...), Pronouns (personal, relative, possessive and demonstrative) and punctuation. Indeed, these words have high frequency in text documents without having a real terminology importance. So it is essential to remove them to avoid hampering the statistical computing and don't induce, subsequently, a noise in the results.

The lemmatization task is performed by "TreeTagger[2]" a part-of-speech tagger having an acceptable performance.

3.2.2 Results evaluation

We apply the sliding window technique on the corpus. Each time, we vary the window size starting with 2 until reaching 10. For each window size, we get a list of collocations ordered by descending order of their Occ_L value. Table 3 contains the first 11 collocations from a list obtained by the use of a window of size 5.

Table 3. Sample of collocations extracted by a window of size 5

Collocation		Occ_L
Fatty	acid	66.488
non-esterified	fatty	28.720
Chronic	hepatitis	28.578
Nephrotic	syndrome	28.359
non-esterified	acid	28.248
Day	life	22.892
Active	hepatitis	22.352
Maternal	plasma	22.002
Maternal	level	21.810
Maternal	fetal	21.632
Blood	glucose	19.700

So, we get 9 lists collocations ordered in descending order (a list for each window size). For each list, we select the top 400 collocations (hereinafter referred to as list-S). List-S contains collocations evaluated as relevant by the system; the other collocations (not belonging to list-S) are evaluated by the system as irrelevant. A collocation belonging to the list-S is seen as a true positive (*TP*) if it belongs to the expert list, else it is considered as false positive (*FP*). A collocation not belonging, at the same time, to the expert list and the list-S is counted as true negative (*TN*). A collocation not belonging to the list-S but it belongs to the expert list is considered as a false negative (*FN*).

Using XLSTAT[3], a statistical and data analysis software, we plot the following ROC curves (Figure: 2, 3, 4, 5, 6, 7, 8, 9 and 10):

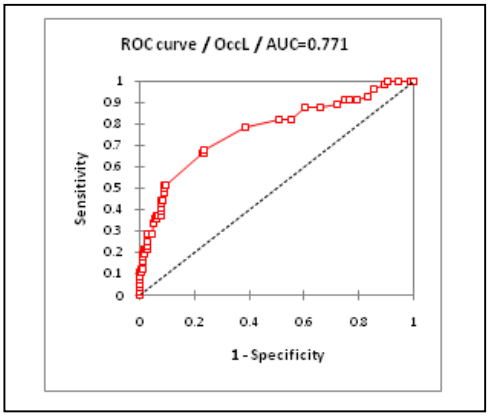

Figure 2. ROC curve corresponding to the window of size 2

[1] ftp://ftp.cs.cornell.edu/pub/smart

[2] http://www.ims.uni-stuttgart.de/projekte/corplex/TreeTagger/

[3] http://www.xlstat.com/fr/

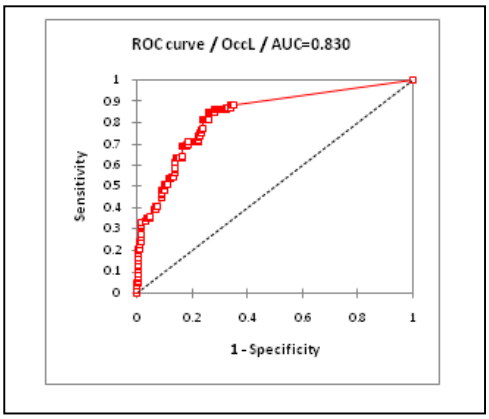

Figure 3. ROC curve corresponding to the window of size 3

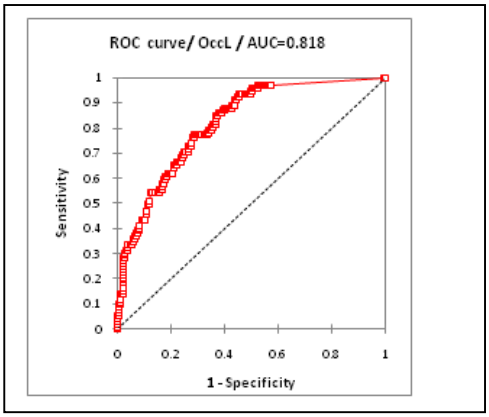

Figure 4. ROC curve corresponding to the window of size 4

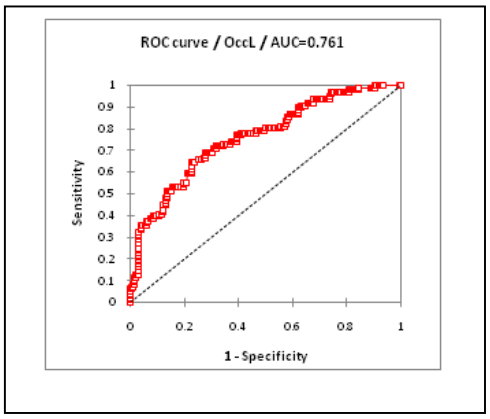

Figure 5. ROC curve corresponding to the window of size 5

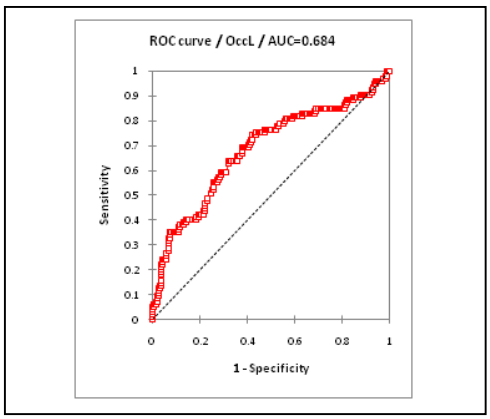

Figure 6. ROC curve corresponding to the window of size 6

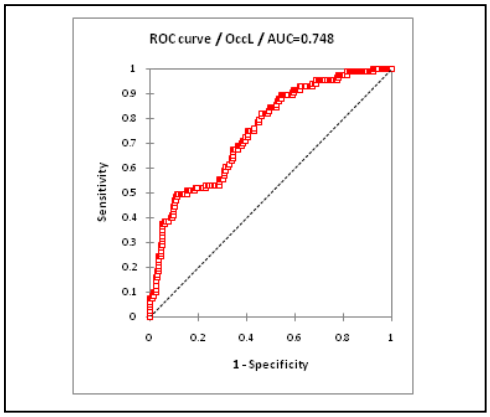

Figure 7. ROC curve corresponding to the window of size 7

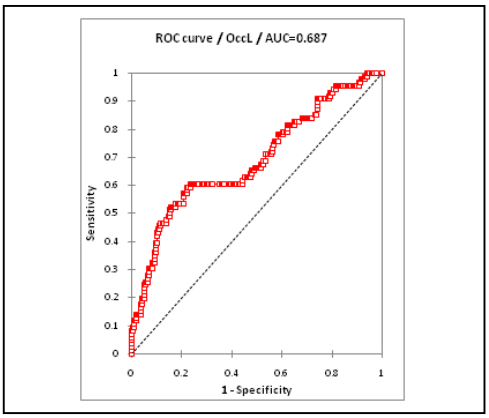

Figure 8. ROC curve corresponding to the window of size 8

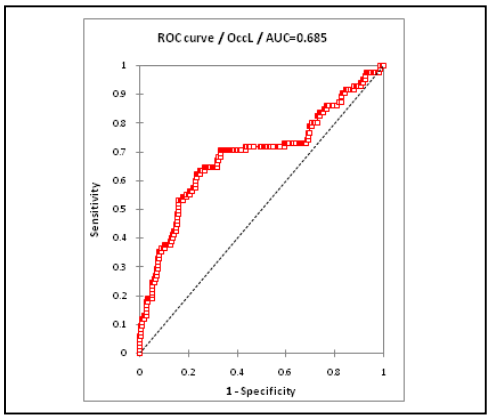

Figure 9. ROC curve corresponding to the window of size 9

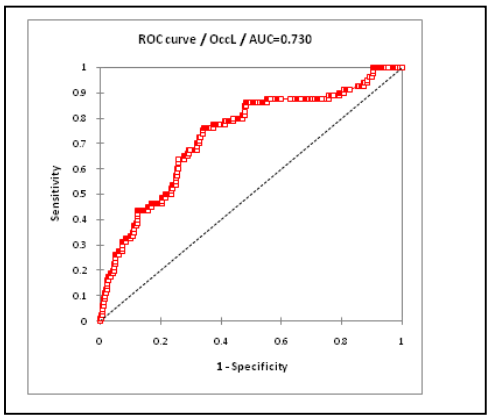

Figure 10. ROC curve corresponding to the window of size 10

To evaluate the 9 ROC curves obtained (see Figure: 2, 3, 4, 5, 6, 7, 8, 9 and 10), we use the Area Under Curve (AUC) as a performance indicator. We recall that the AUC informs about the probability that the test results allows to provide a correct judgment, for two different classes (relevant and irrelevant) of collocations.

As well, when the test is perfectly discriminative, the area under the curve (AUC) is 1. This means that, given two collocations (relevant and irrelevant) the test distinguishes, in 100% of cases, between relevant and irrelevant collocation.

Conversely, when the test is not discriminative, the probability of distinguishing between the relevant and the irrelevant collocation is 50% (chance). In this case, the area under the ROC curve is 0.5.

In the table (Table 4) we sort the windows by their AUC values, greater to the smaller.

Table 4. AUC for each window size

Window Size	3	4	2	5	7
AUC	0.830	0.818	0.771	0.761	0.748
Window Size	10	8	9	6	
AUC	0.730	0.687	0.685	0.684	

According to the table 4, we can classify the results into three groups:

1. Windows having an AUC between 0.8 and 1: The windows of size 3 and 4 have the highest AUC values that exceed (0.8). We can conclude that these window sizes are the more suitable for collocations extraction. The majority of extracted collocations are idioms, named entities and nominal group.
2. Windows having an AUC between 0.7 and 0.8: the majority of windows (2, 5, 7 and 10) belong to this group, which has a medium discriminative capacity, but they are useful for extracting collocations which refers to deep semantic relationships.
3. Windows having an AUC less than 0.7: this group includes windows of size 8, 9 and 6. These window sizes weaken the discriminative power of the system and reduce the importance of testing.

For collocations extraction from a textual corpus of medical field, a window of size 4 can be a good compromise between “fixed” and “semantic” collocations.

4 Conclusion

In this paper, we proposed an approach based on ROC curve for learning the size of the sliding window used in the statistical approach for the extraction of collocations. The choice of the window size, the most appropriate for a given knowledge field, is still a problem without a clear and precise solution. So it's original to propose a practical solution based on experimental studies to circumvent this problem.

Our approach based on ROC curves showed the influence of the various choices of window size on the overall performance of collocations extraction system, to avoid the sizes that weakens the discriminative power of the system and favored the one which gives the optimal discriminative power.

5 References

[1] K. Church, and P. Hanks, "Word association norms, mutual information and lexicography," Computational Linguistics Volume 16, Number 1, March 1990.

[2] M. Benson, "Collocations and general-purpose dictionaries," International Journal of Lexicography Volume 3, Issue 1, Pp. 23-34, 1990.

[3] F. Smadja, "Retrieving Collocations from Text: Xtract," Columbia University, 1993.

[4] R. Fano, "Transmission of Information: A Statistical Theory of Communications," MIT Press, Cambridge, MA, 1961.

[5] C. E. Shannon, "A mathematical theory of communication," Bell System Tech., 27, 379-423, 623-656, 1948.

[6] T. Dunning, "Accurate Methods for the Statistics of Surprise and Coincidence," Vol.19, n1, Mars 1993.

[7] B. Daille, E. Gaussier, and J. Langé, "An evaluation of statistical scores for word association," In (Ginzburg et al., 1998), pages 177–188, 1998.

[8] F. Xu, D. Kurz, J. Piskorski, and S. Schmeier, "A Domain Adaptive Approach to Automatic Acquisition of Domain Relevant Terms and their Relations with Bootstrapping," In LREC 2002, Third international conference on language resources and evaluation, 2002.

[9] M. Roche, J. Azé, O. Matte-Tailliez, and Y. Kodratoff, "Mining texts by association rules discovery in a technical corpus," In Proceedings of IIPWM'04 (Intelligent Information Processing and Web Mining), pages 89–98, 2004.

[10] M. Roche, T. Heitz, O. Matte-Tailliez, and Y. Kodratoff, "EXIT : Un système itératif pour l'extraction de la terminologie du domaine à partir de corpus spécialisés," In Actes de JADT'04 (Les journées internationales d'analyse statistique des données textuelles), Louvain-la-Neuve, Belgique, 2004.

[11] M. Roche, J. Azé, Y. Kodratoff, and M. Sebag, "Learning Interestingness Measures in Terminology Extraction A ROC based approach," In Proceedings of ROC Analysis in AI Workshop (ECAI 2004). Valencia, Espagne, 2004.

[12] K. Church, W. Gale, P. Hanks and D. Hindle, "Parsing, word associations and typical predicate-argument relations," Proceeding HLT '89 Proceedings of the workshop on Speech and Natural Language. Association for Computational Linguistics Stroudsburg, PA, USA, 1989.

[13] A.P. Bradley, "The use of the area under the roc curve in the evaluation of machine learning algorithms," Pattern Recognition, 30(7), 1145– 1159, 1997.

[14] T. Fawcett, "ROC Graphs: Notes and Practical Considerations for Researchers," Pattern Recognition Letters, 27(8):882-891. March 16, 2004.

[15] J. Fogarty, R. S, Baker and S. E. Hudson, "Case Studies in the use of ROC Curve Analysis for Sensor-Based Estimates in Human Computer Interaction," GI '05 Proceedings of Graphics Interface 2005.

Agent-Based Computing Application and its Importance to Digital Forensic Domain

Inikpi O. Ademu[1], Chris O. Imafidon[2]
[1]School of Architecture, Computing and Engineering, University of East London, Docklands Campus, London, United Kingdom
[2]*School* of Architecture, Computing and Engineering, University of East London, Docklands Campus, London, United Kingdom,
[2]Former Head of Management Unit, Queen Mary, University of London, London, United Kingdom

Abstract- *The advancement of the digital forensic investigation requires a new design, improved mechanism and processes. Forensic experts are faced with growth in data. Huge amount of data has expanded and grown in recent years attempts to consume the storage space available. The problem created by this trend is that our ability to analyse and filter data hasn't grown at nearly the same pace. Computing resources are improving, distributed computing field has made major contribution for improvement. By coding tools that can harness the resources of computers. The aim of the research is to identify the main application areas in which agent application has been successfully used currently and to recognise the importance of building digital forensic tool with intelligent agent techniques.*

Keywords- Agent, Intelligent Agent, Autonomy, Automated Tools, Digital Forensic

1. Introduction

Intelligent agent is a new concept for developing software appliactions. Currently, agents are the focus of intense interest on the part of many fields of computer science and artificial intelligence. Agent are used in an increasingly wide variety of applications, from email filters to large open, complex mission criticl system such as air traffic control, in both system the key abstraction used is that of an agent (Jennings and Wooldridge, 1998). Russell and Norvig (2010) describe an agent as anything that can perceive its environment through sensors and act upon that environment through actuators. For instance a human agent has eyes, ears for sensors and hands, legs, for actuators, a robotic agent might have cameras and infrared range finders for sensors and various motor for actuators. A typical example is Letizia, an intelligent agent used for reading documents off the World Wide Web (WWW). Most of the time when the user is accessing the WWW, the computer is idle, waiting for instructions from the user to retrieve a new document. Letizia uses this otherwise idle time to look for other documents somehow related to the document being read, so that the user, after having read the document, will get suggestions for other documents that might be of interest. Letizia thus bases its searching on the contents of relatively recently read documents (Lohani and Jeevan, 2007). Wallace (1997) defined Intelligent Software Agent as software that uses Artificial Intelligence (AI) in the pursuit of the goals for its clients. AI is the limitation of human intelligence by mechanical means. In the terms of this research the word agent generally indicates intelligent agent (IA).

According to Williams (2004) an agent is anything that can perceive its environment through sensors and act upon that environment through effectors. The criterion that is used to evaluate and draw conclusion whether an agent is successful or not is performance measure and a critical success factor is based on how an agent could perform a particular task. The intrinsic part of an agent is being autonomous, adaptive and cooperative in the environment which it operates. The most desirable attribute of an agent is autonomous meaning the agent should not be under the control of another agent (Ademu et al, 2012). The aim of the research is to identify the main application areas in which agent application has been successfully used currently and to recognise the importance of building digital forensic tool with agent technology.

2. Properties of Intelligent Agent

Agent is a computer system put in some environment, that is capable of autonomous action in this environment on order to meet its design objectives (Jennings and Wooldridge, 1998). The system should be able to act without the direct intervention of humans or other agents and should have control over its own

actions and internal state. In drawing a correlation between the notion of autonomy with respect to agents and encapsulation with respect to object oriented systems. An object encapsulates some state, and have some control over this state so that it can only be modified through the methods that the object provides. Agent encapsulate state in the same way but it can also be thought that agent encapsulate behavior in addition to the state but object cannot encapsulate behavior. Due to this distinction (Jennings and Wooldridge, 1998) do not think of agents as invokig actions or methods on agent rather they think of them requesting actions to be performed. The authors identified intelligent agent as a computer system that is capable of flexible autonomous action in order to meet its design objectives. The properties of intelligent agent are:

- **Autonomy:** The agent possesses the capacity to act independently from its user, both in chronological terms and in the sense of adding intelligence to the user's instructions, and exercising control over its own actions (Williams, 2004).

- **Reactivity:** The agent senses in and acts in its own surroundings. The agent also reacts to changes in the surroundings that are the result of its own actions (Bradshaw, 1997).

- **Proactivity:** This refers to the agent's ability to exhibit goal-directed behaviour and take initiatives by itself to get closer to the defined goal, out of an external instruction by its user (Russell and Norvig, 2010). It can predict, or at least make good guesses about the consequences of its own actions, and in this way use its reactivity to come closer to its goal. This should happen simultaneously, and on a periodical basis, which makes their use of enormous help in saving time.

- **Adaptability:** The agent's capacity to learn and change according to the experiences accumulated. This has to do with the feature of having memory, and learning. An agent learns from its user, from the external world and even from other agents, and progressively improves in performing its tasks, independently from external instructions (Lohani and Jeevan, 2007).

- **Continuity:** An agent doesn't necessarily work only when its owner is sitting by the computer, it can be active at all times. It is thus a temporally continuous process (Lohani and Jeevan, 2007).

- **Social ability:** An agent is social software, which interact to other agents to do its job. It can be talking to other similar agents to exchange information, or it can talk to other kinds of agents to request and offer services. Communication with the owner is also important. It is through this the agent is praised or punished for its work, and the owner can give further directions to the agent for how it can do its job better (Herman, 1997).

- **Flexibility:** The agent works proactively, that is directed by goals, but how it goes about to reach these goals may vary. As opposed to a script that performs the same sequence of commands each time it is run, an agent can do the same job in many different ways, depending on the situation and the surroundings (Lohani and Jeevan, 2007).

- **Cooperation:** The notion of cooperation with its user also seems to be fundamental in defining an agent, different from the one-way flow of information of ordinary software; intelligent agents are therefore true interactive tools (William, 2004).

3. Classification of Agent

According to (Jennings and Wooldridge, 1998) agent can be classified by the type of the agent, by the technology used to implement the agent, or by the application domain itself. For the purpose of this research, agent application will be classified as follows:

3.1 Classification by the Type of Agent

Nienaber and Barnard (2005) classified an agent into two namely, stationary agents and mobile agents. A stationary agent can be seen as autonomous software that permanently resides on a particular host. Example of such an agent is one that performs task on its host

machine such as accepting mobile agents, allocating resources, performing specific task etc. A good example of stationary agent is Clippie, the Microsoft Office Assistant where its settings are for programs in Microsoft Office Suite. A mobile agent is a software agent that has the ability to transport itself from one host to another in a network. The ability to travel allows a mobile agent to move to a host that contains an object with which the agent wants to interact, and then to take advantage of the computing resources of the object's host in order to interact with that object. An example of a mobile agent is a flight booking system where a logged request is transferred to a mobile agent that on its part negotiates the web seeking suitable flight information quotations as well as itineraries.

3.2 Classification by Agent Application Domain

- **Commercial Application**

Shopping Assistant: Shopping Assistant uses intelligent agent technology to help the internet shopper to find the desired item quickly without having to browse from one page to the other. A good example is the trading and negotiation agent which negotiate with other agents to buy or sell shares on behalf of their users and the auction agent at EBay (Patel et al, 2010).

Information Management Agents: These agents help to selectively retrieve appropriate information (Bradshaw, 1997). For instance instead of hiring help desk consultant of helping the customers search through the internet for an answer, with intelligent agent, the customer describes the problem and the agent automatically searches the appropriate databases e.g. CD-ROM, or Internet then present a united answer with the most likely first. The diversity of information available to us has increased, the need to manage this information has also grown. The large volume of information availabel throught he internet and World Wide Web (WWW) represents a very real problem. Even though an end user is required to constantly direct the management process there is need for such searches to b carried out by agents, acting autonomously to search the web on behalf of some users this is so important in the digital forensic investigation Ademu, et al, 2011).

Intelligent agent has been proposed in some distributed application as a useful mechanism. Intelligent agent is very applicable in digital forensic investigation. As Solomon and Lattimore (2006) mentioned, in many digital crimes, the procedures of accomplishing forensic are neither consistent nor standardized, instead there are some elementary guidelines for specific situations. Rekhis et al (2009) mentioned that digital investigation should integrate the use of formal techniques that are useful to develop results and proof that should not be disapproved and avoid errors that could be introduced by manual interpretation. There is need to consider the development of automated tools for collection and analysis of digital evidence before presentation.

Web Browser Agent: This is an intelligent agent which helps keep track of what website is visited and customizes ones view of the web by automatically keeping a bookmark list, ordered by how often and how recent one visit the site. It also let you know by notifying you when sites you like are updated, and it could also automatically download pages for browsing offline. A good example is the IBM web browser intelligent, web spider which is used for collecting data to build indexes to be used by a search engine.

Data Mining – This is where information-specific agents provide a context for data searches in vast databases or other information sources (like the web for example) from which cooperating intelligent personal agents will extract a selection of useful information. This field is one of the fastest-evolving ones at the moment given the explosive growth of the amount of accessible information via networks and communications Ralha (2009).

Broker agents: Another types of agent that act as mediators or facilitators by matching user requests against information or known solutions in databases or provided by database agents (Lohani and Jeevan, 2007).

3.3 Classification by Technology used to implement the Agent

Interface Agent: Interface agent emphasize autonomy and learning in order to perform tasks for their owners. Interface agents support and provide proactive assistance to a user learning to use a particular application such as a spreadsheet or an operating system (Jennings and Wooldridge, 1998). The user's agent observes and monitors the actions taken by the user in the interface, learns new short-cuts and suggests better ways of doing the task.

Personal assistant agents: This is an agent that contains personalized learning algorithms developed for a single, specialized application or task. Information filters for browsing tasks belong to this class of agents (Bradshaw, 1997).

Network management – This is where collaborative agents collect and exchange local information on network statistics in order to achieve automation and optimization of decisions on network administration tasks like routing, access, service provisions, monitoring and statistical evaluation, within a global view (Ralha, 2009).

4. Intelligent Agent applied to Digital Foresic Investigation

The New Technologies Inc. (NTI) developed an intelligent Filter program known as the Filter_1 which has the ability to make binary data printable and to extract potentially useful data from a large volume of binary data (Middleton, 2004). The intelligent filter program or Filter_1 tool help to reduce the size of the bitstream files without sacrificing useful information. IP Filter is possibly the most interesting and useful of the Forensic Utilities. It was developed by NTI to help law enforcement track down and investigate child pornography cases. It has a simple DOS user interface and is used in almost the same way as the Filter_1 (Stephenson, 2002). The difference is that it searches for instances of email addresses, Web URLs, and graphic or Zip file names. TextSearch Plus is a utility for searching a disk for text strings. It can search both allocated space and unallocated space (slack space). When used to search the physical disk, it can be used against any file system. TextSearch Plus makes an excellent tool for parsing very large logs in an internet backtracing investigation. It uses fuzzy logic and is designed to process a large amount of data in a relatively short time.

Rekhis et al (2009) developed a system for digital investigation of network security incident using techniques known as intrusion response probabilistic cognitive maps that are constructed to analyse the attacks performed against the network. In their work the authors emphasized that focusing merely on restoring the system as disadvantageous, valuable information and traces that allow understanding the attack could be removed, if the compromised system is formatted or reinstalled, this weakness point up the need for conducting a post - incident digital forensic investigation. And in dealing with the problem faced with collecting and analysing of large amount of data, digital forensic investigation should reconcile both the expertise of the incident response team and the use of formal reasoning techniques, this allows the better filtering of the data to be analysed and source of evidence to be explored and also validate the result of the formal techniques by the incident response team before presenting them. The recommendation by this authors relates to this present research where emphasizes is made for intelligent and reasoning techniques to be applied to digital forensic.

Conclusion

The research identifies the current state of the art in applied agent system. Agents where classified into types, application domain and technology used. The research discussed a wide variety of agent application. This research has pinched from different literature in order to discuss the rapidlly evolving area of software agents and emphasized on the importance of building digital forensic tool with intelligent agent techniques.

Acknowledgement

The authors would like to thank Dr David Preston and the University of Cambridge Computer laboratory for providing support during this research.

Reference

[1] Ademu, I. Imafidon, C. Preston, D., (2012) Intelligent Software Agent applied to Digital Forensic and its Usefulness Vol. 2 (1) Available at: http://interscience.in/IJCSI_Vol2Iss1/IJCSI_Paper_21.pdf (Accessed 10 April 2012)

[2] Ademu, I. Imafidon, C. I. Preston, D. (2011) A New Approach of Digital Forensic Model for Digital Forensic Investigation Vol. 2, (12) Available at: http://thesai.org/Downloads/Volume2No12/Paper%2026-A%20New%20Approach%20of%20Digital%20Forensic%20Model%20for%20Digital%20Forensic%20Investigation.pdf (Accessed 28 April 2012)

[3] Bradshaw, J. (1997) Software Agent p 347 London: MIT Press

[4] Hermans, B. (1997). Intelligent software agents on the internet: An inventory of currently offered functionality in the information society and a prediction of (near) future developed. Available at: http://www.firstmonday.dk/issues/issues2_3/ch_123/ (Accessed 1 April 2012)

[5] Jennings, N. Wooldridge, M. (1997) Agent Technology: Foundations, Applications and Markets Pp 12-14 Berlin: Springer

[6] Lohani, M, Jeevan, V. (2006) intelligent software agents for library application Vol. 28 (3) Available at: www.emeraldinsight.com/0143-5124.htm (Accessed 18 April 2012)

[7] Nienaber, R. Barnard, A. (2005) Software quality management supported by software agent technology. Available at: http://www.informingscience.org/proceedings/InSITE2005/I53f40Nien.pdf (Accessed 13 April 2012)

[8] Patel, A. Qi, W. Wills, C. (2010) A review and future research directions of secure and trustworthy mobile agent-based e-marketplace systems Vol. 28 (3) Available at: www.emeraldinsight.com/0968-5227.htm Accessed 15 April 2012

[9] Ralha, C. (2009) Towards the integration of multi-agent application and data mining.

Available at: http://www.springer.com/cda/content/9781441905215.ci.pdf Accessed 22 April 2012

[10] Rekhis, S. Krichene, J. Boudriga, N. (2009). Forensic investigation in communication networks using incomplete digital evidence Vol. 2 (9). Available at: http://www.sciRP.org/journal/ijens/ (Accessed 20 April 2011)

[11] Russell, S. Norvig, P. (2010) Artificial Intelligence: A modern approach. 3rd Edition. P 34 New Jersey: Prentice Hall

[12] Solomon, J. Lattimore, Erik. (2006) Computer forensics Available at: http://citeseerx.ist.psu.edu/ (Accessed 10 February 2011)

[13] Stephenson, P. (2000) Investigating Computer-Related Crime Florida: CRC p 32

[14] Wallace, D. (1997). Intelligent software agents: Definitions and applications. Available at: http://alumnus.caltech.edu/~croft/research/agent/definition/ (Accessed 25 August 2012).

[15] Williams, G. (2004) Synchronizing E-Security Kluwer Academic Publishers. Pp 34-35

Neural Network Based Modeling and Fuzzy Control of A Chemical Plant for Automatic Gas Yield Control

Su-Yeon Jeong[1] , Bok-Jin Oh[1] , and Doo-Hyun Choi[2]
[1]School of Electronics Engineering and Computer Science, Kyungpook National Univ, Daegu, S. Korea
[2]School of Electronics Engineering, Kyungpook National Univ, Daegu, S. Korea

Abstract — *In this paper, a rectifying tower of a chemical plant is modeled using neural networks and human experts in charge of production control are modeled by fuzzy logic. The neural network models and fuzzy controllers are interconnected for automatic O2 production simulation. Standard multilayer perceptron architecture and backpropagation learning algorithm are used to model a rectifying tower. Real data gathered from operating rectifying tower are used to train and test the neural network models. Two widely used increase and decrease cases of O2 production quantity from 3,000 to 5,000 Nm3/h in rectifying tower is selected in this study. After implementing neural network based rectifying tower, fuzzy logic is used to model human experts and used as a controller instead of human experts. Through experiments using 35 real increase and decrease cases of gas production quantity, the neural network models and fuzzy controller show some possibility to mimic complex real plants and verify that those can be used as useful tools to train unskillful engineers and novices in chemical plants.*

Keywords – rectifying tower; chemical plant; artificial neural network; Fuzzy system; modeling and control

1 Introduction

There are so many plants in a steel company. One of them is chemical plants that are in charge of providing high purity oxygen and nitrogen gases needed to producing steel production. Oxygen and nitrogen production plants are one of the huge energy consuming facilities in steel companies. Efficient production control of chemical plants saves much energy and reduces manufacturing cost as a result. Currently, human experts are controlling production levels of chemical plants between 3000 and 5000Nm3/h considering energy consumption and gases' necessities of other plants in steel companies. The control algorithms of gas production quantity is different from experts to experts and the consumption of energy is different each other and each time. It is necessary to standardize the control process of gas production in order to get effective production control and reduce energy consumption substituting current control paradigm depending on individuals' experience and insights.

There are many approaches to model and control complex real plants having many uncertainties and ambiguities using soft computing algorithms such as neural networks, fuzzy logic, evolutionary algorithms, etc. Some of them use MLPs to model nonlinear systems [1-4] and some try to use fuzzy logic as control algorithms [5-7]. Combination of both neural networks and fuzzy logic systems is also suggested to model and control chemical contents [8-9]. In this paper, neural networks are used to model rectifying towers and fuzzy logic is used to model human experts. The neural network models can be substituted with real plants for training unskillful engineers and fuzzy controllers may be substituted with human experts or used for monitoring human mistakes.

This paper is organized as follower. A chemical plant and a rectifying tower are overviewed and the principle of Claude type gas production is introduced. Proposed artificial chemical plant and fuzzy controller is summarized in section III. Neural network based rectifying tower modeling and its modeling performance is explained in section IV. In section V, fuzzy controllers and simulation result using real data are explained.

2 Overview of a Chemical plant and a rectifying Tower

In 1902, Georges Claude, a French engineer and inventor, devised the Claude system for liquefying air. The system enabled the production of liquid nitrogen (N), oxygen (O_2) and argon (Ar). The system produces liquid air through the processes of air inhaling – air compression – heat exchange – expansion engine – rectifying column. Fig. 1 shows the Claude system.

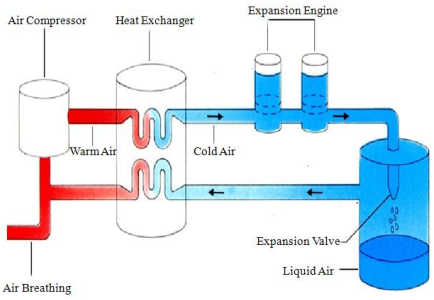

Fig. 1. The Claude system for liquid air production [1].

This study tried to model a rectifying tower in chemical plants and a human expert in charge of controlling the chemical plant. The chemical plant of attention is a high-purity liquid oxygen (O_2), argon (Ar) and nitrogen(N) gas production plant. The plant is built based on the Claude system similar to Fig. 1 and additional processes are used to enhance production efficiency. At first atmospheric air is inhaled and then the inhaled air passes through air filters to reduce dust in the air. Air compressor compresses the air and then heat exchanger using water decreases the air temperature again. Absorber is used to eliminate unnecessary constituents such as moisture, CO_2, carbon, hydrogen, etc. Expansion turbine is used to decrease further the air temperature to near absolute zero degrees. Finally, rectifying towers are used to get liquid gases of N, O_2 and Ar. Fig. 2 shows the block diagram of an O_2 and N production plant. This paper is focused to control of a rectifying tower based on fuzzy inference engine.

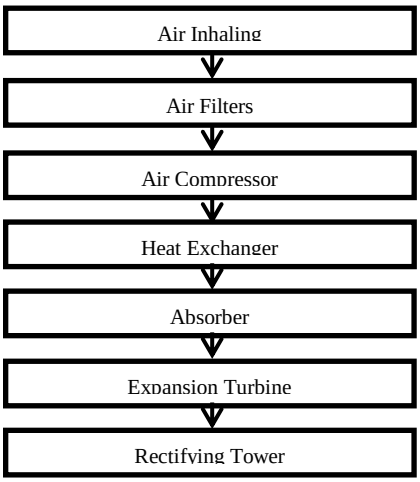

Fig. 2. Block diagram of liquid gas production sequences [1].

3 Overview of the proposed Chemical Plant modeling and Controller

The final goal of this paper is implementing fuzzy controller of a chemical plant using soft-computing algorithms. In order to do this a rectifying tower, the most important process of gas production, is modeling using standard multilayer perceptrons (MLPs) and backpropagation (BP) learning algorithm. Then we tried to model human experts having skills of increase and decrease of gas production using fuzzy systems. The fuzzy models are used as a controller of rectifying tower and directly control the quantity of gas production. Fig. 3 shows the block diagram of neural network modeling and fuzzy control of rectifying towers. Fig. 3(a) shows the block diagram of rectifying tower modeling using neural networks. After modeling process, that is, neural network learning has been finished, the rectifying tower can be replace using neural network models of the rectifying tower as shown in Fig. 3(b). After then the model is used as an education tools for unskillful engineers. To make a fuzzy controller for controlling the quantity of gas production, human experts should be modeled at this time. The human experts use rules based on their experiences and handed down information. These rules are rough and incomplete in general and it is hard or sometimes impossible to model using strict computational tools. We try to apply the fuzzy system to model these rules of human experts. Fig. 3(c) shows the block diagram of modeling of human experts and Fig. 3(d) shows replaced version of chemical plants. Rectifying towers can be replaced to neural networks and human experts to fuzzy controllers using well modeled neural networks and fuzzy controllers. Those may be good educational tools for novices in chemical plants.

4 Neural network modeling of a Rectifying tower

To model a rectifying tower, MLPs are selected and standard BP algorithms are used as their learning algorithms. The real operating data for most frequently used ranges of 3000 and 5000 Nm^3/h increases and decreases of production are used to train neural networks. For 3000 and 5000 Nm^3/h increases and decreases, 30 sequences are gathered. Among the sequences, 27 sequences are used for learning and 3 sequences are used for test. Among many sensing and control data of a rectifying tower 27 data is selected as inputs and outputs of neural networks by analyzing operation history during past 6 months. 27 data include 22 inputs and 10 outputs. In 22 inputs, 5 inputs are fed back from outputs to inputs. All the input data are normalized 0 to 2. Table I summarized every inputs and outputs used rectifying tower modeling in the experiments. Signals used as both input and output are represented using italic font. "(Set)" represents control signals used by human experts. Fig. 4 shows average learning error and final error is 0.0107 after 50,000 iterations. Fig. 5 shows a modeling result for 5000 Nm^3/h decrease of production quantity. In Fig. 5, solid line represents the data from real rectifying tower and dashed line does the data from neural network models.

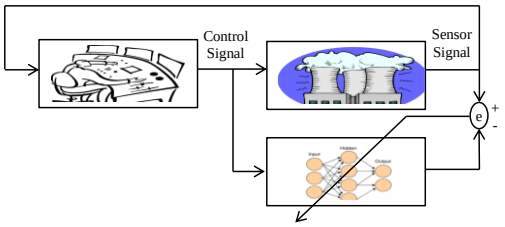

(a)

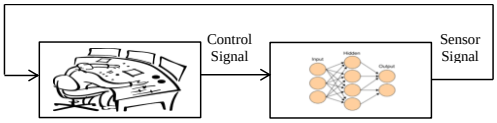

(b)

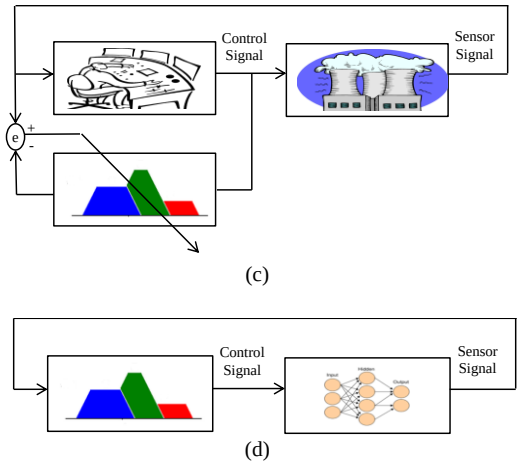

Fig. 3. Neural network based modeling and fuzzy controller for a rectifying tower
(a) NN plant based modeling, (b) NN plant, (c) Fuzzy controller (d) Fuzzy controller with a NN plant

TABLE I. INPUTS AND OUTPUTS FOR RECTIFYING TOWER MODELING [1]

Inputs	**Outputs**
BT/C Output Pressure Liquid O_2 Recycle Pressure Liquid O_2 Level Upper O_2 Purity Upper Liquid Air Quantity Lower Liquid Air Quantity Cooling Tower Height 1 Cooling Tower Height 2 Expansion Turbine Valve Status Expansion Turbine Bypass Quantity *Lean Liquid Quantity* *Expansion Turbine Quantity* *O_2 Output* *N Output* *Lower Air Quantity* Output O_2 Level Output N Level Expansion Turbine Quantity(Set) O_2 Output (Set) N Output (Set) Lower Air Quantity (Set) Lean Liquid Quantity(Set)	*Lean Liquid Quantity* *Expansion Turbine Quantity* *O_2 Output* *N Output* *Lower Air Quantity*

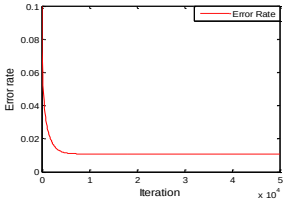

Fig. 4. Learning curve of NN based rectifying tower modeling (0.0107 after 50,000 iterations)

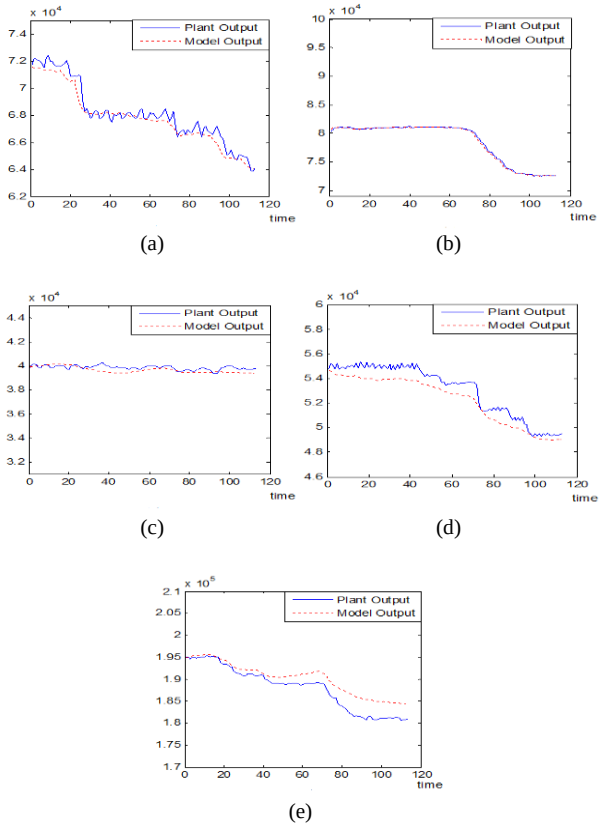

Fig. 5. Neural modeling result for 5000 Nm^3/h decrease of production quantity
(a) Lean Liquid, (b) Expansion Turbine Quantity, (c) N Output, (d) O_2 Output, (e) Lower Air Quantity

5 Fuzzy based controller for increase and decrease of production quantity

Fuzzy system is used to model human experts as mentioned in section III. Several best operation histories of increase and decrease of production quantity are selected with human experts actually working in the chemical plant. Also, several control signals are selected based on data mining of operation history during past 6 months which are same as the period used in rectifying tower modeling. Rules provided by human experts and data mining is used as rule base for fuzzy systems and membership functions are designed for each input and output data. To defuzzify, center of mass (COM) is used after aggregating each rules' outputs. Fig. 6 shows some of the membership functions on sensor data, O_2 Output, N Output, and Lower Air Quantity. Outputs of fuzzy controller are O_2 Output (Set), N Output (Set), Lower Air Quantity (Set), and Lean Liquid Quantity (Set) and these data are used as control signals for the rectifying tower. Fig. 7 shows the result of 5000 Nm^3/h decrease of production quantity using a fuzzy controller and neural network models of a rectifying tower. Solid line represents real output and dashed line represents simulation result. It is obvious that the controller and models can be used in real situation.

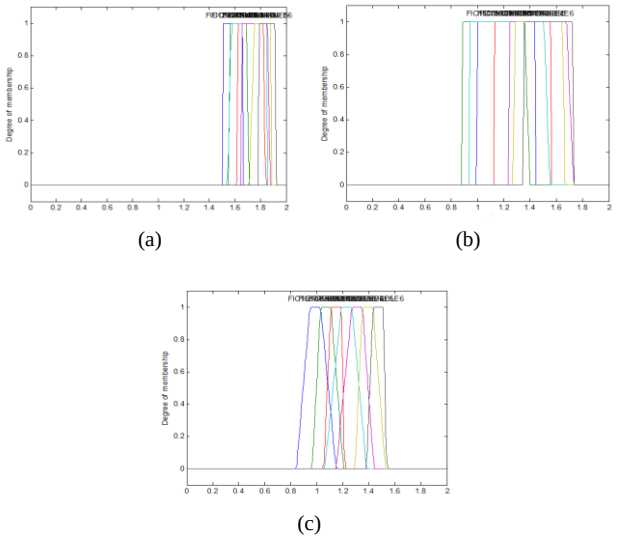

Fig. 6. Fuzzy controller membership functions.
(a) Lower Air Quantity, (b) O_2 Output, (c) Lean Liquid Quantity

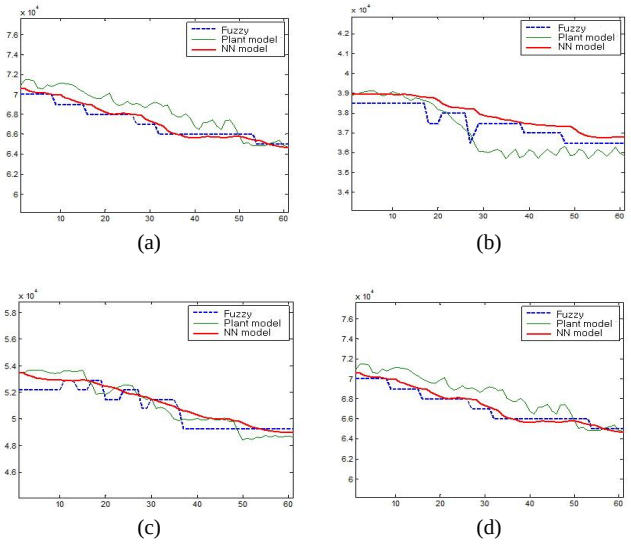

Fig. 7. 5000 Nm^3/h decrease of production quantity using a fuzzy controller and neural network models
(a) N Output, (b) O_2 Output, (c)Lower Air Quantity, (d) Lean Liquid Quantity

6 Conclusion

A fuzzy based controller to control the production quantity of high purity O_2 and N is implemented in this paper. To implement the controller, at first, a rectifying tower is modeled using neural networks using a real data gathered from a rectifying tower on the job during past six months. Total 30 periods of production increase and decrease is selected for training and testing of neural network models with the aid of human experts. The performance of the modeling of rectifying tower is verified using trained data and the other data which is not used to train the neural networks. Then a human expert controlling the production of O_2 and N is also modeled using fuzzy system since the human experts use their experience based rules even though they do not recognize. After composing a fuzzy controller the neural network model for the rectifying tower is interconnected to the fuzzy controller. The performance of the implemented fuzzy controller is tested using 21 production increase period and 14 production decrease periods. Several results for neural network modeling and fuzzy based control are presented in the section IV and V. Small errors exist in the result and so more rules and real data from the site is needed to make elaborate fuzzy controller and neural network models. Even though some minor errors exist it is better than unskillful engineers and in near future human experts may be substituted with soft computing controllers.

7 References

[1] Jong-Hwa Kim, Doo-Hyun Choi, Su-Yeon Jeong, Bok-Jin Oh, Jinhee Lee, "Modeling of Chemical Plant's Rectifying Towers Using Artificial Neural Networks," CICSyN2011, Vol.1, No.1, pp. 152-157, Jul. 2011.

[2] S. Haykin, *Neural networks and learning machines*, Prentice Hall, 2009.

[3] S. Haykin, *Neural Networks: A Comprehensive Foundation*, 2nd ed, Prentice Hall, 1998.

[4] A. K. Singh and P. Gaur, "Adaptive control for non-linear systems using artificial neural network and its application applied on inverted pendulum," IICPE 2010, pp. 1-8, 2010.

[5] K. Indrani, P. Prem Kumar, and B. Laxmidhar, "On identication and stabilization of nonlinear plants using Fuzzy Neural Network," ICSMC 2005, pp. 474-479, 2005.

[6] C. Kriger and R. Tzoneva, "Neural networks for prediction of wastewater treatment plant influent disturbances," ARFICON 2007, pp. 1-7, 2007.

[7] Luolong, Luofei, Zhouliyou, Yehongtao, and Xuyuge, "Predicting wastewater sludge recycle performance based on fuzzy neural network," IEEE Int. Conf. on Networking, Sensing and Control, pp. 266-269, 2011.

[8] S. Zheying, Z. Yingbao, Xueling Song, and L. Chaoying, " Research on prediction model of optimal coagulant dosage in water purifying plant based on nerual network," *CCCM 2009*, pp. 258-261, 2009.

[9] B. J. Tiew, M. Shuhaimi, and H. Haslenda, "CO2 emissions reduction targeting for existing plant through heat exchanger network retrofit and fuel switching with MINLP," Int. Conf. on Modelling, Simulation and Applied Optimization, pp. 1-7, 2011.

[10] F. M. Soares and R. C. L. Oliveira, "Modelling of temperature in the aluminium smelting process using Neural Networks," IJCNN 2010, pp. 1-7, 2010.

[11] K. Salahshoor and R. Khalil Arjomandi, "Comparative evaluation of control loop performance assessment schemes in an industrial chemical process plant," *CCDC 2010*, pp. 2603-2608. 2010.

[12] H. S. Truong, I. Ismail, and R. Razali, "Fundamental modeling and simulation of a binary continuous distillation column," *ICIAS 2010*, pp. 1-5, 2011.

[13] M. Garcia, M. Kessler, M. C. Buseo, and J. A. Fuentes, "Modeling aluminum smelter plants using sliced inverse regression with a view towards load flexibility," IEEE Trans. on Power Systems, vo. 26, no. 1, pp. 282-293, 2011.

Parallel Texts Alignment Strategies

E. B. Kozerenko
Institute of Informatics Problems of the Russian Academy of Sciences, Moscow, Russia

Abstract - *The paper focuses on the problems of design and development of the linguistically motivated mechanisms for parallel texts alignment and grammatical (functional semantic) matches extraction for design of statistical language portraits to be further incorporated into the hybrid models of machine translation. By hybrid models we mean those employing both statistical and rule-based mechanisms within one framework for natural language processing. Our approach consists in the use of the starting ("seed") grammar to be further enriched by the matches discovered in parallel texts. The seed grammar is used featuring the cognitive and functional characteristics of phrase structures. The grammar formalism employed is the Cognitive Transfer Grammar based on the transfemes (bilingual phrase structures).*

Keywords: Alignment, Syntax, Semantics, Phrase Structure, Hybrid Machine Translation, Parallel Texts

1 Introduction

The problem of parallel texts alignment is considered in this paper in connection with the task of developing linguistically sound mechanisms for the learning components of machine translation and knowledge extraction systems. The present state of research and developments in the field of natural language processing is characterized by the "hybridization" of approaches and models. There can be two ways of bringing the stochastic and symbolic paradigms together: either augment an existing formalism with statistical data, or introduce linguistic expertise, i.e. syntax and semantics into statistical mechanisms. Introduction of statistics into the rule-based systems allows to capture the dynamics and variety of language forms and meanings generated in the process of speech activity, and linguistic knowledge in statistical frameworks serves as the means of their "intellectualization".

The objective of our parallel texts studies is to extract the phrase structures conveying the same meaning in different laguages for enhancing the seed grammar component for the tasks of machine translation and for multilingual knowledge extraction from domain-oriented texts. The seed grammar we use features the cognitive and functional characteristics of phrase structures. The grammar formalism employed is the Cognitive Transfer Grammar (CTG) [1] based on the *transfemes* (bilingual phrase structures). The CTG formalism captures the paradigmatic characteristics of the languages under study, i.e. *language* as a *system*, while the parallel texts we align are the realization of *speech, i.e. language* as *activity*. This activity is characterized by syntagmatics and dynamics. Considering the syntagmatic features of the parallel texts under study we focus on sentences as the basic unit of study.

For sentence and word alignments we turn to statistical tools. So, the first step is employment of instruments for sentence alignment to obtain the sentence-aligned parallel corpora. The next step is the word-based alignment which conjectures as to what word of a source sentence corresponds to what word of the target sentence. The word-based alignment methods range from simple 1:1 correspondence establishment to more sophisticated methods attempting to capture some structural differencies in the aligned texts. A further step is phrase-based alignment, however the term *phrase* in statistical alignment does not mean a well-formed non-terminal of any grammar formalism, but rather an arbitrary sequence of words. An overview of statistical alignment methods is presented in section 4.

Major problems in parallel texts alignment and consequently in training statistical language processing tools are caused by the existence of transformations in the source and target sentences which result from the action of specific mechanisms of each particular natural language to describe the referential situation. These phenomena are studied and described in translation theory and linguistics as interpretational transformations. Our efforts are directed at discovery of the most typical and relevant transformations in the parallel texts under study and enriching the typology of transformations already represented in the seed CTG formalism. Thus, we have to design and employ such strategies and instruments that provide maximal adequacy for language structures representation and extraction.

In our research and development we make certain difference between the task of machine translation by transfer method which is performed at the level of syntactic structures with functional semantic motivation [1] which we call *transfemes* and the task of multilingual knowledge extraction based on the interlingua representation mechanism of extended semantic networks (ESN). Hence, we employ two types of alignment strategies:1) transfeme-based alignment; 2) concept-based alignment. The former is founded on the notion of *transfeme* and the latter rests on the concept of *entities* and *links* of the ESN knowledge-based approach. These strategies are presented in sections 2 and 3. The related works are discussed in sections 4 and 5. The functional semantic alignment methods supplied with examples and statistics are given in section 6. The paper is concluded by section 7 containing further research directions.

2 Transfeme-based alignment

A *transfeme* is a unit of cognitive transfer establishing the functional semantic correspondence between the structures of the source language and the structures of the target language.

Definition. Transfeme is a unit of cognitive transfer, the translatable meaningful integral structure of mental-lingual plane taken in the unity of its categorial and functional characteristics that establishes semantic correspondence between text and speech segments belonging to different language levels and systems.

For the alignment of parallel texts the *transfemes* are given as the rewrite rules in which the left part is a nonterminal symbol, and in the right part there are aligned pairs of chains of terminal and nonterminal symbols belonging to the source and target languages :

$T \to \langle \rho, \alpha, \sim \rangle$, (1)

where T is a nonterminal symbol, ρ and α are chains of terminal and nonterminal symbols which belong to the Russian and English languages, and $\sim$ is a symbol of correspondence between the nonterminal symbols occuring in ρ and the nonterminal symbols occuring in α. In the course of parallel texts alignment on the basis of the Cognitive Transfer Grammar (CTG) [1] the derivation process begins with a pair of the linked starting symbols S_ρ and S_α, then at each step the linked nonterminal symbols are rewritten pairwise with the use of the two components of a single rule.

The objectives of parallel texts alignment are as follows :

- extract the phrase structures conveying the same meaning in different laguages – *transfemes ;*
- enhance the seed grammar component for the tasks of machine translation and for multilingual knowledge extraction ;
- develop the *typology of matches*, explore the contextual characteristics of *transfemes* and crosslingual matches.

Of primary concern for our research are the interpreters' transformations existing in parallel texts, and the typology of these transformations has been designed comprising the statistics as to the preferences of particular structures (matched configurations of tokens sequences) for each language under study (Russian, English and French). Of special interest for us is the situation of the categorial shift in translating a syntactic pattern. The category of a syntactic pattern, i.e. phrase structure, is determined by the category of the head word of this phrase structure. Thus, when transfer employs conversion, and the category of the head word shifts to another category, the whole structure is assigned the feature of the new category. Thus a Nominal modifier of a Nominal Phrase becomes an Adjective in translation; a Verbal unit acting as a Verbal modifier becomes an Adverbial clause containing the Finite Verbal form, etc.

We observed 34 major types of transformations, the most statistically relevant being verbal – nominal transformations; nonfinite – finite verbal transformations; passivization with various methods of passivization expression in Russian, English and French. We explored the synonymous ways of conveying the same functional semantic meanings, this phenomenon is frequently addressed as paraphrasing.

We consider morphological-syntactic features of the conversed verbs and nouns:

e.g. *read – reading (chitat'- chtenie – Russian)*

In our studies we focus on functional semantic (transfeme) alignment. The results of alignment are employed for developing the linguistic knowledge base to be used in machine translation. The object of our research is the high quality phrasal transformations extraction from bilingual corpora. We also consider monolingual phrasal and sentential synonyms, transformations, including nominalization, passivization, dative shift, and topicalization.

The *dynamic* alignment is realized in *matches* and is based on Semiotic (Categorial) Grammar mechanism [2,3].

The whole alignment process we employ is carried out in two stages : the preliminary alignment and the functional transfer alignment. The preliminary alignment includes sentence alignment, word alignment, sub-trees alignment, structures alignment and and concordances formation. For preliminary alignment the following instrumental systems are employed: sentence alignment - ABBYY aligner [4]; word alignment - Verbalizator (tokenizer), Berkeley aligner [5]; sub-trees alignment - Cognitive Dwarf [6]; structures alignment and concordances formation: Sketch Engine [7].

The functional semantic stage of alignment is based on the notions of *Transfeme* and *Match*, it is also called a Transfeme-based alignment.

Definition. Transfeme is a paradigmatic unit, i.e. relating to *Language*, Match is a syntagmatic unit, i.e. a unit of *Speech* (*Discourse*), thus *transfemes* are realized in *matches*.

The functional semantic alignment consists in

- head-driven structures establishment,
- head words alignment.

The formalism employed for the functional semantic alignment is Cognitive Transfer Grammar (CTG) [1],

$$G_{CT} = \{T_{L_1}, T_{L_2}, N_{L_1}, N_{L_2}, P_{CA}, P_{CT}, S_{L_1}, S_{L_2}, M, D\} \quad (2)$$

where T_{L_1} and T_{L_2} are the sets of terminal symbols of the languages L_1 and L_2, N_{L_1} and N_{L_2} are the sets of non-terminal symbols of the languages L_1 *and* L_2, P_{CA} and P_{CT}, are the sets of the analysis and transfer rules respectively, M is the function of establishing the correlations between the structures of the languages L_1 and L_2, D is the function assigning the probability values to each rule from the sets P_{CA} and P_{CT}.

• Transfeme is a paradigmatic unit, i.e. relating to *Language*, Match is a syntagmatic unit, i.e. a unit of *Speech* (*Discourse*).

A *match* can be broader than a *tranfeme* and often comprises the context. The core unit of the CTG formalism is the *Transfemes Lexicon* which belongs to the set of non-terminal symbols.

3 Concept-based alignment of parallel texts

The *concept-based* alignment of parallel texts is aimed at entities and links alignment in parallel texts for developing multilingual knowledge bases to be further used in analytical intelligent systems for knowledge processing. The instrument employed for this type of alignment is the Semantix processor. The process of concept-based alignment consists in entities alignment, actions (predicates) alignment and links alignment. For entities alignment phrases with nominal heads are matched in parallel texts; for the links alignment genitive and of- phrases are aligned. In the process of actions (predicates) alignment verbal phrases are aligned taking into account finite-nonfinite and verbal-nominal transformations.

The concept-based alignment mechanism is based on the extended semantic networks (ESN) [8] which have the sufficient expressive power for presenting the highly embedded structures of natural language and plays the role of an *interlingua*. The basic structural element of the ESN is the named N-ary predicate, called "fragment". ESN is the development of this type of networks in the direction of the descriptive power increase with the retention of uniformity. The ESN basis is the set of vertices (V), from which the following elementary fragments are comprised: *V0(V1,V2,...,Vk/Vk+1), where V0,V1,V2,...,Vk,Vk+1 V, k > 0.*

This fragment represents a *k*-ary relation. The fragments are assigned their roles. The vertex V0 corresponds to the name of relation, the vertices V1, V2,…, Vk correspond to the objects which are linked by the relation, and the vertex Vk+1 separated by the line (/) from the entire structure corresponds to the vertex of connection. The Vk+1 is called a C-vertex, and all these elements form the extended semantic network (ESN).

The whole set of language objects are given in the form of predicate-argument structures. The uniformity of language presentations is a very important factor, and in the process of analysis of natural language sentences the unification grammar is used. With this approach the words and the constructions, which perform the role of predicates in the sentence, serve as the "support" elements, and the result of the analysis of a sentence is one "extended" predicate, which corresponds to the predicate of a sentence (i.e. to the basic verb in the tensed form or to another basic predicate expression). The government models and transformation features are given in the vocabulary entries of verbs:

e.g. *shoot the ducks from the rifle – strelyat' utok iz ruzh'ia/ strelyat' po utkam iz ruzh'ia*

shooting the ducks from the rifle – strel'ba po utkam iz ruzh'ia / strelyaiuschii po utkam iz ruzh'ia/ strelyaia po utkam iz ruzh'ia / strelyaiuschii po utkam iz ruzh'ia/ strelyaia po utkam iz ruzh'ia /

The transformations result in the shift of the government models. Special attention in our research is given to the cases of nominalization and changes from prepositional government models to those without prepositions: *strelyat' po utkam - shoot the ducks.*

Hence, the concept-based alignment is the process of multilingual knowledge extraction and subject knowledge base population resulting in subject domain expert systems.

4 Statistical approaches to alignment of parallel texts overview

The statistical approaches to parallel texts alignment are aimed at establishing the most probable alignment *A* for the two given parallel texts *S* and *T*:

$$\arg\max_A P(A \mid S,T) = \arg\max_A P(A,S,T) \qquad (3)$$

For estimation of the probability values indicated in this expression the most frequently used methods present the parallel texts in the form of aligned sentence sequences $(B_{1,\dots,}B_K)$. The probability of each sequence is independent from the probabilities of other sequences, and it depends on the sentences in the given sequence only [9]. Then

$$P(A,S,T) \approx \prod_{k=1}^{K} P(B_k) \qquad (4)$$

This method takes into account the length of sentences in the source language and in the target language measured in symbols. The longer sentence in one languages will correspond to the longer sentence in the other language. This approach gives stable results for similar languages and literal translation. The more finely tuned mechanisms of matching are provided by the methods of lexical alignment. Thus in [10] the method of alignment by means of creating the model for consecutive word-by-word translation is presented. The best alignment result will be the one which maximizes the probability of a corpus generation with the given translation model. For the alignment of the two texts *S* and *T* they should be split into the sequences of sentence chains. A chain contains zero or more sentences in each of the two languages, and the sequence of chains covers the whole corpus

$$B_k = (S_{a_k},\dots,S_{b_k};t_{c_k},\dots,t_{d_k}) \qquad (5)$$

Then the most probable alignment $A = B_1,\dots,B_{m_A}$ of the given corpus is determined by the following expression, and the chains of sentences do not depend on each other:

$$\arg\max_A P(S,T,A) = \arg\max_A P(L)\prod_{k=1}^{m_A} P(B_k), \quad (6)$$

where $P(L)$ denotes the probability of the L chains being generated. The translation model employed in this approach is extremely simplified and does not take into account the factor of the word order in a sentence and the possibility of the fact that a word in the source text can correspond to more than one word in the text of translation. In this model the word chains are used, and they are limited to the 1:1, 0:1 и 1:0 matches. The translation model based on the word-by-word alignment (we employ this model for the Russian and English parallel texts) will be as follows:

$$P(r \mid e) = \frac{1}{Z}\sum_{a_1=0}^{l}\ldots\sum_{a_m=0}^{l}\prod_{j=1}^{m} P(r_j \mid e_{a_j}), \quad (7)$$

where e is a sentence in English; l is the length of e expressed in words; r is a sentence in Russian; m is the length of r; r_j is the j-th word in r; a_j is the position in e, with which the r_j is aligned; $P(w_r \mid w_e)$ is the probability of translation, i.e. the probability of the w_r appearing in the Russian sentence if the corresponding w_e occurs in the English sentence, and Z is the normalization constant.

For a particular alignment m probabilities of translations are multiplied, and the individual translations are independent one from another.

However, there are certain structural differencies between these languages, and in translation there can be considerable transformations. If the languages under consideration are structurally different, the methods are used oriented at the introduction of grammar knowledge, for example, the alignment methods based on the words that belong to particular parts of speech [11] are employed. In this case the auxiliary words are not taken into account. For the employment of these methods the part of speech tagging of the parallel texts should be performed. It is necessary to take into account various transpositions of words, omissions, insertions, and the alignments between different language levels: when a word in the source text corresponds to a phrase in the target text, and the opposite situation. The most general definition of the word-based alignment is given in [12]. Suppose the two word chains are given, one in the source text (for example, in Russian – r) $r_1^J = r_1,\ldots,r_j,\ldots,r_J$, and the other one is in the target language (English – e) $e_1^I = e_1,\ldots,e_i,\ldots,e_I$, and for these chains it is necessary to establish the alignment. The alignment between the two chains of words is a subset of a Cartesian product of the positions of words, i.e. the alignment A is defined as follows:

$$A \subseteq \{(j,i): j = 1,\ldots,J; i = 1,\ldots,I\}. \quad (8)$$

In machine translation based on statistical methods an attempt is made to construct a model of the translation probability $P(r_1^J \mid e_1^I)$, which describes the correlation between some chain r_1^J in the source language and the chain e_1^I in the target language. In statistical texts alignment model $P(r_1^J, a_1^J \mid e_1^I)$ a "hidden" alignment a_1^J is introduced which describes the mapping from the source position j into the target position a_j. The correlation between the translation model and the alignment model is given in the following way:

$$P(r_1^J \mid e_1^I) = \sum_{a_1^J} P(r_1^J, a_1^J \mid e_1^I). \quad (9)$$

The alignment a_1^J can contain the alignments $a_j = 0$ with the empty word e_0 for the words of the source language which had not been aligned with any word in the source language. On the whole the statistical model depends on the set of unknown parameters θ which are extracted from the training data set in the course of learning. The following presentation is used to express the dependence of the model on the set of parameters:

$$P(r_1^J, a_1^J \mid e_1^I) = p_\theta(r_1^J, a_1^J \mid e_1^I) \quad (10)$$

For detection of the unknown parameters θ a training corpus of parallel texts is given containing S sentence pairs $(\mathrm{r}_s, \mathrm{e}_s): s = 1,\ldots,S$. For each pair (r s (the alignment variable is designated by $a = a_1^J$. The unknown parameters are established by means of maximization of the parallel texts similarity in the corpus:

$$\theta = \arg\max_\theta \prod_{s=1}^{S}\sum_{\mathrm{a}} p_\theta(\mathrm{r}_s, \mathrm{a} \mid \mathrm{e}_s). \quad (11)$$

As a rule the maximization for such models is performed on the basis of the expectation maximization algorithm [13] or the similar ones. Such algorithm is useful for the solution of the parameters estimation problem, but it is not indispensable for the statistical approach. Hence despite the fact that there exist a large number of alignments for a given pair of sentences, it is always possible to find the best alignment:

$$a_1^J = \arg\max_{a_1^J} p_\theta(r_1^J, a_1^J \mid e_1^I). \quad (12)$$

The alignment a_1^J is also called the Viterbi alignment for the pair of sentences (r_1^J, e_1^I). The estimation of the Viterbi alignment quality is performed by means of comparison with some reference alignment carried out manually. The parameters of statistical alignment models are optimized with the consideration of the maximal likelihood criterion which does not always reflect the quality of alignment.

5 Related work

The problem of paraphrasing is very topical and it is considered in the works of the leading computational linguistics research teams [14,15,16,17,18,19]. The paraphrase model described in the work [17] was trained using the Europarl corpus. The authors used ten parallel corpora between English and (each of) Danish, Dutch, Finnish, French, German, Greek, Italian, Portuguese, Spanish, and Swedish, with approximately 30 million words per language for a total of 315 million English words. Automatic word alignments were created for these using Giza++ [19]. The English side of each parallel corpus was parsed using the Bikel parser [20]. A total of 1.6 million unique sentences were parsed. A trigram language model was trained on these English sentences using the SRI language modeling toolkit [21]. The toolkit supports creation and evaluation of a variety of language model types based on N-gram statistics, as well as several related tasks, such as statistical tagging and manipulation of N-best lists and word lattices.

Paraphrase extraction using bilingual parallel corpora was proposed by Bannard and Callison-Burch [22] who induced paraphrases using techniques from phrase-based statistical machine translation [23]. Furthermore, by introducing *complex syntactic labels* instead of solely relying on non-terminal symbols in the parse trees, the authors were able to keep the broad coverage of the baseline method. Syntactic constraints significantly improve the quality of this paraphrasing method. The paper [24] presents a novel approach to paraphrasing with bilingual parallel corpora, the author demonstrates that a significantly higher performance can be achieved by constraining paraphrases to have the same syntactic type as the original phrase. The paper proposed constraints on paraphrases at two stages: when deriving them from parsed parallel corpora and when substituting them into parsed test sentences, the author introduced syntactic constraints by labeling all phrases and paraphrases (even non-constituent phrases) with CCG-inspired slash categories. The author did not formally define a synchronous grammar, nor discuss decoding, since his presentation did not include hierarchical rules. Synchronous grammar rules for translation are extracted from sentence pairs in a bixtext which have been automatically parsed and word-aligned. Extraction methods vary on whether they extract only minimal rules for phrases dominated by nodes in the parse tree, or more complex rules that include non-constituent phrases [25].

A key motivation for the use of syntactic paraphrases over their phrasal counterparts is their potential to capture meaning-preserving linguistic transformations in a more general fashion. A syntactic paraphrasing system intuitively should be able to learn well-formed and generic patterns that can be easily applied to unseen data.

6 Transformations in parallel texts alignment

For developing the *typology of transformations* we consider the following Simultaneous Interpretation Techniques (SIT):

1) Full translation of lexical grammatical forms (LGF) *completely correspond to each other both in the source and the target languages as to their form, function and meaning*

(2) Null translation (LGF is used differently)

(3) Partial translation (several content functions)

(4) Functional substitution (functional identity of different LGF)

(5) Assimilation (LGF combinability features differ)

(6) Conversion (substituting a form of one category by a form of another category)

(7) Antonyms employment (is used for eliminating a conflict between lexical and grammatical combinability of LFG)

The transformations in focus are singled out on the basis of their counts in parallel texts, these are:

Nominalization (35% in the English-Russian language pair);

Passivization (18-24% in the Russian-English direction);

Adjectival – Adverbial structures (12-14% in both directions;

Subject – Object transformations (28% in both directions).

Consider some examples:

Indirect Object → Subject

Ser'oznymi raznoglasiyami byla otmechena vstrecha storon – Serious disagreements arose during the meeting of the sides

Direct Object → Subject

Novuiu planetu nazvali v tchest' ieio otkryvatelia – The new planet was named after its discoverer.

Prepositional phrase → Subject

Na vstreche dogovorilis' – The meeting reached the conclusion.

Regular semantic shifts are as follows:

Substituting a predicate of action by the predicate of state.

He is a member of the college team. (A predicate of state).

On igraet v studencheskoi komande. (He plays in the students' team. A predicate of action).

Functional motivation of phrase structures is represented in the set of non-terminals with their counts in a text, e.g.:

("Objective infinitive", 400.0)

("Objective be-infinitive", 600.0)

("Subjective infinitive with participlePast",600.0)

("Subjective infinitive with adjective", 600.0)

("Subjective participle", 600.0)

We employ match typing and statistical portraits of transformations. The Russian language is about 35% more "nominative" than English:

In vacuum molecules have large space in which to move (V)

V vakuume molekuly imeiut bol'shoe prostranstvo dlia dvizhenia. (Rus.-translit)

dlia dvizhenia - for movement

in which to move (V) → *dlia dvizhenia* (N)

The most productive types of verbal-nominal transformations correlate with the following functional values

- Adverbial modifier of purpose and of consequence, expressed by infinitive (58%),
- Composite predicate with the infinitive (be + infinitive) (51%).

This statistics is taken into account in the multivariant cognitive transfer rules. The matches, or *events* comprise well-formed nonterminals and dynamic syntactic contexts represented in categorial grammar (SUG) notation [2,3]. For disambiguation procedures Vector spaces of events are employed. The main technique of phrase matching is heads alignment which is carried out at present semiautomatically, and the fully automated procedure is under development:

phrase head elements are aligned and structures are compared). It is important to emphasize that *Transfeme* is a paradigmatic unit, i.e. relating to *Language*, *Match* is a syntagmatic unit, i.e. a unit of *Speech* (*Discourse*). Transfeme is realized in Matches.

We distinguish two types of Matches: the direct matches without transformation M^d and the matches employing transformations M^t. M^d display direct correspondence of categorial features of head elements of the matched structures (S_s and S_o), i.e. a noun in the source text will correspond to the noun in the objective text, and the phrase structures will be similar, e.g. a NP in the source text will correspond to the NP in the objective text.

M^t will employ transformations, e.g. a noun in the source text will correspond to a verbal element in the objective text, and the phrase structures will differ,

e.g. NP → VP

Match strategies are employed taking into account the possible transformations $M^t_{s\to o}$, where *M* is *Match*, *t* is *transformation*, *s* is a *source* language, *o* is an *objective* language; $S^{CT}_M = \sum M^t_{s\to o}$ forms the space of cognitive transfer matches (S^{CT}_M).

The goal of semantic alignment is the establishment of matches (rules) for training data collections of the machine learning components for the machine translation systems based on statistical and symbolic approaches.

Examples of the English – Russian texts alignment:

The second step of the above described process is conducted in the presence of a metal catalyst.

NP (Subj) PP VP (Passive) PP (English).

Vtoruju (Adj, F, Sg, Acc) stadiju (N, F, Sg, Acc) vysheopisannogo (N, F, Sg, Acc) sposoba (N, M, Sg, Gen) provodiat (V, Pl, 3-d Person, Pres) v (P) prisutstvii (N, Neutr, Sg, Prep) metallicheskogo (Adj, M, Sg, Gen) katalizatora(N, M, Sg, Gen) .

NP(Accusative) NP(Gen) VP (Person Undefined – Plural) PP (Russian).

The transformation will be as follows :

NP (Subj) PP VP (Passive) PP →

NP(Accusative) NP(Gen) VP (Person Undefined – Plural) PP

134 types of matches were established classified into Cognitive Transfer Spaces (CTS)	
Primary Predication	Orientation
Secondary Predication	Partition
Nomination and Relativity	Determination
Modality and Mood	Existentiality
Connectivity	Negation
Attributiveness	Reflexivity
Metrics and Parameters	Emphasis
	Dispersion

Machine learning methods [26,27] provide the system ability to extract meanings that are expected to be heared or read in a given context. Therefore, it is natural to apply statistical data extracted from large amounts of existing textual information and use it to calculate the probability of a certain meaning in a specific context.

The success of a probabilistic model depends, among other things, on an adequate definition of *event.* A common type of event in probabilistic NLP is the occurrence of one or more words in a specific context. Here *word* usually means not a word-form (i.e. a character string as it appears in a text) but rather a stem or *lemma*. The context is in turn defined as an ordered set of adjacent words on both sides of each word occurrence and the length of such context window is usually set to an arbitrary integer value. While equating a stem with a lexical unit *(lexeme)* may be a reasonable if not ideal way of representing meanings, the definition of context commonly used in statistical NLP is a clear oversimplification, which obscures important linguistic relationships. It is indeed reasonable to assume that the probability of a word having a specific sense depends on other words located in its proximity. However, this "bag of words" approach hides underlying complexities that require more precise discovery procedures.

7 Conclusions

In this paper the English-Russian language pair is considered, however our experiments show that major conclusions hold for Byelorussian and Ukrainian languages that are closely related to Russian, as the syntactical transformation processes are similar in these languages. Introduction of statistics into the rule-based systems allows to capture the dynamics and variety of language forms and meanings generated in the process of speech activity.

Functional and cognitive motivation of the seed grammar rules increases the precision of matches by 23% - 42% depending on the text type (the evaluation of human experts). Further developments will comprise the French and German languages and will focus on the texts of scientific and economic domains

Acknowledgements

The work presented in the paper is supported by the Russian Foundation for Basic Research, grant 11-06-00476-a.

References

[1] Kozerenko, E.B. Cognitive Approach to Language Structure Segmentation for Machine Translation Algorithms // Proceedings of the International Conference on Machine Learning, Models, Technologies and Applications, June, 23-26, 2003, Las Vegas, USA.// CSREA Press, pp. 49-55, 2003.

[2] Shaumyan, S. Categorial Grammar and Semiotic Universal Grammar. In Proceedings of The International Conference on Artificial Intelligence, IC-AI'03, Las Vegas, Nevada, CSREA Press, 2003.

[3] Kozerenko, E.B., Shaumyan, S. Discourse Projections of Semiotic Universal Grammar // Proceedings of the International Conference on Machine Learning, Models, Technologies and Applications, June, 27-30, 2005, Las Vegas, USA.// CSREA Press, pp. 3-9, 2005.

[4] The web site for ABBYY Aligner: http://aligner.abbyyonline.com/ru

[5] The web site for Berkeley Aligner: http://snap.cs.berkeley.edu/

[6] The description of Cognitive Dwarf: http://www.isa.ru/proceedings/images/documents/2008-38/91-109.pdf

[7] The web site for Sketch Engine: http://www.sketchengine.co.uk/

[8] Kuznetsov, I.P., Kozerenko, E.B., Matskevich, A.G. Intelligent extraction of knowledge structures from natural language texts // Proceedings - 2011 IEEE/WIC/ACM International Joint Conferences on Web Intelligence and Intelligent Agent Technology - Workshops, WI-IAT 2011, P. 269-272.

[9] Gale W. A., Church K. W. A program for aligning sentences in bilingual corpora // Computational Linguistics, 1993. Vol. 19. P. 75–102.

[10] Chen S. F. Aligning sentences in bilingual corpora using lexical information // Proceedings of the 31st Annual Conference of the Association for Computational Linguistics, 1993. P. 9–16.

[11] Masahiko H., Yamazaki T. High-performance bilingual text alignment using statistical and dictionary information // ACL 34, 1996. P. 131–138.

[12] Och F. J., Ney H. A comparison of alignment models for statistical machine translation // COLING'00: The 18th International Conference on Computational Linguistics. Saarbrucken, Germany, 2000. P. 1086–1090.

[13] Dempster A. P., Laird N. M., Rubin D. B. Maximum likelihood from incomplete data via the EM algorithm // Journal of the Royal Statistical Society. Ser. B, 1977. Vol. 39. No. 1. P. 1–22.

[14] Pang B., K. Knight, and D. Marcu.Syntax-based alignment of multiple translations: Extracting paraphrases and generating new sentences // Proceedings of HLT/NAACL 2003.

[15] Galley M., M. Hopkins, K. Knight, and D. Marcu. What's in a translation rule? // Proceedings of HLT/NAACL 2004.

[16] Koehn P. A parallel corpus for statistical machine translation // Proceedings of MT-Summit, Phuket, Thailand. 2005.

[17] Koehn P. Statistical Machine Translation. Cambridge University Press. 2009.

[18] Och F.J. and Ney H. A Systematic Comparison of Various Statistical Alignment Models // *Computational Linguistics*, volume 29, number 1, pp. 19-51 March 2003. 2003.

[19] The web site for GIZA++: http://www.statmt.org/moses/giza/GIZA++.html).

[20] Bikel D. Design of a multi-lingual, parallel processing statistical parsing engine // Proceedings of HLT-2002. 2002.

[21] Stolcke A. SRILM - an extensible language modeling toolkit // Proceedings of the International Conference on Spoken Language Processing, Denver, Colorado, September, 2002. 2002.

[22] Bannard C. and Callison-Burch C. Paraphrasing with bilingual parallel corpora. In Proceedings of ACL. 2005.

[23] Koehn P., Och F.J., and Marcu D. Statistical phrase-based translation. In Proceedings of HLT/NAACL 2003.

[24] Callison-Burch C. Syntactic Constraints on Paraphrases Extracted from Parallel Corpora // Proceedings of EMNLP-2008. 2008.

[25] Ganitkevitch, Ju., Callison-Burch, C., Napoles, C., Van Durme, B. Learning Sentential Paraphrases from Bilingual Parallel Corpora for Text-to-Text Generation Proceedings of the 2011 Conference on Empirical Methods in Natural Language Processing – 2011.

[26] Bogatyrev, K. In defense of symbolic NLP// Proceedings of the International Conference on Machine Learning, Models, Technologies and Applications, MLMTA'06, Las Vegas, Nevada, USA, June 26-29, 2006, P. 63-68.

[27] Malkov, K.V. Tunitsky, D.V. On Extreme Principles of Machine Learning in Anomaly and Vulnerability Assessment // Proceedings of the International Conference on Machine Learning, Models, Technologies and Applications, MLMTA'06, Las Vegas, Nevada, USA, June 26-29, 2006, P. 24-29.

Domain term relevance through *tf-dcf*

Lucelene Lopes
PPGCC - FACIN
PUCRS University
Porto Alegre - Brazil
lucelene.lopes@pucrs.br

Paulo Fernandes
PPGCC - FACIN
PUCRS University
Porto Alegre - Brazil
paulo.fernandes@pucrs.br

Renata Vieira
PPGCC - FACIN
PUCRS University
Porto Alegre - Brazil
renata.vieira@pucrs.br

***Abstract*—This paper proposes a new index for the relevance of terms extracted from domain corpora. We call it term frequency, disjoint corpora frequency (*tf-dcf*), and it is based on the absolute term frequency of each term tempered by its frequency in other (contrasting) corpora. Conceptual differences and mathematical computation of the proposed index are discussed in respect with other similar approaches that also take the frequency in contrasting corpora into account. To illustrate the efficiency of the *tf-dcf* index, this paper evaluates the application of this index and other similar approaches.**

I. Introduction

The automatic extraction of terms from texts is a well mapped task, but the automatic choice of which extracted terms are relevant for a specific domain is a much more defiant task. Finding the most relevant terms for a domain, *i.e.*, the domain concepts, is an important step for knowledge engineering tasks such as ontology learning from texts [1].

Some classical linguistic-based work in this area suggest the use of distributional analysis [2] to associate terms and then, establish which of them are good concept candidates. A different approach, but yet following the same idea of inferring concepts from term association, is made by Chemudugunta *et al.* [3], where the identification of concepts is made through pure statistical measures tempered by previous inserted human information. Titov and Kozhevnikov [4] work also follows this line of research by inferring semantic relations among terms in order to identify different terms representing a same concept in sets of small documents (weather forecasts) with no linguistic annotation.

The work of Bosma and Vossen [5] presents a similar effort to establish term relevance measures considering a multiple corpora resource. This work proposes different relevance measures of terms to each corpus, but, Bosma and Vossen's relevance measure of a term in a given corpus do not affect the relevance of this same term in other corpora. In fact, the methodology proposed in their work access WORDNET [6] in order to validate the term candidates according to their measures, but also to establish relations (hypernym, hyponym, meronym, *etc.*) among them.

In opposition to these efforts, this paper proposes an approach that is not linguistic-based, but it relies only the on statistical information gather from the domain corpus to establish a numerical measure to term relevance in this corpus. Therefore, this paper approach is aligned with works that take into account the term frequency on documents to compute a relevance index to establish how representative a term extracted from a corpus will be for the domain represented by this corpus. Some examples of such statistical-based approaches are the works of Dunning in 1993 [7] which proposes the use of log likelihood ratio, Manning and Schultz in 1999 [8] which proposes a composition of *tf-idf* (term-frequency, inverse document frequency [9] adapted for term relevance in a corpus), and other initiatives based on computing indexes from one specific corpus only.

However, our claim is that those typical indices fail to rule out those terms which are not particularly relevant to a target domain. The basic idea behind approaches like the one in our paper is the assumption that a term relevance to a specific domain can only be established by comparison with corpora from other domains, called contrasting corpora.

One of the first examples of similar previous work like our own was the work of Chung in 2003 [10]. But recently, more sophisticated versions were proposed by Park *et al.* in 2008 [11] with domain specificity index, by Kit and Liu in 2008 with termhood index [12], and by Kim *et al.* in 2009 with term frequency, inverse domain frequency index [13]. These approaches brought some quality to the term extraction, as was verified by the works of Teixeira *et al.* [14], as well as, Rose *et al.* [15].

Similar to our proposal, all these previous works followed the same principle to compute a relevance index that is directly proportional to the term absolute frequency in the corpus and inversely proportional to the term absolute frequency in other corpora. The main difference among these similar previous works [11], [12], [13] and our own is the specific formula to weight the influence of other corpora frequency.

This paper first contribution resides in drawing a panorama of options of indices to express the relevance of extracted term from a domain corpus, focusing on indices that take into account also corpora of other domains (contrasting corpora). Some experiments illustrate the benefits of approaches using contrasting corpora over traditional indices.

Secondly, and most important, this paper contributes with the proposal of a new relevance index, called *tf-dcf*, that is, according to our experiments, superior to the other indexes based on contrasting corpora. This contribution is enhanced by the analysis of the *tf-dcf* behavior against different options of contrasting corpora.

It is not the goal of this paper to analyze techniques to improve the quality of term extraction itself, since we assume that a previously performed extraction provides a set of extracted terms. It is also out of the scope of this paper to analyze how many terms should be considered concepts of a domain. Our purpose is to present arguments and experiments showing that the proposed index is effective to rank extracted terms according to their relevance for the domain, thus allowing to identify domain concept candidates.

This paper is organized as follows: Section II describes the existent statistical measures that are compared to our proposed *tf-dcf* index; Section III presents our paper main contribution, which is the proposal of a term relevance index based on the inclusion of a "disjoint corpora frequency" (*dcf*) component; Section IV evaluates the existing and proposed indices. Finally, Conclusion stress the contributions and limitations of this paper, leading to the proposition of future works.

II. Existing measures for relevance estimation

The most elementary way to establish the statistical relevance of terms extracted from a domain specific corpus is to compute the absolute frequency of terms, *i.e.*, how many times each term occurs in the corpus. Obviously, this simple approach is very fragile, since not necessarily a very frequent term is relevant for the domain. This fact is specially noticeable with simple extraction methods, although even sophisticated linguistic-based methods also suffer from using such simple criteria.

For example, pure statistical methods require the adoption of a list of highly frequent grammatical words (*stop list*). Without a stop list, any pure statistical method delivers terms with very low significance such as prepositions and usual expressions. However, it might be very difficult to establish an exhaustive stop list in advance for different domain and genre.

The use of term frequency as relevance measure is a little less harmful for extraction methods taking into account linguistic information. For example, the syntactic annotation of a corpus allows the extraction procedure to avoid terms that are unsuitable for concept names, such as verbs and pronouns. In fact, more sophisticated linguistic analysis, as the identification of noun phrases, may improve significantly the quality of extraction, but even in these cases the use of term frequency do not prevent the incorrect extraction of common expressions which are not domain specific. For example, the quite common expression "*future work*" may be found in several academic texts, but it is hardly considered a defining concept to any scientific domain.

Nevertheless, the starting point of all sophisticated indices is the simple absolute frequency. Assuming, $tf_{t,d}$ as the number of occurrences of term t in document d, and $\mathcal{D}^{(c)}$ the set of all documents belonging to the corpus c referring to a specific domain, the absolute term frequency of a term t in corpus c is expressed by:

$$tf_t^{(c)} = \sum_{\forall d \in \mathcal{D}^{(c)}} tf_{t,d} \tag{1}$$

A. Term frequency and inverse document frequency - tf-idf

An alternative for plain term frequency is to take into account the frequency of the term among documents. The seminal work of Spärck-Jones [9] shows the importance to consider frequent terms, but also non-frequent ones in order to retrieve documents. These ideas lead to the well-known Robertson and Spärck-Jones probabilistic model to term relevance to specific documents [16]. Croft and Harper [17], and later Robertson and Walker [18], proposed formulations to a popular index that takes positively into account the term frequency (*tf*), *i.e.*, the number of occurrences of a given term t in a document d; and also considers negatively the number of documents of the corpus where term t appears at least once, *i.e.*, the inverse document frequency (*idf*).

This index, called *tf-idf* has many formulations, *e.g.*, [19], [20], [8], but in this paper we will consider the formulation adopted by Bell *et al.* [21]. The *tf-idf* index is mathematically defined for each term t to each document d belonging to a corpus c that has at least one occurrence of t as follows:

$$tf\text{-}idf_{t,d} = \underbrace{(1 + \log(tf_{t,d}))}_{tf \text{ part}} \times \underbrace{\log\left(1 + \frac{\mid \mathcal{D}^{(c)} \mid}{\mid \mathcal{D}_t^{(c)} \mid}\right)}_{idf \text{ part}} \tag{2}$$

where $tf_{t,d}$ is the number of occurrences of term t in document d; $\mathcal{D}^{(c)}$ is the set of all document of a given corpus c; and $\mathcal{D}_t^{(c)}$ is the subset of these documents where t appears at least once.

Observing equation (2) it is possible to observe the term frequency (*tf*) and the inverse document frequency (*idf*) parts. The *tf* part considers the logarithmic frequency of the term, since the variation of term occurrences of terms approaches an exponential distribution, *i.e.*, a term t that occurs 10 times is not 10 times more important than a term t' that appears only once. Nevertheless, term t is an order of magnitude more important than term t'. The *idf* part represents a value that varies from $\log(2)$ for a term that appears in all documents, until $\log(1+ \mid \mathcal{D}^{(c)} \mid)$ for a document that appears in only one document.

The idea behind *tf-idf* formulation is that a term t is more relevant as a keyword for a document d if it appears many times in this document and very few times (or ideally none) in other documents. This is an important distinction for information retrieval. The popularity of this index is justified mostly because it prevents frequent terms spread in many documents to be considered more relevant than they should. Indeed, *tf-idf* is an effective measure to identify the defining terms of documents, because it spots terms that are good for document indexation.

The use of *tf-idf* to establish relevance of terms to domain corpora was proposed by Manning and Schütze [8]. According to these authors, a possible index to express the relevance of a term t in a corpus c is expressed by:

$$tf\text{-}idf_t^{(c)} = \sum_{\forall d \in \mathcal{D}_t^{(c)}} tf\text{-}idf_{t,d} \tag{3}$$

B. Term domain specificity - tds

The first initiatives to consider the relevance of terms to a domain corpus taking into account contrastive generic corpus, or corpora, include the works made by Chung in 2003 [10] and Drouin in 2004 [22]. However, at the authors best knowledge, it is the work of Park *et al.* [11], in 2008, one of the first formulations of an index to express term relevance to a specific domain. In that work, such index is called *domain specificity*, and it is expressed as the ratio between the probability of occurrence of a term t in a domain corpus c and the probability of this same term in a generic corpus. Park *et al.* definition of term t domain specificity to a specific domain corpus c, considering a generic domain corpus g was expressed as:

$$tds_t^{(c)} = \frac{p_t^{(c)}}{p_t^{(g)}} = \frac{\frac{tf_t^{(c)}}{N^{(c)}}}{\frac{tf_t^{(g)}}{N^{(g)}}} \tag{4}$$

where $p_t^{(c)}$ express the probability of occurrence of term t in corpus c; and $N^{(c)}$ is the total number of terms in corpus c, *i.e.*, $N^{(c)} = \sum_{\forall t'} tf_{t'}^{(c)}$.

C. Termhood - thd

Following the approach to consider, besides the domain corpus of interest, a contrasting corpus, the work of Kit and Liu in 2008 [12] proposes an index called termhood. This index, as for Park *et al.*'s term domain specificity, follows the idea that a term relevant to a domain is more frequent in the corpus domain than in other corpora. The main difference brought by this work is to consider the term rank in the corpus vocabulary (the set of all terms in the corpus), instead of the term absolute frequency. Kit and Liu definition of term t termhood index for a corpus c, a generic domain corpus g (called background corpus by them) was expressed by:

$$thd_t^{(c)} = \underbrace{\frac{r_t^{(c)}}{\mid V^{(c)} \mid}}_{\text{norm. rank value in } c} - \underbrace{\frac{r_t^{(g)}}{\mid V^{(g)} \mid}}_{\text{norm. rank value in } g} \tag{5}$$

where $V^{(c)}$ is the vocabulary of corpus c, *i.e.*, $\mid V^{(c)} \mid$ is the cardinality of the set of all terms in the corpus c, and $r_t^{(c)}$ is the rank value of term t expressed as $\mid V^{(c)} \mid$ for the more frequent term, $\mid V^{(c)} \mid -1$ for the second most frequent, and so on until the less frequent term as $r_t^{(c)} = 1$.

Observing the termhood index we can see it as the difference between the normalized rank value of the term in the domain corpus c and the generic domain corpus g. Actually, the division of the rank value by the vocabulary size is intended to keep the normalized rank value within the interval $(0, 1]$, with a value equal to 1 to the more frequent term, and the other terms decaying, according to their frequency, asymptotically toward 0.

As a result, the termhood index will be whitin the interval $[1, -1]$, having the more frequent term in c having a value equal to 1, if it does not belong to vocabulary $V^{(g)}$, until a value -1 for the more frequent term in g, if it does not belong to vocabulary $V^{(c)}$.

D. Term frequency, inverse domain frequency - TF-IDF

Recently, Kim *et al.* [13] have proposed in 2009 another index to rank term relevance considering the original idea of the *tf-idf* index, which was to identify whereas a term is suitable to represent a document. In such way, Kim *et al.* did not actually proposed a new index, but instead, they proposed the use of the same *tf-idf* formulation, but considering the set of documents of a corpus as a single document. To avoid confusion, we will refer to this index with the acronym *TF-IDF* in uppercase, to differentiate it from the term frequency, inverse document frequency (*tf-idf*).

The *TF-IDF* index for term t at corpus c, considering a set of corpora $\mathcal{G}$ as proposed by Kim *et al.* is numerically expressed by:

$$TF\text{-}IDF_t^{(c)} = \underbrace{\frac{tf_t^{(c)}}{\sum_{\forall t'} tf_{t'}^{(c)}}}_{TF \text{ part}} \times \underbrace{\log\left(\frac{\mid \mathcal{G} \mid}{\mid \mathcal{G}_t \mid}\right)}_{IDF \text{ part}} \tag{6}$$

where $tf_t^{(c)}$ is the term frequency of term t in corpus c; $\mathcal{G}$ is the set of all domain corpora; and $\mathcal{G}_t$ is the subset of $\mathcal{G}$ where the term t appears at least once.

It is important to notice that the basic formulation of *tf-idf* used as inspiration by Kim *et al.* proposal is not as robust as the one of Bell *et al.* (Eq. 3). For instance, if a term t appears in all corpora, the *IDF* part of Eq. 6 will become 0, and therefore, such term t will have a *TF-IDF* index also equal to 0, *i.e.*, it will be considered less relevant than any other term, regardless its number of occurrences. Another important difference between Equations 3 and 6 is that Bell *et al.*'s (Eq. 3) uses the log of absolute term frequency in the *tf* part, while Kim *et al.*'s (Eq. 6) considers directly a relative term frequency.

III. Proposed Index

The goal of all indices presented in the previous section is to obtain higher numeric values for terms that are relevant to a given domain, or for more recent knowledge engineering tasks [14], [15], terms that are suitable candidates for concepts of an ontology. The raw term absolute frequency (Eq. 1), obviously indicates a relevance, since a term that is very frequent is likely to be important to the domain. Also the *tf-idf* (Eq. 3) index can be an indicative of relevance, since terms that are very distinctive to some documents of the corpus are also likely to be representative of the domain.

The *tds* (Eq. 4), *thd* (Eq. 5) and *TF-IDF* (Eq. 6) indices have better chance to identifying concepts of a domain because they use contrasting corpora. Nevertheless, these indices adopt different approaches that reveals distinct empirical initiatives to tackle the concept identification problem.

The first difference is how these indices take the occurrences of terms in the domain corpus into account. The *tds* (Eq. 4) and *TF-IDF* (Eq. 6) indices compute a relative frequency of the term, since the term probability ($p_t^{(c)}$) for *tds* and the *tf* part for *TF-IDF* are computed as the absolute frequency divided

by the total number of terms in the domain corpus. The *thd* (Eq. 5) index, however, computes a normalized rank value, that, even though being computed according to the absolute frequency, delivers a linear relation[1] among all terms.

The second difference resides in the effect brought by the occurrence of terms in contrasting corpora. The *tds* (Eq. 4) index penalizes the terms that occurs in the contrasting corpora by dividing its probability in the domain corpus by the probability in the contrasting corpora. The *thd* (Eq. 5) index also penalizes the terms that occurs in the contrasting corpora, but in this case it subtracts the normalized rank value in the domain corpus by the normalized rank value in the contrasting corpora. The approach for *TF-IDF* (Eq. 6) index is quite different, since it rewards the terms that are unique to the domain corpus by multiplying the relative frequency by the log of the number of corpora. Such reward decreases as the term appears in other contrasting corpora, until it drops to 0 when the term appears in all corpora. It is important to notice that this reward decreases proportionally to the number of corpora, but it is independent to the number of term occurrences in contrasting corpora.

We propose a new index to estimate the term relevance to a domain following the same idea of contrasting corpora, but we propose differences in the way term occurrences in the domain corpus are taken into account, and most of all, in the effect brought by occurrences in the contrasting corpora. Specifically, we propose a representation to this effect called "disjoint corpora frequency" (*dcf*), which is a mathematical way to penalize terms that appear in contrasting corpora proportionally to its number of occurrences, as well as the number of contrasting corpora in which the term appears.

A. Term frequency, disjoint corpora frequency - tf-dcf

Our proposal, like other contrasting corpora approaches, is based on a primary indication of term relevance and a reward/penalization mechanism. The basis of *tf-dcf* index is to consider the absolute frequency as the primary indication of term relevance. Then, we choose to penalize terms that appear in the contrasting corpora by dividing its absolute frequency in the domain corpus by a geometric composition of its absolute frequency in each of the contrasting corpora. The *tf-dcf* index is mathematically expressed, for term t in corpus c, considering a set of contrasting corpora $\mathcal{G}$, as:

$$\textit{tf-dcf}_t^{(c)} = \frac{\textit{tf}_t^{(c)}}{\prod_{\forall g \in \mathcal{G}} 1 + \log\left(1 + \textit{tf}_t^{(g)}\right)} \tag{7}$$

The choice of absolute frequency as primary indication of term t relevance for corpus c, instead of using a relative frequency (like *tds* and *TF-IDF*) or term rank (like *thd*), aims the simplicity of the measure for two main reasons:

- We do not consider that there is a need for linearization brought by the use of the term rank, as for *thd* index, nor there is a need to make explicit the normalization according to the corpus size, as for *tds* and *TF-IDF*; In fact, any normalization according to the corpus size still remain possible after the *tf-dcf* computation;
- We consider that keeping a relation with the absolute term frequency preserves the index intuitive comprehension, since the *tf-dcf* index numeric value will be smaller (if the term appears in the contrasting corpora) or equal to *tf* (if the term does not appear in the contrasting corpora).

The geometric composition of absolute frequencies in the contrasting corpora chosen to express the penalization, *i.e.*, the divisor in Eq. 7, tries to encompass the following assumptions:

- The number of occurrences of a term in each of the contrasting corpora is distributed according to a Zipf law [23], and to correctly estimated this importance, a linearization of this number of occurrences must be made;
- A term that appears only in the domain corpora should not be penalized at all, *i.e.*, terms that do not occur in the contrasting corpora must have the divisor equal to 1; and
- A term that appears in many corpora is more likely to be irrelevant to the domain corpus, than those terms that appears in fewer corpora.

Because of the first assumption, we choose to consider a log function to compute the absolute frequency in each contrasting corpora ($\textit{tf}_t^{(g)}$). This decision follows the same principle adopted in the original proposition of *tf-idf* measure proposed by Robertson and Spärck-Jones [16].

The second assumption made us adapt this log function with the addition of value 1 inside and outside the log function in order to deliver a value equal to 1 when the number of occurrences of a term in a contrasting corpora is equal to 0. This decision follows the same principle adopted to the Bell *et al.* [21] to express their formulation of *tf-idf* measure.

Finally, the third assumption led us to employ the product of the log of occurrences in each contrasting corpora. The product represents that the importance of occurrences grows geometrically as it appears in other corpora. In fact, according to our formulation a term is more likely to be irrelevant for a domain corpus when it appears few times in many multiple contrasting corpora, than if it appears many times in just few contrasting corpora. Additionally, the product is compatible with the idea to have a divisor equal to 1 when a term appears only in the domain corpus.

IV. Practical Results

The practical application of the proposed index is meant to illustrate its effectiveness and some basic characteristics of *tf-dcf* according to the contrasting corpora used. The experiments were conducted over Brazilian Portuguese corpora, using a linguistic-based term extraction tool to provide terms and their number of occurrences. Nevertheless, corpora in any language submitted to any kind of extraction could be employed without any loss of generality.

[1]It is important to recall, that the distribution of absolute frequency values is likely to follow a Zipf law [23], *i.e.*, the most frequent term is likely to have twice the number of occurrences as the second, three times the number of occurrences of the third, and so on.

A. The chosen corpora

The chosen test bed was one corpus from Pediatrics domain [24] with 281 documents from The Brazilian Journal on Pediatrics. This corpus (PED) was chosen because of the availability of reference lists of relevant terms.

Four other scientific corpora were used as support for definition of specific Pediatrics terms. These corpora have approximatively 1 million words each and their domains are: Stochastic modeling (SM), Data mining (DM), Parallel processing (PP) and Geology (GEO) [25]. Tab. I summarizes the information about these corpora.

Table I
CORPORA CHARACTERISTICS.

		documents	sentences	words
Pediatrics	PED	281	27,724	835,412
Stochastic Modeling	SM	88	44,222	1,173,401
Data Mining	DM	53	42,932	1,127,816
Parallel Processing	PP	62	40,928	1,086,771
Geology	GEO	234	69,461	2,010,527

B. Extraction tools

The extraction procedure of terms and their frequencies was made by a two step process. First the documents were annotated by the Portuguese parser PALAVRAS [26]. Then the PALAVRAS output, *i.e.*, a set of TigerXML files, was submitted to ExATOlp term extractor [27].

PALAVRAS and ExATOlp joint application delivers high quality term lists, since the extracted terms are noun phrases found in the corpus and their frequencies. The extracted noun phrases were filtered according to ExATOlp heuristic rules aiming the output of noun phrases as meaningful as possible. These heuristics goes from simple exclusion of articles, but also quite ingenious ones like detection of implicit noun phrases[2] [28].

C. Extracted terms and reference lists

The extracted terms were divided in two lists, bigrams and trigrams. Single terms and those with more than three words were not considered in the evaluation, since they were not included in the hand-made reference list constructed by terminology laboratory TEXTECC (http://www6.ufrgs.br/textecc/).

The reference lists were produced by a careful and laborious process that involved terminologists, domain specialists (Pediatricians) and academic students. These lists are available for download at TEXTECC website and they have been used for practical applications including glossary construction, translation aid, and even ontology construction. These reference lists are composed by 1,534 bigrams and 2,660 trigrams and they can also be consulted at http://ontolp.inf.pucrs.br/ontolp/downloads-ontolplista.php.

The full extracted term lists delivered by PALAVRAS and ExATOlp for the Pediatrics corpus were composed by 15,483 distinct bigrams and 18,171 distinct trigrams. To each of these lists the computed indices were:

- *tf* the absolute term frequency (Eq. 1);
- *tf-idf* the term frequency, inverse document frequency (Eq. 3) with the basic formulation from Bell *et al.* [21] aggregated with the sum proposed by Manning and Schütze [8] to be used as an example of index not using contrasting corpora;
- *tds* the term domain specificity (Eq. 4) proposed by Park *et al.* [11];
- *thd* the termhood (Eq. 5) proposed by Kit and Liu [12];
- *TF-IDF* the term frequency, inverse domain frequency (Eq. 6) proposed by Kim *et al.* [13]; and
- *tf-dcf* the term frequency, disjoint corpora frequency (Eq. 7) proposed in the previous section of this paper.

D. The impact of different measures on frequent terms

Observing in detail some terms in the extracted lists it is possible to have a better understanding of the effect of each index, and, therefore, the benefits brought by *tf-dcf* as relevance index. Tab. II presents the top ten frequent terms, *i.e.*, the ten terms with more absolute occurrences in the Pediatrics corpus. In this table it is shown the number of occurrences of the term in each corpora, *i.e.*, Pediatrics (PED), Stochastic modeling (SM), Data mining (DM), Parallel processing (PP) and Geology (GEO). Additionally, the last column (ref. list) indicates wether the term belongs ("IN") or not ("OUT") to the reference list.

Table II
OCCURRENCES FOR FREQUENT TERMS FROM PEDIATRICS CORPUS.

term in Portuguese	(translation)	PED	SM	DM	PP	GEO	ref. list
aleitamento materno	(breast feeding)	306	0	0	0	0	IN
recém nascido	(new born)	299	0	0	0	0	IN
faixa etária	(age slot)	234	0	6	0	0	IN
presente estudo	(current study)	188	4	1	0	67	OUT
leite materno	(mother's milk)	163	0	0	0	0	IN
idade gestacional	(gestacional age)	144	0	0	0	0	IN
ventilação mecânica	(mechanical ventilation)	138	0	0	0	0	IN
via aérea	(airway)	120	0	0	0	0	IN
pressão arterial	(blood pressure)	112	0	0	0	0	IN
sexo masculino	(male sex)	109	7	8	0	0	OUT

The same ten more frequent terms are also shown in Tab. III with the values for the six presented indices, as well as their rank according to each of them. For example, in the third row of Tab. III, the term "faixa etária" ("age slot" in English) belongs to the reference list and it is ranked as the third term in the lists sorted with the term frequency (*tf* - Eq. 1) and with the term frequency, inverse document frequency (*tf-idf* - Eq. 3). In the lists sorted with the other indices this term is ranked as the $13{,}281^{th}$ (for *tds* - Eq. 4), the fourth (for *thd* - Eq. 5), the sixth (for *TF-IDF* - Eq. 6), and the fifteenth (for *tf-dcf* - Eq. 7).

Observing the rank differences between the lists sorted with the term frequency (*tf* - Eq. 1) and the term frequency, inverse document frequency (*tf-idf* - Eq. 3), we noticed an important

[2]Implicit noun phrases are, for example, "sick children" and "healthy children" that can be extracted from the sentence "Sick and healthy children can be treated.".

Table III
ANALYSIS OF FREQUENT TERMS FROM PEDIATRICS CORPUS.

term in Portuguese (translation)	*tf* Eq. 1	*tf-idf* Eq. 3	*tds* Eq. 4	*thd* Eq. 5	*TF-IDF* Eq. 6	*tf-dcf* Eq. 7
aleitamento materno (breast feeding)	306 1^{st}	199.18 1^{st}	1.00 1^{st}	1.00 1^{st}	0.0027 1^{st}	306.00 1^{th}
recém nascido (new born)	299 2^{nd}	184.98 2^{nd}	1.00 1^{st}	0.99 2^{nd}	0.0027 2^{nd}	299.00 2^{nd}
faixa etária (age slot)	234 3^{rd}	169.18 3^{rd}	0.98 $13{,}281^{st}$	0.93 4^{th}	0.0012 6^{th}	61.46 15^{th}
presente estudo (current study)	188 4^{th}	167.78 4^{th}	0.73 $13{,}429^{th}$	0.50 42^{nd}	0.0002 57^{th}	3.99 $1{,}276^{th}$
leite materno (mother's milk)	163 5^{th}	143.23 5^{th}	1.00 1^{st}	0.94 3^{rd}	0.0015 3^{rd}	163.00 3^{rd}
idade gestacional (gestacional age)	144 6^{th}	135.60 7^{th}	1.00 1^{st}	0.93 5^{th}	0.0013 4^{th}	144.00 4^{th}
ventilação mecânica (mechanical ventilation)	138 7^{th}	140.85 6^{th}	1.00 1^{st}	0.91 6^{th}	0.0012 5^{th}	138.00 5^{th}
via aérea (airway)	120 8^{th}	132.72 8^{th}	1.00 1^{st}	0.90 7^{th}	0.0011 7^{th}	120.00 6^{th}
pressão arterial (blood pressure)	112 9^{th}	93.27 19^{th}	1.00 1^{st}	0.88 8^{th}	0.0010 8^{th}	112.00 7^{th}
sexo masculino (male sex)	109 10^{th}	125.70 9^{th}	0.88 $13{,}318^{th}$	0.77 14^{th}	0.0003 35^{th}	6.53 543^{th}

similarity. The only significantly change occurs for the term "pressão arterial" ("blood pressure") that drops from the 9^{th} to the 19^{th} position. However, this change does not correspond to a meaningful downgrade, since this term ("blood pressure") seems to be as relevant to Pediatrics as, for instance, "via aérea" ("airway"). In contrast, the quite generic term "presente estudo" ("current study") is not affected at all by *tf-idf*.

Observing the effect brought by the term domain specificity index (*tds* - Eq. 4), we realize the lack of precision, since it assigns an equally important rank to all terms that are not exclusive to the Pediatrics corpus. Consequently, the terms that appears in other corpora are cast out of any list of relevant terms, since, giving the contrasting corpora (SM, DM, PP and GEO), there is more than 13,000 terms appearing only in the Pediatrics corpus. The terms "faixa etária" ("age slot"), "presente estudo" ("current study") and "sexo masculino" ("male sex") are all ranked beyond the $13{,}000^{th}$ position.

The list sorted with the termhood index (*thd* - Eq. 5) shows the downgrade effect on the three terms appearing in the contrasting corpora (grey rows in Tabs. II and III). However, these terms are not sent very low, since even the term "presente estudo" ("current study"), which is very frequent in the contrasting corpora (72 occurrences), is downgraded only to the 42^{th} position.

The list sorted according to term frequency, inverse domain frequency index (*TF-IDF* - Eq. 6) shows a stronger effect than the termhood (*thd* - Eq. 5), since it is based on the number of contrasting corpora the term appear. In consequence, the term "faixa etária" ("age slot") drops to the sixth position because it appears also in the Data Mining corpus, while the term "presente estudo" ("current study") drops to the 57^{th} position because it appears in all corpora, but Geology.

It is important to call the reader attention that our proposed index (*tf-dcf* - Eq. 7) is the only one that takes into account both the number of occurrences in the contrasting corpora (as termhood and term domain specificity), and the number of corpora in which the term appears (as term frequency, inverse corpus frequency). For that reason, the downgrade effect in the list sorted according to our index is the stronger one. Our index casts out the term "presente estudo" ("current study") to the $1{,}276^{th}$ position, while it downgrades significantly the term "sexo masculino" ("male sex") to the 543^{th} position. In opposition, the term "faixa etária" ("age slot") is mildly downgraded from the third to the fifteenth position.

V. CONCLUSION

This paper presented a novel numerical index to estimate the relevance of extracted terms with respect to a specific domain. The inclusion of disjoint corpora frequency (*dcf*) component successfully improved the precision of extracted lists in comparison with the traditional *tf* and *tf-idf*, but also other indices based on comparison with contrasting corpora, namely term domain specificity [11], termhood [12] and term frequency, inverse domain frequency [13].

The proposed *dcf* approach was described here in composition with the absolute frequency (*tf*) and it has the advantage to keep an analogue semantic of the original absolute frequency index. If a given term does not appear in other corpora, its *tf-dcf* index will be equal to the term frequency, *i.e.*, only terms appearing in other corpora will be numerically downgraded. This is not the case of any of the other pre-existent measures.

Our proposal is the follow up to initial studies based on the comparison with contrasting corpora. Such intuitive idea was initially proposed during the last 10 years [10], [22], [29], [11], [12], [13], [15], but, at the authors best knowledge, our proposal is the first one to pay attention to an correct weighting of the influence of occurrences of terms in contrasting corpora.

Specifically, our *tf-dcf* index formulation consider the product of the log of the number of occurrences in other corpora as reductive factor for the domain corpus absolute term frequency. This choice is justified by the fact that term occurrences are likely to be distributed by a Zipf law [23]. In Park *et al.* [11] this fact was ignored. In Kit and Liu [12] this fact was approached by the rank difference. In Kim *et al.* [13] this fact was approached by term relative frequency and the logarithm in the *IDF* part. Therefore, our formulation seems to be mathematically more robust.

The main limitation of the current study is the lack of thorough experiments with other corpora. We had choose to limit our experiments to the studied corpora because there were no sign of availability of data sets previously employed by other authors. Nevertheless, since the objective of this paper is to propose the *tf-dcf* index, it remains as a natural future work the experimentation of our proposal to a statistically significant set of corpora. Such future work will demand the analysis of the proposed *tf-dcf* index, in comparison with other indices, in terms of numerical measures, as precision, and the gathering of corpora and corresponding lists of references.

Another valid future work is the study of heuristics to choose a good cut-off point to apply in the extracted term lists. With the use of a simple index of relevance, like the absolute term frequency, the cut-off point choice seems simple, since it is enough to define a minimum number of term occurrences. However, with a more sophisticated one, as the *tf-dcf* index proposed here, it is a little less obvious to define a meaningful and effective cut-off point [30].

REFERENCES

[1] P. Cimiano, *Ontology learning and population from text: algorithms, evaluation and applications*. Springer, 2006.

[2] D. Bourigault and G. Lame, "Analyse distributionnelle et structuration de terminologie. application a la construction d'une ontologie documentaire du droit," *Traitement automatique des langues*, vol. 43, no. 1, 2002.

[3] C. Chemudugunta, A. Holloway, P. Smyth, and M. Steyvers, "Modeling documents by combining semantic concepts with unsupervised statistical learning," in *The Semantic Web - ISWC 2008*, ser. Lecture Notes in Computer Science, A. Sheth, S. Staab, M. Dean, M. Paolucci, D. Maynard, T. Finin, and K. Thirunarayan, Eds. Springer Berlin / Heidelberg, 2008, vol. 5318, pp. 229–244.

[4] I. Titov and M. Kozhevnikov, "Bootstrapping semantic analyzers from non-contradictory texts," in *Proceedings of the 48th Annual Meeting of the Association for Computational Linguistics*, ser. ACL '10. Morristown, NJ, USA: Association for Computational Linguistics, 2010, pp. 958–967.

[5] W. Bosma and P. Vossen, "Bootstrapping language neutral term extraction," in *Proceedings of the Seventh conference on International Language Resources and Evaluation (LREC'10)*, N. C. C. Chair), K. Choukri, B. Maegaard, J. Mariani, J. Odijk, S. Piperidis, M. Rosner, and D. Tapias, Eds. Valletta, Malta: European Language Resources Association (ELRA), may 2010.

[6] C. Fellbaum, "Wordnet," in *Theory and Applications of Ontology: Computer Applications*, R. Poli, M. Healy, and A. Kameas, Eds. Springer Netherlands, 2010, pp. 231–243.

[7] T. Dunning, "Accurate methods for the statistics of surprise and coincidence," *Computational Linguistics*, vol. 19, pp. 61–74, March 1993. [Online]. Available: http://dl.acm.org/citation.cfm?id=972450.972454

[8] C. D. Manning and H. Schütze, *Foundations of statistical natural language processing*. MIT Press, 1999.

[9] K. Spärck-Jones, "A statistical interpretation of term specificity and its application in retrieval," *Journal of Documentation*, vol. 28, no. 1, pp. 11–21, 1972. [Online]. Available: http://www.emeraldinsight.com/journals.htm?articleid=1649768&show=abstract

[10] T. Chung, "A corpus comparison approach for terminology extraction," *Terminology*, vol. 9, pp. 221–246, 2003. [Online]. Available: http://www.ingentaconnect.com/content/jbp/term/2003/00000009/00000002/art00004

[11] Y. Park, S. Patwardhan, K. Visweswariah, and S. C. Gates, "An empirical analysis of word error rate and keyword error rate," in *INTERSPEECH*, 2008, pp. 2070–2073.

[12] C. Kit and X. Liu, "Measuring mono-word termhood by rank difference via corpus comparison," *Terminology*, vol. 14, no. 2, pp. 204–229, 2008.

[13] S. N. Kim, T. Baldwin, and M.-Y. Kan, "Extracting domain-specific words - a statistical approach," in *Proceedings of the 2009 Australasian Language Technology Association Workshop*, L. Pizzato and R. Schwitter, Eds. Sydney, Australia: Australasian Language Technology Association, December 2009, pp. 94–98. [Online]. Available: www.alta.asn.au/events/alta2009/proceedings/pdf/ALTA2009_12.pdf

[14] L. Teixeira, G. Lopes, and R. Ribeiro, "Automatic extraction of document topics," in *Technological Innovation for Sustainability*, ser. IFIP Advances in Information and Communication Technology, L. Camarinha-Matos, Ed. Springer Boston, 2011, vol. 349, pp. 101–108. [Online]. Available: http://dx.doi.org/10.1007/978-3-642-19170-1_11

[15] G. Rose, M. Holland, S. Larocca, and R. Winkler, "Semi-automated methods for refining a domain-specific terminology base," U. S. Army Research Laboratory, Adelphi, MD, USA, Tech. Rep. ARL-RP-0311, 2011.

[16] S. Robertson and K. Spärck-Jones, "Relevance weighting of search terms," *Journal of American Society for Information Science*, vol. 27, no. 3, pp. 129–146, 1976.

[17] W. B. Croft and D. J. Harper, "Using probabilistic models of document retrieval without relevance information," *Journal of documentation*, vol. 35, no. 4, pp. 285–295, 1979.

[18] S. E. Robertson and S. Walker, "On relevance weights with little relevance information," *SIGIR Forum*, vol. 31, pp. 16–24, July 1997. [Online]. Available: http://doi.acm.org/10.1145/278459.258529

[19] A. Lavelli, F. Sebastiani, and R. Zanoli, "Distributional term representations: an experimental comparison," in *CIKM*, 2004, pp. 615–624.

[20] A. Maedche and S. Staab, "Learning ontologies for the semantic web," in *SemWeb*, 2001.

[21] T. Bell, I. Witten, and A. Moffat, *Managing Gigabytes: Compressing and Indexing Documents and Images*. San Francisco: Morgan Kaufmann, 1999. [Online]. Available: http://ontology.csse.uwa.edu.au/reference/browse_paper.php?pid=233281449

[22] P. Drouin, "Detection of domain specific terminology using corpora comparison," in *Proceedings of the 4th International Conference on Language Resources and Evaluation (LREC) 2004*, M. T. Lino, M. F. Xavier, F. Ferreira, R. Costa, and R. Silva, Eds., ELRA. Lisbon, Portugal: European Language Resources Association, May 2004, pp. 79–82.

[23] G. K. Zipf, *The Psycho-Biology of Language - An Introduction to Dynamic Philology*. Boston, USA: Houghton-Mifflin Company, 1935.

[24] R. J. Coulthard, "The application of Corpus Methodology to Translation: the JPED parallel corpus and the Pediatrics comparable corpus," Ph.D. dissertation, UFSC, 2005.

[25] L. Lopes and R. Vieira, "Building Domain Specific Corpora in Portuguese Language," Pontifícia Universidade Católica do Rio Grande do Sul (PUCRS), Porto Alegre, Brasil, Tech. Rep. TR 062, Dezembro 2010.

[26] E. Bick, "The parsing system PALAVRAS: automatic grammatical analysis of portuguese in constraint grammar framework," Ph.D. dissertation, Arhus University, 2000.

[27] L. Lopes, P. Fernandes, R. Vieira, and G. Fedrizzi, "ExATO lp – An Automatic Tool for Term Extraction from Portuguese Language Corpora," in *Proceedings of the 4th Language & Technology Conference: Human Language Technologies as a Challenge for Computer Science and Linguistics (LTC '09)*. Faculty of Mathematics and Computer Science of Adam Mickiewicz University, November 2009, pp. 427–431.

[28] L. Lopes and R. Vieira, "Heuristics to improve ontology term extraction," in *PROPOR 2012 – International Conference on Computational Processing of Portuguese Language*, 2012, submitted.

[29] J. Wermter and U. Hahn, "You can't beat frequency (unless you use linguistic knowledge): a qualitative evaluation of association measures for collocation and term extraction," in *Proceedings of the 21st International Conference on Computational Linguistics and the 44th annual meeting of the Association for Computational Linguistics*, ser. ACL-44. Stroudsburg, PA, USA: Association for Computational Linguistics, 2006, pp. 785–792.

[30] L. Lopes, R. Vieira, M. Finatto, and D. Martins, "Extracting compound terms from domain corpora," *Journal of the Brazilian Computer Society*, vol. 16, pp. 247–259, 2010, 10.1007/s13173-010-0020-4. [Online]. Available: http://dx.doi.org/10.1007/s13173-010-0020-4

Temporal Term Frequency Analysis of Technology

Aviv Segev
Department of Knowledge Service Engineering
KAIST
Daejeon, Korea
aviv@kaist.edu

***Abstract* — The paper suggests a method for analyzing cause and effect of technology. The process can be identified as a flowchart of technologies over time. The method analyzes term frequency of technological terms in patents to identify the prior technologies that lead to a new technology and the identified technology outcome. The analysis was performed on 4,354,054 patents from the US Patent Office from 1975 until today.**

I. INTRODUCTION

The problem of identifying new technologies has implementations in the area of stock prediction, technology venture funds, and government research investment planning. The current work presents a method for analyzing technology trends and identifying the cause and effect of a given technology. The method is based on temporal term frequency analysis and identification of similar technologies that present exponential growth. These technologies are compared to the analyzed technology to identify cause and effect according to the prediction ability of each technology based on their coefficient of determination value over a delta time difference from the original technology.

II. RELEATED WORK

Previous work in Information Retrieval (IR) has targeted patent documents. During the NTCIR Workshops [1], [2] a patent retrieval task was organized in which a test collection of patent documents was produced and used to evaluate a number of participating IR systems. In the NTCIR-3 Patent Retrieval Task, participant groups were required to submit a list of relevant patent documents in response to a search topic consisting of a newspaper article and a supplementary description. Search topics were in four languages. All topics were initially written in Japanese and were manually translated into English, Korean, and traditional or simplified Chinese. In NTCIR-4 the search topic files were Japanese patent applications that were rejected by the Japanese Patent Office. The English patent abstracts were human translations of the Japanese patent abstracts. Currently, the NTCIR tasks aim at machine translation of sentences and claims from Japanese to English. Other work analyzed Japanese-English cross-language patent retrieval using Kernel Canonical Correlation Analysis (KCCA), a method of correlating linear relationships between two variables in the kernel defined by feature spaces [3].

The Workshop of Cross-Language Evaluation Forum (CLEF 2009) [4] gave separate topic sets for the language tasks, when the document language of the topics was English, German, and French. CLEF-IP included Prior Art Candidate Search task (PAC) and Classification task (CLS). Participants in the PAC task were asked to return documents in the corpus that could constitute prior art for a given topic patent. Participants in the CLS task were given patent documents that had to be classified using the International Patent Classification codes. In addition, evaluations were performed on chemical datasets in chemical IR in general and chemical patent IR in particular. A chemical IR track in TREC (TREC-CHEM) [5] addressed the challenges in chemical and patent IR.

Previous work analyzes automatic patent retrieval, while this work describes a method that involves a manual decision process assisted by an automatic suggestion of relevant concepts related to patent technology evolution over time.

III. TECHNOLOGY TEMPORAL ANALAYSIS METHOD

The technology temporal analysis method is based on analyzing a large data set of technology-based documents such as patents. The data set is assumed to be organized sequentially by date of issue. The method includes identifying the main terms related to a given, the next step involves extracting the sequential graph describing the frequency of the terms, followed by an elimination of graphs with different behavior, and finally identification of graphs with closest delta distance that represent the cause and effect of the analyzed technology.

A. Extracting Related Terms

The first step identifies all the terms related to the technology being analyzed. A method to extract the relevant terms can include extracting all of the linked terms that appear in the technology term description in Wikipedia. The extracted term list can be filtered and additional terms can be added manually.

B. Extracting All Graphs

The second step involves extracting values that represent term frequency in a large data set of documents that can represent the different technologies. An example of such data sets can be patents or research publications. The term frequency uses simple keyword search in either the subject, abstract, full description of the document, or all of these options. The time slot being analyzed usually involves a year since smaller time slots can entail high incidents seasonal noise. The term frequency has to be weighted since the

extraction searches for an increase in term frequency rather than just elevated values. The weight method analyzed used $max_j\ (tf_j)$ value on all technology term frequencies. Other terms such as $(tf_i - tf_{i-1})/max_j\ (tf_j)$ were also evaluated. An example of the results of term frequency of related terms to *email* technology is presented in Figure 1 (top).

C. Elimination Process

The elimination process includes identifying all the graphs that do not represent exponential growth of a new technology. The following types of regression functions were analyzed to identify the best fitting function for technology growth including linear, quadric, cubic, quadratic, exponential, and mixed. The best matching function based on a predefined set of sample of existing technologies was an exponential regression and the values selected as coefficients were based on the average values of the sample technology functions:

$$y= 0.055558046* 1.160450815^x -0.084088217$$

For all technologies, the coefficient of determination R^2 was calculated as the square of the sample correlation coefficient between the outcomes and their predicted values in the matching function y. If the value of $R^2<0.94$, then the technology was discarded as not representing new technology exponential growth.

D. Graph Distance

Once all of the exponential growth technologies have been identified, the next step includes classifying technologies that are cause, effect, or non-related to the technology being analyzed. The coefficient of determination is used again to identify the distance between the technology being analyzed and all other technologies. A similar process is used based on predefined Δt time difference. The Δt represents the possible prediction time of one technology affected by the other. The last step identifies the number of data samples that appear before and after the analyzed technology. If the majority of the data samples are before, then the current technology is a predictive cause of the current technology (Figure 1 - middle). If the majority of samples are after the technology, then the current technology is a cause of the new technology, or an effect of the analyzed technology (Figure 1 - bottom).

IV. Technology Temporal Analysis Experiences

The analysis was performed on 4,354,054 patents from the US Patent Office from 1975 until today. An example of *email* technology is displayed in Figure 1. The method allows an identification of contributing technologies which led to the fast growth of the *email* technology. In addition, the method enables the elimination of possible irrelevant technologies that existed at the time but did not directly contribute directly to the analyzed technology. Additional work is currently being performed to create an ongoing flow chart of all technologies that presented exponential growth and their contribution to other new technologies.

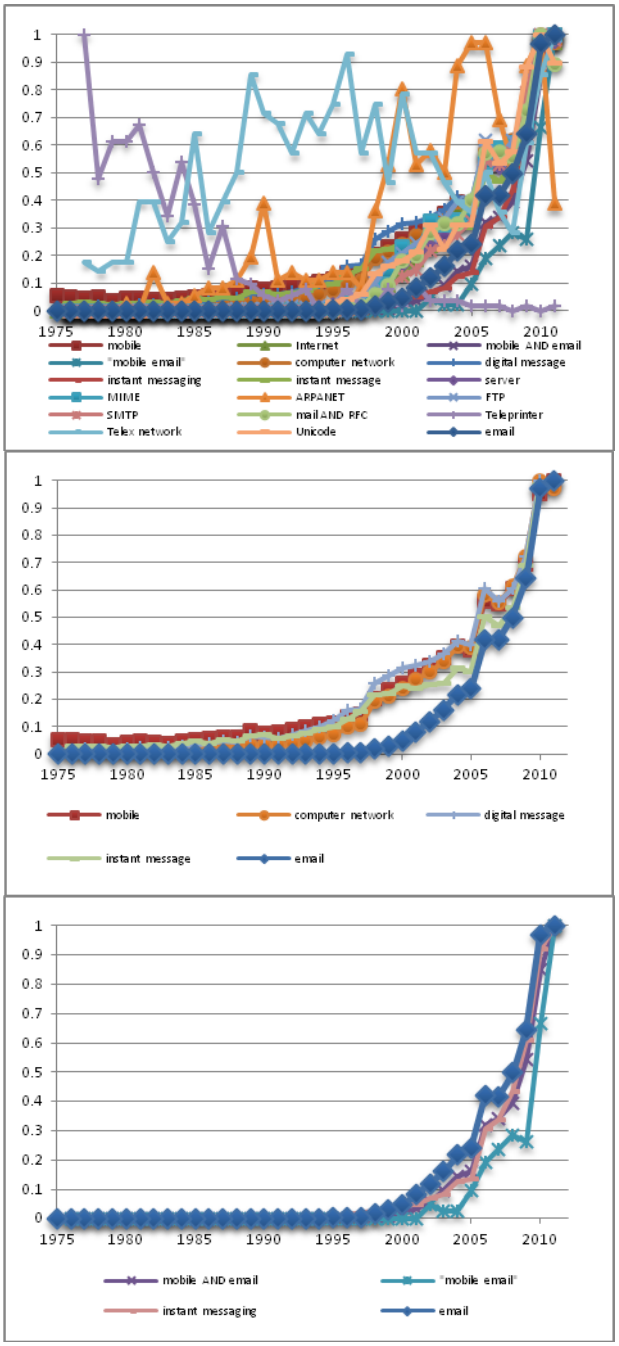

Figure 1. E-Mail Temporal Technologies (Top) Technology Identified Cause (Middle) and Technology Identified Effects (Bottom)

References

[1] M. Iwayama, A. Fujii, N. Kando, Y. Marukawa, Evaluating patent retrieval in the third NTCIR workshop, Information Processing and Management 42 (2006) 207-221.

[2] A. Fujii, M. Iwayama, N. Kando, The patent retrieval task in the fourth NTCIR workshop, in: Proceedings of the SIGIR-04, 2004, pp. 560-561.

[3] Y. Li, J. Shawe-Taylor, Advanced learning algorithms for cross-language patent retrieval and classification, Information Processing and Management, 43 (5), 2007, pp. 1183-1199.

[4] G. Roda, J. Tait, F. Piroi, V. Zenz, CLEF-IP 2009: retrieval experiments in the intellectual property domain, in: Proceedings of the 10th Workshop of the Cross-Language Evaluation Forum (CLEF 2009), 2010, pp. 385-409.

[5] M. Lupu, J. Huang, J. Zhu, J. Tait, TREC-CHEM: large scale chemical information retrieval evaluation at trec, SIGIR Forum 43 (2), 2009, pp. 63-70.

Enhancing Syntactic Models in the Set-Phrase Machine Translation

A. Khoroshilov, E. Kozerenko
Institute of Informatics Problems of the Russian Academy of Sciences, Moscow, Russia

Abstract - *The paper focuses on the issues of introducing syntactic expertise into the example-based machine translation framework largely based on automatically compiled set-phrase dictionaries and translation memory. The functionally motivated syntactic semantic rules are incorporated into the heuristic language processing tools. Machine learning techniques are used for expansion of seed rules and templates.*

Keywords: Machine Translation, Syntax, Semantics, Set-phrase Dictionaries, Machine Learning, Translation Memory

1 Introduction

The paper deals with the problem of enhancing the example-based (set-phrase) machine translation by linguistic expertise representing the syntactic rules of parse and transfer of the whole sentence structures. The main thesis of the set-phrase translation is the statement that the concept names in texts are determined by word combinations rather than single words, the meaning of units of higher level cannot be fully reduced to the sum of meanings of the lower level units comprising them [1-6]. Usual approaches to machine translation concentrate on the study of words and modes of their combinations, being unaware of the two-level structure of languages and its crucial implications both for linguistic theory and for the construction of the models for machine translation. A greater part of the expertise of our system resides outside the lexicon, in a body of knowledge about how meanings and operations on meanings are distributed with reference to the symbolic expressions of language.

The basic method of the set-phrase machine translation is single-step compiling of bilingual frequency dictionaries of words and set-phrase word combinations (Fig. 1).

The systems of machine translation of texts simulate operation of a human translator. Their efficiency depends on how the nature of language operation and mentation are taken into account, and this nature has not yet been adequately studied. Therefore, developers, dealing with the problem of machine translation, must take into account the experience in international communication and translation that has been accumulated by human and machine translators. That experience testifies that in the process of text translation the phraseological word combinations expressing the concepts rather than single words are the basic units of sense. The concepts are the elementary intellectual images, by the use of which it is possible to create more complex intellectual image corresponding to translated text.

In this case, the single words were considered to be basic units of sense expressing the concepts, and the sense of larger speech units (word combinations, phrases and utterance-length units) was supposed to be determined on the base of the sense of words comprising them. In dictionaries the use of word combinations along with single words was also admitted. But these combinations were mainly the idiomatic expressions, and their amount in dictionaries of machine translation systems was negligible in comparison with the amount of single words. Statistical machine translation allows to select the variant for the word combination translation based on matching frequency of the language pair elements.

A weak point of statistical systems is partial or total absence of a mechanism of grammatical rules analysis for the source and target languages. A system which does not analyze the text from the point of view of grammar is unable to release the correct translation of semantically complex texts.

2 Method and implementation of the set phrase machine translation

The starting point of our semantic operators establishment is the phrase structure level. The structures are segmented on the semantic principle of functional transferability, i.e. these structures should be "translatable" which is not always the case if the existing phrase structure grammars are employed. The orientation at the semantic-syntactic and mainly word-by-word translation alone could not lead to the solution of the basic problems of machine translation, because within language and speech the sense of units of higher level, as a rule, cannot be reduced or fully reduced to the sense of the lower level units comprising them. Almost all known systems related to traditional machine translation systems, developed in that direction. Later the developers of traditional systems began to include more terminological word combinations into their dictionaries.

The concept of translation memory (sentence memory) appeared as an alternative to traditional machine translation. That concept can be regarded as an attempt to realize the

idea of Japanese computer scientist Makoto Nagao, that in the process of machine translation it is necessary to use the large corpora of parallel texts, earlier translated by humans [7-10]. A more adequate approach is based on the concept of statistical machine translation (statistics-based machine translation), which is defined by some authors as a "sort of machine translation of texts, based on comparing of large corpora of language pairs". In contrast to traditional machine translation, statistical approach is based on statistical computation of matching probability and does not use the linguistic algorithms. Large corpora of parallel texts are necessary for operation of this system. A statistical mechanism of text analysis is used in the process of translation. This mechanism allows to select the variant for the word combination translation based on matching frequency of the language pair elements. A weak point of statistical systems is partial or total absence of a mechanism of grammatical rules analysis for source and target languages.

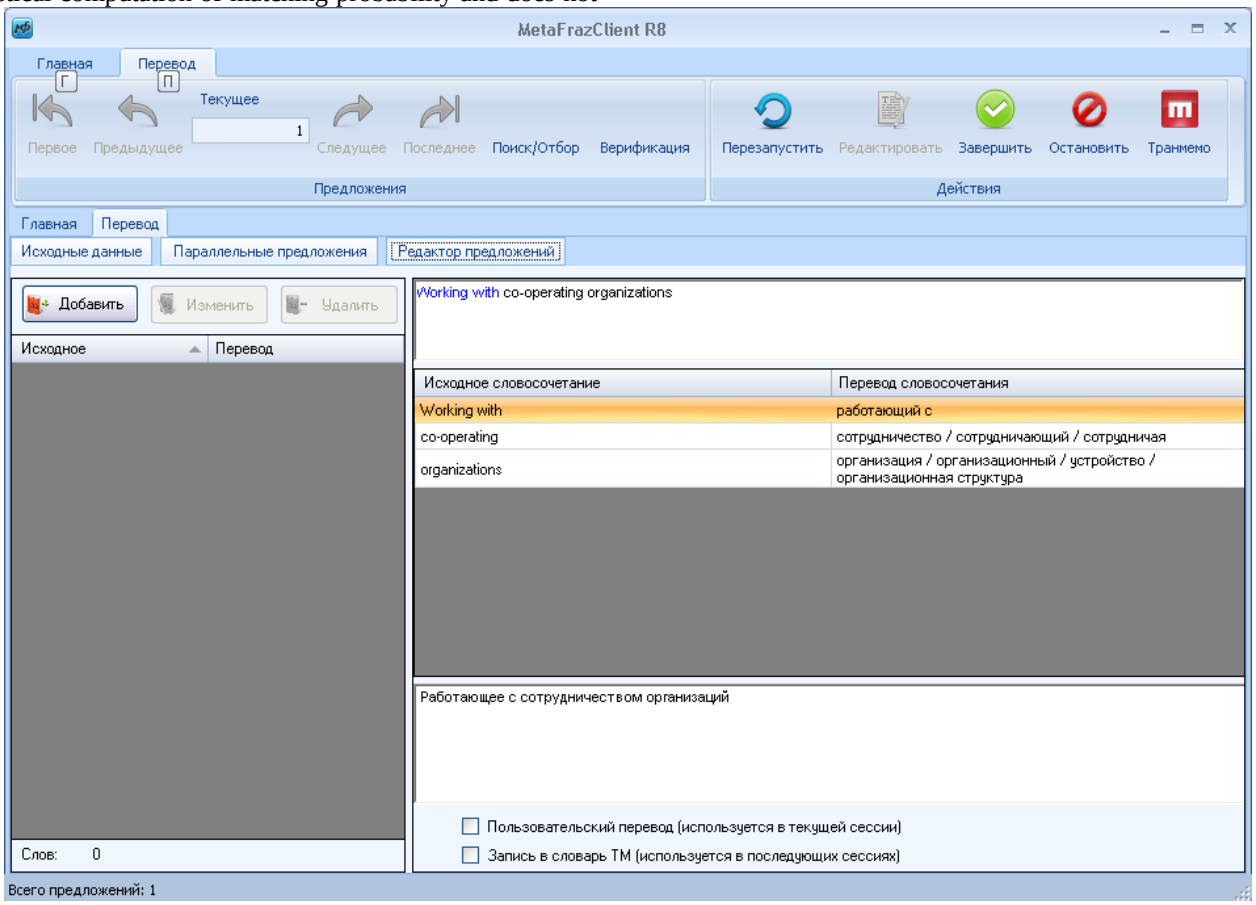

Fig. 1. The MetaPhrase translation system environment: set phrases with translations from parallel texts.

3 Translation memory and example-based translation

A translation memory, or TM, is a database that stores so-called "segments", which can be sentences, paragraphs or sentence-like units (headings, titles or elements in a list) that have previously been translated, in order to aid human translators. The translation memory stores the source text and its corresponding translation in language pairs called “translation units”. The idea to create machine translation systems on the base of previously translated texts presented in the form of "large corpora of language pairs" is not objectionable. It can be realized in different ways. The first way provides text translation with the use of statistic analysis of large corpora of bilingual texts in the process of translation. This way is "statistical machine translation". The second way is connected with a single-step compiling of bilingual frequency dictionaries of words and phraseological word combinations. The creators of the systems of the set-phrase machine translations follow the second way. This way excludes the fatal dependence of the translation process on availability of large volumes of parallel texts and quality of their translation.

The systems of phraseological machine translation are based on the theoretical concept, the main thesis of which is a statement that the concept names in texts are determined by word combinations rather than single words. Therefore, in the process of text translation from one language to another, it is necessary to use the phraseological combinations expressing the concepts, relationships between concepts and the typical situations rather than single words

as basic units of sense. The single words may also be used if the translation with the help of the phraseological word combinations fails.

In compliance with that thesis, the system of phraseological machine translation must comprise the knowledge base of translation equivalents for most frequent phrases, phraseological combinations and single words. In the process of text translation the system should use the translation equivalents stored in its knowledge base in the following order: at first, an attempt to translate the successive sentence of the source text as the integral phraseological unit is made; then, if this attempt fails, words combinations being a part of the sentence should be translated; and, finally, if both above-mentioned attempts fail, word-by-word translation of the text fragments is performed. The fragments of the target text translated with the use of all three approaches, must grammatically agree with one another with the help of procedures of morphological and syntactic synthesis). Let's give consideration to this conception in detail. It is necessary to apply the following principles in the process of development of phraseological machine translation systems:

1. The phraseological units (word combinations and phrases).are basic language and speech units, which should be primarily included in the computerized dictionary.

2. Along with the phraseological units composed of continual word sequences, so called "speech models", phraseological units with slots that may be filled with different words and word combinations, generating meaningful segments of speech, may be used in machine translation systems.

3. Real texts, without regard to their subject area, tend to be polythematic, if they have sufficiently large size. These texts differ from each other not so much by word stock as by probability distribution of occurrence of different words and word combinations from national word stock in them. Therefore, the computerized dictionary designed for translation of the text belonging to a single subject area must be polithematic, not to speak of translation of texts belonging to different subject areas.

4. Systems of phraseological translation need high-volume computerized dictionaries. Such dictionaries should be created on the base of computer-aided processing of parallel texts - bilingual texts, which are translations of each other, and in the process of translation system operation.

5. Along with the main high-volume polithematic dictionary, it is also reasonable to use a set of additional small-volume highly specialized dictionaries in systems of phraseological machine translation. The additional dictionaries should only contain information missing from the main dictionary (for example, data on priority translation equivalents of word combinations and words for different subject areas, if these equivalents are not equal to priority translation equivalents of the main dictionary).

6. The main means for solution of the problem of words polysemy in phraseological translation systems is their use in phraseological word combinations. The additional means is a set of additional specialized dictionaries, where the priority translation equivalent specific for subject area in question is identified for each multiple-meaning word or word combination.

7. The procedures of morphological and syntactic analysis and synthesis of texts that are built on the base of linguistic analogy may play a major role in the systems of phraseological machine translation of texts. These procedures allow us to give up storing large amounts of grammatical information in dictionaries and generate it automatically in the process of translation when the need arises. They make the translation system open - able to process texts with "new" words.

8. Along with text translation in automatic mode, it is reasonable to provide for an interactive mode of operation for the systems of phraseological machine translation. In that mode the user should have potentiality to intervene in the translation process and adapt the additional computerized dictionaries for the subject area of the translated text.

4 Adult learning memory metaphor

Human cognitive systems are likely to be conditioned by principles of efficiency. It is best to concentrate on frequency in search for repeating patterns. There is a clear theoretical justification in associationist psychology for regarding frequency as an important variable in learning. The importance of frequency was recognized in [11, 12, 13].

Actually, our approach takes into account the following principal conclusions:

- human language mechanisms employ a number of complementary techniques, the core being the demand for generalization which is presented in the system of grammar rules;
- the disambiguation process, as well as picking out the particular sense of a given language unit in a given context, is to a great extent similar to the way parallel texts in different languages are aligned, the “statistical mechanisms” incorporated into human brain being at work;
- operation by ready patterns which have been successfully learned at previous stages of a human language activity, and which are stored in the human memory without being subjected to further analysis. This mechanism is simulated in a number of modern machine translation systems, and is known as “translation memory”.

Hence, the computational simulation of language processing mechanisms should employ procedures for all these activities to be more adequate to the complicity of the task. The “adult learning memory” (ALM) means that the system will be supplied with the “adult rule kit” – a starter set of about 300 rules stating the structural semantic correspondences between source and target languages.

The machine translation technique will comprise analysis, transfer and generation across the functional –

categorial values of language units. The core set of language structures designed for the transfer will be upgraded taking into account the cases of categorial shifts and structural polysemy in accordance with the Generalized Nucleus Law [14].

The process of structural patterns recognition will be performed basing on the multiple transfer rule set and the probabilistic functional tree substitution grammar (PFTSG) [15]. New language patterns will be acquired with the employment of machine learning methods.

The rule system design is a sophisticated task, and will employ the following techniques:

"Didactic Expertise" (DE) which includes didactical competence and sufficient language structures coverage: singling out and stating first the most important (highly relevant) rules covering the systems of the source and target languages on the basis of functional similarity.

"Interpreter Expertise" (IE) consists in bridging the gap and establishment of correspondences between the source and target language structures. A very important interpretation technique employing the segmentation of structures will be carried out on the basis of the functional transfer principle. Segmentation and unification of utterances in the course of translation is a major task for human professional interpreters. The selectivity of languages as to the choice of specific characteristics of description of one and the same situation results in numerous distinctions, and one of the most crucial of them is the degree of particularity in conveying a referential situation. Therefore, a situation which in one language is described by means of one specific feature, in another language may require two or more characteristics.

5 Syntactic rules in digital dictionaries

Syntactic rules in the set-phrase machine translation are part of the dictionary enties representing the syntactic information as the sequeces of the categorial tags for the phrasal segments acquired by the system from parallel texts. At first glance, the machine translation concept offered by professor Makoto Nagao in 1984 [7-10] fundamentally differs from the concept, formulated by professor G.G. Belonogov [1-6] nine years earlier. But this is not true. Indeed, in the process of practical realization of Makoto Nagao's concept, it is difficult to imagine that the text written in any language is completely the same as another text written earlier and translated into foreign language. It is not to be expected that this text contains long fragments (chapters, paragraphs and etc.), that are the same as the fragments of the text written and translated earlier but, as our investigations showed, the continuous texts fragments including over ten words repeat on rare occasions - their total frequency doesn't exceed 1%. It is necessary to use only short sentences, single words and text fragments (word combinations) including less than 10-12 words. This is the semantic-syntactic phraseological translation (see Fig. 2).

Of course, along with the translation equivalents of the relatively short fragments of texts, it is possible to include the translation equivalents of longer fragments in the computerized dictionaries. But in this case one should keep in mind, that the computerized dictionaries will be filled with "dead" ballast, i.e. with the dictionary entries, which will be used on rare occasions or will not be used at all in the process of text translation.

When developing the systems of phraseological machine translation, most difficult and time-consuming problem is a problem of compiling sufficiently high-volume computerized dictionaries. The quality of translation depends on the volume of these dictionaries and on the quantity of the phraseological word combinations in them. And those volumes need to be sufficiently large to provide the good covering of texts.

It is known, that in modern languages of the world (for example, in Russian or English) the amount of different words exceeds one million, and the amount of concept names determined by word combinations exceeds hundreds of millions. The authors of this article came to this conclusion on the basis of many years' experience of the statistical study of texts. Confirmation of such viewpoint is the report of All-European terminological centre "Infoterm" (Vienna, Austria, 1998), in which it was found that in modern languages of the world, such as English and German, a total amount of different terms exceeds 50 million, and nomenclature of goods exceeds 100 million. It is well known, that the connected texts consist of not only terms and names of goods.

The computerized dictionaries of such volume cannot be created quickly, but as experience shows, it is possible to achieve satisfactory quality of translation at the first stage in the presence of only several millions of entries in dictionaries, at least 80% of which should be word combinations. In this case the polithematic texts have the coverage of about 99, 7%.

Thereafter, the volume of dictionaries must be constantly increased and with the growth in amount of phraseological combinations, the quality of machine translation should improve. This problem cannot be solved by manual methods. For its solution, a system of computerized compiling and maintenance of the computerized dictionaries was created.

The systems of phraseological machine translation should be orientated at translation of texts on business, science, technologies, politics and economy. Translation of literary texts is a more complex task. But success can be also achieved in this area in future, if modern technological means are used to compile huge phraseological dictionaries for these texts.

6 Well-formed nonterminals and dynamic rules

Conventional machine translation systems use rules as the knowledge. This framework is called Rule-Based Machine Translation (RBMT). The translation mechanism which retrieves similar examples from the database, adapting the examples to the new source text is called Example-Based Machine Translation (EBMT). Enhancment of the set-phrase translation with the syntactic parse and transfer rules consists in the process of grammar formalism design over the set of cognitive transfer structures. In our case a generative unification grammar will be employed incorporating the feature-value structures into the hybrid system of context-free (and partly context-sensitive) productions. The parse and generation will be performed on the basis of these rule systems. We assume a computationally practical approach of feature-valued head-driven phrase structure rules for all the languages included.

The further development of the rules set will be carried out on the basis of Semiotic Universal Grammar (SUG) principles: the ordering of the tree structures and the head features inheritance will be determined by the Nucleus Law (stating that the nucleus of a configuration takes on the function of this configuration on top of its own function of the nucleus of this configuration), and the multiple transfers will be supported by the typing strategy proposed in the SUG approach [14].

The rule systems for functional transfer [15] will comprise about 350 well-formed nonterminals : grammar rules capturing the paradigmatic syntactic structures of the Russian and English languges, and the dynamic rules represented in the SUG categorial grammar formalism will be automatically generated by the system in the course of operation and reflect the dynamic character of the actual speech (discourse).

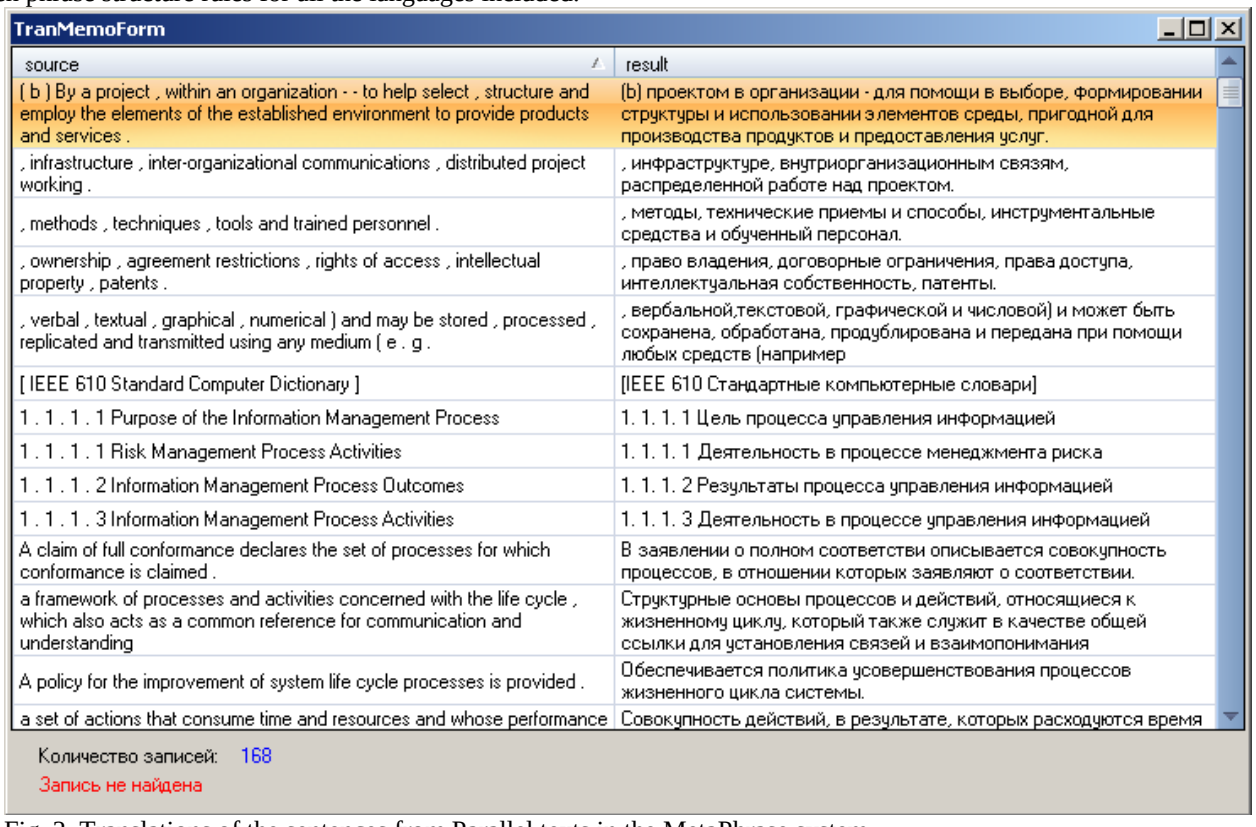

Fig. 2. Translations of the sentences from Parallel texts in the MetaPhrase system.

7 System performance

The implementation of the computerized phraseological text translation from one language into another must have three stages. At first stage, the semantic-syntactic analysis of the source text is carried out. During that analysis the text is split into sentences and then their conceptual and syntactic structure is determined. At the second stage (at the transfer stage) the concept names of the source text are substituted by the concept names in target language and the information on the syntactic structure of the source text is transformed into information required for the target text synthesis. At the final stage (the stage of semantic-syntactic synthesis of the target text) the text in the target language is formed.

The stages listed above are present in the process of translation of texts from any language to any other language, but their specific content for different pairs of languages has

a specific character. This specific character can be seen in procedures of semantic-syntactic analysis and synthesis of texts, which include the procedures of morphological, syntactic and conceptual analysis and synthesis [1-6].

The set-phrase machine translation based on the multilingual dictionaries will operate in the same way, but these systems should be complemented with the procedures of semantic-syntactic and conceptual analysis and synthesis of all languages, which will be included in the system. The authors developed the effective technology based on the use of principles of linguistic analogy for creation of these procedures.

The computerized dictionaries are the most important part of the systems of phraseological machine translation. They should have sufficiently large volume, in order to cover texts, and should contain mainly word combinations. The authors developed the original methods, algorithms and programs for automated compiling and maintaining dictionaries for the system of phraseological machine translation. In cooperation with other specialists, the large-volume Russian-English and English-Russian phraseological computerized dictionaries containing 2, 6 million dictionary entries each were compiled. These dictionaries cover 99, 7% of the lexical content of modern texts and they represent the powerful bilingual conceptual model for a wide range of fields of human activity .

8 Generation of dictionaries

The experience in creation of the large-volume Russian-English and English-Russian computerized dictionaries convinced authors, that Russian and English texts, which are translations to each other (for example, bilingual titles of the documents), can serve as the most reliable source for dictionaries compiling.

The compiling of the computerized dictionaries with the use of bilingual texts was carried out both manually and with the assistance of computers. The manual dictionary making requires huge expenditures of human labour. Therefore the authors of the article developed the procedure for automated dictionary making [3].This procedure is based on the hypothesis, that in numerous bilingual pairs of sentences, which are translations to each other and which contain the same word or word combination of one of the languages, the word or word combination of another language, which is the translation of this word or word combination has maximal occurence frequency.

The procedure was used for processing bilingual (Russian and English) titles of the documents from the databases of VINITI (All-Union Scientific and Technical Information Institute). In this case more than one million pairs of the document titles were processed. The computerized dictionaries of MetaPhrase system can be corrected and completed in the process of text translation in the interactive mode. In that mode there is an opportunity to identify the words and word combinations, which have no translation equivalents in the dictionary or these equivalents do not comply with the context or several equivalents are given, but the first equivalent does not comply with the context. These equivalents can be replaced by the equivalents complying with the textual context.

In compliance with the method described above, the large-scale experiment on compiling English-Russian frequency dictionaries on the base of the automated concept analysis of English and Russian titles of the documents, which are translations to each other, was carried out. For this purpose, the corpus of English titles of the polithematical documents and their Russian translations having the volume of about 2 million pairs of sentences from the VINITI's databases (1994-1999) were processed. The total volume of the corpus of texts is 390 Mb.

In the process of research three English-Russian frequency dictionaries were created:

1. The dictionary, items of which are the combinations of fragments of English and Russian titles of documents, between which the translation equivalents were determined with the assistance of MetaPhrase system;

2. The dictionary, items of which are fragments of titles of documents, between which the translation equivalents were not determined, but they are surrounded by the other fragments, between which such equivalents were determined , or by signs of beginning or end-of-the title;

3. The dictionary, items of which are fragments of English and Russian titles of documents, between which translation equivalents were determined on the initial stage of titles processing.

The first frequency dictionary includes bilingual phraseological word combinations containing 2 to 16 words. It had 3.127.363 dictionary entries.

The value of the dictionary in question is that it contains translation equivalents between English and Russian fragments of titles of documents, which are longer than their fragments selected at the first stage of conceptual analysis of titles. Each of the newly formed dictionary entries practically has just one translation version of English word combination (the percentage of dictionary entries having more than one version of translation is less than 0.1).

The second frequency dictionary includes translation equivalents between fragments of titles of documents that were not found at the initial stage of conceptual analysis of these titles. This dictionary contains 1.825.612 dictionary entries. The most frequent dictionary entries have the frequency of 1.008, and infrequent dictionary entries have the frequency equal to one. 87% of dictionary entries have the frequency equal to one. A spot-check of the dictionary showed that about 50 % of translation equivalents were incorrect. The quantity of such translation equivalents can be reduced at the final stage of dictionary making, if the procedure of semantic-syntactic checking is applied. After that, the dictionary must be edited by humans.

The third frequency dictionary contains translation equivalents between fragments of English and Russian titles

of documents that were found at the initial stage of processing of these titles. It contains 387.025 dictionary entries. The most frequent dictionary entries have the frequency of 4.985, and most infrequent dictionary entries have the frequency equal to one. 56% of dictionary entries had the frequency equal to one.

This dictionary contains only translation equivalents of English concept names, which are found in Russian titles of documents. Therefore, it proved to be tuned to the subject field of translated titles. It allows to consider the compiling procedure of such a dictionary as a means for automated creation of thematically oriented dictionaries.

9 Conclusion

The modern multilingual machine translation systems should be based on set-phrase translation enhanced by functionally motivated grammar. The extensive application of the means for automation allowed the authors to essentially reduce expenditures of human labour in the process of creation of the MetaPhrase system, and therefore, to reduce the creation cost of such systems. The main method for syntactic model enhancement in the set-phrase machine translation is including well-formed non-terminals in the general system of sentence analysis. The non-terminals constitute the complete parse tree of a sentence comprising set-phrase models. The dynamic formation of syntactic structures is supported by alternative categorial grammar parse on the basis of the rules dynamically extracted from parallel corpora.

Further research and development is connected with the expansion and semantic structuring of dictionaries and syntactic transformations introduction. The synergistic approach built on the joint employment of the rule-based and example-based approaches will provide new insights into the language processing theory and practice. This will also be important in developing more efficient educational programs for computer science and computational linguistics courses.

10 References

[1] Belonogov, G. G., Khoroshilov, Alexander A., Khoroshilov, Alexei. A. Phraseological Machine Translation of Texts from Natural Languages to Other Natural Languages. Col:"Scientific-Technical Information", Series 2. - M.: VINITI, 2010, № 10.

[2] Belonogov, G. G., Khoroshilov, Alexander A., Khoroshilov, Alexei A. Automatization of compiling of English-Russian bilingual phraseological dictionary using the corpora of bilingual texts. Col.: “Scientific Technical Information”, Series 2. - M, VINITI, 2010, № 5.

[3] Belonogov, G. G., Gilyarevskij, R. S., Khoroshilov, A.A. On the nature of information. Col.:"Scientific Technical Information”, Series 2. - 2009. - № 1.

[4] Belonogov, G. G., Kalinin, Yu. P., Khoroshilov, Alexander A., Khoroshilov, Alexei A. Systems of Phraseological Machine Translation of Texts. Theoretical Preconditions and Experience in the Development. - M. 2007.

[5] Belonogov, G. G., Kalinin, Yu. P., Khoroshilov, A. A. Computational linguistics and Advanced Information Technologies. Theory and Practice of Constructing of Automatic Text Processing Systems. - M. 2004.

[6] Belonogov, G. G., Bystrov, I. I., Kozachuk, M V., Novoselov, A. P., Khoroshilov A.A. Automated Conceptual Text Analysis. Col. :” Scientific Technical Information”, Series 2. - 2002. № 10.

[7] Nagao, M. A Framework of a Mechanical Translation between Japanese and English byAnalogy Principle. In A. Elithom and R. Banerji (ed.), Artificial and Human Intelligence, North-Holland, P. 173-180. 1984.

[8] Nagao, M. 1988 "Language Engineering: The Real Bottleneck of Natural Language Processing", Proceedings of the 12th International Conference on Computational Linguistics.Nirenburg, S. 1987 Machine Translation, Cambridge University Press, 350.

[9] Sato, S. and Nagao, M. Toward Memory-Based Translation. Proceedings of the 13th International Conference on Computational Linguistics. 1990.

[10] Sumita, E., Iida, H. and Kohyama, H. Translating with Examples: A New Approach to Machine Translation", Proceedings of The Third International Conference on Theoretical and Methodological Issues in Machine Translation of NaturalLanguages, Texas, 203-212. 1990.

[11] Wolff, J. G. Frequency, conceptual structure and pattern recognition. British Journal of Psychology, 67, 377-390, 1976.

[12] Wolff, J. G. Language acquisition and the discovery of phrase structure. Language & Speech, 23, 255-269, 1980.

[13] Wolff, J. G. Cognitive development as optimization. In L. Bolc (Ed.), Computational models of learning. Heidelberg: Springer-Verlag 1987.

[14] Shaumyan, S. Categorial Grammar and Semiotic Universal Grammar. In Proceedings of The International Conference on Artificial Intelligence, IC-AI’03, Las Vegas, Nevada, CSREA Press, 2003.

[15] Kozerenko, E.B. Cognitive Approach to Language Structure Segmentation for Machine Translation Algorithms // Proceedings of the International Conference on Machine Learning, Models, Technologies and Applications, June, 23-26, 2003, Las Vegas, USA.// CSREA Press, pp. 49-55, 2003.